FINAL REPORT

LAX Air Quality and Source Apportionment Study

Volume 2. Phase III Sections 1 through 10

Prepared and Submitted to:

Los Angeles World Airports

Los Angeles World Airports
Environmental Services Division

by:

Tetra Tech, Inc.

June 18, 2013

LAX Air Quality and Source Apportionment Study

Volume 2. Phase III Sections 1 through 10

Prepared and Submitted to:

Los Angeles World Airports

Prepared by:

Tetra Tech, Inc.
Desert Research Institute
KB Environmental Services, Inc.
SCS Tracer Environmental
T&B Systems
Sarav Arunachalam, Ph.D.
Charles Blanchard, Ph.D.
Ron Henry, Ph.D.
Ivar Tombach, Ph.D.

ACRONYMS

AC – automated calibration
AERMOD – American Meteorology Society/Environmental Protection Agency Regulatory Model
ANOMS – Aircraft Noise and Operations Monitoring System
APU – auxiliary power units
AQ site – SCAQMD Hastings site
ASOS – Automated Surface Observation System
ASPM – Aviation System Performance Metrics
ATCT – Air Traffic Control Tower
BAAQMD – Bay Area Air Quality Management District
BAM – beta attenuation monitor
BC – black carbon
Be – beryllium
BOAC –Board of Airport Commissioners
BTEX – benzene, toluene, ethyl benzene, and xylenes
BTS – Bureau of Transportation Statistics
CalTrans – California Department of Transportation
CARB – California Air Resources Board
CBA – Community Benefits Agreement
CDM Smith – Camp, Dresser, and McKee, Smith
CE site – Community East site
CEMs – Continuous Emission Monitors
CHAPIS – Community Health Air Pollution Information System
CMAQ – Community Multiscale Air Quality
CMB – Chemical Mass Balance
CN site – Community North site
CNG – compressed natural gas
CO – carbon monoxide
CO_2 – carbon dioxide
CPC – condensation particle counter
CS site – Community South site
CTA – Central Terminal Area
Cu – copper
DNPH - 2,4-Dinitrophenylhydrazine
DRI – Desert Research Institute
EC – elemental carbon
EDMS – Emissions and Dispersion Monitoring System
EIR – Environmental Impact Report
EIS – Environmental Impact Statement
ESD – Environmental Service Department
FAA – Federal Aviation Administration
FID – flame ionization detector
FIND – Facility Information Detail
FMPS – Fast Mobility Particle Sizer

FOA – First Order Approximation Method
GA – general aviation
GC/MS – gas chromatography/mass spectrometry
GPS – global positioning system
GPU – ground power units
GSE – ground service equipment
HCMS – Harbor Communities Monitoring Study
HPLC – high performance liquid chromatography
Hz – Hertz
IMC – instrument meteorological conditions
INV – invalid
LADOT – Los Angeles Department of Transportation
LADWP – Los Angeles Department of Water and Power
LAWA – Los Angeles World Airports
LAX – Los Angeles International Airport
LAX AQSAS – LAX Air Quality and Source Apportionment Study
LPG – liquefied petroleum gas
LTO – landing/take-off
Man 0/S – manual calibration
MAP – Modeling and Analysis Protocol
MATES II – Multiple Air Toxics Exposure Study II
MMBTU – Million British Thermal Units
Mn – manganese
MP – multi-point calibration
MQAPP – Monitoring and Quality Assurance Project Plan
MRI – Midwest Research Institute
Na – sodium
NA – not available
NCDC – National Climatic Data Center
NDIR – non-dispersive infrared sensor
ng/m^3 – nanograms per cubic meter
Ni – nickel
NMHC – non methane hydrocarbons
NO – nitric oxide
NO_2 – nitrogen dioxide
NO_x – nitrogen oxides
NTA – nonparametric trajectory analysis
NWS – National Weather Service
QA – quality assurance
QC – quality control
OC – organic carbon
OEHHA – Office of Environmental Health Hazard Assessment
PAH – polycyclic aromatic hydrocarbons
PAMS – Photochemical Assessment Monitoring Station
PCA – pre-conditioned air
pDR – personal DataRAM

PeMS – Performance Measurement System
PM_{10} – particulate matter equal to or less than 10 micrometers
$PM_{2.5}$ – particulate matter 2.5 um in diameter
ppb – parts per billion
ppbv – parts per billion by volume
ppm – parts per million
ppt – parts per trillion
PSD – particle size distribution
PST – Pacific Standard Time
R^2 – coefficient of determination
RECLAIM – Regional Clean Air Incentives Market
RH – relative humidity
ROG – reactive organic gases
SCAG – Southern California Association of Governments
SCAQMD – South Coast Air Quality Management District
SCE – source contribution estimates
SFS – sequential filter sampler
SMPS – scanning mobility particle sizer
SO_2 – sulfur dioxide
SO_x – sulfur oxides
SOA – secondary organic aerosols
SoCAB – South Coast Air Basin
SODAR – sonic detecting and ranging
SP – span
SPAS – Specific Plan Amendment Study
SR site – South Runway site
SVHC – semi-volatile hydrocarbons
SVOC – semi-volatile compounds
TC – total $PM_{2.5}$ carbon
TD – thermal denuder
THC – total hydrocarbons
TIGF – Teflon-impregnated glass fiber filters
TLCS – Trinity Lutheran Church School
TOG – total organic gases
TWG – Technical Working Group
$\mu g/m^3$ – micrograms per cubic meter
U – uranium
UFP – ultrafine particulates
UHP – ultra-high purity
UNID – unidentified component in CMB analysis
USC – University of Southern California
U.S. EPA – United States Environmental Protection Agency
USGS – United States Geological Society
UTM – Universal Transverse Mercator
UW – upwind
VMC – visual meteorological conditions

VOC – volatile organic compounds
VTDMA – volatility tandem differential mobility analyzer
WOMS – West Oakland Monitoring Study
χ^2 – chi-square
XRF – x-ray fluorescence
Z – zero

LAX AIR QUALITY AND SOURCE APPORTIONMENT STUDY

Volume 1 – Executive Summary

- Foreword
- Overview
- Introduction
- Scope of the LAX AQSAS
- Meteorological Considerations
- Study Results
- Conclusions

Volume 2 – Phase III Sections 1 through 10

Section 1	Introduction
Section 2	Background
Section 3	Phase III Technical Approach
Section 4	Quality Control/Quality Assurance
Section 5	Phase III Air Monitoring Results - Time Series and Spatial Analysis
Section 6	Chemical Mass Balance
Section 7	Nonparametric Trajectory Analysis
Section 8	Emissions Inventory
Section 9	Source-Based Dispersion Modeling: AERMOD and CMAQ
Section 10	Key Findings and Conclusion of the LAX AQSAS
Appendix A	Responses to Public Feedback

Volume 3 – Phase I and Phase II Technology and Methodology Feasibility Demonstration Project

Final Demonstration Project Report

Module A	Quality Assurance Program Plan
Module B	Source Apportionment Protocol
Module C	Literature Review
Module D	Off-Airport Inventory
Module E	Fuel Analysis
Module F	On-Airport Inventory
Module G	Monitoring and Sampling Report
Module H	Quality Assurance Audits
Module I	Analysis of Air Quality Emissions Data
Module J	Source-Oriented Air Dispersion Modeling
Module K	Receptor Modeling
Module L	Gas Chromatograph/Mass Spectrometer Analysis

(This page is intentionally blank)

Section 1

INTRODUCTION

(This page is intentionally blank)

Table of Contents

List of Figures

(This page is intentionally blank)

1. INTRODUCTION

In July 2011, Los Angeles World Airports (LAWA) contracted with Tetra Tech, Inc. (Tetra Tech) to perform Phase III of the Los Angeles International Airport Air Quality and Source Apportionment Study in accordance with the proposal submitted by Tetra Tech and approved by LAWA.

The Los Angeles International Airport (LAX) is surrounded by the Pacific Ocean to the west and residential neighborhoods to the north, south, and east. In 1999, as a response to concerns expressed among local residents on the potential impact of air emissions from LAX operations on the air quality within the local neighborhoods, LAWA initiated a study to evaluate the LAX contributions to area emissions. In 2000, LAWA voluntarily proposed to conduct an Air Quality and Source Apportionment Study (AQSAS) to evaluate concentrations and sources of potential air pollutants near the LAX. Due to the terrorists' attacks of September 11, 2001, the LAX AQSAS was suspended. In 2002, efforts to resume the study began. The LAX AQSAS is a requirement in the LAX Master Plan Mitigation Monitoring and Reporting Program (MMRP), Community Benefits Agreement (CBA), and the LAX Stipulated Settlement Agreement. In 2008, the LAWA Board of Airport Commissioners (BOAC) approved resumption of the Study.

The LAX AQSAS consisted of three phases. Phase I (Preparation) and Phase II (Demonstration Project or Pilot Study) were conducted between 2008 and 2011 by Jacobs Consultancy (later LeighFisher, Inc.) and included evaluation of measurement techniques in Phase III. Phase III, which was the core study of the LAX AQSAS, was conducted by Tetra Tech between 2011 and 2013. The information presented herein includes results from all three phases, with emphasis on Phase III core study results, presented in this volume of the report, and Phase I and Phase II findings summarized in Volume 3 of the report.

1.1 OBJECTIVE OF THE LAX AQSAS

The overall primary objective of the LAX AQSAS was to assess potential air impacts from the airport-related sources and operations on the local ambient air quality of the adjacent communities.

The primary objectives for the Phase I and Phase II of the Study were to assess the type of monitoring/sampling equipment to be used, the proper siting locations, and the feasibility of completing accurate and comprehensive source apportionment.

The primary objective of Phase III was to conduct source apportionment to assess the potential contribution of LAX operations on local air quality. In short, the LAX AQSAS is a source apportionment study to examine the contribution of LAX to pollutants in the surrounding area; the health effects of these pollutants are not within the scope of this study.

1.2 STUDY AREA

The Phase III Study Area was defined by the Pacific Ocean on the west, Inglewood Avenue on the east, West 120th Street on the south, and Manchester Avenue on the north, with an area of

approximately 35 km^2. The Study Area for Phase III provided a focused area within which detailed air quality monitoring and modeling analyses could occur with particular attention given to the adjacent communities immediately to the north, east, and south of LAX. Figure 1-1 depicts the Study Area used in Phase III.

1.3 ROLES AND RESPONSIBILITIES

The LAX AQSAS was performed under the direction and oversight of the Environmental Services Division (ESD) of LAWA. Norene Hastings, Environmental Supervisor, was LAWA's Project Manager. Ms. Hastings was responsible for the successful execution of this project, acted as the technical regulatory liaison, directed all project-related activities, and maintained close communication with the Project Team through routine meetings and progress reports. Ms. Hastings performed her responsibilities in communication and under the direction from Karin Christie, Environmental Affairs Officer. Both Ms. Hastings and Ms. Christie performed responsibilities under the direction of Robert Freeman, Airport Environmental Manager II.

CDM Smith served in a scientific advisory role to LAWA management. CDM Smith conducted technical review of the reports on behalf of LAWA. Anthony Skidmore was the CDM Smith liaison, and John Pehrson and Dr. Richard Countess were the primary technical reviewers of the reports, reporting directly to LAWA.

Tetra Tech was the general consultant and the lead for the performance of Phase III, directing the project and working closely with a number of technical sub-consultants and subject matter experts. The Tetra Tech's Technical Project Manager was Dr. Charng-Ching Lin, assisted by Erica Alvarado, both working under the direction of Dr. Salar Niku, Program Manager. Tetra Tech's technical sub-consultants and subject matter experts included:

- Desert Research Institute (DRI). DRI was responsible for conducting source profile sampling, chemical analyses, and chemical mass balance (CMB) receptor modeling. The primary lead for DRI was Dr. Eric Fujita, Research Professor at DRI, assisted by David Campbell and Dr. Xiaoliang Wang.

- SCS Tracer Environmental (SCS). SCS was responsible for site preparation, ambient air monitoring, field sampling, and field management. The primary lead for SCS was Paul Schafer, CIEC, Air Monitoring Specialist.

- T&B Systems, Inc. (T&B). T&B was responsible for conducting quality assurance (QA) and system/performance audits. The primary lead for T&B was Robert Baxter, CCM.

- K&B Environmental Sciences, Inc. (KBE). KBE was responsible for the emissions inventory. The primary lead for KBE was Michael Ratte, Senior Air Quality Scientist, working under the direction of Michael Kenney.

- Dr. Ronald Henry, Professor at the University of Southern California (USC) was responsible for Nonparametric Trajectory Analysis (NTA).

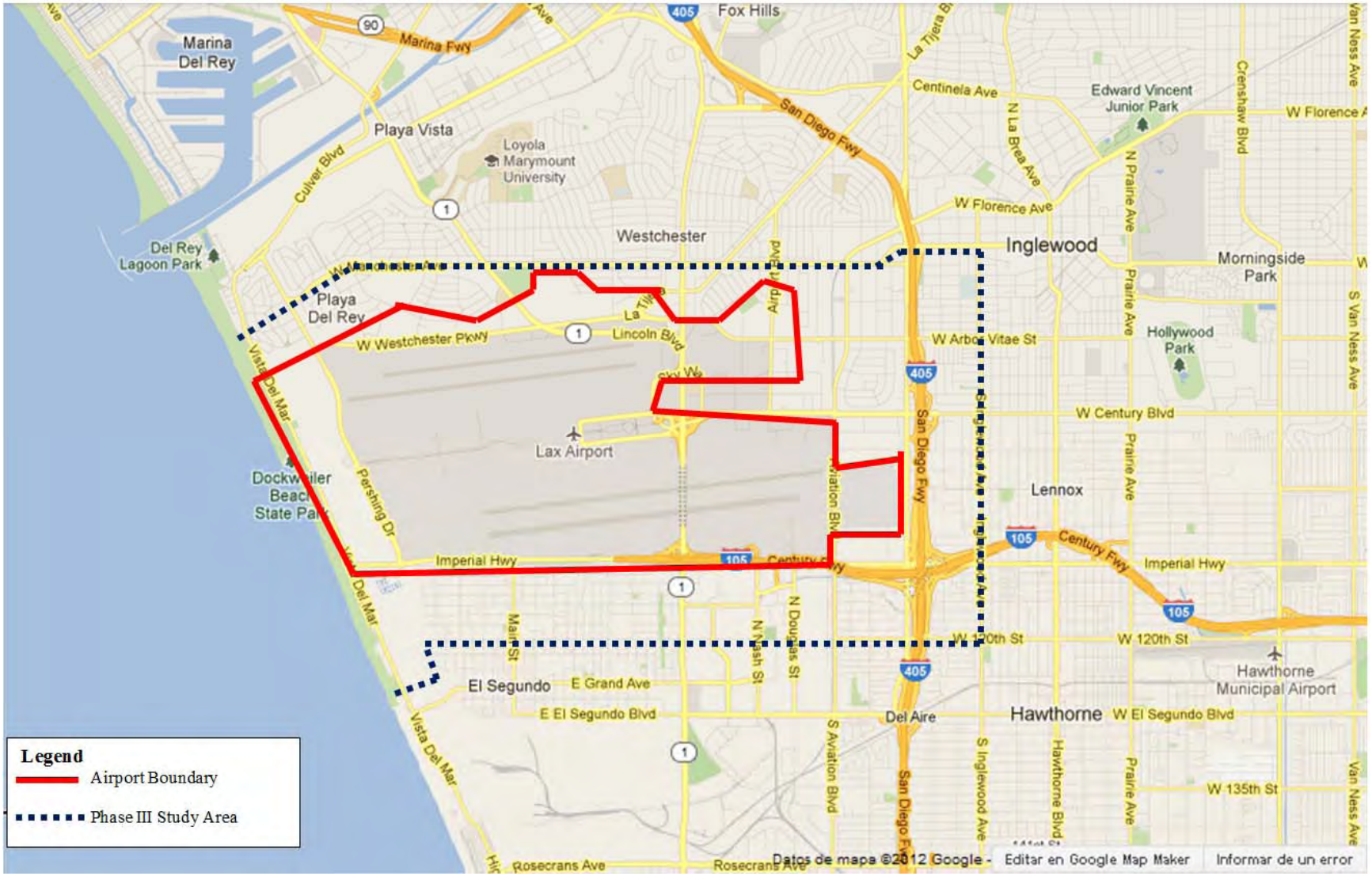

Figure 1-1. Study Area for Phase III.

- Dr. Sarav Arunachalam, Research Professor at the University of North Carolina at Chapel Hill, was responsible for dispersion modeling using American Meteorology Society/ Environmental Protection Agency (EPA) Regulatory Model (AERMOD) and Community Multiscale Air Quality (CMAQ) software programs.

- Dr. Charles Blanchard of Envair and Dr. Ivar Tombach, QEP, were technical advisors to Tetra Tech team and performed internal technical review of the documents. Dr. Eddy Huang, Director of the Air Quality Group at Tetra Tech also performed QA/QC of the field work as well as technical documents.

A Technical Working Group (TWG) served in an advisory role for this Study. The TWG is comprised of experts from the U.S. EPA, California Air Resources Board (CARB), South Coast Air Quality Management District (SCAQMD), Federal Aviation Administration (FAA), Desert Research Institute (DRI), University of Southern California (USC), California Office of Environmental Health Hazard Assessment (OEHHA), and community organizations. The composition of the TWG provided an opportunity for a variety of viewpoints to provide input and share perspectives regarding different aspects of the Study including work plans, monitoring and modeling protocols, data collected and analyzed for the Study, and conclusions and recommendations of those data. Please note that while DRI and USC served on the TWG for Phases I and II, they were sub-consultants to Tetra Tech during Phase III of the LAX AQSAS.

1.4 COMMUNICATIONS

LAWA and its consultant team had primary responsibility for the direction and completion of the LAX AQSAS. LAWA and the TWG worked closely toward consensus-based decision-making and seeking agreement among the respective participants on the scientific methods and processes being used to conduct the Study. During Phase III of the LAX AQSAS, LAWA staff and the Tetra Tech Team interacted with the TWG, providing updates as to the progress of the field monitoring, presenting the preliminary results, and responding to the inquiries of the TWG.

LAWA staff has maintained a project website for the LAX AQSAS, which includes information about the Study background, the project schedule and status updates, project materials, maps/graphics/photos, and an avenue to submit public comments. All final project reports will be placed on LAWA's project website, which is accessible to the public (http://www.lawa.org/airqualitystudy).

Section 2

BACKGROUND

(This page is intentionally blank)

Table of Contents

List of Figures

(This page is intentionally blank)

2. BACKGROUND

2.1 HISTORY OF THE LAX AQSAS

Los Angeles International Airport (LAX) is located within the South Coast Air Basin (Basin or SoCAB). Air quality within the Basin is designated by the United States Environmental Protection Agency (U.S. EPA) as a non-attainment area for several "criteria" air pollutants including ozone (O_3) and particulates.

Between the spring of 1998 and winter of 1999, the South Coast Air Quality Management District (SCAQMD) conducted a seasonal air toxics monitoring program near LAX as part of its Multiple Air Toxics Exposure Study II[1] (MATES II). The results of MATES II indicated that air pollutant levels in these adjacent neighborhoods were similar in magnitude to those found elsewhere in the SoCAB. However, the SCAQMD study did not provide data that could be used to determine LAX's contribution to air pollutants. Within the study area for MATES II, other potential sources of air pollutants were included, such as, but not limited to, three major freeways, several heavily traveled major arterial routes, and numerous industrial facilities including: the Chevron El Segundo refinery, Hyperion Wastewater Treatment Plant, the Department of Water and Power's Scattergood Generating Station, and NRG's El Segundo Generating Station.

In late September 1999, Ms. Lydia Kennard, Executive Director of LAWA, directed staff and a consultant team to develop a study to provide more detailed information about the contribution of LAX in emitting air pollutants and the total concentrations of these pollutants in surrounding neighborhoods. The data collected from the full study (i.e., Phases I, II, and III) were to be used to assess the effectiveness of various methods for reducing airport-related emissions.

2.2 LAX AQSAS TIMELINE

The general approach to conducting the LAX Air Quality and Source Apportionment Study (AQSAS) was originally proposed in the 2000 Technical Work Plan. The Work Plan included the scheduling of a Pilot Study to characterize aircraft emissions and to evaluate measurement methods. The Study was terminated in September of 2001 due to events of September 11. The Study was resumed in mid-2008 with the updated Pilot Study (the Demonstration Project). At the conclusion of the Demonstration Project, it was determined that the appropriate compounds for use in source apportionment techniques could be measured to help identify potential airport contributions at surrounding locations. Thus, the final Scope of Work for Phase III of the LAX AQSAS was developed utilizing a number of recommendations for sampling techniques and locations identified in the Demonstration Project. The overall timeline of the entire LAX AQSAS is shown in Figure 2-1.

[1] SCAQMD MATES II Study. Accessed on January 9, 2013 from http://www.aqmd.gov/matesiidf/matestoc.htm

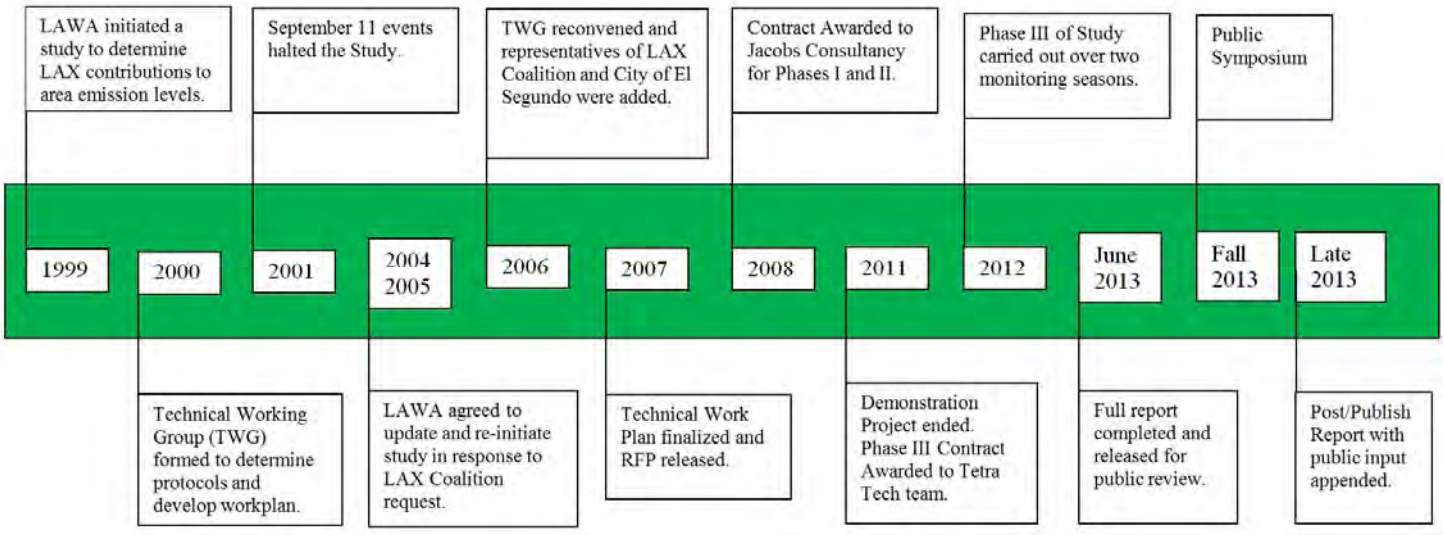

Figure 2-1. LAX AQSAS Timeline

2.3 OBJECTIVES OF THE LAX AQSAS

As mentioned in Section 1.1, the AQSAS clearly identified the primary objective for Phase III, which was to conduct source apportionment specifically to assess the incremental impact or overall contribution of LAX operations on air quality. This objective was achieved by:

1) Quantifying ambient air concentrations of gases and particles as well as particle deposition in neighborhoods near LAX and determining how these vary in space and time;

2) Determining the contribution of various airport-related activities on selected air pollutant concentrations relative to total air quality concentrations in surrounding areas; and

3) Applying receptor and source models used in source apportionment evaluations to LAX and estimating air pollutant emissions from other, non-airport sources near the airport.

2.4 PHASE I AND PHASE II

2.4.1 Implementation

The primary objectives for the Demonstration Project (Phase I and Phase II) were to determine the type of monitoring/sampling equipment to be used for Phase III, assess the proper siting locations, and assess feasibility of completing an accurate and comprehensive source apportionment. The main components of the Demonstration Project (Phase I and Phase II) included development of protocols for both field measurements and modeling. Forty-two days of field measurements were completed and the data were analyzed for the feasibility of using receptor and dispersion modeling techniques, such as nonparametric trajectory analysis and AERMOD, to conduct a comprehensive source apportionment. The Demonstration Project was conducted between March and December of 2008 with the monitoring portion occurring between June and September of 2008.

During the field measurements portion of the Demonstration Project, data were first collected at a location adjacent to the South Airfield Runway 25R blast fence (i.e., the area near the east end of the runway where aircraft begin their takeoff roll) for a total of 27 days to obtain information on aircraft-related emissions. Air pollutants measured by continuous monitors at the South Airfield Runway site included particulate matter 2.5 µm in diameter and less ($PM_{2.5}$), particulate matter 10 µm in diameter or less (PM_{10}), carbon dioxide (CO_2), carbon monoxide (CO), sulfur dioxide (SO_2), nitrogen oxides (NO_x), ozone (O_3), non-methane hydrocarbons (NMHC), black carbon (BC), ultrafine particles (UFP), polycyclic aromatic hydrocarbons (PAHs), and light scattering. Diurnal cycles for other parameters were taken, including, but not limited to, heavy and light hydrocarbons and particulate elements. After data were collected at the South Airfield Runway site, selected monitoring equipment was moved sequentially to four other locations on LAX property to gather information on additional sources, including, but not limited to, local stationary, traffic and parking, and ground support equipment sources. Collection occurred over a seven day period at each of the four locations. A subset of the approaches undertaken at the South Airfield Runway was carried out at the remaining four sites including continuous measurements of $PM_{2.5}$, PM_{10}, CO_2, CO, SO_2, light scattering, BC, UFP, and PAHs.

2.4.2 Overall Findings of Phases I and II by Jacobs Consultancy/LeighFisher

The Demonstration Project findings helped to determine the feasibility of conducting a comprehensive field measurement and modeling program to provide information for source apportionment in Phase III. Overall, the Demonstration Project was able to verify that source apportionment was attainable provided that an appropriate data collection program was implemented in Phase III.

In addition to the preliminary findings of the Demonstration Project, three subsequent reports analyzing these findings and their ability to address the overall source apportionment objectives of Phase III were prepared by Countess Environmental. Utilizing information from these reports, as well as the Demonstration Project findings, recommended modifications were suggested for improving monitoring methodologies used in the Phase III Study.

The entire Demonstration Project report as well as the three reports by Countess Environmental can be found in Volume 3.

2.4.3 Recommended Modifications to the Work Plan for Phase III

The main components of the Phase III project included: quantifying ambient pollutant concentration, conducting source apportionment analysis via receptor (CMB and NTA) and source-based modeling (Emission Inventory, AERMOD, and CMAQ), and source emissions characterization. The following modifications were undertaken for the Phase III Study:

1. The originally proposed year-long study was modified to include two distinct monitoring seasons, Winter and Summer, which were chosen to represent seasonal flight activity levels and meteorological conditions. The scope of work, both time-wise and financially, was unable to support a year-long study.

The 2010/2011 surface wind data collected at the SCAQMD LAX upper air station, located west of the intersection of Pershing Drive and World Way West, indicated there are two distinct wind patterns that affect the airport area. The first pattern encompassed November to March, with variable wind directions but predominantly NE and SW winds. The second pattern encompassed April to October, with predominantly WSW and westerly winds. Considering the local unique wind patterns, it was suggested to include two six-week monitoring periods (Winter and Summer) to capture representative wind patterns in the airport area. Additionally, the 2011 flight data for LAX collected on a monthly basis also depicted a period of lower activity in winter (January to March), with an average of 42,192 takeoffs/landings in 2011 and higher activity in summer (June to August), with an average of 49,483 takeoffs/landings in 2011.[2]

The two-season sampling study could help achieve the measurements of the parameters identified in the Demonstration Project and the Phase III Scope of Work and meet the goals originally proposed for the year-long study. The two season study had the ability to provide measurements over an intensive study period with a sufficient, manageable, and cost effective set of data. In addition, this update to the Scope of Work helped create an intensive study that encompassed: 1) two distinct wind patterns, and 2) a general period of lower flight activity and higher flight activity in the Winter and Summer Season, respectively.

2. Samples were collected concurrently at all sites chosen for the Phase III Study. This would enable spatial and temporal comparisons to be made between sites and between monitoring seasons. Time Series Analysis and Spatial Gradient Analysis, which were included in the overall Study, were not originally conducted during the Demonstration Project. The reason these two analyses were not conducted was because pollutants were not measured concurrently at multiple locations during the Demonstration Project. However, this is a requirement of both the Time Series and Spatial Gradient Analyses. Even though both analyses were not included in the Demonstration Project, they were recommended, and ultimately conducted, for the Phase III Study.

3. A meteorological station capable of providing wind speed and direction that were representative of the Study meteorological conditions was included. This was important, as local meteorology, such as wind speed and direction, affect dispersion of air pollutants and the resultant ambient concentrations. Measurements of meteorological parameters are an integral part of modeling the source of pollutants and in conducting overall source apportionment. For example, winds during the Summer Season were predominantly from the east in the morning hours and the west in the afternoon hours. This would cause the definition of "downwind of the airport" to change depending on the wind direction. As determined in the Demonstration Project, "data collected from the South Airfield Runway site were valuable in searching for pollutants that were present in aircraft exhaust; however, monitoring data from the South Airfield Runway site were recommended not to be used in modeling that includes regional wind data. It was also apparent that meteorological data taken at the South Airfield Runway site were not useful." Therefore, as stated above, it was recommended that meteorology data, in particular wind speed and direction, be collected

[2] ATADS: Airport Operations: Standard Report. http://aspm.faa.gov/opsnet/sys/opsnet-server-x.asp and LAX Flight Activity Data.

during the Phase III Study to help determine which measurements were from the direction of LAX and which were from other source areas.

4. During the Demonstration Project, it was observed that pollutant concentrations decreased quickly as the pollutants dispersed downwind. Therefore, the originally proposed monitoring site locations at varying distances downwind of the South Airfield Runway 25R were re-evaluated. Sites that would be useful in developing a profile of taxiing and idling aircraft engines, which differ in composition compared with emissions from aircraft engines in takeoff mode, were identified. Sites were chosen to best represent the proposed Study Area and to provide the best possible location to measure the pollutants of interest. Further explanation of site location selection is provided in Section 3.3 (Phase III Technical Approach – Monitoring Network Design and Objectives) and Section 5.2 (Time Series and Spatial Analysis – LAX AQSAS Winter and Summer Monitoring Season Data) of this report.

5. During the Demonstration Project, speciated organic lab analyses had been conducted using standard detection limits, which led to a large number of non-detects in the samples. Organics and, more specifically, the ratios of individual organic compounds in a plume, were recognized as having the potential to provide a unique characterization of an aircraft turbine plume compared to a diesel engine plume. Therefore, in Phase III, it was recommended that samples be analyzed in the laboratory using a method that has lower detection limits.

6. Appropriate methodology and instruments, were re-evaluated and certain pollutants or methods that would not provide useful information to the Study were identified (i.e., discontinued measurement of CO_2, NMHC, and the use of deposition plates) and replaced with alternative metrics. For example, using CO, which is a good indicator for gasoline-powered vehicle exhaust, instead of CO_2, which would provide limited value due to the limited incremental concentrations of CO_2 measured above the global background during the Demonstration Project was suggested. For measurement of ultrafine particles (UFP), it was recommended to use particle counters with less than 32 channels, which were used in the Demonstration Project, to provide sufficient results for the purpose of the Phase III Study.

7. As previously mentioned, a primary objective of the Demonstration Project was to determine the best methodologies (field measurements and modeling techniques) to conduct the source apportionment in the Phase III Study. This was done by conducting preliminary measurements to identify the best methodologies to use. Field measurements that were not originally included in the Demonstration Project, but that were identified in Countess Environmental reports (2011a; 2011b; 2011c) and the Preliminary Results from the SCAQMD Taxiway Study at LAX were recommended to benefit the Phase III scope.

   The main purpose of the modeling analysis conducted during the Demonstration Project was to see if the types of models chosen were feasible and applicable to the Phase III Study. From the Demonstration Project results, recommendations were provided on the types of modeling techniques to undertake for the Phase III Study. The NTA receptor model was evaluated in the Demonstration Project and recommended for use in Phase III. However, the use of NTA during the Demonstration Project "was presented solely to demonstrate its capabilities and not to deduce any information about the location of sources in the

communities surrounding LAX, nor to provide any source apportionment." The application limitations of the CMB receptor modeling were discussed but not evaluated. Methodologies that had not been evaluated (e.g., Time Series Analysis, Spatial Gradient Analysis, and CMB) were also recommended for the Phase III Study to provide a comprehensive source apportionment.

2.5 EXTERNAL DATA SOURCES

External data for the AQSAS were obtained from numerous sources and used primarily for the emission inventory and air dispersion modeling portion of the Phase III Study. The following external data were obtained and used.

2.5.1 Meteorological Data

Meteorological data were obtained from the National Weather Service (NWS), the Photochemical Assessment Monitoring Station (PAMS), the Sonic Detection and Ranging (SODAR) station located just to the west of LAX, and from the SCAQMD's AQ site.

2.5.2 CMAQ Data

CMAQ data used for air dispersion modeling for the time period encompassing the Summer Season were obtained from SCAQMD. These data included basin-wide emission inventories developed by SCAQMD. Air toxics inventory reports and pollutant data (CO, SO_2, and NO_x) for the AQ site were obtained from SCAQMD.

2.5.3 Flight Activity

Flight activity data, which included aircraft takeoff and landing data from the North and South Airfields, were obtained from LAWA Airport Noise and Operations Monitoring Systems (ANOMS). Data on the number and layout of the major airport aprons and the major runways were obtained from LAWA staff. Fuel usage was obtained by LAWA from the two primary fuel providers used on the LAX property. A complete ground support equipment (GSE) inventory survey was provided by LAWA that included fuel type, model year, horsepower, and manufacturer for GSE at the airport. Fuel usage was provided by Atlantic Aviation and ASIG/LAXFuel, which track usage of Jet A.

2.5.4 Traffic

On-airport traffic data for the Central Terminal Area roadway loop were obtained from LAWA. Parking facilities ticket counts were obtained for the time period overlapping with the Winter and Summer Seasons. Data for traffic apportionment in the Study Area were obtained from the 2007 LAWA Technical Memorandum regarding Data Analysis of Vehicle License Plate Survey Results for Los Angeles International Airport Arrival Traffic[3]. Off-airport traffic data during the

[3] Fehr and Peers. 2007. Technical Memorandum: Data Analysis of Vehicle License Plate Survey Results for Los Angeles International Airport Arrival Traffic. Prepared for LAWA.

study period were obtained from CalTrans and the Los Angeles Department of Transportation (LADOT).

2.5.5 Marine

Marine vessel emissions were obtained from the Port of Los Angeles' consultant, Starcrest Consulting. However, since the emissions data provided were similar to the California Air Resources Board (CARB) Marine Emissions Model, the CARB model was used in this report.

2.5.6 Stationary Sources

On-airport stationary source emissions reports were obtained from LAWA including the turbine continuous emissions monitoring system for the Central Utility Plant and the quarterly SCAQMD emissions reports for the time periods encompassed by the Study. Off-airport stationary source emissions in close proximity to the Study Area, including the Scattergood and El Segundo Power Plants and the Chevron Refinery, were obtained from each respective company.

2.6 REFERENCES

Countess Environmental. 2011a. Evaluation of Hydrocarbon Data from the LAX Air Quality Source Apportionment Study's Demonstration Project. Report prepared for CDM.

Countess Environmental. 2011b. Evaluation of Monitoring Data from the LAX Air Quality Source Apportionment Study's Demonstration Project. Report prepared for CDM.

Countess Environmental. 2011c. Evaluation of Sampling Data from the LAX Air Quality Source Apportionment Study's Demonstration Project. Report prepared for CDM.

Fehr and Peers. 2007. Technical Memorandum: Data Analysis of Vehicle License Plate Survey Results for Los Angeles International Airport Arrival Traffic. Prepared for LAWA.

Jacobs Consultancy. 2009. Los Angeles International Airport Air Quality and Source Apportionment Study Final Demonstration Project Report. Report prepared for Los Angeles World Airports.

SCAQMD. 2011. Preliminary Findings from the SCAQMD Taxiway Samples at LAX. Prepared by SCAQMD April 2011.

Section 3

PHASE III TECHNICAL APPROACH

(This page is intentionally blank)

Table of Contents

List of Tables

List of Figures

3. PHASE III TECHNICAL APPROACH

3.1 PHASE III SCOPE

The Scope of Work for the Phase III Study contained multiple approaches to air pollutant source apportionment to enhance the ability to draw appropriate conclusions. The use of multiple approaches allowed for identification and reconciliation of differences between source contribution estimates from varying approaches. The Study scope clearly defined data types or parameters, time resolution, and the amount of data required to perform a meaningful source apportionment to meet the Study objective of identifying an accurate estimate of source contributions from airport operations to adjacent communities. The Final Scope of Work for Phase III of the Study can be found in Appendix 3-1.

3.2 MODIFICATIONS TO PHASE III OF THE LAX AQSAS SCOPE OF WORK

In Section 2, modifications to the Work Plan derived from Phases I and II were listed. As discussed below, supplemental studies were also performed to collect additional data to enhance the Study.

3.2.1 Mobile Survey and Pollutant Gradient Study

A mobile survey was conducted to characterize the spatial variations in pollutant concentrations within the communities and buffer zones[1] surrounding LAX and near airport operations (e.g., the Central Terminal Area and aircraft takeoffs, landings, and taxiing). This survey was used to guide the selection of air monitoring sites for Phase III and was used as the basis for developing suggested modifications to the originally proposed air monitoring plan, which are listed below. The following summarizes the approach to the mobile surveys. Additional details are provided in Section 5.1.

The mobile surveys were conducted during the week of September 19, 2011, using the Bay Area Air Quality Management District (BAAQMD) mobile monitoring van, either alone or in combination with the Desert Research Institute (DRI) portable cart-mounted monitoring system. In addition to a GPS, the van was equipped with continuous instruments to monitor nitric oxide (NO), carbon monoxide (CO), volatile organic compounds (VOCs), black carbon (BC), particulate matter 2.5 μm or less in diameter ($PM_{2.5}$), and ultrafine particulates (UFP number concentrations with time resolutions of 10 seconds). Continuous instruments operated in the BAAQMD mobile monitoring van and portable cart-mounted monitoring system are identified in Table 3-1. Sulfur dioxide (SO_2) was not measured due to inadequate sensitivity of the analyzer for calculation of averages. The cart-mounted monitoring system included a GPS and measurements of NO, CO, CO_2, $PM_{2.5}$, and UFP counts. BC was not measured in the cart due to the photoacoustic instrument's high power draw.

[1] "Buffer zones" are defined as LAWA-owned properties located along the periphery of LAX. These include vacant land, such as along Westchester Parkway and at the western edge of the airport, and land developed for airport purposes, such as parking lots at the east end of the airport and cargo/ancillary uses along the southern edge of the airport.

The monitors in the van were used to measure pollutant concentrations within the communities of El Segundo, Playa del Rey, Westchester, Lennox, Hawthorne, and Inglewood. These surveys also included routes near industrial facilities in El Segundo (wastewater treatment plant and power generating plant), the eastern-end of the LAX North and South Airfield runways, cargo terminals on both the north and south sides of LAX, and the Central Terminal Area. The community surveys were scheduled during the morning and evening periods under varying meteorological conditions and traffic patterns. The van and the cart were used simultaneously to determine spatial gradients in pollutant concentrations near and downwind of the takeoff and taxiing areas of South Airfield Runway 25R and near the I-405 freeway along Lennox Boulevard from Inglewood Boulevard to La Cienega Boulevard. Depending upon logistical considerations, either the van or the cart remained stationary during the gradient measurements while the other unit was mobile. The pollutant gradient measurements were made during mid-day, while winds were from the west.

Table 3-1. Continuous Instruments Utilized for the Mobile Survey

Parameters	**CO**	**NO**	**BC**	**CO, CO_2, T, RH**	**"VOC"**	**PM2.5 Mass**	**Ultra-Fine Particles**
Application	Van	Van Cart	Van	Cart	Van	Van Cart	Van Cart
Manufacturer:	Teledyne	2B Technologies	Pat Arnott, UNR	TSI	RAE Systems	TSI	Kanomax
Model:	ML9830	400	photoacoustic	8554 (Q-Trak Plus)	ppbRAE	8520 DustTrak	3800
Lower Detectable Limit:	0.05 ppm	20 ppb	0.2 ug/m3 for 1 min	~ 1 ppm	~30 ppb (1)	~ 1 ug/m3	< 1 particle/cm3
Range :	0-200ppm	up to 200 ppm		0-500 ppm	> 1000 ppm	0.001 to 100 mg/m3	0.015 - 1 um, 0 - 100,000 particles/cm3
Resolution:	0.01 ppm	2 ppb	0.1 ug/m3	0.1 ppm	1 ppb	0.1% + 0.001 mg/m3	
Min sampling interval:	1 sec	10" for NO or NOx only, 5 min for NO2	1 sec	1 sec	1 sec		
Response Time:	<40 secs		1 sec	<60 secs	~10 sec	1 sec	
Precision:	1%+0.1 ppm	3%+2 ppbv	<10%	3%+3ppm	10%+20 ppb	1 ug/m3	
Power Requirements:	200W @ 110/220 VAC	analyzer:11W @12VDC	150 W at 110VAC, plus pump (<100W @ 12VDC)	4 AA batteries (20 hr run time), or 110VAC	rechargeable battery or AC (100W @ 110VAC).	4 C batteries (16 hr run time), or AC adapter for continuous operation	6 AA-size batteries (5-8 hrs run time), or AC adapter (100 – 240V)

Based upon the results from the mobile survey, the following modifications were made to the Technical Work Plan for Phase III of the LAX AQSAS:

- Saturation sampling was expanded from 10 sites to 17 sites to provide gradient and spatial analyses.

- A condensation particle counter (CPC) was used for measuring UFP counts instead of using a Fast Mobility Particle Sizer (FMPS). Scanning Mobility Particle Sizer/Condensation Particle Counter's (SMPS/CPCs) were installed at the CE, CS, and CN sites to measure particle size distribution.

- The thermal desorption gas chromatography/mass spectrometry (GC/MS) analytical method for stable organic compounds collected on a Teflon-impregnated glass fiber (TIGF)/XAD sampler was replaced with an enhanced analytical technique to provide better sensitivity and speciation, including PAHs, alkanes, hopanes, steranes, and polar compounds.

- For $PM_{2.5}$ samples collected at core sites[2], the sampling frequency was changed from twelve-hour to twenty-four hour integrated samples to reduce analytical costs without sacrificing data quality for subsequent analyses.

- Meteorological data collection frequency was increased from a five-minute average to a one-minute average to provide sufficient time resolution for nonparametric trajectory analysis (NTA) to achieve required temporal resolution.

- Continuous CO_2 monitors were not included at the three core sites. This was due to the relatively low contribution of an urban area to the global background levels of CO_2. An exception is for close proximity to combustion sources. Measurements of CO_2 were of limited value as levels would have been fairly consistent with time at the three core sites. CO measurements were substituted for CO_2, as CO is a good tracer for gasoline-powered vehicle emissions.

- Non-methane hydrocarbon (NMHC) emissions at the three core sites were not measured because this measurement lacks high time resolution and sensitivity. The minimum time resolution is one hour, which has limited value for temporal analysis and NTA. Additionally, NMHC data from the continuous instruments were not necessary for receptor analysis.

- Continuous PM sampling with beta attenuation monitors (BAM) for $PM_{2.5}$ mass was determined to have minimal value for this Study. The time resolution of the instrument is one hour and does not provide good precision below $10\mu g/m^3$. Therefore, it was suggested to add pDR25 data measurements of light scattering data on a one-minute time period as well. Also, average $PM_{2.5}$ concentrations measured during the Demonstration Project were relatively uniform at all sites. Urban and regional background is typically a major component of PM concentrations with local sources having minimal impact, except in close proximity to the actual source.

[2] Core sites were originally referred to as "baseline sites" in the draft Scope of Work, Work Plan, Monitoring and Quality Assurance Project Plan (MQAPP), Modeling and Analysis Protocol (MAP). They have been updated to "core sites" or "core monitoring sites" in conjunction with preparation of the AQSAS report to reflect the actual Function of those monitoring sites.

- Video recordings of aircraft activities were not used in the modeling analysis in the Demonstration Project. In Phase III, LAX flight activities data were obtained from the ANOMS. Source profile information was collected behind the blast fence for receptor modeling use.

- Visible particle deposition was not used in the modeling analysis as it targets large particles, such as fine and coarse sand, gravel, pollen, etc., which were not the primary targeted particle measurements of the Study. Therefore, it was not included at the core sites.

3.3 MONITORING NETWORK DESIGN AND OBJECTIVES

The Draft Technical Work Plan was prepared by CDM Smith for Phase III of the LAX AQSAS (CDM, April 2011) and originally described specifications for air quality monitoring at three core sites (with the option for two additional sites) and two satellite sites during two monitoring seasons, each lasting six weeks. The proposed core sites outlined in the original Work Plan included a source site at the east-end of the LAX South Airfield Runway 25R, a community site east of LAX (CE), an upwind site (UW) with the option for an upwind background site either north or south of the LAX runway path (BG), and a downwind site south of the runway (FS). An additional proposed core site included the existing SCAQMD Hastings site (AQ), located at the northwest boundary of LAX. This network of monitoring sites was proposed in the Work Plan for analysis of the spatial and temporal variations of pollutant concentrations in the communities surrounding the airport and for multivariate receptor analysis of source contributions. The following sections summarize the approach to the air quality monitoring conducted in Phase III. Additional details are provided in Section 5.2

3.3.1 Site Selection (core, satellite, and gradient sites)

The Scope of Work for Phase III was developed by LAWA and CDM Smith and reviewed by the Technical Working Group (TWG). The Scope of Work included improvements identified under the Demonstration Project to enhance the overall performance of the Phase III Study. Initially the Tetra Tech team proposed two core sites (SR and CE) with continuous monitoring and collection of time-integrated samples with methods that would ensure quantitative analysis of relevant marker species used in VOC and PM source apportionment for the Phase III Study. Continuous measurements were also proposed for a limited time at an upwind site using a mobile monitoring van. After review of the Scope of Work and after conducting the mobile surveys (see Section 3.2.1), the following recommendations were made and incorporated into the Study design. The results of the mobile survey were used to guide the selection of core and saturation monitoring sites used in Phase III. Modifications to the Scope of Work included:

- The South Airfield Runway 25R (SR) site sampling scheme was replaced with short-term sampling using integrated and continuous samplers to collect source profiles and emission factors for aircraft takeoff and taxiing emissions.

- A gradient study was conducted east of the SR site in the open field to characterize concentration gradients and characteristics of air pollutant dispersions.

- Passive and MiniVol samplers were deployed within LAX source areas, at the perimeter of buffer zones, and within adjacent communities for subsequent gradient and spatial analyses.

- The station originally intended for the SR site was not used. The station hardware was used at the Community South (CS) site, located at the former Imperial Avenue School in El Segundo, to represent air quality in the communities south of the airport.

- Of the four core sites, the AQ site was considered as a background site due to its location.

- The originally proposed location of the upwind (UW) site located in the Dunes west of the airport was changed to another local community site, located at the intersection of Airport Boulevard and Arbor Vitae Street, as the CN site.

In determining the core, satellite, and gradient sites, other factors that were major considerations included:

- Attainment of data relative to study objectives;
- Availability of electrical power;
- Site security;
- Site access;
- Proximity to local pollution sources;
- Lack of obstructions at the site location;
- Obtaining FAA and other necessary permits; and
- The willingness of property owners to provide the necessary space.

Locating sites that were favorable to all of the above mentioned criteria led the Project Team to extensively survey the areas around LAX and to consider multiple potential locations for several sites. Based upon the considerations listed above, the best available sites for the core, satellite, and gradient monitoring locations were identified. A list of these locations is found in Table 3-2.

The three core sites included a community site east of LAX (CE) at La Feria Restaurant in Lennox, a community site south of LAX (CS) at the former Imperial Avenue School in El Segundo, and a community site northeast of LAX (CN) in Westchester. Existing monitoring at the SCAQMD station site (AQ) was augmented with appropriate continuous gas and particulate matter monitors to provide a fourth site in the area with a near comparable set of continuous monitoring data. The components measured at each of the core sites are found in Table 3-3.

Table 3-2. List of Sites for Phase III of the LAX AQSAS Study

Site ID	***Site Type***	***Site ID***	***Site Location***
CE	Core	Community East	La Feria Restaurant, Lennox
CS	Core	Community South	Imperial Ave School, El Segundo
CN	Core	Community North	NE of LAX, Westchester
AQ	Core/Satellite	Upwind Northwest	91st and Hastings, Playa del Rey
UW*	Satellite	Upwind West	W of LAX between SR and NR
CS2	Satellite	Community South #2	El Segundo
CN2	Satellite	Community North #2	Westchester
CE2	Satellite	Community East #2	Hawthorne
BN	Gradient	Buffer Zone North	N of Westchester Parkway
BS	Gradient	Buffer Zone South	Imperial Terminal
SRN	Gradient	South Runway North	Intersection of Century Blvd and Aviation – SW corner
SRE	Gradient	South Runway East	40 m directly east of Runway 25R blast fence
NR	Gradient	North Runway	Fence at east end of NR
BSR	Gradient	Buffer Zone S Runway	Lot B near La Cienega Blvd.
BNR	Gradient	Buffer Zone N Runway	Lot C near Jenny Avenue.
CT	Gradient	LAX Central Terminal	Roof of Parking Garage
R405	Gradient	Freeway I-405 East Edge	East edge of Freeway I-405

* Only limited sampling using passive samplers was conducted at this site to represent air quality in upwind location.

Table 3-3. Core Monitoring Sites, Parameters and Frequencies

Parameters	Site	AQ	CE	CS	CN	Sampling		
	Type	C	C	C	C	Avg Time	Frequency	Period
Continuous Measurements	CO	[redacted]	v	v	v	1-min	Continuous	Duration of monitoring campaign
	NO_x	[redacted]	v	v	v	1-min	Continuous	Duration of monitoring campaign
	SO_2	[redacted]	v	v	v	1-min	Continuous	Duration of monitoring campaign
	$PM_{2.5}$ (BAM)	v	v	v	v	1-hr	Daily	Duration of monitoring campaign
	Light scattering	v	v	v	v	1-min	Continuous	Duration of monitoring campaign
	Black Carbon	v	v	v	v	1-min/5-min	Continuous	Duration of monitoring campaign
	UFP/Size	[redacted]	v	v	v	1-min	Continuous	Duration of monitoring campaign
$PM_{2.5}$ Samples	Mass/ Carbon	v	v	v	v	24-hr	Once daily/14-day	Seasonal intensive periods
	Elements	[redacted]	v	v	v	24-hr	Once daily/14-day	Seasonal intensive periods
	Ions	[redacted]	v	v	v	24-hr	Once daily/14-day	Seasonal intensive periods
	Ammonia	[redacted]	v	v	v	24-hr	Once daily/14-day	Seasonal intensive periods
Others	Semivolatiles (TIGF/XAD)	[redacted]	v	v	v	24-hr	Once daily/14-day	Seasonal intensive periods
	Carbonyls (DNPH)	[redacted]	v	v	v	24-hr	Once daily/14-day	Seasonal intensive periods
	L-HC (Canister)	[redacted]	v	v	v	24-hr	Once daily/14-day	Seasonal intensive periods
	H-HC (Tenax)	[redacted]	v	v	v	24-hr	Once daily/14-day	Seasonal intensive periods
Meteorological Measurements	Wind Speed	[redacted]	v	v	[redacted]	1-min	Continuous	Duration of monitoring campaign
	Wind Direction	[redacted]	v	v	[redacted]	1-min	Continuous	Duration of monitoring campaign
	Temperature	[redacted]	v	v	[redacted]	1-min	Continuous	Duration of monitoring campaign
	Relative Humidity	[redacted]	v	v	[redacted]	1-min	Continuous	Duration of monitoring campaign
	Solar Radiation	[redacted]	v		[redacted]	1-min	Continuous	Duration of monitoring campaign

Footnote: v: measured parameter C: Core; AQ: SCAQMD station; CE: Community East; CS: Community South; CN: Community North
CO: carbon monoxide; NO_x: nitrogen oxides; SO_2: sulfur dioxide; $PM_{2.5}$: particulate matter 2.5µm aerodynamic diameter

3.3.2 Community East (CE) Site Location and Setup

The initial site visit indicated that the proposed CE site (Felton Elementary School) was not suitable to meet siting criteria due to potential obstruction of air flow by the adjacent elevated I-405 Freeway and nearby trees. On September 1, 2011 an alternative site (La Feria Restaurant) located at 10903 South Inglewood Avenue in Lennox, approximately 405 meters east of the I-405 Freeway and 1,560 meters east from South Airfield Runway 25R, was selected (Figure 3-1).

At this site, parking lot space was leased from the owner of the restaurant, which included the provision of electrical services. To get power from the restaurant to the site, a conduit from the restaurant to the site location was installed. Upon delivery of the site trailer and connection of electricity, fencing was installed around the site trailer for security purposes.

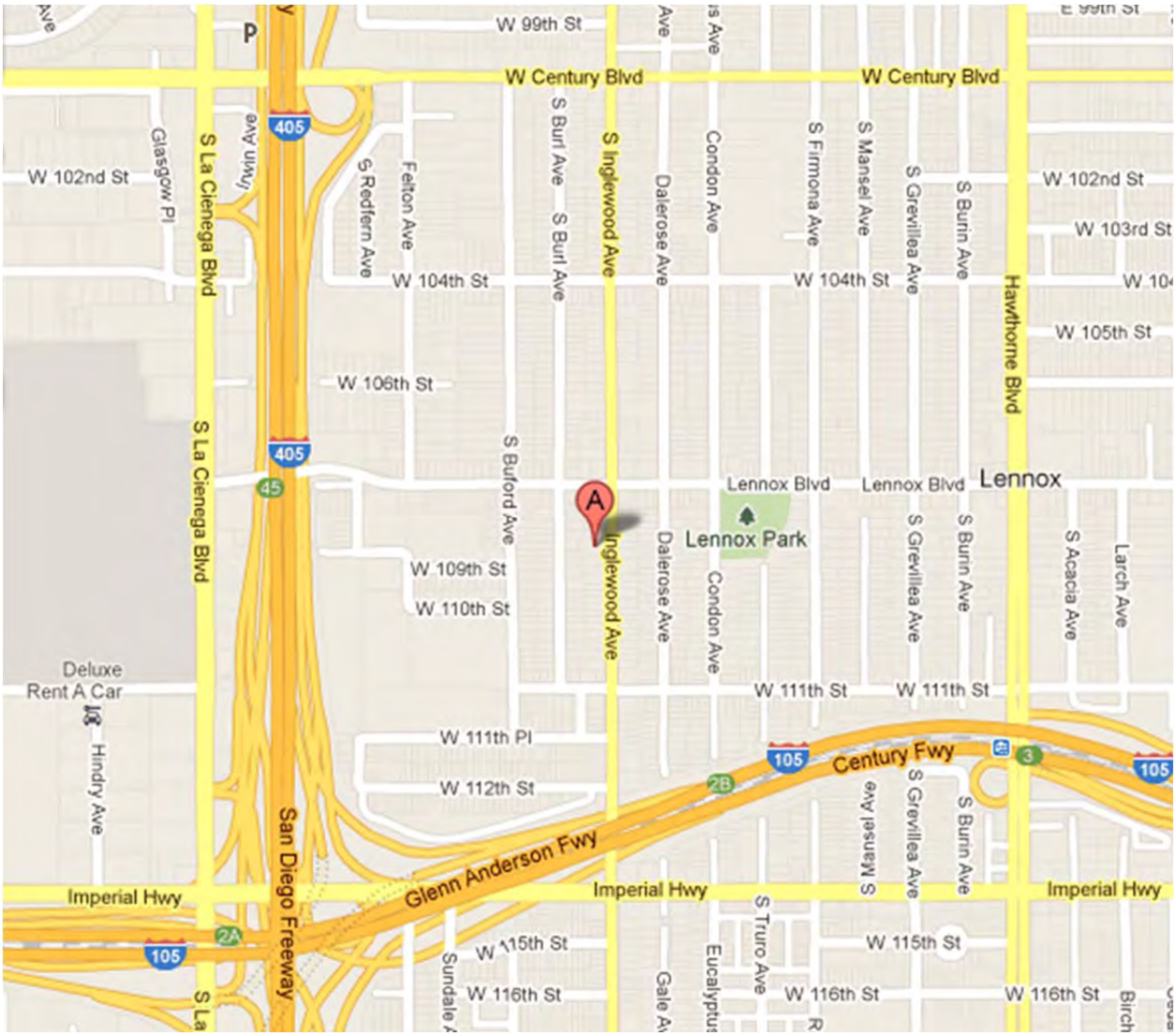

Figure 3-1: Community East Site Location

3.3.3 Community South (CS) Site Location and Setup

The location of the monitoring site on the south side of LAX was constrained due to the limitations on locations of available power sources as well as surrounding topographical features. The originally proposed location for the CS site was on the top of a hill; however, it was suggested by the TWG to seek a location that was more level and closer to Main Street to provide better monitoring results. A site visit was conducted to examine which of the two locations would best represent the El Segundo community. After examining both sites, it was found that the original CS site location was appropriate, as the surrounding area is hilly. Also, the location closer to Main Street would most likely have been more influenced by traffic in the vicinity of the Main Street location.

Power to the CS site location (see Figure 3-2) was via a temporary power pole installed within 75 feet of an existing transformer and was contracted through Southern California Edison (Permit Required – El Segundo Department of Building and Safety). Electrical power was brought from the temporary power pole to the site trailer. The site trailer was delivered and electrical service was connected. Fencing was also installed around the site trailer for security purposes.

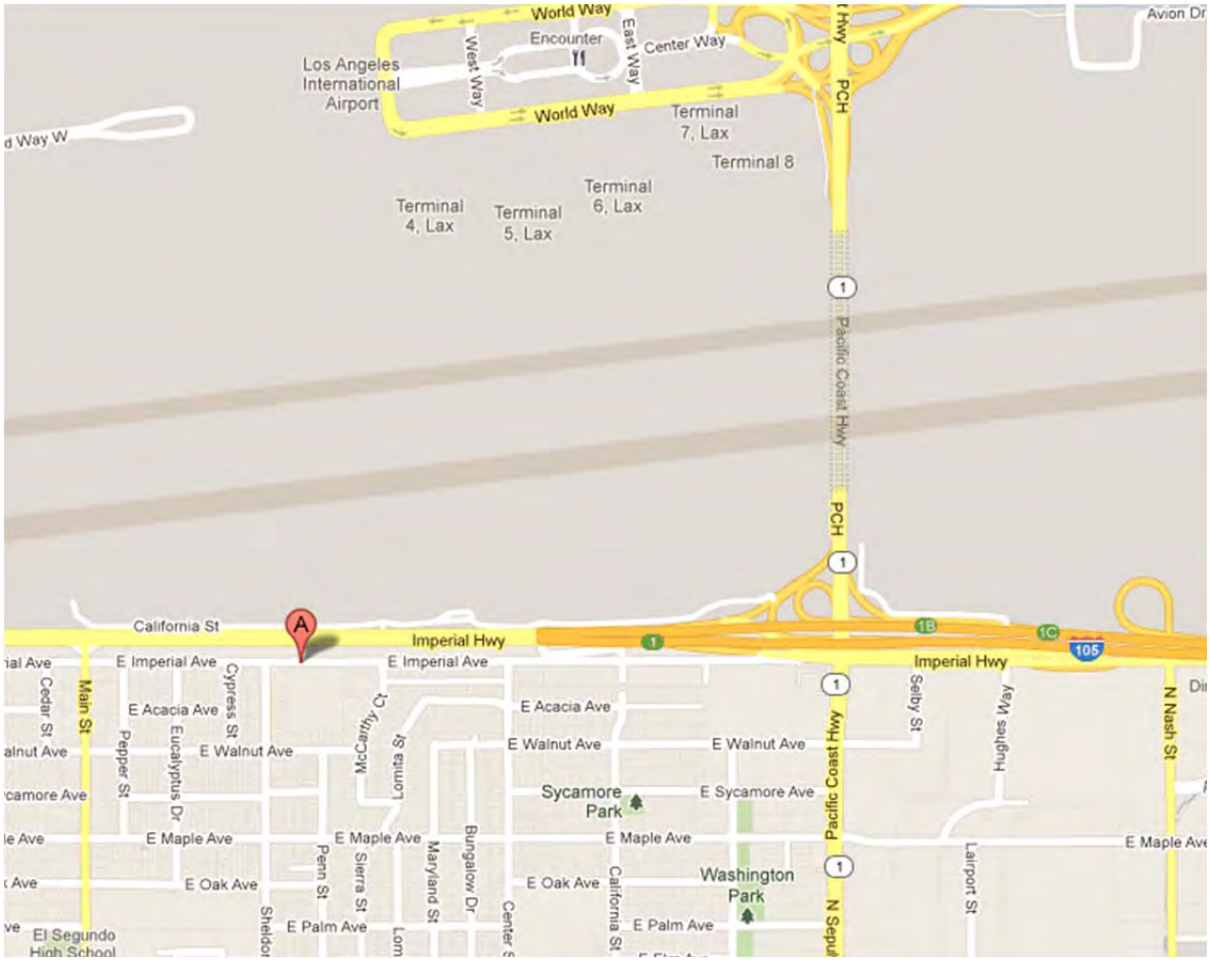

Figure 3-2: Community South Site Location

3.3.4 Community North (CN) Site Location and Setup

An initial site survey identified a property owned by LAWA located at the intersection of Airport Boulevard and Arbor Vitae Street, west of I-405 Freeway as a potential monitoring site. However, this location was not suitable to be used due to its residential zoning designation. An alternative location, also owned by LAWA, at Belford Avenue and West 95th Street was determined to be a more appropriate alternative. This location was designated as the CN site (Figure 3-3) and the DRI trailer was used at this site.

A temporary power pole (permit required through Los Angeles Department of Building and Safety) was installed and electrical service was provided by the Los Angeles Department of Water and Power. Power to the DRI trailer was provided by connecting a Recreational Vehicle pigtail to the power pole. Security fencing was also installed.

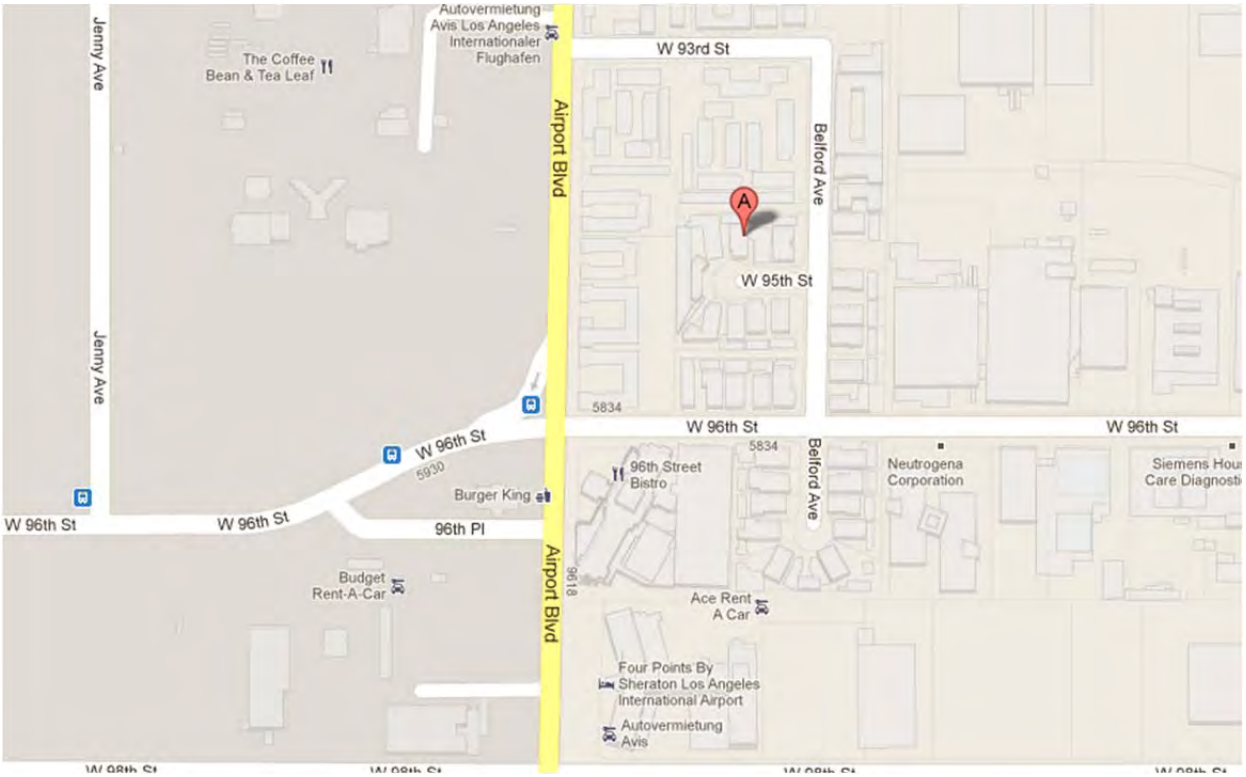

Figure 3-3: Community North Site Location

3.3.5 Saturation Sites

Gradient and spatial analyses were conducted at 17 sites within the community and around the airport perimeter. The full list of these sites is found and the parameters measured are found in Table 3-3 and Table 3-4. The sites are described in greater detail in Section 5.

3.3.6 Sampling and Monitoring Equipment

For the core monitoring sites (CE, CS, and CN, and the background AQ site), monitors taking continuous measurements were located at each location and were supplemented with integrated samplers for analysis of chemical species of interest (see Table 3-5).

During the Winter and Summer Seasons, in addition to continuous measurements and integrated samples at the fixed sites, saturation sampling was conducted using passive samplers and integrated samplers at the CE, CS, CN, and AQ sites as well as 13 other locations. Of the 13 other locations, 10 gradient samplers were located at the areas surrounding the airport including buffer zones, terminal areas, and adjacent to the I-405 freeway and three were collocated at the fixed sites.

3.3.7 Parameters Measured

Table 3-3 and Table 3-4 list parameters measured at each monitoring site. The site identification codes (Site ID) shown in Table 3-4 are representative of samplers located at that particular location. During Phase III of the LAX AQSAS, the following air pollutants of interest and meteorological parameters were measured for analysis and source apportionment modeling:

- Gaseous pollutants: carbon monoxide (CO); nitrogen oxides (NO_x); and sulfur dioxide (SO_2)
- Particulate matter: particulate matter 2.5 µm or less in diameter ($PM_{2.5}$); number concentration and size distribution of ultrafine particles (UFP); black carbon (BC); elemental carbon and organic carbon (EC and OC); and light scattering
- Ions: chloride; nitrate; ammonium; sodium; sulfate
- Metals: sodium to uranium
- Organic Compounds: aldehydes including formaldehyde and acetaldehyde; light hydrocarbons including 1,3-butadiene, benzene, toluene, ethylbenzene, xylenes, styrene; heavy hydrocarbons; semi-volatile and particulate alkanes, polycyclic aromatic hydrocarbons (PAHs), steranes, hopanes, and polar organic compounds.
- Meteorological data: wind speed; wind direction; ambient temperature; solar radiation; and relative humidity

Table 3-4. Monitoring Locations and Number of Measurements During Phase III of the LAX AQSAS

					7-day Samples During 6-Week Intensives										Daily 24-hr for 14 Consecutive Days							
					Passive						Mini-VolPM			Can	Tenax	DNPH	Med-VolPM				SVOC	
Site ID	Site Type	Site Name	Location	Cont	NOx	NO_2	SO_2	BTEX	1,3-BD	Carb	Tef	Tef/Qtz	Qtz	Light HC	Hvy HC	Carb	Tef	Tef/Qtz	Qtz	Qtz/NaCl	TIGF/XAD
CE	Core	Community East	La Feria Restaurant, Lennox	1	2	2	2	2	2	2		1	1	1	1	1		1		1	1
CS	Core	Community South	Imperial Ave School, El Segundo	1				1	1	1	1		1	1	1	1	1		1		1
CN	Core	Community North	NE of LAX, Westchester	1				1	1	1	1		1	1	1	1	1		1		1
AQ	Core	Upwind Northwest	91st & Hastings, Playa del Rey	AQMD+	1	1	1	1	1	1	1		1								
UW	Satellite	Upwind West	W of LAX between SR and NR		1	1	1	1	1	1	1		1								
CS2	Satellite	Community South #2	El Segundo		1	1	1	1	1	1	1		1								
CN2	Satellite	Community North #2	Westchester		1	1	1	1	1	1	1		1								
CE2	Satellite	Community East #2	Hawthorne		1	1	1	1	1	1	1		1								
BN	Gradient	Buffer Zone North	N of Westchester Parkway		1	1	1	1	1	1											
BS	Gradient	Buffer Zone South	Imperial Terminal		1	1	1	1	1	1											
SR	Gradient	South Runway	Fence on east end of SR, Aviation		1	1	1	1	1	1											
NR	Gradient	North Runway	Fence at east end of NR		1	1	1	1	1	1											
BSR	Gradient	Buffer Zone S Runway	Lot B near La Cienega Blvd.		1	1	1	1	1	1											
BNR	Gradient	Buffer Zone N Runway	Lot C near Jenny Ave.		1	1	1	1	1	1											
CT	Gradient	LAX Central Terminal	Roof of Parking Garage		1	1	1	1	1	1											
C&A	Gradient	Century and Aviation	Near intersection		1	1	1	1	1	1											
405E	Gradient	I-405 East Edge	East edge of I-405		1	1	1	1	1	1											
				3+	16	16	16	18	18	18	7	1	8	3	3	3	2	1	2	1	3
			Samplers																		
			Core		3	3	3	5	5	5	3	1	4	3	3	3	2	1	2	1	3
			Satellite		4	4	4	4	4	4	4		4								
			Gradient		9	9	9	9	9	9											
			Total Samples per Season																		
			Core		18	18	18	30	30	30	18	6	24	42	42	42	28	14	28	14	42
			Satellite		24	24	24	24	24	24	24		24								
			Gradient		54	54	54	54	54	54											
			Field Blanks		5	5	5	5	5	5	5		5		4	4	4		4		4
			Total Samples per Season		101	101	101	113	113	113	47	6	53	42	46	46	32	14	32	14	46

Cont: continuous; BTEX: benzene, toluene, ethylbenzene, xylenes; 1,3 BD: 1,3 butadiene; Carb: carbonyls; Tef: teflon; Qtz: quartz; HC: hydrocarbon, TIGF: teflon-impregnated glass fiber; DNPH: 2,4-Dinitrophenylhydrazine; SVOC: semivolatile organic compounds

Table 3-5: Monitoring Network – Core Monitoring Sites

Symbol	***Site Title and Type***	***Location and Type of Measurements***	***Components Analyzed***
CE	Community East. Core site for spatial, time series, and multivariate receptor analyses	La Feria Restaurant, ~1.56 km ESE of Runway 25R. Community exposure – aircraft, freeway, and area emissions.	Continuous analysis of CO, NO_x, SO_2, $PM_{2.5}$, light scattering, black carbon, ultrafine particle number and size distribution. Substrate analysis of $PM_{2.5}$ mass, elements, ions, carbon, ammonia, and organics; as well as gaseous carbonyls, light HC, and heavy HC. TIGF/XAD for semi-volatiles and particulate organic compounds (PAH, alkanes, hopanes, steranes, and polar compounds). 24-hour integrated samples.
CS	Community South. Core site for spatial, time series, and multivariate receptor analyses	Former Imperial Avenue School, ~ 0.5 km south of the South Airfield. Near-field crosswind site - Aircraft, roadway, GSE, stationary & area emissions.	Continuous analysis of CO, NO_x, SO_2, $PM_{2.5}$, light scattering, black carbon, ultrafine particle number and size distribution. Substrate analysis of $PM_{2.5}$ mass, elements, ions, carbon, ammonia, and organics; as well as gaseous carbonyls, light HC, and heavy HC. TIGF/XAD for semi-volatiles and particulate organic compounds (PAH, alkanes, hopanes, steranes, and polar compounds). 24-hour integrated samples.
CN	Community North – Belford Avenue and West 95th Street. Core site for spatial, time series, and multivariate receptor analyses.	Northeast of airport, west of I-405 Freeway. Community exposure – aircraft, freeway, and area emissions.	Continuous analysis of CO, NO_x, SO_2, $PM_{2.5}$, light scattering, black carbon, ultrafine particle number and size distribution. Substrate analysis of $PM_{2.5}$ mass, elements, ions, carbon, ammonia, and organics; as well as gaseous carbonyls, light HC, and heavy HC. TIGF/XAD for semi-volatiles and particulate organic compounds (PAH, alkanes, hopanes, steranes, and polar compounds). 24-hour integrated samples.
AQ	SCAQMD SW Coastal LA County Site: Standard SCAQMD multiple pollutant monitoring site. This site is used as a Background site for spatial, and time series analyses	~0.5 km North of North Airfield Runway 24R (west end of runway). May be impacted by some airport and area sources.	SCAQMD site collects SO_2, NO_x, TSP particulate for lead and sulfate, PM_{10} (filter, not continuous), wind speed and direction, temperature, and humidity. Due to limited available power, the station upgrade included continuous analysis of $PM_{2.5}$, light scattering, and black carbon. Substrate analysis of $PM_{2.5}$ mass, elemental and organic carbon using a MiniVol sampler to provide 24-hour integrated samples.

3.4 STUDY PERIODS

Sampling for Phase III of the LAX AQSAS was carried out over two six-week periods. The Winter Sampling Season was conducted from January 31 to March 13, 2012. The Second Sampling Season was conducted from July 18 to August 28, 2012. The rationale for the two sampling seasons was to capture an accurate representation of the two distinct wind patterns observed in the South Coast Air Basin. During the Winter Season, the wind is predominantly from the east to northeast and while during the Summer Season, the wind is predominantly from the west. These two sampling seasons accurately captured the wind patterns, which have a significant impact on the dispersion of pollutants in the area. A Supplemental Study was conducted from September 4, 2012 through September 11, 2012 to further examine the chemical nature of UFP in jet exhaust and source contributions of UFP in communities east of LAX.

The two sampling seasons were also originally chosen to represent aircraft traffic patterns during the winter and summer. Generally, the summer tends to have slightly higher takeoff and landing frequencies than the winter. During the 42-day Winter Monitoring Season in Phase III, there were 70,696 arrivals and departures (in total) at LAX. During the 42-day Summer Monitoring Season in Phase III, there were 74,072 arrivals and departures (in total) at LAX. Therefore, the Winter and Summer Monitoring Seasons had similar arrival and departure rates during the dates encompassing the study period, with summer having a slightly higher number of arrival and departures.

3.5 MEASUREMENT METHODS

Measurement methods used during Phase III are described below. Analysis of their performance can be found in detail in Section 4 of this report.

3.5.1 Continuous Monitoring

The continuously monitored parameters are shown in both Table 3-3 and Table 3-5. Further detailed descriptions are included below and in Appendix 3-2.

3.5.2 Elemental Carbon (Black Carbon)

Black carbon (BC) was measured with the Magee Scientific Aethalometer, which uses a continuous filtration and optical measurement method to provide a continuous readout of BC concentration. The Aethalometer was equipped with a BGI Model SCC 1.197 particle size-selective inlet port. Air was sampled at a flow rate of approximately 5 liter per minute (lpm), using a mass flow meter and internal pump. The cut point of the inlet used for the Study was 1 micron (PM_1). The flow rate was monitored by an internal mass flow meter. Samples were collected on a quartz fiber filter tape, and a continuous optical analysis was performed during sample collection. The Magee Aethalometer filter tape advances automatically once the filtered spot reaches a manufacturer specified density (degree of attenuation). This ranged anywhere from multiple times per day to two days. The analysis provided a new reading for every defined base time period (two monitors with 1-min and two monitors with 5-min resolution). The 5 minute resolution data were collected at the CN and CS sites. The data were stored to media

(diskette or memory card) and produced as an analog voltage, which was continuously measured by a dedicated data logger.

The principle of the Aethalometer is to measure the attenuation of a beam of light transmitted through a filter while it is continuously collecting an air sample. The BC content of the aerosol collected at each measurement time can be determined by using the appropriate value of the specific attenuation for that particular combination of filter and optical components. An increase in optical attenuation from one time period to the next is due to the increment of aerosol BC collected during the period. This increment is divided by the volume of air sampled during that time, which is then used to calculate the mean BC concentration for the period.

The Aethalometer was operated on the 0-1,000 $\mu g/m^3$ range with a sensitivity of less than 0.1 $\mu g/m^3$.

3.5.3 Continuous Measurement of Light Scattering

The nephelometer (pDR-1200AN) measures the light scattering in an airflow passing through the instrument's scattering chamber. The instrument reading, which is proportional to the light-scattering coefficient, indicates the total amount of light scattered into all directions by the air sample.

The scattering volume is illuminated from the side by a diffuse light source. The photomultiplier detector views a dark trap through a conical scattering volume defined by a series of baffles containing circular holes. The baffles prevent the photomultiplier from viewing any surface illuminated by the light source, except for the internal span calibration chopper.

Light falling on the photomultiplier is approximately proportional to the light-scattering coefficient of the air sample in the scattering chamber, which is a measure of the total amount of light scattered at all angles by the air sample. The nephelometer processes these data to subtract light scattering by the air to obtain a measure of the scattering coefficient b_{sp}. The nephelometer is calibrated to read zero when filled with particle-free air.

3.5.4 Continuous Carbon Monoxide Monitoring

Carbon monoxide (CO) concentrations were measured using a Thermo Scientific Model (TSI) 48 analyzer. The TSI 48 uses infrared detection and the gas filter correlation principle of operation for measurement of CO. The basic components of the gas correlation system are: infrared (IR) source, chopper and rotating gas filter wheels, multiple optical pass sample cell, band pass filter, IR detector and electronic signal processor. Radiation from the IR source is chopped and then passed through a gas filter that alternates between CO and nitrogen (N_2) due to rotation of the filter wheel. The radiation then passes through a narrow band pass filter and a multiple optical-pass sample cell and falls on a solid state IR detector. The CO gas filter produces a reference beam that cannot be further affected by CO in the sample chamber. The N_2 side of the filter wheel, which is transparent to IR radiation, produces a measure beam that can be absorbed by CO. The chopped detector signal is modulated by the alteration between the two gas filters with amplitude proportional to the concentration of CO in the sample chamber. Other gases do not

cause modulation of the detector signal since they absorb the reference and measure beams equally; therefore, the gas filter correlation system responds solely to CO.

The CO analyzers were operated on the 0-50 ppm range with a minimum detection level of 0.1 ppm. Analyzer outputs were time averaged at an interval of one minute.

3.5.5 Continuous Oxides of Nitrogen

Ambient levels of NO_x were monitored continuously using Thermo Scientific (TSI) Corporation Model 42C and 42I NO_x analyzers. This instrument is sensitive, interference free, and provides long-term zero and span stability for continuous monitoring of NO, NO_2, and NO_x.

The TSI 42 series monitors detect NO in ambient air by reacting NO with ozone. The resulting chemiluminescent reaction is monitored through an optical filter by a photo-multiplier tube (PMT) located at the end of the reaction chamber. The optical filter limits the wavelength of light measured by the PMT, so that it corresponds specifically to the wavelength of the chemiluminescent reaction between NO and O_3.

Total NO_x was measured by passing the sample gas through a catalytic converter, which converts NO_2 quantitatively into NO, where it was measured by the detector. The microprocessor-controlled analyzer directs sample flow either through the catalytic converter (measuring NO_x) or by passing the sample directly into the detector (measuring NO). Signals from the PMT are conditioned and fed to the microprocessor where a mathematical algorithm is utilized to calculate three independent outputs: NO, NO_2, and NO_x.

The NO_x analyzer was operated on the 0-0.500 ppm range, with a minimum detection level of 0.001 ppm. Analyzer outputs were averaged at an interval of one minute.

3.5.6 Continuous Trace Level Sulfur Dioxide

Ambient levels of SO_2 were monitored continuously by using Thermo Model 43i TLE SO_2 analyzers at the CS, CN, CE, and AQ sites. The Model 43i TLE is capable of measuring the amount of SO_2 in the air as low as 50 parts per trillion (ppt). Dual sets of reflective band pass filters are less subject to photochemical degradation and more selective in wavelength, which results in increased detection specificity and long term stability. The Model 43i TLE uses pulsed fluorescent radiation of SO_2 molecules. A reaction chamber is irradiated by UV light and the fluorescent radiation is detected by a sensitive PMT. Associated electronics amplify the output from the PMT. The output voltage is proportional to SO_2 concentrations.

The SO_2 analyzer was operated on the 0-500 ppb range during the Winter Season and 0-50 ppb range during the Second Season, with a minimum detection level of 0.05 ppb for both seasons. Analyzer outputs were averaged at an interval of one minute.

3.5.7 Continuous Measurement of $PM_{2.5}$

Continuous monitoring of $PM_{2.5}$ was performed using a Met One BAM-1020, which is a beta-attenuation monitor manufactured by Met One Instruments, Inc. (Met One).

The beta attenuation process uses a small source of beta particles (carbon-14, 60 microcuries) coupled to a sensitive detector that counts the emitted beta particles. The dust particles are collected on glass fiber filter tape placed between the beta source and the detector. Dust on the filter intercepts some of the beta particles. The BAM-1020 automatically advances the filter tape at the end of each hour. The air stream is heated to reduce the relative humidity of the sample stream to below 60 percent to reduce positive artifact measurement due to condensation on the filter. The reduction of beta particles is proportional to the amount of dust on the filter, which allows the mass of dust to be determined from the beta particle counts. The dust mass is divided by the air volume collected during the filter exposure time to determine the PM concentration.

The BAM-1020 monitor was equipped with particle size selective inlets, which are designed to remove particles larger than the desired size range from the airflow, based on the flow rate. Sampling flow rate is critical in maintaining the proper particle size cut points of the inlets. Flow rates were maintained at 16.7 liters per minute (LPM) in the BAM-1020 using an integral flow meter, pressure sensor, and ambient temperature sensor on board each monitor.

Data from the BAM-1020 unit were recorded by digital data loggers and each unit's internal data logger, at an averaging interval of 60 minutes. The detection level of the BAM-1020 is 1 $\mu g/m^3$ and the instruments were operated on the 0-1 mg/m^3 (0-1000 $\mu g/m^3$) range.

3.5.8 Continuous Measurement of Ultrafine Particulates

Scanning Mobility Particle Sizers (SMPS) were operated at the three core sites (CE, CN, and CS) to measure particle size distributions continuously. The types of instruments provided by DRI were the SMPS 3936N25A (TSI Inc., Shoreview, MN), SMPS 3936L10 (TSI Inc., Shoreview, MN), and Grimm SMPS+C (Grimm Aerosol Technik, Ainring, Germany). A SMPS system typically consists of three major components: bipolar charger, mobility classifier, and condensation particle counter (CPC). Particles first pass through a bipolar charger to establish an equilibrium charge distribution and then enter an electrical mobility classifier in which they are separated according to their electrical mobility. The CPC measures the particle concentration at each mobility size range. The TSI SMPS 3936N25A has the capability of measuring size distributions in the range of 2.5 to 80 nm in 96 channels, the TSI SMPS 3936L10 can measure 10 to 700 nm in 96 channels, and the Grimm SMPS+C can measure 5.4 to 358 nm in 44 channels. Thirty-two channels were used in Phase III as recommended. Time resolutions of these measurements are 2 to 3 minutes.

3.5.8.1 Sequential Filter Samples

The sequential filter sampler allows air to be drawn through a size-selective inlet and through two different sets of filter media. Solenoid valves controlled by a timer have the ability to switch between up to six sets of filters at preset intervals.

There are three versions of the sequential filter sampler. The samplers configured for $PM_{2.5}$, which were acquired through a Bendix 240 cyclone, were used in this Study. The $PM_{2.5}$ units also contain a bundle of aluminum oxide treated denuders between the inlet and the plenum to remove nitric acid gas from the air stream.

Open-faced filter packs located inside each plenum are connected to solenoid valves, which open when a sample is exposed. A vacuum pump draws air through these filters when the valves are open. The flow rate is controlled by maintaining constant pressure across a valve with a differential pressure regulator.

The $PM_{2.5}$ samples were taken on numbered filter packs in Nuclepore polycarbonate filter holders labeled FT and FQ. The FT filter packs are placed in sampling Ports 1 through 5 and consist of a Gelman (Ann Arbor, MI) polyolefin ringed, 2.0 micron pore size, 47 mm diameter PTFE Teflon membrane filter (#R2PJ047), a Nuclepore (Pleasanton, CA) 47 mm diameter fiber drain disk (#231100), and a Pre-fired Pallflex 47 mm diameter quartz fiber filter. FQ filter packs (Quartz/Nylon) on Ports 7 through 11 contain a pre-fired Pallflex 47 mm diameter quartz fiber filter (#2500QAOT-UP) and NaCl impregnated cellulose backup filter.

The Teflon membrane removes particles for gravimetric, light absorption, and x-ray fluorescence analyses. The drain disk prevents the physical contact of the Teflon and the quartz back-up filter, and the quartz back-up filter is analyzed for organic and elemental carbon to provide an estimate of gaseous organic carbon artifact. The FT and FQ quartz fiber substrates collect samples which can be analyzed for chloride, nitrate, and sulfate by ion chromatography, for potassium and sodium by atomic absorption spectrophotometry, and for organic and elemental carbon by thermal/optical reflectance. The backup cellulose/NaCl substrate measures the volatilized nitrate by ion chromatography.

Each filter pack has air drawn through it at 56.5 lpm. If a lower flow rate is desired, makeup flow through a separate Port to provide the 113 lpm flow rate is required by the inlets to maintain particle cut point of 2.5 µm. All flow rates were measured before and after sampling with a rotameter transfer standard. Elapsed time meters on each channel measure the sample duration. The timing sequence is set for continuous sampling so following completion of sampling on Ports 5 and 11, the SFS automatically switches to Ports 1 and 7. Dynamic field blanks are located in Port 6 for FT ($PM_{2.5}$ Teflon / quartz), TT (PM_{10} Teflon), or GK (Glass fiber / citric acid impregnated, cellulose / potassium carbonate, impregnated cellulose) filter packs and in Port 12 for FQ, FT or GK filter packs.

3.5.9 Saturation and Gradient Monitoring

3.5.9.1 Passive Sampling

The ability of passive samplers to collect analytes over extended periods of time allowed for potentially high sensitivity for low pollutant concentrations. Sensitivity is limited only by the amount of time a sampler can be exposed and the blank value of the analyte on an unexposed adsorbent surface. Five different types of passive samplers were used, each having a unique adsorbent and method of analysis. The analysis methods that were used are listed in Table 3-6.

Table 3-6. Passive Sampling Analysis Methods

Manufacturer	***Target Pollutant***	***Analysis Method***
Ogawa	NO_2/NO_x	Colorimetry for nitrite
Ogawa	SO_2	Ion Chromatography
Radiello	VOC (BTEX)	Thermal Desorption/GC/MS
Radiello	Aldehyde	HPLC/UV

Pollutants accumulate over time via diffusion of the gaseous pollutants across a surface to an adsorbing material. The continual adsorption of the pollutant from the air maintained a concentration gradient near the surface that allowed uptake of the pollutant to occur without any forced air movement (i.e., no pump or fan required). Unlike other samplers that use axial diffusion from one surface to another, Radiello samplers use radial diffusion over a microporous cylinder into an absorbing inner cylinder, which gives about a 100 times higher uptake rate.

After sampling, the collected pollutant was desorbed from the sampling media by thermal or chemical means and analyzed quantitatively. The average concentration of the pollutant in the air the sampler was exposed to can be calculated from the following relationship:

$$\text{Concentration} = \frac{\text{Mass of Analyte}}{\text{Sampling Rate} * \text{Sampling Time}}$$

The sampling rate for every analyte was calculated experimentally as pumps are not used in passive collection. Radiello[3] and Ogawa and Company[4] supply sampling rates for numerous commonly collected compounds. These sampling rates have been validated by DRI in chamber experiments for NO_x, formaldehyde, acrolein and BTEX. Mass of the analyte was calculated as the average blank result subtracted from the analytical result. Sampling time was the amount of time the sampler was exposed. While lengthening the exposure time corresponded to an increase in sensitivity, it should be noted that exposure time was generally limited to a maximum of 14 days due to the capacity of the adsorbents.

Further information about Ogawa Passive Samplers and Radiello Diffusive Samplers can be found in Section B2.3 of the Monitoring and Quality Assurance Project Plan (MQAPP) (Appendix 3-3).

3.5.10 Chemical Speciation

3.5.10.1 Carbon Speciation Sampling

Aerosol samples were collected using a MiniVol Portable air sampler manufactured by Airmetrics. The MiniVols collected $PM_{2.5}$ which was analyzed for elements, ammonia, carbon (using the IMPROVE method), ions, volatile nitrate and select organics (method TO-13A).

[3] Information about Radiello Passive Samplers can be found at http://www.radiello.com.
[4] Information and sales for Ogawa passive samplers can be found at http://www.ogawausa.com/.

The Airmetrics MiniVol is equipped with an inlet impactor capable of separating particulate matter by size. The impactors had a $PM_{2.5}$ cut point and were designed to operate at a fixed flow rate of 5 LPM at actual conditions. The units were also equipped with a flow control device, which maintained a specified flow rate, and a flowmeter to measure the flow rate during the sampling period. An elapsed time meter and a programmable timer allowed the sampler to run unattended. To allow longer unattended sampling durations, a direct power system using a switch-mode 12V power supply in place of the battery system, which had been tested and proved reliable over a period of five weeks of continuous operation, was used. The new systems are also much lighter in weight and require only about 300 mA of 110V line power to operate (less than a 40W light bulb). This allowed for multiple complete twenty-four hour sampling periods.

3.5.10.2 Hydrocarbons Sampling

Heavy Hydrocarbons
Sampling of heavy hydrocarbons (VOCs) was conducted by drawing air through Tenax sorbent tubes. The VOCs in the sample were then desorbed/extracted and analyzed. The sampling apparatus included an in-line particulate filter, a sampling tube and a flow controller/pump combination. Twenty four-hour integrated samples starting at 12:00 AM PST were collected on ten consecutive days at a flow rate of 1.0 liter per minute (lpm).

A check of the flow controller was made by placing the sorbent sample tube on the sampling train and making flow adjustments using a mass flow meter. At the end of the sampling period the flow was checked a second time to ensure the flow rate has not deviated more than 10 percent.

Light Hydrocarbons
SUMMA canisters, six liters in volume, were cleaned prior to sampling by repeated evacuation and pressurization with humidified zero air, as described in the U.S. EPA "Technical Assistance Document for Sampling and Analysis of Ozone Precursors" (October 1991, EPA/600-8-91/215). Six repeatable cycles of evacuation to ~0.5 mm Hg absolute pressure, followed by pressurization with ultra-high purity (UHP) humid zero air to ~15 psig were used. One canister out of the 10 per lot was filled with humidified UHP zero air and analyzed by the GC/MS/FID method TO-15 method (DRI SOP 704.2). The canisters were considered clean when the target compound concentrations were less than 0.05 ppbv each. The canister sampling systems were cleaned prior to field sampling by purging with humidified zero air for forty-eight hours, followed by purging with dry UHP zero air for one hour.

After cleaning, air from the canisters was evacuated. The canisters had a six-liter capacity and an initial vacuum of approximately negative 30 inches Hg. A seven micron pre-filter was installed prior to the inlet of the canister to minimize entry of particulates.

A vacuum gauge was used to measure the initial and final vacuum of the canister and monitor the filling of the canister during the actual sampling. The gauges were used to provide a relative measure of pressure change between the initial and final vacuum of the canister to assure no leaks during the sampling. Prior to sampling, the gauge was used to confirm the pressure read between negative 29 inches and negative 30 inches Hg for each canister.

Fixed-rate flow controllers and micron particulate filters were placed on the canister after measurement of initial canister pressure using a vacuum gauge. The flow-controllers were pre-set to meter the flow of air into the canister at a relatively constant rate over the course of a 24-hour sampling period to fill the canister to positive pressure.

3.5.11 Carbonyl Sampling

Waters, Inc.'s 2,4-dinitrophenylhydrazine (DNPH) impregnated Sep-Pak cartridge was used to collect carbonyls, such as formaldehyde, acetaldehyde, and acrolein, according to the U.S. EPA Method TO-11A. When air was drawn through the cartridge at a rate of one liter per minute for a 24-hour period, carbonyls in the sample were captured by reacting with DNPH to form hydrazones. The hydrazones were eluted from the sampling cartridges using acetone-free acetonitrile (CAN) and were quantified using reverse-phase high performance liquid chromatography (HPLC) with ultraviolet absorption detection at 360 nm. The sample pump flow rate was measured pre- and post- sample with an NIST traceable device.

3.5.12 Meteorology

3.5.12.1 Horizontal Wind Speed and Wind Direction Measurements

Horizontal wind speed and direction sensors were installed on a 10-meter tower at the CE and CS sites. The sensors were Met One Model 010 and 020 Series wind speed and wind direction sensors, respectively. Wind speed was measured using an anemometer, which operates based on a magnetically induced AC current that produces a frequency proportional to wind speed. The wind direction sensor was a lightweight vane that senses position by a precision potentiometer. The wind sensors were installed at the 10-meter level. The standard deviation (sigma-theta) of the wind direction was calculated by the data logger using the U.S. EPA-preferred Yamartino method (U.S. EPA, 2000). Data were recorded for both wind speed and wind direction on a 1-minute time-averaged basis.

3.5.12.2 Ambient Temperature Measurements

Ambient air temperature at the CE and CS sites was measured at two levels (8-meter and 2-meter) on the 10-meter tower using Met One Model 060A temperature probes housed in aspirated enclosures.

This sensor configuration is designed to provide complete signal wire compensation and eliminate any measurement errors resulting from signal cable resistance. The motorized aspirator was mechanically ventilated with a fan to prevent conductive interference from precipitation and radiation from solar and terrestrial sources. Temperature data were recorded in units of degrees Celsius for both elevations on a 1-minute time-averaged basis.

3.5.12.3 Solar Radiation Measurements

At the CE Site, solar radiation measurements were made using an Eppley Model 8-48 pyranometer located at about the 2-meter level. The sensor is designed for the measurement of

global (sun and sky) radiation. The detector is a differential thermopile made of plated copper on constantan junctions. Hot-junction receivers are covered with a stable black coating and cold junction receivers are whitened with non-hygroscopic barium sulfate. The sensor is temperature compensated using thermistor circuitry to within 1.5 percent of the range of -20 °C to +40 °C. The sensor is sensitive to wavelengths of 0.285 to 2.800 µm. Solar radiation data were recorded in kilowatts per meter squared (KW/m^2) on a 1-minute time-averaged basis. These data were used for dispersion modeling purposes.

3.5.12.4 Relative Humidity Measurements

The relative humidity (RH) sensor was housed in an aspirated radiation shield at the CE site. RH measurements were made using the Met One Model 083E RH sensor, which measures the variance in the capacitance change of a one-micron thick dielectic polymer layer. The film absorbs water molecules through a metal electrode and causes capacitance changes proportional to RH. RH data were recorded in percent on a 1-minute time-averaged basis. These data were used for dispersion modeling purposes.

3.6 SAMPLING FOR CMB RECEPTOR MODELING

Ambient speciation measurements were collected for fourteen sets of 24-hour VOC and $PM_{2.5}$ samples. These measurements were conducted at the CE, CN, and CS sites for both the Winter and Summer Monitoring Periods. The sets of speciation samples included: Teflo®, 2.0 µm pore size, 47 mm diameter Teflon filters (RPJ047), and Pallflex 47 mm diameter pre-fired quartz filters (2500 QAT-UP) collected with medium-volume sequential filter samplers (SFS) at 56.6 liters per minute for each filter channel for $PM_{2.5}$ mass, organic carbon (OC), elemental carbon (EC), elements (Na to U), and nitrate, sulfate, ammonium, sodium, and chloride ions; Teflon-impregnated glass fiber filters (TIGF) with backup XAD resin cartridges for separate analysis of 49 particulate and semi-volatile phase alkanes, 95 polycyclic aromatic hydrocarbons (PAH), 15 hopanes and steranes, and 99 polar organic compounds; whole air canister samples for 71 C_2-C_{11} hydrocarbons; Tenax cartridges for 66 C_8-C_{28} hydrocarbons; and Waters Sep-Pak 2,4-dinitrophenylhydrazine (DNPH) cartridges for 14 C_1-C_8 aldehydes and ketones.

SUMMA canisters, six liters in volume, were cleaned prior to sampling by repeated evacuation and pressurization with humidified zero air, as described in the U.S. EPA "Technical Assistance Document for Sampling and Analysis of Ozone Precursors" (October 1991, EPA/600-8-91/215). Six repeatable cycles of evacuation to approximately 0.5 mm Hg absolute pressure, followed by pressurization with ultra-high purity (UHP) humid zero air to approximately 15 psig were used. One canister out of the 10 per lot was filled with humidified UHP zero air and analyzed by the gas chromatography/mass spectrometry flame ion detection (GC/MS/FID) method (DRI SOP 704.1). The canisters are considered clean if the target compound concentrations are less than 0.05 ppbv each. The canister sampling systems were cleaned prior to field sampling by purging with humidified zero air for forty-eight hours, followed by purging with dry UHP zero air for one hour. After cleaning, air from the canisters was evacuated. The canisters have a six-liter capacity and an initial vacuum of approximately -30 inches Hg. A seven micron pre-filter was installed prior to the inlet of the canister to minimize entry of particulates. A vacuum gauge was used to measure the initial and final vacuum of the canister and monitor the filling of the

canister. The flow-controllers will be pre-set to meter the flow of air into the canister at a relatively constant rate over the course of a twelve-hour sampling period to fill the canister to positive pressure. After sampling the samples were packaged and shipped to the DRI laboratory for analysis.

Sampling of C_8-C_{28} heavy hydrocarbons (VOCs) and carbonyl compounds was conducted by drawing air through Tenax sorbent tubes and DNPH cartridges, respectively. The VOCs in the sample were desorbed/extracted and analyzed. The sampling apparatus included an in-line particulate filter, a sampling tube, and a critical orifice to control the flow rate. A single pump and timer were used for all VOC sampling media at each site. Samples were collected over a 24-hour period at a flow rate of approximately 1.0 lpm[5]. Checks of the flow controller were made by placing the sorbent sample tube on the sampling train and making flow adjustments using a mass flow meter. At the end of the sampling period the flow was checked a second time to ensure the flow rate had not deviated more than 10 percent.

The Teflon filters were weighed on a Mettler Toledo MT5 electro microbalance and analyzed for elements by energy dispersive X-ray fluorescence (EDXRF) analysis on a PANalytical Epsilon 5 EDXRF analyzer. PM samples were also analyzed by inductively coupled plasma-mass spectrometry (ICP-MS) for total Mg, Al, Ca, V, Cr, Mn Fe, Ni, Cu, Zn, Mo, Ba, Ce, Hg, and Pb. The quartz filters were analyzed for EC and OC by thermal optical reflectance (TOR) method (Chow et al., 2001) using the IMPROVE_A (Interagency Monitoring of Protected Visual Environments) temperature/oxygen cycle protocol (Chow et al., 2007).

Speciated C_2-C_{11} hydrocarbon compounds were measured using gas chromatography/mass spectrometry (GC/MS) technique according to EPA Method TO-15 (EPA, 1999a). The GC-FID/MS system includes a Lotus Consulting Ultra-Trace Toxics sample preconcentration system (Lotus Consulting, Long Beach, CA) built into a Varian 3800 GC with FID coupled to a Varian Saturn 2000 ion trap MS. Light hydrocarbons (C_2-C_4) are separated on a Chrompack Al_2O_3/KCl column (25m x 0.53mm x 10µm) leading to FID. The mid-range and heavier hydrocarbons (C_4-C_{11}) are deposited to a J&W DB-1 column (60m x 0.32mm x 1µm) connected to the ion trap MS. The GC initial temperature is 5 ºC held for approximately 9.5 minutes, then ramps at 3 ºC/min to 200 ºC for a total run time of 80 minutes. Calibration of the system is conducted with a mixture that contained the most commonly found hydrocarbons (75 compounds from ethane to n-undecane, purchased from Air Environmental) in the range of 0.2 to 10 ppbv.

C_1-C_7 carbonyl compounds were measured as their hydrazone derivative according to EPA Method TO-11A (EPA, 1999b) using a high performance liquid chromatograph (Waters 2690 Alliance HPLC System with 996 Photodiode Array Detector). After sampling, the cartridges were eluted with acetonitrile. An aliquot of the eluent was transferred into a 2-ml septum vial and injected with an autosampler into a Polaris C_{18}-A 3µm 100 x 2.0 mm HPLC column.

Tenax samples were analyzed by thermal desorption GC/MS based on the EPA Method T0-17 (EPA, 1999c). The GC/MS system includes a Gerstel TDS3 with TDSA autosampler mounted on a Varian 3800 GC coupled to a Varian Saturn 4000 ion trap MS. The TDS3 has a thermal

[5] The flow rate for Tenax samples was reduced to approximately 100 cc/min halfway through the Winter Monitoring Period to reduce breakthrough losses for the lighter MW compounds.

desorption chamber where Tenax samples are heated while being flushed with helium. A deactivated steel transfer line connects the desorption chamber to a cryo-focusing injection system (CIS) cooled by liquid nitrogen. A Varian VF-1MS (60m x 0.32mm x 1.0µm) column in the GC connects the TDS3 to the MS. The initial temperature of the Gerstel TDS is 20 ºC for 1 minute, then ramps 60 ºC/min to 320 ºC and holds for 8 minutes. During this time, the temperature of the transfer line is held at 300 ºC and the cryogenically cooled injection liner is held at -150 ºC. After the desorption hold time is complete, the GC run begins and the CIS temperature ramps at 10 ºC/second to 300 ºC and holds for 2.25 minutes. A 20:1 split flow is set at the CIS to provide split injections to the GC column. The initial temperature of the GC oven of 30 ºC is held for 3 minutes and then it ramps at 5 ºC/min to a final temperature of 320 ºC, where it is held for 4 minutes. From 9 to 64 minutes the MS scans from 50 to 300 atomic mass unit (a.m.u). Calibration of the system is performed by spiking unsampled Tenax tubes with mixtures of C_8-C_{28} hydrocarbons at increasing concentrations.

Semi-volatile and condensed-phase organic species that were identified and quantified from the TIGF filters and XAD-4 resin samples included 55 polycyclic aromatic hydrocarbons (PAH), 23 hopanes and steranes, and 50 alkanes and cycloalkanes in the C_{12} to C_{40} range using a modified EPA Method TO-13A (EPA, 1999c; Wang et al., 1994a; Wang et al., 1994b). The higher molecular weight ~C_{20} to C_{35} alkanes and cycloalkanes in lubricating oils appear as a single hump on the gas chromatograms. These compounds were quantified together based on the ions with mass-to-charge ratios (m/z) of 57 and 55, which are characteristic aliphatic hydrocarbons, and reported as total unresolved complex mixture (UCM) of alkanes. The TIGF filters and XAD-4 resins were extracted separately using the Dionex ASE with dichloromethane followed by hexane extraction under 1500 psi at 70 ^{o}C. Prior to extraction, the following deuterated internal standards were added to each filter and XAD-4 sorbent: naphthalene-d8, biphenyl-d10, acenaphthene-d10, phenanthrene-d10, anthracene-d10, pyrene-d10, benz(a)anthracene-d12, chrysene-d12, benz(k)fluoranthene-d12, benzo[e]pyrene-d12, benzo[a]pyrene-d12, perylene-d12, benzo[g,h,i]perylene-d12, coronene-d12, cholestane-d6, hexadecane-d34, eicosane-d42, tetracosane-d50, octacosane-d58, and triacontane-d62. All extracts were concentrated by rotary evaporation at 35°C under gentle vacuum to approximately1 mL and filtered through 0.2 µm polytetrafluoroethylene (PTFE) disposal filter (Whatman Pura discTM 25TF), rinsing the flask three times with 1 ml dichloromethane and hexane (50/50 by volume) each time. The solvent was exchanged to toluene under ultra-high purity nitrogen.

The TIGF filters and XAD-4 extracts were analyzed separately by GC/MS, using a Varian CP-3800 GC equipped with a CP8400 autosampler and interfaced to a Varian 4000 ion trap for analysis of all semi-volatile and condensed-phase organic compounds except hopanes and steranes, as described before (Fujita et al., 2007). Hopanes and steranes were analyzed using the Varian 1200 triple quadrupole gas chromatograph/mass spectrometer (GC/MS/MS) system with CP-8400 autosampler due to the higher sensitivity of this system. Quantification of the individual compounds was obtained by the SIM technique, monitoring the molecular (or the most characteristic) ion of each compound of interest and the corresponding deuterated internal standard.

Fuel samples were analyzed by both gas chromatography/flame ionization detection (GC-FID) and GC/MS to get the range of analytes from C_4-C_{30}. For the most volatile hydrocarbons, C_4-C_6

range, a Varian 3800 GC equipped with liquid nitrogen coolant for the oven and an FID for detection was necessary. Mid-range and heavy hydrocarbons, C_6-C_{30}, were quantified with a Varian 3800 GC coupled to a Varian Saturn 4000 ion trap mass spectrometer. Both GC's had a Varian 8400 auto sampler for making 1µl liquid injections of fuel samples. The GC/FID had a J&W DB-1 (60m x 0.32mm x 1.0µm) column connecting the 1177 liquid injector to the FID. The injector temperature was maintained at 320 ºC and 300:1 split/splitless injections were made. The GC oven initial temperature of 5 ºC was held for 9.5 minutes and then ramped to 200 ºC at 5 ºC/min, then to 320 ºC at 20 ºC/min. The range of the FID was set to 12. Calibration of the FID for analytes was achieved by injecting a standard solution of C_6-C_{30} hydrocarbons and observing the detector response in units of peak size/µmol.C for several compounds and applying that to hydrocarbons that were not present in the standard, the C_4-C_6 range, but were present in fuel samples and needed for source profiles.

The GC/MS had a Phenomenex Inferno ZB-5HT (60m x 0.25mm x 0.25 µm) column connecting the 1177 liquid injector to the MS. The injector temperature was maintained at 320 ºC and 100:1 split/splitless injections were made. The GC oven initial temperature of 60 ºC was held for 3 minutes before ramping to 350 ºC at 10 ºC/min with a final hold time of 3 minutes. The MS scanned 50-200 a.m.u. from 4.0-34 minutes. Calibration of the MS for each analyte was achieved by injecting standard solutions of varying concentrations of C_6-C_{30} hydrocarbons. Some overlap of hydrocarbons reported by both GC/FID and GC/MS allowed comparison between the methods for assurance that results between detection techniques were comparable.

3.7 SUPPLEMENTAL STUDY FOR ULTRAFINE PARTICLE SOURCES AND COMPOSITION

Preliminary analysis of the monitoring data and the NTA results for the Winter Monitoring Season indicated that airport operations were potentially large contributors to UFP concentrations in adjacent communities located downwind. UFP and SO_2 concentrations at the CE site showed different diurnal and day-of-week patterns as compared to other pollutants (CO, NO_x, etc.). Weekday levels of CO, NO_x, and BC peaked during the morning commute periods at the CE and CN sites, but SO_2 and UFP showed steady increases during the day. While CO, NO_x, and BC, which are mainly associated with on-road motor vehicles, were substantially lower on Sundays relative to weekdays, SO_2 and UFPs showed less day-of-week dependence. In contrast, SO_2 and UFP concentrations peaked during the morning commute period at the CS site and were very low during the day. The observed temporal and spatial variations in pollutant concentrations in the Winter Monitoring Season and diurnal variations in wind direction, with northeast wind in the morning and west winds in the afternoon, suggested jet exhaust may be a significant source of SO_2 and UFPs in areas downwind of LAX. NTA results also supported these initial findings.

As a result of the preliminary observations from the Winter Monitoring Season, a three-part Supplemental Study was conducted. The main goals of this supplemental study were to further examine UFP composition as well as the potential source contributions to areas located downwind of LAX.

The Supplemental Study A study plan included operation of two SMPS at full scan, one with and one without a thermal denuder (TD) at the CE site followed by the Trinity Lutheran Church/School (TLCS) located 1.5 miles directly south of the CE site and out of the LAX flight path. The TD temperatures used for the study were: 25 ºC (ambient), 125 ºC (evaporation of sulfuric acid and low molecular weight organics), 175 ºC (evaporation of ammonium sulfate, bisulfate, and higher molecular weight organics), and 300 ºC (what remains is refractory material) (Burtscher et al., 2001).

The Supplemental Study B study plan included the operation of two SMPS at both the CE and TLCS sites with each measuring a single particle size bin, one at 15 nm and a second at 50 nm. Measurement of a single size bin rather than the entire range allowed for operation with time averages as short as one second rather than two to three minutes for full scans. The objective of this portion of the Supplemental Study was to simultaneously monitor very fine particles that may be associated with jet exhaust and larger particles that may be associated with on-road vehicle exhaust. Finer time resolution allowed for detection of possible brief peaks in UFP concentrations that may be associated with the two sources to be revealed. Measurements were made at both sites over one weekend and on two weekdays to allow for examination of diurnal and day-of-week variations of 15 nm versus 50 nm particle number concentrations.

The Supplemental Study C study plan included the operation of two SMPS, both measuring a single particle size bin at 15 nm, one with and one without a TD and a third SMPS measuring a single particle size bin at 50 nm at the blast fence at the east end of South Airfield Runway 25R. The monitors were installed behind the blast fence, using the existing power and shelter to operate.

3.8 DATA MANAGEMENT – DATA REDUCTION

3.8.1 Minute and Hourly Data

Data for NO_x, SO_2, CO, and BC were collected in one-minute intervals. BC data were collected at the CN and CS sites in five-minute intervals and at the CE and AQ sites in one-minute intervals. $PM_{2.5}$ data were collected on both a minute (pDR2.5 light scattering) and hourly (BAM $PM_{2.5}$) basis. All raw data were subjected to quality control/quality assurance procedures by both SCS Tracer and by T&B Systems. Due to potential measurement issues, such as problems during calibration or measurement time periods resetting to default settings, these raw data were adjusted, if necessary. This was done for CO and SO_2 during the Winter and Summer Seasons. After the data were appropriately reviewed, they were uploaded to an FTP site.

3.8.2 Database – Share Point

A database, located on a shared site (SharePoint), was created to house data from Phase III Study on the Tetra Tech server. All data received from the field sampling during the Winter and Summer Monitoring Periods, laboratory analysis, the quality control/quality assurance reports, and all final modeling results including: CMB, NTA, emissions inventory, AERMOD, and CMAQ files, were uploaded to the SharePoint site. All data collected from outside sources, as mentioned in Section 2.5 were also uploaded to the SharePoint site. All individuals involved in

the Study were given access to the SharePoint site and had the ability to upload their data results directly or download any uploaded data. This was to allow any team member who required any data from another member of the team to have immediate access. The SharePoint site also included all reports required as part of the Scope of Work for Phase III of the LAX AQSAS including: the Modeling and Analysis Protocol, Winter Monitoring Season Report, the TWG presentation for the Winter Monitoring Season, and reports drafted by team members.

3.9 MODELING ANALYSIS PROTOCOL

A Modeling and Analysis Protocol (MAP) was drafted to use as a guide for source apportionment analysis during receptor-oriented modeling during the Winter and Summer Monitoring Seasons. It also provided guidance for source-oriented modeling conducted that used the emissions inventory and the AERMOD dispersion modeling technique.

The MAP was used to provide general methodology on how to conduct receptor and source modeling. The receptor modeling portion consisted of Chemical Mass Balance (CMB), spatial gradient and time series analysis, and nonparametric trajectory analysis (NTA). The source modeling portion consisted of estimates of Study Area emissions (both on- and off-airport) and dispersion modeling (AERMOD and CMAQ).

For a full copy of the MAP, please see Appendix 3-4.

3.10 REFERENCES

Burtscher, H.; Baltensperger, U.; Bukowiecki, N.; Cohn, P.; Hüglin, C.; Mohr, M.; Matter, U.; Nyeki, S.; Schmatloch, V.; Streit, N.; Weingartner, E. (2001). Separation of volatile and non-volatile aerosol fractions by thermodesorption: instrumental development and applications. *Journal of Aerosol Science*, 32(4):427-442. http://www.sciencedirect.com/science/article/pii/S0021850200000896.

Chow, J.C., J.G. Watson, L-W.A. Chen, M.C.O. Chang, N.F. Robinson, D. Trimble, S.D Kohl. 2007. The IMPROVE_A temperature protocol for thermal/optical carbon analysis: maintaining consistency with a long-term database. J. Air Waste Manage. Assoc. 57: 1014-1023.

Chow, J. C., Watson, J. G., Crow, D., Lowenthal, D. H., and Merrifield, T.: 2001. Comparison of IMPROVE and NIOSH carbon measurements, Aerosol Sci. Technol., 34 (1), 23–34.

Fujita, E.M., B. Zielinska, D.E. Campbell, W.P. Arnott, J. Sagebiel, J.C. Chow, L.R. Rinehart, P.A. Gabele, W. Crews, R. Snow, N.N. Clark, S. Wayne, D.R. Lawson. 2007. Variations in speciated emissions from spark-ignition motor vehicles in the California's South Coast Air Basin. J. Air Waste Manage. 57:705-720.

U.S. Environmental Protection Agency. 1999a. Compendium Method TO-15 determination of volatile organic compounds (VOCs) in air collected in specially-prepared canisters and analyzed by gas chromatography/mass spectrometry (GC/MS); EPA/625/R-96/010b, Cincinnati OH, January 1999.

U.S. Environmental Protection Agency. 1999b. Compendium method TO-11A determination of formaldehyde in ambient air using adsorbent cartridges followed by high pressure liquid chromatography (HPLC); EPA/625/R-96/010b, Cincinnati OH, January 1999.

U.S. Environmental Protection Agency. 1999c. Compendium Method TO-13A determination of polycyclic aromatic hydrocarbons (PAHs) in ambient air using gas chromatography/mass spectrometry (GC/MS); EPA/625/R-96/010b, Cincinnati OH, January 1999.

Wang, Z., M. Fingas, K. Li. 1994a. Fractionation of a light crude oil and identification and quantification of aliphatic, aromatic, and biomarker compounds by GC-FID and GC-MS, Part I. J. Chromatograph. Sci., 32: 361-366.

Wang, Z., M. Fingas, K. Li. 1994b. Fractionation of a light crude oil and identification and quantification of aliphatic, aromatic, and biomarker compounds by GC-FID and GC-MS, Part II, J. Chromatograph. Sci., 32: 367-382.

APPENDICES

Appendix 3-1: Los Angeles International Airport Air Quality and Source Apportionment Study Phase III

Appendix 3-2: Continuous Monitoring Equipment and Recovery Rates
Daily Calibration Response of Gaseous Pollutants

Appendix 3-3: Monitoring and Quality Assurance Project Plan

Appendix 3-4: Modeling and Analysis Protocol

(This page is intentionally blank)

Appendix 3-1

FINAL SCOPE OF WORK

(This page is intentionally blank)

Los Angeles International Airport
Air Quality and Source Apportionment Study
Phase III

Final Scope of Work

November 16, 2011

Prepared for:

Los Angeles World Airports
Environmental Services Division
7301 World Way West
Los Angeles, California 90045

Prepared by:

Tetra Tech, Inc.
3475 E. Foothill Boulevard,
Pasadena, California 91107

(This page is intentionally blank)

PREFACE

This Final Scope of Work for Phase III of the Los Angeles International Airport (LAX) Air Quality and Source Apportionment Study was developed based on the "Air Quality and Source Apportionment Study (AQSAS) of the Area Surrounding Los Angeles International Airport: Technical Work Plan Revision 5, April 21, 2011," prepared by Camp Dresser & McKee, Inc. (CDM).

This Final Scope of Work incorporates a multi-tiered sampling strategy proposed by the Tetra Tech Project Team to achieve the project goals and objectives within budget constraints. The final plan combines fully-instrumented monitoring stations consisting of high time resolution monitors and comprehensive chemical speciation with supplemental saturation monitoring using passive and active low-volume aerosol samplers for subsequent gradient and spatial analyses. Additionally, the Final Scope of Work includes an evaluation of sampling locations proposed in the draft Work Plan and recommendations for potential relocation of one or more fixed stations. The Final Scope of Work also includes source characterization measurements to develop fuel-based emission factors and chemical profiles for jet aircraft emissions for application in source apportionment analysis and for evaluation of emission inventory estimates.

The Tetra Tech Project Team (Desert Research Institute, SCS Tracer, T&B Systems, Dr. Ron Henry, University of South Carolina-Chapel Hill, and K&B Environmental) will perform tasks described in the Final Scope of Work to collect required data and conduct subsequent analysis for Phase III of the LAX Air Quality and Source Apportionment Study. Dr. Charles Blanchard and Dr. Ivar Tombach will serve as special technical advisors to the Project Team.

(This page is intentionally blank)

Contents

List of Figures

List of Tables

(This page is intentionally blank)

List of Acronyms

AA	Atomic absorption
AERMOD	AMS/EPA Regulatory Model
AMS	American Meteorological Society
APU	Auxiliary power unit
AQ	Air Quality sampling site (SCAQMD Hastings Monitoring Station)
BAM	Beta attenuation monitor
BC	Black carbon
BG	Background site
C_2	Hydrocarbon compounds containing two carbon atoms
C_{12}	Hydrocarbon compounds containing twelve carbon atoms
C_{20}	Hydrocarbon compounds containing twenty carbon atoms
CARB	California Air Resources Board
CCSEM	Computer Automated Scanning Electron Microscopic
CDM	Camp Dresser & McKee Inc.
CE	Community East site
CMB	Chemical mass balance
CO	Carbon monoxide
CO_2	Carbon dioxide
Cr	Chromium
CRPAQS	Central California Particulate Air Quality Study
CS	Community South site
DNPH	2,4-dinitrophenylhydrazine
DRI	Desert Research Institute
DWP	Department of Water and Power (City of Los Angeles)
EC	Elemental carbon
EOF	Empirical orthogonal function
EPA	Environmental Protection Agency
FAA	Federal Aviation Administration
FID	Flame ionization detector

FIND	Facility Information Detail (SCAQMD emissions database)
FS	Freeway South sampling site
FTIR	Fourier Transform Infrared Spectroscopy
GC	Gas chromatography
GSE	Ground support equipment
HC	Hydrocarbon
HPLC	High-pressure liquid chromatography
ICP	Inductively Coupled Plasma
LAWA	Los Angeles World Airports
LAX	Los Angeles International Airport
MS	Mass spectrometry
MQAPP	Monitoring and Quality Assurance Program Plan
NaCl	Sodium chloride
Ni	Nickel
NMHC	Non-methane hydrocarbon
NO	Nitric oxide
NO_2	Nitrogen dioxide
NO_x	Oxides of nitrogen (or nitrogen oxides)
NTA	Nonparametric trajectory analysis
O_3	Ozone
OC	Organic carbon
OEHHA	Office of Environmental Health Hazard Assessment (State of California)
PAMS	Photochemical assessment monitoring stations
Pb	Lead
PM	Particulate matter
PM_{10}	Particulate matter with aerodynamic diameters less than or equal to 10 micrometers
$PM_{2.5}$	Particulate matter with aerodynamic diameters less than or equal to 2.5 micrometers
PMF	Positive matrix factorization
PN	Park North site
PS5	Potable Station (Demonstration Project) site No. 5
QA	Quality assurance
QC	Quality control

RFP	Request for proposal
SCAQMD	South Coast Air Quality Management District
SCE	Southern California Edison
SCOS	Southern California Ozone Study
SFS	Sequential filter sampler
SO_2	Sulfur dioxide
SO_x	Sulfur oxides
SR	South Airfield or Runway 25R sampling site
TEOM	Tapered element oscillating microbalance
TWG	Technical Working Group (for the Air Quality and Source Apportionment Study)
UFP	Ultrafine particulates
UNMIX	A multivariate receptor model (maintained by U.S. EPA)
USC	University of Southern California
U.S. EPA	United States Environmental Protection Agency
UW	Upwind site
VOC	Volatile organic compounds
XRF	X-Ray Fluorescence Analysis

(This page is intentionally blank)

Section 1
Introduction

1.1 Background

Los Angeles International Airport (LAX) is located within the South Coast Air Basin (Basin). Air quality within the Basin is widely regarded as among the poorest in the nation, and fails to attain state and federal standards for several "criteria" air pollutants including: ozone (O_3), coarse particulate matter (particles with aerodynamic diameters less than 10 μm or PM_{10}), and fine particulate matter (particles with aerodynamic diameters less than 2.5 μm or $PM_{2.5}$). Increased attention has recently been given to "toxic air pollutants" (air toxics) and "ultrafine particles" (UFP, particles with diameters less than 0.1 μm, often measured by number instead of mass) within the Basin. Although ambient levels of air toxics and UFP are not regulated in the same way as criteria pollutants, regulatory agencies have begun to examine ambient levels of air toxics and public concern over possible health effects of air toxics and UFP is increasing. LAX is adjacent to residential neighborhoods to the north, south and east. Significant concern has been expressed among local residents questioning if the airport is contributing to unhealthy air quality within their neighborhoods.

During the summer of 1999, the South Coast Air Quality Management District (SCAQMD) conducted a short-term air toxics monitoring program in the areas around LAX. The results of the study indicated that air toxics levels in the neighborhoods surrounding LAX were consistent with those found elsewhere in the Basin. However, the SCAQMD study was limited in extent and duration and did not provide data that could be used to determine either long-term impacts or LAX's contribution to toxic air pollutants. Additional potential sources of toxic air pollutants within the area include three major freeways, several heavily traveled major arterial routes, and numerous industrial facilities including: the Chevron El Segundo refinery, Hyperion Wastewater Treatment Plant, Department of Water and Power (DWP) Scattergood Generating Station, and NRG Energy's El Segundo Generating Station.

In late September 1999, Lydia Kennard, Executive Director of Los Angeles World Airports (LAWA), directed her staff and a consultant team to develop a study to provide more detailed information about the role of LAX in emitting air toxics and the total concentrations of air toxics in the surrounding neighborhoods. It is intended that the data collected from the current study will be used to assess the effectiveness of various methods for reducing airport-related emissions.

In 2000, LAWA proposed to conduct an Air Quality and Source Apportionment Study (Study), as described in the November 2000 Technical Work Plan, to increase understanding of concentrations and sources of air toxics near the airport. The November 2000 Work Plan was developed with the assistance of a Technical Working Group (TWG, see Section 1.2 below for TWG member organizations) specifically formed to oversee and provide guidance on the technical aspects of the Study. As part of the November 2000 Work Plan, a Pilot Study was scheduled to characterize aircraft emissions and to evaluate measurement methods behind the blast fence on Runway 25R. The Pilot Study was terminated on September 11, 2001 for security reasons.

In 2003, U.S. Environmental Protection Agency (U.S. EPA) conducted a peer review workshop on the 2000 Study design. The peer-review panelists concluded the Study design and technical approach met the Study's stated technical objectives and all goals and objectives were proper. In addition, the panelists provided a number of suggestions and recommendations to improve the Study's ability to meet the stated objectives. Many of the recommendations focused on utilization of newer technology that had evolved since development of the original Study Work Plan. Technology has progressed further since the peer review workshop, primarily as a result of the U.S. EPA's supersites program and research associated with homeland security.

During 2006 and 2007, the TWG was reconvened to update the Work Plan to be used as the basis for a request for proposal (RFP) to conduct the Study. The revised Work Plan was completed in May 2007, with several of the new developments identified during the peer review incorporated into the Study design. A RFP for the Study was issued in 2007 and the team led by Jacobs Consultancy (now named LeighFisher Inc.) was selected and placed under contract in early 2008.

In the summer of 2008, the Jacobs Consultancy team conducted a Technology and Methodology Demonstration Project (Demonstration Project), formerly called the Pilot Study, to provide verification that measurement methods identified in the Work Plan would work at LAX and source apportionment methods could be applied to the results. At the conclusion of the measurement phase of the Demonstration Project, it was proposed that the appropriate compounds for use in source apportionment techniques could be measured to help identify potential airport contributions at surrounding locations. Additional evaluation of the Demonstration Project data was necessary to better determine which compounds should be measured in Phase III of the Study. This additional evaluation was completed in June of 2011. The findings from this effort were used to supplement the development of the final scope of work for Phase III.

The TWG felt that several issues should be resolved before the Phase III monitoring started. Specifically, the data from the Demonstration Project should be analyzed more thoroughly to determine if trends or compositions could be identified that would help focus on appropriate compounds to measure in the Phase III Study.

In addition, the speciated organic lab analyses had been conducted using standard detection limits which led to a large number of non-detects in the samples. Organics and, more specifically, the ratios of individual organic compounds in a plume may provide a unique characterization of an aircraft turbine plume compared to a diesel engine plume. Therefore, the TWG recommended that future sampling be conducted with lower detection limits in the lab analysis. Included in the TWG recommendation was that sampling near the south airfield taxiway be conducted to develop a profile of taxiing and idling aircraft engines, which are different in composition compared to emissions from aircraft engines in takeoff mode. SCAQMD completed the taxiway sampling in April 2011 and the collected volatile organics data were provided to Countess Environmental for analysis and making recommendations to be considered in the Phase III Study.

In March 2011, Jacob Consultancy's three-year contract with LAWA for work associated with the Air Quality and Source Apportionment Study expired. Continuation of the Study work effort now occurs through one of the LAWA's on-call environmental services contractors - Tetra Tech, Inc. and its subcontractors, with the understanding that the technical work will need to be completed by the end of 2012 and the final report completed no later than April 1, 2013.

1.2 TWG Members

The original members of the TWG included air quality and aviation experts from the U.S. EPA, California Air Resources Board (CARB), SCAQMD, Federal Aviation Administration (FAA), LAWA, Desert Research Institute (DRI), University of Southern California (USC), and Camp Dresser & McKee Inc. (CDM). In 2006, the current composition of the TWG was expanded to include experts from the California Office of Environmental Health Hazard Assessment (OEHHA), the City of El Segundo, and the LAX Coalition for Economic, Environmental, and Educational Justice. The expanded composition of the TWG provided the opportunity for a variety of viewpoints to provide input and share perspectives regarding a potential work plan and monitoring and modeling protocols proposed for the Study. In addition to TWG participation in meetings over four years, the TWG was, and continues to be, provided the opportunity to review draft reports and deliverables developed for this Study.

1.3 Existing Air Quality

Acceptable ambient levels of carbon monoxide (CO), O_3, PM_{10}, $PM_{2.5}$, sulfur dioxide (SO_2), nitrogen dioxide (NO_2), sulfates, and lead (Pb) are set on a federal level by U.S. EPA and on the state level by CARB. The Basin is currently in compliance with federal and state standards for SO_2, CO, and sulfates. Both federal and state O_3, $PM_{2.5}$, and PM_{10} standards are exceeded in the Basin, but exceedances have been decreasing in number and magnitude, which indicates that control actions are succeeding. Higher pollutant concentrations are most prevalent in the central and eastern parts of the Basin rather than near the Pacific coast. The Basin is also designated as nonattainment (i.e., does not meet the standard) for the federal Pb standard and the state NO_2 standard. The Pb concentrations exceed the 2008 federal standard near two lead-acid battery recycling facilities, one in Vernon and the other in the City of Industry.

(This page is intentionally blank)

Section 2
Objectives

The objectives of this Study covered both technical and non-technical issues. The objectives, as originally defined in the 2000 draft Technical Work Plan, are presented below.

2.1 Technical Objectives

The primary focus of the remaining work effort to be completed is on the air quality impacts from LAX activities on the surrounding community. This focus takes into consideration the budget and staff resources available and the basic purposes of the Study as well as the refined details of the Phase III Study associated with the Work plan.

2.1.1 Primary Objective

The primary objective is source apportionment, specifically to assess the incremental impact or "fair-share" contribution of LAX operations on local air quality. This objective will be achieved by:

- Quantifying spatial and temporal variations in ambient air concentrations of gases and particles at LAX and adjacent communities.

- Determining fuel-based emission factors and chemical composition of jet exhaust and taxiing emissions and updating the emissions inventory of airport and non-airport sources within and near LAX. The emissions inventory will be developed primarily from previously published reports and data.

- Determining the contributions of various airport-related activities and non-airport sources to the concentrations of selected air pollutants within communities adjacent to LAX using both source and receptor modeling.

2.1.2 Secondary Objective

The secondary objective is to provide data for future studies, in terms of outdoor human exposures, meteorological effects on pollutant transport, dispersion and chemical transformation and development of a baseline for evaluating effectiveness of control strategies.

Due to the complexity of emission sources and the atmospheric environment, it is well-known that it is a major challenge to accurately quantify contributions from various emission sources and their subsequent potential impacts on air quality in adjacent communities. The LAWA Technical Work Plan provides a general overview of the receptor-oriented modeling tools that will be used to quantify the air quality impacts of airport operations and activities to the adjacent community with their respective strengths and limitations.

(This page is intentionally blank)

Section 3
Technical Approach Overview

This section describes the technical approach for accomplishing the study objectives to acquire ambient measurements that permit receptor-oriented methods to be applied, and to potentially improve emission inventories used in source-oriented source apportionment methods. The program design applies multiple approaches to the source-apportionment objective providing a higher probability of success. Deficiencies in one method are compensated for by other methods. It also permits differences between source contribution estimates from varying approaches to be identified and reconciled. A general discussion of the proposed methods and approaches follows. More specific refinements to the monitoring plan in the Draft Technical Work Plan (Version 5, dated April 21, 2011) are described in Section 4.

3.1 Quantifying Ambient Pollutant Concentration and Deposition

The primary objective of this study is to collect chemical concentrations in ambient air by operating a monitoring network over a sufficient period of time. The general layout for the originally proposed network for Phase III is presented in **Figure 3-1**[1]. Descriptions of each potential monitoring site are provided in **Table 3-1**[1].

The Draft Technical Work Plan (Version 5) prepared by CDM for Phase III of the LAX AQSAS (CDM, April 2011) described specifications for air quality monitoring at three "core" sites (with option for two additional sites) and two "satellite" sites during two seasons, each lasting six weeks. Measurements at the core sites include: continuous (1 to 5 minute resolution) measurements of carbon dioxide (CO_2), nitric oxide (NO), oxides of nitrogen (NO_x), sulfur dioxide (SO_2), black carbon (BC), particle size distributions, ultrafine particle (UFP) number concentrations and light scattering; semi-continuous (hourly) non-methane hydrocarbons (NMHC) and $PM_{2.5}$ mass; and two twelve-hour average samples during ten consecutive days within each of the two six-week sampling periods for chemical speciation of light hydrocarbons (C_2-C_{11}), heavy hydrocarbons (C_{10}-C_{18}), carbonyl compounds (C_1-C_7), and particulate organic compounds (by thermal desorption of quartz filters). Proposed core sites included a "source" site at the east end of the LAX south runway (SR), i.e., Runway 25R, a community site east of LAX (CE), an upwind site (UW) with options for an upwind background site either north or south of the LAX runway path (BG) and a downwind site south of the runway (FS) (Figure 3-1). Measurements at satellite sites included: continuous light scattering and PM size distributions and UFP number concentrations; and the same set of two twelve-hour speciation samples collected at core sites. Satellite sites were proposed within the community south (CS) and at the northeast edge (PN) of LAX. An existing SCAQMD air monitoring site (AQ) is located at the northwest boundary of the Airport. This network of monitoring sites was proposed for analysis of the spatial and temporary variations of pollutant concentrations in the communities surrounding the airport and for multivariate receptor analysis of source contributions.

[1] Figure 3-1 and Table 3-1 represent the sampling plan as described in the draft Technical Work Plan,Version 5. The revised sampling plan is presented in Section 4.

The Request for Work Task Proposal issued by LAWA for Phase III of the LAX AQSAS solicited proposals based upon the Draft April 2011 Technical Work Plan. In its successful bid, the Tetra Tech Inc. team proposed two core sites (SR and CE) with continuous monitoring and collection of time-integrated samples with methods that would ensure quantitative analysis of relevant marker species used in VOC and PM source apportionment. Continuous measurements were also proposed for a limited time at an upwind site using a mobile monitoring van. The monitoring program originally proposed by the Tetra Tech team also included saturation monitoring consisting of seven-day integrated nitrogen dioxide (NO_2), oxides of nitrogen (NO_x) and sulfur dioxide (SO_2) using Ogawa passive samplers, and VOC (benzene, toluene, ethylbenzene and xylenes) and carbonyl compounds using Radiello passive samplers during six consecutive weeks in two seasons. Additionally, the Tetra Tech team proposed seven-day integrated Teflon and quartz filters to be collected with portable Airmetrics MiniVol samplers and analyzed for $PM_{2.5}$ mass, elements and organic carbon (OC) and elemental carbon (EC). Saturation monitoring would also include additional "gradient" sites consisting of passive-only sampling for NO_2, NO_x, and SO_2 to characterize the zones of influence near emission sources (e.g., near the east end of the Runway 25R or both prevailing upwind and downwind edges of the roadside along freeways and major arterials.

Spatial surveys of pollutant concentrations were conducted prior to the Phase III main study using a mobile monitoring van to guide the selection of saturation monitoring sites. The results of the mobile surveys (see Appendix A) were considered in determining further refinements to the originally proposed monitoring plan given existing resources and project budget. The rationale for these changes and specific refinements are described in Section 4.1.

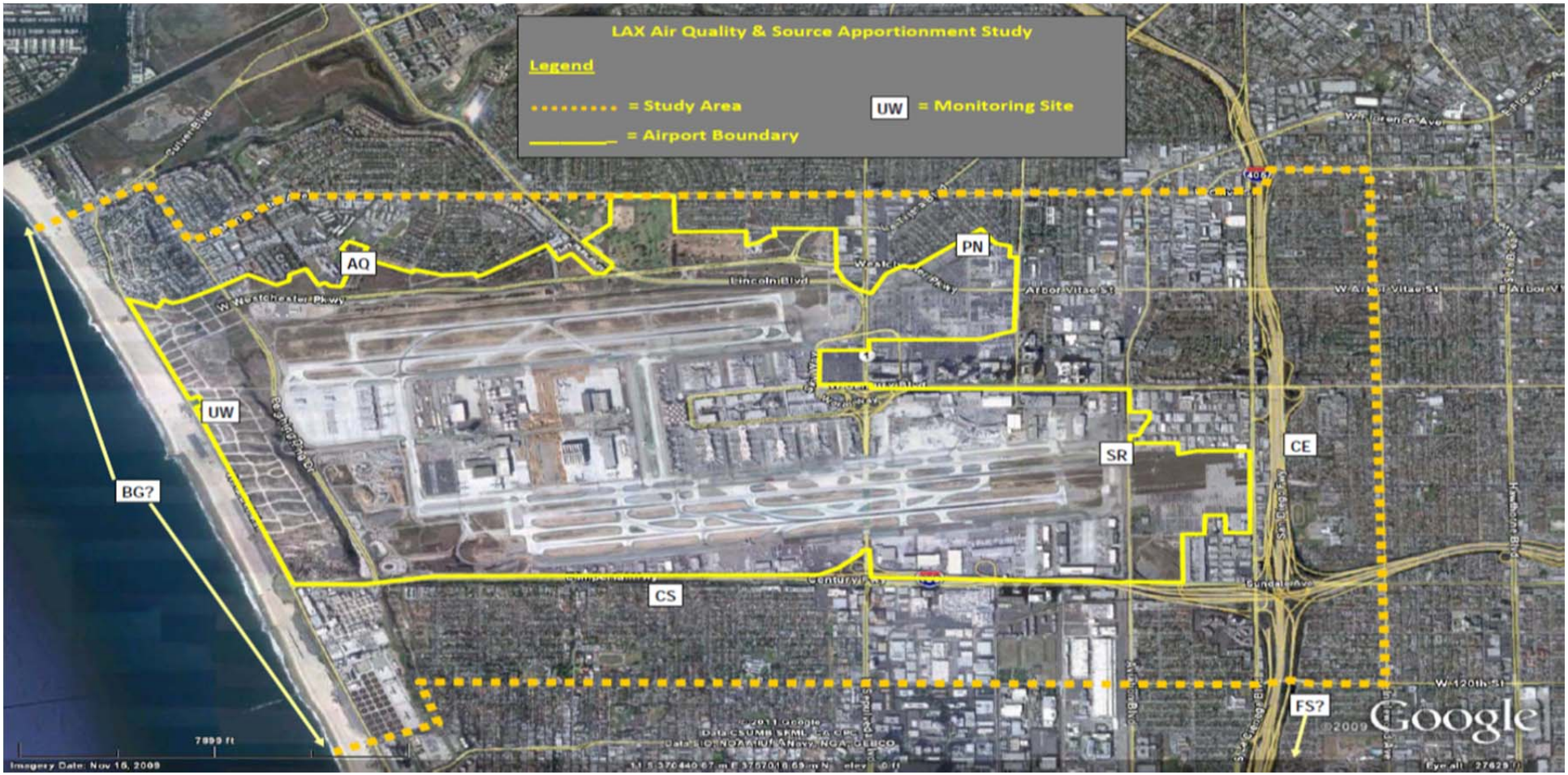

Figure 3-1. The Study Area and Originally Proposed Monitoring Locations

Table 3-1
Originally Proposed Monitoring Site Name and Purpose

Symbol	*Site Title and Type*	*Location and Purpose*	*Components Analyzed*
SR	South Runway: Core site for spatial, time series, and multivariate receptor analyses.	Behind blast fence on Runway 25R*. Source-dominated – aircraft taxiing & takeoffs, & some roadway emissions. *This site may be located outside of the Airport security fence instead of behind the Runway 25R blast fence.	Continuous analysis of CO_2, NO_x, SO_2, $PM_{2.5}$, PM_{10}, light scattering, black carbon, ultrafine particle number and size distribution. Substrate analysis of $PM_{2.5}$ mass, elements, ions, carbon, ammonia, and organics; as well as gaseous carbonyls, light HC, and heavy HC. Visible particle deposition sampling.
CE	Community East. Core site for spatial, time series, and multivariate receptor analyses	Felton Elementary School, ~1.25 km ENE of Runway 25R. Community exposure – aircraft, freeway, and area emissions.	Continuous analysis of CO_2, NO_x, SO_2, $PM_{2.5}$, PM_{10}, light scattering, black carbon, ultrafine particle number and size distribution. Substrate analysis of $PM_{2.5}$ mass, elements, ions, carbon, ammonia, and organics; as well as gaseous carbonyls, light HC, and heavy HC. Visible particle deposition sampling.
CS	Community South. Satellite site for spatial and time series analyses.	Former Imperial Avenue School, ~ 0.5 km south of the South Airfield. Near-field crosswind site - Aircraft, roadway, GSE, stationary & area.	Continuous analysis of light scattering. Substrate analysis of $PM_{2.5}$ mass, elements, ions, carbon, ammonia, organics, and volatile nitrate, stable PAH and source markers. Ultrafine particle count and size distribution measurements.
PN	Park North. Satellite site for spatial and time series analyses.	Carl Nielson Youth Park. ~1.3 km ENE of the North Airfield. Community exposure – aircraft, traffic and area emissions.	Continuous analysis of light scattering. Substrate analysis of $PM_{2.5}$ mass, elements, ions, carbon, ammonia, organics, and volatile nitrate, stable PAH and source markers Ultrafine particle count and size distribution measurements.

Table 3-1
Originally Proposed Monitoring Site Name and Purpose

Symbol	*Site Title and Type*	*Location and Purpose*	*Components Analyzed*
UW	Upwind Site: Core site for spatial, time series, and multivariate receptor analyses	Dunes west of airport, between north and south airfields. Some airport activity and construction sources.	Continuous analysis of CO_2, NO_x, SO_2, $PM_{2.5}$, PM_{10}, light scattering, black carbon, ultrafine particle number and size distribution. Substrate analysis of $PM_{2.5}$ mass, elements, ions, carbon, ammonia, and organics; as well as gaseous carbonyls, light HC, and heavy HC. Visible particle deposition sampling.
AQ	SCAQMD SW Coastal LA County Site: Standard SCAQMD multiple pollutant monitoring site.	~0.5 km North of Runway 24R (west end of runway). Some airport and area sources. Possible background site.	SO_2, NO_x, TSP particulate for lead and sulfate, PM_{10} (filter, not continuous), wind speed and direct, temperature and humidity. Ozone precursor hydrocarbons are measured July through September on a one in three day basis. Collecting both twenty-four hour integrated samples as well as 3 eight-hour integrated samples. During the non-PANS season data was collected on a one in six day basis and only over a twenty four-hour period.
BG (Optional) Not shown on Fig 3-1	Background Site: Core site for spatial, time series, and multivariate receptor analyses	This potential site would be near the coast but not directly under the LAX flight path.	Continuous analysis of CO_2, NO_x, SO_2, $PM_{2.5}$, PM_{10}, light scattering, black carbon, ultrafine particle number and size distribution. Substrate analysis of $PM_{2.5}$ mass, elements, ions, carbon, ammonia, and organics; as well as gaseous carbonyls, light HC, and heavy HC. Visible particle deposition sampling.

Table 3-1
Originally Proposed Monitoring Site Name and Purpose

Symbol	*Site Title and Type*	*Location and Purpose*	*Components Analyzed*
FS (Optional) Not shown on Fig 3-1	Freeway South: Core site for spatial, time series, and multivariate receptor analyses	Potentially located at Lloyde High School (Lawndale), located just east of I-405 Freeway, but not downwind of LAX. Results would be compared to Felton School site.	Continuous analysis of CO_2, NO_x, SO_2, $PM_{2.5}$, PM_{10}, light scattering, black carbon, ultrafine particle number and size distribution. Substrate analysis of $PM_{2.5}$ mass, elements, ions, carbon, ammonia, and organics; as well as gaseous carbonyls, light HC, and heavy HC. Visible particle deposition sampling.

3.2 Source Apportionment Techniques

This section describes a specific recommended approach; however, flexibility will be required in the application of these techniques. Multiple methods and technologies will be utilized to ensure the study objectives described in Section 2 are met. Dynamic, near real-time data interpretation will ensure measurements are being conducted to achieve the desired objectives, and alternative measurements will be initiated if necessary, after review and acceptance by LAWA, within the confines of the project budget and schedule.

Source apportionment can be accomplished in a number of ways, including:

- Chemical Mass Balance (CMB) receptor modeling
- Multivariate analysis (UNMIX and Positive matrix factorization)
- Spatial gradient and time series analysis
- Nonparametric trajectory analysis
- Source-based modeling (Air dispersion modeling)
- Emissions inventory scaling

Each of these techniques, which will require their own specific inputs, has the ability to determine LAX's contributions to air pollutant concentrations around the airport. These approaches have different sets of strengths and uncertainties and are thus complementary. Using multiple techniques has several advantages which include: 1) providing alternative or backup source apportionment analysis in case one of the data collection systems fails, 2) identification and reconciliation of different source contribution estimates from the different approaches, and 3) providing the ability to calibrate dispersion analysis of airport sources with reasonable accuracy (i.e., improve the inputs and assumptions used in dispersion models to produce results that better match measured concentration patterns). This last advantage is important for assessing

the benefit of potential mitigation measures. An overview of each of these methods is provided in the following discussion.

3.2.1 Receptor Modeling

Receptor-based models are designed to use the measured data at receptor locations to determine source or source-type emission characterizations. Several general reviews of receptor modeling include Watson and Chow (2004), Henry (2002), and Blanchard (1999). Descriptions of receptor modeling techniques follow.

Chemical Mass Balance

The Chemical Mass Balance (CMB) receptor model expresses each chemical concentration as the sum of a source contribution multiplied by the abundance of that chemical in each source type. Upon measurement of ambient concentrations and appropriate source profiles (fractional abundances of the chemical in the source), these equations can be solved for the source contributions. This approach requires knowledge of the number of sources contributing to the observed ambient concentration of VOC or PM and chemical species, and also the chemical composition ("fingerprint") of the VOC or PM emitted from each source.

Positive Matrix Factorization and Edge Detection

The positive matrix factorization (PMF) and UNMIX solutions estimate the number of factors and the chemical constituents of these factors from the receptor concentrations. These analyses require multiple sampling periods and therefore, unlike CMB, cannot be implemented with only one or a few ambient samples. Approximately 100 observations of 20 or more species are needed for the PMF and UNMIX solutions. These factors must then be associated with source types through comparison with measured source profiles. Henry et al. (1997) gave an example of the application of a multivariate receptor model to volatile organic compounds (VOC) data in the Houston Ship Channel that identified major omissions and inaccuracies in the emission inventory for the area.

Spatial Gradient Analysis

Spatial gradients are determined by analyzing observations of a single pollutant measured simultaneously at multiple sites. Spatial gradient analysis is based on the idea that if a source is located between two or more sampling sites, then there may be changes or gradients between the source and the downwind sites that can be associated with the emission source. The multivariate technique of Empirical Orthogonal Functions (EOFs) can be used to generalize this concept to many observations at many sites (Henry et al., 1991). Local, unidentified sources of particles can be determined and separated from the general urban background with EOF analysis. Spatial gradient analysis can also help identify the location of the source and its radius of influence. This is of special interest to those estimating the health impacts of a specific source. The multi-tiered monitoring approach in this Study provides air quality data at multiple locations with varying time resolution and overlapping spatial coverage.

Time Series Analysis

Time series analysis is similar to spatial gradient analysis because a single pollutant or marker (e.g., particle light scattering and/or black carbon) is monitored simultaneously at several sites. The time increment between measurements may be on the order of seconds or minutes (e.g., continuous/semi-continuous measurements of gas phase criteria pollutants), or may be as long as one hour (e.g., tapered element oscillating microbalance (TEOM) or beta attenuation monitor (BAM) measurements of PM_{10} and $PM_{2.5}$), or longer (e.g., twenty four-hour or seven-day integrated VOC and aerosol samples). This type of analysis is useful in identifying the regional diurnal fluctuations as well as source or event-specific emissions (e.g., Watson et al., 2000). The event-specific emissions show up as sharp peaks or spikes on the time series chart. The peaks for a given event show up at different times at each of the monitoring sites. The time difference between the peaks, coupled with local meteorological data (wind speed and wind direction) measured concomitantly with the marker, are used to determine the approximate source location and emission characteristics. Additional information can be found in Watson et al. (2000). For this Study, variations in NO/NO_x, CO, SO_2, black carbon, light scattering and ultrafine particle number concentrations measured at several locations around the airport will be potential impacts of local emissions sources.

Nonparametric Trajectory Analysis

Nonparametric trajectory analysis (NTA) is a relatively new method that has been applied to highly time-resolved monitored concentration and meteorological data (Henry 2008). The approach uses these one or two minute averaged ambient concentrations, wind speed and wind direction data to estimate the average concentration of a pollutant at a receptor for air passing over a given geographic location.

3.2.2 Source-Based Modeling

Emissions Inventory Improvement

Emissions factors and activity levels have improved substantially for on-road sources and industrial facilities. Emission factors are being improved for certain non-road sources, such as aircraft exhaust (U.S. EPA 2009a, b, and c). However, more accurate non-road emissions estimates allow for an independent estimate of relative contributions from different sources and may serve as the basis for the development of an airport emission control strategy. An accurate current inventory that includes spatial and temporal characteristics as well as emission rates and composition will provide insight into which compounds are likely to be found at levels that may be of community concern. In addition, inventories of specific compounds may provide potential markers for certain point sources while the ratios of emitted pollutants, which undergo little or no chemical reaction between the source and potential receptors, may also provide signature data.

The emission inventory for the Phase III study will focus on updating the inventory developed in the Demonstration Project such as updating ground supporting equipment emissions, on- and off-road vehicular emissions, and marine vessel emissions. Details of source inventory development will be described in Task 4 – Prepare Modeling and Analysis Protocol.

Air Dispersion Modeling

Atmospheric dispersion modeling provides a method to estimate ambient concentrations at downwind receptor sites from known emission inventories. The advantage to dispersion modeling is its ability to provide concentration results at virtually any location, provided that sufficient emission data and other model inputs, such as wind speed and direction, are available. Since this analysis is conducted through the use of software, it is much less expensive than collecting and analyzing monitored data. However, to be useful as a planning tool, modeled concentrations must be compared with monitored results, which help refine the emissions inventories used as inputs to the dispersion model.

AERMOD is U.S. EPA's currently approved air dispersion model. AERMOD is a Gaussian model capable of analyzing point, area and volume sources directly, and can be utilized to analyze line sources (such as roadways). Inputs to the model include hourly emission rates and meteorological data, source and receptor locations and data to calculate particulate deposition rates for different sized particles. The model output provides spatial concentration estimates or deposition rates from gridded receptor data for each averaging period analyzed.

Air dispersion modeling for the Phase III study will use the updated emission inventory and surface and upper air meteorological data to simulate air pollutant emissions in the Study Area. Details of the air dispersion modeling approach will be developed in Task 4 – Prepare Modeling and Analysis Protocol.

3.2.3 Source Emissions Characterization

Source emissions can be characterized by assembling existing information regarding on-airport, airport neighborhood, and Study Area emissions from a variety of sources. This information can be supplemented with new emissions estimates specific to LAX sources. Existing emissions inventories include: 1) the SCAQMD Facility Information Detail (FIND) web database; 2) the California State AB2588 inventory; 3) the SCOS-97 ozone modeling inventory; 4) the CARB emissions trends inventory for Los Angeles County and the Basin; 5) the CARB OFFROAD model emission estimates for ground support equipment at LAX; 6) the federal Toxic Release Inventory; and 7) the U.S. EPA National Emissions Inventory. These inventories have different spatial, temporal and species resolutions as well as different methods of compilation. Emissions methods and estimates will be documented and reconciled with the methods used to estimate LAX emissions so that the fraction of LAX emissions for each source type can be identified.

Original emissions rate estimates are made of LAX source types by location, time and source type, including those caused by traffic into and out of the Airport, within-airport (on- and off-road) vehicle use, food preparation in airport restaurants, power generation and cooling, aircraft maintenance, aircraft fueling, and aircraft exhaust from taxiing, take-offs and landings. These estimates use published emissions factors coupled with concurrent activity levels provided by the LAX operations managers. Aircraft exhaust emissions during approach and climb out modes also depend on the atmospheric mixing height, which is spatially and temporally dependent. Recent LAX-specific mixing height data will be used when calculating aircraft exhaust emissions.

Emissions will be characterized with respect to their chemical composition to address pollutants of concern and identify chemical markers for different source types. Source profiles, the fraction of each chemical in particulate matter (PM) or volatile organic compound (VOC) mass, have been measured for most of the common urban-scale source types identified above, but they are insufficient for aircraft exhaust and fueling. Existing particulate and VOC source profiles will be compiled from previous studies relevant to the Basin and will be supplemented by original source tests of LAX-specific sources. Many of the LAX emissions originate from gasoline- and diesel-fueled vehicles that likely have profiles similar to those used on non-LAX roadways in the neighborhoods. Only aircraft exhaust and fueling might have compositions that differ from those of the other source types common to on-airport and off-airport emitters. Some studies have identified emission profiles for military aircraft engines fueled with JP-8, a fuel similar to Jet A fuel used in commercial turbofan engines (Pleil et al., 2000). To characterize these emitters, a variety of aircraft fuel samples will be taken and analyzed for organic compounds and elements. Evaporated fuel will also be analyzed for VOCs in the headspace above these samples to represent re-fueling profiles. Monitored results at one source-dominated site using a canister sampler, $PM_{2.5}$ collected on Teflon and quartz filters and TIGF/XAD samplers, will provide exhaust emission component characterization for aircraft taxi and take-off operations. To accomplish this, this source-dominated site needs to be located as close to the east-end of the runways as safety and applicable regulations allow.

Source influence and apportionment can be accomplished by the receptor-oriented approaches of: 1) time series correlation; 2) advanced analysis of dependence of concentrations on wind direction and speed; 3) spatial gradients; and 4) chemical markers. Source-oriented approaches include: 1) source category emissions inventory scaling; and 2) emissions dispersion modeling. Results from these six approaches can be used to complement and verify each other.

Time series correlation can examine the relationship between spikes in pollutant concentrations at the runway and community exposure core sites. Short-term spikes at the runway site can be associated with events such as aircraft take-off, idling, and taxiing, based on wind direction and visual observations. These spikes can be filtered out of the measurement data set and compared with longer period averages of the remaining contributions that vary more slowly in time due to the urban emissions/meteorology cycle. The same can be done with the community exposure measurements. Correspondence between light scattering spikes at the runway sites and at the downwind satellite sites can be used to determine the extent to which short-term emissions are attenuated with distance. The attenuation of specific chemical components when wind vectors line up between the runway and the receptor site can be obtained. Temporal variations in activity levels at the airport, such as week day to weekend, will also be developed by comparisons of data among the core sites. The Environmental Services Division at LAWA will obtain aircraft departure and arrival records, and the Facilities Planning Division, Landside Improvements Section, will provide estimates from previous studies for traffic temporal patterns and volumes and this data will be provided to the Tetra Tech team.

Spatial gradients will be estimated from measurement data collected at saturation sampling locations. The gradients will be superimposed on spatial emissions maps that identify the highest airport and non-airport point, area and mobile emissions locations. Spatial gradients will be

estimated for different meteorological transport regimes using high time resolution measurements and by measurement campaign periods for the integrated sample measurements. Sharp gradients between source areas will indicate incremental contributions from those sources.

Unique chemical markers, if they exist, will be used in the different receptor models to quantify the contributions of different source types to receptor concentrations at the runway and community exposure sites. The chemical markers approach makes use of high time resolution data as well as one hour and twelve-hour averaged data, where appropriate. Source contributions will be estimated for $PM_{2.5}$ and VOCs, and selected chemical components of concern. Based on recent literature, distinguishable source categories for either PM or VOC are: 1) gasoline vehicle exhaust from well-maintained, poorly maintained and cold-start operating modes; 2) diesel exhaust; 3) cooking; 4) wood burning; 5) fugitive dust; 6) solvent use; 7) evaporated diesel fuel and gasoline; 8) marine aerosols; and 9) secondary sulfate and nitrate. While a receptor model may be able to distinguish secondary sulfate and nitrate as formed from NO_x and sulfur oxides (SO_x) in the atmosphere, no available receptor model is able to apportion such secondary pollutants back to the primary sources of NO_x and SO_x. (Note: Due to the limited size of the Study domain, there will likely be minimal secondary formation of pollutants in the Study domain from sources of primary emissions in the domain.)

Published source profiles for aircraft refueling and exhaust will be used to determine the extent to which these can be distinguished from more common vehicle fuel and exhaust emissions by chemical markers. As of 2007, all on-road and non-road diesel fuels in the Basin (and in California) were to contain less than 15 ppm sulfur by weight. One of the most important indicators of jet exhaust is concentration of SO_2. The ratio of SO_2 to other pollutants ($PM_{2.5}$, ultrafines, CO_2 and speciated hydrocarbons) in source-dominated plumes may also assist in estimating the contributions of those sources, such as aircraft refueling and exhaust, to measured ambient concentrations.

The source category emissions scaling method will allow estimates of the fraction of total emissions within a source category constituted by airport emissions. These emissions fractions are specific to the pollutants of concern and can be applied to the source category contributions determined by the receptor models to estimate absolute concentrations from each source category, on or off the airport. Ratios of the species of concern to aircraft SO_2 emissions will be estimated from aircraft source-dominated (end of runway) sites and from emissions testing, as reported in the technical literature, and the amount of sulfur in the jet fuel. The amount of species of concern from aircraft will be estimated by multiplying the ratio of the species of concern to aircraft SO_2 emissions by the twenty-four hour averaged aircraft SO_2 emissions. This is standard procedure assuming the ratio of the species of concern to SO_2 does not vary much from source to receptor. Fine particulate matter (i.e., $PM_{2.5}$) was mentioned as a pollutant of concern and will be measured on a one minute basis. Thus, the ratio of fine particle concentration to aircraft SO_2 should be determined. Using the ratio and measurement of SO_2 and fine particulate matter concentrations, the apportionment of a twenty-four hour average particulate concentration from aircraft will be calculated.

The emissions dispersion modeling method will utilize the AERMOD dispersion model to select LAX and non-airport emission sources in the Study Area, to the extent they can be quantified on a spatial and temporal scale consistent with the neighborhood scale Study domain. This modeling will account for emissions by transport direction and dispersion, thereby providing a more precise impact of source contribution estimates than the emissions-scaling method. The greatest uncertainty resides in the ability to obtain off-airport emissions with spatial resolution of less than 0.5 km for the chemical species of concern. Emissions and dispersion modeling will be conducted for intensive monitoring periods (i.e., two sampling seasons during the study period) that have the highest resolution data available from the network sites.

In addition to the source apportionment methods described above, the nonparametric trajectory analysis (NTA) method developed by Dr. Ronald Henry at USC will be applied to the monitoring data collected with high time resolution. Details of NTA methodology will be discussed in Section 4, Task 4: Prepare Modeling and Analysis Protocol.

Section 4
General Scope of Work

LAWA expects to complete the following tasks to accomplish the technical objectives in this Work Plan. However, it is understood that the actual task scope may change as the program progresses with the ultimate goal to provide the best scientific data possible to respond to those objectives within the schedule and budget parameters of the study.

Task 1	Finalize Detailed Scope of Work with LAWA
Task 2	Finalize Monitoring Site Assessments and Permission from Site Owners, and Install Necessary Power and Security Systems
Task 3	Prepare Monitoring and Quality Assurance Program Plan (MQAPP)
Task 4	Prepare Modeling and Analysis Protocol
Task 5	Procure and Install Monitoring Equipment
Task 6	Sample and Characterize Mobile Source Fuels Used On and Around the Airport
Task 7	Conduct QA/QC Evaluation of Monitoring and Sampling Systems
Task 8	Commence 1st Season of Ambient Monitoring and Sample Collection and Analysis
Task 9	Compile 1st Season Monitoring and Analysis Data, and Prepare 1st Season Report of Findings and Lessons Learned
Task 10	Begin Receptor Modeling, Time Series Analysis, Spatial Analysis and Nonparametric Trajectory Analysis on 1st Season Data
Task 11	Commence 2nd Season of Ambient Monitoring and Sample Collection and Analysis
Task 12	Compile 2nd Season Monitoring and Analysis Data and Prepare 2nd Season Report of Findings and Lessons Learned
Task 13	Continue Receptor Modeling, Time Series Analysis, Spatial Analysis and Nonparametric Trajectory Analysis on 1st and 2nd Season Data
Task 14	Develop Refined Emission Inventories of Study Area Sources
Task 15	Conduct Air Dispersion Modeling of Refined Emission Inventories

Task 16	Prepare Preliminary Draft Project Report and Database
Task 17	Prepare Draft Final Project Report and Database
Task 18	Prepare Final Project Report and Database
Task 19	Prepare Presentation Materials for, and Participate in Public Meeting
Task 20	On-Going Coordination with CDM/Owner's Representative
Task 21	On-Going Coordination with TWG

The general scope of work contains twenty-one individual tasks. Each task is described below along with the technical approach as presented in TetraTech's technical proposal. Please note, since the beginning of the program, several modifications to the technical approach have been made according to recent findings, to more accurately reflect the program requirements and meet program objectives. These modifications are also discussed under each associated task.

4.1 (Task 1) Finalize Detailed Scope of Work with LAWA

The draft detailed scope of work was developed by LAWA and CDM, and reviewed by the TWG. The first task is to finalize the detailed scope of work, which will clearly define data types or parameters, time resolution, and the amount of data required to perform meaningful source apportionment modeling to meet the study objective of identifying a reasonable estimate of source contributions from airport operations to adjacent communities. The final scope of work includes issues and improvements identified under the Demonstration Project to enhance overall performance. The finalized detailed scope of work will serve as technical guidance to lead the field measurement activities and subsequent data analysis and modeling.

Mobile Survey

To better understand that the proposed locations can truly represent the ambient air pollutants in the Study Area, Tetra Tech's team member – DRI - conducted a mobile survey of the Study Area from September 20 to 23, 2011 at locations within the communities, buffer zones, and near airport operations. This mobile survey provides insights of ambient air quality at the proposed monitoring locations, in the local communities, and guides the selection of sampling sites for spatial and gradient analysis in the Phase III Study. Details of the mobile survey are presented in Appendix A.

The mobile survey was conducted using a mobile monitoring van borrowed from the Bay Area Air Quality Management District (BAAQMD). The van included instruments to measure CO, NO, BC, $PM_{2.5}$ and UFP and a cart-mounted monitoring system built by DRI to measure NO, CO, CO_2, $PM_{2.5}$ and UFP. The two systems measured air pollutant concentrations simultaneously to provide gradient and spatial distribution information. Nine survey routes were conducted including: locations at neighboring communities, LAX terminals, the runway and taxiway at different times (e.g., morning hours versus evening hours) on the same survey day.

The mobile survey results are summarized below:

- Air pollutant concentrations are relatively low and uniform at north and south neighboring communities and boundaries of LAX.
- High spots are identified at LAX terminals and downwind locations to the east of the Airport.
- Survey at the South Airfield or Runway 25R (SR) site located at north of Runway 25R at Walsh Austin laydown area, which was originally intended to be used as a source-oriented monitoring site, shows that airplane takeoff emissions have minimal impact on this location.
- Survey east of the SR site in the open field of landing guide posts shows that NO and BC in the plume from takeoff emissions are fairly concentrated along the north guide light posts and west of the SR blast fence. However, $PM_{2.5}$ and UFP profiles do not show the same pattern. In general, spikes in NO concentrations correspond with plane takeoffs. The air pollutant concentration profiles of NO, BC, and UFP indicate that these concentrations are aircraft-specific.

As a result, the following recommendations are made:

- Replace the SR site sampling scheme with short-term sampling using integrated and continuous samplers to collect source profiles and emission factors for aircraft takeoff and taxiing emissions.
- Conduct a gradient study east of the SR site in the open field to characterize concentration gradients and characteristics of air pollutant dispersions.
- Deploy passive and MiniVol samplers within LAX source areas, at the perimeter of buffer zones and within adjacent communities for subsequent gradient and spatial analyses.
- Relocate the stations originally intended for the SR site to another community location, such as the former Imperial Avenue School in El Segundo as the community south (CS) site.
- The AQMD Hastings (or AQ) site is considered as a background site due to its location. This site can be upgraded with specific instruments to serve as the Playa del Rey community site.
- Relocate the originally proposed location of the upwind (UW) site located in the Dunes west of the Airport to another local community site, located at the intersection of Airport Boulevard and Arbor Vitae Street. This site will be considered as the community north (CN) site.

Furthermore, the mobile survey study results allow a ranking of the priority of alternate monitoring strategy and parameters based on required inputs for modeling and analysis, and the following additional recommendations are made:

- Highest priority measurements include:
    - Source sampling behind the blast fence at Runway 25R and northeast of end of runway to collect engine exhausts from aircraft takeoffs and taxiing, respectively.

These source profile measurements are required for Chemical Mass Balance Receptor modeling. LAWA will provide aircraft activity logs such as numbers and timing of takeoffs and landings.

- Continuous measurements of NO, NO_2, SO_2, black carbon, ultrafine and fine particle concentrations and size distributions, CO (substitute for CO_2), and wind speed and direction with at -1-minute or less time resolution for time-series analysis and nonparametric trajectory analysis. CO will be a good indicator for gasoline-powered vehicles exhausts.
- Ambient 24-hour VOC and $PM_{2.5}$ samples (two seven consecutive days or 14 consecutive days during two seasons) with comprehensive chemical speciation at three core sites (CE, CS, CN). 24-hour integrated sample will provide better analytical detection sensitivity.
- Ambient 7-day integrated passive samples (6 consecutive weeks during two seasons) for NO_x, NO_2, SO_2, and volatile air toxics (benzene, toluene, xylenes, ethylbenzene, formaldehyde, acetaldehyde) at six community sites (3 core and 3 satellite), one upwind site, four LAX buffer zone sites, and six near source sites for analysis of spatial variations of gas-phase pollutant concentrations.
- Ambient 7-day integrated mini-volume aerosol samples (6 consecutive weeks during two seasons) for $PM_{2.5}$ mass, elements, ions, organic carbon and elemental carbon at the three core sites, AQMD site, and three satellite sites for analysis of spatial variations of particle-phase pollutant concentrations.

- High Priority
  - Gradient measurements during source sampling at Runway 25R to characterize zone of influence of jet exhaust emissions.
- Lower Priority
  - Continuous measurements of CO_2 at the three core sites, which will provide limited value to the program due to limited incremental concentration above global background. CO measurements should be substituted for CO_2, since CO is a good tracer for gasoline-powered vehicle emissions.
  - Non-methane hydrocarbon emissions at the three core sites, which will be of limited value for source apportionment modeling analysis and nonparametric trajectory analysis.
  - Continuous PM sampling with beta attenuation monitors (BAM) for PM_{10} and $PM_{2.5}$ mass with 1-hour resolution and a precision with a large uncertainty for PM concentrations below 10 $\mu g/m^3$ will not be of great value to the project since the major component of PM concentration is urban and regional background, and local sources have minimal impact expect very near the source.
- Lowest Priority
  - Particle deposition
  - Video recordings

CE Site

The initial site visit indicated the proposed CE site (Felton Elementary School) could not meet siting criteria due to potential obstruction of air flow by the adjacent elevated I-405 Freeway and nearby trees. On September 1, 2011 an alternative site (La Feria Restaurant) located at 10903 S.

Inglewood Avenue in Lennox, approximately 405 meters east of the I-405 Freeway and 1,560 meters east from Runway 25R, was selected.

CN Site

An initial site survey identified a property owned by LAWA located at the intersection of Airport Boulevard and Arbor Vitae Street, west of I-405 Freeway. This location was designated as the CN site using the DRI trailer originally intended for UW site.

Refined Sampling Plan

Based on findings from the mobile survey and visits to CE and UW sites, LAWA staff and –CDM,- LAWA's technical advisor concurred with Tetra Tech team that the draft sampling plan should be refined. Tables 4-1 and 4-2 list the refined sampling plan.

Table 4-1 Revised Monitoring Network – Fixed Station

Symbol	*Site Title and Type*	*Location and Purpose*	*Components Analyzed*
CE	Community East. Core site for spatial, time series, and multivariate receptor analyses	La Feria Restaurant, ~1.56 km ESE of Runway 25R. Community exposure – aircraft, freeway, and area emissions.	Continuous analysis of CO, NO_x, SO_2, $PM_{2.5}$, light scattering, black carbon, ultrafine particle number and size distribution. Substrate analysis of $PM_{2.5}$ mass, elements, ions, carbon, ammonia, and organics; as well as gaseous carbonyls, light HC, and heavy HC. TIGF/XAD for semi-volatiles and particulate organic compounds (PAH, alkanes, hopanes, steranes and polar compounds). 24-hour integrated samples.
CS	Community South. Core site for spatial, time series, and multivariate receptor analyses	Former Imperial Avenue School, ~ 0.5 km south of the South Airfield. Near-field crosswind site - Aircraft, roadway, GSE, stationary & area emissions.	Continuous analysis of CO, NO_x, SO_2, $PM_{2.5}$, light scattering, black carbon, ultrafine particle number and size distribution. Substrate analysis of $PM_{2.5}$ mass, elements, ions, carbon, ammonia, and organics; as well as gaseous carbonyls, light HC, and heavy HC. TIGF/XAD for semi-volatiles and particulate organic compounds (PAH, alkanes, hopanes, steranes and polar compounds). 24-hour integrated samples.

Symbol	***Site Title and Type***	***Location and Purpose***	***Components Analyzed***
CN	Community North – Airport/Arbor Vitae. Core site for spatial, time series, and multivariate receptor analyses.	North east of airport, west of I-405 Freeway. Community exposure – aircraft, freeway, and area emissions.	Continuous analysis of CO, NO_x, SO_2, $PM_{2.5}$, light scattering, black carbon, ultrafine particle number and size distribution. Substrate analysis of $PM_{2.5}$ mass, elements, ions, carbon, ammonia, and organics; as well as gaseous carbonyls, light HC, and heavy HC. TIGF/XAD for semi-volatiles and particulate organic compounds (PAH, alkanes, hopanes, steranes and polar compounds). 24-hour integrated samples.
AQ	SCAQMD SW Coastal LA County Site: Standard SCAQMD multiple pollutant monitoring site. This site is used as a Background site for spatial, and time series analyses	~0.5 km North of Runway 24R (west end of runway). May be impacted by some airport and area sources.	SCAQMD site collects SO_2, NO_x, TSP particulate for lead and sulfate, PM_{10} (filter, not continuous), wind speed and direct, temperature, and humidity. Due to limited available power the station upgrade will include continuous analysis of $PM_{2.5}$, light scattering, and black carbon. Substrate analysis of $PM_{2.5}$ mass, elemental and organic carbon using a MiniVol sampler to provide 24-hour integrated samples.

Table 4-2 Revised Monitoring Network – Source Profile and Saturation Monitoring

Source Profile Sampling			
Symbol	***Site Title and Type***	***Location and Purpose***	***Components Analyzed***
SR	South Runway and Taxiway (SR): Source Profile site for source profiles and emission factors from aircraft takeoffs and taxiing	Behind blast fence on Runway 25R and Taxiway. Source-dominated – aircraft taxiing, takeoffs, and some roadway emissions from Aviation Blvd.	Canister samplers for light hydrocarbons (C_2-C_{11}), methane, CO and CO_2. Tenax samplers for heavy hydrocarbons (C_{10}-C_{20}). DNPH cartridge samplers for carbonyl compounds. TIGF/XAD for semi-volatiles and particulate organic compounds (PAH, alkanes, hopanes, steranes, and polar compounds). Teflon filter for $PM_{2.5}$ mass and metals, quartz filter for OC, EC and sulfate. Continuous NO and sound monitors to record activity. Wind speed and wind direction.
	Downwind of Runway: plume dispersion.	Gradient sampling in the open field east of Runway 25R and Aviation Boulevard to determine plume dispersion from aircraft takeoffs, taxiing, and landings.	4 to 6-hr passive samplers for NO_2, NO_x, SO_2, VOC and carbonyls. MiniVol samplers with Teflon filters for $PM_{2.5}$ mass and metals and quartz filter for OC, EC and sulfate.
Saturation Sampling			
Symbol	***Site Title and Type***	***Location and Purpose***	***Components Analyzed***
SS	Saturation sampling at community locations and airport perimeters	Three communities locations (core sites: CE, CN, CS) adjacent to airport and four satellite sites at airport perimeters and seven gradient sites	7-day passive sampling for NO_2, NO_x, SO_2, VOC and carbonyls. 7-day integrated sample during 14-day intensive periods in each sampling season.
		Three core sites (CE, CS, CN) and four satellite locations at airport perimeters (CE2, CN2, CS2, and AQ)	MiniVol samplers with Teflon filters for $PM_{2.5}$ mass and metals and quartz filter for OC, EC and sulfate. 7-day integrated sample during intensive periods.

Deviations from the Draft Work Plan

Listed below are deviations from the original draft sampling and analytical scheme and the rationale for each deviation.

- Expanded saturation sampling from 10 sites to 17 sites, is proposed to provide gradient and spatial analyses.
- As suggested by the review report prepared by Countess Environmental, a condensation particle counter (CPC) is proposed for measuring ultrafine particle counts instead of using a Fast Mobility Particle Sizer (FMPS). SMPS-CPCs will be installed at three core sites to measure particle size distribution.
- The thermal desorption GC/MS analytical method for stable organic compounds collected on a TIGF/XAD sampler is replaced with an enhanced analytical technique to provide better sensitivity and speciation including PAHs, alkanes, hopanes, steranes, and polar compounds.
- For $PM_{2.5}$ samples collected at fixed sites, the sampling frequency is changed from twelve-hour to twenty four-hour integrated samples to reduce expensive analytical costs without sacrificing data quality for subsequent analyses.
- Meteorological data collection frequency is increased from a five-minute average to a one-minute average to provide sufficient time resolution for non-parametric trajectory analysis to achieve required spatial resolution.
- Continuous CO_2 monitors at the three core sites are not included. This is due to incremental contributions of emission sources within an urban area to the global background levels of CO_2 are relatively low except in close proximity to combustion sources. Measurements will be of limited value as CO_2 levels will be fairly constant with time at the three community core sites. CO measurements are substituted for CO_2, since CO is a good tracer for gasoline-powered vehicle emissions.
- Measurements of non-methane hydrocarbon (NMHC) emissions at the three core sites are not included. This measurement lacks high time resolution and sensitivity as the minimum time resolution is one hour, thus has limited value for temporal analysis and nonparametric trajectory analysis. Additionally, NMHC data from the continuous instruments are not necessary for receptor analysis.
- Continuous PM sampling with beta attenuation monitors (BAM) for PM_{10} and $PM_{2.5}$ mass has minimal value. The time resolution of the instrument is 1-hour and does not have good precision below 10 $\mu g/m^3$. The average $PM_{2.5}$ and PM_{10} concentrations measured during the Demonstration Project were relatively uniform at all four sites. Urban and regional background is typically a major component of PM concentrations and local source have minimal impact expect very near the source.
- Video recording of aircraft activities will not be used in the modeling analysis, and are replaced by LAX operations data and NO measurements as proposed for the source sampling (SR) location.
- Visible particle deposition will not be used in the modeling analysis, therefore, sampling and analysis at the core site is not included based on recommendation from the mobile survey.

Tables 4-3, 4-4 and 4-5 show fixed, source profile and saturation sampling sites and proposed measurements, respectively.

Table 4-3. Fixed Monitoring Sites, Parameters and Frequencies

Parameters	Site	AQ	CE	CS	CN	Sampling		
	Type	BG	C	C	C	Avg Time	Frequency	Period
Continuous Measurements	CO		v	v	v	5-min	Continuous	Duration of monitoring campaign
	NO_x	v	v	v	v	5-min	Continuous	Duration of monitoring campaign
	SO_2	v	v	v	v	5-min	Continuous	Duration of monitoring campaign
	$PM_{2.5}$ (BAM)	v	v	v	v	1-hr	Daily	Duration of monitoring campaign
	Light scattering	v	v	v	v	5-min	Continuous	Duration of monitoring campaign
	Black Carbon	v	v	v	v	5-min	Continuous	Duration of monitoring campaign
	UFP/Size		v	v	v	5-min	Continuous	Duration of monitoring campaign
$PM_{2.5}$ Samples	Mass/ Carbon	v	v	v	v	24-hr	Once daily/14-day	Seasonal intensive periods
	Elements		v	v	v	24-hr	Once daily/14-day	Seasonal intensive periods
	Ions		v	v	v	24-hr	Once daily/14-day	Seasonal intensive periods
	Ammonia		v	v	v	24-hr	Once daily/14-day	Seasonal intensive periods
Others	Semivolatiles (TIGF/XAD)		v	v	v	24-hr	Once daily/14-day	Seasonal intensive periods
	Carbonyls (DNPH)		v	v	v	24-hr	Once daily/14-day	Seasonal intensive periods
	L-HC (Canister)		v	v	v	24-hr	Once daily/14-day	Seasonal intensive periods
	H-HC (Tenax)		v	v	v	24-hr	Once daily/14-day	Seasonal intensive periods
Meteorological Measurements	WS		v	v		1-min	Continuous	Duration of monitoring campaign
	WD		v	v		1-min	Continuous	Duration of monitoring campaign
	T		v	v		1-min	Continuous	Duration of monitoring campaign
	RH		v	v		1-min	Continuous	Duration of monitoring campaign
	Solar Radiation		v			1-min	Continuous	Duration of monitoring campaign

Footnote: v: measured parameter AQ: AQMD station; CE: Community East; CS: Community South; CN: Community North; C: Core; BG: Background

Table 4-4 Source Profile Monitoring Sites and Parameters

Site ID	Site Name	Location	Continuous	Number of Sample: 4 to 6-hour Samples at Each Site During 4-days of Source Measurements													
				Passive					Mini-Vol $PM_{2.5}$		Canister		Tenax	DNPH	Med-Vol $PM_{2.5}$		Semi Volatile Organic Compounds (SVOC)
				NO_x	NO_2	SO_2	Benzene, Toluene, Ethylbenzene, Xylenes (BTEX)	Carbonyl	mass, metals	OC, EC	Light HC	CH_4, CO, CO_2	Heavy HC	Carbonyl	Teflon	Quartz	TIGF/ XAD
SRB	Runway 25R Blast Fence	Behind Blast Fence	NO, BC, PM, sound	1	1	1	1	1			1	1	1	1	1	1	1
SR2	South Runway Taxiway	Taxiway		1	1	1	1	1			1	1	1	1	1	1	1
SR3	South Runway #3	~25m east of Aviation	WS, WD	1	1	1	1	1	1	1							
SR4	South Runway #4	~125m east of Aviation	NO, BC, PM, CPC	1	1	1	1	1	1	1							
SR5	South Runway #5	~325m east of Aviation		1	1	1	1	1	1	1							
BSR	Buffer Zone S Runway	Lot B near La Cienega Boulevard		1	1	1	1	1	1	1							
CE	Community East	La Feria Restaurant, Lennox	1														
Total number of sample per sampling day				6	6	6	6	6	4	4	2	2	2	2	2	2	2
Number of days per season			4														
Total number of samples/season				24	24	24	24	24	16	16	8	8	8	8	8	8	8

Table 4-5 Saturation Monitoring Sites and Parameters

Site ID	Site Type	Site Name	Location	Continuous	Number of 7-day Samples During LAX-AQSAS Six-Week Intensives							Number of Daily 24-hr Sample for 2 7-day or 14 Consecutive Days					
					Passive					Mini-Vol $PM_{2.5}$		Canister	Tenax	DNPH	Med-Vol $PM_{2.5}$		SVOC
					NO_x	NO_2	SO_2	BTEX	Carbonyl	mass, metals	OC, EC	Light HC	Heavy HC	Carbonyl	Teflon	Quartz	TIGF/ XAD
CE	Core	Community East	La Feria Restaurant, Lennox	1	1	1	1	1	1	1	1	1	1	1	1	1	1
CS	Core	Community South	Former Imperial Ave School, El Segundo	1	1	1	1	1	1	1	1	1	1	1	1	1	1
CN	Core	Community North	Northeast of LAX, Westchester	1	1	1	1	1	1	1	1	1	1	1	1	1	1
AQ	Background	Upwind Northwest	91st & Hastings, Playa del Rey	1	1	1	1	1	1	1	1						
CS2	Satellite	Community South #2	El Segundo		1	1	1	1	1	1	1						
CN2	Satellite	Community North #2	Westchester		1	1	1	1	1	1	1						
CE2	Satellite	Community East #2	Hawthorne		1	1	1	1	1	1	1						
BN	Gradient	Buffer Zone North	North of Westchester Parkway		1	1	1	1	1								
BS	Gradient	Buffer Zone South	Imperial Terminal		1	1	1	1	1								
SR	Gradient	South Runway	Fence on east end of SR, Aviation		1	1	1	1	1								
NR	Gradient	North Runway	Fence at east end of NR		1	1	1	1	1								
BSR	Gradient	Buffer Zone S Runway	Lot B near La Cienega Boulevard		1	1	1	1	1								
BNR	Gradient	Buffer Zone N Runway	Lot C near Jenny Avenue		1	1	1	1	1								
CT	Gradient	LAX Central Terminal	Roof of Parking Garage		1	1	1	1	1								
C&A	Gradient	Century and Aviation	Near intersection		1	1	1	1	1								
405W	Gradient	I-405 West Edge	West edge of I-405		1	1	1	1	1								
405E	Gradient	I-405 East Edge	East edge of I-405		1	1	1	1	1								
Subtotal				3	17	17	17	17	17	7	7	3	3	3	3	3	3
Core					3	3	3	3	3	3	3	3	3	3	3	3	3
Satellite (including one background)					4	4	4	4	4	4	4						
Gradient					10	10	10	10	10								

Figure 4-1. Phase III of the LAX AQSAS Revised Sampling Locations Map

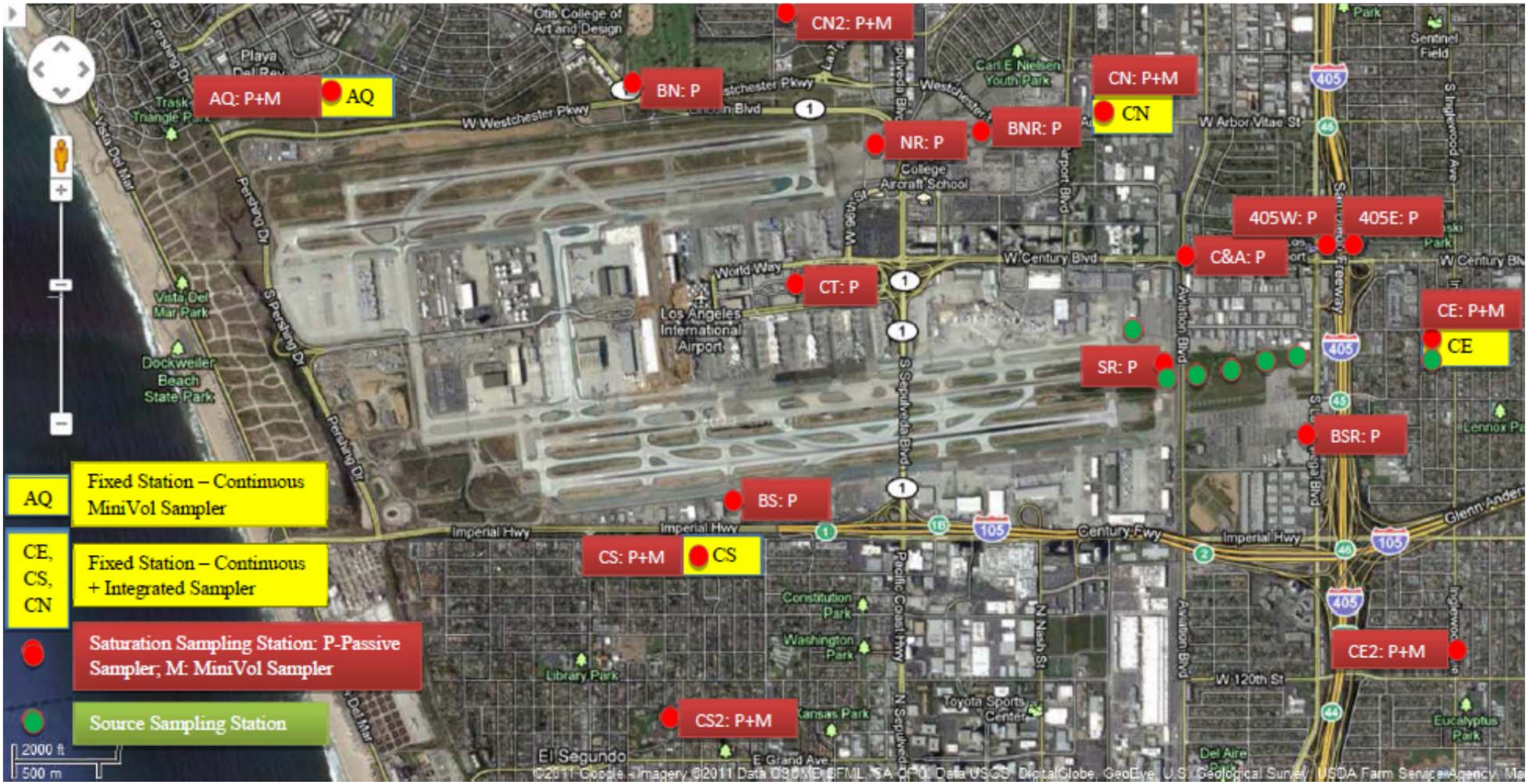

Monitoring Period

The 2010/2011 wind data collected at the SCAQMD LAX upper air station, located west of the intersection of Pershing Drive and World Way West, indicate there are two distinct wind patterns in the airport area. Figure 4-2 shows monthly wind rose from October 2010 to September 2011. The first pattern encompassed November to March, with variable wind directions but predominantly ENE to NE and WSW to westerly winds. The second pattern encompassed April to October, with predominantly WSW and westerly winds. Considering the local unique wind patterns, it is suggested the monitoring period include two seasons – winter to spring and summer to fall. The two proposed monitoring periods should provide representative wind patterns in the airport area. Therefore, it is recommended that Task 8 and Task 11 - 1st season and 2nd season of ambient monitoring and sample collection and analysis should start approximately in January 2012 and July 2012, respectively.

4.2 (Task 2) Finalize Monitoring Site Assessments and Securing Permission from Site Owners, and Install Necessary Power and Security Systems

LAWA and the TWG have identified several potential monitoring sites including three core sites: South Runway (SR), Community East (CE) and Upwind (UW) sites, two optional core sites: Background (BG) and Freeway South (FS), and two satellite sites: Community South (CS) and Park North (PN), for the Phase III ambient measurements (see Figure 1.1). LAWA has begun contacting the property owners for those sites not on LAWA property. LAWA also conducted a survey of potential power supply at five additional locations – 104th Street and Aviation; Vista Del Mar Park, Nielsen Park, and Parking Lots C and D.

As discussed in Task 1, the actual number of sites and locations has been revised according to the findings and recommendations from the mobile survey study. In summary,

- The originally proposed location of CE site is moved from the Felton Elementary School to the La Feria Restaurant located at 10903 S. Inglewood Avenue in Lennox due to air flow obstruction from the elevated freeway and nearby tree lines, and security concerns. The supply power for this location has been negotiated with the owner and an agreement is being developed. The site location is located at the northwest corner of the parking lot. Trimming of nearby palm trees will be performed to provide sufficient free air flow for sampling to meet siting criteria. A security fence will be installed.
- The remaining fixed sites, UW (Dunes site) and CS (former Imperial Avenue School, El Segundo) were visited in the beginning of the program. Power for the CS site needs to be arranged through the Southern California Edison. Power supply for the AQ (AQMD Hastings) site has been assessed and only three additional continuous monitors will be installed because of limited power available. The CN site (Airport Boulevard/Arbor Vitae Street) will require power supply from the Los Angeles Department Water and Power. The AQ site will not require security fences; however, the CE, CS and CN sites need security fences.
- The power supply for the SR (source sampling) site at the South Runway will be provided by the existing power connection near the Runway 25R blast fence.

- Passive samplers will not require any power. Active samplers (i.e., MiniVol) will either be powered by battery and/or a portable gas-powered generator, depending on sampling duration.

Figure 4-2 AQMD LAX UA Site Monthly Wind Rose (October 2010 to September 2011)

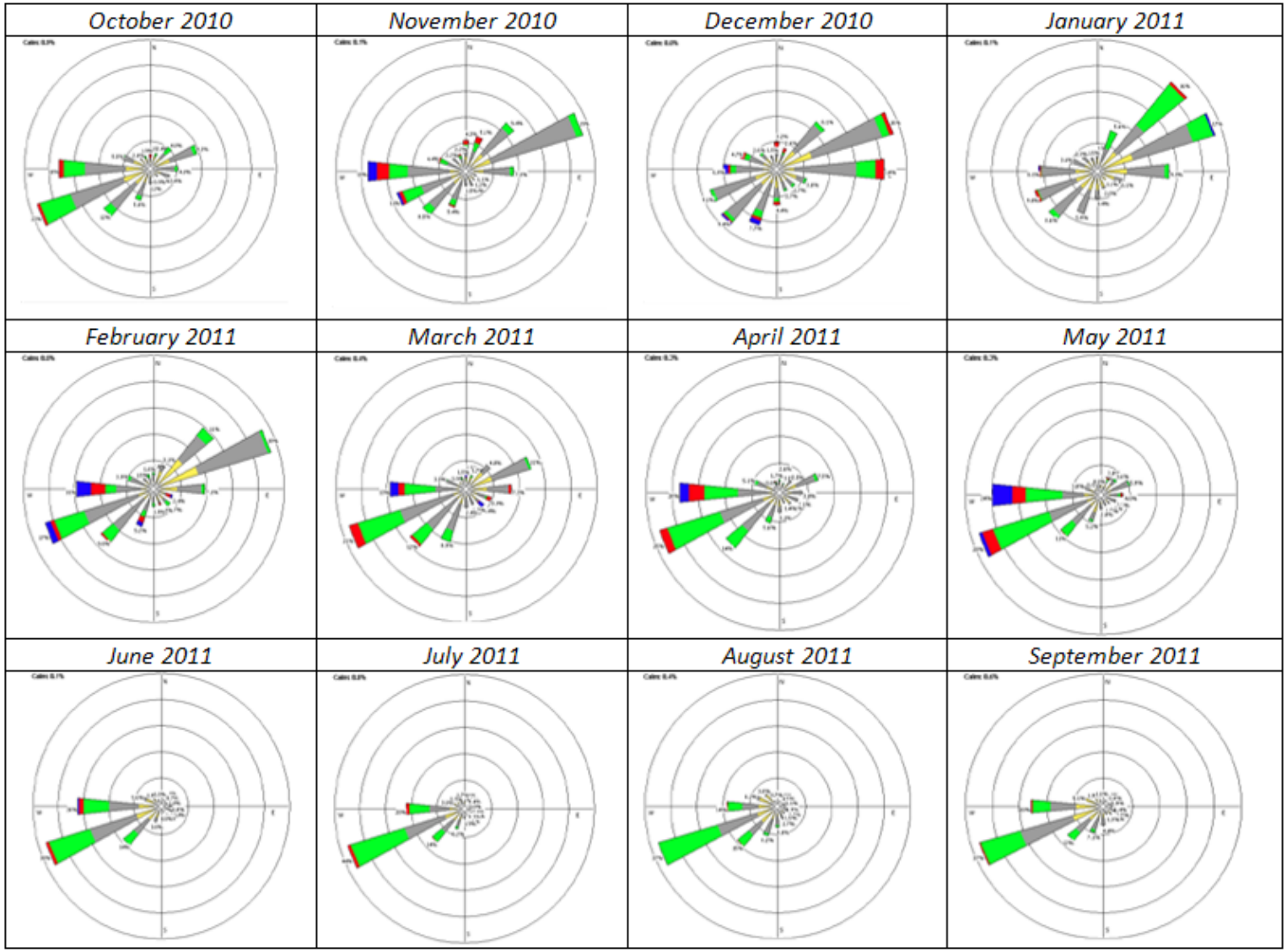

Upon finalization of the number and location of monitoring sites, the Project Team conducted site visits to previously unevaluated sites to assess access, power supply and site security. The Project Team has verified sufficient power is available for equipment operated at the fixed locations. If additional power is needed, the Project Team will be responsible for obtaining this power including all costs, and coordination with the owner, utility company, licensed electricians and LAWA to have this power installed. The Project Team will also be responsible for the purchase, installation and removal of security fencing, and for complying with site access agreements or conditions, and requirements. If an equipment staging area is necessary, the Project Team will be responsible for providing, maintaining, and securing the staging area. Finally, the Project Team will be responsible for maintaining that the site is in good operating condition for the duration of the study and decommissioning the site when the study is completed

The Project Team fully understands the critical nature of this task, specifically site access and utility services. It is the intention of the Project Team to work through any potential delays to ensure timely implementation of the project.

4.3 (Task 3) Prepare Monitoring and Quality Assurance Program Plan (MQAPP)

Integral to the planning process is the development of a comprehensive and complete Monitoring and Quality Assurance Project Plan (MQAPP). This document provides the road map for the project execution and defines the measurements to be made, data quality goals and the means to verify that the goals are being achieved. The MQAPP will provide details on the ambient air quality measurements, sample analysis and quality assurance procedures that will be followed during the Phase III Study. The MQAPP will be prepared collectively by the Project Team to assure that procedures are in place for meeting the data collection objectives.

The MQAPP will be prepared according to the requirements as outlined in the U.S. EPA – "EPA Requirements for Quality Assurance Project Plan" (QA/ R5 - EPA/240/B-01/003, March 2001), and the following key elements as outlined in the RFP. Essentially, the MQAPP will include the following key components:

- Project Management: This section will clearly define the project team organization as well as the roles and responsibilities for each team member. Additionally, this section will describe study objectives, data quality objectives, training requirements, and documentation/reporting requirements, etc.

- Measurement/Data Acquisition: This section will define the parameters that will be measured, describe sampling strategies and methods, describe analytical techniques used to collect the data and identify the corresponding data quality objectives. Prior to preparing the MQAPP, the Project Team will thoroughly review the U.S. EPA National Air Toxics Trends Station (NATTS) reporting requirements, including the non-detect (ND) levels, reporting limits (RL) and minimum detection limits (MDL) for each compound to be analyzed. This section will also describe the definition of the ND level for analytical methods. It is expected that the reporting and detection limits will be at least one order of magnitude lower, in the part per trillion/volume (ppt-v) ranges, than

standard method detection limits. Furthermore, this section will describe all measurement methods including: continuous ambient monitoring systems, discrete air sample collection and laboratory analysis, meteorological data collection, airport activity data collection and data acquisition and telemetry.

- Data Management: Measurement data including: methods and systems used to collect continuous monitoring data, laboratory analysis results and meteorological data will be organized, reviewed, validated and archived using a commercially available standard database programs (such as Microsoft Excel or Access). The MQAPP will describe details of data structure, organization and management. The MQAPP will also discuss database development logics, data access and reporting. The Project Team will use commercially available software (i.e., Microsoft Office – Word, Excel, Access, etc.) for document preparation and data processing and storage. No proprietary programs will be used in the preparation and delivery of final databases, documents and/or other deliverables.

- Quality Management: Data quality is critical to the success of this project. The MQAPP will describe QA/QC processes to ensure the data quality objectives are met. QC testing, inspection, maintenance requirements and instrumentation calibration and frequency will be discussed. The MQAPP will include system and performance audit procedures for the proposed monitoring sites and the laboratory providing analytical services.

For field measurements, sampling periods for the intensive monitoring periods will be determined in conjunction with LAWA. Actual start and stop times for sampling for each season will be included in the MQAPP based upon the historical seasonal wind flow pattern as discussed in Task 1.

Detection limits for discrete samples are dependent upon sample volumes and analytical methods. The Team will work with LAWA to define the most applicable combination of sample volumes and analytical methods relative to each sampling parameter in order to achieve appropriate detection limits.

In addition to the main body of the MQAPP, this document will also include extensive appendices containing standard operating procedures and calibration procedures for all monitoring and sampling equipment.

The Project Team will ensure that all ambient air quality data generated meeting specific data quality objectives (DQOs). In some cases, such as for monitoring of criteria pollutants (including $PM_{2.5}$), data quality objectives have been established by the U.S. EPA. These DQOs have been used to establish data quality indicators (DQIs) for various phases of the monitoring process. The DQIs that will be used to characterize measurements for this project are listed below.

Precision: Precision represents the reproducibility of measurements as determined by collocated sampling using the same methods or by propagation of individual measurements precision determined by replicate analysis, blank analysis and performance tests. The project goal for

precision is ±10 percent, expressed as the coefficient of variation (CV), for values that exceed ten times their lower quantifiable limits. The precision goal for gravimetric mass is ±5 percent CV as determined from replicate weighings.

Accuracy: Accuracy is the correctness of data and refers to the degree of difference between a measured value and a known or "true" value. For particulate measurements, there are no known true values. Sampler accuracy is measured by performance (flow rate) checks and audits between the sampler and a certified flow meter. The goal is ± 5 percent relative percent difference (RPD) or better. Since no true reference samples exist for the chemistry of airborne particulate matter, the accuracy of other speciated atmospheric components cannot be inherently determined. Analytical accuracy of the analytes will be determined by analyzing known reference materials in the laboratory.

Representativeness: Representativeness is the degree to which data accurately and precisely represents a characteristic of a population, parameter variations at a sampling point, a process condition or an environment condition. For this project, spatial and temporal data representativeness are achieved by following U.S. EPA siting criteria for particulate monitoring sites and by comparing measurements with those from other monitoring stations (e.g., LAX-Hastings, West Los Angeles, Long Beach) in the region, including those operated and maintained by the SCAQMD.

Completeness: Completeness is the percentage of valid data compared to the total expected data. For this project, in which many of the instruments are prototypes or are newer technology, the completeness objective for all species and measurements is 75 percent of all attempted measurements.

Comparability: Comparability reflects the extent to which measurements of the same observable agree among different methods. Comparability may vary by method, aerosol composition and meteorological conditions.

Additionally, bias and detectability will also be addressed in the MQAPP.

Bias: Bias is the systematic or persistent distortion of a measurement process that causes error in one direction. Bias is determined through performance audits and/or by inter-comparisons of the performance of similar instruments. Quantifiable biases that exceed precision intervals are corrected as part of the data validation process.

Detectability: Detectability is the low range critical value that a method-specific procedure can reliably discern. The minimum detection level (MDL) for Study measurements is determined as three times the standard deviation of field blanks or three times the standard deviation of the noise of an instrument when subjected to clean air.

The Tetra Tech Team has taken great care to establish an independent reporting structure for QA of the measurements and of the collected and reported data. This will provide LAWA with assurances that a proper set of checks and verifications are in place to most efficiently and effectively collect the required data of known quality.

Project Team member - T&B Systems - will conduct the quality assurance for this project to manage and handle the external quality assurance for this program. T&B's role will be independent of the internal quality management performed by the Tetra Tech measurement team and will provide the oversight, review and verification of all aspects of the data specification, collection and reporting process. T&B's expertise will be applied directly to this project to help guide the program to collection of data that is usable in the modeling and analysis efforts.

The quality management program will include two areas. The first area is in independent quality assurance audits of the measurement and data validation tasks. More details on the audits to be conducted will be discussed in the Task 7 - Conduct QA/QC Evaluations of Monitoring and Sampling Systems. The second, and related area, is in real-time review of the on-going measurement systems. Through the existing data management and display systems, the QA task team will routinely poll and make available the continuous monitoring data through a simple to use and effective web based data display system. This will allow both project personnel and technical management to completely understand the quality of the data being collected. It will allow prompt recognition of out-of-control conditions and lead to the rapid response and correction of issues. This is extremely important given the relatively short nature of the data collection efforts.

The MQAPP will be used to assure quality of monitoring data collected during the 1st and 2nd field measurement seasons.

4.4 (Task 4) Prepare Modeling and Analysis Protocol

The Project Team will develop protocols for receptor and source apportionment modeling and analysis. The modeling protocol will provide general methodology that will be used to:

- Conduct receptor modeling
  - CMB and multivariate analysis (UNMIX)
  - Spatial gradient analysis (such as Empirical Orthogonal Function)
  - Time series analysis
  - Non-parametric trajectory hybrid modeling
- Conduct source modeling
  - Estimates of Study Area emissions (both on- and off-airport)
  - Dispersion modeling

Receptor Modeling

Receptor models have been widely used to estimate the contributions of various sources to measured VOC and particulate matter concentrations. The CMB approach requires knowledge of the number of sources contributing to the observed concentrations of VOCs or PM and chemical species as well as the composition of the emitted VOCs or PM from each source. The contributions of fugitive dust, sea salt and secondary inorganic components of PM (e.g., ammonium nitrate and ammonium sulfate) are straightforward. More recent applications of this

method for PM apportionment have explored the use of particulate organic tracers to provide greater resolution of the contributions of various combustion sources of carbonaceous PM. Project Team member - DRI - has conducted many of the recent major source characterization and organic tracer-based CMB studies, including an evaluation of this approach for quantifying the contribution of diesel and gasoline exhaust to fine carbonaceous PM in the South Coast Air Basin. Chemical composition of VOC and PM emissions from commercial jets has been examined by a team of investigators lead by the University of Missouri. These and other available source of relevant data, including the chemical composition data that will be obtained during this project for gasoline, diesel and jet fuels will be used to supplement the existing library of available source composition compiled by DRI.

The same model can be solved for source contributions without prior knowledge of the source composition profiles using several different multivariate factor analytic algorithms, such as the UNMIX and positive matrix factorization (PMF). These analyses require multiple sampling periods and therefore, unlike CMB, cannot be implemented with only one or a few ambient samples. This is a potential limitation of multivariate methods since detailed organic speciation of PM is costly. However, the sample collection approach for this project, which emphasizes temporal and spatial (near-source vs. community) differences in ambient VOC and PM composition, could improve the ability of these multivariate methods to yield useful results given the relatively small sample size. The factors derived by the multivariate methods are often a mixture of covariant sources. These results are complementary to the source apportionments from CMB and will be interpreted together with meteorological variables and other spatially and temporally varying air quality data from the saturation monitoring and surveys with the mobile monitoring van. Analysis of the air quality and meteorological data from the proposed air quality monitoring program will be used to develop a conceptual explanation of the potential impacts of airport operations and activities on the communities adjacent to LAX and will provide the necessary data for operational evaluation of the source modeling and associated emissions inventory.

Nonparametric Trajectory Analysis

Additionally, the non-parametric trajectory analysis (NTA) will be used to separate the impact of LAX from other sources in the immediate area. The NTA protocol will include:

- Monitoring data requirements, especially the importance of accurate time stamps and synchronization for data reported every one to five minutes.
- Required information on runway maintenance and activity and aircraft takeoff and landing records.
- Airport operations data will be obtained from the LAWA.
- Wind speed and directional data requirements from Phase III stations. The sources of meteorological data include National Weather Service Automated Surface Observing System (ASOS) one minute data from LAX, Hawthorne, and Santa Monica Airports.
- The importance of simultaneous measurements from upwind and downwind stations and how these will be used to estimate the impact of the Airport and other local sources.
- The relationship of NTA to other receptor modeling methods.

For NTA modeling, the data will be screened by examining time series and looking for variations in the concentrations and wind data that are not consistent with expectations based on knowledge of the sources and past experience. This "level 3" type screening will be done rapidly by the modeler so that any possible problems with the monitors or their location can be reviewed by the team and, if necessary, corrected as soon as possible.

To allow for the timely application of NTA, the preliminary back-trajectories will be calculated for each monitoring station using wind speed and direction data from all available monitoring stations that are part of the study. The National Weather Service ASOS one minute wind data from LAX, Hawthorne, and Santa Monica Airports are generally not available until the following month. The final NTA will use back-trajectories calculated using all the available ASOS data.

NTA will be applied to one minute concentrations of all primary air pollutants from all the active monitoring stations. The species are expected to include nitrogen oxides, sulfur dioxide, black carbon, and ultrafine particles. The NTA analysis will include upwind – downwind analysis for all appropriate pairs of stations. The NTA will also be applied to data from the SCAQMD station near LAX if monitoring data are made available.

Emission Inventory and Source-Oriented Modeling

Before source-oriented modeling can be performed, the Project Team will prepare an updated emission inventory for emissions from airport activities as well as from the Study Area, including mobile source emissions from local traffic and vessel emissions in the coastal waters.

The emission inventory will be built on the FAA Emissions and Dispersion Monitoring System (EDMS) version 5.1.3, which is updated from the previous version. Additionally, other major stationary sources and mobile emissions near the airport will also be included. More discussion of the EDMS emission inventory protocol is presented in Task 14.

For source-oriented modeling, Project Team member - UNC Institute for the Environment - will prepare a modeling protocol focused on source-based dispersion modeling. The protocol will include the following components and further discussion of the proposed approaches is presented in Task 15.

- Model name, version, configuration with choice of various options
- Meteorological datasets that will be used
- Emissions inputs that will be used
- Ambient air quality measurements both from Phase III and from routine air quality monitors in the region, such as AQMD stations, AQS, STN, IMPROVE, etc.
- Methodology for analyses and model evaluation, using both current standard practices as well as innovative approaches that will be relevant from the perspective of an airport study

This Modeling and Analysis Protocol will be used to guide data analysis for source apportionment analysis using receptor-oriented modeling during the 1st and 2nd field

measurement seasons and source-oriented modeling using updated emission inventory and AERMOD dispersion modeling technique.

4.5 (Task 5) Monitoring Equipment Procurement and Installation

During the course of the study, data may indicate that a specific type of sampling/monitoring is not providing relative value to the Project. For this reason, it is necessary that the sampling program be dynamic. In this case, funds for measurement of this parameter may be shifted to another parameter or site.

As discussed in Task 1 - Finalize Detailed Work Scope - a revised sampling plan was developed based on preliminary mobile survey results. The revised sampling plan specifies three "core" sites and one background site: 1) upwind of LAX (UW) using the AQMD Hastings site with an equipment upgrade, 2) a community site downwind of the Airport and the I-405 freeway (CE), 3) a community site south of the Airport (CS), and, 4) a site in the community northeast of the Airport (CN) before the I-405 freeway. The parameters to be monitored or sampled at these sites are shown in Tables 4-1 and 4-2.

Additionally, for measurement periods, the revised sampling plan specifies six consecutive weeks of monitoring in two seasons using continuous monitors and collection of twenty four-hour integrated gas and PM samples for ten consecutive days in each season. The proposed sampling seasons based on past wind patterns are presented in Task 1 – Monitoring Period.

Fixed Station and Saturation Sampling

The full-scale (six sites) monitoring network as specified in the original draft Work Plan has been revised and the Team proposed a smaller number (three community sites and one AQMD site) of fully-instrumented monitoring sites, with more sensitive analytical methods than specified in the LAWA Technical Work Plan to provide detailed organic speciation information for receptor modeling. These sites will be augmented with a combination of saturation monitoring sites utilizing passive diffusive samplers and mini-volume aerosol samplers, and spatial surveys. As discussed in detail in Task 1, the mobile monitoring van was used to conduct spatial surveys of pollutant concentrations within and around LAX to characterize spatial gradients in pollutant concentrations and guide the selection of fixed and saturation monitoring sites. The original sampling plan was then revised.

The core component of the saturation monitoring networks will consist of six seven-day time-integrated samples during each seasonal monitoring period at seven sites (three at core stations and four at local community sites) using a combination of passive diffusive samplers for NO_2, NO_x, SO_2, VOCs (benzene, toluene, xylenes, ethylbenzene), and carbonyl compounds (formaldehyde, acetaldehyde, and acrolein), and mini-volume aerosol sampling for $PM_{2.5}$ mass, elements and organic and elemental carbon. The source site monitoring will be conducted using short-term sampling with active samplers, three to four days in each sampling season for four to six hours a day, to collect source profile and emission factors information for the receptor modeling.

Additional, seven-day integrated NO_2, NO_x and SO_2 samples will be collected at ten (10) additional locations to establish pollutant gradients downwind of the east end of the Runway 25R and major roadways (e.g., I-405 freeway, Aviation Boulevard and La Cienega Boulevard.).

Field Measurements at Fixed Sites

At the time of field deployment, establishment of the sites will include the following steps:

- Finalize site preparation including permit, power supply and security;
- Procure required equipment;
- Movement of the monitoring station (equipment shelter) and instruments on site;
- Build-out of instrument racks, plumbing, electrical and sampling platform;
- Installation and checkout of communications and data polling equipment;
- Installation of instruments;
- Initial calibration and collocated sampling; and
- Operational dry run.

The Project Team has a large inventory of equipment to support this program. Any monitors, samplers, etc. needed for the project that are not in the current inventory will be procured from reputable manufacturers and dealers. The team will provide all necessary equipment along with spares to meet program requirements.

Selected instrumentation will meet or exceed the specifications provided in the RFP. The equipment shelters located at the core sites will remain on-site for the duration of the study.

With proper planning, each station will have sufficient lead time to allow for the QA/QC evaluation prior to the commencement of monitoring and sampling operations.

Data from each continuous analyzer will be stored in a local data logger. Depending on the number of parameters recorded and the frequency of recording, data from each monitoring station, it may require downloading data from each station on a frequent basis. This will be accomplished remotely via telephone modem. Either dedicated landline or cellular telephone (preferred method) modems will be used to provide these communications. A remotely located computer will poll each monitoring station data logger on a daily basis and provide for on-demand retrieval of instantaneous analyzer data.

Quality Control of Real-Time Data

Because of the fixed time period in which data will be collected, it is critical to be able to identify any issues with the measurements being made and be able to make corrections or changes to the systems as rapidly as possible. To aid in this rapid identification, and as part of the external quality assurance program, a real-time data monitoring system will be provided to key team members. This system will be independent of the measurement team, but it will tie into the data systems used by the team through polling of the station data systems to provide real-time quality control of collected data. The real-time system is based on the Vista Data Vision web based software package that provides access to all data, both real-time and historical, with the

ability to perform analyses of the collected data through a browser based web interface. This information will allow on-going review of collected information to rapidly identify any instrument problems as well as review the collected data to determine if it is meeting the goals set forth in the MQAPP. As this information will be made available to the measurement team and independent QA team so that Project Team, will have the ability to review and provide feedback on the measurement program progress. Login to the system is user and password controlled with the ability to provide select data sets to individual groups. This approach will select and implement the most reliable and cost-effective method to ensure consistently high data recovery.

Saturation Sampling and Source Profile Sampling

Saturation sampling will require mainly passive samplers and active PM samplers. The Project Team member - DRI - maintains a sufficient inventory of required samplers and, if needed, additional samplers will be procured to meet project needs.

Source profile sampling will require active samplers for VOC and SVOC analysis, including canister, DNPH sampler, Tenax and TIFG/XAD samplers, and active PM MiniVol samplers.

Prior to deployment to the field, all equipment will be bench tested for proper operation and calibrated with known standards according to the field monitoring protocol.

4.6 (Task 6) Sample and Characterize Mobile Source Fuels Used On and Around the Airport

Mobile sources fuel combustion represents the single most significant source of emissions in the Study Area. A substantial fraction of VOC emissions from combustion sources is unburned fuel. Another significant emissions source is the non-combustion emissions, which are generated from fuel transfer into stationary storage tanks and from storage tanks into mobile source fuel tanks. For emission-estimation purposes, the Project Team will use SCAQMD-approved methods to calculate these volatile losses. Definitive characterization of the fuels used in and around the airport (e.g., off-airport rent-a-car facilities, commercial gasoline stations on or adjacent to LAX) is crucial for the ultimate success of the Study.

Jet A specification fuel has been used in the United States since the 1950s and is only available in the United States, whereas Jet A-1 is the standard specification fuel used in the rest of the world. Kerosene-type jet fuel (including Jet A and Jet A-1) has a carbon number distribution between about 8 and 16, which is heavier range than gasoline and lighter range than diesel. Aviation fuels consist of blends of over a thousand chemicals, primarily hydrocarbons (paraffins, olefins, naphthenes, and aromatics) as well as additives such as antioxidants to prevent gumming (alkyl phenols), antistatic agents to dissipate static electricity and prevent sparking (e.g., dinonylnaphthylsulfonic acid), and metal deactivators. Jet fuel typically has much higher sulfur content than gasoline or diesel fuel, which will result in higher SO_2, elemental sulfur and sulfate exhaust emission rates.

Diesel fuel is produced from the fractional distillation of crude oil between 200°C and 350°C at atmospheric pressure, resulting in a mixture of carbon chains that typically contain between 8 and 21 carbon atoms per molecule. It is composed of about 75 percent saturated hydrocarbons (primarily paraffins including n-, iso-, and cyclo-paraffins), and 25 percent aromatic hydrocarbons (including naphthalenes and alkylbenzenes).

Typical gasoline consists of hydrocarbons with between 4 and 12 carbon atoms per molecule and is enhanced with iso-octane or the aromatic hydrocarbons toluene and benzene to increase its octane rating. Small quantities of various additives are common, for purposes such as tuning engine performance or reducing harmful exhaust emissions. Gasoline sold in California contains 5 to 10 percent ethanol by volume and 30 ppm sulfur by weight.

The Project Team will collect and analyze 15 fuel samples, including: Jet A (3), diesel (3) and gasoline (9). This task will be accomplished at the beginning of the Phase III. The Project Team will develop a sampling and analysis protocol (including candidate sampling locations). The liquid fuel samples will be analyzed at DRI using a 100-m Petrocol DH (Supelco, Inc.), 0.25-mm i.d. column with a 0.5-µm poly-methyl siloxane phase. This column is designed to speciate liquid fuel (which does not contain C_2 compounds and only a very small amount of C_3 compounds). The method is consistent with the analysis protocol developed for the Auto/Oil program.[2] The compositions of fuel headspace vapors can be predicted from the measured composition of liquid fuel. This method is based on the proportionality between the equilibrium headspace partial pressure for each compound identified in gasoline with its mole fraction in liquid gasoline times the vapor pressure of the pure species. The individual vapor pressures are determined using the Wagner equation.[3]

The Project Team will secure the access required for fuel sampling, and for labeling, storage, and delivery of samples to the DRI lab for analysis. Sampling and analytical data will be properly documented as part of the final project report.

4.7 (Task 7) Conduct QA/QC Evaluations of Monitoring and Sampling Systems

The QC testing of monitoring and sampling equipment and quality assurance auditing/data validation of monitoring and sampling results will be conducted after installation of the equipment and before collection of data for the 1st season monitoring and sampling campaign. The procedures described in the MQAPP developed under Task 3 will be followed when conducting these evaluations. The quality control and quality assurance procedures will be repeated at the beginning of the 2nd Season campaign.

The independent QA activities will be conducted by T&B Systems, who are not involved in the field measurements and laboratory analysis. As part of the external QA program, independent

[2] Society of Automotive Engineers. 1993. Auto-Oil Air Quality Improvement Research Program. Society of Automotive Engineers Inc. p: 1-308.
[3] Kirchstetter TW et al. 1999. Impact of California Reformulated Gasoline on Motor Vehicle Emissions. 2. Volatile Organic Compound Speciation and Reactivity. Environ. Sci. Technol. 33: 329-336.

audits will be conducted at various stages of the program to identify any issues that may affect the data quality, capture rates or usability of the collected information. These audits will test the entire data collection process against the standards and goals established in the MQAPP. The audits to be conducted will include the following:

Monitoring Station System Audits. The systems audits will be conducted once the monitoring stations are up and running and the program is collecting data considered to be meeting the program goals. The system audit includes a review of the entire data collection process at the site level, including factors that may affect the quality of the data collected. This includes the siting relative to the U.S. EPA siting criteria and any other issues that may affect the measurement quality objectives (MQOs). This is an important step because the station locations will be a compromise between "ideal" sites and measurement conditions and the reality of the available locations to collect the data meeting security, power and other considerations. The system audit will identify where compromises were necessary and what effect they may have on the collected data. The system audit will clearly identify what, if any, siting criteria were compromised and what effect it will have on the data collected. Results of each site system audit will be discussed with the site operator immediately at the conclusion of the audit and a summary provided within 30 days of the audit conclusion. Any identified critical issues will be corrected immediately (if possible) and reported within one day of the audit to the measurement team manager.

Monitoring Station Performance Audits. Within two weeks of the monitoring initiation, performance audits of each monitoring station will be conducted using personnel, equipment and audit standards independent of the measurements team. The goal of the performance audits will be to, when possible, establish the accuracy of the measurements made and identify any measurement processes that may not meet the program MQOs. The audit procedures will follow standard audit protocols consistent with U.S. EPA guidance for air quality and meteorological measurements. The audit procedures for the continuous and discrete sampling methodologies are detailed in the MQAPP, as will the certification process for all of the audit standards. Preliminary results of the performance audits will be provided on-site to the site operator with an audit summary to follow within 30 days of the audit completion. Critical issues identified during the performance audit will be corrected immediately (if possible) and reported within one day to the measurement team manager. As the data collection efforts are divided into discrete seasons of limited duration, this rapid identification and correction is essential to the collection of a usable data set for the source/receptor analysis.

Laboratory Audits. Following the start of the measurement program, the laboratories performing the analyses will be audited to assess compliance with the standards and procedures set forth in the MQAPP. As indicated above, sampling is divided into discrete seasons and rapid identification of issues is essential to assure any potential problems are identified and rectified quickly. This will minimize the potential for collection of data that do not meet the quality objectives of the program. If the laboratories already participate in U.S. EPA audit programs and the sensitivities of analytical methods used meet this project's requirements, then this process may only involve a review of the audit status and any issues identified during those audits. This program will, however, likely be using improved analytical procedures to enhance compound

resolution and help achieve lower detection limits. The audit will therefore focus on the necessary procedures to achieve these lower levels.

Data Audits. To verify the integrity of the collected data, the data audit will follow the entire process from the raw Level 0 data collected by the data systems, through the validation process and into the final database, considered to be Level 1. This will verify any corrections made as a result of needed calibrations to the data. Additionally, laboratory data will be reviewed to assure the proper application of blank and pre-analysis information. The goal of the data audits will be to verify that the final data set includes properly validated Level 1 information and that the stated accuracy and precision is verifiable. Any deviations from the quality objectives stated in the MQAPP will be noted. The data audits will be conducted once the first set of data for each season is prepared and ready for use in the modeling and analysis.

Quality Control of Real-Time Data. As discussed in Task 5, the capability of reviewing real-time data will allow on-going review of collected information to rapidly identify any instrument problems as well as review the collected data to determine if they are meeting the goals set forth in the MQAPP. This system will be run independent of the measurements team and also serve as an independent collection process to aid in the data integrity audits to be performed.

4.8 (Task 8) Commence 1st Season of Ambient Monitoring, and Sample Collection and Analysis

The Project Team's field measurement task member - SCS Tracer - will oversee the logistic aspects of the monitoring program for the fixed monitoring sites and confirm all equipment and power supplies are in place and operating for the 1st season measurement campaign. The Project Team will operate, maintain, repair, and calibrate the equipment as detailed in the Task 3: MQAPP. This work effort will include:

- Furnish routine calibration gases
- Synchronize monitors' internal clocks
- Visit monitoring sites as necessary to change calibration gases
- Perform routine field calibrations of the monitoring equipment at each site
- Remotely interrogate each site to download data each normal working day
- Provide first level quality control by reviewing the data each normal working day
- Document calibrations and field activities
- Incorporate quality-controlled data into project database
- Provide a summary report of activities and issues to project management team

In addition to collecting filter and canister samples, SCS Tracer will be responsible for labeling, storage, and delivery of samples to the DRI laboratory for analysis.

Once the establishment of the air monitoring sites is completed, monitoring and sampling will take place over two seasonal periods of six weeks each. The 1st season of air monitoring is anticipated to start approximately in January 2012. There will also be an intensive sampling period of ten days with selected twenty-four hour integrated samples collected daily. This period

will take place within the seasonal air monitoring period and will be coincidental with continuous monitoring efforts. Due to the shorter-term nature of this monitoring program, maximum data recovery becomes even more important. To facilitate this, a greater level-of-effort in terms of field manpower will be required. Rather than sites being visited two to three times per week on a normal long-term monitoring effort, each site in this program will be visited at the rate of four to five times per week. During the 10-day intensive periods, site visits will occur every day including weekends. The shorter-term nature of this program will also mandate strict procedures for troubleshooting and/or replacement of faulty equipment. Problems identified through data review or site visits will initiate a troubleshooting process aimed at minimizing down time for all instruments.

The monitoring and sampling program will be supported by a vigorous QA/QC protocol as detailed in the MQAPP that includes the following:

- Strict chain-of-custody procedures for collection and shipment of samples;
- Daily automated performance checks on continuous analyzers;
- Biweekly precision checks on continuous analyzers;
- Conduct flow checks on samplers during sampling seasons;
- Thorough documentation of all onsite activities; and
- A comprehensive laboratory QA/QC program.

Additionally, raw data from the continuous instruments will be reviewed daily. The main purpose of the review will be the early detection of instrument problems. Problems noted in the review will mandate communication with field personnel for immediate rectification. A secondary purpose will be the detection of any trends in the data. To ensure compliance with the QC program, a set of established procedures has been developed for the onsite operator to follow. Station operation not only includes many procedures to follow but redundant documentation of these activities. These procedures are described further below.

Activities can be separated into two different categories. These include activities that need to be performed on each and every site visit and those that are regularly scheduled. The activities that need to be accomplished each and every site visit including the following:

- Completion of station logbook;
- Completion of operator checklists;
- Checking for satisfactory gas cylinder pressures;
- Checking for correct air flow settings;
- Checking for instrument malfunctions; and
- Notation of any unusual activities, odors or sounds.

A number of specific tasks need to be accomplished prior to completing the checklists. These are discussed below.

Scheduled activities include calibrations, preventive maintenance, preparation and collection of sampling media, and collection of data.

Site Logs. A bound station logbook is kept at each station and is used to record all activities of the site operator. The site operator first enters the time and date of his or her arrival. Any subsequent activities such as calibrations or maintenance are recorded along with their beginning and ending times. Any problems in site operation or performance of any piece of equipment are also recorded in the site log.

Operator Checklists. The Operator Checklist consists of two pages of checks that need to be completed by the site technician upon each visit to the monitoring station. The checklist contains a number of key questions concerning the operational status of air quality analyzers, calibration equipment, meteorological sensors, and data systems as well as general checks. Most entries require only a yes/no response while there are a few that require specific information. Any discrepancies noted during the checks mandated by the checklist are entered in the site logs.

Checking for Satisfactory Gas Cylinder Pressures. The pressures of the gas cylinders are checked and logged. A replacement cylinder is ordered when the supply pressure drops below 500 psig (300 psig for superblends) or one month before the certification expiration date (whichever comes first). The minimum usable pressure for zero air cylinders is 200 psig. Excessive drops in cylinder pressures are also investigated.

Checking for Correct Air Flow Settings. All instruments are checked for correct air flow. Any deviation in flow is immediately diagnosed and corrected.

Checking for Instrument Malfunctions. Instruments are inspected for obvious malfunctions. Temperature control, mode cycling, timing, pump operation, meteorological instrument operation, and data logging are just a few of the functions checked for correct operation.

Notation of Any Unusual Activities, Odors or Sounds. Any unusual activities around the site will be recorded. Any unusual odor may indicate a point source of a pollutant or a malfunctioning instrument. A new noise or absence of a usual noise can also indicate a malfunction in the equipment.

Any malfunctions noted by the site operator are corrected if possible. Regardless of the operator's ability to remedy the problem, the problem is documented in the site logs and operator's checklist. For problems that the site operator cannot correct on the spot, a Corrective Action Request Form is filled out and provided it to the field manager for review. This form ensures that problems are taken care of in a timely manner and provides the documentation to show completion. The form specifically documents:

- The Malfunction;
- The Time of Occurrence;
- The Time of Correction;
- The Corrective Action; and
- The Person Correcting the Malfunction.

The form can also be submitted by data processing personnel if problems are noted during processing and review of data.

There are times when there are unusual circumstances surrounding data collection that may have an influence on the data. These unusual situations include weather events, fires in the area, local construction, etc. Any events that have the potential to affect data are documented on the Unusual Occurrence Form. The form is filled out by the site operator and forwarded to data processing personnel. Data processing personnel make judgments concerning the effects these occurrences had on the data.

On a daily basis, each station will automatically be polled and the previous twenty-four hours of data retrieved. An air quality scientist reviews the data to verify the proper operation of the air quality analyzers, meteorological sensors, and data logger. The review entails scanning the data for reasonableness. The reviewer is verifying that the data collected by the data logger make sense. The automated zero, precision, and span check data are also reviewed to ensure that the checks fall within control limits. Any problems noted are brought to the attention of field personnel. The previously discussed Corrective Action Request Form is completed to provide documentation on any problems discovered.

Spatial Survey with Mobile Monitoring Van

As discussed in Task 1, the spatial survey was conducted prior to the 1st monitoring season over a four-day period. The survey included the LAX perimeter, with traverses through the surrounding residential areas, fixed site locations in the communities, terminal area, and other areas with potential elevated pollutant concentrations. The mobile survey also investigated the areas near and downwind of the blast fence at the east end of Runway 25R, and nearby roadways. The survey results were used to refine the Work Scope, finalize locations for fixed stations, and refine the draft monitoring plan.

Saturation Monitoring

As part of the revised sampling plan, the Project Team will conduct six-week saturation monitoring in both seasons to determine gradient in pollutant concentrations within communities adjacent to LAX.

In the saturation monitoring program, the sampling locations will include seven core sampling locations - the three core and four community sites. Measurements at these sites will include seven-day integrated passive samples for NO, NO_x, SO_2, BTEX, and aldehydes (formaldehyde, acetaldehyde, and acrolein) using the passive samplers described in Appendix D. Additionally, seven-day integrated quartz filter samples will be collected with portable Airmetrics MiniVol samplers and analyzed for $PM_{2.5}$ mass, elements, organic carbon (OC) and elemental carbon (EC). The Project Team will also measure NO, NO_x and SO_2, at ten additional locations to characterize the spatial variations in pollutant concentrations near and downwind of the blast fence at the east end of Runway 25R and along the upwind and downwind edges of the I-405 freeway, Aviation Boulevard and La Cienega Boulevard.

Based on past experience, the Ogawa and Radiello passive sampling methods have replicate precisions of better than 10 percent.

Source Profile Sampling

During the sampling seasons, source profile sampling will be conducted behind the blast fence of Runway 25R to collect air pollutants for source profile characterization to be used in the subsequent CMB receptor modeling. The Project Team will collect samples using active samplers for VOC, SVOC, EC and OC analysis near Runway 25R and the open field east of Aviation Boulevard.

4.9 (Task 9) Compile 1st Season Monitoring and Analysis Data, and Prepare 1st Season Report of Findings and Lessons Learned

The Project Team's field measurement task member - SCS Tracer - will compile all continuous monitoring data from air quality and meteorological monitors and all discrete sample analysis data into an appropriate database. The format of the database is described in the MQAPP developed under Task 3. The compiled data will be validated to both Level 1 (observations have received quantitative and qualitative reviews for accuracy, completeness and internal consistency). DRI will compile all chemical data from the time-integrated samples and fuel analysis and perform Level 2 (measurements are compared for external consistency against other independent data sets) data validation levels for all measurement data. DRI will also compile all analytical data from samples collected using passive and active PM samplers during saturation sampling and source profile sampling campaigns.

The Project Team will prepare the 1st Season Report, which describes the findings and lessons learned during the measurement campaign. The report will summarize the equipment and methods used, the issues and challenges encountered and how these were resolved or addressed, a summary of the measurement results and comparisons of the various measurements over time and by location. From these results, the Project Team will recommend to LAWA any adjustments in the monitoring methods and approach to better achieve the desired project objectives.

All measurement data will be compiled into a database along with relevant information from each sample run such as start and stop times, flow rates, sampler pressure, analysis results and corresponding concentrations. In addition to the database, all field-generated supporting data will be submitted. This includes calibration forms, operator checklists, sampling logs and chain-of-custody forms. The data validation process encompasses all aspects of the air monitoring programs. Data validation procedures begin in the field and continue until the final report is prepared for submission. Below are examples of data validation check procedure:

Internal and Historical Consistency Checks

Internal consistency checks are designed to identify values that are too high or too low compared with the rest of the data (identification of outliers). Discrepancies are investigated and further verified to ensure that any problems are isolated and not widespread. Historical consistency checks involve the use of an air quality scientist to review the data with respect to previously recorded and anticipated patterns. The qualified scientist searches for anomalies that include measured pollutant concentrations being recorded during hours when none are expected or pollutant levels below an established baseline, etc. In short, the scientist is checking for major deviations from the climatology of the site. Any anomalies found are investigated and a determination of the validity of the data is made.

Review of Calibration Data

The next level of validation is performed by reviewing the calibration data. Review of the calibration data consists of verifying the following:

- Calibrations and precision checks were performed within the required intervals.
- Verification of calibration results.
- Determination of data validity based on calibration results.
- Take corrective action if necessary.

Performance of Required Calibrations

The reviewer ensures that all of the required checks are performed within the proper time intervals. The reviewer verifies that precision and manual Level 1 checks are conducted as required and that multipoint calibrations are performed in the beginning of each sampling season. In cases where the data logger's automated Level 1 system fails, the weekly performance of manual Level 1 checks is verified. Performance of nonscheduled calibrations such as those required before and after maintenance activities are also verified. Nonperformance of any required calibrations is assessed for its effect on the validity of the data. The following rules apply to the nonperformance of required calibrations:

- Data not bracketed by valid Level 1 checks greater than seven days apart will be flagged.
- Instrument adjustments performed without performing a Level 1 check prior to the adjustment will invalidate data back to the last automated or manual valid Level 1 check.
- Failure to perform any calibrations prior to maintenance or repair on an analyzer will invalidate data back to the last calibration.

Calibration Results and Data Validation

Since calibrations give a measure of the performance of an analyzer, there must be guidelines for determining whether the data collected by an analyzer are acceptable. For example, in the standard ambient air measurements, data are invalidated whenever the following occur:

- Zero checks exceed +3 percent of the full scale range of the analyzer.
- Span outputs exceed +15 percent of the input concentration.
- The slope of the linear regression curve derived from the multipoint calibration results is less than 0.85 or greater than 1.15.

- The intercept of the linear regression curve derived from the multipoint calibration results exceeds +3 percent of the full scale range of the analyzer.
- The correlation coefficient of the linear regression curve derived from the multipoint calibration results is less than 0.9950.

These criteria need to be modified for the more sensitive measurements proposed to be used in this study. Should any of these conditions occur, data are invalidated back to the last check or calibration that had acceptable results.

Laboratory Data Validation

Analytical data generated from chemical analysis in the laboratory will be reviewed and validated. The focus will include linearity of the calibration curve, instrument noise, method detection limits, field and laboratory blanks, etc. to assure accuracy of the chemical analysis of collected samples. Data will be reviewed by the analyst and laboratory supervisor. If applicable, data will be stored in the laboratory information management system to generate either hardcopy or electronic reports.

4.10 (Task 10) Begin Receptor Modeling, Time Series Analysis, Spatial Analysis, and Nonparametric Trajectory Analysis on 1st Season Data

The Project Team's modeling experts will use various receptor-oriented methods, including CMB, UNMIX (a multivariate method) and a non-parametric trajectory hybrid model to analyze the collected air quality and meteorological measurements for source apportionment. The analyses will also include time-series analysis and gradient spatial analysis. A general description of these models and the time series and spatial gradient analyses is included in Task 3.

Receptor Modeling, Time Series Analysis and Spatial Analysis

The collected measurements will be reviewed by DRI as part of Level 2 validation in Task 9. Level 2 data validation takes place after data from various measurement methods have been assembled in the master database. Level 2 validation is the first step in data analysis. Level 2A tests involve comparisons of collocated measurements (e.g., filter and continuous mass, passive and continuous NO_x and SO_2) and internal consistency tests (e.g., the sum of measured aerosol species does not exceed measured mass concentrations). Level 2 tests also involve the testing of measurement assumptions, comparisons of collocated measurements and internal consistency tests. Based on the review of the data, any problems with applying the data in each of the models can be identified and suggestions of alternative receptor models can be made if the data review indicates another model would be better for producing source apportionment results.

Pertinent findings from these analyses will be summarized in a modeling report. The expected outputs of the receptor modeling analysis are source contributions to the measured ambient VOC and $PM_{2.5}$ concentrations at the community monitoring sites. These source contribution estimates will be combined with the observed gradients in pollutant concentrations obtained from the saturation monitoring and mobile surveys, which will define the zone of influence of identified

emission hotspots related to airport operations and activities. The gradients measured over longer time averages (twelve- or twenty four-hour and seven-day) will be related to the observed diurnal and day-of-week variations in pollutant concentrations that affect known temporal variations in airport operations, vehicular traffic related to flight departures and arrival and regional traffic patterns. The temporal and spatial variations measured at and near LAX will be placed in context with similar pollutant measurements from other SCAQMD air monitoring stations in the South Coast Air Basin with particular emphasis on stations located in the western basin (e.g., West Los Angeles, North Long Beach, Compton, and Central Los Angeles). Additionally, measured ultrafine particle concentrations will be compared to similar measurements that have been made recently in the Port area for the Harbor Communities Monitoring Study (HCMS), LAX, and the Van Nuys and Santa Monica Airports. Results of this study will also be compared to previous monitoring by SCAQMD downwind of LAX at Felton and Lloyde Schools and the 2006-07 Multiple Air Toxics Exposure Study (MATES-III) data base. It is anticipated that the District will soon conduct MATES-IV. If there is overlap in timing with this study, the Project Team will explore opportunities to coordinate the objectives of the Phase III of the LAX Air Quality and Source Apportionment Study with the planned monitoring program for MATES-IV. The combined results of this analysis will be used to develop a conceptual explanation of the potential impact of airport operations on the air quality of the surrounding community. This conceptual explanation, source contributions and the temporal and spatial variations in pollutant concentrations near LAX will be used for operational evaluation of the dispersion modeling and for top-down evaluation of the associated emissions inventory.

The modeling and analysis conducted here should follow the Modeling Protocol developed under Task 4. Pertinent findings from these analyses will be summarized in a modeling report.

Any issues encountered in conducting the receptor modeling, time series and spatial gradient analyses of the 1st Season data could be used to help refine the monitoring and sampling for the 2nd Season measurement campaign. Therefore, issues or problems in applying the models to the data will be presented to LAWA while the modeling is still being conducted.

Nonparametric Trajectory Analysis

NTA is a receptor model that, given upwind – downwind data, can remove the effects of nearby sources so that the airport contribution to observed concentrations can be estimated. At the same time, NTA locates the sources of the background pollutants and estimates the impact of these on the concentrations at the monitoring sites. It does this by using one minute average pollutant concentrations and one minute average wind measurements to calculate back-trajectories. Making use of nonparametric regression, NTA at a point (X,Y) estimates the conditional expected value of a pollutant at the receptor given that the air has passed through (X,Y) before reaching the receptor. An intuitive, graphical explanation of how NTA is calculated is provided in Figure 4-3.

Assume there are n back-trajectories with m points equally spaced in time on each trajectory. Let the points on the back-trajectories be given by (x_{ij},y_{ij}) where i = 1,…,m and j = 1,…,n. Further, let C_j be the concentration at the receptor at the start of the jth back–trajectory. The NTA at point (X,Y) is a weighted sum of the observed concentrations given by:

$$E(C \mid \text{air passes over point } (X,Y)) = \frac{\sum_{i=1}^{m}\sum_{j=1}^{n} C_j W_{ij}}{\sum_{i=1}^{m}\sum_{j=1}^{n} W_{ij}} \qquad (1)$$

where

$$W_{ij} = K\left(\frac{X - x_{ij}}{h}\right) K\left(\frac{Y - y_{ij}}{h}\right) \qquad (2)$$

and

$$K(u) = 0.75(1 - u^2) \quad \text{for } |u| \le 1$$
$$K(u) = 0 \quad \text{otherwise} \qquad (3)$$

Note that the weights W_{ij} are all nonnegative and have a maximum value of $0.75^2 = 0.5625$.

The NTA model is unique in its use of back-trajectories on the scale of a few kilometers and meteorological data on the time scale of minutes to identify local source-receptor relationships. These back-trajectories are estimated using wind speed and direction observations that have both measurement error and natural variability. The effect of this uncertainty in wind speed and direction is uncertainty in the back-trajectories and an associated increase in the uncertainty of the NTA results. The effect of the errors in the trajectories is to increase the NTA error by about 25 to 35 percent.

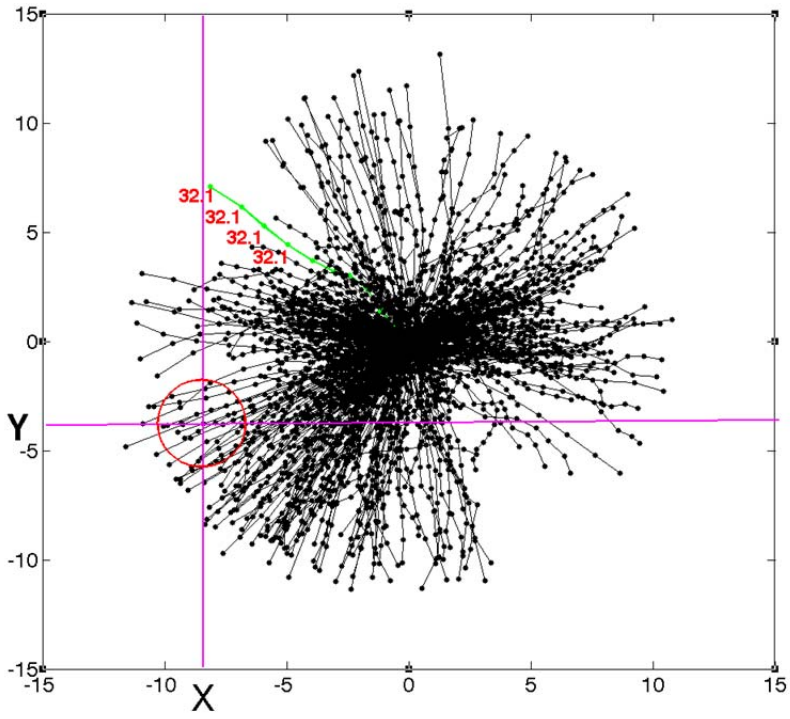

Figure 4-3. How NTA Works

The back–trajectories are shown as black lines and points at five-minute intervals. Each point on a trajectory is associated with the concentration observed when the trajectory arrives at the receptor. For example, each point on the trajectory shown in green is associated with the concentration 32.1 ppb shown as numerical values in red. The NTA value for point (X,Y) is the weighted sum of the values associated with the trajectory points inside the red circle. The weights for each trajectory point are based on the distance of the point from (X,Y). The radius of the circle is the smoothing parameter or scaling factor for probability density.

4.11 (Task 11) Commence 2nd Season of Ambient Monitoring, and Sample Collection and Analysis

This task will be undertaken using the same approach as for the 1st season of ambient monitoring and sample collection and analysis (Task 8). However, this season of sampling is anticipated to take place at the start of July or August 2012.

4.12 (Task 12) Compile 2nd Season Monitoring and Analysis Data, and Prepare 2nd Season Report of Findings, and Lessons Learned

This task will be undertaken using the same approach as for the 1st season of monitoring and analysis data (Task 9). However, the data analysis and report will be about the sampling that took

place beginning in July or August. The 2nd season report would integrate the findings of the 1st and 2nd seasons, and would be the basis for developing the final report.

4.13 (Task 13) Continue Receptor Modeling, Time Series Analysis, Spatial Analysis, and Nonparametric Trajectory Analysis on 1st and 2nd Season Data

The Project Team will continue with the various methods of analyzing the collected air quality and meteorological measurements for source apportionment started under Task 10 and described in the Modeling Protocol developed under Task 4. The collected measurements from the 2nd Season will first be reviewed by the receptor modelers to determine if there are sufficient valid data to be used in each of these models. Based on the review of the data, the Project Team will note any problems with applying the data in each of the models to LAWA and suggest alternative receptor models if the data review indicates another model would be better for producing source apportionment results.

Receptor Modeling, Time Series Analysis, Spatial Analysis, and Nonparametric Trajectory Analysis

The same technical approach and methodology for receptor modeling, time series and spatial analysis and NTA as described in Task 10 for the 1st season monitoring data will be used in modeling the 2nd season data.

4.14 (Task 14) Develop Refined Emission Inventories of Study Area Sources

The draft Demonstration Project documents include emission estimates for 2008, which will be used as a starting point. However, the Project Team will update the inventories to best reflect current activity levels, including on-airport and off-airport sources.

The on-airport sources will include:

- Aircraft engines
- Ground support equipment (GSE)
- Auxiliary power units (APU)
- Parking lots
- On-airport roadways
- Stationary Sources

The off-airport sources will include:

- Off-airport roadways
- Off-airport parking lots
- Off-road equipment
- Stationary sources
- Marine vessel emissions

The emission modeling methods will be developed in the Task 4 - Modeling and Analysis Protocol. Emissions source activity levels that occur during the sampling campaigns will be provided by LAWA and incorporated in the inventory and the resulting emission inventories will be used as input to the dispersion modeling analysis conducted under Task 15.

It is anticipated that the 1st season data analysis and receptor modeling analysis may provide results that could be used to adjust the emission inventories specifically developed from activity levels and other databases. If those results are applicable to the emission inventory analysis, they will be incorporated into the inventories.

Emission Inventory

During the Demonstration Project, FAA's EDMS Version 5.0.2 was used to produce a three-month inventory of all airport-related emissions, including aircraft, APUs, ground support equipment (GSE), roadways, parking facilities and stationary sources at LAX. In this task, these emissions will be updated to a 2011 inventory, using the EDMS 5.1.3. This newest version of EDMS includes patches for some model bugs found during the Demonstration Project and incorporates hazardous air pollutants (HAPs) from aircraft and PM from APU engines into the emission inventory. The AERMOD input files developed by EDMS will be used for dispersion modeling.

It is expected that a single inventory will be prepared and that there will not be iterations associated with reconciliation or calibration of the dispersion model (and associated emission inventory) with the monitoring data.

Project Team member - K&B Environmental - will use aircraft activity data from the LAX's operation division and EDMS input files to generate emission inventory for airport operations. Additionally, real-time marine emissions, real-time highway emissions and detailed inventories within a 1,000 foot radius of each monitoring site will be prepared. LAWA is seeking to provide the Project Team with an updated version of a GSE Inventory Survey. If this is available, the updated GSE inventory will be incorporated in the 2011 inventory.

Documentation will be provided for all assumptions and methodologies used in developing the inventory. The Project Team will revise the documentation based on resulting comments.

SCAG Mobile Source Emissions

The Project Team will develop EDMS input files for real-time roadway activity of the I-405 and I-105 freeways. This can be accomplished by substituting hourly Freeway Performance Measurement System (PeMS) data in place of the Southern California Association of Governments (SCAG) Transportation Model Summer 2008 forecast link flow and speed data for the I-405 and I-105 traffic links. The SCAG data should still be used as necessary to augment missing vehicle types or other specific data not available from PeMS.

Mobile source emissions are determined using emission factors in CARB's EMission FACtors (EMFAC) model. On September 29, 2011, CARB released the EMFAC 2011 model with a web-

based data access platform (http://www.arb.ca.gov/msei/modeling.htm). The Project Team will use this new release to obtain mobile emission factors for this project.

Marine Emissions

Marine emissions from ocean-going vessels in the nearby harbors and along coastal shipping lanes off the coast of California near LAX are important emission sources that could have significant impacts to the air quality in the Study Area.

The marine emissions will be developed using CARB Marine Model Version 2.3G dated April 28, 2011 (http://www.arb.ca.gov/msei/categories.htm#ogv_category). Shipping lane and El Segundo Buoy forecast emissions data will be used as part of the model inputs. The marine emission inventory will be updated by obtaining shipping data from the Marine Exchange of Southern California, including transit data and emission factor from Ports of Los Angeles and Long Beach Air Emission Inventory Reports.

Monitor Site Refinement

The Project Team expects to complete EDMS input files associated with all activities near each monitoring site. . This effort will include identification of all stationary sources and emission estimates for the surrounding roadway network. Once the refinement is done, detailed emission inventory data from the associated SCAG emission inventory grid squares inventory will be removed to avoid double counting.

4.15 (Task 15) Conduct Air Dispersion Modeling of Refined Emission Inventories

The Project Team will conduct air dispersion modeling of Study Area emissions as described in the Modeling and Analysis Protocol developed under Task 4. The resulting concentrations for the key compounds being modeled will be compared to the monitored values to determine if the emissions/dispersion analysis provides similar results to what is being measured. The comparisons will review the relative ranking of receptor locations for a given pollutant, the relative ranking of the key pollutants at a given receptor and the absolute magnitude range of concentrations for a given pollutant across all receptors.

The Project Team's dispersion modeling expert - UNC Institute for the Environment - will conduct dispersion modeling of the Study Area emissions as outlined in the Modeling and Analysis Protocol developed in Task 4.

UNC performed air dispersion modeling using AERMOD and emission inventory developed in Phase II of the LAX Air Quality and Source Apportionment Study – Demonstration Project. The results were compared to measurements taken during the July to September 2008 period. The air dispersion simulations used the following set of receptors in AERMOD:

- Polar grid, every 5-km up to 50-km radius
- Square grid, every 500-m up to 5-km

- Five measurement locations from LAX AQSAS Phase II
- Use flag-pole receptors at heights of 2, 7, 12, 17 and 22m

Additionally, the dispersion model exercises used flag-pole receptors aloft to identify whether AERMOD has higher concentrations aloft than at the surface. The results indicated that AERMOD under-predicted as shown in some studies, such as at Providence T.F. Green Airport with the presence of a high concentration plume aloft rather than at the surface. [4]

Conduct Air Dispersion Modeling of Refined Emission Inventories

The Project Team will use the latest version of AERSURFACE, AERMET, and AERMOD from the U.S. EPA for this task. The Project Team will obtain representative meteorological data from available sources for the study periods 1 (January/February 2012) and 2 (July/August 2012), including on-site data from LAX and from upper air data from a local location, such as the AQMD Upper Air station located west of the Airport. A potential concern with the NWS or FAA data; however, has been the presence of calms (wind speed less than three knots) and variable wind conditions at most stations. Since AERMOD cannot simulate dispersion under calm or missing wind conditions, U.S. EPA has developed a new tool called AERMINUTE to process one minute archived wind data for the Automated Surface Observing System (ASOS) stations. If available, ASOS data available at one minute frequencies from the National Climatic Data Center (NCDC) will be used. The land characteristics around the selected meteorological stations will be determined and applied in the AERSURFACE model. AERMET will be used to process the available meteorological data for input into AERMOD. From past experience, several problems were found with the default meteorological fields that come out of AERMET. Therefore, in this study the meteorological data will undergo extensive screening to ensure there are no anomalous values that may possibly impact model performance. For instance, to address abnormal values of both heat flux and surface friction velocity (U*) from AERMET in recent AERMOD applications, the meteorological fields were carefully screened to fix abnormal values, or remove those hours in the final analyses.

The dispersion model will use the complete AERMOD-ready emissions inventories, as prepared in Task 14.

- The Project Team will create a receptor network similar to the modeling effort for the LAX Phase II Demonstration Project work, but replace the measurement locations with the ones corresponding to the Phase III. Then, AERMOD will be performed to predict concentrations of all study pollutants at the four sets of receptors discussed above including: polar grid every 5-km up to 50-km radius, square grid every 500-m up to 5-km, five measurement locations from LAX AQSAS Phase II, and use of flag-pole receptors at heights of 2, 7, 12, 17 and 22m

.

[4] Partnership for Air Transportation Noise and Emission Reduction. 2008. MCIP2AERMOD: A Prototype Tool for Preparing Meteorological Inputs for AERMOD. Accessed from: www.cmascenter.org/conference/.../davis_mcip2**aermod**_cmas08.ppt on November 11, 2011.

The outputs in the form of time-series, scatter plots, Q-Q plots, box-and-whisker plots and violin plots for different averaging periods (depending on the pollutant) will be analyzed to understand model performance. For $PM_{2.5}$ and its components (such as $EC_{2.5}$, $OC_{2.5}$), daily averages will be computed but will retain hourly averages for all gaseous species.

Figure 4-4 is an example of AERMOD outputs on a polar grid stretching out up to 50-km from the Airport, with receptors placed every 5-km. The analysis shows the impact of the Airport beyond 5-km radius is minimal. Most impacts are east of the Airport, except for SO_2, which has a strong signal southwest of the Airport from port activity.

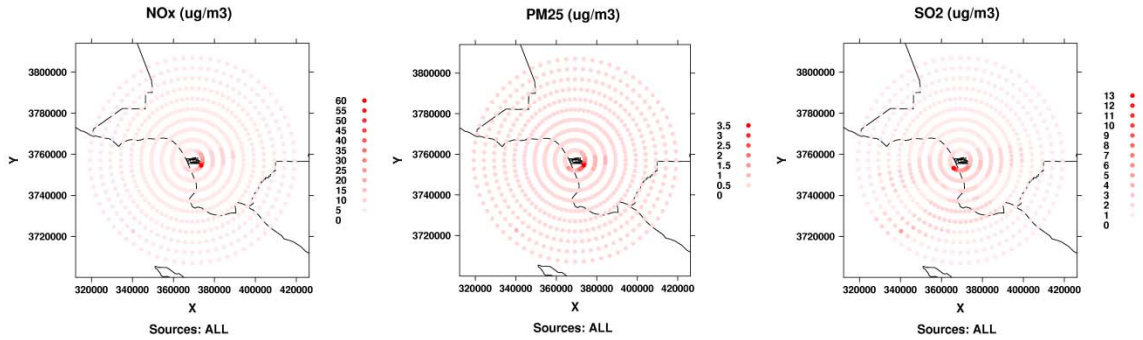

Figure 4-4. AERMOD predictions of NO_x, $PM_{2.5}$ and SO_2 concentrations for LAX, on a 50-km polar grid of receptors

Figure 4-5 shows an example of AERMOD predictions for LAX on a 5x5-km uniform grid (with receptors every 500m) for NO_x, $PM_{2.5}$ and SO_2. While most NO_x impacts are east of the south runway, both $PM_{2.5}$ and SO_2 show impacts to the east and the south of runways from off-airport sources.

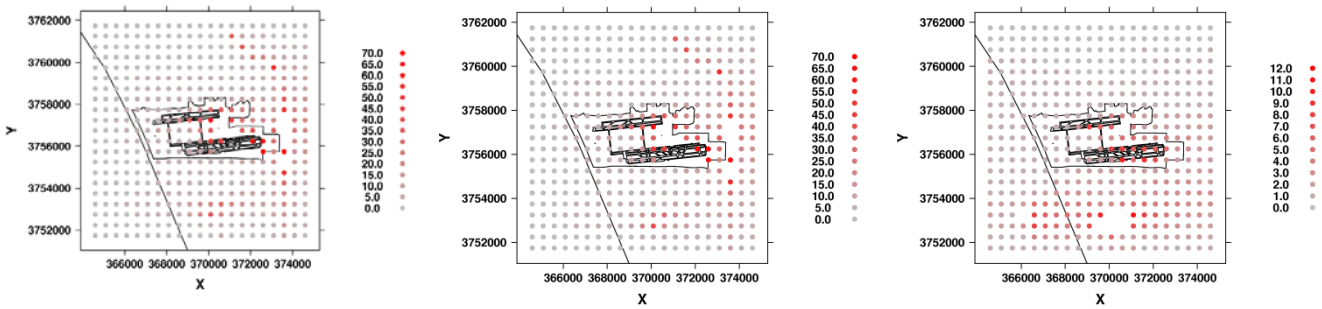

Figure 4-5 AERMOD predictions of NO_x, $PM_{2.5}$ and SO_2 concentrations for LAX on a 5x5-km grid

CMAQ Modeling

To supplement the AERMOD dispersion simulation, the Project Team proposes to use the CMAQ model. CMAQ is a state-of-the-art, comprehensive, multi-scale one-atmosphere air quality modeling system that treats gas-phase chemistry, PM and HAPs. The "one-atmosphere" capability indicates that oth ozone and PM can be predicted using a single modeling system.

CMAQ simulates the numerous physical and chemical processes involved in the formation, transport and destruction of air pollutants using an Eulerian modeling system.

The Project Team's modeler will explore the possibility of relying on a standard application of CMAQ for the Los Angeles region at the appropriate horizontal resolution performed either by UNC from other on-going studies, or from the U.S. EPA or CARB. It is important that the results from this task be extensively evaluated against ambient monitoring data and that model performance is consistent with other regional-scale model applications.

If the standard application can be identified, the Project Team will use the Sparse Matrix Operator Kernel Emissions (SMOKE) modeling system to process all LAX study emissions (discussed above) and prepare CMAQ-ready inputs at the model grid resolution. The Project Team proposes to perform two CMAQ simulations for each of the two monitoring periods:

- Base case with all emissions (LAX and all other anthropogenic and biogenic sources) included, and

- Zero-out case where LAX study emissions are subtracted from the base case.

The CMAQ model outputs will be analyzed by plotting absolute and relative differences of the two scenarios to assess the incremental contributions from LAX on ambient air quality.

4.16 (Task 16) Prepare Preliminary Draft Project Report and Database

The Project Team will prepare the Preliminary Draft Project Report that summarizes the findings from the 1st and 2nd Season measurement campaigns and the source-oriented and receptor-oriented modeling. The Preliminary Draft Database will also be prepared with appropriate data qualifiers. The Preliminary Draft Project Report and Database will be submitted to LAWA for review and comment. Revised versions of the report and database will be prepared, incorporating LAWA comments, for submittal to the TWG for review and comment.

The Preliminary Draft Project Report will include discussions of the project background; selection of sites; air quality and meteorological parameters observed; methods used and results of monitoring, sampling and laboratory analysis; methods used and results of source and receptor modeling; and conclusions of the source apportionment analysis addressing the primary objectives of the Study.

4.17 (Task 17) Prepare Final Draft Project Report and Database

Upon completion of the technical analyses, the Project Team will prepare a Final Draft Project Report documenting the technical approach, findings and conclusions of the study. The Final Draft Project Report will incorporate comments received from LAWA and the TWG on the Preliminary Draft Project Report prepared under Task 16. The Final Draft Project Report will be written in easily understood language and will be comprehensive, describing all the work done

on the project. The project's findings and any recommendations will be included as its own section of the report. The Final Draft Report will be submitted to LAWA and the TWG for final review and comment by November 19, 2012.

Depending on the type of monitoring data, file format such as text or ASCII file, MS Excel and Access will be used to record and compile collected data into a project database as part of the Final Draft Project Report.

4.18 (Task 18) (Task 21) Prepare Final Project Report and Database

The Project Team will incorporate changes into the Final Project Report and Database that address the comments received from LAWA and the TWG on the Final Draft Project Report and Database.

4.19 (Task 19) (Prepare Presentation Materials for, and Participate in Public Meeting(s)

The Project Team will support LAWA in preparing presentation materials and participating in public meeting(s).

If requested, the Project Team will prepare presentation materials for the meeting(s) and submit them to LAWA for approval prior to the meeting(s). Additionally, the Project Team personnel will participate in the meeting(s) to support LAWA staff.

4.20 (Task 20) On-Going Coordination with CDM/Owner's Representative

The Project Team key personnel will update and coordinate activities with CDM (Owner's Representative) and LAWA. It is anticipated that regular periodic conference calls between the Project Team, CDM, and LAWA will be scheduled to review progress, discuss logistics, resolve issues, and verify remaining budget. Any technical submittals submitted to LAWA by the Project Team will be copied to CDM at the same time.

4.21 (Task 21) On-Going Coordination with TWG

To ensure this Project is conducted in accordance with the objectives set forth in the LAWA Technical Work Plan, the Project Team will provide updates and coordinate activities with the TWG. Occasional scheduled conference calls among the Project Team, CDM, LAWA, and the TWG may be carried out to review progress and brainstorm potential solutions to issues and problems, as needed.

Anticipated coordination activities may include:

- Work Plan review meeting with LAWA, the Project Team and the TWG.

- 1st Season Measurement campaign review meeting – to review results and problems encountered during 1st campaign. This meeting should be conducted far enough in advance of the start of the 2nd Season Measurement campaign to incorporate suggested improvements in the 2nd campaign.

- Preliminary Draft Project Report review meeting – provides a discussion forum for comments and concerns with the findings to date from the TWG.

- If the opportunity arises, one or more TWG member organizations may conduct monitoring on or near the Airport. This monitoring could be used to enhance or expand the findings to different pollutants or additional receptors in the Study Area. However, the Project Team will need to coordinate the collection, analysis and presentation of this material with the TWG organization(s) conducting the analysis and incorporate it into the Study's Final Report.

The actual number of conference calls and meetings with the TWG will be discussed and finalized between the Project Team and LAWA.

Section 5
Schedule

The anticipated schedule is summarized in Figure 5-1. Although the schedules for individual tasks may change, the end date is fixed at April 1, 2013. All final project deliverables will be completed and submitted to LAWA on or prior to this date.

Figure 5-1. Proposed Schedule

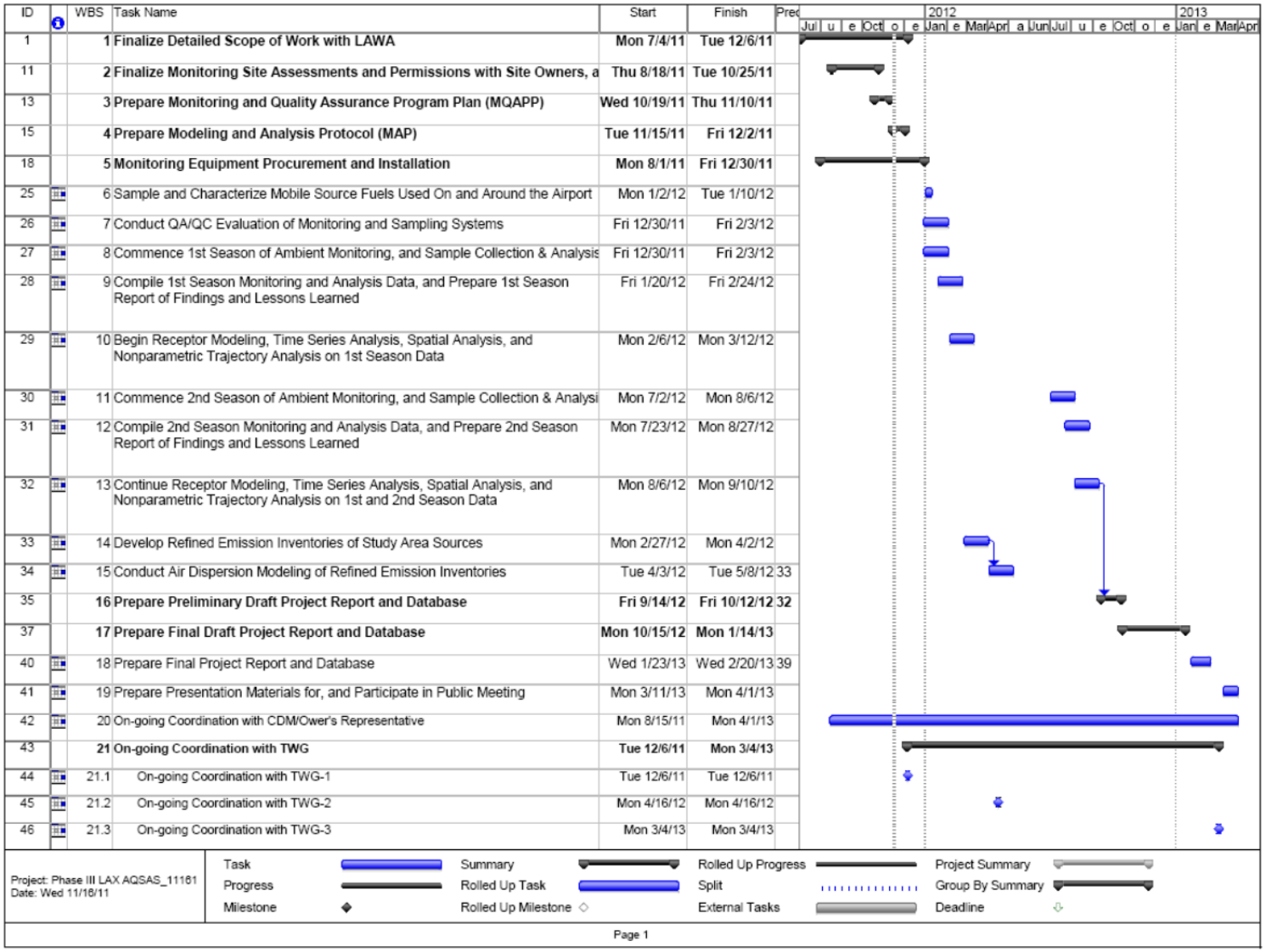

ID	WBS	Task Name	Start	Finish	Pred
1	**1**	**Finalize Detailed Scope of Work with LAWA**	**Mon 7/4/11**	**Tue 12/6/11**	
11	**2**	**Finalize Monitoring Site Assessments and Permissions with Site Owners, a**	**Thu 8/18/11**	**Tue 10/25/11**	
13	**3**	**Prepare Monitoring and Quality Assurance Program Plan (MQAPP)**	**Wed 10/19/11**	**Thu 11/10/11**	
15	**4**	**Prepare Modeling and Analysis Protocol (MAP)**	**Tue 11/15/11**	**Fri 12/2/11**	
18	**5**	**Monitoring Equipment Procurement and Installation**	**Mon 8/1/11**	**Fri 12/30/11**	
25	6	Sample and Characterize Mobile Source Fuels Used On and Around the Airport	Mon 1/2/12	Tue 1/10/12	
26	7	Conduct QA/QC Evaluation of Monitoring and Sampling Systems	Fri 12/30/11	Fri 2/3/12	
27	8	Commence 1st Season of Ambient Monitoring, and Sample Collection & Analysis	Fri 12/30/11	Fri 2/3/12	
28	9	Compile 1st Season Monitoring and Analysis Data, and Prepare 1st Season Report of Findings and Lessons Learned	Fri 1/20/12	Fri 2/24/12	
29	10	Begin Receptor Modeling, Time Series Analysis, Spatial Analysis, and Nonparametric Trajectory Analysis on 1st Season Data	Mon 2/6/12	Mon 3/12/12	
30	11	Commence 2nd Season of Ambient Monitoring, and Sample Collection & Analysi	Mon 7/2/12	Mon 8/6/12	
31	12	Compile 2nd Season Monitoring and Analysis Data, and Prepare 2nd Season Report of Findings and Lessons Learned	Mon 7/23/12	Mon 8/27/12	
32	13	Continue Receptor Modeling, Time Series Analysis, Spatial Analysis, and Nonparametric Trajectory Analysis on 1st and 2nd Season Data	Mon 8/6/12	Mon 9/10/12	
33	14	Develop Refined Emission Inventories of Study Area Sources	Mon 2/27/12	Mon 4/2/12	
34	15	Conduct Air Dispersion Modeling of Refined Emission Inventories	Tue 4/3/12	Tue 5/8/12	33
35	**16**	**Prepare Preliminary Draft Project Report and Database**	**Fri 9/14/12**	**Fri 10/12/12**	**32**
37	**17**	**Prepare Final Draft Project Report and Database**	**Mon 10/15/12**	**Mon 1/14/13**	
40	18	Prepare Final Project Report and Database	Wed 1/23/13	Wed 2/20/13	39
41	19	Prepare Presentation Materials for, and Participate in Public Meeting	Mon 3/11/13	Mon 4/1/13	
42	20	On-going Coordination with CDM/Ower's Representative	Mon 8/15/11	Mon 4/1/13	
43	**21**	**On-going Coordination with TWG**	**Tue 12/6/11**	**Mon 3/4/13**	
44	21.1	On-going Coordination with TWG-1	Tue 12/6/11	Tue 12/6/11	
45	21.2	On-going Coordination with TWG-2	Mon 4/16/12	Mon 4/16/12	
46	21.3	On-going Coordination with TWG-3	Mon 3/4/13	Mon 3/4/13	

Section 6
References

Blanchard, C.L., 1999. "Methods for Attributing Ambient Air Pollutants to Emission Sources," *Annual Review of Energy and the Environment*, **24**: 329-365.

Henry, R.C., Y.J. Wang, and K.A. Gebhart, 1991. "The Relationship Between Empirical Orthogonal Functions and Sources of Air Pollution," *Atmospheric Environment*, **25A**: 503-509.

Henry, R.C. and C. Spiegelman, 1997. "Reported Emissions of Volatile Organic Compounds are not Consistent with Observations," *Proceedings of the National Academy of Sciences*, **94**: 6596-6599.

Henry, R.C., 2002. "Receptor Modeling," *Encyclopedia of Environmetrics,* **3:** 1706-1721.

Henry, R.C., 2008. "Locating and Quantifying the Impact of Local Sources of Air Pollution," *Atmospheric Environment,* **42:** 358-363.

Pleil, J.D., L.B. Smith, and S.D. Zelnick, 2000. "Personal Exposure to JP-8 Jet Fuel and Exhaust at Air Force Bases," *Environmental Health Perspectives*, 108(3): 183-192.

South Coast Air Quality Management District, 2001. "Air Monitoring Study at Felton and Lloyde Schools," Diamond Bar. September.

U.S. Environmental Protection Agency, 2009a. "Recommended Best Practice for Quantifying Speciated Organic Gas Emissions from Aircraft Equipped with Turbofan, Turbojet, and Turboprop Engines," EPA-420-R-09-901, Office of Transportation and Air Quality. May.

U.S. Environmental Protection Agency, 2009b. "Aircraft Engine Speciated Organic Gases: Speciation of Unburned Organic Gases in Aircraft Exhaust," EPA-420-R-09-902, Office of Transportation and Air Quality. May.

U.S. Environmental Protection Agency, 2009c. "Characterization of Emissions from Commercial Aircraft Engines during the Aircraft Particle Emissions eXperiment (APEX) 1 to 3," EPA-600/R-09/130, Office of Research and Development. October.

Watson, J.G., J.C. Chow, J.L. Brown, D.H. Lowenthal, S. Herring, P. Ouchida, and W. Oslund, 2000. "Air Quality Measurements from the Fresno Supersite," *Journal of the Air and Waste Management Association*, **50**(8): 1321-1334.

Watson, J.G. and J.C. Chow, 2004. "Receptor Models for Air Quality Management," *Environmental Manager,* (A&WMA, October 2004), pp. 15-24.

Yu, K.N., Y.P. Cheung, T. Cheung, R.C. Henry, 2004. "Identifying the impact of large urban airports on local air quality by nonparametric regression." *Atmospheric Environment*, **38**(27): 4501-4507.

Appendix A

Mobile Survey Results

(This bank intentionally left blank)

Desert Research Institute

Phase III of the LAX Air Quality Source and Apportionment Study

Mobile Survey Results and Recommended Monitoring Program

For Discussion Purposes Only

Prepared for:

Los Angeles World Airports (LAWA)

Prepared by

Eric M. Fujita and David E. Campbell
Division of Atmospheric Sciences
Desert Research Institute,
Nevada System of Higher Education
2215 Raggio Parkway
Reno, NV 89512

Subcontract to Tetra Tech Inc.
Pasadena, CA

October 31, 2011

TABLE OF CONTENTS

1. INTRODUCTION

The Los Angeles International Airport (LAX) Air Quality and Source Apportionment Study (AQSAS) is being conducted to assess the impact of LAX operations on local air quality. This objective will be achieved by determining the spatial and temporal variations in ambient air concentrations of gases and particulate matter (PM) and by a combination of source and receptor modeling. This document describes the results of initial mobile surveys conducted by the Desert Research Institute (DRI) to characterize the spatial variations in pollutant concentrations within the communities and buffer zones surrounding LAX and near airport operations (e.g., Central Terminal area and aircraft takeoffs, landings and taxiing). These surveys are used to guide the selection of air monitoring sites during Phase III of the LAX AQSAS and as the basis for developing suggested refinement to the proposed air monitoring plan. A recommended air monitoring plan is included at the end of this document.

1.1 Background

Various air monitoring and modeling studies indicate that higher pollutant concentrations may exist in close proximity to roadways, industrial facilities, airport runways and other sources of emissions. Following the inverse-square law that a specified quantity or strength is inversely proportional to the square of the distance from the source, the gradients in pollutant concentrations near major roadways are steep with concentrations typically dropping to the community average within 300 meters away from the roadway (Zhu et al., 2002; Fujita et al, 2010). Emissions from roadways and other major sources of emissions mix with the surrounding neighborhood background pollutant concentrations, which exhibit large diurnal variations due to changing meteorological conditions (mixing heights and winds), and regional emission patterns (e.g., total traffic volume and vehicle mix). Roadside concentrations of nitrogen oxides (NOx), carbon monoxide (CO) and volatile organic compounds (VOC) are typically about a factor of 2 to 4 higher than the community average ambient concentrations if gasoline-powered vehicles are the dominant local source of emissions (Fujita et al., 2003; Fujita et al., 2008). Presence of diesel vehicles may increase these ratios to as much as 10 for NOx and black carbon (BC) (Fujita et al., 2010; Westerdahl et al. 2005). Even higher ratios may be measured for NOx, sulfur dioxide (SO_2), BC and ultrafine particles (UFP) downwind of the Airport runway during jet takeoffs (Westerdahl et al. 2007). The corresponding ratios for fine particulate matter ($PM_{2.5}$) are usually lower by comparison because of their larger background concentrations and the proportionately greater contributions of secondary components of $PM_{2.5}$ (e.g., ammonium nitrate, ammonium sulfate, secondary organic aerosol) and other area sources such as wind-blown dust (Fujita et al, 2009).

A few widely-spaced fixed monitoring stations have limited capacity to characterize higher pollutant concentrations and accompanying concentration gradients near local emission sources, and additional air quality data of finer spatial resolution (e.g., "saturation monitoring") are needed to determine the zones of influence of local emissions on adjacent communities. However, the costs and logistical requirements of traditional monitoring technologies pose constraints on the numbers and locations of monitoring stations that can be established. Thus, the proposed air monitoring plan for Phase III of the LAX AQSAS included a supplemental saturation monitoring program consisting of passive and longer-time average mini-volume aerosol samples. The saturation monitoring program for Phase III the LAX AQSAS will apply the approaches that have successfully been used in the 2007 Harbor Community Monitoring

Study (HCMS) (Fujita et al. 2009) sponsored by the California Air Resources Board and the 2009 West Oakland Monitoring Study (WOMS) (Fujita et al. 2010) sponsored by the Bay Area Air Quality Management District (BAAQMD).

2. MOBILE SURVEYS

2.1 Experimental

The mobile surveys were conducted during the week of September 19, 2011 using the Bay Area Air Quality Management District (BAAQMD) mobile monitoring van, either alone or in combination with the DRI portable cart-mounted monitoring system (Figure 1). In addition to a Global Positions System (GPS), the van was equipped with continuous instruments to monitor NO, CO, VOC (est), black carbon (BC), $PM_{2.5}$ mass, and ultrafine particle (UFP) number concentrations with time resolutions of 10 seconds. Sulfur dioxide (SO_2) was not measured due to inadequate sensitivity of the analyzer for few minute averages. The cart-mounted monitoring system included a GPS and measurements of NO, CO, CO_2, $PM_{2.5}$, and UFP counts. BC was not measured in the cart due to the photoacoustic instrument's high power draw. Instrument specifications are summarized in Table 1 and the associated methods are described in Attachment A.

The monitors in the van were used to measure pollutant concentrations within the communities of El Segundo, Playa del Rey, Westchester, Lennox, Hawthorne and Inglewood. These surveys also included routes near industrial facilities in El Segundo (waste water treatment plant and power generating plant), the eastern end of the LAX north and south airfields, cargo terminals on both north and south sides of LAX, and the Central Terminal Area. The community surveys were scheduled during the morning and evening periods under varying meteorological conditions and traffic patterns. The van and cart were used simultaneously to determine spatial gradients in pollutant concentrations near and downwind of the takeoff and taxiing areas of Runway 25R and near the I-405 freeway along Lennox Boulevard from Inglewood Boulevard to La Cienega Boulevard. Depending upon logistical considerations, either the van or cart remained stationary during the gradient measurements while the other unit was mobile. The pollutant gradient measurements were made during midday with winds from the west. Table 2 shows the dates and times for each of the mobile surveys along with the type of survey, location(s) and average prevailing wind directions and speed. Relevant specific details are summarized with the results.

Figure 1. BAAQMD Mobile Monitoring Van (left) and DRI Portable Cart-Mounted Monitoring System.

Table 1. Continuous Instruments Operated in the BAAQMD Mobile Van and Portable Cart.

Parameters	**CO**	**NO**	**BC**	**CO, CO_2, T, RH**	**"VOC"**	**PM2.5 Mass**	**Ultra-Fine Particles**
Application	Van	Van Cart	Van	Cart	Van	Van Cart	Van Cart
Manufacturer:	Teledyne	2B Technologies	Pat Arnott, UNR	TSI	RAE Systems	TSI	Kanomax
Model:	ML9830	400	photoacoustic	8554 (Q-Trak Plus)	ppbRAE	8520 DustTrak	3800
Lower Detectable Limit:	0.05 ppm	20 ppb	0.2 ug/m3 for 1 min	~ 1 ppm	~30 ppb (1)	~ 1 ug/m3	< 1 particle/cm3
Range :	0-200ppm	up to 200 ppm		0-500 ppm	> 1000 ppm	0.001 to 100 mg/m3	0.015 - 1 um, 0 - 100,000 particles/cm3
Resolution:	0.01 ppm	2 ppb	0.1 ug/m3	0.1 ppm	1 ppb	0.1% + 0.001 mg/m3	
Min sampling interval:	1 sec	10" for NO or NOx only, 5 min for NO2	1 sec	1 sec	1 sec		
Response Time:	<40 secs		1 sec	<60 secs	~10 sec	1 sec	
Precision:	1%+0.1 ppm	3%+2 ppbv	<10%	3%+3ppm	10%+20 ppb	1 ug/m3	
Power Requirements:	200W @ 110/220 VAC	analyzer:11W @12VDC	150 W at 110VAC, plus pump (<100W @ 12VDC)	4 AA batteries (20 hr run time), or 110VAC	rechargeable battery or AC (100W @ 110VAC).	4 C batteries (16 hr run time), or AC adapter for continuous operation	6 AA-size batteries (5-8 hrs run time), or AC adapter (100 – 240V)

Table 2. Phase III LAX AQSAS – Initial Spatial Survey

No	Run ID	Date	Start Time	End Time	Survey Type	Locations	Wind Dir	WS (mph)
1	CS20	20-Sep	9:10	11:30	Community/LAX	See Community Survey	calm/variable/W	0/4/6
2	RG20	20-Sep	14:00	15:20	25R Runway Gradient	Van at Walsh Austin laydown area, cart in open field	W	13
3	TW21A	21-Sep	8:47	10:45	Taxiway Gradient	Van at end of International Rd, cart to Century and back		0
4	LX21A	21-Sep	11:37	13:08	Lennox Gradient	From La Feria to La Cienega and back with cart, Van at La Feria	W	8-10
5	LX21P	21-Sep	17:40	18:52	Lennox Gradient	From La Feria to La Cienega and back with cart, Van at La Feria	W	7-10
6	TX21P	21-Sep	19:22	19:50	Taxiway Gradient	Van at end of International Rd, cart to north end of cargo terminal area. Very clean	W	7
7	CS22A	22-Sep	8:39	11:26	Community/LAX	See Community Survey	calm/W/W	0/6/6.5
8	CS22P	22-Sep	19:21	21:13	Community/LAX	See Community Survey	W/W/var	9/8/4
9	RG23	23-Sep	11:40	14:00	25R Runway Gradient	Van and cart in open field	WSW/W	8-12

2.2 Survey Results

Surveys #1, 7 and 8 – Spatial Surveys of Community and LAX

Surveys of LAX and adjacent communities were conducted on September 20, 2011 from 9:10 am to 11:30 am (Survey #1) and on September 22, 2011 from 8:39 am to 11:26 am (Survey #7) and 7:21 pm to 9:13 pm (Survey #8). The surveys were conducted with the monitoring van beginning at the LAX maintenance yard located at the west end of LAX and covering the communities of El Segundo, Playa del Rey, Westchester, Hawthorne, Lennox and Inglewood. The survey route also included the industrial facilities in El Segundo, LAX Central Terminal Area, the Sepulveda Tunnel, and near the LAX south runways. The specific routes varied slightly for each survey. However, each survey nominally included the following sequence of locations.

1) El Segundo south of LAX including nearby industrial facilities (e.g., Hyperion Sewage Treatment Plant, LADWP Scattergood Power Plant, Chevron El Segundo Refinery.
2) Imperial Highway from Sepulveda Boulevard though the Imperial Cargo Terminal area to Vista del Mar.
3) Vista del Mar from El Segundo to Playa del Rey and Westchester north of LAX.
4) LAX Central Terminal area, upper and lower levels.
5) Sepulveda Boulevard through the tunnel, Imperial Highway, Aviation Boulevard past the LAX south runways.
6) Lennox east of LAX and east of I-405 Freeway
7) South end of International Road near Runway 25R taxiway.

The results of the LAX/Community surveys are presented in a series of spatial maps in Figures 2, 3 and 4. Each dot represents a 1-minute average concentration and is located at the GPS position that is the midpoint in the 1-minute period. The spatial maps show the variations in concentrations of CO (ppm), NO (ppb), BC ($\mu g/m^3$) and UFP (10^3 particles per cc). The BAAQMD portable condensation particles counter malfunctioned during the first survey and was inoperable for the remainder of the mobile surveys. The highest pollutant levels were generally measured near high traffic areas at the LAX Central Terminal Area and on main arterial streets (e.g., Century Boulevard, Sepulveda Boulevard and Imperial Highway). Higher NO and BC were also measured near the east end of the LAX south airfield. Though data are not available, higher UFP concentrations are likely as well at this location. With very few exceptions, the pollutant levels along the north and south boundaries of LAX and within the adjacent communities of El Segundo and Westchester were uniformly low. These measurements will be compared to corresponding data from nearby SCAQMD monitoring stations. The spatial plots are short snapshots in time and should be interpreted with appropriate caution. Although the van did not follow other vehicles too closely, occasionally higher pollutant concentrations may have been measured during brief stops at intersections or while behind a diesel truck or high-polluting passenger car or light truck.

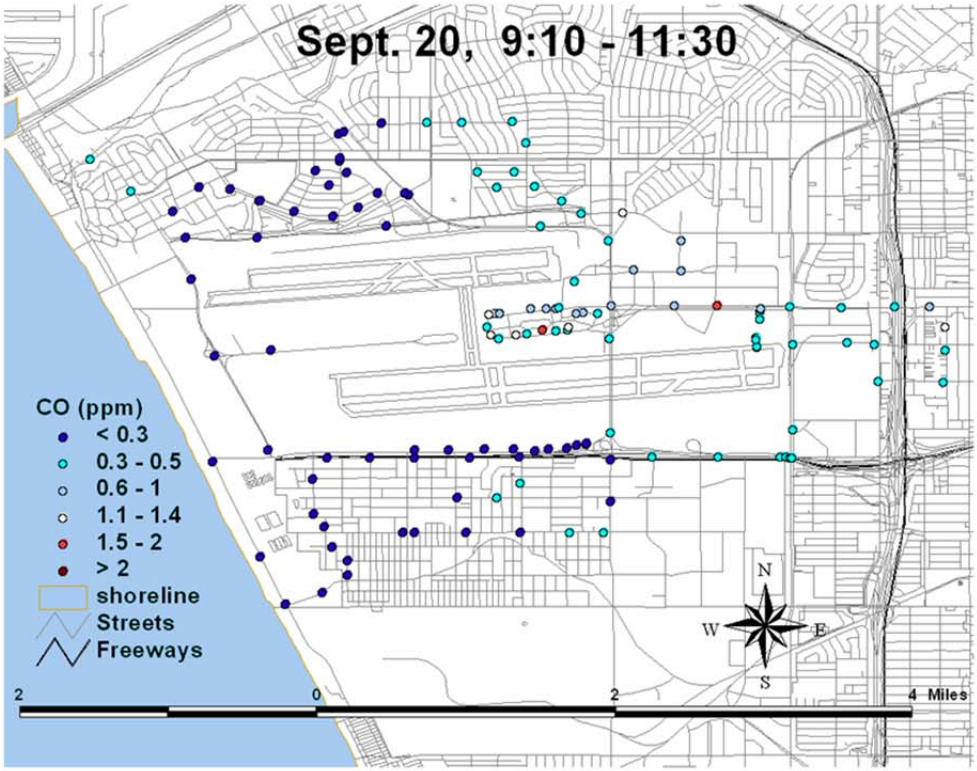

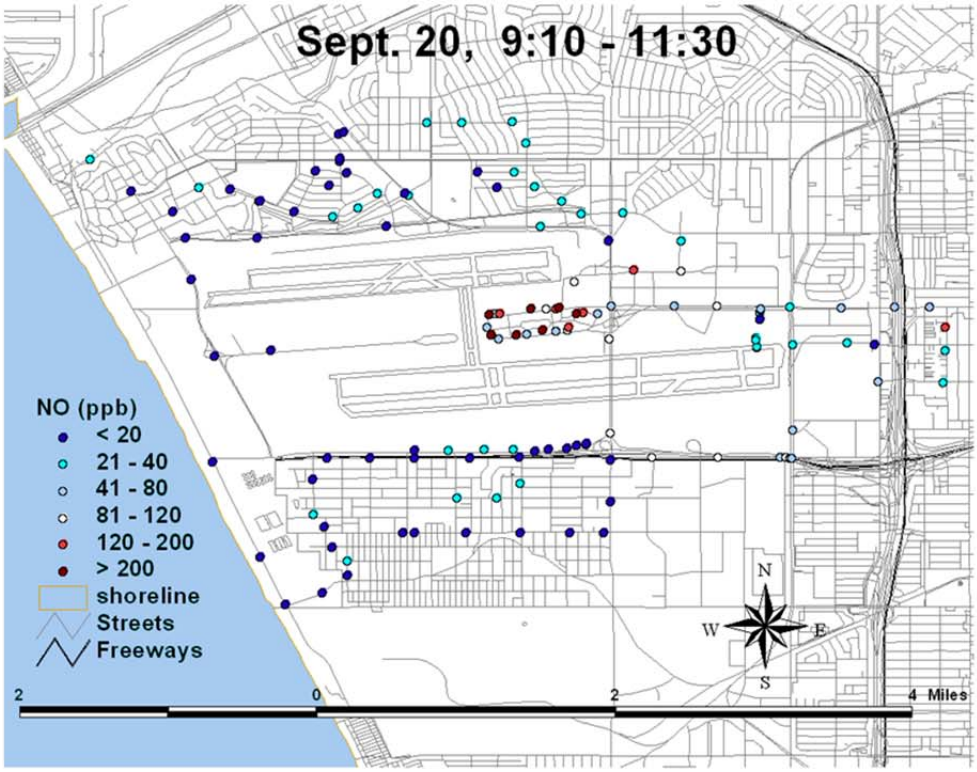

Figure 2a. Spatial Variations in CO (ppm) and NO (ppb) during Community Survey on September 20, 2011 from 9:10 to 11:30 am.

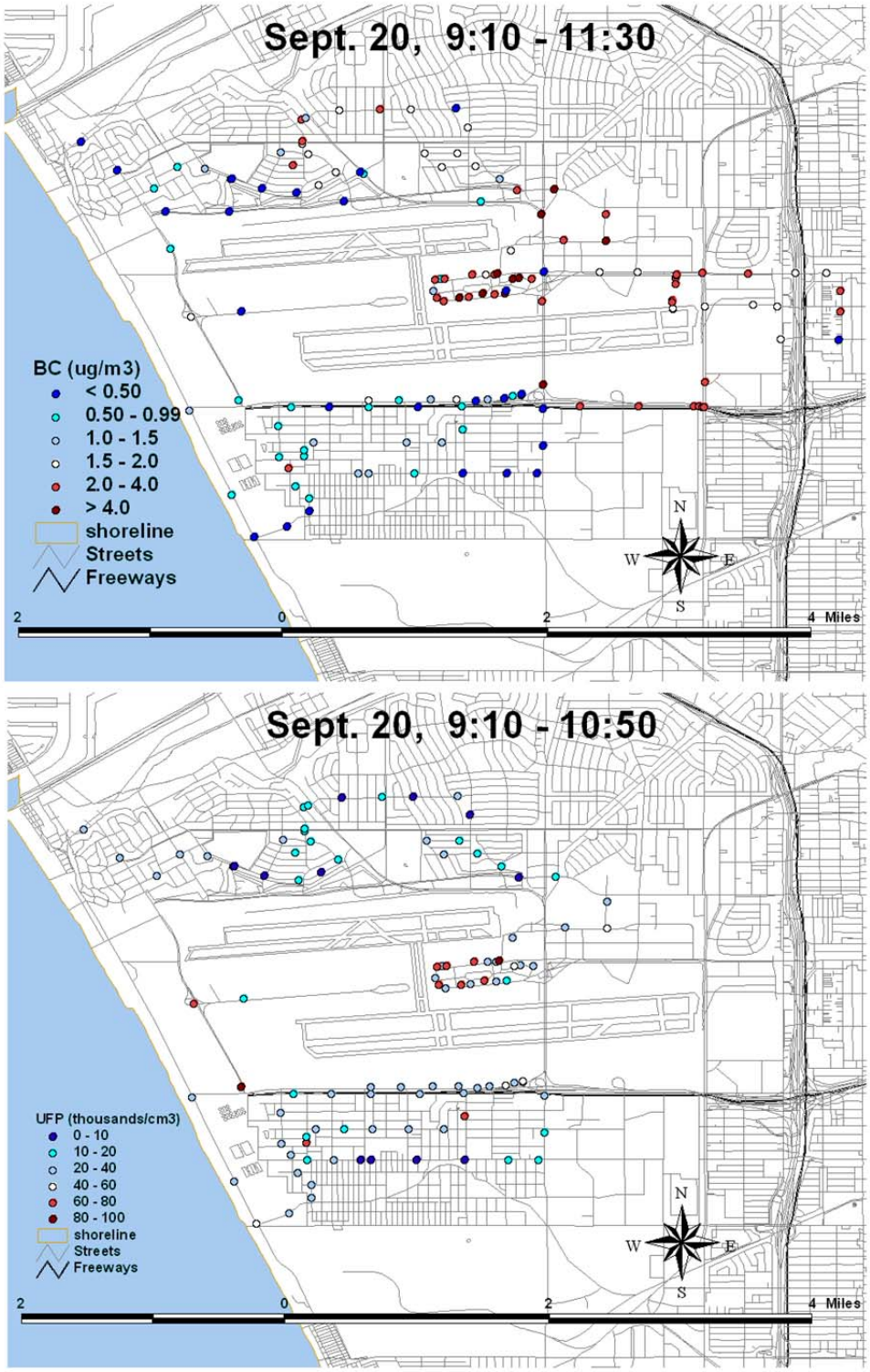

Figure 2b. Spatial Variations in BC (µg/m^3) and UFP (thousands/cm^3) during Community Survey on September 20, 2011 from 9:10 to 11:30 am.

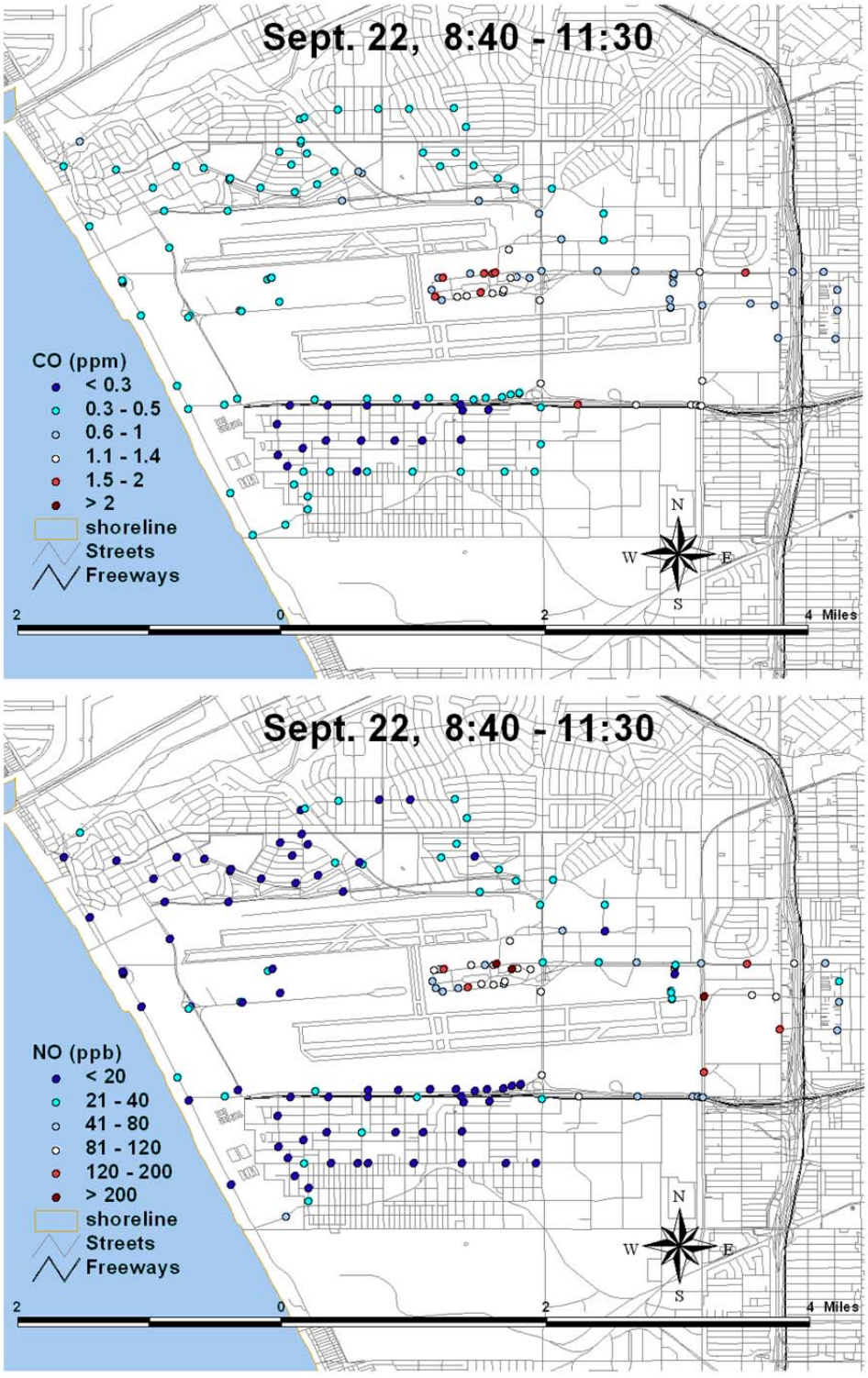

Figure 3a. Spatial Variations in CO (ppm) and NO (ppb) during Community Survey on September 22, 2011 from 8:40 to 11:30 am.

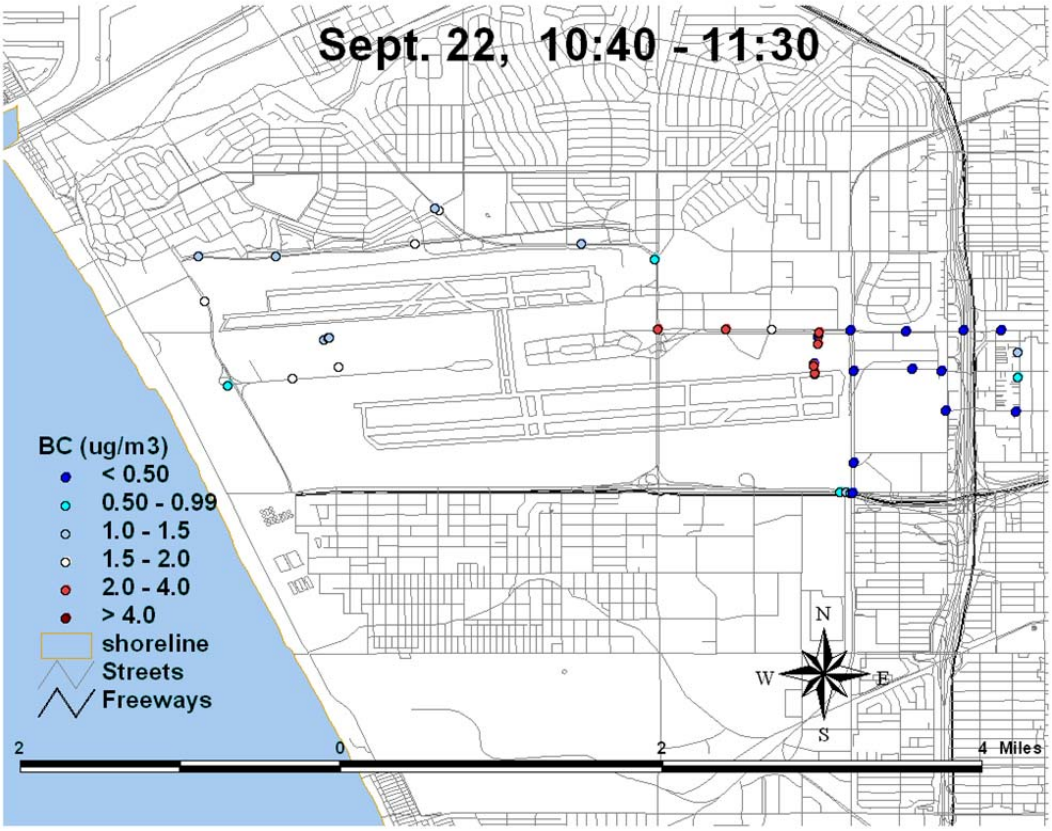

Figure 3b. Spatial Variations in BC (µg/m^3) during Community Survey on September 22, 2011 from 8:40 to 11:30 am. BAAQMD CPC was Inoperable.

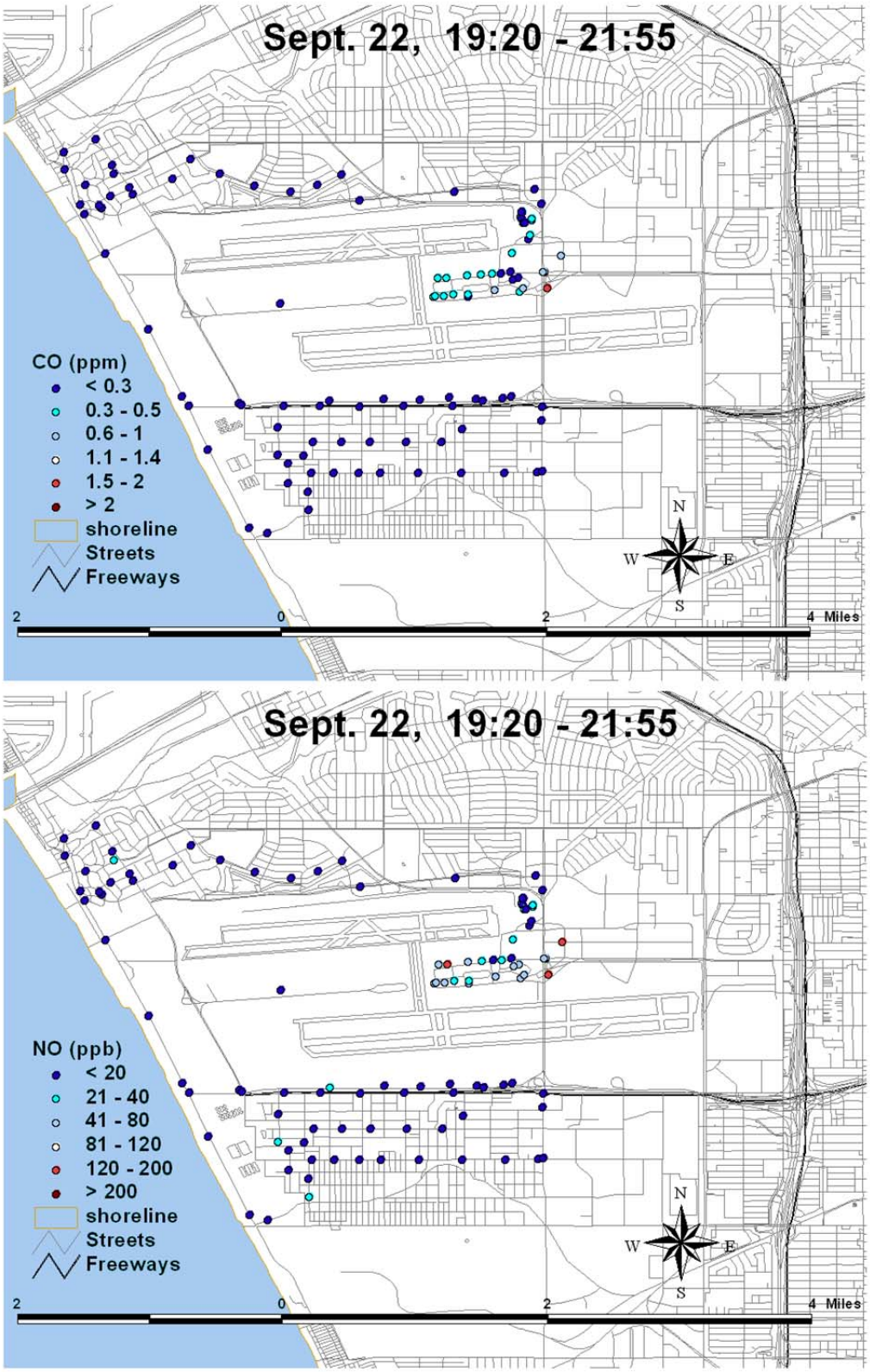

Figure 4a. Spatial Variations in CO (ppm) and NO (ppb) during Community Survey on September 22, 2011 from 7:20 to 9:55 pm.

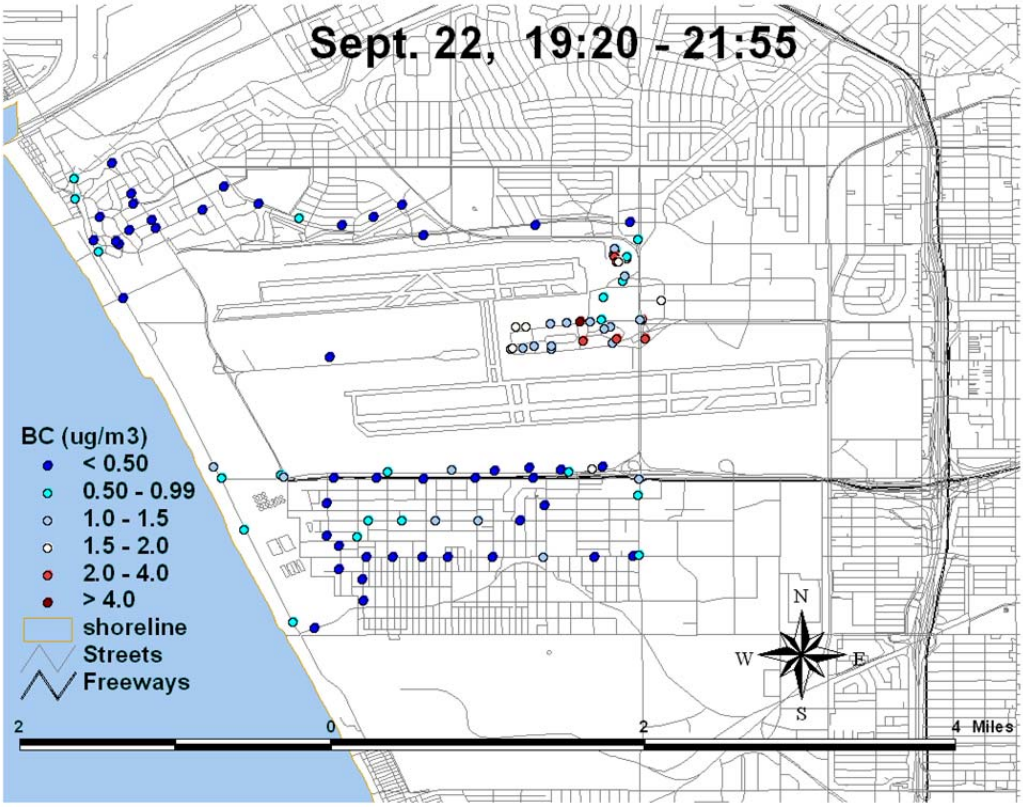

Figure 4b. Spatial Variations in BC (µg/m^3) during Community Survey on September 22, 2011 from 7:20 to 9:55 pm. BAAQMD CPC was Inoperable.

Survey #2 – Gradient Measurements at Runway 25R

The measurements for gradient survey #2 (Runway 25R) were made on September 20, 2011 for about 1.5 hours beginning at 2:00 pm. The mobile monitoring van was located at the proposed SR site in the Walsh Austin laydown area. Measurements included CO, CO_2, $PM_{2.5}$, NO, UFP on the cart and CO, $PM_{2.5}$, NO, BC in the van. The BAAQMD CPC in the van was inoperable. Prior to start of the gradient measurements, the instruments were run with both cart and van located at the Walsh Austin laydown area. Measurements were made with the cart for 10 minutes at varying distances east of Aviation Boulevard starting with the location nearest the roadway. After reaching the farthest location about halfway into the experiment, the cart began its return trip to the starting location while making a second set of measurements at each sampling location. DRI was informed about half-way into the experiment that runway operations had been suspended at 2:40 pm for maintenance. This was serendipitous, since the return trip with the cart occurred during no takeoffs (i.e. impact of traffic on Aviation Boulevard only without jet emissions). Winds reported by LAX during this time were from the west at ~ 14 mph (hourly average). The cart passive CO data were adjusted based on collocated measurements with the van NDIR measurements. Otherwise the data have received minimal QA at this time. Out-of-range CPC values were included in the averages, thus UFP number concentrations represent lower-limit values.

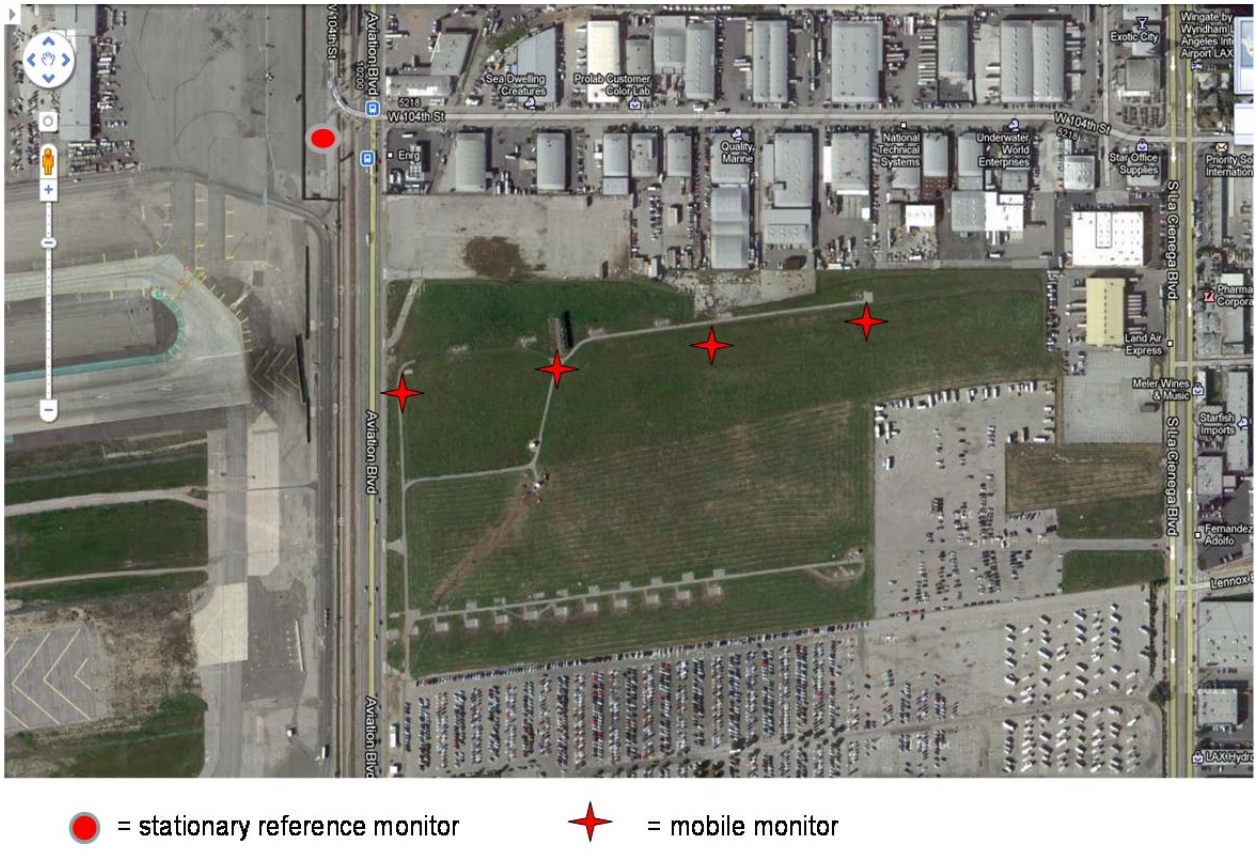

Figure 5. Survey #2 - South Runway/Aviation Boulevard West-East Gradient. Field between Aviation and La Cienega is 160 to 800 meters east of the east end of Runway 25R.

The following time series are plots of 1-minute averages of data from the cart (in dashed red) and the van (in solid blue). X-axis also indicates the cart's locations beginning with collocated measurements at the SR site and various distances in meters east of Aviation Boulevard, NO, BC, UFP are the measured pollutants mainly associated with jet aircraft takeoffs. CO was minor in comparison. The time-series plots of NO and $PM_{2.5}$ clearly show that the SR site (van) missed most of higher concentrations measured at the runway approach location (cart). BC concentration measured at the SR site did decrease when the runway shut down, but the differences were not as dramatic as would be expected from the cart NO and $PM_{2.5}$ data. During April 2011, the SCAQMD made measurements very near the proposed SR location. The intent of their measurements was to capture taxing emissions as the jets made the turn at the end of the runway (Fine, 2011). Grab samples were collected when the odor of aviation fuel was detected. The role of SR site as one of the three permanent fixed monitoring sites during Phase III of the LAX AQSAS needs to be reexamined given the results of the survey measurements and previous work by SCAQMD at the same location.

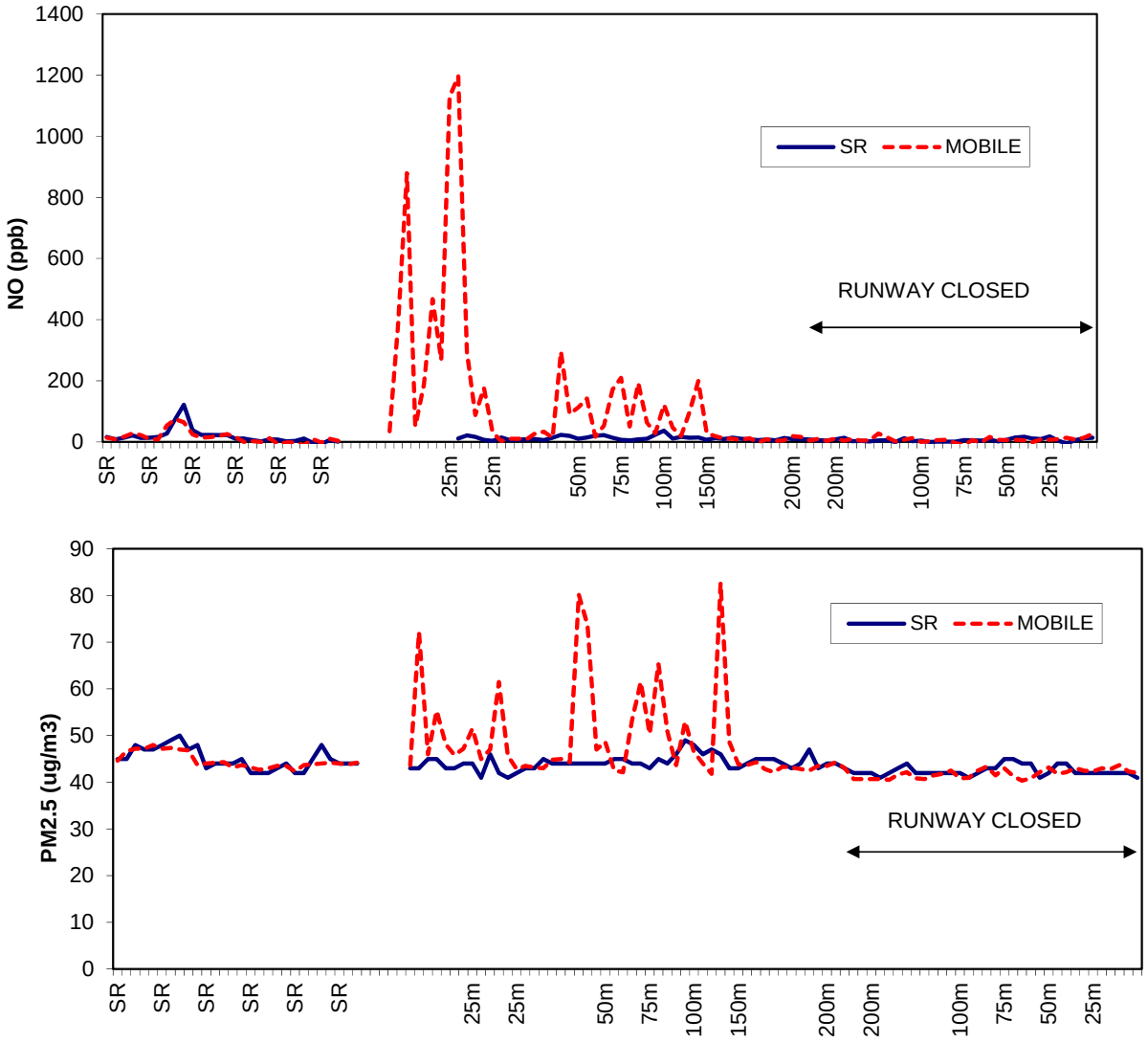

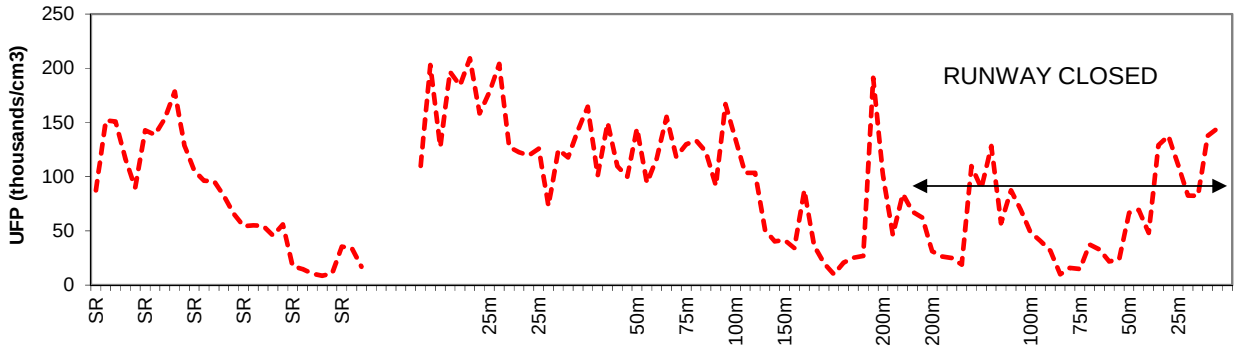
UFP (thousands/cm3)
250
200
150
100
50
0
RUNWAY CLOSED
SR
SR
SR
SR
SR
SR
25m
25m
50m
75m
100m
150m
200m
200m
100m
75m
50m
25m

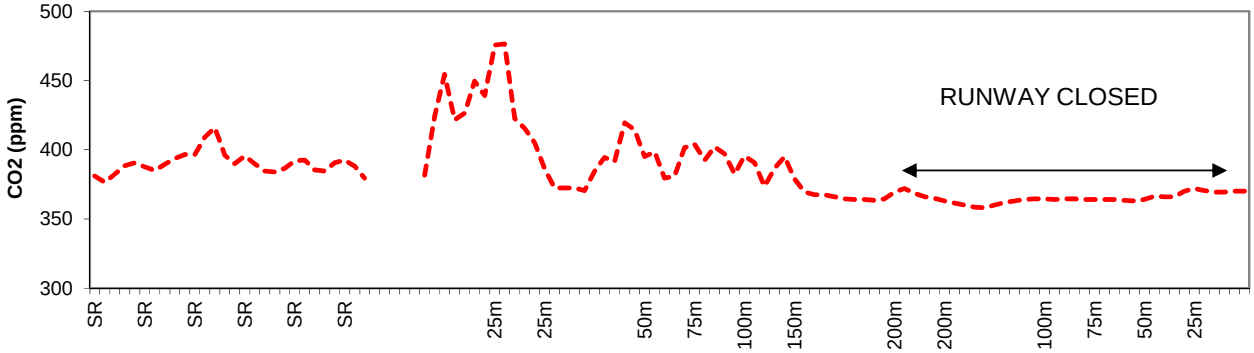
CO2 (ppm)
500
450
400
350
300
RUNWAY CLOSED
SR
SR
SR
SR
SR
SR
25m
25m
50m
75m
100m
150m
200m
200m
100m
75m
50m
25m

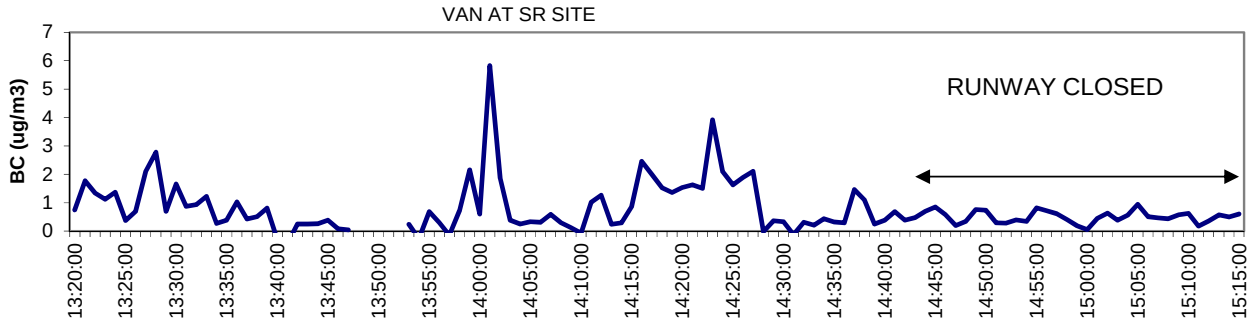
VAN AT SR SITE
BC (ug/m3)
7
6
5
4
3
2
1
0
RUNWAY CLOSED
13:20:00
13:25:00
13:30:00
13:35:00
13:40:00
13:45:00
13:50:00
13:55:00
14:00:00
14:05:00
14:10:00
14:15:00
14:20:00
14:25:00
14:30:00
14:35:00
14:40:00
14:45:00
14:50:00
14:55:00
15:00:00
15:05:00
15:10:00
15:15:00

Survey #9 – Gradient Measurements at Runway 25R

Following review of the preliminary results from Gradient Survey #2, a follow up experiment was conducted on September 23, 2011 to determine the spatial extent of the jet exhaust plume east of the Runway 25R. Figure 6 shows the sampling locations and times during Gradient Survey #9. The experiment began at 11:42 am after the winds had shifted from S-SW to W. The cart monitoring system remained stationary at location #1 about 101 m east of the blast fence and 20 m from the east edge of Aviation Boulevard. Measurements were made in the van for 5 minutes each at various distances east (50, 115, 180, 243, 313, and 447 m; locations #2 through #7) of location #1 along the runway approach light service road on the north side of the approach field. Measurements were also made 68 m (location #8) and 82 m (location #9) south of location #1 and at various distances east (115, 220 and 388 m; locations #10, #10b and #11) of location #9 along the runway approach light service road on the south side of the approach field. There were 81 and 50 takeoffs and landings, respectively, during the 2 hour 17 minute duration of the experiment or approximately 3 takeoffs and slightly less than 2 landings every five minutes.

Figure 7 shows time series of 1-minute average CO (ppm), NO (ppb), and PM2.5 (μg/m3) concentrations downwind of Runway 25R from 11:42 am to 2:00 pm. X-axis is labeled with locations of the van at 5 minute intervals. Large spikes in NO levels were measured, which coincided with aircraft takeoffs. The larger spikes were associated with larger aircrafts and accompanied by sudden gusts of wind at Location #1 lasting about a minute. Note the decreasing NO levels measured in the van relative to the cart and time delay in peak concentrations with increasing distance between sampling locations. CO levels were consistently low during the entire experiment. The occasions when higher CO was measured by the cart monitor, the van was collocated with the cart and idling for some time. $PM_{2.5}$ show a steady decrease over time in the baseline concentrations corresponding to the diurnal changes in the surrounding background levels. The spikes in PM2.5 concentrations were correlated to takeoffs, but the ratios of the peak to baseline levels were considerably smaller than for NO.

Figure 8 shows NO, BC and UFP together in the same time series plot. Correlations among these three parameters were expected and, in some cases, the associations are obvious. However, closer examination shows that relationship among the three pollutants are aircraft specific with some emitting considerably more BC and UFP relative to NO than other aircraft. As a result, the three parameters measured at the L1 sites were not well correlated as shown in Figure 11.

Measured pollutant concentrations with increasing distance downwind of the L1 reference site are shown in Figure 9 and 10. The NO plumes from jet exhaust are not evident 300 m downwind of the reference site. The plume also appears to be confined along the approach light on the north side of the field. BC shows similar decreases in concentration with distance, but with a greater background levels. Jet exhaust contributions to the measured $PM_{2.5}$ concentrations are relatively small relative to the urban background. UFP concentrations are also more widespread than NO or BC and more persistent between takeoffs. It is not clear whether this is due to persistence of the UFP that are emitted by the jets during takeoffs and landings or from contributions of other nearby combustion sources (e.g., gasoline and diesel vehicles).

Figure 6. Map Showing Sampling Locations and Times During Gradient Survey #9 on September 23, 2011.

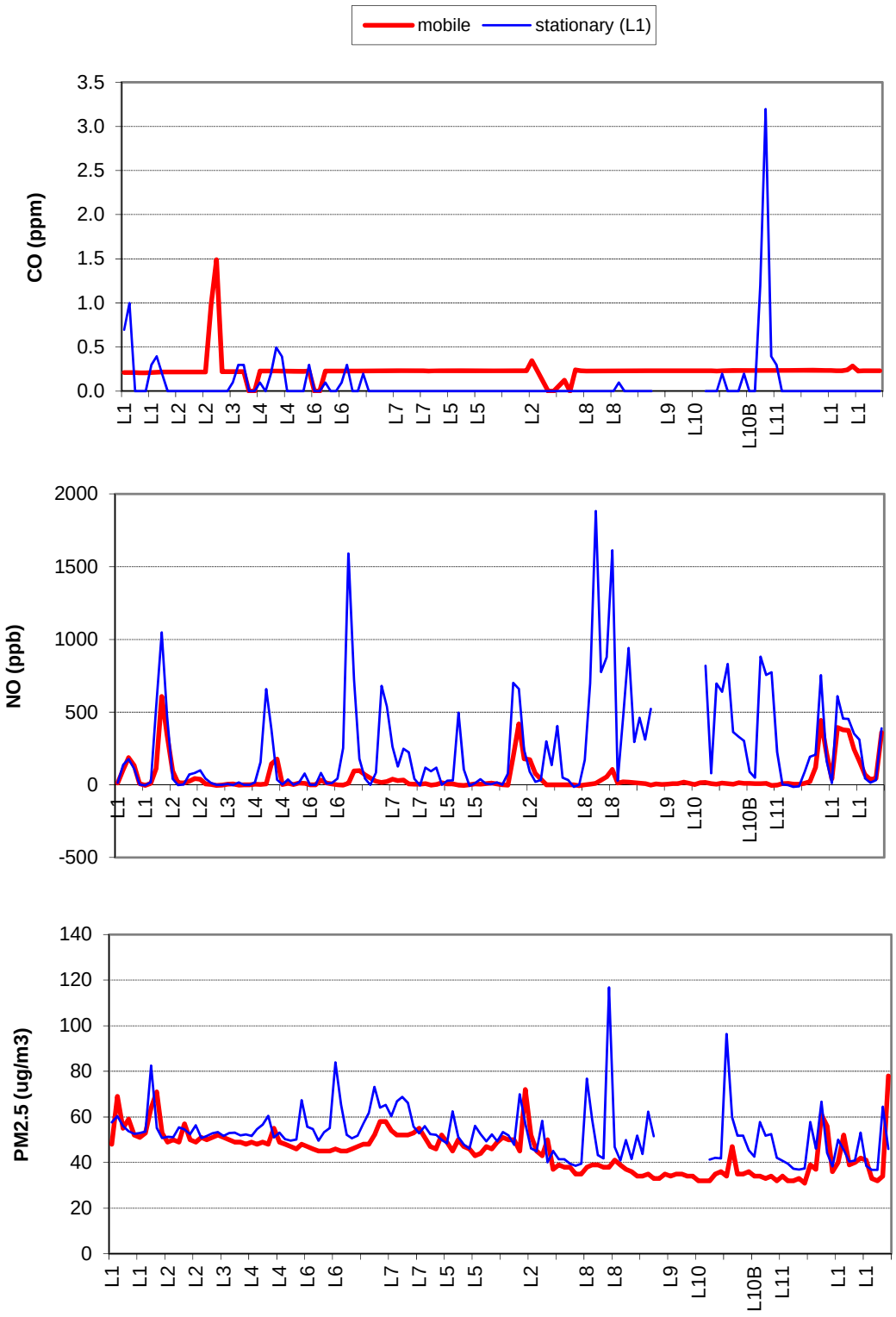

Figure 7. Time Series of 1-Minute Average CO (ppm), NO (ppb), and $PM_{2.5}$ ($\mu g/m^3$) Concentrations Downwind of Runway 25R on September 23, 2011 from 11:42 am to 2:00 pm. X-Axis is labeled with Locations (see Figure 6) of the Van at 5 Minute Intervals.

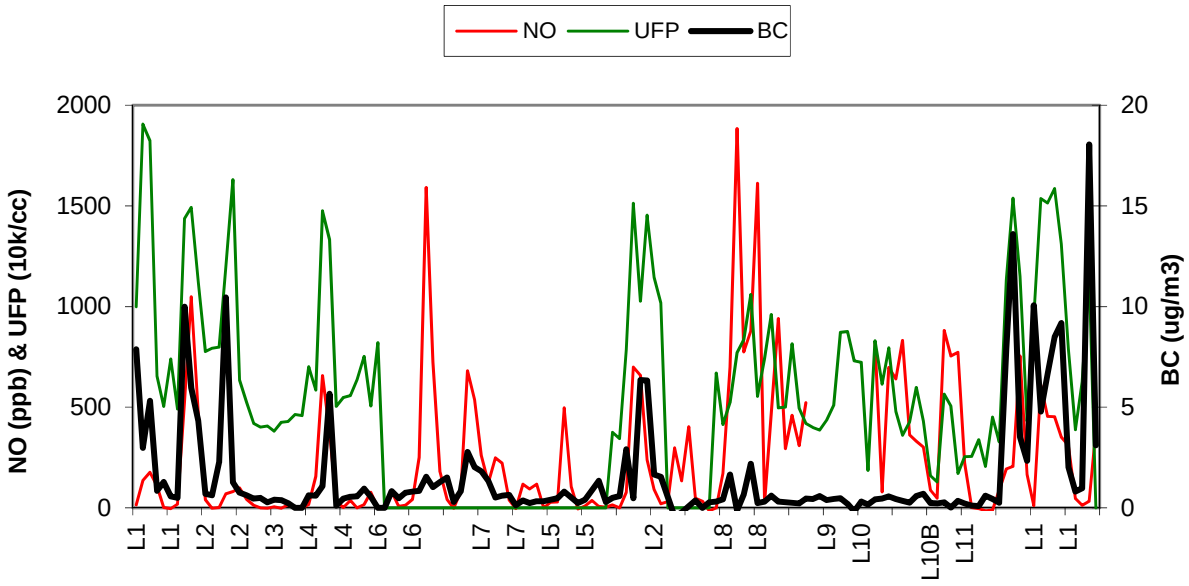

Figure 8. Time Series of NO, UFP and BC Concentrations.

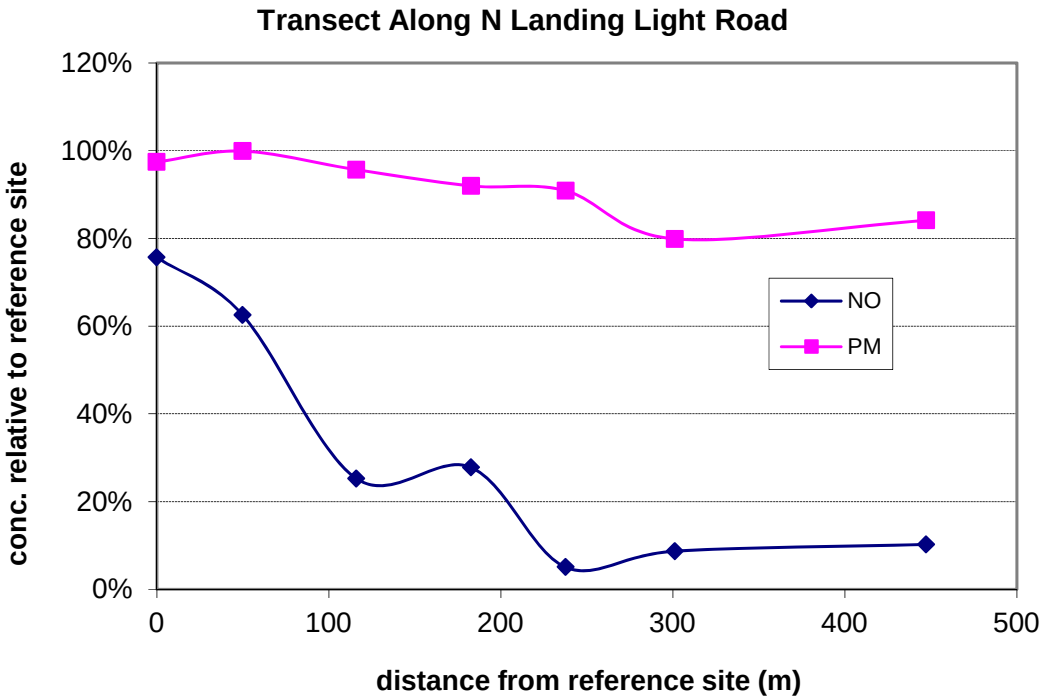

Figure 9. Variations in NO and PM Concentrations with Distance as Ratios of the Reference Site.

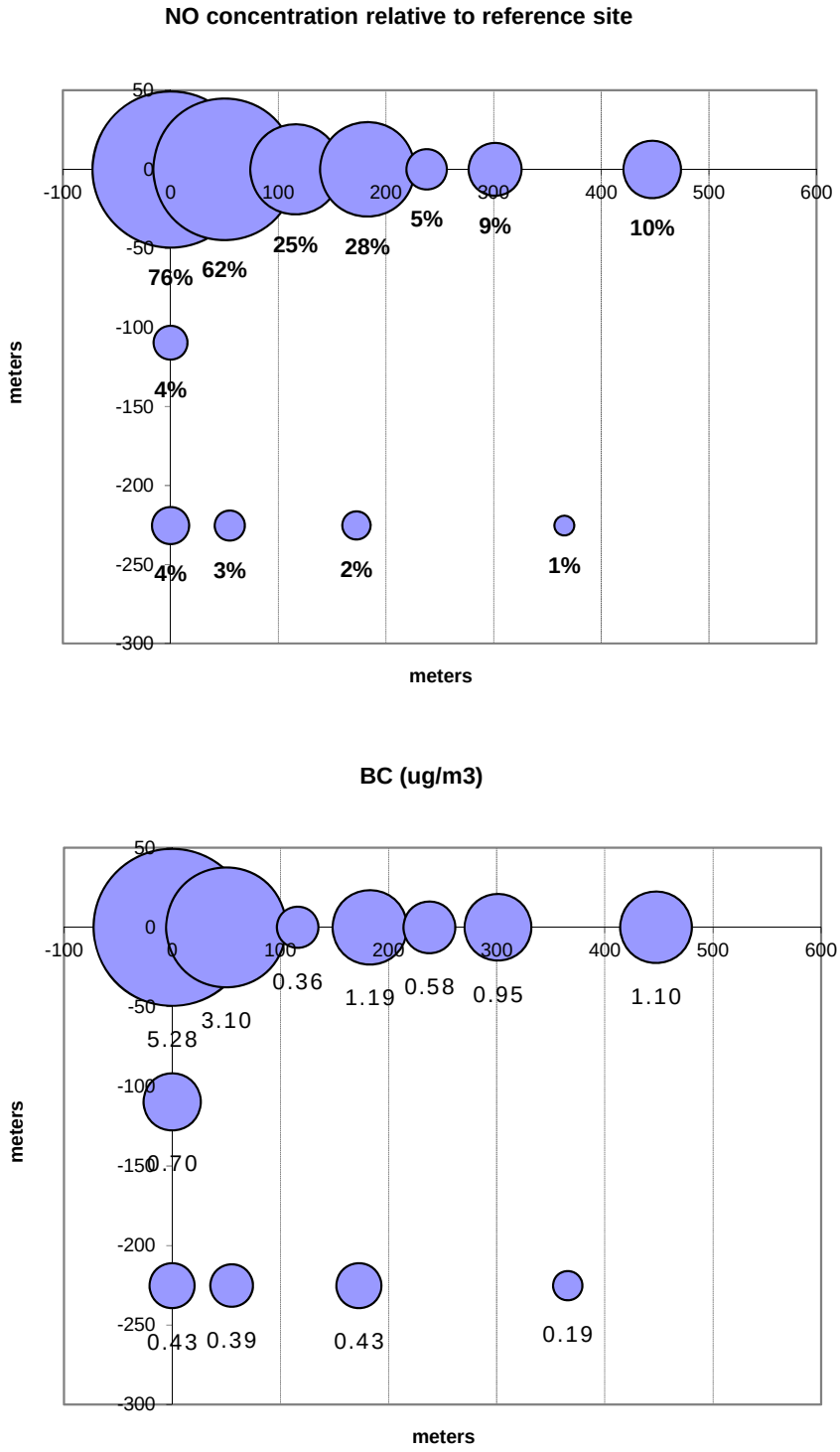

Figure 10a. Spatial Variations in NO and BC Concentrations Relative to the Reference Site.

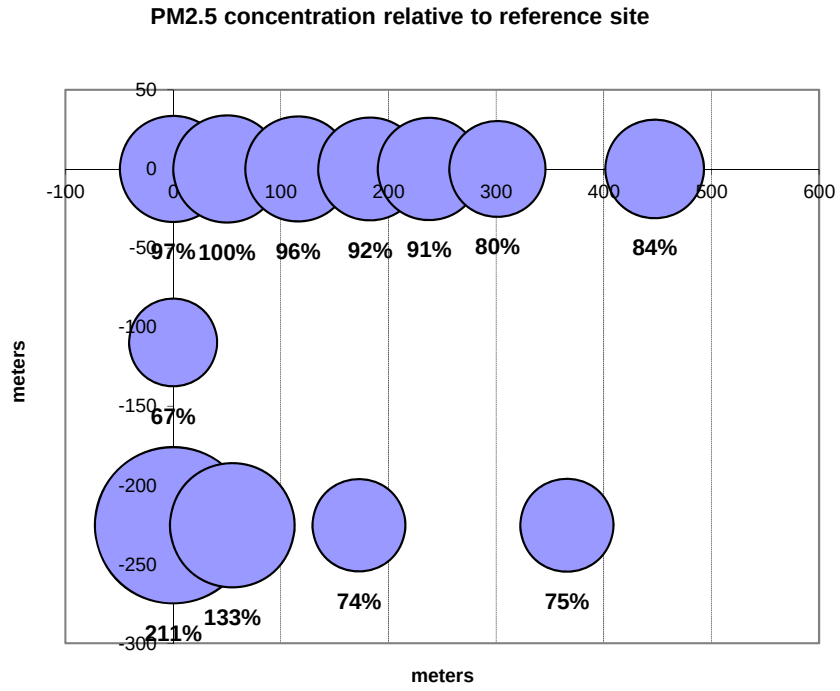

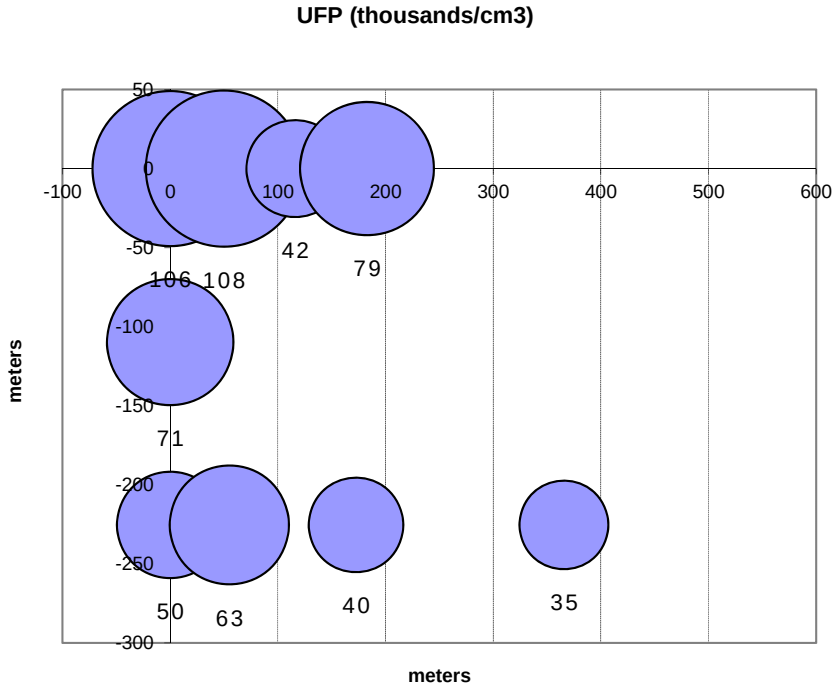

Figure 10b. Spatial Variations in $PM_{2.5}$ and UFP Number Concentrations Relative to the Reference Site.

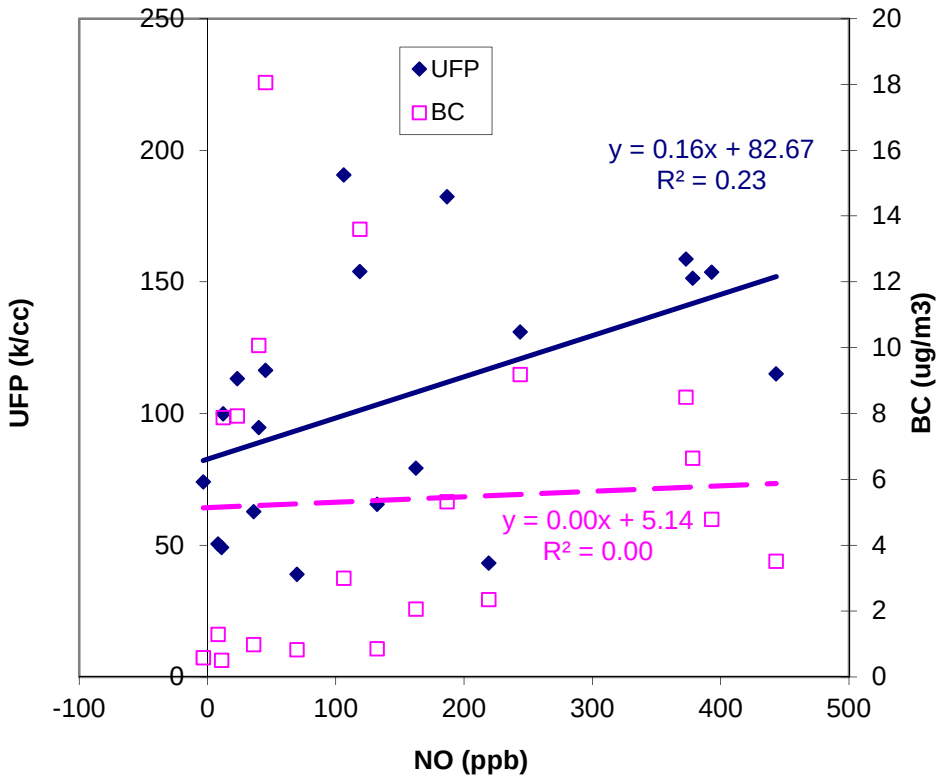

Figure 11. Scatter Plot of 1-Minute Average Data from Van at Location #1 (L1)

Survey #3 and 6 - Gradient Measurement North of Runway 25R Taxiway

The two surveys were made during the morning and evening of September 21, 2012. Measurements were made with the van at a fixed location at the end of International Road about 10 m from the airport boundary fence and measurements were made with the cart along International Road starting from this location and 340 m and 190 m north toward Century Boulevard.

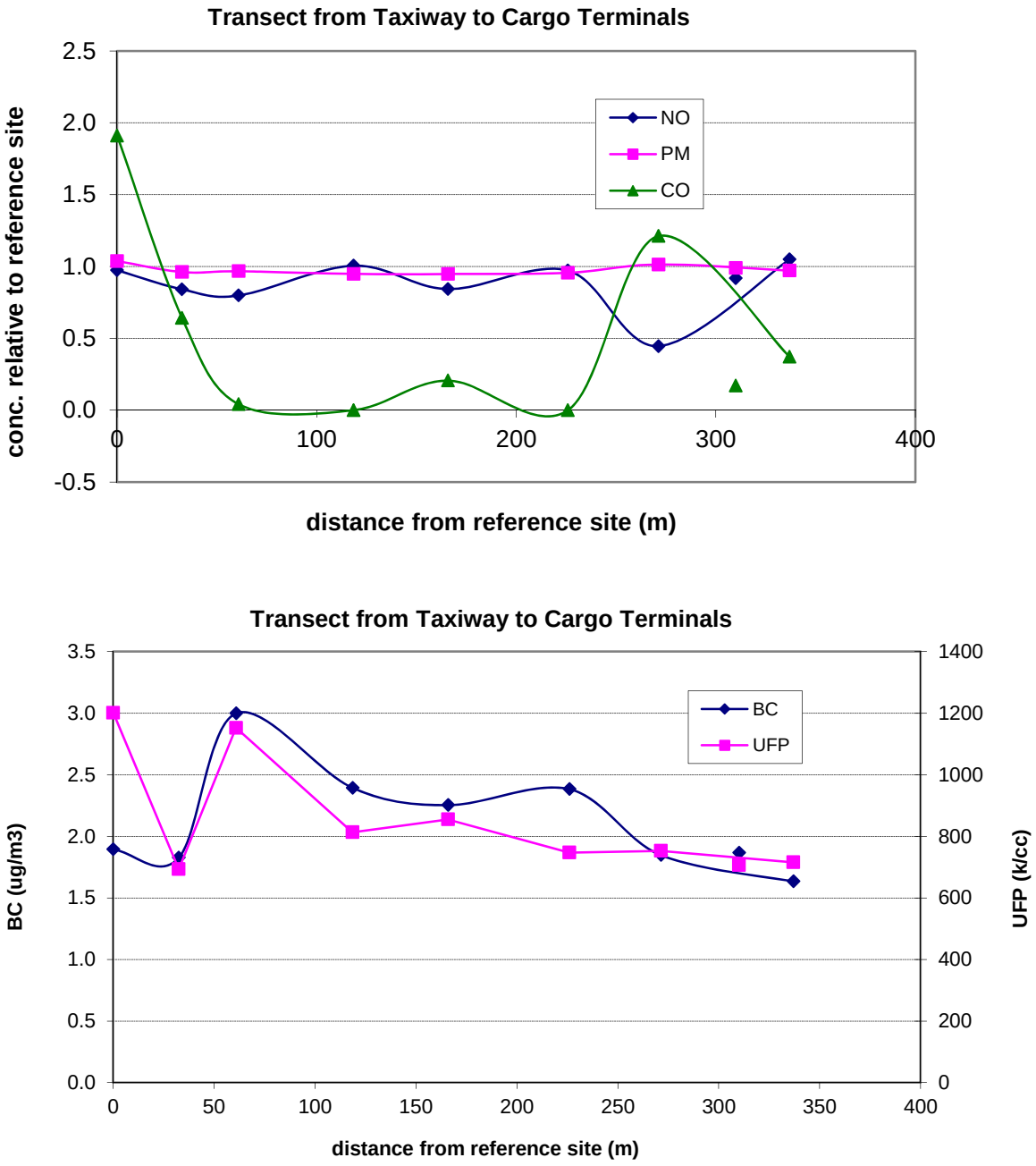

Figure 12a. Variations in BC Concentrations (bottom) and Relative to Reference Site (top) during Transect from South End of International Road Toward Century Boulevard during Morning of September 21, 2011.

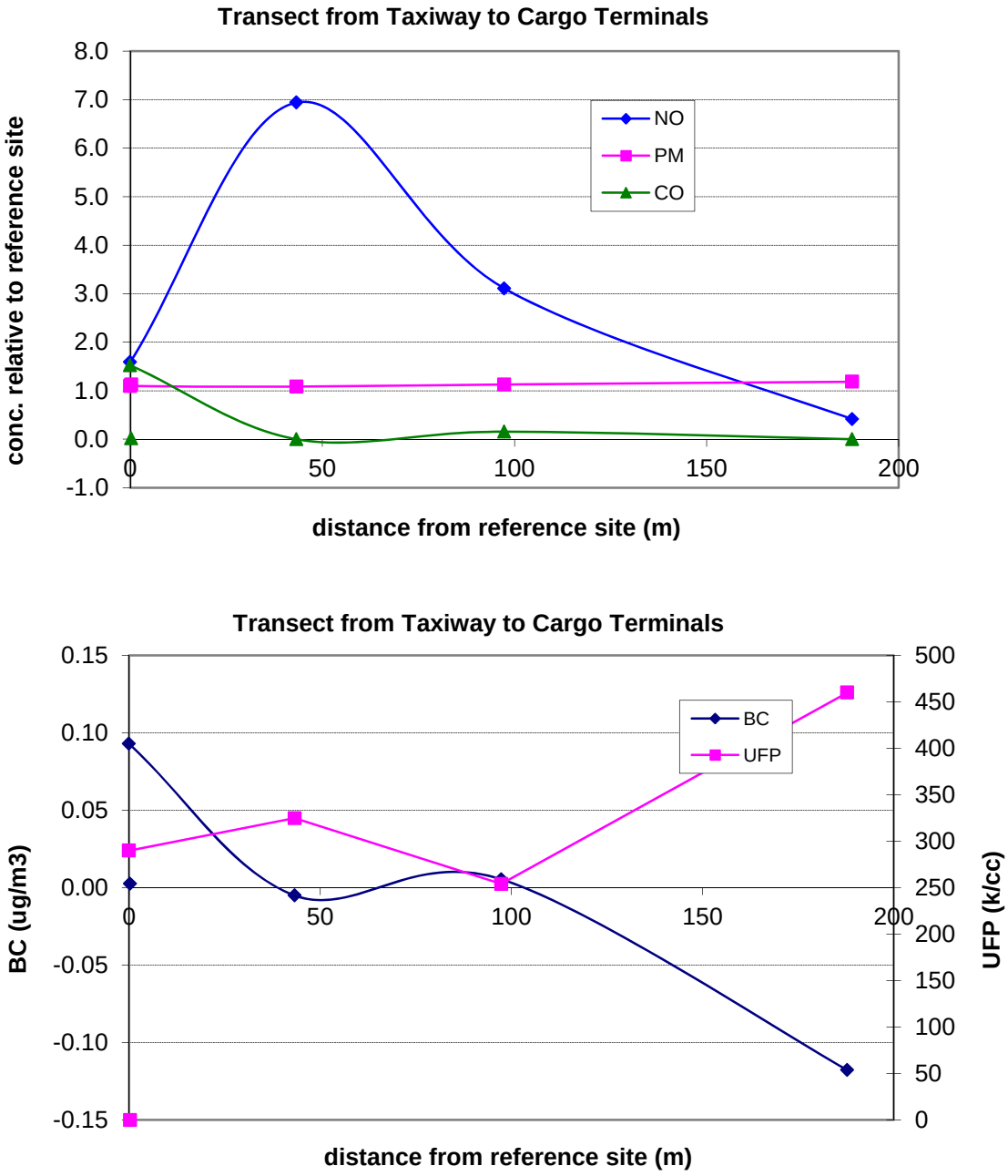

Figure 12b. Variations in BC Concentrations (bottom) and Relative to reference site (top) during Transect from South End of International Rd Toward Century Boulevard during Evening of September 21, 2011.

Gradient Survey #4 and #5 – I-405 Freeway in Lennox

1) West to east gradient along Lennox Boulevard from west of La Cienega Boulevard, underneath I-405 and continuing into community of Lennox about 1 km east of I-405 as shown in Figure 5. The van is shown as the stationary reference monitor at Felton Elementary School. An analogous route will be substituted if another community background site is selected in place of Felton Elementary School.

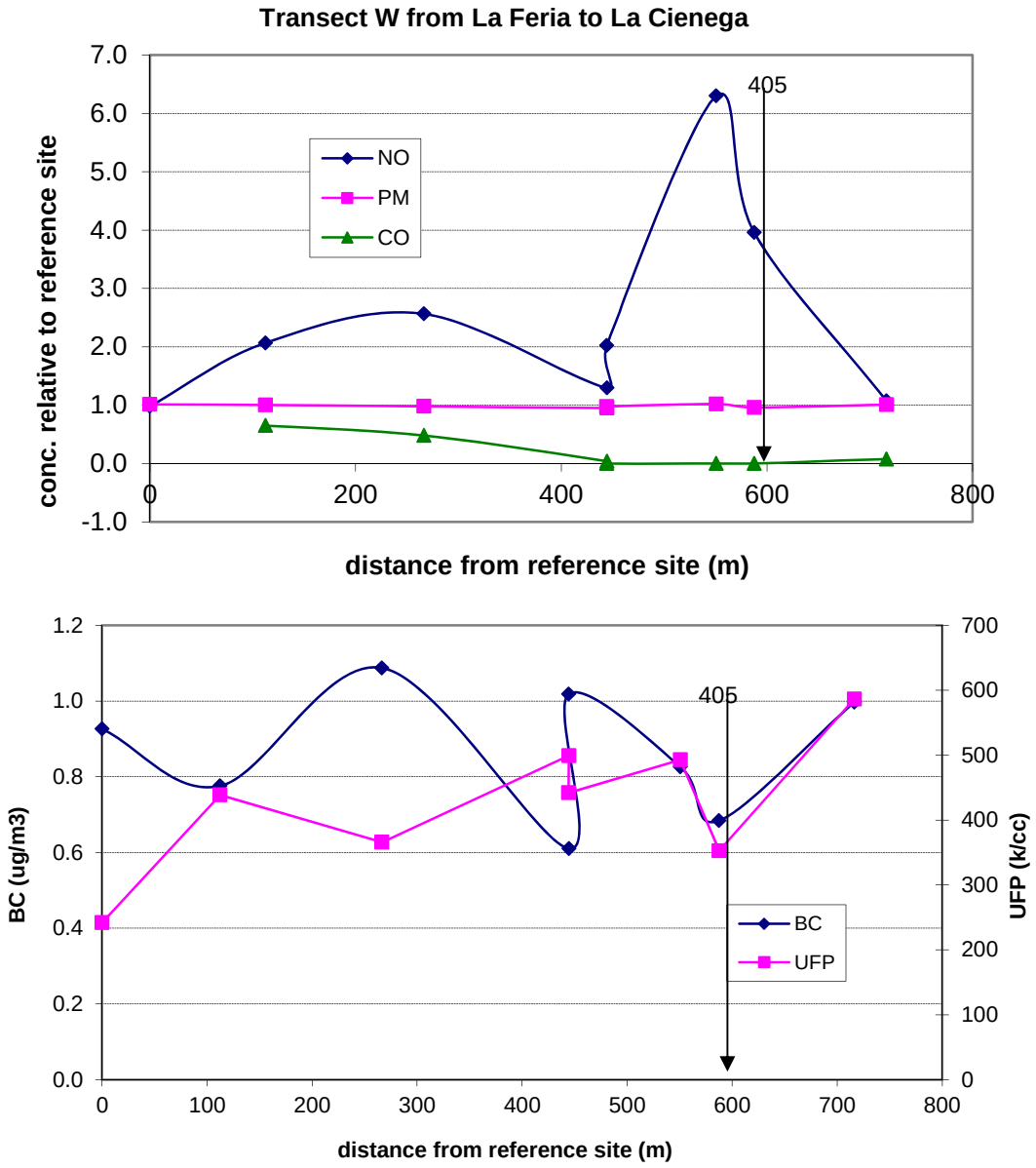

Figure 13a. Lennox Midday

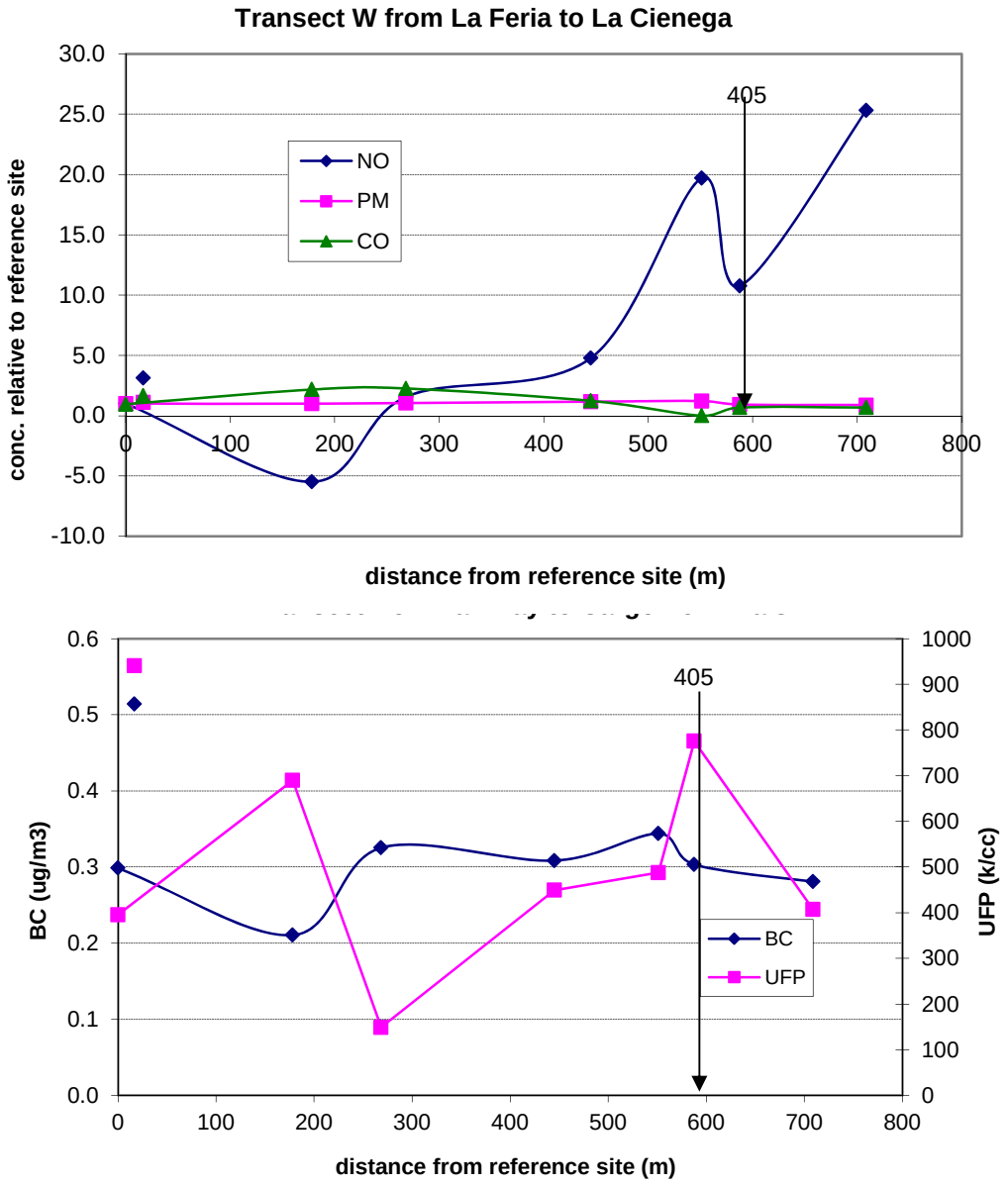
Transect W from La Feria to La Cienega
conc. relative to reference site
distance from reference site (m)
NO
PM
CO
405
BC (ug/m3)
UFP (k/cc)
BC
UFP

Figure 13b.

2.3 Conclusions

Results of gradient survey #2 showed that the proposed SR sites was minimally influenced by emissions during aircraft takeoff when winds were from the west, which is the predominant direction throughout the year except during late fall and winter. Additionally, the results of survey #9 showed that most of the exhaust emissions from aircraft takeoffs were transported directly east along the runway centerline. The impact of takeoff emissions at the SR site will likely be minimal during late-fall and winter as well when the predominant prevailing winds are from the northeast. Given these results, measurements at the SR site during Phase III of the LAX AQSAS will likely reflect dilute taxiway emissions with minimal contributions from takeoff emissions. Therefore, the LAX AQSAS Project Team should reevaluate the purpose of the SR site in the context of the primary study objective, which is to apportion the contributions of air operations to air quality in communities adjacent to LAX.

3. RECOMMENDED MONITORING PLAN FOR PHASE III OF THE LAX AQSAS

This section describes suggested modifications to the draft Technical Work Plan for Phase III of the LAX AQSAS based upon results of the mobile surveys conducted by the Desert Research Institute during the week of September 21, 2011.

3.1 Background

The draft Technical Work Plan (Version 5) prepared by CDM for Phase III of the LAX AQSAS (CDM, April 2011) described specifications for air quality monitoring at three "core" sites (with an option for two additional sites) and two "satellite" sites during two seasons, each lasting six weeks. Measurements at the core sites include: continuous (1 to 5 minute resolution) measurements of carbon dioxide (CO_2), nitric oxide (NO), oxides of nitrogen (NOx), sulfur dioxide (SO_2), black carbon (BC), particle size distributions, ultrafine particle (UFP) number concentrations and light scattering; semi-continuous (hourly) non-methane hydrocarbons (NMHC) and $PM_{2.5}$ mass; and two 12-hour average samples during ten consecutive days within each two six-week season for chemical speciation of light hydrocarbons (C_2-C_{11}), heavy hydrocarbons (C_{10}-C_{18}), carbonyl compounds (C_1-C_7), and particulate organic compounds (by thermal desorption of quartz filters). Proposed core sites include a "source" site at the east end of Runway 25R (SR), a community site east of LAX (CE) and an upwind site (UW) with options for an upwind background site either north or south of the LAX runway path (BW) and a downwind site south of the runway (FS) (Figure 1). Measurements at satellite sites include: continuous light scattering and PM size distributions and UFP number concentrations; and the same set of two 12-hour speciation samples collected at core sites. Satellite sites were proposed within the community south (CS) and at the northeast edge (PN) of LAX. An existing SCAQMD air monitoring site (AQ) is located at the northwest boundary of the Airport. This network of monitoring sites was proposed for analysis of the spatial and temporary variations of pollutant concentrations in the communities surrounding the Airport and for multivariate receptor analysis of source contributions.

The Request for Work Task Proposals issued by LAWA for Phase III of the LAX AQSAS solicited proposals based upon the April 2011 draft Technical Work Plan. In its successful bid the Tetra Tech Inc. team proposed two core sites (SR and CE) with continuous monitoring and collection of time-integrated samples with methods that would ensure quantitative analysis of relevant marker species used in VOC and PM source apportionment. Continuous measurements were also proposed for a limited time at an upwind site using a mobile monitoring van. The monitoring program originally proposed by the Tetra Tech team also included saturation monitoring consisting of 7-day integrated nitrogen dioxide (NO_2), oxides of nitrogen (NOx) and sulfur dioxide (SO_2) using Ogawa passive samplers, and VOC (benzene, toluene, ethylbenzene and xylenes) and carbonyl compounds using Radiello passive samplers during six consecutive weeks in two seasons. Additionally, 7-day integrated Teflon and quartz filters will be collected with portable Airmetrics MiniVol samplers and analyzed for $PM_{2.5}$ mass, elements and organic carbon (OC) and elemental carbon (EC). Saturation monitoring will also include additional "gradient" sites consisting of passive-only sampling for NO_2, NOx, and SO_2 to characterize the zones of influence near emission sources (e.g., near the east end of the Runway 25R or roadside along freeways and major arterials (both prevailing upwind and downwind

edges). Spatial surveys of pollutant concentrations were conducted prior to the main study using a mobile monitoring van to guide the selection of saturation monitoring sites.

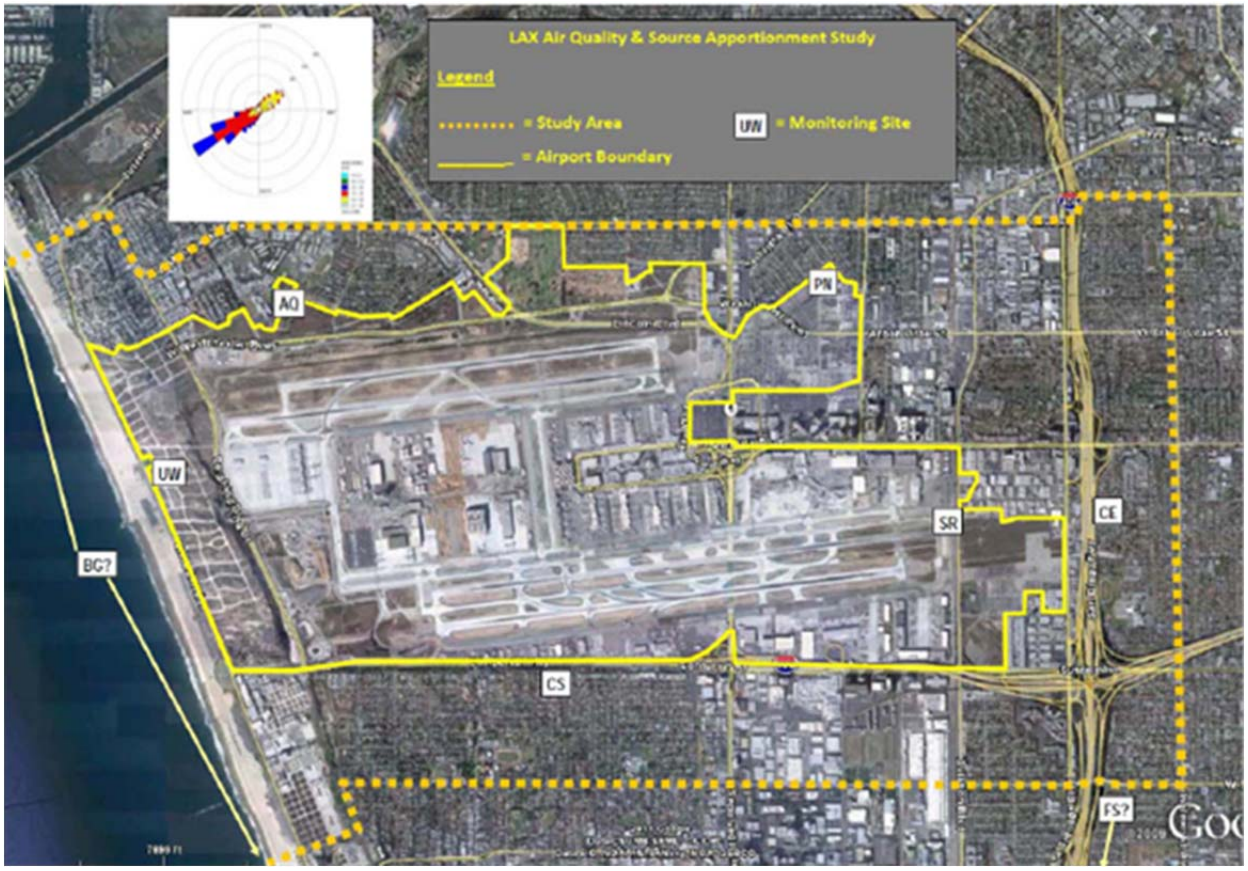

Figure 14. Study Area and Originally Proposed Monitoring Locations.

The proposed source-dominated SR site is located about 75 m north-northeast of the east end of Runway 25R. The gradient survey #2 showed that this site was minimally influenced by emissions during aircraft takeoff when winds were from the west, which is the predominant direction throughout the year except during late fall and winter. Additionally, the results of survey #9 showed that most of the exhaust emissions from aircraft takeoffs were transported directly east along the runway centerline. Consistent with this expectation, the SCAQMD sampled at a location about 25 m northeast of the proposed SR site in April 2011 to capture taxiway emissions as the jets made the turn at the end of Runway 25R. The impact of takeoff emissions at the proposed SR site will likely be minimal during late-fall and winter as well when the predominant prevailing winds are from the northeast. Given these results, measurements at the proposed SR site during Phase III of the LAX AQSAS will likely reflect dilute taxiway emissions with minimal contributions from takeoff emissions. Therefore, the purpose of the proposed SR site should be reevaluated in the context of the primary study objective, which is to

apportion the contributions of airport operations to air quality in communities adjacent to LAX.

Receptor modeling will be one of several methods that will be used to achieve the study objectives. Receptor models infer contributions from different source types using multivariate measurements taken at receptor locations. Receptor models use ambient concentrations and the abundances of chemical components in source emissions to quantify source contributions. For example, the Chemical Mass Balance (CMB) model consists of a least-squares solution to a set of linear equations that expresses each receptor concentration of a chemical species as a linear sum of products of source profile species and source contributions. The source profile species (the fractional amount of the species in the PM or VOC emissions from each source type) and the receptor concentrations, each with uncertainty estimates, serve as input data to the CMB model. The output consists of the contributions for each source type to the total ambient PM or VOC as well as to individual species concentrations. Thus ambient measurements at receptor locations are the primary focus of monitoring programs in the context of source attribution of pollutant concentrations. Measurements at "source-dominated" locations are typically made to develop source composition profiles only when direct source measurements (e.g., vehicle exhaust testing on chassis dynamometers or in-stack testing) are not possible or practical. While measurements at source-dominated locations have utility in analysis of spatial variations in pollutant concentrations, many sampling locations (i.e., saturation monitoring) are required and is usually cost prohibitive.

In the summer of 2008, the Jacobs Consultancy (now named LeighFisher Inc.) team conducted a Demonstration Project to evaluate potential measurement methods and to characterize the spatial gradients in pollutant concentrations downwind of the blast fence at the east end of Runway 25R. Fuels (gasoline, diesel, and aviation fuels) and source-dominated ambient samples were collected and analyzed to develop source composition profiles that could be applied in source apportionment analysis during the main study using the Chemical Mass Balance (CMB) receptor model. However, after review of the data from the Demonstration Project, the Study's Technical Work Group (TWG) concluded that the sensitivity and breadth of the chemical analysis were not adequate for this purpose. The TWG also recommended sampling near the south airfield taxiway to develop a profile of taxiing and idling aircraft engines, which are produce relatively greater emissions of VOC and CO relative to NOx, SO_2, BC and UFP. This taxiway sampling was conducted in April 2011 through in-kind support from the SCAQMD. Given the remaining data gaps relative to applicable source composition profiles for receptor modeling, DRI recommends that this work be integrated into the Phase III work.

3.2 Recommended Modifications to the Phase III LAX AQSAS Air Monitoring Plan

The following modifications are suggested for discussion by the Project Team. The alternative air monitoring plan places greater emphasis on community monitoring for the core sites and utilizes saturation monitoring to compare pollutant concentrations within adjacent communities to corresponding measurements at the airport buffer zones, and near airport operations and high-traffic areas. The recommended monitoring plan is summarize in Tables 3 (seasonal saturation monitoring) and 4 (source characterization). The following gives the objectives and approaches for the main components of the recommended monitoring plan.

- Redirect emphasis of the SR site from seasonal ambient monitoring to source characterization for subsequent application in source apportionment analysis.

Replace the seasonal monitoring at the SR site with a short-term sample collection and monitoring effort that is specifically designed to obtain relevant source composition profiles and emission factors for jet exhaust during takeoffs and taxiing. Deploy integrated samplers and continuous monitors for 4 days for 4-6 hour during the day behind the blast fence (takeoffs) and at the former SCAQMD taxiway sampling location (Table 4). Samples for chemical speciation should parallel the samples that will be collected at the three core monitoring sites during Phase III of the LAX AQSAS. These samples include: canisters for C_2-C_{11} hydrocarbons; tenax tubes for C_{10}-C_{20} hydrocarbons; DNPH cartridges for carbonyl compound; TIGF/XAD for semi-volatile and particulate organic compounds (polycyclic aromatic compounds, alkanes, hopanes and steranes and polar compounds, Teflon filters for PM mass and metals, and quartz filters OC, EC, and sulfate. Also analyze canister samples for methane, CO and CO_2 for use in deriving fuel-based emission factors. Include continuous NO and sound monitors to document activity (timing and duration of emissions impact). If line power is not available behind the blast fence, all samplers can be run by gasoline-powered generators located downwind of the sampling locations.

Simultaneously with collection of source samples described above, conduct a pollutant gradient study downwind of Runway 25R. Deploy a set of passive and battery-operated mini-volume aerosol samplers behind the blast fence and in the open field east of the Runway 25R at various distances from east edge of Aviation Boulevard (e.g., 25, 125, 325 m, and at the east end of the open field ~500-600m). Collect 4-6 hour integrated passive samples for NO_2, NOx, SO_2, VOC and carbonyl compounds and mini-volume Teflon filter samples for $PM_{2.5}$ mass and metals, and quartz samples for OC, EC and sulfate. Samplers would be attached to the runway approach light posts. If the light posts cannot be used, all samplers can be attached to a tripod posts secured with sand bags. Add continuous measurements of NO and BC by photoacoustic instrument, UFP by CPC with adequate upper range and $PM_{2.5}$ at the blast fence location. Deploy the same set of continuous monitors at the site 125 m east of Aviation Boulevard. Measure WS and WD at this location to document prevailing winds between takeoffs as well as the timing and duration of intermittent increases in wind speed from the jet exhaust wash during takeoffs relative to time of takeoff as indicated by the sound meter and spikes in NO concentrations measured at the blast fence.

The work described above should be done following the first seasonal intensive period of the main study with operation of all continuous monitors at the CE sites continued until completion of source characterization work. The time series of the four pollutant concentrations, WS and sound measured at the blast fence will be compared to the corresponding time series obtained at the site 125 m from the east edge of Aviation Boulevard and the CE core monitoring site in Lennox located about 1.5 km east of the end of Runway R25. Compile a comprehensive speciation profile for takeoff and taxing emissions. The taxiing samples will be used for background subtraction of the takeoff samples. A third background site will be necessary to collect samples for background subtraction of taxiing emissions.

- Increase spatial coverage of core monitoring sites within the communities adjacent to LAX and change sampling schedule for

First DRI suggests moving the proposed SR fixed monitoring site to the Community South (CS) location at the former Imperial Avenue Elementary School. Secondly, consider whether the SCAQMD monitoring site (AQ) can serve as an upwind site in place of the Vista del Mar background (UW) site. If so, the core monitoring station previously proposed for the UW site can be deployed in Westchester at a location further east of the AQ site (e.g., PN site in the draft Work Plan prepared by CDM or an alternate site in the area). Including the CE core site (La Feria Restaurant) located east of LAX in Lennox, communities adjacent to LAX in all three directions (north, east and south) will be represented by a core monitoring site, which will provide the maximum possible temporal resolution in pollutant concentrations and the comprehensive chemical speciation necessary for source apportionment analysis.

Informal conversations with SCAQMD staff suggest that the AQMD Hastings air monitoring site (AQ) is more characteristic of a background site than an urban neighborhood-scale monitoring site. Pollutant concentrations at this site are expected to be low during most of the year based upon its location and predominant westerly wind direction. However, occasionally higher pollutant concentrations may be measured during northeasterly or easterly winds in the late fall and winter, which are less likely to be related to airport operations. Available data from the monitoring station should be reviewed to better characterize this monitoring site. This site should be augmented with appropriate continuous gas and PM monitors as the available budget, space and electrical power allow in order to provide a fourth site in the area with a comparable set of continuous monitoring data. At a minimum, BC and UFP number concentrations should be added to the existing measurements of CO, SO_2, and NO_x. Collection of comprehensive speciation samples will not be possible with the existing available power, but it is less of a priority at this site as VOC and PM concentrations are expected to be low with correspondingly greater analytical uncertainties. However, basic chemical speciation at the level of a satellite site (i.e., 7-day integrated passive and mini-volume aerosol samples) is possible and should be obtained at this site.

Consideration should be given to changing the comprehensive speciation sampling at the three core sites from two 12-hour samples per day for ten days (60 sets of samples total) to one 24-hour sample per day for 14 consecutive days (42 sets of samples). Savings associated with this change offsets the additional cost for source characterization and pollutant gradient work. Furthermore, the 14 consecutive samples can be averaged into two 7-day averages that can be compared directly at the three core sites with the corresponding 7-day passive NO_2, NO_x, SO_2, VOC and carbonyl compound samples and $PM_{2.5}$ mass, metal, OC, EC, and sulfate from the 7-day integrated mini-volume aerosol samples. Besides the quality assurance provided by these comparisons, the Chemical Mass Balance receptor modeling results utilizing the full speciation data obtained at the three core sites can be compared with the more limited speciation data obtained at the four satellite sites. The potential contributions of differences in sampling and analytical methods at core and satellite sites on the source apportionment results can be evaluated. DRI believes the benefits of this change outweigh the objective of obtaining separate daytime and nighttime speciation samples. These differences can be evaluated by examining diurnal variations in continuously measured pollutants such as CO, BC, UFP, SO_2, NO_x, or their combinations, that can serve as surrogates of emission sources. Ambient data from the three core sites and source composition data from the source characterization experiment and other literature sources will be used to examine the relationships between these species and potential source markers (e.g., molecular and elemental markers).

- Deploy a network of saturation monitoring sites to determine spatial variations in pollutant concentrations within adjacent communities relative to locations near airport operations and the buffer zone surrounding the Airport.

The proposed air monitoring plan for Phase III of the LAX AQSAS is summarize in Table 3. The monitoring network consists of three categories of monitoring sites: core, satellite, and gradient. In the recommended monitoring plan, the three fully-instrumented core sites are intended to determine the temporal variations and average daily source contributions to VOC and PM within the communities adjacent to LAX, Lennox to the east, El Segundo to the south and Westchester to the north. Core sites include both 24-hour integrated sampling on 14 consecutive days for comprehensive chemical speciation and six consecutive 7-day passive samples for NO_2, NO_x, SO_2, VOC, carbonyl compounds and mini-volume aerosol samples for $PM_{2.5}$ mass, metals, OC, EC, and sulfate. The four satellite sites, consisting of 7 day passive and mini-volume aerosol samples, provide chemical data at three additional community sites (El Segundo, Hawthorne, and Westchester) and a background site. The CMB receptor modeling for the core sites will include organic molecular markers, while the analysis for satellite sites will be based on elements and OC and EC. The combination of core and satellite sites provides analysis of the spatial variations of pollutant concentrations for VOC, PM, and air toxics within the communities adjacent to LAX. The three community satellite sites should be located within the center of each community and at least 200 m away from the nearest arterial surface street. Private residences are usually the best choice for such sites.

The ten gradient sites consisting of 7-day passive samples on six consecutive weeks for NO_2, NO_x, SO_2, VOC, and carbonyl compounds will be located at the perimeter of LAX buffer zones and near airport operations (north and south airfields, and the Central Terminal Area) and at high traffic areas (near intersection of Century Boulevard and Aviation Boulevard, and the west and east edges of the I-405 freeway). Sampling at the runways will include a set of samples on the wire fence at the east edges of the Runway 25 and Runway 24 and a sampling location about 500 m east of the near-runway sampling locations. All gradient samples will be located in publicly accessible areas and will not require coordination of access with LAX Operations.

Table 3. Monitoring Locations and Measurements during Phase III of the LAX AQSAS.

					7-day Samples During 6-Week Intensives									Daily 24-hr for 14 Consecutive Days							
					Passive						Mini-VolPM			Can	Tenax	DNPH	Med-VolPM				SVOC
Site ID	Site Type	Site Name	Location	Cont	NOx	NO_2	SO_2	BTEX	1,3-BD	Carb	Tef	Tef/Qtz	Qtz	Light HC	Hvy HC	Carb	Tef	Tef/Qtz	Qtz	Qtz/NaCl	TIGF/XAD
CE	Core	Community East	La Feria Restaurant, Lennox	1	2	2	2	2	2	2		1	1	1	1	1		1		1	1
CS	Core	Community South	Imperial Ave School, El Segundo	1				1	1	1	1		1	1	1	1	1		1		1
CN	Core	Community North	NE of LAX, Westchester	1				1	1	1	1		1	1	1	1	1		1		1
AQ	Core	Upwind Northwest	91st & Hastings, Playa del Rey	AQMD+	1	1	1	1	1	1	1		1								
UW	Satellite	Upwind West	W of LAX between SR and NR		1	1	1	1	1	1	1		1								
CS2	Satellite	Community South #2	El Segundo		1	1	1	1	1	1	1		1								
CN2	Satellite	Community North #2	Westchester		1	1	1	1	1	1	1		1								
CE2	Satellite	Community East #2	Hawthorne		1	1	1	1	1	1	1		1								
BN	Gradient	Buffer Zone North	N of Westchester Parkway		1	1	1	1	1	1											
BS	Gradient	Buffer Zone South	Imperial Terminal		1	1	1	1	1	1											
SR	Gradient	South Runway	Fence on east end of SR, Aviation		1	1	1	1	1	1											
NR	Gradient	North Runway	Fence at east end of NR		1	1	1	1	1	1											
BSR	Gradient	Buffer Zone S Runway	Lot B near La Cienega Blvd.		1	1	1	1	1	1											
BNR	Gradient	Buffer Zone N Runway	Lot C near Jenny Ave.		1	1	1	1	1	1											
CT	Gradient	LAX Central Terminal	Roof of Parking Garage		1	1	1	1	1	1											
C&A	Gradient	Century and Aviation	Near intersection		1	1	1	1	1	1											
405E	Gradient	I-405 East Edge	East edge of I-405		1	1	1	1	1	1											
				3+	16	16	16	18	18	18	7	1	8	3	3	3	2	1	2	1	3
			Samplers																		
			Core		3	3	3	5	5	5	3	1	4	3	3	3	2	1	2	1	3
			Satellite		4	4	4	4	4	4	4		4								
			Gradient		9	9	9	9	9	9											
			Total Samples per Season																		
			Core		18	18	18	30	30	30	18	6	24	42	42	42	28	14	28	14	42
			Satellite		24	24	24	24	24	24	24		24								
			Gradient		54	54	54	54	54	54											
			Field Blanks		5	5	5	5	5	5	5		5		4	4	4		4		4
			Total Samples per Season		101	101	101	113	113	113	47	6	53	42	46	46	32	14	32	14	46

Table 4. Locations and Measurements during Source Characterization at Runway 25R.

				4-6 hour Samples during 4-day Source Measurements													
				Passive					Mini-Vol PM		Can		Tenax	DNPH	Med-Vol PM		SVOC
Site ID	Site Name	Location	Cont	NOx	NO2	SO2	BTEX	Carb	mass, metals	OC, EC	Light HC	CH4, CO, CO2	Heavy HC	Carb	Tef	Qtz	TIGF/ XAD
SRB	South Runway Blast	Behind Blast Fence	NO, BC, PM, sound	1	1	1	1	1			1	1	1	1	1	1	1
SR2	South Runway Taxiway	Taxiway		1	1	1	1	1			1	1	1	1	1	1	1
SR3	South Runway #3	~25m east of Aviation	WS, WD	1	1	1	1	1	1	1							
SR4	South Runway #4	~125m east of Aviation	NO, BC, PM, CPC	1	1	1	1	1	1	1							
SR5	South Runway #5	~325m east of Aviation		1	1	1	1	1	1	1							
BSR	Buffer Zone S Runway	Lot B near LaCienega Blvd.		1	1	1	1	1	1	1							
CE	Community East	LaFeria Restaurant, Lennox	1														
				6	6	6	6	6	4	4	2	2	2	2	2	2	2
		Number of days per season	4														
		Total number of samples/season		24	24	24	24	24	16	16	8	8	8	8	8	8	8

3.3 Recommended Measurement Priority

Considering the input data required for source apportionment modeling study, the following assessment of measurement priorities is provided to facilitate discussions by the Project team and LAWA about possible budget adjustment that may be required.

Highest Priority

- Source sampling behind the blast fence at Runway 25R and northeast of end of runway to develop composition profiles and fuel-based emission factors for commercial jet exhaust and taxiing emissions for use in Chemical Mass Balance Receptor modeling.
- Ambient 24-hour VOC and PM samples (14 consecutive days during two seasons) with comprehensive chemical speciation at three core sites for source apportionment of ambient VOC (including air toxics) and PM at the three community sites located east, north and south of LAX.
- Continuous measurements of NO, NO_2, SO_2, black carbon, ultrafine and fine particle concentrations and size distributions, CO (substitute for CO_2), and wind speed and direction with at least 1-minute time resolution for time-series analysis and nonparametric trajectory analysis. LAWA will provide aircraft activity logs such as numbers and timing of takeoffs and landings.
- Ambient 7-day integrated passive samples (6 consecutive weeks during two seasons) for NO_2, NO_x, SO_2, and volatile air toxics (benzene, toluene, xylenes, ethylbenzene, formaldehyde, acetaldehyde) at six community sites (3 core and 3 satellite), one upwind site, four LAX buffer zone sites, and six near source sites for analysis of spatial variations of gas-phase pollutant concentrations.
- Ambient 7-day integrated mini-volume aerosol samples (6 consecutive weeks during two seasons) for $PM_{2.5}$ mass, elements, organic carbon and elemental carbon at the three core site, AQMD site, and three satellite sites for analysis of spatial variations of particle-phase pollutant concentrations.

High Priority

- Gradient measurements during source sampling at Runway 25R to characterize zone of influence of jet exhaust emissions. While not essential for the source apportionment analysis, this information will provide corroborative information that will be useful in interpreting the temporal analysis of the continuous measurements at the CE core site and spatial analysis of the passive measurements. This experiment will be required to examine the relative importance of jet and on-road motor vehicle exhaust to the ultrafine particle number concentrations measured at the CE core site.

Lower Priority

- Continuous measurements of CO_2 at the three core sites. The incremental contributions of emission sources within an urban area to the global background levels of CO_2 are relatively low except in close proximity to combustion sources. Measurements will be of limited value as CO_2 levels will be fairly constant with time at the three community core sites. CO_2 measurements should be substituted with CO, which is a good tracer for gasoline-powered vehicle emissions.

- Non-methane hydrocarbon emissions at the three core sites. This measurement lacks high time resolution and sensitivity, thus will be of limited value temporal analysis and nonparametric trajectory analysis. NMHC data from the continuous instruments are not necessary for receptor analysis.
- Continuous PM sampling with beta attenuation monitors (BAM) for PM_{10} and $PM_{2.5}$ mass. Cannot provide less than 1-hour resolution and do not have good precision below 10 $\mu g/m^3$. Urban and regional background is typically a major component of PM concentrations and local source have minimal impact expect very near the source. Coarse particles ($PM_{2.5}$ to PM_{10}) are typically higher near sources of fugitive dust and during high wind conditions. Salt from sea spray also contribute at coastal locations.

Lowest Priority

- Particle deposition
- Video recordings

REFERENCES

Arnott WP, Moosmüller H, Rogers CF, Jin T, Bruch R. (1999). Photoacoustic spectrometer for measuring light absorption by aerosols: Instrument description. Atmos Environ 33:2845-2852.

Arnott, W. P., K. Hamasha, H. Moosmüller, P.J. Sheridan and J.A. Ogren (2005). "Towards Aerosol Light Absorption Measurements with a 7-Wavelength Aethalometer: Evaluation with a Photoacoustic Instrument and 3-Wavelength Nephelometer." Aerosol Sci. and Technol. 39:17-29.

Fujita EM., Campbell DE, Zielinska B, Sagebiel JC, Bowen JL, Goliff W, Stockwell WR, and Lawson DR. 2003. Diurnal and weekday variations in source contributions of ozone precursors in California's south coast air basin. J Air Waste Manage Assoc 53:844-863.

Fujita, EM., Zielinska B, Campbell DE, Arnott WP. 2007. Evaluations of source apportionment methods for determining contributions of gasoline and diesel exhaust to ambient carbonaceous aerosols. J Air Waste Manage Assoc, 57:721-740.

Fujita, E.M., D.E. Campbell, B. Zielinska, W.P. Arnott, J.C. Chow (2008). Concentrations of Air Toxics in Motor Vehicle Dominated Microenvironments. Final report submitted to the Health Effects Institute, HEI contract 4704-RFA03-1/02-16, Boston, MA, January 13, 2008.

Fujita, E.M., D.E. Campbell, B. Mason, B. Zielinska (2009). Harbor Community Monitoring Study (HCMS) Saturation Monitoring. Final report submitted to the California Air Reesources Board, Sacramento, CA, May 15, 2009.

Fujita, E.M. and D.E. Campbell (2010). West Oakland Monitoring Study. Final report prepared for the Bay Area Air Quality Management District, San Francisco, CA, October 7, 2010.

Fine, P. (2011). Personal communication on September 22, 2011.

Westerdahl D, Fruin S, Sax T, Fine P, Sioutas C. 2005. Mobile platform measurements of ultrafine particles and associated pollutant concentrations on freeways and residential streets in Los Angeles. Atmos Envir 39:3597-3610.

Westerdahl D, Fruin S, Fine P, Sioutas C. 2007. The Los Angeles International Airport as a source of ultrafine particle and other pollutants to nearby communities. Atmos Envir 42:3143-3155.

Zhu, Y.F, Hinds, W.C, Kim, S, Shen, S, Sioutas, C. (2002) Study of ultrafine particles near a major highway with heavy-duty diesel traffic; Atmospheric Environment, 36, 4323-4335.

ATTACHMENT

Measurement Methods

(This page is intentionally blank)

A.1 Gaseous Pollutants

2B Technologies Model 400 NO Monitor. This monitor is designed for measurement of NO in the range of 2 to 2000 ppbv. In combination with the Model 401 NO2 converter, NOx and NO2 (by difference) are also measured. The detection method uses UV absorption technology to determine the depletion of ozone by NO and calculates the NO concentration by assuming a 1:1 stoichiometric ratio for the NO/O_3 reaction cycle. It is compact (3.5 x 8.5 x 11 inches), light weight (6.4 lbs) and runs on 12 V dc or 120 V ac (11 watts in low power mode. No calibration gas is required and the instrument is calibrated annually.

Carbon Monoxide and Carbon Dioxide. CO will be monitored continuously in the van using an NDIR CO monitor such as the Teledyne/Monitor Labs 9830 or a TEI model 48 gas-filter correlation CO monitor. These rack-mounted EPA reference method instruments have a resolution of 0.1 ppm. CO will be monitored on the cart by a TSI Model 8854 CO_2/CO monitor. This portable, passive sampling instrument has a resolution of 1 ppm and accuracy of 3%+3 ppm from 0 to 500 ppm for CO.

Volatile Organic Compounds. A RAE Systems Model PGM-7240 (ppbRAE) portable PID monitor could be used to continuously monitor ambient VOC levels. The monitor is equipped with a 10.6 eV photoionization (PID) detector and responds to certain organic and inorganic gases that have an ionization potential of less than 10.6 eV, which includes aromatic hydrocarbons, olefins, and higher molecular weight alkanes. It does not respond to light hydrocarbons such as methane, ethane, and propane or to acetylene, formaldehyde or methanol. The monitor has < 5-second response and lower detection limit of ~20 ppb. Because the total response of the PID depends upon the specific mix of VOC's, the response must be calibrated to the expected mix of VOC. Isobutylene is the normal calibration gas but the PID response can be adjusted to one of several specific VOC species or a standard mixtures of VOC such as gasoline. DRI has developed empirical relationships between the PID response to urban air and the sum of VOC species from the canister VOC data. Instruments utilizing flame ionization detection (FID) are sensitive to a broader range of hydrocarbons, but do not provide the sensitivity and rapid response time required for ambient air monitoring.

A.2 Continuous PM Mass and Black Carbon

PM2.5 Mass. The TSI DustTrak is a portable, battery-operated, laser-photometer that measures 90° light scattering (different from the total light scattering measured by an integrating nephelometer) and reports it as PM mass concentration. Because it is sensitive, requires low flow rates, offers good time resolutions, and is portable and relatively inexpensive, the TSI DustTrak nephelometer may be well suited for continuous onboard PM measurements in this study. It can be fitted with inlets of varying size-cuts. DRI will equip the monitor for this project with a $PM_{2.5}$ inlet. The reported PM mass concentration is factory-calibrated using the respirable fraction of an Arizona Road Dust standard (ISO 12103-1, A1), which consists of primarily silica particles (70%) that are provided with some particle size specifications. The mass scattering efficiency depends on particle shapes, size distribution, and composition (index of refraction). By volume, the standard consists of 1–3% particles with diameter less than 1000 nm (1 μm), 36–44% with diameter less than 4000 nm (4 μm), 83–88% with diameter less than 7000 nm (7 μm), and 97–100% with diameter less than 10,000 nm (10 μm). This standard contains a larger quantity of

coarse 2500 nm (>2.5 μm) particles than are usually found in ambient aerosol. $PM_{2.5}$ has a higher mass scattering efficiency, so the DustTrak overestimates $PM_{2.5}$ for smaller, chain aggregate soot particles. The laser diode used by the DustTrak has a wavelength of 780 nm, which limits the smallest detectable particle to about 100 nm. Combustion aerosols typically have a mass median diameter between 100 nm and 300 nm. Although direct optical light scattering of particles in this size range is limited, it has been shown to correlate reasonably well with gravimetric mass from vehicle exhaust samples. In the recent Gasoline/Diesel PM Split Study, the DustTrak was found to exceed gravimetric mass concentrations of the motor vehicle-dominated ambient samples by a factor of 2.24 with an R^2 of 0.75 (Fujita et al., 2005). To determine the appropriate relationship between light scattering measurements and actual $PM_{2.5}$ mass concentrations DRI proposes collecting simultaneous filter samples for gravimetric analysis in each microenvironment. Samples would be collected on Teflon membrane filters using an Airmetrics mini-vol sampler. This sampler can operate on battery at flow rates of about 5 lpm for up to 24 hours and has a size-selective inlet or impactor.

Black Carbon (soot). The photoacoustic instrument has been developed at DRI and has been described in several publications (Arnott, Moosmüller et al. 1999; Arnott, Moosmüller et al. 2000). Briefly, light from a 1047 nm laser is power-modulated at the operating frequency of an acoustical resonator. Sample air is continuously drawn through the resonator at a flow rate of 1 to 3 lpm. Light absorbing aerosol (black carbon) will absorb some of the laser power, slightly heating the aerosol (typically much less than 1 C). The heat transfers very rapidly from the aerosol to the surrounding air, and the local pressure increases, contributing to the standing acoustic wave in the resonator. The acoustic wave is measured with a microphone as a measure of the light absorption. For the operating conditions of the resonator, and the laser wavelength used, the light absorption measurement is linearly proportional to the mass concentration of the black carbon aerosol in the sample air. The constant of proportionality has been inferred from correlations of black carbon measurements with elemental carbon as determined by the TOR method, and an efficiency factor of 5 square meters per gram is used to go from aerosol light absorption to estimated black carbon mass concentration. No filters are needed for the photoacoustic measurement, and the flow rate is not used in the calculation of aerosol mass concentration. The flow rate must only be sufficient to adequately sample the air with minimal particle loss in the instrument and sample lines. The resolution of the instrument for a 3 second averaging time is usually 2.5 inverse Mm for light absorption, corresponding to 0.5 microgram per cubic meter for black carbon mass concentration. The resolution scales as the square root of sampling time, so for example, a resolution of 0.25 micrograms per cubic meter can be obtained for a 9 second averaging time. The photoacoustic measurement does not receive interference from exhaust gases, in DRI's experience so far, and it is a zero-based measurement when no light absorbing aerosols are present.

Ultrafine Particle Number Concentrations. For detecting particles smaller than 0.3 μm in aerodynamic diameter, a condensation particle counter (CPC) would be required. These instruments pass aerosol through a humidification chamber, typically containing an alcohol or ethylene glycol bath, which causes the particles to grow in size due to condensation so that they can be counted by an OPC or other optical method. Portable units that could be operated in a vehicle or on a cart are available from TSI and Kanomax. Although these instruments can detect ultra-fine particles as small as 10 nm in diameter, they cannot distinguish between particle sizes. A CPC combined with a Scanning Mobility Particle Sizer (SMPS) will also give size distribution information, but such instruments are not suited for mobile sampling applications.

A.3 Meteorological Parameters

A Davis Instruments meteorology package will be deployed to measure wind speed, wind direction, relative humidity, and temperature during sampling at fixed locations unless data is available from existing meteorological equipment. Time-integrated data will be recorded at 10-minute intervals by a dedicated datalogger.

(This page is intentionally blank)

Appendix 3-2

CONTINUOUS MONITORING EQUIPMENT AND RECOVERY RATES

DAILY CALIBRATION RESPONSE OF GASEOUS POLLUTANTS

(This page is intentionally blank)

Contents

List of Tables

(This page is intentionally blank)

Table 3A-1. Continuous Monitoring Equipment at Core Sites

Site	Parameter	Equipment Type	Make	Model	Serial #	Operating Range	Detection Limit
CE	Black Carbon Aethalometer	Monitor	Magee Scientific	AE 21	639	0-1000 µg/m^3	0-0.1 µg/m^3
CE	Carbon Monoxide	Monitor	Thermo Scientific	48i	-363	0-50 ppm	0.1 ppm
CE	NOx	Monitor	Thermo Scientific	42i	-1039	0-500 ppb	1.0 ppb
CE	$PM_{2.5}$, BAM 1020	Monitor	Met One	1020	F5131	0-1000 µg/m^3	1.0 µg/m^3
CE	SO_2	Monitor	Thermo Scientific	43iTLE	-1043	0-500 ppb Winter Season 0-50 ppb Summer Season	0.1 ppb
CE	Wind Speed w/ Cable	Sensor	Met One	010C	M10593	0-100 mph	0.5 mph (Starting Threshold)
CE	Wind Direction w/ Cable	Sensor	Met One	020C	M10654	0-540 deg	0.5 mph (Starting Threshold)
CE	Ambient Temp (2 heights)	Sensor	Met One	060A	M8799, M8807	-50.0 – 50.0 C	0.1 C
CE	pDR 1200 AN for cont. $PM_{2.5}$	Monitor	Thermo Scientific	1200 AN	7566	0-4000 µg/m^3	1.0 µg/m^3
CS	Black Carbon Aethalometer	Monitor	Magee Scientific	AE 21	637	0-1000 µg/m3	0-0.1 µg/m^3
CS	Carbon Monoxide	Monitor	Thermo Scientific	48C	-362	0-50 ppm	0.1 ppm
CS	NOx	Monitor	Thermo Scientific	42C	-350	0-500 ppb	1.0 ppb
CS	$PM_{2.5}$, BAM 1020	Monitor	Met One	1020	P5134	0-1000 µg/m^3	1.0 µg/m^3
CS	SO_2	Monitor	Thermo Scientific	43iTLE	1136151042	0-500 ppb Winter Season 0-50 ppb Summer Season	0.1 ppb
CS	Wind Speed w/ Cable	Sensor	Met One	010C	F1077	0-100 mph	0.5 mph (Starting Threshold)
CS	Wind Direction w/ Cable	Sensor	Met One	020C	A1178	0-540 deg	0.5 mph (Starting Threshold)
CS	Ambient Temp (2 heights)	Sensor	Met One	060A	D8475, D7113	-50.0 – 50.0 C	0.1 C
CS	pDR 1200 AN for cont. $PM_{2.5}$	Monitor	Thermo Scientific	1200 AN	7565	0-4000 µg/m_3	1.0 µg/m^3
CN	Black Carbon Aethalometer	Monitor	Magee Scientific	AE 21	636	0-1000 µg/m^3	0-0.1 µg/m^3
CN	Carbon Monoxide	Monitor	Thermo Scientific	48C	-349	0-50 ppm	0.1 ppm
CN	NO_x	Monitor	Thermo Scientific	42C	325981773	0-500 ppb	1.0 ppb
CN	$PM_{2.5}$, BAM 1020	Monitor	Met One	1020	F5132	0-1000 µg/m^3	1.0 µg/m^3
CN	SO_2	Monitor	Thermo Scientific	43iTLE	-1104	0-500 ppb Winter Season	0.1 ppb

						0-50 ppb Summer Season	
CN	pDR 1200 AN for cont. $PM_{2.5}$	Monitor	Thermo Scientific	1200 AN	6626	0-4000 µg/m^3	1.0 µg/m^3
AQ	Black Carbon Aethalometer	Monitor	Magee Scientific	AE 21	683	0-1000 µg/m^3	0-0.1 µg/m^3
AQ	$PM_{2.5}$, BAM 1020	Monitor	Met One	1020	F5133	0-1000 µg/m^3	1.0 µg/m^3
AQ	pDR 1200 AN for cont. $PM_{2.5}$	Monitor	Thermo Scientific	1200 AN	6627	0-4000 µg/m^3	1.0 µg/m^3

Table 3A-2. Recovery Rates of Continuous Parameters

Parameter	CE site Winter Season	CS site Winter Season	CN site Winter Season	AQ site Winter Season	CE site Summer Season	CS site Summer Season	CN site Summer Season	AQ site Summer Season
Carbon Monoxide	94.0%	92.8%	93.4%	NA	95.5%	95.5%	95.0%	NA
Nitrogen Dioxide	94.0%	92.9%	87.1%	NA	95.5%	92.4%	82.1%	NA
Sulfur Dioxide	94.0%	93.1%	93.4%	NA	95.5%	94.8%	94.8%	NA
Wind Speed	98.4%	97.3%	NA	NA	100.0%	100.0%	NA	NA
Wind Direction	97.9%	97.0%	NA	NA	100.0%	100.0%	NA	NA
Sigma Theta of WD	85.1%	80.6%	NA	NA	92.6%	100.0%	NA	NA
Outside Temperature (8m)	98.4%	97.3%	NA	NA	100.0%	100.0%	NA	NA
Outside Temperature (2m)	98.4%	97.3%	NA	NA	100.0%	100.0%	NA	NA
Relative Humidity	84.0%	NA	NA	NA	92.5%	NA	NA	NA
Solar Radiation	98.4%	NA	NA	NA	100.0%	NA	NA	NA
Light Scattering - $PM_{2.5}$	98.3%	97.0%	49.5%	93.5%	96.7%	100.0%	97.9%	93.0%
BAM 1020 - $PM_{2.5}$	95.9%	97.0%	99.4%	98.3%	99.2%	99.3%	99.2%	99.4%
Black Carbon	99.4%	98.7%	91.2%	99.4%	99.6%	99.6%	98.2%	99.9%

Table 3A-3. Winter Monitoring Season - Community East Daily Calibration Response of Gaseous Pollutants

Parameter				CO		NO		NO_x		NO_2		SO_2	
Date	Time	Calibration Type	Adjusted	Zero % Full Scale	Span % Error	Zero % Full Scale	Span % Error	Zero % Full Scale	Span % Error	Zero % Full Scale	Span % Error	Zero % Full Scale	Span % Error
2/1/2012	2-3:00	AC	N	0.06%	-0.07%	0.21%	1.55%	0.18%	1.75%	0.25%	-0.52%	0.00%	-1.29%
2/2/2012	2-3:00	AC	N	0.15%	-0.24%	0.17%	0.89%	0.14%	1.11%	0.26%	-0.79%	0.02%	-1.55%
2/3/2012	2-3:00	AC	N	0.28%	0.12%	0.24%	0.17%	0.25%	0.35%	0.28%	-1.02%	0.05%	-0.93%
2/4/2012	2-3:00	AC	N	0.31%	0.01%	0.18%	-1.66%	0.19%	-1.64%	0.28%	-1.69%	0.01%	-0.59%
2/5/2012	2-3:00	AC	N	0.36%	-0.02%	0.30%	-2.80%	0.33%	-2.65%	0.31%	-2.14%	0.02%	-0.13%
2/6/2012	2-3:00	AC	N	0.32%	-0.10%	0.21%	-3.71%	0.22%	-3.60%	0.29%	-2.61%	0.02%	-0.29%
2/7/2012	2-3:00	AC	N	0.35%	-0.14%	0.18%	-6.07%	0.23%	-6.00%	0.33%	-2.89%	0.02%	-2.96%
2/8/2012	2-3:00	AC	N	INV	INV	INV	INV	INV	INV	INV	INV	INV	INV
2/8/2012	14:08-14:45	Man 0/S	N	0.40%	3.17%	0.20%	0.47%	0.20%	0.95%	NA	NA	0.03%	-1.24%
2/9/2012	2-3:00	AC	N	0.24%	0.80%	0.26%	0.00%	0.27%	0.18%	0.28%	0.15%	-0.01%	0.86%
2/10/2012	2-3:00	AC	N	0.46%	0.46%	0.21%	-0.17%	0.20%	0.08%	0.28%	0.26%	0.04%	1.00%
2/11/2012	2-3:00	AC	N	0.57%	1.56%	0.18%	0.41%	0.12%	0.59%	0.23%	0.03%	0.02%	2.05%
2/12/2012	2-3:00	AC	N	0.53%	1.24%	0.17%	-1.29%	0.14%	-1.14%	0.25%	-1.52%	0.05%	1.98%
2/13/2012	2-3:00	AC	N	0.56%	1.11%	0.18%	-2.47%	0.14%	-2.35%	0.24%	-2.54%	0.03%	1.93%
2/14/2012	2-3:00	AC	N	0.70%	1.53%	0.16%	0.03%	0.08%	0.19%	0.19%	0.09%	0.03%	2.29%
2/15/2012	2-3:00	AC	N	0.77%	1.56%	0.24%	-0.11%	0.22%	0.05%	0.26%	0.35%	0.02%	2.56%
2/16/2012	2-3:00	AC	N	0.95%	2.16%	0.16%	0.53%	0.10%	0.66%	0.23%	0.61%	0.03%	3.19%
2/17/2012	2-3:00	AC	N	0.78%	1.26%	0.16%	-1.88%	0.10%	-1.84%	0.20%	-0.87%	0.01%	2.34%
2/18/2012	2-3:00	AC	N	0.88%	1.50%	0.23%	-0.58%	0.22%	-0.38%	0.27%	0.22%	0.03%	2.63%
2/19/2012	2-3:00	AC	N	0.89%	1.46%	0.18%	-1.04%	0.15%	-0.72%	0.25%	-0.20%	0.02%	2.57%
2/20/2012	2-3:00	AC	N	0.93%	1.51%	0.21%	-1.36%	0.15%	-1.13%	0.24%	-0.41%	0.02%	2.45%
2/21/2012	2-3:00	AC	N	1.00%	1.76%	0.20%	-1.38%	0.16%	-1.23%	0.24%	-0.18%	0.02%	2.89%
2/21/2012	13:20-14:35	MP	N	1.20%	2.56%	0.14%	-0.40%	0.12%	0.09%	0.18%	-5.10%	0.02%	2.64%
2/22/2012	2-3:00	AC	N	1.32%	1.69%	0.22%	-1.42%	0.21%	-1.37%	0.27%	3.01%	-0.03%	3.04%
2/23/2012	2-3:00	AC	N	1.32%	1.60%	0.21%	-1.83%	0.22%	-1.61%	0.29%	2.70%	0.02%	2.16%

Parameter				CO		NO		NO_x		NO_2		SO_2	
Date	Time	Calibration Type	Adjusted	Zero % Full Scale	Span % Error	Zero % Full Scale	Span % Error	Zero % Full Scale	Span % Error	Zero % Full Scale	Span % Error	Zero % Full Scale	Span % Error
2/24/2012	2-3:00	AC	N	1.41%	1.85%	0.17%	-1.90%	0.14%	-1.54%	0.26%	2.72%	0.00%	2.56%
2/25/2012	2-3:00	AC	N	1.47%	INV	0.17%	INV	0.14%	INV	0.26%	INV	-0.01%	INV
2/26/2012	2-3:00	AC	N	1.50%	INV	0.18%	INV	0.17%	INV	0.28%	INV	0.03%	INV
2/27/2012	2-3:00	AC	N	1.51%	INV	0.18%	INV	0.16%	INV	0.27%	INV	0.01%	INV
2/28/2012	2-3:00	AC	N	1.77%	INV	0.17%	INV	0.09%	INV	0.19%	INV	0.00%	INV
2/28/2012	11:20-12:00	Man 0/S	N	1.78%	3.04%	0.20%	-1.18%	0.20%	-1.18%	0.20%	NA	-0.03%	2.94%
2/29/2012	2-3:00	AC	N	1.77%	2.55%	0.19%	-2.22%	0.17%	-2.05%	0.26%	2.93%	-0.01%	3.49%
3/1/2012	2-3:00	AC	N	1.67%	2.16%	0.18%	-2.99%	0.12%	-2.60%	0.22%	2.35%	0.00%	2.81%
3/2/2012	2-3:00	AC	N	1.73%	2.23%	0.16%	-2.92%	0.11%	-2.67%	0.24%	2.41%	0.00%	2.88%
3/3/2012	2-3:00	AC	N	1.92%	1.34%	0.33%	-4.19%	0.52%	-4.08%	0.48%	2.02%	0.38%	2.04%
3/4/2012	2-3:00	AC	N	1.86%	1.17%	0.28%	-4.59%	0.23%	-4.21%	0.32%	1.85%	0.05%	1.74%
3/5/2012	2-3:00	AC	N	1.94%	1.34%	0.27%	-4.29%	0.33%	-4.09%	0.32%	1.74%	0.01%	2.15%
3/6/2012	2-3:00	AC	N	1.80%	1.79%	0.16%	-4.28%	0.17%	-4.02%	0.29%	1.83%	0.00%	1.92%
3/7/2012	2-3:00	AC	N	2.08%	1.72%	0.17%	-4.04%	0.09%	-3.82%	0.18%	2.38%	-0.04%	2.32%
3/8/2012	2-3:00	AC	N	2.16%	2.05%	0.20%	-4.40%	0.16%	-4.27%	0.25%	2.24%	-0.01%	2.27%
3/9/2012	2-3:00	AC	N	2.14%	1.67%	0.23%	-5.18%	0.25%	-4.95%	0.29%	1.65%	-0.03%	1.85%
3/10/2012	2-3:00	AC	N	2.10%	1.91%	0.22%	-4.87%	0.30%	-4.91%	0.35%	1.49%	0.00%	1.89%
3/11/2012	2-3:00	AC	N	2.26%	1.98%	0.17%	-5.07%	0.19%	-4.79%	0.30%	1.18%	0.00%	2.13%
3/12/2012	2-3:00	AC	N	2.32%	2.03%	0.16%	-5.20%	0.14%	-5.15%	0.24%	1.54%	0.00%	2.01%
3/13/2012	2-3:00	AC	N	2.36%	2.20%	0.18%	-5.32%	0.13%	-5.00%	0.23%	1.50%	0.00%	2.01%
3/14/2012	2-3:00	AC	N	2.82%	2.25%	0.17%	-5.65%	0.14%	-5.38%	0.25%	-1.65%	0.00%	2.59%
3/15/2012	2-3:00	AC	N	2.94%	2.34%	0.16%	-5.70%	0.12%	-5.38%	0.22%	-0.54%	0.00%	2.69%
3/16/2012	2-3:00	AC	N	3.00%	2.75%	0.16%	-5.51%	0.12%	-5.13%	0.23%	-1.68%	0.00%	2.09%
3/16/2012	11:45-13:00	MP	N	3.20%	2.75%	0.16%	-4.64%	0.10%	-4.57%	0.00%	-3.59%	0.00%	2.40%

Footnote: AC = automated calibration, Man 0/S = manual calibration; Z = zero, SP = span, MP =multi-point calibration, INV = invalid; NA = not available; Y = yes, N = no

Table 3A-4. Winter Monitoring Season - Community South Daily Calibration Response of Gaseous Pollutants

Parameter:				CO		NO		NO_x		NO_2		SO_2	
Date	Time	Calibration Type	Adjusted	Zero % Full Scale	Span % Error	Zero % Full Scale	Span % Error	Zero % Full Scale	Span % Error	Zero % Full Scale	Span % Error	Zero % Full Scale	Span % Error
1/31/12	2-3:00	AC	N	0.11%	0.61%	-0.10%	0.83%	0.06%	0.80%	-0.48%	-0.58%	0.04%	0.87%
2/1/12	2-3:00	AC	N	-0.09%	-1.56%	-0.07%	-1.76%	0.09%	-1.57%	-0.26%	-0.54%	0.03%	-1.80%
2/2/12	2-3:00	AC	N	-0.46%	-1.67%	-0.12%	-2.98%	0.11%	-2.96%	-0.50%	-1.45%	0.03%	-2.15%
2/3/12	2-3:00	AC	N	0.14%	2.82%	-0.07%	0.08%	0.02%	-0.15%	-0.17%	-0.90%	0.01%	1.05%
2/4/12	2-3:00	AC	N	0.14%	0.82%	-0.17%	-0.98%	0.04%	-1.54%	-0.29%	-0.22%	0.01%	-0.78%
2/5/12	2-3:00	AC	N	0.10%	2.31%	-0.06%	-1.69%	0.11%	-2.27%	-0.22%	-0.73%	0.02%	-0.85%
2/6/12	2-3:00	AC	N	-0.01%	2.33%	-0.18%	-3.01%	0.02%	-3.79%	-0.55%	-1.72%	0.01%	-1.27%
2/7/12	2-3:00	AC	N	0.13%	1.77%	-0.19%	-3.37%	0.20%	-4.05%	-0.48%	-1.87%	0.01%	-1.81%
2/8/12	2-3:00	AC	N	INV	INV	INV	INV	INV	INV	INV	INV	INV	INV
2/8/12	16:37-17:08	Z/SP	N	0.80%	-0.24%	0.10%	-7.67%	0.16%	-7.97%	NA	NA	0.02%	-2.20%
2/9/12	2-3:00	AC	N	0.74%	2.00%	-0.17%	-4.99%	0.10%	-5.73%	-0.49%	-3.12%	0.02%	-1.42%
2/10/12	2-3:00	AC	N	0.44%	0.55%	-0.18%	-5.71%	0.05%	-6.00%	-0.94%	-2.58%	0.01%	-2.20%
2/11/12	2-3:00	AC	N	0.80%	2.52%	-0.23%	-5.44%	0.00%	-6.20%	-0.75%	-3.63%	0.01%	-1.10%
2/12/12	2-3:00	AC	N	1.10%	3.72%	-0.21%	-5.11%	0.03%	-5.90%	-0.68%	-3.43%	0.02%	-0.90%
2/13/12	2-3:00	AC	N	1.16%	4.22%	-0.20%	-4.88%	0.03%	-5.67%	-0.66%	-2.94%	0.01%	-0.93%
2/14/12	2-3:00	AC	N	1.17%	3.59%	-0.21%	-5.72%	0.01%	-6.45%	-0.69%	-3.60%	0.01%	-1.92%
2/15/12	2-3:00	AC	N	1.15%	4.26%	-0.21%	-4.66%	0.13%	-5.72%	-0.72%	-2.24%	0.00%	-1.91%
2/16/12	2-3:00	AC	N	1.30%	5.10%	-0.18%	-5.02%	0.05%	-5.84%	-0.70%	-2.65%	0.00%	-2.20%
2/17/12	2-3:00	AC	N	1.29%	2.45%	-0.21%	-5.98%	0.00%	-6.11%	-0.89%	-2.40%	0.00%	-3.10%
2/18/12	2-3:00	AC	N	0.78%	5.19%	-0.19%	-3.98%	0.06%	-4.79%	-0.62%	-3.94%	0.01%	-2.51%
2/19/12	2-3:00	AC	N	0.91%	4.97%	-0.21%	-5.48%	0.04%	-6.23%	-0.67%	-5.10%	-0.01%	-3.19%
2/20/12	2-3:00	AC	N	1.06%	5.91%	-0.19%	-5.80%	0.05%	-6.67%	-0.72%	-5.53%	-0.01%	-2.15%
2/21/12	2-3:00	AC	N	1.45%	6.44%	-0.13%	-5.67%	0.05%	-6.29%	-0.43%	-5.75%	-0.01%	-1.37%
2/21/12	16:20-18:00	MP	Y - CO	1.40%	9.18%	-0.20%	-7.55%	0.20%	-7.31%	-0.20%	-9.87%	-0.05%	-2.80%

Parameter:				CO		NO		NO_x		NO_2		SO_2	
Date	Time	Calibration Type	Adjusted	Zero % Full Scale	Span % Error	Zero % Full Scale	Span % Error	Zero % Full Scale	Span % Error	Zero % Full Scale	Span % Error	Zero % Full Scale	Span % Error
2/21/12	16:20-18:00	MP	Y - CO	1.20%	-6.04%	NA	NA	NA	NA	NA	NA	NA	NA
2/22/12	2-3:00	AC	N	1.31%	-5.02%	-0.19%	-6.57%	0.05%	-7.44%	-0.77%	-6.30%	-0.03%	-2.02%
2/22/12	14:00-14:40	Z/SP	N	1.32%	-0.87%	-0.18%	-7.10%	0.05%	-7.13%	NA	NA	-0.02%	-0.46%
2/23/12	2-3:00	AC	N	0.24%	-1.45%	-0.19%	-7.77%	0.05%	-8.53%	-0.63%	-7.80%	-0.02%	-1.96%
2/24/12	2-3:00	AC	N	-0.60%	-1.38%	-0.19%	-9.75%	0.11%	-10.11%	-0.67%	-8.92%	-0.02%	-2.37%
2/24/12	17:45-18:15	Z/SP	Y - NO,NO_x	NA	NA	-0.20%	-8.73%	0.60%	-8.73%	NA	NA	NA	NA
2/24/12	17:45-18:15	Z/SP	Y - NO,NO_x	NA	NA	0.00%	-0.24%	0.00%	-0.71%	NA	NA	NA	NA
2/25/12	2-3:00	AC	N	-0.54%	-0.12%	-0.19%	-0.53%	0.05%	-2.19%	-1.46%	-0.26%	-0.03%	-2.03%
2/26/12	2-3:00	AC	N	-0.46%	0.44%	-0.37%	0.20%	-0.05%	-1.71%	-1.41%	0.09%	-0.01%	-2.02%
2/27/12	2-3:00	AC	N	-0.24%	0.00%	-0.29%	-1.64%	0.05%	-3.76%	-1.63%	-0.97%	-0.01%	-2.68%
2/28/12	2-3:00	AC	N	0.64%	1.04%	-0.13%	-1.02%	-0.40%	-2.17%	-1.26%	-2.00%	-0.02%	-1.57%
2/29/12	2-3:00	AC	N	-0.18%	1.55%	-0.21%	0.39%	0.03%	-1.19%	-1.30%	0.26%	-0.01%	-1.94%
3/1/12	2-3:00	AC	N	-0.07%	1.68%	-0.22%	2.73%	0.72%	0.77%	-0.56%	1.66%	-0.02%	-2.25%
3/2/12	2-3:00	AC	N	-0.26%	1.33%	-0.27%	2.23%	0.05%	0.48%	-1.43%	2.87%	-0.02%	-2.67%
3/3/12	2-3:00	AC	N	0.12%	0.10%	INV	INV	INV	INV	INV	INV	N/A	N/A
3/4/12	2-3:00	AC	N	-0.06%	-0.09%	INV	INV	INV	INV	INV	INV	0.00%	-3.94%
3/5/12	2-3:00	AC	N	0.08%	-1.78%	-0.12%	-3.93%	0.10%	-4.91%	-1.54%	-2.29%	-0.02%	-4.66%
3/6/12	2-3:00	AC	N	0.05%	-0.50%	-0.21%	-0.29%	0.04%	-1.73%	-1.33%	0.24%	-0.03%	-4.22%
3/7/12	2-3:00	AC	N	1.18%	1.32%	-0.24%	2.69%	-0.05%	1.25%	-1.34%	7.53%	-0.03%	-3.98%
3/8/12	2-3:00	AC	N	1.19%	1.71%	-0.17%	4.84%	0.03%	3.24%	-1.36%	10.16%	-0.03%	-3.53%
3/9/12	2-3:00	AC	N	1.18%	1.10%	-0.20%	6.72%	0.16%	5.11%	-1.25%	12.04%	-0.03%	-4.53%
3/9/12	11:13-12:16	Z/SP	Y - CO, SO_2	1.60%	-4.56%	-0.20%	-0.23%	0.00%	-0.94%	NA	NA	-0.03%	-5.74%
3/9/12	11:13-12:16	Z/SP	Y - CO, SO_2	1.00%	-3.84%	0.00%	-0.47%	0.20%	-1.17%	NA	NA	0.06%	-0.55%

Parameter:				CO		NO		NO_x		NO_2		SO_2	
Date	Time	Calibration Type	Adjusted	Zero % Full Scale	Span % Error	Zero % Full Scale	Span % Error	Zero % Full Scale	Span % Error	Zero % Full Scale	Span % Error	Zero % Full Scale	Span % Error
3/10/12	2-3:00	AC	N	0.76%	-1.63%	-0.18%	3.57%	0.04%	2.57%	-0.31%	7.83%	0.07%	0.13%
3/11/12	2-3:00	AC	N	0.73%	-0.74%	-0.21%	4.56%	0.05%	3.80%	-0.36%	8.72%	0.03%	-0.33%
3/12/12	2-3:00	AC	N	0.77%	-0.71%	-0.24%	3.54%	0.05%	2.87%	-0.35%	7.50%	0.02%	0.19%
3/13/12	2-3:00	AC	N	0.83%	-0.58%	-0.21%	1.34%	0.05%	0.34%	-0.36%	5.07%	0.03%	0.35%
3/14/12	2-3:00	AC	N	0.96%	-0.60%	-0.19%	-0.95%	0.04%	-1.90%	-0.36%	2.89%	0.03%	-0.01%
3/15/12	2-3:00	AC	N	0.93%	1.04%	-0.16%	1.60%	0.03%	0.36%	-0.35%	5.18%	0.02%	0.36%
3/16/12	2-3:00	AC	N	1.02%	-0.22%	-0.18%	1.64%	0.05%	0.43%	-0.36%	4.96%	0.02%	-0.03%
3/16/12	13:45-14:50	MP	N	1.40%	-0.96%	-0.20%	3.75%	-0.20%	4.22%	-0.20%	5.45%	0.02%	-0.26%

Footnote: AC = automated calibration, Man 0/S = manual calibration; Z = zero, SP = span, MP =multi-point calibration, INV = invalid; NA = not available; Y = yes, N = no

Table 3A-5. Winter Monitoring Season - Community North Daily Calibration Response of Gaseous Pollutants

Parameter:				CO		NO		NO_x		NO_2		SO_2	
Date	Time	Calibration Type	Adjusted	Zero % Full Scale	Span % Error	Zero % Full Scale	Span % Error	Zero % Full Scale	Span % Error	Zero % Full Scale	Span % Error	Zero % Full Scale	Span % Error
2/2/12	2-3:00	AC	N	-0.27%	-0.33%	0.47%	-3.66%	0.63%	-3.59%	-0.16%	2.31%	0.32%	INV
2/3/12	2-3:00	AC	N	-0.27%	-0.79%	0.42%	6.29%	0.63%	6.01%	0.01%	4.53%	0.29%	-10.70%
2/4/12	2-3:00	AC	N	-0.52%	-0.91%	0.49%	14.14%	0.55%	14.19%	0.00%	7.77%	0.27%	-10.42%
2/5/12	2-3:00	AC	N	-0.64%	-1.14%	0.85%	16.84%	0.92%	17.03%	0.17%	10.41%	0.31%	-8.56%
2/6/12	2-3:00	AC	N	-0.81%	-1.68%	0.72%	17.68%	0.59%	17.67%	0.03%	12.96%	0.35%	-7.65%
2/6/12	11:32-12:05	Z/Sp	Y - NO_x	NA	NA	0.40%	15.13%	0.40%	17.02%	NA	NA	NA	NA
2/6/12	11:32-12:05	Z/Sp	Y - NO_x	NA	NA	0.40%	0.00%	0.40%	-0.71%	NA	NA	NA	NA
2/7/12	2-3:00	AC	N	-0.89%	-2.11%	0.61%	0.79%	0.58%	-0.88%	0.17%	-4.18%	0.36%	-3.90%
2/8/12	2-3:00	AC	N	-0.97%	-2.40%	0.58%	0.08%	0.49%	-1.78%	0.14%	-4.92%	0.40%	-2.48%
2/9/12	2-3:00	AC	N	-0.99%	-2.32%	0.16%	-0.47%	0.59%	-2.24%	-0.15%	-3.54%	0.40%	-0.16%
2/10/12	2-3:00	AC	N	-1.01%	-2.27%	-0.10%	-2.19%	0.39%	-3.77%	-0.21%	-3.98%	0.39%	2.20%
2/11/12	2-3:00	AC	N	-1.06%	-2.36%	0.92%	-5.46%	0.52%	-7.24%	0.30%	-6.10%	0.38%	2.12%
2/12/12	2-3:00	AC	N	-1.06%	-2.24%	0.91%	-4.48%	0.50%	-6.05%	0.26%	-3.71%	0.37%	4.51%
2/13/12	2-3:00	AC	N	-1.04%	-2.38%	0.88%	-6.15%	0.46%	-7.52%	0.21%	-4.70%	0.36%	6.13%
2/14/12	2-3:00	AC	N	-0.98%	-1.79%	-0.79%	-9.16%	0.26%	-10.78%	-0.69%	-7.86%	0.34%	7.73%
2/15/12	2-3:00	AC	N	-0.93%	-1.57%	-0.87%	-9.00%	0.36%	-10.83%	-0.90%	-7.63%	0.31%	9.56%
2/15/12	12:43-13:20	Z/Sp	Y - NO_x, CO, SO_2	-1.00%	2.17%	1.00%	-9.69%	1.60%	-11.58%	NA	NA	0.34%	8.51%
2/15/12	12:43-13:20	Z/Sp	Y - NO_x, CO, SO_2	0.20%	0.72%	0.80%	0.00%	1.40%	-0.95%	NA	NA	0.00%	1.20%
2/16/12	2-3:00	AC	N	0.21%	0.98%	1.11%	-1.05%	1.44%	-2.08%	-0.13%	1.59%	0.03%	2.88%
2/17/12	2-3:00	AC	N	0.06%	0.29%	0.60%	-0.05%	1.06%	-1.09%	0.02%	2.03%	0.04%	2.94%
2/18/12	2-3:00	AC	N	0.15%	0.61%	1.24%	-3.52%	1.42%	-4.42%	0.03%	-0.81%	0.02%	4.09%
2/19/12	2-3:00	AC	N	0.10%	0.12%	0.60%	-3.47%	0.95%	-4.33%	-0.14%	-0.71%	0.03%	4.69%
2/20/12	2-3:00	AC	N	0.16%	0.31%	0.91%	-4.85%	1.13%	-5.97%	-0.09%	-2.22%	0.01%	5.48%
2/21/12	2-3:00	AC	N	0.22%	0.75%	1.47%	-5.50%	1.57%	-6.37%	-0.04%	-2.77%	-0.03%	6.63%
2/21/12	09:39-10:45	MP	N	0.26%	0.41%	1.00%	-7.09%	1.00%	-5.20%	0.20%	-2.11%	-0.02%	5.81%

Parameter:				CO		NO		NO_x		NO_2		SO_2	
Date	Time	Calibration Type	Adjusted	Zero % Full Scale	Span % Error	Zero % Full Scale	Span % Error	Zero % Full Scale	Span % Error	Zero % Full Scale	Span % Error	Zero % Full Scale	Span % Error
2/22/12	2-3:00	AC	N	0.23%	0.34%	-2.73%	-14.27%	-1.18%	-14.82%	-2.48%	-12.13%	-0.04%	7.04%
2/23/12	2-3:00	AC	N	0.17%	0.43%	-2.76%	-13.21%	-1.19%	-13.82%	-2.30%	-10.66%	-0.05%	7.36%
2/24/12	2-3:00	AC	N	0.18%	0.34%	-2.82%	-9.45%	-1.12%	-10.41%	-2.16%	-6.63%	-0.07%	7.27%
2/24/12	09:30-10:35	Z/Sp	Y - NO_x, SO_2	0.20%	0.72%	-2.00%	-3.78%	-0.60%	-5.67%	NA	NA	-0.02%	7.73%
2/24/12	09:30-10:35	Z/Sp	Y - NO_x, SO_2	NA	NA	0.20%	-0.47%	0.80%	-1.18%	NA	NA	-0.02%	0.27%
2/25/12	2-3:00	AC	N	0.21%	0.79%	0.56%	-0.55%	0.91%	-1.80%	-0.05%	2.33%	-0.07%	0.48%
2/26/12	2-3:00	AC	N	0.28%	0.55%	0.20%	-1.89%	0.75%	-3.04%	-0.11%	1.14%	-0.04%	0.84%
2/27/12	2-3:00	AC	N	0.24%	0.36%	0.26%	-2.34%	0.78%	-3.76%	0.09%	0.83%	-0.06%	0.68%
2/28/12	2-3:00	AC	N	0.46%	1.72%	-1.23%	-3.94%	-0.06%	-5.51%	-0.99%	-0.67%	-0.07%	2.59%
2/29/12	2-3:00	AC	N	0.21%	1.12%	-1.37%	-3.04%	-0.03%	-4.55%	-1.03%	-1.80%	-0.04%	2.37%
3/1/12	2-3:00	AC	N	0.16%	0.95%	-1.46%	-2.89%	-0.22%	-4.04%	-1.06%	-1.58%	-0.08%	1.97%
3/2/12	2-3:00	AC	N	0.16%	0.92%	-1.37%	-4.90%	-0.16%	-5.86%	-1.06%	-3.10%	-0.08%	2.63%
3/3/12	2-3:00	AC	N	0.18%	0.23%	-1.39%	-5.94%	0.00%	-7.24%	-1.26%	-2.66%	0.10%	2.29%
3/4/12	2-3:00	AC	N	0.16%	-0.20%	-1.95%	-6.24%	-0.06%	-7.56%	-1.39%	-2.81%	-0.05%	1.71%
3/5/12	2-3:00	AC	N	0.14%	-0.36%	-2.00%	-5.29%	0.00%	-6.51%	-1.29%	-3.46%	-0.08%	1.22%
3/6/12	2-3:00	AC	N	0.18%	0.00%	-1.89%	-6.95%	-0.11%	-8.33%	-1.34%	-3.87%	-0.08%	1.72%
3/6/12	11:20-11:55	Z/Sp	N	NA	NA	1.00%	-1.87%	0.40%	-1.17%	NA	NA	NA	NA
3/7/12	2-3:00	AC	N	0.29%	0.56%	0.49%	-4.92%	0.23%	-5.52%	-0.77%	-1.09%	-0.11%	2.94%
3/8/12	2-3:00	AC	N	0.39%	0.94%	0.42%	-5.88%	0.32%	-6.87%	-0.79%	-2.12%	-0.10%	3.13%
3/9/12	2-3:00	AC	N	0.35%	0.51%	0.60%	-5.64%	0.81%	-6.57%	-0.80%	-1.70%	-0.09%	2.64%
3/10/12	2-3:00	AC	N	0.34%	0.05%	0.69%	-6.38%	0.90%	-7.37%	-0.64%	-2.44%	-0.10%	2.06%
3/11/12	2-3:00	AC	N	0.31%	-0.10%	0.60%	-8.00%	0.53%	-9.03%	-0.21%	-4.70%	-0.10%	1.63%
3/12/12	2-3:00	AC	N	0.39%	0.09%	0.59%	-7.72%	0.50%	-8.76%	-0.41%	-4.19%	-0.11%	2.28%
3/13/12	2-3:00	AC	N	0.42%	0.00%	0.41%	-7.88%	0.31%	-9.05%	0.14%	-3.87%	-0.10%	2.01%
3/14/12	2-3:00	AC	N	0.51%	0.49%	0.45%	-14.79%	0.26%	-16.06%	0.18%	-11.70%	-0.12%	2.62%
3/15/12	2-3:00	AC	N	0.48%	0.04%	0.38%	-16.14%	0.27%	-17.59%	0.14%	-13.13%	-0.12%	2.01%
3/16/12	2-3:00	AC	N	0.43%	-0.27%	0.43%	-13.80%	0.37%	-15.09%	0.23%	-10.59%	-0.11%	1.58%
3/16/12	10:05-	MP	N	0.26%	-0.62%	0.80%	-7.73%	1.00%	-6.09%	0.20%	-2.11%	-0.02%	4.80%

Parameter:				CO		NO		NO_x		NO_2		SO_2	
Date	Time	Calibration Type	Adjusted	Zero % Full Scale	Span % Error	Zero % Full Scale	Span % Error	Zero % Full Scale	Span % Error	Zero % Full Scale	Span % Error	Zero % Full Scale	Span % Error
	11:10												

Footnote: AC = automated calibration, Man 0/S = manual calibration; Z = zero, SP = span, MP =multi-point calibration, INV = invalid; NA = not available; Y = yes, N = no

Table 3A-6. Summer Monitoring Season - Community East Daily Calibration Response of Gaseous Pollutants

Parameter				CO		NO		NOx		NO2		SO2	
Date	Time	Calibration Type	Adjusted	Zero % Full Scale	Span % Error	Zero % Full Scale	Span % Error	Zero % Full Scale	Span % Error	Zero % Full Scale	Span % Error	Zero % Full Scale	Span % Error
7/18/2012	2-3:00	AC	N	-0.88%	-0.25%	0.20%	-2.27%	0.00%	-2.50%	0.20%	-4.93%	-0.10%	-3.43%
7/19/2012	2-3:00	AC	N	-0.82%	-1.17%	0.20%	-2.27%	0.00%	-2.27%	0.20%	-0.55%	-0.18%	-5.12%
7/20/2012	2-3:00	AC	N	-0.60%	-1.31%	0.20%	-2.50%	0.00%	-2.27%	0.20%	-0.27%	-0.16%	-4.09%
7/21/2012	2-3:00	AC	N	-0.84%	-1.06%	0.20%	-2.95%	0.00%	-2.95%	0.20%	-0.82%	-0.14%	-4.12%
7/22/2012	2-3:00	AC	N	-0.82%	-0.99%	0.20%	-3.18%	0.00%	-2.73%	0.00%	-0.82%	-0.16%	-3.52%
7/23/2012	2-3:00	AC	N	-0.62%	-1.31%	0.20%	-3.41%	0.00%	-3.41%	0.20%	-0.82%	-0.22%	-2.88%
7/24/2012	2-3:00	AC	N	-0.72%	-0.88%	0.20%	-3.41%	0.00%	-3.41%	0.20%	-0.82%	-0.22%	-2.70%
7/25/2012	2-3:00	AC	N	-0.66%	-0.61%	0.20%	-3.41%	0.00%	-3.41%	0.20%	-0.82%	-0.18%	-2.26%
7/26/2012	2-3:00	AC	N	-0.62%	-0.77%	0.20%	-3.41%	0.00%	-3.64%	0.20%	-0.82%	-0.18%	-2.72%
7/27/2012	2-3:00	AC	N	-0.60%	-0.68%	0.20%	-3.64%	0.00%	-3.86%	0.20%	-1.10%	-0.20%	-2.58%
7/28/2012	2-3:00	AC	N	-0.58%	-0.86%	0.20%	-4.09%	0.00%	-3.86%	0.20%	-1.10%	-0.16%	-1.97%
7/29/2012	2-3:00	AC	N	0.00%	0.47%	0.20%	-2.05%	0.00%	-2.05%	0.20%	-0.82%	-0.20%	-0.96%
7/30/2012	2-3:00	AC	N	0.00%	0.47%	0.20%	-2.05%	0.00%	-1.82%	0.20%	-0.82%	-0.20%	-0.96%
7/31/2012	2-3:00	AC	N	0.00%	2.88%	0.20%	0.00%	0.00%	0.00%	0.20%	0.27%	-0.20%	-1.10%
8/1/2012	2-3:00	AC	N	0.10%	2.97%	0.20%	-0.23%	0.00%	-0.23%	0.20%	0.00%	-0.16%	-1.92%
8/2/2012	2-3:00	AC	N	0.08%	3.00%	0.20%	-0.23%	0.00%	0.00%	0.20%	0.00%	-0.18%	0.41%
8/3/2012	2-3:00	AC	N	0.16%	3.11%	0.20%	-0.23%	0.00%	0.00%	0.20%	0.27%	-0.28%	0.23%
8/4/2012	2-3:00	AC	N	0.20%	3.29%	0.20%	-0.23%	0.00%	-0.23%	0.20%	0.00%	-0.20%	-1.14%
8/5/2012	2-3:00	AC	N	0.20%	3.29%	0.20%	-0.45%	0.00%	-0.23%	0.20%	0.00%	-0.12%	0.14%
8/6/2012	2-3:00	AC	N	0.28%	3.38%	0.20%	-0.45%	0.00%	-0.23%	0.20%	0.00%	-0.16%	-0.66%
8/7/2012	2-3:00	AC	N	0.52%	3.38%	0.20%	-0.23%	0.00%	0.00%	INV	INV	-0.18%	INV
8/8/2012	2-3:00	AC	N	0.44%	3.24%	0.20%	-0.23%	0.20%	-0.23%	0.20%	-3.56%	-0.12%	-2.06%
8/9/2012	2-3:00	AC	N	0.46%	3.29%	0.20%	-0.23%	0.20%	-0.23%	0.20%	-3.56%	-0.16%	-2.08%
8/10/2012	2-3:00	AC	N	0.52%	3.40%	0.20%	-0.23%	0.00%	0.00%	0.20%	-3.56%	-0.20%	-0.69%

Parameter				CO		NO		NOx		NO2		SO2	
Date	Time	Calibration Type	Adjusted	Zero % Full Scale	Span % Error	Zero % Full Scale	Span % Error	Zero % Full Scale	Span % Error	Zero % Full Scale	Span % Error	Zero % Full Scale	Span % Error
8/11/2012	2-3:00	AC	N	0.56%	3.54%	0.20%	-0.23%	0.00%	0.00%	0.20%	-3.84%	-0.18%	-4.37%
8/12/2012	2-3:00	AC	N	0.60%	3.67%	0.20%	-0.23%	0.00%	-0.23%	0.20%	-4.11%	-0.20%	-3.96%
8/13/2012	2-3:00	AC	N	0.62%	3.72%	0.20%	-0.23%	0.00%	-0.23%	0.20%	-4.11%	-0.20%	-4.16%
8/14/2012	2-3:00	AC	N	0.70%	3.74%	0.20%	-0.45%	0.00%	-0.23%	0.20%	-4.11%	-0.24%	-2.40%
8/15/2012	2-3:00	AC	N	0.74%	3.65%	0.20%	-0.68%	0.00%	-0.45%	0.20%	-4.38%	-0.16%	-0.75%
8/16/2012	2-3:00	AC	N	0.78%	3.69%	0.20%	-1.14%	0.00%	-0.91%	0.20%	-4.38%	-0.16%	-1.53%
8/17/2012	2-3:00	AC	N	0.82%	4.03%	0.20%	-1.14%	0.00%	-0.91%	0.20%	-4.11%	-0.16%	-0.82%
8/18/2012	2-3:00	AC	N	0.90%	4.01%	0.20%	-1.36%	0.00%	-1.14%	0.20%	-4.38%	-0.16%	-2.22%
8/19/2012	2-3:00	AC	N	0.94%	4.12%	0.20%	-1.36%	0.00%	-1.36%	0.20%	-4.38%	-0.20%	-2.38%
8/20/2012	2-3:00	AC	N	INV	INV	INV	INV	INV	INV	INV	INV	INV	INV
8/21/2012	2-3:00	AC	N	INV	INV	INV	INV	INV	INV	INV	INV	INV	INV
8/22/2012	2-3:00	AC	N	1.02%	4.30%	0.20%	-1.59%	0.00%	-1.59%	0.20%	-4.38%	-0.20%	-1.69%
8/23/2012	2-3:00	AC	N	1.06%	4.53%	0.20%	-1.82%	0.20%	-2.05%	0.20%	-4.93%	-0.16%	-2.77%
8/24/2012	2-3:00	AC	N	1.08%	4.62%	0.20%	-1.82%	0.00%	-1.82%	0.20%	-4.93%	-0.16%	-1.26%
8/24/2012	8:18-8:26	Z/SP	Y	0.38%	NA	NA	NA	NA	NA	NA	NA	NA	NA
8/25/2012	2-3:00	AC	N	0.28%	2.93%	0.20%	-2.05%	0.00%	-1.82%	0.20%	-5.48%	-0.22%	-1.23%
8/26/2012	2-3:00	AC	N	0.30%	2.77%	0.20%	-2.27%	0.00%	-2.27%	0.20%	-5.48%	-0.20%	-1.07%
8/27/2012	2-3:00	AC	N	0.32%	2.61%	0.20%	-2.50%	0.20%	-2.73%	0.20%	-5.75%	-0.22%	0.23%
8/28/2012	2-3:00	AC	N	0.36%	2.93%	0.20%	-2.27%	0.00%	-2.27%	0.20%	-5.75%	-0.20%	-0.18%
8/29/2012	2-3:00	AC	N	0.46%	3.22%	0.20%	-1.82%	0.20%	-2.27%	0.20%	-5.48%	-0.20%	-1.28%

Footnote: AC = automated calibration, Man 0/S = manual calibration; Z = zero, SP = span, MP =multi-point calibration, INV = invalid; NA = not available; Y = yes, N = no

Table 3A-7. Summer Monitoring Season - Community South Daily Calibration Response of Gaseous Pollutants

Parameter				CO		NO		NO_x		NO_2		SO_2	
Date	Time	Calibration Type	Adjusted	Zero % Full Scale	Span % Error	Zero % Full Scale	Span % Error	Zero % Full Scale	Span % Error	Zero % Full Scale	Span % Error	Zero % Full Scale	Span % Error
7/18/2012	2-3:00	AC	N	-0.34%	0.30%	-0.20%	-5.37%	0.00%	-6.07%	-0.20%	-4.85%	0.04%	-1.18%
7/19/2012	2-3:00	AC	N	-0.38%	0.05%	-0.20%	-4.44%	0.20%	-6.31%	-0.20%	-5.45%	0.12%	-2.68%
7/20/2012	2-3:00	AC	N	-0.30%	0.23%	-0.20%	-4.21%	0.20%	-7.24%	-0.20%	-4.55%	0.08%	-3.35%
7/21/2012	2-3:00	AC	N	-0.26%	0.19%	-0.20%	-4.67%	0.20%	-6.78%	-0.20%	-5.15%	0.08%	-3.21%
7/22/2012	2-3:00	AC	N	-0.24%	0.44%	-0.20%	-3.50%	0.20%	-5.61%	-0.20%	-5.45%	0.20%	-4.43%
7/23/2012	2-3:00	AC	N	-0.06%	0.32%	0.00%	-7.48%	0.20%	-5.84%	-0.20%	-5.76%	0.10%	-4.75%
7/24/2012	2-3:00	AC	N	-0.10%	0.49%	-0.20%	-14.25%	0.20%	-11.92%	-0.20%	-13.33%	0.10%	-5.11%
7/24/2012	7:50-08:45	Z/SP	Y	-0.10%	0.28%	INV	INV	INV	INV	INV	INV	0.24%	-0.02%
7/25/2012	2-3:00	AC	N	-0.04%	1.23%	INV	INV	INV	INV	INV	INV	0.10%	0.36%
7/25/2012	12:40-13:10	Z/SP	N	NA	NA	-0.20%	0.00%	0.00%	-0.23%	INV	INV	NA	NA
7/26/2012	2-3:00	AC	N	-0.02%	1.44%	-0.20%	-1.64%	-0.20%	-2.10%	-0.20%	-0.30%	0.08%	-0.51%
7/27/2012	2-3:00	AC	N	-0.04%	1.39%	-0.20%	0.23%	0.20%	2.10%	-0.20%	0.00%	0.10%	-1.52%
7/28/2012	2-3:00	AC	N	0.10%	0.79%	-0.20%	-0.70%	0.20%	3.97%	-0.20%	1.21%	0.14%	-2.96%
7/29/2012	2-3:00	AC	N	0.10%	0.93%	-0.20%	0.47%	0.20%	4.44%	-0.20%	1.21%	0.14%	-2.96%
7/30/2012	2-3:00	AC	N	0.18%	1.25%	-0.20%	-0.93%	0.20%	1.87%	-0.20%	1.21%	0.08%	-2.43%
7/31/2012	2-3:00	AC	N	0.38%	1.16%	-0.20%	-0.47%	0.00%	2.57%	-0.20%	0.91%	-0.08%	-1.28%
8/1/2012	2-3:00	AC	N	0.38%	1.14%	-0.20%	1.40%	0.20%	4.91%	-0.20%	1.21%	0.02%	-0.72%
8/2/2012	2-3:00	AC	N	0.38%	1.16%	-0.20%	0.00%	0.20%	3.50%	-0.20%	1.52%	0.00%	-2.51%
8/3/2012	2-3:00	AC	N	0.44%	1.23%	-0.20%	0.23%	0.20%	5.14%	-0.20%	0.91%	0.00%	-2.15%
8/4/2012	2-3:00	AC	N	0.44%	1.30%	-0.20%	2.57%	0.20%	7.01%	-0.20%	2.12%	-0.08%	-2.72%
8/5/2012	2-3:00	AC	N	0.44%	1.58%	-0.20%	2.57%	0.20%	6.31%	-0.20%	3.94%	0.06%	-1.81%
8/6/2012	2-3:00	AC	N	0.54%	1.51%	-0.20%	4.91%	0.20%	8.18%	-0.20%	4.55%	0.06%	-2.17%
8/7/2012	2-3:00	AC	N	0.64%	1.34%	-0.20%	6.31%	0.20%	9.11%	-0.20%	4.85%	-0.04%	-2.46%
8/7/2012	11:30-12	Z/SP	Y	NA	NA	0.00%	-0.70%	0.20%	-1.17%	NA	NA	NA	NA

Parameter				CO		NO		NO_x		NO_2		SO_2	
Date	Time	Calibration Type	Adjusted	Zero % Full Scale	Span % Error	Zero % Full Scale	Span % Error	Zero % Full Scale	Span % Error	Zero % Full Scale	Span % Error	Zero % Full Scale	Span % Error
8/8/2012	2-3:00	AC	N	0.62%	1.60%	-0.20%	1.17%	0.20%	2.80%	-0.20%	1.82%	0.00%	-1.30%
8/9/2012	2-3:00	AC	N	0.64%	1.67%	-0.20%	3.04%	0.20%	6.31%	-0.20%	3.33%	-0.08%	-2.17%
8/10/2012	2-3:00	AC	N	0.64%	1.65%	-0.20%	0.93%	0.20%	5.14%	-0.20%	0.30%	0.02%	-2.36%
8/11/2012	2-3:00	AC	N	0.74%	1.69%	-0.20%	4.21%	0.20%	9.11%	-0.20%	2.12%	0.00%	-3.18%
8/12/2012	2-3:00	AC	N	0.80%	1.92%	-0.20%	2.57%	0.20%	7.24%	-0.20%	1.82%	0.00%	-2.36%
8/13/2012	2-3:00	AC	N	0.86%	1.99%	-0.20%	1.40%	0.20%	3.97%	-0.20%	1.52%	-0.04%	-1.93%
8/14/2012	2-3:00	AC	N	0.82%	2.06%	-0.20%	0.00%	0.20%	2.10%	-0.20%	0.30%	0.02%	-2.63%
8/15/2012	2-3:00	AC	N	0.86%	1.88%	-0.20%	0.00%	0.20%	2.10%	-0.20%	2.12%	0.00%	-2.72%
8/16/2012	2-3:00	AC	N	0.94%	1.83%	-0.20%	0.47%	0.20%	2.34%	-0.20%	2.73%	0.04%	-2.19%
8/17/2012	2-3:00	AC	N	0.98%	1.85%	-0.20%	-0.47%	0.20%	0.70%	-0.20%	1.52%	-0.06%	-3.13%
8/18/2012	2-3:00	AC	N	1.02%	1.79%	-0.20%	0.23%	0.20%	1.40%	-0.20%	2.12%	-0.04%	-3.11%
8/19/2012	2-3:00	AC	N	1.06%	1.90%	-0.20%	0.23%	0.20%	2.10%	-0.20%	2.73%	-0.08%	-3.11%
8/20/2012	2-3:00	AC	N	1.06%	2.04%	-0.20%	0.47%	0.20%	0.93%	-0.20%	2.73%	0.00%	-3.35%
8/21/2012	2-3:00	AC	N	1.06%	1.99%	-0.20%	0.23%	0.20%	1.17%	-0.20%	3.03%	-0.08%	-2.29%
8/22/2012	2-3:00	AC	N	1.06%	2.13%	-0.20%	2.57%	0.20%	3.04%	-0.20%	5.45%	-0.08%	-3.11%
8/23/2012	2-3:00	AC	N	1.06%	2.13%	-0.20%	2.57%	0.20%	2.80%	-0.20%	5.45%	0.04%	-2.96%
8/24/2012	2-3:00	AC	N	1.06%	2.11%	-0.20%	2.57%	0.20%	2.80%	-0.20%	5.15%	-0.08%	-3.09%
8/24/2012	09:38-09:48	Z	Y	0.40%	NA	NA	NA	NA	NA	NA	NA	NA	NA
8/25/2012	2-3:00	AC	N	0.20%	-0.14%	-0.20%	2.80%	0.20%	2.80%	-0.20%	5.45%	-0.08%	-2.53%
8/26/2012	2-3:00	AC	N	0.20%	-0.07%	-0.20%	2.57%	0.20%	2.10%	-0.20%	5.76%	0.04%	-3.49%
8/27/2012	2-3:00	AC	N	0.20%	0.00%	-0.20%	3.74%	0.20%	3.27%	-0.20%	6.67%	-0.04%	-2.29%
8/28/2012	2-3:00	AC	N	0.26%	0.16%	-0.20%	3.97%	0.20%	3.50%	-0.20%	6.97%	-0.02%	-2.82%
8/29/2012	2-3:00	AC	N	0.40%	0.02%	-0.20%	4.67%	0.20%	4.21%	-0.20%	7.27%	0.04%	-3.11%

Footnote: AC = automated calibration, Man 0/S = manual calibration; Z = zero, SP = span, MP =multi-point calibration, INV = invalid; NA = not available; Y = yes, N = no

Table 3A-8. Summer Monitoring Season - Community North Daily Calibration Response of Gaseous Pollutants

Parameter				CO		NO		NO_x		NO_2		SO_2	
Date	Time	Calibration Type	Adjusted	Zero % Full Scale	Span % Error	Zero % Full Scale	Span % Error	Zero % Full Scale	Span % Error	Zero % Full Scale	Span % Error	Zero % Full Scale	Span % Error
7/18/2012	2-3:00	AC	N	-0.44%	-1.99%	-1.20%	3.07%	-0.40%	2.84%	-0.80%	1.39%	0.01%	INV
7/19/2012	2-3:00	AC	N	-0.20%	-1.46%	-1.00%	3.78%	-0.20%	3.07%	-0.80%	2.78%	0.00%	INV
7/20/2012	2-3:00	AC	N	-0.20%	-1.53%	-1.20%	-1.89%	-0.20%	-2.36%	-0.60%	-1.94%	0.01%	INV
7/21/2012	2-3:00	AC	N	-0.28%	-2.41%	-1.60%	-5.20%	-0.60%	-5.44%	-0.60%	-5.00%	0.00%	INV
7/22/2012	2-3:00	AC	N	-0.28%	-2.27%	-1.60%	-11.58%	-0.40%	-11.58%	-0.60%	-10.83%	0.00%	INV
7/23/2012	2-3:00	AC	N	-0.24%	-2.15%	-1.40%	-18.44%	-0.40%	-18.20%	-0.60%	-16.39%	0.00%	INV
7/24/2012	2-3:00	AC	N	-0.30%	-2.01%	-1.40%	-23.64%	-0.40%	-23.40%	-0.60%	-21.11%	0.01%	INV
7/24/2012	09:48-10:30	Z/SP	Y	NA	NA	-1.40%	-5.67%	-0.40%	-6.62%	NA	NA	NA	NA
7/25/2012	2-3:00	AC	N	-0.34%	-1.11%	-1.60%	18.68%	-0.40%	17.73%	-0.80%	38.61%	0.00%	INV
7/25/2012	11:55-12:XX	Z/SP	Y	NA	NA	-1.20%	1.89%	0.00%	1.89%	NA	NA	NA	NA
7/26/2012	2-3:00	AC	N	-0.30%	-1.04%	-1.60%	1.89%	-0.40%	2.13%	-0.60%	1.94%	0.00%	INV
7/27/2012	2-3:00	AC	N	-0.20%	-1.09%	-1.60%	2.13%	-0.40%	2.60%	-0.60%	2.50%	0.00%	INV
7/28/2012	2-3:00	AC	N	-0.16%	-0.93%	-1.60%	3.31%	-0.40%	3.31%	-0.60%	3.06%	0.00%	INV
7/29/2012	2-3:00	AC	N	-0.06%	-0.76%	-1.40%	2.60%	-0.40%	2.84%	-0.80%	3.33%	0.01%	INV
7/30/2012	2-3:00	AC	N	-0.08%	-0.74%	-1.80%	1.65%	-0.60%	2.36%	-0.60%	2.50%	0.01%	INV
7/31/2012	2-3:00	AC	N	-0.02%	0.44%	-1.80%	-1.42%	-0.60%	-1.18%	-0.80%	-0.28%	-0.01%	INV
7/31/2012	16:15-17:11	Z/SP	Y	NA	NA	NA	NA	NA	NA	NA	NA	-0.01%	-0.25%
8/1/2012	2-3:00	AC	N	-0.04%	-0.23%	-2.00%	-1.65%	-0.60%	-1.65%	-0.60%	0.00%	-0.01%	-3.48%
8/2/2012	2-3:00	AC	N	0.02%	-0.63%	-2.00%	-3.07%	-0.60%	-2.84%	-0.60%	-1.11%	0.01%	INV
8/3/2012	2-3:00	AC	N	0.08%	-0.81%	-2.00%	-2.84%	-0.60%	-1.89%	-0.60%	-6.39%	0.01%	INV
8/3/2012	12:17-12:40	Z/SP	N	NA	NA	NA	NA	NA	NA	NA	NA	0.01%	-0.09%
8/4/2012	2-3:00	AC	N	0.08%	-0.16%	0.60%	-2.84%	1.20%	-2.60%	0.80%	-2.50%	0.01%	-5.28%
8/5/2012	2-3:00	AC	N	0.06%	-0.30%	-1.60%	-5.20%	-0.40%	-4.73%	-0.40%	-3.06%	0.01%	-5.07%
8/6/2012	2-3:00	AC	N	0.04%	-0.72%	1.40%	-4.49%	1.60%	-4.96%	0.00%	-5.83%	0.00%	-5.67%

Parameter				CO		NO		NO_x		NO_2		SO_2	
Date	Time	Calibration Type	Adjusted	Zero % Full Scale	Span % Error	Zero % Full Scale	Span % Error	Zero % Full Scale	Span % Error	Zero % Full Scale	Span % Error	Zero % Full Scale	Span % Error
8/7/2012	2-3:00	AC	N	-0.04%	-1.32%	1.80%	-5.20%	2.20%	-4.96%	0.80%	-5.00%	0.01%	-8.35%
8/8/2012	2-3:00	AC	N	0.12%	-0.16%	-1.20%	-5.44%	-0.20%	-5.67%	0.00%	-4.17%	0.00%	-2.84%
8/9/2012	2-3:00	AC	N	0.06%	-0.49%	-1.40%	-12.06%	-0.40%	-12.06%	0.00%	-10.28%	0.00%	-4.75%
8/10/2012	2-3:00	AC	N	0.10%	-0.05%	-1.40%	-9.46%	-0.20%	-9.69%	-0.20%	-7.50%	0.00%	-3.41%
8/10/2011	07:19-08:20	Z/SP	Y	NA	NA	-1.00%	-1.42%	0.00%	-2.13%	NA	NA	0.00%	0.00%
8/11/2012	2-3:00	AC	N	0.16%	-2.15%	1.60%	-1.18%	3.80%	-0.24%	-0.60%	-1.11%	0.03%	-0.07%
8/12/2012	2-3:00	AC	N	0.16%	-2.48%	1.80%	-0.71%	2.60%	-0.95%	-0.20%	0.83%	0.03%	-3.28%
8/13/2012	2-3:00	AC	N	0.20%	-2.08%	1.80%	-4.02%	3.40%	-2.84%	-0.60%	-3.89%	0.03%	0.83%
8/14/2012	2-3:00	AC	N	0.20%	-1.78%	1.80%	-7.57%	2.60%	-8.51%	0.00%	-8.06%	0.03%	0.42%
8/15/2012	2-3:00	AC	N	0.34%	-1.88%	1.40%	-10.40%	3.00%	-7.57%	-0.80%	-9.72%	0.03%	0.55%
8/16/2012	2-3:00	AC	N	0.40%	-1.44%	1.60%	-15.84%	4.00%	-14.89%	-0.80%	-15.56%	0.02%	0.16%
8/16/2012	09:28-11:00	Z/SP	Y	NA	NA	0.00%	-5.44%	0.00%	-5.20%	NA	NA	NA	NA
8/17/2012	2-3:00	AC	N	0.42%	-1.53%	-0.80%	-13.00%	-1.00%	-12.06%	0.00%	-13.33%	0.03%	0.85%
8/17/2012	06:58-07:35	Z/SP		NA	NA	-0.20%	2.60%	0.00%	2.84%	NA	NA	NA	NA
8/18/2012	2-3:00	AC	N	0.50%	-1.16%	-0.40%	-0.71%	-0.60%	0.47%	0.00%	-0.56%	0.01%	1.48%
8/19/2012	2-3:00	AC	N	0.44%	-1.53%	-0.80%	1.18%	-0.80%	2.36%	0.00%	1.67%	0.02%	-2.77%
8/20/2012	2-3:00	AC	N	0.42%	-1.50%	-0.60%	3.07%	-0.60%	4.26%	0.00%	3.33%	0.02%	-0.14%
8/21/2012	2-3:00	AC	N	0.46%	-1.57%	-0.60%	4.02%	-0.60%	4.96%	0.00%	4.17%	0.03%	0.83%
8/22/2012	2-3:00	AC	N	0.58%	-1.55%	-0.40%	5.20%	-0.40%	6.38%	0.00%	5.56%	0.03%	0.58%
8/23/2012	2-3:00	AC	N	0.62%	-1.23%	-0.40%	3.31%	-0.40%	4.73%	0.00%	4.17%	0.02%	0.90%
8/24/2012	2-3:00	AC	N	0.68%	-1.11%	2.00%	2.60%	2.00%	4.49%	0.20%	3.89%	0.03%	1.11%
8/25/2012	2-3:00	AC	N	0.72%	-0.63%	-0.60%	1.42%	-0.60%	2.84%	0.00%	2.78%	0.02%	1.08%
8/26/2012	2-3:00	AC	N	0.76%	-0.35%	-0.60%	-0.95%	-0.60%	0.24%	0.00%	0.56%	0.03%	-2.12%
8/27/2012	2-3:00	AC	N	0.96%	0.09%	-0.60%	-1.65%	-0.60%	-0.71%	0.00%	-0.83%	0.02%	0.16%
8/27/2012	09:28-09:48	Z	Y	-0.40%	-1.13%	NA	NA	NA	NA	NA	NA	NA	NA
8/28/2012	2-3:00	AC	N	-0.40%	-0.79%	-0.60%	-4.49%	-0.60%	-3.07%	0.00%	-3.33%	0.03%	1.48%

Parameter				CO		NO		NO_x		NO_2		SO_2	
Date	Time	Calibration Type	Adjusted	Zero % Full Scale	Span % Error	Zero % Full Scale	Span % Error	Zero % Full Scale	Span % Error	Zero % Full Scale	Span % Error	Zero % Full Scale	Span % Error
8/29/2012	2-3:00	AC	N	0.20%	-1.00%	-0.60%	-5.20%	-0.60%	-4.49%	0.00%	-5.00%	0.01%	1.43%
8/30/2012	2-3:00	AC	N	0.06%	-1.25%	-0.60%	-2.13%	-0.60%	-0.71%	0.00%	-1.39%	0.02%	-0.07%

Footnote: AC = automated calibration, Man 0/S = manual calibration; Z = zero, SP = span, MP =multi-point calibration, INV = invalid; NA = not available; Y = yes, N = n

Appendix 3-3

MONITORING AND QUALITY ASSURANCE PROJECT PLAN (MQAPP)

(This page is intentionally blank)

LOS ANGELES WORLD AIRPORTS

Monitoring and Quality Assurance Project Plan
for
Phase III of the LAX
Air Quality and Source Apportionment Study

Prepared for
Los Angeles World Airports
Environmental Services Division

Prepared by
Tetra Tech, Inc.

Desert Research Institute
SCS-Tracer Technologies
T&B Systems

December 9, 2011

(This Page is Intentionally Blank)

A1. Quality Assurance Project Plan Identification and Approval

Title: *Phase III of the LAX Air Quality and Source Apportionment Study*

The attached Quality Assurance Project Plan for the Phase III of the LAX Air Quality and Source Apportionment Study is hereby recommended for approval and commits the following individuals to follow the elements described within.

Salar Niku, Ph.D.	Program Manager	Tetra Tech, Inc.
Charng-Ching Lin, Ph.D.	Project Manager	Tetra Tech, Inc.
Eddy Huang, Ph.D.	QA/QC Officer (internal)	Tetra Tech, Inc.
Eric Fujita, D.Env.	Senior Scientist	Desert Research Institute
Paul Schafer	Field Manager – Air Monitoring	SCS-Tracer Environmental
Bob Baxter	Quality Assurance Manager	T&B Systems

A2. Table of Contents

B2.4 Analytical Methods

A3. List of Acronyms

AA	Atomic absorption
AERMOD	AMS/EPA Regulatory Model
AMS	American Meteorological Society
APU	Auxiliary power unit
AQ	Air Quality sampling site (SCAQMD Hastings Monitoring Station)
BAM	Beta attenuation monitor
BC	Black carbon
BG	Background site
C_2	Hydrocarbon compounds containing two carbon atoms
C_{12}	Hydrocarbon compounds containing twelve carbon atoms
C_{20}	Hydrocarbon compounds containing twenty carbon atoms
CARB	California Air Resources Board
CCSEM	Computer Automated Scanning Electron Microscopic
CDM	Camp Dresser & McKee Inc.
CE	Community East site
CMB	Chemical mass balance
CO	Carbon monoxide
CO_2	Carbon dioxide
Cr	Chromium
CRPAQS	Central California Particulate Air Quality Study
CS	Community South site
DNPH	2,4-dinitrophenylhydrazine
DRI	Desert Research Institute
DWP	Department of Water and Power (City of Los Angeles)
EC	Elemental carbon
EOF	Empirical orthogonal function
EPA	Environmental Protection Agency
FAA	Federal Aviation Administration
FID	Flame ionization detector

FIND	Facility Information Detail (SCAQMD emissions database)
FS	Freeway South sampling site
FTIR	Fourier Transform Infrared Spectroscopy
GC	Gas chromatography
GSE	Ground support equipment
HC	Hydrocarbon
HPLC	High-pressure liquid chromatography
ICP	Inductively Coupled Plasma
LAWA	Los Angeles World Airports
LAX	Los Angeles International Airport
MS	Mass spectrometry
MQAPP	Monitoring and Quality Assurance Program Plan
NaCl	Sodium chloride
Ni	Nickel
NMHC	Non-methane hydrocarbon
NO	Nitric oxide
NO_2	Nitrogen dioxide
NO_x	Oxides of nitrogen (or nitrogen oxides)
NTA	Nonparametric trajectory analysis
O_3	Ozone
OC	Organic carbon
OEHHA	Office of Environmental Health Hazard Assessment (State of California)
PAMS	Photochemical assessment monitoring stations
Pb	Lead
PM	Particulate matter
PM_{10}	Particulate matter with aerodynamic diameters less than or equal to 10 micrometers
$PM_{2.5}$	Particulate matter with aerodynamic diameters less than or equal to 2.5 micrometers
PMF	Positive matrix factorization
PN	Park North site
PS5	Potable Station (Demonstration Project) site No. 5
QA	Quality assurance

QC	Quality control
RFP	Request for proposal
SCAQMD	South Coast Air Quality Management District
SCE	Southern California Edison
SCOS	Southern California Ozone Study
SFS	Sequential filter sampler
SO_2	Sulfur dioxide
SO_x	Sulfur oxides
SR	South Airfield or Runway 25R sampling site
TEOM	Tapered element oscillating microbalance
TWG	Technical Working Group (for the Air Quality and Source Apportionment Study)
UFP	Ultrafine particulates
UNMIX	A multivariate receptor model (maintained by U.S. EPA)
USC	University of Southern California
U.S. EPA	United States Environmental Protection Agency
UW	Upwind site
VOC	Volatile organic compounds
XRF	X-Ray Fluorescence Analysis

A4. Distribution List

A hardcopy of this MQAPP has been distributed to the individuals in Table A4-1.

Table A4-1. Distribution List

Name	Title	Organization
Robert Freeman	Airport Environmental Manager II	LAWA ESD
Karin Christie	Environmental Affairs Officer	LAWA ESD
Norene Hastings	Environmental Specialist/Project Manager	LAWA ESD
Salar Niku, Ph.D.	Program Manager	Tetra Tech, Inc.
Charng-Ching Lin, Ph.D.	Project Manager	Tetra Tech, Inc.
Eddy Huang, Ph.D.	QA/QC Officer (internal)	Tetra Tech, Inc.
Eric Fujita, D.Env.	Senior Scientist	Desert Research Institute
Paul Schafer	Field Manager – Air Monitoring	SCS-Tracer Environmental
Bob Baxter	Quality Assurance Manager	T&B Systems

A5. Project Organization/ Roles and Responsibilities

The proposed Phase III of the LAX Air Quality and Source Apportionment Study team organization is shown on Figure A5-1, including the specialties of key technical personnel and anticipated service areas from the subcontractors.

Ms. Norene Hastings, Environmental Specialist with ESD, is LAWA's Project Manager on this project. She will be the primary LAWA staff responsible for the successful execution of this project. She will represent LAWA and provide technical and regulatory liaison. Ms. Hastings will direct all project-related issues and the team performance to ensure that all work performed adheres to the schedule and budget while meeting the overall project goals. Ms. Hastings will maintain close communications with the Project Team on all project activities through routine project meetings and monthly progress reports.

Ms. Hastings will perform her responsibilities under the direction from Ms. Karin Christie, Officer of Environmental Affairs, and both Ms. Hastings and Ms. Christie will perform under the direction of Mr. Robert Freeman, Airport Environmental Manager.

The role of CDM is as a scientific advisor to LAWA.

The Project Team includes Tetra Tech, Inc.'s Program Manager – Dr. Salar Niku, Project Manager – Dr. Charng-Ching Lin, and QA/QC officer – Dr. Eddy Huang; Desert Research Institute's (DRI) Task Manager – Dr. Eric Fujita; SCS-Tracer Technologies Task Manager – Mr. Paul Schafer; T&B Systems Task Manager – Mr. Bob Baxter; Technical Advisor - Ivan Tombach, Technical Advisor - Charlie Blanchard; Non-Parametric Trajectory Analysis - Ron Henry; UNC Dispersion Modeling – Sarav Arunachalem; and K&B Environmental Emission Inventory – Michael Kenney.

Tetra Tech staff will have the overall responsibility of implementing the field measurements. Team Members – DRI and SCS-Tracer will perform actual field measurements, data collection and analysis; and, T&B Systems will conduct third party independent quality assurance audits of the field sampling, data collection and laboratory analysis.

Figure A5-1. Project organization for Phase III of the LAX Air Quality and Source Apportionment Study

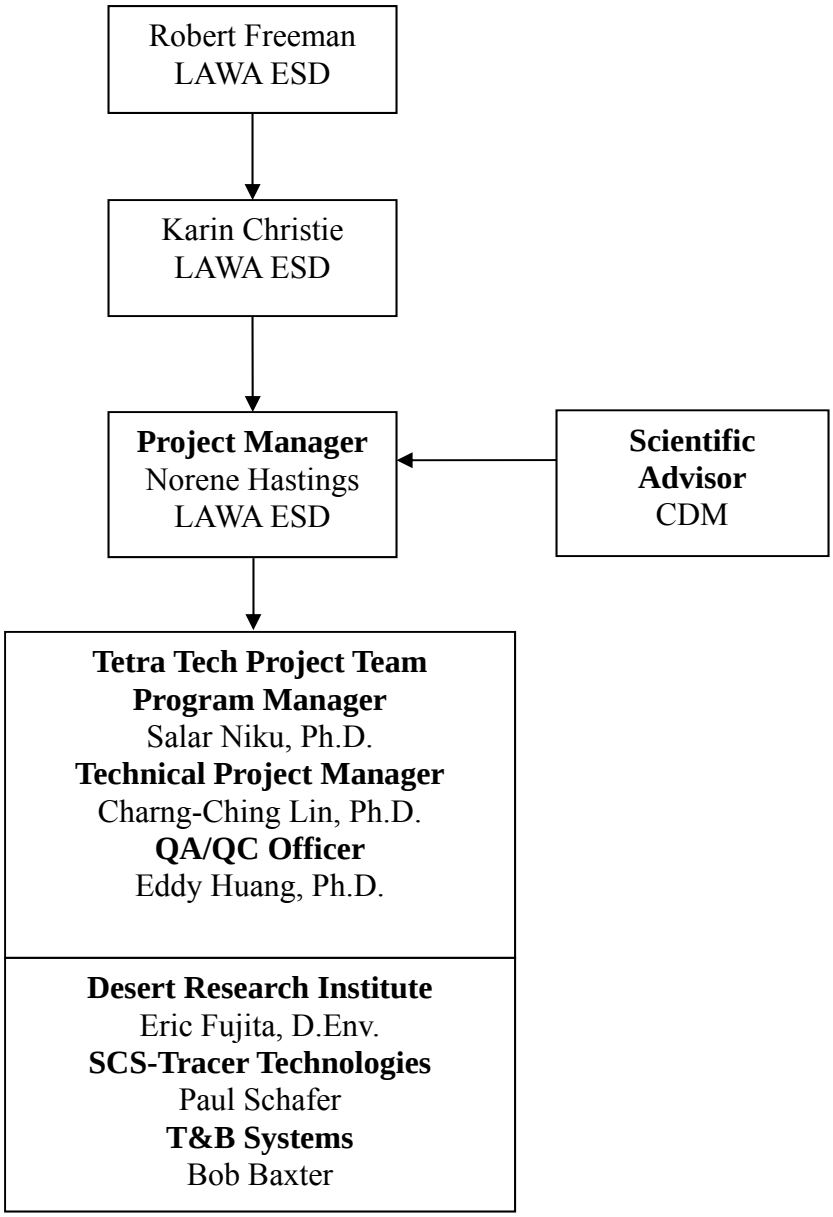

A6. Background

A6.1 Project Background

Los Angeles International Airport (LAX) is located within the South Coast Air Basin (Basin). Air quality within the Basin is widely regarded as among the poorest in the nation, and fails to attain state and federal standards for several "criteria" air pollutants including: ozone (O_3), coarse particulate matter (particles with aerodynamic diameters less than 10 μm or PM_{10}), and fine particulate matter (particles with aerodynamic diameters less than 2.5 μm or $PM_{2.5}$). Increased attention has recently been given to "toxic air pollutants" (air toxics) and "ultrafine particles" (UFP, particles with diameters less than 0.1 μm, often measured by number instead of mass) within the Basin. Although ambient levels of air toxics and UFP are not regulated in the same way as criteria pollutants, regulatory agencies have begun to examine ambient levels of air toxics and public concern over possible health effects of air toxics and UFP is increasing. LAX is adjacent to residential neighborhoods to the north, south and east. Significant concern has been expressed among local residents questioning if the airport is contributing to unhealthy air quality within their neighborhoods.

During the summer of 1999, the South Coast Air Quality Management District (SCAQMD) conducted a short-term air toxics monitoring program in the areas around LAX. The results of the study indicated air toxics levels in the neighborhoods surrounding LAX were consistent with those found elsewhere in the Basin. However, the SCAQMD study was limited in extent and duration and did not provide data that could be used to determine either long-term impacts or LAX's contribution to toxic air pollutants. Additional potential sources of toxic air pollutants within the area include three major freeways, several heavily traveled major arterial routes, and numerous industrial facilities including: the Chevron El Segundo refinery, Hyperion Wastewater Treatment Plant, Department of Water and Power (DWP) Scattergood Generating Station, and Southern California Edison (SCE) El Segundo Generating Station.

In late September 1999, Lydia Kennard, Executive Director of Los Angeles World Airports (LAWA), directed her staff and a consultant team to develop a study to provide more detailed information about the role of LAX in emitting air toxics and the total concentrations of air toxics in the surrounding neighborhoods. It is intended that the data collected from the current study will be used to assess the effectiveness of various methods for reducing airport-related emissions.

In 2000, LAWA proposed to conduct an Air Quality and Source Apportionment Study (Study), as described in the November 2000 Technical Work Plan, to increase understanding of concentrations and sources of air toxics near the airport. The November 2000 Work Plan was developed with the assistance of a Technical Working Group specifically formed to oversee and provide guidance on the technical aspects of the Study. As part of the November 2000 Work Plan, a Pilot Study was scheduled to characterize aircraft emissions and to evaluate measurement methods was scheduled to begin operating behind the blast fence on Runway 25R. The Pilot Study was terminated on September 11, 2001 for security reasons.

In 2003, U.S. Environmental Protection Agency (U.S. EPA) reviewed the pilot study design and concluded that the study design and technical approach met the goals and objectives; and, provided suggestions and recommendations, such as using newer technology, to improve the study's ability to meet the objectives.

In 2007, a team led by Jacobs Consultancy (now named LeighFisher Inc.) was selected to implement the second phase of the study – Technology and Methodology Demonstration study to verify measurement methods identified in the Work Plan would work at LAX and source apportionment methods could be applied to the results. At the conclusion of the Demonstration Project, the findings from this effort were used to supplement the development of the final scope of work for Phase III. Considering aircraft exhaust characteristics are different in compositions during taxiing, idling and takeoff modes, SCAQMD conducted a taxiway sampling project in April 2011 and the collected volatile organics data were provided to Countess Environmental for analysis and making recommendations to be considered in the Phase III study.

In July 2011, Tetra Tech, Inc. and its subcontractors were selected to implement the Phase III of the study. The Phase III study will be completed by the end of 2012 and the final report completed no later than April 1, 2013.

A6.2 List of Pollutants

The Phase III of the LAX Air Quality and Source Apportionment Study will measure the following air pollutants of interest for subsequent analysis and source apportionment modeling:

- Gaseous pollutants: CO, NO_x and SO_2
- Particulate matter: $PM_{2.5,}$ ultrafine particles, black carbon, elemental carbon, organic carbon
- Ions: sulfate
- Metals
- Organics: carbonyls, light hydrocarbons, heavy hydrocarbons, polyaromatic hydrocarbons, steranes, and hopanes

Additionally, meteorological parameters such as wind direction, wind speed, relative humidity and temperature will be measured at two locations and solar radiation will be measured at one of the two locations.

A7. Project Description

A7.1 Project Scope and Field Activities

The Project Scope encompasses measuring air pollutant concentrations in the Study area including adjacent communities and perimeters of the LAX and subsequent modeling using source apportionment techniques to understand potential impacts of air emissions from airport operations on air quality of local communities. This section describes field sampling and analysis to be performed in the Phase III of the LAX Air Quality and Source Apportionment Study.

Field Sampling Plan

Based on findings from the mobile survey, notably the unique aircraft exhaust plume characteristics and dispersion, the Tetra Tech team in consultation with LAWA and their technical advisor - CDM - concurred that the original sampling plan should be revised to reflect the mobile study findings. The revised field sampling plan is comprised of three components: Fixed Stations, Saturation Sampling and Source Profile Sampling.

There are a total of three fixed stations in the community – Community East (CE) located at the La Feria Restaurant on Inglewood Avenue, Community South (CS) located at the Imperial Avenue School, and Community North (CN) which is a LAWA-owned property located at the intersection of Airport Blvd. and Arbor Vitae Street. The South Coast Air Quality Management District Hastings Site (AQ) is designated as the background site with additional equipment to augment the existing list of sensors. All fixed sites are equipped with continuous monitors and supplemented with integrated samplers for analysis of chemical species of interest.

During the two sampling seasons, in addition to continuous measurements and integrated samples at the fixed stations, saturation samplings are conducted using passive samplers and integrated samplers at three community sites, the background (AQ) site, and thirteen other locations. Of the thirteen other locations, ten gradient samplers are located at the areas surrounding the airport including buffer zones, terminal areas and adjacent to the I-405 Freeway and three are collocated at the fixed sites.

To obtain chemical characteristics of aircraft exhaust emissions for subsequent source apportionment analysis, source sampling using passive and integrated samplers is conducted at the South Runway and Taxiway location, including the locations behind the blast fence and the Walsh Austin laydown area adjacent to the taxiway. Additionally, samplers for gradient analysis are located at the CE site and the open field east of Airport Blvd. to characterize plume patterns from aircraft takeoffs.

Tables A7-1 to A7-2 list the revised sampling plans for fixed stations, and source and saturation sampling, respectively. Figure A7-1 shows the field sampling locations. Tables A7-3 to A7-5 show sampling locations, parameters and frequency for fixed stations, source, and saturation sampling, respectively.

Table A7-1
Revised Monitoring Network – Fixed Station

Symbol	*Site Title and Type*	*Location and Purpose*	*Components Analyzed*
CE	Community East. Core site for spatial, time series, and multivariate receptor analyses	La Feria Restaurant, ~1.56 km ESE of southern airfield. Community exposure – aircraft, freeway, and area emissions.	Continuous analysis of CO, NO_x, SO_2, $PM_{2.5}$, light scattering, black carbon, ultrafine particle number and size distribution. Substrate analysis of $PM_{2.5}$ mass, elements, ions, carbon, ammonia, and organics; as well as gaseous carbonyls, light HC, and heavy HC. TIGF/XAD for semi-volatiles and particulate organic compounds (PAH, alkanes, hopanes, steranes and polar compounds). 24-hour integrated samples.
CS	Community South. Core site for spatial, time series, and multivariate receptor analyses	Imperial Ave. School, ~ 0.5 km south of southern runways. Near-field crosswind site - Aircraft, roadway, GSE, stationary & area.	Continuous analysis of CO, NO_x, SO_2, $PM_{2.5}$, light scattering, black carbon, ultrafine particle number and size distribution. Substrate analysis of $PM_{2.5}$ mass, elements, ions, carbon, ammonia, and organics; as well as gaseous carbonyls, light HC, and heavy HC. TIGF/XAD for semi-volatiles and particulate organic compounds (PAH, alkanes, hopanes, steranes and polar compounds). 24-hour integrated samples.
CN	Community North – Airport/Arbor Vitae. Core site for spatial, time series, and multivariate receptor analyses.	North east of airport, West of I-405 Freeway. Community exposure – aircraft, freeway, and area emissions.	Continuous analysis of CO, NO_x, SO_2, $PM_{2.5}$, light scattering, black carbon, ultrafine particle number and size distribution. Substrate analysis of $PM_{2.5}$ mass, elements, ions, carbon, ammonia, and organics; as well as gaseous carbonyls, light HC, and heavy HC. TIGF/XAD for semi-volatiles and particulate organic compounds (PAH, alkanes, hopanes, steranes and polar compounds). 24-hour integrated samples.
AQ	SCAQMD SW Coastal LA County Site: Standard SCAQMD multiple pollutant monitoring site. This site is used as a Satellite or Background site for spatial, and time series analyses	~0.5 km North of Runway 24R (west end of runway). Some airport and area sources. Possible background site.	SCAQMD site collects SO_2, NO_x, TSP particulate for lead and sulfate (filter, not continuous), wind speed and direct, temperature and humidity. Due to limited available power the station upgrade will include continuous analysis of $PM_{2.5}$, light scattering, and black carbon. Substrate analysis of $PM_{2.5}$ mass, elemental and organic carbon using a MiniVol sampler. 7-day integrated samples during intensive periods.

Table A7-2
Revised Monitoring Network – Source Profile and Saturation Monitoring

Source Profile Sampling			
Symbol	***Site Title and Type***	***Location and Purpose***	***Components Analyzed***
SR	South Runway and Taxiway (SR): Source Profile site for source profiles and emission factors from aircraft takeoffs and taxiing	Behind blast fence on Runway 25R and Taxiway. Source-dominated – aircraft taxiing, takeoffs, and some roadway emissions.	Canister samplers for C_2-C_{11} hydrocarbons, methane, CO and CO_2. Tenax samplers for C_{10}-C_{20} hydrocarbons. DNPH cartridge samplers for carbonyl compounds. TIGF/XAD for semi-volatiles and particulate organic compounds (PAH, alkanes, hopanes, steranes and polar compounds). Teflon filter for PM mass and metals, quartz filter for OC, EC and sulfate. Continuous NO and sound monitors to record activity. Wind speed and wind direction.
	Downwind of Runway: plume dispersion.	Gradient sampling in the open field east of South Runway and Aviation Blvd. to determine plume dispersion from aircraft takeoffs, taxiing and landings.	4 to 6-hr passive samplers for NO_2, NO_x, SO_2, VOC and carbonyls. MiniVol samplers with Teflon filters for PM mass and metals and quartz filter for OC, EC and sulfate.
Saturation Sampling			
Symbol	***Site Title and Type***	***Location and Purpose***	***Components Analyzed***
SS	Saturation sampling at community locations and airport perimeters	Three communities locations (core sites: CE, CN, CS) adjacent to airport and four satellite sites at airport perimeters and seven gradient sites	7-daypassive sampling for NO_2, NO_x, SO_2, VOC and carbonyls. 7-day integrated sample during intensive periods.
		Three core sites (CE, CS, CN) and four satellite locations at airport perimeters (CE2, CN2, CS2 and AQ)	MiniVol samplers with Teflon filters for PM mass and metals and quartz filter for OC, EC and sulfate. 7-day integrated sample during intensive periods.

Figure A7-1. Phase III of the LAX AQSAS Revised Sampling Locations Map

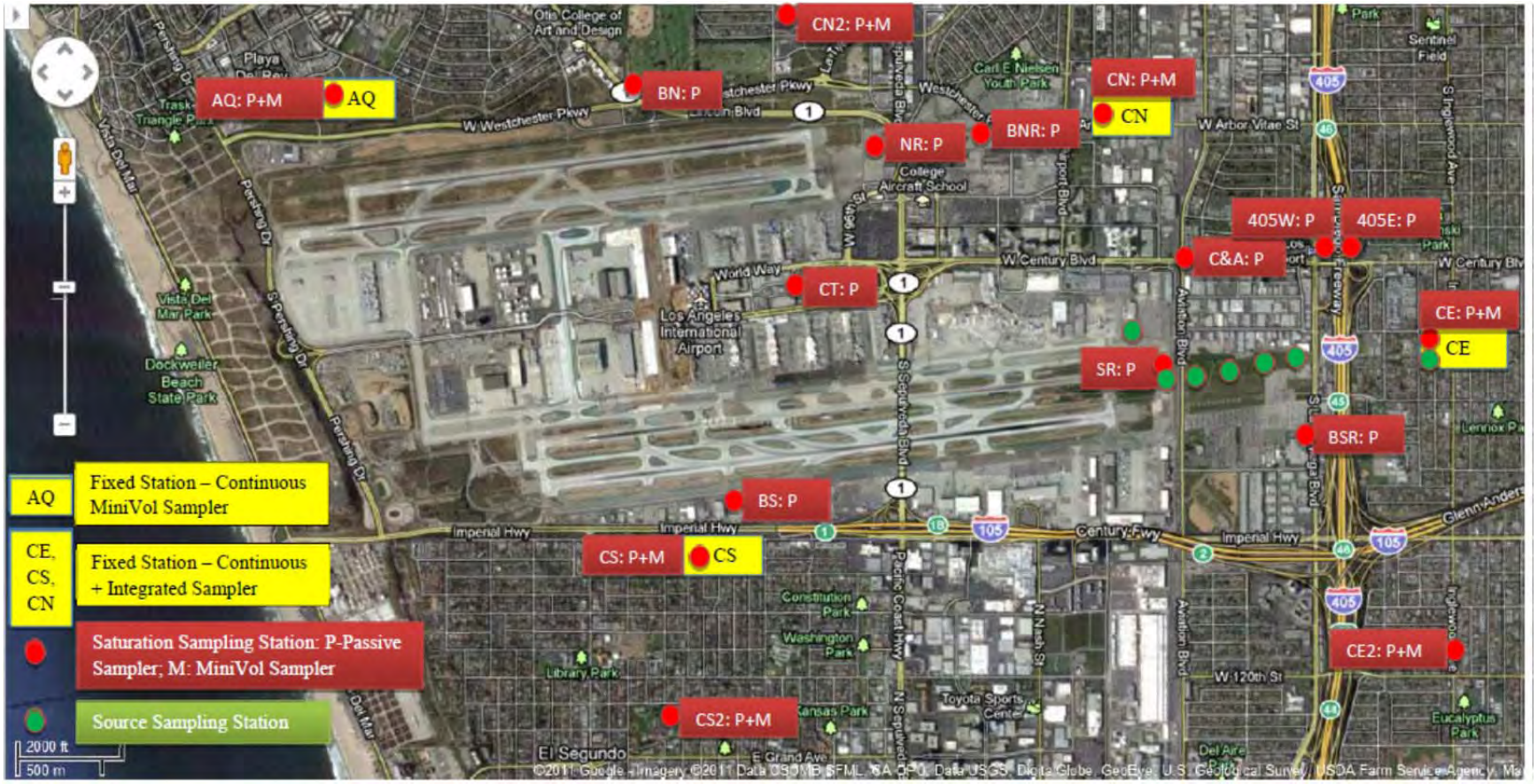

Table A7-3. Fixed Monitoring Sites, Parameters and Frequencies

Parameters	Site	AQ	CE	CS	CN	Sampling		
	Type	BG	C	C	C	Avg Time	Frequency	Period
Continuous Measurements	CO		v	v	v	5-min	Continuous	Duration of monitoring campaign
	NO_x	v	v	v	v	5-min	Continuous	Duration of monitoring campaign
	SO_2	v	v	v	v	5-min	Continuous	Duration of monitoring campaign
	$PM_{2.5}$ (BAM)	v	v	v	v	1-hr	Daily	Duration of monitoring campaign
	Light scattering	v	v	v	v	5-min	Continuous	Duration of monitoring campaign
	Black Carbon	v	v	v	v	5-min	Continuous	Duration of monitoring campaign
	UFP/Size		v	v	v	5-min	Continuous	Duration of monitoring campaign
$PM_{2.5}$ Samples	Mass/ Carbon	v	v	v	v	24-hr	Once daily/14-day	Seasonal intensive periods
	Elements		v	v	v	24-hr	Once daily/14-day	Seasonal intensive periods
	Ions		v	v	v	24-hr	Once daily/14-day	Seasonal intensive periods
	Ammonia		v	v	v	24-hr	Once daily/14-day	Seasonal intensive periods
Others	Semivolatiles (TIGF/XAD)		v	v	v	24-hr	Once daily/14-day	Seasonal intensive periods
	Carbonyls (DNPH)		v	v	v	24-hr	Once daily/14-day	Seasonal intensive periods
	L-HC (Canister)		v	v	v	24-hr	Once daily/14-day	Seasonal intensive periods
	H-HC (Tenax)		v	v	v	24-hr	Once daily/14-day	Seasonal intensive periods
Meteorological Measurements	WS		v	v		1-min	Continuous	Duration of monitoring campaign
	WD		v	v		1-min	Continuous	Duration of monitoring campaign
	T		v	v		1-min	Continuous	Duration of monitoring campaign
	RH		v	v		1-min	Continuous	Duration of monitoring campaign
	Solar Radiation		v			1-min	Continuous	Duration of monitoring campaign

Footnote: v: parameter measured. AQ: AQMD station CE: Community East; CS: Community South; CN: Community North; C: Core; BG: Background

Table A7-4. Source Profile Monitoring Sites and Parameters

Site ID	Site Name	Location	Continuous	Number of Sampler: 4 to 6-hour Samples During 4-day Source Measurement												
				Passive					Mini-Vol PM		Canister		Tenax	DNPH	Med-Vol PM		SVOC
				NO_x	NO_2	SO_2	BTEX	Carbonyl	mass, metals	OC, EC	Light HC	CH_4, CO, CO_2	Heavy HC	Carbonyl	Teflon	Quartz	TIGF/ XAD
SRB	South Runway Blast	Behind Blast Fence	NO, BC, PM, sound	1	1	1	1	1	-	-	1	1	1	1	1	1	1
SR2	South Runway Taxiway	Taxiway	-	1	1	1	1	1	-	-	1	1	1	1	1	1	1
SR3	South Runway #3	~25m east of Aviation	WS, WD	1	1	1	1	1	1	1	-	-	-	-	-	-	-
SR4	South Runway #4	~125m east of Aviation	NO, BC, PM, CPC	1	1	1	1	1	1	1	-	-	-	-	-	-	-
SR5	South Runway #5	~325m east of Aviation	-	1	1	1	1	1	1	1	-	-	-	-	-	-	-
BSR	Buffer Zone S Runway	Lot B near La Cienega Blvd.	-	1	1	1	1	1	1	1	-	-	-	-	-	-	-
CE	Community East	La Feria Restaurant, Lennox	1	-	-	-	-	-	-	-	-	-	-	-	-	-	-
Total number of sampler per sampling dal				6	6	6	6	6	4	4	2	2	2	2	2	2	2
Number of days per season			4														
Total number of samples/season				24	24	24	24	24	16	16	8	8	8	8	8	8	8

Table A7-5. Saturation Monitoring Sites and Parameters

Site ID	Site Type	Site Name	Location	Continuous	Number of 7-day Samples During LAX-AQSAS Six-Week Intensives							Number of Daily 24-hr Sample for 14 Consecutive Days					
					Passive					Mini-Vol PM		Canister	Tenax	DNPH	Med-Vol PM		SVOC
					NO_x	NO_2	SO_2	BTEX	Carbonyl	mass, metals	OC, EC	Light HC	Heavy HC	Carbonyl	Teflon	Quartz	TIGF/ XAD
CE	Core	Community East	La Feria Restaurant, Lennox	1	1	1	1	1	1	1	1	1	1	1	1	1	1
CS	Core	Community South	Imperial Ave School, El Segundo	1	1	1	1	1	1	1	1	1	1	1	1	1	1
CN	Core	Community North	NE of LAX, Westchester	1	1	1	1	1	1	1	1	1	1	1	1	1	1
AQ	Core/Satellite	Upwind Northwest	91st and Hastings, Playa de Rey	1	1	1	1	1	1	1	1	1	1	1	1	1	1
UW*	Satellite	Upwind West	W of LAX between SR and NR	-	1	1	1	1	1	-	-	-	-	-	-	-	-
CS2	Satellite	Community South #2	El Segundo	-	1	1	1	1	1	1	1	-	-	-	-	-	-
CN2	Satellite	Community North #2	Westchester	-	1	1	1	1	1	1	1	-	-	-	-	-	
CE2	Satellite	Community East #2	Hawthorne	-	1	1	1	1	1	-	-	-	-	-	-	-	-
BN	Gradient	Buffer Zone North	N of Westchester Parkway	-	1	1	1	1	1	-	-	-	-	-	-	-	-
BS	Gradient	Buffer Zone South	Imperial Terminal	-	1	1	1	1	1	-	-	-	-	-	-	-	-
SRN	Gradient	South Runway North	Intersection of Century Blvd and Aviation – SW corner	-	1	1	1	1	1	-	-	-	-	-	-	-	-
SRE	Gradient	South Runway East	40 m directly east of Runway 25R blast fence	-	1	1	1	1	1	-	-	-	-	-	-	-	-
NR	Gradient	North Runway	Fence at east end of NR	-	1	1	1	1	1	-	-	-	-	-	-	-	-
BSR	Gradient	Buffer Zone S Runway	Lot B near La Cienega Blvd.	-	1	1	1	1	1	-	-	-	-	-	-	-	-
BNR	Gradient	Buffer Zone N Runway	Lot C near Jenny Avenue.	-	1	1	1	1	1	-	-	-	-	-	-	-	-
CT	Gradient	LAX Central Terminal	Roof of Parking Garage	-	1	1	1	1	1	-	-	-	-	-	-	-	-
R405	Gradient	Freeway I-405 East Edge	East edge of Freeway I-405	-	1	1	1	1	1	-	-	-	-	-	-	-	-
Subtotal				4	17	17	17	17	17	6	6	4	4	4	4	4	4
Core					4	4	4	4	4	4	4	4	4	4	4	4	4
Satellite					4	4	4	4	4	4	4	-	-	-	-	-	-
Gradient					9	9	9	9	9	-	-	-	-	-	-	-	-

Monitoring Period

The 2010/2011 wind data collected at the SCAQMD LAX upper air station located west of the intersection of Pershing Drive and World Way West indicate two distinct wind patterns in the airport area. Figure A7-2 shows a monthly wind rose from October 2010 to September 2011. The first pattern encompassed November to March, with variable wind directions but predominantly ENE to NE and WSW to westerly winds. The second pattern encompassed April to October, with predominantly WSW and westerly winds. Considering the local unique wind patterns and the available budget for the program, it is suggested the monitoring period include two seasons – winter to spring and summer to fall. The two proposed monitoring periods should provide representative wind patterns in the airport area.

A7.2 Project Schedule

Based upon the project end date of April 1, 2013, sampling will occur over two seasons. The first will take place over six weeks, starting in January and finishing in February, 2012. The second sampling period will take place over six weeks, starting in July and finishing in mid-August, 2012.

Figure A7-2. AQMD LAX UA Site – Monthly Wind Rose (October 2010 to September 2011)

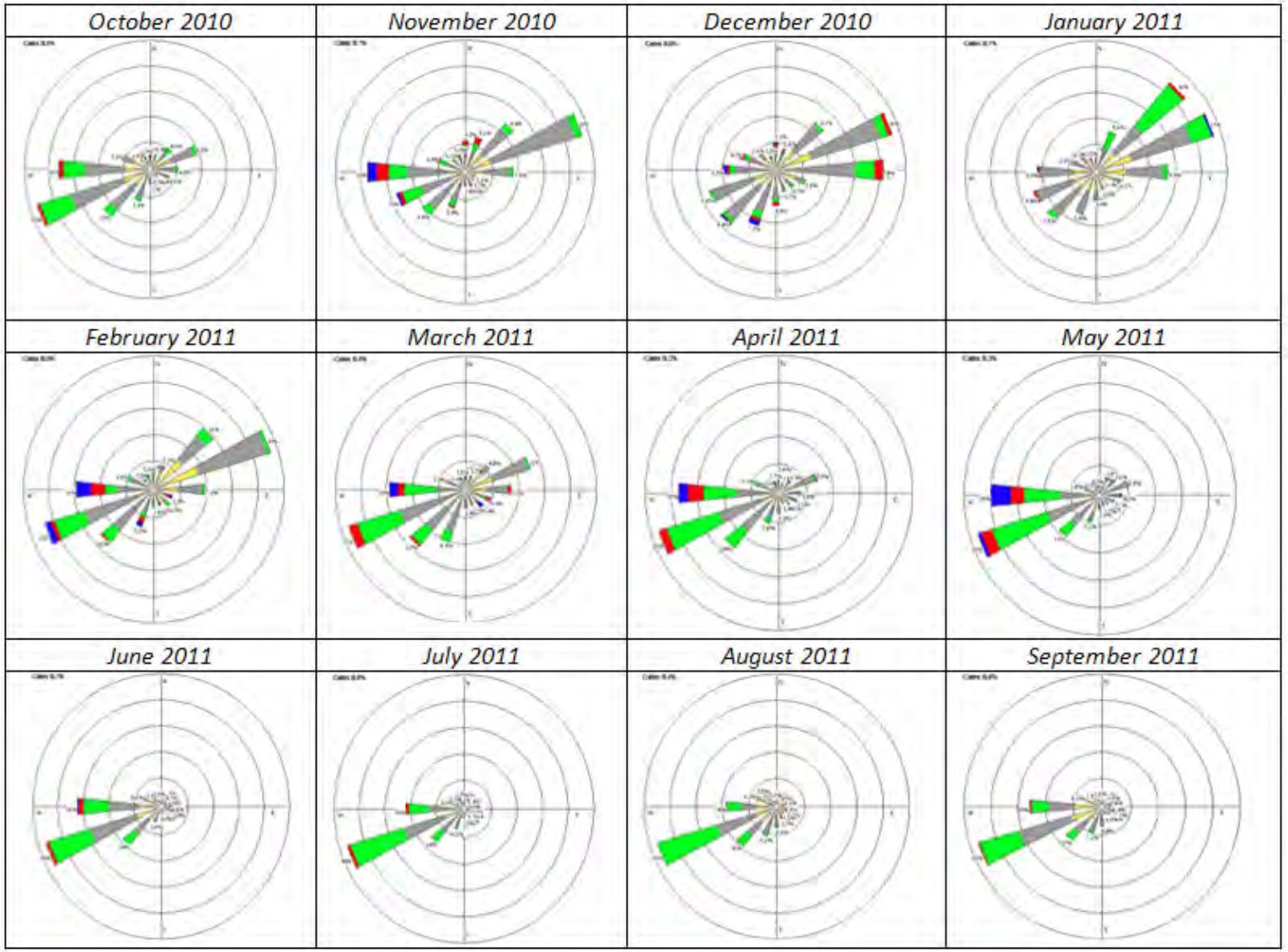

A8. Quality Objectives and Criteria for Measurement Data

A8.1 Data Quality Objectives

Quality assurance (QA) and quality control (QC) are an integral part of any measurement program. The purpose and objective of the QA/QC program is to standardize the procedures within the monitoring program and allow a thorough assessment of the precision, accuracy and validity of the data collected.

- Quality Control: The system of activities to provide a quality product.

- Quality Assurance: The system of activities to provide assurance that the quality control system is performing adequately.

The QC program consists of a variety of tasks and operational procedures designed to best ensure the collection of high quality data. The QA portion of the program uses the QC procedures to assess the quality of the data in terms of precision, accuracy and validity.

Accuracy – The degree of agreement between the measured and true concentrations of air pollutants in the ambient air. Accuracy may be expressed as a percentage or absolute difference between measured and true values.

Precision – The variability in a set of measurements of air pollutant performed under the same conditions with the same sampling and analytical procedures and equipment. Precision may be expressed as average difference, standard deviation (SD), or relative standard deviation (RSD) of a set of measurements.

Completeness – The number of air pollutant measurements actually obtained relative to the number of measurements expected if no loss of data occurred. Data completeness (also called data recovery or data capture) is usually express as a percentage.

Comparability – The ability to compare air pollutant monitoring data obtained at different time, at different geographical locations,, and by different organizations. Data comparability is dependent on the measurement methods, data processing techniques, reporting formats and units, and quality control/quality assurance procedures employed to perform the measurements.

Tetra Tech and its team members, DRI, SCS Tracer and T&B Systems, are fully committed to an effective QA/QC program for Phase III of the LAX Air Quality and Source Apportionment Study. The Project Team will ensure all ambient air quality and research measurement data generated meeting specific data quality objectives (DQOs). The U.S. EPA has established DQOs for actions, such as monitoring criteria pollutants. These DQOs have been used to establish data quality indicators (DQIs) for various phases of the monitoring process. Efforts are made to compare the same measurements on multiple instruments used for the LAX Study to assess the quality,

reliability and comparability of measured pollutant concentrations. Table A8-1 lists data quality objectives for selected parameters for the LAX study.

Table A8-1. Data Quality Objectives for Selected Parameters Measured During the Study

Parameters	***Data Quality Objectives***		
	Accuracy/Bias	***Precision***	***Completeness***
NO_x	95% CL ≤10%	90% CL CV≤10%	75%
SO_2	95% CL ≤10%	90% CL CV≤10%	75%
CO	95% CL ≤10%	90% CL CV≤10%	75%
$PM_{2.5}$ (BAM)	±10%	CV≤10%	75%
Hydrocarbons, Carbonyls	±10%	CV≤10%	75%
Elements (XRF)	±5%	±10% or within ±3 times the analytical uncertainties for each element	75%
Wind speed	±5%	±0.2 m/s	75%
Wind direction	±5°	±2°	75%
Temperature	±1°C	-	75%
Humidity	±10 % RH	-	75%

CL - Confidence Level; CV – Confidence Value

Success of the project will be evaluated in terms of: 1) accuracy, precision, validity and completeness of acquired data and 2) the extent to which data can be used to meet stated project objectives. Regular flow and calibration checks will be conducted by field operators. In addition, DRI routinely conducts inter-laboratory comparisons with CARB and the South Coast Air Quality Management District. A final report by the Project team will discuss accomplishments with respect to data qualification. The Tetra Teach project team is fully committed to an effective QA/QC program for this project and ensures that data meet specific DQOs.

A8.2 Measurement Quality Objectives

The Project Team recognizes the need to provide products and services of optimum quality. A comprehensive program of quality management and quality assurance has been established to identify requirements and provide procedural guidance for achieving quality objectives through proper planning, guidance, control, review, communication, auditing, reporting, and corrective action.

A major objective of the QA Program is to plan to reduce or eliminate errors, improve efficiency and achieve better quality in a cost-effective manner. Another major objective is to ensure, assess and document that all information and work produced meets known standards of quality such as completeness, comparability, precision, accuracy, representativeness and traceability.

QA objectives for tasks involving measurements and support functions include the following:

* Implement an appropriate written QA plan for all tasks that involve data collection or characterization activities

- Ensure implemented QA plans are reviewed regularly and updated as needed
- Produce data that meet DQOs and management quality objectives (MQOs)
- Provide quality products and services on time and cost-effectively
- Inform LAWA representatives of the status of product quality regularly
- Ensure that all project team personnel have the training and resources to meet project objectives, standards for product quality and other requirements
- Review all data to ensure DQOs, MQOs and contract specifications and requirements are met
- Provide software development and system acceptance tests to ensure that such items meet CARB or U.S. EPA requirements for functionality and system performance
- Apply standard operating and review procedures to data transfer, security and storage to ensure the integrity of any measurement or environmental data collection or characterization of spreadsheets or databases
- Maintain a continuing assessment of the quality of data generated by analysts working in the DRI's Organic Analytical Laboratory and Environmental Analytical Facility.
- Provide a permanent record of instrument performance as a basis for validating data and projecting repairs and replacement needs.
- Ensure sample integrity.
- Ensure rigorous record keeping.
- Produce analytical results that can withstand scientific and legal scrutiny.

The project will involve two laboratories within DRI's Division of Atmospheric Science, the Environmental Analysis Facility (EAF), and the Organic Analytical Laboratory (OAL). The Environmental Analysis Facility (EAF) quantifies trace substances of atmospheric contaminants collected on substrates. EAF conducts gravimetric analysis, carbon analysis by thermal optical reflectance and transmittance (TOR and TOT), elemental analysis by XRF, and ions by ion chromatography and colorimetry. The Organic Analytical Laboratory (OAL) provides collection and analysis of trace organic contaminants and hazardous air pollutants in ambient and source samples using gas chromatography (GC), mass spectrometry (MS), Fourier transform infrared spectroscopy (FTIR) and high performance liquid chromatography (HPLC). Each laboratory maintains a complete QA/QC program.

QA is a project management responsibility that integrates quality control, quality auditing, measurement method validation and sample validation into the measurement process. Quality auditing is an external function performed by personnel not involved in normal operations. The purpose of quality audits is to determine whether the QC procedures are adequate and adhered to and whether the tolerances for accuracy and precision are being achieved. The quality auditing function consists of: 1) systems audits and 2) performance audits. Systems audits include review of the operational and QC procedures to assess whether they are adequate to assure valid data meet the specified levels of accuracy and precision. All phases of measurement and data processing activities are examined during the systems audit to determine if procedures are being

followed and operating personnel are properly trained. Performance audits establish whether the predetermined specifications for accuracy are being achieved. For measurements, the performance audit involves challenging the measurement/analysis system with a known standard sample traceable to a primary standard. Performance audits of data processing involve independent processing of raw data and comparison of results with reports generated by routine data processing.

QA personnel for this project will function independently of the groups responsible for the routine work or environmental data collection activities. Dr. Steve Kohl, the DRI EAF QA Manager and Mr. David Campbell, the DRI OAL QA Manager, will have the overall responsibility for the QA/QC program for their respective laboratories. Each of the QA Managers report directly to the Executive Director of DRI's Division of Atmospheric Sciences (DAS) for DRI'S internal QA-related activities.

QA management for the project is the joint responsibility of the Project Principal Investigator, Laboratory Directors and the Quality Assurance (QA) Manager. The QA Manager must ensure the program design contains adequate QC procedures and adequate external checks to assure data obtained will be adequate for the intended purposes. It is the responsibility of the Laboratory Director to monitor the QA activities during the project and to ensure problems are rapidly identified and solved. DRI maintains a complete QA/QC program, which includes:

Daily calibration. Calibration checks are completed each day on all laboratory instruments to be used in this study. These checks will confirm response factors and retention times for continuous and time-integrated instruments.

Daily instrument blank. An appropriate blank will be run daily for each instrument. Typically, this occurs after the calibration check and before any sample is analyzed. This confirms no carryover exists from the calibration check as well as confirms the blank or zero level of the instrument.

Duplicate analysis for every 10 samples. Protocols employed by DRI request 10 percent replicate analysis leading to duplicate analysis every 10 samples. This is an important component of the QA/QC program since the protocols are used to determine replicate precision, which allows for calculation of sample uncertainty.

Control samples. DRI labs analyze a variety of control samples for QA/QC purposes. These include calibration, replicate, colocated and blind QA samples.

Recovery tests for selected analytes. For carbonyls (2,4-Dinitrophenylhydrazine (DNPH)) analyses, internal standards are also added.

Determine and report minimum trapping efficiency. For solid adsorbent samples (DNPH for carbonyls and Tenax for C_{12}-C_{20} hydrocarbons), backup traps are used to confirm that no quantifiable levels of compounds are moving through the first trap.

Every measurement consists of a value, a precision, an accuracy, and a validity (e.g., Hidy, 1985). Validity applies to both the measurement method and to each measurement taken with that method. The validity of each measurement is indicated by appropriate flagging within the database and the validity of the methods used in this study is evaluated. The measurement methods described in the previous section are used to obtain the value. QA is the complementary part of the measurement process, which provides the precision, accuracy and validity estimates and guarantees these attributes are within acceptable limits.

QA for the project is the joint responsibility of the laboratory manager and the QA manager. It is the responsibility of the laboratory manager to monitor the QA activities during the project and to ensure problems are rapidly identified and solved. The QA manager must ensure the program design contains adequate QC procedures and external checks to assure data obtained will be acceptable for their intended purposes.

(Please note that project QA performed by T&B System is discussed in Section C.)

A9. Special Training/Certification

The roles of principal investigators, QA manager, field and lab supervisors, operators and coordinators, data base managers, and data analysts are clearly defined. Each person possesses extensive research experience in his or her assigned tasks. The Project team ensures project participants are properly trained to perform individual tasks. Additional guidance about actual site operations for this project is provided to the site operators in the form of checklists, forms, SOPs and other material comprising the MQAPP.

A10. Documentation and Records

The MQAPP summarizes the LAX Study measurements, defines data quality indicators and specifies data quality objectives. Laboratory records, including written and computerized, are maintained to provide documentation for data during the Study. Field and laboratory standard operating procedures (SOPs) developed for the LAX Study measurements are followed and revised as needed for the duration of the Study. Procedures for advanced monitoring methods created and reviewed by the Project Team. Revisions made to SOPs during the study period are noted and archived for traceability. Remedial actions taken as a result of field, laboratory or data audits are also to be documented. Procedural summaries will also be published in appropriate handbooks and manuals.

Field records

Site Logs

A bound logbook is kept at each station and is used to record all site operator activities. The site operator first enters the time and date of his or her arrival. Any subsequent activities, such as calibrations or maintenance are recorded along with their beginning and ending times. Any problems in site operation or in the performance of any piece of equipment are also recorded in the site log.

Operator Checklists

The Operator Checklists consist of pages of checks to be completed by the site technician upon each visit to the monitoring station. The checklists contain a number of key questions concerning the operational status of air quality analyzers, calibration equipment, meteorological sensors and data systems as well as general checks. Most entries require only a yes/no response while others require specific information.

Any discrepancies noted during the mandated checks are entered in the site logs. Serious problems noted during the checks will also be documented on additional forms.

Laboratory Records

Several forms of laboratory records are routinely maintained. Written records include shipping and receiving log books, chain-of-custody forms, project log books, instrument log books, instrument service log books, calibration records (including a calibration standard log book) and graphs of response factors vs. time, a canister cleaning log book, and sampler maintenance and cleaning log books. Computerized records include method, calibration, raw data, processed data, and combined data files.

Written records are maintained in the appropriate location in the laboratory in non-erasable ink so any alteration is easily noted. Project log books record sample information, including arrival

time. Instrument log books record each sample run, including all pertinent information and calibration runs. Other calibration records include the calibration log book where all standard solutions made in the laboratory are logged, a graph of all calibration checks, and the computerized calibration files. Service log books show services and/or modifications of the instruments. The canister cleaning log book records each canister number, the project the canister was used for, date of last cleaning, and certification information. Each entry is signed and dated.

Computerized records are maintained on a central computer at DRI (the LIMS file server). The data collection system includes a history record that maintains a list of created or modified files and the individual who entered the file. Each sample has an original report printed at the time the sample run is completed, which indicates the method and calibration file used and the last modification date of the file. Backups of computerized records, including removable media (floppy disks) and tapes, are stored in the LIMS manager's office at an off-site storage area.

Standard Operating Procedures (SOPs)

Standard operating procedures (SOPs) codify the actions taken to implement a measurement process over a specified time period. State-of-the-art scientific information is incorporated into the SOP with each revision. SOPs include the following elements:

* A brief summary of the measurement method, its principles of operation, its expected accuracy and precision, and the assumptions which must be met for it to be valid.
* A list of materials, equipment, reagents and suppliers. Specifications are given for each expendable item and its storage location.
* A general traceability path, the designation of primary standards or reference materials, tolerances for transfer standards, and a schedule for transfer standard verification.
* Start-up, routine and shut-down operating procedures and an abbreviated checklist.
* Copies of data forms with examples of filled out forms.
* Routine maintenance schedules, maintenance procedures and troubleshooting tips.
* Internal calibration and performance testing procedures and schedules.
* External performance auditing schedules.
* References to relevant literature and related SOPs.

Table A10-1 lists the SOPs applicable to the Air Quality and Source Apportionment Study measurements and their current status. For criteria pollutant and meteorological measurements, CARB QA procedures and SOPs are followed to assure continuity and consistency of data with other data collected within the state. SOPs are provided as a separate volume. The method detection limits (MDLs) for the equipment used to measure the analytes listed in Table A10-1 are contained in Table A10-2.

Table A10-1: Summary of SOPs Applied to Source Apportionment Study

Measurement Parameter	*Method*	*Make and Model Number*	*Applicable SOP*
Black Carbon	Optical Absorption	Magee Scientific Aethalometer Model AE 21-HS-P3-FO-MCr	ARB-AQSB SOP 407
Carbon Monoxide	Gas Filter Correlation with IR Absorption	Thermo Environmental Instruments Model 48 or Teledyne API	ARB-AMQA Volume II, Appendix Y
Light Scattering	Light Scattering	Radiance M903 or Equivalent	ARB-AMQA Volume II, Appendix L
Carbon Speciation	GC/MS	MiniVol Sampler	DRI 2-204.4
Thermal/Optical Carbon Analysis (Quartz Fiber Filter)	TOR/TOT	Quartz fiber filters 2500 QAT-UP and Muffle Oven (Model 51894	DRI 2-106r6
CO, CO_2, CH_4	GC with FID	Shimatzu GC 17-A	DRI 2-701-2
NO_x	Chemiluminescence	Thermo Environmental Instruments Model 42 or Teledyne API Model 200	ARB-AMQA Volume II, Appendix W
SO_2- Trace Level	Pulsed Fluorescence	Thermo Environmental Instruments Model 43i TLE or Equivalent	ARB-AMQA Volume II, Appendix C
Passive $NO/NO_2/NO_x$ and SO_2	Passive Sampler	Ogawa 3300 Sampler	Ogawa Sampling Protocol Version 6
$PM_{2.5}$	Beta Attenuation	MetOne BAM 1020 or Equivalent with Sharp Cut Cyclone	ARB-AQSB SOP 400
$PM_{2.5}$ Gravimetry	Gravimetric Analysis	Mettler Toledo XP6 Microbalance	DRI 2-114.8
Particulate Elements $PM_{2.5}$, (Ni, - U)	X-Ray Fluorescence and ICP-MS	DRI Med-Vol Sequential Sampler	SCS SOP Draft and DRI SOP #2-209.6 and #2-220r0
$PM_{2.5}$ carbon (EC/OC)	Thermal Optical Reflectance	DRI Med-Vol Sequential Sampler	DRI SOP2-216r2
$PM_{2.5}$ anions (NO_3, SO_4)	Ion Chromatography	DRI Med-Vol Sequential Sampler with Nitric Acid Denuder	DRO SOP 2-203r7
Particulate Matter	Portable $PM_{2.5}$ Sampler Airmetrics impactor	Field Operations	DRI 1-210r4
Ultrafine Particulates	SMPS/CPC	Scanning Mobility Particle Sizer (Bipolar Charger, Mobility Classifier, Condensation Particle Counter) Grimm SMPS (Model 5.400) and TSI Nano-SMPS (Model 3936N25A)	DRI 1-750.4; DRI TSI Nano, Regular and Grimm SMPS Instructions
Carbonyls	Sampling Followed by HPLC	Sequential Sampler w/ DNPH Cartridge; Waters (WAT047205)	EPA Method TO-11A (DRI 2-710.4)

Measurement Parameter	*Method*	*Make and Model Number*	*Applicable SOP*
Heavy Hydrocarbons	Tenax Sampling Followed by Laboratory Analysis	Sequential Tenax (Charcoal) Sampler	SCS SOP Draft DRI 1-720.3
Light Hydrocarbons	SUMMA Canister Sampling Followed by Laboratory Analysis	Sequential Canister Sampler	SCS SOP Draft
VOC (C_8-C_{20}) Range	GC with MSD Detection	Varian CP-3800 gas chromatograph equipped with an 8200 CX Autosampler and interfaced to a Vairan Saturn 2000 Ion Trap Mass Spectrometer	DRI 2-750.5
Semi-Volatile Organic Compounds (SVOCs)	GC/MS	Varian CP-3800 gas chromatograph, 8200 CX Autosampler and Varian Saturn 2000 Ion Trap Mass Spectrometer	EPA Method TO-13 (DRI 750.5)
Fine Particulates/SVOCs	Sequential Sampler	4 Channel Sequential Sampler	DRI 1-750.4
Ambient VOC	GC/MS	Varian 3800 gas chromatograph and Varian Saturn 2000 Ion Trap Mass Spectrometer	Modified TO-15 method (DRI 2-704.1)
Passive VOC/Carbonyl	Passive Sampler	Radiello 145/165 Sampler	DRI SOP1-Passive 3
Aerosols	X-Ray Fluorescence	PANalytical Epsilon 5 XRF	DRI 2-304.4
	TOR/TOT Method IMPROVE A	DRI Model 2001 Thermal/Optical Carbon Analyzer	DRI 2-216.2
Anions	Ion Chromatography	Dionex Series 500 Ion Chromatography (IC) System	DRI 2-203r7
Wind Speed w/ Cable	Anemometer	Met One Model 010	ARB-AMQA Volume II, Appendix T
Wind Direction w/ Cable	Potentiometer	Met One Model 020	ARB-AMQA Volume II, Appendix V
Ambient Temp (2 heights)	Precision Thermistor	Met One Model 060A	ARB-AMQA Volume II, Appendix AA
Solar Radiation	Pyranometer	Eppley Model 8-48	ARB-AMQA Volume II, Appendix U
Relative Humidity	Hygroscopic Capacitor	Met One 083C %RH	
Filter Packs	Processing	Filter Holders, Filter Media, Barcode Labels	DRI 2-111.4
Chain of Custody	Shipping and Receiving	Sample Shipping, Receiving and Chain of Custody	DRI 2-209.4

A10-2: Method Detection Limits for Analytes Measured

Analyte	*Analytical Method*	*Method*	*Detection Limit(s)*
Black Carbon	Aethalometer	ARB-AQSB SOP 407	~>50 ng/m^3
Carbon Monoxide	IR Absorpotion	ARB-AMQA Volume II, Appendix Y	0.04 ppm (30 second averaging time)[1]
Light Scattering	Nephelometer	ARB-AMQA Volume II, Appendix L	<0.3 Mm-1 (60 second averaged data)
Carbon Speciation	GC/MS	DRI 2-204.4	total OC 0.39 µg/cm^2 total EC 0.01 µg/cm^2 TC 0.42 µg/cm^2
Thermal/Optical Carbon Analysis (Quartz Fiber Filter)	Quartz Fiber Filter	DRI 2-106r6	Upper limit for organic carbon levels is 1.5 µg/cm^2, Elemental carbon levels is 0.5 µg/cm^2, and total carbon levels is 2.0 µg/cm^2. The upper limit for ions is <1.0 µg/filter.
CO, CO_2, CH_4	GC/MS – Flame Ion Detector	DRI 2-701.2	Est. 0.01% by volume
NO_x	Chemiluminescence	ARB-AMQA Volume II, Appendix W	50 ppb (lower detection limit)[2]
SO_2 – Trace Level	Pulsed Fluorescence	ARB-AMQA Volume II, Appendix C	0.5 ppb of SO_2
Passive $NO/NO_2/NO_x$ and SO_2	Ogawa Passive Sampler	Ogawa Sampling Protocol Version 6	1.3 ppb [3]
$PM_{2.5}$	Beta Attenuation	ARB-AQSB SOP 400	< 1 ug/m^3 (at 24 hours); <4.8 ug/m^3 (at 1 hour)
$PM_{2.5}$ Gravimetry	Mettler Toledo XP6 Microbalance	DRI 2-202.4 (DRI 2-114r7)	Min Weight: 1.2 mg + 9x(10^{-5}) Rgr (gross weight)
Particulate Elements $PM_{2.5}$ (Ni – U)	X-Ray Fluorescence (XRF)	DRI 2-209.6	In µg/cm^2 Na 0.204; Mg 0.125 Al 0.016, Si 0.018 P 0.006 S 0.006 Cl 0.004 K 0.006 Ca 0.015 Sc 0.083 Ti 0.004 V 0.001 Cr 0.001 Mn 0.007 Fe 0.002 Co 0.002 Ni 0.002 Cu 0.004 Zn 0.003 Ga 0.014 As 0.001 Se 0.004 Br 0.003 Rb 0.002 Sr 0.003 Y 0.002 Zr 0.008 Nb 0.004 Mo 0.005 Pd 0.006 Ag 0.007 Cd 0.012 In 0.010 Sn 0.015 Sb 0.018 Cs 0.050 Ba 0.031 La 0.051 Ce 0.033 Sm 0.087 Eu 0.071 Tb 0.071 Hf 0.032 Ta 0.018 W 0.022 Ir 0.006 Au 0.007 Hg 0.006

			Tl 0.004 Pb 0.005 U 0.005
$PM_{2.5}$ carbon (EC/OC)	Thermal Optical Reflectance	DRI 2-216r2	total OC 0.39 µg/cm^2 total EC 0.01 µg/cm^2 TC 0.42 µg/cm^2
$PM_{2.5}$ anions (NO_3, SO_4)	Ion Chromatography	DRI 2-203r7	Lower Quantifiable Limit (µg/m^3) F^- 0.0017 Cl^- 0.0017 NO_2- 0.0017 NO_3- 0.0017 SO_4- 0.0017 Br^- 0.0017 $PO_4^=$ 0.0017
Particulate Matter	Portable PM sampler	DRI 1-210r4	6 to 300 μg/m^3 (range) 3 to 6 μg/m^3 (lower quantifiable limit)
Carbonyls	High Performance Liquid Chromatography	U.S. EPA Method TO-11A (DRI 2-710.4)	est. ~ 0.1 ppbv
Heavy Hydrocarbons	Tenax Sampling	SCS SOP Draft (U.S. EPA Method TO-15)	0.01-0.05 ppbv
Light Hydrocarbons	SUMMA Canister sampling	SCS SOP Draft (U.S. EPA Method TO-15)	0.01-0.05 ppbv
VOC ($C_8 - C_{20}$) range	GC with MSD Detection	DRI 2-750.5	HC: 0.12 ppb carbon; Method: 0.04 ppb carbon. 0.5 to 25 parts per billion (ppbv) concentration (TO-17)
Semi-VOCs	GC/MS	U.S. EPA Method TO-13 (DRI 2-750.5)	0.01-0.03 ng/µl for PAH, hopane and sterane, and alkane compounds, and 0.03-0.04 ng/µl for polar compounds
Ambient VOCs	GC/MS	U.S. EPA Method TO-15 (DRI 2-704.2)	0.01-0.05 ppbv
Passive VOC	Radiello Passive Sampler	DRI SOP 1-Passive 3	0.05-1.0 μg/m^3 [4]
Aerosols	X-Ray Fluorescence (XRF) and Thermal/Optical Carbon Analysis	2-209.6 (2-304.4)	In µg/cm^2 Na 0.204; Mg 0.125 Al 0.016, Si 0.018 P 0.006 S 0.006 Cl 0.004 K 0.006 Ca 0.015 Sc 0.083 Ti 0.004 V 0.001 Cr 0.001 Mn 0.007 Fe 0.002 Co 0.002 Ni 0.002 Cu 0.004 Zn 0.003 Ga 0.014 As 0.001 Se 0.004 Br 0.003 Rb 0.002 Sr 0.003 Y 0.002 Zr 0.008 Nb 0.004

			Mo 0.005 Pd 0.006 Ag 0.007 Cd 0.012 In 0.010 Sn 0.015 Sb 0.018 Cs 0.050 Ba 0.031 La 0.051 Ce 0.033 Sm 0.087 Eu 0.071 Tb 0.071 Hf 0.032 Ta 0.018 W 0.022 Ir 0.006 Au 0.007 Hg 0.006 Tl 0.004 Pb 0.005 U 0.005 IMPROVE Method: total OC 0.39 µg/cm^2 total EC 0.01 µg/cm^2 TC 0.42 µg/cm^2
Anions	Ion Chromatography	DRI 2-203r7	LQL: 10 - 30 ppb range (in µg/m^3) F^- 0.0017 Cl^- 0.0017 NO_2- 0.0017 NO_3- 0.0017 SO_4- 0.0017 Br^- 0.0017 $PO_4^=$ 0.0017

[1]http://www.thermoscientific.com/ecomm/servlet/productsdetail?navigationId=L10403&categoryId=89577&productId=11961392&&storeId=11152

[2]http://cmbcontrol.com/pdf/thermo_analizador42ihl_no_no2_y_nox.pdf

[3]http://www.ogawausa.com/pdfs/fieldmethod.pdf

[4]http://www.sigmaaldrich.com/etc/medialib/docs/Supelco/The_Reporter/1/t211003-radiello.Par.0001.File.tmp/t211003-radiello.pdf

(This page is intentionally blank)

B. Measurement / Data Acquisition

B1. Site Selection

Two types of sites were selected, 1) community areas and 2) sites for spatial gradient analysis. These sites will be used to identify air quality impacts from LAX activities on the surrounding community areas. For this reason, community sites were chosen. Sites for spatial gradient analysis will allow for the determination of which types of pollutants are located at which distances from LAX.

Community Sites include:

Community East (CE). Community exposure site looking at aircraft, freeway, and area emission will serve as a core site for spatial, time series and multivariate receptor analyses. The site will be located at La Feria Restaurant about 1.5 km ESE of the southern airfield.

Community South (CS). Near-field crosswind site looking at aircraft, roadway, ground support equipment, stationary and area emission and will serve as a core site for spatial, time series and multivariate receptor analyses. The site will be located at the Imperial Avenue School approximately 0.5 km south of the southern runways.

Community North (CN). Community exposure site looking at aircraft, freeway, and area emissions will serve as a core site for spatial, time series and multivariate analyses. An initial site survey identified a property owned by LAWA located at the intersection of Airport Boulevard and Arbor Vitae Street, west of I-405 Freeway. This location was designated as the CN site using the DRI trailer originally intended for UW site.

SCAQMD Hastings (AQ). Standard SCAQMD multiple pollutant monitoring site looking at some airport and area sources, located northwest of LAX (AQ). This site is used as a Background site for spatial, and time series analyses

Spatial Gradient Analysis Sites include:

Source Profile. 1) Source-dominated site looking at aircraft taxiing, takeoffs and some roadway emissions will serve to provide source profiles and emissions factors. 2) Gradient sampling site located in the open field east (downwind) of the South Runway and Aviation Blvd and will be used to determine plume dispersion from aircraft takeoffs, taxiing and landings.

Saturation Sampling. Multiple sites will be located within the community and around the airport perimeter to conduct gradient and spatial analyses.

Table B1-1: List of Sites for Phase III of the LAX AQSAS Study

Site ID	***Site Type***	***Site ID***	***Site Type***
CE	Core	Community East	La Feria Restaurant, Lennox
CS	Core	Community South	Imperial Ave School, El Segundo
CN	Core	Community North	NE of LAX, Westchester
AQ	Core/Satellite	Upwind Northwest	91st and Hastings, Playa del Rey
UW*	Satellite	Upwind West	W of LAX between SR and NR
CS2	Satellite	Community South #2	El Segundo
CN2	Satellite	Community North #2	Westchester
CE2	Satellite	Community East #2	Hawthorne
BN	Gradient	Buffer Zone North	N of Westchester Parkway
BS	Gradient	Buffer Zone South	Imperial Terminal
SRN	Gradient	South Runway North	Intersection of Century Blvd and Aviation – SW corner
SRE	Gradient	South Runway East	40 m directly east of Runway 25R blast fence
NR	Gradient	North Runway	Fence at east end of NR
BSR	Gradient	Buffer Zone S Runway	Lot B near La Cienega Blvd.
BNR	Gradient	Buffer Zone N Runway	Lot C near Jenny Avenue.
CT	Gradient	LAX Central Terminal	Roof of Parking Garage
R405	Gradient	Freeway I-405 East Edge	East edge of Freeway I-405

* Only limited sampling using passive samplers will be conducted at this site to represent air quality in upwind location.

For further information, please reference Tables A7-1 and A7-2.

B2. Sampling Method

B2.1 Continuous Measurements

B2.1.1 Gaseous Pollutants

Continuous Carbon Monoxide Monitoring

CO concentrations will be measured using a Thermo Environmental Model (TEI) 48 analyzer. The TEI 48 uses infrared detection and the gas filter correlation principle of operation for measurement of CO. The basic components of the gas correlation system are: infrared (IR) source, chopper and rotating gas filter wheels, multiple optical pass sample cell, band pass filter, IR detector and electronic signal processor. Radiation from the IR source is chopped and then passed through a gas filter that alternates between CO and N_2 due to rotation of the filter wheel. The radiation then passes through a narrow band pass filter and a multiple optical-pass sample cell and falls on a solid state IR detector. The CO gas filter produces a reference beam that cannot be further affected by CO in the sample chamber. The N_2 side of the filter wheel, which is transparent to IR radiation, produces a measure beam that can be absorbed by CO. The chopped detector signal is modulated by the alteration between the two gas filters with amplitude proportional to the concentration of CO in the sample chamber. Other gases do not cause modulation of the detector signal since they absorb the reference and measure beams equally; therefore, the gas filter correlation system responds solely to CO.

The CO analyzer will be operated on the 0-50 ppm range with a minimum detection level of 0.1 ppm. Analyzer outputs will be averaged at a minimum interval of five minutes.

Continuous Measurement of Light Scattering

The nephelometer (Radiance Research Model 903 or equivalent) measures the light scattering in an airflow passing through the instrument's scattering chamber. The instrument reading, which is proportional to the light-scattering coefficient, indicates the total amount of light scattered into all directions by the air sample.

The scattering volume is illuminated from the side by a diffuse light source. The photomultiplier detector views a dark trap through a conical scattering volume defined by a series of baffles containing circular holes. The baffles prevent the photomultiplier from viewing any surface illuminated by the light source, except for the internal span calibration chopper.

Light falling on the photomultiplier is approximately proportional to the light-scattering coefficient of the air sample in the scattering chamber, which is a measure of the total amount of light scattered at all angles by the air sample. The nephelometer processes these data to subtract light scattering by the air to obtain a measure of the scattering coefficient b_{sp}. The nephelometer is calibrated to read zero when filled with particle-free air. A calibration span gas (Freon 134A SUVA), which has a larger scattering coefficient than air, is used to adjust the span of the nephelometer so the data are recorded directly in engineering units of m^{-1}.

Continuous Oxides of Nitrogen

Ambient levels of NO_x will be monitored continuously using Thermo Electron (TEI) Corporation Model 42C NO_x analyzer. This instrument is sensitive, interference free, and provides long-term zero and span stability for continuous monitoring of NO, NO_2 and NO_x.

The TEI 42C detects NO in ambient air by reacting NO with O_3. The resulting chemiluminescent reaction is monitored through an optical filter by a photo-multiplier tube (PMT) located at the end of the reaction chamber. The optical filter limits the wavelength of light measured by the PMT, so that it corresponds specifically to the wavelength of the chemiluminescent reaction between NO and O_3.

Total NO_x will be measured by passing the sample gas through a catalytic converter, which converts NO_2 quantitatively into NO, where it is measured by the detector. The microprocessor-controlled analyzer directs sample flow either through the catalytic converter (measuring NO_x) or by passing the sample directly into the detector (measuring NO). Signals from the PMT are conditioned and fed to the microprocessor where a sophisticated mathematical algorithm is utilized to calculate three independent outputs: NO, NO_2 and NO_x.

The NO_x analyzer will be operated on the 0-0.500 ppm range, with a minimum detection level of 0.001 ppm. Analyzer outputs will be averaged at a minimum interval of one minute.

Continuous Trace Level Sulfur Dioxide

Ambient levels of SO_2 will be monitored continuously by using a Thermo Model 43i TLE SO_2 analyzer. The Model 43i TLE is capable of measuring the amount of SO_2 in the air as low as 50 ppt. Dual sets of reflective band pass filters are less subject to photochemical degradation and more selective in wavelength, which results in increased detection specificity and long term stability. The Model 43i TLE uses pulsed fluorescent radiation of SO_2 molecules. A reaction chamber is irradiated by UV light and the fluorescent radiation is detected by a sensitive PMT. Associated electronics amplify the output from the PMT. The output voltage is proportional to SO_2 concentrations.

The SO_2 analyzer will be operated on the 0-0.500 ppm range, with a minimum detection level of 0.001 ppm. Analyzer outputs will be averaged at a minimum interval of one minute.

B2.1.2 Continuous Measurement of $PM_{2.5}$

Continuous monitoring of $PM_{2.5}$ will be performed using a beta-attenuation monitor (BAM) manufactured by Met One Instruments, Inc. (Met One). Met One BAM-1020 monitor will be used for continuous $PM_{2.5}$ measurements to provide hourly $PM_{2.5}$ concentrations.

The beta attenuation process uses a small source of beta particles (carbon-14, 60 microcuries) coupled to a sensitive detector that counts the emitted beta particles. The dust particles are collected on glass fiber filter tape placed between the beta source and the detector. Dust on the filter will intercept some of the beta particles. The air stream is heated to reduce the relative humidity of the sample stream to below 60 percent to reduce positive artifact measurement due to

condensation on the filter. The reduction of beta particles is proportional to the amount of dust on the filter, which allows the mass of dust to be determined from the beta particle counts. The dust mass is divided by the air volume collected during the filter exposure time to determine the PM concentration.

The BAM-1020 monitor will be equipped with particle size selective inlets, which are designed to remove particles larger than the desired size range from the air flow, based on the flow rate. Sampling flow rate is critical to maintain the proper particle size cut points of the inlets. Flow rates are maintained at 16.7 liters per minute (LPM) in the BAM-1020 using an integral flow meter, pressure sensor and ambient temperature sensor on board each monitor.

Data from the BAM-1020 unit will be recorded by digital data loggers, using the analog signal outputs of the monitors at a minimum averaging interval of 60 minutes. The detection level of the BAM-1020 is 1 $\mu g/m^3$ and the instrument will be operated on the 0-1 mg/m^3 (0-1000 $\mu g/m^3$) range.

B2.1.3 Continuous Measurement of Ultrafine Particulates

Scanning Mobility Particle Sizers (SMPS) for Particle Size Distribution

SMPS systems will operate at the three core sites to measure particle size distributions continuously. The types of instruments provided by DRI will be SMPS 3936N25A (TSI Inc., Shoreview, MN), SMPS 3936L10 (TSI Inc., Shoreview, MN), and Grimm SMPS+C (Grimm Aerosol Technik, Ainring, Germany). A SMPS system typically consists of three major components: bipolar charger, mobility classifier and condensation particle counter (CPC). Particles first pass through a bipolar charger to establish an equilibrium charge distribution and then enter an electrical mobility classifier in which they are separated according to their electrical mobility. The CPC measures the particle concentration at each mobility size range. The TSI SMPS 3936N25A measures size distributions in the range of 2.5–80 nm in 96 channels, the TSI SMPS 3936L10 measures 10–700 nm in 96 channels, and the Grimm SMPS+C measures 5.4–358 nm in 44 channels. Time resolutions of these measurements are 2–3 minutes.

Sequential Filter Samples

The sequential filter sampler allows air to be drawn through a size-selective inlet and through two different sets of filter media. Solenoid valves controlled by a timer switch between up to six sets of filters at preset intervals. The sequential sampling makes it unnecessary to have a person present at every sample changing interval.

There are three versions of the sequential filter sampler. For this project we will use the one for configured for $PM_{2.5}$ which are acquired through a Bendix 240 cyclone. The $PM_{2.5}$ units also contain a bundle of aluminum oxide treated denuders between the inlet and the plenum to remove nitric acid gas from the air stream.

Open faced filter packs located inside each plenum are connected to solenoid valves which open when a sample is to be exposed. A vacuum pump draws air through these filters when the valves are open. The flow rate is controlled by maintaining a constant pressure across a valve with a differential pressure regulator.

The $PM_{2.5}$ samples are taken on numbered filter packs in Nuclepore polycarbonate filter holders labeled FT and FQ. The FT filter packs are placed in sampling Ports 1 through 5 and consist of a Gelman (Ann Arbor, MI) polyolefin ringed, 2.0 micron pore size, 47 mm diameter PTFE Teflon membrane filter (#R2PJ047), a Nuclepore (Pleasanton, CA) 47 mm diameter fiber drain disk (#231100), and a Pre-fired Pallflex 47 mm diameter quartz fiber filter. FQ filter packs (Quartz/Nylon) on Ports 7 through 11 contain a pre-fired Pallflex 47 mm diameter quartz fiber filter (#2500QAOT-UP) and NaCl impregnated cellulose backup filter.

The Teflon membrane removes particles for gravimetric, light absorption, and x-ray fluorescence analyses. The drain disk prevents the physical contact of Teflon and quartz back-up filter, and the quartz back-up filter is analyzed for organic and elemental carbon to provide an estimate of gaseous organic carbon artifact. The TQ and FQ quartz fiber substrates collect samples which can be analyzed for chloride, nitrate and sulfate by ion chromatography, for potassium and sodium by atomic absorption spectrophotometry, and for organic and elemental carbon by thermal/optical reflectance. The backup cellulose/NaCl substrate measures the volatilized nitrate by ion chromatography.

Each filter pack has air drawn through it at 56.5 lpm. If a lower flow rate is desired, makeup flow through a separate Port to provide the 113 lpm flow rate required by the inlets to maintain particle cut points of 2.5 and 10 m. All flow rates are measured before and after sampling with a rotameter transfer standard. Elapsed time meters on each channel measure the sample duration. The timing sequence is set for continuous sampling so following completion of sampling on Ports 5 and 11, the SFS automatically switches to Ports 1 and 7. Dynamic field blanks are located in Port 6 for FT, TT or GK filter packs and in Port 12 for FQ, TQ or GQ filter packs.)

B2.1.4 Black Carbon

Elemental Carbon (Black Carbon)

The Magee Aethalometer Model AE-21 uses a continuous filtration and optical measurement method to provide a continuous readout of the concentration of black carbon (BC). The aethalometer will be equipped with a BGI Model SCC 1.197 particle size-selective inlet port. Air is sampled at a flow rate of 5 lpm, using a mass flow meter and internal pump. The cut point of the inlet used for the Study will be 1 micron (PM_1). The flow rate is monitored by an internal mass flow meter. Samples are collected on quartz fiber filter tape (containing 1500 filtered spots) and a continuous optical analysis is performed during sample collection. The analysis gives a new reading every defined base time period. The Magee Aethalometer filter tape advances automatically once the filtered spot reaches a manufacturer specified density (degree of attenuation). This could range from multiple times a day to two days. The data is stored to media (diskette or memory card), transmitted via serial data port and produced as an analog voltage.

The principle of the aethalometer is to measure the attenuation of a beam of light transmitted through a filter while it is continuously collecting an air sample. The Model AE-21 series aethalometer measures at two different wavelengths (800 nm and 370 nm). The 880 nm (IR-1) is designed for the measurement of Black Carbon (Elemental Carbon). The 370 nm (UV) is more specific to aromatic organic species such as those found in tobacco smoke, wood fire smoke and fresh diesel exhaust. The BC content of the aerosol collected at each measurement time can be determined by using the appropriate value of the specific attenuation for that particular combination of filter and optical components. An increase in optical attenuation from one time period to the next is due to the increment of aerosol BC collected during the period. This increment is divided by the volume of air sampled during that time and is used to calculate the mean BC concentration for the period.

The aethalometer will be operated on the 0-1,000 $\mu g/m^3$ range and has a sensitivity of <0.1 $\mu g/m^3$. The aethalometer will be set up with a one-minute time period to provide averaged data over one-minute.

B2.1.5 Meteorological Measurements

Horizontal Wind Speed and Wind Direction Measurements
Horizontal wind speed and direction on the tower will be measured continuously at the proposed monitoring sites using Met One Model -010 and 020 Series wind speed and wind direction sensors respectively. Both scalar and vector wind direction values will be collected. Wind speed will be measured using an anemometer whose operation is based on a magnetically induced AC current that produces a frequency proportional to wind speed. The wind direction sensor will be a lightweight vane that senses position by a precision potentiometer. The wind sensors will be installed at 10 meter (or the maximum feasible height given site restrictions). The standard deviation (sigma-theta) of the wind direction is calculated by the data logger using the U.S. EPA-preferred Yamartino method (U.S. EPA 2000).

Relative Humidity Measurements
The RH sensor will be housed in as aspirated radiation shield at the CS monitoring site. Relative humidity (RH) measurements will be made using the Met One Model 083E relative humidity sensor. This sensor measures the variance in the capacitance change of a one-micron thick dielectic polymer layer. The film absorbs water molecules through a metal electrode and causes capacitance changes proportional to RH.

Ambient Temperature Measurements
Ambient air temperature at the proposed monitoring sites will be measured at two levels on the tower using Met One Model 060A temperature probes housed in aspirated enclosures.

This sensor configuration is designed to provide complete signal wire compensation and eliminate any measurement errors resulting from signal cable resistance. The motorized aspirator is mechanically ventilated with a fan to prevent conductive interference from precipitation and radiation from solar and terrestrial sources.

Solar Radiation Measurements
At the proposed monitoring sites, solar radiation measurements will be made using an Eppley Model 8-48 pyranometer located at about the 2m level. The sensor is designed for measurement of global (sun and sky) radiation. The detector is a differential thermopile made of plated copper on constantan junctions. Hot-junction receivers are covered with a stable black coating and cold junction receivers are whitened with non-hygroscopic barium sulfate. The sensor is temperature compensated using thermistor circuitry to within 1.5 percent of the range of -20 °C to +40 °C. The sensor is sensitive to wavelengths of 0.285 to 2.800 µm.

B2.2 Integrated Sampling

B2.2.1 Carbon Speciation Sampling

Aerosol samples will also be collected using a MiniVol Portable air sampler manufactured by Airmetrics. The MiniVols will collect $PM_{2.5}$ to be analyzed for elements, ammonia, carbon (using the IMPROVE method), ions, volatile nitrate and select organics (method TO-13A)

The Airmetrics MiniVol is equipped with an inlet impactor capable of separating particulate matter by size. The impactors will have a $PM_{2.5}$ cut point and are designed to operate at a fixed flow rate of 5 LPM at actual conditions. The units are also equipped with a flow control device, which will maintain a specified flow rate, and a flowmeter to measure the flow rate during the sampling period. An elapsed time meter and a programmable timer allow the sampler to run unattended. To allow longer unattended sampling durations, a direct power system using a switch-mode 12V power supply in place of the battery system, was tested and proved reliable over a period of five weeks of continuous operation. The new systems are also much lighter in weight and require only about 300 mA of 110V line power to operate (less than a 40W light bulb). This can allow for multiple complete twenty-four hour sampling periods.

B2.2.2 Hydrocarbons Sampling

Heavy Hydrocarbons
Sampling of heavy hydrocarbons (VOCs) will be conducted by drawing air through Tenax sorbent tubes. The VOCs in the sample are then desorbed/extracted and analyzed. The sampling apparatus will include an in-line particulate filter, a sampling tube and a flow controller/pump combination. 24-hour integrated samples will be collected during ten consecutive days at a flow rate of 1.0 liter per minute (lpm).

A check of the flow controller will be made by placing the sorbent sample tube on the sampling train and making flow adjustments using a mass flow meter. At the end of the sampling period the flow will be checked a second time to ensure that the flow rate has not deviated more than 10 percent.

Light Hydrocarbons

SUMMA canisters, six liters in volume, will be cleaned prior to sampling by repeated evacuation and pressurization with humidified zero air, as described in the U.S. EPA "Technical Assistance Document for Sampling and Analysis of Ozone Precursors" (October 1991, EPA/600-8-91/215). Six repeatable cycles of evacuation to ~0.5 mm Hg absolute pressure, followed by pressurization with ultra-high purity (UHP) humid zero air to ~15 psig will be used. One canister out of the 10 per lot will be filled with humidified UHP zero air and analyzed by the GC/MS/FID method TO-15 method (DRI SOP 704.1). The canisters are considered clean if the target compound concentrations are less than 0.05 ppbv each. The canister sampling systems are cleaned prior to field sampling by purging with humidified zero air for forty-eight hours, followed by purging with dry UHP zero air for one hour.

After cleaning, air from the canisters will be evacuated. The canisters will have a six-liter capacity and an initial vacuum of approximately negative 30 inches Hg. A seven micron pre-filter will be installed prior to the inlet of the canister to minimize entry of particulates.

A vacuum gauge will be used to measure the initial and final vacuum of the canister and monitor the filling of the canister during the actual sampling. The gauges will be used to provide a relative measure of change. Before sampling, the gauge will confirm that pressure reads between negative 29 inches and negative 30 inches Hg for each canister.

Fixed-rate flow controllers and micron particulate filters will be placed on the canister after measurement of initial canister pressure (normally between negative 29 and negative 30 inches Hg using a vacuum gauge). The flow-controllers will be pre-set to meter the flow of air into the canister at a relatively constant rate over the course of a twelve hour sampling period to fill the canister to positive pressure.

The samples will be packaged and shipped to the laboratory for analysis. The final vacuum will be noted on the Chain of Custody form, which will allow the lab to compare the sampling vacuum with the receipt vacuum. The sample integrity is ensured if the final field and lab receipt readings are similar. If the readings significantly differ, the sample may have been compromised during shipment. Custody seals will also be affixed across box entry points to provide another method of determining if samples were tampered with during shipment to the laboratory.

SUMMA canisters and analysis of their contents will be provided by DRI

B2.2.3 Carbonyl Sampling

Waters, Inc.'s 2,4-dinitrophenylhydrazine (DNPH) impregnated Sep-Pak cartridge will be used to collect carbonyls, such as formaldehyde, acetaldehyde and acrolein, according to the U.S. EPA Method TO-11A. When air is drawn through the cartridge at a rate of one liter per minute for a twelve hour period, carbonyls in the sample are captured by reacting with DNPH to form hydrazones. The hydrazones are eluted from the sampling cartridges using acetone-free

acetonitrile (CAN) and are quantified using reverse-phase HPLC with ultraviolet absorption detection at 360 nm.

The sample pump flow rate will be measured pre- and post- sample with an NIST traceable device such as a Bios Dry Cal. Sep-Pak cartridges and laboratory analysis of these cartridges will be provided by DRI.

B2.3 Saturation Sampling

B2.3.1 Passive Sampling

The ability of passive samplers to collect analytes over extended periods of time allows for potentially high sensitivity for low pollutant concentrations. Sensitivity is limited only by the amount of time a sampler can be exposed and the blank value of the analyte on an unexposed adsorbent surface. Five different types of passive samplers will be used, each with a unique adsorbent and method of analysis. The analysis methods are listed in the table below:

Table B2-2: Passive Sampling Analysis Methods

Manufacturer	***Target Pollutant***	***Analysis Method***
Ogawa	NO_2/NO_x	Colorimetry for nitrite
Ogawa	SO_2	Ion Chromatography
Radiello	VOC (BTEX)	Thermal Desorption/GC/MS
Radiello	Aldehyde	HPLC/UV

Pollutants will accumulate over time via diffusion of the gaseous pollutants across a surface to an adsorbing material. The continual adsorption of the pollutant from the air maintains a concentration gradient near the surface that allows uptake of the pollutant to occur without any forced air movement (i.e., no pump or fan required). Unlike other samplers that use axial diffusion from one surface to another, Radiello samplers use radial diffusion over a microporous cylinder into an absorbing inner cylinder, which gives about a 100 times higher uptake rate.

After sampling, the collected pollutant is desorbed from the sampling media by thermal or chemical means and analyzed quantitatively. The average concentration of the pollutant in the air the sampler was exposed to can be calculated from the following relationship:

$$\text{Concentration} = \frac{\text{Mass of Analyte}}{\text{Sampling Rate} * \text{Sampling Time}}$$

The sampling rate for every analyte is calculated experimentally since pumps are not used in passive collection. Radiello[1] and Ogawa and Company[2] supply sampling rates for numerous

[1] Information about Radiello Passive Samplers can be found at http://www.radiello.com.
[2] Information and sales for Ogawa passive samplers can be found at http://www.ogawausa.com/.

commonly collected compounds. These sampling rates have been, or will be, validated by DRI in chamber experiments for NO_x, formaldehyde, acrolein and BTEX. Mass of the analyte is calculated as the average blank result subtracted from the analytical result. Sampling time is the amount of time the sampler was exposed. While lengthening the exposure time corresponds to an increase in sensitivity, it should be noted that exposure time is generally limited to a maximum of 14 days due to the capacity of the adsorbents.

Ogawa Passive Samplers for NO_x, NO_2 and SO_2

Ogawa Passive Sampling Systems (Ogawa & Co., USA, Inc.) will be used for monitoring NO_x, NO_2 and SO_2. NO_x, and SO_2 will be collected over weeklong periods using precoated 14.5 mm sampling pads deployed in personal sampling bodies. NO concentrations will be calculated by subtracting NO_2 from NO_x concentrations. Sampling and analysis are performed according to manufacturer protocols (http://www.rpco.com/assets/lit/lit03/amb3300_00312_protocolno.pdf).

For the Ogawa samplers the sampling rate conversion factor α (ppb-min/ng) is given by the equations:

$$\alpha_{NO} = \frac{10000}{(-0.78 \cdot P \cdot RH) + 220} \qquad \alpha_{NO2} = \frac{10000}{(0.677 \cdot P \cdot RH) + (2.009 \cdot T) + 89.8}$$

$$P = \left(\frac{2P_N}{P_T + P_N} \right)^{2/3}$$

where P_N and P_T are the vapor pressure of water in mmHg at 20 C and ambient temperature, respectively. α_{SO2} is determined from tables provided by the manufacturer, and varies from 44-35 ppb-min/ng for the temperature range 0 –40º C. The Ogawa NO_2 and NO_x pads are extracted and mixed with a solution of sulfanilamide and N-(1-Naphthyl)-ethylenediamine dihydrochloride to produce a colored nitrite solution, which is analyzed on a Technicon (Tarrytown, NY) TRAACS 800 Automated Colorimetric System (AC). The Ogawa SO_2 pads are extracted in 8 mL of deionized-distilled water (DDW) to which 1.75 percent hydrogen peroxide is added and sulfates are measured with the Dionex 2020i (Sunnyvale, CA) ion chromatograph (IC). These analyses will be performed by the Environmental Analysis Facility (EAF) of DRI.

Radiello Diffusive Samplers for VOCs

Radiello diffusive samplers (adsorbing cartridge code 145) will be used for passive sampling of benzene, toluene, ethylbenzene, xylenes (BTEX) and possibly 1,3-butadiene (if quantitative measurement of this compound is confirmed during laboratory evaluations). VOC samples will be collected over weeklong periods using stainless steel net cylinders (3x8 µm mesh, 4.8 mm diameter x 60 mm length) packed with Carbograph 4 (350 mg) and deployed in the diffusive sampling bodies, according to the manufacturer's instruction (http://www.radiello.com). The Radiello samplers are insensitive to humidity within the range 10-90 percent RH and wind speed

between 0.1 and 10 m/s. The actual value used for the sampling rate is calculated based on ambient temperature during sampling using the following equation:

$$Q_T = Q_{298}(T/298)^{1.5}$$

where Q_T is the sampling rate at ambient temperature T in ^{o} K and Q_{298} is the reference value at 25^o C. This produces a variation of ± 5 percent for ± 10^o C variation from 25^o C.

All VOC passive samples are analyzed by the thermal desorption-cryogenic preconcentration method, followed by high-resolution gas chromatographic separation and mass spectrometric detection (GC/MS) of individual compounds. The Gerstel ThermoDesorption System (TDS) unit, equipped with a 20–position autosampler, attached to the Varian Saturn 2000 GC/MS system, is used for the purpose of sample desorption and cryogenic preconcentration. A 60 m (0.32 mm i.d., 0.25 mm film thickness) DB-1 capillary column (J&W Scientific, Inc.) is used to achieve separation of the target species. For calibration of the GC/MS, a set of standard Carbograph 4 cartridges are prepared by spiking the cartridges with a known amount of gaseous calibration mixture of benzene, toluene, ethylbenzene, o-, m- and p- xylene (BTEX) and 1, 3–butadiane, prepared from authentic standards (Aldrich, Inc). Three different concentrations (plus one blank) are used to construct calibration curves.

Radiello Diffusive Samplers for Carbonyl Compounds

Radiello diffusive samplers will be used to passively collect carbonyl compounds. A stainless steel net cartridge filled with 2,4-dinitrophenylhydrazine (2,4-DNPH) coated florisil (Code 165) will be used. Carbonyl compounds react with 2,4-DNPH forming corresponding 2,3-dinitrophenylhydrazones. Sampling rate varies from value at 25^o C according to the following equation:

$$Q_T = Q_{298}(T/298)^{0.35}$$

This produces a variation of ± 1percent for ± 10^o C variation from 25^o C. The hydrazones are extracted and analyzed by HPLC with UV detection (Waters 2690 Alliance System with 996 Photodiode Array Detector). The VOC and carbonyl compound analyses are performed by the Organic Analytical Laboratory (OAL) of DRI. Detailed SOPs for these methods are available upon request.

B2.3.2 MiniVol filter sampling

MiniVol portable $PM_{2.5}$ air samplers from AirMetrics Corporation will be used for particle sampling at each site for seven continuous days coinciding with the passive samples. The sampler is equipped with an inlet containing an impactor unit with 2.5-μm particle cut point and a flow control system capable of maintaining a constant flow rate within the design specifications of the inlet. The impactor is designed for 50 percent collection efficiency for particles of aerodynamic diameter of 2.5 μm at a flow rate of five liters per minute. The following substrates will be used:

- Gelman (Ann Arbor, MI) polymethylpentane ringed, 2.0 mm pore size, 47 mm diameter PTFE Teflon-membrane Teflo filters (#RPJ047) for particle gravimetric mass and elements.
- Pallflex (Putnam, CT) 47 mm diameter pre-fired quartz-fiber filters (#2500 QAT-UP) for organic and elemental carbon measurements

The samplers are designed to operate from rechargeable battery packs to allow for continuous field sampling up to twenty four hours on a single charge. To allow longer unattended sampling durations, a direct power system using a switch-mode 12V power supply in place of the battery system, was tested and proved reliable over a period of five weeks of continuous operation. The new systems are also much lighter in weight and require only about 300 mA of 110V line power to operate (less than a 40W light bulb).

DRI SVOC Sampler

The DRI semi-volatile organic compound (SVOC) sampler is used to collect aerosol samples on 100 mm diameter Teflon-impregnated quartz fiber filters with backup XAD adsorbant cartridges to capture material volatilized from the filters. These samplers are equipped with a $PM_{2.5}$ cyclone inlet requiring flow rates of approximately 113 lpm controlled by needle valves downstream from the filters. An electronic flow meter monitors the air flow rate through the filter during sampling.

B2.4. Analytical Methods

Analytical methods are listed in Table A10-1. MDLs vary by analyte and are dependent on sampling volumes and filter loadings. See SOPs for MDLs in terms of mass density available in the Appendix.

Laboratory Analysis of VOC Samples

Canister and passive samples will be analyzed for BTEX and other VOC species using gas chromatography (GC)/mass spectrometry (MS) according to U.S. EPA Method TO-15. The analysis will be run in SIM mode with an MDL of approximately 10 pptV. The GC-FID/MS system includes a Lotus Consulting Ultra-Trace Toxics sample pre-concentration system built into a Varian 3800 gas chromatograph with flame ionization detector (FID) coupled to a Varian Saturn 2000 ion trap mass spectrometer. The Lotus pre-concentration system consists of three traps. Mid- and heavier weight hydrocarbons are trapped on the front trap consisting of 1/8 inch nickel tubing packed with multiple adsorbents. Trapping is performed at 55º C and eluting is performed at 200º C. The rear traps are comprised of two traps: empty 0.040 inch ID nickel tubing for trapping light hydrocarbons and a cryo-focusing trap for mid and higher weight hydrocarbons isolated in the front trap. The cryo-focusing trap is built from 6 foot by 1/8 inch nickel tubing filled with glass beads. Trapping of both rear traps occurs at 180º C and eluting at 200º C. Light hydrocarbons are deposited to a Varian CP-Sil5 column (15m x 0.32mm x 1µm) plumbed to a column-switching valve in the GC oven, then to a Chrompack Al_2O_3/KCl column (25m x 0.53mm x 10µm) leading to the flame ionization detector for quantitation of light hydrocarbons. The mid-range and heavier hydrocarbons cryo-focused in the rear trap are deposited to a J&W DB-1 column (60m x 0.32mm x 1µm) connected to the ion trap mass

spectrometer. The GC initial temperature is 5º C held for approximately 9.5 minutes, then ramps at 3º C/min to 200º C for a total run time of 80 minutes.

Calibration of the system is conducted with a mixture that contains commonly found hydrocarbons (75 compounds from ethane to n-undecane, purchased from Air Environmental) in the range of 0.2 to 10 ppbv. Three point external calibrations are run prior to analysis, and one calibration check is run every twenty four- hours. If the response of an individual compound is more than 10 percent off, the system is recalibrated. Replicate analysis is conducted at least twenty four-hours after the initial analysis to allow re-equilibration of the compounds within the canister.

The VOC analysis system (GC-MS for $C_4 - C_{12}$ and GC-FID for $C_2 - C_5$) is calibrated with a 74 component blend of hydrocarbons (including aromatics) in nitrogen at mixing ratios between 0.5 and 2 ppb. The standard is supplied by Apel-Riemer Environmental Inc. (Bloomfield, CO). For halogenated compound measurements, an NIST-traceable standard mixture of 39 compounds will be purchased from Scott Specialty Gases and diluted by DRI scientists for calibration. For VOC measurements by GC/MS system, 74 compound mixture in low ppb level (Air Environmental, Inc., Denver, CO), traceable to the NIST SRM 1805, will be used for calibration. For PAH measurements NIST SRM 1647, with the addition of other compounds not present in the mixture, will be used.

Gas cylinders of helium, nitrogen, hydrogen and ultra-zero air (all UHP grade) will be used for the GC/FID, GC/MS and GC/IRD/MSD. From a single analysis, the GC/IRD/MSD system provides three dimensions of data for positive compound identification: retention times, infrared spectra and mass spectra. Identification of individual compounds is based upon matching corresponding data for authentic samples. The current inventory of reference samples at DRI's Organic Analytical Laboratory consists of over 250 single- and multi-component reference samples.

Laboratory Analysis of DNPH Cartridges for Carbonyl Compounds

The hydrazones are separated and quantified per U.S. EPA Method TO-11A using a high performance liquid chromatograph (Waters 2690 Alliance HPLC System with 996 Photodiode Array Detector). After sampling, the cartridges are eluted with acetonitrile. An aliquot of the eluent is transferred into a 2 mL septum vial and injected with an autosampler into a Polaris C18-A 3µm 100 x 2.0 mm HPLC column. Since the HPLC system is equipped with the photodiode array detector, the identification of carbonyl compounds is more accurate than with standard UV/VIS detector. Also, the sensitivity of the analysis is enhanced by using the photodiode array detector.

Acrolein is known to rearrange on DNPH cartridges to an unknown degradation product (acrolein-x) (Tejada, 1986). This process of rearrangement is sufficiently rapid that most of the acrolein converts to acrolein-x, unless the sample is analyzed within a few hours. Acrolein-x also co-elutes in the HPLC analysis with butyraldehyde, which provides substantial overlap in the chromatographic retention time of acrolein-x with butyraldehyde. Thus, the sum of acrolein and

butyraldehyde represents an upper-bound estimate of the acrolein originally present in the sample.

DRI's Organic Analytical Laboratory determined if a more accurate measurement of acrolein could be obtained by post-analysis reprocessing of the HPLC spectra. An acrolein-x standard was generated by collecting a known concentration of acrolein onto a DNPH cartridge and allowing part of the acrolein to convert to acrolein-x. The concentration of acrolein-x was calculated as the difference between the known amount of acrolein deposited on the DNPH cartridge and concentration determined from HPLC analysis. The apparent concentration of acrolein-x (from the peak identified as butyraldehyde) detected in the analysis was equivalent to the concentration of acrolein collected on the DNPH cartridge, which allowed for generation of a 'standard' for acrolein-x. Several mixtures containing varying relative amounts of acrolein-x and butyraldehyde were analyzed to obtain spectra for the known correct proportions. Then, using an iterative solution process, peaks from the spectra of the two pure compounds were added together to obtain the closest match to the spectrum of each mixture. The scaling factors applied to the spectra from the acrolein-x and butyraldehyde spectra to obtain the best fit indicated the estimated amounts of each compound in the mixture.

Results from the experiment yielded agreement to within 20 percent of the actual concentrations for all mixtures except those where the concentration of butyraldehyde was much higher (e.g., 10x) than acrolein. Comparing the sum of the two separated compounds to the original concentration of unresolved acrolein-x and butyraldehyde for each sample showed very strong correlations and good agreement.

Laboratory Analysis of Time-integrated PM Samples for PM Mass and Carbon

Batch samples collected during the field study will be retrieved within 24 hours from the end of the sampling period, placed in climate-controlled storage, and periodically returned to DRI for analysis by the Environmental Analysis Facility or Organic Analysis Laboratory.

Gravimetric Analysis. The Mettler Toledo XP6 Microbalance is used to weigh filters to the nearest 0.001 milligram before and after sampling to determine collected aerosol mass. The following quality control protocols are used to assure accuracy:

- New filters are removed from their sealed packages and equilibrated in a clean, open atmosphere for a sufficient time to allow the filter weights to stabilize before use (typically 3 to 6 weeks).

- Humidity changes affect the mass of filters and their deposits by changing the amount of absorbed water on the sample. To minimize this effect, filters are equilibrated and weighed in a temperature and humidity controlled environment (20 to 23 °C and 30% to 40% RH acceptable, 21.5 ± 2 °C and 35% ± 5% RH preferred). Twenty four-hour and current temperature and humidity conditions are checked prior to starting weighing procedures and compared to control charts produced from an Access database of weighing room conditions.

- Contamination from airborne particles or from particles that have accumulated on instrument and workbench surfaces is also possible. The balance resides in a laminar flow hood and filters are handled only with clean tweezers to reduce the likelihood of contamination.

- Static electrical charge on the filters, which may be significant after air is pulled through the filters during sampling, is dissipated by placing the filters over a radioactive 210Po ionizing radiation source for 30 to 60 seconds prior to weighing.

- Replicate weighing's are performed on 100 percent of the filters weighed before sampling (initial weights or pre-weights), and on 30 percent of the filters weighed after sampling (final weights or post-weights). Replicate pre-sampling (initial) weights must be within ± 0.010 mg of the original weights. Replicate post-sampling (final) weights on ambient samples must be within ± 0.015 mg; post-sampling weights on heavily loaded (i.e., greater than 1 mg) samples must be within 2 percent of the net weight.

- All balance calibration (zero and span) and replicate data points are checked before and after each weighing session. If any measurement is not within specified limits, samples are re-weighed.

Elemental and Organic Carbon. Elemental carbon (EC) and organic carbon (OC) will be measured by thermal optical reflectance (TOR) method using the IMPROVE (Interagency Monitoring of Protected Visual Environments) temperature/oxygen cycle (IMPROVE TOR) (Chow et al., 1993; Chow et al., 2001). Samples are collected on quartz filters and a section of the filter is placed in the carbon analyzer oven to monitor the optical reflectance of He-Ne laser light (632.8 nm). The filter is heated under oxygen-free helium purge gas. Volatilized or pyrolyzed carbonaceous gases are carried to the oxidizer catalyst where all carbon compounds are converted to CO_2, which is then reduced to methane and quantified by a flame ionization detector (FID). The carbon evolved during the oxygen-free heating stage is defined as "organic carbon." The sample is then heated in the presence of helium gas containing two percent oxygen and the carbon evolved during this stage is defined as "elemental carbon." Some organic compounds pyrolyze when heated during the oxygen-free stage of the analysis and produce additional EC, which is defined as pyrolyzed carbon (PC). The formation of PC is monitored during the analysis by the sample reflectance. EC and OC are distinguished based upon the refractory properties of EC using a thermal evolution carbon analyzer with optical correction to compensate for the pyrolysis (charring) of OC. Carbon fractions in the IMPROVE method correspond to temperature steps of 120^{o} C (OC1), 250^{o} C (OC2), 450^{o} C (OC3), and 550^{o} C (OC4) in a nonoxidizing helium atmosphere, and at 550^{o} C (EC1), 700^{o} C (EC2), and 850^{o} C (EC3) in an oxidizing atmosphere. The IMPROVE method uses variable hold times of 150-580 seconds at each heating stage so carbon responses return to baseline values. In this study, total OC, total EC, total carbon will be reported. No pyrolyzed carbon will be reported due to complexity of data interpretation.

Laboratory Analysis of Time-integrated PM Samples for Semi-volatile Organic Compounds (SVOC).

Samples are extracted by the accelerated solvent extraction (ASE) method, using Dionex ASE 300. Prior to extraction, deuterated internal standards are added to each sample. Filters are extracted with dichloromethane followed by acetone. The extracts are combined and concentrated by rotary evaporation at 20 °C under gentle vacuum to ~1 ml, and filtered through 0.45 mm Acrodiscs (Gelman Scientific). Approximately 200 µl of acetonitrile is added to the sample and the solvent evaporated under a gentle stream of nitrogen. The sample was then split into two fractions: the first fraction is analyzed without further alteration for non-polar compounds (i.e. PAH, hopanes/steranes, alkanes), and the second fraction is derivatized to convert polar compounds to their trimethylsilyl derivatives for GC/MS analysis.

Calibration curves for GC/MS quantification are made for the molecular ion peaks of compounds of interest using the corresponding deuterated species (or the deuterated species most closely matched in volatility and retention characteristics) as internal standards. Individual neat standards will be used to make calibration solutions. A four to six level calibration will be performed for each compound of interest and the calibration check (using a median calibration solution of standards) is run every ten samples to check for accuracy of the analyses. If the relative accuracy of measurement (defined as a percentage difference from the standard value) is less than 20%, the instrument is recalibrated and samples are reanalyzed.

Laboratory Analysis of Elements

Nitrate and Sulfate Ions. Soluble anions will be extracted from the Teflon and quartz filters and analyzed by ion chromatography (IC) using the Dionex 500, a liquid chromatographic technique based on an ion exchange mechanism and suppressed conductivity detection for the separation and determination of anions. Its separation principle is similar to that of all chromatographic methods. Each ion's affinity for the exchange site, known as its selectivity quotient, is largely determined by its radius and its valence. As a consequence of differences in the equilibrium distribution of sample components between the mobile (sample/eluent flow) and stationary (ion exchange column) phases, the sample ions elute from the column as discrete bands based upon their migration velocities. Each ion is identified by its retention time within the ion exchange column.

During routine operation, a filtered aliquot of sample is pumped through an ion exchange column where the ions are separated. The eluent ions from this separator column are then neutralized in the anion self-regenerating suppressor (ASRS) Ultra, and the sample ions are converted to their corresponding strong acids for detection with a conductivity detector. The conductivity responses are associated with ionic species by their elution times. Ionic concentrations are quantitatively determined from conductivity peak heights or area.

Elements by XRF. Analysis of aerosol filter samples using the PANalytical Epsilon 5 XRF analyzer is based on energy dispersive x ray fluorescence of elemental components in a thin film sample. The emissions of x ray photons from the sample are integrated over time and yield quantitative measurements of elements ranging from aluminum (Al) through uranium (U) and

semi quantitative measurements of sodium (Na) and magnesium (Mg). A spectrum of X-ray counts versus photon energy is acquired and displayed during analysis, with individual peak energies corresponding to each element and peak areas corresponding to elemental concentrations. The advantages of XRF analysis include high sensitivity for a number of elements, the ability to analyze small quantities of sample, and the non destructive nature of the analysis. In addition, because x ray fluorescence depends on the quantum absorption and emission of photons at the M, L, and K orbitals, the technique is insensitive to the chemical state of the elements. Disadvantages include the subjection of the sample to a vacuum, resulting in loss of some volatile species such as hydrocarbons, ammonia, nitrate, chlorine, and bromine.

The source of x rays in the PANalytical Epsilon 5 analyzer is a side window dual anode x ray tube with both Scandium (Sc) and Tungsten (W) anodes. X-rays are focused on one of 11 secondary targets which in turn emit polarized x-rays used to excite a sample. X rays from a secondary target or the tube are absorbed by the sample, exciting electrons to high level orbitals. As the electrons return to their ground state, photons are emitted which are characteristic of the quantum level jumps made by the electron; the energy of the emitted photons are, therefore, characteristic of the elements contained in the sample. The fluoresced photons are detected in a solid state Germanium X-ray detector. Each photon that enters the detector generates an electrical charge whose magnitude is proportional to the photon's energy. The electrical signals from the detector are sorted into energy channels, counted, and displayed. A sample spectrum consists of characteristic peaks superimposed on a background caused by the scatter of x-rays from the tube into the detector. Spectra are collected for a specified length of time and stored on disk for later processing.

DRI uses eight different analysis conditions during a single analysis run to maximize sensitivity to the full range of elements reported. Each of the analysis conditions, which correspond to different secondary targets, x-ray tube voltage and current, and energy detection range, is designed for a specific group of elements.

ICP-MS. In Inductively Coupled Plasma Mass Spectrometry analysis the aerosol deposit on a Teflon filter is digested in an acidic solution, then a pump is used to draw a liquid sample solution into a nebulizer. The nebulized solution is then passed through a plasma torch, which ionizes the dissolved metals. The ionized metals pass through a skimmer and sampler cone and then enter a quadrupole magnet which filters out all ions except for those within a narrow range of mass-to-charge ratio. The ion within this mass-to-charge ratio is then detected by a dynode detector (electron photomultiplier). The quadrupole is controlled to allow a series of ions with different mass-to-charge ratios pass through it, permitting a series of different elements to be detected. The ion signal detected by the dynode detector is proportional to the amount of the element present in the solution.

The Thermo Elemental ICPMS analyzer running under DRI's analysis protocol uses up to 7 different analysis conditions to maximize sensitivity to select groups of elements. Two types of standards are used with the DRI ICPMS: stock standards of individual elements from Inorganic Ventures, Inc. (comes in 1000 ppm) and a multi-element external standard (currently 56 elements) also from Inorganic Ventures, Inc. (comes in 1 pm) called DRI Cal4. A multi-element

stock solution of 10 pm is made from the individual elemental solutions, which are used to make the standards for the calibration curve. The calibration curve minimum and maximum concentration varies, depending on the elements, but the maximum range (and typically used range) is 0.001 – 500 ppb.

Laboratory Instrument Maintenance

All of the major equipment (the GC/IRD/MSD, GC/MS and GC/FID) is on a service contract with the original manufacturer. This contract calls for biannual routine service by a Hewlett-Packard or Varian service technician, and immediate response to any service call. The contract specifically states that any problem will be corrected within forty eight-hours of notification of the manufacturer.

Several of DRI's laboratory personnel have extensive experience working with all the major laboratory equipment and DRI has extensive support facilities (electronics and machine shops, QA lab with standard reference materials, etc.). These personnel and facilities ensure the continued smooth operation of all analytical instruments.

Laboratory Instrument Calibration

The GC/FID, HPLC, GC/MS and GC/IRD/MSD systems are calibrated initially by multipoint calibration (i.e., three levels plus humid zero air), and regularly checked by a one-point calibration, using appropriate NIST SRM or other standard. The day-to-day reproducibility of ±10 percent is acceptable for either standard. Control charts are used for assessing analytical system performance.

Samples that fall outside the calibration range are diluted until bracketed by the calibration curve. Instrument responses to calibration standards for each parameter are analyzed using a least squares linear regression. The calibration must generate a correlation co-efficient (R^2) of 0.995 to be acceptable. During the course of analysis, calibration standards are routinely analyzed to ensure the instrument response has not changed. The criterion of within 10 percent of expected response is used by the analyst to determine whether the instrument must be recalibrated.

In addition, DRI routinely conducts inter-laboratory comparisons with CARB and the South Coast Air Quality Management District

B.3 Sample Handling and Custody

Strict sample custody procedures are employed to ensure collected samples are shipped to laboratories in accordance with the specific limitations for each method and to provide a documented record of the custody of the collected sample and its transport.

All samples have a unique number for identification purposes. The sample ID is affixed to the sample media and recorded in the sample log sheets maintained by the site operator and on the Chain of Custody form submitted with the sample to the laboratory. Sampling log sheets will include information such as sampling date, duration, flow rate or volume collected, and vacuum for canister, etc. The laboratory also includes the sample ID with the analysis. Field labeling of samples will follow the convention of "Site Location-Analyte-Number" (example CE-VOCs-001).

Packing and transport of collected samples depend on the method used, which can have time or temperature restrictions for shipment. Each sample is packed and shipped according to its method requirements. The specifics for each method can be found in the appropriate SOP.

For the QA plan, a sample is considered in custody upon receipt by the DRI-DAS receiving department. At this time, it is logged into the general receiving department's log book and the laboratory is notified of the package's arrival. A laboratory representative signs for the package and opens it upon return to the laboratory room. The samples are logged into the laboratory’s receiving log book, the Chain-of-Custody form is updated, and the samples are stored appropriately. At this time, any unusual situations (damaged shipping container, evidence of damage and/or tampering, etc.) are brought to the attention of the laboratory manager. If necessary, a review will be initiated to determine if the damage compromised the integrity and/or quality of the sample.

Samples are stored at the DRI Northern Nevada Science Center (2215 Raggio Parkway, Reno, NV). All condensed phase samples and sample extracts are stored in the freezers. The rooms are locked when not in use and the building has limited access (i.e., it is locked from 17:30 to 07:30 weekdays and all weekend to ensure access only to authorized personnel).

When a sample is analyzed, the identification number (sample number) is recorded in the written logbook for each instrument and in the Laboratory Information Management System (LIMS) file created for that analysis. The sample number serves as a tracking number, as does the LIMS file itself. Canisters will not be cleaned until each sample has passed initial validation.

Condensed phase samples (e.g., filter samples) and sample extracts will be maintained for at least one year following the completion of the project. Samples will be stored in refrigerators or freezers. Long term storage or archiving of project samples may be requested.

Data Handling and Sample Custody

Strict, well documented data handling and sample custody procedures are adhered to in the monitoring program. The procedures are designed for data to flow in an organized manner and to ensure the integrity of samples and data collected. A data flow schematic is provided in Figure B3-1.

Figure B3-1. Data Flow Schematic

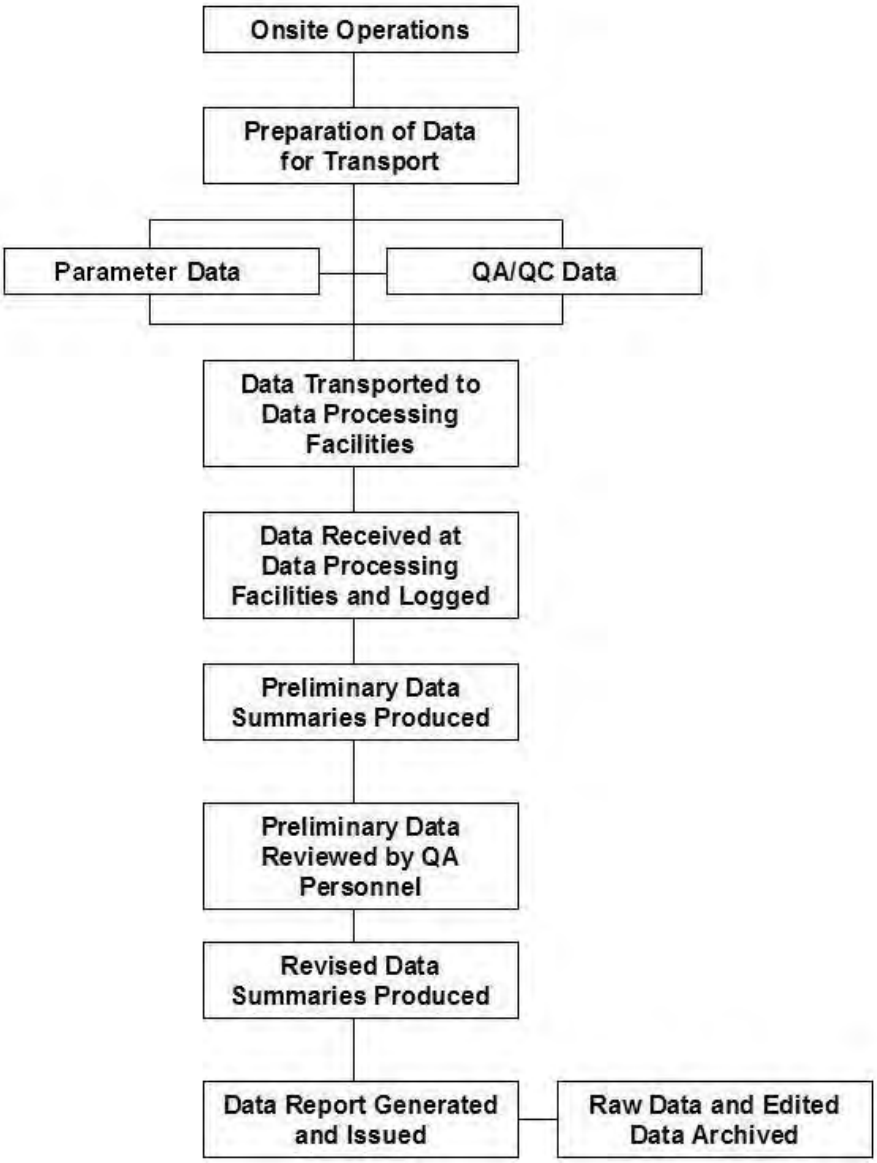

The Chain of Custody form is the primary tool used to maintain sample custody and accompanies all field data, including:

- Digital chart recordings.
- Site logs and operator checklists.
- Calibration data.
- Certification forms.

All data are clearly marked for identification. The original Chain of Custody record is filed at the monitoring station and a copy is enclosed with the shipment of all data.

Upon receipt of the data, the contents of the shipment are verified against the enclosed Chain of Custody record, which is filed in the monthly data file. If discrepancies are noted, they are brought to the attention of field personnel.

B4. Quality Control Requirements

B4.1 Quality Control

Performance tolerances and standards to be implemented for the LAX Study are summarized in Table B4-1. Detailed quality control (QC) and quality assurance (QA) procedures are specified in each listed SOP.

Each continuous air quality analyzer used on the monitoring program must meet or exceed the criteria provided in Table B4-1. In addition, the analyzers should also meet the following criteria:

- Have a Reference or Equivalent Method Designation except where U.S. EPA has not provided a designation for the particular parameter
- Be able to operate unattended for a minimum of one week
- Have a sample flow rate that does not exceed five liters per minute
- Have a rise time less than five minutes for 90 percent span response.

Table B4-1. Performance Tolerances and Standards

Performance Parameter	*Units*	*NO_x*	*CO*	*SO_2 (units are in ppb)*
Range	ppm	0-0.5	0-50	0-500
Noise	ppm	0.005	0.50	0.025
Lower Detectable Limit	ppm	0.01	1.0	0.05
Interference Equivalent				
Each Interferant	ppm	0.02	1.0	3
Total Interference	ppm	0.04	1.5	5
Zero Drift, 12 and 24 hours	ppm	0.02	1.0	0.2
Span Drift, 24 hour				
20% of Upper Limit	%	± 20	± 10	± 5
80% of Upper Limit	%	± 5	± 2.5	± 5
Lag Time	min	20	10	5
Rise Time	min	15	5	15
Fall Time	min	15	5	15
Precision				
20% of Upper Limit	ppm	0.02	0.5	0.2
80% of Upper Limit	ppm	0.03	0.5	0.2

The meteorological equipment used in the Study must meet or exceed the specifications listed in Table B4-2. Each piece of ancillary equipment should be of sufficient industrial quality so that a minimum level of maintenance is required.

Table B4-2. Minimum Performance Specifications for Meteorological Instrumentation

Parameter	*Starting Threshold*	*Accuracy*	*Distance Constant*	*Damping Ratio*
Wind Speed	< 0.5 m/s	± 5% or .25 m/s	≤ 5.0 m	NA
Wind Direction	< 0.5 m/s	≤ 5°	≤ 5.0 m	0.4 – 0.65
Temperature	NA	≤ 1.0° C	NA	NA
Solar Radiation	NA	± 5% or 25 Watts/m^2	NA	NA
Relative Humidity	NA	±2% from 0-100%	NA	NA

The Project Team is committed to the implementation of an effective Quality Control (QC) program on all ambient monitoring projects. An effective QC program ensures all samples and data are gathered in accordance with guidelines set forth by U.S. EPA and any local agencies. The QC program consists of activities in the following areas:

- Data Handling and Sample Custody
- Calibrations and Precision Checks
- Preventive Maintenance
- Routine Station Operation
- Data Validation
- Data Correction

B4.2 Weekly Check (Operator Visits)

To ensure compliance with the Study's QC program, a set of established procedures have been developed for the onsite operator to follow.

Activities can be separated into two different categories; those that need to be performed on each and every site visit and those that are regularly scheduled. The activities that need to be accomplished each and every site visit follow.

Site Logs
Please reference Section A7. Project Description.

Operator Checklists
Please reference Section A7. Project Description.

Review of Digital Charts
The site operator reviews the digital chart since the last site visit. The traces are inspected for any unusual spikes, which may indicate a pollution episode, and for noticeable span and zero drift. The nightly auto-calibrations are also examined for any unusual occurrences. The chart is also examined for indications of malfunctions, proper timing and agreement with DAS values. The chart time is maintained at Pacific Standard Time throughout the year.

Checking for Satisfactory Gas Cylinder Pressures
The pressures of the gas cylinders are checked and logged. A replacement cylinder is ordered when the supply pressure drops below 500 psig (300 psig for superblends) or one month before the certification expiration date (whichever comes first). The minimum usable pressure for zero air and hydrogen cylinders is 200 psig. Excessive drops in cylinder pressures are also investigated.

Checking for Correct Air Flow Settings
All instruments are checked for correct air flow. Any deviation in flow is immediately diagnosed and corrected.

Notation of Any Unusual Odors or Sounds or Unusual Occurrences
Any unusual odor may indicate a point source of a pollutant or a malfunctioning instrument. A new noise or absence of a usual noise can also indicate a malfunction in the equipment.

There are times when unusual circumstances surround data collection that may have an influence on the data. These unusual situations include weather events, fires in the area, local construction, etc. Any events that have the potential to affect data are documented on the Unusual Occurrence Form. The form is filled out by the site operator and forwarded to data processing personnel, who make judgments concerning the effects that these occurrences had on the data.

Checking for Instrument Malfunctions
Instruments are inspected for obvious malfunctions. Temperature control, mode cycling, timing, pump operation, meteorological instrument operation, and data logging are just a few of the functions that are checked for correct operation.

Any malfunctions noted by the site operator are corrected if possible. Regardless of the operator's ability to remedy the problem, it is documented in the site logs and operator's checklist. For problems the site operator cannot correct on the spot, a Corrective Action Request Form is filled out. This form ensures problems are taken care of in a timely manner and provides the documentation to show completion. The form specifically documents:

- The Malfunction
- The Time of Occurrence
- The Time of Correction
- The Corrective Action
- The Person Correcting the Malfunction

The form can also be submitted by data processing personnel if problems are noted during processing and review of data. Figure B4-1 shows a flowchart of the corrective action that occurs when malfunctions are noted.

Any problems noted are brought to the attention of field personnel. The previously discussed Corrective Action Request Form is completed to provide documentation on any problems discovered.

Figure B4-1. Corrective Action Flowchart

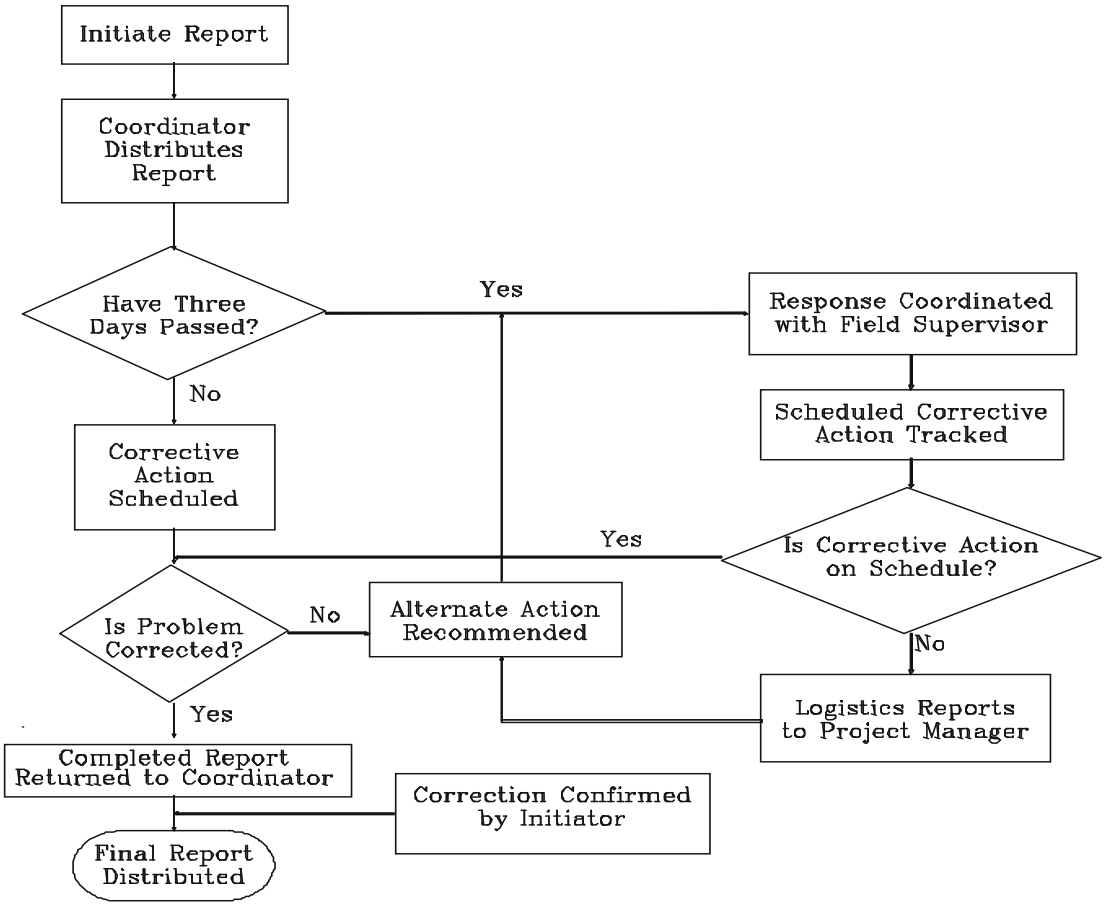

B5. Sampling Equipment Inspection, Testing and Maintenance

B.5.1 Sampling Equipment Inspection

All sampling equipment will be cleaned and tested for proper operation and leaks at DRI prior to deployment. Prior to the start of the field study, all samplers will be checked for leaks and the in-line flow meters will be cross checked using reference flow measurement devices. Leak testing will be performed by capping the inlet lines leading to each sampler and turning on the pumps. The system is considered as leak-free if the flow meter readings decrease to less than 10 percent of the nominal sampling flow rate in a reasonably short time, for example, 5 minutes. If not, the source of the leak will be identified and fixed, and then the test repeated.

B.5.1 Sampling Equipment Testing

Operational testing will be repeated after installation at the sampling sites. Prior to commencement of sample collection, sample trains will be tested for air leaks and sampling flow rates will be validated with transfer standards.

B.5.3 Sampling Equipment Maintenance

All of equipment is on a preventative maintenance schedule. Systematic performance checks are important preventative maintenance tools. When an instrument is not performing up to standards, it is investigated and most problems are identified before they become significant.

Given the duration of the planned sampling periods, no routine maintenance should be required for the filter samplers during this study. Nevertheless, a supply of spare parts will be provided and replacement units will be made available for the MiniVol samplers. All samplers will be cleaned and tested between the two planned sampling seasons and any necessary maintenance will be performed at that time.

Prior to deployment in the field, each sampler is bench-tested and inspected in the laboratory. Maintenance frequency varies (weekly, monthly, quarterly, or semiannually) depending on the sampler. Equipment testing, inspection and maintenance requirements are discussed in detail in the SOPs.

MiniVol Flow Checks

The transfer standard for sampler flow rates is an external (independent) rotameter which has been calibrated against a primary flow standard (Roots meter or electronic bubble meter) prior to the beginning of the sampling program. Flow rates will be measured for each sampler at the start and end of each sample using this transfer standard connected to the top of the inlet to assure consistency.

SMPS Flow and Leak Checks

The transfer standard for sampler flow rates is an external (independent) thermal flow meter which has been calibrated against a primary flow standard (Roots meter or electronic bubble meter) prior to the beginning of the sampling program. Flow rates at the inlet of the CPC and the

SMPS will be measured once a week. SMPS leak check will be performed once a week by turning off the SMPS voltage and reading the CPC concentration.

B6. Field Instrument Calibration and Frequency

Several types of standards are needed for calibration, auditing and performance tests. Primary standards are well characterized and protected. All other standards are traceable to these standards. Transfer standards, which are also traceable to primary standards, are often more easily produced or are more commonly available. These are used for calibration, performance testing and auditing. The same standards may be used for calibration and performance testing, however, audit standards should be independently traceable to primary standards. When transfer standards for the primary observable parameter are lacking, performance tests may measure instrument response rather than response to a specific value of an observable parameter.

The following sections identify the primary and transfer standards and their application for calibration, performance testing and auditing. The method for delivering these standards to the instrument is dependent upon the instrument. Flow rates are relatively simple to verify, but evaluating continuous monitoring responses to particle size is impractical under field conditions.

Calibration, performance testing and auditing methods for laboratory operations are largely based on the preparation of standard solutions from mineral salts. The National Institute of Standards and Testing (NIST) does not provide these types of standards. Standard solutions in a large range of concentrations are commercially available for inorganic monoatomic and polyatomic ions. The VOC analysis system (GC-MS for C_4-C_{12} and GC-FID for C_2-C_5) with a 74 component blend of hydrocarbons (including aromatics) in nitrogen at mixing ratios between 0.5 and 2 ppb. The standard is supplied by Apel-Riemer Environmental, Inc (Bloomfield, CO).

Gas and meteorological monitors are often used in compliance networks because common procedures and standards have been developed for their calibration and auditing. Some of the novel measurements in Table B6-1 will be evaluated by comparison with other measurements that have traceable standards and audit trails.

The QA Manager conducts field and laboratory systems audits, a laboratory performance audit and/or interlaboratory comparisons, and field performance audits. Systems audits examine all phases of measurement and data processing to determine SOPs are followed and to ensure operational staff is properly trained. The systems audit is intended to be a cooperative assessment resulting in improved data. Performance audits establish the extent to which data specifications are being achieved in practice and evaluate measurement accuracy against independent standards. The field systems audit is conducted at the beginning of the Study after all equipment is installed and operating and is followed by the first field performance audit. These audits will identify deficiencies and implement remedial actions. Subsequent field performance audit results will be used to define the accuracy of field measurements.

B6.1 Calibrations and Precision Checks

Calibrations establish the relationship between actual pollutant inputs and the analyzer response. Calibrations are performed by challenging analyzers with known concentrations of gas and recording the response.

Different types of calibrations and quality control checks are performed at varying intervals and include:

- Automated Zero and Span Checks
- Manual Zero, Precision and Span Checks
- Multipoint Calibrations on Continuous Analyzers
- Multipoint Calibrator Flow Checks
- Checks of Calibrator Ozone Standard
- Calibrations of Meteorological Sensors

Checks are performed during hours where exceedances of standards are not anticipated in order to avoid a failure to monitor during an anticipated or actual exceedance of a standard for any pollutant parameter. This includes scheduling of the automated checks, which take place at night.

For photochemical species (NO_x, efforts are made to avoid conducting the QC checks during the peak photochemical hours of the day. Whenever possible, most of these checks will be performed in the early morning hours.

Precision checks are a one point check using an input concentration of 16-20 percent of the full scale range of the analyzer. The results of precision checks, which are conducted on at least a bi-weekly basis, are used to assess the precision of the data collected by an analyzer. Therefore, it is important for the check to be conducted under conditions closely resembling actual sampling conditions. To accomplish this, the precision checks are conducted “as-is” (prior to any adjustment to the analyzer). Additionally, the input gas passes through all filters and sampling lines the ambient air passes through.

Automated zero and span checks are performed on each of the air quality analyzers on a nightly basis between midnight and 5:00 AM LST. These nightly checks are completely automated and controlled by the station's data logger. The zero and span checks are two point calibrations consisting of input concentrations of zero and 80 - 90 percent of the full scale range of each analyzer.

Manual zero, precision and span checks are conducted prior to any adjustments (zero adjustments, etc.) made to the analyzer. This "as-is" check provides a record of analyzer performance and data validity prior to the adjustments. Results of these checks are also recorded on the QA Data Sheet (see the SOPs). After adjustments, a manual zero and span check is conducted. The input gas for these checks must pass through all filters and sampling lines ambient air is normally drawn through.

The results of both the manual and automated zero and span checks have important implications in

terms of data validation, adjustment or determining the need for analyzer adjustment. The control limits and required actions based on the results of these checks are given in Table B6-1.

Table B6-1. Zero and Span Check Control Limits

Required Action	***Zero Check Results***	***Span Check Results***
No Action	$\leq$ 1% of full scale	$\leq$ 8% error from true
Adjust Analyzer	> 1% and $\leq$ 3% of full scale	> 8% and < 15% error from true
Adjust Analyzer and Invalidate Data	> 3% of full scale	$\geq$ 15 % error from true

Multipoint calibrations of field monitoring equipment consist of four points (zero point and three upscale points). The upscale points consist of the precision point (16-20 percent of full scale), a midpoint (35-40 percent of full scale) and the span point (80-90 percent of full scale). Multipoint calibrations are performed manually every two weeks by a lead technician or engineer. In addition to this scheduled calibration, multipoint calibrations are also performed under the following circumstances:

- Upon analyzer installation or replacement.
- Physical relocation of the analyzer.
- Prior to, and following any maintenance activity on major analyzer assemblies that affect analyzer response.
- Zero drift exceeds 3 percent of full scale.
- Span drift exceeds 15 percent of true.
- After a power or thermal breakdown that causes a change in analyzer response.
- Prior to the cessation of monitoring.
- Any time an analyzer has been off line for more than twenty four-hours.

The results of multipoint calibrations are recorded on an analyzer specific Multipoint Calibration Form. The technician also calculates the linear regression results of the multipoint calibration.

Multipoint Calibrator Flow Checks

Certifications of the station calibrator mass-flow controllers will be performed prior to each seasonal sampling period. These are multipoint calibrations performed at SCS Tracer's Air Monitoring Laboratory using flow standards in addition to the "in-house" equipment. The results of the calibrator flow checks are recorded on the calibrator's Multipoint Flow Form.

Checks of Calibrator Ozone Standard in Dynamic Dilution Calibrator

Quarterly checks of the station calibrator's ozone generator and delivery system will be performed. These are multipoint certifications performed at SCS Tracer's Air Monitoring Laboratory using an ozone primary standard to directly measure the ozone generator's output at multiple set points. The results of the calibrator ozone certifications are recorded on the calibrator's Multipoint Ozone Form. Step by step instructions for performing these checks are also found in the calibrators respective Appendix.

Calibration of Meteorological Sensors

Calibration of meteorological sensors normally occurs on at least a semiannual basis. Multipoint calibration of meteorological sensors will be performed prior to the commencement of this Study and prior to and immediately after each intensive monitoring period. Calibration of meteorological sensors requires a minimum of the following equipment:

- Digital Multimeter
- Synchronous Motor (300 and 600 RPM reversible)
- Transit, Theodolite or Compass
- Torque Measurement Device
- NIST Traceable Thermometer

Calibrations are also performed on meteorological sensors whenever any of the following occur:

- Installation of sensors.
- Repair or maintenance of sensors.
- Prior to cessation of monitoring.

Relative humidity and solar radiation sensors will be installed with current factory calibration certifications. Verification of the proper operation of these sensors in the field will be established during the field audits performed by T&B Systems.

B7. Inspection/Acceptance of Supplies and Consumables

Field/laboratory supplies, consumables, quantities, cost, frequency of replacement, catalog number and vendor information are listed in detail in each SOP. Lab and field coordinators are responsible for checking/replenishing supplies prior to and following each seasonal sampling period.

All sampling media for this project will be procured by DRI, inspected for damage or defects by analytical laboratory personnel, and repackaged in labeled batches designed to meet the sampling plan, before sending them to the project site. For commercial cartridges, e.g., Waters Si-DNPH, DRI shall analyze 5 percent of the purchase initially to ascertain the blank variability. Another 5 percent will be analyzed if the initial data show the blank variability is marginally acceptable (at or slightly higher than 1/3 of the desired lower quantifiable limits (LQL)). This is necessary because, unless cartridges are prepared in-house, there is no other indication of the quality of the product, such as how pure the reagent or the blank cartridges are. In some measurements, e.g., carbonyl compounds, the blank variability is the single most important factor in determining the lower quantifiable limit of the measurement. The other factors, such as flow rate and analytical variabilities are secondary in importance.

B8. Data Acquisition

B8.1 Continuous Analyzers

Data are gathered at each ambient monitoring station by a data logger and strip chart recorders. The primary method is by use of a data logger (a computer based data collection system; in this case an ESC 8800), which records the voltage output of the continuous analyzers and sensors every second. The logger converts the voltages to engineering units and calculates auxiliary one-minute averages. The auxiliary one-minute averages are used by the data logger to calculate hourly averages. The data logger also performs calculations for sigma and vector parameters. To minimize the potential for data loss, the data loggers used should have the following capabilities:

- Storage of data files with a storage capacity in excess of twenty-four hours.
- Performance of calculations consistent with the specifications of regulatory agencies.
- Ability to link with a PC for continuous archiving of data files.
- Allow site operator access through a user friendly keyboard.
- Have a scan rate of once per second for all channels.
- Remote telemetry via telephone modem.
- Ability to flag questionable data values.
- Self-diagnostics.
- Control of automated zero and span check sequence.
- Battery powered clock to maintain correct time during power outages and automatic program reload.

The secondary means of data collection is strip chart recorders (Monarch, Datachart 2000). The digital chart recorders can provide data in case of data logger malfunction for specific instrumentation. The digital charts also serve as a powerful quality assurance tool for verifying data from the data logger.

B9. Data Management

Data management activities, and the QA/QC procedures that govern them, are involved in all aspects of the ambient monitoring programs. From field data collection to preparation and issuance of final reports, strict procedures relating to data processing must be followed. This section will describe the procedures used to collect, process and report the data and how they relate to the overall QA/QC program.

B9.1 Data Acquisition and Recording

Each continuous analyzer and sensor produces a voltage output directly proportional to the amount of what is being measured. The voltages from each analyzer and sensor are converted to engineering units (ppm, m/s, etc.) using an analog to digital board. The conversion is represented by equation B9-1.

$$Y = Y_{max}\left(\frac{V}{V_{max}}\right) + Y_o \qquad \text{(Equation B9-1)}$$

where Y is the instrument response in engineering units, Y_{max} is the full scale setting of the instrument in engineering units, V is the instrument response in voltage units, V_{max} is the full scale voltage of the instrument and Y_o is the zero offset of the instrument in engineering units.

Each data channel is sampled by the data logger once per second for continuous gaseous monitor and per hour for measurements of particulates. The data logger stores the values in its memory for the calculation of hourly averages (the data logger can be programmed to calculate averages of any length of time desired). The data logger also calculates a number of derived parameters.

In addition to collecting ambient data, the data logger is programmed to initiate, control and record results of the nightly autocalibration sequence. The data logger also marks down all of the channels prior to initiation of the autocalibration sequence. This will flag the affected data in the hourly and daily summary files.

All sample and analysis data are tracked and collated using unique media identification codes assigned prior to sampling. Bar coded stickers with unique media IDs are attached to all media and their corresponding log sheets for tracking. Immediately after the conclusion of each sampling period the media are repacked with the log sheets and stored in an insulated container. Field personnel will fill in all requested information on pre-printed log sheets which accompany each set of sampling media. For each integrated sample, the run number, start and stop time, elapsed time, initial and final flow rate, and any exceptional occurrences will be recorded on log sheets which are kept with the media at all times. Information from those log sheets will be entered into an existing database when media are returned to DRI laboratory.

B9.2 Data Processing, Reporting and Reduction

Data processing procedures fall into the following general categories:

- Field Collection, Review and Shipment of Data
- Data Editing
- Report Compilation and Review

B9.2.1 Field Collection, Review and Shipment

SCS Tracer will be providing raw data to an FTP site for all continuous parameters on an hourly basis. Only T&B Systems and SCS Tracer will have access to the raw data.

At the conclusion of each monitoring period (e.g., day, week, intensive period, etc.), the site operator is responsible for the collection, review and shipment of data. In this instance, data refer to the raw ambient data as well as supporting materials. The operator is responsible for the following items:

- Digital chart recordings of continuously monitored parameters.
- QC documentation (calibration and precision results, site logs, operator checklists, strip chart review forms, etc.).

The above items are transported to SCS Tracer's data processing center. Prior to shipment of the data package, many of the items are backed up to prevent possible loss. Copies of the data disk are made and all of the QC documentation is photocopied and kept at the data processing center. A Chain of Custody form is filled out detailing the contents of the data package, photocopied and enclosed with the package.

B9.2.2 Data Editing

The raw data from the monitoring site are corrected during data review and processing whenever any of the following occur:

1. Zero value exceeds ± 1 percent of the full-scale range of the analyzer.
2. Span value of any parameter exceeds 10 percent and is less than or equal to 15 percent of true.

Precision check data must be adjusted when data corrections are made. This assures that calculated confidence limits are representative of the corrected data.

Zero adjustments are linearly interpolated between calibration points, where a zero value, which is determined by linear interpolating between the surrounding autocal zero checks, is subtracted from the raw data as shown in Equation B9-2.

$$Y_{adj} = Y_{raw} - Z \qquad \text{(Equation B9-2)}$$

where Y_{adj} is the adjusted value, Y_{raw} is the raw value and Z is the zero value.

Level 1 adjustments are made in conjunction with zero adjustments as shown in Equation B9-3,

$$Y_{adj} = \frac{Y_{raw} - Z}{(1 + LI)} \qquad \text{(Equation B9-3)}$$

where Z is again the zero value and LI is the percent difference of the Level 1 check divided by 100. As is the case for the zero value, the Level 1 percent difference is determined by applying a linear interpolation using the two surrounding Level 1 checks.

If the result of a correction of an air quality data value is negative, but is within the adjustment criteria described above, then the data value is set to zero. For Level 1 data review, the negative value will be reported as zero.

The raw data from the monitoring site is invalidated during data review and processing whenever any of the following occur:

1. Zero value exceeds ±3 percent of the full-scale value of the analyzer.
2. Span value of any parameter exceeds 15 percent of true value (i.e., less than 85 percent or greater than 115 percent).

All corrections, edits and invalidations to the data set are documented and included in the data submittal.

When the editing process is completed, the data set is then ready for review.

B9.2.3 Report Compilation and Review

The electronic report of continuous data in spreadsheet form is supported by a hardcopy report. This report consists of the following:

- A summary of all invalid and flagged data, and hand reduced data and the reason for each period of missing data.
- Any departures from normal procedures that occurred during the sampling period and their effect on the data.
- Quality control information including results of manual calibrations.
- Operator checklists and site logs.

Sample analysis data are processed using proprietary software developed at DRI. These systems perform blank subtractions, calibration corrections and estimates of uncertainty from replicate analyses in a pre-defined, consistent manner. Additionally, they utilize sample tracking codes to

combine raw data from laboratory instruments with measurement information (e.g., sample date, flow rates, etc.) to provide tables of field results in appropriate units for individual samples. Data tables are generated and stored after each processing step for examination by QA personnel and traceability.

Level 1 data will be provided to Tetra Tech and T&B Systems in a spreadsheet or CSV file once a week containing the previous week's data.

B9.3 Data Storage and Retrieval

Electronic data files including raw and edited data will be archived in duplicate. Primary storage of continuous data will be on SCS Tracer's network server, which is backed up on tape every evening. Secondary storage will be on CD-ROM.

Supporting data such as site logs and calibration forms will also be stored in duplicate. Hard copies will be kept in the project file with back-up pdfs created prior to filing.

The primary functions of laboratory data management are to have data stored in a consistent fashion that is both secure and available. To serve this need DRI has established a file server system that provides a central storage area for all laboratory and field data. The databases have defined structures maintained in one area so all field names will be consistent, which permits easy merging and comparison of the various databases. Locating all data on a central file server prevents the problems associated with having multiple copies of the same data set, and allows the individuals charged with data processing, security, validation, and QA access to the same database. All sample analysis results and subsequent data treatment will be stored on DRI's secure internal network, which is firewall protected and backed up weekly. On request, data may be accessed by LAWA and CDM via a public FTP site

C. Assessment and Corrective Actions

C.1 Assessment

Key elements of a quality assurance project plan (MQAPP) for air quality monitoring are identified in U.S. EPA (1999) and include the following:

- Project Management: Includes the roles and responsibilities of the participants.
- Data Generation and Acquisition: Maintenance, data handling and sample custody, calibrations and quality control activities and the overall data quality objectives.
- Assessment and Oversight: Includes the activities for assessing the effectiveness of the implementation of the project and associated QA and QC activities. This includes the assessment and response actions and reports to management.
- Data Validation and Usability. Includes the activities that occur after the data collection or generation phase of the project is completed and includes the steps to validate the collected data and assess the usability for the intended purpose.

System and performance audits will be conducted using an independent entity (T&B Systems), to verify the site operations and data accuracy. These audits will be conducted for both the air quality and meteorological measurements and will review the data collection efforts to assess the compliance with the stated project Data Quality Objectives in Section A8.1. Audits will be conducted for both monitoring seasons, within the first week of monitoring if possible. The review and assessment will then continue through the data processing and validation stage to provide the independent assessment of the overall data produced by the monitoring program. Comments and recommendations resulting from the audits will be discussed immediately with measurement personnel at the time of the audit, with a formal audit report to project management as soon as possible, no later than 30 days of the audit.

The following sections present the overall QA program procedures for Phase III of the LAX Study and provide details on how audits will be conducted and how the results will be integrated into the overall monitoring program. Audits will be conducted at all study-related sites, including core, satellite and, if it occurs, mobile monitoring efforts. All study-specific audits will be conducted within two weeks of the commencement of operations.

C1.1 System Audit Procedures

The purpose of the system audit is to assess consistency of measurements with the applicable Standard Operating Procedures (SOPs) and program Data Quality Objectives (DQOs). A system audit form/checklist is used to ensure the pertinent items of the audit are covered and to report the audit findings. The audit procedures employed are consistent with *Meteorological Monitoring*

Guidance for Regulatory Modeling Applications (EPA-454/R-99-005), February 2000 and the U.S. EPA *Quality Assurance Handbook for Air Pollution Measurement Systems, Volumes I, II and IV* (U.S. EPA, 1994, 2008, 2008).

The subjects that are addressed by the system audits include:

Network design and siting
- network size and design
- sensor exposure
- review of station

Resources and facilities
- instruments and methods
- staff and facilities
- standards and traceability

Quality assurance (QA) and quality control (QC)
- status of QA program
- audit participation
- precision and accuracy checks

Additionally, once the system audits of all sites in a network are complete, the auditor checks for possible differences in operation among the various sites.

Each of the system audits conducted will have specific system audit forms that will be filled out over the course of the audit. These forms will become part of the final audit documentation.

Gaseous Air Quality and Particulate Measurements. The system audit of air quality monitoring systems consists of an inspection to determine if the sampling and data acquisition system (DAS) equipment are operational, sample lines are clean and secure, and reviews the station check logs and onsite forms to determine if the documentation conforms to the specifications of the plan. The system audit of particulate samplers consists of an inspection to determine if the samplers are operational and clean, the spatial distribution of the samplers at each site conforms to the siting criteria and flow records and QC checks appear reasonable. Specifically designed system audit forms are used to document the system audit results and are included in the final audit report.

An evaluation of the QA/QC plan procedures, including preventive maintenance, is performed. Reviews of calibration records and maintenance logs are checked for consistency, frequency and accuracy. Equipment settings including flow rates and zero/span settings are evaluated to determine if ranges are acceptable.

Surface Meteorological Measurements. The system audit of the surface meteorological sensing systems consists of an inspection of the site to assess proper siting of the instrument sensors, a review of the station check logs and other site documentation, as well as an interview with the

site operator concerning his or her knowledge of the MQAPP and applicable SOP sections. Sensor siting criteria for meteorological sensors are specified in the U.S. EPA *Quality Assurance Handbook for Air Pollution Measurement Systems, Volume IV* (U.S. EPA, 2008) and *Meteorological Monitoring Guidance for Regulatory Modeling Applications* (U.S. EPA, 2000). On-site forms and site logs are reviewed to check that the documentation conforms to the specifications of the plan.

Laboratory. An audit of the DRI laboratory will be conducted through an on-site visit and review of the operations. This will include observing the sample preparation and handling procedures, sample custody, QC checks, analysis procedures, and data integrity through the process of receiving the samples to the analysis and reporting of the final results. This includes a review of the sample media preparation and cleaning process for the media transported to the field for collection of ambient samples. Any recent audits of the laboratories will be reviewed.

Data Management. The system audit of the data management will have several integral parts. Data will be collected, processed and validated by the groups responsible for their respective monitoring roles with the validated data transferred to Project Team for integration into the project database. The audit will be conducted in an electronic form by obtaining the raw initial data, in the format originally collected, and validating it against the final generated database. This system audit will be conducted prior to the final release of the database for analysis. No travel to the individual data providers is anticipated for this audit. In addition to the above system audit, an independent polling and real-time data display system will be operated by the audit staff, allowing on-going review of collected information to rapidly identify any instrument problems as well as review the collected data to determine if goals set forth in the MQAPP are being met. This system audit will be run independently of the measurements team and also serve as an independent collection process to aid in the auditing of data integrity.

C1.2 Performance Audit Procedures

Performance audits will be conducted on all applicable measurement equipment. Table C2-1 provides a summary of performance audit procedures and criteria. Details on the performance audit procedures for each audit are provided below.

Table C1-1. Summary of independent audit criteria and procedures.

Measurement Variable	*Audit Criteria*	*Procedure Reference*	*General Procedure*
Time	±5 seconds	Audit clock synchronized to either WWV or to the satellite GPS network	Comparison check to the data logging clocks.
Horizontal Wind Speed	Accuracy ±(0.2 m/s + 5% of observed). Equivalent wind speed starting torque to meet the wind speed starting thresholds for the respective sensors.	EPA-454/B-08-002	Three wind speeds within the expected range of operation. If any points are outside of criteria then corrective action is necessary.
Horizontal Wind Direction	Accuracy ±3 degrees for linearity, ±2 degrees for alignment to known direction. Equivalent wind speed starting torque to meet the wind speed starting thresholds for the respective sensors.	EPA-454/B-08-002	Depending on the mechanical sensor type from 4 to 36 points equally spaced around the compass are compared. If any points are outside of criteria then corrective action is necessary. Torque measurements are made to determine the mechanical sensor starting threshold. Sensor alignment is verified using solar or GPS methods.
Temperature	±0.5°C (monitoring criteria)	EPA-454/B-08-002	Three temperatures within the expected range of temperatures (0 to 40°C). If any points are outside of criteria then corrective action is necessary.
Temperature Difference (ΔT)	±0.1°C	EPA-454/B-08-002	Three temperatures within the expected range of temperatures (0 to 40°C). If any points are outside of criteria then corrective action is necessary. The criteria refer to the tracking of the two sensors at two heights at the same site over the range of audit temperatures.
Solar Radiation	± 5% of observed + 10 w/m^2	EPA-454/B-08-002	Five measurements within the range of operations on a given audit day are made. If any points are outside of criteria then corrective action is necessary.

Measurement Variable	***Audit Criteria***	***Procedure Reference***	***General Procedure***
Relative Humidity	±1.5°C equivalent dew point	EPA-454/B-08-002	Three comparisons are made of the station sensor to an aspirated psychrometer. If any points are outside of criteria then corrective action is necessary. The preferred method uses a self-contained RH/Temperature data logging system, which is collocated with a site sensor, recording data over the audit period. These data are compared to several observed station readings. If any points are outside of criteria then corrective action is necessary.
Gaseous Air Quality Response	Slope – 1.00 ±0.15 (all points within ±15%) Intercept -- ±3% (full-scale) NO_2 GPT Efficiency -- ≥96%	EPA-454/B-08-003	Dilution of known traceable concentrations of gas. Zero air to be provided by a CO-scrubbing zero air system.
Particulate Matter MiniVol	$PM_{2.5}$ Filter -- ±10% (5 lpm)	EPA-454/B-08-003 and experience. No audit criteria exists specifically for the minivol. Methods also developed during the 2000 CRPAQS program.	Measurement of inlet flow using a certified Gilibrator flow device
Particulate Matter BAM $PM_{2.5}$	±10% of 16.67 lpm	EPA-454/B-08-003	Measurement of the inlet flow using a certified flow device
Ultrafine particle number and sizer	±10% of audit flow – (procedures and criteria distributed to participants in memo prior to first audit)		Measurement of the inlet flow using a certified flow device
Light Scattering (Nephelometer)	±10% response to Specific Ultraviolet Absorbance SUVA ±1°C temperature ±5% RH ±3 mb pressure	CRPAQS Audit Methods	HEPA filter to zero the instrument and SUVA for the span check. Audit by comparison of the internal pressure, temperature and relative humidity sensors.
Black Carbon (Aethalometer)	±10% of audit flow ±10% flow difference from design flow		Measurement of the inlet flow using a certified Gilibrator flow device. Check of zero using a HEPA filter
PM2.5 mass and speciation	±4% of audit flow ±5% flow difference from design flow ±2°C temperature ±10mm Hg pressure	EPA-454/B-08-003	Measurement of the inlet flow using a certified dry test meter. Comparison of the available temperature sensors to the audit standard. Comparison of the internal pressure measurement to the audit standard.

Measurement Variable	***Audit Criteria***	***Procedure Reference***	***General Procedure***
Carbonyls	±5% of audit flow		Measurement of the inlet flow using a certified Gilibrator flow device
Passive Samplers	- Difference between data from passive sampler and fixed site analyzer		Evaluation of results versus collocated continuous gas analyzers at fixed sites

C1.3 Gaseous Air Quality Measurements

- **$NO/NO_x/NO_2$, SO_2, CO**

The entire sample train of the analyzer is connected to a certified dilution system output port via a glass manifold. Care is taken to introduce the audit span gas through as much of the normal sampling train (i.e., filters and scrubbers) as possible. The analyzers are challenged with three specific concentrations of span gas as shown in Table C1-2. Audit concentrations will be dependent on the final selected operational range and typical ambient concentrations anticipated at the sites.

Table C1-2. Audit concentrations.

Audit Level	*Concentration Range – PPM*		
	NO_2	***SO_2***	***CO***
1	0.0003 to 0.0029	0.0003 to 0.0029	0.020 to 0.059
2	0.0030 to 0.0049	0.0030 to 0.0049	0.060 to 0.199
3	0.0050 to 0.0079	0.0050 to 0.0079	0.200 to 0.899
4	0.0080 to 0.0199	0.0080 to 0.0199	0.900 to 2.999
5	0.0200 to 0.0499	0.0200 to 0.0499	3.000 to 7.999
6	0.0500 to 0.0999	0.0500 to 0.0999	8.000 to 15.999
7	0.1000 to 0.2999	0.1000 to 0.2999	16.000 to 30.999
8	0.3000 to 0.4999	0.3000 to 0.4999	31.000 to 39.999
9	0.5000 to 0.7999	0.5000 to 0.7999	40.000 to 50.000
10	0.8000 to 1.000	0.8000 to 1.000	50.000 to 60.000

Nitric oxide (NO), sulfur dioxide (SO_2), and carbon monoxide (CO) and carbon dioxide (CO_2) concentrations are generated using National Institute of Standards and Testing (NIST) traceable U.S. EPA protocol cylinders and gas dilution. Zero air is used to dilute the concentrations of cylinder gas. The zero air is provided by Scott Marrin Inc., Riverside, California, or by a zero air generator. Zero air for the CO_2 dilution is provided by a cylinder of CO_2 free air or by using a soda lime scrubber in conjunction with the zero air generator.

Nitrogen dioxide concentrations are introduced into a $NO/NO_2/NO_x$ analyzer by gas-phase titration (GPT) of NO with O_3. Nitric oxide reacts completely with ozone to produce nitrogen dioxide and oxygen.

The NO_2 input concentration is determined by:

$$[NO_2 \text{ input}] = \frac{[\text{NO initial}] - [\text{NO final}]}{\text{NO slope}}$$

[NO initial] = analyzer's NO channel response to the NO span prior to the addition of O_3
[NO final] = analyzer's NO response after the addition of O_3
NO slope = slope of the curve generated by linear regression of the NO concentrations versus the analyzer's response during the audit of the NO channel, where the NO input is the abscissa and the response is the ordinate

The final stage of the $NO/NO_2/NO_x$ analyzer audit is to determine the converter efficiency from the following relationships:

$$[NO_2 \text{ converted}] = [NO_2 \text{ input}] - \frac{[NO_x \text{ initial}] - [NO_x \text{ final}]}{NO_x \text{ slope}}$$

[NO_x initial] = analyzer's NO_x channel response before the addition of O_3
[NO_x final] = analyzer's NO_x response after the input sample of NO is titrated with O_3
NO_x slope = slope obtained from the audit of the NO_x channel

The converter efficiency for each audit point is:

$$\frac{[NO_2 \text{ converted}]}{[NO_2 \text{ input}]} \times 100$$

The analyzer converter efficiency is defined as the slope of the linear regression using the NO_2 source versus the NO_2 converted x 100. The converter efficiency must be greater than or equal to 96 percent to pass the audit.

Canister sampling. The canister sampling will be audited by measuring the flow rate with a certified flow device in the sampler inlet and verifying the rate is appropriate to fill the canister in a linear manner over the integrated sampling period.

Carbonyls. The carbonyl samplers will be audited by measuring the flow rate with the audit Gilibrator in the sampler inlet and comparing it to the sampler set point. As the key component is the total flow through the sampling media, the audit will only compare the sampler set point flow to the measured audit flow.

Light Scattering (Nephelometer). The nephelometer zero is audited using particle free air generated by scrubbing the inlet with a HEPA filter. The response of the instrument is then verified by flooding the chamber with Freon 134a gas, also known as SUVA. The upscale response is then compared to the calculated response for the gas at the station altitude. The instrument RH, pressure and temperature sensors are then compared to the audit standards.

Particulate Matter Air Quality Measurements

MiniVols. MiniVol samplers are turned on and allowed to warm up and the flow to stabilize with the sample filter in place. The rain cap is removed and an adapter used to connect the audit Gilibrator to the sample inlet. The readings from the Gilibrator are used as-is because the flow is provided at actual conditions. The measured audit flow rate is compared to the operator provided sampler flow rate as well as the manufacturer specified 5 lpm flow rate.

Beta Attenuation Monitors (BAMs). $PM_{2.5}$ BAM sampler flow rates are audited at the sample inlet by removing the sample head and using an adaptor to connect the audit Gilibrator at the sampler cyclone. Readings obtained from the Gilibrator are used as-is because the flow is provided at actual conditions. The measured audit flow rate is compared to the operator provided sampler flow rate as well as the manufacturer specified 16.67 lpm flow rate.

PM Speciation Samplers. PM Speciation samplers are audited first by performing a leak check in accordance with the manufacturer's procedures. An audit filter cassette is then loaded into the sampler with the calibration/leak check adapter placed on the sampler inlet. The audit dry test meter is then connected to the sample inlet, via an adapter, and the sampler started and allowed to stabilize. Timing of the sampler total flow is then initiated and the audit flow rate is calculated from the audit dry test meter registered total flow and elapsed time. The measured audit flow is compared to the operator provided sampler flow as well as the manufacturer specified 16.67 lpm flow rate. The ambient temperature probe is audited by comparison of a collocated NIST-traceable digital thermometer. The audit probe is placed within the ambient temperature radiation shield. When both the audit and sampler temperature probe readings stabilized, a one-point comparison is made. A one-point comparison of the sampler barometric sensor is conducted by comparing average audit standard and sampler readings based on three separate readings performed at 10-minute intervals.

Ultrafine Particles. The audit method looked at the sampler flow rate for UFP measurements.

Aethalometer. As there are no practical field methods to audit the precision or accuracy of the aethalometer measurements, the only audit that will be performed is of the flow rate. This flow rate will be specific to the cut point of the sample inlet. The flow rate will be audited using the Gilibrator and the measured flow compared to both the sampler set point and specified flow to achieve the proper sampler cut point.

Passive Samplers. Collocated passive samplers will be collected at the fixed sites for evaluation with data collected by the continuous analyzers. Samples will be collected for the duration of the satellite site monitoring, using procedures and schedules identical to those used for the satellite sites. Comparison criteria will be based on measurement quality objectives assigned by the end-users of the data.

Surface Meteorological Measurements

Wind Speed. The wind speed audit begins with the inspection of the wind speed cups or propeller(s) to ensure that they are intact. The cups are then removed to produce a zero point. Next, the R.M. Young selectable speed anemometer drive is connected to the sensor shaft to simulate wind speeds of approximately 5, 15 and 35 m/s. Actual values depend on the sensor model and are determined by multiplying the motor speed by a cup or propeller transfer coefficient supplied by the manufacturer. The data logger responses are compared to the calculated actual values and the differences compared to the audit criteria.

The sensor bearings are then checked for excessive wear by manually turning the sensor shaft to determine whether there is any bearing drag. Next, the sensor is removed from the crossarm and the R.M. Young torque disk mounted on the sensor shaft. The starting torque is determined using the manufacturer-recommended procedures.

Wind Direction. The wind sensor crossarm alignment relative to true north is checked using a GPS unit or a tripod mounted Brunton surveyor compass. The angle of declination is taken into account when performing this check. This angle is verified using a solar siting. The wind direction vane is then pointed toward at least the four cardinal directions and the responses of the data logger and chart recorder are noted and differences calculated and compared with the criteria. The sensor bearings are then checked for excessive wear, first by manually turning the sensor shaft to determine whether bearing drag is present and then by using an R.M. Young vane bearing torque gauge according to the manufacturer-recommended procedures.

Ambient Temperature. The temperature-sensing system is audited by immersing the system sensor and a calibrated precision digital thermometer, which is certified against a NIST-traceable mercury-in-glass thermometer in the same water bath. The thermometer readings are compared with the data logger and chart recorder outputs at approximately zero, 20° and 40° C. The difference calculated for each point is compared with the audit criteria.

Temperature Difference (ΔT). The temperature difference-sensing system is audited by immersing the two system probes in the same water bath and comparing the readings of the probes at each of the audit temperatures. The difference in readings between the probes is calculated for each point and compared with the audit criteria. This audit is performed in conjunction with the ambient temperature audit described above.

Relative Humidity and Dew-point Temperature. A self-contained mobile data logger is collocated with the station sensor and records data for the duration of the audit. The data are downloaded and time averaged to match the interval reported by the station sensor. If readings do not agree, a psychrometer is used for backup verification. The muslin wick of the wet bulb thermometer of the motorized psychrometer is wetted with distilled water. The motorized psychrometer is then placed in close proximity to the relative humidity or dew point sensor and allowed to run for at least five minutes or until the thermometer readings stabilize. Once the readings stabilize, the audit psychrometer wet and dry bulb temperatures, the audit barometric pressure and the station relative humidity and ambient temperature or dew-point temperature are read simultaneously. These readings are used, along with a measure of pressure, to calculate the audit relative humidity and dew-point temperature. If the station reports relative humidity, it is converted to an equivalent dew-point temperature for comparison with the calculated audit dew-point temperature. If dew-point temperature is measured directly, the station value is directly compared with the calculated audit value. The difference between the station equivalent or measured dew-point temperature and the calculated audit dew-point temperature is compared with the audit criteria.

Solar Radiation. A certified LiCor pyranometer is collocated with the station solar radiation sensor and at least five simultaneous readings over the course of the audit are collected and the differences compared with the audit criteria. Similarly, the audit pyranometer may be hooked up to an audit data logger, and the audit readings can be averaged into periods comparable to those collected by the station.

D. Data Validation and Usability

D1. Data Review, Verification and Validation

Data will be examined for compliance with all QC requirements for the methods used for analysis. Notations will be made concerning any deviations from these criteria. Outliers will be tested and appropriate notations will be made in the summary report concerning the rejection of any data as outliers.

D2. Verification and Validation Methods

Data validation will be performed by DRI personnel according to SOPs. This validation will begin with examination of the raw data, summary data, and field and laboratory validation codes. DRI will ensure all required data are included, sample calculations are complete, and summary data accurately represent raw data. The validation data will be assembled with the reduced laboratory notations and data validation notations, and a report will be prepared.

Mueller (1980), Mueller et al., (1983), and Watson et al. (1983, 1989, 1995) define a three-level data validation process for an environmental measurement study. Data records are designated as having passed these levels by entries in the column of each data file. These levels, and the validation codes that designate them, are defined as follows:

Level 0 (ZERO). These data are obtained directly from the data loggers that acquire the data in the field. Averaging times represent the minimum intervals recorded by the data logger, which do not necessarily correspond to the averaging periods specified for the database files. Level 0 data have not been edited for instrument downtime, nor have procedural adjustments been applied for baseline and span changes. Level 0 data are not contained in the database; although they are consulted on a regular basis to ascertain instrument functionality and to identify potential episodes prior to receipt of Level 1A data.

Level 1 (1). These data have passed several validation tests applied by the measurement investigator prior to data submission. The general features of Level 1 are: 1) no removal of data values and use of flagging data when monitoring instruments did not function within procedural tolerances; 2) flagging measurements when significant deviations from measurement assumptions have occurred; 3) verifying computer file entries against data sheets; 4) replacement of data from a backup data acquisition system in the event of failure of the primary system; 5) adjustment of measurement values for quantifiable baseline and span or interference biases; and 6) identification, investigation, and flagging of data that are beyond reasonable bounds or that are unrepresentative of the variable being measured.

Level 2 (2): Level 2 data validation occurs after data from various measurement methods have been assembled in the master database. Level 2 validation is the first step in data analysis. Level 2 tests involve the testing of measurement assumptions (e.g., internal sampler temperatures do not significantly exceed ambient temperatures), comparisons of collocated measurements, and internal consistency tests (e.g., the sum of measured aerosol species does not exceed measured mass concentrations). Level 2 tests also involve the testing of measurement assumptions, comparisons of collocated measurements and internal consistency tests.

Level 3 (3). Level 3 is applied during the model reconciliation process, when the results from different modeling and data analysis approaches are compared with each other and with measurements. The first assumption upon finding a measurement, which is inconsistent with physical expectations, is that the unusual value is due to a measurement error. If, upon tracing the path of the measurement, nothing unusual is found, the value can be assumed to be a valid

result of an environmental cause. The Level 3 designation is applied only to those variables that have undergone this reexamination after the completion of data analysis and modeling. Level 3 validations continue for as long as the database is maintained.

A higher validation level assigned to a data record indicates that those data have gone through, and passed a greater level of scrutiny than data at a lower level.

D3. Reconciliation with Data Quality Objectives

For QA purposes, substantial comparisons among measurements will be made to determine their predictability, comparability and equivalence. Although the different observables measured are diverse, it is possible they may be highly correlated due to their quantification of related particle properties or to large fluctuations caused by emissions and meteorology. Relationships between variables will depend on the composition of the aerosol as well as meteorological conditions. Measures of predictability, comparability and equivalence are applied to data sets stratified by aerosol composition and season. Predictability requires a consistent and reliable relationship between measurements, even if they are of different quantities.

(This page is intentionally blank)

APPENDIX

List of Available Standard Operating Procedures

(This page is intentionally blank)

List of SOPs (available upon request)

1. 4 Channel Sequential FP/SVOC Sampler (DRI 1-750.4)
2. Analysis of Carbonyl Compounds by High Performance Liquid Chromatography (DRI 2-710.4)
3. Analysis of Semi-Volatile Organic Compound by GC/MS (DRI 2-750.5)
4. Analysis of VOC in Ambient Air by Gas Chromatography and Mass Spectrometry (DRI 2-704.2)
5. Anion Analysis of Filter Extracts and Precipitation Samples by Ion Chromatography (DRI 2-203r7)
6. Filter Pack Assembly, Disassembly and Cleaning (DRI 2-111.4)
7. Grimm SMPC Setup, Operation, and Maintenance Procedure (DRI SOP)
8. Inside/Outside Temperature Sensors (ARB-AMQA Volume II, Appendix AA)
9. Magee Scientific Aethalometer (ARB-AQSB SOP 407)
10. Met-One Instruments Beta Attenuation Mass Monitor (BAM-1020) (ARB-AQSB SOP 400)
11. Meteorological Parameter Procedures for Wind Direction Sensors (ARB-AMQA Volume II, Appendix V)
12. Meteorological Parameter Procedures for Wind Speed Sensors (ARB-AMQA Volume II, Appendix T)
13. Nephelometer (ARB-AQMA Volume II, Appendix L)
14. NO, NO_2, NO_x and SO_2 Sampling Protocol Using The Ogawa Sampler (Ogawa)
15. Passive Sampling for Volatile Organic Compounds (DRI Radiello Sampling v2)
16. $PM_{2.5}$ FRM Gravimetric Analysis (DRI 2-114.8)
17. Pre-firing and Acceptance Testing of Quartz Fiber Filters For Aerosol and Carbonaceous Material Sample (DRI 2-106r6)
18. Sample Shipping, Receiving and Chain-of-Custody (DRI 2-209.4)
19. Thermal/Optical Carbon Analysis (TOR/TOT) of Aerosol Filter Samples – Method IMPROVE_A (DRI 216r2)
20. TECO 42 Oxides of Nitrogen Analyzer (ARB-AMQA Volume II, Appendix W)
21. TECO Model 48 Carbon Monoxide Analyzer (ARB-AQMA Volume II, Appendix Y)

22. Thermo Electron Model 43 Sulfur Dioxide Analyzer (ARB-AMQA Volume II, Appendix C)
23. Thermo Environmental Instruments Model 43C Trace Level Pulsed Fluorescence Sulfur Dioxide Analyzer (ARB-AMQA Volume II, Appendix C)
24. TSI Nano Scanning Mobility Particle Sizer (Nano-SMPS) Setup, Operation, and Maintenance Procedure (DRI SOP)
25. TSI Regular Scanning Mobility Particle Sizer (RSMPS) Setup, Operation, and Maintenance Procedure (DRI SOP)
26. X-Ray Fluorescence (XRF) Analysis of Aerosol Filter Samples (PANalytical Epsilon 5) (DRI 2-209.6)
27. Meteorological Parameters Percent Relative Humidity Sensors. (ARB – AMQA Volume II, Appendix UU)
28. Carbonyl Sampler (DRI 1-710r4)
29. Airmetrics MiniVol Portable PM Survey Sampler Field Operations. (DRI 1-210r4)
30. Canister-Based Analysis of CO/CO2/CH4 by Gas Chromatography with Flame Ionization Detection (DRI 2-701.2)
31. Procedure for Collecting Tenax Samples. (DRI 1-720.3)
32. Determination of VOCs in Ambient Air Using Active Sampling onto Sorbent Tubes. Method TO-17. EPA/625/R-96/010b
33. Digital Datalogging Sound Level Meter Model HD 600. Extech Instruments.
34.

Appendix 3-4

MODELING AND ANALYSIS PROTOCOL (MAP)

(This page is intentionally blank)

Los Angeles
World Airports

Los Angeles International Airport
Air Quality and Source Apportionment Study
Phase III

Final Scope of Work for Modeling and Analysis Protocol

June 13, 2012

Prepared for:

Los Angeles World Airports
Environmental Services Division
7301 World Way West
Los Angeles, California 90045

Prepared by:

Tetra Tech, Inc.
3475 E. Foothill Boulevard,
Pasadena, California 91107

(This page is intentionally blank)

PREFACE

The Modeling and Analysis Protocol (MAP) was developed as part of the requirements described in the "Draft Scope of Work" for Phase III of the Los Angeles International Airport Air Quality and Source Apportionment Study (LAX AQSAS). The MAP was developed to provide the protocols and methodologies that were used in conducting the receptor and source apportionment modeling and analysis portion of the LAX AQSAS.

The MAP was developed by Tetra Tech, in collaboration with the following project team members:

- Dr. Eric Fujita of the Desert Research Institute for spatial and temporal analysis of ambient pollutant concentrations and receptor modeling by Chemical Mass Balance;
- Dr. Ron Henry for non-parametric trajectory analysis;
- Mr. Mike Ratte of KB Environmental Sciences for on- and off-airport air emission inventory; and
- Dr. Sarav Arunachalam for source-oriented air dispersion modeling.

The MAP provides a roadmap as to how the modeling and analysis portion of the LAX AQSAS is conducted; explains each of the modeling techniques; and identifies information required for the analyses. Additionally, the MAP will be used to cross check the modeling analyses with the field measurements collected during the 1st and 2nd monitoring seasons to evaluate the results from the field sampling and modeling. This approach of using multiple techniques to determine LAX contributions to air pollutant concentrations in the areas surrounding the airport will provide the following advantages:

- Providing backup information and the ability to continue source apportionment analysis if one of the data collection systems fails;
- Identification and reconciliation of difference source contribution estimates from the multiple approaches; and
- Providing the ability to calibrate dispersion analysis of airport sources with reasonable accuracy, such as improving the inputs and assumptions used in dispersion models to produce results that better match measured concentration patterns

In summary, the project team expects that through this approach of using multiple modeling techniques, the primary objective of the LAX AQSAS, to assess the incremental impact of LAX operations on local air quality, can be achieved.

(This page is intentionally blank)

Contents

List of Tables

List of Figures

List of Acronyms

ACES – Advance Collaborative Emissions Study
AER – Annual Emission Reporting
ANOMS – Aircraft Noise and Operations Monitoring System
APU – auxiliary power unit
AQSAS – Air Quality and Source Apportionment Study
ASOS – Automated Surface Observing System
ASPM – Aviation System Performance Metrics
ATCT – Air Traffic Control Tower
CalTrans – California Department of Transportation
CARB – California Air Resources Board
CB05 – Carbon Bond 2005 Chemical Mechanism
CEIDARS – California Emission Inventory Development and Reporting System
CEMS – Continuous Emissions Monitoring System
CHAPIS – Community Health Air Pollution Information System
CLOSE – Collaborative Lubricating Oil Study on Emissions
CMAQ – Community Multiscale Air Quality Model
CMB – Chemical Mass Balance
CNG – compressed natural gas
CO – carbon monoxide
CO_2 – carbon dioxide
CTA – Central Terminal Area
DNPH - 2,4-Dinitrophenylhydrazine
DPM – diesel particulate matter
DRI – Desert Research Institute
EC – elemental carbon
EDMS – Emissions and Dispersion Monitoring System
EPAct – Effect of Gasoline Properties on Exhaust Emissions from Tier 2 Light-Duty Vehicles
FAA – Federal Aviation Administration
FIND – Facility Information Detail
GC/MS – gas chromatography/mass spectrometry
GPU – ground power unit
GSE – ground support equipment
HAP – hazardous air pollutant
HONO – nitrous acid
HPLC/UV – High-Pressure Liquid Chromatography with UV Detector
Hz - Hertz
ICP-MS – inductively coupled plasma mass spectroscopy
IMC – instrument meteorological conditions
LAWA – Los Angeles World Airports
LAX – Los Angeles International Airport
LPG – liquefied petroleum gas
LTO – landing and takeoff cycle
MDL – method detection limit

NCDC – National Climatic Data Center
NMHC – nonmethane hydrocarbon
NO_x – oxide of nitrogen
NO_2 – nitrogen dioxide
NTA – Nonparametric Trajectory Analysis
OC – organic carbon
PAH – polycyclic aromatic hydrocarbons
PAMS – Photochemical Assessment Monitoring Station
PCA – pre-conditioned air
PeMS – Freeway Performance Maintenance System
$PM_{2.5}$ – particulate matter 2.5μm in diameter
PM_{10} – particulate matter 10 μm in diameter
POC – particulate organic carbon
ppb – part per billion
ROG – reactive organic gas
SCAG – Southern California Association of Governments
SCAQMD – South Coast Air Quality Management District
SCE – source contribution estimates
SMOKE – Sparse Matrix Operator Kernel Emissions Modeling System
SO_2 – sulfur dioxide
SO_x – sulfur oxides
SOA – secondary organic aerosols
SVHC – semi-volatile hydrocarbons
TC – total carbonaceous aerosols
THC – total hydrocarbons
TOG – total organic compounds
UNC – University of North Carolina
UNID – unidentified
UNMIX – multivariate analysis
USC – University of Southern California
U.S. EPA – United States Environmental Protection Agency
UTM – Universal Transverse Mercator
VALE – Voluntary Airport Low Emissions
VMC – visual meteorological conditions
VOC – volatile organic compounds
WRF – Weather Research Forecast Model
XRF – X-Ray fluorescence

Section 1
Introduction

The Modeling and Analysis Protocol (MAP) will be used to guide data analysis for source apportionment analysis using receptor-oriented modeling during the 1st and 2nd field measurement seasons and source-oriented modeling using updated emission inventory and AERMOD dispersion modeling technique.

The primary objective of Phase III of the LAX Air Quality and Source Apportionment Study (AQSAS) is source apportionment, specifically to assess the incremental impact or "fair-share" contribution of LAX operations on local air quality.

This objective will be achieved by:

- Quantifying spatial and temporal variations in ambient air concentrations of gases and particles at LAX and adjacent communities.
- Determining fuel-based emission factors and chemical composition of jet exhaust and taxiing emissions and updating the emissions inventory of airport and non-airport sources within and near LAX. The emissions inventory will be developed primarily from previously published reports and data.
- Determining the contributions of various airport-related activities and non-airport sources to the concentrations of selected air pollutants within communities adjacent to LAX using both source and receptor modeling.

These objectives will be achieved using a combination of descriptive data analysis and both receptor and source-oriented modeling and analysis to identify significant sources of pollutant and the types of pollutants they emit, as shown in Figure 1. The modeling conducted will also help identify the potential contributions of LAX emissions to the surrounding communities.

Receptor modeling techniques were to originally include chemical mass balance (CMB) modeling, positive matrix factorization (PMF), multivariate receptor modeling (UNMIX), and non-parametric trajectory analysis (NTA). However, to provide a meaningful analysis of the data, both PMF and UNMIX require a larger speciation sample size (i.e., minimal 80 to 100 samples)[1]. However, only 14 complete speciation samples will be collected in this study. Therefore, the use of PMF and UNMIX in receptor modeling for this study will not be performed. Furthermore, receptor modeling analysis by CMB and NTA should be sufficient to provide source apportionment information at receptor sites.

The modeling protocol will provide general methodology that will be used to:

[1] Personal communication with Drs. Eric Fujita and Ronald Henry. May 29, and May 30, 2012

- Conduct receptor modeling
  - Chemical Mass Balance (CMB)
  - Spatial gradient and time series analysis
  - Non-parametric trajectory hybrid modeling

- Conduct source modeling
  - Estimates of Study Area emissions (both on- and off-airport)
  - Dispersion modeling

The receptor modeling using CMB and multivariate analysis will be conducted by Dr. Eric Fujita of Desert Research Institute (DRI). Receptor modeling using non-parametric trajectory hybrid modeling will be conducted by Dr. Ron Henry of USC. Source modeling emissions inventory will be conducted by Mr. Michael Ratte of KB Environmental Sciences. Source modeling using the AERMOD and CMAQ models will be conducted by Dr. Sarav Arunachalam of the University of North Carolina at Chapel Hill (UNC).

Figure 1. Schematic summary of the Phase III LAX AQSAS Data Analysis Plan Showing the Connections Between Measurements (in red) and the Modeling and Data Analysis Approaches.

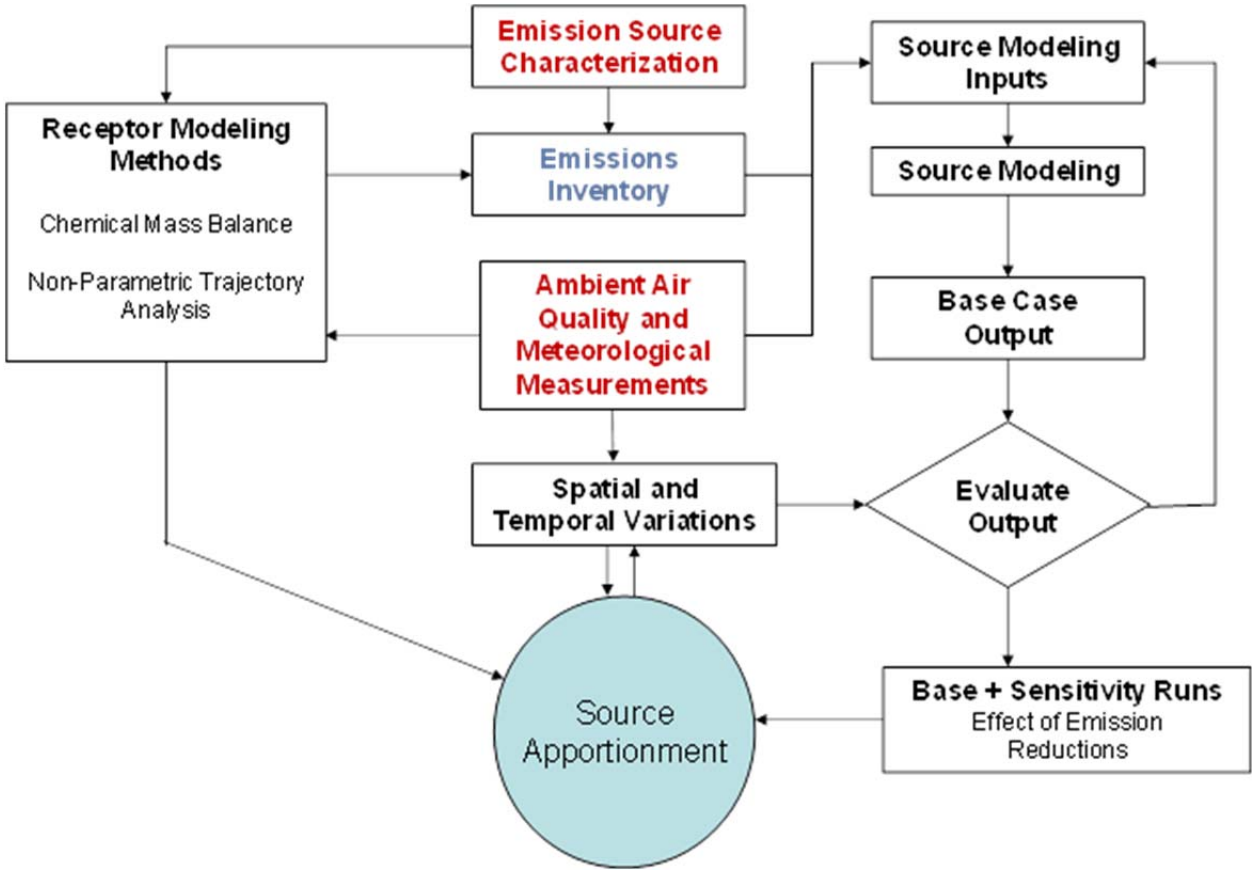

Section 2
Receptor Modeling

2.1 Chemical Mass Balance Receptor Model

The Chemical Mass Balance (CMB) receptor model will be applied to LAX AQSAS community monitoring data to estimate the source contributions to measured ambient concentrations of volatile organic compounds (VOC), specific gaseous air toxics (e.g., benzene, toluene, ethylbenzene and xylenes), total carbonaceous aerosols (TC) and $PM_{2.5}$. The CMB receptor model consists of a least-squares solution to a set of linear equations. The solution expresses each receptor concentration of a chemical species as a linear sum of products of source profile species and receptor contributions. The source profile species (the fractional amount of each species in the VOC or PM emissions from a given source type) and the receptor concentrations, each with uncertainty estimates, serve as input data to the CMB model. Input data uncertainties are used to weight the relative importance of the input data to the model solution and to estimate uncertainties of the source contributions. The output consists of the contributions of each source type to both total and individual ambient VOC and PM concentrations. The model calculates values and uncertainties for each source contribution.

The CMB procedure requires: 1) identification of the contributing source types; 2) selection of chemical species to be included; 3) estimation of the fractions of each chemical species contained in each source type; 4) estimation of the uncertainties to ambient concentrations and source compositions; and 5) solution of the CMB equations. The CMB model assumes: 1) compositions of source emissions are constant over the period of ambient and source sampling; 2) chemical species do not react with each other, i.e., they add linearly; 3) all sources with a potential for significant contribution to the receptor have been identified and have had their emissions characterized; 4) the source compositions are linearly independent of each other; 5) the number of source categories is less than or equal to the number of chemical species; and 6) measurement uncertainties are random, uncorrelated and normally distributed. While these assumptions are fairly restrictive, it is necessary to keep in mind that all assumptions will not be able to be completely adhered to within an actual practice. Deviations from these assumptions increase the uncertainties of the source contribution estimates.

The review by Watson et al. (2001) examined how the CMB receptor model has been applied to quantify ambient VOC source contributions to ambient concentrations of organic gases. DRI also prepared a guidance document for applying the CMB receptor model to the Photochemical Assessment Monitoring Station (PAMS) VOC data and for evaluating and interpreting model outputs (Fujita and Campbell, 2004). The document includes a summary of the fundamentals of CMB and descriptions of the features of CMB Version 8 (CMB8). Sample VOC source and ambient input data files, default source and fitting species selection files and a library of available source VOC composition profiles in CMB8-ready format are also included. More recent applications of CMB for PM apportionment have used particulate organic tracers to provide greater resolution of the contributions of various combustion sources of carbonaceous particles (Schauer et al., 1996; Watson et al., 1998; Fujita et al., 1998, Fujita et al., 2007; Lough

et al., 2007; Lough and Schauer, 2007). The model assumes the composition of the particles does not change from source to receptor. Therefore, its ability to resolve secondary organic aerosols (SOA) is limited. The residual PM mass not apportioned to specific sources in the CMB calculation is commonly used to estimate SOA.

Normalization of Source Composition Profiles and Uncertainties

The source composition profiles used in the CMB calculations for apportionment of VOC are expressed as weight percentages of the sum of the PAMS target species shown in Table 1 or total nonmethane hydrocarbons (NMHC). The PAMS target compounds typically account for about 80 percent of the ambient hydrocarbons in urban areas. Heavier gas-phase hydrocarbons and semi-volatile hydrocarbons (SVHC) in the C_{12} to C_{18} range, from an analysis of the Tenax samples, typically account for less than 10 percent of the total sum of VOC and SVHC. However, they serve as useful markers for diesel exhaust and, potentially, for jet exhaust. The source profile data reported in units of ppbC are converted to $\mu g/m^3$ prior to calculating the weight percentages using species-specific conversion factors. Source profiles used in PM apportionment are expressed as weight percent of total carbon or $PM_{2.5}$ mass. The speciation of particulate and semi-volatile organic compounds (SVOC) includes heavy alkanes, polycyclic aromatic hydrocarbons (PAH), hopanes, steranes, polar organic compounds, and metals that can be used as source tracers. One-sigma uncertainties are derived from variations among multiple measurements for a particular source type or a nominal analytical uncertainty of 10 percent with a minimum uncertainty of 0.001. The assigned uncertainties are the larger of the two values.

Selection of Fitting Species

A prerequisite for using receptor models is that the relative proportions of chemical species change little between source and receptor. Most ambient NMHCs are oxidized in the lowest two kilometers of the troposphere with lifetimes ranging from hours to days. Nominal afternoon summertime residence times for a reactive environment (e.g., Los Angeles) are estimated in Table 2-1. These estimates provide indications of which components are likely to remain relatively stable between source and receptor, thereby qualifying as a fitting species for CMB source apportionment of VOC. An exception is isoprene, which is included as a fitting species despite its high reactivity because it serves as a marker for biogenic emissions. The source contribution estimates tend to underestimate the actual source contributions of biogenic emissions, i.e., they provide a lower limit to biogenic contributions. Table 1 lists three sets of default fitting species, by site type and time of day.

Type 1, 2 and 4 sites are in upwind background, downwind edge and extreme downwind locations, respectively, and a list of 11 photochemically stable compounds are used as fitting species for these sites. Type 2 PAMS sites are located in areas of maximum precursor emissions and are typically placed near the central business district. An expanded list of hydrocarbons (36 species) may be used as fitting species at Type 2 sites for samples collected in the morning hours prior to 9:00 a.m. (i.e., Type 2 AM) since the emissions are largely unreacted. A shorter list of more stable species (20 species) is used for samples collected between 9:00 a.m. and 6:00 p.m. (i.e., Type 2 PM). Reactive species are retained in the CMB modeling as “floating species”, and provide useful diagnostic information. The predicted concentrations for these species exceed the measured values by margins that increase proportionally with reactivity of the species. We anticipate the expanded list of 36 species can be used for the LAX AQSAS twenty-four hour

VOC samples because LAX is in the upwind edge of the urban areas of the South Coast Air Basin. The predicted versus measured concentration differences will be examined to confirm which fitting species to retain in the final CMB calculations.

Model Output and Diagnostic Information

CMB software applies the effective variance solution, which gives greater influence to chemical species that are measured more precisely in both source and receptor samples. The software also calculates uncertainties for source contributions from both the source and receptor uncertainties. Source contribution estimates (SCE) are the main output of the CMB model. The sum of these concentrations approximates the total mass concentrations. Negative SCE are not physically meaningful, but can occur when a source profile is collinear with another profile or when the source contribution is close to zero. When the SCE is less than its standard error, the source contribution is undetectable. The upper limit of the SCE in this case may be taken to be two or three times the standard error. There is approximately a 66 percent probability the true source contribution is within one standard error and approximately a 95 percent probability the true concentration is within two standard errors of the SCE.

The reduced chi square (χ^2), R^2, and percent mass are goodness of fit measures for the least-squares calculation. The χ^2 is the weighted sum of squares of the differences between calculated and measured fitting species concentrations. The weighting is inversely proportional to the squares of the precision in the source profiles and ambient data for each species. A value of less than one indicates a very good fit to the data, while values between 1 and 2 are acceptable. χ^2 values greater than 4 indicate that one or more of the fitting species concentrations are not well-explained by the source contribution estimates. R^2 is determined by the linear regression of the measured versus model-calculated values for the fitting species. R^2 ranges from 0 to 1. The closer the value is to 1.0, the better the SCEs explain the measured concentrations. The SCEs do not explain the observations with the given source profiles well when R^2 is less than 0.8. Percent mass is the percent ratio of the sum of model-calculated SCEs to the measured mass concentration. This ratio should equal 100 percent, though values ranging from 80 to 120 percent are acceptable.

Table 1. Photochemical Assessment Monitoring Station (PAMS) Target Species and Their Reactivity.

	Mnemonics[1]	Names	Formula	AIRS Code	convert to ug/m3	MW	Group	k_{OH} at 298 K	Lifetime hours	CMB Fitting Species Type 2 AM	Type 2 PM	Types 1,3, & 4
1	ETHENE	ethene	C2H4	43203	0.5736	28.05	O	8.52	6.52	*		
2	ACETYL	acetylene	C2H2	43206	0.5325	26.04	Y	0.90	61.73	*	*	*
3	ETHANE	ethane	C2H6	43202	0.6149	30.07	P	0.27	207.30	*	*	*
4	PROPE	Propene	C3H6	43205	0.5737	42.08	O	26.30	2.11			
5	N_PROP	n-propane	C3H8	43204	0.6012	44.10	P	1.15	48.31	*	*	*
6	I_BUTA	isobutane	C4H10	43214	0.5943	58.12	P	2.34	23.74	*	*	*
7	LBUT1E	1-butene	C4H8	43280	0.5737	56.11	O	31.40	1.77			
8	N_BUTA	n-butane	C4H10	43212	0.5943	58.12	P	2.54	21.87	*	*	*
9	T2BUTE	t-2-Butene	C4H8	43216	0.5737	56.11	O	64.00	0.87			
10	C2BUTE	c-2-butene	C4H8	43217	0.5737	56.11	O	56.40	0.99			
11	IPENTA	isopentane	C5H12	43221	0.5902	72.15	P	3.90	14.25	*	*	*
12	PENTE1	1-pentene	C5H10	43224	0.5737	70.13	O	31.40	1.77			
13	N_PENT	n-pentane	C5H12	43220	0.5902	72.15	P	3.94	14.10	*	*	*
14	I_PREN	isoprene	C5H8	43243	0.5571	68.11	O	101.00	0.55	+	+	+
15	T2PENE	t-2-Pentene	C5H10	43226	0.5737	70.13	O	67.00	0.83			
16	C2PENE	c-2-pentene	C5H10	43227	0.5737	70.13	O	65.00	0.85			
17	BU22DM	2,2-dimethylbutane	C6H14	43244	0.5874	86.17	P	2.32	23.95	*	*	*
18	CPENTA	cyclopentane	C5H10	43242	0.5737	70.13	P	5.16	10.77	*	*	
19	BU23DM	2,3-dimethylbutane	C6H14	43284	0.5874	86.17	P	6.20	8.96	*		
20	PENA2M	2-methylpentane	C6H14	43285	0.5874	86.17	P	5.60	9.92	*	*	
21	PENA3M	3-methylpentane	C6H14	43230	0.5874	86.17	P	5.70	9.75	*	*	
22	P1E2ME	2-methyl-1-pentene	C6H12	43246	0.5737	84.16	O	31.40	1.77			
23	N_HEX	n-hexane	C6H14	43231	0.5874	86.17	P	5.61	9.90	*	*	
24	MCYPNA	Methylcyclopentane	C6H12	43262	0.5737	84.16	P	8.81	6.31	*		
25	PEN24M	2,4-dimethylpentane	C7H16	43247	0.5855	100.20	P	5.10	10.89	*	*	
26	BENZE	benzene	C6H6	45201	0.5324	78.11	A	1.23	45.17	*	*	*
27	CYHEXA	cyclohexane	C6H12	43248	0.5737	84.16	P	7.49	7.42	*		
28	HEXA2M	2-methylhexane	C7H16	43263	0.5737	98.19	P	6.79	8.18	*		
29	PEN23M	2,3-dimethylpentane	C7H16	43291	0.5855	100.20	P	4.87	11.41	*	*	
30	HEXA3M	3-methylhexane	C7H16	43249	0.5855	100.20	P	7.16	7.80	*	*	
31	PA224M	2,2,4-trimethylpentane	C8H18	43250	0.584	114.23	P	3.68	15.10	*	*	*
32	N_HEPT	n-heptane	C7H16	43232	0.5855	100.20	P	7.15	7.77	*		
33	MECYHX	methylcyclohexane	C7H14	43261	0.5737	98.19	P	10.40	5.34	*		
34	PA234M	2,3,4-trimethylpentane	C8H18	43252	0.584	114.23	P	7.00	7.94	*		
35	TOLUE	toluene	C7H8	43202	0.5384	92.14	A	5.96	9.32	*	*	
36	HEP2ME	2-methylheptane	C8H18	43260	0.5829	114.23	P	8.18	6.80	*	*	
37	HEP3ME	3-methylheptane	C8H18	43253	0.584	114.23	P	8.56	6.49	*		
38	N_OCT	n-octane	C8H18	43233		114.22	P	8.68	6.40	*		
39	ETBZ	ethylbenzene	C8H10	45203	0.5427	106.16	A	7.10	7.82	*		
40	MP_XYL	mp-xylene	C8H10	45109	0.5427	106.16	A	18.95	4.71			
41	STYR	styrene	C8H8	45220	0.5324	104.14	A	58.00	0.96			
42	O_XYL	o-xylene	C8H10	45204	0.5428	106.17	A	13.70	4.06			
43	N_NON	n-nonane	C9H20	43235	0.5829	128.26	P	10.20	5.45	*		
44	IPRBZ	isopropylbenzene	C9H12	45210	0.5462	120.20	A	6.50	8.55	*		
45	N_PRBZ	n-propylbenzene	C9H12	45209	0.5462	120.20	A	6.00	9.26	*		
46	M_ETOL	m-ethyltoluene	C9H12	45212	0.5462	120.20	A	19.20	2.89			
47	P_ETOL	p-ethyltoluene	C9H12	45213	0.5462	120.20	A	12.10	4.59			
48	BZ135M	1,3,5-trimethylbenzene	C9H12	45207	0.5462	120.20	A	57.50	0.97			
49	O_ETOL	o-ethyltoluene	C9H12	45211	0.5462	120.20	A	12.30	4.52			
50	BZ124M	1,2,4-trimethylbenzene	C9H12	45208	0.5462	120.20	A	32.50	1.71			
51	N_DEC	n-decane	C10H22	43238	0.582	142.29	P	11.60	4.79	*		
52	BZ123M	1,2,3-trimethylbenzene	C9H12	45225	0.5462	120.20	A	32.70	1.70			
53	DETBZ1	m-diethylbenzene	C10H14	45218		134.22	A	14.20	3.90			
54	DETBZ2	p-diethylbenzene	C10H14	45219		134.22	A	14.20	3.90			
55	N_UNDE	n-undecane	C11H24	43954		156.30	P	13.20	4.20	*		
	TNMOC											
	PAMHC											
	UNID											
	MTBE											

A = aromatic, AL = Aldehyde, O = alkene (olefin), P = parafin, Y = alkyne, K = ketone, E = ether, X = haogenated, OH = alcohol

Note: Rate constants k at 298 K for the reaction of OH radicals with VOCs.

Unit: 1012 x k cm3 molecule-1 s-1

While the application of the CMB receptor model is relatively straightforward given the input data, assessment of the validity of source contribution estimates is not. The uncertainties derived by the CMB model alone are insufficient to assess the true validity of the apportionment results. The uncertainty in the source composition profile may only account for measurement uncertainties in the selected profile and may not reflect the actual variability of the source composition among alternative profiles for the same source category. Testing and sampling protocols and a number of other factors affect the emission rates and chemical composition of gaseous and particulate pollutants from various combustion sources. Sampling and analytical methods also affect ambient measurements. Ambient PM measured at the receptor location may not be able to be differentiated from a similar source nearby. Ambient PM measured at receptor locations may also result from: (1) particulates transported from multiple areas with similar sources that may have differing chemical profiles and (2) gaseous pollutants that have undergone atmospheric transformation during transport. CMB results can also vary with the specific procedures used to derive the composite profiles and uncertainties as well as the choice of source profiles and fitting species.

The emissions inventory is the starting point for a CMB source apportionment to identify potential contributors to ambient concentrations. Air monitoring and modeling studies have shown that the zone of influence of an emission source is inversely proportional to the square of the distance from the source. Concentrations typically drop to the community average within a relatively short distance from the source. The contributions of emission sources to the community-scale pollutant concentrations depend on the temporal and spatial variations in the numbers and emission rates of sources in the upwind vicinity of the monitoring location. Urban air quality monitoring sites consistently reflect vehicle-related emissions, including exhaust and evaporated fuel, which are ubiquitous in all urban areas. Architectural emissions, other surface coatings and industrial solvent use are also common, but highly variable. Cooking, Petrochemical production, oil refining and other industrial plants are more specific to certain urban areas where these facilities exist. Emissions from meat cooking and vegetative burning typically have large diurnal and seasonal variations and widely varying composition profiles.

2.2 Source Composition Profiles of Primary Emission Sources

To address the contribution of airport operations to air quality in the surrounding community, we will use area specific source composition profiles for gasoline vehicle exhaust, evaporative emissions and diesel exhaust. The need for adding additional source categories will be assessed by examining the residual VOC and PM mass and compositions not accounted for by these sources. The source composition profiles used in receptor modeling and as input to photochemical air quality models should be current and regionally specific. This will allow for the profiles to account for temporal and regional variations in fuel formulations and distribution of area and point sources. Updated profiles will be developed for major sources for this project including commercial jet exhaust (both takeoff and taxiing), and fuel composition for gasoline (regular, mid-grade and premium), Jet-A, and #2 diesel. The source samples proposed for this project are described in Phase III of the LAX AQSAS.

2.2.1 VOC Source Composition Profiles

Vehicle Exhaust. Diesel and gasoline exhaust profiles are similar with respect to the composition of light hydrocarbons, and are often collinear in CMB calculations. Ethene, acetylene, 1-butene, iso-butene, propane, propene, isopentane, n-pentane, 2,2 dimethylbutane, 2-methylpentane, n-hexane, benzene, 3-methyhexane, toluene, ethylbenzene, m- and p-xylene, m-ethyltoluene, and 1,2,4-trimethylbenzene, are the most abundant compounds in either or both of these emissions. Several of these are short-lived and are only used in CMB calculations where fresh emissions are expected. Major differences between these two exhaust profiles are evident for: 1) acetylene, iso-butene, isopentane, n-hexane, and 2-methylhexane, which are most abundant in gasoline exhaust; and 2) for propene, propane, 2,2 dimethylbutane, n-decane, and n-undecane which are more abundant in diesel exhaust. Previous studies have shown that source attributions between tailpipe and evaporative emissions from receptor modeling can vary greatly depending on the particular profile chosen for tailpipe emissions (Harley et al., 1992; Fujita et al., 1994; Pierson et al., 1996). This is because tailpipe emissions are a mixture of hydrocarbons produced during combustion (e.g., acetylene, ethene, propene and benzene) along with unburned gasoline resulting from incomplete combustion. The relative abundances of combustion by-products in the exhaust profile vary with emission control technology, level of vehicle maintenance and operating mode. In the CMB calculation, liquid gasoline represents the additional unburned gasoline (due to misfiring and other engine malfunctions) that is not included in the exhaust profile, plus evaporative emissions from gasoline spillage, hot soaks, and a portion of resting losses (leaks, permeation). The profile for gasoline headspace vapor is taken to represent fuel tank vapor losses (e.g., migration of fuel vapor from the canister).

Gasoline Liquid and Vapor. Running and resting losses are the two sources of evaporative loss from vehicles travelling on the road. Running losses are releases of gasoline vapor from the fuel system during vehicle operation as a result of the heating of the fuel tank. Vapors are released when the rate of fuel vapor formation exceeds the capacity of the vapor storage and purge systems. The composition of running losses tends to resemble headspace vapors if the canister is saturated and butane-enriched vapors if the canister is not saturated. The canister similarly affects the composition of diurnal evaporative emissions. Resting loss evaporative emissions are due to migration of fuel vapors from the evaporative canister, leaks, and fuel permeation through joints, seals and polymeric components of the fuel system. Most of these losses, as well as hot soaks, tend to appear more like whole liquid gasoline. Liquid gasoline contains many compounds in common with gasoline-vehicle exhaust. It is depleted in combustion products, such as ethane, ethene, acetylene, propene, and to some extent, benzene. Evaporated gasoline and heavier hydrocarbons that volatilize more slowly from liquid fuels are also depleted in these combustion compounds. Isobutane, n-butane, t-2 butene, and especially isopentane are enriched in evaporated gasoline. These differences are sufficient for CMB separation of gasoline exhaust from liquid and evaporated gasoline, and often from diesel exhaust, in ambient air.

Surface Coatings. Although solvents from paints and industrial uses are large components of VOC inventories, they have few reported profiles. The most comprehensive data are those of Censullo et al. (1996), which included analyses of eleven categories of coating. Detailed species profiles were obtained for a total of 106 samples of water-based and solvent-based coating samples. Surface coating profiles for solvent-based industrial maintenance coatings, solvent-

based medium gloss/high gloss, solvent-based primers and sealers, quick dry primers and enamels, and thinning solvent were applied in the apportionments. These are largely depleted in the species common to fuel use and production, with larger abundances of styrene, n-decane, and "other" VOCs, which are oxygenated compounds and differ substantially among the different coatings tested.

Regional Background and Biogenic Emissions. Regional upwind, background VOC's typically contain higher abundances of relatively nonreactive hydrocarbons, such as ethane and propane and oxidized species, primarily aldehydes. In addition to urban background, both compressed natural gas (CNG) and liquefied petroleum gas (LPG) are potential sources of ethane and propane. Since CNG and LPG cannot be distinguished from urban background, these source contributions will be combined.

Unidentified. Most source profiles contain a UNID component, which represents the fractional compositions of NMHC not assigned to individual, identified species in the gas chromatographic analysis. A single constituent source profile, where the UNID component is assumed to comprise 100 percent of NMHC, has been used in the past (Fujita et al., 1994b) to account for NMHC contributions. The difference between the measured total NMHC and the sum of the source contributions from fitted sources is named as "unexplained". The "unexplained" source contributions in this report refer to the differences between the measured NMHC and the sum of the predicted contributions from those identified source categories. Nearly all of the unexplained mass is related to UNID not assigned to the identified categories. The fraction of UNID is consistently higher in downwind and afternoon samples, which suggests that much of this residual UNID could be secondary organic species produced by photochemical reactions.

2.2.2 PM Source Composition Profiles

The main sources of primary carbonaceous aerosols in urban areas include motor vehicle exhaust (diesel and gasoline), off-road vehicles and equipment, wood combustion, and restaurant grills and residential cooking. Inorganic constituents, including trace elements, sulfate, nitrate, ammonium, and total particulate organic carbon (OC) and elemental carbon (EC), are typically measured in PM source apportionment studies. However, source contributions of carbonaceous particles are difficult to distinguish solely on the basis of these constituents. EC and OC are present in motor vehicle exhaust, wood-smoke, and other combustion-related emissions in varying proportions within the same source type.

Since organic compounds are emitted from all combustion sources, certain organic compounds such as polycyclic aromatic hydrocarbons (PAH), hopanes, steranes, sterols, methoxyphenols and other types of organic species have been used to obtain more selective apportionment of various combustion sources. Highly specific molecular markers exist for wood combustion (e.g., levoglucosan and methoxyphenols) and meat cooking (sterols). In contrast, particle emissions from gasoline and diesel-powered vehicles share many molecular markers. The apportionments for these sources are based upon differences in the relative amounts of the molecular markers and EC. However, the variations in abundances of these markers among profiles within a source category can vary greatly, resulting in a range of source contribution estimates and uncertainties that depend upon the profiles selected. In addition to emissions from combustion sources, OC

can be directly entrained into the atmosphere by abrasion of leaf and plant wax (during summer months) and decomposition of vegetative detritus (fall). High molecular n-alkanes with strong odd carbon number predominance may serve as markers for this source.

The organic compounds most suitable for serving as source tracers in receptor modeling studies should be:

- Emitted in relatively high concentration, to allow small sample sizes and short sampling times;
- Relatively easy to distinguish from other classes of organic compounds;
- Relatively easy to identify and quantify on the basis of the chromatographic and spectral properties of its members;
- Either be chemically stable or of quantifiable reactivity;
- Emitted in reasonably stable proportion to the amount of $PM_{2.5}$ and total carbon mass.
- Present in different levels of emissions when compared to one or more of the sources of interest.

The following list summarizes the major chemical types and specific organic compounds related to emission sources and species that may be indicative of SOA formation.

Vehicle Exhaust

- Higher abundance of EC relative to OC in diesel exhaust. However, newer diesel engines have lower abundances of EC than older model year engines. EC abundances in PM emissions of gasoline vehicle are very low but can be higher during hard accelerations and during cold starts.
- Sum of hopanes and sum of steranes (both diesel and gasoline).
- High-molecular weight PAH such as benzo(ghi)perylene, ideno(1,2,3-cd)pyrene, and coronene (gasoline)
- dimethylnaphthalenes, methyl- and dimethylphenanthrenes, and methylfluorenes (diesel emissions contained higher proportions but these are mostly semi-volatile).

Commercial Jet Exhaust

- Naphthalene, methylnaphthalene,
- Sulfate and Elemental sulfur
- Elemental carbon
- Heavy hydrocarbons

Vegetative Burning

- dehydroabietic, abietic or pimaric acid (resin acids that are biosynthesized mainly by conifers)
- retene (1-methyl-7-isopropylphenanthrene) (derived by thermal degradation of abietic acid, but is semi-volatile)
- methoxy phenols: guaiacol (2-methoxyphenol) and its derivatives (wood lignin pyrolysis product in similar ratio for all woods, but mostly semi-volatile).
- dimethoxy phenols: syringol (2,6 dimethoxyphenols) and its derivatives (wood lignin pyrolysis product in almost two orders of magnitude higher in hardwoods).
- Levoglucosan (1,6-anhydro-β-D-glucose) (product of decomposition of cellulose). Pine needles, grasses and scrubs produce much higher abundances of levoglucosan than burning wood (Mazzoleni et al., 2007). This can be an important distinction between residential wood burning versus wildfires.

Meat Cooking (Charbroiling of hamburger meat with 20 percent fat).

- C_7 to C_{22} n-alkanoic acids (saturated n-fatty acids) with no odd or even carbon number predominance. C_7 to C_{12} n-alkanoic acids are predominantly in the gas phase. Fatty acids make up about five percent of OC with hexadecanoic (palmitic) and octadecanoic (stearic) acids accounting for 2.6 and 1.5 percent, respectively.
- n-alkenoic acids account for about four percent of particulate OC with 9-octadecenoic (oleic), 9-hexadecenoic (palmitoleic) acids accounting for 3.4 and 0.3 percent, respectively.
- C_1 to C_{29} n-alkanes. Volatile under C_{13} and semi-volatile from C_{13} to C_{25}. Alkanes in the particulate phase accounted for 0.1 percent of OC.
- Cholesterol is a specific organic marker for meat cooking. However it typically accounts for a small fraction (0.1 percent or less) of particulate OC.

Leaf Abrasion and Vegetative Detritus. Green and dead leaves from 62 plant species from the Los Angeles area. Leaf composites were agitated in a Teflon bag with pure air flowed through. Fine particles shed from leaf surfaces were extracted and analyzed.

- C_8 to C_{32} n-alkanoic acids (saturated n-fatty acids) with even carbon number predominance (approximately one to two orders of magnitude higher abundance for even carbon number). About uniform distribution among even carbon number n-alkanoic acid with hexadecanoic acid (palmitic acid) and undecanoic acids, the two most abundant. This group accounted for 4.5 and 12.3 percent of the leaf abrasion products for green leaf and dead leaf, respectively. Abrasion products from dead leaves have 5-15 times greater abundances of C_{20} to C_{32} fatty acids.

- C_{19} to C_{36} n-alkanes, mostly in the range of C_{27} to C_{33} with odd carbon number predominance (4, 1, 25, 2, 41, 3, 20 for green leaf and 3, 1, 20, 1, 29, 3, 17 for dead leaf). This group accounted for 2.3 and 2.5 percent of the leaf abrasion products for green leaf and dead leaf, respectively.

- n-alkenoic acids (oleic, linoleic and linolenic acids). Accounted for about 0.03 and 0.01 percent for green and dead leaves, respectively.

Other Sources of Secondary Organic Aerosol

- pinonic acid (ozonlysis of α-pinene and β-pinene).

- butanedioic (succinic) acid, pentanedioic (glutaric) acid and hexanedioic (adipic) acids (mostly SOA, but also directly emitted)

- 1,2-benzene dicarboxylic acid (phthalic acid) and 1,3-benzene dicarboxylic acid (isophthalic acid) (SOA from with primary vehicular emissions)

- dicarbonyls, carboxylic acids, hydroxy carbonyl and organic nitrate compounds.

- It is important to note that emissions from vegetative burning are highly reactive and can produce SOA in addition to SOA produced from anthropogenic and biogenic sources.

2.3 Apportionment of VOC and PM by CMB

The CMB receptor model will be applied to the ambient speciated VOC and $PM_{2.5}$ data using appropriate source composition profiles. Both ambient and source composition data will consist of the species listed in Tables 2 to 8. The CMB analysis will consist of the following sequence of steps.

2.3.1 (Step 1) Compile Available and Supplemental Source Composition Profiles

Appropriate chemical composition profiles of gaseous and particulate emissions will be compiled for gasoline and diesel vehicles from the most recent and relevant vehicle emission testing programs. These studies include: the Gas/Diesel Split Study (Fujita et al., 2007), Heavy-Duty Vehicle Chassis Dynamometer Testing for Emission Inventory, Air Quality Modeling, Source Apportionment, and Air Toxic Inventory (CRC E-55), EC Diesel Fuel Emission Characterization Study (Lev-On et al., 2002), Kansas City Light-Duty Gasoline Vehicle PM Emissions Characterization Study (U.S. EPA, 2006) Advance Collaborative Emissions Study (ACES) of new technology diesel engines, the Collaborative Lubricating Oil Study on Emissions (CLOSE) of the contributions of lubrication oil to exhaust emissions from gasoline and diesel engines, and the Effect of Gasoline Properties on Exhaust Emissions from Tier 2 Light-Duty Vehicles (EPAct) study of the impacts of ethanol-blended gasoline on emission rates of regulated pollutants. These studies collectively represent the most comprehensive set of investigations to

date of emission rates and composition of PM, VOC and SVOC emissions from gasoline and diesel-powered motor vehicles. The most recent studies are focused on the effects of lubricating oils and ethanol content of fuels on the exhaust emission rates of regulated pollutants and the chemical composition of VOC, SVOC and POC.

The source composition data that will be compiled specifically for the LAX AQSAS include commercial jet exhaust during takeoffs and taxiing, and local samples of Jet-A, gasoline and #2 diesel fuels. The jet exhaust samples were collected in early March 2012 at the end of the first season of ambient sampling. Composite gasoline profiles will be derived based on weighted averages of the three grades of gasoline according to the relative sales volumes. The compositions of gasoline headspace vapors will be predicted for varying temperatures from the measured composition of liquid gasoline using the method described by Kirchstetter et al. (1999). This method is based on the proportionality between the equilibrium headspace partial pressure for each compound identified in gasoline with its mole fraction in liquid gasoline multiplied by the vapor pressure of the pure species. The individual vapor pressures are determined using the Wagner equation.

The emissions inventory for the LAX AQSAS area will be examined to identify any other significant primary source of VOC or $PM_{2.5}$ OC other than commercial aircraft, gasoline and diesel vehicles. Ranges in the abundance of potential marker compounds among the relevant profiles will be compared among alternative profiles for each source category to determine an initial list of potential fitting species for the CMB analysis.

2.3.2 (Step 2) Conduct Sensitivity Analysis Of Alternative Profiles and Potential Fitting Species

The appropriate individual and VOC and PM composite profiles for sensitivity testing will be selected. A subset of samples from each of the three core community sites (Community North, Community South, and Community East) with the highest VOC and particulate OC concentrations will then be selected and a series of CMB analyses with alternative source composition profiles will be performed to determine the ranges in source contribution estimates and model performance. Identification and characterization of any site differences will be done with respect to suitability of various sets of default profiles that would be applied to the entire dataset.

Potential fitting species that have analytically significant ambient levels will be evaluated and species that may not fit due to documented reasons (e.g., semi-volatile compounds that have different phase distributions in ambient and source samples, reactive species) will be removed. The MPIN (Marketing Partner ID Number**)** matrix will be reviewed to confirm species that influence the apportionment. Spatial and seasonal variations in the magnitude of the unexplained fraction of particulate OC will be examined and this fraction will be correlated with species associated with SOAs.

2.3.3 (Step 3) CMB Analysis of the Full Data Set

The CMB analysis will be conducted in autofit mode using the default sets of profiles and fitting species developed in Step 2. A review of the source contributions to VOC, $PM_{2.5}$, TC and OC and related performance statistics will be done and the analysis repeated, if necessary, for individual samples with poor results by adjusting the fitting species used.

2.3.4 (Step 4) Summarize and Analyze CMB analysis Results

A summary table of CMB results and performance statistics will be prepared by site and season. Time-series of the attributions will be examined and significant seasonal and spatial variations among primary sources of OC and the unexplained OC will be characterized. The composition of the residual OC and the relative concentrations of potential marker species for SOA from anthropogenic and biogenic sources will be examined.

Table 2. List of Hydrocarbons (canister with gas chromatography/mass Spectrometry (GC/MS)) and Carbonyl Compounds (DNPH cartridges with HPLC/UV) for Phase III of the LAX AQSAS.

Hydrocarbons			Carbonyl Compounds
Sum C2s	2,4-DiMePentane	m/p-xylene	Formaldehyde
propene	223TriMeButane	2MeOctane	Acetaldehyde
propane	1MeCypentene	3MeOctane	Acetone
isoButane	Benzene	Styrene+heptanal	Acrolein
1Butene+iButylene	CycloHexane	o-xylene	Propionaldehyde
1,3-Butadiene	4MeHexene	Nonene-1	Crotonaldehyde
n-Butane	2MeHexane	n-Nonane	Methyl Ethyl Ketone
t-2-Butene	23DiMePentane	iPropBenzene	Methacrolein
c-2-Butene	Cyclohexene	iPropCyHexane	Butyraldehyde/Acrolein RP
3-Me-1-Butene	3MeHexane	26DiMeOctane	Benzaldehyde
isopentane	3EtPentane	alpha-pinene	Glyoxal
1-Pentene	1-Heptene	36DiMeOctane	Valeraldehyde
2-Me-1-Butene	224TrMePentane	nPropBenzene	m-Tolualdehyde
n-Pentane	t-3-Heptene	mEtToluene	Hexanaldehyde
Isoprene	n-Heptane	pEtToluene	
t-2-Pentene	244TMe-1-Pentene	135TriMeBenzene	
c-2-Pentene	MeCyHexane	oEtToluene	
2-Me-2-Butene	25DiMeHexane	beta-pinene	
22DiMeButane	24DiMeHexane	124TriMeBenzene	
CycloPentene	234TrMePentane	n-Decane	
CycloPentane	Toluene	iButBenzene	
23DiMeButane	23DiMeHexane	sButBenzene	
MTBE	2MeHeptane	123TriMeBenzene	
2-MePentane	4MeHeptane	Limonene	
22-DiMePentane	3MeHeptane	Indan	
3-MePentane	225TMHexane	13diethylbenzene	
2-Me-1-Pentene	Octene-1	14diethylbenzene	
1-Hexene	11DMeCyHexane	12diethylbenzene	
n-Hexane	n-Octane	2-propylToluene	
t-2-Hexene	235TriMeHexane+Bgr.	iPrToluene	
2-Me-2-Pentene	24DiMeHeptane	n-Undecane	
c-3-Me-2-Pentene	44DiMeHeptane	1245tetraMeBenzene	
c-3-Hexene	26DiMeHeptane	1235tetraMeBenzene	
c-2-Hexene	25DiMeHeptane	1234tetraMeBenzene	
t-3-Me-2-Pentene	33DiMeHeptane	Naphthalene+Decanal	
MeCyPentane	EtBenzene	n-Dodecane	

a. Canister/GC-FID or MS with MDL = 0.1 ppbC
b. DNPH cartridges/HPLC-UV with MDL = 0.1 ppbv
Acrolein RP – rearrangement product of acrolein coelutes with butryaldehyde

Table 3. List of Heavy Hydrocarbons (Tenax with GC/MS) for the Phase III of the LAX AQSAS.

toluene	2-methylindan
n-octane	diethylmethylbenzene
ethylbenzene	1-methylindan
m&p-xylene	1,2,3,4-tetramethylbenzene
methyloctane	naphthalene.
styrene	dimethylindan
o-xylene	dimethylindan
1-nonene	n-dodecane
n-nonane	2-methylnaphthalene
isopropylbenzene	1-methylnaphthalene
benzaldehyde	n-tridecane
a-pinene	biphenyl
dimethyloctane	1-ethylnaphthalene
n-propylbenzene	2-ethylnaphthalene
m-ethyltoluene	2,6-dimethylnaphthalene
p-ethyltoluene	2,7-dimethylnaphthalene
1,3,5-trimethylbenzene	n-tetradecane
phenol	1,3-dimethylnaphthalene
b-pinene	1,4-dimethylnaphthalene
1,2,4-trimethylbenzene	2,3-dimethylnaphthalene
para-dichlorobenzene	1,5-dimethylnaphthalene
iso-butylbenzene	acenaphthylene
n-decane	1,2-dimethylnaphthalene
1,2,3-trimethylbenzene	dimethylnaphthalene
indan	1,8-dimethylnaphthalene
limonene	acenaphthene
indene	n-pentadecane
1,3-diethylbenzene	fluorene
acetophenone	n-hexadecane
1,4-diethylbenzene	n-heptadecane
dimethylethylbenzene	C18-paraffin
1,2-diethylbenzene	phenanthrene
tolualdehyde	n-octadecane
methylindan+C4-benzene	methylanth+methylphenanth
methylindan	methylanth+methylphenanth
nonanal	n-nonadecane
n-undecane	n-eicosane
1,2,4,5-tetramethylbenzene	n-heneicosane
1,2,3,5-tetramethylbenzene	

MDL = 0.1 $\mu g/m^3$

Table 4. List of Ions and Metals (XRF) for Phase III of the LAX AQSAS.

Species	Analysis Method[a]	MDL[b] (µg/filter)	Species	Analysis Method[a]	MDL[b] (µg/filter)
Chloride (Cl^-)	IC	1.5005	Zinc (Zn)	XRF	0.0144
Nitrate (NO_3^-)	IC	1.5005	Gallium (Ga)	XRF	0.0259
Sulfate ($SO_4^{=}$)	IC	1.5005	Arsenic (As)	XRF	0.0230
			Selenium (Se)	XRF	0.0173
Organic Carbon (OC)	TOR	2.7590	Bromine (Br)	XRF	0.0144
Elemental Carbon (EC)	TOR	2.7590	Rubidium (Rb)	XRF	0.0144
			Strontium (Sr)	XRF	0.0144
Sodium (Na)	XRF	0.9533	Yttrium (Y)	XRF	0.0173
Magnesium (Mg)	XRF	0.3456	Zerconium (Zr)	XRF	0.0230
Aluminum (Al)	XRF	0.1382	Molybdenum (Mo)	XRF	0.0374
Silicon (Si)	XRF	0.0864	Palladium (Pd)	XRF	0.1526
Phosphorus (P)	XRF	0.0778	Silver (Ag)	XRF	0.1670
Sulfur (S)	XRF	0.0691	Cadmium (Cd)	XRF	0.1670
Chlorine (Cl)	XRF	0.1382	Indium (In)	XRF	0.1786
Patassium (K)	XRF	0.0835	Tin (Sn)	XRF	0.2333
Calcium (Ca)	XRF	0.0634	Antimony (Sb)	XRF	0.2477
Titanium (Ti)	XRF	0.0403	Barium (Ba)	XRF	0.7171
Vanadium (V)	XRF	0.0346	Lanthanum (La)	XRF	0.8554
Chromium (Cr)	XRF	0.0259	Gold (Au)	XRF	0.0432
Manganese (Mn)	XRF	0.0230	Mercury (Hg)	XRF	0.0346
Iron (Fe)	XRF	0.0202	Thallium (Tl)	XRF	0.0346
Cobalt (Co)	XRF	0.0115	Lead (Pb)	XRF	0.0403
Nickel (Ni)	XRF	0.0115	Uranium (U)	XRF	0.0317
Copper (Cu)	XRF	0.0144			

[a] IC=ion chromatography. AC=automated colorimetry. AAS=atomic absorption spectrophotometry. TOR=thermal/optical reflectance. XRF=x-ray fluorescence.

[b] Minimum detectable limit (MDL) is the concentration at which instrument response equals three times the standard deviation of the response to a known concentration of zero.

Table 5. Relative Detection Limits for XRF and ICP-MS Elemental Analysis.

		XRF			ICP-MS
Species	ICP/XRF sensitivity	Protocol A MDL[b] (µg/filter)	Protocol B MDL[b] (µg/filter)	Protocol C MDL[b] (µg/filter)	mdl ug/sample
Boron (B)		na	na	na	na
Sodium (Na)		na	na	na	0.1000
Aluminum (Al)	1.1920	0.1192	0.0858	0.0429	0.1000
Phosphorus (P)		0.0668	0.0477	0.0238	na
Sulfur (S)		0.0596	0.0417	0.0215	na
Chlorine (Cl)		0.1192	0.0882	0.0441	na
Silicon (Si)		0.0751	0.0524	0.0262	na
Calcium (Ca)	0.5364	0.0536	0.0381	0.0191	0.1000
Chromium (Cr)	2.2648	0.0226	0.0167	0.0080	0.0100
Manganese (Mn)	9.5360	0.0191	0.0131	0.0067	0.0020
Iron (Fe)	0.0894	0.0179	0.0131	0.0064	0.2000
Nickel (Ni)	0.5304	0.0106	0.0075	0.0037	0.0200
Copper (Cu)	3.2780	0.0131	0.0091	0.0045	0.0040
Zinc (Zn)	6.5560	0.0131	0.0091	0.0045	0.0020
Arsenic (As)	9.5360	0.0191	0.0131	0.0067	0.0020
Mercury (Hg)	30.9920	0.0310	0.0215	0.0108	0.0010
Lead (Pb)	89.4000	0.0358	0.0262	0.0131	0.0004
K		0.0727	0.0513	0.0262	
Ti		0.0346	0.0250	0.0119	
V		0.0298	0.0203	0.0104	
Co		0.0105	0.0074	0.0037	
Ga		0.0226	0.0167	0.0081	
Se		0.0143	0.0103	0.0051	
Br		0.0119	0.0086	0.0043	
Rb		0.0119	0.0081	0.0041	
Sr		0.0131	0.0093	0.0046	
Y		0.0155	0.0110	0.0055	
Zr		0.0203	0.0143	0.0070	
Mo		0.0322	0.0226	0.0113	
Pd		0.1311	0.0906	0.0453	
Ag		0.1430	0.1025	0.0513	
Cd		0.1430	0.1025	0.0513	
In		0.1550	0.1132	0.0572	
Sn		0.2026	0.1430	0.0739	
Sb		0.2146	0.1550	0.0763	
Ba		0.6198	0.4410	0.2146	
La		0.7390	0.5245	0.2622	
Au		0.0370	0.0262	0.0131	
Tl		0.0298	0.0215	0.0105	
U		0.0274	0.0203	0.0099	

[b] Minimum detectable limit (MDL) is the concentration at which instrument response equals three times the standard deviation of the response to a known concentration of zero.

na - not available

Table 6. List of Polycyclic Aromatic Hydrocarbons for Phase III of the LAX AQSAS.

Polycyclic Aromatic Hydrocarbons (PAH) [a]	
Naphthalene	Anthrone
2-methylnaphthalene	9-methylanthracene
1-methylnaphthalene	Anthraquinone
Biphenyl	3,6-dimethylphenanthrene
2-Methylbiphenyl	A-dimethylphenanthrene
3-Methylbiphenyl	B-dimethylphenanthrene
4-Methylbiphenyl	C-dimethylphenanthrene
1+2ethylnaphthalene	D-dimethylphenanthrene
2,6+2,7-dimethylnaphthalene	E-dimethylphenanthrene
1,3+1,6+1,7dimethylnaphth	1,7-dimethylphenanthrene
1,4+1,5+2,3-dimethylnaphth	Fluoranthene
1,2-dimethylnaphthalene	Pyrene
Acenaphthylene	9-Anthraaldehyde
Acenaphthene	Retene
Dibenzofuran	1-MeFl+C-MeFl/Py
A-trimethylnaphthalene	B-MePy/MeFl
B-trimethylnaphthalene	C-MePy/MeFl
C-trimethylnaphthalene	D-MePy/MeFl
E-trimethylnaphthalene	4-methylpyrene
F-trimethylnaphthalene	1-methylpyrene
2,3,5+I-trimethylnaphthalene	Benzonaphthothiophene
J-trimethylnaphthalene	Benzo(c)phenanthrene
2,4,5-trimethylnaphthalene	Benz(a)anthracene
1,4,5-trimethylnaphthalene	Chrysene/Triphenylene
Fluorene	Benzanthrone
A-methylfluorene	Benz(a)anthracene-7,12-dione
1-methylfluorene	5+6-methylchrysene
B-methylfluorene	7-methylbenz(a)anthracene
9-fluorenone	Benzo(b+j+k)fluoranthene
Phenanthrene	BeP
Anthracene	BaP
Xanthone	Perylene
Perinaphthenone	7-methylbenzo(a)pyrene
Acenaphthenequinone	9,10-dihydrobenzo(a)pyrene-7(8H)-one
A-methylphenanthrene	Indeno[123-cd]pyrene
2-methylphenanthrene	Dibenzo(ah+ac)anthracene
B-methylphenanthrene	Benzo(ghi)perylene
C-methylphenanthrene	Coronene
1-methylphenanthrene	

a. TIGF/XAD and GC/MS with MDL = 0.02 ug/sample

b. TIGF/XAD and GC/MS with MDL = 0.01 ug/sample

Table 7. List of Hopanes, Steranes and Alkanes for Phase III of the LAX AQSAS.

Hopanes and Steranes [a]	Alkanes [b]
C27-20S5a(H),14a(H)-cholestane	norfarnesane
C27-20R5a(H),14ß(H)-cholestane	heptylcyclohexane
C27-20S5a(H),14ß(H),17ß(H)-cholestane	farnesane
C27-20R5a(H),14a(H),17a(H)-cholestane & C29-20S13ß(H),17a(H)-diasterane	octylcyclohexane
C28-20S5a(H),14a(H),17a(H)-ergostane	nonylcyclohexane
C28-20R5a(H),14ß(H),17ß(H)-ergostane	norpristane
C28-20S5a(H),14ß(H),17ß(H)-ergostane	hexadecane
C28-20R5a(H),14a(H),17a(H)-ergostane	heptadecane
C29-20S5a(H),14a(H),17a(H)-stigmastane	decylcyclohexane
C29-20R5a(H),14ß(H),17ß(H)-stigmastane	pristane
C29-20S5a(H),14ß(H),17ß(H)-stigmastane	undecylcyclohexane
18a(H),21ß(H)-22,29,30-Trisnorhopane	octadecane
17a(H),18a(H),21ß(H)-25,28,30-Trisnorhopane	nonadecane
C29-20R5a(H),14a(H),17a(H)-stigmastane	phytane
17a(H),21ß(H)-22,29,30-Trisnorhopane	dodecylcyclohexane
17a(H),21ß(H)-30-Norhopane	tridecylcyclohexane
17b(H),21a(H)-30-Norhopane	tetradecylcyclohexane
17a(H),21ß(H)-Hopane	eicosane
17ß(H),21a(H)-hopane	heneicosane
22S-17a(H),21ß(H)-30-Homohopane	pentadecylcyclohexane
22R-17a(H),21ß(H)-30-Homohopane	hexadecylcyclohexane
17ß(H),21ß(H)-Hopane	docosane
22S-17a(H),21ß(H)-30,31-Bishomohopane	triacosane
22R-17a(H),21ß(H)-30,31-Bishomohopane	heptadecylcyclohexane
22S-17a(H),21ß(H)-30,31,32-Trisomohopane	octadecylcyclohexane
22R-17a(H),21ß(H)-30,31,32-Trishomohopane	tetracosane
	pentacosane
	hexacosane
	nonadecylcyclohexane
	eicosylcyclohexane
	heptacosane
	octacosane
	nonacosane
	triacontane
	hentriacontane
	dotriacontane
	tritriacontane
	tetratriacontane
	pentatriacontane
	hexatriacontane

a. TIGF/XAD and GC/MS with MDL = 0.02 ug/sample
a. TIGF/XAD and GC/MS with MDL = 0.1 ug/sample

Table 8. List of Polar Organics for Phase III of the LAX AQSAS.

Analytical Standards	Classification	Potential Organic Marker Type	MDL microgram/sample
hexanoic acid	alkanoic acid		0.05
heptanoic acid	alkanoic acid		0.05
methylmalonic	alkanedioic acid	secondary aerosol	0.05
guaiacol	methoxy phenol	wood smoke	0.05
benzoic acid	aromatic acid		0.05
octanoic acid	alkanoic acid		0.05
butenedioic (maleic) acid	alkenedioic acid	secondary aerosol	0.05
butanedioic (succinic) acid	alkanedioic acid	secondary aerosol	0.05
4-me-guaiacol	methoxy phenol	wood smoke	0.05
me-succinic acid	alkanedioic acid	secondary aerosol	0.05
nonanoic acid	alkanoic acid		0.05
4-ethyl-guaiacol	methoxy phenol	wood smoke	0.05
syringol	methoxy phenol	wood smoke	0.05
glutaric acid	alkanedioic acid	secondary aerosol	0.05
2-methylglutaric	alkanedioic acid	secondary aerosol	0.05
3-methylglutaric acid	alkanedioic acid	secondary aerosol	0.05
decanoic acid	alkanoic acid		0.05
4-allyl-guaiacol (eugenol)	methoxy phenol	wood smoke	0.05
4-methyl-syringol	methoxy phenol	wood smoke	0.05
hexanedioic (adipic) acid	alkanedioic acid	secondary aerosol	0.05
cis-pinonic acid	aromatic acid		0.05
3-methyladipic acid	alkanedioic acid	secondary aerosol	0.05
4-formyl-guaiacol (vanillin)	methoxy phenol	wood smoke	0.05
undecanoic acid	alkanoic acid		0.05
isoeugenol	methoxy phenol	wood smoke	0.05
heptanedioic (pimelic) acid	alkanedioic acid	secondary aerosol	0.05
acetovanillone	methoxy phenol	wood smoke	0.05
dodecanoic (lauric) acid	alkanoic acid		0.05
phthalic acid	aromatic diacid		0.05
suberic acid	alkanedioic acid	secondary aerosol	0.05
levoglucosan	carbohydrate	wood smoke	0.05
syringaldehyde	methoxy phenol	wood smoke	0.05
tridecanoic acid	alkanoic acid		0.05
isophthalic acid	aromatic diacid		0.05
vanillic acid	methoxy acid	wood smoke	0.05
homovanillic acid	methoxy acid	wood smoke	0.05
azelaic acid	alkanedioic acid	secondary aerosol	0.05
myristoleic acid	alkenoic acid	meat cooking	0.05
myristic acid	alkanoic acid		0.05
sebacic acid	alkanedioic acid	secondary aerosol	0.05
syringic acid	methoxy acid		0.05
pentadecanoic acid	alkanoic acid		0.05
undecanedioic acid	alkanedioic acid	secondary aerosol	0.05
palmitoleic acid	alkenoic acid	meat cooking	0.05
palmitic acid	alkanoic acid		0.05
isostearic acid	alkanoic acid		0.05
dodecanedioic acid	alkanedioic acid	secondary aerosol	0.05
heptadecanoic acid	alkanoic acid		0.05
traumatic acid	alkenoic acid		0.05
1,11-undecanedicarboxylic acid	alkanedioic acid	secondary aerosol	0.05
oleic acid	alkenoic acid		0.05
elaidic acid	alkenoic acid		0.05
stearic acid	alkanoic acid		0.05
1,12-dodecanedicarboxylic acid	alkanedioic acid	secondary aerosol	0.05
8,15-pimaradien-18-oic acd	resin acid	wood smoke	0.05
pimaric acid	resin acid	wood smoke	0.05
nonadecanoic acid	alkanoic acid		0.05
isopimaric acid	resin acid	wood smoke	0.05
dehydroabietic acid	resin acid	wood smoke	0.05
abietic acid	resin acid	wood smoke	0.05
eicosanoic acid	alkanoic acid		0.05
heneicosanoic acid	alkanoic acid		0.05
docosanoic acid	alkanoic acid		0.05
tricosanoic acid	alkanoic acid		0.05
tetracosanoic acid	alkanoic acid		0.05
cholesterol	sterol	meat cooking	0.05

2.4 Nonparametric Trajectory Analysis

Nonparametric Trajectory Analysis (NTA) is a receptor-oriented model that uses ambient wind and concentration data to quantify the effects of nearby sources on local air quality. It was developed by Dr. Ronald Henry with the assistance of Drs. Gary Norris and Ram Vedantham of the U.S. EPA. The model has undergone in-house review by U.S. EPA and has been documented, with applications, in the peer-reviewed literature (Henry, 2007; Henry et al., 2011).

An example NTA result for black carbon data from Henry et al. (2011) is provided in Figure 1. The receptor is located slightly east of the freeway at the origin *(0,0)*. Air arriving at the receptor from the west must first pass over the freeway where high concentrations of black carbon are picked up prior to reaching the receptor. The airport is located east of the receptor and its impact on black carbon is less than the freeway.

The gray contour lines are the 5-sigma errors in the NTA estimates. The monitoring stations are located along the rail spur shown as a dashed line crossing north-south freeway

Figure 2. NTA Map for Black Carbon (µg/m^3) at Station 2 (0.135 km east of the freeway).

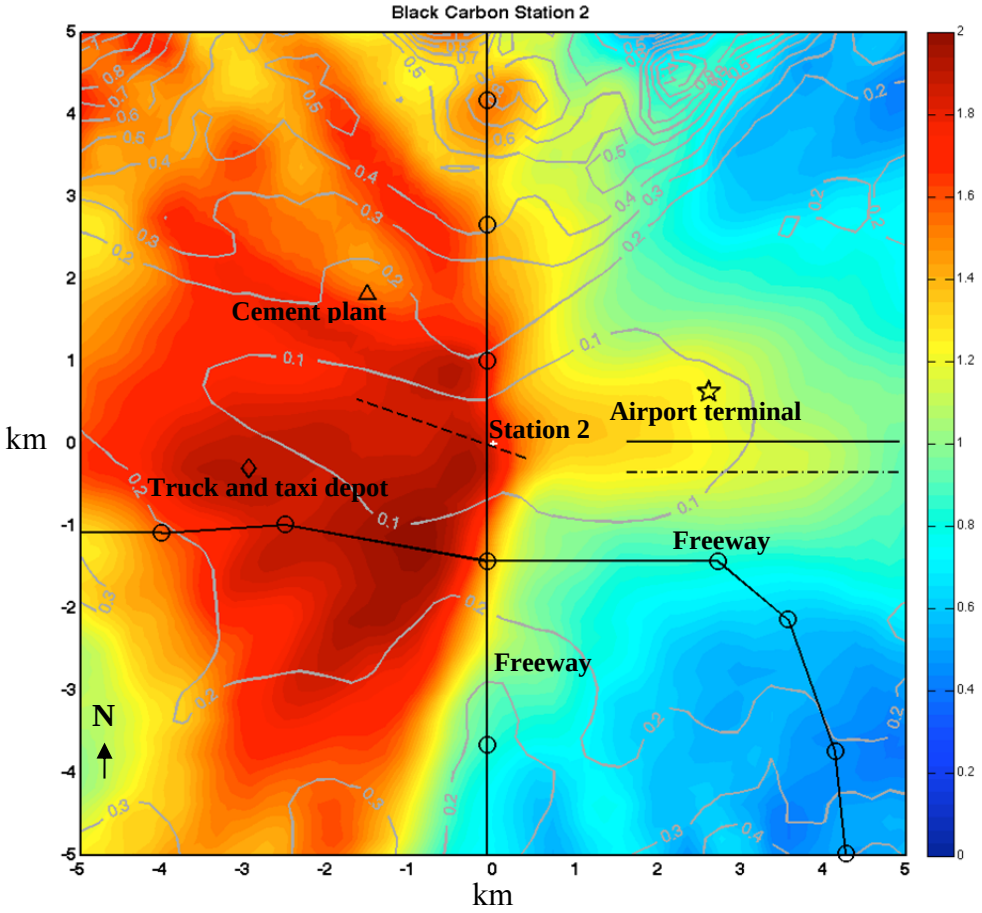

.

The NTA model uses relatively short time-resolution data (1 to 5 minute averages) of pollutant concentrations and wind speed and direction to estimate the conditional expected value of an pollutant concentration at a receptor. The model requires air to have first passed over a nearby location before reaching the receptor. NTA also estimates errors in the results based on the observed variability of the pollutant concentration and wind data. Locations of high NTA values are often associated with local sources of the pollutant.

NTA requires measurements of only one pollutant concentration, such as black carbon or sulfur dioxide. No assumptions about the sources are necessary. The pollutant may react chemically or deposit to the ground. NTA has the unique ability to identify the impact of unexpected sources. For example, an early version of NTA identified the offshore oil tanker terminal of the El Segundo refinery as a source affecting the community around LAX. Thus, NTA acts as a top-down check on the results of the other receptor and source oriented model results.

2.4.1 NTA Methodology

The NTA model is unique among air quality models in its use of back-trajectories, on the scale of a few kilometers, and meteorological data, on the time scale of minutes, to identify local source-receptor relationships. To use the model, assume *n* back-trajectories with *m* points equally spaced in time along each trajectory arriving at a receptor. Let the points on the back-trajectories be given by (x_{ij},y_{ij}) where $i = 1,\ldots,m$ and $j = 1,\ldots,n$, further let C_j be the concentration at the receptor at the start of the *jth* back–trajectory. The NTA value at point *(X,Y)* is the expected value of concentration *C*, given that air passes over point *(X,Y)* before reaching the monitoring station and is given by:

$$\frac{\sum_{i=1}^{m}\sum_{j=1}^{n} C_j W_{ij}}{\sum_{i=1}^{m}\sum_{j=1}^{n} W_{ij}} \qquad \textbf{(1)}$$

where

$$W_{ij} = K\left(\frac{X - x_{ij}}{h}\right) K\left(\frac{Y - y_{ij}}{h}\right) \qquad \textbf{(2)}$$

and

$$\begin{aligned} K(u) &= 0.75(1-u^2) \quad \text{for } |u| \le 1 \\ K(u) &= 0 \qquad\qquad\quad \text{otherwise} \end{aligned} \qquad \textbf{(3)}$$

Note that the weights W_{ij} are all nonnegative and have a maximum value of $0.75^2 = 0.5625$. The smoothing parameter *h* is the radius of a circle centered at *(X,Y)*. The expected value of concentration *C* is contained within the circle and is determined based on empirical data observed at a receptor (see Figure 3). The NTA value for point *(X,Y)* is the weighted sum of the values associated with the trajectory points within a radius of *h* (red circle in Figure 3). The weights for each trajectory point are based on the distance of the point from *(X,Y)*.

Figure 3. Back–Trajectories (black lines) of Air Parcels Arriving at a Receptor Site Located at the Origin *(0, 0)*.

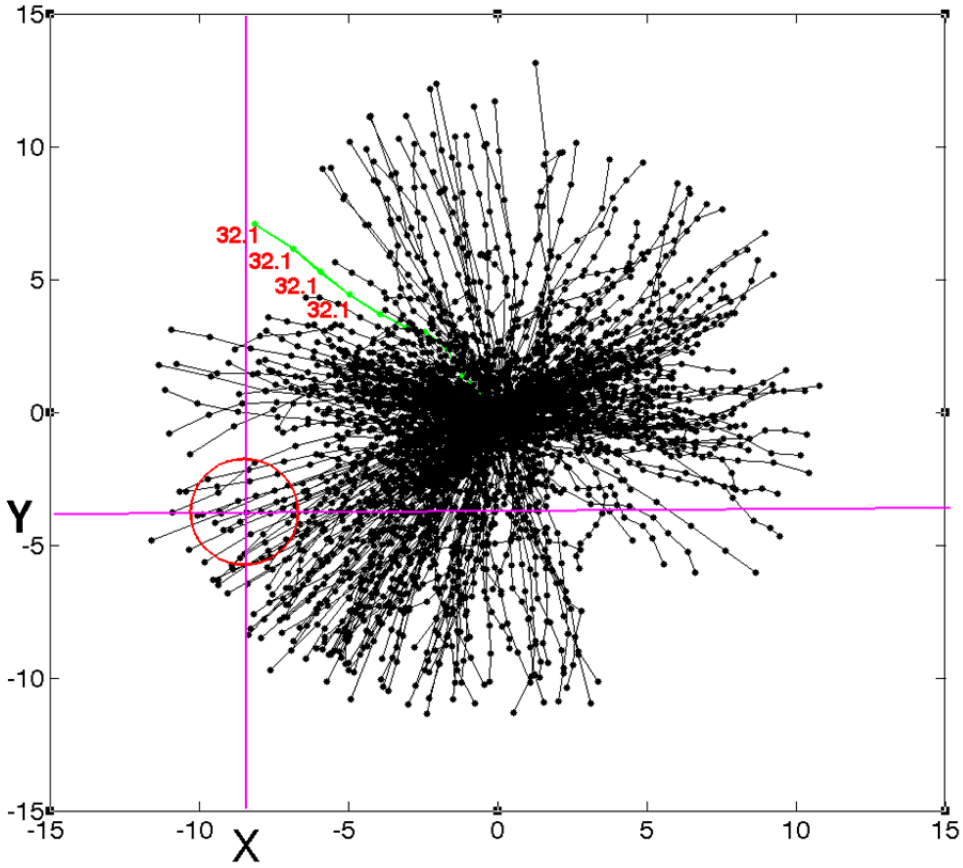

Each point along a trajectory represents the location of the air parcel at five-minute intervals and is associated with the concentration observed when the trajectory arrives at the receptor site. The green line illustrates the two dimensional trajectory of an air parcel arriving at the receptor site and the corresponding air pollutant concentration, in this example 32.1 ppb. The NTA value for point *(X,Y)* is the weighted sum of the values associated with the trajectory points inside the red circle whose radius is the smoothing parameter *h*.

In addition to the smoothing parameter, the NTA model has a matrix of *x* coordinates and a matrix of corresponding *y* coordinates of the points on the back-trajectories. These matrices are configured so that each column of the matrix represents a trajectory. The concentration of the pollutant at the receptor at the time the trajectory reaches the receptor is associated with each column of the matrix.

Back-trajectories are constructed using wind speed and direction observations that have measurement error and natural variability, which result in uncertainty in the back-trajectories and an associated increase in the uncertainty of the NTA results. The effect of the errors in the trajectories is to increase the overall error of NTA results by about 25 to 35 percent.

2.4.2 NTA Application in Phase III

NTA will be applied to all five-minute average measurements of CO, NO_x, SO_2, light scattering, black carbon and ultrafine particle number taken at the four fixed stations (Community North, Community South, Community East, and AQMD Hastings Sites). For NTA modeling, the input data will be screened by examining time series and looking for variations in the concentrations and wind data that are not consistent with expectations based on knowledge of the sources and past experience.

To allow for the timely application of NTA, the preliminary back-trajectories will be calculated for each monitoring station using wind speed and direction data from all available monitoring stations that are part of the study. The National Weather Service Automated Surface Observing System (ASOS) one-minute wind data from LAX, Hawthorne and Santa Monica Airports are generally unavailable until the following month. The final NTA will use back-trajectories calculated with all available ASOS data and wind observations from this study.

The primary user-defined parameter for NTA is smoothing because it defines the effective spatial resolution of the results. There are several statistical methods to estimate an optimum smoothing parameter. However, experience shows trial and error is quick and provides a reasonable approach when compared with statistical procedures. Once determined, the same smoothing parameter will be used throughout to assure that all the NTA results can be compared. The smoothing parameter controls the analysis grid spacing for the NTA. Once determined, the same grid spacing will be used for all NTA runs. Finally, the grid size will be determined by the how far back the trajectories are taken. Experience shows one-hour back trajectories are usually the maximum, but this will be investigated as part of the initial NTA modeling. Once determined, the length of the back-trajectories will be fixed for all the NTA runs. All steps of the back trajectory calculations have an exception for special studies.

While most of the air quality data are one minute averages, some are five minute averages. One minute averages will be estimated from these by cubic spline interpolation.

The NTA analysis will include upwind – downwind analysis for the four fixed stations. This can provide estimates of the impact of sources that lie between the four sites. Individual source areas inside the airport property line may be located and their impact on the receptors may be estimated.

Runway maintenance and activity and aircraft takeoff and landing records will be used to evaluate the NTA results. For example, periods of runway closures offer opportunities to test the validity model estimates of runway and taxiway impacts.

The NTA results will be compared qualitatively and quantitatively with the CMB and source-oriented model results. NTA will be applied to data from the time periods covered by the CMB and multivariate model results.

(This page is intentionally blank)

Section 3
Source Modeling

3.1 Emission Inventory

For Phase III of the LAX AQSAS, the Project Team will prepare an updated emissions inventory for both airport-related activities as well as other emissions sources within the Study Area but beyond the Airport property. These are defined as on-airport and off-airport sources, respectively. On-airport activities include aircraft operations, auxiliary power units (APU), ground support equipment (GSE), motor vehicles traveling along on-airport roadways and within parking facilities, and stationary sources such as boilers, generators, fuel storage, and cooling towers. Off-airport sources include motor vehicle traffic on off-airport roadways, stationary sources including the Chevron El Segundo Refinery, Scattergood Power Plant, and El Segundo Power Plant, marine vessels in coastal waters, and other aggregate and area sources.

The Project Study Area is shown in Figure 3, generally bounded by Inglewood Avenue on the east, the Pacific Ocean on the west, West 120th Street on the south, and Manchester Avenue on the north. Emission sources located outside these bounds (with the exception of marine vessels in coastal waters and the larger stationary sources) will not be included in the emissions inventory; as a result of the Phase II Study, these sources are considered too distant/too insignificant to have a measurable impact on the area near LAX.

Figure 4. Phase III Study Area

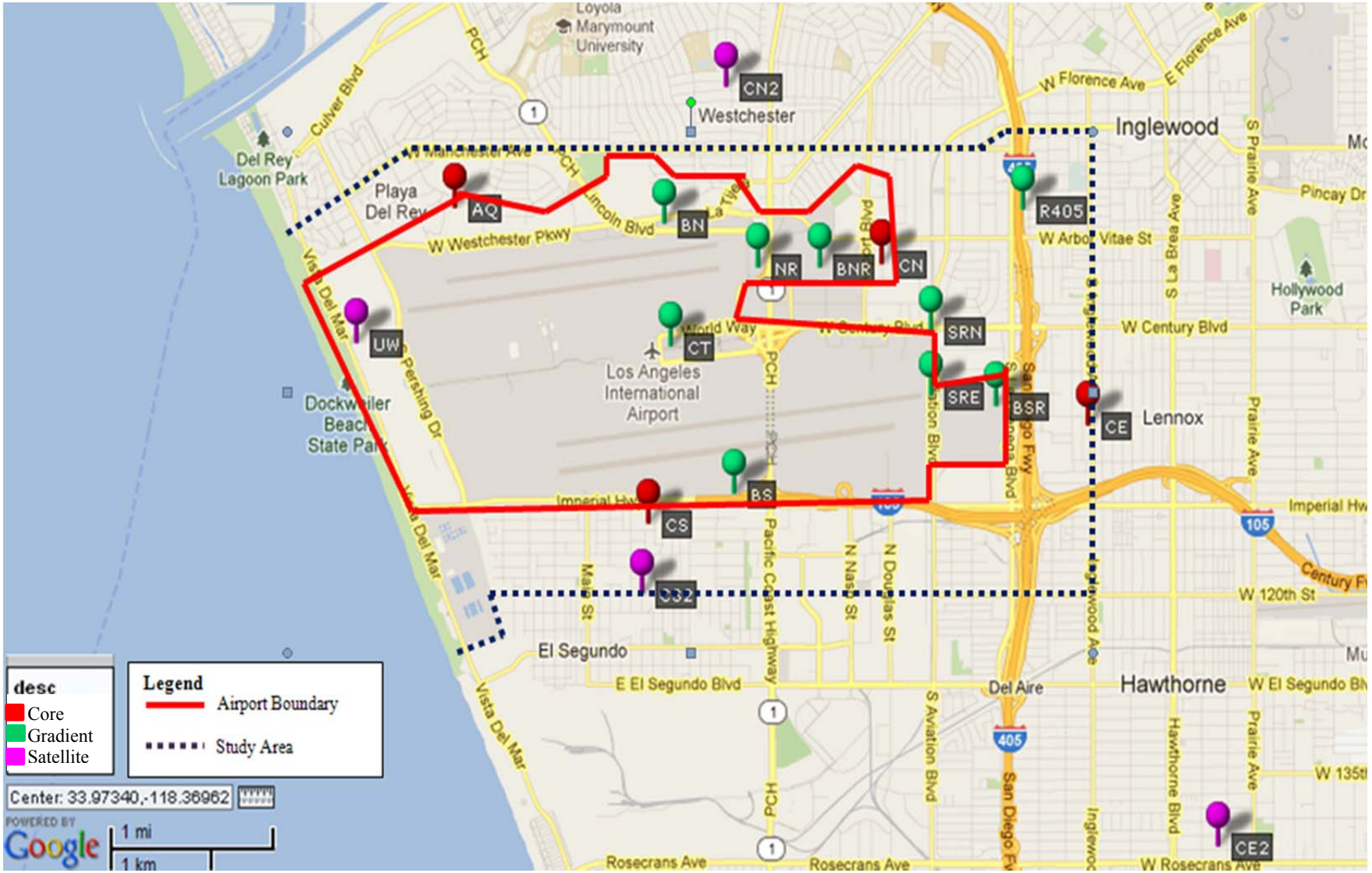

The on-airport emissions inventory will be compiled using the Federal Aviation Administration (FAA) Emissions and Dispersion Monitoring System (EDMS) (Version 5.1.3). Several improvements have been made to the latest version of EDMS, including the ability to estimate hazardous air pollutant (HAP) emissions[2], PM emissions from APUs, and volatile and non-volatile PM emissions from aircraft via the FAA's First Order Approximation (FOA3a). The latest EDMS also includes updates to the aircraft fleet database.

EDMS provides the ability to estimate airport-related emissions of carbon monoxide (CO), total hydrocarbons (THC), non-methane hydrocarbons (NMHC), volatile organic compounds (VOC), total organic gases (TOG), nitrogen dioxide (NO_2), sulfur dioxide (SO_2), particulate matter equal to or less than 10 micrometers (coarse particulates or PM_{10}), and particulate matter equal to or less than 2.5 micrometers (fine particulates or $PM_{2.5}$).

The on-airport emissions inventory will focus on emissions that occur at LAX during two ambient monitoring campaigns, the 1st season during January/February/March 2012 and the 2nd season during July/August/September 2012. Where available, the emission inventory for the ambient monitoring campaigns will use activity levels, meteorological data, and other information from each specific time period; otherwise data form previous years will be used and adjusted accordingly.

In addition, various databases, models, programs, and references will be used to gather data related to both on- and off-airport source operations, source emissions, spatial and temporal profiles, and other supporting data for the emissions inventory and source modeling. These data will be developed from information gathered through coordination with Los Angeles World Airports (LAWA), the U.S. Environmental Protection Agency (U.S. EPA), the California Air Resources Board (CARB), South Coast Air Quality Management District (SCAQMD), the Southern California Association of Governments (SCAG), California Department of Transportation (CalTrans), and other pertinent facilities and entities associated with emission sources within the Study Area.

The following sections describe the source and type of data that will be gathered for the emissions inventory, the emission assessment methodology and how any recommendations from the Phase II Demonstration Project[3] will be implemented. The improvements to the Phase II analysis will focus on those emissions sources with the greatest contributions to the emissions and dispersion concentration results, such as aircraft during taxi, GSE and APU within aircraft apron gates, off-airport roadways, and the Chevron El Segundo Refinery.

[2] In September of 2009, FAA released guidance for quantifying speciated organic compounds and HAP emissions from airport sources. The guidance provides detailed recommendations on the preparation of the analysis and references HAPs speciation profiles for airport emission sources. EDMS 5.1.3 includes 394 speciated organic gases; 45 of them are considered to be HAPs (such as acetaldehyde, benzene, 1,3-butadiene, formaldehyde, and toluene). EDMS includes HAP emissions for all airport sources including aircraft, APU, GSE, stationary sources, and motor vehicles.

[3] Los Angeles International Airport Air Quality and Source Apportionment Study, Draft Final Demonstration Project Report, April 2009.

3.1.1 On-Airport Emissions

The on-airport emissions inventory will be developed for airport-related sources at LAX using the FAA's EDMS 5.1.3 program. Airport emission sources include aircraft, APU, GSE (such as aircraft tugs, belt loaders, baggage tractor, fuel trucks, and service trucks), roadways, parking facilities, and stationary sources such as boilers, generators, fuel storage, and cooling towers. Figure 4 displays the runways, taxiways, aprons, roadways, and parking lots at LAX.

Figure 5. On-Airport Emission Sources

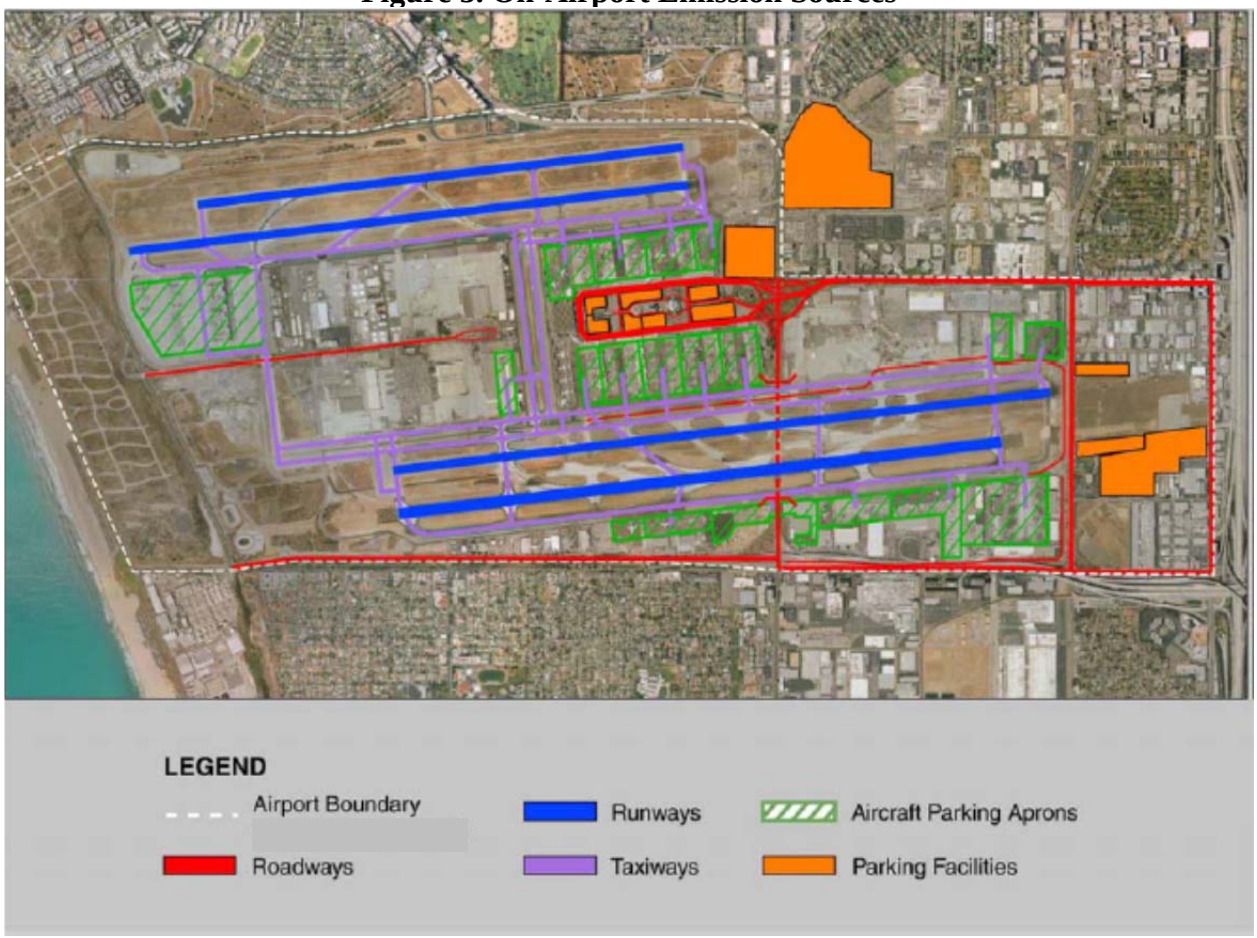

Data essential to the on-airport emissions inventory include aircraft operational levels, aircraft fleet mix, runway utilization, aircraft taxi/delay times, assigned taxipaths (ground path between runway ends and apron position), GSE surveys, traffic volumes, vehicle fleet mix, and stationary source emission estimates.

Table 9 presents a list of the on-airport emissions sources, the data used to develop the emissions inventory, and sources from which the data will be acquired.

Table 9. Sources of Emission Data for On-Airport Sources

Emissions Source	Data	Data Source
Aircraft	Aircraft operations and fleet mix	LAWA's Noise Monitoring Office Aircraft Noise and Operations Monitoring System
	Aircraft weights	FAA's T-100 Air Carrier database
	Aircraft/engine combination	*JP Airline-Fleets International* database
	Emission factors	Emissions and Dispersion Monitoring System (EDMS)
	Taxi travel and queue time	EDMS Delay and Sequence Model
	Airfield capacity	FAA's Aviation System Performance Metrics
	Mixing height and hourly meteorological data	National Climatic Data Center
	Airfield layout	FAA's Airport Master Record database
	Taxipaths	Air Traffic Control Tower
Auxiliary power units	Availability of 400 Hz gate power and pre-conditioned air	Los Angeles World Airports
Ground support equipment (GSE)	GSE inventory survey	Los Angeles World Airports
	GSE operating time survey	Phase III Team
	Availability of hydrant fueling system	Los Angeles World Airports
	Emission factors	CARB OFFROAD emissions model
Roadways	Central Terminal Area, local, and service roadway volumes, speeds, vehicle types, temporal profiles	LAWA Transportation Planning Department
	Emission factors	CARB EMFAC2011 emissions model
Parking facilities	Ticket counts	LAWA's Parking Operations Department
	Emission factors	CARB EMFAC2011 emissions model
Airport stationary sources	Fuel usage, location, stack parameters	Los Angeles World Airports
	Tank dimensions, fuel type	Los Angeles World Airports
Tenant stationary sources	Emission estimates	SCAQMD Facility Information Detail

3.1.1.1 Aircraft Operations

Aircraft are the largest emission source at the airport. Aircraft emissions occur during approach, taxi in (from runway to apron including landing roll), engine startup at the apron, taxi out (from

apron to runway), takeoff, and climb-out[4]. To estimate emissions from aircraft sources, a series of model inputs are needed including: aircraft fleet mix, aircraft engine assignment, aircraft runway and apron assignments, and generalized aircraft taxipath (a series of taxiways depicting an aircraft's travel path across the airfield). Temporal distributions of aircraft operations (by hour, day and month) are also necessary.

Emissions Methodology

An EDMS aircraft schedule specifies the aircraft/engine combination, runway, operation type (i.e., arrival/departure), the specific apron where the operation initiated or terminated its ground movement, and date/time[5]. For Phase II, an aircraft schedule was developed from data provided by LAWA's Noise Monitoring Office using a data set obtained from the Aircraft Noise and Operations Monitoring System (ANOMS). The data set included aircraft operations of commercial, cargo, and general aviation operators; and operation details such as airline, aircraft type, operation type (i.e., arrival/departure), date and time of operation, and runway. Of note, this system can give false positives. Therefore, for Phase III, the aircraft stage length and/or flight origin/destination (if available) will also be used as a means to adjust aircraft weight (especially important for cross-country and international flights) instead of using EDMS default values. During Phase III, data from FAA's T-100 Air Carrier database will also be consulted to determine appropriate aircraft weights.

The aircraft/engine combination is essential to accurately estimate aircraft emissions and will be developed specifically for this project. The actual mixture of aircraft/engine combinations for each airline and/or aircraft tail number that utilizes LAX will be acquired using the *JP Airline-Fleets International* 2011/2012 database (JP Fleets)[6].

Based on the ANOMS data, each scheduled flight will be assigned an engine based on the distribution of engines used by a particular airline for that particular aircraft. The distribution of engine types for each operator's aircraft fleet is contained within JP Fleets.

Emission Factors and Operating Time per Mode

EDMS 5.1.3 contains a database of aircraft/engine-specific criteria pollutant emission factors based on engine manufacturer, model and operational mode. Aircraft emissions will be

[4] Taxi/delay includes the time an aircraft taxis between the runway and a terminal, and all ground-based delay incurred through the aircraft route. The taxi/idle-delay mode includes the landing roll, which is the movement of an aircraft from touchdown through deceleration to taxi speed or full stop. Approach begins when an aircraft descends below the atmospheric mixing height and ends when an aircraft touches down on a runway. Takeoff begins when full power is applied to an aircraft and ends when an aircraft reaches approximately 500 to 1,000 feet. At this altitude, pilots typically power back for a gradual ascent. Climb out begins when an aircraft powers back from the takeoff mode and ascends above the atmospheric mixing height. Aircraft emissions (of THC, NMHC, VOC, and TOC) also account for the period of engine startup which occurs within the apron area prior to departure.

[5] Temporal profiles for aircraft are not used when using the aircraft schedule.

[6] These data (found at http://www.buchair.com/JPAF.htm) comprise a comprehensive reference of the aircraft fleet for all known commercial aircraft operators including the current registration, type, serial number, previous identity, date of manufacture, date of delivery, engine type and number, maximum take-off weight, configuration, fleet number, name, etc. for every aircraft weighing over 3,000 pounds. The database represents more than 6,000 operators and over 50,000 aircraft.

calculated using emission factors specific to aircraft/engine combinations, accounting for the number of engines the aircraft has as well as the time spent in each of the operational modes. EDMS default information (adjusted for mixing height) will be used to represent the time spent in takeoff, climb-out, approach, and landing roll. Takeoff, climb-out, and approach will be further adjusted by aircraft weight. Time spent in arrival taxiing (taxi-in), departure taxiing (taxi-out), and apron/taxiway idling (idle/queue) modes will be simulated by the Delay and Sequence Model within EDMS.

The EDMS Delay and Sequence Model simulates each aircraft's ground movements using the aircraft operations schedule, the assigned aircraft speed within taxiways, and the overall capacity of the airport. The Delay and Sequence Model then estimates the time it takes each individual aircraft to taxi between apron and runway endpoints based on user-specified taxipaths.

The EDMS Delay and Sequence Model estimates time spent at idle, which is added to taxi time-in-mode using a queuing algorithm that assesses departure queuing delays. Inputs to the algorithm include the estimated hourly capacities of an airport's runway system, runway use configurations, weather conditions, and the temporal distribution of aircraft operations from the user-specified flight schedule. The algorithm produces estimates of departure delays attributable to each runway departure end. The Delay and Sequence Model results will be reviewed against the taxi times from FAA's Aviation System Performance Metrics (ASPM) ASPM and/or Bureau of Transportation Statistics (BTS) during the measurement period, with adjustments to taxiway speeds if necessary.

Airfield Capacity and Configurations

EDMS requires the capacity of runway use configurations as inputs to the Delay and Sequence Model. For Phase II, two runway use configurations and two weather conditions were considered in the LAX runway capacity development. LAX typically operates in a westerly flow, with arrivals using Runways 24R and 25L and departures using Runways 24L and 25R. Overnight and wind-permitting, LAX operates in a "head-to-head" configuration with arrivals landing to the east of the airport and departures taking off to the west. During periods of high offshore winds, which rarely occur, LAX operates in an easterly flow, with arrivals using Runways 6L and 7R and departures using Runway 6R and 7L.

One of the many factors that affect runway capacity is weather, particularly visibility and cloud ceiling. For Phase II, two weather conditions were considered—visual meteorological conditions (VMC) and instrument meteorological conditions (IMC). VMC was defined as visibility at LAX at least three statute miles and cloud ceiling at least 3,000 feet above ground level. IMC was defined as either the visibility or cloud ceilings at LAX were below the aforementioned levels. For the Phase III Study, the FAA's Aviation System Performance Metrics (ASPM) database will be used to establish the hourly capacity of LAX's runway system in VMC and IMC conditions.

The percent of time the various runways are used for departures/arrivals, will be provided by LAWA based on the ANOMS data. These percentages will be used to distribute the landing-takeoff cycles to each runway end point. To accommodate EDMS, the runway utilization will be developed by aircraft size (small, large and heavy) for each configuration.

Meteorological Data and Atmospheric Mixing Height

Estimated aircraft operating times within the approach and climb-out modes account for the site-specific atmospheric mixing height[7] per EDMS methodology. In marine climates, mixing heights tend to be lower compared to desert or continental climates and lower during the morning compared to the afternoon. Mixing height also varies with season. Historical data from the LAX area report an average annual mixing height of 1,780 and 2,670 feet (542 and 814 meters) for the morning and afternoon, respectively. The Phase II emissions inventory used a value of 1,806 feet (550 meters).

EDMS Delay and Sequence Module (which is the case for this project) requires hourly meteorological data to conduct an emissions inventory. Information for the time period of the monitoring campaigns will be inferred using data provided by the NCDC and/or SCAQMD. Surface data will be provided by the LAX surface station and upper air data will be provided by the San Diego Airport station.

Spatial and Temporal Allocation

EDMS incorporates specific details on source location (airport layout and roadway network) and activity variation to develop a spatial and temporal representation of each emission source. The location of emission sources will be represented in the Universal Transverse Mercator (UTM) coordinate system. The LAX location (known as the airport reference point[8]) is approximately 369,874.86 meters East and 3,756,677.41 meters North (UTM Zone 11N) with North American Datum of 1983. All emissions sources will be located and defined within this same coordinate system.

Aircraft ground activity locations include runways, aprons and taxiways as current during the Phase III Study. The locations of runway endpoints will be taken from the FAA's Airport Master Record. To localize aircraft emissions at and near aircraft parking positions, 21 different aprons will be defined. To estimate the emissions from aircraft taxi and idle modes, and for precision in locating the taxi/idle emissions around the airfield, eight major taxiways and 52 taxiways will be modeled. Aircraft taxi speeds will be assigned based on the type of taxiway: high speed exit (46 mph), reverse high speed exit[9] (29 mph), crossfield (17 mph), and terminal area (12 mph).

The route an aircraft takes in taxiing to/from the runway plays a large role in the amount of taxi/idle emissions attributable to that aircraft. These routes, often referred to as taxipaths, are assigned to the aircraft by the Air Traffic Control Tower. However, these all-purpose taxipaths are often circumvented to accommodate real-time requirements. Within the Phase II Demonstration Project, only one path from each terminal to each runway end and from each runway exit to each terminal was modeled. These taxipaths will be reviewed and modified, if appropriate, for the Phase III Study.

[7] Mixing heights (also referred to as mixing depths) are used by meteorologists to quantify the vertical height of pollutant mixing that occurs in the atmosphere.
[8] The airport reference point is a point of an airport located at the geometric center of all the usable runways.
[9] ICAO defines high speed exit as a taxiway connected at an acute angle and designed to allow a landing airplane to turn off at higher speeds than are achieved on other exit taxiways.

Temporal profiles will be used to describe the relationship of one time period to another (i.e., the relationship of the activity during one-hour to the activity during a twenty-four hour period). In EDMS, temporal profiles are used to represent varying levels of activity as a fraction of a peak hour (a scale of 0 to 1). The use of temporal factors gives the model the ability to more accurately reflect real world conditions. The profiles are also used to evaluate the level of emissions expected to occur during a specific period within a year. Quarter-hour, day, and month factors will be developed to simulate aircraft activity during the analysis period. Distinct temporal profiles will be developed for air carrier, cargo, commuter, general aviation, and military operations during arrival and departure conditions. For the Phase III Study, the FAA's Aviation System Performance Metrics (ASPM) database will be used to establish the operational profiles for aircraft operations. These profiles will correspond to the measurement campaign periods.

Aircraft emissions can be temporally allocated in two ways, (1) by way of operational profiles (user specified quarter-hour, day, and month factors), and (2) by way of a simulated schedule of operations for the study period. For Phase II, the simulated schedule option was used to better control the distribution of flight operations among the runways. As part of Phase III, the flight schedule versus the use of operational profiles will be reviewed.

Phase III Modifications and Improvements
The following recommendations and modifications pertaining to aircraft emissions from Phase II will be incorporated and/or investigated for the Phase III Study:

- Review airfield capacity metrics to account for any changes to airfield usage and layout.
- Review runway, taxiway, and apron coordinates and taxipath designations for any changes to airfield usage and layout.
- Review the use of operational profiles versus the flight schedule.
- Evaluate sequence modeling versus aircraft operational profiles to better align EDMS internal assignments of runway exit paths with actual airfield usage.
- Include helicopter operations by assigning a specific gate/apron area.
- Utilize estimated takeoff weights rather than EDMS default values.
- Use aircraft tail number to identify aircraft engine assignment.

3.1.1.2 Auxiliary Power Units

Auxiliary power units (APU) are small turbine engines used by many commercial jet aircraft to start the main engines; provide electrical power to aircraft radios, lights, and other equipment; and to power the onboard air conditioning (heating and cooling) system. When an aircraft arrives at an apron, the pilot can opt to shut off power to the main jet engines and operate the onboard APU, which is fueled by the aircraft's jet fuel. However, APU must be run for a period of time (approximately seven minutes during arrival/departure) to allow warm-up/cool down. Alternately, an aircraft can utilize fixed gate infrastructure to receive 400 Hertz (Hz) of gate power and pre-conditioned air (PCA) from mobile ground power unit (GPU) and air conditioning equipment or from gate connections that provide electrical power and PCA. In most

cases, gate power connections are built into the passenger loading bridge used to connect the terminal building to the aircraft for loading and unloading of passengers.

Emissions Methodology
EDMS 5.1.3 has a database of APU typically assigned to aircraft and contains emission factors (in kilograms per hour of operation) for each model of APU. Of note, EDMS 5.1.3 has the ability to estimate PM emissions from APU, which was unavailable at the time of the Phase II emissions inventories. It is generally difficult to develop specific aircraft/APU assignments based on information from the airlines. Thus, for this study, the EDMS default aircraft/APU assignments will be used. Therefore, the APU emissions will be generated per operation as a product of the emission factor (based on default assignments) and operating time (based on the existence of 400 Hz gate power and/or PCA).

In accordance with FAA guidelines, the recommended APU operating time is seven minutes per landing and takeoff cycle (LTO) for all aircraft parked at gates that provide 400 Hz gate power and PCA.[10] For those gates without 400 Hz gate power and PCA, the recommended APU operating time is between 26 and 60 minutes per LTO 45 minutes was used during Phase II). [11]

Spatial and Temporal Allocation
Spatially, EDMS allocates APU emissions to a defined aircraft apron. The temporal allocations for APUs are defined within EDMS and the emissions are applied to each operation, which includes the time between arrival and departure from the gate in a manner consistent with any assigned operational profiles for the aircraft or flight schedule.

Phase III Modifications and Improvements
The following recommendations and modifications pertaining to APU emissions from Phase II will be incorporated and/or investigated for the Phase III Study:

- Better estimate the availability and usage of 400 Hz gate power and PCA per apron area.
- Use EDMS 5.1.3 to provide PM emissions estimation from APU.

3.1.1.3 Ground Service Equipment
Ground support equipment (GSE) includes the equipment that service aircraft after arrival and before departure at an airport and the vehicles that support airport operation. GSE at LAX includes: aircraft tugs, baggage tugs, fuel trucks, hydrant carts, catering trucks, cargo tractors, GPU, water trucks, lavatory trucks, cabin service, belt loaders, cargo loaders, and others. Different types of aircraft operations require different services, such as catering trucks or forklifts. Depending on aircraft category or size, different GSE are required. GSE operating times are a function of the airline and the aircraft category or size. GSE emissions are a function of its fuel type, model year and horsepower rating.

[10] During Phase II, it was noted that there are many ground power units in use at LAX, and therefore it is uncertain that this is the case in reality. This condition will be reviewed within the Phase III Study.
[11] Consistent with the Voluntary Airport Low Emissions *(VALE) Technical Report* Version 7 (dated December 2, 2010), block times are capped at 60 minutes for narrow body aircraft and at 90 minutes for wide body aircraft. Block times are defined as the time the aircraft resides in its "parking position" (from the Airport CDM Implementation Manual).

Emissions Methodology
EDMS 5.1.3 has a database of GSE emission factors (in grams-horsepower per hour) based on U.S. EPA's NONROAD2005 emissions model. However, the Phase III Study will use emissions factors developed by CARB within the OFFROAD2011 emissions model and/or In-Use Off-Road Equipment emissions model. EDMS also provides default information related to GSE type, horsepower, load factor, and operating times and their assignment to particular aircraft.

EDMS offers the operations-based method (using operating time per aircraft LTO) or the population-based method (using annual hours of operation) for estimating GSE emissions. The operations-based method assigns GSE to aircraft on an LTO basis (e.g., a 190 horsepower aircraft tug is assigned to a Boeing 757-200 and operates for eight minutes during departure). These GSE operations occur within the apron the aircraft is assigned to. The population-based method assigns GSE by number or amount (e.g., six aircraft tugs operate in an apron area for 500 hours annually each).

The Phase III Study will use the LAX GSE inventory survey (October, 2006) and determine GSE emissions based on the population-based method; as it most closely corresponded to the information available in the LAX GSE Inventory Survey. Phase III will use EDMS default hours of operation, load factors, and equipment age distributions. The Phase III Study will conduct a survey of GSE operations with site observations at the terminal apron areas during aircraft arrival and departure. The purpose of this survey will be to identify the types of GSE typically used at LAX, by airline and aircraft type (narrow, wide and commuter).

Spatial and Temporal Allocation
EDMS allocates GSE emissions to aircraft terminal aprons. Phase III will include 21 apron areas (i.e., Terminals 1 through 8, Bradley Terminal, cargo areas, and general aviation areas). GSE will be assigned as population-based on site survey results, GSE type and its prominence at particular aircraft apron areas, the percent of total aircraft operations at particular aircraft apron areas, and the type of aircraft operations (i.e., passenger, cargo, and general aviation) performed at particular gates.

GSE activities will be allocated throughout the hours, days, and months of the study period with the use of operational profiles. The same operational profiles used for aircraft operations will be used for GSE operations.

Phase III Modifications and Improvements
The following recommendations and modifications pertaining to GSE emissions from Phase II will be incorporated and/or investigated for the Phase III Study:

- Use CARB OFFROAD2011 emissions model and supporting databases instead of U.S. EPA's NONROAD2005 emissions model to determine GSE emission factors.
- Use population-based GSE as a function of their usage within the apron area or throughout the airport.
- Conduct a GSE operations survey during aircraft arrival/departure.

3.1.1.4 Roadways

For Phase II, on-airport roadways were included in three categories; (1) Central Terminal Area (CTA) roadways, (2) cargo routes, and (3) service roads. CTA roadways consist of five roadways in the center of the LAX terminal buildings and the connector ramps that connect West Century Boulevard and South Sepulveda Boulevard to World Way for inbound and outbound traffic. The same on-airport roadway network will be used for Phase III. Several service roadways and cargo routes will also be included. Traffic volumes associated with the CTA, cargo routes, and services will be considered 100 percent related to LAX operations.

Emissions Methodology

Emission levels from the operation of airport-related motor vehicles depend on several factors including: the vehicle volume, vehicle fleet mix (vehicle and fuel type), the emission factor, travel distance, speed, the level of congestion/delay, the year of analysis (and model year distribution), and meteorological factors.

CTA roadway volumes will be determined using traffic counters (loop detectors) that are permanently positioned in the inbound and outbound connector ramps for the CTA roadways. The loop detectors provide a basis to estimate the total number of vehicles on CTA roadways during the Study time periods.

Criteria pollutant emissions associated with on-airport vehicles will be calculated by combining the activity information with emissions factors derived using the CARB EMFAC2011 on-road emissions model.[12] Of note, emission factors from U.S. EPA's MOBILE6.2 emissions model are built into the EDMS but are not specifically applicable to California.

Spatial and Temporal Allocation

The on-airport roadways will be located in the project UTM coordinate system. Quarter-hour, day, and monthly profiles for CTA roadways will be estimated from the above mentioned traffic counters and/or aircraft operational profiles.

Phase III Modifications and Improvements

The following recommendations and modifications pertaining to traffic-related emissions from Phase II will be incorporated and/or investigated for the Phase III Study:

- Use EMFAC2011 to determine motor vehicle emissions factors.
- Update roadway locations, traffic volume, fleet mix, and traveling speed for the Phase III monitoring period.
- Review temporal profiles.
- Consider including on-airport service roadways to the north and west end of airfield.

3.1.1.5 Parking Facilities

Twelve parking facilities were included in the Phase II analysis. These facilities include seven public LAWA-owned parking garages in the CTA (LAX lots 1-7), two public LAWA-owned

[12] CARB EMFAC2011 On-road Emissions Model, http://www.arb.ca.gov/msei/msei.htm.

surface lots (LAX lots B and C), one LAWA-owned employee surface lot (LAX lot E), one public off-airport parking surface lot east of the CTA, and one trucking depot lot located east of Runway 25R. These parking facilities were chosen because of their close proximity to the air monitoring locations, which can measure emissions from vehicles entering or exiting these facilities and the same facilities will be included in the Phase III Study.

Emissions Methodology

Emissions occurring at parking facilities will be calculated using estimates of the number of vehicles accessing the facility, the amount of time a vehicle spends idling (typically 1.5 minutes), the travel time within the facility at a given speed (typically between ten miles per hour), vehicle type, facility geometry and spatial characteristics, and the emission factors.

The total volume of vehicles entering and exiting each LAWA-owned public parking facility will be estimated using parking data from the monitoring periods. Total traffic volume for the LAWA-owned employee lot (Lot E) will also be estimated using seven days of automated traffic counts. Traffic volumes in the public off-airport parking lot located east of the CTA on Century Boulevard (known as Park One) will be estimated using volumes from a LAWA-owned long-term surface lot (Lot C) scaled by the ratio of the number of parking spaces available in each lot.

Average distance traveled within the parking facility will be calculated independently for each facility. Per convention, the distance traveled will be based on the equivalent diagonal of the square area of the parking facility. Average occupancy and differences in facility characteristics will be taken considered in the calculation.

For the Phase II Study, public parking lots used a vehicle class distribution consistent with the default fleet mix option offered in EDMS. However, the Phase III Study will review this distribution and evaluate its use in CARB's EMFAC2011 with an adjustment specific to parking facilities.[13] Emissions associated with parking facilities will be calculated by combining the activity information with emissions factors, in grams per mile and grams per minute, derived using the EMFAC2011 emissions model.

Spatial and Temporal Allocation

The parking facilities will be located in the project UTM coordinate system. Each parking garage will be analyzed as one area source per garage level, that is stacked to simulate a parking garage. The number of levels in each garage and the average separation between levels will be accounted for.

Quarter-hour, day, and month- operational profiles will use aircraft profiles for quarter hour and daily. Monthly temporal data will be provided by LAWA's Parking Operations Department to represent actual motor vehicle emissions from parking facilities at the Airport.

[13] Parking facilities typically have a larger percentage of passenger automobiles and trucks and a lower percentage of heavy duty trucks and buses.

Phase III Modifications and Improvements
The following recommendations and modifications pertaining to parking facility emissions from Phase II will be incorporated and/or investigated for the Phase III Study:

- Use EMFAC2011 to determine motor vehicle emissions factors.
- Update parking facility locations, traffic volume, and fleet mix for the Phase III monitoring period.

3.1.1.6 Stationary Sources

Emissions inventories of LAWA-owned on-airport stationary sources will be developed based on various resources. Tenant-owned on-airport stationary source emissions will also be developed.

Phase III will include LAWA-owned on-airport stationary sources that include 30 stationary internal combustion engines, two turbines, and four boilers. In addition, the four cooling towers for the Central Utility Plant will be included in the Phase III Study. There are also several tenant-owned on-airport stationary sources (i.e., American Airlines, Skychefs and U.S. Post Office).

The Phase II Study did not include fuel storage tanks for Jet A, aviation gasoline, motor gasoline, and motor diesel fuels. The Phase III Study will request a list of fuel storage tanks, location, fuel type, dimensions, capacity, and annual throughout and consider including the resulting emissions.

Emissions from aircraft parts painting/degreasing facilities, dry cleaning facilities, food kitchens, and terminal-based food concessions will not be included, as these emission sources are minor and not easily quantified. However, these emissions will be included in the Community Health Air Pollution Information System (CHAPIS) database for area sources. The inclusion of training fires will be evaluated based on the schedule of training fire activities during the monitoring campaigns.

Emissions Methodology
The annual emissions for on-airport stationary sources will be calculated based on fuel usage during the two ambient monitoring campaigns for the stationary sources and the appropriate emission factors (via permits of U.S. EPA databases). The actual fuel usage for each of the stationary sources will be obtained from the *Air Toxics Inventory Report for the Los Angeles International Airport*, LAX fuel records, and other appropriate references. The fuel based emission factors will be chosen based on: stationary source type (engine, turbine, boiler etc.), combustion fuel type (diesel, natural gas, etc.), rated capacity (horsepower, heated capacity, etc.), and air-fuel ratio (lean-burn or rich-burn).

Spatial and Temporal Allocation
For Phase II, spatial allocation of each on-airport sources was based on street addresses and/or UTM coordinates provided by LAWA's environmental staff. The Phase III Study will review and augment this data as necessary. In many cases, Phase II used default stack parameters (i.e., stack height, exhaust temperature, exit velocity) for each unit type. Actual data on these parameters will depend on data availability.

For Phase II, no temporal allocation of the on-airport stationary source emissions was made because hourly, weekly, monthly or seasonal data were not available to allocate the emissions over time. Therefore, a constant emission rate was assumed for each hour of the modeling period based on the annual average data. The Phase III Study will review the availability of temporal profiles especially with respect to monthly or seasonal variations in usage and incorporate as appropriate.

Phase III Modifications and Improvements
The following recommendations and modifications pertaining to stationary source emissions from Phase II will be incorporated and/or investigated for the Phase III Study:

- The spatial allocation of many of the sources used in Phase II was not field verified. A review of the stationary source locations will be conducted as part of Phase III.
- The use of temporal allocation data will be examined. The use of temporal profiles may make the analysis a better representation of actual conditions. This is especially relevant for the emergency/backup engines, which would typically be operated only for selected periods of time, and boilers, which typically experience a seasonal differential in operation.
- Emissions from fuel storage facilities at LAX will be included in the analysis. A data request for a list of fuel storage tanks, location, fuel type, dimensions, capacity, and annual throughout will be developed.
- The inclusion of airport cooling tower emissions will be evaluated.
- In many cases, Phase II used default stack parameters (i.e., stack height, exhaust temperature, exit velocity) for each unit type. Actual data on these parameters will be determined to the extent possible.

3.1.2 Off-Airport Emissions

The off-airport emissions inventory will include off-airport onshore emission sources within the defined study area and major offshore emission sources located west of the study area. Sources include stationary sources, on-road traffic, off-road equipment, area sources, aggregated stationary sources,[14] and marine sources.

Data related to off-airport emissions will be retrieved from information gathered through interaction with U.S. EPA, CARB, SCAQMD, CalTrans, and other pertinent sources and entities associated with emission sources within the Study Area. These data from these sources typically contain criteria pollutant emissions and in some cases, air toxics emissions.

Table 10 presents a list of the off-airport emissions sources, the data which will be used to develop the emissions inventory, and the sources from which the data will be acquired.

[14] Aggregated stationary sources are those small point sources, such as restaurants, gas stations, etc. that do not have available separate emission source data.

Table 10. Sources of Emission Data for Off-Airport Sources

Emissions Source	Data	Data Source
Major Arterial Roadways	Volumes	SPAS Environmental Documentation
	Emission factors	CARB EMFAC2011 emissions model
	Temporal profiles	LA Department of Transportation
	Traffic Source Apportionment	LAX Master Plan
Interstate 405 and 105	Volumes	CalTrans Performance Maintenance System
	Emission factors	CARB EMFAC2011 emissions model
	Temporal profiles	CalTrans Performance Maintenance System
	Roadway entrained dust emission factors	U.S. EPA AP-42 Section 13.2.1
	Traffic Source Apportionment	LAX Master Plan
Major Stationary sources	Emission estimates, fuel usage, location, stack parameters, temporal profiles	SCAQMD Annual Emission Reporting
		SCAQMD Facility Information Detail
		Scattergood Power Plant Continuous Emissions Monitoring System (CEMs)
		Chevron El Segundo Refinery CEMs
		Los Angeles World Airports CEMs
Marine vessels and harbor craft	Emission estimates, location, temporal profiles	CARB Marine Emissions Model
	Exhaust release parameters	CARB *2007 Oceangoing Ship Survey Summary of Results*
Off-road equipment, area sources, and aggregate stationary sources	Emission estimates	CARB Community Health Air Pollution Information System
	Temporal profiles	U.S. EPA's Emissions Modeling Clearinghouse Temporal Allocation CARB EMFAC Emissions model

3.1.2.1 Roadways

On-road emissions will be calculated for major roadway links within the Phase III study area such as Century West, Imperial, Airport, Aviation, Sepulveda, La Cienage, Manchester, and Westchester based on data collected for the LAX SPAS project, LA DOT, or other traffic studies. Emissions will be determined separately for each of the I-405 and I-105 links that overlay the study area based on CalTrans PeMS.

Sepulveda Boulevard travels in two tunnels under the runways of the south airfield—one three-lane tunnel in each direction. Therefore, it will be modeled separately from all other roadways to estimate the total emissions produced by vehicles inside the tunnel, while ensuring that the roadway emissions are not included in the dispersion model.

Based on information developed for the LAX Master Plan, the portion of traffic related to LAX will be determined for each roadway segment. For example, on-airport and off-airport roadways closer to LAX tend to have a higher percentage of traffic related to the airport. The LAX Master Plan provides a survey of traffic at select intersections (for example, Sepulveda and imperial) near LAX. These surveys include an estimate of the percentage LAX-related traffic. These percentages will be assigned to each of the off-airport roadways as well as I-405 and I-105 as a means to estimate LAX-related and background traffic volumes within the roadway network. This methodology provides a general, broad assessment of traffic apportionment and will not utilized Traffic Demand Modeling analysis.

Emissions Methodology

CalTrans PeMS will be used to obtain traffic volumes, link coordinates, traffic times for each link, and vehicle class information for portions of I-405 and I-105 that are within the Phase III Study Area. The EMFAC2011 emissions model will be used to determine emission factors. $PM_{2.5}$ emissions will be estimated using size fraction data from California Emission Inventory Development and Reporting System (CEIDARS).

Spatial and Temporal Allocation

The off-airport roadways will be located in the project UTM coordinate system. On-road temporal factors will be based on the SCAG Transportation model, CalTrans Performance Measurement System (PeMS) data for the freeway links, and/or EMFAC.

Phase III Modifications and Improvements

The following recommendations and modifications pertaining to off-airport roadway emissions from Phase II will be incorporated and/or investigated for the Phase III Study:

- Improve temporal profiles based on best available data.
- Apportion traffic to LAX-related and background.
- Expand off-airport roadway network based on recent traffic studies.

3.1.2.2 Stationary Sources

There are a total of eighteen non-LAWA stationary sources within the Phase III Study area. Facilities with emissions over five tons per year for any single criteria pollutant will be included in Phase III Study. During Phase II, the following sources were found to contribute the majority of the off-site stationary source emissions: Chevron El Segundo Refinery, Scattergood Power Plant, El Segundo Power Plant, and So Cal Gas Playa Vista. During Phase III, additional sources will include Delta Airlines, Garrett Aviation, Continental Airlines, United Airlines, Boeing Systems, Northrop Grumman, and others.

Emissions Methodology

Data related to off-airport emissions will be retrieved from information gathered through coordination with U.S. EPA, CARB, SCAQMD, and other pertinent facilities and entities associated with emission sources within the Study Area. Data including, but are not limited to, National Emissions Inventory (NEI) facility emissions from U.S. EPA (2008), CHAPIS facility and area wide emissions from CARB (2001), and Annual Emission Reporting (AER) facility emissions and equipment and Facility Information Detail (FIND) from SCAQMD. Active

emission sources will be determined (e.g., those that have not been modified or replaced since the Phase II study). The references used to develop the stationary source emissions are shown in Table 10.

Table 11. Stationary Source Emission Inventory References

Stationary Source Data Reference
U.S. EPA National Emissions Inventory
U.S. EPA Clean Air Markets
CARB Community Health Air Pollution Information System
SCAQMD Annual Emission Reporting
SCAQMD Facility Information Detail
Chevron El Segundo Refinery Continuous Emissions Monitoring System (CEMs)
Scattergood Power Plant CEMs
El Segundo Power Plant CEMs

For some of the larger off-airport stationary sources, direct contact will be initiated to obtain additional data and/or clarification of data. However, during Phase II these efforts found some of the requested data were unavailable to the public. Exceptions were the Scattergood Power Plant and El Segundo Power Plant, which agreed to supply available hourly emissions and fuel use data through CEMS. A similar request will be made for the Phase III monitoring campaign periods.

Spatial and Temporal Allocation

The location of the stationary sources will be determined based on available information. Most of the stationary source databases do not provide enough information to develop temporal profiles and will therefore be assumed to operate at a constant continuous rate. The exception would be the hourly emissions and fuel use data for Chevron El Segundo Refinery and El Segundo Power Plant and the other larger sources, where available.

Phase III Modifications and Improvements

The following recommendations and modifications pertaining to off-airport stationary source emissions from Phase II will be incorporated and/or investigated for the Phase III Study:

- Revisit data sources to remove those facilities no longer in the reduced (from Phase II boundaries) study area and account for retirement/creation of new sources since the original study
- Obtain updated source data from AER/FIND SCAQMD, especially the Chevron El Segundo Refinery.

3.1.2.3 Marine Sources

Marine sources are represented by marine vessels within coastal waters west of LAX. Cargo handling emissions will not be included in the Phase III Study. Although the marine sources represented a significant contribution to the emissions (i.e., 86 percent of SO_2, 47 percent of $PM_{2.5}$, and 42 percent of NO_x) in the Phase II analysis, the contribution to the concentration results was much less significant (i.e., less than one percent of the total).

Emissions Methodology
CARB has developed separate emission models for marine vessels, providing each marine source with an Access database containing updated emissions information.

The marine vessel emissions will be developed based on CARB output from their Marine Emissions Model (dated May 2011). For a baseline year of 2006, the Marine Emissions Model produces daily emissions by specific shipping lane link for CO, NO_x, ROG, SO_x, and $PM_{2.5}$. Emissions are calculated by multiplying the emission factors by vessel-specific activity parameters, such as number of vessel calls, horsepower, operating load, hours of operation, and fuel sulfur content and are characterized by the activities of marine vessels (e.g., vessel transit, reduce speed zone, maneuvering, and hotelling activities for propulsion engines, auxiliary engines, and auxiliary boilers). Shipping lane links will be limited to the lanes north of Point Vicente, south of the extended Los Angeles County border, and east of the Channel Islands.

Spatial and Temporal Allocation
Marine emissions will be selected based on proximity to the study area. The locations of ship sources include the El Segundo buoys as well as a selected number of shipping lanes nearest the study area. For the buoys, locations will be determined by mapping historical aerial photographs that had vessels stationed at both buoys. Emissions will be assumed to be constant throughout the study period unless temporal data for ship and buoy operations are available. Source release parameters may use data from the CARB *2007 Oceangoing Ship Survey Summary of Results.*

Phase III Modifications and Improvements
The following recommendations and modifications pertaining to marine emissions from Phase II will be incorporated and/or investigated for the Phase III Study:

- Incorporate shipping lanes to the west of the airport.
- Improve temporal profiles based on best available data.

3.1.2.4 Offroad Equipment, Area Sources, and Aggregated Stationary Sources
The CARB CHAPIS provides emissions data on one-kilometer by one-kilometer grid cells for the following:

- *Off-road Sources* – non-road mobile sources such as construction equipment, trains and lawn mowers.
- *Area Sources* – widely dispersed sources such as the use of consumer products (hairspray, home automotive products, home cleaners, etc.) and other dispersed solvent uses, such as painting.
- *Aggregated Stationary Source* – small industrial facilities and businesses.

Any one-kilometer grid cell included in the Phase II Study which is located entirely outside the Phase III study area will not be included in the Phase III emissions inventory.

Emissions Methodology

Off-road equipment, area source, and aggregated stationary source emissions will be separately obtained from CARB's CHAPIS (based on information from 2001) within the one-kilometer grid square system. The emissions will be adjusted as a function of population within Los Angeles to reflect the monitoring campaign time period. Off-road equipment data within CHAPIS grids within LAX will not be included as to not double count GSE emissions. Aggregated stationary sources emissions will be reviewed to ensure that airport cooling tower emissions and airport (including tenant sources) stationary sources are not double counted within the resultant respective one-kilometer grid square.

Spatial and Temporal Allocation

Sources will be located in the project UTM coordinate system within the one-kilometer grid square system. Temporal factors for off-road, area-wide and aggregated point sources will be taken from U.S. EPA's Emissions Modeling Clearinghouse Temporal Allocation (dated February 2005).

3.2 AERMOD Modeling

In this task, dispersion modeling of the LAX airport emissions as discussed in Section 3.1 will be conducted using the latest versions of AERSURFACE (v08009), AERMINUTE ((v10300), AERMET (v11059) and AERMOD (v12060) (Cimorelli et al., 2005) from U.S. EPA. Lessons learned by University of North Carolina during work previously performed applying and evaluating AERMOD against measurements taken during the LAX Phase II AQSAS during the July-September 2008 period (Arunachalam et al., 2011b) will be leveraged. The various inputs that will be used for AERMOD are discussed below.

3.2.1 Input meteorology

Representative meteorological data from available sources will be obtained for the two study periods in Winter/Spring 2012 and Summer 2012, including on-site data from the LAX airport and from upper air data from Miramar (San Diego). However, a potential concern with the National Weather Service (NWS) or FAA data has been the presence of calms (wind speed less than 3 knots) and variable wind conditions at most stations. Since AERMOD cannot simulate dispersion under calm or missing wind conditions, U.S. EPA has developed a new tool called AERMINUTE to process one-minute archived wind data for the ASOS stations. If available, ASOS data available at one-minute frequency from the National Climatic Data Center (NCDC) will be used. Land characteristics around the selected meteorological stations will be determined and the AERSURFACE model will be applied AERMET (v11059) will then be used to process the available meteorological data for input into AERMOD. This version of AERMET has the following capabilities:

- Process one-minute ASOS wind data (TD-6405) to compute hourly averages:
    - Allows filling for missing values in standard NWS data due to calm or variable winds
    - Adjustments of ASOS winds by 0.5 knot to account for bias
- Few other enhancements related to processing onsite data (e.g., precipitation, relative humidity, etc.)
- Flexibility in selecting most appropriate upper air sound data

From past experience, several problems with the default meteorological fields that come out of AERMET have been found. Extensive screening of the meteorological data will be performed to make sure there are no anomalous values that may possibly impact model performance. For instance, to address abnormal values of both heat flux and U* (surface friction velocity) from AERMET in recent AERMOD applications for airport and other urban studies, screening analyses of the meteorological fields were performed to fix such values, or those hours were removed in the final analyses.

3.2.2 Input emissions

Emissions inventories developed in AERMOD-ready format for LAX Phase III AQSAS as described in detail in Section 3.1 of this document will be used directly in AERMOD.

3.2.3 Receptors

AERMOD will be instrumented with the following set of receptors:

- Polar grid, every 5-km up to 50-km radius
- Square grid, every 500-m up to 5-km
- All measurement locations from LAX AQSAS Phase III
- Flag-pole receptors at heights of 2, 7, 12, 17, 22m

The model will be instrumented with flag-pole receptors aloft to determine if AERMOD has higher concentrations aloft than at the surface. In previous modeling and analyses performed for the Providence T.F. Green airport (Arunachalam et al., 2011a), it was found that underprediction by AERMOD was due to the presence of a high concentration plume aloft rather than at the surface.

3.2.4 Output Analyses

Outputs will be analyzed in the form of time-series, X-Y scatter plots, Q-Q plots, box-and-whisker plots and violin plots for different averaging periods (depending on the pollutant) to understand model performance. For $PM_{2.5}$ and its components (such as $EC_{2.5}$, $OC_{2.5}$), daily averages will be computed and hourly averages for all gaseous species will be retained. An aggregate analysis will be performed as follows:

- relative ranking of receptor locations for each pollutant to identify the top 10 receptor locations
- relative ranking of key pollutants at a given receptor for all time periods modeled, and
- absolute magnitude range (minimum to maximum) of concentrations for a given pollutant across all receptors.

Note: The receptor locations for this analysis will include all four (4) sets of receptors defined in Section 3.2.3 above (i.e., LAX AQSAS Phase III sites are a subset of this group).

In Figure 5, AERMOD outputs are presented on a polar grid stretching out up to 50-km from the airport (illustrative results from LAX AQSAS Phase II) (Arunachalam et al., 2011b) with receptors placed every 5-km. From this analysis, it is seen that the impact of airport beyond 5-km radius is minimal. Most impacts are east of the airport, except for SO_2, which has a strong signal southwest of the airport due to marine port activity.

Figure 6. AERMOD Predictions of NO_x, $PM_{2.5}$ and SO_2 Concentrations for the LAX Airport, on a 50-km Polar Grid of Receptors.

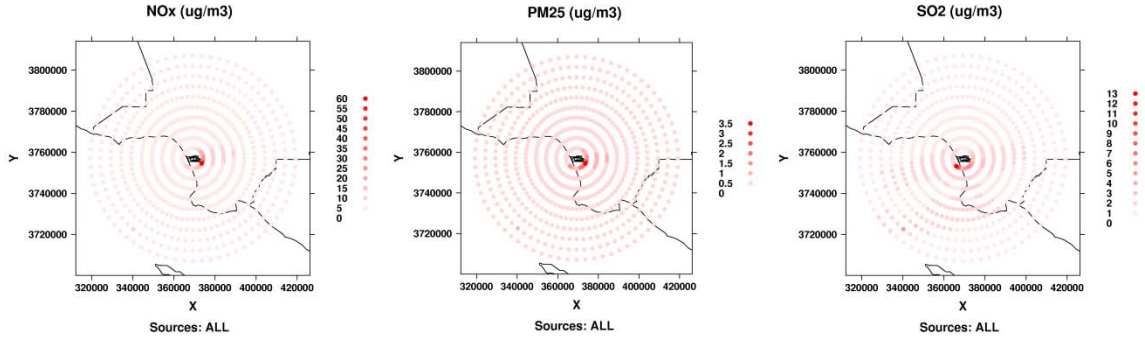

In Figure 6, AERMOD predictions for the LAX airport are presented on a 5x5-km uniform grid, with receptors every 500m (illustrative results from LAX Phase II AQSAS) for NO_x, $PM_{2.5}$ and SO_2. While most NO_x impacts are east of the South runway, both $PM_{2.5}$ and SO_2 show impacts to the east and south of runways from off-airport sources.

Figure 7. AERMOD Predictions of NO_x, $PM_{2.5}$ and SO_2 Concentrations for the LAX Airport on a 5x5-km grid.

a) NO_x b) $PM_{2.5}$ c) SO_2

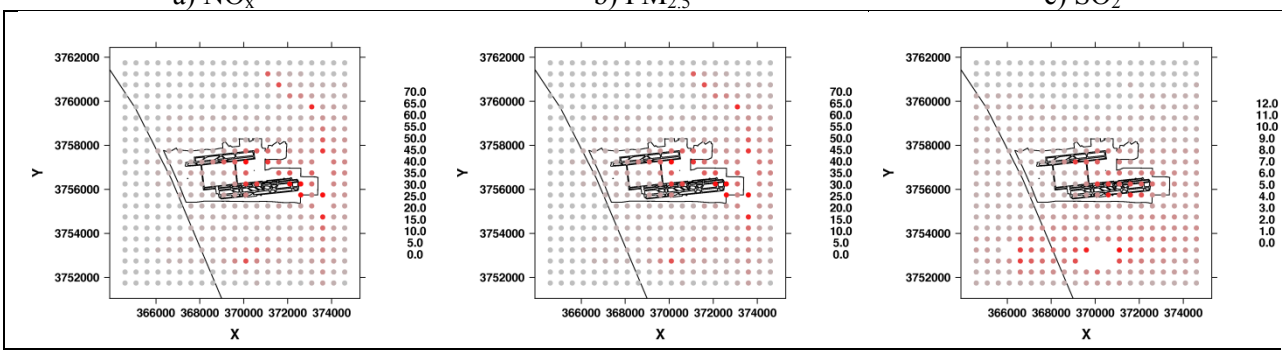

3.3 CMAQ Modeling

For this sub-task, the Community Multiscale Air Quality (CMAQ) (Byun and Ching, 1999; Byun and Schere, 2006; Foley et al, 2010) model will be used. CMAQ is a state-of-the-art, comprehensive, multiscale one-atmosphere air quality modeling system that identifies gas-phase chemistry, PM, and hazardous air pollutants (HAPs). The "one-atmosphere" capability indicates that ozone, PM and air toxics can be predicted using a single modeling system. CMAQ simulates the numerous physical and chemical processes involved in the formation, transport, and destruction of air pollutants using an Eulerian modeling system. Figure 7 shows a sample CMAQ modeling domain for the Continental U.S. at a 36-km horizontal model resolution.

Figure 8. Sample 3-D Modeling Domain Depicting Terrain Height (meters).

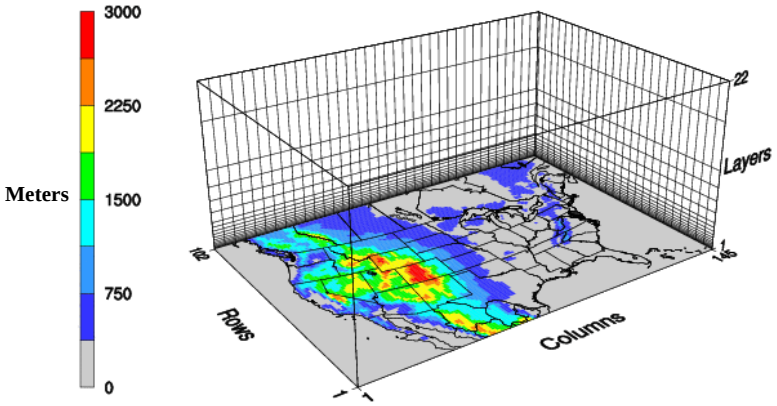

For the LAX AQSAS Phase III study, a standard application of CMAQ will be used for the Los Angeles region at a suitable horizontal resolution that has been conducted by the U.S. EPA, CARB or the SCAQMD. Arunachalam et al. (2011c) modeled three different airports using CMAQ at multiple horizontal grid resolutions of 36, 12, and 4-km to perform source apportionment of airport-related air quality impacts, and showed that in spite of significant differences in maximum concentrations attributable to aviation emissions, total air quality impacts over the entire model domain were largely unaffected by model horizontal grid resolution, with a 2 percent difference in air quality impacts between the 36-km and 12-km resolution outputs. Analyses of model scale indicated that a 108 x 108 km domain centered on the airport captured most population exposure for primary components of $PM_{2.5}$, however, secondary ammonium sulfate and nitrate were found to occur more than 300 km from the airports.

Since the air quality impacts from a source such as LAX includes both primary (directly emitted) as well as secondary (formed due to atmospheric reactions) pollutants, a source apportionment study like the one being undertaken for LAX, needs to rely on a detailed chemistry-transport model like CMAQ for a comprehensive assessment. Models like AERMOD can only provide source apportionment due to primary pollutants, and lack the treatment of atmospheric chemistry to assess secondary pollutants. As has been shown in previous work for assessment of air quality impacts of aviation, secondary pollutants play a large role.

Depending on the specific configuration of the base application, if possible, the latest version of CMAQ (Version 5) that was released by U.S. EPA via UNC's Center for Modeling and Analyses System (CMAS) in February 2012 will be used. Upon receipt of the base application from U.S. EPA or SCAQMD, the configuration will be reviewed completely to ensure it is suitable for use in this study. Before using the CMAQ application from SCAQMD (or other agency), we will ensure that this base application has been extensively evaluated against ambient monitoring data for the LAX region by the developers of this application, and that model performance has been established to be consistent with other regional-scale model applications.

3.3.1 Emissions Processing

The Sparse Matrix Operator Kernel Emissions (SMOKE) modeling system (Houyoux et al., 2000) and EDMS2Inv (Baek et al, 2007) will then be used to process all LAX airport study emissions (discussed earlier in detail in Section 3.1) and prepare CMAQ-ready inputs at the model grid resolution. EDMS2Inv is a new interface developed specifically to support processing EDMS emissions for CMAQ. SMOKE is an emissions modeling system that performs chemical speciation, temporal allocation and spatial allocation for inputs to CMAQ.

In processing aircraft emissions from LAX, refined methodology developed in processing aircraft emissions for other FAA-sponsored studies at UNC will be adopted. Specifically, NO_x speciation profiles specific to aircraft activity mode will be used (Wood et al., 2008), which correspond to 76 percent NO, 23 percent NO_2, and one percent HONO for landing-takeoff (LTO) emissions. VOC estimates will be converted to total organic compounds (TOG) and the latest chemical speciation profiles from a joint recent study by the FAA and U.S. EPA (FAA, 2009) will be utilized, paying attention to distinction to aircraft engine types (turbofan, turbojet, turboprop, etc.). The mass fraction of various species in TOG for turbo engines is provided in Appendix A. The actual speciation to the model chemical species will be based upon the choice of the chemical mechanism, most likely the Carbon Bond 2005 with extensions (Yarwood et al., 2005). Use of EDMS2Inv ensures aircraft emissions are represented in a true 4-D varying pattern within the model, as opposed to treating all airport emissions as surface layer emissions, in other routine air quality modeling practices.

The chemical speciation and temporal allocation of non-aircraft sources will be based upon standard profiles provided by U.S. EPA in the NEI modeling platform, and which UNC has used in several model applications to-date.

3.3.2 CMAQ Simulations

Two CMAQ simulations for the corresponding AQSAS Phase III modeling periods from Spring 2012 and Summer 2012 will then be performed, including:

- *base case* with all emissions (LAX airport and all other background sources - anthropogenic and biogenic sources) included, and
- *zero-out* case where the LAX airport study emissions will be subtracted from the base case. This scenario is intended to capture the broad regional background of air pollution in the LAX region from all other sources.

To support the source apportionment, a simple difference of these two simulations will provide an assessment of the total air quality impacts of all airport-related emissions sources that are included in the “base case”, but not in the “zero-out case”. The specific analyses that will be performed are discussed in detail below.

3.3.3 CMAQ Analyses

While CMAQ outputs are usually hourly, the model results will be used to compute daily and period averages. Further analyses of the CMAQ model outputs include plotting absolute and relative differences of the two scenarios (base case and zero-out case) to assess the incremental contributions from LAX airport on ambient air quality. An aggregate analysis, similar to what was outlined for AERMOD, will be performed as follows:

- relative ranking of receptor locations for each pollutant to identify the top 10 receptor locations
- relative ranking of key pollutants at a given receptor for all time periods modeled, and
- absolute magnitude range of concentrations for a given pollutant across all receptors.

Since AERMOD does not treat chemical transformation, but CMAQ does, comparative analyses of modeled contributions from the LAX airport similar to previous work we performed for the T.F. Green airport in Providence, Rhode Island (Arunachalam et al., 2011a) will be performed. Spatial maps of CMAQ-based LAX contributions to ambient air quality will be provided for all pollutants modeled. The strengths and weaknesses of the two modeling approaches compared to data from the field measurements will be highlighted.

Section 4 References

Arunachalam, S., A. Valencia, D. Yang, N. Davis, BH Baek, R Dodson, EA Houseman and JI Levy, 2011a. Comparing monitoring-based and modeling-based approaches for evaluating Black Carbon contributions from a U.S. airport. D.G. Steyn and S.T. Castelli (eds.), *Air Pollution Modeling and its Application XXI, NATO Science for Peace and Security Series C: Environmental Security 4*, DOI 10.1007/978-94-007-1359-8_102, Springer, The Netherlands, 2011.

Arunachalam, S., N. Davis, K. Talgo, 2011b. EDMS/AERMOD Evaluation for the Los Angeles International (LAX) Airport, *Presented at the 9th Annual Meeting of the FAA Aviation Emissions Characterization (AEC) Roadmap Meeting,* Washington, D.C., May 2011.

Arunachalam, S., Wang, B., Davis, N., Baek, B.H., Levy, J.I., 2011c. Effect of Chemistry-Transport Model Scale and Resolution on Population Exposure to PM2.5 from Aircraft Emissions during Landing and Takeoff, *Atmospheric Environment*, 45(19):3294-3300, doi:10.1016/j.atmosenv.2011.03.029

Baek, B.H., S. Arunachalam, A. Holland, Z. Adelman, A. Hanna, T. Thrasher, and P. Soucacos (2007). *Development of an Interface for the Emissions Dispersion and Modeling System (EDMS) with the SMOKE Modeling System*. In Proceedings of the 16th Annual Emissions Inventory Conference - "Emissions Inventories: Integration, Analyses and Communication", Raleigh, NC, May 2007.

Byun, D.W., and Ching, J.K.S., 1999. Science algorithms of the EPA Models-3 Community Multiscale Air Quality (CMAQ) modeling system. EPA/600/R-99/030, Office of Research and Development, U.S. EPA, Washington, D.C.

Byun, D.W., and Schere, K.L., 2006. Review of the Governing Equations, Computational Algorithms, and Other Components of the Models-3 Community Multiscale Air Quality (CMAQ) Modeling System. *J. Applied Mechanics Reviews*, Vol. 59 (2):51-77.

Censullo, A.C., D.R. Jones, and M.T. Wills (1996). Improvement of Speciation Profiles for Architectural and Industrial Maintenance Coating Operations. Final report prepared by California Polytecnic State University, San Luis Obispo, CA for the California Air Resources Board, June 30, 1996.

Cimorelli, Alan J.; Perry, Steven G.; Venkatram, Akula; Weil, Jeffrey C.; Paine, Robert J.; Wilson, Robert B.; Lee, Russell F.; Peters, Warren D.; Brode, Roger W., 2005. AERMOD: A Dispersion Model for Industrial Source Applications. Part I: General Model Formulation and Boundary Layer Characterization. J. ***Applied Met.*** 44 (5): 682-693. (AN 17406372)

Foley, K. M., Roselle, S. J., Appel, K. W., Bhave, P. V., Pleim, J. E., Otte, T. L., Mathur, R., Sarwar, G., Young, J. O., Gilliam, R. C., Nolte, C. G., Kelly, J. T., Gilliland, A. B., and Bash, J. O.: Incremental testing of the Community Multiscale Air Quality (CMAQ)

modeling system version 4.7, *Geosci. Model Dev.,* 3, 205-226, doi:10.5194/gmd-3-205-2010, 2010.

FAA/U. S. EPA. Recommended Best Practice for Quantifying Speciated Organic Gas Emissions From Aircraft Equipped with Tubofan, Turbojet and Turboprop Engines. Version 1.0, May **2009**. Available from:

http://www.faa.gov/regulations_policies/policy_guidance/envir_policy/media/FAA_EPA_RBP_Speciated%20OG_Aircraft_052709.pdf.

Fujita, E., J.G. Watson, J.C. Chow, N. Robinson, L. Richards, and N. Kumar (1998). Northern Front Range Air Quality Study. Volume C: Source Apportionment and Simulation Methods and Evaluation. Final report prepared for Colorado State University, Fort Collins, CO, June 30, 1998.

Fujita, E.M. and D. Campbell (2003). Validation and Application Protocol for Source Apportionment of Photochemical Assessment Monitoring Stations (PAMS) Ambient Volatile Organic Compound (VOC) Data. Final report prepared for the U.S. Environmental Protection Agency under EPA Star Grant #GR826237-01-0, August 31, 2003.

Fujita, E. (2005). Validation of the U.S. EPA MOBILE6 Highway Vehicle Emission Factor Model, Task 4: Guidance Document for Validation of On-Road Vehicle Emissions Inventory. Final report submitted to the Lake Michigan Air Directors Consortium, April 24, 2005

Fujita, E.M., B. Zielinska, D.E. Campbell, W.P. Arnott, J. Sagebiel, L. Mazzoleni, J.C. Chow, N. P.A. Gabele, W. Crews, R. Snow, N. Clark, S. Wayne and D.R. Lawson (2007). Variations in speciated emissions from spark-ignition and compression ignition motor vehicles in the California's South Coast Air Basin. J. Air Waste Manage. Assoc. 57: 705-720.

Fujita, E.M.; Campbell, D.E.; Arnott, W.P.; Zielinska B. Evaluations of Source Apportionment Methods for Determining Contributions of Gasoline and Diesel Exhaust to Ambient Carbonaceous Aerosols. J. Air & Waste Manage. Assoc. 2007, 57, 721-740.

Harley, R.A., M.P. Hannigan, G.R. Cass (1992). Respeciation of Organic Gas Emissions and the Detection of Excess Unburned Gasoline in the Atmosphere. Environ. Sci. Technol. 26:2395.

Henry, R. C. 2007. Locating and Quantifying the Impact of Local Sources of Air Pollution. *Atmospheric Environment* 42, 358-363. DOI: 0.1016/j.atmosenv.2007.09.039

Henry, R.C. Norris, G., Vedantham, R. 2011 Air Quaity Impact of a Major Highway and Nearby Sources By NonParametric Trajectory. *Environ. Sci. & Technol.,* 45, 10471–10476, DOI: 10.1021/es202070k

Houyoux, M.R., Vukovich, J.M., Coats, C.J., Jr., Wheeler, N.J.M., and Kasibhatla, P.S., 2000. Emission inventory development and processing for the seasonal model for regional air quality (SMRAQ) project. *J. Geophys. Res.*, Vol. 105(D7): 9079-9090.

Kirchstetter, T.W., B.C. Singer, R.A. Harley, G.R. Kendall, and J.M. Hesson (1999). Impact of California Reformulated Gasoline on Motor Vehicle Emissions: 2. Volatile Organic Compound Speciation and Reactivity. Environ. Sci. Technol., 33:329-336.

Lev-On, M.; LeTavec, C.; Uihlein, J.; Kimura, K.; Alleman, T. L.; Lawson, D. R.; Vertin,K;. Thompson, G. J.; Clark, N.; Gautam, M.; Wayne, S.; Okamoto, R.; Rieger, P.; Yee, G.; Zielinska, B.; Sagebiel, J.; Chatterjeee, S.; Hallstrom K. Chemical Speciation of Exhaust Emissions from Trucks and Buses Fueled on Ultra-Low Sulfur Diesel and CNG. SAE Technical Paper 2002-01-0432.

Lough, G.C., C.G. Christensen, J.J. Schauer, J. Tortorelli, E. Mani, D.R. Lawson, N.N. Clark, and P.a. Gabele (2007a). Development of molecular maker source profiles for emissions from on-road gasoline and diesel vehicle fleets, J. Air Waste Manage. Assoc. 57: 1190-1199.

Lough, G.C. and J.J. Schauer (2007b). Sensitivity of source apportionment of urban particulate matter to uncertainties in motor vehicle emissions profiles, J. Air Waste Manage. Assoc. 57: 1200-1213.

Pierson, W.R., D.R. Lawson, D.E. Schorran, E.M. Fujita, J.C. Sagebiel, and R.L. Tanner (1997). Assessment of Non-Tailpipe Hydrocarbon Emissions from Motor Vehicles. Final Report prepared for the Coordinating Research Council (CRC Project No. VE-11-7), Atlanta, GA, by the Desert Research Institute, Reno, NV. March 1997.

Schauer, J.J.; Christensen, C.G.; Kittelson, D.B.; Johnson, J.P.; Watts, W.F. Impact of Ambient Temperatures and Driving Conditions on the Chemical Composition of Particulate Matter Emissions from Non-Smoking Gasoline-Powered Motor Vehicles, Aerosol Science and Technology, 2008, 42, 210-223.

U.S. Environmental Protection Agency (2008a). Kansas City PM Characterization Study. Final Report, EPA420-R-08-009. Assessment and Standards Division Office of Transportation and Air Quality U.S. Environmental Protection Agency Ann Arbor, MI, EPA Contract No. GS 10F-0036K, October 27, 2006, Revised April 2008 by EPA staff.

Watson, J., E. Fujita, J.C. Chow, B. Zielinska, L. Richards, W. Neff, and D. Dietrich (1998). Northern Front Range Air Quality Study. Final report prepared for Colorado State University, Fort Collins, CO, June 30, 1998.

Watson, J.G., N.F. Robinson, E.M. Fujita, J.C. Chow, T.G. Pace, C. Lewis, and T. Coulter (1998). CMB8 Applications and Validation Protocol for PM2.5 and VOCs. Prepared for U.S. Environmental Protection Agency, Research Triangle Park, NC, by Desert Research Institute, Reno, NV.

Watson, J., J.C. Chow, and E. Fujita (2001). Review of Volatile Organic Compound Source Apportionment by Chemical Mass Balance. Atmos. Environ. 35:1567-1584.

Watson, J.G., N.F. Robinson, J.C. Chow, R.C. Henry, B.M. Kim, T.G. Pace, E.L. Meyer, and Q. Nguyen (1990). "The USEPA/DRI Chemical Mass Balance receptor model, CMB 7.0." Environ. Software, 5, 1, 38-49.

Wood, E. C.; Herndon, S. C.; Timko, M. T.; Yelvington, P. E.; Miake-Lye, R. C. Speciation and Chemical Evolution of Nitrogen Oxides in Aircraft Exhausts Near Airports. *Environmental Science and Technology.* 2008**,** *42*,1884-1891.

Yarwood, G., S. Rao, M. Yocke, G.Z. Whitten, 2005: Updates to the Carbon Bond Mechanisms: CB05 Report to the U.S. Environmental Protection Agency, Available at: http://www.camx.com/publ/pdfs/CB05_Final_Report_120805.pdf

Yarwood, G., R. Morris, S. Rao, S. Lau, E.M. Fujita, D.E. Campbell and W. White (2005). Evaluating VOC Receptor Models Using Grid-Model Simulations CRC Project A-34. Final report submitted to Coordinating Research Council, Alpharetta, GA, April 27, 2005.

Appendix A

Speciation of Total Organic Gases for Turbo Engines
(Also available at: http://www.epa.gov/oms/regs/nonroad/aviation/420r09903.xls)

Species	Mass Fraction	MW (from SPECIATE) [g/mol]
Ethylene	0.15458986	28.05316
Acetylene	0.039385952	26.03728
Ethane	0.005214505	30.06904
Propylene	0.045336437	42.07974
Propane	0.000780871	44.09562
Isobutene/1-Butene	0.017538274	56.10632
1,3-Butadiene	0.016869627	54.09044
cis-2-Butene	0.002104593	56.10632
3-Methyl-1-butene	0.001403439	70.1329
1-Pentene	0.007760686	70.1329
2-Methyl-1-butene	0.001744648	70.1329
n-Pentane	0.00198433	72.14878
trans-2-Pentene	0.003593968	70.1329
cis-2-Pentene	0.002757017	70.1329
2-Methyl-2-butene	0.001846216	70.1329
4-Methyl-1-pentene	0.000858179	84.15948
2-Methylpentane	0.004084956	86.17536
2-Methyl-1-pentene	0.000428122	84.15948
1-Hexene	0.00736025	84.15948
trans-2-Hexene	0.000371141	84.15948
Benzene	0.01681482	78.11184
1-Heptene	0.004384568	98.18606
n-Heptane	0.000638894	100.20194
Toluene	0.006421156	92.13842
1-Octene	0.002757017	112.21264
n-Octane	0.000624801	114.22852
Ethylbenzene	0.001742866	106.165
m-Xylene/p-Xylene	0.002821783	106.165
Styrene	0.003094253	104.14912
o-Xylene	0.001659872	106.165
1-Nonene	0.002455358	126.23922
n-Nonane	0.000623583	128.2551
Isopropylbenzene	3.96117E-05	120.19158
n-Propylbenzene	0.00066586	120.19158
m-Ethyltoluene	0.001926704	120.19158
p-Ethyltoluene	0.000802048	120.19158
1,3,5-Trimethylbenzene	0.000675821	120.19158
o-Ethyltoluene	0.000817972	120.19158
1,2,4-Trimethylbenzene	0.004377359	120.19158

1-Decene	0.001846216	137.1921245
n-Decane	0.003201988	142.28168
1,2,3-Trimethylbenzene	0.001327673	120.19158
n-Undecane	0.004441511	156.30826
n-Dodecane	0.004615541	170.33484
n-Tridecane	0.005354028	184.36142
C14-alkane	0.00186031	198.388
C15-alkane	0.00177053	212.41458
n-tetradecane	0.00416355	198.388
C16-alkane	0.001459826	226.44116
n-pentadecane	0.001726267	212.41458
n-hexadecane	0.000486609	226.44116
C18-alkane	1.76775E-05	254.49432
n-heptadecane	8.84283E-05	240.46774
phenol	0.007261785	94.11124
naphthalene	0.00541181	128.17052
2-methyl naphthalene	0.002061886	142.1971
1-methyl naphthalene	0.002466177	142.1971
dimethylnapthalenes	0.000898492	156.22368
C4-Benzene + C3-aroald	0.006564325	134.21816
C5-Benzene+C4-aroald	0.003241136	148.24474
Methanol	0.018051895	32.04186
Formaldehyde (FAD)	0.123081099	30.02598
Acetaldehyde (AAD)	0.042718224	44.05256
Acetone	0.003693477	58.07914
Propionaldehyde	0.007265856	58.07914
Crotonaldehyde	0.012909514	70.08984
Butyraldehyde	0.001481767	72.10572
Benzaldehyde	0.004695067	106.12194
Isovaleraldehyde	0.000406083	86.1323
Valeraldehyde	0.003064793	86.1323
o-Tolualdehyde	0.002872119	120.14852
m-Tolualdehyde	0.003471951	120.14852
p-Tolualdehyde	0.000602286	120.14852
Methacrolein	0.005362609	70.09
Glyoxal	0.018164641	58.03608
Methylglyoxal	0.015032806	72.06266
acrolein	0.024493139	56.06326
C-10 paraffins*	0.141565	142.28168
C-10 oleffins*	0.056626	140.2658
Decanal*	0.056626	156.2652
Dodecenal*	0.028313	184.31836
	1.000120509	

* 29% of unidentified mass was assigned based on judgment [*FAA/EPA*, 2009].

Section 4

QUALITY ASSURANCE / QUALITY CONTROL

(This page is intentionally blank)

Table of Contents

List of Tables

List of Figures

Appendices

Appendix 4-1 - System Audit Checklist

Appendix 4-2 - Laboratory System Audit Checklist

Appendix 4-3 - Siting and System Records

Appendix 4-4 - Performance Audit Reports – Winter Season

Appendix 4-5 - Performance Audit Reports – Summer Season

Appendix 4-6 - Audit Result Summary

4. QUALITY CONTROL/QUALITY ASSURANCE

4.1 QUALITY ASSURANCE APPROACH AND OBJECTIVES

Quality control (QC) and quality assurance (QA) were conducted to assure the project data quality objective was met. QC activities were performed by the monitoring sub-consultants (SCS Tracer and the Desert Research Institute (DRI)), with general oversight by Tetra Tech, to ensure all samples and data are gathered in accordance with guidelines set forth by U.S. Environmental Protection Agency (U.S. EPA) and relevant local air quality agencies. The QC program consisted of the following activities:

- Standard operating procedures
- Calibrations and precision checks
- Preventive maintenance
- Data handling and sample custody
- Data validation
- Data correction

The QA program consisted of an independent assessment of data quality, performed by a third party, T&B Systems Inc., to assure that the QC program was implemented properly and the collected data met the stated Data Quality Objectives (DQOs) as stated in the Monitoring and Quality Assurance Project Plan (MQAPP).

Tetra Tech was responsible for the QA program, which began with the development and implementation of the MQAPP (please see Appendix 3-3). T&B Systems conducted the QA assessment to verify that the MQAPP had been successfully implemented. T&B Systems operated independently from the other sub-consultants, and was not involved in any of the routine monitoring activities. Consequently, standards used during the assessment effort were independent from those used by the monitoring sub-consultant, SCS Tracer.

4.2 QUALITY ASSURANCE APPROACH

The overall QA program was presented in detail in the MQAPP; a copy of this report is included in Appendix 3-3.

QA assessment efforts consisted of two principal categories: 1) system audits, and 2) performance audits. System audits are systematic, on-site qualitative audits of facilities, equipment, personnel, training, procedures, recordkeeping, data validation, data management, and reporting. Performance audits quantitatively assess the performance of the monitoring equipment using known standards and measurement inputs.

Audits were conducted for both the air quality and meteorological measurements by reviewing the data collection efforts to assess the compliance with the stated project DQOs in Section A8.1 and Table A8-1 of the MQAPP. Table B4-1 (Performance Tolerances and Standards for Gaseous Monitors) and Table B4-2 (Minimum Performance Specifications for Meteorological Instrumentation) of the MQAPP provide additional information regarding study data monitoring objectives. A combination of the objectives from these three tables was used to define the audit criteria used for the performance audits.

4.3 AUDIT METHODS

The following sections provide a brief description of the audit types and methods used during the Study. Additional details regarding system audit procedures can be found in Appendix 3-3.

4.3.1 System Audits of Monitoring Activities

The purpose of the system audits was to assess consistency of measurements with the applicable Standard Operating Procedures (SOPs) and DQOs. The audit procedures employed are consistent with the *Meteorological Monitoring Guidance for Regulatory Modeling Applications* (EPA-454/R-99-005), February 2000, and the U.S. EPA *Quality Assurance Handbook for Air Pollution Measurement Systems, Volumes I, II, and IV* (U.S. EPA, 1994, 2008, 2008). Elements checked during the system audit can be found in the system audits form/checklist that was used to ensure that the necessary items have been covered and to also record the audit findings. The audit forms/checklists are included in Appendix 4-1.

4.3.2 Performance Audits

Performance audits were conducted on all applicable measurement equipment. Table 4-1 provides a summary of performance audit procedures and criteria. Details on the performance audit procedures for each audit can be found in the Appendix 3-3. Audits were conducted for both the Winter and Summer Monitoring Seasons, within the first couple of weeks of monitoring. The review and assessment were carried out through the data processing and validation stage to provide an independent assessment of the quality of the overall data produced by the monitoring program. Comments and recommendations resulting from the audits were discussed immediately with personnel who were performing the measurements, at the time of the audit, with a summary audit report provided to the project management (Tetra Tech) within 30 days of the audit.[1]

[1] The comments and recommendations were discussed and addressed immediately with project management. However, the actual report was completed within 30 days.

Table 4-1. Summary of Audit Procedures and Criteria

Measurement Variable	***Audit Criteria***	***Procedure Reference***	***General Procedure***
Time	±5 seconds	Audit clock synchronized to either NIST Radio Station to the satellite GPS network	Comparison check to the data logging clocks.
Horizontal Wind Speed	Accuracy ±0.25 m/s (WS < 5 m/s) or ± 5% of observed (WS > 5 m/s). Equivalent wind speed starting torque to meet the wind speed starting thresholds for the respective sensors.	EPA-454/B-08-002	Three wind speeds within the expected range of operation. If any points are outside of the criteria, then corrective action is necessary.
Horizontal Wind Direction	Accuracy ±3 degrees for linearity, ±2 degrees for alignment to known direction. Equivalent wind speed starting torque to meet the wind speed starting thresholds for the respective sensors.	EPA-454/B-08-002	Depending on the mechanical sensor type, between 4 to 36 points equally spaced around the compass are compared. If any points are outside of the criteria, then corrective action is necessary. Torque measurements are made to determine the mechanical sensor starting threshold. Sensor alignment is verified using solar or GPS methods.
Temperature	±0.5°C (monitoring criteria)	EPA-454/B-08-002	Three temperatures within the expected range of temperatures (0 to 40°C). If any points are outside of the criteria, then corrective action is necessary.
Temperature Difference (ΔT)	±0.1°C	EPA-454/B-08-002	Three temperatures within the expected range of temperatures (0 to 40°C). If any points are outside of the criteria, then corrective action is necessary. The criteria refer to the tracking of the two sensors at two heights at the same site over the range of audit temperatures.
Solar Radiation	± 10% of observed	EPA-454/B-08-002 as modified through discussions with U.S. EPA	Five measurements within the range of operations on a given audit day are made. If any points are outside of the criteria, then corrective action is necessary.

Measurement Variable	*Audit Criteria*	*Procedure Reference*	*General Procedure*
Relative Humidity (RH)	±10% RH	EPA-454/B-08-002	Three comparisons are made of the station sensor to an aspirated psychrometer. If any points are outside of the criteria, then corrective action is necessary. The preferred method uses a self-contained RH/Temperature data logging system, which is collocated with a site sensor, recording data over the audit period. These data are compared to several observed station readings. If any points are outside of the criteria, then corrective action is necessary.
Gaseous Air Pollutant Monitor Response	Slope: 1.00 ±0.15 (all points within ±15%) Intercept:- ±2% (full-scale) NO_2 GPT Efficiency: ≥96%	EPA-454/B-08-003	Dilution of known traceable concentrations of gas. Zero air to be provided by a CO-scrubbing zero air system.
Particulate Matter MiniVol Flowrate	$PM_{2.5}$ Filter: ±10% (0.5 lpm)	EPA-454/B-08-003 and experience. No audit criteria exist specifically for the MiniVol. Methods also developed during the 2000 California Regional Particulate Air Quality Study (CRPAQS) program.	Measurement of inlet flow using a certified bubble flow or piston flow device. The method was revised to use a certified rotameter, as the backpressure of the automated methods created flow issues in some samplers.
Particulate Matter BAM $PM_{2.5}$ Flowrate	±10% of 16.67 lpm	EPA-454/B-08-003	Measurement of the inlet flow using a certified flow device
Ultrafine particle number and sizer Flowrate	±10% of audit flow	N/A – No reference EPA procedure available	Measurement of the inlet flow using a certified flow device
Light Scattering based Particulate Matter (pDR) Flowrate	±10% of audit flow	N/A – No reference EPA procedure available	HEPA filter to zero the instrument. Certified flow device to determine flow rate. Leak check performed on sample inlet to evaluate inlet integrity.
Black Carbon (Aethalometer) Flowrate	±10% of audit flow ±10% flow difference from design flow	N/A – No reference EPA procedure available	Measurement of the inlet flow using a certified flow device. Check of zero BC concentration using a High-Efficiency Particulate Air (HEPA) filter
$PM_{2.5}$ mass and speciation (DRI SFS) Flowrate	±10% of audit flow ±10% flow difference from design flow	N/A – No reference EPA procedure available	Measurement of the inlet flow using a certified flow device.
Semi-volatile	±10% of audit flow	N/A – No reference	Measurement of the inlet flow using

Measurement Variable	*Audit Criteria*	*Procedure Reference*	*General Procedure*
organics (DRI SVOC) Flowrate	±10% flow difference from design flow	EPA procedure available	a certified flow device.
Carbonyls Flowrate	±5% of audit flow	N/A – No reference EPA procedure available	Measurement of the inlet flow using a certified flow device
Passive Samplers	Difference between data from passive sampler and fixed site analyzer	N/A – No reference EPA procedure available	Evaluation of results versus collocated continuous gas analyzers at fixed sites (conducted during analyses of field data)
Monitoring site coordinates	Not applicable	GPS operating manual	Reported coordinates of monitoring site are checked by a GPS instrument

4.3.3 Laboratory Audits

A system audit of the DRI laboratories was conducted during an on-site visit and review of the operations. This included observing the sample preparation and handling procedures, sample custody, QC checks, analysis procedures, and data integrity. No actual laboratory performance audit was performed. The laboratory system audit began with the process of receiving the samples and continued through the analysis and reporting of the final results. A review was also conducted of the sample media preparation and cleaning process for the media used in the field for collection of ambient samples. Any recent audits of the laboratories were also reviewed. The laboratory system audit consisted of the following:

- Review of SOPs for all analyses, concentrating on QA/QC procedures
- Review of recent external reviews/audits of laboratory operations, including the following:
    - Technical Systems Audit of DRI's Environmental Analysis Facility report dated June 1, 2011 by the U.S. EPA, pertaining to speciated particulate analyses
    - Experimental Inter-comparison of Speciation Laboratories report dated June 15, 2010 by the U.S. EPA, pertaining to speciated particulate analyses
    - Evaluation of Passive Samplers for Assessment of Community Exposure to Toxic Air Contaminants and Related Pollutants, a peer reviewed article in Environmental Science & Technology published February 15, 2011
    - Intercomparison Program for Organic Speciation in $PM_{2.5}$ Air Particulate Matter published in 2005 and 2006, which include DRI's Organic Analytical Laboratory
- Interviews of key personnel associated with the laboratory analysis for the Study
- A tour of each of the DRI analytical facilities with DRI personnel, with an emphasis on reviewing chain-of-custody and QA/QC procedures for each of the analytical methods

- Review of data management procedures, including review of files collected for the Study, focusing on calibrations, QC check data, and replicate analysis data.

Appendix 4-2 provides the laboratory system audit checklist used as a guide to conduct the audit.

4.3.4 Data Audits

Data audits were conducted by obtaining the raw data electronically and comparing it against the final data files within a couple of weeks of being available on the project ftp site. Additionally, instrument zero/span data were reviewed. Data audits were conducted for both the Winter and Summer Monitoring Seasons. Data audits consisted of the following:

- Review of time-series graphs produced on T&B Systems' web-based data management and display system for data reasonableness
- Review of all final data files submitted by SCS Tracer
- Spot check of final files against original data logger/chart/instrument files
- Review of zero/span data for the air quality parameters
- Comparison of performance checks against study DQOs

4.4 AUDIT RESULTS

4.4.1 System Audits

A system audit of the air monitoring efforts was conducted at the beginning of the Winter Monitoring Season, with correction of any noted issues verified during the Summer Monitoring Season. Siting forms generated as part of the system audits are included in Appendix 4-3.

Issues identified during system audits included:

- Insufficient temperature sampling probe height above the ground
- Meteorological tower not plumb
- Monitoring equipment malfunction
- Potential air flow obstruction by nearby building structure
- Inaccurate site coordinates

The height of the sampling probe on the roof of the DRI's motorhome at CN site was less than the one meter height recommended by the U.S. EPA siting criteria. This issue was corrected by extending the probe at least one meter above the roof of the shelter before the Summer Monitoring Season. Additionally, the slightly tilting meteorological tower at the CE site was adjusted to be vertical to the ground before the Summer Monitoring Season began. The insufficient probe height and slightly tilting meteorological tower would not affect the data quality of air pollutant measured.

Temperature probes were relocated to the required height on the tower immediately after the audit. Malfunctioning monitors were replaced with a spare. Inaccurate site coordinates were corrected in the site logs. Potential air flow obstruction by nearby building structures was noted and was considered as a compromise due to site availability. Generally, these issues were resolved or corrected immediately or soon after the system audit was completed to minimize any potential adverse impacts on overall data quality.

4.4.2 Performance Audits

Performance audits of the air monitoring efforts were conducted at the beginning of both the Winter and Summer Monitoring Seasons. Results of the audits for each monitoring season are described below.

Winter Monitoring Season Performance Audit Results

Detailed audit results are listed in Appendix 4-4. Due to unique nature of the sequential filter sampler (SFS), audit results of the SFS were recorded separately and also are presented in Appendix 4-4.

Issues identified during the Winter Monitoring Season performance audits included:

- Air leaks in the sampling lines
- Incorrect sample air flow rate
- Monitoring instrument baseline drift
- Monitoring instrument internal clock time differed from standard time

The monitoring instrument that was identified with an air leak was corrected immediately by replacing with a new spare monitor. Monitors with incorrect air flow rate were corrected either by readjusting and balancing bypass air flow rates or simply replacing with a new monitor. Baseline drift issues could not be corrected during the measurement and were corrected by SCS Tracer by adjusting the raw data during data post-processing. Data were adjusted by subtracting the offset from the raw data values during periods where zero checks indicated that the offset had exceeded DQOs for accuracy, as specified in the MQAPP. The internal clock was corrected by resetting the data logger time. Data quality impacts were minimized by immediately taking corrective action.

Summer Monitoring Season Performance Audit Results

Detailed audit results, including those for the SFS units, are presented in Appendix 4-5. Issues identified during the Summer Monitoring Season performance audits included:

- SO_2 calibration gas was scrubbed by the regulator and caused over calibration of the analyzer at the CN site
- Minor air leaks in the sampling lines

- Incorrect internal time stamp in data logger
- Incorrect sample air flow rate
- Monitoring instrument malfunction

The regulator that caused SO_2 calibration gas scrubbing problem at the CN site was replaced. Additionally, frequent purges of the regulator prior to introducing calibration gas into the analyzer were conducted to correct the problem. The affected monitoring data were corrected during the post-processing of the data by SCS Tracer. The monitoring instrument identified with a minor air leak was corrected immediately. Monitors with incorrect air flow rate were corrected by recalibrating sample air flow rate. The internal clock was corrected by resetting the data logger time. Malfunctioning monitors were replaced with a spare or corrected by replacing the non-operational parts with a new part. These issues were corrected immediately to minimize negative impacts on overall data quality.

Please note, not all saturation MiniVol sites were visited during the Summer Monitoring Season performance audit, as the siting and exposure were addressed during the first round of audits. Performance checks were conducted during the Summer Monitoring Season audits by verifying that sampler flows of units coincided with MiniVol flow rates at the four core sites. This check provided an adequate verification that the flow standards used by the auditor, DRI and SCS Tracer were in agreement without the need to check each individual sampler. In some cases, the samplers audited at these sites were found to have timer or other issues, which are typical items noted during the weekly site visits by DRI while changing the sample media. For the samplers found to be operating properly, the flow verifications showed a high level of agreement between the audit and operator flow standards.

Issues noted during the audit, as well as their resolution, are presented in Table 4-2 for the Winter Season and Table 4-3 for the Summer Season.

Table 4-2. System and Performance Audit Comments and Corrective Action – Winter Monitoring Season

No.	Date	Issues identified during audits	Corrective Action(s) Taken
1	2/1-2/3/2012	The temperature sensors at the CE and CS sites were located at 3.3 meters and 8.2 meters. In addition, the lower sensor at both sites was located very close to the trailer, which is a potential radiative source, particularly during morning hours. It was recommended that the lower sensor be moved down to 2 meters (a more conventional height for the low level of delta-T and potentially less impacted by the trailer wall) and away from the shelter as far as the supporting boom would allow. This was done following the audit at both sites.	Relocated the temperature sensors before the Winter Monitoring Season began.
2		The tower at CE site was noticeably tilting by 1 or 2 degrees. SCS Tracer indicated that the top support of the tower was temporary, and that a more secure and adjustable support was to be installed to straighten the tower.	The tower support to the shelter was replaced and the tower was adjusted prior to the Summer Monitoring Season. The meteorological data were not appreciably affected by the very slight tilt.
3		The lower level temperature aspirator fan at the CS site was failing and was replaced. The replacement fan was a 230 volt model that should be replaced with a 120 volt model as soon as possible. That way the delta-T would use aspirators with the same flows.	Replacing the aspirator necessitated tilting the tower down to ground level. It was replaced prior to the summer season.
4		The Grimm particle size classifier at the CE site was not operating at the time of the audit. In addition, the SMPS particle size classifier at the CN site was producing suspicious data, and appeared to have an incorrect sample or sheath flow. Concerns were passed on to DRI.	The instrument was relocated from the CS to the CE site. A stand-alone CPC to collect UFP data was subsequently installed with the desired particle size range.

No.	Date	Issues identified during audits	Corrective Action(s) Taken
5	2/1-2/3/2012	The pDR 1200 has a design issue that makes sealing of systems equipped with a $PM_{2.5}$ cyclone difficult. A significant amount of air was leaking downstream of the cyclone at the CE site and, to an even greater extent, at the CS site, where very little of the sample was going through the cyclone. The operator indicated that systems with this issue would be temporarily replaced with a spare sampler to allow for the leak in the affected systems to be properly sealed.	On 2/8/12 the pDR 1200 at the CS site was replaced with a spare. The spare had a measured flow through the cyclone of 3.6 lpm compared to a flow set point of 4.0 lpm. This was significantly better than the flow rate through the cyclone of the replaced pDR 1200. The replaced spare never achieved an adequate flow rate through the cyclone and therefore was never placed back in service during the Winter Monitoring Season. The unit was repaired prior to the Summer
6		One of the MiniVols at the CN site was found to not be operating when audited, apparently due to a flow fault. The auditor reset the sampler, and the flow rate was measured at 5 lpm (nominal flow rate).	Sampler was replaced after another unexplained shut-down occurred.
7		Though the SO_2 analyzer at the CN site read 0.0 ppb on the analyzer meter, the site data logger read 1.1 ppb when challenged with zero air. Given that the intent is to collect trace SO_2 levels, this difference was significant. SCS Tracer noted this issue and planned to correct the data during post-processing.	Raw data collected by the data logger were adjusted based upon response to calibrations using the criteria in the MQAPP during post processing.
8		Similar to the above issue, the zero for the CO analyzer was negative at all sites, as low as - 0.5 ppm. The nightly station zero/span checks confirmed these values. While meeting overall audit criteria, post processing of the data to account for the zero offsets may be required in order to meet study objectives.	Raw data collected by the data logger were adjusted based upon response to calibrations using the criteria in the MQAPP during post processing.
9		When auditing MiniVol flows, it became apparent that using either a Bios piston flow meter or BGI Challenger pressure differential flow meter produced a sufficient pressure drop to influence the pump's ability to maintain the 5 lpm flow rate for some of the samplers audited. This brings into question the ability of the MiniVols to maintain flow rates over a seven-day period of filter loading and high humidity. Measured end flow rates should be carefully reviewed to evaluate the issue.	Initial and final flow rates were provided to T&B Systems for the samplers in question. There was no indication of reduced flow rates.

No.	Date	Issues identified during audits	Corrective Action(s) Taken
		Siting	
10		During the February 1, 2, 3 audits, data logger times were compared against the GPS time at each of the sites. Some differences up to 20 seconds were noted and it was emphasized that agreement to within 5 seconds was required in order to make 1-minute data comparable between the sites. During the audit, SCS set the data logger times to agree with GPS time. During the February 21 audit, all sites were found to be within 5 seconds.	Reset data logger time to agree GPS time. Issues were corrected.
11		Noted during the February 1, 2, 3 audits, but not included in the initial summary, the U.S. EPA siting criteria for air quality sample inlets state that the sample inlet should be at least 1 meter from supporting structures (typically the roof of the monitoring shelter). This is the case except for the CN site, where the inlets were generally below 1 meter (only about 0.4 meters for the gaseous parameters inlet). It was recommended that the sampling height be adjusted for the Summer Monitoring Season.	The sample inlets at each site were adjusted to at least 1 meter above the roof line of the shelters for the Summer Monitoring Season.
12	2/21/2012	Also noted during the February 1, 2, 3 audits, but not included in the initial summary, the samplers for Tenax, canister and DNPH samples are located on the ground, with the sample inlets located at a height below that of the wind/security fence at each site. We acknowledged that logistics and security issues limit the placement of these samplers. However, we recommend that the sample canes be extended before the second round of sampling to the point where they are sampling air above the top of the fence, at a height of at least 2 meters.	The sample canes for the Tenax, canister and DNPH samplers were extended for the Summer Monitoring Season to the point where they are sampling air above the top of the fence, at a height of at least 2 meters.
13		Similar to the above sampler inlet height issues, the SVOC samplers audited during the February 21 audits also had sample inlet heights at or near the height of the wind/security fencing. While they are close to breathing height, we recommend the sample inlet height to be above the top of the fencing and at a height of at least 2 meters. This adjustment should be performed before the Summer Monitoring Season.	The inlet heights were extended for the Summer Monitoring Season to the point where they are sampling air above the top of the fence, at a height of at least 2 meters.
14		At the CS site, the building complex to the southwest may present some blockage to flow from that direction. This possible influence should be recognized during the analysis of meteorological data.	The airport and airport related sources are all located to the north of the sampling site. The blockage to flow from the southwest direction should not influence study objectives

No.	Date	Issues identified during audits	Corrective Action(s) Taken
15	2/21/2012	At the CN2 site, a tree to the west was in a pollination stage at the time of the audit. This tree, in combination with other plants surrounding the site, will likely produce pollen in the samples.	This was taken into consideration by analysts when working with the data.
16		At the SRE site, the coordinates differed from the audit values. As this site location may be critical for modeling with relation to the blast fence. The coordinates should be checked and verified by the Site Operator.	Site coordinates were checked for accuracy prior to use in modeling.
17		At the BSR site, the site coordinates differed from the audit values. Like the SRE site, this location may be critical for modeling with relationship to the runway. The coordinates should therefore be checked and verified by the Site Operator.	Site coordinates were checked for accuracy prior to use in modeling.
18		At the NR site, the site coordinates differed from the audit values. Like the other identified sites, this location may be critical for modeling with the relationship to the runway. The coordinates should therefore be checked and verified by the Site Operator.	Site coordinates were checked for accuracy prior to use in modeling.
19		At the BNR site, the site coordinates differed from the audit values. Like the other identified sites, this location may be critical for modeling with the relationship to the runway. The coordinates should therefore be checked and verified by the Site Operator.	Site coordinates were checked for accuracy prior to use in modeling.
20		At the CT site, there were passive samples that either fell out of the sampler housing or were knocked out of the housing. Modifications were made to assure the samples would not accidentally fall out of the housing, but not much could be done if this was vandalism. If this does happen repeatedly, then consideration should be given to moving the sampling location.	Sampler housing was reinforced to prevent the samples from falling out.
		MiniVol	
21		At the CS2 site, no flow issues were found with the samples that had been collected during the previous week. However, when the new filter was loaded into sampler s/n 1217, it could not maintain the required flow rate of 5 lpm. This was verified by DRI, and the sampler was replaced with s/n 1296. Flows were found to be within criteria with the filter installed in this replacement unit.	Replaced sampler. Note that the cutpoint may have been significantly affected and was corrected for in data analysis of samples.
		SVOC	
22		At the CN site, the measured audit flow for Channel 2 of the SVOC sampler was 125 lpm. While the assumed site flow of 113 lpm was within the ±10 percent audit criteria of the audit flow, the flow rate of 125 lpm was outside of the criteria for maintaining the proper cut point for the sampler inlet (113 ±11 lpm, 10%).	When concentrations of SVOCs were calculated, the actual flow rate was used.

No.	Date	Issues identified during audits	Corrective Action(s) Taken
		SFS	
23		At the CE site, the paired samples at positions 2 and 8 had a total flow of 126 lpm, which was outside of the design flow rate audit criteria of 113 ±11 lpm.	Flow rates were adjusted.
24		At the CS site, the paired samples 1&7 and 5&11 had total flows of 93 and 87 lpm, respectively. These flow rates were outside of the design flow rate audit criteria of 113 ±11 lpm	Bypass flow was added to make total inlet flow ~113 lpm.
25	2/21/2012	At the CN site, four sets of paired samples were audited. Because the pump at the site could not be shut off, one flow channel was used for makeup flow to prevent the pump from drawing a vacuum when all channels were closed. When the makeup flow rate was added to the paired sample flows, the total flow for each of the sample pairs was outside of the design flow rate criteria of 113 ±11 lpm. The total flows were 133, 132, 132 and 132 lpm for 1&7, 2&8, 3&9 and 4&10, respectively. The makeup flow was adjusted from 38 to 21 lpm following the audit.	Bypass flow was reduced to make total inlet flow ~113 lpm.

Table 4-3. System and Performance Audit Comments and Corrective Action – Summer Monitoring Season

No.	Date	Issues identified during performance audits	Corrective Action(s) Taken
1	7/30-7/31/2012	The response of the SO_2 analyzer at the CN site was approximately 18 percent higher relative to the audit input concentrations, though station span data were showing no issues. Further testing conducted during the audit revealed that the regulator on the station's span cylinder was scrubbing SO_2, producing lower span concentrations than expected and resulting in the analyzer response being adjusted high. Two possible corrections to the calibration system were discussed during the audit – replacing the regulator or conducting frequent purges of the regulator (which were shown during the audit to correct the problem).	Based on new span checks, SO_2 data obtained prior to the audit were adjusted during data processing. Station operations were modified by incorporating automatic purging of the regulator prior to span and calibration checks.
2		At the CN site, the Environmental Systems Corporation (ESC) logger was 10 seconds slow and the chart recorder was 15 seconds slow. It was recommended that the clock accuracy on each of the data systems be monitored to keep the time accuracy within the project specified ±5 sec.	These clocks were corrected during the audit.
3		The BAM at the AQ site had a minor leak that was corrected during the audit.	The leak did not appear to affect the data collected.
4		At the CN site, MiniVol sampler s/n 0987 was found not to be working.	The sampler was replaced with s/n 1018 and the flows found to be within audit criteria.
5		At the AQ site, the CNC sampler had been moved to an outdoor environmentally controlled shelter as the prior location, where the sampler was during the Winter Monitoring Season, was now in use by other sampling equipment. The as-found audit did find the flow to be approximately 27 percent high.	The operator recalibrated the flow to the design set point of 1.5 lpm. The as-left flow was found to be within 2 percent of the calibration set point.
6		At the CS site, the GRIMM instrument had failed at the time of the audit and could not be audited. The instrument needed at least a day to have any water in the system evaporate before any further checks could be made.	As confidence in the site flow standards was obtained through other audits, the on-site flow checks were deemed adequate to verify the proper instrument operation.

No.	Date	Issues identified during performance audits	Corrective Action(s) Taken
7	7/30-7/31/2012	At both the CS and CN sites the SFS sampler was not operational and needed the internal tubing replaced.	As there was reasonable agreement between the operator and audit flow standards, as demonstrated during both the CE site, audit of this sampler and the SVOC audits, audits of the CS and CN site samplers were not warranted, once repairs had been made.
8		At the CN site, the SMPS was operating in the low flow mode. The sample inlet from the roof was shared with the site Aethalometer. Thus, the total flow measured at roof level was the sum of the SMPS and Aethalometer flows. Individual instrument flow rate audits were therefore performed at the location in the shelter where the flow was split to the respective instruments. The mass flow controlled flow in the SMPS appeared to be sensitive to the piston type flow technology used by the BIOS Defender audit device so the direct results from this audit could not be used.	A comparison was then made of the SMPS flow to the on-site TSI flow calibrator with the results obtained within 2 percent. A check of the on-site flow calibrator and the audit BIOS was made on an instrument that was not sensitive to the piston technology and agreement of better than 4 percent was obtained. Thus, it was concluded there were no problems with the SMPS flows.

4.4.3 Laboratory Audits

DRI's laboratory procedures are well documented and carefully followed. The results from U.S. EPA's recent technical systems audits and inter-comparison performance audits conducted in 2010 and 2011 revealed no problems with DRI laboratory operations and performance consistent with other National Laboratories. No issues were noted during the on-site review of the DRI analytical facilities by T&B Systems. However, the following observation related to the laboratory effort, though not pertaining directly to laboratory operations, was noted during the audit.

- Of the speciated measurements conducted for the Study, TENAX sampling was the only measurement that did not have a collocated sampler due to the requirement of an additional sampler. Collocated samples provide data from which measurement uncertainty can be estimated. It was recommended that collocated TENAX measurements be conducted during the Summer Monitoring Season to estimate measurement uncertainty. Per recommendation, a collocated sample was collected during the Summer Monitoring Season.

4.4.4 Data Audits

Data audit results specific to each of the monitoring seasons, issues identified, and recommended corrective actions are summarized below.

For both sampling seasons, solar radiation at the CE site was labeled as Langleys when it is actually kilowatts per square meter in the data provided. This issue has been resolved, and the unit of "watt/m^2" was used for solar radiation data for both seasons.

Winter Monitoring Season

In general, the data were found to be complete and representative; however, the following identified issues and corrective actions were taken:

- Review of the nightly zero/span data showed zero data were generally within the lower detection limits (LDLs) noted above for both the CE and CS sites. However, the zero data for the trace SO_2 analyzer at the CN site frequently deviated from zero by over 0.5 ppb, with some zero check values as high as 2 ppb. It was recommended that all SO_2 data for the CN site be systematically adjusted by subtracting the nightly zero check value for the day. SO_2 data for all sites were adjusted based on the nightly zero check as recommended.

- Zero check data for the CE site were generally good, but the nightly zero for CO from March 3 to 16, 2012 was greater than 1.0 ppm. It was recommended that CO data for this period be adjusted by subtracting the nightly zero check value for the day. The data were adjusted as recommended.

- The CN site daily span check data from February 4 to 6, 2012 at the beginning of the Winter Monitoring Season showed the span responses for the NO_x compounds were approximately 15 percent high. It is difficult to determine a corresponding span response DQO from Table B4-1, as was done for the zero response. However, Volume II of the U.S. EPA Quality Assurance Handbook (EPA-454/B-08-003, 2008) states a critical criterion of ±10 percent for QC checks. It was recommended the NO, NO_x, and NO_2 data be adjusted for these three days using a suitable factor based on the nightly span data. These data were adjusted as recommended.

- One-minute BC data obtained from the aethalometer at the AQ site had occasional large negative spikes (-1400 ng/m^3 and lower), which are flagged as invalid. In addition, the response from this aethalometer was found to be inherently much noisier than those at the other sites, particularly for the one-minute data. Figure 4-1 shows one-minute data from late February 2012, indicating that the response is characterized by a periodic high spike followed by a low spike. However, it appears that hourly averages are not significantly affected, since the high and the low spikes tend to offset one another. The time-series plot indicates these fluctuations are potentially caused by the on-off cycling of an air-conditioner. The aethalometer manufacturer, Magee Scientific, has indicated the effect is due to variations in RH of air surrounding the equipment and not due to temperature variations. When the RH is moderately high, the air exiting from the air conditioner will have passed over cold refrigeration coils with a substantially lower humidity level than the general surrounding air. The variations in RH create a very small change in the optical properties of the filter material. This, in turn, is interpreted by the algorithm in the aethalometer as an artifact on the data. The artifact is amplified because the instrument is being operated on a one-minute time-base. Data users were made aware of the potential impacts of RH on the one-minute BC data.

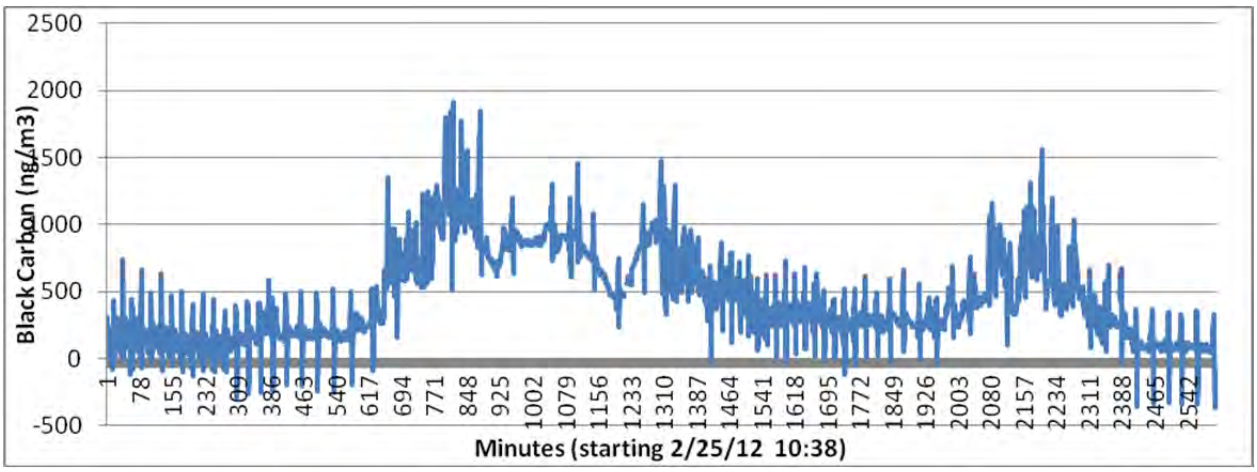

Figure 4-1. Aethalometer One-Minute Data from the AQ Site for a 2600-Minute Period.

- Delta-temperature readings from the two meteorological sites (CE and CS) are quite large, particularly during sunny days. This was especially noticeable at the CS site, where the temperature at the 2-meter level was frequently 5°C higher than at the 10-meter level, and occasionally as much as 6°C higher. The differences between levels during mid-day at the CE site typically were 2°C to 3°C. These high delta-T readings were

likely due to the siting of the 2-meter sensors, which were subject to siting limitations, including proximity to the eastern shelter wall. The location of the 10-meter tower at the CE site may have experienced radiative heating, especially in the morning, as well as decreased ventilation during daytime westerly winds. A possible explanation for the significantly higher daytime readings from the CS site is that the aspirator used at this level was utilizing a 220 volt fan and was operating at only half of the design flow rate. The issue appeared to be limited to the 2-meter temperature readings, as there was good agreement between the 10-meter measurements at the CE and CS sites. It was recommended that the data user carefully review the 2-meter temperature data at the CS site before use. If delta-T is being used for stability estimates, the sigma theta measurements may prove to be more representative. The CS site 2-meter aspirator fan was changed prior to the Summer Monitoring Season during which the CS site delta-T data were more consistent with CE site data, with both sites showing delta-T values typically around 3°C during midday.

Summer Monitoring Season

With one notable exception, the data were essentially complete and provided good representation for the Summer Monitoring Season. SCS Tracer had addressed issues noted in the review of the Winter Monitoring Season data regarding adjustment of data for analyzer zero drift.

NO and NO_x data for the CN site appear to have been significantly affected by zero baseline drift associated with high interior station temperatures. To understand this issue, it is useful to view typical valid data for the study. Figure 4-2 shows an example of raw measurement data for two representative days, August 27 to August 28 at the CE site. CO and SO_2 data, which often are correlated to NOx data, are included for comparison. Note that the large, offscale spikes at the beginning of each day are the result of automatic calibrations checks of the analyzers. The NOx data are characterized by rising NO and NO_x concentrations in the morning, with lower concentrations during the afternoon, which has better mixing. NO and NO_x profiles have a spiky appearance. NO_2 values are defined by available ambient ozone to convert NO to NO_2. This was fairly uniform in the morning, when excess NO was present, but was limited by available ozone. The NO_2 concentrations were essentially equal to NO_x in the afternoon, when there was excess ozone. Data observed at the CN site showed this pattern from July 18 through August 3, 2012.

Figure 4-3 shows CN site raw measurement data for the same two-day period, August 27 to August 28. While the morning activity is similar, data observed in the afternoon were very different. Instead of near-zero readings, NO and NO_x values are consistently high. In addition, these elevated NO values have a very smooth profile. This pattern is consistent with basically near-zero NO concentrations, such as those at the CE site, with the upward baseline drift caused by elevated station temperature resulting in elevated analyzer readings for NO and NO_x. Additionally, strong correlation was observed between maximum ambient temperature (using CE site data as a surrogate, since ambient temperature was not measured at the CN site) and the relative magnitude of this baseline rise. On some days, the baseline drifts were observed to be above 100 ppb.

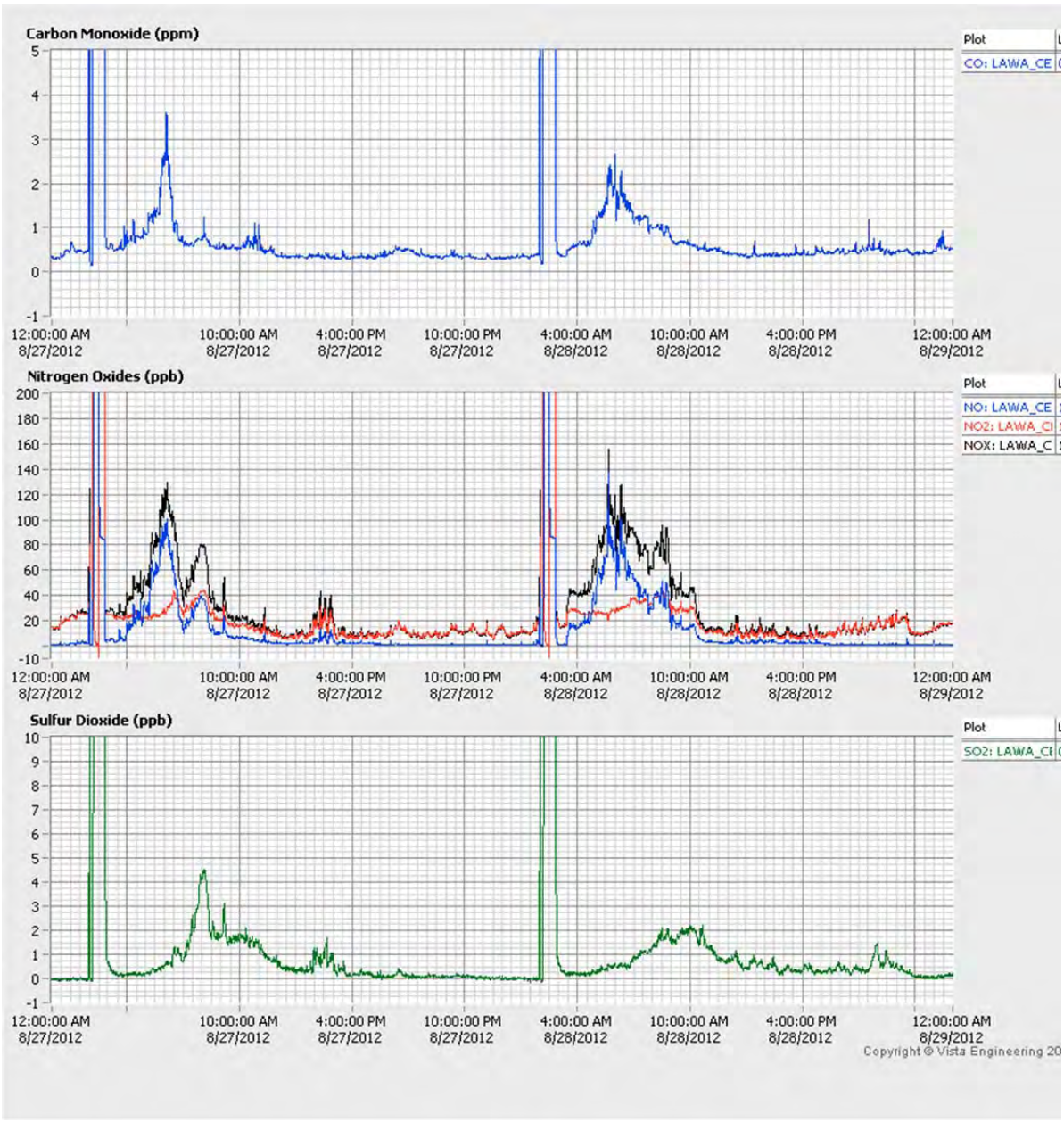

Figure 4-2. Summer Monitoring Season One-Minute Invalidated Gaseous Data from CE Site.

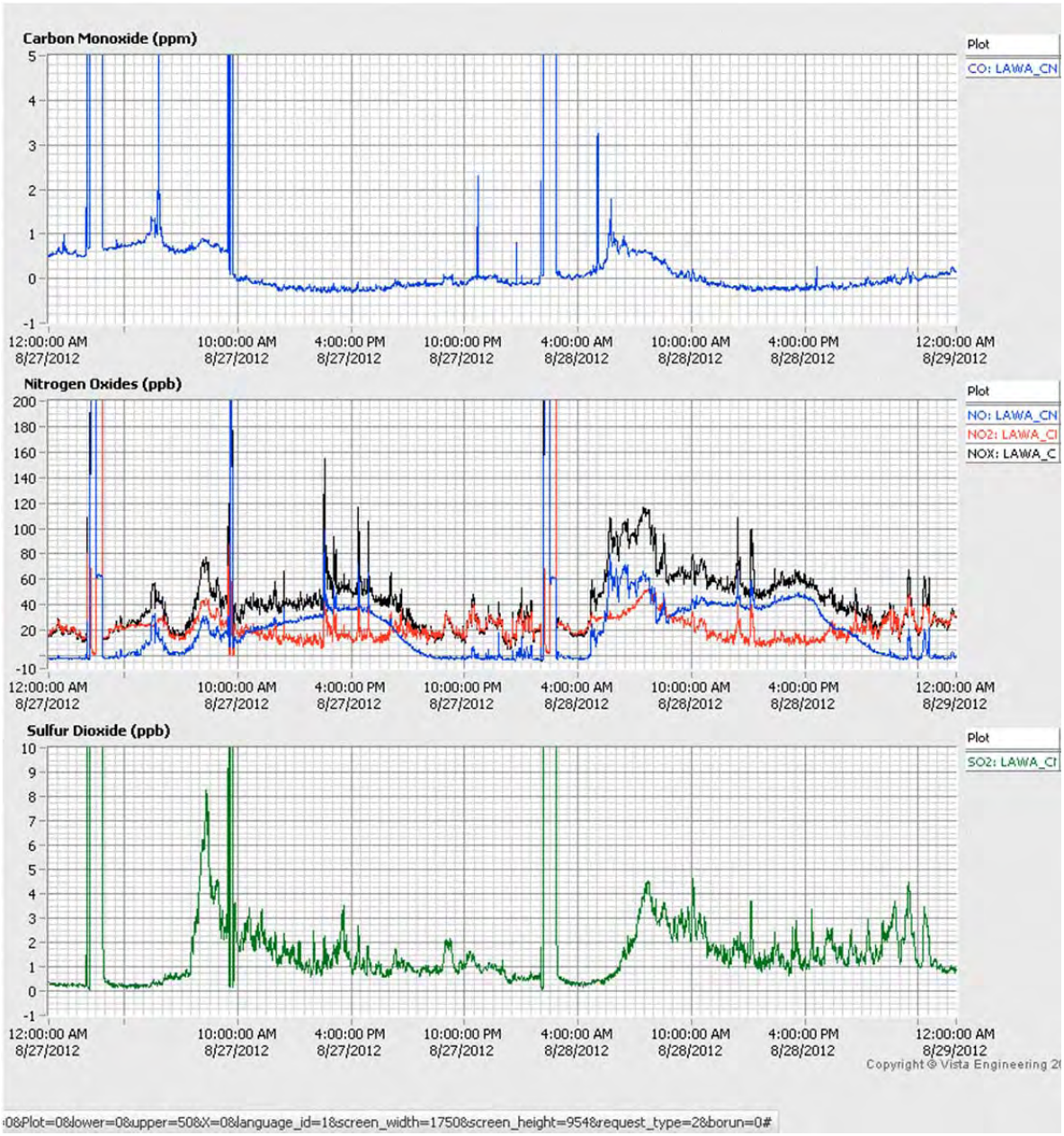

Figure 4-3. Summer Monitoring Season One-Minute Raw Measurement Data from CN Site. Time period is the same as for Figure 4-2.

Figure 4-4 shows the post-monitoring season and calibration data, August 29 and 30, at the CN site. The plot shows that a zero air check was run for approximately one hour mid-day on August 29. SO_2, CO, and NO_2 values all go to zero, but the NO and NO_x readings remain elevated at about 55 ppb. This observation indicated the analyzer had an elevated baseline issue. This check also confirms the NO and NO_x baselines appear to be identical, which means the NO_2 data are likely representative.

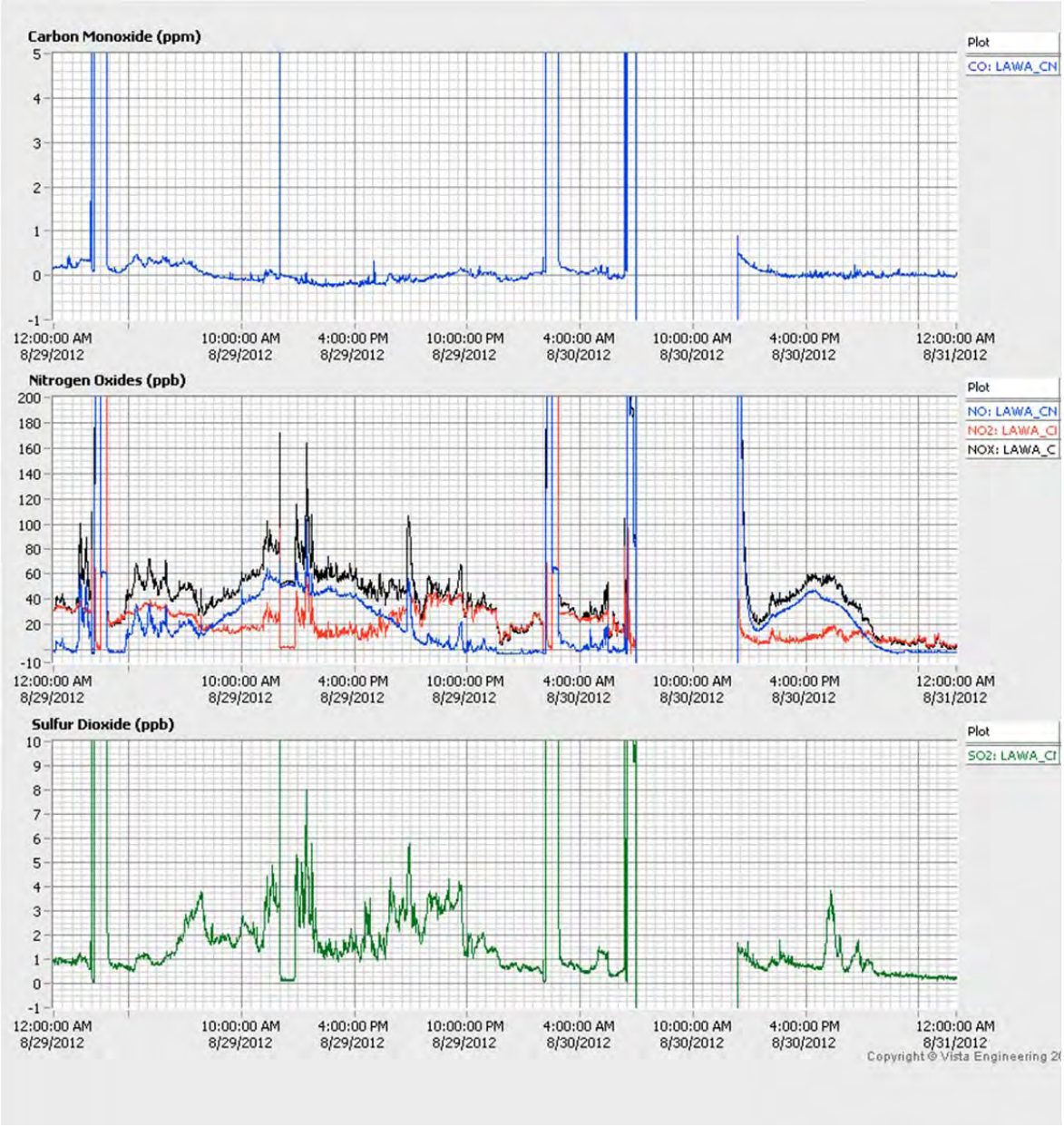

Figure 4-4. Summer Monitoring Season Gaseous Data from the CN Site Showing Zero Check On August 29, 2012.

As previously noted, the problem at the CN site started on August 3, as shown in Figure 4-5. The CO data also appear to be similarly affected, but in the opposite direction with lower values during the daytime. There is an obvious diurnal pattern that becomes more pronounced when the NO pattern also becomes more pronounced. There is a slight decrease in the CO zero response over the course of the hour of zero gas, as seen in Figure 4-3, that occurs when a rise in the NO zero response was observed. However, the change in CO zero response is well within the DQOs stated in the MQAPP.

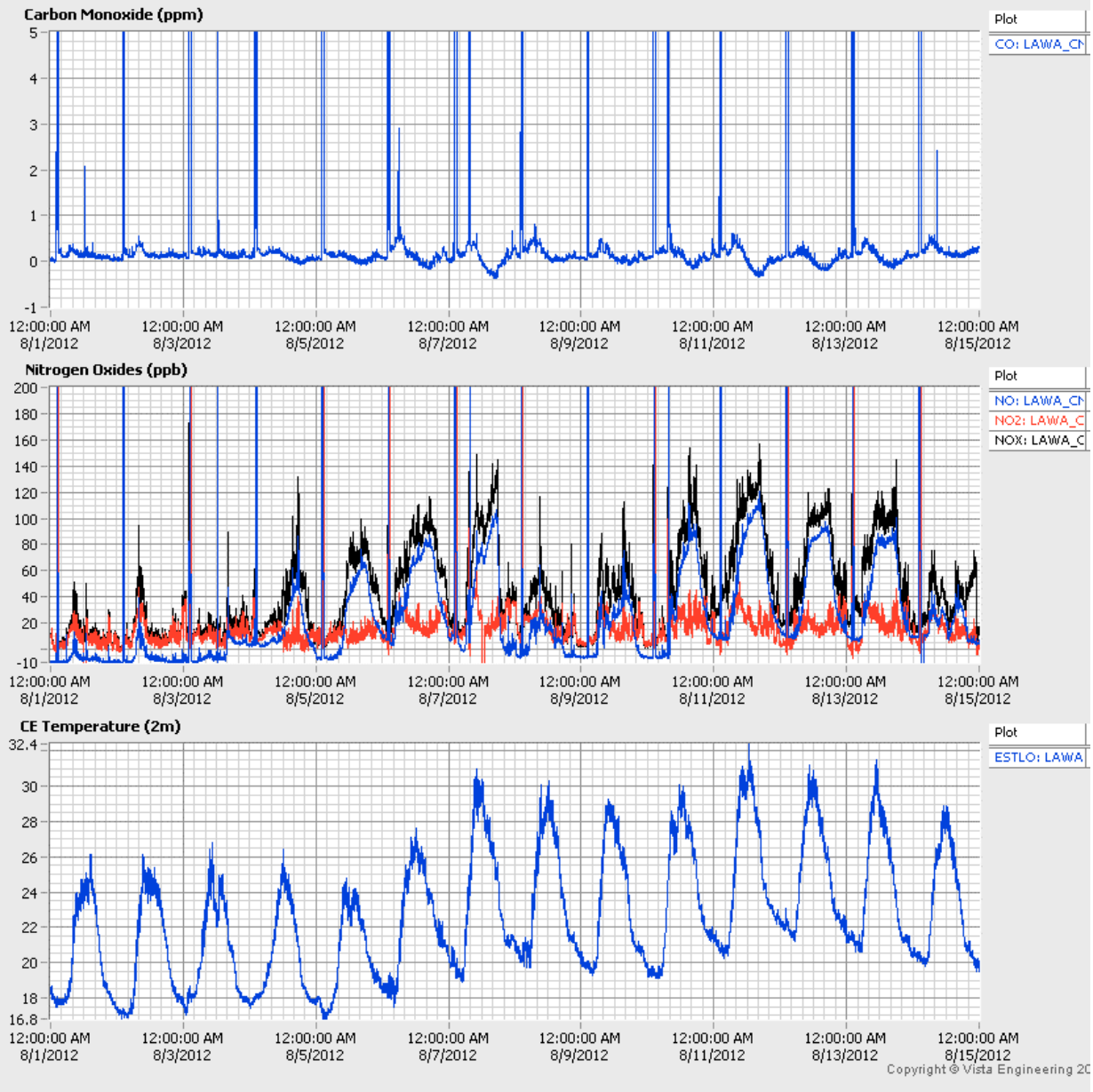

Figure 4-5. Summer Monitoring Season - Two Weeks of NO_x and CO Data from the CN Site. Bottom graph is 2-meter ambient temperature at CE site, demonstrating correlation of increasing baseline drift with increasing temperature.

As a result of the data audit, it was recommended the NO and NO_x data for the CN site be invalidated beginning on August 3, 2012, while the NO_2 data be retained but flagged appropriately to alert data users of the noted issues regarding data quality. The audit noted that, if desired, NO and NO_x data for some night-time and morning hours can potentially be salvaged by determining when the NO baseline is within an acceptable range of zero; however, there is notable day-to-day variation even in the nighttime zero readings (as can be seen in Figure 4-5), so the data user should be aware of the usefulness of such a data set. Based on the data audit recommendation, NO and NO_x data during periods when the baseline drift exceeded the data monitoring objective of ±10 ppb were invalidated by SCS Tracer.

- pDR data at the CE site prior to July 20 were near zero and unusually stable. It was initially thought that this may imply the sampler was not in operation during this period; however, further investigation by SCS Tracer showed no changes in monitoring status and operations over the period, and the data were considered "valid."

- There is an outlier BAM $PM_{2.5}$ value (0.995 mg/m^3) reported for the CS site on August 27 at 09:00 hour. The total flow for this hour is shown as "0", therefore, the value was considered invalid.

- Gaseous pollutant data at the AQ site contain daily zero/span checks conducted at about 03:45 – 04:55. These daily zero/span check data should be removed and flagged as such. In some cases, high NO values were noted when NO_x was reported as "0." These data were supplied by the SCAQMD.[2] Data were reviewed by all data users prior to use.

- As noted in the review of the Winter Monitoring Season data, one-minute BC data obtained from the aethalometer at the AQ site continued to show occasional large negative spikes (-2000 ng/m^3 and lower). The response from this aethalometer is inherently noisy, with variations of ±500 ng/m^3 commonly occurring when looking at the one-minute data. In addition, data from the aethalometer at the CE site showed similar noise during the Summer Monitoring Season, as did the aethalometer at the CS site, although to a lesser extent (~ ±200 ng/m^3). Based on T&B System's review, it appeared that hourly averages were not significantly affected, since the high and the low spikes seem to offset one another. However, the data user was made aware of the unusual noisy one-minute data and took this into account when using the data.

[2] Monitoring data at the AQ station were provided by the SCAQMD during the Study periods. These data were reviewed and invalid data (i.e., data collected during calibration data and outliers) were flagged following SCAQMD QA/QC guideline and were excluded from subsequent data analysis.

APPENDICES

Appendix 4-1 - System Audit Checklist

Appendix 4-2 - Laboratory System Audit Checklist

Appendix 4-3 - Siting and System Records

Appendix 4-4 - Performance Audit Reports – Winter Season

Appendix 4-5 - Performance Audit Reports – Summer Season

Appendix 4-6 - Audit Result Summary

SECTION 4

APPENDICES

(This page is intentionally blank)

Appendix 4-1
System Audit Checklist

(This page is intentionally blank)

T&B SYSTEMS

SITING AND SYSTEM AUDIT FORM

STATE OR PROJECT:

MONITORING ORGANIZATION:

SITE NAME AND LOCATION:

AUDITOR:

DATE:

SITE OPERATOR:

Revision 4.1

(This page is intentionally blank)

I. Parameters Monitored

A. Air Quality

	Parameter	Method	Manufacturer	Model	Serial #	Range	DAS	SOP Date
1								
2								
3								
4								
5								
6								
7								
8								
9								
10								
11								
12								
13								
14								
15								

Data Acquisition Systems (DAS): A – digital, with telemetry; B – analog or digital, downloaded at site; C - stripcharts

(1) B. Meteorological

	Parameter	Method	Manufacturer	Model	Serial #	Range	DAS	SOP Date
1								
2								
3								
4								
5								
6								
7								
8								
9								
10								

Data Acquisition Systems (DAS): A – digital, with telemetry; B – analog or digital, downloaded at site; C - stripcharts

Are there any required parameters that are not monitored?
Are any methods and equipment unacceptable?
Are any operating ranges improper?

Are there any significant differences between instrumentation on site and the monitoring plan?

Comments:

C. Auxiliary Equipment

	Manufacturer	Model	Serial #	Calibration/ Certification Freq.	Last Calibration/ Certification Date
Dilution Calibrator					
O_3 Transfer Standard					
DAS System					
Chart Recorder					
Chart Recorder					
Chart Recorder					
Chart Recorder					
Met Tower					
Monitor Shelter					
Computer					
Power Conditioner					
A/C Unit					
Flow meter					
Bubblemeter					
Cylinder					
Cylinder					
Zero Air System					

(2) D. Station Check Equipment

	Manufacturer	Model	Serial #	Calibration/ Certification Freq.	Last Calibration/ Certification Date
WS Motors					
Compass					
Thermometer					
Psychrometer					
Precipitation Gauge					
Solar Radiation					
Flow Standards					
Miscellaneous					

Comments:

II. Sensor/Probe height and Exposure

A. Air Quality (compare against attached table)

	Response	Meet QAPP and MP (Yes/No)
1. Height of sampling cane above ground		
2. Height of sampling cane above roof		
3. Distance of sampling cane from supporting structures		
4. Distance of sampling cane to obstacles		
5. Arc of unrestricted air flow		
6. Distance to nearest road		
7. Volume of traffic on road		
8. Distance to nearest trees		
9. Height of trees		
10. Distance to nearest possible source		

A. Particulate Samplers (compare against attached table)

	Response	Meet QAPP and MP (Yes/No)
1. Height of samplers above ground		
2. Height of samplers above structure		
3. Distance of samplers from obstruction		
4. Arc of unrestricted air flow		
5. Distance to nearest road		
6. Volume of traffic on road		
7. Distance to nearest trees		
8. Height of trees		
9. Distance to nearest possible source		

Comments:

A. Meteorology

	Response	Meet QAPP and MP (Yes/No)
(3) Wind Sensors		
1. Height of WS sensor above ground		
2. Height of WD sensor above ground		
3. Height of VWS sensor above ground		
4. Distance to nearest obstacle		
5. Is obstacle separation at least 10X obstruction height?		
6. Are instruments on a rooftop?		
7. If so, are instruments 1.5X the height above the roof?		
8. Arc of unrestricted flow?		
(4) Temperature/dew point/RH sensors		
9. Height of temperature sensor above ground		
10. Distance of temperature sensor from obstruction		
11. Height of RH sensor above ground.		
12. Distance of RH sensor from obstruction		
13. Are the sensor distances 4X from obstruction height?		
14. Are sensors shielded/motor aspirated?		
15. Are sensors above representative terrain?		
Additional information		
16. Height of solar radiation above structure		
17. Distance of solar radiation to nearest obstacle		
18. Will solar radiation sensor fall within a shadow?		
19. Are there any significant differences between the on-site equipment and the monitoring plan?		

Comments:

(5) III. Operations

(6) A. Air Quality

	Response	Meet QAPP and MP (Yes/No)
1. Are all analyzers operational?		
2. Is the sampling inlet intact?		
3. Is sampling inlet system and manifold clean?		
4. How often is manifold cleaned?		
5. How is manifold cleaned?		
6. Are unused ports securely plugged?		
7. Is manifold SS, Pyrex or Teflon?		
8. Is a manifold blower required?		
9. Is the manifold blower operational?		
10. Is it in accordance with EPA guidance?		
11. Are all desiccants blue?		
12. Is automatic zero-span operational?		
13. Are all sampling lines Teflon?		
14. Are sample lines clean?		
15. How frequently are sample lines replaced?		
16. Are the autocalibration responses stable?		
17. Are calibration cylinders present?		
18. Has the cylinder been certified within 24 months?		
19. Who certifies cylinders?		
20. Are the cylinders properly secured?		
21. Are flow rates for analyzers normal?		
22. Are analyzer filter holders intact?		
23. How often are inlet filters changed?		
24. Are EPA stickers on all Criteria Samplers?		
25. Are the chart traces clear and readable?		
26. Are all chart recorders times correct?		
27. Is DAS operational?		
28. Is the printer functional?		
29. Is hard copy available?		
30. Are precision checks performed at least biweekly?		
31. Overall, is the site well maintained?		
32. Please provide data logger software version.		

Comments:

(7) B. Meteorology

	Response	Meet QAPP and MP (Yes/No)
1. Are all WS, WD sensors operational?		
2. Is the temp probe and aspirator operational?		
3. Is the Dew pt/RH probe and aspirator operational?		
4. Is solar radiation sensor operational?		
5. Is met tower perpendicular to the ground?		
6. Are all cables secured?		
7. Are connections clean and rust-free?		
8. Are vanes/cups/propellers intact?		
9. Are S/Ns available?		
10. Are WS/WD bearings free?		
11. Are the chart traces clear?		
12. Are all chart recorders times correct?		
13. Is DAS operational?		
14. Are the sigma values being collected?		
15. Sigma averaging periods?		
16. Are vector values being collected?		
17. Are scalar WS/WD values being collected?		
18. Is the printer functional?		
19. Is hard copy available?		
20. Are torque tests being performed on WS and WD sensors?		
21. Overall, is the site well maintained?		
22. Are met calibrations performed every six months?		

(8) C. Auxiliary Equipment

	Response	Meet QAPP and MP (Yes/No)
1. Is the A/C unit operational?		
2. Is the station temperature system operational?		
3. Is site temperature recorded on chart?		
4. Is site temperature maintained at 20-30 deg. C?		
5. Is site clean?		
6. Does modem work?		
7. Does telephone work?		
8. Is the site secure?		
9. Overall, is auxiliary equipment well maintained?		

Comments:

(9) D. Station Check Procedures and Documentation

	Response	Meet QAPP and MP (Yes/No)
1. Are the station logs present?		
2. Are the station logs up to date?		
3. Are station logs detailed?		
4. Are routine checklists used?		
5. Are the routine checklists detailed?		
6. Are the calibration forms present?		
7. Are the calibration forms detailed?		
8. Are zero/span/calibration criteria documented?		
9. Are instrument adjustment procedures well defined?		
10. Are all adjustments performed after required precision checks?		
11. Are SOPs present?		
12. Is the Quality Assurance Project Plan present?		
13. Are the analyzer/sensor manuals present?		
14. Is the site technician well trained?		
15. How frequently is the site visited?		
16. Are correct source values listed?		
17. Are certification forms for cylinders present?		
18. Are the strip charts annotated each visit?		
19. Are charts annotated with date and time?		

Comments:

Please provide the frequency of calibration for the following:

	Calibration	Precision Freq / Level	Level I Freq / Level	Acceptance Criteria	Last Cal. Date
Air quality analyzers					
Meteorological sensors					
Particulate samplers					
Site temperature					

Comments:

(10) E. Chain of Custody

1. Review paper work for chain of custody from field to data processing.
   Comments:

2. How are data stored?

3. How often is the data logger dumped?

Comments:

(11)IV. Preventive Maintenance

	Response	Meet QAPP and MP (Yes/No)
1. Is preventive maintenance discussed in the QA plan or SOPs?		
2. Is preventative maintenance being performed on all parameters?		
3. Are field operators given special training for preventive maintenance?		
4. Is the training reinforced?		
5. Please provide preventative maintenance worksheets and paperwork. Is this acceptable?		
6. Are control charts implemented?		
7. Are tools and spare parts adequate?		
8. Are preventative maintenance logbooks maintained?		
9. How often are they reviewed?		
10. By whom?		

Comments:

(12)V. Overall Comments

	Response	Meet QAPP and MP (Yes/No)
1. Overall, is the station well maintained?		
2. Overall, is the data quality good?		
3. Are QA/QC maintained?		
4. Is site and equipment in good working order?		
5. Overall, is the site tech well trained?		
6. Overall, do meteorological patterns agree with topography?		
7. Are the meteorological readings reasonable for large-scale meteorological patterns?		
8. Are the ambient readings reasonable for large-scale meteorological patterns?		
9. Does inlet and sensor exposure correspond with the type of monitoring performed? (i.e. Micro, Middle, Neighborhood, Urban, or Regional?)		
10. Is the station well sited? If not, why?		

Comments:

Pollutant	Scale (maximum monitoring path length, meters)	Height from ground to probe or 80% of monitoring path [A] (meters)	Horizontal and vertical distance from supporting structures to probe or 90%[B] monitoring path [A] (meters)	Distance from trees to probe of monitoring path [A] (meters)
SO_2 (C, D, E, F)	Middle (300m), Neighborhood, Urban, and Regional (1 km)	3 – 15	>1	>10
CO (D, E, G)	Micro; Middle (300m), Neighborhood (1 km)	3 ± 0.5 (micro); 3 – 15 (all others)	>1	>10
O_3 (C, D, E)	Middle (300m), Neighborhood, Urban, and Regional (1 km)	3 – 15	>1	>10
Ozone precursors for (PAMS) (C, D, E)	Neighborhood, and Urban (1 km)	3 – 15	>1	>10
NO_2 (C, D, E)	Middle (300m), Neighborhood, and Urban (1 km)	3 – 15	>1	>10
Pb (C, D, E, F, H)	Micro, Middle, Neighborhood, Urban, and Regional (1 km)	2-7 (micro); 2-15 (all other scales)	>2 (all scales, horizontal distance only)	>10 (all scales)
PM_{10} (C, D, E, F, H)	Micro, Middle, Neighborhood, Urban, and Regional	2-7 (micro); 2-15 (all other scales)	>2 (all scales, horizontal distance only)	>10 (all scales)
$PM_{2.5}$ (C, D, E, F, H, I)	Micro, Middle, Neighborhood, Urban, and Regional	2-7 (micro); 2-15 (all other scales)	>2 (all scales, horizontal distance only)	>10 (all scales)

A - Monitoring Path for open path analyzers is applicable only to middle or neighborhood scale CO monitoring and all applicable scales for monitoring SO_2, O_3, O_3 precursors, and NO.
B - When probe is located on a rooftop, this separation distance is in reference to walls, parapets, or penthouses located on roof.
C - Should be > 20 meters from the dripline of tree(s) and must be 10 meters from the dripline when the trees (s) act as an obstruction.
D - Distance from sampler, probe, or 90% of monitoring path to obstacle, such as a building, must be at least twice the height the obstacle protrudes above the sampler, probe or monitoring path. Sites not meeting this criterion may be classified as middle scale.
E - Must have unrestricted air flow 270 around probe or sampler; 180 if the probe is on the side of a building
F - The Probe, sampler, or monitoring path should be away from minor sources, such as a furnace or incineration flues. The separation distance is dependent on the height of the minor source's emission point (such as a flue), the type of fuel or waste bed, and the quality of fuel (sulfur, ash, or lead content). This criterion is designed to avoid undue influences from minor sources.
G - For microscale CO monitoring sites, he probe must be >10 meters from a street intersection and preferably at a midblock location.
H - For collocated Pb and PM-10 samplers, a 2-4 meter separation distance between collocated samplers must be met.
I - For collocated PM-2.5 samplers, a 1-4 meter separation distance between collocated samplers must be met.

B. Minimum separation distance in meters between roadways and probes or monitoring paths at various scales.

Roadway ave. daily traffic vehicles per day	**O_3** Neighbor. & Urban	**NO_2** Neighbor. & Urban	**(13) CO** Neighbor.	**(14) Pb** Micro	**(15) Pb** Middle	**(16) Pb** Neighbor., Urban, Reg.	**(17) PAMS**
≤10,000	10	10	10	5-15	>15-50	>50	>10
15,000	20	20	25				20
20,000	30	30	45	5-15	>15-75	>75	30
30,000			80				
≥40,000				5-15	>15-100	>100	
40,000	50	50	115				50
50,000			135				
≥60,000			150				
70,000	100	100					100
≥110,000	250	250					250

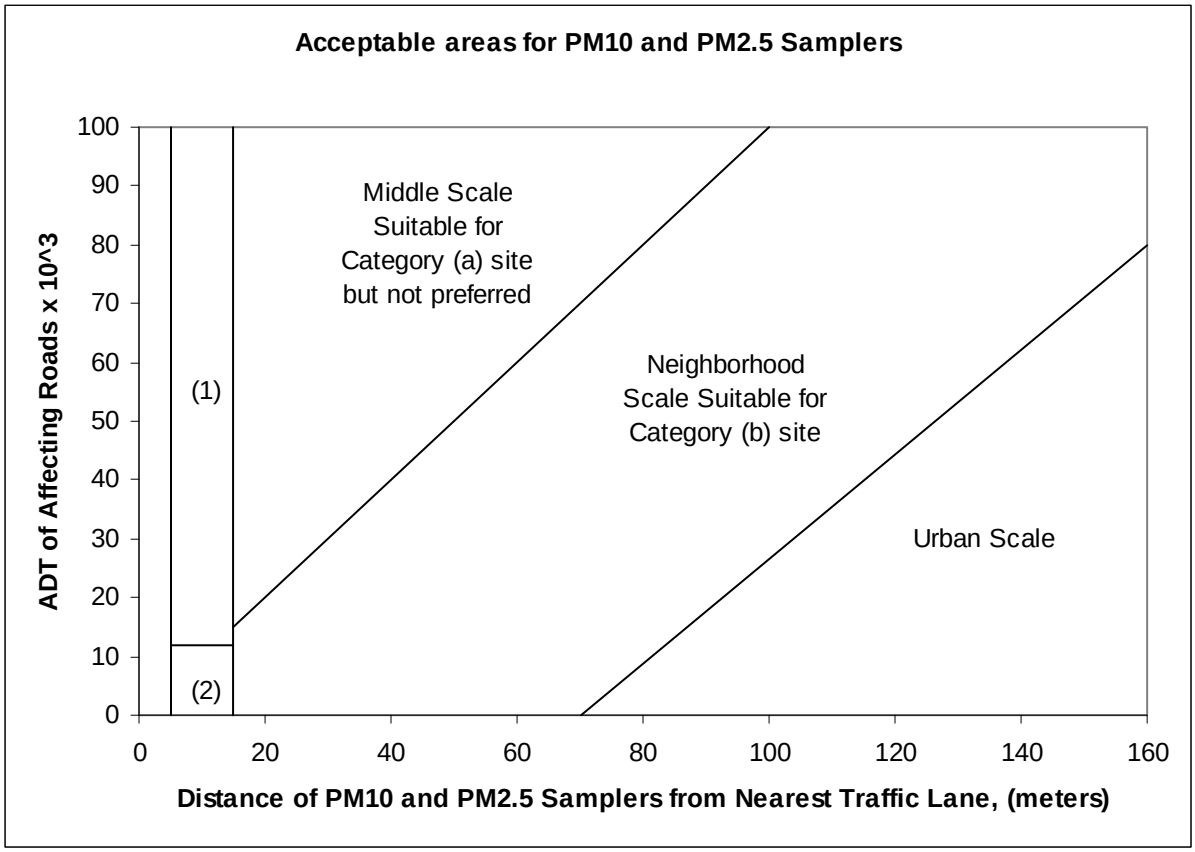

(1) Preferred area for Category (a) site microscale if monitor is 2 – 7 meters high, middle scale otherwise.
(2) Not Category (a) sites

Appendix 4-2
Laboratory System Audit Checklist

(This page is intentionally blank)

LABORATORY SYSTEMS AUDIT

AUDIT LOCATION:

AUDIT DATE:

AUDITOR: David Bush

(This page is intentionally blank)

Laboratory System Audit
Page 1

A. Measurement Program: Laboratory understanding of project goals, including sample collection and analysis

1. Number of samples to be processed (per month, year or project, as appropriate)
2. Type of sample media
3. Method of analysis
4. Reporting frequency

B. Organization

1. Provide an organizational chart.
2. Is the QA/QC plan fully implemented?
3. Is the QA/QC plan, monitoring plan, and all SOPs available to the staff? Provide the laboratory copy.
4. Provide the names of the following personnel:

   Organization director

   QA manager

   QC manager

   Sample clerk

   Lab supervisor

   Data management

   Report supervisor

C. Training and Qualifications

1. What is the general awareness of the project sampling plan?
2. What training is provided for project staff?
3. Is training documented?
4. Is the staff sufficiently qualified and trained to perform the work? (Provide education, work experience and training for each project staff member.)

D. SOPS and Workplans

1. Does the laboratory have SOPs? .
2. Does the laboratory have a QA/QC plan? *Yes* Is it current?

E. Instrumentation

1. What instrumentation is used for sample processing? (Include extraction apparatus, sample loaders, chromatograph columns, electronic processors and integrators and post analysis processors and software.)

F. Sample Preparation and Analysis

1. Briefly describe the sample preparation and analysis steps. Include sample media preparation prior to sampling, sample media work-up for analysis and the sample analysis.

G. Standards

1. Are laboratory grade chemicals used?
2. Are all chemicals clearly marked with dates and concentrations?
3. Are pure standard materials used?
4. Describe the secondary dilution standards setup.
5. Are all chemicals stored in a safe manner? Are hoods available?
6. Are standards for GC/MS/AA bought from a vendor? Provide complete traceability documentation for the last year. Are all standards acceptable?
7. If standards are made, show all calibration documentation. Are all standards acceptable?
8. Are standard Methods available and used for all lab techniques? If not, what references are available*? .*
9. Water supply: Describe the system to produce pure water and the water purity criteria. Is the system adequate?

H. QA/QC

1. What is the frequency of duplicates, blanks, standards, and spikes? Show all QC/QA documentation.
2. Describe lab blank analysis.
3. Explain acceptance/nonacceptance limits.
4. How does lab use spike data?
5. Explain acceptable percent recovery and precision.
6. How are upper and lower control limits derived?
7. Are upper and lower control limit charts used?
8. Are the UCL/LCL limits R+/-3s?
9. How does the lab define and calculate accuracy (R +/-S)?
10. How are MDLs calculated? Describe in detail. *.*
11. Explain duplicate data analysis.
12. Does lab use NIST-SRMs? If no, please provide all traceability documentation for last year.
13. Provide calibration levels.
14. Are they in normal ambient range?

15. Overall, how is the QC?
16. Is the lab clean? Are records in good order? Are calibration data accessible?
17. Are all personnel competent? *Yes.* Knowledgeable?
18. Are QA/QC plan, manual, and handbooks accessible? .
19. Explain the QA manager's duties.
20. Is there a QA/QC implementation plan?
21. Are QA/QC internal audits performed? How often? Please provide a copy.
22. Have the problems in the internal audit report been resolved? If not, why?
23. Has a systems audit been performed? When? Have the problems in the report been resolved? If not, why?
24. Are OSHA regulations concerning handling of chemicals used throughout the lab?
25. Are NIOSH/MESA approved gas respirators available?
26. Are all samples iced or refrigerated?
27. Are all bottles sealed with minimal bubbles?
28. How often are Tenax traps, Methyl silicone packing, or silica gel cleaned or replaced?
29. Is TFE plastic tubing used in all lines?
30. Are field reagent blanks prepared from reagent water and carried through sampling and handling protocol?
31. Does the state audit this facility? If so, please provide the documentation.
32. Are state-certified standards tested in this lab? . Please provide the most recent results.
33. Does the lab participate in EPA interlaboratory testing? Please provide the results.
34. How many internal calibration points are used for the daily calibrations?
35. Please provide the last five calibration curves.
36. Are any of the last five calibration points beyond +/- 10% from the source value? Were new standards made?

I. Sample Custody

1. How do the samples reach the sample custodian (how does the lab insure that the samples are not mishandled by their shipping and receiving department?)
2. How does the laboratory custodian check in the samples and compare to the chain of custody?

3. Are the samples kept in a secure area?
4. Who has access to the samples? (Who has a key to the sample refrigerator/sample vault?) .
5. Describe sample login procedure.
6. Are all samples assigned login numbers with the date?
7. Trace a sample through the lab.
8. Are all raw results kept in bound log books?
9. Explain how reported values are transformed from raw data.
10. Do the raw data log books include:
    - equipment used -
    - daily calibrations -
    - maintenance -
    - blanks -
    - spikes -
    - duplicates -
    - QA samples -
    - Initials -
11. How are log books archived? How long?
12. Show chain of custody forms. Do they travel with the sample?
13. Overall, discuss the operation.
14. Are the procedures congruent with the QA/QC plan?

J. Preventive Maintenance

1. Who is responsible for preventive maintenance? Please provide a copy of the preventive maintenance schedule.

K. Equipment Testing and General Maintenance

1. Explain in detail the new equipment testing procedures.
2. Show documentation.
3. Briefly describe inventory system.

L. Overall Comments

Appendix 4-3
Siting and System Records

AUDIT RECORD

SITING and SYSTEM

T&B Systems
26074 Avenue Hall Unit 9
Valencia, CA 91355
(661) 294-1103

Date: **2/1/12 and 2/21/12**
Auditor: **D. Bush/R. Baxter**

Site name: **CE**
Project: **LAX AQSAS**

Ind. Site Location
Latitude (°): **33.93751**
Longitude (°): **-118.36185**

Audit Site Location
Latitude (°): **33.93742**
Longitude (°): **-118.36185**

Difference
Latitude (°): **0.00009**
Longitude (°): **0.00000**
Approximate Distance (m): **10**

North

East

South

West

Comments: Palm trees adjacent to the site could influence the measurements. The tower was not completely vertical, tilting by 1 to 2°. The lower temperature sensor was at 3.3m and was moved to 2m. Ground mounted sampers had the inlets just at the security fence height. While at breathing height, the flow may be blocked by the screening. The inlets were not mounted higher for security reasons.

AUDIT RECORD

SITING and SYSTEM

T&B Systems
26074 Avenue Hall Unit 9
Valencia, CA 91355
(661) 294-1103

Date: **2/2/12**
Auditor: **D. Bush/R. Baxter**

Site name: **CS**
Project: **LAX AQSAS**

Ind. Site Location
Latitude (°): **33.92952**
Longitude (°): **-118.40951**

Audit Site Location
Latitude (°): **33.92948**
Longitude (°): **-118.40951**

Difference
Latitude (°): **0.00004**
Longitude (°): **0.00000**
Approximate Distance (m): **4**

North

East

South

West

Comments: Reasonable exposure for air quality but with some blockage of flow for the wind sensor when the wind is from the southwest. Ground mounted samplers may be shielded from general air flow but are at that height (at the fence top) for security reasons. The lower temperature sensor was moved to 2m following the audit.

AUDIT RECORD

SITING and SYSTEM

T&B Systems
26074 Avenue Hall Unit 9
Valencia, CA 91355
(661) 294-1103

Date: **2/21/12**
Auditor: **D. Bush/R. Baxter**

Site name: **CN**
Project: **LAX AQSAS**

Ind. Site Location
Latitude (°): **33.95066**
Longitude (°): **-118.38422**

Audit Site Location
Latitude (°): **33.95057**
Longitude (°): **-118.38429**

Difference
Latitude (°): **0.00009**
Longitude (°): **0.00007**
Approximate Distance (m): **12**

North

East

South

West

Comments: Well sited with good exposure. Ground mounted samplers may be shielded from general air flow but are at that height (at the fence top) for security reasons.

AUDIT RECORD

SITING and SYSTEM

T&B Systems
26074 Avenue Hall Unit 9
Valencia, CA 91355
(661) 294-1103

Date: **2/2/12**
Auditor: **D. Bush/R. Baxter**

Site name: **AQ**
Project: **LAX AQSAS**

Ind. Site Location
Latitude (°): **33.95511**
Longitude (°): **-118.43041**

Audit Site Location
Latitude (°): **33.95509**
Longitude (°): **-118.43043**

Difference
Latitude (°): **0.00002**
Longitude (°): **0.00002**
Approximate Distance (m): **3**

North

East

South

West

Comments: Well sited with good exposure.

AUDIT RECORD

SITING and SYSTEM

T&B Systems
26074 Avenue Hall Unit 9
Valencia, CA 91355
(661) 294-1103

Date: **2/21/12**
Auditor: **R. Baxter**

Site name: **CE2**
Project: **LAX AQSAS**

Ind. Site Location
Latitude (°): **33.90338**
Longitude (°): **-118.34780**

Audit Site Location
Latitude (°): **33.90340**
Longitude (°): **-118.34779**

Difference
Latitude (°): **-0.00002**
Longitude (°): **-0.00001**
Approximate Distance (m): **2**

North

East

South

West

Comments: Good exposure to the surrounding community with some trees surrounding the site.

AUDIT RECORD

SITING and SYSTEM

T&B Systems
26074 Avenue Hall Unit 9
Valencia, CA 91355
(661) 294-1103

Date: **2/21/12**
Auditor: **R. Baxter**

Site name: **CS2**
Project: **LAX AQSAS**

Ind. Site Location
Latitude (°): **33.92379**
Longitude (°): **-118.41018**

Audit Site Location
Latitude (°): **33.92381**
Longitude (°): **-118.41018**

Difference
Latitude (°): **-0.00002**
Longitude (°): **0.00000**
Approximate Distance (m): **2**

North

East

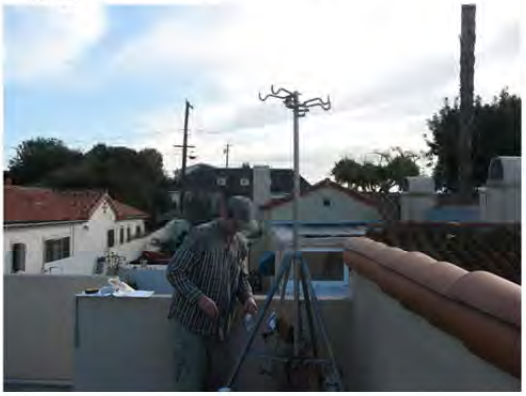

South

West

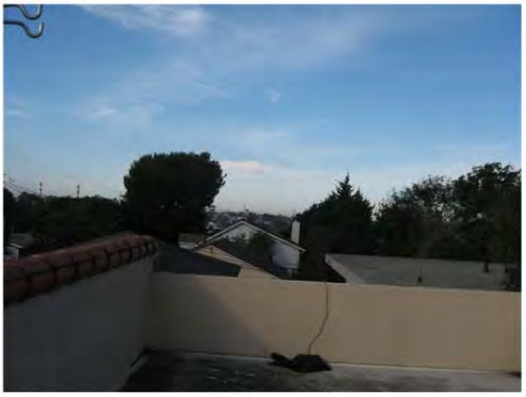

Comments: Good expsure to the surrounding community.

AUDIT RECORD

SITING and SYSTEM

T&B Systems
26074 Avenue Hall Unit 9
Valencia, CA 91355
(661) 294-1103

Date: **2/21/12**
Auditor: **R. Baxter**

Site name: **CN2**
Project: **LAX AQSAS**

Ind. Site Location
Latitude (°): **33.96504**
Longitude (°): **-118.40097**

Audit Site Location
Latitude (°): **33.96505**
Longitude (°): **-118.40097**

Difference
Latitude (°): **-0.00001**
Longitude (°): **0.00000**
Approximate Distance (m): **1**

North

East

South

West

Comments: Tall trees and vegetation surround the site, but it is representative of the surrounding community. Sampler may get tree pollen in the sample during west winds.

AUDIT RECORD

SITING and SYSTEM

T&B Systems
26074 Avenue Hall Unit 9
Valencia, CA 91355
(661) 294-1103

Date: **2/21/12**
Auditor: **R. Baxter**

Site name: **UW**
Project: **LAX AQSAS**

Ind. Site Location
Latitude (°): **33.94420**
Longitude (°): **-118.44100**

Audit Site Location
Latitude (°): **33.94415**
Longitude (°): **-118.44105**

Difference
Latitude (°): **0.00005**
Longitude (°): **0.00005**
Approximate Distance (m): **8**

North

East

South

West

Comments: Exposure is good.

AUDIT RECORD

SITING and SYSTEM

T&B Systems
26074 Avenue Hall Unit 9
Valencia, CA 91355
(661) 294-1103

Date: **2/21/12**
Auditor: **R. Baxter**

Site name: **BN**
Project: **LAX AQSAS**

Ind. Site Location
Latitude (°): **33.95392**
Longitude (°): **-118.40766**

Audit Site Location
Latitude (°): **33.95404**
Longitude (°): **-118.40764**

Difference
Latitude (°): **-0.00012**
Longitude (°): **-0.00002**
Approximate Distance (m): **13**

North

East

South

West

Comments: Exposure is good.

AUDIT RECORD

SITING and SYSTEM

T&B Systems
26074 Avenue Hall Unit 9
Valencia, CA 91355
(661) 294-1103

Date: **2/2/12**
Auditor: **R. Baxter**

Site name: **BS**
Project: **LAX AQSAS**

Ind. Site Location
Latitude (°): **33.93198**
Longitude (°): **-118.40013**

Audit Site Location
Latitude (°): **33.93200**
Longitude (°): **-118.40014**

Difference
Latitude (°): **-0.00002**
Longitude (°): **0.00001**
Approximate Distance (m): **2**

North

East

South

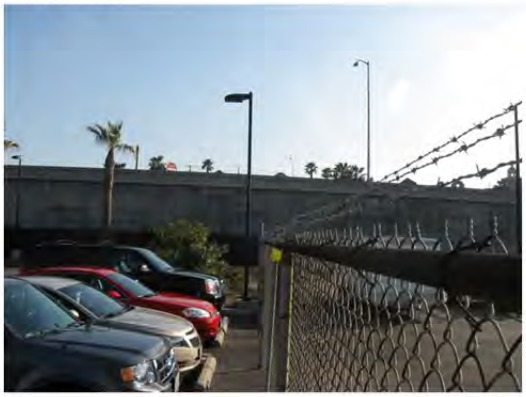

West

Comments: Exposure is good.

AUDIT RECORD

SITING and SYSTEM

T&B Systems
26074 Avenue Hall Unit 9
Valencia, CA 91355
(661) 294-1103

Date: **2/21/12**
Auditor: **R. Baxter**

Site name: **SRE**
Project: **LAX AQSAS**

Ind. Site Location
Latitude (°): **33.93997**
Longitude (°): **-118.37882**

Audit Site Location
Latitude (°): **33.94023**
Longitude (°): **-118.37876**

Difference
Latitude (°): **-0.00026**
Longitude (°): **-0.00006**
Approximate Distance (m): **28**

North

East

South

West

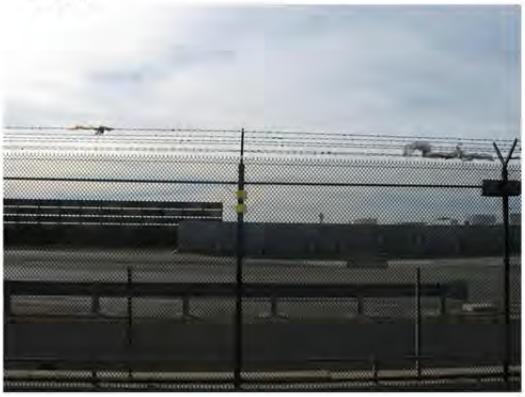

Comments: Exposure is good but the lat/lon differed from the audit values. The operator should verify the site coordinates.

AUDIT RECORD

SITING and SYSTEM

T&B Systems
26074 Avenue Hall Unit 9
Valencia, CA 91355
(661) 294-1103

Date: **2/21/12**
Auditor: **R. Baxter**

Site name: **SRN**
Project: **LAX AQSAS**

Ind. Site Location
Latitude (°): **33.94523**
Longitude (°): **-118.37893**

Audit Site Location
Latitude (°): **33.94523**
Longitude (°): **-118.37890**

Difference
Latitude (°): **0.00000**
Longitude (°): **-0.00003**
Approximate Distance (m): **3**

North

East

South

West

Comments: Exposure is good and at a very busy intersection.

AUDIT RECORD

SITING and SYSTEM

T&B Systems
26074 Avenue Hall Unit 9
Valencia, CA 91355
(661) 294-1103

Date: **2/2/12**
Auditor: **R. Baxter**

Site name: **BSR**
Project: **LAX AQSAS**

Ind. Site Location
Latitude (°): **33.93911**
Longitude (°): **-118.37187**

Audit Site Location
Latitude (°): **33.93929**
Longitude (°): **-118.37187**

Difference
Latitude (°): **-0.00018**
Longitude (°): **0.00000**
Approximate Distance (m): **19**

North

East

South

West

Comments: Exposure is good. The reported lat/lon appeared slightly different from the audit values and should be rechecked by the operator.

AUDIT RECORD

SITING and SYSTEM

T&B Systems
26074 Avenue Hall Unit 9
Valencia, CA 91355
(661) 294-1103

Date: **2/21/12**
Auditor: **R. Baxter**

Site name: **NR**
Project: **LAX AQSAS**

Ind. Site Location
Latitude (°): **33.95034**
Longitude (°): **-118.39762**

Audit Site Location
Latitude (°): **33.95034**
Longitude (°): **-118.39791**

Difference
Latitude (°): **0.00000**
Longitude (°): **0.00029**
Approximate Distance (m): **31**

North

East

South

West

Comments: The latitude/longitude should be verified by the operator as it differed from the audit location. Exposure at the location was good.

AUDIT RECORD

SITING and SYSTEM

T&B Systems
26074 Avenue Hall Unit 9
Valencia, CA 91355
(661) 294-1103

Date: **2/21/12**
Auditor: **R. Baxter**

Site name: **BNR**
Project: **LAX AQSAS**

Ind. Site Location
Latitude (°): **33.95037**
Longitude (°): **-118.39094**

Audit Site Location
Latitude (°): **33.95115**
Longitude (°): **-118.39093**

Difference
Latitude (°): **-0.00078**
Longitude (°): **-0.00001**
Approximate Distance (m): **83**

North

East

South

West

Comments: Appears that the site lat/lon my be off and has been identified in the adjacent parking lot. This should be verified by the operator. Exposure is good.

AUDIT RECORD

SITING and SYSTEM

T&B Systems
26074 Avenue Hall Unit 9
Valencia, CA 91355
(661) 294-1103

Date: **2/21/12**
Auditor: **R. Baxter**

Site name: **CT**
Project: **LAX AQSAS**

Ind. Site Location
Latitude (°): **33.94400**
Longitude (°): **-118.40710**

Audit Site Location
Latitude (°): **33.94398**
Longitude (°): **-118.40717**

Difference
Latitude (°): **0.00001**
Longitude (°): **0.00007**
Approximate Distance (m): **8**

North

East

South

West

Comments: Good exposure. At the time of the audit with the change of samples there were badges that either fell out of the sampler housing or were knocked out of the housing. Modifications were made to assure the samples would not fall out of the housing.

AUDIT RECORD

SITING and SYSTEM

T&B Systems
26074 Avenue Hall Unit 9
Valencia, CA 91355
(661) 294-1103

Date: **2/21/12**
Auditor: **R. Baxter**

Site name: **R405**
Project: **LAX AQSAS**

Ind. Site Location
Latitude (°): **33.95506**
Longitude (°): **-118.36896**

Audit Site Location
Latitude (°): **33.95506**
Longitude (°): **-118.36891**

Difference
Latitude (°): **0.00000**
Longitude (°): **-0.00005**
Approximate Distance (m): **5**

North

East

South

West

Comments: Site located at the closed bridge over the 405 freeway.

AUDIT RECORD

SITING and SYSTEM

T&B Systems
26074 Avenue Hall Unit 9
Valencia, CA 91355
(661) 294-1103

Date: **7/30/12**
Auditor: **R. Baxter**

Site name: **BSR1**
Project: **LAX AQSAS**

Ind. Site Location
Latitude (°): **33.93852**
Longitude (°): **-118.37322**

Audit Site Location
Latitude (°): **33.93851**
Longitude (°): **-118.37321**

Difference
Latitude (°): **0.00001**
Longitude (°): **-0.00001**
Approximate Distance (m): **2**

North

East

South

West

Comments: Exposure is good. This site was moved for the summer study due to the additional activity at the original BSR site.

(This page is intentionally blank)

Appendix 4-4
Performance Audit Reports – Winter Season

(This page is intentionally blank)

AUDIT RECORD

NITRIC OXIDE

T & B Systems
26074 Avenue Hall Unit 9
Valencia, CA 91355
(661) 294-1103

Date: **02/01/12**
Start: **08:45 PST**
Finish: **13:00 PST**
Auditor: **David Gemmill / David Bush**
Witness: **Paul Schafer**

Site Name: **Community East**
Operator: **SCS Tracer**
Project: **LAWA**

Analyzer make: **TEI**
Serial No.: **1136151039**
Sample flow: **0.65 lpm**
Range: **0.5** **PPM**

Model: **42i**
Filter: **Bi-Weekly**
Span setting: **1.002**
Zero setting: **1.8**
Last Calibrated: **01/31/12**

NO Audit Point	PPM Input (X)	PPM DAS (Y)	PPM Dif (%)
1	0.000	0.002	
2	0.030	0.030	0.0
3	0.070	0.070	0.0
4	0.119	0.119	0.0
5	0.221	0.224	1.4
6	0.397	0.402	1.3

Linear Regression: (Y=PPM Corrected, X=PPM Input)

Audit Statisitics	
Slope:	1.011
Intercept:	0.000
Correlation:	1.0000

Comments: None.

Audit Equipment	Make	Model	ID	Certification Date
Dilution System:	API	M700EU	58	12/4/11
Zero Air System:	CSI	205	974830001	NA
Calibration Gas:	SMI	Multi	JJ8550	04/22/10

AUDIT RECORD

OXIDES OF NITROGEN

T&B Systems
26074 Avenue Hall Unit 9
Valencia, CA 91355
(661) 294-1103

Date: **02/01/12**
Start: **08:45 PST**
Finish: **13:00 PST**
Auditor: **David Gemmill / David Bush**
Witness: **Paul Schafer**

Site Name: **Community East**
Organization: **SCS Tracer**
Project: **LAWA**

Analyzer make: **TEI**
Serial No.: **1136151039**
Sample flow: **0.65 lpm**
Range: **0.5** **PPM**

Model: **42i**
Filter: **Bi-Weekly**
Span setting: **0.008**
Zero setting: **2.3**
Last cal.: **01/31/12**

NO_X Audit Point	PPM Input (X)	PPM DAS (Y)	PPM Dif (%)
1	0.000	0.001	
2	0.030	0.030	0.0
3	0.069	0.070	1.4
4	0.118	0.119	0.8
5	0.221	0.224	1.4
6	0.397	0.401	1.0

Linear Regression: (Y=PPM Corrected, X=PPM Input)

Audit Statisitics	
Slope:	1.010
Intercept:	0.000
Correlation:	1.0000

Comments: None.

Audit Equipment	Make	Model	ID	Certification Date
Dilution System:	API	M700EU	58	12/4/11
Zero Air System:	CSI	205	974830001	NA
Calibration Gas:	SMI	Multi	JJ8550	04/22/10

AUDIT RECORD

NITROGEN DIOXIDE

T & B Systems
26074 Avenue Hall Unit 9
Valencia, CA 91355
(661) 294-1103

Date: **02/01/12**
Start: **08:45 PST**
Finish: **13:00 PST**
Auditor: **David Gemmill / David Bush**
Witness: **Paul Schafer**

Site Name: **Community East**
Operator: **SCS Tracer**
Project: **LAWA**

Analyzer make: **TEI**
Serial No.: **1136151039**
Sample flow: **0.65 lpm**
Range: **0.5** **PPM**

Model: **42i**
Converter T.: **317 Deg C**
Last cal.: **01/31/12**

NO_2 Audit Point	PPM Input (X)	PPM DAS (Y)	PPM Dif (%)
1	0.000	0.001	
2	0.016	0.016	0.0
3	0.035	0.033	-5.7
4	0.057	0.059	3.5
5	0.150	0.150	0.0

Linear Regression: (Y=PPM Corrected, X=PPM Input)

Audit Statisitics	
Slope:	0.999
Intercept:	0.000
Correlation:	0.9997

Converter Efficiency
100.0%

Comments: None.

Audit Equipment	Make	Model	ID	Certification Date
Dilution System:	API	M700EU	58	12/4/11
Zero Air System:	CSI	205	974830001	NA
Calibration Gas:	SMI	Multi	JJ8550	04/22/10

AUDIT RECORD

CARBON MONOXIDE

T&B Systems
26074 Avenue Hall Unit 9
Valencia, CA 91355
(661) 294-1103

Date: **02/01/12**
Start: **08:45 PST**
Finish: **13:00 PST**
Audited by: **David Gemmill / David Bush**
Witness: **Paul Schafer**

Site name: **Community East**
Operator: **SCS Tracer**
Project: **LAWA**

Analyzer make: **TEI**
Serial No.: **1136151040**
Sample flow: **1.052**
Zero setting: **-0.201**
Range: **50** **PPM**

Model: **48i**
Filter: **Bi-Weekly**
Span setting: **1.041**
Pressure: **752.5 mm Hg**
Last cal.: **1/31/12**

CO Audit Point	PPM Input (X)	PPM DAS (Y)	PPM Dif (%)
1	0.00	-0.13	NA
2	1.00	0.86	-14.0
3	2.51	2.39	-4.8
4	6.98	6.76	-3.2
5	14.98	15.15	1.1

Linear Regression: (Y=PPM Corrected, X=PPM Input)

	DAS
Slope:	1.0187
Intercept:	-0.18
Correlation:	0.9999

Comments: Low zero confirmed by station checks. Data can be post-processed to achieve higher accuracy at low levels.

Audit Equipment	Make	Model	ID	Certification Date
Dilution System:	API	700	225	12/4/11
Zero Air System:	Cylinder	SMI	NA	NA
Calibration Gas:	SMI	Multi	JJ24295	01/25/12

AUDIT RECORD

TRACE LEVEL SULFUR DIOXIDE

T&B Systems
26074 Avenue Hall Unit 9
Valencia, CA 91355
(661) 294-1103

Date: **02/01/12**
Start: **08:45 PST**
Finish: **13:00 PST**
Audited by: **David Gemmill / David Bush**
Witness: **Paul Schafer**

Site name: **Community East**
Operator: **SCS Tracer**
Project: **LAWA**

Analyzer make: **TEI**
Serial No.: **1136151043**
Sample flow: **0.505 lpm**
Zero setting: **1.46**
Range: **0.5** **PPM**

Model: **43iTLE**
Filter: **Bi-Weekly**
Span setting: **0.854**
Vacuum: **NA**
Last cal.: **1/31/12**

SO_2 Audit Point	PPM Input (X)	PPM DAS (Y)	PPM Dif (%)
1	0.0000	0.0003	NA
2	0.0020	0.0019	-5.0
3	0.0041	0.0039	-4.9
4	0.0070	0.0068	-2.9
5	0.0150	0.0148	-1.3

Linear Regression: (Y=PPM Corrected, X=PPM Input)

	DAS
Slope:	0.9768
Intercept:	0.0001
Correlation:	0.9996

Comments: No problems were noted.

Audit Equipment	Make	Model	ID	Certification Date
Dilution System:	API	M700EU	58	12/4/11
Zero Air System:	CSI	205	2427	NA
Calibration Gas:	SMI	Multi	JJ24295	01/25/12

AUDIT RECORD

HORIZONTAL WIND SPEED

T&B Systems
26074 Avenue Hall Unit 9
Valencia, CA 91355
(661) 294-1103

Date: **02/01/12**
Start: **08:20 PST**
Finish: **10:00 PST**
Auditor: **David Gemmill / David Bush**
Witness: **Paul Schafer**

Site Name: **Community East**
Operator: **SCS Tracer**
Project: **LAWA**

Manufacturer: **Met One**
Serial No.: **M10593**
K factor: **1.4**
Range: **0-50** **m/s**
Last Calibrated: **01/31/12**

Model: **010C**
Sensor Ht.: **10 meters**
Starting torque: **0.1** **gm cm**
Starting threshold: **0.27** **m/s**
Starting threshold criteria: **0.5** **m/s**

Audit Point	Input m/s	DAS m/s	Diff. m/s
1	0.27	0.26	-0.01
2	3.47	3.45	-0.02

Audit Criteria: ±.25 m/s; ws ≤ 5 m/s

Audit Point	Input m/s	DAS m/s	Diff. %
3	8.27	8.25	-0.2
4	16.26	16.24	-0.1
5	24.26	24.24	-0.1

Audit Criteria: ± 5%; ws > 5 m/s

Comments: No problems noted.

AUDIT RECORD

HORIZONTAL WIND DIRECTION

T&B Systems
26074 Avenue Hall Unit 9
Valencia, CA 91355
(661) 294-1103

Date: **02/01/12**
Start: **08:20 PST**
Finish: **10:00 PST**
Auditor: **David Gemmill / David Bush**
Witness: **Paul Schafer**

Site Name: **Community East**
Operator: **SCS Tracer**
Project: **LAWA**

Manufacturer: **Met One**
Serial No.: **M10654**
K factor: **30**
Range: **0 - 540**
Crossarm: **182°**
Last Calibrated: **01/31/12**

Model: **020C**
Sensor Ht.: **10 meters**
Starting torque: **4.2** **gm cm**
Starting threshold: **0.37** **m/s**
Starting threshold criteria: **0.5** **m/s**

Audit Point	Degrees Reference	Degrees DAS	Diff. Degrees
1	92	96	4
2	182	186	4
3	272	277	5
4	362	363	1
5	452	455	3

Audit Criteria: ± 5 degrees

Comments: No problems noted.

AUDIT RECORD

AMBIENT TEMPERATURE

T&B Systems
26074 Avenue Hall Unit 9
Valencia, CA 91355
(661) 294-1103

Date: **02/01/12**
Start: **08:20 PST**
Finish: **10:00 PST**
Auditor: **David Gemmill / David Bush**
Witness: **Paul Schafer**

Site Name: **Community East**
Operator: **SCS Tracer**
Project: **LAWA**

Manufacturer: **Met One**
Serial No.: **M8807**
Lower Range: **-30** **Deg C**
Upper Range: **50** **Deg C**
Last Calibrated: **01/31/12**

Model: **060A-2**
Sensor Ht.: **3.4 meters**

Audit Point	Input Deg C	DAS Deg C	Diff. Deg C
1	0.2	0.1	-0.1
2	16.3	16.2	-0.1
3	36.2	36.1	-0.1

Audit Criteria: ± 1.0 degree Celsius

Comments: No problems were noted.

AUDIT RECORD

TEMPERATURE DIFFERENCE (DELTA-T)

T&B Systems
26074 Avenue Hall Unit 9
Valencia, CA 91355
(661) 294-1103

Date: **02/01/12**
Start: **08:20 PST**
Finish: **10:00 PST**
Auditor: **David Gemmill / David Bush**
Witness: **Paul Schafer**

Site Name: **Community East**
Operator: **SCS Tracer**
Project: **LAWA**

Manufacturer: **Met One**
Serial No.: **M8799**
Lower Range: **-30** **Deg C**
Upper Range: **50** **Deg C**
Last Calibrated: **01/31/12**

Model: **060A-2**
Sensor Ht.: **8.2 meters**

Audit Point	Input Deg C	2-9 Temp Diff Deg C
1	0.2	-0.08
2	16.3	-0.08
3	36.2	-0.08

Audit Criteria: ± 0.1°C

Comments: No problems were noted.

AUDIT RECORD

SOLAR RADIATION

T&B Systems
26074 Avenue Hall Unit 9
Valencia, CA 91355
(661) 294-1103

Date: **2/1/12**
Start: **10:00 PST**
Finish: **15:00 PST**
Auditor: **David Gemmill / David Bush**
Witness: **Paul Schafer**

Site name: **Community East**
Operator: **SCS Tracer**
Project: **LAWA**

Sensor Mfg: **Met One**
Serial No.: **NA**
Range: **0 - 1500 W/m2**
Last Calibrated: **1/31/2012**

Model: **095**
Sensor Ht.: **3.5 m**

Audit Point	Input W/m2	DAS W/m2	Diff. % W/m2
11:00	624	641	2.7%
12:00	644	650	0.8%
13:00	588	598	1.5%
14:00	467	483	3.3%

Criteria: ± 10%

Comments: Comparison with collocated transfer standard. Hourly averages (hour beginning) based on 1-minute data.

AUDIT RECORD

RELATIVE HUMIDITY

T&B Systems
26074 Avenue Hall Unit 9
Valencia, CA 91355
(661) 294-1103

Date: **02/02/12**
Start: **12:00 PST**
Finish: **23:00 PST**
Auditor: **David Gemmill / David Bush**
Witness: **Paul Schafer**

Site name: **Community East**
Operator: **SCS Tracer**
Project: **LAWA**

Sensor Mfg: **Met One**
Serial No.: **M10919**
Range: **0-100 %**
Last Calibrated: **1/31/12**

Model: **083E-0-6**
Sensor Ht.: **3 m**

Audit Point	Input RH (%)	DAS RH (%)	Diff. %
12:00	52.8	58.7	5.9
13:00	60.8	69.0	8.2
16:00	68.7	74.2	5.5
17:00	75.2	78.5	3.3
18:00	82.3	83.2	0.9
23:00	88.9	88.8	-0.1

Criteria: ± 10%

Comments: Comparison of hourly averages versus Hobo Pro audit transfer standard over available ambient range.

AUDIT RECORD

BAM

T&B Systems
26074 Avenue Hall Unit 9
Valencia, CA 91355
(661) 294-1103

Date: **02/01/12**
Start: **11:10 PST**
Finish: **11:25 PST**
Auditor: **David Gemmill / David Bush**
Witness: **Paul Schafer**

Site name: **Community East**
Operator: **SCS Tracer**
Project: **LAWA**

Sampler: **BAM (PM2.5)**
Serial No.: **F5131**
Last Calibrated.:

Make: **Met One**
Model: **1020**

Amb. Press: **29.96** **in. Hg**
Amb. Temp.: **19.0** **°C**
Leak Check: **0.3** **LPM**

Flowmeters
Model: **BGI Challenger**

	Audit	Site	Diff.
Flow	16.66 lpm	16.70 lpm	0.2%
Amb T (^{o}C)	19.3 ^{o}C	18.8 ^{o}C	-0.5
Amb P (mm)	763 mm Hg	763 mm Hg	0

Audit Criteria: Flow - ± 10%; Total 15.0 - 18.4 lpm
Amb T - ± 2^{o}C
Amb P - ± 15 mm

Comments: No problems noted.

AUDIT RECORD

AETHALOMETER

T&B Systems
26074 Avenue Hall Unit 9
Valencia, CA 91355
(661) 294-1103

Date: **02/01/12**
Start: **11:30 PST**
Finish: **11:35 PST**
Auditor: **David Gemmill / David Bush**
Witness: **Paul Schafer**

Site name: **Community East**
Operator: **SCS Tracer**
Project: **LAWA**

Manufacturer: **Mcgee Scientific**
Serial No.:

Model: **AE 21**
Sensor Ht.: **5 m**

Last Calibrated:

Audit device: Bios Defender

Audit Point	Audit lpm	Sampler lpm	%diff.
1	3.44	3.30	-4.1

Audit Criteria: ± 10%

Comments: Ambient reading during audit: ~1400 ng/m3
Reading with Hepa filter on inlet: 0 ng/m3

AUDIT RECORD

SMPS

T&B Systems
26074 Avenue Hall Unit 9
Valencia, CA 91355
(661) 294-1103

Date: **02/01/12**
Start: **14:50 PST**
Finish: **15:40 PST**
Auditor: **David Gemmill / David Bush**
Witness: **Paul Schafer**

Site name: **Community East**
Operator: **SCS Tracer**
Project: **LAWA**

Manufacturer: **Grimm**
Serial No.:

Model: **SMPS**
Sensor Ht.: **6 m**

Last Calibrated:

Audit device: Bios Defender

Audit Point	Audit lpm	Sampler lpm	%diff.
1			

Audit Criteria: ± 10%

Comments: Not operating at time of audit.

AUDIT RECORD

NEPHELOMETER

T&B Systems
26074 Avenue Hall Unit 9
Valencia, CA 91355
(661) 294-1103

Date: **02/01/12**
Start: **11:25 PST**
Finish: **11:30 PST**
Auditor: **David Gemmill / David Bush**
Witness: **Paul Schafer**

Site name: **Community East**
Operator: **SCS Tracer**
Project: **LAWA**

Manufacturer: **Thermo**
Serial No.:

Model: **pDR-1200**
Sensor Ht.: **4.5 m**

Last Calibrated:

Audit device: Bios Defender

Audit Point	Audit lpm	Sampler lpm	%diff.
1	2.92	4.00	37.0

Audit Criteria: ± 10%

Comments: Leak in plenum. Requires corrective action.

AUDIT RECORD

NITRIC OXIDE

T&B Systems
26074 Avenue Hall Unit 9
Valencia, CA 91355
(661) 294-1103

Date: **02/02/12**
Start: **08:45 PST**
Finish: **13:00 PST**
Auditor: **David Bush / Bob Baxter**
Witness: **Paul Schafer**

Site Name: **Community South**
Operator: **SCS Tracer**
Project: **LAWA**

Analyzer make: **TEI**
Serial No.: **65762-350**
Sample flow: **0.691 lpm**
Range: **0.5** **PPM**

Model: **42i**
Filter: **Bi-Weekly**
Span setting: **1.172**
Zero setting: **3.3**
Last Calibrated: **01/31/12**

NO Audit Point	PPM Input (X)	PPM DAS (Y)	PPM Dif (%)
1	0.000	-0.001	
2	0.030	0.029	-3.3
3	0.069	0.067	-2.9
4	0.118	0.117	-0.8
5	0.221	0.228	3.2
6	0.397	0.407	2.5

Linear Regression: (Y=PPM Corrected, X=PPM Input)

Audit Statisitics	
Slope:	1.032
Intercept:	-0.003
Correlation:	0.9999

Comments: None.

Audit Equipment	Make	Model	ID	Certification Date
Dilution System:	API	M700EU	58	12/4/11
Zero Air System:	CSI	205	974830001	NA
Calibration Gas:	SMI	Multi	JJ8550	04/22/10

AUDIT RECORD

OXIDES OF NITROGEN

T&B Systems
26074 Avenue Hall Unit 9
Valencia, CA 91355
(661) 294-1103

Date: **02/02/12**
Start: **08:45 PST**
Finish: **13:00 PST**
Auditor: **David Bush / Bob Baxter**
Witness: **Paul Schafer**

Site Name: **Community South**
Organization: **SCS Tracer**
Project: **LAWA**

Analyzer make: **TEI**
Serial No.: **65762-350**
Sample flow: **0.691 lpm**
Range: **0.5** **PPM**

Model: **42i**
Filter: **Bi-Weekly**
Span setting: **0.997**
Zero setting: **4**
Last cal.: **01/31/12**

NO_X Audit Point	PPM Input (X)	PPM DAS (Y)	PPM Dif (%)
1	0.000	0.001	
2	0.030	0.030	0.0
3	0.069	0.069	0.0
4	0.118	0.118	0.0
5	0.221	0.228	3.2
6	0.397	0.405	2.0

Linear Regression: (Y=PPM Corrected, X=PPM Input)

Audit Statisitics	
Slope:	1.023
Intercept:	0.000
Correlation:	0.9999

Comments: None.

Audit Equipment	Make	Model	ID	Certification Date
Dilution System:	API	M700EU	58	12/4/11
Zero Air System:	CSI	205	974830001	NA
Calibration Gas:	SMI	Multi	JJ8550	04/22/10

AUDIT RECORD

NITROGEN DIOXIDE

T&B Systems
26074 Avenue Hall Unit 9
Valencia, CA 91355
(661) 294-1103

Date: **02/02/12**
Start: **08:45 PST**
Finish: **13:00 PST**
Auditor: **David Bush / Bob Baxter**
Witness: **Paul Schafer**

Site Name: **Community South**
Operator: **SCS Tracer**
Project: **LAWA**

Analyzer make: **TEI**
Serial No.: **65762-350**
Ozone flow: **0.105 lpm**
Range: **0.5** **PPM**

Model: **42i**
Converter T.: **317 Deg C**
Last cal.: **01/31/12**

NO_2 Audit Point	PPM Input (X)	PPM DAS (Y)	PPM Dif (%)
1	0.000	0.000	
2	0.014	0.014	0.0
3	0.031	0.032	3.2
4	0.054	0.056	3.7
5	0.144	0.148	2.8

Linear Regression: (Y=PPM Corrected, X=PPM Input)

Audit Statisitics	
Slope:	1.029
Intercept:	0.000
Correlation:	1.0000

Converter Efficiency
100.0%

Comments: None.

Audit Equipment	Make	Model	ID	Certification Date
Dilution System:	API	M700EU	58	12/4/11
Zero Air System:	CSI	205	974830001	NA
Calibration Gas:	SMI	Multi	JJ8550	04/22/10

AUDIT RECORD

CARBON MONOXIDE

T&B Systems
26074 Avenue Hall Unit 9
Valencia, CA 91355
(661) 294-1103

Date: **02/02/12**
Start: **08:45 PST**
Finish: **13:00 PST**
Audited by: **David Bush / Bob Baxter**
Witness: **Paul Schafer**

Site name: **Community South**
Operator: **SCS Tracer**
Project: **LAWA**

Analyzer make: **TEI**
Serial No.: **69154-362**
Sample flow: **1.141**
Zero setting: **-0.166**
Range: **50** **PPM**

Model: **48i**
Filter: **Bi-Weekly**
Span setting: **1.107**
Pressure: **776.2 mm Hg**
Last cal.: **1/31/12**

CO Audit Point	PPM Input (X)	PPM DAS (Y)	PPM Dif (%)
1	0.00	-0.38	NA
2	1.03	0.64	-37.9
3	2.51	2.09	-16.7
4	6.98	6.60	-5.4
5	15.12	15.15	0.2

Linear Regression: (Y=PPM Corrected, X=PPM Input)

	DAS
Slope:	1.0277
Intercept:	-0.45
Correlation:	0.9999

Comments: Low zero confirmed by station checks. Data should be post-processed to achieve higher accuracy at low levels.

Audit Equipment	Make	Model	ID	Certification Date
Dilution System:	API	700	225	12/4/11
Zero Air System:	Cylinder	SMI	NA	NA
Calibration Gas:	SMI	Multi	JJ24295	01/25/12

AUDIT RECORD

TRACE LEVEL SULFUR DIOXIDE

T&B Systems
26074 Avenue Hall Unit 9
Valencia, CA 91355
(661) 294-1103

Date: **02/02/12**
Start: **08:45 PST**
Finish: **13:00 PST**
Audited by: **David Bush / Bob Baxter**
Witness: **Paul Schafer**

Site name: **Community South**
Operator: **SCS Tracer**
Project: **LAWA**

Analyzer make: **TEI**
Serial No.: **1136151042**
Sample flow: **0.450 lpm**
Zero setting: **1.82**
Range: **0.5** **PPM**

Model: **43iTLE**
Filter: **Bi-Weekly**
Span setting: **1.079**
Vacuum: **NA**
Last cal.: **1/31/12**

SO_2 Audit Point	PPM Input (X)	PPM DAS (Y)	PPM Dif (%)
1	0.0000	0.0000	NA
2	0.0020	0.0020	0.0
3	0.0070	0.0070	0.0
4	0.0150	0.0148	-1.3

Linear Regression: (Y=PPM Corrected, X=PPM Input)

	DAS
Slope:	0.9866
Intercept:	0.0000
Correlation:	1.0000

Comments: No problems were noted.

Audit Equipment	Make	Model	ID	Certification Date
Dilution System:	API	M700EU	58	12/4/11
Zero Air System:	Cylinder	SMI	NA	NA
Calibration Gas:	SMI	Multi	JJ24295	01/25/12

AUDIT RECORD

HORIZONTAL WIND SPEED

T&B Systems
26074 Avenue Hall Unit 9
Valencia, CA 91355
(661) 294-1103

Date: **02/02/12**
Start: **09:30 PST**
Finish: **12:00 PST**
Auditor: **David Bush / Bob Baxter**
Witness: **Paul Schafer**

Site Name: **Community South**
Operator: **SCS Tracer**
Project: **LAWA**

Manufacturer: **Met One**
Serial No.: **F1077**
K factor: **1.4**
Range: **0-50** **m/s**
Last Calibrated: **01/31/12**

Model: **010C**
Sensor Ht.: **10 meters**
Starting torque: **0.2** **gm cm**
Starting threshold: **0.38** **m/s**
Starting threshold criteria: **0.5** **m/s**

Audit Point	Input m/s	DAS m/s	Diff. m/s
1	0.27	0.26	-0.01
2	3.47	3.45	-0.02

Audit Criteria: ±.25 m/s; ws ≤ 5 m/s

Audit Point	Input m/s	DAS m/s	Diff. %
3	8.27	8.25	-0.2
4	16.26	16.24	-0.1
5	24.26	24.24	-0.1

Audit Criteria: ± 5%; ws > 5 m/s

Comments: No problems noted.

AUDIT RECORD

HORIZONTAL WIND DIRECTION

T&B Systems
26074 Avenue Hall Unit 9
Valencia, CA 91355
(661) 294-1103

Date: **02/02/12**
Start: **09:30 PST**
Finish: **12:00 PST**
Auditor: **David Bush / Bob Baxter**
Witness: **Paul Schafer**

Site Name: **Community South**
Operator: **SCS Tracer**
Project: **LAWA**

Manufacturer: **Met One**
Serial No.: **A1178**
K factor: **30**
Range: **0 - 540**
Crossarm: **180°**
Last Calibrated: **01/31/12**

Model: **020C**
Sensor Ht.: **10 meters**
Starting torque: **5** **gm cm**
Starting threshold: **0.41** **m/s**
Starting threshold criteria: **0.5** **m/s**

Audit Point	Degrees Reference	Degrees DAS	Diff. Degrees
1	90	92	2
2	180	180	0
3	270	274	4
4	360	360	0
5	450	451	1

Audit Criteria: ± 5 degrees

Comments: No problems noted.

AUDIT RECORD

AMBIENT TEMPERATURE

T&B Systems
26074 Avenue Hall Unit 9
Valencia, CA 91355
(661) 294-1103

Date: **02/02/12**
Start: **09:30 PST**
Finish: **12:00 PST**
Auditor: **David Bush / Bob Baxter**
Witness: **Paul Schafer**

Site Name: **Community South**
Operator: **SCS Tracer**
Project: **LAWA**

Manufacturer: **Met One**
Serial No.: **D7113**
Lower Range: **-30** **Deg C**
Upper Range: **50** **Deg C**
Last Calibrated: **01/31/12**

Model: **060A-2**
Sensor Ht.: **3.4 m**

Audit Point	Input Deg C	DAS Deg C	Diff. Deg C
1	2.6	2.6	0.0
2	18.3	18.1	-0.2
3	37.9	37.7	-0.2

Audit Criteria: ± 1.0 degree Celsius

Comments: No problems were noted.

AUDIT RECORD

TEMPERATURE DIFFERENCE (DELTA-T)

T&B Systems
26074 Avenue Hall Unit 9
Valencia, CA 91355
(661) 294-1103

Date: **02/02/12**
Start: **09:30 PST**
Finish: **12:00 PST**
Auditor: **David Bush / Bob Baxter**
Witness: **Paul Schafer**

Site Name: **Community South**
Operator: **SCS Tracer**
Project: **LAWA**

Manufacturer: **Met One**
Serial No.: **D8475**
Lower Range: **-30** **Deg C**
Upper Range: **50** **Deg C**
Last Calibrated: **01/31/12**

Model: **060A-2**
Sensor Ht.: **8.2 m**

Audit Point	Input Deg C	2-9 Temp Diff Deg C
1	2.6	-0.06
2	18.3	0.00
3	37.9	0.00

Audit Criteria: ± 0.1°C

Comments: No problems were noted.

AUDIT RECORD

BAM

T&B Systems
26074 Avenue Hall Unit 9
Valencia, CA 91355
(661) 294-1103

Date: **02/02/12**
Start: **12:45 PST**
Finish: **12:50 PST**
Auditor: **David Bush / Bob Baxter**
Witness: **Paul Schafer**

Site name: **Community South**
Operator: **SCS Tracer**
Project: **LAWA**

Sampler: **BAM (PM2.5)**
Serial No.:
Last Calibrated.:

Make: **Met One**
Model: **1020**

Amb. Press: **23.15** **in. Hg**
Amb. Temp.: **-8.5** **°C**
Leak Check: **0.2** **LPM**

Flowmeters
Model: **BGI Challenger**

	Audit	Site	Diff.
Flow	16.72 lpm	16.70 lpm	-0.1%
Amb T (^{o}C)	#N/A ^{o}C	#N/A ^{o}C	#N/A
Amb P (mm)	757 mm Hg	757 mm Hg	0

Audit Criteria: Flow - ± 10%; Total 15.0 - 18.4 lpm
Amb T - ± 2^{o}C
Amb P - ± 15 mm

Comments: No problems noted.

AUDIT RECORD

AETHALOMETER

T&B Systems
26074 Avenue Hall Unit 9
Valencia, CA 91355
(661) 294-1103

Date: **02/02/12**
Start: **11:35 PST**
Finish: **12:30 PST**
Auditor: **David Bush / Bob Baxter**
Witness: **Paul Schafer**

Site name: **Community South**
Operator: **SCS Tracer**
Project: **LAWA**

Manufacturer: **Mcgee Scientific**
Serial No.:

Model: **AE 21**
Sensor Ht.: **5 m**

Last Calibrated:

Audit device: Bios Defender

Audit Point	Audit lpm	Sampler lpm	%diff.
1	3.80	3.50	-7.9

Audit Criteria: ± 10%

Comments: Ambient reading during audit: ~1200 ng/m3
Reading with Hepa filter on inlet: -55 ng/m3

AUDIT RECORD

SMPS

T&B Systems
26074 Avenue Hall Unit 9
Valencia, CA 91355
(661) 294-1103

Date: **02/02/12**
Start: **14:50 PST**
Finish: **15:40 PST**
Auditor: **David Bush / Bob Baxter**
Witness: **Paul Schafer**

Site name: **Community South**
Operator: **SCS Tracer**
Project: **LAWA**

Manufacturer: **TSI**
Serial No.:

Model: **RSMPS**
Sensor Ht.: **6 m**

Last Calibrated:

Audit device: Bios Defender

Audit Point	Audit lpm	Sampler lpm	%diff.
1	0.91	1.00	9.9

Audit Criteria: ± 10%

Comments: Ambient particle distribution looks appropriate.
With Hepa filter on inlet, average particle count per bin drops frop from 30000 to 20/cm2.

AUDIT RECORD

NEPHELOMETER

T&B Systems
26074 Avenue Hall Unit 9
Valencia, CA 91355
(661) 294-1103

Date: **02/02/12**
Start: **12:50 PST**
Finish: **13:00 PST**
Auditor: **David Bush / Bob Baxter**
Witness: **Paul Schafer**

Site name: **Community South**
Operator: **SCS Tracer**
Project: **LAWA**

Manufacturer: **Thermo**
Serial No.:

Model: **pDR-1200**
Sensor Ht.: **4.5 m**

Last Calibrated:

Audit device: Bios Defender

Audit Point	Audit lpm	Sampler lpm	%diff.
1	0.90	4.00	344.4

Audit Criteria: ± 10%

Comments: Large leek in plenum. Requires corrective action.

AUDIT RECORD

OXIDES OF NITROGEN

T&B Systems
26074 Avenue Hall Unit 9
Valencia, CA 91355
(661) 294-1103

Date: **02/03/12**
Start: **08:00 PST**
Finish: **15:30 PST**
Auditor: **David Bush**
Witness: **Paul Schafer**

Site Name: **Community North**
Organization: **SCS Tracer**
Project: **LAWA**

Analyzer make: **TEI**
Serial No.: **325981773**
Sample flow: **0.485 lpm**
Range: **0.5** **PPM**

Model: **42C**
Filter: **Bi-Weekly**
Span setting: **1.039**
Zero setting: **52**
Last cal.: **02/01/12**

NO_X Audit Point	PPM Input (X)	PPM DAS (Y)	PPM Dif (%)
1	0.000	0.001	
2	0.030	0.033	10.0
3	0.069	0.076	10.1
4	0.118	0.130	10.2
5	0.221	0.249	12.7
6	0.397	0.442	11.3

Linear Regression: (Y=PPM Corrected, X=PPM Input)

Audit Statisitics	
Slope:	1.115
Intercept:	0.000
Correlation:	1.0000

Comments: None.

Audit Equipment	Make	Model	ID	Certification Date
Dilution System:	API	M700EU	58	12/4/11
Zero Air System:	CSI	205	974830001	NA
Calibration Gas:	SMI	Multi	JJ8550	04/22/10

AUDIT RECORD

NITROGEN DIOXIDE

T&B Systems
26074 Avenue Hall Unit 9
Valencia, CA 91355
(661) 294-1103

Date: **02/03/12**
Start: **08:00 PST**
Finish: **15:30 PST**
Auditor: **David Bush**
Witness: **Paul Schafer**

Site Name: **Community North**
Operator: **SCS Tracer**
Project: **LAWA**

Analyzer make: **TEI**
Serial No.: **325981773**
Sample flow: **0.485 lpm**
Range: **0.5** **PPM**

Model: **42C**
Converter T.: **317 Deg C**
Last cal.: **02/01/12**

NO_2 Audit Point	PPM Input (X)	PPM DAS (Y)	PPM Dif (%)
1	0.000	0.000	
2	0.014	0.015	7.1
3	0.031	0.033	6.5
4	0.056	0.061	8.9
5	0.143	0.159	11.2

Linear Regression: (Y=PPM Corrected, X=PPM Input)

Audit Statisitics	
Slope:	1.115
Intercept:	-0.001
Correlation:	0.9999

Converter Efficiency
99.1%

Comments: None.

Audit Equipment	Make	Model	ID	Certification Date
Dilution System:	API	M700EU	58	12/4/11
Zero Air System:	CSI	205	974830001	NA
Calibration Gas:	SMI	Multi	JJ8550	04/22/10

AUDIT RECORD

NITRIC OXIDE

T&B Systems
26074 Avenue Hall Unit 9
Valencia, CA 91355
(661) 294-1103

Date: **02/03/12**
Start: **08:00 PST**
Finish: **15:30 PST**
Auditor: **David Bush**
Witness: **Paul Schafer**

Site Name: **Community North**
Operator: **SCS Tracer**
Project: **LAWA**

Analyzer make: **TEI**
Serial No.: **325981773**
Sample flow: **0.485 lpm**
Range: **0.5** **PPM**

Model: **42C**
Filter: **Bi-Weekly**
Span setting: **1.405**
Zero setting: **49.0**
Last Calibrated: **02/01/12**

NO Audit Point	PPM Input (X)	PPM DAS (Y)	PPM Dif (%)
1	0.000	0.002	
2	0.030	0.034	13.3
3	0.070	0.077	10.0
4	0.119	0.131	10.1
5	0.221	0.248	12.2
6	0.397	0.439	10.6

Linear Regression: (Y=PPM Corrected, X=PPM Input)

Audit Statisitics	
Slope:	1.105
Intercept:	0.001
Correlation:	1.0000

Comments: None.

Audit Equipment	Make	Model	ID	Certification Date
Dilution System:	API	M700EU	58	12/4/11
Zero Air System:	CSI	205	974830001	NA
Calibration Gas:	SMI	Multi	JJ8550	04/22/10

AUDIT RECORD

CARBON MONOXIDE

T&B Systems
26074 Avenue Hall Unit 9
Valencia, CA 91355
(661) 294-1103

Date: **02/03/12**
Start: **08:00 PST**
Finish: **15:30 PST**
Audited by: **David Bush**
Witness: **Paul Schafer**

Site name: **Community North**
Operator: **SCS Tracer**
Project: **LAWA**

Analyzer make: **TEI**
Serial No.: **1136151041**
Sample flow: **1.085**
Zero setting: **0.056**
Range: **50** **PPM**

Model: **48i**
Filter: **Bi-Weekly**
Span setting: **1.085**
Pressure: **743.1 mm Hg**
Last cal.: **2/1/12**

CO Audit Point	PPM Input (X)	PPM DAS (Y)	PPM Dif (%)
1	0.00	-0.53	NA
2	1.03	0.53	-48.5
3	2.51	2.06	-17.9
4	6.98	6.63	-5.0
5	15.12	15.37	1.7

Linear Regression: (Y=PPM Corrected, X=PPM Input)

	DAS
Slope:	1.0509
Intercept:	-0.58
Correlation:	0.9999

Comments: Low zero confirmed by station checks. Data should be post-processed to achieve higher accuracy at low levels.

Audit Equipment	Make	Model	ID	Certification Date
Dilution System:	API	700	225	12/4/11
Zero Air System:	Cylinder	SMI	NA	NA
Calibration Gas:	SMI	Multi	JJ24295	01/25/12

AUDIT RECORD

TRACE LEVEL SULFUR DIOXIDE

T&B Systems
26074 Avenue Hall Unit 9
Valencia, CA 91355
(661) 294-1103

Date: **02/03/12**
Start: **08:00 PST**
Finish: **15:30 PST**
Audited by: **David Bush**
Witness: **Paul Schafer**

Site name: **Community North**
Operator: **SCS Tracer**
Project: **LAWA**

Analyzer make: **TEI**
Serial No.: **1136151044**
Sample flow: **0.485 lpm**
Zero setting: **2.58**
Range: **0.5** **PPM**

Model: **43iTLE**
Filter: **Bi-Weekly**
Span setting: **1.398**
Pressure: **731.8 mm Hg**
Last cal.: **2/1/12**

SO_2 Audit Point	PPM Input (X)	PPM DAS (Y)	PPM Dif (%)
1	0.0000	-0.0003	NA
2	0.0020	0.0029	45.0
3	0.0070	0.0079	12.9
4	0.0150	0.0156	4.0

Linear Regression: (Y=PPM Corrected, X=PPM Input)

	DAS
Slope:	1.0336
Intercept:	0.0003
Correlation:	0.9972

Comments: Low zero confirmed by station checks.
Data should be post-processed to achieve higher accuracy at low levels.

Audit Equipment	Make	Model	ID	Certification Date
Dilution System:	API	M700EU	58	12/4/11
Zero Air System:	CSI	205	2427	NA
Calibration Gas:	SMI	Multi	JJ24295	01/25/12

AUDIT RECORD

BAM

T&B Systems
26074 Avenue Hall Unit 9
Valencia, CA 91355
(661) 294-1103

Date: **02/03/12**
Start: **10:15 PST**
Finish: **10:30 PST**
Auditor: **David Bush**
Witness: **Paul Schafer**

Site name: **Community North**
Operator: **SCS Tracer**
Project: **LAWA**

Sampler: **BAM (PM2.5)**
Serial No.:
Last Calibrated.:

Make: **Met One**
Model: **1020**

Amb. Press: **29.90** **in. Hg**
Amb. Temp.: **19.0** **°C**
Leak Check: **0.2** **LPM**

Flowmeters
Model: **BGI Challenger**

	Audit	Site	Diff.
Flow	16.71 lpm	16.70 lpm	-0.1%
Amb T (^{o}C)	#N/A ^{o}C	#N/A ^{o}C	#N/A
Amb P (mm)	758 mm Hg	757 mm Hg	-1

Audit Criteria: Flow - ± 10%; Total 15.0 - 18.4 lpm
Amb T - ± 2^{o}C
Amb P - ± 15 mm

Comments: No problems noted.

AUDIT RECORD

AETHALOMETER

T&B Systems
26074 Avenue Hall Unit 9
Valencia, CA 91355
(661) 294-1103

Date: **02/03/12**
Start: **09:10 PST**
Finish: **10:00 PST**
Auditor: **David Bush**
Witness: **Paul Schafer**

Site name: **Community North**
Operator: **SCS Tracer**
Project: **LAWA**

Manufacturer: **Mcgee Scientific**
Serial No.:

Model: **AE 21**
Sensor Ht.: **3.5 m**

Last Calibrated:

Audit device: Bios Defender

Audit Point	Audit lpm	Sampler lpm	%diff.
1	4.05	4.10	1.2

Audit Criteria: ± 10%

Comments: Ambient reading during audit: ~1500 ng/m3
Reading with Hepa filter on inlet: -115 ng/m3

AUDIT RECORD

SMPS

T&B Systems
26074 Avenue Hall Unit 9
Valencia, CA 91355
(661) 294-1103

Date: **02/03/12**
Start: **09:10 PST**
Finish: **10:00 PST**
Auditor: **David Bush**
Witness: **Paul Schafer**

Site name: **Community North**
Operator: **SCS Tracer**
Project: **LAWA**

Manufacturer: **TSI**
Serial No.:

Model: **3080**
Sensor Ht.: **3.5 m**

Last Calibrated:

Audit device: Bios Defender

Audit Point	Audit lpm	Sampler lpm	%diff.
1	0.27	0.34	25.9

Audit Criteria: ± 10%

Comments: Sampler does not appear to be working properly. Unusual distributions displayed. Anticipated that sample flow should have been set to 1.0 lpm. Operator not present to discuss results.

AUDIT RECORD

NEPHELOMETER

T&B Systems
26074 Avenue Hall Unit 9
Valencia, CA 91355
(661) 294-1103

Date: **02/03/12**
Start: **11:25 PST**
Finish: **11:30 PST**
Auditor: **David Bush**
Witness: **Paul Schafer**

Site name: **Community North**
Operator: **SCS Tracer**
Project: **LAWA**

Manufacturer: **Thermo**
Serial No.:

Model: **pDR-1200**
Sensor Ht.: **2.5 m**

Last Calibrated:

Audit device: Bios Defender

Audit Point	Audit lpm	Sampler lpm	%diff.
1	3.70	4.00	8.1

Audit Criteria: ± 10%

Comments: No problems were noted.
Ambient reading during audit: 0.023 mg/m3
Reading with Hepa filter on inlet: 0 mg/m3

AUDIT RECORD

BAM

T&B Systems
26074 Avenue Hall Unit 9
Valencia, CA 91355
(661) 294-1103

Date: **02/02/12**
Start: **17:00 PST**
Finish: **17:10 PST**
Auditor: **David Bush / Bob Baxter**
Witness: **Paul Schafer**

Site name: **SCAQMD AQ**
Operator: **SCS Tracer**
Project: **LAWA**

Sampler: **BAM (PM2.5)**
Serial No.:
Last Calibrated.:

Make: **Met One**
Model: **1020**

Amb. Press: **29.96** **in. Hg**
Amb. Temp.: **19.0** **°C**
Leak Check: **0.0** **LPM**

Flowmeters
Model: **BGI Challenger**

	Audit	Site	Diff.
Flow	16.50 lpm	16.70 lpm	1.2%
Amb T (^{o}C)	#N/A ^{o}C	#N/A ^{o}C	#N/A
Amb P (mm)	#N/A mm Hg	#N/A mm Hg	#N/A

Audit Criteria: Flow - ± 10%; Total 15.0 - 18.4 lpm
Amb T - ± 2^{o}C
Amb P - ± 15 mm

Comments: No problems noted.

AUDIT RECORD

AETHALOMETER

T&B Systems
26074 Avenue Hall Unit 9
Valencia, CA 91355
(661) 294-1103

Date: **02/02/12**
Start: **16:35 PST**
Finish: **17:20 PST**
Auditor: **David Bush / Bob Baxter**
Witness: **Paul Schafer**

Site name: **SCAQMD AQ**
Operator: **SCS Tracer**
Project: **LAWA**

Manufacturer: **Mcgee Scientific**
Serial No.:

Model: **AE 21**
Sensor Ht.: **1.5 m**

Last Calibrated: **08/28/11**

Audit device: Bios Defender

Audit Point	Audit lpm	Sampler lpm	%diff.
1	4.14	4.20	1.4

Audit Criteria: ± 10%

Comments: Ambient reading during audit: ~370 ng/m3
Reading with Hepa filter on inlet: 70 ng/m3

AUDIT RECORD

CPC

T&B Systems
26074 Avenue Hall Unit 9
Valencia, CA 91355
(661) 294-1103

Date: **02/02/12**
Start: **16:50 PST**
Finish: **17:20 PST**
Auditor: **David Bush / Bob Baxter**
Witness: **Paul Schafer**

Site name: **SCAQMD AQ**
Operator: **SCS Tracer**
Project: **LAWA**

Manufacturer: **TSI**
Serial No.:

Model: **CPC**
Sensor Ht.: **1.5 m**

Last Calibrated:

Audit device: Bios Defender

Audit Point	Audit lpm	Sampler lpm	%diff.
1	1.75		

Audit Criteria: ± 10%

Comments: Ambient reading during audit: ~5000 p/cm3
Reading with Hepa filter on inlet: 2.8 p/cm3

AUDIT RECORD

NEPHELOMETER

T&B Systems
26074 Avenue Hall Unit 9
Valencia, CA 91355
(661) 294-1103

Date: **02/02/12**
Start: **16:50 PST**
Finish: **17:00 PST**
Auditor: **David Bush / Bob Baxter**
Witness: **Paul Schafer**

Site name: **SCAQMD AQ**
Operator: **SCS Tracer**
Project: **LAWA**

Manufacturer: **Thermo**
Serial No.:

Model: **pDR-1200**
Sensor Ht.: **1.5 m**

Last Calibrated:

Audit device: Bios Defender

Audit Point	Audit lpm	Sampler lpm	%diff.
1	3.80	4.00	5.3

Audit Criteria: ± 10%

Comments: No problems were noted.
Reading with Hepa filter on inlet: 0 mg/m3

AUDIT RECORD

DRI SVOC

T&B Systems
26074 Avenue Hall Unit 9
Valencia, CA 91355
(661) 294-1103

Date: **2/21/12**
Time: **~11:30**
Auditor: **R. Baxter**

Site name: **CE**
Project: **LAX AQSAS**
Operator: **DRI**
Site Operator: **D. Campbell**

Sensor Mfg: **DRI**
Serial No.: **N/A**

Model: **DRI SVOC**
Sensor Height: **2 m**
Ambient Pressure (in Hg): **29.94**
Ambient Temperature (°C): **27**

Last cal. date: **Unknown**

Audit Device: **Teledyne Hastings NAHL-5**
Serial No.: **11614**
Last Cert.: **1/20/12**

	Channel 1	Channel 2
Operator provided sampler flow in l/m:	**113**	**113**
Audit flow in l/m:	**122**	**121**
Sampler Flow Diff (l/m):	**-9**	**-8**
Sampler Flow % Diff.:	**-7.6%**	**-6.8%**

Audit Criteria: 113 ±11 l/m ±10% from audit flow

Comments: The audit flow was measured in SLPM and converted to actual conditions using the ambient pressure and temperature. No problems noted.

AUDIT RECORD

DRI SVOC

T&B Systems
26074 Avenue Hall Unit 9
Valencia, CA 91355
(661) 294-1103

Date: **2/21/12**
Time: **~10:30**

Auditor: **R. Baxter**

Sensor Mfg: **DRI**
Serial No.: **N/A**

Site name: **CS**
Project: **LAX AQSAS**
Operator: **DRI**
Site Operator: **D. Campbell**

Model: **DRI SVOC**
Sensor Height: **2 m**
Ambient Pressure (in Hg): **30.04**
Ambient Temperature (°C): **20**

Last cal. date: **Unknown**

Audit Device: **Teledyne Hastings NAHL-5**
Serial No.: **11614**
Last Cert.: **1/20/12**

	Channel 1	Channel 2
Operator provided sampler flow in l/m:	**113**	**113**
Audit flow in l/m:	**117**	**120**
Sampler Flow Diff (l/m):	**-4**	**-7**
Sampler Flow % Diff.:	**-3.5%**	**-5.9%**

Audit Criteria: 113 ±11 l/m ±10% from audit flow

Comments: The audit flow was measured in SLPM and converted to actual conditions using the ambient pressure and temperature. No problems noted.

AUDIT RECORD

DRI SVOC

T&B Systems
26074 Avenue Hall Unit 9
Valencia, CA 91355
(661) 294-1103

Date: **2/21/12**
Time: **~15:45**

Auditor: **R. Baxter**

Sensor Mfg: **DRI**
Serial No.: **N/A**

Site name: **CN**
Project: **LAX AQSAS**
Operator: **DRI**
Site Operator: **D. Campbell**

Model: **DRI SVOC**
Sensor Height: **2 m**
Ambient Pressure (in Hg): **30.00**
Ambient Temperature (°C): **21**

Last cal. date: **Unknown**

Audit Device: **Teledyne Hastings NAHL-5**
Serial No.: **11614**
Last Cert.: **1/20/12**

	Channel 1	Channel 2
Operator provided sampler flow in l/m:	**113**	**113**
Audit flow in l/m:	**122**	**125**
Sampler Flow Diff (l/m):	**-9**	**-12**
Sampler Flow % Diff.:	**-7.1%**	**-9.3%**

Audit Criteria: 113 ±11 l/m ±10% from audit flow

Comments: The audit flow was measured in SLPM and converted to actual conditions using the ambient pressure and temperature. No problems noted.

AUDIT RECORD

DRI SFS

T&B Systems
26074 Avenue Hall Unit 9
Valencia, CA 91355
(661) 294-1103

Date: **2/21/12**
Time: **~11:30**

Auditor: **R. Baxter**

Site name: **CE**
Project: **LAX AQSAS**
Operator: **DRI**
Site Operator: **D. Campbell**

Sensor Mfg: **DRI**
Serial No.: **N/A**

Model: **DRI SVOC**
Sensor Height: **2 m**
Ambient Pressure (in Hg): **29.94**
Ambient Temperature (°C): **27**

Last cal. date: **Unknown**

Audit Device: Teledyne Hastings NAHL-5
Serial No.: 11614
Last Cert.: 1/20/12

	Flow (l/m)		Total Flow (l/m)		Pos. Flow Difference		Total Flow Difference		Design Flow Difference	
Position	Audit	Sampler	Audit	Sampler	l/m	%	l/m	%	l/m	%
Makeup										
1	52	49	119	111	-3	-5.7%	-8	-6.9%	6	5.5%
7	67	62			-5	-7.8%				
2	62		126						13	11.9%
8	64									
NA										
NA										
NA										
NA										

Audit Criteria: 113 ±11 l/m total flow ±10% from audit flow

Comments: While the position flow comparison showed results within criteria, the total measured audit flow with positions 2 and 8 running were outside the design flow criteria. For this configuration, postions 1 & 7 are paired, and 2 & 8 are paired. The total flow with the paired positions should be at the total design flow of 113 lpm. No makeup flow was provided, as indicated by DRI.

AUDIT RECORD

DRI SFS

T&B Systems
26074 Avenue Hall Unit 9
Valencia, CA 91355
(661) 294-1103

Date: **2/21/12**
Time: **~10:30**

Auditor: **R. Baxter**

Site name: **CS**
Project: **LAX AQSAS**
Operator: **DRI**
Site Operator: **D. Campbell**

Sensor Mfg: **DRI**
Serial No.: **N/A**

Model: **DRI SVOC**
Sensor Height: **2 m**
Ambient Pressure (in Hg): **30.04**
Ambient Temperature (°C): **20**

Last cal. date: **Unknown**

Audit Device: Teledyne Hastings NAHL-5
Serial No.: 11614
Last Cert.: 1/20/12

	Flow (l/m)		Total Flow (l/m)		Pos. Flow Difference		Total Flow Difference		Design Flow Difference	
Position	Audit	Sampler	Audit	Sampler	l/m	%	l/m	%	l/m	%
Makeup										
1	40	38	93	88	-2	-4.3%	-5	-5.7%	-20	-17.5%
7	54	50			-4	-6.7%				
5	35	38	87	88	3	9.4%	1	0.8%	-26	-22.7%
11	53	50			-3	-4.9%				
NA										
NA										
NA										
NA										

Audit Criteria: 113 ±11 l/m total flow ±10% from audit flow

Comments: While the position flow comparison showed results within criteria, the total measured audit flow with both pairs were outside of the audit criteria. No makeup flow was provided, as indicated by DRI.

AUDIT RECORD

DRI SFS

T&B Systems
26074 Avenue Hall Unit 9
Valencia, CA 91355
(661) 294-1103

Date: **2/21/12**
Time: **~15:45**

Auditor: **R. Baxter**

Site name: **CS**
Project: **LAX AQSAS**
Operator: **DRI**
Site Operator: **D. Campbell**

Sensor Mfg: **DRI**
Serial No.: **N/A**

Model: **DRI SVOC**
Sensor Height: **2 m**
Ambient Pressure (in Hg): **30.00**
Ambient Temperature (°C): **21**

Last cal. date: **Unknown**

Audit Device: Teledyne Hastings NAHL-5
Serial No.: 11614
Last Cert.: 1/20/12

	Flow (l/m)		Total Flow (l/m)		Pos. Flow Difference		Total Flow Difference		Design Flow Difference	
Position	Audit	Sampler	Audit	Sampler	l/m	%	l/m	%	l/m	%
Makeup	38									
1	46		133						20	17.3%
7	49									
2	46		132						19	16.5%
8	48									
3	46		132						19	16.5%
9	48									
4	46		132						19	16.5%
10	48									

Audit Criteria: 113 ±11 l/m total flow ±10% from audit flow

Comments: Makeup flow was used at this site to minimize the issue with the pump that was running continuously. When the makeup flow was added to each of the flow pairs, the resulting total flow was outside of the audit criteria. This was confirmed by DRI at the time of the audit and the makeup flow was adjusted from 38 l/m to about 21. The result was to place the flows well within the audit criteria.

AUDIT RECORD

MINIVOL

T&B Systems
26074 Avenue Hall Unit 9
Valencia, CA 91355
(661) 294-1103

Date: **2/1/12**
Start: **11:45**
Finish: **11:55**
Auditor: **D. Bush**

Site name: **CE-1**
Project: **LAX AQSAS**
Operator: **DRI**
Site Operator: **D. Campbell**

Sensor Mfg: **Airmetrics**
Serial No.: **1141**

Model: **Minivol**
Sensor Height: **4 m**

Last cal. date: **Unknown**

Audit Device: **Dwyer**
Serial No.: **TBS-1**
Last Cert.: **2/21/12**

Minivol rotameter reading:	**N/A**
Operator provided sampler flow in l/m:	**5.0**
Audit flow in l/m:	**5.0**
Sampler Flow Diff (l/m):	**0.0**
Sampler Flow % Diff.:	**0.0%**

Audit Criteria: 5.0 ±0.5 l/m ±10% from audit flow

Comments: None

AUDIT RECORD

MINIVOL

T&B Systems
26074 Avenue Hall Unit 9
Valencia, CA 91355
(661) 294-1103

Date: **2/1/12**
Start: **11:45**
Finish: **11:55**
Auditor: **D. Bush**

Site name: **CE-2**
Project: **LAX AQSAS**
Operator: **DRI**
Site Operator: **D. Campbell**

Sensor Mfg: **Airmetrics**
Serial No.: **0989**

Model: **Minivol**
Sensor Height: **4 m**

Last cal. date: **Unknown**

Audit Device: **Dwyer**
Serial No.: **TBS-1**
Last Cert.: **2/21/12**

Minivol rotameter reading:	**N/A**
Operator provided sampler flow in l/m:	**5.0**
Audit flow in l/m:	**5.1**
Sampler Flow Diff (l/m):	**-0.1**
Sampler Flow % Diff.:	**-2.0%**

Audit Criteria: 5.0 ±0.5 l/m ±10% from audit flow

Comments: None

AUDIT RECORD

MINIVOL

T&B Systems
26074 Avenue Hall Unit 9
Valencia, CA 91355
(661) 294-1103

Date: **2/2/12**
Start: **11:10**
Finish: **11:20**
Auditor: **B. Baxter/D. Bush**

Site name: **CS-1**
Project: **LAX AQSAS**
Operator: **DRI**
Site Operator: **D. Campbell**

Sensor Mfg: **Airmetrics**
Serial No.: **1106**

Model: **Minivol**
Sensor Height: **4 m**

Last cal. date: **Unknown**

Audit Device: **Dwyer**
Serial No.: **TBS-1**
Last Cert.: **2/21/12**

Minivol rotameter reading:	**N/A**
Operator provided sampler flow in l/m:	**5.0**
Audit flow in l/m:	**4.8**
Sampler Flow Diff (l/m):	**0.2**
Sampler Flow % Diff.:	**4.2%**

Audit Criteria: 5.0 ±0.5 l/m ±10% from audit flow

Comments: Note that the Bios flow check also read 4.72 and the audit rotameter was 4.8

AUDIT RECORD

MINIVOL

T&B Systems
26074 Avenue Hall Unit 9
Valencia, CA 91355
(661) 294-1103

Date: **2/2/12**
Start: **11:10**
Finish: **11:20**
Auditor: **B. Baxter/D. Bush**

Site name: **CS-2**
Project: **LAX AQSAS**
Operator: **DRI**
Site Operator: **D. Campbell**

Sensor Mfg: **Airmetrics**
Serial No.: **1270**

Model: **Minivol**
Sensor Height: **4 m**

Last cal. date: **Unknown**

Audit Device: **Dwyer**
Serial No.: **TBS-1**
Last Cert.: **2/21/12**

Minivol rotameter reading:	**N/A**
Operator provided sampler flow in l/m:	**5.0**
Audit flow in l/m:	**5.0**
Sampler Flow Diff (l/m):	**0.0**
Sampler Flow % Diff.:	**0.0%**

Audit Criteria: 5.0 ±0.5 l/m ±10% from audit flow

Comments: Audit rotameter reading was 5.0, Bios flow check was 4.87 but intermittent.

AUDIT RECORD

MINIVOL

T&B Systems
26074 Avenue Hall Unit 9
Valencia, CA 91355
(661) 294-1103

Date: **2/3/12**
Start: **10:30**
Finish: **10:45**
Auditor: **D. Bush**

Site name: **CN-1**
Project: **LAX AQSAS**
Operator: **DRI**
Site Operator: **D. Campbell**

Sensor Mfg: **Airmetrics**
Serial No.: **1276**

Model: **Minivol**
Sensor Height: **4 m**

Last cal. date: **Unknown**

Audit Device: **Dwyer**
Serial No.: **TBS-1**
Last Cert.: **2/21/12**

Minivol rotameter reading:	**N/A**
Operator provided sampler flow in l/m:	**5.0**
Audit flow in l/m:	**4.6**
Sampler Flow Diff (l/m):	**0.4**
Sampler Flow % Diff.:	**8.7%**

Audit Criteria: 5.0 ±0.5 l/m ±10% from audit flow

Comments: None

AUDIT RECORD

MINIVOL

T&B Systems
26074 Avenue Hall Unit 9
Valencia, CA 91355
(661) 294-1103

Date: **2/3/12**
Start: **10:30**
Finish: **10:45**
Auditor: **D. Bush**

Site name: **CN-2**
Project: **LAX AQSAS**
Operator: **DRI**
Site Operator: **D. Campbell**

Sensor Mfg: **Airmetrics**
Serial No.: **1018**

Model: **Minivol**
Sensor Height: **4 m**

Last cal. date: **Unknown**

Audit Device: **Dwyer**
Serial No.: **TBS-1**
Last Cert.: **2/21/12**

Minivol rotameter reading:	**N/A**
Operator provided sampler flow in l/m:	**5.0**
Audit flow in l/m:	**5.2**
Sampler Flow Diff (l/m):	**-0.2**
Sampler Flow % Diff.:	**-3.8%**

Audit Criteria: 5.0 ±0.5 l/m ±10% from audit flow

Comments: Sampler not operating upon arrival at site. It was reset and then audited.

AUDIT RECORD

MINIVOL

T&B Systems
26074 Avenue Hall Unit 9
Valencia, CA 91355
(661) 294-1103

Date: **2/2/12**
Start: **16:40**
Finish: **16:50**
Auditor: **D. Bush**

Site name: **AQ-1**
Project: **LAX AQSAS**
Operator: **DRI**
Site Operator: **D. Campbell**

Sensor Mfg: **Airmetrics**
Serial No.: **1005**

Model: **Minivol**
Sensor Height: **4 m**

Last cal. date: **Unknown**

Audit Device: **Dwyer**
Serial No.: **TBS-1**
Last Cert.: **2/21/12**

Minivol rotameter reading:	**N/A**
Operator provided sampler flow in l/m:	**5.0**
Audit flow in l/m:	**5.1**
Sampler Flow Diff (l/m):	**-0.1**
Sampler Flow % Diff.:	**-2.0%**

Audit Criteria: 5.0 ±0.5 l/m ±10% from audit flow

Comments: None

AUDIT RECORD

MINIVOL

T&B Systems
26074 Avenue Hall Unit 9
Valencia, CA 91355
(661) 294-1103

Date: **2/2/12**
Start: **16:40**
Finish: **16:50**
Auditor: **D. Bush**

Site name: **AQ-2**
Project: **LAX AQSAS**
Operator: **DRI**
Site Operator: **D. Campbell**

Sensor Mfg: **Airmetrics**
Serial No.: **1313**

Model: **Minivol**
Sensor Height: **4 m**

Last cal. date: **Unknown**

Audit Device: **Dwyer**
Serial No.: **TBS-1**
Last Cert.: **2/21/12**

Minivol rotameter reading:	**N/A**
Operator provided sampler flow in l/m:	**5.0**
Audit flow in l/m:	**5.1**
Sampler Flow Diff (l/m):	**-0.1**
Sampler Flow % Diff.:	**-2.0%**

Audit Criteria: 5.0 ±0.5 l/m ±10% from audit flow

Comments: None

AUDIT RECORD

MINIVOL

T&B Systems
26074 Avenue Hall Unit 9
Valencia, CA 91355
(661) 294-1103

Date: **2/21/12**
Start: **10:50**
Finish: **10:55**
Auditor: **B. Baxter**

Site name: **CE2-1**
Project: **LAX AQSAS**
Operator: **DRI**
Site Operator: **D. Campbell**

Sensor Mfg: **Airmetrics**
Serial No.: **1172**

Model: **Minivol**
Sensor Height: **4 m**

Last cal. date: **Unknown**

Audit Device: **Dwyer**
Serial No.: **TBS-1**
Last Cert.: **2/21/12**

	Exposed Filter	New Filter
Minivol rotameter reading:	**N/A**	**N/A**
Operator provided sampler flow in l/m:	**5.0**	**5.0**
Audit flow in l/m:	**4.8**	**4.9**
Sampler Flow Diff (l/m):	**0.2**	**0.1**
Sampler Flow % Diff.:	**4.2%**	**2.0%**

Audit Criteria: 5.0 ±0.5 l/m ±10% from audit flow

Comments: None

AUDIT RECORD

MINIVOL

T&B Systems
26074 Avenue Hall Unit 9
Valencia, CA 91355
(661) 294-1103

Date: **2/21/12**
Start: **10:50**
Finish: **10:55**
Auditor: **B. Baxter**

Site name: **CE2-2**
Project: **LAX AQSAS**
Operator: **DRI**
Site Operator: **D. Campbell**

Sensor Mfg: **Airmetrics**
Serial No.: **1275**

Model: **Minivol**
Sensor Height: **4 m**

Last cal. date: **Unknown**

Audit Device: **Dwyer**
Serial No.: **TBS-1**
Last Cert.: **2/21/12**

	Exposed Filter	New Filter
Minivol rotameter reading:	**N/A**	**N/A**
Operator provided sampler flow in l/m:	**5.0**	**5.0**
Audit flow in l/m:	**4.8**	**4.9**
Sampler Flow Diff (l/m):	**0.2**	**0.1**
Sampler Flow % Diff.:	**4.2%**	**2.0%**

Audit Criteria: 5.0 ±0.5 l/m ±10% from audit flow

Comments: None

AUDIT RECORD

MINIVOL

T&B Systems
26074 Avenue Hall Unit 9
Valencia, CA 91355
(661) 294-1103

Date: **2/21/12**
Start: **08:42**
Finish: **08:47**
Auditor: **B. Baxter**

Site name: **CS2-1**
Project: **LAX AQSAS**
Operator: **DRI**
Site Operator: **D. Campbell**

Sensor Mfg: **Airmetrics**
Serial No.: **1194**

Model: **Minivol**
Sensor Height: **5 m**

Last cal. date: **Unknown**

Audit Device: **Dwyer**
Serial No.: **TBS-1**
Last Cert.: **2/21/12**

	Exposed Filter	New Filter
Minivol rotameter reading:	**N/A**	**N/A**
Operator provided sampler flow in l/m:	**5.0**	**5.0**
Audit flow in l/m:	**4.9**	**5.0**
Sampler Flow Diff (l/m):	**0.1**	**0.0**
Sampler Flow % Diff.:	**2.0%**	**0.0%**

Audit Criteria: 5.0 ±0.5 l/m ±10% from audit flow

Comments: None

AUDIT RECORD

MINIVOL

T&B Systems
26074 Avenue Hall Unit 9
Valencia, CA 91355
(661) 294-1103

Date: **2/21/12**
Start: **08:42**
Finish: **08:47**
Auditor: **B. Baxter**

Site name: **CS2-2**
Project: **LAX AQSAS**
Operator: **DRI**
Site Operator: **D. Campbell**

Sensor Mfg: **Airmetrics**
Serial No.: **1217 & 1296**

Model: **Minivol**
Sensor Height: **5 m**

Last cal. date: **Unknown**

Audit Device: **Dwyer**
Serial No.: **TBS-1**
Last Cert.: **2/21/12**

	Exposed Filter	New Filter
Minivol rotameter reading:	**N/A**	**N/A**
Operator provided sampler flow in l/m:	**5.0**	**5.0**
Audit flow in l/m:	**4.7**	**4.9**
Sampler Flow Diff (l/m):	**0.3**	**0.1**
Sampler Flow % Diff.:	**6.4%**	**2.0%**

Audit Criteria: 5.0 ±0.5 l/m ±10% from audit flow

Comments: When the new filter was loaded into sampler 1217 it could not generate the required flow. The samler was replaced with s/n 1296 and the flow was found to be correct.

AUDIT RECORD

MINIVOL

T&B Systems
26074 Avenue Hall Unit 9
Valencia, CA 91355
(661) 294-1103

Date: **2/21/12**
Start: **13:12**
Finish: **13:17**
Auditor: **B. Baxter**

Site name: **CN2-1**
Project: **LAX AQSAS**
Operator: **DRI**
Site Operator: **D. Campbell**

Sensor Mfg: **Airmetrics**
Serial No.: **1204**

Model: **Minivol**
Sensor Height: **3 m**

Last cal. date: **Unknown**

Audit Device: **Dwyer**
Serial No.: **TBS-1**
Last Cert.: **2/21/12**

	Exposed Filter	New Filter
Minivol rotameter reading:	**N/A**	**N/A**
Operator provided sampler flow in l/m:	**5.0**	**5.0**
Audit flow in l/m:	**4.8**	**4.9**
Sampler Flow Diff (l/m):	**0.2**	**0.1**
Sampler Flow % Diff.:	**4.2%**	**2.0%**

Audit Criteria: 5.0 ±0.5 l/m ±10% from audit flow

Comments: None

AUDIT RECORD

MINIVOL

T&B Systems
26074 Avenue Hall Unit 9
Valencia, CA 91355
(661) 294-1103

Date: **2/21/12**
Start: **13:12**
Finish: **13:17**
Auditor: **B. Baxter**

Site name: **CN2-2**
Project: **LAX AQSAS**
Operator: **DRI**
Site Operator: **D. Campbell**

Sensor Mfg: **Airmetrics**
Serial No.: **1187**

Model: **Minivol**
Sensor Height: **3 m**

Last cal. date: **Unknown**

Audit Device: **Dwyer**
Serial No.: **TBS-1**
Last Cert.: **2/21/12**

	Exposed Filter	New Filter
Minivol rotameter reading:	**N/A**	**N/A**
Operator provided sampler flow in l/m:	**5.0**	**5.0**
Audit flow in l/m:	**4.8**	**4.8**
Sampler Flow Diff (l/m):	**0.2**	**0.2**
Sampler Flow % Diff.:	**4.2%**	**4.2%**

Audit Criteria: 5.0 ±0.5 l/m ±10% from audit flow

Comments: None

AUDIT RECORD

MINIVOL

T&B Systems
26074 Avenue Hall Unit 9
Valencia, CA 91355
(661) 294-1103

Date: **2/21/12**
Start: **08:19**
Finish: **08:24**
Auditor: **B. Baxter**

Site name: **UW-1**
Project: **LAX AQSAS**
Operator: **DRI**
Site Operator: **D. Campbell**

Sensor Mfg: **Airmetrics**
Serial No.: **0986**

Model: **Minivol**
Sensor Height: **2 m**

Last cal. date: **Unknown**

Audit Device: **Dwyer**
Serial No.: **TBS-1**
Last Cert.: **2/21/12**

	Exposed Filter	New Filter
Minivol rotameter reading:	**N/A**	**N/A**
Operator provided sampler flow in l/m:	**5.0**	**5.0**
Audit flow in l/m:	**5.0**	**5.0**
Sampler Flow Diff (l/m):	**0.0**	**0.0**
Sampler Flow % Diff.:	**0.0%**	**0.0%**

Audit Criteria: 5.0 ±0.5 l/m ±10% from audit flow

Comments: None

AUDIT RECORD

MINIVOL

T&B Systems
26074 Avenue Hall Unit 9
Valencia, CA 91355
(661) 294-1103

Date: **2/21/12**
Start: **08:19**
Finish: **08:24**
Auditor: **B. Baxter**

Site name: **UW-2**
Project: **LAX AQSAS**
Operator: **DRI**
Site Operator: **D. Campbell**

Sensor Mfg: **Airmetrics**
Serial No.: **1017**

Model: **Minivol**
Sensor Height: **2 m**

Last cal. date: **Unknown**

Audit Device: **Dwyer**
Serial No.: **TBS-1**
Last Cert.: **2/21/12**

	Exposed Filter	New Filter
Minivol rotameter reading:	**N/A**	**N/A**
Operator provided sampler flow in l/m:	**5.0**	**5.0**
Audit flow in l/m:	**5.0**	**5.0**
Sampler Flow Diff (l/m):	**0.0**	**0.0**
Sampler Flow % Diff.:	**0.0%**	**0.0%**

Audit Criteria: 5.0 ±0.5 l/m ±10% from audit flow

Comments: None

(This page is intentionally blank)

Appendix 4-5
Performance Audit Reports – Summer Season

(This page is intentionally blank)

AUDIT RECORD

NITRIC OXIDE

T & B Systems
26074 Avenue Hall Unit 9
Valencia, CA 91355
(661) 294-1103

Date: **07/30/12**
Start: **09:00 PST**
Finish: **15:45 PST**
Auditor: **Bob Baxter / David Bush**
Witness: **Paul Schafer**

Site Name: **Community East**
Operator: **SCS Tracer**
Project: **LAWA**

Analyzer make: **TEI**
Serial No.: **1136151039**
Sample flow: **0.59 lpm**
Range: **0.5** **PPM**

Model: **42i**
Filter: **Bi-Weekly**
Span setting: **1.084**
Zero setting: **1.9**
Last Calibrated: **07/15/12**

NO Audit Point	PPM Input (X)	PPM DAS (Y)	PPM Dif (%)
1	0.000	0.001	
2	0.040	0.039	-2.5
3	0.080	0.078	-2.5
4	0.132	0.128	-3.0
5	0.256	0.249	-2.7
6	0.402	0.393	-2.2

Linear Regression: (Y=PPM Corrected, X=PPM Input)

Audit Statisitics	
Slope:	0.976
Intercept:	0.000
Correlation:	1.0000

Comments: None.

Audit Equipment	Make	Model	ID	Certification Date
Dilution System:	API	M700E	643	07/30/12
Zero Air System:	API	701	2973	NA
Calibration Gas:	SMI	Multi	JJ8550	04/23/12

AUDIT RECORD

OXIDES OF NITROGEN

T&B Systems
26074 Avenue Hall Unit 9
Valencia, CA 91355
(661) 294-1103

Date: **07/30/12**
Start: **09:00 PST**
Finish: **15:45 PST**
Auditor: **Bob Baxter / David Bush**
Witness: **Paul Schafer**

Site Name: **Community East**
Organization: **SCS Tracer**
Project: **LAWA**

Analyzer make: **TEI**
Serial No.: **1136151039**
Sample flow: **0.59 lpm**
Range: **0.5** **PPM**

Model: **42i**
Filter: **Bi-Weekly**
Span setting: **0.992**
Zero setting: **2.5**
Last cal.: **07/15/12**

NO_X Audit Point	PPM Input (X)	PPM DAS (Y)	PPM Dif (%)
1	0.000	0.000	
2	0.040	0.038	-5.0
3	0.080	0.077	-3.8
4	0.132	0.127	-3.8
5	0.256	0.247	-3.5
6	0.402	0.388	-3.5

Linear Regression: (Y=PPM Corrected, X=PPM Input)

Audit Statisitics	
Slope:	0.966
Intercept:	0.000
Correlation:	1.0000

Comments: None.

Audit Equipment	Make	Model	ID	Certification Date
Dilution System:	API	M700E	643	07/30/12
Zero Air System:	API	701	2973	NA
Calibration Gas:	SMI	Multi	JJ8550	04/23/12

AUDIT RECORD

NITROGEN DIOXIDE

T&B Systems
26074 Avenue Hall Unit 9
Valencia, CA 91355
(661) 294-1103

Date: **07/30/12**
Start: **09:00 PST**
Finish: **15:45 PST**
Auditor: **Bob Baxter / David Bush**
Witness: **Paul Schafer**

Site Name: **Community East**
Operator: **SCS Tracer**
Project: **LAWA**

Analyzer make: **TEI**
Serial No.: **1136151039**
Sample flow: **0.59 lpm**
Range: **0.5** **PPM**

Model: **42i**
Converter T.: **317 Deg C**
Last cal.: **07/15/12**

NO_2 Audit Point	PPM Input (X)	PPM DAS (Y)	PPM Dif (%)
1	0.000	-0.001	
2	0.029	0.028	-3.4
3	0.068	0.066	-2.9
4	0.113	0.110	-2.7
5	0.235	0.228	-3.0

Linear Regression: (Y=PPM Corrected, X=PPM Input)

Audit Statisitics	
Slope:	0.973
Intercept:	0.000
Correlation:	1.0000

Converter Efficiency
100.0%

Comments: None.

Audit Equipment	Make	Model	ID	Certification Date
Dilution System:	API	M700E	643	07/30/12
Zero Air System:	API	701	2973	NA
Calibration Gas:	SMI	Multi	JJ8550	04/23/12

AUDIT RECORD

CARBON MONOXIDE

T&B Systems
26074 Avenue Hall Unit 9
Valencia, CA 91355
(661) 294-1103

Date: **07/30/12**
Start: **09:00 PST**
Finish: **15:45 PST**
Audited by: **Bob Baxter / David Bush**
Witness: **Paul Schafer**

Site name: **Community East**
Operator: **SCS Tracer**
Project: **LAWA**

Analyzer make: **TEI**
Serial No.: **1136151040**
Sample flow: **1.052**
Zero setting: **-0.201**
Range: **50** **PPM**

Model: **48i**
Filter: **Bi-Weekly**
Span setting: **1.041**
Pressure: **752.5 mm Hg**
Last cal.: **1/31/12**

CO Audit Point	PPM Input (X)	PPM DAS (Y)	PPM Dif (%)
1	0.00	-0.20	NA
2	1.08	0.87	-19.4
3	2.63	2.46	-6.5
4	8.09	7.72	-4.6
5	16.77	16.39	-2.3

Linear Regression: (Y=PPM Corrected, X=PPM Input)

	DAS
Slope:	0.9873
Intercept:	-0.19
Correlation:	1.0000

Comments:

Audit Equipment	Make	Model	ID	Certification Date
Dilution System:	API	700	225	07/30/12
Zero Air System:	Cylinder	SMI	NA	NA
Calibration Gas:	SMI	Multi	JJ24295	09/21/12

AUDIT RECORD

TRACE LEVEL SULFUR DIOXIDE

T&B Systems
26074 Avenue Hall Unit 9
Valencia, CA 91355
(661) 294-1103

Date: **07/30/12**
Start: **09:00 PST**
Finish: **15:45 PST**
Audited by: **Bob Baxter / David Bush**
Witness: **Paul Schafer**

Site name: **Community East**
Operator: **SCS Tracer**
Project: **LAWA**

Analyzer make: **TEI**
Serial No.: **1136151043**
Sample flow: **0.501 lpm**
Zero setting: **1.08**
Range: **0.05** **PPM**

Model: **43iTLE**
Filter: **Bi-Weekly**
Span setting: **0.826**
Pressure: **730.4**
Last cal.: **7/17/12**

SO_2 Audit Point	PPM Input (X)	PPM DAS (Y)	PPM Dif (%)
1	0.0000	0.0001	NA
2	0.0034	0.0031	-8.8
3	0.0100	0.0102	2.0
4	0.0300	0.0295	-1.7

Linear Regression: (Y=PPM Corrected, X=PPM Input)

	DAS
Slope:	0.9841
Intercept:	0.0000
Correlation:	0.9998

Comments: No problems were noted.

Audit Equipment	Make	Model	ID	Certification Date
Dilution System:	API	M700E	643	07/30/12
Zero Air System:	CSI	205	2427	NA
Calibration Gas:	SMI	Multi	JJ24295	09/21/12

AUDIT RECORD

HORIZONTAL WIND SPEED

T&B Systems
26074 Avenue Hall Unit 9
Valencia, CA 91355
(661) 294-1103

Date: **07/30/12**
Start: **08:00 PST**
Finish: **10:00 PST**
Auditor: **Bob Baxter / David Bush**
Witness: **Paul Schafer**

Site Name: **Community East**
Operator: **SCS Tracer**
Project: **LAWA**

Manufacturer: **Met One**
Serial No.: **M10593**
K factor: **1.4**
Range: **0-50** **m/s**
Last Calibrated: **01/31/12**

Model: **010C**
Sensor Ht.: **10 meters**
Starting torque: **0.1** **gm cm**
Starting threshold: **0.27** **m/s**
Starting threshold criteria: **0.5** **m/s**

Audit Point	Input m/s	DAS m/s	Diff. m/s
1	0.27	0.25	-0.02
2	2.94	2.93	-0.01

Audit Criteria: ±.25 m/s; ws ≤ 5 m/s

Audit Point	Input m/s	DAS m/s	Diff. %
3	8.27	8.29	0.3
4	16.26	16.31	0.3
5	24.26	24.35	0.4

Audit Criteria: ± 5%; ws > 5 m/s

Comments: No problems noted.

AUDIT RECORD

HORIZONTAL WIND DIRECTION

T&B Systems
26074 Avenue Hall Unit 9
Valencia, CA 91355
(661) 294-1103

Date: **07/30/12**
Start: **08:00 PST**
Finish: **10:00 PST**
Auditor: **Bob Baxter / David Bush**
Witness: **Paul Schafer**

Site Name: **Community East**
Operator: **SCS Tracer**
Project: **LAWA**

Manufacturer: **Met One**
Serial No.: **M10654**
K factor: **30**
Range: **0 - 540**
Crossarm: **0°**
Last Calibrated: **01/31/12**

Model: **020C**
Sensor Ht.: **10 meters**
Starting torque: **4** **gm cm**
Starting threshold: **0.37** **m/s**
Starting threshold criteria: **0.5** **m/s**

Audit Point	Degrees Reference	Degrees DAS	Diff. Degrees
1	360	361	1
2	90	93	3
3	180	182	2
4	270	272	2
5	360	362	2
6	450	453	3

Audit Criteria: ± 5 degrees

Comments: No problems noted.

AUDIT RECORD

AMBIENT TEMPERATURE

T&B Systems
26074 Avenue Hall Unit 9
Valencia, CA 91355
(661) 294-1103

Date: **07/30/12**
Start: **08:00 PST**
Finish: **10:00 PST**
Auditor: **Bob Baxter / David Bush**
Witness: **Paul Schafer**

Site Name: **Community East**
Operator: **SCS Tracer**
Project: **LAWA**

Manufacturer: **Met One**
Serial No.: **M8807**
Lower Range: **-30** **Deg C**
Upper Range: **50** **Deg C**
Last Calibrated: **01/31/12**

Model: **060A-2**
Sensor Ht.: **3.4 meters**

Audit Point	Input Deg C	DAS Deg C	Diff. Deg C
1	3.1	3.2	0.1
2	19.6	19.5	-0.1
3	39.5	39.6	0.1

Audit Criteria: ± 1.0 degree Celsius

Comments: No problems were noted.

AUDIT RECORD

AMBIENT TEMPERATURE

T&B Systems
26074 Avenue Hall Unit 9
Valencia, CA 91355
(661) 294-1103

Date: **07/30/12**
Start: **08:00 PST**
Finish: **10:00 PST**
Auditor: **Bob Baxter / David Bush**
Witness: **Paul Schafer**

Site Name: **Community East**
Operator: **SCS Tracer**
Project: **LAWA**

Manufacturer: **Met One**
Serial No.: **M8799**
Lower Range: **-30** **Deg C**
Upper Range: **50** **Deg C**
Last Calibrated: **01/31/12**

Model: **060A-2**
Sensor Ht.: **8.2 meters**

Audit Point	Input Deg C	DAS Deg C	Diff. Deg C
1	3.1	3.1	0.0
2	19.6	19.4	-0.2
3	39.5	39.5	0.0

Audit Criteria: ± 1.0 degree Celsius

Comments: No problems were noted.

AUDIT RECORD

TEMPERATURE DIFFERENCE (DELTA-T)

T&B Systems
26074 Avenue Hall Unit 9
Valencia, CA 91355
(661) 294-1103

Date: **07/30/12**
Start: **08:00 PST**
Finish: **10:00 PST**
Auditor: **Bob Baxter / David Bush**
Witness: **Paul Schafer**

Site Name: **Community East**
Operator: **SCS Tracer**
Project: **LAWA**

Manufacturer: **Met One**
Serial No.: **M8799**
Lower Range: **-30** **Deg C**
Upper Range: **50** **Deg C**
Last Calibrated: **01/31/12**

Model: **060A-2**
Sensor Ht.: **8.2 meters**

Audit Point	Input Deg C	2-9 Temp Diff Deg C
1	3.1	-0.10
2	19.6	-0.02
3	39.3	-0.13

Audit Criteria: ± 0.1°C

Comments: No problems were noted.

AUDIT RECORD

SOLAR RADIATION

T&B Systems
26074 Avenue Hall Unit 9
Valencia, CA 91355
(661) 294-1103

Date: **7/30/12**
Start: **10:00 PST**
Finish: **15:00 PST**
Auditor: **Bob Baxter / David Bush**
Witness: **Paul Schafer**

Site name: **Community East**
Operator: **SCS Tracer**
Project: **LAWA**

Sensor Mfg: **Met One**
Serial No.: **NA**
Range: **0 - 1500 W/m2**
Last Calibrated: **1/31/2012**

Model: **095**
Sensor Ht.: **3.5 m**

Audit Point	Audit W/m2	DAS W/m2	Diff. % W/m2
9:00	796	786	-1.3%
10:00	890	910	2.2%
11:00	1006	962	-4.4%
12:00	1010	969	-4.1%
13:00	947	911	-3.8%

Criteria: ± 10%

Comments: Comparison with collocated transfer standard. Hourly averages (hour beginning) based on 1-minute data.

AUDIT RECORD

RELATIVE HUMIDITY

T&B Systems
26074 Avenue Hall Unit 9
Valencia, CA 91355
(661) 294-1103

Date: **02/02/12**
Start: **12:00 PST**
Finish: **23:00 PST**
Auditor: **Bob Baxter / David Bush**
Witness: **Paul Schafer**

Site name: **Community East**
Operator: **SCS Tracer**
Project: **LAWA**

Sensor Mfg: **Met One**
Serial No.: **M10919**
Range: **0-100 %**
Last Calibrated: **1/31/12**

Model: **083E-0-6**
Sensor Ht.: **3 m**

Audit Point	Input RH (%)	DAS RH (%)	Diff. %
10:00	54.7	61.7	7.0
11:00	52.9	59.8	6.9
12:00	52.4	58.9	6.5
13:00	52.3	59.4	7.1

Criteria: ± 10%

Comments: Comparison with collocated transfer standard. Hourly averages (hour beginning) based on 1-minute data.

AUDIT RECORD

BAM

T&B Systems
26074 Avenue Hall Unit 9
Valencia, CA 91355
(661) 294-1103

Date: **07/30/12**
Start: **10:10 PST**
Finish: **10:25 PST**
Auditor: **Bob Baxter / David Bush**
Witness: **Paul Schafer**

Site name: **Community East**
Operator: **SCS Tracer**
Project: **LAWA**

Sampler: **BAM (PM2.5)**
Serial No.: **F5131**
Last Calibrated.:

Make: **Met One**
Model: **1020**

Amb. Press: **29.89** **in. Hg**
Amb. Temp.: **22.3** **°C**
Leak Check: **0.2** **LPM**

Flowmeters
Model: **Bios Defender**

	Audit	Site	Diff.
Flow	16.80 lpm	16.70 lpm	-0.6%
Amb T (^{o}C)	22.3 ^{o}C	22.2 ^{o}C	-0.1
Amb P (mm)	759 mm Hg	759 mm Hg	0

Audit Criteria: Flow - ± 10%; Total 15.0 - 18.4 lpm
Amb T - ± 2^{o}C
Amb P - ± 15 mm

Comments: No problems noted.

AUDIT RECORD

AETHALOMETER

T&B Systems
26074 Avenue Hall Unit 9
Valencia, CA 91355
(661) 294-1103

Date: **07/30/12**
Start: **9:45 PST**
Finish: **9:50 PST**
Auditor: **Bob Baxter / David Bush**
Witness: **Paul Schafer**

Site name: **Community East**
Operator: **SCS Tracer**
Project: **LAWA**

Manufacturer: **Mcgee Scientific**
Serial No.:

Model: **AE 21**
Sensor Ht.: **5 m**

Last Calibrated:

Audit device: **Bios Defender**

Audit Point	Audit lpm	Sampler lpm	%diff.
1	3.24	3.20	-1.2

Audit Criteria: ± 10%

Comments: Ambient reading during audit: ~885 ng/m3
Reading with Hepa filter on inlet: 0 ng/m3

AUDIT RECORD

SMPS

T&B Systems
26074 Avenue Hall Unit 9
Valencia, CA 91355
(661) 294-1103

Date: **07/31/12**
Start: **17:00 PST**
Finish: **17:05 PST**
Auditor: **Bob Baxter / David Bush**
Witness: **Paul Schafer**

Site name: **Community East**
Operator: **SCS Tracer**
Project: **LAWA**

Manufacturer: **TSI**
Serial No.: **010220**

Model: **3080**
Sensor Ht.: **6 m**

Last Calibrated:

Audit device: **Bios Defender**

Audit Point	Audit lpm	Sampler lpm	%diff.
Sample	1.00	1.02	2.0

Audit Criteria: ± 10%

Comments: Sheath flow 10.0 lpm indicated versus 9.7 lpm measured.

AUDIT RECORD

NEPHELOMETER

T&B Systems
26074 Avenue Hall Unit 9
Valencia, CA 91355
(661) 294-1103

Date: **07/30/12**
Start: **09:55 PST**
Finish: **10:00 PST**
Auditor: **Bob Baxter / David Bush**
Witness: **Paul Schafer**

Site name: **Community East**
Operator: **SCS Tracer**
Project: **LAWA**

Manufacturer: **Thermo**
Serial No.:

Model: **pDR-1200**
Sensor Ht.: **4.5 m**

Last Calibrated:

Audit device: **Bios Defender**

Audit Point	Audit lpm	Sampler lpm	% diff.
1	4.33	4.00	-7.6

Audit Criteria: ± 10%

Comments: No problems were noted.
Ambient reading during audit: 13 ug/m3
Reading with Hepa filter on inlet: 2 ug/m3

AUDIT RECORD

NITRIC OXIDE

T&B Systems
26074 Avenue Hall Unit 9
Valencia, CA 91355
(661) 294-1103

Date: **07/31/12**
Start: **06:20 PST**
Finish: **11:30 PST**
Auditor: **David Bush / Bob Baxter**
Witness: **Paul Schafer**

Site Name: **Community South**
Operator: **SCS Tracer**
Project: **LAWA**

Analyzer make: **TEI**
Serial No.: **65762-350**
Sample flow: **0.625 lpm**
Range: **0.5** **PPM**

Model: **42i**
Filter: **Bi-Weekly**
Span setting: **1.363**
Zero setting: **3.5**
Last Calibrated: **07/25/12**

NO Audit Point	PPM Input (X)	PPM DAS (Y)	PPM Dif (%)
1	0.000	0.000	
2	0.035	0.034	-2.9
3	0.075	0.071	-5.3
4	0.125	0.119	-4.8
5	0.250	0.242	-3.2
6	0.400	0.391	-2.3

Linear Regression: (Y=PPM Corrected, X=PPM Input)

Audit Statisitics	
Slope:	0.978
Intercept:	-0.001
Correlation:	1.0000

Comments: None.

Audit Equipment	Make	Model	ID	Certification Date
Dilution System:	API	M700E	643	07/30/12
Zero Air System:	API	701	2973	NA
Calibration Gas:	SMI	Multi	JJ8550	04/23/12

AUDIT RECORD

OXIDES OF NITROGEN

T&B Systems
26074 Avenue Hall Unit 9
Valencia, CA 91355
(661) 294-1103

Date: **07/31/12**
Start: **06:20 PST**
Finish: **11:30 PST**
Auditor: **David Bush / Bob Baxter**
Witness: **Paul Schafer**

Site Name: **Community South**
Organization: **SCS Tracer**
Project: **LAWA**

Analyzer make: **TEI**
Serial No.: **65762-350**
Sample flow: **0.625 lpm**
Range: **0.5** **PPM**

Model: **42i**
Filter: **Bi-Weekly**
Span setting: **0.977**
Zero setting: **3.5**
Last cal.: **07/25/12**

NO_X Audit Point	PPM Input (X)	PPM DAS (Y)	PPM Dif (%)
1	0.000	0.001	
2	0.035	0.034	-2.9
3	0.075	0.070	-6.7
4	0.125	0.117	-6.4
5	0.250	0.237	-5.2
6	0.400	0.380	-5.0

Linear Regression: (Y=PPM Corrected, X=PPM Input)

Audit Statisitics	
Slope:	0.949
Intercept:	0.000
Correlation:	1.0000

Comments: None.

Audit Equipment	Make	Model	ID	Certification Date
Dilution System:	API	M700E	643	07/30/12
Zero Air System:	API	701	2973	NA
Calibration Gas:	SMI	Multi	JJ8550	04/23/12

AUDIT RECORD

NITROGEN DIOXIDE

T&B Systems
26074 Avenue Hall Unit 9
Valencia, CA 91355
(661) 294-1103

Date: **07/31/12**
Start: **06:20 PST**
Finish: **11:30 PST**
Auditor: **David Bush / Bob Baxter**
Witness: **Paul Schafer**

Site Name: **Community South**
Operator: **SCS Tracer**
Project: **LAWA**

Analyzer make: **TEI**
Serial No.: **65762-350**
Ozone flow: **0.103 lpm**
Range: **0.5** **PPM**

Model: **42i**
Converter T.: **319 Deg C**
Last cal.: **07/25/12**

NO_2 Audit Point	PPM Input (X)	PPM DAS (Y)	PPM Dif (%)
1	0.000	-0.001	
2	0.020	0.018	-10.0
3	0.064	0.060	-6.3
4	0.105	0.099	-5.7
5	0.232	0.221	-4.7

Linear Regression: (Y=PPM Corrected, X=PPM Input)

Audit Statisitics	
Slope:	0.957
Intercept:	-0.001
Correlation:	1.0000

Converter Efficiency
100.0%

Comments: None.

Audit Equipment	Make	Model	ID	Certification Date
Dilution System:	API	M700E	643	07/30/12
Zero Air System:	API	701	2973	NA
Calibration Gas:	SMI	Multi	JJ8550	04/23/12

AUDIT RECORD

CARBON MONOXIDE

T&B Systems
26074 Avenue Hall Unit 9
Valencia, CA 91355
(661) 294-1103

Date: **07/31/12**
Start: **06:20 PST**
Finish: **11:30 PST**
Audited by: **David Bush / Bob Baxter**
Witness: **Paul Schafer**

Site name: **Community South**
Operator: **SCS Tracer**
Project: **LAWA**

Analyzer make: **TEI**
Serial No.: **69154-362**
Sample flow: **1.143**
Zero setting: **1.885**
Range: **50** **PPM**

Model: **48i**
Filter: **Bi-Weekly**
Span setting: **1.129**
Pressure: **781.1 mm Hg**
Last cal.: **7/17/12**

CO Audit Point	PPM Input (X)	PPM DAS (Y)	PPM Dif (%)
1	0.00	-0.25	NA
2	1.08	0.90	-16.7
3	2.65	2.48	-6.4
4	8.40	8.17	-2.7
5	17.03	17.42	2.3

Linear Regression: (Y=PPM Corrected, X=PPM Input)

	DAS
Slope:	1.0334
Intercept:	-0.28
Correlation:	0.9998

Comments: No problems noted.

Audit Equipment	Make	Model	ID	Certification Date
Dilution System:	API	700	225	07/30/12
Zero Air System:	Cylinder	SMI	NA	NA
Calibration Gas:	SMI	Multi	JJ24295	09/21/12

AUDIT RECORD

TRACE LEVEL SULFUR DIOXIDE

T&B Systems
26074 Avenue Hall Unit 9
Valencia, CA 91355
(661) 294-1103

Date: **07/31/12**
Start: **06:20 PST**
Finish: **11:30 PST**
Audited by: **David Bush / Bob Baxter**
Witness: **Paul Schafer**

Site name: **Community South**
Operator: **SCS Tracer**
Project: **LAWA**

Analyzer make: **TEI**
Serial No.: **1136151042**
Sample flow: **0.461 lpm**
Zero setting: **1.32**
Range: **0.05 PPM**

Model: **43iTLE**
Filter: **Bi-Weekly**
Span setting: **1.182**
Pressure: **738.9 mm Hg**
Last cal.: **7/17/12**

SO_2 Audit Point	PPM Input (X)	PPM DAS (Y)	PPM Dif (%)
1	0.0000	0.0003	NA
2	0.0049	0.0052	6.1
3	0.0118	0.0127	7.6
4	0.0324	0.0350	8.0

Linear Regression: (Y=PPM Corrected, X=PPM Input)

	DAS
Slope:	1.0754
Intercept:	0.0001
Correlation:	0.9999

Comments: No problems were noted.

Audit Equipment	Make	Model	ID	Certification Date
Dilution System:	API	M700E	643	07/30/12
Zero Air System:	Cylinder	SMI	NA	NA
Calibration Gas:	SMI	Multi	JJ24295	09/21/12

AUDIT RECORD

HORIZONTAL WIND SPEED

T&B Systems
26074 Avenue Hall Unit 9
Valencia, CA 91355
(661) 294-1103

Date: **07/30/12**
Start: **15:00 PST**
Finish: **16:00 PST**
Auditor: **David Bush / Bob Baxter**
Witness: **Paul Schafer**

Site Name: **Community South**
Operator: **SCS Tracer**
Project: **LAWA**

Manufacturer: **Met One**
Serial No.: **F1077**
K factor: **1.4**
Range: **0-50** **m/s**
Last Calibrated: **01/31/12**

Model: **010C**
Sensor Ht.: **10 meters**
Starting torque: **0.1** **gm cm**
Starting threshold: **0.27** **m/s**
Starting threshold criteria: **0.5** **m/s**

Audit Point	Input m/s	DAS m/s	Diff. m/s
1	0.27	0.26	-0.01
2	2.94	2.94	0.00

Audit Criteria: ±.25 m/s; ws ≤ 5 m/s

Audit Point	Input m/s	DAS m/s	Diff. %
3	8.27	8.31	0.5
4	16.26	16.38	0.7
5	24.26	24.45	0.8

Audit Criteria: ± 5%; ws > 5 m/s

Comments: No problems noted.

AUDIT RECORD

HORIZONTAL WIND DIRECTION

T&B Systems
26074 Avenue Hall Unit 9
Valencia, CA 91355
(661) 294-1103

Date: **07/30/12**
Start: **15:00 PST**
Finish: **16:00 PST**
Auditor: **David Bush / Bob Baxter**
Witness: **Paul Schafer**

Site Name: **Community South**
Operator: **SCS Tracer**
Project: **LAWA**

Manufacturer: **Met One**
Serial No.: **A1178**
K factor: **30**
Range: **0 - 540**
Crossarm: **180°**
Last Calibrated: **01/31/12**

Model: **020C**
Sensor Ht.: **10 meters**
Starting torque: **4** **gm cm**
Starting threshold: **0.37** **m/s**
Starting threshold criteria: **0.5** **m/s**

Audit Point	Degrees Reference	Degrees DAS	Diff. Degrees
1	0	0	0
2	180	180	0
3	270	275	5
4	360	363	3
5	450	451	1

Audit Criteria: ± 5 degrees

Comments: 90 deg point not achievable for an unkwonn reason.
However, this should not affect data capture.

AUDIT RECORD

AMBIENT TEMPERATURE

T&B Systems
26074 Avenue Hall Unit 9
Valencia, CA 91355
(661) 294-1103

Date: **07/30/12**
Start: **15:00 PST**
Finish: **16:00 PST**
Auditor: **David Bush / Bob Baxter**
Witness: **Paul Schafer**

Site Name: **Community South**
Operator: **SCS Tracer**
Project: **LAWA**

Manufacturer: **Met One**
Serial No.: **D7113**
Lower Range: **-30** **Deg C**
Upper Range: **50** **Deg C**
Last Calibrated: **01/31/12**

Model: **060A-2**
Sensor Ht.: **2 m**

Audit Point	Input Deg C	DAS Deg C	Diff. Deg C
1	1.9	1.8	-0.1
2	21.3	20.9	-0.4
3	39.2	38.6	-0.6

Audit Criteria: ± 1.0 degree Celsius

Comments: No problems were noted.

AUDIT RECORD

AMBIENT TEMPERATURE

T&B Systems
26074 Avenue Hall Unit 9
Valencia, CA 91355
(661) 294-1103

Date: **07/30/12**
Start: **15:00 PST**
Finish: **16:00 PST**
Auditor: **David Bush / Bob Baxter**
Witness: **Paul Schafer**

Site Name: **Community South**
Operator: **SCS Tracer**
Project: **LAWA**

Manufacturer: **Met One**
Serial No.: **D8475**
Lower Range: **-30** **Deg C**
Upper Range: **50** **Deg C**
Last Calibrated: **01/31/12**

Model: **060A-2**
Sensor Ht.: **8.2 m**

Audit Point	Input Deg C	DAS Deg C	Diff. Deg C
1	1.9	1.7	-0.2
2	21.3	20.8	-0.5
3	39.2	38.6	-0.6

Audit Criteria: ± 1.0 degree Celsius

Comments: No problems were noted.

AUDIT RECORD

TEMPERATURE DIFFERENCE (DELTA-T)

T&B Systems
26074 Avenue Hall Unit 9
Valencia, CA 91355
(661) 294-1103

Date: **07/30/12**
Start: **15:00 PST**
Finish: **16:00 PST**
Auditor: **David Bush / Bob Baxter**
Witness: **Paul Schafer**

Site Name: **Community South**
Operator: **SCS Tracer**
Project: **LAWA**

Manufacturer: **Met One**
Serial No.: **D8475**
Lower Range: **-30** **Deg C**
Upper Range: **50** **Deg C**
Last Calibrated: **01/31/12**

Model: **060A-2**
Sensor Ht.: **8.2 m**

Audit Point	Input Deg C	2-9 Temp Diff Deg C
1	1.7	-0.03
2	20.8	-0.05
3	38.4	-0.05

Audit Criteria: ± 0.1°C

Comments: No problems were noted.

AUDIT RECORD

BAM

T&B Systems
26074 Avenue Hall Unit 9
Valencia, CA 91355
(661) 294-1103

Date: **07/31/12**
Start: **7:00 PST**
Finish: **7:05 PST**
Auditor: **David Bush / Bob Baxter**
Witness: **Paul Schafer**

Site name: **Community South**
Operator: **SCS Tracer**
Project: **LAWA**

Sampler: **BAM (PM2.5)**
Serial No.: **20024885**
Last Calibrated.:

Make: **Met One**
Model: **1020**

Amb. Press: **29.89** **in. Hg**
Amb. Temp.: **16.0** **°C**
Leak Check: **0.8** **LPM**

Flowmeters
Model: **Bios Defender**

	Audit	Site	Diff.
Flow	16.33 lpm	16.70 lpm	2.3%
Amb T (^{o}C)	16.0 ^{o}C	15.7 ^{o}C	-0.3
Amb P (mm)	759 mm Hg	758 mm Hg	-1

Audit Criteria: Flow - ± 10%; Total 15.0 - 18.4 lpm
Amb T - ± 2^{o}C
Amb P - ± 15 mm

Comments: No problems noted.

AUDIT RECORD

AETHALOMETER

T&B Systems
26074 Avenue Hall Unit 9
Valencia, CA 91355
(661) 294-1103

Date: **07/31/12**
Start: **11:35 PST**
Finish: **12:30 PST**
Auditor: **David Bush / Bob Baxter**
Witness: **Paul Schafer**

Site name: **Community South**
Operator: **SCS Tracer**
Project: **LAWA**

Manufacturer: **Mcgee Scientific**
Serial No.: **20024761**

Model: **AE 21**
Sensor Ht.: **5 m**

Last Calibrated:

Audit device: **Bios Defender**

Audit Point	Audit lpm	Sampler lpm	%diff.
1	4.40	4.20	-4.5

Audit Criteria: ± 10%

Comments: Ambient reading during audit: ~300 ng/m3
Reading with Hepa filter on inlet: -29 ng/m3

AUDIT RECORD

SMPS

T&B Systems
26074 Avenue Hall Unit 9
Valencia, CA 91355
(661) 294-1103

Date: **07/31/12**
Start: **14:50 PST**
Finish: **15:40 PST**
Auditor: **David Bush / Bob Baxter**
Witness: **Paul Schafer**

Site name: **Community South**
Operator: **SCS Tracer**
Project: **LAWA**

Manufacturer: **GRIMM**
Serial No.:

Model: **Series 5.400**
Sensor Ht.: **6 m**

Last Calibrated:

Audit device: **Bios Defender**

Audit Point	Audit lpm	Sampler lpm	%diff.
1			

Audit Criteria: ± 10%

Comments: Instrument problems at time of audit. Not audited.

AUDIT RECORD

NEPHELOMETER

T&B Systems
26074 Avenue Hall Unit 9
Valencia, CA 91355
(661) 294-1103

Date: **07/31/12**
Start: **7:20 PST**
Finish: **7:25 PST**
Auditor: **David Bush / Bob Baxter**
Witness: **Paul Schafer**

Site name: **Community South**
Operator: **SCS Tracer**
Project: **LAWA**

Manufacturer: **Thermo**
Serial No.:

Model: **pDR-1200**
Sensor Ht.: **4.5 m**

Last Calibrated:

Audit device: **Bios Defender**

Audit Point	Audit lpm	Sampler lpm	% diff.
1	4.34	4.00	-7.8

Audit Criteria: ± 10%

Comments: No problems were noted.
Ambient reading during audit: 49 ug/m3
Reading with Hepa filter on inlet: 4 ug/m3

AUDIT RECORD

NITRIC OXIDE

T&B Systems
26074 Avenue Hall Unit 9
Valencia, CA 91355
(661) 294-1103

Date: **07/31/12**
Start: **12:30 PST**
Finish: **17:15 PST**
Auditor: **David Bush / Bob Baxter**
Witness: **Paul Schafer**

Site Name: **Community North**
Operator: **SCS Tracer**
Project: **LAWA**

Analyzer make: **TEI**
Serial No.: **325981773**
Sample flow: **0.505 lpm**
Range: **0.5** **PPM**

Model: **42C**
Filter: **Bi-Weekly**
Span setting: **1.446**
Zero setting: **51.0**
Last Calibrated: **07/25/12**

NO Audit Point	PPM Input (X)	PPM DAS (Y)	PPM Dif (%)
1	0.000	-0.001	
2	0.040	0.040	0.0
3	0.081	0.081	0.0
4	0.133	0.132	-0.8
5	0.256	0.257	0.4
6	0.403	0.406	0.7

Linear Regression: (Y=PPM Corrected, X=PPM Input)

Audit Statisitics	
Slope:	1.009
Intercept:	-0.001
Correlation:	1.0000

Comments: None.

Audit Equipment	Make	Model	ID	Certification Date
Dilution System:	API	M700E	643	07/30/12
Zero Air System:	API	701	2973	NA
Calibration Gas:	SMI	Multi	JJ8550	04/23/12

AUDIT RECORD

OXIDES OF NITROGEN

T&B Systems
26074 Avenue Hall Unit 9
Valencia, CA 91355
(661) 294-1103

Date: **07/31/12**
Start: **12:30 PST**
Finish: **17:15 PST**
Auditor: **David Bush / Bob Baxter**
Witness: **Paul Schafer**

Site Name: **Community North**
Organization: **SCS Tracer**
Project: **LAWA**

Analyzer make: **TEI**
Serial No.: **325981773**
Sample flow: **0.505 lpm**
Range: **0.5** **PPM**

Model: **42C**
Filter: **Bi-Weekly**
Span setting: **1.024**
Zero setting: **52.7**
Last cal.: **07/25/12**

NO_X Audit Point	PPM Input (X)	PPM DAS (Y)	PPM Dif (%)
1	0.000	0.000	
2	0.040	0.040	0.0
3	0.081	0.080	-1.2
4	0.133	0.131	-1.5
5	0.256	0.254	-0.8
6	0.403	0.401	-0.5

Linear Regression: (Y=PPM Corrected, X=PPM Input)

Audit Statisitics	
Slope:	0.995
Intercept:	0.000
Correlation:	1.0000

Comments: None.

Audit Equipment	Make	Model	ID	Certification Date
Dilution System:	API	M700E	643	07/30/12
Zero Air System:	API	701	2973	NA
Calibration Gas:	SMI	Multi	JJ8550	04/23/12

AUDIT RECORD

NITROGEN DIOXIDE

T&B Systems
26074 Avenue Hall Unit 9
Valencia, CA 91355
(661) 294-1103

Date: **07/31/12**
Start: **12:30 PST**
Finish: **17:15 PST**
Auditor: **David Bush / Bob Baxter**
Witness: **Paul Schafer**

Site Name: **Community North**
Operator: **SCS Tracer**
Project: **LAWA**

Analyzer make: **TEI**
Serial No.: **325981773**
Sample flow: **0.505 lpm**
Range: **0.5** **PPM**

Model: **42C**
Converter T.: **317 Deg C**
Last cal.: **07/25/12**

NO_2 Audit Point	PPM Input (X)	PPM DAS (Y)	PPM Dif (%)
1	0.000	0.000	
2	0.024	0.024	0.0
3	0.067	0.066	-1.5
4	0.108	0.107	-0.9
5	0.217	0.214	-1.4

Linear Regression: (Y=PPM Corrected, X=PPM Input)

Audit Statisitics	
Slope:	0.986
Intercept:	0.000
Correlation:	1.0000

Converter Efficiency
99.5%

Comments: None.

Audit Equipment	Make	Model	ID	Certification Date
Dilution System:	API	M700E	643	07/30/12
Zero Air System:	API	701	2973	NA
Calibration Gas:	SMI	Multi	JJ8550	04/23/12

AUDIT RECORD

CARBON MONOXIDE

T&B Systems
26074 Avenue Hall Unit 9
Valencia, CA 91355
(661) 294-1103

Date: **07/31/12**
Start: **12:30 PST**
Finish: **17:15 PST**
Audited by: **David Bush / Bob Baxter**
Witness: **Paul Schafer**

Site name: **Community North**
Operator: **SCS Tracer**
Project: **LAWA**

Analyzer make: **TEI**
Serial No.: **1136151041**
Sample flow: **1.069**
Zero setting: **0.096**
Range: **50** **PPM**

Model: **48i**
Filter: **Bi-Weekly**
Span setting: **1.072**
Pressure: **747.5 mm Hg**
Last cal.: **7/17/12**

CO Audit Point	PPM Input (X)	PPM DAS (Y)	PPM Dif (%)
1	0.00	-0.32	NA
2	1.08	0.80	-25.9
3	2.64	2.39	-9.5
4	8.37	7.91	-5.5
5	17.11	16.68	-2.5

Linear Regression: (Y=PPM Corrected, X=PPM Input)

	DAS
Slope:	0.9900
Intercept:	-0.29
Correlation:	1.0000

Comments: Low zero confirmed by station checks. Data should be post-processed to achieve higher accuracy at low levels.

Audit Equipment	Make	Model	ID	Certification Date
Dilution System:	API	700	225	07/30/12
Zero Air System:	Cylinder	SMI	NA	NA
Calibration Gas:	SMI	Multi	JJ24295	09/21/12

AUDIT RECORD

TRACE LEVEL SULFUR DIOXIDE

T&B Systems
26074 Avenue Hall Unit 9
Valencia, CA 91355
(661) 294-1103

Date: **07/31/12**
Start: **12:30 PST**
Finish: **17:15 PST**
Audited by: **David Bush / Bob Baxter**
Witness: **Paul Schafer**

Site name: **Community North**
Operator: **SCS Tracer**
Project: **LAWA**

Analyzer make: **TEI**
Serial No.: **1136151044**
Sample flow: **0.455 lpm**
Zero setting: **1.62**
Range: **0.05 PPM**

Model: **43iTLE**
Filter: **Bi-Weekly**
Span setting: **1.356**
Pressure: **733.8 mm Hg**
Last cal.: **7/17/12**

SO_2 Audit Point	PPM Input (X)	PPM DAS (Y)	PPM Dif (%)
1	0.0000	0.0001	NA
2	0.0047	0.0053	12.8
3	0.0118	0.0138	16.9
4	0.0330	0.0390	18.2

Linear Regression: (Y=PPM Corrected, X=PPM Input)

	DAS
Slope:	1.1831
Intercept:	-0.0001
Correlation:	1.0000

Comments: Low zero confirmed by station checks.
Data should be post-processed to achieve higher accuracy at low levels.

Audit Equipment	Make	Model	ID	Certification Date
Dilution System:	API	M700E	643	07/30/12
Zero Air System:	CSI	205	2427	NA
Calibration Gas:	SMI	Multi	JJ24295	09/21/12

AUDIT RECORD

TRACE LEVEL SULFUR DIOXIDE

T&B Systems
26074 Avenue Hall Unit 9
Valencia, CA 91355
(661) 294-1103

Date: **07/31/12**
Start: **12:30 PST**
Finish: **17:15 PST**
Audited by: **David Bush / Bob Baxter**
Witness: **Paul Schafer**

Site name: **Community North**
Operator: **SCS Tracer**
Project: **LAWA**

Analyzer make: **TEI**
Serial No.: **1136151044**
Sample flow: **0.455 lpm**
Zero setting: **1.62**
Range: **0.05 PPM**

Model: **43iTLE**
Filter: **Bi-Weekly**
Span setting: **1.356**
Pressure: **733.8 mm Hg**
Last cal.: **7/17/12**

SO_2 Audit Point	PPM Input (X)	PPM DAS (Y)	PPM Dif (%)
1	0.0000	0.0001	NA
2	0.0047	0.0046	-2.2
3	0.0118	0.0120	1.4
4	0.0330	0.0338	2.5

Linear Regression: (Y=PPM Corrected, X=PPM Input)

	DAS
Slope:	1.0257
Intercept:	-0.0001
Correlation:	1.0000

Comments: Low zero confirmed by station checks.
Data should be post-processed to achieve higher accuracy at low levels.

Audit Equipment	Make	Model	ID	Certification Date
Dilution System:	API	M700E	643	07/30/12
Zero Air System:	CSI	205	2427	NA
Calibration Gas:	SMI	Multi	JJ24295	09/21/12

AUDIT RECORD

BAM

T&B Systems
26074 Avenue Hall Unit 9
Valencia, CA 91355
(661) 294-1103

Date: **07/31/12**
Start: **8:00 PST**
Finish: **8:05 PST**
Auditor: **David Bush / Bob Baxter**
Witness: **Paul Schafer**

Site name: **Community North**
Operator: **SCS Tracer**
Project: **LAWA**

Sampler: **BAM (PM2.5)**
Serial No.: **20024884**
Last Calibrated.:

Make: **Met One**
Model: **1020**

Amb. Press: **29.91** **in. Hg**
Amb. Temp.: **21.0** **°C**
Leak Check: **0.4** **LPM**

Flowmeters
Model: **Bios Defender**

	Audit	Site	Diff.
Flow	16.50 lpm	16.70 lpm	1.2%
Amb T (^{o}C)	21.0 ^{o}C	20.4 ^{o}C	-0.6
Amb P (mm)	760 mm Hg	760 mm Hg	0

Audit Criteria: Flow - ± 10%; Total 15.0 - 18.4 lpm
Amb T - ± 2^{o}C
Amb P - ± 15 mm

Comments: No problems noted.

AUDIT RECORD

AETHALOMETER

T&B Systems
26074 Avenue Hall Unit 9
Valencia, CA 91355
(661) 294-1103

Date: **07/31/12**
Start: **09:05 PST**
Finish: **09:10 PST**
Auditor: **David Bush / Bob Baxter**
Witness: **Paul Schafer**

Site name: **Community North**
Operator: **SCS Tracer**
Project: **LAWA**

Manufacturer: **Mcgee Scientific**
Serial No.: **636:0509**

Model: **AE 21**
Sensor Ht.: **3.5 m**

Last Calibrated:

Audit device: **Bios Defender**

Audit Point	Audit lpm	Sampler lpm	%diff.
1	4.26	4.00	-6.1

Audit Criteria: ± 10%

Comments: Ambient reading during audit: ~3300 ng/m3
Reading with Hepa filter on inlet: -6 ng/m3

AUDIT RECORD

SMPS

T&B Systems
26074 Avenue Hall Unit 9
Valencia, CA 91355
(661) 294-1103

Date: **07/31/12**
Start: **12:40 PST**
Finish: **12:45 PST**
Auditor: **David Bush / Bob Baxter**
Witness: **Paul Schafer**

Site name: **Community North**
Operator: **SCS Tracer**
Project: **LAWA**

Manufacturer: **TSI**
Serial No.:

Model: **3080**
Sensor Ht.: **3.5 m**

Last Calibrated:

Audit device: **Bios Defender**

Audit Point	Audit lpm	Sampler lpm	%diff.
1	0.30	0.37	21.8

Audit Criteria: ± 10%

Comments: Sheath flow 3.0 lpm set point, 2.71 lpm audit
Sampler running in low flow mode. Site flow device showed 2.93 lpm - Audit piston flow measurement device may have affected flows.

AUDIT RECORD

NEPHELOMETER

T&B Systems
26074 Avenue Hall Unit 9
Valencia, CA 91355
(661) 294-1103

Date: **07/31/12**
Start: **08:00 PST**
Finish: **08:05 PST**
Auditor: **David Bush / Bob Baxter**
Witness: **Paul Schafer**

Site name: **Community North**
Operator: **SCS Tracer**
Project: **LAWA**

Manufacturer: **Thermo**
Serial No.:

Model: **pDR-1200**
Sensor Ht.: **2.5 m**

Last Calibrated:

Audit device: **Bios Defender**

Audit Point	Audit lpm	Sampler lpm	% diff.
1	4.30	4.00	-7.0

Audit Criteria: ± 10%

Comments: No problems were noted.
Ambient reading during audit: 54 ug/m3
Reading with Hepa filter on inlet: 5 ug/m3

AUDIT RECORD

BAM

T&B Systems
26074 Avenue Hall Unit 9
Valencia, CA 91355
(661) 294-1103

Date: **07/30/12**
Start: **12:40 PST**
Finish: **12:50 PST**
Auditor: **David Bush / Bob Baxter**
Witness: **Paul Schafer**

Site name: **SCAQMD AQ**
Operator: **SCS Tracer**
Project: **LAWA**

Sampler: **BAM (PM2.5)**
Serial No.:
Last Calibrated.:

Make: **Met One**
Model: **1020**

Amb. Press: **29.83** **in. Hg**
Amb. Temp.: **20.1** **°C**
Leak Check: **2.8** **LPM**

Flowmeters
Model: **BGI Challenger**

	Audit	Site	Diff.
Flow	16.30 lpm	16.70 lpm	2.5%
Amb T (^{o}C)	20.1 ^{o}C	20.1 ^{o}C	0.0
Amb P (mm)	758 mm Hg	757 mm Hg	-1

Audit Criteria: Flow - ± 10%; Total 15.0 - 18.4 lpm
Amb T - ± 2^{o}C
Amb P - ± 15 mm

Comments: Minor leak repaired during audit. Reaudit values: Leak check 0.0 lpm, Flow 16.4 lpm.

AUDIT RECORD

AETHALOMETER

T&B Systems
26074 Avenue Hall Unit 9
Valencia, CA 91355
(661) 294-1103

Date: **07/30/12**
Start: **13:00 PST**
Finish: **13:10 PST**
Auditor: **David Bush / Bob Baxter**
Witness: **Paul Schafer**

Site name: **SCAQMD AQ**
Operator: **SCS Tracer**
Project: **LAWA**

Manufacturer: **Mcgee Scientific**
Serial No.:

Model: **AE 21**
Sensor Ht.: **3 m**

Last Calibrated:

Audit device: Bios Defender

Audit Point	Audit lpm	Sampler lpm	%diff.
1	2.59	2.50	-3.5

Audit Criteria: ± 10%

Comments: Ambient reading during audit: ~330 ng/m3
Reading with Hepa filter on inlet: 0 ng/m3

AUDIT RECORD

CPC

T&B Systems
26074 Avenue Hall Unit 9
Valencia, CA 91355
(661) 294-1103

Date: **07/31/12**
Start: **14:40 PST**
Finish: **14:50 PST**
Auditor: **David Bush / Bob Baxter**
Witness: **Dave Campbell**

Site name: **SCAQMD AQ**
Operator: **SCS Tracer**
Project: **LAWA**

Manufacturer: **TSI**
Serial No.:

Model: **CPC**
Sensor Ht.: **1.5 m**

Last Calibrated:

Audit device: Bios Defender

Audit Point	Audit lpm	Sampler lpm	%diff.
1	1.90	1.90	0.0

Audit Criteria: ± 10%

Comments: Located in outside enclosure.
Ambient reading during audit: ~1900 p/cm3.
Reading with Hepa filter on inlet: 0.1 p/cm3
Adjusted during audit: Audit 1.47 lpm, Sampler 1.5 lpm.

AUDIT RECORD

NEPHELOMETER

T&B Systems
26074 Avenue Hall Unit 9
Valencia, CA 91355
(661) 294-1103

Date: **07/30/12**
Start: **13:00 PST**
Finish: **13:10 PST**
Auditor: **David Bush / Bob Baxter**
Witness: **Paul Schafer**

Site name: **SCAQMD AQ**
Operator: **SCS Tracer**
Project: **LAWA**

Manufacturer: **Thermo**
Serial No.:

Model: **pDR-1200**
Sensor Ht.: **3 m**

Last Calibrated:

Audit device: Bios Defender

Audit Point	Audit lpm	Sampler lpm	%diff.
1	4.20	4.00	-4.8

Audit Criteria: ± 10%

Comments: No problems were noted.
Ambient reading during audit: 8 ug/m3
Reading with Hepa filter on inlet: 0 ug/m3

AUDIT RECORD

DRI SVOC

T&B Systems
26074 Avenue Hall Unit 9
Valencia, CA 91355
(661) 294-1103

Date: **7/31/12**
Time: **~17:20 PST**
Auditor: **R. Baxter**

Site name: **CE**
Project: **LAX AQSAS**
Operator: **DRI**
Site Operator: **D. Campbell**

Sensor Mfg: **DRI**
Serial No.: **N/A**

Model: **DRI SVOC**
Sensor Height: **2 m**
Ambient Pressure (in Hg): **29.81**
Ambient Temperature (°C): **22.7**

Last cal. date: **Unknown**

Audit Device: **Teledyne Hastings NAHL-5**
Serial No.: **11614**
Last Cert.: **1/20/12**

	Channel 1	Channel 2
Operator provided sampler flow in l/m:	**114**	**113**
Audit flow in l/m:	**123**	**119**
Sampler Flow Diff (l/m):	**-9**	**-6**
Sampler Flow % Diff.:	**-7.4%**	**-5.1%**

Audit Criteria: 113 ±11 l/m ±10% from audit flow

Comments: The audit flow was measured in SLPM and converted to actual conditions using the ambient pressure and temperature. No problems noted.

AUDIT RECORD

DRI SVOC

T&B Systems
26074 Avenue Hall Unit 9
Valencia, CA 91355
(661) 294-1103

Date: **7/31/12**
Time: **~13:00 PST**

Auditor: **R. Baxter**

Sensor Mfg: **DRI**
Serial No.: **N/A**

Site name: **CN**
Project: **LAX AQSAS**
Operator: **DRI**
Site Operator: **D. Campbell**

Model: **DRI SVOC**
Sensor Height: **2 m**
Ambient Pressure (in Hg): **29.91**
Ambient Temperature (°C): **27.6**

Last cal. date: **Unknown**

Audit Device: **Teledyne Hastings NAHL-5**
Serial No.: **11614**
Last Cert.: **1/20/12**

	Channel 1	Channel 2
Operator provided sampler flow in l/m:	**113.3**	**113**
Audit flow in l/m:	**122**	**122**
Sampler Flow Diff (l/m):	**-8**	**-9**
Sampler Flow % Diff.:	**-6.9%**	**-7.1%**

Audit Criteria: 113 ±11 l/m ±10% from audit flow

Comments:

AUDIT RECORD

DRI SVOC

T&B Systems
26074 Avenue Hall Unit 9
Valencia, CA 91355
(661) 294-1103

Date: **7/31/12**
Time: **~16:07 PST**

Auditor: **R. Baxter**

Sensor Mfg: **DRI**
Serial No.: **N/A**

Site name: **CS**
Project: **LAX AQSAS**
Operator: **DRI**
Site Operator: **D. Campbell**

Model: **DRI SVOC**
Sensor Height: **2 m**
Ambient Pressure (in Hg): **29.87**
Ambient Temperature (°C): **25.0**

Last cal. date: **Unknown**

Audit Device: **Teledyne Hastings NAHL-5**
Serial No.: **11614**
Last Cert.: **1/20/12**

	Channel 1	Channel 2
Operator provided sampler flow in l/m:	**113**	**113**
Audit flow in l/m:	**122**	**118**
Sampler Flow Diff (l/m):	**-9**	**-5**
Sampler Flow % Diff.:	**-7.2%**	**-4.0%**

Audit Criteria: 113 ±11 l/m ±10% from audit flow

Comments: The audit flow was measured in SLPM and converted to actual conditions using the ambient pressure and temperature. No problems noted.

AUDIT RECORD

DRI SFS

T&B Systems
26074 Avenue Hall Unit 9
Valencia, CA 91355
(661) 294-1103

Date: **7/31/12**
Time: **~17:30 PST**

Auditor: **R. Baxter**

Site name: **CE**
Project: **LAX AQSAS**
Operator: **DRI**
Site Operator: **D. Campbell**

Sensor Mfg: **DRI**
Serial No.: **N/A**

Model: **DRI SVOC**
Sensor Height: **2 m**
Ambient Pressure (in Hg): **29.87**
Ambient Temperature (°C): **25**

Last cal. date: **Unknown**

Audit Device: Teledyne Hastings NAHL-5
Serial No.: 11614
Last Cert.: 1/20/12

	Flow (l/m)		Total Flow (l/m)		Pos. Flow Difference		Total Flow Difference		Design Flow Difference	
Position	Audit	Sampler	Audit	Sampler	l/m	%	l/m	%	l/m	%
Makeup										
1	60	55.5	124	114.2	-4	-7.3%	-10	-7.8%	11	9.6%
7	64	58.7			-5	-8.2%				
2	58	54.6	121	113.3	-3	-5.6%	-7	-6.2%	8	6.9%
8	63	58.7			-4	-6.7%				
3	59	55.0			-4	-6.6%				
9	63	58.4	122	113.4	-5	-7.2%	-8	-6.9%	9	7.8%
4	59	55.4			-3	-5.9%				
10	63	58.9	122	114.3	-4	-6.4%	-7	-6.2%	9	7.8%

Audit Criteria: 113 ±11 l/m total flow ±10% from audit flow

Comments: All Positions are operational. No issues noted.

AUDIT RECORD

DRI SFS

T&B Systems
26074 Avenue Hall Unit 9
Valencia, CA 91355
(661) 294-1103

Date: **7/31/12**
Time: **13:30 PST**

Auditor: **R. Baxter**

Site name: **CN**
Project: **LAX AQSAS**
Operator: **DRI**
Site Operator: **D. Campbell**

Sensor Mfg: **DRI**
Serial No.: **N/A**

Model: **DRI SVOC**
Sensor Height: **2 m**
Ambient Pressure (in Hg): **NA**
Ambient Temperature (°C): **NA**

Last cal. date: **Unknown**

Audit Device: Teledyne Hastings NAHL-5
Serial No.: 11614
Last Cert.: 1/20/12

	Flow (l/m)		Total Flow (l/m)		Pos. Flow Difference		Total Flow Difference		Design Flow Difference	
Position	Audit	Sampler	Audit	Sampler	l/m	%	l/m	%	l/m	%
Makeup										
1	#VALUE!		#VALUE!	0.0	#VALUE!	#VALUE!	#VALUE!	#VALUE!	#VALUE!	#VALUE!
7	#VALUE!				#VALUE!	#VALUE!				
2	#VALUE!		#VALUE!	0.0	#VALUE!	#VALUE!	#VALUE!	#VALUE!	#VALUE!	#VALUE!
8	#VALUE!				#VALUE!	#VALUE!				
3	#VALUE!				#VALUE!	#VALUE!				
9	#VALUE!		#VALUE!	0	#VALUE!	#VALUE!	#VALUE!	#VALUE!	#VALUE!	#VALUE!
4	#VALUE!				#VALUE!	#VALUE!				
10	#VALUE!		#VALUE!	0	#VALUE!	#VALUE!	#VALUE!	#VALUE!	#VALUE!	#VALUE!

Audit Criteria: 113 ±11 l/m total flow ±10% from audit flow

Comments: Initially there were no filters at the site to test. After retrieving the filters there was a flow issue identified with the sample lines that were collapsing under vacuum. No further audits were attempted as the sampler required repair.

AUDIT RECORD

DRI SFS

T&B Systems
26074 Avenue Hall Unit 9
Valencia, CA 91355
(661) 294-1103

Date: **7/31/12**
Time: **NA**

Auditor: **R. Baxter**

Site name: **CS**
Project: **LAX AQSAS**
Operator: **DRI**
Site Operator: **D. Campbell**

Sensor Mfg: **DRI**
Serial No.: **N/A**

Model: **DRI SVOC**
Sensor Height: **2 m**
Ambient Pressure (in Hg): **NA**
Ambient Temperature (°C): **NA**

Last cal. date: **Unknown**

Audit Device: Teledyne Hastings NAHL-5
Serial No.: 11614
Last Cert.: 1/20/12

	Flow (l/m)		Total Flow (l/m)		Pos. Flow Difference		Total Flow Difference		Design Flow Difference	
Position	Audit	Sampler	Audit	Sampler	l/m	%	l/m	%	l/m	%
Makeup										
1	#VALUE!		#VALUE!	0.0	#VALUE!	#VALUE!	#VALUE!	#VALUE!	#VALUE!	#VALUE!
7	#VALUE!				#VALUE!	#VALUE!				
2	#VALUE!		#VALUE!	0.0	#VALUE!	#VALUE!	#VALUE!	#VALUE!	#VALUE!	#VALUE!
8	#VALUE!				#VALUE!	#VALUE!				
3	#VALUE!				#VALUE!	#VALUE!				
9	#VALUE!		#VALUE!	0	#VALUE!	#VALUE!	#VALUE!	#VALUE!	#VALUE!	#VALUE!
4	#VALUE!				#VALUE!	#VALUE!				
10	#VALUE!		#VALUE!	0	#VALUE!	#VALUE!	#VALUE!	#VALUE!	#VALUE!	#VALUE!

Audit Criteria: 113 ±11 l/m total flow ±10% from audit flow

Comments: Initially there were no filters at the site to test. After retrieving the filters there was a flow issue identified with the sample lines that were collapsing under vacuum. No further audits were attempted as the sampler required repair.

AUDIT RECORD

MINIVOL

T&B Systems
26074 Avenue Hall Unit 9
Valencia, CA 91355
(661) 294-1103

Date: **7/31/12**
Start: **15:23**
Finish: **15:23**
Auditor: **R. Baxter**

Site name: **AQ-1**
Project: **LAX AQSAS**
Operator: **DRI**
Site Operator: **D. Campbell**

Sensor Mfg: **Airmetrics**
Serial No.: **1005**

Model: **Minivol**
Sensor Height: **4 m**

Last cal. date: **Unknown**

Audit Device: **Dwyer**
Serial No.: **TBS-1**
Last Cert.: **2/21/12**

Minivol rotameter reading:	**N/A**
Operator provided sampler flow in l/m:	**5.0**
Audit flow in l/m:	**5.0**
Sampler Flow Diff (l/m):	**0.0**
Sampler Flow % Diff.:	**0.0%**

Audit Criteria: 5.0 ±0.5 l/m ±10% from audit flow

Comments: None

AUDIT RECORD

MINIVOL

T&B Systems
26074 Avenue Hall Unit 9
Valencia, CA 91355
(661) 294-1103

Date: **7/31/12**
Start: **15:23**
Finish: **15:23**
Auditor: **R. Baxter**

Site name: **AQ-2**
Project: **LAX AQSAS**
Operator: **DRI**
Site Operator: **D. Campbell**

Sensor Mfg: **Airmetrics**
Serial No.: **1313**

Model: **Minivol**
Sensor Height: **4 m**

Last cal. date: **Unknown**

Audit Device: **Dwyer**
Serial No.: **TBS-1**
Last Cert.: **2/21/12**

Minivol rotameter reading:	**N/A**
Operator provided sampler flow in l/m:	**4.9**
Audit flow in l/m:	**4.9**
Sampler Flow Diff (l/m):	**0.0**
Sampler Flow % Diff.:	**0.0%**

Audit Criteria: 5.0 ±0.5 l/m ±10% from audit flow

Comments: None

AUDIT RECORD

MINIVOL

T&B Systems
26074 Avenue Hall Unit 9
Valencia, CA 91355
(661) 294-1103

Date: **7/31/12**
Start: **17:45**
Finish: **17:45**
Auditor: **R. Baxter**

Site name: **CE-1**
Project: **LAX AQSAS**
Operator: **DRI**
Site Operator: **D. Campbell**

Sensor Mfg: **Airmetrics**
Serial No.: **1172**

Model: **Minivol**
Sensor Height: **4 m**

Last cal. date: **Unknown**

Audit Device: **Dwyer**
Serial No.: **TBS-1**
Last Cert.: **2/21/12**

Minivol rotameter reading:	**N/A**
Operator provided sampler flow in l/m:	**5.0**
Audit flow in l/m:	**5.0**
Sampler Flow Diff (l/m):	**0.0**
Sampler Flow % Diff.:	**0.0%**

Audit Criteria: 5.0 ±0.5 l/m ±10% from audit flow

Comments: None

AUDIT RECORD

MINIVOL

T&B Systems
26074 Avenue Hall Unit 9
Valencia, CA 91355
(661) 294-1103

Date: **7/31/12**
Start: **17:45**
Finish: **17:45**
Auditor: **R. Baxter**

Site name: **CE-2**
Project: **LAX AQSAS**
Operator: **DRI**
Site Operator: **D. Campbell**

Sensor Mfg: **Airmetrics**
Serial No.: **1275**

Model: **Minivol**
Sensor Height: **4 m**

Last cal. date: **Unknown**

Audit Device: **Dwyer**
Serial No.: **TBS-1**
Last Cert.: **2/21/12**

Minivol rotameter reading:	**N/A**
Operator provided sampler flow in l/m:	**5.1**
Audit flow in l/m:	**5.1**
Sampler Flow Diff (l/m):	**0.0**
Sampler Flow % Diff.:	**0.0%**

Audit Criteria: 5.0 ±0.5 l/m ±10% from audit flow

Comments: None

AUDIT RECORD

MINIVOL

T&B Systems
26074 Avenue Hall Unit 9
Valencia, CA 91355
(661) 294-1103

Date: **7/31/12**
Start: **13:59**
Finish: **13:59**
Auditor: **R. Baxter**

Site name: **CN-1**
Project: **LAX AQSAS**
Operator: **DRI**
Site Operator: **D. Campbell**

Sensor Mfg: **Airmetrics**
Serial No.: **1315**

Model: **Minivol**
Sensor Height: **4 m**

Last cal. date: **Unknown**

Audit Device: **Dwyer**
Serial No.: **TBS-1**
Last Cert.: **2/21/12**

Minivol rotameter reading:	**N/A**
Operator provided sampler flow in l/m:	**5.0**
Audit flow in l/m:	**5.0**
Sampler Flow Diff (l/m):	**0.0**
Sampler Flow % Diff.:	**0.0%**

Audit Criteria: 5.0 ±0.5 l/m ±10% from audit flow

Comments: None

AUDIT RECORD

MINIVOL

T&B Systems
26074 Avenue Hall Unit 9
Valencia, CA 91355
(661) 294-1103

Date: **7/31/12**
Start: **14:00**
Finish: **14:00**
Auditor: **R. Baxter**

Site name: **CN-2**
Project: **LAX AQSAS**
Operator: **DRI**
Site Operator: **D. Campbell**

Sensor Mfg: **Airmetrics**
Serial No.: **0987 (not working)**
Replaced with s/n 1018

Model: **Minivol**
Sensor Height: **4 m**

Last cal. date: **Unknown**

Audit Device: **Dwyer**
Serial No.: **TBS-1**
Last Cert.: **2/21/12**

Minivol rotameter reading:	**N/A**
Operator provided sampler flow in l/m:	**5.2**
Audit flow in l/m:	**5.2**
Sampler Flow Diff (l/m):	**0.0**
Sampler Flow % Diff.:	**0.0%**

Audit Criteria: 5.0 ±0.5 l/m ±10% from audit flow

Comments: Sampler 0987 not working replaced with sampler s/n 1018. Elasped time on old sampler 1298.6. S/N 0987 was as-found, s/n 1018 was as left. The results reflect the audit on s/n 1018.

AUDIT RECORD

MINIVOL

T&B Systems
26074 Avenue Hall Unit 9
Valencia, CA 91355
(661) 294-1103

Date: **7/31/12**
Start: **16:35**
Finish: **16:35**
Auditor: **R. Baxter**

Site name: **CS-1**
Project: **LAX AQSAS**
Operator: **DRI**
Site Operator: **D. Campbell**

Sensor Mfg: **Airmetrics**
Serial No.: **1270**

Model: **Minivol**
Sensor Height: **5 m**

Last cal. date: **Unknown**

Audit Device: **Dwyer**
Serial No.: **TBS-1**
Last Cert.: **2/21/12**

Minivol rotameter reading:	**N/A**
Operator provided sampler flow in l/m:	**5.0**
Audit flow in l/m:	**5.0**
Sampler Flow Diff (l/m):	**0.0**
Sampler Flow % Diff.:	**0.0%**

Audit Criteria: 5.0 ±0.5 l/m ±10% from audit flow

Comments: None

AUDIT RECORD

MINIVOL

T&B Systems
26074 Avenue Hall Unit 9
Valencia, CA 91355
(661) 294-1103

Date: **7/31/12**
Start: **16:35**
Finish: **16:35**
Auditor: **R. Baxter**

Site name: **CS-2**
Project: **LAX AQSAS**
Operator: **DRI**
Site Operator: **D. Campbell**

Sensor Mfg: **Airmetrics**
Serial No.: **1106**

Model: **Minivol**
Sensor Height: **5 m**

Last cal. date: **Unknown**

Audit Device: **Dwyer**
Serial No.: **TBS-1**
Last Cert.: **2/21/12**

Minivol rotameter reading:	**N/A**
Operator provided sampler flow in l/m:	**5.2**
Audit flow in l/m:	**5.1**
Sampler Flow Diff (l/m):	**0.1**
Sampler Flow % Diff.:	**2.0%**

Audit Criteria: 5.0 ±0.5 l/m ±10% from audit flow

Comments: None

Appendix 4-6

Audit Result Summary

(This page is intentionally blank)

Table A4-6.1. First Monitoring Season Audit Result Summary – Continuous Gas Monitors, CE Site

Site: Community East
Project: LAWA
Operator: SCS Tracer

AMBIENT AIR QUALITY MONITORS

Audit Date	Parameter	Max Diff. (%)	DAS* Slope	DAS Intercept	DAS Correlation
2/1/2012	**Nitric Oxide**	1.4	1.0114	0.0001	1.0000
2/1/2012	**Total Oxides of Nitrogen**	1.4	1.0095	0.0003	1.0000
2/1/2012	**Nitrogen Dioxide**	-5.7	0.9995	0.0002	0.9997
2/1/2012	**Carbon Monoxide**	-14.0	1.0187	-0.1830	0.9999
2/1/2012	**Sulfur Dioxide (Trace)**	-5.0	0.9768	0.0001	0.9996

Audit Criteria: Max Diff ±15%, Slope 1.000 ± 0.10: Intercept 0 ± 0.010 ppm (CO 0 ± 1.0 ppm); Correlation > 0.9950; Trace SO_2 (Audit levels 1 - 3): Max Diff ±15%, Slope 1.000 ± 0.15 OR ±0.5 ppb (Whichever is greater)

* Data Analysis System

Table A4-6.2. First Monitoring Season Audit Result Summary – Meteorological Sensors, CE Site

Site: Community East
Project: LAWA
Operator: SCS Tracer

METEOROLOGICAL SENSORS

Audit Date	Sensor	Audit Input	DAS Diff.	Audit Criteria
2/1/2012	**Wind Speed (10 meters)**	**m/s** 0.27 3.47 **m/s** 8.27 16.26 24.26	**m/s** 0.0 0.0 **%** -0.2 -0.1 -0.1	±.25 m/s < 5 m/s ± 5%; ws > 5 m/s
2/1/2012	**Wind Direction (10 meters)**	**Deg** 92 182 272 362 452	**Deg** 4 4 5 1 3	± 5 degrees
2/1/2012	**Temperature (2 meters)**	**Deg C** 0.2 16.3 36.2	**Deg C** -0.1 -0.1 -0.1	± 1.0 degree Celsius
2/1/2012	**Solar Radiation**	**W/m2** 623.6 644.2 588.4 467.2	**%** 2.7 0.8 1.5 3.3	±10%
2/2/2012	**Relative Humidity**	**%** 52.8 60.8 75.2 82.3 88.9	**%** 5.9 8.2 3.3 0.9 -0.1	± 10%
2/1/2012	**Temperature (Delta T 2-10 meters)**	**Deg C** 0.2 16.3 36.2	**Deg C** -0.08 -0.08 -0.08	± 0.1°C

Table A4-6.3. First Sampling Season Audit Result Summary – Additional Samplers, CE Site

Site: Community East
Project: LAWA
Operator: SCS Tracer / DRI

PARTICULATE AND SVOC SAMPLERS

Audit Date	Sensor	Audit Flow (lpm)	% Diff.	Audit Criteria
2/1/2012	BAM ($PM_{2.5}$)	16.66	0.2	±10%
2/1/2012	Aethalometer	3.44	-4.1	
2/1/2012	SMPS	N/A	N/A	
2/1/2012	Nephelometer (pDR)	2.92	37.0	
2/21/2012	SVOC Ch1	122	-7.6	±10%
2/21/2012	SVOC Ch2	121	-6.8	113 lpm ± 12 lpm

Table A4-6.4. First Sampling Season Audit Result Summary – Continuous Gas Monitors, CS Site

Site: Community South
Project: LAWA
Operator: SCS Tracer

AMBIENT AIR QUALITY MONITORS

Audit Date	Parameter	Max Diff. (%)	DAS Slope	DAS Intercept	DAS Correlation
2/2/2012	Nitric Oxide	-3.3	1.0324	-0.0025	0.9999
2/2/2012	Total Oxides of Nitrogen	3.2	1.0227	-0.0005	0.9999
2/2/2012	Nitrogen Dioxide	3.7	1.0288	0.0000	1.0000
2/2/2012	Carbon Monoxide	-37.9	1.0277	-0.4500	0.9999
2/2/2012	Sulfur Dioxide (Trace)	-1.3	0.9866	0.0000	1.0000

Audit Criteria: Max Diff ±15%, Slope 1.000 ± 0.10: Intercept 0 ± 0.010 ppm (CO 0 ± 1.0 ppm); Correlation > 0.9950; Trace SO_2 (Audit levels 1 - 3): Max Diff ±15%, Slope 1.000 ± 0.15 OR ±0.5 ppb (Whichever is greater)

Table A4-6.5. First Monitoring Season Audit Result Summary – Meteorological Sensors, CS Site

Site: Community South
Project: LAWA
Operator: SCS Tracer

METEOROLOGICAL SENSORS

Audit Date	Sensor	Audit Input	DAS Diff.	Audit Criteria
2/2/2012	**Wind Speed (10 meters)**	**m/s** 0.27 3.47 **m/s** 8.27 16.26 24.26	**m/s** 0.0 0.0 **%** -0.2 -0.1 -0.1	±.25 m/s < 5 m/s ± 5%; ws > 5 m/s
2/2/2012	**Wind Direction (10 meters)**	**Deg** 90 180 270 360 450	**Deg** 2 0 4 0 1	± 5 degrees
2/2/2012	**Temperature (2 meters)**	**Deg C** 2.6 18.3 37.9	**Deg C** 0.0 -0.2 -0.2	± 1.0 degree Celsius
2/2/2012	**Temperature (Delta T 2-10 meters)**	**Deg C** 2.6 18.3 37.9	**Deg C** -0.06 0.00 0.00	± 0.1°C

Table A4-6.6. First Monitoring Season Audit Result Summary – Additional Samplers, CS Site

Site: Community South
Project: LAWA
Operator: SCS Tracer / DRI

PARTICULATE AND SVOC SAMPLERS

Audit Date	Sensor	Audit Flow (lpm)	% Diff.	Audit Criteria
2/2/2012	**BAM ($PM_{2.5}$)**	16.72	-0.1	±10%
2/2/2012	**Aethalometer**	3.80	-7.9	
2/2/2012	**SMPS**	0.91	9.9	
2/2/2012	**Nephelometer (pDR)**	0.90	344.4	
2/21/2012	**SVOC Ch1**	117	-3.5	±10%
2/21/2012	**SVOC Ch2**	120	-5.9	113 lpm ± 12 lpm

Table A4-6.7. First Monitoring Season Audit Result Summary – Continuous Gas Monitors, CN Site

Site: Community North
Project: LAWA
Operator: SCS Tracer

AMBIENT AIR QUALITY MONITORS

Audit Date	Parameter	Max Diff. (%)	DAS Slope	DAS Intercept (ppm)	DAS Correlation
2/3/2012	**Nitric Oxide**	13.3	1.1055	0.0010	1.0000
2/3/2012	**Total Oxides of Nitrogen**	12.7	1.1155	-0.0001	1.0000
2/3/2012	**Nitrogen Dioxide**	11.2	1.1148	-0.0008	0.9999
2/3/2012	**Carbon Monoxide (Trace)**	-48.5	1.0509	-0.5769	0.9999
2/3/2012	**Sulfur Dioxide (Trace)**	45.0	1.0336	0.0003	0.9972

Audit Criteria: Max Diff ±15%, Slope 1.000 ± 0.10: Intercept 0 ± 0.010 ppm (CO 0 ± 1.0 ppm); Correlation > 0.9950; Trace SO_2 (Audit levels 1 - 3): Max Diff ±15%, Slope 1.000 ± 0.15 OR ±0.5 ppb (Whichever is greater)

Table A4-6.8. First Monitoring Season Audit Result Summary – Additional Samplers, CN Site

Site: Community North
Project: LAWA
Operator: SCS Tracer / DRI

PARTICULATE AND SVOC SAMPLERS

Audit Date	Sensor	Audit Flow (lpm)	% Diff.	Audit Criteria
2/3/2012	**BAM ($PM_{2.5}$)**	16.71	-0.1	±10%
2/3/2012	**Aethalometer**	4.05	1.2	
2/3/2012	**SMPS**	0.27	25.9	
2/3/2012	**Nephelometer (pDR)**	3.70	8.1	
2/21/2012	**SVOC Ch1**	122	-7.1	±10%
2/21/2012	**SVOC Ch2**	125	-9.3	113 lpm ± 12 lpm

Table A4-6.9. First Monitoring Season Audit Result Summary – Additional Samplers, AQ Site

Site: SCAQMD AQ
Project: LAWA
Operator: SCS Tracer / DRI

PARTICULATE SAMPLERS

Audit Date	Sensor	Audit Flow (lpm)	% Diff.	Audit Criteria
2/2/2012	**BAM (PM2.5)**	16.50	1.2	±10%
2/2/2012	**Aethalomter**	4.14	1.4	
2/2/2012	**CPC**	1.75		
2/2/2012	**Nephelometer (pDR)**	3.80	5.3	

Table A4-6.10. First Monitoring Season Audit Result Summary – MiniVols

Project: LAWA
Operator: DRI

MINIVOL PARTICULATE MATTER SAMPLERS

Audit Date	Site	Audit Flow (lpm)	% Diff.	Audit Criteria
2/1/2012	CE-1	5.0	0.0	±10%
2/1/2012	CE-2	5.1	-2.0	5 lpm ± 0.5 lpm
2/2/2012	CS-1	4.8	4.2	
2/2/2012	CS-2	5.0	0.0	
2/3/2012	CN-1	4.6	8.7	
2/3/2012	CN-2	5.2	-3.8	
2/2/2012	AQ-1	5.1	-2.0	
2/2/2012	AQ-2	5.1	-2.0	
2/21/2012	CE2-1	4.8	4.2	
2/21/2012	CE2-2	4.8	4.2	
2/21/2012	CS2-1	4.9	2.0	
2/21/2012	CS2-2	4.7	6.4	
2/21/2012	CN2-1	4.8	4.2	
2/21/2012	CN2-2	4.8	4.2	
2/21/2012	UW-1	5.0	0.0	
2/21/2012	UW-2	5.0	0.0	

Table A4-6.11. Second Monitoring Season Audit Result Summary – Continuous Gas Monitors, CE Site

Site: Community East
Project: LAWA
Operator: SCS Tracer

AMBIENT AIR QUALITY MONITORS

Audit Date	Parameter	Max Diff. (%)	DAS Slope	DAS Intercept	DAS Correlation
7/30/2012	**Nitric Oxide**	-3.0	0.9755	0.0000	1.0000
7/30/2012	**Total Oxides of Nitrogen**	-5.0	0.9659	-0.0003	1.0000
7/30/2012	**Nitrogen Dioxide**	-3.4	0.9733	-0.0004	1.0000
7/30/2012	**Carbon Monoxide (Trace)**	-19.4	0.9873	-0.1932	1.0000
7/30/2012	**Sulfur Dioxide (Trace)**	-8.8	0.9841	0.0000	0.9998

Audit Criteria: Max Diff ±15%, Slope 1.000 ± 0.10: Intercept 0 ± 0.010 ppm (CO 0 ± 1.0 ppm); Correlation > 0.9950; Trace SO_2 (Audit levels 1 - 3): Max Diff ±15%, Slope 1.000 ± 0.15 OR ±0.5 ppb (Whichever is greater)

Table A4-6.12. Second Monitoring Season Audit Result Summary – Meteorological Sensors, CE Site

Site: Community East
Project: LAWA
Operator: SCS Tracer

METEOROLOGICAL SENSORS

Audit Date	Sensor	Audit Input	DAS Diff.	Audit Criteria
7/30/2012	**Wind Speed (10 meters)**	**m/s** 0.27 2.94 **m/s** 8.27 16.26 24.26	**m/s** 0.0 0.0 **%** 0.3 0.3 0.4	±.25 m/s < 5 m/s ± 5%; ws > 5 m/s
7/30/2012	**Wind Direction (10 meters)**	**Deg** 360 90 180 270 360	**Deg** 1 3 2 2 2	± 5 degrees
7/30/2012	**Temperature (2 meters)**	**Deg C** 3.1 19.6 39.5	**Deg C** 0.1 -0.1 0.1	± 1.0 degree Celsius
7/30/2012	**Solar Radiation**	**W/m2** 796 890 1006 1010 947	**%** -1.3 2.2 -4.4 -4.1 -3.8	±10%
2/2/2012	**Relative Humidity**	**%** 54.7 52.9 52.4 52.3	**%** 7.0 6.9 6.5 7.1	± 10%
7/30/2012	**Temperature (Delta T 2-10 meters)**	**Deg C** 3.1 19.6 39.3	**Deg C** -0.10 -0.02 -0.13	± 0.1°C

Table A4-6-13. Second Monitoring Season Audit Result Summary – Additional Samplers, CE Site

Site: Community East
Project: LAWA
Operator: SCS Tracer / DRI

PARTICULATE AND SVOC SAMPLERS

Audit Date	Sensor	Audit Flow (lpm)	% Diff.	Audit Criteria
7/30/2012	BAM ($PM_{2.5}$)	16.80	-0.6	±10%
7/30/2012	Aethalometer	3.24	-1.2	
7/31/2012	SMPS	1.00	2.0	
7/30/2012	Nephelometer (pDR)	4.33	-7.6	
7/31/2012	SVOC Ch1	123	-7.4	±10%
7/31/2012	SVOC Ch2	119	-5.1	113 lpm ± 12 lpm

Table A4-6.14. Second Monitoring Season Audit Result Summary – Continuous Gas Monitors, CS Site

Site: Community South
Project: LAWA
Operator: SCS Tracer

AMBIENT AIR QUALITY MONITORS

Audit Date	Parameter	Max Diff. (%)	DAS Slope	DAS Intercept	DAS Correlation
7/31/2012	Nitric Oxide	-5.3	0.9777	-0.0014	1.0000
7/31/2012	Total Oxides of Nitrogen	-6.7	0.9487	-0.0001	1.0000
7/31/2012	Nitrogen Dioxide	-10.0	0.9570	-0.0012	1.0000
7/31/2012	Carbon Monoxide	-16.7	1.0334	-0.2826	0.9998
7/31/2012	Sulfur Dioxide (Trace)	8.0	1.0754	0.0001	0.9999

Audit Criteria: Max Diff ±15%, Slope 1.000 ± 0.10: Intercept 0 ± 0.010 ppm (CO 0 ± 1.0 ppm); Correlation > 0.9950; Trace SO_2 (Audit levels 1 - 3): Max Diff ±15%, Slope 1.000 ± 0.15 OR ±0.5 ppb (Whichever is greater)

Table A4-6.15. Second Monitoring Season Audit Result Summary – Meteorological Sensors, CS Site

Site: Community South
Project: LAWA
Operator: SCS Tracer

METEOROLOGICAL SENSORS

Audit Date	Sensor	Audit Input	DAS Diff.	Audit Criteria
7/30/2012	**Wind Speed (10 meters)**	**m/s** 0.27 2.94 **m/s** 8.27 16.26 24.26	**m/s** 0.0 0.0 **%** 0.5 0.7 0.8	±.25 m/s < 5 m/s ± 5%; ws > 5 m/s
7/30/2012	**Wind Direction (10 meters)**	**Deg** 0 180 270 360 450	**Deg** 0 0 5 3 1	± 5 degrees
7/30/2012	**Temperature (2 meters)**	**Deg C** 1.9 21.3 39.2	**Deg C** -0.1 -0.4 -0.6	± 1.0 degree Celsius
7/30/2012	**Temperature (Delta T 2-10 meters)**	**Deg C** 1.7 20.8 38.4	**Deg C** -0.03 -0.05 -0.05	± 0.1°C

Table A4-6.16. Second Monitoring Season Audit Result Summary – Additional Samplers, CS Site

Site: Community South
Project: LAWA
Operator: SCS Tracer / DRI

PARTICULATE AND SVOC SAMPLERS

Audit Date	Sensor	Audit Flow (lpm)	% Diff.	Audit Criteria
7/31/2012	BAM ($PM_{2.5}$)	16.33	2.3	±10%
7/31/2012	Aethalometer	4.40	-4.5	
7/31/2012	SMPS	N/A	N/A	
7/31/2012	Nephelometer (pDR)	4.34	-7.8	
7/31/2012	SVOC Ch1	122	-7.2	±10%
7/31/2012	SVOC Ch2	118	-4.0	113 lpm ± 12 lpm

Table A4-6.17. Second Monitoring Season Audit Result Summary – Continuous Gas Monitors, CN Site

Site: Community North
Project: LAWA
Operator: SCS Tracer

AMBIENT AIR QUALITY MONITORS

Audit Date	Parameter	Max Diff. (%)	DAS Slope	DAS Intercept (ppm)	DAS Correlation
7/31/2012	Nitric Oxide	-0.8	1.0089	-0.0010	1.0000
7/31/2012	Total Oxides of Nitrogen	-1.5	0.9948	-0.0004	1.0000
7/31/2012	Nitrogen Dioxide	-1.5	0.9860	0.0002	1.0000
7/31/2012	Carbon Monoxide	-25.9	0.9900	-0.2895	1.0000
7/31/2012	Sulfur Dioxide (Trace)	18.2	1.1831	-0.0001	1.0000

Audit Criteria: Max Diff ±15%, Slope 1.000 ± 0.10: Intercept 0 ± 0.010 ppm (CO 0 ± 1.0 ppm); Correlation > 0.9950; Trace SO_2 (Audit levels 1 - 3): Max Diff ±15%, Slope 1.000 ± 0.15 OR ±0.5 ppb (Whichever is greater)

Table A4-6.18. Second Monitoring Season Audit Result Summary – Additional Samplers, CN Site

Site: Community North
Project: LAWA
Operator: SCS Tracer / DRI

PARTICULATE MATTER SAMPLERS

Audit Date	Sensor	Audit Flow (lpm)	% Diff.	Audit Criteria
7/31/2012	BAM ($PM_{2.5}$)	16.50	1.2	±10%
7/31/2012	Aethalometer	4.26	-6.1	
7/31/2012	SMPS	0.30	21.8	
7/31/2012	Nephelometer (pDR)	4.30	-7.0	
7/31/2012	SVOC Ch1	122	-6.9	±10%
7/31/2012	SVOC Ch2	122	-7.1	113 lpm ± 12 lpm

Table A4-6.19. Second Monitoring Season Audit Result Summary – Additional Samplers, AQ Site

Site: SCAQMD AQ
Project: LAWA
Operator: SCS Tracer

PARTICULATE MATTER SAMPLERS

Audit Date	Sensor	Audit Flow (lpm)	% Diff.	Audit Criteria
7/30/2012	BAM ($PM_{2.5}$)	16.30	2.5	±10%
7/30/2012	Aethalometer	2.59	-3.5	
7/31/2012	CPC	1.90	0.0	
7/30/2012	Nephelometer (pDR)	4.20	-4.8	

Table A4-6.20. Second Monitoring Season Audit Result Summary – MiniVols

Project: LAWA
Operator: DRI

MINIVOL PARTICULATE MATTER SAMPLERS

Audit Date	Site	Audit Flow (lpm)	% Diff.	Audit Criteria
7/31/2012	CE-1	5.0	0.0	±10%
7/31/2012	CE-2	5.1	0.0	5 lpm ± 0.5 lpm
7/31/2012	CS-1	5.0	0.0	
7/31/2012	CS-2	5.1	2.0	
7/31/2012	CN-1	5.0	0.0	
7/31/2012	CN-2	5.2	0.0	
7/31/2012	AQ-1	5.0	0.0	
7/31/2012	AQ-2	4.9	0.0	

Section 5

PHASE III AIR MONITORING RESULTS - TIME SERIES AND SPATIAL ANALYSIS

(This page is intentionally blank)

Table of Contents

List of Tables

List of Figures

5. THE PHASE III AIR QUALITY MONITORING RESULTS

Air quality monitoring for the Phase III of the LAX Air Quality and Source Apportionment Study (AQSAS) consisted of two six-week field measurement campaigns: "Winter Monitoring Season" from 1/31/12 to 3/13/12 and "Summer Monitoring Season" from 7/18/12 to 8/28/12. The monitoring network consisted of three types of monitoring sites (core, satellite and gradient) with different combinations of continuous monitors and time-integrated (24-hour and 7-day) samples to optimize the temporal and spatial resolution of the monitoring data and the variety of chemical species that could be measured. Prior to the Winter Monitoring Season, the Desert Research Institute (DRI) conducted mobile surveys to characterize the spatial variations of pollutant concentrations within the communities and buffer zones surrounding LAX, as well as near airport operations (e.g., Central Terminal Area and aircraft takeoffs, landings, and taxiing) as shown in Figure 5-1. These surveys were used to develop the air quality monitoring plan for Phase III of the LAX AQSAS and guide the selections of appropriate monitoring locations. Following the Summer Monitoring Season, additional ambient measurements were made from 9/5/12 to 9/11/12, referred to as "Supplemental Monitoring," to further examine the chemical nature of ultrafine particles (UFP) in jet exhaust and source contributions of UFP in communities east of LAX. This section describes the detail of, and results from, the Phase III air quality monitoring

5.1 INITIAL MOBILE SURVEY AND POLLUTANT GRADIENT STUDY AT SOUTH AIRFIELD RUNWAY 25R

The mobile surveys were conducted during the week of September 20 to 23, 2011 and included equipment loaned to the team from the Bay Area Air Quality Management District (BAAQMD) as well as equipment owned by team members. Air monitors in the BAAQMD mobile monitoring van were used either alone or in combination with the DRI portable cart-mounted monitoring system (both shown in Figure 5-2). The van was equipped with a Global Positioning System (GPS) as well as continuous instruments to monitor nitric oxide (NO), carbon monoxide (CO), volatile organic compounds (VOC - estimated by photoionization detector), black carbon (BC), $PM_{2.5}$ mass (estimated by light scattering), and UFP number concentrations with time resolutions of 10 seconds. Sulfur dioxide (SO_2) was not measured due to inadequate sensitivity of the BAAQMD analyzer for the required time resolution. The cart-mounted monitoring system also included a GPS and was used to take measurements of NO, CO, CO_2, $PM_{2.5}$, and UFP number concentrations. BC was not measured on the cart due to the photoacoustic instrument's high power draw. The measurement methods for the instruments as listed in Table 5-1 were previously described in Section 3.

Mobile surveys were conducted within the communities of El Segundo, Marina del Rey, Westchester, Lennox, Hawthorne, and Inglewood. These surveys also included routes near industrial facilities in El Segundo (Hyperion Treatment Plant and LA DWP Scattergood Generating Station), the eastern-end of the LAX North and South Airfields, cargo terminals on both north and south sides of LAX, and the LAX Central Terminal Area. The community surveys were scheduled during the morning and evening periods under varying meteorological conditions and traffic patterns. Table 5-2 shows the dates and times for each mobile survey along with the type of survey, location, and average prevailing wind direction and speed. Due to gusty

wind conditions and low overall concentrations, the Taxiway and Lennox Street gradient measurements were inconclusive and will not be discussed in this report.

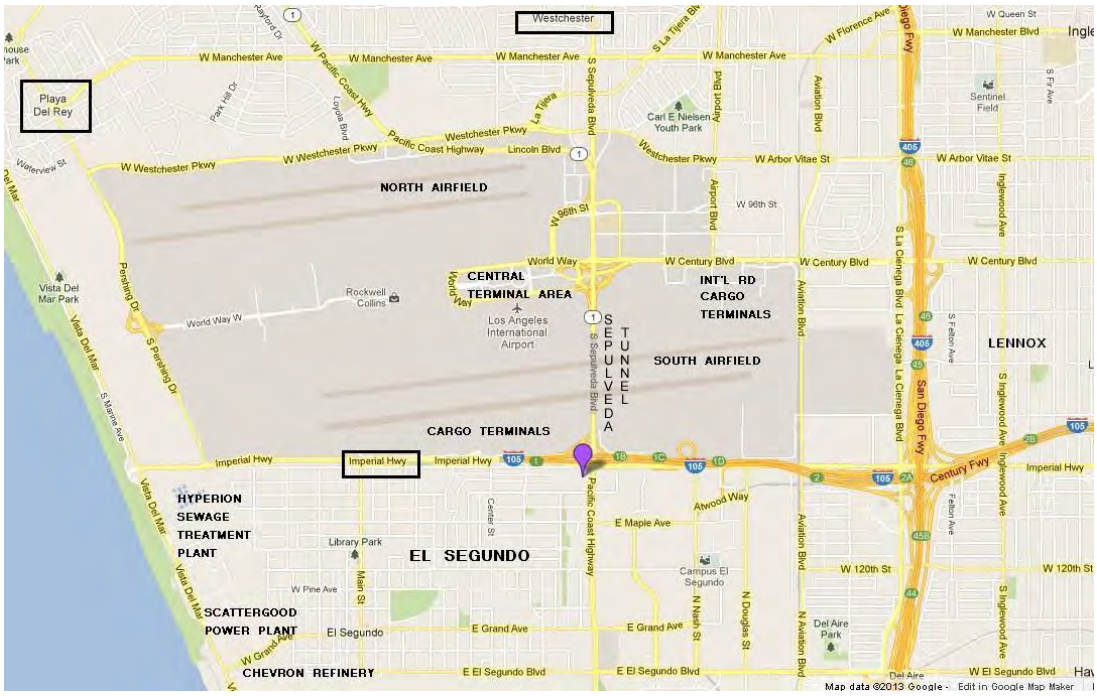

Figure 5-1. Map of LAX area.

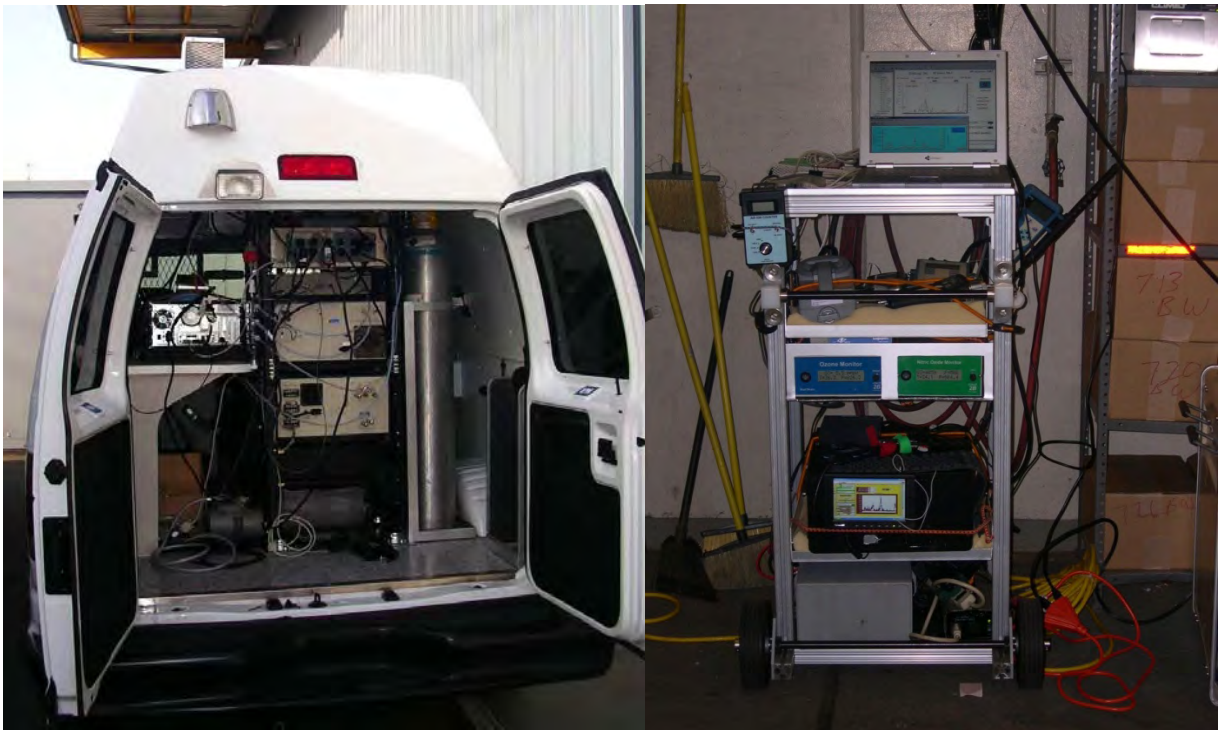

Figure 5-2. BAAQMD mobile monitoring van and DRI cart-mounted monitoring system.

Table 5-1. Continuous instruments operated in the BAAQMD mobile van and portable cart.

Parameters	**CO**	**NO**	**BC**	**CO, CO_2, Temp, RH**	**"VOC"**	**PM2.5 Mass**	**Ultra-Fine Particles**
Application	Van	Van Cart	Van	Cart	Van	Van Cart	Van Cart
Manufacturer:	Teledyne	2B Technologies	Pat Arnott, UNR	TSI	RAE Systems	TSI	Kanomax
Model:	ML9830	400	photoacoustic	8554 (Q-Trak Plus)	ppbRAE	8520 DustTrak	3800
Lower Detectable Limit:	0.05 ppm	20 ppb	0.2 ug/m3 for 1 min	~ 1 ppm	~30 ppb [(1)]	~ 1 ug/m3	< 1 particle/cm3
Range :	0-200ppm	up to 200 ppm		0-500 ppm	> 1000 ppm	0.001 to 100 mg/m3	0.015 - 1 um, 0 - 100,000 particles/cm3
Resolution:	0.01 ppm	2 ppb	0.1 ug/m3	0.1 ppm	1 ppb	0.1% + 0.001 mg/m3	1 particle/cm3
Min sampling interval:	1 sec	10 sec for NO or NOx only, 5 min for NO_2	1 sec	1 sec	1 sec	1 sec	10 sec
Response Time:	<40 secs	10 sec	1 sec	<60 secs	~10 sec	1 sec	2 sec
Precision:	1%+0.1 ppm	3%+2 ppbv	<10%	3%+3ppm	10%+20 ppb	1 ug/m3	
Power Requirements:	200W @ 110/220 VAC	analyzer:11W @12VDC	150 W at 110VAC, plus pump (<100W @ 12VDC)	4 AA batteries (20 hr run time), or 110VAC	rechargeable battery or AC (100W @ 110VAC).	4 C batteries (16 hr run time), or AC adapter for continuous operation	6 AA-size batteries (5-8 hrs run time), or AC adapter (100 – 240V)

[1] Based on prior experience.

Table 5-2. Phase III of the LAX AQSAS – initial spatial surveys.

No	Run ID	Date	Start Time	End Time	Survey Type	Locations	Wind Dir	WS (mph)
1	CS20	20-Sep	9:10	11:30	Community/LAX	See Community Survey	calm/variable/ W	0/4/6
2	RG20	20-Sep	14:00	15:20	LAX South Airfield Runway Gradient	NE of 25R just outside airport operation area, cart in open field	W	13
3	TW21A	21-Sep	8:47	10:45	Taxiway Gradient	Van at end of International Rd, cart to Century and back		0
	LX21A	21-Sep	11:37	13:08	Lennox Gradient	From La Feria to La Cienega and back with cart, Van at La Feria	W	8-10
4	LX21P	21-Sep	17:40	18:52	Lennox Gradient	From La Feria to La Cienega and back with cart, Van at La Feria	W	7-10
5	TX21P	21-Sep	19:22	19:50	Taxiway Gradient	Van at end of International Rd, cart to north end of cargo terminal area. Very clean	W	7
3	CS22A	22-Sep	8:39	11:26	Community/LAX	See Community Survey	calm/W/W	0/6/6.5
4	CS22P	22-Sep	19:21	21:13	Community/LAX	See Community Survey	W/W/var	9/8/4
5	RG23	23-Sep	11:40	14:00	25R Runway Gradient	Van and cart in open field	WSW/W	8-12

5.1.1 Spatial Surveys of the LAX Airport and Adjacent Communities

Surveys of the LAX and adjacent communities were conducted with the monitoring van beginning at the maintenance yard in the west-end of the LAX and covering the communities of El Segundo, Marina del Rey, Westchester, Hawthorne, Lennox and Inglewood. The survey route

included industrial facilities in El Segundo, the LAX Central Terminal Area, Sepulveda Tunnel, and areas near the east-end of the LAX South Airfield runways. While there were slight variations in the routes, all three community surveys nominally included the following sequence of locations.

1) El Segundo south of LAX including nearby industrial facilities (e.g., Hyperion Sewage Treatment Plant, LADWP Scattergood Power Plant, Chevron El Segundo Refinery).
2) West on Imperial Highway from Sepulveda Boulevard though the Imperial Cargo Terminal area to Vista del Mar.
3) North on Vista del Mar from El Segundo to Playa del Rey and Westchester north of LAX.
4) LAX Central Terminal area, upper and lower levels.
5) South on Sepulveda Boulevard through the Sepulveda Tunnel, east on Imperial Highway, north on Aviation Boulevard past the LAX South Airfield runways.
6) Lennox east of LAX and east of I-405 Freeway.
7) South-end of International Road near South Airfield Runway 25R taxiway.

The results of the LAX/Community surveys are presented in the spatial maps in Figure 5-3 through Figure 5-8. Each dot on the maps represents a 1-minute average concentration at the midpoint GPS position during a 1-minute measurement period. The spatial maps show the variations in concentrations of CO (ppm), NO (ppb), BC ($\mu g/m^3$), and UFP (10^3 particles/cm^3). The portable condensation particles counter (CPC) malfunctioned during the first survey and was inoperable for the remainder of the mobile surveys and the handheld PID monitor for VOC exhibited excessive baseline drift during the surveys, making data from it unusable.

The highest pollutant levels were generally measured near high traffic areas at the LAX Central Terminal Area and on main arterial streets (e.g., Century Boulevard, Sepulveda Boulevard, and Imperial Highway). Although following other vehicles too closely was avoided, higher pollutant concentrations were occasionally measured during brief stops at intersections or while behind a diesel truck or high-polluting passenger car or light truck. Higher NO and BC were measured near the east-end of the LAX South Airfield runways. Due to the proximity of measurements to the LAX's runways, it was expected that UFP concentrations would be higher at this location similar to the findings in Westerdahl et al (2007). With very few exceptions, the pollutant levels along the north and south boundaries of LAX and within the adjacent communities of El Segundo and Westchester were uniformly low.

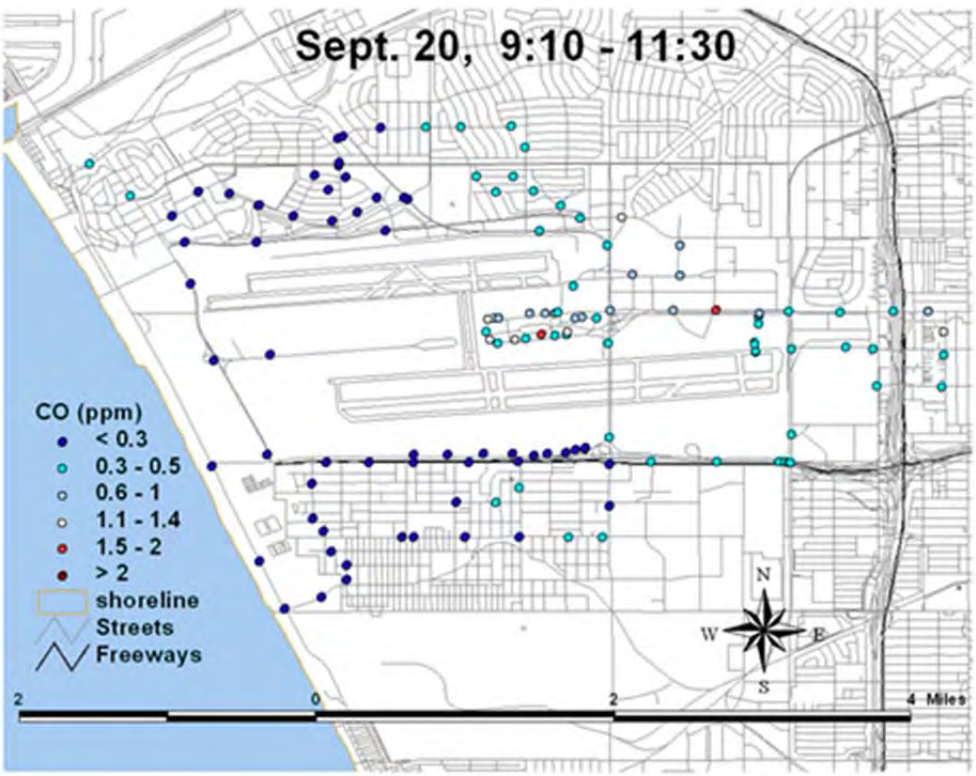

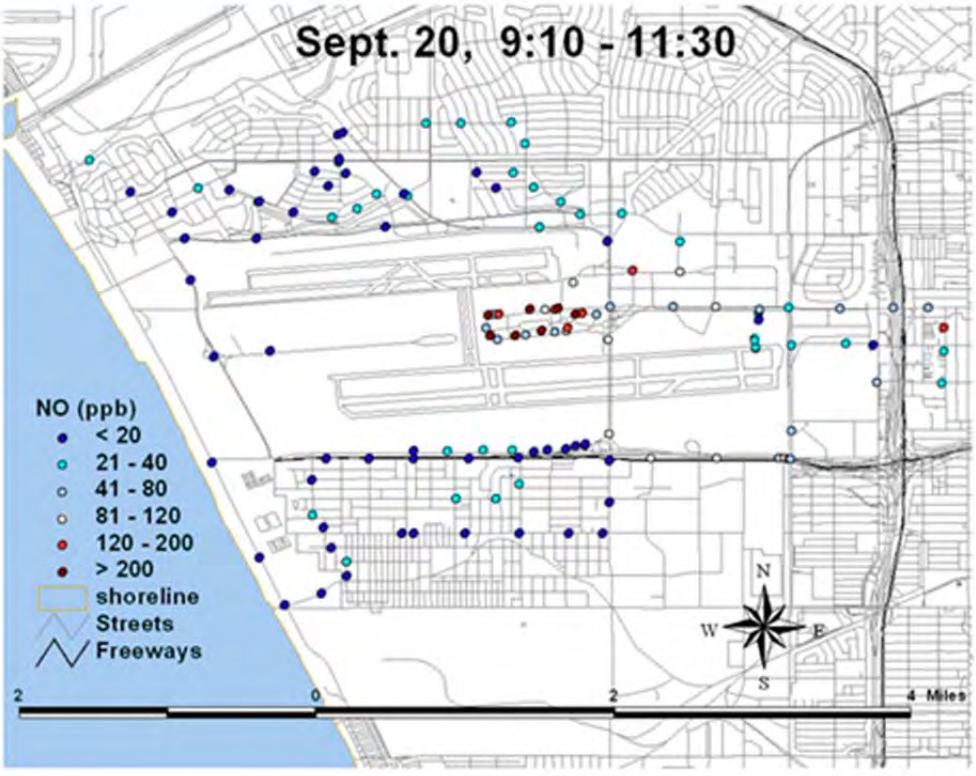

Figure 5-3. Spatial variations in CO (ppm) and NO (ppb) during community survey on 9/20/11 from 9:10 to 11:30.

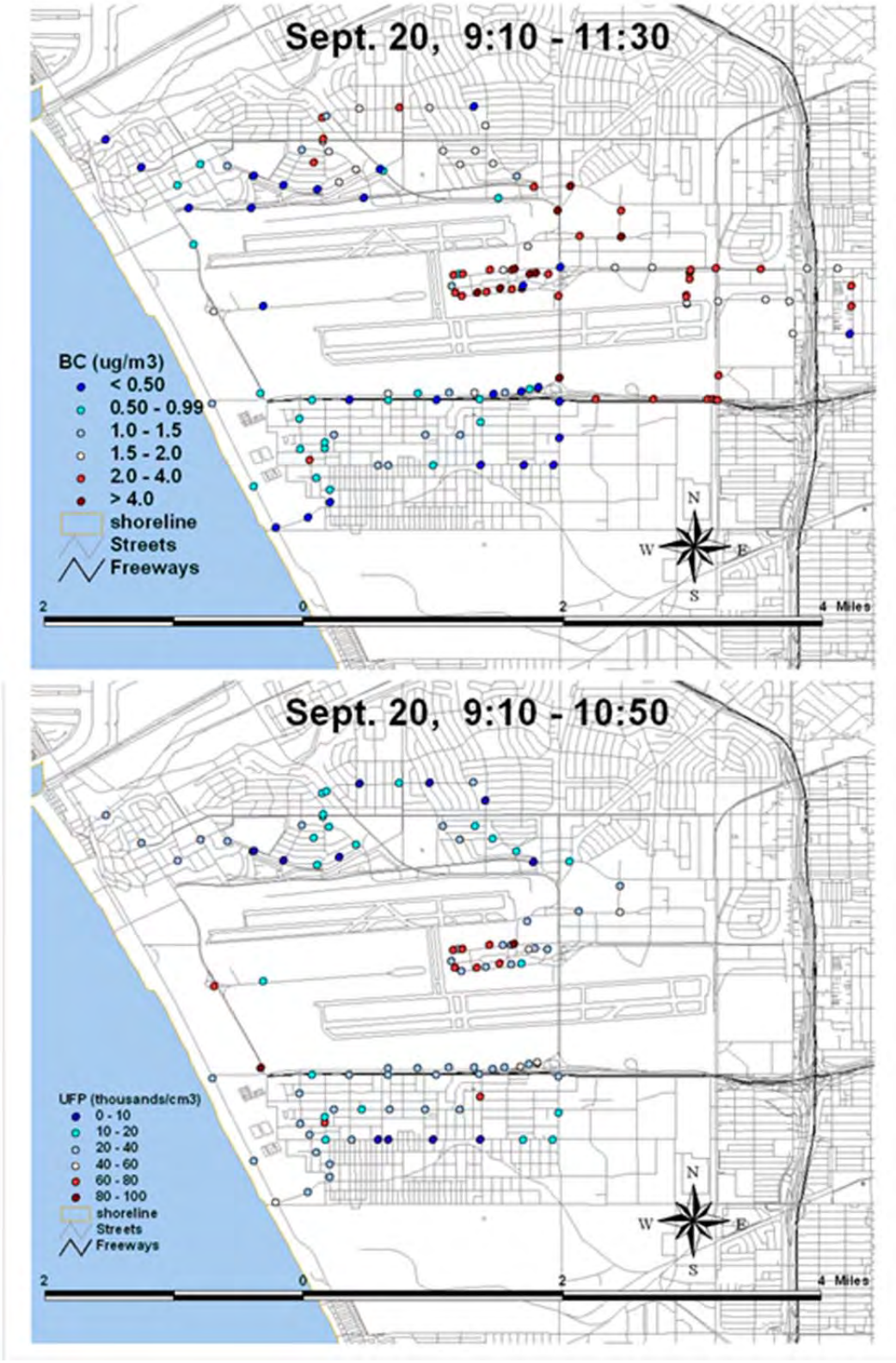

Figure 5-4. Spatial variations in BC (μg/m^3) and UFP (thousands/cm^3) during community survey on 9/20/11 from 9:10 to 11:30.

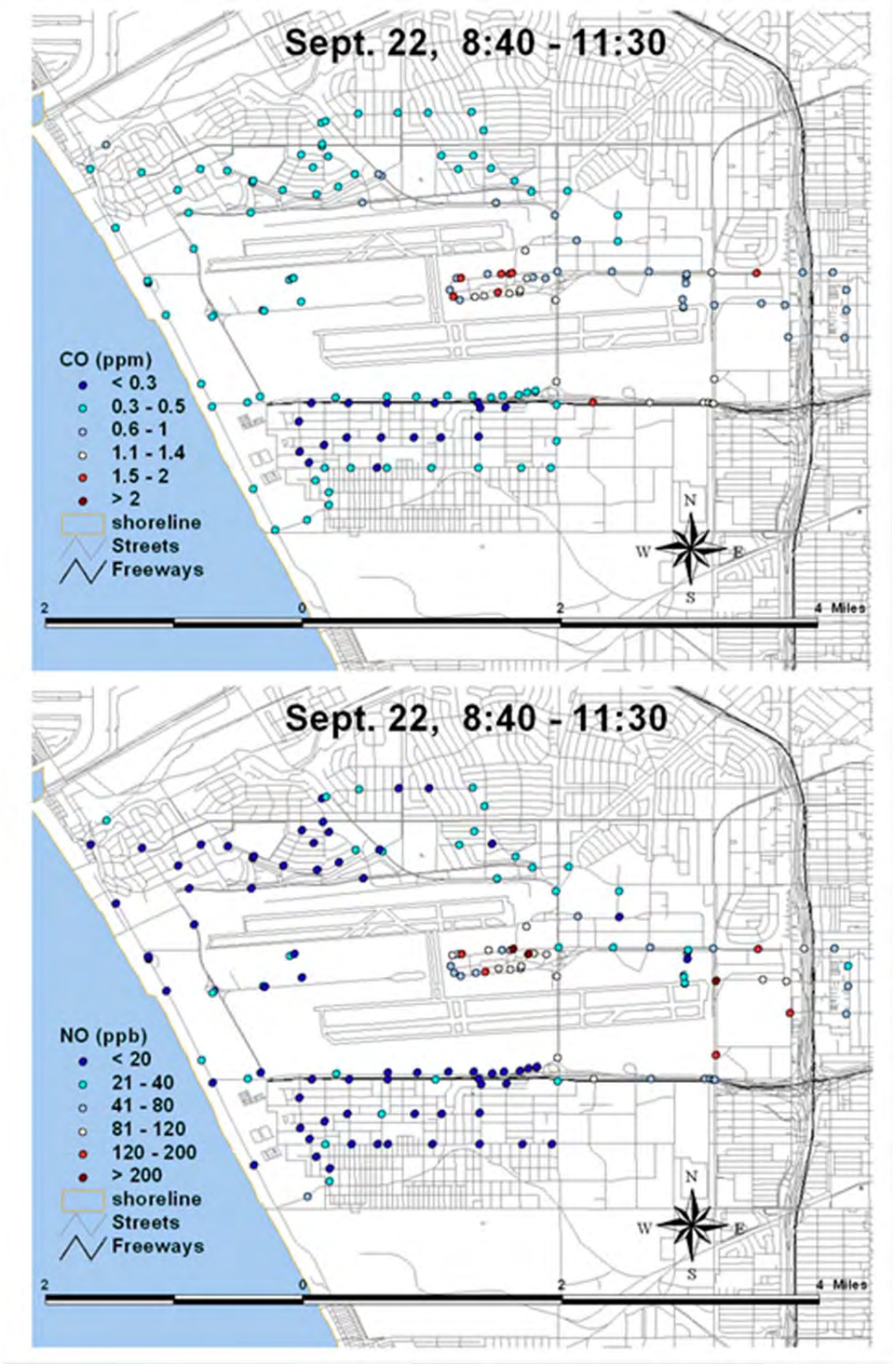

Figure 5-5. Spatial variations in CO (ppm) and NO (ppb) during community survey on 9/22/11 from 8:40 to 11:30.

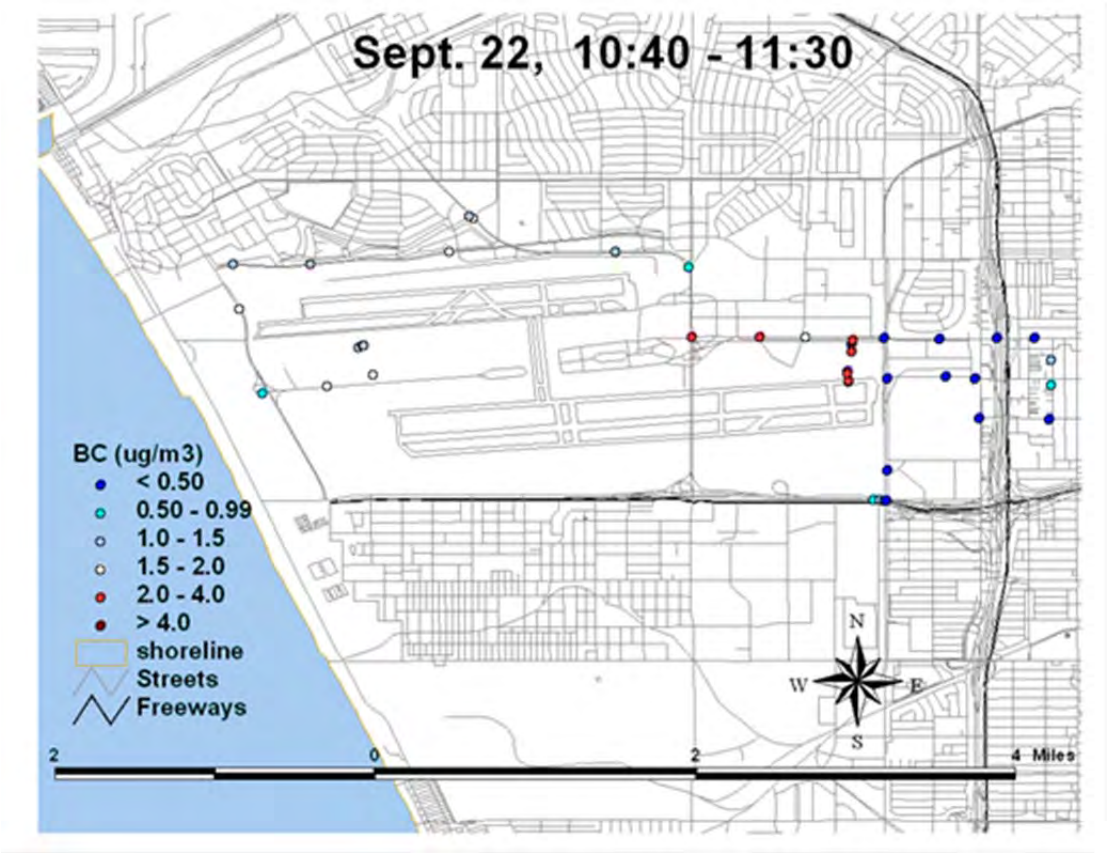

Figure 5-6. Spatial variations in BC (µg/m^3) during community survey on 9/22/11 from 10:40 to 11:30. BAAQMD CPC was inoperable.

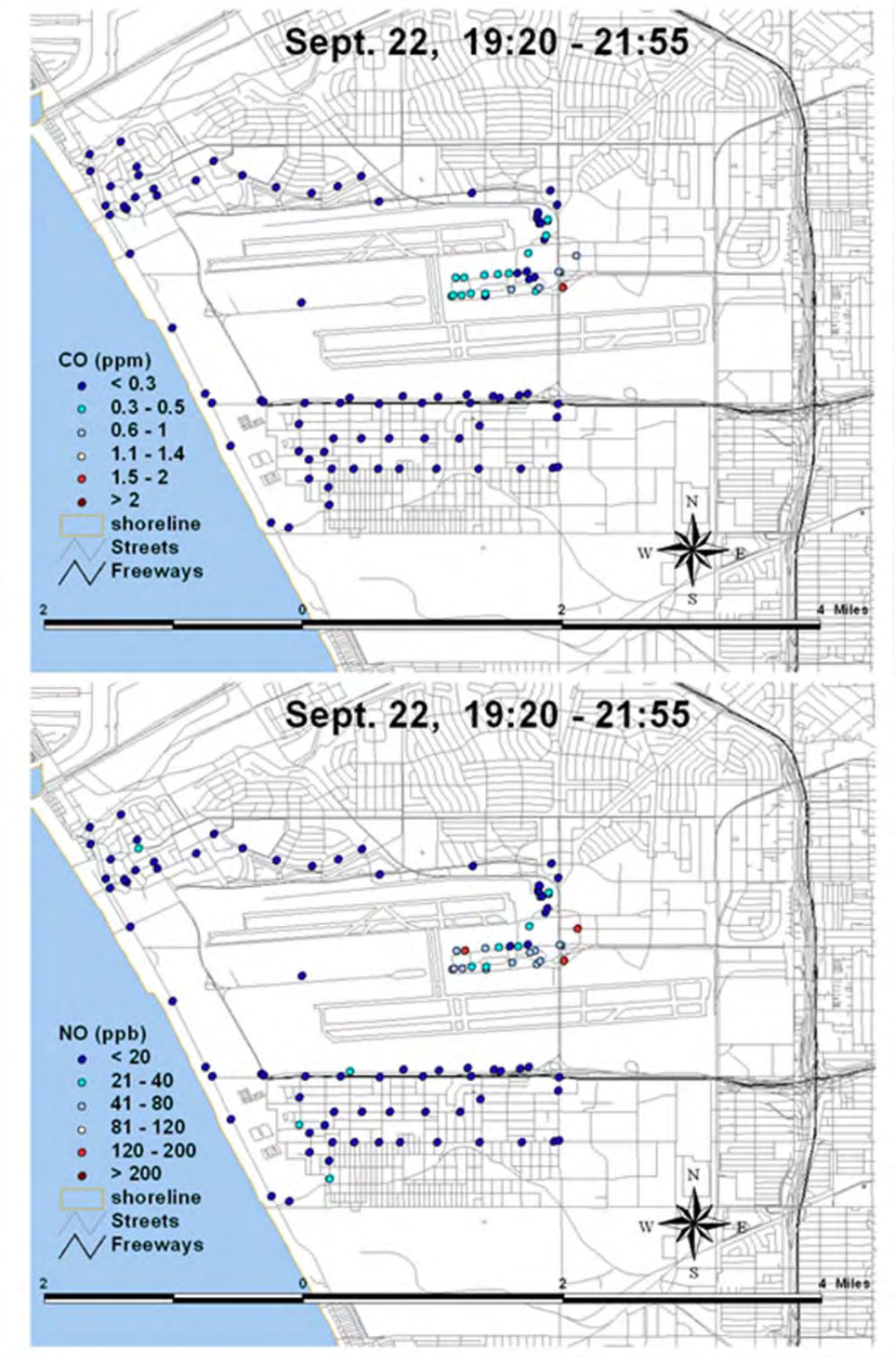

Figure 5-7. Spatial variations in CO (ppm) and NO (ppb) during community survey on 9/22/11 from 19:20 to 21:55.

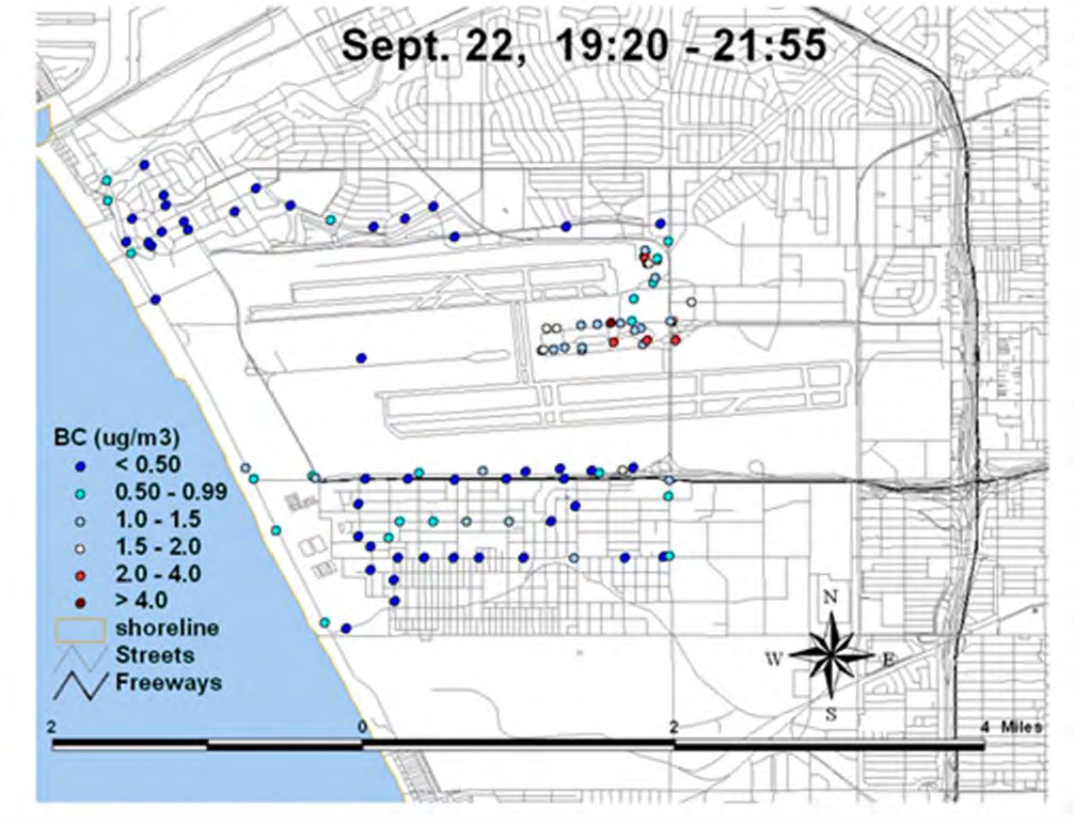

Figure 5-8. Spatial variations in BC (µg/m^3) during community survey on 9/22/11 from 19:20 to 21:55. BAAQMD CPC was inoperable.

5.1.2 Gradient Measurements at LAX South Airfield Runway 25R

The gradients in pollutant concentrations were measured near the South Airfield Runway 25 R on 9/20/11 for about 1.5 hours beginning at 2:00 P.M. The mobile monitoring van remained stationary at the northeast edge of Runway 25R just outside the airport operational area ("NE edge of 25R" indicated by the red circle in Figure 5-9) while the cart was positioned at varying distances (red crosses) east of Aviation Boulevard. Measurements on the cart included CO, CO_2, $PM_{2.5}$, NO, and UFP. CO, $PM_{2.5}$, NO, and BC were measured in the van. The BAAQMD CPC in the van was inoperable during this survey. The NE edge of 25R was previously proposed as one of the core monitoring sites in the Study Plan prepared during Phase II of the LAX AQSAS.

Prior to the start of the gradient measurements, the instruments were run with both cart and van positioned at the same location northeast of Runway 25R. After the collocated measurements, the cart was positioned at varying distances from Aviation Boulevard. Measurements were made for 10 minutes at each location (to allow the measurements to stabilize) starting with the one nearest to the roadway. After reaching the farthest location, approximately halfway into the experiment, the cart began its return trip to the starting location while making a second set of measurements at each previous sampling location. The field staff was informed about half-way into the experiment that the runway operations on South Airfield Runway 25R had been suspended for maintenance at 14:40. Therefore, during the return trip with the cart, no takeoffs

occurred (i.e., only impact of traffic on Aviation Boulevard, without jet emissions). Winds reported by LAX during this time were from the west at approximately 14 mph or 6.26 m/s (hourly average). The cart CO data were adjusted based on collocated measurements with the van non-dispersive infrared sensor (NDIR) measurements. Out-of-range CPC values were included in the averages, thus UFP number concentrations represent lower-limit values.

Figure 5-9. South Runway/Aviation Boulevard. West-East Gradient. Field between Aviation Boulevard and La Cienega Boulevard is 160 to 800 meters east of the east-end of South Airfield Runway 25R.

The time-series plots of NO and $PM_{2.5}$ presented in Figure 5-10 show that the SR site (van) did not capture most of the higher concentrations measured at the runway approach location (cart). The time series are plots of 1-minute averages of data from the cart (in dashed red) and the van (in solid blue). The x-axis indicates the cart's locations beginning with collocated measurements at the SR site and various distances in meters east of Aviation Boulevard. NO, BC, and UFP are the measured pollutants mainly associated with jet aircraft takeoffs. BC and UFP concentrations measured at the SR site did decrease when the runway shut down, but the differences were not as pronounced as would have been expected from the cart-measured NO and $PM_{2.5}$ data (Figure 5-11).

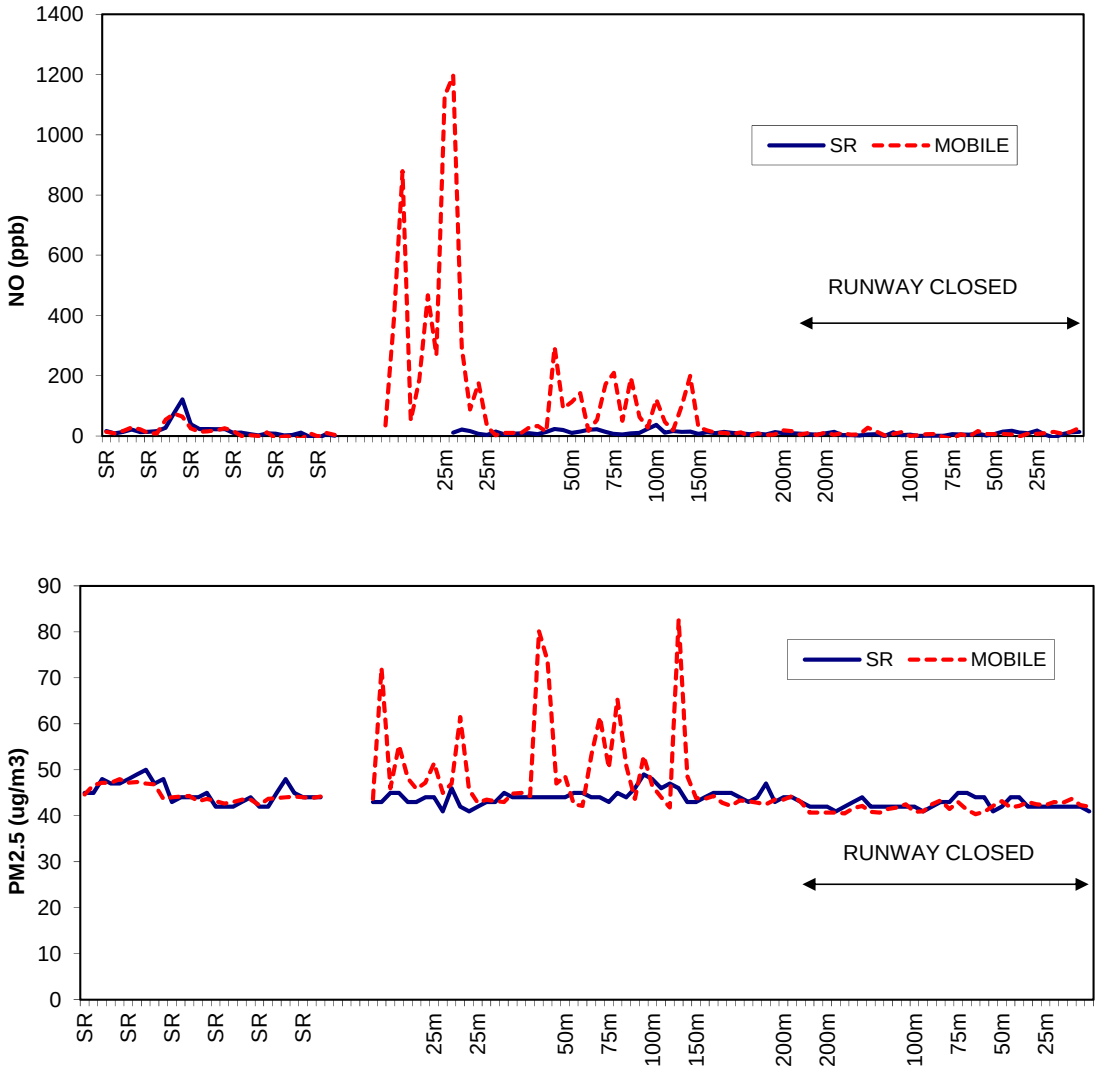

Figure 5-10. Time series of 1-minute average NO and $PM_{2.5}$ data from the cart (in dashed red) and the van (in solid blue). X-axis indicates the cart's locations beginning with collocated measurements at the SR site and various distances in meters east of Aviation Boulevard.

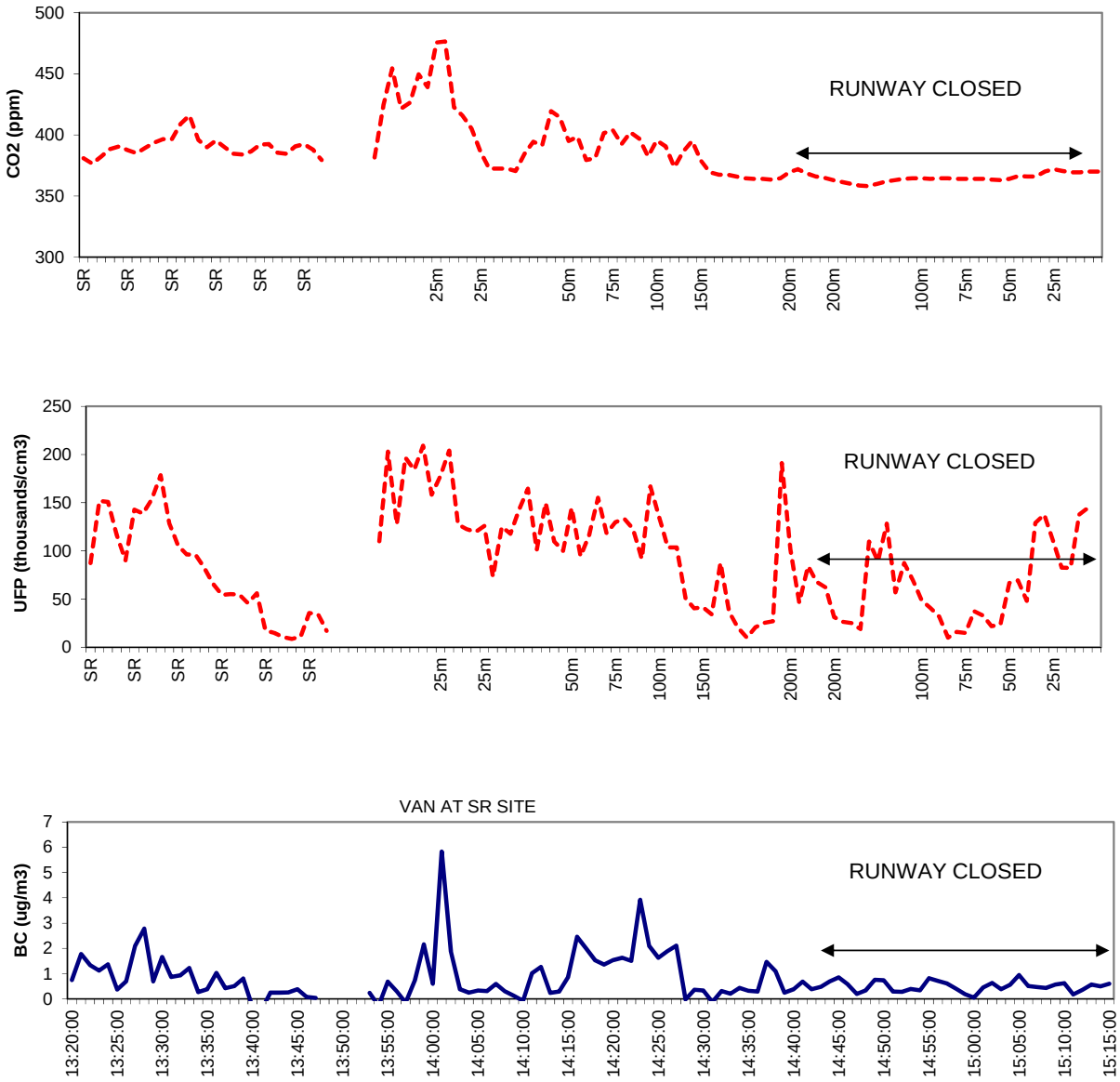

Figure 5-11. Time series of 1-minute average CO2, UFP and BC concentrations from the cart (in dashed red) and the van (in solid blue). X-axis indicates the cart's locations beginning with collocated measurements at the SR site and various distances in meters east of Aviation Boulevard.

A second experiment was conducted on 9/23/11 to determine the spatial extent of the jet exhaust plume east of the South Airfield Runway 25R. Figure 5-12 shows the sampling locations and times. The experiment began at 11:42 after the winds had shifted from south-southwest to west and ended at 14:00. The cart monitoring system remained stationary at location #1 about 100 m east of the blast fence and 20 m from the east edge of Aviation Boulevard. Measurements were made in the van for five minutes each at various distances east of location #1 (50, 115, 180, 243, 313 and 447 m; locations #2 through #7) along the South Airfield Runway 25R approach light service road on the north side of the approach field. Sampling duration at each location allowed

for inclusion of at least two takeoffs and completion of the experiment within reasonable length of time. Measurements were also made 68 m (location #8) and 82 m (location #9) south of location #1 and at various distances east of location #9 (115, 220 and 388 m; locations #10, #10b and #11) along the runway approach light service road on the south side of the approach field.

There were 81 takeoffs and 50 landings during the 2 hour 17 minute duration of the experiment or approximately three takeoffs and slightly less than two landings every five minutes.

Figure 5-12. Map showing sampling locations and times on September 23, 2011. Locations 2-7 are located at north landing light road, and Locations 9-11 are located at south landing light road.

Figure 5-13 shows time series of 1-minute average CO, NO, and $PM_{2.5}$ concentrations downwind of South Airfield Runway 25R from 11:42 to 14:00. The x-axis is labeled with locations of the van at five minute intervals. Large spikes in NO levels coincided with aircraft takeoffs. The larger spikes were associated with larger aircraft and accompanied by sudden gusts of wind at Location #1 lasting about one minute. Note the decreasing NO levels measured by the mobile van relative to the stationary cart and the time delay in peak concentrations with increasing distance between sampling locations. CO levels were consistently low during the entire experiment. The large spike in CO measured by the stationary cart monitor occurred while the van was collocated upwind of the cart and idling for some time and should be disregarded. $PM_{2.5}$ shows a steady decrease over time in the baseline concentrations corresponding to the diurnal changes in the surrounding background levels. The spikes in $PM_{2.5}$ concentrations measured by the stationary cart were correlated to takeoffs, but the ratios of the peak to baseline levels were considerably smaller than for NO.

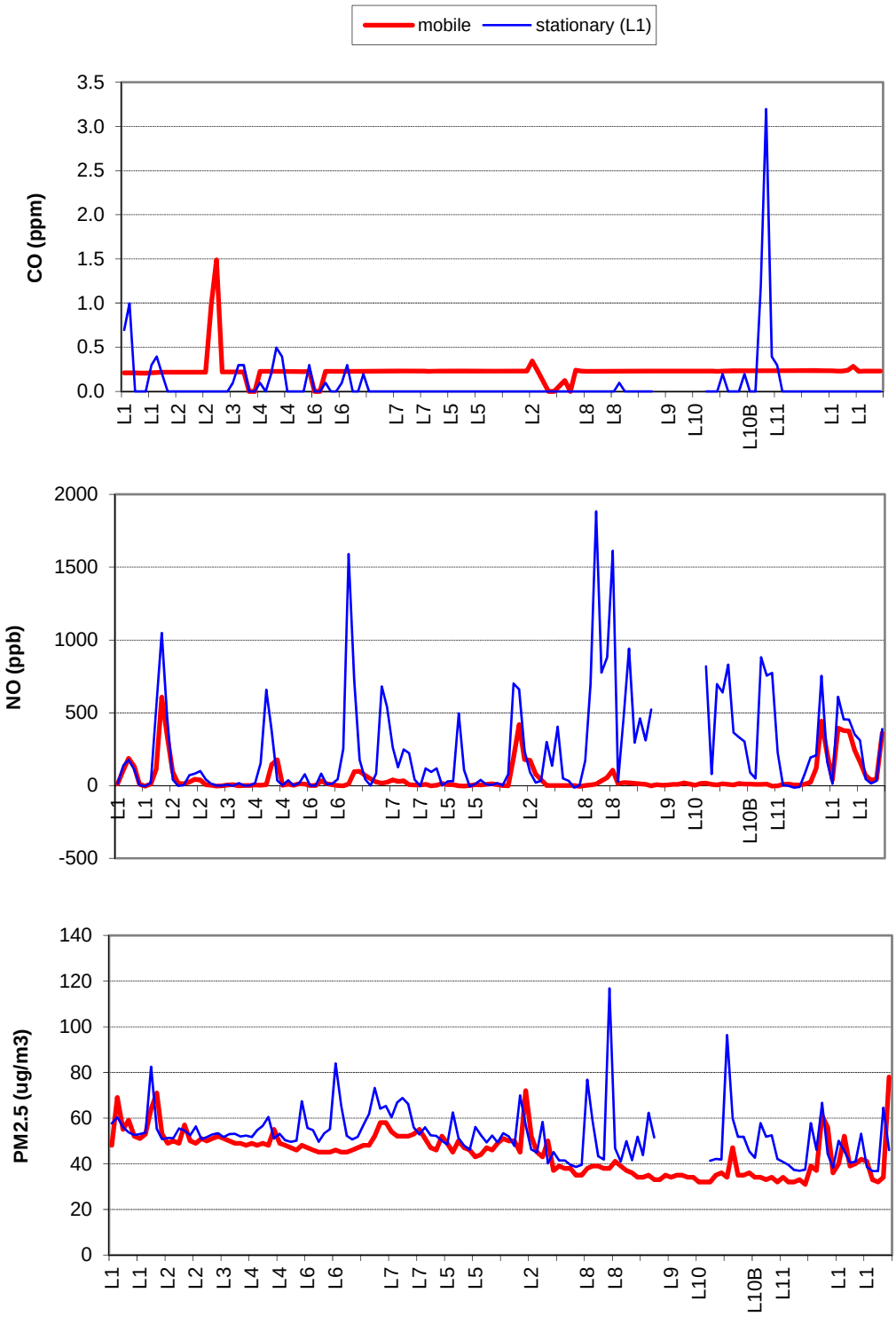

Figure 5-13. Time series of 1-minute average CO (ppm), NO (ppb), and $PM_{2.5}$ ($\mu g/m^3$) concentrations downwind of LAX South Airfield Runway 25R on 9/23/11 from 11:42 to 14:00. The x-axis is labeled with locations (see Figure 5-12) of the van at five minute intervals.

Figure 5-14 shows NO, BC and UFP together in the same time series plot. While spikes in NO concentrations corresponded to plane takeoffs, large variations in the relative concentrations of NO, BC, and UFP indicated that the exhaust emission profiles are aircraft-specific. As a result, the three parameters measured at location #1 (L1) were not well correlated as shown in Figure 5-15.

Measured pollutant concentrations with increasing distance downwind of the L1 reference site are shown in Figure 5-16 through Figure 5-18. The NO plumes from jet exhaust are not evident 300 m downwind of the reference site. The plume also appears to be confined along the approach lights on the north side of the field. BC shows similar decreases in concentration with distance, but with higher background levels. Jet exhaust contributions to the measured $PM_{2.5}$ concentrations are small relative to the urban background. UFP concentrations are also more widespread than NO or BC and more persistent between takeoffs. It is not clear whether this is due to persistence of the UFP that are emitted by the jets during takeoffs and landings or from contributions of other nearby combustion sources (e.g., gasoline and diesel vehicles).

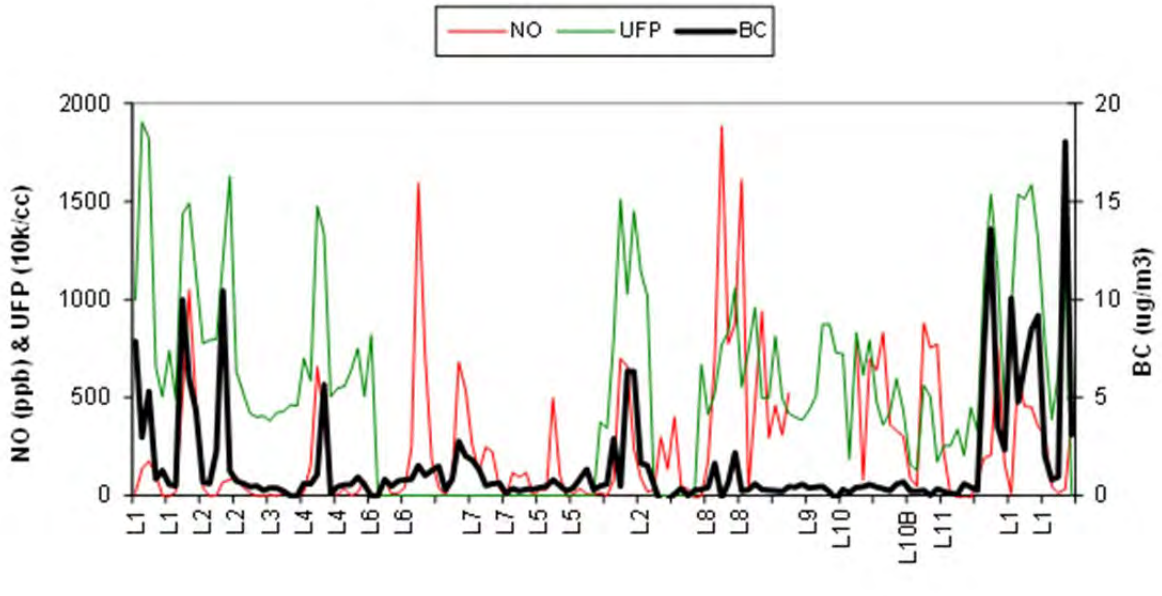

Figure 5-14. Time series of NO, UFP, and BC concentrations downwind of LAX South Airfield Runway 25R on 9/23/11 from 11:42 to 14:00.

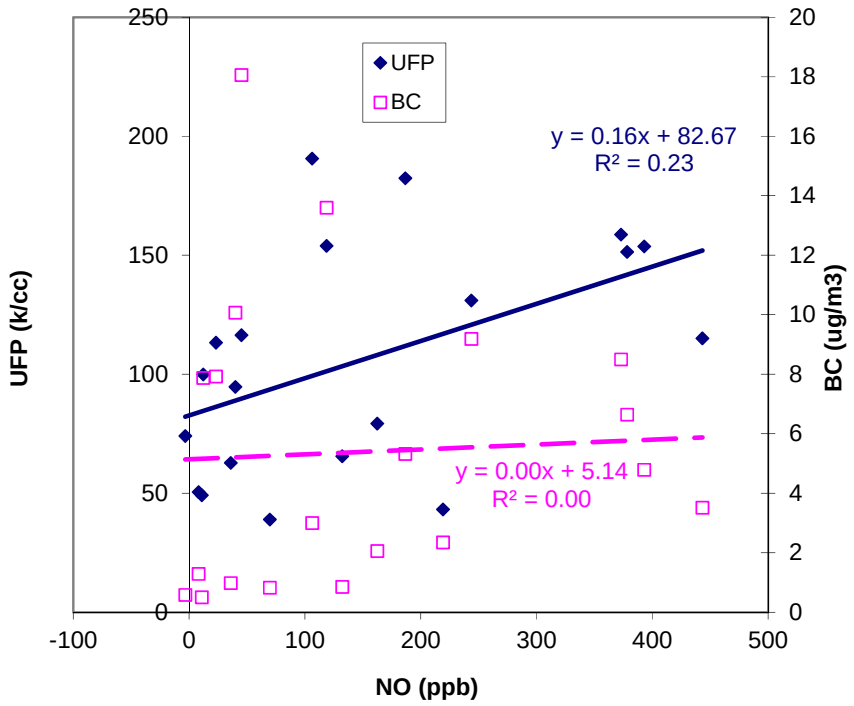

Figure 5-15. Scatter plot of 1-minute average data from van at Location #1 (L1)

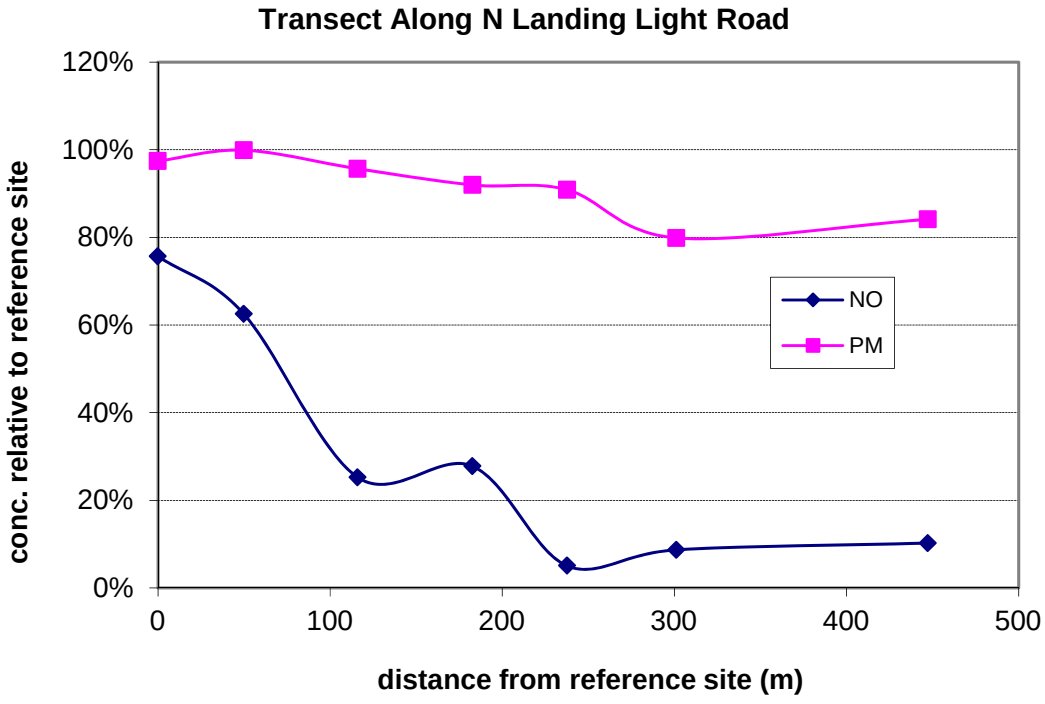

Figure 5-16. Variations in NO and $PM_{2.5}$ concentrations with respect to distance and presented as percentages relative to the reference site concentration.

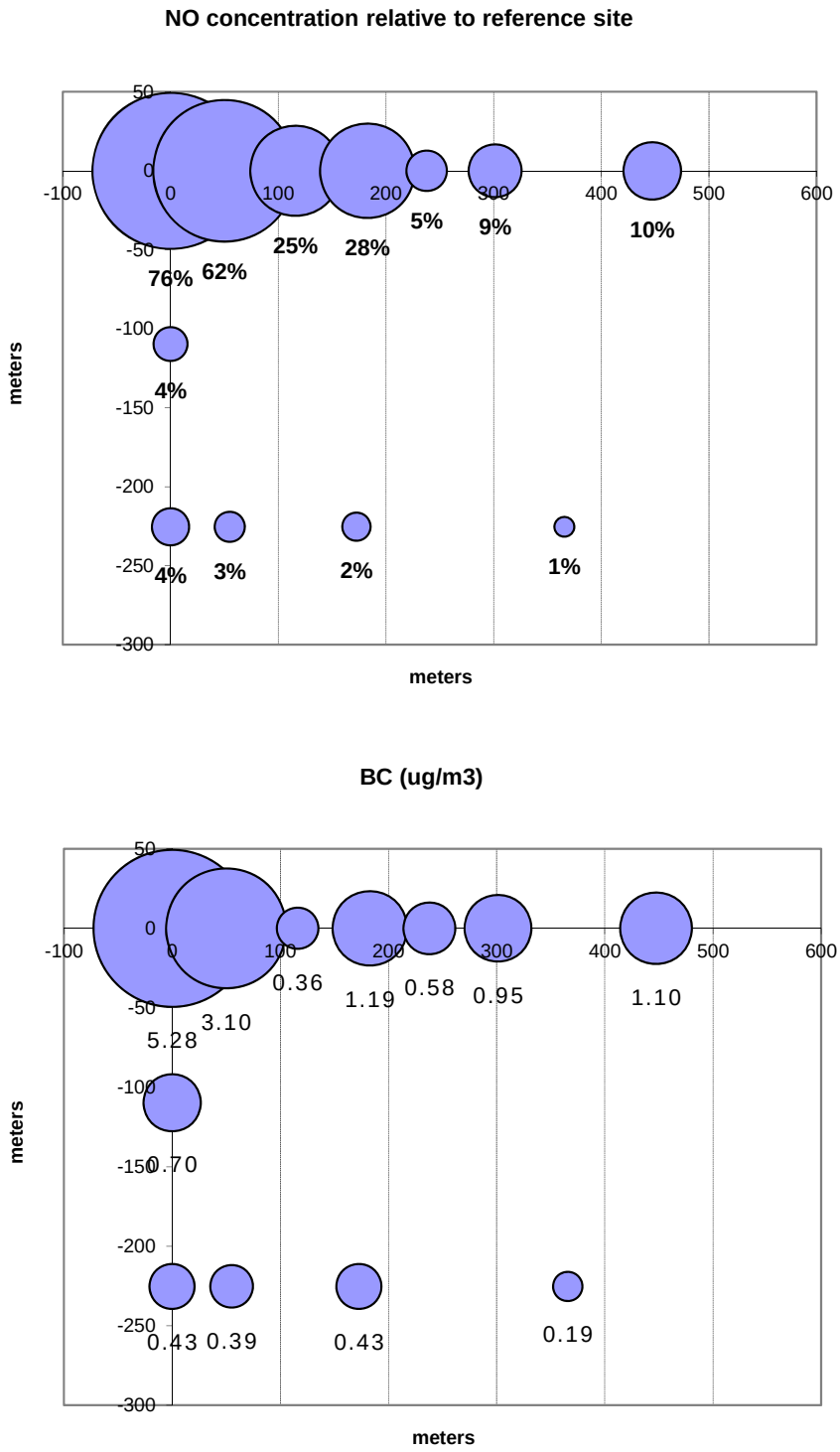

Figure 5-17. Spatial variations in NO concentrations presented as percentages relative to the reference site concentration, and in measured BC concentrations.

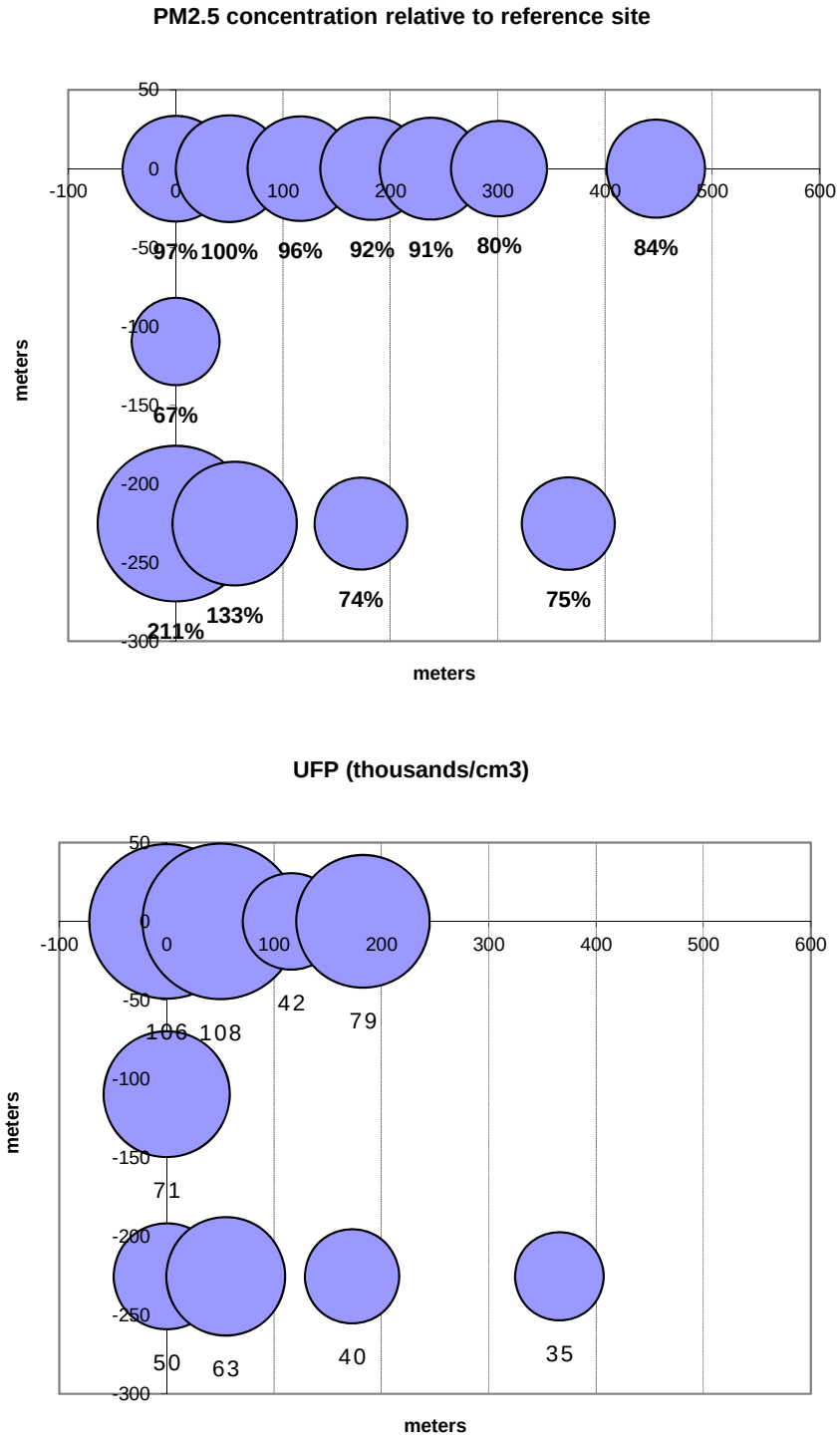

Figure 5-18. Spatial variations in $PM_{2.5}$ concentrations presented as percentages of the reference site concentration, and in measured UFP number concentrations.

5.1.3 Conclusions from the Mobile Surveys and Recommendations

The results of the mobile and gradient surveys described above provided the basis for certain refinements to the work statement originally proposed for Phase III of the LAX AQSAS. The original work statement for Phase III was based on the Study Plan developed during Phase II. The Study Plan specified three fully equipped "core" monitoring stations: one located upwind in the dunes west of the airport between the North and South Airfields (UW), a source-dominated site near the end of the South Airfield runways (SR), and a downwind community site located east of LAX in Lennox (CE). The existing SCAQMD LAX Hastings monitoring station was proposed for the fourth core site (AQ) with addition of supplemental time-integrated speciation sampling. The Study Plan also called for a minimum of two additional "satellite" sites with speciation sampling but with fewer continuous measurements than the core sites. The first two satellite sites were to be located east-northeast of the North Airfield (CN) and in the community south of the airport (CS). As described in Section 3, the monitoring program proposed by the Tetra Tech team included the UW, SR and CE core monitoring sites, the AQ site, and a supplemental saturation monitoring network consisting of four community satellite sites and nine "Gradient" monitoring sites conducting only passive sampling.

Results of the mobile and gradient surveys indicated elevated pollutant concentrations near high-traffic areas including the LAX Central Terminal Area and near airport operations, especially at the end of the North and South Airfields with sharp gradients in pollutant concentrations from the source of emissions. Pollutant concentrations were relatively low and uniform within the communities north and south of LAX. The South Runway (SR) site located at the Walsh Austin laydown area was originally intended to be used as a source-oriented monitoring site; however, measurements showed this location was minimally impacted by airplane takeoff emissions when winds were from the west. This is the predominant direction throughout the year except during late fall and winter. In contrast, the gradient surveys in the open field along the landing guide light posts east of the South Airfield Runway 25R showed that jet exhaust emissions from takeoffs were transported directly east along the runway centerline with sharp measured gradients in NO, BC and possibly UFP, but not $PM_{2.5}$. The impact of takeoff emissions at the SR site are likely minimal during late-fall and winter as well, when the predominant prevailing winds are from the northeast. These results indicate that measurements at the SR sites likely reflect dilute taxiway emissions with minimal contributions from takeoff emissions. Mobile survey results indicate that measurements at the Walsh Austin laydown area would not necessarily correlate with impacts from aircraft operations measured at the CE site. As such, rather than committing only half of the core monitoring resources to measurements within the community, an alternative monitoring approach was adopted to commit all of the core sites to monitoring within communities and to deploy a larger network of lower-cost passive samplers to characterize the spatial variations in pollutant concentrations from emission sources to the community.

5.2 LAX AQSAS WINTER AND SUMMER MONITORING SEASON DATA

Air quality monitoring for Phase III of the LAX AQSAS consisted of two six-week field measurement campaigns during winter and summer of 2012. The 17 sites in the air monitoring network are listed in Table 5-3 and identified by location in Figure 5-19. The applicable

sampling and laboratory analysis methods were specified in Section 3 and more fully described in the November 11, 2011 Monitoring and Quality Assurance Project Plan (MQAPP) prepared for Phase III of the LAX AQSAS (presented in Appendix 3-2).

Table 5-3. Phase III of the LAX AQSAS – Monitoring Sites[1]

Site Code	Site Type	Site Name	Address or Location	Latitute	Longitude
UW	Satellite	Upwind West (West of LAX)	Near east edge of Vista Del Mar Park	33.94420	-118.44100
AQ	Core/ Satellite	Upwind Northwest (AQMD Hastings Monitoring Station	9106 Hastings Avenue, Los Angeles, CA 90293	33.95511	-118.43041
CN2	Satellite	Community North #2 (Westchester)	6460 West 81st St, Westchester, CA 90045	33.96504	-118.40097
BN	Gradient	Buffer Zone North	Between Westchester Pkwy and Lincoln Blvd ~80m east of S. McConnell Ave.	33.95392	-118.40766
CT	Gradient	Central Terminal	Top level of parking structure P-3	33.94400	-118.40710
NR	Gradient	North Runway	100m directly east of Runway 24L	33.95034	-118.39762
BNR	Gradient	Buffer Zone North Runway	LAX Lot C ~ 600m east of Site NR	33.95037	-118.39094
CN	Core	Community North (Westchester)	5843 W. 95th St, Los Angeles, CA 90045	33.95066	-118.38422
R405	Gradient	Roadway I-405	East edge of I-405 at end of W. Spruce Ave.	33.95506	-118.36896
CS2	Satellite	Community South #2 (El Segundo)	535 East Mariposa Ave, El Segundo, CA 90245	33.92379	-118.41018
CS	Core	Community South (El Segundo)	559 E. Walnut Ave., El Segundo, CA	33.92952	-118.40951
BS	Gradient	Buffer Zone South	Cargo Terminal off Imperial Hwy ~ 300 m west of Sepulveda	33.93198	-118.40013
SRN	Gradient	South Runway North	Intersection of Century Blvd and Aviation Blvd. - SW corner	33.94523	-118.37893
SRE	Gradient	South Runway East	40m directly east of Runway 25R blast fence	33.93997	-118.37882
BSR	Gradient	Buffer Zone South Runway	LAX Lot B ~ 600m east of Site SRE and 150m west of La Cienega Blvd.	33.93911	-118.37187
CE	Core	Community East (Lennox)	10903 S. Inglewood Ave, Inglewood, CA 90304	33.93751	-118.36185
CE2	Satellite	Community East #2 (Hawthorne)	4151 W. 142nd St, Hawthorne, CA	33.90338	-118.34780

[1] The sites are listed according to two transects from west to east: 1) coast (UW) to east of the North Airfield including the communities north of LAX (R405); and 2) near coast (CS2) to east of the South Airfield including communities south of LAX (CE2).

Figure 5-19. Locations of Phase III monitoring sites of the LAX AQSAS. The emissions inventory for Phase 3 of the AQSAS was developed for the area bounded by the study area.

The core of the monitoring program consisted of three community-scale "core" monitoring sites: one located east of the South Airfield Runways 25R and 25L and I-405 in Lennox (CE site), a second site located east of the North Airfield Runways 24R and 24L in Westchester (CN site) and a third site located south of LAX in El Segundo (CS site). Each site was comparably equipped with continuous instruments for measuring 1-minute average NO/NO_x, SO_2, and CO concentrations, 5-minute average ultrafine and fine particle number concentrations and size distributions, 5-minute average light scattering, 1-minute average black carbon, and 1-hour average $PM_{2.5}$ mass concentrations. Meteorological data at the CE and CS sites included 1-minute measurements of wind speed and direction, temperature (2 and 10 m height), relative humidity and solar radiation. The Project Team added measurements of $PM_{2.5}$ mass, BC, light scattering and ultrafine particle number concentrations (CPC only) to the existing measurements (NO/NO_x, SO_2, and CO) at the AQ site. This monitoring station, located north of LAX in Playa del Rey, served as a fourth core site. Six consecutive 7-day integrated samples were collected at the four baseline sites for VOC (benzene, toluene, ethylbenzene and xylenes), 1,3-butadiene, and carbonyl compounds using Radiello passive samplers and for $PM_{2.5}$ mass, elements (Na to U), organic carbon (OC) and elemental carbon (EC) using portable Airmetrics MiniVol samplers.

Fourteen 24-hour (midnight to midnight) chemical speciation samples were collected during both monitoring seasons at the CE, CN, and CS sites for application in Chemical Mass Balance (CMB) receptor modeling. The sets of speciation samples included: canisters for 71 C_2-C_{11}

hydrocarbons; Tenax cartridges for 66 C_7-C_{28} hydrocarbons; 2,4-Dinitrophenylhydrazine (DNPH) cartridges for 14 C_1-C_8 aldehydes and ketones; Teflon and quartz filters collected with medium-volume sequential filter samplers (SFS) for $PM_{2.5}$ mass, OC, EC, elements Na to U, nitrate, sulfate, ammonium, sodium, chloride; and Teflon-impregnated glass fiber filters (TIGF) with backup XAD resin cartridges for separate analysis of particulate and semi-volatile phase alkanes, polycyclic aromatic hydrocarbons, hopanes and steranes, and polar compounds. In addition to ambient chemical speciation measurements, DRI collected and analyzed local source samples for application receptor modeling. These included the composition of local fuel samples (gasoline, diesel and Jet-A). DRI also collected comparable sets of speciation samples behind the blast fence at the end of the South Airfield Runways 25R during March 14-15, 2012 to derive source composition profiles of jet exhaust during takeoffs. Companion sets of speciation samples were simultaneously collected at the CS site and used to subtract an urban background from the blast fence samples. The chemical speciation data are summarized with the chemical mass balance (CMB) results in Section 6.

Satellite sites provided 7-day integrated measurements of gases and particles at one upwind site (UW) west of LAX between the North and South Airfield Runways and at three additional community-scale sampling sites in El Segundo (CS2), Westchester (CN2), and Hawthorne (CE2). The set of measurements included NO_2, NO_x, and SO_2 using Ogawa passive samplers and VOC (benzene, toluene, ethylbenzene and xylenes) and carbonyl compounds using Radiello passive samplers. Seven-day integrated Teflon and quartz filters were collected with portable Airmetrics MiniVol samplers and analyzed for $PM_{2.5}$ mass, elements, and OC and EC. Table 5-4 provides a summary of the criteria pollutant concentrations at the core monitoring sites along with the means of the Mini-Vol sampler samples.

Passive samplers were also deployed at nine additional sites located in close proximity to sources or within the buffer zones separating LAX from the adjacent communities (gradient sites). The passive sampling at 17 sites (4 core, 4 satellite, and 9 gradient sites) comprised the saturation monitoring component of the monitoring program for Phase III of the LAX AQSAS. The nine gradient sampling sites were intended to characterize potentially higher concentrations that may exist within several meters to 100 meters of emission sources (e.g., near roadways and airport runways) and near edges of the buffer zones separating areas of active airport operations from the adjacent communities. Measurements at these sites included only passive measurements (NO_2, NO_x, SO_2, BTEX, 1,3 butadiene, and carbonyl compounds) to allow maximum siting flexibility and the greatest number of sampling sites within the project constraints. Criteria pollutant levels are also shown for three SCAQMD monitoring sites for comparable monitoring periods.

Additional samples were collected for quality assurance purposes at the CE site. Samples collected on NaCl-impregnated cellulose filters behind the 24-hour medium-volume quartz filters were analyzed to determine nitrate volatilized off the primary quartz filter. Samples collected on quartz filters behind both 24-hour medium-volume and 7-day low-volume Teflon filters were analyzed to determine positive adsorption artifacts of OC from the primary quartz filters. NO_2, NO_x, and SO_2 were also measured with Ogawa passive samplers for comparisons with time-averages of the continuous measurements at the CE site in winter and at all core sites in summer.

All passive samples at the CE sites were collected in duplicate to assess the measurement precision. These results along with data capture rates are summarized in Section 5.2.1.

Table 5-4. Summary of criteria pollutant concentrations at the Core monitoring sites.

	CO		NO_2		SO_2	$PM_{2.5}$ BAM		7-day Filter [1]
	1hr max ppm	8hr max ppm	1-hr max ppb	mean ppb	1-hr max ppb	24-hr max $\mu g/m^3$	mean $\mu g/m^3$	mean $\mu g/m^3$
NAAQS [2]	35	9	100	53	75	35	12	12
LAX AQSAS [3]								
CE	4.9	< 1hr max	62	19.5	3.8	33	17	10.9
CN	2.2		73	20.8	6.1	31	16	8.0
CS	1.8		70	12.6	5.7	27	11	8.4
AQ	1.6		62	10.4	4.0	30	15	8.2
SCAQMD [3]								
Burbank	2.3	< 1hr max	57	22.9	8	34	17	
Central LA	1.9		69	21.5	8	43	18	
Long Beach [4]	2.0		59	17.2	9	28	11	

[1] Six consecutive 7-day Mini-Vol Teflon samples in each Phase 3 LAX AQSAS monitoring season.
[2] NAAQS standards for max NO_2, SO_2, and $PM_{2.5}$ are for the 3-year running average of the annual 98th (99th for SO2) percentile value.
[3] Statistics are based upon Phase 3 LAX AQSAS monitoring seasons (1/21/12 to 3/13/12 and 7/18/12 to 8/28/12).
[4] N. Long Beach site, except for PM from S. Long Beach. One outlier (=370 ppb NOx at Long Beach) was excluded since it occurred just before a period of missing data

5.2.1 Data Recovery Statistics and Data Quality Assessments

Data recovery statistics are summarized for various measurements in the following tables and figures. Data recovery for the time-integrated samples was quite high overall during both monitoring seasons, with the exception of the 24-hour Teflon and quartz filter samples at the core sites. Power problems during the Winter Season, and a series of equipment failures during the Summer Season resulted in a significant loss of samples at the CN site. In addition, a high level of breakthrough for some analytes negatively impacted the VOC samples collected on Tenax cartridges during the first half of the Winter Season. The problem was corrected by reducing sampling flow rates on 2/26 at CS and CE sites and on 2/29 at the CS site.

During the Winter Monitoring Season, the Grimm SMPS was initially installed at the CE site and began having flow problem after 1/27/2012. On 2/10/2012, this SMPS was exchanged with the TSI RSMPS at the CS site. The Grimm SMPS at the CS site continued to have a flow problem during most of the Winter Season. Consequently the data recovery for this sampler was low. The aerosol pump was replaced after the Winter Monitoring Season. During the Summer Monitoring Season, the Grimm SMPS sheath flow pumps failed on 7/29/2012. The TSI CPC at the CN site began to have a leak on 8/9/2012, causing data lost at the CN site till the end of the monitoring season. Consequently the data recovery for this sampler was low.

Table 5-5. Data recovery statistics for time-integrated samples during the Winter Monitoring Season.

	Samples Planned	Samples Collected	Samples Analyzed	Valid Data
Passive SO2	96	98%	98%	98%
Passive NOx	96	99%	99%	99%
Passive BTEX	108	100%	100%	100%
Passive 1,3 butadiene	108	100%	98%	98%
Passive Aldehydes	108	100%	100%	100%
7day PM2.5 & Elements	48	88%	88%	88%
7day EC/OC & Ions	48	94%	94%	94%
24hr PM2.5 & Elements	42	83%	83%	83%
24hr EC/OC & Ions	42	83%	83%	83%
24hr Aldehydes	42	100%	100%	100%
24hr VOC (C2-C11)	42	100%	100%	100%
24hr VOC (C12-C20)	42	100%	100%	52%
24hr SVOC	42	95%	95%	95%

Table 5-6. Data recovery statistics for time-integrated samples during the Summer Monitoring Season.[1]

	Samples Planned	Samples Collected	Samples Analyzed	Valid Data
Passive SO2	108	98%	98%	98%
Passive NOx	108	96%	96%	94%
Passive BTEX	108	98%	98%	98%
Passive 1,3 butadiene	108	96%	96%	96%
Passive Aldehydes	108	98%	98%	98%
7day PM2.5 & Elements	48	100%	98%	94%
7day EC/OC & Ions	48	100%	100%	96%
24hr PM2.5 & Elements	42	88%	83%	67%
24hr EC/OC & Ions	42	88%	83%	67%
24hr Aldehydes	42	100%	100%	95%
24hr VOC (C2-C11)	42	102%	102%	95%
24hr VOC (C12-C20)	42	105%	105%	95%
24hr SVOC	42	100%	100%	93%

[1] Passive sampling of NO_2/NO_x and SO_2 was added to all core sites during the Summer Monitoring Season for comparison with time-averaged data from the continuous analyzers. These samples were not collected at the core sites during the Winter Monitoring Season.

Day	Mon	Tue	Wed	Thu	Fri	Sat	Sun	Mon	Tue	Wed	Thu	Fri	Sat	Sun
Site/Date	1/30	1/31	2/1	2/2	2/3	2/4	2/5	2/6	2/7	2/8	2/9	2/10	2/11	2/12
CN	No Data		Sheath flow wrong, but data correctable						SMPS					
CS	SMPS							No Data			SMPS		No Data	
CE	No Data		CPC										SMPS	No Data
Site/Date	2/13	2/14	2/15	2/16	2/17	2/18	2/19	2/20	2/21	2/22	2/23	2/24	2/25	2/26
CN	SMPS									No Data				
CS	CPC		SMPS		No Data					CPC				
CE	SMPS								CPC flow clogged, data cannot be used					
Site/Date	2/27	2/28	2/29	3/1	3/2	3/3	3/4	3/5	3/6	3/7	3/8	3/9	3/10	3/11
CN	No Data	SMPS												
CS	CPC		NoData		SMPS-Bad Data		No Data					SMPS		
CE	CPC clogged	SMPS												
Site/Date	3/12	3/13	3/14	3/15	3/16									
CN	SMPS													
CS	SMPS	No Data												
CE	SMPS													

Figure 5-20. Summary of SMPS operation and data capture during the Winter Monitoring Season. Yellow bars indicate that the SMPS operated as a stand-alone CPC when the differential mobility analyzer (DMA) was not operable.

Day	Mon	Tue	Wed	Thu	Fri	Sat	Sun	Mon	Tue	Wed	Thu	Fri	Sat	Sun
Site/Date	7/16	7/17	7/18	7/19	7/20	7/21	7/22	7/23	7/24	7/25	7/26	7/27	7/28	7/29
CN		SMPS												
CS			SMPS						No Data	SMPS				No Data
CE		SMPS												No Data
Site/Date	7/30	7/31	8/1	8/2	8/3	8/4	8/5	8/6	8/7	8/8	8/9	8/10	8/11	8/12
CN	SMPS										No Data			
CS	No Data								CPC					
CE	SMPS													
Site/Date	8/13	8/14	8/15	8/16	8/17	8/18	8/19	8/20	8/21	8/22	8/23	8/24	8/25	8/26
CN	No Data (CPC Leak)													
CS	CPC										No Data			
CE	SMPS													
Site/Date	8/27	8/28												
CN	No Data													
CS	No Data													
CE	SMPS													

Figure 5-21. Summary of SMPS operation and data capture during the Summer Monitoring Season. Yellow bars indicate that the SMPS operated as a stand-alone CPC when the differential mobility analyzer (DMA) was not operable.

Table 5-7. Data recovery statistics of SMPS measurements during the Winter and Summer Monitoring Seasons.

Site	Winter		Summer	
	Measurements Planned	Valid Data	Measurements Planned	Valid Data
CN	21,502	83.5%	19,711	49.2%
CS	17,108	49.8%	15,683	22.7%
CE	21,860	60.2%	20,040	95.7%

Assessment of data quality is essential for proper interpretation of the LAX AQSAS data. This is especially important for passive measurements, which are not routinely used in national and local air quality monitoring programs. These passive measurements were evaluated by DRI during the recently completed Harbor Communities Monitoring Study (HCMS; Mason et al., 2011). The HCMS was conducted to characterize the spatial variations in concentrations of toxic air contaminants and their co-pollutants within the communities adjacent to the Ports of Los Angeles and Long Beach (Fujita et al., 2009), and had study objectives similar to the LAX AQSAS. The passive monitors were also used by DRI investigators in the West Oakland Monitoring Study (WOMS; Fujita et al., 2010) as well as an exposure assessment study of the Barnet Shale natural gas production area (Zielinska et al., 2010).

The precision results of the passive measurements for these prior studies were better than 10 percent for compounds with ambient levels greater than five times the limit of detection. The passive samples for BTEX were stable for storage times of up to 14 days at -18º C and measured values were generally within ± 15 percent of corresponding samples collected by active sampling methods commonly used in state and local monitoring programs. The experimentally-determined sampling rates (rate of specific pollutant absorption) for toluene and xylenes were within 10 percent of those published by Radiello. DRI's experimentally-determined sampling rates for benzene and ethylbenzene of 22.4 and 37.4 ml/min, respectively, were used rather than 27.8 and 25.7 ml/min values published by Radiello. These substitutions result in concentrations that are a factor of 1.24 higher for benzene and 0.69 lower for ethylbenzene. Passive measurements of formaldehyde and acetaldehyde were in good agreement with diluted standards for the laboratory evaluations. Acetaldehyde measured by the passive sampler was 43 percent lower than values obtained by active sampling on DNPH cartridges. Acetaldehyde had poor accuracy most likely due to low collection efficiencies over extended sampling times, which may also apply to "reference" samples collected actively on DNPH cartridges. The accuracy of passive measurements of acrolein could not be evaluated during the HCMS as their ambient concentrations were often below the limits of detection. Radiello diffusive samplers (Carbograph 4 adsorbing cartridge code R145) were used in the LAX AQSAS for passive sampling of benzene, toluene, ethylbenzene, xylenes (BTEX). Radiello samplers with Carbopack X (R141), which have been shown to significantly reduce the inaccuracy due to desorption of 1,3-butadiene[1], were introduced for sampling 1,3-butadiene for the LAX AQSAS.

[1] http://www.sigmaaldrich.com/etc/medialib/docs/Supelco/Brochure/reporte37_radiello_butadiene.Par.0001.File.tmp/reporte37_radiello_butadiene.pdf

Precision of the LAX AQSAS passive measurements is provided in Table 5-8 through Table 5-10. The results include seasonal means of the six 7-day samples at the CE site and the mean percent relative differences between the individual replicates and mean of the three replicates. The precision of the passive measurements are generally consistent with the estimates of precision obtained during the HCMS and WOMS, which are also presented for comparison in the tables. The mean ambient concentrations measured during the LAX AQSAS were well above the detection limits for all compounds with the exception of SO_2 and acrolein. The practical consequence of these results is that any spatial differences in pollutant concentrations within the monitoring network that are greater than two times the mean relative difference between replicates are significant with respect to the precision of the measurement, as stated in the MQAPP.

Simultaneous measurements by both passive sampling and continuous monitors at the CE site showed agreement between the two sets of measurements to within ± 15 percent for both NO and NO_2 (Figure 5-22) with good correlation (R^2 of 0.97 for NO and 0.85 for NO_2) during the Winter Season. The 7-day average ambient SO_2 levels were typically near or below the limits of detection for both the passive measurements (0.5 ppb) at most sites as well as the trace-level SO_2 monitors (0.1 ppb). Consequently, poorer correlations between the passive and continuous SO_2 measurements were expected. However, good agreement for the highest passive sample (0.36 ppb) with the corresponding average of the continuous monitor (0.34 ppb) suggests that the two methods may yield comparable values at higher SO_2 levels. Higher average SO_2 levels occurred during the Summer Season, but correlation between the passive and continuous methods is still poor. However, the differences are generally within the precision, as seen in Table 5-8. The internal temperatures in the motorhome at the CN site were higher than the allowable range during the Summer Season resulting in invalid high NO_x readings on most days. Although corrections for the high temperatures were made, the adjusted values were uncertain and were not used in the subsequent data analysis.

Strong correlations between EC concentrations obtained from the 7-day MiniVol sampler quartz filters and the corresponding average of BC measured continuously by the Aethalometers were observed at all three core sites during the Winter Season (EC and BC concentrations at the AQ site were too low to generate a correlation). The significantly different slope (see Figure 5-22) at the CN site may be due to data losses during two weeks for the Aethalometer at this site, however, the Aethalometer BC data at the CN site seems too high relative to the BC data from CS and CE as well as the corresponding quartz TOR EC data so there may have been an unrecognized malfunction at CN. Despite much lower average concentrations during the Summer Season, the two methods (i.e., EC versus BC measurements) still compare well, except at the CN site where there was a significant negative bias evident in the Aethalometer data. The comparison of $PM_{2.5}$ mass concentration measured by gravimetric analysis of the Teflon filters and the reconstructed sum of species, which accounts for common oxide forms of the major soil components, yielded similar results for all sites and both seasons Figure 5-24). The higher intercepts of the Summer Season regression lines are attributed to increased volatilization of ammonium nitrate from the Teflon filters (ionic species measured from the quartz filter, which retains nitrate better, are used to calculate reconstructed mass).

Table 5-8. Precision of passive NO_2, NO_x, and SO_2 measurements at the CE site during Phase III of the LAX AQSAS compared to results from the West Oakland Monitoring Study (WOMS) and Harbor Communities Monitoring Study (HCMS).

	MDL [1]	Mean [2]	Differences of Replicates	
	ppb	ppb	Mean (ppb) [3]	%RD [4]
LAX AQSAS Winter 2012				
Nitric Oxide (NO)	0.32	30.6	1.3	4.8%
Nitrogen Oxides (NO_2)	0.32	25.6	0.6	2.5%
Sulfur Dioxide (SO_2)	0.54	0.07	0.10	142%
LAX AQSAS Summer 2012				
Nitric Oxide (NO)	0.32	7.0	1.5	20.0%
Nitrogen Oxides (NO_2)	0.32	15.4	1.5	9.0%
Sulfur Dioxide (SO_2)	0.54	0.8	0.80	85%
WOMS Summer 2009				
Nitrogen Dioxide (NO_2)	0.32	9.0	1.3	14.0%
Nitrogen Oxides (NOx)	0.32	17.5	0.7	4.2%
Sulfur Dioxide (SO_2)	0.54	0.09	0.03	33.9%
WOMS Winter 2009/10				
Nitrogen Dioxide (NO_2)	0.32	5.7	0.1	1.7%
Nitrogen Oxides (NOx)	0.32	25.9	0.8	3.1%
Sulfur Dioxide (SO_2)	0.54	1.0	0.79	81.5%
HCMS Summer 2007				
Nitrogen Dioxide (NO_2)	0.32	19.5	1.0	4.9%
Nitrogen Oxides (NOx)	0.32	29.4	0.6	2.2%
Sulfur Dioxide (SO_2)	0.54	1.0	0.20	19.8%
HCMS Winter 2007				
Nitrogen Dioxide (NO_2)	0.32	28.5	1.5	5.3%
Nitrogen Oxides (NOx)	0.32	73.0	2.0	2.8%
Sulfur Dioxide (SO_2)	0.54	1.1	0.11	9.8%

[1] Minimum detection limits (MDL) are based upon manufacturer's specification for 7-day exposure.
[2] Seasonal means of six 7-day sampling periods for LAX AQSAS and four 7-day sampling periods for WOMS and HCMS.
[3] Mean of the absolute differences between duplicate samples for LAX AQSAS (up to 6 values per season) and mean of the triplicates and individual sample for WOMS and HCMS (up to 12 values per season).
[4] Mean of the absolute differences normalized to mean of the duplicates or triplicates in percent.

Table 5-9. Precision of passive BTEX measurements at the CE site during Phase III of the LAX AQSAS compared to results from the West Oakland Monitoring Study (WOMS) and Harbor Communities Monitoring Study (HCMS).

	MDL [1]	Mean	Differences of Replicates	
	ppb	ppb	Mean (ppb) [2]	%RD [3]
LAX AQSAS Winter 2012				
benzene	0.015	1.37	0.18	12.2%
toluene	0.002	1.78	0.24	13.3%
ethylbenzene	0.002	0.20	0.03	16.5%
xylenes	0.002	1.17	0.18	15.2%
LAX AQSAS Summer 2012				
benzene	0.015	0.30	0.15	68.0%
toluene	0.002	0.41	0.11	51.0%
ethylbenzene	0.002	0.04	0.02	58.0%
xylenes	0.002	0.30	0.14	65.0%
WOMS Summer				
benzene	0.015	0.16		
toluene	0.002	0.19	Not Available.	
ethylbenzene	0.002	0.08	See text for explanation.	
xylenes	0.002	0.36		
WOMS Winter				
benzene	0.015	0.26	0.02	7.8%
toluene	0.002	0.78	0.04	5.1%
ethylbenzene	0.002	0.15	0.01	5.1%
xylenes	0.002	0.63	0.03	5.0%
HCMS Summer				
benzene	0.015	0.35	0.03	7.5%
toluene	0.002	1.05	0.04	4.2%
ethylbenzene	0.002	0.21	0.01	6.7%
xylenes	0.002	0.69	0.06	9.2%
HCMS Winter				
benzene	0.015	0.61	0.01	2.3%
toluene	0.002	1.73	0.04	2.3%
ethylbenzene	0.002	0.34	0.01	2.4%
xylenes	0.002	1.41	0.03	2.2%

[1] Minimum detection limits (MDL) are based upon manufacturer's specification for 7-day exposure.
[3] Mean of the absolute differences between duplicate samples for LAX AQSAS (up to 6 values per season) and mean of the triplicates and individual sample for WOMS and HCMS (up to 12 values per season).
[3] Mean of the absolute differences normalized to mean of the duplicates or triplicates in percent.

Table 5-10. Precision of passive carbonyl compounds and 1,3-butadiene measurements at the CE site during Phase III of the LAX AQSAS compared to results from the West Oakland Monitoring Study (WOMS) and Harbor Communities Monitoring Study (HCMS).

	MDL [1]	Mean	Differences of Replicates	
	ppb	ppb	Mean (ppb) [2]	%RD [3]
LAX AQSAS Winter 2012				
Formaldehyde	0.07	2.2	0.13	5.8%
Acetaldehyde	0.05	1.4	0.09	6.5%
Acrolein	0.12	0.31	0.48	170%
1,3-butadiene		0.13	0.01	5.7%
LAX AQSAS Summer 2012				
Formaldehyde	0.07	1.34	0.26	19.0%
Acetaldehyde	0.05	0.43	0.10	24.0%
Acrolein	0.12			
1,3-butadiene		0.015	0.010	80.0%
WOMS Summer				
Formaldehyde	0.07	1.4	0.03	1.8%
Acetaldehyde	0.05	0.55	0.03	4.7%
Acrolein	0.12	0.009	0.005	57.7%
WOMS Winter				
Formaldehyde	0.07	1.3	0.1	5.1%
Acetaldehyde	0.05	0.5	0.1	18.9%
Acrolein	0.12	0.028	0.009	65.5%
HCMS Summer				
Formaldehyde	0.07	1.76	0.12	6.7%
Acetaldehyde	0.05	0.73	0.03	4.7%
Acrolein	0.12	0.010	0.005	47.4%
HCMS Winter				
Formaldehyde	0.07	2.65	0.06	2.2%
Acetaldehyde	0.05	1.88	0.05	2.8%
Acrolein	0.12	0.028	0.015	52.0%

[1] Minimum detection limits (MDL) are based upon manufacturer's specification for 7-day exposure. None provided for 1,3 butadiene.

[2] Mean of the absolute differences between duplicate samples for LAX AQSAS (up to 6 values per season) and mean of the triplicates and individual sample for WOMS and HCMS (up to 12 values per season).

[3] Mean of the absolute differences normalized to mean of the duplicates or triplicates in percent.

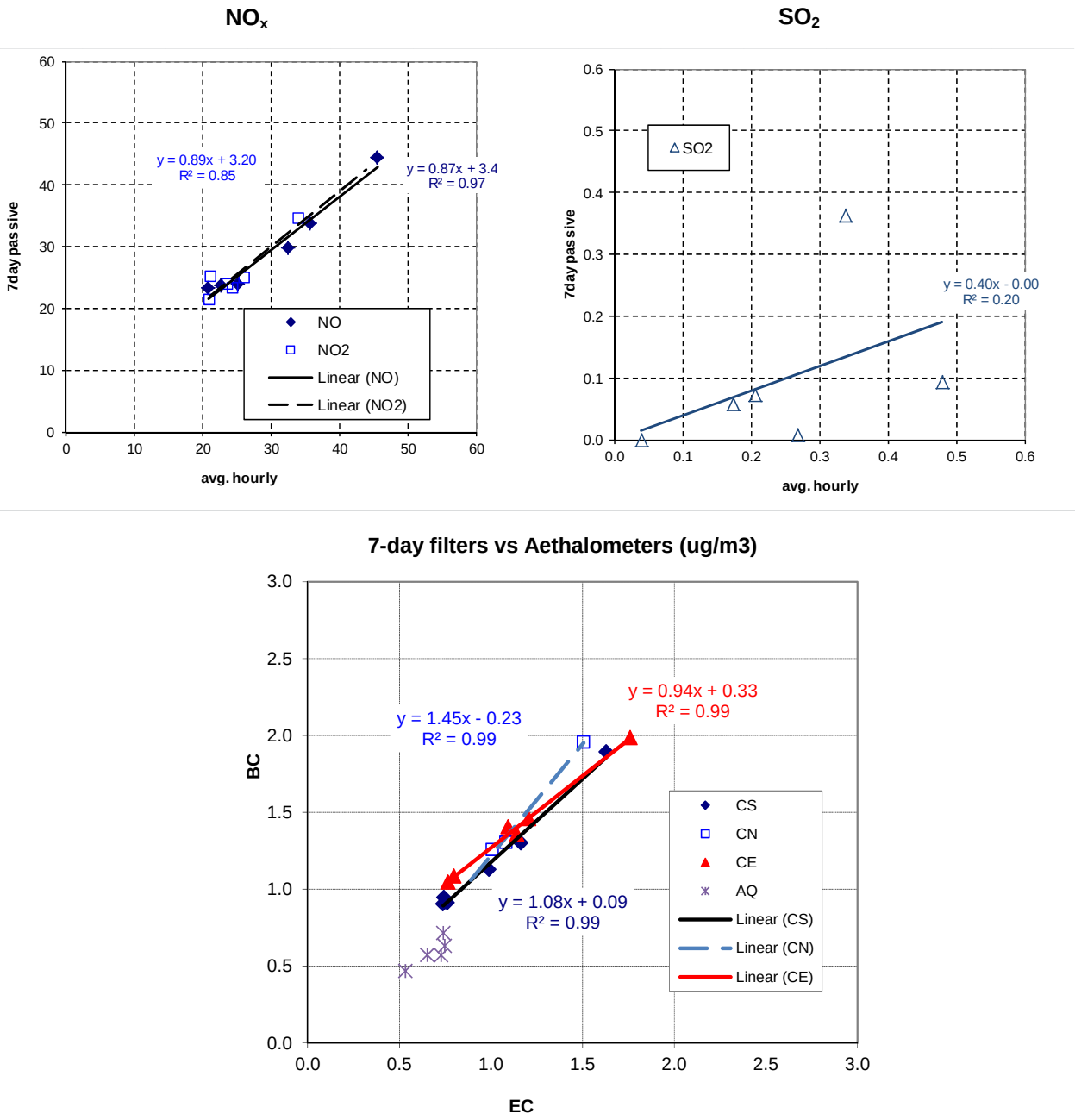

Figure 5-22. Scatterplots of 7-day integrated samples versus time-integrated continuous measurements during Winter Monitoring Season: NO and NO_2 (ppb) and SO_2 (ppb) at the CE site; and BC and EC at the four core sites.

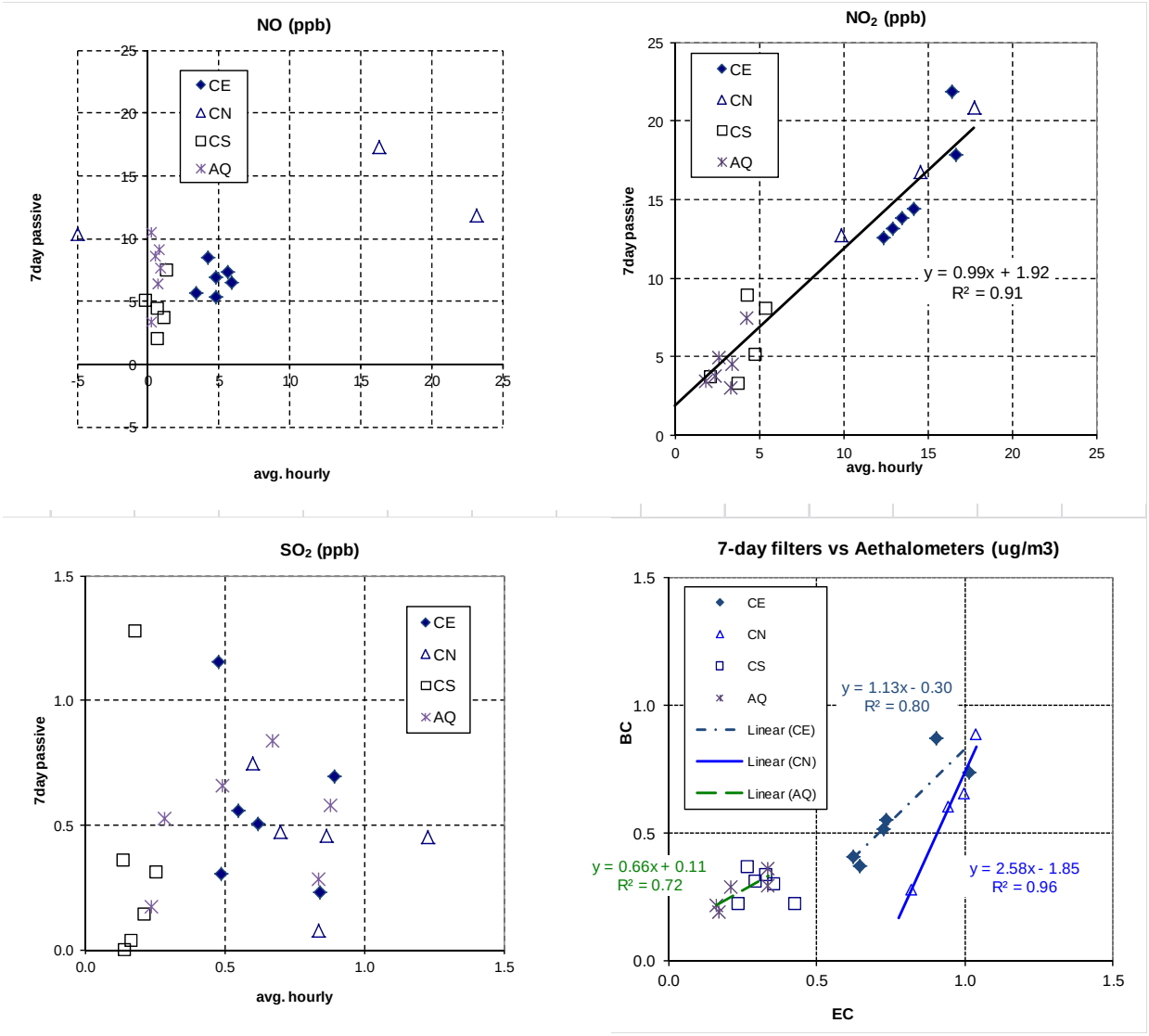

Figure 5-23. Scatterplots of 7-day integrated samples versus time-integrated continuous measurements during Summer Monitoring Season: NO and NO_2, SO_2, and BC and EC at the four core sites.

Backup quartz filters were included for PM sampling at the CE site to evaluate the breakthrough of nitrate and organic carbon due to volatilization of particles collected on the primary (front) filter. The results in Table 5-11 and Table 5-12 show that the amounts of nitrate and semi-volatile organic carbon (OC1 and OC2 fractions) on the backup filters were substantial relative to the concentrations measured on the primary filters. Since the amount of breakthrough relative to that on the primary filter was highly variable we were not able to account for it with any accuracy at the other sites, where no backup filters were collected. Therefore, the reported nitrate and organic carbon concentrations for the CN, CS and AQ sites should be considered lower bounds that may noticeably underestimate the true ambient concentrations.

Collocated tests were conducted in the laboratory at DRI prior to the Winter Monitoring Season to ensure the comparability of the three SMPS with different manufacturers and models. In these tests, all three SMPS sampled nebulized sodium chloride (NaCl) particles. Figure 5-25 shows the NaCl particle size distribution measured by the three collocated SMPS agreed reasonably well. The TSI RSMPS showed somewhat narrower distribution with higher concentration at the peak. Collocated SMPS comparison was also conducted onsite during the Supplemental Study and in a DRI laboratory after the Study as shown in Table 5-13.

Table 5-11. Backup/primary filter ratios[1] and concentrations for nitrate and carbon[2]– Winter Monitoring Season.

backup/primary	nitrate	OC	EC	TC	O1TC	O2TC	O3TC	O4TC	OPTTC	OPTRC	E1TC	E2TC	E3TC
SFS 24HR													
median	72%	54%	8%	44%		73%	48%	17%	9%	0%	0%	34%	0%
stdev	669%	7%	3%	6%		15%	16%	7%	13%	0%	0%	67%	0%
MiniVol 7day													
median		47%	17%	41%		55%	61%	34%	6%	0%	0%	49%	
stdev		6%	9%	5%		7%	10%	11%	26%	0%	1%	17%	

(μg/m^3)	nitrate	OC	EC	TC	O1TC	O2TC	O3TC	O4TC	OPTTC	OPTRC	E1TC	E2TC	E3TC
SFS 24HR													
mean primary	0.65	1.91	0.51	2.42	0.09	0.95	0.46	0.29	0.19	0.13	0.52	0.11	0.00
mean backup	0.73	1.05	0.04	1.09	0.06	0.73	0.21	0.05	0.02	0.00	0.00	0.04	0.00
MiniVol 7day													
mean primary		1.80	0.58	2.38	0.07	0.60	0.58	0.35	0.30	0.21	0.62	0.17	0.00
mean backup		0.83	0.10	0.93	0.07	0.60	0.58	0.35	0.30	0.21	0.62	0.17	0.00

[1] Backup quartz filters were included at CE site to assess loss of semi-volatile particles from primary filters.
[2] Carbon fractions in the IMPROVE method correspond to temperature steps of 120^o C (O1TC), 250^o C (O2TC), 450^o C (O3TC), and 550^o C (O4TC) in a nonoxidizing helium atmosphere, and at 550^o C (E1TC), 700^o C (E2TC), and 850^o C (E3TC) in an oxidizing atmosphere. Some organic compounds pyrolyze when heated during the oxygen-free stage of the analysis and produce additional EC, which is defined as pyrolyzed carbon (OP).

Table 5-12. Backup/primary filter ratios[1] for nitrate and carbon – Summer Monitoring Season

backup/primary	nitrate	OC	EC	TC	O1TC	O2TC	O3TC	O4TC	OPTTC	OPTRC	E1TC	E2TC	E3TC
SFS 24HR													
median	112%	40%	4%	25%		60%	20%	13%	1%	0%	0%	49%	
stdev	125%	20%	4%	22%		38%	14%	5%	7%	0%	1%	28%	
MiniVol 7day													
median		16%	8%	16%	0%		35%		0%		1%	101%	
stdev		5%	2%	4%	0%		10%		5%		2%	33%	

($\mu g/m^3$)	nitrate	OC	EC	TC	O1TC	O2TC	O3TC	O4TC	OPTTC	OPTRC	E1TC	E2TC	E3TC
SFS 24HR													
mean primary	0.74	1.81	1.18	2.98	0.02	0.49	0.80	0.53	0.36	0.08	1.17	0.08	0.00
mean backup	0.90	0.74	0.05	0.76	0.17	0.32	0.20	0.07	0.02	0.00	0.01	0.04	0.00
MiniVol 7day													
mean primary		3.66	1.40	3.67	11.62	0.70	0.60	0.14	1.03	0.00	1.43	0.09	0.00
mean backup		0.58	0.11	0.64	0.03	0.11	0.31	0.17	0.05	0.00	0.03	0.09	0.00

[1] No data shown if primary filter concentration is less than two times measurement uncertainty.

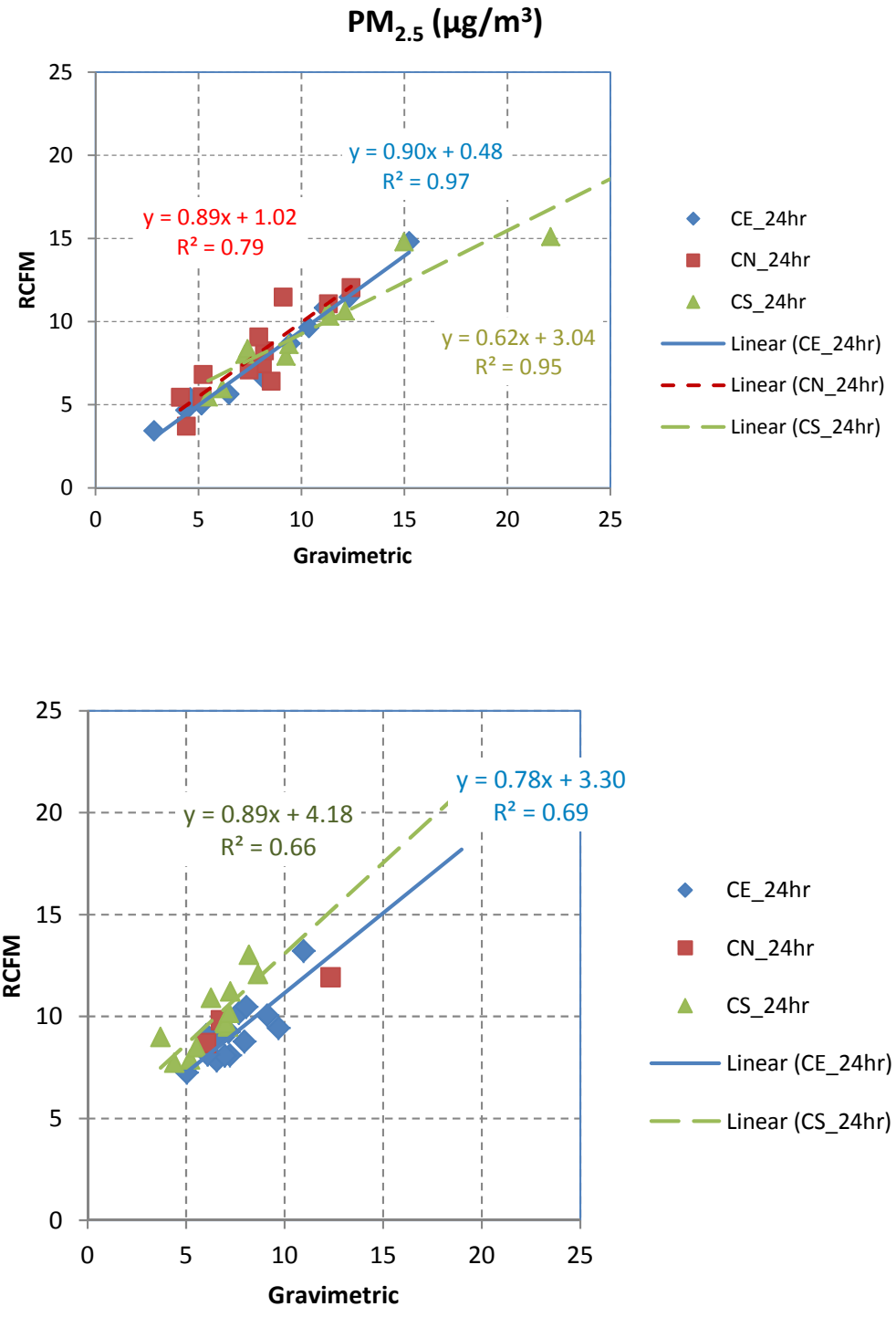

Figure 5-24. Scatterplots of 24-hour $PM_{2.5}$ mass concentrations (µg/m^3) and reconstructed fine mass (RCFM, i.e., sum of PM components) for Winter Monitoring (top) and Summer Monitoring Seasons (bottom) for three core sites. No linear regression is shown for the Summer Season at the CN site, due to low sample recovery.

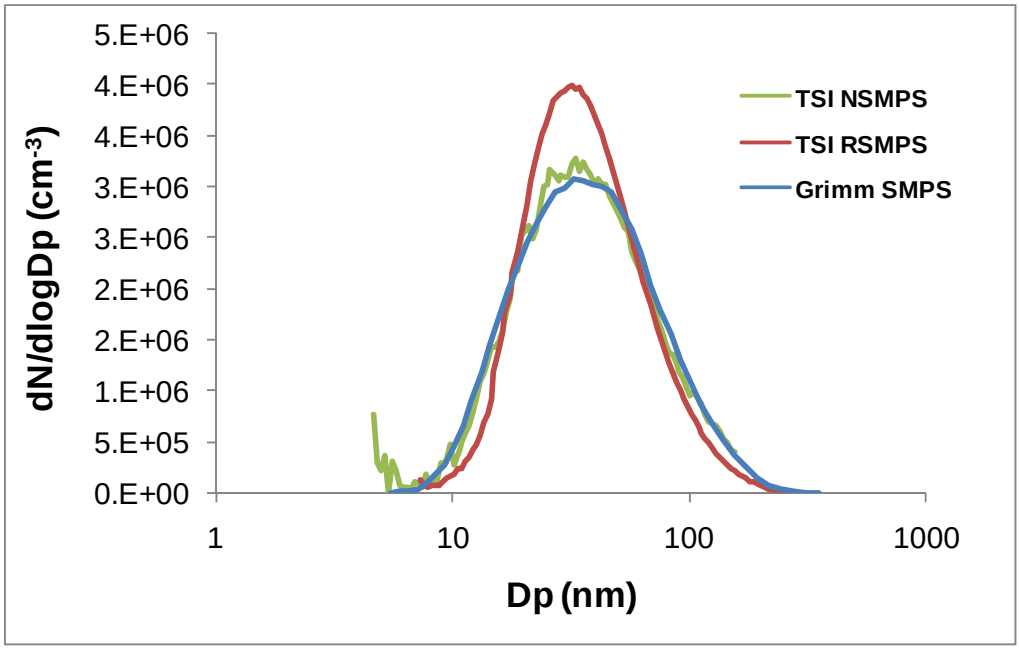

Figure 5-25. NaCl particle size distribution measured in the DRI laboratory by the three collocated SMPS.

Table 5-13. Configurations of collocated SMPS comparisons

Site	Date	SMPS	Particle type
TLCS	9/4/2012 (ambient) 9/6/2012 (car exhaust)	RSMPS_CE, NSMPS_CN, NSMPS_AQ	Ambient aerosols, car exhaust
DRI	9/25/2012	RSMPS_CE, NSMPS_CN, Grimm	Candle smoke

Figure 5-26 shows the particle size distributions (PSD) measured by the three SMPS at the Trinity Lutheran Church School (TLCS) site during the Supplemental Study for ambient aerosols and car exhaust during ignition. For ambient aerosols, the size distributions by the three SMPS agreed very well, with a peak around 18 nm. The RSMPS showed somewhat higher concentrations for particles approximately 9 nm in diameter, most likely due to its higher sampling flow rate resulting in lower diffusional losses of small particles. These size distributions were measured around 15:00, which coincided with parents coming to pick up students from the TLCS site. Cars entering, idling, and leaving the parking lot were most likely the source of the nanoparticles peaking at approximately 18 nm. Figure 5-26 (b) shows that the three SMPS had different peak sizes and concentrations for car ignition exhaust taken directly from the tailpipe of a rental gasoline-powered SUV. The size distribution measured by SMPS is not accurate because the particle generation duration was much shorter than the SMPS scan time (2 minutes). The observed size distribution difference is likely caused by different residence times in the sampling plumbing. Nevertheless, the peak sizes of 18–25 nm from car exhaust confirms their contributions to the ambient concentrations observed in Figure 5-26 (a).

a)

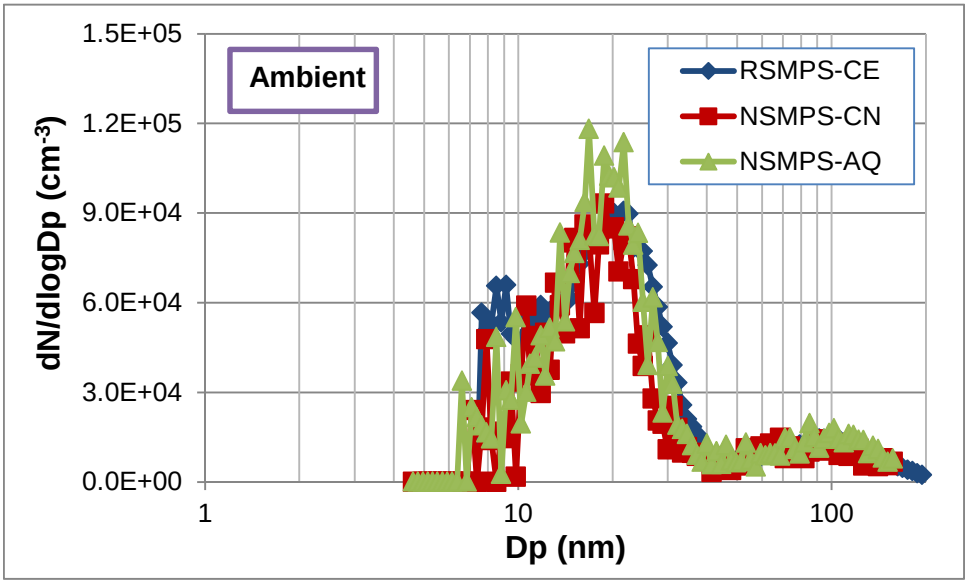

b)

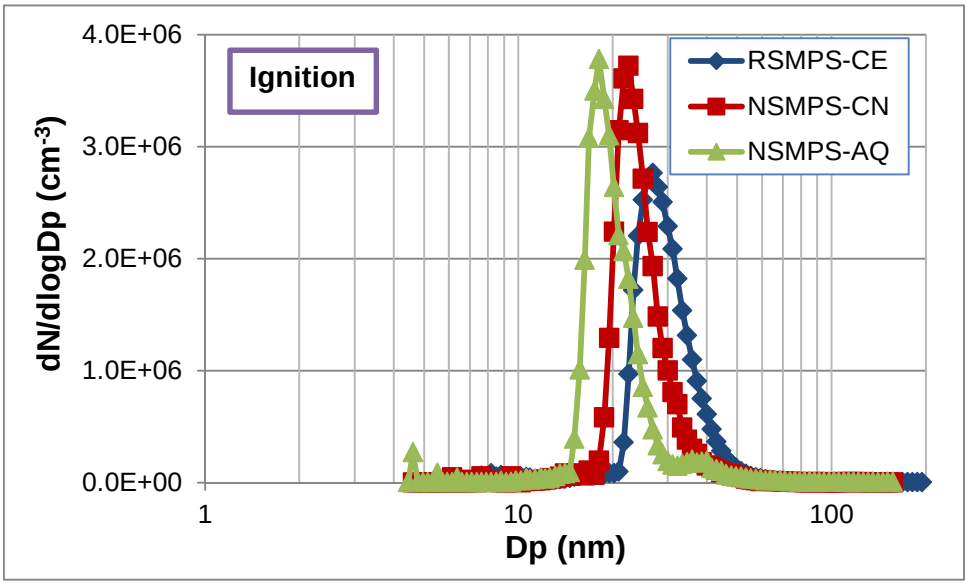

Figure 5-26. Collocated comparison for RSMPS_CE, NSMPS_CN, and NSMPS_AQ at the TLCS site for ambient aerosol and car exhaust during ignition.

Figure 5-27 shows size distribution comparison for candle smoke measured in a DRI laboratory after the Supplemental Study. The tube length to each SMPS was set to have the same flow residence time for all three SMPS. Size distributions by the three SMPS agreed very well.

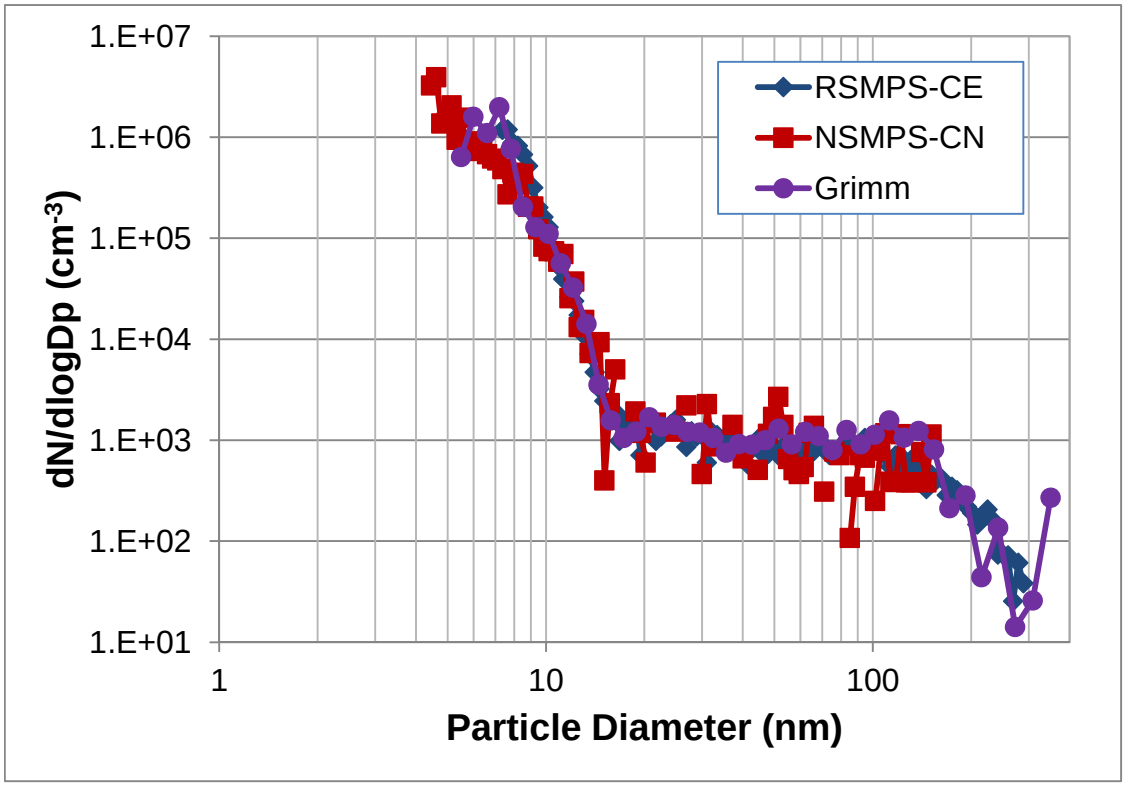

Figure 5-27. Collocated comparison for RSMPS_CE, NSMPS_CN, and Grimm in a DRI laboratory for candle smoke (conducted after the Supplemental Study).

5.2.2 Spatial Variations of Average Pollutant Concentrations Observed from the Saturation Monitoring Network

The saturation air quality monitoring for the LAX AQSAS included 7-day time-integrated passive sampling of NO_2, NO_x, SO_2, BTEX, 1,3-butadiene, and carbonyl compounds for six consecutive weeks during the Winter and Summer monitoring seasons at 17 locations at LAX and the adjacent communities of Westchester, Inglewood, Lennox, Hawthorne, and El Segundo (see Figure 5-19). The sampling locations were selected to determine pollutant gradients from the LAX operations areas, airport buffer zones and the surrounding communities. The measured ambient pollutant concentrations depended upon the proximity, magnitude and mix of local emission sources, and meteorological conditions that affect dispersion and transport of emissions. Higher concentrations are expected near high traffic locations and near the airport runways.

The SRE site is located on the fence line bordering the east edge of the South Airfield and is 95 m directly east of the South Airfield Runway 25R (40 m from the blast fence). BSR and CE are located 710 m and 1620 m east of South Airfield Runway 25R, respectively. The corresponding three sites east of the North Airfield, NR, BNR and CN, are located 350 m, 970 m and 1590 m east of North Airfield Runway 24L, respectively. The fence line of the North Airfield is further away from the active runway area than the South Airfield. Consequently the NR site was about 250 m further from the runway than the SRE site and may receive more influence from other sources since it also borders an employee parking lot. It is important to note that the CN site was

located west of I-405, while the CE site was located east of the freeway. The near-road locations included R405 on the east edge of I-405, SRN at the SW corner of Century Boulevard and Aviation Avenue, and CT on the top level of parking structure P-3 in the Central Terminal Area.

The monitoring results are presented in Tables 5-14 through 5-21. Passive NO_x and SO_2 samples were not collected during the Winter Season at the CN and CS sites and the mean NO_x and SO_2 values for these two sites in Table 5-14 were derived from the continuous monitoring data. Measurement uncertainties for the passive sampling are propagated precision errors based on the average absolute differences of replicate samples collected at the CE site. Uncertainties for the mini-volume (MiniVol) aerosol samples are based upon the root mean squares of the one standard deviation of the analytical replicates, sample volume, and blank uncertainties. These estimates of measurement uncertainty provide benchmarks for evaluating whether differences in pollutant concentrations among the sampling sites are significant. The line plots in Figure 5-28 through Figure 5-33 show the six week means, and symbols show the individual weekly measurements. Sampling sites are listed in the tables and similarly arranged in the plots to facilitate examinations of spatial variations in pollutant concentrations. The sites are roughly arranged along two west to east transects: 1) coast to east of the North Airfield including the communities north of LAX; and 2) coast to east of the South Airfield including communities south of LAX. Although the R405 site is east of the North Airfield, it represents the same freeway source as between the BSR and CE sites, so it is more relevant to that transect and is presented there. Figure 5-34 and Figure 5-35 show the six-week mean NO, NO_2, SO_2, and BTEX concentrations above the background levels measured at the UW sampling site (site minus UW), Figure 5-36 shows the Winter Season plots with and without ("adjusted") a single SO_2 outlier at the R405 site during the Winter Season. As in the tables, the error bars are propagated precision errors based on the average absolute differences of replicate samples collected at the CE site.

Consistent with the mobile monitoring survey of September 2011, the highest NO concentrations during both monitoring seasons were measured near high traffic areas (R405, SRN, and CT) and near the takeoff areas of the North and South Airfields (NR and SRE). The seasonal mean NO concentrations at SRE (173 ppb in Winter Season and 278 ppb in Summer Season) are substantially higher than at the NR site (36 ppb in Winter Season and 25 ppb in Summer Season). While the use of the South Airfield by larger planes may be a contributing factor, closer proximity to the runway is likely the main reason for the higher NO concentrations at the SRE site based upon the results of the runway gradient study. Compared to the Winter Season, NO and NO_2 concentrations were lower during the Summer Season due to greater atmospheric dispersion. More rapid chemical transformation of NO_x to nitric acid and particulate nitrate during the Summer Season would also account for the lower NO_x levels.

The SO_2 concentrations were highest by a wide margin at the SRE site compared to other sites (12.7 ppb during the Winter Season and 17.1 ppb during the Summer Season). The SO_2 value (20.1 ppb) for one of the 7-day Winter Season samples (3/6/12 to 3/13/12) from the R405 site was unusually high compared to the other five weekly samples, which were consistently much lower. Removing this one sample reduces the average SO_2 at R405 from 3.4 to 0.1 ppb. The reason for the single high value is unknown. SO_2 levels were below the measurement uncertainty of 0.4 ppb at approximately half of the sites and below twice the uncertainty at the remaining sites. Higher ambient SO_2 levels were mostly correlated with proximity to the airport. As shown

in Figure 5-37, aircraft emissions account for a substantial fraction (45%) of the total SO_2 emission from the combined basin-wide emissions of SO_2 from aircraft and on-road motor vehicles. The data from the saturation monitoring results and the emissions inventory indicate ambient concentrations of SO_2 may be a potential tracer for jet exhaust near LAX and should correlate well with diurnal and day of week variations in jet takeoffs and landings.

In contrast to SO_2, aircraft emissions account for only 3.7 percent of the combined basin-wide aircraft and on-road motor vehicle NO_x emissions. Although the NO_x emission rates of commercial jets are high, their emissions mix with those from other local and regional sources that have combined area-wide emissions far exceeding the total contributions from jet exhaust. Therefore, the highest NO levels were measured at roadside locations (e.g., R405 and SRN) as well as at the SRE site next to South Airfield Runway 25R. The NO levels at community sampling locations near the coast away from traffic (e.g., AQ, CS2, and CN2) were comparable to those measured at the upwind (UW) site.

On-road gasoline-powered vehicles are the main source of BTEX. Emission rates of BTEX from commercial jets are very low. Therefore, the spatial variations in ambient concentrations of BTEX levels are more uniform with higher levels near roadways. Similarly, aldehydes, EC, OC, and $PM_{2.5}$ were higher near on-road vehicle traffic, but with less spatial variations than NO and SO_2.

Table 5-14. Mean NO, NO_2, and SO_2 concentrations (ppb) of the six 7-day integrated passive samples and EC, OC, and $PM_{2.5}$ concentrations ($\mu g/m^3$) from six 7-day integrated mini-volume aerosol samples during the Winter Monitoring Season with propagated measurement uncertainties.

Site	NO (ppb)	NO_2 (ppb)	SO_2 (ppb)	EC ($\mu g/m^3$)	OC ($\mu g/m^3$)	$PM_{2.5}$ ($\mu g/m^3$)
UW	18.8 ± 0.5	18.9 ± 0.4	0.1 ± 0.4	0.76 ± 0.08	1.95 ± 0.17	10.76 ± 0.56
AQ	16.3 ± 0.5	19.1 ± 0.4	0.1 ± 0.4	0.76 ± 0.08	2.22 ± 0.18	9.30 ± 0.49
CN2	16.2 ± 0.5	19.0 ± 0.4	0.2 ± 0.4	0.81 ± 0.08	2.19 ± 0.18	9.32 ± 0.49
BN	19.6 ± 0.5	20.1 ± 0.4	0.1 ± 0.4			
CT	42.2 ± 0.9	33.0 ± 0.6	0.4 ± 0.4			
NR	36.2 ± 0.8	30.5 ± 0.6	0.7 ± 0.4			
BNR	29.8 ± 0.8	31.1 ± 0.6	0.2 ± 0.4			
CN	23.2*	27.3*	1.1*	1.13 ± 0.10	2.61 ± 0.18	10.11 ± 0.52
R405 [1]	43.3 ± 0.9	31.7 ± 0.6	3.4 ± 0.4			
CS2	16.2 ± 0.5	21.0 ± 0.4	0.1 ± 0.4	0.73 ± 0.07	1.89 ± 0.16	9.26 ± 0.49
CS	37.7*	16.6*	0.3*	1.01 ± 0.10	2.42 ± 0.19	9.74 ± 0.51
BS	27.1 ± 0.7	25.0 ± 0.5	0.1 ± 0.4			
SRN	53.1 ± 1.0	33.2 ± 0.6	0.2 ± 0.4			
SRE	172.5 ± 2.3	50.2 ± 0.9	12.7 ± 0.5			
BSR	31.8 ± 0.7	26.8 ± 0.5	0.6 ± 0.4			
CE	29.8 ± 0.7	25.6 ± 0.5	0.1 ± 0.4	1.13 ± 0.11	2.92 ± 0.22	11.97 ± 0.62
CE-r	30.8 ± 0.7	25.2 ± 0.4	0.1 ± 0.4			
CE2	26.9 ± 0.6	22.1 ± 0.4	0.1 ± 0.4	0.93 ± 0.10	2.75 ± 0.21	11.25 ± 0.59

* Values are based upon time-averages of continuous NO_x and SO_2 measurements at the CN and CS sites.

[1] SO_2 value at R405 is unusually high for one 7-day sample (3/6/12 to 3/13/12). Other pollutants for this sampling period are close to the average values. Reason for this high SO_2 values has not been identified. Removing this one sample reduces the average SO_2 at R405 from 3.4 to 0.1 ppb.

Table 5-15. Mean NO, NO_2, and SO_2 concentrations (ppb) of the six 7-day integrated passive samples and EC, OC, and $PM_{2.5}$ concentrations ($\mu g/m^3$) from six 7-day integrated mini-volume aerosol samples during the Summer Monitoring Season with propagated measurement uncertainties.

Site	NO (ppb)	NO_2 (ppb)	SO_2 (ppb)	EC ($\mu g/m^3$)	OC ($\mu g/m^3$)	$PM_{2.5}$ ($\mu g/m^3$)
UW	6.0 ± 0.1	3.9 ± 0.1	0.4 ± 0.4	0.76 ± 0.08	1.95 ± 0.17	10.76 ± 0.56
AQ	7.6 ± 0.2	4.5 ± 0.1	0.5 ± 0.4	0.76 ± 0.08	2.22 ± 0.18	9.30 ± 0.49
CN2	3.4 ± 0.2	7.1 ± 0.1	0.4 ± 0.3	0.81 ± 0.08	2.19 ± 0.18	9.32 ± 0.49
BN	4.8 ± 0.2	10.8 ± 0.2	1.5 ± 0.4			
CT	19.7 ± 0.5	18.5 ± 0.3	0.2 ± 0.4			
NR	25.0 ± 0.5	19.1 ± 0.3	0.8 ± 0.4			
BNR	9.1 ± 0.4	18.5 ± 0.3	0.4 ± 0.4			
CN	16.7 ± 0.3	13.5 ± 0.2	0.6 ± 0.4	1.13 ± 0.10	2.61 ± 0.18	10.11 ± 0.52
R405	29.6 ± 0.7	26.3 ± 0.4	0.8 ± 0.4			
CS2	5.1 ± 0.2	5.6 ± 0.1	0.3 ± 0.4	0.73 ± 0.07	1.89 ± 0.16	9.26 ± 0.49
CS	4.5 ± 0.5	5.8 ± 0.3	0.4 ± 0.4	1.01 ± 0.10	2.42 ± 0.19	9.74 ± 0.51
BS	6.7 ± 0.2	10.4 ± 0.2	0.4 ± 0.4			
SRN	27.5 ± 0.6	23.4 ± 0.4	0.5 ± 0.4			
SRE	278.2 ± 3.1	67.1 ± 1.0	17.1 ± 0.8			
BSR	11.5 ± 0.3	16.3 ± 0.2	0.5 ± 0.4			
CE	6.7 ± 0.3	15.6 ± 0.3	0.6 ± 0.4	1.13 ± 0.11	2.92 ± 0.22	11.97 ± 0.62
CE-r	7.6 ± 0.3	14.7 ± 0.2	1.0 ± 0.4			
CE2	5.3 ± 0.2	6.9 ± 0.1	0.3 ± 0.4	0.93 ± 0.10	2.75 ± 0.21	11.25 ± 0.59

Table 5-16. Seven-day mean concentrations (ppb) of 1,3-butadiene and BTEX during the Winter Monitoring Season with propagated measurement uncertainties.

Site	1,3-butadiene	benzene	toluene	ethylbenzene	m&p-xylene	o-xylene
UW	0.000 ± 0.001	0.29 ± 0.11	0.31 ± 0.15	0.03 ± 0.02	0.10 ± 0.08	0.05 ± 0.04
AQ	0.003 ± 0.001	0.27 ± 0.11	0.23 ± 0.15	0.01 ± 0.02	0.05 ± 0.08	0.02 ± 0.04
CN2	0.005 ± 0.001	0.71 ± 0.11	0.83 ± 0.15	0.08 ± 0.02	0.32 ± 0.08	0.13 ± 0.04
BN	0.005 ± 0.001	0.62 ± 0.11	0.72 ± 0.15	0.06 ± 0.02	0.25 ± 0.08	0.11 ± 0.04
CT	0.006 ± 0.001	0.54 ± 0.11	0.65 ± 0.15	0.06 ± 0.02	0.25 ± 0.08	0.11 ± 0.04
NR	0.005 ± 0.001	0.77 ± 0.11	0.67 ± 0.15	0.04 ± 0.02	0.18 ± 0.08	0.08 ± 0.04
BNR	0.010 ± 0.001	0.66 ± 0.11	0.82 ± 0.15	0.08 ± 0.02	0.33 ± 0.08	0.14 ± 0.04
CN	0.004 ± 0.001	0.82 ± 0.11	1.14 ± 0.15	0.10 ± 0.02	0.41 ± 0.08	0.17 ± 0.04
R405	0.005 ± 0.001	1.36 ± 0.11	1.79 ± 0.15	0.19 ± 0.02	0.79 ± 0.08	0.33 ± 0.04
CS2	0.006 ± 0.001	0.22 ± 0.11	0.27 ± 0.15	0.02 ± 0.02	0.08 ± 0.08	0.04 ± 0.04
CS	0.008 ± 0.001	0.64 ± 0.11	0.73 ± 0.15	0.06 ± 0.02	0.26 ± 0.08	0.11 ± 0.04
BS	0.009 ± 0.001	0.74 ± 0.11	1.02 ± 0.15	0.10 ± 0.02	0.40 ± 0.08	0.17 ± 0.04
SRN	0.007 ± 0.001	1.16 ± 0.11	1.42 ± 0.15	0.15 ± 0.02	0.64 ± 0.08	0.27 ± 0.04
SRE	0.008 ± 0.001	0.84 ± 0.11	0.98 ± 0.15	0.09 ± 0.02	0.38 ± 0.08	0.16 ± 0.04
BSR	0.006 ± 0.001	1.06 ± 0.11	1.35 ± 0.15	0.12 ± 0.02	0.50 ± 0.08	0.21 ± 0.04
CE	0.006 ± 0.001	1.39 ± 0.11	1.64 ± 0.15	0.17 ± 0.02	0.72 ± 0.08	0.30 ± 0.04
CE-r	0.014 ± 0.001	1.48 ± 0.11	1.85 ± 0.15	0.20 ± 0.02	0.85 ± 0.08	0.37 ± 0.04
CE2	0.006 ± 0.001	1.37 ± 0.11	1.65 ± 0.15	0.14 ± 0.02	0.55 ± 0.08	0.23 ± 0.04

Table 5-17. Seven-day mean concentrations (ppb) of 1,3-butadiene and BTEX during the Summer Monitoring Season with propagated measurement uncertainties.

Site	1,3-butadiene	benzene	toluene	ethylbenzene	m&p-xylene	o-xylene
UW	0.000 ± 0.100	0.03 ± 0.11	0.01 ± 0.10	0.00 ± 0.10	0.00 ± 0.10	0.00 ± 0.10
AQ	0.000 ± 0.100	0.05 ± 0.11	0.04 ± 0.10	0.00 ± 0.10	0.02 ± 0.10	0.01 ± 0.10
CN2	0.005 ± 0.100	0.17 ± 0.11	0.18 ± 0.10	0.02 ± 0.10	0.08 ± 0.10	0.03 ± 0.10
BN	0.001 ± 0.100	0.16 ± 0.11	0.14 ± 0.10	0.02 ± 0.10	0.07 ± 0.10	0.03 ± 0.10
CT	0.000 ± 0.100	0.24 ± 0.11	0.33 ± 0.10	0.04 ± 0.10	0.20 ± 0.10	0.08 ± 0.10
NR	0.007 ± 0.100	0.30 ± 0.11	0.25 ± 0.10	0.03 ± 0.10	0.13 ± 0.10	0.05 ± 0.10
BNR	0.015 ± 0.100	0.19 ± 0.11	0.17 ± 0.10	0.03 ± 0.10	0.11 ± 0.10	0.05 ± 0.10
CN	0.015 ± 0.100	0.30 ± 0.11	0.25 ± 0.10	0.03 ± 0.10	0.16 ± 0.10	0.07 ± 0.10
R405	0.004 ± 0.100	0.41 ± 0.11	0.46 ± 0.10	0.06 ± 0.10	0.29 ± 0.10	0.12 ± 0.10
CS2	0.000 ± 0.100	0.17 ± 0.11	0.15 ± 0.10	0.02 ± 0.10	0.08 ± 0.10	0.03 ± 0.10
CS	0.003 ± 0.100	0.11 ± 0.11	0.13 ± 0.10	0.01 ± 0.10	0.06 ± 0.10	0.02 ± 0.10
BS	0.003 ± 0.100	0.29 ± 0.11	0.26 ± 0.10	0.03 ± 0.10	0.10 ± 0.10	0.04 ± 0.10
SRN	0.012 ± 0.100	0.22 ± 0.11	0.18 ± 0.10	0.02 ± 0.10	0.09 ± 0.10	0.04 ± 0.10
SRE	0.013 ± 0.100	0.24 ± 0.11	0.19 ± 0.10	0.03 ± 0.10	0.13 ± 0.10	0.06 ± 0.10
BSR	0.001 ± 0.100	0.31 ± 0.11	0.19 ± 0.10	0.02 ± 0.10	0.07 ± 0.10	0.03 ± 0.10
CE	0.016 ± 0.100	0.25 ± 0.11	0.39 ± 0.10	0.04 ± 0.10	0.22 ± 0.10	0.08 ± 0.10
CE-r	0.013 ± 0.100	0.36 ± 0.11	0.44 ± 0.10	0.05 ± 0.10	0.22 ± 0.10	0.09 ± 0.10
CE2	0.000 ± 0.100	0.21 ± 0.11	0.24 ± 0.10	0.02 ± 0.10	0.06 ± 0.10	0.03 ± 0.10

Table 5-18. Seven-day mean concentrations (ppb) of carbonyl compounds during the Winter Monitoring Season with propagated measurement uncertainties.

Site	formaldehyde	acetaldehyde	acrolein	propionaldehyde	butyraldehyde	valeraldehyde	hexaldehyde
UW	1.62 ± 0.03	0.74 ± 0.02	0.00 ± 0.01	0.07 ± 0.01	0.00 ± 0.01	0.22 ± 0.01	0.02 ± 0.01
AQ	1.52 ± 0.03	0.81 ± 0.02	0.00 ± 0.01	0.07 ± 0.01	0.00 ± 0.01	0.21 ± 0.01	0.03 ± 0.01
CN2	1.48 ± 0.03	0.84 ± 0.02	0.00 ± 0.01	0.07 ± 0.01	0.00 ± 0.01	0.22 ± 0.01	0.05 ± 0.01
BN	1.55 ± 0.03	0.83 ± 0.02	0.00 ± 0.01	0.07 ± 0.01	0.00 ± 0.01	0.22 ± 0.01	0.03 ± 0.01
CT	2.42 ± 0.05	1.17 ± 0.02	0.11 ± 0.01	0.08 ± 0.01	0.00 ± 0.01	0.38 ± 0.01	0.05 ± 0.01
NR	2.01 ± 0.04	1.10 ± 0.02	0.09 ± 0.01	0.09 ± 0.01	0.00 ± 0.01	0.29 ± 0.01	0.04 ± 0.01
BNR	1.86 ± 0.04	1.10 ± 0.02	0.09 ± 0.01	0.09 ± 0.01	0.00 ± 0.01	0.28 ± 0.01	0.05 ± 0.01
CN	2.24 ± 0.05	1.14 ± 0.02	0.30 ± 0.02	0.18 ± 0.01	1.03 ± 0.11	0.30 ± 0.01	0.06 ± 0.01
R405	2.12 ± 0.04	1.21 ± 0.03	0.00 ± 0.01	0.10 ± 0.01	0.00 ± 0.01	0.32 ± 0.01	0.05 ± 0.01
CS2	1.77 ± 0.04	0.86 ± 0.02	0.00 ± 0.01	0.08 ± 0.01	0.00 ± 0.01	0.24 ± 0.01	0.03 ± 0.01
CS	1.72 ± 0.04	0.88 ± 0.02	0.13 ± 0.01	0.10 ± 0.01	0.13 ± 0.03	0.24 ± 0.01	0.04 ± 0.01
BS	1.96 ± 0.04	1.00 ± 0.02	0.06 ± 0.01	0.08 ± 0.01	0.00 ± 0.01	0.31 ± 0.01	0.04 ± 0.01
SRN	2.25 ± 0.05	1.24 ± 0.03	0.00 ± 0.01	0.10 ± 0.01	0.00 ± 0.01	0.35 ± 0.01	0.03 ± 0.01
SRE	2.50 ± 0.05	1.29 ± 0.03	0.05 ± 0.01	0.10 ± 0.01	0.02 ± 0.01	0.38 ± 0.01	0.05 ± 0.01
BSR	2.27 ± 0.05	1.19 ± 0.03	0.00 ± 0.01	0.10 ± 0.01	0.00 ± 0.01	0.34 ± 0.01	0.04 ± 0.01
CE	2.14 ± 0.04	1.36 ± 0.03	0.15 ± 0.02	0.12 ± 0.01	0.05 ± 0.01	0.34 ± 0.01	0.06 ± 0.01
CE-r	2.04 ± 0.04	1.30 ± 0.03	0.44 ± 0.02	0.12 ± 0.01	0.16 ± 0.03	0.31 ± 0.01	0.05 ± 0.01
CE2	1.86 ± 0.04	1.20 ± 0.03	0.00 ± 0.01	0.11 ± 0.01	0.00 ± 0.01	0.27 ± 0.01	0.05 ± 0.01

Table 5-19. Seven-day mean (ppb) of carbonyl compounds during the Summer Monitoring Season with propagated measurement uncertainties.

Site	formaldehyde	acetaldehyde	acrolein	propionaldehyde	butyraldehyde	valeraldehyde	hexaldehyde
UW	0.92 ± 0.10	0.25 ± 0.10	0.00 ± 0.10	0.00 ± 0.10	0.00 ± 0.10	0.05 ± 0.10	0.00 ± 0.10
AQ	1.03 ± 0.10	0.29 ± 0.10	0.00 ± 0.10	0.00 ± 0.10	0.00 ± 0.10	0.07 ± 0.10	0.00 ± 0.10
CN2	1.08 ± 0.10	0.27 ± 0.10	0.00 ± 0.10	0.00 ± 0.10	0.00 ± 0.10	0.07 ± 0.10	0.00 ± 0.10
BN	1.08 ± 0.10	0.32 ± 0.10	0.00 ± 0.10	0.00 ± 0.10	0.00 ± 0.10	0.08 ± 0.10	0.00 ± 0.10
CT	1.44 ± 0.10	0.39 ± 0.10	0.00 ± 0.10	0.00 ± 0.10	0.00 ± 0.10	0.11 ± 0.10	0.00 ± 0.10
NR	1.58 ± 0.10	0.42 ± 0.10	0.00 ± 0.10	0.00 ± 0.10	0.00 ± 0.10	0.14 ± 0.10	0.00 ± 0.10
BNR	1.43 ± 0.10	0.41 ± 0.10	0.00 ± 0.10	0.01 ± 0.10	0.00 ± 0.10	0.12 ± 0.10	0.00 ± 0.10
CN	1.53 ± 0.10	0.37 ± 0.10	0.00 ± 0.10	0.03 ± 0.10	0.00 ± 0.10	0.12 ± 0.10	0.00 ± 0.10
R405	1.75 ± 0.10	0.50 ± 0.10	0.00 ± 0.10	0.03 ± 0.10	0.00 ± 0.10	0.16 ± 0.10	0.00 ± 0.10
CS2	1.04 ± 0.10	0.31 ± 0.10	0.00 ± 0.10	0.00 ± 0.10	0.00 ± 0.10	0.07 ± 0.10	0.00 ± 0.10
CS	1.08 ± 0.10	0.32 ± 0.10	0.00 ± 0.10	0.00 ± 0.10	0.00 ± 0.10	0.08 ± 0.10	0.00 ± 0.10
BS	1.13 ± 0.10	0.33 ± 0.10	0.00 ± 0.10	0.00 ± 0.10	0.00 ± 0.10	0.09 ± 0.10	0.00 ± 0.10
SRN	1.67 ± 0.10	0.45 ± 0.10	0.00 ± 0.10	0.00 ± 0.10	0.00 ± 0.10	0.14 ± 0.10	0.00 ± 0.10
SRE	2.61 ± 0.10	0.61 ± 0.10	0.00 ± 0.10	0.03 ± 0.10	0.00 ± 0.10	0.23 ± 0.10	0.00 ± 0.10
BSR	1.32 ± 0.10	0.40 ± 0.10	0.00 ± 0.10	0.03 ± 0.10	0.00 ± 0.10	0.12 ± 0.10	0.00 ± 0.10
CE	1.34 ± 0.10	0.44 ± 0.10	0.00 ± 0.10	0.02 ± 0.10	0.00 ± 0.10	0.12 ± 0.10	0.00 ± 0.10
CE-r	1.35 ± 0.10	0.44 ± 0.10	0.00 ± 0.10	0.03 ± 0.10	0.00 ± 0.10	0.10 ± 0.10	0.00 ± 0.10
CE2	1.08 ± 0.10	0.38 ± 0.10	0.00 ± 0.10	0.03 ± 0.10	0.00 ± 0.10	0.10 ± 0.10	0.00 ± 0.10

Table 5-20. Seven-day mean and max concentration (µg/m^3) of $PM_{2.5}$ mass, OC, EC, and select elements during the Winter Monitoring Season.

	UW	AQ	CS2	CS	CN2	CN*	CE	CE2
PM2.5 mass	10.76 (12.94)	9.30 (12.60)	9.26 (12.08)	9.74 (12.16)	9.32 (12.18)	10.11	11.97 (16.15)	11.25 (15.39)
Total Organic Carbon	1.95 (2.15)	2.22 (3.06)	1.89 (2.18)	2.42 (3.17)	2.19 (3.06)	2.61 (3.23)	2.92 (4.22)	2.75 (3.94)
Total Elemental Carbon	0.76 (0.86)	0.76 (1.12)	0.73 (0.89)	1.01 (1.63)	0.81 (1.22)	1.13 (1.51)	1.13 (1.76)	0.93 (1.56)
Total Carbon	2.71 (3.00)	2.97 (4.17)	2.62 (3.06)	3.42 (4.79)	3.00 (4.27)	3.73 (4.73)	4.04 (5.97)	3.67 (5.49)
Sodium (qualitative only)	0.68 (1.34)	0.35 (0.67)	0.28 (0.44)	0.46 (0.80)	0.33 (0.49)	0.51	0.40 (0.80)	0.41 (0.60)
Magnesium (qualitative only)	0.08 (0.22)	0.02 (0.05)	0.01 (0.03)	0.02 (0.06)	0.02 (0.04)	0.00	0.02 (0.07)	0.01 (0.04)
Aluminum	0.07 (0.10)	0.04 (0.08)	0.05 (0.07)	0.06 (0.11)	0.05 (0.10)	0.10	0.06 (0.13)	0.05 (0.09)
Silicon	0.13 (0.27)	0.10 (0.24)	0.11 (0.25)	0.11 (0.28)	0.12 (0.28)	0.31	0.16 (0.37)	0.14 (0.29)
Phosphorous	0.00 (0.00)	0.00 (0.00)	0.00 (0.00)	0.00 (0.00)	0.00 (0.00)	0.00	0.00 (0.00)	0.00 (0.00)
Sulfur	0.45 (0.67)	0.41 (0.64)	0.42 (0.64)	0.40 (0.62)	0.40 (0.63)	0.54	0.47 (0.71)	0.43 (0.61)
Chlorine	0.446 (1.188)	0.146 (0.421)	0.159 (0.335)	0.186 (0.370)	0.109 (0.184)	0.11	0.206 (0.407)	0.193 (0.347)
Potassium	0.070 (0.084)	0.063 (0.080)	0.050 (0.069)	0.056 (0.076)	0.057 (0.078)	0.08	0.077 (0.097)	0.070 (0.079)
Calcium	0.073 (0.112)	0.054 (0.097)	0.058 (0.095)	0.063 (0.114)	0.062 (0.109)	0.12	0.086 (0.144)	0.076 (0.106)
Scandium	0.000 (0.001)	0.001 (0.005)	0.000 (0.000)	0.000 (0.000)	0.000 (0.002)	0.00	0.000 (0.003)	0.000 (0.002)
Titanium	0.011 (0.013)	0.008 (0.012)	0.008 (0.011)	0.008 (0.012)	0.010 (0.013)	0.01	0.014 (0.019)	0.013 (0.017)
Vanadium	0.001 (0.002)	0.001 (0.001)	0.001 (0.001)	0.001 (0.001)	0.001 (0.002)	0.00	0.001 (0.002)	0.001 (0.002)
Chromium	0.000 (0.001)	0.000 (0.001)	0.000 (0.001)	0.000 (0.001)	0.000 (0.001)	0.00	0.001 (0.001)	0.001 (0.001)
Manganese	0.002 (0.003)	0.002 (0.003)	0.002 (0.003)	0.001 (0.003)	0.002 (0.003)	0.00	0.003 (0.004)	0.004 (0.005)
Iron	0.128 (0.161)	0.108 (0.154)	0.108 (0.130)	0.114 (0.143)	0.131 (0.169)	0.18	0.189 (0.218)	0.166 (0.226)
Cobalt	0.000 (0.000)	0.000 (0.000)	0.000 (0.000)	0.000 (0.000)	0.000 (0.000)	0.00	0.000 (0.000)	0.000 (0.000)
Nickel	0.000 (0.001)	0.000 (0.001)	0.000 (0.001)	0.000 (0.001)	0.000 (0.001)	0.00	0.001 (0.001)	0.001 (0.001)
Copper	0.007 (0.010)	0.006 (0.010)	0.007 (0.008)	0.007 (0.009)	0.008 (0.011)	0.01	0.011 (0.014)	0.010 (0.014)
Zinc	0.009 (0.013)	0.008 (0.011)	0.009 (0.010)	0.009 (0.011)	0.009 (0.011)	0.01	0.014 (0.016)	0.015 (0.020)
Lead	0.002 (0.003)	0.002 (0.002)	0.001 (0.002)	0.001 (0.002)	0.002 (0.003)	0.00	0.002 (0.004)	0.002 (0.004)

*Only one valid Teflon filter sample was collected at the CN site due to equipment malfunctions.
Concentrations are presented as mean (max) values.

Table 5-21. Seven-day mean and max concentration (µg/m^3) of $PM_{2.5}$ mass, OC, EC, and select elements during the Summer Monitoring Season.

SITE	UW	AQ	CS2	CS	CN2	CN	CE	CE2
PM2.5 mass	7.54 (9.02)	7.06 (8.59)	7.14 (8.17)	7.17 (8.63)	7.84 (8.78)	7.31 (9.82)	9.80 (12.03)	8.40 (9.95)
Total Organic Carbon	1.24 (1.62)	1.18 (1.67)	1.21 (1.70)	1.44 (1.73)	1.45 (1.96)	1.66 (2.05)	1.80 (2.75)	1.66 (2.82)
Total Elemental Carbon	0.27 (0.39)	0.23 (0.34)	0.26 (0.46)	0.29 (0.37)	0.38 (0.54)	0.57 (0.89)	0.58 (0.87)	0.32 (0.46)
Total Carbon	1.51 (2.01)	1.41 (2.00)	1.46 (2.16)	1.73 (2.06)	1.83 (2.31)	2.23 (2.93)	2.38 (3.62)	1.99 (3.28)
Sodium (qualitative)	0.81 (0.97)	0.81 (1.04)	0.80 (1.30)	0.75 (0.96)	0.82 (1.06)	0.77 (1.54)	0.93 (1.69)	0.94 (1.32)
Magnesium (qualitative)	0.10 (0.14)	0.11 (0.23)	0.07 (0.13)	0.09 (0.25)	0.08 (0.10)	0.06 (0.08)	0.08 (0.13)	0.07 (0.13)
Aluminum	0.03 (0.04)	0.02 (0.05)	0.02 (0.04)	0.02 (0.03)	0.01 (0.03)	0.02 (0.03)	0.02 (0.04)	0.03 (0.06)
Silicon	0.01 (0.03)	0.01 (0.02)	0.01 (0.02)	0.02 (0.02)	0.02 (0.04)	0.01 (0.03)	0.03 (0.05)	0.03 (0.04)
Phosphorous	0.00 (0.00)	0.00 (0.00)	0.00 (0.00)	0.00 (0.00)	0.00 (0.00)	0.00 (0.00)	0.00 (0.00)	0.00 (0.00)
Sulfur	0.88 (1.08)	0.86 (1.05)	0.87 (1.09)	0.86 (1.08)	0.93 (1.10)	0.84 (1.26)	1.03 (1.35)	0.95 (1.26)
Chlorine	0.207 (0.664)	0.098 (0.482)	0.073 (0.351)	0.080 (0.396)	0.044 (0.147)	0.045 (0.180)	0.073 (0.322)	0.073 (0.347)
Potassium	0.045 (0.055)	0.037 (0.049)	0.038 (0.049)	0.038 (0.051)	0.039 (0.049)	0.034 (0.049)	0.049 (0.065)	0.044 (0.058)
Calcium	0.042 (0.056)	0.037 (0.059)	0.039 (0.053)	0.038 (0.048)	0.041 (0.049)	0.036 (0.059)	0.053 (0.074)	0.047 (0.064)
Scandium	0.001 (0.002)	0.000 (0.002)	0.001 (0.005)	0.001 (0.004)	0.001 (0.002)	0.001 (0.004)	0.001 (0.006)	0.001 (0.003)
Titanium	0.002 (0.003)	0.001 (0.002)	0.002 (0.003)	0.001 (0.001)	0.003 (0.003)	0.002 (0.003)	0.004 (0.006)	0.003 (0.006)
Vanadium	0.001 (0.002)	0.001 (0.002)	0.001 (0.002)	0.001 (0.002)	0.001 (0.002)	0.001 (0.002)	0.001 (0.002)	0.001 (0.001)
Chromium	0.000 (0.000)	0.000 (0.001)	0.000 (0.000)	0.000 (0.000)	0.000 (0.000)	0.000 (0.000)	0.000 (0.001)	0.000 (0.001)
Manganese	0.001 (0.001)	0.000 (0.001)	0.000 (0.001)	0.000 (0.001)	0.000 (0.001)	0.001 (0.002)	0.001 (0.002)	0.001 (0.002)
Iron	0.028 (0.045)	0.021 (0.041)	0.025 (0.033)	0.022 (0.029)	0.031 (0.054)	0.033 (0.052)	0.064 (0.087)	0.043 (0.061)
Cobalt	0.000 (0.000)	0.000 (0.000)	0.000 (0.000)	0.000 (0.000)	0.000 (0.000)	0.000 (0.000)	0.000 (0.000)	0.000 (0.000)
Nickel	0.000 (0.001)	0.000 (0.000)	0.000 (0.001)	0.000 (0.001)	0.000 (0.001)	0.000 (0.001)	0.001 (0.001)	0.000 (0.001)
Copper	0.001 (0.002)	0.001 (0.001)	0.001 (0.002)	0.001 (0.001)	0.002 (0.003)	0.002 (0.003)	0.004 (0.005)	0.002 (0.003)
Zinc	0.002 (0.004)	0.002 (0.003)	0.003 (0.006)	0.003 (0.004)	0.003 (0.004)	0.003 (0.005)	0.005 (0.010)	0.004 (0.004)
Lead	0.001 (0.002)	0.001 (0.002)	0.000 (0.001)	0.000 (0.001)	0.000 (0.001)	0.000 (0.001)	0.000 (0.001)	0.000 (0.001)

Concentrations are presented as mean (max) values.

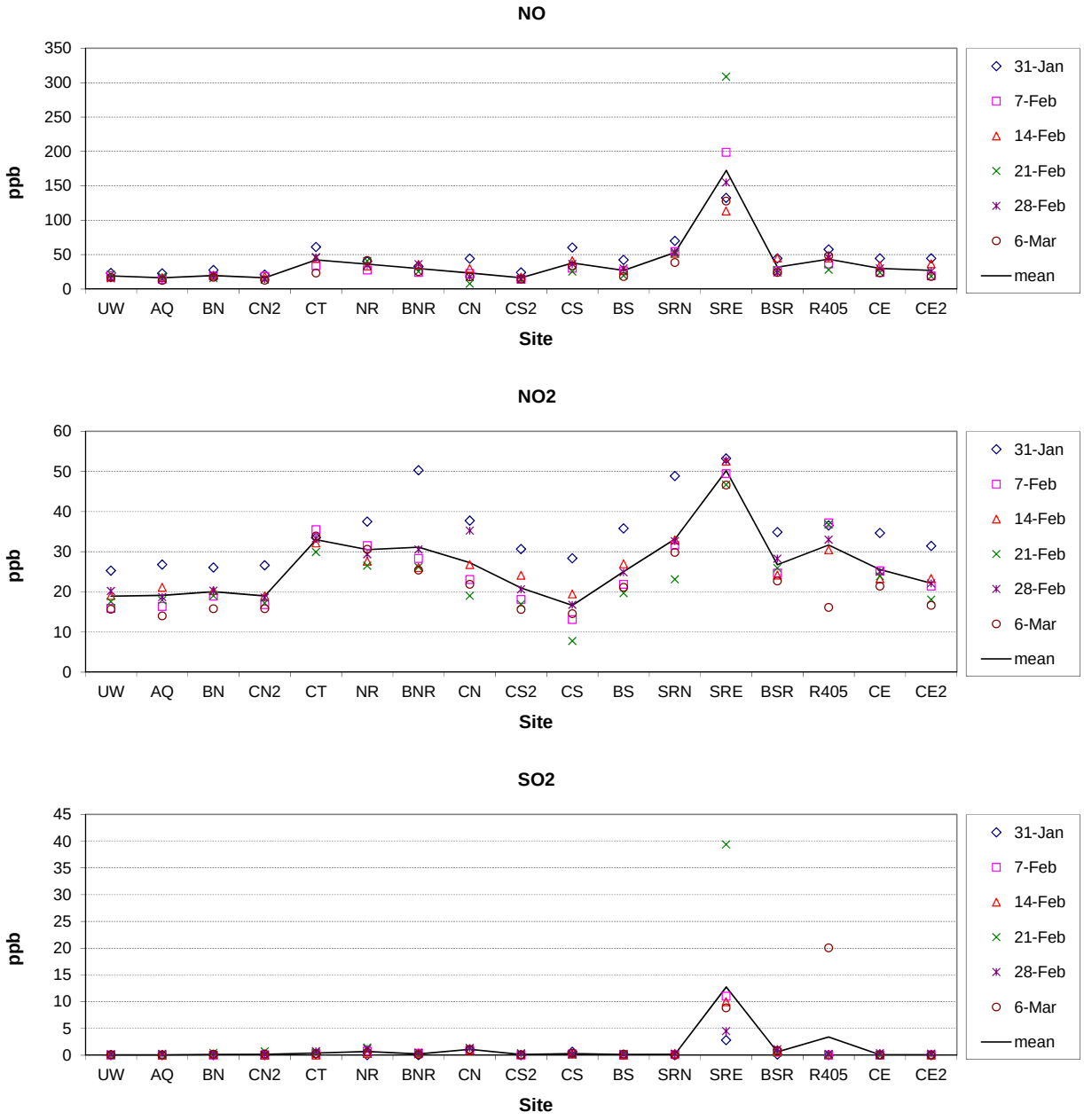

Figure 5-28. Seven-day passive measurements of NO (by NO_x-NO_2), NO_2, and SO_2 by site and week during the Winter Monitoring Season. Sites are arranged approximately along two west to east traverses: north of LAX from UW to CN and south of LAX from CS2 to CE2.

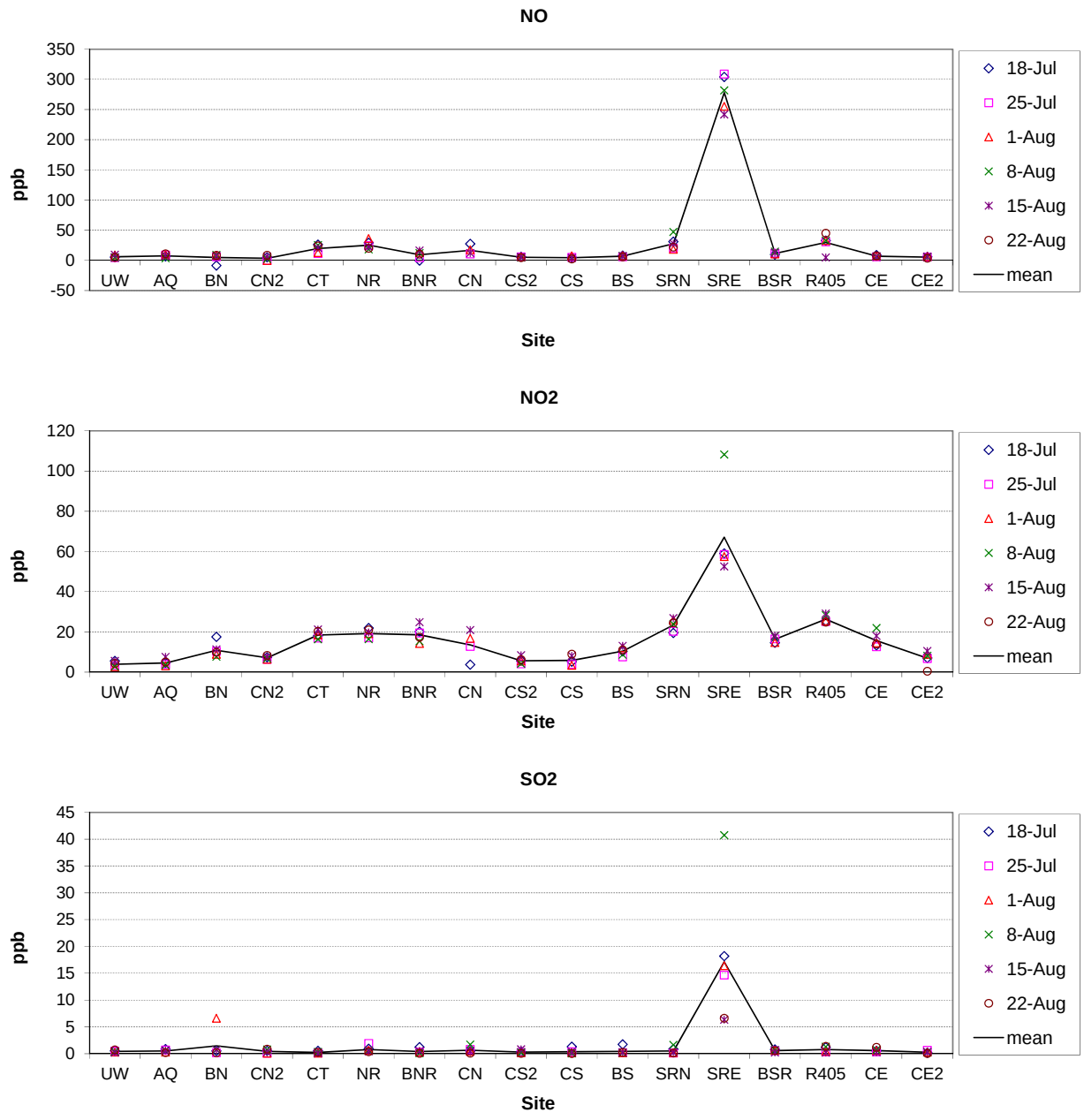

Figure 5-29. Seven-day passive measurements of NO (by NO_x-NO_2), NO_2, and SO_2 by site and week during the Summer Monitoring Season. Sites are arranged approximately along two west to east traverses: north of LAX from UW to CN and south of LAX from CS2 to CE2.

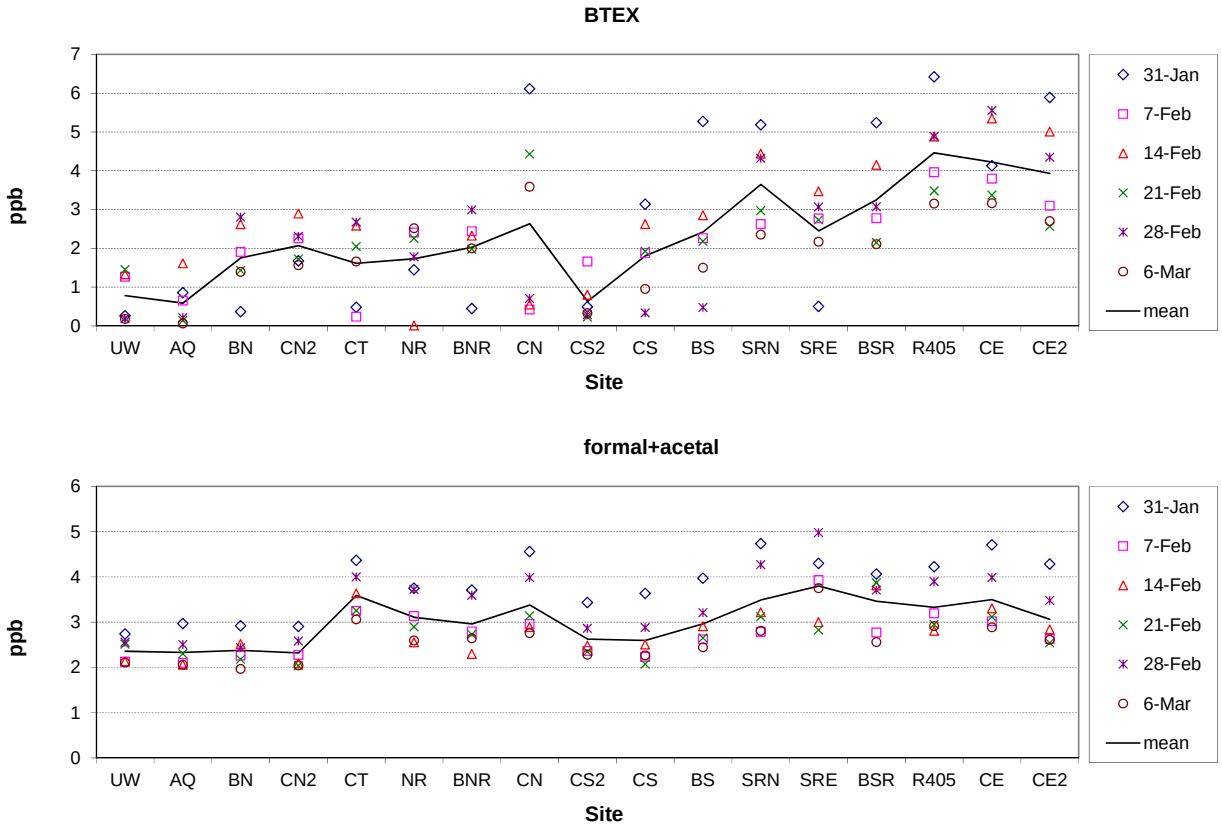

Figure 5-30. Seven-day passive measurements of BTEX and formaldehyde + acetaldehyde by site and week during the Winter Monitoring Season. Sites are arranged approximately along two west to east traverses: north of LAX from UW to CN and south of LAX from CS2 to CE2.

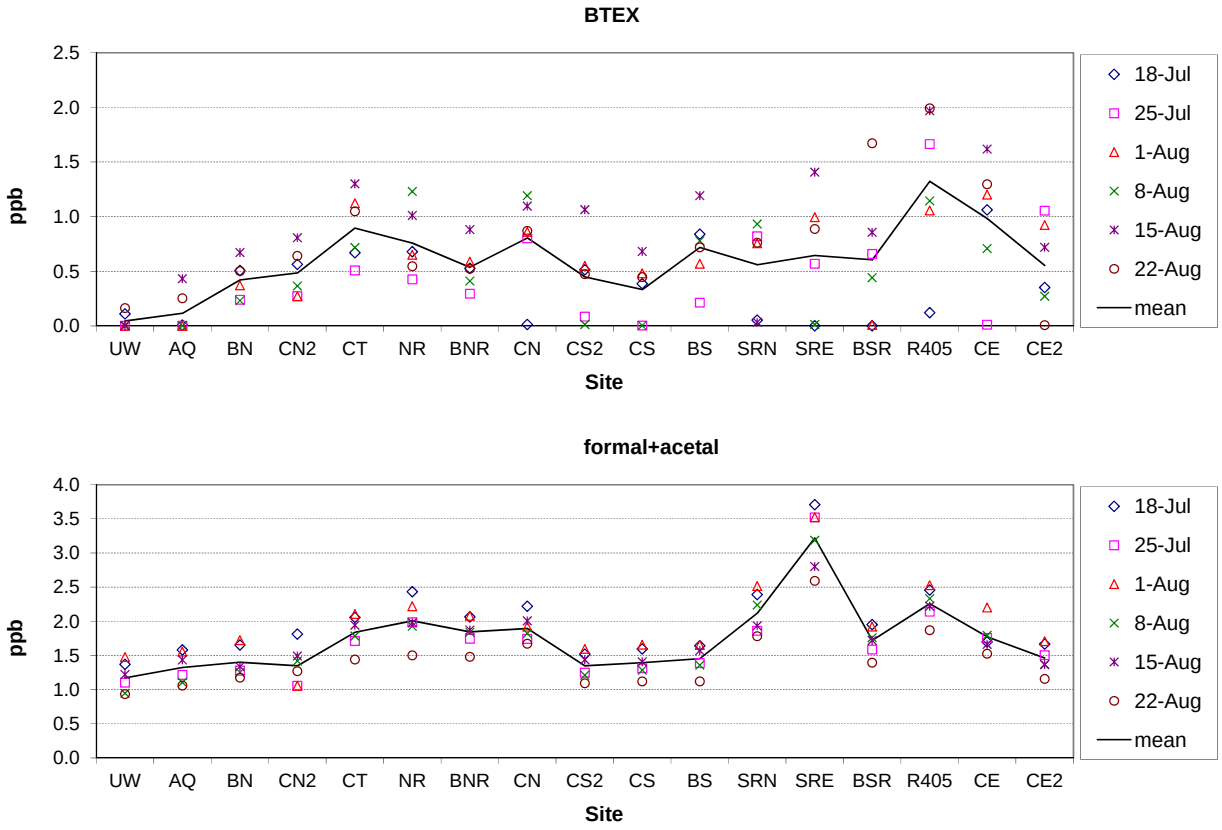

Figure 5-31. Seven-day passive measurements of BTEX and formaldehyde + acetaldehyde by site and week during the Summer Monitoring Season. Sites are arranged approximately along two west to east traverses: north of LAX from UW to CN and south of LAX from CS2 to CE2.

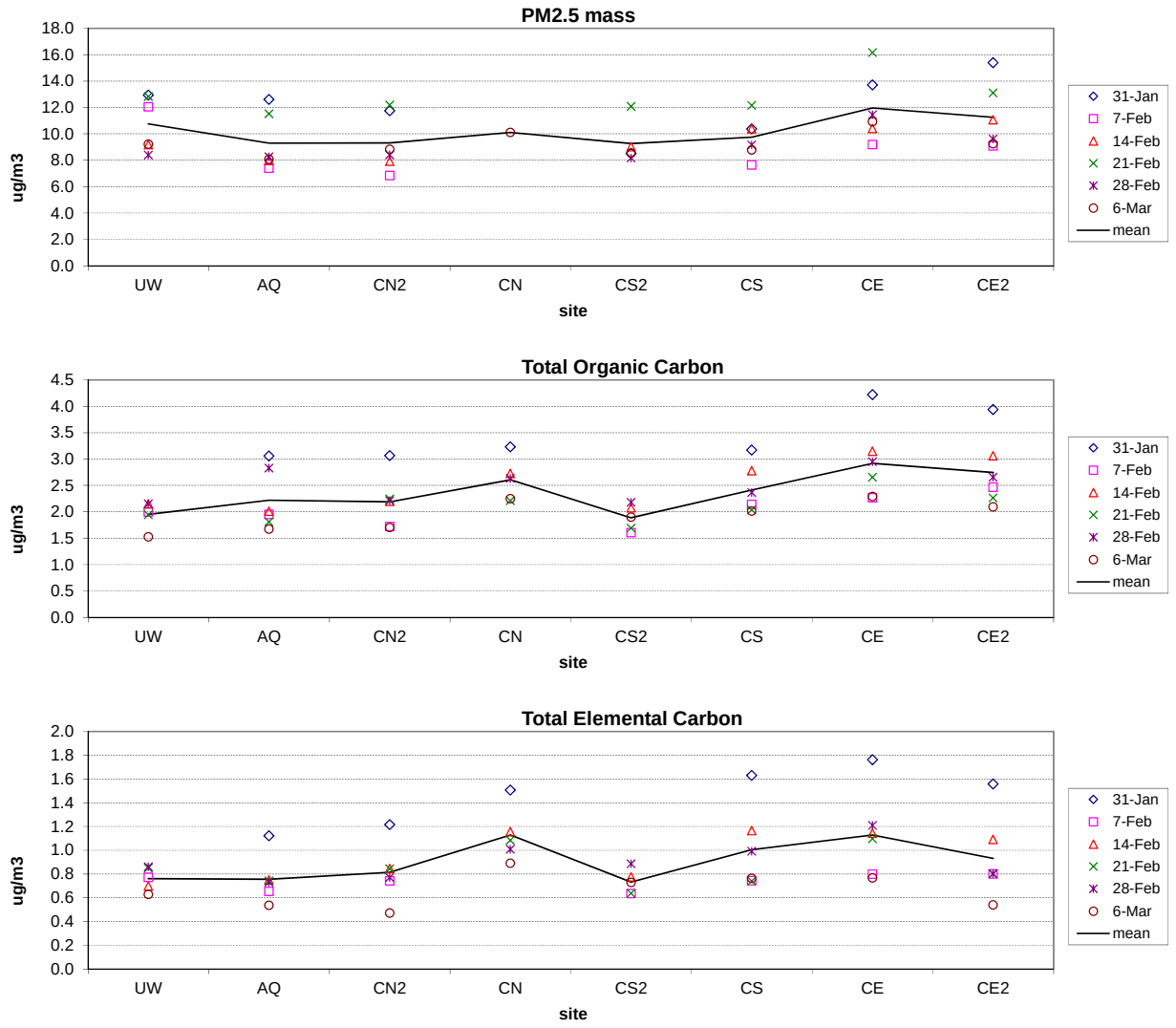

Figure 5-32. Seven-day $PM_{2.5}$ mass, OC, and EC by site and week during the Winter Monitoring Season.

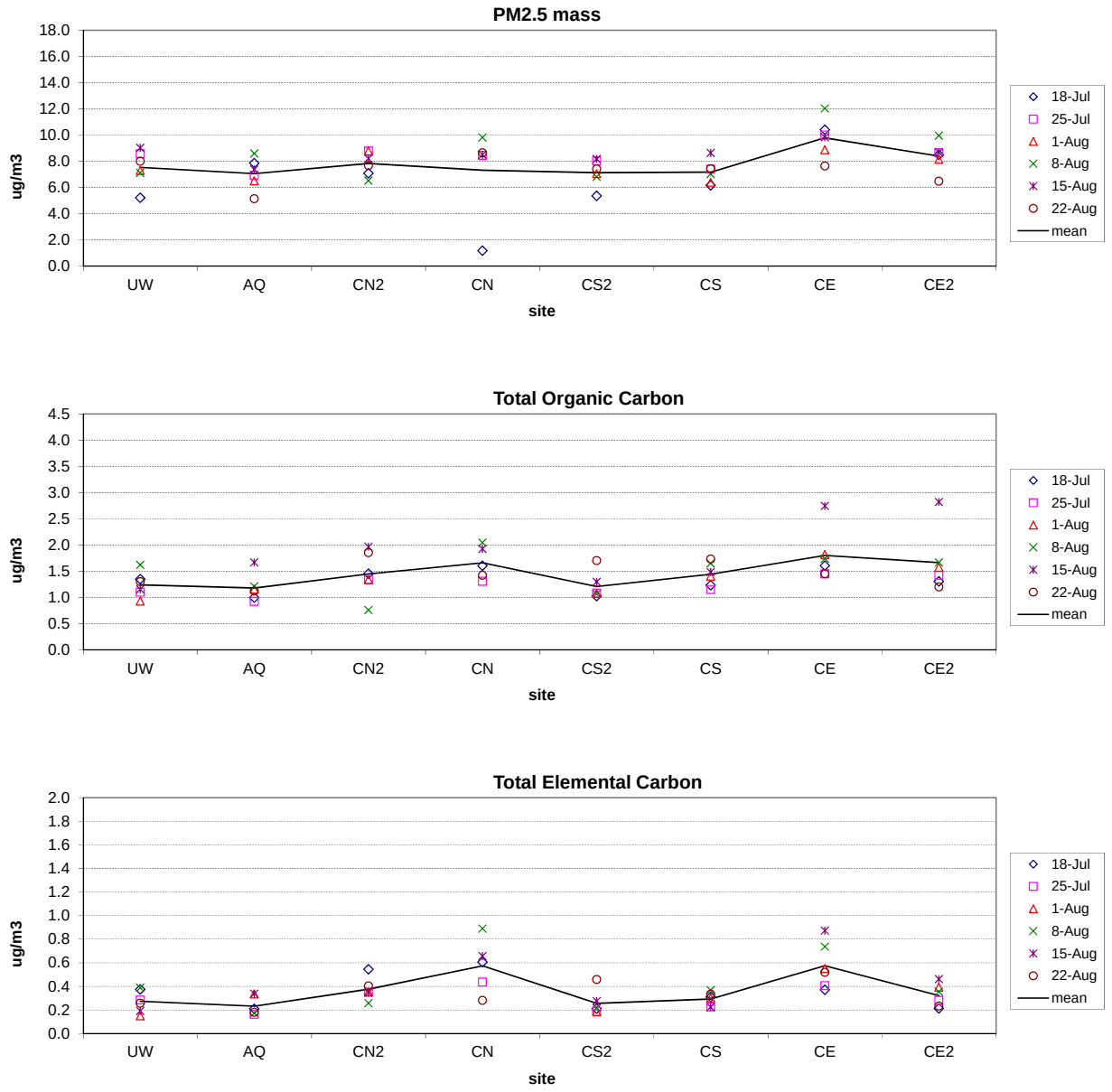

Figure 5-33. Seven-day $PM_{2.5}$ mass, OC, and EC by site and week during the Summer Monitoring Season.

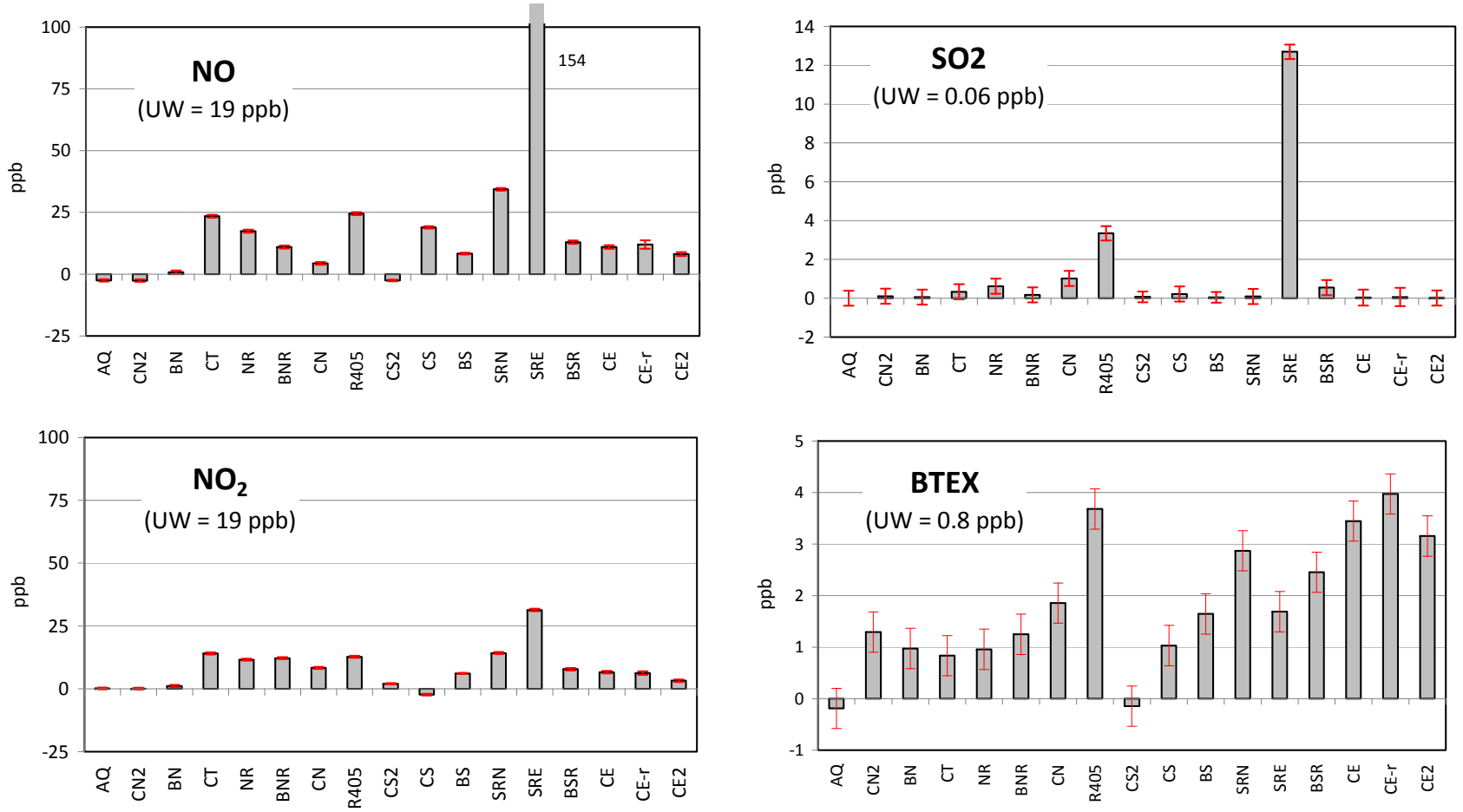

Figure 5-34. Net mean pollutant concentrations (site minus UW) measured during the Winter Monitoring Season. Sites are arranged approximately along two west to east traverses: north of LAX from UW to CN and south of LAX from CS2 to CE2

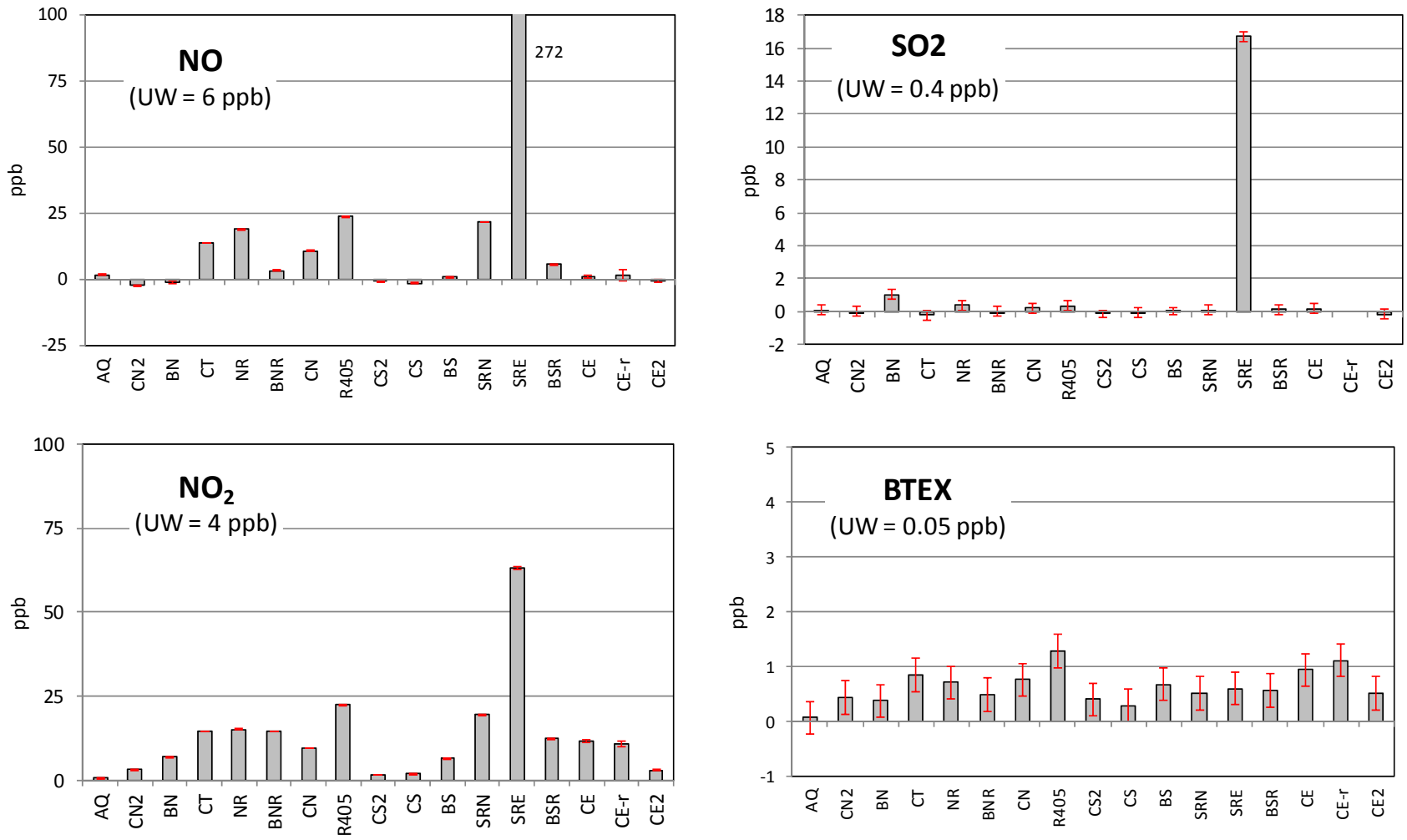

Figure 5-35. Net mean pollutant concentrations (site minus UW) measured during the Summer Monitoring Season. Sites are arranged approximately along two west to east traverses: north of LAX from UW to CN and south of LAX from CS2 to CE2

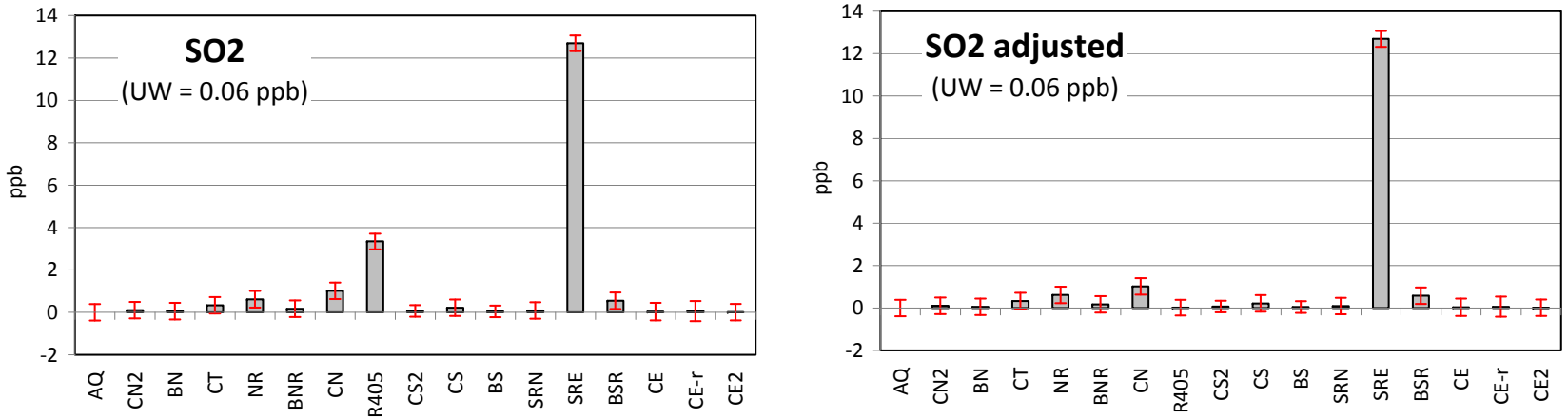

Figure 5-36. Net mean NO and SO_2 (site minus UW) measured during the Winter Monitoring Season with and without inclusion (adjusted) of a single outlier sample at the R405 site. Sites are arranged approximately along two west to east traverses: north of LAX from UW to CN and south of LAX from CS2 to CE2

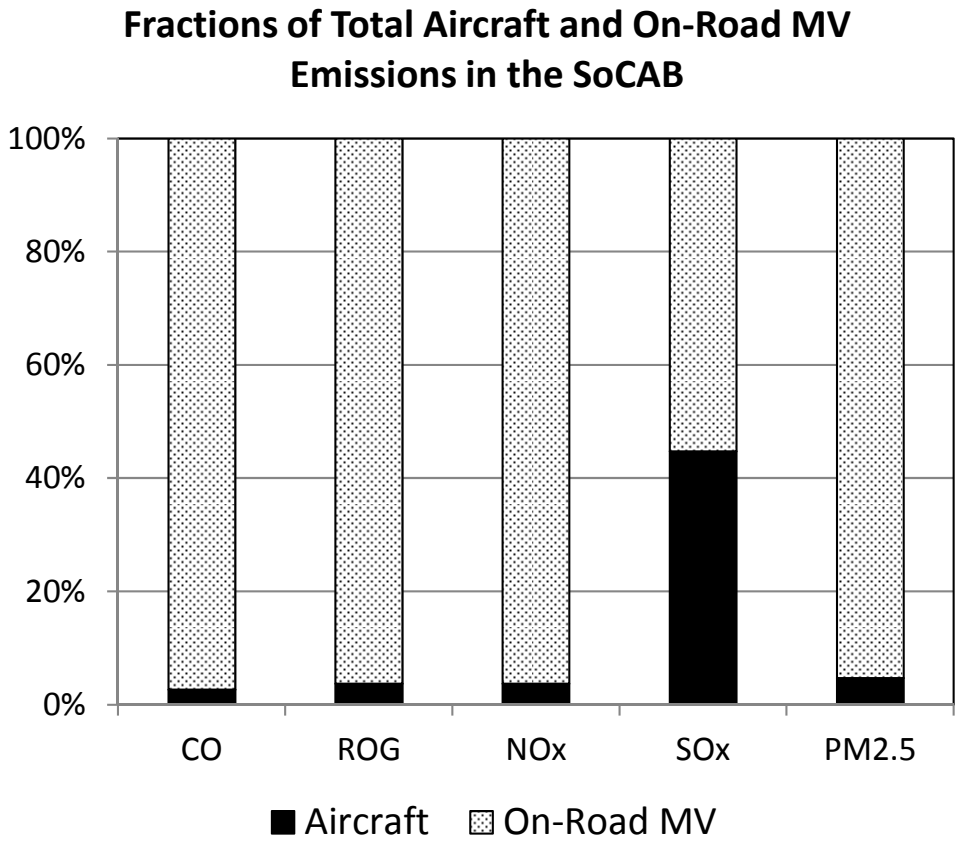

Figure 5-37. Relative contributions of aircraft and on-road motor vehicle emissions in the South Coast Air Basin (SoCAB) in 2010. Adapted from data obtained from the California Air Resources Board emission inventory database: http://www.arb.ca.gov/app/emsinv/emssumcat_query.php?F_YR=2008&F_DIV=0&F_SEASON=A&SP=2009&F_AREA=AB&F_AB=SC, accessed 07/12/12.

5.2.3 Diurnal and Day of Week Variations at Community Core Monitoring Sites

The continuous monitoring data from the core sites were used to examine short-term variations in pollutant concentrations relative to temporal variations in local emission sources contributions and changes in wind direction and mixing heights. This section presents the diurnal variations in the hourly average pollutant concentrations during the LAX AQSAS at the four core sites. The mean diurnal variations in NO, NO_2, CO, BC, SO_2 and UFP number concentrations are shown in Figure 5-38 through Figure 5-45. Figure 5-46 and Figure 5-47 show the average numbers of landing and takeoffs on the South Airfield and North Airfield at LAX by hour and day of week during the Winter and Summer Monitoring Seasons, respectively.

Figure 5-48 and Figure 5-49 show the average diurnal variations in wind speed and resultant wind directions at the CE, CS, and AQ sites (met data from the AQ site for the winter season were invalidated by SCAQMD, so data from their nearby PAMS LAX meteorological station are presented instead). The winds were typically from the northeast in the early morning during the Winter Season. LAX was downwind of all core sites during this time of the day, except the CS site. The CE and CN sites were downwind of LAX during consistent westerly winds from about 10:00 A.M. to 9:00 P.M. Winds were consistently from the west during the Summer Season throughout the day and most of the overnight period. Both the CE and CN sites were almost always downwind of LAX during the Summer Season, while the CS and AQ sites were consistently upwind of the eastern end of the North and South Airfields. The diurnal variations in pollutant concentrations at the four core sites were consistent with these seasonal and diurnal differences in wind direction and the temporal variations in vehicle traffic and airport activity. Note that the winds depicted in Figure 5-48 and Figure 5-49 may appear to be erratic when direction is near due north due to the presentation of polar data on a linear scale.

Similar diurnal patterns were observed at the CE site during the summer for NO_x, CO, and BC with concentrations peaking in the morning, very low at midday and increasing during the evening beginning around sunset. The peak concentrations in the morning coincided with lower mixing heights, especially during the winter months, and peak traffic volumes during the morning commute period. Increasing mixing heights and wind speeds result in greater dispersion of emissions and lower midday pollutant concentrations. Greater atmospheric stability and traffic volumes during the evening commute period resulted in increasing pollutant levels after sunset. These are typical diurnal patterns in ambient pollutant concentrations in the South Coast Air Basin (SoCAB) and most urban areas throughout the country where on-road motor vehicles are the major sources of these pollutants. While the diurnal variations were similar between the two monitoring seasons for NO_2 and BC, the morning and especially the evening peaks, were substantially lower during the Summer Season for NO and CO because sunset and the development of stable atmospheric conditions occur after the evening commute period during the summer. The substantially lower NO_x, CO, and BC levels at the CE site during weekend mornings in both seasons are strong indications that on-road motor vehicles are the predominant source of these pollutants at this site.

In contrast, SO_2 and UFP concentrations at the CE site were generally lowest during the early morning and steadily increased throughout the day and into the evening hours during the Winter Season. The difference between weekday and weekend was less for SO_2 compared to NO_x, CO, and BC. UFP number concentrations showed no difference by day of week. Both SO_2 and UFP

are significant components of jet exhaust and the highest concentrations are measured during westerly winds when emissions from LAX can be transported to the CE site. Peak UFP levels during the day at the CE site were about 160 k/cm^3 during the Winter Season and peak SO_2 levels were about 0.6 ppb. In contrast to the Winter Season, in the Summer Season both SO_2 and UFPs peaked between the morning commute period and midday and gradually decreased throughout the afternoon with a second evening peak. These late morning peaks may be related to earlier onset of westerly winds during the summer combined with greater vertical mixing during the day. The late morning SO_2 peak of approximately 1.5 ppb was about three times greater than the evening peak. The two peaks for UFP were approximately the same with a value of about 100 k/cm^3.

The diurnal variations in pollutant concentrations during the Winter Season at the CN site were similar to the CE site, with SO_2 and UFP showing increasing concentrations during the day and minimal weekday variations. While the reported peak SO_2 levels during the Winter Season were approximately 1.7 ppb, these levels are comparable to those measured at the CE site after adjusting for the baseline shift of about 0.8 ppb. However, the hourly average UFP number concentrations peaked at about 40 k/cm^3, which is substantially lower than values measured at the CE site. The summertime diurnal pattern for SO_2 at the CN site was also similar to the CE site, with a late morning peak but with a more gradual decrease through the day. A late morning UFP number concentration peak of 50k/cm^3 was also observed, which remained flat at that level through the day and evening. Similar to the CE site, the diurnal and day of week variations in NO_x, CO, and BC concentrations at the CN site indicate that on-road vehicle emissions were the predominant source of these pollutants impacting this site during the Winter Season. This conclusion also applies to CO and BC data for the Summer Season. The continuous NO_x data at the CN site, shown in Figure 5-41 for the Summer Season, are invalid due to a baseline shift caused by high temperatures inside the monitoring station (i.e., motorhome) that exceeded specifications of the NO_x analyzer.

The diurnal variations are similar for all five pollutants at the CS site with morning and evening peaks in concentrations. However, while NO_x, CO, and BC concentrations were lower during weekend than weekday mornings, there are no significant weekday differences for SO_2 and UFP. The UFP data are incomplete at the CS site due to a malfunctioning pump. However, the limited data indicate that peak UFP number concentrations in the morning are only slightly lower than peak afternoon concentrations at the CE site. Peak SO_2 concentrations were approximately 0.8 ppb in the morning from about 07:00-09:00, and consistently lower during other times of the day. Winds were from the northeast during the early morning during the Winter Season, which potentially transported airport-related emissions to the CS site during this period. However, the winds were more consistently from the west throughout the day and most of the night. The seasonal differences in wind directions may explain the substantially lower concentrations for all pollutants at the CS site during the Summer Season, when transport from the South Airfield was predominately to the east, compared to the Winter Season when it was more variable.

Pollutant concentrations measured at the AQ site showed a peak during the morning commute period, but were much lower than the concentrations measured at the other three core sites during the Winter Season. A second smaller peak was observed to build after sunset. UFP number concentrations peaked in the morning at about 40 k/cm^3 and averaged about 22 k/cm^3 for a 24-hour period.

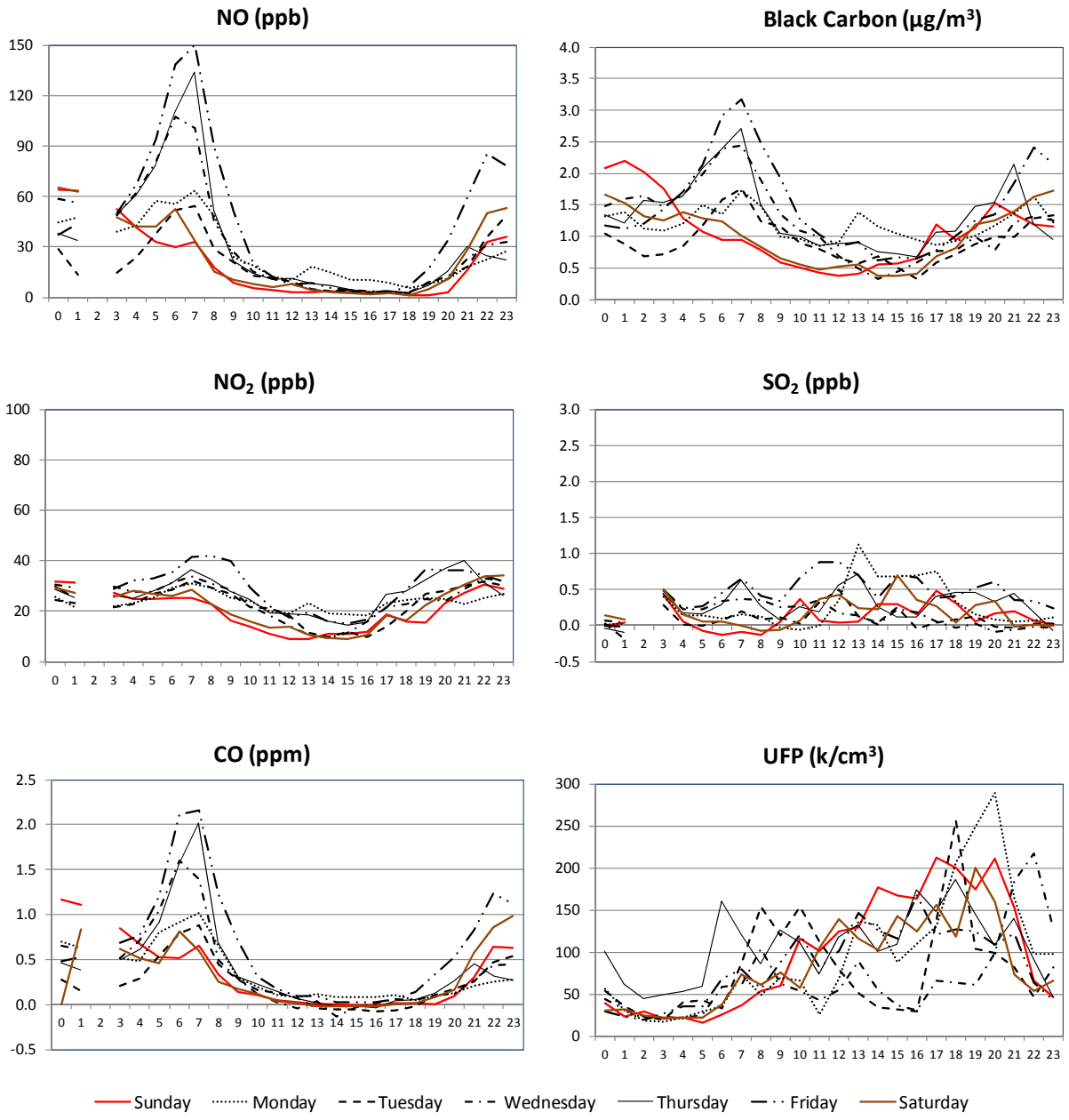

Figure 5-38. Mean diurnal variations in NO, NO_2, CO, BC, SO_2, and UFP number concentrations during the Winter Monitoring Season at the CE Site.

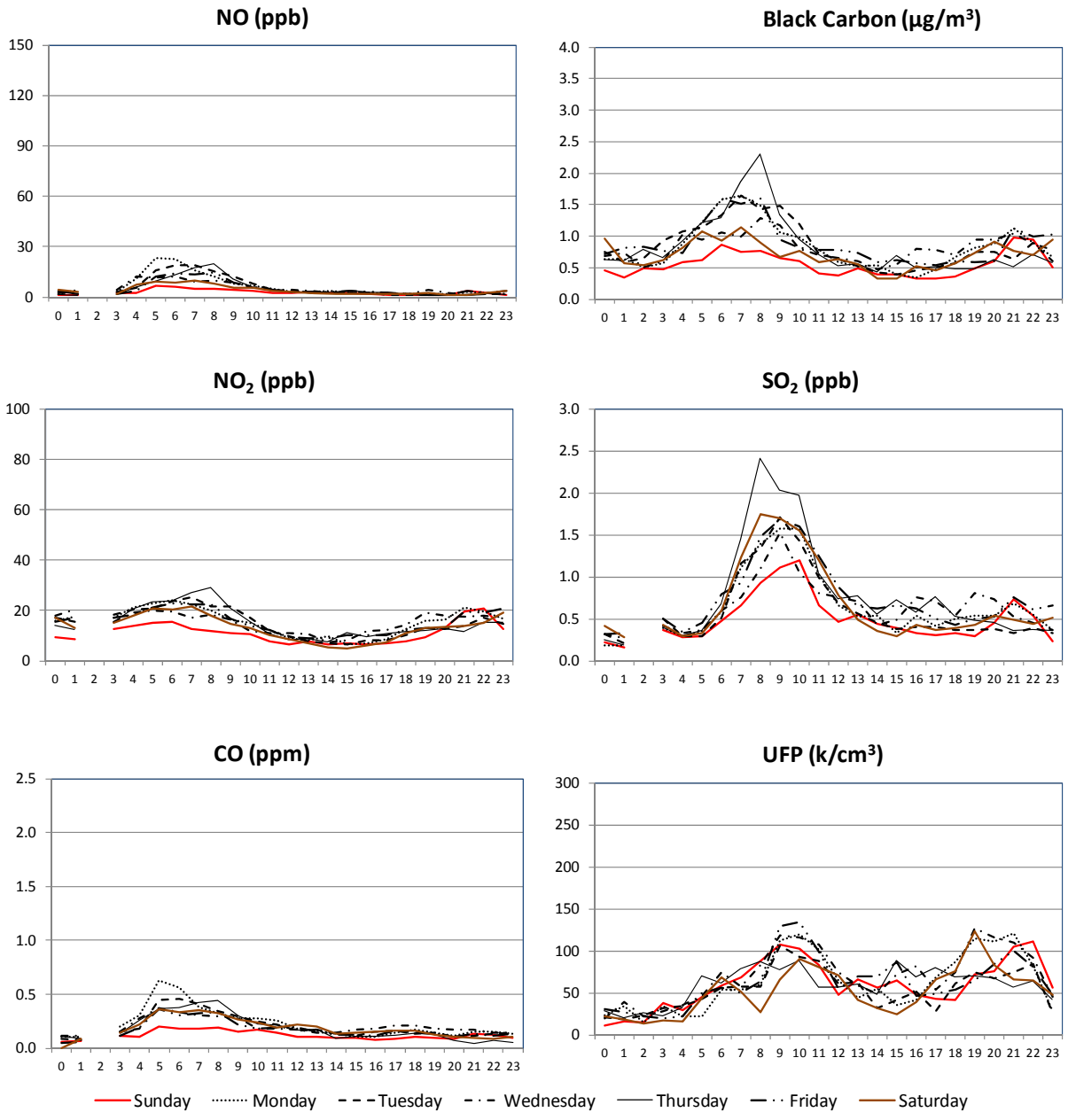

Figure 5-39. Mean diurnal variations in NO, NO_2, CO, BC, SO_2, and UFP number concentrations during the Summer Monitoring Season at the CE Site. Times are Pacific Standard Time (local time is one hour ahead).

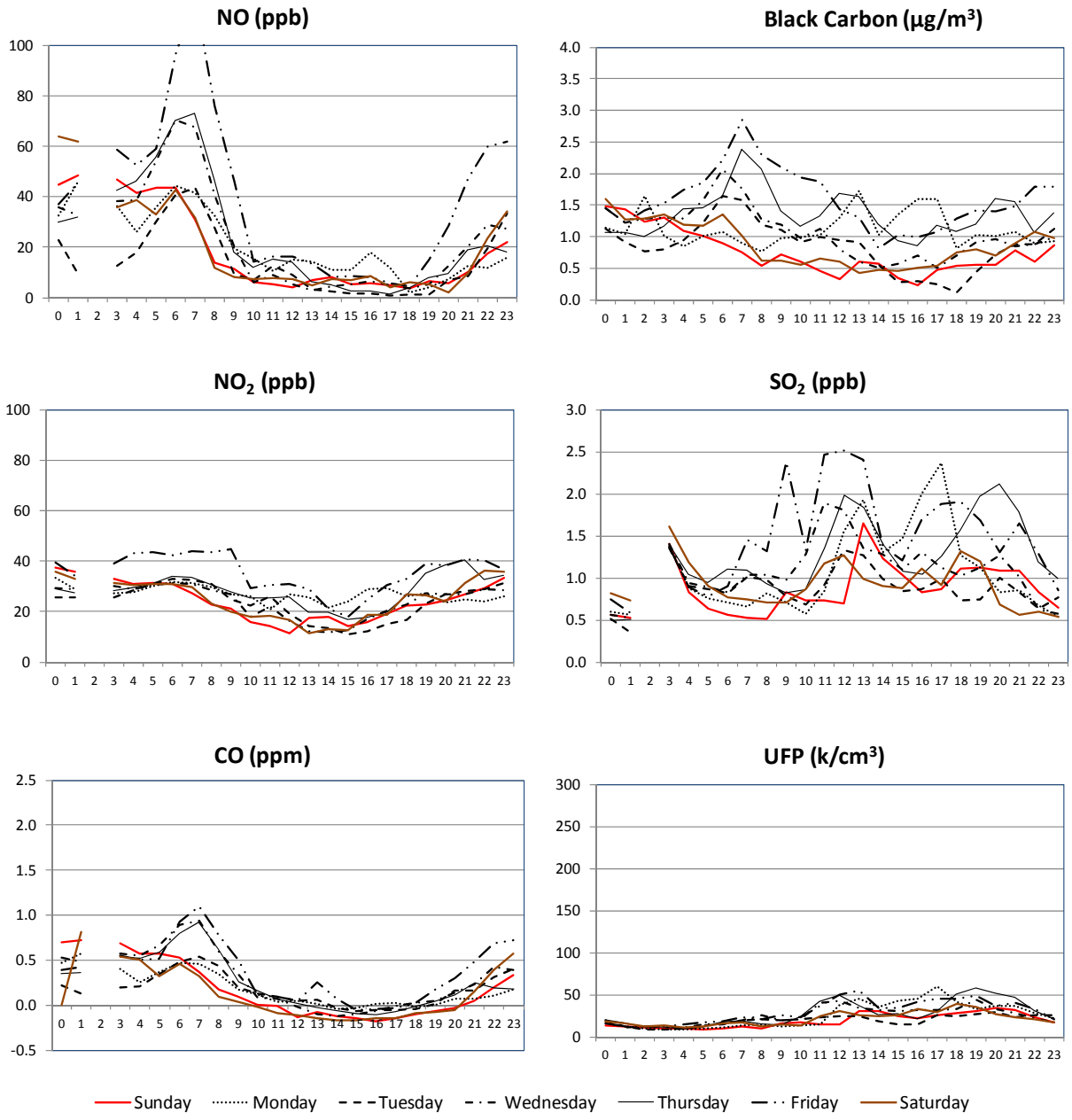

Figure 5-40. Mean diurnal variations in NO, NO_2, CO, BC, SO_2, and UFP number concentrations during the Winter Monitoring Season at the CN Site.

Note: A baseline shift of about 0.8 to 1.0 ppb for SO_2 was observed.

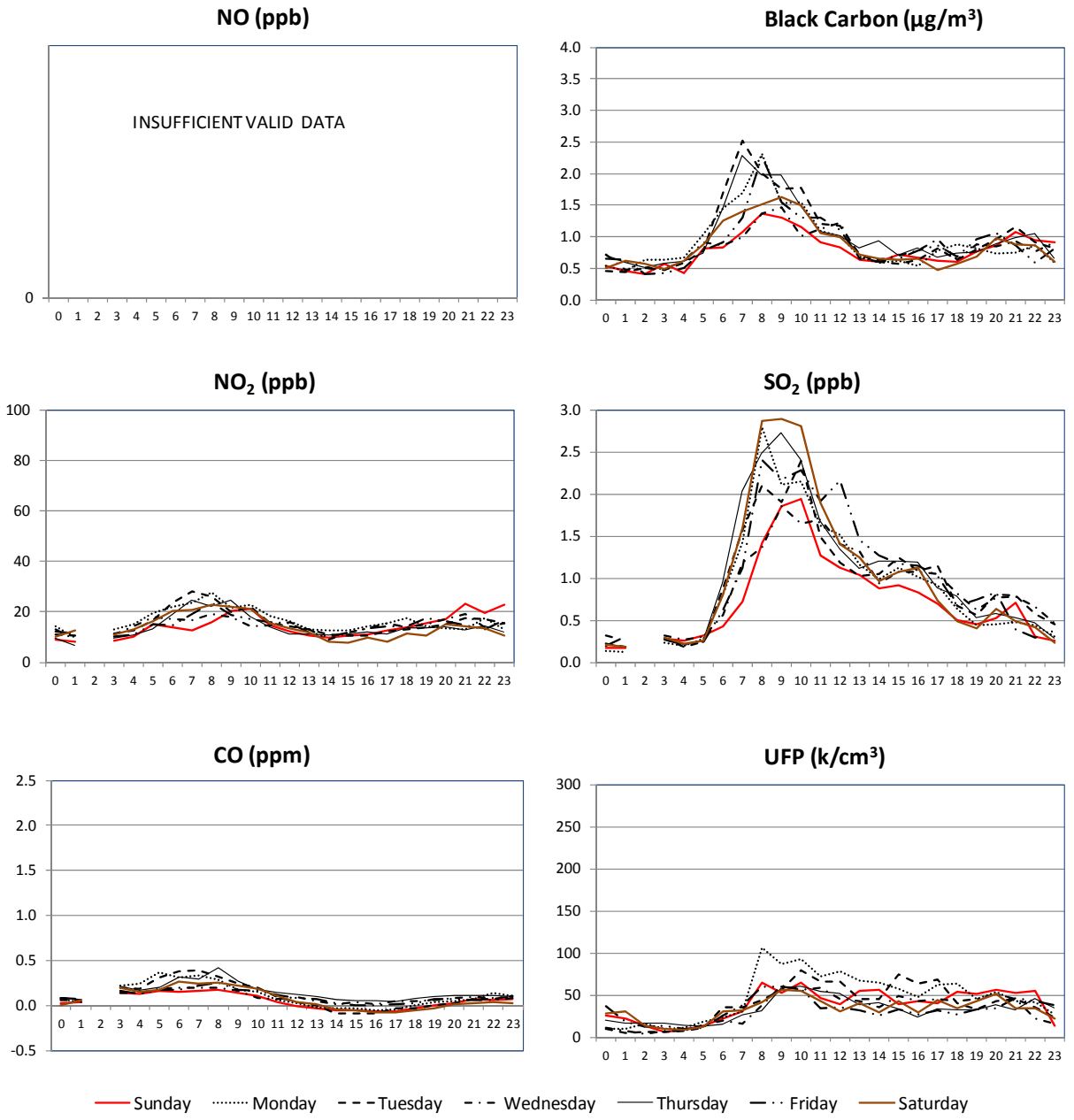

Figure 5-41. Mean diurnal variations in NO, NO_2, CO, BC, SO_2, and UFP number concentrations during the Summer Monitoring Season at the CN Site.

Note: NO data were found to have a significant baseline shift when the shelter temperatures exceeded instrument specification.

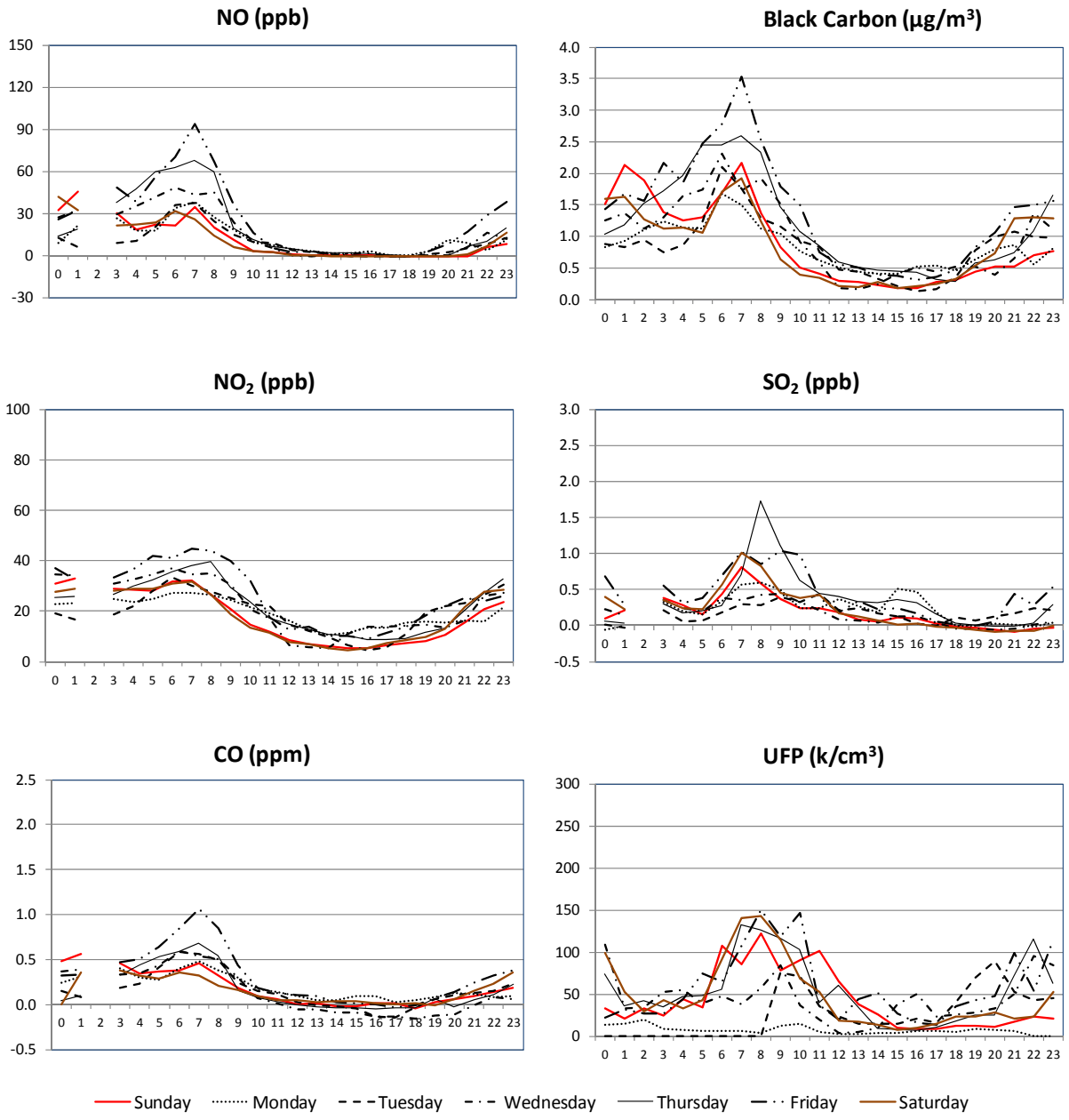

Figure 5-42. Mean diurnal variations in NO, NO_2, CO, BC, SO_2, and UFP number concentrations during the Winter Monitoring Season at the CS Site.

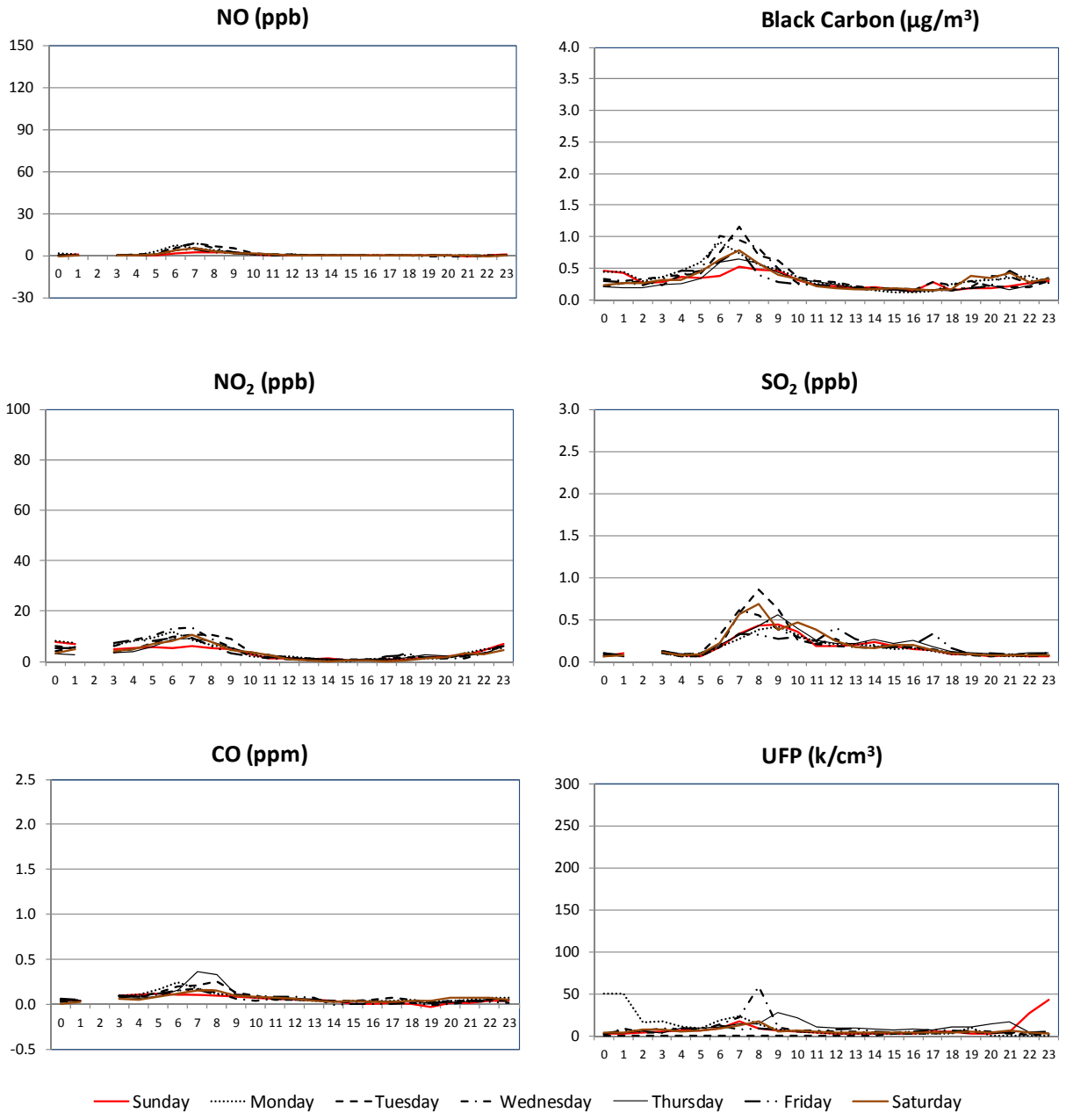

Figure 5-43. Mean diurnal variations in NO, NO_2, CO, BC, SO_2, and UFP number concentrations during the Summer Monitoring Season at the CS Site.

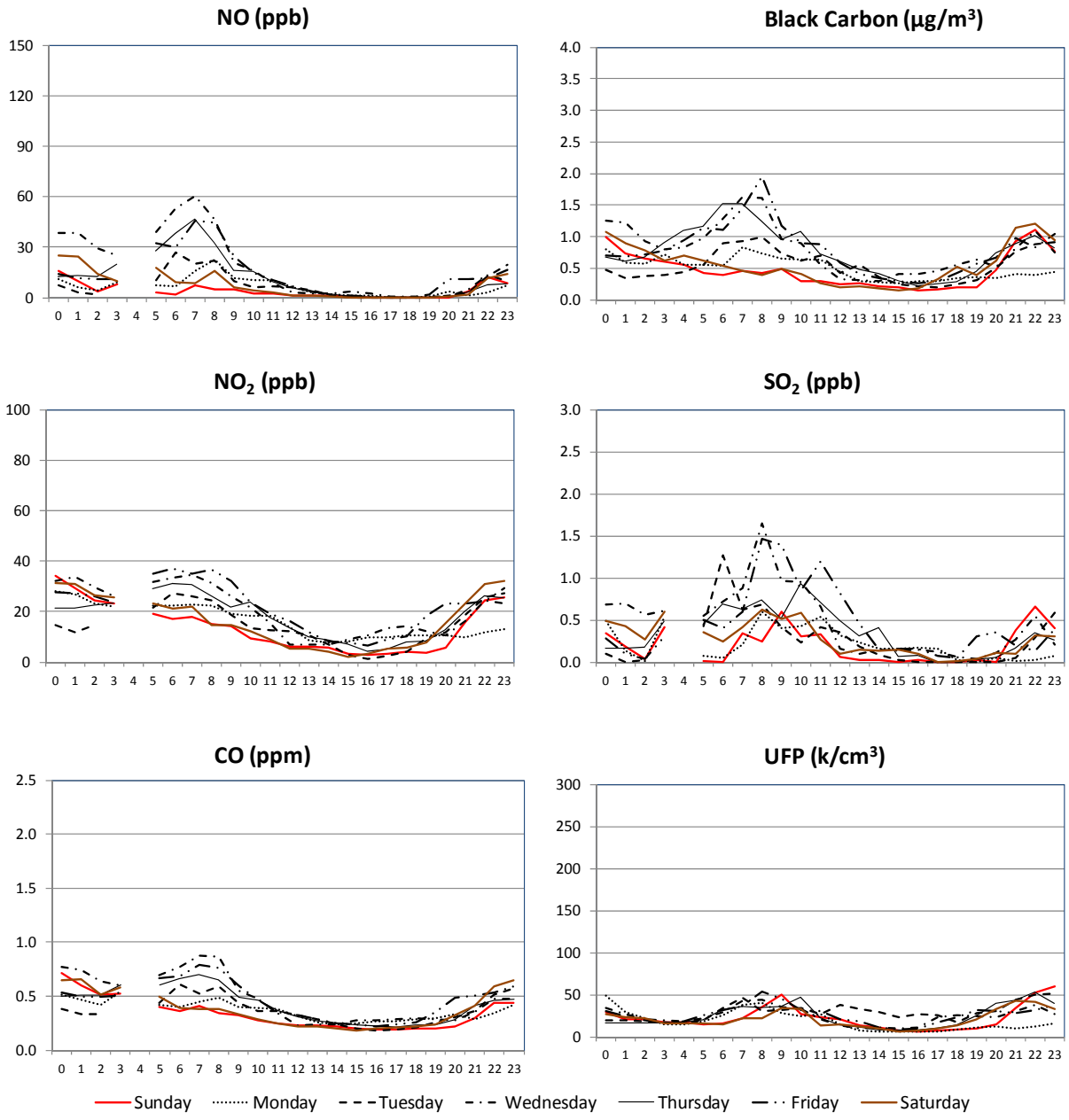

Figure 5-44. Mean diurnal variations in NO, NO_2, CO, BC, SO_2, and UFP number concentrations during the Winter Monitoring Season at the AQ Site.

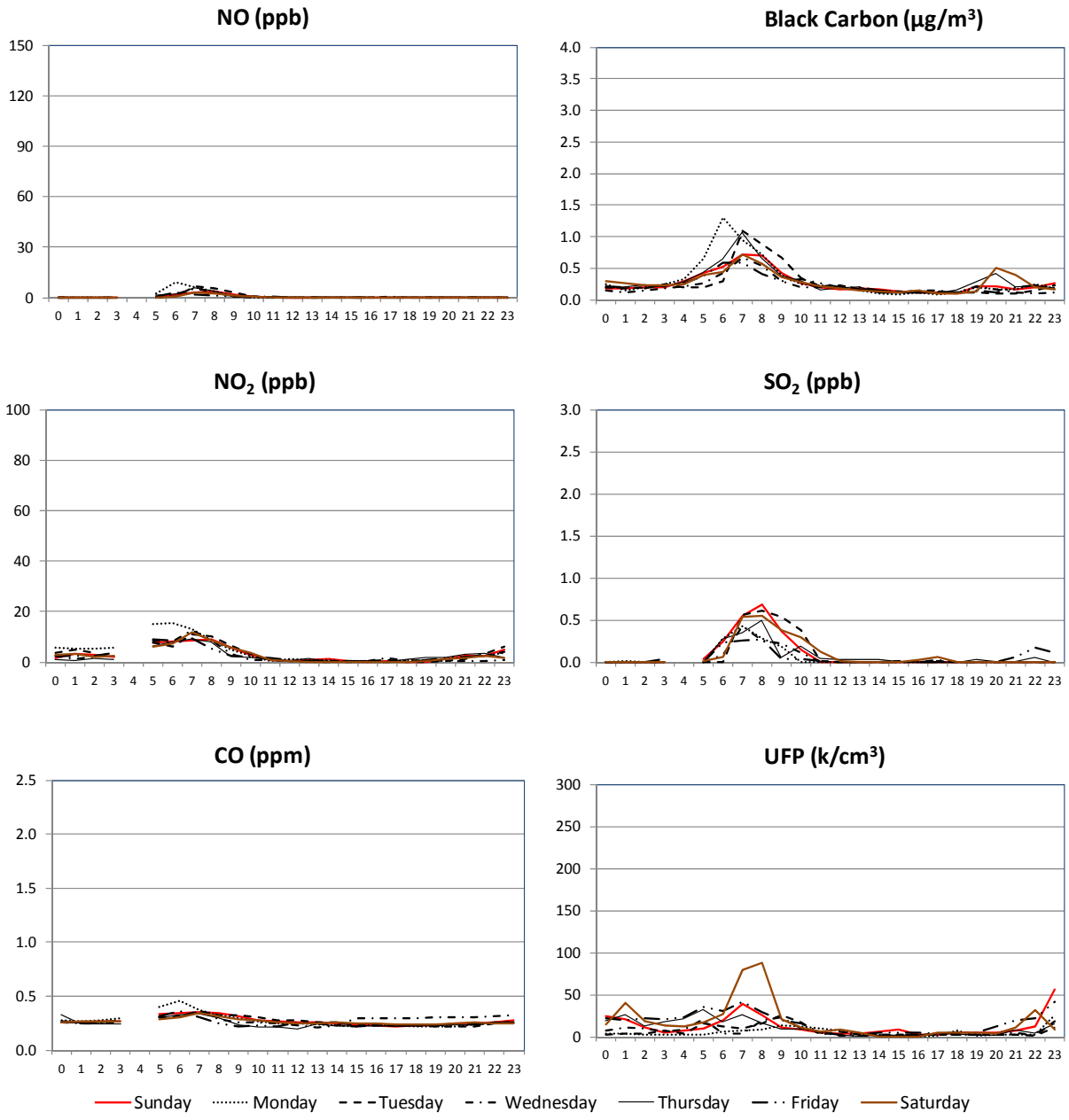

Figure 5-45. Mean diurnal variations in NO, NO_2, CO, BC, SO_2, and UFP number concentrations during the Summer Monitoring Season at the AQ Site.

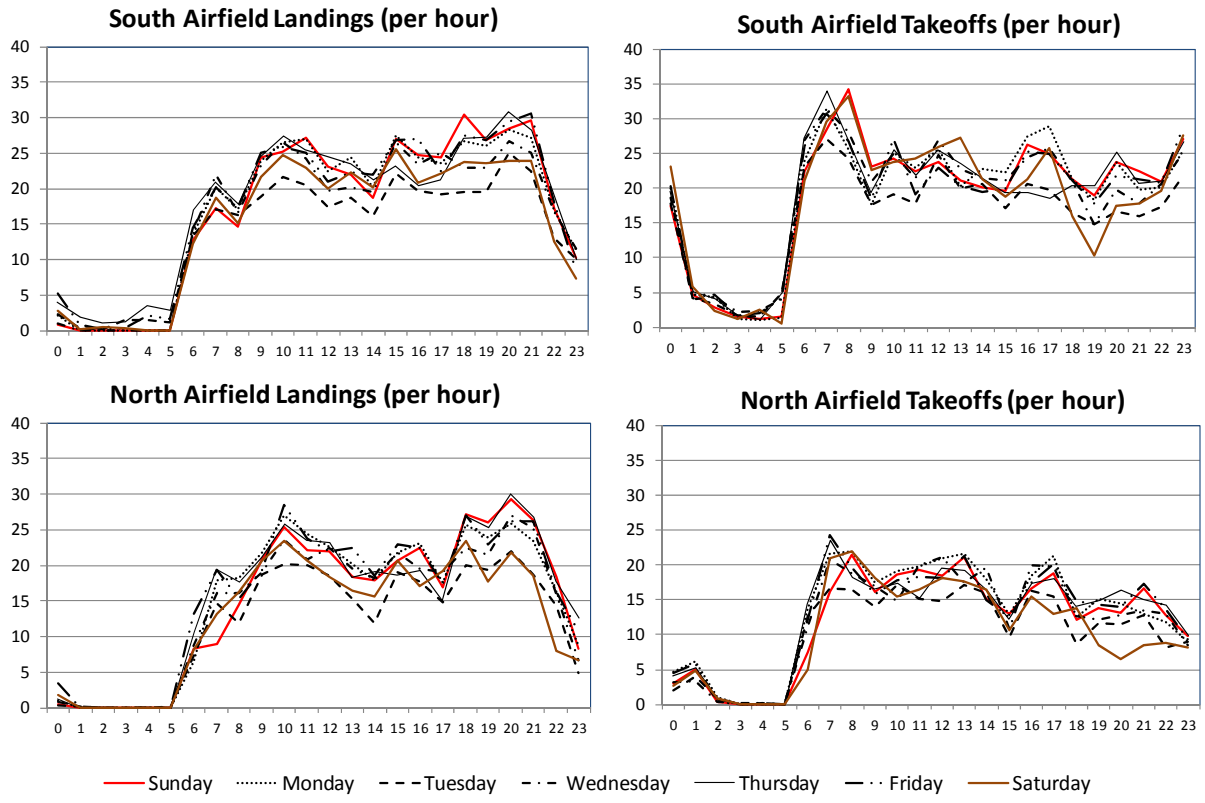

Figure 5-46. Average number of aircraft landings and takeoffs per hour by day of the week at the LAX South and North Airfields during the Winter Monitoring Season.

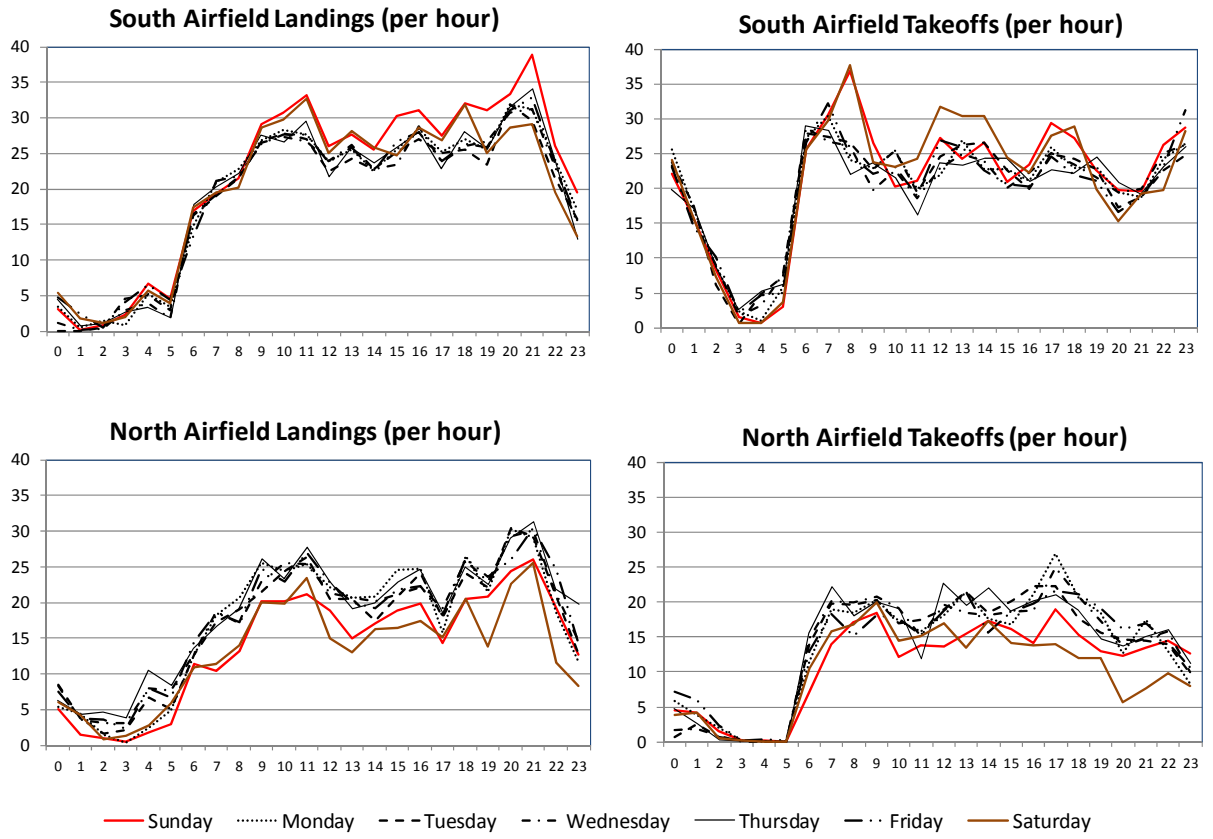

Figure 5-47. Average number of aircraft landings and takeoffs per hour by day of the week at the LAX South and North Airfields during the Summer Monitoring Season.

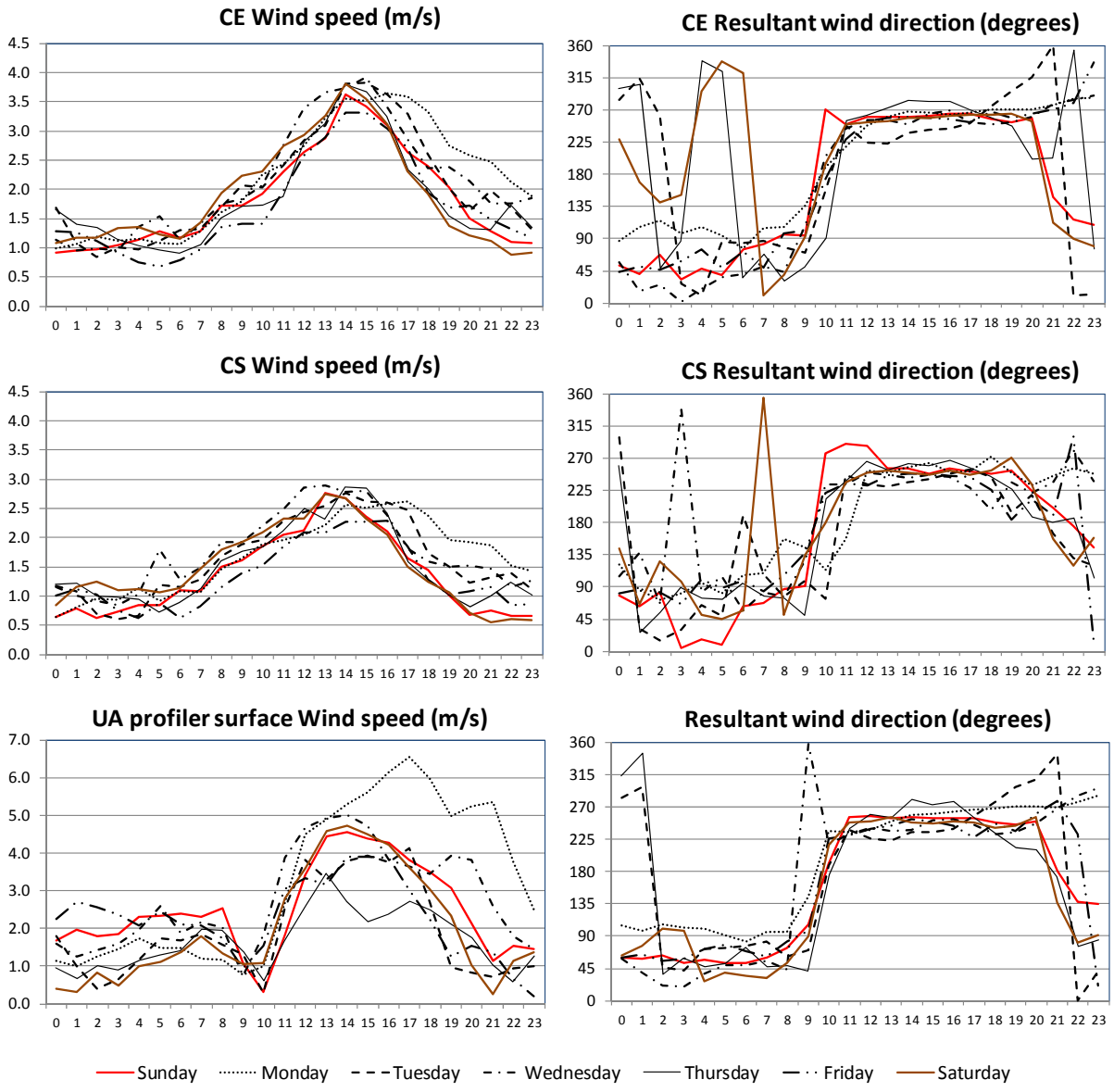

Figure 5-48. Average diurnal variations in hourly wind speed and resultant wind directions at the CE, CS, and LAX Upper Air Profiler sites during the Winter Monitoring Season.

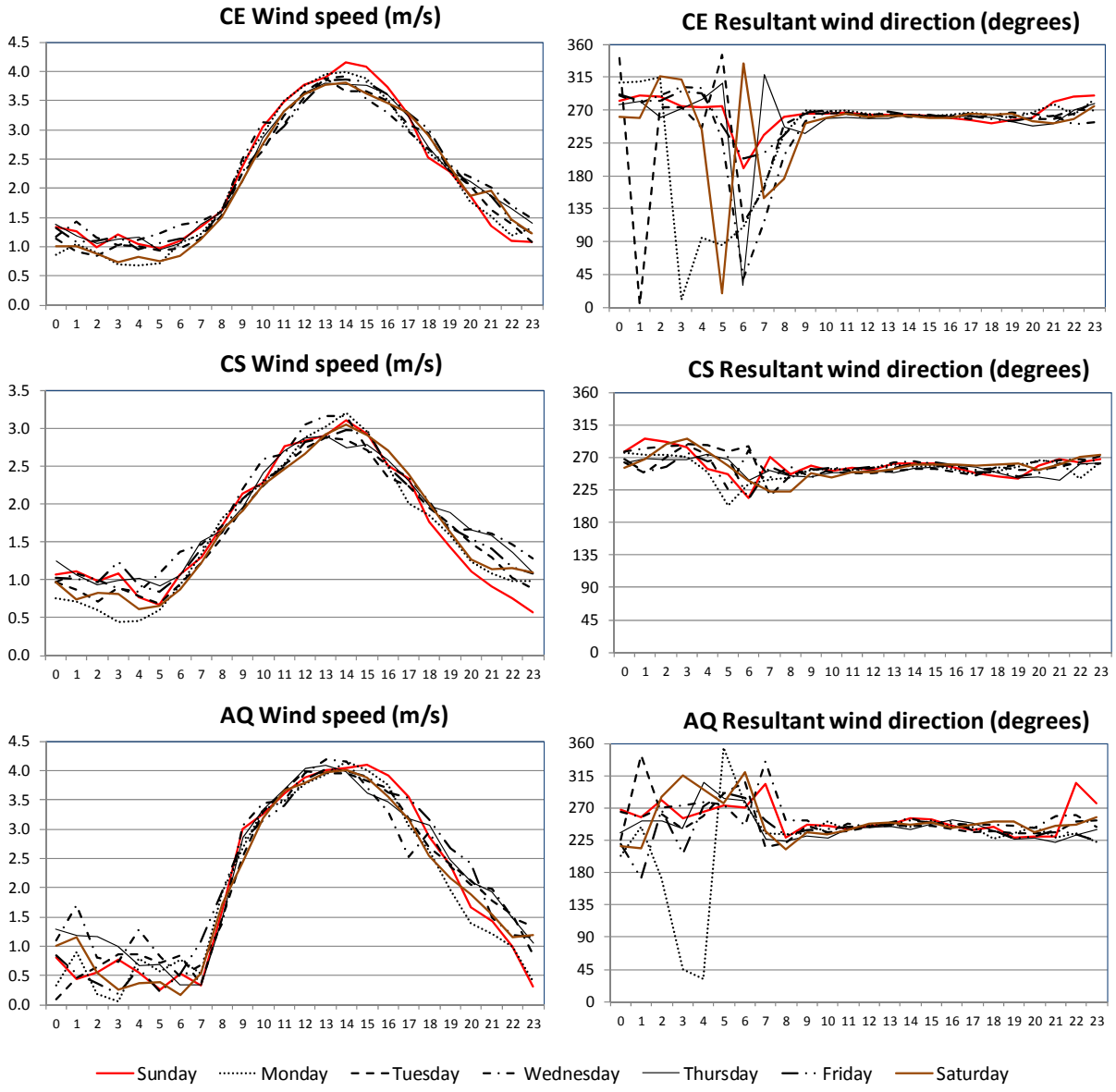

Figure 5-49. Average diurnal variations in hourly wind speed and resultant wind directions at the CE, CS, and AQ sites during the Summer Monitoring Season.

5.2.4 Ultrafine Particle Size Distributions and Correlations with Other Pollutants

Diurnal variations in ultrafine particle size distributions (PSD) can provide useful insight to the relative importance of freshly emitted and secondary particles. Furthermore, the diurnal variations of PSD, which depend on day of the week, and the correlations of specific particle size ranges with other pollutants, may be related to the relative contributions of different emission sources.

Figure 5-50 plots PSD (7-160 nm) measured at the CE site during low activity hours (01:00 to 04:00) and morning traffic hours (06:00 to 09:00) for each day of a week during the entire Winter Monitoring Season. The PSDs reflect local background levels during 01:00 to 04:00 when both vehicle traffic and airport activity were low. During 06:00 to 09:00, airport activities increased from low to normal operation levels, and vehicular traffic increased with the start of the morning rush hour during workdays. Therefore, during the weekday 06:00 to 09:00 period, the PSD may be influenced by both airport operations and vehicle traffic, depending upon wind trajectories. Traffic volumes were lower on the weekends, especially on Sundays while airport activities remained quite similar to weekdays. During the 01:00 to 04:00 time period, the PSDs at the CE site were bimodal with one peak occurring at less than 10 nm and another between 40 nm and 100 nm. The 7-30 nm UFP concentrations were lowest between 01:00 to 04:00 due to low amounts of fresh emissions, while the larger mode was related to particle aging and growth. The 7-30 nm UFP concentrations increased 2.7 to 5.0 fold during the morning commute period relative to the overnight period on both weekdays and weekends. This observation indicates airport activities are probably a major source of the 7-30 nm UFP, since reduced vehicle traffic during weekend mornings did not cause a significant reduction in the 7-30 nm UFP concentrations. The 30-160 nm particle concentrations increased 1.1 to 2.2 fold over the same time period on weekdays, but decreased by a factor of 0.6-0.9 on weekends. Therefore, we conclude that the larger particles at the CE site consist primarily of background aerosols and less so of fresh emissions.

Figure 5-51 shows the analogous series of PSD plots for the Summer Monitoring Season. One major difference from the Winter Season PSD (Figure 5-50) is the much smaller accumulation mode (~30-100 nm) in the Summer Season. This was most likely caused by lower temperatures and wind speeds in the Winter Season favored particle growth. Similar to the Winter Season, concentrations of 7-30 nm particles increased by a factor of 2.5 to 4.0 between 01:00-04:00 to 06:00-09:00. The differences between weekdays and weekends in these increases were not significant. Concentrations of 30-160 nm particles increased 2.0 to 3.5-fold between the low activity and morning traffic hours and differences between weekdays and weekends were not significant when compared to the Winter Season.

The seasonal differences in the diurnal and weekday variations in the PSD are likely due to different wind patterns during winter and summer. In the winter, the winds were calm and from the north/northeast during 06:00-09:00 (Figure 5-48). UFP concentrations at the CE site were mainly affected by diffusion, which results in higher increases in the 7-30 nm particles compared to the 30-160 nm particles. In summer, the winds are stronger and from the west during 06:00-09:00 (Figure 5-49) and UFP concentrations at the CE site were affected by transport from LAX and the freeways, resulting in increases in concentrations of both the 7-30 and the 30-160 nm particles on weekdays and weekends.

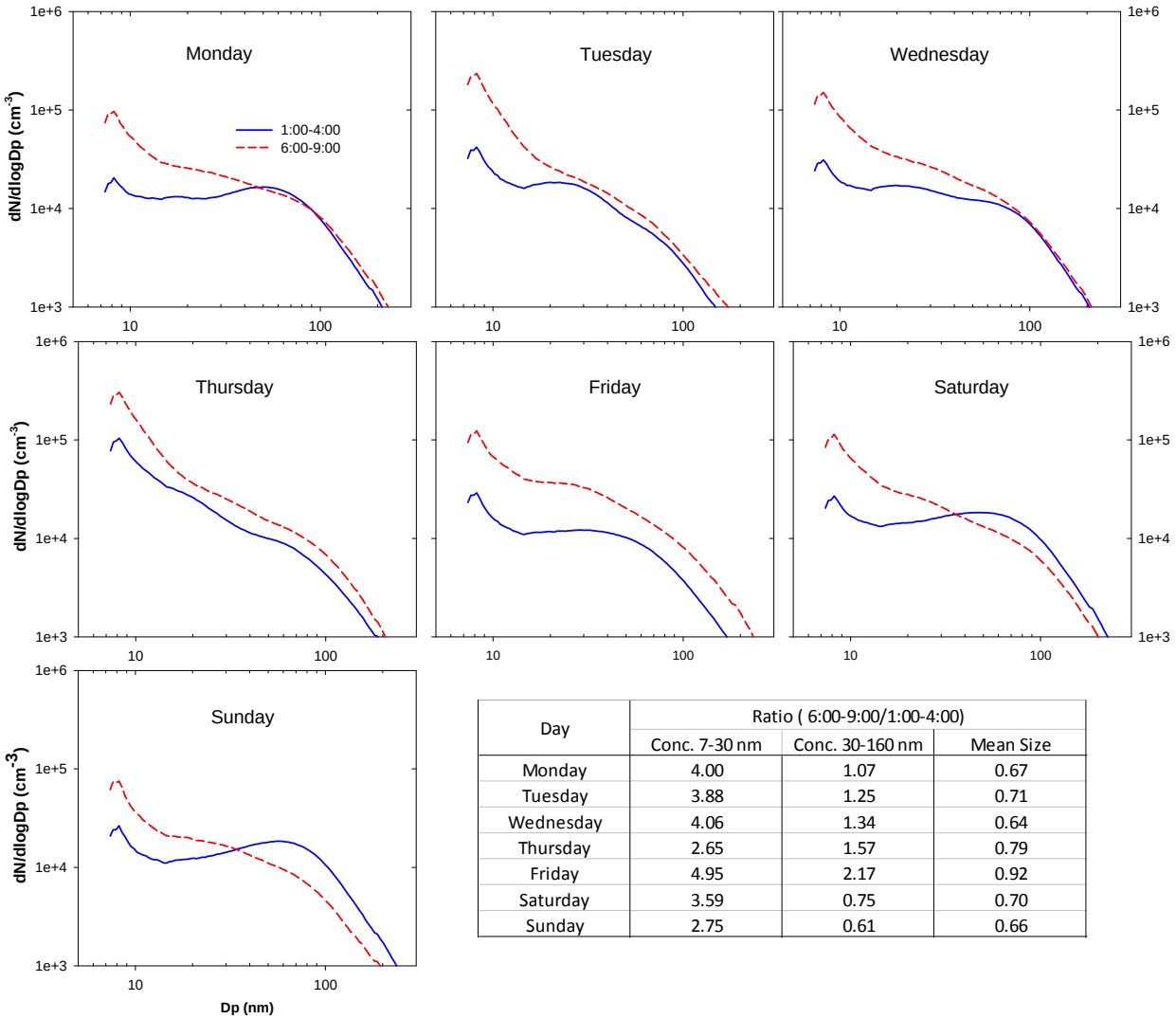

Day	Ratio (6:00-9:00/1:00-4:00)		
	Conc. 7-30 nm	Conc. 30-160 nm	Mean Size
Monday	4.00	1.07	0.67
Tuesday	3.88	1.25	0.71
Wednesday	4.06	1.34	0.64
Thursday	2.65	1.57	0.79
Friday	4.95	2.17	0.92
Saturday	3.59	0.75	0.70
Sunday	2.75	0.61	0.66

Figure 5-50. UFP size distributions at the CE site during the Winter Monitoring Season for low activity hours (01:00-04:00) and morning rush hours (06:00-09:00). The inserted table lists ratios during these two periods (06:00-09:00 over 01:00-04:00) for 7-30 nm and 30-160 nm particles and mean particle size. The y-axis indicates particle number concentrations over logarithm interval of particle size range on the x-axis.

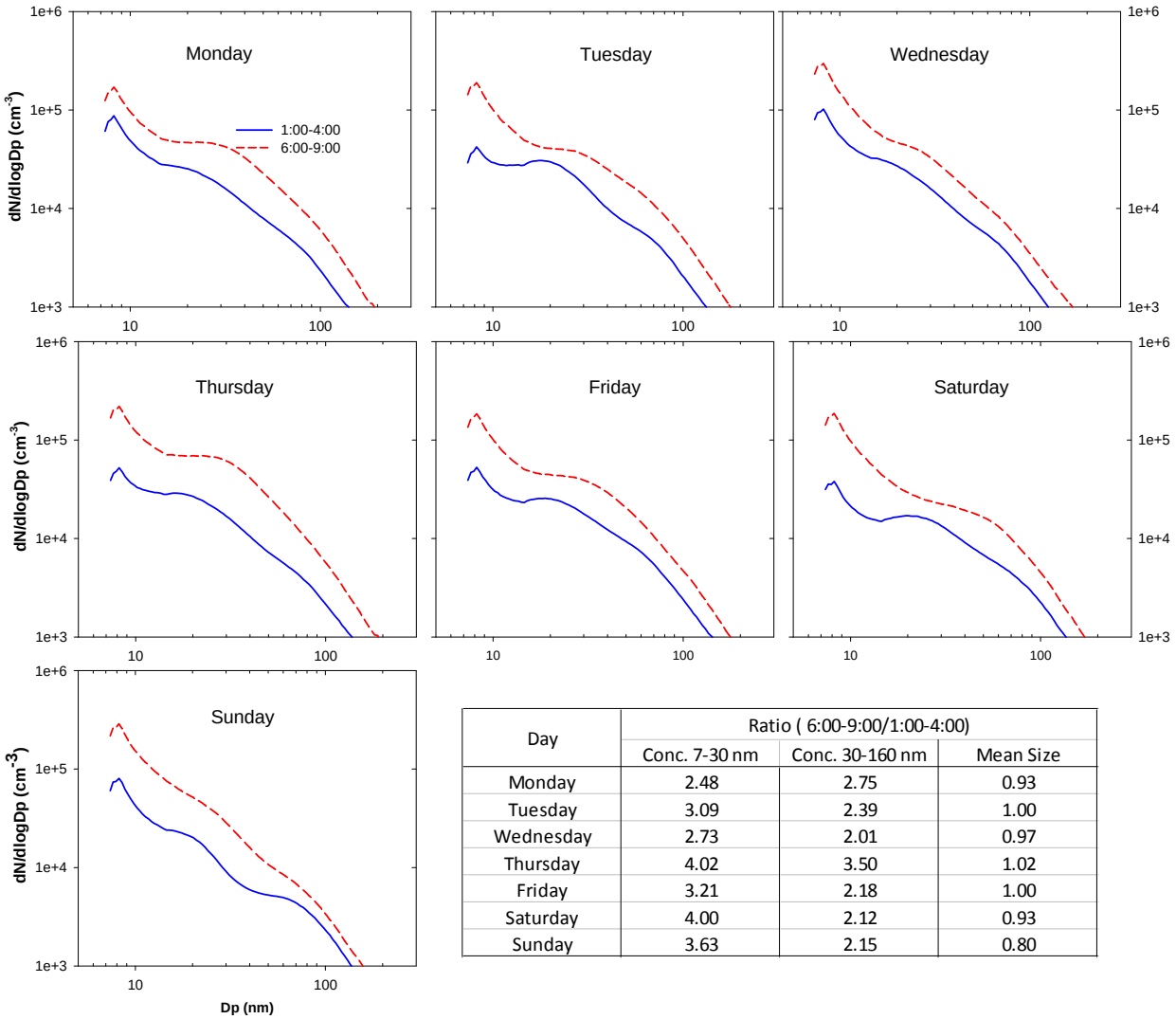

Day	Ratio (6:00-9:00/1:00-4:00)		
	Conc. 7-30 nm	Conc. 30-160 nm	Mean Size
Monday	2.48	2.75	0.93
Tuesday	3.09	2.39	1.00
Wednesday	2.73	2.01	0.97
Thursday	4.02	3.50	1.02
Friday	3.21	2.18	1.00
Saturday	4.00	2.12	0.93
Sunday	3.63	2.15	0.80

Figure 5-51. Particle size distributions (PSD) at the CE site during the Summer Monitoring Period for low activity hours (01:00-04:00) and morning rush hours (06:00-09:00). The inserted table lists ratios during these two periods (06:00-09:00 over 01:00-04:00) for 7-30 nm and 30-160 nm particles and mean particle size.

The squares of the correlation coefficient (R^2) between UFP number and volume concentration with other pollutants measured are plotted in Figure 5-52 through Figure 5-54 for the CE, CN, and CS sites. UFPs were separated into two size categories: 7-30 nm as the freshly emitted or newly formed particles and 30-160 nm as the relatively "aged" particles. Correlations between measured particle and gas species for all wind directions are listed in Table 5-22.

Figure 5-52 (a) and (b) show that at the CE site, 7-30 nm particles were best correlated with NO_2, SO_2, and BC when wind was from the west both in the Winter Season (R^2 = 0.29-0.49) and in the Summer Season (R^2 = 0.37-0.46). However, 7-30 nm particles and CO had poor correlations, especially during the Winter Season. Since CO is an indicator of gasoline-powered vehicle emissions, the low correlation with CO indicates that 7-30 nm particles at the CE site were influenced more by airport activities than vehicle traffic. Figure 5-52 (c) and (d) show that the 30-160 nm particles were correlated with CO, NO, NO_2, SO_2, and BC, with much less dependence on the wind direction. Zhang et al. (2002) suggested that UFP less than 30 nm in size resulting from road traffic dramatically decrease to background level at distances greater than 300 m away from roads, with the rates of decrease greater than for the larger 30-160 nm particles. The fact that 30-160 nm particles were better correlated with CO, NO, and BC indicates a portion of these particles at the CE site are from vehicle traffic and airport activities. The less wind direction dependent correlations and higher correlations with NO_2 and SO_2 indicate that secondary aerosols may also contribute to this size fraction. The correlation between 7-160 particle volume (Figure 5-52 (e) and (f)) and 30-160 particle number were similar. This is expected since the 7-160 nm particle volume was dominated by the 30-160 nm size range. The average UFP concentration in the size range of 7-160 nm was only approximately 10 percent of $PM_{2.5}$, and poor correlations were found between the BAM and the personal DataRAM (PDR). These two factors contributed to the poor correlation between UFP and PDR.

Figure 5-53 shows the R^2 at the CN site was very similar to the CE site. The 7-30 nm particles were correlated with NO_2, SO_2, and BC, as was also seen at the CE site. In the Winter Season, the correlations were stronger with westerly winds; while in the Summer Season, the correlations were less wind direction dependent. The 7-30 nm particles were not correlated with CO, again indicates less direct contributions from vehicle exhaust. The 30-160 nm particles were correlated with all species, except PDR, with weak dependence on wind direction, indicating multiple source contributions.

Figure 5-54 shows the correlations at the CS site. Time series of CO, NO_x, SO_2, BC, and UFP in different size ranges, with resolution of 1 to 3 minutes, were examined for potential correlations between airport activity at the South Airfield runways and variations in pollutant concentrations at the CE and CN sites. The 7-30 nm particles had the best correlation (R^2 = 0.75) with SO_2 under northern wind conditions in the Winter Season (a); while in the Summer Season (b), these particles were better correlated with NO, NO_2, SO_2, and BC under north, west, and easterly winds. The CS site can be impacted by airport activities under north and easterly winds, while the jet exhaust from takeoffs could impact this site under westerly wind.

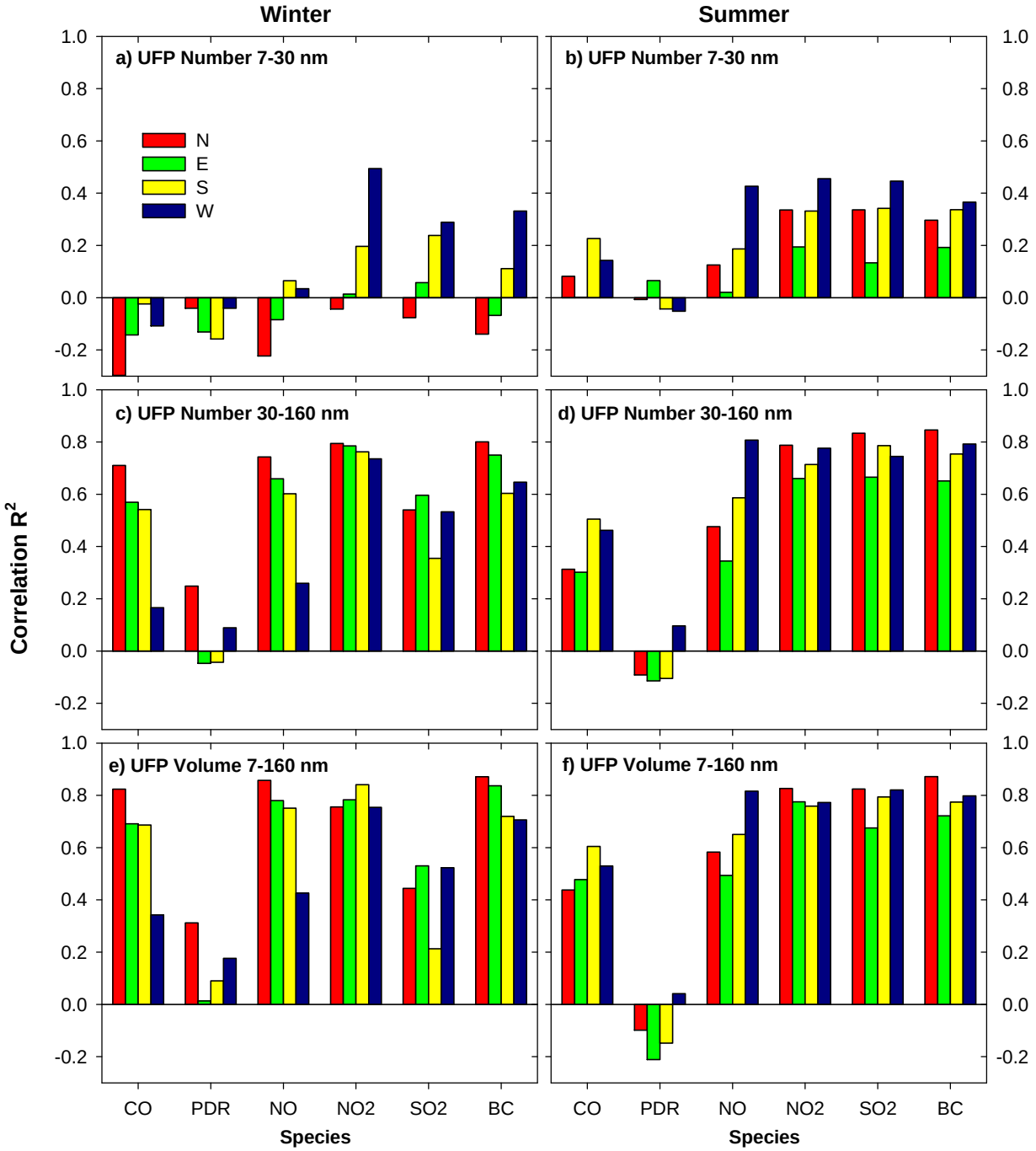

Figure 5-52. Correlation between UFP and other species at the CE site for the four wind directions for the Winter and Summer Monitoring Seasons. The UFP volume concentration is calculated from number concentration assuming particles are spherical.

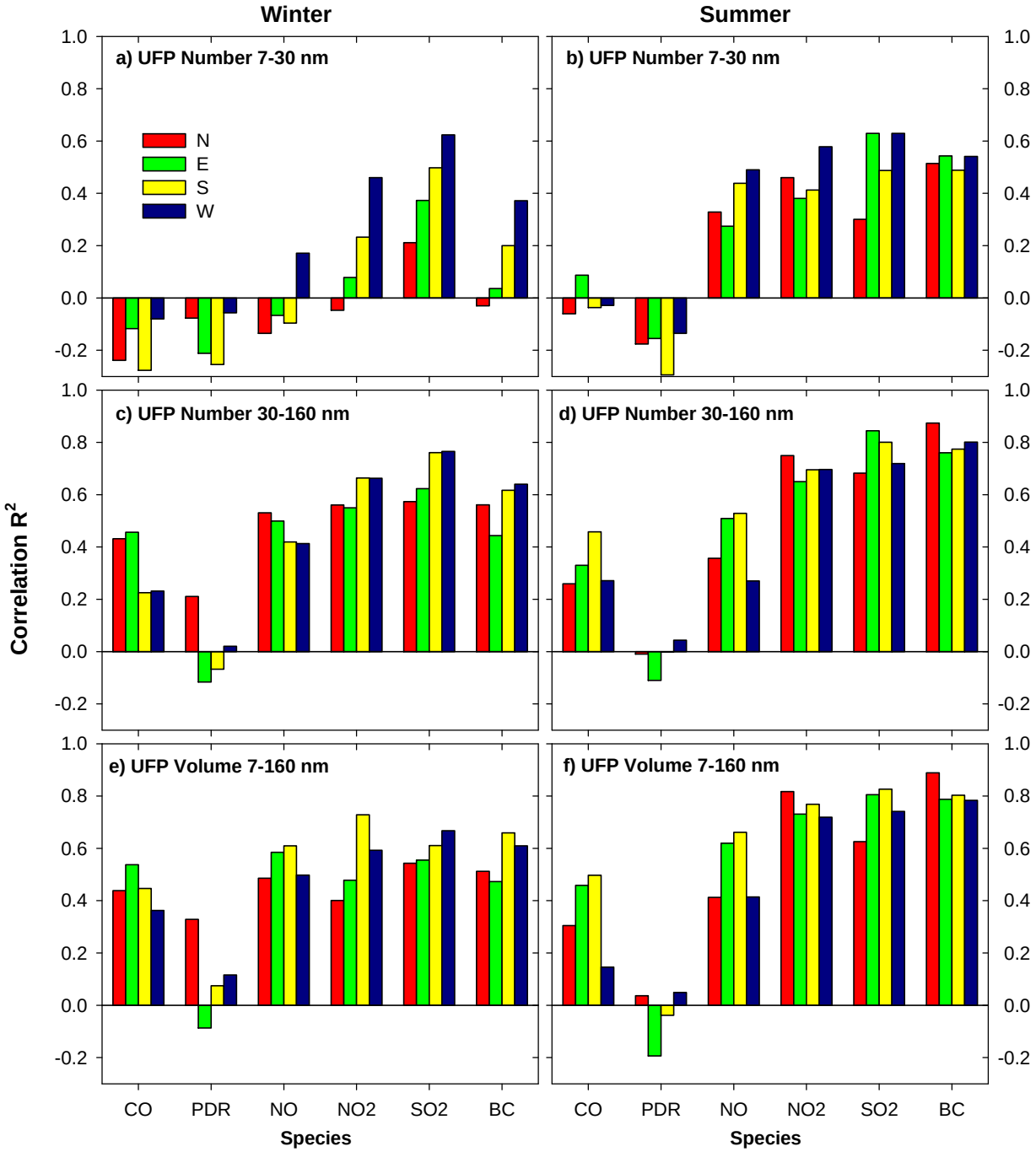

Figure 5-53. Correlation between UFP and other species at the CN site under the four wind directions for the Winter and Summer Monitoring Seasons.

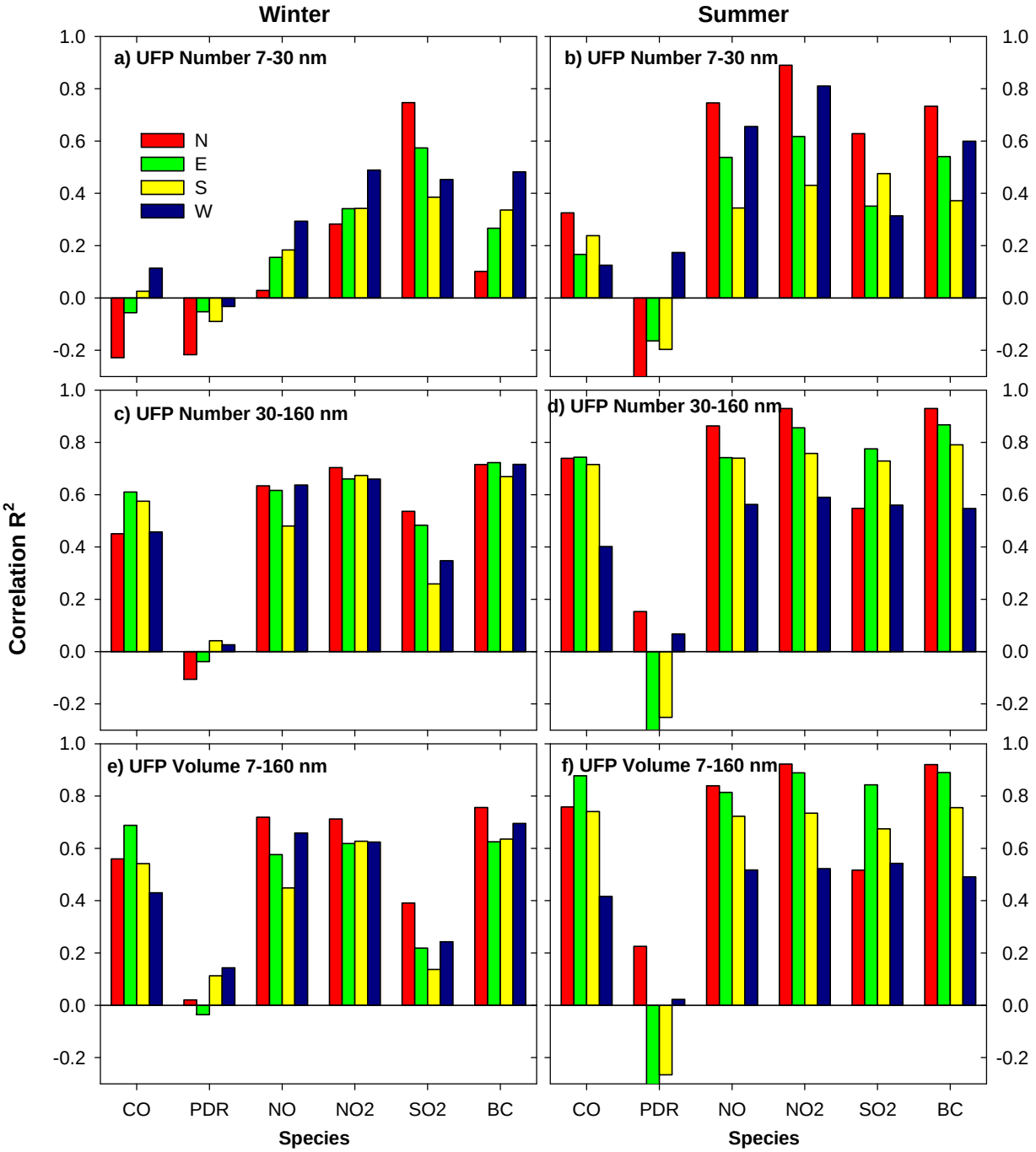

Figure 5-54. Correlation between UFP and other species at the CS site under the four wind directions for the Winter and Summer Monitoring Seasons.

Table 5-22. Correlations (R^2 values) of UFP with other pollutants for a) Winter and b) Summer Sampling Seasons

a) Winter Season

Site	Parameter		Ultrafine Particles				CO	PDR	NO_x	NO	NO_2	SO_2	BC
			7-160 nm	7-30 nm	30-160 nm	Volume							
CE	Ultrafine Particles	7-160 nm	1										
		7-30 nm	1.00	1									
		30-160 nm	0.34	0.24	1								
		Volume	0.16	0.07	0.88	1							
	CO		-0.21	-0.27	0.46	0.70	1						
	PDR		-0.09	-0.11	0.11	0.21	0.25	1					
	NO_x		-0.03	-0.10	0.63	0.82	0.93	0.19	1				
	NO		-0.11	-0.16	0.53	0.75	0.94	0.17	0.98	1			
	NO_2		0.20	0.13	0.75	0.79	0.55	0.18	0.79	0.65	1		
	SO_2		0.34	0.30	0.44	0.28	-0.10	-0.19	0.08	0.02	0.26	1	
	BC		0.13	0.07	0.71	0.80	0.66	0.26	0.77	0.71	0.72	0.22	1
CN	Ultrafine Particles	7-160 nm	1										
		7-30 nm	0.97	1									
		30-160 nm	0.69	0.50	1								
		Volume	0.41	0.22	0.82	1							
	CO		-0.18	-0.30	0.23	0.44	1						
	PDR		-0.12	-0.14	0.00	0.10	0.15	1					
	NO_x		0.05	-0.09	0.48	0.60	0.89	0.17	1				
	NO		-0.05	-0.17	0.36	0.52	0.89	0.14	0.96	1			
	NO_2		0.23	0.09	0.57	0.56	0.57	0.16	0.81	0.63	1		
	SO_2		0.67	0.57	0.70	0.52	0.03	-0.07	0.29	0.20	0.40	1	
	BC		0.21	0.07	0.54	0.57	0.59	0.23	0.75	0.68	0.71	0.42	1
CS	Ultrafine Particles	7-160 nm	1										
		7-30 nm	0.91	1									
		30-160 nm	0.56	0.16	1								
		Volume	0.48	0.08	0.98	1							
	CO		0.18	0.10	0.63	0.67	1						
	PDR		-0.02	-0.03	0.05	0.10	0.10	1					
	NO_x		0.46	0.39	0.75	0.72	0.78	0.24	1				
	NO		0.34	0.27	0.67	0.65	0.82	0.18	0.97	1			
	NO_2		0.55	0.48	0.75	0.71	0.57	0.29	0.88	0.74	1		
	SO_2		0.71	0.69	0.53	0.33	0.24	-0.09	0.50	0.44	0.49	1	
	BC		0.47	0.38	0.77	0.71	0.69	0.28	0.92	0.87	0.85	0.46	1

b) Summer Season

Site	Parameter		Ultrafine Particles				CO	PDR	NO_x	NO	NO_2	SO_2	BC
			7-160 nm	7-30 nm	30-160 nm	Volume							
CE	Ultrafine Particles	7-160 nm	1.00										
		7-30 nm	1.00	1.00									
		30-160 nm	0.48	0.41	1.00								
		Volume	0.50	0.44	0.93	1.00							
	CO		0.07	0.04	0.36	0.46	1.00						
	PDR		-0.08	-0.08	0.04	-0.02	0.05	1.00					
	NO_x		0.31	0.26	0.70	0.74	0.70	0.13	1.00				
	NO		0.16	0.13	0.51	0.57	0.79	0.02	0.88	1.00			
	NO_2		0.38	0.33	0.73	0.75	0.48	0.20	0.90	0.59	1.00		
	SO_2		0.44	0.40	0.74	0.80	0.31	-0.16	0.53	0.43	0.52	1.00	
	BC		0.37	0.32	0.78	0.80	0.46	0.12	0.80	0.63	0.79	0.56	1.00
CN	Ultrafine Particles	7-160 nm	1.00										
		7-30 nm	0.99	1.00									
		30-160 nm	0.77	0.67	1.00								
		Volume	0.75	0.66	0.93	1.00							
	CO		-0.03	-0.10	0.29	0.27	1.00						
	PDR		-0.19	-0.22	0.00	0.00	0.20	1.00					
	NO_x		0.57	0.55	0.50	0.62	-0.03	-0.12	1.00				
	NO		0.47	0.47	0.32	0.45	-0.19	-0.18	0.95	1.00			
	NO_2		0.49	0.42	0.67	0.72	0.42	0.04	0.63	0.38	1.00		
	SO_2		0.65	0.59	0.75	0.76	0.25	-0.08	0.50	0.39	0.49	1.00	
	BC		0.58	0.49	0.80	0.80	0.39	0.03	0.48	0.26	0.76	0.64	1.00
CS	Ultrafine Particles	7-160 nm	1.00										
		7-30 nm	0.96	1.00									
		30-160 nm	0.71	0.48	1.00								
		Volume	0.63	0.41	0.92	1.00							
	CO		0.33	0.19	0.53	0.58	1.00						
	PDR		0.06	0.08	-0.01	-0.06	-0.02	1.00					
	NO_x		0.73	0.63	0.67	0.65	0.64	0.10	1.00				
	NO		0.58	0.47	0.58	0.60	0.66	-0.02	0.91	1.00			
	NO_2		0.76	0.67	0.67	0.64	0.59	0.17	0.97	0.80	1.00		
	SO_2		0.47	0.35	0.59	0.57	0.36	-0.25	0.37	0.40	0.32	1.00	
	BC		0.66	0.55	0.66	0.63	0.49	0.13	0.82	0.73	0.82	0.33	1.00

Examples of hourly average particle size distributions measured at the CE and CN sites on a weekday (2/17/2012, Friday) and a weekend day (2/19/2012, Sunday) are plotted in Figure 5-55. Hourly averages of the PSD at 0:00-1:00 6:00-7:00, 12:00-13:00, 18:00-19:00, and 23:00-00:00 plotted in Figure 5-56 show that particles at CE had bimodal distributions, with one peak below 10 nm and another greater than or equal to 50 nm. The relative concentration of these two modes varies over the course of a day. On Friday, 2/17/12 (Plot (a) in Figure 5-56), particle concentrations were low during 00:00-01:00, but increased by factors of 2 to 10 over the entire particle size range by 06:00-07:00. The PSD during 12:00-13:00 showed higher concentrations of UFP less than about 10 nm, but lower concentrations of UFP greater than about 10 nm as compared to those during 6:00-7:00. This is most likely due to increased emissions of UFP less than 10 nm, increased mixing depths and the westerly wind direction. The PSD during 18:00-19:00 had lower concentrations of particles less than 10 nm compared to 12:00-13:00, but higher concentrations of particles greater than 10 nm. While the UFP less than 10 nm stayed about the same from 18:00 to midnight, significant growth of the larger mode was observed. Figure 5-56(b) shows the smaller mode was the highest around 12:00-13:00, and particle growth was evident in the evening.

Figure 5-56(c) and (d) show that the particle distributions at the CN site had a single mode in the morning periods with one peak centered at about 20 nm. Total particle concentrations were much lower at the CN site than the CE site. Particle number concentrations were substantially higher during the daytime than the nighttime hours on both weekdays and weekends with particle growth evident for both weekdays and weekends as well. The concentrations of particles greater than 30 nm were higher during the overnight period during weekends compared to weekdays. This is likely due to increased late-night traffic on Fridays and Saturdays.

Figure 5-57 shows the time series (1 to 3 minute resolution) of wind, particles, and gases on 2/17/2012 (Friday) measured at the CE site. The wind data was broken down into east (E) and north (N) vectors. UFP, BC, CO, NO, and NO_2 gradually started to increase around 03:00, probably due to low wind speeds and accumulation of pollutants near the ground. Peak concentrations of BC, CO, and NO were observed between 6:00 and 10:00, when flight activities and morning traffic increased. A similar concentration change was observed for 30-160 nm particles, while the 7-30 nm particles did not show as much of an increase during this time period. The 7-30 nm particles increased by a factor of 1.6 (from $23\times10^3/cm^3$ to $38\times10^3/cm^3$) from 05:00-06:00 to 07:00-08:00. The wind switched to a direction between west and southwest at around 10:00, which reduces BC, PDR, CO, NO, and NO_2 to near zero levels at the CE site. At the same time, there were sharp increases of SO_2 and 7-30 nm particles. At around 13:00, the south winds were weaker, and SO_2 concentrations also decreased to near zero until around 16:30 when high concentrations of SO_2 were again observed. High concentration peaks of 7-30 nm particles were observed from 13:00 to 16:30 while SO_2 and all other gaseous species were low. The origin of the UFP during this period is not clear. After the westerly wind subsided around 18:30, BC, CO, NO, NO_2, and 30-160 nm particles gradually increased, which also coincided with increased evening traffic. Spikes of 30-160 nm particles, BC, CO, NO, and NO_2 were observed over a steadily increasing baseline during 20:00-00:00. The 7-30 nm particle number concentration baseline and SO_2 baseline remained relatively flat.

Figure 5-58 shows the times series on 2/19/2012 (Sunday) at the CE site. Winds were very light prior to 09:00 and increases in 30-170 nm particles, BC, CO, and NO were more gradual than

those presented in Figure 5-57, which is most likely due to the lack of a morning commute traffic on Sunday, although the air flight activities were similar between Friday and Sunday. These observations indirectly indicate that vehicle traffic was likely the major source of 30-160 nm particles, BC, CO, and NO. The 7-30 nm particles increased by a factor of 4.3 (from 7×10^3/cm^3 to 30×10^3/cm^3) from 05:00-06:00 to 07:00-08:00. When westerly winds began around 9:00, BC, PDR, CO, NO, and NO_2 decreased to near zero, while SO_2 showed a peak during 09:00-11:00. This peak coincided with a minor peak of 7-30 nm particles. During 12:00-17:00 and 19:30-22:30, there were two periods with high and variable concentrations of 7-30 nm particles.

Figure 5-59 shows that 7-30 nm particle concentrations were moderately correlated with NO_2 during 12:00-17:00 (R^2 = 0.65). However, high concentrations of 7-30 nm particles during 19:30-22:30 were not correlated with NO_2 or other measured species. The high concentration UFP persists even after the westerly winds died down after 21:00. Around 22:45, there were peaks of UFP, PDR, CO, and NO, which are most likely vehicle traffic related.

Figure 5-60 shows the times series of wind, particles, and gases on 2/17/2012 (Friday) measured at the CN site. Similar to the CE site (Figure 5-57), UFP, BC, CO, NO, and NO_2 at the CN site gradually began to increase around 03:00, reaching a high concentration period between 06:00 and 10:00. The UFP concentration showed an increase by a factor of 2.2 (from 11×10^3/cm^3 to 24×10^3/cm^3) from 05:00-06:00 to 07:00-08:00, which was similar to the CE site observations. However, unlike the CE site where the high SO_2 concentration only appeared around 10:00 when southwest wind started, the SO_2 concentration at the CN site increased around 08:00. UFP, CO, NO, NO_2, and SO_2 showed similar temporal changes during 8:00-10:00. Between the time period marked by westerly winds (10:00-18:00), CO, NO, SO_2 and NO_2 concentrations were low, while UFP concentration remained high and variable. There was a high CO period during 13:00-15:00, which did not seem to affect UFP concentration significantly.

Figure 5-61 shows the time series of wind, particles, and gases on 2/19/2012 (Sunday) measured at the CN site. The 7-30 nm particle number concentration moderately increased 1.6 fold (from 4×10^3 to 7×10^3 cm^{-3}) from 05:00-06:00 to 07:00-08:00. The high concentrations of CO and NO between 05:00 and 08:00 did not coincide with high UFP concentrations. However, high concentrations of UFP, BC, SO_2, and NO_2 were observed from 09:00-10:00, which coincided with the start of winds from the west. UFP concentration remained high until 23:00.

Table 5-23 lists the average concentrations of particles and gases for 2/17/12 (Friday) and 2/19/12 (Sunday) at the CE and CN sites. At the CE site, CO and NO on Sunday were less than 50 percent of those on Friday, most likely due to a reduction in vehicle traffic. The 7-30 nm particles were 35 percent greater on Sunday than on Friday, indicating UFP sources other than traffic. At the CN site, CO and NO on Sunday were approximately 50 percent of those on Friday. The 7-30 nm and 30-160 nm particles were 70 percent and 61 percent of Friday's measurements, respectively. CO and NO concentrations were higher on Friday at the CE site than the CN site, while their concentrations were closer in value on Sunday. This is expected since the CE site has a greater influence from vehicle traffic than the CN site.

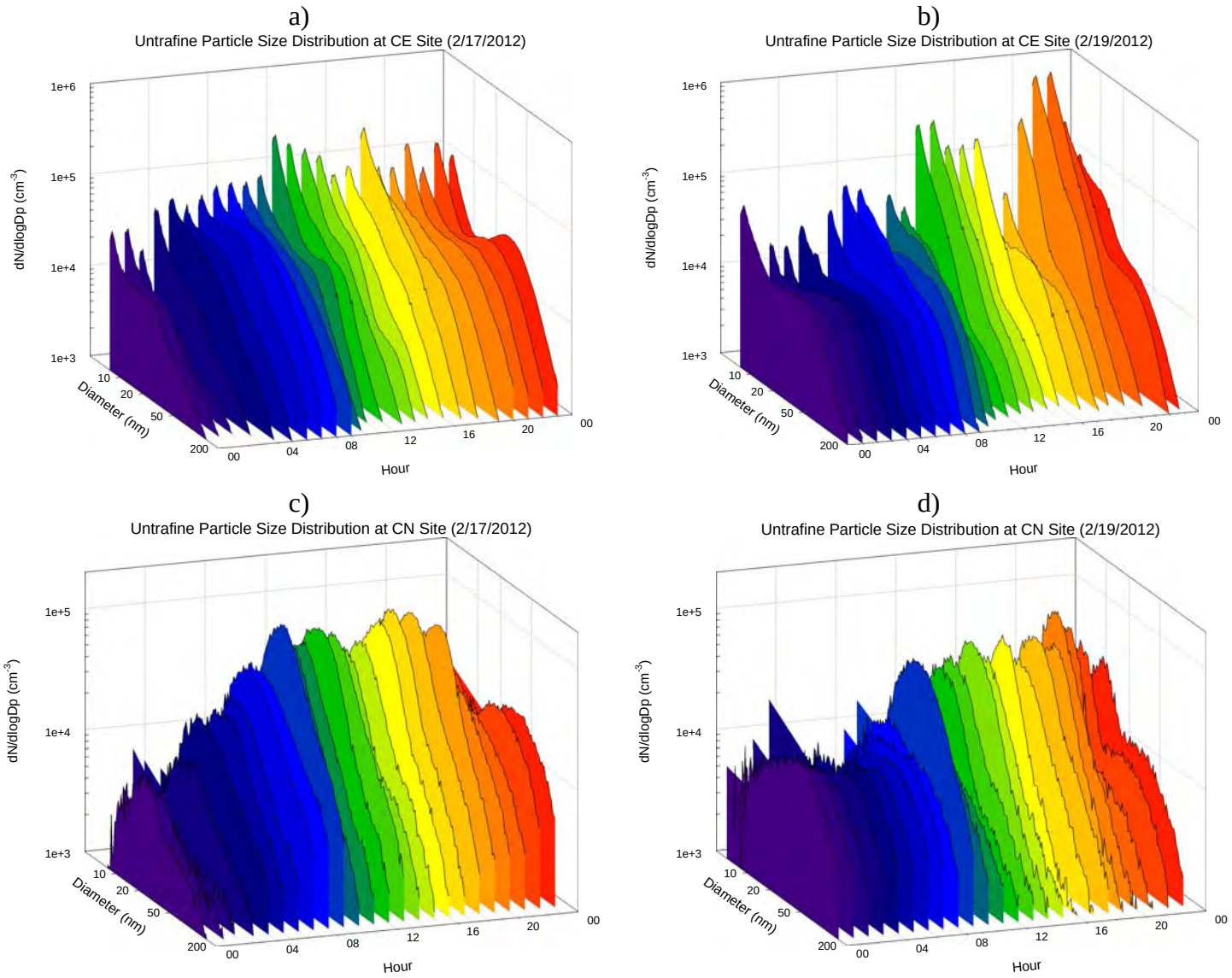

Figure 5-55. Diurnal variations in particle size distributions (dN/dlogDp) at the CE and CN sites on 2/17/2012 (Friday) and 2/19/2012 (Sunday).

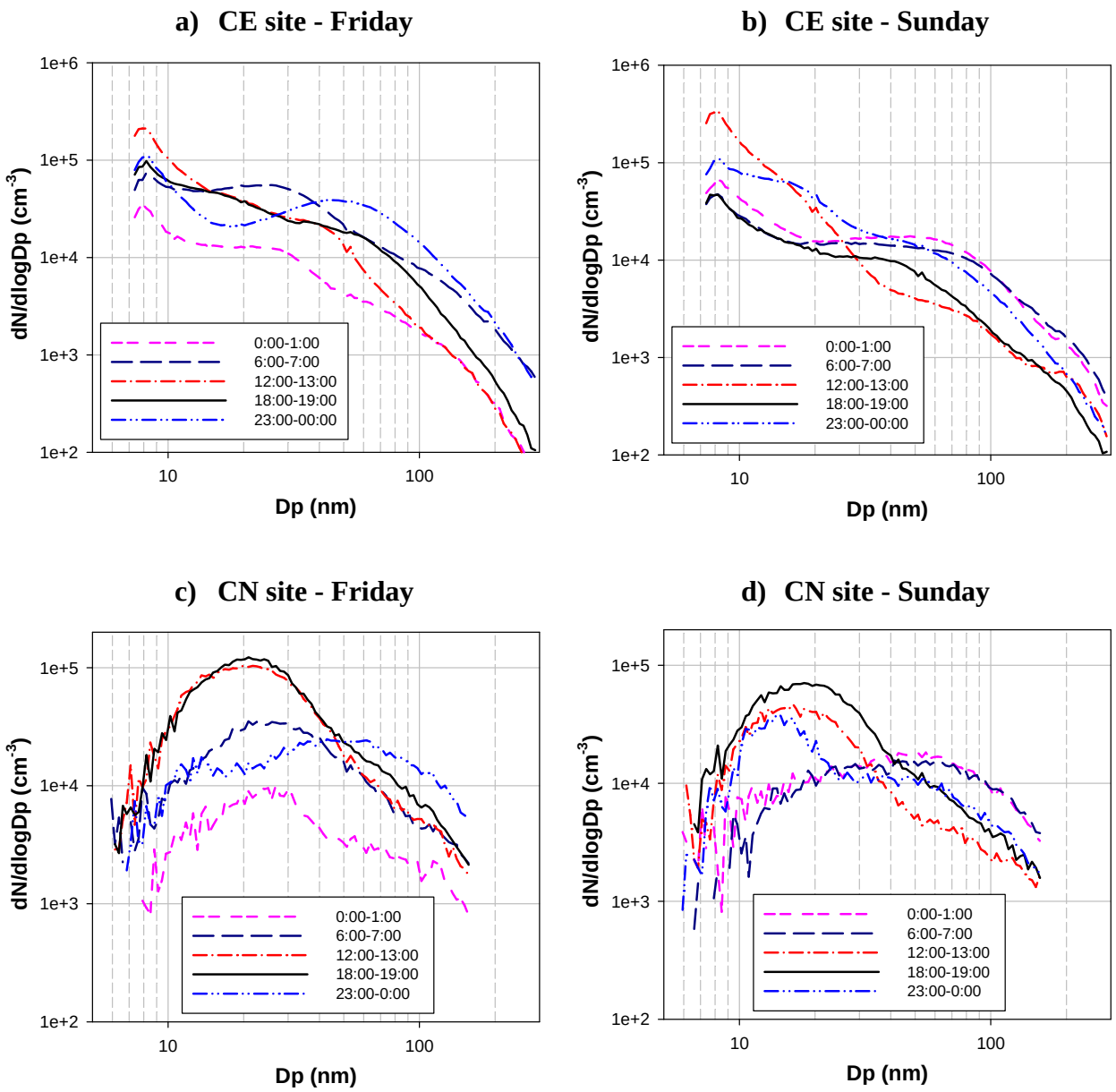

Figure 5-56. Average particle size distributions at the CE and CN sites on 2/17/2012 (Friday) and 2/19/2012 (Sunday) for different time periods of the day.

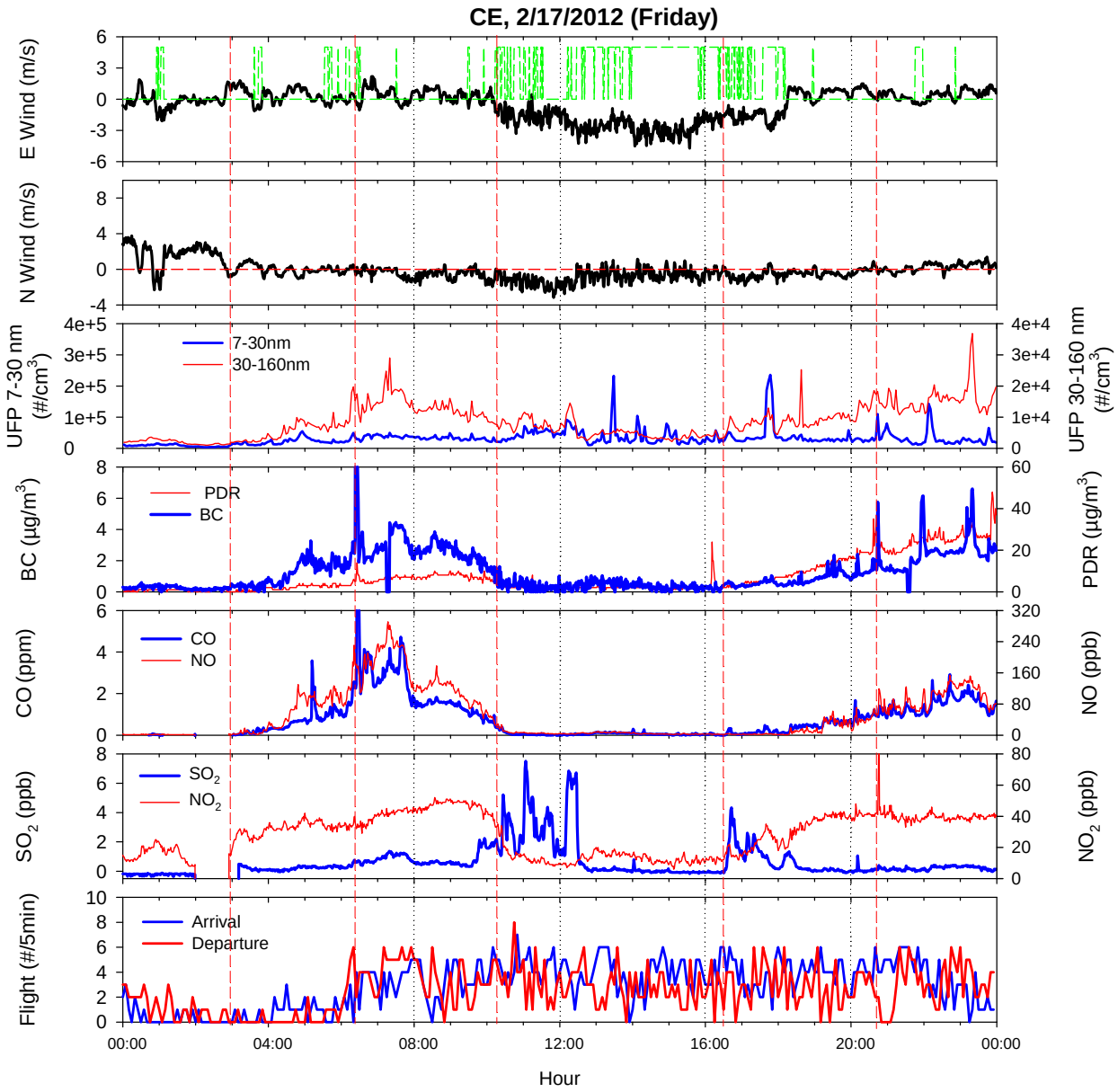

Figure 5-57. Time series of wind speed, wind direction, UFP, BC and PDR, SO_2 and NO_2, CO and NO, and flight activities on 2/17/2012 (Friday) at the CE site. Wind speeds are shown as east and north wind vectors. The green lines in the top panel indicate westerly wind direction of 240-300 degrees.

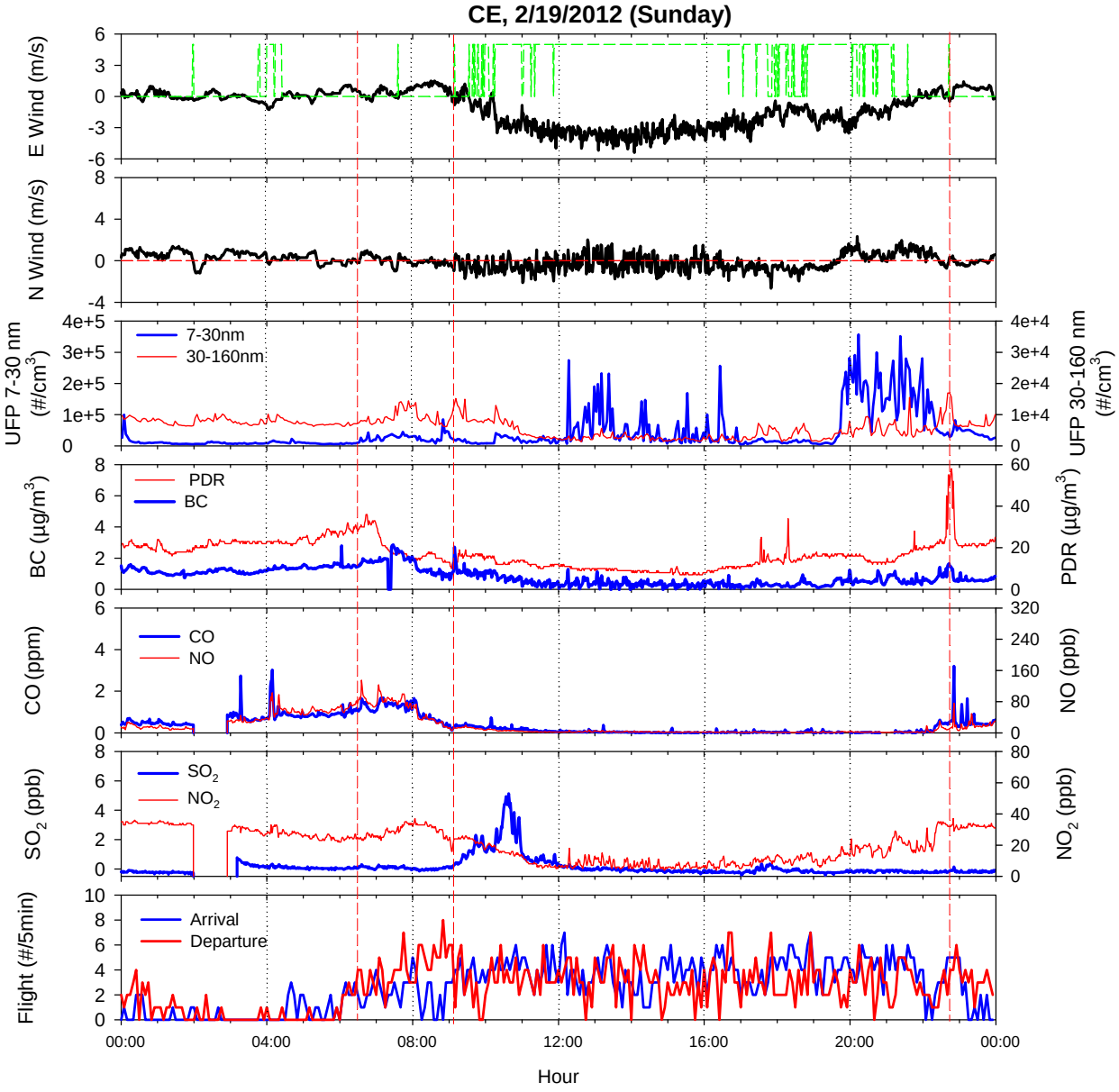

Figure 5-58. Time series of wind speed, wind direction, UFP, BC and PDR, SO_2 and NO_2, CO and NO, and flight activities on 2/19/2012 (Sunday) at the CE site. Wind speeds are shown as east and north wind vectors. The green lines in the top panel indicate westerly wind direction of 240-300 degrees.

a)

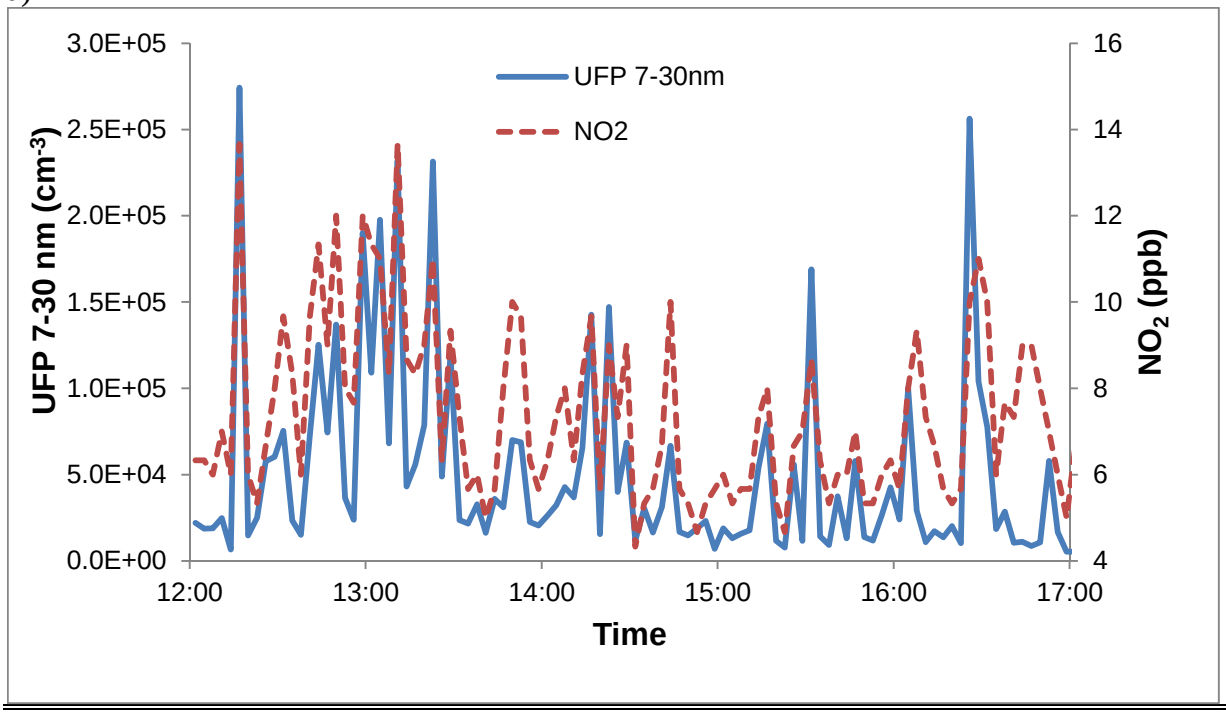

b)

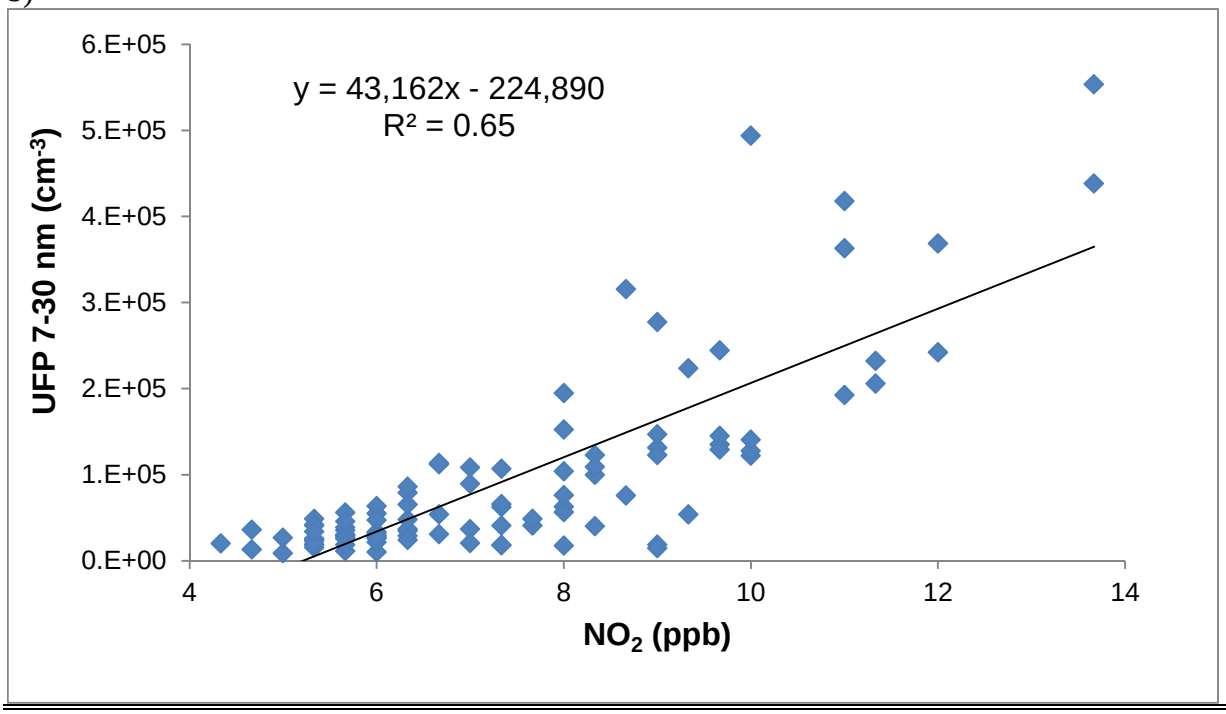

Figure 5-59. a) Time series of 7-30 nm UFP and NO_2 and b) correlation between 7-30 nm UFP and NO_2 during 12:00-17:00 on 2/19/12 (Sunday) at the CE site.

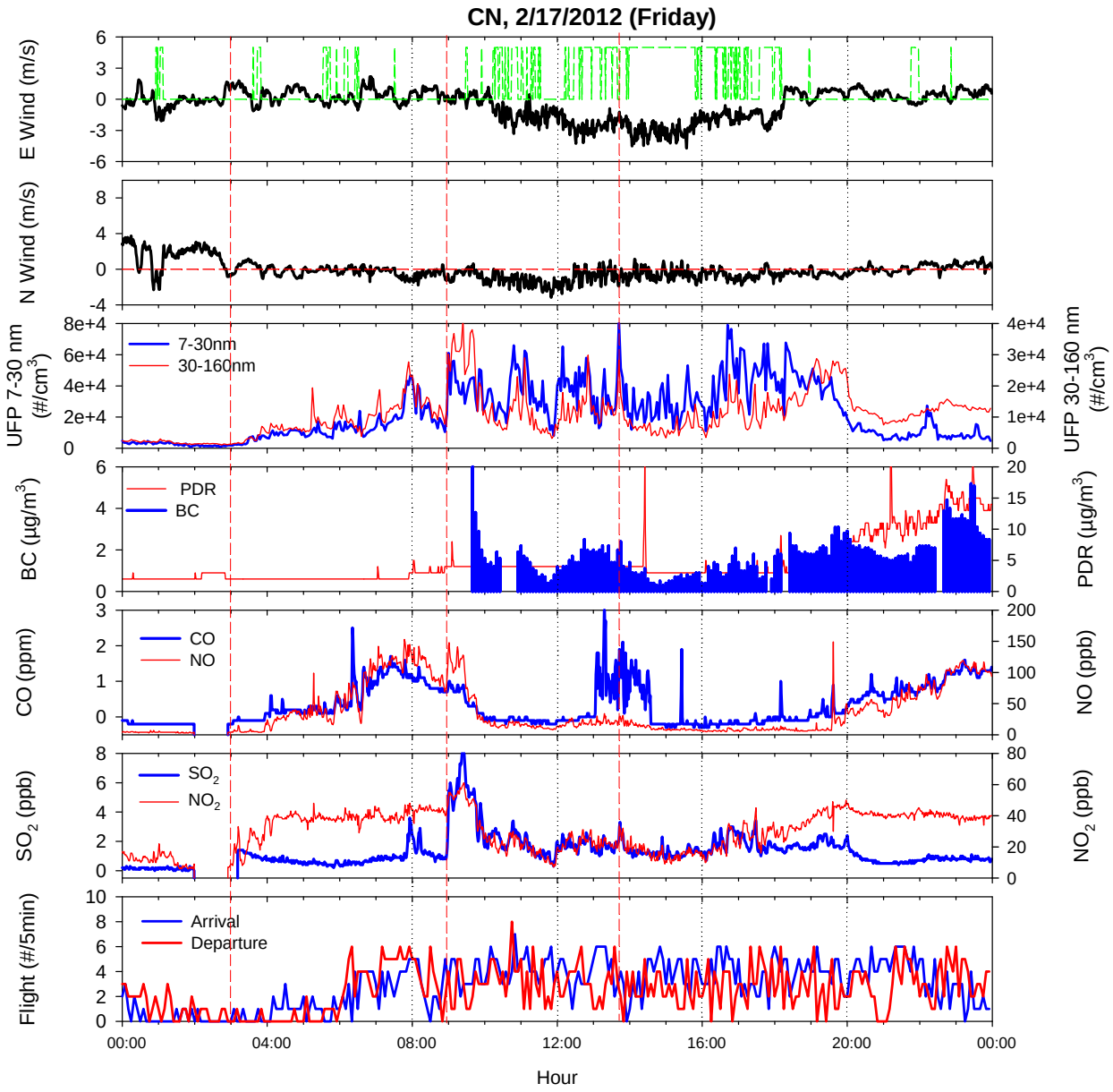

Figure 5-60. Time series of wind speed, wind direction, UFP, BC and PDR, SO_2 and NO_2, CO and NO, and flight activities on 2/17/2012 (Friday) at the CN site. Wind speeds are shown as east and north wind vectors. The green lines in the top panel indicate westerly wind direction of 240-300 degrees.

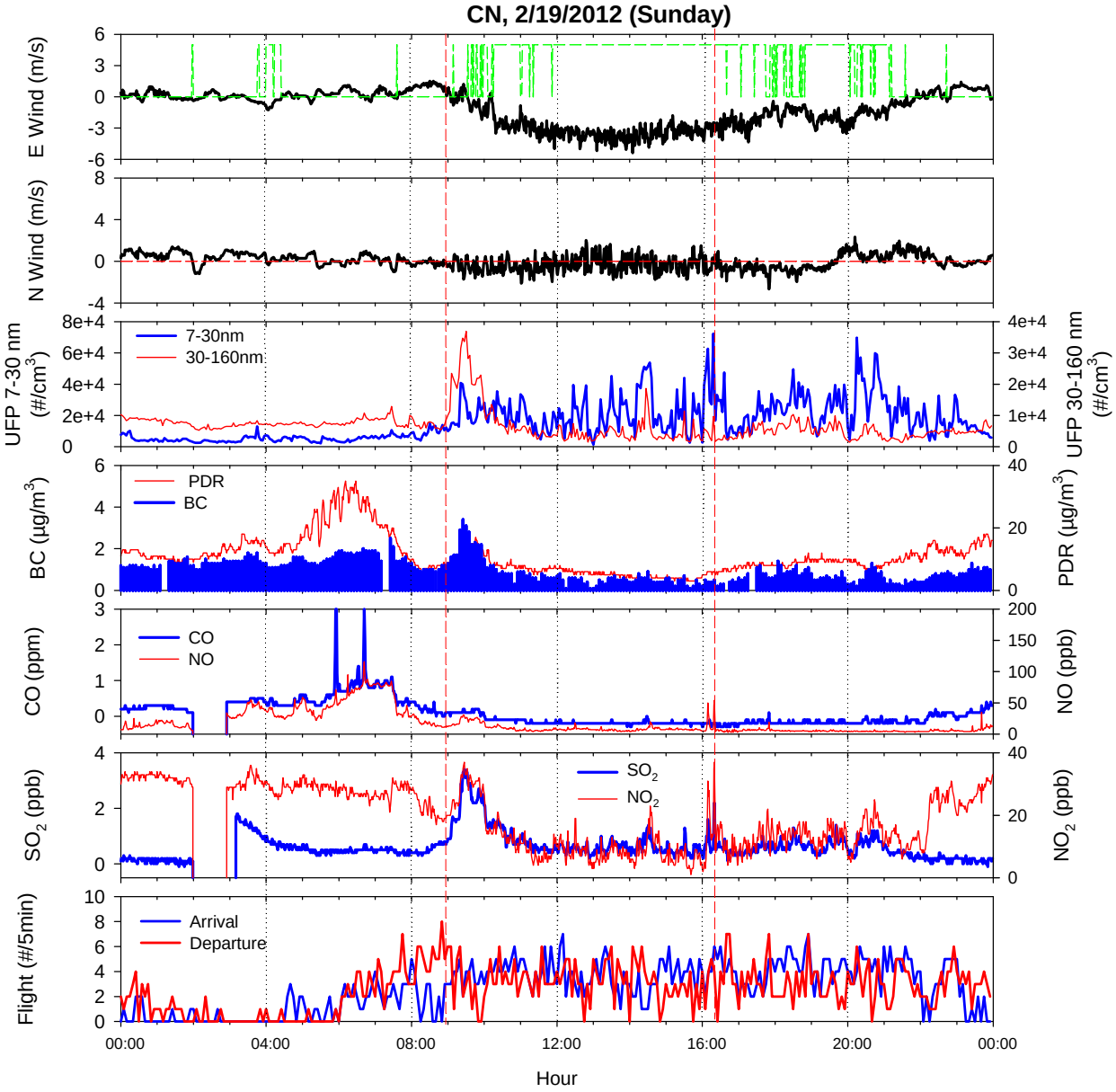

Figure 5-61. Time series of wind speed, wind direction, UFP, BC and PDR, SO_2 and NO_2, CO and NO, and flight activities on 2/19/2012 (Sunday) at the CN site. Wind speeds are shown as east and north wind vectors. The green line in the top panel indicates westerly wind direction of 240-300 degrees.

Table 5-23. Average particle and gas concentrations on 2/17/12 (Friday) and 2/19/12 (Sunday) at the CE and CN sites. See text in Section 5.2-4 for discussions regarding the values highlighted in red.

Concentration/Site	CE Site			CN Site		
Species/Date	2/17/2012	2/19/2012	Ratio (S/F)*	2/17/2012	2/19/2012	Ratio (S/F)*
UFP 7-30 nm (#/cm^3)	3.12E+04	4.21E+04	1.35	2.25E+04	1.56E+04	0.70
UFP 30-160 nm (#/cm^3)	8.48E+03	5.93E+03	0.70	1.07E+04	6.57E+03	0.61
BC (µg/m^3)	1.25	0.82	0.65	1.76	0.98	0.56
CO (ppm)	0.81	0.40	0.49	0.64	0.35	0.55
NO (ppm)	50.93	19.09	0.37	37.80	17.59	0.47
NO_2 (ppm)	28.41	19.63	0.69	30.06	19.16	0.64
SO_2 (ppm)	0.79	0.46	0.58	1.33	0.62	0.47

*Ratio (S/F) is Sunday/Friday

5.2.5 Pollutant Concentrations by Wind Direction and LAX Activity

The diurnal variations in the percentage of cumulative pollutant concentrations by wind direction during the six-week Winter Monitoring Season are shown in Figure 5-62 through Figure 5-69 for the four core monitoring sites. Each segment of the stacked bar is the relative contribution of each wind condition: west (airfield upwind), east (airfield downwind), other, or calm) to the mean concentrations. These were calculated by adding together the hourly mean concentrations that were measured whenever the indicated wind condition occurred, and dividing the total by the number of available measurements for the season during the specified 3-hour time slot. The lower right plot in each of the figures shows the distribution of wind conditions for each three-hour period and the average numbers of aircraft landings and takeoffs.

The percentage of the total daily cumulative pollutant concentration at the CE site during the Winter Season when the winds were from the west are 0, 7, 25, 46 and 57 percent during the Summer Season for CO, NO, BC, SO_2, and UFP, respectively. At the CN site, these contributions were 0, 9, 24, 42, and 42 percent, respectively. The airport runways are located north and northeast of the CS monitoring site. In contrast to the CE and CN sites, the cumulative contributions at the CS site are low for SO_2 and UFP during the Summer Season when the winds were from the west and much higher for other wind directions, especially from the north and northeast. All pollutants had similar wind-directional dependence in cumulative contributions to measured concentrations at the AQ site. Highest contributions were from the north and northeast, indicating that the low concentrations of SO_2 and UFP are likely related to on-road motor vehicle emissions located north and east of the CS site.

The contributions of transport from the west to total cumulative pollutant concentrations were high for all pollutants at the CE and CN sites during the Summer Season with winds coming more consistently from the west during the day. While winds were much weaker during the overnight hours, they were still primarily from the west. This explains the greater contributions of SO_2 and UFP during west winds occurring in the morning hours compared to the Winter

Season. More variable and weaker overnight and early morning winds account for greater contributions from other wind directions during this time period.

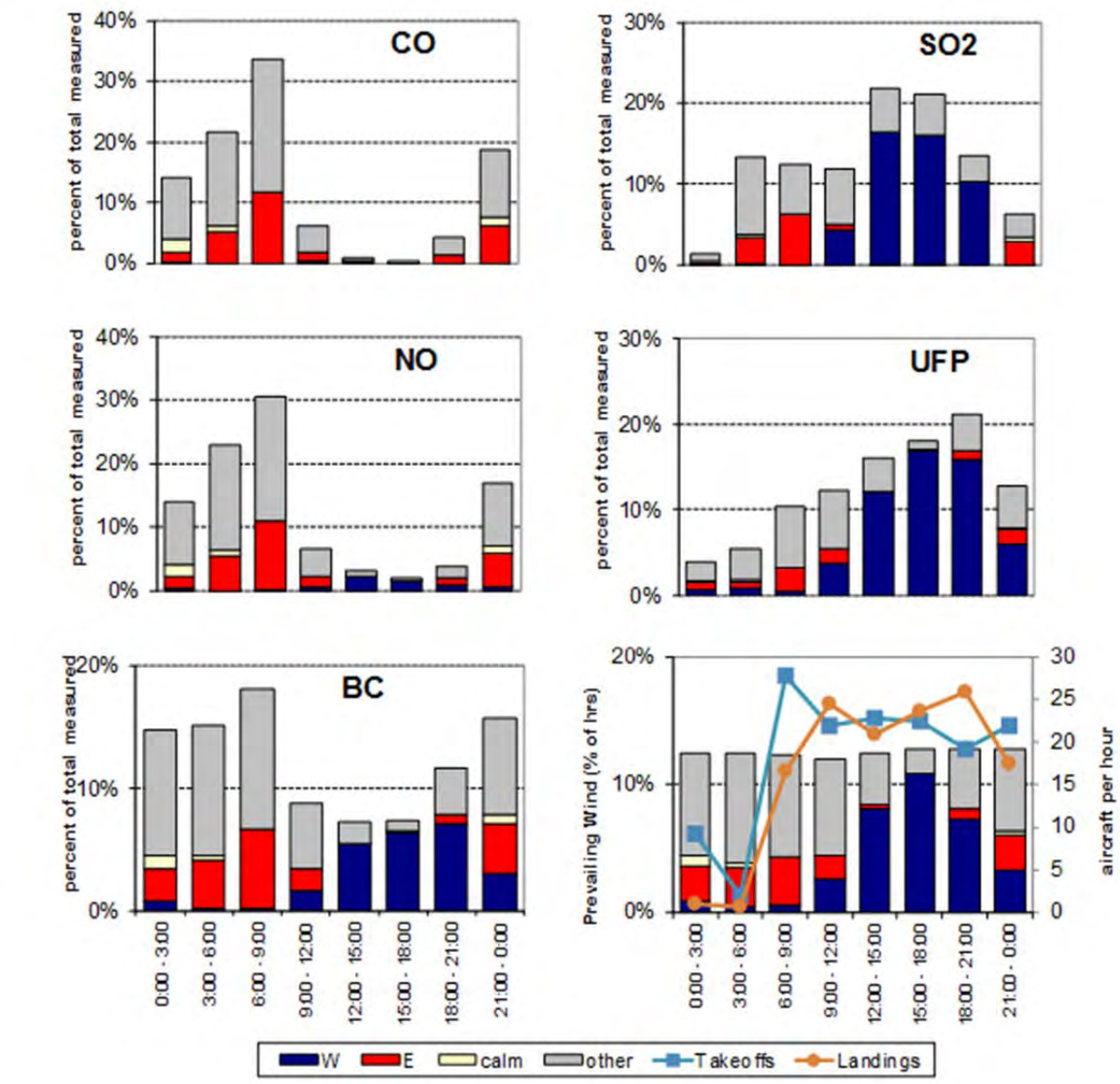

Figure 5-62. Diurnal variations in the percentage of cumulative pollutant concentrations by wind direction during the Winter Monitoring Season at the CE Site for each 3-hour time period. West and east directions are 45 degree segments. Calm conditions are defined as below a threshold of 0.5 m/sec. The lower right plot shows each wind condition percentage (based on hours per time period) and the number of aircraft landings and takeoffs from the South Airfield.

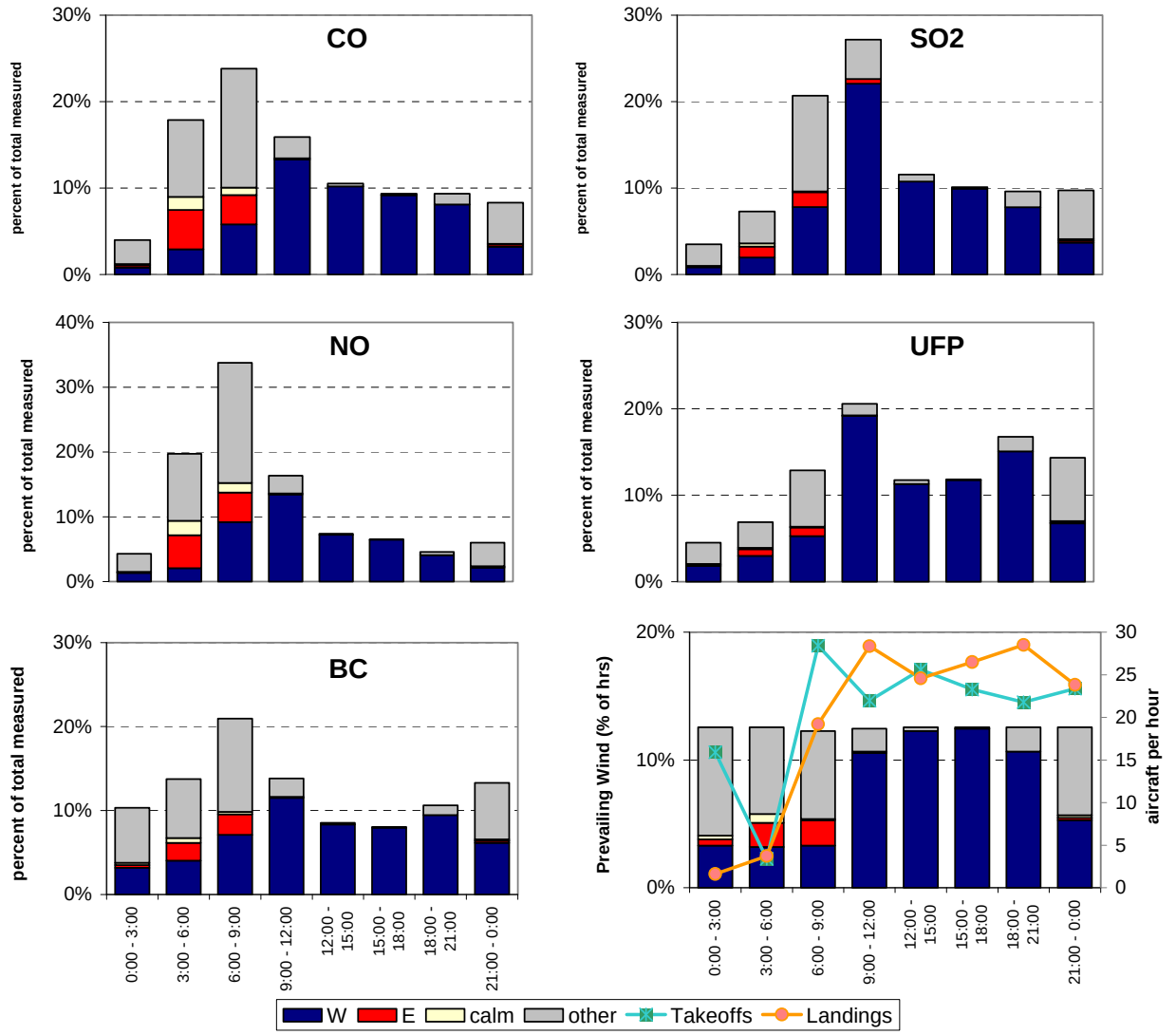

Figure 5-63. Diurnal variations in the percentage of cumulative pollutant concentrations by wind direction during the Summer Monitoring Season at the CE Site. West and east directions are 45 degree segments. Calm conditions are defined as below a threshold of 0.5 m/sec. The lower right plot shows each wind condition percentage (based on hours per time period) and the number of aircraft landings and takeoffs from the South Airfield.

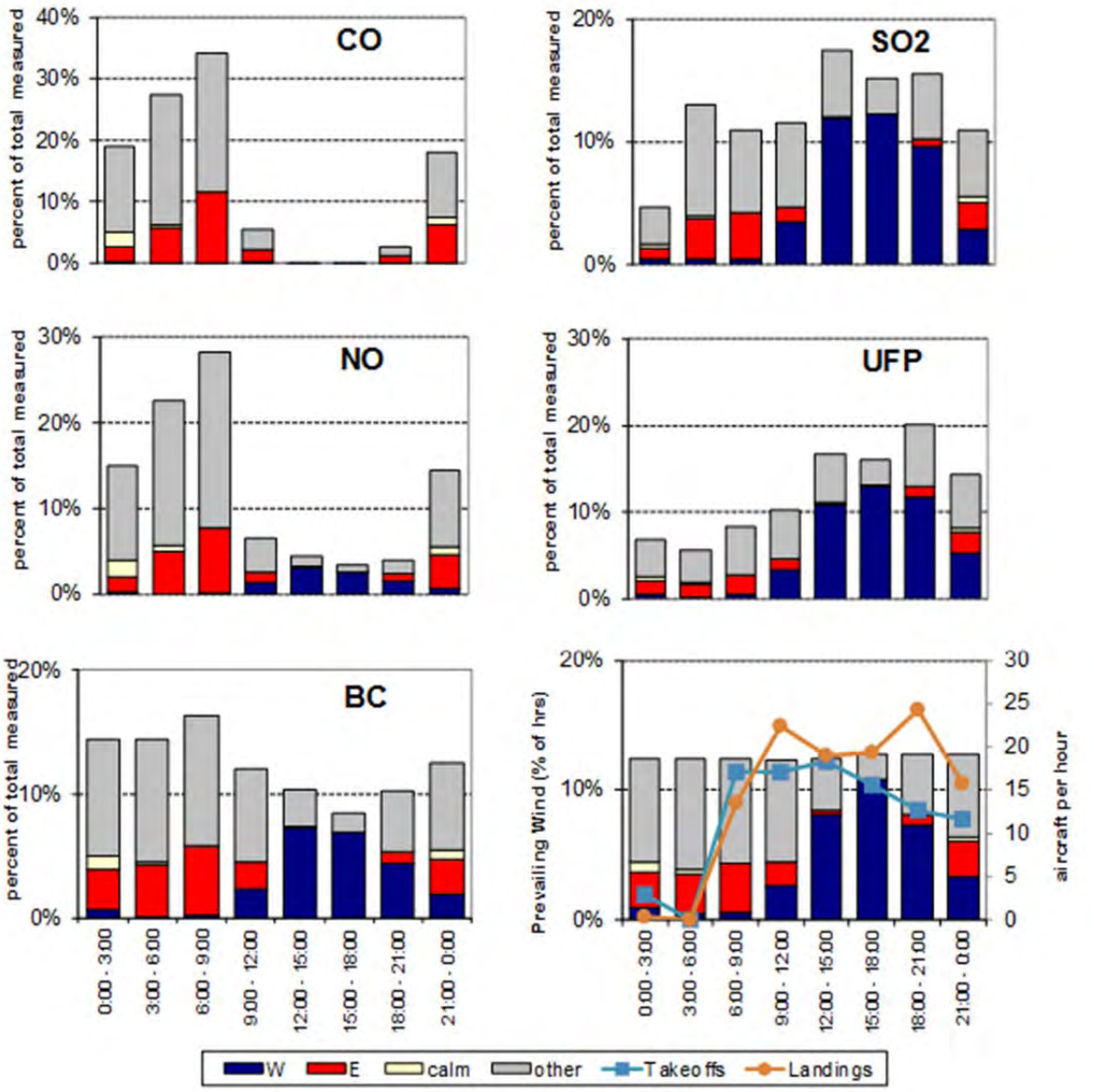

Figure 5-64. Diurnal variations in the percentage of cumulative pollutant concentrations by wind direction during the Winter Monitoring Season at the CN Site. West and east directions are 45 degree segments. Calm conditions are defined as below a threshold of 0.5 m/sec. The lower right plot shows each wind condition percentage (based on hours per time period) and the number of aircraft landings and takeoffs from the North Airfield.

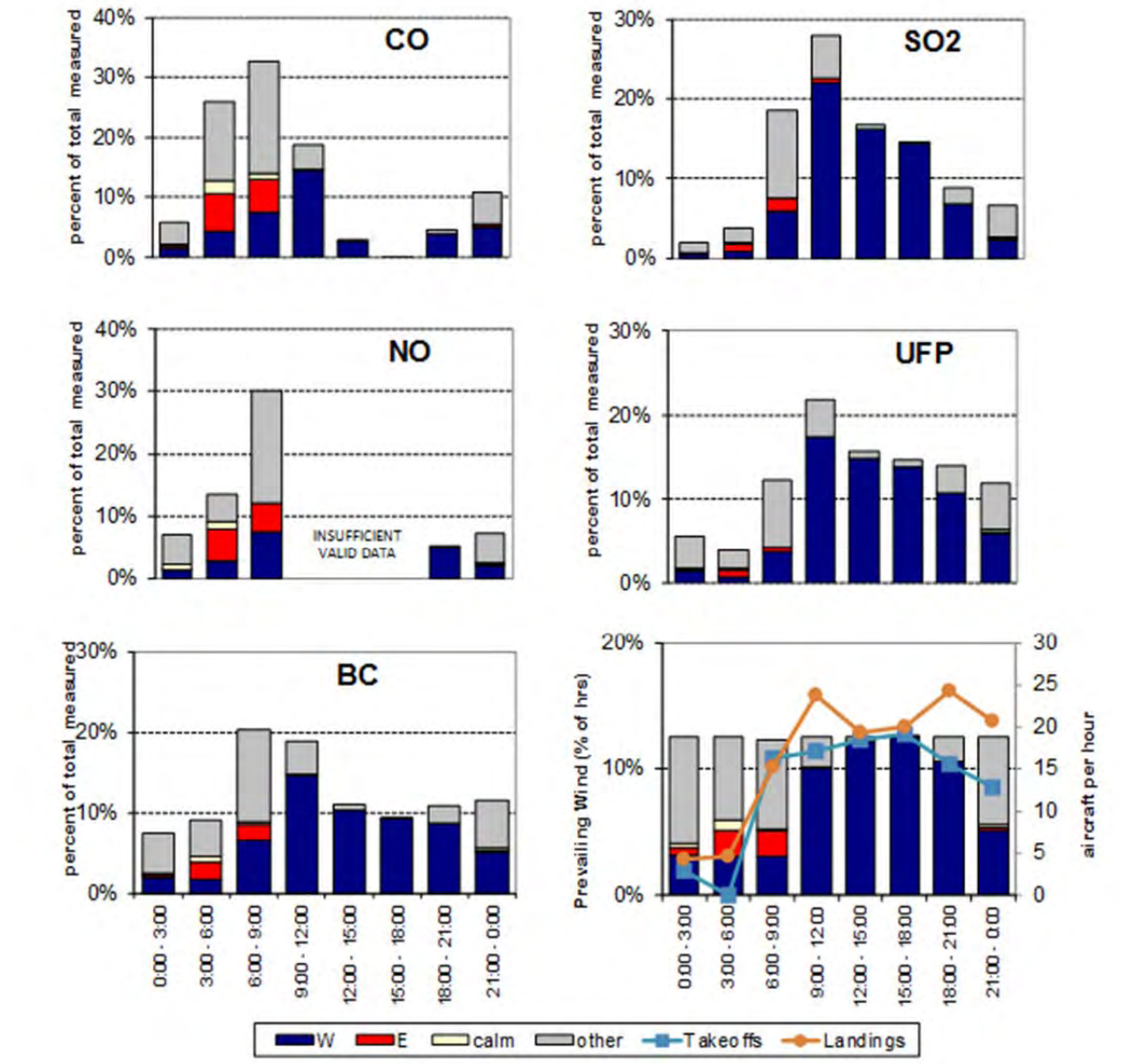

Figure 5-65. Diurnal variations in the percentage of cumulative pollutant concentrations by wind direction during the Summer Monitoring Season at the CN Site. West and east directions are 45 degree segments. Calm conditions are defined as below a threshold of 0.5 m/sec. The lower right plot shows each wind condition percentage (based on hours per time period) and the number of aircraft landings and takeoffs from the North Airfield.

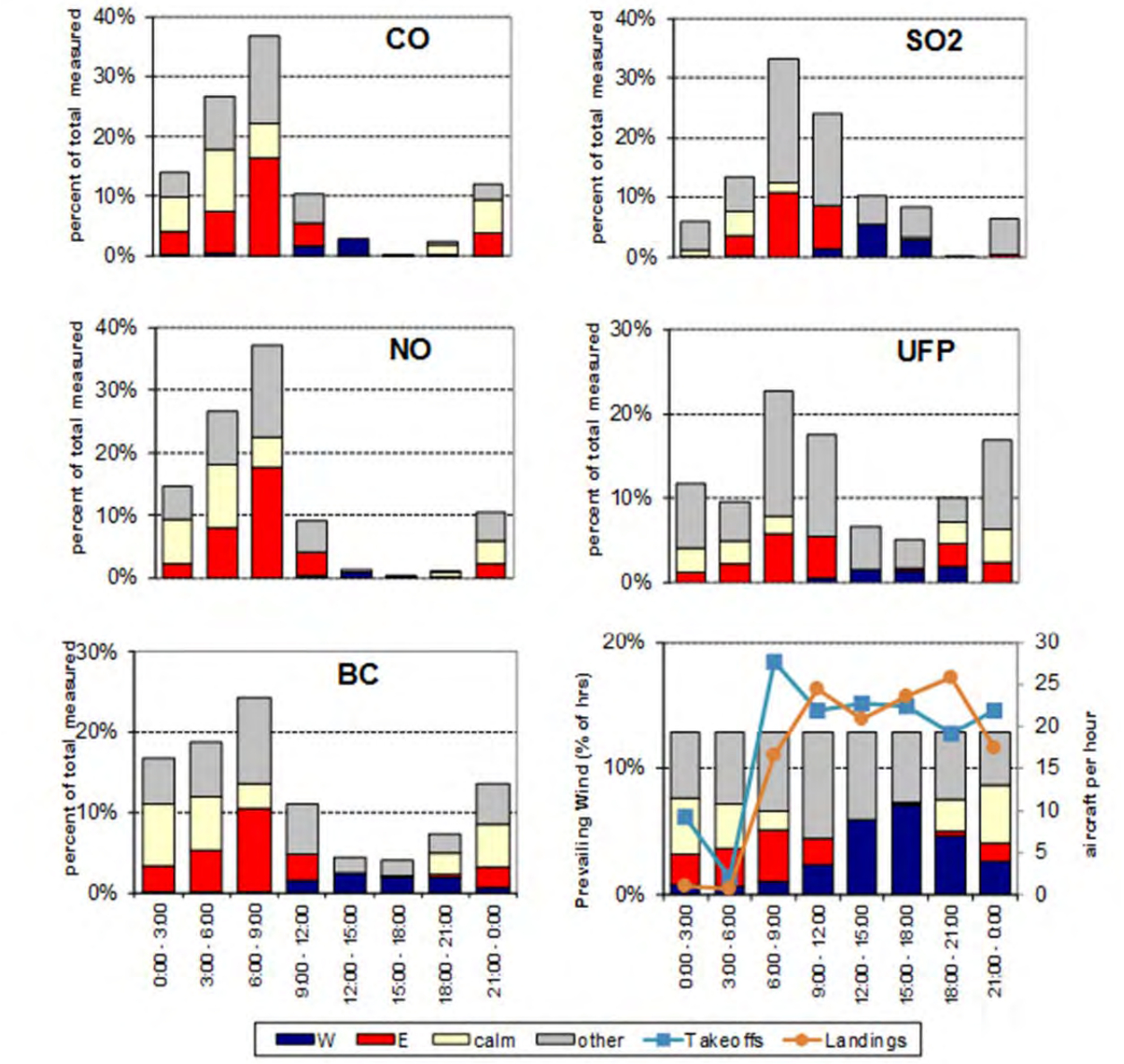

Figure 5-66. Diurnal variations in the percentage of cumulative pollutant concentrations by wind direction during the Winter Monitoring Season at the CS Site. West and east directions are 45 degree segments. Calm conditions are defined as below a threshold of 0.5 m/sec. The lower right plot shows each wind condition percentage (based on hours per time period) and the number of aircraft landings and takeoffs from the South Airfield.

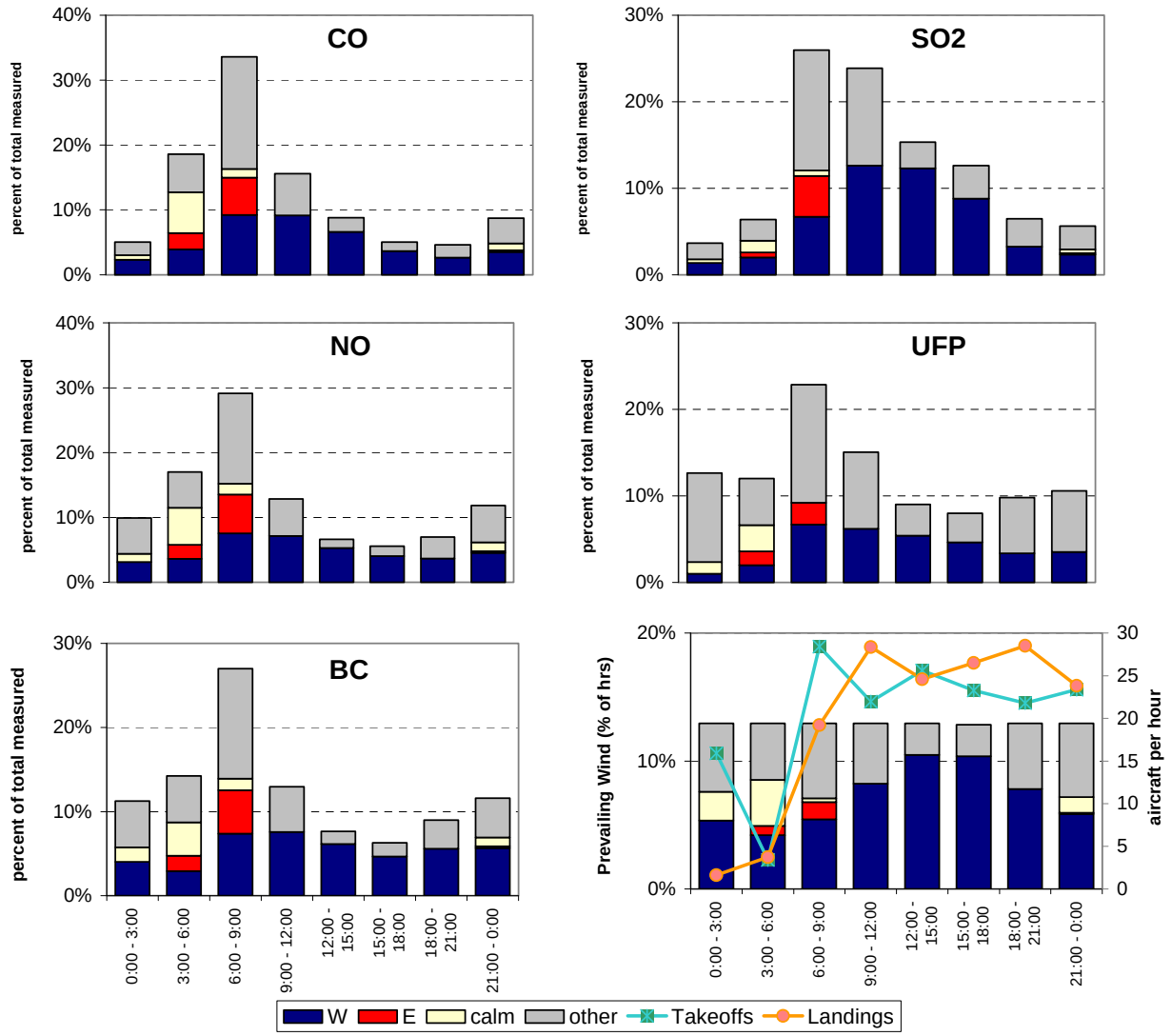

Figure 5-67. Diurnal variations in the percentage of cumulative pollutant concentrations by wind direction during the Summer Monitoring Season at the CS Site. West and east directions are 45 degree segments. Calm conditions are defined as below a threshold of 0.5 m/sec. The lower right plot shows each wind condition percentage (based on hours per time period) and the number of aircraft landings and takeoffs from the South Airfield

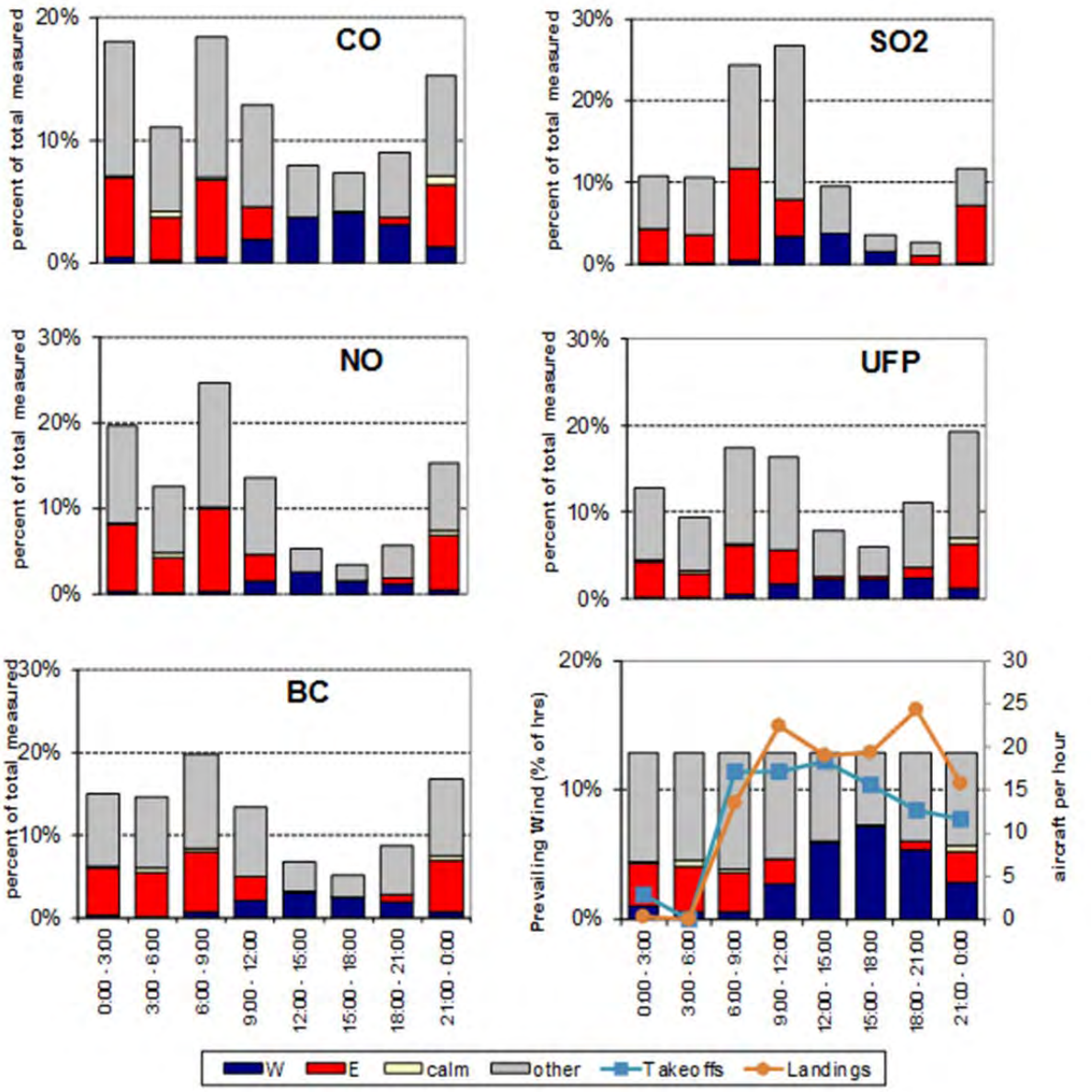

Figure 5-68. Diurnal variations in the percentage of cumulative pollutant concentrations by wind direction during the Winter Monitoring Season at the AQ Site. West and east directions are 45 degree segments. Calm conditions are defined as below a threshold of 0.5 m/sec. The lower right plot shows each wind condition percentage (based on hours per time period) and the number of aircraft landings and takeoffs from the North Airfield.

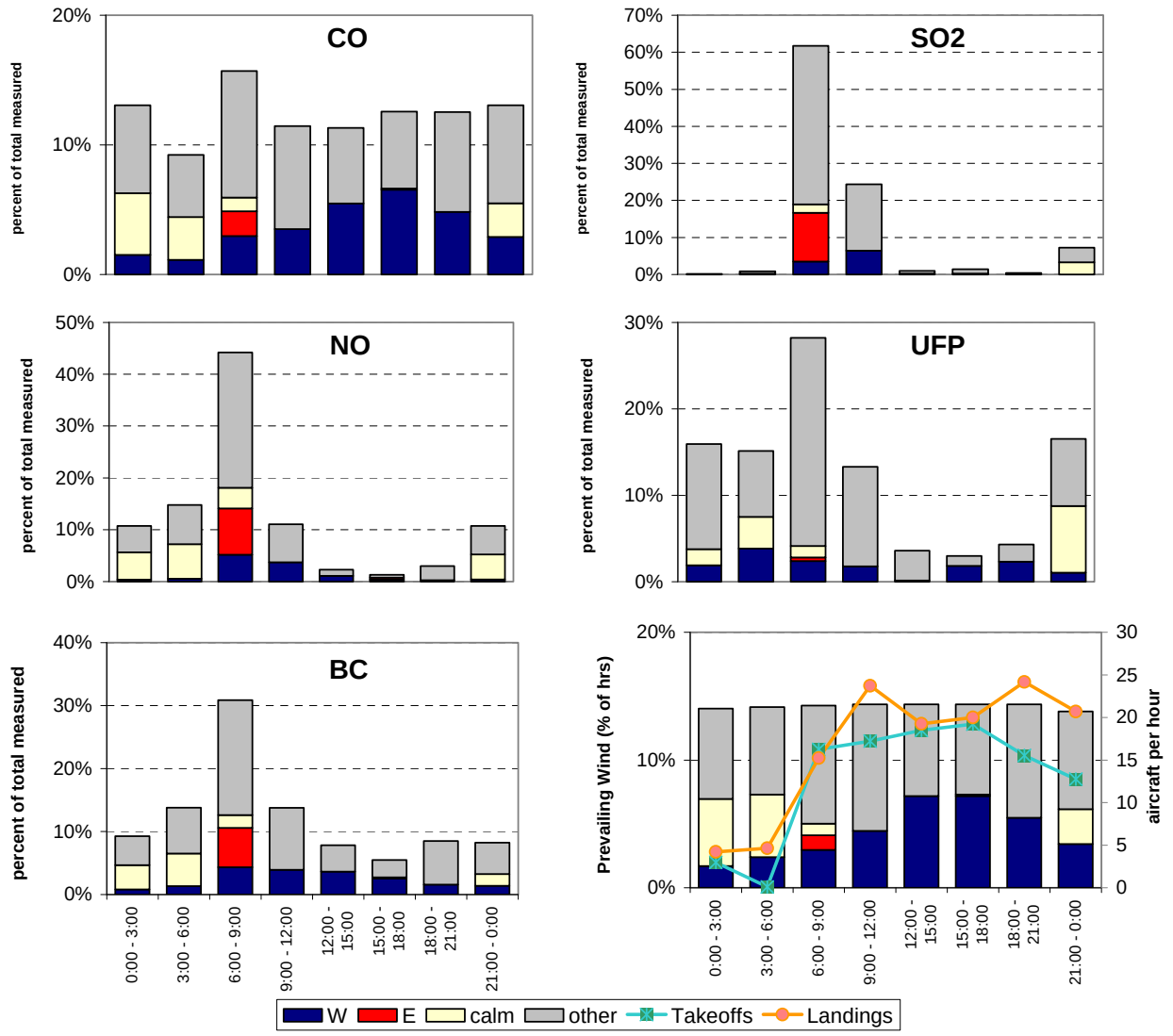

Figure 5-69. Diurnal variations in the percentage of cumulative pollutant concentrations by wind direction during the Summer Monitoring Season at the AQ Site. West and east directions are 45 degree segments. Calm conditions are defined as below a threshold of 0.5 m/sec. The lower right plot shows each wind condition percentage (based on hours per time period) and the number of aircraft landings and takeoffs from the North Airfield.

5.3 CHEMICAL NATURE AND SOURCE CONTRIBUTIONS OF ULTRAFINE PARTICLES - SUPPLEMENTAL EXPERIMENT

Analysis of the monitoring data and the Nonparametric Trajectory Analysis (NTA) from the Winter Monitoring Season indicated airport operations are potentially major contributors to the UFP concentrations in downwind communities. Weekday levels of CO, NO_x, and BC peaked during the morning commute periods at the CE and CN sites, but SO_2 and UFPs steadily increased throughout the day. CO, NO_x, and BC, which are mainly associated with on-road motor vehicles, were substantially lower on Sundays relative to weekdays. SO_2 exhibited less weekday dependence by comparison. UFP had the same diurnal pattern on weekdays and weekends at the CE and CN sites. In contrast, SO_2 and UFP concentrations peaked during the morning commute period at the CS site, which was characterized by northeast winds. The SO_2 and UFP concentrations were very low during the day, which had winds predominantly from the west. These observations from the Winter Season, which are consistent with the initial NTA results for the Winter Season, indicate that jet exhaust contributes to SO_2 and UFPs measured in downwind locations near LAX. The particle size distribution (PSD) data from the Winter Season indicates the 7-30 nm particles are likely associated with jet exhaust while the 30-160 nm particles were likely associated with aged aerosol and directly emitted vehicle exhaust emissions.

UFPs contain both volatile and non-volatile particles. A quick review of other studies measuring UFP near airports reveals that only particle number concentrations were measured in most studies and no extensive chemical measurements were made to determine chemical constituents of the measured UFP. A literature review indicates that the volatile and smallest particle fractions may contain mostly sulfuric acid, with soot or elemental carbon comprising the larger non-volatile fraction. Particulate organic carbon and semi-volatile organic compounds from combustion sources are typically found in the smaller size fractions.

5.3.1 Supplemental Experiment Description

A three-part supplemental monitoring study (Parts A, B, and C) was conducted in September 2012, following the end of the Summer Monitoring Season, to examine the chemical nature and source contributions of UFPs in downwind areas. The schedule and measurement for the supplemental work is summarized in Table 5-24.

Supplemental Study A (Volatility Measurement)
This experiment examined volatility of the UFPs by measuring PSD changes when heated to different temperatures. As shown in Figure 5-70, two SMPS were operated in parallel scanning full size distributions, one with and one without a thermal denuder (TD), first at the CE site and then at the Trinity Lutheran Church/School (TLCS). The TLCS site was located 1.5 miles directly south of the CE site and out of the LAX flight path. The TD consists of a heater and a denuder filled with activated charcoal. Previous studies indicate that sulfuric acid (H_2SO_4) and ammonium sulfate ($[NH_4]_2SO_4$) decompose and evaporate around 125 °C and 175 °C, respectively, along with some organics (Burtscher et al., 2001). After heating to 300 °C, only refractory materials are left. To infer particle chemical composition based on their volatility, the TD heater temperature was set at approximately 25 °C (ambient), and then at 125°C, 175°C, and 300°C. Temperatures of 50°C and 400°C were also used for several tests. The TD was designed

to operate at a flow rate of 0.3 L/min. In the field, it was found that this low flow rate was insufficient for adequate counting statistics in the CPC readings; therefore, the heater flow was increased to 1.5 L/min. This change altered the flow temperature and residence time in the heater leading the particle evaporation behavior to differ from the design expectations determined earlier in the laboratory. The actual TD performance was tested and confirmed in the laboratory after the study.

Table 5-24. Schedule and measurement during the three-part supplemental study.

a) Supplemental Study A: Volatility Measurement		
Site\Date	9/4 15:00 - 9/5 15:00	9/5 16:00 - 9/6 16:00
CE	TD-NSMPS: 25, 50, 125, 175, 300, 400 °C; 3-79 nm	NSMPS: 4.6-157 nm; every 180 s
	RSMPS: 7.3-289 nm; every 180 s	
	CO, NO_x, SO_2, BC, DustTrak DRX PM_1, $PM_{2.5}$, PM_4, PM_{10}, and PM_{15}	
TLC	NSMPS: 4.6-157 nm; every 180 s	TD-NSMPS: 25, 50, 125, 175, 300, 400 °C; 3-79 nm
	Grimm: 5.5-350 nm; every 230 s	
	CO, NO_x, SO_2, BC, DustTrak DRX PM_1, $PM_{2.5}$, PM_4, PM_{10}, and PM_{15}	

b) Supplemental Study B: High Time Resolution PSD	
Site\Date	9/6 18:00 - 9/10 12:00
CE	NSMPS: 10-53 nm, every 40 s
	RSMPS: 14.5 nm, every 1 s
	CO, NO_x, SO_2, BC, DustTrak DRX PM_1, $PM_{2.5}$, PM_4, PM_{10}, and PM_{15}
TLC	NSMPS: 10-53 nm, every 40 s
	Grimm: 14.5 nm, every 1 s
	CO, NO_x, SO_2, BC, DustTrak DRX PM_1, $PM_{2.5}$, PM_4, PM_{10}, and PM_{15}

c) Supplemental Study C: Blast Fence Measurement		
Site\Date	9/10 17:00 - 9/11 9:00	9/11 9:00 - 15:00
Blast Fence	VTDMA: 14.5 nm; 125 °C	VTDMA: 5, 14.5, 30, 50 nm; 25, 125, 175, 300, 400 °C
	RSMPS: 10-53 nm, every 40 s	
	Grimm: 14.5 nm, every 1 s	
	CO, NO_x, SO_2, BC, DustTrak DRX PM_1, $PM_{2.5}$, PM_4, PM_{10}, and PM_{15}	
CE	CO, NO_x, SO_2, BC, DustTrak DRX PM_1, $PM_{2.5}$, PM_4, PM_{10}, and PM_{15}	

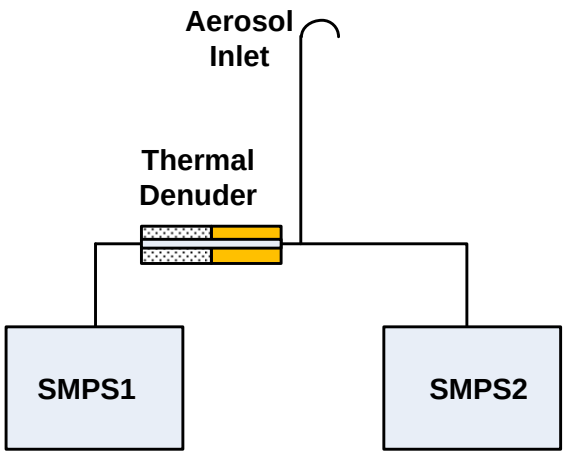

Figure 5-70. Schematic of particle volatility measurement setup during Supplemental Study A.

The TSI NSMPS measured the PSD passing through the TD while the TSI RSMPS measured the unheated PSD at the CE site from 9/4/12 (Tuesday) at approximately 15:00 to 9/5/12 (Wednesday) at approximately 15:00. During this period, the Grimm SMPS and the other TSI NSMPS were operated without a TD to evaluate comparability of the two SMPS at the TLCS site. From 9/5/12 (Wednesday) at approximately16:00 to 9/6/12 (Thursday) at approximately 16:00, the TD was positioned at the TLCS site and connected to the TSI NSMPS to measure the heated PSD, while the Grimm SMPS measured the unheated PSD for reference. During this period, the two SMPS at the CE site were run for a collocated comparison. Additional measured parameters at each site included continuous measurement of CO, NO_x, SO_2, BC, and DustTrak DRX PM_1, $PM_{2.5}$, PM_4, PM_{10}, and PM_{15}.

Supplemental Study B (High Time Resolution PSD)

Two SMPS were operated at the CE and TLCS sites for high time resolution measurement (without TD). At the CE site, the TSI RSMPS was set to measure 14.5 nm particle concentrations every second, while the TSI NSMPS was set to scan 10-53 nm PSD every 40 seconds. At the TLCS site, the Grimm SMPS was set to measure 14.5 nm particle concentrations every second, while the TSI NSMPS was set to scan 10-53 nm PSD every 40 seconds. Measuring a single size bin and a narrower size range rather than the entire range allowed operation with time resolution as short as one second rather than two to three minutes for full scans. The objective of this measurement was to simultaneously monitor very fine particles that may be associated with jet exhaust and larger particles that may be associated with on-road vehicle exhaust. Finer time resolution may reveal brief peaks in UFP concentrations that may be associated with the two sources. Measurements were made at both sites from 9/6/12 (Thursday) at approximately 18:00 to 9/10/12 (Monday) at approximately 12:00. UFP concentrations over the weekend and weekdays allowed for examination of diurnal and day-of-week variations. Additional measured parameters at each site included continuous measurement of CO, NO_x, SO_2, BC, and DustTrak DRX PM_1, $PM_{2.5}$, PM_4, PM_{10}, and PM_{15}.

Supplemental Study C (Blast Fence)

All four SMPS were used at the blast fence to measure different parameters (as shown in Figure 5-71). The Grimm SMPS measured 14.5 nm every second; the TSI RSMPS scanned 10-53 nm every 40 seconds; and the two TSI NSMPS were configured as a volatility tandem differential mobility analyzer (VTDMA) to measure particle volatility. As shown in Figure 5-71, in the VTDMA setup, the DMA1 selected a size of interest (5, 15, 30, or 50 nm), and the CPC1 measured the monodisperse particle concentration prior to heating. Particles passed through a heater set at ambient temperature, 50°C, 125°C, 175°C, 300°C, and 400°C. The residual particle size distribution was measured by DMA2 and CPC2 with time resolution of 40-135 s depending on the initial particle size. The 14.5 nm single size and 10-53 nm scan were measured continuously from 9/10/12 (Monday) at 16:40 to 9/11/12 (Tuesday) at 15:00. The VTDMA was set to measure changes to the 14.5 nm size particle at 125 °C from 9/10/12 (Monday) at 16:44 to 9/11/12 (Tuesday) at 08:37. On 9/11/12 from 09:00 to 15:00, size changes of 5, 15, 30, and 50 nm were measured at heater set temperatures of ambient, 50 °C, 125 °C, 175 °C, 300 °C, and 400 °C. Additional measured parameters including continuous measurement of CO, NO_x, SO_2, BC, and DustTrak DRX PM_1, $PM_{2.5}$, PM_4, PM_{10}, and PM_{15} were made at the blast fence and CE site.

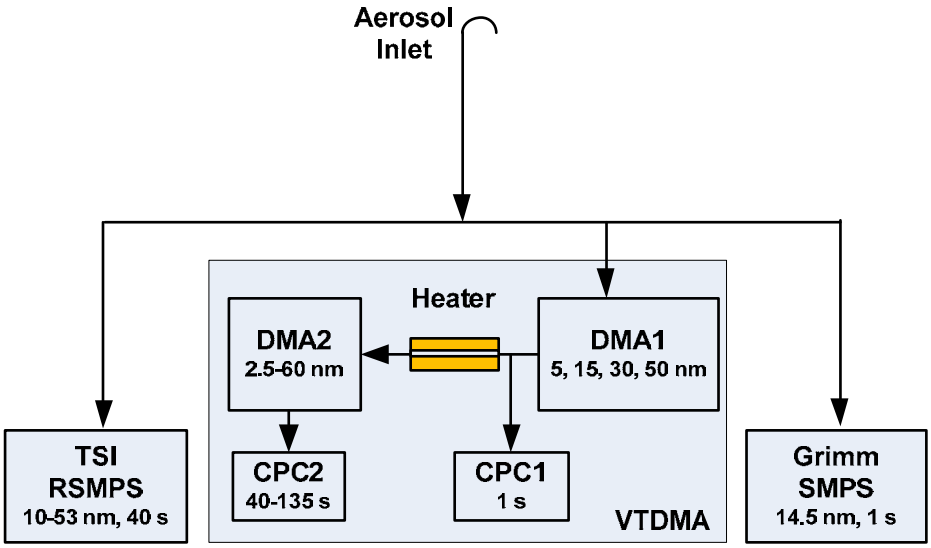

Figure 5-71. Schematic diagram of SMPS configuration at the blast fence during Supplemental Study C.

5.3.2 Particle Volatility Results for the CE and TLCS sites (Supplemental Study A)

Figure 5-72 shows particle size distributions with and without passing through the TD at various temperatures during one set of measurements. The particle size change was not significant at 50°C and 125°C, but was apparent at 175-400°C. Figure 5-73 plots the size-dependent ratio of particle concentrations that passed the TD to that did not pass the TD. The data were averaged from a total of 13 to 15 sets of TD-SMPS measurements, each set containing ambient temperature, 125°C, 175°C, and 300°C, and 3 to 4 sets containing addition temperature steps at 50°C and 400°C. Particle evaporation behaviors at the two sites were very similar. For particles

in the size range of 20-80 nm, the average concentration decreased by 10-15 percent at 125-175°C, while the reduction was 40-70 percent at 300-400 °C. Measurements for less than 20 nm were less reliable due to lower counting statistics. However, excessive increases (up to a factor of 20) in concentration of particles less than 20 nm after passing through the TD were observed during two runs (9/5/2012: 01:27:17 and 02:48:15) at the CE site. This was most likely due to breakdown of larger particles and/or renucleation of evaporated vapors. These reductions in particles sized 20-80 nm were much lower than the reductions in H_2SO_4 and $(NH_4)_2SO_4$ (Figure 5-78) and those observed at the blast fence Figure 5-79). Due to transformation and transport, particles at the CE and TLCS sites were quite different from those at the blast fence, which was dominated by fresh emissions.

5.3.3 High Time Resolution PSD Measurement Results (Supplemental Study B)

Figure 5-74 shows the concentrations of 14.5 nm particles measured at the CE and TLCS sites with a one second time resolution between 9/6/2012 at 18:00 to 9/10/2012 at 12:00. The CE site concentration showed more spikes than the TLCS, which indicates the direct influence of frequent intermittent sources such as jet exhaust. The average 14.5 nm concentration during this period was 2844 particle/cm^3 at the CE site, which was approximately three times that of the TLCS site (973 particle/cm^3). The TLCS concentration showed a clear pattern with higher concentrations from 12:00-18:00, probably due to activities in and around the TLCS site. The average particle size distribution measured during this period is shown in Figure 5-75. UFP concentrations at the CE site were 1.5-2.5 times higher than the TLCS site, confirming a greater impact from UFP sources.

One specific event of interest was observed at the TLCS site on Sunday 9/9/2012, as shown in Figure 5-76. From 6:00 to 18:00, there were very high concentrations of SO_2 and its temporal pattern was highly correlated (R^2=0.52-0.74) with UFP of all size ranges (10-20, 20-30, 30-40, and 40-50 nm), indicating a common source. During this period, on-road vehicle emission indicators (CO, NO, and BC) remained low and stable. Therefore, the SO_2 and UFP were most likely from a source other than vehicle traffic.

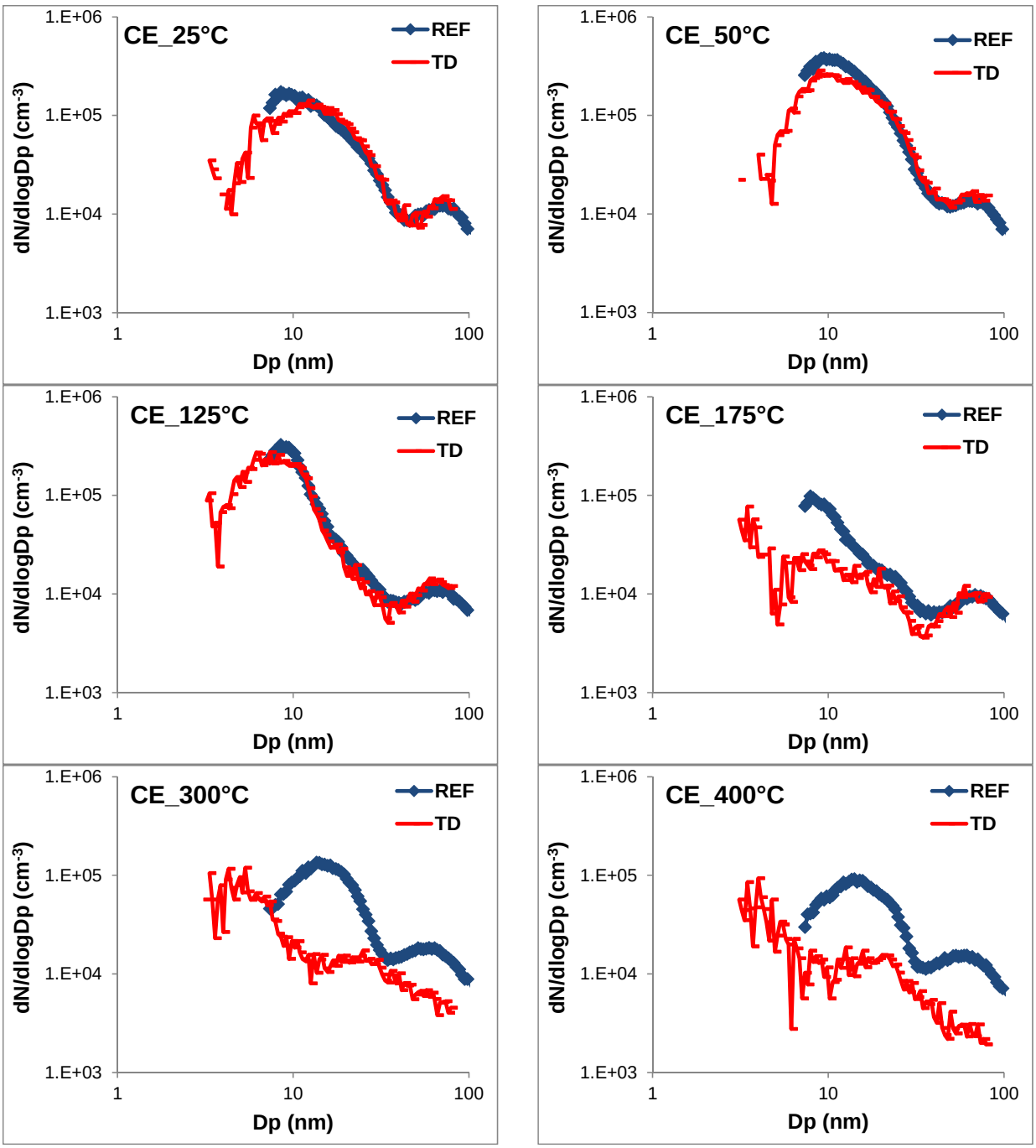

Figure 5-72. Example of particle size distribution with (TD) and without (REF) passing through the thermal denuder (TD) at the CE site during a series of scans (9/5/2012: 14:12-15:31).

a) CE

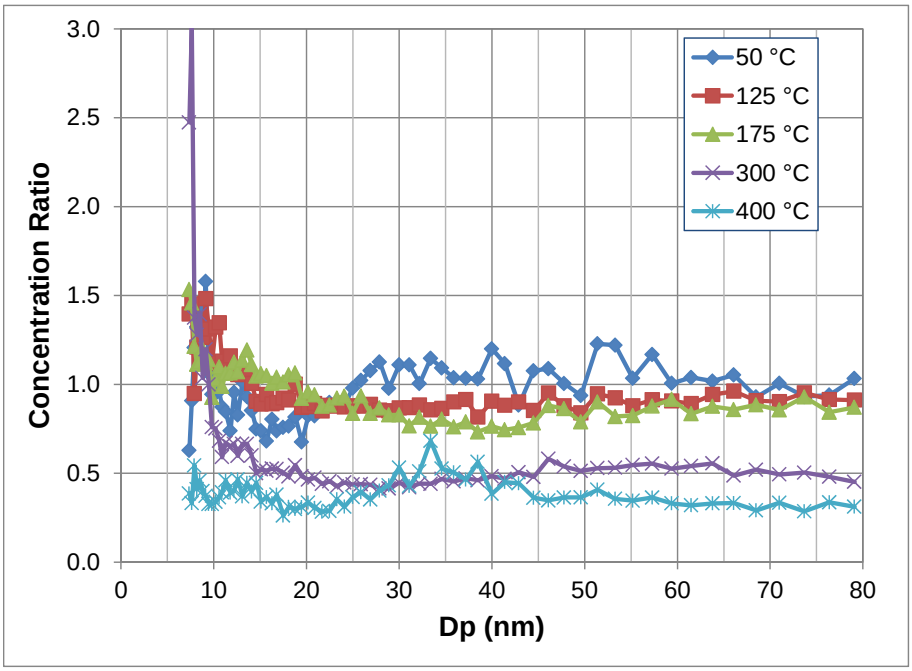

b) TLCS

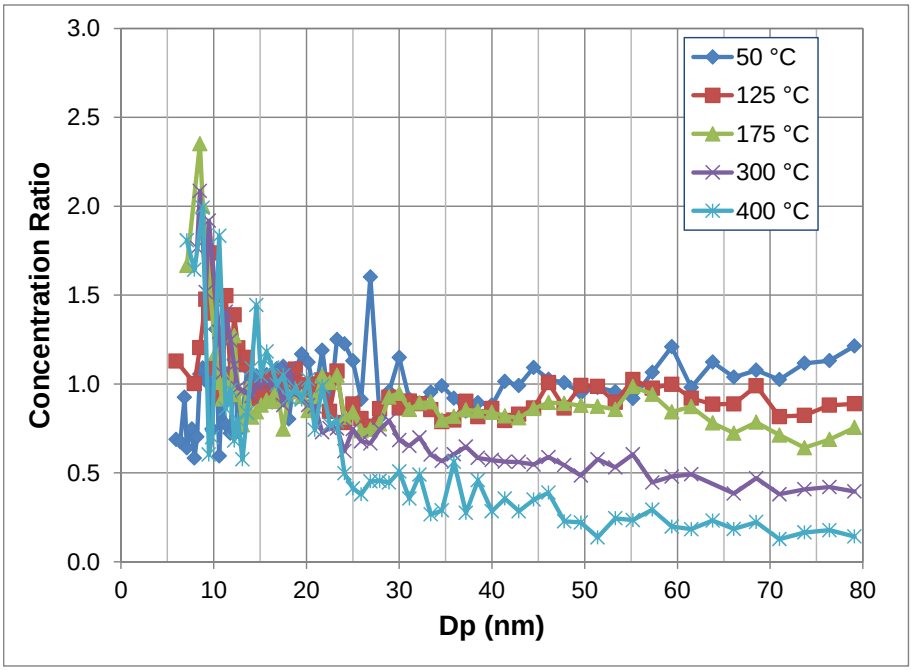

Figure 5-73. Ratio of size-dependent particle concentrations with and without passing through the thermal denuder (TD) at different temperatures at a) the CE and b) TLCS sites.

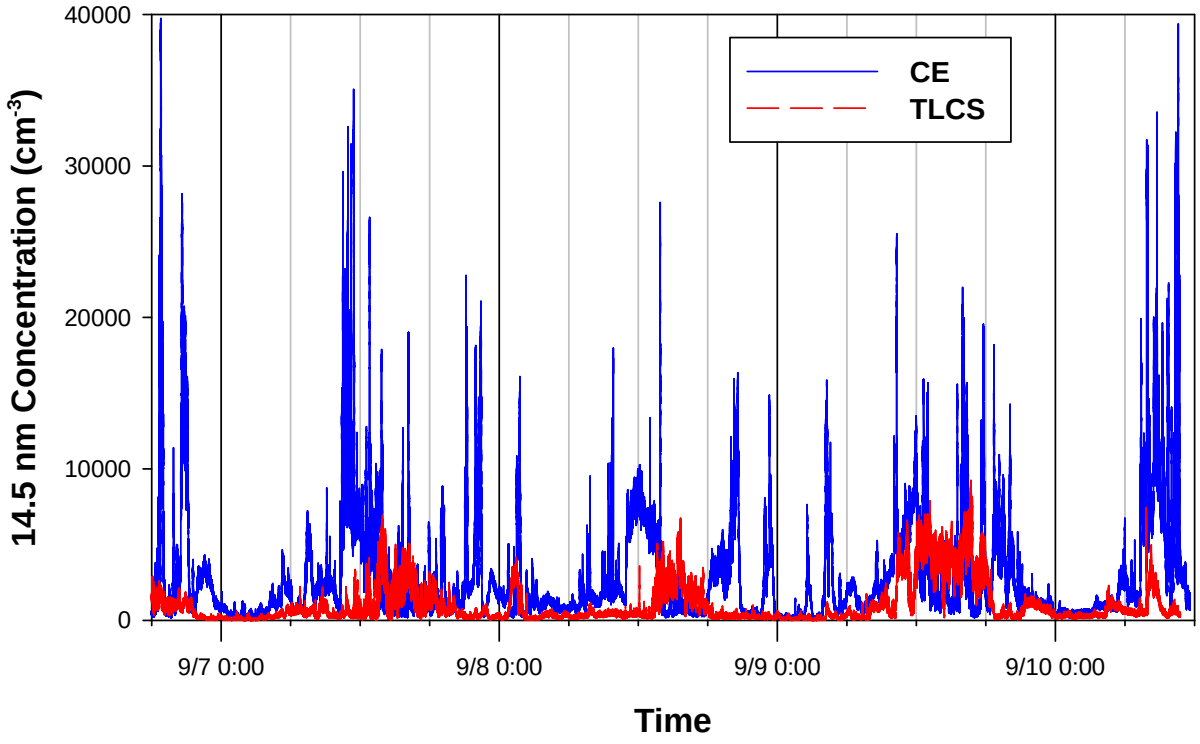

Figure 5-74. Concentrations of 14.5 nm particles at the CE and TLCS sites during 9/6/2012 18:00 to 9/10/2012 12:00.

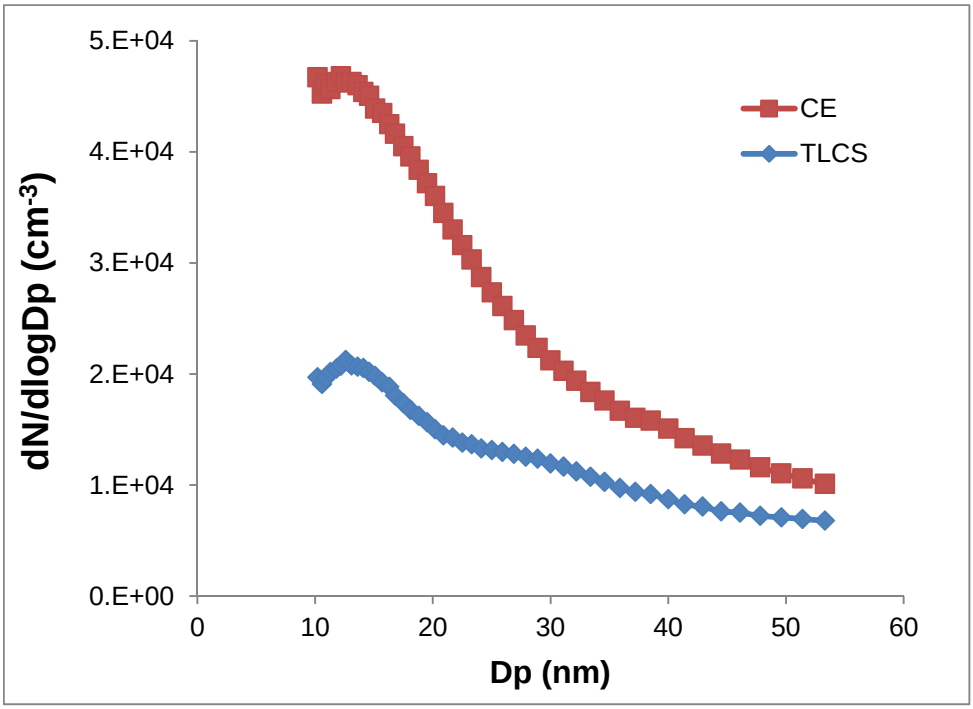

Figure 5-75. Average particle size distribution measured at the CE and TLCS sites during 9/6/2012 18:00 to 9/10/2012 12:00.

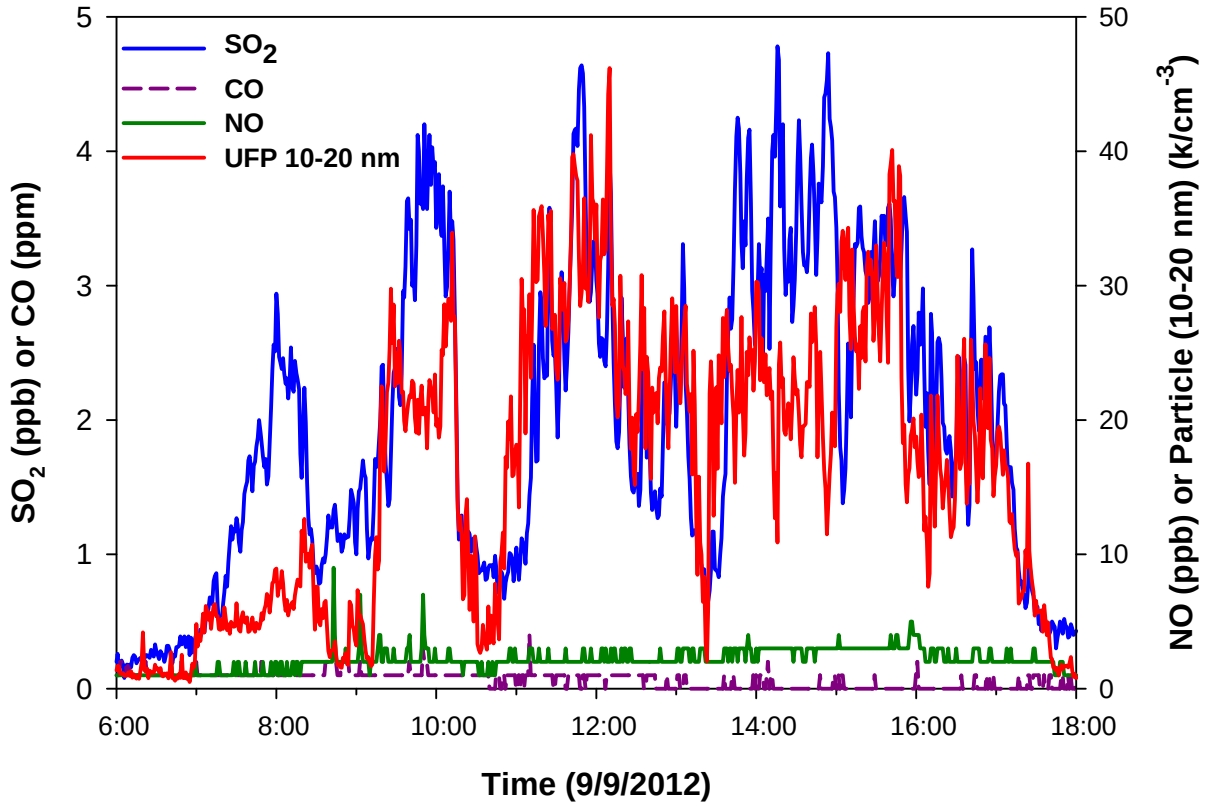

Figure 5-76. SO_2 and UFP event at the TLCS sites on 9/9/2012 (Sunday). The 10-20 nm range is plotted.

5.3.4 Blast Fence Experiment (Supplemental Study C)

Temporal Variations of Ultrafine Particle Size Bins Relative to Other Pollutants

Figure 5-77 shows times series plots of UFP 10-20 nm, UFP 30-50 nm, $PM_{2.5}$, PM_{10}, BC, CO, and SO_2 measured at the blast fence as well as the flight activity data. All pollutants showed similar temporal patterns because they were dominated by airport emissions. The 10-20 nm particle concentrations were approximately 15 times higher than 20-30 nm particle concentrations and approximately 100 times higher than 30-50 nm particle concentrations. Therefore, airport activities emit significantly higher numbers of smaller UFP. During 00:00 – 02:00, there were only airplane departures and no arrivals. All pollutants still showed spikes in concentrations, indicating departures contribute significantly to blast fence concentrations. During 02:00 – 06:00, there were very few arrivals or departures, and all pollutants dropped to very low levels, indicating that blast fence concentrations were dominated by airport operations.

Blast Fence Volatility Tandem Differential Mobility Analyzer Results

Figure 5-78 shows that laboratory-measured particle volume concentration changed after passing monodisperse 14.5 nm and 50 nm NaCl, H_2SO_4, and $(NH_4)_2SO_4$ particles through the heater at different temperatures. The laboratory test provides a volatility reference for field measurement. While NaCl particles did not evaporate, even at a heater set temperature of 300°C, H_2SO_4 and

$(NH_4)_2SO_4$ particles showed continuous evaporation at varying temperatures. At 50-175°C, the remaining particle volume was 50-70 percent of initial volume. At 300°C, almost all H_2SO_4, and $(NH_4)_2SO_4$ particles had evaporated. For an unknown reason, the H_2SO_4 and $(NH_4)_2SO_4$ had similar volatility behavior in this heater.

Figure 5-79 shows the particle volume concentration ratio at the blast fence after passing the monodisperse particles (ranging from 5 nm to 50 nm) through the thermal denuder at different set temperatures. The volatility tandem differential mobility analyzer (VTDMA) measurement requires the inlet PSD to be stable for 40-135 seconds during the size scan. However, the PSD at the blast fence changed significantly every few seconds due to landing and departing activities. Therefore, accurate measurement of the particle size distribution after passing the heater was not possible. Furthermore, the number of tests at each condition was limited. Therefore, the data in Figure 5-79 only provide a qualitative picture of particle volatility. Comparing the 14.5 nm particle measurements presented on Figure 5-78(a) and Figure 5-79(b) indicate that some particles at the blast fence were more volatile than H_2SO_4 and $(NH_4)_2SO_4$ since less than 20 percent of the particle volume remained after heating to 125 -175 °C. This is also true for 50 nm particles, although the limited amount of data together with a large amount of scatter that occurred made the information less definitive. The 30 nm particle measurements at the blast fence (Figure 5-79c) have a volatility similar to H_2SO_4 and $(NH_4)_2SO_4$. It was observed that particles of the same size had different volatility. For example, 5 nm particles at 125°C showed a range in the amounts of residual particles, although this may be partially caused by changes in ambient concentrations. However, 14.5 nm and 50 nm showed residual particles even at heater set temperature of 400 °C, indicating some particles are refractory (e.g., soot and ash).

Figure 5-80 shows an example of different residual particle size distributions after heating 14.5 nm to 400°C during two different scans after passing through the TD (indicated as W/TD-1 and W/TD-2) The PSD upstream of the heater (indicated as W/O TD) calculated from TDMA theory (Rader and McMurry, 1986) is plotted for comparison. The first distribution with TD (W/TD-1) showed the residual particles had a bimodal distribution, with one more volatile and the other less so. The W/TD-2 distribution showed these particles were mostly volatile with only a few particles left after heating. These results show particles of the same size are comprised of different chemical compositions, which change with time.

The heterogeneous nature of particle volatility is also shown in the overnight VTDMA measurement of 14.5 nm heated to 125 °C. As shown in Figure 5-81, the volume ratio varied from 0 to 2.5, with an average of 0.57, which were similar to those of H_2SO_4 and $(NH_4)_2SO_4$ presented in Figure 5-78. The ratios larger than one were due to VTDMA measurement error when the ambient PSD changed during the size scan or when the particle concentrations were very low.

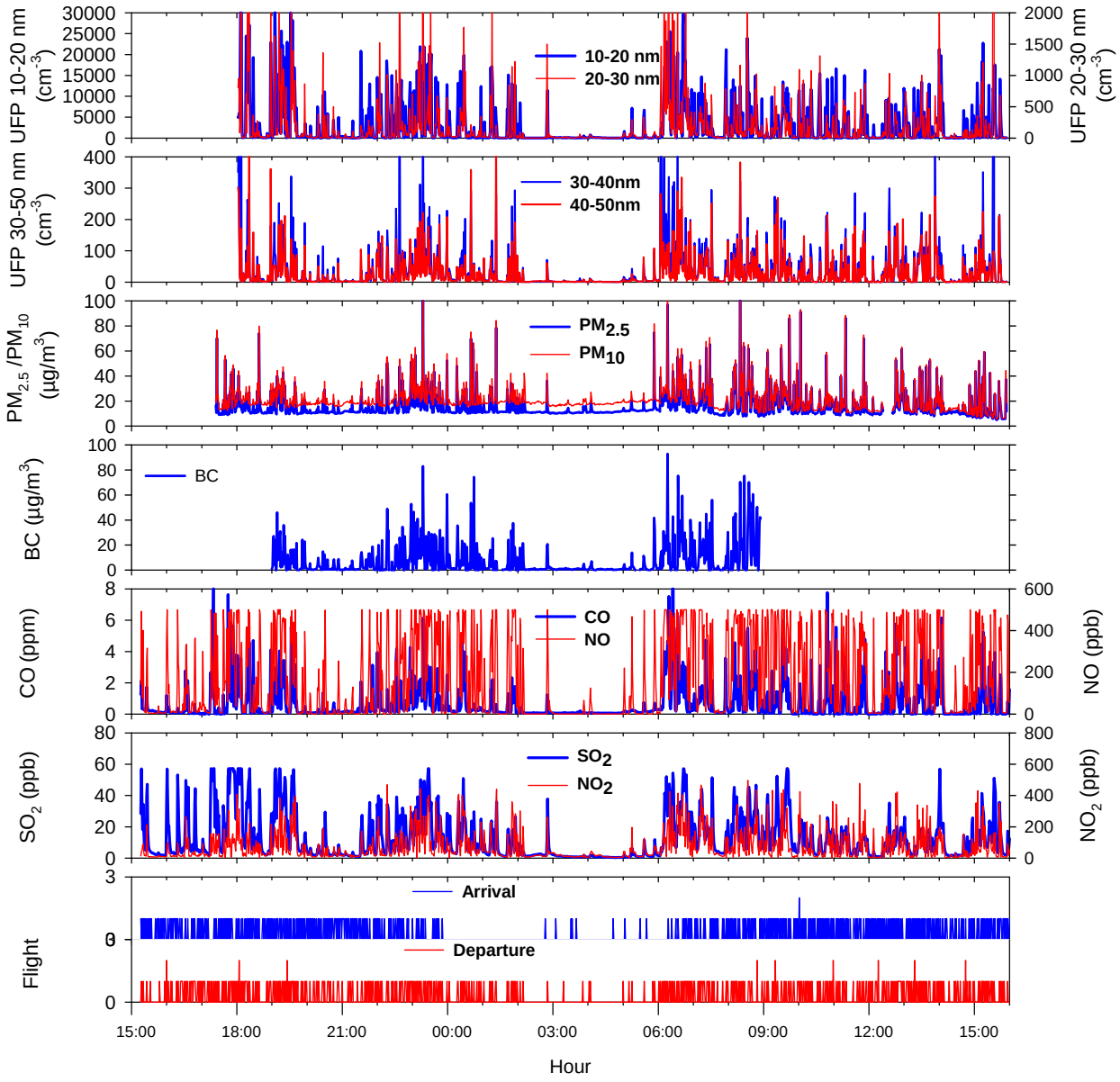

Figure 5-77. Time series of blast fence measurement during 9/10/2012 15:00 to 9/11/2012 16:00.

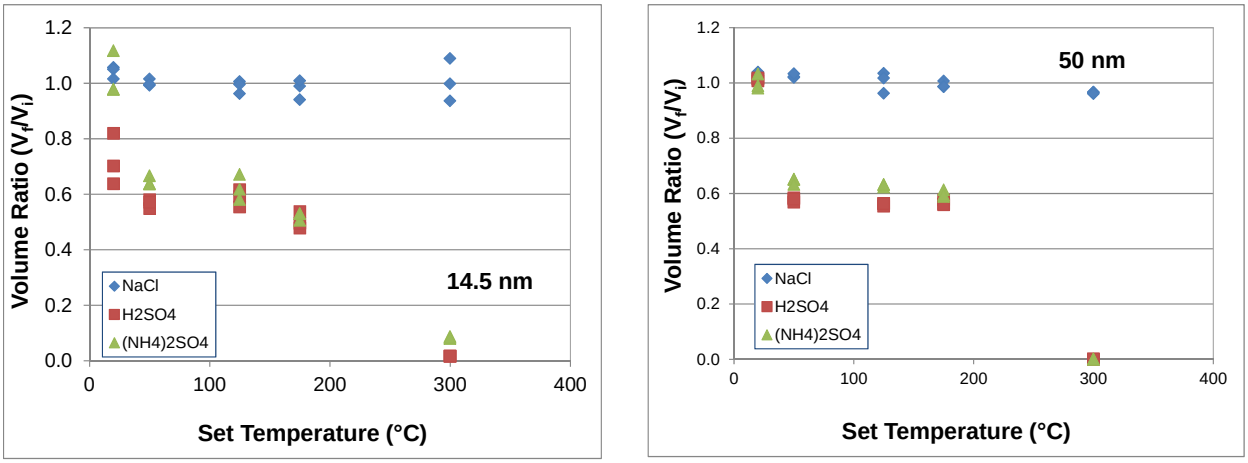

Figure 5-78. Laboratory-measured ratio of final (V_f) and initial (V_i) particle volume concentrations of NaCl, H_2SO_4, and $(NH_4)_2SO_4$ particles after being heated up to 300°C for initial sizes of a) 14.5 nm and b) 50 nm.

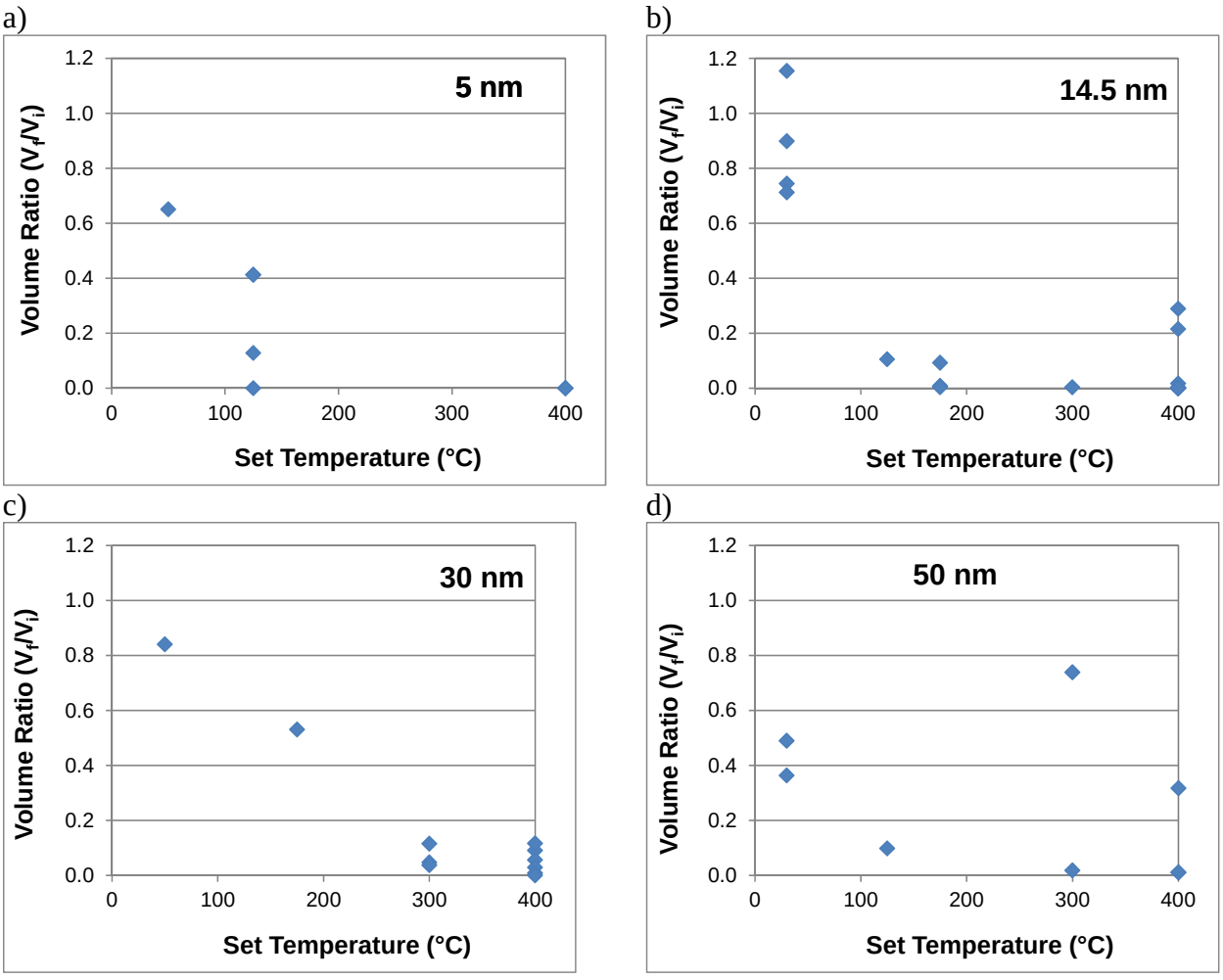

Figure 5-79. Particle volume concentration ratios at the blast fence after passing through the VTDMA heater set at different temperatures for initial sizes of a) 5 nm, b) 14.5 nm, c) 30 nm, and d) 50 nm.

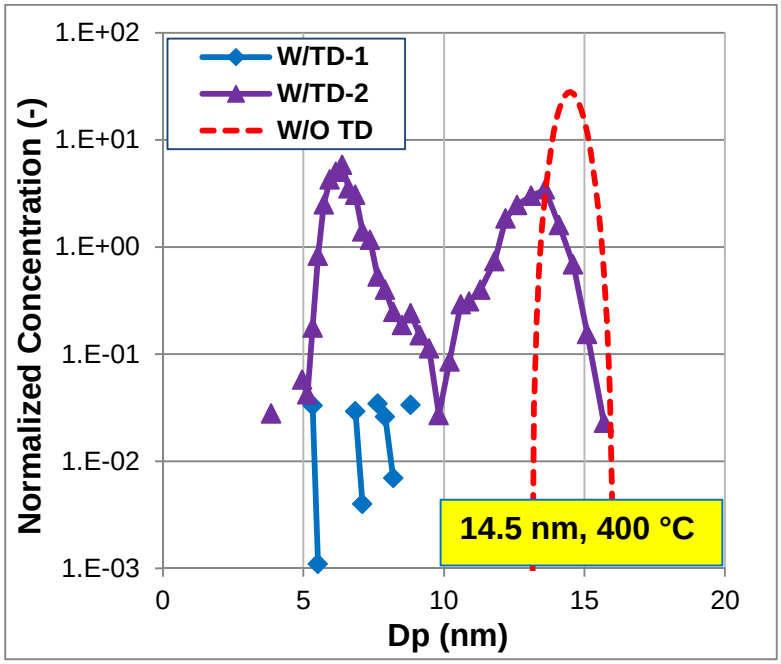

Figure 5-80. Illustration of 14.5 nm particle size distributions before and after heating to 400°C.

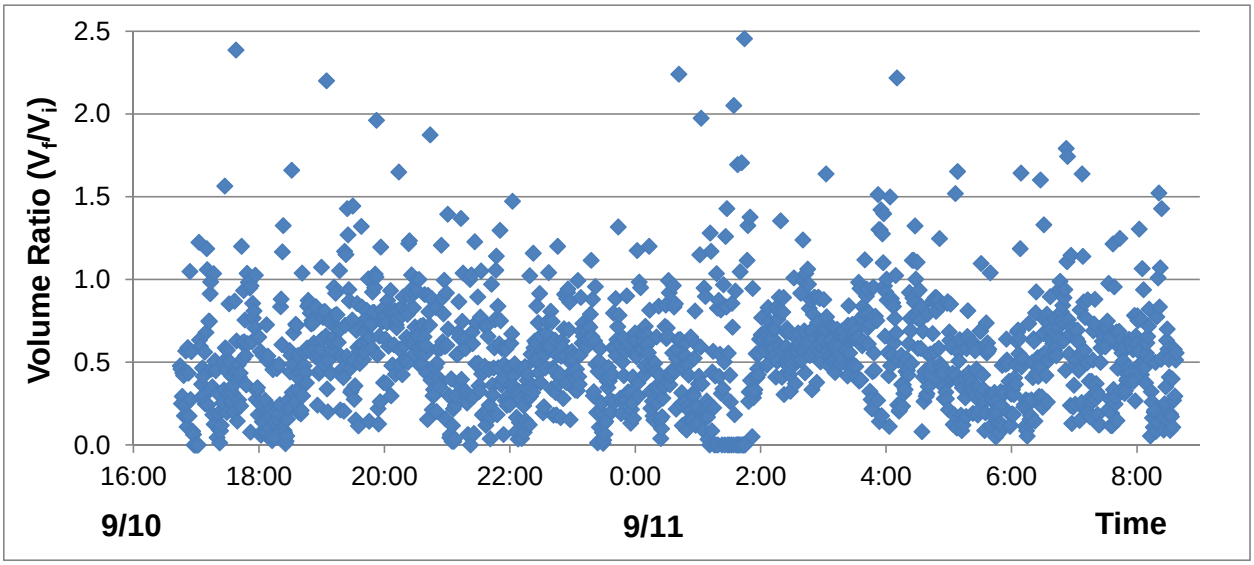

Figure 5-81. Particle volume concentration ratio at the blast fence after passing 14.5 nm particles through the VTDMA heater set at 125 °C during the period of 9/10/12 16:44 to 9/11/12 08:37.

5.4 FINDINGS AND CONCLUSIONS

The ambient air quality monitoring for the Phase III of the LAX AQSAS was designed to measure the spatial variations in seasonal average pollutant concentrations in the buffer zones and communities bordering LAX relative to near-source locations. Monitoring was also designed to characterize the diurnal and day-of-week variations in pollutant concentrations relative to source activity and changes in meteorological conditions. Special emphasis was given to the temporal variations in size distributions of UFP and correlations to other pollutants by time of day, day of week, varying meteorological conditions, and emission source activity. The associations between the spatial and temporal variations in pollutant concentrations with emission source activity and transport are qualitative indications of the impacts of airport emissions on local air quality relative to other emission sources. These results provide context and complement the source apportionment results obtained by CMB, NTA and dispersion modeling discussed in Sections 6, 7, and 9, respectively.

The time-integrated saturation monitoring data showing the highest pollutant concentrations were measured near airport runways and roadways. Although NO_x emission rates from commercial jets are high, they mix with NO_x emissions from other sources, which have total area-wide emissions that substantially exceed the contributions of jet exhaust. While higher NO_x concentrations were measured near both roadways and runways, most of the higher SO_2 concentrations were measured in close proximity to the airport runways. These results, along with the emission inventory data, indicate that ambient concentrations of SO_2 may serve as a tracer for jet exhaust near LAX and should correlate well with temporal variations in airport activity after accounting for the effects of pollutant transport. However, the hourly-average SO_2 levels measured at the four core sites were all well below the national and state air quality standards. BTEX emission rates from commercial jets were found to be relatively low and the spatial variations indicated that on-road gasoline-powered vehicles are likely the main source of BTEX. Therefore, spatial variations in BTEX levels were more uniform with higher levels near roadways. Ambient concentrations of aldehydes are spatially uniform because on-road vehicle are the main directly-emitting source of aldehydes along with the atmospheric formation from oxidation of precursor hydrocarbons, especially during the summer.

The diurnal and day-of-week variations in ambient pollutant concentrations and meteorological conditions were combined with the spatial and temporal patterns of pollutant emissions to examine potential impacts of local emission sources to pollutant concentrations at monitoring locations. During the Winter Season, morning winds were from the northeast until about 10:00, resulting in greater contributions from non-airport emissions at the CE and CN sites. The simultaneous peaks in CO, NO_x, and BC concentrations at these sites during the weekday (M-F) morning commute period can be attributed to on-road vehicle emissions. The significantly lower concentrations during the same time period on Sundays provide additional confirmation of this source attribution. In contrast, the SO_2 and UFP concentrations were low during this period at the CE, CN, and AQ sites, but substantially higher at the CS site. SO_2 and UFP concentrations gradually increased throughout the day at both the CE and CN sites after 10:00 when the wind direction changed from northeast to west, while concentrations near background levels were measured at both the CS and AQ sites. These results, coupled with the minimal weekday dependences for both SO_2 and UFP, indicate airport emissions were the main source of SO_2 and

UFP measured at the core monitoring sites during the Winter Monitoring Season. It appears that the CN and CE sites were potentially impacted by airport emissions from late morning to evening during the Winter Monitoring Season. The CS site was impacted during a relatively brief period from about 06:00 to 10:00. The monitoring data from the AQ site show little evidence of impact from airport emissions.

The potential impacts of local sources within the Study Area during the Summer Season differ from the Winter Season due to seasonal changes in pollutant transport patterns. Winds during the summer were more consistently from the west. Light to calm (< 1 m/sec) overnight winds from the west changed to west-southwest between daybreak and about 09:00 to 10:00. Wind speeds during midday were from the west at a maximum average speed of about 3 to 4 m/sec. Airport emissions were potentially transported to the CN and CE sites at all hours of the day and night during the Summer Season in contrast to the Winter Season when this did not occur during the overnight and early morning hours when the winds were from the northeast. Consequently, SO_2 and UFP concentrations were higher earlier in the day during the Summer Season at both the CE and CN sites, while SO_2 and UFP concentrations at the CS site were much lower compared to the Winter Season. Pollutant concentrations were very low at both the CS and AQ sites throughout the day and night due to the persistent west winds during the Summer Season. Diurnal patterns for NO_x, CO, and BC were similar during the Winter Season at the CE and CN sites with concentrations observed to have morning peaks, very low midday levels and increasing during the evening starting at about sunset. Daytime and early evening concentrations were lower for all pollutants at the CE and CN sites during the Summer Season due to greater vertical mixing and later development of the stable nocturnal inversion layer, which occurs in the summer after the evening commute. The substantially lower NO_x, CO, and BC levels at the CE and CN sites during the weekend mornings in both seasons are indications that on-road motor vehicles are likely the predominant source of these pollutants. Differences between the weekday and weekend were comparatively less for SO_2. UFP number concentrations showed no day-of-week dependence. This indicates these pollutant concentrations are associated primarily with jet exhaust.

Diurnal variations in PSD can provide useful insight regarding the relative importance of both freshly emitted and secondary particles. Furthermore, the day-of-week dependence on diurnal variations of PSD and correlations of specific particle size ranges with other pollutants may be related to the relative contributions of different emission sources. Differences in correlations of UFP with other pollutants and day-of-week variations in diurnal profiles in 7-30 nm and 30-160 nm particles suggest that particles in the two size ranges may have different origins. Good correlations of the 30-160 nm particles with CO, NO, and BC and strong weekday dependence of diurnal variations indicate an association of these particles with vehicle emissions. In contrast, the poorer correlation of 7-30 nm particles with these mobile source pollutants and stronger correlations with SO_2 and NO_2 suggest contributions of jet exhaust and possibly secondary particles. The VTDMA measurements behind the blast fence at the end of the South Airfield Runway 25R provided evidence of volatile sulfuric acid and ammonium sulfate in the smallest UFP size range. On average, about 30 to 50 percent of the UFP were not nonvolatile.

5.5 REFERENCES

Arnott WP, Moosmüller H, Rogers CF, Jin T, Bruch R. (1999). Photoacoustic spectrometer for measuring light absorption by aerosols: Instrument description. Atmos Environ 33:2845-2852.

Arnott, W. P., K. Hamasha, H. Moosmüller, P.J. Sheridan and J.A. Ogren (2005). "Towards Aerosol Light Absorption Measurements with a 7-Wavelength Aethalometer: Evaluation with a Photoacoustic Instrument and 3-Wavelenght Nephelometer." Aerosol Sci. and Technol. 39:17-29.

Burtscher, H.; Baltensperger, U.; Bukowiecki, N.; Cohn, P.; Hüglin, C.; Mohr, M.; Matter, U.; Nyeki, S.; Schmatloch, V.; Streit, N.; Weingartner, E. (2001). Separation of volatile and non-volatile aerosol fractions by thermodesorption: instrumental development and applications. *Journal of Aerosol Science*, 32(4):427-442. http://www.sciencedirect.com/science/article/pii/S0021850200000896.

California Air Resources Board. (2008). "Diesel Particulate Matter Health Risk Assessment for the West Oakland Community." Available on-line at http://www.arb.ca.gov/ch/communities/ra/westoakland/documents/westoaklandreport.pdf

Chow, J.; Watson, J.; Crow, D.; Lowenthal, D.; Merrifield. T. Comparison of IMPROVE and NIOSH Carbon Measurements. *Aerosol Science and Technology*, 2001, 34(1): 23-34.

Chow J.C.; Watson, J.G.; Chen, A.L.-W.; Arnott, W.P; Moosmuller H.; Fung, K. Equivalence of Elemental Carbon by Thermal/Optical Reflectance and Transmittance with Different Temperature Protocols. *Environ. Sci. Technol***.** 2004. 38, 4414-4422.

Fine, P. (2011). Personal communication on September 22, 2011.

Fujita EM., Campbell DE, Zielinska B, Sagebiel JC, Bowen JL, Goliff W, Stockwell WR, and Lawson DR. 2003. Diurnal and weekday variations in source contributions of ozone precursors in California's south coast air basin. J Air Waste Manage Assoc 53:844-863.

Fujita, E.M.; Zielinska, B.; Campbell D.E.; Arnott, W.P.; Sagebiel, J.C.; Reinhart, L.; Chow, J.C.; Gabele, P.A.; Crews, W.; Snow, R.; Clark, N.N.; Wayne, W.S.; and Lawson D.R. Variations in speciated emissions from spark-ignition and compression-ignition motor vehicles in California's South Coast Air Basin. *J. Air Waste Manage. Assoc.*, 2007, 57: 705-720.

Fujita, EM., Zielinska B, Campbell DE, Arnott WP. 2007. Evaluations of source apportionment methods for determining contributions of gasoline and diesel exhaust to ambient carbonaceous aerosols. *J Air Waste Manage Assoc*, 57:721-740.

Fujita, E.M., B. Mason, D.E. Campbell and B. Zielinska (2009). Harbor Community Monitoring Study – Saturation Monitoring. Final report submitted to the California Air Resources Board, Sacramento, CA, May 15, 2009.

Fujita, E.M., D.E. Campbell, B. Zielinska, W.P. Arnott, J.C. Chow (2008). Concentrations of Air Toxics in Motor Vehicle Dominated Microenvironments. Final report submitted to the Health Effects Institute, HEI contract 4704-RFA03-1/02-16, Boston, MA, January 13, 2008.

Fujita, E.M., D.E. Campbell, B. Mason, B. Zielinska (2009). Harbor Community Monitoring Study (HCMS) Saturation Monitoring. Final report submitted to the California Air Reesources Board, Sacramento, CA, May 15, 2009.

Fujita, E.M. and D.E. Campbell (2010). West Oakland Monitoring Study. Final report prepared for the Bay Area Air Quality Management District, San Francisco, CA, October 7, 2010.

Mason, J. Brooks E.M. Fujita, D.E. Campbell and B. Zielinska (2011): Evaluation of Passive Samplers for Assessment of Community Exposure to Toxic Air Contaminants and Related Pollutants, *Environ. Sci. Technol*. 2011, 45, 2243–2249.

Rader, D.J.; McMurry, P.H. (1986). Application of the Tandem Differential Mobility Analyzer to Studies of Droplet Growth or Evaporation. *J. Aerosol Sci*., 17(5):771-787.

Westerdahl D, Fruin S, Sax T, Fine P, Sioutas C. 2005. Mobile platform measurements of ultrafine particles and associated pollutant concentrations on freeways and residential streets in Los Angeles. Atmos Envir 39:3597-3610.

Westerdahl D, Fruin S, Fine P, Sioutas C. 2007. The Los Angeles International Airport as a source of ultrafine particle and other pollutants to nearby communities. Atmos Envir 42:3143-3155.

Zhu, Y.F, Hinds, W.C, Kim, S, Shen, S, Sioutas, C. (2002) Study of ultrafine particles near a major highway with heavy-duty diesel traffic; Atmospheric Environment, 36, 4323-4335.

(This page is intentionally blank)

Section 6

CHEMICAL MASS BALANCE

(This page is intentionally blank)

Table of Contents

List of Tables

List of Figures

6. RECEPTOR MODELING RESULTS – CHEMICAL MASS BALANCE

The Chemical Mass Balance (CMB) receptor model was used to estimate the source contributions to the ambient concentrations of particulate matter 2.5 µm or less in diameter ($PM_{2.5}$), organic carbon (OC), elemental carbon (EC), volatile organic compounds (VOC), and gaseous air toxics (e.g., benzene, toluene, ethylbenzene and xylenes) measured at the core community monitoring sites in Westchester, Lennox, and El Segundo. No speciated VOC or PM samples were collected at the AQ site, so it is not included in the source apportionment. The source composition profiles used in the CMB analysis included several profiles developed by the Desert Research Institute (DRI) in prior emission source characterization and receptor modeling studies. Supplemental source profiles were developed as part of the LAX AQSAS for fuels (Jet-A, diesel, and gasoline) and jet exhaust from samples collected at the end of the South Airfield Runway 25R. This section describes the ambient speciation data, compiled source composition profiles, and results of the source contribution estimates derived from the CMB analysis.

6.1 CHEMICAL MASS BALANCE RECEPTOR MODEL

Receptor models have been widely used to estimate the contributions of various sources to measured volatile organic compounds and particulate matter concentrations (Hopke, 1997; Henry, 1997; Watson et al. 2001a; Watson et al., 2001b). The ambient source apportionments were obtained for this study using Version 8.0 of the CMB receptor model (Watson et al. 1984). The CMB model infers contributions from different source types. This is done by using multivariate measurements taken at receptor locations and the abundances of chemical components in source emissions. The model consists of a least-squares solution to a set of linear equations that expresses each receptor concentration of a chemical species as a linear sum of products of source profile species and source contributions. The source profile species and the receptor concentrations, each with uncertainty estimates, serve as input data to the CMB model. The CMB software applies the effective variance solution, which gives greater influence in the solution to chemical species that are measured more precisely in both source and receptor samples. The software also calculates uncertainties for source contributions from both the source and receptor uncertainties.

The source contribution estimates (SCE) are the main output of the CMB model. The sum of these concentrations approximates the total mass concentrations. When the SCE is less than its standard error, the source contribution is undetectable. Negative SCE values do not provide meaningful data, but can occur when a source profile is collinear with another profile or when the source contribution is close to zero. The reduced chi square (χ^2), coefficient of determination (R^2), and percent mass are degree of fit measures for the least-squares calculation. The χ^2 is the weighted sum of squares of the differences between calculated and measured fitting species concentrations. The weighting is inversely proportional to the squares of the precision in the source profiles and ambient data for each species. χ^2 values greater than 4 indicate one or more of the fitting species concentrations are not well-explained by the source contribution estimates. An R^2 value ranging from 0 to 1 is determined by the linear regression of the measured versus model-calculated values for the fitting species. The closer the value is to 1, the better the SCEs explain the measured concentrations. Percent mass is the percent ratio of the sum of model-calculated SCEs to the measured mass concentration.

Secondary pollutants, which are formed by atmospheric reactions of primary pollutants, often constitute a major fraction of $PM_{2.5}$. The contributions of ammonium nitrate and ammonium sulfate to $PM_{2.5}$ were determined directly from measurements of ammonium, nitrate, and sulfate ions in the aerosol samples. Receptor models cannot apportion these secondary pollutants to specific sources of the gaseous precursors (i.e., sulfur dioxide, nitrogen oxides, and ammonia). Similarly, it is not possible to apportion secondary organic aerosols (SOA), which are derived from chemical reactions and gas-to-particle conversion of VOC and semi-volatile organic compounds (SVOC) emitted by both anthropogenic and natural sources. SOA can subsequently form new aerosol particles by nucleation, adsorption or absorption on preexisting aerosols or cloud particles. Under conditions where there is high confidence that all important direct primary sources of particulate matter are incorporated into the molecular marker CMB models, the residual (or unexplained) OC mass provides an upper limit estimate of the secondary organic aerosol contribution.

The VOC source composition profiles used in the CMB calculations were expressed as weight fractions of the sum of the 55 Photochemical Assessment Monitoring Station (PAMS) target hydrocarbon species shown in Table 6-1. These compounds typically account for about 80 percent of the ambient hydrocarbons in urban areas. The source profile data reported in units of ppbC were converted to $\mu g/m^3$ prior to calculating the weight fractions using species-specific conversion factors. One-sigma uncertainties were derived from variations among multiple measurements for a particular source type or the propagated analytical uncertainty. The assigned uncertainties are the larger of the two values.

A prerequisite for using receptor models is that the relative proportions of chemical species change little between source and receptor. Most ambient NMHCs are oxidized with tropospheric lifetimes ranging from hours to several months.[1] Estimates of nominal afternoon summertime residence times for a reactive environment (e.g., Los Angeles) are presented in Table 6-1. These estimates provide indications of which components are likely to remain relatively stable between source and receptor, thereby qualifying as fitting species for CMB source apportionment. Table 6-1 lists three sets of default fitting species for the four types of PAMS sites, which are characterized by their location relative to emission sources and patterns of pollutant transport in the atmosphere. Type 2 PAMS sites are located within or immediately downwind of the area of maximum precursor emissions. All three LAX AQSAS core sites would be classified as Type 2 sites. An expanded list of hydrocarbons (36 species) is used as fitting species at Type 2 sites for samples collected in the morning hours prior to 09:00, since the emissions are largely unreacted. A shorter list of more stable species (20 species) is used for samples collected at these sites during the afternoon or over a 24 hour period. The other three types of PAMS sites are not relevant to this study. Type 1 sites characterize upwind background, Type 3 sites monitor maximum ozone concentrations downwind from the fringe of the urban area, and Type 4 sites characterize the extreme downwind transported ozone and its precursor concentrations exiting the area.

[1] The atmospheric lifetime for a compound in the air is typically the time necessary for the compound concentration to decay to a value that is approximately 0.37 (37 percent) of its initial concentration.

Table 6-1. Photochemical Assessment Monitoring Station (PAMS) target species and their reactivity.

	Mnemonics[1]	Names	Formula	AIRS Code	convert to ug/m3	MW	Group	k_{OH} at 298 K	Lifetime hours	CMB Fitting Species Type 2 AM	Type 2 PM	Types 1,3, & 4
1	ETHENE	ethene	C2H4	43203	0.5736	28.05	O	8.52	6.52	*		
2	ACETYL	acetylene	C2H2	43206	0.5325	26.04	Y	0.90	61.73	*	*	*
3	ETHANE	ethane	C2H6	43202	0.6149	30.07	P	0.27	207.30	*	*	*
4	PROPE	Propene	C3H6	43205	0.5737	42.08	O	26.30	2.11			
5	N_PROP	n-propane	C3H8	43204	0.6012	44.10	P	1.15	48.31	*	*	*
6	I_BUTA	isobutane	C4H10	43214	0.5943	58.12	P	2.34	23.74	*	*	*
7	LBUT1E	1-butene	C4H8	43280	0.5737	56.11	O	31.40	1.77			
8	N_BUTA	n-butane	C4H10	43212	0.5943	58.12	P	2.54	21.87	*	*	*
9	T2BUTE	t-2-Butene	C4H8	43216	0.5737	56.11	O	64.00	0.87			
10	C2BUTE	c-2-butene	C4H8	43217	0.5737	56.11	O	56.40	0.99			
11	IPENTA	isopentane	C5H12	43221	0.5902	72.15	P	3.90	14.25	*	*	*
12	PENTE1	1-pentene	C5H10	43224	0.5737	70.13	O	31.40	1.77			
13	N_PENT	n-pentane	C5H12	43220	0.5902	72.15	P	3.94	14.10	*	*	*
14	I_PREN	isoprene	C5H8	43243	0.5571	68.11	O	101.00	0.55	+	+	+
15	T2PENE	t-2-Pentene	C5H10	43226	0.5737	70.13	O	67.00	0.83			
16	C2PENE	c-2-pentene	C5H10	43227	0.5737	70.13	O	65.00	0.85			
17	BU22DM	2,2-dimethylbutane	C6H14	43244	0.5874	86.17	P	2.32	23.95	*	*	*
18	CPENTA	cyclopentane	C5H10	43242	0.5737	70.13	P	5.16	10.77	*	*	
19	BU23DM	2,3-dimethylbutane	C6H14	43284	0.5874	86.17	P	6.20	8.96	*		
20	PENA2M	2-methylpentane	C6H14	43285	0.5874	86.17	P	5.60	9.92	*	*	
21	PENA3M	3-methylpentane	C6H14	43230	0.5874	86.17	P	5.70	9.75	*	*	
22	P1E2ME	2-methyl-1-pentene	C6H12	43246	0.5737	84.16	O	31.40	1.77			
23	N_HEX	n-hexane	C6H14	43231	0.5874	86.17	P	5.61	9.90	*	*	
24	MCYPNA	Methylcyclopentane	C6H12	43262	0.5737	84.16	P	8.81	6.31	*		
25	PEN24M	2,4-dimethylpentane	C7H16	43247	0.5855	100.20	P	5.10	10.89	*	*	
26	BENZE	benzene	C6H6	45201	0.5324	78.11	A	1.23	45.17	*	*	*
27	CYHEXA	cyclohexane	C6H12	43248	0.5737	84.16	P	7.49	7.42	*		
28	HEXA2M	2-methylhexane	C7H16	43263	0.5737	98.19	P	6.79	8.18	*		
29	PEN23M	2,3-dimethylpentane	C7H16	43291	0.5855	100.20	P	4.87	11.41	*	*	
30	HEXA3M	3-methylhexane	C7H16	43249	0.5855	100.20	P	7.16	7.80	*	*	
31	PA224M	2,2,4-trimethylpentane	C8H18	43250	0.584	114.23	P	3.68	15.10	*	*	*
32	N_HEPT	n-heptane	C7H16	43232	0.5855	100.20	P	7.15	7.77	*		
33	MECYHX	methylcyclohexane	C7H14	43261	0.5737	98.19	P	10.40	5.34	*		
34	PA234M	2,3,4-trimethylpentane	C8H18	43252	0.584	114.23	P	7.00	7.94	*		
35	TOLUE	toluene	C7H8	43202	0.5384	92.14	A	5.96	9.32	*	*	
36	HEP2ME	2-methylheptane	C8H18	43260	0.5829	114.23	P	8.18	6.80	*	*	
37	HEP3ME	3-methylheptane	C8H18	43253	0.584	114.23	P	8.56	6.49	*		
38	N_OCT	n-octane	C8H18	43233		114.22	P	8.68	6.40	*		
39	ETBZ	ethylbenzene	C8H10	45203	0.5427	106.16	A	7.10	7.82	*		
40	MP_XYL	mp-xylene	C8H10	45109	0.5427	106.16	A	18.95	4.71			
41	STYR	styrene	C8H8	45220	0.5324	104.14	A	58.00	0.96			
42	O_XYL	o-xylene	C8H10	45204	0.5428	106.17	A	13.70	4.06			
43	N_NON	n-nonane	C9H20	43235	0.5829	128.26	P	10.20	5.45	*		
44	IPRBZ	isopropylbenzene	C9H12	45210	0.5462	120.20	A	6.50	8.55	*		
45	N_PRBZ	n-propylbenzene	C9H12	45209	0.5462	120.20	A	6.00	9.26	*		
46	M_ETOL	m-ethyltoluene	C9H12	45212	0.5462	120.20	A	19.20	2.89			
47	P_ETOL	p-ethyltoluene	C9H12	45213	0.5462	120.20	A	12.10	4.59			
48	BZ135M	1,3,5-trimethylbenzene	C9H12	45207	0.5462	120.20	A	57.50	0.97			
49	O_ETOL	o-ethyltoluene	C9H12	45211	0.5462	120.20	A	12.30	4.52			
50	BZ124M	1,2,4-trimethylbenzene	C9H12	45208	0.5462	120.20	A	32.50	1.71			
51	N_DEC	n-decane	C10H22	43238	0.582	142.29	P	11.60	4.79	*		
52	BZ123M	1,2,3-trimethylbenzene	C9H12	45225	0.5462	120.20	A	32.70	1.70			
53	DETBZ1	m-diethylbenzene	C10H14	45218		134.22	A	14.20	3.90			
54	DETBZ2	p-diethylbenzene	C10H14	45219		134.22	A	14.20	3.90			
55	N_UNDE	n-undecane	C11H24	43954		156.30	P	13.20	4.20	*		
	TNMOC											
	PAMHC											
	UNID											
	MTBE											

A = aromatic, AL = Aldehyde, O = alkene (olefin), P = parafin, Y = alkyne, K = ketone, E = ether, X = haogenated, OH = alcohol

Note: Rate constants k at 298 K for the reaction of OH radicals with VOCs.

Unit: 1012 x k cm3 molecule-1 s-1

\+ - a marker for biogenic emissions

Hydrocarbons with lifetimes generally greater than approximately 8 hours were used as fitting species for CMB analysis of the LAX AQSAS ambient VOC data. An exception is isoprene,

which is included as a fitting species despite its high reactivity because it serves as a marker for biogenic emissions. The larger alkanes, n-tetradecane, n-pentadecane, n-hexadecane, n-heptadecane and n-octadecane were also included with the Type 2 PM list of 20 fitting species to potentially provide better discrimination among gasoline, diesel, and jet fuel combustion exhaust. These longer-chain alkanes are more reactive than the Type 2 AM threshold used in Table 6-1. Their ambient concentrations were generally low and influences on the CMB apportionments were relatively small. Since the CMB model calculations are based upon non-reactive fitting species, the predicted concentrations typically exceed the measured values by margins that increase with increasing reactivity of the species. Several of the reactive species were retained in the CMB modeling as "floating species" to verify these expectations. Compounds with potential analytical problems, such as coelution of peaks during gas chromatographic analysis, were excluded as fitting species.

6.2 AMBIENT SPECIATION MEASUREMENTS FOR PHASE III OF THE LAX AQSAS

Up to 14 sets of 24-hour (midnight to midnight) VOC and $PM_{2.5}$ samples were collected at each core monitoring site (CE, CN and CS) during both winter 2012 (Winter Monitoring Season) and summer 2012 (Summer Monitoring Season) and were analyzed at the DRI laboratory (see Table 6-2). Samples were collected during the Winter Season on 2/15 (W), 2/16 (Th), 2/19 (Su), 2/20 (M), 2/22 (W), 2/23 (Th), 2/26 (Su), 2/27 (M), 2/29 (W), 3/1 (Th), 3/4 (Su), 3/5 (M), 3/7 (W), and 3/8 (Th), and during the Summer Season on 8/1 (W), 8/2 (Th), 8/5 (Su), 8/6 (M), 8/8 (W), 8/9 (Th), 8/12 (Su), 8/13 (M), 8/15 (W), 8/16 (Th), 8/19 (Su), 8/20 (M), 8/22 (W), and 8/23 (Th). The sets of speciation samples included:

- Teflon and quartz filters collected with medium-volume sequential filter samplers (SFS) for $PM_{2.5}$ mass, OC, EC, elements (sodium [Na] to uranium [U] by XRF and Mg, Al, Ca, V, Fe, Cr, Mn, Ni, Cu, Zn, Mo, Ag, Cd, Sn, Ba, Ce, Hg and Pb by ICPMS), and nitrate, sulfate, ammonium, sodium, and chloride ions;

- Teflon-impregnated glass fiber filters (TIGF) with backup XAD resin cartridges for separate analysis of 49 particulate and semi-volatile phase alkanes, 95 polycyclic aromatic hydrocarbons (PAHs), 15 hopanes and steranes, and 99 polar organic compounds;

- whole air canister samples for 71 C_2-C_{11} hydrocarbons; Tenax cartridges for 66 C_8-C_{28} hydrocarbons; and

- DNPH cartridges for 14 C_1-C_8 aldehydes and ketones.

Sampling and analytical methods are described in Section 3.

In addition to the spatial density and rates of pollutant emissions, meteorology is the dominant factor controlling air quality from one day to the next and from one location to the next. Synoptic and mesoscale meteorological features govern the transport of emissions between sources and receptors. This affects the dilution and dispersion of pollutants during transport and

the time available during which pollutants can react to form secondary pollutants. Southern California is in the semi-permanent high pressure zone of the eastern Pacific. In the summer, frequent and persistent temperature inversions occur during periods of maximum solar radiation, which create daytime mixed layers of approximately 1000 meters. The sea-land breeze is strong during daytime in summer with a nighttime weak land-sea breeze. The land surface sufficiently cools overnight to create surface inversions, with depths as shallow as 50 meters. Surface heating usually erodes the surface and marine layers within a few hours after sunrise each day. Summertime wind flow patterns are from the west and south during the morning and change to predominantly westerly winds by afternoon. The land-sea breeze circulation moves air back and forth between the South Coast Air Basin (SoCAB) and the Pacific Ocean. The semi-permanent combination of Pacific anticyclone and 'thermal' low pressure that extends up from Mexico into the California Valley in summer begins to break down in fall. Typically, by late September, the mid-latitude transient weather systems start to move toward the California coastline – influencing the northern California coastline first and, later in the season, the southern California coastline. These transient systems continue to impact the coast until early April. The very cold/dry penetrations that affect the southern California coast do not typically begin until early December (late fall). These cold/dry penetrations are usually associated with northwesterly wind flow, and the pollutants tend to be purged from the SoCAB during these episodes. The synoptic weather situations that favor increases in pollution (as measured by $PM_{2.5}$ concentrations) appear to be the quiescent periods where steady-state high pressure covers the southern half of California.

6.2.1 Ambient Fine Particulate Matter

The concentrations of $PM_{2.5}$ components and certain organic compounds in Table 6-2 provide information regarding the likely sources of fine particles in the Study Area. The table includes the seasonal averages of up to fourteen 24-hour samples for each sampling site and monitoring season, along with the standard errors of the mean. Concentrations of $PM_{2.5}$ mass, sulfate, nitrate and ammonium ions, and elemental and organic carbon for individual 24-hour samples during the Winter and Summer Monitoring Seasons are found in Figure 6-1 and Figure 6-2, respectively. The combined mean $PM_{2.5}$ mass concentrations for the Winter and Summer Season samples were well below (i.e., better than) the new annual National Ambient Air Quality Standards (NAAQS) for $PM_{2.5}$ of 12 $\mu g/m^3$ at all three core monitoring sites.[2] The individual 24-hour samples were also all below the 24-hour average $PM_{2.5}$ NAAQS of 35 $\mu g/m^3$. The alternating periods of frontal passages followed by stable conditions during the Winter Monitoring Season are seen in Figure 6-1. By comparison, Figure 6-2 shows little day-to-day variation in PM concentrations, reflecting the more stable meteorological conditions during the Summer Monitoring Season.

During the Winter Monitoring Season, total carbon (TC) comprised 36, 34, and 23 percent of $PM_{2.5}$ mass at the CE, CN, and CS sites, respectively. The corresponding $TC/PM_{2.5}$ ratios during the Summer Monitoring Season were 26, 23, and 33 percent at the CE, CN, and CS sites, respectively. The OC/EC ratios were 1.5 at the CE site, 1.7 at the CN site, and 1.8 and the CS

[2] On December 14, 2012, the U.S. Environmental Protection Agency revised the annual average National Ambient Air Quality Standard (NAAQS) for $PM_{2.5}$ from 15.0 $\mu g/m^3$ to 12.0 $\mu g/m^3$.

site during winter and significantly larger during summer with values of 3.0 at the CE site, 2.7 at the CN site, and 5.3 at the CS site. EC, and a portion of OC, are emitted directly from combustion sources, such as on-road motor vehicles, wood combustion, meat cooking, and jet aircraft exhaust emissions. Possible sources of non-combustion sources of OC include vegetative detritus and leaf abrasion. The larger OC/EC ratios during the summer indicate greater contributions of SOA. SOA is derived from SVOCs produced by gas-phase reactions that subsequently form new aerosol particles by nucleation, adsorption, or absorption on preexisting aerosols or cloud particles. High molecular weight alkenes, aromatics, and SVOCs may react with hydroxyl radical, ozone or nitrate radicals to produce SOA (Fuentes et al., 2000; Stockwell et al., 2012). These reactions produce a host of low volatility dicarbonyls, carboxylic acids, hydroxy carbonyl, and organic nitrate compounds that can exist both in the gas and aerosol phase. It is important to note that the CMB apportionments are based on carbon, not organic matter (OM). The apportionment of OM can be estimated by multiplying OC by the appropriate source-specific OM/OC ratios (1.4 for gasoline, 1.5 for diesel, 1.8 for all other primary sources, and 2.2 for SOA-anthropogenic and SOA-biogenic) that have been reported in the literature (e.g. El-Zanan et al., 2009; Turpin and Lim, 2001).

Ammonium nitrate and ammonium sulfate are also major components of fine particles comprising a combined 20-25 percent of $PM_{2.5}$ mass during the Winter Monitoring Season and 44-65 percent during the Summer Monitoring Season. Nitrate and sulfate particles are also secondary pollutants formed from the oxidation of SO_2 and NOx to sulfuric acid and nitric acid, respectively, and subsequent neutralization of the acids with ammonia. The contributions of nitrate and sulfate to fine particles are greater during summer because gas-phase conversions of SO_2 and NO_x to acids, which are the main reaction pathways, are more rapid during the hot summer months. However, aqueous-phase conversion to sulfates in clouds and fogs may be an important chemical pathway along coastal areas of the SoCAB during late fall and early summer.

Road-dust and other fugitive dust from soil can be significant contributors to ambient PM concentrations during windy conditions. Figure 6-3 shows significantly higher concentrations of $PM_{2.5}$, along with the soil-related elements of calcium, silicon, iron, and aluminum, at the CS site on March 7 and 8. As shown in Figure 6-4, such extreme values did not occur during the Summer Monitoring Season. While the concentrations of soil-related elements vary one day to the next as well as between seasons, their relative abundances are similar for all three sites during both monitoring seasons. Chemical profiles were developed from samples of road dust collected near each of the three core site and were used in the CMB analysis.

Figure 6-5 and Figure 6-6 show the concentrations and relative abundances of benzo(ghi)perylene, indeno(1,2,3-cd)pyrene, coronene, 17A(H),21B(H)-30-norhopane (hop17), and 17A(H),21B(H)-hopane (hop19) for the winter and summer seasons, respectively. The high-molecular weight polycyclic aromatic hydrocarbons (PAH) are produced during combustion of hydrocarbon fuels and are especially indicative of gasoline vehicle engine exhaust. Hopanes and steranes are emitted in diesel and gasoline engine exhaust. They are indicative of unburned lubricating oils and are emitted mainly from smoking gasoline vehicles and older technology diesel engines. The relative abundances of these compounds are generally similar among all samples and the sums of their concentrations are well correlated with total carbon.

Data for samples collected at the end of the South Airfield Runway 25R, and the associated background samples collected at the CS site, at the end of the Winter Season are also shown in the Figure 6-1, Figure 6-3, and Figure 6-5. The influence of jet exhaust resulted in higher concentrations of carbonaceous particles and greater abundance of EC, shown in Figure 6-1. The greater contributions of copper and zinc in Figure 6-3 suggest these elements may serve as potential markers of jet exhaust. The concentrations of PAH and hopanes and steranes in the runway and background samples were comparable, as seen in Figure 6-5, which indicates jet exhaust is not a significant source of these compounds.

Table 6-2. Number of observations (obs.), means and standard errors of the ambient concentrations of $PM_{2.5}$ components and potential source markers in ng/m^3 at the three core sites.

	Winter Season			Summer Season		
	CE	CN	CS	CE	CN	CS
Obs. PM mass, elem, ions, OC, EC	12	12	12	14	7 (10) *	13
Obs. speciated organic compounds	14	12	14	12	14	13
PM 2.5 mass	8183 ± 1065	7665± 751	12328 ±2054	7517 ±421	7635± 1093	6380 ±405
nitrate	741 ± 210	672± 90	1077 ±210	589 ±120	922± 205	705± 142
sulfate	876 ± 192	966 ± 203	1049 ±189	2195 ±221	1984± 210	2720 ±275
ammonium	361 ± 125	287± 75	365 ± 127	610 ±90	451± 97	690± 111
elemental carbon	1179 ±179	957 ± 189	1022 ±145	493 ±27	467± 46	332 ±25
organic carbon	1812 ±263	1645± 225	1847 ±258	1467 ± 69	1248± 154	1770 ±103
Elements	1134± 110	1421 ± 99	2360 ±501	1955 ±117	2172± 102	1782 ±146
silicon	116.0 ±26.8	101.4± 22.3	408.6 ± 180.6	36.7 ±4.0	53.3± 17.2	23.1 ±4.9
aluminum	50.5 ±6.6	37.0± 5.6	146.2 ±51.5	25.2 ±2.0	35.6± 9.3	18.2 ±4.6
calcium	56.3 ±7.9	57.2± 6.3	176.4 ±62.8	40.8 ±4.3	60.4± 17.2	31.9 ±4.4
iron	136.1 ±21.1	138.1± 26.2	254.7 ±72.5	49.5 ±4.2	52.5± 10.0	21.0 ±3.0
copper	7.95 ± 1.29	9.08 ± 1.87	11.43 ±2.33	2.94 ±0.31	4.03± 1.89	0.76± 0.19
zinc	16.64 ±3.21	17.72± 2.93	24.74 ±3.71	5.68 ±1.18	12.82± 1.22	5.76± 0.81
molybdenum	0.80 ± 0.15	0.58 ± 0.13	0.88 ± 0.18	0.26 ±0.06	0.21± 0.09	0.17± 0.06
Sum semi-volatile alkanes	827 ± 132	604 ± 124	594 ±82	723 ±57	552± 86	367 ±37
Sum particulate alkanes	139.6 ±28.5	129.9± 30.2	129.0 ±18.9	50.3 ±5.1	96.9± 9.8	62.6 ±3.4
heptacosane, n-C27	1.777 ± 0.634	1.453 ± 0.378	1.332 ± 0.275	0.397 ±0.082	4.150± 0.599	0.347± 0.074
octacosane, n-C28	1.199 ± 0.562	0.819 ± 0.198	0.683 ± 0.170	0.181 ±0.041	0.953± 0.300	0.086± 0.024
nonacosane, n-C29	2.231 ± 0.529	1.398 ± 0.372	1.015 ± 0.121	0.232 ±0.064	1.388± 0.280	0.253± 0.044
triacontane, n-C30	1.485 ± 0.399	1.359 ± 0.261	0.821 ± 0.122	0.448 ±0.062	1.358± 0.194	0.059± 0.019
hentriacontane, n-C31	1.967 ± 0.374	1.172 ± 0.194	1.151 ± 0.134	0.382 ±0.037	0.958± 0.184	0.308± 0.040
dotriacontane, n-C32	0.804 ± 0.214	0.464 ± 0.091	0.551 ± 0.086	0.147 ±0.022	0.462± 0.099	0.068± 0.019
tritriacontane. n-C33	1.162 ± 0.209	0.784 ± 0.124	0.769 ± 0.087	0.243 ±0.024	0.492± 0.081	0.164± 0.023
UCM (C19-C35)	102 ±22	92 ± 23	96 ± 16			
Sum hopanes and steranes	0.709 ± 0.128	1.067 ± 0.222	0.762 ± 0.089	0.850 ±0.113	0.919± 0.118	0.846± 0.129
17A(H),21B(H)-30-Norhopane (hop17)	0.107 ± 0.021	0.181 ± 0.059	0.116 ± 0.017	0.121 ±0.021	0.100± 0.012	0.100± 0.018
17A(H),21B(H)-Hopane (hop19)	0.160 ± 0.035	0.214 ± 0.056	0.143 ± 0.024	0.019 ±0.005	0.073± 0.016	0.052± 0.010
Sum semi-volatile PAH	510 ±72	396± 61	328 ±38	247 ±16	198± 31	160 ±21
Sum particulate PAH	4.3 ± 0.5	2.7 ± 0.4	4.0 ± 0.5	2.5 ±0.2	1.5± 0.2	1.5± 0.1
benzo(ghi)pyrelene	0.450 ± 0.056	0.269 ± 0.047	0.266 ± 0.039	0.051 ±0.010	0.034± 0.006	0.018± 0.003
indeno[123-cd]pyrene	0.158 ± 0.021	0.088 ± 0.015	0.105 ± 0.015	0.016 ±0.005	0.010± 0.002	0.005± 0.001
coronene	0.189 ± 0.024	0.116 ± 0.020	0.109 ± 0.016	0.027 ±0.004	0.016± 0.003	0.011± 0.002
Sum polar organic compounds	1594 ±145	1408± 148	1530 ±126	1528 ±143	1155± 102	1321 ±165
dehydroabietic acid	57.24 ± 13.64	38.97 ± 10.60	77.76 ± 23.21	5.92 ±4.14	1.14± 0.51	0.60± 0.36
pimaric acid	0.606 ± 0.197	0.634 ± 0.290	2.109 ± 0.504	0.309 ±0.112	0.259± 0.115	0.214± 0.095
abietic acid	0.140 ± 0.024	0.143 ± 0.031	0.280 ± 0.045	0.046 ±0.015	0.050± 0.017	0.054± 0.016
levoglucosan	279.1 ±40.8	181.1± 34.2	232.2 ±32.8	26.3 ±4.0	18.8± 2.8	29.1 ±4.9
syringaldehyde	0.608 ± 0.202	0.227 ± 0.045	0.255 ± 0.108	0.342 ±0.157	0.413± 0.114	0.874± 0.292
4-formyl-guaiacol	20.7 ±3.0	9.8 ± 1.2	16.4 ±1.0	19.9 ±1.7	14.1± 0.7	23.3 ±3.0
isoeugenol	0.528 ± 0.117	0.248 ± 0.058	0.762 ± 0.100	0.188 ±0.050	0.257± 0.102	0.328± 0.076
palmitic acid	90.1 ± 10.5	86.8 ± 13.6	49.8 ±6.3	53.9 ±11.9	59.3± 14.7	48.4± 10.7
oleic acid	7.520 ± 4.558	8.137 ± 4.718	0.357 ± 0.215	0.526 ±0.360	0.056± 0.040	2.777± 1.972
stearic acid	66.7 ±8.2	55.9± 7.5	51.5 ±5.8	19.3 ±2.7	18.3± 2.5	17.4 ±2.2
cholesterol	2.627 ± 0.918	2.212 ± 0.741	0.763 ± 0.217	0.063 ±0.063	0.241± 0.154	0.000± 0.000
cis-pinonic acid	87.1 ±8.8	87.1 ± 11.8	107.5 ±11.9	42.7 ±6.2	32.0± 5.0	40.8 ±5.1
succinic acid	70.8 ± 12.9	104.7± 17.5	90.1 ±9.1	258.3 ±24.4	260.3± 23.9	212.1 ±21.3

* One of the samples from CN during Summer Season is a media composite of four days (8/8, 8/9, 8/12, and 8/13).

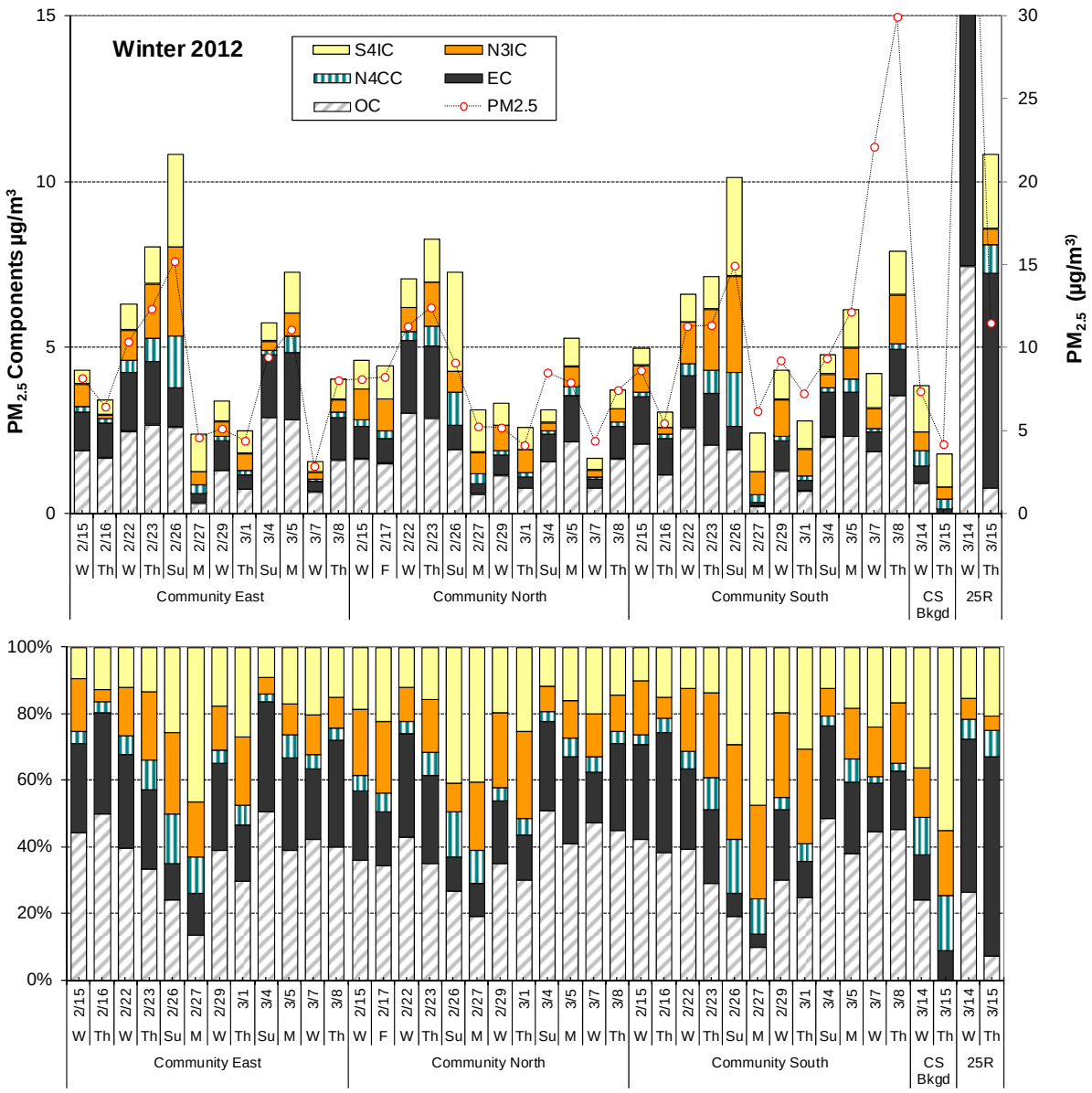

Figure 6-1. Twenty four-hour average concentrations (µg/m^3) of $PM_{2.5}$, sulfate (S4IC), nitrate (N3IC), ammonium ion (N4CC), and elemental carbon (EC) and organic carbon (OC) during the Winter Season at the three core sampling sites. Paired samples were also collected on 3/14 and 3/15 at the end of South Airfield Runway 25R and the CS site, which was used to subtract an urban background from the runway samples. Off-scale values for 25R on 3/14 are 50.5 µg/m^3 for $PM_{2.5}$ and 28.2 µg/m^3 for the sum of species (13.0 for EC alone).

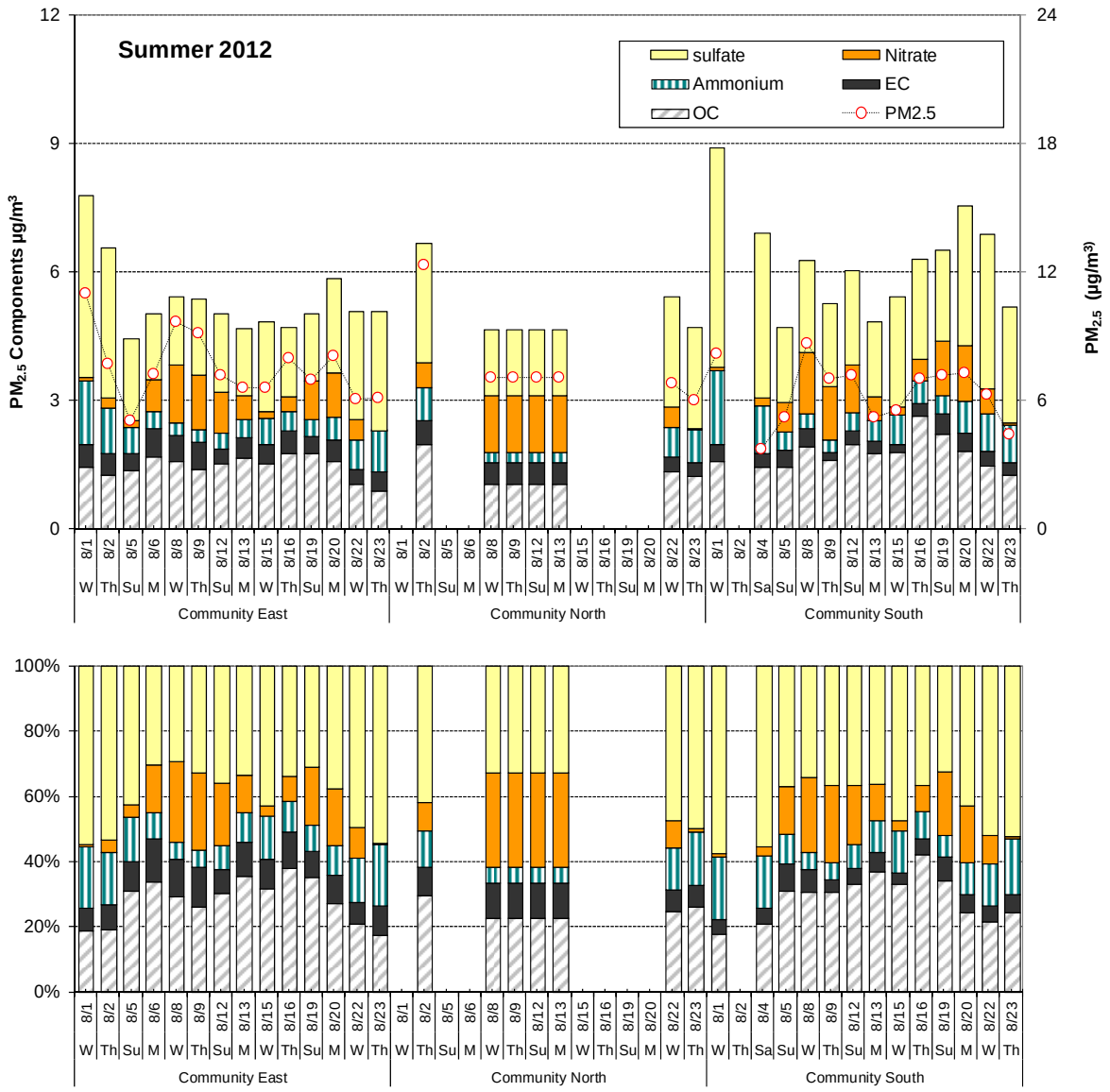

Figure 6-2. Twenty four-hour average concentrations (µg/m^3) of $PM_{2.5}$, sulfate, nitrate, and ammonium ion, and elemental and organic carbon during Summer Season at the three core sampling sites. One of the samples from CN is a media composite of four days (8/8, 8/9, 8/12, and 8/13).

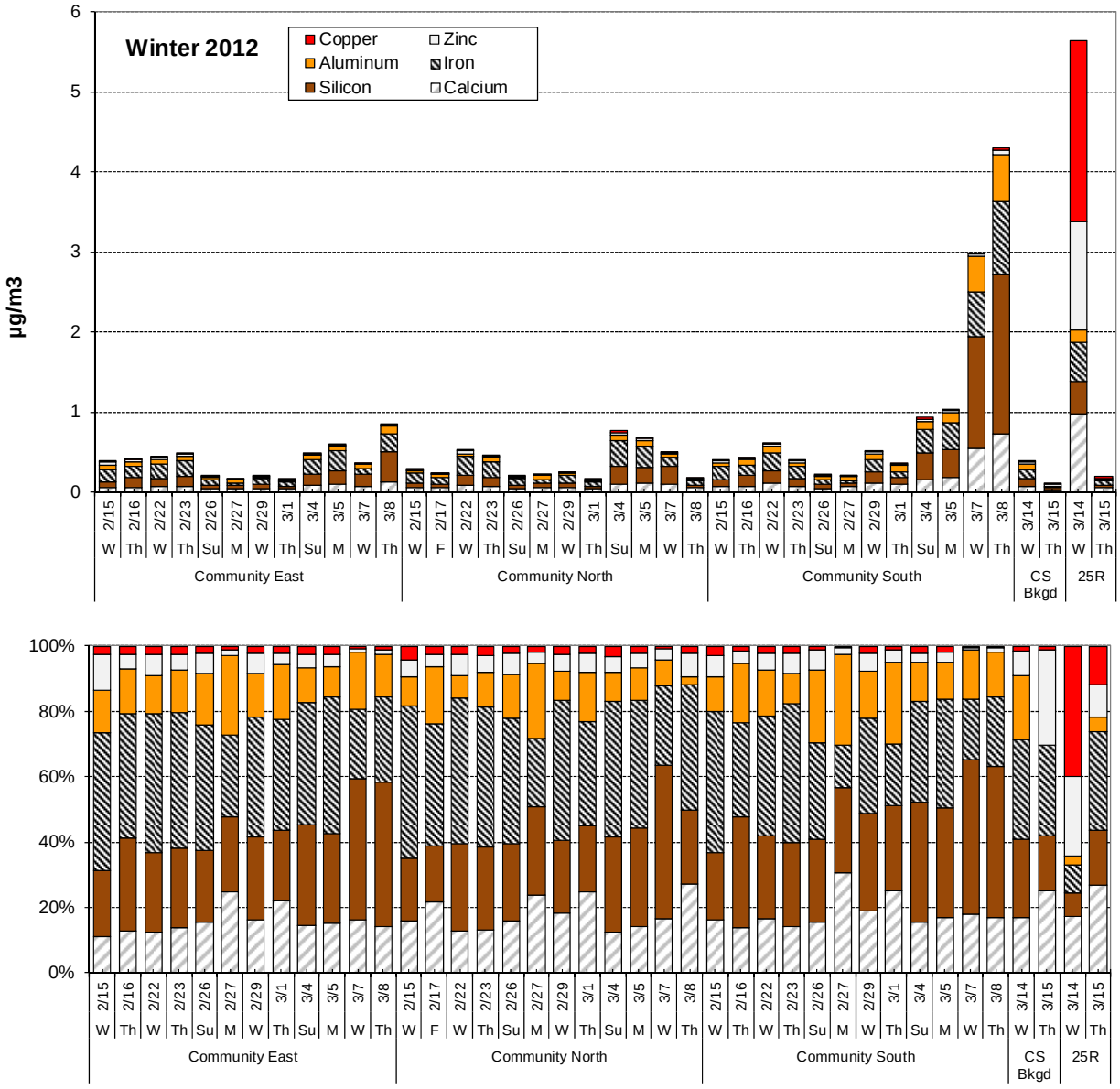

Figure 6-3. Twenty four-hour average concentrations (µg/m^3) of calcium, silicon, iron, aluminum, zinc, and copper during Winter Season at the three core sampling sites. Paired samples were also collected on 3/14 and 3/15 at the end of South Airfield Runway 25R and the CS site, which was used to subtract an urban background from the runway samples.

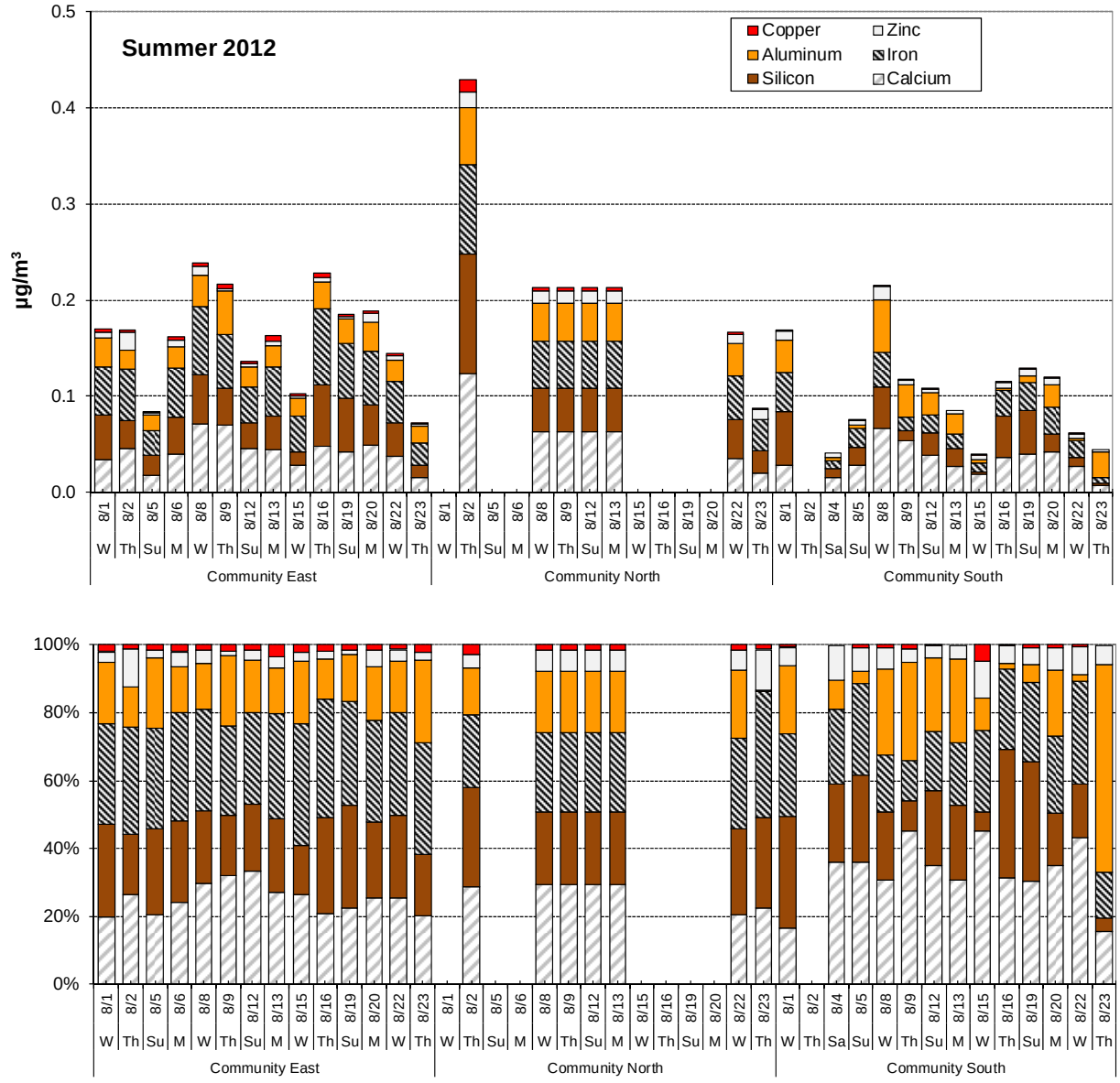

Figure 6-4. Twenty four-hour average concentrations (µg/m^3) of calcium, silicon, iron, aluminum, zinc, and copper during Summer Season at the three core sampling sites. One of the samples from CN is a media composite of four days (8/8, 8/9, 8/12, and 8/13).

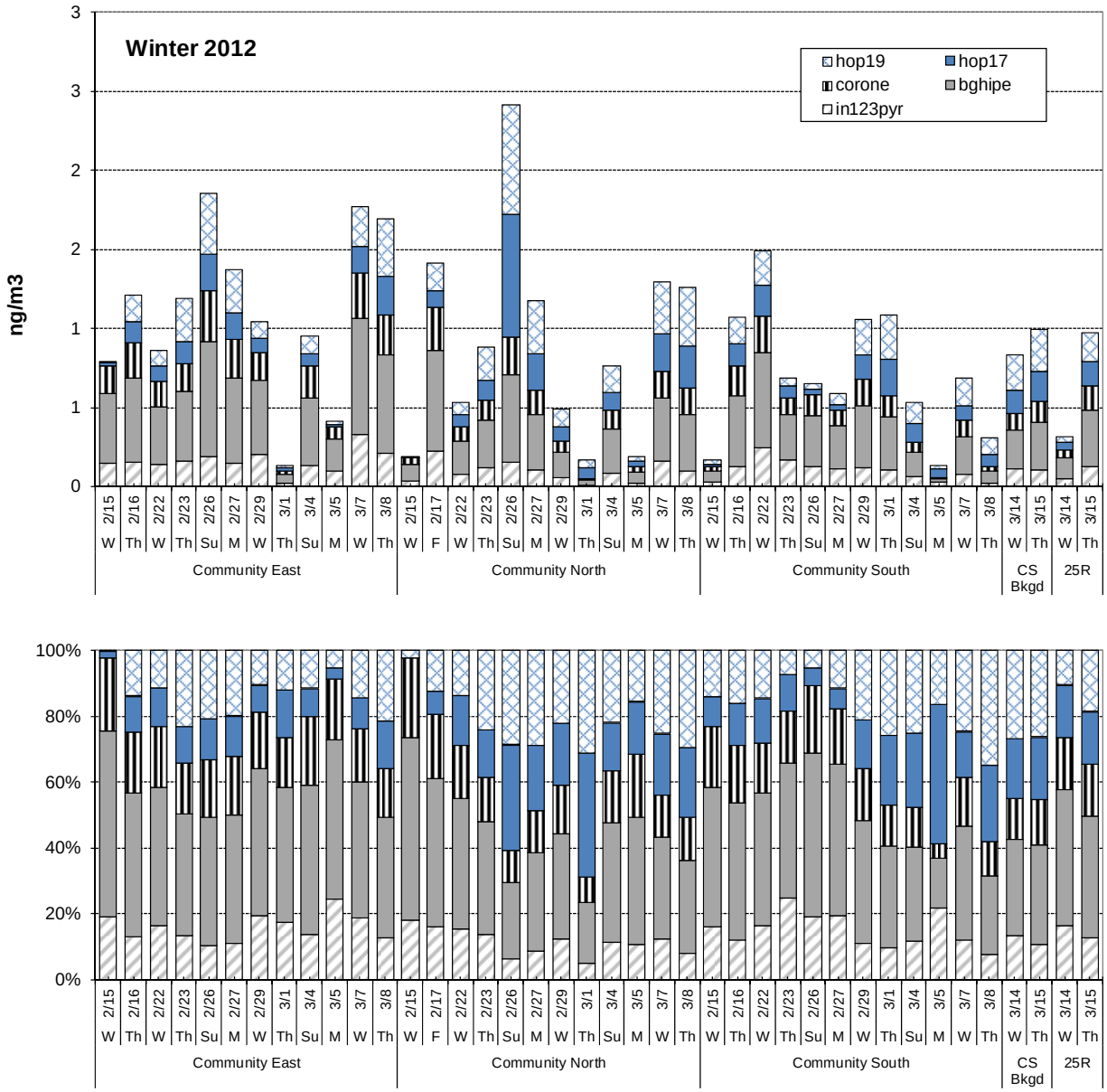

Figure 6-5. Twenty four-hour average concentrations (µg/m^3) of benzo(ghi)perylene (bghipe), indeno(1,2,3-cd)pyrene (in123pyr), coronene (corone), 17A(H),21B(H)-30-norhopane (hop17), and 17A(H),21B(H)-hopane (hop19) during Winter Season at the three core sampling sites. Paired samples were also collected on 3/14 and 3/15 at the end of South Airfield Runway 25R and the CS site, which was used to subtract an urban background from the runway samples.

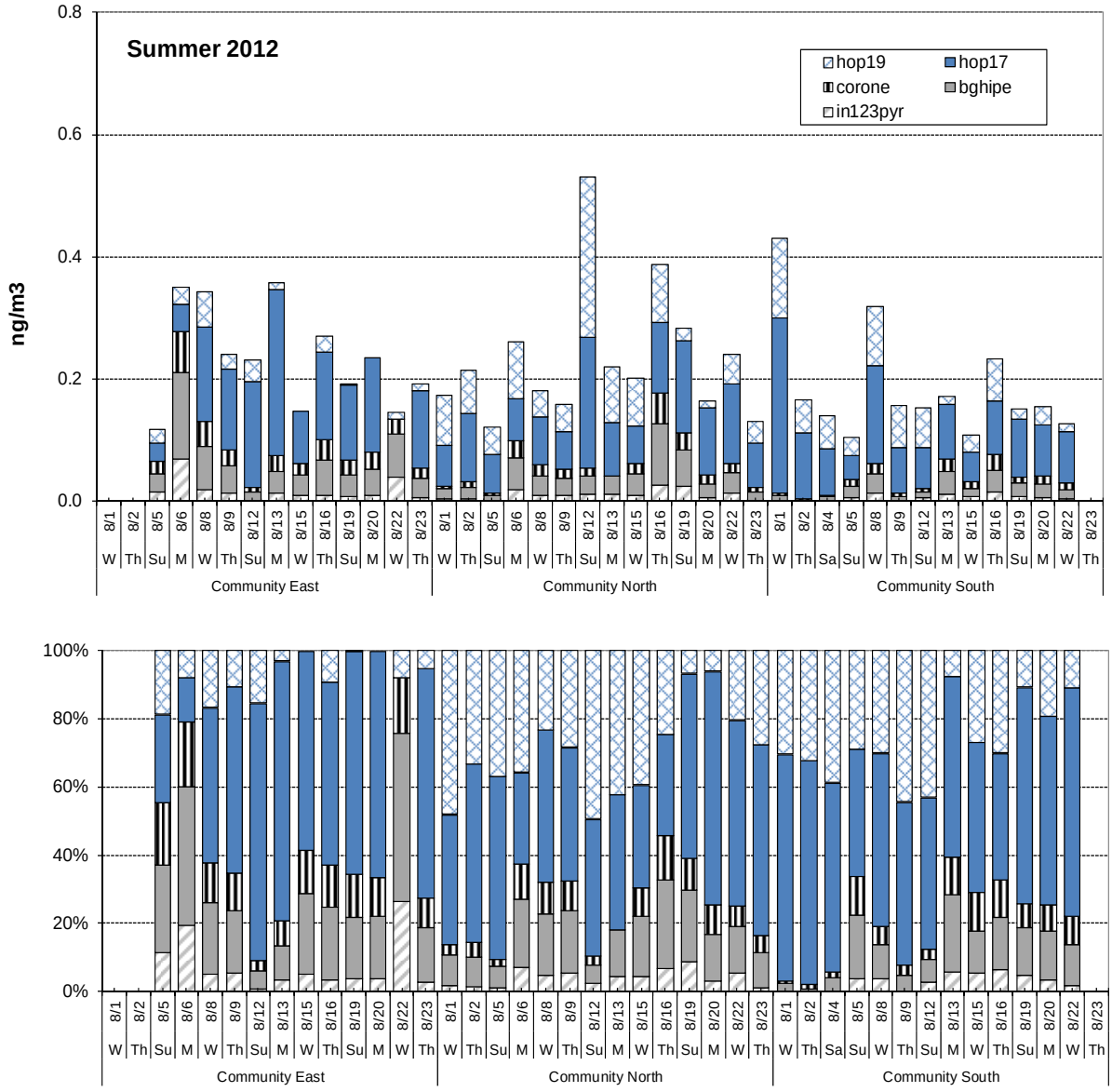

Figure 6-6. Twenty four-hour average concentrations (µg/m3) of benzo(ghi)perylene (bghipe), indeno(1,2,3-cd)pyrene (in123pyr), coronene (corone), 17A(H),21B(H)-30-norhopane (hop17), and 17A(H),21B(H)-hopane (hop19) during Summer Season at the three core sampling sites.

6.2.2 Ambient Volatile and Semi-Volatile Organic Compounds

Ambient measurements of speciated C_2-C_{11} hydrocarbons, C_1-C_7 carbonyl compounds, and C_8-C_{18} hydrocarbons were acquired at the three core monitoring sites. Table 6-3 presents seasonal averages for identified hydrocarbons from ethane to n-undecane and the totals as well as the totals of the PAMS target compounds, which are indicated by an asterisk in Table 6-3. The compounds 2-methylhexane and 2,3-dimethylpentane were unable to be core resolved during gas chromatographic analysis of the samples from the Summer Monitoring Season. While the mass spectral response factors are similar for 2-methylhexane and 2,3-dimethylpentane, the combined total concentration is not reported since the data were not used in the CMB analysis.

The plots of seasonal mean concentrations of speciated C_2 to C_{11} hydrocarbons in Figure 6-7 show similar patterns for the three monitoring sites. However, unusually high levels of the same small group of hydrocarbons at two sites (CE and CS) suggest the possibility of a local source. Therefore, day-to-day variations in the concentrations of toluene, n-octane, n-nonane, 2-methylheptane, and 3-methylheptane at the CE site are presented in Figure 6-8. On February 16, 2012 the concentrations of all five hydrocarbons were simultaneously much higher than the seasonal average. After a steep reduction by February 19, 2012 the concentrations of the five hydrocarbons continued to gradually decline over the next two weeks. The concentrations were substantially lower during the Summer Season for all five hydrocarbons. The same pattern was observed at the CS site, however, initial concentrations were lower than at the CE site. Unusually high concentrations were not observed for the five aforementioned hydrocarbons at the CN site during the Winter Season. After learning that the monitoring shelters at the CE and CS sites were freshly painted a day before they were installed at the sites in late-January, DRI obtained and analyzed a sample of the acrylic semi-gloss paint to confirm whether it contained the five hydrocarbons. Samples of the paint can headspace vapors were analyzed as well as the residual vapors from painted boards that were left to dry for three days. Based on the vapor composition, it is unlikely that this paint was the cause of the unusual composition of the ambient hydrocarbons at the CE and CS sites. A profile for the unknown local source composition was derived from the abundances of the five hydrocarbons above their seasonal averages after the contamination was no longer apparent in the ambient hydrocarbon composition. This profile was included in the CMB analysis.

Other apparent anomalies in Figure 6-7 are the high concentrations of n-butane and isopentane at the CN site. The n-butane/acetylene and isopentane/acetylene ratios at the CN site range from ~3.5 to 42 and ~3 to 37, respectively, compared to ranges at the CE and CS sites of ~1.5 to 4 and ~1 to 4, respectively. While less visible in the plots, concentrations of other light hydrocarbons were significantly greater at the CN site relative to either CE or CS sites. The significantly higher ratios of these hydrocarbons to acetylene suggest greater contributions of gasoline vapors at the CN site. This conclusion is further supported by the plots in Figure 6-9, which show the day-to-day variations in the concentrations of n-butane, isopentane, and 2-methylpentane are generally correlated to daily maximum temperature. Unlike the portable shelters used at the CE and CS sites, a motorhome was used at the CN site. The motorhome's fuel tank is the most likely source of the apparent excess gasoline vapors at CN. The motorhome was completely fenced in for security purposes and tarp covering on the fence restricted ventilation around the motorhome.

Table 6-3. Mean ambient concentrations and standard errors in ng/m^3 of volatile organic compounds from 24-hour canister samples at the three core sites.

			Winter Season			Summer Season		
Species	Mnemonic	PAMS	CE	CN	CS	CE	CN	CS
No. Observations			14	14	14	12	14	14
C2-C11 NMHC	NMHC		223846 ± 45528	173943 ± 28021	104756 ± 15196	66242 ± 7316	52736 ± 6726	25644 ± 3527
PAMS	PAMS		216409 ± 45048	167614 ± 27038	101245 ± 14702	62301 ± 6856	50004 ± 6512	23124 ± 3325
acetylene	ACETYL	*	2385 ± 442	3477 ± 580	1858 ± 293	888 ± 83	759 ± 62	402 ± 55
ethene	ETHENE	*	4771 ± 780	6367 ± 1067	3675 ± 554	2305 ± 205	2274 ± 276	1054 ± 131
ethane	ETHANE	*	12721 ± 3276	18464 ± 3074	11579 ± 1538	9112 ± 1953	4044 ± 534	3979 ± 678
propene	LPROPE	*	2713 ± 374	3455 ± 572	2180 ± 276	1154 ± 102	1192 ± 94	712 ± 110
propane	LPROPA	*	10164 ± 1966	18734 ± 3426	9287 ± 1371	7524 ± 1213	4591 ± 986	2946 ± 548
1,3-butadiene	LBUD13		332 ± 55	418 ± 72	243 ± 40	141 ± 12	137 ± 15	75 ± 24
1-butene	LBUT1E	*	585 ± 75	945 ± 130	456 ± 55	304 ± 34	341 ± 39	208 ± 45
c-2-butene	LC2BUT	*	165 ± 30	616 ± 101	107 ± 17	56 ± 19	145 ± 28	35 ± 11
isobutylene	LIBUTE		2942 ± 537	1546 ± 182	1401 ± 166	1494 ± 339	801 ± 159	809 ± 114
t-2-butene	LT2BUT	*	205 ± 36	764 ± 124	138 ± 20	138 ± 50	191 ± 30	76 ± 10
n-butane	LBUTAN	*	6171 ± 1103	26935 ± 4694	4979 ± 758	2136 ± 329	4988 ± 1198	1411 ± 275
iso-butane	LIBUTA	*	2891 ± 573	7363 ± 1178	2348 ± 338	1638 ± 271	1297 ± 263	919 ± 168
iso-pentane	LIPENT	*	6610 ± 1369	24833 ± 4471	4691 ± 817	3641 ± 594	7881 ± 1904	1710 ± 344
n-pentane	LNPENT	*	2300 ± 437	5796 ± 1020	1823 ± 299	1485 ± 230	1826 ± 383	743 ± 161
1-pentene	PENTE1	*	206 ± 40	399 ± 68	179 ± 35	111 ± 11	190 ± 31	83 ± 16
2-methyl-1-butene	B1E2M		287 ± 65	768 ± 146	163 ± 35	136 ± 25	228 ± 48	32 ± 9
isoprene	I_PREN	*	200 ± 38	216 ± 42	129 ± 21	386 ± 75	82 ± 11	200 ± 23
t-2-pentene	T2PENE	*	221 ± 49	648 ± 119	121 ± 25	97 ± 16	225 ± 50	36 ± 6
c-2-pentene	C2PENE	*	126 ± 29	363 ± 69	66 ± 14	58 ± 10	133 ± 30	18 ± 4
2-methyl-2-butene	B2E2M		346 ± 106	801 ± 153	132 ± 28	144 ± 62	301 ± 66	38 ± 7
2,2-dimethylbutane	BU22DM	*	510 ± 106	1214 ± 234	312 ± 64	198 ± 37	321 ± 72	69 ± 15
cyclopentene	CPENTE		91 ± 19	191 ± 35	54 ± 9	40 ± 5	70 ± 12	19 ± 4
cyclopentane	CPENTA	*	222 ± 48	537 ± 101	159 ± 28	162 ± 24	217 ± 45	80 ± 17
2,3-dimethylbutane	BU23DM	*	700 ± 155	1845 ± 349	462 ± 91	383 ± 62	594 ± 127	150 ± 34
2-methylpentane	PENA2M	*	1921 ± 409	4131 ± 780	1228 ± 219	1115 ± 173	1341 ± 273	454 ± 92
3-methylpentane	PENA3M	*	1181 ± 240	2497 ± 467	817 ± 142	729 ± 107	863 ± 164	342 ± 65
2-methyl-1-pentene	P1E2ME	*	242 ± 49	316 ± 53	221 ± 39	98 ± 14	121 ± 21	41 ± 9
n-hexane	N_HEX	*	1044 ± 185	1791 ± 346	764 ± 123	706 ± 89	626 ± 101	328 ± 66
t-2-hexene	T2HEXE		72 ± 19	149 ± 30	38 ± 12	67 ± 11	54 ± 11	15 ± 4
c-2-hexene	C2HEXE		36 ± 10	82 ± 17	23 ± 7	16 ± 3	17 ± 6	6 ± 2
1,3-hexadiene (trans)	HXDI13		14 ± 7	35 ± 16	22 ± 8	13 ± 6	14 ± 7	3 ± 2
methylcyclopentane	MCYPNA	*	1171 ± 247	2216 ± 426	815 ± 149	736 ± 120	731 ± 145	352 ± 81
2,4-dimethylpentane	PEN24M	*	547 ± 129	1368 ± 262	369 ± 73	358 ± 52	534 ± 106	169 ± 21
benzene	BENZE	*	2661 ± 369	2132 ± 321	1488 ± 163	1479 ± 243	857 ± 80	510 ± 67
cyclohexane	CYHEXA	*	399 ± 92	1155 ± 217	872 ± 201	68 ± 27	255 ± 65	54 ± 34
2-methylhexane	HEXA2M	*	866 ± 153	1280 ± 255	484 ± 91		Coeluting peaks	
2,3-dimethylpentane	PEN23M	*	1320 ± 224	2091 ± 403	741 ± 140			
cyclohexene	CYHEXE		40 ± 7	74 ± 14	29 ± 5	31 ± 5	24 ± 3	36 ± 6
3-methylhexane	HEXA3M	*	1143 ± 183	1391 ± 273	597 ± 109	1018 ± 247	401 ± 67	182 ± 37
1,3-dimethylcyclopentane (cis)	CPA13M		259 ± 50	419 ± 81	171 ± 30	180 ± 27	131 ± 26	71 ± 20
1-heptene	HEP1E		537 ± 83	912 ± 243	297 ± 50	862 ± 107	691 ± 122	338 ± 74
2,2,4-trimethylpentane	PA224M	*	2158 ± 494	4382 ± 892	1457 ± 271	1154 ± 173	1377 ± 269	472 ± 83
n-heptane	N_HEPT	*	1162 ± 146	1038 ± 192	733 ± 138	594 ± 91	342 ± 42	201 ± 36
2,3-dimethyl-2-pentene	P2E23M		87 ± 29	4 ± 2	30 ± 9	26 ± 17	3 ± 1	6 ± 2
methylcyclohexane	MECYHX	*	2350 ± 396	1065 ± 210	1296 ± 287	460 ± 78	285 ± 43	148 ± 47
2,3,4-trimethylpentane	PA234M	*	477 ± 115	807 ± 187	290 ± 62	260 ± 43	216 ± 32	106 ± 19
toluene	TOLUE	*	96320 ± 31008	6996 ± 1116	28519 ± 5741	8324 ± 1543	3632 ± 810	1032 ± 155
2-methylheptane	HEP2ME	*	3663 ± 1376	578 ± 101	1300 ± 288	318 ± 36	224 ± 26	138 ± 18
4-methylheptane	HEP4ME		1269 ± 491	204 ± 35	419 ± 95	101 ± 12	73 ± 8	39 ± 6
3-methylheptane	HEP3ME	*	3816 ± 1528	477 ± 96	1189 ± 273	219 ± 30	123 ± 19	59 ± 13
n-octane	N_OCT	*	11345 ± 5424	857 ± 140	2841 ± 613	520 ± 79	326 ± 31	156 ± 20
ethylbenzene	ETBZ	*	1589 ± 200	697 ± 139	804 ± 107	739 ± 113	337 ± 46	154 ± 23
m&p-xylene	MP_XYL	*	6869 ± 956	2580 ± 476	3547 ± 433	2807 ± 417	1303 ± 188	540 ± 89
styrene	STYR	*	2728 ± 390	714 ± 116	2159 ± 137	5102 ± 725	1982 ± 454	1446 ± 243
o-xylene	O_XYL	*	2125 ± 300	887 ± 161	1095 ± 134	931 ± 126	480 ± 54	229 ± 32
n-nonane	N_NON	*	12303 ± 7021	476 ± 85	1229 ± 266	318 ± 31	302 ± 29	86 ± 25

Table 6-3 (continued). Mean ambient concentrations and standard errors in ng/m^3 of volatile organic compounds from 24-hour canister samples at the three core sites.

			Winter Season			Summer Season		
Species	Mnemonic	PAMS	CE	CN	CS	CE	CN	CS
isopropylbenzene	IPRBZ	*	73 ± 10	39 ± 8	36 ± 5	51 ± 9	29 ± 3	15 ± 2
n-propylbenzene	N_PRBZ	*	251 ± 29	167 ± 27	133 ± 16	320 ± 39	228 ± 23	140 ± 20
alpha-pinene	A_PINE		212 ± 46	77 ± 15	142 ± 25	764 ± 112	281 ± 51	1078 ± 284
3-ethyltoluene	M_ETOL	*	491 ± 53	397 ± 65	277 ± 35	613 ± 55	469 ± 36	278 ± 36
4-ethyltoluene	P_ETOL	*	457 ± 63	312 ± 58	212 ± 31	365 ± 60	263 ± 36	143 ± 26
1,3,5-trimethylbenzene	BZ135M	*	387 ± 73	252 ± 57	145 ± 25	170 ± 23	123 ± 12	58 ± 9
o-ethyltoluene	O_ETOL	*	246 ± 39	169 ± 36	102 ± 16	136 ± 15	106 ± 11	54 ± 7
n-decane	N_DEC	*	501 ± 77	479 ± 108	367 ± 46	437 ± 51	487 ± 33	189 ± 37
1,2,3-trimethylbenzene	BZ123M		195 ± 32	181 ± 39	118 ± 18	152 ± 17	113 ± 11	63 ± 9
indan	INDAN	*	95 ± 15	89 ± 19	47 ± 7	67 ± 9	45 ± 4	30 ± 6
1,3-diethylbenzene	DETBZ13	*	50 ± 8	57 ± 11	30 ± 6	36 ± 4	27 ± 5	15 ± 3
1,4-diethylbenzene	DETBZ14	*	33 ± 5	50 ± 10	24 ± 5	50 ± 4	73 ± 11	61 ± 8
n-undecane	N_UNDE	*	126 ± 32	203 ± 48	154 ± 26			

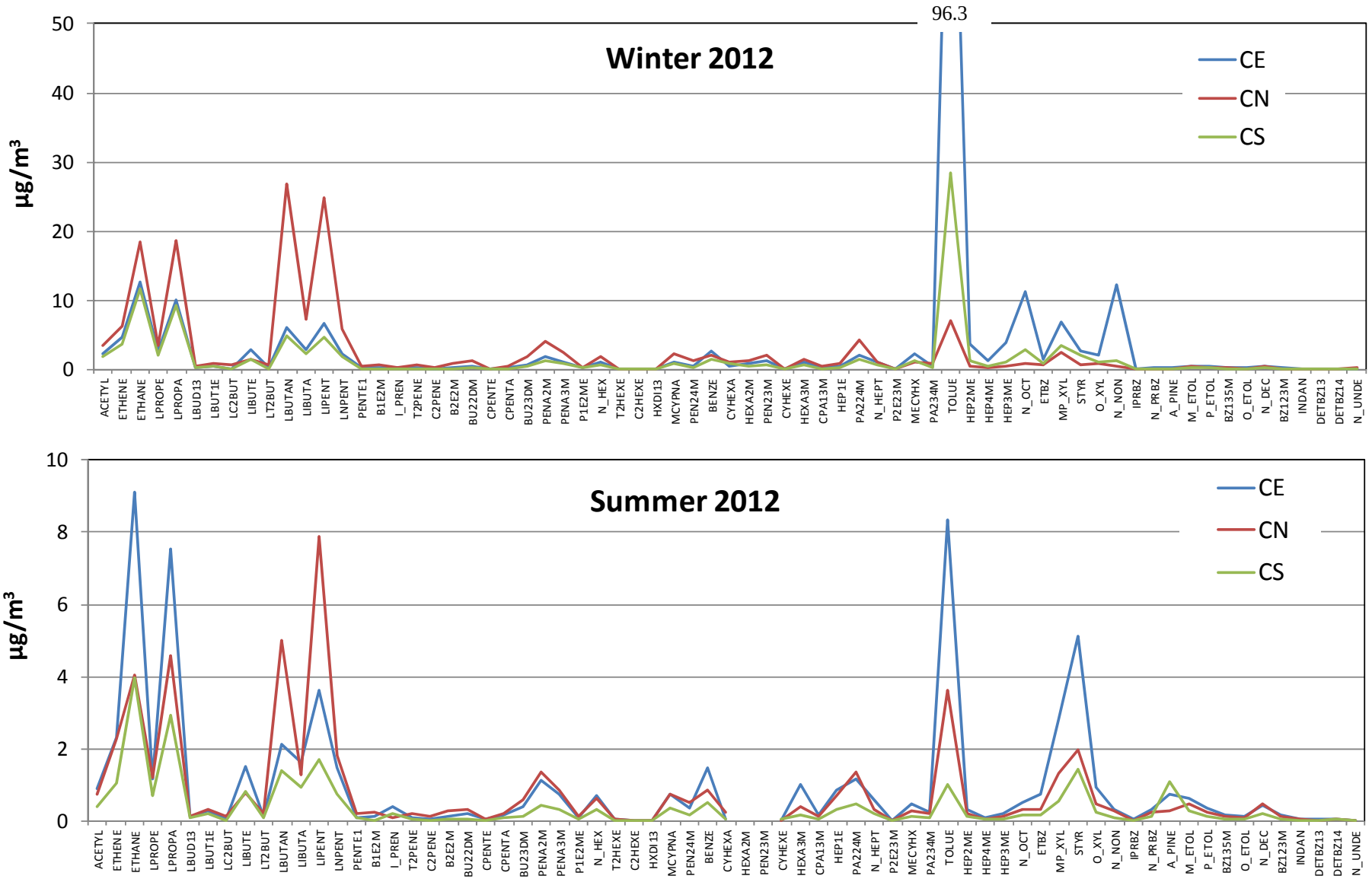

Figure 6-7. Seasonal mean concentrations of speciated hydrocarbon from 24-hour canister samples at the three core monitoring sites.

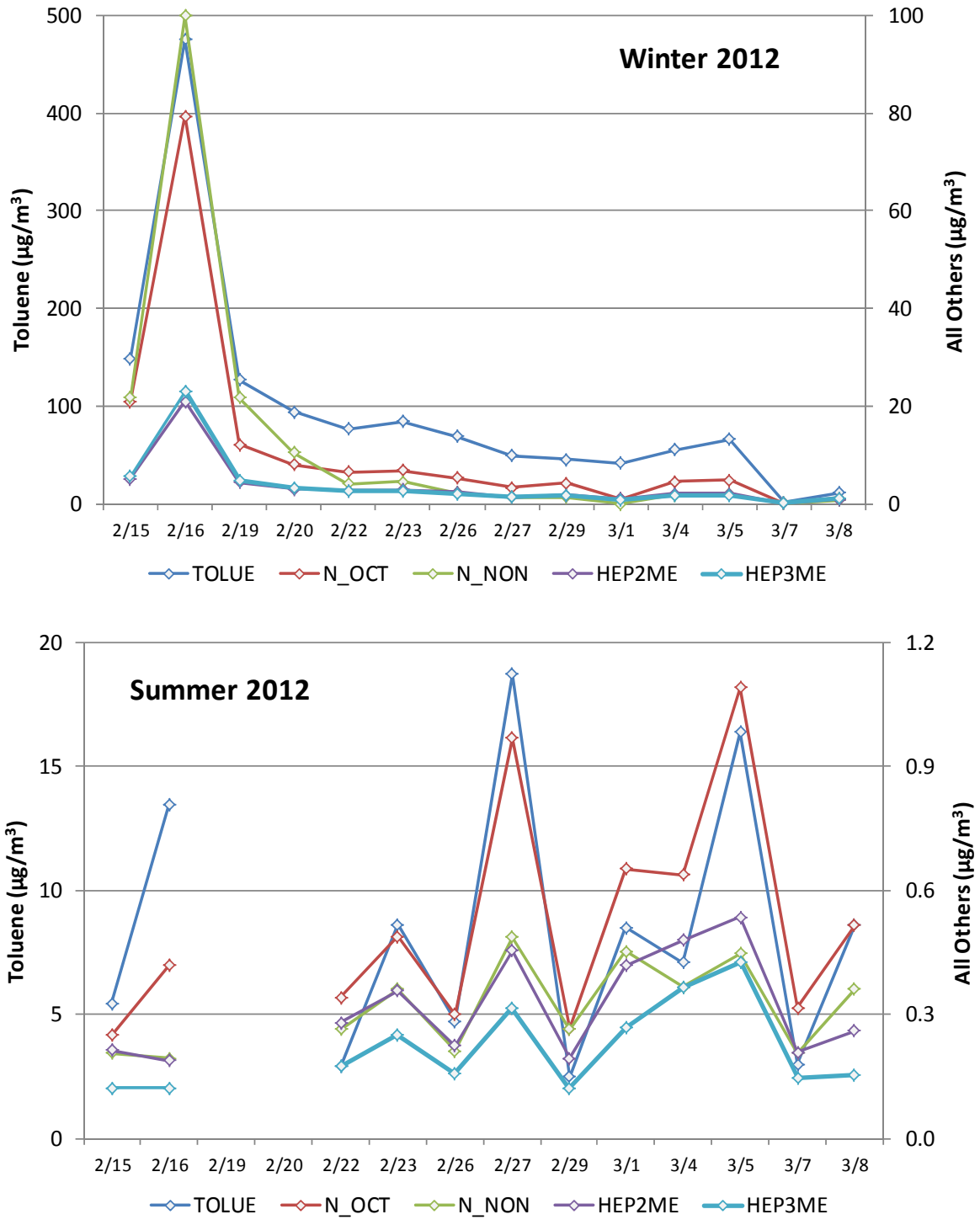

Figure 6-8. Daily variations in the concentrations of toluene, n-octane, n-nonane, 2-methylheptane, and 3-methylheptane at the CE site during the Winter and Summer Monitoring Seasons.

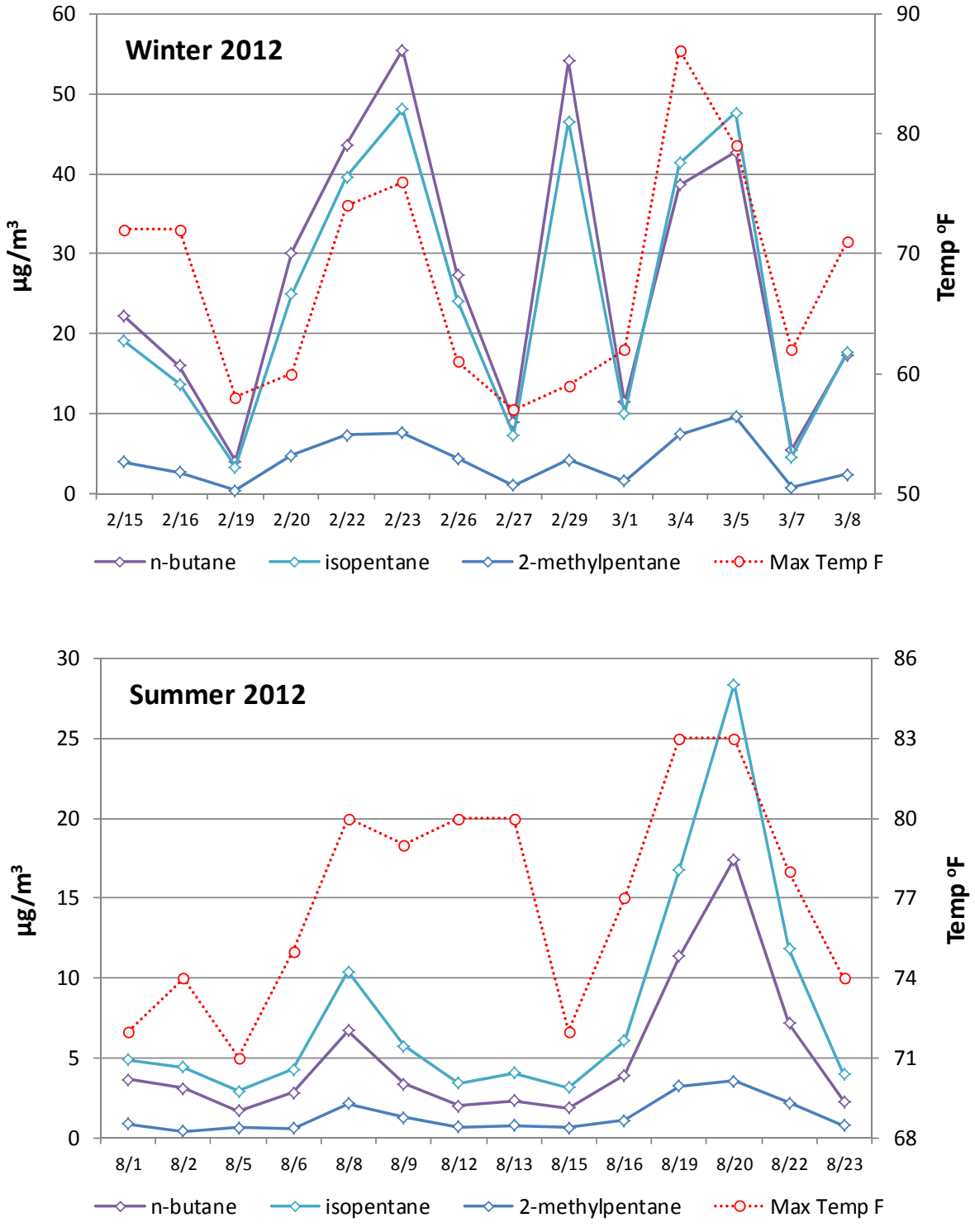

Figure 6-9. Daily variations in the concentrations of n-butane, isopentane and 2-methylpentane at the CN sites and daily maximum temperature during the Winter and Summer Monitoring Seasons.

The mean ambient concentrations at the three core sites of carbonyl compounds and semi-volatile hydrocarbons are shown in Table 6-4 and Table 6-5, respectively. Carbonyl compounds were approximately four times higher during the Winter Season than the Summer Season. The lower levels during the Summer Season reflect the influence of persistent onshore flow in reducing the accumulation of carbonyl compounds near the coast, despite greater contributions of atmospheric formation of carbonyl compounds during the summer.

The daily variations in the sum of hydrocarbons from ethane to n-decane and greater than decane to n-octadecane are shown in Figure 6-10. The contributions of the semi-volatile hydrocarbons (SVHC) measured from the Tenax samples generally ranged from 1 to 3 percent of the total C_2-C_{18} hydrocarbons during the Winter Season and from 2 to 10 percent during Summer Season. One exception was a sample collected at CS on 8/22/12, in which SVHC represented 24 percent of the total C_2-C_{18} hydrocarbons. One of the samples collected at the takeoff end of the South Airfield Runway had 20 percent SVHC. Greater abundances of SVHC may result from contributions of jet exhaust during gate idling and runway taxiing. Diesel exhaust is also an important source of SVHC.

Table 6-4. Mean ambient concentrations and standard errors in ng/m^3 of carbonyl compounds from 24-hour DNPH cartridge samples at the three core sites.

		Winter Season			Summer Season		
Species	Mnemonic	CE	CN	CS	CE	CN	CS
No. Observations		14	14	14	12	14	14
Sum Carbonyl Compounds		4812 ± 921	4012 ± 698	2570 ± 405	943 ± 190	917 ± 117	664 ± 148
formaldehyde	FORMAL	1794 ± 278	1702 ± 271	999 ± 112	565 ± 121	448 ± 84	247 ± 79
acetaldehyde	ACETAL	1020 ± 247	761 ± 179	349 ± 94	70 ± 28	23 ± 11	57 ± 37
acrolein	ACROLN	56 ± 12	45 ± 11	22 ± 7	3 ± 3	2 ± 2	0 ± 0
glyoxal	GLYOXL	469 ± 44	481 ± 36	408 ± 38	388 ± 30	376 ± 25	291 ± 30
acetone	ACETO	785 ± 317	486 ± 223	494 ± 272	0 ± 0	0 ± 0	0 ± 0
propionaldehyde	PROAL	173 ± 38	150 ± 36	67 ± 21	10 ± 5	3 ± 2	15 ± 9
crotonaldehyde	CROTON	0 ± 0	2 ± 2	0 ± 0	4 ± 1	6 ± 2	7 ± 3
methacrolein	MACROL	0 ± 0	0 ± 0	0 ± 0	0 ± 0	0 ± 0	0 ± 0
n-butyraldehyde	BUTAL	159 ± 32	112 ± 33	56 ± 18	1 ± 1	0 ± 0	2 ± 2
2-butanone (MEK)	MEK	84 ± 44	89 ± 38	35 ± 16	1 ± 1	8 ± 4	11 ± 5
valeraldehyde	VALAL	113 ± 20	87 ± 19	55 ± 11	32 ± 4	27 ± 3	29 ± 3
benzaldehyde	BENZAL	158 ± 45	97 ± 34	84 ± 25	25 ± 8	25 ± 7	6 ± 4

Table 6-5. Mean ambient concentrations and standard errors in ng/m^3 of semi-volatile hydrocarbons from 24-hour Tenax cartridge samples at the three core sites.

		Winter Season			Summer Season		
Species	Mnemonic	CE	CN	CS	CE	CN	CS
No. Observations		8	8	6	12	14	14
1-decene	DEC1E	24 ± 16	20 ± 12	48 ± 14	18 ± 10	8 ± 5	24 ± 17
1,2,4-Trimethylbenzene_tert-Butylbezene	TM_TBBZ	498 ± 122	360 ± 89	322 ± 54	206 ± 17	177 ± 21	140 ± 23
decane	N_DEC	230 ± 66	198 ± 54	171 ± 48	314 ± 35	320 ± 38	253 ± 56
isobutylbenzene	I_BUBZ	24 ± 5	16 ± 3	15 ± 3	16 ± 5	10 ± 3	6 ± 1
sec-butylbenzene	S_BUBZ	17 ± 4	12 ± 3	13 ± 2	10 ± 1	11 ± 1	5 ± 1
1-methyl-3-Isopropylbenzene	M1IPR3BZ	29 ± 7	17 ± 4	18 ± 3	15 ± 2	14 ± 1	8 ± 2
1-methyl-4-Isopropylbenzene	M1IPR4BZ	95 ± 28	50 ± 13	66 ± 17	49 ± 6	33 ± 6	51 ± 9
1-methyl-2-Isopropylbenzene	M1IPR2BZ	5 ± 2	2 ± 1	1 ± 0	0 ± 0	2 ± 0	1 ± 0
1-methyl-3-n-Propylbenzene	M1NP3BZ	159 ± 39	100 ± 24	85 ± 15	46 ± 4	40 ± 4	21 ± 4
1Me4nP_nB_13dMe5Ebenzene	MPBMEBZ	281 ± 69	175 ± 42	145 ± 26	107 ± 14	96 ± 9	52 ± 10
1,2-diethylbenzene	DEBZ12	145 ± 40	95 ± 26	64 ± 16	47 ± 3	47 ± 4	29 ± 3
1-methyl-2-n-Propylbenzene	M1NP2BZ	52 ± 13	34 ± 8	31 ± 5	23 ± 2	22 ± 2	10 ± 2
1,4-dimethyl-2-Ethylbenzene	M14E2BZ	121 ± 30	67 ± 15	66 ± 9	64 ± 6	53 ± 6	24 ± 5
1,2-dimethyl-4-Ethylbenzene	M12E4BZ	159 ± 39	96 ± 22	81 ± 14	55 ± 6	43 ± 4	26 ± 5
undecane	N_UNDE	176 ± 44	146 ± 39	168 ± 24	208 ± 22	220 ± 20	119 ± 20
1,3-dimethyl-2-Ethylbenzene	M13E2BZ	13 ± 3	8 ± 2	7 ± 1	5 ± 0	4 ± 0	2 ± 1
1,2-dimethyl-3-Ethylbenzene	M12E3BZ	44 ± 11	28 ± 6	26 ± 4	18 ± 1	15 ± 1	8 ± 2
2Mbutyl_1245tMebenzene	MB2TMBZ	89 ± 22	55 ± 13	48 ± 8	31 ± 3	23 ± 2	14 ± 3
tert-1-butyl-2-Methylbenzene	T1BM2BZ	19 ± 5	14 ± 4	11 ± 1	5 ± 1	3 ± 1	4 ± 1
n-pentylbenzene	NPTBZ	23 ± 5	20 ± 6	16 ± 3	15 ± 5	11 ± 3	4 ± 1
t-1-butyl-3,5-dimethylbenzene	T1BM35BZ	6 ± 4	2 ± 2	2 ± 2	2 ± 1	2 ± 1	0 ± 0
tert-1-Butyl-4-Ethylbenzene	T1BE4BZ	25 ± 15	24 ± 12	2 ± 2	16 ± 3	13 ± 2	6 ± 1
dodecane	DODEC	118 ± 26	91 ± 22	116 ± 15	109 ± 8	108 ± 11	49 ± 11
1,3,5-triethylbenzene	E135BZ	12 ± 4	6 ± 3	3 ± 2	6 ± 1	5 ± 1	1 ± 0
1,2,4-triethylbenzene	E124BZ	0 ± 0	0 ± 0	0 ± 0	0 ± 0	0 ± 0	0 ± 0
n-hexylbenzene	NHXBZ	10 ± 2	9 ± 2	9 ± 2	8 ± 3	4 ± 2	2 ± 1
norfarnesane	NORFARN	32 ± 8	22 ± 5	30 ± 4	23 ± 2	22 ± 2	14 ± 3
tridecane	TRIDEC	81 ± 18	58 ± 13	84 ± 13	94 ± 9	80 ± 8	47 ± 9
farnesane	FARNES	15 ± 3	13 ± 3	16 ± 2	15 ± 1	16 ± 1	9 ± 2
tetradecane	TDEC	194 ± 55	86 ± 24	85 ± 16	217 ± 42	93 ± 14	45 ± 9
pentadecane	PENTAD	79 ± 21	44 ± 10	48 ± 8	103 ± 17	55 ± 7	39 ± 15
hexadecane	HEXAD	30 ± 7	24 ± 5	24 ± 4	49 ± 6	35 ± 4	18 ± 4
heptadecane	HEPTAD	21 ± 5	17 ± 3	17 ± 3	35 ± 4	27 ± 3	24 ± 10
pristane	PRIST	10 ± 2	8 ± 2	7 ± 1	14 ± 2	12 ± 2	7 ± 1
octadecane	OCTAD	9 ± 3	11 ± 2	10 ± 2	22 ± 4	17 ± 2	8 ± 3
phytane	PHYTAN	3 ± 1	2 ± 1	3 ± 1	7 ± 1	5 ± 1	2 ± 1
nonadecane	NONAD	2 ± 2	4 ± 1	4 ± 1	28 ± 13	12 ± 4	13 ± 9
eicosane	EICOSA	1 ± 1	3 ± 1	0 ± 0	16 ± 5	9 ± 3	4 ± 2
henicosane	HENEIC	0 ± 0	2 ± 1	6 ± 6	20 ± 8	14 ± 7	10 ± 7
docosane	DOCOSA	1 ± 1	2 ± 1	1 ± 1	38 ± 12	18 ± 10	102 ± 89
tricosane	TRICOSA	2 ± 1	1 ± 1	0 ± 0	44 ± 14	21 ± 9	12 ± 9
tetracosane	TETCOS	1 ± 1	1 ± 1	0 ± 0	85 ± 41	37 ± 25	13 ± 11
pentacosane	PENCOS	4 ± 4	0 ± 0	0 ± 0	63 ± 32	29 ± 20	203 ± 202
hexacosane	HEXCOS	10 ± 10	2 ± 2	0 ± 0	58 ± 30	31 ± 19	19 ± 19
heptacosane	HEPCOS	16 ± 16	16 ± 16	0 ± 0	71 ± 37	38 ± 22	222 ± 220
octacosane	OCTCOS	14 ± 14	2 ± 2	0 ± 0	52 ± 27	34 ± 19	14 ± 14

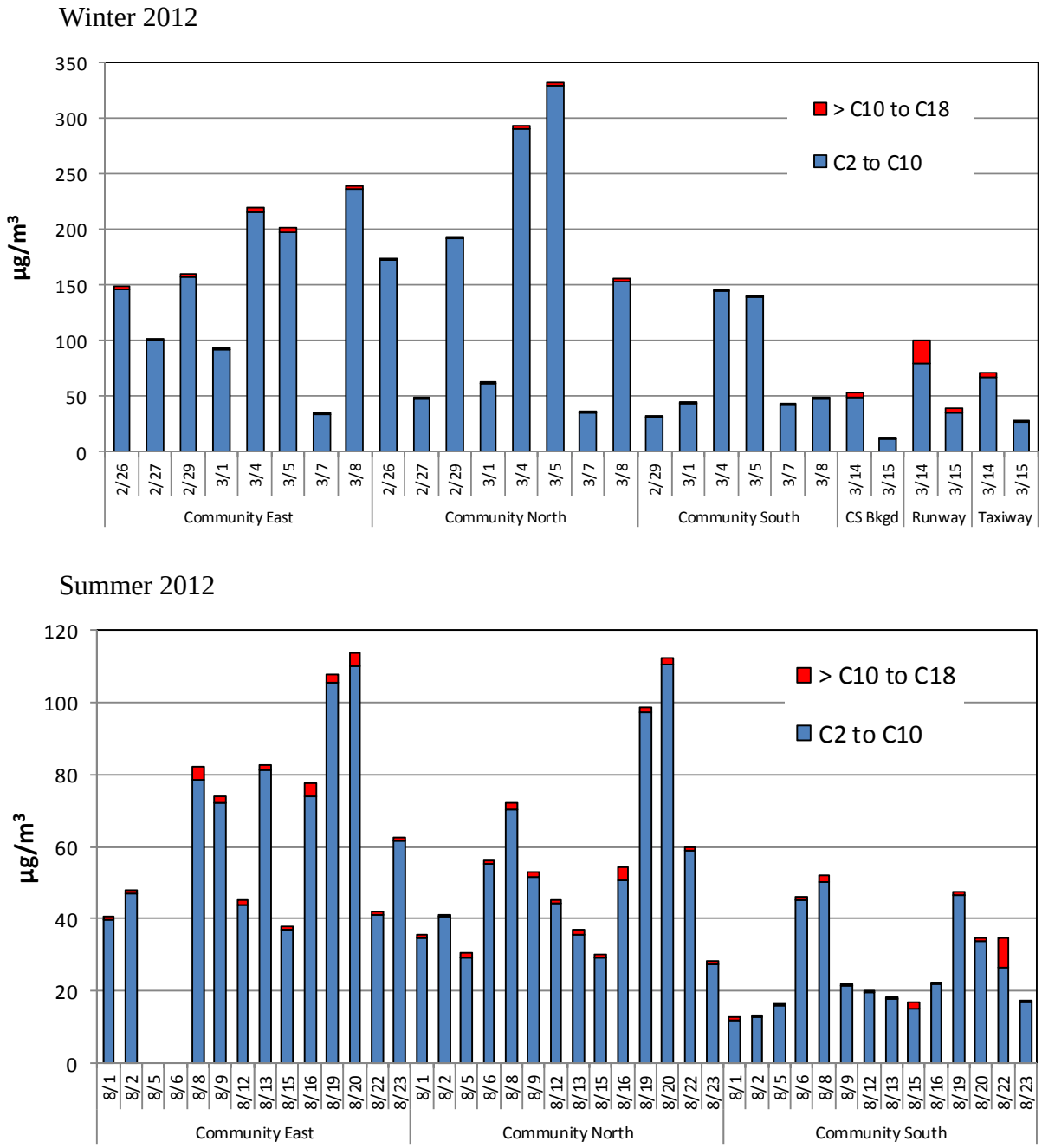

Figure 6-10. Daily variations in the sum of hydrocarbons from ethane to n-decane (C2 to C10) and greater than decane to n-octadecane (>C10 to C18) at the three core monitoring sites Winter and Summer Monitoring Seasons.

6.3 SOURCE COMPOSITION PROFILES

The concentrations and composition of pollutants measured at a community-scale air quality monitoring site depend on the temporal and spatial variations in the numbers and emission rates of sources in the vicinity of the monitoring location. These local emissions are superimposed on an urban background with a pollutant mix that varies with changes in regional pollutant transport patterns. The VOC and $PM_{2.5}$ emission inventory for the SoCAB in Table 6-6 is helpful in identifying the major emission sources that may contribute to ambient pollutant concentrations. In addition to jet exhaust emissions, the CMB analysis included other sources that could potentially impact the monitoring locations. The impact of on-road motor vehicles are expected since they are ubiquitous sources. Although area sources such as wild fires and fugitive dust may impact a wide area, these are intermittent events. Surface coating and solvent use are also common sources, but their emissions are more variable in space and time. Emissions from meat cooking and vegetative burning typically have large diurnal and seasonal variations and widely varying composition profiles. Petrochemical production, oil refining, and other industrial plants are specific to locations where these facilities exist.

6.3.1 PM Source Composition Profiles from Previous Studies

The source composition profiles that have been assembled for this Study for use in CMB analysis of the LAX AQSAS ambient data are listed in Table 6-7. An initial list of 17 chemical profiles (13 fossil fuel combustion, two vegetative burning, and two meat cooking) were compiled from previous emissions characterization studies. Multiple profiles representing most source categories were included during initial model runs to determine which were most appropriate and evaluate the sensitivity to variations in profile composition. Profiles that consistently resulted in poor model performance were eliminated from the profile set used in the final run. Most of these profiles are composites of multiple source measurements within a category. Six additional profiles were created for this study: two jet exhaust, two mineral dust (soil), and two for major secondary aerosols (ammonium nitrate and ammonium sulfate). Table 6-8 shows the distributions of organic compounds by class in weight percent of total $PM_{2.5}$ mass for each profile. The profiles are grouped according to source types to facilitate comparisons among profiles within and between source categories. Table 6-8 shows there are substantial variations in abundances of molecular markers within a source category, depending upon the fuel that is burned, conditions of the tests, and other factors.

The following summary identifies the major chemical types and specific organic compounds that are typically found in PM emissions from motor vehicles, vegetative burning, meat cooking, leaf abrasion and vegetative detritus, and species that may be indicative of secondary organic aerosol (SOA) formation. This summary is for illustrative purposes and is not meant to be comprehensive. Where abundances of specific organic compounds or groups of compounds are given, as in the case for meat cooking, they apply to specific tests or composites.

Vehicle Exhaust

- Higher abundance of EC in diesel exhaust. However, newer diesel engines have lower abundances of EC than older model year engines. EC abundances in PM emissions of

gasoline vehicle are very low but can be higher during hard accelerations and during cold starts.

- Hopanes and sum of steranes are very stable components of petroleum feedstocks and are found with similar composition in lubricating oils used by both diesel and gasoline vehicles.
- benzo(ghi)perylene, ideno(1,2,3-cd)pyrene, and coronene (gasoline)
- dimethylnaphthalenes, methyl- and dimethylphenanthrenes, and methylfluorenes (diesel emissions contained higher proportions but these are mostly semi-volatile and are not quantitatively collected on quartz filters).

Vegetative Burning

- dehydroabietic, abietic, or pimaric acid (resin acids that are biosynthesized mainly by conifers)
- retene (1-methyl-7-isopropylphenanthrene) (derived by thermal degradation of abietic acid, but is semi-volatile).
- methoxy phenols: guaiacol (2-methoxyphenol) and its derivatives (wood lignin pyrolysis product in similar ratio for all woods, but mostly semi-volatile).
- dimethoxy phenols: syringol (2,6 dimethoxyphenols) and its derivatives (wood lignin pyrolysis product in almost two orders of magnitude higher in hardwoods).
- Levoglucosan (1,6-anhydro-β-D-glucose) (product of decomposition of cellulose): Pine needles, grasses, and scrubs produce much higher abundances of levoglucosan than burning wood (Mazzoleni et al., 2007). This can be an important distinction between residential wood burning versus wildfires and prescribed fires.

Meat Cooking (Charbroiling of hamburger meat with 20% fat)

- C_7 to C_{22} n-alkanoic acids (saturated n-fatty acids) with no odd or even carbon number predominance. C_7 to C_{12} n-alkanoic acids are predominantly in the gas phase. Fatty acid make up about 5 percent of OC with hexadecanoic (palmitic) and octadecanoic (stearic) acids accounting for 2.6 and 1.5 percent, respectively.
- n-alkenoic acids account for about 4 percent of particulate OC with 9-octadecenoic (oleic), 9-hexadecenoic (palmitoleic) acids accounting for 3.4 and 0.3 percent, respectively.
- C_1 to C_{29} n-alkanes. Volatile under C_{13} and semi-volatile from C_{13} to C_{25}. Alkanes in the particulate phase accounted for 0.1 percent of OC.
- Cholesterol is a specific organic marker for meat cooking. However it typically accounts for a small fraction (0.1 percent or less) of particulate OC.

Table 6-6. 2010 VOC and $PM_{2.5}$ emission inventory (annual average day) for the South Coast Air Basin in tons/day (TPD) and percent of total (Pct).

		VOC		PM2.5	
TYPE	SOURCE CATEGORY	TPD	Pct	TPD	Pct
STATIONARY	FUEL COMBUSTION	5.8	1.0%	5.43	5.3%
	WASTE DISPOSAL	9.1	1.6%	0.32	0.3%
	CLEANING AND SURFACE COATINGS				
	Coatings and related process solvents	19.6	3.4%	0.54	0.5%
	Degreasing	10.8	1.9%	0.00	0.0%
	Printing	5.5	0.9%	0.00	0.0%
	Adhesives and Sealants	3.8	0.7%	0.00	0.0%
	Laundering and Other Cleaning	1.0	0.2%	0.01	0.0%
	PETROLEUM PRODUCTION AND MARKETING				
	Petroleum Marketing	27.1	4.7%	0.00	0.0%
	Petroleum Refining	4.6	0.8%	2.06	2.0%
	Oil and Gas Production	1.5	0.3%	0.01	0.0%
	INDUSTRIAL PROCESSES	20.2	3.5%	7.05	6.9%
AREAWIDE	SOLVENT EVAPORATION				
	Consumer Products	103.6	18.0%	0.00	0.0%
	Architectural Coating and Related Process Solvents	23.1	4.0%	0.00	0.0%
	Pesticide, Fertilizers, Paving, Roofing	2.6	0.5%	0.02	0.0%
	MISCELLANEOUS PROCESSES				
	Paved Road Dust	0.0	0.0%	18.54	18.2%
	Cooking	2.0	0.3%	14.40	14.1%
	Residential Fuel CombustionBUSTION	4.1	0.7%	8.35	8.2%
	Construction and DemolitionION	0.0	0.0%	5.28	5.2%
	Managed Burning and disposal	3.6	0.6%	4.64	4.6%
	All other misc processes	5.0	0.9%	1.86	1.8%
MOBILE	ON-ROAD MOTOR VEHICLES				
	Light-Duty Autos, Motocycles & Trucks	131.3	22.8%	8.17	8.0%
	Med to Heavy Duty Gas Trucks, Buses, Motorhomes	37.1	6.4%	1.67	1.6%
	All Diesel Trucks & Buses	13.6	2.4%	7.61	7.5%
	School and Other Buses	0.7	0.1%	0.19	0.2%
	OTHER MOBILE SOURCES				
	Aircraft	8.7	1.5%	0.93	0.9%
	Trains	2.4	0.4%	0.77	0.8%
	Ocean Going Vessels	0.9	0.2%	1.29	1.3%
	Commercial Harbor Craft	0.4	0.1%	0.24	0.2%
	Recreational Boats	37.7	6.5%	2.36	2.3%
	Off-Road Recreational Vehicles	7.0	1.2%	0.04	0.0%
	Off-Road Equipment	72.9	12.7%	9.77	9.6%
	Farm Equipment	1.2	0.2%	0.34	0.3%
	Fuel Storage and Handing	8.7	1.5%	0.00	0.0%
TOTAL STATIONARY		109.0	18.9%	15.4	15.1%
TOTAL AREAWIDE		144.1	25.0%	53.1	52.1%
TOTAL MOBILE		322.9	56.1%	33.4	32.8%
TOTAL		576.0		101.9	

Source: http://www.arb.ca.gov/app/emsinv/

Table 6-7. Source composition profiles compiled for use in source apportionment of PM.

Profile Name	Source Category	Description	Reference	selected
RWAY_TC1	Jet Exhaust	Background subtracted source measurements from behind blast fence, Runway 25R	LAXAQSAS	Y
RWAY_TC2	Jet Exhaust	Background subtracted source measurements from behind blast fence, Runway 25R	LAXAQSAS	
CI_HCS	Diesel Exhaust	Heavy HD truck exhaust composite, city/suburban drive cycle	Fujita, et al. 2007	Y
CI_HDD	Diesel Exhaust	Heavy HD truck exhaust composite, composite drive cycles	Fujita, et al. 2007	
CI_HW	Diesel Exhaust	Heavy HD truck exhaust composite, highway drive cycle	Fujita, et al. 2007	Y
MDD	Diesel Exhaust	Medium HD truck exhaust composite, city/suburban drive cycle	Fujita, et al. 2007	
Fleet_avg	Gasoline Exhaust	LD Gasoline vehicle exhaust, fleet average	EPA Kansas City PM Characterization Study, 2008	Y
BlkSmoker	Gasoline Exhaust	LD Gasoline vehicle exhaust, high emitters with high EC/TC ratio	Kansas City PM Study	Y
OilBurner	Gasoline Exhaust	LD Gasoline vehicle exhaust, high emitters with high OC/TC ratio	Kansas City PM Study	Y
NormEm	Gasoline Exhaust	LD Gasoline vehicle exhaust, normal emitters	Kansas City PM Study	
SI_BC	Gasoline Exhaust	LD Gasoline vehicle exhaust, high emitters with high EC/TC ratio, UDC cold start	Fujita, et al. 2007	
SI_BW	Gasoline Exhaust	LD Gasoline vehicle exhaust, high emitters with high EC/TC ratio, UDC warm start	Fujita, et al. 2007	
SI_HC	Gasoline Exhaust	LD Gasoline vehicle exhaust, normal emitters, UDC cold start	Fujita, et al. 2007	
SI_HW	Gasoline Exhaust	LD Gasoline vehicle exhaust, normal emitters, UDC warm start	Fujita, et al. 2007	
Hardwood	Biomass Combustion	Residential wood stove emissions, hardwood fuel	Mazzolini, et al. 2007	Y
Softwood	Biomass Combustion	Residential wood stove emissions, softwood fuel	Mazzolini, et al. 2007	
Charbroil	Cooking	Meat cooking, charcoal broiling composite	Fitz, et al. 2003	Y
GasGrill	Cooking	Meat cooking, propane fired grill	Fitz, et al. 2003	Y
ORDsl	Diesel Exhaust	Off-road diesel vehicle exhaust composite	Fujita, et al. 2007	
RwayDust	Resuspended Dust	resuspended dust from behind blast fence, Runway 25R	LAXAQSAS	
avgSoil	Resuspended Dust	resuspended dust from baseline sites, composite	LAXAQSAS	Y
NH4SO4	Secondary Aerosol	Ammonium Sulfate		Y
NH4NO3	Secondary Aerosol	Ammonium Nitrate		Y

Table 6-8. Distributions of marker compounds as mass fractions of total $PM_{2.5}$ by type of available source profiles*.

Profile Name	OC	EC	AL	SI	CU	ZN	PB	PAH gasoline markers	Hopanes & Steranes	cyclo-hexanes	guiacol +iseug+ acvan	cholesterol	eledaic acid
RWAY_TC1	0.1646	0.3062	0.0001	0.0001	0.0547	0.0319	0.0042	0.0000	0.0000	0.0000	0.0000	0.0000	0.0000
CI_HCS	0.1112	0.7931	0.0016	0.0016	0.0003	0.0045	0.0002	0.0000	0.0003	0.0046	0.0000	0.0000	0.0000
CI_HW	0.0841	0.8289	0.0011	0.0011	0.0002	0.0038	0.0001	0.0000	0.0003	0.0088	0.0000	0.0000	0.0000
Fleet_avg	0.5169	0.3122	0.0016	0.0016	0.0006	0.0038	0.0004	0.0029	0.0012	0.0014	0.0010	0.0000	0.0001
BlkSmoker	0.2391	0.6646	0.0001	0.0001	0.0004	0.0012	0.0002	0.0063	0.0007	0.0001	0.0001	0.0000	0.0000
OilBurner	0.6651	0.2092	0.0004	0.0004	0.0001	0.0012	0.0001	0.0031	0.0018	0.0010	0.0005	0.0000	0.0000
Hardwood	0.6272	0.0445	0.0011	0.0011	0.0001	0.0006	0.0001	0.0003	0.0001	0.0000	0.0437	0.0000	0.0011
Charbroil	0.6764	0.0260	0.0002	0.0002	0.0001	0.0001	0.0002	0.0001	0.0000	0.0000	0.0002	0.0021	0.0051
GasGrill	0.6609	0.1078	0.0001	0.0001	0.0001	0.0001	0.0000	0.0007	0.0000	0.0000	0.0002	0.0030	0.0053
SeaSalt	0.0000	0.0000	0.0000	0.0000	0.0000	0.0000	0.0000	0.0000	0.0000	0.0000	0.0000	0.0000	0.0000
NH4SO4	0.0000	0.0000	0.0000	0.0000	0.0000	0.0000	0.0000	0.0000	0.0000	0.0000	0.0000	0.0000	0.0000
NH4NO3	0.0000	0.0000	0.0000	0.0000	0.0000	0.0000	0.0000	0.0000	0.0000	0.0000	0.0000	0.0000	0.0000

*profile names are defined in Table 6-7

Leaf Abrasion and Vegetative Detritus.

- C_8 to C_{32} n-alkanoic acids (saturated n-fatty acids) with even carbon number predominance (~ 1 to 2 order of magnitude higher abundance for even carbon number). About uniform distribution among even carbon number n-alkanoic acid with hexadecanoic acid (palmitic acid) and undecanoic acids the two most abundant. This group accounted for 4.5 and 12.3 percent of the leaf abrasion products for green leaf and dead leaf, respectively. Abrasion products from dead leaves have 5-15 times greater abundances of C_{20} to C_{32} fatty acids.
- C_{19} to C_{36} n-alkanes, mostly in the range of C_{27} to C_{33} with odd carbon number predominance (4, 1, 25, 2, 41, 3, 20 for green leaf and 3, 1, 20, 1, 29, 3, 17 for dead leaf). This group accounted for 2.3 and 2.5 percent of the leaf abrasion products for green leaf and dead leaf, respectively.
- n-alkenoic acids (oleic, linoleic and linolenic acids). Accounted for about 0.03 and 0.01 percent for green and dead leaves, respectively.

Secondary Organic Aerosol

- pinonic acid (ozonlysis of α-pinene and β-pinene).
- butanedioic (succinic) acid, pentanedioic (glutaric) acid and hexanedioic (adipic) acids (mostly SOA, but also directly emitted).
- 1,2-benzene dicarboxylic acid (phthalic acid) and 1,3-benzene dicarboxylic acid (isophthalic acid) (SOA from primary vehicular emissions)
- dicarbonyls, carboxylic acids, hydroxy carbonyl and organic nitrate compounds.
- It is important to note that emissions from vegetative burning are highly reactive and can produce SOA in addition to SOA produced from anthropogenic and biogenic sources.

6.3.2 PM Source Composition Profiles Developed for LAX AQSAS

The total particle number in jet exhaust is dominated by the nucleation-mode particles comprised of sulfuric acid and other volatile species, which are approximately 10-20 nm in diameter (Timko et al., 2010; Corporan et al., 2007). Johnson et al. (2008) reported fuel-based emission factor estimates for total particle number of 9.0×10^{15} and 3.5×10^{16} per kg of fuel consumed during takeoffs and taxiing, respectively. The corresponding fuel-based $PM_{2.5}$ mass emission rates were 0.1 and 0.2 g/kg, respectively. Although organic PM emissions were low, the aforementioned studies confirmed lubricating oil was the predominant component of emitted particulate matter from modern aircraft engines (Timko et al., 2010; Yu et al., 2010). Aviation lubricants are synthetic oils consisting of a mixture of C_5-C_{10} fatty acid esters of pentaerythritol and dipentaerythritol (95%), tricresyl phosphate (3%), phenyl-alpha-naphthylamine (1%), benzamine, 4-Octyl-N-(4-Octylphenyl), and other minor ingredients. The in-use oil also contains several metals such as copper (Cu), beryllium (Be), nickel (Ni), and manganese (Mn) from wear of engine seals and bearings that may be contained in the emitted PM.

Supplemental source profiles that were developed as part of Phase III of the LAX AQSAS included jet exhaust from samples collected at the end of the South Airfield Runway 25R behind the blast fence near Aviation Boulevard. PM samples collected behind the blast fence during normal daytime runway operations were adjusted to remove local background concentrations of all analytes. This was done by subtracting the ambient concentrations measured at the CS site during the same time period. PM profiles were also adjusted to remove resuspended surface material based on the analysis of surface dust samples collected at the blast fence.[3] The remainder should represent only emissions from runway operations. Since winds were westerly during the source sampling period, the only activity upwind of the sampling area was departing flights. Therefore, resulting background subtracted pollutant concentrations can reasonably be considered to be representative of the PM emissions in jet aircraft exhaust.

Aerosol components that were significantly above background levels in the runway samples included sulfate, EC, and several metals that may be related to wear of engine seals and bearing (e.g., copper, nickel, manganese). Copper was especially prominent and is a key marker compound since it is much less abundant in other source profiles.

6.3.3 VOC Source Composition Profiles

Source profiles were selected to represent the major sources of VOCs in the LAX area. The major source categories represented and the provenance of the profiles chosen are shown in Table 6-9. Table 6-10 shows the distributions of selected species as weight percent of the sum of 55 PAMS target compounds for each profile used in the CMB analysis. The weight fractions are normalized to the sum of the 55 PAMS species listed in Table 6-1. To the extent possible, the most regionally specific and current profiles were selected for each source category. Alternative profiles were also included to evaluate their specificity and the sensitivity of the apportionment to variations in profile composition. Profiles that consistently resulted in poor model performance were eliminated from the profile set used in the final run. Those profiles that were ultimately selected by CMB as producing the best fit to ambient data are indicated as 'selected' in Table 6-9.

Vehicle Exhaust

Diesel and gasoline exhaust profiles are similar with respect to the composition of light hydrocarbons, and are often collinear in CMB calculations. Ethene, acetylene, 1-butene, iso-butene, propane, propene, isopentane, n-pentane, 2,2 dimethylbutane, 2-methylpentane, n-hexane, benzene, 3-methyhexane, toluene, ethylbenzene, m- and p-xylene, m-ethyltoluene, and 1,2,4-trimethylbenzene, are the most abundant compounds in both diesel and gasoline emissions. Several of these are short-lived and are only used in CMB calculations where fresh emissions are expected. Major differences between these two exhaust profiles are evident for: 1) acetylene, iso-butene, isopentane, n-hexane, and 2-methylhexane, which are most abundant in gasoline

[3] The resuspended dust correction was made by normalizing the mass of all analytes in the $PM_{2.5}$ fraction of surface dust samples to mass of silicon, and then subtracting silicon and proportional amounts of other analytes from the ambient $PM_{2.5}$ measured behind the blast fence. The concentrations of inorganic components of the surface dust were determined by resuspending the dust in a specially designed chamber and collecting it on filters, which were subjected to the same gravimetric, IC, and XRF analysis as the ambient samples.

exhaust; and 2) for propene, propane, 2,2 dimethylbutane, n-decane, and n-undecane which are more abundant in diesel exhaust. Previous studies have shown that source attributions between tailpipe and evaporative emissions from receptor modeling can vary greatly depending on the particular profile chosen for tailpipe emissions (Harley et al., 1992; Fujita et al., 1994; Pierson et al., 1999). This is because tailpipe emissions are a mixture of hydrocarbons produced during combustion (e.g., acetylene, ethene, propene, and benzene), along with unburned gasoline, resulting from incomplete combustion. The relative abundances of combustion by-products in the exhaust profile vary with emission control technology, level of vehicle maintenance, and operating mode. In the CMB calculation, liquid gasoline represents the additional unburned gasoline (due to misfiring and other engine malfunctions) that is not included in the exhaust profile, plus evaporative emissions from gasoline spillage, hot soaks, and a portion of resting losses (leaks, permeation). The profile for gasoline headspace vapor is taken to represent fuel tank vapor losses (e.g., migration of fuel vapor from the canister).

The most relevant contemporary profile for on-road vehicle exhaust is from the on-road mobile emission study by the DRI at the traffic tunnel on Sherman Way in Van Nuys, California in August 2010 (Fujita et al., 2012). The Tunnel Study measured fleet-averaged emission rates of regulated and unregulated pollutants. The measured emission factors were compared to corresponding fleet-average emission factors estimated using MOVES2010a, MOBILE6.2, and EMFAC2007 for ambient temperature and traffic conditions observed during the Tunnel Study. Additionally, integrated canister, DNPH cartridge, and Teflon-impregnated glass fiber filter (with backup XAD cartridges) samples were obtained during two 3-hour sampling periods each day (09:00 -12:00 and 12:15 -15:15) on August 20, 21, 22, 24, 25, 26, 28, and 29 (two Saturdays, two Sundays, and four weekdays) in 2010. The fraction of diesel vehicles ranged from 0.9 percent on Sundays to 4.2 percent on weekdays. The profiles developed from the tunnel measurements represent a varying composite of emissions from diesel and gasoline vehicles, including running evaporative losses.

Fuel, Liquid, and Vapor

Running and resting losses are the two sources of evaporative loss from vehicles travelling on the road. Running losses are releases of gasoline vapor from the fuel system during vehicle operation as a result of the heating of the fuel tank. Vapors are released when the rate of fuel vapor formation exceeds the capacity of the vapor storage and purge systems. The composition of running losses tends to resemble headspace vapors if the carbon canister is saturated and butane-enriched vapors if the canister is not saturated. The canister similarly affects the composition of diurnal evaporative emissions. Resting loss evaporative emissions are due to migration of fuel vapors from the evaporative canister, leaks, and fuel permeation through joints, seals and polymeric components of the fuel system. Most of these losses, as well as hot soaks, tend to appear more like whole liquid gasoline. Liquid gasoline contains many compounds in common with gasoline-vehicle exhaust. It is depleted in combustion products, such as ethane, ethene, acetylene, propene, and to some extent, benzene. Evaporated gasoline and heavier hydrocarbons that volatilize more slowly from liquid fuels are also depleted in these combustion compounds. Isobutane, n-butane, t-2 butene, and especially isopentane are enriched in evaporated gasoline. These differences are sufficient for CMB separation of gasoline exhaust from liquid and evaporated gasoline, and often from diesel exhaust, in ambient air.

Surface Coatings

Although solvents from paints and industrial uses are large components of VOC inventories, they have few reported profiles. The most comprehensive data are those of Censullo et al. (1996), which included analyses of 11 categories of coating. Detailed species profiles were obtained for a total of 106 samples of water-based and solvent-based coating samples. Surface coating profiles for solvent-based industrial maintenance coatings, solvent-based medium gloss/high gloss, solvent-based primers and sealers, quick dry primers and enamels, and thinning solvent were applied in the apportionments. These are largely depleted in the species common to fuel use and production, with larger abundances of styrene, n-decane, and "other" VOCs, which are oxygenated compounds and differ substantially among the different coatings tested.

High concentrations of toluene, nonane, and methyl-heptanes observed at the CE and CS sites during the first week of speciated VOC sample collection are suspected to be indicative of local emissions from some type of surface coating, adhesive, or solvent. However, these VOCs do not match any of the profiles in DRI's library or samples of the paint used on the shelters. To avoid skewing the apportionment of other sources containing these compounds, a synthetic profile was created by subtracting the relative amounts of all hydrocarbon species found in a sample collected at the CE site on a day when ventilation was high from the high concentrations observed during the first week of the Winter Season, and using the remainder as a profile for the unidentified local source (CEloc).

Regional Background and Biogenic Emissions

Regional upwind, background VOC's typically contain higher abundances of relatively nonreactive hydrocarbons, such as ethane and propane, and oxidized species, primarily aldehydes. In addition to urban background, both compressed natural gas (CNG) and liquefied petroleum gas (LPG) are potential sources of ethane and propane. However, since CNG and LPG cannot be distinguished from urban background, these source contributions may be combined to represent urban background VOC.

Biomass Combustion

Emissions from burning of natural vegetation (e.g. wildfires, prescribed burns, yard waste incineration, and wood-fueled residential heating) are extremely variable due to their sensitivity to fuel composition and combustion conditions, which makes them difficult to apportion accurately. However, these emissions tend to be enriched in the C_2 compounds when compared to more efficient fuel combustion sources (heaters, boilers, engines, etc.). Several profiles derived from a variety of fire types, mentioned above, were included in the apportionment. Meat cooking also produces a wide range of emissions, which depend on the method, fat content, and fuel used. This makes identification of these sources difficult to identify. Composite profiles representing commercial cooking of beef and chicken using charcoal and propane fuels were included because one of the sites was located close to a restaurant. However, there is potential for these profiles to be overrepresented in some cases due to the similarity with other types of fuel combustion.

Unidentified

Most source profiles used in this study contain an unidentified (UNID) component, which represents the fractional compositions of non-methane hydrocarbons (NMHC) not assigned to individual, identified species in the gas chromatographic analysis. A single constituent source profile (UNID is taken to constitute 100 percent of NMHC) has been used in the past (Fujita et al., 1994) to account for the contributions from this component. The difference between the measured total NMHC and the sum of the source contributions from fitted sources is named as "unexplained." The "unexplained" source contributions in this report refer to the differences between the measured NMHC and the sum of the predicted contributions from those identified source categories. Nearly all of the unexplained mass is related to UNID and not assigned to the identified categories. The fraction of UNID is consistently higher in downwind and afternoon samples, which suggests that much of this residual UNID could be secondary organic species produced by photochemical reactions.

6.3.4 VOC Source Composition Profiles Developed for LAX AQSAS

Supplemental source profiles that were developed as part of the LAX AQSAS included jet exhaust from samples collected at the end of the South Airfield Runway 25R behind the blast fence near Aviation Boulevard and analysis of fuel (gasoline, diesel and Jet-A) samples from the study area. VOC samples collected behind the blast fence during normal daytime runway operations were adjusted to remove local background concentrations of all analytes by subtracting the ambient concentrations measured at the CS site during the same time period.

Since gasoline composition has been modified substantially in recent years to meet air quality regulations, new profiles were created from analysis of fuel samples collected from local stations on and near LAX. Three grades and several brands of gasoline were analyzed and the results composited according to the fractions of premium and regular grade sold in LA County. The compositions of gasoline headspace vapors were predicted from the measured composition of liquid gasoline using the method described by Kirchstetter et al. (1999). This method is based on the proportionality between the equilibrium headspace partial pressure for each compound identified in gasoline with its mole fraction in liquid gasoline multiplied by the vapor pressure of the pure species. The individual vapor pressures are determined using the Wagner equation. Older fuel profiles from the LA area were also included for comparison, but were not selected for the final source apportionment.

Source profiles were also created from analysis of samples of liquid diesel fuel and Jet-A fuel collected during this Study. However it was not possible to accurately estimate the composition of evaporative emissions since a substantial fraction of the total NMHC are higher molecular weight compounds that were not identified by the analysis. An archived profile for the jet fuel evaporative emissions obtained from the California Air Resources Board was included instead.

Table 6-9. Source composition profiles tested for use in source apportionment of VOC.

Profile Name	Source Category	Description	Reference	Selected
VNT_WD	On-road vehicles	mixed vehicle exhaust, Van Nuys Tunnel, Weekday	Fujita, et al. 2012	Y
VNT_SUa	On-road vehicles	mixed vehicle exhaust, Van Nuys Tunnel, Sunday AM	Fujita, et al. 2012	
VNT_SUp	On-road vehicles	mixed vehicle exhaust, Van Nuys Tunnel, Sunday PM	Fujita, et al. 2012	Y
VNT_SAT	On-road vehicles	mixed vehicle exhaust, Van Nuys Tunnel, Saturday	Fujita, et al. 2012	
TuS96	On-road vehicles	mixed vehicle exhaust, Sepulveda Tunnel	Fujita, et al. 1997	
LiqGas	On-road vehicles	liquid gasoline, LAX area composite	LAXAQSAS	Y
VapGas	On-road vehicles	gasoline headspace vapor, LAX area composite	LAXAQSAS	Y
Gas00VRPC	On-road vehicles	gasoline headspace vapor, LA area composite	Fujita, et al. 2007	
LiqDiesl	On-road vehicles	liquid diesel fuel, LAX area composite	LAXAQSAS	
TuMchHDc	On-road vehicles	Diesel Profile, Ft McHenry Tunnel, Baltimore, 1992	Gertler et al, 1996	Y
Runway1	Aircraft Emissions	Jet Exhaust, LAX runway 25R	LAXAQSAS	Y
Runway2	Aircraft Emissions	Jet Exhaust, LAX runway 25R	LAXAQSAS	
TaxiWay1	Aircraft Emissions	Mixed runway operations, LAX south airfield	LAXAQSAS	
TaxiWay2	Aircraft Emissions	Mixed runway operations, LAX south airfield	LAXAQSAS	
Jet5exh_	Aircraft Emissions	Composite jet exhaust JP-5 (EPA 1097-1099)	Spicer 1984; EPA 1988	Y
Jet4evap	Aircraft Emissions	Jet fuel evaporation (jp-4)	CARB	Y
LiqJetA	Aircraft Emissions	liquid Jet A fuel, LAX	LAXAQSAS	
CNG	CNG/LPG	Commercial Natural Gas from Los Angeles	Mayrsohn et al 1976	Y
GNG	CNG/LPG	Geogenic Natural Gas from Los Angeles	Mayrsohn et al 1976	
LPG	CNG/LPG	Liquefied Petroleum Gas from Los Angeles	Mayrsohn et al 1976	Y
COATcomp	Surface Coatings	composite of 10 coatings, weighted by total U.S. sales	Censullo, 1991	
CEloc	Surface Coatings	excess C7 & C8 HC observed at CE site.	LAXAQSAS	Y
i-butane	Unidentified	iso-butane	single species profile	Y
n-butane	Unidentified	butane	single species profile	Y
i-pentane	Unidentified	iso-pentane	single species profile	Y

Table 6-10. Distributions of selected species as percentage of sum of 55 PAMS species in VOC source profiles.

	Profile Name*										
	VNT_WD	VNT_SUp	LiqGas	VapGas	TuMchHDc	Runway1	Jet5exh_	Jet4evap	CNG	LPG	CEloc
acetylene	5.52%	7.97%			1.80%	7.80%	11.49%				
ethane	4.40%	4.98%			1.19%	11.66%	2.53%		69.19%	4.11%	
propane	1.57%	3.15%			2.23%	12.79%	0.54%		21.23%	90.58%	
iso-butane	1.39%	0.90%	0.70%	0.97%	0.28%	2.82%			2.09%	0.20%	
n-butane	4.24%	4.00%	7.30%	10.09%	0.64%	4.86%			3.10%		
iso-pentane	28.01%	33.90%	12.30%	13.69%	1.32%	5.65%			0.69%		
n-pentane	8.60%	10.61%	5.85%	6.51%	1.53%	2.20%	0.59%		0.69%		
isoprene	0.75%	0.11%				0.25%					
2,2-dimethylbutane	1.96%	2.14%			2.64%	0.44%					
cyclopentane	0.77%	0.82%	0.69%	0.79%	0.32%	0.21%					
2-methylpentane	7.25%	7.92%	5.96%	5.56%	1.98%	1.57%	1.06%		0.30%		
3-methylpentane	4.29%	4.65%	3.63%	3.39%	0.92%	1.09%			0.10%		
n-hexane	3.05%	3.53%	3.62%	3.37%	0.97%	0.90%			0.40%		
2,4-dimethylpentane	2.70%	2.25%	1.38%	1.11%	0.36%	0.49%					
benzene	4.53%	3.78%	1.37%	1.41%	3.21%	2.52%	5.39%	1.09%			
2,3-dimethylpentane	4.39%	2.99%			0.91%	1.04%					
3-methylhexane	2.74%	2.85%	2.51%	2.01%	2.32%	0.67%			0.20%		
toluene	10.13%	11.33%	11.60%	10.12%	4.52%	3.96%	1.45%	5.47%			74.09%
ethylbenzene	1.77%	1.83%	2.34%	1.77%	2.86%	0.49%	0.47%	1.09%			
n-nonane	0.72%	0.28%	0.56%	0.35%	1.13%	0.56%	0.39%	9.63%			10.88%
m&p-xylene	6.30%	6.80%	9.59%	7.26%	11.05%	1.60%					
o-xylene	2.22%	2.48%	2.97%	2.25%	3.76%	0.59%	0.54%				
2-methylheptane	1.12%	1.05%	1.11%	0.78%		0.36%			0.40%		2.53%
Tetradecane	0.61%	0.38%			9.25%	0.52%	1.65%	23.85%			
Pentadecane	0.35%	0.03%			7.05%	0.37%	0.74%	14.66%			
Hexadecane	0.23%	0.04%			4.25%	0.20%	0.37%				
Heptadecane	0.32%	0.10%			2.24%	0.06%	0.02%				
Octadecane	0.09%	0.07%			0.94%						

* profile names are defined in Table 6-9

6.4 CMB SOURCE APPORTIONMENT RESULTS

The CMB receptor model was used to estimate the contributions of jet exhaust and other emission sources to the ambient concentrations of $PM_{2.5}$, OC, EC, VOC and gaseous air toxics (e.g., benzene, toluene, ethylbenzene and xylenes) at the core monitoring sites.

6.4.1 Fine Particulate Matter

The seasonal mean source contribution estimates (SCE) to ambient concentrations of $PM_{2.5}$, OC, and EC, along with the propagated errors of the estimates, are presented by site and season in Table 6-8, Table 6-9, and Table 6-10, respectively. The daily variations in SCEs of $PM_{2.5}$, with and without secondary aerosol contribution, are plotted in Figure 6-11 and in Figure 6-13 respectively. $PM_{2.5}$ was apportioned to four combustion sources, jet exhaust, diesel vehicle exhaust, gasoline-vehicle exhaust, and wood combustion. Meat cooking was also separately apportioned, but since it was highly uncertain, it was combined with unidentified OC and included in Table 6-8 as unidentified organic matter (OM).

Ammonium sulfate, ammonium nitrate, and residual organic matter that were not apportioned to combustion sources comprised approximately half of the $PM_{2.5}$ mass at the CE, CN and CS sites during the Summer Season and greater than two-third during the Winter Season. Sulfate ion is normally derived from the chemical conversion of gaseous SO_2 in the atmosphere to sulfuric acid (H_2SO_4) and subsequent neutralization by ammonia and cannot be apportioned by CMB to specific sources of SO_2. A small fraction (from < 1 to a few percent) of SO_2 is oxidized to H_2SO_4 in jet exhaust and directly emitted as the acid. The estimated contributions of jet exhaust to sulfate in $PM_{2.5}$ are 2.0% at the CE site, 7.1% at the CN site, and 1.3% at the CS, assuming a conversion rate of SO_2 to H_2SO_4 in jet exhaust of approximate one percent. This rate is consistent with the mass ratios of sulfate to the sum of SO_2 and sulfate (all background subtracted) from measurements behind the blast fence at the South Airfield Runway 25R. Soil was generally a minor component (< 5 percent) of $PM_{2.5}$, except on windy days. Soil accounted for about 30 percent of $PM_{2.5}$ mass at the CS site during a strong wind event on March 7 and 8, 2012. The soil contributions were also higher at the other two sites, which accounts for the higher mean soil contributions during the Winter Season at all three core sites.

The contributions of jet exhaust at the three core sites during both seasons were between 1 and 2.5 percent of $PM_{2.5}$ mass. In contrast, the diurnal and day-of-week variations in particle size distributions (PSD) described in Section 5 suggest that jet exhaust was a significant contributor to UFP number concentrations for sizes smaller than 30 nm. These seemingly contradictory conclusions can both be true because the contributions of UFP < 30 nm to $PM_{2.5}$ mass are negligible. This is illustrated in Figure 6-14., which shows the PSD measured at the CE and Trinity Lutheran Church School (TLCS) sites during the Supplemental Study on 9/5/12 through 9/6/12. While the number concentrations of UFP < 30 nm were much higher at the CE, the distribution of volume concentrations, which are proportional to mass concentrations, were similar at the two sites and the contributions of UFP< 30 nm are negligible in the volume distribution.

Table 6-11. CMB fit quality (R^2) and source contribution estimates to $PM_{2.5}$ mass (µg/m^3) by site and season.

Site	Season	$PM_{2.5}$ mass (ug/m3)	number samples	R^2	Jet Exhaust	Diesel Exh	Gasoline Exh	Wood Smoke	Soil	Am Sulfate[1]	Am Nitrate[2]	unid OM[3]
CE	Winter	8.18	12	0.88	0.151 + 0.013	1.453 + 0.143	0.172 + 0.149	0.395 + 0.028	0.524 + 0.036	1.14	0.95	2.16
	Summer	7.41	11	0.79	0.055 + 0.005	0.571 + 0.054	0.022 + 0.056	0.283 + 0.024	0.171 + 0.013	2.60	0.91	2.22
CN	Winter	7.57	10	0.90	0.182 + 0.016	1.239 + 0.129	0.149 + 0.080	0.155 + 0.013	0.502 + 0.041	1.29	0.79	2.22
	Summer	8.06	4	0.78	0.110 + 0.025	0.646 + 0.058	0.024 + 0.047	0.217 + 0.018	0.319 + 0.072	3.16	0.78	2.07
CS	Winter	12.33	12	0.88	0.218 + 0.020	1.300 + 0.141	0.125 + 0.146	0.346 + 0.026	1.970 + 0.248	1.37	1.38	2.37
	Summer	6.80	11	0.74	0.029 + 0.006	0.512 + 0.049	0.014 + 0.028	0.409 + 0.032	0.101 + 0.010	3.58	1.05	2.72

[1] ammonium sulfate = (measured SO_4^{2-} - apportioned SO_4^{2-}) *1.375
[2] ammonium nitrate = (measured NO_3^- - apportioned NO_3^-) *1.29
[3] unidentified organic mass = (measured OC - apportioned OC) *1.8

Table 6-12. CMB fit quality (R^2) and source contribution estimates to total organic carbon (µg/m^3) by site and season.

Site	Season	OC conc. (ug/m3)	number samples	R^2	Jet Exhaust	Diesel Exh	Gasoline Exh	Wood Smoke	Soil
CE	Winter	1.95	12	0.89	0.027 + 0.004	0.169 + 0.048	0.115 + 0.020	0.265 + 0.025	0.014 + 0.002
	Summer	1.50	11	0.79	0.009 + 0.001	0.058 + 0.021	0.014 + 0.002	0.178 + 0.017	0.004 + 0.001
CN	Winter	1.66	10	0.90	0.030 + 0.004	0.137 + 0.037	0.096 + 0.018	0.097 + 0.009	0.013 + 0.002
	Summer	1.40	4	0.78	0.018 + 0.004	0.072 + 0.019	0.014 + 0.003	0.136 + 0.013	0.008 + 0.002
CS	Winter	1.99	12	0.91	0.039 + 0.005	0.156 + 0.041	0.088 + 0.016	0.226 + 0.022	0.055 + 0.009
	Summer	1.85	11	0.74	0.005 + 0.001	0.057 + 0.015	0.008 + 0.001	0.257 + 0.025	0.003 + 0.001

Table 6-13. CMB performance statistics and source contribution estimates to total elemental carbon (µg/m^3) by site and season.

Site	Season	EC conc. (ug/m3)	number samples	R^2	Jet Exhaust	Diesel Exh	Gasoline Exh	Wood Smoke	Soil
CE	Winter	1.18	12	0.88	0.046 + 0.005	1.157 + 0.054	0.046 + 0.010	0.018 + 0.002	0.000 + 0.001
	Summer	0.50	11	0.79	0.017 + 0.002	0.460 + 0.021	0.005 + 0.001	0.013 + 0.001	0.000 + 0.001
CN	Winter	0.98	10	0.90	0.056 + 0.006	0.983 + 0.081	0.034 + 0.008	0.007 + 0.001	0.000 + 0.001
	Summer	0.43	4	0.78	0.034 + 0.008	0.512 + 0.024	0.006 + 0.001	0.010 + 0.001	0.000 + 0.001
CS	Winter	1.02	12	0.88	0.067 + 0.007	1.031 + 0.045	0.028 + 0.006	0.015 + 0.002	0.001 + 0.002
	Summer	0.34	11	0.74	0.009 + 0.001	0.406 + 0.017	0.004 + 0.001	0.018 + 0.002	0.000 + 0.001

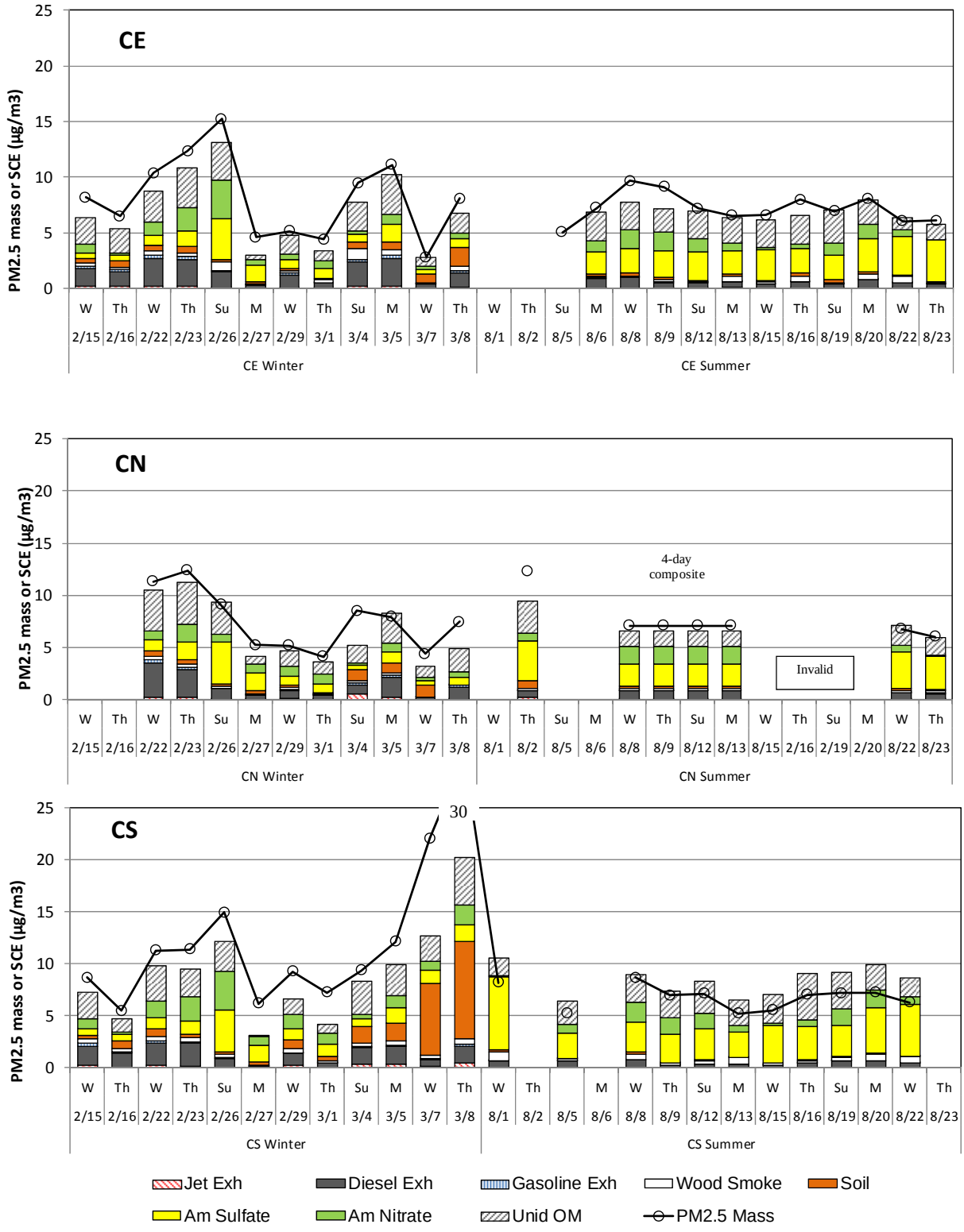

Figure 6-11. Chemical Mass Balance source contribution estimates (SCE) of 24-hour $PM_{2.5}$ during Winter and Summer Seasons at the three LAX AQSAS core monitoring sites.

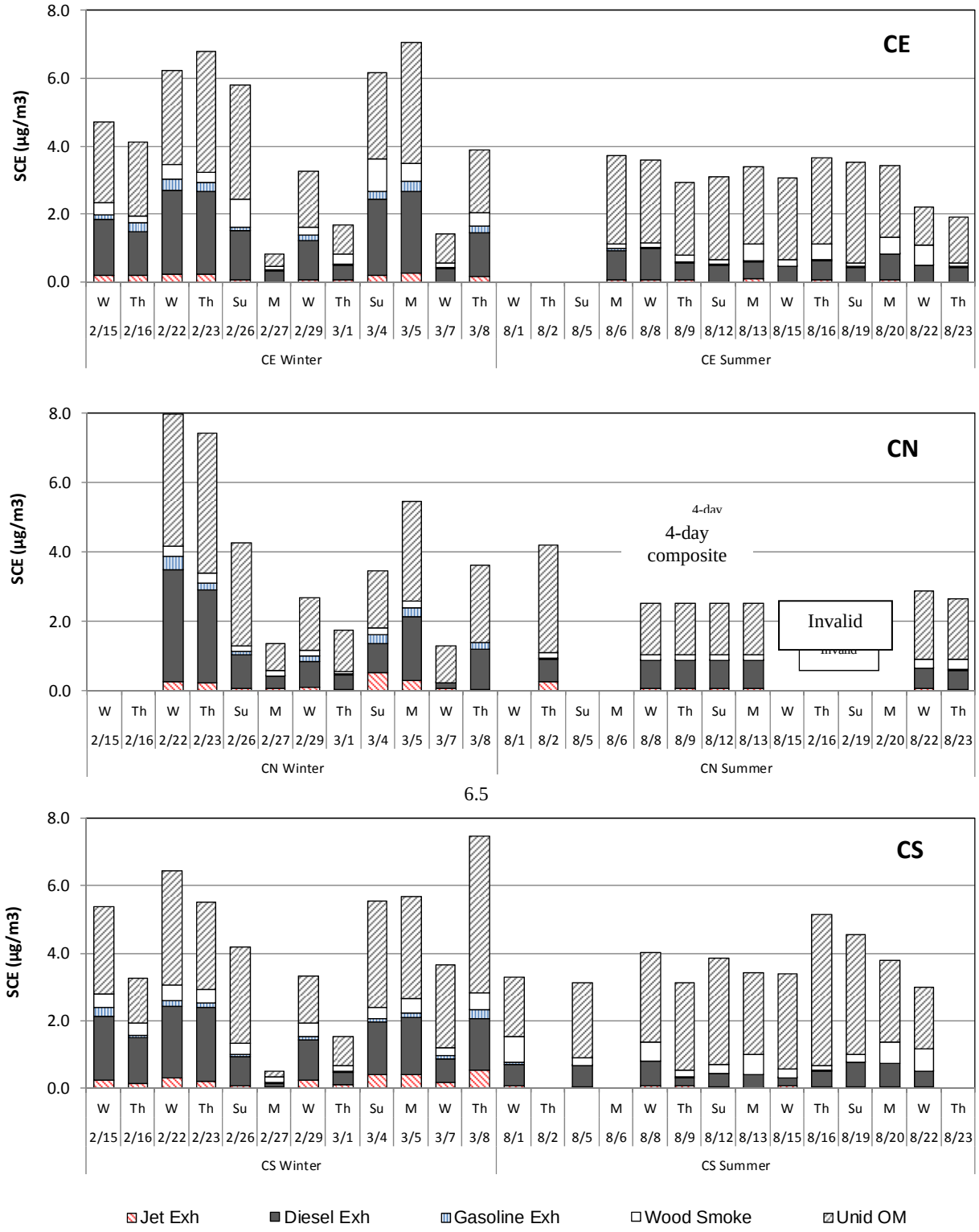

Figure 6-12. Chemical Mass Balance source contribution estimates (SCE) of 24-hour $PM_{2.5}$ during Winter and Summer Seasons at the three LAX AQSAS core monitoring sites excluding soil, ammonium sulfate, and ammonium nitrate.

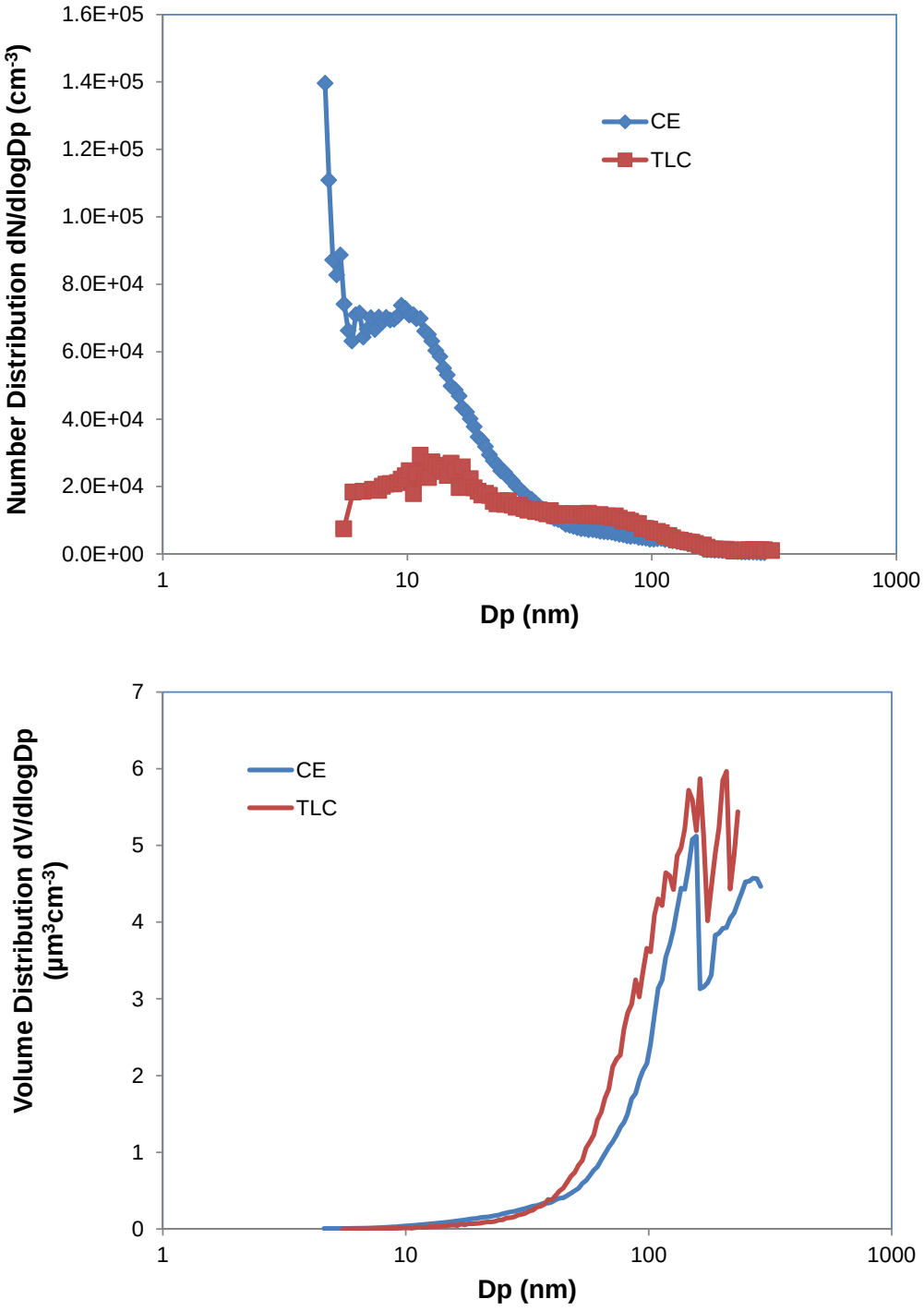

Figure 6-13. Average particle size distributions (PSD) measured at the CE and TLCS sites during 9/5/12 through 9/6/12. PSD at the CE site had much higher number concentrations for particles less than 25 nm. Volume concentrations were comparable for the two sites.

6.4.2 Volatile Organic Compounds

The seasonal mean SCE to ambient concentrations (in $\mu g/m^3$) of the sums of the PAMS target hydrocarbons, benzene, and toluene are presented by site and season in Table 6-14, Table 6-15, and Table 6-16, respectively, and the day-to-day variations in SCE are plotted in Figure 6-14. through Figure 6-16. 16. The sums of the PAMS hydrocarbons were apportioned to jet exhaust, on-road vehicles, gasoline vapor, CNG/LPG, local unidentified sources, excess butanes and isopentanes, and a residual unidentified fraction that was not apportioned to any of the direct sources. The seasonal mean SCEs by sites are summarized in Figure 6-17.

The mean contributions of jet exhaust to the sum of PAMS species ranged from a few percent to as much as 20 percent. The contributions were greater during the Winter Season with SCEs of 12.3 $\mu g/m^3$ at the CE site, 12.7 $\mu g/m^3$ at the CS site, and 4.0 $\mu g/m^3$ at the CN site. The contributions were generally lower during the Summer Season, with mean contributions of about 3 $\mu g/m^3$ at both the CE and CN sites, and less than 1 $\mu g/m^3$ at the CS site. The substantially lower contributions of jet exhaust during the Summer Season at the CS site was due to more persistent west winds compared to the morning northeast wind during the Winter Season. About 3 to 4 percent of the sum of PAM species attributed to jet exhaust was benzene. Apportionment of toluene to jet exhaust was not significant.

As described in Section 6.3.4, the chemical composition profiles for jet exhaust were based on ambient samples collected at the east end of the South Airfield Runway 25R. The runway profile was background subtracted using corresponding samples collected at the CS site. The impact on these profiles from vehicle exhaust emissions from traffic on Aviation Boulevard is believed to be small given the prevailing westerly winds. However, the apportionment of jet exhaust may be overestimated to the extent that influences of vehicle exhaust were not completely removed by the background subtraction. Acetylene is a major by-product of the combustion of all hydrocarbon-based fuels and a precursor to formation of PAHs and EC soot in the exhaust. Fuel combustion in modern jet engines is extremely efficient and VOC emissions from unburned fuel are typically very low, especially during takeoffs. Accordingly, the fitting species with greater influence for jet exhaust included acetylene and benzene, which was likely from dealkylation of various alkylbenzenes in jet fuel. While exhaust from gasoline and diesel engines also includes acetylene and benzene, their abundances are lower. As shown in Table 6-9, alternative profiles from Spicer et al (1984) and the California Air Resources Board were also included in the CMB analysis. These alternate profiles were used to apportion the runway sample as a validation of the jet exhaust profile (see Figure 6-17).

The vehicle exhaust profiles that were used in the CMB analysis were from the 2010 Van Nuys Tunnel Study conducted by the DRI. These profiles are background subtracted and are representative of a mixed fleet of gasoline and diesel vehicles in an urban area of the SoCAB. This tunnel study provided contemporary on-road vehicle exhaust profiles that are regionally relevant to the LAX AQSAS. The fractions of diesel traffic in the samples collected ranged from about 1 percent on Sunday to 4 percent on weekdays. Thus, these profiles are representative of on-road vehicle exhaust from a mixed fleet of predominantly gasoline-powered vehicles, with a smaller fraction of diesel-powered vehicles. The mix of traffic within the LAX AQSAS area

varies by time of day and day of week. However, since the total contributions of gasoline exhaust to VOC emissions greatly outweigh diesel exhaust, the combined source composition profile should provide a reasonable estimate of the sum of SCEs from separate apportionment of gasoline and diesel exhaust. On-road vehicles accounted for 25-40 percent of the sum of PAM species and about 50-75 percent of the measured benzene. The relative contribution to toluene varied greatly depending on the influence of a local unidentified source.

Higher ratios of light hydrocarbons to acetylene on warm days indicated the tunnel profile also included varying amounts of running evaporative losses. However, these losses would not include hot-soaks and diurnal evaporative losses. To account for these other sources, a gasoline vapor profile was included in the CMB analysis. This profile, as previously described, was derived from gasoline samples collected at service stations near LAX. Additionally, the excessively high butane and isopentane levels at the CN site may have been related to gasoline vapor losses from the motorhome used to house equipment at this site, especially during the Winter Season. Single-species source profiles for these hydrocarbons were included in the CMB analysis to account for this potential local source of evaporative emission. Separate contributions of these profiles are likely to overlap due to possible colinearity. Therefore, they were combined to represent the total contributions of gasoline vapor. This contribution was twice as high at the CN site during the Winter Season than at the other two sites.

Unusually high levels of the same small group of hydrocarbons (toluene, n-octane, n-nonane, 2-methylheptane, and 3-methylheptane) at the CE and CS sites suggested the possibility of a local source. Although this source was suspected to be related to painting or other material used in the monitoring shelter prior to their deployment in the field, the source could not be conclusively identified. Therefore, a source profile was constructed from the proportions of the concentrations for each of the five hydrocarbons in excess of their ratios to other compounds in samples that did not appear to contain the unidentified source. The contributions of this source to the sum of the PAMS species were about 40 and 15 percent at CE and CS, respectively, during the Winter Season and much smaller during the Summer Season. Contributions of this unidentified source to toluene were substantial at the CE and CS sites during the Winter Season (> 80%) and zero at the CN site. The residual effect of the local source at the CE site remained significant at the CE site during the Summer Season for toluene, but less so at the other two sites. The hydrocarbon concentrations during the Summer Season were about a third of the Winter Season levels and the CMB apportionments had a higher degree of uncertainty.

Regional background or aged VOC's typically contain higher abundances of relatively nonreactive hydrocarbons, such as ethane and propane and oxidized species, primarily aldehydes. Since CNG and LPG cannot be distinguished from urban background, these source contributions are interpreted as combinations of CNG, LPG plus aged vehicle emissions. The greater contributions of this source category during the Winter Season are meteorologically driven. More persistent west winds during the summer do not allow aged emissions to return to the coast.

Table 6-14. CMB apportionments of VOC (sum of 55 PAMS species) in µg/m^3 averaged by site and study period.

Season /Site	PAMS conc. (ug/m3)	number of samples	R^2	Jet Exhaust	On-road vehicles	Gasoline Evap	CNG & LPG	Unid local source	Butanes and Isopentane *	Unid. Sources
winter										
CE	141	8	0.96	12.3 + 4.1	30.8 + 9.4	3.1 + 6.3	24.5 + 1.8	49.4 + 1.8	13.7	7.4
CN	155	8	1.00	4.0 + 1.7	54.0 + 8.1	20.4 + 5.1	31.7 + 1.9	0.2 + 0.2	40.5	4.1
CS	62	8	1.00	12.7 + 2.2	14.0 + 2.7	5.0 + 1.6	15.5 + 0.9	9.3 + 0.5	5.8	-0.7
summer										
CE	65	10	0.93	2.8 + 2.3	21.6 + 2.3	2.1 + 1.4	17.3 + 1.0	8.0 + 0.5	8.3	4.7
CN	51	14	0.98	3.3 + 1.2	19.9 + 2.7	8.8 + 1.9	9.2 + 0.4	2.7 + 0.2	10.4	-3.6
CS	26	14	0.95	0.6 + 0.3	10.7 + 1.2	3.0 + 0.8	6.9 + 0.3	0.2 + 0.1	5.4	-0.7

* See Section 6.2.2 for discussion of excess unapportioned butanes and isopentane.

Table 6-15. CMB apportionments of benzene in µg/m^3 averaged by site and study period.

Season /Site	benzene (ug/m3)	No. of samples	R^2	Jet Exhaust	On-road vehicles	Gasoline Evap	Unid local source	Unid. Sources
winter								
CE	3	8	0.96	0.55 + 0.05	1.07 + 0.19	0.04 + 0.01	0.00 + 0.01	1.3
CN	2	8	1.00	0.10 + 0.01	1.62 + 0.21	0.29 + 0.03	0.00 + 0.01	-0.1
CS	1	8	1.00	0.38 + 0.04	0.42 + 0.08	0.07 + 0.01	0.00 + 0.01	0.2
summer								
CE	2	10	0.93	0.11 + 0.02	0.86 + 0.15	0.03 + 0.01	0.00 + 0.01	0.5
CN	1	14	0.98	0.12 + 0.01	0.60 + 0.12	0.12 + 0.01	0.00 + 0.01	0.1
CS	1	14	0.95	0.02 + 0.01	0.38 + 0.05	0.04 + 0.01	0.00 + 0.01	0.1

Table 6-16. CMB apportionments of toluene in µg/m^3 averaged by site and study period.

Season /Site	Toluene (ug/m3)	No. of samples	R^2	Jet Exhaust	On-road vehicles	Gasoline Evap	Unid local source	Unid. Sources
winter								
CE	43	8	0.96	0.28 + 0.03	3.26 + 0.46	0.31 + 0.03	36.57 + 3.66	2.2
CN	6	8	1.00	0.16 + 0.02	5.74 + 0.59	2.06 + 0.21	0.16 + 0.02	-2.1
CS	9	8	1.00	0.45 + 0.04	1.45 + 0.19	0.51 + 0.05	6.86 + 0.69	-0.3
summer								
CE	9	10	0.93	0.07 + 0.01	2.21 + 0.37	0.21 + 0.02	5.94 + 0.82	0.4
CN	4	14	0.98	0.10 + 0.01	2.03 + 0.34	0.89 + 0.09	2.01 + 0.20	-0.9
CS	1	14	0.95	0.02 + 0.01	1.08 + 0.11	0.31 + 0.03	0.14 + 0.12	-0.4

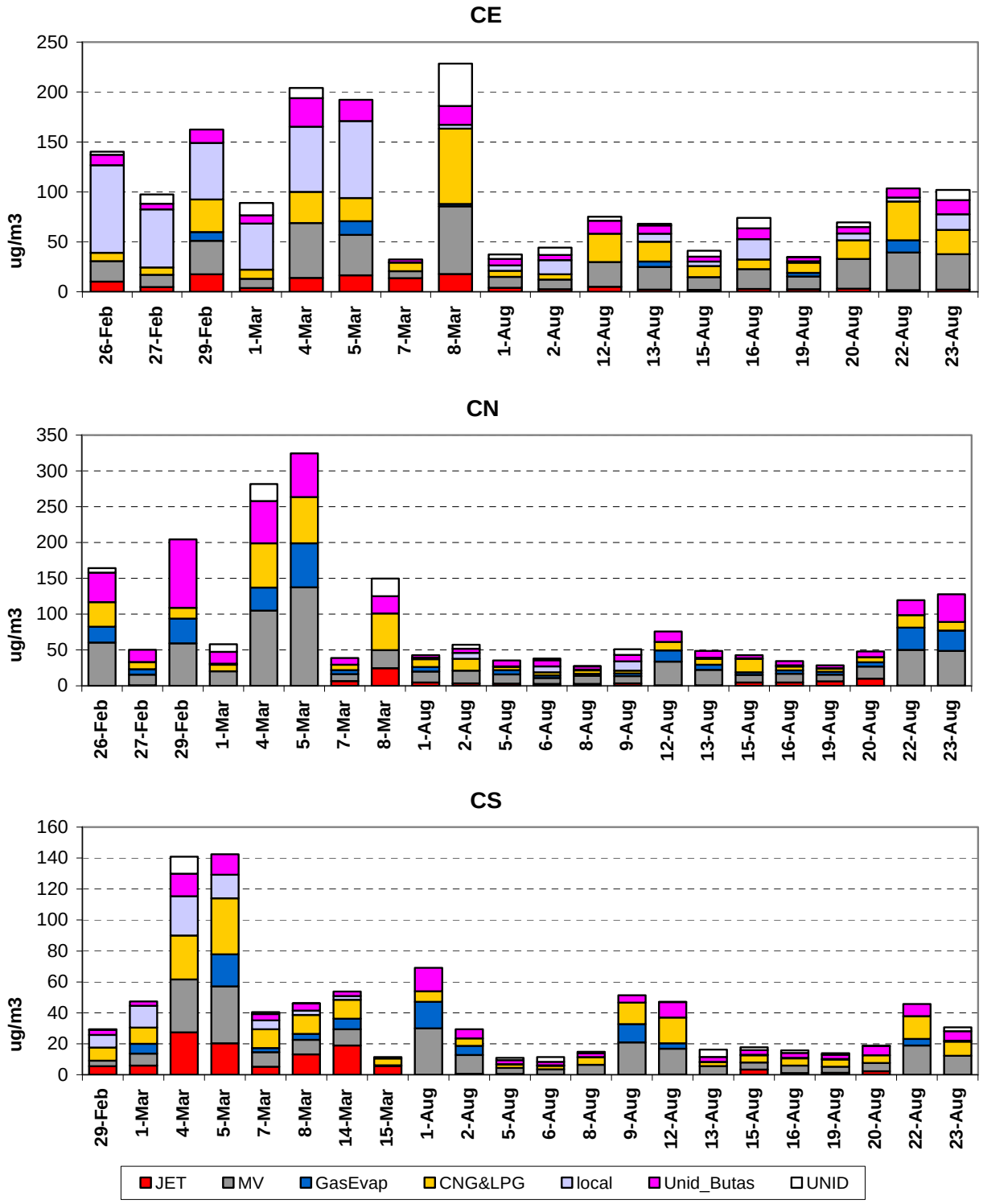

Figure 6-14. CMB apportionments of VOC (sum of 55 PAMS species) for individual 24-hr samples at the CE, CN, and CS sites. See Section 6.2.2 for discussion of excess unidentified butanes and isopentane (Unid_Butas).

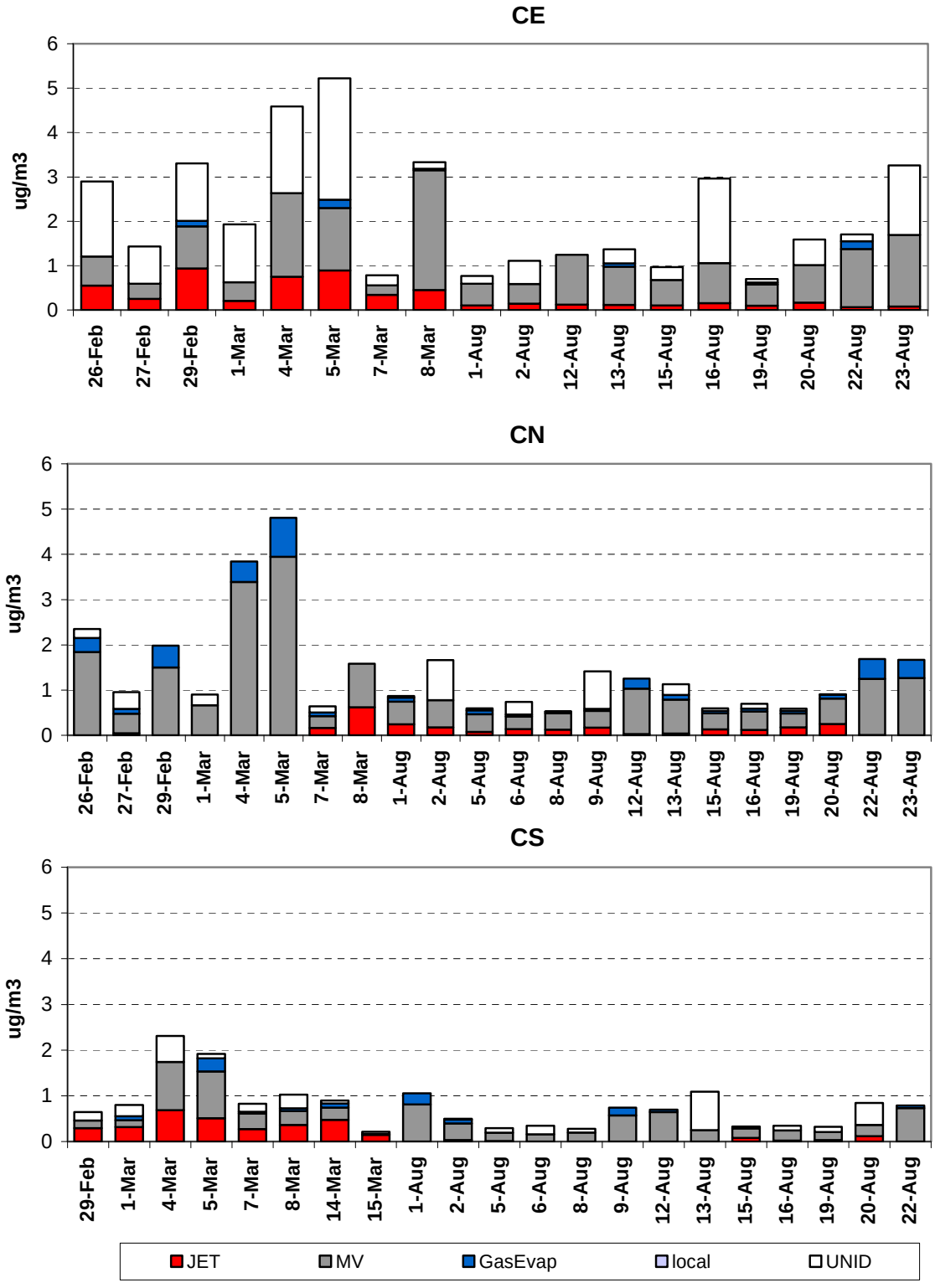

Figure 6-15. CMB apportionments of benzene for individual 24-hr samples at the CE, CN, and CS sites.

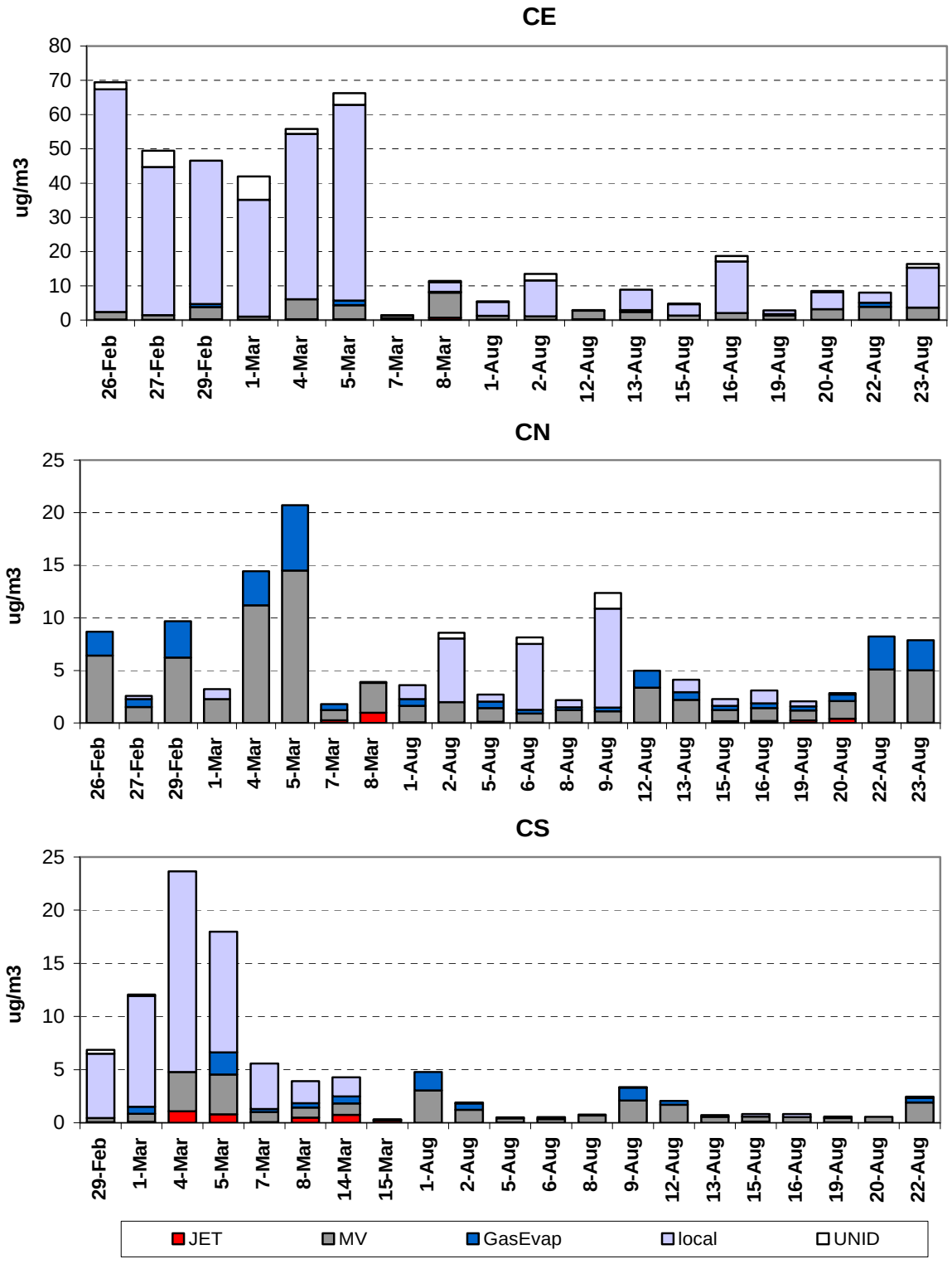

Figure 6-16. CMB apportionments of toluene for individual 24-hr samples at the CE, CN, and CE sites.

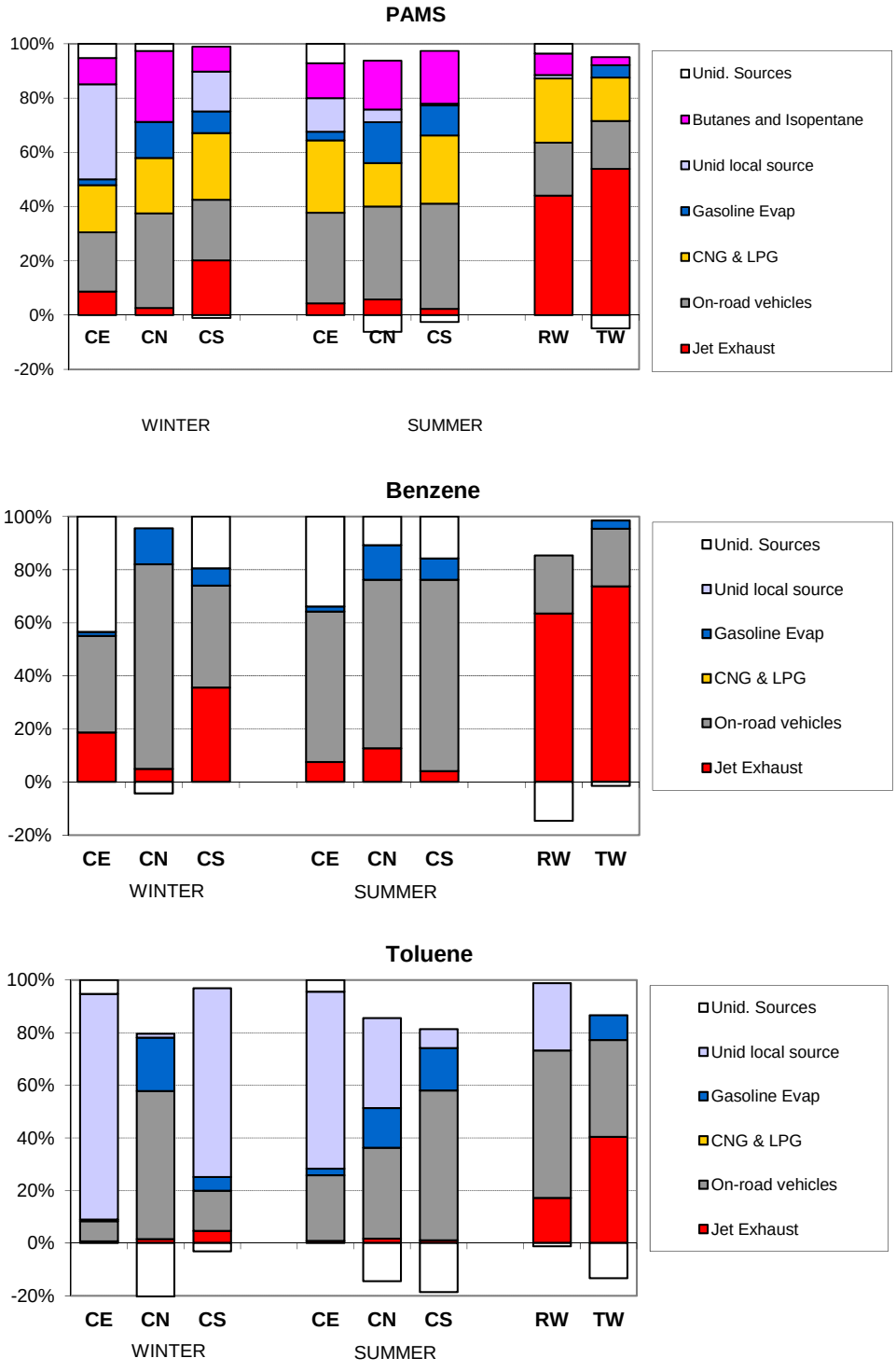

Figure 6-17. CMB apportionments of VOC averaged by site and study period. Apportionment of samples from downwind of a runway (RW) and taxiway (TW) are included for comparison. Negative values for 'Unid Sources' indicate over-apportionment.

6.5 FINDINGS AND CONCLUSIONS

The Chemical Mass Balance (CMB) receptor model was used to estimate the source contributions to the ambient concentrations of $PM_{2.5}$, organic carbon (OC), elemental carbon (EC), volatile organic compounds (VOC), and gaseous air toxics (e.g., benzene, toluene, ethylbenzene and xylenes) measured at the three core community monitoring sites in Lennox (CE), Westchester (CN), and El Segundo (CS). Up to 14 sets of 24-hour (midnight to midnight) ambient air samples were collected at each core monitoring site (CE, CN and CS) during both Winter and Summer Monitoring Seasons and analyzed to characterize the chemical composition of volatile organic compounds (VOC) and particulate matter 2.5 µm or less in diameter ($PM_{2.5}$).

Chemical analysis of ambient $PM_{2.5}$ showed that:

- The combined mean $PM_{2.5}$ mass concentrations for the Winter and Summer Season samples were well below (i.e., better than) the new annual National Ambient Air Quality Standards (NAAQS) for $PM_{2.5}$ of 12 µg/m^3 at all three core monitoring sites.[4] The individual 24-hour samples were also all below the 24-hour average $PM_{2.5}$ NAAQS of 35 µg/m^3.

- Total carbon (TC) comprised 36, 34, and 23 percent of $PM_{2.5}$ mass at the CE, CN, and CS sites, respectively, during the Winter Monitoring Season. The OC/EC ratios were 1.5 at the CE site, 1.7 at the CN site, and 1.8 and the CS site. The corresponding TC/$PM_{2.5}$ ratios during the Summer Monitoring Season were 26, 23, and 33 percent at the CE, CN, and CS sites, respectively. The OC/EC ratios were significantly larger during the Summer Monitoring Season with values of 3.0 at the CE site, 2.7 at the CN site, and 5.3 at the CS site. The larger OC/EC ratios during the summer indicate greater contributions of secondary organic aerosol (SOA).

- Ammonium nitrate and ammonium sulfate are also major components of fine particles comprising a combined 20-25 percent of $PM_{2.5}$ mass during the Winter Monitoring Season and 44-65 percent during the Summer Monitoring Season. Nitrate and sulfate particles are also secondary pollutants formed from the oxidation of SO_2 and NOx to sulfuric acid and nitric acid, respectively, and subsequent neutralization of the acids with ammonia. Nitrate contributions are lower-bound estimates due to volatilization of ammonium nitrate during sampling.

- Road-dust and other fugitive dust from soil can be significant contributors to ambient PM concentrations during windy conditions. Significantly higher concentrations of $PM_{2.5}$, along with soil-related elements (calcium, silicon, iron, and aluminum) were measured at the CS site on March 7 and 8, 2012. While the concentrations of soil-related elements vary one day to the next as well as between seasons, their relative abundances are similar for all three sites during both monitoring seasons. Chemical profiles were developed

[4] On December 14, 2012, the U.S. Environmental Protection Agency revised the annual average National Ambient Air Quality Standard (NAAQS) for $PM_{2.5}$ from 15.0 µg/m^3 to 12.0 µg/m^3.

from samples of soil collected near each of the three core site and used in the CMB analysis.

- The relative abundances of benzo(ghi)perylene, indeno(1,2,3-cd)pyrene, coronene, 17A(H),21B(H)-30-norhopane (hop17), and 17A(H),21B(H)-hopane (hop19) were generally similar among all samples and the sums of their concentrations are well correlated with total carbon. The high-molecular weight polycyclic aromatic hydrocarbons (PAH) are produced during combustion of hydrocarbon fuels and are especially indicative of gasoline vehicle engine exhaust. Hopanes and steranes are emitted in diesel and gasoline engine exhaust. They are indicative of unburned lubricating oils and are emitted mainly from smoking gasoline vehicles and older technology diesel engines.

- Samples collected at the end of the South Airfield Runway 25R had higher concentrations of carbonaceous particles and greater abundance of EC than the associated background samples collected at the CS site. The greater abundances of copper and zinc in the runway samples suggest these elements may serve as potential markers of jet exhaust. The concentrations of PAH and hopanes and steranes in the runway and background samples were comparable, which indicates jet exhaust is not a significant source of these compounds.

Chemical analysis of ambient volatile and semi-volatile hydrocarbons showed that:

- The seasonal mean concentrations of speciated C_2 to C_{11} hydrocarbons showed similar patterns for the three core monitoring sites. However, unusually high levels of the same group of hydrocarbons at two sites suggested the possible influences of local sources. An unknown local source composition was derived from the abundances of the five hydrocarbons (toluene, n-octane, n-nonane, 2-methylheptane, and 3-methylheptane) above the regional background (estimated from their concentrations on a day with very high ventilation). This profile was included in the CMB analysis.

- Other apparent anomalies in hydrocarbon composition data were the high concentrations of n-butane and isopentane at the CN site. Concentrations of other light hydrocarbons were also significantly greater at the CN site relative to either CE or CS sites. The significantly higher ratios of these hydrocarbons to acetylene suggested greater contributions of gasoline vapors at the CN site. This conclusion is further supported by the observation that day-to-day variations in the concentrations of n-butane, isopentane, and 2-methylpentane were generally correlated with daily maximum temperature. Unlike the portable shelters used at the CE and CS sites, a motorhome was used at the CN site. The motorhome's fuel tank is the most likely source of the apparent excess gasoline vapors at CN. Source profiles were included in the CMB analysis to account for this local source of evaporative hydrocarbon emissions.

- Carbonyl compounds were approximately four times higher during the Winter Season than the Summer Season. The lower levels during the Summer Season reflect the influence of persistent onshore flow in reducing the accumulation of carbonyl compounds

near the coast, despite greater contributions of atmospheric formation of carbonyl compounds during the summer.

- The contributions of the semi-volatile hydrocarbons generally ranged from one to three percent of the total C_2-C_{18} hydrocarbons during the Winter Season and from two to ten percent during Summer Season. One exception was a sample collected at CS on 8/22/12, in which SVHC accounted for 24 percent of the total C_2-C_{18} hydrocarbons. One of the samples collected at the takeoff end of the South Airfield Runway had 20 percent SVHC. Greater abundances of SVHC may result from contributions of jet exhaust during gate idling and runway taxiing. Diesel exhaust is also an important source of SVHC.

The CMB receptor model was used to estimate the contributions of jet exhaust and other emission sources to the ambient concentrations of $PM_{2.5}$, organic carbon (OC), elemental carbon (EC), volatile organic compounds (VOC), and gaseous air toxics (e.g., benzene, toluene, ethylbenzene, and xylenes) at the CE site in Lennox, the CN site in Westchester, and the CS site in El Segundo. CMB fit quality (R^2) and source contribution estimates (%) by site and season are shown in Table 6-17 for measured $PM_{2.5}$, OC and EC and in Table 6-19 for the measured sum of PAMS species, benzene and toluene. The mean contributions of jet exhaust by site and season are summarized in Table 6-18 and Table 6-20 for $PM_{2.5}$ and non-methane hydrocarbons (NMHC), respectively.

The CMB analysis of $PM_{2.5}$ showed that:

- Ammonium sulfate, ammonium nitrate, and residual organic matter (OM) not apportioned to combustion sources comprised approximately half of the PM2.5 mass at the CE, CN and CS sites during the Summer Season and about two-thirds during the Winter Season. The unapportioned OM was estimated by multiplying OC by the appropriate source-specific OM/OC ratios (1.4 for gasoline, 1.5 for diesel, 1.8 for all other primary sources, and 2.2 for SOA-anthropogenic and SOA-biogenic species) that have been reported in the literature (e.g. El-Zanan et. al., 2009; Turpin and Lim, 2001).

- Sulfate ion is normally derived from the chemical conversion of gaseous SO_2 in the atmosphere to sulfuric acid (H_2SO_4) and subsequent neutralization by ammonia and cannot be apportioned by CMB to specific sources of SO_2. A small fraction (from < 1 to a few percent) of SO_2 is oxidized to H_2SO_4 in jet exhaust and directly emitted as the acid. The estimated contributions of jet exhaust to sulfate in $PM_{2.5}$ are 2.0% at the CE site, 7.1% at the CN site, and 1.3% at the CS, assuming a conversion rate of SO_2 to H_2SO_4 in jet exhaust of approximate one percent. This rate is consistent with the mass ratios of sulfate to the sum of SO_2 and sulfate (all background subtracted) from measurements behind the blast fence at the South Airfield Runway 25R.

Table 6-17. CMB source contribution estimates (%) of measured $PM_{2.5}$, OC and EC by site and season. Uncertainties are the larger of either the mean of individual uncertainties or standard deviation of individual sample apportionments.

Site	Season	Number Samples	conc. (µg/m^3)	R^2	Sum SCE/Measured Sum CMB SCE	Sum SCE/Measured CMB SCE + Secondary	Jet Exhaust	Diesel Exh	Gasoline Exh	Wood Smoke	Soil	Unapportioned Secondary PM Am Sulfate [1]	Am Nitrate [2]	unid OM [3]
PM2.5														
CE	winter	12	8.2	0.88	39.3	102.8	1.84 ± 0.16	17.75 ± 1.74	2.11 ± 1.82	4.82 ± 0.34	6.40 ± 0.44	14.0	11.6	37.9
	summer	11	7.4	0.79	14.9	92.4	0.74 ± 0.07	7.70 ± 0.73	0.29 ± 0.76	3.82 ± 0.32	2.31 ± 0.17	35.1	12.3	30.1
CN	winter	10	7.6	0.90	33.8	98.4	2.41 ± 0.21	16.38 ± 1.70	1.97 ± 1.06	2.05 ± 0.17	6.64 ± 0.54	17.0	10.5	37.1
	summer	4	8.1	0.78	16.3	90.9	1.36 ± 0.31	8.02 ± 0.72	0.30 ± 0.58	2.69 ± 0.22	3.96 ± 0.89	39.2	9.7	25.7
CS	winter	12	12.3	0.88	32.3	74.1	1.77 ± 0.16	10.54 ± 1.15	1.01 ± 1.18	2.80 ± 0.21	15.98 ± 2.01	11.1	11.2	19.5
	summer	11	6.8	0.74	16.1	125.1	0.42 ± 0.09	7.53 ± 0.71	0.21 ± 0.41	6.02 ± 0.48	1.48 ± 0.15	52.6	15.5	40.9
Organic Carbon														
CE	winter	12	1.9	0.89	50.0		1.37 ± 0.18	8.67 ± 2.47	5.88 ± 1.05	13.58 ± 1.30	0.74 ± 0.12			
	summer	11	1.5	0.79	17.9		0.60 ± 0.08	3.87 ± 1.37	0.91 ± 0.17	11.87 ± 1.14	0.30 ± 0.07			
CN	winter	10	1.7	0.90	36.0		1.81 ± 0.24	8.27 ± 2.21	5.79 ± 1.07	5.88 ± 0.56	0.78 ± 0.13			
	summer	4	1.4	0.78	17.7		1.29 ± 0.30	5.11 ± 1.35	1.02 ± 0.19	9.71 ± 0.93	0.59 ± 0.13			
CS	winter	12	2.0	0.91	29.0		1.96 ± 0.26	7.83 ± 2.07	4.40 ± 0.80	11.36 ± 1.09	2.75 ± 0.44			
	summer	11	1.8	0.74	18.9		0.25 ± 0.05	3.08 ± 0.81	0.41 ± 0.08	13.91 ± 1.33	0.14 ± 0.05			
Elemental Carbon														
CE	winter	12	1.2	0.88	108.6		3.92 ± 0.42	98.13 ± 4.54	3.92 ± 0.81	1.49 ± 0.15	0.02 ± 0.08			
	summer	11	0.5	0.79	99.9		3.37 ± 0.36	92.88 ± 4.19	1.06 ± 0.23	2.54 ± 0.25	0.02 ± 0.20			
CN	winter	10	1.0	0.90	111.1		5.70 ± 0.61	100.30 ± 8.31	3.45 ± 0.80	0.70 ± 0.10	0.02 ± 0.10			
	summer	4	0.4	0.78	129.7		7.75 ± 1.79	118.28 ± 5.57	1.44 ± 0.33	2.22 ± 0.23	0.03 ± 0.23			
CS	winter	12	1.0	0.88	111.7		6.54 ± 0.70	100.83 ± 4.36	2.73 ± 0.63	1.50 ± 0.15	0.08 ± 0.15			
	summer	11	0.3	0.74	129.9		2.59 ± 0.30	120.41 ± 5.14	1.21 ± 0.30	5.39 ± 0.53	0.01 ± 0.30			

[1] ammonium sulfate = (measured SO_4^{2-} - apportioned SO_4^{2-})*1.375

[2] ammonium nitrate = (measured NO_3^- - apportioned NO_3^-)*1.29. Nitrate contributions are lower-bound estimates due to volatilization of ammonium nitrate during sampling.

[3] unidentified organic mass = (measured OC - apportioned OC)*1.8

Table 6-18. Average source contribution estimates for jet exhaust (µg/m^3) by site and season. Uncertainties are the larger of either the mean of individual uncertainties or standard deviation of individual sample apportionments.

	First Season (Winter 2012)			Second Season (Summer 2012)		
PM Components	**CE**	**CN**	**CS**	**CE**	**CN**	**CS**
Ambient Conc (ng/m3)						
PM 2.5 mass	8183 ± 3689	7567 ± 2866	12328 ± 7115	7412 ± 1188	8056 ± 2892	6799 ± 1131
organic carbon	1179 ± 622	980 ± 718	1022 ± 501	496 ± 112	433 ± 121	337 ± 95
elemental carbon	1948 ± 819	1656 ± 861	1993 ± 772	1496 ± 285	1400 ± 408	1845 ± 351
sulfate	876 ± 665	974 ± 775	1049 ± 654	1913 ± 429	2322 ± 557	2620 ± 1020
copper	7.95 ± 4.49	9.14 ± 7.04	12.40 ± 7.71	3.10 ± 1.17	4.73 ± 4.98	1.30 ± 0.45
zinc	16.64 ± 11.13	18.96 ± 10.62	24.74 ± 12.86	4.90 ± 2.51	12.50 ± 3.21	6.19 ± 2.93
manganese	2.53 ± 1.65	2.08 ± 2.05	4.39 ± 4.74	0.73 ± 0.32	1.40 ± 1.44	0.47 ± 0.26
chromium	0.79 ± 0.77	0.56 ± 0.50	0.88 ± 0.87	0.17 ± 0.25	0.20 ± 0.17	0.20 ± 0.24
vanadium	0.67 ± 0.83	0.62 ± 0.85	0.95 ± 1.13	0.37 ± 0.34	0.48 ± 0.15	0.47 ± 0.39
lead	2.00 ± 1.10	1.77 ± 1.14	1.65 ± 0.65	0.44 ± 0.31	0.75 ± 0.31	0.24 ± 0.21
POM (PAH)	0.41 ± 0.25	0.22 ± 0.16	0.25 ± 0.14	0.14 ± 0.11	0.03 ± 0.05	0.02 ± 0.06
Jet Exhaust SCE (ng/m3)						
PM 2.5 mass	150.8 ± 88.1	182.4 ± 157.9	218.3 ± 150.4	54.5 ± 21.4	109.7 ± 101.2	28.5 ± 16.0
organic carbon	26.6 ± 13.7	30.0 ± 26.0	39.0 ± 23.5	9.0 ± 3.5	18.1 ± 16.6	4.7 ± 2.6
elemental carbon	46.2 ± 27.0	55.8 ± 48.4	66.9 ± 46.1	16.7 ± 6.5	33.6 ± 31.0	8.8 ± 4.9
sulfate	10.5 ± 6.2	12.7 ± 11.0	15.2 ± 10.5	3.8 ± 1.5	7.7 ± 7.1	2.0 ± 1.1
copper	8.23 ± 4.82	9.97 ± 8.65	12.95 ± 7.81	2.98 ± 1.18	6.03 ± 5.52	2.06 ± 0.68
zinc	4.82 ± 2.80	5.84 ± 5.04	6.98 ± 4.82	1.75 ± 0.67	3.53 ± 3.23	0.93 ± 0.51
manganese	0.13 ± 0.09	0.14 ± 0.12	0.17 ± 0.12	0.03 ± 0.05	0.08 ± 0.10	0.00 ± 0.01
chromium	0.13 ± 0.08	0.16 ± 0.14	0.19 ± 0.13	0.05 ± 0.02	0.10 ± 0.09	0.02 ± 0.02
vanadium	0.00 ± 0.01	0.00 ± 0.01	0.00 ± 0.01	0.00 ± 0.01	0.00 ± 0.01	0.00 ± 0.01
lead	0.63 ± 0.37	0.74 ± 0.65	0.92 ± 0.61	0.23 ± 0.09	0.48 ± 0.42	0.12 ± 0.08
POM (PAH)	0.00 ± 0.01	0.00 ± 0.01	0.00 ± 0.01	0.00 ± 0.01	0.00 ± 0.01	0.00 ± 0.01
Jet Exhaust SCE (%)						
PM 2.5 mass	1.8%	2.4%	1.8%	0.7%	1.4%	0.4%
organic carbon	1.4%	1.8%	2.0%	0.6%	1.3%	0.3%
elemental carbon	3.9%	5.7%	6.5%	3.4%	7.8%	2.6%
sulfate	1.2%	1.3%	1.5%	0.2%	0.3%	0.1%
copper	103.6%	109.1%	104.5%	96.2%	127.5%	158.2%
zinc	28.9%	30.8%	28.2%	35.6%	28.2%	15.0%
manganese	5.0%	6.7%	3.8%	3.8%	5.4%	0.0%
chromium	16.9%	29.1%	21.4%	28.7%	49.2%	12.4%
vanadium	0.0%	0.2%	0.0%	0.0%	0.0%	0.0%
lead	31.3%	42.0%	55.6%	52.1%	63.3%	50.0%
POM (PAH)	0.0%	0.0%	0.0%	0.0%	0.0%	0.0%

.

- The contribution of jet exhaust to $PM_{2.5}$ mass were consistently small with Winter Season means ranging from two percent at the CE and CS sites and 2.5 percent at the CN site. Contribution during the Summer Season was below one percent at the CE and CS sites and slightly higher than one percent at the CN site. These results appear to contradict the particle size distribution (PSD) measurements showing that jet exhaust was a significant contributor to number concentrations of UFP smaller than 30 nm. However, these very small particles contribute little to $PM_{2.5}$ mass.

- At the CE, CN, and CS sites, the average contributions to $PM_{2.5}$ mass of emissions from diesel vehicles accounted for 15 and 8 percent of the ambient $PM_{2.5}$ mass concentrations during the Winter and Summer Seasons, respectively. Emissions of gasoline vehicles accounted for 1.7 percent of the Winter Season and 0.3 percent of the Summer Season concentrations. While it is not possible for CMB to separately apportion airport- and non-airport-related vehicle emissions, the temporal and spatial analysis of ambient data suggests greater contributions from non-airport related traffic emissions.

- Jet exhaust contributed over half of the measured ambient lead and about quarter of chromium concentrations. However, these contributions were generally below 1-2 ng/m^3 and have high uncertainties. Vanadium and PAH contributions were below detection.

- Soil was generally a minor component (< 5 percent) of $PM_{2.5}$, except on windy days. Soil accounted for about 30 percent of $PM_{2.5}$ mass at the CS site during a strong wind event on March 7 and 8. The soil contributions were also higher at the other two sites during these days.

The CMB analysis of VOC showed that:

- The mean contributions of jet exhaust to the sum of PAMS target hydrocarbons ranged from a few percent to as much as 20 percent. The contributions were greater during the Winter Season with SCEs of 12.3 µg/m3 at the CE site, 12.7 $\mu g/m^3$ at the CS site, and 4.0 µg/m3 at the CN site.

- The hydrocarbon concentrations during the Summer Season were about a third of the Winter Season levels, so the CMB apportionments had a higher degree of uncertainty. The contributions of jet exhaust to the sum of PAMS target hydrocarbons were generally lower during the Summer Season, with mean contributions of about 3 $\mu g/m^3$ at both CE and CN sites, and less than 1 $\mu g/m^3$ at the CS site. The substantially lower contributions of jet exhaust during the Summer Season at the CS site is due to more persistent west winds compared to the morning northeast wind during the Winter Season.

- About three to four percent of the sum of PAMS species attributed to jet exhaust was benzene. Apportionment of toluene to jet exhaust was not significant. The apportionment results indicate that jet exhaust may contribute a significant fraction of the measured 1,3-butadiene in some cases with high uncertainty.

- On-road vehicles accounted for 25-40 percent of the sum of PAMS species and about 50-75 percent of the measured benzene. CMB cannot distinguish between on- and off-airport vehicle emissions, so an unknown fraction of the on-road vehicle apportionment is associated with airport ground support vehicles and vehicle traffic to and from the airport. However, vehicles in closer proximity to the monitoring sites can be expected to have greater influence on the measured VOC levels.

Table 6-19. CMB performance statistics and source contribution estimates (%) of measured VOC, benzene and toluene by site and season. Uncertainties are the larger of either the mean of individual uncertainties or standard deviation of individual sample apportionments.

Site	Season	Conc. (ug/m^3)	Number Samples	R^2	ΣSCE/ Meas	Jet Exhaust	On-road vehicles	Gasoline Evap	CNG & LPG	Unid local source	Butanes and Isopentane *	Unid. Sources
Sum of PAMS												
CE	winter	141.0	8	0.96	0.95	8.7 + 2.9	21.8 + 6.6	2.2 + 4.4	17.4 + 1.3	35.0 + 1.3	9.7	5.3
CE	summer	64.8	10	0.93	0.93	4.3 + 3.6	33.4 + 3.6	3.3 + 2.2	26.6 + 1.5	12.4 + 0.8	12.8	7.2
CN	winter	154.8	8	1.00	0.97	2.6 + 1.1	34.9 + 5.3	13.2 + 3.3	20.5 + 1.2	0.1 + 0.1	26.1	2.6
CN	summer	50.8	14	0.98	1.07	6.6 + 2.3	39.1 + 5.4	17.3 + 3.7	18.2 + 0.8	5.3 + 0.4	20.5	-7.1
CS	winter	61.7	8	1.00	1.01	20.6 + 3.6	22.8 + 4.4	8.2 + 2.5	25.2 + 1.5	15.0 + 0.8	9.3	-1.1
CS	summer	26.0	14	0.95	1.03	2.4 + 1.1	40.9 + 4.6	11.6 + 3.2	26.5 + 1.2	0.7 + 0.6	20.6	-2.7
Benzene												
CE	winter	2.94	8	0.96	0.57	18.64 + 1.86	36.45 + 6.58	1.48 + 0.34				43.4
CE	summer	1.52	10	0.93	0.66	7.47 + 1.16	56.71 + 10.15	1.96 + 0.66				33.9
CN	winter	1.92	8	1.00	1.05	5.39 + 0.54	84.47 + 11.06	14.92 + 1.49				-4.8
CN	summer	0.94	14	0.98	0.89	12.68 + 1.27	63.48 + 12.87	13.08 + 1.31				10.8
CS	winter	1.08	8	1.00	0.81	35.54 + 3.55	38.49 + 7.61	6.56 + 0.93				19.4
CS	summer	0.53	14	0.95	0.84	4.11 + 1.89	72.06 + 8.89	8.06 + 1.89				15.8
Toluene												
CE	winter	2.94	8	0.96	0.95	0.65 + 0.06	7.65 + 1.09	0.73 + 0.07		85.73 + 8.57		5.2
CE	summer	1.52	10	0.93	0.96	0.84 + 0.11	24.98 + 4.21	2.43 + 0.24		67.31 + 9.31		4.4
CN	winter	1.92	8	1.00	1.34	2.58 + 0.26	94.95 + 9.75	34.16 + 3.42		2.57 + 0.26		-34.3
CN	summer	0.94	14	0.98	1.20	2.40 + 0.24	48.61 + 8.07	21.29 + 2.13		48.13 + 4.81		-20.4
CS	winter	1.08	8	1.00	1.03	5.00 + 0.50	16.17 + 2.08	5.68 + 0.57		76.47 + 7.65		-3.3
CS	summer	0.53	14	0.95	1.30	1.66 + 0.84	90.72 + 9.07	25.68 + 2.57		11.51 + 10.42		-29.6

* See Section 6.2.2 for discussion of excess unapportioned butanes and isopentane.

Table 6-20. Average source contribution estimates for jet exhaust (µg/m^3) by site and season. Uncertainties are the larger of either the mean of individual uncertainties or standard deviation of individual sample apportionments.

	First Season (Winter 2012)			Second Season (Summer 2012)		
VOC Components	**CE**	**CN**	**CS**	**CE**	**CN**	**CS**
Ambient Conc (ng/m3)						
sum of PAMS	141026 ± 65565	154843 ± 106867	61659 ± 48546	64811 ± 24908	50765 ± 23658	26041 ± 15050
1,3 butadiene	369 ± 248	363 ± 294	206 ± 201	148 ± 42	141 ± 53	68 ± 78
Benzene	2936 ± 1519	1923 ± 1310	1080 ± 689	1522 ± 907	945 ± 349	529 ± 247
Toluene	42652 ± 24426	6044 ± 4705	8975 ± 7770	8832 ± 5610	4175 ± 3207	1193 ± 714
EthylBenzene	1448 ± 624	619 ± 605	529 ± 438	769 ± 416	388 ± 201	169 ± 94
Xylenes	7990 ± 3731	3025 ± 2899	3020 ± 2480	3886 ± 2170	2022 ± 1127	858 ± 536
Jet Exhaust SCE (ng/m3)						
sum of PAMS	12253 ± 5525	4002 ± 8609	12728 ± 8618	2812 ± 1024	3328 ± 2665	631 ± 1009
1,3 butadiene	443 ± 311	39 ± 73	199 ± 77	88 ± 43	81 ± 67	14 ± 30
Benzene	547 ± 286	104 ± 215	384 ± 169	114 ± 32	120 ± 81	22 ± 37
Toluene	276 ± 229	156 ± 342	449 ± 394	75 ± 60	100 ± 112	20 ± 36
EthylBenzene	58 ± 27	20 ± 42	62 ± 43	15 ± 6	17 ± 13	3 ± 5
Xylenes	63 ± 117	62 ± 138	168 ± 172	15 ± 28	34 ± 49	8 ± 15
Jet Exhaust SCE (%)						
sum of PAMS	8.7%	2.6%	20.6%	4.3%	6.6%	2.4%
1,3 butadiene	120.3%	10.6%	96.5%	59.0%	57.4%	20.5%
Benzene	18.6%	5.4%	35.5%	7.5%	12.7%	4.1%
Toluene	0.6%	2.6%	5.0%	0.8%	2.4%	1.7%
EthylBenzene	4.0%	3.2%	11.7%	1.9%	4.4%	2.1%
Xylenes	1.6%	2.8%	8.0%	0.8%	2.7%	1.4%

- The relative contribution of the local unidentified source suspected to be related to painting or other material used in the monitoring shelters prior to their deployment in the field were variable, but substantial in some samples. The contributions of this local source to the sum of the PAMS species were about 40 and 15 percent at the CE and CS sites, respectively, during the Winter Season and much smaller during the Summer Season. Contributions of this unidentified source to toluene were substantial at the CE and CS sites during the Winter Season (> 80%) and zero at the CN site. The residual effect of the local source at the CE site remained significant at the CE site during the Summer Season for toluene and less so at the other two sites.

- The contribution of gasoline vapor was twice as high at the CN site during the Winter Season than at the other two sites. The higher contributions at the CN site during the Winter Season may have been related to gasoline vapor losses from the motorhome used to house the monitoring equipment at this site.

The lower contributions of regional background or aged VOC's during the Summer Season were due to more persistent west wind that did not allow aged emissions to return to the coast with off-shore winds after sunset. Regional upwind, background VOC's typically contain higher abundances of relatively nonreactive hydrocarbons, such as ethane and propane, and oxidized species, primarily aldehydes. In addition to urban background, both compressed natural gas (CNG) and liquefied petroleum gas (LPG) are potential sources of ethane and propane. Since CNG and LPG cannot be distinguished from urban background, these source contributions were combined.

6.6 REFERENCES

Corporan, E.; DeWitt, M.J.; Belovich, V.; Pawlik, R.; Lynch, A.C., Gord, J.R.; Meyer, T.R. Emission characteristics of a turbine engine and research combustor burning a fischer-tropsch jet fuel. *Energy Fuels* 2007, 21, 2615-2626.

El-Zanan, H.S., B. Zielinska, and Lynn R. Mazzoleni (2009). Analytical Determination of the Aerosol Organic Mass-to-Organic Carbon Ratio. *J. Air Waste Manage. Assoc.*, 59:58-69.

Fuentes, J.D., M. Lerdau, R. Atkinson, D. Baldocchi, J.W. Botteneheim, P. Ciccioli, B. Lamb, C. Gercon, L. Gu, A. Guenther, T.D. Sharkey and W.R. Stockwell (2000). Biogenic Hydrocarbons in the Atmospheric Bounday Layer. A Review, *Bull. Amer. Meteor. Soc*., 81, 1537-1575, 2000.

Fujita, E.M., J.G. Watson, J.C. Chow and Z. Lu (1994). Validation of the Chemical Mass Balance Receptor Model Applied to Hydrocarbon Source Apportionment in the Southern California Air Quality Study. *Environ. Sci. Technol*., 28, 1633-1649.

Fujita, E.M., J.G. Watson, J.C. Chow and K.L. Magliano (1995c). Receptor Model and Emissions Inventory Source Apportionments of Nonmethane Organic Gases in California's San Joaquin Valley and San Francisco Bay Area. *Atmos. Environ*., 29(21), 3019-3035.

Fujita, E.M.; Campbell, D.E.; Zielinska, B.; Chow, J.C.; Lindhjem, C.E.; DenBleyker, A; Bishop, G.A; Schuchmann B.G.; Stedman, D.H.; Lawson, D.L. (2012). Comparison of the MOVES2010a, MOBILE6.2 and EMFAC2007 Mobile Source Emissions Models with On-Road Traffic Tunnel and Remote Sensing Measurements. *J. Air & Waste* Manage. Assoc. 2012, 62(10):1134–1149.

Harley, R.A., M.P. Hannigan, G.R. Cass (1992). Respeciation of Organic Gas Emissions and the Detection of Excess Unburned Gasoline in the Atmosphere. *Environ. Sci. Technol.* 26:2395.

Henry, R.C., History and fundamentals of multivariate air duality receptor models. *Chemometrics and Intelligent Laboratory Systems*, 1997. 37(1): p. 37-42.

Hopke, P.K., Receptor Modeling for Air Quality Management. *Environ. Sci. Technol.*, 1997. 8: 95-117.

Johnson, G.R.; Mazaheri, M.; Ristovski, Z.D.; Morawska, L. A plume capture technique for the remote characterization of aircraft engine emissions. *Environ. Sci. Technol.*, 2008. 42: 4850-4856.

Kirchstetter, T.W., B.C. Singer, R.A. Harley, G.R. Kendall, and J.M. Hesson (1999). Impact of California Reformulated Gasoline on Motor Vehicle Emissions: 2. Volatile Organic Compound Speciation and Reactivity. *Environ. Sci. Technol.*, 33:329-336.

Mayrsohn, H. and Crabtree, J.H. (1976). Source reconciliation of atmospheric hydrocarbons. *Atmos.Environ*., 10:137-43.

Mayrsohn, H., Crabtree, J.H., Kuramoto, M., Sothern, R.D., Mano, S.H. (1977). Source reconciliation of atmospheric hydrocarbons 1974. *Atmos.Environ*., 11:189-92.

Pierson, W., E. Schorran, E. Fujita, J. Sagebiel, D. Lawson, and R. Tanner (1999). Assessment of Non-Tailpipe Hydrocarbon Emissions from Motor Vehicles. *J. Air Waste Manage. Assoc.*, 49: 498-519.

Stockwell, W.R., C.V. Lawson, E. Saunders, W.S. Goliff. 2012. A review of tropospheric atmospheric chemistry and gas-phase chemical mechanisms for air quality modeling. *Atmosphere* 3: 1-32.

Timko, M.T.; Onasch, T.B.; Northway, M.J.; Jayne, J.T.; Canagaratna, M.R.; Herndon, S.C.; Wood, E.C.; Miake-Lye R.C.; Knighton, W.B. Gas turbine engine emission – PartII: Chemical properties of particulate matter. *J. Eng. Gas Turbine Power*. 2010. 132, 061505/1-15.

Turpin, B.J. and H.J. Lim (2001). Contributions to PM2.5 mass concentrations: revisiting common assumptions for estimating organic mass. Aerosol Sci. Technol. 2001, 35,1, 602-610.

Watson, J., J.C. Chow, and E. Fujita (2001a). Review of Volatile Organic Compound Source Apportionment by Chemical Mass Balance. Atmos. Environ. 35:1567-1584.

Watson, J.G., T. Zhu, J.C. Chow, J. Engelbrecht, E.M. Fujita, and W.W. Wilson (2001b). Receptor Models for Particulate Source Apportionment. *Atmos. Environ.* 35, 1567-1584.

Yu, Z.; Liscinsky, D.S.; Rue, B.S.; Timko, M.T.; Bhargava, A.; Herndon, S.C.; Miake-Lye R.C.; Anderson, B.E. Characterization of lubricating oil emissions from aircraft engines. *Environ. Sci. Technol.*, 2010, 44, 9530-9534.

Section 7

NONPARAMETRIC TRAJECTORY ANALYSIS

(This page is intentionally blank)

Table of Contents

List of Figures

7. NONPARAMETRIC TRAJECTORY ANALYSIS AND SOURCE APPORTIONMENT

7.1 NONPARAMETRIC TRAJECTORY ANALYSIS

Nonparametric Trajectory Analysis (NTA) is applied to air quality data to determine the location and contribution of nearby sources to air quality at one or more of the monitoring sites for Phase III of the LAX AQSAS. In general, for this study, NTA has been projected to provide useful information for sources up to ten kilometers from a monitoring location. NTA relies on observations of airborne emittant concentrations as well as wind speed and direction values averaged over one to five minutes. It is important for the wind data to be representative of air movement in the local region at or near ground level.

NTA was applied to all continuous monitoring data (one or five minute averages) from the Community East (CE), Community North (CN), and Community South (CS) sites operated as part of Phase III of the LAX AQSAS Winter and Summer Monitoring Seasons. The species concentration data analyzed included: carbon monoxide (CO), nitrogen oxides (NO_x), sulfur dioxide (SO_2), black carbon (BC), and ultrafine particulates (UFP). NTA was also applied to the data from the AQ site operated by South Coast Air Quality Management District (SCAQMD). The species measured at the AQ site that were analyzed by NTA were CO, NO_x, SO_2, and BC. The UFP data were not suitable for this analysis due to the gaps in the data. The continuous data from all stations and seasons were subjected to the following data screening procedures:

- Five-minute average data is linearly interpolated to one-minute data and is then treated the same as one-minute data.

- Time series plots of all data from each station were examined. Based on examination of the time series, all large outliers of several minutes (one to ten minutes) duration were removed unless there was another species that showed outliers at the same time. An outlier is defined as a value that is more than five times the surrounding values. Many of the species showed multiple small negative values, often due to some degree of baseline drift. These data were run through an algorithm that removed the baseline drift and small negative values. For removal of small negative values, the baseline drift algorithm estimates the baseline as a minimum over the previous one and a half hours.

- Due to a fault in the air conditioning starting August 3, 2012, the NO and NO_x data at the CN station suffered from severe baseline drift as temperature in the shelter increased during the day. The baseline drift algorithm was applied to the NO_x. For the CN site NO_x, the baseline is determined as the minimum of the previous six hours. Corrected NO data is corrected NO_x minus NO_2.

- Some of the BC data showed small amplitude cycling with a period of tens of minutes caused by the cycling of the station air conditioning. Because of the short period and small amplitude of the changes in the BC data, it was determined that any errors in source

apportionment would cancel out. Thus, no corrections to BC data for this effect were made.

- The SO_2 monitor for the AQ site has a resolution of 1 ppb. About 19 percent of the AQ site SO_2 data is missing (about the same as CO and NO_x) and about 59 percent of the SO_2 data is 0. Thus, almost 80 percent of the SO_2 data at the AQ site is zero or missing. While this does not present any special problems for the source apportionment algorithm; it does imply the source apportionment for SO_2 at AQ will be small compared to the other stations.

The meteorological data for the Winter and Summer Monitoring Seasons were obtained from the Automated Surface Observation System (ASOS) stations located at LAX, the Hawthorne Airport, and the Santa Monica Airport. The wind speed and direction data are running averages of the previous two minutes, reported every minute. Wind speeds are reported as whole numbers in the unit of "knots" and wind directions are reported in whole numbers in the unit of "degrees."

Back trajectories are calculated from wind data for all three ASOS stations using inverse squared distance interpolation. Wind data from the community monitoring sites were not used because it was unavailable for the AQ and CN sites or the wind monitors were located such that the data were not representative of general transport winds for the CE and CS sites.

7.2 BACK TRAJECTORY SOURCE APPORTIONMENT

7.2.1 Methodology

For each minute of the period of interest, in this instance the two 43-day monitoring seasons, a 1-hour back-trajectory arriving at the sampling site is calculated. For source apportionment purposes, the trajectories are parsed into three mutually exclusive categories:

- R is the set of trajectories with 1-hr average wind speeds less than 1 knot
- H is the set of trajectories not in R that pass over the source region.
- M is the set of trajectories not in R that do not pass over the source region.

For the Winter Monitoring Season, the three sets of trajectories for the four monitoring sites are shown in Figure 7-1 to Figure 7-4. For the Summer Season, two sets of trajectories for the four monitoring sites are shown in Figure 7-5 to Figure 7-8. There were no trajectories with vector average wind speed of less than 1 knot for the Summer Monitoring Season. The frequency of winds with direction and speed for each monitoring season can be seen in the wind roses in Figures 9-2 through 9-7.

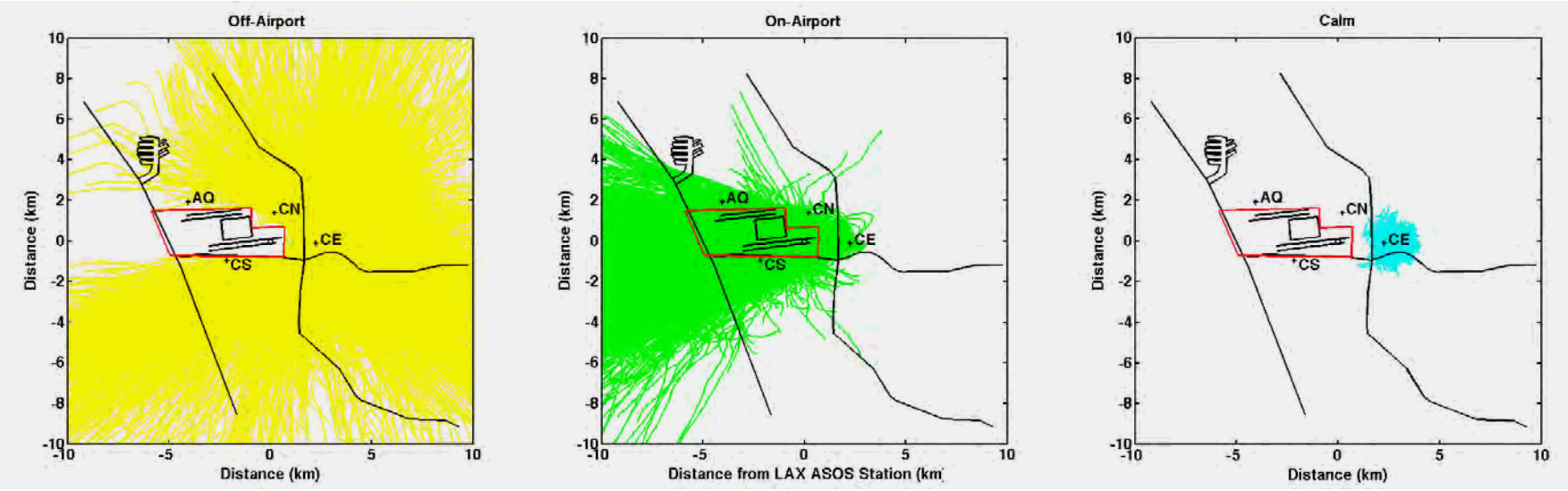

(1) **(2)** **(3)**

Figure 7-1. Three sets of trajectories for CE site for the Winter Season. 1) off-airport (yellow), does not pass over the airport and wind speed is greater than 1 knot; 2) on airport (green), passes over the airport and wind speed is greater than 1 knot; 3) low wind speed (blue), 1-hour average wind speed is less than or equal to 1 knot. Units on the axes are km from the LAX ASOS station. The North and South Airfields and Central Terminal Area are shown in black. The airport boundary is in red. "Calm" is defined as wind speeds less than 1 knot.

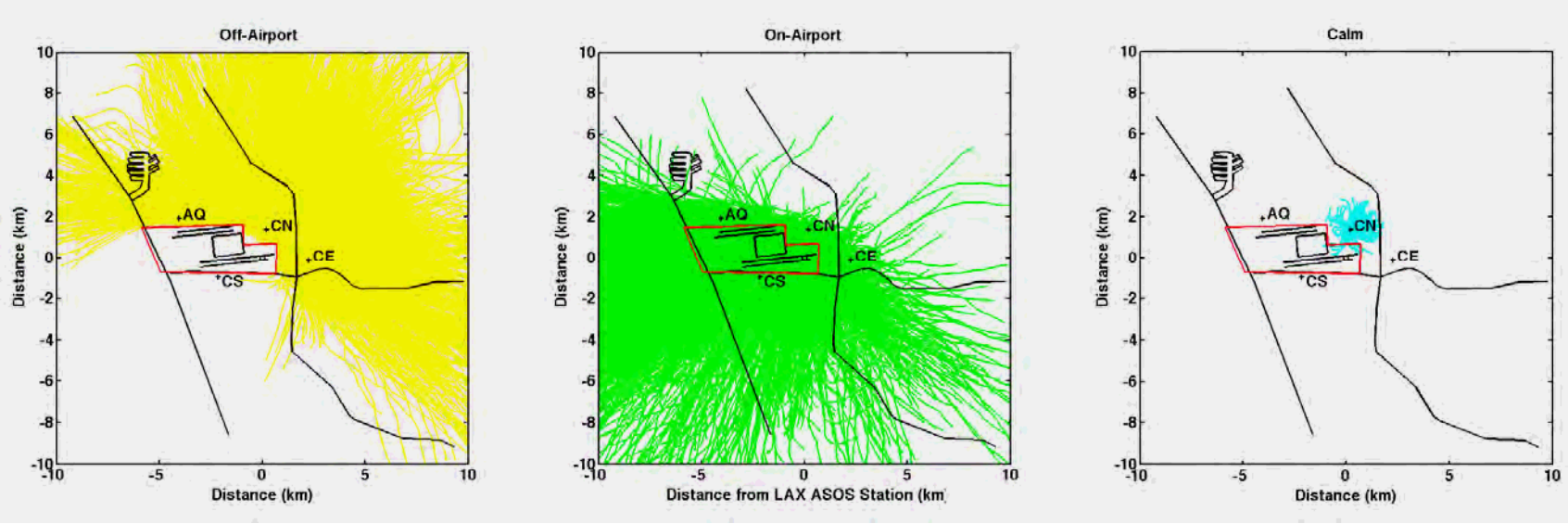

(1) **(2)** **(3)**

Figure 7-2. Three sets of trajectories for CN site for the Winter Season. 1) off-airport (yellow), does not pass over the airport and wind speed is greater than 1 knot; 2) on airport (green), passes over the airport and wind speed is greater than 1 knot; 3) low wind speed (blue), 1-hour average wind speed is less than or equal to 1 knot. Units on the axes are km from the LAX ASOS station. The North and South Airfields and Central Terminal Area are shown in black. The airport boundary is in red. "Calm" is defined as wind speeds less than 1 knot.

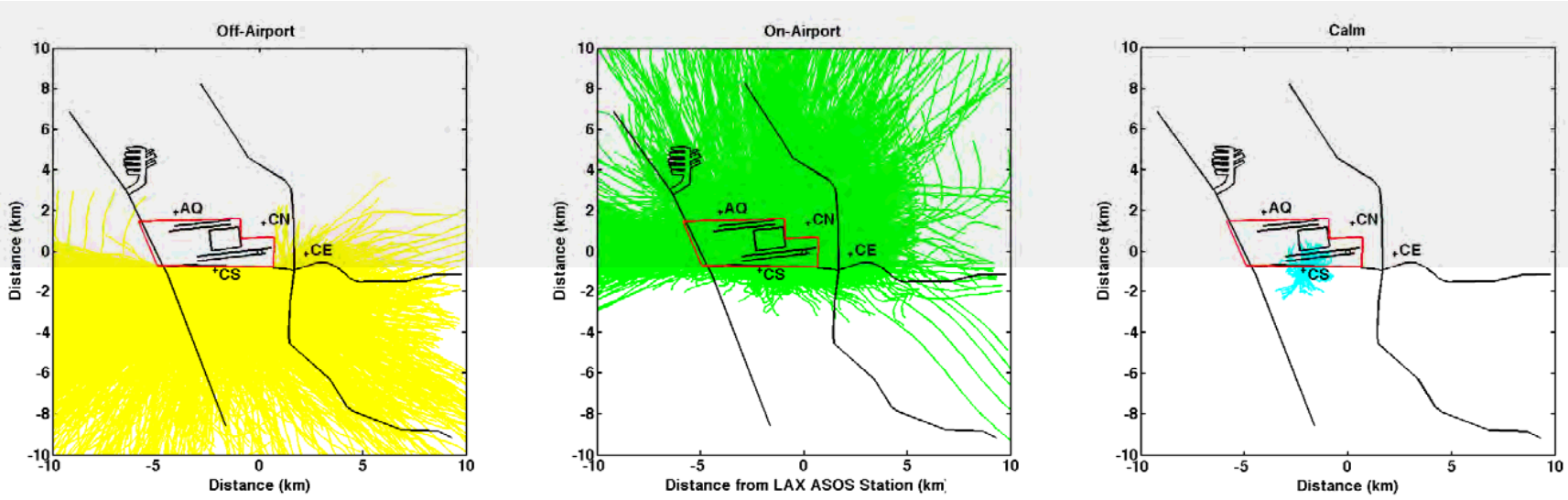

(1) **(2)** **(3)**

Figure 7-3. Three sets of trajectories for CS site for the Winter Season. 1) off-airport (yellow), does not pass over the airport and wind speed is greater than 1 knot; 2) on airport (green), passes over the airport and wind speed is greater than 1 knot; 3) low wind speed (blue), 1-hour average wind speed is less than or equal to 1 knot. Units on the axes are km from the LAX ASOS station. The North and South Airfields and Central Terminal Area are shown in black. The airport boundary is in red. "Calm" is defined as wind speeds less than 1 knot.

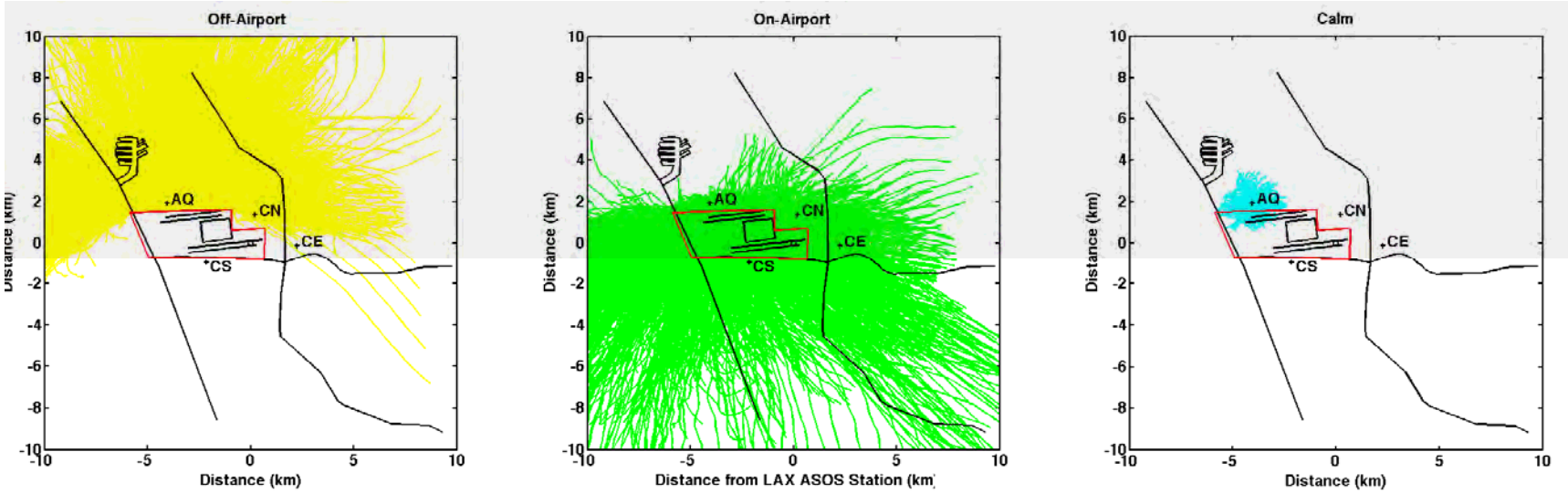

Figure 7-4. Three sets of trajectories for AQ site for the Winter Season. 1) off-airport (yellow), does not pass over the airport and wind speed is greater than 1 knot; 2) on airport (green), passes over the airport and wind speed is greater than 1 knot; 3) low wind speed (blue), 1-hour average wind speed is less than or equal to 1 knot. Units on the axes are km from the LAX ASOS station. The North and South Airfields and Central Terminal Area are shown in black. The airport boundary is in red. "Calm" is defined as wind speeds less than 1 knot.

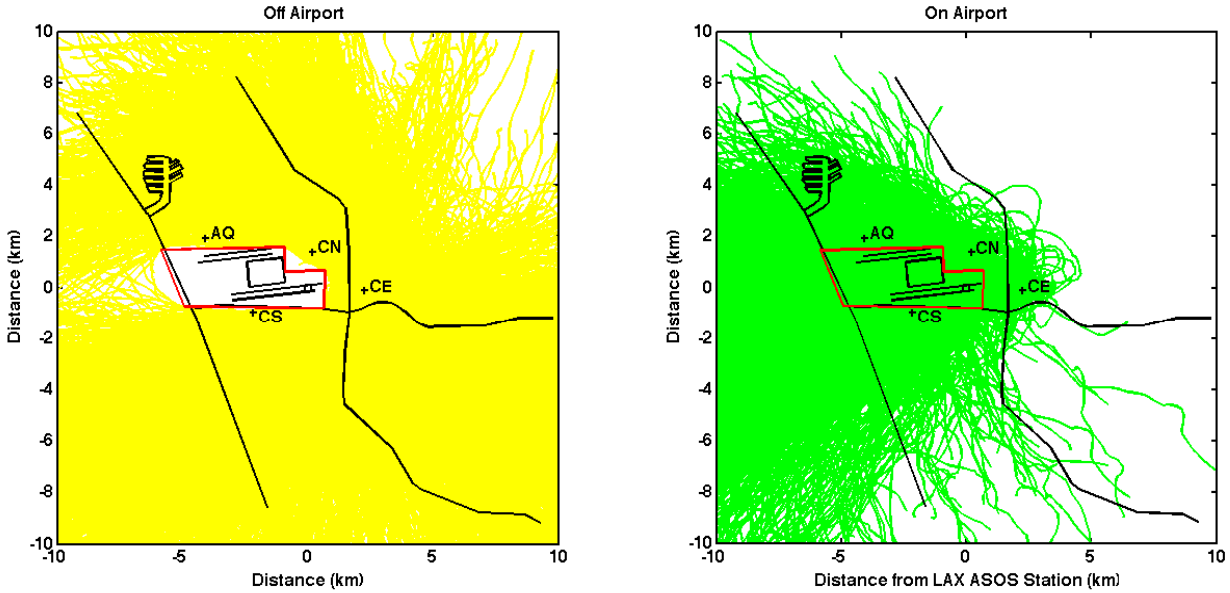

Figure 7-5. Two sets of back trajectories for CE site for the Summer Season. 1) off-airport (yellow), does not pass over the airport and wind speed is greater than 1 knot; 2) on airport (green), passes over the airport and wind speed is greater than 1 knot. There were no trajectories with1-hour average wind speed is less than or equal to 1 knot. Units on the axes are km from the LAX ASOS station. The North and South Airfields and Central Terminal Area are shown in black. The airport boundary is in red.

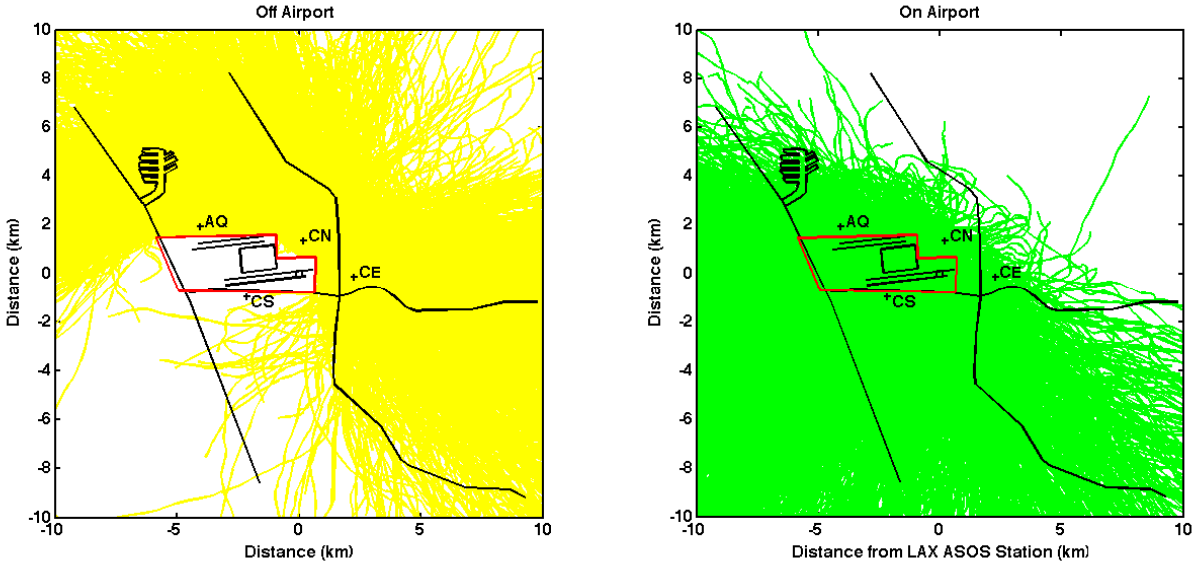

Figure 7-6. Two sets of back trajectories for CN site for the Summer Season. 1) off-airport (yellow), does not pass over the airport and wind speed is greater than 1 knot; 2) on airport (green), passes over the airport and wind speed is greater than 1 knot. There were no trajectories with1-hour average wind speed is less than or equal to 1 knot. Units on the axes are km from the LAX ASOS station. The North and South Airfields and Central Terminal Area are shown in black. The airport boundary is in red.

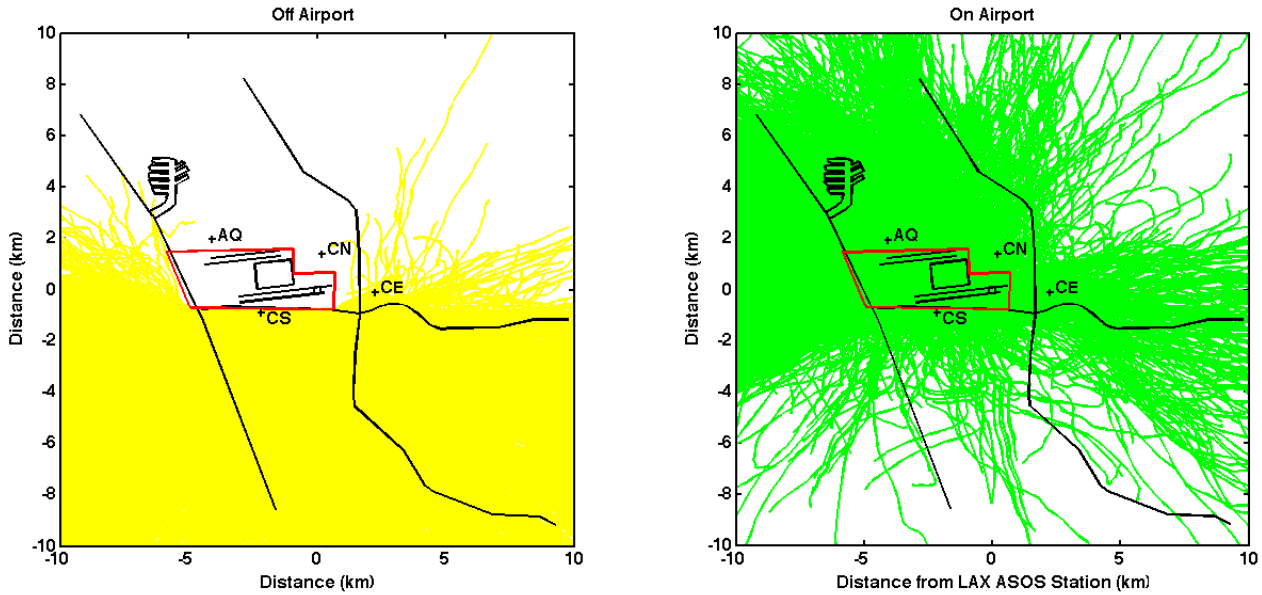

Figure 7-7. Two sets of back trajectories for CS site for the Summer Season. 1) off-airport (yellow), does not pass over the airport and wind speed is greater than 1 knot; 2) on airport (green), passes over the airport and wind speed is greater than 1 knot. There were no trajectories with1-hour average wind speed is less than or equal to 1 knot. Units on the axes are km from the LAX ASOS station. The North and South Airfields and Central Terminal Area are shown in black. The airport boundary is in red.

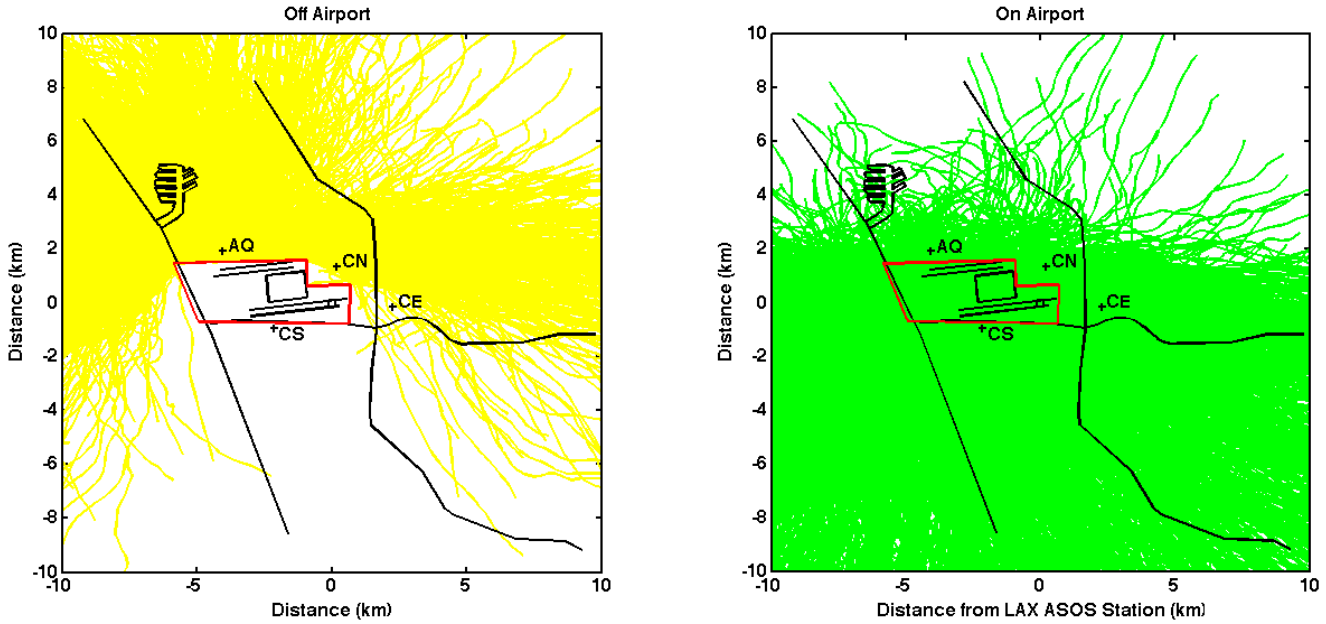

Figure 7-8. Two sets of back trajectories for AQ site for the Summer Season. 1) off-airport (yellow), does not pass over the airport and wind speed is greater than 1 knot; 2) on airport (green), passes over the airport and wind speed is greater than 1 knot. There were no trajectories with1-hour average wind speed is less than or equal to 1 knot. Units on the axes are km from the LAX ASOS station. The North and South Airfields and Central Terminal Area are shown in black. The airport boundary is in red.

Consider an air sample collected at a monitoring site starting at time t_i, $i = 1 \ldots N$, where N is the number of observations. Let the concentration resulting from the source area during this period be s_i, then the average source contribution is given by:

$$\overline{S} = N^{-1}\left(\sum_{i\in H} s_i + \sum_{i\in M} s_i + \sum_{i\in R} s_i\right) \quad (1)$$

For $i \in H$, (in which i is a member of H, which is the set of trajectories not in R that pass over the source region) let the observed concentration be c_i, which can be split between the portion due to the source area and the portion due to background sources, b_i. Thus, s_i can be written as:

$$\begin{aligned} c_i &= s_i + b_i \\ s_i &= c_i - b_i \end{aligned} \quad (2)$$

For $i \in M$, the source contribution can be assumed to be zero, since the air has not passed over the source area within the past hour.

$$s_i = 0 \quad (3)$$

However, this may not be assumed if the air has been moving slowly without a well-defined direction. This case is discussed below.

For $i \in R$, the average air speed during the previous hour was less than or equal to 1 knot. Thus, the air had not traveled more than 1.85 km during the hour. The trajectories in this project are calculated using data from the ASOS stations at LAX, Hawthorne, and Santa Monica airports. ASOS wind speeds are reported in "knots" as whole numbers. Thus, the lowest nonzero wind speed is 1 knot. Below this value, the wind direction does not provide useful information, which indicates the resulting back trajectories are not reliable. For this reason, it is not possible to apportion the concentrations associated with these trajectories in a similar manner to the two other sets of trajectories. The contribution of the source is taken to be an unknown fraction f_i of the observed concentration:

$$s_i = f_i c_i, \quad 0 \le f_i \le 1 \quad (4)$$

Where f_i corrects for other sources:

$$\overline{S} = N^{-1}\sum_{i\in H}(c_i - b_i) + N^{-1}\sum_{i\in R} f_i c_i \quad (5)$$

The lower limit for the average source contribution of the source area (S_L) is calculated using the high estimate of the background (as defined in the next section) and $f_i = 0$,

$$\overline{S}_L = N^{-1}\sum_{i\in H}(c_i - b_i^{hi}) \quad (6)$$

The upper limit (S_U) is found by using the low estimate of the background and $f_i = 1$,

$$\overline{S}_U = N^{-1}\sum_{i\in H}(c_i - b_i^{lo}) + N^{-1}\sum_{i\in R} c_i \quad (7)$$

The best estimate (S_M) is the average of the upper and lower bounds,

$$\overline{S}_M = 0.5(\overline{S}_L + \overline{S}_U) \quad (8)$$

The errors in these sums are calculated by the standard rules that the variance of the sum is the sum of the variances and that the variance of the mean of a sample is the variance of the sample divided by the number of terms.

7.2.2 Background Estimation

The high and low estimates of the background concentration of any species at a site are determined using the two lowest values at the three other sites. UFPs are an exception because they are measured in particle number, which is not an unchanging quantity. Significant numbers of particles can, and often are, formed and lost in a matter of minutes in transit between the background sites and the monitoring site. While NO_x and SO_2 may be lost (but not formed), the time required to make a significant change is usually on the order of an hour or more.

The algorithm to determine the background concentration is:

> The low background estimate is the minimum of the three other sites over the previous 15 minutes. The high background estimate is the second lowest of the other sites over the previous 15 minutes. If the concentration at the site being analyzed is lower than the background determined as stated above, the background is set to the site's concentration.

Missing background values are due to the necessity for all four sites to have simultaneous non-missing data for the background to be calculated. Relaxing the requirement that all the stations have data is possible, but would lead to greater uncertainty in the results and, for this analysis, would not greatly increase the number of data points used in the final analysis.

7.3 NONPARAMETRIC TRAJECTORY ANALYSIS MODEL

7.3.1 Methodology

NTA is a receptor model that can show the effects of nearby sources on the data and, at the same time, the sources of background pollutants can be located and quantified. This is completed by using one to five minute average pollutant concentrations and back-trajectories calculated using one to five minute average wind data. Averaging times on the order of minutes are needed to be able to separate the effects of local sources. NTA estimates the conditional expected value of a pollutant at the receptor, given that the air has passed through *(X, Y)* prior to reaching the receptor. Graphical representation of how NTA is calculated is provided in Figure 7-9.

Assume there are *n* back-trajectories with *m* points equally spaced in time along each trajectory. Let the points on the back-trajectories be given by (x_{ij},y_{ij}) where $i = 1,\ldots,m$ and $j = 1,\ldots,n$. Let C_j be the concentration at the receptor when the trajectory arrives at that monitor. Therefore, the NTA at point *(X,Y)* is a weighted sum of the observed concentrations given by:

$$E(C \mid \text{air passes over point } (X,Y)) = \frac{\sum_{i=1}^{m}\sum_{j=1}^{n} C_j W_{ij}}{\sum_{i=1}^{m}\sum_{j=1}^{n} W_{ij}} \quad (9)$$

where,

$$W_{ij} = K\left(\frac{X - x_{ij}}{h}\right) K\left(\frac{Y - y_{ij}}{h}\right) \quad (10)$$

and,

$$\begin{aligned} K(u) &= 0.75(1-u^2) \quad \text{for } |u| \le 1 \\ K(u) &= 0 \qquad\qquad\quad \text{otherwise} \end{aligned} \quad (11)$$

The smoothing parameter *h* is the radius of the circle in Figure 7-9. Further details can be found in Henry (2007).

The NTA model is unique in its use of back-trajectories on the scale of a few kilometers, and meteorological data on the time scale of minutes, to identify local source-receptor relationships. These back-trajectories are estimated using wind speed and direction, which have both measurement error and natural variability. The effect of this uncertainty in wind speed and direction is an uncertainty in the back-trajectories and an associated increase in the uncertainty of the NTA results. The errors in the NTA estimates for the Study include the effects of errors in the trajectories, which cause errors in the weighting factors W_{ij} in Eq. 9. The standard formulae for errors assume the W_{ij} are error free. The effect of the errors in the trajectories is to increase the error by approximately 25 to 35 percent and to make the errors increase toward the edges of the grid.

In this work, the smoothing parameter *h* is 0.707 km. This value was derived empirically. Results are not sensitive to the exact value. The NTA analysis points *(X, Y)* are defined on a grid of 100 by 100 cells with a width of 140 m each and the origin at the receptor (a monitoring site) and *X* and *Y* limits of -7 km and +7 km. These limits are chosen as the back trajectories are most likely not reliable beyond this region.

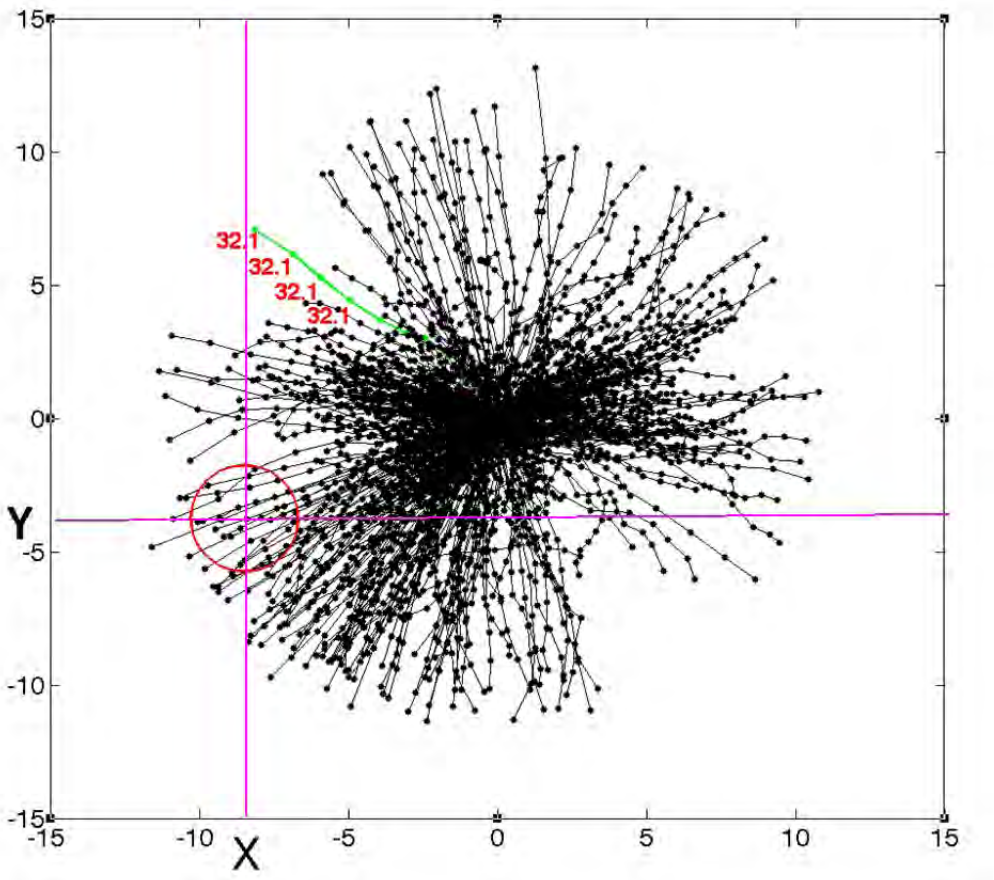

Figure 7-9. Visual representation of NTA. The back-trajectories are shown as black lines and points at 5-minute intervals. Each point on a trajectory is associated with the concentration observed when the trajectory arrives at the receptor. For example, each point on the trajectory shown in green is associated with the concentration 32.1 shown as red values. The NTA value for point (X,Y) is the weighted sum of the values associated with the trajectory points inside the red circle. The weights for each trajectory point are based on the distance of the point from (X,Y). The diameter of the circle is related to the smoothing parameter.

7.4 RESULTS AND INTERPRETATION

One of the primary goals of NTA is to identify the potential locations of emission sources within the Study Area. NTA was carried out for all continuous data at each of the three core sites. The base map that covers the area used in NTA is shown in Figure 7-10. A compilation of the main results for the Winter Monitoring Season is found in Figure 7-11. Each plot contained within the figure is comprised of the combined NTA results for the three community sites (CE, CN, and CS), which are influenced by similar sources. The mapped values are the minimum concentrations for the three sites. The green areas on the figure represent areas that are high concentrations for all the sites and are likely to be the source of the emittant in question. The AQ site was observed to have been potentially influenced by a different set of non-airport related sources. The NTA results for the Summer Monitoring Season are found in Figure 7-12.

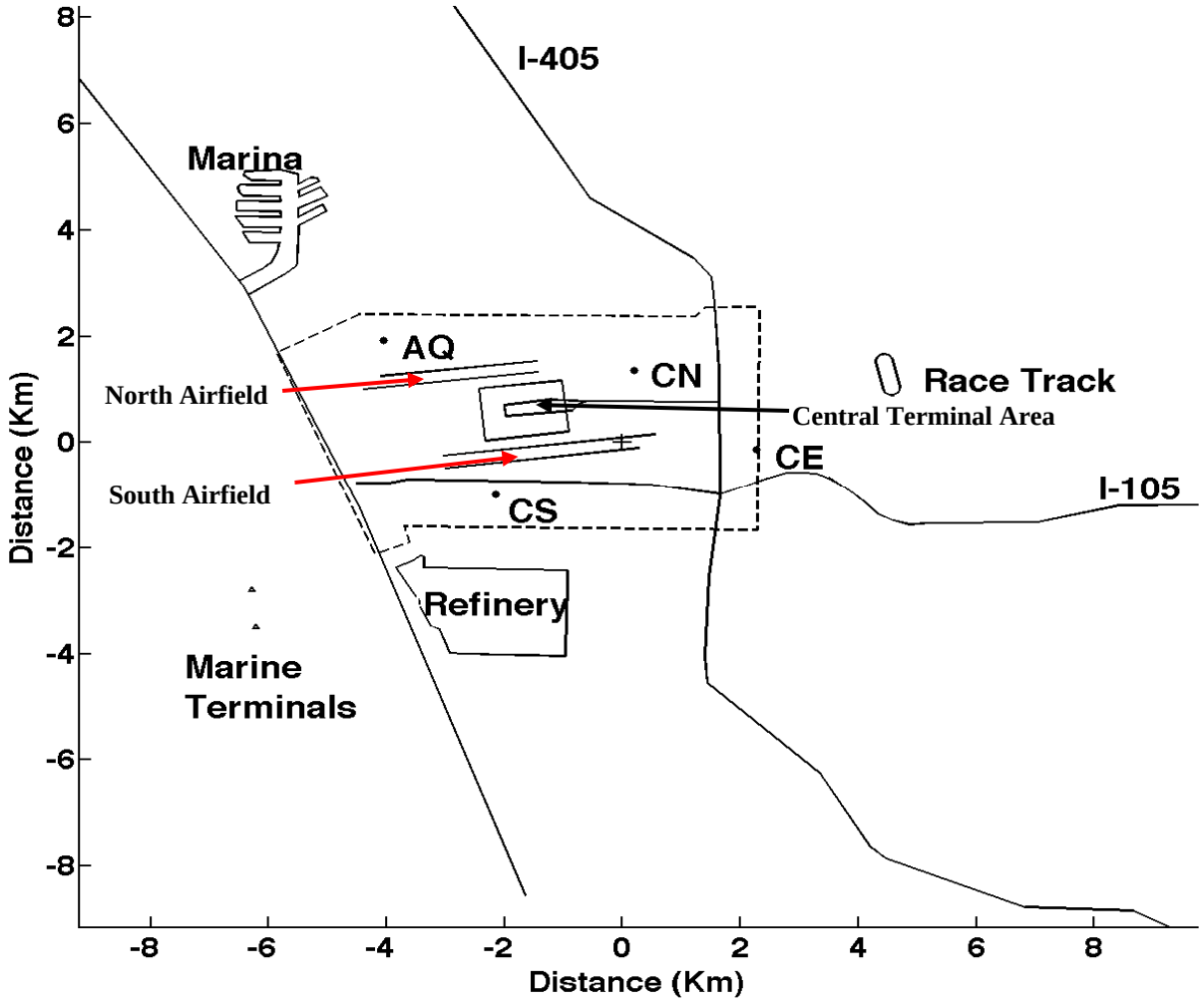

Figure 7-10. Base map for NTA results at the LAX airport. The dotted line encompasses the Study Area boundary for Phase III of the LAX AQSAS. The LAX ASOS station is located at the origin marked by +.

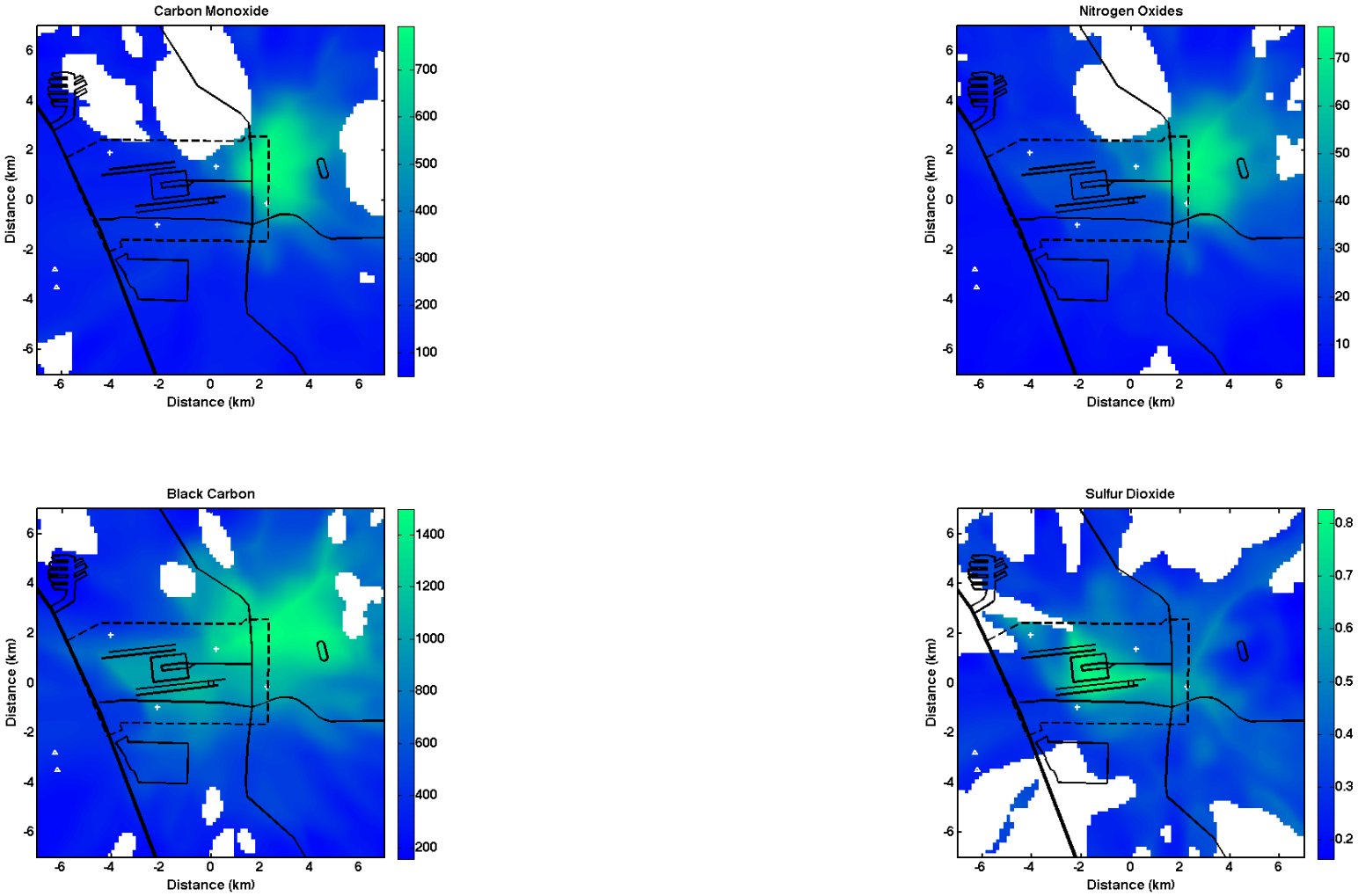

Figure 7-11. Composite NTA results for CE, CN, and CS sites during the Winter Season. Regions colored green are likely the location of the main sources of the species affecting the monitoring sites. Regions colored blue are unlikely to have major sources. The white areas represent locations that had an insufficient number of data points to be statistically significant. Units for BC are ng m^{-3}, all others are in ppb. The four sites are indicated by the white plus signs. Please see Figure 7-10 for indication of site names.

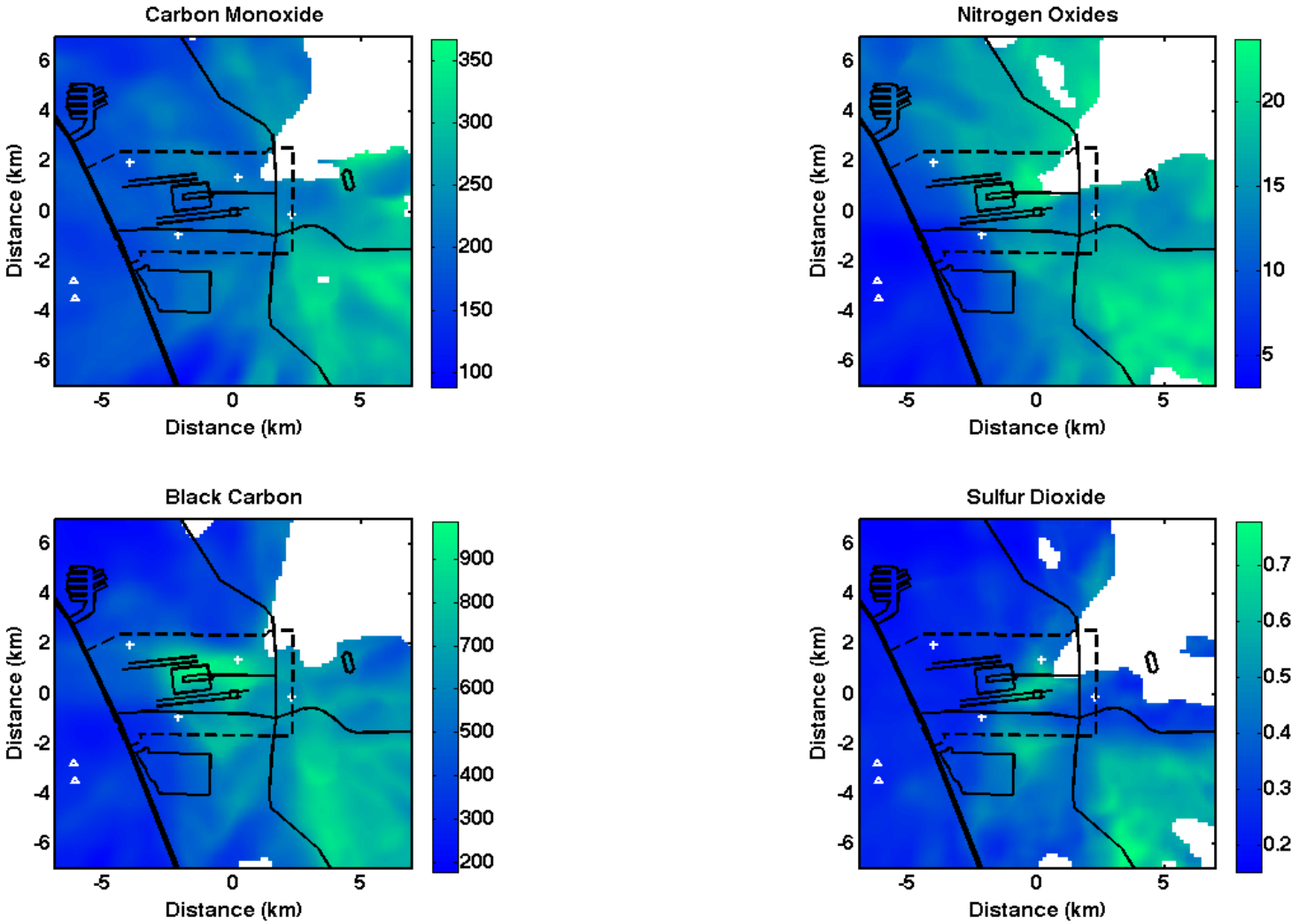

Figure 7-12. Composite NTA results for CE, CN, and CS sites during the Summer Season. Regions colored green are likely the location of the main sources of the species affecting the monitoring sites. Regions colored blue are unlikely to have major sources. The white areas represent locations that had too few data points to be statistically significant. Units for BC are ng-m^{-3}; all others are ppb. The four sites are indicated by the white plus signs. Please see Figure 7-10 for indication of site names.

Data for the Winter Monitoring Season show that:

- The main sources of high concentrations of NO_x and CO are local traffic in the region north of the I-105 and east of the I-405 freeways.

- The main source areas for SO_2 are the Central Terminal Area and North and South Airfields of the airport, with other sources potentially including offshore and roadway.

- The highest concentrations of BC are associated with the same regions as CO and NO_x. The airport is also found to be a source area.

- The NTA results indicate only a possible minor offshore source of SO_2.

Data for the Summer Monitoring Season show that:

- The main sources of high CO concentrations are from air passing over the region located south of the I-105 freeway and east of the I-405 freeway. This region is also a source of high concentrations of NO_x, BC, and SO_2. Since this region southeast of LAX is associated with high concentrations of all the species measured, and no obvious large sources are located within several kilometers of this region, the NTA results indicate a flow of the abovementioned pollutants into the Study Area from sources to the southeast of the airport. During the Summer Monitoring Season, the air flow came from this southeast region about ten percent of the time. Potential contributors in this direction include refineries and seaports. Although it is a rare occurrence during this period, the possibility exists that some of the polluted burden of the southeastern flow is recirculated airport emissions from early morning flow from the north and northeast.

- Main sources for high NO_x concentrations include the polluted southeast flow as well as all regions more than one or two km inland from the coast, including LAX and the commercial districts near the Study Area.

- The main source areas for SO_2 are the Central Terminal Area; the South Airfield, and the polluted southeast flow. A region of possible high emissions was located to the south of the Study Area and northeast of the El Segundo Refinery. The nature of possible sources in this area is not known at this time.

- Elevated concentrations of BC are associated with the Central Terminal Area and North and South Airfields and, as noted above, with flow from the southeast.

Inferences from the NTA analysis:

- For the Winter Monitoring Season, high concentrations of the measured pollutants were associated with sources within several kilometers of LAX. There was no indication of the monitoring stations being influenced by sources located at a distance greater than several kilometers. For the Summer Monitoring Season, this phenomenon was not observed. High concentrations of the measured pollutants were associated with sources

to the southeast of the LAX ASOS, some of which were most likely greater than five to ten kilometers from LAX.

- For the Winter Monitoring Season, the elevated concentrations of CO, NO_x, and BC were associated with late night and early morning periods of stagnation and drainage flow from the elevated terrain located to the northeast of the monitoring sites. Local traffic was the most likely source. During the Summer Monitoring Season, air parcels were very rarely from this direction.

- For the Summer Monitoring Season, high concentrations of CO, NO_x, SO_2, and BC were associated with a broad region located to the southeast of the monitoring sites. This was possibly due in part to local traffic sources. However, the diffuse nature on the NTA maps is indicative of transport from more distant sources. During the Summer Monitoring Season, the onshore sea breeze was strong and often did not weaken until midnight or later, if at all. The flow then was directed to the north or, more often, to the south and east as it reversed. Wind speeds dropped, thus creating the potential for high concentrations as the flow reverses. The offshore winds often come from the southeast early in the morning, between 7:00 to 9:00 PST.

- For the Winter Monitoring Season, CO and NO_x at all the monitoring sites were most likely dominated by off-airport sources. BC had both significant on- and off-airport sources. SO_2 was primarily from airport sources.

- For the Summer Monitoring Season, the relative roles of on-airport and off-airport sources were less clear than for the Winter Monitoring Season. While there are off-airport sources for all species, it is difficult to judge their importance since the frequency of the winds from the southeast is quite low. The Summer Monitoring Season NTA results support the observation that the on- and off-airport sources were much more balanced for the Summer Monitoring Season than the Winter Monitoring Season, especially for CO and NO_x.

7.5 QUANTITATIVE SOURCE APPORTIONMENT

The goal of source apportionment is to identify the upper and lower bounds that pertain to the impact of the airport. This is done by using observed minute by minute concentrations at the monitoring sites and one-hour back-trajectories calculated for each minute. Assumptions include:

- If the back trajectory for that particular measured pollutant does not pass over the airport, the contribution of the airport is zero for that minute.

- If the trajectory from a monitoring site does pass over the airport, the contribution of the airport equals the observed concentration at that minute minus the background concentration as estimated from the other three monitoring sites.

- If the average wind speed for the trajectory is less than 1 knot (1.15 mph or 0.514 m/s), the wind direction and the corresponding trajectory may not represent actual transport. In this instance, the impact of the airport is unknown and assumed to be all or none of the observed concentration, as explained below.

The estimate of the low airport impact assumes a high estimate of background concentration, which is given by the second lowest of the three monitoring sites. Also, none of the concentrations observed at low wind speeds are apportioned to the airport. The estimate of the high airport impact assumes a low estimate of background concentration given by the lowest of the three monitoring stations. Also, all of the concentrations observed at low wind speeds are apportioned to the airport. The estimate of the average airport impact is given as the average of the low and high estimates. The high and low source contribution values are estimates of the bias in the method.

The key to this method of source apportionment is in determining which trajectories pass over the airport (on-airport) and which do not (off-airport), class one and class two, respectively. The trajectories with very low average wind speeds of less than one knot constitute the third class. The three classes of trajectories for the CN site are found in Figure 7-2. If the line connecting any two trajectory points intersects the airport boundary, it is counted as an on-airport trajectory, even if all of the trajectory points lie outside the airport boundary. For the Summer Monitoring Season, there were no periods with an hourly average wind speed of less than one knot.

7.6 SOURCE APPORTIONMENT RESULTS

The average contribution of on-airport and off-airport sources to CO, NO_x, SO_2, and BC at the four monitoring sites for the Winter and Summer Monitoring Seasons are seen in Figure 7-13. The main features of these results are:

- The average concentrations of all species at all sites were lower for the Summer Monitoring Season than the Winter Monitoring Season. Lower concentrations during the Summer Monitoring Season are expected since there is increased dilution of emittants due to higher wind speeds and mixing heights in the summer than the winter. However,

this was not true for the peak hourly concentrations of SO_2, which were actually higher during the Summer than the Winter Monitoring Season.

- During the Winter Monitoring Season, the off-airport contributions were generally much larger than the on-airport contributions. The main exceptions being SO_2 at the CE and CN sites, and BC at the CN site where the on- and off-airport contributions are very similar.

- During the Summer Monitoring Season, at the CE and CN sites, the on-airport source contribution was similar to or greater than the off-airport source contributions for all the species. However, at the CS and AQ sites, off-airport sources were more dominant than on-airport sources.

Since the concentrations for the Winter and Summer Monitoring Seasons differ greatly, it is customary in source apportionment studies to normalize the results by the total concentration and to express source contributions as a percentage of the total. This is seen in Figure 7-14 for the on-airport source contributions. The on-airport source contributions are approximately 50 percent or greater for the two sites that most often lie downwind of the airport (CE and CN sties) and those emittants associated with aircraft operations (SO_2 and BC). While it is beneficial to examine the average values for source contributions for the two monitoring seasons, the hourly average source contributions for each season are able to provide more detailed information.

Hourly on- and off-airport source contributions averaged over the Winter Monitoring Season are shown in Figure 7-15. The range of uncertainty due to random errors and assumptions of the method for the on-airport source contributions is shown, along with the emittant total hourly average concentration.

- The concentrations of all emittants peak in the early morning and are at a minimum during midday. The only exception to this observation is SO_2 at the CE and CN sites where the highest concentrations occurred in the middle of the day. This hourly pattern can be explained by a combination of the variation in the dilution effects and source emissions. The lowest dilution occurs in the late night and early morning hours when wind speeds and mixing heights are low. This is especially true during the winter season. The main source of all the emittants, other than SO_2, is vehicular traffic, which peaks strongly in the morning hours and less strongly in the late afternoon. The major source of SO_2 is from aircraft with a broad peak observed during the day. This differs from the other emittants which observe peaks due to vehicular traffic in the morning hours and, less strongly, in the late afternoon hours.

- At the CE and CN sites, the on-airport source contributions are larger than the off-airport contributions only during the middle of the day when total concentrations are low (with SO_2 as the exception).

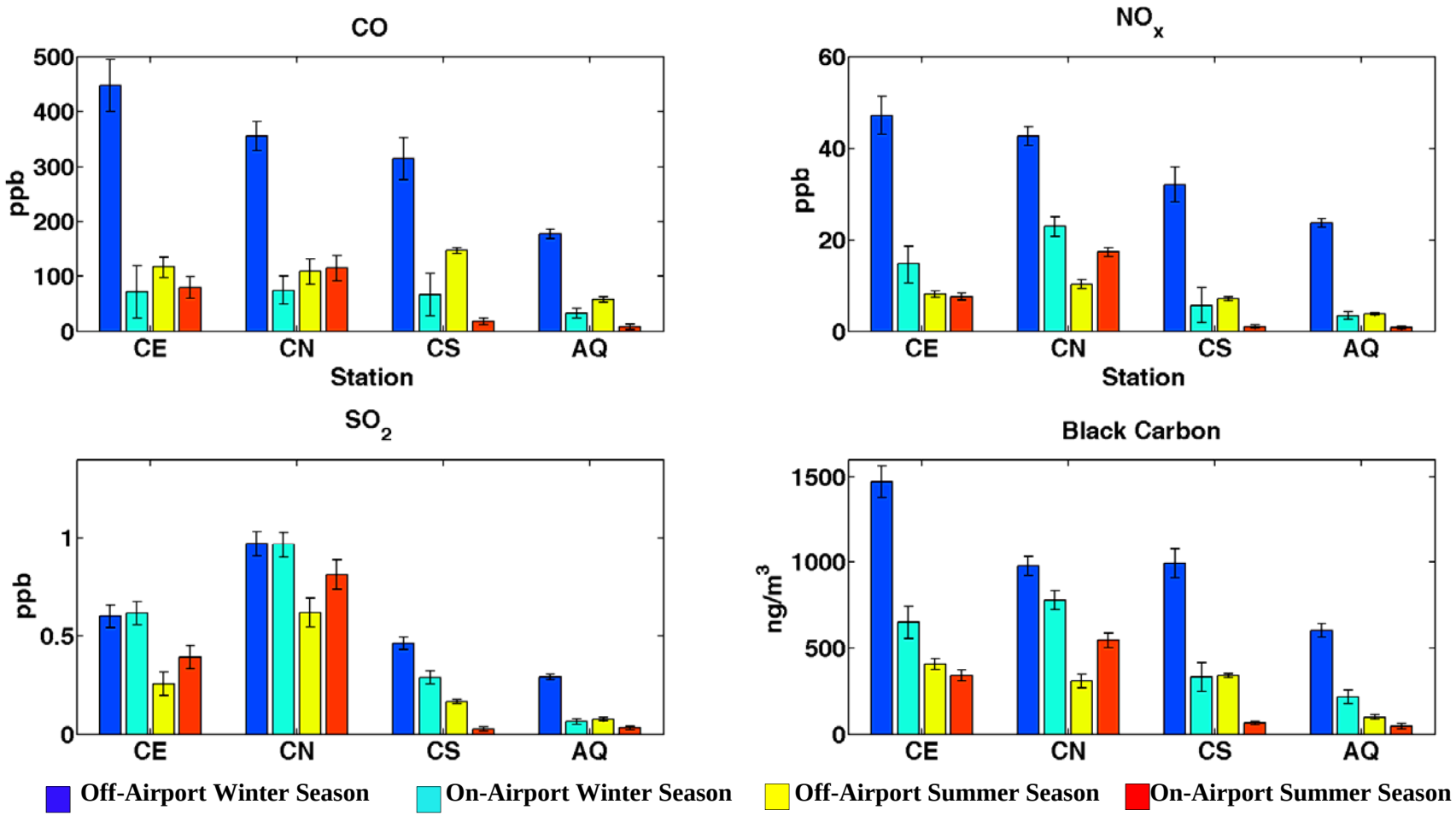

Figure 7-13. Average NTA source apportionment for the Winter and Summer Seasons (the ranges shown at the top of the bar are inclusive of both random error and errors in assumptions in the computations).

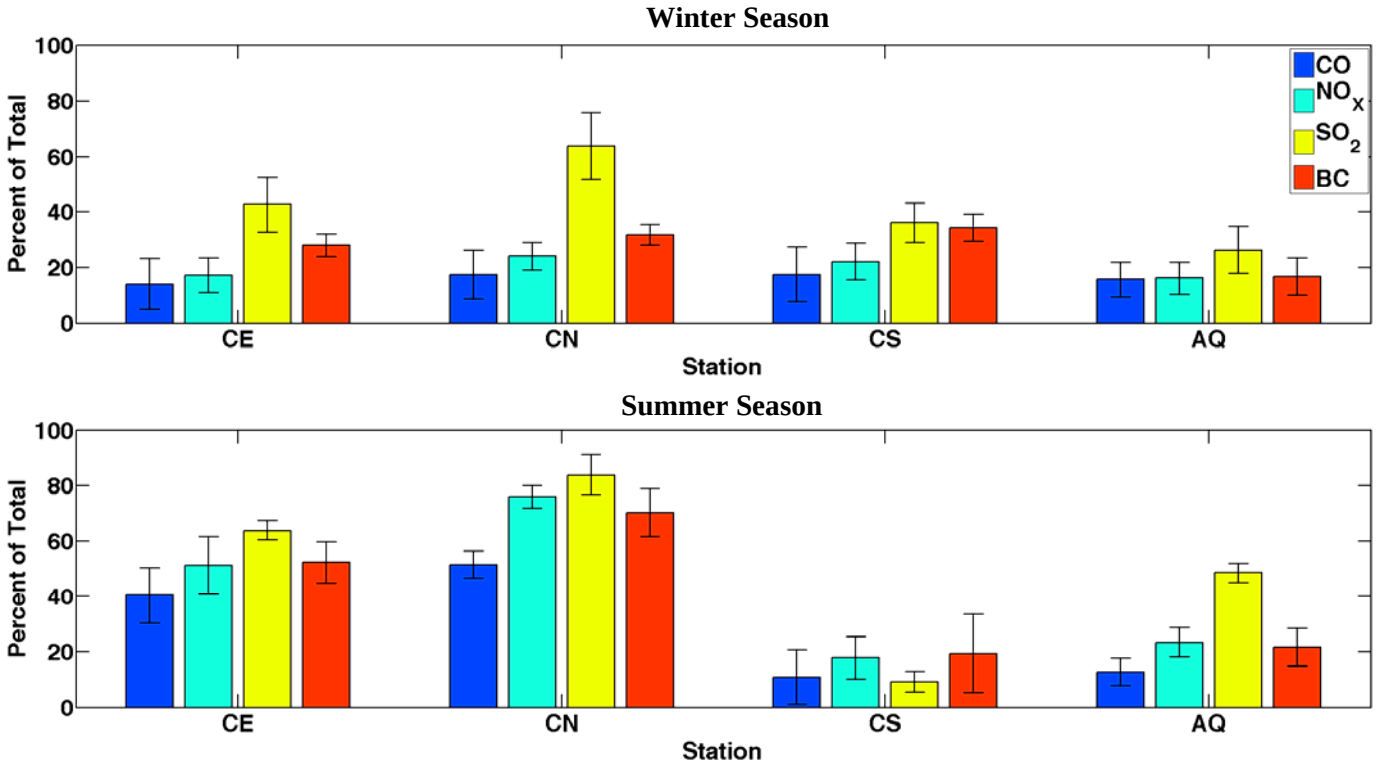

Figure 7-14. Average NTA on-airport source apportionment for the Winter and Summer Seasons expressed as a percentage of the total observed average concentration. (The ranges shown at the top of the bar are inclusive of both random error and errors in assumptions in the computations.)

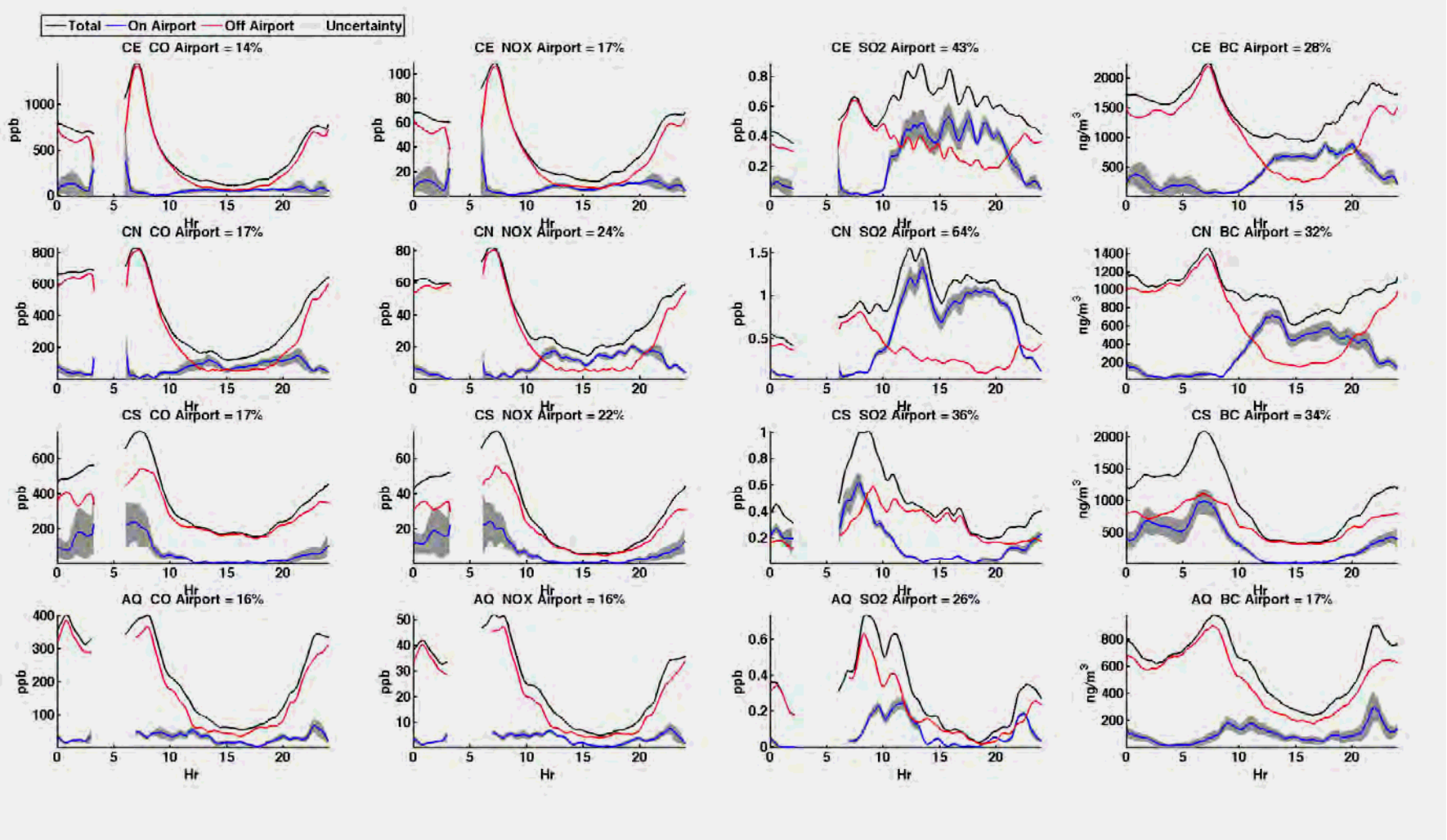

Figure 7-15. Hourly trajectory-based NTA source apportionment for the Winter Season. The black line is the total contribution, red is the off-airport contribution, and blue is the on-airport contribution. The on-airport contribution line contains the upper and lower limits (gray shaded), which include the estimated effects of random error and assumptions made in the computations. Breaks in the lines occur in the early morning hours when automatic calibration of the gas monitors occurs.

- The high estimate of airport contribution is less than 50 percent for all except SO_2 at CE and CN sites as evidenced by the times when the blue line is above the red line in the figure.

- At the CS site, the highest concentrations occur in the early morning. Outside of a few exceptions, airport source contributions are less than 50 percent.

- The airport source contributions at the AQ site are low and have two peaks, one in the morning and one in the evening.

- The range of uncertainty in the calculations is relatively small and does not affect the above conclusions.

The hourly average source contributions for the Summer Monitoring Season are in Figure 7-16, which show that:

- The peak concentrations for all species, except SO_2, are less than during the Winter Monitoring Season. SO_2 peak concentrations are lower at the AQ and CS sites, but higher at the CE and CN stations.

- All species have peak concentrations in the morning, but generally later than during the Winter Monitoring Season.

- At the CE and CN sites, the on-airport source contributions are higher than the off-airport contributions for a majority of the time, except for a few hours in the very early morning.

- The CS site is little impacted by airport sources for all species.

- The AQ site had little impact from on-airport sources of CO and moderate impacts by NO_x, BC, and SO_2, with peaks occurring about 8:00.

7.7 ULTRAFINE PARTICLE SOURCE APPORTIONMENT

The UFP concentrations for the Winter Monitoring Season were for total particle number per cubic centimeter. No sufficiently complete size distribution data were available to allow quantitative source apportionment by size. During the Winter Monitoring Season, only the CE and CN sites had ultrafine particle (UFP) number data that allowed for hourly average source apportionment to be conducted. Figure 7-17 shows the hourly source apportionment for the UFP number concentration with SO_2 and BC for comparison. These pollutants are shown because the main sources of UFP are diesel vehicles and jet engines and BC is primarily from diesel vehicles and SO_2 is primarily from jet engines.

No background subtraction has been done for the UFP source apportionment because UFP particle number is a constantly changing quantity. Particles form and are lost on a relatively short time scale of minutes, making it impossible to infer a reasonable background concentration.

It was observed that a diurnal pattern for UFP resembles a combination of the BC and SO_2 on-airport contributions, which is seen in Figure 7-16. Approximately 52 and 69 percent of the total UFP particle numbers at the CE and CN sites, respectively, are apportioned to on-airport sources for the Winter Monitoring Season. These percentages are evidenced by the times when the blue line is above the red line in the figure, as was done for CO, SO_2, NO_x and BC. However, this is an overestimate due to no background subtraction. The diurnal pattern for the off-airport source contributions resembles local vehicle traffic, especially for the CE station, which is the station with the greatest traffic impact.

For the Summer Monitoring Season several size ranges as well as the total volume of the UFP were analyzed. Size-resolved UFP numbers were unavailable from the AQ site. The volume of the UFP particles is used to represent mass. The small size range is from 7.37 to 30 nm, while the large size range is from 30 to 160 nm. The results are shown in Figure 7-18. All the UFP-related numbers at the CE and CN sites show a distinct pattern with two identifiable peaks, one in the morning and one in late evening. The only other pollutant measured that shows a similar pattern to the one observed for UFP was BC at the CE and CN sites, as seen in Figure 7-167. The diurnal pattern for the total particle number is similar to the 7.37 to 30 nm size range. Since the smaller particles dominate the total particle number, this is to be expected. The diurnal pattern for the UFP volume is similar to the 30 to 160 nm particles, which is also expected because this size range dominates the volume.

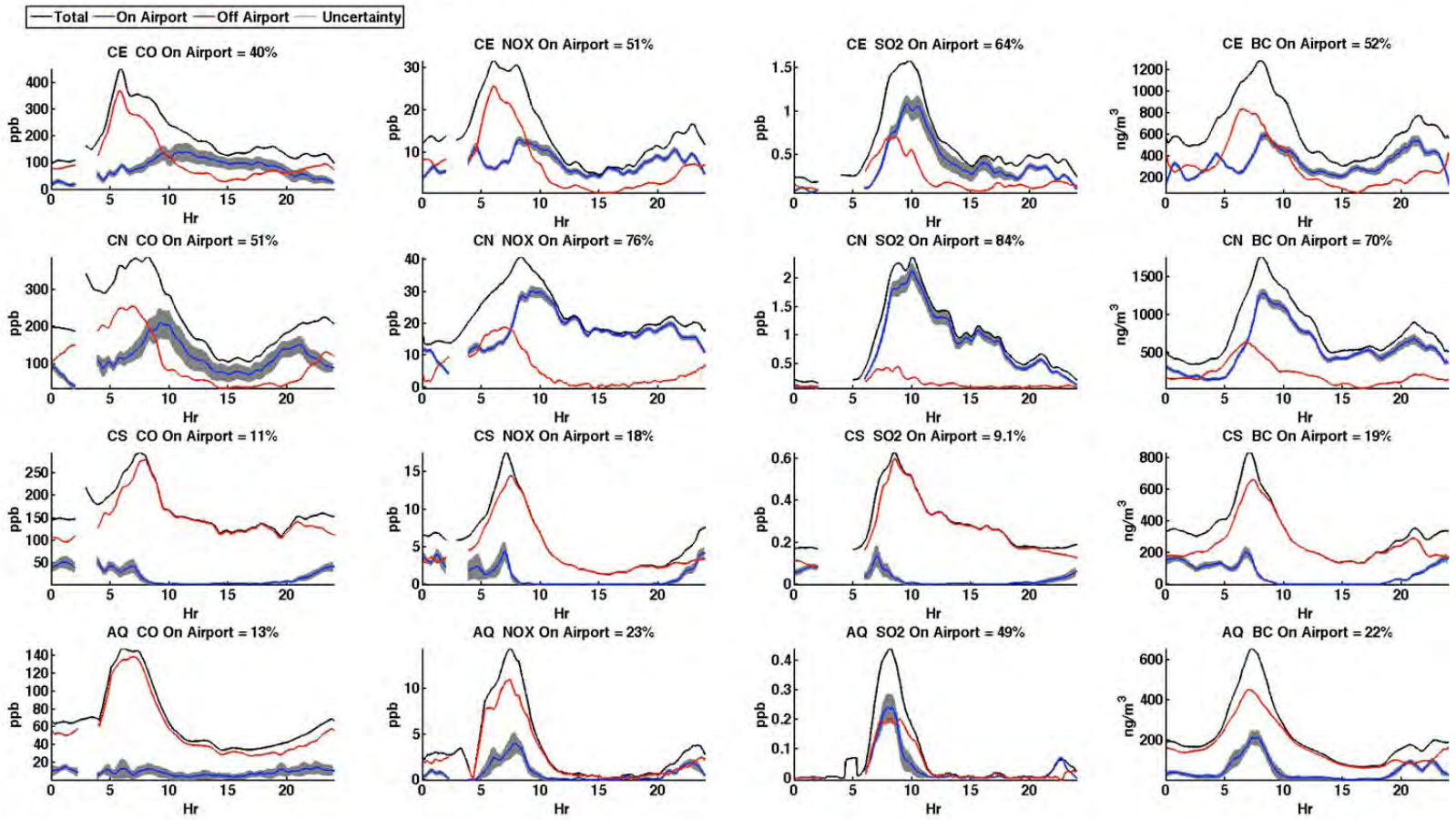

Figure 7-16. Hourly trajectory-based NTA source apportionment for the Summer Season. The black line is the total contribution, red is the off-airport contribution, and blue is the on-airport contribution. The on-airport contribution line contains the upper and lower limits (gray shaded), which include the estimated effects of random error and assumptions made in the computations. Breaks in the lines occur in the early morning hours when automatic calibration of the gas monitors occurs.

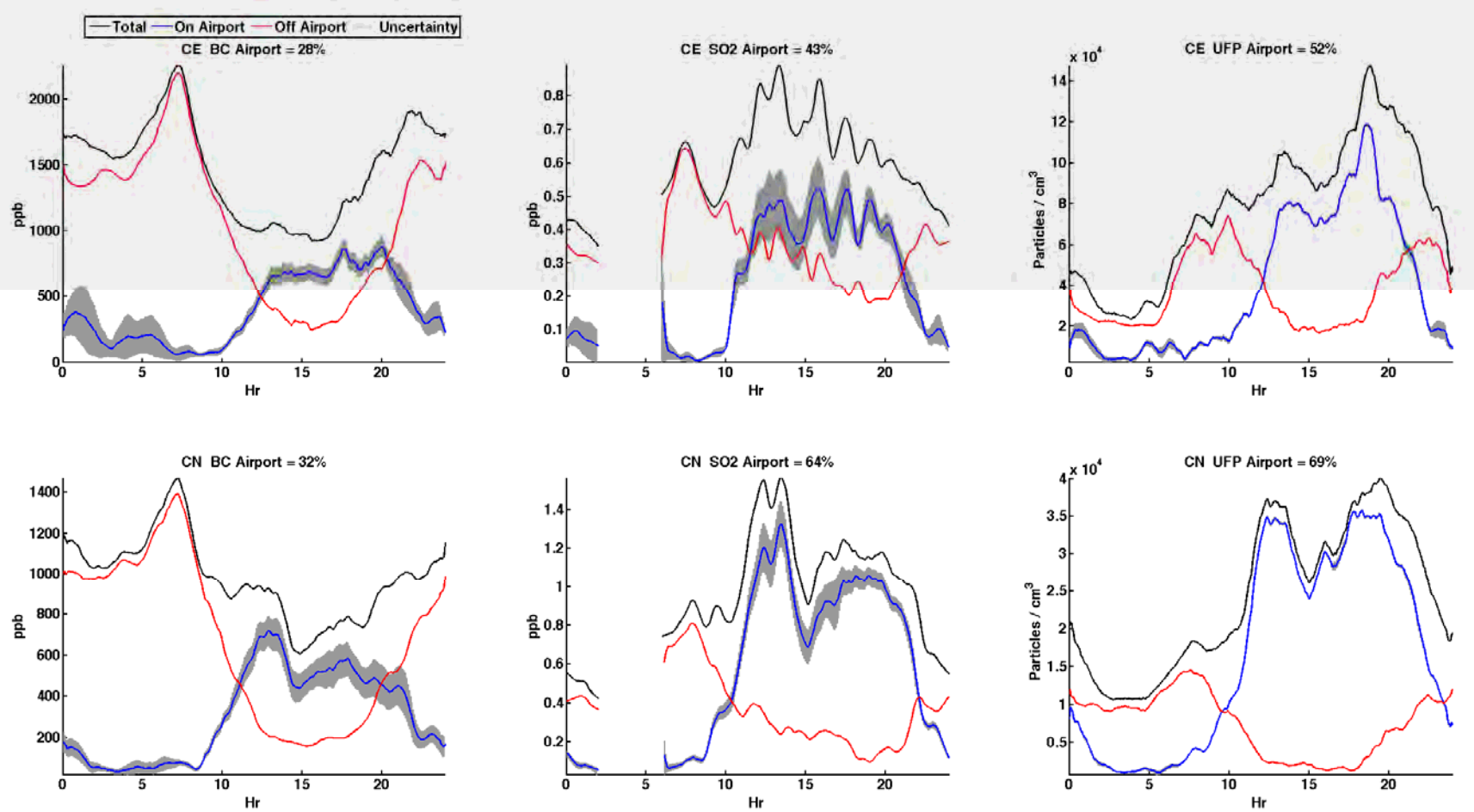

Figure 7-17. Winter Monitoring Season NTA source apportionment of UFP for CE and CN sites. The black line is the total contribution, red is the off-airport contribution, and blue is the on-airport contribution. The on-airport contribution line contains the upper and lower limits (gray shaded), which include the estimated effects of random error and assumptions made in the computations.

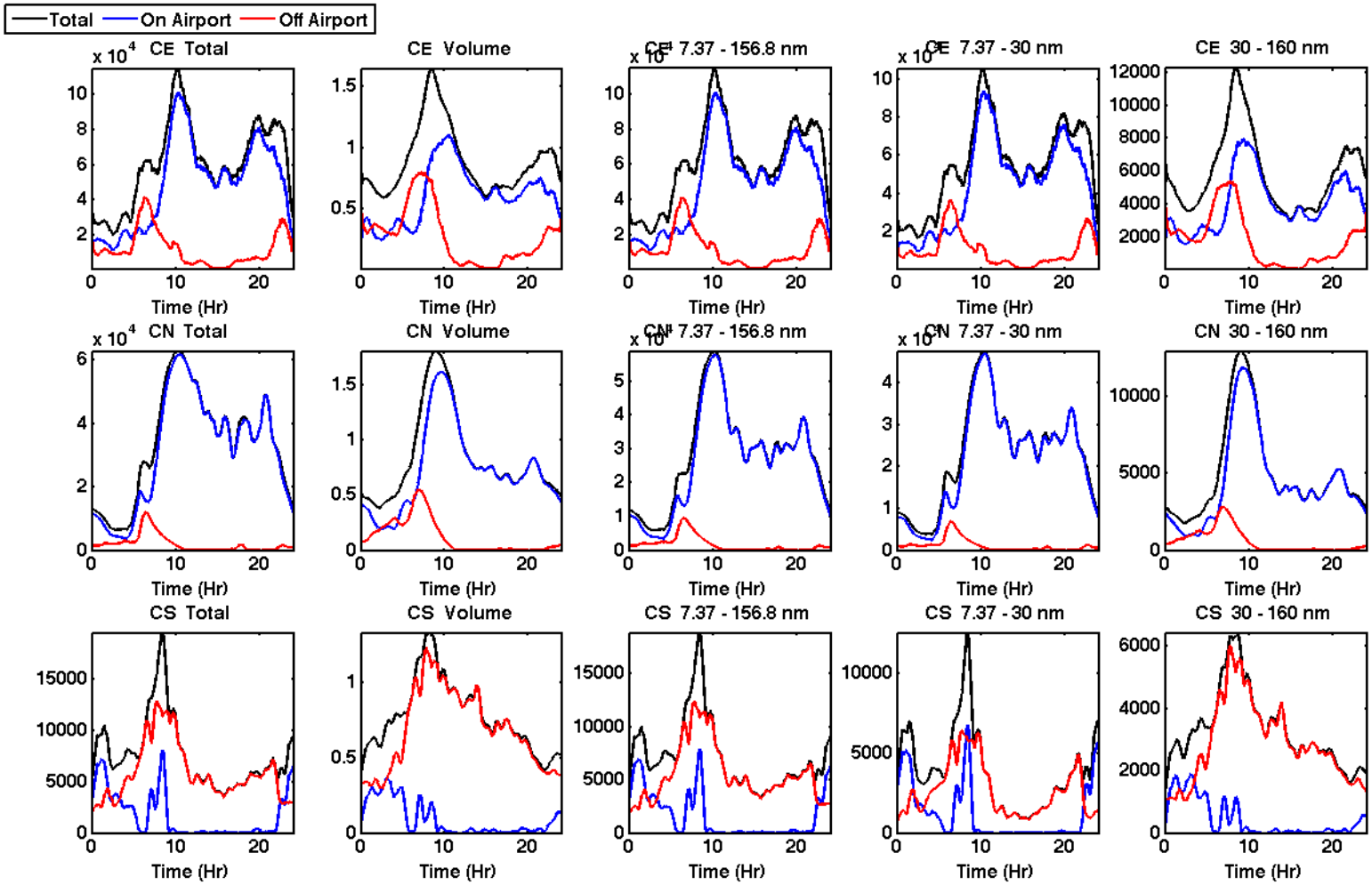

Figure 7-18. Summer Season NTA source apportionment of UFP for the CE, CN, and CS sites. The black line is the total contribution, red is the off-airport contribution, and blue is the on-airport contribution. No background subtraction was done for UFP, so there is no range of uncertainty given (the range due to random error is usually too small to be shown). The units of the total are particles per cm^3, volume is cm^3 per cm^3 of air, the remaining units are particles per cm^3 of air.

7.8 COMBINING NTA RESULTS

The results of the NTA analysis in Phase III of the LAX AQSAS are presented as combined NTA maps and explained in the above sections. The NTA was performed for all of the continuous monitoring data for all four core monitoring sites for the Winter and Summer Monitoring Seasons. The NTA maps for BC at the CE, CN, and CS sites for the Summer Monitoring Season are shown in Figure 7-19 through 7-21. The combined NTA map at each site is the minimum value of the NTA maps at that point over all three sites. Areas in the NTA figure located inside the contours labeled 3 have large statistical uncertainty and were excluded from the combined NTA map. The final results in this case were presented earlier in Figure 7-11 and Figure 7-12 for the Winter and Summer Monitoring Seasons, respectively.

7.9 IMPORTANCE OF ONE MINUTE METEOROLOGICAL DATA ON NTA

National and state ambient air quality standards are set for averages of at least one hour. Consequently, air quality monitoring studies have traditionally used one hour average pollutant concentrations and one hour average wind speed and direction. As shown in Figure 7-22, relying on one hour data does not allow for a complete view of transport winds, which largely determine the concentrations at the monitoring sites. Wind patterns can shift rapidly in the course of one hour. Typically, one hour average wind speeds are calculated as vector averages, which can obscure the true wind patterns if the winds vary rapidly in direction. For example, if the wind blows from the north at 5 m/s for 30 minutes and then from the south for 30 minutes at 5 m/s, the average vector wind speed would be 0 m/s. For the wind data used in this Study, if the hourly vector average wind speed was less than one knot, the wind speed for that hour was reported as calm with no wind direction. At times, this gives the false impression of light variable winds when, in fact, the wind speeds may have been relatively high and the winds shifted during the hour to the opposite direction.

The above mentioned occurrence was observed on the morning of August 7, 2012 during the Second Season. The first panel in Figure 7-22 shows that the winds at all the monitoring stations are predominately from the north from 06:04 to 07:04 A.M. (the time 06:34 shown provides the middle of this period). The second panel shows the winds shifting rapidly to the south from 06:40 to 07:40 A.M. Finally, the third panel shows the winds are from the south and southeast. The LAX hourly winds are reported as calm from 06:00 to 09:00 A.M. while hourly winds at Hawthorne and Santa Monica airports were reported as calm from Midnight through 08:00 A.M. These hourly winds do not capture the dynamic nature of the winds during the morning hours of August 7. A similar wind pattern was observed on multiple other mornings during the two monitoring season. In the second panel (07:10) of Figure 7-22, the CS site shows the highest SO_2, while in the third panel (07:40) the AQ site shows the highest levels of SO_2. This is consistent with the winds veering from the north to the south, as shown by the 1-minute data. The reported hourly wind data are all calm for this period and do not allow for these types of changes in the SO_2 at the CN and AQ sites to be observed. These rapid changes in wind direction are the result of a transition from an off-shore wind with the formation and passage of the sea breeze front over the Study Area. Rapid changes in concentrations at the monitors are often associated with the passage of the sea breeze front, as demonstrated in the lower three panels in Figure 7-22. For example, in the middle panel for 10:08, the SO_2 at the CN site more

than doubles from a value of three ppb to over six ppb in just five minutes as the sea breeze veers from the south to the west directly down the north runway.

While airport operations are a major source of SO_2, the data clearly show high concentrations of SO_2 are sometimes associated with transport from areas other than the airport. Figure 7-23 shows the back-trajectories for the one hour period centered at 08:15 A.M. on August 18, 2012. SO_2 concentrations at the CS, CN, and CE sites were higher while at the AQ site the concentrations were relatively low, even though the AQ site is directly downwind of the central terminal.

The data show some impact of offshore sources of SO_2 for the Summer Monitoring Season and, more so for the Winter Monitoring Season. This is shown in Figure 7-24. Transport of SO_2 from the El Segundo Marine Terminal (ESMT) is the most likely explanation for the data in Figure 7-24, for the one-hour period centered on 04:57 PM of March 5, 2012. The back trajectories in the figure show that the air arriving at the CS site is coming from the region of the ESMT. The air is also passing over the power plant on the coast located to the south of the airport. However, the emissions of the power plant are from an elevated stack and most likely are not impacting CS site. There is a broad peak of high SO_2 concentrations at the CS site that is consistent with the ESMT as the source of the peak. A similar peak is seen passing the CE site approximately 20 minutes later. The distance between the monitors is 2.8 miles, which implies a transport wind speed of about 8 miles per hour (mph). The reported hourly average wind speed for the period was about 8 mph. There is also a peak in the CN site SO_2 concentrations approximately 5 minutes after the peak at the CE site. The peaks measured at the CE and CN sites are a bit higher in concentration than the CS peak. This is most likely the result of additional SO_2 being picked up after the peak passed the CS site. For the AQ site, an offshore background concentration of 0 for SO_2 was measured.

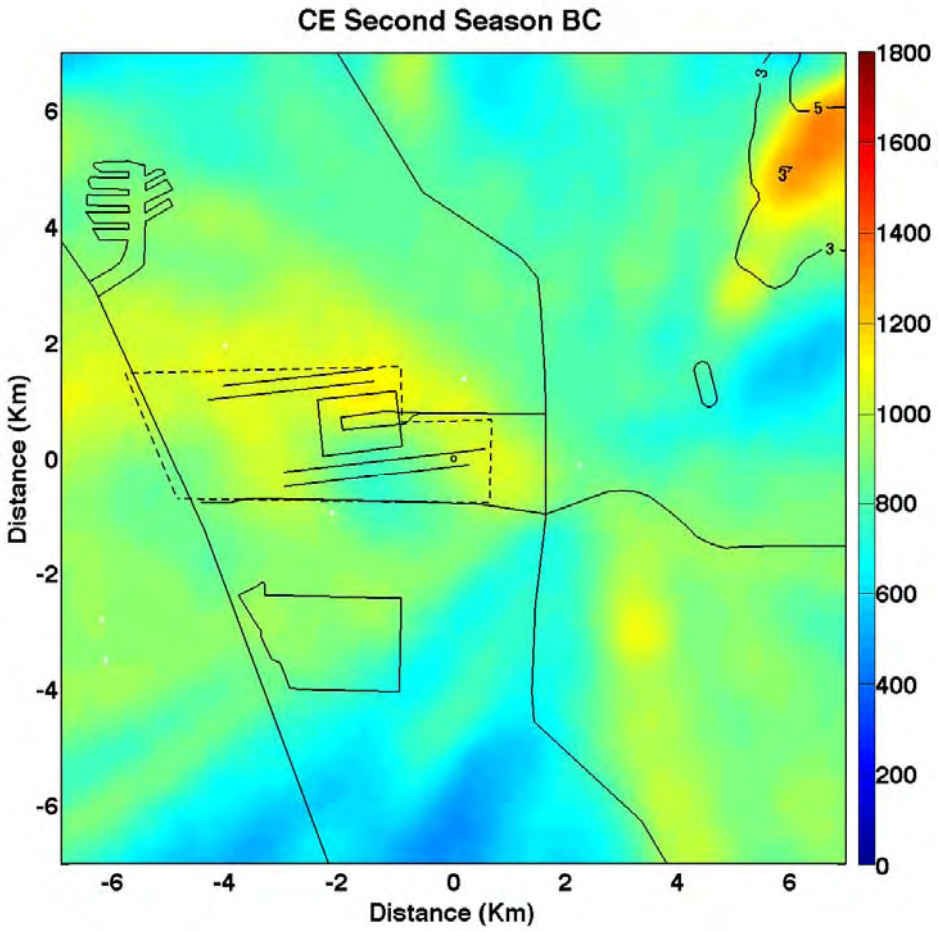

Figure 7-19. NTA map for BC at the CE site during the Summer Season. Units are in ng-m^{-3}. The contours show areas with large statistical uncertainty.

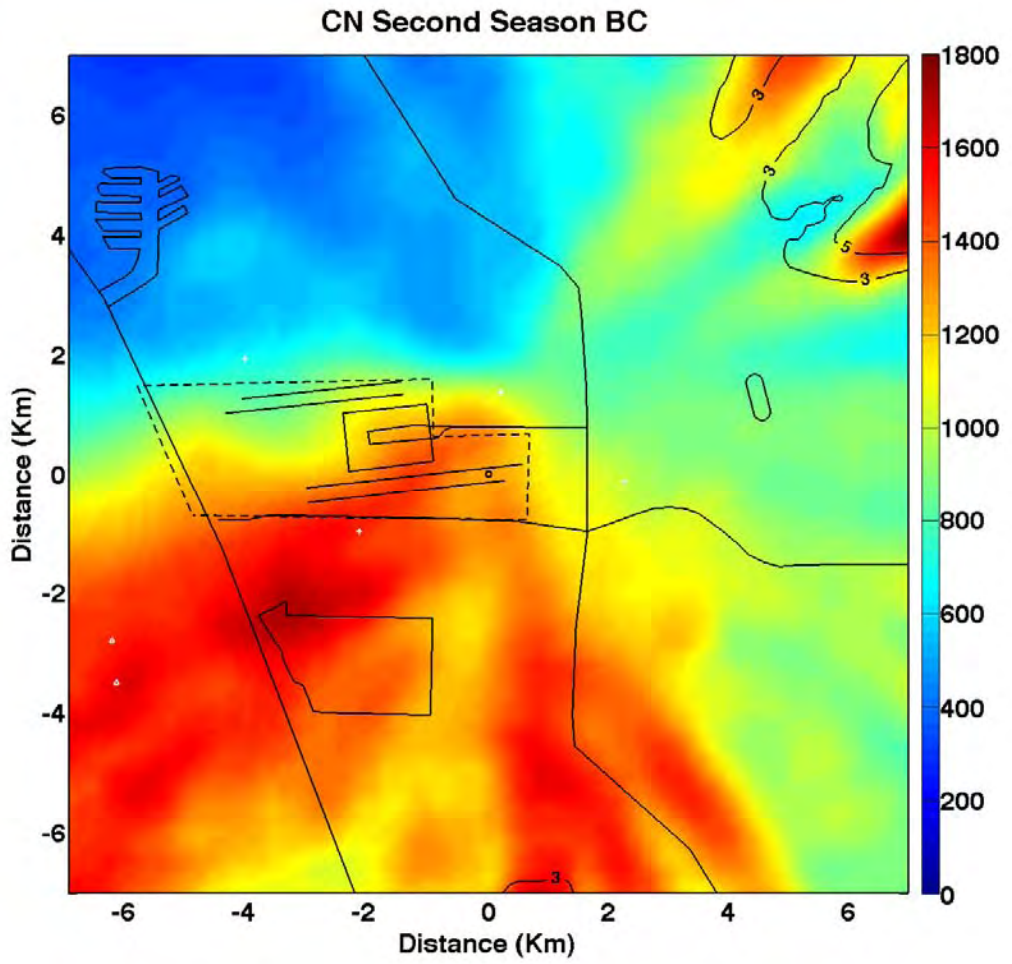

Figure 7-20. NTA map for BC at the CN site during the Summer Season. Units are in ng-m^{-3}. The contours show areas with large statistical uncertainty.

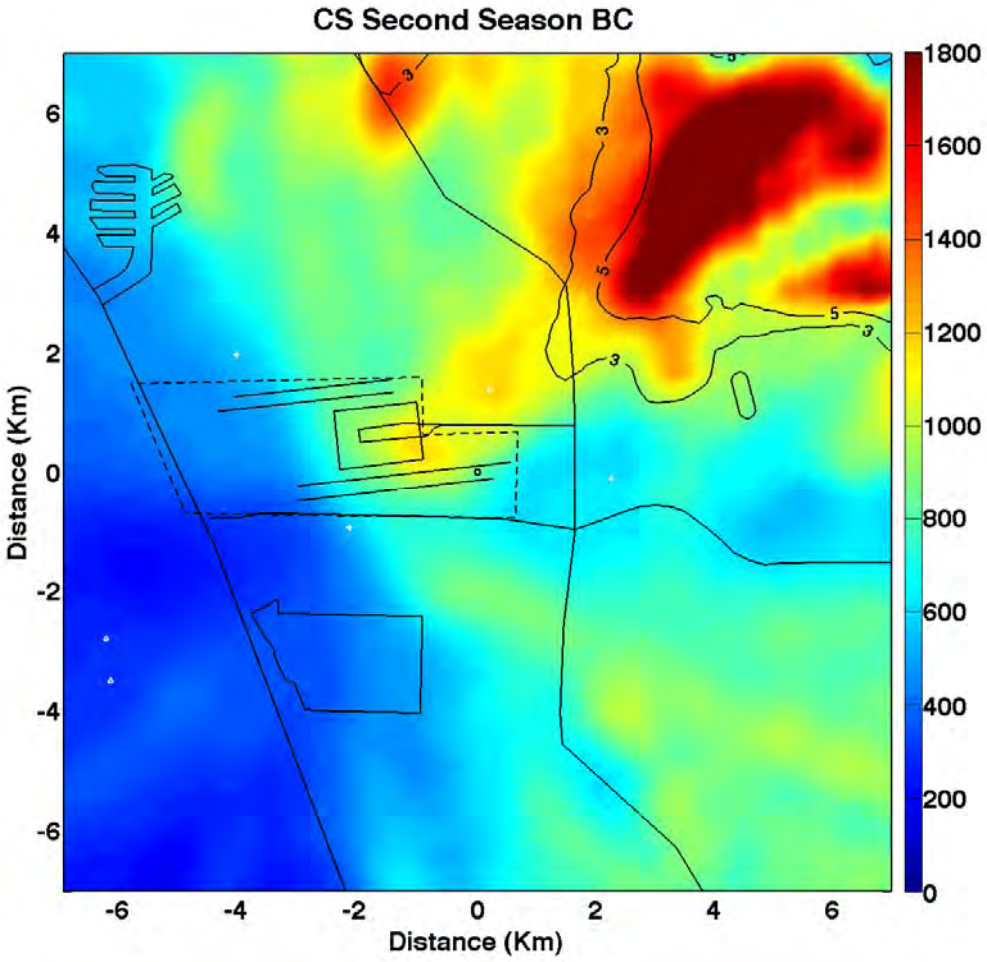

Figure 7-21. NTA map for BC at the CS site during the Summer Season. Units are in ng-m^{-3}. The contours show areas with large statistical uncertainty.

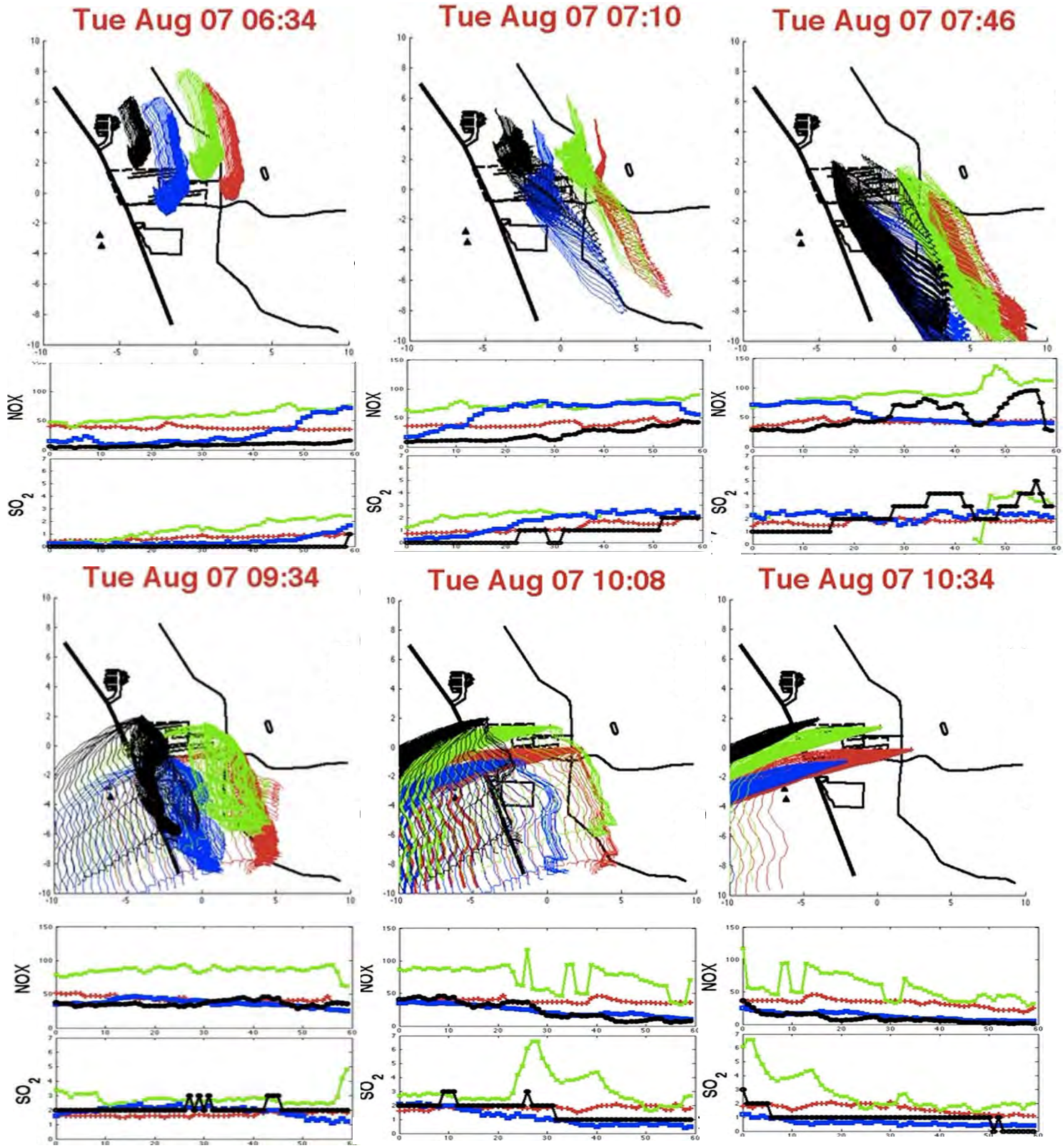

Figure 7-22. Wind direction and corresponding pollutant concentrations for SO_2 and NO_x at the four core sites. Black is for the AQ site, green is for the CN site, red is for the CE site, and blue is for the CS site

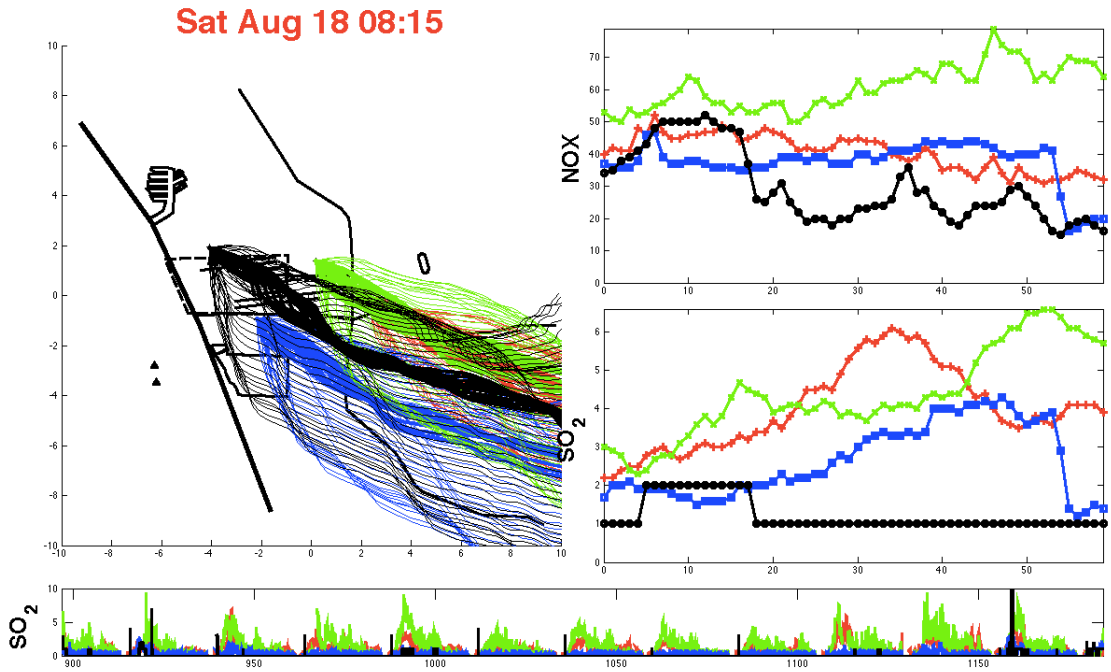

Figure 7-23. Back trajectories for SO_2 concentrations for one-hour period. High concentrations of SO_2 at CS, CN, and CE sites. The concentrations observed at these three sites are not associated with transport from the airport, but from a broad region to the southeast. Black is for the AQ site, green is for the CN site, red is for the CE site, and blue is for the CS site.

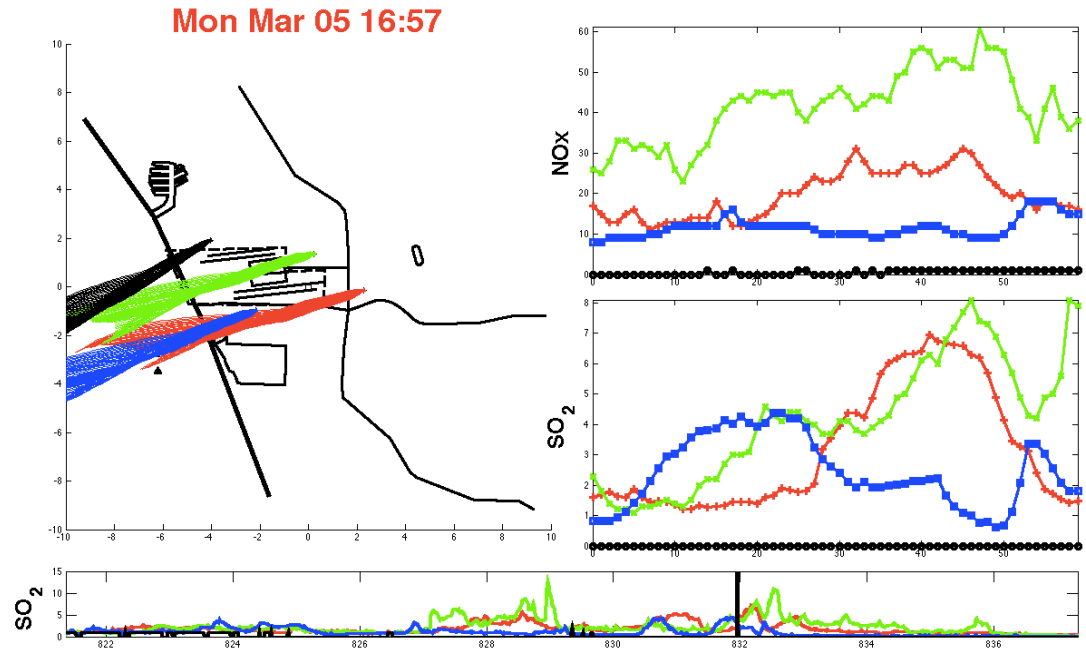

Figure 7-24. High concentrations of SO_2 at the CS, CN, and CE sites associated with transport from the El Segundo Marine Terminal.

7.10 REFERENCES

Henry, R. C. 2007. Locating and Quantifying the Impact of Local Sources of Air Pollution. Atmos. Environ., 42, 358-363. DOI: 0.1016/j.atmosenv.2007.09.039

Henry, R.C. Norris, G., Vedantham, R. Air Quality Impact of a Major Highway and Nearby Sources By NonParametric Trajectory. Environ. Sci. & Technol., 45, 10471–10476, DOI: 10.1021/es202070k

(This page is intentionally blank)

Section 8

EMISSIONS INVENTORY

(This page is intentionally blank)

Table of Contents

List of Figures

List of Tables

(This page is intentionally blank)

8. EMISSIONS INVENTORY

The primary purpose of this emissions inventory was to quantify airport-related (emissions coming from airport operations) and non-airport related (or background) emissions that occur both on and off the airport for Phase III of the LAX AQSAS. The results of the emissions inventory were used to: 1) aid in the apportionment of LAX emissions to total emissions within the Study Area, and 2) to assess the effects of these emissions on pollutant concentrations in the neighboring areas during the Winter and Summer Monitoring Seasons.

The Phase III Study Area was generally bounded by Inglewood Avenue to the east, the Pacific Ocean to the west, West 120th Street to the south, and Manchester Avenue to the north (see Figure 8-1). Generally, emission sources located outside the Study Area boundaries were not included in the emissions inventory, except for major emission sources located outside but adjacent to the Study Area. Based on the Phase II Study conclusion, these excluded sources were considered too distant or too small to have a measurable impact on the area near LAX. Marine vessels in coastal waters to the west, Scattergood Generating Station, El Segundo Energy Center, and the Chevron El Segundo Refinery, were large emitters and near enough to the Study Area to be included in the analysis.

The emissions inventories for both airport-related activities, as well as other emissions sources within the Study Area but beyond the LAX property boundary, have been prepared. These activities are defined as airport and non-airport (or background) sources, respectively.

Airport sources include aircraft engines, auxiliary power units (APU), ground support equipment (GSE), motor vehicles traveling along on-airport roadways and within parking facilities, fuel storage tanks, Los Angeles International Airport (LAX) and tenant operated stationary sources such as turbines, boilers, generators, fuel storage, and cooling towers, and aggregate stationary sources,[1] and area wide sources[2] located on the airport.

Aircraft operations occur within six modes of operation; taxi-out, takeoff, climb-out, approach, landing roll, and taxi-in.[3] Aircraft emissions are distributed along runways, taxiways, terminal area gates (and apron areas), and the flight tracks aircraft follow into and out of the airspace around the airport. APU and GSE activities occur within the specific apron areas (i.e., aircraft parking/holding areas where aircraft are parked, unloaded or loaded, refueled, or boarded) associated with air carrier, air taxi, cargo, general aviation (GA) and military operations.

[1] Aggregated stationary sources are small point sources, such as restaurants, gas stations, etc. that do not have available separate emission source data.

[2] Area-wide sources are widely dispersed sources such as the use of consumer products (hairspray, home automotive products, home cleaners, etc.) and other dispersed solvent uses, such as painting.

[3] Taxi-out and taxi-in include the time an aircraft taxis between the runway and a terminal, and all ground-based delay incurred through the aircraft route. The taxi-in mode also includes the landing roll with reverse thrust, which is the movement of an aircraft from touchdown through deceleration to taxi speed or full stop. Approach begins when an aircraft descends below the atmospheric mixing height and ends when an aircraft touches down on a runway. Takeoff begins when full power is applied to an aircraft and ends when an aircraft reaches approximately 500 to 1,000 feet. At this altitude, pilots typically power back for a gradual ascent. Climb out begins when an aircraft powers back from the takeoff mode and ascends above the atmospheric mixing height.

Figure 8-1. Study Area for Phase III of the LAX AQSAS.

Off-airport sources include motor vehicle traffic along off-airport roadways and freeways, major stationary sources[4] including the Chevron El Segundo refinery, Scattergood Generating Station, and El Segundo Energy Center, marine vessels in coastal waters, aggregate and area-wide sources, and off-road equipment[5] beyond the airport boundary. Emission source types included in the emissions inventory are listed in Table 8-1Table 8-1.

Table 8-1**.** Emission Inventory Sources

Airport	**Off-Airport**
Aircraft	Roadways
Auxiliary Power Units	Stationary Sources
Ground Support Equipment	Marine Vessels
Roadways	Area-wide Sources
Parking Facilities	Aggregate Stationary Sources
Stationary Sources	Off-road Equipment

Off-airport roadways such as the major arterials of Century West, Imperial, Airport, Aviation, Sepulveda, La Cienega, Manchester, and Westchester Boulevards, and the I-105 and I-405 freeways were included. Apportionment of traffic on and around the airport was conducted to estimate emissions from motor vehicles traveling to/from the airport along nearby roadways and freeways. Apportionment of roadway traffic to airport-related activity was estimated using a gravity feed traffic model algorithm, assuming the airport contribution was greatest along access roads closest to the airport and decreases further from the airport. The airport traffic apportionment was based on data collected from a driver survey[6] and a license plate survey[7] performed by others and includes intersections and roadways within the Study Area. Roadway emissions include motor vehicle running exhaust, brake and tire wear, and entrained road dust.

[4] Those sources having a Title V operating permit and/or required to provide SCAQMD with an annual emissions inventory (i.e., greater than 4 tons per year of a criteria pollutant or any amount of a hazardous air pollutant).

[5] Non-road mobile sources such as construction equipment, trains and lawn mowers.

[6] LAX Master Plan EIS/EIR, Off-Airport Surface Transportation Technical Report (Section 7.3.2), dated January 2001.

[7] A license plate survey (*Data Analysis of Vehicle License Plate Survey Results for Los Angeles International Airport Arrival Traffic*, dated April 26, 2007) was conducted on August 18, 2006. The survey locations were at six off-airport gateway locations (such as westbound on Century West to the west of La Cienega Boulevard), two principal airport parking lot driveways, and five immediate airport access locations. The license plate survey used high-resolution digital video camcorders to record images of vehicle license plates passing the survey locations as a means to determine if vehicles were accessing the airport (i.e., traveling from a gateway location to an airport access location).

8.1 EMISSION CALCULATION METHODOLOGY

The emissions inventory was compiled using the Federal Aviation Administration (FAA) Emissions and Dispersion Monitoring System (EDMS) (Version 5.1.3)[8] and numerous other databases and emissions models. EDMS served as a platform to spatially allocate emissions from mobile sources based on emission factors using California Air Resource Board (CARB) OFFROAD2011[9] for GSE and EMFAC2011[10] for motor vehicles. Several improvements have been made, by the FAA, to the version of EDMS used during the Phase II Demonstration Project[11], including the ability to estimate PM emissions from APUs, and volatile and non-volatile particulate matter (PM) emissions from aircraft via the FAA's First Order Approximation (FOA3a). EDMS5.1.3 also includes updates to the aircraft fleet database.

EDMS has a database of emission factors for pollutant sources found at airports. These emission factors are in units of mass per unit of time, material usage or distance (e.g., grams/second, grams/mile, or grams/gallon). The EDMS database of emission factors is able to account for the differences in emissions from fuel type, fuel burn, engine power load, manufacture year, and manufacturer, among many other characteristics. These emission factors are used by EDMS to calculate total emissions for a specified time period. This is done by multiplying the emission factor for the particular source by the time, distance, or usage, resulting in total emissions for each source group and ultimately total emissions for the time period. Other models, such as CARB's EMFAC2011 and OFFROAD2011, provide emission factors for roadway vehicles and off-road equipment, respectively.

In addition, various databases, models, programs, and references, as listed in Table 8-2, were used to gather data related to both on- and off-airport operations, source emissions, exhaust release characteristics, spatial and temporal profiles, and other supporting data for the emissions inventory and dispersion modeling. These data were developed from information gathered through coordination with LAWA, the U.S. Environmental Protection Agency (U.S. EPA), the California Air Resources Board (CARB), Los Angeles Department of Transportation (LADOT), South Coast Air Quality Management District (SCAQMD), the Southern California Association of Governments (SCAG), California Department of Transportation (CalTrans), and other pertinent facilities and entities associated with emission sources within the Study Area.

The pollutants inventoried include: carbon monoxide (CO), volatile organic compounds (VOC), total organic gases (TOG), nitrogen oxides (NO_x), sulfur oxides (SO_x), and particulate matter

[8] FAA developed EDMS in the mid-1980s in cooperation with the United States Air Force. The model has become increasingly sophisticated over time and provides users with the ability to conduct emission inventories and dispersion analysis for all of the major emission sources in the airport environment. EDMS develops time- and location varying emissions from aircraft engines, APUs, GSE, ground access vehicles, training fires, and stationary sources such as generators, cooling towers, boilers, and fuel storage tanks. EDMS incorporates specific details on types of aircraft and typical aircraft schedules for taxi, take-off, and landing to develop a robust temporal and spatial representation of airport emissions.

[9] OFFROAD 2011. http://www.arb.ca.gov/msei/categories.htm#offroad_motor_vehicles

[10] EMFAC2011, http://www.arb.ca.gov/msei/categories.htm

[11] Los Angeles International Airport Air Quality and Source Apportionment Study, Draft Final Demonstration Project Report, April 2009.

equal to or less than ten micrometers (coarse particulates or PM_{10}), and particulate matter equal to or less than 2.5 micrometers (fine particulates or $PM_{2.5}$).

The Winter Monitoring Season emission inventory was conducted from January 31 through March 16 of 2012 (a total of 46 days) and the Summer Monitoring Season emission inventory was conducted from July 18 through August 28 of 2012 (a total of 42 days). Whenever possible, the emission inventories used activity levels, meteorological data, and other information from the Winter and Summer season time periods; otherwise data from previous years were used and adjusted accordingly as a function of data such as aircraft operations and passenger counts. A list of the airport and non-airport emissions sources, the data used to develop the emissions inventory, and the sources from which the data were acquired are included in Table 8-2 and Table 8-3.

There are a number of important limitations and uncertainties commonly associated with emission inventories of this nature. The EDMS contains a comprehensive list of aircraft engines, GSE, APU, vehicular, and stationary source emission factor data with emission indices (in grams per kilogram of fuel) based on the International Civil Aviation Organization (ICAO) Aircraft Engine Exhaust Databank. However, there may be cases where the EDMS database does not contain a specific data element (e.g. a newly available emission factor). In these cases, EDMS makes allowances for the user to enter their own data and will perform parameter validation where possible. Other emission factors are based on widely accepted publications, database, and models which have been verified through source testing and detailed examination. The activity levels, spatial allocation, and temporal allocation of activities are better known for some activities than for others. Generally, detailed site-specific data (e.g., fuel usage, traffic volumes, emission estimates, aircraft activity) for the exact measurement periods were used and provides the best available data.

Table 8-2. Sources of Emission Data for Airport Sources

Emissions Source	Data	Data Source
Aircraft	Aircraft Noise and Operations Monitoring System	LAWA's Noise Monitoring Office
	Aircraft weights	FAA's T-100 Air Carrier database
	Aircraft/engine combination	*JP Airline-Fleets International* database
	Emission factors	Emissions and Dispersion Monitoring System
	Taxi travel and queue time	EDMS Delay and Sequence Model
	Airfield capacity	FAA's Aviation System Performance Metrics
	Mixing height and meteorological data	National Climatic Data Center SCAQMD
	Airfield layout	FAA's Airport Master Record database
	Taxipaths	Air Traffic Control Tower
Auxiliary power units (APU)	Availability of 400 Hertz (Hz) gate power and pre-conditioned air	LAWA
Ground support equipment (GSE)	GSE inventory survey	LAWA
	GSE operating time survey	LAWA
	Availability of hydrant fueling system	LAWA
	Emission factors	CARB OFFROAD2011 emissions model
Roadways	Central Terminal Area, local, and service roadway volumes, speeds, vehicle types, temporal profiles	LAWA Transportation Planning Department
	Emission factors	CARB EMFAC2011 emissions model
Parking facilities	Ticket counts	LAWA Parking Operations Department
	Emission factors	CARB EMFAC2011 emissions model
Airport stationary sources	Fuel usage, location, stack parameters	LAWA
	Tank dimensions, fuel type	LAWA
Tenant stationary sources	Emission estimates	SCAQMD Facility Information Detail (FIND)

Table 8-3. Sources of Emission Data for Non-Airport Sources

Emissions Source	Data	Data Source
Major Roadways	Volumes, speeds, vehicle types, temporal profiles	LAX Specific Plan Amendment Study EIR LADOT
	Emission factors	CARB EMFAC2011 emissions model
	Roadway entrained dust emission factors	U.S. EPA AP-42 Section 13.2.1
Interstate 405 and 105	Volumes, speeds, vehicle types, temporal profiles	California Department of Transportation Freeway Performance Measurement System (PeMS)
	Emission factors	CARB EMFAC2011 emissions model
	Roadway entrained dust emission factors	U.S. EPA AP-42 Section 13.2.1
Stationary sources	Emission estimates, fuel usage, location, stack parameters, temporal profiles	SCAQMD Annual Emission Reporting (AER)
		SCAQMD Facility Information Detail (FIND)
		Scattergood Generating Station Continuous Emissions Monitoring System (CEMS)
		El Segundo Energy Center CEMS
		Chevron El Segundo Refinery CEMS
Marine vessels and harbor craft	Emission estimates, location, temporal profiles	CARB Marine Emissions Model
	Exhaust release parameters	CARB, Diesel Particulate Matter Exposure Assessment Study for the Ports of Los Angeles and Long Beach, April 2006.
Off-road equipment, area sources, and aggregate stationary sources	Emission estimates	CARB Community Health Air Pollution Information System (CHAPIS)
	Temporal profiles	U.S. EPA's Emissions Modeling Clearinghouse Temporal Allocation

8.2 SPATIAL ALLOCATION

All emission sources were located spatially within the Study Area. Source locations were determined using high resolution, geo-referenced, aerial photographs, maps, available databases, and/or site visits.

EDMS incorporates specific details on source location (airport layout and roadway network) and activity variation to develop a spatial representation of each emission source. The locations of emission sources were represented in the Universal Transverse Mercator (UTM) coordinate system. The airport reference point[12] is approximately 369,874.86 meters East and 3,756,677.41 meters North (UTM Zone 11N) with North American Datum of 1983. All emissions sources were located and defined within this same coordinate system. This airport reference point was also the origin for the dispersion modeling analysis (see Section 9).

Depending on the source category (e.g., stationary, taxiway, or roadway), EDMS constructs a point, area, or volume source for use in dispersion modeling. Point sources are used to model stacks from boilers, turbines, generators, and cooling towers. Area sources are used to model emissions from aircraft gates aprons (i.e., aircraft at startup, GSE operations, and APU activity), aircraft taxiing, queuing, accelerating on the runway, and in climb-out and approach modes. Volume sources were used to model any source that has an area and height element. The fuel storage facilities were modeled as volume sources.

8.3 TEMPORAL ALLOCATION

Temporal (or operational) profiles were used to describe the relationship of one time period to another (i.e., the relationship of the activity during one-hour to the activity during a twenty-four hour period). In EDMS, temporal profiles are used to represent varying levels of activity as a fraction of a peak period (a scale of zero to one: unitless values denoted as fraction of peak values). Thus, if the peak hour traffic volume is 1,000 vehicles and the temporal profile for 06:00 is 0.5, then the estimated traffic volume is 500 vehicles. The use of temporal factors gives the model the ability to more accurately reflect real world conditions. The profiles are also used to evaluate the level of emissions expected to occur during a specific period within a year.

These profiles provide a method to realistically distribute activity levels throughout the day, week, and month of the study period. Operational profiles are used throughout the EDMS program to account for fluctuations in emissions from all sources. Based on a peak quarter hour value (such as traffic volume), the operational profiles are used to estimate values for each hour of the measurement campaigns. EDMS uses quarter-hour intervals (data representing 15-minute periods), which are then averaged into hourly values. For brevity, hourly profiles are presented below instead of the quarter hour profiles. Each emission source has a temporal distribution unique to that emission source.

[12] The airport reference point is a point of an airport located at the geometric center of all the usable runways.

8.4 AIRCRAFT OPERATIONS

Aircraft are the largest emission source at the airport. Aircraft emissions occur during approach, taxi in (from runway to apron, including landing roll), engine startup at the apron, taxi out (from apron to runway), takeoff, and climb-out, known collectively as operating modes. To estimate emissions from aircraft sources, a series of inputs are needed including: aircraft fleet mix[13], aircraft engine assignment, aircraft runway and apron assignments, and generalized aircraft taxipath (a series of taxiways depicting an aircraft's travel path across the airfield). This information is coupled with emission factors and operating times for each aircraft operating mode. Spatial allocation and temporal distributions of aircraft operations (by hour, day, and month) are also necessary to locate the emission sources and distribute the emissions throughout the Phase III Study period.

8.4.1 Emission Calculation Methodology

An EDMS aircraft schedule specifies the aircraft/engine combination, runway, operation type (i.e., arrival/departure), the specific apron where the operation initiated or terminated its ground movement, and date/time. An aircraft schedule was developed from data provided by LAWA's Noise Monitoring Office, which used data from the Aircraft Noise and Operations Monitoring System (ANOMS). The data set included: aircraft operations of air carrier, air taxi, cargo, general aviation (GA) and military operators, and operation details such as airline, aircraft type (e.g., B737-500), operation type (i.e., arrival/departure), date and time of operation, and runway utilization. The aircraft stage length (i.e., a measure of the flight distance) and/or flight origin/destination (if available) were also used as a means to adjust aircraft weight instead of using EDMS default values. This was especially important for cross country and international flights. Data from FAA's T-100 Air Carrier database were consulted to determine appropriate aircraft weights, which were adjusted based on the aircraft stage length. Aircraft destinations further from LAX require greater amounts of fuel and thus, are of greater weight as denoted with a larger stage length.

The aircraft/engine combination was essential to accurately estimate aircraft emissions and was developed specifically for this analysis. The actual mixture of aircraft/engine combinations for each airline and/or aircraft tail number that utilizes LAX were acquired using the *JP Airline-Fleets International* 2011/2012 database (JP Fleets)[14]. Based on the ANOMS data, each

[13] The type of aircraft (i.e., Boeing 737-700) and the number of operations (i.e., a landing or a takeoff).

[14]These data (found at http://www.buchair.com/JPAF.htm) comprise a comprehensive reference of the aircraft fleet for all known commercial aircraft operators including: the current registration, type, serial number, previous identity, date of manufacture, date of delivery, engine type and number, maximum take-off weight, configuration, fleet number, name, etc. for every aircraft weighing over 3,000 pounds. The database represents more than 6,000 operators and over 50,000 aircraft.

scheduled flight was assigned an engine based on the distribution of engines used by a particular airline for that particular aircraft. The distribution of engine types for each operator's aircraft fleet is contained within JP Fleets. Table 8-4 presents the generalized aircraft fleet mix for the Winter and Summer Monitoring Seasons. The aircraft fleet mix was similar for each monitoring season; while the Summer Monitoring Season provides slightly greater aircraft activity as the result of summertime travel. The Boeing 727/737, Airbus 318/319/320/321, and regional jets are the most frequently operating aircraft at LAX. The category labeled "other" includes a number of miscellaneous air carrier, cargo, and GA operations.

Table 8-4. Aircraft operations by aircraft type

	Winter Monitoring Season		**Summer Monitoring Season**	
Aircraft Type	**Number of Operations**	**Percent of Operations**	**Number of Operations**	**Percent of Operations**
Airbus 300/310	421	0.6%	367	0.5%
Airbus 318/319/320/321	9,928	14.0%	11,510	15.5%
Airbus 330/340	1,344	1.9%	1,215	1.6%
Airbus 380	321	0.5%	376	0.5%
Boeing 727/737	17,935	25.4%	19,399	26.2%
Boeing 747	1,981	2.8%	2,221	3.0%
Boeing 757	6,681	9.5%	8,417	11.4%
Boeing 767	3,480	4.9%	2,393	3.2%
Boeing 777	3,036	4.3%	3,430	4.6%
Boeing MD 81/82/83/87/88/90	1,296	1.8%	2,239	3.0%
CRJ 100/200/700/900	9,251	13.1%	9,473	12.8%
Embraer 120	4,774	6.8%	4,376	5.9%
Embraer 135	4,272	6.0%	3,459	4.7%
Embraer 140/170/190	921	1.3%	730	1.0%
Other	5,055	7.2%	4,467	6.0%
Total	**70,696**		**74,072**	

8.4.1.1 Emission Factors and Operating Time per Mode

EDMS contains a database of aircraft/engine-specific emission factors based on engine manufacturer, model and operational mode (i.e., climb-out, takeoff, approach, and taxi). Aircraft emissions were calculated using emission factors specific to aircraft/engine combinations, accounting for the number of engines as well as the time spent in each of the operational modes. EDMS default information (adjusted for mixing height) was used to represent the time spent in takeoff, climb-out, approach, and landing roll. Takeoff, climb-out, and approach were further adjusted by aircraft weight. Time spent in arrival taxiing (taxi-in), departure taxiing (taxi-out), and apron/taxiway idling (idle/queue) modes was simulated by the Delay and Sequence Module within EDMS.

The level of aircraft-related emissions is reflective of the time an aircraft operates in each of the operational modes with the entire cycle referred to as a landing/take-off (LTO) cycle. An LTO cycle consists of the following operational modes:

- "Taxi/idle" includes the time an aircraft taxis between the runway and a terminal for either an arrival or a departure, and all ground-based delays incurred through the aircraft route. The taxi/idle mode also includes the landing roll with reverse thrust, which is the movement of an aircraft from touchdown through deceleration to taxi speed or full stop.

- "Approach" begins when an aircraft descends below the atmospheric mixing height and ends when an aircraft touches down on a runway.

- "Takeoff" begins when full power is applied to an aircraft and ends when an aircraft reaches approximately 500 to 1,000 feet. At this altitude, pilots typically power back for a gradual ascent.

- "Climb-out" begins when an aircraft powers back from the takeoff mode and ascends above the atmospheric mixing height.

- Aircraft emissions (of VOC and TOG) also account for the period of engine startup which occurs within the gate terminal area prior to departure.

$PM_{10/2.5}$ emission factors were developed using the FAA's FOA3a for turbine engines. For turboprop and piston engines, $PM_{10/2.5}$ emission factors were developed using other appropriate references (e.g., AP-42[15], U.S. Air Force [16], and FOCA[17]). For aircraft, 100 percent of the PM_{10} emissions were considered $PM_{2.5}$ emissions per EDMS. EDMS's conservative fuel sulfur content of 0.068 percent for $PM_{10/2.5}$ emissions, which equates to a fuel sulfur content of 1.292 grams per kilogram, was assumed. TOG emissions were based on both the calculated VOC emission factors and U.S. EPA conversion factors (e.g., VOC to THC and THC to TOG)[18].

The EDMS Delay and Sequence Module simulates each aircraft's ground movements using the aircraft operations schedule, the assigned aircraft speed within taxiways, and the overall capacity of the airport. The Delay and Sequence Module then estimates the time it takes each individual aircraft to taxi between apron and runway endpoints, based on airport-specified taxipaths.

The EDMS Delay and Sequence Module estimates time spent at idle. This is added to taxi time-in-mode using a queuing algorithm that assesses departure queuing delays (i.e., delays at the runway end, gate, and runway crossings). Inputs to the algorithm include: the estimated hourly capacities of an airport's runway system, runway use configurations, weather conditions, and the temporal distribution of aircraft operations from the specified flight schedule. The algorithm produces estimates of departure delays attributable to each runway departure end. The Delay and Sequence Module results were reviewed against the measured taxi times from FAA's

[15] Unites States Environmental Protection Agency, Compilation of Air Pollution Emission Factors, January 1995.

[16] Unites States Air Force, Aircraft Engine and Auxiliary Power Unit Emissions Testing: Volumes 1 through 3, March 1999.

[17] *Aircraft Piston Engine Emissions Summary Report*, Report 33-05-003, Federal Office of Civil Aviation (FOCA), Switzerland, June 2007.

[18] Federal Aviation Administration, Guidance for Quantifying Speciated Organic Gas Emissions from Airport Sources, September 2, 2009

Aviation System Performance Metrics (ASPM) [19] and Bureau of Transportation Statistics (BTS)[20] during the measurement campaigns, with adjustments to taxiway speeds, as appropriate. Table 8-5 displays the airfield average taxi times for the Winter and Summer Monitoring Seasons based on the BTS. However, the emissions inventory was based on the taxi times calculated within the Delay and Sequence Module. The taxi time during the Summer Monitoring Season was approximately ten percent greater than the taxi time during the Winter Monitoring Season, which corresponds to slightly greater aircraft operations during the summertime.

Table 8-5. Average aircraft taxi times (minutes)

Winter Monitoring Season		**Summer Monitoring Season**	
Taxi In	**Taxi Out**	**Taxi In**	**Taxi Out**
9.35	14.87	10.69	16.73

8.4.1.2 Aircraft Capacity and Configurations

EDMS requires the capacity of runway use configurations as inputs to the Delay and Sequence Module. Two runway use configurations and two weather conditions were considered in the LAX runway capacity determination. LAX typically operates in a westerly flow, with arrivals using North Airfield Runway 24R and South Airfield Runway 25L and departures using North Airfield Runway 24L and South Airfield Runway 25R. Overnight and wind-permitting, LAX operates in a "head-to-head" configuration with arrivals landing to the east of the airport and departures taking off to the west. During periods of high offshore winds, which rarely occur, LAX operates in an easterly flow, with arrivals using North Airfield Runway 6L and South Airfield 7R and departures using North Airfield Runway 6R and South Airfield Runway 7L.

Table 8-6 displays the airfield configurations and capacity for use in the analysis. Airfield capacity is directly correlated to ground delays, which correlate to aircraft taxi emissions. A lower airfield capacity may result in greater delays and higher emissions.

One of the many factors that affect runway capacity is weather, particularly visibility and cloud ceiling. Two weather conditions were considered for the capacity configuration - visual meteorological conditions (VMC) and instrument meteorological conditions (IMC). VMC was defined as the visibility at LAX of at least three statute miles and a cloud ceiling of at least 3,000 feet above ground level. IMC was defined as either the visibility or cloud ceilings at LAX were below the aforementioned levels. The FAA's ASPM database was used to establish the hourly capacity of LAX's runway system in VMC and IMC conditions.

[19] The Aviation System Performance Metrics (ASPM) online access system provides detailed data on flights to and from the ASPM airports (currently 77); and all flights by the ASPM carriers (currently 22), including flights by those carriers to international and domestic non-ASPM airports. All instrument flight rules (IFR) traffic and some visual flight rules (VFR) traffic are included. ASPM also includes airport weather, runway configuration, and arrival and departure rates. This combination of data provides a robust picture of air traffic activity for these airports and air carriers. http://aspmhelp.faa.gov/index.php/ASPM_System_Overview

[20] Bureau of Transportation Statistics, http://www.bts.gov/xml/ontimesummarystatistics/src/index.xml

Table 8-6. Airfield configurations and capacity

Runway Configuration	Weather Conditions	Ceiling (feet)	Visibility (mile)	Hourly arrival capacity	Hourly departure capacity
West flow	Visual approach conditions	3,000	3	84	88
	Instrument approach conditions	0	0	68	75
East flow	Visual approach conditions	3,000	3	68	75
	Instrument approach conditions	0	0	58	70

The percent of time the various runways are used for departures/arrivals was provided by LAWA based on the ANOMS data. These percentages were used to distribute the aircraft operations to each runway endpoint. To accommodate EDMS, the runway utilization was developed by aircraft size (small, large and heavy) for each airfield configuration. The runway utilization also assigns the spatial location of aircraft arrival and departure emissions for use in dispersion modeling.

Generally, aircraft arrive using North Airfield Runway 24R and South Airfield Runway 25L. Heavier aircraft also arrive using South Airfield Runway 7L. Aircraft depart using North Airfield Runway 24L and South Airfield 25R and to a less extent South Airfield 25L. Table 8-7 contains the runway utilization percentages (by runway and arrival/departure operation) for the Winter and Summer Monitoring Seasons. The runway utilization was similar for each measurement campaign, except for greater frequency of arrivals at North Airfield Runway 24L and greater frequency of departures at North Airfield Runway 24R during the Summer Monitoring Season due to a greater frequency of westerly winds.

Table 8-7. Runway utilization (Percent by aircraft size)

		Winter Monitoring Season		Summer Monitoring Season	
Aircraft Size	**Runway**	**Arrival**	**Departure**	**Arrival**	**Departure**
Small	06L	1.17	0.08	0.56	0.00
Small	06R	0.76	0.95	1.47	0.03
Small	07L	1.03	1.01	0.34	0.03
Small	07R	1.88	0.25	0.16	0.06
Small	24L	0.93	28.55	5.25	31.88
Small	24R	32.76	1.99	31.37	7.13
Small	25L	58.45	10.19	58.15	6.84
Small	25R	3.02	56.96	2.69	54.02
Large	06L	1.10	0.33	0.53	0.01
Large	06R	0.85	0.69	2.07	0.03
Large	07L	1.01	1.24	0.53	0.00
Large	07R	1.52	0.06	0.13	0.00
Large	24L	1.17	43.01	6.28	36.53
Large	24R	45.80	1.25	37.26	5.75
Large	25L	46.36	1.90	50.71	1.01

Aircraft Size	Runway	Arrival	Departure	Arrival	Departure
Large	25R	2.20	51.52	2.50	56.67
Heavy	06L	1.77	0.31	1.06	0.00
Heavy	06R	3.64	0.20	5.70	0.00
Heavy	07L	6.55	1.84	3.06	0.02
Heavy	07R	2.66	0.10	0.39	0.00
Heavy	24L	1.03	18.24	8.05	17.58
Heavy	24R	35.11	0.09	33.77	1.21
Heavy	25L	46.78	8.94	45.46	7.84
Heavy	25R	2.46	70.28	2.52	73.34

Note: Heavy equates to a maximum takeoff weight of greater than 255,000 pounds, Large equates to a maximum takeoff weight of between 41,001 and 255,000 pounds, and Small equates to a maximum takeoff weight of less than 41,000 pounds.

8.4.2 Spatial Allocation

The aircraft operations were located in the project UTM coordinate system. Aircraft ground activity locations include runways, parking aprons, and taxiways. The location of runway endpoints was taken from the FAA's Airport Master Record. As depicted in Figure 8-2, there is a North Airfield (Runway 6L/24R and Runway 6R/24L) and a South Airfield (Runway 7L/25R and Runway 7R/25L). Each runway is utilized for arrivals and departures per instructions by the Air Traffic Control Tower (ATCT) as a function of meteorological conditions, aircraft size, airfield capacity, and assigned gate/apron position.

Figure 8-2. The North and South Airfields for LAX. The North Airfield consists of Runways 6R/6L and 24R/24L. The South Airfield consists of Runways 7R/7L and 25R/L.

To estimate the emissions from aircraft taxi and idle modes, and for precision in locating the taxi/idle emissions around the airfield, eight major taxiways and 52 minor taxiways were included in the emissions inventory. Aircraft taxi speeds were assigned based on the type of taxiway: high speed exit (46 mph), reverse high speed exit[21] (29 mph), crossfield (17 mph), and terminal area (12 mph). Figure 8-3 displays the taxiways used in the analysis. These taxiways are used by aircraft to move between the runway ends and the assigned apron area. The taxiways define the spatial location of aircraft taxi in and out emissions for use in dispersion modeling.

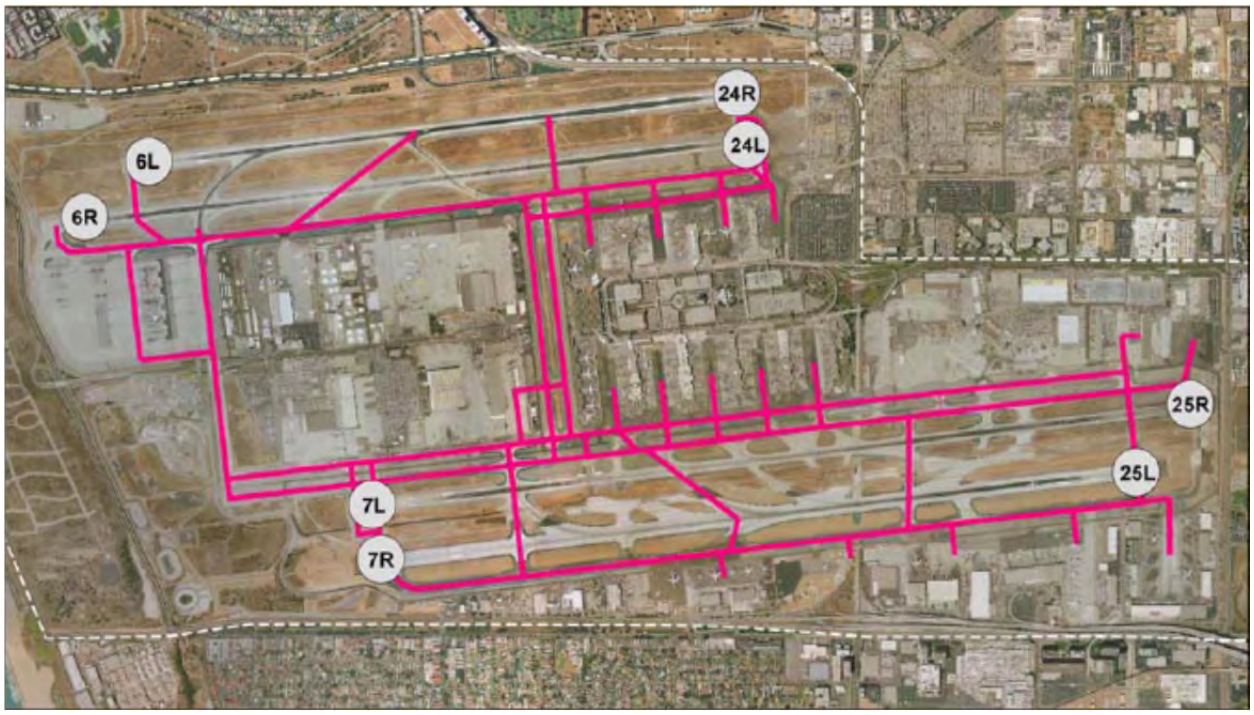

Figure 8-3. Taxiways used in Phase III of the LAX AQSAS.

To localize aircraft emissions at and near aircraft parking positions (i.e., terminal gates, GA hangers, cargo holds), 21 different apron areas were defined. These apron areas define the locations of aircraft operations such as unloading and loading of cargo and passengers. Thus, these locations also represent activities associated with APU, GSE and other supporting operations. Figure 8-4 presents the locations of the aircraft apron areas within this analysis. The aircraft apron areas include the following:

- Terminal apron east of Terminal 1 (A1)
- Terminal apron between Terminal 1 and Terminal 2 (A2)
- Terminal apron between Terminal 2 and Terminal 3 (A3)
- Terminal apron between Terminal 3 and the Bradley International Terminal (A4)
- Terminal apron between Bradley International Terminal and Terminal 4 (A5)

[21] The International Civil Aviation Organization (ICAO) defines a reverse high speed exit as a taxiway connected at an acute angle and designed to allow a landing airplane to turn off at higher speeds than are achieved on other exit taxiways.

- Terminal apron between Terminal 4 and Terminal 5 (A6)
- Terminal apron between Terminal 5 and Terminal 6 (A7)
- Terminal apron between Terminal 6 and Terminal 7 (A8)
- Terminal apron between Terminal 7 and Terminal 8 (A9)
- Terminal apron for American Eagle (A10) – located to the east of A9
- Terminal apron at Bradley International Terminal (A11) – located to the west of A5
- Cargo terminal apron at Imperial Terminal, west of Sepulveda Boulevard (CG1)
- Cargo terminal apron west of Federal Express (CG2)
- Cargo terminal apron affiliated with Federal Express operations (FX)
- GA terminal apron at Imperial Terminal, west of Sepulveda Boulevard (GA1)
- GA terminal apron adjacent to Sepulveda Boulevard (GA2)
- Imperial Cargo Center terminal apron on the corner of Aviation Boulevard/Imperial Highway (ICC)
- UPS terminal apron (UPS)

The following aircraft apron areas were included in the analysis; however, operations associated with these areas were minimal and/or difficult to determine:

- Remote terminal apron for American Airlines west of taxiways Q and S (RMA)
- Remote terminal apron for International Flights west side of Airport Property (RMW)
- U.S. Postal Service terminal apron (USM)

Terminal gate (apron) assignments were made based on the airline associated with each aircraft within the flight schedule. For example, Southwest Airlines operations were assigned to Terminal 1 (A1). Table 8-8 presents the distribution of gate/apron utilization for the Winter and Summer Monitoring Seasons. There were only minor differences in the gate utilization between each measurement campaign. The largest percent of aircraft operations were associated with the North Terminal at A1 and A3 and the South Terminal at A5, A8, and A9. Larger aircraft (such as the Airbus 380) tended to be associated with international flights at the Bradley International Terminal (A11). Cargo, charter, and GA operations are located at the South Airfield. The spatial location of these operations was used in the dispersion modeling to associate the APU, GSE, and other aircraft supporting activities.

Figure 8-4. Aircraft apron areas used in analysis for Phase III of the LAX AQSAS.

Table 8-8. Gate utilization

	Winter Monitoring Season		Summer Monitoring Season	
Apron	**Operations**	**% of Total**	**Operations**	**% of Total**
A1	9,948	14.07	10,487	14.16
A2	3,906	5.53	4,593	6.20
A3	7,244	10.25	7,967	10.76
A4	1,912	2.70	2,233	3.01
A5	7,456	10.55	7,773	10.49
A6	4,661	6.59	5,127	6.92
A7	1,701	2.41	1,724	2.33
A8	7,988	11.30	9,209	12.43
A9	12,737	18.02	11,997	16.20
A10	5,415	7.66	5,205	7.03
A11	2,342	3.31	2,356	3.18
CG1	14	0.02	171	0.23
CG2	566	0.80	366	0.49
FX	1,006	1.42	902	1.22
GA1	1,095	1.55	1,364	1.84
GA2	1,957	2.77	1,793	2.42
ICC	619	0.88	691	0.93
UPS	129	0.18	114	0.15
Total	**70,696**	**100**	**74,072**	**100**

The route an aircraft takes in taxiing to/from the runway ends plays a large role in the amount of taxi/idle emissions attributable to that aircraft and the spatial location of the emissions for dispersion modeling. These routes, often referred to as taxipaths (i.e., a series of taxiways), are assigned to the aircraft by the ATCT. However, these all-purpose taxipaths are often circumvented to accommodate real-time requirements. EDMS Delay and Sequence Module assigns a taxipath based on the runway utilization and assigned apron area.

Assumptions made on departure taxipaths from the North passenger terminals are provided in Figure 8-5. Assumptions made on arrivals to the South passenger terminals are provided in Figure 8-6. Taxipaths were also assigned to connect the North passenger terminal, South passenger terminal, cargo and general aviation terminals, and the remote west terminal to each of the eight runway-ends for departures and arrivals.

Figure 8-5. North Terminal Aprons – Departure taxipaths.

Figure 8-6. South Terminal Aprons – Arrival taxipaths.

8.4.3 Temporal Allocation

Distinct temporal (or operational) profiles were developed for air carrier, cargo, commuter, general aviation, and military aircraft operations during arrival and departure conditions. Aircraft temporal profiles were developed for quarter hour of the day, day of the week, and month. The FAA's ASPM database was used to establish the profiles for aircraft operations. These temporal profiles correspond to the specific measurement campaign periods. These temporal profiles represent the variation in aircraft operations. Figure 8-7 displays the hourly aircraft operational profiles (unitless values from 0 to 1 denoted as fraction of peak values) during the Winter and Summer Monitoring Season for all aircraft categories. In addition, temporal profiles were established individually for air carrier, cargo, commuter, general aviation, and military aircraft operations during each of the arrival and departure conditions. The profiles for cargo and air carrier are quite different as cargo operations tend to arrive in the morning hours and depart in the evening. The operational pattern of arrivals and departures for each category of aircraft operations was similar in both monitoring seasons.

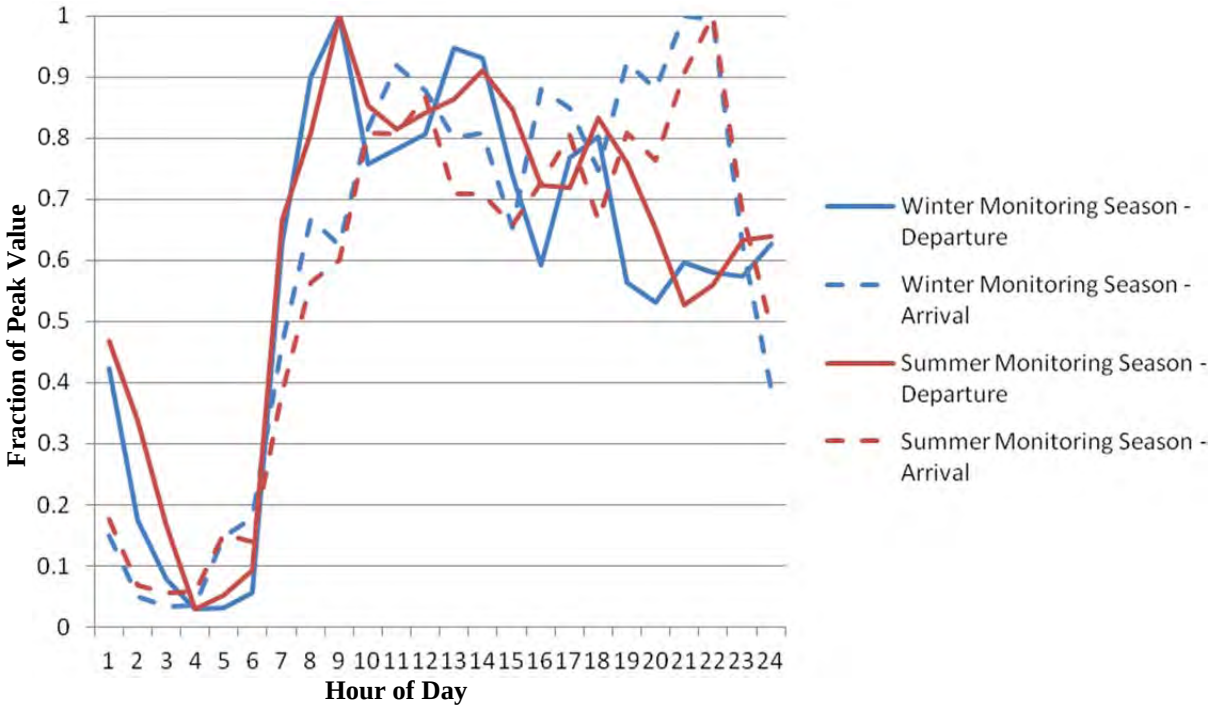

Figure 8-7. Hourly profiles of aircraft operations (Unitless values denoted as fraction of peak values).

Figure 8-8 displays the aircraft temporal data by day of the week (unitless values from zero to one denoted as fraction of peak values). As shown, the peak day of the week was Thursday. There were only slight differences in daily profiles between the Winter and Summer Monitoring Seasons. Along with the greater number of operations, the Summer Monitoring Season was operating closer to the peak daily profile during each day of the week compared to the Winter Monitoring Season**.**

The monthly profiles for aircraft show that March is the busiest month during the Winter Monitoring Season and July is slightly busier than August during the Summer Monitoring Season.

Aircraft emissions can be temporally allocated in two ways: 1) by way of operational profiles (user specified quarter-hour, day, and month factors), and 2) by way of a simulated schedule of operations for the study period. The operational profiles provide relative comparisons from hour to hour, day to day, and month to month and the peak or annual operational data is estimated for each period based on the profile. The simulated schedule uses the actual aircraft activity and contains the following fields: aircraft type, engine type, identification, call sign, airline, date/time, stage length, operation type, gate, runway, and weight (in pounds). For this project, the simulated schedule option was used to more precisely model the distribution of flight operations among the runways.

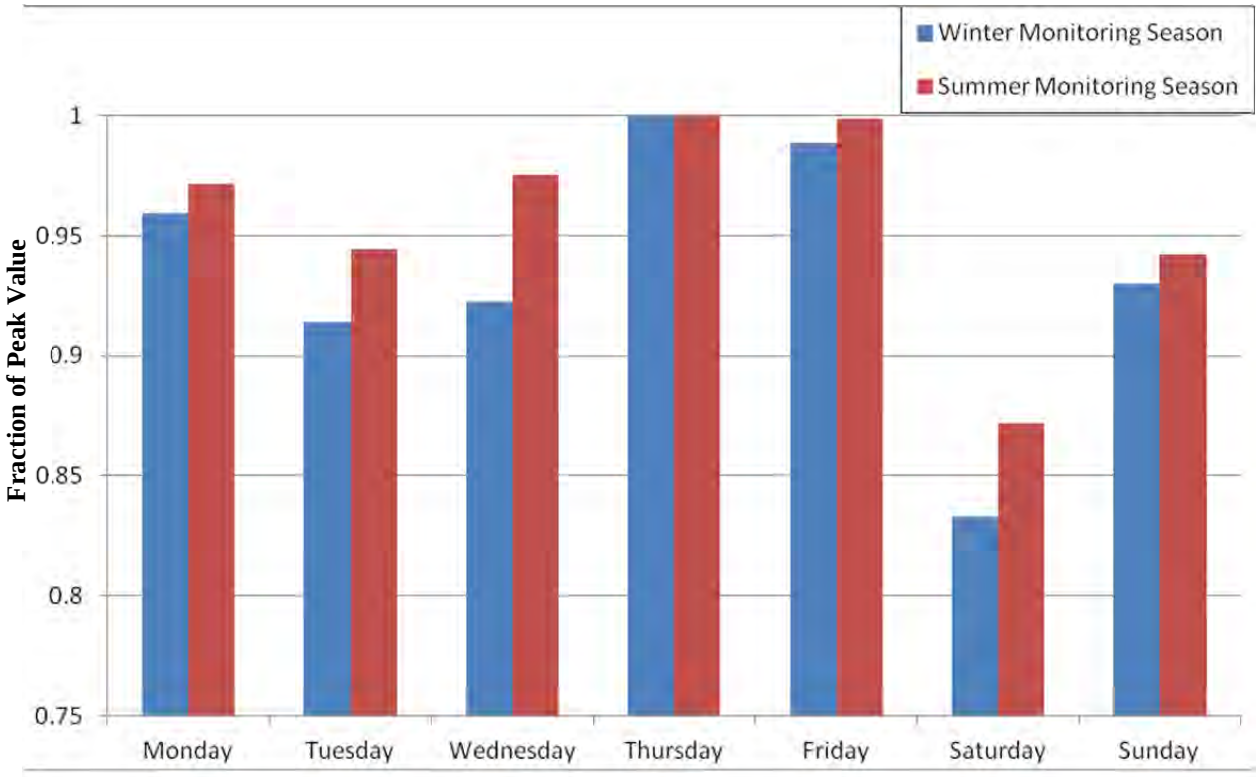

Figure 8-8. Daily profiles of aircraft operations (Unitless values denoted as fraction of peak values).

8.5 AUXILIARY POWER UNITS

Auxiliary power units (APU) are small turbine engines used by many commercial jet aircraft to start the main engines; provide electrical power to aircraft radios, lights, and other equipment; and to power the onboard air conditioning (heating and cooling) system. When an aircraft arrives at an apron, the pilot can opt to shut off power to the main jet engines and operate the onboard APU, which is fueled by the aircraft's jet fuel. However, APU must be run for a period of time (approximately seven minutes during arrival/departure) to allow for engine warm-up/cool down. Alternately, aircraft can utilize fixed gate infrastructure to receive 400 Hertz (Hz) gate power and pre-conditioned air (PCA) from mobile ground power units (GPU) and air conditioning equipment or from gate connections that provide electrical power and PCA. In most cases, gate power connections are built into the passenger loading bridge used to connect the terminal building to the aircraft for loading and unloading of passengers. The APU is, in effect, a small jet engine. The calculations for the emissions generated by an APU are similar to those of an aircraft engine operating in only one power setting.

8.5.1 Emission Calculation Methodology

EDMS has a database of APU assigned to specific aircraft and contains emission factors (in kilograms per hour of operation) for each model. The newest version of EDMS (5.1.3) has the ability to estimate PM_{10} and $PM_{2.5}$ emissions from APU. This feature was unavailable at the time of the Phase II emissions inventories. It is generally difficult to develop specific aircraft/APU assignments based on information (often proprietary) from the airlines. Therefore, for this analysis, the EDMS default aircraft/APU assignments were used. The APU emissions were generated per operation as a product of the emission factor (based on default assignments) and operating time (based on the availability of 400 Hz gate power and/or PCA).

In accordance with FAA guidelines, the recommended APU operating time is seven minutes per landing and takeoff cycle (LTO) for all aircraft parked at gates providing 400 Hz gate power and PCA. For those gates without 400 Hz gate power and PCA, the recommended APU operating time is 26 minutes per LTO for narrow body aircraft and 60 minutes for wide body aircraft. Approximately 55 percent of the terminal gates at LAX provide PCA and all terminal gates have 400 Hz gate power. Thus, the estimate weighted APU operating time for commercial aircraft was estimated at 15.6 minutes (i.e., 26 minutes times 45 percent plus 7 minutes times 55 percent). The apron areas associated with cargo, GA, and remote aircraft parking do not provide gate infrastructure (i.e., gate power and PCA). Thus, the APU operating time associated with aircraft at cargo and remote parking was set to 26 minutes, as a majority of these operations tend

to be narrow body aircraft. Of note, many GA and some smaller commuter aircraft do not contain APU.

All PM_{10} emissions from APU are considered to be $PM_{2.5}$ and EDMS uses conversation factors to determine TOG emissions as a function of VOC emissions. These conversion factors were the same as for aircraft operations per EDMS.

8.5.2 Spatial Allocation

The APU operations were located in the project UTM coordinate system. EDMS spatially allocates APU emissions to a defined aircraft apron. The APU operations within the aircraft apron area were designated an area source with a height of 1.5 meters and an initial vertical distribution of 3 meters.

8.5.3 Temporal Allocation

The temporal allocations for APUs were defined within EDMS. The emissions were applied to each operation, which includes the time between arrival and departure from the gate in a manner consistent with any assigned operational profiles for aircraft operations.

8.6 GROUND SUPPORT EQUIPMENT

Ground support equipment (GSE) include the equipment that service aircraft after arrival and before departure at an airport and the equipment that supports general airport operations that includes: aircraft tugs, baggage tugs, forklifts, fuel trucks, hydrant carts, catering trucks, cargo tractors, GPU, water trucks, lavatory trucks, cabin service, belt loaders, cargo loaders, and others. Different types of aircraft operations require different services. For example, passenger airlines require catering trucks, while cargo operations require loaders. GSE can be directly associated with an aircraft LTO cycle, (such as baggage tractors and belt loaders unloading/loading cargo) or as part of the general operations of the airport (such as generators, sweepers, and deicers). GSE can be fueled by diesel, gasoline, propane, CNG or electric powered.

The type of GSE required depends on aircraft category or size. Wide body aircraft tend to require a greater number of catering equipment and commuter aircraft tend to require less equipment operating for shorter durations. GSE operating times are a function of the airline procedures and the aircraft category or size. Larger aircraft tend to require more GSE and low cost airlines tend to conduct operations in less turnaround time. GSE emissions are a function of the emission factors (in units of grams per horsepower-hour), fuel type, model year, horsepower rating, operating time, and load factor (percent of full throttle).

8.6.1 Emission Calculation Methodology

EDMS offers two methods for estimating GSE emissions: operations-based or population-based method. In the operations-based method, EDMS can assign specific levels of GSE activity to each aircraft specified in the model, thereby providing an emissions estimate based on the number of operations and the type of service each aircraft would likely require. In the population-based method, an inventory of equipment is developed and linked with hours of usage to calculate an emissions inventory from emissions factors. For this project, the population-based method was chosen because it most closely corresponded to the information available in the GSE Inventory Survey conducted at LAX.

A complete GSE inventory survey from October 2006 was provided by LAWA that included fuel type, model year, horsepower, and manufacturer for GSE at the airport. This list of a total of 1,991 pieces of equipment, shown in Table 8-9, was the basis for the GSE emissions inventory. EDMS default hours of operation, load factors, and equipment age distributions were used.

Table 8-9. GSE Inventory

GSE Type	Fuel Type	Number of Pieces	Annual Hours of Operation	GSE Type	Fuel Type	Number of Pieces	Annual Hours of Operation
Air Conditioner	Diesel	8	808	Generator	Diesel	11	1630
Air Start	Diesel	32	333		Gasoline	6	1630
Aircraft Tractor	Diesel	157	800	GPU	Diesel	96	1600
	Gasoline	3	800		Gasoline	16	1600
Baggage Tractor	Diesel	55	1500	Hydrant Truck	Diesel	15	1527
	Gasoline	79	1500		Gasoline	11	1527
	Propane	173	1500	Lavatory Truck	Diesel	10	1492
Belt Loader	Diesel	49	1300		Gasoline	35	1492
	Gasoline	94	1300	Lift	Diesel	32	341
	Propane	34	1300		Gasoline	46	341
Bobtail	Diesel	4	1867		Propane	22	341
	Gasoline	26	1867	Other	Diesel	34	1646
Cargo Loader	Diesel	156	1100		Gasoline	34	1646
	Gasoline	7	1100		Propane	1	1646
Cargo Tractor	Diesel	21	1349	Passenger Stand	Diesel	4	188
	Gasoline	110	1349		Gasoline	27	188
	Propane	95	1349		Propane	1	188
Cart	Gasoline	2	100	Service Truck	Diesel	30	840
Catering Truck	Diesel	41	1600		Gasoline	140	840
	Propane	21	1600		Propane	2	840
Deicer	Gasoline	1	500	Sweeper	Diesel	3	12
Forklift	Diesel	29	976		Gasoline	4	12
	Gasoline	15	976		Propane	1	12
	Propane	153	976	Water Service	Gasoline	9	960
Fuel Truck	Diesel	28	564				
	Gasoline	6	564				
	Propane	2	564				

Notably, a load factor of 0.60 equates to 60 percent of throttle capacity during operation. Typically, load factors range from 20 to 80 percent depending on the type of GSE. Equipment age distribution is typically a normal bell curve with a specified equipment lifetime. Typical equipment lifetime is 5 to 15 years.

Table 8-9 also displays the default annual hours of operation. These values represent the annual hours of operation per each piece of equipment based on nationwide surveys of GSE operations. The GSE hours of operation during the Winter Monitoring Season was based on the duration of the monitoring campaign for the emissions inventory (46 days). During the Winter Monitoring Season, the air conditioner units were assumed to operate for 102 hours (or 808 hours per year for 46 days out of 365 days annually).

In the LAX GSE Inventory Survey, ten percent of the equipment was listed as "other on-road equipment." It was assumed this category was composed of vehicles used for unscheduled transportation of employees and goods around the airfield, which utilize the service roadways that are not closely tied to aircraft operations.

EDMS 5.1.3 has a database of GSE emission factors (in grams-horsepower per hour) based on U.S. EPA's NONROAD[22] emissions model. However, this analysis used emissions factors developed by CARB within the OFFROAD2011 emissions model and/or In-Use Off-Road Equipment emissions model because this is the valid model in California. Table 8-10 provides the data, including assigned horsepower and load factor for the GSE fleet, which lead to the determination of the emission factors. The emission factors also vary per fuel type. Gasoline tends to have a higher emission rate of CO and VOC, and diesel tends to have a higher emission rate of NO_x and $PM_{2.5}$.

Table 8-10. GSE Fleet Horsepower and Load Factor

GSE Type	Fuel Type	HP	Load Factor	GSE Type	Fuel Type	HP	Load Factor
Air Conditioner	Diesel	155	0.75	Generator	Diesel	229	0.78
Air Start	Diesel	384	0.9		Gasoline	107	0.78
Aircraft Tractor	Diesel	178	0.8	GPU	Diesel	163	0.75
	Gasoline	130	0.8		Gasoline	150	0.75
Baggage Tractor	Diesel	71	0.37	Hydrant Truck	Diesel	175	0.7
	Gasoline	100	0.55		Gasoline	122	0.7
	Propane	100	0.55	Lavatory Truck	Diesel	168	0.25
Belt Loader	Diesel	54	0.34		Gasoline	130	0.25
	Gasoline	60	0.5	Lift	Diesel	115	0.5
	Propane	60	0.5		Gasoline	100	0.5
Bobtail	Diesel	113	0.37		Propane	100	0.5
	Gasoline	100	0.55	Other	Diesel	140	0.34
Cargo Loader	Diesel	101	0.34		Gasoline	50	0.5
	Gasoline	70	0.5		Propane	50	0.5
Cargo Tractor	Diesel	88	0.36	Passenger Stand	Diesel	100	0.4
	Gasoline	95	0.54		Gasoline	125	0.59
	Propane	100	0.55		Propane	165	0.59
Cart	Gasoline	12	0.5	Service Truck	Diesel	174	0.2
Catering Truck	Diesel	240	0.52		Gasoline	180	0.2
	Propane	204	0.52		Propane	180	0.2
Deicer	Gasoline	93	0.95	Sweeper	Diesel	51	0.51
Forklift	Diesel	156	0.3		Gasoline	53	0.51
	Gasoline	50	0.3		Propane	45	0.51
	Propane	50	0.3	Water Service	Gasoline	150	0.2
Fuel Truck	Diesel	189	0.25				
	Gasoline	130	0.25				

[22] NONROAD2008 updates NONROAD2005 to include new non-road emission standards promulgated in 2008 related to small gasoline engines and pleasure craft http://www.epa.gov/oms/nonrdmdl.htm

GSE Type	Fuel Type	HP	Load Factor	GSE Type	Fuel Type	HP	Load Factor
	Propane	140	0.25				

8.6.2 Spatial Allocation

The GSE were located in the project UTM coordinate system. Spatially, EDMS allocates GSE emissions to a defined aircraft apron based on the assignment for each aircraft. The GSE operations within the aircraft apron area were designated an area sources with a height of 1.5 meters and an initial vertical distribution of 3 meters.

8.6.3 Temporal Allocation

The temporal allocations for GSE are defined within EDMS. The emissions are applied to each operation, which includes the time between arrival and departure from the gate in a manner consistent with any assigned operational profiles for aircraft operations.

8.7 AIRPORT ROADWAYS

As shown in Figure 8-9, on-airport roadways were included in three categories: 1) the Central Terminal Area (CTA) roadways, 2) cargo routes, and 3) service roads. The CTA consists of five roadways in the center of the LAX terminal buildings and the ramps that connect West Century Boulevard and South Sepulveda Boulevard to World Way for inbound (lower) and outbound (upper) traffic. Traffic volumes associated with the CTA, cargo routes, and service roads as well as traffic on World Way West were considered 100 percent related to LAX operations and apportioned as airport emissions.

Figure 8-9. Airport roadways.

Service roadways consist of two Airport service roads:

- Airfield Service Road F – This service road allows transport of GSE and automobile traffic around parts of the south runways. The roadway runs north/south behind the ends of South Airfield Runways 25R and 25L, and runs east/west just south of Terminals 4, 5, 6, 7, and 8.

- South Cargo Complex Access Road – This service road allows transport around the south cargo complex buildings and parking lots, on the landside (to the east). This roadway runs parallel to Aviation Boulevard and Imperial Highway along the east and south perimeters of the South Cargo Complex east of Sepulveda Boulevard.

8.7.1 Emission Calculation Methodology

Emission levels from the operation of motor vehicles for airport roadways is dependent on several factors including: the vehicle volume, fleet mix (i.e., vehicle type, age, and fuel), the emission factors (in grams per mile traveled), travel distance, speed, and meteorological factors, such as temperature and relative humidity.

Emissions associated with airport vehicles were calculated by combining the activity information with emissions factors derived using the CARB EMFAC2011 on-road emissions model.[23] Emission factors from U.S. EPA's MOBILE6.2 emissions model are built into EDMS but are not specifically applicable to California and were therefore overwritten with more applicable emission factors from EMFAC.

CTA roadway volumes were determined using traffic counters (loop detectors) that are permanently positioned in the inbound and outbound connector ramps for the CTA roadways. The loop detectors provide a basis to estimate the total number and types of vehicles on CTA roadways during the Winter and Summer Monitoring Seasons. Table 8-11 presents the traffic volumes for the CTA roadways during the Winter and Summer Monitoring Seasons. The Summer Monitoring Season recorded greater traffic volumes as a result of greater summertime activities.

Table 8-11. Central Terminal Area traffic volumes

Monitoring Season	Departures	Arrival	Total
Winter Monitoring Season	2,465,206	2,774,401	5,239,607
Summer Monitoring Season	2,504,518	3,856,185	6,360,703

World Way West, service roadways, and cargo route volumes were estimated using traffic data from numerous sources including: the LAWA Transportation Planning Department, CalTrans, and traffic data collected in June 2008 for the Phase II study. These sources provided daily and/or weekly traffic volumes. Weekly totals from other locations were used to scale up the daily volumes into a weekly volume if only daily volumes were available. Once the weekly volume was determined, the volume for the entire Phase III monitoring period was estimated. The 2008 traffic data were adjusted to represent the 2012 monitoring periods utilizing the actual passenger enplanements during the two monitoring seasons.

The vehicle classifications (e.g., percent of fleet which is light duty automobile, heavy duty diesel truck, etc.) required as input to the EMFAC emissions model were collected in two ways. CTA roadway classifications were estimated using the Airport's Automatic Vehicle Identification (AVI) system for commercial vehicles. This system allowed for an estimation of commercial gasoline vehicles (such as taxicabs and limousines), small buses, large buses, and LAX-owned shuttle buses. Commercial gasoline vehicles were assumed to be made up of a default public roadway mix; small buses were classified as single unit trucks due to limitations of EMFAC; large buses were classified as urban diesel and Compressed Natural Gas (CNG) buses; and LAX parking lot shuttle buses were included and are fueled by Liquid Natural Gas (LNG).

[23] CARB EMFAC2011 On-road Emissions Model, http://www.arb.ca.gov/msei/msei.htm.

Table 8-12 displays the CTA motor vehicle class distribution for airport roadways, except the cargo routes for which a majority of the vehicles were assumed to be medium duty diesel trucks. The motor vehicle class distribution for the CTA is assumed to be representative of all airport roadways except the cargo routes.

Table 8-12. Central Terminal Area (CTA) motor vehicle class distribution (percentage)

CTA	Rental Car	Hotel Shuttle	Private Parking Shuttle	Scheduled Service	Shared Ride	Light Duty Shared Ride	Charter	Taxi	LAX Shuttle	Fly-away	Passenger Drop-off
Winter Monitoring Season											
Lower	6.87	2.69	7.05	0.51	2.87	0.20	6.03	12.22	2.07	0.33	59.17
Upper	5.40	2.65	5.34	0.18	1.97	0.18	9.09	6.63	2.89	0.32	65.36
Both	6.18	2.67	6.25	0.36	2.44	0.19	7.47	9.59	2.46	0.32	62.08
Summer Monitoring Season											
Lower	4.51	2.01	4.61	0.31	2.23	0.17	4.59	8.88	1.22	0.19	71.29
Upper	4.36	2.48	4.60	0.14	1.83	0.19	7.80	5.46	2.05	0.23	70.86
Both	4.45	2.22	4.61	0.23	2.05	0.18	5.99	7.39	1.58	0.21	71.10

The EMFAC emissions model used average speed and vehicle class distribution data to produce emission factors in grams per vehicle-mile for CO, VOC, TOG, NO_x, SO_x, PM_{10}, and $PM_{2.5}$. The assumed traffic speeds were estimated from observations (during June of 2008) of each roadway segment that showed the average speed tended to be about half of the speed limit on the roadway. An estimated average speed (between 15 and 25 mph depending on roadway) used in the analysis for airport roadways came from these observations. Table 8-13 displays the emission factors for airport roadway motor vehicles.

Table 8-13. Motor vehicle emission factors (g/mile)

Speed	**CO**	**VOC**	**TOG**	**NO_x**	**SO_x**	**PM_{10}**	**$PM_{2.5}$**
	Winter Monitoring Season						
Idle (g/hour)	26.9	2.67	3.41	6.52	0.060	0.218	0.200
5	5.38	0.534	0.682	1.30	0.012	0.044	0.040
10	4.47	0.366	0.463	1.04	0.009	0.031	0.029
15	3.67	0.243	0.307	0.794	0.007	0.021	0.020
20	3.10	0.165	0.211	0.672	0.006	0.017	0.015
25	2.73	0.124	0.158	0.522	0.005	0.011	0.010
30	2.46	0.103	0.130	0.528	0.004	0.010	0.009
35	2.28	0.093	0.116	0.614	0.004	0.012	0.011
40	2.13	0.086	0.107	0.685	0.004	0.013	0.012
45	2.03	0.081	0.101	0.714	0.004	0.015	0.014
50	1.98	0.079	0.098	0.729	0.004	0.016	0.015
55	1.99	0.083	0.102	0.813	0.004	0.020	0.019
60	2.07	0.095	0.116	1.06	0.004	0.030	0.027
65	2.30	0.117	0.142	1.49	0.005	0.051	0.046
	Summer Monitoring Season						
Idle (g/hour)	28.7	2.74	3.51	6.16	0.060	0.218	0.200
5	5.75	0.547	0.702	1.23	0.012	0.044	0.040
10	4.83	0.375	0.477	0.98	0.009	0.031	0.029
15	3.98	0.248	0.315	0.746	0.007	0.021	0.020
20	3.38	0.169	0.216	0.630	0.006	0.017	0.015
25	2.99	0.126	0.162	0.486	0.005	0.011	0.010
30	2.69	0.104	0.133	0.493	0.004	0.010	0.009
35	2.45	0.093	0.118	0.576	0.004	0.012	0.011
40	2.32	0.087	0.109	0.644	0.004	0.013	0.012
45	2.24	0.082	0.103	0.674	0.004	0.015	0.014
50	2.16	0.080	0.100	0.688	0.004	0.016	0.015
55	2.13	0.083	0.104	0.768	0.004	0.020	0.019
60	2.08	0.093	0.115	1.00	0.004	0.030	0.027
65	2.27	0.115	0.140	1.42	0.005	0.051	0.046

EMFAC2011 includes PM_{10} and $PM_{2.5}$ emissions from exhaust as well as brake and tire wear. Estimates of entrained roadway dust were also included in the emission inventory. The entrained roadway dust includes emissions of fugitive PM_{10} and $PM_{2.5}$ entrained by vehicular travel on paved roads. In areas such as Los Angeles (i.e., drier climate), entrained dust can be an important contributor to local and regional levels of PM_{10} and $PM_{2.5}$. The emission factors for entrained paved road dust were obtained using U.S. EPA's methodology (Section 13.2.1 of AP-42, dated January 2011).

The equation for deriving the paved road dust emission factor is shown below:

$$E = K * [(sL)^{0.91} * (W)^{1.02}] * (1-P/4N)$$

where:

E= Particulate emission factor in units of grams per vehicle mile traveled.
K = Particle size multiplier (used to compute PM_{10} and $PM_{2.5}$ in the units of the emission factor).
sL = Roadway silt loading in grams/square meter
W = Average weight (tons) of vehicles on the road
P = Number of "wet" days with at least 0.254 mm (0.01 in) of precipitation
N = Number of days in the averaging period (e.g., 365 days for an annual estimate)

The final term in the equation (1-P/4N) is the rainfall correction factor, which effectively reduces the emission factor based on the number of rain days within the period of estimation (i.e., 46 days per year). The factor of "4" in the denominator accounts for the drying of paved roads during the rainy days (greater than 0.01 inches of rain) and for days when rain does not occur over a full 24-hour period.

Inputs to the paved road dust equation were developed from area-specific roadway silt loading and average vehicle weight data measured by Midwest Research Institute (MRI). The statewide average vehicle weight for California was assumed to be 2.4 tons. This estimate is based on an informal traffic count estimated by MRI while they were performing California silt loading measurements. Road dust emissions for the following four classes of roads: 1) freeways/expressways, 2) major streets/highways, 3) collector streets, and 4) local streets. The following silt loadings were assumed for the four road categories: 0.02 g/m^2 for freeways, 0.035 g/m^2 for major roads, and 0.32 g/m^2 for both collector and local roads. The $PM_{2.5}/PM_{10}$ ratio for paved road dust is 0.169 (or 16.9 percent of PM_{10} is considered $PM_{2.5}$). Table 8-14 presents the entrained roadway dust emission factors for various vehicle speeds and roadway classifications.

Table 8-14. Entrained roadway dust motor vehicle emission factors (g/mile)

	PM_{10}			$PM_{2.5}$		
Speed	**Freeway**	**Major**	**Local/Collector**	**Freeway**	**Major**	**Local/Collector**
5	0.133	0.178	0.904	0.065	0.076	0.258
10	0.121	0.165	0.892	0.054	0.065	0.247
15	0.111	0.155	0.882	0.045	0.056	0.237
20	0.106	0.151	0.877	0.040	0.051	0.233
25	0.100	0.145	0.872	0.035	0.046	0.228
30	0.099	0.144	0.871	0.034	0.045	0.227
35	0.101	0.146	0.872	0.035	0.047	0.228
40	0.102	0.147	0.874	0.037	0.048	0.230
45	0.104	0.149	0.876	0.038	0.050	0.231
50	0.106	0.150	0.877	0.040	0.051	0.233
55	0.109	0.154	0.881	0.043	0.055	0.236
60	0.119	0.164	0.890	0.052	0.063	0.245
65	0.140	0.184	0.911	0.071	0.082	0.264

8.7.2 Spatial Allocation

The airport roadways were located in the project UTM coordinate system. Performing dispersion modeling of emissions (see Section 9) requires the specification of x and y coordinates with associated elevation, width, and release height for each roadway. The roadway coordinates spatially locate the roadway in the airport configuration and provide information on roadway dimensions. The default width is 20 meters (65.6 feet). However, roadway-specific widths were determined based on aerial photographs and maps. The initial vertical dispersion parameter was specified as 3 meters. The roadway width determines the width of the area sources used to model the roadway emissions. A roadway is defined as a series of connected line segments, which are identified by their endpoints and is modeled as an area source derived from the length and width of each segment.

8.7.3 Temporal Allocation

Temporal (or operational) profiles for the airport roadways were estimated from the CTA loop traffic counters. The peak hour for the CTA departure level (Upper) was 11:00 (for the Winter Monitoring Season) and 07:00 for the Summer Monitoring Season. The peak hour for the CTA-arrival level (Lower) was 23:00 for the Winter Monitoring Season and 12:00 for the Summer Monitoring Season. Figure 8-10 displays the hourly operational profiles for the CTA roadways, which was also used for the World Way West. During the Winter Monitoring Season, Wednesday was the peak day of the week; while during the Summer Monitoring Season, the peak days of the week were Monday and Sunday. Operational profiles for the cargo route and service roadways were used for the operational profiles associated with cargo and air carrier aircraft operations, respectively, as these roadways more closely follow the pattern of aircraft operations and not air passenger traffic movements.

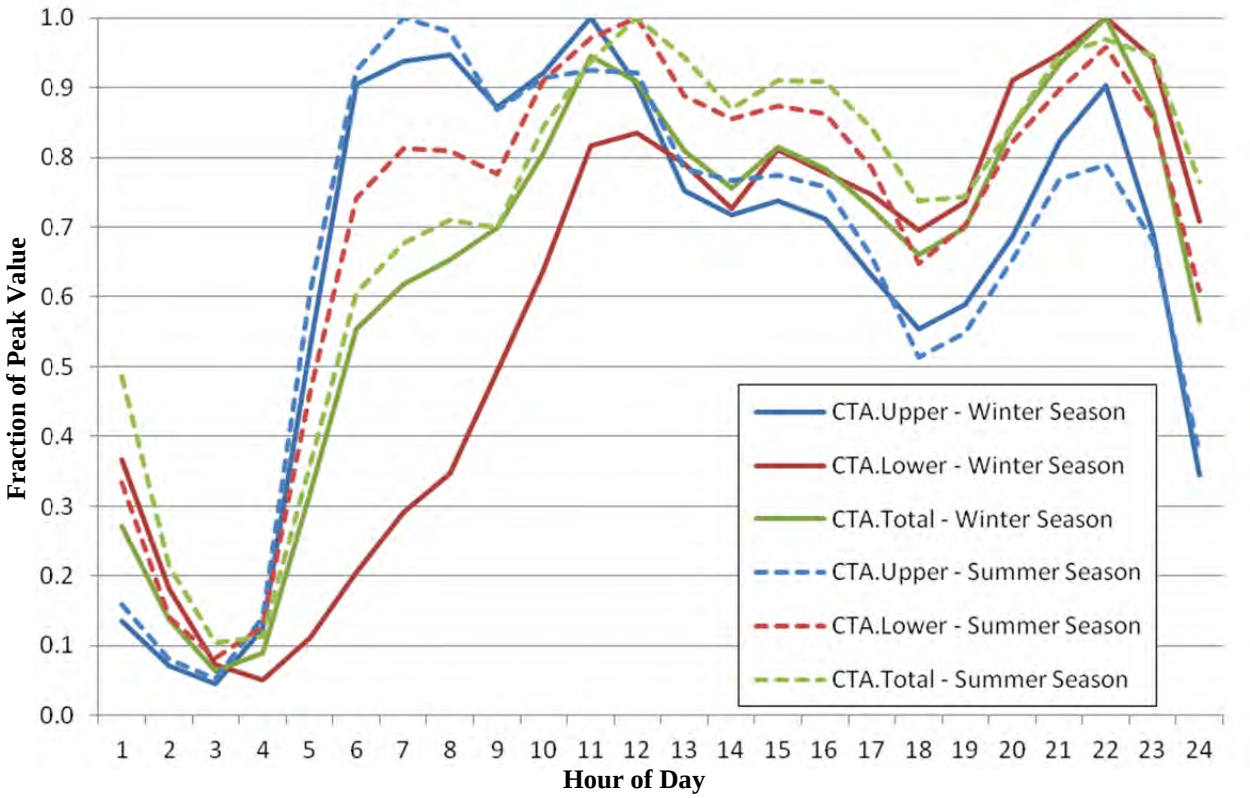

Figure 8-10. Hourly profiles of CTA roadways used to represent non-cargo airport roadways (Unitless values denoted as fraction of peak values).

8.8 PARKING FACILITIES

Twelve parking facilities were included in the analysis as shown in Figure 8-11. These facilities include seven public LAWA-owned parking garages (with multiple levels) in the CTA (LAX lots 1-7), two public LAWA-owned surface lots (LAX lots B and C), one LAWA-owned employee surface lot (LAX lot E), one public off-airport parking surface lot east of the CTA, and one trucking depot lot located east of South Airfield Runway 25R.

Figure 8-11. Parking facilities utilized in Phase III of the LAX AQSAS.

8.8.1 Emission Calculation Methodology

Emissions were estimated using similar methodology for all parking facilities except for the trucking depot east of South Airfield Runway 25R, which is frequented by a greater percentage of trucks than automobiles. Emissions occurring at parking facilities were calculated using estimates of the number of vehicles accessing the facility, the amount of time a vehicle spends idling (typically 1.5 minutes), the travel time within the facility at a given speed (typically ten miles per hour), the vehicle type distribution, facility geometry and spatial characteristics, and emission factors.

The total volume of vehicles entering and exiting each LAWA-owned public parking facility was estimated using parking ticket data from the seasonal measurement campaigns as shown in Table 8-15. Total traffic volume for the LAWA-owned employee lot (Lot E) was estimated using seven days of automated traffic counts obtained during Phase II of the LAX AQSAS. Traffic volumes in the public off-airport parking lot located east of the CTA on Century Boulevard (known as Park One) were estimated using volumes from a LAWA-owned long-term surface lot (Lot C) scaled by the ratio of the number of parking spaces available in each lot.

Table 8-15. Parking facilities ticket count and travel parameters

Parking Facility	Winter Monitoring Season	Summer Monitoring Season	Travel Distance (meters)	Idle Time (min)
Lot 1	147,120	202,592	214	1.5
Lot 2	210,356	240,419	310	1.5
Lot 3	298,024	270,445	199	1.5
Lot 4	289,048	360,076	199	1.5
Lot 5	80,495	100,521	136	1.5
Lot 6	145,774	179,074	176	1.5
Lot 7	136,166	193,021	359	1.5
Lot B	Did not operate			
Lot C	60,940	66,000	607	1.5
Lot E	34,626	31,615	379	1.5
Park One	35,236	32,172	277	1.5
Trucking	16,599	15,155	250	1.5

Average distance traveled was calculated independently for each facility. Average occupancy and differences in facility characteristics were taken into account in estimating the average distance traveled within each parking facility. Average occupancy plays a role in average distance traveled as fuller facilities require more driving to locate parking spaces. Other attributes that affect distance traveled are locations of entrances and exits, location of pedestrian access, number of levels in the garage, and how the ramp system within the garage is designed. All of these attributes have been identified from observations, interviews with LAWA staff, and professional experience.

Public parking lots used a vehicle class distribution consistent with airport roadways. One exception was the trucking depot, which was weighted more towards medium duty diesel trucks. Emissions from vehicles idling within the parking facilities were calculated by using the vehicle idle time and the idle emissions factors, in grams per hour, derived from the EMFAC2011 emissions model, as shown in Table 8-16. Emissions from vehicles driving within the parking facilities were calculated by using the vehicle travel distance and the running emissions factors, in grams per mile, derived from the EMFAC2011 emissions model. PM_{10} and $PM_{2.5}$ emission factors include exhaust, brake and tire wear, as well as paved road dust.

8.8.2 Spatial Allocation

The parking facilities were located in the project UTM coordinate system. Each parking garage was treated as one area source per garage level, which was stacked to simulate a parking garage. The number of levels in each garage (between three and five, depending on the garage) and the average separation between levels (approximately 4 meters or 13 feet) was accounted for in the calculation of the emissions. Performing dispersion modeling (see Section 9) requires the x, y coordinates and associated elevations for each level of the parking facilities. The x, y coordinates which determine the size of the area source were determined for each parking facility based on aerial photographs and maps. The initial vertical dispersion parameter was specified as

three meters. The size of the area source is defined by the x, y coordinates for the facility. A parking facility was modeled as an area source derived from the segments and the width.

Table 8-16. Parking facilities motor vehicle emission factors (g/hour and g/mile)

Parking Facility	Speed	CO	VOC	TOG	NO_x	SO_x	PM_{10}	$PM_{2.5}$
Winter Monitoring Season								
Parking Lots	Idle	26.9	2.67	3.41	6.52	0.060	0.218	0.200
	10 mph	4.47	0.366	0.463	1.04	0.009	0.892	0.246
Trucking Depot	Idle	43.4	22.0	25.1	132	5.000	0.896	0.824
	10 mph	5.44	2.56	2.92	19.6	1.182	1.16	1.15
Summer Monitoring Season								
Parking Lots	Idle	28.7	2.74	3.51	6.16	0.060	0.218	0.200
	10 mph	4.83	0.375	0.477	0.978	0.009	0.892	0.246
Trucking Depot	Idle	43.4	22.0	25.1	127	5.000	0.896	0.824
	10 mph	5.44	2.56	2.92	18.8	1.18	1.16	1.15

8.8.3 Temporal Allocation

Hour of the day, day of the week, and monthly profiles were developed to simulate parking activity during the two seasonal measurement campaigns. The traffic volumes were estimated for each hour of both monitoring seasons based on the parking ticket counts during the measurement campaigns and these operational profiles. As shown in Table 8-17, the hourly profiles for the parking facilitates show the peak hour was 17:00 for Lot 2, 21:00 for Lots 1, B, and C, 22:00 for Lots 3, 4 5, and 19:00 and 23:00 for Lot 6. The peak day was Saturday. These hourly profiles represent average profiles during both monitoring periods as detailed data was not available.

Table 8-17. Hourly profiles of parking facilities

Hour	Lot 1	Lot 2	Lot 3	Lot 4	Lot 5	Lot 6	Lot 7	Lot B	Lot C
1	0.162	0.450	0.469	0.491	0.288	0.494	0.296	0.668	0.632
2	0.107	0.219	0.167	0.211	0.058	0.289	0.184	0.528	0.445
3	0.038	0.071	0.042	0.054	0.013	0.089	0.047	0.775	0.279
4	0.078	0.057	0.021	0.302	0.058	0.032	0.056	0.315	0.262
5	0.155	0.113	0.066	0.111	0.201	0.080	0.255	0.796	0.610
6	0.362	0.320	0.141	0.252	0.357	0.242	0.308	0.958	0.878
7	0.446	0.358	0.233	0.333	0.300	0.278	0.393	0.865	0.875
8	0.535	0.325	0.334	0.361	0.288	0.304	0.445	0.747	0.833
9	0.629	0.403	0.397	0.437	0.467	0.399	0.421	0.806	0.817
10	0.785	0.521	0.516	0.534	0.606	0.624	0.631	0.737	0.844
11	0.941	0.801	0.660	0.740	0.701	0.658	0.755	0.763	0.858
12	0.969	0.814	0.795	0.846	0.617	0.626	0.763	0.788	0.916
13	0.970	0.682	0.751	0.811	0.542	0.548	0.648	0.837	0.873
14	0.754	0.708	0.714	0.796	0.444	0.401	0.520	0.917	0.909
15	0.816	0.882	0.778	0.900	0.462	0.401	0.589	0.867	0.922
16	0.756	0.461	0.784	0.870	0.394	0.361	0.577	0.904	0.907
17	0.767	**1.000**	0.691	0.805	0.379	0.345	0.451	0.925	0.869
18	0.770	0.751	0.627	0.690	0.382	0.353	0.442	0.857	0.913
19	0.838	0.695	0.576	0.705	0.481	0.476	0.424	0.818	0.907
20	0.947	0.820	0.618	0.812	0.602	0.645	0.649	0.836	0.893
21	**1.000**	0.818	0.795	0.948	0.844	0.699	0.795	**1.000**	**1.000**
22	0.874	0.915	**1.000**	**1.000**	**1.000**	0.868	**1.000**	0.938	0.925
23	0.710	0.951	0.966	0.960	0.960	**1.000**	0.872	0.883	0.947
24	0.439	0.814	0.754	0.828	0.623	0.961	0.439	0.812	0.929

Note: Bold values represent peak hourly period. Unitless values representing fractions of the peak value.

8.9 AIRPORT STATIONARY SOURCES AND FUEL STORAGE TANKS

LAX operates several airport stationary sources including: 30 stationary internal combustion engines (generators), two turbines, and four boilers; all of which were included in this analysis.

Figure 8-12 presents the location of the airport stationary sources. The generators are either natural gas or diesel fired. The turbines and boilers are natural gas fired. The turbines are rated at 50 MMBTU and the boilers are rated at 27.5 MMBTU. In addition, the Central Utility Plant, along with the turbines, contains four cooling towers. Of note, there are several tenant-owned airport stationary sources associated with various airlines. The analysis also included VOC and TOG emissions from airport fuel storage tanks for Jet A, motor gasoline, and diesel fuels. Of note, aviation gasoline is not stored at the Airport.

Emissions from aircraft parts painting/degreasing facilities, dry cleaning facilities, food kitchens, and terminal-based food concessions were not included, as these emission sources are minor and not easily quantified. Training fires were not included as these operations were not performed during the Winter or Summer Monitoring Seasons.

8.9.1 Emission Calculation Methodology

Emissions for LAX-operated airport stationary sources were based on reported values within the SCAQMD Regional Clean Air Incentives Market (RECLAIM) *Quarterly Certification of Emissions Report* and the 2011 Annual Emissions Report. An annual report is required to be submitted by LAWA because LAX is designated as a major source and contains a Title V operating permit. The generators, turbines, and boilers emissions are required to be reported quarterly; thus, these quarterly reports formed the basis for the emissions estimates calculated for each measurement campaigns, and were scaled based on the number of days for each measurement campaign. The quarterly report is not required to include the cooling tower emissions. Thus, its emissions were based on the 2011 Annual Emissions Report and were scaled based on the actual number of days for each measurement campaign.

The turbines associated with the Central Utility Plant are required to also monitor emissions through the use of hourly Continuous Emissions Monitors (CEMs). These CEMs measure hourly NO_x emissions, natural gas flow, stack flow, and production rate. Emissions of CO, VOC, TOG, SO_x, PM_{10}, and $PM_{2.5}$ were estimated as a function of the reported quarterly values within RECLAIM and assumed to vary in a manner similar to the hourly production rate. A large majority of the emissions associated with LAX-operated airport stationary sources was due to the operation of the two turbines associated with the Central Utility Plant.

The sources of VOC and TOG emissions from the storage of fuel included breathing and working losses for storage tanks. VOC emissions from fuel storage were calculated using the EDMS 5.1.3. Fuel usage was provided by Atlantic Aviation and ASIG/LAXFuel, which tracks usage of Jet A. LAX does not have any aviation gasoline (Avgas) usage since this fuel is only required for piston aircraft. Diesel and gasoline usage were estimated based on GSE operations and fuel usage rates within EDMS and U.S. EPA's NONROAD emissions model.

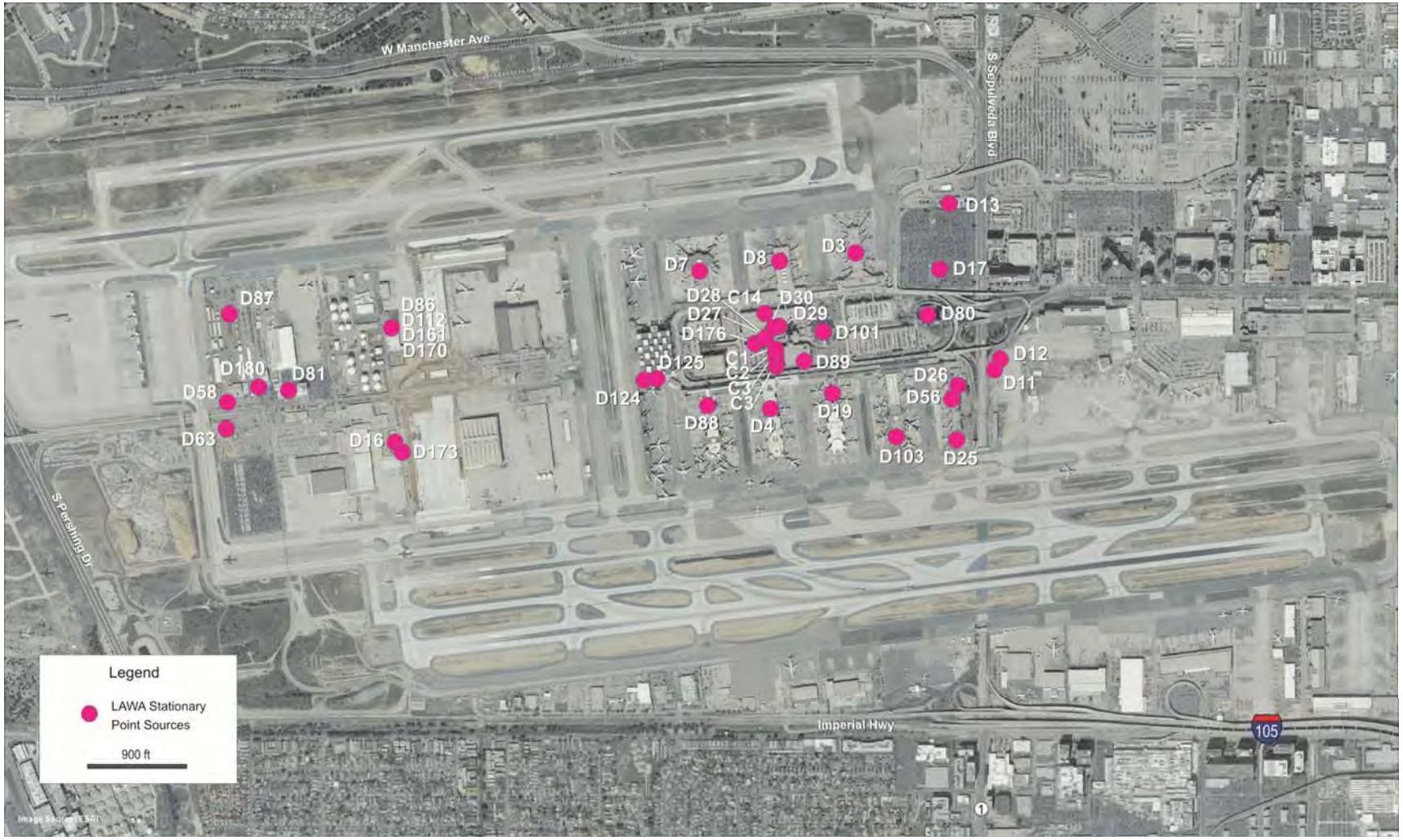

Figure 8-12. Stationary sources at LAX. C## denotes and cooling towers and D## denotes generators (except D27/28 – boilers and D29/30 – turbines).

8.9.2 Spatial Allocation

The LAX-operated airport stationary sources were located in the project UTM coordinate system. The locations were based on the LAX Title V Operating Permit, aerial photographs and maps. Stack release parameters such as height, diameter, temperature and velocity for the generators were based on default data and engineering judgment. Table 8-18 presents a list of generators at LAX. Stack release parameters for the turbines, boilers, and cooling towers were based on the LAX Title V Operating Permit and other published data.

Table 8-18. List of LAX generators

ID	Fuel	Size (hp)	ID	Fuel	Size (hp)
D3	Diesel	375	D80	Diesel	474
D4	Diesel	269	D81	Diesel	1199
D7	Natural Gas	69	D86	Diesel	349
D8	Diesel	355	D87	Diesel	823
D11	Diesel	245	D88	Diesel	349
D12	Diesel	420	D89	Diesel	166
D13	Natural Gas	210	D101	Diesel	465
D14	Diesel	264	D103	Diesel	300
D16	Diesel	390	D112	Diesel	33
D17	Diesel	141	D124	Diesel	2220
D19	Diesel	191	D125	Diesel	2220
D25	Diesel	92	D161	Diesel	500
D26	Diesel	535	D170	Diesel	500
D56	Diesel	60	D173	Diesel	755
D58	Diesel	150	D176	Diesel	422
D63	Diesel	750	D180	Diesel	822

Table 8-19 presents the source release parameters for the boilers, turbines, and cooling tower stacks. The boilers and turbines are natural gas fired. Fifteen Jet A storage tanks were treated as vertical fixed roof tanks while diesel and gasoline tanks (two each) were treated as horizontal tanks with dimensions based on aerial photographs, maps, and site visits.

Table 8-19. LAX major stationary source release parameters

ID	Source Type	Height (m)	Temperature (K)	Velocity (m/s)	Diameter (m)
D27	Turbine	55	422	20.3	1.524
D28	Turbine	55	422	20.3	1.524
D29	Boiler	55	422	6.65	0.853
D30	Boiler	55	422	6.65	0.853
C1	Cooling Tower	40	293	3.40	7.01
C2	Cooling Tower	40	293	3.40	7.01
C3	Cooling Tower	40	293	3.40	7.01
C4	Cooling Tower	40	293	3.40	7.01

8.9.3 Temporal Allocation

Except for the turbines, no temporal allocation of the airport stationary source emissions was made. This was because hourly, day of the week, and monthly data were not available to allocate the emissions over time. Therefore, a constant emission rate was assumed for each hour for the generators, boilers and cooling towers. The turbines used temporal data within the CEMs to estimate hourly emissions throughout the measurement campaigns. Figure 8-13 presents an example of the CEMs data for the D28 turbine during the Winter Monitoring Season.

Figure 8-13. Continuous Emissions Monitor data for D28 turbine during the Winter Monitoring Season for NOx emissions (average daily pounds/hour).

8.10 OFF-AIRPORT MAJOR ARTERIAL ROADWAYS

Off-airport roadways included the major arterials surrounding the airport and were comprised of Century West, Imperial, Airport, Aviation, Sepulveda, La Cienega, Manchester, and Westchester Boulevards. Of note, Sepulveda Boulevard travels in two tunnels under the runways of the South Airfield and includes one three-lane tunnel in each direction. Emissions were also determined separately for each of the I-405 and I-105 links that overlay the Study Area (See Section 8.12). Figure 8-14 displays the off-airport major arterial roadways included in the emissions inventory. These roadways included:

- 96th Street from Sepulveda Boulevard to Airport Boulevard
- 111th Street from Aviation Boulevard to La Cienega Boulevard
- Airport Boulevard from Century West Boulevard to Manchester Avenue
- Aviation Boulevard from West 120th Street to Manchester Avenue
- Century West Boulevard from Sepulveda Boulevard to Inglewood Avenue
- Douglas Street from Mariposa Avenue to Imperial Highway
- Imperial Highway from Pershing Avenue to Inglewood Avenue
- Inglewood Avenue from Imperial Highway to Manchester Avenue
- La Tijera Boulevard from Lincoln Boulevard to Sepulveda Boulevard
- Lincoln Boulevard from Manchester Avenue to Sepulveda Boulevard
- Manchester Avenue from Pershing Drive to Inglewood Avenue
- Mariposa Avenue from Sepulveda Boulevard to Douglas Street
- Nash Street from Mariposa Avenue to Imperial Highway
- Pershing Drive from Imperial Highway to Manchester Avenue
- Sepulveda Boulevard from Mariposa Avenue to Manchester Avenue
- West 120th Street from Aviation Boulevard to Inglewood Avenue
- Westchester Parkway from Pershing Avenue to Inglewood Avenue

Each roadway was separated into link segments from one major (or signalized) intersection to the next major intersection to represent an individual roadway portion. For example, Airport Boulevard was separated into four segments: 1) from Century West Boulevard to 98th Street, 2) from 98th to 96th Street, 3) from 96th to Westchester Parkway, and 4) from Westchester Parkway to Manchester Avenue. Each of these segments was represented with different traffic conditions and characteristics such as traffic volumes, vehicle speed, roadway width, roadway coordinates, elevations, and the percentage of traffic volume associated with LAX. Emissions from vehicles driving to and from LAX on off-airport roadways are classified as airport related emissions.

Figure 8-14. Major arterial roadways within Study Area.

Traffic volumes on the off-airport roadways for this analysis were based on data collected and compiled for the LAX Specific Plan Amendment Study (SPAS) EIR (dated July 2012). The SPAS collected traffic counts at over 200 intersections with 57 of these intersections located within the Phase III Study Area. For SPAS, intersection turning movement counts were collected in July and August 2010 during the weekday morning, mid-day, and afternoon time periods; a total of three 2-hour periods. July and August are considered to be the peak months for airport-related traffic. These data were considered representative but conservative (i.e., overestimate traffic volumes) for the Summer Monitoring Season. Seasonal adjustments were made to the data to better represent the Winter Monitoring Season and lower traffic volumes.

The peak quarter hour traffic movements for each traffic direction (e.g., east, west, north, and south) at the 57 applicable intersections were used in this analysis. Table 8-20 presents the peak quarter hour traffic movements at these intersections. These cardinal direction traffic volumes were best matched with each roadway segment within the off-airport roadway network. These traffic volumes, along with the appropriate temporal profiles, allowed for the simulation of traffic volumes throughout the two seasonal measurement campaigns.

Table 8-20. Off-airport roadways peak quarter hour traffic volumes by direction from intersection

SPAS ID	North/South Roadway	East/West Roadway	East	North	West	South
6	Airport Boulevard	Westchester Parkway	345	473	311	511
7	Airport Boulevard	Century West Boulevard	1024	464	1054	66
9	Airport Boulevard	Manchester Avenue	631	317	573	424
10	Aviation Boulevard	Arbor Vitae Street	283	313	356	415
11	Inglewood Avenue	Arbor Vitae Street	281	145	296	214
13	La Cienega Boulevard	Arbor Vitae Street	291	356	264	405
14	Aviation Boulevard	Century West Boulevard	1038	635	1136	712
16	Aviation Boulevard	Imperial Highway	681	587	610	496
17	Aviation Boulevard	Manchester Avenue	552	338	716	363
19	Aviation Boulevard	111th Street	169	581	98	578
20	Aviation Boulevard	West 120th Street	160	440	49	459
35	Inglewood Avenue	Century West Boulevard	665	292	682	281
36	La Cienega Boulevard	Century West Boulevard	782	541	957	570
38	Sepulveda Boulevard	Century West Boulevard	244	1586	78	1650
39	NB I-405 Ramps	Century West Boulevard	709	58	907	430
47	Douglas Street	Imperial Highway	572	76	514	206
48	Douglas Street	Mariposa Avenue	32	369	227	448
66	Inglewood Avenue	Imperial Highway	690	558	670	522
67	La Cienega Boulevard	Imperial Highway	680	502	605	390
68	Main Street	Imperial Highway	684	6	561	485
69	Pershing Drive	Imperial Highway	533	419	269	12
71	Sepulveda Boulevard	Imperial Highway	721	1370	316	1488
72	Vista del Mar	Imperial Highway	264	384	34	516
73	Nash Street/WB I-105	Imperial Highway	501	567	525	423

SPAS ID	North/South Roadway	East/West Roadway	East	North	West	South
	Ramps					
74	I-105 Ramps/Aviation	Imperial Highway	588	146	677	395
75	I-405 NB Ramps/La Cienega	Imperial Highway	657	139	648	164
76	Inglewood Avenue	Lennox Boulevard	185	277	150	319
77	Inglewood Avenue	Manchester Avenue	560	143	593	152
89	La Cienega Boulevard	Lennox Boulevard	141	478	0	463
90	La Cienega Boulevard	Manchester Avenue	674	515	450	430
94	La Cienega Boulevard	111th Street	0	441	214	489
95	La Cienega Boulevard	West 120th Street	363	405	206	304
96	La Cienega Boulevard	SB I-405 Ramps/Century West	301	448	0	549
97	La Cienega Boulevard	SB I-405 Ramps/Century West	272	623	5	381
98	La Cienega Boulevard	SB I-405 Ramps/Imperial Highway	135	442	13	450
99	Lincoln Boulevard	La Tijera Boulevard	28	834	82	844
100	La Tijera Boulevard	Manchester Avenue	551	358	579	340
101	Sepulveda Boulevard	La Tijera Boulevard	342	936	268	981
105	Lincoln Boulevard	Manchester Avenue	394	951	379	880
108	Sepulveda Boulevard	Lincoln Boulevard	83	920	861	1830
113	Pershing Drive	Manchester Avenue	275	377	257	335
114	Sepulveda Boulevard	Manchester Avenue	544	990	557	847
115	Ash Avenue	Manchester Avenue	726	127	805	371
116	Nash Street	Mariposa Avenue	161	384	241	287
117	Sepulveda Boulevard	Mariposa Avenue	283	1381	191	1337
123	Pershing Drive	Westchester Parkway	158	308	0	393
135	Sepulveda Boulevard	Westchester Parkway	290	909	268	979
139	Sepulveda Boulevard	I-105 WB Ramps/Imperial Highway	627	2156	695	1447
141	Airport Boulevard	96th Street	79	510	161	460
142	Jenny Avenue	96th Street	163	87	205	0
143	Vicksburg Avenue	96th Street	196	220	158	69
144	Airport Boulevard	98th Street	185	511	192	461
145	Jenny Avenue	Westchester Parkway	312	36	271	82
146	Sepulveda Boulevard	Westchester Parkway	324	166	278	88
157	La Cienega Boulevard	104th Street	28	393	144	416
158	Vista del Mar	Waterview Street	19	396	0	396
159	Hindry Avenue	Manchester Avenue	554	55	552	71

To estimate airport-related emissions from motor vehicles traveling to/from the airport on nearby roadways and freeways, consideration was given to apportioning traffic (i.e., percentage of traffic related to the airport) in and around the airport area. Apportionment of roadway traffic to

airport-related activity was estimated using a gravity feed traffic model algorithm[24], assuming the airport contribution was greatest along access roads closest to the airport. The LAX traffic apportionment was based on a driver survey[25] and a license plate survey,[26] which included data for intersections and roadways within the Study Area.

A driver survey was conducted during March of 1995 as part of the LAX Master Plan EIS/EIR and includes several intersections and roadways within the Study Area. A total of 18 intersections were included in this survey. Each intersection was surveyed for two hours during the morning peak period (7:00 to 9:00) and two hours during the afternoon peak period (16:00 to 18:00). Each approach of the intersection was surveyed for 30 minutes or approximately 20 signal cycles. Drivers were queried as to whether they were going to the Airport and asked to respond with thumbs up or down. Thus, the results of the driver survey indicate the percentage of traffic associated with the airport. However, the driver survey does not include all intersections and roadways analyzed as part of the Phase III off-airport roadway network. Gaps in data were filled by using the gravity feed traffic model algorithm. Lastly, the driver survey included numerous intersections and roadways outside the Study Area; these data were used to estimate the traffic apportionment (approximately seven percent related to the airport) for local roadways.

The following information was also considered in developing the traffic apportionment:

- 2011 Airport Passenger Survey
- 2011 Los Angeles International Airport Traffic Generation Report (dated August 2011)
- Data Analysis of Vehicle License Plate Survey Results for Los Angeles International Airport Arrival Traffic (dated April 26, 2007)

The license plate survey was conducted at 13 locations during August 18, 2006 during three peak periods: 08:00 to 09:00, 11:00 to 12:00, and 17:00 to 18:00. The license plate survey used high-resolution digital video camcorders to record images of vehicle license plates passing the survey locations as a means to determine if vehicles were accessing the airport (i.e., traveling from a gateway location to an airport access location).

[24] Gravity feed traffic models assume that the traffic exchanged between locations is proportional to the volumes entering and exiting at those locations and that the traffic associated with a given source is greatest nearest the entrance and exit location of the source.

[25] LAX Master Plan EIS/EIR, Off-Airport Surface Transportation Technical Report (Section 7.3.2), dated January 2001.

[26] A license plate survey was conducted on August 18, 2006. The survey locations were at six off-airport gateway locations (such as westbound on Century West to the west of La Cienega Boulevard), two principal airport parking lot driveways, and five immediate airport access locations. The license plate survey used high-resolution digital video camcorders to record images of vehicle license plates passing the survey locations as a means to determine if vehicles were accessing the airport (i.e., traveling from a gateway location to an airport access location). Data Analysis of Vehicle License Plate Survey Results for Los Angeles International Airport Arrival Traffic, dated April 26, 2007.

The driver survey and license plate survey do not provide data for every intersection and roadway segment within the Study Area. Therefore, the traffic apportionment for roadways with data unavailable was based on a gravity feed traffic model algorithm, which assumes airport contribution was greatest along access roads closest to the airport and decreased further from the airport.

Figure 8-15 displays the relative percentage of airport-related traffic contributions for each segment of nearby roadways including: major arterials, minor arterials, and collectors within the Study Area. For example, 16 percent of motor vehicle traffic along Pershing Drive was considered airport-related; while 24 percent of the total traffic along Century West between La Cienega and Aviation; and, 6 percent of total traffic along I-405 Freeway are considered related to LAX.

8.10.1 Emission Calculation Methodology

The EMFAC2011 emissions model was used to determine emission factors for off-airport roadways. Emission factors for the off-airport roadways were determined in a manner similar to airport roadways (see Section 8.8), while considering vehicle speeds and distribution. Entrained roadway dust for the off-airport roadways was also determined in a manner similar to airport roadways (see Section 8.8). Appropriate entrained roadway dust emission factors were determined based on the four classes of roads: 1) freeways/expressways, 2) major streets/highways, 3) collector streets, and 4) local streets. For example, Century West Boulevard was considered a major street while Nash Street was considered a collector street.

The vehicle classifications for off-airport roadways were based on default classifications pertaining to Los Angeles County within the CARB EMFAC2011 emissions model. This classification displays the mixture (percentage) of vehicle type and fuel type. The EMFAC emissions model used average speed and vehicle class distribution data to produce emission factors in grams per vehicle-mile for CO, VOC, TOG, NO_x, SO_x, PM_{10}, and $PM_{2.5}$. The traffic speeds were based on data prepared for the LAX SPAS EIR (dated July 2012). The emission factors presented in Table 8-12 in Section 8.7 were also used for motor vehicles traveling on off-airport roadways.

Figure 8-15. LAX traffic apportionment. Units are in percentages.

8.10.2 Spatial Allocation

The off-airport roadways were located in the project UTM coordinate system. Performing a dispersion analysis requires the specification of x, y coordinates with associated elevations, width, and release height for each roadway. The roadway coordinates locate the roadway spatially within the network and provide information on roadway dimensions. The default width is 20 meters (65.6 feet). However, roadway-specific widths were determined based on aerial photographs and maps. The initial vertical dispersion parameter was specified as 3 meters. The roadway width determines the width of the area sources used to model the roadway. Height is the distance above the ground elevation at which emissions are released. A roadway was defined as a series of connected line segments identified by their endpoints. A roadway was designated an area source derived from the segments and the width.

8.10.3 Temporal Allocation

The SPAS traffic data only provides the peak quarter hour and peak hour values during three 2-hour periods; not for the entire day. Temporal profiles were not determined based on this data because the counts were only conducted during these periods during a single day.

Different temporal profiles were used for airport-related traffic on off-airport roadways versus non-airport related traffic on off-airport roadways. Thus, for airport-related traffic on off-airport roadways, the temporal profiles associated with the CTA (both upper and lower or arrivals and departures) were used. These traffic patterns more closely corresponded to airport-related vehicle activities for airport roadways instead of non-airport related traffic on off-airport roadways. Non-airport traffic on off-airport roadways used temporal profiles developed from short-term and 24-hour traffic counts for several of the intersections and roadways within the Study Area collected by LADOT. These data represent conditions in July and August during 2009 through 2011 and were applied to the two monitoring seasons. A composite hourly profile from all available intersections and roadways data collected by LADOT was used to determine the non-airport traffic temporal profile for off-airport roadways.

The peak hour for the airport-related traffic (based on the CTA counters) was 22:00 for the Winter Monitoring Season and 12:00 for the Summer Monitoring Season. The peak hour for the non-airport traffic (based on LADOT data) was 18:00 for both seasons.

Figure 8-16 displays the hourly operational profiles for the airport-related and non-airport related traffic for off-airport roadways. As shown, the airport-related traffic was more reflective of aircraft operations and background traffic was more reflective of the typical morning, lunchtime, and evening rush hours. Table 8-21 presents the daily operational profiles for the off-airport roadways. Weekday profiles do not show much difference between on-airport related traffic and off-airport traffic but weekend profiles show that the airport-related traffic is highest on Sunday and non-airport related traffic is highest on Saturday.

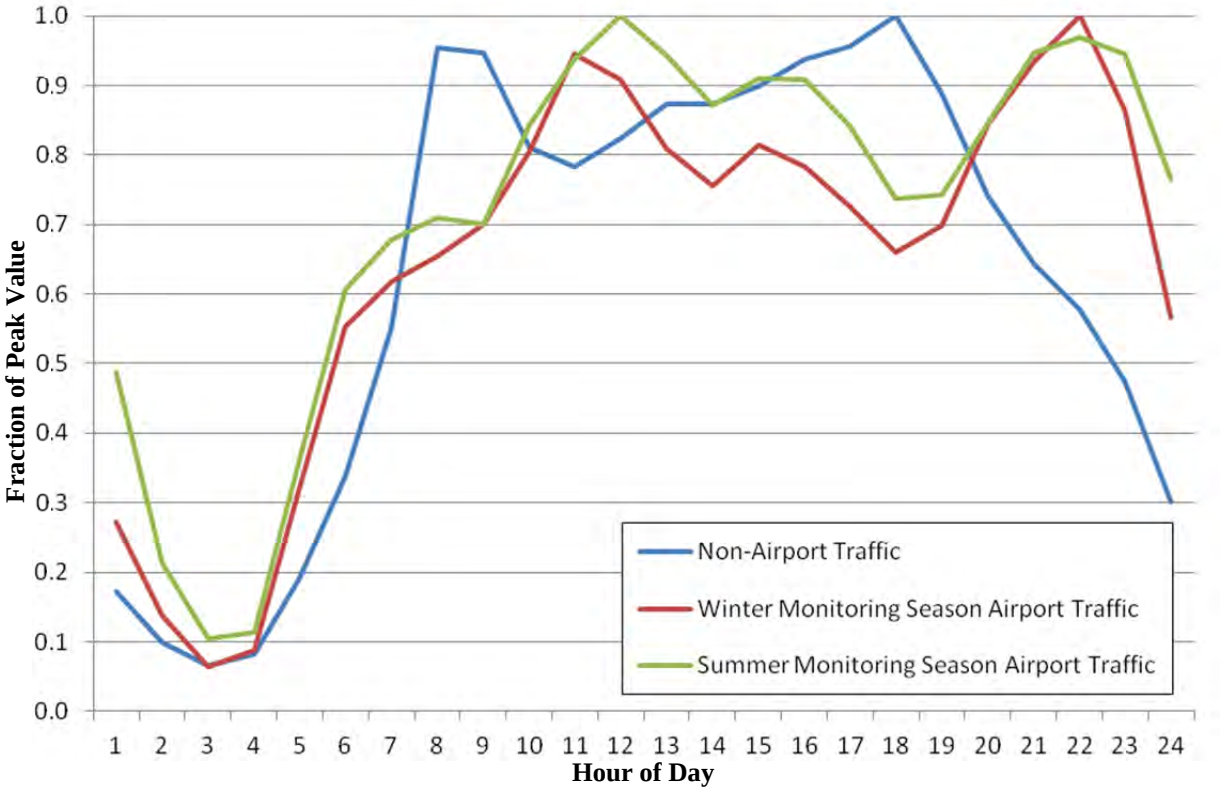

Figure 8-16. Hourly profiles of off-airport major arterial roadways (Unitless values denoted as fraction of peak values).

Table 8-21. Daily profiles of off-airport major arterial roadways

Day	Airport	Non-Airport
Winter Monitoring Season		
Monday	0.920	0.926
Tuesday	0.964	0.941
Wednesday	**1.000**	0.958
Thursday	0.919	0.978
Friday	0.923	**1.000**
Saturday	0.780	0.908
Sunday	0.892	0.788
Summer Monitoring Season		
Monday	**1.000**	0.939
Tuesday	0.924	0.950
Wednesday	0.958	0.972
Thursday	0.963	0.985
Friday	0.989	**1.000**
Saturday	0.866	0.929
Sunday	0.989	0.821

Notes: Bold values represent peak hourly period. These are unitless values representing fraction of the peak value.

8.11 FREEWAYS

The I-405 and I-105 freeways were included in the analysis as they traverse the Study Area (see Figure 8-20). Similar to off-airport roadways, each freeway was separated into segments to represent individual freeway portions from one major interchange to another. For example, the I-405 from Westchester Parkway to Manchester Avenue was designated as a freeway segment. Each segment was represented with different traffic conditions and characteristics, such as traffic volumes, vehicle speed, roadway width, roadway coordinates, elevations, and the percentage of traffic volume related to LAX. Traffic apportionment along the I-405 and I-105 were based on driver survey data at intersections of freeway ramps with roadways, which provide key access to LAX (such as Century West Boulevard).

8.11.1 Emission Calculation Methodology

CalTrans Performance Measurement System (PeMS)[27] was used to obtain traffic volumes for portions of the I-405 and I-105 freeways within the Study Area. The traffic data within PeMS is collected in real-time from over 25,000 individual detectors throughout California. These sensors span the freeway system across all major metropolitan areas of the state including the I-405 and I-105 freeways within the Study Area. PeMS provides hourly traffic counts and time series data for each day of the week during the measurement campaigns.

The EMFAC2011 emissions model was used to determine emission factors. Exhaust emission factors for freeways were determined in a manner similar to off-airport roadways (see Section 8.11) and considered vehicle speeds. Entrained roadway dust for the freeways was also determined in a manner similar to off-airport roadways (see Section 8.11). Appropriate entrained roadway dust emission factors were determined based on the freeways/expressways roadway type.

The vehicle classifications for freeways were based on default classifications pertaining to Los Angeles County within the EMFAC2011 emissions model. This classification displays the mixture (percentage) of vehicle and fuel types. The EMFAC2011 emissions model used average speed and vehicle class distribution data to produce emission factors in grams per vehicle-mile for CO, VOC, TOG, NO_x, SO_x, PM_{10}, and $PM_{2.5}$. The emission factors for motor vehicles are listed in Table 8-12.

Apportioning traffic in and around the airport area was carried out to estimate airport-related emissions from motor vehicles while traveling on freeways to and from the airport. Apportionment of roadway traffic to airport-related activity was estimated in a manner similar to off-airport roadways. SPAS gathered data at intersections between freeway ramps and arterial roadways with access to the airport but did not conduct traffic counts on the freeways (see Table 8-20). SPAS traffic counts for the freeway ramps and arterial roadways, along with its assigned airport-related apportionment based on the driver survey and a license plate survey, were compared to freeway counts within PeMS to determine an apportionment of airport-related traffic on the freeways. The percentage of the ramp traffic and the resultant ramp volumes were compared to the total freeway traffic and the difference was considered through traffic (i.e., non-

[27] California Department of Transportation Performance Measurement System, http://pems.dot.ca.gov/

airport related traffic). As shown in Figure 8-15, the airport apportionment for the I-405 was determined to be 6 percent and for the I-105 was determined to be 11 percent.

8.11.2 Spatial Allocation

The freeways were located in the project UTM coordinate system. Performing a dispersion analysis requires the specification of x, y coordinates with associated elevations, width, and release height for each roadway. The roadway coordinates locate the roadway spatially in the airport configuration and provide information on roadway dimensions. The default width is 20 meters (65.6 feet). However, roadway-specific widths were determined based on aerial photographs and maps. The initial vertical dispersion parameter was specified as 3 meters. The roadway width determines the width of the area sources used to model the roadway. Height is the distance above the ground elevation at which emissions are released. A roadway is defined as a series of connected line segments, which are identified by their endpoints. A roadway was designated an area source derived from the segments and the width.

8.11.3 Temporal Allocation

As with the off-airport roadways, for airport-related traffic within freeways, the temporal profiles associated with the CTA were used. Again, these traffic patterns more closely correspond to airport-related vehicle activities. Non-airport traffic on freeways used temporal profiles developed from data collected within the PeMS, which allows for the determination of temporal profiles for each traffic direction (e.g., northbound and southbound on the I-405 freeway).

The peak hour for the non-airport traffic on the freeways was between 15:00 and 17:00 depending on freeway location.

Figure 8-17 displays the hourly operational profiles (unitless values representing fraction of the peak value) for the freeways. As shown, these data were reflective of the typical morning and evening rush hours. Table 8-22 presents the daily (day of the week) operational profiles for the freeways. The peak traffic day of the week was Friday for each freeway segment and all directions of traffic for each measurement campaign and Sunday had the lowest daily traffic volume. The non-airport freeway traffic was reflective of typical background traffic patterns in urban areas while the airport-related traffic was reflective of airport operations (using the CTA temporal profiles).

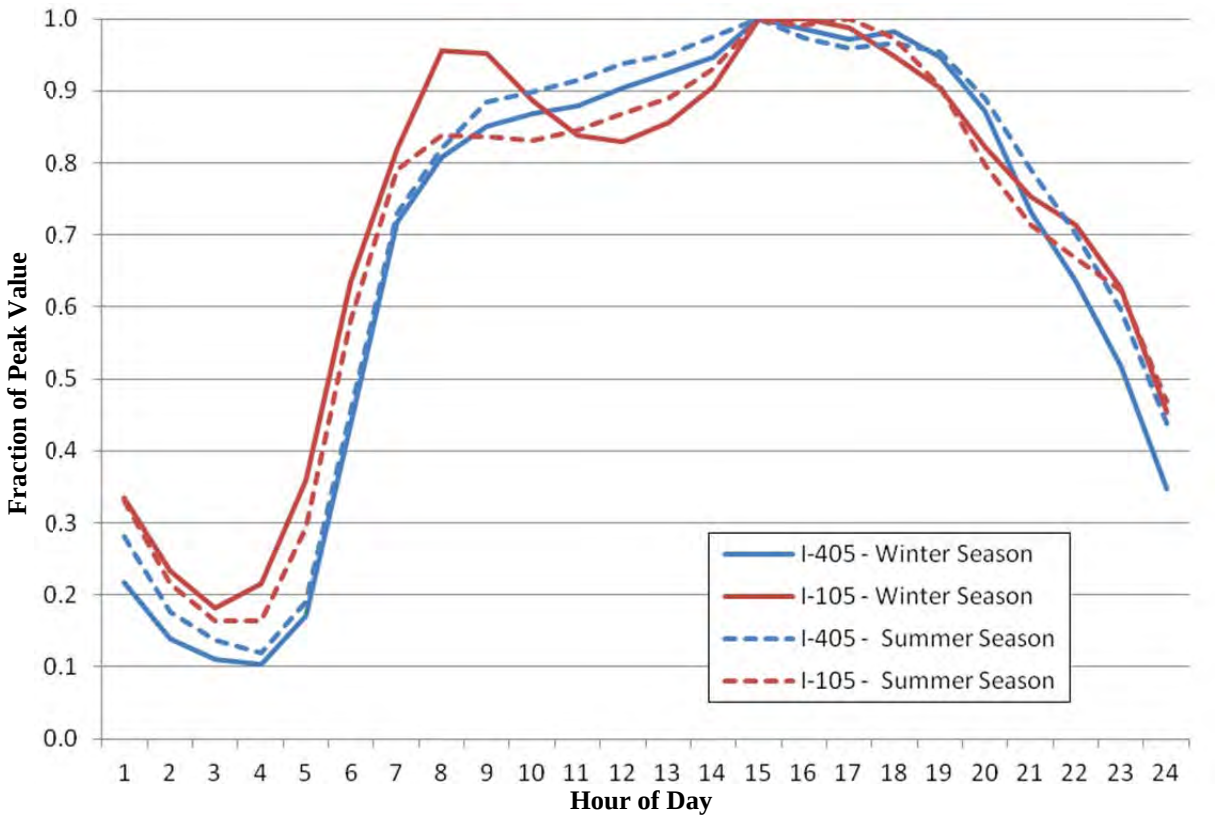

Figure 8-17. Hourly traffic profiles for the I-405 and I-105 freeways (Unitless values denoted as fraction of peak values).

Table 8-22. Daily Traffic Profiles for Freeways

Day	I-405S	I-405N	I-405 (North and South)	I-105E	I-105W	I-105 (North and South)
Winter Monitoring Season						
Monday	0.917	0.937	0.927	0.926	0.924	0.925
Tuesday	0.934	0.949	0.941	0.943	0.936	0.939
Wednesday	0.957	0.963	0.960	0.951	0.951	0.951
Thursday	0.975	0.981	0.978	0.979	0.974	0.977
Friday	**1.000**	**1.000**	**1.000**	**1.000**	**1.000**	**1.000**
Saturday	0.913	0.908	0.910	0.918	0.882	0.899
Sunday	0.778	0.798	0.788	0.801	0.775	0.787
Summer Monitoring Season						
Monday	0.933	0.947	0.940	0.937	0.936	0.936
Tuesday	0.942	0.956	0.949	0.954	0.954	0.954
Wednesday	0.969	0.976	0.972	0.967	0.973	0.970
Thursday	0.982	0.989	0.986	0.983	0.978	0.980
Friday	**1.000**	**1.000**	**1.000**	**1.000**	**1.000**	**1.000**
Saturday	0.926	0.930	0.928	0.937	0.905	0.921
Sunday	0.810	0.839	0.824	0.815	0.799	0.807

Note: Bold values represent peak hourly period. Unitless values representing fraction of the peak value.

8.12 MAJOR STATIONARY SOURCES

There are a total of 18 stationary sources within the Study Area not owned or operated by LAX, four of which are located on airport property and are associated with airline operations. The emissions associated with these airline operations were included as airport-related emissions. The 18 sources were included in the analysis based on their inclusion in the SCAQMD Facility Information Detail (FIND) database.[28] FIND is a database of SCAQMD-regulated facilities, which are required to have a permit to operate equipment emitting pollutants into the air. The FIND database reports annual emissions based on annual facility reporting requirements. The latest available data are for 2011.

The 18 facilities include: Chevron El Segundo Refinery, Scattergood Generating Station, El Segundo Energy Center, So Cal Gas Playa Vista, Delta Airlines, Garrett Aviation, Continental Airlines, United Airlines, Boeing Systems, Northrop Grumman, and others. These facilities include such sources as boilers, generators, processing units, reformers, painting operations, and other emissions sources. While some of these sources are located within the Airport boundary, a majority are located beyond the boundary. The locations for these major stationary sources are found in Figure 8-18. The list of major stationary sources included in the analysis can be found in Table 8-23.

8.12.1 Emission Calculation Methodology

Emissions for the majority of the off-airport and tenant stationary sources were based on the reported values within the FIND database and scaled to represent the duration of the measurement campaigns. Three facilities (Chevron El Segundo Refinery, Scattergood Generating Station, and El Segundo Energy Center) are also required to provide CEMs of hourly emissions to SCAQMD and U.S. EPA on a periodic basis. CEMs data for Chevron El Segundo Refinery, Scattergood Generating Station, and El Segundo Energy Center were provided by the specific facility and through the U.S. EPA Air Markets Program Data tool.[29] Similar to the CEMs for the LAX turbines, the CEMs for the stationary sources measure hourly parameters such as SO_x and NO_x emissions, steam load, and heat input. Emissions of CO, VOC, TOG, PM_{10}, and $PM_{2.5}$ were estimated as a function of the reported annual values within FIND and assumed to vary in a manner similar to the hourly heat input. The Chevron El Segundo Refinery includes combustion sources and fugitive sources.

[28] SCAQMD Facility Information Detail, http://www.aqmd.gov/webappl/fim/default.htm
[29] U.S. EPA Air Markets Program Data tool, http://ampd.epa.gov/ampd/QueryToolie.html

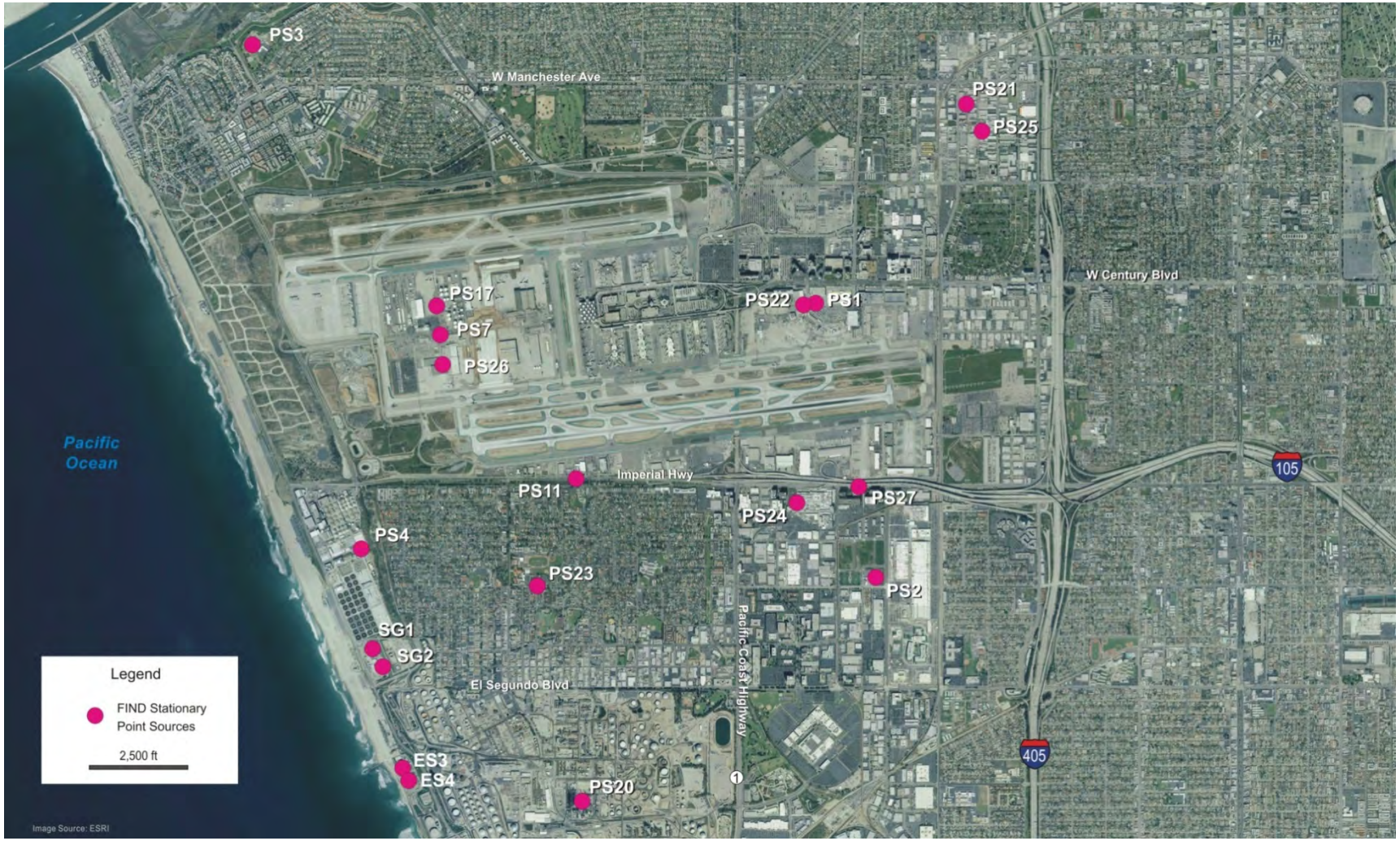

Figure 8-18. Airport tenant and non-airport major stationary sources. (See Table 8-23 for source identification)

Table 8-23 presents the reported 2011 annual emissions for the off-airport stationary sources within the Study Area. For many of these sources, the annual emissions were scaled to represent the monitoring seasons. Actual monitored emissions from the measurement campaign periods were used for the Chevron El Segundo Refinery, Scattergood Generating Station, and El Segundo Energy Center. Although these sources (as well as marine sources) are often located downwind or crosswind of LAX, these sources potentially contribute to the pollutants impacts within the Study Area and thus were included in the emission inventory.

Table 8-23. Off-airport stationary source annual emissions for 2011 (tons)

ID	Source Type	CO	VOC	NO_x	SO_x	TSP
ES3&4	El Segundo Energy Center	107	7.12	10.8	0.76	9.65
SG1&2	Scattergood Generating Station	409	50.6	52.0	41.7	29.9
PS1	United Airlines	6.94	3.12	11.4	0.01	1.22
PS2	Northrop Grumman	5.59	27.3	8.89	0.07	0.82
PS3	So Cal Gas/Playa Del Rey	1.08	16.8	21.4	0.02	0.95
PS4	Los Angeles Sanitation Bureau	1.79	19.9	2.43	0.01	2.88
PS7	American Airlines	1.69	6.64	3.60	0.05	1.75
PS11	Garrett Aviation Services	1.15	0.55	1.53	0.06	0.08
PS20A	Air Liquide	4.36	14.3	18.3	0.85	3.28
PS20B	Chevron El Segundo Refinery	753	542	628	367	208
PS21	Rho-Chem	0.02	0.01	0.03	-	0.01
PS22	Delta Airlines	0.54	0.24	1.87	0.03	0.13
PS23	Glentek Inc	0.01	0.02	0.01	-	-
PS24	Boeing Satellite Systems	8.06	4.16	4.71	0.06	1.00
PS25	Multichrome/Microplate	0.14	0.12	0.22	0.11	0.12
PS26	Continental Airlines	0.04	1.62	0.19	-	0.01
PS27	Boeing Satellite Systems	1.35	0.31	1.70	0.01	0.11

8.12.2 Spatial Allocation

The off-airport major stationary sources were located in the project UTM coordinate system. Performing a dispersion analysis requires the specification of x, y coordinates with associated elevations and source release parameters (such as stack height, diameter, exit velocity, and exit temperature). These data were obtained from operating permits (for Chevron El Segundo Refinery, Scattergood Generating Station, and the El Segundo Energy Center). Stationary sources were treated as point sources. Table 8-24 displays the off-airport stationary source release parameters. There are also numerous fugitive sources at the Chevron El Segundo Refinery which were represented as a surface-based source with ambient release conditions and minimal momentum. Table 8-25 displays the stationary sources release parameters for the Chevron El Segundo Refinery, which are based on the Title V Operating Permits.

Table 8-24. Off-airport stationary source exhaust release parameters

ID	Source Type	Height (m)	Temperature (K)	Velocity (m/s)	Diameter (m)
ES3	El Segundo Energy Center (Unit 3)	65.6	391	15.4	6.45
ES4	El Segundo Energy Center (Unit 4)	65.6	391	15.4	6.45
SG1	Scattergood Generating Station (Units 1 and 2)	91.4	419	16.9	6.10
SG2	Scattergood Generating Station (Unit 3)	101	406	13.5	7.16
PS1	United Airlines	9	500	20	0.5
PS2	Northrop Grumman	12	330	4	2
PS3	So Cal Gas/Playa Del Rey Storage Facility	12	600	20	0.7
PS4	Los Angeles Sanitation Bureau	11	330	4	2
PS7	American Airlines	9	500	20	0.5
PS11	Garrett Aviation Services	8	310	4	1
PS20A	Air Liquide	3.05	295	0	0.0009
PS20B	Chevron El Segundo Refinery	Large number of point and fugitive sources			
PS21	Rho-Chem	9	500	20	0.5
PS22	Delta Airlines	9	500	20	0.5
PS23	Glentek Inc	9	500	20	0.5
PS24	Boeing Satellite Systems	9	500	20	0.5
PS25	Multichrome/Microplate	9	500	20	0.5
PS26	Continental Airlines	9	500	20	0.5
PS27	Boeing Satellite Systems	9	500	20	0.5

Table 8-25. Chevron El Segundo Refinery stationary source exhaust release parameters

ID	Height (m)	Temperature (K)	Velocity (m/s)	Diameter (m)
82	47.2	640	8.23	3.05
83	47.2	478	5.66	2.90
84	62.8	516	1.74	3.72
115	29.6	644	1.16	4.11
159	44.4	550	14.1	2.15
160	44.2	551	12.7	2.13
161	44.2	551	12.7	2.13
328	45.1	589	12.1	4.27
389	31.1	745	0.85	1.33
390	30.5	866	2.22	1.32
398	31.0	715	1.33	1.28
428	46.6	745	4.08	1.22
451	50.0	450	2.42	2.29
453	24.7	616	6.04	1.37
466	55.2	616	12.7	1.31
467	36.3	599	3.87	1.36
468	55.2	616	12.5	1.31
471	36.7	647	8.15	2.59
472	36.6	576	1.98	2.59
473	36.6	576	1.98	2.59

ID	Height (m)	Temperature (K)	Velocity (m/s)	Diameter (m)
502	25.0	489	3.23	1.37
504	25.0	664	2.01	1.41
580	35.7	516	2.72	1.55
583	35.4	570	7.76	1.54
614	35.4	570	7.76	1.54
615	35.4	570	7.76	1.54
617	35.1	566	5.12	1.89
618	35.1	566	5.12	1.89
619	35.1	566	5.12	1.89
620	35.1	566	5.12	1.89
623	39.3	560	1.63	1.91
625	39.3	560	1.28	1.91
641	51.8	544	5.12	3.84
643	54.8	583	2.69	3.92
1698	28.4	316	12.2	0.58
1767	28.4	316	12.2	0.58
1781	28.4	316	12.2	0.58
1795	28.4	316	12.2	0.58
1805	28.4	316	12.2	0.58
1822	28.4	316	12.2	0.58
3031	36.6	576	1.98	2.59

8.12.3 Temporal Allocation

Most of the stationary sources do not provide enough information to develop temporal profiles and were therefore assumed to operate at a constant and continuous rate. The exceptions are the hourly emissions for Chevron El Segundo Refinery, and El Segundo Energy Center, and Scattergood Generating Station, which used data from the CEMs.

8.13 MINOR ROADWAYS, AGGREGATE STATIONARY SOURCES, AREAWIDE SOURCES, AND OFF-ROAD EQUIPMENT

The CARB Community Health Air Pollution Information System (CHAPIS)[30] was used to estimate emissions from a wide variety of miscellaneous sources for which data are more generalized and the variety of sources are numerous and spread out geographically over the entire Study Area. CHAPIS provides emissions data on one-kilometer by one-kilometer grid cells for the following sources:

- *Minor Roadways* – minor arterial and local roadways.
- *Aggregated Stationary Source* – small industrial facilities and businesses.
- *Area-wide Sources* – widely dispersed sources, such as the use of consumer products (hairspray, home automotive products, home cleaners, etc.) and other dispersed solvent uses, such as painting.
- *Off-road Equipment* – non-road mobile sources, such as construction equipment, trains and lawn mowers.

Any one-kilometer grid cell, which is located within the Study Area, was included in the emissions inventory. Figure 8-19 displays the one-kilometer by one-kilometer CHAPIS grid cells. CHAPIS provides emission estimates of CO, ROG, NO_x, SO_x, and PM_{10} for each of the grid cells and is representative of 2001 conditions, which were adjusted to better reflect 2012 conditions. Although a portion of the CHAPIS emissions may be double counting emissions from previously described sources, care was taken to limit this condition (e.g., some CHAPIS emissions within the LAX boundary were not included as these emissions are fully represented by the GSE emissions).

8.13.1 Emission Calculation Methodology

Minor roadways, off-road equipment, area-wide, and aggregated stationary source emissions were obtained from CARB's CHAPIS database (i.e., one-kilometer grid square system). A number of adjustments were made to the CHAPIS emission estimates to better reflect the monitoring season's conditions. First, the CHAPIS data were adjusted from 2001 to 2012 using linear interpolation of the CARB emissions estimates for Los Angeles County for 2000 and 2010.[31] Grid cells located within airport property were assigned as airport-related sources, while grid cells outside airport property were assigned as non-airport sources. Off-road equipment emissions located within airport property were not used, as these emissions are more appropriately captured by APU and GSE data. Vehicle traffic on the minor roadways (both on and off-airport) was apportioned as seven percent attributed to LAX based on traffic surveys for the region.

[30]CARB Community Health Air Pollution Information System, http://www.arb.ca.gov/ch/chapis1/chapis1.htm

[31] California Emissions Inventory and Reporting Data, http://www.arb.ca.gov/ei/emissiondata.htm

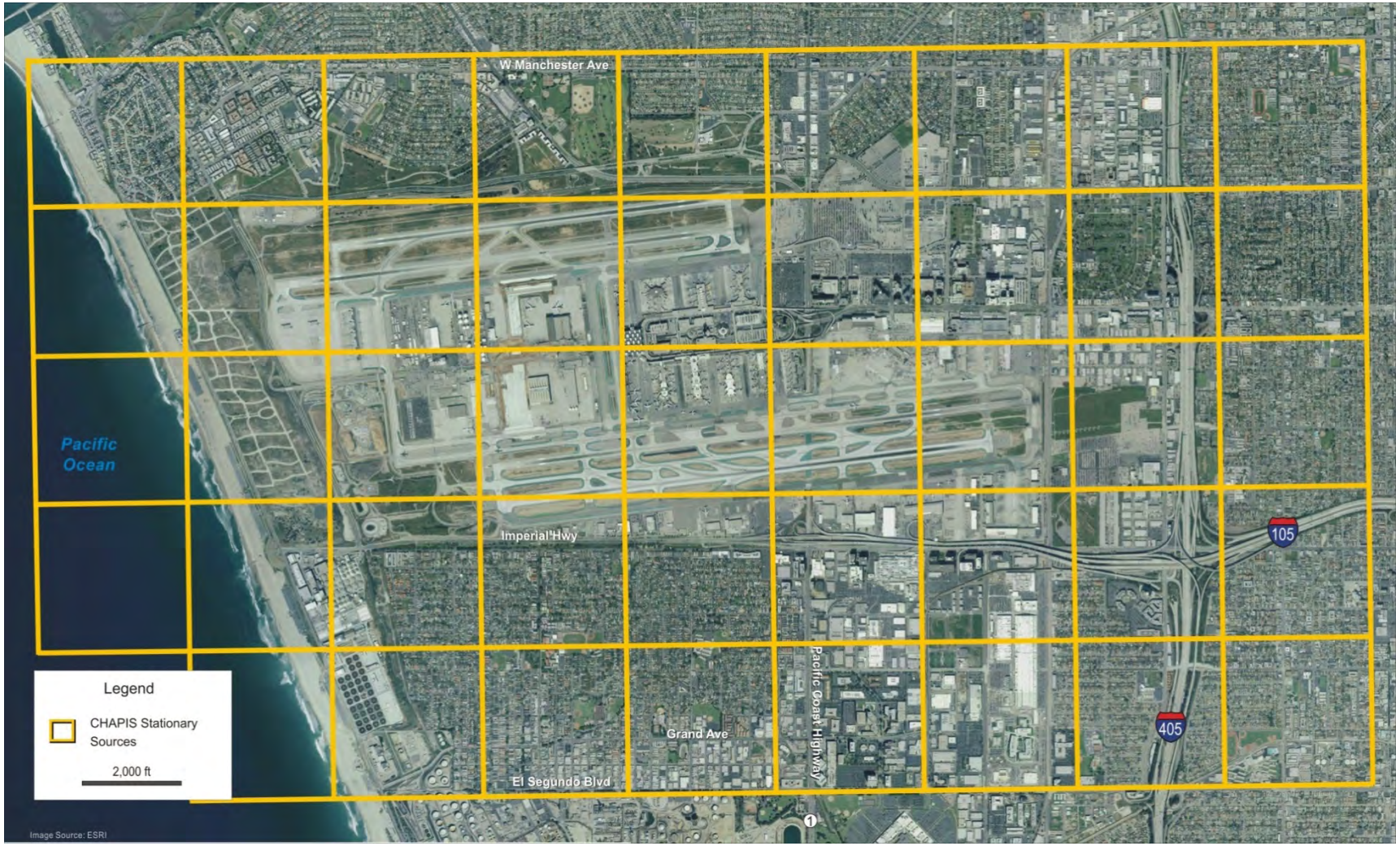

Figure 8-19. Grid cells for Minor roadways, aggregate stationary sources, area-wide sources, and off-road equipment.

The California Emission Inventory Data and Reporting System (CEIDERS) was used to develop conversion factors to estimate $PM_{2.5}$ as a function of PM_{10} emissions because CHAPIS does not provide $PM_{2.5}$ emission estimates. TOG emissions were estimated as a function of CHAPIS-reported ROG emissions using a conversion factor also based on the CEIDERS. Table 8-26 presents the conversion factors used to derive $PM_{2.5}$ as a function of PM_{10} emissions and TOG emissions as a function of ROG emissions. The $PM_{2.5}/PM_{10}$ ratio represents exhaust emissions only.

Table 8-26. CHAPIS Pollutant Conversion Factors

Pollutants	On-road Vehicles	Area-wide	Aggregate Sources	Off-road Equipment
$PM_{2.5}/PM_{10}$	0.73	0.23	0.39	0.90
TOG/ROG	1.24	1.53	1.13	1.10

8.13.2 Spatial Allocation

CHAPIS grid cells were located in the project UTM coordinate system within the one-kilometer grid square system. The CHAPIS grids were treated as area sources. The initial vertical dispersion parameter was specified as 1.4 meters. A height of 3 meters was used.

8.13.3 Temporal Allocation

Hourly temporal factors for area-wide, aggregated stationary sources, and off-road equipment were based on Profile 26 within U.S. EPA's Emissions Modeling Clearinghouse Temporal Allocation (dated February 2005).[32] Hourly temporal factors for minor roadways were based on CARB's EMFAC2011 emissions model. Table 8-27 presents the hourly profiles for the CHAPIS sources. Daily temporal profiles were assumed not to vary.

[32] U.S. EPA Emissions Modeling Clearinghouse Temporal Allocation http://www.epa.gov/ttnchie1/emch/temporal/,

Table 8-27. Hourly profiles of CHAPIS sources

Hour	Onroad Vehicles	Area-wide	Aggregate Sources	Off-road Equipment
1	0.146	0.312	0.312	0.312
2	0.055	0.293	0.293	0.293
3	0.062	0.287	0.287	0.287
4	0.040	0.295	0.295	0.295
5	0.066	0.331	0.331	0.331
6	0.120	0.394	0.394	0.394
7	0.469	0.490	0.490	0.490
8	0.947	0.611	0.611	0.611
9	0.881	0.735	0.735	0.735
10	0.550	0.832	0.832	0.832
11	0.582	0.899	0.899	0.899
12	0.730	0.951	0.951	0.951
13	0.757	0.976	0.976	0.976
14	0.746	0.994	0.994	0.994
15	0.859	**1.000**	**1.000**	**1.000**
16	0.875	0.983	0.983	0.983
17	0.916	0.935	0.935	0.935
18	**1.000**	0.863	0.863	0.863
19	0.695	0.836	0.836	0.836
20	0.520	0.802	0.802	0.802
21	0.399	0.669	0.669	0.669
22	0.404	0.515	0.515	0.515
23	0.301	0.405	0.405	0.405
24	0.229	0.343	0.343	0.343

Note: Bold values represent peak hourly period. Unitless values representing fraction of the peak value.

8.14 MARINE SOURCES

Marine sources are represented by marine vessels within coastal waters west of LAX. Cargo handling, hotelling, and harborcraft emissions associated with operations at the Port of Los Angeles and Port of Long Beach were not included in this analysis as these facilities are well beyond the Study Area. Marine vessel transit within coastal waters may include vessels moving within or through the area or arriving/departing a specific port. Figure 8-20 displays the marine vessel points for which emissions were determined. These points represent points along specific shipping lanes. For this analysis, shipping lane links were limited to the lanes north of Point Vicente, south of the extended Los Angeles County border, and east of the Channel Islands. This area and shipping lanes represents the offshore area associated with the South Coast Air Basin, although marines sources would be expected to have minimal air quality impacts within the Study Area.

Marine vessels periodically spend time positioned at the El Segundo buoys (located offshore to the west of LAX), and transit via the Eastern, Northern, and Western shipping lanes. The El Segundo buoys are denoted as ELSEGUN and ELSEGUS in Figure 8-20. The Eastern route is denoted as passing by locations denoted as S42, S43, and S44. The Western route is denoted as passing by locations denoted as S564, S816, S92, and S408. The Northern route is separated into two portions: the arrival on the northern side of the Coast Guard Separation Zone and the departure on the southern side of the Coast Guard Separation Zone. The arrival Northern route is denoted as passing by locations denoted as S287, S404, and S403. The departure Northern route is denoted as passing by locations denoted as S285 and S405.

Although the marine sources represent a significant contribution to the Study Area emissions (i.e., 31 percent of SO_2, 15 percent of $PM_{2.5}$, and 40 percent of NO_x), their contribution to the concentration impacts within the Study Area are much less significant (See Section 9) due to the distance from the sources to the monitoring stations. Notably, marine vessel emissions of SO_x and $PM_{2.5}$ have decreased significantly during the past seven years with the regulatory requirement of lower sulfur fuels usage.

Figure 8-20. Marine sources off the coast of Los Angeles County.

8.14.1 Emission Calculation Methodology

CARB has developed an emission model for marine vessels, providing each marine source with an Access database containing updated emissions information. The marine vessel emissions were developed based on CARB output from the Marine Emissions Model (dated May 2011)[33]. For a baseline year of 2006, the Marine Emissions Model produces daily emissions by specific shipping lane links for CO, NO_x, ROG, SO_x, and $PM_{2.5}$. Emissions of TOG, VOC, and PM_{10} were estimated based on available conversion factors. Emissions are calculated by multiplying the emission factors by vessel-specific activity parameters, such as number of vessel calls, horsepower, operating load, hours of operation, and fuel sulfur content and are characterized by the activities of marine vessels (e.g., vessel transit, reduce speed zone, maneuvering, and hotelling activities for propulsion engines, auxiliary engines, and auxiliary boilers). The Marine Emissions Model also estimates, based on forecasted information, the 2012 annual emissions for marine vessels at specific shipping lane links. These 2012 annual emissions were used in the emissions inventory and scaled to reflect the durations of the measurement campaigns. Table 8-28 displays the estimated annual emissions during 2012 for the marine vessel locations included in the analysis. A majority of the emissions (except the El Segundo buoys, located about one mile offshore) are within shipping lanes which are located 20 to 40 miles offshore and would be expected to have minimal air quality impacts within the Study Area.

Table 8-28. 2012 Annual marine vessel emissions (tons)

Location	CO	VOC	TOG	NO_x	SO_x	PM_{10}	$PM_{2.5}$
ELSEGUS	8.07	3.40	4.96	90.1	26.7	3.26	3.14
ELSEGUN	8.07	3.40	4.96	90.1	26.7	3.26	3.14
S285	143	65.4	83.1	1,508	31.8	24.1	23.5
S287	125	56.8	72.2	1,318	27.8	21.0	20.4
S403	45.4	20.9	26.6	464	9.82	7.56	7.36
S404	13.2	6.05	7.71	134	2.85	2.19	2.13
S405	15.6	7.23	9.21	160	3.40	2.62	2.55
S408	2.90	1.29	1.65	33.9	0.73	0.53	0.51
S42	2.86	1.24	1.58	36.0	0.76	0.53	0.52
S43	2.22	0.97	1.24	28.2	0.60	0.42	0.41
S44	0.01	0.00	0.00	0.07	0.00	0.00	0.00
S564	6.93	2.97	3.77	89.0	53.7	7.63	7.44
S816	15.0	6.41	8.15	192	116	16.5	16.1
S92	15.6	6.67	8.51	183	4.08	2.90	2.83
Total	**404**	**183**	**234**	**4,327**	**305**	**92.4**	**90.0**

[33] Marine Emissions Model, http://www.arb.ca.gov/msei/categories.htm#offroad_motor_vehicles

The Port of Los Angeles and the Port of Long Beach conduct an annual emissions inventory to estimate emissions associated with activity levels at each Port. The inventories include: ocean-going vessels, harbor craft, cargo handling equipment, locomotives, and heavy-duty vehicles[34] associated with activities at the two Ports and within transit (along shipping lanes to the Ports). The most recent published emissions inventories are for 2011 activities.[35]

Although the Ports' emissions inventories for 2012 are currently under development, a preliminary estimate of the two Port's 2012 emissions associated with marine vessels within the pertinent shipping lanes was compared to the CARB Marine Emissions Model data. Notably, the Ports' emissions inventories do not include data associated with activities at the El Segundo buoys nor do the inventories include activities for marine vessels which are not associated with the Ports. The comparison with the Ports' emissions inventories and the CARB Marine Emissions Model found that the use of the CARB Marine Emissions Model data was appropriate, reasonable, and comprehensive in its representation of the marine vessel emissions during the measurement campaigns.

8.14.2 Spatial Allocation

Marine emissions were selected based on proximity to the Study Area. The locations of marine vessels include the El Segundo buoys as well as a select number of shipping lanes nearest the Study Area out to 24 nautical miles from the shoreline (defined as in-state for regulatory purposes). Marine vessels in open waters are simulated with a release height of 50 meters and an initial vertical dimension of 23.3 meters. For the Study, marine sources were initially analyzed as line sources, within open waters, and point sources at the buoy locations. Subsequent to review of initial results, all marine sources were modeled as point sources. Model parameters[36] for marine vessels in hotelling conditions at the El Segundo buoys include: stack height, diameter, exhaust temperature, and exhaust exit velocity as shown in Table 8-29.

Table 8-29. Marine vessels emission parameters at El Segundo Buoys

Height (m)	Temperature (K)	Velocity (m/s)	Diameter (m)
37.6	495	25.8	2.01

8.14.3 Temporal Allocation

Temporal factors were used to describe the relationship of activity levels in one period of time to another (i.e., the relationship of the activity during one-hour to the activity during a 24-hour

[34] Cargo handling, hotelling, locomotives, and harborcraft emissions associated with operations at the Port of Los Angeles and Port of Long Beach were not included in this analysis as these facilities are well beyond the Study Area.

[35] Starcrest Consulting Group, LLC, Port of Los Angeles Inventory of Air Emissions – 2011, July 2012, http://www.portoflosangeles.org/environment/studies_reports.asp and Starcrest Consulting Group, LLC, Port of Long Beach Air Emissions Inventory - 2011, July 2012, http://www.polb.com/environment/air/emissions.asp

[36] California Air Resources Board, Diesel Particulate Matter Exposure Assessment Study for the Ports of Los Angeles and Long Beach, April 2006.

period). The use of temporal factors gives dispersion modeling the ability to more accurately reflect real world conditions. For marine vessels, there was assumed to be no difference in emissions from one day to the next; however, hourly emissions varied such that 80 percent of the emissions occur between 04:00 and 20:00 and the remaining 20 percent occur between 20:00 and 04:00. [37]

[37] California Air Resources Board, Diesel Particulate Matter Exposure Assessment Study for the Ports of Los Angeles and Long Beach, April 2006.

8.15 RESULTS

As previously stated, airport-related emission sources include: aircraft, APU, GSE, airport stationary sources (i.e., generators, cogeneration units, boilers, cooling towers, and fuel storage), parking facilities, airport-related motor vehicles traveling to/from the airport on nearby off-airport roadways and freeways as well as on roadways within the LAX property, aggregate stationary sources, and area-wide sources. Figure 8-21 shows the relative percentage of airport-related traffic contributions for each segment of nearby off-airport roadways (including major arterials, minor arterials, collectors, and local) and freeways within the Study Area.

For example, 16 percent of motor vehicle traffic along Pershing Drive (along the western edge of the airport) was considered airport-related; while, between 17 and 47 percent of traffic along Aviation Boulevard was considered airport-related, and 100 percent of the Central Terminal Area was considered airport-related. Of note, traffic volumes along local roadways within the Study Area are represented as seven percent airport-related traffic. Although these roadways have lower volumes, they are more numerous and thus, were an important subset of traffic emissions. Traffic apportionment for freeways was estimated based on survey data for a number of freeway exit/entrance ramps and was estimated at 6 percent as airport-related.

8.15.1 Airport Sources

Airport sources include aircraft operations, APU, GSE, motor vehicles traveling along on-airport roadways, freeways, and within parking facilities, fuel storage tanks, LAWA and tenant operated stationary sources such as boilers, turbines, generators, and cooling towers, as well as aggregate stationary sources[38] and area wide sources[39] located on the airport property.

8.15.1.1 Winter Monitoring Season

The airport-related emissions inventory for the Winter Monitoring Season is summarized in Table 8-30. Airport-related emissions totaled: 709 tons of CO, 85.3 tons of VOC, 93.4 tons of TOG, 499 tons of NO_x, 32 tons of SO_x, 30 tons of PM_{10}, and 18 tons of $PM_{2.5}$.

Figure 8-22 through Figure 8-26 show the results of emission percentage and source contribution for the Winter Monitoring Season. Aircraft emissions represent the largest source of VOC, TOG, NO_x, and SO_x among the various airport-related source groups. GSE, airport roadways, and stationary sources comprise the largest airport-related emission sources for CO, PM_{10}, and $PM_{2.5}$, respectively. Aircraft operations account for CO (32 percent), VOC (49 percent), TOG (45 percent), NO_x (72 percent), SO_x (94 percent), PM_{10} (11 percent), and $PM_{2.5}$ (18 percent) of the total airport-related emissions.

[38] Aggregated stationary sources are small point sources, such as restaurants, gas stations, etc. that do not have available separate emission source data.

[39] Area-wide sources are widely dispersed sources such as the use of consumer products (hairspray, home automotive products, home cleaners, etc.) and other dispersed solvent uses, such as painting.

The airport-related traffic emissions (both on- and off-airport) comprise between 10 and 12 percent of the total traffic-related emissions within the Study Area for CO, VOC, TOG, NO_x, and SO_x and 37 to 29 percent for PM_{10} and $PM_{2.5}$, respectively.

Table 8-30. Airport-related emissions inventory (tons per period) – Winter Monitoring Season

	CO	**VOC**	**TOG**	**NO_x**	**SO_x**	**PM_{10}**	**$PM_{2.5}$**
On-airport Sources							
Aircraft	225	41.5	41.7	362	29.7	3.31	3.31
GSE	349	19.9	21.5	94.6	0.14	3.40	3.29
APU	9.50	0.83	0.83	9.25	1.27	1.34	1.34
Parking Facilities	2.20	0.21	0.27	0.63	0.01	0.23	0.07
Airport Roadways	35.5	1.68	2.14	7.01	0.07	11.1	2.90
Fuel Storage	-	2.19	2.28	-	-	-	-
Major Stationary Sources (LAWA)	7.51	0.76	1.25	3.37	0.09	4.94	4.94
Major Stationary Sources (Tenants)	1.16	1.46	1.82	2.15	0.01	0.39	0.36
Aggregate Stationary Source	3.93	6.02	6.78	2.64	0.05	0.97	0.38
Area Sources	1.18	5.05	7.71	0.68	0.01	0.36	0.08
Off-airport Sources							
Major Roadways	22.4	0.91	1.14	6.57	0.04	3.12	0.89
Freeways	6.45	0.26	0.32	2.27	0.01	0.33	0.12
Minor Roadways	45.1	4.50	5.60	8.46	0.12	0.50	0.36
Total	**709**	**85.3**	**93.4**	**499**	**31.6**	**29.9**	**18.0**

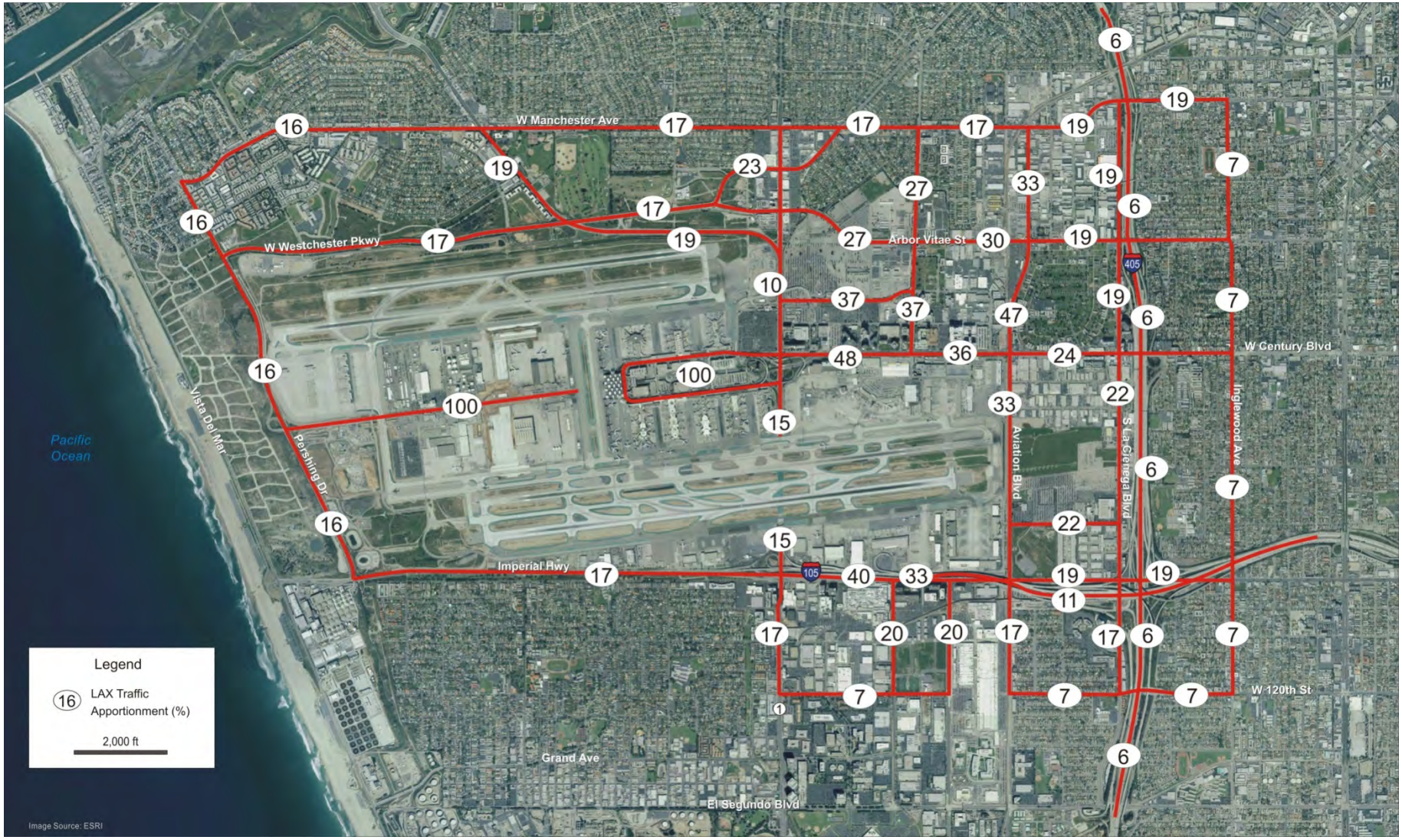

Figure 8-21. LAX traffic apportionment. Numbers listed are percent of traffic on that particular roadway that may be characterized as airport-related.

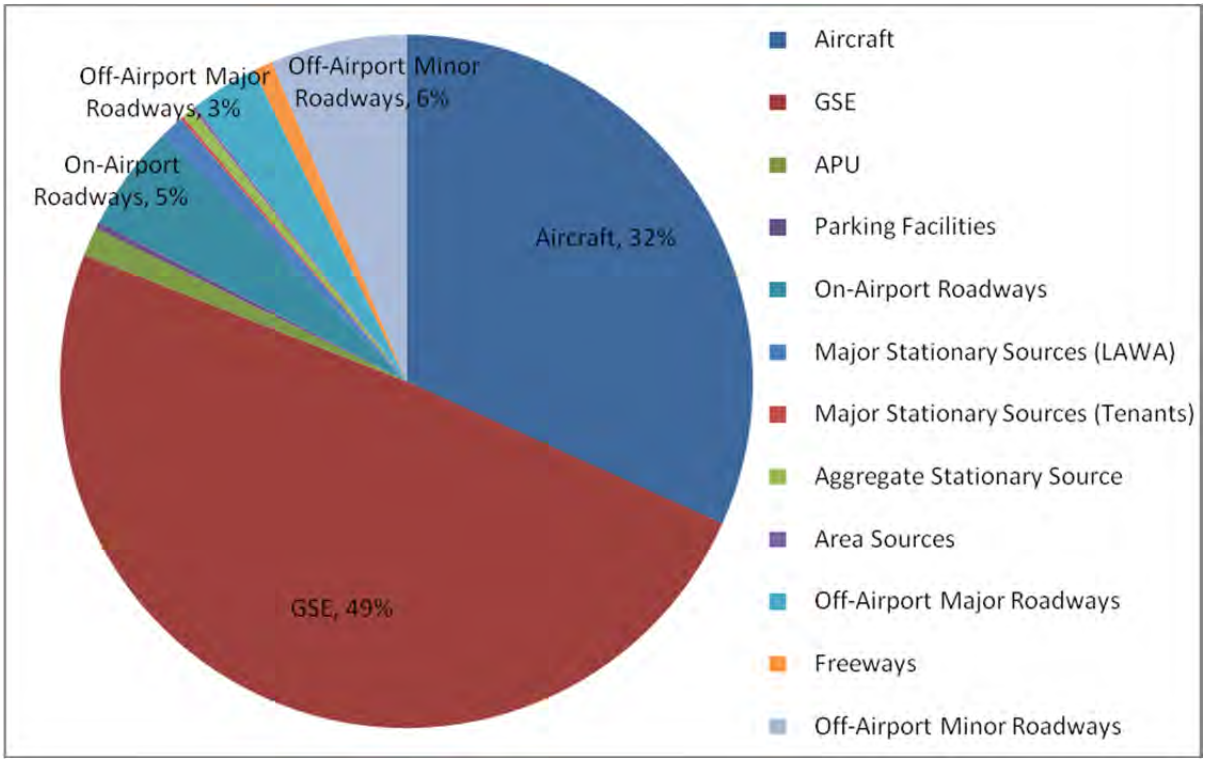

Figure 8-22. Airport-related CO emissions contribution by source group.

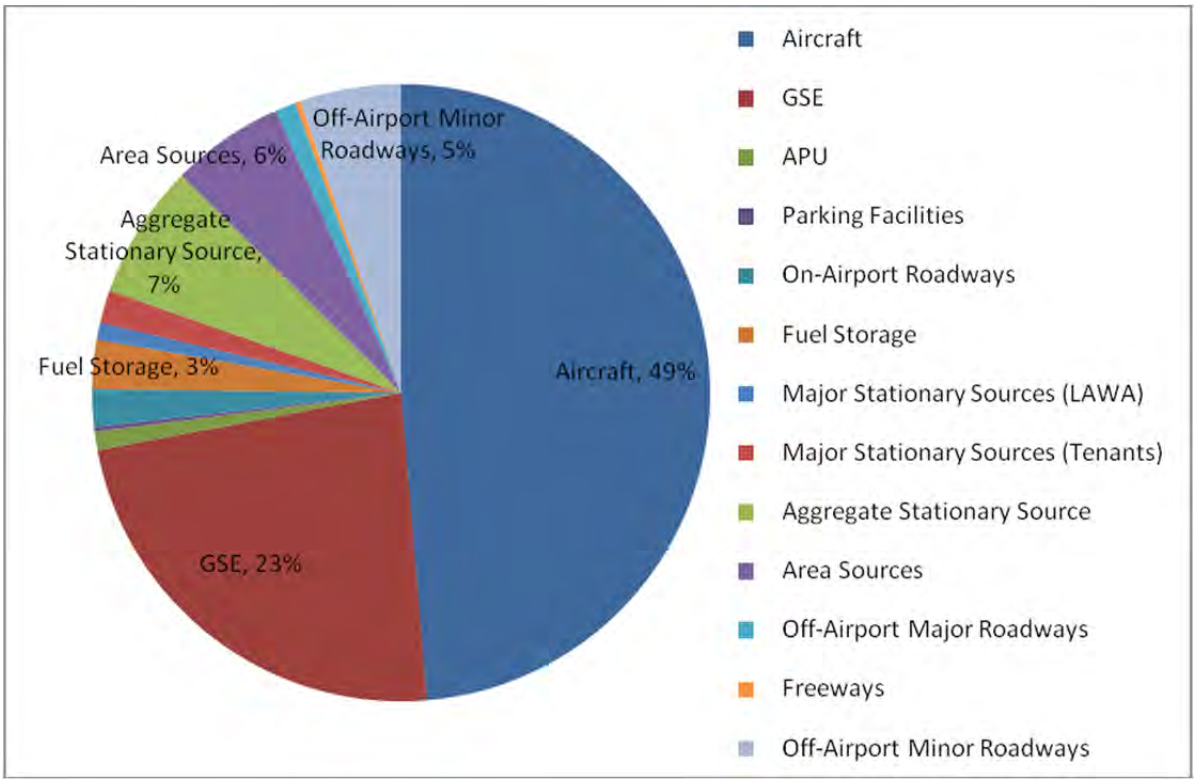

Figure 8-23. Airport-related VOC emissions contribution by source group.

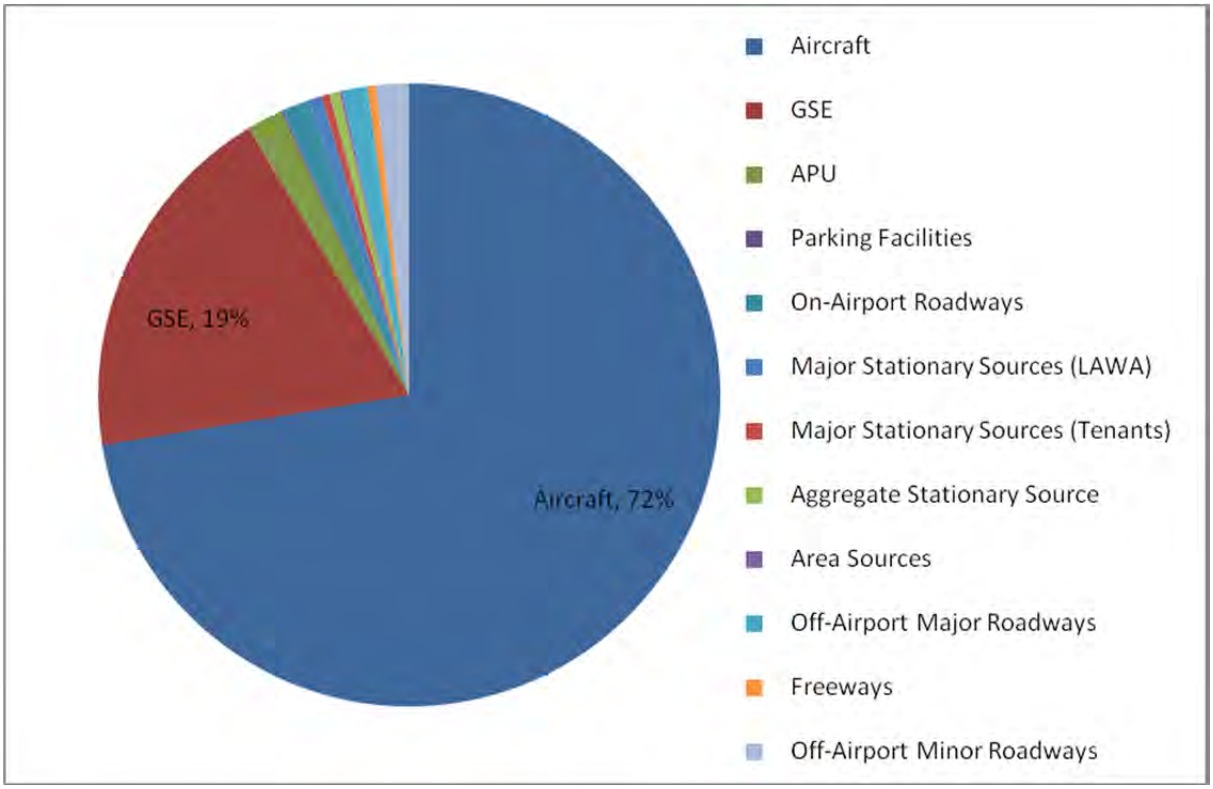

Figure 8-24. Airport-related NOx emissions contribution by source group.

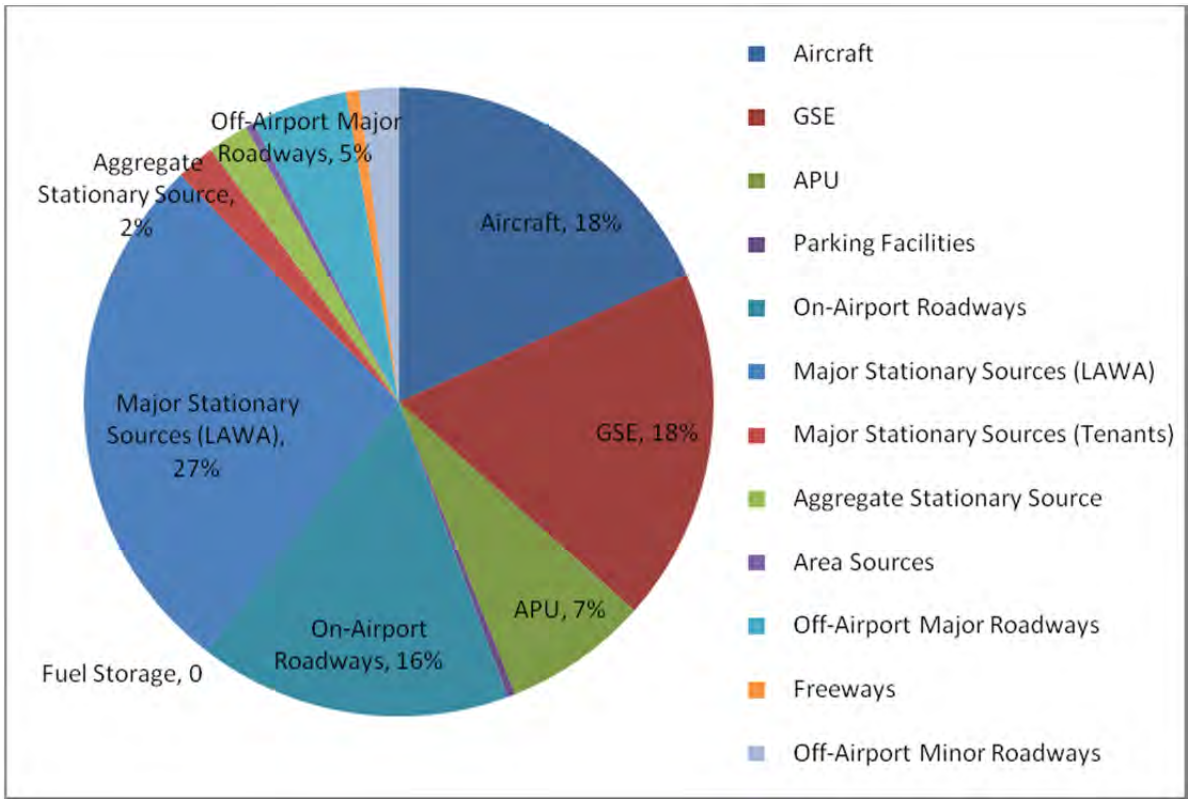

Figure 8-25. Airport-related PM2.5 emissions contribution by source group.

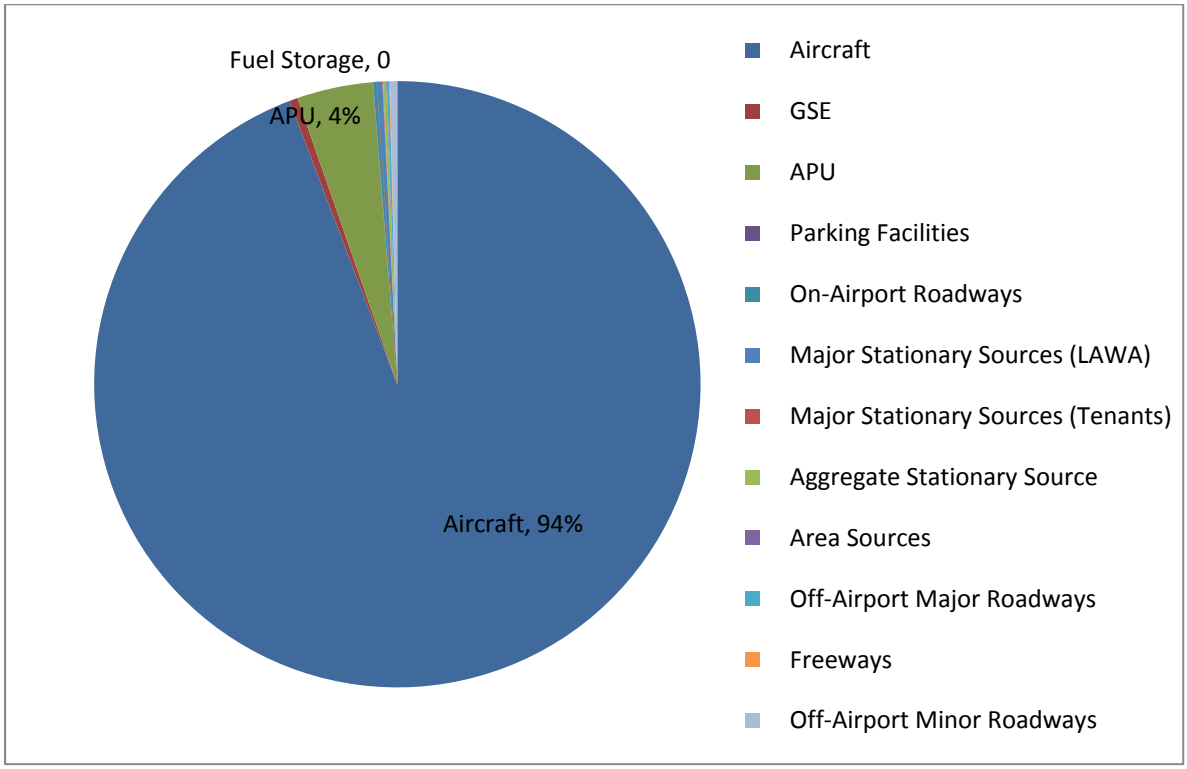

Figure 8-26. Airport-related SOx emissions contribution by source group.

8.15.1.2 Summer Monitoring Season

The airport-related emissions inventory for the Summer Monitoring Season is summarized in Table 8-31. Airport-related emissions totaled 698 tons of CO, 84 tons of VOC, 91 tons of TOG, 465 tons of NO_x, 31 tons of SO_x, 32 tons of PM_{10}, and 18 tons of $PM_{2.5}$. The percentage and source contribution for the Summer Monitoring Season were similar to the Winter Monitoring Season.

Aircraft emissions represent the largest source of VOC, TOG, NO_x, and SO_x among the various airport-related source groups. GSE, airport roadways, and stationary sources comprise the largest airport emission sources for CO, PM_{10}, and $PM_{2.5}$, respectively. Aircraft operations account for CO (33 percent), VOC (51 percent), TOG (46 percent), NO_x (72 percent), SO_x (94 percent), PM_{10} (11 percent), and $PM_{2.5}$ (19 percent) of the total airport-related emissions.

The airport-related traffic emissions (both on and off-airport) comprise 11 to 14 percent of the total traffic-related emissions within the Study Area for CO, VOC, TOG, NO_x, and SO_x and 40 to 32 percent for PM_{10} and $PM_{2.5}$, respectively.

Table 8-31. Airport-related emissions inventory (tons per period) – Summer Monitoring Season

	CO	VOC	TOG	NO_x	SO_x	PM_{10}	$PM_{2.5}$
On-airport Sources							
Aircraft	228	42.2	42.4	336	29.5	3.42	3.42
GSE	319	18.2	19.7	86.4	0.13	3.10	3.00
APU	9.88	0.85	0.86	9.44	1.29	1.39	1.39
Parking Facilities	2.75	0.25	0.32	0.67	0.01	0.27	0.08
Airport Roadways	45.3	1.98	2.54	7.59	0.08	12.9	3.38
Fuel Storage	-	2.33	2.42	-	-	-	-
Major Stationary Sources (LAWA)	6.86	0.69	1.21	2.24	0.03	4.51	4.51
Major Stationary Sources (Tenants)	1.06	1.34	1.66	1.96	0.01	0.36	0.33
Aggregate Stationary Source	3.59	5.49	6.19	2.41	0.05	0.88	0.35
Area Sources	1.08	4.61	7.04	0.62	0.01	0.33	0.07
Off-airport Sources							
Major Roadways	30.9	1.18	1.48	7.96	0.05	3.99	1.14
Freeways	8.58	0.32	0.39	2.58	0.02	0.40	0.15
Minor Roadways	41.2	4.11	5.11	7.73	0.11	0.46	0.33
Total	**698**	**83.5**	**91.3**	**465**	**31.3**	**32.0**	**18.2**

8.15.2 Non-Airport Sources

Non-airport related emission sources include major off-airport stationary sources such as the Chevron El Segundo Refinery, Scattergood Generating Station, and El Segundo Energy Center; motor vehicles (not attributed to the airport) traveling on nearby roadways and freeways; marine vessels; off-road equipment; aggregate stationary sources; and area-wide sources located beyond the airport boundary.

8.15.2.1 Winter Monitoring Season

The emission inventory for non-airport sources for the Winter Monitoring Season is summarized in Table 8-32. As shown, these non-airport emissions within the Study Area were estimated to be 1,269 tons of CO, 267 tons of VOC, 497 tons of TOG, 911 tons of NO_x, 91 tons of SO_x, 80 tons of PM_{10}, and 59 tons of $PM_{2.5}$.

Table 8-32. Non-airport emissions inventory (tons per period) – Winter Monitoring Season

Source Category	CO	VOC	TOG	NO_x	SO_x	PM_{10}	$PM_{2.5}$
Off-Airport Major Roadways	85.8	3.48	4.36	24.8	0.15	13.9	3.89
Freeways	93.4	3.71	4.62	32.8	0.18	4.79	1.77
Off-Airport Minor Roadways	635	63.3	78.8	119	1.71	7.05	5.12
Chevron El Segundo Refinery	96.3	68.2	194	81.7	47.8	25.4	24.9
Scattergood Generating Station	26.6	6.38	31.2	2.59	1.30	3.77	3.77
El Segundo Energy Center	13.4	0.90	4.39	0.59	0.01	1.22	1.22
Other Major Stationary Sources	2.74	8.02	38.6	7.16	0.15	0.76	0.75
Aggregate Stationary Source	14.8	25.3	28.6	10.2	0.21	3.65	1.44
Area Sources	9.57	37.3	56.9	4.44	0.08	3.12	0.71

Source Category	CO	VOC	TOG	NO_x	SO_x	PM_{10}	$PM_{2.5}$
Off-Road Equipment	241	23.4	25.8	82.3	1.32	4.50	4.04
Marine	51.0	26.5	29.4	545	38.4	11.6	11.3
Total	**1,269**	**267**	**497**	**911**	**91.3**	**79.8**	**58.9**

As shown, the largest contributors to non-airport emissions of CO were off-airport freeways and other roadways (approximately 64 percent). The Chevron facility was the largest contributor of VOC, TOG, SO_x, PM_{10}, and $PM_{2.5}$, while marine sources were the largest contributor of NO_x (approximately 60 percent) emissions.

8.15.2.2 Summer Monitoring Season

The emission inventory for non-airport sources for the Summer Monitoring Season is summarized in Table 8-33. As shown, non-airport emissions within the Study Area were estimated to be 1,209 tons of CO, 245 tons of VOC, 458 tons of TOG, 811 tons of NO_x, 84 tons of SO_x, 76 tons of PM_{10}, and 54 tons of $PM_{2.5}$.

Table 8-33. Non-airport emissions inventory (tons per period) – Summer Monitoring Season

Source Category	CO	VOC	TOG	NO_x	SO_x	PM_{10}	$PM_{2.5}$
Off-Airport Major Roadways	101	3.87	4.87	25.8	0.17	15.3	4.29
Freeways	109	3.99	4.99	32.6	0.19	5.05	1.86
Off-Airport Minor Roadways	580	57.8	71.9	109	1.56	6.44	4.67
Chevron El Segundo Refinery	87.9	62.3	177	74.6	43.6	23.2	22.7
Scattergood Generating Station	26.6	6.38	31.2	2.59	1.30	3.77	3.77
El Segundo Energy Center	13.4	0.90	4.39	0.59	0.01	1.22	1.22
Other Major Stationary Sources	2.50	7.32	35.2	6.54	0.14	0.70	0.69
Aggregate Stationary Source	13.5	23.1	26.1	9.35	0.19	3.34	1.32
Area Sources	8.74	34.0	52.0	4.05	0.07	2.85	0.65
Off-Road Equipment	220	21.4	23.5	75.1	1.20	4.11	3.69
Marine	46.5	24.2	26.9	471	35.1	9.57	9.38
Total	**1,209**	**245**	**458**	**811**	**83.6**	**75.6**	**54.3**

The largest portion of non-airport emissions of CO is the result of off-airport freeways and other roadways (approximately 71 percent). The Chevron facility was the largest contributor of VOC, TOG, SO_x, PM_{10}, and $PM_{2.5}$, while marine sources are the largest portion of the NO_x (approximately 58 percent) emissions from background sources.

8.15.3 Emissions Inventory Summary

Table 8-34 and Table 8-35 combine (in total tons per period) the airport-related and non-airport emissions inventories for the Winter and Summer Monitoring Seasons, respectively. Similarly, Table 8-36 and Table 8-37 display the summary (in tons per day) of the airport-related and non-airport emissions inventories for the Winter and Summer Monitoring Seasons, respectively. The average daily emissions for the Summer Monitoring Season are slightly higher than the Winter Monitoring Season. This greater value was largely due to greater aircraft and motor vehicle

activity during the summertime and higher emissions from the El Segundo Energy Center, which had been operating at lower capacity as a result of maintenance activities during the Winter Monitoring Season.

As shown, when compared to non-airport sources within the Study Area, the airport-related emissions approximate the following overall percentages for each pollutant: CO (36 percent), VOC (24 percent), TOG (16 percent), NO_x (35 percent), SO_x (26 percent), PM_{10} (27 percent) and $PM_{2.5}$ (23 percent).

Table 8-34. Airport-related and non-airport emissions inventory (tons per period) – Winter Monitoring Season

Source Category	**CO**	**VOC**	**TOG**	**NO_x**	**SO_x**	**PM_{10}**	**$PM_{2.5}$**
Airport	709	85.3	93.4	499	31.6	29.9	18.0
Non-Airport	1,269	267	497	911	91.3	79.8	58.9
Grand Total	**1,978**	**352**	**590**	**1,410**	**123**	**110**	**77.0**
Percentage of Total	**CO**	**VOC**	**TOG**	**NO_x**	**SO_x**	**PM_{10}**	**$PM_{2.5}$**
Airport	36	24	16	35	26	27	23
Non-Airport	64	76	84	65	74	73	77

Table 8-35. Airport-related and non-airport emissions inventory (tons per period) – Summer Monitoring Season

Source Category	**CO**	**VOC**	**TOG**	**NO_x**	**SO_x**	**PM_{10}**	**$PM_{2.5}$**
Airport	698	83.5	91.3	465	31.3	32.0	18.2
Non-Airport	1,209	245	458	811	83.6	75.6	54.3
Grand Total	**1,907**	**329**	**550**	**1,276**	**115**	**108**	**72.4**
Percentage of Total	**CO**	**VOC**	**TOG**	**NO_x**	**SO_x**	**PM_{10}**	**$PM_{2.5}$**
Airport	37	25	17	36	27	30	25
Non-Airport	63	75	83	64	73	70	75

Table 8-36. Airport-related and non-airport daily emissions inventory (tons per day) – Winter Monitoring Season

Source Category	**CO**	**VOC**	**TOG**	**NO_x**	**SO_x**	**PM_{10}**	**$PM_{2.5}$**
Airport	15.4	1.85	2.03	10.9	0.69	0.65	0.39
Non-Airport	27.6	5.80	10.8	19.8	1.99	1.74	1.28
Grand Total	**43.0**	**7.65**	**12.8**	**30.7**	**2.67**	**2.39**	**1.67**

Table 8-37. Airport-related and non-airport daily emissions inventory (tons per day) – Summer Monitoring Season

Source Category	**CO**	**VOC**	**TOG**	**NO_x**	**SO_x**	**PM_{10}**	**$PM_{2.5}$**
Airport	16.6	1.99	2.17	11.1	0.75	0.76	0.43
Non-Airport	28.8	5.84	10.9	19.3	1.99	1.80	1.29
Grand Total	**45.4**	**7.83**	**13.1**	**30.4**	**2.73**	**2.56**	**1.72**

The emissions inventory is unable to determine the potential airport contribution to ambient air quality impacts; however, it provides necessary data for dispersion modeling. When combined with the dispersion modeling results, these data aid in the apportionment of airport emissions to the pollutant concentrations in the neighboring areas. The downwind concentrations from each emission source are also a function of their location, temporal conditions, dispersion characteristics, and meteorological data.

(This page is intentionally blank)

Section 9

SOURCE-BASED DISPERSION MODELING

AERMOD AND CMAQ

(This page is intentionally blank)

Table of Contents

List of Tables

List of Figures

9. SOURCE-BASED DISPERSION MODELING

Atmospheric dispersion modeling provides a method to estimate ambient concentrations at downwind receptor sites utilizing known emission inventories. With sufficient emission data and other model inputs, such as wind speed and direction, dispersion modeling has the ability to provide concentration results at any location. For Phase III, source-based dispersion modeling was used to perform source attribution of air quality impacts due to the airport compared to non-airport related activities. Source-based dispersion modeling was performed for Phase III of the Los Angeles Airport Air Quality and Source Apportionment Study (LAX AQSAS) using two different models and using the emissions inventories described in Section 8. The two dispersion models used for Phase III included the American Meteorological Society/Environmental Protection Agency Regulatory Model (AERMOD) and the Community Multiscale Air Quality (CMAQ) modeling. Both these models have been recommended for use in recently issued guidance[1] for quantifying the contribution of airport emissions to local air quality (Kim et al, 2012). AERMOD is a Gaussian steady-state plume dispersion model used to estimate impacts from numerous sources, such as which airport-related sources contribute to ambient air quality in the communities surrounding the airport. AERMOD takes the impact of local terrain into account, which helps in determining movement of pollutants and vertical mixing. CMAQ is an Eulerian grid-based chemical transport model based on a 3-dimensional grid, which is used for urban and regional scale simulations and can help states assess necessary actions to meeting National Ambient Air Quality Standards (NAAQS). The CMAQ model helps to understand atmospheric trace gas transformations and distributions.[2]

9.1 AERMOD MODELING

9.1.1 General Description

The American Meteorological Society/U.S. Environmental Protection Agency Regulatory MODel (AERMOD) is the U.S. EPA's regulatory dispersion model. AERMOD is a comprehensive model for sources of various types including point, area, and volume-type sources in stable and convective atmospheric conditions using Monin-Obhukov similarity theory to vertically scale the winds and turbulence (Cimorelli et al., 2005; Perry et al., 2005). The Federal Aviation Administration (FAA) Emissions and Dispersion Modeling System (EDMS) is the required model (Federal Register, 1998) for performing air quality analysis of aviation sources in the United States and is typically used to analyze changes to local air quality in the vicinity of individual airports. In the public release, EDMS computes spatially and temporally allocated emissions for use with AERMOD for estimating pollutant concentrations. The EDMS/AERMOD models have been used extensively to perform several airport-related air quality studies in the U.S., including Phase II of the LAX AQSAS.

Source-based dispersion modeling was conducted using AERMOD, based on the emissions inventory described in Section 8, for the following pollutants: carbon monoxide (CO), nitrogen

[1] Transportation Research Board's Airport Cooperative Research Program (ACRP) Report 71: Guidance for Quantifying the Contribution of Airport Emissions to Local Air Quality addresses procedures for using air quality models in combination with on-site measurement equipment to prepare a comprehensive assessment of air pollution concentrations in the vicinity of airports.
[2] Community Multiscale Air Quality. CMAQ Overview. Access on 3/14/2013 from: http://www.cmaq-model.org/overview.cfm

oxides (NO_x), particulate matter 2.5 µm or less in diameter ($PM_{2.5}$), sulfur dioxides (SO_x), total organic gases (TOG), and volatile organic gases (VOC) for the Winter and Summer Monitoring Seasons. The AERMOD dispersion modeling accounts for the source emissions, the source release parameters, source location, the temporal distribution of the emissions as well as meteorological and terrain data and receptor location.

9.1.2 Model Inputs and Options

In April of 2000, U.S. EPA proposed that AERMOD be adopted to replace ISC3 as part of the *Guideline on Air Quality Models* (Code of Federal Regulations; April 21, 2000). On November 9 of 2005, AERMOD was adopted by the U.S. EPA and promulgated as their preferred regulatory model, effective as of December 9 of 2005. As such, upon final action, AERMOD became U.S. EPA's preferred regulatory model for both simple and complex terrain.

AERMOD[3] (version 12060) is a steady-state dispersion model designed for short-range (up to 50 kilometers) dispersion of air pollutant emissions from point, area and volumes sources. The model contains a meteorological data preprocessor, AERMET[4] (version 11059), that accepts surface meteorological data, upper air soundings, and data from on-site instrument towers (optional). (Note however that since the time of this modeling, EPA released updated versions [version 12345] of both AERMOD and AERMET.) Atmospheric parameters needed by the dispersion model, such as atmospheric turbulence characteristics, mixing heights, friction velocity, Monin-Obukov length, and surface heat flux are then calculated. The model also includes a terrain preprocessor, AERMAP[5] (version 11103), which provides a physical relationship between terrain features and the behavior of air pollution plumes. AERMAP generates location and height data for each receptor and source location. It also provides information that allows the dispersion model to simulate the effects of air flowing over hills or splitting flow around hills. AERMOD includes PRIME (Plume Rise Model Enhancements), which is an algorithm for modeling the effects of downwash created by the pollution plume flowing over nearby buildings.

In 1998, the Federal Aviation Administration (FAA) revised its policy on air quality modeling procedures to identify Emissions and Dispersion Modeling System (EDMS) as the required model to perform air quality analyses for aviation sources. This revised policy ensures the consistency and quality of aviation analyses performed for FAA. The FAA continues to enhance the model under the guidance of its government/industry advisory board to more effectively determine emission levels and concentrations generated by typical airport emission sources. The current model version is 5.1.3, released in November of 2010.[6] EDMS provides a means to input and organize aviation emission sources for use in AERMOD. EDMS provides two outputs, an

[3] United States Environmental Protection Agency, *AERMOD User's Guide*, September 2004.

[4] United States Environmental Protection Agency, User's Guide for the AERMOD Meteorological Preprocessor (AERMET), November 2004.

[5] United States Environmental Protection Agency, User's Guide for the AERMOD Terrain Preprocessor (AERMAP, October 2004.

[6] *Emissions and Dispersion Modeling System (EDMS)*. U.S. Department of Transportation, Federal Aviation Administration, Office of Environment and Energy. Washington, DC. Version 5.1.3. November 2010.

AERMOD input file and the hourly emission rate file for each emissions source. The airport-related emissions sources included within EDMS were combined with the non-airport-related sources into a single AERMOD input file.

AERMOD can simulate point, area, volume, and line sources and has the capability to include simple, intermediate, and complex terrain. It also predicts both short-term (1 to 24 hours) and long-term (quarterly or annual) average concentrations. The model was executed using the regulatory default options (stack-tip downwash, elevated terrain effects, calm wind speeds processing routine, missing data processing routine, buoyancy-induced dispersion, and final plume rise), default wind speed profile categories, default potential temperature gradients, and no pollutant decay. Lastly, the dispersion modeling did not account for building downwash effects. No gas or particle deposition or wet/dry depletion of the plume was employed. AERMOD was executed to yield one hour and season average concentrations (in microgram per cubic meter or $\mu g/m^3$) at each receptor. These concentrations were output in plot files and receptor files showing the results at each receptor for tabular and graphical display.

The selection of the appropriate dispersion coefficients depends on the land use within three kilometers (km) of the project site. The land use typing was based on the classification method defined by Auer (1978); using pertinent United States Geological Survey (USGS) 1:24,000 scale (7.5 minute) topographic maps of the area. If the Auer land use types of heavy industrial, light-to-moderate industrial, commercial, and compact residential account for 50 percent or more of the total area, the U.S. EPA *Guideline on Air Quality Models* recommends using urban dispersion coefficients; otherwise, the appropriate rural coefficients are used. Based on observation of the area surrounding the project site, rural dispersion coefficients were applied in the analysis (urban areas were only designated within dense city centers such as downtown Los Angeles).

The South Coast Air Quality Management District (SCAQMD) modeling guidance for AERMOD states the urban modeling option should be executed. The guidance also states that if the rural modeling option is utilized, the analysis should provide discussion to support this change, per U.S. EPA *Guideline on Air Quality Models*. The AERMOD Implementation Guide (March 19, 2009) states that there may be sources located within an urban area, but located close enough to a body of water or to other non-urban land use categories to result in a predominately rural land use classification within three kilometers of the source following the *Guideline on Air Quality Models*. Secondly, the use of the urban option may not be appropriate for elevated sources, since the actual plume is likely to be transported over the urban boundary layer. Given the location of LAX, its proximity to water, the relationship between the water and the predominate fetch of wind direction, and the importance of elevated sources (i.e., aircraft above the ground during takeoff, climbout, and approach) in the analysis, rural dispersion coefficients are appropriate.

9.1.2.1 Sources and Source Parameters

The dispersion modeling was conducted for both airport-related activities (located within the LAX property boundary and along roadways within the Study Area) and non-airport activities located beyond the LAX property boundary. These activities are defined as airport-related and non-airport (or background) sources, respectively.

Airport sources include aircraft engines (see Section 8.4), auxiliary power units (APU) (See Section 8.5), ground service equipment (GSE) (see Section 8.6), motor vehicles traveling along on-airport roadways (see Section 8.7) and within parking facilities (see Section 8.8), fuel storage tanks, LAX and tenant operated stationary sources such as turbines, boilers, generators, fuel storage, and cooling towers (see Section 8.9), and aggregate stationary sources, and area wide sources located on the airport. Aircraft operations occur within six modes of operation; taxi-out, takeoff, climb-out, approach, landing roll, and taxi-in. APU and GSE activities occur within the specific apron areas (i.e., aircraft parking/holding areas where aircraft are parked, unloaded or loaded, refueled, or boarded). Of note, some airport-related sources (such as roadway traffic traveling to/from the airport) are located beyond the airport boundary (see Sections 8.10 and 8.11).

Off-airport sources include motor vehicle traffic along off-airport roadways and freeways, major stationary sources (see Section 8.12) including the Chevron El Segundo refinery, Scattergood Generating Station, and El Segundo Energy Center, marine vessels in coastal waters (see Section 8.14), aggregate and area-wide sources, and off-road equipment (see Section 8.13) beyond the airport boundary. Nearly 6,000 sources, within 30 source groups, were included in the AERMOD dispersion modeling analysis. Section 8 contains a detailed discussion of the sources, their release parameters, spatial and temporal profiles, and emission estimates.

As mentioned above, for the AERMOD dispersion modeling analysis, the emissions sources were divided into two main groups: airport-related (comprised of 16 individual source categories) and non-airport-related or background (comprised of 11 individual source categories). In addition to these two main groups (with 27 individual source categories), three AERMOD source groups: AIRPORT (for all on-airport sources combined), BACKGROUND (for all non-airport or background sources combined), and ALL (AIRPORT plus BACKGROUND) were created to summarize the results. The 27 individual source categories and the three AERMOD source groups are listed in Table 9-1. The “Source Group” column of this table lists the specific keyword used to track this emissions group in the model and in all post-processing performed.

Depending on the source category (e.g., stationary, taxiway, or roadway), AERMOD/EDMS constructs a point, area, or volume source for use in dispersion modeling. Point sources are used to model stacks from boilers, turbines, generators, and cooling towers. Area sources are used to model emissions from aircraft gates aprons (i.e., aircraft at startup, GSE operations, and APU activity), aircraft taxiing, queuing, accelerating on the runway, and in climb-out and approach modes. Roadways were also classified as area sources. Volume sources were used to model any source that has an area and height element. The fuel storage facilities were modeled as volume sources.

Table 9-1. Emissions Source Groups Modeled in AERMOD

ID	Source Group	Description	Airport-Related or Background	Model	Source Location Figure (Sect. 8)
1	APPROACH	Aircraft Approach	AIRPORT	EDMS	Figure 8-2
2	TAKEOFF	Aircraft Takeoff	AIRPORT	EDMS	Figure 8-2
3	LANDING	Aircraft Landing	AIRPORT	EDMS	Figure 8-2
4	TAXIQ	Aircraft Taxi/Queue	AIRPORT	EDMS	Figures 8-5 & 8-6
5	GATES	APU, GSE, and Aircraft Startup	AIRPORT	EDMS	Figure 8-4
6	PARKING	On-airport Parking	AIRPORT	EDMS	Figure 8-11
7	STATSRCS	On-airport LAWA-owned Stationary Sources except COGEN	AIRPORT	EDMS	Figure 8-12
10	CAONRDAP	Minor On-road Sources	AIRPORT	AERMOD	Figure 8-19
12	CAOFFAP	Off-road Equipment	AIRPORT	AERMOD	Figure 8-19
14	CAAGGAP	Aggregate Stationary Sources	AIRPORT	AERMOD	Figure 8-19
16	COGEN	LAWA Cogeneration Units	AIRPORT	AERMOD	Figure 8-12
17	CAAREAAP	Area wide Sources	AIRPORT	AERMOD	Figure 8-19
20	SSTENAP	Airport Tenant Sources	AIRPORT	AERMOD	Figure 8-18
23	ROADOFAP	Off-airport Major Roadway	AIRPORT	EDMS	Figure 8-15
25	ROADONAP	On-airport Roadway	AIRPORT	EDMS	Figure 8-9
26	FREEWYAP	Freeway	AIRPORT	EDMS	Figure 8-15
28	AIRPORT	ALL AIRPORT-RELATED SOURCES	AIRPORT		See figures listed above
8	CHEVRON	Chevron Products Co. (El Segundo Refinery)	BACKGROUND	AERMOD	Figure 8-18
9	MARINE	Marine Vessels	BACKGROUND	AERMOD	Figure 8-20
11	CAONRDBK	Minor On-road Sources	BACKGROUND	AERMOD	Figure 8-19
13	CAOFFBK	Off-road Equipment	BACKGROUND	AERMOD	Figure 8-19
15	CAAGGBK	Aggregate Stationary Sources	BACKGROUND	AERMOD	Figure 8-19
18	CAAREABK	Area wide Sources	BACKGROUND	AERMOD	Figure 8-19
19	SEGUNDO	El Segundo Power Plant	BACKGROUND	AERMOD	Figure 8-18
21	SSOTHBK	Other Non-Airport Related Stationary Sources	BACKGROUND	AERMOD	Figure 8-18
22	SCTRGOOD	Scattergood Power Plant	BACKGROUND	AERMOD	Figure 8-18
24	ROADOFBK	Off-airport Major Roadway	BACKGROUND	EDMS	Figure 8-15
27	FREEWYBK	Freeway	BACKGROUND	EDMS	Figure 8-15
29	BACK-GROUND	ALL BACKGROUND SOURCES	BACKGROUND		See figures listed above
30	ALL	ALL AIRPORT & BACKGROUND SOURCES MODELED IN AERMOD	ALL		see figures listed above

9.1.2.2 Meteorology and Mixing Height

Air quality is a function of both the rate and location of pollutant emissions under the influence of meteorological conditions and topographic features affecting pollutant movement and dispersal. Atmospheric conditions, such as wind speed, wind direction, atmospheric stability, and air temperature gradients interact with the physical features of the landscape to determine the movement and dispersal of air pollutants, which affect air quality. The emissions inventory and dispersion modeling analysis used representative meteorological data to simulate conditions at and above the surface.

Local meteorology can affect pollutant concentrations depending on the severity of temperature inversions that characterize the South Coast Air Basin (SoCAB). A temperature inversion occurs when the upper air is warmer than the air near the ground, as seen in Figure 9-1. This causes air pollutants released at the surface to be trapped beneath the level where the air begins to warm.

The temperature inversion is also related to mixing height. The term atmospheric mixing height generally describes the height above ground level where atmospheric mixing of most air pollutants occurs. Within the atmosphere, this height (expressed in meters or feet above ground level) is determined by multiple environmental factors including: air temperature, humidity, solar radiation, wind speed, and topographic features on the ground. The atmospheric mixing height is dynamic, moving up and down spatially and temporally throughout the day, season, and year due to corresponding changes in the abovementioned factors.

The determination of the atmospheric mixing height is based on measurements made by weather balloons, instrumented aircraft, and/or ground-based remote sensing. These data, which are collected over extended periods of time, are used for weather forecasting, aeronautical and military purposes, and air quality assessments. In air quality assessments (i.e., emissions inventories and dispersion modeling) the atmospheric mixing height is used to define the vertical limit(s) of a particular study area. In simple terms, this is the height of a figurative box within which airport-related emissions are assumed to occur and disperse, with the ground representing the bottom and the horizontal distances representing the sides of the box.

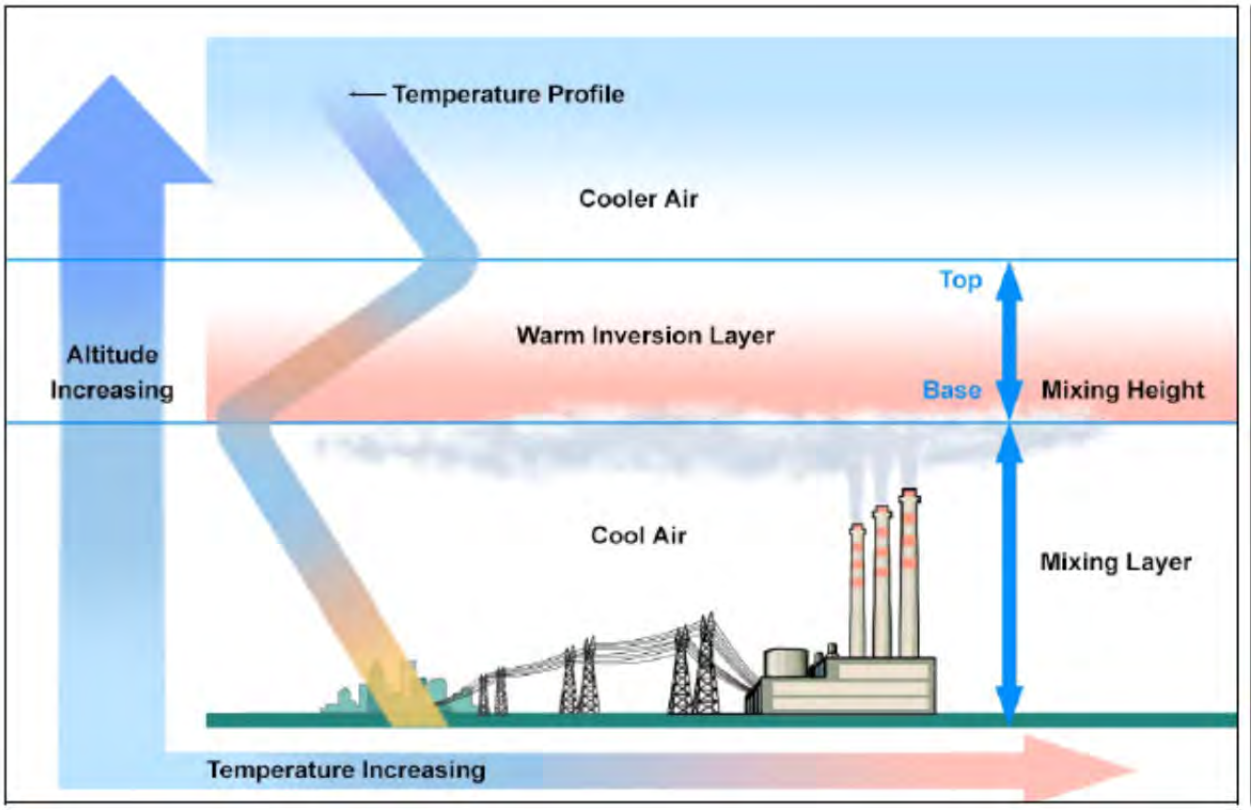

Figure 9-1. Temperature inversion diagram.

Unstable air tends to have a higher mixing height than in stable air. The height of the mixing zone varies by time of day and by season. Typically, during summer daylight hours, the mixing height can be 2,000 meters while during the winter the mixing height may only be 200 to 900 meters. In marine climates, mixing heights tend to be lower compared to desert or continental climates and lower during the morning compared to the afternoon. Historical data from the LAX area report an average annual mixing height of 1,780 and 2,670 feet (542 and 814 meters) for the morning and afternoon, respectively. An average mixing height of 1,806 feet (550 meters) was used in this analysis.

Meteorological data for use in EDMS and dispersion modeling were processed using AERMET. AERMET processes commercially available (typically from the National Climatic Data Center [NCDC] or National Weather Service [NWS]) or on-site meteorological data and creates two files: a surface data file and a profile data file. AERSURFACE[7] was used to assess the land use cover and determine the appropriate surface roughness length[8], Bowen ratio[9], and albedo[10] based

[7] AERSURFACE is a tool that processes land cover data to determine the surface characteristics for use in AERMET.

[8] The roughness length is approximately one-tenth of the height of the surface roughness elements. For example, short grass of height 0.01m has a roughness length of approximately 0.001m. Surfaces are rougher if they have more protrusions. Forests have much larger roughness lengths than tundra, for example. Roughness length is an important concept in urban meteorology as the building of tall structures, such as skyscrapers, has an effect on roughness length and wind patterns.

[9] The Bowen ratio is used to describe the type of heat transfer in a water body. The Bowen ratio is the mathematical method generally used to calculate heat lost (or gained) in a substance; it is the ratio of energy fluxes from one state to another by sensible and latent heating respectively.

[10] The ratio of reflected radiation from the surface to incident radiation upon it or reflecting power of a surface.

on land use cover, soil moisture, and seasonal conditions. The appropriate surface roughness length, Bowen ratio, and albedo for the analysis were estimated on AERSURFACE, which calculated values of 0.172, 1.27, and 0.18, respectively, indicative of a land use containing desert shrubland, water surfaces, and significant areas of pavement. These values were compared to the SCAQMD values, which are estimated as 0.256 meters, 1.0, and 0.16, respectively, based on conditions at LAX.[11] The SCAQMD values do differ from the AERSURFACE estimates but are more applicable to the land use cover in the area around LAX and were therefore used in this analysis. AERMOD is more sensitive to surface roughness, which tends to be higher in urban environments due to greater obstructions and thus, greater turbulence. Bowen ratio has little effect on the AERMOD results, while albedo can have a slight effect on the results. Higher surface roughness lengths may produce lower concentrations for surface-based emissions but higher concentrations for elevated emission sources.

Hourly surface meteorological data for both the Winter and Summer Seasons were obtained from the LAX NWS station located at the southeast portion of the airport. Automated Surface Observation System (ASOS) 1-minute data were also obtained from the LAX NWS station.[12] Upper air data were obtained from the Miramar Station near San Diego.[13] SCAQMD[14] also operates a Sonic Detection and Ranging (SODAR) station to the west of LAX. This instrument provides continuous vertical profiles of wind and virtual temperature that were used to better define the upper air conditions for the Winter and Summer Seasons. The SODAR data including wind speed and direction at heights above ground level from 30 to 200 meters (in intervals of 10 meters), were used along with the upper air data from Miramar for the Study. The meteorological data were processed in accordance with the AERMET and SCAQMD guidance.[15,16]

The AERMET output files contain meteorological parameters such as wind speed, wind direction, temperature, precipitation, relative humidity, atmospheric pressure, and a number of parameters defining the turbulence and stability of the atmosphere. For example, during the daytime, the Monin-Obukhov length is a rough measure of the height above which turbulence is

[11] South Coast Air Quality Management District, Surface Characteristics of Meteorological Sites Used in AETMET, May 21, 2009 (accessed April 26, 2012) and The Development of AERMOD-Ready Meteorological Data for the South Coast Air Basin and the Coachella Valley, Volume I April 17, 2009 and The Development of AERMOD-Ready Meteorological Data for the South Coast Air Basin and the Coachella Valley, Volume II: Appendices" April 17, 2009.

[12] The U.S. EPA's AERMINUTE program processes 1-minute ASOS wind data available from the NCDC to generate hourly averaged wind speed and wind direction to supplement the standard hourly NWS observations. The hourly averaged wind speed and direction generated by the AERMINUTE program are merged with data from standard surface data along with upper air and site-specific data (if available) within the AERMET processing. ftp://ftp.ncdc.noaa.gov/pub/data/asos-onemin/

[13] National Oceanic and Atmospheric Administration, ftp://ftp3.ncdc.noaa.gov/pub/data/noaa

[14] 2008 through 2010 SCAQMD Upper-Air Station Data Summary, August 2011. ftp://ftp.aqmd.gov/pub/rw/...Analysis/SCAQMDReport_final.pdf

[15] The Development of AERMOD-Ready Meteorological Data for the South Coast Air Basin and the Coachella Valley, Volume I April 17, 2009 and The Development of AERMOD-Ready Meteorological Data for the South Coast Air Basin and the Coachella Valley, Volume II: Appendices" April 17, 2009.

[16] SCAQMD Meteorological Data for AERMOD, http://www.aqmd.gov/smog/metdata/AERMOD.html and SCAQMD Modeling Guidance for AERMOD http://www.aqmd.gov/smog/metdata/AERMOD_ModelingGuidance.html.

generated more by buoyancy than by wind shear. It is a measure of the relative importance of mechanical and thermal forcing on atmospheric turbulence.[17]

Figure 9-2 displays the wind rose for the Winter Monitoring Season and Figure 9-3 displays the wind rose for the Summer Monitoring Season. The wind measurement height is 30 feet above ground level. During the Winter Monitoring Season, the average wind speed was 2.77 m/s or 5.34 knots and the wind direction was predominately from the west-southwest. The west winds occurred during the day at higher wind speed and the east winds occurred during the night at lower wind speed. The average temperature was 57.3 degrees Fahrenheit with a relative humidity of 60 percent. During the Summer Monitoring Season, the average wind speed was 2.62 m/s or 5.09 knots and the wind direction was predominately from the west. The average temperature was 69.4 degrees Fahrenheit with a relative humidity of 75 percent.

Figure 9-4 displays the wind rose for the daytime during the Winter Monitoring Season and Figure 9-5 displays the wind rose for the nighttime during the Winter Monitoring Season. Figure 9-6 displays the wind rose for the daytime during the Summer Monitoring Season and Figure 9-7 displays the wind rose for the nighttime during the Summer Monitoring Season. These wind roses display the typical sea breeze during the day (average wind speed of 3.09 m/s) and land breeze during the nighttime (average wind speed of 2.40 m/s). Of note, the Summer Monitoring Season had frequent (especially during evenings) winds from the northwest and, unlike the Winter Season, limited wind conditions from the east. The northwest winds may be indicative of eddies and northerly flow along the coast during the summertime. When these wind patterns occur, winds from the northwest are measured only between 20:00 and 08:00. These winds tend to last between one and ten hours, are generally lighter in speed, and appear to be confined to the surface or only the lower levels (the winds above 60 meters tend to be from the southwest during this condition).

Please note that the Nonparametric Trajectory Analysis (discussed in Section 7) used one minute wind data, which showed that during the Summer Season, the wind speeds can be much higher during these shorter durations, and show shifting direction every few minutes. However, these when averaged to an hourly basis as required by AERMOD, result in low hourly wind speeds.

[17] Air quality models, such as AERMOD, use the Monin-Obukhov Similarity Theory to characterize turbulence and other planetary boundary layer (PBL) processes. Turbulence is produced by two primary mechanisms: wind shear and buoyancy. There are equations for many PBL parameters, such as the friction velocity, convective velocity, and the Monin-Obukhov length, that are solved iteratively by the model. The friction velocity is a measure of the shear contribution to turbulence. The convective velocity is a measure of the contribution due to buoyancy. The theoretical height at which these two scales become equal is known as the Monin-Obukhov length.

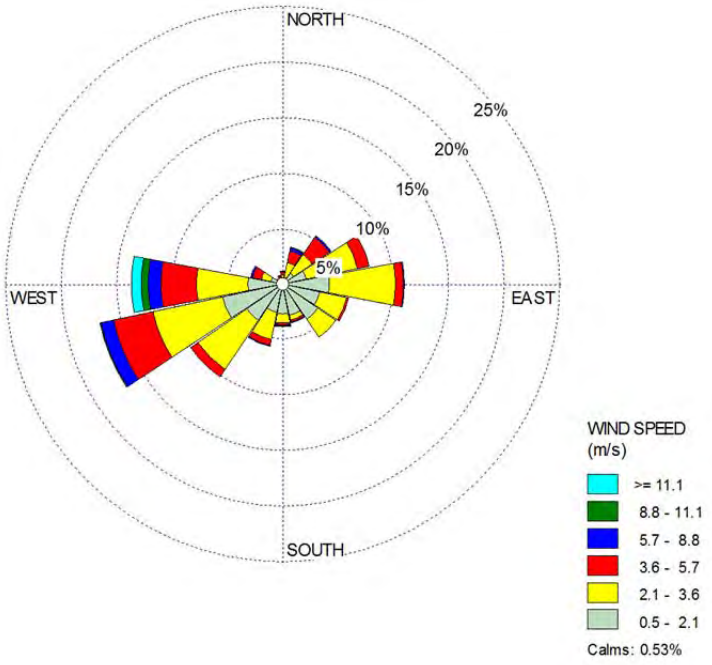

Figure 9-2. Meteorological wind rose – Winter Monitoring Season.

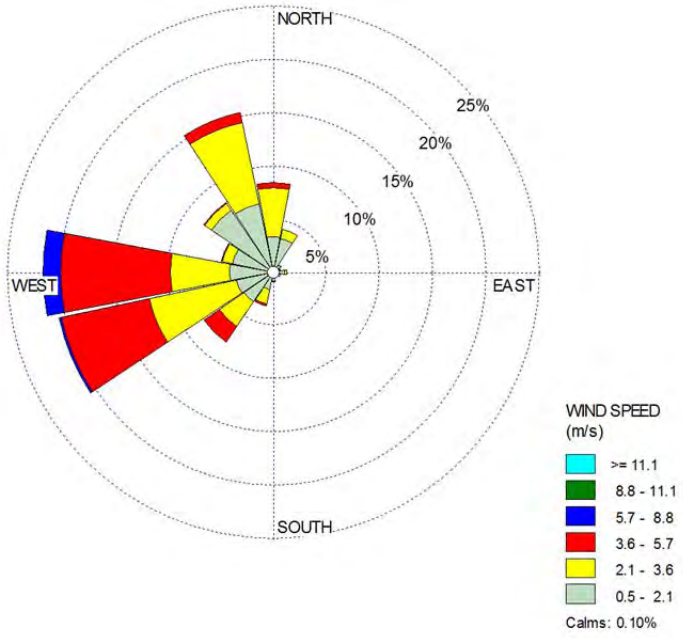

Figure 9-3. Meteorological wind rose – Summer Monitoring Season.

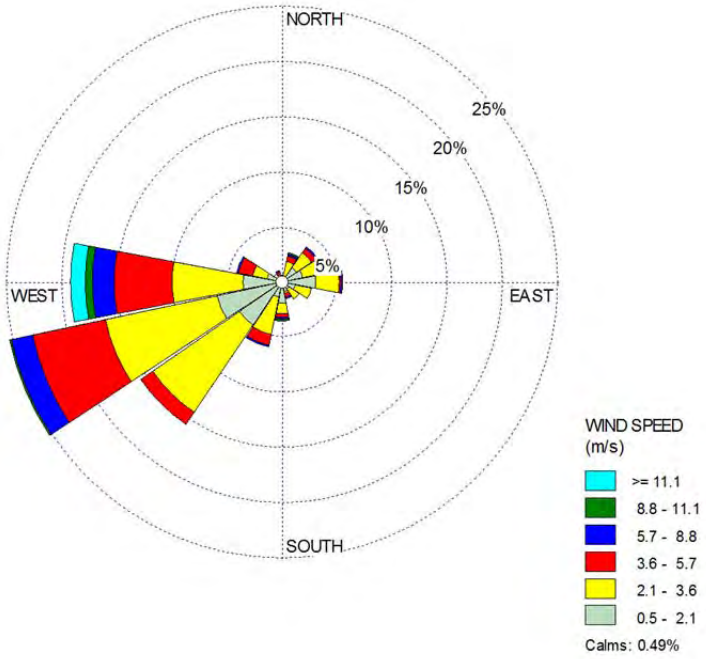

Figure 9-4. Meteorological wind rose – Winter Daytime Monitoring Season.

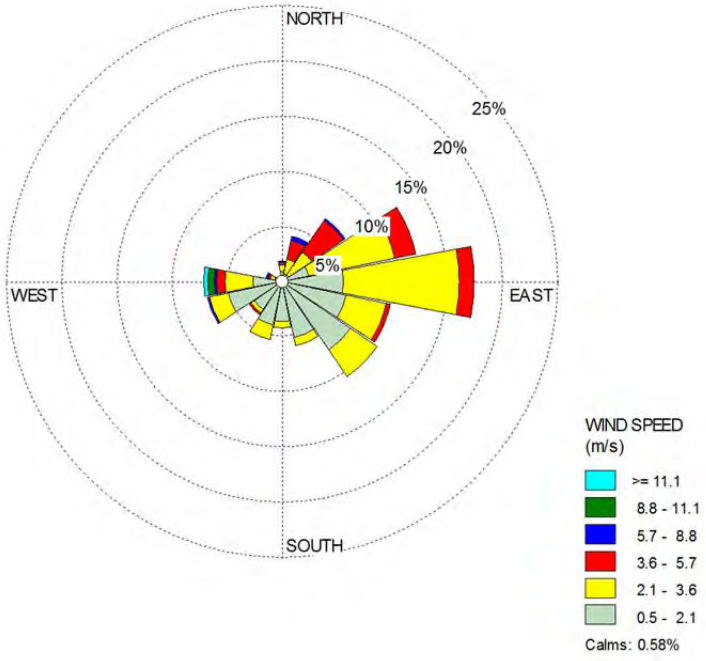

Figure 9-5. Meteorological wind rose – Winter Nighttime Monitoring Season.

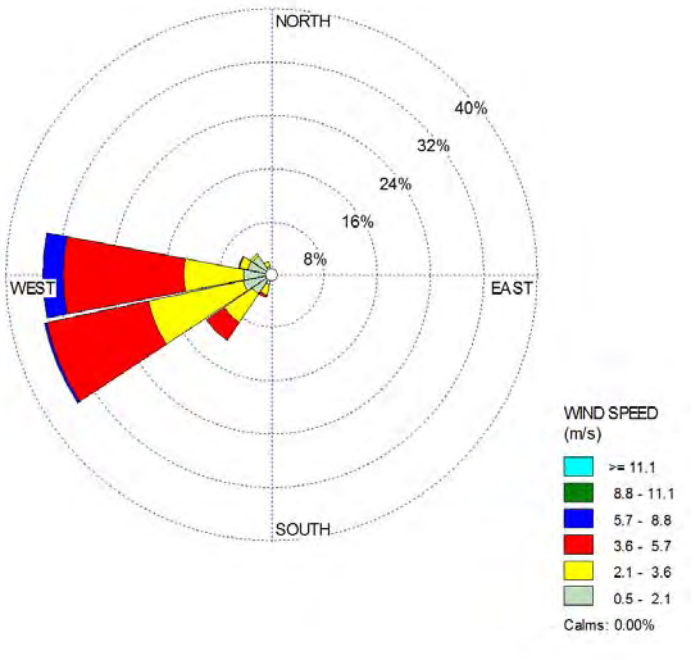

Figure 9-6. Meteorological wind rose - Summer Daytime Monitoring Season

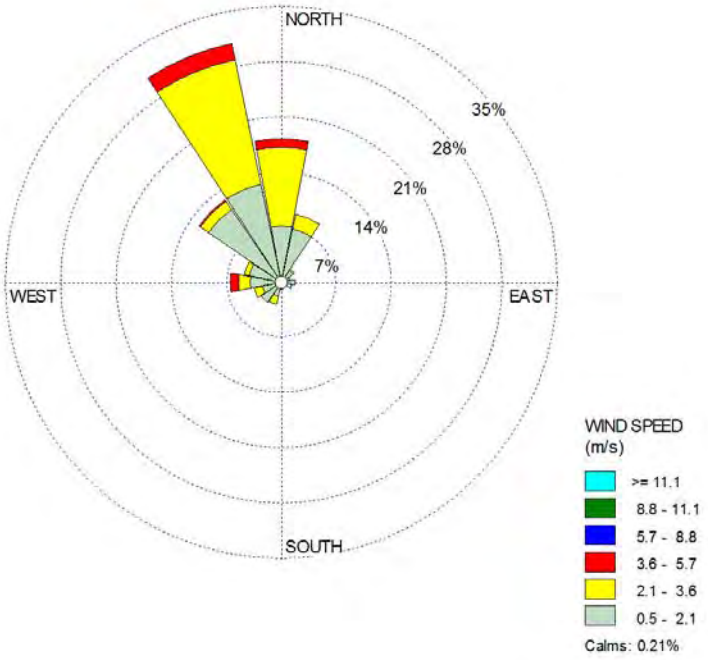

Figure 9-7. Meteorological wind rose - Summer Nighttime Monitoring Season

9.1.2.3 Terrain Data

AERMAP is a terrain preprocessor used in dispersion modeling. AERMAP processes United States Geological Society (USGS) Digital Elevation Model (DEM) data and creates a file of elevation and hill-height scaling factors. DEM data consisted of 7.5 minute series for the east and west quadrangle for Long Beach, Los Angeles, San Bernardino, and Santa Ana. These elevations are used to determine the elevation for each emission source and receptor. The data represent a general elevation of 32 meters at the Airport, higher elevations to the south within El Segundo, slightly higher elevations to the north, and gradually lower elevations to the Pacific Ocean. Figure 9-8 represents the terrain contours within the Study Area.

The locations of emission sources and receptors were represented in the Universal Transverse Mercator (UTM) coordinate system. The airport reference point[18] is approximately 369,874.86 meters East and 3,756,677.41 meters North (UTM Zone 11N) with North American Datum of 1983.

Figure 9-8. Terrain Elevation Map.

[18] The airport reference point is a point of an airport located at the geometric center of all the usable runways.

9.1.2.4 Receptors

A receptor network was developed to capture and adequately define the area of maximum impact and concentration distribution of the Study Area emission sources as well as comparison to the sampling site measurements. Cartesian and polar receptor grids were developed to estimate concentrations. These grids were designed to provide sufficient receptor coverage to capture the maximum concentrations.

The receptor network includes discrete receptors at the 17 monitoring sites in the Phase III Study. Secondly, a Cartesian grid was developed with a spacing of 500 meters to a distance of 5 kilometers (km) (i.e., covering the near field) from the airport reference point. Lastly, a polar grid was developed to contain 36 radii spaced at 10-degree intervals. The polar grid extends from 5 to 50 kilometers (i.e., covering the far field) from the airport reference point. A total of 1,028 receptors were included in the AERMOD analysis.

The following groups of receptors were created and hourly concentrations were predicted for each hour of the Winter and Summer Monitoring Seasons:

- Cartesian grid of receptors centered on the airport, and spaced every 500 meters up to 5 km from the airport reference point
- Polar grid, every 5-km out to a 50-km radius, along directions ranging from 10 to 360 degrees at 10 degree intervals, centered on the airport reference point
- Seventeen discrete receptors representing the monitoring sites (
- Table 9-2) including the four core measurement locations
    - SCAQMD Hastings site (AQ)
    - Community North site (CN)
    - Community South site (CS)
    - Community East site (CE)
- Flag-pole receptors at heights of 2 (typical breathing height as well as approximate height of monitoring probes), 7, 12, 17, and 22 meters above the ground level.

The Cartesian grid of receptors centered on the airport, and spaced every 500 meters up to 5-kilometers (km), is shown in Figure 9-9 and coordinates provided in Table 9-3. The Polar grid centered on the airport, and spaced every 5-km up to a 50-km radius, is shown in Figure 9-10 and coordinates provided in Table 9-4. As seen in the figures, the Polar grid extends 50 kilometers beyond the Study Area, and the Cartesian grid extends five kilometers beyond the Study Area. Thus, while the Cartesian grid has a much denser network of receptors in the immediate vicinity of the airport (the focus region for the LAX Phase III Study), the polar grid covers a larger region beyond the Study Area, albeit at a coarser resolution. The objective of making the AERMOD receptor modeling domain extend beyond the Study Area is to identify strengths and weaknesses of the modeling approach by assessing potentially high ranges of concentrations that may be predicted beyond the boundaries of the Study Area. The objective of the flag-pole receptors is to understand the nature of elevated plumes that are not brought down to the surface

due to potential issues related to the model or prevalent meteorological conditions. A LIDAR study of aircraft plume rise and spread at LAX by Wayson et al. (2004) and at Hartsfield-Jackson Atlanta International Airport (ATL) and Denver International by Wayson et al. (2008) showed that substantial plume rise of buoyant plumes from jet exhaust occurs. This application was examined in AERMOD modeling for Phase III to understand if this phenomenon of plume rise was exhibited, since it would have additional implications on the results of source apportionment.

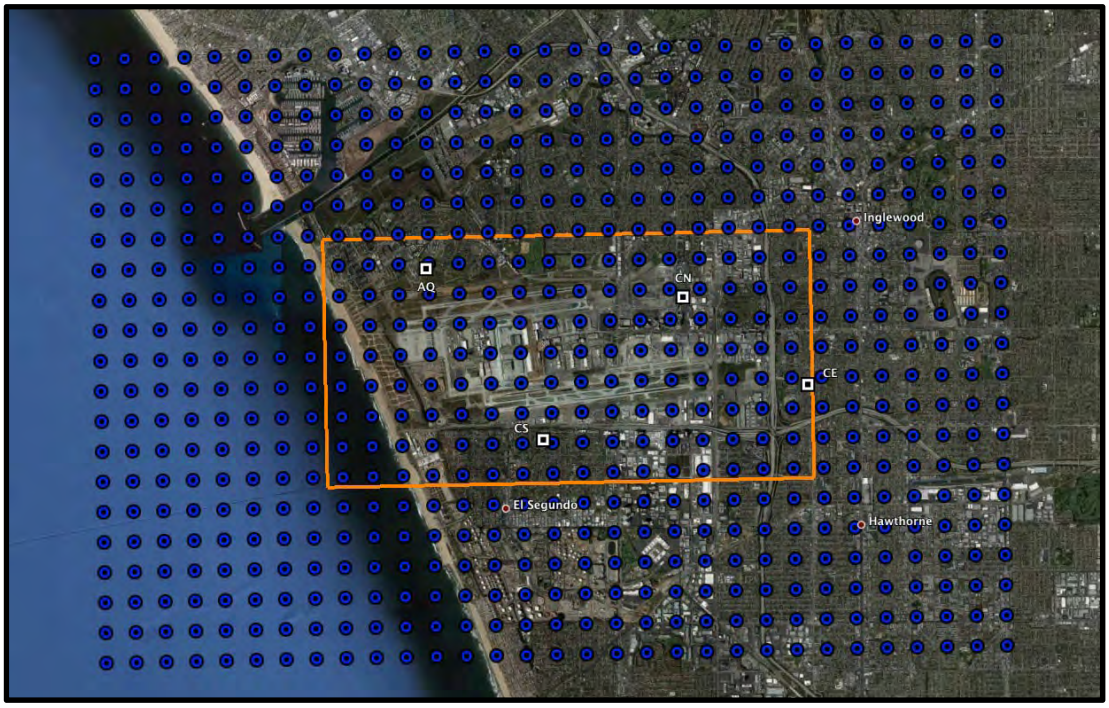

Figure 9-9. Cartesian grid of receptors around the airport. The rectangle represents the approximate Study Area.

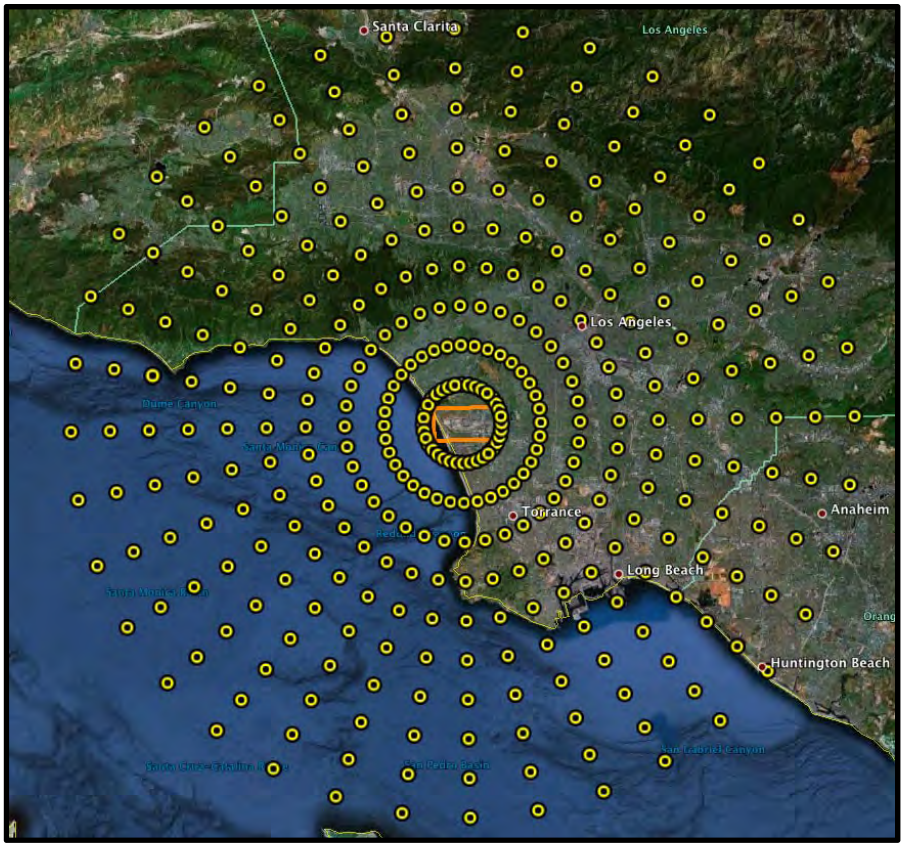

Figure 9-10. Polar grid of receptors centered on the airport. The rectangle represents the approximate Study Area.

Table 9-2. AERMOD Discrete Receptors

ID	Code	Description	UTM-E	UTM-N
1	CE	Community East	374,140	3,756,062
2	CS	Community South	369,722	3,755,236
3	CN	Community North	372,092	3,757,548
4	AQ	Upwind Northwest	367,830	3,758,100
5	CE2	Community East #2	375,388	3,752,261
6	CS2	Community South #2	369,652	3,754,601
7	CN2	Community North #2	370,566	3,759,164
8	UW	Upwind West	366,834	3,756,904
9	BN	Buffer Zone North	369,931	3,757,939
10	BS	Buffer Zone South	370,593	3,755,497
11	SRE	South Runway East	372,575	3,756,356
12	SRN	South Runway North	372,572	3,756,940
13	BSR	Buffer Zone South Runway	373,216	3,756,252
14	NR	North Runway	370,853	3,757,530
15	BNR	Buffer Zone North Runway	371,470	3,757,525
16	CT	Central Terminal	369,967	3,756,839
17	R405	Roadway I-405	373,508	3,758,017

Table 9-3. AERMOD Cartesian Grid Receptors.

Parameter Description	Value
Origin x-axis grid location (meters)	362375.0
Origin y-axis grid location (meters)	3751680.0
Number of x-axis receptors	31
Number of y-axis receptors	21
Spacing in meters between x-axis receptors	500.00
Spacing in meters between y-axis receptors	500.00

Table 9-4. AERMOD Polar Grid Receptors

Parameter Description	Value
X-coordinate for origin of polar network (meters)	369875.0
Y-coordinate for origin of polar network (meters)	3756680.0
Number of rings of polar coordinates	10
Distance of between each ring in meters	5000.00
Number of directions that define the polar system	36
Starting direction of the polar system	10.0
Increment (in degrees) for defining directions	10.0

9.1.2.5 AERMOD Model Options

The following pollutants were modeled: carbon monoxide (CO), nitrogen oxides (NO_x), particulate matter 2.5 µm or less in diameter ($PM_{2.5}$), sulfur dioxides (SO_x), total organic gases (TOG), and volatile organic gases (VOC) for the Winter and Summer Monitoring Seasons. Although PM_{10} emissions were estimated, they were not modeled in AERMOD since field measurements of PM_{10} were not conducted in Phase III. A list of key model options used is provided in Table 9-5 below. A sample input file is included at the end of Appendix 9-1.[19]

Table 9-5. AERMOD Configuration

Version	12060
Dispersion Options	CONC FASTALL ELEV
Averaging Time Options	1 24 MONTH PERIOD
Pollutants	CO, NO_x, $PM_{2.5}$, SO_x, TOG, VOC
Flagpole Heights (meters)	02, 07, 12, 17, 22, 27
Year	2012
Simulation Duration	Winter Period: Jan 31 – Mar 13 Summer Period: Jul 18 – Aug 28

9.1.3 AERMOD Analyses and Results

The AERMOD model outputs were analyzed in three distinct ways:

- Spatial analyses of model outputs

[19] Appendix 9-1 includes supplemental material from the AERMOD modeling section.

- Model evaluation against Phase III measurements
- Source apportionment using model outputs

While predictions of CO, NO_x, $PM_{2.5}$, SO_x and TOG were analyzed using spatial patterns across the entire modeling domain, the model evaluation and source apportionment using AERMOD were performed only from CO, NO_x, $PM_{2.5}$ and SO_x to match the measurements available from the four core monitoring locations for Phase III. The three AERMOD model output analyses are described in detail below.

9.1.3.1 Spatial Analyses

Spatial analysis of AERMOD outputs was performed by generally comparing spatial patterns of predictions across all receptors in the Polar and Cartesian grids, from three major source groups:

- Airport-related sources
- Background sources
- All (Airport-related and background) sources

For each pollutant modeled, summary statistics were computed for the Winter and Summer Monitoring Seasons for maximum one-hour concentrations and maximum of period-average concentrations amongst all receptors for each source group. These calculations were performed twice.

- The first calculation used AERMOD outputs only from the lowest elevation receptors (at a height of two meters, and which roughly corresponds to the heights of monitors used in Phase III), and
- The second calculation used AERMOD outputs from all flag-pole receptors (2, 7, 12, 17, and 22 meters) to characterize elevated plumes that are not brought down to the surface due to potential issues related to the model or prevalent meteorological conditions.[20]

By performing this calculation twice, it was possible to separate out the maximum impacts that affect surface air quality, as well as identify potential model performance issues that may keep the plume at elevated heights in the atmosphere. This second calculation was performed based upon findings from prior studies where AERMOD evaluation from Phase II of the LAX AQSAS and at Providence T.F. Green airport (Arunachalam et al., 2008) showed an elevated plume aloft that was not being brought down to the surface in the model.

Overall characterization of air quality modeled by AERMOD is performed by first looking at spatial patterns of pollutants across each group of receptors in the LAX airport area and beyond, and then comparing concentrations across vertical layers of atmosphere by looking at predictions from the flag-pole receptors.

[20] It is important to understand the information of the elevated plume; however, it was not used directly for source apportionment.

All the spatial maps are included in Appendix 9-1 organized by Winter and Summer Seasons. Within each season, the figures are organized by pollutants in the following order: CO, NO_x, $PM_{2.5}$, SO_2, and TOG. The spatial maps in Appendix 9-1 include:

- Spatial map of maximum one-hour and season average concentrations for Polar grid from each of airport-related, background-related, and all emissions groups (shown for CO during the Winter Season in Figure 9A-1)

- Spatial map of maximum one-hour and season average concentrations for Cartesian grid from each of airport-related, background-related, and all emissions groups (shown for CO during the Winter Season in Figure 9A-2)

- Spatial map of maximum one-hour concentrations for Polar grid from airport-related sources at different flag-pole heights of 2, 7, 12, 17, and 22 m (shown for CO during the Winter Season in Figure 9A-3)

- Spatial map of period average concentrations for Polar grid from airport-related sources at different flag-pole heights of 2, 7, 12, 17, and 22 m (shown for CO during the Winter Season in Figure 9A-4)

- Spatial map of maximum one-hour concentrations for Cartesian grid from airport-related sources at different flag-pole heights of 2, 7, 12, 17, and 22 m (shown for CO during the Winter Season in Figure 9A-5)

- Spatial map of season average concentrations for Cartesian grid from airport-related sources at different flag-pole heights of 2, 7, 12, 17, and 22 m (shown for CO during the Winter Season in Figure 9A-6)

- Spatial map of maximum one-hour concentrations for Cartesian grid from airport-related sources (broken down by each source group) at different flag-pole heights of 2, 7, 12, 17, and 22 m (shown for CO during the Winter Season in Figure 9A-7)

- Spatial map of maximum one-hour concentrations for Cartesian grid from background sources (broken down by each source group) at different flag-pole heights of 2, 7, 12, 17, and 22 m (shown for CO during the Winter Season in Figure 9A-8)

- Spatial map of season average concentrations for Cartesian grid from airport-related sources (broken down by each source group) at different flag-pole heights of 2, 7, 12, 17, and 22 m (shown for CO during the Winter Season in Figure 9A-9)

- Spatial map of season average concentrations for Cartesian grid from background-related sources (broken down by each source group) at different flag-pole heights of 2, 7, 12, 17, and 22 m (shown for CO during the Winter Season in Figure 9A-10)

Corresponding spatial maps for the Polar Grid for the Winter Season are shown for NO_x in Figures 9A-11 to 9A-20, for $PM_{2.5}$ in Figures 9A-21 to 9A-30, for SO_2 in Figures 9A-31 to 9A-40, and for TOG in Figures 9A-41 to 9A-50.

Corresponding spatial maps for the Polar Grid for the Summer Season are shown for CO in Figures 9A-102 to 9A-112, for NO_x in Figures 9A-113 to 9A-112, for $PM_{2.5}$ in Figures 9A-123 to 9A-132, for SO_2 in Figures 9A-133 to 9A-142, and for TOG in Figures 9A-143 to 9A-152.

9.1.4 Discussion of AERMOD Results

The analyses of spatial fields provide a good overview of the contribution of Study emissions to the overall ambient air quality in the vicinity of the airport, both in terms of magnitude and spatial extents within which the model shows impacts. This is one of the advantages of using a model, since measurements, while potentially more accurate, are limited in the spatial coverage they offer.

Analyses of the Polar grid of receptors showed that based upon AERMOD predictions, the contribution of Phase III study emissions did not reach much beyond the immediate vicinity of the airport for all pollutants (See Figures 9A-1, 11, 21, 31, and 41 in Appendix 9-1.). The remainder of the discussion will focus only on the Cartesian grid of receptors.

9.1.4.1 Carbon Monoxide

During the Winter Season, from the Cartesian grid of receptors, a CO plume was observed from the maximum one-hour concentrations due to airport-related sources that extend from the eastern end of the airport to the south and east. Similarly, the impacts of I-405 can be easily seen east of the airport moving north-south, while fairly large CO impacts are seen due to background sources east of the airport. During the Summer Season; however, the CO plume, based on maximum one-hour concentrations, appears to be fairly more widespread, showing that the short-term impacts of CO are observed more often around the airport than the season averages.

9.1.4.2 Nitrogen Oxides

During the Winter Season, from the Cartesian grid of receptors, a NO_x plume was observed from the maximum one-hour concentrations that extend from the eastern end of the airport to the south and east, due to airport-related sources. Similar to CO, a fairly large NO_x impacts are seen east of the airport due to background sources. During the Summer Season; however, the NO_x plume, based on maximum one-hour concentrations, seems to be fairly more widespread, showing that the short-term impacts of NO_x are observed more often around the airport (similar to CO) than the season averages.

9.1.4.3 Fine Particulate Matter

From the Cartesian grid of receptors during the Winter Season, a $PM_{2.5}$ plume was observed from the maximum one-hour concentrations that extend from the eastern end of the airport to the south and east. Similar to CO and NO_x, the impact of background sources in the immediate vicinity of the airport to the east and north was observed. During the Summer Season, the $PM_{2.5}$ plume, while generally more widespread than during the Winter Season, does not have as much spatial impact when compared to CO or NO_x as discussed above.

9.1.4.4 Sulfur Oxides

From the Cartesian grid of receptors during the Winter Season, a SO_2 plume from the maximum one-hour concentration that extends in all directions from the airport was observed. However, the impacts on the season average seem to be generally contained with the airport region. Again during the Summer Season, the SO_2 plume from the maximum 1-hour concentration appeared to be generally more widespread with a strong localized impact seen east of the airport due to airport-related activity.

9.1.4.5 Analyses of Elevated Receptors

Ratios of modeled concentrations at the lowest elevation (at 2m height) to other elevations (anywhere from 7, 12, 17 and 22 m) were computed for each pollutant, using both maximum one-hour and season average concentrations for each of the two periods. These ratios were computed for each of the 27 source groups modeled and are presented in Table 9A-1 and Table 9A-2 for the Winter Season and in Table 9A-5 and Table 9A-6 for the Summer Season.

The source groups related to landing and takeoff (LTO) activity predicted the highest concentrations aloft rather than at the surface. The ratios of the maximum values at the lowest elevation (2m) to all elevations ranged from 0.09 to 0.18 (amongst the five pollutants) for "Aircraft approach," from 0.81 to 0.99 for "Aircraft Takeoff," from 0.48 to 0.86 for "Aircraft landing" and from 0.71 to 0.97 for "Aircraft Taxi/Queue." Other airport-related stationary sources also show higher values aloft, with the ratios ranging from 0.08 to 0.62.

From the background sources, the ratios for "marine vessels" ranged from 0.57 to 0.76 and from 0.27 to 0.91 for "El Segundo Power plant." The ratios for "Chevron" were 1.0 for all pollutants except for VOCs, which had a ratio of 0.86 for the Winter Season and 0.33 for the Summer Season maximum one-hour concentration.

The actual elevations where the maximum concentrations were predicted by AERMOD are presented in Table 9A-3 and Table 9A-4 for the Winter Season and Table 9A-7 and Table 9A-8 for the Summer Season. These elevations are depicted as "heat maps"[21] where the actual elevations are color-coded from green to red and vary in intensity based upon flag-pole altitude.

From the "heat maps," it is seen that the highest concentrations for aircraft approach were seen at an elevation of 22m for all pollutants, and for LTO at 12m. The airport-related stationary sources predicted the highest one-hour maxima at the 7m receptor for all pollutants except for $PM_{2.5}$ and VOCs. However, for the season averages, only VOC concentrations were highest at 22m, and all other pollutants had the highest concentrations at 7m. Overall, when looking at all airport-related activity, the highest modeled predictions were seen at the 2m elevation for all pollutants except for SO_2 during both seasons for both metrics and for maximum one-hour NO_x during the Winter Season when the highest values were modeled at 12m. The SO_2 and NO_x anomaly is attributed to emissions from aircraft during their LTO cycles. Similarly, when

[21] A heat map is a graphical representation of data where the individual values contained in an array are represented as colors, and the color-coding represents ranges of values in a hierarchy.

looking at background sources within the study domain, the highest modeled predictions were always seen at the 2m elevation for all pollutants.

9.1.4.6 Model Evaluation

AERMOD model predictions were evaluated by comparing total predictions (due to all source groups, i.e. from airport-related and background sources) at the four core sites (AQ, CE, CN, and CS) where measurements of CO, NO_x, $PM_{2.5}$ and SO_2 were made during Phase III of the LAX AQSAS. Detailed characteristics of these sites are discussed in Section 3.3. The locations of these four core sites are shown in Figure 9-11.

Figure 9-11. Location of Phase III core monitoring sites: AQ, CE, CN, and CS. Sites are represented by pink squares. Blue circles identify the Cartesian grid receptors.

The AERMOD model evaluation included both quantitative and qualitative approaches.

Quantitative Evaluation:

The quantitative model performance measures used here are the observed mean, modeled mean, mean bias (MB), mean error (ME), the correlation coefficient (R), and the fraction of estimates within a factor of two of the measured value (FAC2). These are standard measures typically used in evaluating dispersion models such as AERMOD (Chang and Hanna, 2004; Kumar et al., 2006). The Atmospheric Model Evaluation Tool (AMET) (Appel et al., 2011) was adapted to perform the AERMOD model evaluation and create several plots included in this section. However, it should be noted that since the metrics defined above are based upon paired statistics (i.e., each pair is generated by matching the model to the observation in space and time), they are

considered to be the most stringent measures of model performance. The definitions of these quantities are:

$$MeanBias = \overline{C_p - C_o}$$

$$MeanError = \overline{abs(C_p - C_o)}$$

$$R = \frac{\overline{\left(C_o - \overline{C_o}\right)\left(C_p - \overline{C_p}\right)}}{\sigma_{C_o}\sigma_{C_p}}$$

and

FAC2: Fraction of model estimates that satisfy

$$0.5 \leq \frac{C_p}{C_o} \leq 2.0$$

where C is the concentration, either observed (subscript 'o') or predicted ('p'), and the overbar indicates an arithmetic average. Mean Bias is a measure of the systematic bias of the model and is ideally equal to zero. Mean Error is an estimate of the mean error, and is smaller for better model performance (= 0, ideally). The correlation coefficient can range from -1 and +1 and reflects the linear relationship between the observed and predicted values (= +1, ideally). Finally, FAC2 measures the fraction of estimates within a factor of two of the observations (= 1, ideally).

These quantitative metrics of model performance (observed mean, model mean, Mean Bias, Mean Error, R and FAC2) are presented as bar charts in Figure 9-12 through Figure 9-15 for the Winter Season and in Figure 9-16 through Figure 9-19 for the Summer Season. Based upon this stringent test of model evaluation paired in space and time at each of the four monitoring locations, the model performance is generally fair to poor. The correlation is less than 0.50 for all sites for all pollutants, with the Summer Season performance marginally better than the Winter Season performance. In other words, AERMOD was able to explain only up to 50 percent of the variability in measured concentrations. The FAC2 metric showed values between 0.10 and 0.36 (NO_x at the CS site) during the Winter Season, and between 0.05 and 0.55 (SO_2 at the AQ site) during the Summer Season. This again showed that most often more than 50 percent of the modeled values differ from the observed values by more than a factor of two. Looking at MB, at all four core sites, AERMOD has a positive bias for NO_x and SO_2, and a negative bias for $PM_{2.5}$. However, for CO, AERMOD has a negative bias at the AQ and CS sites during the Winter Season and at the AQ site during the Summer Season. The negative bias in $PM_{2.5}$ is likely attributed to the lack of treatment of secondary aerosols in AERMOD, and the possibility that the measurements at the four core sites are capturing impacts from sources beyond the Study Area.

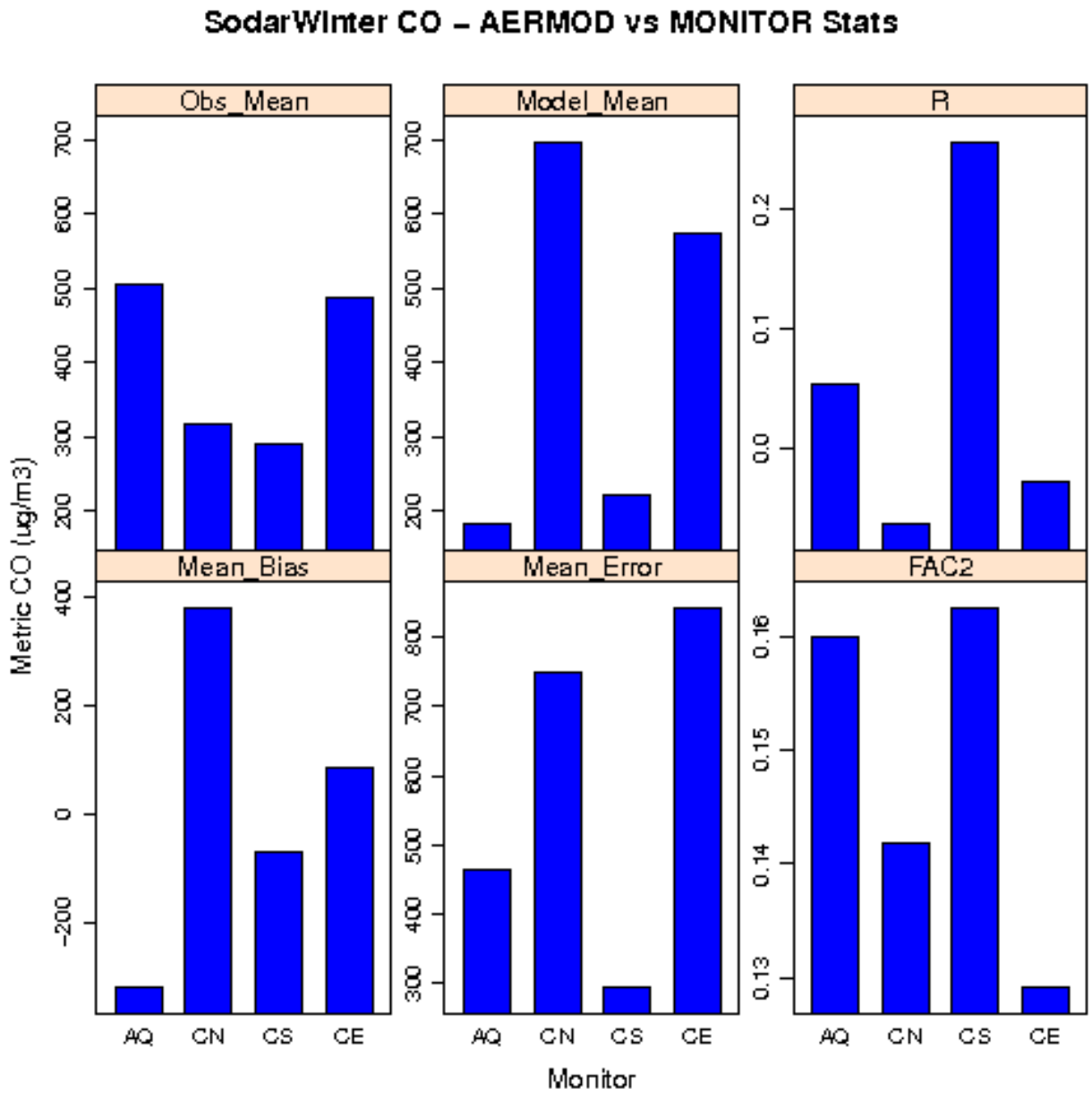

Figure 9-12. . Summary statistics of AERMOD model evaluation for CO concentrations at each core site from ALL (both airport-related and background) sources during the Winter Season. [Note that Mean, Bias and Error have units of µg/m^3, while R and FAC2 are unitless]

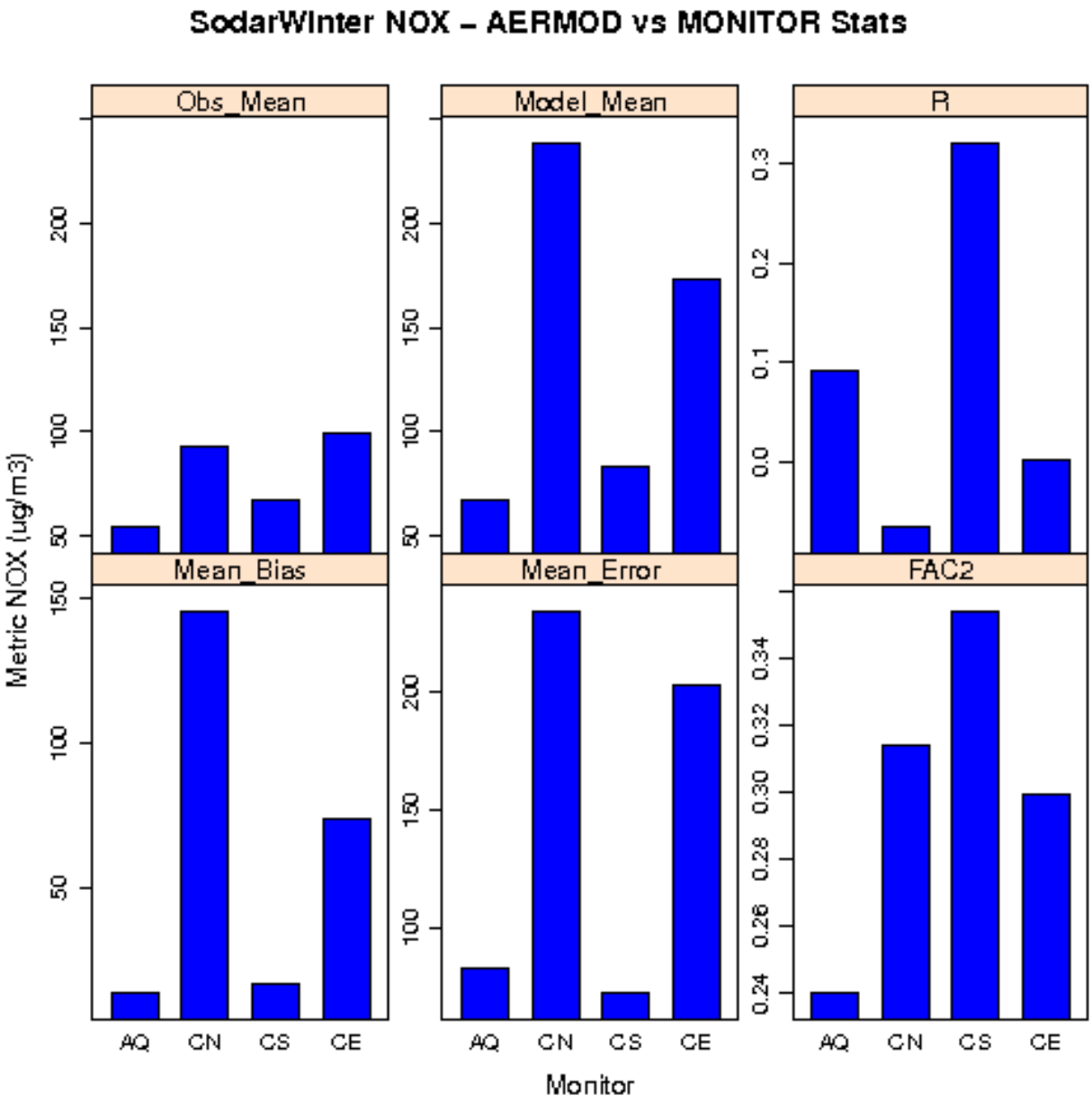

Figure 9-13. Summary statistics of AERMOD model evaluation for NO_x concentrations at each core site from ALL (both airport-related and background) sources during the Winter Season. [Note that Mean, Bias and Error have units of $\mu g/m^3$, while R and FAC2 are unitless]

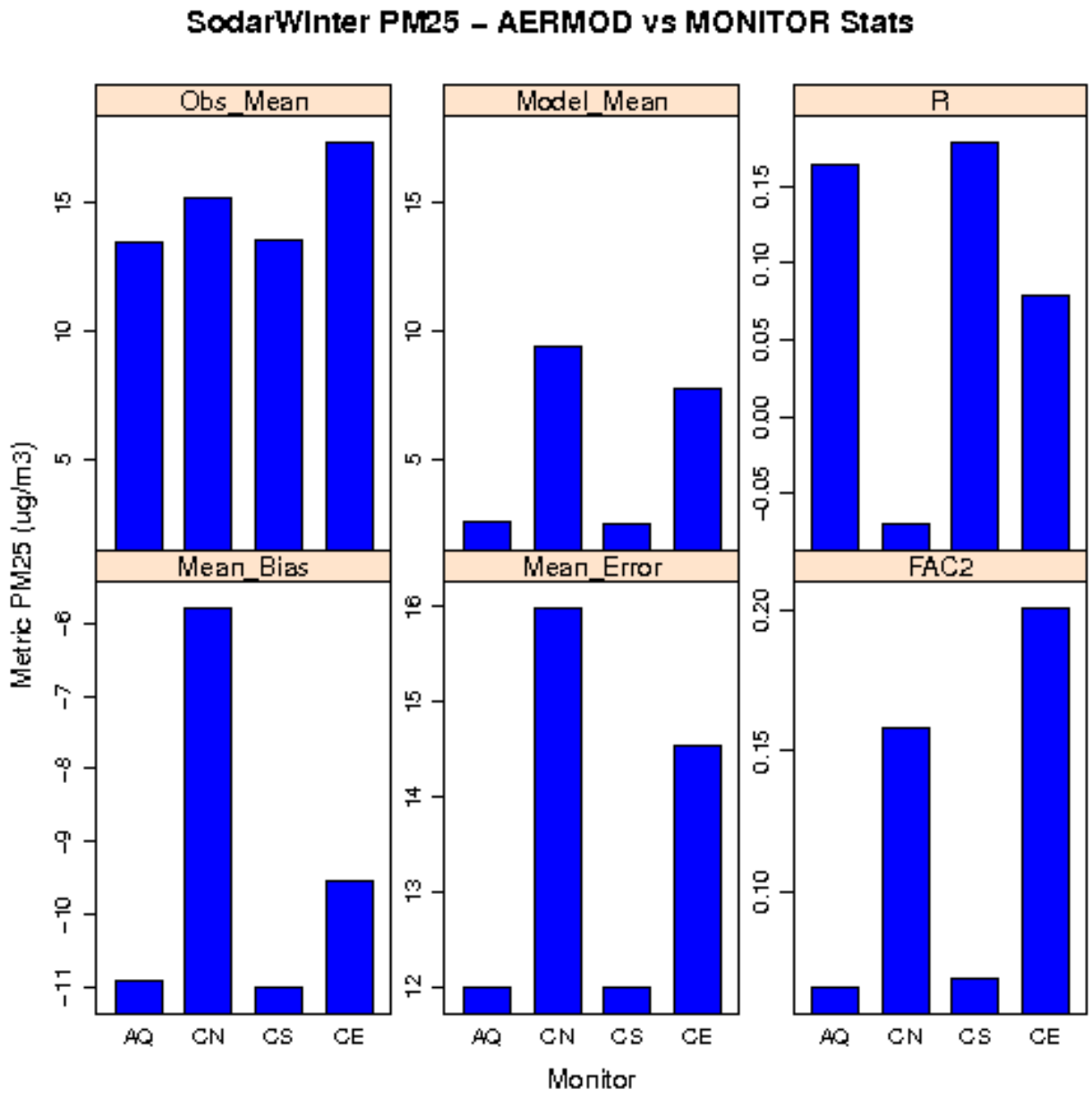

Figure 9-14. Summary statistics of AERMOD model evaluation for $PM_{2.5}$ concentrations at each core site from ALL (both airport-related and background) sources during the Winter Season. [Note that Mean, Bias and Error have units of $\mu g/m^3$, while R and FAC2 are unitless]

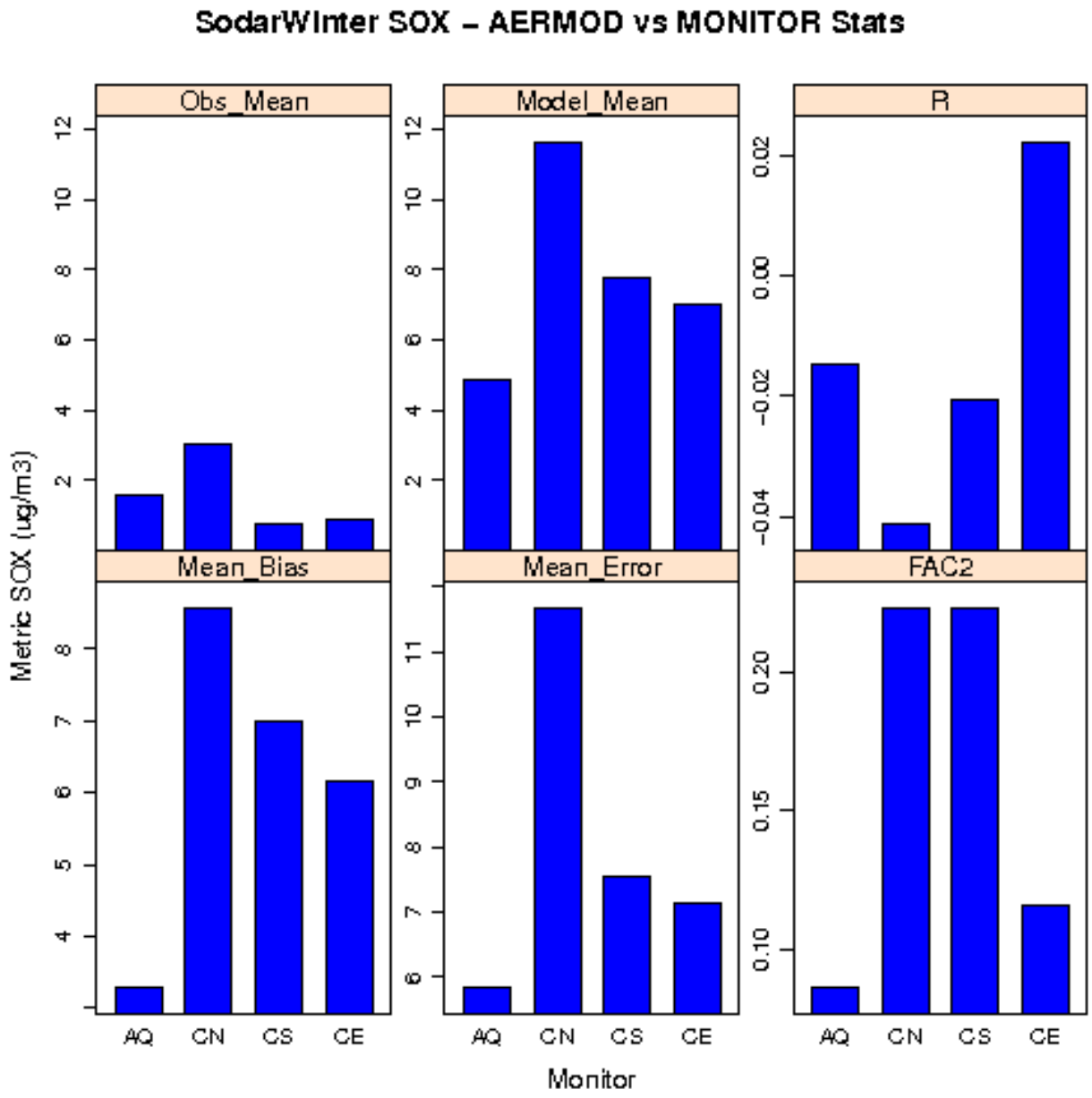

Figure 9-15. Summary statistics of AERMOD model evaluation for SO_x concentrations at each core site from ALL (both airport-related and background) sources during the Winter Season. [Note that Mean, Bias and Error have units of $\mu g/m^3$, while R and FAC2 are unitless]

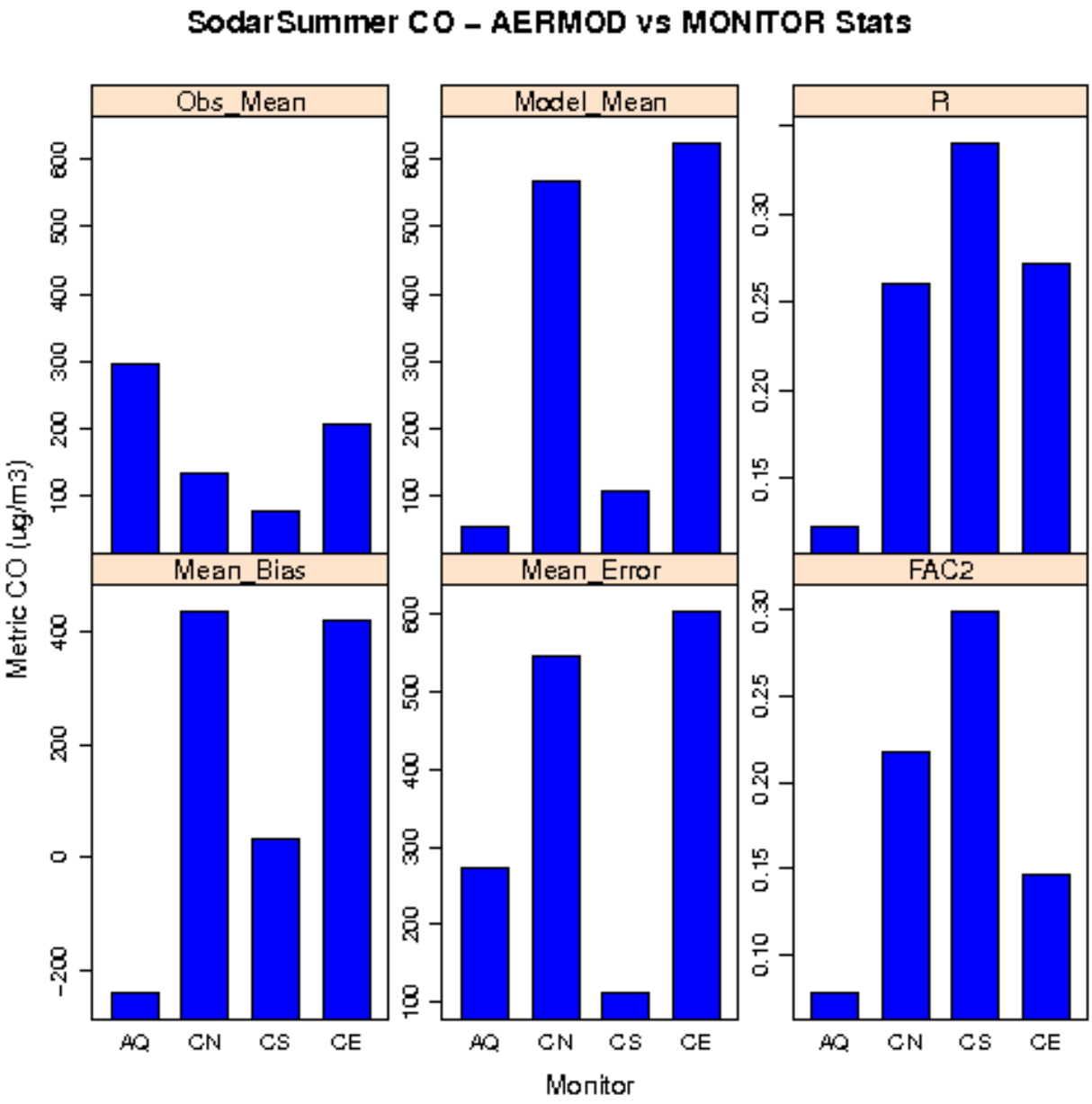

Figure 9-16. Summary statistics of AERMOD model evaluation for CO concentrations at each core site from ALL (both airport-related and background) sources during the Summer Season. [Note that Mean, Bias and Error have units of $\mu g/m^3$, while R and FAC2 are unitless]

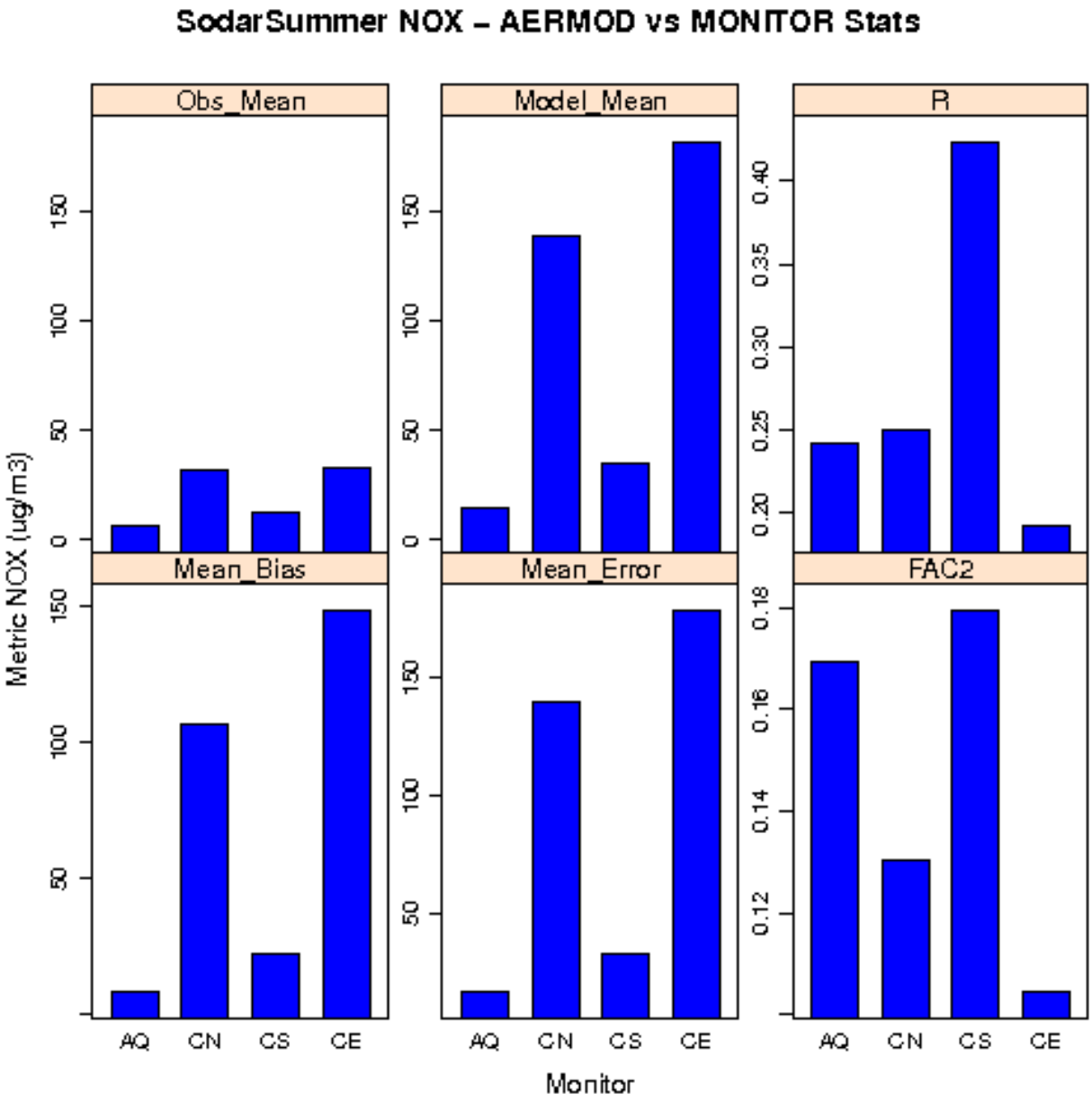

Figure 9-17. Summary statistics of AERMOD model evaluation for NO_x concentrations at each core site from ALL (both airport-related and background) sources during the Summer Season. [Note that Mean, Bias and Error have units of $\mu g/m^3$, while R and FAC2 are unitless]

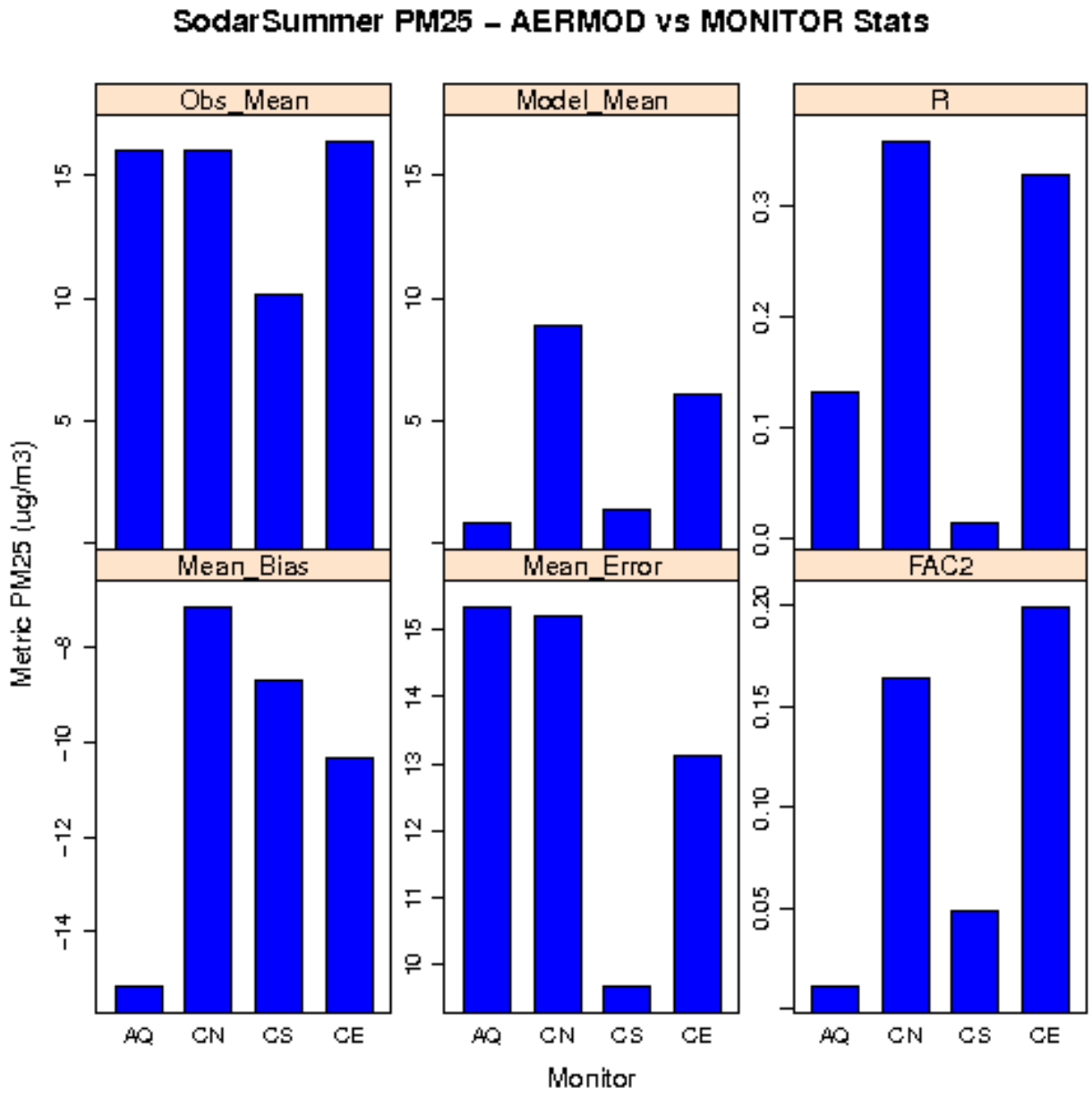

Figure 9-18. Summary statistics of AERMOD model evaluation for $PM_{2.5}$ concentrations at each core site from ALL (both airport-related and background) sources during the Summer Season. [Note that Mean, Bias and Error have units of $\mu g/m^3$, while R and FAC2 are unitless]

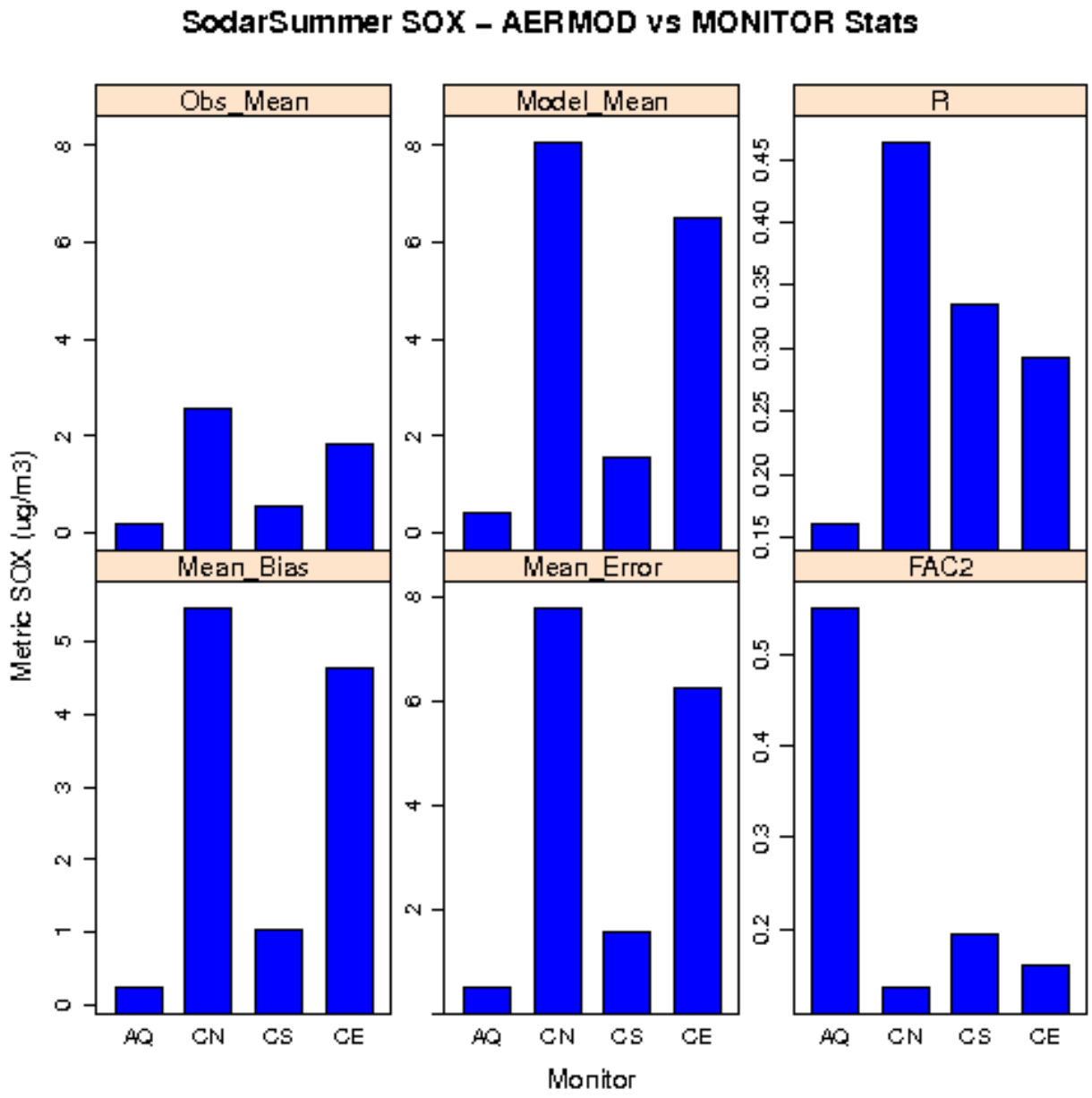

Figure 9-19. Summary statistics of AERMOD model evaluation for SO_x concentrations at each core site from ALL (both airport-related and background) sources during the Summer Season. [Note that Mean, Bias and Error have units of $\mu g/m^3$, while R and FAC2 are unitless]

Qualitative Evaluation:

The following qualitative analyses were performed comparing AERMOD outputs against observations at the four core sites:

1. Quantile-quantile (Q-Q) plots were used to rank order the modeled and observed concentrations unpaired in time, but paired in space at the monitored location, and plot them for each site. The Q-Q plots start with the same paired data as scatter plots, but remove the pairing and ranks observed and modeled from lowest to highest. In doing this, for example, the fifth highest modeled concentration will be plotted against the fifth highest observed concentration. In an ideal case, all the points lie close to the 1:1 line or, at least between the 1:2 and 2:1 lines that are shown parallel to the 1:1 line and lie on either side of this line. A quantile refers to the point below which a given fraction (or percent) of the points lie. That is, the 0.3 (or 30%) quantile is the point at which 30 percent of the data fall below and 70 percent fall above that particular value. Q-Q plots help to assess if the distributions of all of the observed and predicted values are comparable as a whole. Q-Q plots also help identify data that have departures from normality, such as when the data are skewed or have heavy tails (biases at the lower or higher concentrations). This type of analysis is recommended for AERMOD (Chang and Hanna, 2004), since it is expected that AERMOD will better perform to capture extreme values unpaired in space and time. However, note that the data used in these Q-Q plots are paired in space to understand model behavior at each of the core sites. Figure 9-21 and Figure 9-22 show Q-Q plots for CO, NO_x, $PM_{2.5}$ and SO_2 for the Winter Season, and Figure 9-23 and Figure 9-24 show Q-Q plots for the Summer Season.

2. Diurnal variability of observed versus modeled concentrations at four different flag-pole receptors (2m, 7m, 12m, 17m) was used to determine if there was a potential elevated plume in AERMOD not being captured by the surface monitor (Figures 9A-51 to 9A-66 for CO, NO_x, $PM_{2.5}$ and SO_2 during Winter Season and Figures 9A-153 to 9A-168 for CO, NO_x, $PM_{2.5}$ and SO_2 during Summer Season). In these figures, diurnal estimates are computed by finding the interquartile ranges (middle 50 percent, or the difference between the upper and lower quartiles of the distribution) of observed and modeled values for each hour and plotting them as bars, while the means of all observed and modeled values for each hour are plotted as lines. An illustration of this diurnal plot is provided in Figure 9-20 below. There are two caveats that should be noted while reviewing these diurnal figures.

    - As shown in Figure 9-20, there are hours when either the model and/or observations have high values (high outliers), when compared to the interquartile range (IQR). In these instances, the means are greater than the 75^{th} percentile, and hence outside the plotted IQRs.

    - Each figure in Appendix 9-1 shows a four-panel plot, comparing observed values to model predictions at each of the four flag-pole receptors. The most accurate comparison is when the observation is compared to AERMOD outputs from the 2m flag-pole receptors (top left panel in each case). In the remaining three panels, comparisons of surface observations are made with AERMOD outputs at elevated locations and are shown strictly for illustrative purposes.

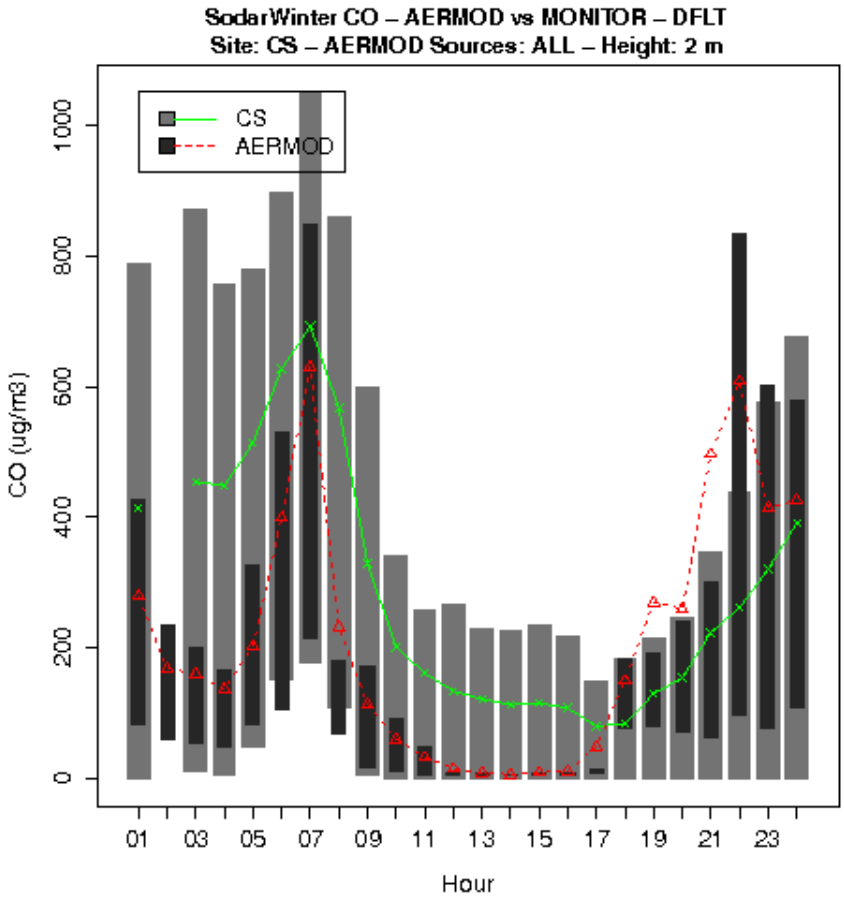

Figure 9-20. Diurnal variability in observed and modeled CO concentrations at the CS site. (Bars represent interquartile ranges and lines represent means of values)

The results from qualitative evaluation focusing on each of the four pollutants measured at the four monitoring locations are discussed below.

Carbon Monoxide

During the Winter Season, AERMOD overpredicted CO at the CN and CE sites for certain hours. However, the model underpredicted at the AQ site, specifically several observed values in the range of 100 – 1000 $\mu g/m^3$ during early morning and late evening hours. Observations at the CE and CS sites had a large scatter with no significant trend. From the diurnal plots (average for each hour during each season), the underprediction at the AQ site was during all hours of the day (Figure 9A-51). At the CE and CN sites, the overpredictions were during the evening hours between 18:00 to 21:00 and underpredictions occurred during early morning hours (Figures 9A-52, 9A-53). At the CS site, the model performed best during early morning and late evening hours, with significant underprediction during mid-day (Figure 9A-54).

As seen in Figure 9-23, during the Summer Season, model performance was similar to the Winter Season (see Figure 9-21). However, upon examining the diurnal plots, different patterns were observed. At the AQ site, the model performed well during a single morning hour (08:00

to 09:00), but largely underpredicted during all other hours of the day (Figure 9A-153). AERMOD overpredicted observations at the CE, CN, and CS sites during the hours between 08:00 and 14:00, (Figures 9A-154, 9A-155 and 9A-156), with a very pronounced peak at 07:00 (at the CS site) and 08:00 to 09:00 (at the CE and CN sites). When comparing the general trends between the Winter and Summer Seasons, the measured values during the Winter Season were much higher than the Summer Season. However, as seen in Figure 9-12 and Figure 9-16, the model did not observe the same order of magnitude differences between the two monitoring seasons.

The Q-Q plots (Figure 9-21 and Figure 9-23) indicate much lower modeled (predicted) CO concentrations than observed concentrations for all hours at the AQ site and for certain hours at the CS site. This clearly indicates the monitor at the AQ site is measuring contributions from other sources or from the regional background not included in AERMOD.

Nitrogen Oxides

The quantitative evaluation showed that the model performance for NO_x was generally poor, with the model R2 less than 0.10 and FAC2 less than 0.35 at all sites. As seen in the diurnal plots presented in Appendix 9-1, model performance at the AQ site was better during early morning and late evening hours (Figure 9A-55) than during the rest of the day. However, at the CE and CN sites, the overpredictions were pronounced during the hours from 18:00 to 22:00, and underpredictions during early morning hours (Figure 9A-56 and 9A-57). AERMOD results for the CS site showed the best diurnal performance (relative to other sites), with modest underprediction during few early morning hours and midday (Figure 9A-58). However, even at the CS site, the range of measured values was generally much greater than predicted by the model, except around 07:00 and between 18:00 and 23:00 hours.

As seen in Figure 9-23, during the Summer Season, the model performance was similar to the Winter Season (Figure 9-21). However, the variations in the tails of the distribution at the AQ site were larger during both seasons. The overpredictions during several hours are an order of magnitude higher. From the diurnal plots, AERMOD overpredicts beginning the early morning hours from 08:00 and through early afternoon to 14:00 at all four core sites (Figures 9A-157 to 9A-160). Comparing the Summer Season diurnal plots to those from the Winter Season, AERMOD overpredicted during late afternoon hours in the Winter Season and during morning hours in the Summer Season, indicating potential problems in AERMOD capturing on-shore versus off-shore effects of winds during the two seasons.

The Q-Q plots for NO_x show much better agreement between AERMOD predicted and observed concentrations, especially during the Winter Season. During the Summer Season, the agreement is best for middle quantiles (between 0.25 and 0.75 of the distribution). However, both ends of the tails show outliers (large deviations from the 1:1 line which leads to overprediction of the highest observations and underprediction of the lowest observations), especially for the AQ site.

Fine Particulate Matter

Except for a few data points, AERMOD underpredicted hourly $PM_{2.5}$ (from the BAM sites) at all four core sites during the Winter and Summer Seasons. Based upon the diurnal plots presented in Appendix 9-1, AERMOD underpredicted observations during all hours of the day at the AQ and CS sites (Figures 9A-59 and 9A-62). However, during the hours from 18:00 to 21:00, the model captured the observed values at site CE (Figure 9A-60), and overpredicted at the CN site by over a factor of two (Figure 9A-61).

During the Summer Season, AERMOD exhibits peaks of overprediction during early morning hours at 08:00 at the CE and CS sites, and from 08:00 to noon at the CN site (Figures 9A-161 to 9A-164), and underprediction during all other hours. The contrast in the timing of the diurnal peaks points to the differences in processes that contribute to $PM_{2.5}$ formation (and likely chemical speciation) during the two seasons.

The Q-Q plots for $PM_{2.5}$ (Figure 9-22 and Figure 9-24) again highlight the drastic underprediction by AERMOD compared to observations at all four core sites. The overall $PM_{2.5}$ underprediction during most hours is related to AERMOD's inability to treat secondary aerosol formation as well as the observations likely capturing impacts from emissions sources outside the Study Area.

Sulfur Oxides

During the Winter Season, AERMOD overpredicted SO_x at the CE and CS sites, but tended to underpredict for several hours at both the AQ and CN sites. From the diurnal analyses, AERMOD overpredicted observations during both early morning and late evening hours at the AQ and CS sites (Figures 9A-63 and 66). At the CE and CN sites, overprediction was observed only during late evening hours from 18:00 to 23:00 (Figures 9A-64 and 9A-65), with a gradual decrease in trend from evening to midnight.

The model performance during the Summer Season was better than the Winter Season. From the diurnal plots presented in Appendix 9-1, AERMOD overpredicted between the hours of 08:00 to 14:00 at the CE and CN sites and 03:00 to 08:00 at the CS site (Figures 9A-165 to 9A-168). At the AQ site, the model performance was much better, with an approximate underprediction of a factor of two of the observed peaks from 07:00 to 08:00.

The Q-Q plots for SO_2 (Figure 9-22 and Figure 9-24) show much better agreement at all four core sites for the middle quantiles (between 0.25 and 0.75 of the distributions) However, the tails are skewed indicating a large underprediction or overprediction of contributions during both seasons, especially for the AQ site.

Discussion of Qualitative Model Performance

There are several reasons why AERMOD performed poorly during Phase III of the LAX AQSAS. Several of these reasons have been recently found in other model applications for modeling aircraft sources with AERMOD (e.g., Phase II of the LAX AQSAS and for the T.F.

Green airport in Providence, Rhode Island (Arunachalam et al., 2008), and some of them are listed below:

- Treatment of aircraft sources as stepped area sources up to 1000 feet and a single area source from 1000 feet to mixing height. Since AERMOD area sources have no plume rise, buoyant plume rise from jet exhausts are not adequately treated, which tend to lead to overprediction by the model.
- Wake impacts on plume behavior in horizontal and vertical directions are not included in AERMOD, which will lead to overprediction
- Lack of treatment of regional background or lack of treatment of regional emissions sources. This is specifically important for $PM_{2.5}$, which leads to underprediction in AERMOD
- $PM_{2.5}$ emissions from First Order Approximation (FOA) treat only primary components, with no provision for treating secondary and volatile components. Since AERMOD is a Gaussian steady-state dispersion model, this will remain a limitation in AERMOD for all airport studies. However, this limitation is overcome for the LAX AQSAS Phase III by utilization of the Community Multiscale Air Quality (CMAQ) model (discussed later in Section 9.2).

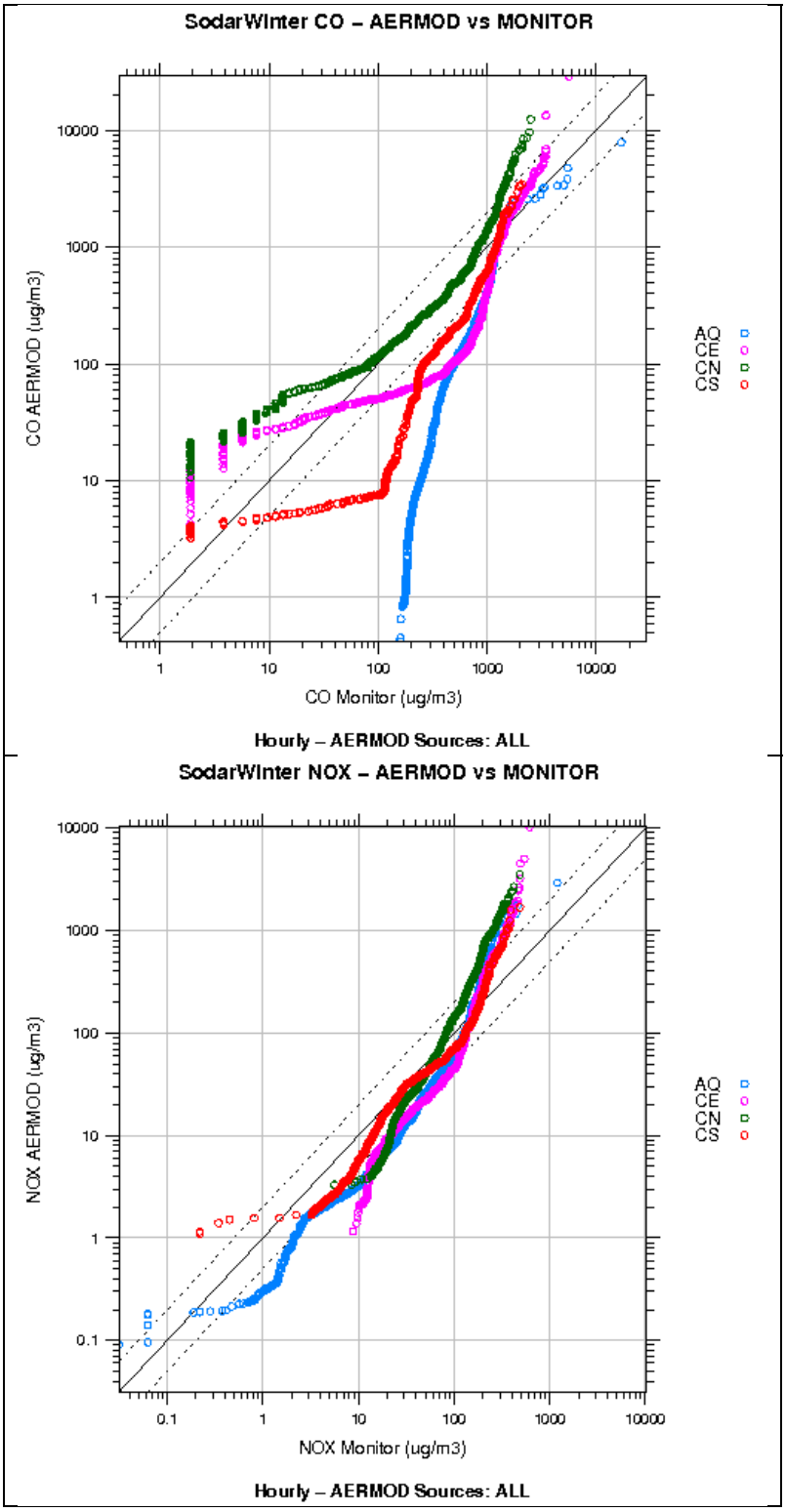

Figure 9-21. Q-Q plots of observed and modeled CO (top) and NO_x (bottom) concentrations at the four core sites during the Winter Season.

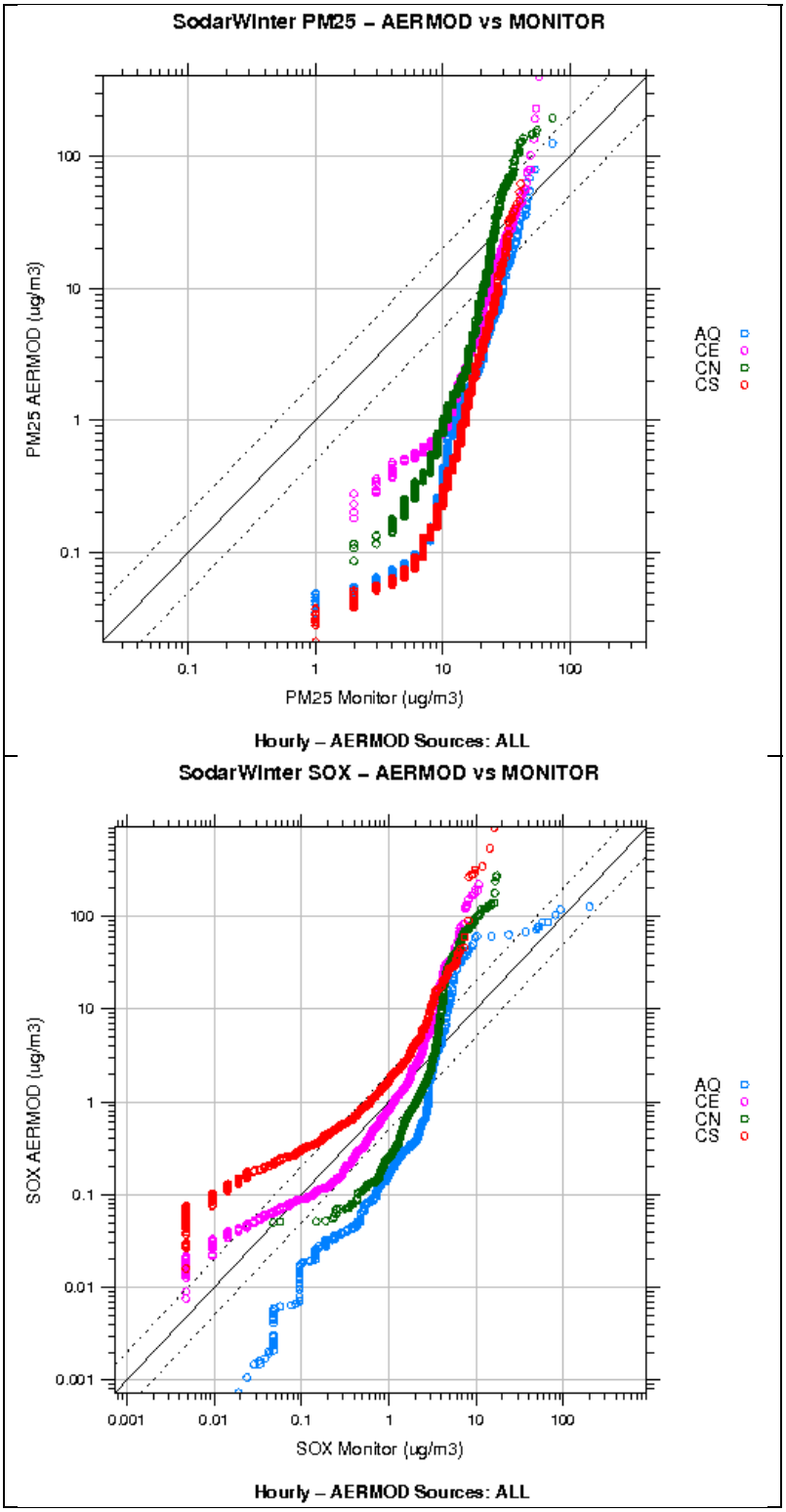

Figure 9-22. Q-Q plots of observed and modeled $PM_{2.5}$ (top) and SO_x (bottom) concentrations at the four core sites during the Winter Season.

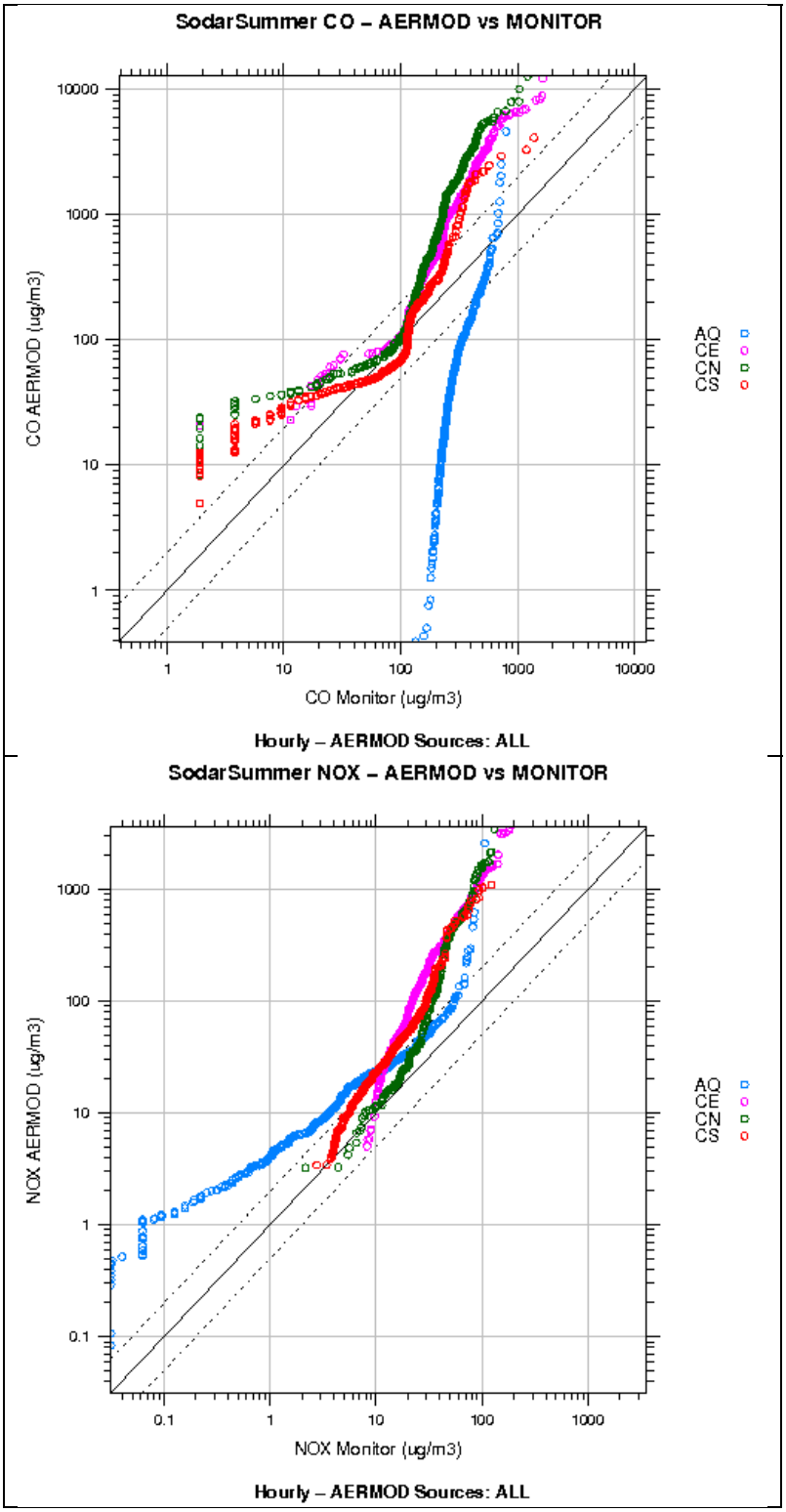

Figure 9-23. Q-Q plots of observed and modeled CO (top) and NO_x (bottom) concentrations at the four core sites during the Summer Season.

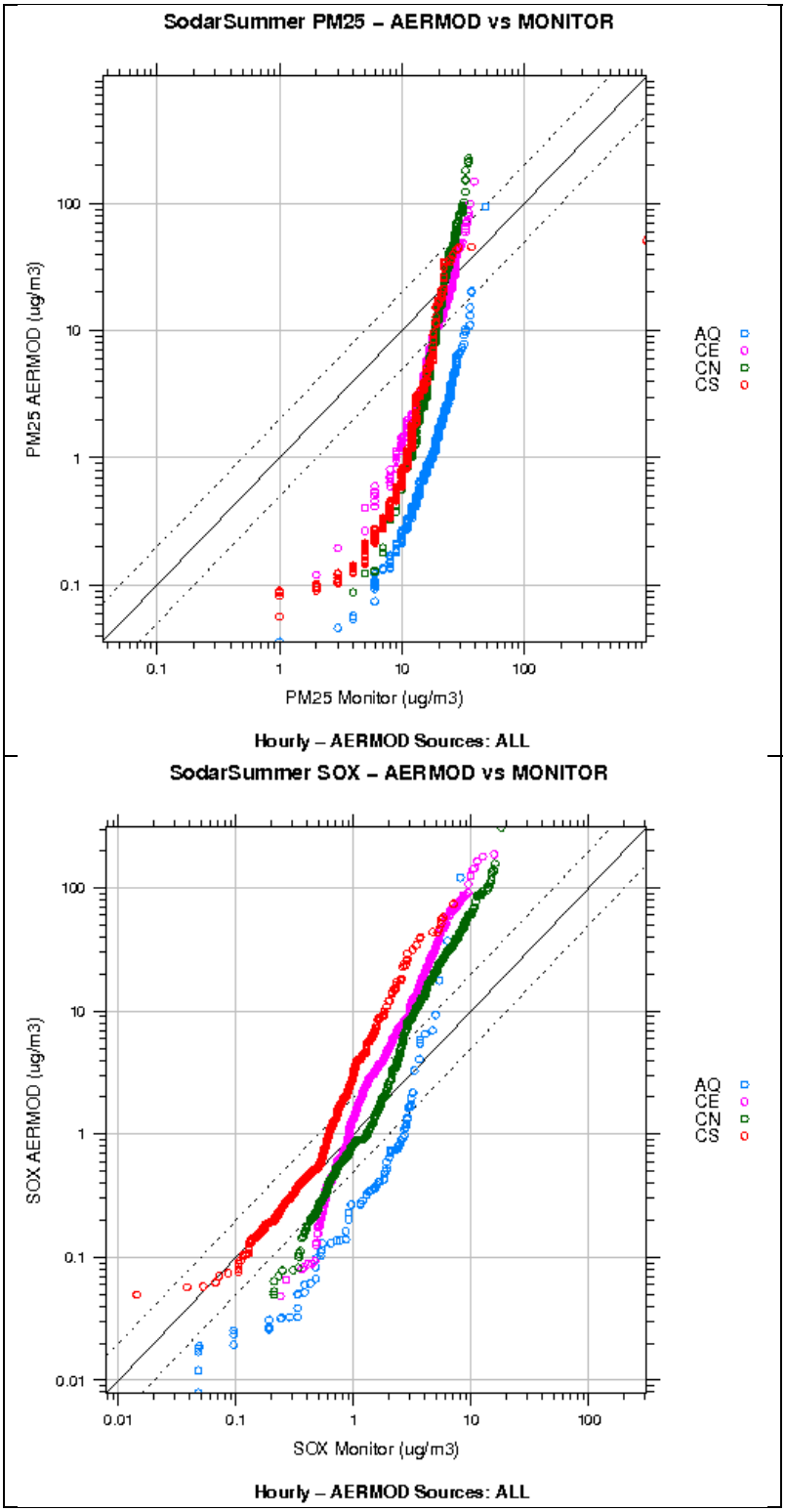

Figure 9-24. Q-Q plots of observed and modeled $PM_{2.5}$ (top) and SO_x (bottom) concentrations at the four core sites during the Summer Season.

9.1.4.7 Source Apportionment

To perform source apportionment using AERMOD results, the model outputs were processed to find the maximum one-hour concentrations at each of the four core sites for both of the measurement periods, and then the concentration predicted by AERMOD for each individual source group during that hour (paired in space and time) was used. This calculation was performed three times – using (1) only airport-related sources, (2) only background sources, and (3) using both airport-related and background sources (all sources), to find the source contribution to hourly maxima for CO, NO_x, $PM_{2.5}$, and SO_2 from each of the three groups.

This calculation was repeated using season averages. AERMOD-predicted season averages for each monitor from each source group were used to find their relative contribution.

Since AERMOD was set up to run for each of the 27 source groups separately, a very detailed source apportionment could be conducted to find the relative contribution from each individual source group to the overall concentrations measured at the four core sites.

The analysis is presented in the form of bar plots and pie charts in the figures listed below, which are presented in Appendix 9-1.

- Bar plots showing source-sector contributions to maximum one-hour and season average concentrations at each monitored location, organized by three major emissions groups (AIRPORT, BACKGROUND, and ALL)
  - Figures 9A-67 to 9A-74 show the CO contribution at the four core sites during the Winter Season
  - Figures 9A-76 to 9A-83 show the NO_x contribution at the four core sites during the Winter Season
  - Figures 9A-85 to 9A-92 show the $PM_{2.5}$ contribution at the four core sites during the Winter Season
  - Figures 9A-94 to 9A-101 show the SO_2 contribution at the four core sites during the Winter season
  - Figures 9A-169 to 9A-176 show the CO contribution at the four core sites during the Summer Season
  - Figures 9A-178 to 9A-185 show the NO_x contribution at the four core sites during the Summer Season
  - Figures 9A-187 to 9A-194 show the $PM_{2.5}$ contribution at the four core sites the during the Summer Season
  - Figures 9A-196 to 9A-203 show the SO_2 contribution at the four core sites during the Summer Season

In the above figures, the time stamp (date and hour) when the maximum one-hour concentration was predicted in each case is shown below the figure.

- Pie charts showing source-sector contributions to season average concentrations at each monitored location from all source groups, aggregated as follows:
    1. Airport/APU/GSE sources
    2. Airport-related traffic sources (both on and off airport property)
    3. Other airport-related sources
    4. Background sources

- Pie charts showing airport-related versus background contributions to season average concentrations at each monitored location. In these analyses, the term "airport-related" refers to the sum of the following three source groups:
    1. Airport/APU/GSE sources
    2. Airport-related traffic sources (both on and off airport property)
    3. Other airport-related sources
    - Figure 9-25 and Figure 9-26 show the aggregated CO contributions by these four sectors at the four core sites during the Winter Season
    - Figure 9-27 and Figure 9-28 show the aggregated NO_x contributions by these four sectors at the four core sites during the Winter Season
    - Figure 9-29 and Figure 9-30 show the aggregated $PM_{2.5}$ contributions by these four sectors at the four core sites during the Winter Season
    - Figure 9-31 and Figure 9-32 show the aggregated SO_2 contributions by these four sectors at the four core sites during the Winter Season
    - Figure 9-33 and Figure 9-34 show the aggregated CO contributions by these four sectors at the four core sites during the Summer Season
    - Figure 9-35 and Figure 9-36 show the aggregated NO_x contributions by these four sectors at the four core sites during the Summer Season
    - Figure 9-37 and Figure 9-38 show the aggregated $PM_{2.5}$ contributions by these four sectors at the four core sites during the Summer Season
    - Figure 9-39 and Figure 9-40 show the aggregated SO_2 contributions by these four sectors at the four core sites during the Summer Season

The information presented in the bar charts for AERMOD-based source apportionment is consolidated and presented as a summary in Table 9-6. This table provides a mapping of the source that had the maximum contribution to each site for pollutant for the season average as well as the maximum one-hour concentrations during each of the two seasons.

Table 9-6. Summary of AERMOD-based source apportionment, indicating the source with maximum contribution to each site/pollutant/metric combination for the two seasons.

Season	Pollutant	Site	Largest Source	
			1-hour max	**Season Avg.**
Winter	CO	AQ	APU/GSE/Aircraft Startup	APU/GSE/Aircraft Startup
		CE	APU/GSE/Aircraft Startup	Minor on-road sources_off
		CN	APU/GSE/Aircraft Startup	APU/GSE/Aircraft Startup
		CS	Minor on-road sources_off	Minor on-road sources_off
	NO_x	AQ	APU/GSE/Aircraft Startup	Aircraft takeoff
		CE	APU/GSE/Aircraft Startup	Minor on-road sources_off
		CN	APU/GSE/Aircraft Startup	APU/GSE/Aircraft Startup
		CS	Chevron	Off-road equipment_off
	$PM_{2.5}$	AQ	APU/GSE/Aircraft Startup	Off airport major roads_off
		CE	APU/GSE/Aircraft Startup	Off airport major roads_off
		CN	APU/GSE/Aircraft Startup	APU/GSE/Aircraft Startup
		CS	On airport roadways	APU/GSE/Aircraft Startup
	SO_2	AQ	Chevron	Chevron
		CE	Aircraft Taxi/Queue	Chevron
		CN	Chevron	Aircraft Taxi/Queue
		CS	Chevron	Chevron
Summer	CO	AQ	APU/GSE/Aircraft Startup	Minor on-road sources_off
		CE	Minor on-road sources_off	Minor on-road sources_off
		CN	APU/GSE/Aircraft Startup	APU/GSE/Aircraft Startup
		CS	Minor on-road sources_off	Minor on-road sources_off
	NO_x	AQ	Aircraft takeoff	Minor on-road sources_off
		CE	APU/GSE/Aircraft Startup	Minor on-road sources_off
		CN	APU/GSE/Aircraft Startup	APU/GSE/Aircraft Startup
		CS	Aircraft takeoff	Off-road equipment_off*
	$PM_{2.5}$	AQ	On airport roadways	Off airport major roads_off
		CE	On airport roadways	Off airport major roads_off
		CN	On airport roadways	APU/GSE/Aircraft Startup
		CS	APU/GSE/Aircraft Startup	On airport roadways
	SO_2	AQ	Aircraft takeoff	Aircraft Taxi/Queue
		CE	Aircraft takeoff	Chevron
		CN	Chevron	Aircraft Taxi/Queue
		CS	Aircraft Taxi/Queue	Aircraft Taxi/Queue

The information in the table listed above is consolidated in Figure 9-25through Figure 9-40below for each pollutant.

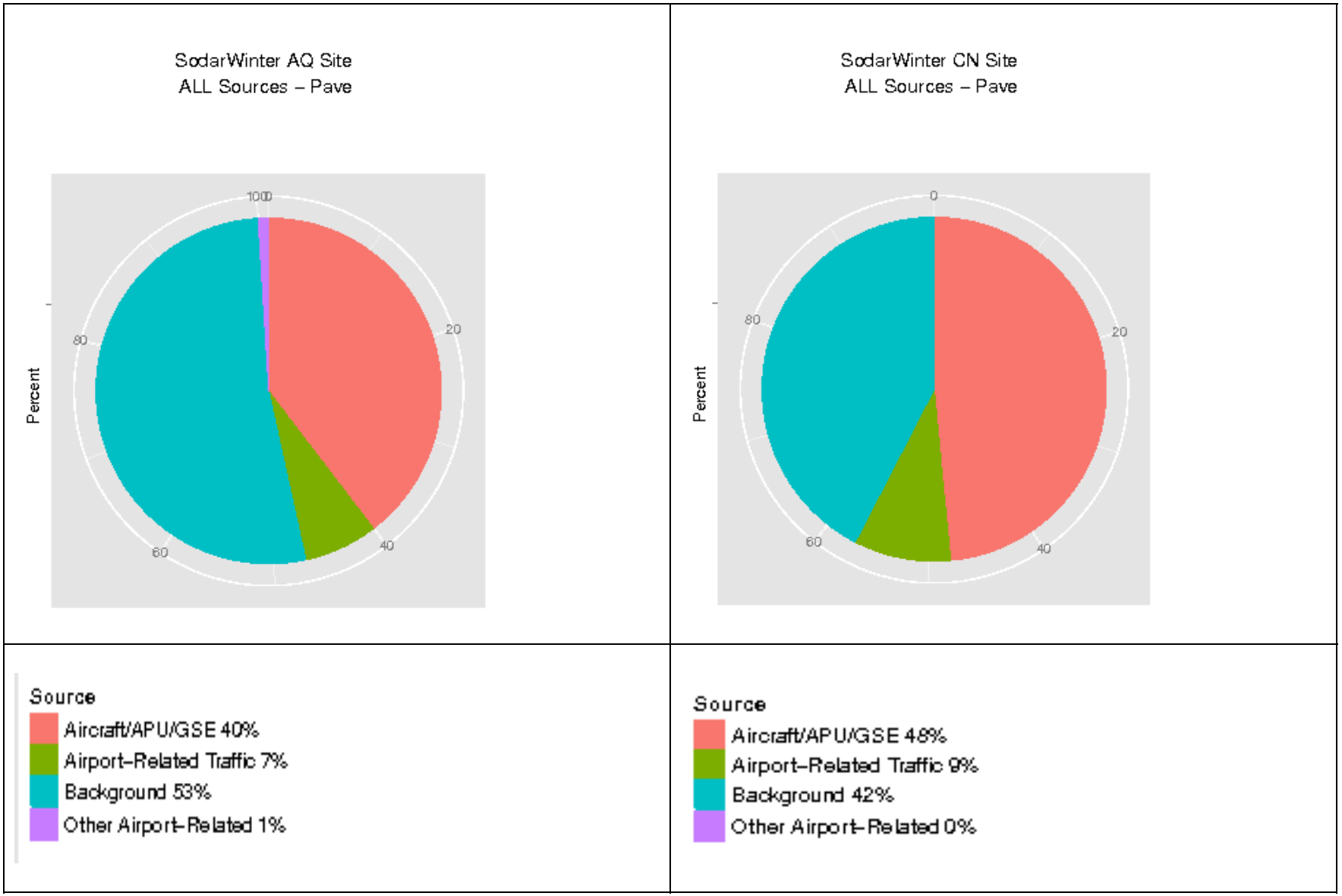

Figure 9-25. Source-sector contributions to period average CO concentrations at AQ and CN sites during Winter Season.

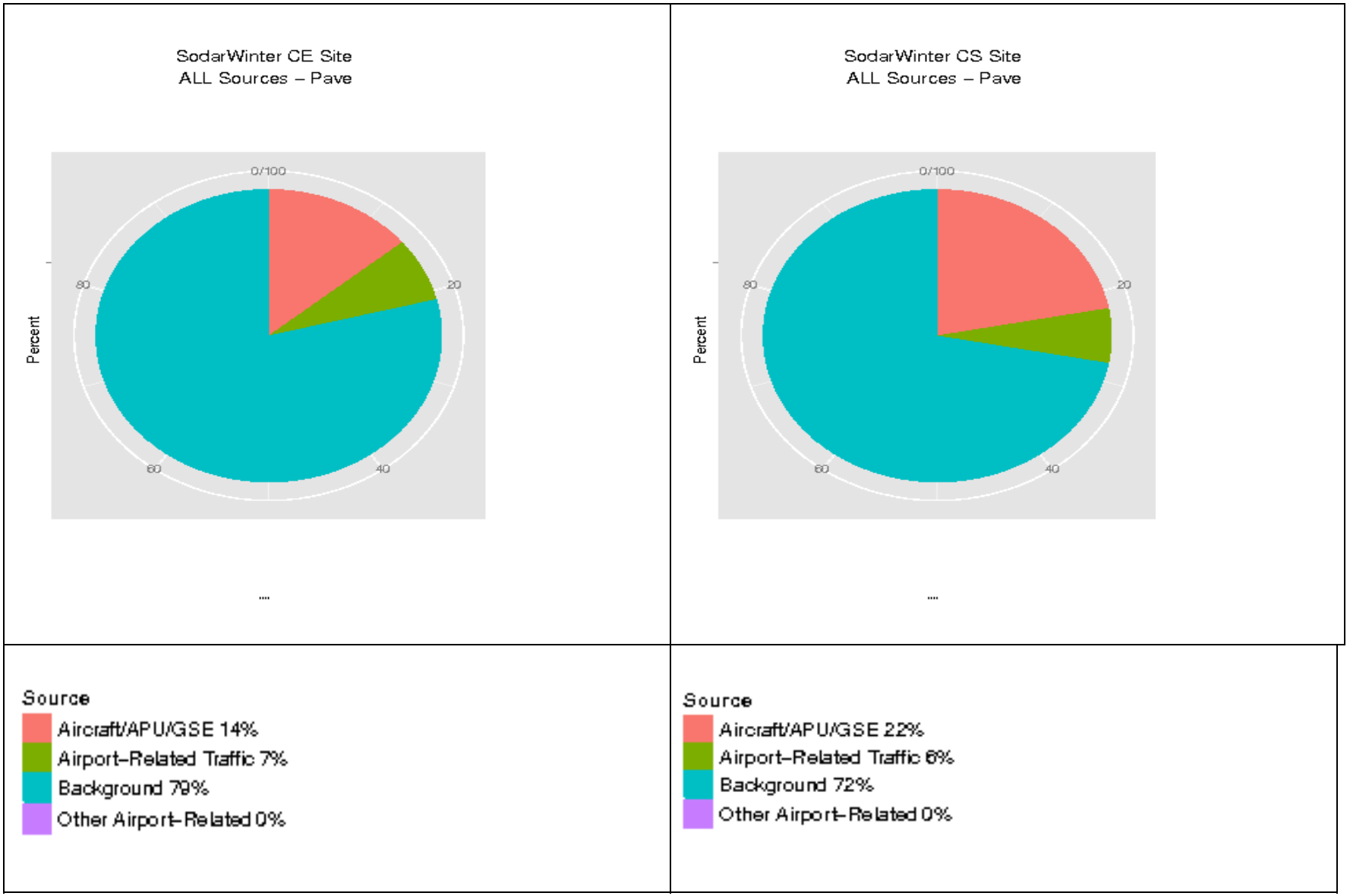

Figure 9-26. Source-sector contributions to period average CO concentrations at CE and CS sites during Winter Season.

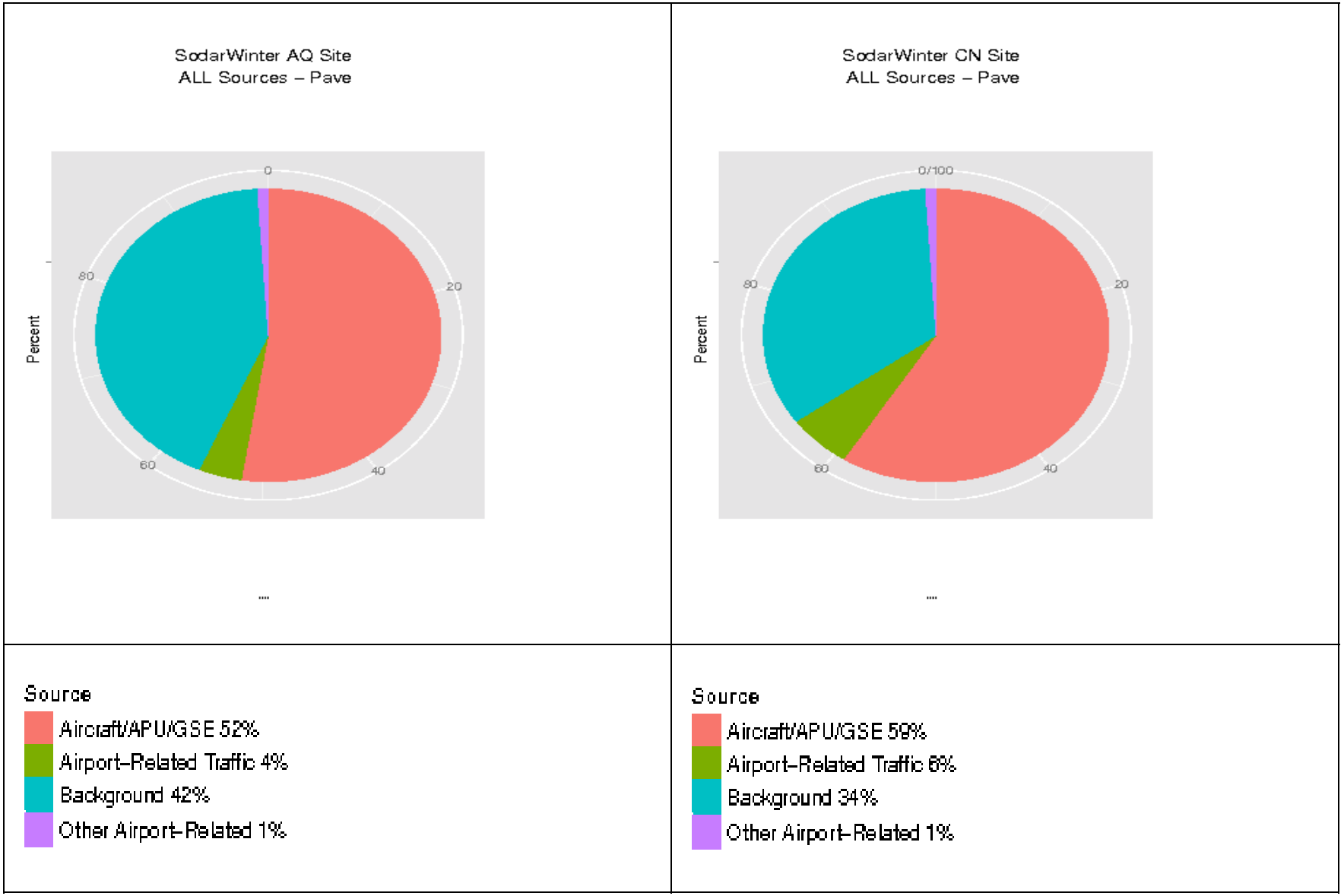

Figure 9-27. Source-sector contributions to period average NO_x concentrations at AQ and CN sites during Winter Season.

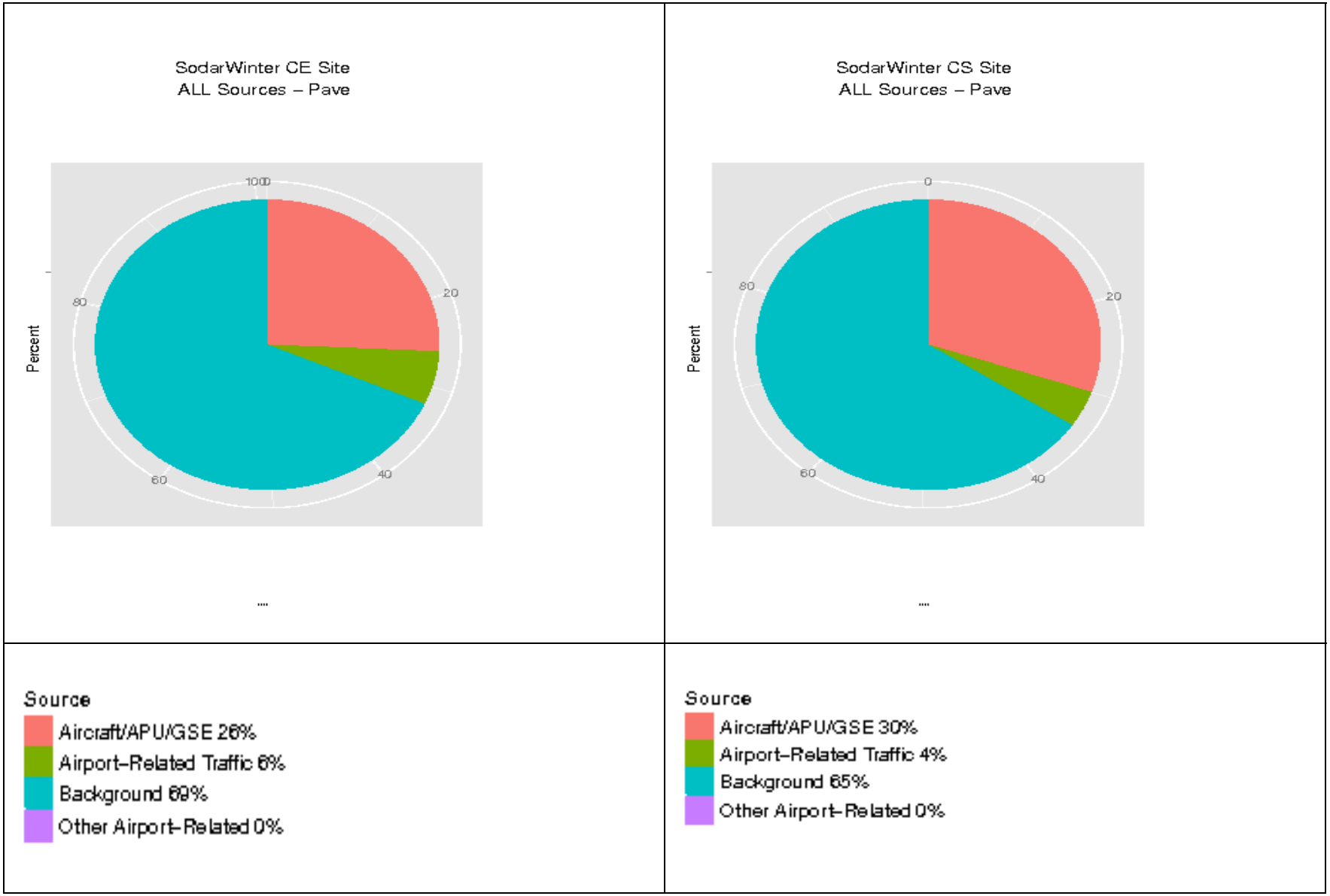

Figure 9-28. Source-sector contributions to period average NO_x concentrations at CE and CS sites during Winter Season.

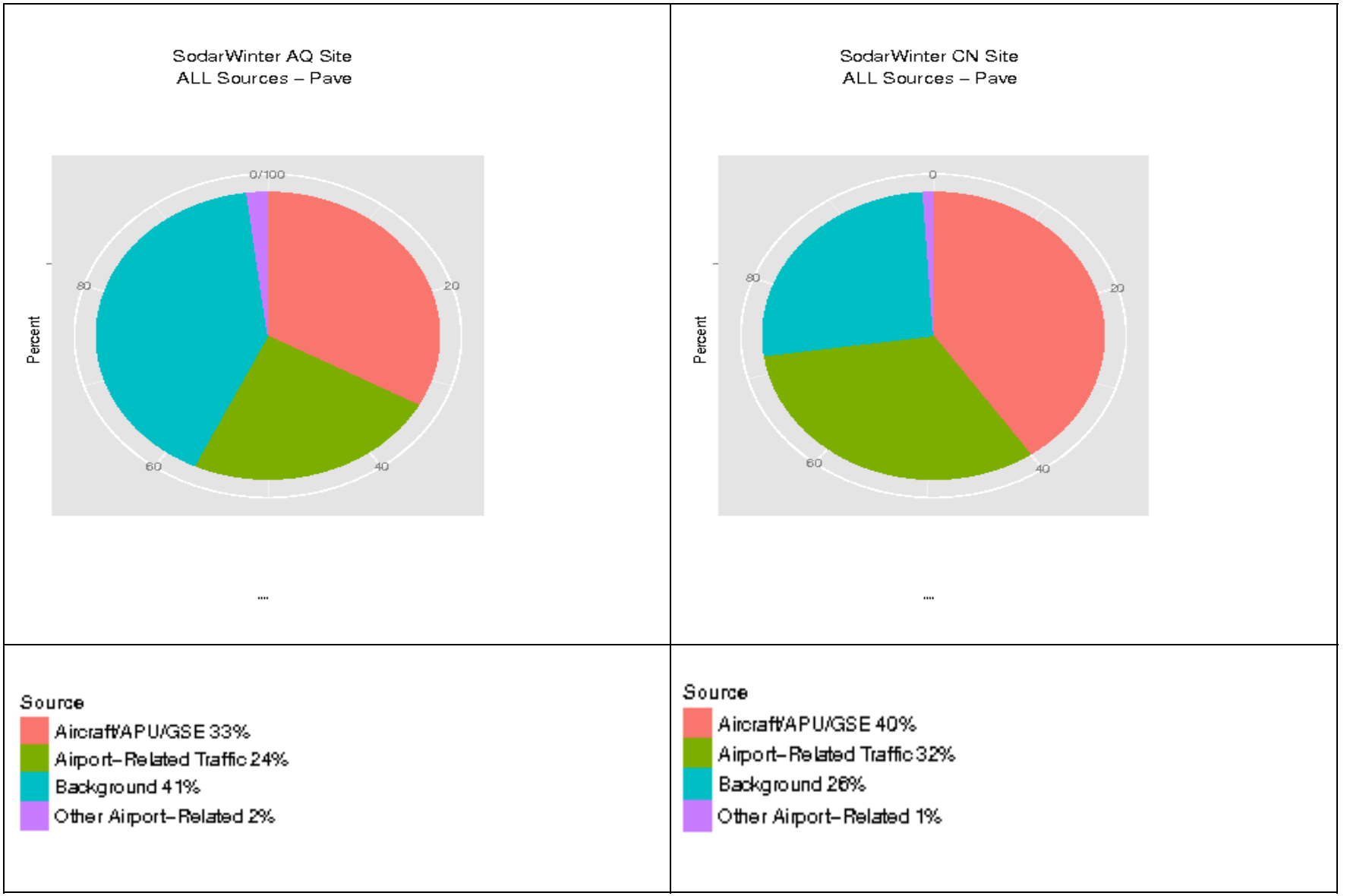

Figure 9-29. Source-sector contributions to period average $PM_{2.5}$ concentrations at AQ and CN sites during Winter Season.

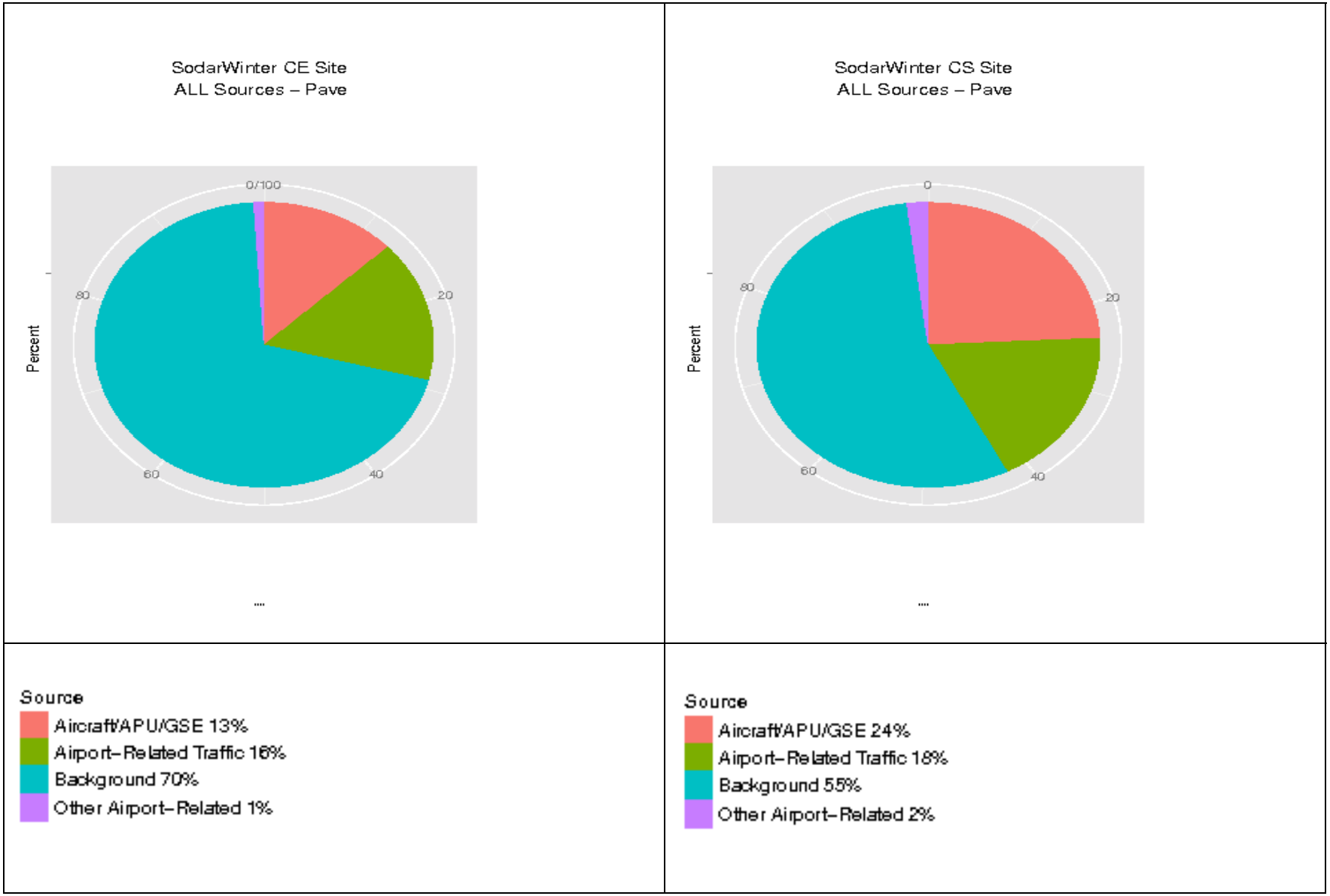

Figure 9-30. Source-sector contributions to period average $PM_{2.5}$ concentrations at CE and CS sites during Winter Season.

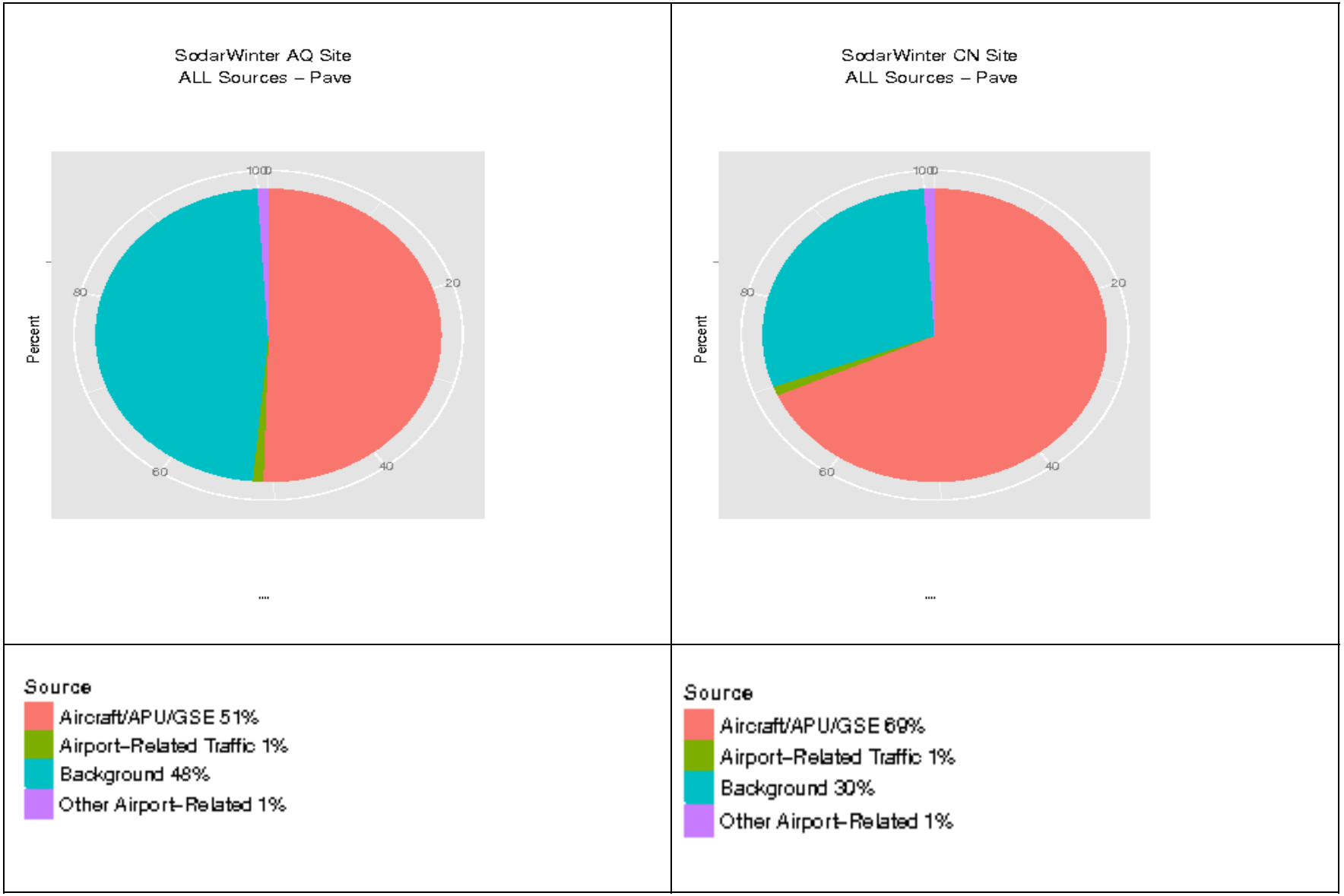

Figure 9-31. Source-sector contributions to period average SO_x concentrations at AQ and CN sites during Winter Season.

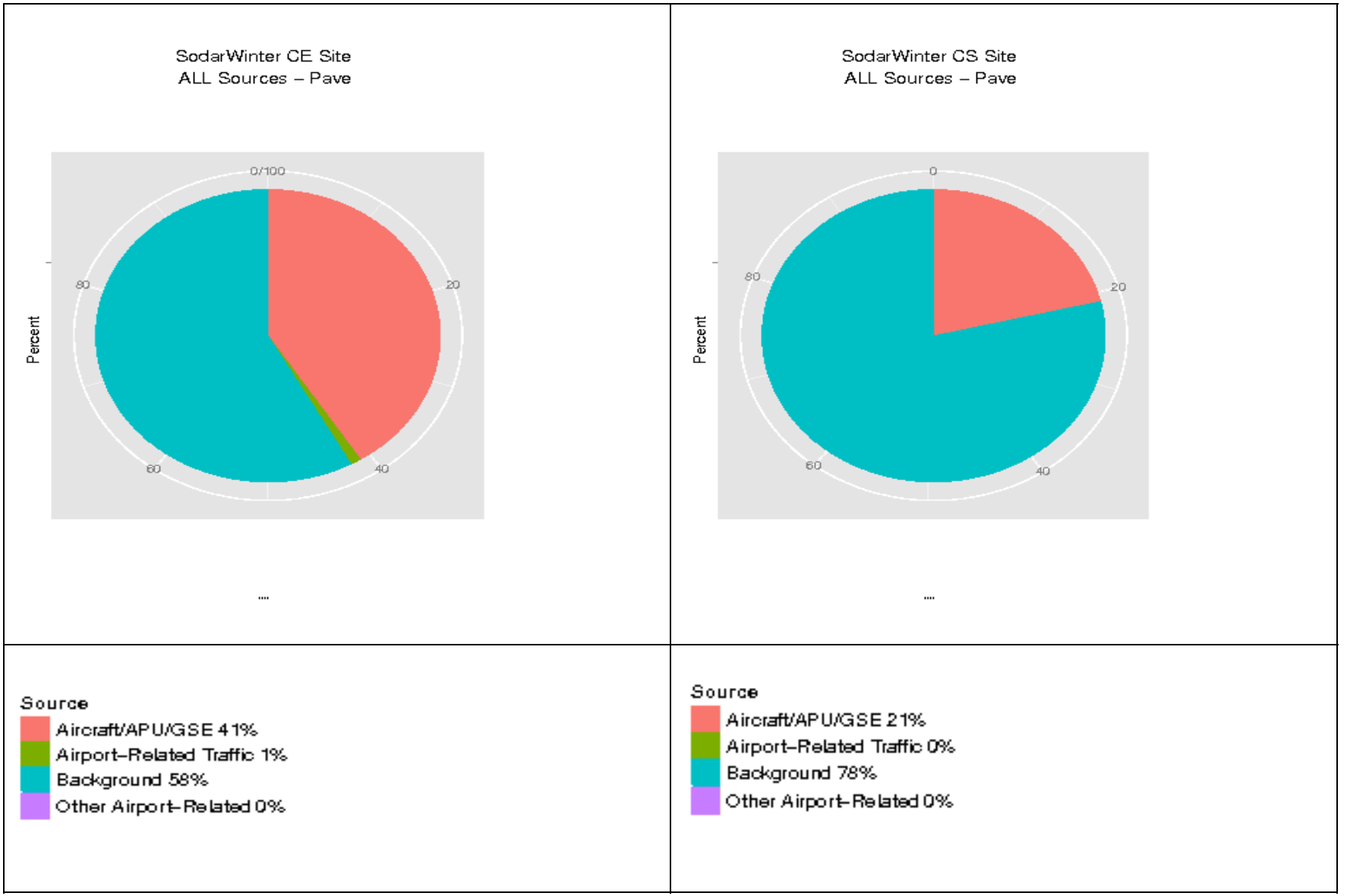

Figure 9-32. Source-sector contributions to period average SO_x concentrations at CE and CS sites during Winter Season.

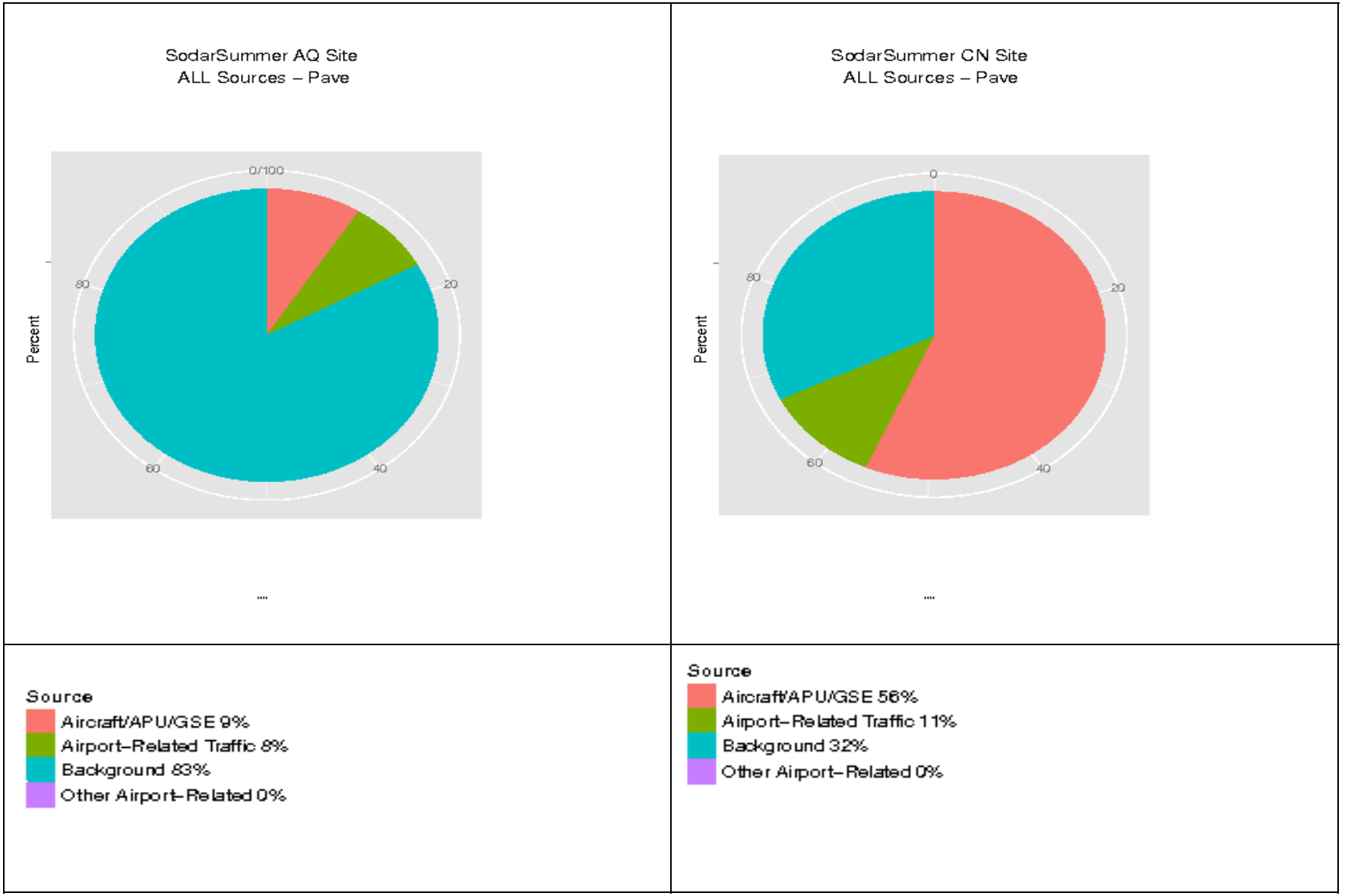

Figure 9-33. Source-sector contributions to period average CO concentrations at AQ and CN sites during Summer Season.

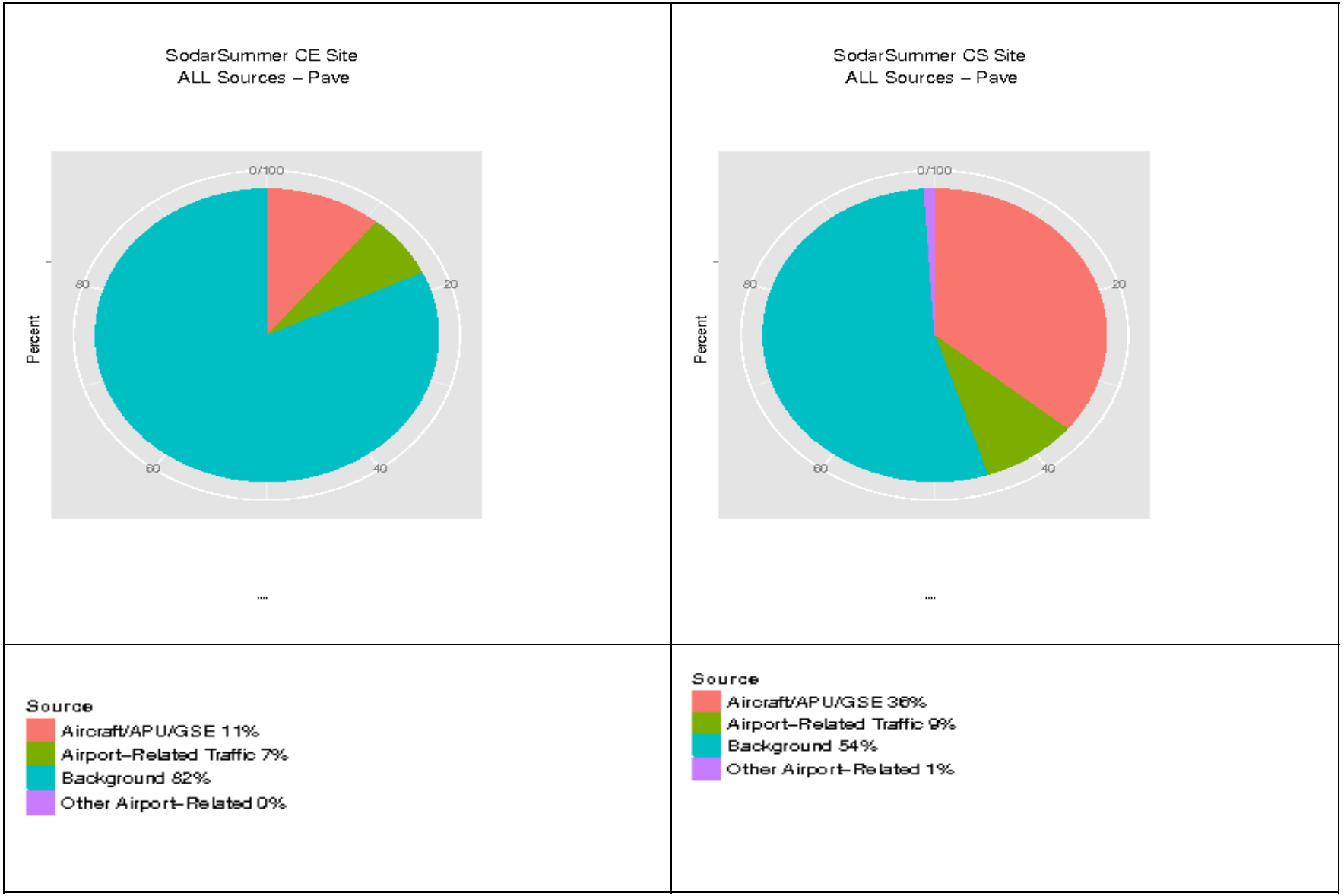

Figure 9-34. Source-sector contributions to period average CO concentrations CE and CS sites during Summer Season.

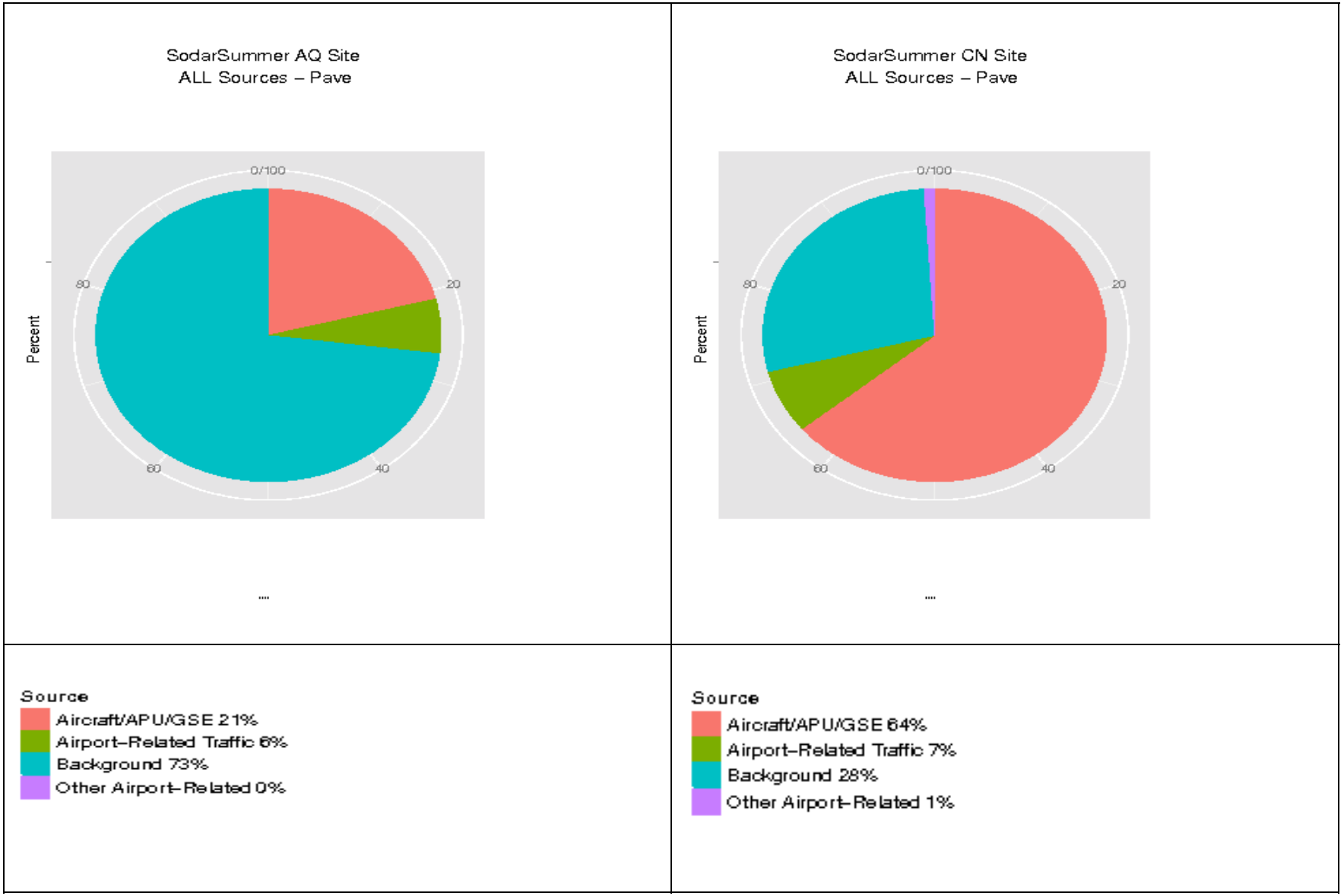

Figure 9-35. Source-sector contributions to period average NO_x concentrations at AQ and CN sites during Summer Season.

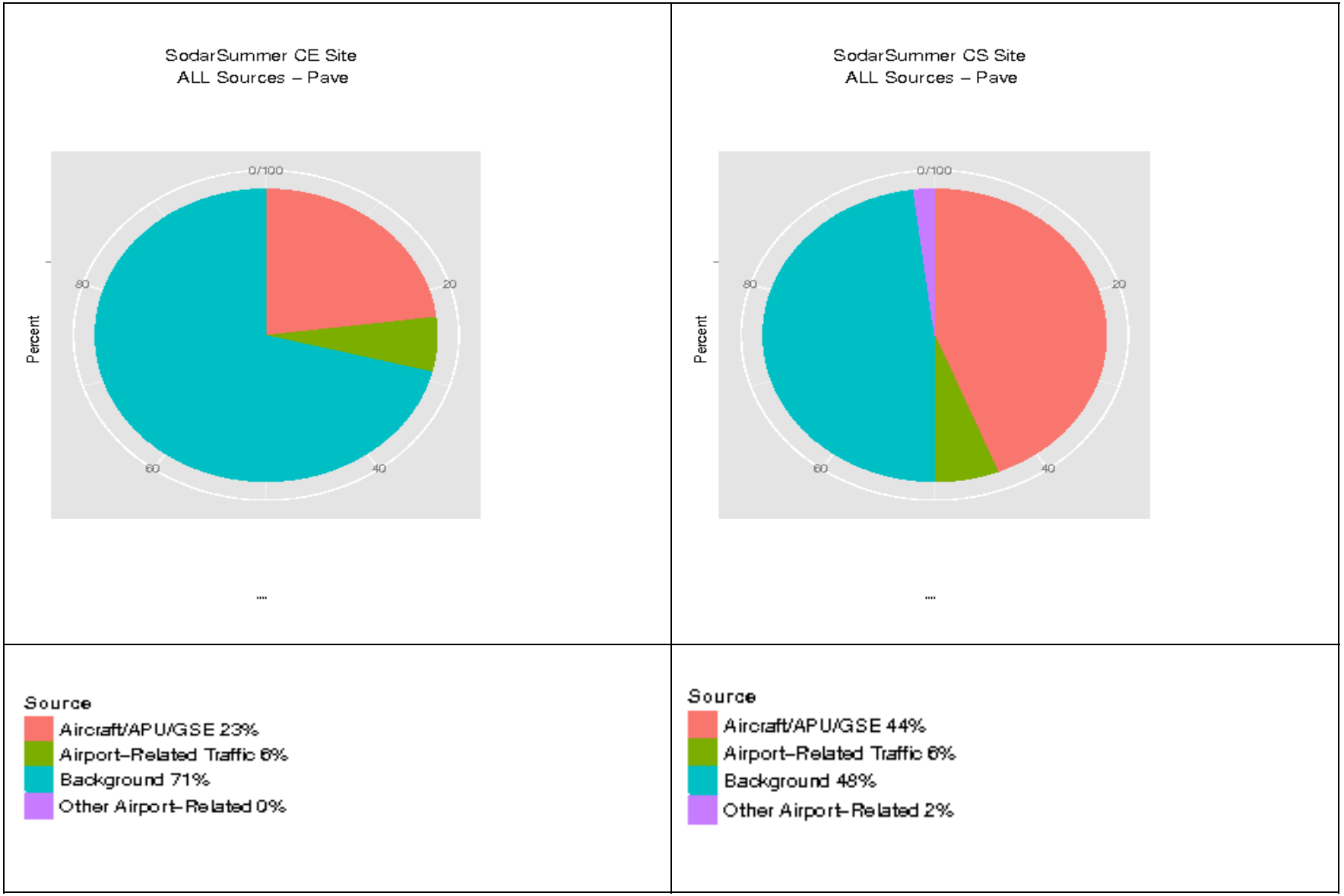

Figure 9-36. Source-sector contributions to period average NO_x concentrations at CE and CS sites during Summer Season.

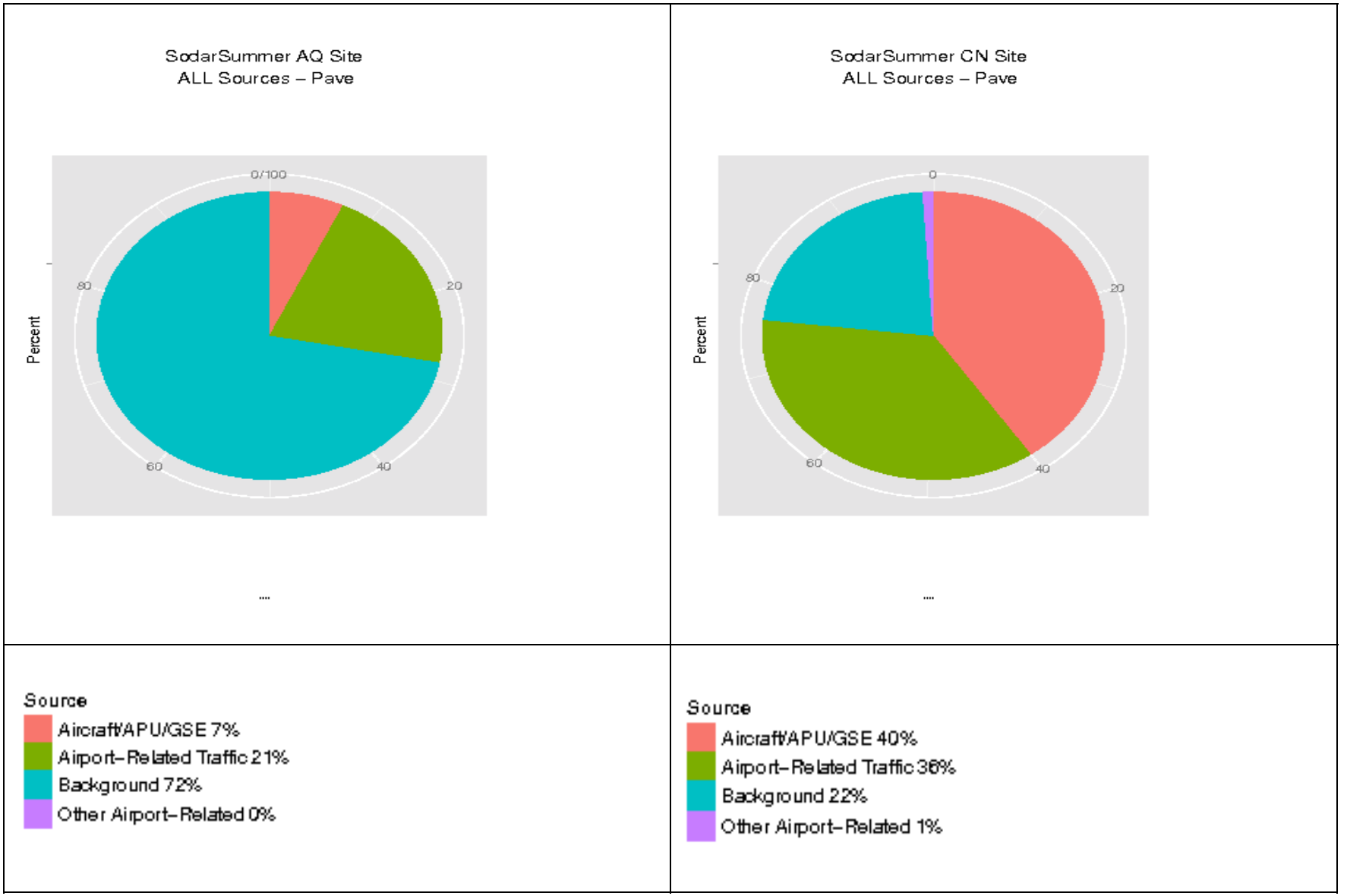

Figure 9-37. Source-sector contributions to period average $PM_{2.5}$ concentrations at AQ and CN sites during Summer Season.

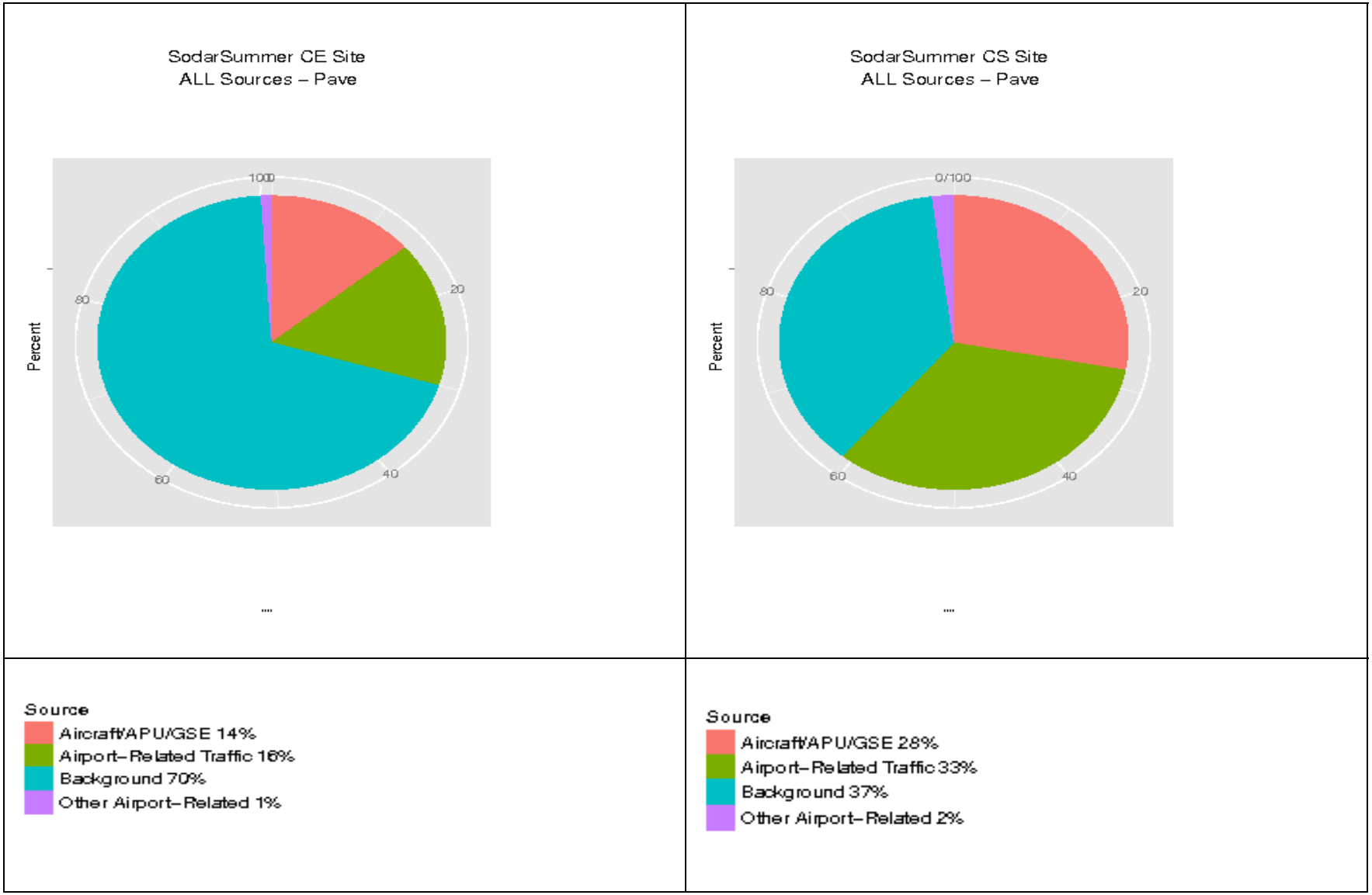

Figure 9-38. Source-sector contributions to period average $PM_{2.5}$ concentrations at CE and CS sites during Summer Season.

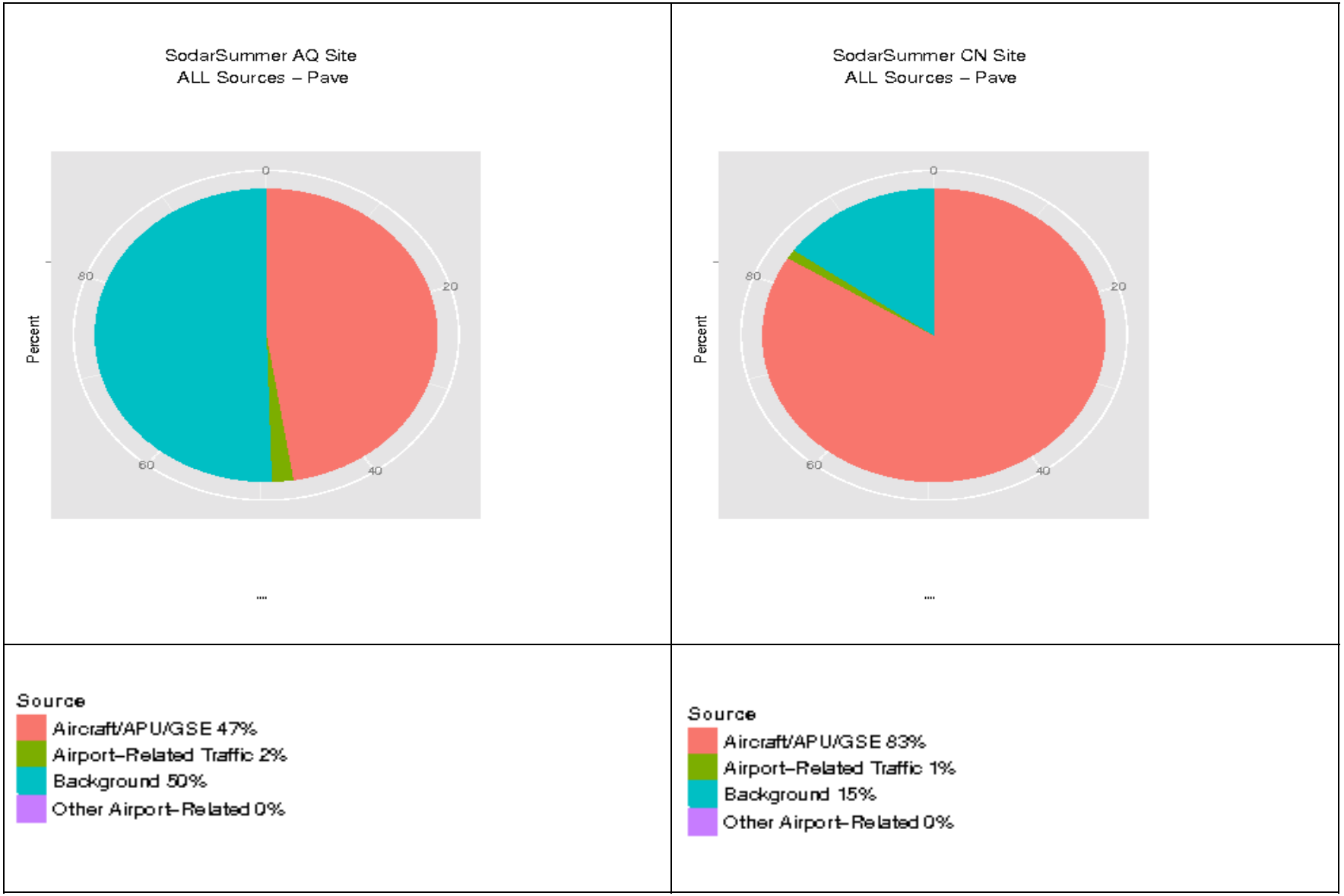

Figure 9-39. Source-sector contributions to period average SO_x concentrations at AQ and CN sites during Summer Season

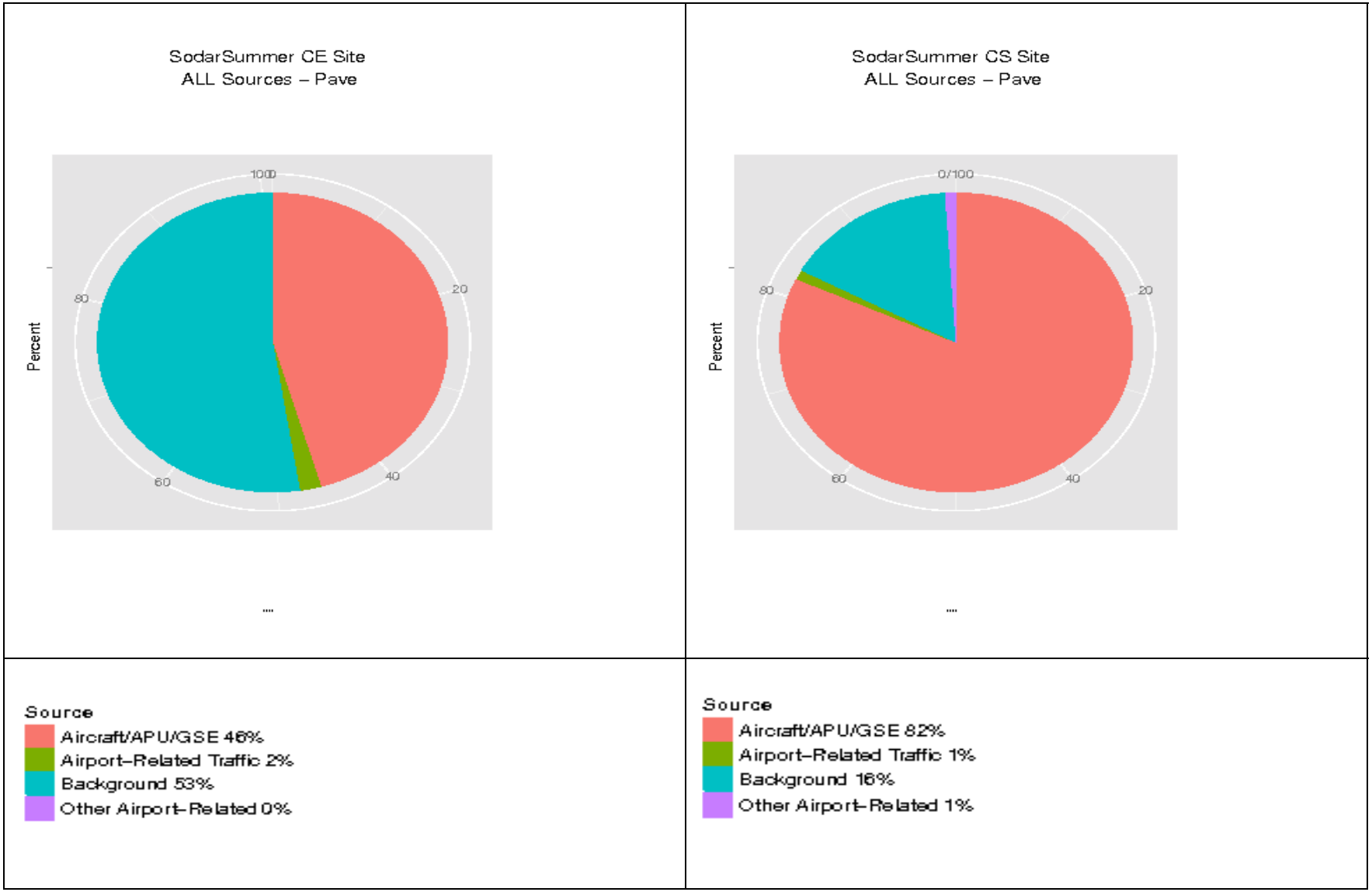

Figure 9-40. Source-sector contributions to period average SO_x concentrations at CE and CS sites during Summer Season

Carbon Monoxide

In summary, during the Winter Season, aircraft sources due to terminal area activity dominated the model predicted season averages of CO at the CN site (48%), while background sources in the Study Area dominated the season averages at the AQ (53%), CE (79%) and CS sites (72%). Similarly during the Summer Season, the general trend was similar, with slightly different magnitudes with aircraft sources dominating CO at the CN site (56%), and background sources comprising the largest contributions at the AQ (83%), CE (82%) and CS sites (54%).

Nitrogen Oxides

In summary, during the Winter Season, aircraft sources due to terminal area activity dominated the model predicted season averages of NO_x at the AQ (52%) and CN sites (59%), while background sources in the study area dominated at the CE (69%) and CS sites (65%). During the Summer Season, aircraft sources due to terminal area activity dominated at the CN site (64%), while background sources in the study area comprised the largest emission sources at the AQ (73%), CE (71%) and CS sites (46%).

Fine Particulate Matter

In summary, during the Winter Season, aircraft sources due to terminal area activity dominated the model predicted season averages of $PM_{2.5}$ concentrations at the CN site (40%), while background sources in the study area dominated at the AQ (41%), CE (70%) and CS sites (55%). The general trend was the same in the Summer Season, with slightly different results, where aircraft activity dominated at the CN site (40%), and background sources are the largest contributing sources at the AQ (72%), CE (70%) and CS sites (37%). Airport-related traffic was the second largest contributor at both the CN and CS sites with contributions of 32 percent and 18 percent during Winter Season and 36 percent and 33 percent during Summer Season, respectively.

Sulfur Oxides

In summary, during the Winter Season, aircraft sources due to terminal area activity dominated the model predicted season averages of SO_2 concentrations at the AQ (51%) and CN sites (69%), while background sources dominated at the CE (58%) and CS sites (78%). During the Summer Season, aircraft activity dominated at the CN (83%) and CS sites (82%), and background sources dominated the modeled season average SO_2 concentrations at the AQ (50%) and CE sites (53%). The aircraft activity contributions to season average SO_2 concentrations at the AQ and CE sites were 47 and 46 percent, respectively.

9.1.5 Summary and Conclusion

Source-based modeling of emissions inventories prepared for Phase III of the LAX AQSAS (as described in Section 8) was performed with the AERMOD model for the two seasons studied – January 31 – March 13 during the Winter Season and from July 18 – August 28, 2012 during the Summer Season.

The modeling outputs were analyzed in three phases:

- Spatial analyses of overall concentration patterns of maximum one-hour concentrations and seasonal averages
- Model evaluation against ambient measurements performed at the four core sites
- Source apportionment of modeled values to modeled maximum one-hour concentrations and seasonal averages generated using AERMOD.

Key findings from source-based modeling include:

- Analyses of results for flag-pole receptors indicate that predictions at two meters above ground are often less than values modeled at higher elevations. Highest concentrations for aircraft takeoff and landing, power plants, and marine sources were often modeled aloft (as high as 22 m, and not at the surface)

- Performance evaluation of AERMOD showed that when using the most stringent paired-in-time-and-space approach, the model performance was generally fair to poor, with the model explaining at most only up to 50 percent of the variability in the observations. Nearly two-thirds of the modeled values were off from the observations by over a factor of two, both above and below the observed values. The Q-Q plots with data paired in space, but not in time, at the four core sites showed generally better performance, especially in the middle quartiles, but had underprediction at the lower ends and overprediction at the higher ends of the distribution.

- During the Winter Season, background sources in the Study Area contribute to more than 50 percent of the modeled CO, NO_x, $PM_{2.5}$, and SO_2 concentrations at the CS and CE sites. Airport-related sources contribute more than 75 percent of the modeled $PM_{2.5}$ and SO_2 concentrations at the AQ and CN sites.

- During the Summer Season, background sources contribute to more than 50 percent of the modeled CO, NO_x, $PM_{2.5}$ and SO_2 concentrations at the AQ and CE sites, with approximately 75 percent at the AQ site for CO, NO_x, and $PM_{2.5}$. Airport-related sources contribute more than 75 percent of the modeled concentrations for all pollutants at the CN site and approximately 50 percent contribution of the modeled concentrations for all pollutants at the CS site.

- Short-term impacts (one-hour maxima) driven by airport-related sources at the AQ, CE, and CN sites during both the Summer and Winter Seasons, while background sources dominate both median and 75^{th} percentile ranges.

- Of all the Airport-related sources, major roadway sources account for the highest contribution at the AQ and CS sites. Aircraft takeoff dominate at the CE site while APU, GSE, and Start-up emissions dominate at the CN site

- Of all the Background sources, Off-road equipment dominate at the AQ, CN, and CS sites, minor on-road sources dominate at the CE site, but also play a major role at the AQ and CN sites

9.2 CMAQ MODELING

The results from modeling performed with the Community Multiscale Air Quality (CMAQ) model for Phase III of the LAX AQSAS Phase III are included in this section. CMAQ was used as a supplement to AERMOD for source-based dispersion modeling of emissions from the Airport.

CMAQ has been used to study air quality impacts of several airports. Arunachalam et al., (2011) modeled aircraft emissions during landing and takeoff (LTO) cycles at the Hartsfield Atlanta, Chicago O'Hare and Providence T.F. Green airports, and concluded that from an air quality and health risk perspective the choice of modeled grid resolution (36-km vs. 12-km vs. 4-km) contributed only a two percent difference in modeled health risk. Kim et al. (2010) modeled the Washington Dulles airport using CMAQ at a 12 km and 4 km grid resolution as part of Federal Aviation Administration sponsored study to provide guidance for airport operators by quantifying the contribution of airport emissions to local air quality. Woody et al. (2011) modeled emissions from the 99 largest U.S. airports to study current and future year air quality impacts utilizing the CMAQ model.

Using a hybrid modeling technique that combines CMAQ and AERMOD, Davis and Arunachalam (2009) showed that a coarser grid resolution CMAQ application, when combined with AERMOD, can provide a very highly resolved field of air quality impacts in the immediate vicinity of the airport. More recently, Rissman et al. (2013) developed an application of using a subgrid scale treatment in CMAQ to model aircraft sources during LTO cycles at the Hartsfield Atlanta airport, and demonstrated the enhanced characterization as well as highly resolved air quality impacts due to this advanced hybrid treatment.

9.2.1 General Description

The CMAQ model is a state-of-the-art, comprehensive, one-atmosphere Eulerian or grid-based air quality modeling system that treats gas-phase chemistry, particulate matter (PM), and hazardous air pollutants (HAPs) (Byun and Schere, 2006). CMAQ simulates the numerous physical and chemical processes involved in the formation, transport, and destruction of air pollutants. Inputs to the model include emissions estimates (from aircraft as well as all other anthropogenic and biogenic sources), meteorological fields, and initial condition and boundary condition data. The meteorological fields are developed from the Weather Research and Forecast (WRF) model (Skamarock et al., 2008), and emissions processed through the Sparse Matrix Operator Kernel Emissions (SMOKE) modeling system (Houyoux et al., 2000). While CMAQ can handle different time resolutions for inputs and outputs, typical applications (like the one used for this Study) are configured to read and process hourly inputs and outputs.

CMAQ currently treats PM formation through a modal approach (Binkowski and Roselle, 2003). Particulate matter 2.5 μm or less in diameter ($PM_{2.5}$) is represented by two sub-distributions or

modes (Whitby, 1978) called the Aitken and accumulation modes. The Aitken mode includes particles with diameters up to approximately 0.1 µm for the mass distribution. The accumulation mode covers the mass distribution in the range from 0.1 to 2.5 µm. CMAQ treats the following components of $PM_{2.5}$ explicitly in each of the Aitken and accumulation modes: sulfate (ASO4), nitrate (ANO3), ammonium (ANH4), organic carbon from anthropogenic sources (AORGA), organic carbon from biogenic sources (AORGB), elemental carbon (AEC), and. other unknown crustal material (A25).

The latest version of CMAQ released to the general public is CMAQ v5.0.1 and includes several updates to the modeling system.

9.2.2 CMAQ Configuration and Inputs

SCAQMD created the 2008 base year modeling database for 2012 State Implementation Plan (SIP) purposes. This modeling is described in detail in the 2012 Air Quality Management Plan (AQMP).[22] SCAQMD provided the following CMAQ-ready inputs for modeling conducted for Phase III of the LAX AQSAS.

- Meteorological outputs from the Weather Research Forecast (WRF) model processed through the Meteorology-Chemistry Interface Processor (MCIP) (Otte et al., 2010)
- Photolysis Rates
- Initial and Boundary Conditions
- Ocean-mask file to define the surf zone
- Emissions inventories that included all anthropogenic sources (including LAX) and natural sources for the region.

The 2012 SIP Platform used CMAQ version 4.7.1 (Foley et al, 2010) with the Statewide Air Pollution Research Center (SAPRC-99) chemical mechanism,[23] and a horizontal grid resolution of 4 km x4 km. While WRF was configured with a 30-layer vertical structure extending to 19.2 km above the surface, SCAQMD used MCIP to collapse the vertical structure to use only 18 layers, with identical mapping in the boundary layer (lowest 10 layers of the atmosphere, extending to 851 meters). Table 9-7 lists the modeling domain configuration, and Figure 9-41 shows the modeling domain.

[22] SCAQMD. 2012. Draft Final 2012 AQMP Appendix V Access on 4/11/2013 from: http://www.aqmd.gov/aqmp/2012aqmp/DraftFinal/AppV.pdf.

[23] SAPRC Atmospheric Chemical Mechanisms and VOC Reactivity Scales Access on 4/11/2013 from: http://www.engr.ucr.edu/~carter/SAPRC/

Table 9-7. CMAQ Modeling Domain Configuration

Projection Parameters	Projection	Lambert Conformal Projection
	Latitude of Origin	37 N
	Central Meridian	120.5 W
	Standard Parallel	30 N, 60 N
	Horizontal Grid Size	4 km x 4 km
	Southwest Origin	(-84 km, -552 km)
	Modeling Domain	156 x 102 x 18
	Vertical Layer Structure	Variable up to 50 hPa (mb)
Model Configuration	Version	4.7.1
	Chemical Mechanism	SAPRC-99
	Horizontal Advection Module	Piecewise Parabolic Method (Hppm)
	Vertical Advection Module	Piecewise Parabolic Method (Vppm)
	Vertical Diffusion Module	Asymmetric Convective Module (ACM2)
	Aerosol Module	Version 5 (Aero5)
	Cloud Treatment	ACM with Aerosol V5 (ACM_AE5)
Periods	Year	2008
	Simulation Duration	Winter: Jan 31 – Mar 16 Summer: Jul 18 - Aug 28

In addition to the 2008 base year, SCAQMD had created emissions inventories and performed future year emissions strategy modeling to demonstrate attainment for $PM_{2.5}$ for 2014, 2017, and 2019. Since the base year emissions estimates are more certain than future year estimates, it was decided to use the 2008 base year modeling platform to model the Winter (January 31 – March 13, 2012) and Summer (July 18 – August 28, 2012) Seasons corresponding to the Phase III Study. SCAQMD performed a detailed evaluation of the WRF and CMAQ base year modeling results by comparing modeled predictions against observations (both meteorological and air quality parameters). This is described in the 2012 AQMP.

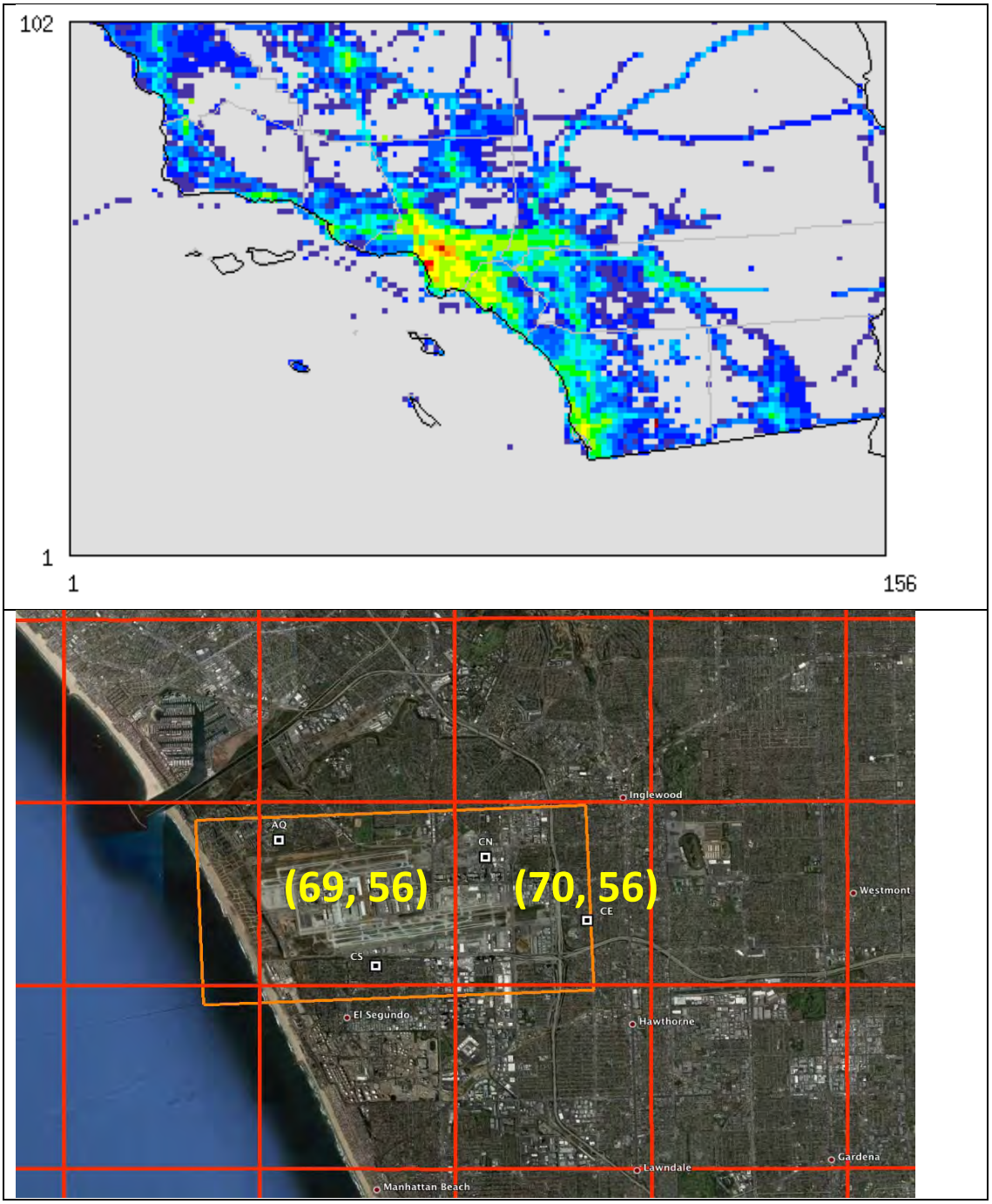

Figure 9-41: CMAQ 4-km x 4-km gridded modeling domain (top) with zoomed-in region around LAX, showing the general airport location and the four core monitoring sites (bottom). Each square represents a 4-km x 4-km grid cell treated in the model.

9.2.2.1 LAX Emissions Inputs from SCAQMD

SCAQMD provided gridded CMAQ-ready hourly emissions inputs that already included SCAQMD estimated emissions from LAX. Details about the Airport inventory were obtained to remove them from the gridded emissions, before Phase III emissions for the Study Area

described in Section 8 could be added. However, note that the off-airport or background emissions in the LAX Phase III Study area are likely double-counted in the modeling, since there was no way to separate those from the SCAQMD provided emissions inventories.

SCAQMD provided two files "nonmed.aircraft_LAX.2008" and "nonmed.airport_GSE.2008," which contained information on the magnitude and location of emissions related to LAX. This information was used to calculate the average daily total emissions for each grid-cell for each pollutant emitted by both aircraft and GSE. Similarly, average daily total emissions for each grid-cell in the airport vicinity (defined as grid-cells containing airport activity) were also computed from the CMAQ-ready base case emissions files provided by SCAQMD, and then reduction factors (RF) computed. These reduction factors were calculated by dividing the average daily totals from aircraft+GSE sources in LAX (estimated by AQMD) by the average daily totals from the SCAQMD provided base case in the corresponding grid-cell for each pollutant, and listed in Table 9-8. Using this information, a revised base case was created, where the emissions for each airport grid-cell were computed as follows:

$$AQMD_{Zero} = AQMD_{Base}(1 - RF)$$

where,

- $AQMD_{Base}$ refers to the original base emissions scenario provided by SCAQMD for this Study,
- RF refers to the emissions reductions factors that were developed, and is the ratio of SCAQMD estimated daily average aircraft emissions to average daily all source emissions from the base case in each grid-cell (higher the RF, higher the portion of AQMD estimated aircraft-related emissions in that grid-cell, and hence smaller the value of $AQMD_{Zero}$ subsequently, and vice-versa; RF is always <= 1.0), and
- $AQMD_{Zero}$ refers to the emissions scenario where SCAQMD estimated aircraft+GSE emissions were removed for this study.

Table 9-8. Emissions reduction factors (RF) developed to remove SCAQMD estimated LAX emissions from CMAQ emission inputs.

COLUMN	ROW	CO	NO_x	SO_x	TOG	NH_3
Winter Season		Reduction Factors				
68	56	0.5253	0.8104	0.9742	0.3318	0.0055
69	55	0.1298	0.2405	0.0579	0.0476	0.0002
69	56	0.3052	0.5303	0.9275	0.2086	0.0027
69	57	0.1681	0.4059	0.8986	0.1025	0.0011
70	56	0.2591	0.5374	0.9179	0.1105	0.0020
Summer Season						
68	56	0.4769	0.8022	0.9510	0.2959	0.0055
69	55	0.1333	0.2523	0.0568	0.0489	0.0003
69	56	0.3021	0.5509	0.9077	0.2163	0.0027
69	57	0.1620	0.4273	0.8799	0.1000	0.0011
70	56	0.2594	0.5640	0.9034	0.1125	0.0020

9.2.2.2 LAX Emissions Inputs from KBE

Phase III emissions inventories described in Section 8 were added to the newly created AQMD_Zero files. KBE provided emissions inventories for the Study Area in AERMOD-ready format, using UTM coordinates and in units of kg/hour. KBE also assigned every source in the Study Area inventory to unique Source Classification Codes (SCC) to help with processing for CMAQ. The U.S. EPA defines SCCs for all source categories that are reported in the National Emissions Inventories (NEI), and these are used in conjunction with SCC-specific chemical speciation and temporal allocation profiles for air quality modeling. Phase III inventories were split into nine sub-sectors to assist with processing as well as for quality assurance (QA), and the EDMS2Inv processor (Baek et al., 2008) was used to convert the emissions to a format that could be used by SMOKE for further use in CMAQ. The nine source sectors were:

- Av Gas
- Jet
- Elsegundo
- LAWA Cogen
- Off Airport Roadway
- On Airport Roadway
- Parking
- Scattergood
- Stationary

EDMS2Inv creates hourly emission estimates for each source, and performs additional conversions as follows, for use in SMOKE:

- from UTM coordinates to latitude/longitude coordinates
- from kg/hour to tons/day
- stack parameters from meters to feet, and temperature from degrees Kelvin to degrees Fahrenheit

All Phase III emissions for the Study Area were then processed with SMOKE to create three different emissions scenarios as follows:

- Jet (only aircraft engines, APUs and GSE)
- Airport (all airport-related sources, these are included in the *.Airport files generated by EDMS, discussed in Section 9.1)
- All (all airport-related and background sources in the Phase III study domain)

The specific sources included in each of these three emissions scenarios are listed in Table 9-9 These scenarios are the same source groups as described in Section 9.1.

Table 9-9. Emissions source groups modeled in CMAQ

ID	Source Group	Description	Scenario		
			Jet	Airport	All
1	APPROACH	Aircraft Approach	✔	✔	✔
2	TAKEOFF	Aircraft Takeoff	✔	✔	✔
3	LANDING	Aircraft Landing	✔	✔	✔
4	TAXIQ	Aircraft Taxi/Queue	✔	✔	✔
5	GATES	APU, GSE, and Aircraft Startup	✔	✔	✔
6	PARKING	On-airport Parking		✔	✔
7	STATSRCS	On-airport LAWA owned Stationary Sources except COGEN		✔	✔
23	ROADOFAP	Off-airport Major Roadway		✔	✔
25	ROADONAP	On-airport Roadway		✔	✔
26	FREEWYAP	Freeway		✔	
24	ROADOFBK	Off-airport Major Roadway		✔	✔
27	FREEWYBK	Freeway		✔	✔
10	CAONRDAP	Minor Onroad Sources			✔
12	CAOFFAP	Off-road Equipment			✔
14	CAAGGAP	Aggregate Stationary Sources			✔
16	COGEN	LAWA Cogeneration Units			✔
17	CAAREAAP	Area wide Sources			✔
20	SSTENAP	Airport Tenant Sources			✔
8	CHEVRON	Chevron Products Co.			✔
9	MARINE	Marine Vessels			✔
11	CAONRDBK	Minor Onroad Sources			✔
13	CAOFFBK	Off-road Equipment			✔
15	CAAGGBK	Aggregate Stationary Sources			✔
18	CAAREABK	Area wide Sources			✔
19	SEGUNDO	El Segundo Power Plant			✔
21	SSOTHBK	Other Off-airport Stationary Source			✔
22	SCTRGOOD	Scattergood Power Plant			✔

A comparison of aircraft+GSE emissions estimates provided by SCAQMD and those generated for the Study is provided in Table 9-10. While total suspended particulate matter (TSP) (or $PM_{2.5}$) is about 50 percent higher, the other pollutants are generally comparable between the two estimates.

CMAQ needs chemical speciation profiles to assign lumped estimates of emissions such as TOG or $PM_{2.5}$ to explicit model chemical species. During this processing, the chemical speciation profiles specific to the SAPRC-99 chemical mechanism were used to be consistent with the SCAQMD created base emission inventories. The TOG speciation profiles for aircraft engines were based upon a recent FAA/U.S. EPA guidance document (U.S. EPA, 2009a), and were adapted for use with the SAPRC-99 chemical mechanism. The specific speciation profiles used for TOG and $PM_{2.5}$ for aircraft (SCC 27502011) and GSEs (SCC 2265008000) are provided in Table 9-11 through Table 9-14. The entire list of speciation profiles used to process emissions inventories for air quality models is available in a query browser[24] along with detailed documentation (U.S. EPA, 2009b).

Table 9-10. Comparison of aircraft+GSE emissions estimated by SCAQMD to those used in LAX Phase III (tons/day).

	CO	NO_X	SO_X	TOG	
SCAQMD Estimates (Average Day)	15.52	10.60	0.92	2.16	
LAX Phase III Estimates (Average Winter Episode Day)	12.62	10.02	0.65	1.36	
LAX Phase III Estimates (Average Summer Episode Day)	12.06	9.61	0.69	1.34	
Ratio of LAX Phase III to SCAQMD Estimates (Ave Winter Day)	81.3%	94.6%	70.1%	63.0%	
Ratio of LAX Phase III to SCAQMD Estimates (Ave Summer Day)	77.7%	90.7%	74.9%	61.9%	

Table 9-11. Chemical speciation profiles for Aircraft TOG (Source: U.S. EPA, 2009a)

Speciation profile code	Pollutant	Species	Molar Fraction	Mass %
5565	TOG	ACET	0.0000637	0.37%
5565	TOG	ALK1	0.0001729	0.52%
5565	TOG	ALK2	0.0015234	4.02%
5565	TOG	ALK4	0.0000812	0.67%
5565	TOG	ALK5	0.0011998	17.65%
5565	TOG	ARO1	0.0001552	1.41%
5565	TOG	ARO2	0.0002535	3.26%
5565	TOG	BALD	0.0000909	1.03%
5565	TOG	CCHO	0.0009693	4.27%
5565	TOG	PHEN	0.0000776	0.73%
5565	TOG	ETHENE	0.0055110	15.46%
5565	TOG	GLY	0.0003136	1.82%
5565	TOG	HCHO	0.0040998	12.31%
5565	TOG	ISOPRENE	0.0001470	1.03%
5565	TOG	MACR	0.0004952	2.88%

[24] SPECIATE Query Browser http://cfpub.epa.gov/si/speciate/

Speciation profile code	Pollutant	Species	Molar Fraction	Mass %
5565	TOG	MEOH	0.0005618	1.80%
5565	TOG	MGLY	0.0002082	1.50%
5565	TOG	OLE1	0.0017515	13.63%
5565	TOG	OLE2	0.0007677	7.49%
5565	TOG	RCHO	0.0005481	6.97%
5565	TOG	NROG	0.0002143	1.18%

Table 9-12. Chemical speciation profiles for Aircraft $PM_{2.5}$ (Source: U.S. EPA, 2009b).

Speciation profile code	Pollutant	Species	Molar Fraction	Mass %
92035	PM2_5	POC	0.1760000	17.60%
92035	PM2_5	PEC	0.7710000	77.10%
92035	PM2_5	PNO3	0.0011400	0.11%
92035	PM2_5	PSO4	0.0029500	0.30%
92035	PM2_5	PMFINE	0.0489100	4.89%

Table 9-13. Chemical speciation profiles for GSE TOG (Source: U.S. EPA, 2009b)

Speciation profile code	Pollutant	Species	Molar Fraction	Mass %
1186	TOG	ALK1	0.0002294646	0.69%
1186	TOG	ALK2	0.0010215054	2.66%
1186	TOG	ALK3	0.0044732224	26.07%
1186	TOG	ALK4	0.0034551829	26.73%
1186	TOG	ALK5	0.0005500539	6.23%
1186	TOG	ARO1	0.0005359661	6.46%
1186	TOG	ARO2	0.0005948167	6.85%
1186	TOG	CH4	0.0015274314	2.45%
1186	TOG	ETHENE	0.0015508021	4.35%
1186	TOG	ISOPRENE	0.0000146800	0.10%
1186	TOG	NROG	0.0006285171	5.61%
1186	TOG	OLE1	0.0008458550	5.38%
1186	TOG	OLE2	0.0008877147	6.44%
1301	TOG	OLE1	0.0011869267	9.96%
9007	TOG	MEOH	0.0005118602	1.64%

Table 9-14. Chemical speciation profile for GSE $PM_{2.5}$ (Source: U.S. EPA, 2009b)

Speciation profile code	Pollutant	Species	Molar Fraction	Mass %
92049	PM2_5	POC	0.475	47.50%
92049	PM2_5	PEC	0.122	12.20%
92049	PM2_5	PNO3	0.001	0.07%

Speciation profile code	Pollutant	Species	Molar Fraction	Mass %
92049	PM2_5	PSO4	0.001	0.05%
92049	PM2_5	PMFINE	0.402	40.18%

These three emissions scenarios were then merged with the AQMD_Zero case to create the following three emissions sensitivity scenarios for CMAQ modeling, for each of the two monitoring seasons:

- AQMD_Zero: AQMD provided Base case adjusted to remove LAX aircraft+GSE emissions, as described in Section 9.2.2.1
- Sens1: AQMD_Zero + Jet/APU/GSE
- Sens2: AQMD_Zero + Airport-related emissions
- Sens3: AQMD_Zero + All[25]

The objective of creating these three CMAQ scenarios was to obtain a lower, middle and upper bound of estimates of the contribution from LAX emissions to ambient air quality.

In Figure 9-42 below, a vertical profile of daily total emissions from Jet emissions (by CMAQ model layer as well as actual atmosphere heights), along with a vertical cross-section of the modeling domain, is shown to illustrate the vertical distribution of emissions in the row that contains the airport (Row 56 in Figure 9-41). These emissions are daily totals for a single day in winter (February 1, 2008). The figures show the vertical extent of the emissions allocation in the CMAQ modeling domain. Each grid-cell in this cross-sectional plot indicates a 4-km x 4-km CMAQ grid-cell. As can be seen from Figure 9-42, the aircraft emissions are represented within the lowest 882 m of the atmosphere resolved into 8 model layers.

[25] Please note that Sens3 may potentially double count the background sources since there was no way to separate those from the SCAQMD provided emissions inventories.

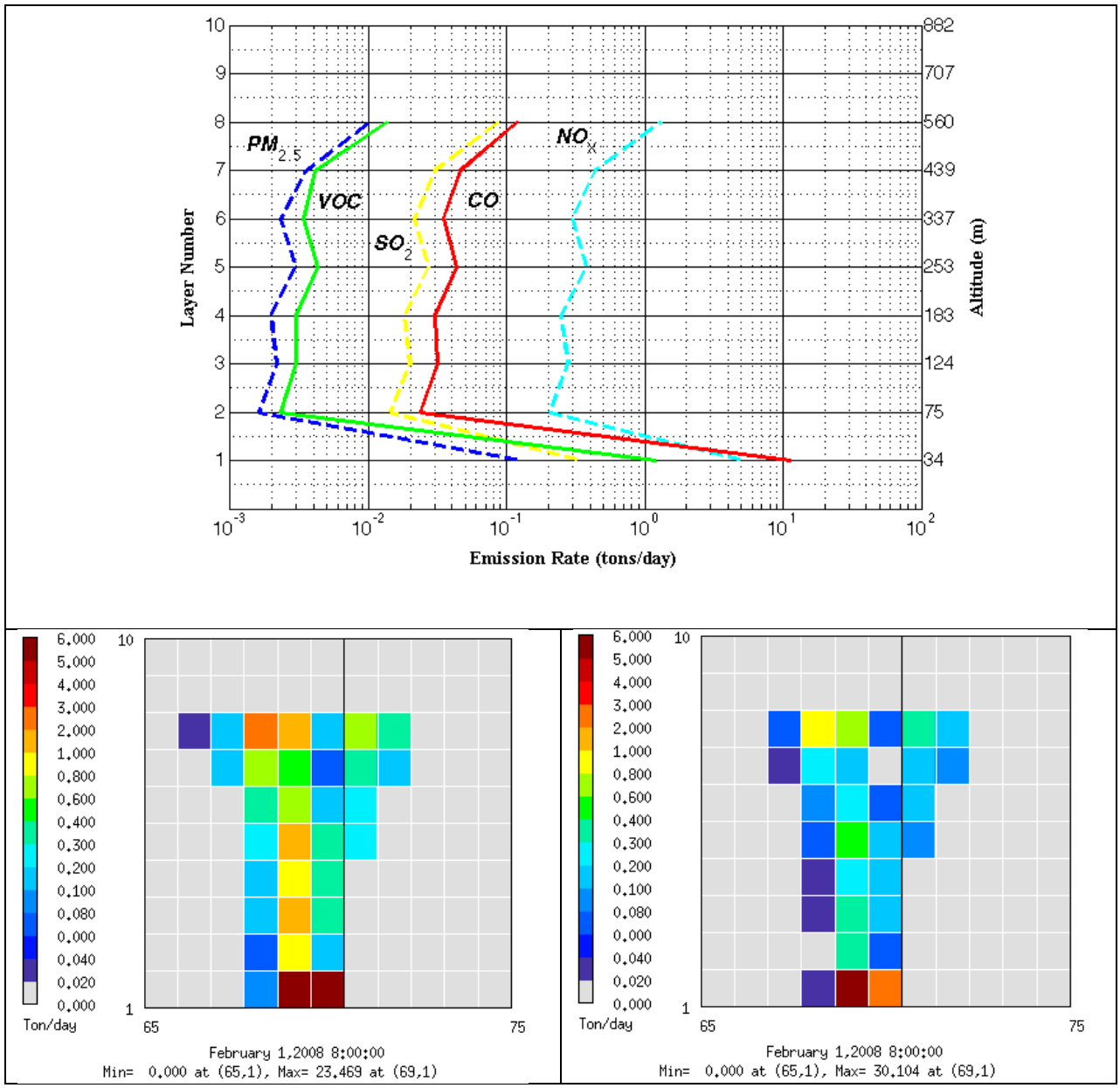

Figure 9-42. Vertical profile of daily total emission (top) and a vertical cross-section of daily total emissions of NO_x (top left) and $PM_{2.5}$ (bottom right) from "Jet" emissions scenario on February 1, 2008.

Typical CMAQ applications such as those used by SCAQMD likely assign all airport emissions to the surface layer; however, the application developed for Phase III of the LAX AQSAS uses this enhanced approach with emissions in elevated grid cells, which is a more realistic representation of these emissions for aircraft takeoff and landing at the airport. Additional details on the algorithms used to process aircraft emissions are described in Baek et al., 2008.

9.2.3 CMAQ Modeling and Analyses

The three emissions scenarios and base case with no LAX emissions (AQMD_Zero) described earlier were used to perform CMAQ modeling for each of the two seasons. The general approach to modeling airport emissions with CMAQ is based on previous work (Arunachalam et al., 2008; 2011). The model outputs were then post-processed to compute differences between each of the three LAX emissions scenarios and the AQMD_Zero scenario to obtain incremental air quality concentrations of these emissions, compared to the broad regional background, as follows:

1. AQMD_Zero

2. Sens1 minus AQMD_Zero, an estimate of contributions from aircraft engine, APUs, and GSE

3. Sens2 minus AQMD_Zero, an estimate of contributions from all airport-related sources

4. Sens3 minus AQMD_Zero, an estimate of contributions from all airport-related sources and background sources in the study domain

During post-processing, the individual CMAQ species were aggregated as shown in Table 9-15 to compute total $PM_{2.5}$. In the table below, AORGPAT indicates total primary organic aerosol, and AORGAT, AORGBT and AORGCT indicate the various components of secondary organic aerosols. In addition to $PM_{2.5}$ and its constituents, CO, NO_x and SO_2 were also analyzed.

Table 9-15. $PM_{2.5}$ species output by CMAQ

Description	Variable	Equation (In terms of CMAQ chemical species)
PM Sulfates	ASO4T	ASO4I + ASO4J
PM Nitrates	ANO3T	ANO3I + ANO3J
PM Ammonium	ANH4T	ANH4I + ANH4J
PM Elemental Carbon	AECT	AECI + AECJ
PM Organics	AOCT	AORGAT + AORGBT + AORGCT + 1.4*AORGPAT
PM Crustal	A25J	A25J
Total $PM_{2.5}$	PM2.5	ASO4T + ANO3T + ANH4T + AECT + AOCT + A25J

Seasonal mean concentrations and seasonal maximum daily concentrations were computed for each of the two seasons modeled for the base case scenario and the three emissions scenarios (AQMD_Zero, AQMD_Jet, AQMD_Airport and AQMD_All). Seasonal maximum daily average concentrations were determined by computing the daily averages for each season and then finding the maximum value for that particular season. Differences between each of the airport emissions scenarios and the AQMD_Zero scenario were computed.

The CMAQ model analysis was performed in two steps as described below.

1. Spatial analyses were performed to understand spatial patterns of air quality impacts due to LAX emissions in a broad area around the airport region

2. Time-series analyses were performed to understand temporal behavior of air quality impacts due to LAX emissions at key grid-cells containing the core sites

9.2.3.1 Spatial Analyses

To perform the spatial analyses, the two metrics mentioned above (seasonal mean and seasonal maximum daily concentrations) were first computed for each of the four scenarios for both seasons. Differences were computed, both on a simple difference (A – B) as well as relative difference (A – B) / A, and were presented on a percent basis, where A refers to any of the three airport emissions scenarios, and B refers to the AQMD_Zero scenario. Thus all numbers presented in this section are relative increases in air quality concentrations compared to the broad regional background modeled by CMAQ.

Since CMAQ has a detailed chemical treatment for $PM_{2.5}$, the results are presented with additional detail to show the individual chemical components. The following metrics were then plotted for a domain zoomed-in around a sub-domain 24-km x 20 km (or 6 x 5 grid-cells) centered on the airport region, and included in Appendix 9-2 of this section. The spatial extent of this zoomed-in domain was chosen to include two rows or columns (or an 8 km by 8 km region) surrounding the airport grid-cells in all four directions.

The specific products from these analyses are listed below:

- Spatial maps of simple and relative (%) differences in seasonal mean CO, NO_x and SO_2 concentrations between AQMD_Jet and AQMD_Zero scenarios during the Winter Season (Figure 9B-1[26])

- Spatial maps of simple and relative (%) differences in seasonal mean CO, NO_x and SO_2 concentrations between AQMD_Airport and AQMD_Zero scenarios during the Winter Season (Figure 9B-2)

- Spatial maps of simple and relative (%) differences in seasonal mean CO, NO_x and SO_2 concentrations between AQMD_All and AQMD_Zero scenarios during the Winter Season (Figure 9B-3)

- Spatial maps of simple and relative (%) differences in seasonal mean total $PM_{2.5}$ concentrations between AQMD_Jet, AQMD_Airport and AQMD_All and AQMD_Zero scenarios during the Winter Season (Figure 9B-4)

- Spatial maps of simple differences in seasonal mean speciated $PM_{2.5}$ concentrations between AQMD_Jet and AQMD_Zero scenarios during the Winter Season (Figure 9B-5)

[26] Figure 9B-xx refers to figures included in Appendix 9-2 of this section.

- Spatial maps of simple differences in seasonal mean speciated $PM_{2.5}$ concentrations between AQMD_Airport and AQMD_Zero scenarios during the Winter Season (Figure 9B-6)

- Spatial maps of simple differences in seasonal mean speciated $PM_{2.5}$ concentrations between AQMD_All and AQMD_Zero scenarios during the Winter Season (Figure 9B-7)

- Spatial maps of relative (%) differences in seasonal mean speciated $PM_{2.5}$ concentrations between AQMD_Jet and AQMD_Zero scenarios during the Winter Season (Figure 9B-8)

- Spatial maps of relative (%) differences in seasonal mean speciated $PM_{2.5}$ concentrations between AQMD_Airport and AQMD_Zero scenarios during the Winter Season (Figure 9B-9)

- Spatial maps of relative (%) differences in seasonal mean speciated $PM_{2.5}$ concentrations between AQMD_All and AQMD_Zero scenarios during the Winter Season (Figure 9B-10)
- Repeat above using seasonal maximum daily average concentrations during the Winter Season (Figures 9B-11 to 9B-20)

- Repeat above using seasonal mean concentrations during the Summer Season (Figures 9B-21 to 9B-30)

- Repeat above using seasonal maximum daily average concentrations during the Summer Season (Figures 9B-31 to 9B-40)

A pollutant-by-pollutant discussion of these figures for CO, NO_x, SO_2 and $PM_{2.5}$ is presented below. While the discussion focuses on the maximum impacts seen in the CMAQ grid-cell (69, 56) shown in Figure 9-41, which contains the bulk of the LAX airport layout, the broader impact of LAX airport emissions on ambient air quality in adjacent grid-cells can also be seen. As more emissions are added into each CMAQ scenario (Jet, Airport, and then All), it is possible to see the increase in the magnitude of the air quality impact for all four pollutants analyzed both at the airport grid-cell level as well as a larger spatial region in several instances, with grid-cells containing at least a 10 percent impact often stretching to the edge of the 24-km x 20 km area shown. Figure 9-43 below illustrates this for incremental NO_x concentrations during the Winter and Summer Seasons due to the three emissions scenarios modeled. Table 9-16 and Table 9-17 present the summary of these estimates for the two seasons.

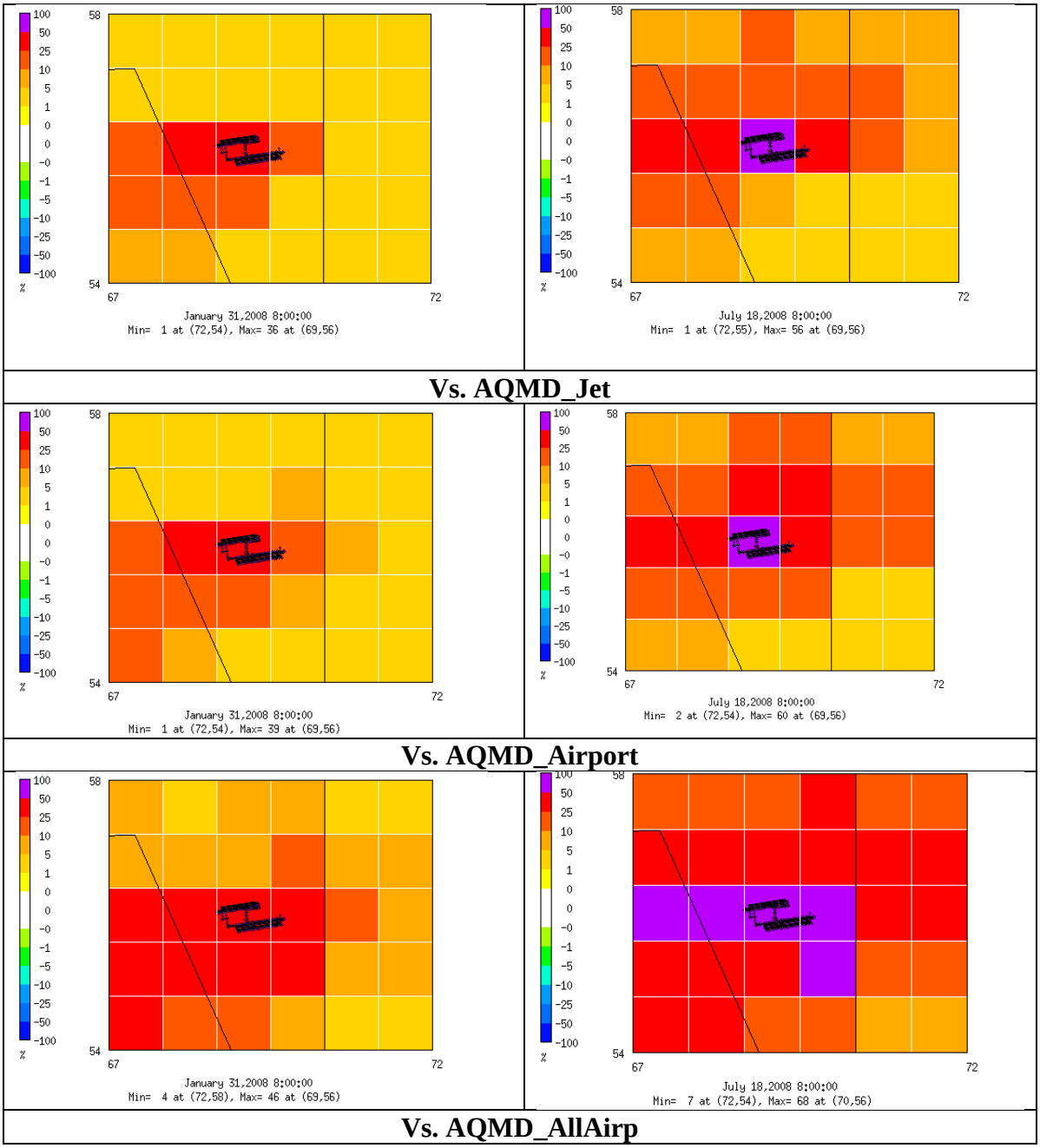

Figure 9-43. Incremental NO_x concentrations due to the three emissions scenarios during Winter (left) and Summer (right) Seasons.

Table 9-16. Maximum Incremental contributions (%) due to various emissions scenarios during the Winter Season.

	Seasonal Average			Seasonal Maximum Daily Average		
	Jet	**Airport**	**All**	**Jet**	**Airport**	**All**
CO	15	18	25	15	18	30
NO_x	36	39	46	32	35	45
$PM_{2.5}$	6	16	17	4	12	14
SO_2	35	36	43	19	25	34

Table 9-17. Maximum Incremental contributions (%) due to various emissions scenarios during the Summer Season.

	Seasonal Average			Seasonal Maximum Daily Average		
	Jet	**Airport**	**All**	**Jet**	**Airport**	**All**
CO	24	30	43	30	36	44
NO_x	56	60	68	61	64	69
$PM_{2.5}$	9	21	26	8	19	22
SO_2	35	35	45	19	19	25

Carbon Monoxide

During the Winter Season, the maximum incremental impacts of mean CO concentrations modeled by CMAQ ranged from 15 percent (in the case of Jet) to 25 percent (in the case of Airport) for the three emissions scenarios, while the maximum incremental impacts of seasonal maximum daily CO range from 15 to 30 percent.

During the Summer Season, the impacts of mean CO concentrations ranged from 24 to 43 percent, while the maximum incremental impacts of seasonal maximum daily ranged from 30 to 44 percent. Overall, the footprint of CO is wider and more intense with the All scenario during the Summer Season for both seasonal mean as well as seasonal maximum daily average concentrations, highlighting the increasing contribution from background sources to the analyses region.

Nitrogen Oxides

During the Winter Season, the maximum incremental impacts of mean NO_x concentrations modeled by CMAQ during the Winter Season ranged from 36 to 46 percent for the three emissions scenarios, while the maximum incremental impacts of seasonal maximum daily NO_x range from 32 to 45 percent.

During the Summer Season, the impacts of mean NO_x values ranged from 56 to 68 percent, while the maximum incremental impacts of seasonal maximum daily ranged from 61 to 69 percent. Overall, the footprint of NO_x, like CO, was also seen to be wider and more intense with the All scenario during the Summer Season for both seasonal mean as well as seasonal maximum

daily average concentrations. Large increases in NO_x contributions in the southwest corner of the region were due to impacts of marine and Chevron El Segundo Refinery emissions.

Sulfur Oxides

During the Winter Season, the maximum incremental impacts of mean SO_2 concentrations modeled by CMAQ during the Winter Season ranged from 35 to 43 percent for the three emissions scenarios, while the maximum incremental impacts of seasonal maximum daily SO_2 ranged from 19 to 34 percent.

During the Summer Season, the impacts of mean SO_2 concentrations ranged from 35 to 45 percent, while the maximum incremental impacts of seasonal maximum daily ranged from 19 to 25 percent. Similar to CO and NO_x, the footprint of SO_2 was also seen to be wider and more intense with the All scenario during the Summer Season for both seasonal mean as well as seasonal maximum daily average concentrations, where the bottom-most row of the 3x3 grid observed impacts increasing from less than one percent up to ten percent.

Fine Particulate Matter

The maximum incremental impacts of seasonal mean $PM_{2.5}$ values modeled by CMAQ during the Winter Season ranged from 35 to 43 percent for the three emissions scenarios, also in the same grid-cell as was seen for CO. These relative impacts translated to a $PM_{2.5}$ concentration range of 1.3 to 4.2 $\mu g/m^3$. The spatial maps of $PM_{2.5}$ chemical components in each case provided additional information. In the case of AQMD_Jet, comparable contributions were seen from elemental carbon (EC), organic carbon (OC), and crustal PM (0.4 $\mu g/m^3$ each). The source of crustal PM is from GSE emissions (see Table 9-14, which assigns approximately 40 percent of PM2.5 emissions to crustal material). When the remaining airport-related emissions were added (from Airport), the largest constituent was OC (1.4 $\mu g/m^3$), followed by EC (1.0 $\mu g/m^3$), and crustal (0.9 $\mu g/m^3$). When the remaining background emissions in the Study Area were added (from All), the largest constituents were OC and crustal (1.4 μg/m3), followed by EC (1.0 μg/m3). It was also observed from these figures that addition of aircraft sources to the AQMD_Zero case resulted in reduced nitrate aerosol concentrations in and around the airport region, due to the nonlinear reaction of the inorganic system of nitrate-sulfate-ammonium aerosols. Specifically, aircraft NOx emissions reduce nighttime NO3 (nitrate radical) concentrations. With the reduction in NO3 concentrations, less HNO3 (nitric acid) and hence less ANO3T (nitrate aerosols) are formed. If the nighttime reduction of ANO3T is larger in magnitude than the daytime increase due to aircraft emissions, the net effect (e.g. daily average) will appear as an overall decrease in ANO3T. This phenomenon was previously observed in multi-resolution modeling performed for the Hartsfield Atlanta airport, and is described in elaborate detail using a diagnostic technique called Process Analyses enabled in CMAQ (Woody and Arunachalam, 2012a).

When looking at the incremental impacts of seasonal maximum daily $PM_{2.5}$ during the Winter Season, the range was from 4 to 14 percent, which translates to a $PM_{2.5}$ concentration range of 1.6 to 7.0 $\mu g/m^3$. The breakdown of speciated components did not provide much different information when compared to the seasonal mean analysis**.**

During the Summer Season, the maximum incremental impacts of seasonal mean $PM_{2.5}$ ranged from 9 to 26 percent (1.4 to 4.5 $\mu g/m^3$) for the three emissions scenarios, and the seasonal maximum daily $PM_{2.5}$ impacts ranged from 8 to 22 percent (2.3 to 7.1 $\mu g/m^3$). Looking at the spatial maps of the speciated components, EC, OC and crustal were the main components, all with comparable contributions of approximately 0.4 $\mu g/m^3$ to AQMD_Jet impacts. In the case of AQMD_Airport, the largest was OC (1.5 $\mu g/m^3$) followed by EC and crustal (0.9 $\mu g/m^3$ each). For the AQMD_All scenario, the key constituents were OC and crustal (approximately 1.5 $\mu g/m^3$ each) followed by sulfate EC (1.0 $\mu g/m^3$), and then sulfate aerosol (20.4 $\mu g/m^3$). The general patterns and relative importance of speciated components when looking at the seasonal maximum daily $PM_{2.5}$ impacts were comparable to those from the seasonal mean impacts, albeit with higher magnitudes during the Summer Season. Also during the Summer Season, both nitrate and ammonium aerosols were decreased in the LAX region due to the addition of Study Area emissions.

In Appendix Figures 9B-41 to 9B-42, the percent differences in seasonal maximum daily average concentrations due to AQMD_Airport impacts are shown for the entire 4-km x 4-km gridded domain for the Winter and Summer Seasons. While the impacts of CO and $PM_{2.5}$, were relatively limited to the first tens of kilometers, e.g., 10, 20, or 30 km, from LAX, the impacts of NO_x and SO_2 were seen much further downwind (up to 10 percent increases in NO_x at distances of 100 km, and up to 5 percent increases in NO_x and SO_2 at distances of 200-250 km). The footprints of these impacts were generally larger during the Winter than during the Summer Season. Since all emissions in the Airport scenario are low-level except for aircraft emissions during landing and takeoff, these downwind impacts are almost all due to aircraft emissions at LAX.

In Appendix Figures 9B-43 to 9B-44, similar percent differences are presented, however, these were all due to AQMD_All emissions. As expected, due to larger emissions present in this scenario, the regional air quality impacts of these emissions in Southern California were higher, as well as more widespread, than impacts due to AQMD_Airport emissions. During both seasons, NO_x impacts were as high as 20 percent at downwind distances up to 100km, 15 percent at distances up to 150 km, and at least 5 percent at distances up to 300 km. Similarly SO_2 impacts of at least 10 percent were seen at distances up to 150 km, and at least 5 percent stretching few hundred kilometers near the eastern edge of the study domain. As with the AQMD_Airport impacts, footprints of AQMD_All impacts were generally larger during the Winter than during the Summer Season.

9.2.3.2 Time-Series Analyses

Of the four core sites, the AQ and CS sites are in grid cell 69, 56 of the CMAQ modeling domain, and the CE and CN sites are in the adjacent grid cell 70, 56 (see Figure 9-41 above). Daily average concentrations of CO, NO_x, $PM_{2.5}$ and SO_2 were computed at these two grid-cells and compared to the monitored data. Since CMAQ has the ability to estimate individual components of $PM_{2.5}$, these components were also extracted to provide an estimate of the major constituents related to airport activity. In the time-series plots discussed below, sens1 refers to AQMD_Jet, sens2 refers to AQMD_Airport and sens3 refers to AQMD_All emissions scenarios.

The time-series analyses are presented in two different ways (Options) for each pollutant for the Winter and Summer Season:

a) Comparing observed concentrations to each of the four modeled emissions scenarios (e.g. Figure 9-36):
    - AQMD_Zero
    - Sens1 or AQMD_Jet
    - Sens2 or AQMD_Airport
    - Sens3 or AQMD_All

b) Comparing observed concentrations to the incremental modeled concentrations defined in the beginning of Section 9.2.3 (e.g. Figure 9-37):
    - Sens1 minus AQMD_Zero
    - Sens2 minus AQMD_Zero
    - Sens3 minus AQMD_Zero

While Option (a) alone is the preferred approach to evaluate model predictions with observations, Option (b) provides insight into understanding the magnitudes of the air quality contributions due to Study Area emissions to the measurements, and also as a way to cross-compare against AERMOD predictions (since AERMOD included only Study Area emissions and no treatment of regional background emissions sources).

Carbon Monoxide

In Figure 9-44, the modeled daily average CO concentrations from the four CMAQ emissions scenarios are presented as time-series plots for the Summer Season at the grid-cell containing the AQ and CS sites, and then in the grid-cell containing the CE and CN sites. On all days modeled, the AQMD_All scenario (i.e., CO_sens3) predicted the highest concentrations compared to the other three scenarios. In Figure 9-45, the modeled differences between the three airport emissions scenarios compared to the AQMD_Zero scenario are compared to the field measurement data. By performing this comparison looking at both measurements versus modeled scenarios and as measurements versus modeled differences between scenarios, a better understanding of the relative contributions using measurements and modeled outputs was provided. Again, the contributions from the All scenario predicted the highest differences. When compared to the monitoring data, the modeled All scenario concentrations compared the best with the AQ site observations, while the contributions due to the Jet emissions scenario compared the best with the CS site. At the CE site however, the differences due to All scenario came closer to matching the measurement data, though the model predicted higher values on several days. The modeled impacts due to the Airport scenario emissions (i.e., CO_sens2) were lower than the values measured at the CN site.

Similar figures during Winter Season are shown in Figure 9-46 and Figure 9-47. During the Winter Season, the CMAQ modeled incremental contributions due to all three emissions

scenarios are much lower than the observed values at all core sites. However, the total concentrations predicted in the scenarios seem to match the field measurements on several days, especially at the AQ and CE sites (up to eight days during Winter Season when the modeled and observed CO concentrations differed by less than 10 percent). This suggests the CO measurements at these sites are more indicative of contributions from all sources in the LAX area rather than just due to modeled airport emissions.

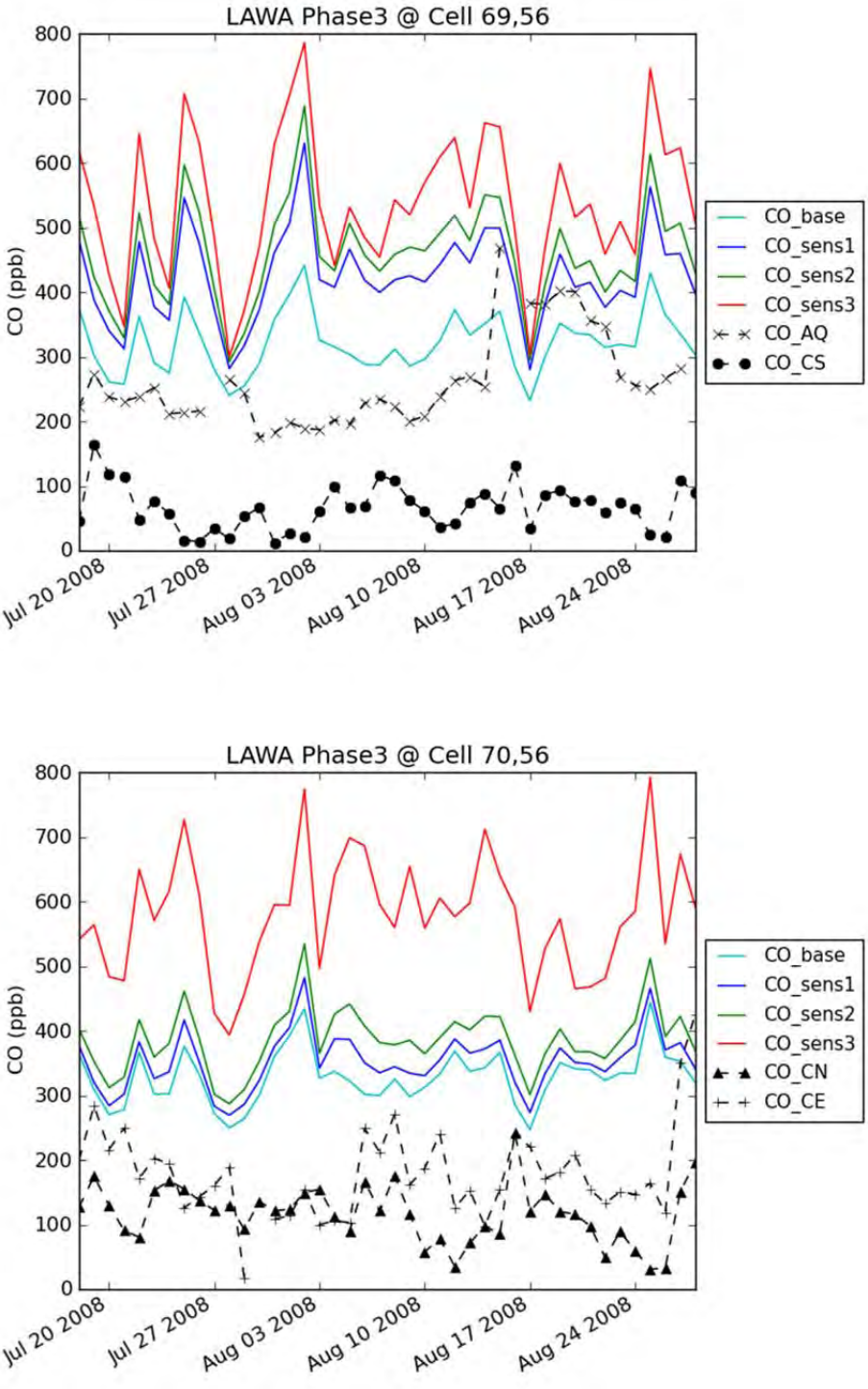

Figure 9-44. Daily average CO concentrations from the four modeling scenarios compared to field measurements at the AQ and CS sites (top) and CN and CE sites (bottom) during the Summer Season.

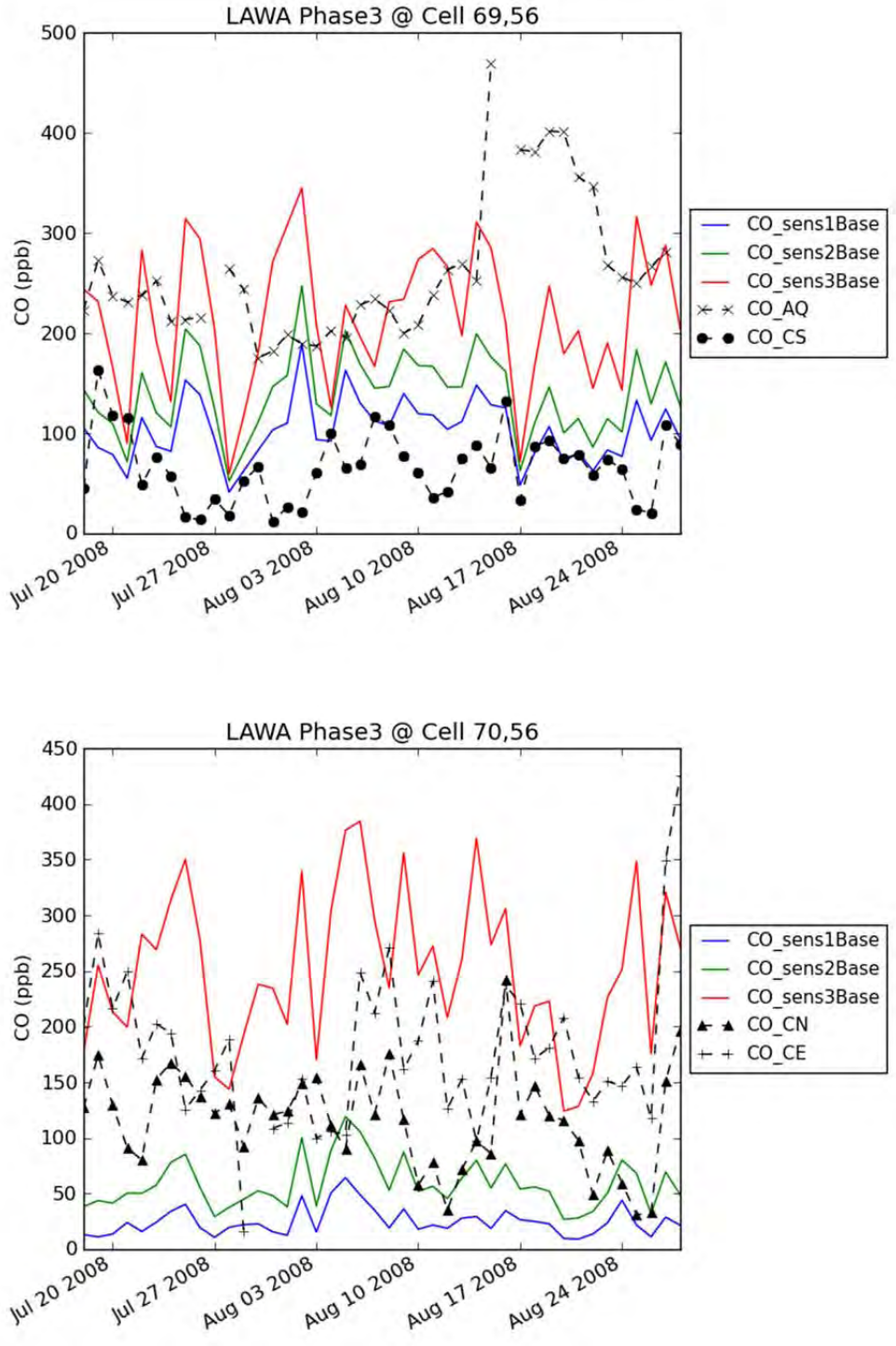

Figure 9-45. Differences in daily average CO concentrations between the three airport emissions scenarios versus base compared to field measurements at the AQ and CS sites (top) and CN and CE sites (bottom) during the Summer Season.

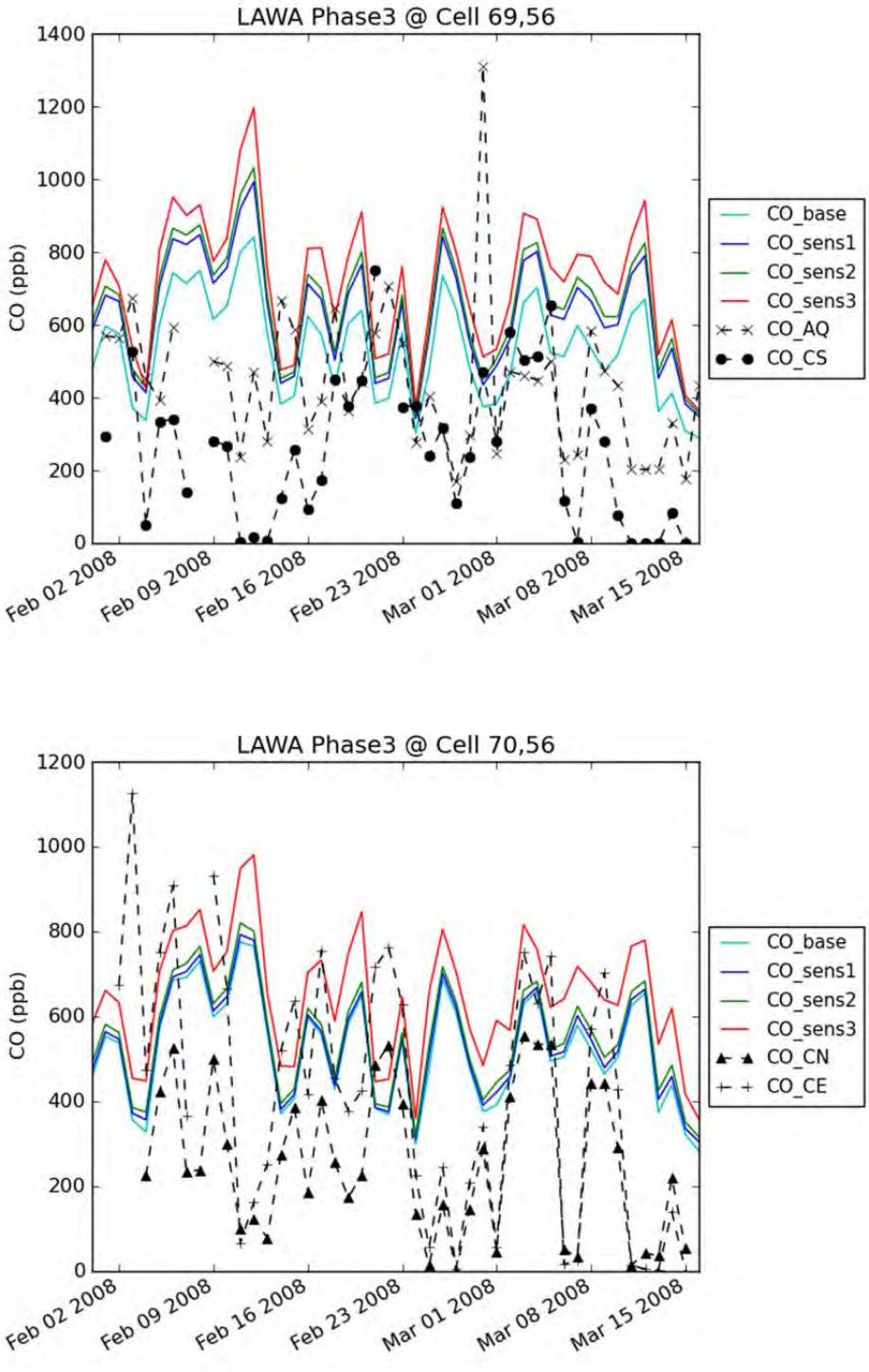

Figure 9-46. Daily average CO concentrations from the four modeling scenarios compared to field measurements at the AQ and CS sites (top) and CN and CE sites (bottom) during the Winter Season.

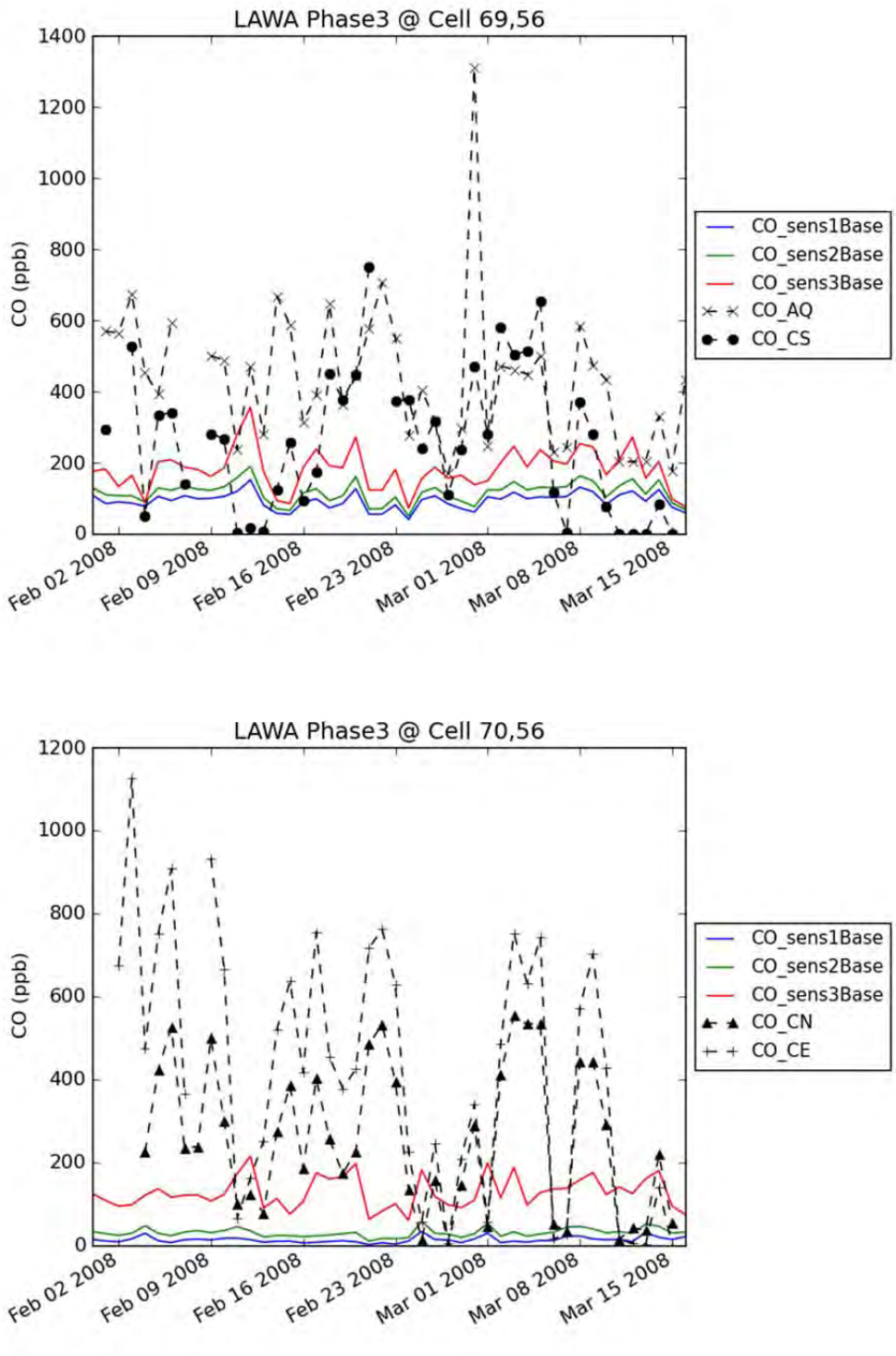

Figure 9-47. Differences in daily average CO concentrations between the three airport emissions scenarios versus base compared to field measurements at the AQ and CS sites (top) and CN and CE sites (bottom) during the Winter Season.

Nitrogen Oxides

In Figure 9-48, the total predicted daily average NOx concentrations from the four CMAQ scenarios are compared to the measurement data from the four core sites during the Summer Season. While the addition of airport emissions for the three scenarios to the AQMD_Zero case shows increased NO_x concentrations, all modeled predictions are much higher than field measurement data from both the AQ and CS sites. In the adjacent grid-cell however, the CMAQ-predicted AQMD_Zero case (i.e., NO_x_base without airport-related sources) compares better with measured values from the CE and CN sites. Adding the airport-related emissions from the three other scenarios shows higher concentrations than AQMD_Zero, since each of the three airport-related emissions scenario included increasingly higher NOx emissions than AQMD_Zero scenario.

In Figure 9-49, the incremental NO_x contributions due to the three airport emissions scenarios are compared to the measurement data from the four core sites. It was observed that the modeled concentrations are higher than the measurement data at the AQ and CS sites. However, at the adjacent grid cell, the CMAQ modeled incremental concentrations due to airport-related jet emissions (i.e., NOx_sens1Base) and Airport emissions (i.e., NOx_sens2Base) tend to match the field measurements at the CE and CN sites (9 days during the Summer Season had less than a 10 percent difference between modeled deltas and observed NO_x concentrations), indicating the effects of terminal area activity being captured by these measurements.

Similar results for the Winter Season are presented in Figure 9-50 and Figure 9-51. CMAQ-predicted AQMD_Zero concentrations pick up the maxima observed at the AQ and CS sites on several days. In the adjacent grid-cell however, all four scenarios predicted comparable values as those measured at the CN and CE sites (five days during the Winter Season had less than a 10 percent difference between modeled and observed NO_x concentrations). Based upon the incremental concentrations predicted by CMAQ, the AQMD_All scenario (i.e., NOx_sens3Base) matches the field measurements at the AQ and CS sites, especially during the latter half of the Winter Season. The model seems to underpredict the observed values during the early period. However, at the CE and CN sites, the modeled differences are much lower than the measurement data, indicating the likelihood of broader contributions from the overall background from the LAX area to these observations.

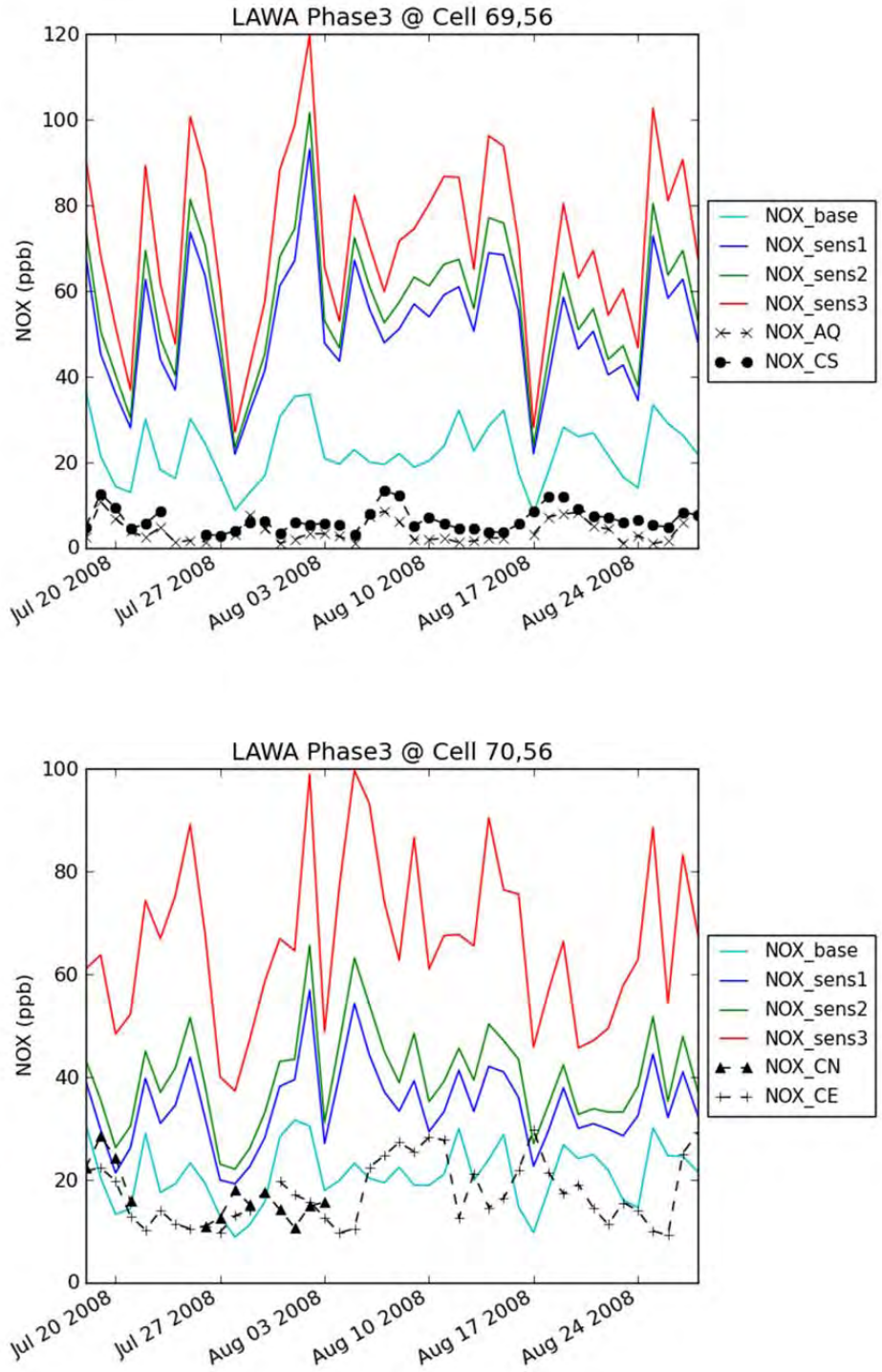

Figure 9-48. Daily average NO_x concentrations from the four modeling scenarios compared to field measurements at the AQ and CS sites (top) and CN and CE sites (bottom) during Summer Season.

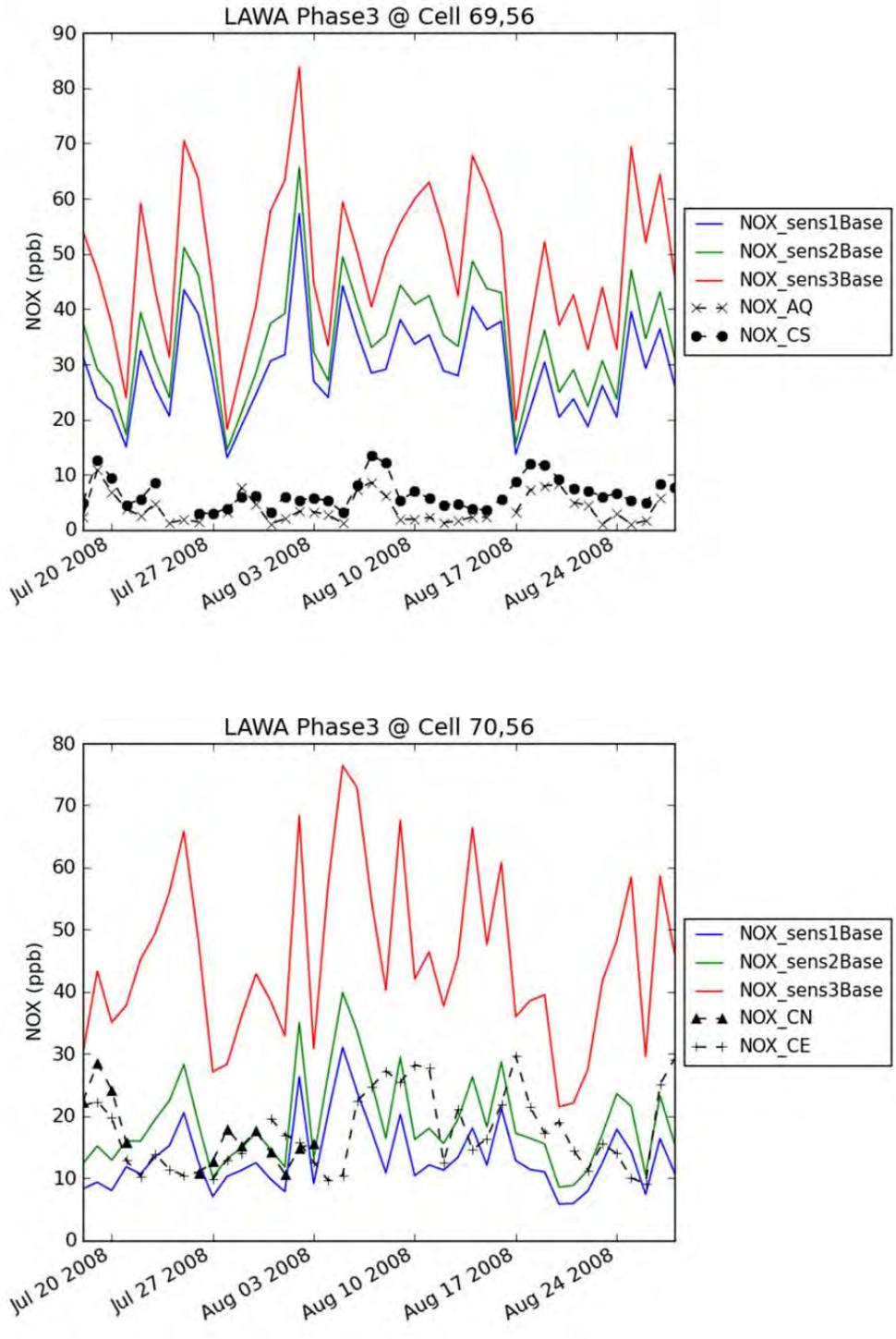

Figure 9-49. Differences in daily average NO_x concentrations between the three airport emissions scenarios versus base compared to field measurements at the AQ and CS sites (top) and CN and CE sites (bottom) during Summer Season.

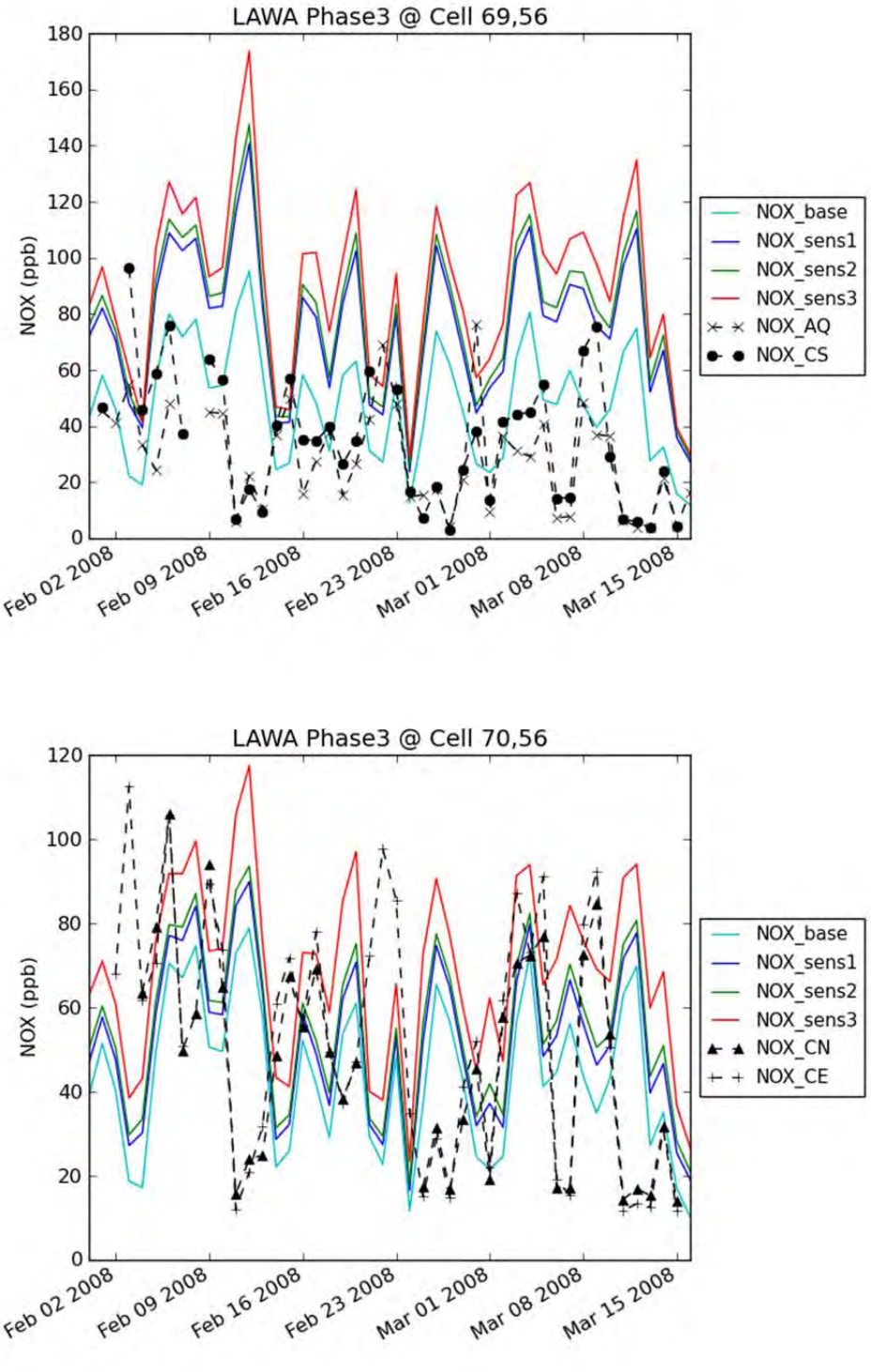

Figure 9-50. Daily average NO_x concentrations from the four modeling scenarios compared to field measurements at the AQ and CS sites (top) and CN and CE sites (bottom) during Winter Season.

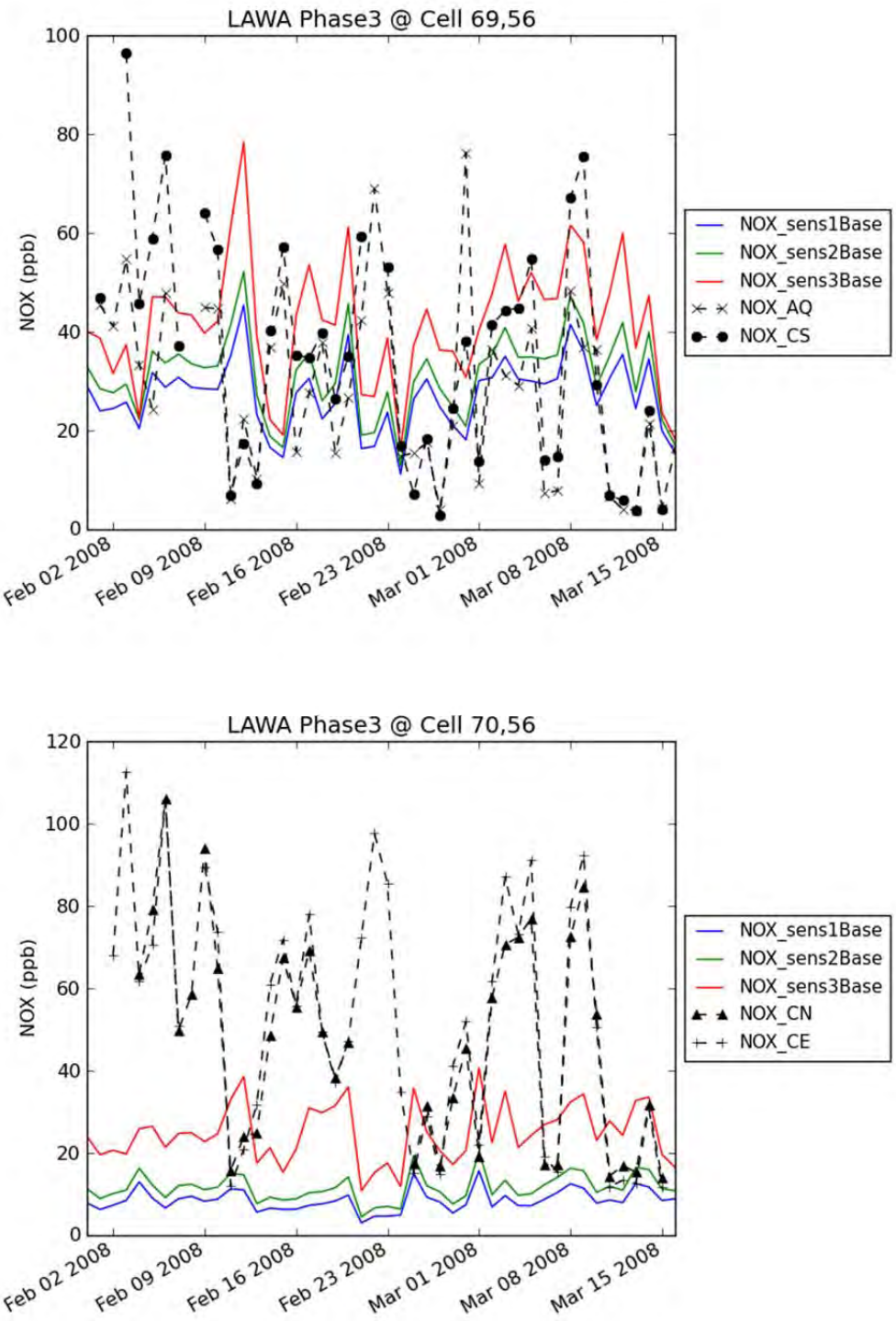

Figure 9-51. Differences in daily average NO_x concentrations between the three airport emissions scenarios versus base compared to field measurements at the AQ and CS sites (top) and CN and CE sites (bottom) during Winter Season.

Sulfur Oxides

In Figure 9-52, the CMAQ modeled daily average SO_2 concentrations from the four scenarios are compared to the measurement data from the four core sites during the Summer Season. The CMAQ predictions for all four scenarios are much higher than the monitoring data collected at the four core sites. The modeled incremental concentrations during the Summer Season are presented in Figure 9-53. At the AQ and CS sites, the predicted increments are higher than the monitoring data, indicating that the measurements were not capturing the contribution from these airport sources during this period. However, at the CE and CN sites, the incremental contributions from the AQMD_All scenario better track the trends at the CN site for several days during the middle of the Summer Season, and again during the end of the season. On other days, the AQMD_Airport scenario better tracks the CN site field data indicating the contribution of these airport related sources at that site.

Similar results for the Winter Season are presented in Figure 9-54 and Figure 9-55. Except for a very high peak observed at site AQ on March 1, 2012 the modeled concentrations from the four scenarios are much higher than those measured at the AQ and CS site. Similar trends are observed in the adjacent grid-cell with the CE and CN sites; however the relative ranges of modeled concentrations are lower than the grid-cell containing the AQ and CS sites. The anomalous spike in SO_2 at the AQ site on March 1, 2012, is not captured by any of the CMAQ-modeled scenarios. The CMAQ-modeled incremental concentrations from the AQMD_All scenario capture the trends from the AQ site during the first half of the season. However, during the second half, the emissions due to Airport sources alone seem to better track the trends from the CS site. The anomalous spike in SO_2 at the CS site on March 1 is not captured by any of the CMAQ-modeled scenarios. In the adjacent grid-cell, the observations at the CN site are higher than all incremental concentrations during several days, indicating the contribution from other background sources in the LAX region to this site. However the observed SO_2 values at the CE site are generally lower than those at the CN site, and match the incremental concentrations from the Airport emissions on several days, confirming the contribution of LAX sources to this location.

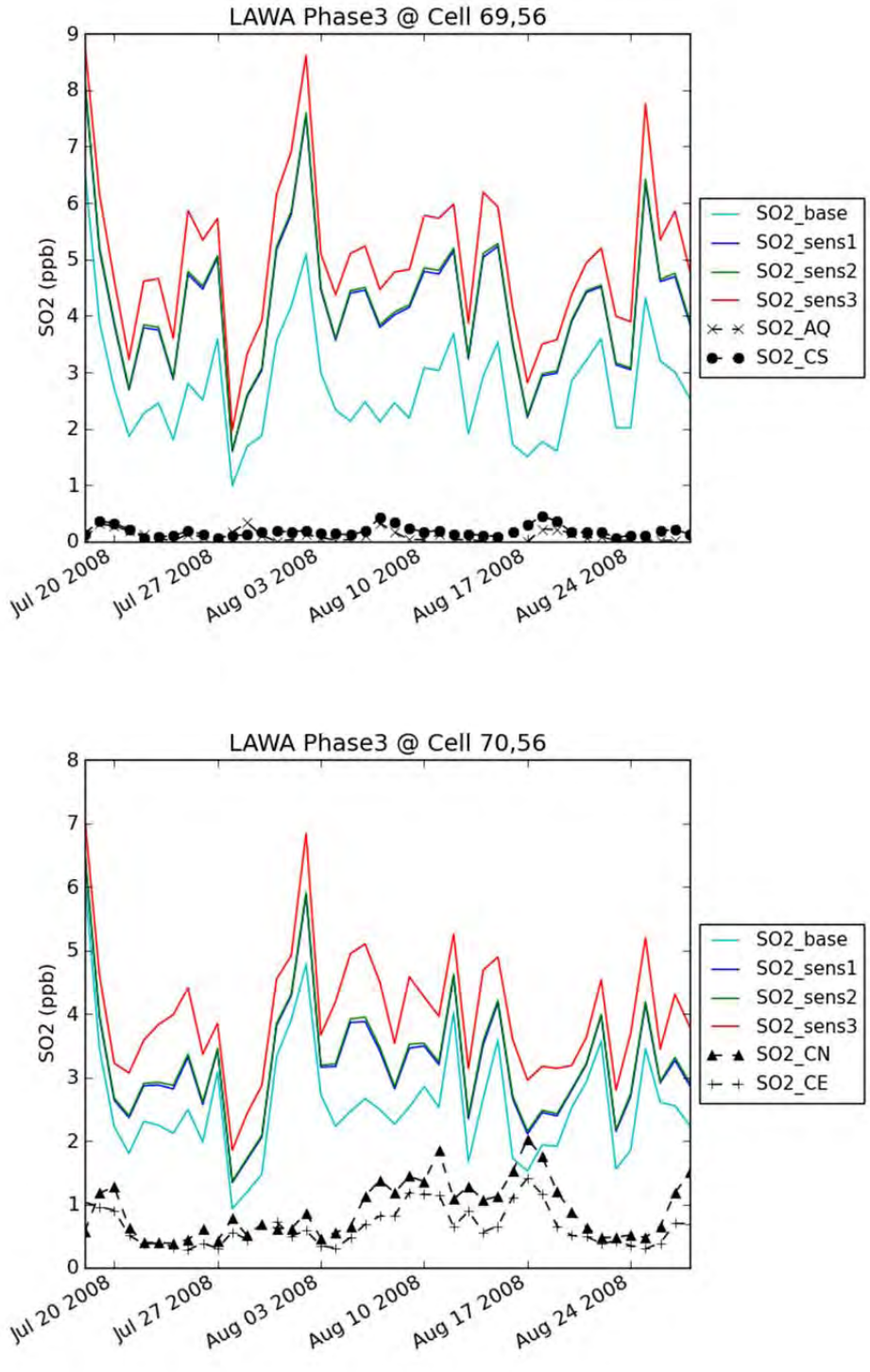

Figure 9-52. Daily average SO_2 concentrations from the four modeling scenarios compared to field measurements at the AQ and CS sites (top) and CN and CE sites (bottom) during Summer Season.

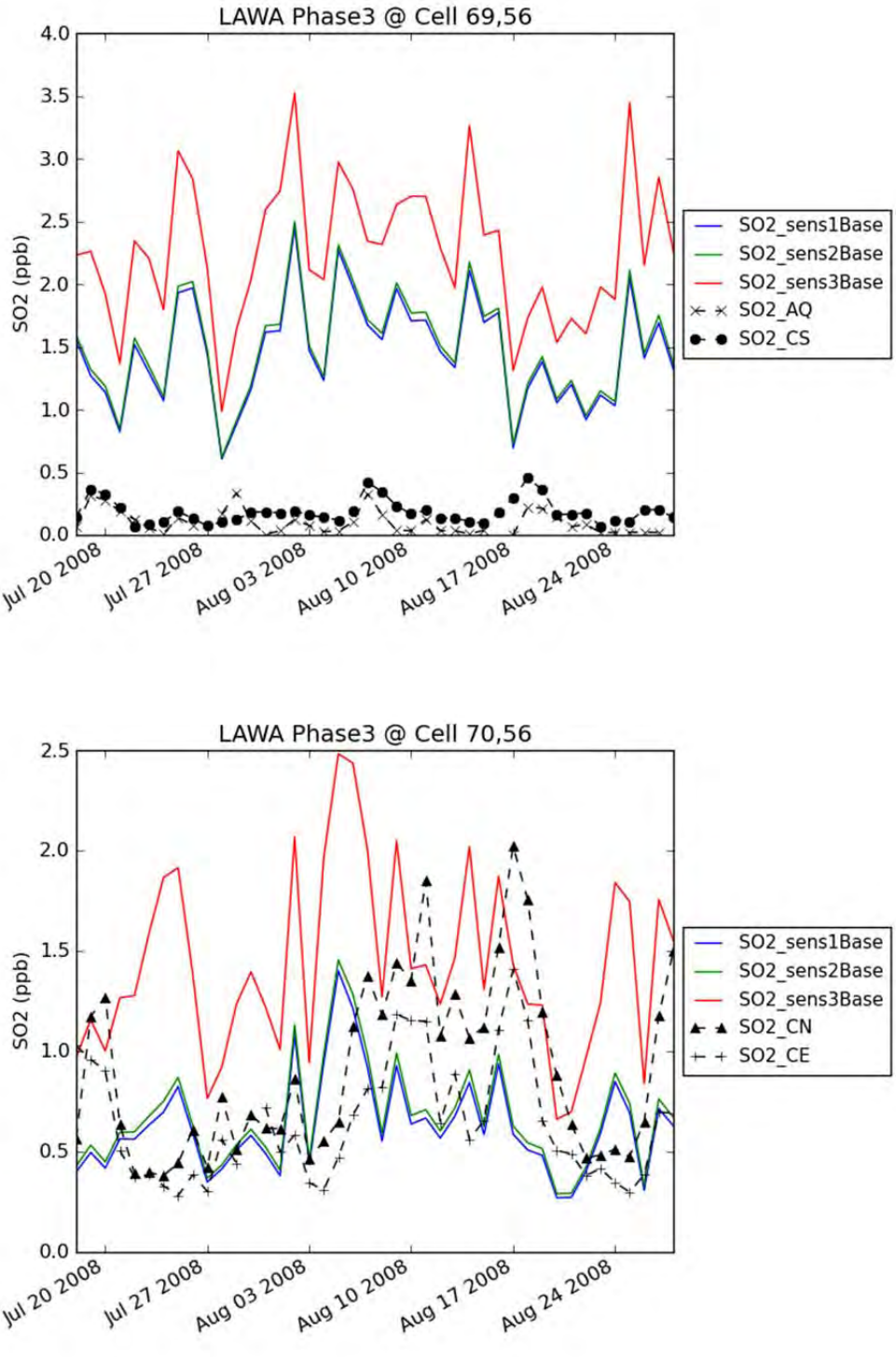

Figure 9-53. Differences in daily average SO_2 concentrations between the three airport emissions scenarios versus base compared to field measurements at the AQ and CS sites (top) and CN and CE sites (bottom) during Summer Season.

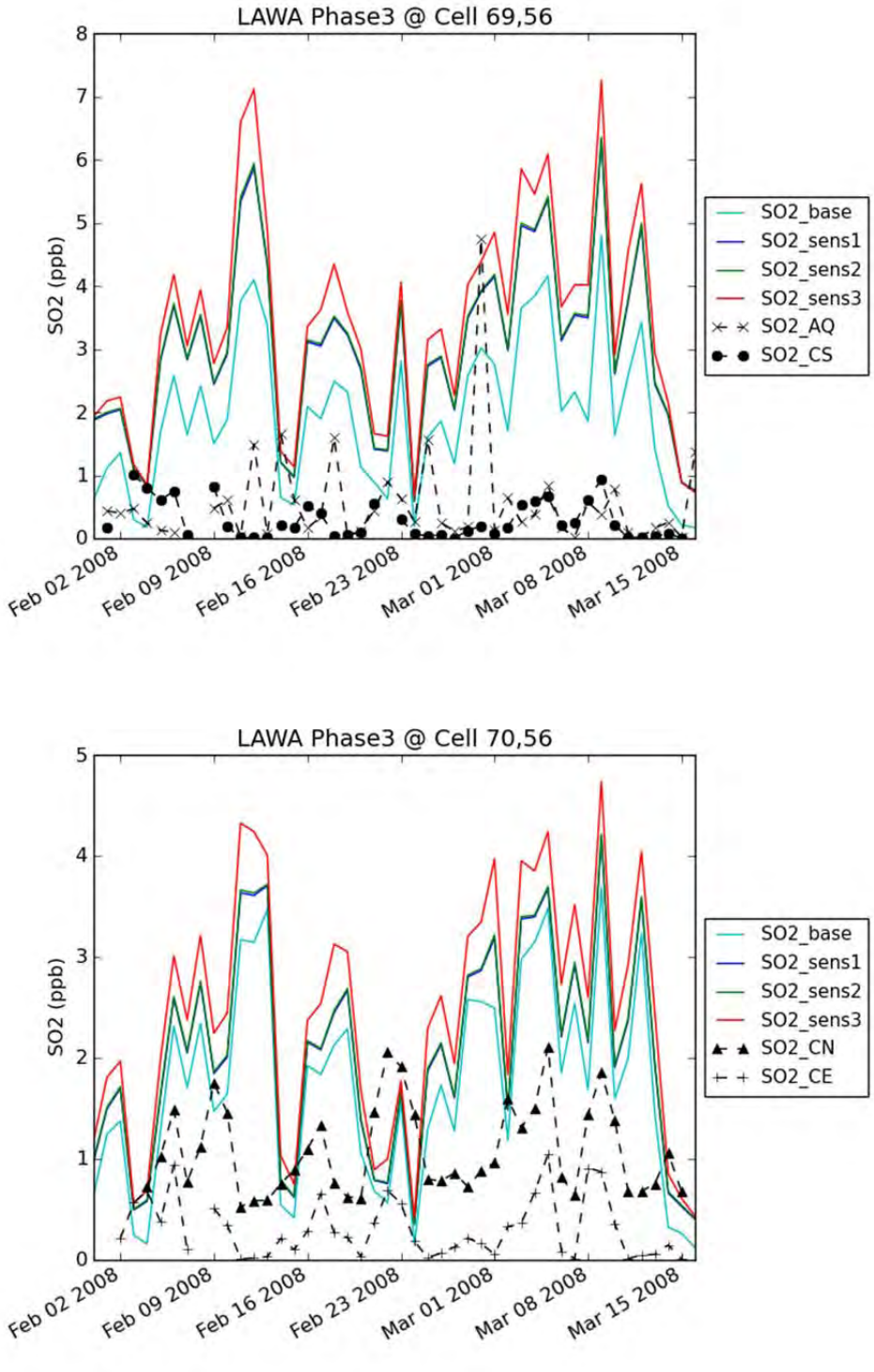

Figure 9-54. Daily average SO_2 concentrations from the four modeling scenarios compared to field measurements at the AQ and CS sites (top) and CN and CE sites (bottom) during Winter Season.

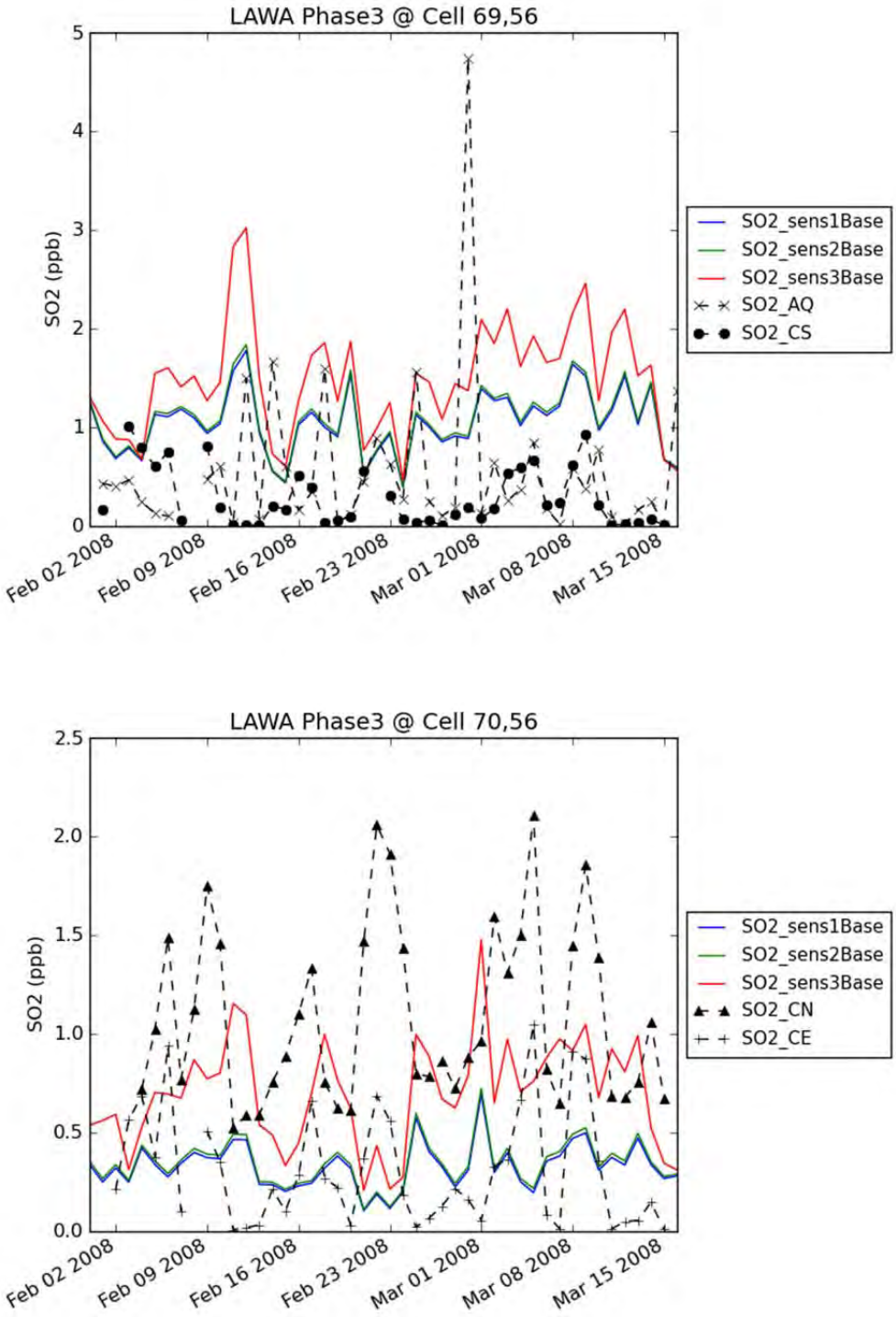

Figure 9-55. Differences in daily average SO_2 concentrations between the three airport emissions scenarios versus base compared to field measurements at the AQ and CS sites (top) and CN and CE sites (bottom) during Winter Season.

Fine Particulate Matter

The $PM_{2.5}$ measurements at the four core sites during the Summer Season are generally high, and in the range of 10-25 $\mu g/m^3$ on a daily average basis, with higher values reaching up to 50 $\mu g/m^3$ toward the end of the season at the CS site, as shown in Figure 9-56. The observations at the CS are generally low compared to those at the other three locations. The four CMAQ-modeled scenarios generally track each other very closely, and appear to match the field measurements at the AQ site, and then in the adjacent grid-cell at the CN and CE sites, which on the average have comparable concentrations. However, CMAQ vastly underpredicts the measured concentrations at the CE and CN sites approximately half of the time.

In Figure 9-57, the incremental contributions to $PM_{2.5}$ at the grid-cell containing the AQ and CS sites are shown. For all three scenarios, the modeled contributions do not exceed 2.6 $\mu g/m^3$ (for jet emissions) and 7.5 $\mu g/m^3$ (for All emissions), showing the generally low incremental contributions predicted by CMAQ compared to the field measurements. This confirms that most of measured values are typical of what is contributed from the broader background sources in the LAX region. CMAQ has the ability to treat $PM_{2.5}$ predictions in a very detailed manner, which allows for additional insight into the relative magnitudes of the specific chemical constituents of $PM_{2.5}$ during these two monitoring periods. This breakdown of $PM_{2.5}$ components is shown in stacked bar plots in the bottom of Figure 9-57 for the incremental Jet emissions scenario, and in Figure 9-58 for the incremental Airport and All scenarios. The three constituents that stand out as having positive contributions in all three emissions scenarios are AECT (primary elemental carbon), AORGPAT (primary organic carbon) and A25 (crustal material). The A25 contribution at the airport comes primarily from GSE emissions. This is justified by the fact that GSE sources constitute 38 percent of $PM_{2.5}$ from Aircraft/APU/GSE, and 16.5 percent from All Study area sources (see Table 8-31 in Section 8) and, taking into consideration that the chemical speciation profile for GSE sources assigns 40 percent to crustal material, this seems reasonable.

As shown in Table 9-12 and Table 9-14, the chemical speciation profile for jet emissions assigns 4.9 percent of $PM_{2.5}$ to PMFINE and GSE sources assign 40.2 percent of $PM_{2.5}$ to PMFINE, which subsequently are assigned as A25 (unknown crustal material) in CMAQ. On several days, it is seen that addition of airport-related emissions to this grid-cell causes a decrease in both ANO3T (nitrate aerosol) and ANH4T (ammonium aerosol). This is caused by the incremental NO_x emissions from aircraft sources. This effect is caused by the same phenomenon as described earlier in the section on spatial analyses which reported that the additions of aircraft NO_x emissions reduce night-time levels of nitrate radicals. With the reduction in nitrate radicals, less nitric acid, and hence less aerosol nitrate is formed. If the nighttime reduction of ANO3T is larger in magnitude than the daytime increase due to aircraft emissions, the net effect (e.g., daily average) will appear as an overall decrease in ANO3T. This would indicate why an increase in ANO3T is observed on some days due to aircraft emissions but a decrease is observed on several others.

A small contribution due to ASO4T (sulfate aerosol) was observed on a few days, however, at a lower magnitude compared to the other three major components related to aircraft emissions.

Similar results for the adjacent grid-cell containing the CE and CN sites are presented in Figure 9-59 and Figure 9-60. Again, the modeled incremental concentrations are much lower compared to the measured values, and do not exceed 1.2 $\mu g/m^3$ (for Jet emissions), 3.6 $\mu g/m^3$ (for Airport emissions) and 5.1 $\mu g/m^3$ (for All emissions) during the Summer Season. For the CE and CN sites, the three major chemical constituents of $PM_{2.5}$ due to the modeled emissions scenarios are A25, AECT, and AORGPAT. It was observed that ASO4T plays a relative larger role in this grid-cell for Jet and All emissions scenarios compared to the adjacent grid-cell containing the AQ and CS sites. With the exception of a few days, both ANO3T and ANH4T have negative contributions in all three scenarios. The phenomenon of negative contributions from inorganic $PM_{2.5}$ components was also observed in other CMAQ modeling applications for airports as described in Arunachalam et al., 2011 and Woody et al., 2011.

Similar analyses as above were also performed for the Winter Season and can be found in Figure 9-61 and Figure 9-65. The ranges of field measurement data during Winter Season at the four core sites are comparable to those in Summer Season, and range between 10 – 25 $\mu g/m^3$. The CMAQ-modeled concentrations for all four scenarios were generally high compared to measurement data and track each other very closely, with the exception of a few days in the middle of the season. The incremental contributions due to the airport emissions scenarios in the grid-cell containing the AQ and CS sites do not exceed 2.3 $\mu g/m^3$ (for Jet emissions), 6.0 $\mu g/m^3$ (for Airport emissions), and 7.2 $\mu g/m^3$ (for All emissions) during the Winter Season. Similar values for the adjacent grid-cell containing the CE and CN sites were 0.9, 2.0, and 2.6 $\mu g/m^3$, respectively.

When looking at the $PM_{2.5}$ speciated components for the Winter Season, the trends were similar to those observed during the Summer Season at the grid-cell containing the AQ and CS sites. AECT, AORGPAT, and A25 were the largest contributors, providing between 30-35 percent each to the total $PM_{2.5}$ levels. A relatively smaller positive contributions from ASO4T and negative contributions from ANO3T and ANH4T were also observed. However, at the adjacent grid-cell containing the CE and CN site, A25 due to jet emissions is comparatively smaller, with increased contributions from ASO4T on several days, indicating the contributions from secondary production of aerosols in the atmosphere.

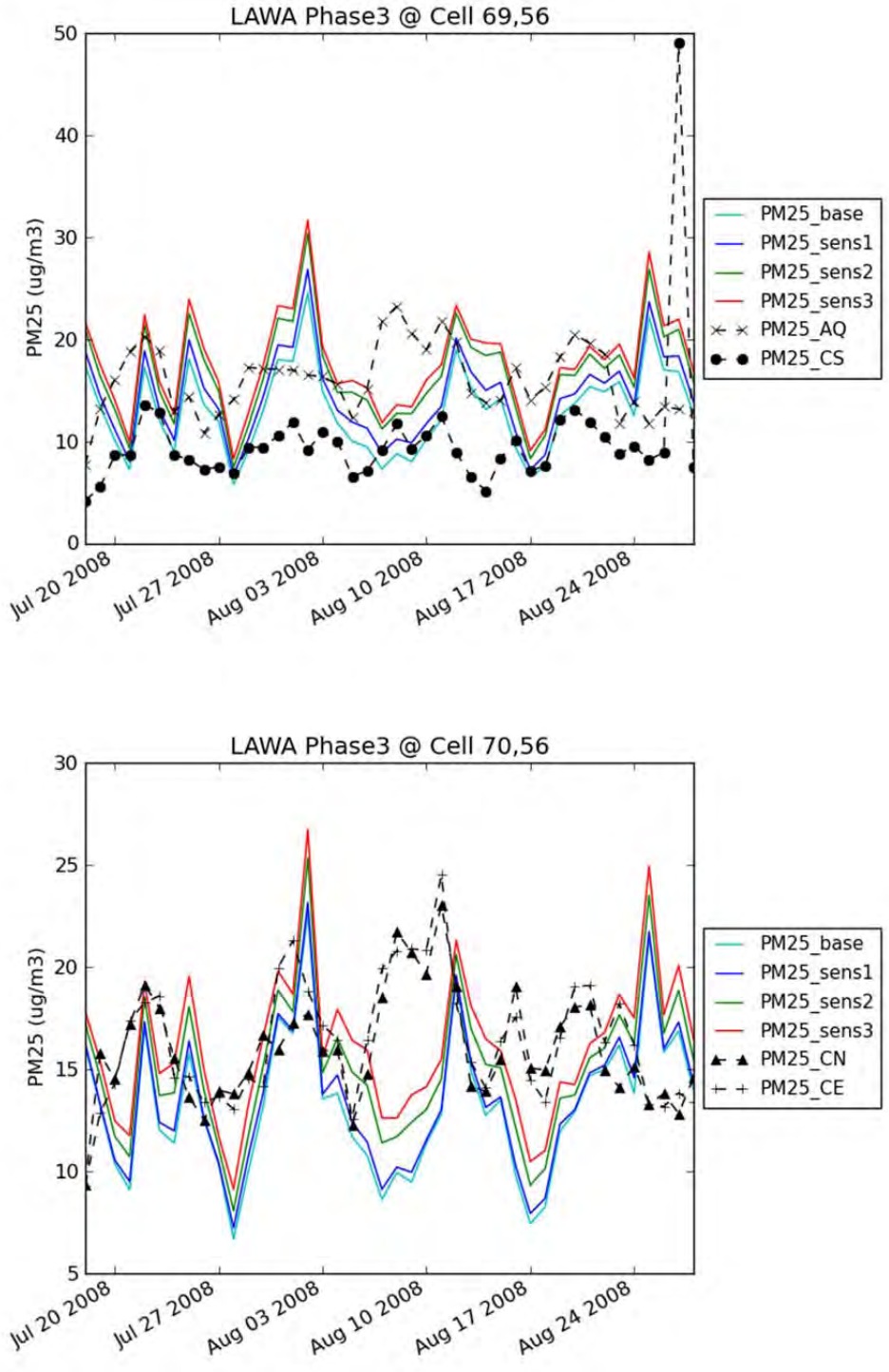

Figure 9-56. Daily average $PM_{2.5}$ concentrations from the four modeling scenarios compared to field measurements at the AQ and CS sites (top) and CN and CE sites (bottom) during Summer Season.

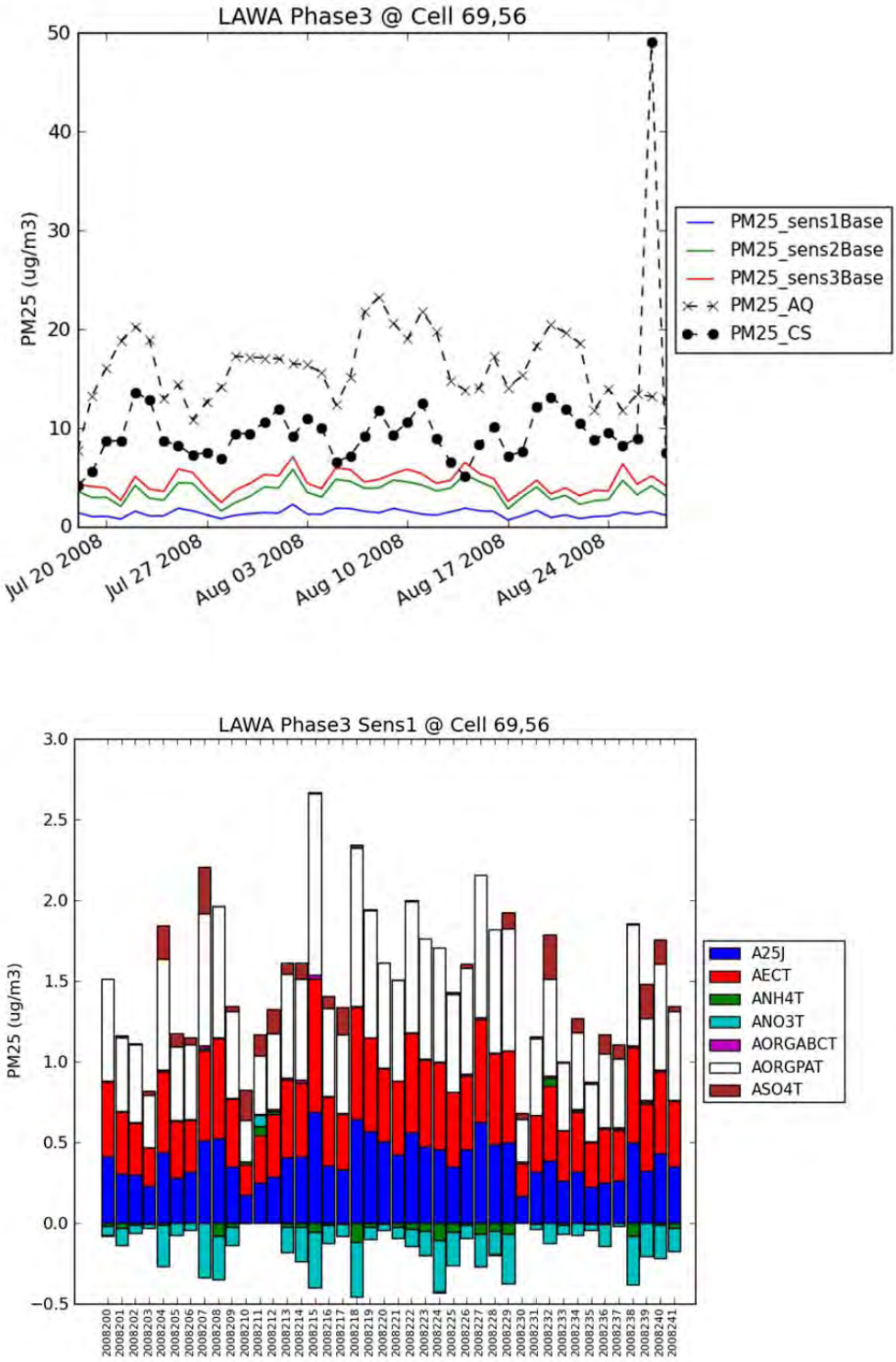

Figure 9-57. Differences in daily average $PM_{2.5}$ concentrations between the three airport emissions scenarios versus base compared to field measurements at the AQ and CS sites (top) and differences in speciated $PM_{2.5}$ concentrations between AQMD_Jet and AQMD_Zero scenarios during Summer Season.

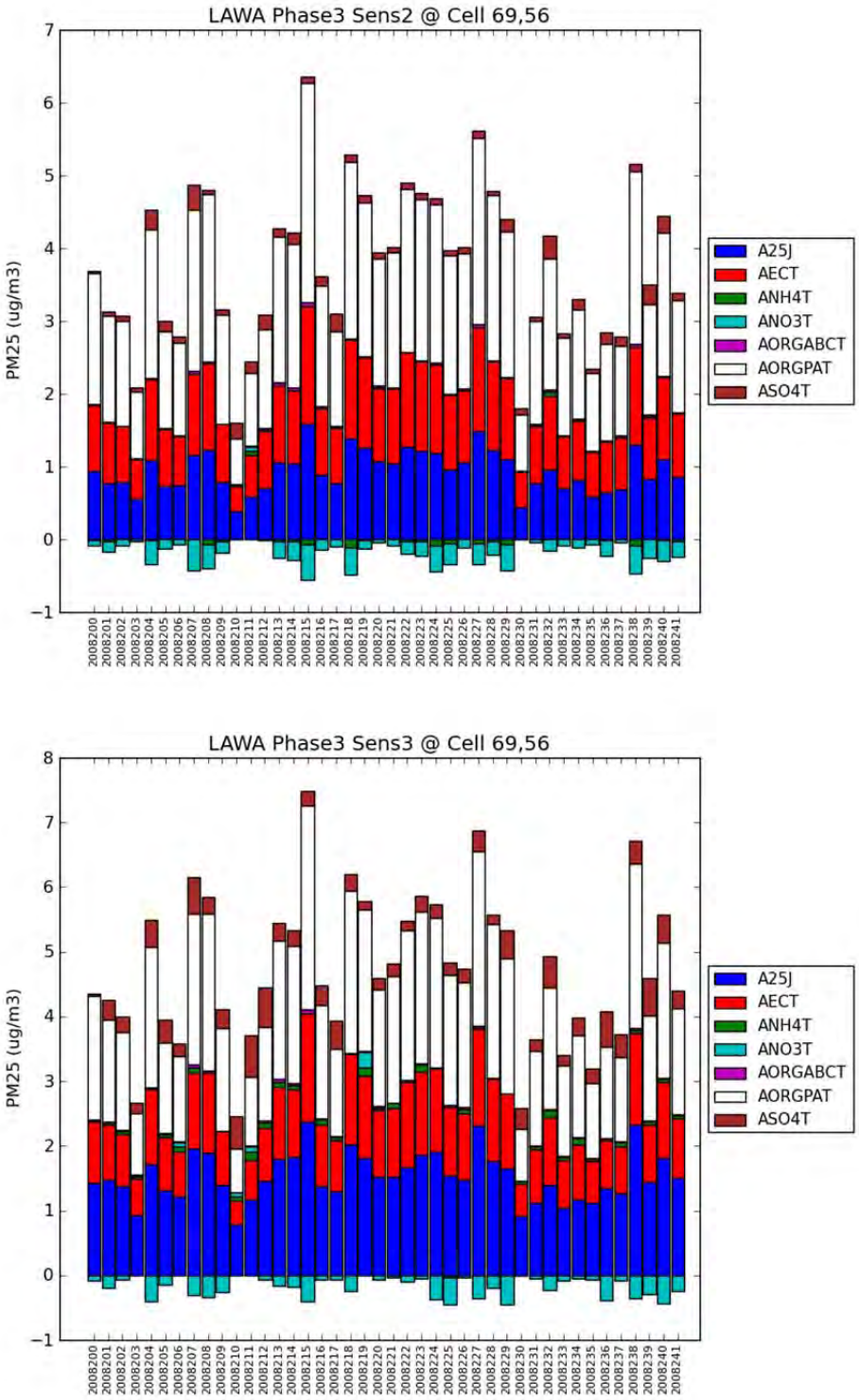

Figure 9-58. Differences in speciated $PM_{2.5}$ concentrations between AQMD_Airport and AQMD_Zero scenarios (top) and between AQMD_All and AQMD_Zero scenarios (bottom) at grid-cell containing the AQ and CS sites during Summer Season.

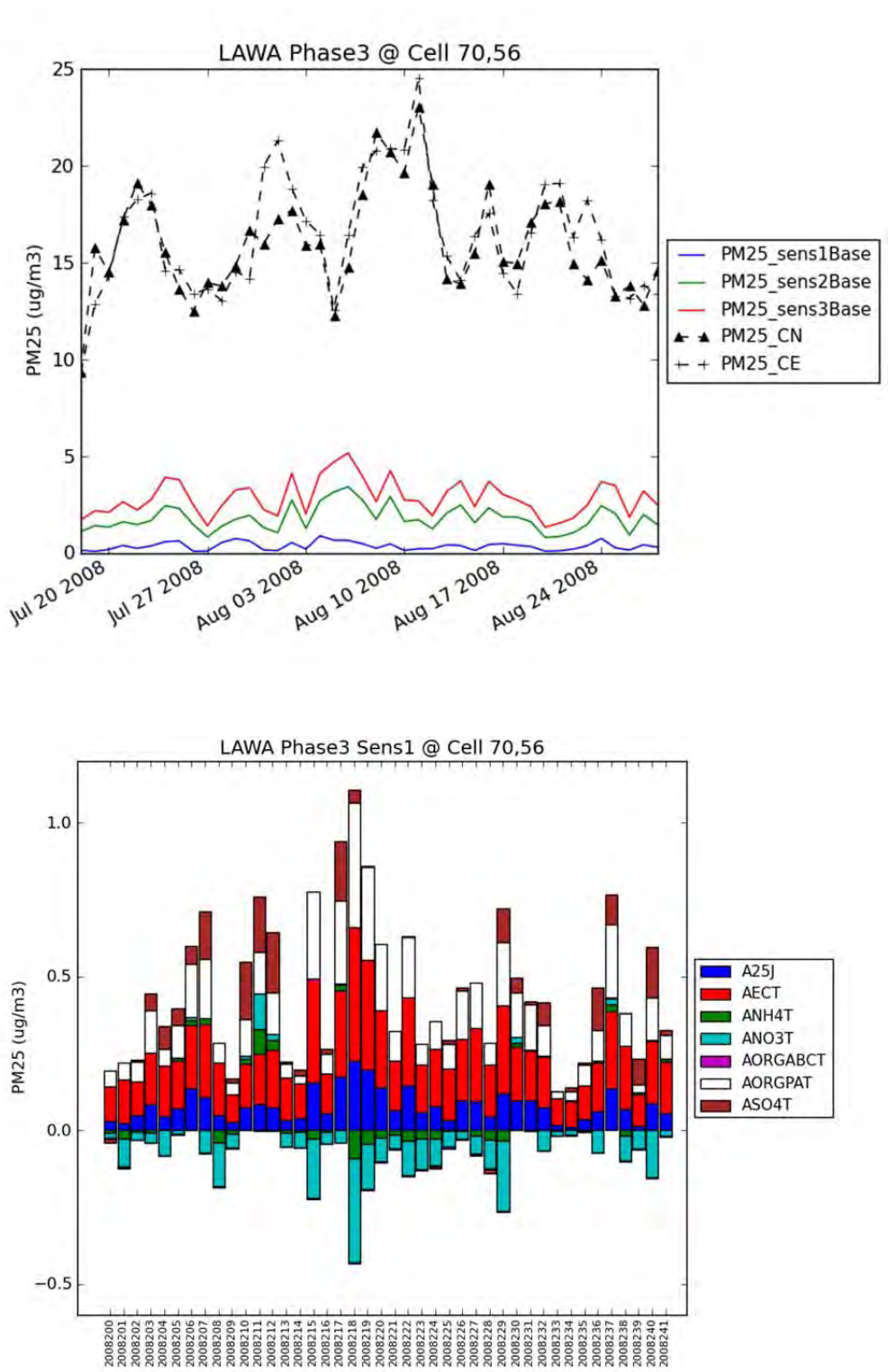

Figure 9-59. Differences in daily average $PM_{2.5}$ concentrations between the 3 airport emissions scenarios versus base compared to field measurements at the CE and CN sites (top) and differences in speciated $PM_{2.5}$ concentrations between AQMD_Jet and AQMD_Zero scenarios during Summer Season.

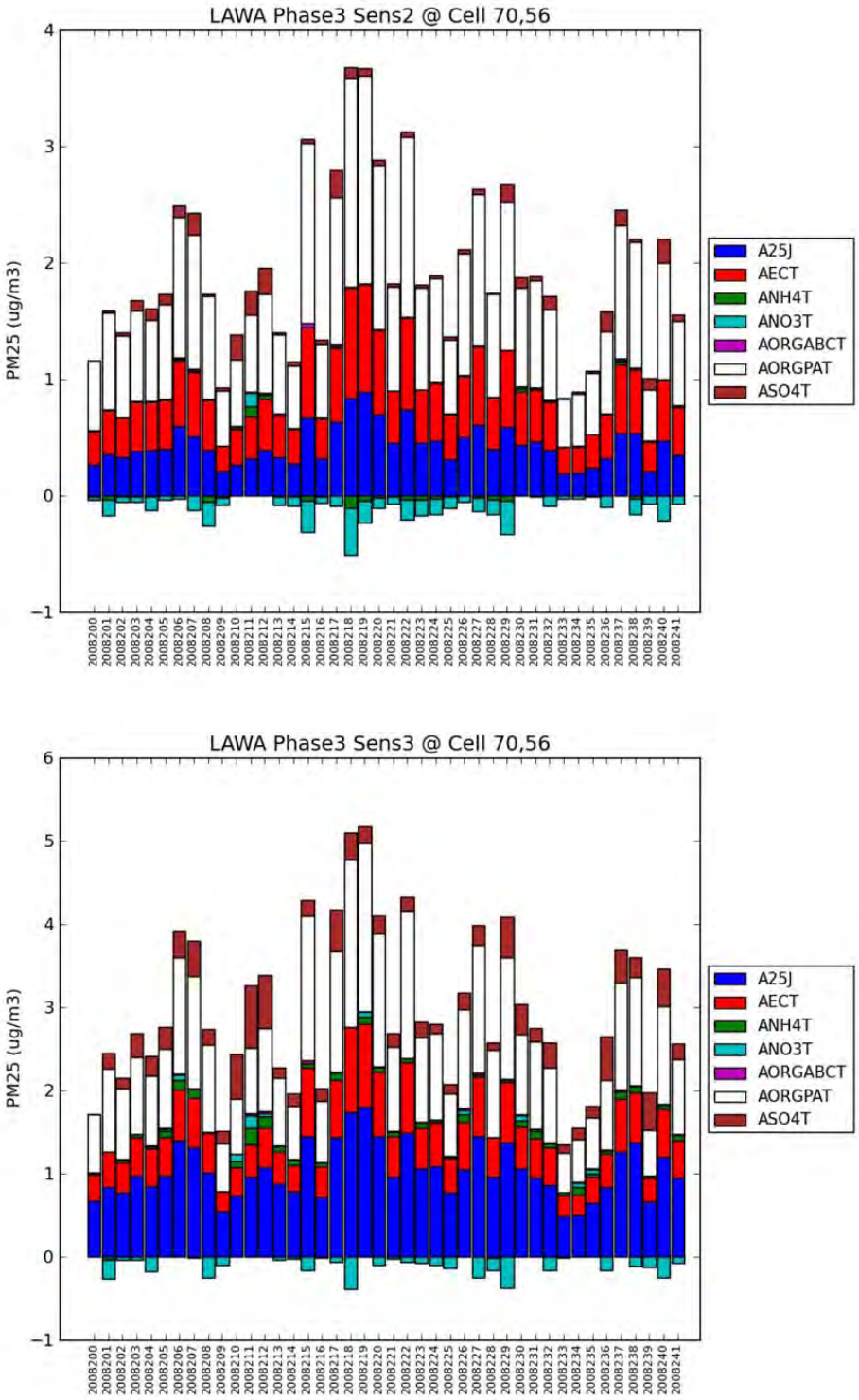

Figure 9-60. Differences in speciated $PM_{2.5}$ concentrations between AQMD_Airport and AQMD_Zero scenarios (top) and between AQMD_All and AQMD_Zero scenarios (bottom) at grid-cells containing CE and CN sites during Summer Season.

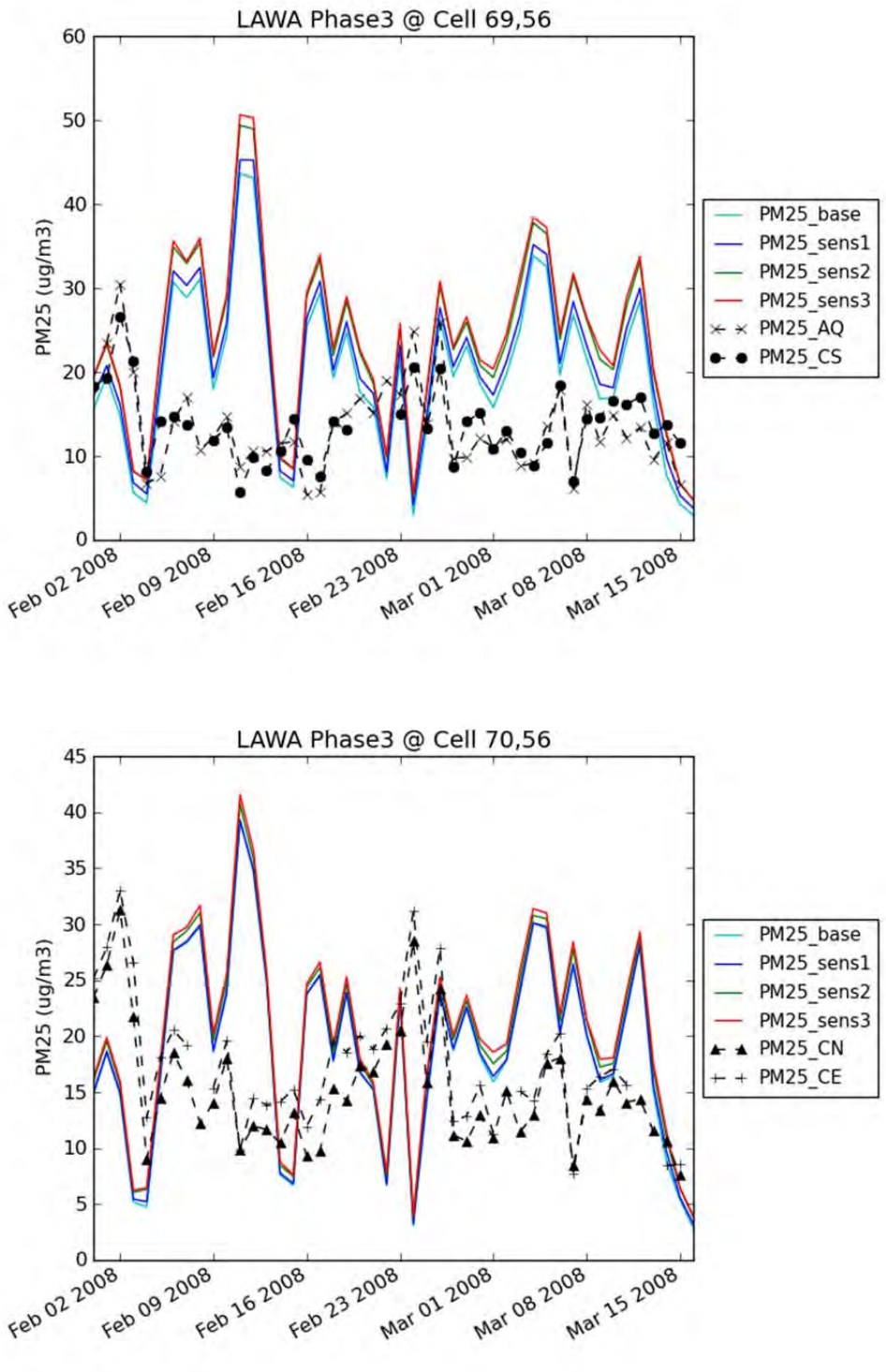

Figure 9-61. Daily average $PM_{2.5}$ concentrations from the four modeling scenarios compared to field measurements at the AQ and CS sites (top) and CN and CE sites (bottom) during Winter Season.

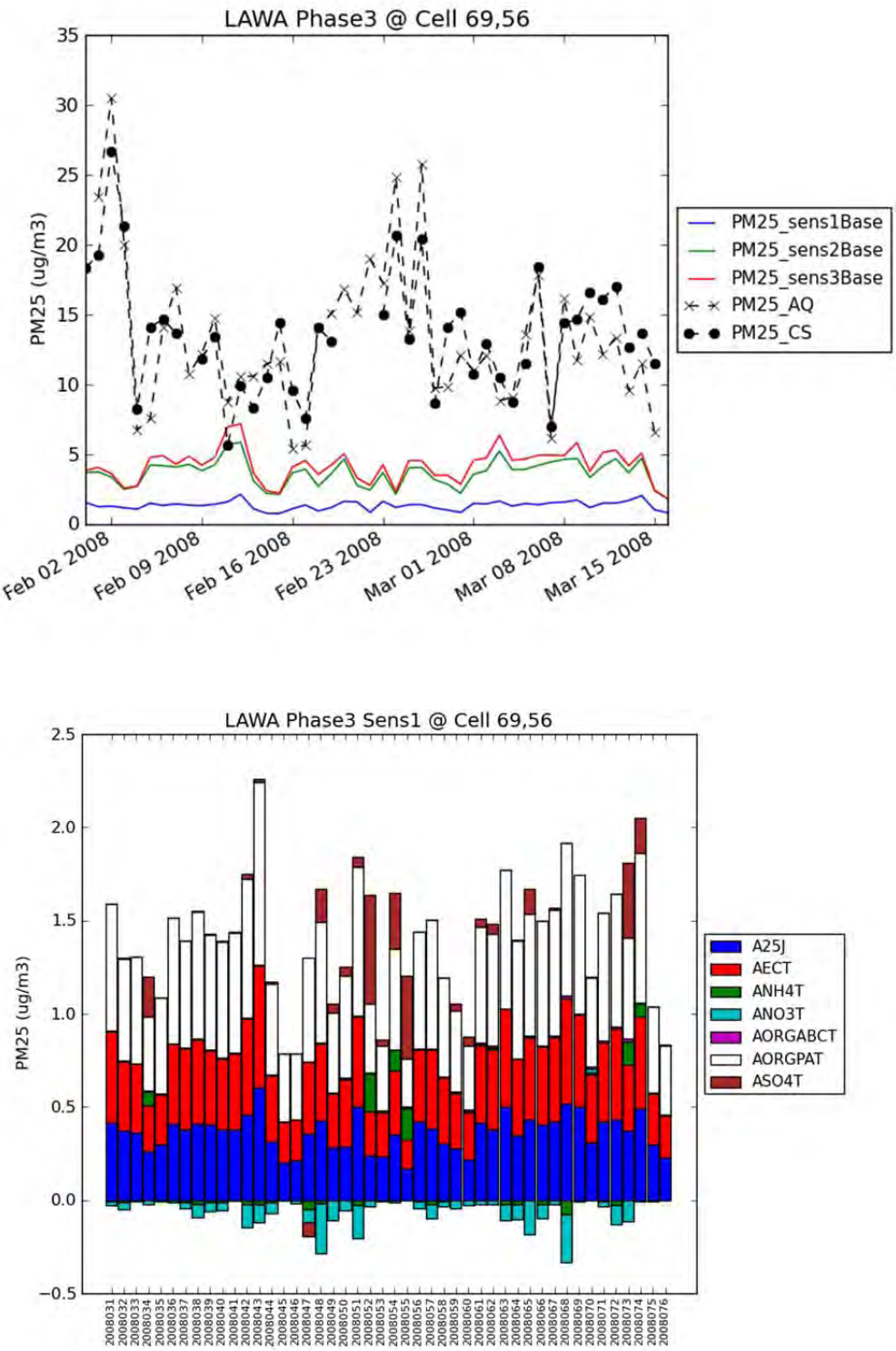

Figure 9-62. Differences in daily average $PM_{2.5}$ concentrations between the three airport emissions scenarios versus base compared to field measurements at the AQ and CS sites (top) and differences in speciated $PM_{2.5}$ concentrations between AQMD_Jet and AQMD_Zero scenarios during Winter Season.

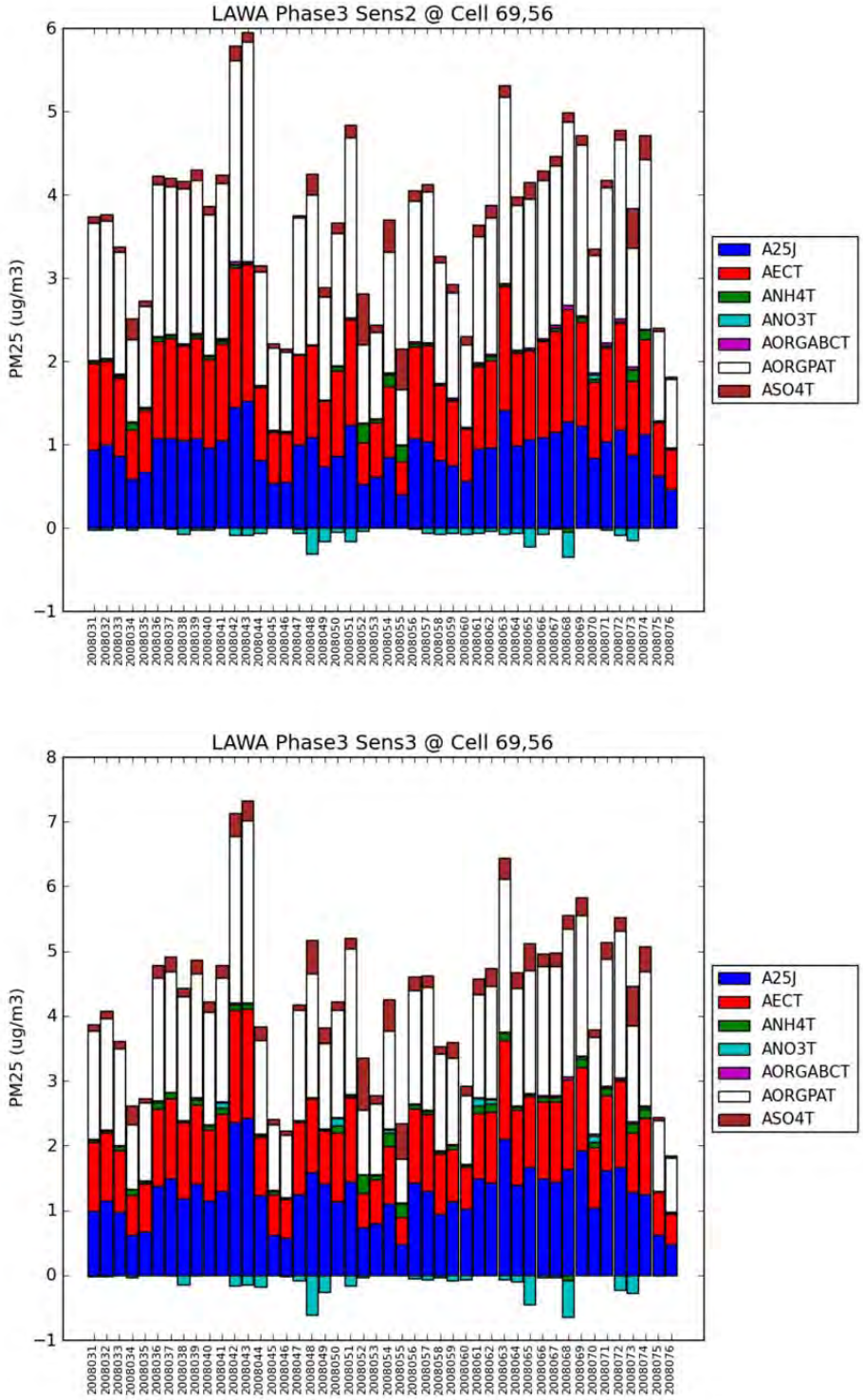

Figure 9-63. Differences in speciated $PM_{2.5}$ concentrations between AQMD_Airport and AQMD_Zero scenarios (top) and between AQMD_All and AQMD_Zero scenarios (bottom) at grid-cell containing AQ and CS sites during Winter Season.

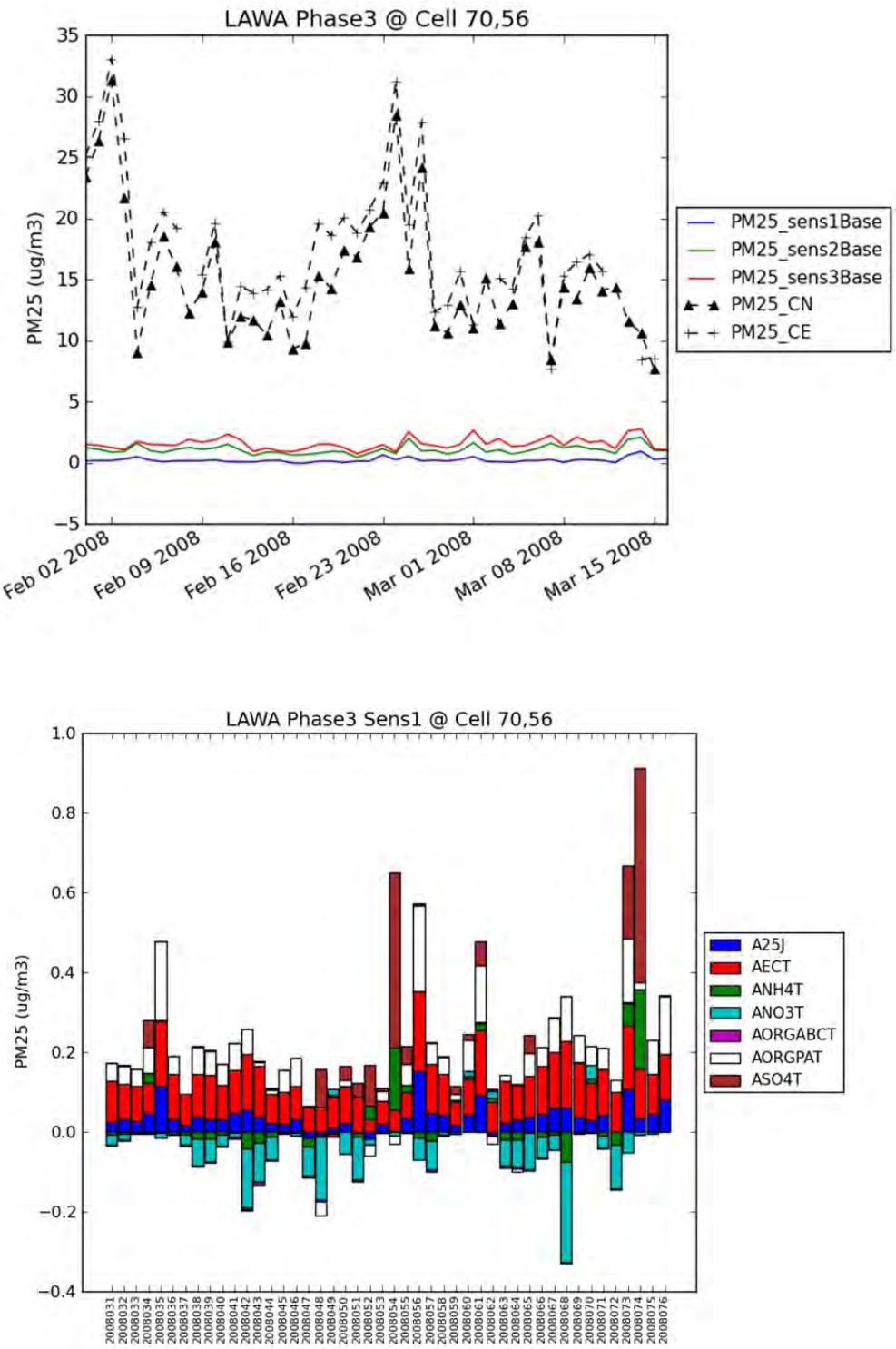

Figure 9-64. Differences in daily average $PM_{2.5}$ concentrations between the three airport emissions scenarios versus base compared to CE and CN sites (top) and differences in speciated $PM_{2.5}$ concentrations between AQMD_Jet and AQMD_Zero scenarios during Winter Season.

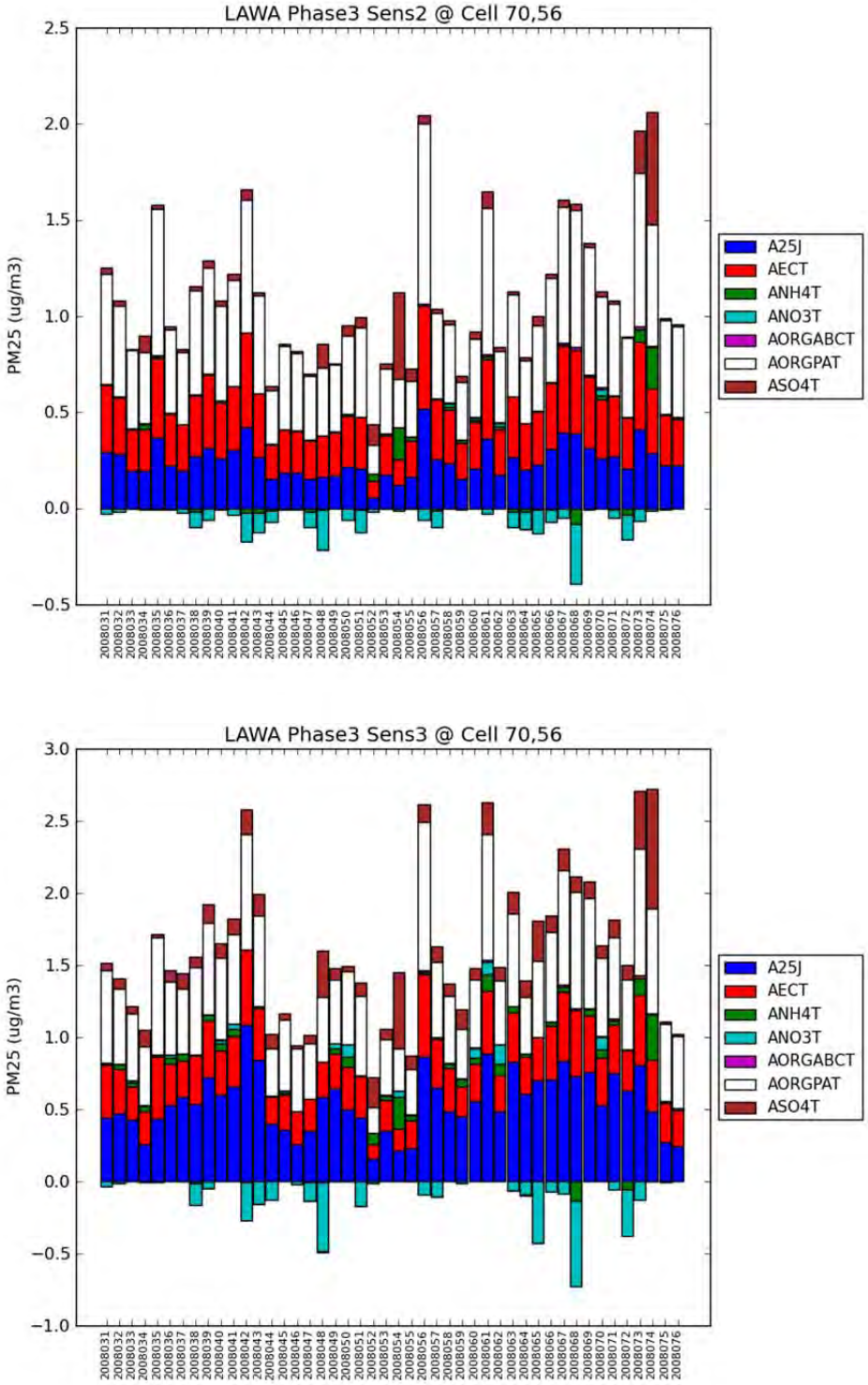

Figure 9-65. Differences in speciated $PM_{2.5}$ concentrations between AQMD_Airport and AQMD_Zero scenarios (top) and between AQMD_All and AQMD_Zero scenarios (bottom) at grid-cells containing CE and CN sites during Winter Season.

9.2.3.3 Source Apportionment

In this section, results from the CMAQ-based source apportionment of the Phase III Study emissions are presented. Source apportionment was performed to understand

a) the incremental contribution of LAX Phase III emissions to total ambient concentrations predicted by CMAQ (referred to as CMAQ-SA1 hereafter), and

b) the relative contribution of airport-related activity to total incremental concentrations due to Phase III emissions (referred to as CMAQ-SA2 hereafter).

It is important to carefully distinguish between the two approaches, CMAQ-SA1 and CMAQ-SA2, defined above. The first provides the incremental contribution of each of the three airport emissions scenarios to total ambient concentration. The second provides the relative contribution of airport-related sources to total air quality impacts due to Study Area emissions in Phase III. Since AERMOD predictions only include the contribution due to Study Area emissions and not contributions from the broad regional background, the CMAQ-calculated source apportionment from the CMAQ-SA2 approach is comparable to the estimates from AERMOD presented in Section 9.1.

Taking into consideration that fact that the four core sites are at the edge of the CMAQ grid-cells, the analysis was extended by looking at the contribution in adjacent grid-cells. A 3x3 array of nine grid-cells centered on the CMAQ grid-cell (70,56) that contains part of the airport was chosen, and the source apportionment metrics are presented in each grid-cell in this section. The four CMAQ emissions scenarios are defined as:

- AQMD_Zero: AQMD Base case with no LAX airport emissions
- AQMD_Sens1: Add Jet + APU + GSE emissions to AQMD_Zero
- AQMD_Sens2: Add other LAX airport-related emissions (from Airport scenario) to AQMD_Sens1
- AQMD_Sens3: Add local background emissions (All) to AQMD Sens2

In the following subsections, results from CMAQ-SA1 are presented in Section 9.2.3.4 and from CMAQ-SA2 are presented in Section 9.2.3.5.

9.2.3.4 Incremental Contributions of Emissions Scenarios compared to Regional Background

For this analysis, the following four metrics were computed in each of the nine grid-cells above, using season average concentrations predicted by CMAQ.

- Jet (Aircraft/APU/GSE contributions) = (AQMD_Sens1 minus AQMD_Zero) * 100 / AQMD_Sens1
- OnAirport1 = (AQMD_Sens2 minus AQMD_Zero) * 100 / AQMD_Sens2

- Off+OnAirport = (AQMD_Sens3 minus AQMD_Zero) * 100 / AQMD_Sens3
- OnAirport2 = (AQMD_Sens2 minus AQMD_Zero) * 100 / AQMD_Sens3

In performing these calculations, the denominator is intended to capture the total predicted concentrations by CMAQ due to the emissions assumption used for that particular scenario, and hence the first three equations are the preferred metrics to understand source apportionment due to CMAQ. However, the fourth metric above was computed to assess the relative contribution of airport-related emissions to total ambient air that includes regional background sources as well as Study Area emissions, and simply provides an alternate approach. Given the non-linearities involved in the atmospheric processes involved, the fourth metric potentially has more uncertainties compared to the first three.

The results are presented as stacked bar charts below and it should be noted that the y-axis scales vary between the two seasons on all these bar charts. In each figure, the grid-cell where the incremental contributions are calculated is shown at the top.

- Incremental percent of CO contributions modeled by CMAQ due to various emissions scenarios during the Winter and Summer Seasons (Figure 9-66.)

- Incremental percent of NO_x contributions modeled by CMAQ due to various emissions scenarios during the Winter and Summer Seasons (Figure 9-67.)

- Incremental percent of $PM_{2.5}$ contributions modeled by CMAQ due to various emissions scenarios during the Winter and Summer Seasons (Figure 9-68.)

- Incremental percent of SO_2 contributions modeled by CMAQ due to various emissions scenarios during the Winter and Summer Seasons (Figure 9-69.)

The actual incremental concentrations corresponding to these percentages in Figure 9-66. through Figure 9-69. are available in a similar layout of the 3x3 array of grid-cells in Appendix Figures 9B-1 to 9B-4.

For all pollutants, except SO_2, the largest contributions are seen in the two grid-cells that contain the airport emissions and the four core sites, (i.e., in grid-cells 69,56 and 70,56). In the case of SO_2 alone, a large contribution from the grid-cell (69,55) that lies directly south of the west airport grid-cell (69,56) was observed during both seasons.

Carbon Monoxide

The largest impacts of CO (15 percent during the Winter Season and 20 percent during the Summer Season) due to Aircraft/APU/GSE sources were seen in grid-cell 69,56. Addition of the remaining Study Area emissions increased this to 25 percent and 40 percent during the two seasons respectively. These increases are attributed primarily to off-airport major and minor roadways. The contributions from LAX are slightly enhanced during the Summer Season in the

two grid-cells directly north of the airport, which was likely due to the effect of the on-shore winds.

Nitrogen Oxides

The relative contribution for NO_x due to the different emissions scenarios did not vary much in the grid-cell 69,56, and were in the range of 35-40 percent. However, the relative contribution of NO_x due to the different emissions scenarios varies quite a bit in the adjacent grid-cell 70,56, where the addition of background emissions sources nearly doubled the contribution from approximately 15 percent to more than 30 percent during the Winter Season and from 40 percent to 70 percent during the Summer Season. In the two grid-cells south of the airport, the airport-related sources contributed only around 10 percent, but adding background sources (primarily marine emissions and Chevron Refinery, to a lesser degree), increases the impacts by over a factor of three to greater than 30 percent during the Winter Season and greater than 40 percent during the Summer Season. Similar to CO, the NO_x contributions from LAX were slightly enhanced during Summer Season in the two grid-cells directly north of the airport, which was likely due to the effect of the on-shore winds.

Fine Particulate Matter

$PM_{2.5}$ contributions due to Aircraft/APU/GSE sources were relatively small (5 percent during the Winter and 10 percent during the Summer Season). However, adding the remaining airport sources nearly doubles the contribution. The addition of off-airport sources did not seem to have a significant impact in the airport grid-cell 69,56, however, it did seem to make a big difference in the adjacent grid-cell 70,56 and in the grid-cells south of the airport. This highlights the contribution from off-airport roadways and the Chevron Refinery located to the south of the airport.

Sulfur Dioxide

Airport-related sources contribute more than 30 percent to SO_2 concentrations in the grid-cell 69,56. The addition of background sources enhances this to nearly 40 percent. However in the adjacent grid-cell 70,56, the impacts of background sources were much more pronounced, with the contribution observed, increasing from approximately 15 percent to 30 percent during both seasons. The SO_2 impacts due to background sources in the two grid-cells south of the airport were in the 20-25 percent range. In absolute terms, (see Figure 9B-44), grid-cell 69,55, located south of the airport, had the largest contribution in the entire Study Area. This enhancement is attributed to the Chevron Refinery and marine sources.

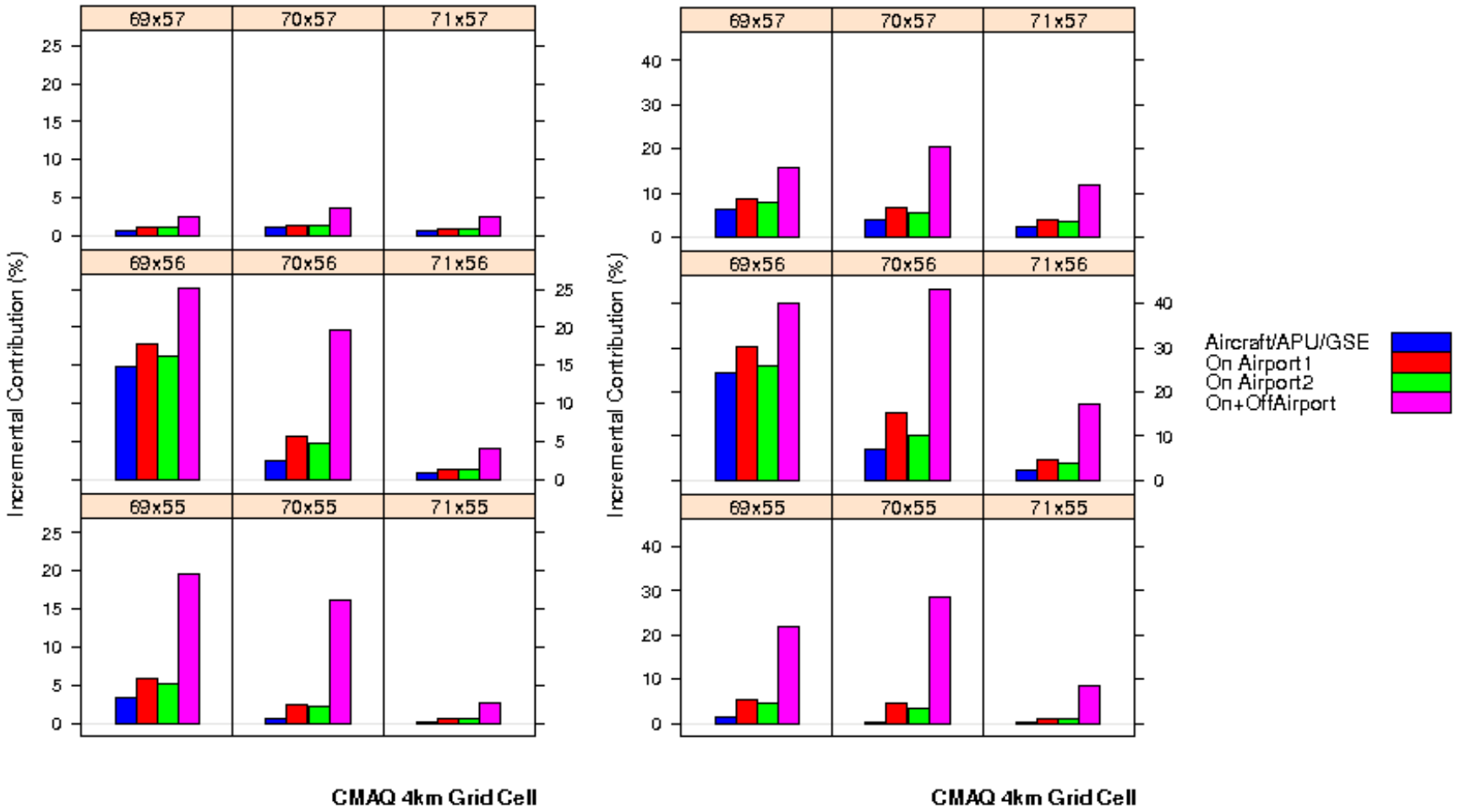

Figure 9-66. Incremental percent of CO contributions modeled by CMAQ due to various emissions scenarios during Winter (left) and Summer (right). [Numbers such as 69x57 indicate the Column, Row index of the CMAQ grid-cell]

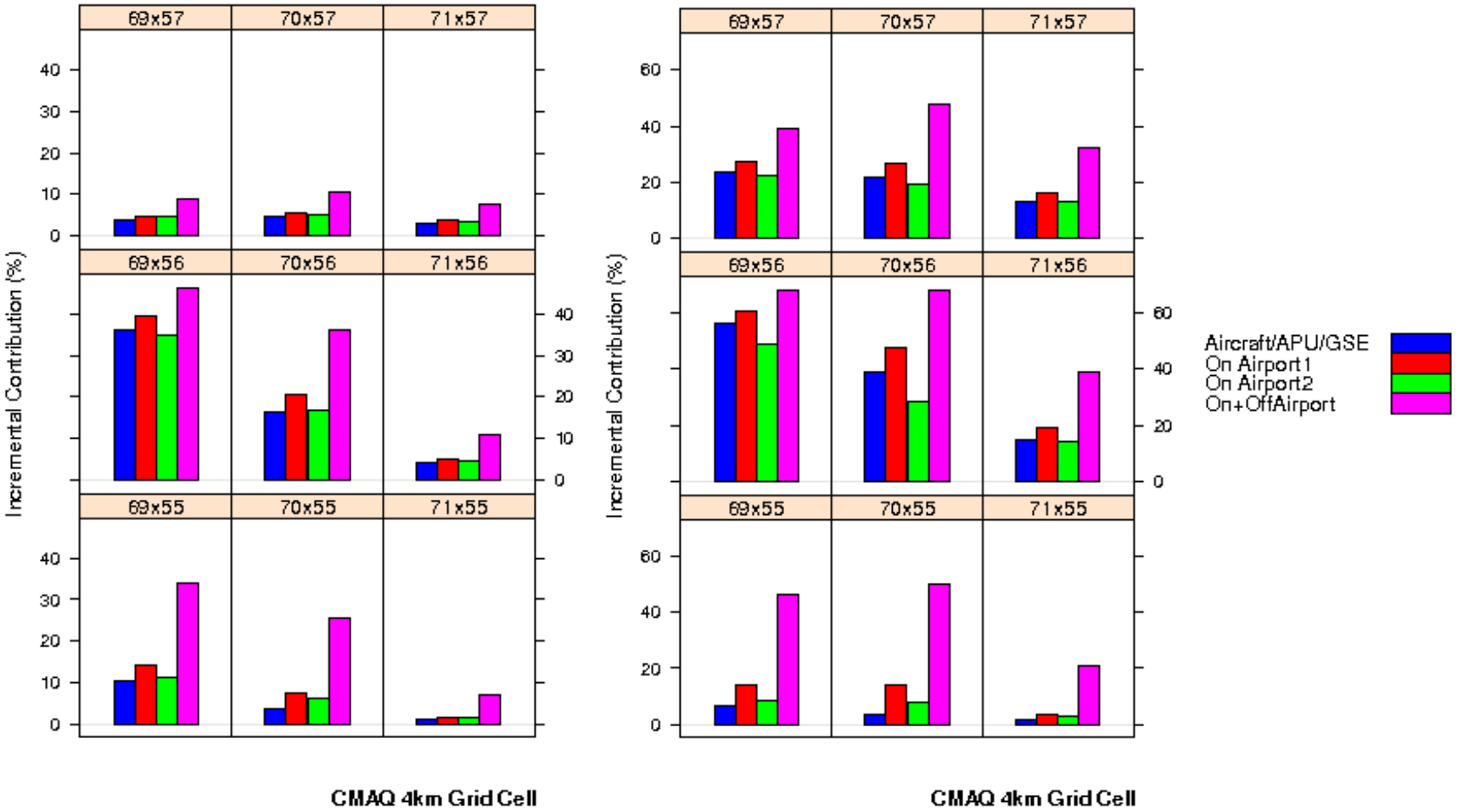

Figure 9-67. Incremental percent of NO_x contributions modeled by CMAQ due to various emissions scenarios during Winter (left) and Summer (right). [Numbers such as 69x57 indicate the Column, Row index of the CMAQ grid-cell]

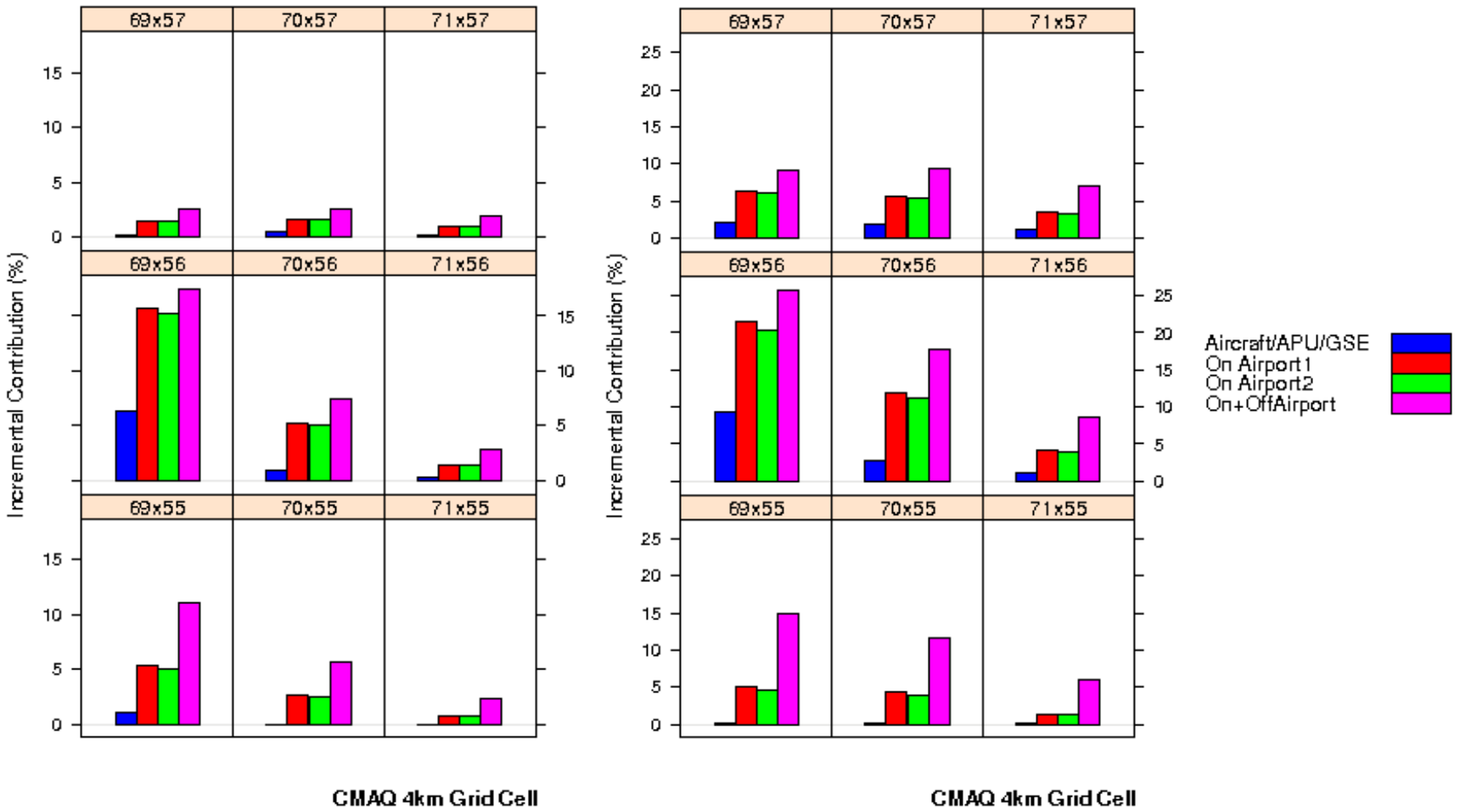

Figure 9-68. Incremental percent of $PM_{2.5}$ contributions modeled by CMAQ due to various emissions scenarios during Winter (left) and Summer (right). [Numbers such as 69x57 indicate the Column, Row index of the CMAQ grid-cell]

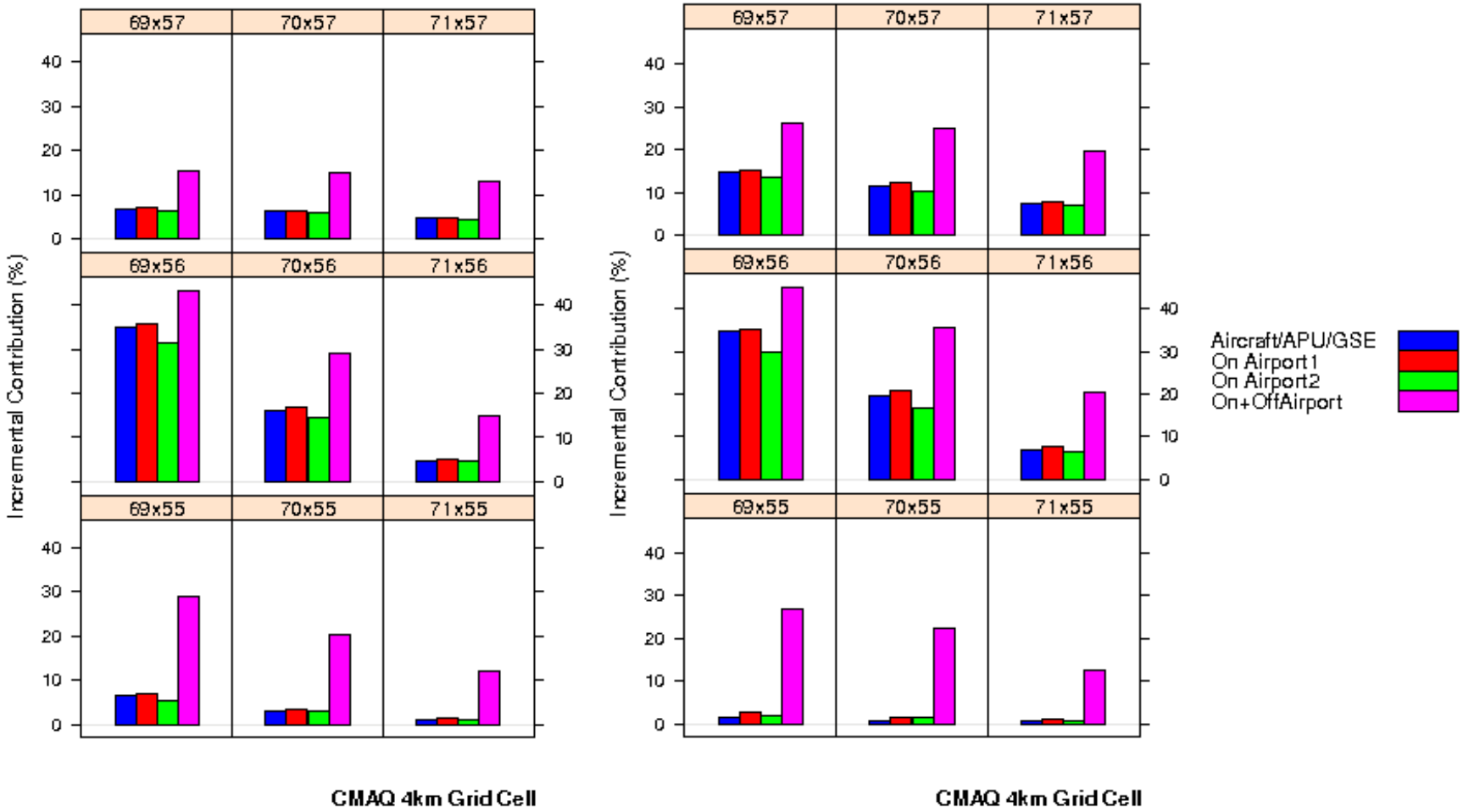

Figure 9-69. Incremental percent of SO_2 contributions modeled by CMAQ due to various emissions scenarios during Winter (left) and Summer (right). [Numbers such as 69x57 indicate the Column, Row index of the CMAQ grid-cell]

9.2.3.5 Relative Contributions of Airport-related vs. Background sources

For the second set of source apportionment calculations, the contributions from AQMD_Sens3 scenario compared to the AQMD_Zero (i.e., AQMD_Sens3 minus AQMD_Zero) were taken and then broken into three components:

- Jet+APU+GSE
- Other Airport-related emissions
- Non-airport emissions (or background emissions) in LAX Study Area

Adding the first two components above is equivalent to assessing the contribution due to all "airport-related" sources. This analysis was performed for each of the same nine grid-cells centered on the airport presented above, and the results from this analysis are presented as pie-charts in the following figures.

- Fractional CO contribution from LAX airport emissions modeled by CMAQ during the Winter Season (Figure 9-70.)
- Fractional CO contribution from LAX airport emissions modeled by CMAQ during the Summer Season (Figure 9-71.)
- Fractional NO_x contribution from LAX airport emissions modeled by CMAQ during the Winter Season (Figure 9-72.)
- Fractional NO_x contribution from LAX airport emissions modeled by CMAQ during the Summer Season (Figure 9-73.)
- Fractional $PM_{2.5}$ contribution from LAX airport emissions modeled by CMAQ during the Winter Season (Figure 9-74.)
- Fractional $PM_{2.5}$ contribution from LAX airport emissions modeled by CMAQ during the Summer Season (Figure 9-75.)
- Fractional SO_2 contribution from LAX airport emissions modeled by CMAQ during the Winter Season (Figure 9-76.)
- Fractional SO_2 contribution from LAX airport emissions modeled by CMAQ during the Summer Season (Figure 9-77.)

In Figure 9-70. to Figure 9-77., "Jet" indicates Aircraft+APU+GSE, "Other-Airport" indicates other airport-related sources such as airport-related traffic and stationary sources, and "Off-Airport" indicates background sources.

Carbon Monoxide

During both the Winter and Summer Seasons, aircraft sources contributed approximately 50 percent of the CO concentrations in grid-cell 69,56. When combined with other airport-related

sources, the contribution was nearly 70 percent. However, in the adjacent grid-cell 70,56, airport-related sources contributed only approximately 25 percent.

Nitrogen Oxides

Total airport-related sources contributed up to 75 percent of the NO_x concentrations in grid-cell 69,56, and were as high as 50 percent in the adjacent grid-cells (70,56 to the east and the two grid-cells north of the airport). In the two grid-cells south of the airport, background sources contributed up to 75 percent of the NO_x concentration, which is attributed primarily to on-roadway sources, the marine sources and, to a relatively smaller degree the Chevron Refinery.

Fine Particulate Matter

The pie-charts for $PM_{2.5}$ are unique compared to the gaseous pollutants. Aircraft sources contributed only around 30 percent of the $PM_{2.5}$ concentrations in the west airport grid-cell (69,56), and even less in the adjacent east airport grid-cell 70,56. However, the other airport-related sources contributed approximately 65 percent of the PM2.5 concentration in the Winter Season and approximately 50 percent in the Summer Season in these two grid-cells, which is attributed to emissions from major stationary sources (owned by LAWA) on airport property as well as on-airport traffic sources. The background sources contributed approximately 55 percent in the Winter Season and approximately 70 percent in the Summer Season in the two grid-cells south of the airport, which could be attributed to the Chevron Refinery and marine sources.

Sulfur Dioxide

The SO_2 pie-charts show that the main contributions were from background (or off-airport) sources in all nine grid-cells except the west airport grid-cell (69,56) where the aircraft sources contributed as much as 70-75 percent during both seasons. Other airport-related sources had a negligible contribution to SO_2 in all nine grid-cells. In the grid-cells south of the airport, the background sources (primarily Chevron and marine sources) contributed as high as 80 percent during the Winter Season and 95 percent during the Summer Season.

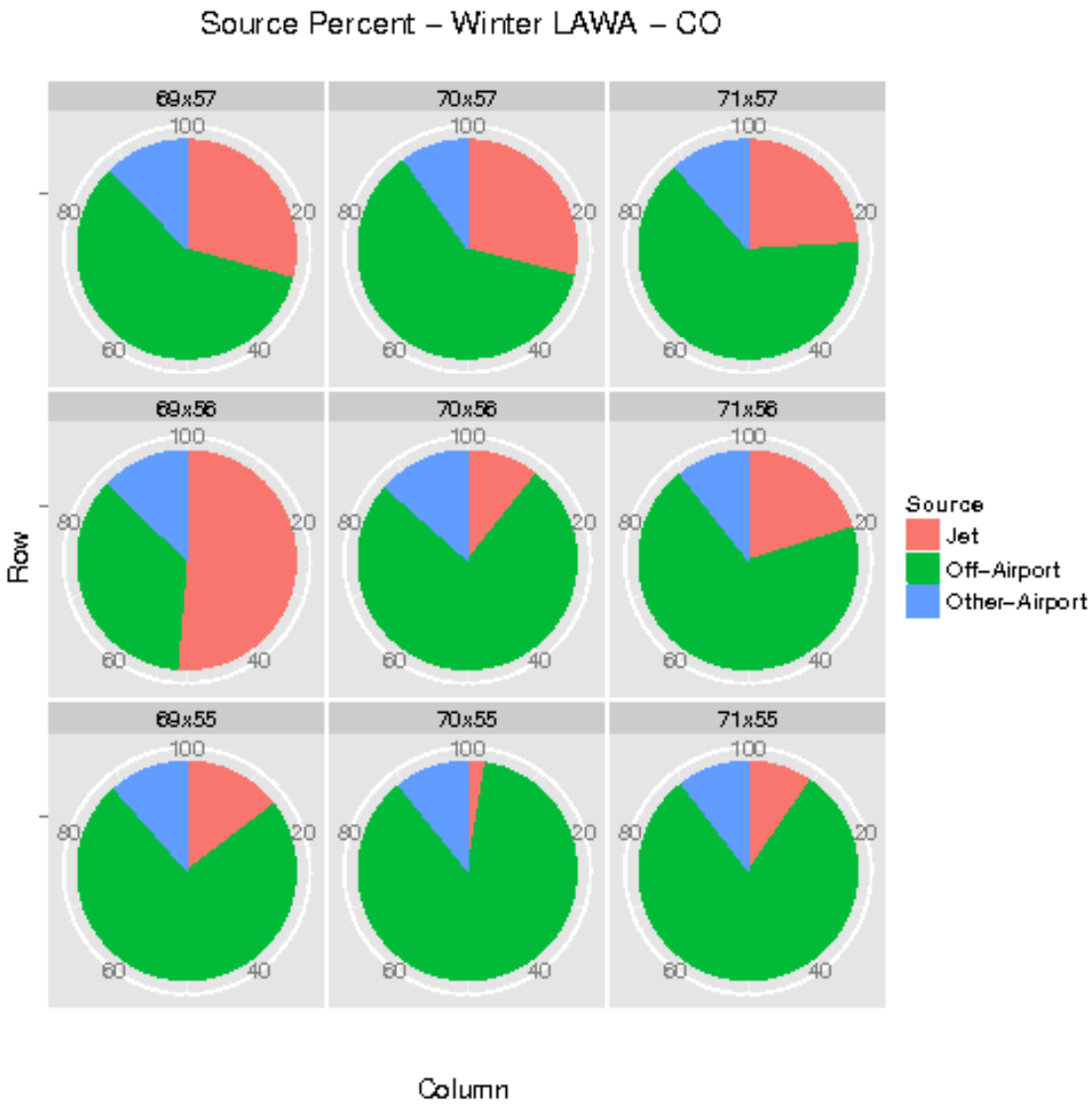

Figure 9-70. Fractional CO contribution from LAX airport emissions modeled by CMAQ during the Winter Season. Numbers such as 69x57 indicate the Column, Row index of the CMAQ grid-cell. "Jet" indicates Aircraft+APU+GSE, "Other-Airport" indicates remaining airport sources such as traffic and stationary, and "Off-Airport" indicates background sources.

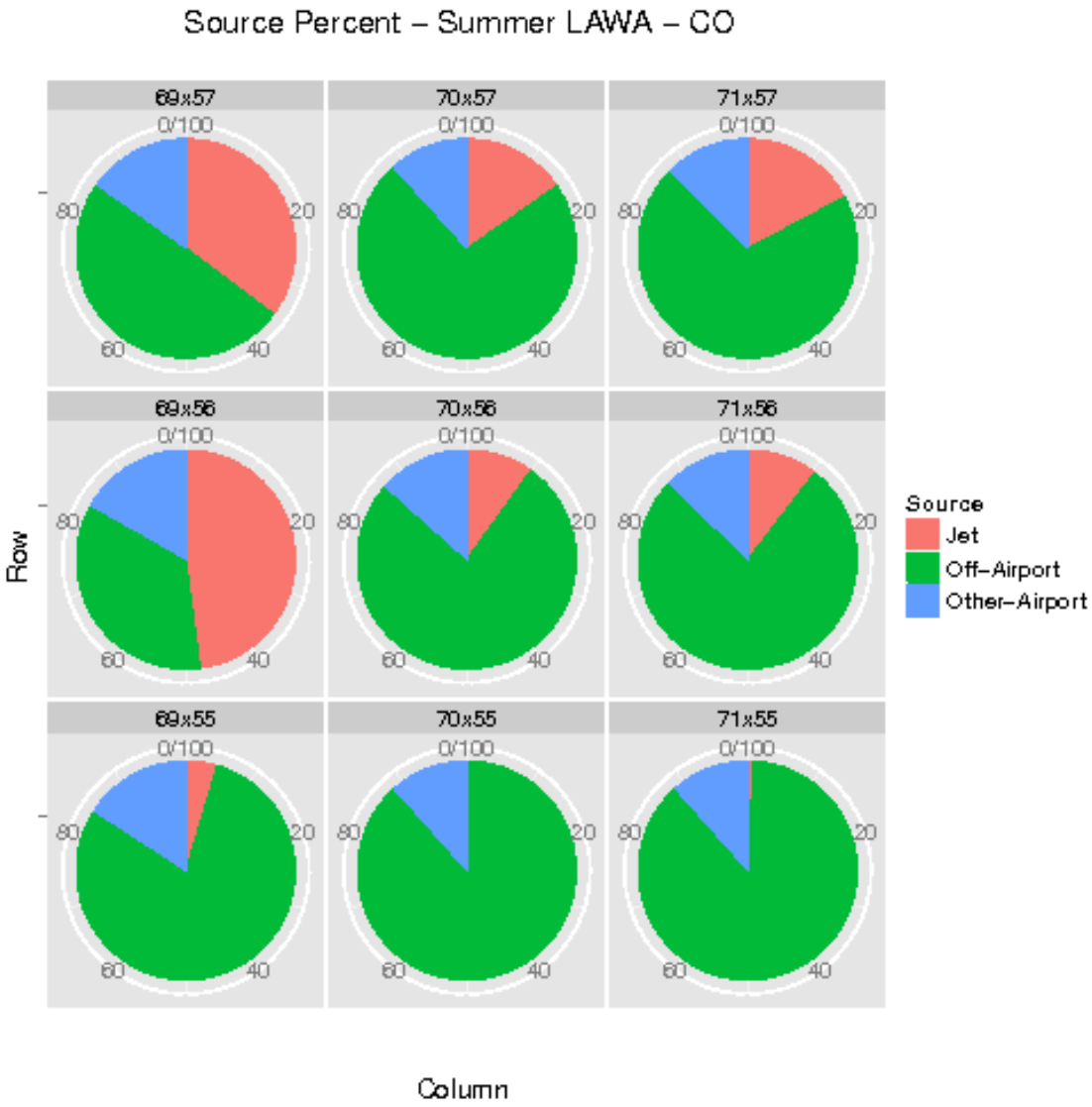

Figure 9-71. Fractional CO contribution from LAX airport emissions modeled by CMAQ during the Summer Season. Numbers such as 69x57 indicate the Column, Row index of the CMAQ grid-cell. Jet" indicates Aircraft+APU+GSE, "Other-Airport" indicates remaining airport sources such as traffic and stationary, and "Off-Airport" indicates background sources.

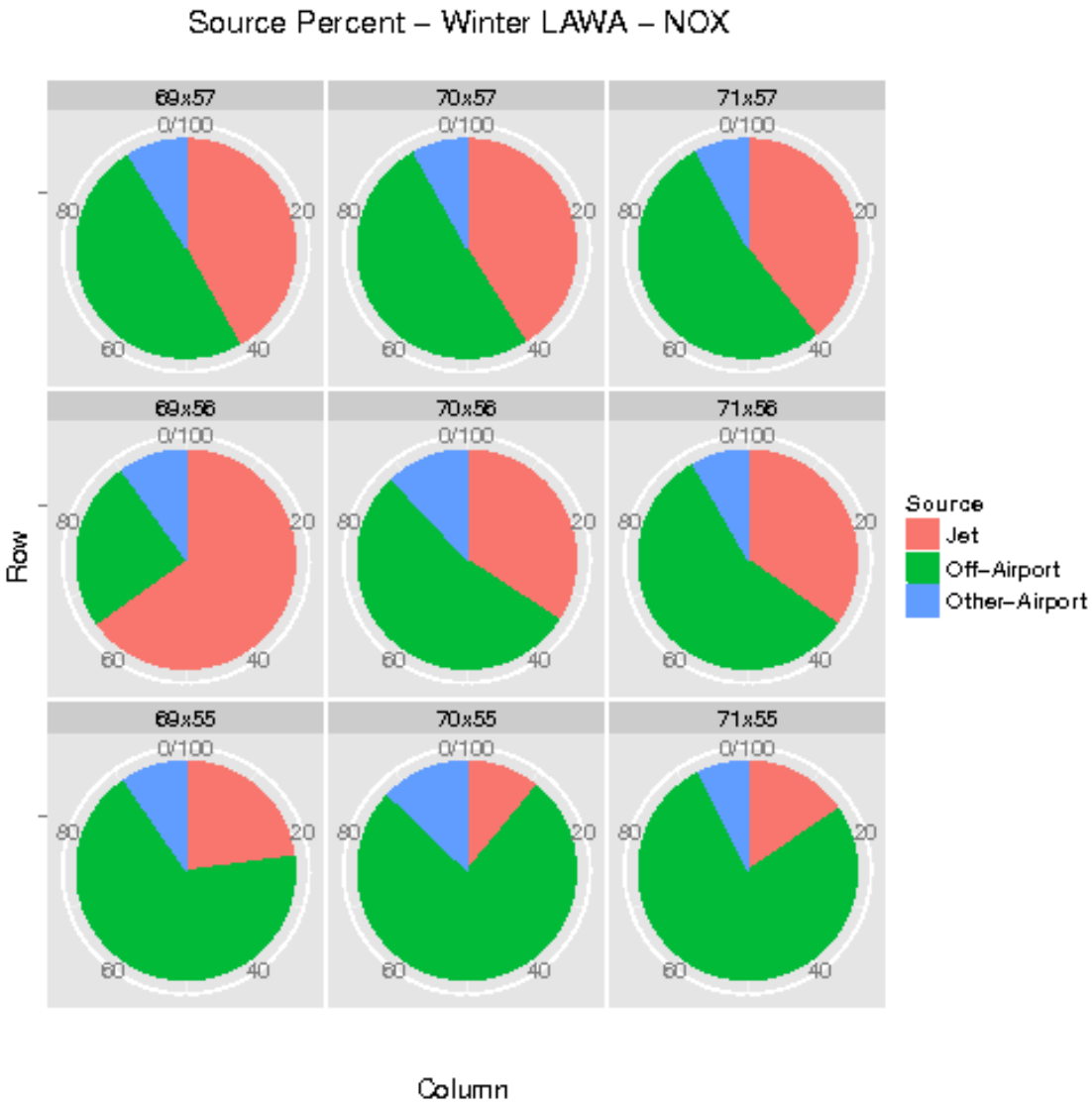

Figure 9-72. Fractional NO_x contribution from LAX airport emissions modeled by CMAQ during the Winter season. Numbers such as 69x57 indicate the Column, Row index of the CMAQ grid-cell. Jet" indicates Aircraft+APU+GSE, "Other-Airport" indicates remaining airport sources such as traffic and stationary, and "Off-Airport" indicates background sources.

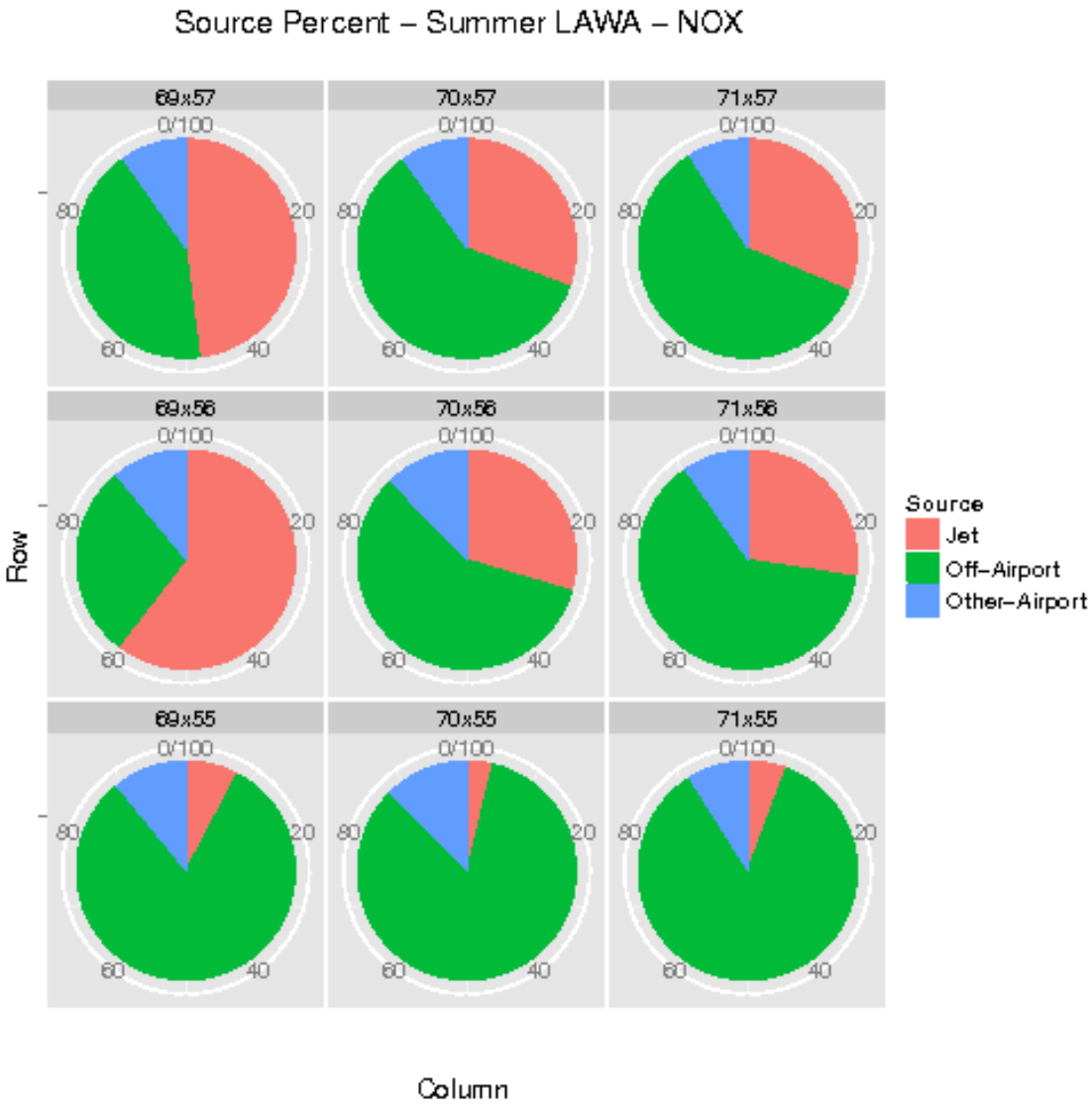

Figure 9-73. Fractional NO_x contribution from LAX airport emissions modeled by CMAQ during the Summer Season. Numbers such as 69x57 indicate the Column, Row index of the CMAQ grid-cell. Jet" indicates Aircraft+APU+GSE, "Other-Airport" indicates remaining airport sources such as traffic and stationary, and "Off-Airport" indicates background sources.

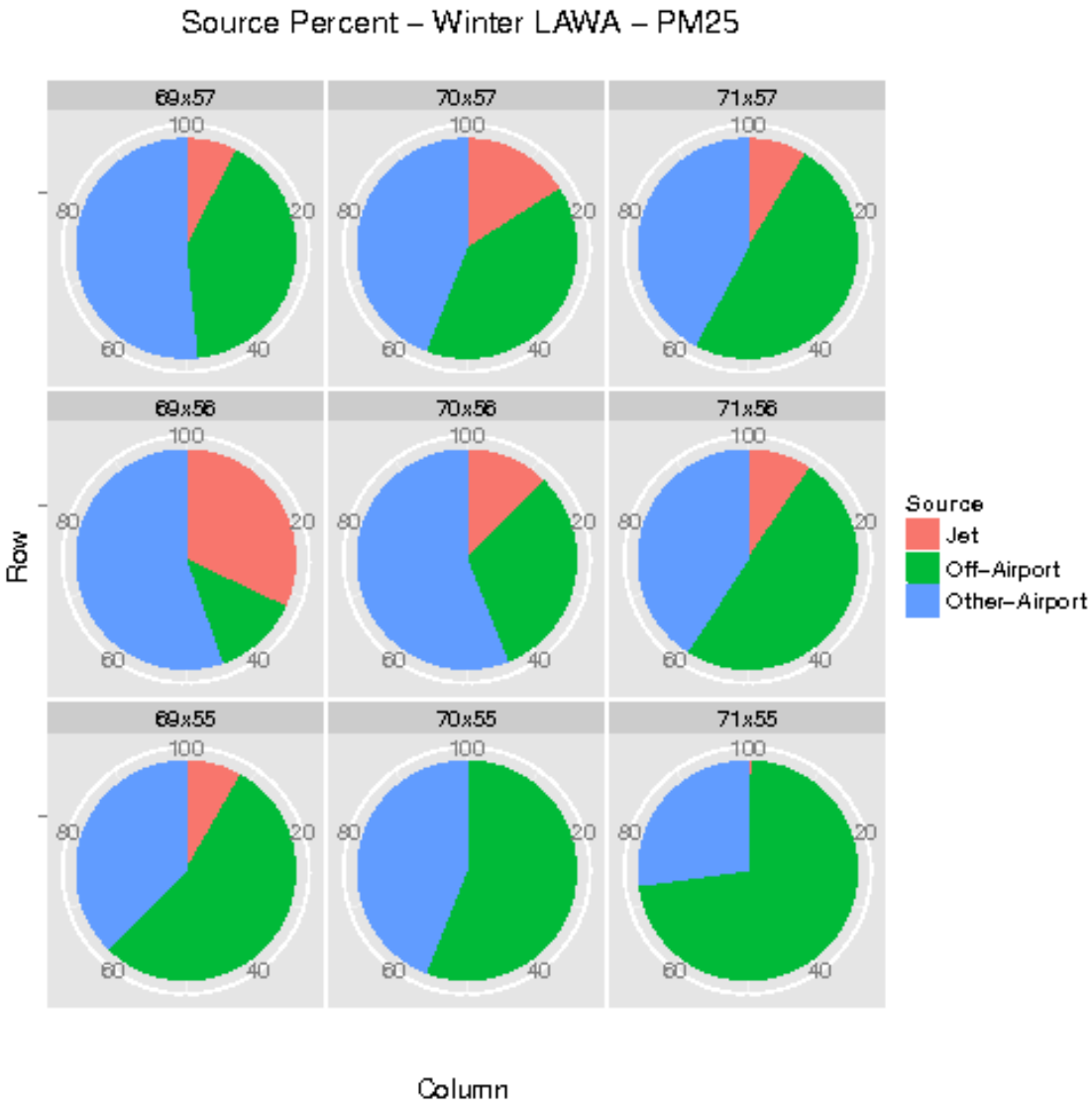

Figure 9-74. Fractional $PM_{2.5}$ contribution from LAX airport emissions modeled by CMAQ during the Winter Season. Numbers such as 69x57 indicate the Column, Row index of the CMAQ grid-cell. Jet" indicates Aircraft+APU+GSE, "Other-Airport" indicates remaining airport sources such as traffic and stationary, and "Off-Airport" indicates background sources.

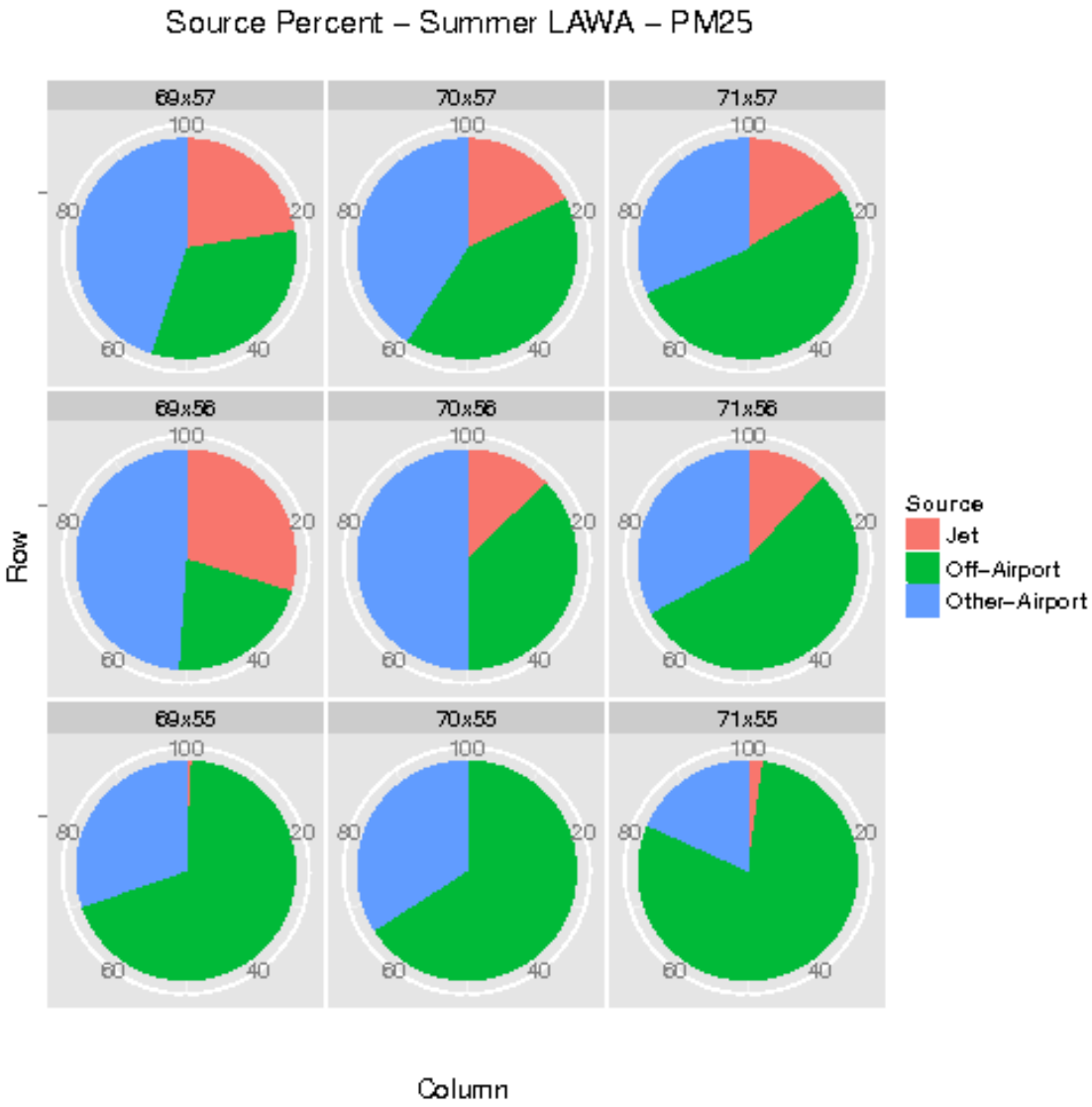

Figure 9-75. Fractional $PM_{2.5}$ contribution from LAX airport emissions modeled by CMAQ during the Summer Season. Numbers such as 69x57 indicate the Column, Row index of the CMAQ grid-cell. Jet" indicates Aircraft+APU+GSE, "Other-Airport" indicates remaining airport sources such as traffic and stationary, and "Off-Airport" indicates background sources.

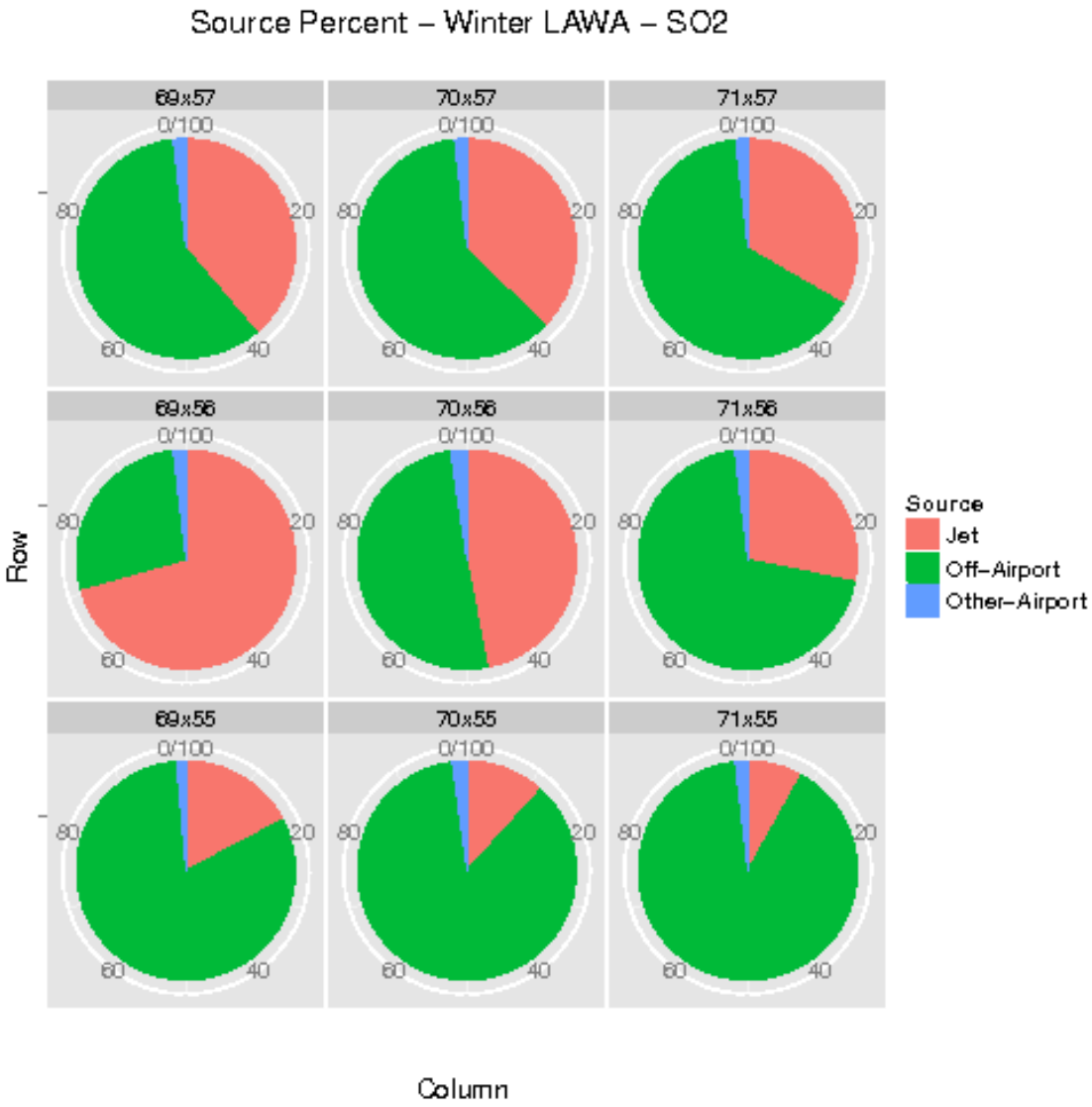

Figure 9-76. Fractional SO_2 contribution from LAX airport emissions modeled by CMAQ during the Winter Season. Numbers such as 69x57 indicate the Column, Row index of the CMAQ grid-cell. Jet" indicates Aircraft+APU+GSE, "Other-Airport" indicates remaining airport sources such as traffic and stationary, and "Off-Airport" indicates background sources.

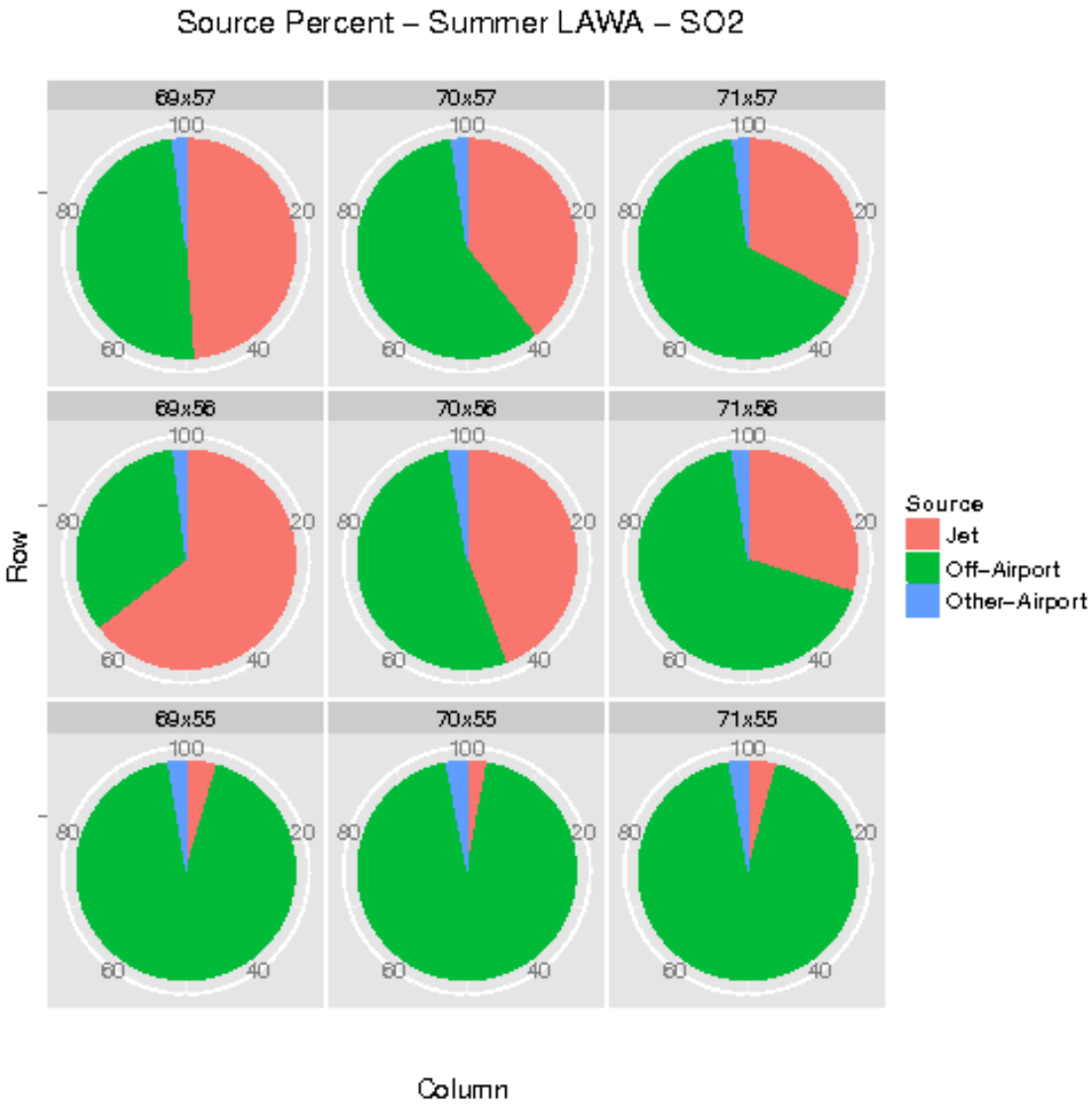

Figure 9-77. Fractional SO_2 contribution from LAX airport emissions modeled by CMAQ during the Summer Season. Numbers such as 69x57 indicate the Column, Row index of the CMAQ grid-cell. Jet" indicates Aircraft+APU+GSE, "Other-Airport" indicates remaining airport sources such as traffic and stationary, and "Off-Airport" indicates background sources.

9.2.4 Summary and Conclusions

Source-based modeling of emissions inventories was performed with the CMAQ model for the Winter and Summer Seasons. The initial application was based upon the SIP model application provided by the SCAQMD for the year 2008, using the WRF-SMOKE-CMAQ system at a four-km grid resolution for Southern California, and using the SAPRC-99 chemical mechanism. After zeroing out SCAQMD-provided estimates of LAX emissions, three new emissions scenarios were modeled and compared with the zeroed-out case to assess incremental contributions from different source groups.

The model predictions of CO, NO_x, $PM_{2.5}$ and SO_2 were analyzed in three phases including: (1) spatial analyses by computing differences between the zeroed-out case and three airport-related emissions scenarios, (2) model evaluation against ambient measurements performed at the four core sites using time-series analyses and (3) source apportionment of modeled values to season average concentrations.

In the first two phases above, the $PM_{2.5}$ analysis was extended to look at speciated components, specifically to understand contributions from primary versus secondary $PM_{2.5}$.

Figure 9-78 and Figure 9-79 show the composite source apportionment results for the Winter and Summer Seasons, respectively, for all four pollutants in the 3x3 array of CMAQ grid-cells. The information in these two figures is the same as that present in Figure 9-70. through Figure 9-77., except that the data are grouped by pollutant in each array with only the "airport-related" contributions presented.

9.2.4.1 Key Findings from Source-Based Modeling with CMAQ

- Modeled incremental concentrations were much lower than the field measurement data at the AQ and CS sites for NO_x and SO_2 in the Summer Season, showing the impacts from broad regional background

- Modeled incremental concentrations from the on-airport sources were generally in agreement with measurement data at the CE and CN sites during the Summer Season, but were less so in the Winter Season.

- Impacts from terminal area activity showed contributions from airport-related emissions to be more than 64 percent for all pollutants in both monitoring seasons. (See Figures 9-70 and 9-71 for grid-cell 69,56.)

- The use of CMAQ is able to highlight the impacts of secondary contributions (such as inorganic aerosol) formed at downwind distances from airport. However, CMAQ does show that some secondarily formed pollutants, such as nitrate aerosols, are reduced in the airport grid-cells. This is due to nighttime reduction of nitrate radicals, which further leads to reduction in nitric acid, and hence nitrate aerosols, as described in detail in Section 9.2.3.2.

- Study Area emissions have air quality impacts much beyond the immediate airport vicinity, sometimes at downwind distances up to 100-150 km from the airport, as shown in Figure 9B-43 and 9B-44. This was observed specifically for NO_x and SO_2 during both seasons, though the Winter Season impacts are generally higher than during the Summer Season. CO and $PM_{2.5}$ impacts are generally in the range of one to two percent at those distances.

Carbon Monoxide Impacts

- Contributions at the AQ and CS site were from both airport-related sources and regional background, while background sources dominate contributions at the CN and CE sites, especially during the Summer Season

- CO impacts due to aircraft sources were dominant in the grid-cell 69,56 and were as high as 65 percent during both seasons. CO impacts due to on-airport sources in grid-cell 70,56 were approximately 25 percent.

Nitrogen Oxides Impacts

- Contributions at the AQ and CS sites were from both airport-related sources and regional background, while both aircraft and other on-airport sources contributed to measurement data at the CE and CN sites during the Summer Season but not during the Winter Season

- NO_x impacts due to aircraft sources were dominant in the grid-cell 69,56 and were as high as 65 percent during both seasons. NO_x impacts due to on-airport sources in grid-cell 70,56 were approximately 45 percent.

- Marine emissions from background sources dominated impacts to regions south of the two airport grid-cells. While these grid-cells also contained Chevron El Segundo Refinery and on-roadway emissions, marine emissions were the largest contributor of NO_x (approximately 60 percent) emissions, as shown in Table 8-32 of Section 8.

Fine Particulate Matter Impacts

- Modeled incremental contributions were generally lower than measurements at the four core sites, indicating contribution from both airport-related and regional background sources to field measurements

- The primary components of $PM_{2.5}$ dominated at monitored locations. However, LAX emissions contributed to enhanced secondary components of $PM_{2.5}$ at distances located downwind of the airport

- Sulfate aerosol (from atmospheric reactions of aircraft emissions) was also produced on several days, therefore, enhancing total $PM_{2.5}$ contributions due to airport-related sources

- Addition of aircraft NO_x emissions did deplete nitrate and ammonium aerosol near the airport, on a few days, due to nonlinear atmospheric chemistry, involving nighttime reduction of nitrate radicals.

- $PM_{2.5}$ impacts from airport-related sources other than aircraft were as high as 50 percent in the two grid-cells containing the airport and the four core sites as shown in Figure 9-74. and Figure 9-75.. These are primarily from stationary and traffic-related sources on airport property.

- The Chevron El Segundo Refinery and marine sources combined contributed nearly 50 percent of the $PM_{2.5}$ in the two grid-cells south of the airport

- Recent studies have shown that non-traditional SOA (secondary organic aerosol) precursors are a missing source of SOA formation due to aircraft emissions (Miracolo et al., 2011; Jathar et al., 2012). Incorporating NTSOA (non-traditional secondary organic aerosol) precursors shows an enhancement of up to 18 percent in SOA due to aircraft at the Hartsfield Atlanta airport (Woody et al., 2012 a,b). The results from this ongoing SOA research were not available in time to implement and enhance the treatment of NTSOA precursors in this study. Hence, the SOA contributions to $PM_{2.5}$ impacts for Phase III of the LAX AQSAS are likely underestimated.

Sulfur Dioxide Impacts

- Modeled impacts at the CN and CE site indicated contributions from both airport-related and background emissions during most days, except during the middle of the Summer Season, when airport sources dominated

- At the AQ and CS sites, both airport and regional background contributed to observed values during the first half of the Winter Season. However, since AQ values are higher CS in the measurements, it is possible that AQ is picking up more of the regional background contributions than CS.

- Field measurements at the CN site were greater than all incremental concentrations during several days, indicating contribution from regional background sources

- Measurement data at the CE site were generally lower than those at CN site, and matched the incremental concentrations from Airport emissions on several days, confirming the contribution of LAX airport sources at the CE site

- The Chevron Refinery and marine sources combined contributed up to 80 percent (during the Winter Season) and 95 percent (during the Summer Season) of SO_2 in the two grid-cells south of the airport

While the grid-resolution used in CMAQ was fairly large, the model results were not able to discern differences between concentrations that were predicted at each of the individual four core sites. However, CMAQ still offered additional information for source apportionment by

providing additional information (compared to AERMOD) on the $PM_{2.5}$ components that were major contributors to $PM_{2.5}$ mass.[27]

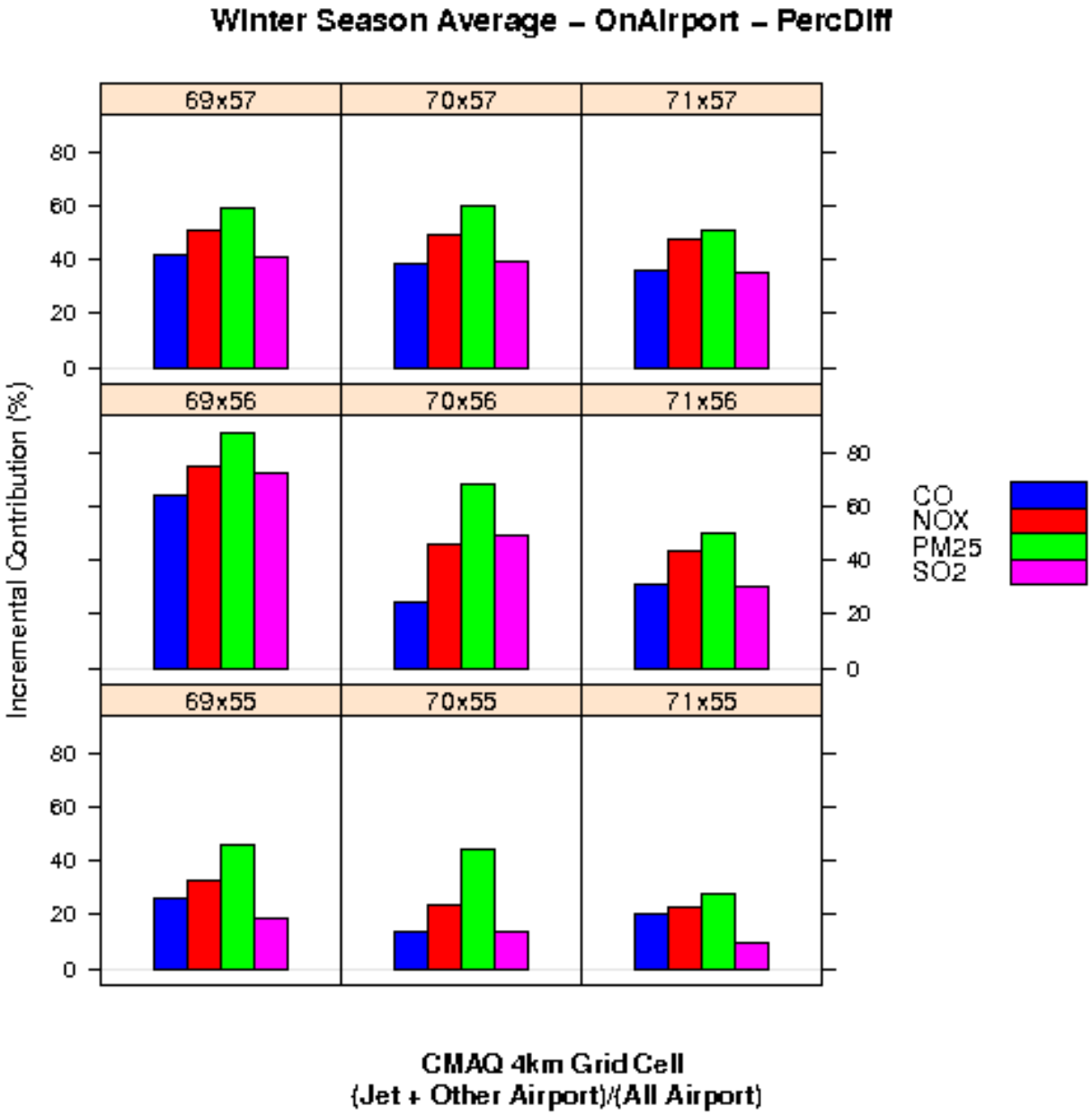

Figure 9-78. Incremental airport-related contributions modeled by CMAQ during the Winter Season. Numbers such as 69x57 indicate the Column, Row index of the CMAQ grid-cell.

[27] CMAQ assumes the emissions in a given grid cell (such as aircraft emissions on the runway) are instantaneously and evenly dispersed within the 4 km x 4 km cell, even though the runway is located at some distance in a cross-wind or even downwind direction from the monitoring station. This is one of the potential shortcomings of CMAQ modeling.

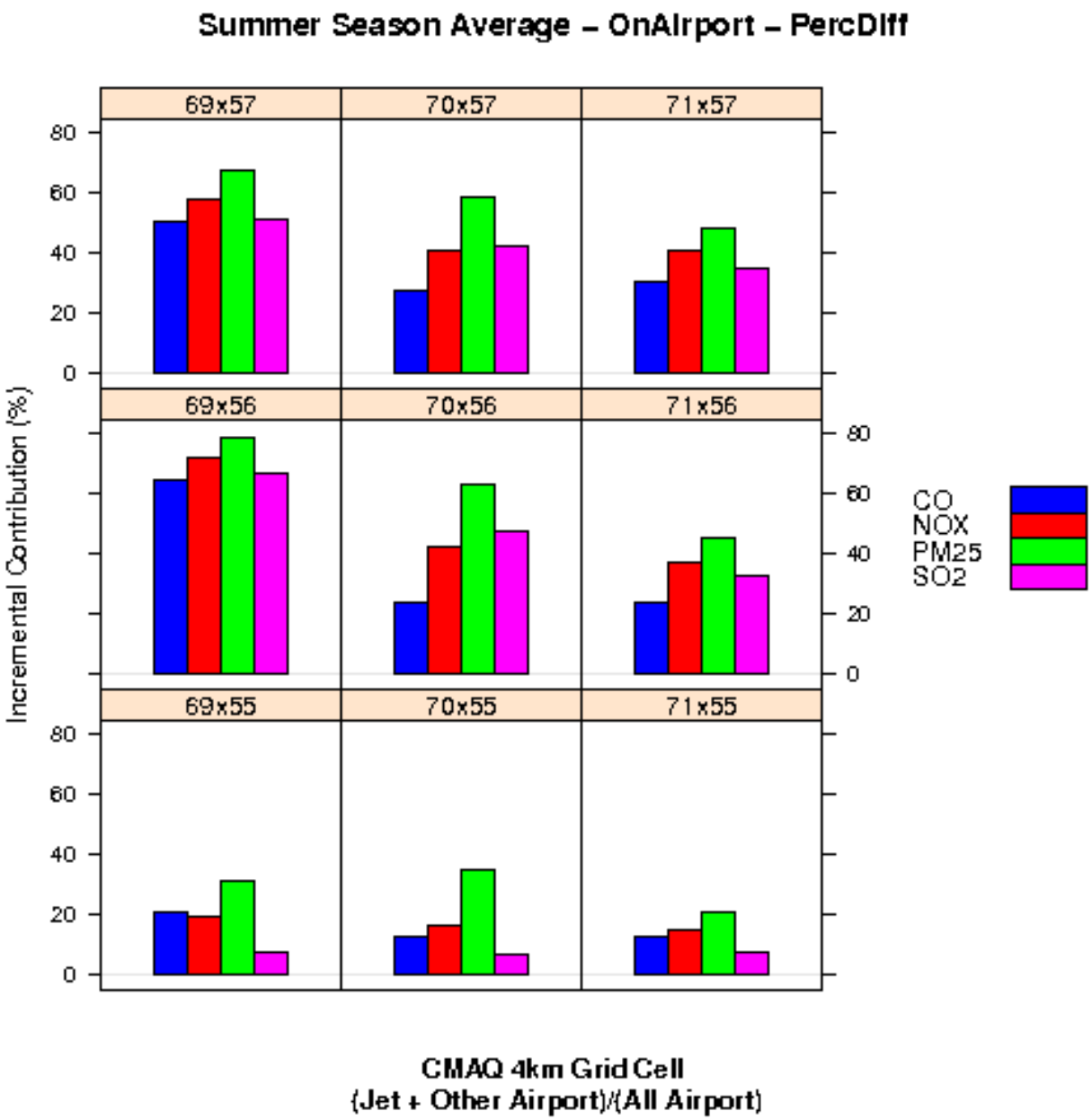

Figure 9-79. Incremental airport-related contributions modeled by CMAQ during the Summer Season. Numbers such as 69x57 indicate the Column, Row index of the CMAQ grid-cell.

9.3 REFERENCES

Appel, K., Wyat, R. C. Gilliam, N. Davis, A. Zubrow, S. C. Howard, 2011.Overview of the atmospheric model evaluation tool (AMET) v1.1 for evaluating meteorological and air quality models, *Environmental Modelling and Software*, 26(4), 434-443.

Arunachalam, S., B.H. Baek, F.S. Binkowski, B. Wang, Neil Davis, A. Hanna, and W. F. Hutzell (2008) A Modeling Study to Assess Air Quality Impacts of Air Toxics from Aircraft and other Sources at an Urban Airport – Case Study for Providence – T.F. Green, presented at the CRC Mobile Source Air Toxics Workshop, Dec 2008

Arunachalam, S., B.H. Baek, A. Holland, Z. Adelman, F.S. Binkowski, A. Hanna, T. Thrasher and P. Soucacos (2008). *An Improved Method to Represent Aviation Emissions in Air Quality Modeling Systems and their Impacts on Air Quality*, In Proceedings of the 13th Conference on Aviation, Range and Aerospace Meteorology, New Orleans, LA, Jan 2008

Arunachalam, S., Wang, B., Davis, N., Baek, B.H., Levy, J.I., 2011. Effect of Chemistry-Transport Model Scale and Resolution on Population Exposure to PM2.5 from Aircraft Emissions during Landing and Takeoff, *Atmos. Environ*, 45(19):3294-3300, doi:10.1016/j.atmosenv.2011.03.029

Arunachalam, S., et al, 2013. An intercomparison of dispersion model and statistically-based regression model approaches for assessing jet exhaust impacts on ambient air quality at a U.S. airport. In preparation.

Baek, B.H., S. Arunachalam, A. Holland, Z. Adelman, A. Hanna, T. Thrasher, and P. Soucacos (2007). *Development of an Interface for the Emissions Dispersion and Modeling System (EDMS) with the SMOKE Modeling System.* In Proceedings of the 16th Annual Emissions Inventory Conference - "Emissions Inventories: Integration, Analyses and Communication", Raleigh, NC, May 2007.

Binkowski, F.S. and Roselle, S.J., 2003. Models-3 Community Multiscale Air Quality (CMAQ) model aerosol component, 1 Model description. *J. Geophys. Res.*, Vol. 108(D6): 4183.

Byun, D. W. and Schere, K. L.: Review of the Governing Equations, Computational Algorithms, and Other Components of the Models-3 Community Multiscale Air Quality (CMAQ) Modeling System, J. Appl. Mech. Rev., 59, 51–77, doi:10.1115/1.2128636, 2006.

Chang, J.C. and S.R. Hanna, 2004. Air Quality Model Performance Evaluation, *Meteorol. Atmos. Phys*., 87, 167-196.

Cimorelli, A.J., Perry, S.G., Venkatram, A., Weil, J.C., Paine, R.J., Wilson, R.B., Lee, R.F., Peters, W.D., Brode, R.W., 2005. AERMOD: a dispersion model for industrial source applications. Part I: general model formulation and boundary layer characterization. J. Appl. Meteorol. 44, 682–693.

Davis, N., and S. Arunachalam, 2009. A Hybrid CMAQ and AERMOD Approach to Investigate the Impact of Airports on Local Air Quality, In Proceedings of the 8th Annual Models-3/CMAS Users Conference, Chapel Hill, NC, Oct 2009.

Federal Register, 1998: Emissions and Dispersion Modeling System (EDMS) Policy for Airport Air Quality Analysis: Interim Guidance to FAA Orders 1050.1D and 5050.4A, 63 Federal Register 70 (30 April 1998), pp. 18068.

Foley, K. M., Roselle, S. J., Appel, K. W., Bhave, P. V., Pleim, J. E., Otte, T. L., Mathur, R., Sarwar, G., Young, J. O., Gilliam, R. C., Nolte, C. G., Kelly, J. T., Gilliland, A. B., and Bash, J. O.: Incremental testing of the Community Multiscale Air Quality (CMAQ) modeling system version 4.7, Geosci. Model Dev., 3, 205–226, doi:10.5194/gmd-3-205-2010, 2010.

Houyoux, M.R., J.M. Vukovich, C.J. Coats Jr., N.W. Wheeler and P.S. Kasibhatla: Emission Inventory Development and Processing for the Seasonal Model for Regional Air Quality (SMRAQ) project, *J. Geophys. Res.*,105:D7:9079-9090, 2000.

Kim, B., J. Rachami, D. Robinson, B. Robinette, K. Nakada, S. Arunachalam, N. Davis, BH Baek, U. Shankar, K. Talgo, D. Yang, A.F. Hanna, R. Wayson, G. Noel, S. Cliff, Y. Zhao, P.K. Hopke and P. Kumar, 2010. Guidance for Quantifying the Contribution of Airport Emissions to Local Air Quality, ACRP Report 71, prepared for the Transportation Research Board's Airport Cooperative Research Program, Washington, D.C., 2012.

Kumar A., Dixit S., Varadarajan C., Vijayan A., and A. Masuraha. 2006. Evaluation of the AERMOD dispersion model as a function of atmospheric stability for an urban area, Environmental Progress, 25(2): 141-151

Jathar, S. H., Miracolo, M. A., Presto, A. A., Donahue, N. M., Adams, P. J., and Robinson, A. L.: Modeling the formation and properties of traditional and non-traditional secondary organic aerosol: problem formulation and application to aircraft exhaust, *Atmos. Chem. Phys*., 12, 9025-9040, doi:10.5194/acp-12-9025-2012, 2012.

Miracolo, M. A., Hennigan, C. J., Ranjan, M., Nguyen, N. T., Gordon, T. D., Lipsky, E. M., Presto, A. A., Donahue, N. M., and Robinson, A. L.: Secondary aerosol formation from photochemical aging of aircraft exhaust in a smog chamber, *Atmos. Chem. Phys*., 11, 4135-4147, doi:10.5194/acp-11-4135-2011, 2011.

Otte, T. L. and Pleim, J. E.: The Meteorology-Chemistry Interface Processor (MCIP) for the CMAQ modeling system: updates through MCIPv3.4.1, Geosci. Model Dev., 3, 243-256, doi:10.5194/gmd-3-243-2010, 2010.

Perry, S.G., Cimorelli, A.J., Paine, R.J., Brode, R.W., Weil, J.C., Venkatram, A., Wilson, R.B., Lee, R.F., Peters, W.D., 2005. AERMOD: A Dispersion Model for Industrial Source

Applications. Part II: Model Performance against 17 Field Study Databases. J. Appl. Meteorol. 44, 694–708.

Rissman, J., Arunachalam, S., Woody, M., West, J. J., BenDor, T., and Binkowski, F. S. (2013). A plume-in-grid approach to characterize air quality impacts of aircraft emissions at the Hartsfield-Jackson Atlanta International Airport, *Atmos. Chem. Phys. Discuss.*, 13, 1089-1132, doi:10.5194/acpd-13-1089-2013.

Skamarock, W. C., J. B. Klemp, J. Dudhia, D. O. Gill, D. M. Barker, M. Duda, X.-Y. Huang, W. Wang and J. G. Powers: A Description of the Advanced Research WRF Version 3, NCAR Technical Note, 2008. [Available from download at: http://www.mmm.ucar.edu/wrf/users/docs/arw_v3.pdf]

Stein, A.F., V. Isakov, J. Godowitch, and R.R. Draxler, 2007. A hybrid modeling approach to resolve pollutant concentrations in an urban area. *Atmos. Environ*, 41:9410-9426.

U.S. Environmental Protection Agency, 2009a. Recommended Best Practice for Quantifying Speciated Organic Gas Emissions from Aircraft Equipped with Turbofan, Turbojet, and Turboprop Engines. U.S. EPA Office of Transportation and Air Quality and FAA Office of Environment and Energy, EPA-420-R-09–901 and 902, May 2009.

U.S. Environmental Protection Agency, 2009b. SPECIATE 4.2, Speciation Database Development Documentation, EPA/600-R-09/038, Prepared for Office of Research and Development, U.S. EPA, June 2009.Whitby, K. T., The physical characteristics of sulfur aerosols, Atmos. Environ., 12, 135– 159, 1978.

Wayson, R. L., Fleming, G. G., Kim, B. Y., Eberhard, W. L., Brewer, W. A., 2004. The use of LIDAR to characterize aircraft initial plume characteristics. Tech. Rep. FAA-AEE-04–01, Federal Aviation Administration.

Wayson, R. L., Fleming, G. G., Noel, G., MacDonald, J., Eberhard, W. L., McCarty, B., Marchbanks, R., Sandberg, S., George, J., 2008. LIDAR measurement of exhaust plume characteristics from commercial jet turbine aircraft at the Denver International Airport. Tech. Rep. FAA-AEE-08–02, Federal Aviation Administration.

Whitby, K. T., 1978. The physical characteristics of sulfur aerosols, *Atmos. Environ.*, 12, 135–159.

Woody, M., Baek, B.H., Adelman, Z., Omary, M., Lam, Y-F., West, J.J., Arunachalam, S. 2011. An Assessment of Aviation's Contribution to Current and Future Fine Particulate Matter in the United States, *Atmos. Environ*, 45(20):3424-3433, doi:10.1016/j.atmosenv.2011.03.041

Woody, M. and S. Arunachalam, 2012a. Secondary Organic Aerosol Produced from Aircraft Emissions at the Atlanta Airport: An Advanced Diagnostic Investigation Using Process Analysis. In Review.

Woody, M., S. Arunachalam, F.S. Binkowski, J.J. West, S. Jathar, and A.L. Robinson, 2012b. Simulating the Contributions from Aircraft Emissions to Organic Aerosols Using the Volatility Basis Set, Presented at the Fall Annual Meeting of the American Geophysical Union, San Francisco, CA, Dec 3-7, 2012

(This page is intentionally blank)

APPENDIX 9-1: Tables and Figures for AERMOD Analyses

(This page is intentionally blank)

LIST OF TABLES

LIST OF FIGURES

Figure 9A-9: Modeled period average CO concentrations from airport-related sources by source sector at flag-pole receptors at heights of 2m, 7m, 12m, 17m, 22m and 27m in Cartesian Grid of receptors during Winter Season.

Figure 9A-10: Modeled period average CO concentrations from background sources by source sector at flag-pole receptors at heights of 2m, 7m, 12m, 17m, 22m and 27m in Cartesian Grid of receptors during Winter Season.

Figure 9A-11a: Modeled hourly max (left) and period average (right) NOx concentrations from airport-related in Polar Grid of receptors during Winter Season.

Figure 9A-11b: Modeled hourly max (left) and period average (right) NOx concentrations from background sources in Polar Grid of receptors during Winter Season.

Figure 9A-11c: Modeled hourly max (left) and period average (right) NOx concentrations from ALL in Polar Grid of receptors during Winter Season.

Figure 9A-12a: Modeled hourly max (left) and period average (right) NOx concentrations from airport-related in Cartesian Grid of receptors during Winter Season.

Figure 9A-12b: Modeled hourly max (left) and period average (right) NOx concentrations from background sources in Cartesian Grid of receptors during Winter Season.

Figure 9A-12c: Modeled hourly max (left) and period average (right) NOx concentrations from ALL in Cartesian Grid of receptors during Winter Season.

Figure 9A-13: Modeled hourly max NOx concentrations from airport-related sources at flag-pole receptors at heights of 2m, 7m, 12m, 17m, 22m and 27m in Polar Grid of receptors during Winter Season.

Figure 9A-14: Modeled period average NOx concentrations from airport-related sources at flag-pole receptors at heights of 2m, 7m, 12m, 17m, 22m and 27m in Polar Grid of receptors during Winter Season.

Figure 9A-15: Modeled hourly max NOx concentrations from airport-related sources at flag-pole receptors at heights of 2m, 7m, 12m, 17m, 22m and 27m in Cartesian Grid of receptors during Winter Season.

Figure 9A-16: Modeled period average NOx concentrations from airport-related sources at flag-pole receptors at heights of 2m, 7m, 12m, 17m, 22m and 27m in Cartesian Grid of receptors during Winter Season.

Figure 9A-17: Modeled hourly maximum NOx concentrations from airport-related sources by source sector at flag-pole receptors at heights of 2m, 7m, 12m, 17m, 22m and 27m in Cartesian Grid of receptors during Winter Season.

Figure 9A-18: Modeled hourly maximum NOx concentrations from background sources by source sector at flag-pole receptors at heights of 2m, 7m, 12m, 17m, 22m and 27m in Cartesian Grid of receptors during Winter Season.

Figure 9A-19: Modeled period average NOx concentrations from airport-related sources by source sector at flag-pole receptors at heights of 2m, 7m, 12m, 17m, 22m and 27m in Cartesian Grid of receptors during Winter Season.

Figure 9A-20: Modeled period average NOx concentrations from background sources by source sector at flag-pole receptors at heights of 2m, 7m, 12m, 17m, 22m and 27m in Cartesian Grid of receptors during Winter Season.

Figure 9A-21a: Modeled hourly max (left) and period average (right) $PM_{2.5}$ concentrations from airport-related in Polar Grid of receptors during Winter Season.

Figure 9A-21b: Modeled hourly max (left) and period average (right) $PM_{2.5}$ concentrations from background sources in Polar Grid of receptors during Winter Season.

Figure 9A-21c: Modeled hourly max (left) and period average (right) $PM_{2.5}$ concentrations from ALL in Polar Grid of receptors during Winter Season.

Figure 9A-22a: Modeled hourly max (left) and period average (right) $PM_{2.5}$ concentrations from airport-related in Cartesian Grid of receptors during Winter Season.

Figure 9A-22b: Modeled hourly max (left) and period average (right) $PM_{2.5}$ concentrations from background sources in Cartesian Grid of receptors during Winter Season.

Figure 9A-22c: Modeled hourly max (left) and period average (right) $PM_{2.5}$ concentrations from ALL in Cartesian Grid of receptors during Winter Season.

Figure 9A-23: Modeled hourly max $PM_{2.5}$ concentrations from airport-related sources at flag-pole receptors at heights of 2m, 7m, 12m, 17m, 22m and 27m in Polar Grid of receptors during Winter Season.

Figure 9A-24: Modeled period average $PM_{2.5}$ concentrations from airport-related sources at flag-pole receptors at heights of 2m, 7m, 12m, 17m, 22m and 27m in Polar Grid of receptors during Winter Season.

Figure 9A-25: Modeled hourly max $PM_{2.5}$ concentrations from airport-related sources at flag-pole receptors at heights of 2m, 7m, 12m, 17m, 22m and 27m in Cartesian Grid of receptors during Winter Season.

Figure 9A-26: Modeled period average $PM_{2.5}$ concentrations from airport-related sources at flag-pole receptors at heights of 2m, 7m, 12m, 17m, 22m and 27m in Cartesian Grid of receptors during Winter Season.

Figure 9A-27: Modeled hourly maximum $PM_{2.5}$ concentrations from airport-related sources by source sector at flag-pole receptors at heights of 2m, 7m, 12m, 17m, 22m and 27m in Cartesian Grid of receptors during Winter Season.

Figure 9A-28: Modeled hourly maximum $PM_{2.5}$ concentrations from background sources by source sector at flag-pole receptors at heights of 2m, 7m, 12m, 17m, 22m and 27m in Cartesian Grid of receptors during Winter Season.

Figure 9A-29: Modeled period average $PM_{2.5}$ concentrations from airport-related sources by source sector at flag-pole receptors at heights of 2m, 7m, 12m, 17m, 22m and 27m in Cartesian Grid of receptors during Winter Season.

Figure 9A-30: Modeled period average $PM_{2.5}$ concentrations from background sources by source sector at flag-pole receptors at heights of 2m, 7m, 12m, 17m, 22m and 27m in Cartesian Grid of receptors during Winter Season.

Figure 9A-31a: Modeled hourly max (left) and period average (right) SOx concentrations from airport-related in Polar Grid of receptors during Winter Season.

Figure 9A-31b: Modeled hourly max (left) and period average (right) SOx concentrations from background sources in Polar Grid of receptors during Winter Season.

Figure 9A-31c: Modeled hourly max (left) and period average (right) SOx concentrations from ALL in Polar Grid of receptors during Winter Season.

Figure 9A-32a: Modeled hourly max (left) and period average (right) SOx concentrations from airport-related in Cartesian Grid of receptors during Winter Season.

Figure 9A-32b: Modeled hourly max (left) and period average (right) SOx concentrations from airport-related background sources in Cartesian Grid of receptors during Winter Season.

Figure 9A-32c: Modeled hourly max (left) and period average (right) SOx concentrations from ALL in Cartesian Grid of receptors during Winter Season.

Figure 9A-33: Modeled hourly max SOx concentrations from airport-related sources at flag-pole receptors at heights of 2m, 7m, 12m, 17m, 22m and 27m in Polar Grid of receptors during Winter Season.

Figure 9A-34: Modeled period average SOx concentrations from airport-related sources at flag-pole receptors at heights of 2m, 7m, 12m, 17m, 22m and 27m in Polar Grid of receptors during Winter Season.

Figure 9A-35: Modeled hourly max SOx concentrations from airport-related sources at flag-pole receptors at heights of 2m, 7m, 12m, 17m, 22m and 27m in Cartesian Grid of receptors during Winter Season.

Figure 9A-36: Modeled period average SOx concentrations from airport-related sources at flag-pole receptors at heights of 2m, 7m, 12m, 17m, 22m and 27m in Cartesian Grid of receptors during Winter Season.

Figure 9A-37: Modeled hourly maximum SOx concentrations from airport-related sources by source sector at flag-pole receptors at heights of 2m, 7m, 12m, 17m, 22m and 27m in Cartesian Grid of receptors during Winter Season.

Figure 9A-38: Modeled hourly maximum SOx concentrations from background sources by source sector at flag-pole receptors at heights of 2m, 7m, 12m, 17m, 22m and 27m in Cartesian Grid of receptors during Winter Season.

Figure 9A-39: Modeled period average SOx concentrations from airport-related sources by source sector at flag-pole receptors at heights of 2m, 7m, 12m, 17m, 22m and 27m in Cartesian Grid of receptors during Winter Season.

Figure 9A-40: Modeled period average SOx concentrations from background sources by source sector at flag-pole receptors at heights of 2m, 7m, 12m, 17m, 22m and 27m in Cartesian Grid of receptors during Winter Season.

Figure 9A-41a: Modeled hourly max (left) and period average (right) TOG concentrations from airport-related in Polar Grid of receptors during Winter Season.

Figure 9A-41b: Modeled hourly max (left) and period average (right) TOG concentrations from background sources in Polar Grid of receptors during Winter Season.

Figure 9A-41c: Modeled hourly max (left) and period average (right) TOG concentrations from ALL in Polar Grid of receptors during Winter Season.

Figure 9A-42a: Modeled hourly max (left) and period average (right) TOG concentrations from airport-related in Cartesian Grid of receptors during Winter Season.

Figure 9A-42b: Modeled hourly max (left) and period average (right) TOG concentrations from background sources in Cartesian Grid of receptors during Winter Season.

Figure 9A-42c: Modeled hourly max (left) and period average (right) TOG concentrations from ALL in Cartesian Grid of receptors during Winter Season.

Figure 9A-43: Modeled hourly max TOG concentrations from airport-related sources at flag-pole receptors at heights of 2m, 7m, 12m, 17m, 22m and 27m in Polar Grid of receptors during Winter Season.

Figure 9A-44: Modeled period average TOG concentrations from airport-related sources at flag-pole receptors at heights of 2m, 7m, 12m, 17m, 22m and 27m in Polar Grid of receptors during Winter Season.

Figure 9A-45: Modeled hourly max TOG concentrations from airport-related sources at flag-pole receptors at heights of 2m, 7m, 12m, 17m, 22m and 27m in Cartesian Grid of receptors during Winter Season.

Figure 9A-46: Modeled period average TOG concentrations from airport-related sources at flag-pole receptors at heights of 2m, 7m, 12m, 17m, 22m and 27m in Cartesian Grid of receptors during Winter Season.

Figure 9A-47: Modeled hourly maximum TOG concentrations from airport-related sources by source sector at flag-pole receptors at heights of 2m, 7m, 12m, 17m, 22m and 27m in Cartesian Grid of receptors during Winter Season.

Figure 9A-48: Modeled hourly maximum TOG concentrations from background sources by source sector at flag-pole receptors at heights of 2m, 7m, 12m, 17m, 22m and 27m in Cartesian Grid of receptors during Winter Season.

Figure 9A-49: Modeled period average TOG concentrations from airport-related sources by source sector at flag-pole receptors at heights of 2m, 7m, 12m, 17m, 22m and 27m in Cartesian Grid of receptors during Winter Season.

Figure 9A-50: Modeled period average TOG concentrations from background sources by source sector at flag-pole receptors at heights of 2m, 7m, 12m, 17m, 22m and 27m in Cartesian Grid of receptors during Winter Season.

Figure 9A-51: Diurnal variability in observed and modeled CO concentrations at AQ Site from flagpole receptors at heights of 2m, 7m, 12m and 17m during Winter Season.

Figure 9A-52: Diurnal variability in observed and modeled CO concentrations at CE Site from flagpole receptors at heights of 2m, 7m, 12m and 17m during Winter Season.

Figure 9A-53: Diurnal variability in observed and modeled CO concentrations at CN Site from flagpole receptors at heights of 2m, 7m, 12m and 17m during Winter Season.

Figure 9A-54: Diurnal variability in observed and modeled CO concentrations at CS Site from flagpole receptors at heights of 2m, 7m, 12m and 17m during Winter Season.

Figure 9A-55: Diurnal variability in observed and modeled NOx concentrations at AQ Site from flagpole receptors at heights of 2m, 7m, 12m and 17m during Winter Season.

Figure 9A-56: Diurnal variability in observed and modeled NOx concentrations at CE Site from flagpole receptors at heights of 2m, 7m, 12m and 17m during Winter Season.

Figure 9A-57: Diurnal variability in observed and modeled NOx concentrations at CN Site from flagpole receptors at heights of 2m, 7m, 12m and 17m during Winter Season.

Figure 9A-58: Diurnal variability in observed and modeled NOx concentrations at CS Site from flagpole receptors at heights of 2m, 7m, 12m and 17m during Winter Season.

Figure 9A-59: Diurnal variability in observed and modeled $PM_{2.5}$ concentrations at AQ Site from flagpole receptors at heights of 2m, 7m, 12m and 17m during Winter Season.

Figure 9A-60: Diurnal variability in observed and modeled $PM_{2.5}$ concentrations at CE Site from flagpole receptors at heights of 2m, 7m, 12m and 17m during Winter Season.

Figure 9A-61: Diurnal variability in observed and modeled $PM_{2.5}$ concentrations at CN Site from flagpole receptors at heights of 2m, 7m, 12m and 17m during Winter Season.

Figure 9A-62: Diurnal variability in observed and modeled $PM_{2.5}$ concentrations at CS Site from flagpole receptors at heights of 2m, 7m, 12m and 17m during Winter Season.

Figure 9A-63: Diurnal variability in observed and modeled SOx concentrations at AQ Site from flagpole receptors at heights of 2m, 7m, 12m and 17m during Winter Season.

Figure 9A-64: Diurnal variability in observed and modeled SOx concentrations at CE Site from flagpole receptors at heights of 2m, 7m, 12m and 17m during Winter Season.

Figure 9A-65: Diurnal variability in observed and modeled SOx concentrations at CN Site from flagpole receptors at heights of 2m, 7m, 12m and 17m during Winter Season.

Figure 9A-66: Diurnal variability in observed and modeled SOx concentrations at CS Site from flagpole receptors at heights of 2m, 7m, 12m and 17m during Winter Season.

Figure 9A-67: Source-sector contributions to Hourly Maximum (left) and Period Average CO concentrations at AQ Site from airport-related sources (top) and background sources (bottom) during Winter Season.

Figure 9A-68: Source-sector contributions to Hourly Maximum (left) and Period Average CO concentrations at AQ Site from ALL sources during Winter Season.

Figure 9A-69: Source-sector contributions to Hourly Maximum (left) and Period Average CO concentrations at CE Site from airport-related sources (top) and background sources (bottom) during Winter Season.

Figure 9A-70: Source-sector contributions to Hourly Maximum (left) and Period Average CO concentrations at CE Site from ALL sources during Winter Season.

Figure 9A-71: Source-sector contributions to Hourly Maximum (left) and Period Average CO concentrations at CN Site from airport-related sources (top) and background sources (bottom) during Winter Season.

Figure 9A-72: Source-sector contributions to Hourly Maximum (left) and Period Average CO concentrations at CN Site from ALL sources during Winter Season.

Figure 9A-73: Source-sector contributions to Hourly Maximum (left) and Period Average CO concentrations at CS Site from airport-related sources (top) and background sources (bottom) during Winter Season.

Figure 9A-74: Source-sector contributions to Hourly Maximum (left) and Period Average CO concentrations at CS Site from ALL sources during Winter Season.

Figure 9A-75: Source-sector contributions to Period Average CO concentrations at each site from airport-related vs. background sources during Winter Season.

Figure 9A-76: Source-sector contributions to Hourly Maximum (left) and Period Average NOx concentrations at AQ Site from airport-related sources (top) and background sources (bottom) during Winter Season.

Figure 9A-77: Source-sector contributions to Hourly Maximum (left) and Period Average NOx concentrations at AQ Site from ALL sources during Winter Season.

Figure 9A-78: Source-sector contributions to Hourly Maximum (left) and Period Average NOx concentrations at CE Site from airport-related sources (top) and background sources (bottom) during Winter Season.

Figure 9A-79: Source-sector contributions to Hourly Maximum (left) and Period Average NOx concentrations at CE Site from ALL sources during Winter Season.

Figure 9A-80: Source-sector contributions to Hourly Maximum (left) and Period Average NOx concentrations at CN Site from airport-related sources (top) and background sources (bottom) during Winter Season.

Figure 9A-81: Source-sector contributions to Hourly Maximum (left) and Period Average NOx concentrations at CN Site from ALL sources during Winter Season.

Figure 9A-82: Source-sector contributions to Hourly Maximum (left) and Period Average NOx concentrations at CS Site from airport-related sources (top) and background sources (bottom) during Winter Season.

Figure 9A-83: Source-sector contributions to Hourly Maximum (left) and Period Average NOx concentrations at CS Site from ALL sources during Winter Season.

Figure 9A-84: Source-sector contributions to Period Average NOx concentrations at each site from airport-related vs. background sources during Winter Season.

Figure 9A-85: Source-sector contributions to Hourly Maximum (left) and Period Average $PM_{2.5}$ concentrations at AQ Site from airport-related sources (top) and background sources (bottom) during Winter Season.

Figure 9A-86: Source-sector contributions to Hourly Maximum (left) and Period Average $PM_{2.5}$ concentrations at AQ Site from ALL sources during Winter Season.

Figure 9A-87: Source-sector contributions to Hourly Maximum (left) and Period Average $PM_{2.5}$ concentrations at CE Site from airport-related sources (top) and background sources (bottom) during Winter Season.

Figure 9A-88: Source-sector contributions to Hourly Maximum (left) and Period Average $PM_{2.5}$ concentrations at CE Site from ALL sources during Winter Season.

Figure 9A-89: Source-sector contributions to Hourly Maximum (left) and Period Average PM2.5 concentrations at CN Site from airport-related sources (top) and background sources (bottom) during Winter Season.

Figure 9A-90: Source-sector contributions to Hourly Maximum (left) and Period Average $PM_{2.5}$ concentrations at CN Site from ALL sources during Winter Season.

Figure 9A-91: Source-sector contributions to Hourly Maximum (left) and Period Average $PM_{2.5}$ concentrations at CS Site from airport-related sources (top) and background sources (bottom) during Winter Season.

Figure 9A-92: Source-sector contributions to Hourly Maximum (left) and Period Average $PM_{2.5}$ concentrations at CS Site from ALL sources during Winter Season.

Figure 9A-93: Source-sector contributions to Period Average $PM_{2.5}$ concentrations at each site from airport-related vs. background sources during Winter Season.

Figure 9A-94. Source-sector contributions to Hourly Maximum (left) and Period Average SOx concentrations at AQ Site from airport-related sources (top) and background sources (bottom) during Winter Season.

Figure 9A-95: Source-sector contributions to Hourly Maximum (left) and Period Average SOx concentrations at AQ Site from ALL sources during Winter Season.

Figure 9A-96: Source-sector contributions to Hourly Maximum (left) and Period Average SOx concentrations at CE Site from airport-related sources (top) and background sources (bottom) during Winter Season.

Figure 9A-97: Source-sector contributions to Hourly Maximum (left) and Period Average SOx concentrations at CE Site from ALL sources during Winter Season.

Figure 9A-98: Source-sector contributions to Hourly Maximum (left) and Period Average SOx concentrations at CN Site from airport-related sources (top) and background sources (bottom) during Winter Season.

Figure 9A-99: Source-sector contributions to Hourly Maximum (left) and Period Average SOx concentrations at CN Site from ALL sources during Winter Season.

Figure 9A-100: Source-sector contributions to Hourly Maximum (left) and Period Average SOx concentrations at CS Site from airport-related sources (top) and background sources (bottom) during Winter Season.

Figure 9A-101: Source-sector contributions to Hourly Maximum (left) and Period Average SOx concentrations at CS Site from ALL sources during Winter Season.

Figure 9A-102: Source-sector contributions to Period Average SOx concentrations at each site from airport-related vs. background sources during Winter Season.

Figure 9A-103a: Modeled hourly max (left) and period average (right) CO concentrations from airport-related in Polar Grid of receptors during Summer Season.

Figure 9A-103b: Modeled hourly max (left) and period average (right) CO concentrations from background sources in Polar Grid of receptors during Summer Season.

Figure 9A-103c: Modeled hourly max (left) and period average (right) CO concentrations from ALL in Polar Grid of receptors during Summer Season.

Figure 9A-104a: Modeled hourly max (left) and period average (right) CO concentrations from airport-related in Cartesian Grid of receptors during Summer Season.

Figure 9A-104b: Modeled hourly max (left) and period average (right) CO concentrations from background sources in Cartesian Grid of receptors during Summer Season.

Figure 9A-104c: Modeled hourly max (left) and period average (right) CO concentrations from ALL in Cartesian Grid of receptors during Summer Season.

Figure 9A-105: Modeled hourly max CO concentrations from airport-related sources at flag-pole receptors at heights of 2m, 7m, 12m, 17m, 22m and 27m in Polar Grid of receptors during Summer Season.

Figure 9A-106: Modeled period average CO concentrations from airport-related sources at flag-pole receptors at heights of 2m, 7m, 12m, 17m, 22m and 27m in Polar Grid of receptors during Summer Season.

Figure 9A-107: Modeled hourly max CO concentrations from airport-related sources at flag-pole receptors at heights of 2m, 7m, 12m, 17m, 22m and 27m in Cartesian Grid of receptors during Summer Season.

Figure 9A-108: Modeled period average CO concentrations from airport-related sources at flag-pole receptors at heights of 2m, 7m, 12m, 17m, 22m and 27m in Cartesian Grid of receptors during Summer Season.

Figure 9A-109: Modeled hourly maximum CO concentrations from airport-related sources by source sector at flag-pole receptors at heights of 2m, 7m, 12m, 17m, 22m and 27m in Cartesian Grid of receptors during Summer Season.

Figure 9A-110: Modeled hourly maximum CO concentrations from background sources by source sector at flag-pole receptors at heights of 2m, 7m, 12m, 17m, 22m and 27m in Cartesian Grid of receptors during Summer Season.

Figure 9A-111: Modeled period average CO concentrations from airport-related sources by source sector at flag-pole receptors at heights of 2m, 7m, 12m, 17m, 22m and 27m in Cartesian Grid of receptors during Summer Season.

Figure 9A-112: Modeled period average CO concentrations from background sources by source sector at flag-pole receptors at heights of 2m, 7m, 12m, 17m, 22m and 27m in Cartesian Grid of receptors during Summer Season.

Figure 9A-113a: Modeled hourly max (left) and period average (right) NOx concentrations from airport-related in Polar Grid of receptors during Summer Season.

Figure 9A-113b: Modeled hourly max (left) and period average (right) NOx concentrations from background sources in Polar Grid of receptors during Summer Season.

Figure 9A-11c3: Modeled hourly max (left) and period average (right) NOx concentrations from ALL in Polar Grid of receptors during Summer Season.

Figure 9A-114a: Modeled hourly max (left) and period average (right) NOx concentrations from airport-related in Cartesian Grid of receptors during Summer Season.

Figure 9A-114b: Modeled hourly max (left) and period average (right) NOx concentrations from background sources in Cartesian Grid of receptors during Summer Season.

Figure 9A-114c: Modeled hourly max (left) and period average (right) NOx concentrations from ALL in Cartesian Grid of receptors during Summer Season.

Figure 9A-115: Modeled hourly max NOx concentrations from airport-related sources at flag-pole receptors at heights of 2m, 7m, 12m, 17m, 22m and 27m in Polar Grid of receptors during Summer Season.

Figure 9A-116: Modeled period average NOx concentrations from airport-related sources at flag-pole receptors at heights of 2m, 7m, 12m, 17m, 22m and 27m in Polar Grid of receptors during Summer Season.

Figure 9A-117: Modeled hourly max NOx concentrations from airport-related sources at flag-pole receptors at heights of 2m, 7m, 12m, 17m, 22m and 27m in Cartesian Grid of receptors during Summer Season.

Figure 9A-118: Modeled period average NOx concentrations from airport-related sources at flag-pole receptors at heights of 2m, 7m, 12m, 17m, 22m and 27m in Cartesian Grid of receptors during Summer Season.

Figure 9A-119: Modeled hourly maximum NOx concentrations from airport-related sources by source sector at flag-pole receptors at heights of 2m, 7m, 12m, 17m, 22m and 27m in Cartesian Grid of receptors during Summer Season.

Figure 9A-120: Modeled hourly maximum NOx concentrations from background sources by source sector at flag-pole receptors at heights of 2m, 7m, 12m, 17m, 22m and 27m in Cartesian Grid of receptors during Summer Season.

Figure 9A-121: Modeled period average NOx concentrations from airport-related sources by source sector at flag-pole receptors at heights of 2m, 7m, 12m, 17m, 22m and 27m in Cartesian Grid of receptors during Summer Season.

Figure 9A-122: Modeled period average NOx concentrations from background sources by source sector at flag-pole receptors at heights of 2m, 7m, 12m, 17m, 22m and 27m in Cartesian Grid of receptors during Summer Season.

Figure 9A-123a: Modeled hourly max (left) and period average (right) $PM_{2.5}$ concentrations from airport-related in Polar Grid of receptors during Summer Season.

Figure 9A-123b: Modeled hourly max (left) and period average (right) $PM_{2.5}$ concentrations from background sources in Polar Grid of receptors during Summer Season.

Figure 9A-123c: Modeled hourly max (left) and period average (right) $PM_{2.5}$ concentrations from ALL in Polar Grid of receptors during Summer Season.

Figure 9A-124a: Modeled hourly max (left) and period average (right) PM2.5 concentrations from airport-related in Cartesian Grid of receptors during Summer Season.

Figure 9A-124b: Modeled hourly max (left) and period average (right) $PM_{2.5}$ concentrations from background sources in Cartesian Grid of receptors during Summer Season.

Figure 9A-124c: Modeled hourly max (left) and period average (right) $PM_{2.5}$ concentrations from ALL in Cartesian Grid of receptors during Summer Season.

Figure 9A-125: Modeled hourly max $PM_{2.5}$ concentrations from airport-related sources at flag-pole receptors at heights of 2m, 7m, 12m, 17m, 22m and 27m in Polar Grid of receptors during Summer Season.

Figure 9A-126: Modeled period average $PM_{2.5}$ concentrations from airport-related sources at flag-pole receptors at heights of 2m, 7m, 12m, 17m, 22m and 27m in Polar Grid of receptors during Summer Season.

Figure 9A-127: Modeled hourly max $PM_{2.5}$ concentrations from airport-related sources at flag-pole receptors at heights of 2m, 7m, 12m, 17m, 22m and 27m in Cartesian Grid of receptors during Summer Season.

Figure 9A-128: Modeled period average $PM_{2.5}$ concentrations from airport-related sources at flag-pole receptors at heights of 2m, 7m, 12m, 17m, 22m and 27m in Cartesian Grid of receptors during Summer Season.

Figure 9A-129: Modeled hourly maximum $PM_{2.5}$ concentrations from airport-related sources by source sector at flag-pole receptors at heights of 2m, 7m, 12m, 17m, 22m and 27m in Cartesian Grid of receptors during Summer Season.

Figure 9A-130: Modeled hourly maximum $PM_{2.5}$ concentrations from background sources by source sector at flag-pole receptors at heights of 2m, 7m, 12m, 17m, 22m and 27m in Cartesian Grid of receptors during Summer Season.

Figure 9A-131: Modeled period average $PM_{2.5}$ concentrations from airport-related sources by source sector at flag-pole receptors at heights of 2m, 7m, 12m, 17m, 22m and 27m in Cartesian Grid of receptors during Summer Season.

Figure 9A-132: Modeled period average $PM_{2.5}$ concentrations from background sources by source sector at flag-pole receptors at heights of 2m, 7m, 12m, 17m, 22m and 27m in Cartesian Grid of receptors during Summer Season.

Figure 9A-133a: Modeled hourly max (left) and period average (right) SOx concentrations from airport-related (top), background sources (middle) and ALL (bottom) in Polar Grid of receptors during Summer Season.

Figure 9A-133b: Modeled hourly max (left) and period average (right) SOx concentrations from airport-related (top), background sources (middle) and ALL (bottom) in Polar Grid of receptors during Summer Season.

Figure 9A-133c: Modeled hourly max (left) and period average (right) SOx concentrations from airport-related (top), background sources (middle) and ALL (bottom) in Polar Grid of receptors during Summer Season.

Figure 9A-134a: Modeled hourly max (left) and period average (right) SOx concentrations from airport-related in Cartesian Grid of receptors during Summer Season.

Figure 9A-134b: Modeled hourly max (left) and period average (right) SOx concentrations from background sources in Cartesian Grid of receptors during Summer Season.

Figure 9A-134c: Modeled hourly max (left) and period average (right) SOx concentrations from ALL in Cartesian Grid of receptors during Summer Season.

Figure 9A-135: Modeled hourly max SOx concentrations from airport-related sources at flag-pole receptors at heights of 2m, 7m, 12m, 17m, 22m and 27m in Polar Grid of receptors during Summer Season.

Figure 9A-136: Modeled period average SOx concentrations from airport-related sources at flag-pole receptors at heights of 2m, 7m, 12m, 17m, 22m and 27m in Polar Grid of receptors during Summer Season.

Figure 9A-137: Modeled hourly max SOx concentrations from airport-related sources at flag-pole receptors at heights of 2m, 7m, 12m, 17m, 22m and 27m in Cartesian Grid of receptors during Summer Season.

Figure 9A-138: Modeled period average SOx concentrations from airport-related sources at flag-pole receptors at heights of 2m, 7m, 12m, 17m, 22m and 27m in Cartesian Grid of receptors during Summer Season.

Figure 9A-139 Modeled hourly maximum SOx concentrations from airport-related sources by source sector at flag-pole receptors at heights of 2m, 7m, 12m, 17m, 22m and 27m in Cartesian Grid of receptors during Summer Season.

Figure 9A-140: Modeled hourly maximum SOx concentrations from background sources by source sector at flag-pole receptors at heights of 2m, 7m, 12m, 17m, 22m and 27m in Cartesian Grid of receptors during Summer Season.

Figure 9A-141: Modeled period average SOx concentrations from airport-related sources by source sector at flag-pole receptors at heights of 2m, 7m, 12m, 17m, 22m and 27m in Cartesian Grid of receptors during Summer Season.

Figure 9A-142: Modeled period average SOx concentrations from background sources by source sector at flag-pole receptors at heights of 2m, 7m, 12m, 17m, 22m and 27m in Cartesian Grid of receptors during Summer Season.

Figure 9A-143a: Modeled hourly max (left) and period average (right) TOG concentrations from airport-related in Polar Grid of receptors during Summer Season.

Figure 9A-143b: Modeled hourly max (left) and period average (right) TOG concentrations from background sources in Polar Grid of receptors during Summer Season.

Figure 9A-143c: Modeled hourly max (left) and period average (right) TOG concentrations from ALL in Polar Grid of receptors during Summer Season.

Figure 9A-144a: Modeled hourly max (left) and period average (right) TOG concentrations from airport-related in Cartesian Grid of receptors during Summer Season.

Figure 9A-144b: Modeled hourly max (left) and period average (right) TOG concentrations from background sources in Cartesian Grid of receptors during Summer Season.

Figure 9A-144c: Modeled hourly max (left) and period average (right) TOG concentrations from ALL in Cartesian Grid of receptors during Summer Season.

Figure 9A-145: Modeled hourly max TOG concentrations from airport-related sources at flag-pole receptors at heights of 2m, 7m, 12m, 17m, 22m and 27m in Polar Grid of receptors during Summer Season.

Figure 9A-146: Modeled period average TOG concentrations from airport-related sources at flag-pole receptors at heights of 2m, 7m, 12m, 17m, 22m and 27m in Polar Grid of receptors during Summer Season.

Figure 9A-147: Modeled hourly max TOG concentrations from airport-related sources at flag-pole receptors at heights of 2m, 7m, 12m, 17m, 22m and 27m in Cartesian Grid of receptors during Summer Season.

Figure 9A-148: Modeled period average TOG concentrations from airport-related sources at flag-pole receptors at heights of 2m, 7m, 12m, 17m, 22m and 27m in Cartesian Grid of receptors during Summer Season.

Figure 9A-149: Modeled hourly maximum TOG concentrations from airport-related sources by source sector at flag-pole receptors at heights of 2m, 7m, 12m, 17m, 22m and 27m in Cartesian Grid of receptors during Summer Season.

Figure 9A-150: Modeled hourly maximum TOG concentrations from background sources by source sector at flag-pole receptors at heights of 2m, 7m, 12m, 17m, 22m and 27m in Cartesian Grid of receptors during Summer Season.

Figure 9A-151: Modeled period average TOG concentrations from airport-related sources by source sector at flag-pole receptors at heights of 2m, 7m, 12m, 17m, 22m and 27m in Cartesian Grid of receptors during Summer Season.

Figure 9A-152: Modeled period average TOG concentrations from background sources by source sector at flag-pole receptors at heights of 2m, 7m, 12m, 17m, 22m and 27m in Cartesian Grid of receptors during Summer Season.

Figure 9A-153: Diurnal variability in observed and modeled CO concentrations at AQ Site from flagpole receptors at heights of 2m, 7m, 12m and 17m during Summer Season.

Figure 9A-154: Diurnal variability in observed and modeled CO concentrations at CE Site from flagpole receptors at heights of 2m, 7m, 12m and 17m during Summer Season.

Figure 9A-155: Diurnal variability in observed and modeled CO concentrations at CN Site from flagpole receptors at heights of 2m, 7m, 12m and 17m during Summer Season.

Figure 9A-156: Diurnal variability in observed and modeled CO concentrations at CS Site from flagpole receptors at heights of 2m, 7m, 12m and 17m during Summer Season.

Figure 9A-157: Diurnal variability in observed and modeled NOx concentrations at AQ Site from flagpole receptors at heights of 2m, 7m, 12m and 17m during Summer Season.

Figure 9A-158: Diurnal variability in observed and modeled NOx concentrations at CE Site from flagpole receptors at heights of 2m, 7m, 12m and 17m during Summer Season.

Figure 9A-159: Diurnal variability in observed and modeled NOx concentrations at CN Site from flagpole receptors at heights of 2m, 7m, 12m and 17m during Summer Season.

Figure 9A-160: Diurnal variability in observed and modeled NOx concentrations at CS Site from flagpole receptors at heights of 2m, 7m, 12m and 17m during Summer Season.

Figure 9A-161: Diurnal variability in observed and modeled $PM_{2.5}$ concentrations at AQ Site from flagpole receptors at heights of 2m, 7m, 12m and 17m during Summer Season.

Figure 9A-162: Diurnal variability in observed and modeled $PM_{2.5}$ concentrations at CE Site from flagpole receptors at heights of 2m, 7m, 12m and 17m during Summer Season.

Figure 9A-163: Diurnal variability in observed and modeled $PM_{2.5}$ concentrations at CN Site from flagpole receptors at heights of 2m, 7m, 12m and 17m during Summer Season.

Figure 9A-164: Diurnal variability in observed and modeled $PM_{2.5}$ concentrations at CS Site from flagpole receptors at heights of 2m, 7m, 12m and 17m during Summer Season.

Figure 9A-165: Diurnal variability in observed and modeled SOx concentrations at AQ Site from flagpole receptors at heights of 2m, 7m, 12m and 17m during Summer Season.

Figure 9A-166: Diurnal variability in observed and modeled SOx concentrations at CE Site from flagpole receptors at heights of 2m, 7m, 12m and 17m during Summer Season.

Figure 9A-167: Diurnal variability in observed and modeled SOx concentrations at CN Site from flagpole receptors at heights of 2m, 7m, 12m and 17m during Summer Season.

Figure 9A-168: Diurnal variability in observed and modeled SOx concentrations at CS Site from flagpole receptors at heights of 2m, 7m, 12m and 17m during Summer Season.

Figure 9A-169: Source-sector contributions to Hourly Maximum (left) and Period Average CO concentrations at AQ Site from airport-related sources (top) and background sources (bottom) during Summer Season.

Figure 9A-170: Source-sector contributions to Hourly Maximum (left) and Period Average CO concentrations at AQ Site from ALL sources during Summer Season.

Figure 9A-171: Source-sector contributions to Hourly Maximum (left) and Period Average CO concentrations at CE Site from airport-related sources (top) and background sources (bottom) during Summer Season.

Figure 9A-172: Source-sector contributions to Hourly Maximum (left) and Period Average CO concentrations at CE Site from ALL sources during Summer Season.

Figure 9A-173: Source-sector contributions to Hourly Maximum (left) and Period Average CO concentrations at CN Site from airport-related sources (top) and background sources (bottom) during Summer Season.

Figure 9A-174: Source-sector contributions to Hourly Maximum (left) and Period Average CO concentrations at CN Site from ALL sources during Summer Season.

Figure 9A-175: Source-sector contributions to Hourly Maximum (left) and Period Average CO concentrations at CS Site from airport-related sources (top) and background sources (bottom) during Summer Season.

Figure 9A-176: Source-sector contributions to Hourly Maximum (left) and Period Average CO concentrations at CS Site from ALL sources during Summer Season.

Figure 9A-177: Source-sector contributions to Period Average CO concentrations at each site from airport-related vs. background sources during Summer Season.

Figure 9A-178: Source-sector contributions to Hourly Maximum (left) and Period Average NOx concentrations at AQ Site from airport-related sources (top) and background sources (bottom) during Summer Season.

Figure 9A-179: Source-sector contributions to Hourly Maximum (left) and Period Average NOx concentrations at AQ Site from ALL sources during Summer Season.

Figure 9A-180: Source-sector contributions to Hourly Maximum (left) and Period Average NOx concentrations at CE Site from airport-related sources (top) and background sources (bottom) during Summer Season.

Figure 9A-181: Source-sector contributions to Hourly Maximum (left) and Period Average NOx concentrations at CE Site from ALL sources during Summer Season.

Figure 9A-182: Source-sector contributions to Hourly Maximum (left) and Period Average NOx concentrations at CN Site from airport-related sources (top) and background sources (bottom) during Summer Season.

Figure 9A-183: Source-sector contributions to Hourly Maximum (left) and Period Average NOx concentrations at CN Site from ALL sources during Summer Season.

Figure 9A-184: Source-sector contributions to Hourly Maximum (left) and Period Average NOx concentrations at CS Site from airport-related sources (top) and background sources (bottom) during Summer Season.

Figure 9A-185: Source-sector contributions to Hourly Maximum (left) and Period Average NOx concentrations at CS Site from ALL sources during Summer Season.

Figure 9A-186: Source-sector contributions to Period Average NOx concentrations at each site from airport-related vs. background sources during Summer Season.

Figure 9A-187: Source-sector contributions to Hourly Maximum (left) and Period Average $PM_{2.5}$ concentrations at AQ Site from airport-related sources (top) and background sources (bottom) during Summer Season.

Figure 9A-188: Source-sector contributions to Hourly Maximum (left) and Period Average $PM_{2.5}$ concentrations at AQ Site from ALL sources during Summer Season.

Figure 9A-189: Source-sector contributions to Hourly Maximum (left) and Period Average $PM_{2.5}$ concentrations at CE Site from airport-related sources (top) and background sources (bottom) during Summer Season.

Figure 9A-190: Source-sector contributions to Hourly Maximum (left) and Period Average $PM_{2.5}$ concentrations at CE Site from ALL sources during Summer Season.

Figure 9A-191: Source-sector contributions to Hourly Maximum (left) and Period Average $PM_{2.5}$ concentrations at CN Site from airport-related sources (top) and background sources (bottom) during Summer Season.

Figure 9A-192: Source-sector contributions to Hourly Maximum (left) and Period Average $PM_{2.5}$ concentrations at CN Site from ALL sources during Summer Season.

Figure 9A-193: Source-sector contributions to Hourly Maximum (left) and Period Average $PM_{2.5}$ concentrations at CS Site from airport-related sources (top) and background sources (bottom) during Summer Season.

Figure 9A-194: Source-sector contributions to Hourly Maximum (left) and Period Average $PM_{2.5}$ concentrations at CS Site from ALL sources during Summer Season.

Figure 9A-195: Source-sector contributions to Period Average $PM_{2.5}$ concentrations at each site from airport-related vs. background sources during Summer Season.

Figure 9A-196: Source-sector contributions to Hourly Maximum (left) and Period Average SOx concentrations at AQ Site from airport-related sources (top) and background sources (bottom) during Summer Season.

Figure 9A-197: Source-sector contributions to Hourly Maximum (left) and Period Average SOx concentrations at AQ Site from ALL sources during Summer Season.

Figure 9A-198: Source-sector contributions to Hourly Maximum (left) and Period Average SOx concentrations at CE Site from airport-related sources (top) and background sources (bottom) during Summer Season.

Figure 9A-199: Source-sector contributions to Hourly Maximum (left) and Period Average SOx concentrations at CE Site from ALL sources during Summer Season.

Figure 9A-200: Source-sector contributions to Hourly Maximum (left) and Period Average SOx concentrations at CN Site from airport-related sources (top) and background sources (bottom) during Summer Season.

Figure 9A-201: Source-sector contributions to Hourly Maximum (left) and Period Average SOx concentrations at CN Site from ALL sources during Summer Season.

Figure 9A-202: Source-sector contributions to Hourly Maximum (left) and Period Average SOx concentrations at CS Site from airport-related sources (top) and background sources (bottom) during Summer Season.

Figure 9A-203: Source-sector contributions to Hourly Maximum (left) and Period Average SOx concentrations at CS Site from ALL sources during Summer Season.

Figure 9A-204: Source-sector contributions to Period Average SOx concentrations at each site from airport-related vs. background sources during Summer Season.

Sample AERMOD Input file

Table 9A-1. Ratios of modeled maximum one-hour concentrations during Winter Season. Ratios are from anywhere among all flag-pole receptors to receptors at 2 meter elevation.*

		Winter Max 1-hr				
Source Group	Description	CO	NO_x	$PM_{2.5}$	SO_x	VOC
ALL	ALL	1.00	1.00	1.00	1.00	1.00
Airport-related Sources						
APPROACH	Aircraft Approach	0.10	0.18	0.16	0.16	0.18
TAKEOFF	Aircraft Takeoff	0.99	0.97	0.94	0.94	0.94
LANDING	Aircraft Landing	0.65	0.59	0.65	0.65	0.67
TAXIQ	Aircraft Taxi/Queue	0.72	0.71	0.80	0.71	1.00
GATES	APU, GSE, and Aircraft Startup	1.00	1.00	1.00	1.00	1.00
PARKING	On-airport Parking	0.38	0.77	0.38	1.00	0.38
STATSRCS	On-airport LAWA-Owned Stationary Sources	0.62	0.32	0.50	0.62	0.07
CAONRDAP	Minor On-road Sources	1.00	1.00	1.00	1.00	1.00
CAOFFAP	Off-road Equipment	1.00	1.00	1.00	1.00	1.00
CAAGGAP	Aggregate Stationary Sources	1.00	1.00	1.00	1.00	1.00
COGEN	LAWA COGEN	0.54	0.53	0.53	0.53	0.54
CAAREAAP	Area wide Sources	1.00	1.00	1.00	1.00	1.00
SSTENAP	AIRPORT TENANT	0.32	0.34	0.36	0.36	0.36
ROADOFAP	Off-airport Major Roadway	1.00	1.00	1.00	1.00	1.00
ROADONAP	On-airport Roadway	1.00	1.00	1.00	1.00	1.00
FREEWYAP	Freeway	1.00	1.00	1.00	1.00	1.00
EDMS	EDMS	1.00	0.97	1.00	0.99	1.00
AIRPORT	All sources within airport boundary	1.00	0.97	1.00	0.99	1.00
Background Sources						
CHEVRON	CHEVRON PRODUCTS CO.	1.00	1.00	1.00	1.00	0.86
MARINE	Marine Vessels	0.71	0.73	0.76	0.70	0.72
CAONRDBK	Minor On-road Sources	1.00	1.00	1.00	1.00	1.00
CAOFFBK	Off-road Equipment	1.00	1.00	1.00	1.00	1.00
CAAGGBK	Aggregate Stationary Sources	1.00	1.00	1.00	1.00	1.00
CAAREABK	Area wide Sources	1.00	1.00	1.00	1.00	1.00
SEGUNDO	El Segundo Power Plant	0.91	0.87	0.91	0.27	0.91
SSOTHBK	OTHER OFF-AIRPORT STATIONARY SOURCE	1.00	1.00	1.00	1.00	1.00
SCTRGOOD	Scattergood Power Plant	0.96	0.94	0.96	0.96	0.96
ROADOFBK	Off-airport Major Roadway	1.00	1.00	1.00	1.00	1.00
FREEWYBK	Freeway	1.00	1.00	1.00	1.00	1.00
BACKGROUND	All sources outside airport boundary	1.00	1.00	1.00	1.00	1.00

* All ratios less than 1.0 are shown shaded in red. When a ratio was less than 1.0, it indicated that the maximum was predicted at flag-pole receptors aloft rather than at the lowest elevation of 2m. The actual receptors where the maxima are predicted are shown in Table 9A-3.

Table 9A-2. Ratios of modeled maximum Winter Season average concentrations. Ratios are from anywhere among all flag-pole receptors to receptors at 2 meter elevation.*

		Winter Max Season Average				
Source Group	Description	CO	NO_x	$PM_{2.5}$	SO_x	VOC
ALL	ALL	1.00	1.00	1.00	1.00	1.00
Airport-related Sources						
APPROACH	Aircraft Approach	0.21	0.23	0.23	0.23	0.23
TAKEOFF	Aircraft Takeoff	0.83	0.79	0.79	0.79	0.78
LANDING	Aircraft Landing	0.68	0.55	0.64	0.56	0.69
TAXIQ	Aircraft Taxi/Queue	0.62	0.60	0.62	0.60	0.65
GATES	APU, GSE, and Aircraft Startup	1.00	1.00	1.00	1.00	1.00
PARKING	On-airport Parking	1.00	1.00	1.00	1.00	1.00
STATSRCS	On-airport LAWA-Owned Stationary Sources	0.70	0.69	0.70	0.69	0.23
CAONRDAP	Minor On-road Sources	1.00	1.00	1.00	1.00	1.00
CAOFFAP	Off-road Equipment	1.00	1.00	1.00	1.00	1.00
CAAGGAP	Aggregate Stationary Sources	1.00	1.00	1.00	1.00	1.00
NOxGEN	LAWA NOxGEN	0.98	0.98	0.98	0.98	0.98
CAAREAAP	Area wide Sources	1.00	1.00	1.00	1.00	1.00
SSTENAP	AIRPORT TENANT	0.31	0.36	0.62	0.62	0.63
ROADOFAP	Off-airport Major Roadway	1.00	1.00	1.00	1.00	1.00
ROADONAP	On-airport Roadway	1.00	1.00	1.00	1.00	1.00
FREEWYAP	Freeway	1.00	1.00	1.00	1.00	1.00
EDMS	EDMS	1.00	1.00	1.00	0.89	1.00
AIRPORT	All sources within airport boundary	1.00	1.00	1.00	0.90	1.00
Background Sources						
CHEVRON	CHEVRON PRODUCTS NOx.	1.00	1.00	1.00	1.00	0.85
MARINE	Marine Vessels	0.97	0.97	0.97	0.98	0.97
CAONRDBK	Minor On-road Sources	1.00	1.00	1.00	1.00	1.00
CAOFFBK	Off-road Equipment	1.00	1.00	1.00	1.00	1.00
CAAGGBK	Aggregate Stationary Sources	1.00	1.00	1.00	1.00	1.00
CAAREABK	Area wide Sources	1.00	1.00	1.00	1.00	1.00
SEGUNDO	El Segundo Power Plant	0.76	0.75	0.76	0.20	0.76
SSOTHBK	OTHER OFF-AIRPORT STATIONARY SOURCE	1.00	1.00	1.00	1.00	1.00
SCTRGOOD	Scattergood Power Plant	0.95	0.97	0.94	0.91	0.94
ROADOFBK	Off-airport Major Roadway	1.00	1.00	1.00	1.00	1.00
FREEWYBK	Freeway	1.00	1.00	1.00	1.00	1.00
BACKGROUND	All sources outside airport boundary	1.00	1.00	1.00	1.00	1.00

* All ratios less than 1.0 are shown shaded in red. When a ratio was less than 1.0, it indicated that the maximum was predicted at flag-pole receptors aloft rather than at the lowest elevation of 2m. The actual receptors where the maxima are predicted are shown in Table 9A-4.

Table 9A-3. Heat map of elevation (meters) where maximum **one-hour** concentration was modeled during Winter Season by AERMOD.*

		Winter Max 1-hr				
Source Group	Description	CO	NO_x	$PM_{2.5}$	SO_x	VOC
ALL	ALL	2	2	2	2	2
Airport-related Sources						
APPROACH	Aircraft Approach	22	22	22	22	22
TAKEOFF	Aircraft Takeoff	12	12	12	12	12
LANDING	Aircraft Landing	12	12	12	12	12
TAXIQ	Aircraft Taxi/Queue	12	12	12	12	12
GATES	APU, GSE, and Aircraft Startup	2	2	2	2	2
PARKING	On-airport Parking	12	12	12	2	12
STATSRCS	On-airport LAWA-Owned Stationary Sources	7	7	27	7	22
CAONRDAP	Minor On-road Sources	2	2	2	2	2
CAOFFAP	Off-road Equipment	2	2	2	2	2
CAAGGAP	Aggregate Stationary Sources	2	2	2	2	2
COGEN	LAWA COGEN	27	27	27	27	27
CAAREAAP	Area wide Sources	2	2	2	2	2
SSTENAP	AIRPORT TENANT	27	27	27	27	27
ROADOFAP	Off-airport Major Roadway	2	2	2	2	2
ROADONAP	On-airport Roadway	2	2	2	2	2
FREEWYAP	Freeway	2	2	2	2	2
EDMS	EDMS	2	12	2	12	2
AIRPORT	All sources within airport boundary	2	12	2	12	2
Background Sources						
CHEVRON	CHEVRON PRODUCTS CO.	2	2	2	2	27
MARINE	Marine Vessels	27	27	27	27	27
CAONRDBK	Minor On-road Sources	2	2	2	2	2
CAOFFBK	Off-road Equipment	2	2	2	2	2
CAAGGBK	Aggregate Stationary Sources	2	2	2	2	2
CAAREABK	Area wide Sources	2	2	2	2	2
SEGUNDO	El Segundo Power Plant	27	27	27	27	27
SSOTHBK	OTHER OFF-AIRPORT STATIONARY SOURCE	2	2	2	2	2
SCTRGOOD	Scattergood Power Plant	27	27	27	27	27
ROADOFBK	Off-airport Major Roadway	2	2	2	2	2
FREEWYBK	Freeway	2	2	2	2	2
BACKGROUND	All sources outside airport boundary	2	2	2	2	2

Legend for flag-pole heights: Green 2m, Yellow 7m, Orange 12m, Red 22m, Deep Red 27m.

*Values in colored cells are the elevations of flag-pole receptors modeled in AERMOD. The 'heat map' indicates the ranges in elevation where the maximum was predicted by AERMOD.

Table 9A-4. Heat map of elevation (meters) where maximum Winter Season average concentration was modeled by AERMOD.*

		Winter Max Season Average				
Source Group	Description	CO	NO_x	$PM_{2.5}$	SO_x	VOC
ALL	ALL	2	2	2	2	2
Airport-related Sources						
APPROACH	Aircraft Approach	22	22	22	22	22
TAKEOFF	Aircraft Takeoff	12	12	12	12	12
LANDING	Aircraft Landing	12	12	12	12	12
TAXIQ	Aircraft Taxi/Queue	12	12	12	12	12
GATES	APU, GSE, and Aircraft Startup	2	2	2	2	2
PARKING	On-airport Parking	2	2	2	2	2
STATSRCS	On-airport LAWA-Owned Stationary Sources	7	7	7	7	22
CAONRDAP	Minor On-road Sources	2	2	2	2	2
CAOFFAP	Off-road Equipment	2	2	2	2	2
CAAGGAP	Aggregate Stationary Sources	2	2	2	2	2
COGEN	LAWA COGEN	27	27	27	27	27
CAAREAAP	Area wide Sources	2	2	2	2	2
SSTENAP	AIRPORT TENANT	27	27	27	27	27
ROADOFAP	Off-airport Major Roadway	2	2	2	2	2
ROADONAP	On-airport Roadway	2	2	2	2	2
FREEWYAP	Freeway	2	2	2	2	2
EDMS	EDMS	2	2	2	12	2
AIRPORT	All sources within airport boundary	2	2	2	12	2
Background Sources						
CHEVRON	CHEVRON PRODUCTS CO.	2	2	2	2	27
MARINE	Marine Vessels	27	27	27	27	27
CAONRDBK	Minor On-road Sources	2	2	2	2	2
CAOFFBK	Off-road Equipment	2	2	2	2	2
CAAGGBK	Aggregate Stationary Sources	2	2	2	2	2
CAAREABK	Area wide Sources	2	2	2	2	2
SEGUNDO	El Segundo Power Plant	27	27	27	27	27
SSOTHBK	OTHER OFF-AIRPORT STATIONARY SOURCE	2	2	2	2	2
SCTRGOOD	Scattergood Power Plant	27	27	27	27	27
ROADOFBK	Off-airport Major Roadway	2	2	2	2	2
FREEWYBK	Freeway	2	2	2	2	2
BACKGROUND	All sources outside airport boundary	2	2	2	2	2

Legend for flag-pole heights: Green 2m, Yellow 7m, Orange 12m, Red 22m, Deep Red 27m.

*Values in colored cells are the elevations of flag-pole receptors modeled in AERMOD. The 'heat map' indicates the ranges in elevation where the maximum was predicted by AERMOD.

Table 9A-5. Ratios of modeled maximum one-hour concentrations for Summer Season Ratios are from anywhere among all flag-pole receptors to receptors at 2 meter elevation.*

		Summer Max 1-hr				
Source Group	Description	CO	NO_x	$PM_{2.5}$	SO_x	VOC
ALL	ALL	1.00	1.00	1.00	1.00	1.00
Airport-related Sources						
APPROACH	Aircraft Approach	0.16	0.09	0.14	0.09	0.16
TAKEOFF	Aircraft Takeoff	0.82	0.82	0.82	0.81	0.81
LANDING	Aircraft Landing	0.86	0.48	0.76	0.61	0.78
TAXIQ	Aircraft Taxi/Queue	0.86	0.86	0.97	0.85	0.78
GATES	APU, GSE, and Aircraft Startup	1.00	1.00	1.00	1.00	1.00
PARKING	On-airport Parking	0.70	1.00	0.76	1.00	0.77
STATSRCS	On-airport LAWA-Owned Stationary Sources	0.28	0.26	0.08	0.28	0.04
CAONRDAP	Minor On-road Sources	1.00	1.00	1.00	1.00	1.00
CAOFFAP	Off-road Equipment	1.00	1.00	1.00	1.00	1.00
CAAGGAP	Aggregate Stationary Sources	1.00	1.00	1.00	1.00	1.00
COGEN	LAWA COGEN	0.39	0.39	0.39	0.39	0.39
CAAREAAP	Area wide Sources	1.00	1.00	1.00	1.00	1.00
SSTENAP	AIRPORT TENANT	0.15	0.15	0.20	0.20	0.20
ROADOFAP	Off-airport Major Roadway	1.00	1.00	1.00	1.00	1.00
ROADONAP	On-airport Roadway	1.00	1.00	1.00	1.00	1.00
FREEWYAP	Freeway	1.00	1.00	1.00	1.00	1.00
EDMS	EDMS	1.00	1.00	1.00	0.86	1.00
AIRPORT	All sources within airport boundary	1.00	1.00	1.00	0.86	1.00
Background Sources						
CHEVRON	CHEVRON PRODUCTS CO.	1.00	1.00	1.00	1.00	0.33
MARINE	Marine Vessels	0.63	0.63	0.57	0.62	0.63
CAONRDBK	Minor On-road Sources	1.00	1.00	1.00	1.00	1.00
CAOFFBK	Off-road Equipment	1.00	1.00	1.00	1.00	1.00
CAAGGBK	Aggregate Stationary Sources	1.00	1.00	1.00	1.00	1.00
CAAREABK	Area wide Sources	1.00	1.00	1.00	1.00	1.00
SEGUNDO	El Segundo Power Plant	0.85	0.85	0.85	0.85	0.85
SSOTHBK	OTHER OFF-AIRPORT STATIONARY SOURCE	1.00	1.00	1.00	1.00	1.00
SCTRGOOD	Scattergood Power Plant	0.99	1.00	0.99	0.99	0.99
ROADOFBK	Off-airport Major Roadway	1.00	1.00	1.00	1.00	1.00
FREEWYBK	Freeway	1.00	1.00	1.00	1.00	1.00
BACKGROUND	All sources outside airport boundary	1.00	1.00	1.00	1.00	1.00

* All ratios less than 1.0 are shown shaded in red. When a ratio was less than 1.0, it indicated that the maximum was predicted at flag-pole receptors aloft rather than at the lowest elevation of 2m. The actual receptors where the maxima are predicted are shown in Table 9A-7.

Table 9A-6. Ratios of modeled maximum Summer Season average concentrations. Ratios are from anywhere among all flag-pole receptors to receptors at two meter elevation.*

		Summer Max Season Average				
Source Group	Description	CO	NO_x	$PM_{2.5}$	SO_x	VOC
ALL	ALL	1.00	1.00	1.00	1.00	1.00
Airport-related Sources						
APPROACH	Aircraft Approach	0.24	0.24	0.24	0.24	0.25
TAKEOFF	Aircraft Takeoff	0.74	0.71	0.72	0.72	0.67
LANDING	Aircraft Landing	0.78	0.73	0.76	0.75	0.82
TAXIQ	Aircraft Taxi/Queue	0.70	0.69	0.72	0.69	0.68
GATES	APU, GSE, and Aircraft Startup	1.00	1.00	1.00	1.00	1.00
PARKING	On-airport Parking	1.00	1.00	1.00	1.00	1.00
STATSRCS	On-airport LAWA-Owned Stationary Sources	0.43	0.43	0.32	0.43	0.10
CAONRDAP	Minor On-road Sources	1.00	1.00	1.00	1.00	1.00
CAOFFAP	Off-road Equipment	1.00	1.00	1.00	1.00	1.00
CAAGGAP	Aggregate Stationary Sources	1.00	1.00	1.00	1.00	1.00
NOxGEN	LAWA NOxGEN	0.52	0.52	0.52	0.52	0.52
CAAREAAP	Area wide Sources	1.00	1.00	1.00	1.00	1.00
SSTENAP	AIRPORT TENANT	0.26	0.22	0.11	0.11	0.11
ROADOFAP	Off-airport Major Roadway	1.00	1.00	1.00	1.00	1.00
ROADONAP	On-airport Roadway	1.00	1.00	1.00	1.00	1.00
FREEWYAP	Freeway	1.00	1.00	1.00	1.00	1.00
EDMS	EDMS	1.00	1.00	1.00	1.00	1.00
AIRPORT	All sources within airport boundary	1.00	1.00	1.00	1.00	1.00
Background Sources						
CHEVRON	CHEVRON PRODUCTS NOx.	1.00	1.00	1.00	1.00	0.26
MARINE	Marine Vessels	0.52	0.51	0.48	0.42	0.52
CAONRDBK	Minor On-road Sources	1.00	1.00	1.00	1.00	1.00
CAOFFBK	Off-road Equipment	1.00	1.00	1.00	1.00	1.00
CAAGGBK	Aggregate Stationary Sources	1.00	1.00	1.00	1.00	1.00
CAAREABK	Area wide Sources	1.00	1.00	1.00	1.00	1.00
SEGUNDO	El Segundo Power Plant	0.55	0.56	0.55	0.56	0.55
SSOTHBK	OTHER OFF-AIRPORT STATIONARY SOURCE	1.00	1.00	1.00	1.00	1.00
SCTRGOOD	Scattergood Power Plant	0.94	0.95	0.94	0.93	0.94
ROADOFBK	Off-airport Major Roadway	1.00	1.00	1.00	1.00	1.00
FREEWYBK	Freeway	1.00	1.00	1.00	1.00	1.00
BACKGROUND	All sources outside airport boundary	1.00	1.00	1.00	1.00	1.00

* All ratios less than 1.0 are shown shaded in red. When a ratio was less than 1.0, it indicated that the maximum was predicted at flag-pole receptors aloft rather than at the lowest elevation of 2m. The actual receptors where the maxima are predicted are shown in Table 9A-8.

Table 9A-7. Heat map of elevation (meters) where maximum one-hour concentration was modeled by AERMOD.*

		Summer Max 1-hr				
Source Group	Description	CO	NO_x	$PM_{2.5}$	SO_x	VOC
ALL	ALL	2	2	2	2	2
Airport-related Sources						
APPROACH	Aircraft Approach	22	22	22	22	22
TAKEOFF	Aircraft Takeoff	12	12	12	12	12
LANDING	Aircraft Landing	12	12	12	12	12
TAXIQ	Aircraft Taxi/Queue	12	12	12	12	12
GATES	APU, GSE, and Aircraft Startup	2	2	2	2	2
PARKING	On-airport Parking	12	2	12	2	12
STATSRCS	On-airport LAWA-Owned Stationary Sources	7	7	27	7	22
CAONRDAP	Minor On-road Sources	2	2	2	2	2
CAOFFAP	Off-road Equipment	2	2	2	2	2
CAAGGAP	Aggregate Stationary Sources	2	2	2	2	2
COGEN	LAWA COGEN	27	27	27	27	27
CAAREAAP	Area wide Sources	2	2	2	2	2
SSTENAP	AIRPORT TENANT	27	27	27	27	27
ROADOFAP	Off-airport Major Roadway	2	2	2	2	2
ROADONAP	On-airport Roadway	2	2	2	2	2
FREEWYAP	Freeway	2	2	2	2	2
EDMS	EDMS	2	2	2	12	2
AIRPORT	All sources within airport boundary	2	2	2	12	2
Background Sources						
CHEVRON	CHEVRON PRODUCTS CO.	2	2	2	2	27
MARINE	Marine Vessels	27	27	27	27	27
CAONRDBK	Minor On-road Sources	2	2	2	2	2
CAOFFBK	Off-road Equipment	2	2	2	2	2
CAAGGBK	Aggregate Stationary Sources	2	2	2	2	2
CAAREABK	Area wide Sources	2	2	2	2	2
SEGUNDO	El Segundo Power Plant	27	27	27	27	27
SSOTHBK	OTHER OFF-AIRPORT STATIONARY SOURCE	2	2	2	2	2
SCTRGOOD	Scattergood Power Plant	27	27	27	27	27
ROADOFBK	Off-airport Major Roadway	2	2	2	2	2
FREEWYBK	Freeway	2	2	2	2	2
BACKGROUND	All sources outside airport boundary	2	2	2	2	2

Legend for flag-pole heights: Green 2m, Yellow 7m, Orange 12m, Red 22m, Deep Red 27m.

*Values in colored cells are the elevations of flag-pole receptors modeled in AERMOD. The 'heat map' indicates the ranges in elevation where the maximum was predicted by AERMOD.

Table 9A-8. Heat map of elevation (meters) where maximum Summer Season average was modeled by AERMOD.*

		Summer Max Season Average				
Source Group	Description	CO	NOx	$PM_{2.5}$	SOx	VOC
ALL	ALL	2	2	2	2	2
Airport-Related Sources						
APPROACH	Aircraft Approach	22	22	22	22	22
TAKEOFF	Aircraft Takeoff	12	12	12	12	12
LANDING	Aircraft Landing	12	12	12	12	12
TAXIQ	Aircraft Taxi/Queue	12	12	12	12	12
GATES	APU, GSE, and Aircraft Startup	2	2	2	2	2
PARKING	On-airport Parking	12	2	12	2	12
STATSRCS	On-airport LAWA-Owned Stationary Sources	7	7	27	7	22
CAONRDAP	Minor On-road Sources	2	2	2	2	2
CAOFFAP	Off-road Equipment	2	2	2	2	2
CAAGGAP	Aggregate Stationary Sources	2	2	2	2	2
COGEN	LAWA COGEN	27	27	27	27	27
CAAREAAP	Area wide Sources	2	2	2	2	2
SSTENAP	AIRPORT TENANT	27	27	27	27	27
ROADOFAP	Off-airport Major Roadway	2	2	2	2	2
ROADONAP	On-airport Roadway	2	2	2	2	2
FREEWYAP	Freeway	2	2	2	2	2
EDMS	EDMS	2	2	2	12	2
AIRPORT	All sources within airport boundary	2	2	2	12	2
Background Sources						
CHEVRON	CHEVRON PRODUCTS CO.	2	2	2	2	27
MARINE	Marine Vessels	27	27	27	27	27
CAONRDBK	Minor On-road Sources	2	2	2	2	2
CAOFFBK	Off-road Equipment	2	2	2	2	2
CAAGGBK	Aggregate Stationary Sources	2	2	2	2	2
CAAREABK	Area wide Sources	2	2	2	2	2
SEGUNDO	El Segundo Power Plant	27	27	27	27	27
SSOTHBK	OTHER OFF-AIRPORT STATIONARY SOURCE	2	2	2	2	2
SCTRGOOD	Scattergood Power Plant	27	27	27	27	27
ROADOFBK	Off-airport Major Roadway	2	2	2	2	2
FREEWYBK	Freeway	2	2	2	2	2
BACKGROUND	All sources outside airport boundary	2	2	2	2	2

Legend for flag-pole heights: Green 2m, Yellow 7m, Orange 12m, Red 22m, Deep Red 27m.

*Values in colored cells are the elevations of flag-pole receptors modeled in AERMOD. The 'heat map' indicates the ranges in elevation where the maximum was predicted by AERMOD.

I. Spatial Analyses

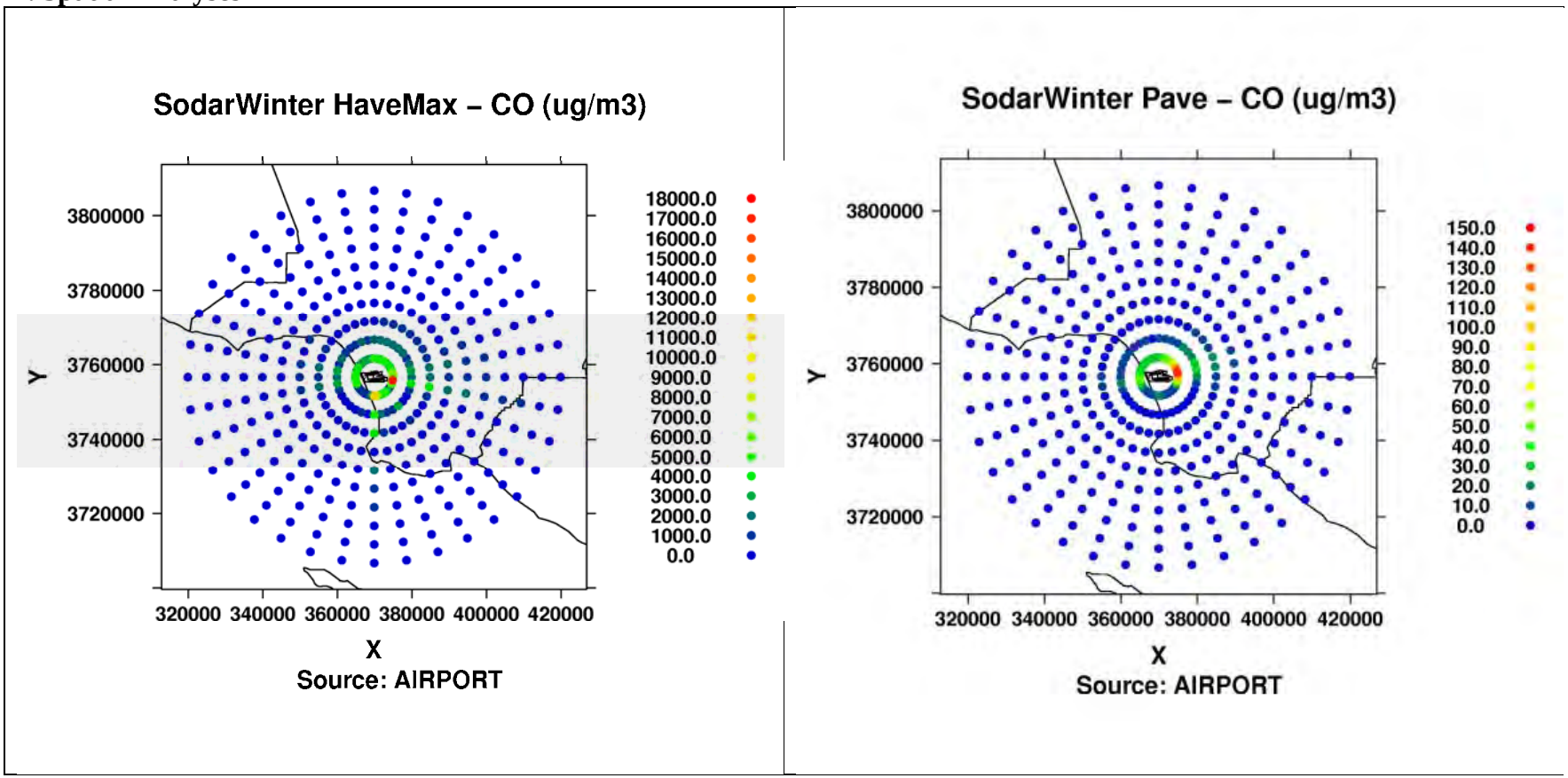

Figure 9A-1a: Modeled hourly max (left) and period average (right) CO concentrations from airport-related in Polar Grid of receptors during Winter Season.

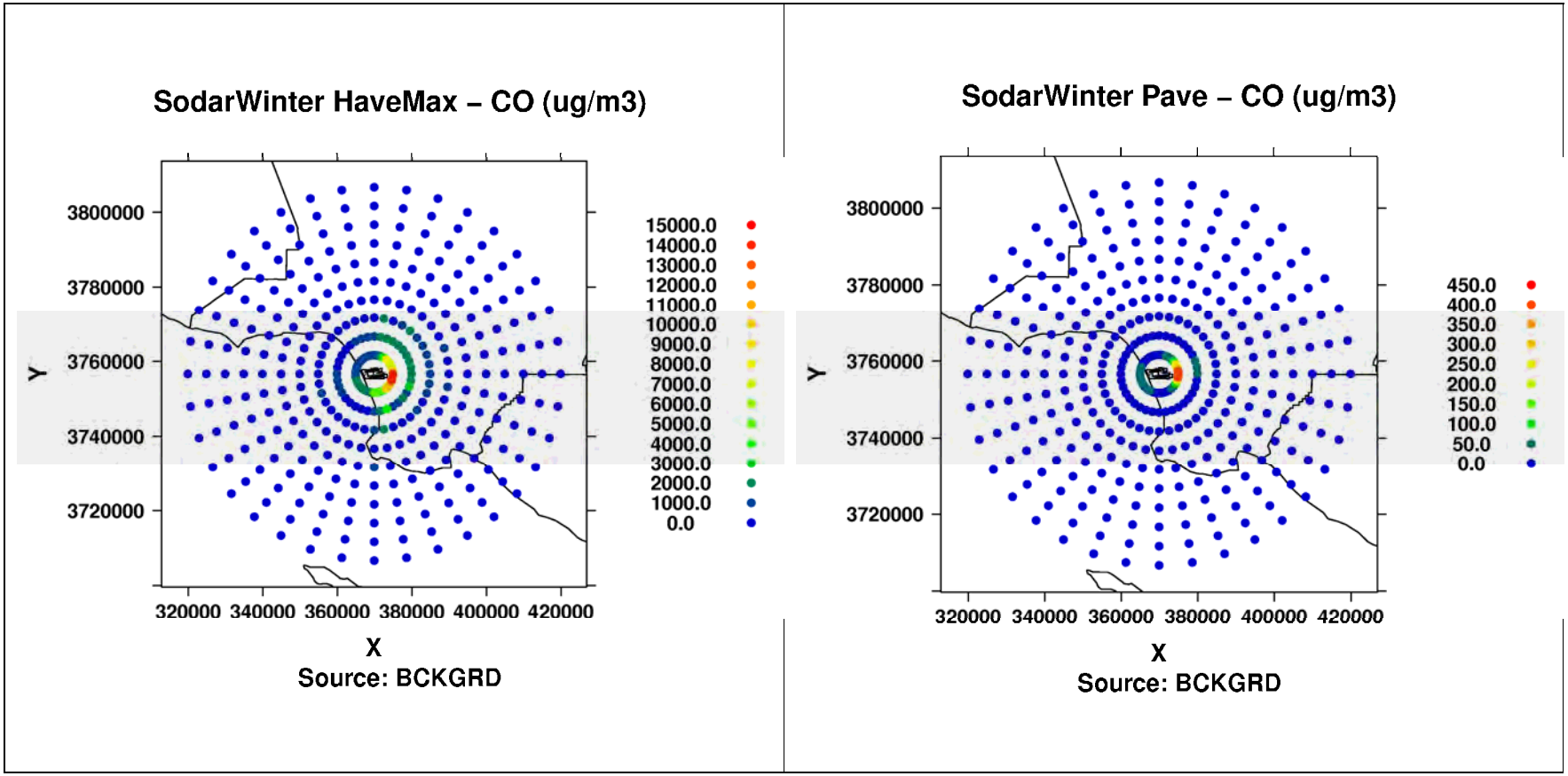

Figure 9A-1b: Modeled hourly max (left) and period average (right) CO concentrations from background sources in Polar Grid of receptors during Winter Season.

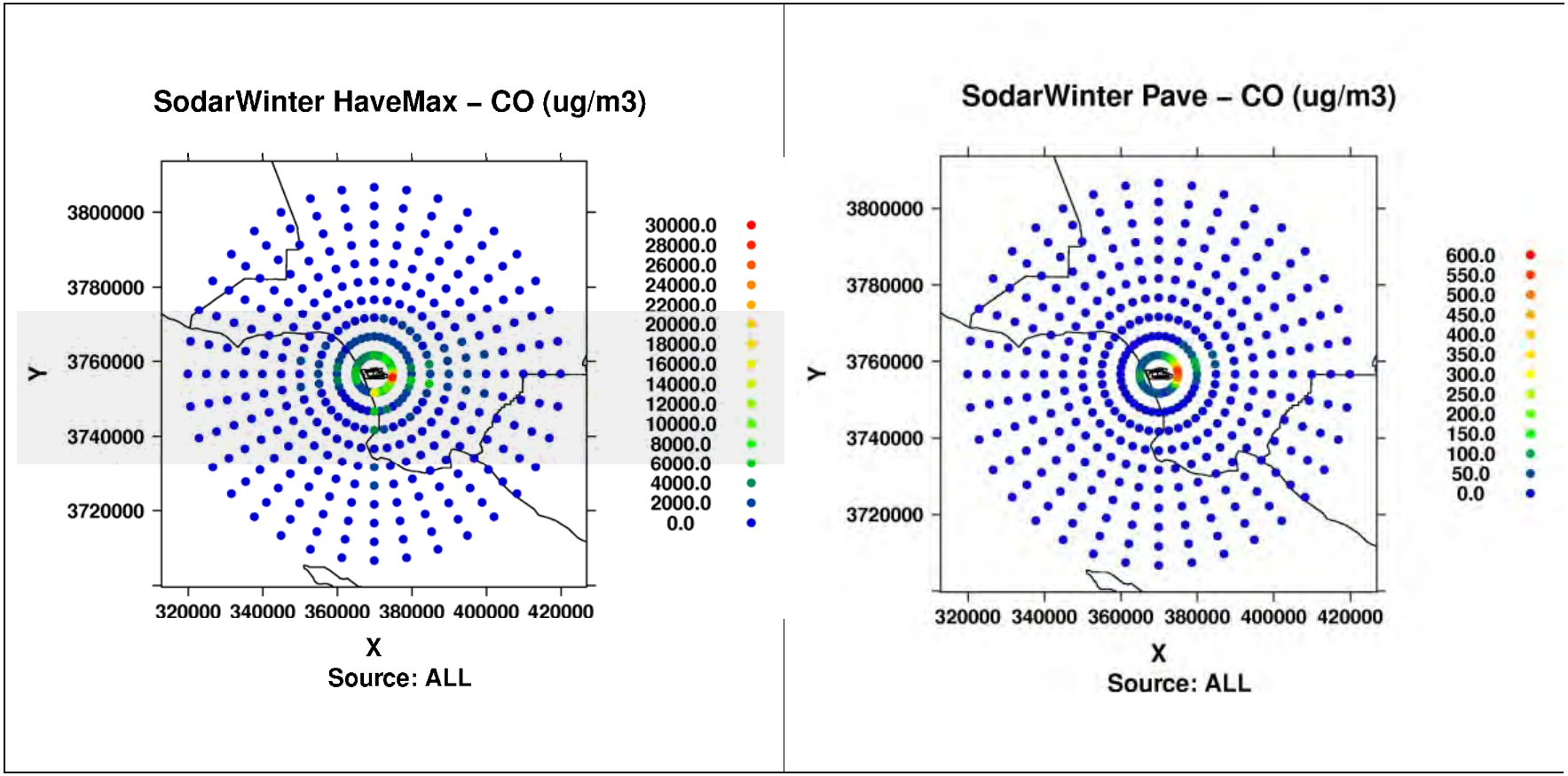

Figure 9A-1c: Modeled hourly max (left) and period average (right) CO concentrations from ALL sources in Polar Grid of receptors during Winter Season.

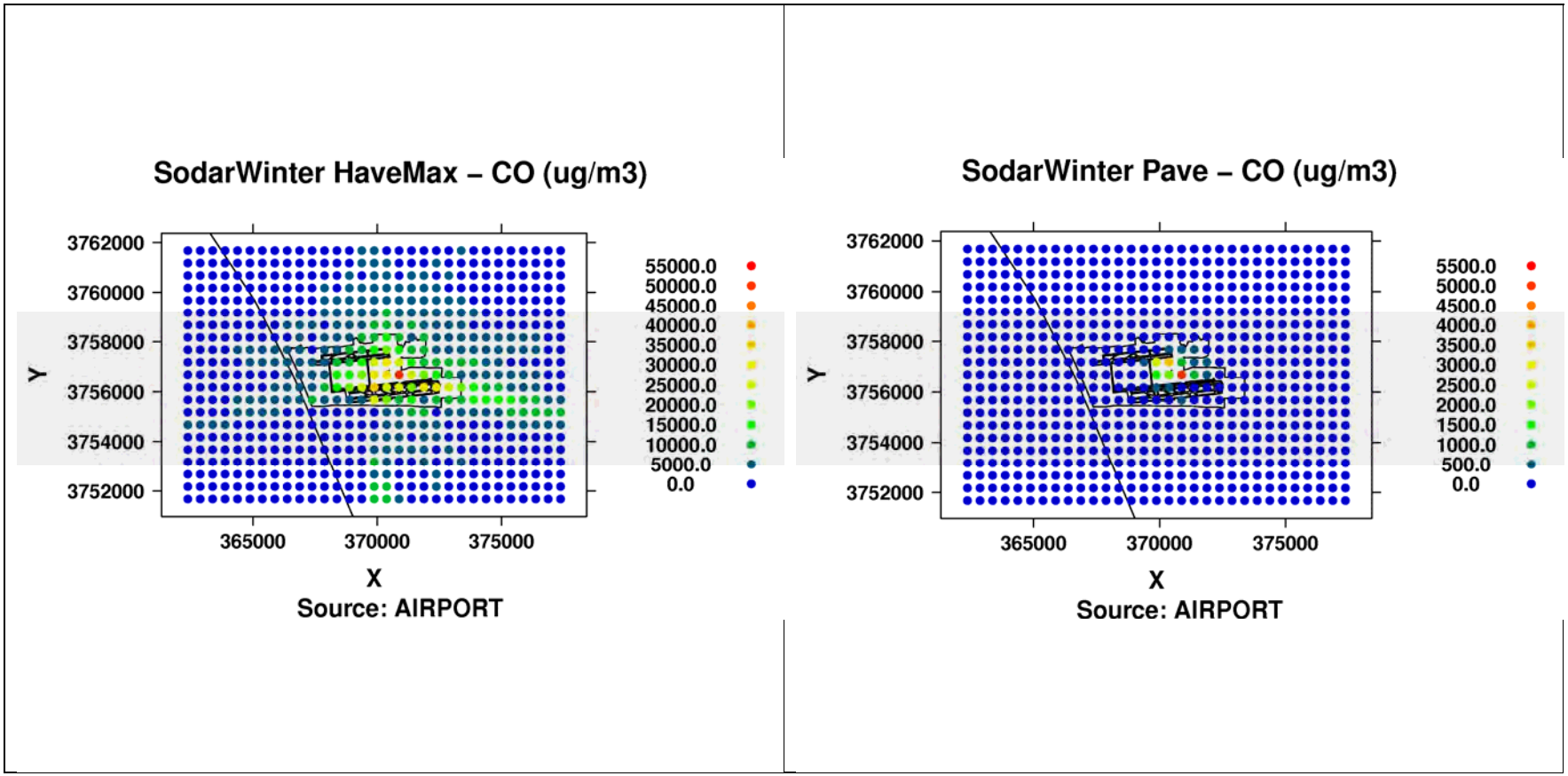

Figure 9A-2a: Modeled hourly max (left) and period average (right) CO concentrations from airport-related in Cartesian Grid of receptors during Winter Season.

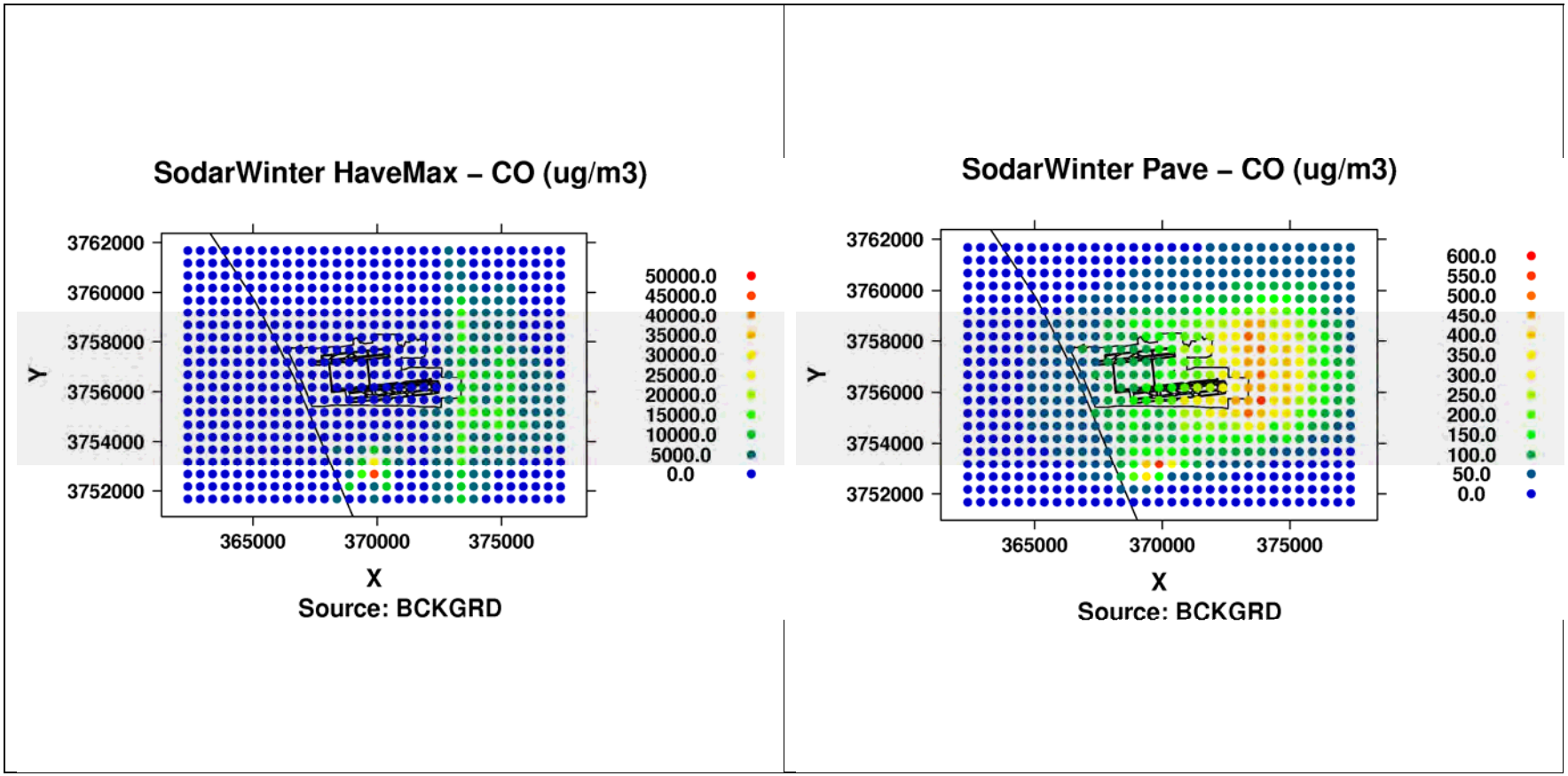

Figure 9A-2b: Modeled hourly max (left) and period average (right) CO concentrations from background sources in Cartesian Grid of receptors during Winter Season.

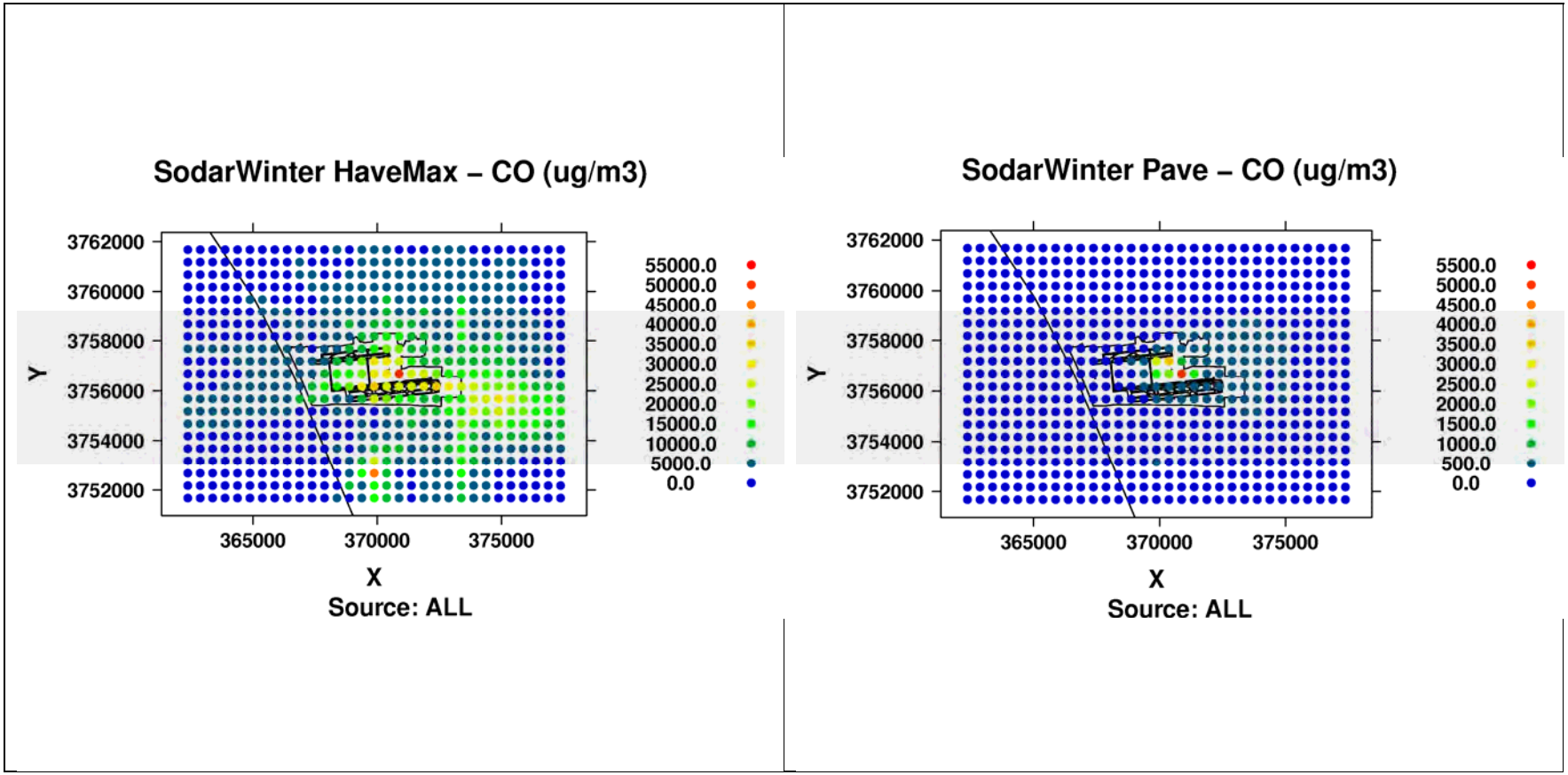

Figure 9A-2c: Modeled hourly max (left) and period average (right) CO concentrations from All sources in Cartesian Grid of receptors during Winter Season.

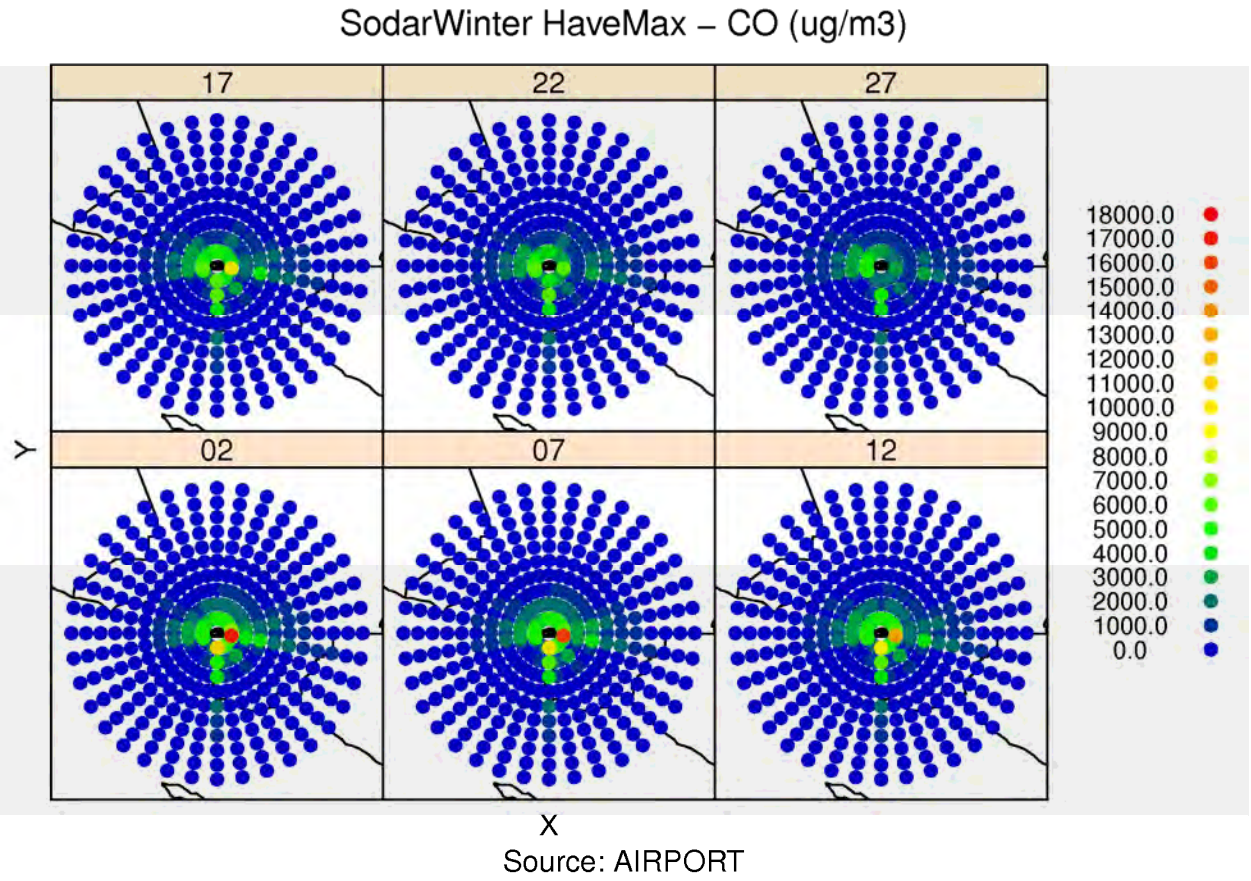

Figure 9A-3: Modeled hourly max CO concentrations from airport-related sources at flag-pole receptors at heights of 2m, 7m, 12m, 17m, 22m and 27m in Polar Grid of receptors during Winter Season.

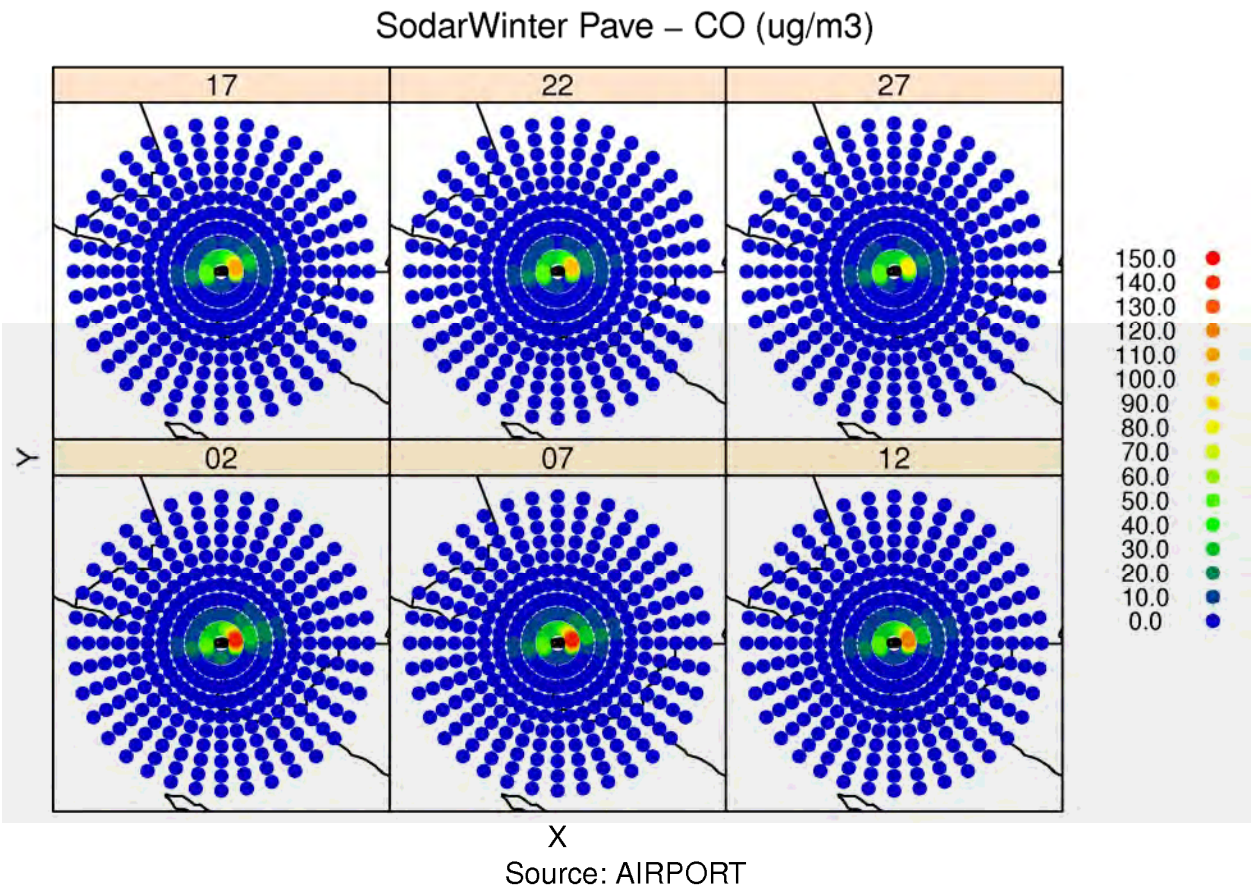

Figure 9A-4: Modeled period average CO concentrations from airport-related sources at flag-pole receptors at heights of 2m, 7m, 12m, 17m, 22m and 27m in Polar Grid of receptors during Winter Season.

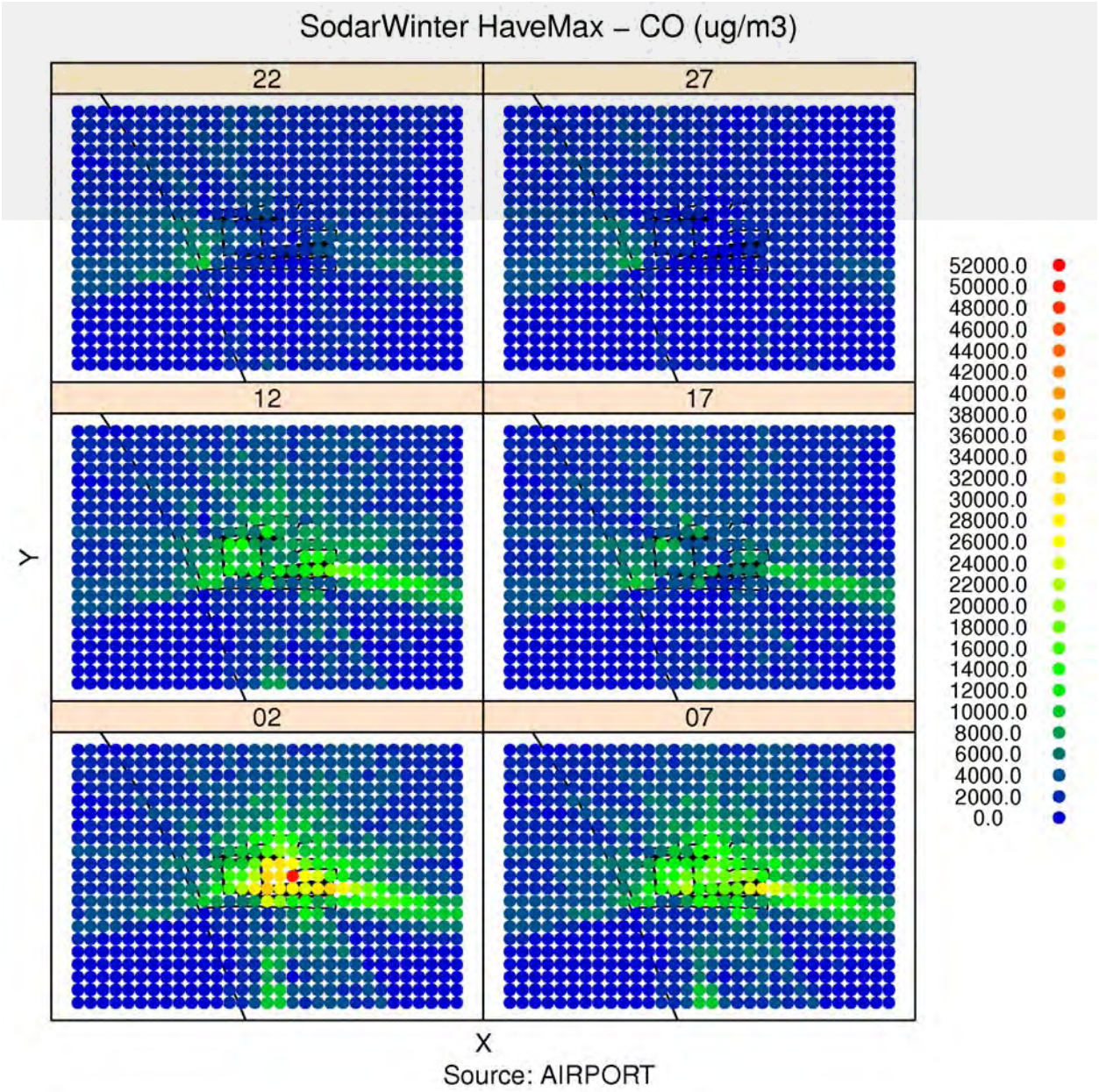

Figure 9A-5: Modeled hourly max CO concentrations from airport-related sources at flag-pole receptors at heights of 2m, 7m, 12m, 17m, 22m and 27m in Cartesian Grid of receptors during Winter Season.

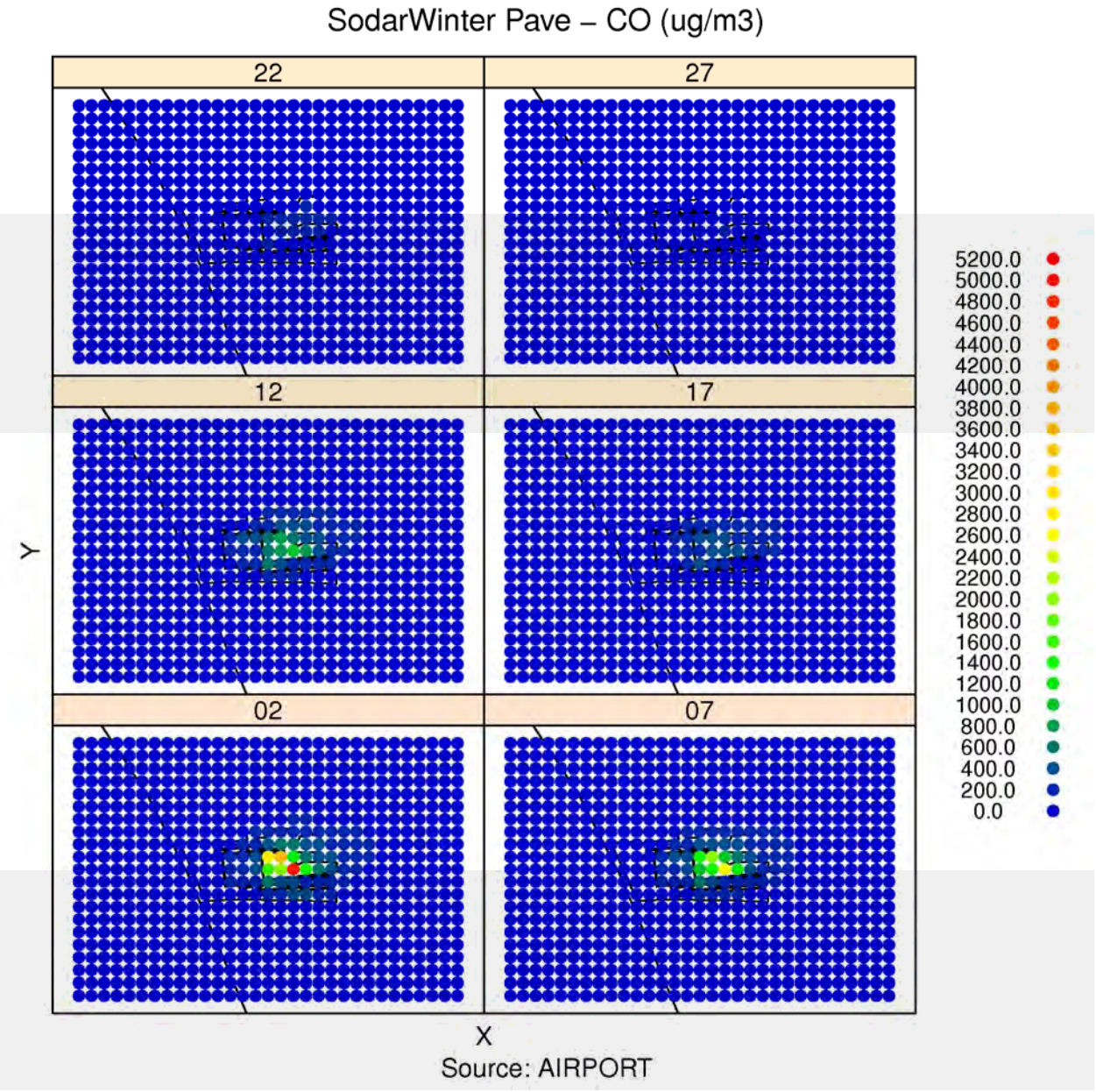

Figure 9A-6: Modeled period average CO concentrations from airport-related sources at flag-pole receptors at heights of 2m, 7m, 12m, 17m, 22m and 27m in Cartesian Grid of receptors during Winter Season.

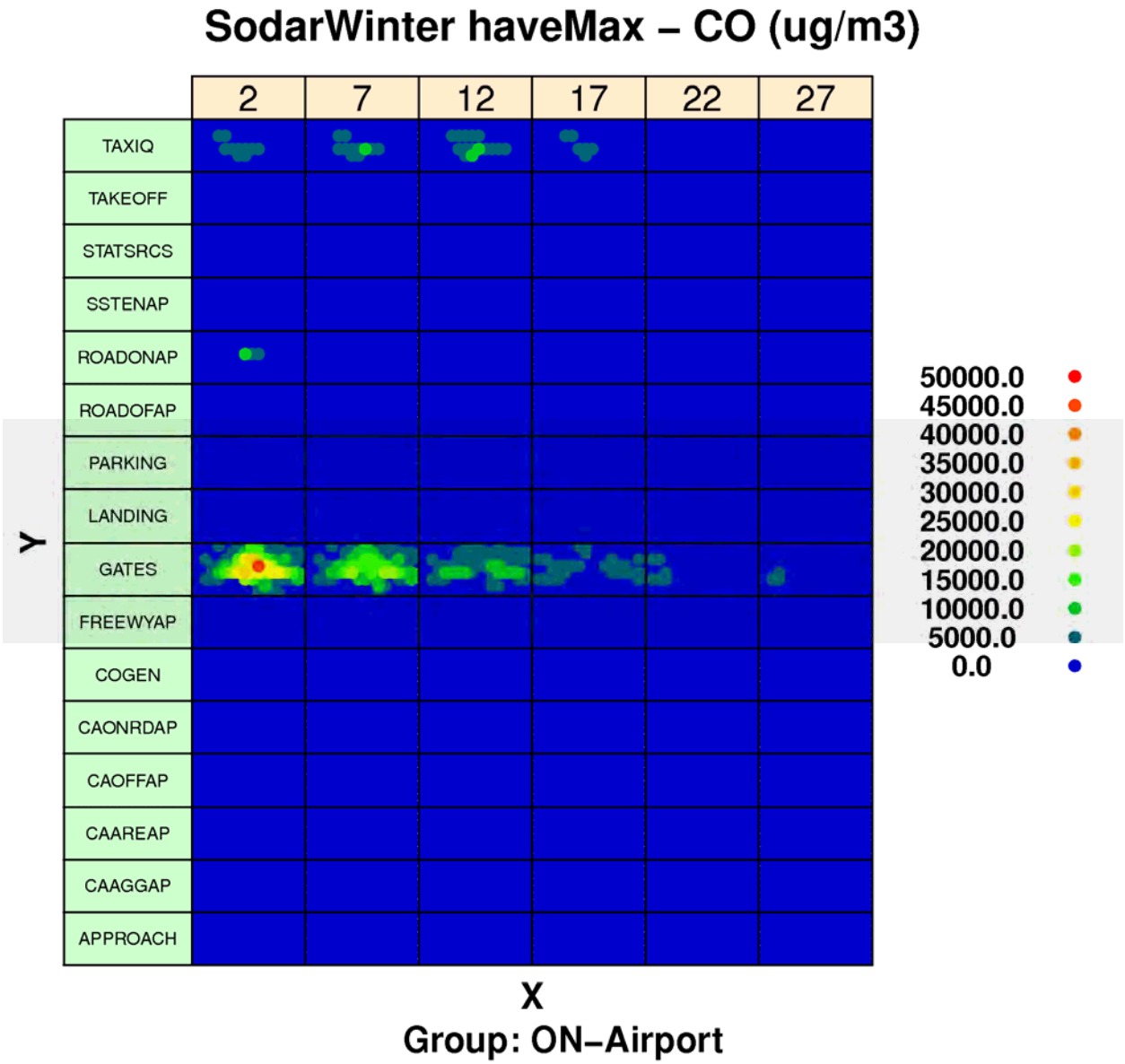

Figure 9A-7: Modeled hourly maximum CO concentrations from airport-related sources by source sector at flag-pole receptors at heights of 2m, 7m, 12m, 17m, 22m and 27m in Cartesian Grid of receptors during Winter Season.

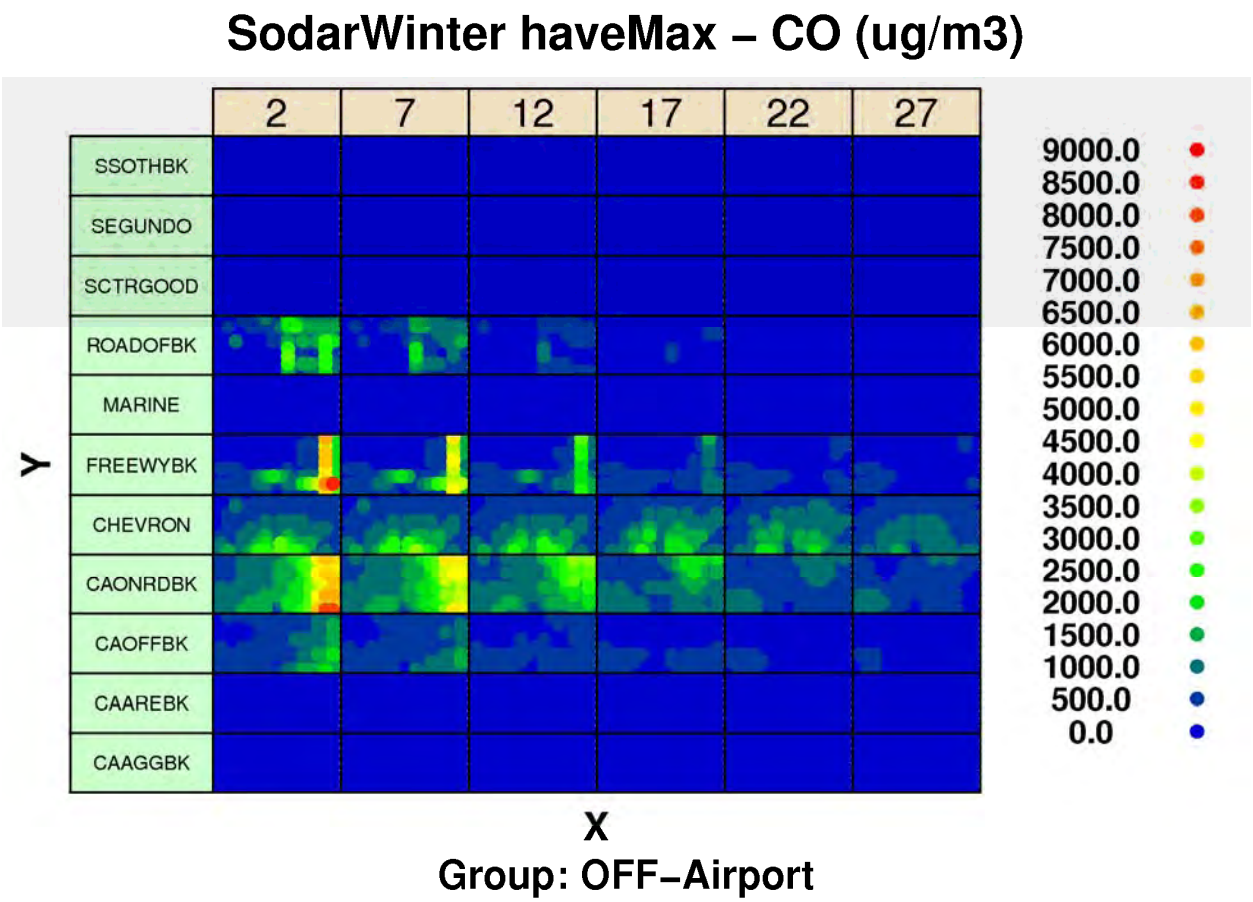

Figure 9A-8: Modeled hourly maximum CO concentrations from background sources by source sector at flag-pole receptors at heights of 2m, 7m, 12m, 17m, 22m and 27m in Cartesian Grid of receptors during Winter Season.

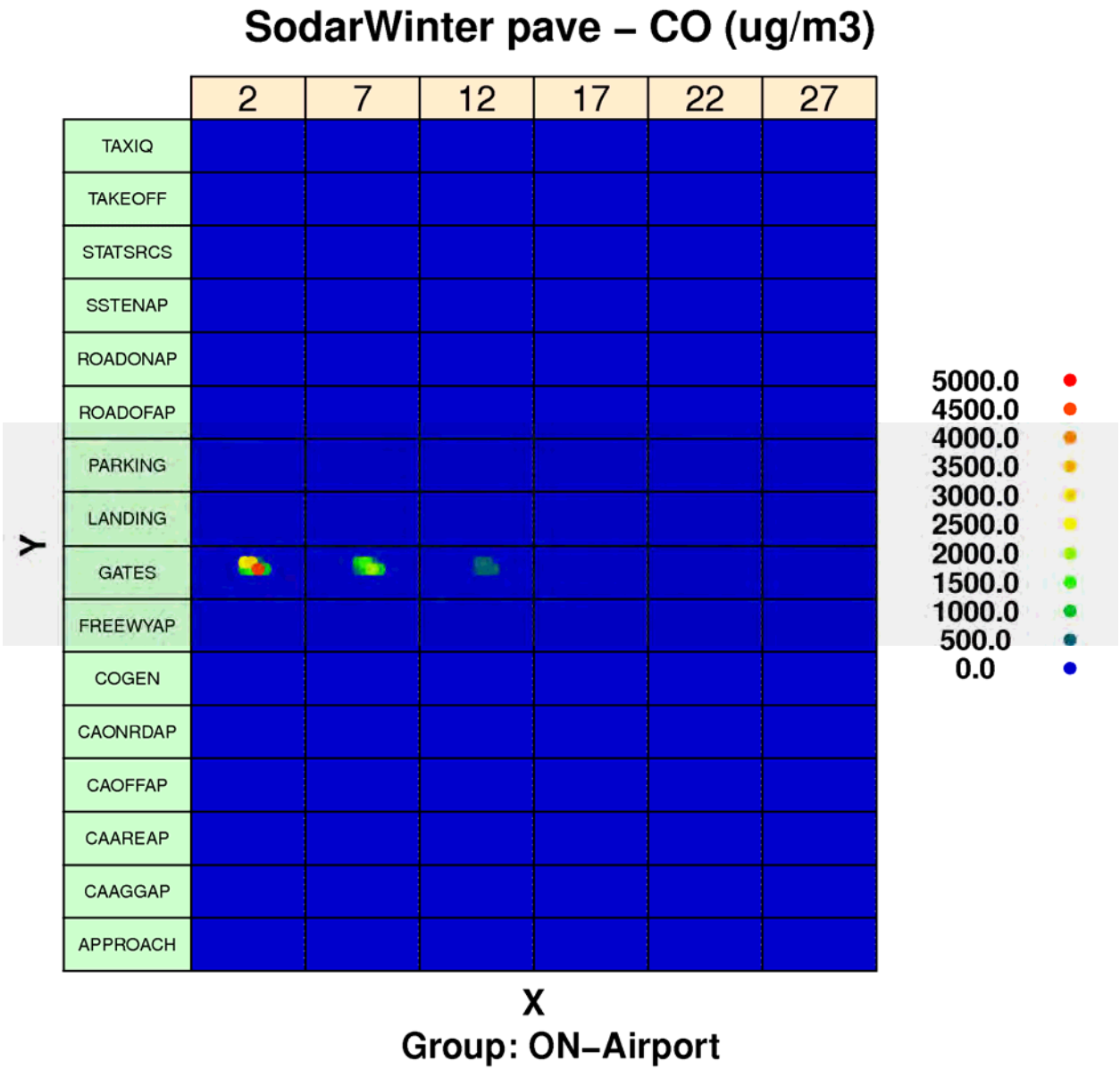

Figure 9A-9: Modeled period average CO concentrations from airport-related sources by source sector at flag-pole receptors at heights of 2m, 7m, 12m, 17m, 22m and 27m in Cartesian Grid of receptors during Winter Season.

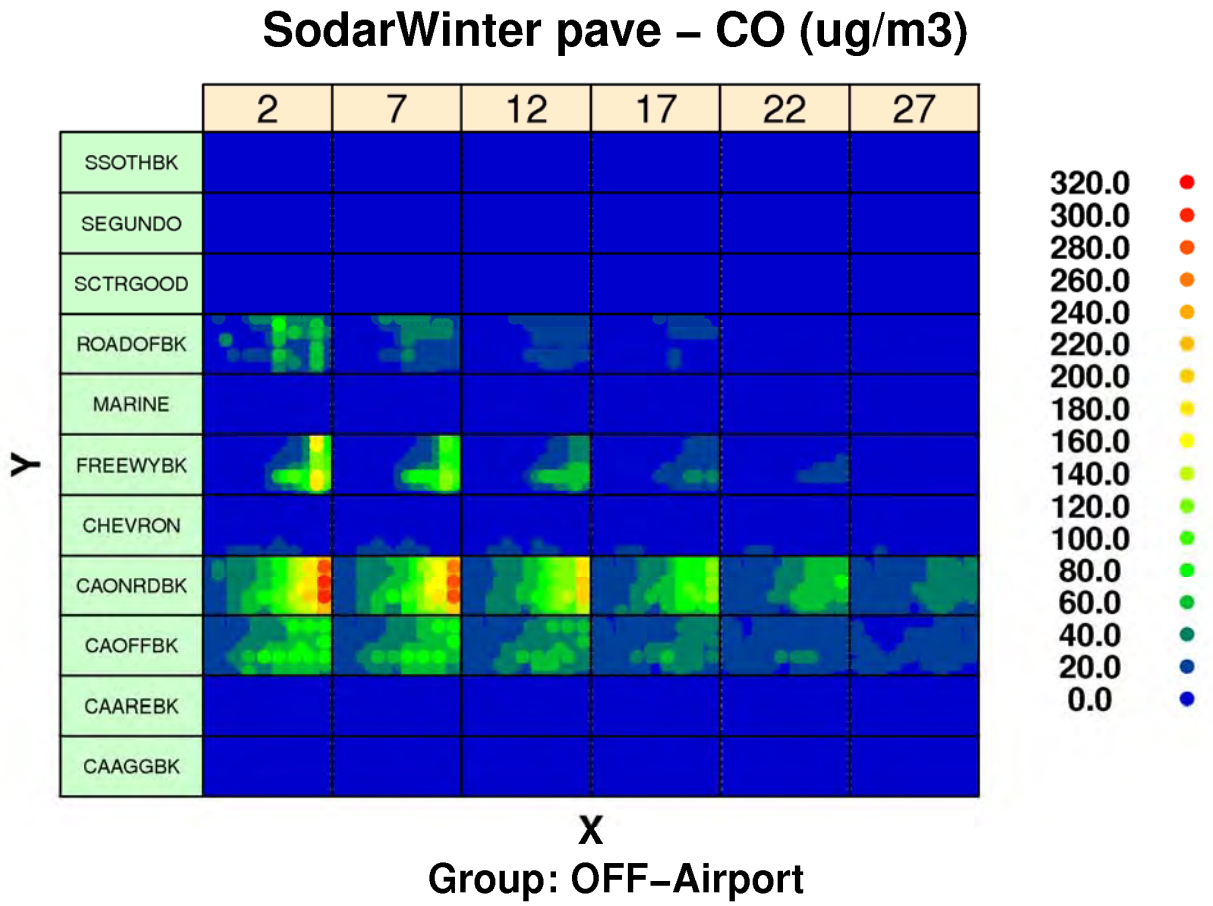

Figure 9A-10: Modeled period average CO concentrations from background sources by source sector at flag-pole receptors at heights of 2m, 7m, 12m, 17m, 22m and 27m in Cartesian Grid of receptors during Winter Season.

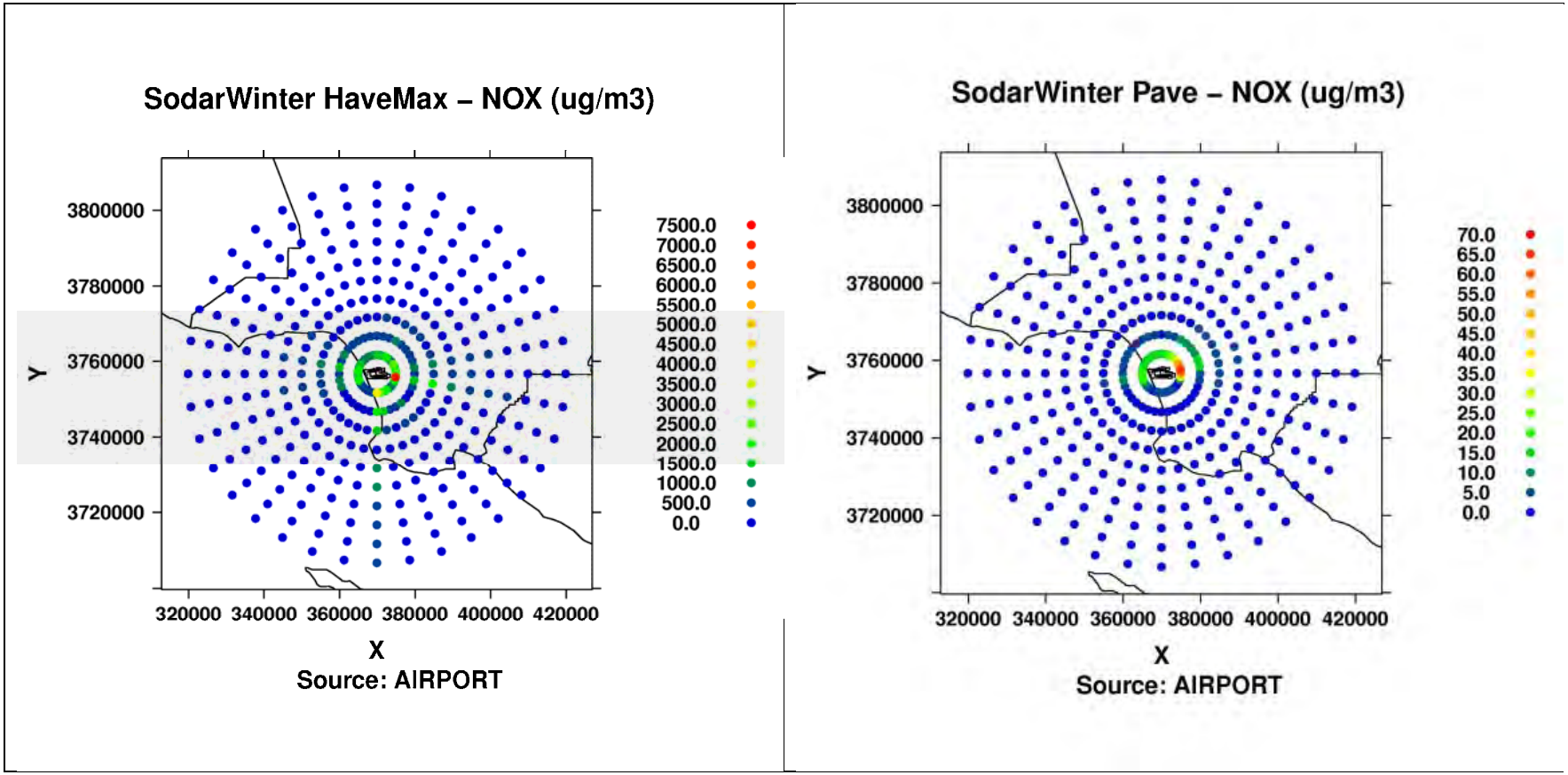

Figure 9A-11a: Modeled hourly max (left) and period average (right) NOx concentrations from airport-related in Polar Grid of receptors during Winter Season.

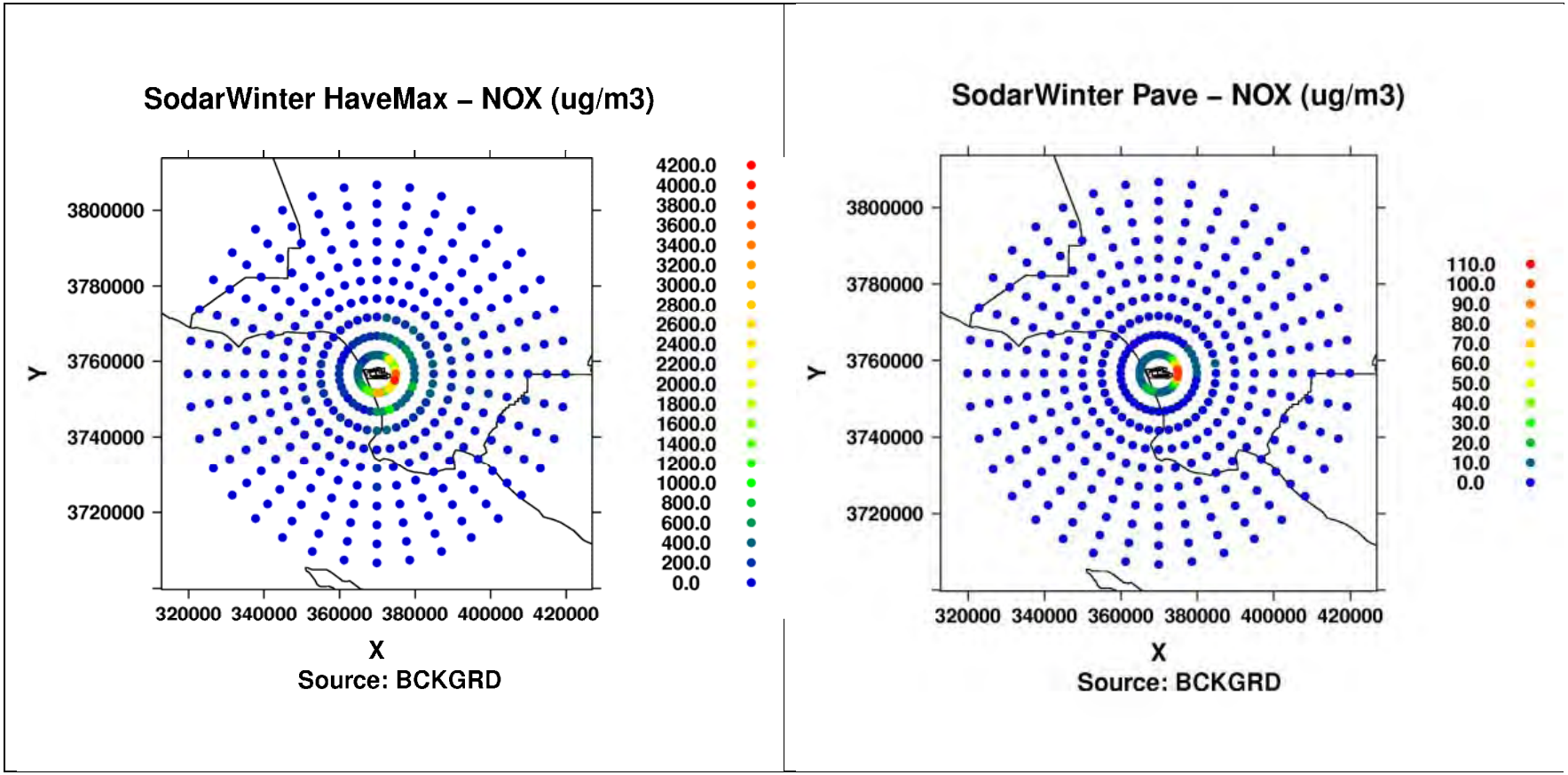

Figure 9A-11b: Modeled hourly max (left) and period average (right) NOx concentrations from background sources in Polar Grid of receptors during Winter Season.

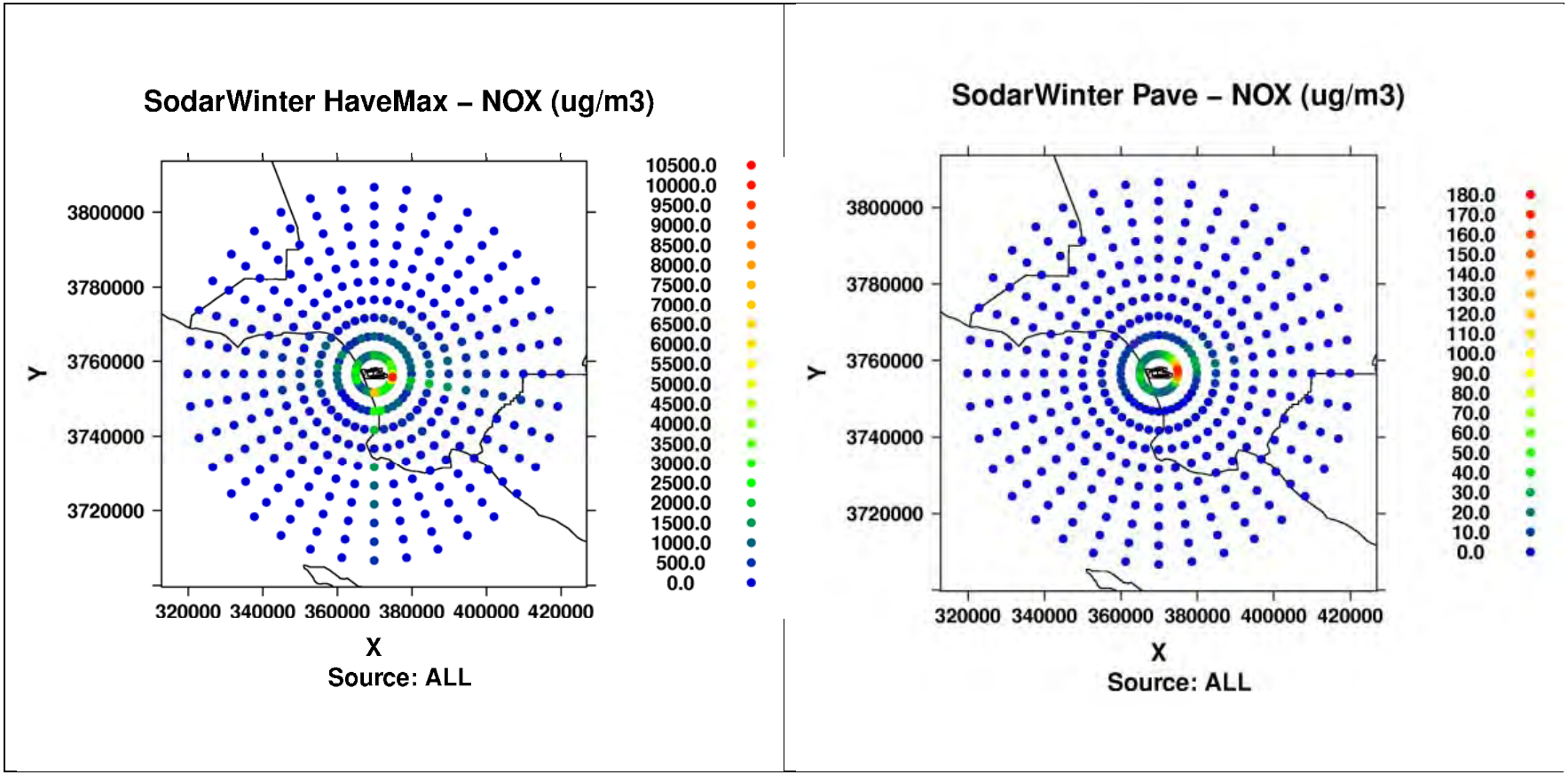

Figure 9A-11c: Modeled hourly max (left) and period average (right) NOx concentrations from airport-related (top), background sources (middle) and ALL (bottom) in Polar Grid of receptors during Winter Season.

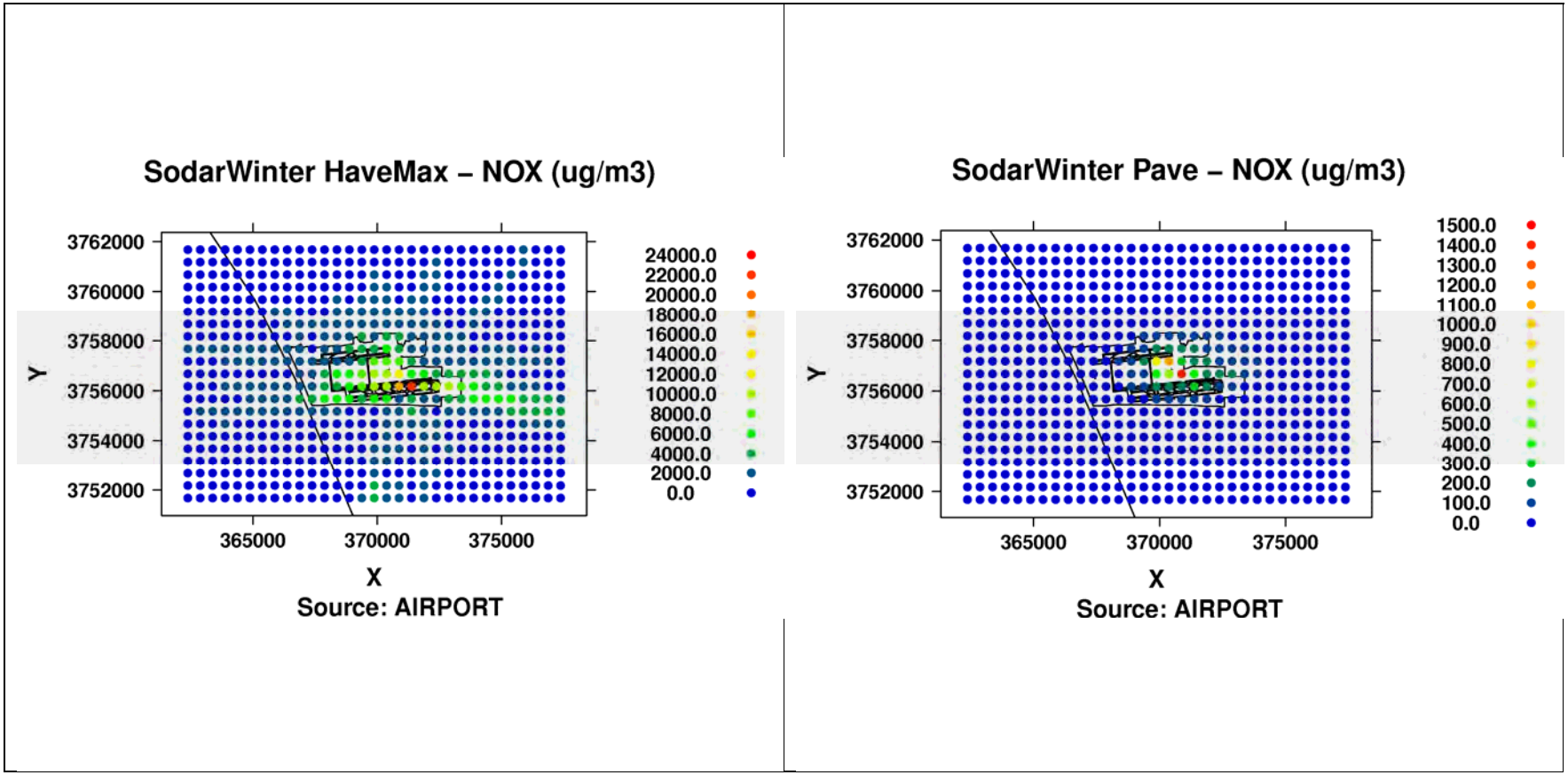

Figure 9A-12a: Modeled hourly max (left) and period average (right) NOx concentrations from airport-related in Cartesian Grid of receptors during Winter Season

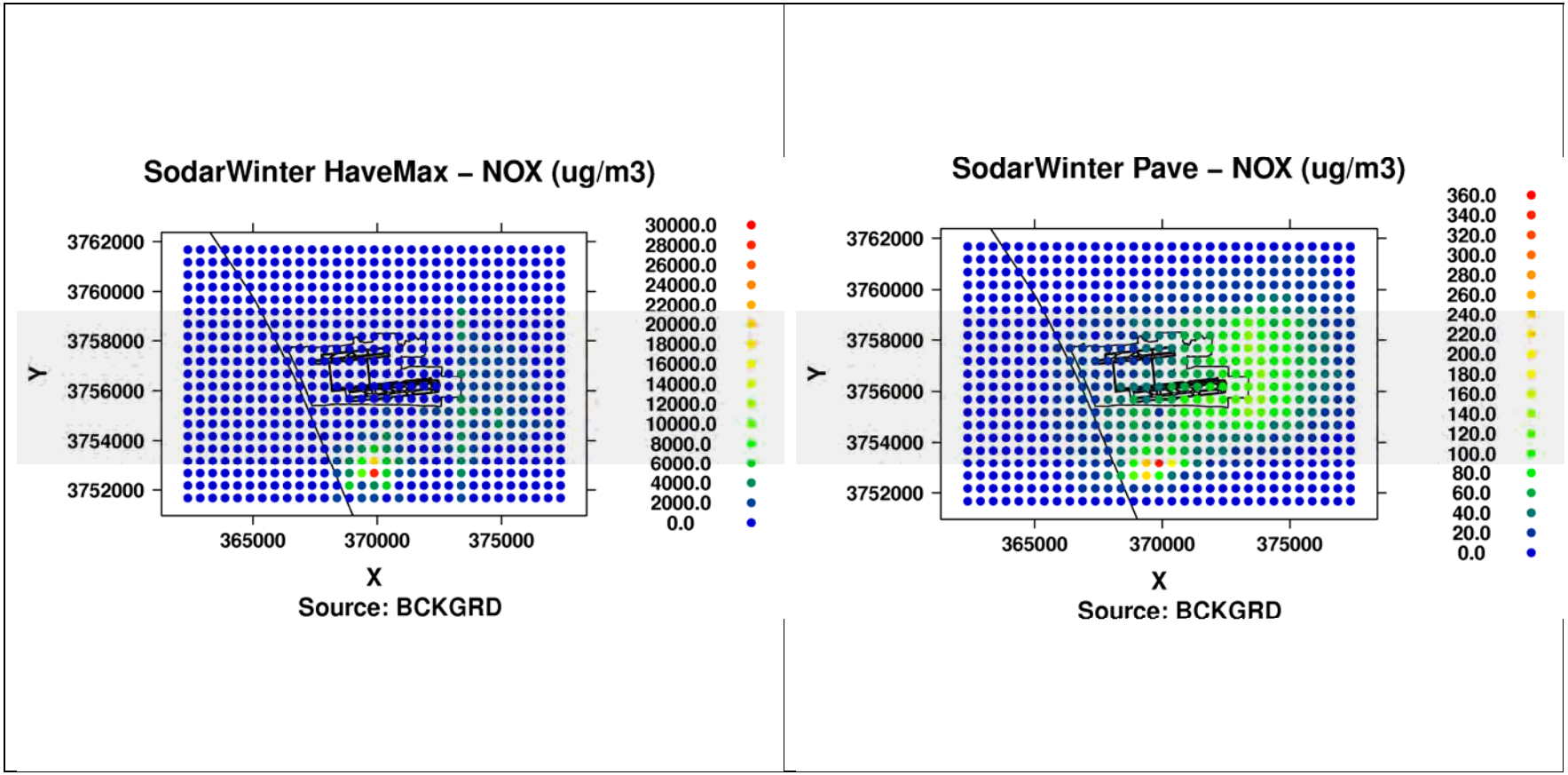

Figure 9A-12b: Modeled hourly max (left) and period average (right) NOx concentrations from background sources in Cartesian Grid of receptors during Winter Season

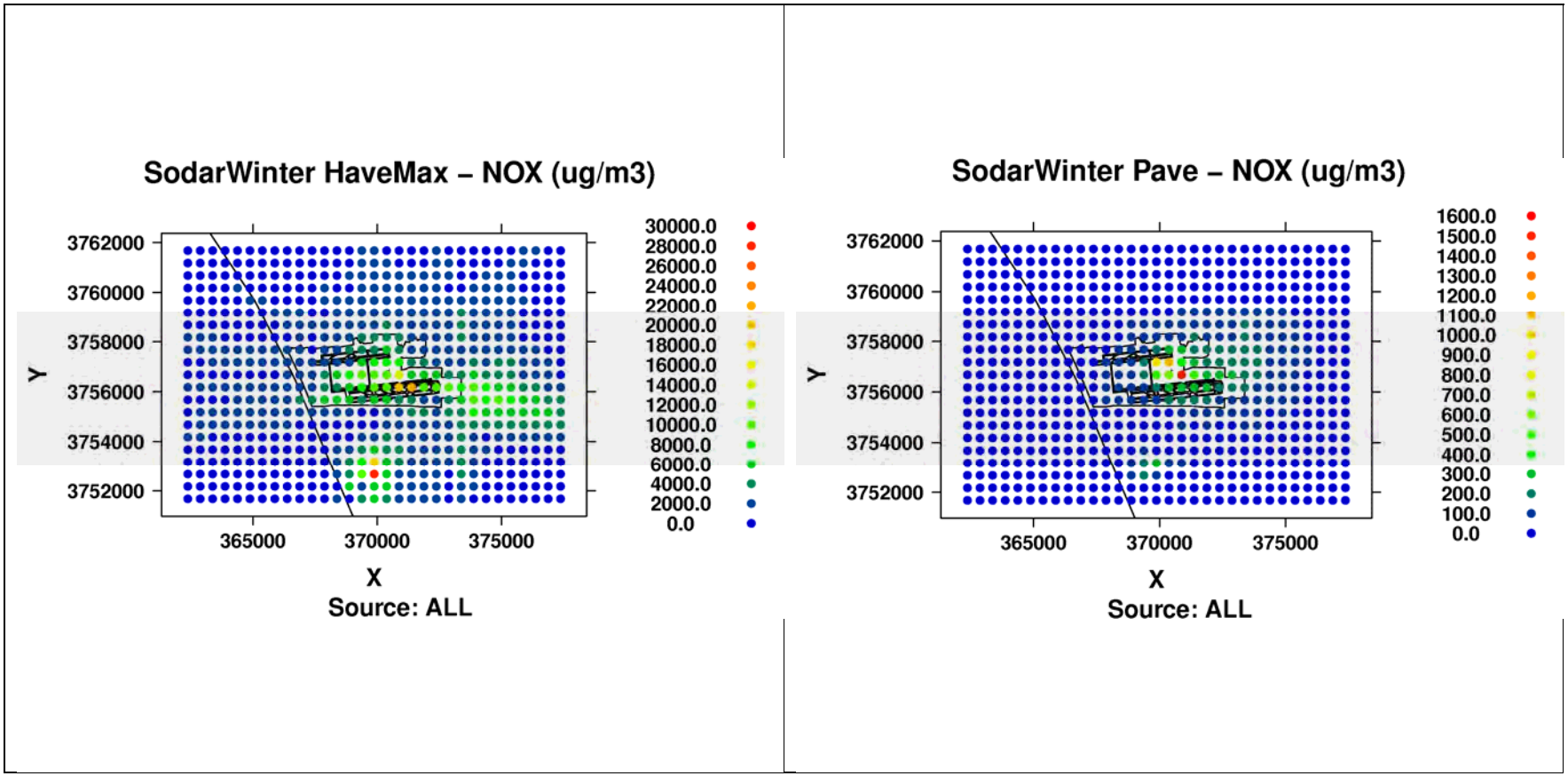

Figure 9A-12c: Modeled hourly max (left) and period average (right) NOx concentrations from ALL in Cartesian Grid of receptors during Winter Season.

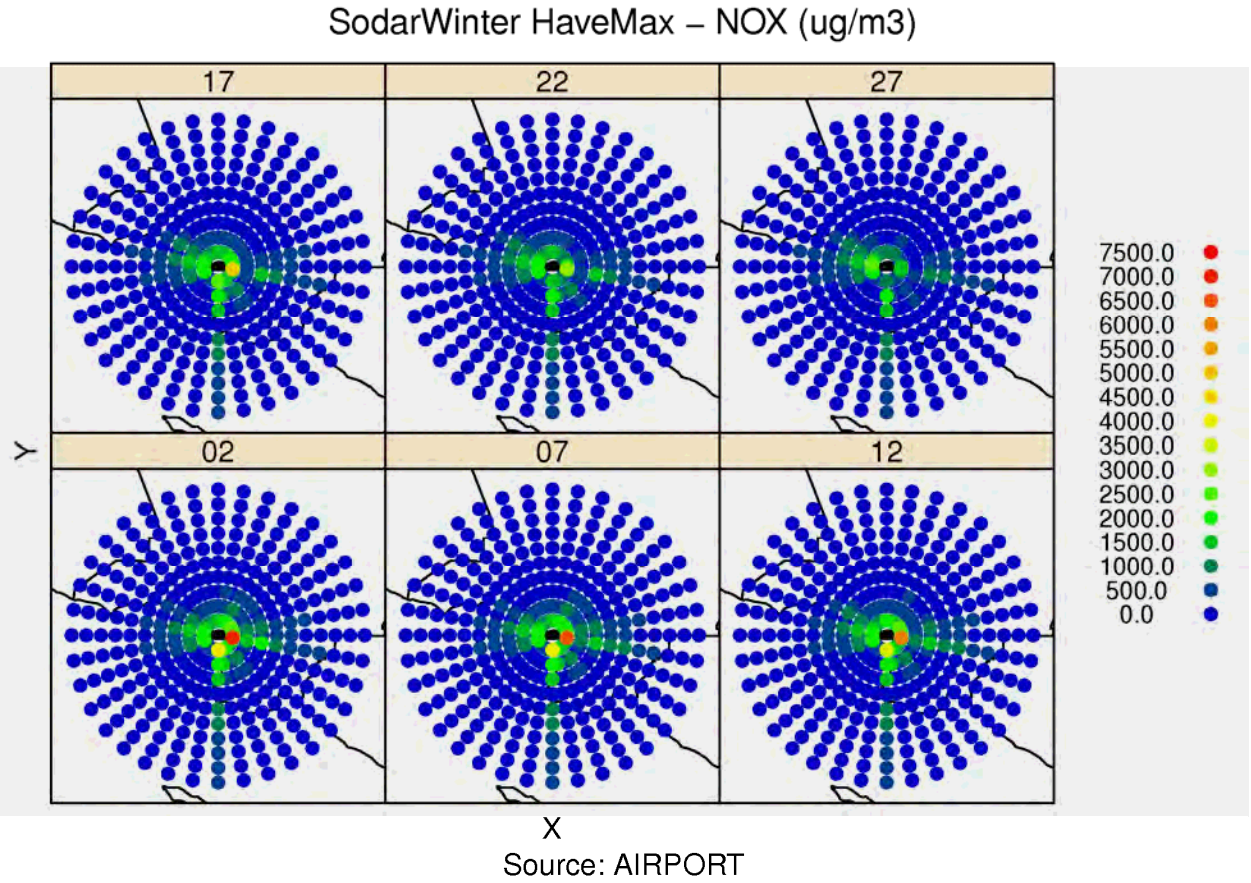

Figure 9A-13: Modeled hourly max NOx concentrations from airport-related sources at flag-pole receptors at heights of 2m, 7m, 12m, 17m, 22m and 27m in Polar Grid of receptors during Winter Season.

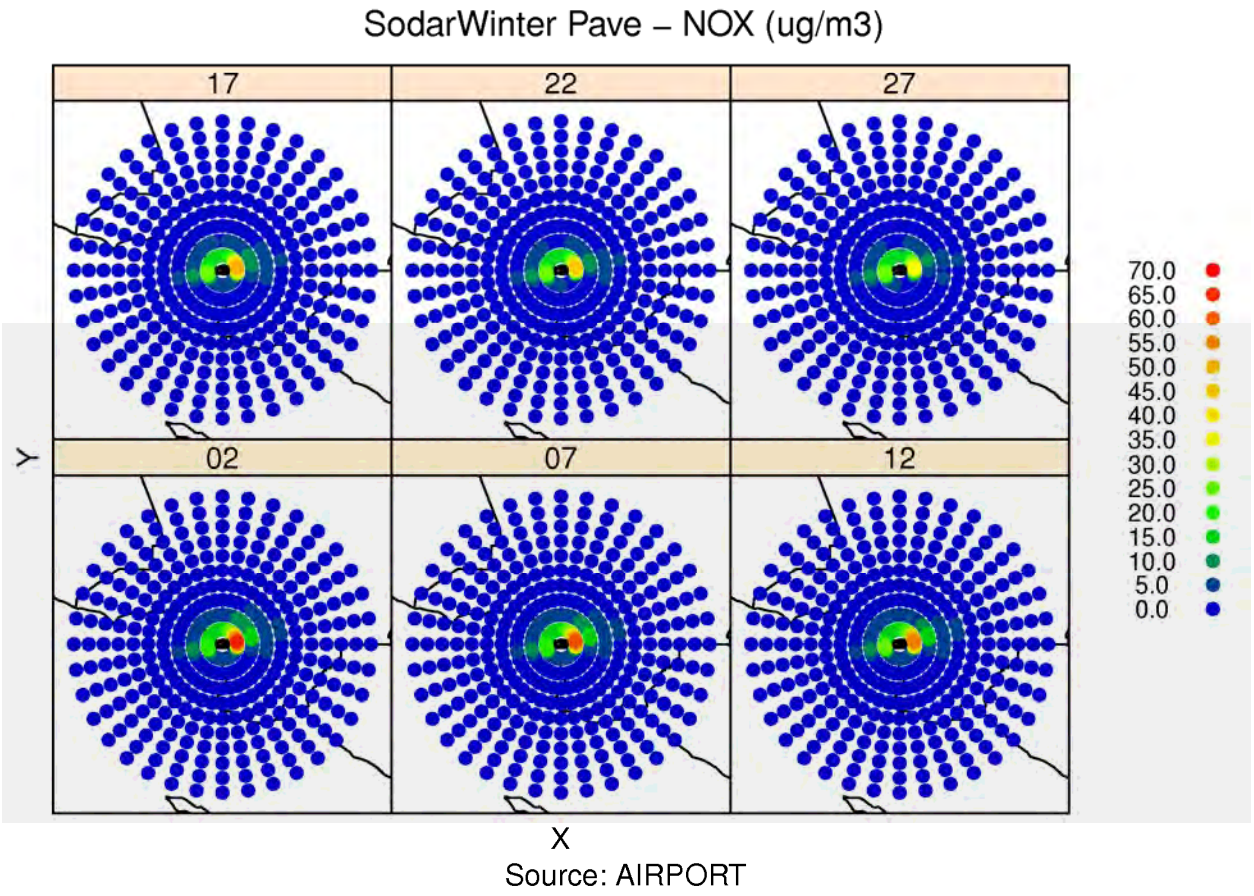

Figure 9A-14: Modeled period average NOx concentrations from airport-related sources at flag-pole receptors at heights of 2m, 7m, 12m, 17m, 22m and 27m in Polar Grid of receptors during Winter Season.

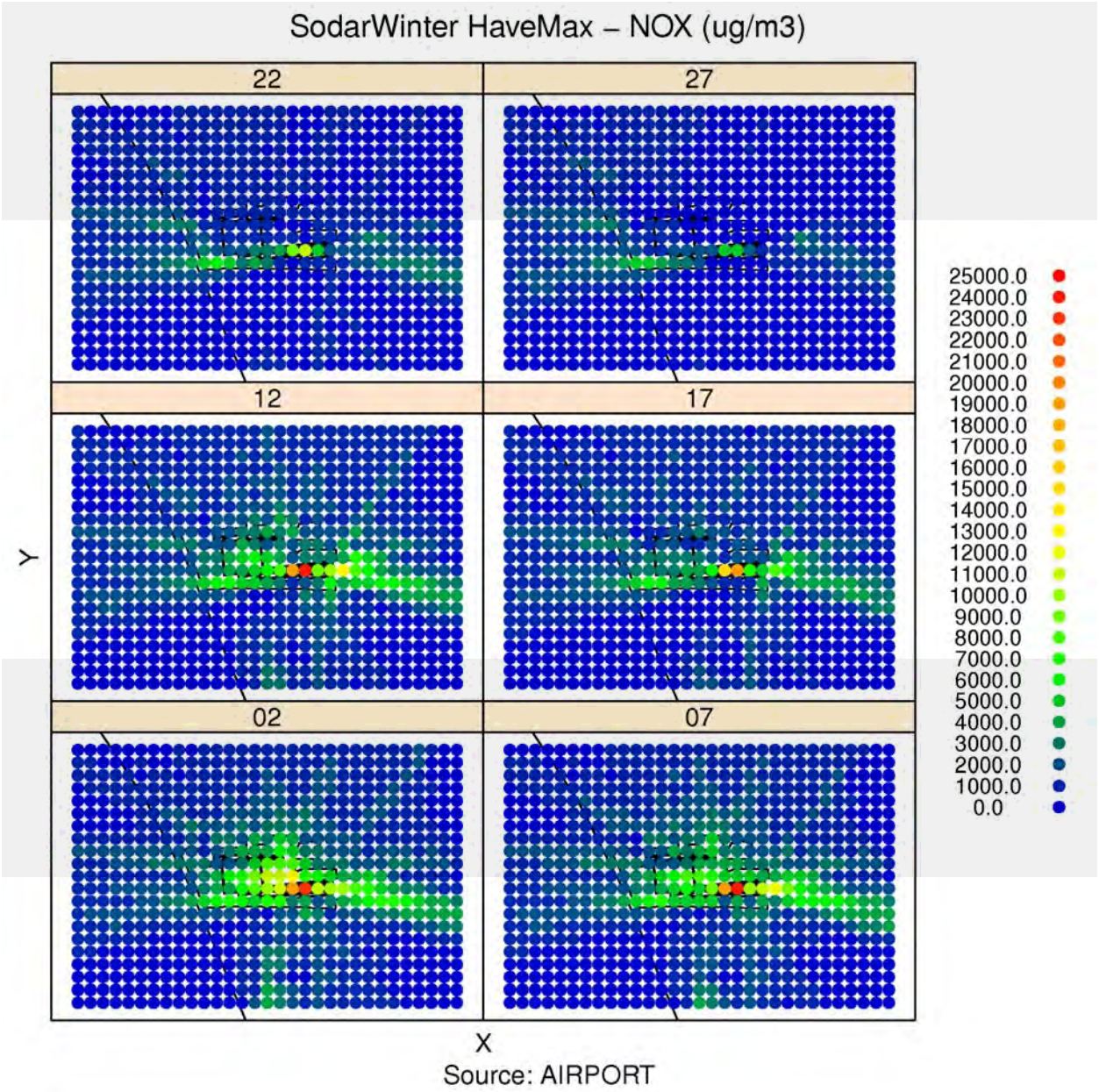

Figure 9A-15: Modeled hourly max NOx concentrations from airport-related sources at flag-pole receptors at heights of 2m, 7m, 12m, 17m, 22m and 27m in Cartesian Grid of receptors during Winter Season.

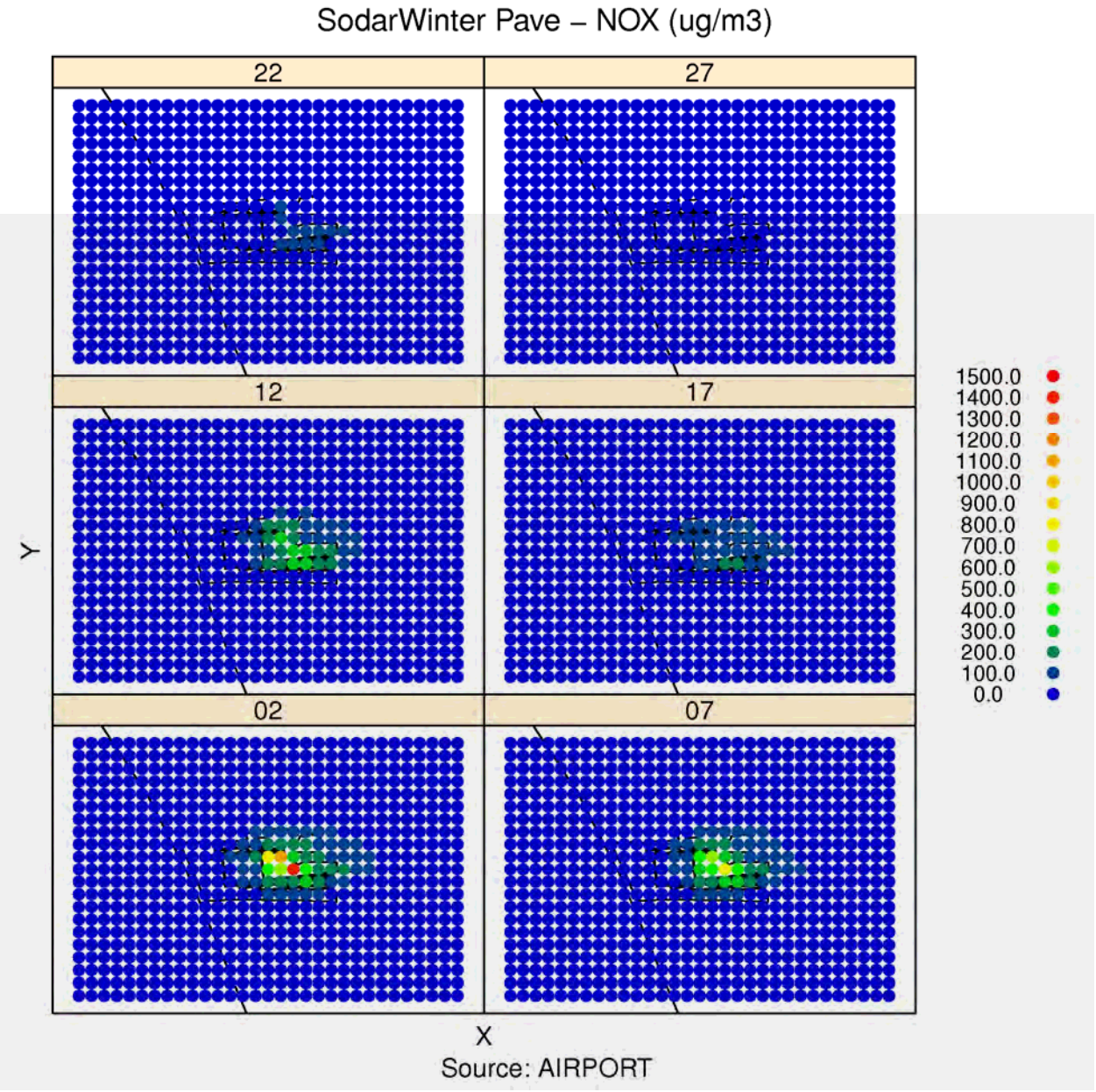

Figure 9A-16: Modeled period average NOx concentrations from airport-related sources at flag-pole receptors at heights of 2m, 7m, 12m, 17m, 22m and 27m in Cartesian Grid of receptors during Winter Season.

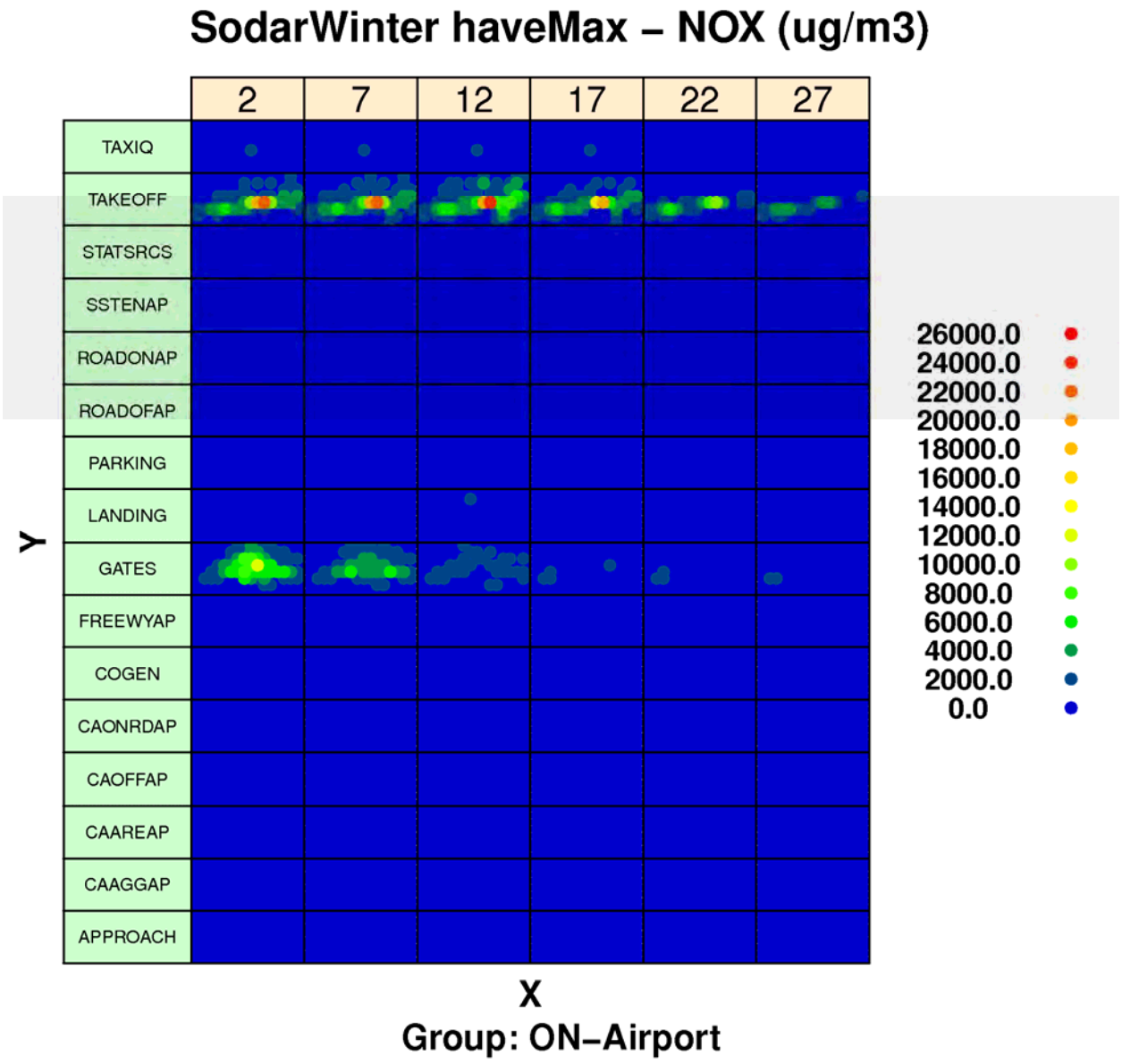

Figure 9A-17: Modeled hourly maximum NOx concentrations from airport-related sources by source sector at flag-pole receptors at heights of 2m, 7m, 12m, 17m, 22m and 27m in Cartesian Grid of receptors during Winter Season.

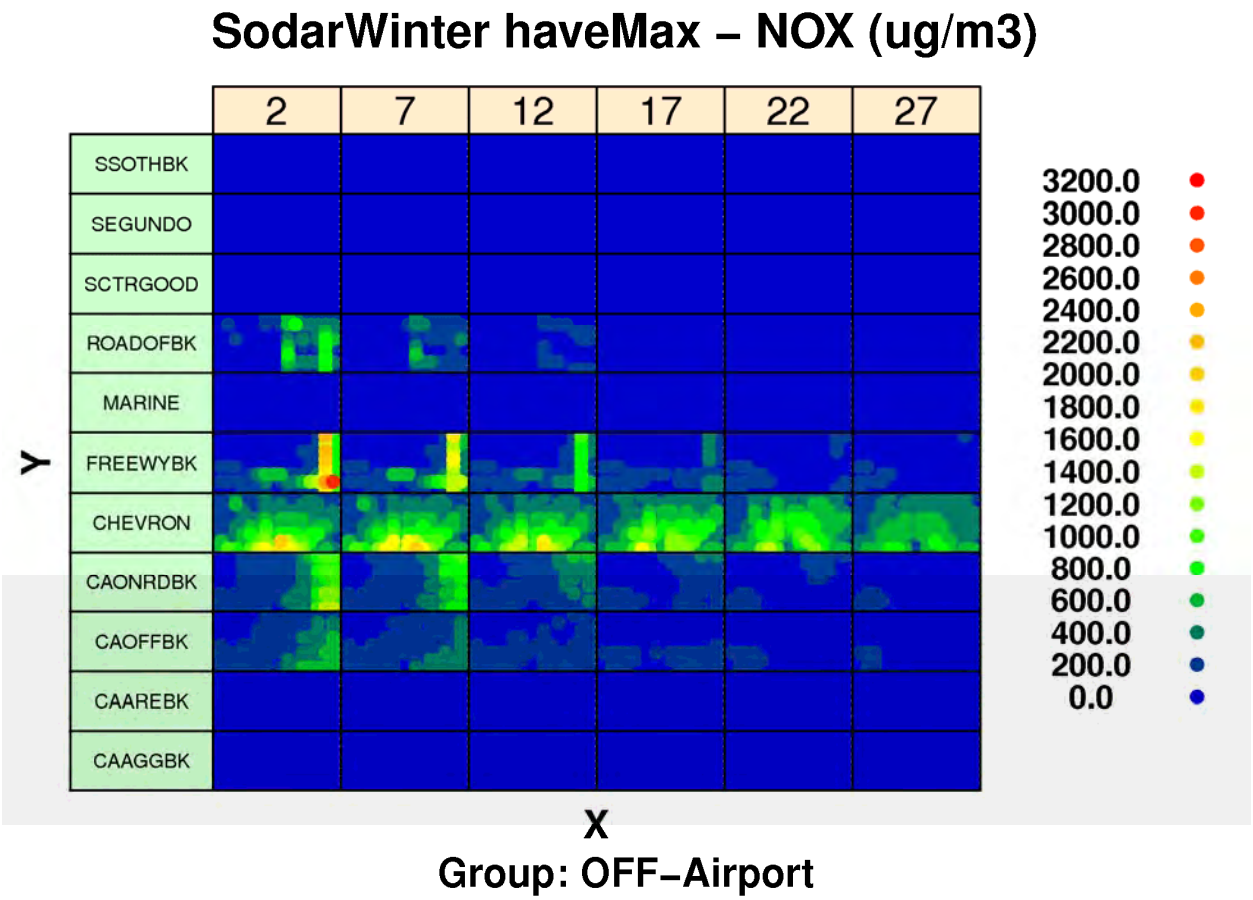

Figure 9A-18: Modeled hourly maximum NOx concentrations from background sources by source sector at flag-pole receptors at heights of 2m, 7m, 12m, 17m, 22m and 27m in Cartesian Grid of receptors during Winter Season.

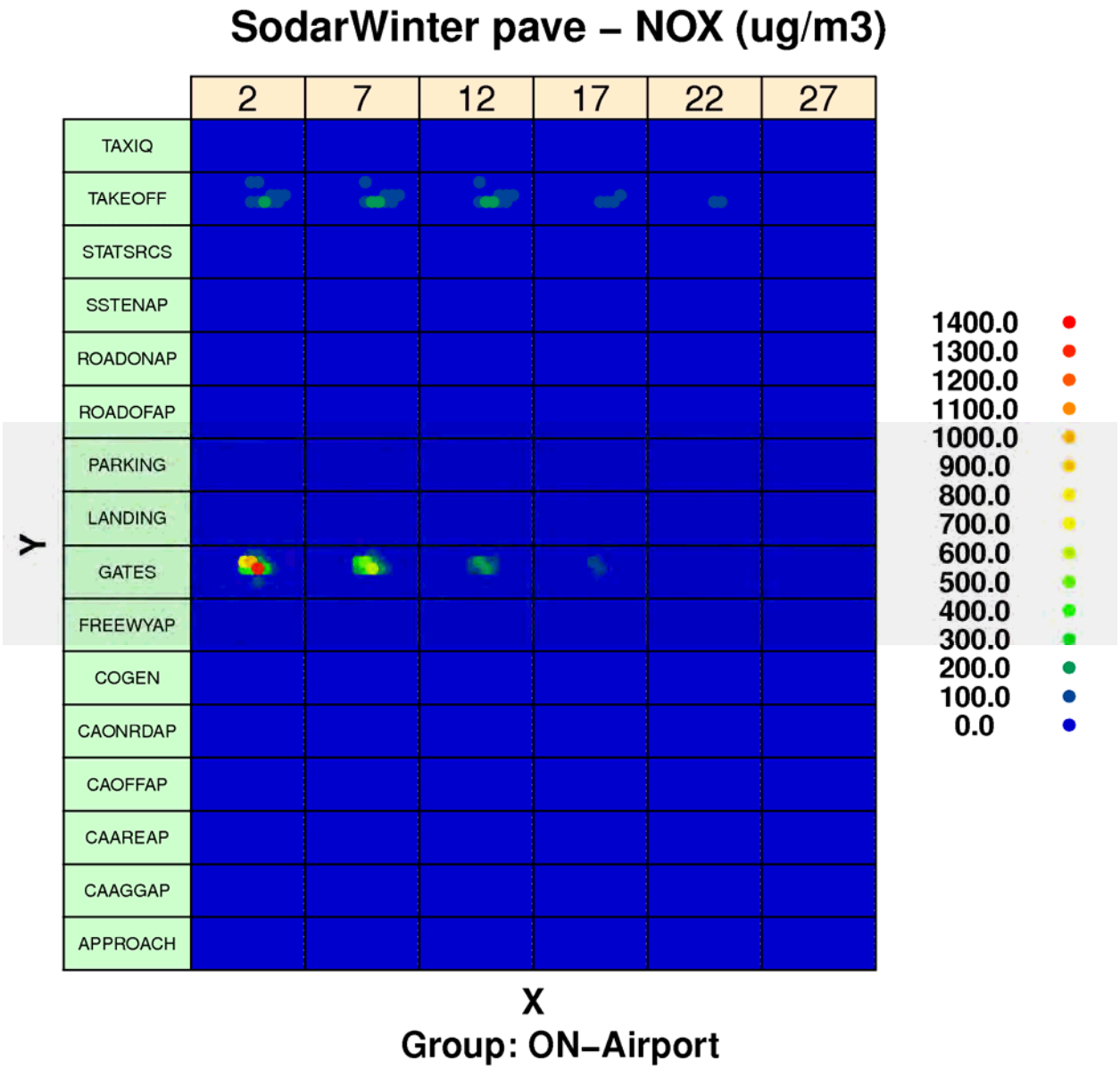

Figure 9A-19: Modeled period average NOx concentrations from airport-related sources by source sector at flag-pole receptors at heights of 2m, 7m, 12m, 17m, 22m and 27m in Cartesian Grid of receptors during Winter Season.

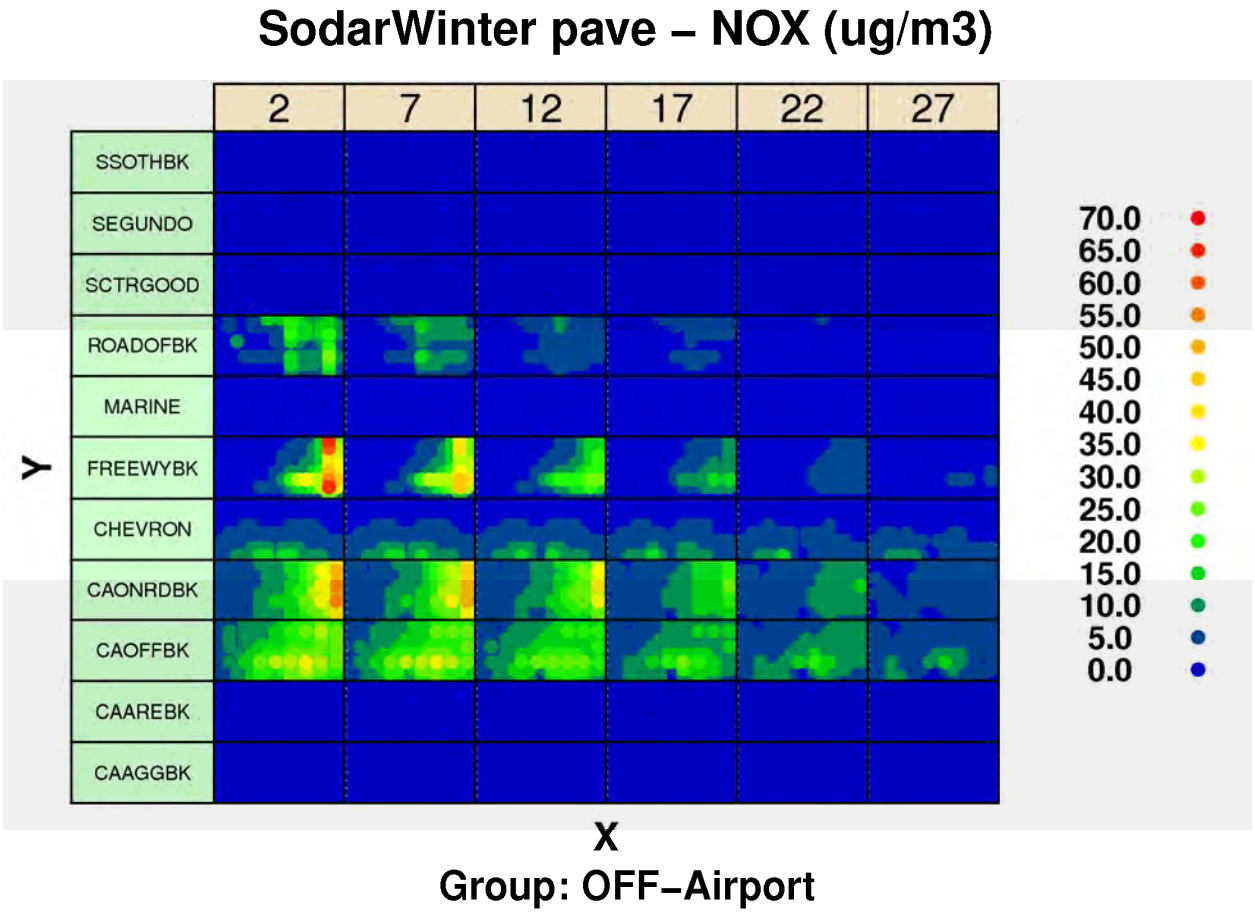

Figure 9A-20: Modeled period average NOx concentrations from background sources by source sector at flag-pole receptors at heights of 2m, 7m, 12m, 17m, 22m and 27m in Cartesian Grid of receptors during Winter Season.

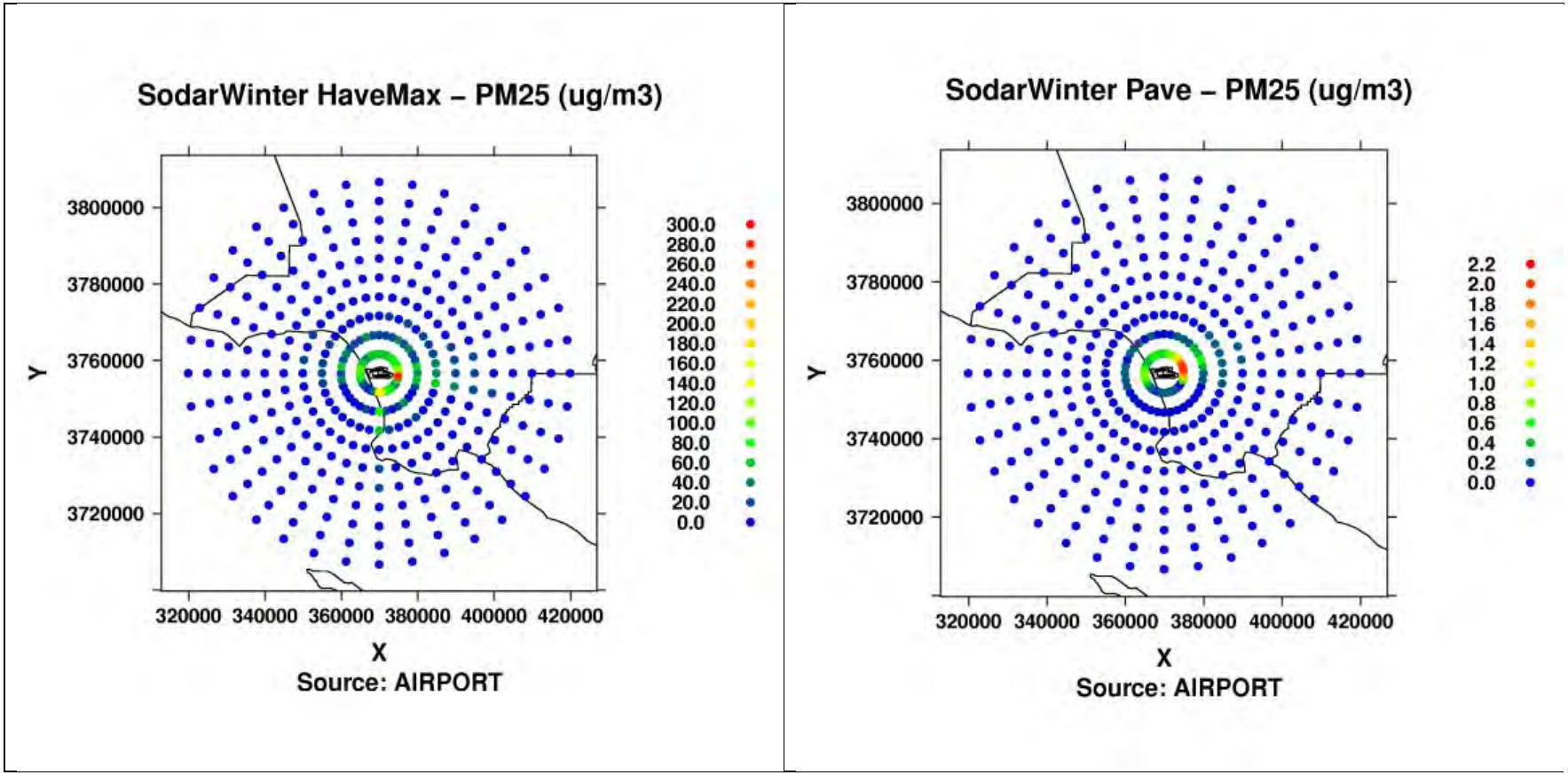

Figure 9A-21a: Modeled hourly max (left) and period average (right) $PM_{2.5}$ concentrations from airport-related in Polar Grid of receptors during Winter Season.

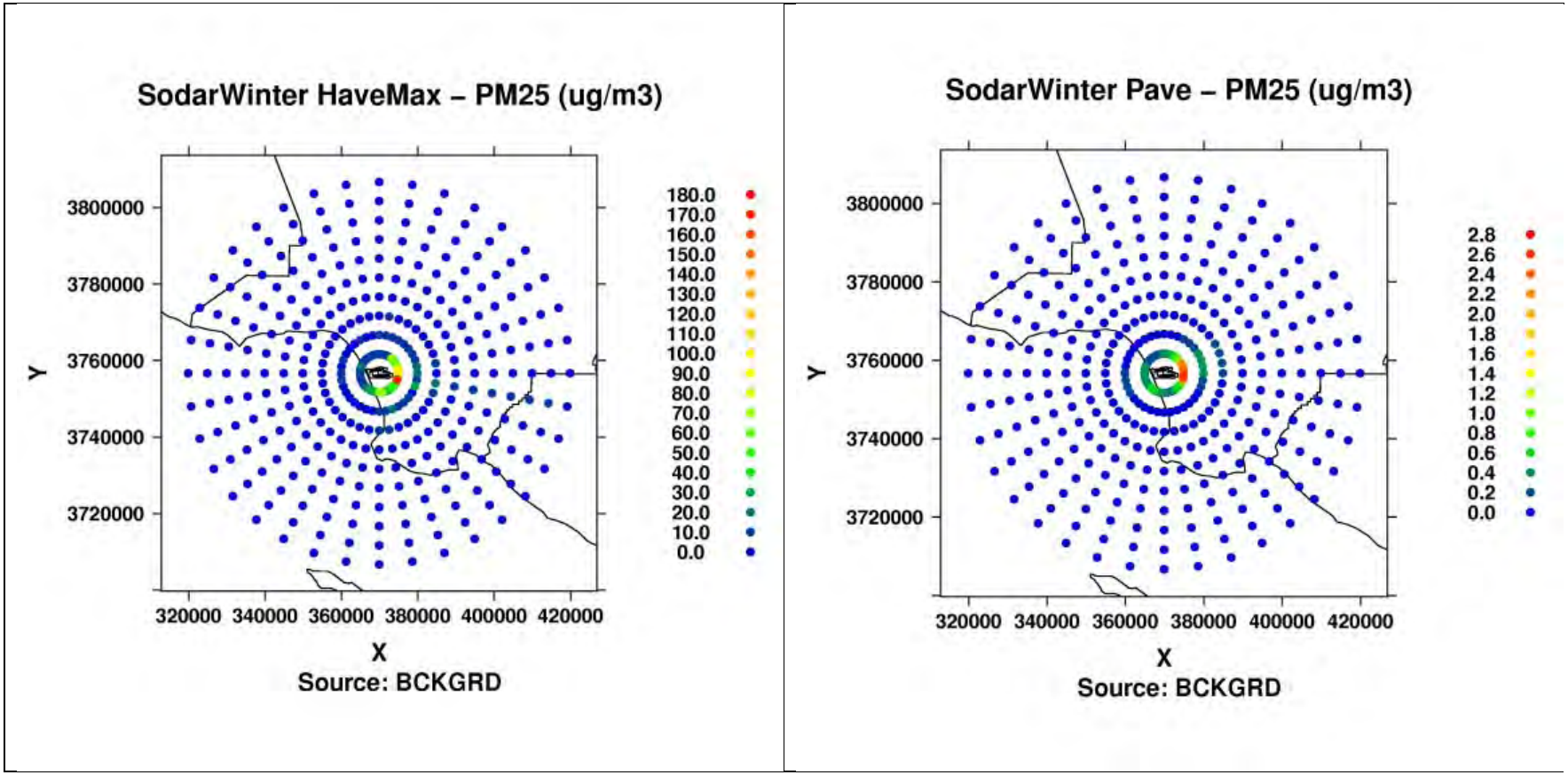

Figure 9A-21b: Modeled hourly max (left) and period average (right) $PM_{2.5}$ concentrations from background sources in Polar Grid of receptors during Winter Season.

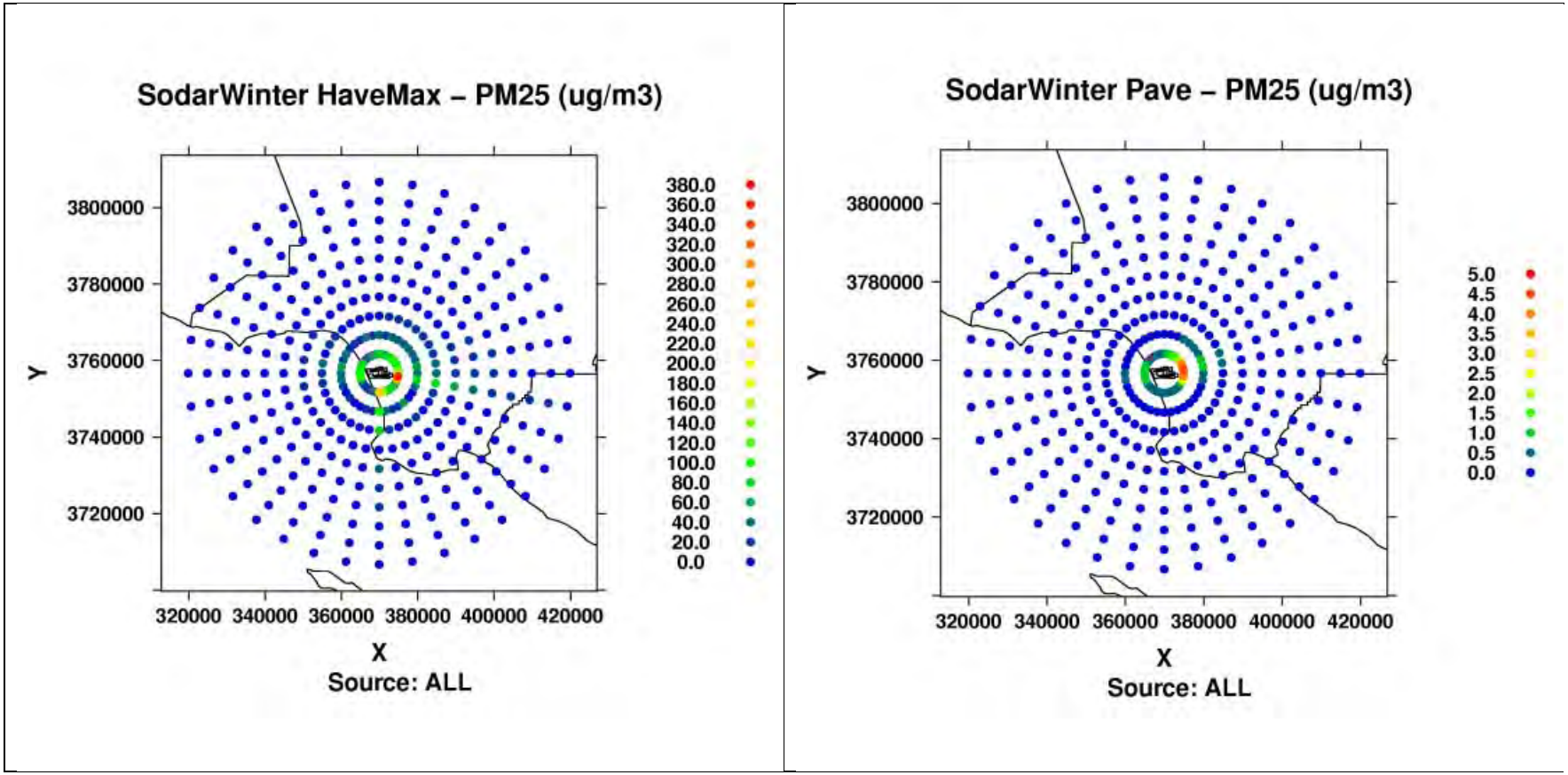

Figure 9A-21c: Modeled hourly max (left) and period average (right) $PM_{2.5}$ concentrations from ALL in Polar Grid of receptors during Winter Season.

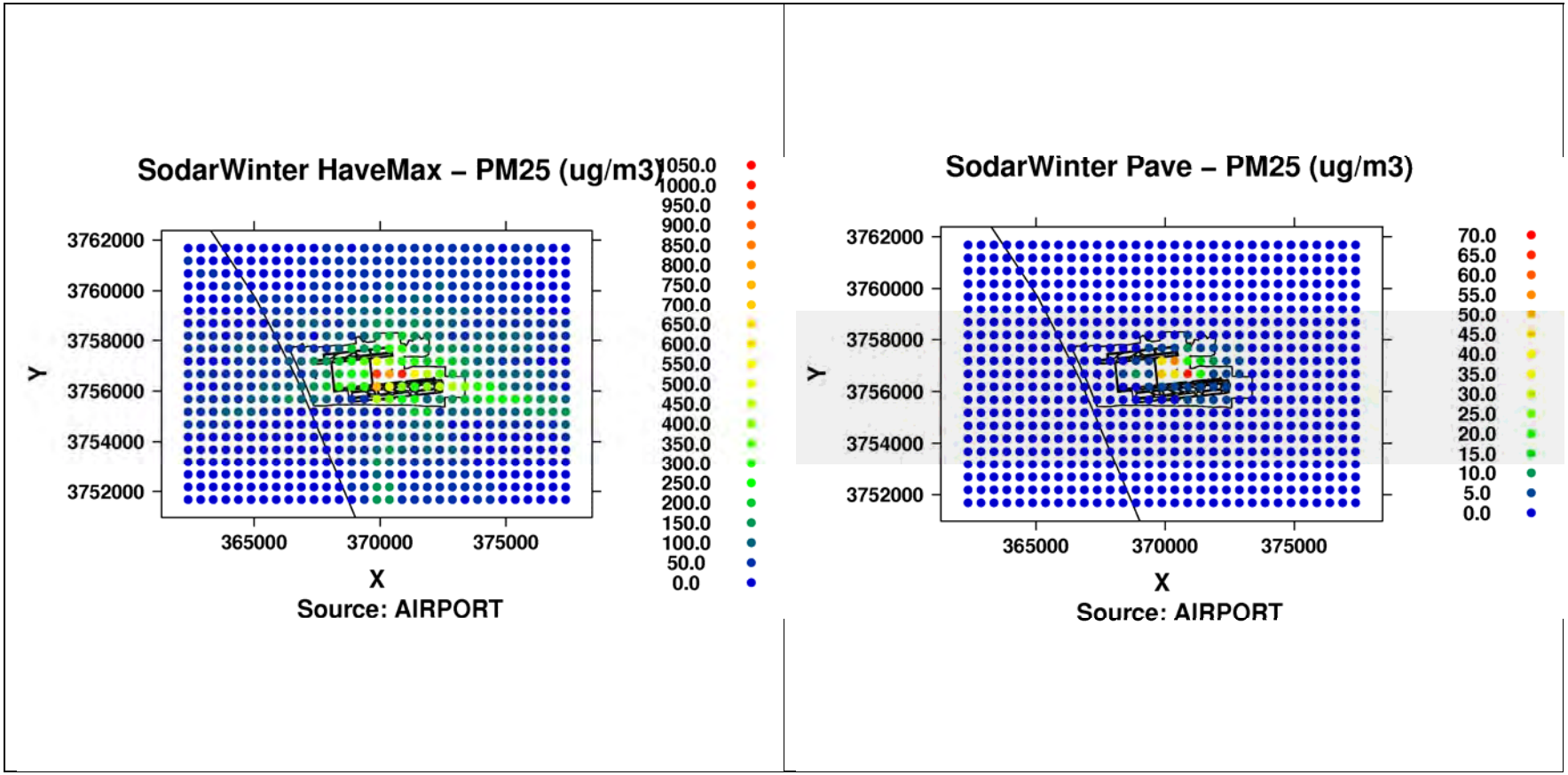

Figure 9A-22a: Modeled hourly max (left) and period average (right) $PM_{2.5}$ concentrations from airport-related in Cartesian Grid of receptors during Winter Season.

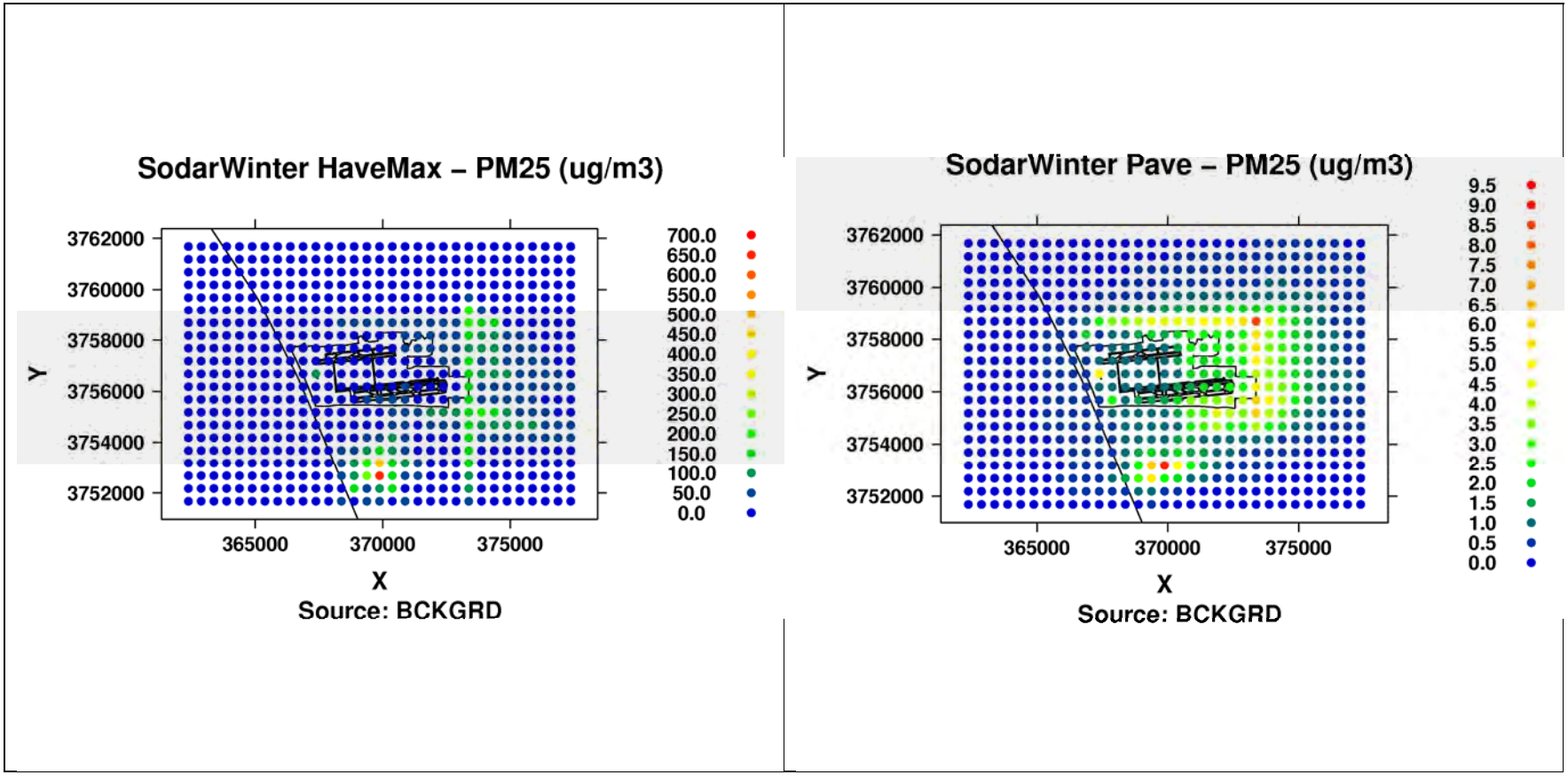

Figure 9A-22b: Modeled hourly max (left) and period average (right) $PM_{2.5}$ concentrations from background sources in Cartesian Grid of receptors during Winter Season.

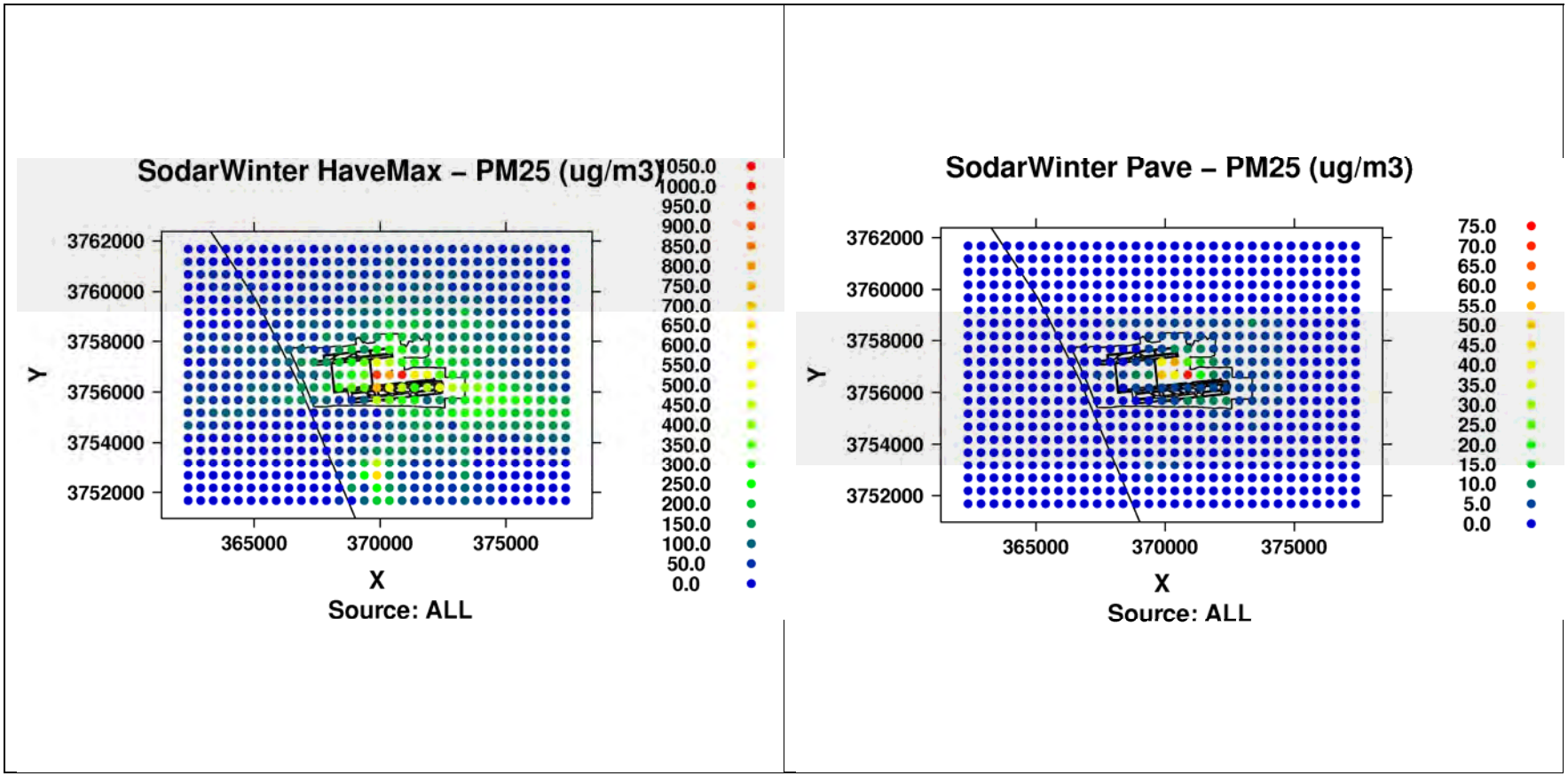

Figure 9A-22c: Modeled hourly max (left) and period average (right) $PM_{2.5}$ concentrations from airport-related ALL in Cartesian Grid of receptors during Winter Season.

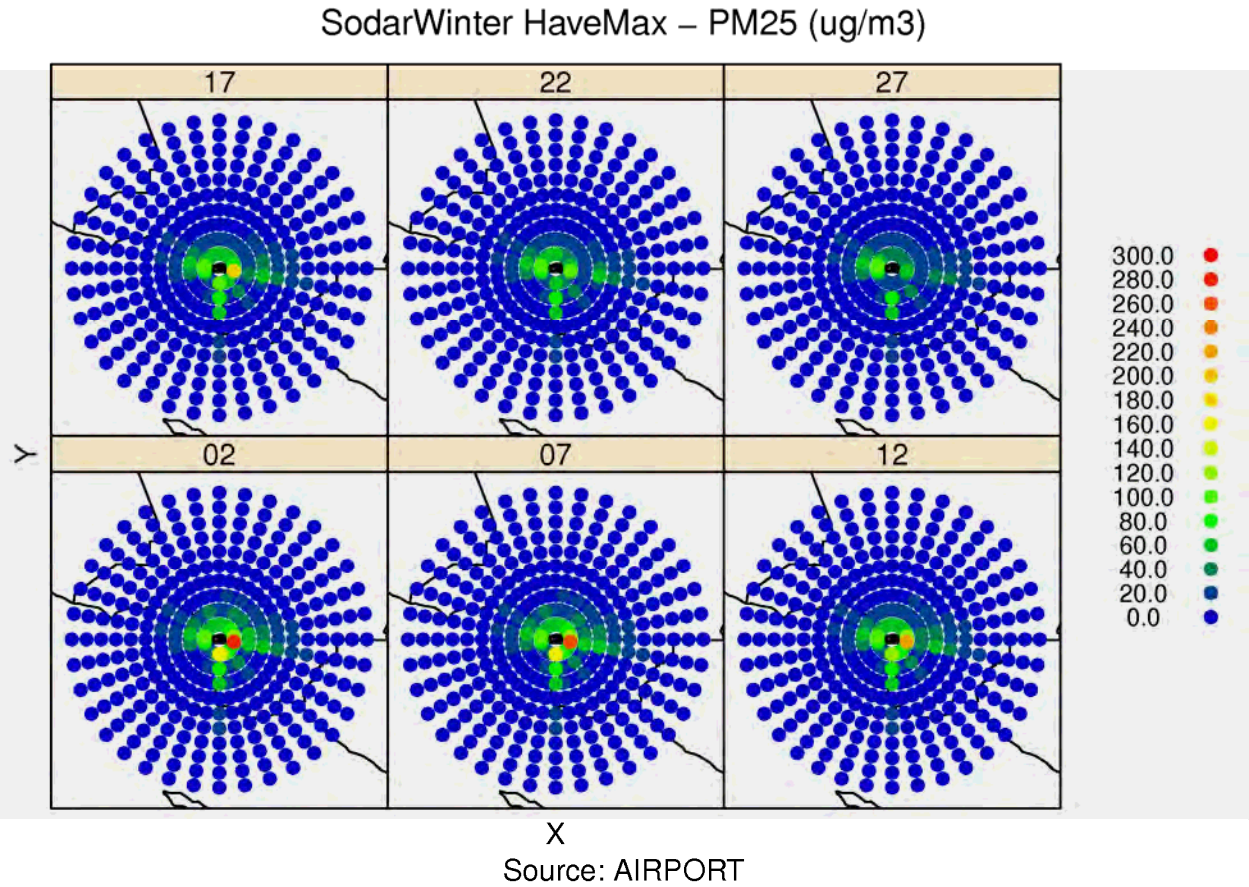

Figure 9A-23: Modeled hourly max $PM_{2.5}$ concentrations from airport-related sources at flag-pole receptors at heights of 2m, 7m, 12m, 17m, 22m and 27m in Polar Grid of receptors during Winter Season.

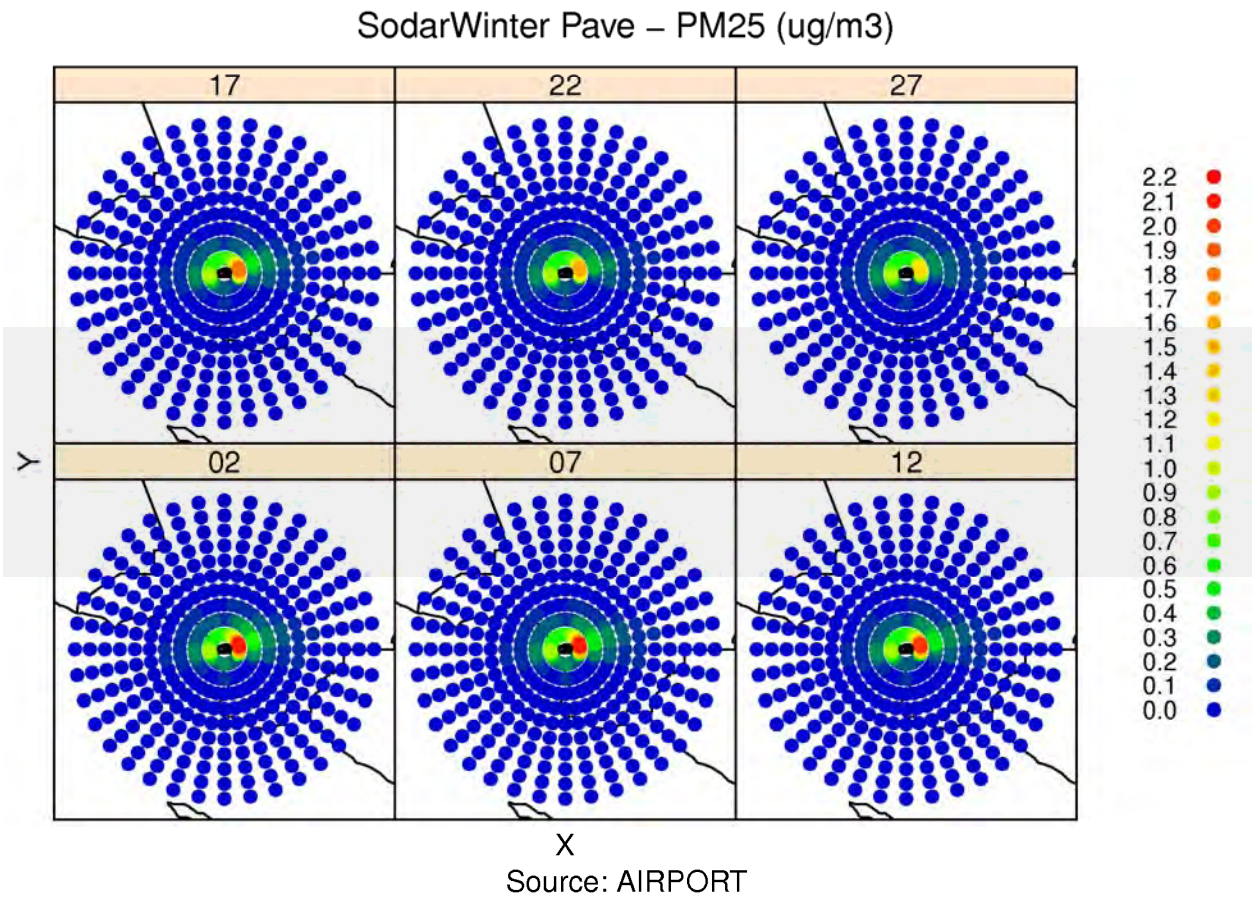

Figure 9A-24: Modeled period average $PM_{2.5}$ concentrations from airport-related sources at flag-pole receptors at heights of 2m, 7m, 12m, 17m, 22m and 27m in Polar Grid of receptors during Winter Season.

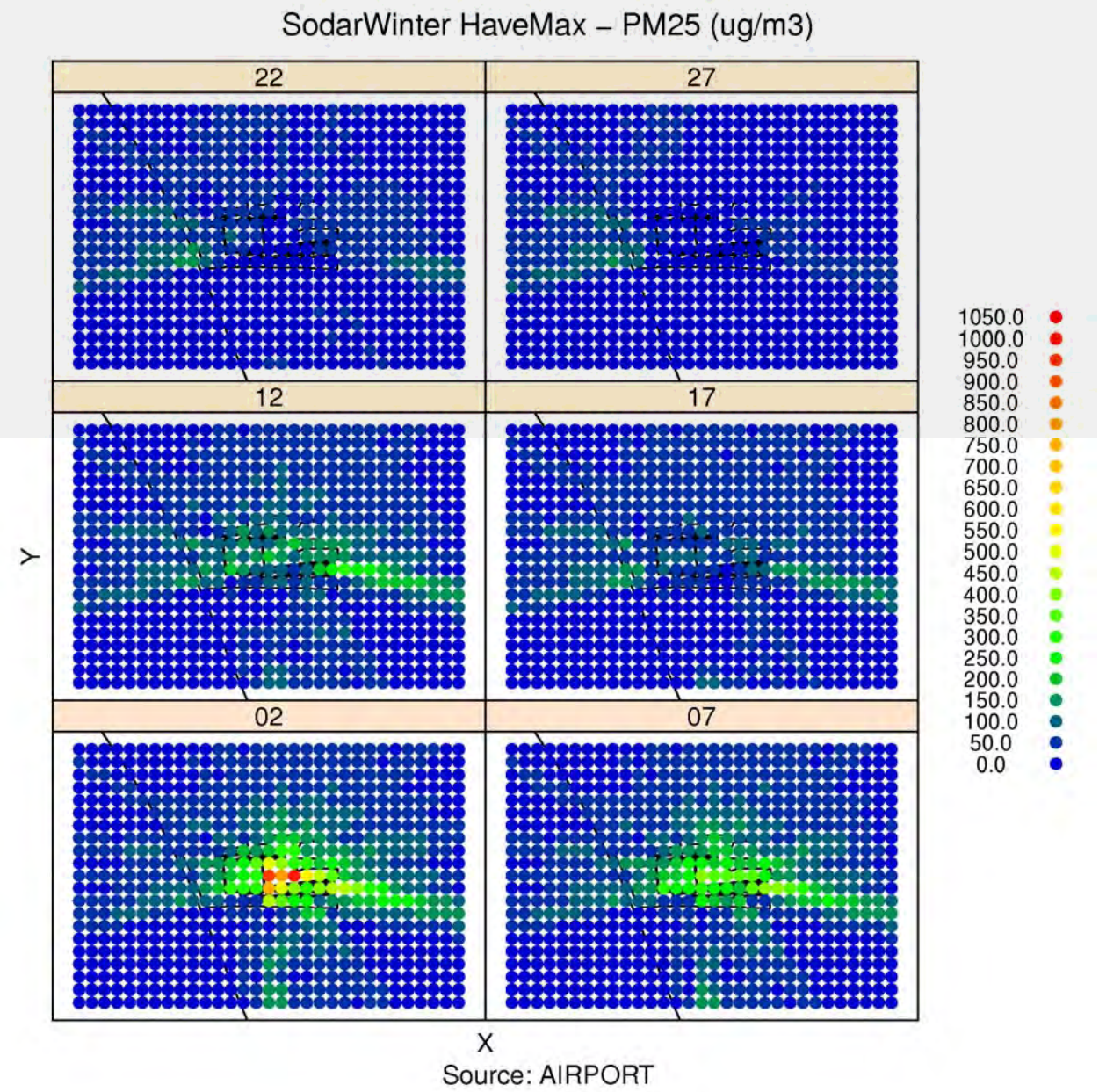

Figure 9A-25: Modeled hourly max $PM_{2.5}$ concentrations from airport-related sources at flag-pole receptors at heights of 2m, 7m, 12m, 17m, 22m and 27m in Cartesian Grid of receptors during Winter Season.

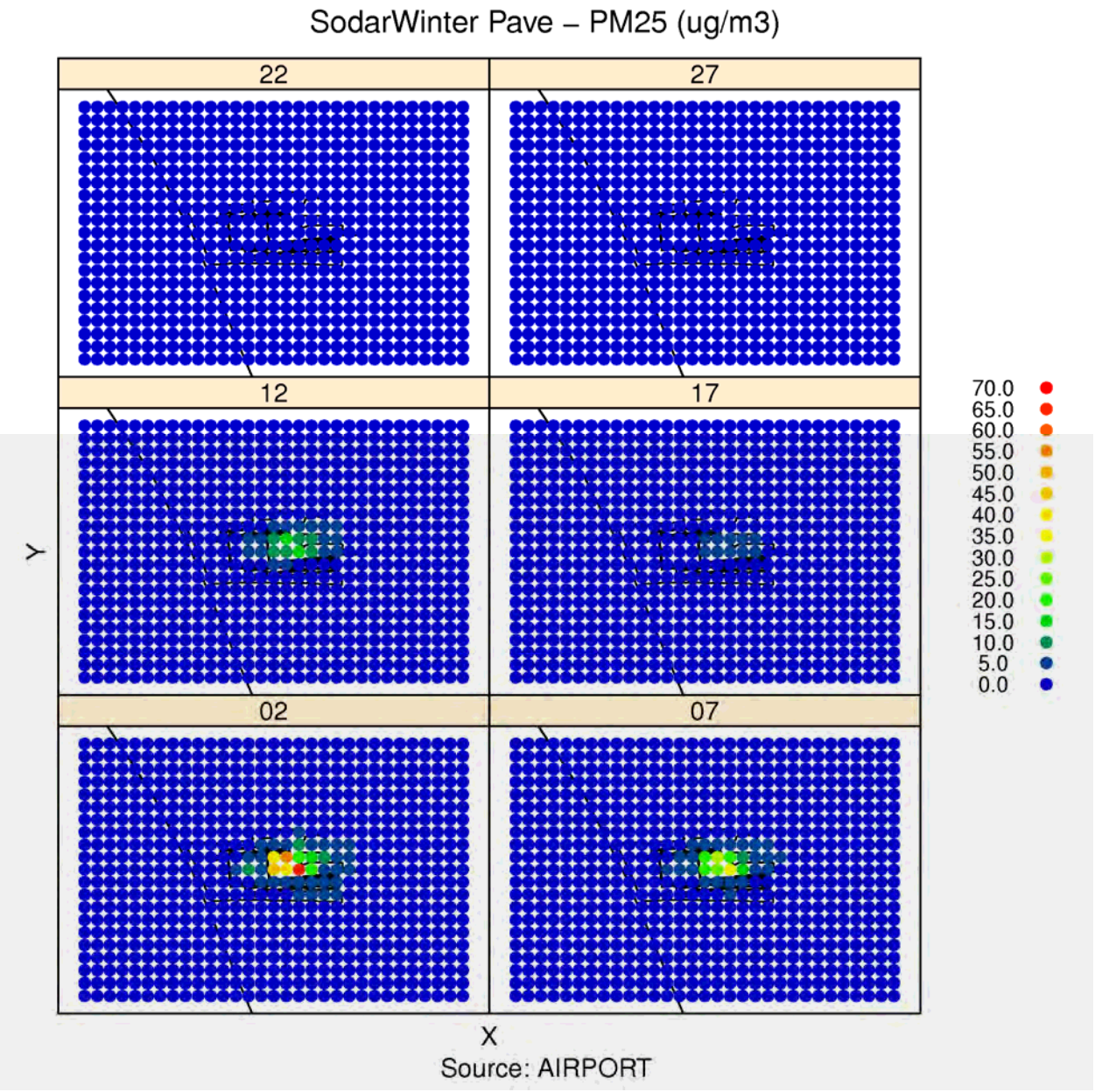

Figure 9A-26: Modeled period average $PM_{2.5}$ concentrations from airport-related sources at flag-pole receptors at heights of 2m, 7m, 12m, 17m, 22m and 27m in Cartesian Grid of receptors during Winter Season.

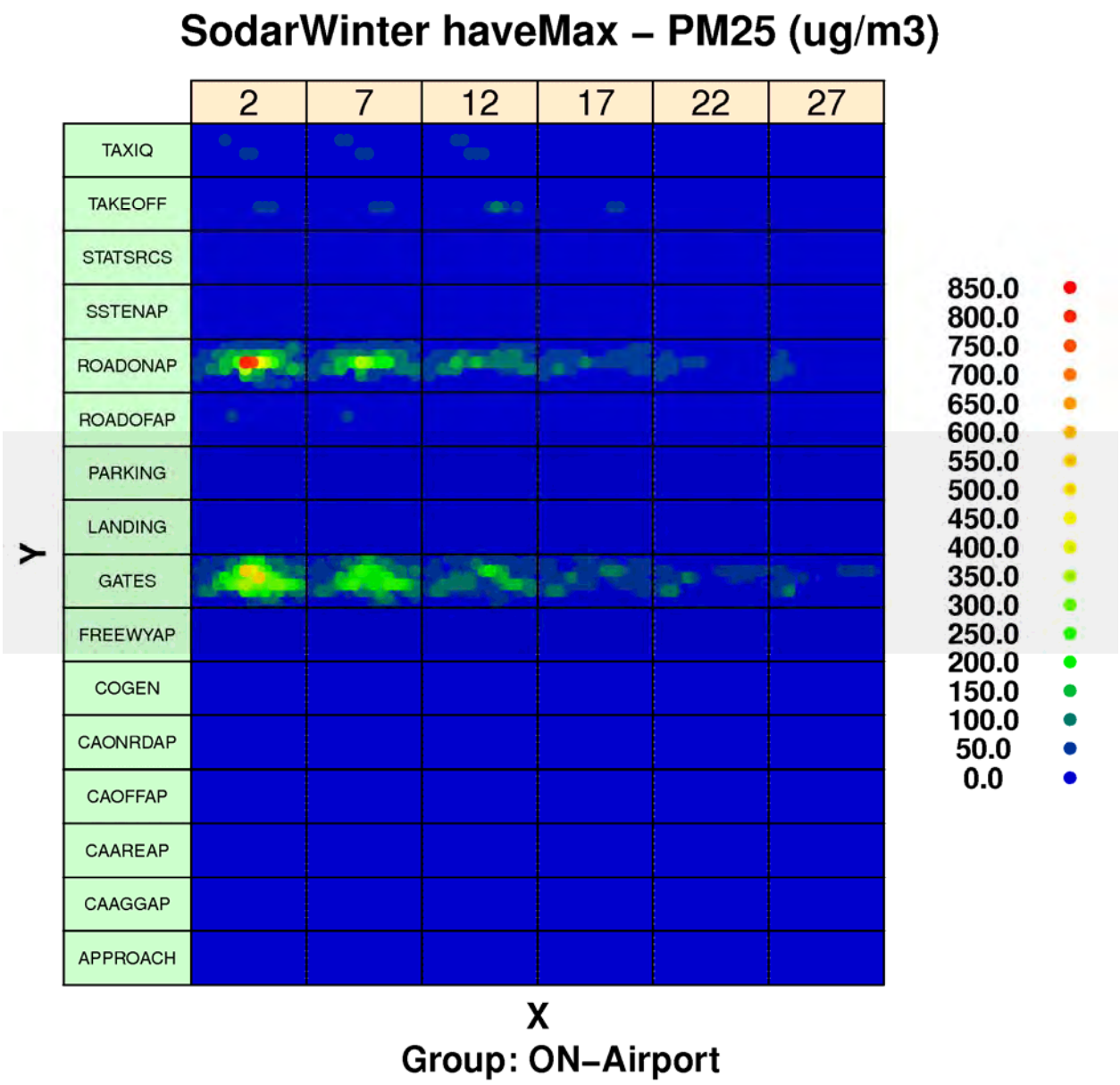

Figure 9A-27: Modeled hourly maximum $PM_{2.5}$ concentrations from airport-related sources by source sector at flag-pole receptors at heights of 2m, 7m, 12m, 17m, 22m and 27m in Cartesian Grid of receptors during Winter Season.

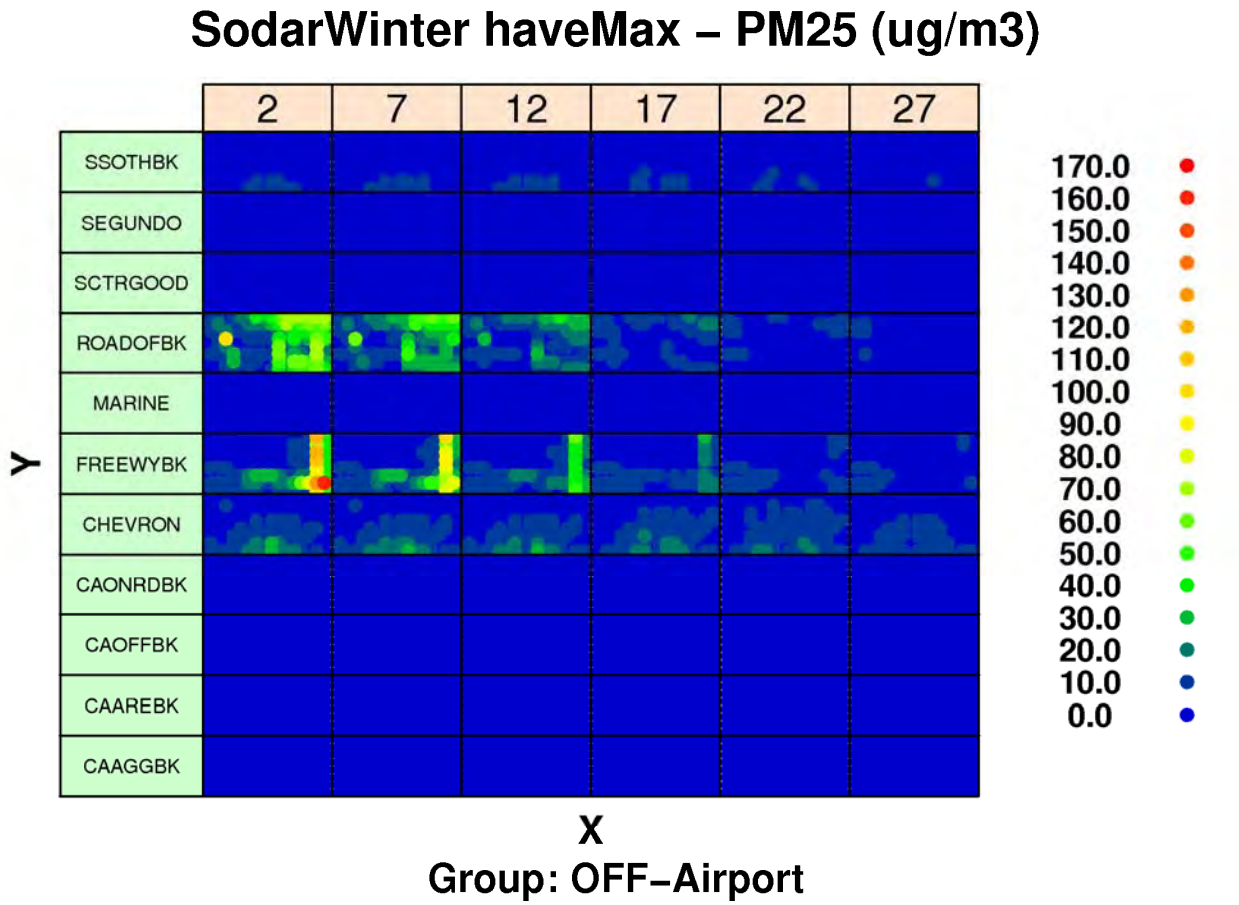

Figure 9A-28: Modeled hourly maximum $PM_{2.5}$ concentrations from background sources by source sector at flag-pole receptors at heights of 2m, 7m, 12m, 17m, 22m and 27m in Cartesian Grid of receptors during Winter Season.

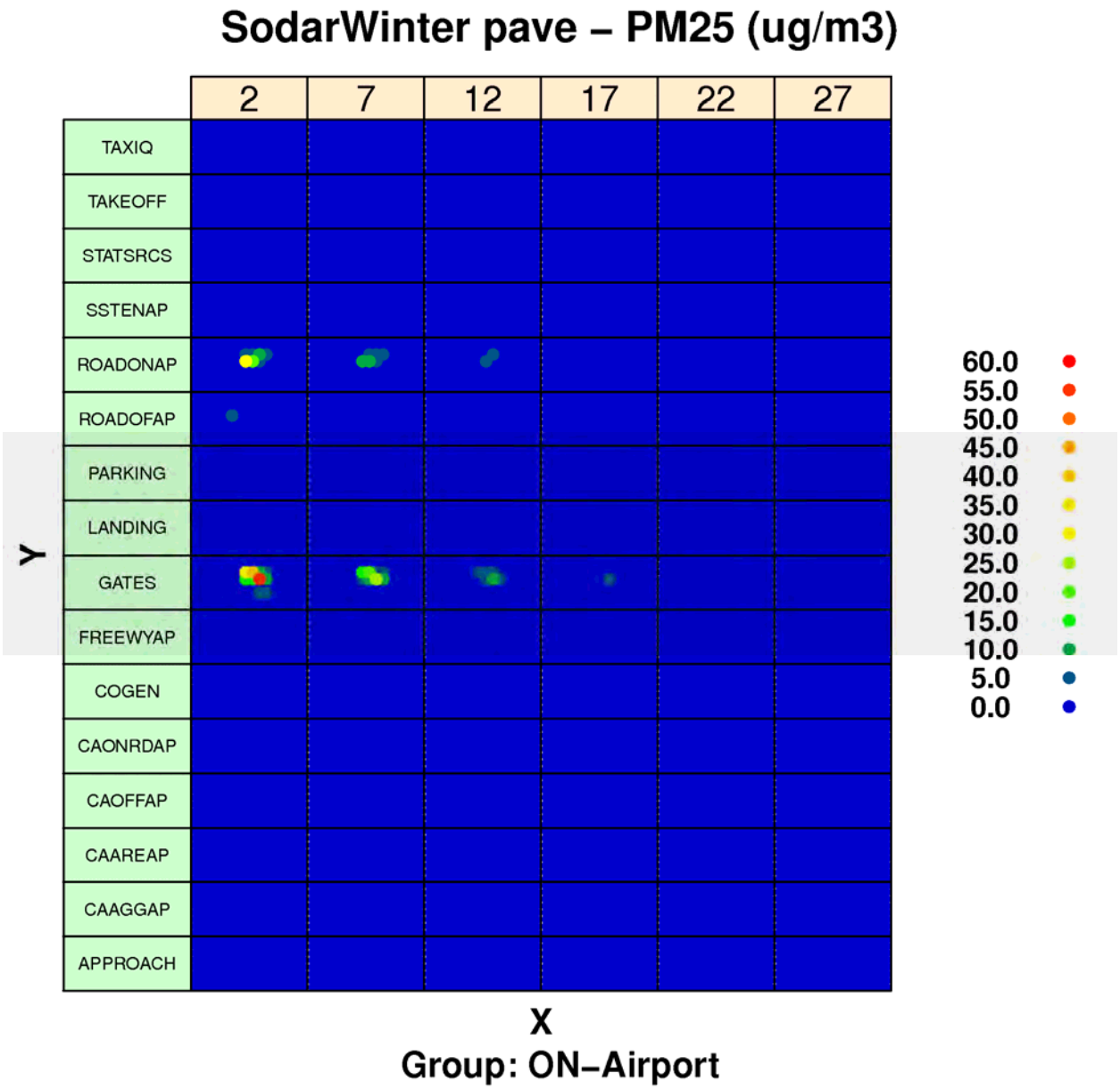

Figure 9A-29: Modeled period average $PM_{2.5}$ concentrations from airport-related sources by source sector at flag-pole receptors at heights of 2m, 7m, 12m, 17m, 22m and 27m in Cartesian Grid of receptors during Winter Season.

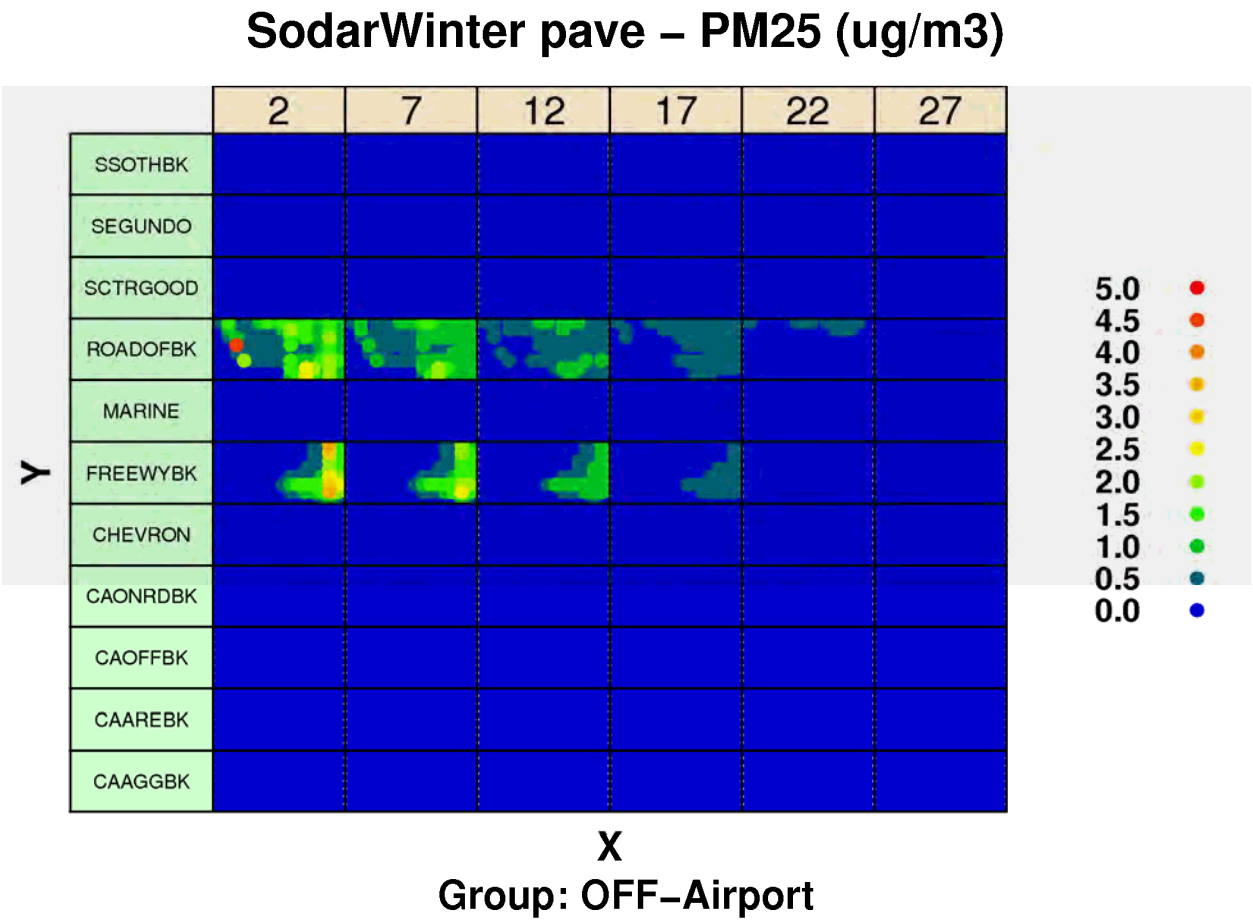

Figure 9A-30: Modeled period average $PM_{2.5}$ concentrations from background sources by source sector at flag-pole receptors at heights of 2m, 7m, 12m, 17m, 22m and 27m in Cartesian Grid of receptors during Winter Season.

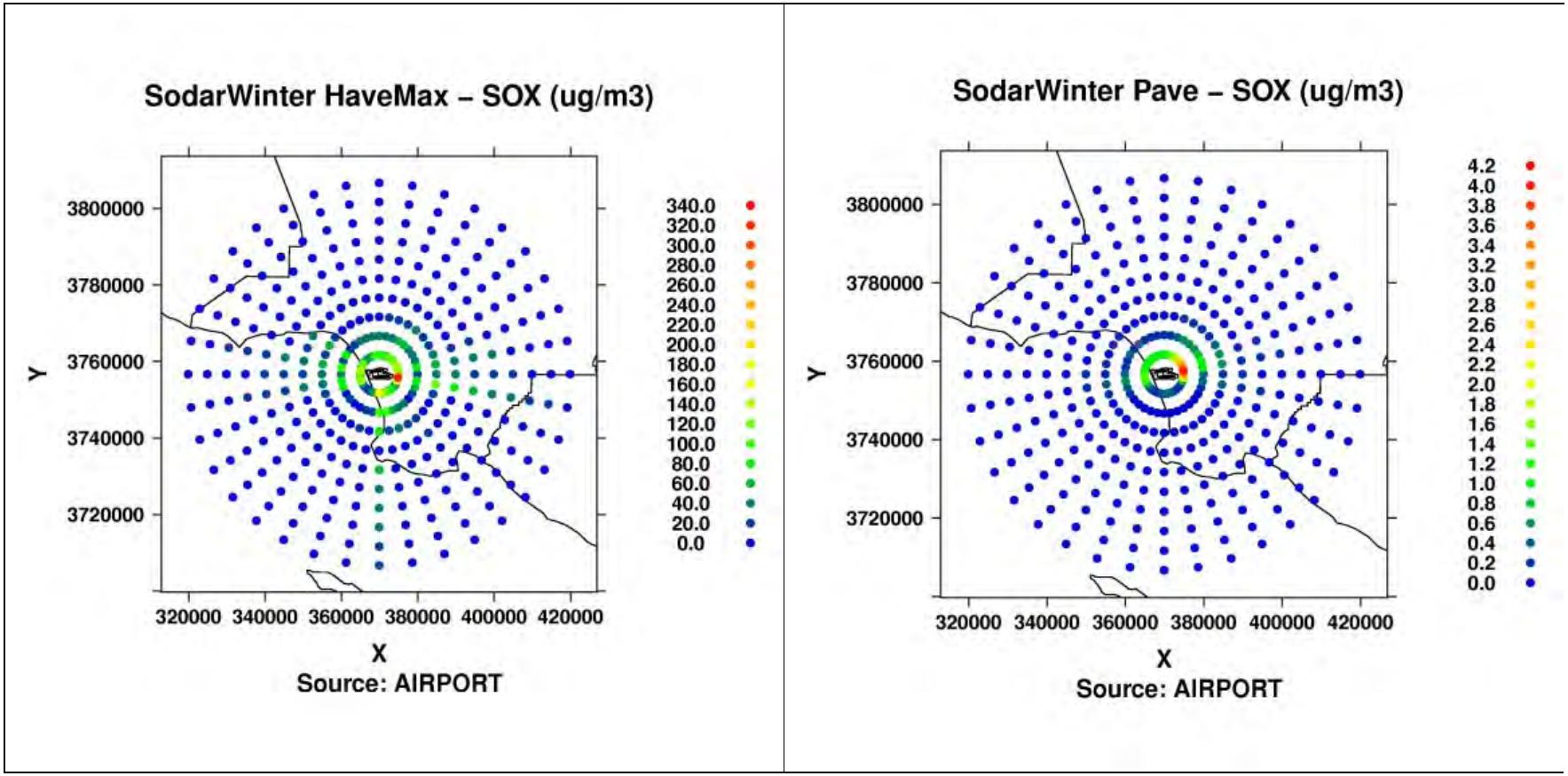

Figure 9A-31a: Modeled hourly max (left) and period average (right) SOx concentrations from airport-related in Polar Grid of receptors during Winter Season.

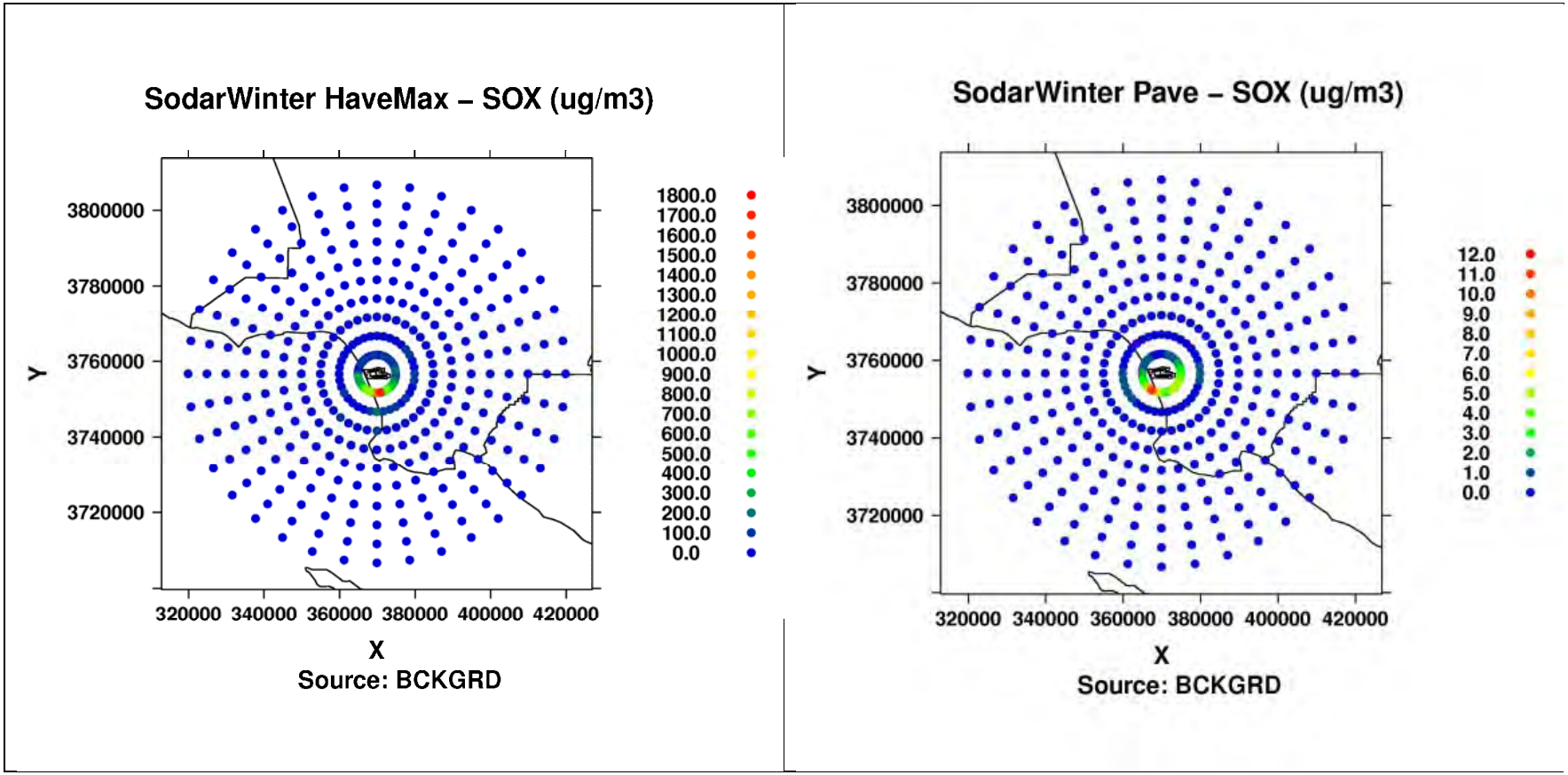

Figure 9A-31b: Modeled hourly max (left) and period average (right) SOx concentrations from background sources in Polar Grid of receptors during Winter Season.

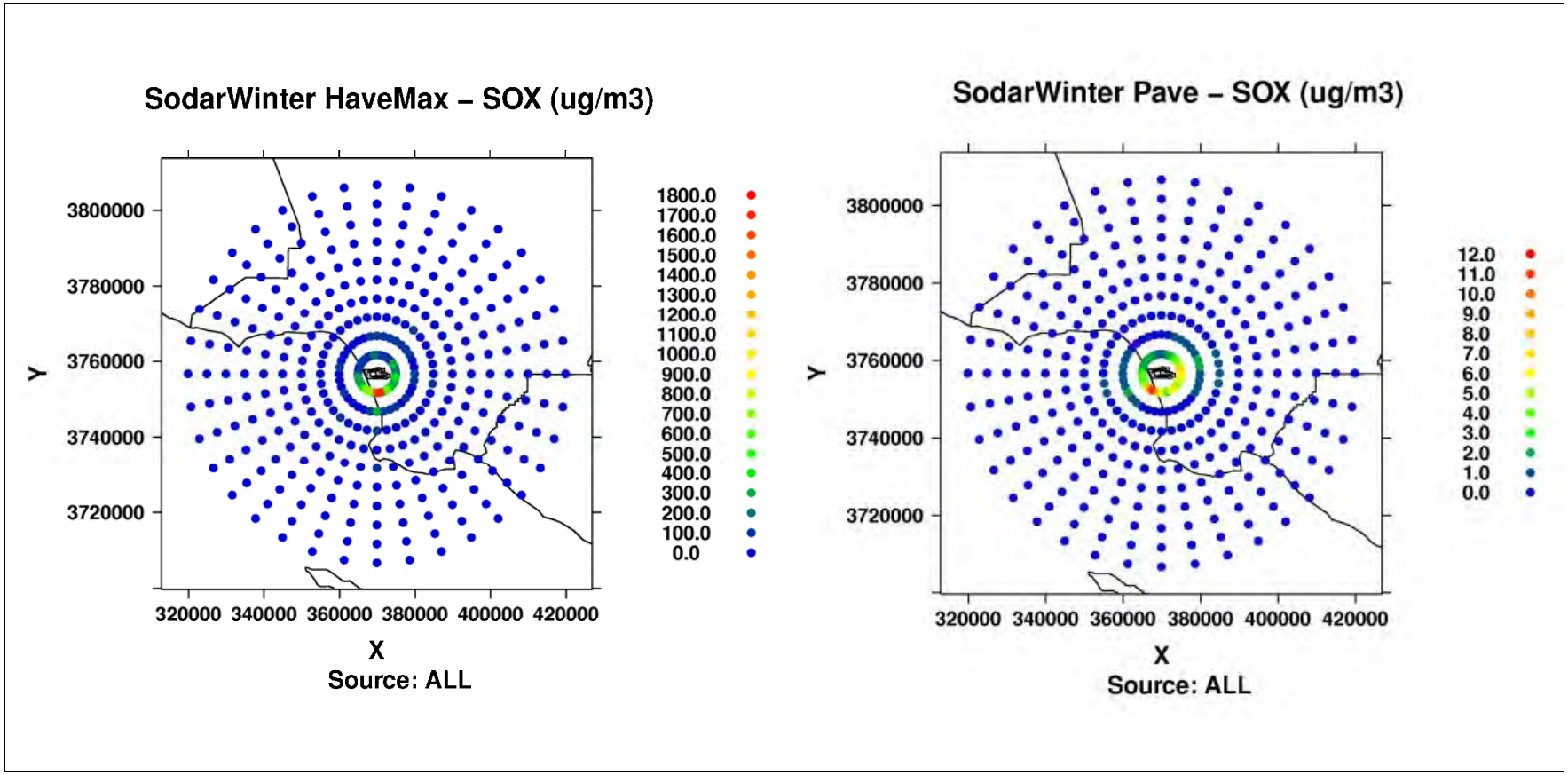

Figure 9A-31c: Modeled hourly max (left) and period average (right) SOx concentrations from ALL in Polar Grid of receptors during Winter Season.

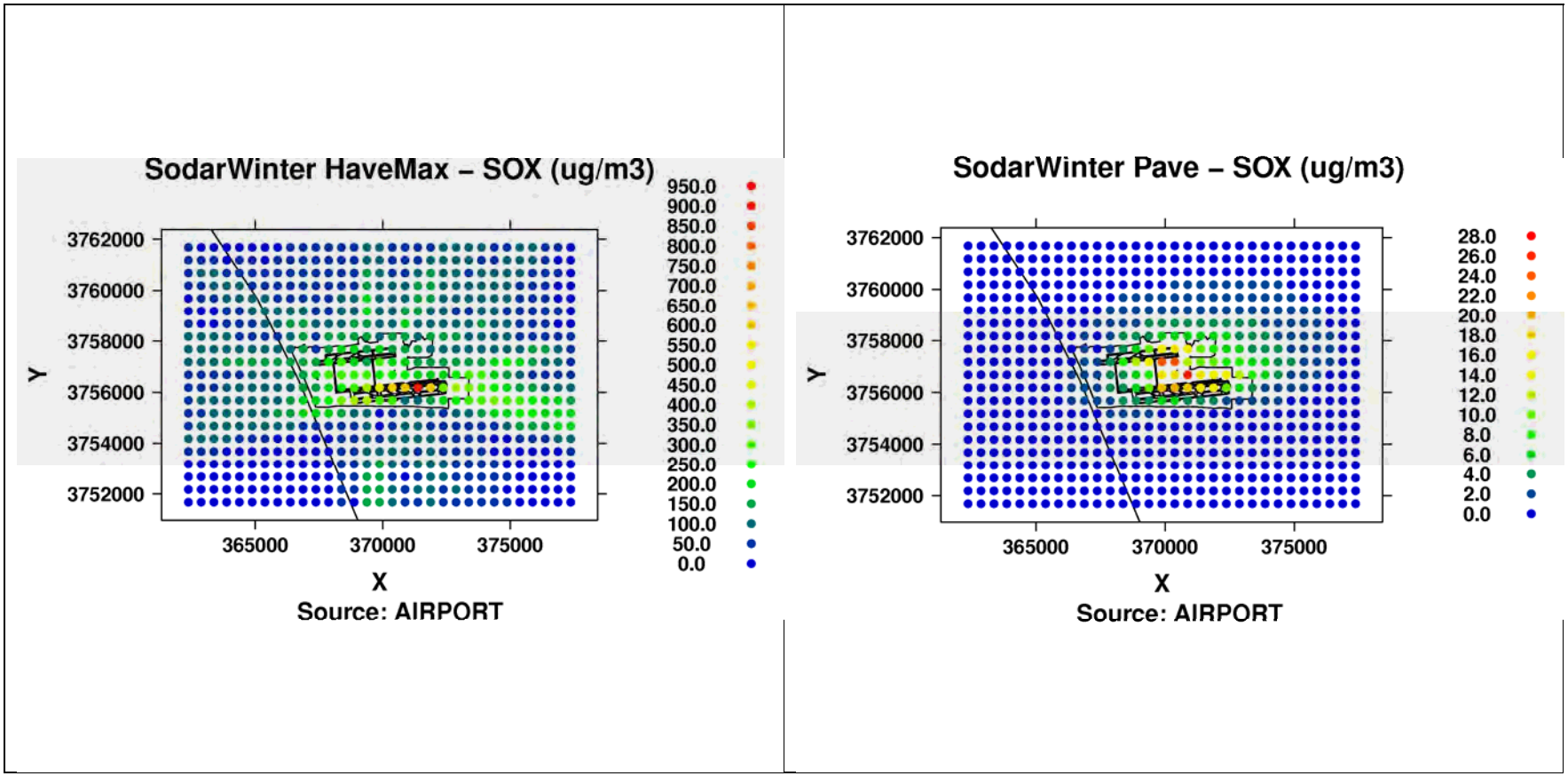

Figure 9A-32a: Modeled hourly max (left) and period average (right) SOx concentrations from airport-related in Cartesian Grid of receptors during Winter Season.

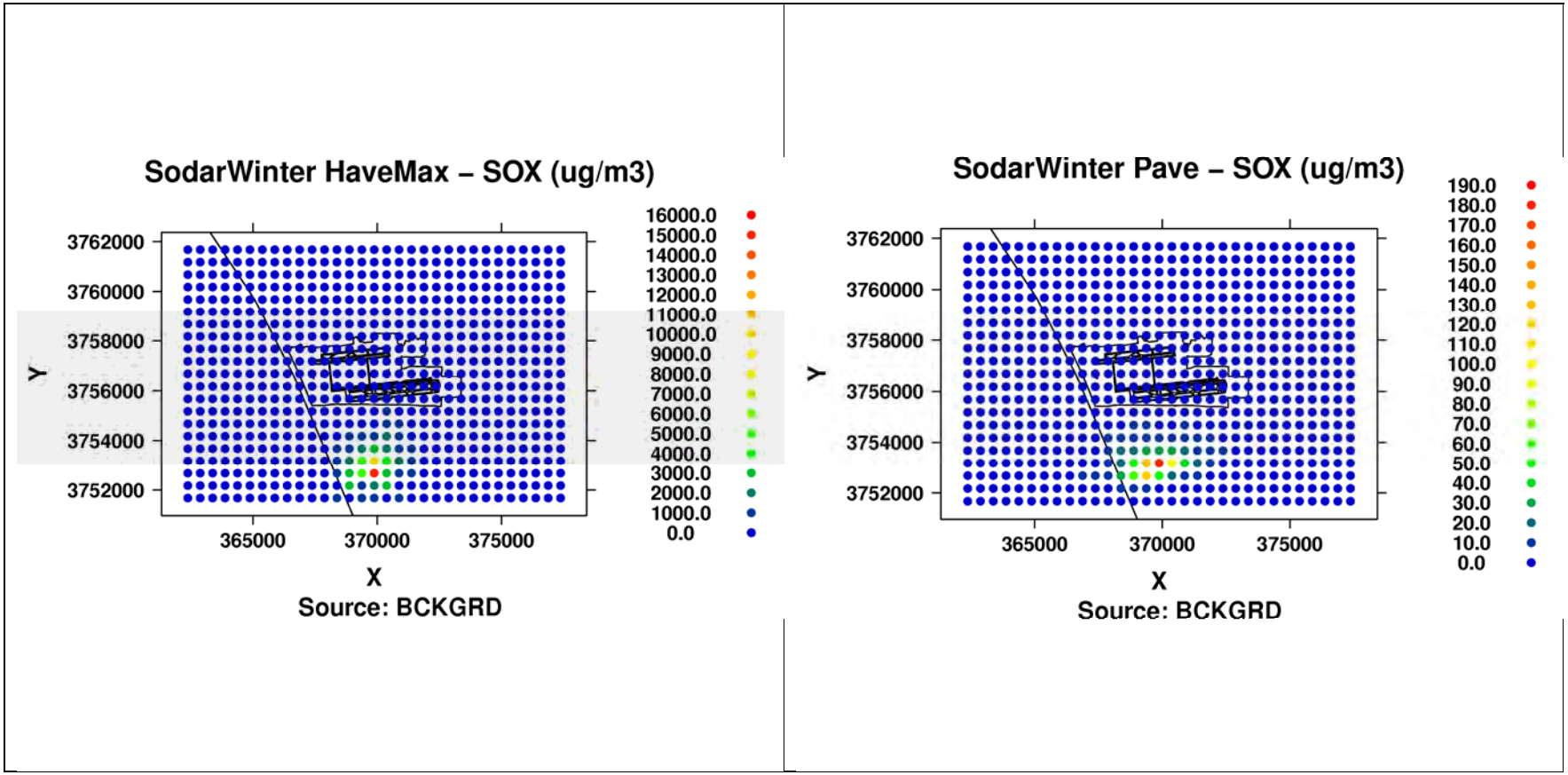

Figure 9A-32b: Modeled hourly max (left) and period average (right) SOx concentrations from background sources in Cartesian Grid of receptors during Winter Season.

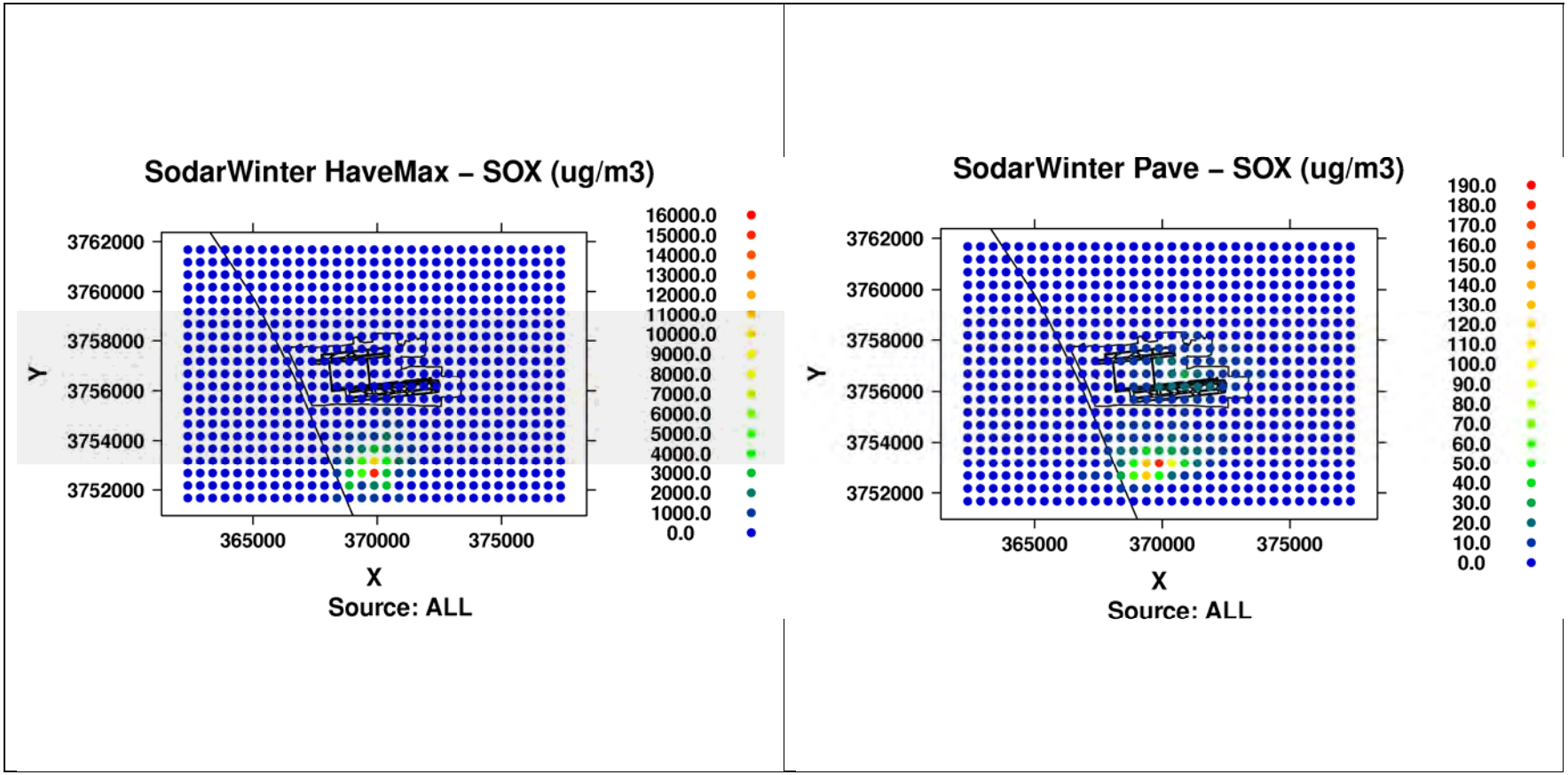

Figure 9A-32c: Modeled hourly max (left) and period average (right) SOx concentrations from ALL in Cartesian Grid of receptors during Winter Season.

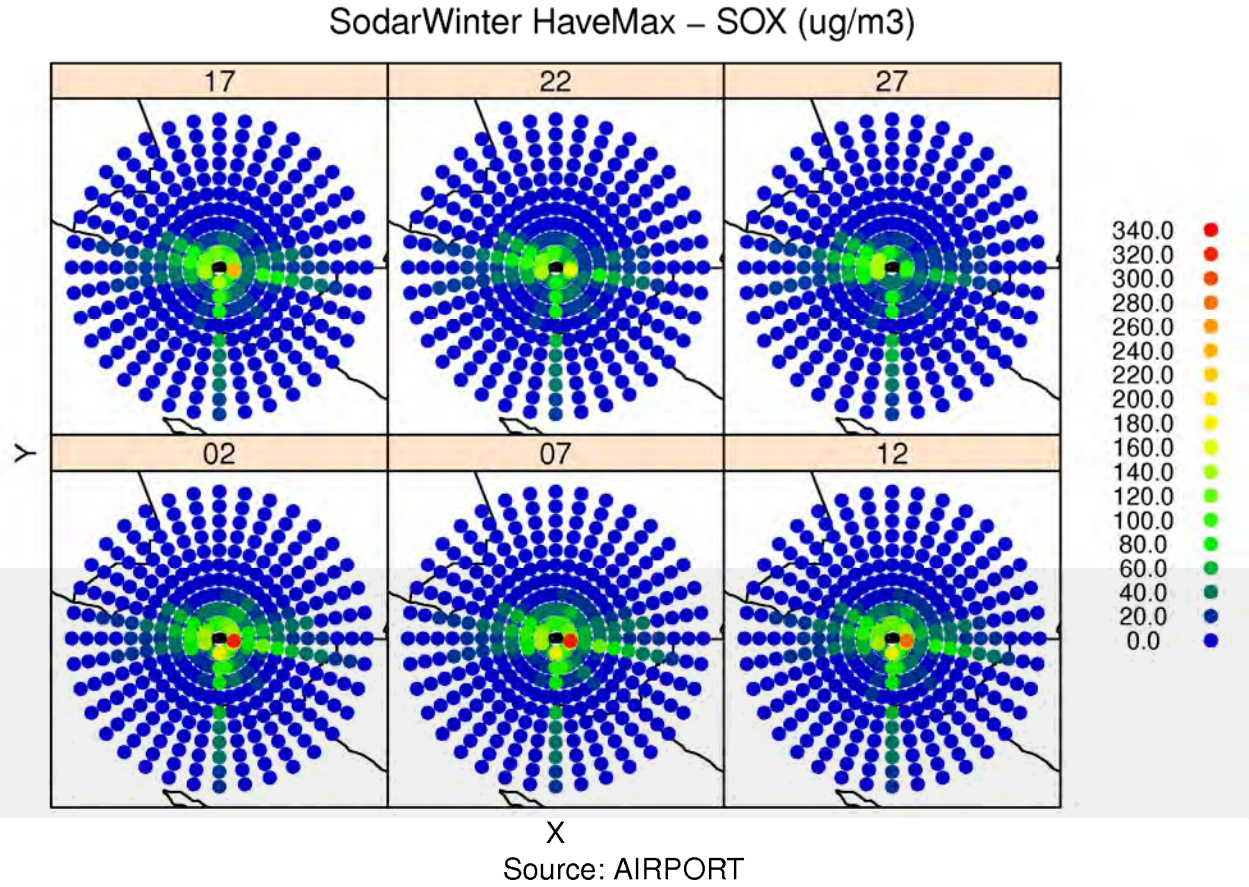

Figure 9A-33: Modeled hourly max SO_X concentrations from airport-related sources at flag-pole receptors at heights of 2m, 7m, 12m, 17m, 22m and 27m in Polar Grid of receptors during Winter Season.

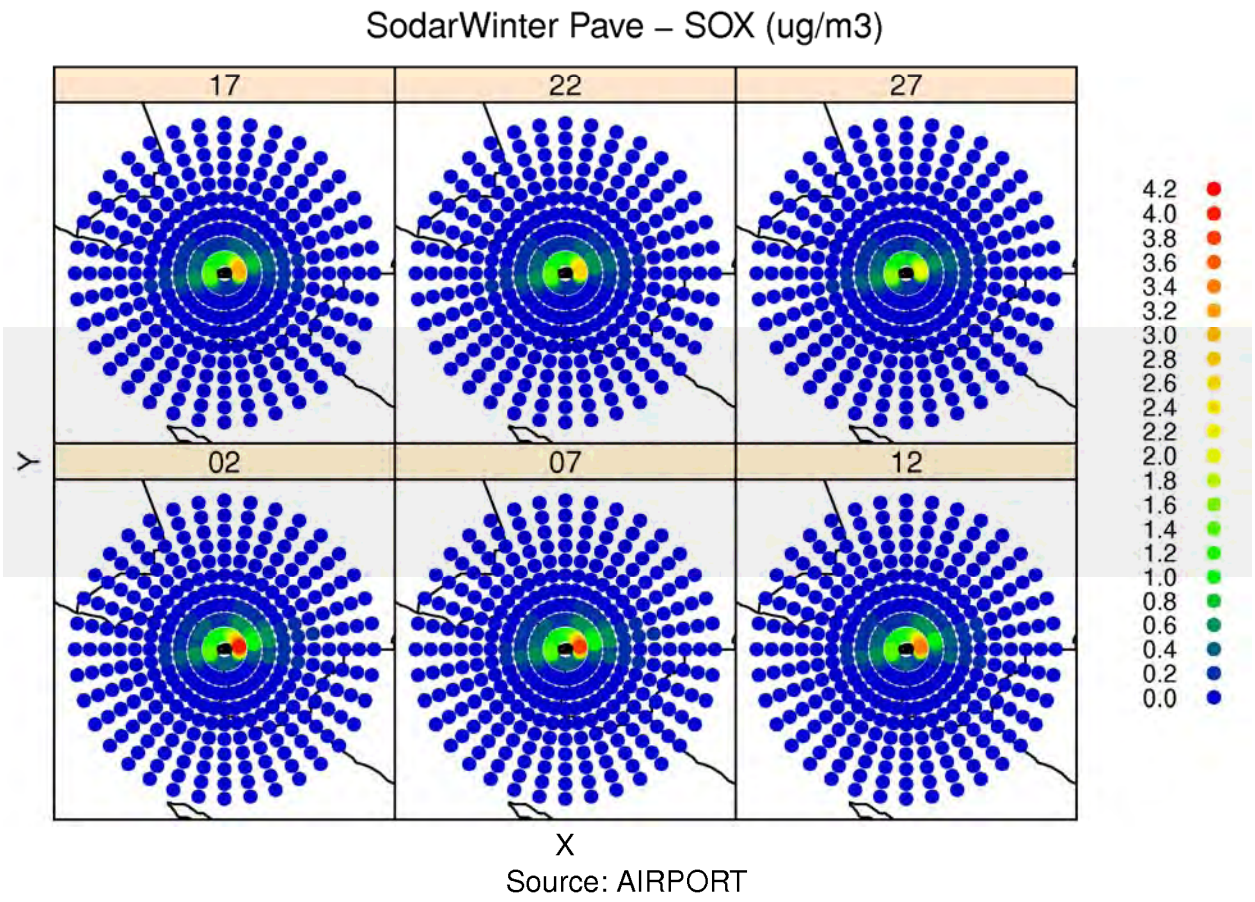

Figure 9A-34: Modeled period average SO_X concentrations from airport-related sources at flag-pole receptors at heights of 2m, 7m, 12m, 17m, 22m and 27m in Polar Grid of receptors during Winter Season.

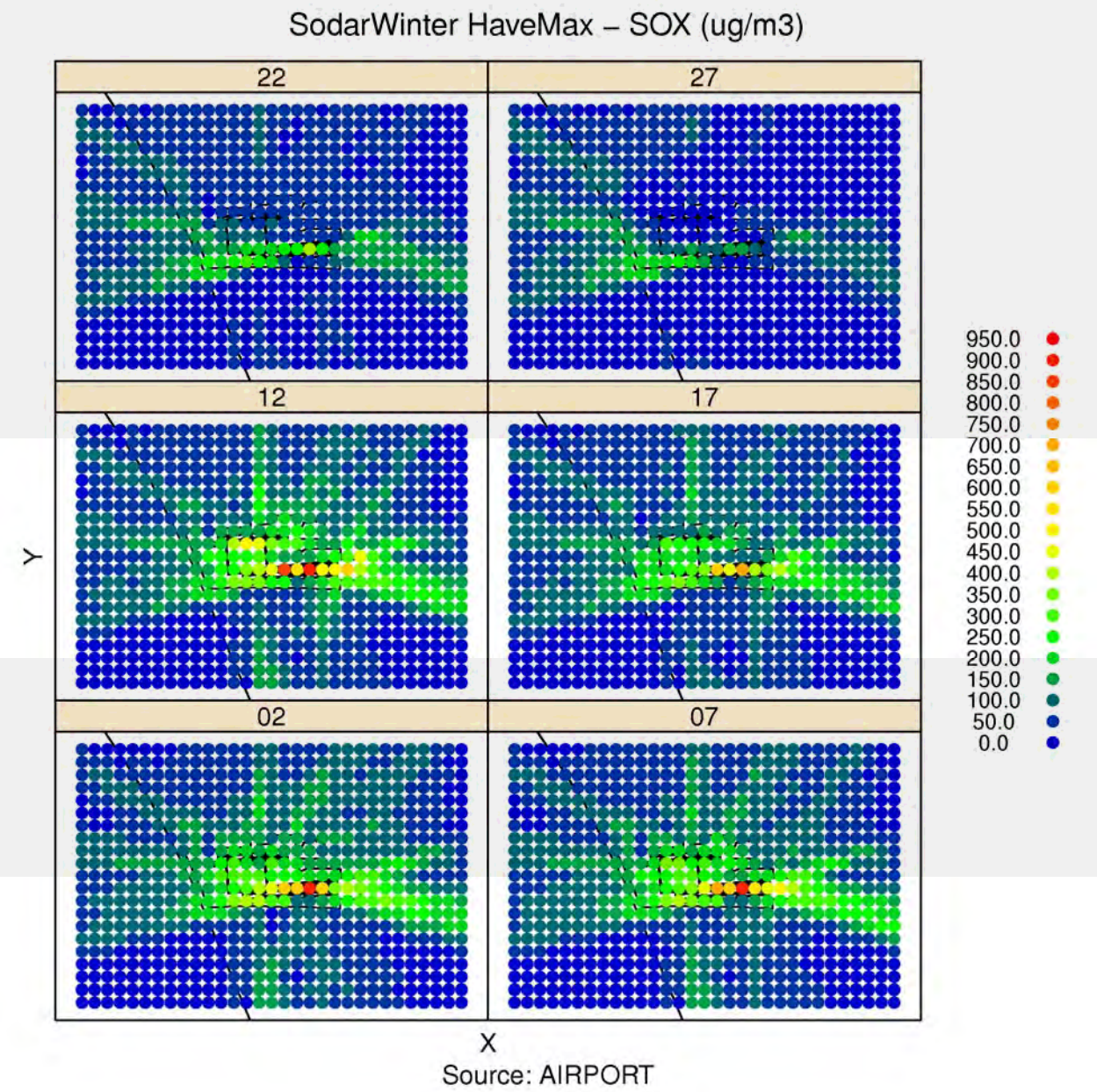

Figure 9A-35: Modeled hourly max SO_X concentrations from airport-related sources at flag-pole receptors at heights of 2m, 7m, 12m, 17m, 22m and 27m in Cartesian Grid of receptors during Winter Season.

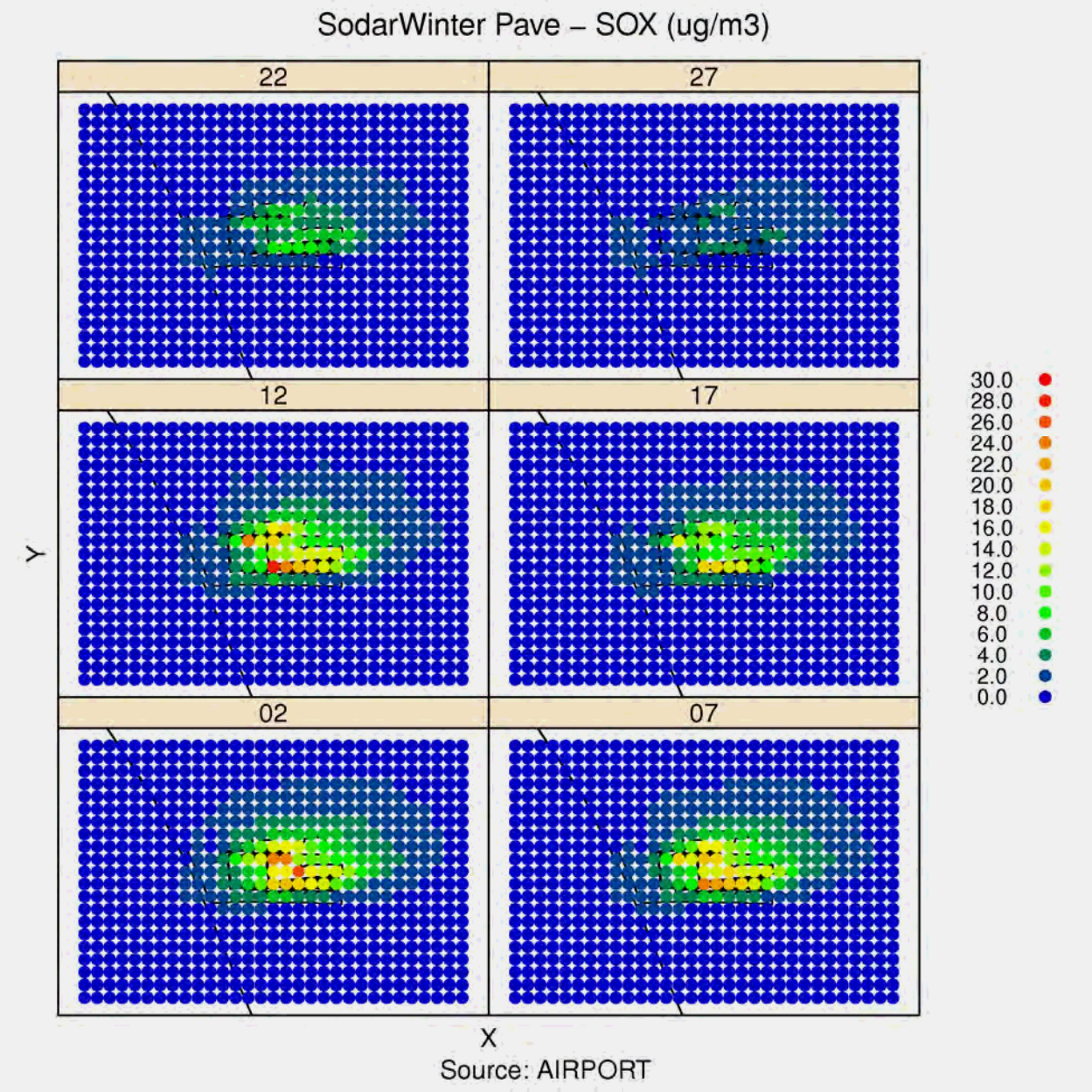

Figure 9A-36: Modeled period average SO_X concentrations from airport-related sources at flag-pole receptors at heights of 2m, 7m, 12m, 17m, 22m and 27m in Cartesian Grid of receptors during Winter Season.

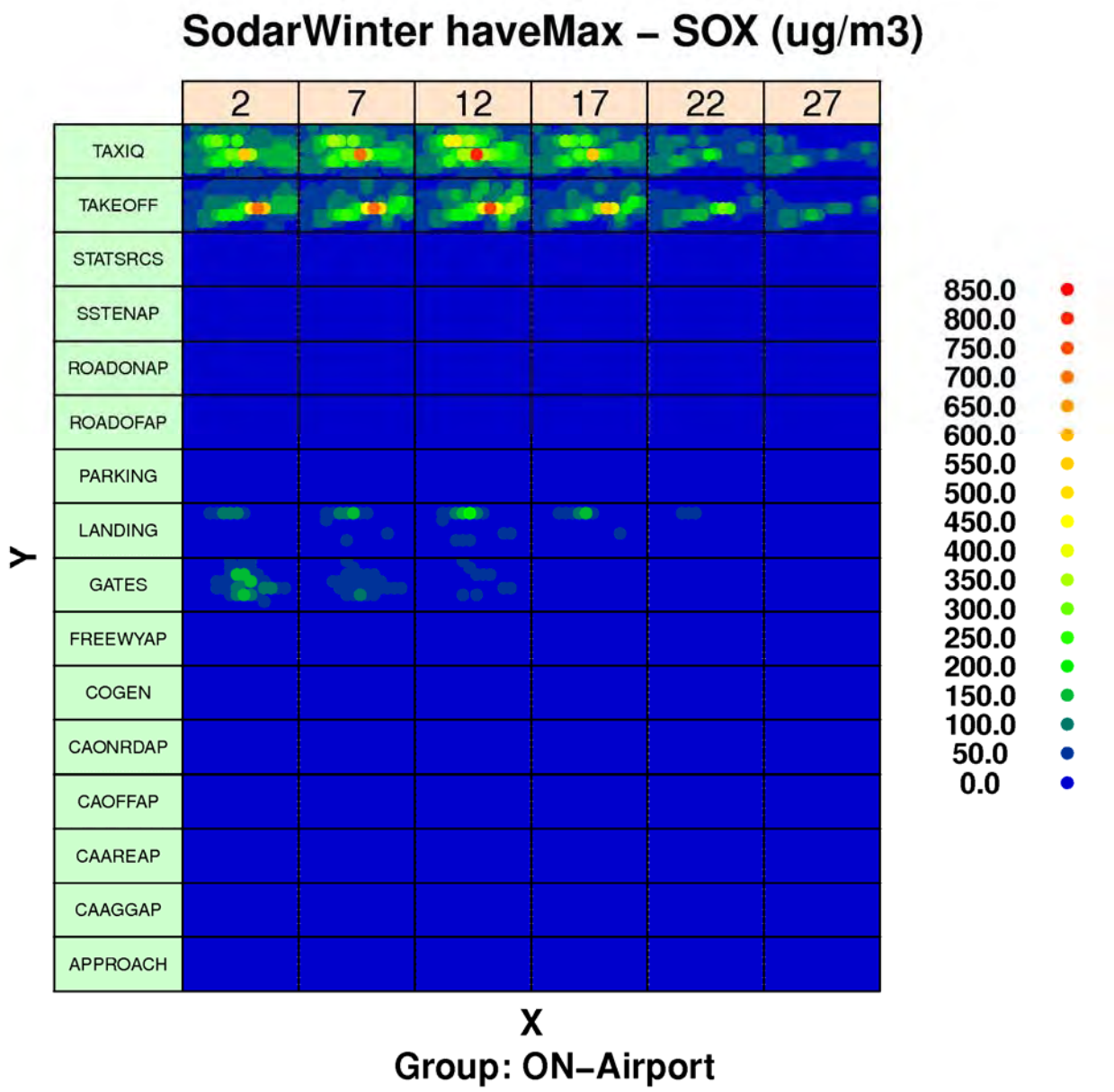

Figure 9A-37: Modeled hourly maximum SOx concentrations from airport-related sources by source sector at flag-pole receptors at heights of 2m, 7m, 12m, 17m, 22m and 27m in Cartesian Grid of receptors during Winter Season.

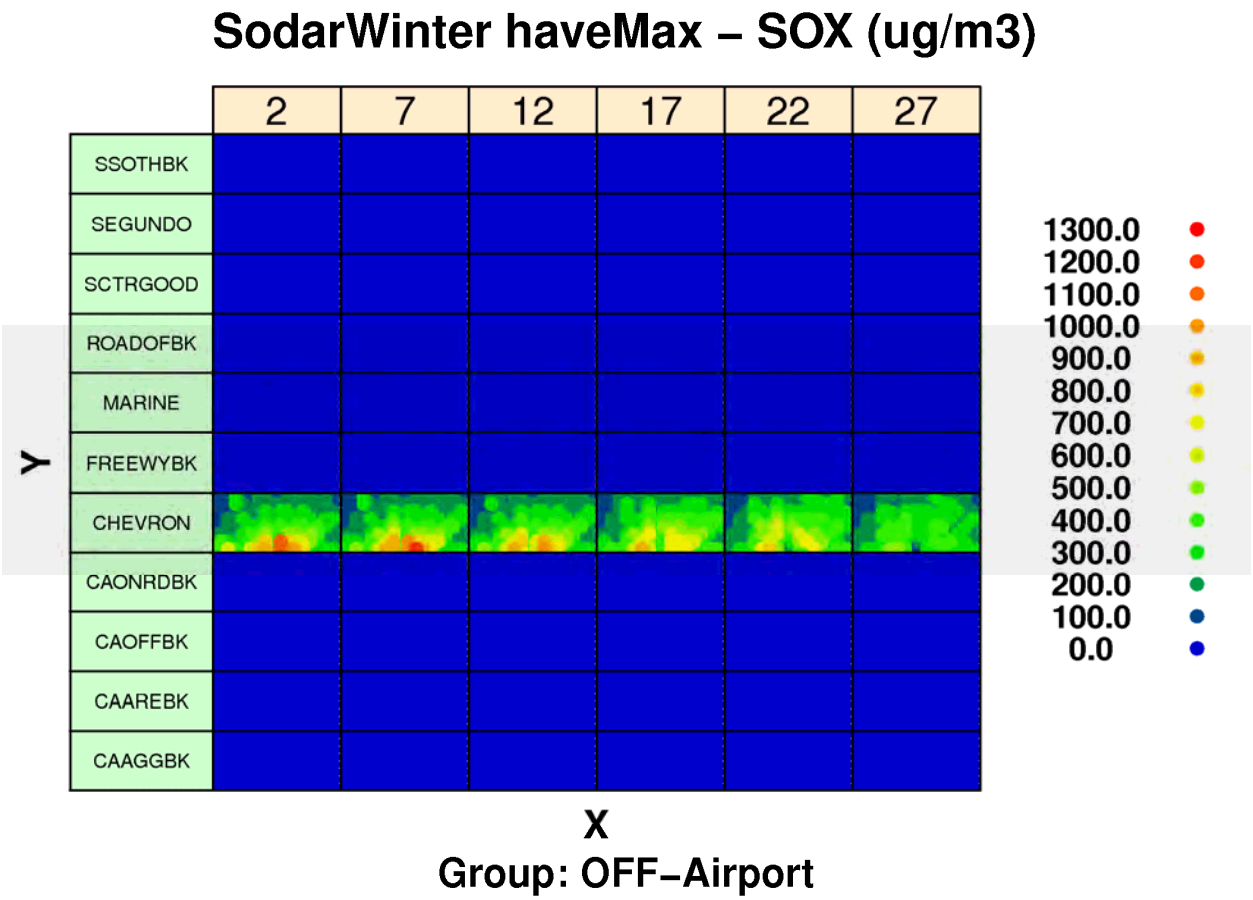

Figure 9A-38: Modeled hourly maximum SOx concentrations from background sources by source sector at flag-pole receptors at heights of 2m, 7m, 12m, 17m, 22m and 27m in Cartesian Grid of receptors during Winter Season.

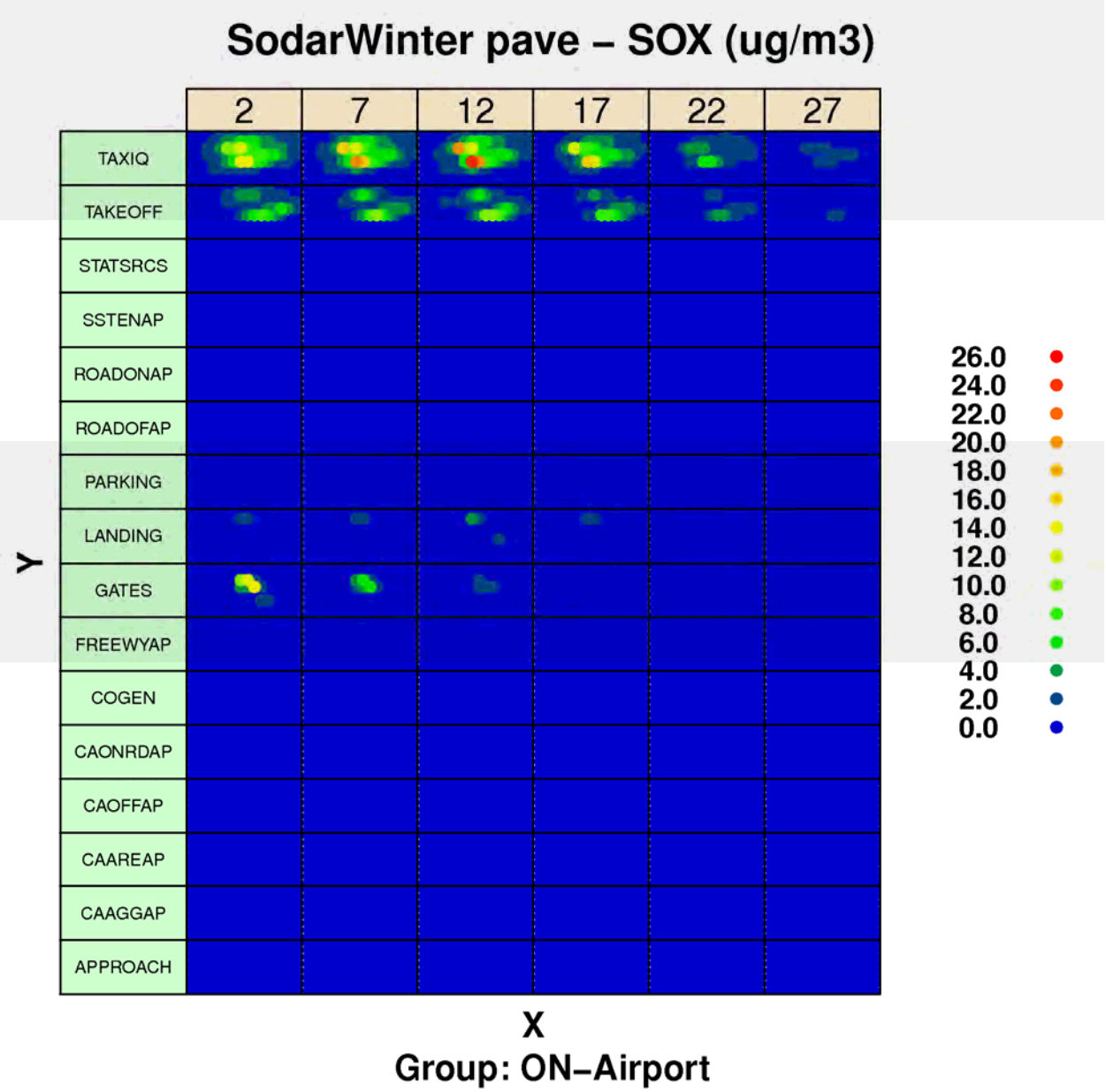

Figure 9A-39: Modeled period average SOx concentrations from airport-related sources by source sector at flag-pole receptors at heights of 2m, 7m, 12m, 17m, 22m and 27m in Cartesian Grid of receptors during Winter Season.

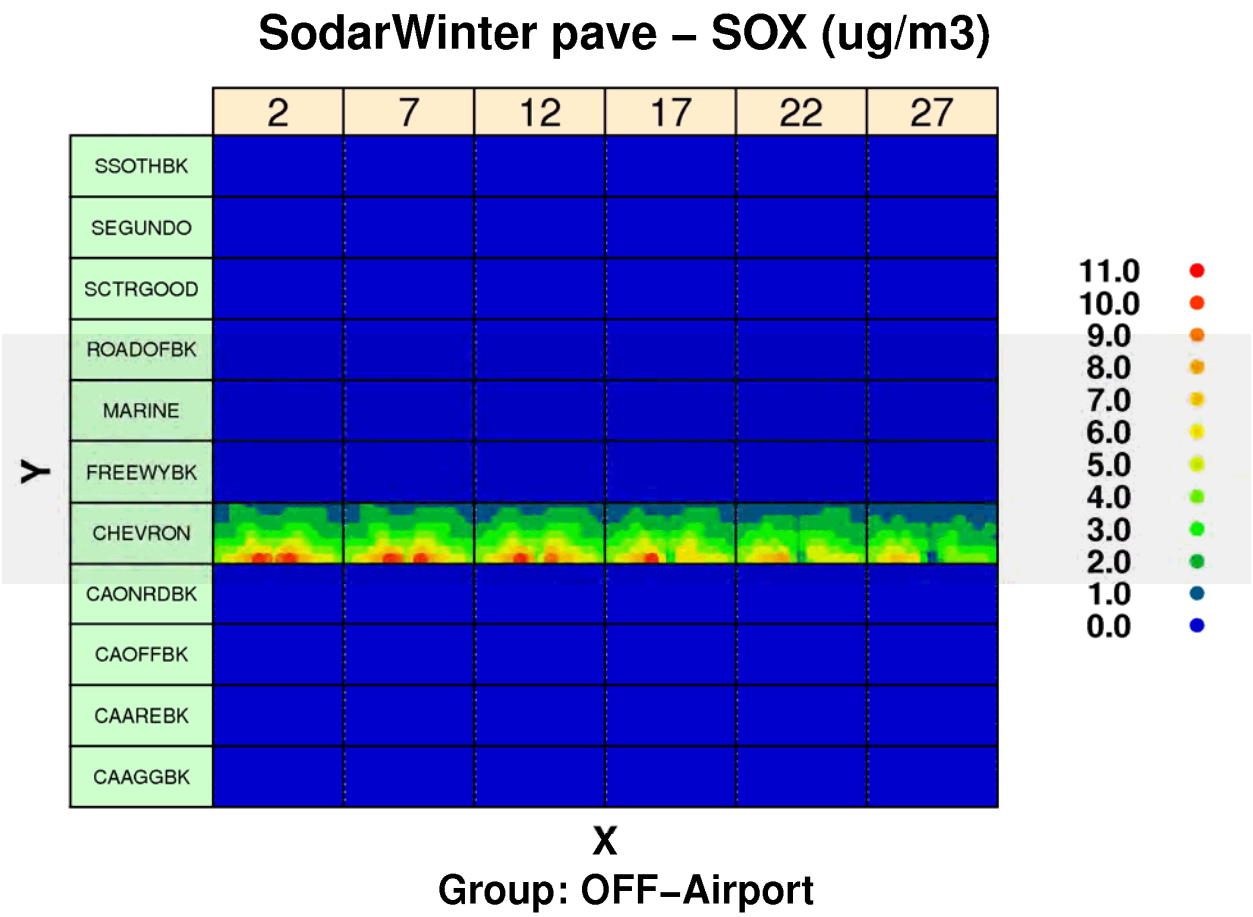

Figure 9A-40: Modeled period average SOx concentrations from background sources by source sector at flag-pole receptors at heights of 2m, 7m, 12m, 17m, 22m and 27m in Cartesian Grid of receptors during Winter Season.

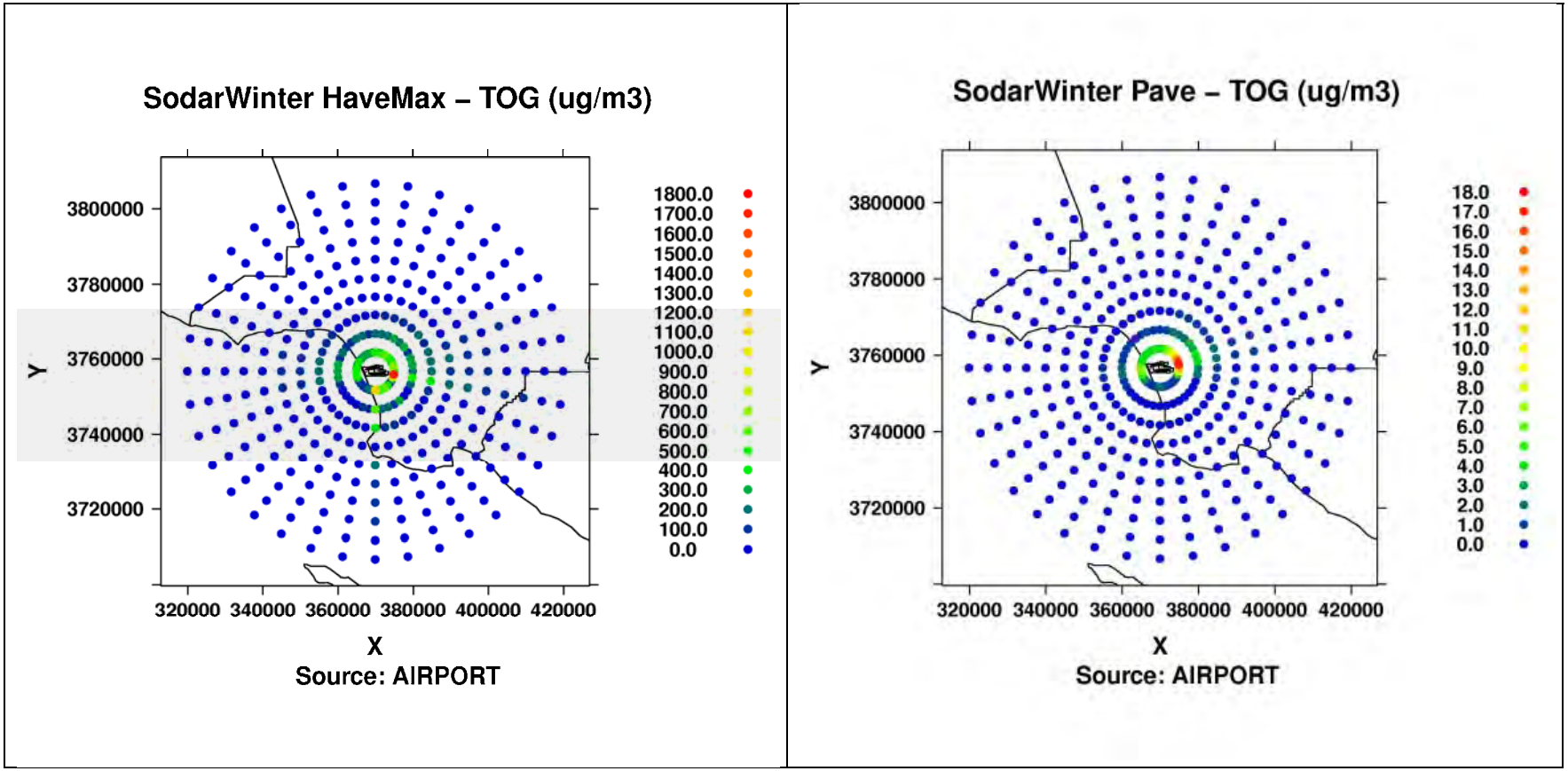

Figure 9A-41a: Modeled hourly max (left) and period average (right) TOG concentrations from airport-related in Polar Grid of receptors during Winter Season.

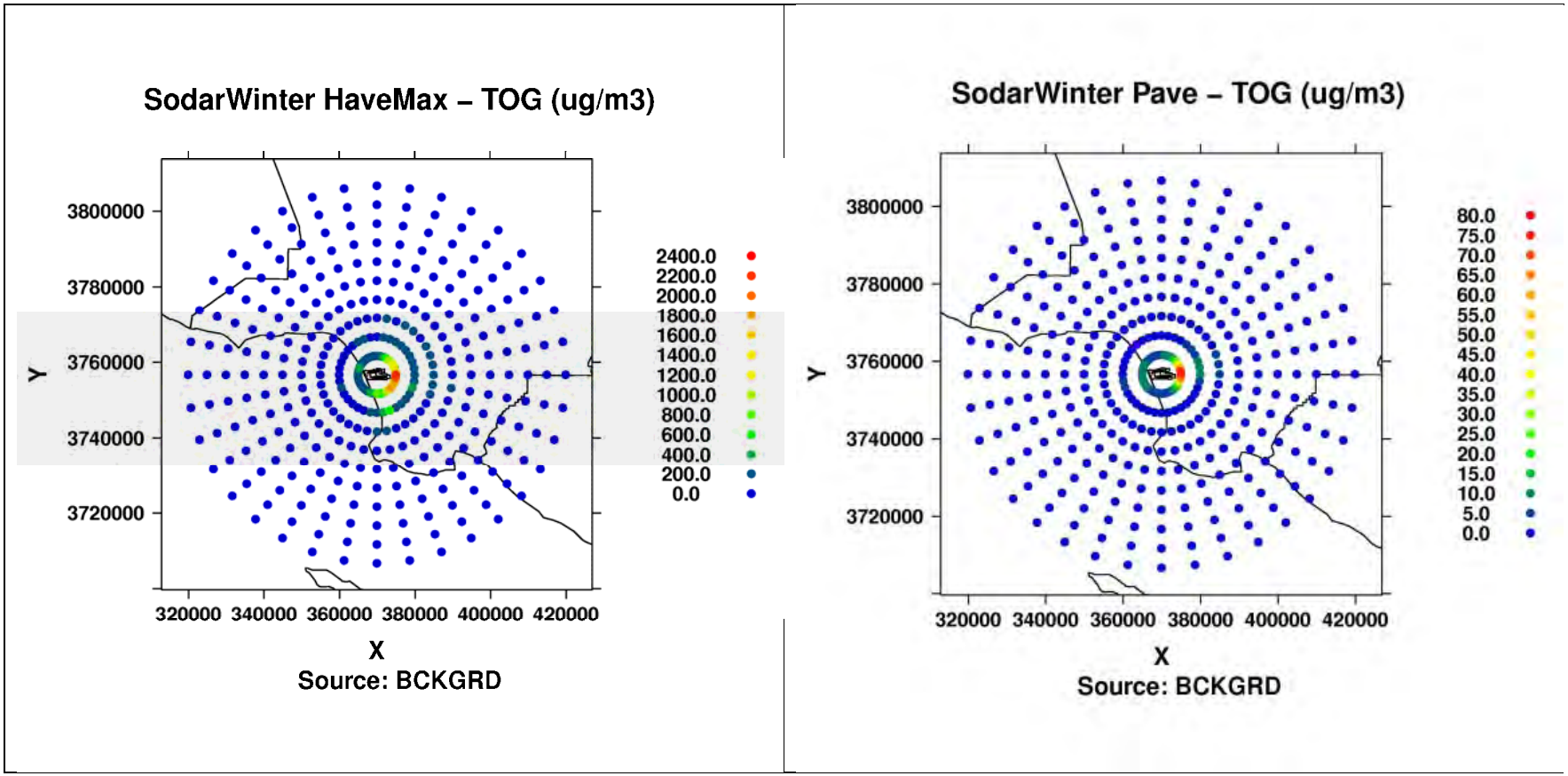

Figure 9A-41b: Modeled hourly max (left) and period average (right) TOG concentrations from background sources in Polar Grid of receptors during Winter Season.

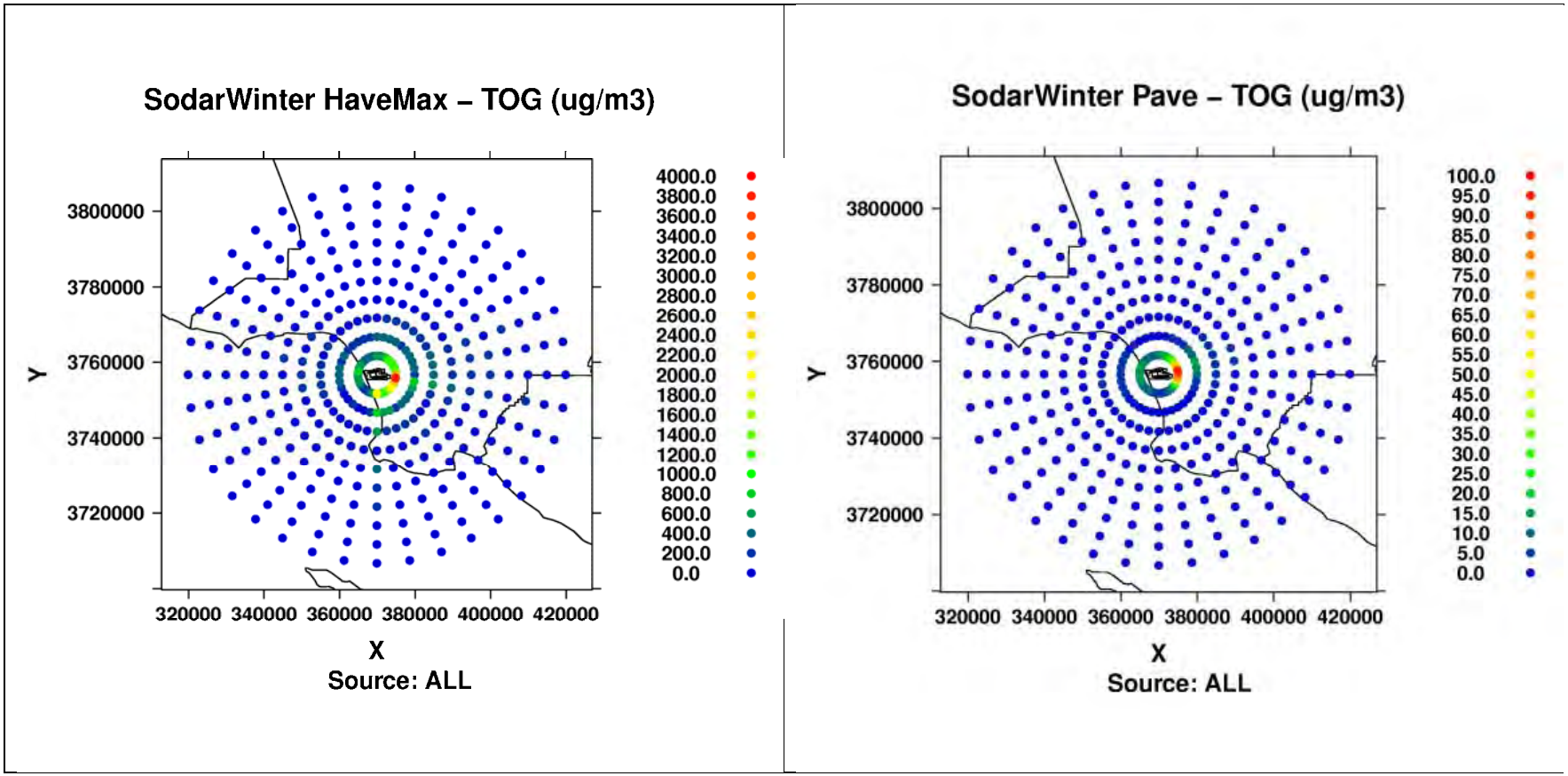

Figure 9A-41c: Modeled hourly max (left) and period average (right) TOG concentrations from ALL in Polar Grid of receptors during Winter Season.

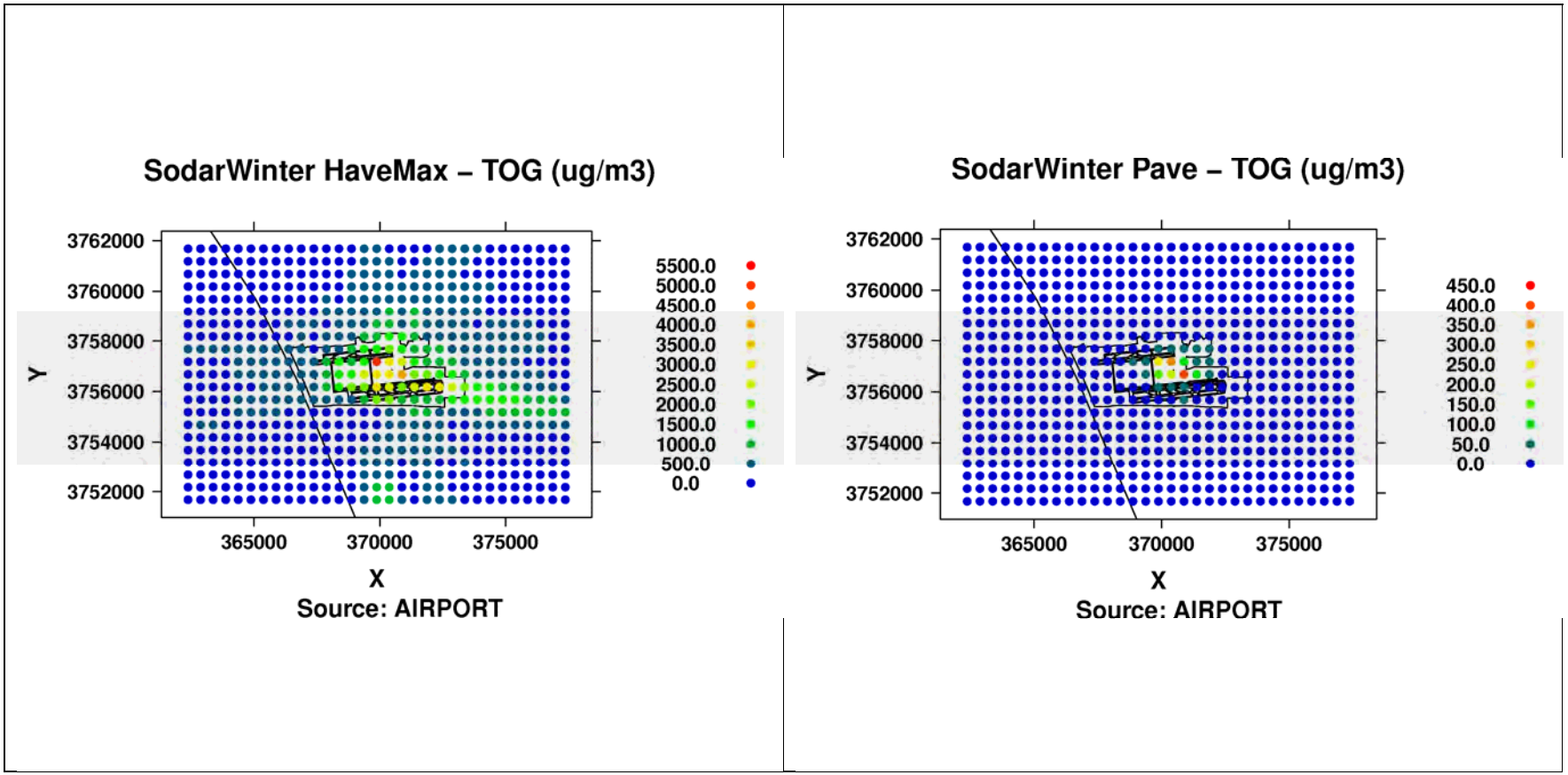

Figure 9A-42a: Modeled hourly max (left) and period average (right) TOG concentrations from airport-related in Cartesian Grid of receptors during Winter Season.

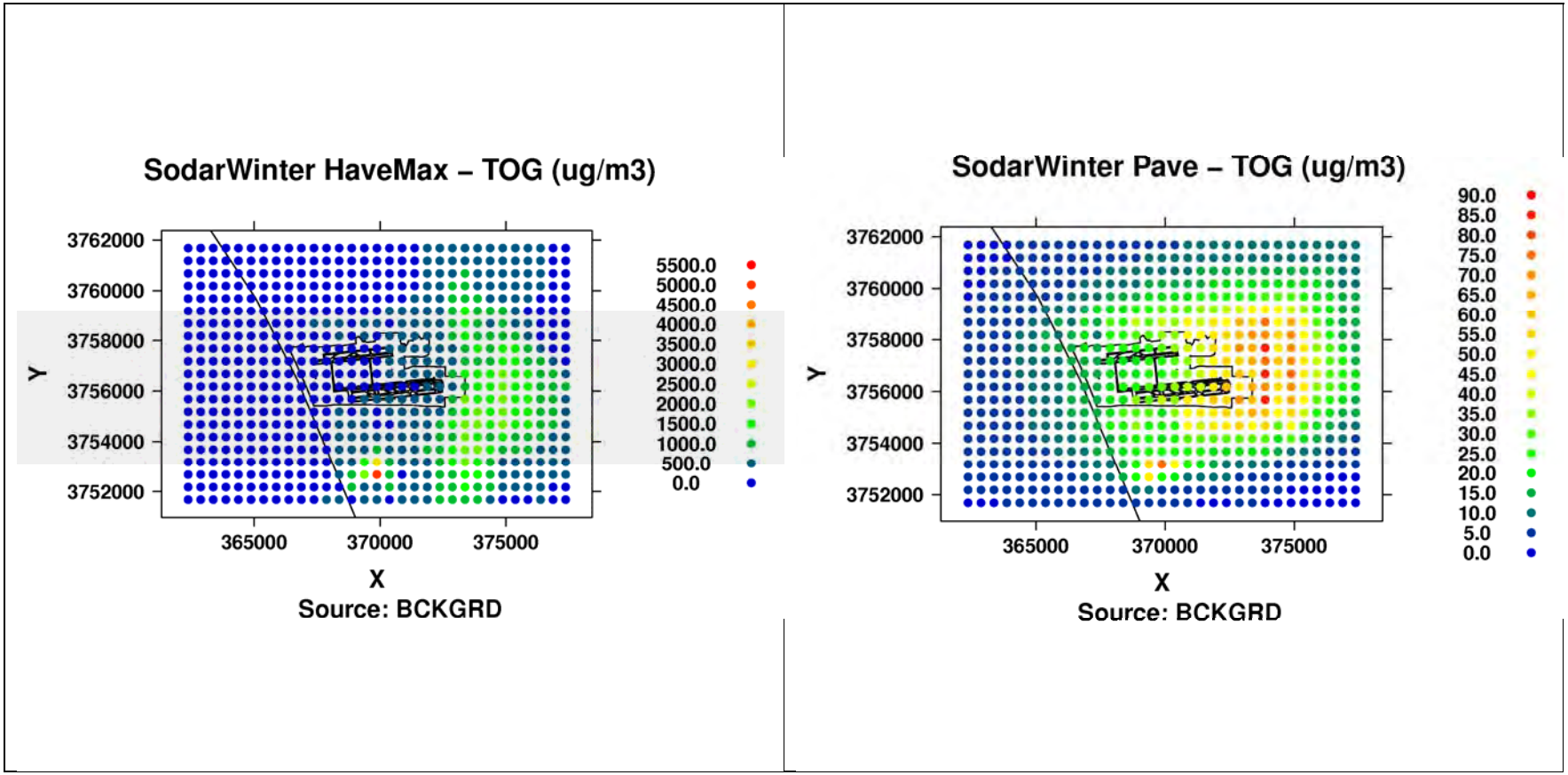

Figure 9A-42b: Modeled hourly max (left) and period average (right) TOG concentrations from background sources in Cartesian Grid of receptors during Winter Season.

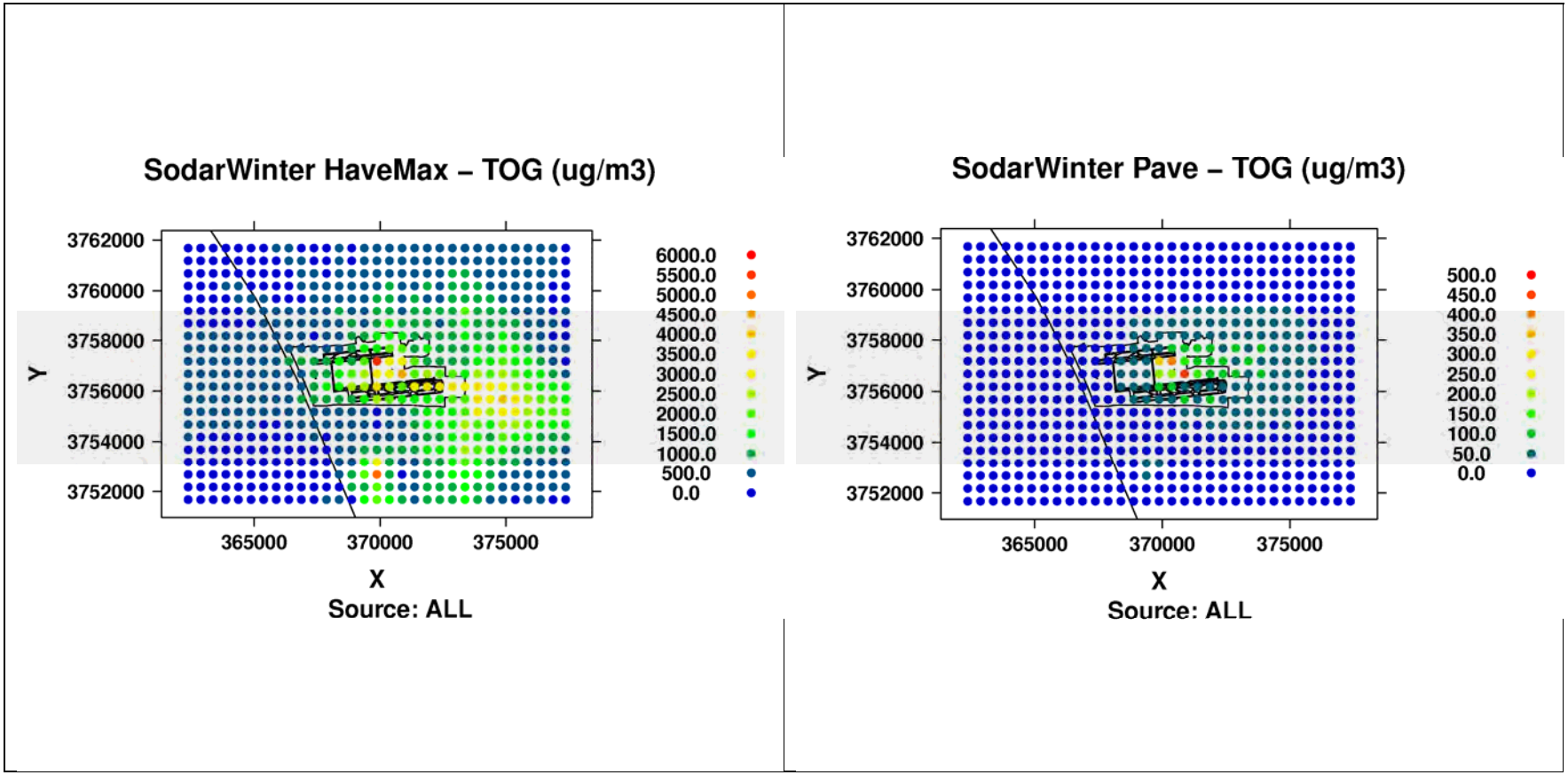

Figure 9A-42c: Modeled hourly max (left) and period average (right) TOG concentrations ALL in Cartesian Grid of receptors during Winter Season.

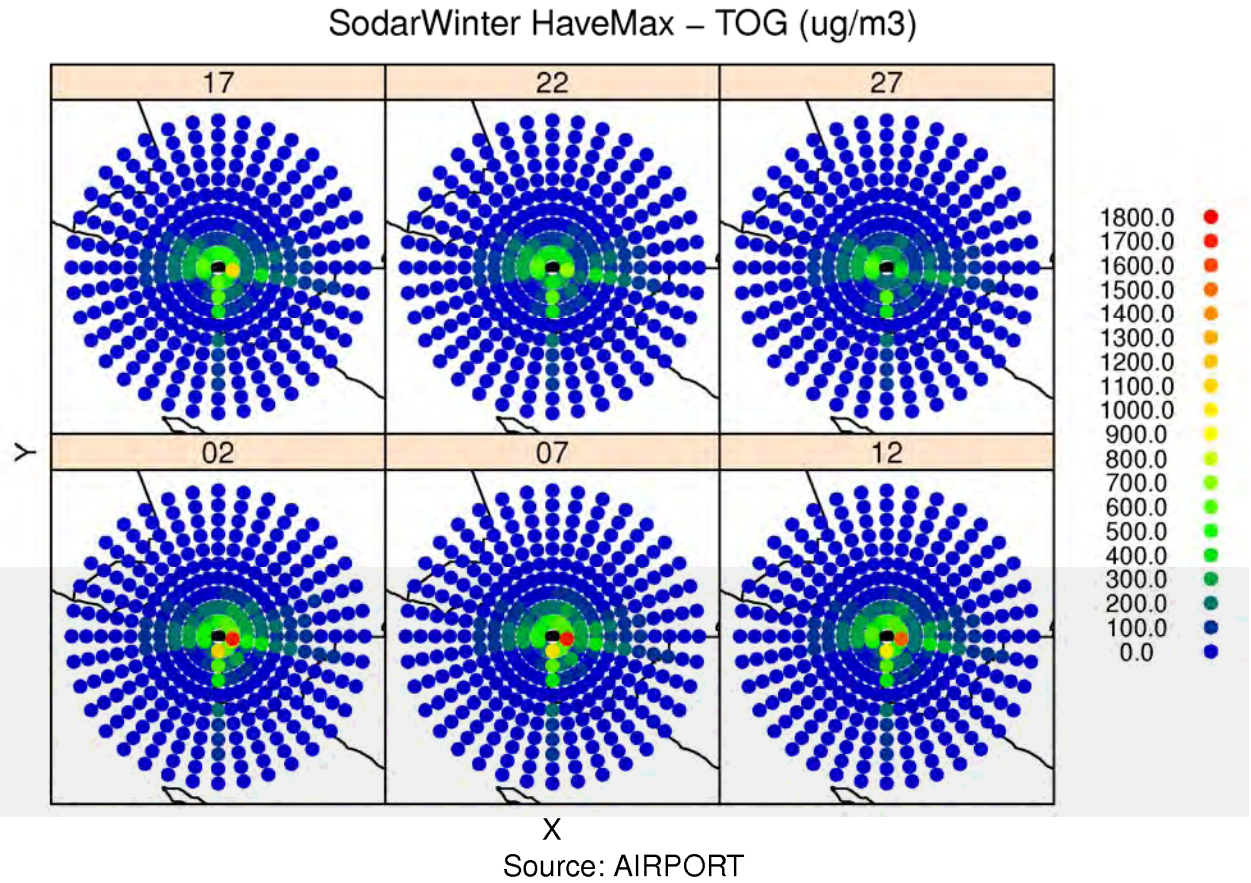

Figure 9A-43: Modeled hourly max TOG concentrations from airport-related sources at flag-pole receptors at heights of 2m, 7m, 12m, 17m, 22m and 27m in Polar Grid of receptors during Winter Season.

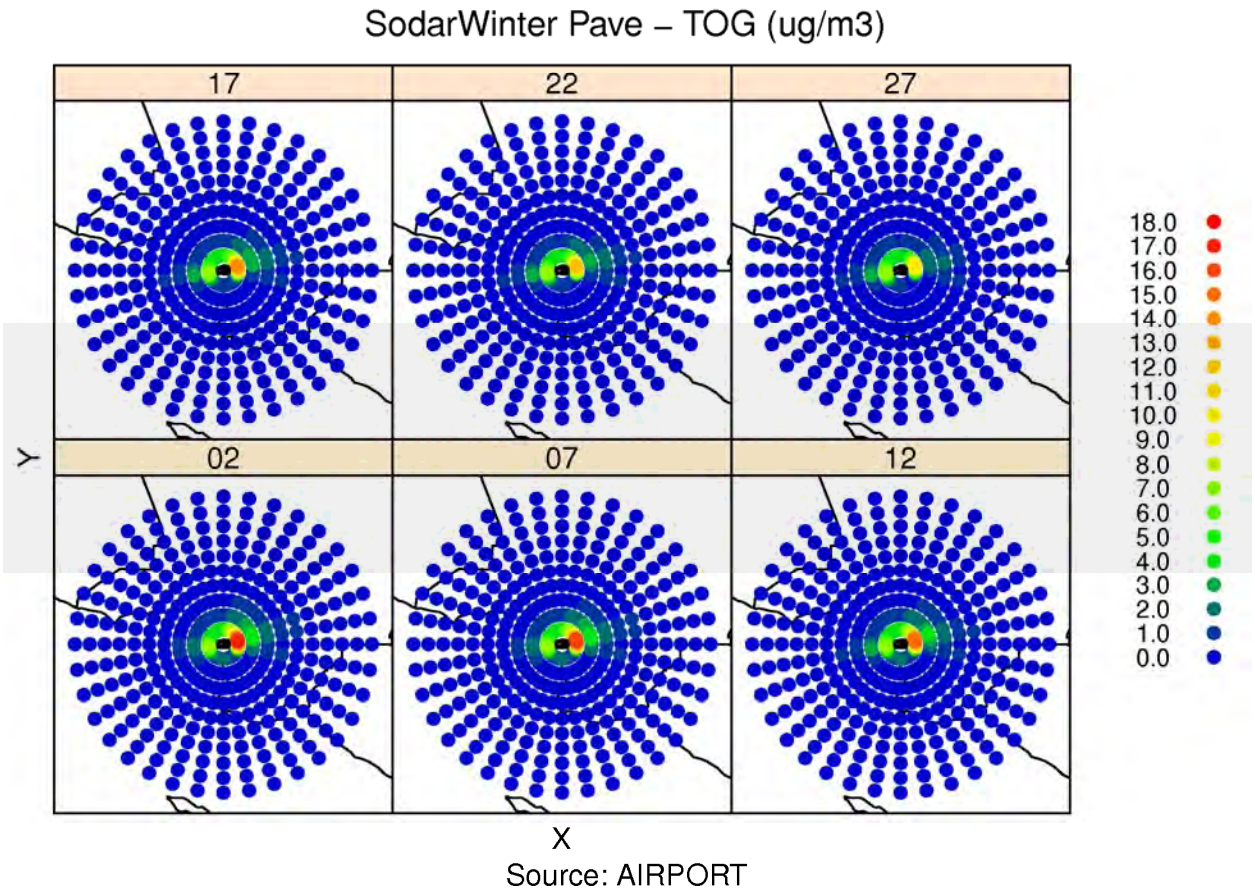

Figure 9A-44: Modeled period average TOG concentrations from airport-related sources at flag-pole receptors at heights of 2m, 7m, 12m, 17m, 22m and 27m in Polar Grid of receptors during Winter Season.

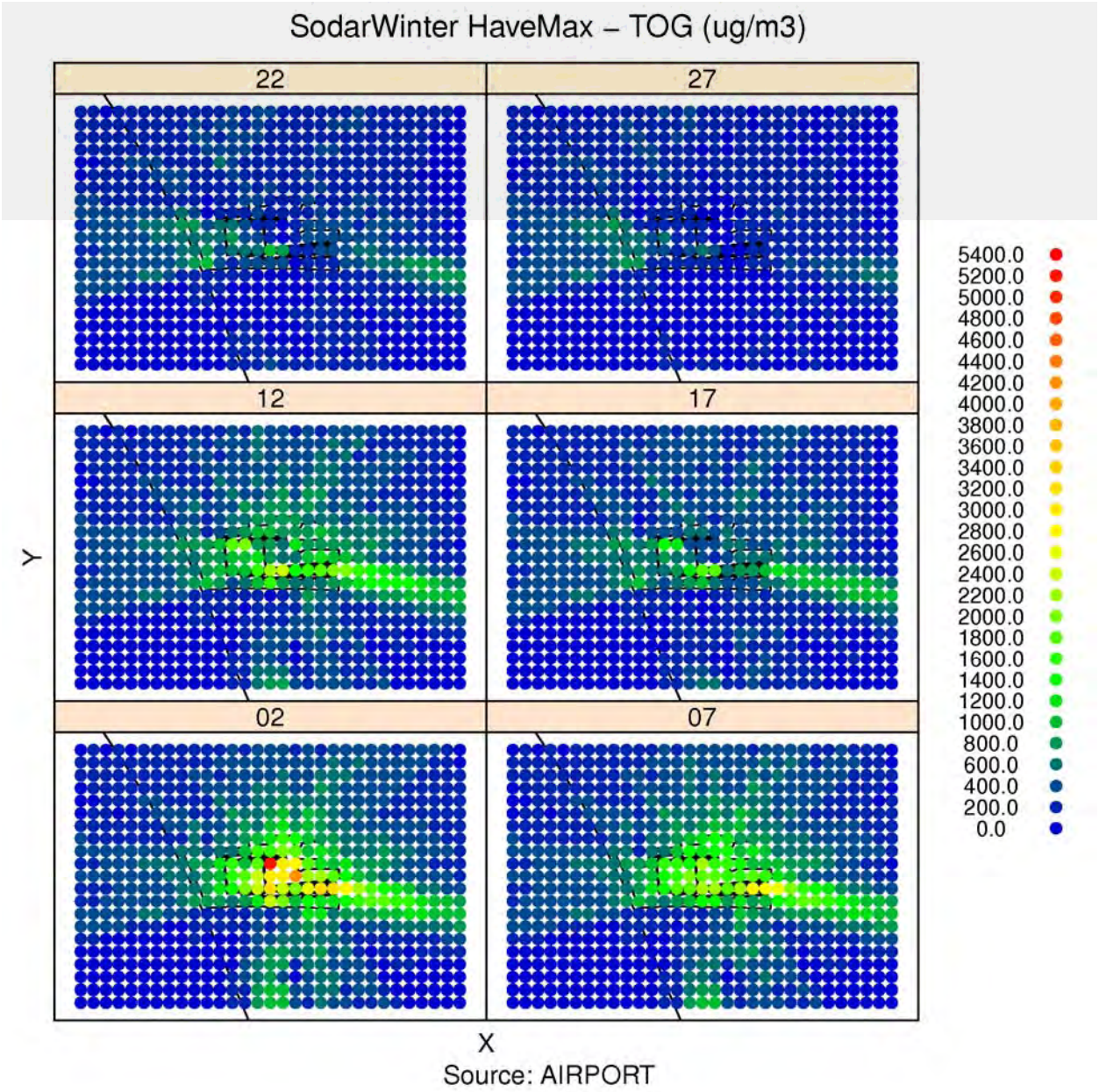

Figure 9A-45: Modeled hourly max TOG concentrations from airport-related sources at flag-pole receptors at heights of 2m, 7m, 12m, 17m, 22m and 27m in Cartesian Grid of receptors during Winter Season.

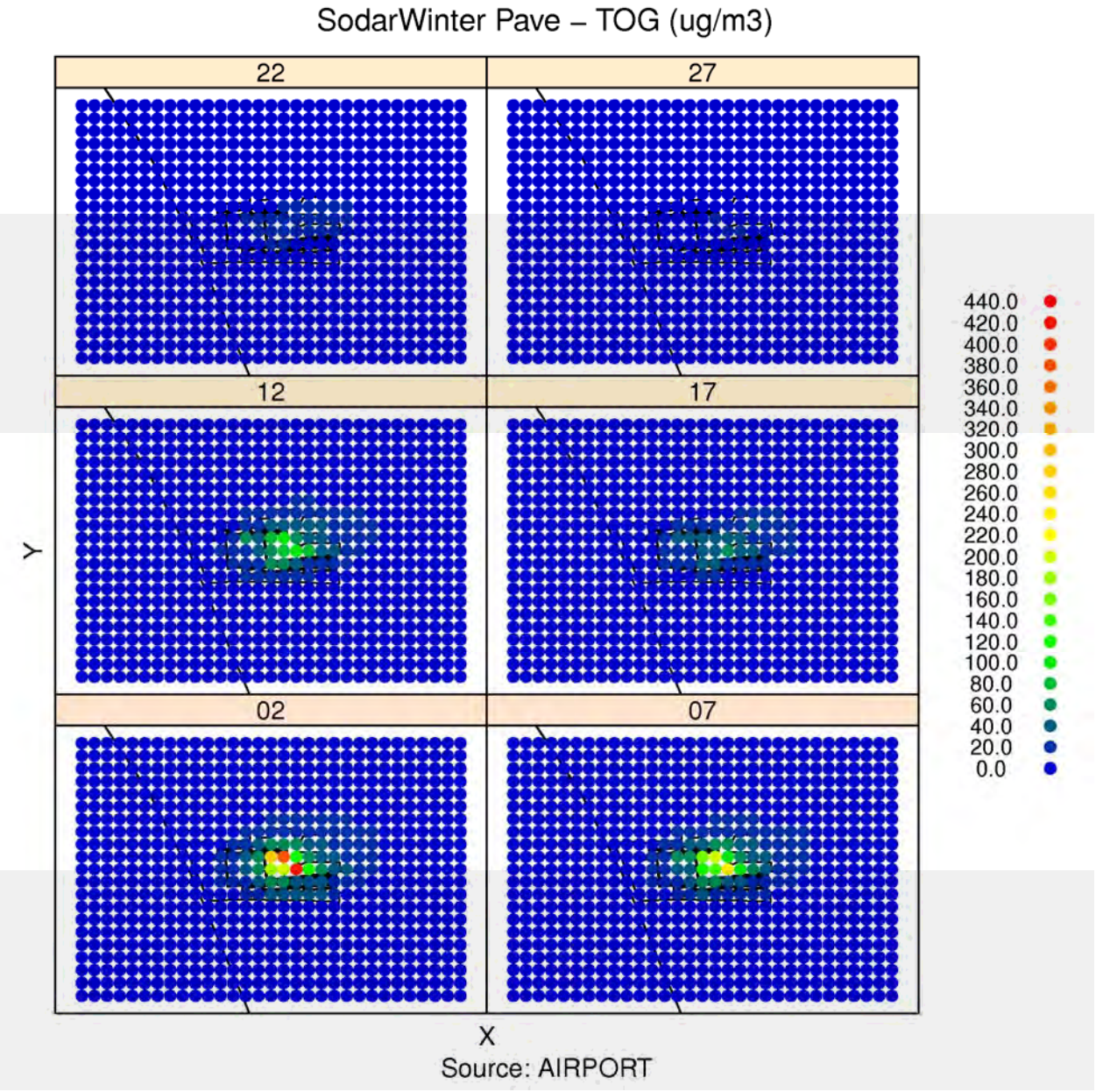

Figure 9A-46: Modeled period average TOG concentrations from airport-related sources at flag-pole receptors at heights of 2m, 7m, 12m, 17m, 22m and 27m in Cartesian Grid of receptors during Winter Season.

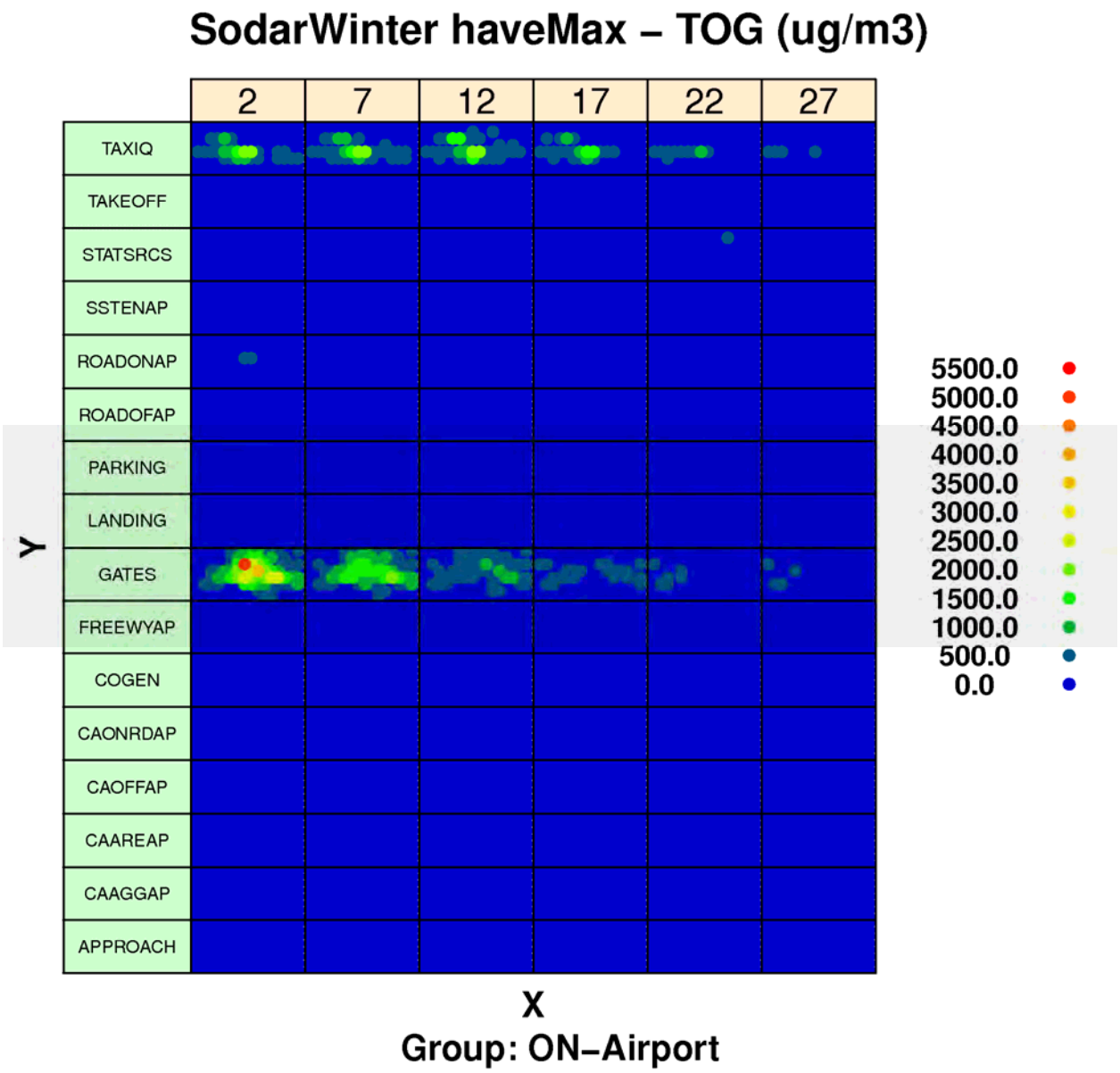

Figure 9A-47: Modeled hourly maximum TOG concentrations from airport-related sources by source sector at flag-pole receptors at heights of 2m, 7m, 12m, 17m, 22m and 27m in Cartesian Grid of receptors during Winter Season.

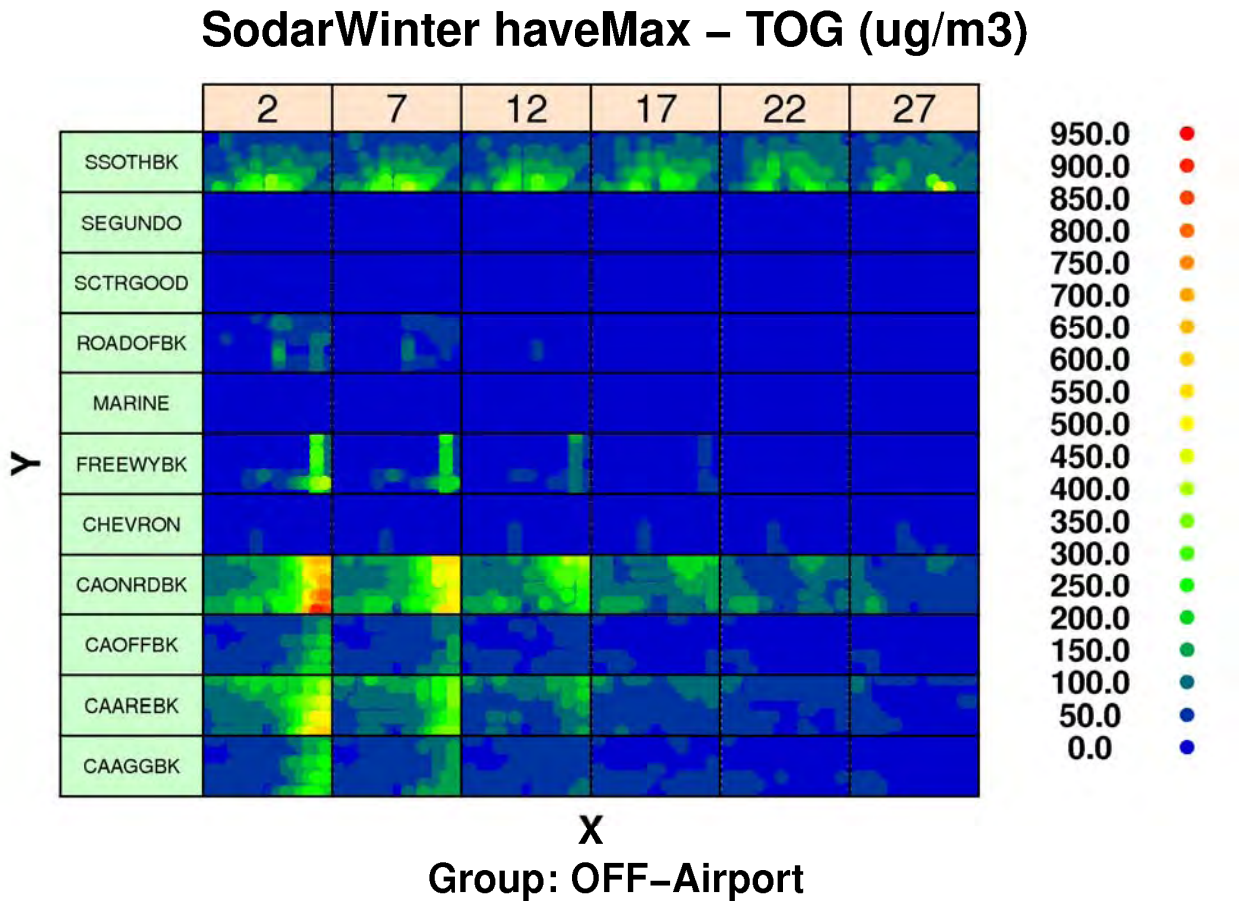

Figure 9A-48: Modeled hourly maximum TOG concentrations from background sources by source sector at flag-pole receptors at heights of 2m, 7m, 12m, 17m, 22m and 27m in Cartesian Grid of receptors during Winter Season.

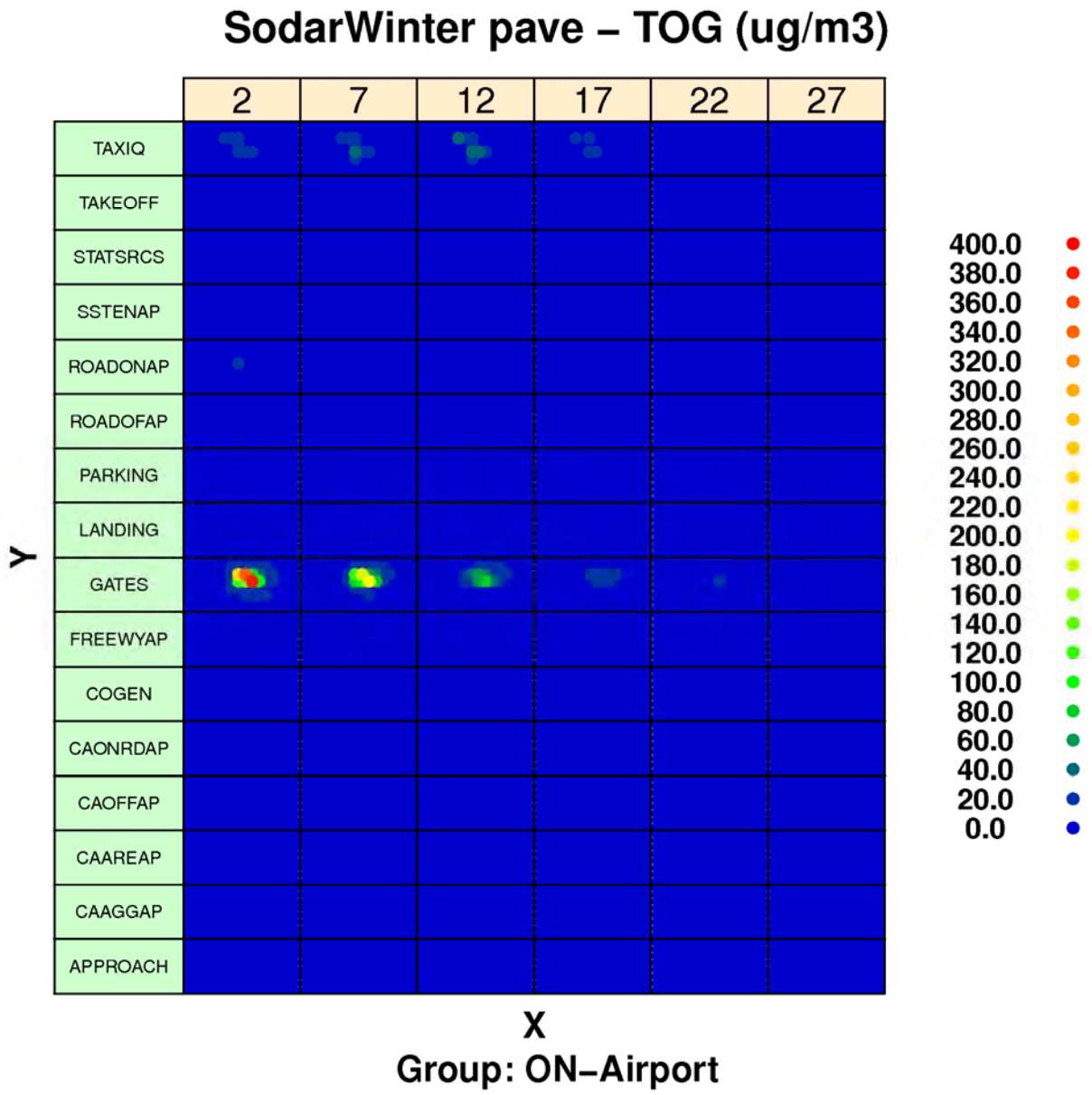

Figure 9A-49: Modeled period average TOG concentrations from airport-related sources by source sector at flag-pole receptors at heights of 2m, 7m, 12m, 17m, 22m and 27m in Cartesian Grid of receptors during Winter Season.

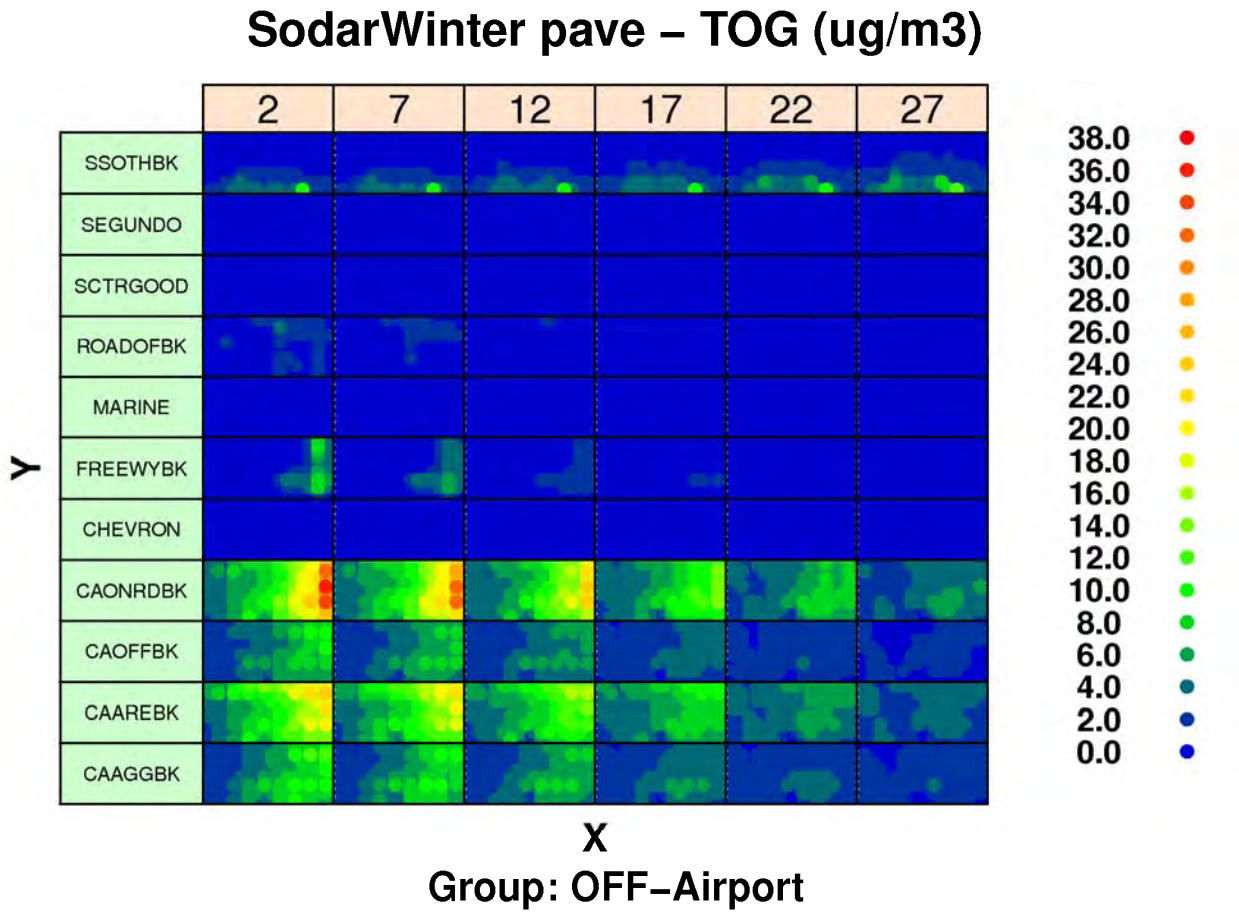

Figure 9A-50: Modeled period average TOG concentrations from background sources by source sector at flag-pole receptors at heights of 2m, 7m, 12m, 17m, 22m and 27m in Cartesian Grid of receptors during Winter Season.

II. Model Evaluation

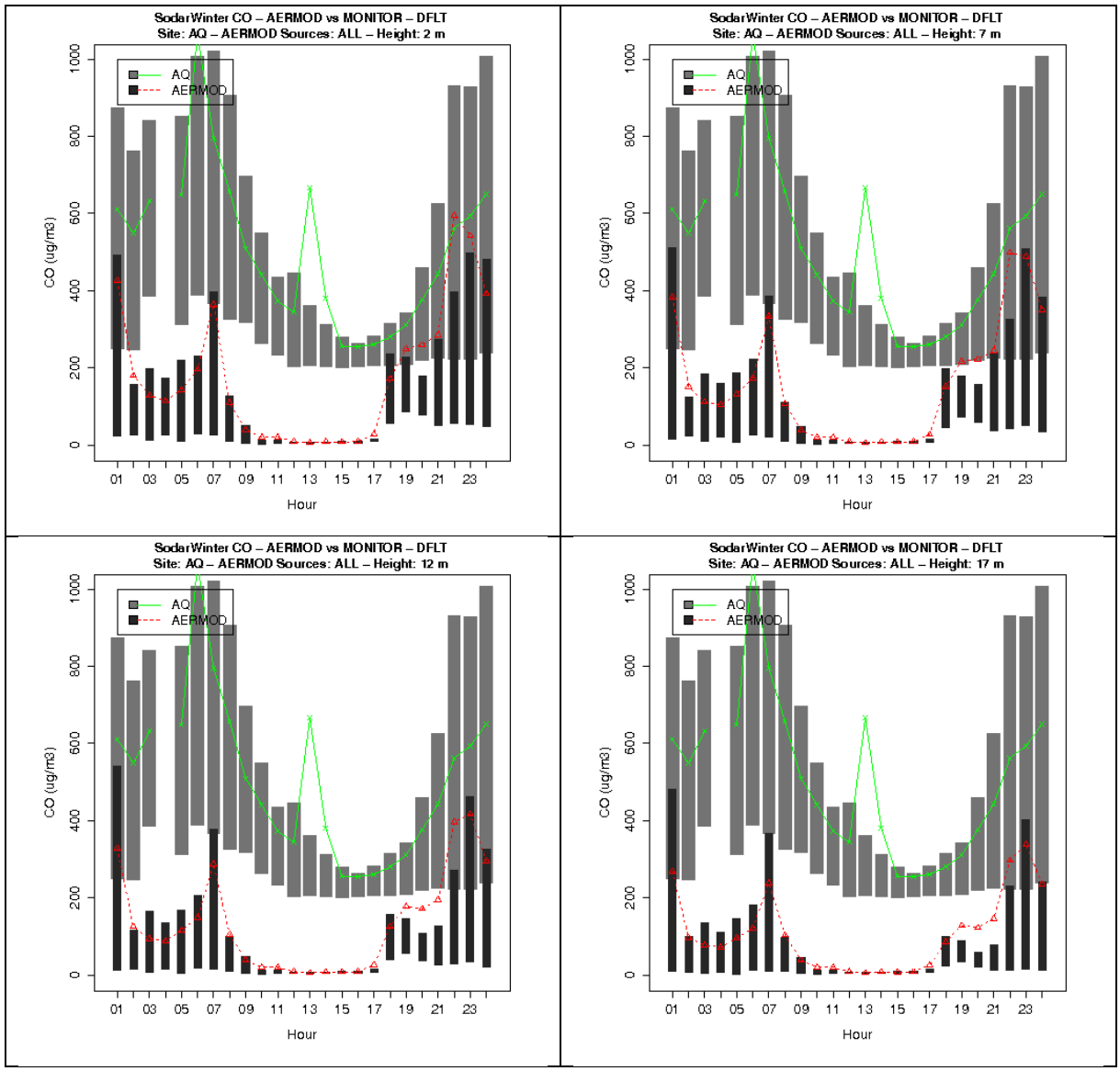

Figure 9A-51: Diurnal variability in observed and modeled CO concentrations at AQ Site from flagpole receptors at heights of 2m, 7m, 12m and 17m during Winter Season.

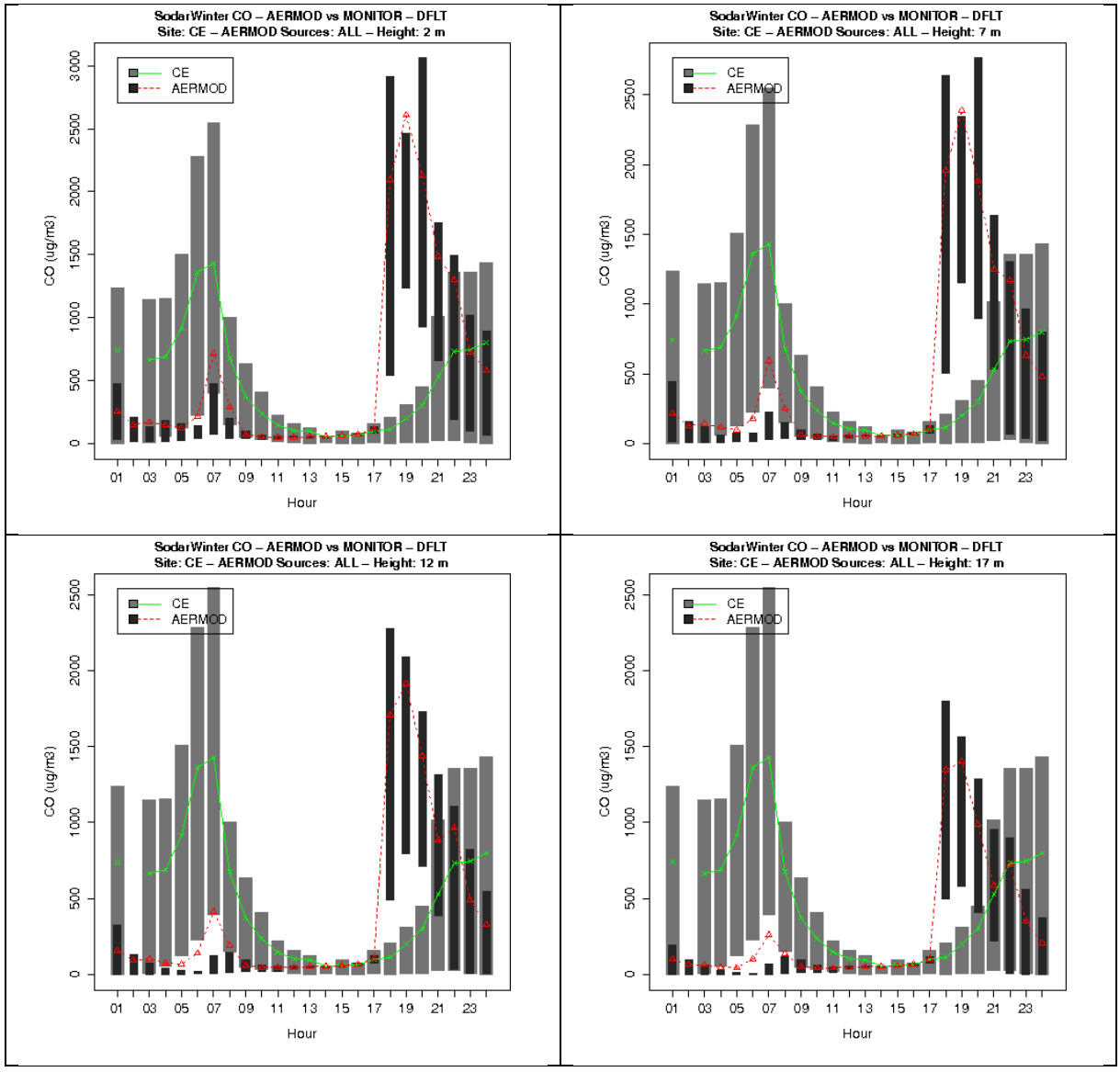

Figure 9A-52: Diurnal variability in observed and modeled CO concentrations at CE Site from flagpole receptors at heights of 2m, 7m, 12m and 17m during Winter Season.

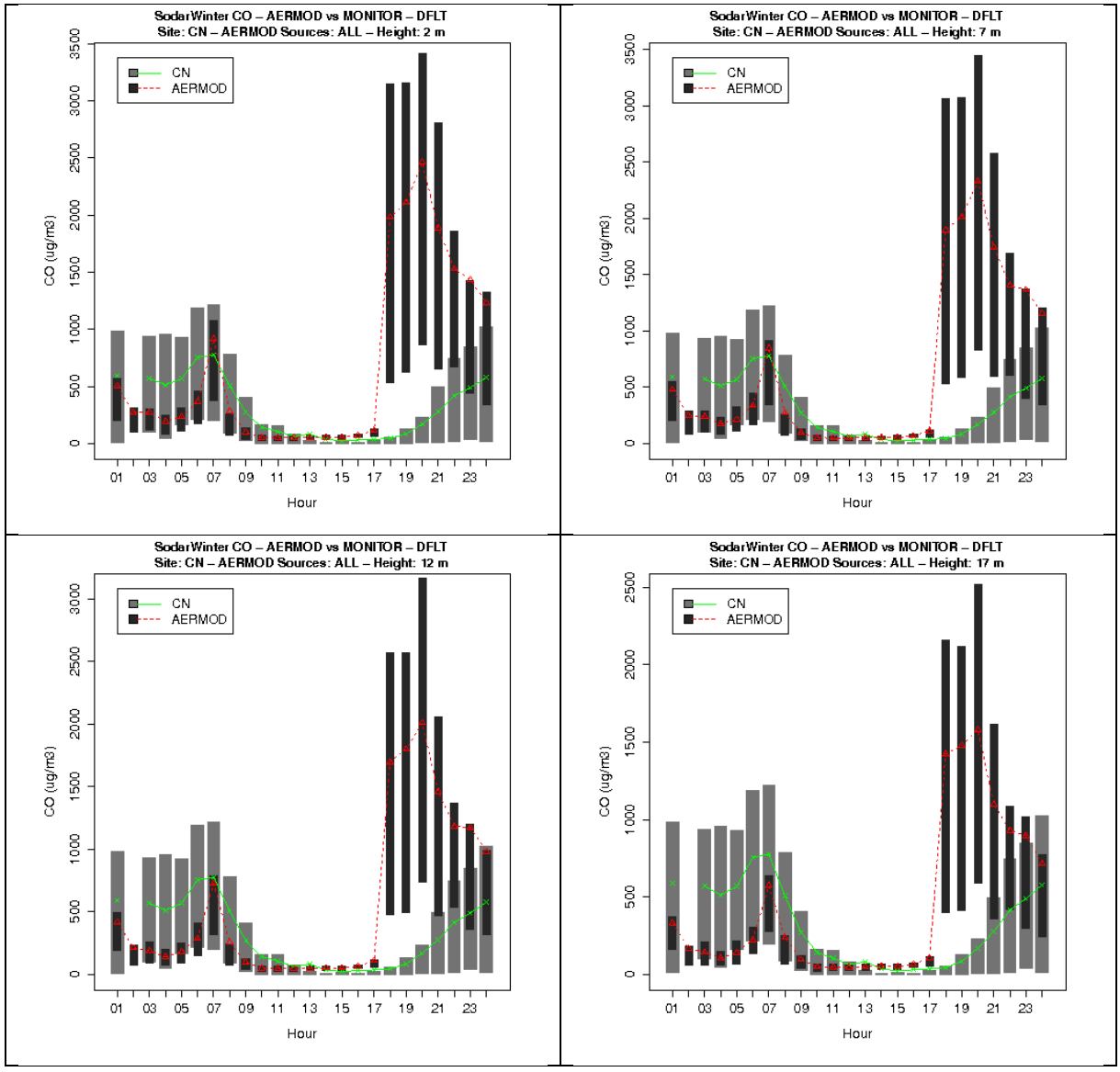

Figure 9A-53: Diurnal variability in observed and modeled CO concentrations at CN Site from flagpole receptors at heights of 2m, 7m, 12m and 17m during Winter Season.

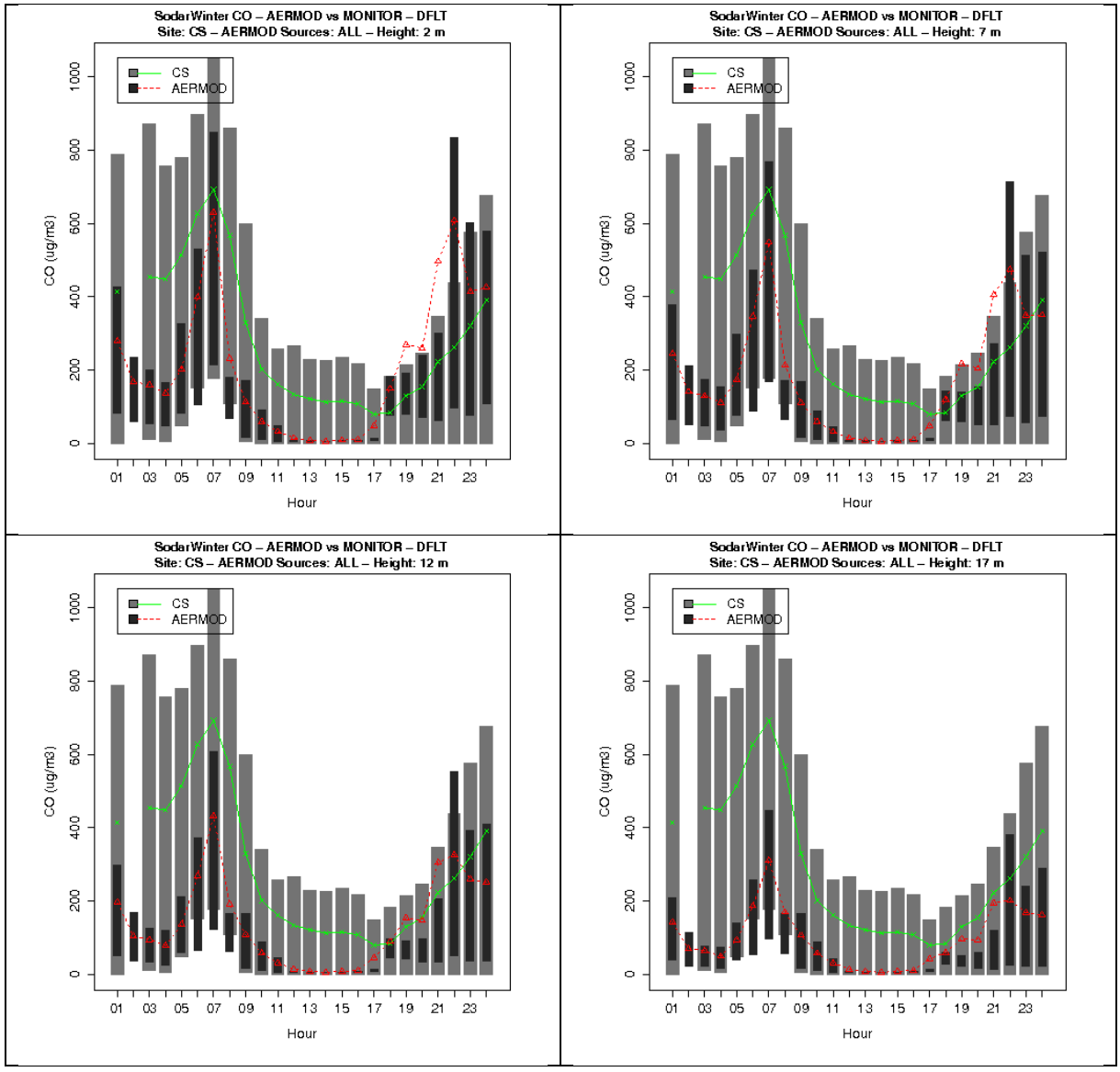

Figure 9A-54: Diurnal variability in observed and modeled CO concentrations at CS Site from flagpole receptors at heights of 2m, 7m, 12m and 17m during Winter Season.

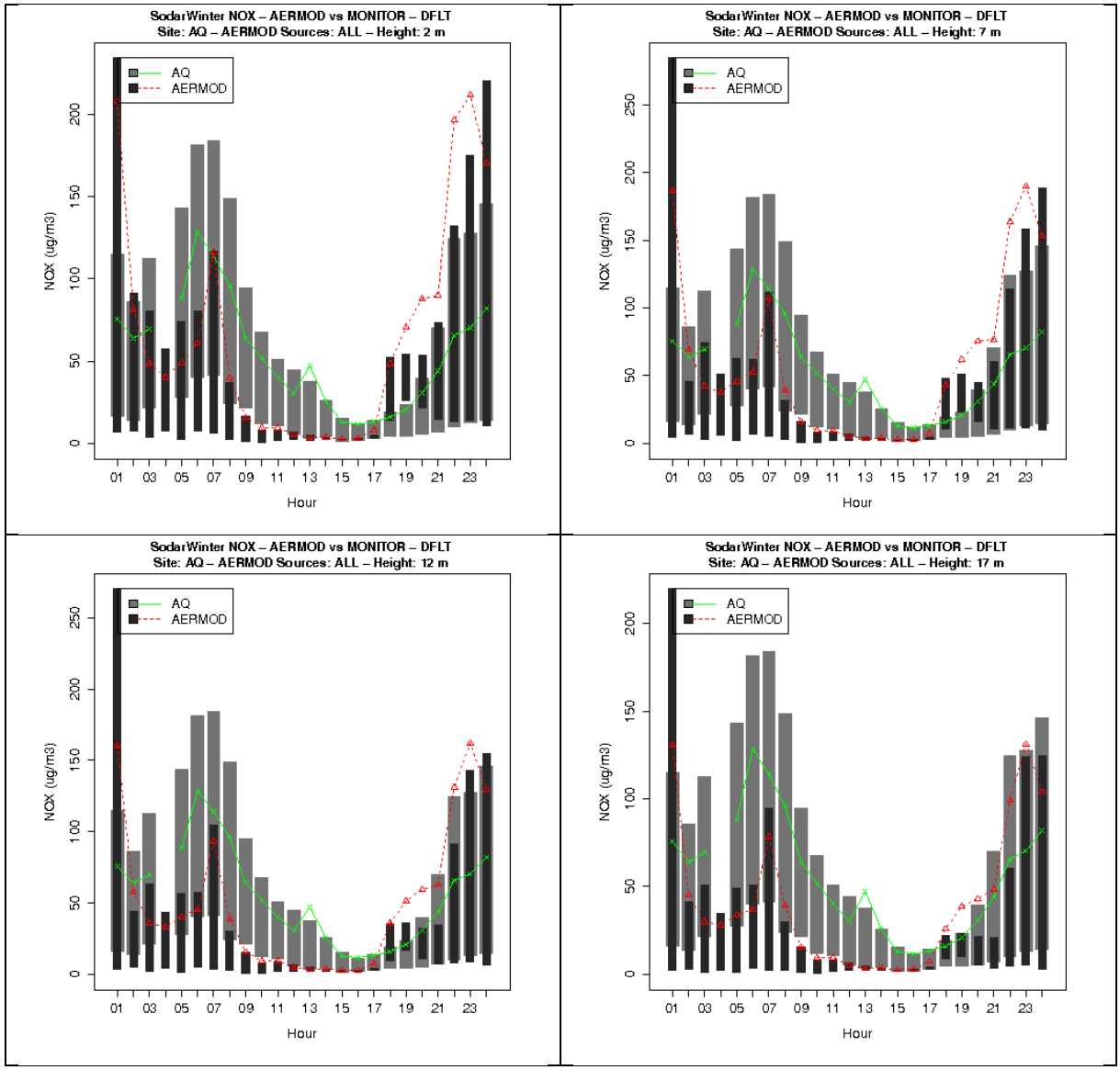

Figure 9A-55: Diurnal variability in observed and modeled NOx concentrations at AQ Site from flagpole receptors at heights of 2m, 7m, 12m and 17m during Winter Season.

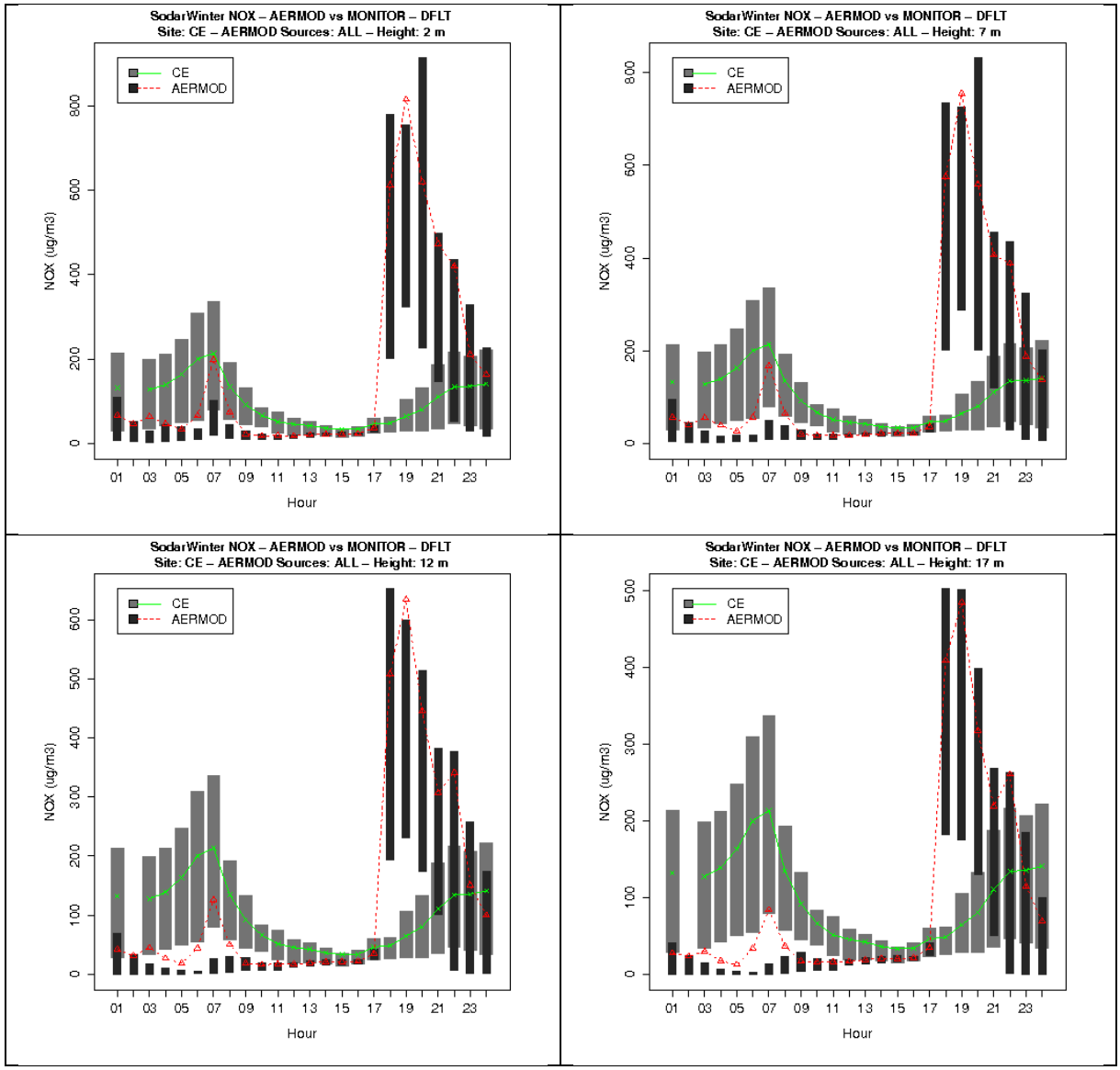

Figure 9A-56: Diurnal variability in observed and modeled NOx concentrations at CE Site from flagpole receptors at heights of 2m, 7m, 12m and 17m during Winter Season.

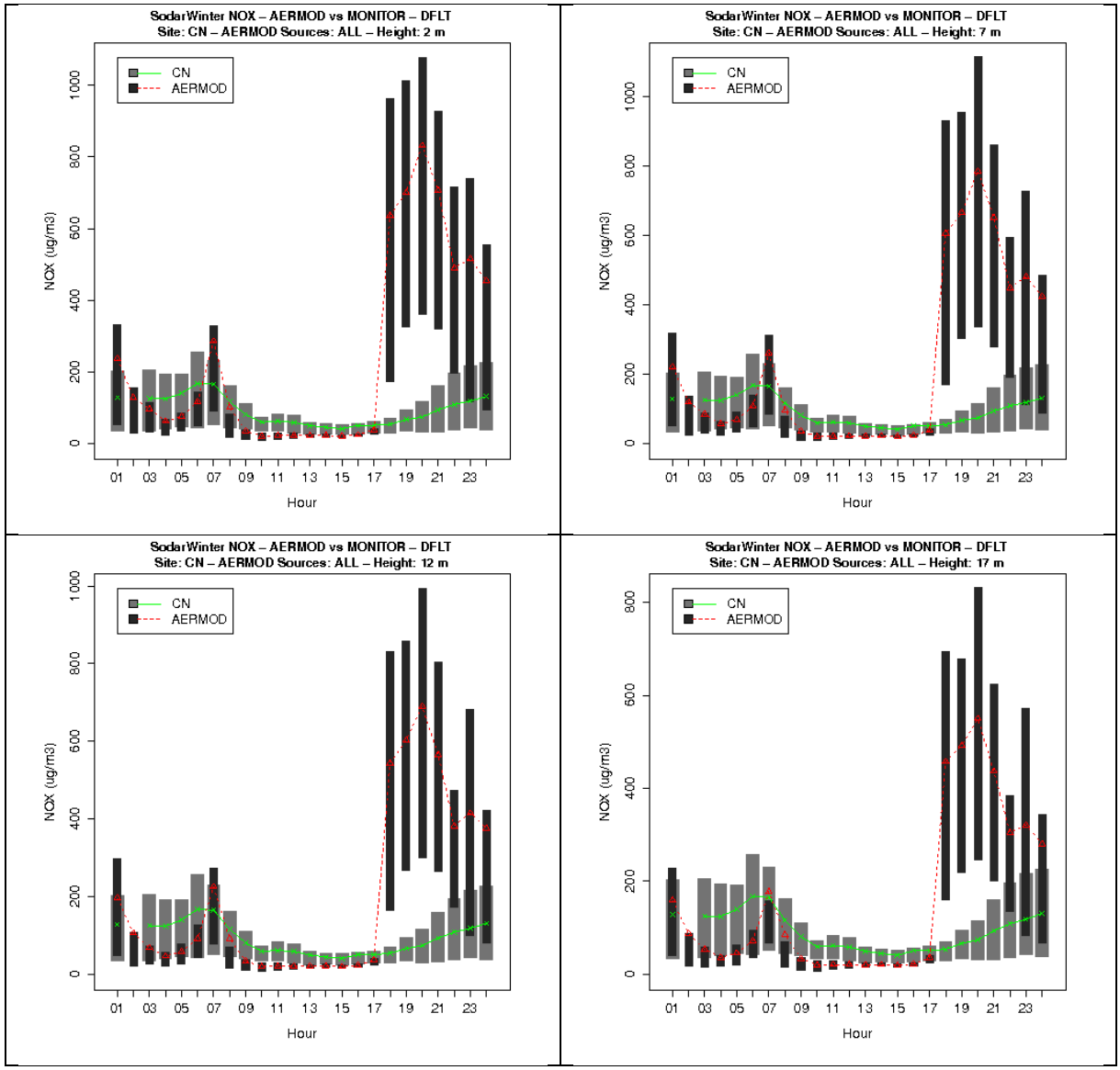

Figure 9A-57: Diurnal variability in observed and modeled NOx concentrations at CN Site from flagpole receptors at heights of 2m, 7m, 12m and 17m during Winter Season.

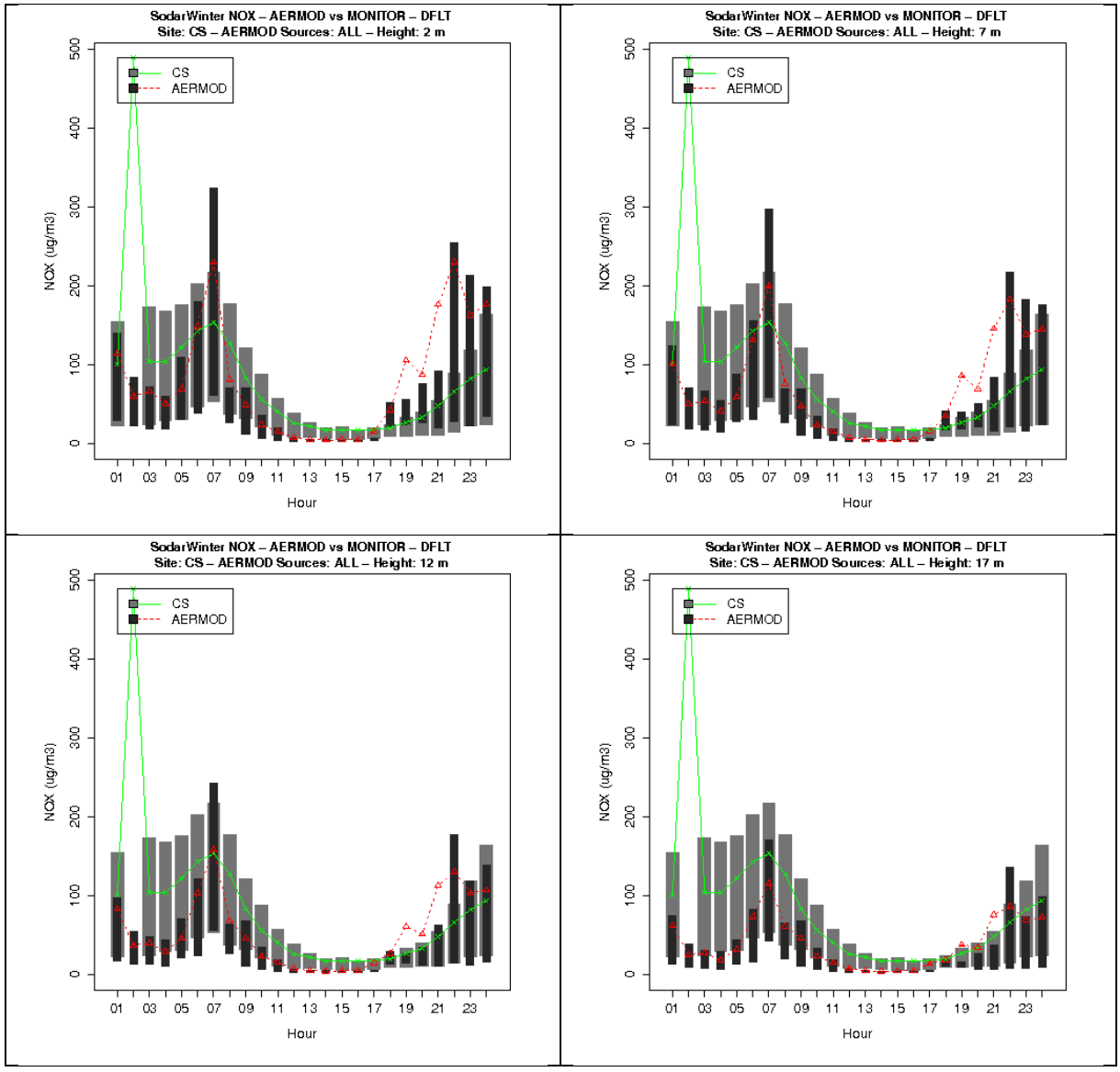

Figure 9A-58: Diurnal variability in observed and modeled NOx concentrations at CS Site from flagpole receptors at heights of 2m, 7m, 12m and 17m during Winter Season.

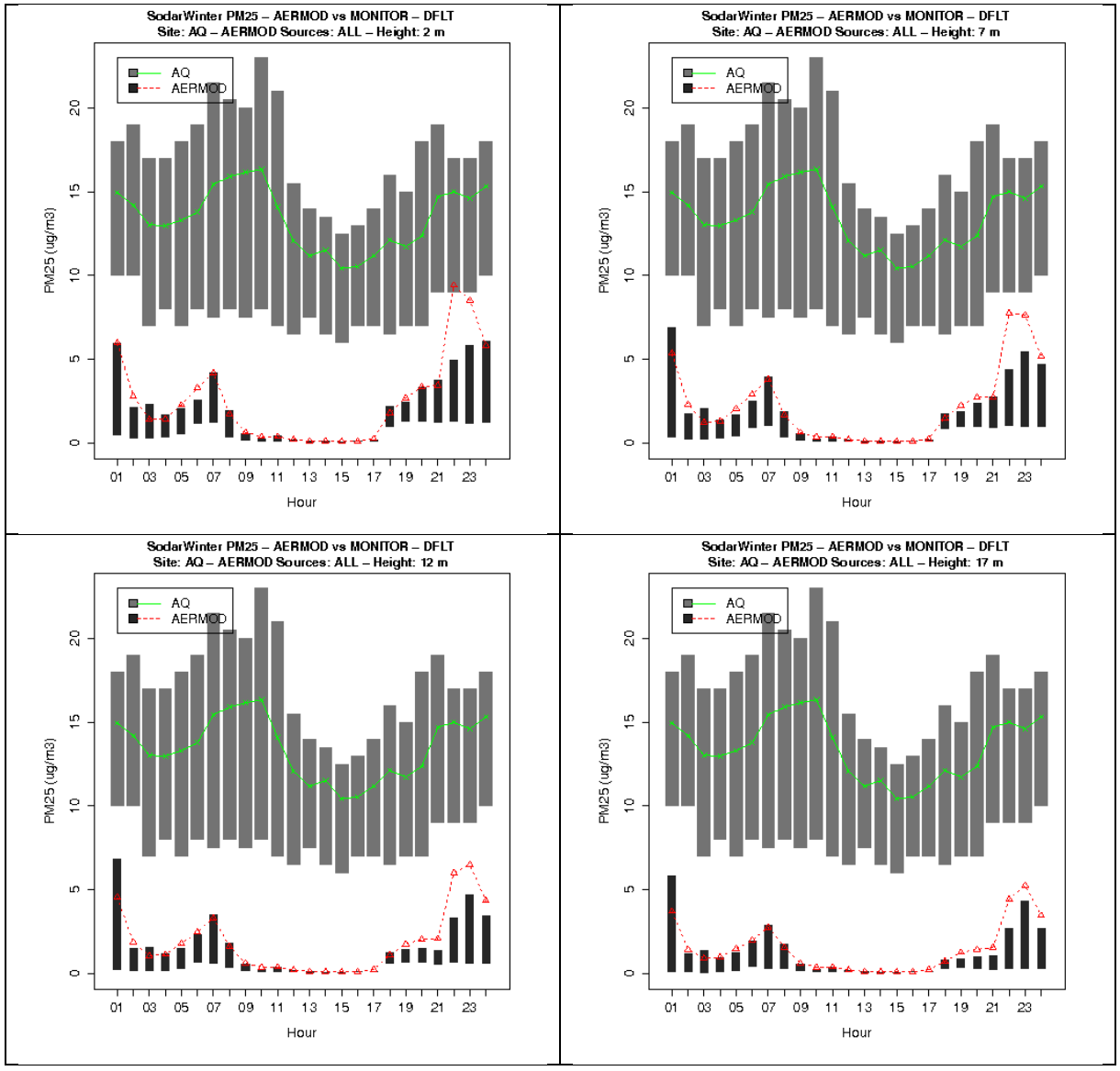

Figure 9A-59: Diurnal variability in observed and modeled $PM_{2.5}$ concentrations at AQ Site from flagpole receptors at heights of 2m, 7m, 12m and 17m during Winter Season.

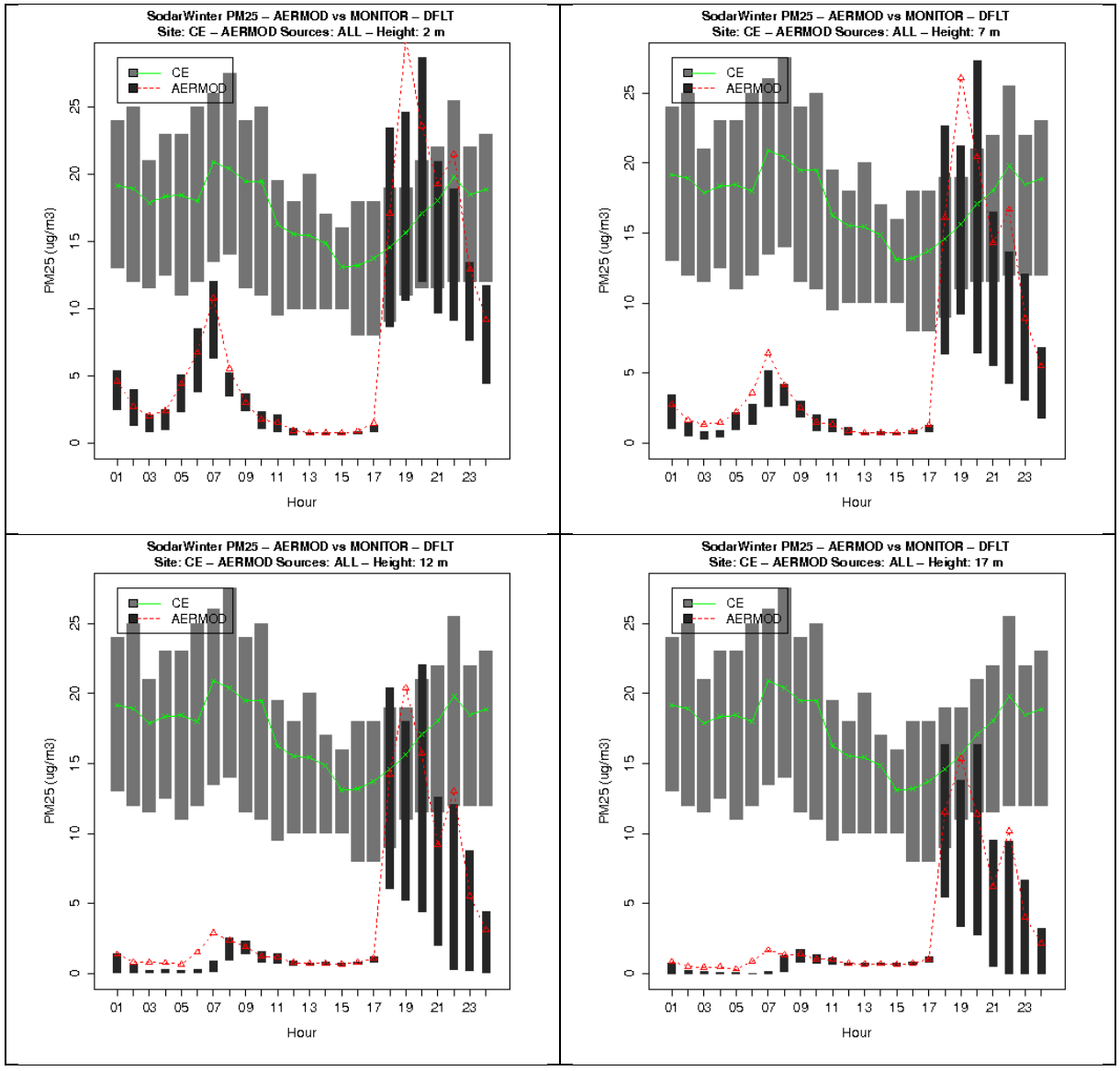

Figure 9A-60: Diurnal variability in observed and modeled $PM_{2.5}$ concentrations at CE Site from flagpole receptors at heights of 2m, 7m, 12m and 17m during Winter Season.

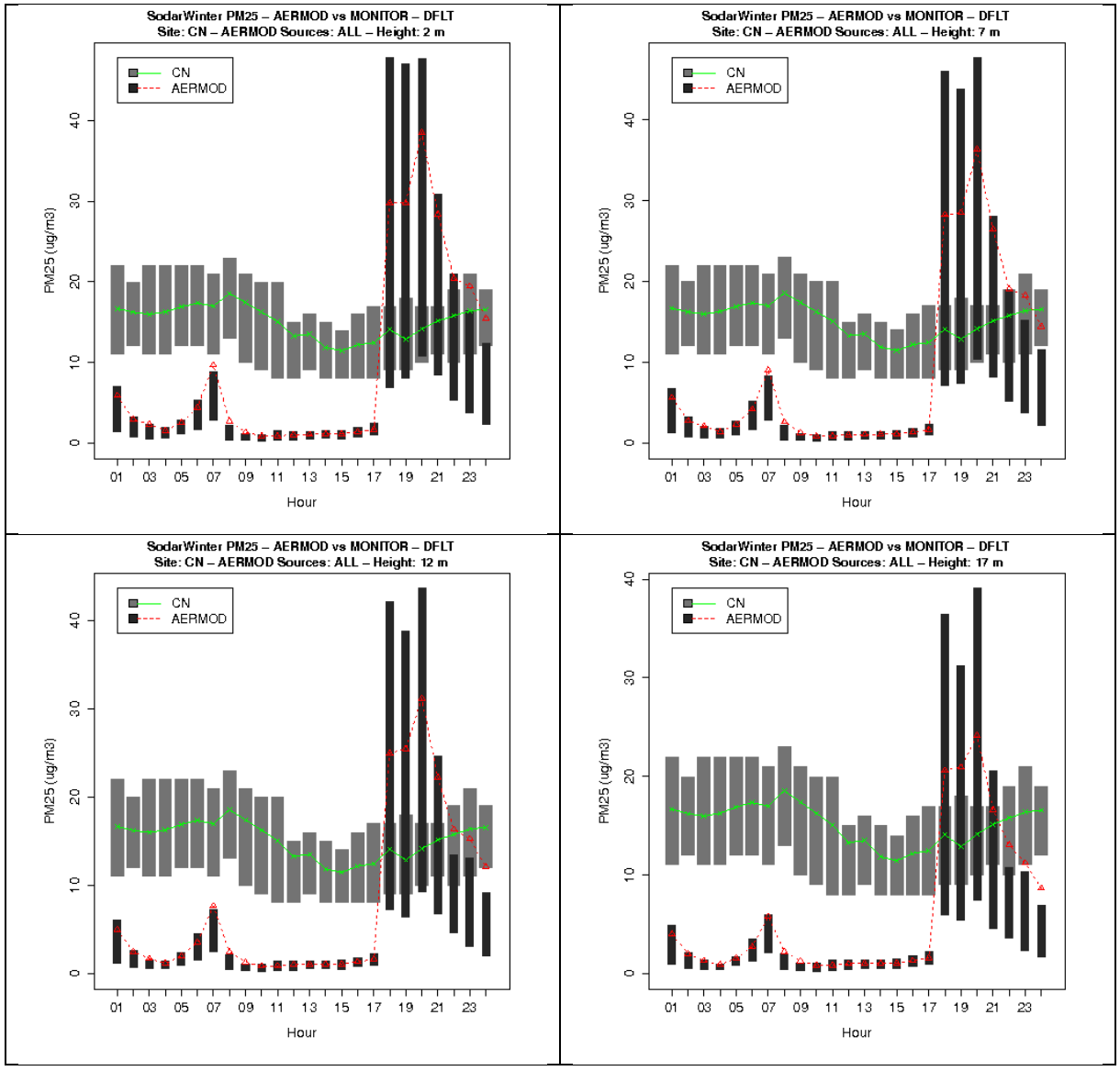

Figure 9A-61: Diurnal variability in observed and modeled $PM_{2.5}$ concentrations at CN Site from flagpole receptors at heights of 2m, 7m, 12m and 17m during Winter Season.

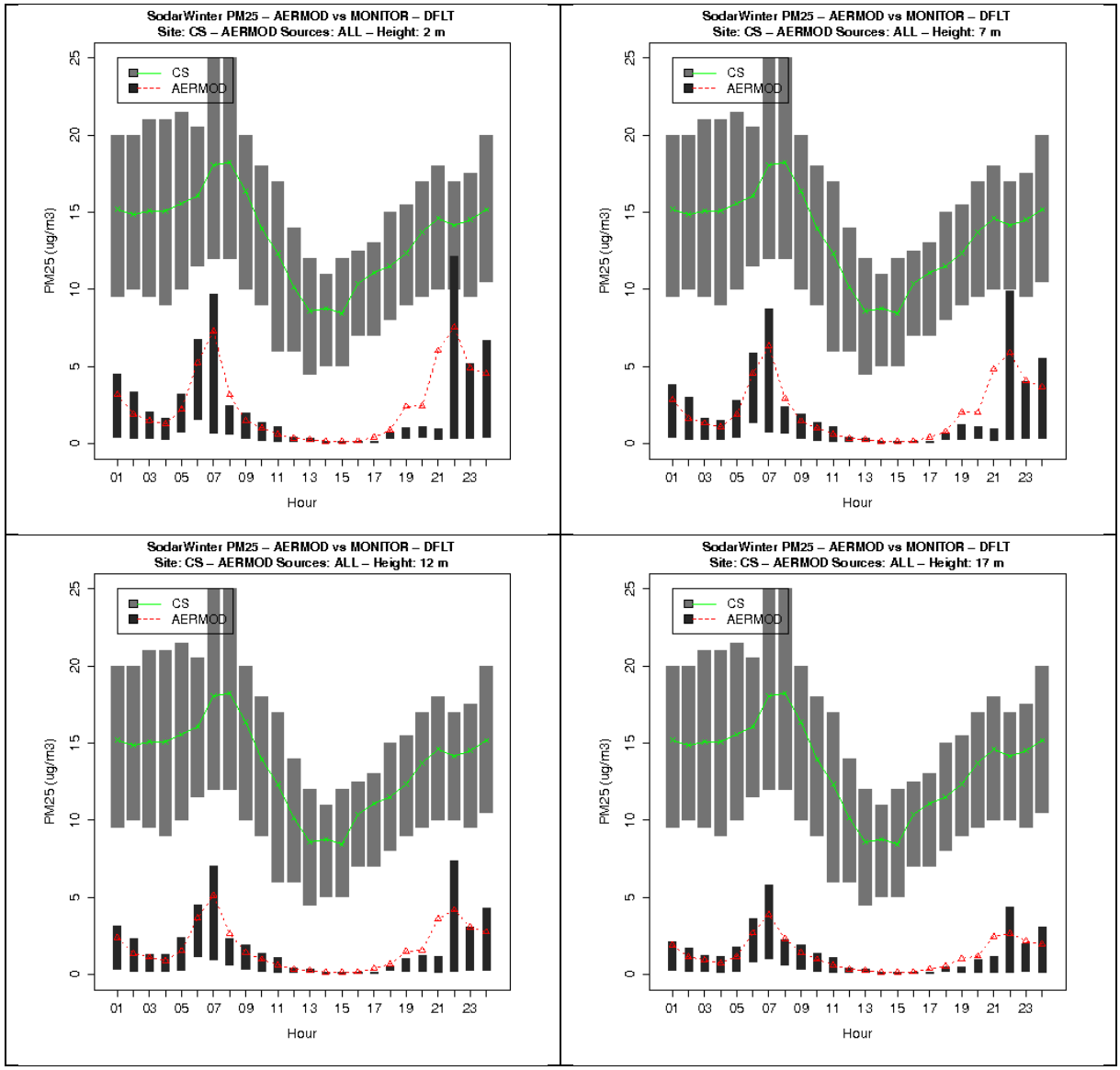

Figure 9A-62: Diurnal variability in observed and modeled $PM_{2.5}$ concentrations at CS Site from flagpole receptors at heights of 2m, 7m, 12m and 17m during Winter Season.

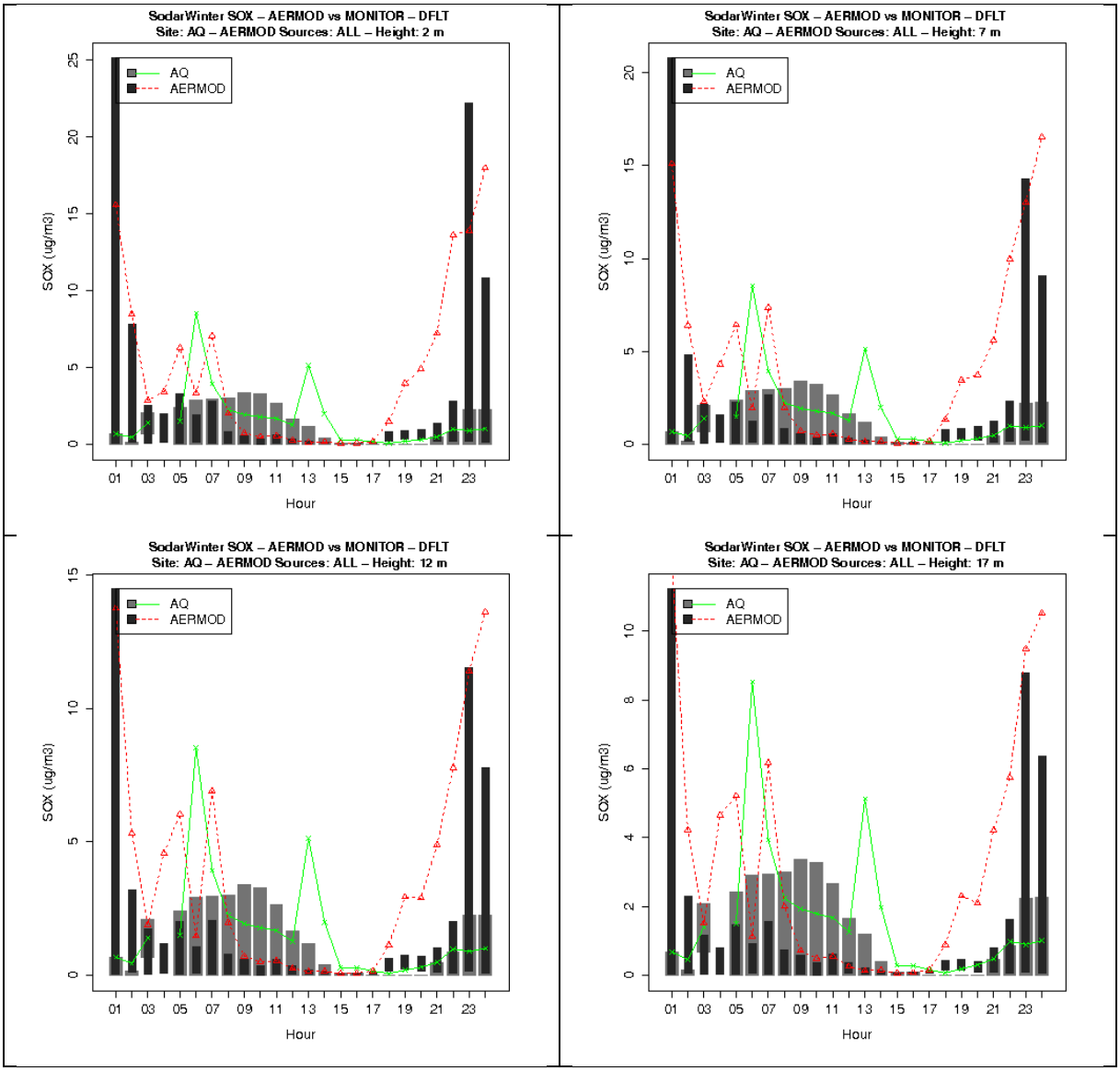

Figure 9A-63: Diurnal variability in observed and modeled SOx concentrations at AQ Site from flagpole receptors at heights of 2m, 7m, 12m and 17m during Winter Season.

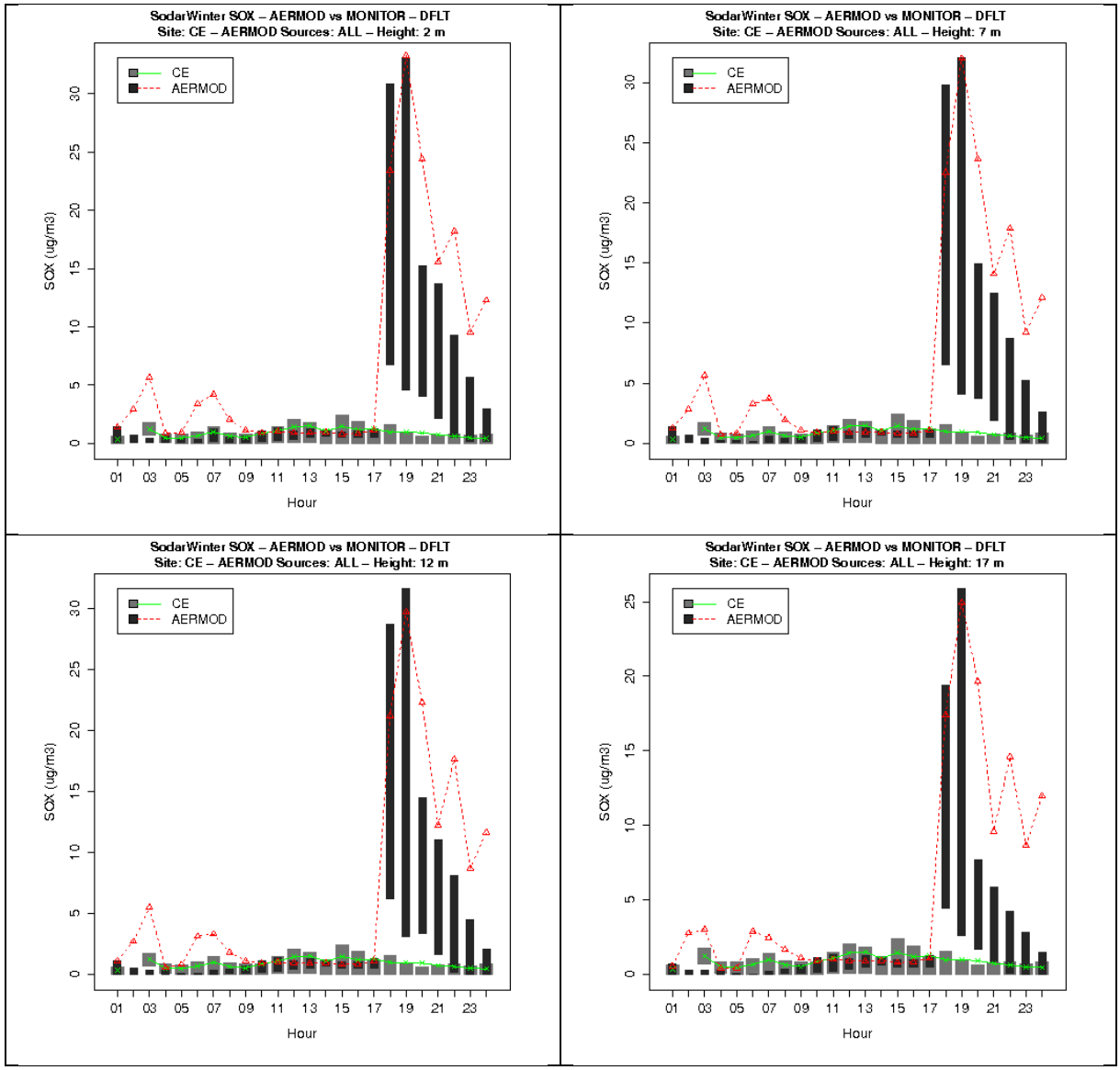

Figure 9A-64: Diurnal variability in observed and modeled SOx concentrations at CE Site from flagpole receptors at heights of 2m, 7m, 12m and 17m during Winter Season.

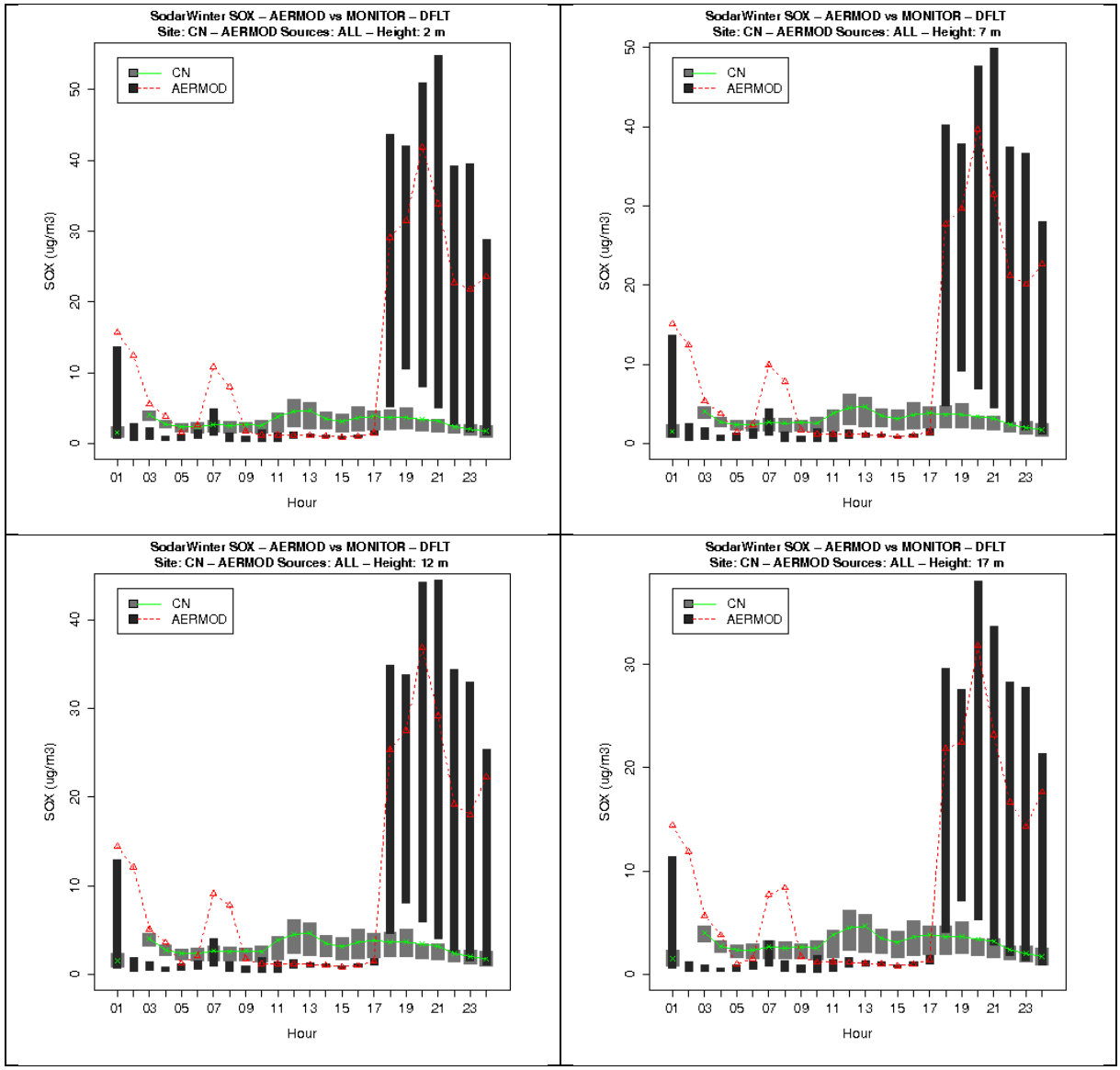

Figure 9A-65: Diurnal variability in observed and modeled SOx concentrations at CN Site from flagpole receptors at heights of 2m, 7m, 12m and 17m during Winter Season.

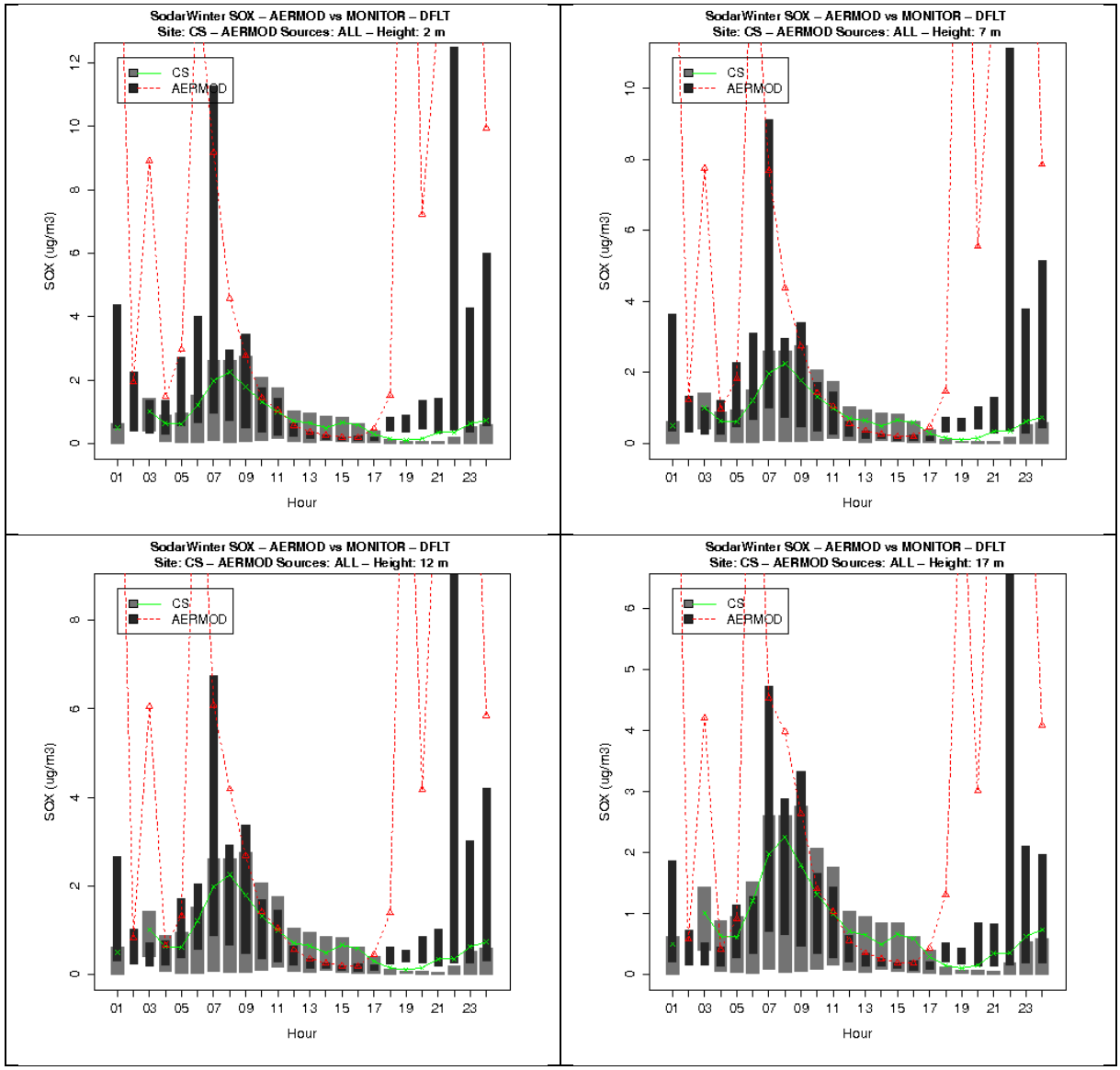

Figure 9A-66: Diurnal variability in observed and modeled SOx concentrations at CS Site from flagpole receptors at heights of 2m, 7m, 12m and 17m during Winter Season.

III. Source Attribution

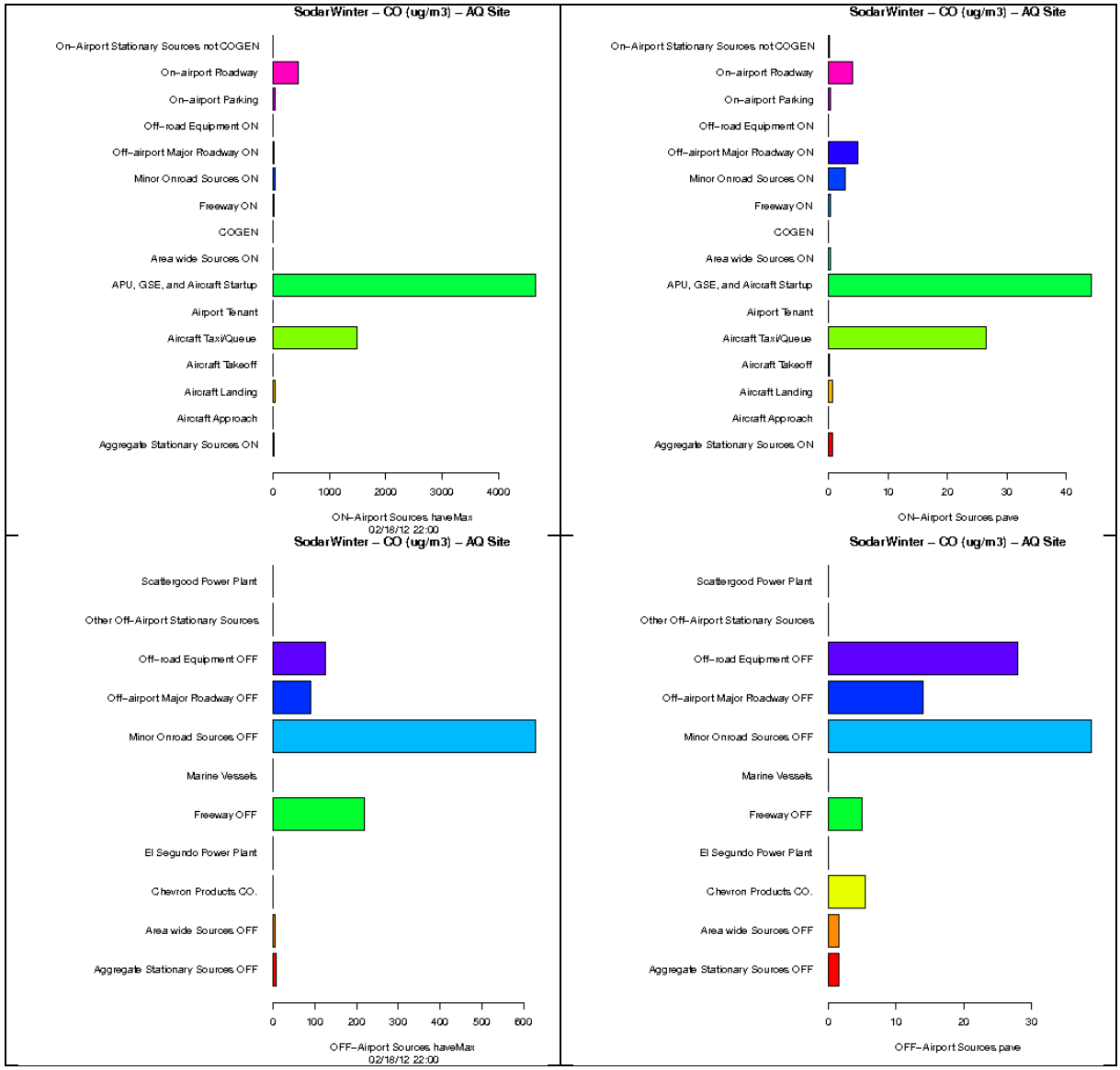

Figure 9A-67: Source-sector contributions to Hourly Maximum (left) and Period Average CO concentrations at AQ Site from airport-related sources (top) and background sources (bottom) during Winter Season.

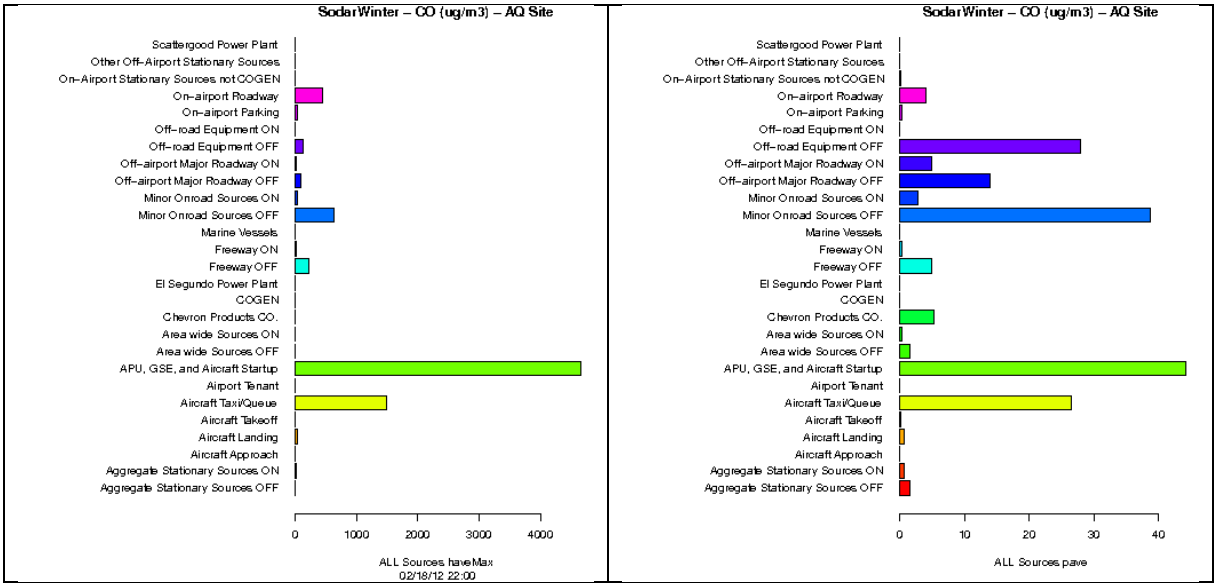

Figure 9A-68: Source-sector contributions to Hourly Maximum (left) and Period Average CO concentrations at AQ Site from ALL sources during Winter Season.

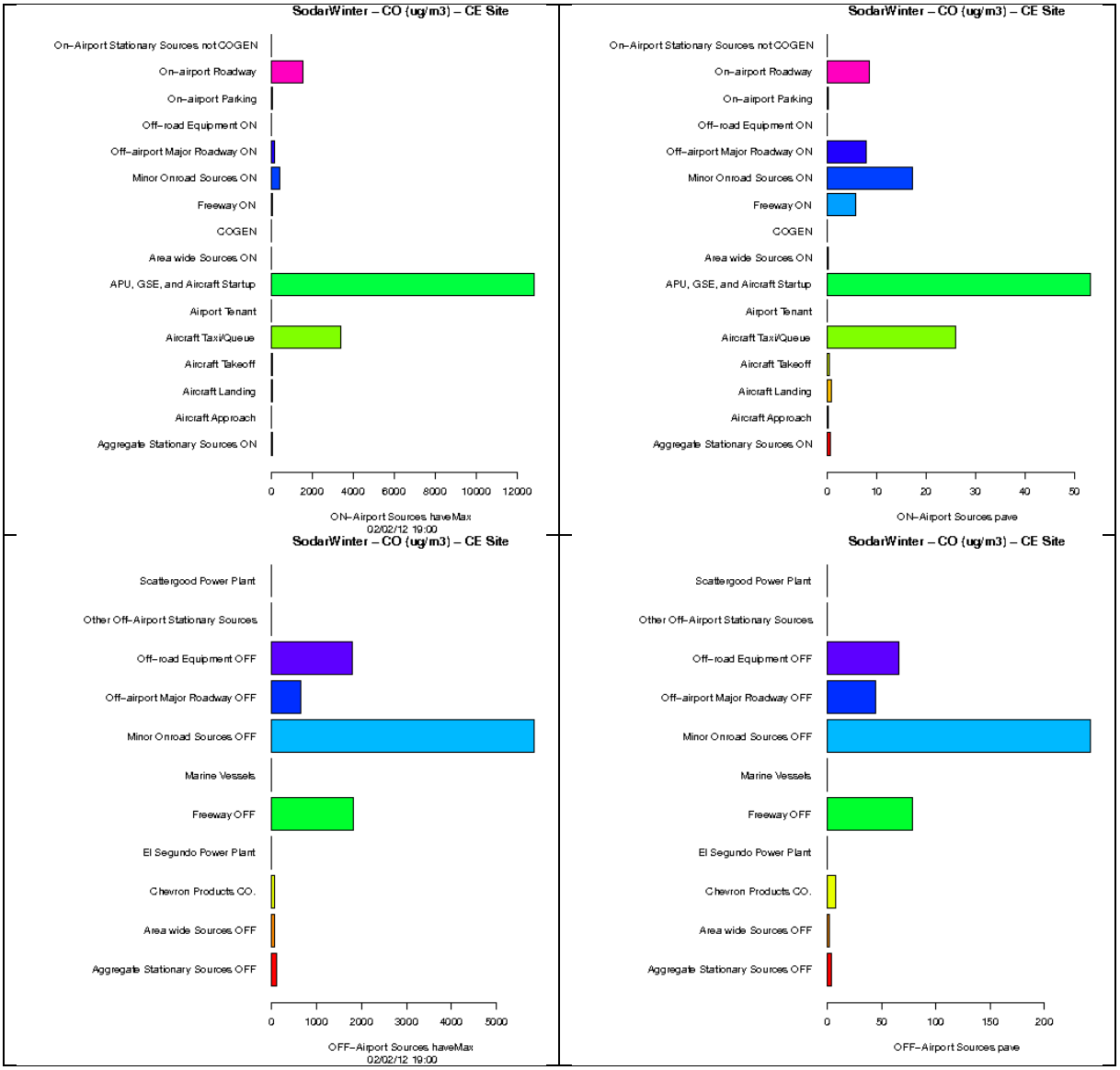

Figure 9A-69: Source-sector contributions to Hourly Maximum (left) and Period Average CO concentrations at CE Site from airport-related sources (top) and background sources (bottom) during Winter Season.

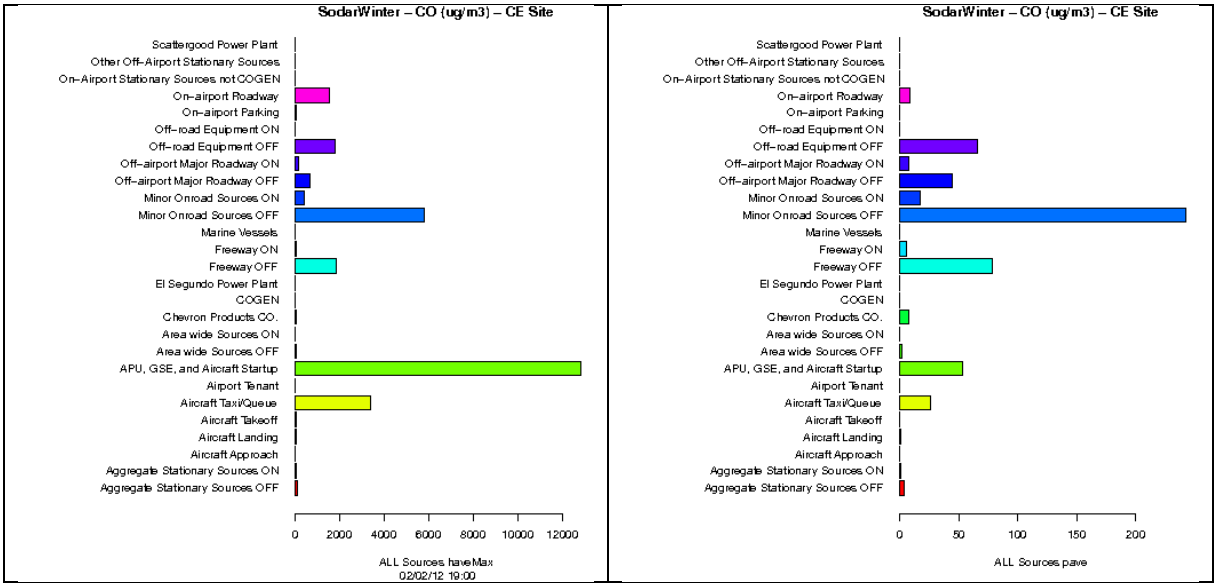

Figure 9A-70: Source-sector contributions to Hourly Maximum (left) and Period Average CO concentrations at CE Site from ALL sources during Winter Season.

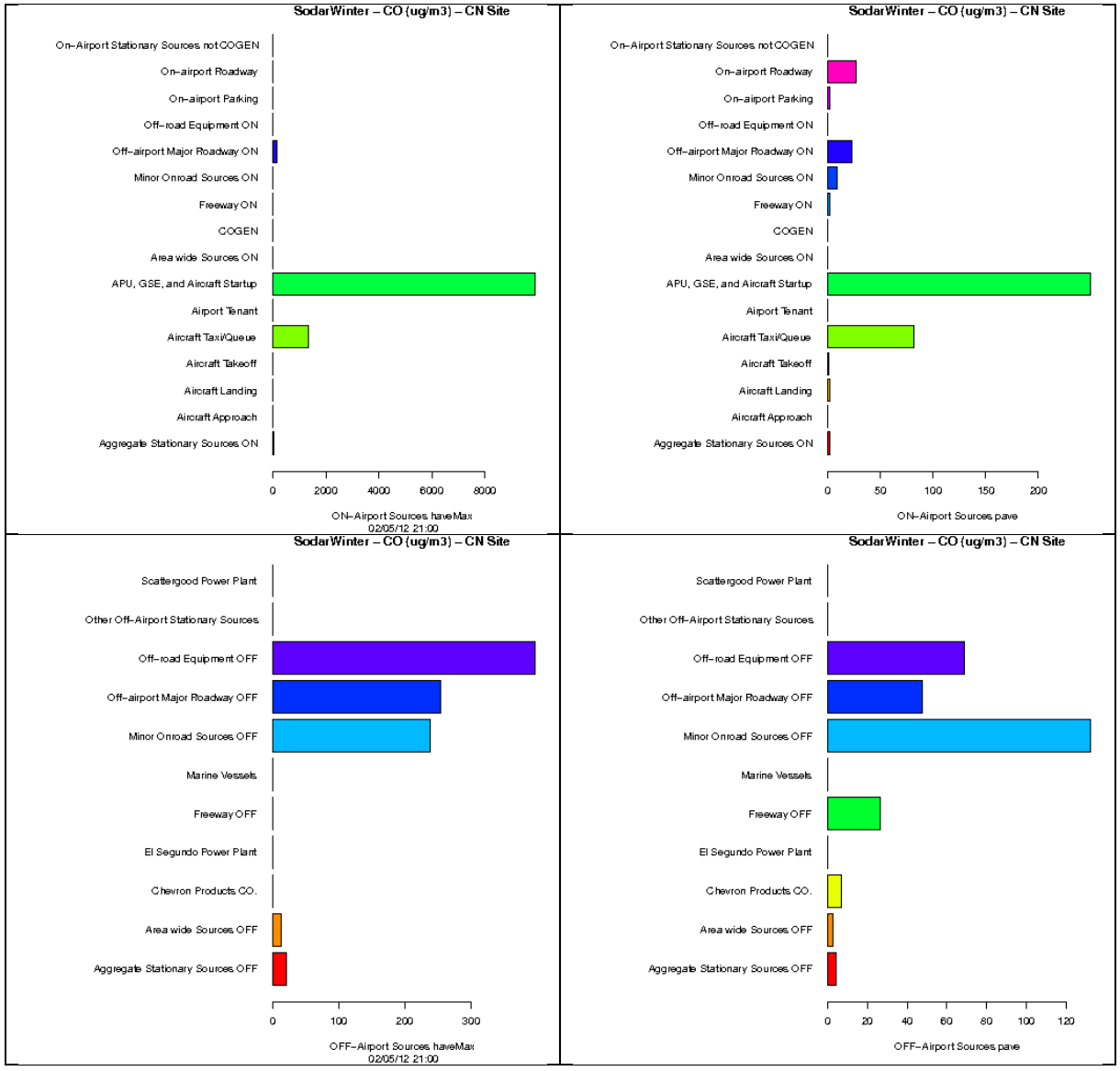

Figure 9A-71: Source-sector contributions to Hourly Maximum (left) and Period Average CO concentrations at CN Site from airport-related sources (top) and background sources (bottom) during Winter Season.

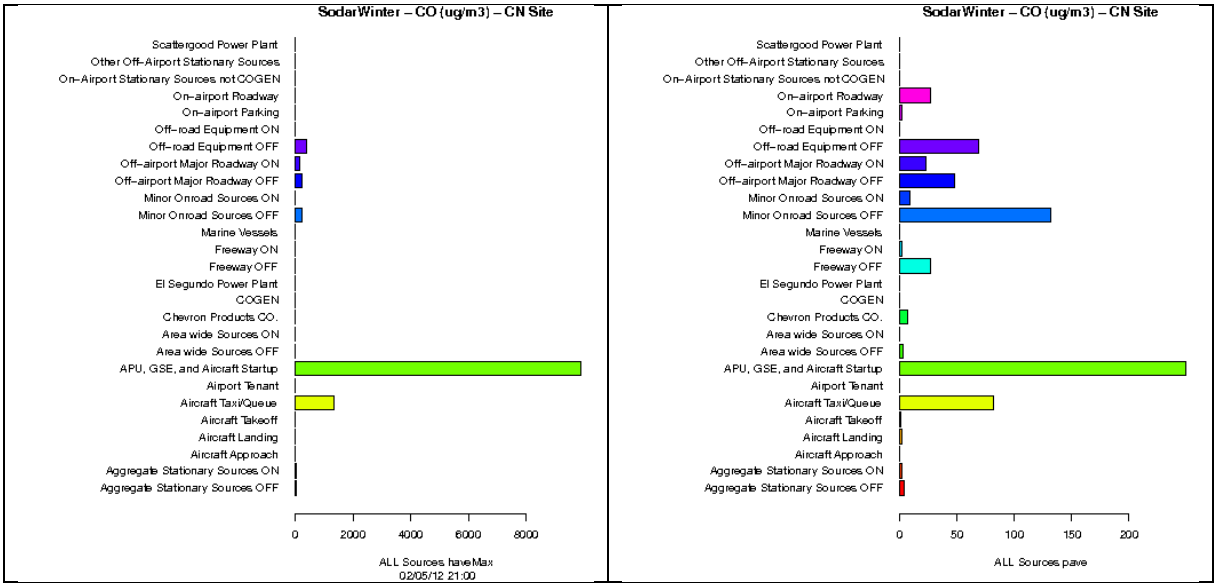

Figure 9A-72: Source-sector contributions to Hourly Maximum (left) and Period Average CO concentrations at CN Site from ALL sources during Winter Season.

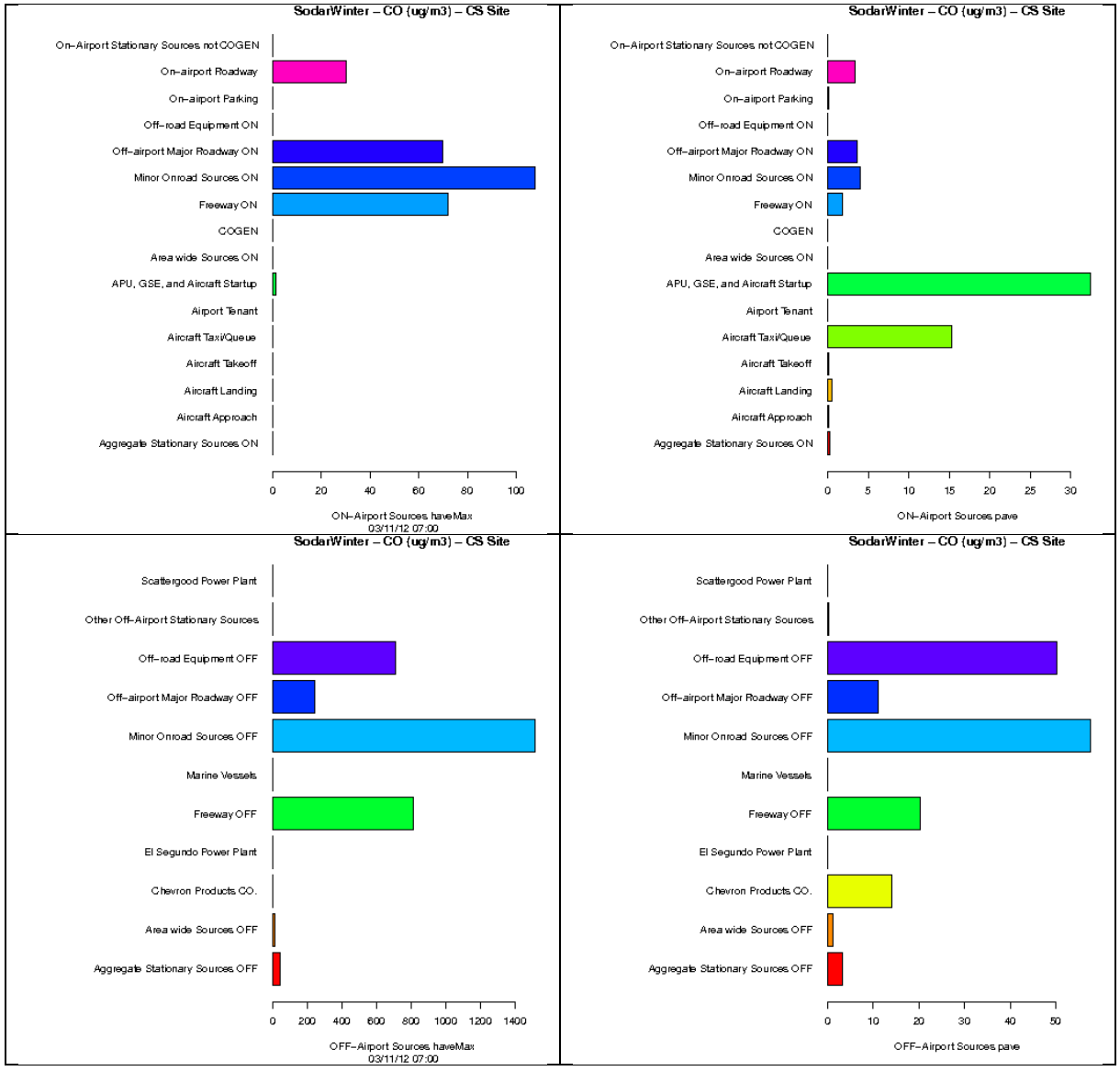

Figure 9A-73: Source-sector contributions to Hourly Maximum (left) and Period Average CO concentrations at CS Site from airport-related sources (top) and background sources (bottom) during Winter Season.

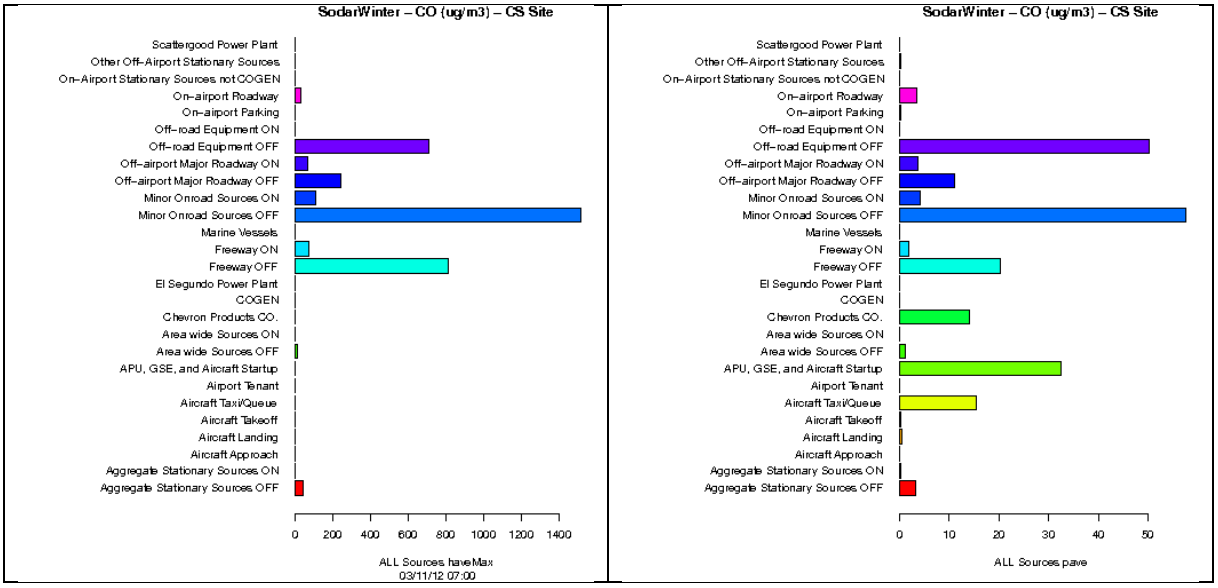

Figure 9A-74: Source-sector contributions to Hourly Maximum (left) and Period Average CO concentrations at CS Site from ALL sources during Winter Season.

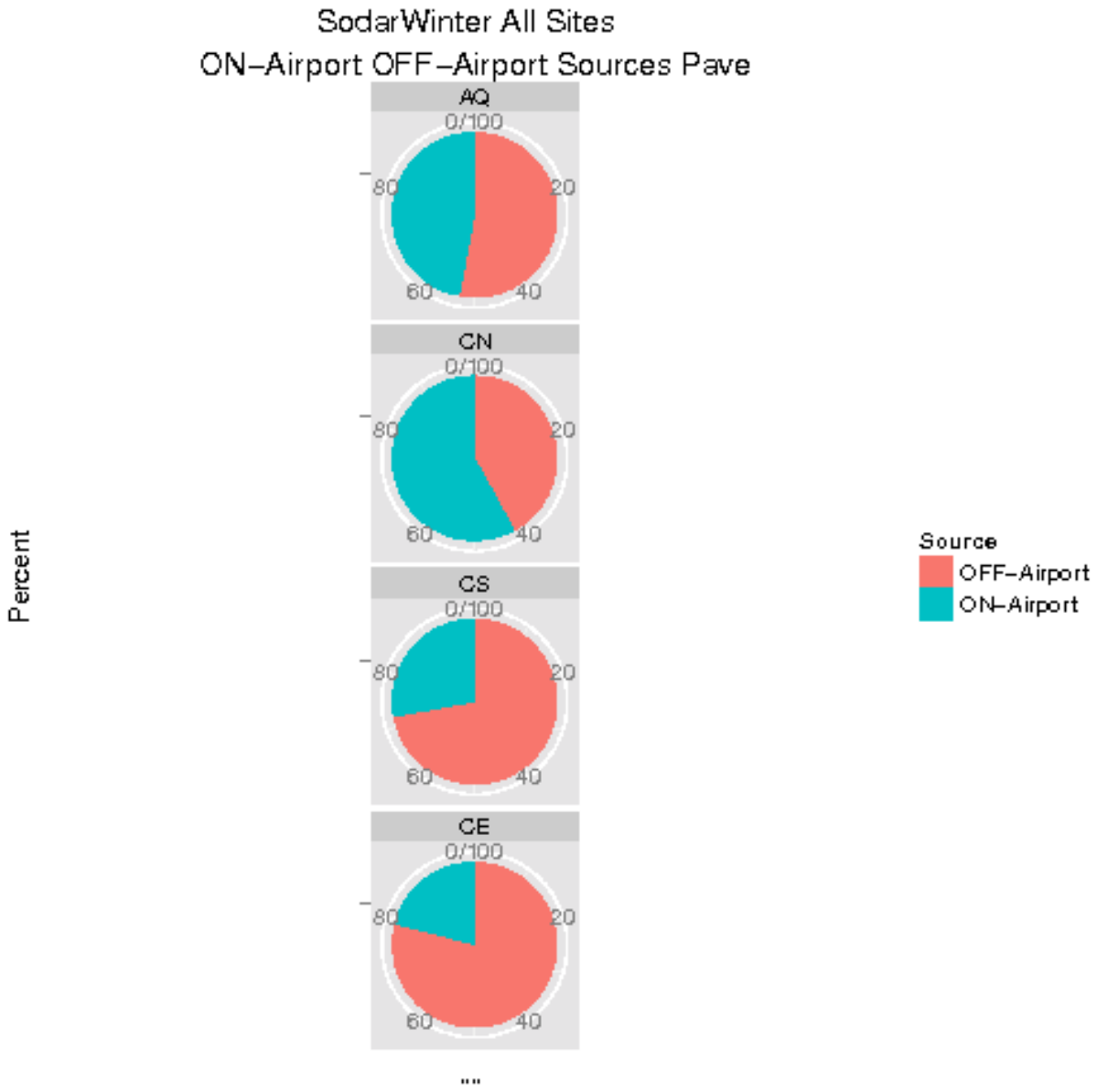

Figure 9A-75: Source-sector contributions to Period Average CO concentrations at each site from airport-related vs. background sources during Winter Season.

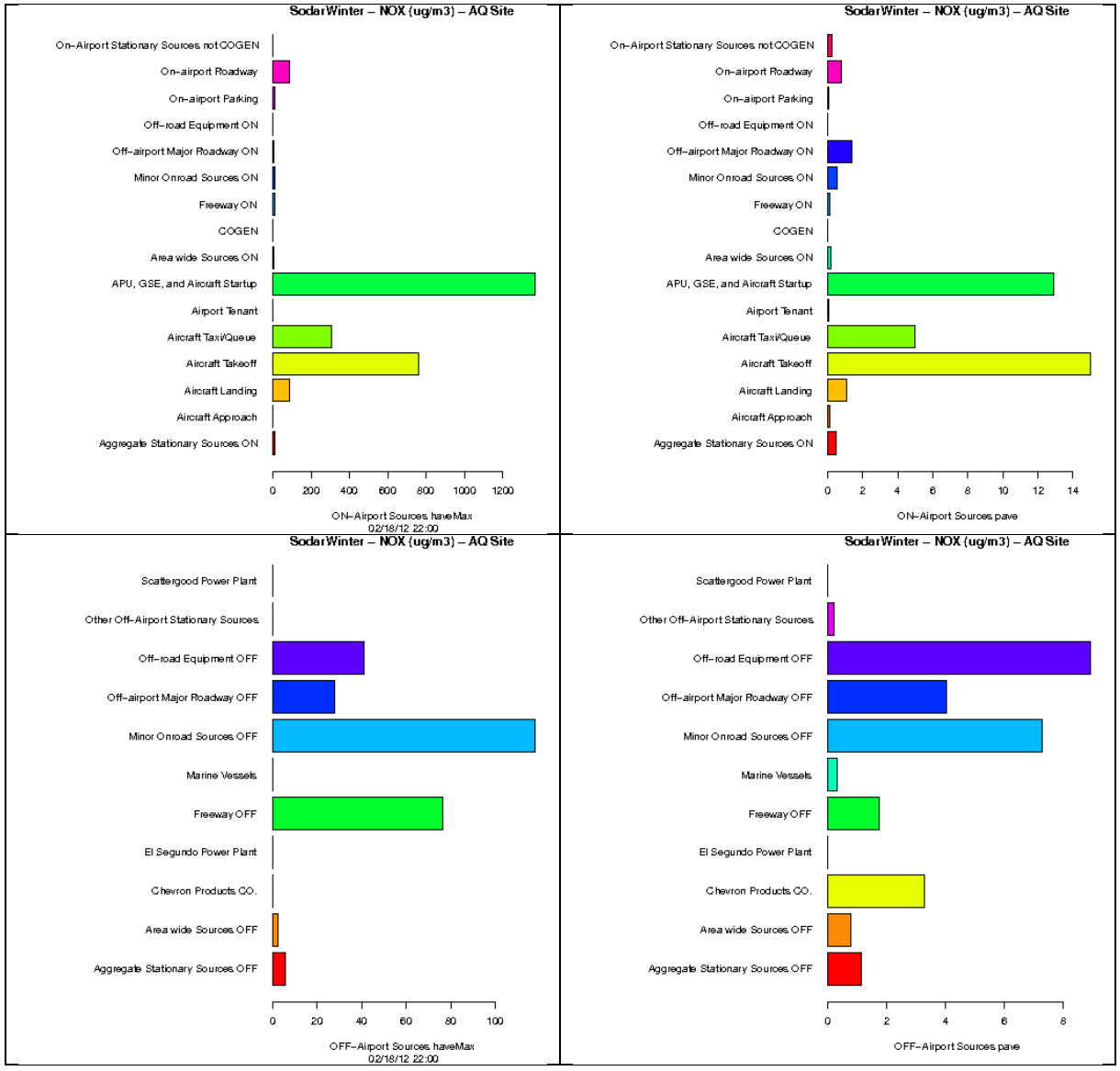

Figure 9A-76: Source-sector contributions to Hourly Maximum (left) and Period Average NOx concentrations at AQ Site from airport-related sources (top) and background sources (bottom) during Winter Season.

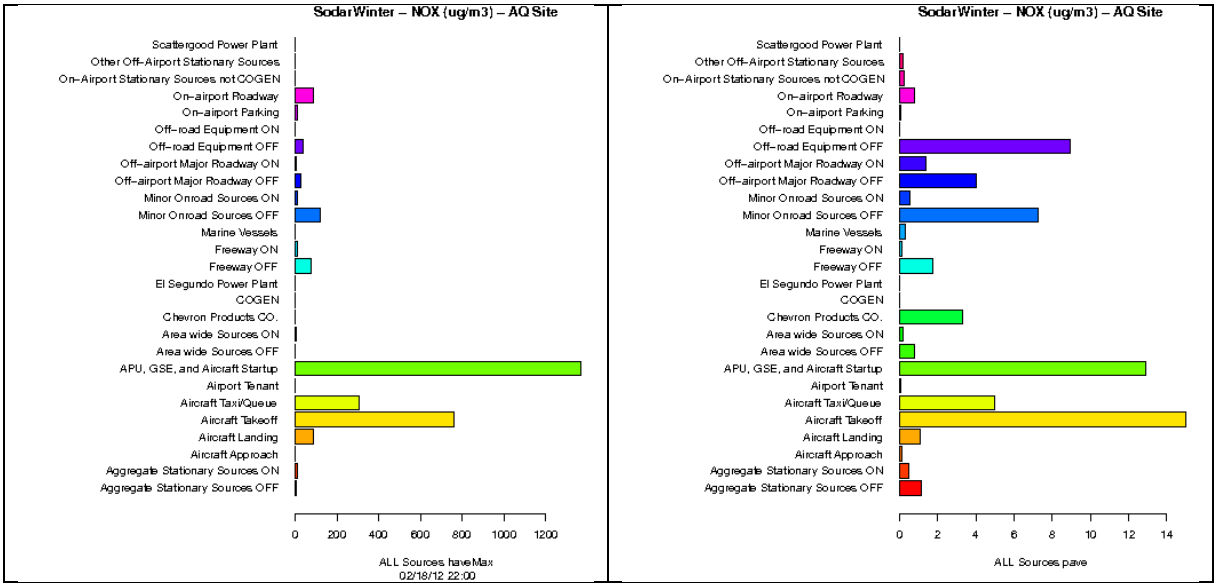

Figure 9A-77: Source-sector contributions to Hourly Maximum (left) and Period Average NOx concentrations at AQ Site from ALL sources during Winter Season.

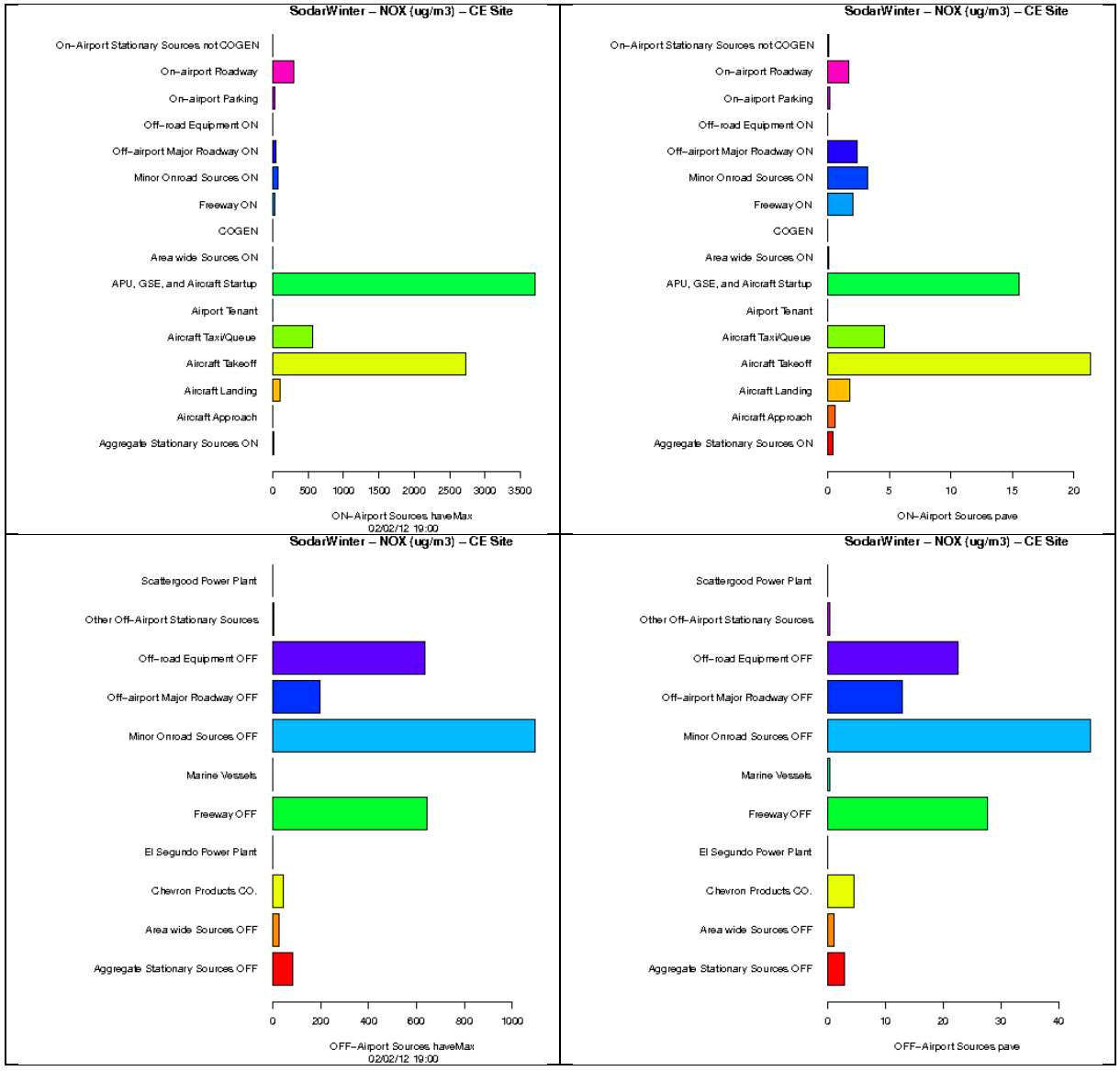

Figure 9A-78: Source-sector contributions to Hourly Maximum (left) and Period Average NOx concentrations at CE Site from airport-related sources (top) and background sources (bottom) during Winter Season.

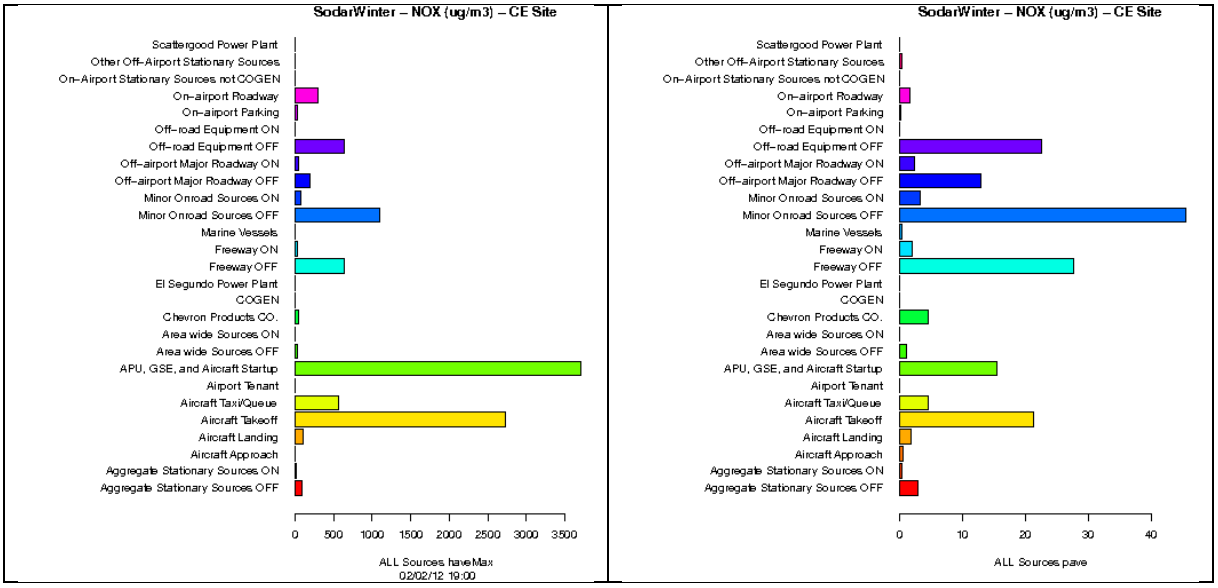

Figure 9A-79: Source-sector contributions to Hourly Maximum (left) and Period Average NOx concentrations at CE Site from ALL sources during Winter Season.

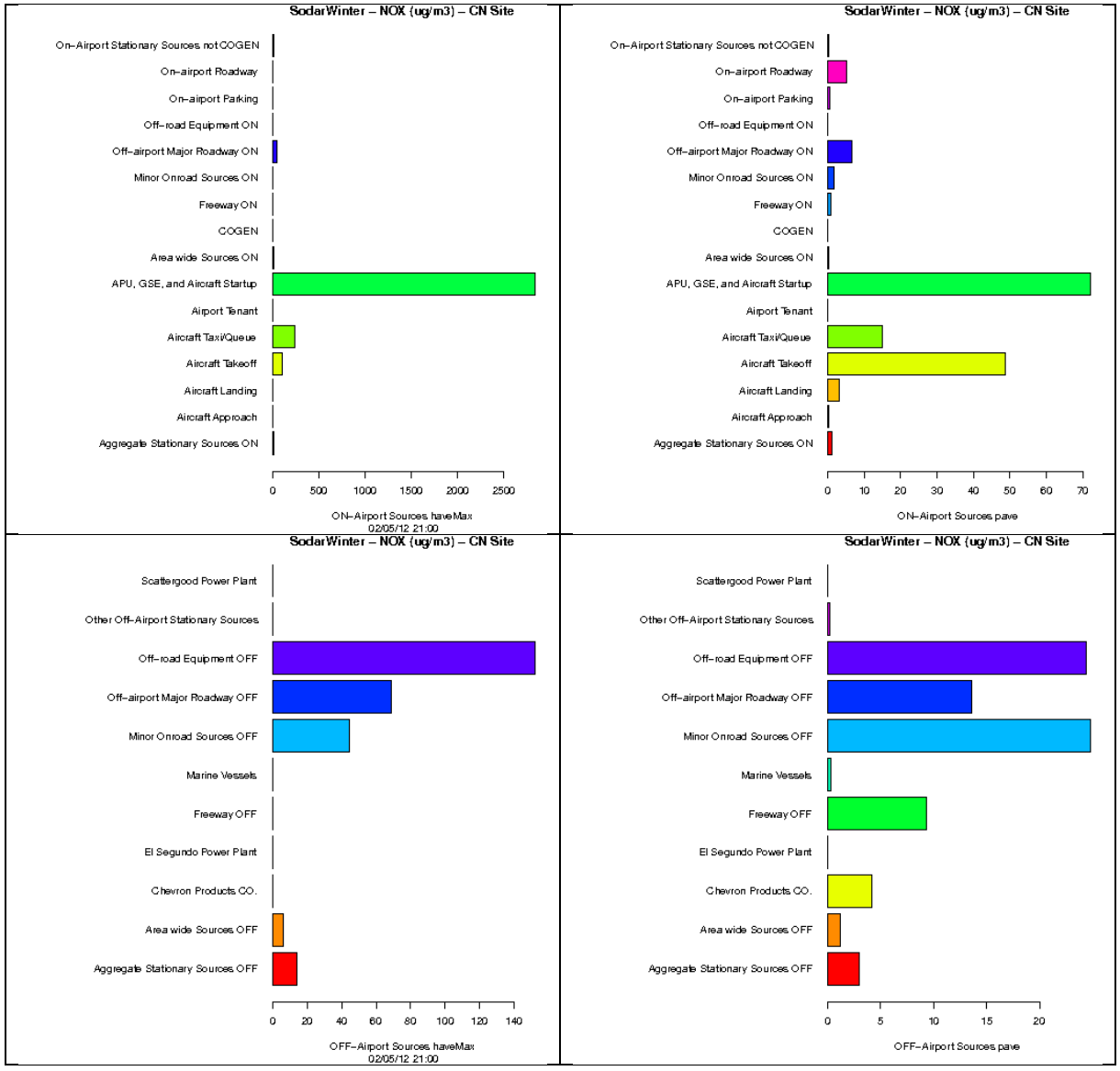

Figure 9A-80: Source-sector contributions to Hourly Maximum (left) and Period Average NOx concentrations at CN Site from airport-related sources (top) and background sources (bottom) during Winter Season.

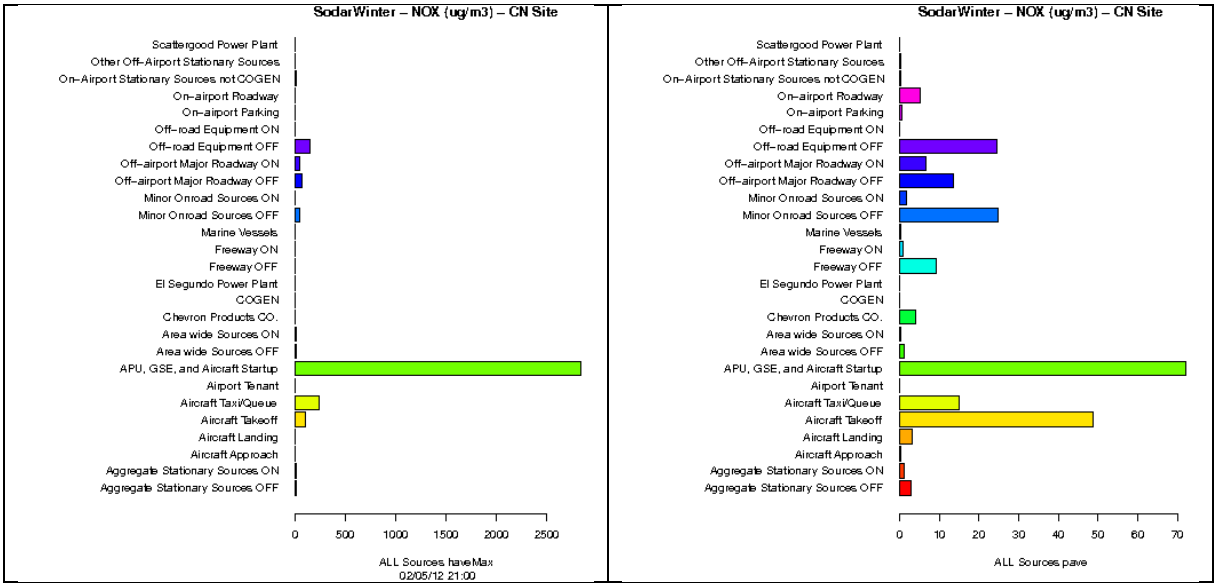

Figure 9A-81: Source-sector contributions to Hourly Maximum (left) and Period Average NOx concentrations at CN Site from ALL sources during Winter Season.

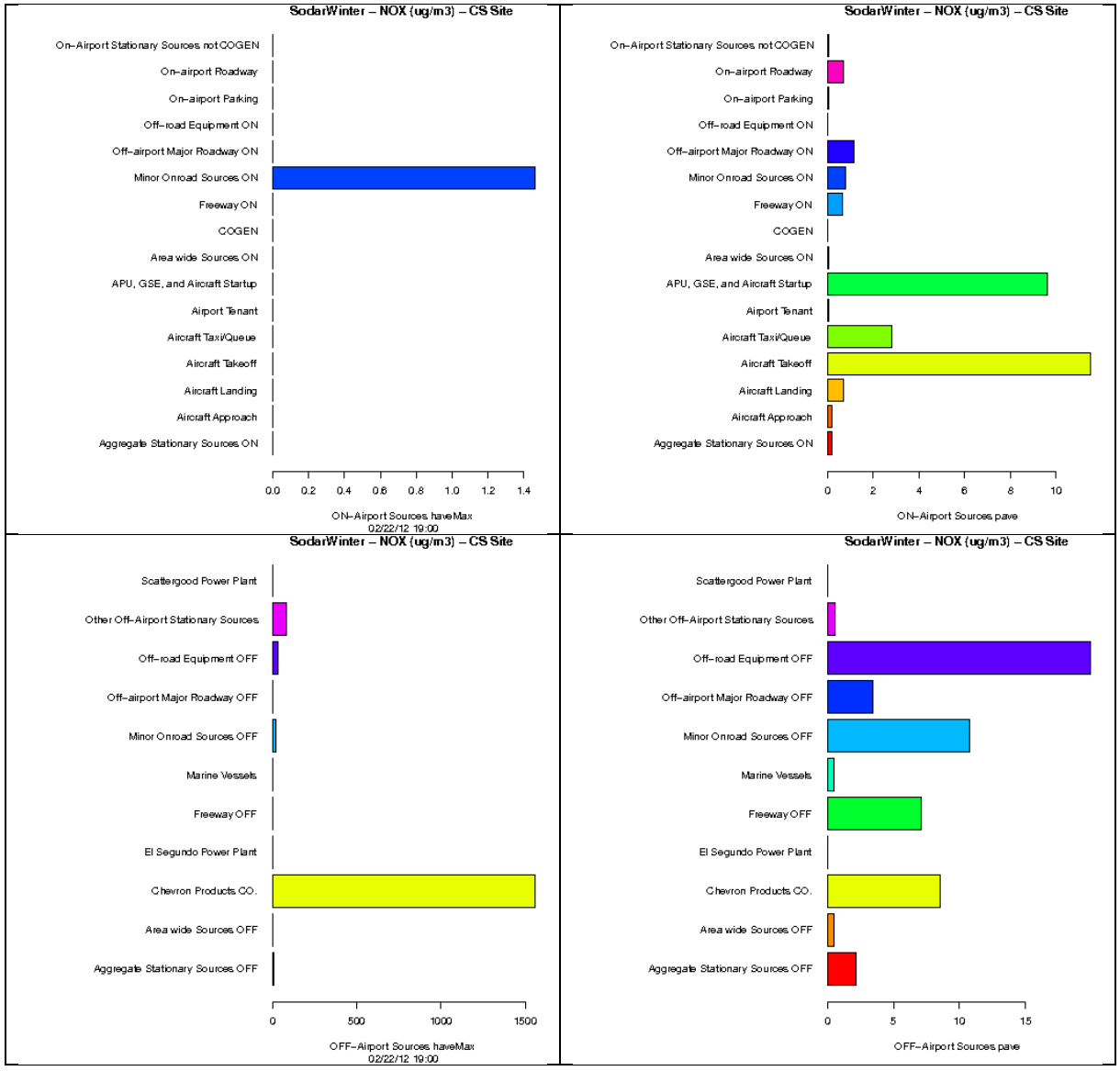

Figure 9A-82: Source-sector contributions to Hourly Maximum (left) and Period Average NOx concentrations at CS Site from airport-related sources (top) and background sources (bottom) during Winter Season.

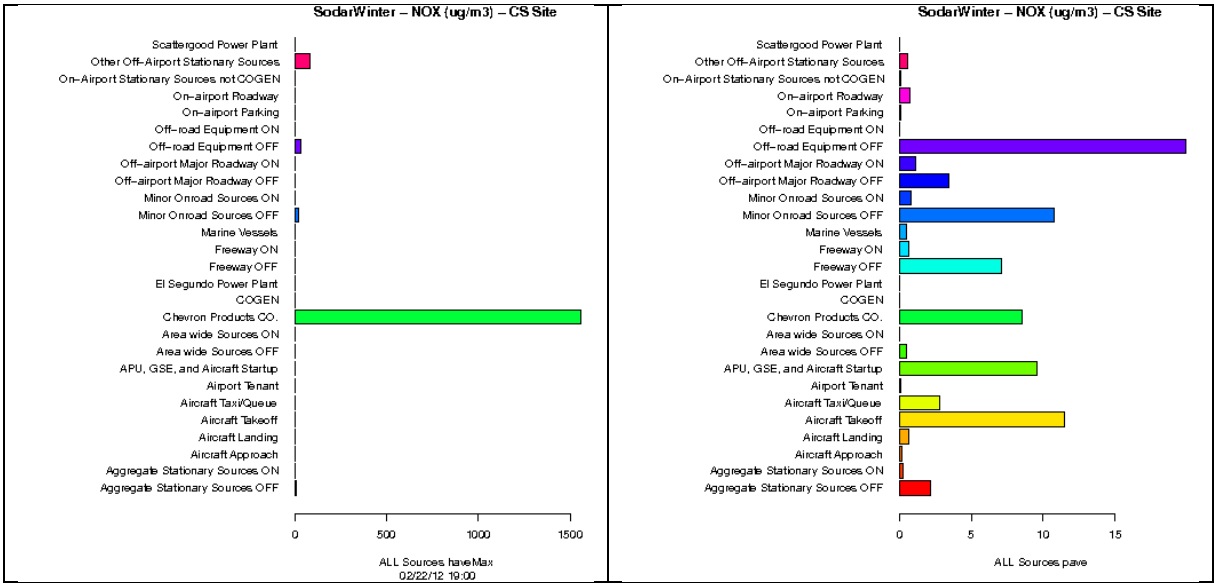

Figure 9A-83: Source-sector contributions to Hourly Maximum (left) and Period Average NOx concentrations at CS Site from ALL sources during Winter Season.

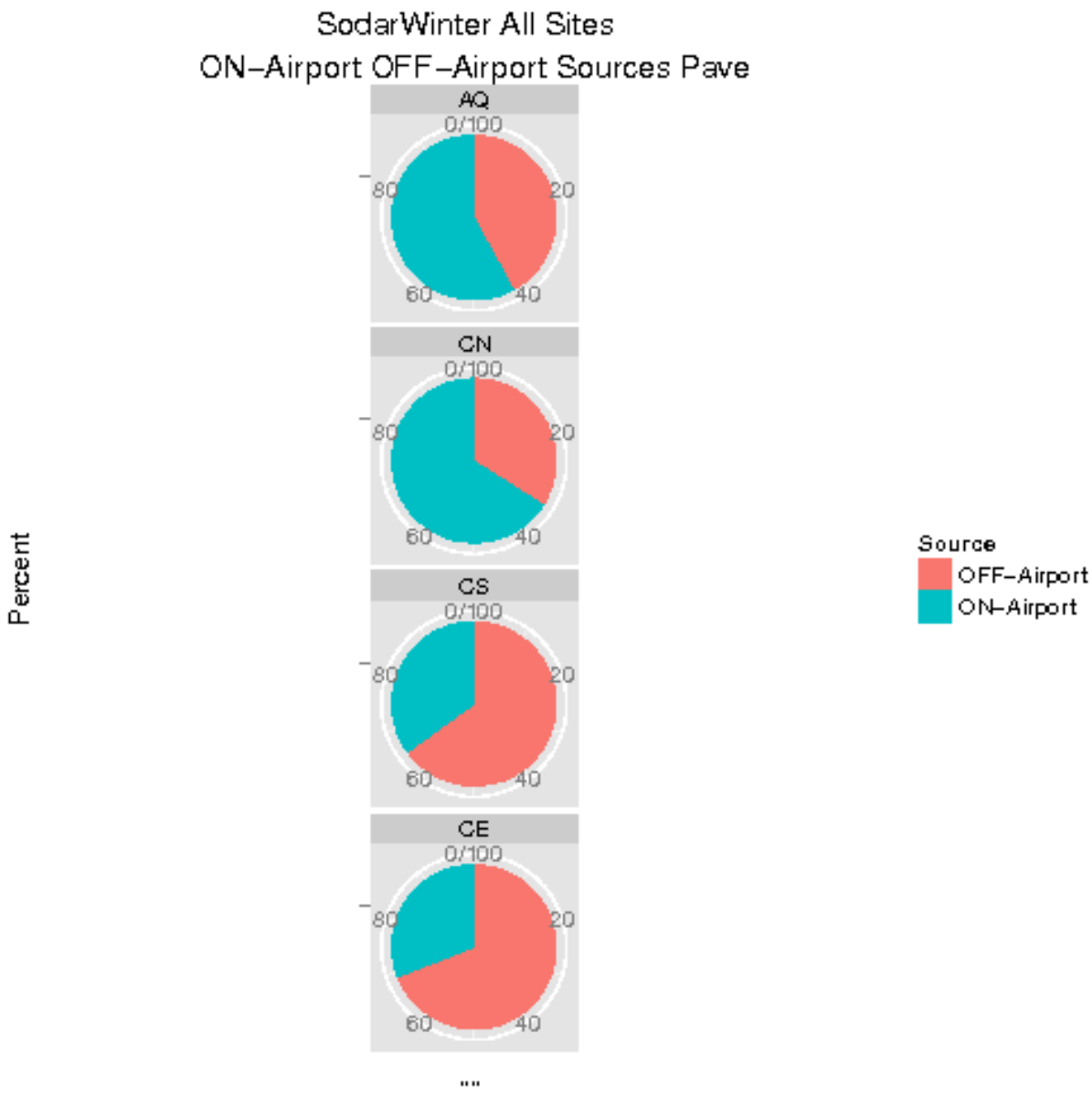

Figure 9A-84: Source-sector contributions to Period Average NOx concentrations at each site from airport-related vs. background sources during Winter Season.

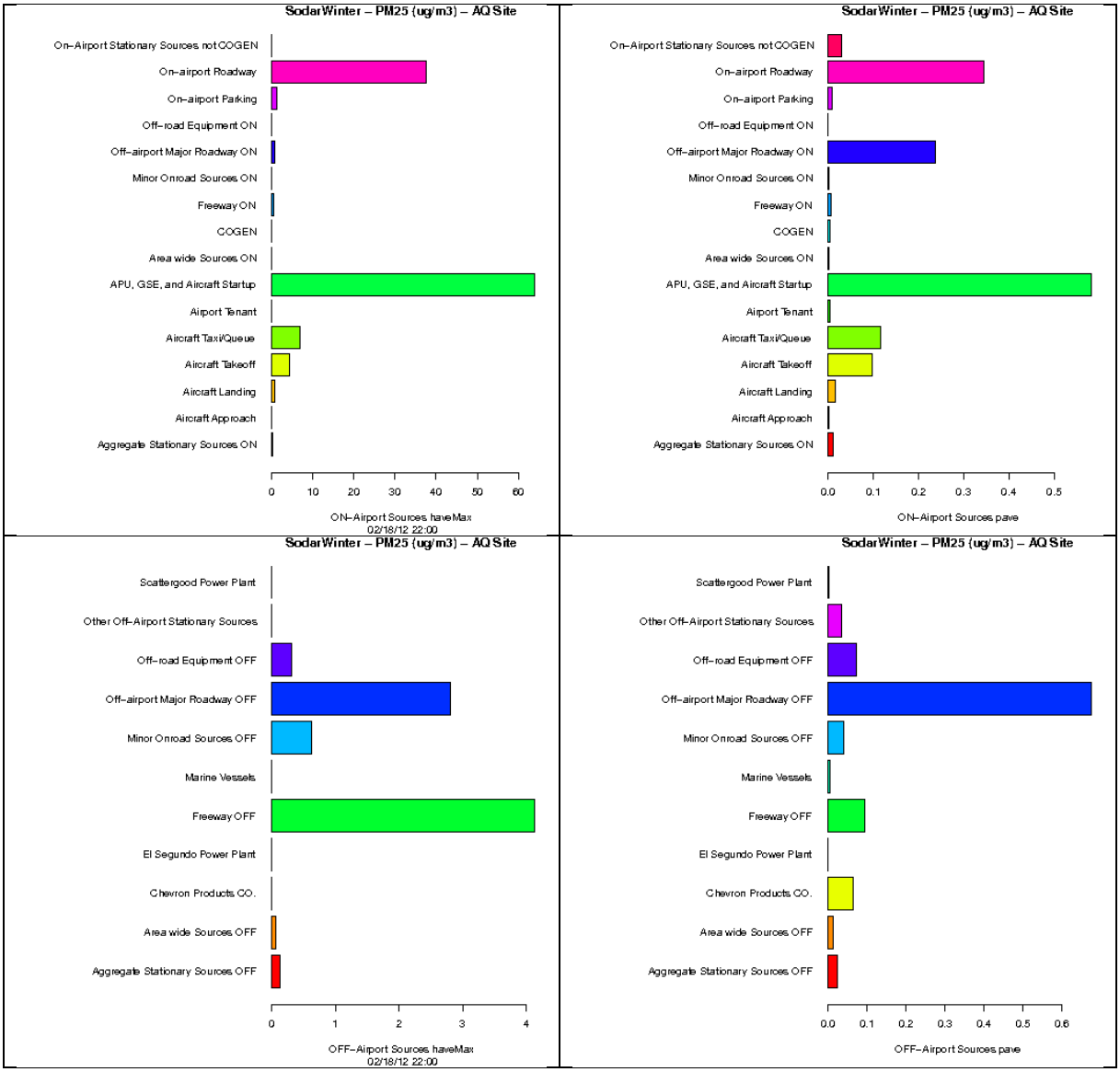

Figure 9A-85: Source-sector contributions to Hourly Maximum (left) and Period Average $PM_{2.5}$ concentrations at AQ Site from airport-related sources (top) and background sources (bottom) during Winter Season.

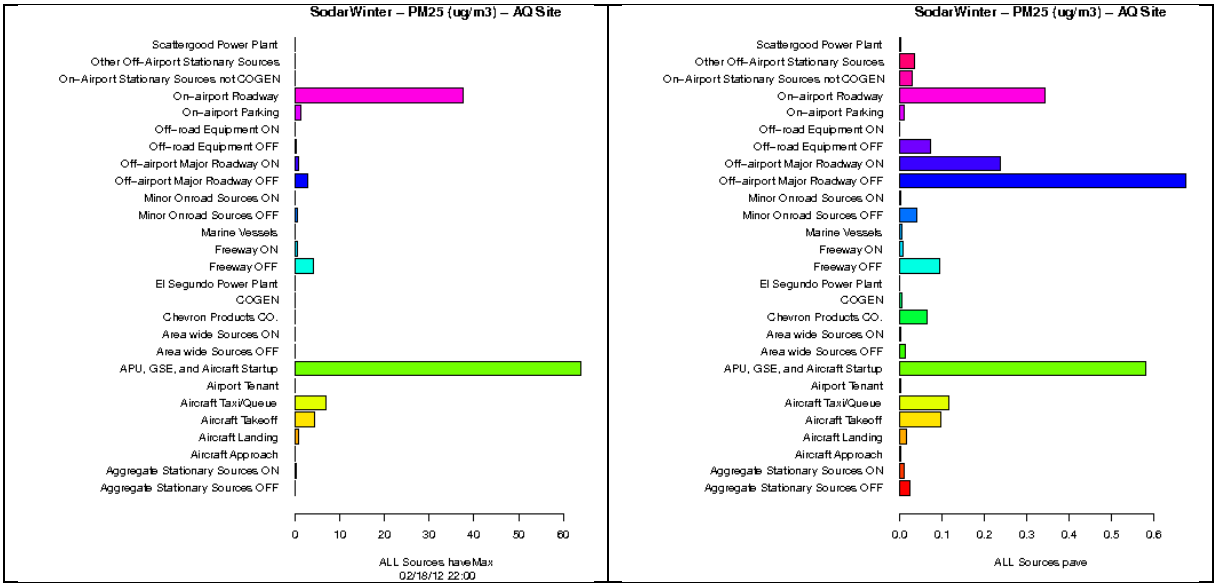

Figure 9A-86: Source-sector contributions to Hourly Maximum (left) and Period Average $PM_{2.5}$ concentrations at AQ Site from ALL sources during Winter Season.

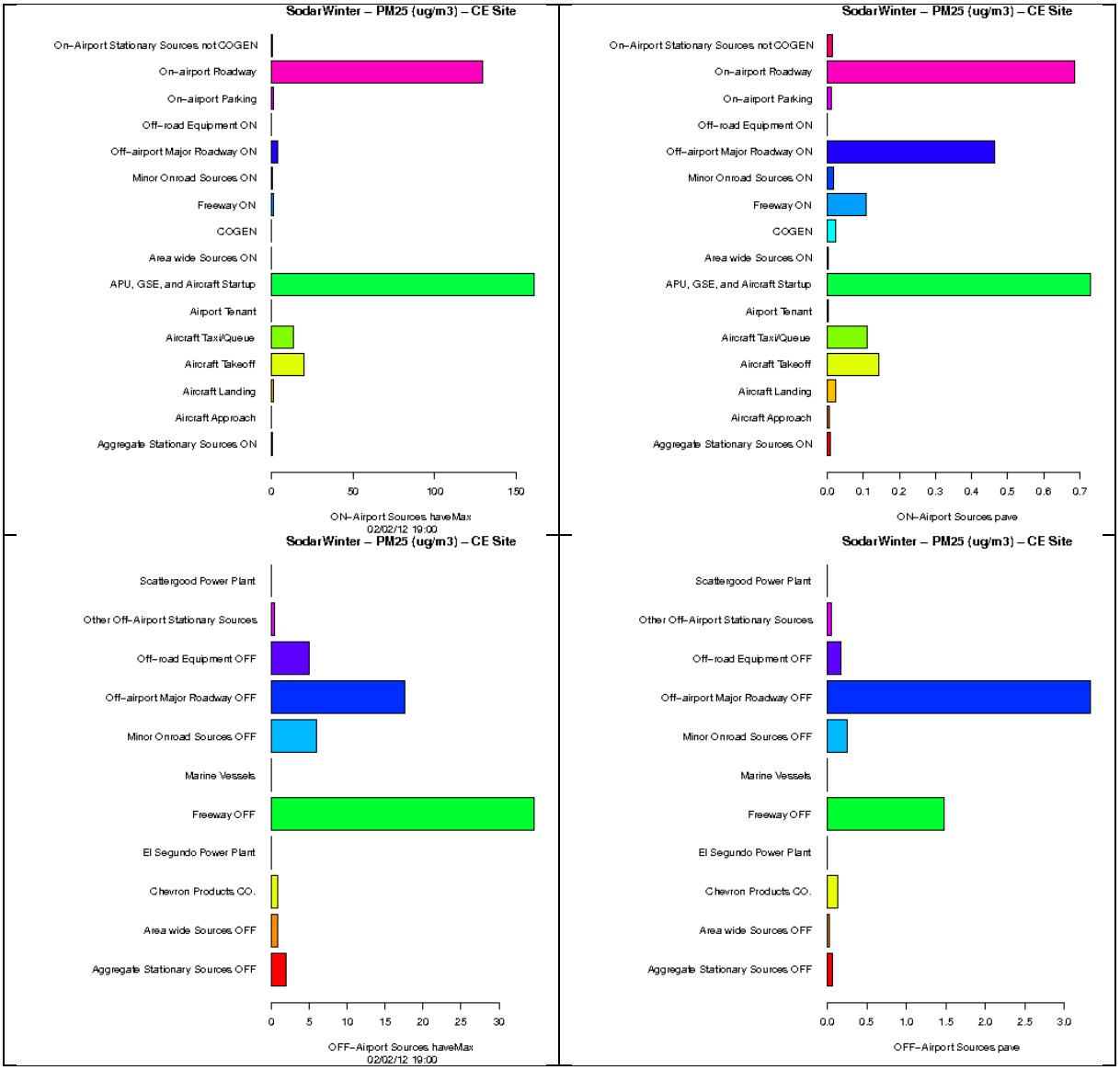

Figure 9A-87: Source-sector contributions to Hourly Maximum (left) and Period Average $PM_{2.5}$ concentrations at CE Site from airport-related sources (top) and background sources (bottom) during Winter Season.

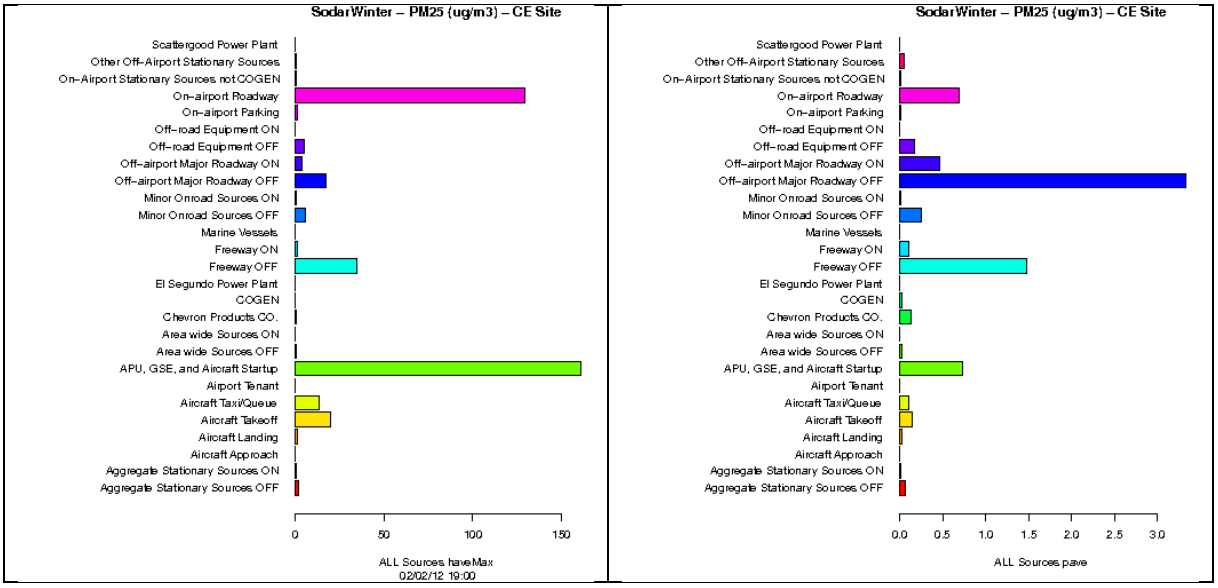

Figure 9A-88: Source-sector contributions to Hourly Maximum (left) and Period Average $PM_{2.5}$ concentrations at CE Site from ALL sources during Winter Season.

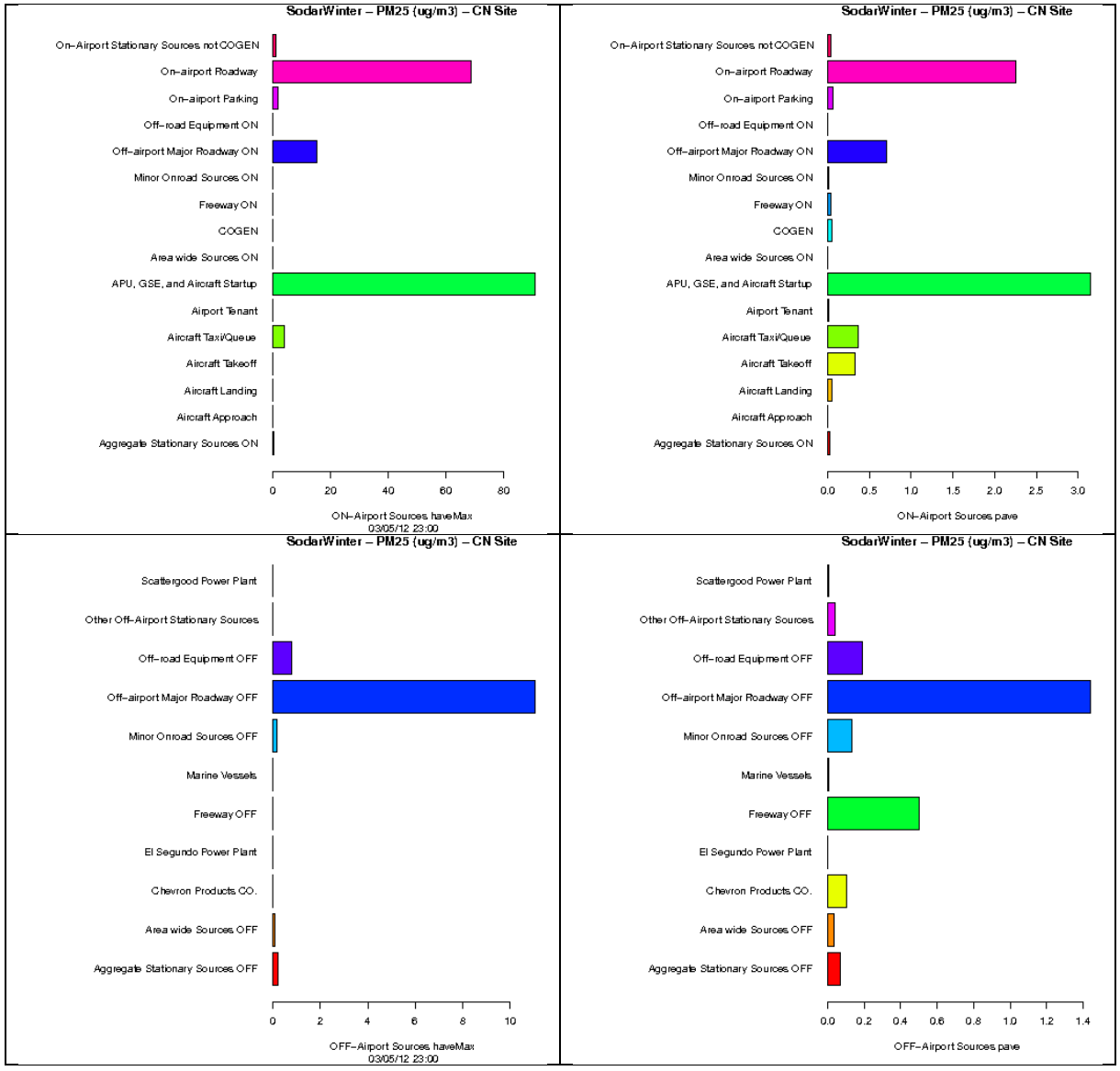

Figure 9A-89: Source-sector contributions to Hourly Maximum (left) and Period Average $PM_{2.5}$ concentrations at CN Site from airport-related sources (top) and background sources (bottom) during Winter Season.

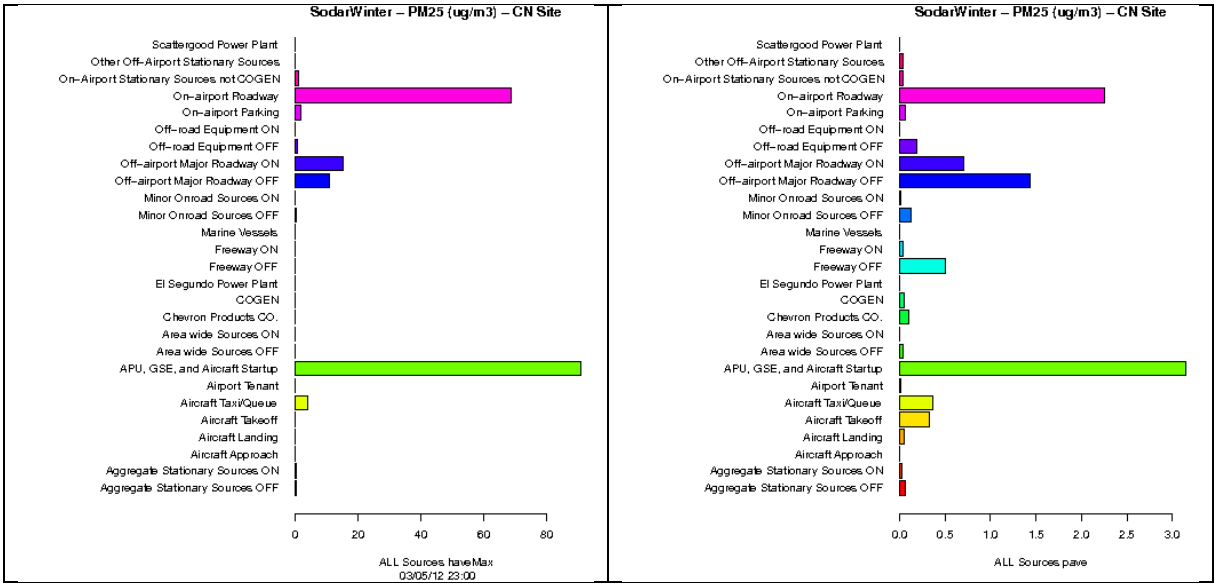

Figure 9A-90: Source-sector contributions to Hourly Maximum (left) and Period Average $PM_{2.5}$ concentrations at CN Site from ALL sources during Winter Season.

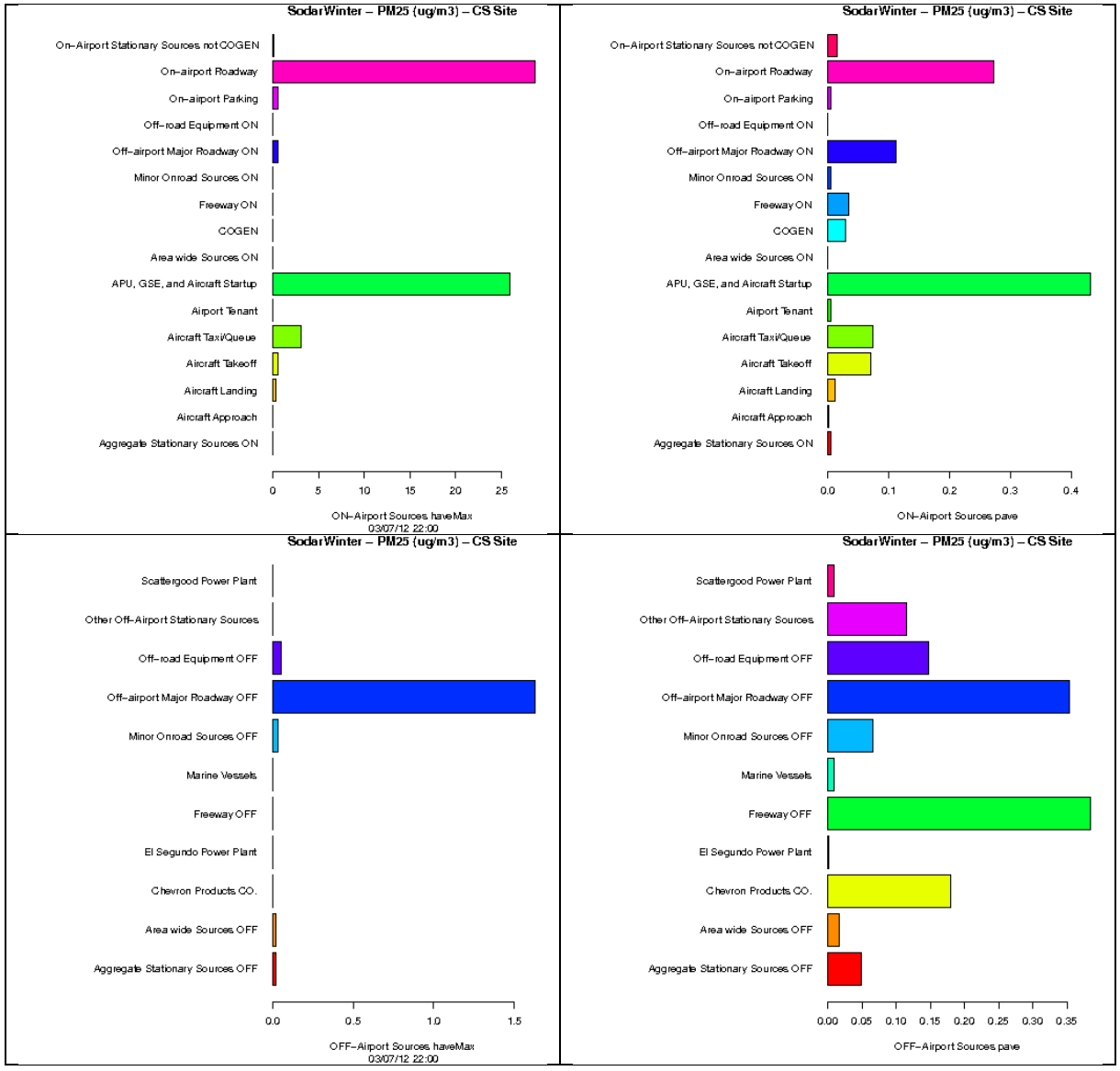

Figure 9A-91: Source-sector contributions to Hourly Maximum (left) and Period Average $PM_{2.5}$ concentrations at CS Site from airport-related sources (top) and background sources (bottom) during Winter Season.

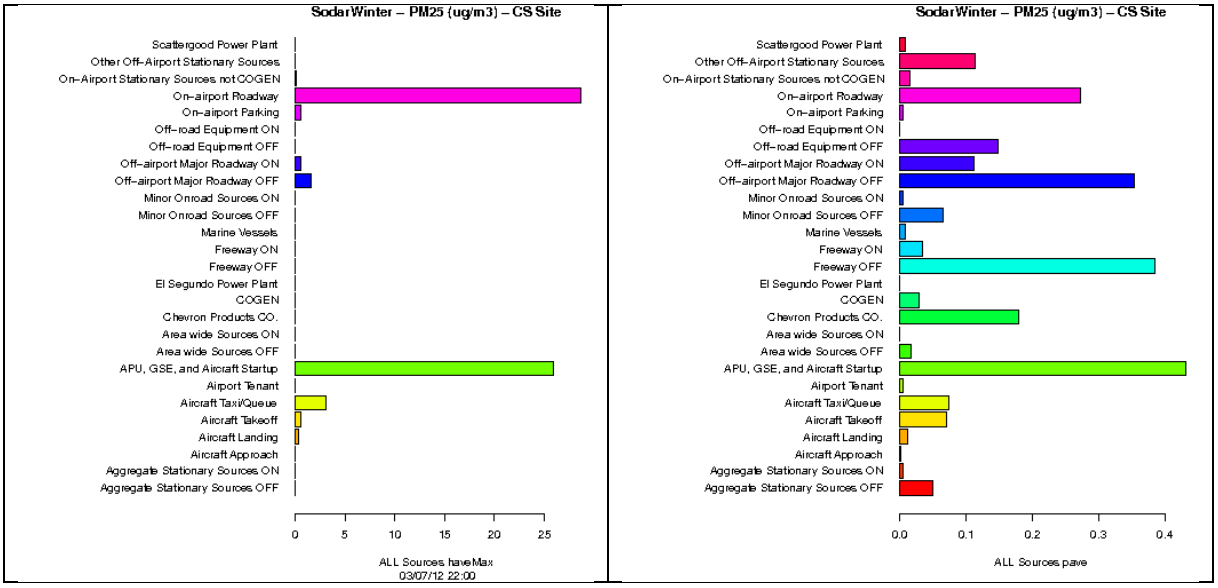

Figure 9A-92: Source-sector contributions to Hourly Maximum (left) and Period Average $PM_{2.5}$ concentrations at CS Site from ALL sources during Winter Season.

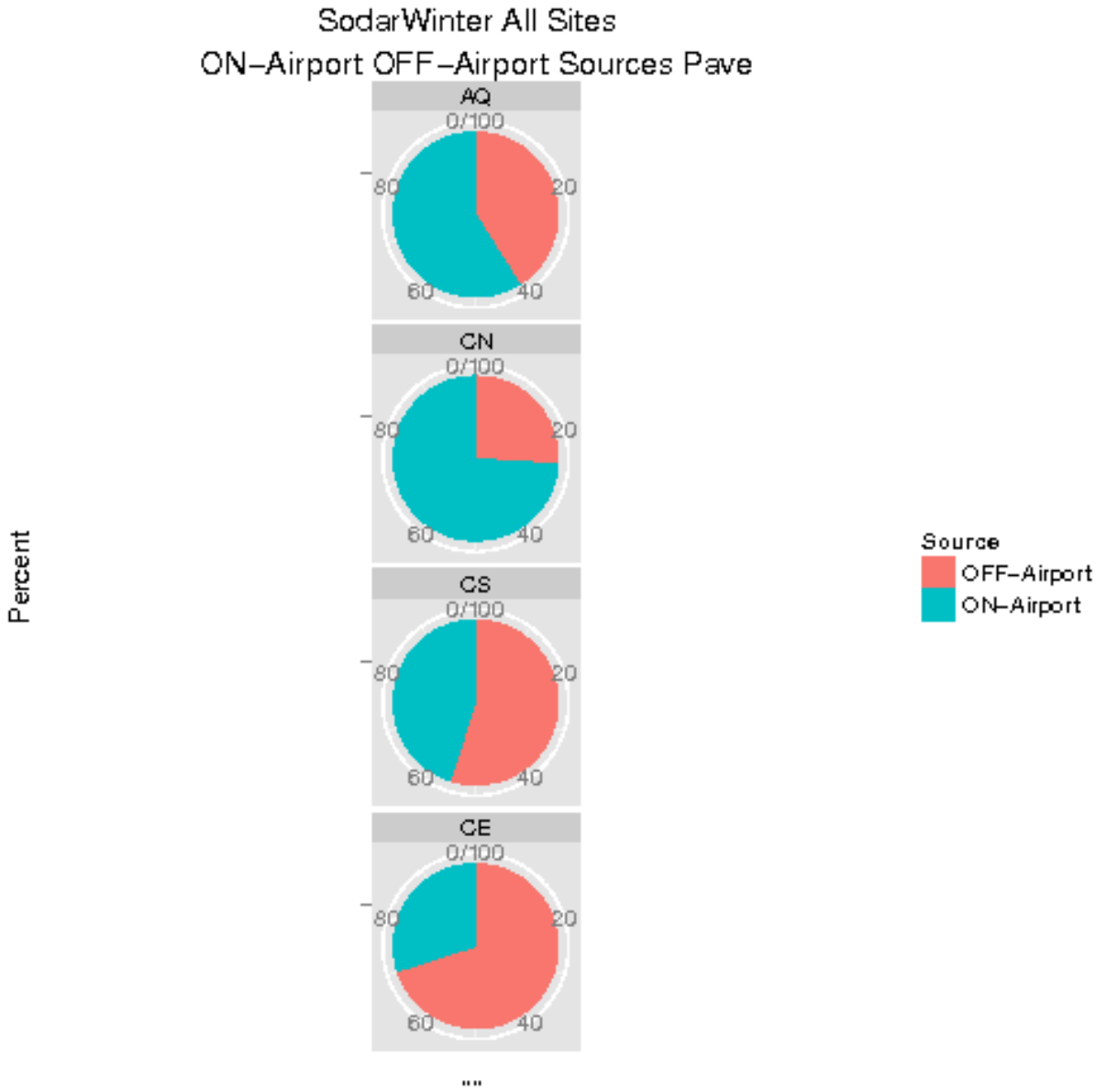

Figure 9A-93: Source-sector contributions to Period Average $PM_{2.5}$ concentrations at each site from airport-related vs. background sources during Winter Season.

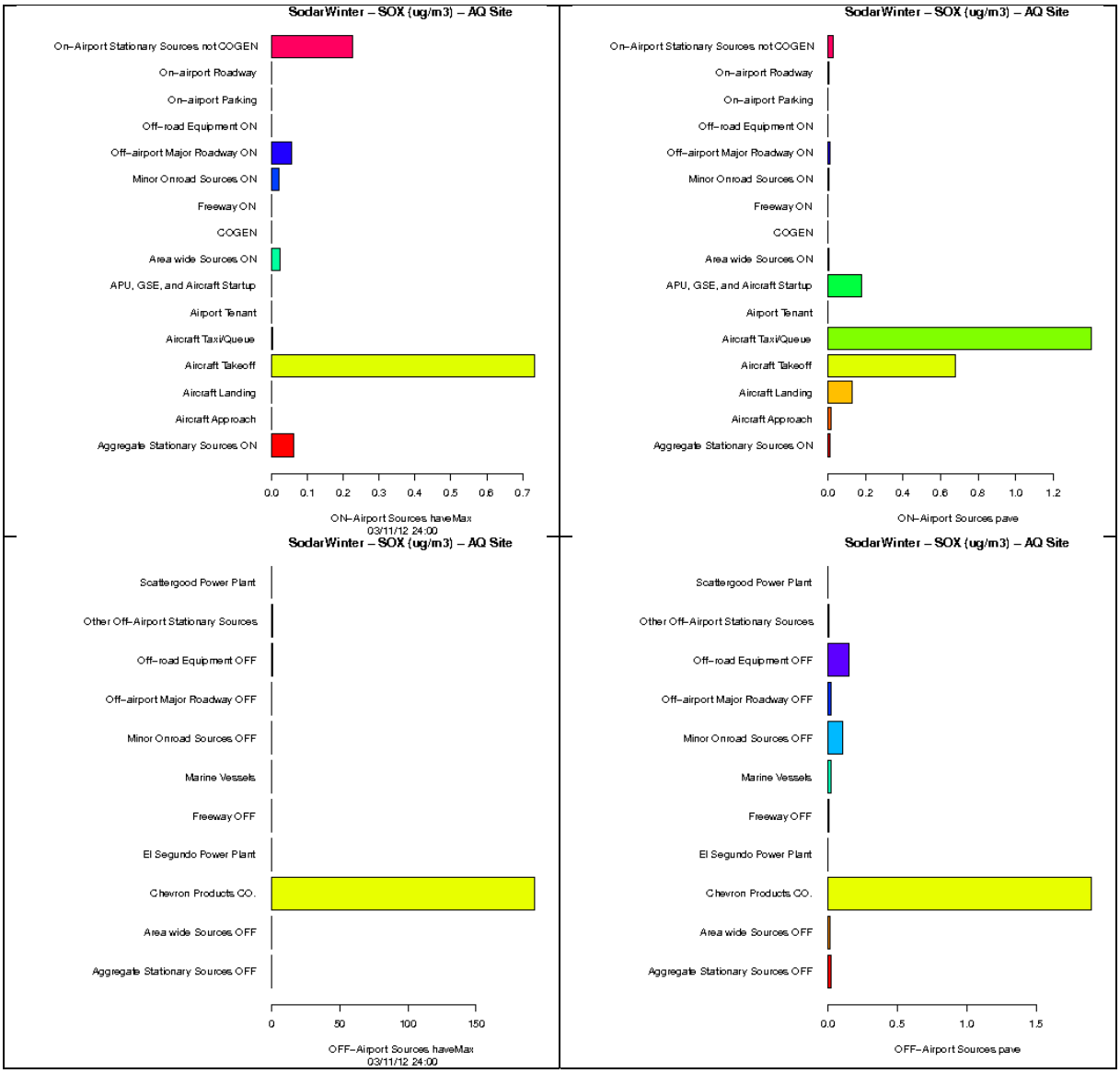

Figure 9A-94: Source-sector contributions to Hourly Maximum (left) and Period Average SOx concentrations at AQ Site from airport-related sources (top) and background sources (bottom) during Winter Season.

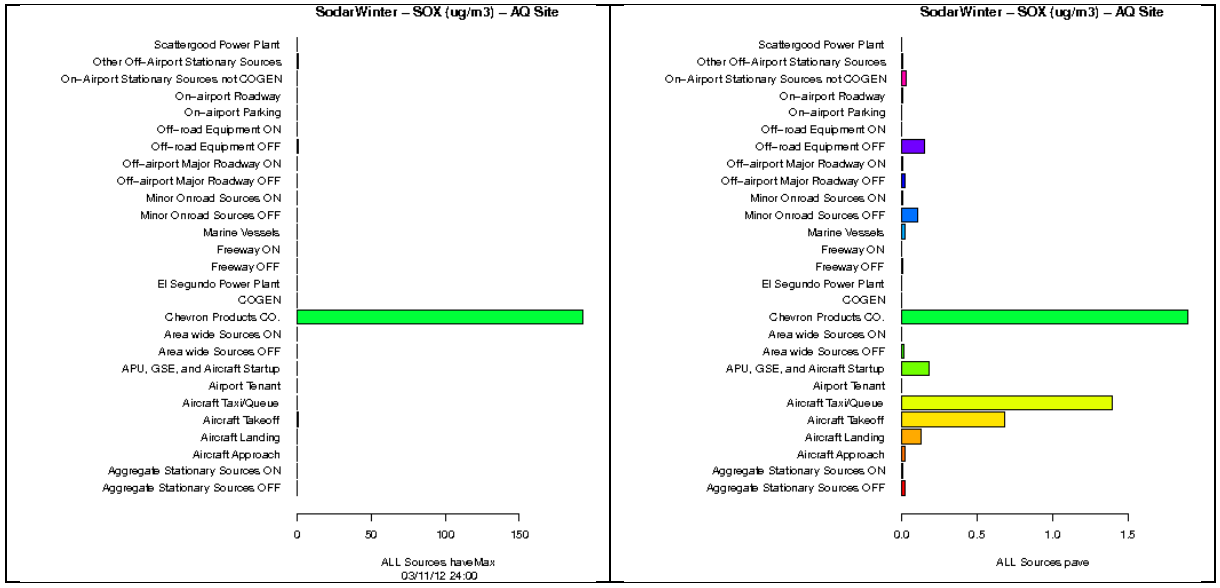

Figure 9A-95: Source-sector contributions to Hourly Maximum (left) and Period Average SOx concentrations at AQ Site from ALL sources during Winter Season.

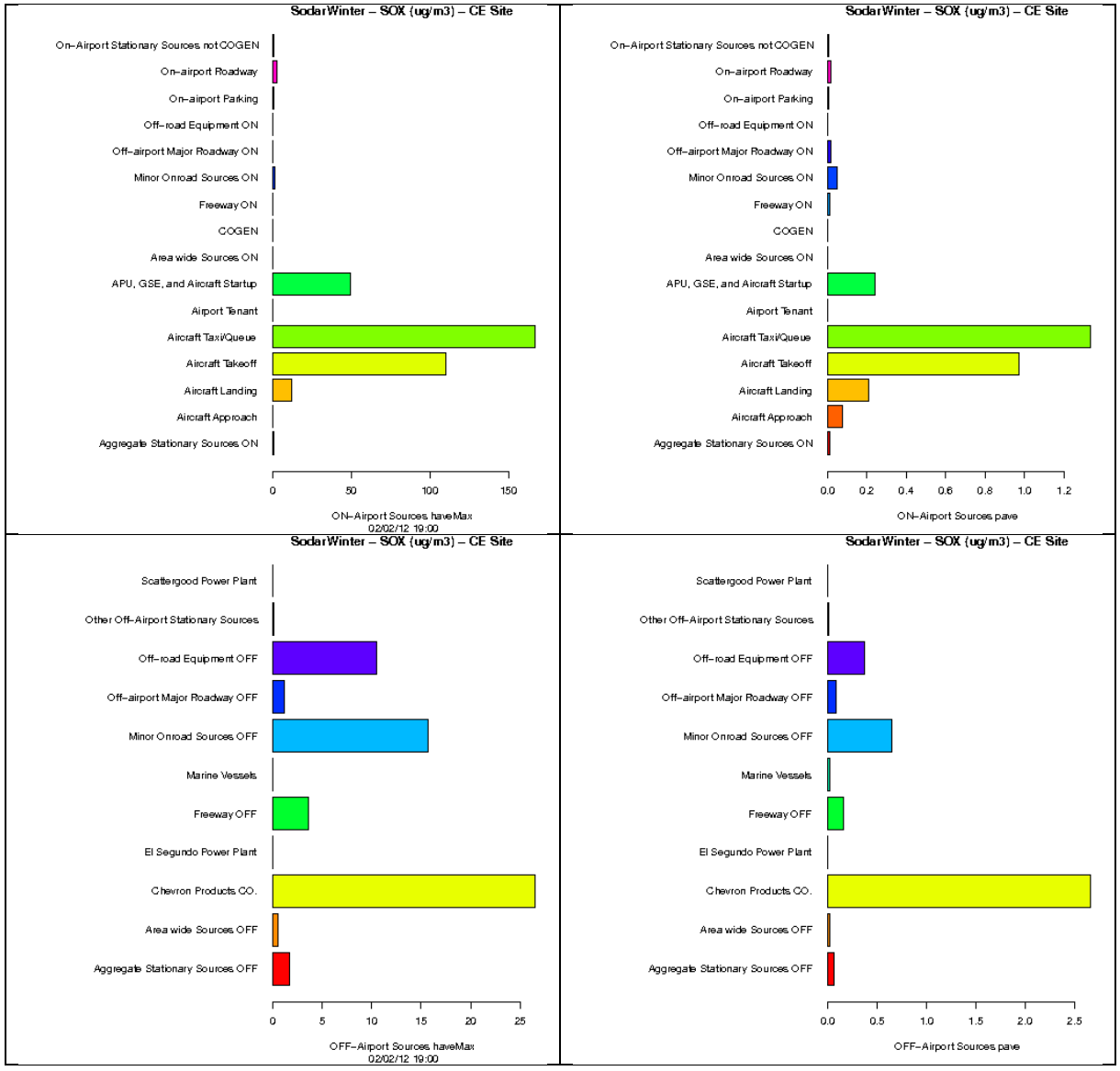

Figure 9A-96: Source-sector contributions to Hourly Maximum (left) and Period Average SOx concentrations at CE Site from airport-related sources (top) and background sources (bottom) during Winter Season.

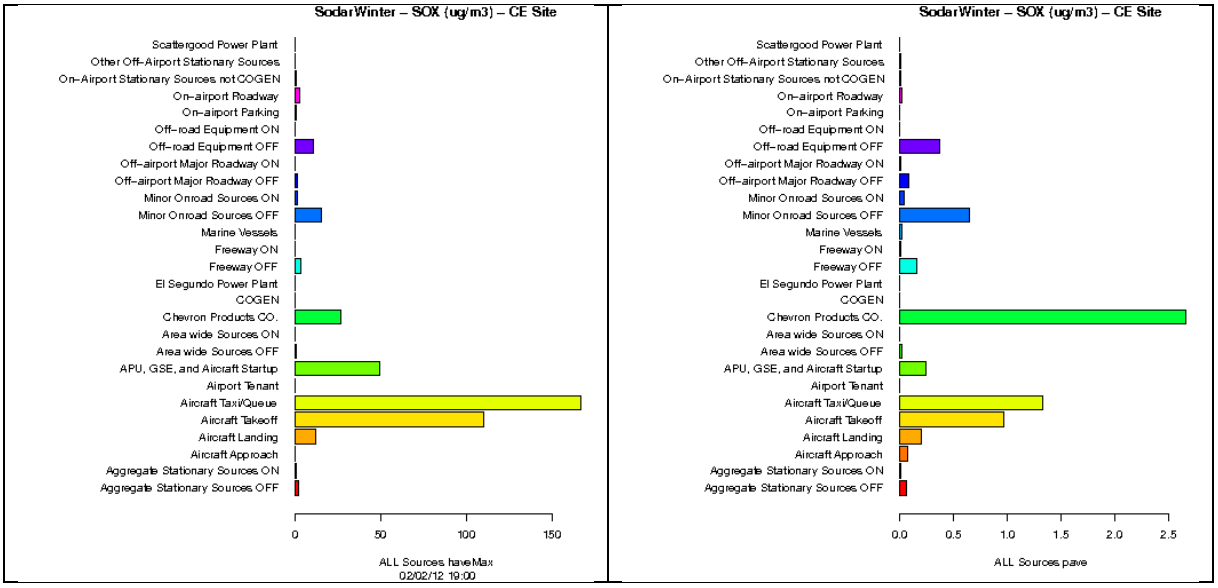

Figure 9A-97: Source-sector contributions to Hourly Maximum (left) and Period Average SOx concentrations at CE Site from ALL sources during Winter Season.

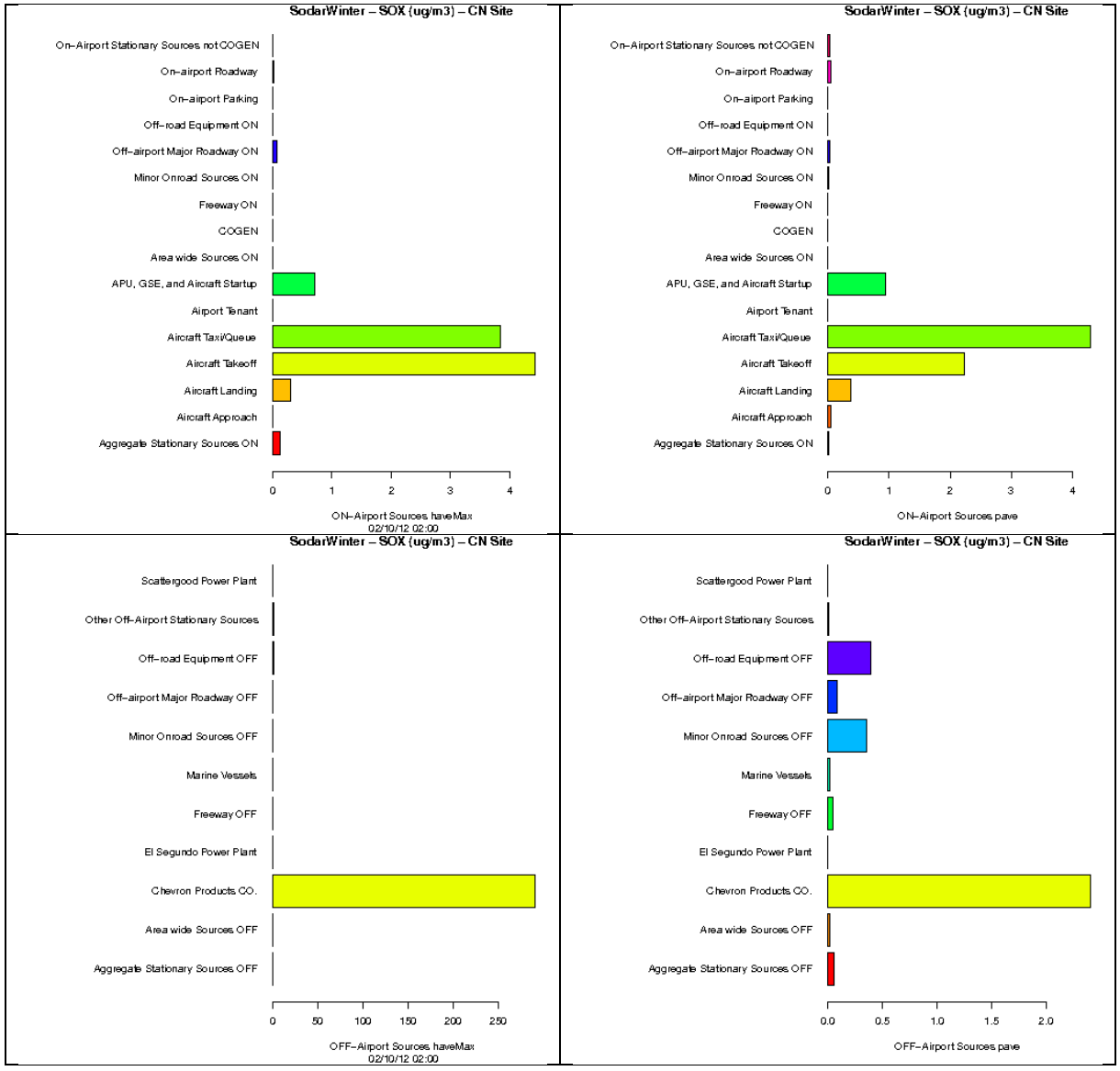

Figure 9A-98: Source-sector contributions to Hourly Maximum (left) and Period Average SOx concentrations at CN Site from airport-related sources (top) and background sources (bottom) during Winter Season.

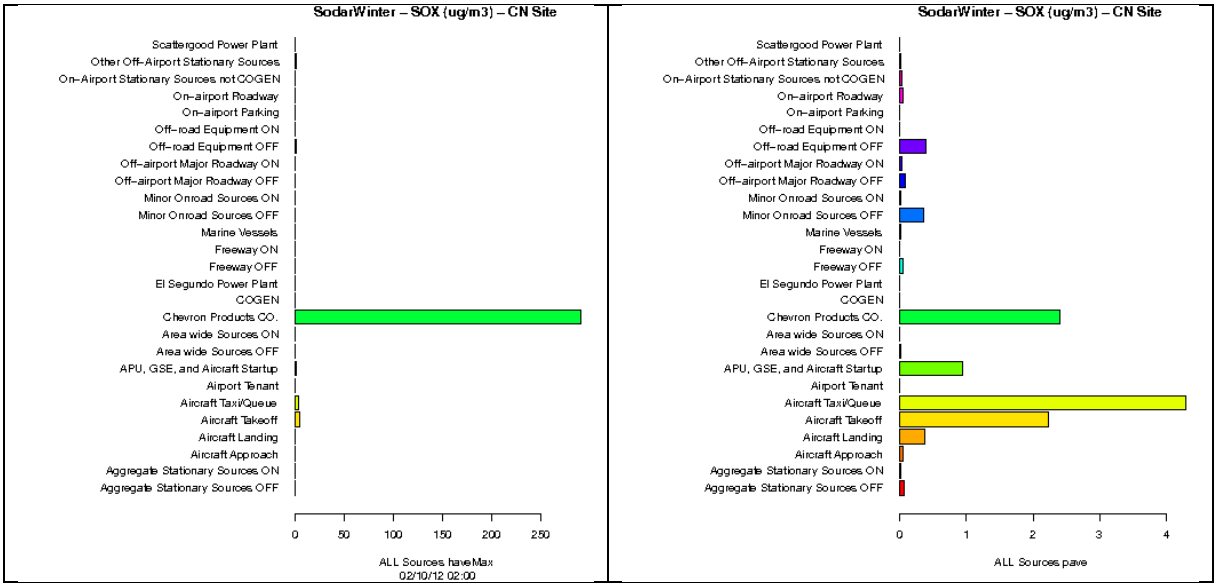

Figure 9A-99: Source-sector contributions to Hourly Maximum (left) and Period Average SOx concentrations at CN Site from ALL sources during Winter Season.

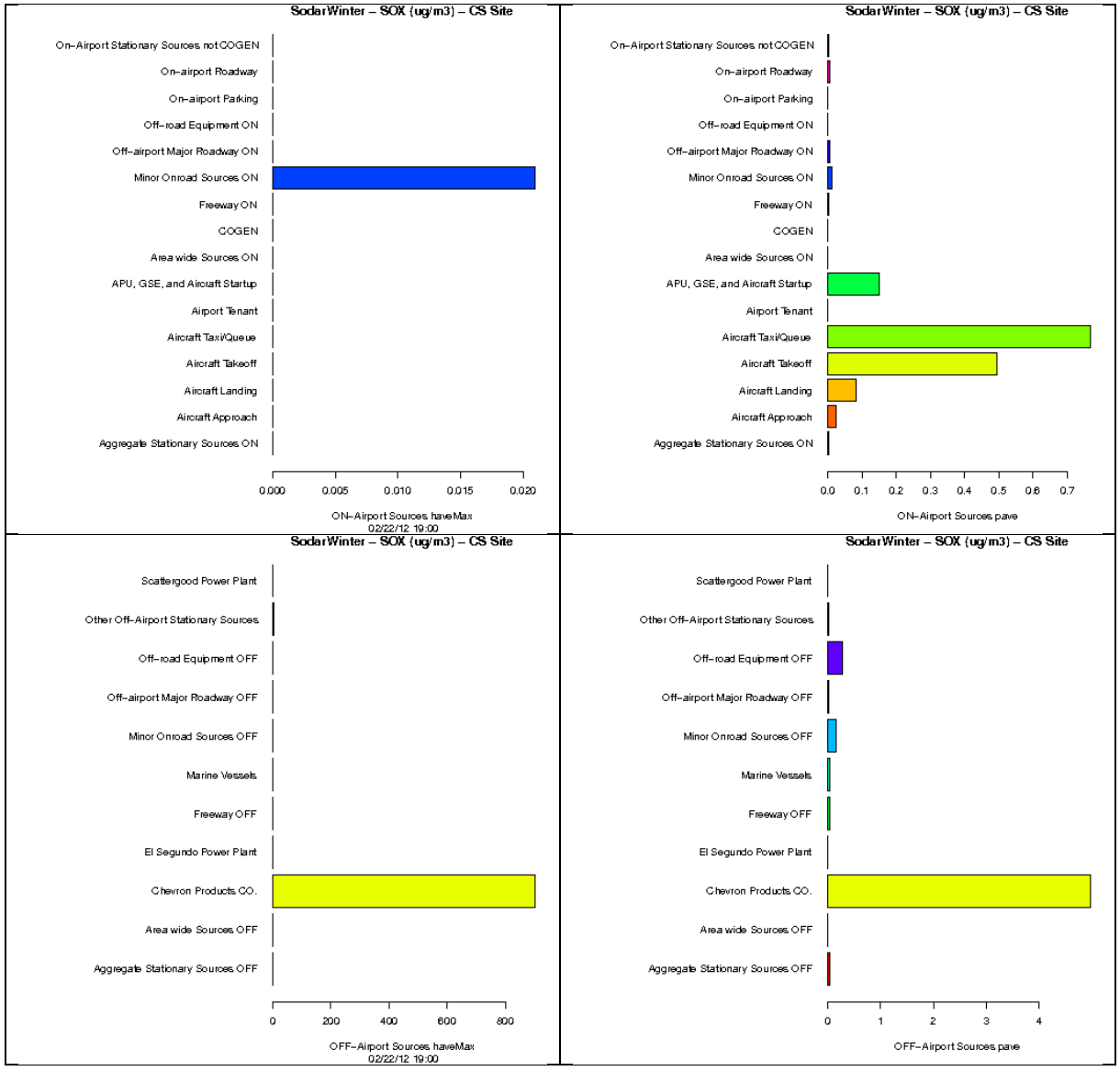

Figure 9A-100: Source-sector contributions to Hourly Maximum (left) and Period Average SOx concentrations at CS Site from airport-related sources (top) and background sources (bottom) during Winter Season.

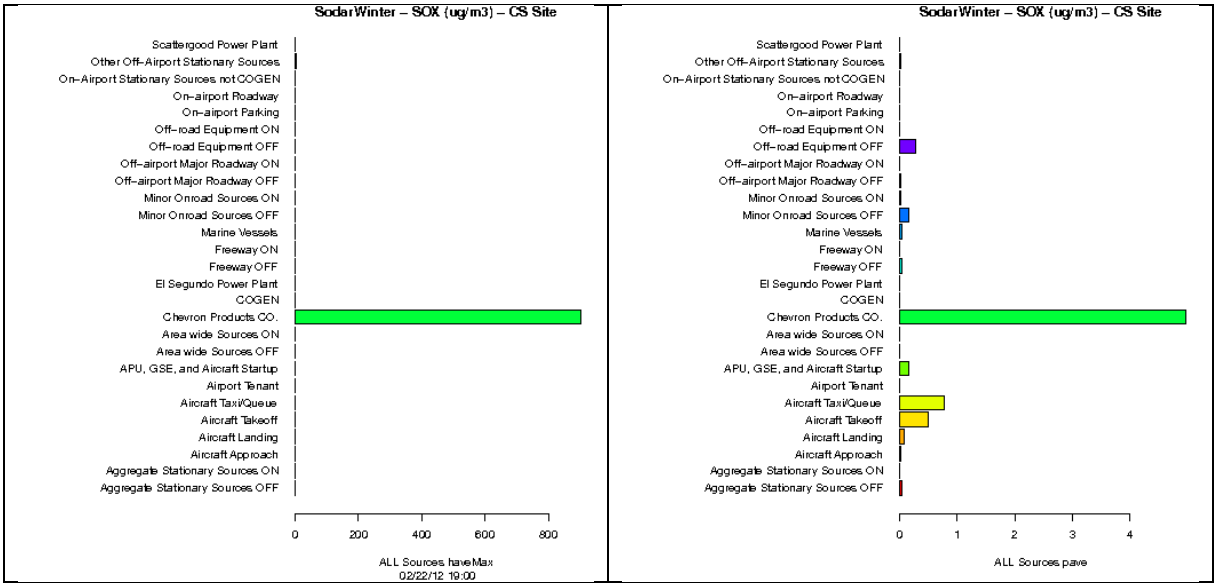

Figure 9A-101: Source-sector contributions to Hourly Maximum (left) and Period Average SOx concentrations at CS Site from ALL sources during Winter Season.

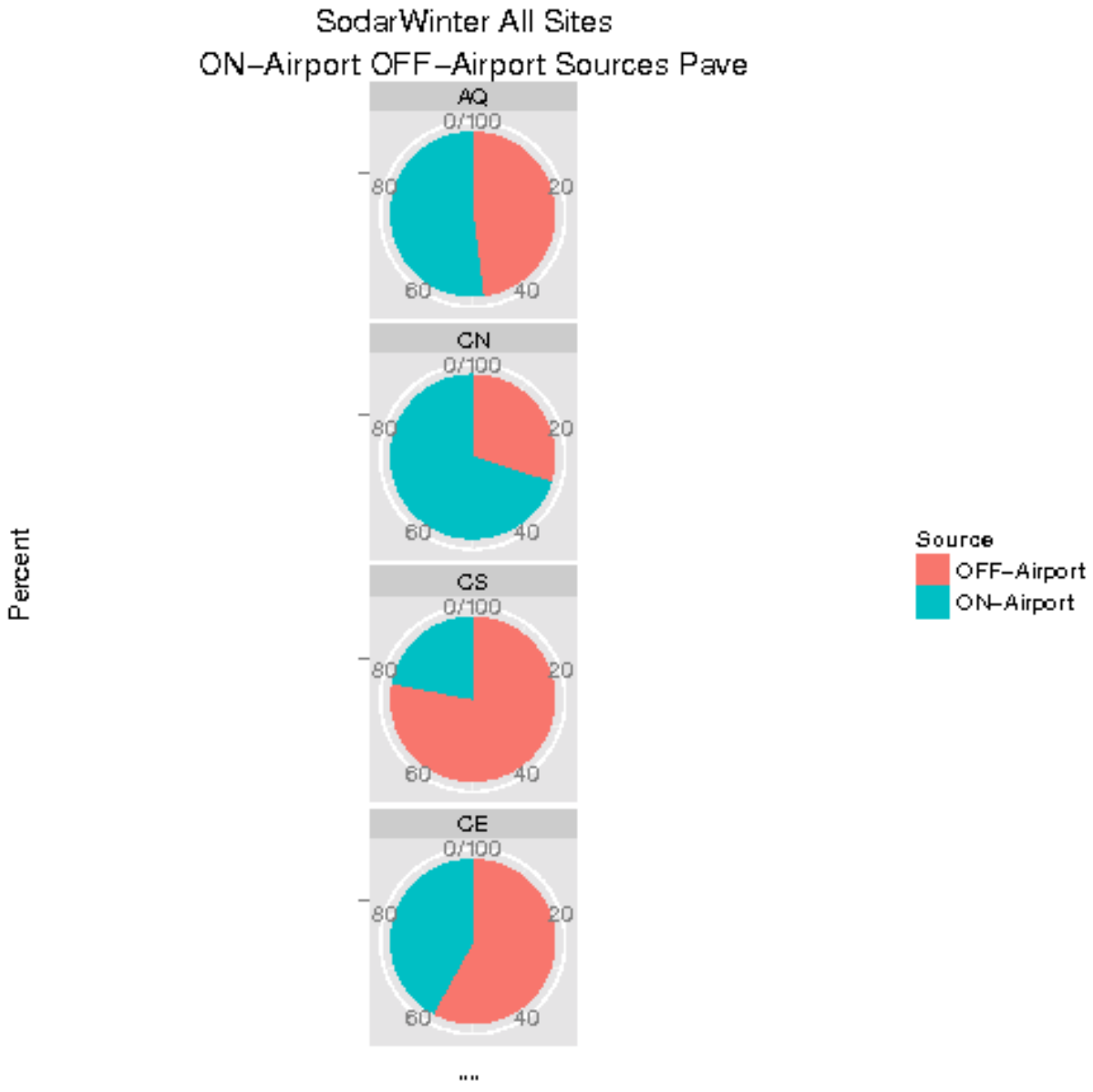

Figure 9A-102: Source-sector contributions to Period Average SOx concentrations at each site from airport-related vs. background sources during Winter Season.

SUMMER SEASON

(This page is intentionally blank)

I. Spatial Analyses

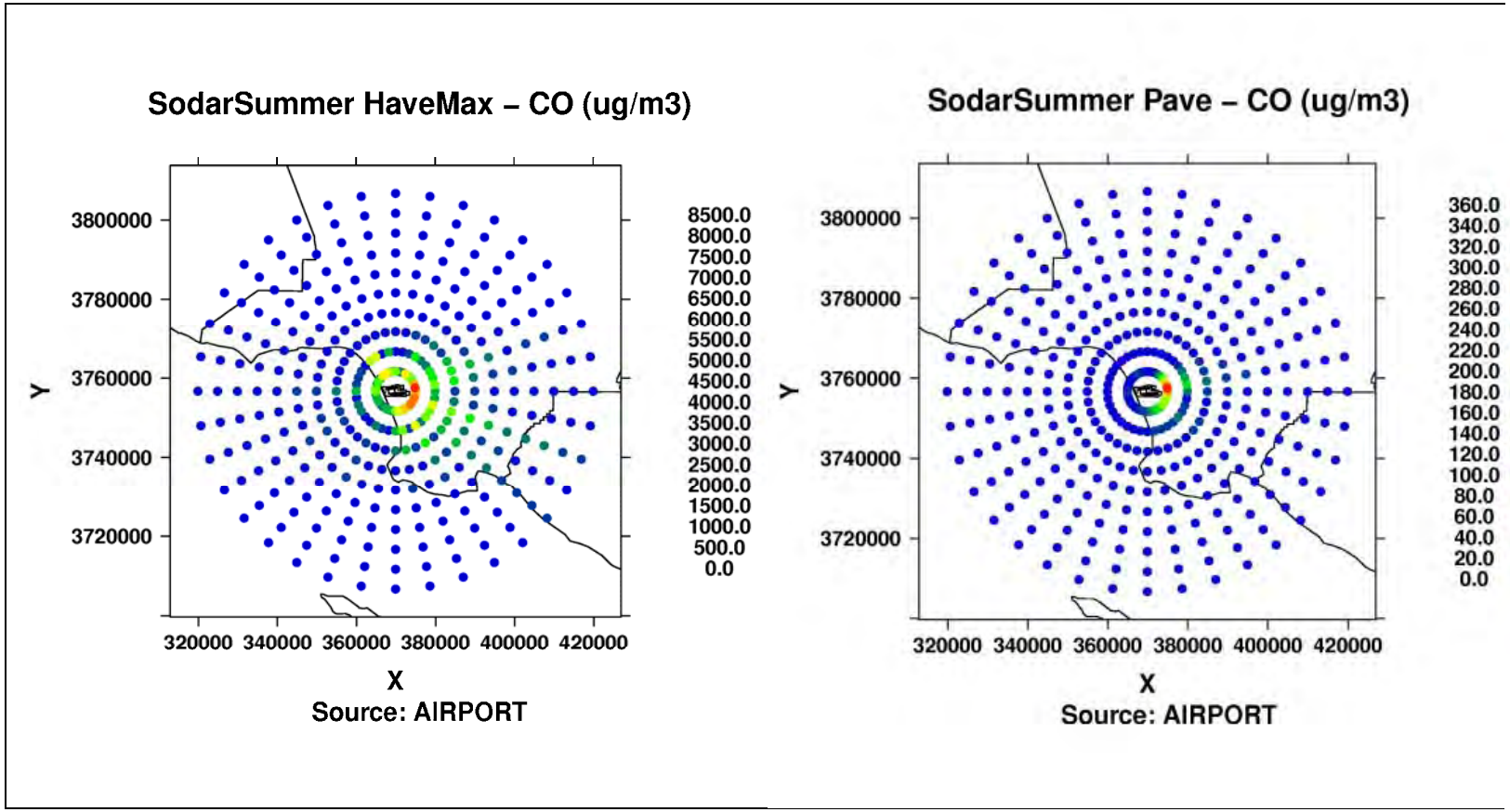

Figure 9A-103a: Modeled hourly max (left) and period average (right) CO concentrations from airport-related in Polar Grid of receptors during Summer Season.

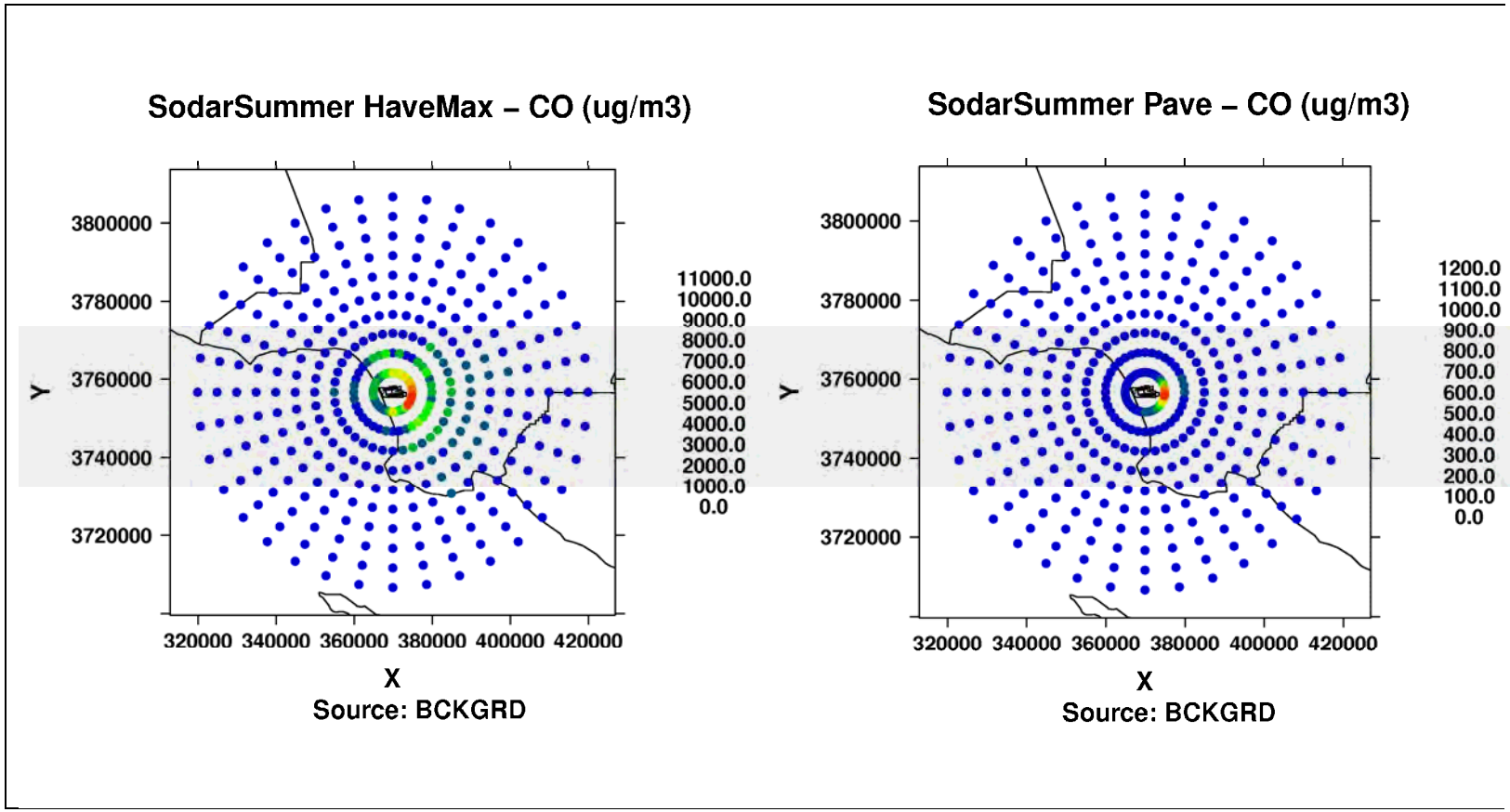

Figure 9A-103b: Modeled hourly max (left) and period average (right) CO concentrations from background sources in Polar Grid of receptors during Summer Season.

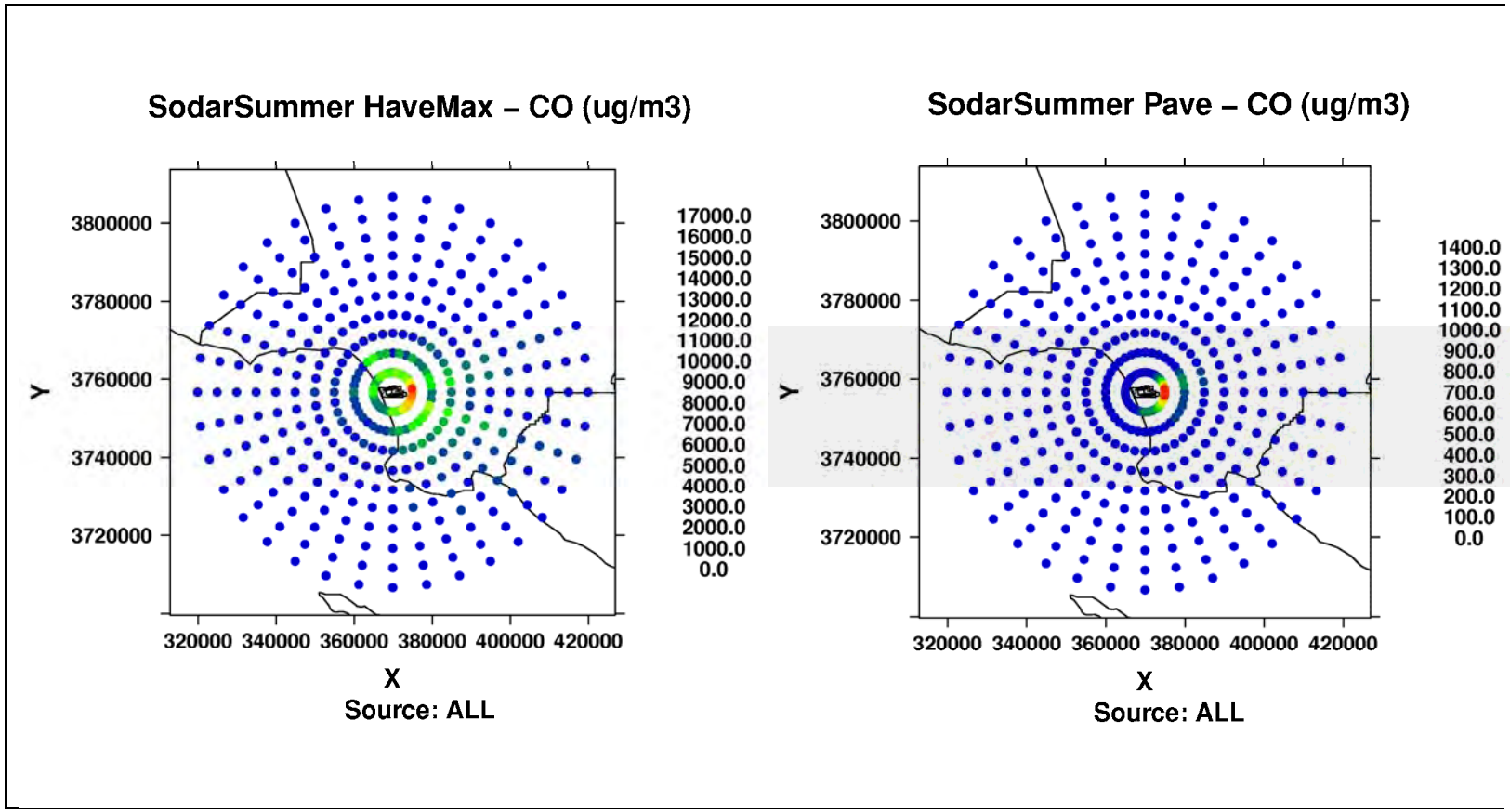

Figure 9A-103c: Modeled hourly max (left) and period average (right) CO concentrations from ALL in Polar Grid of receptors during Summer Season.

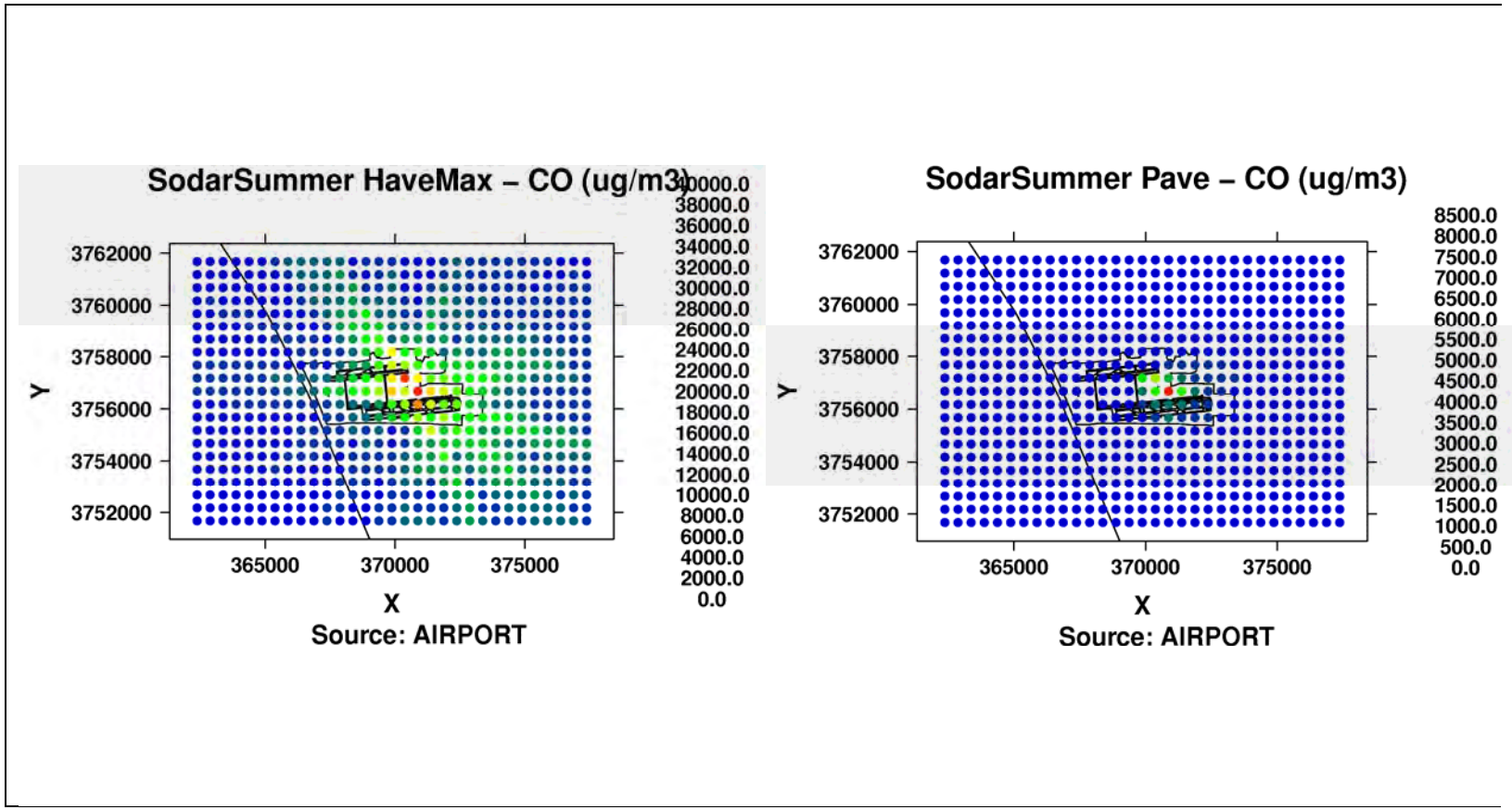

Figure 9A-104a: Modeled hourly max (left) and period average (right) CO concentrations from airport-related in Cartesian Grid of receptors during Summer Season.

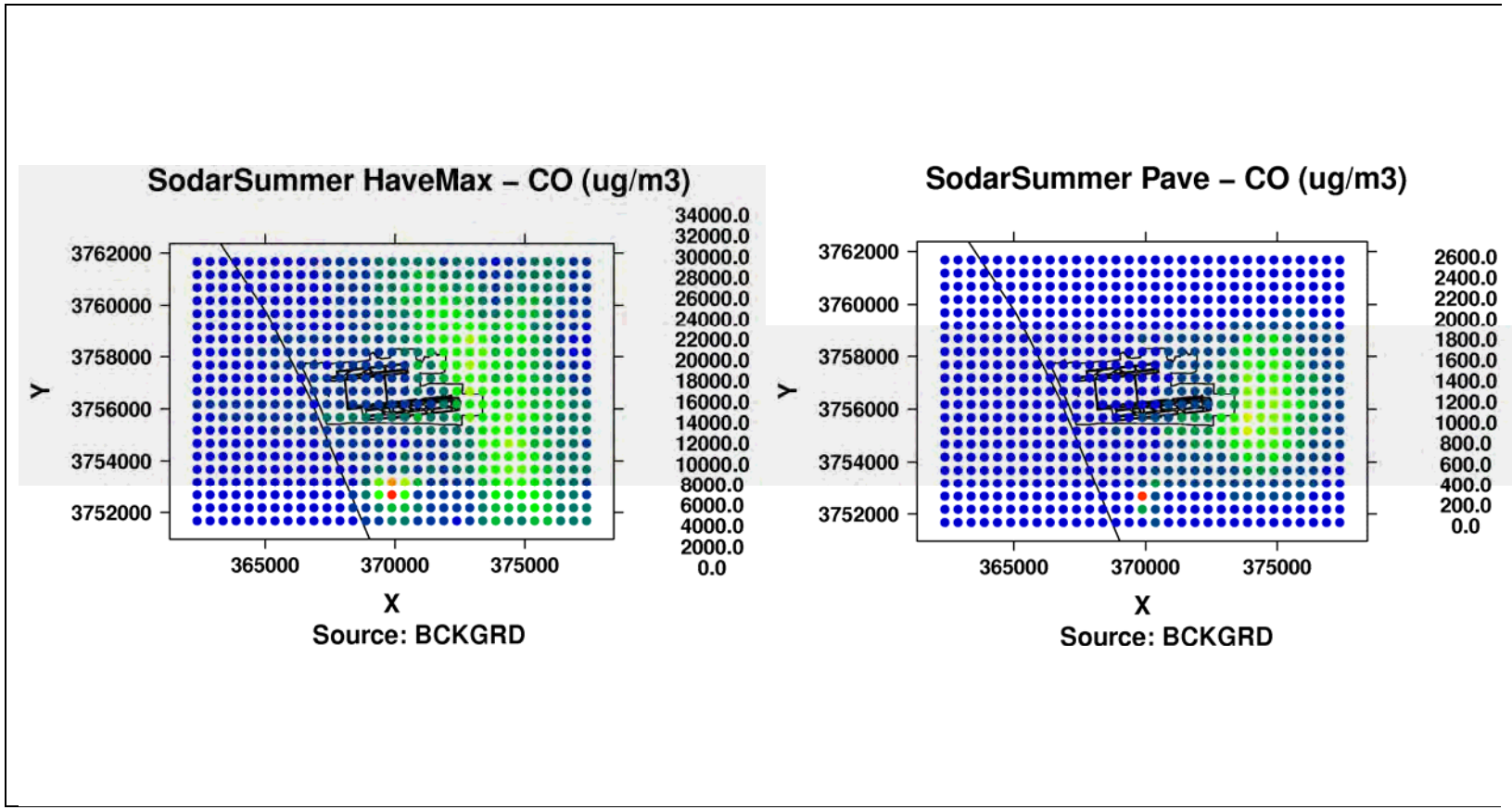

Figure 9A-104b: Modeled hourly max (left) and period average (right) CO concentrations from background sources in Cartesian Grid of receptors during Summer Season.

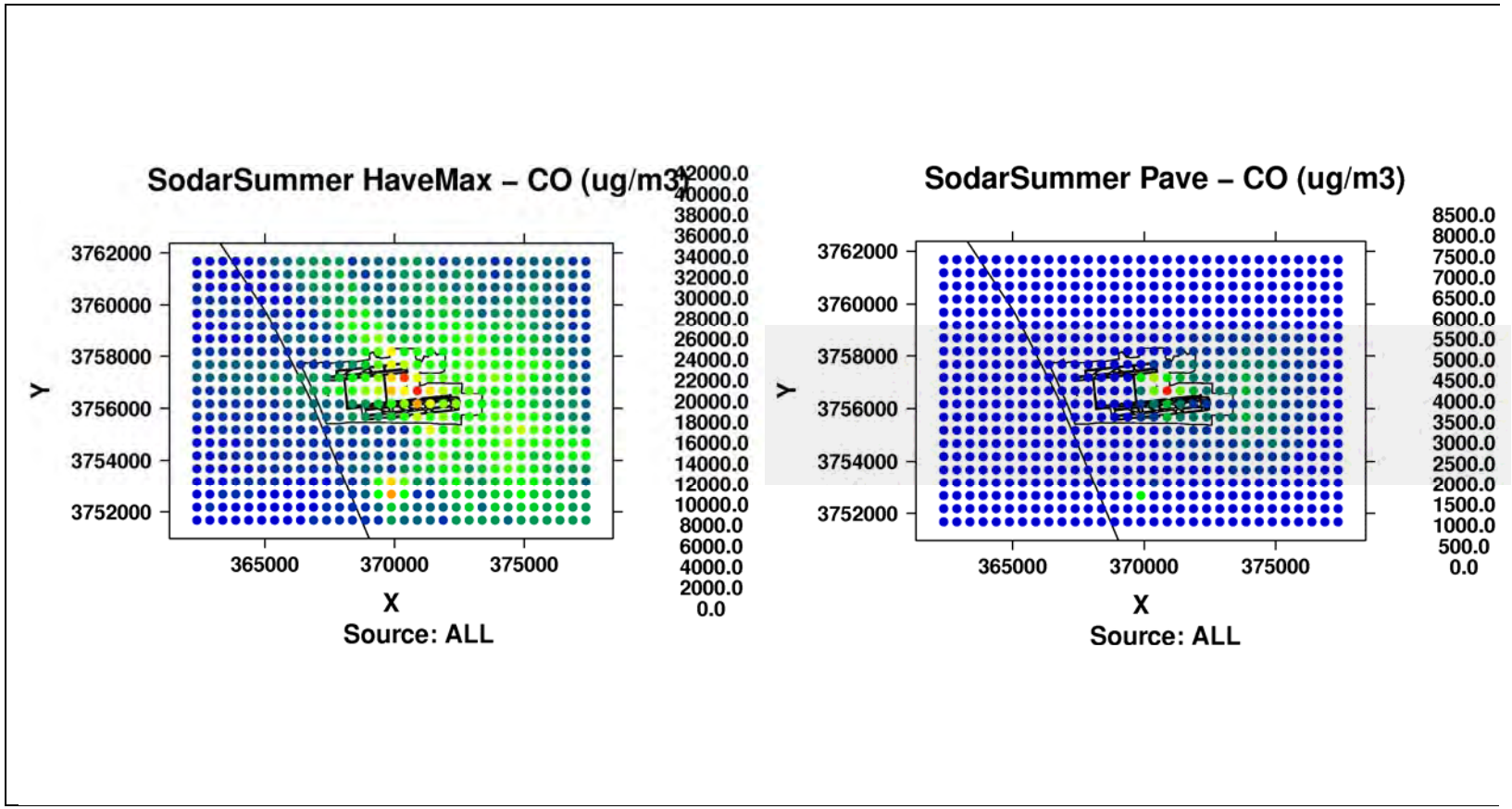

Figure 9A-104c: Modeled hourly max (left) and period average (right) CO concentrations from airport-related (top), background sources (middle) and ALL (bottom) in Cartesian Grid of receptors during Summer Season.

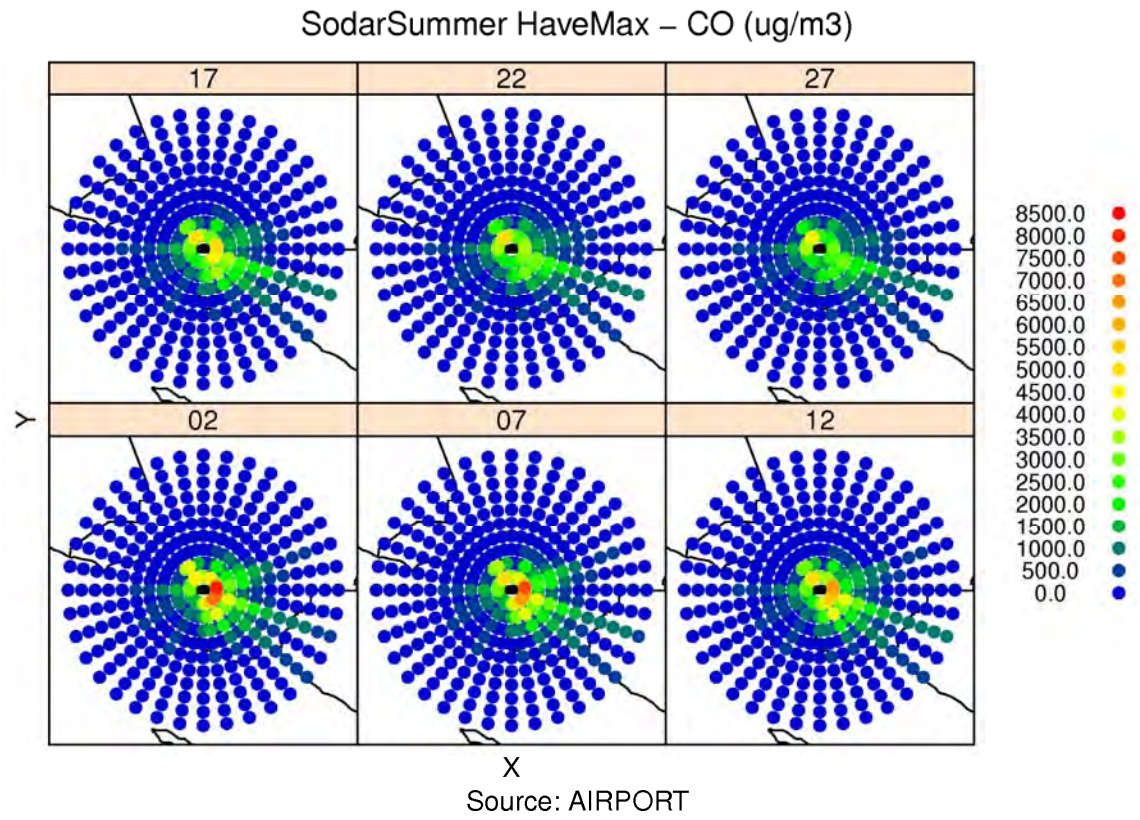

Figure 9A-105: Modeled hourly max CO concentrations from airport-related sources at flag-pole receptors at heights of 2m, 7m, 12m, 17m, 22m and 27m in Polar Grid of receptors during Summer Season.

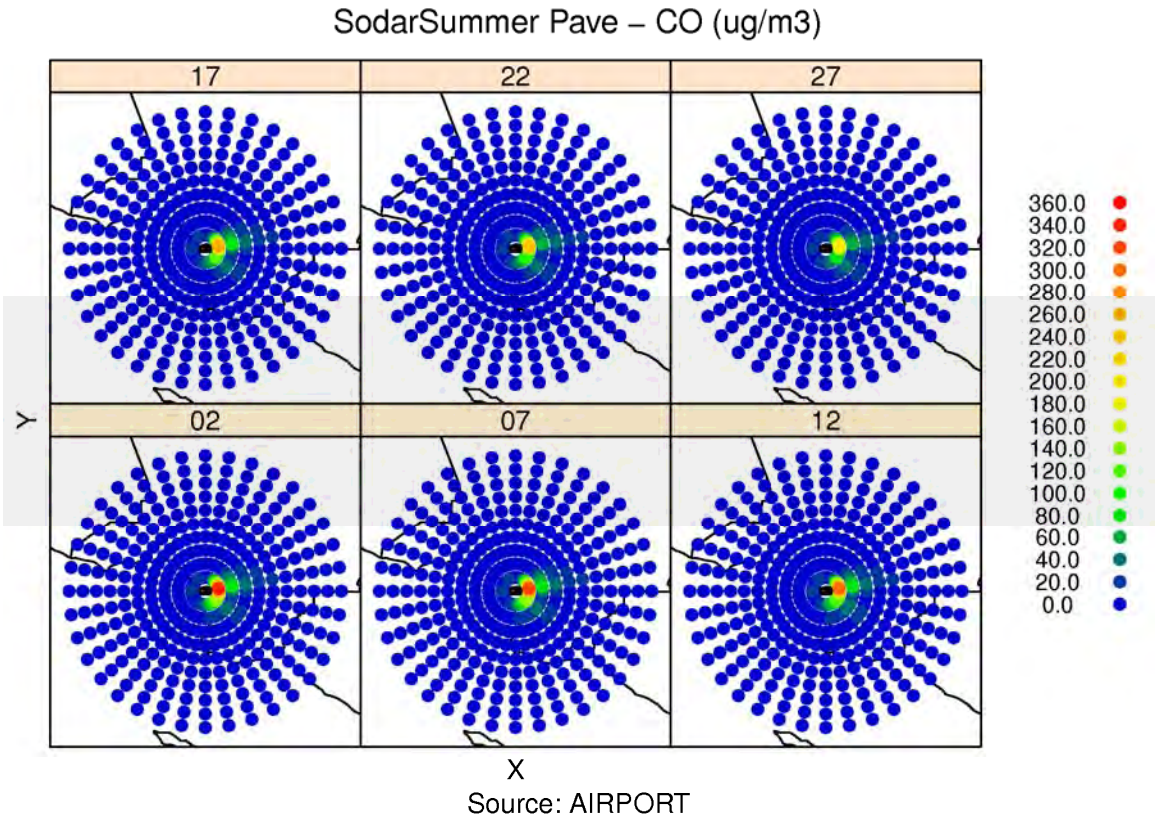

Figure 9A-106: Modeled period average CO concentrations from airport-related sources at flag-pole receptors at heights of 2m, 7m, 12m, 17m, 22m and 27m in Polar Grid of receptors during Summer Season.

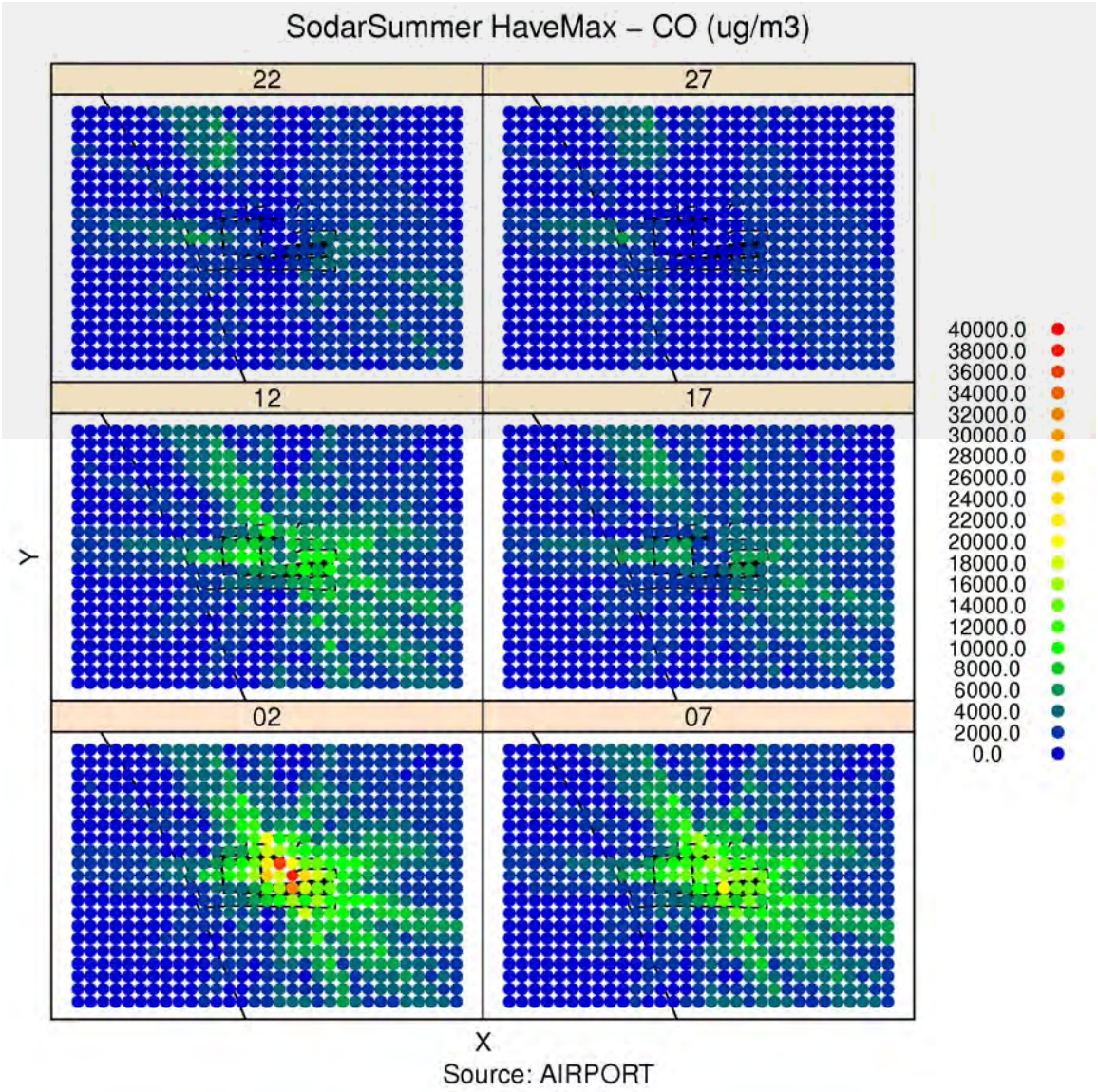

Figure 9A-107: Modeled hourly max CO concentrations from airport-related sources at flag-pole receptors at heights of 2m, 7m, 12m, 17m, 22m and 27m in Cartesian Grid of receptors during Summer Season.

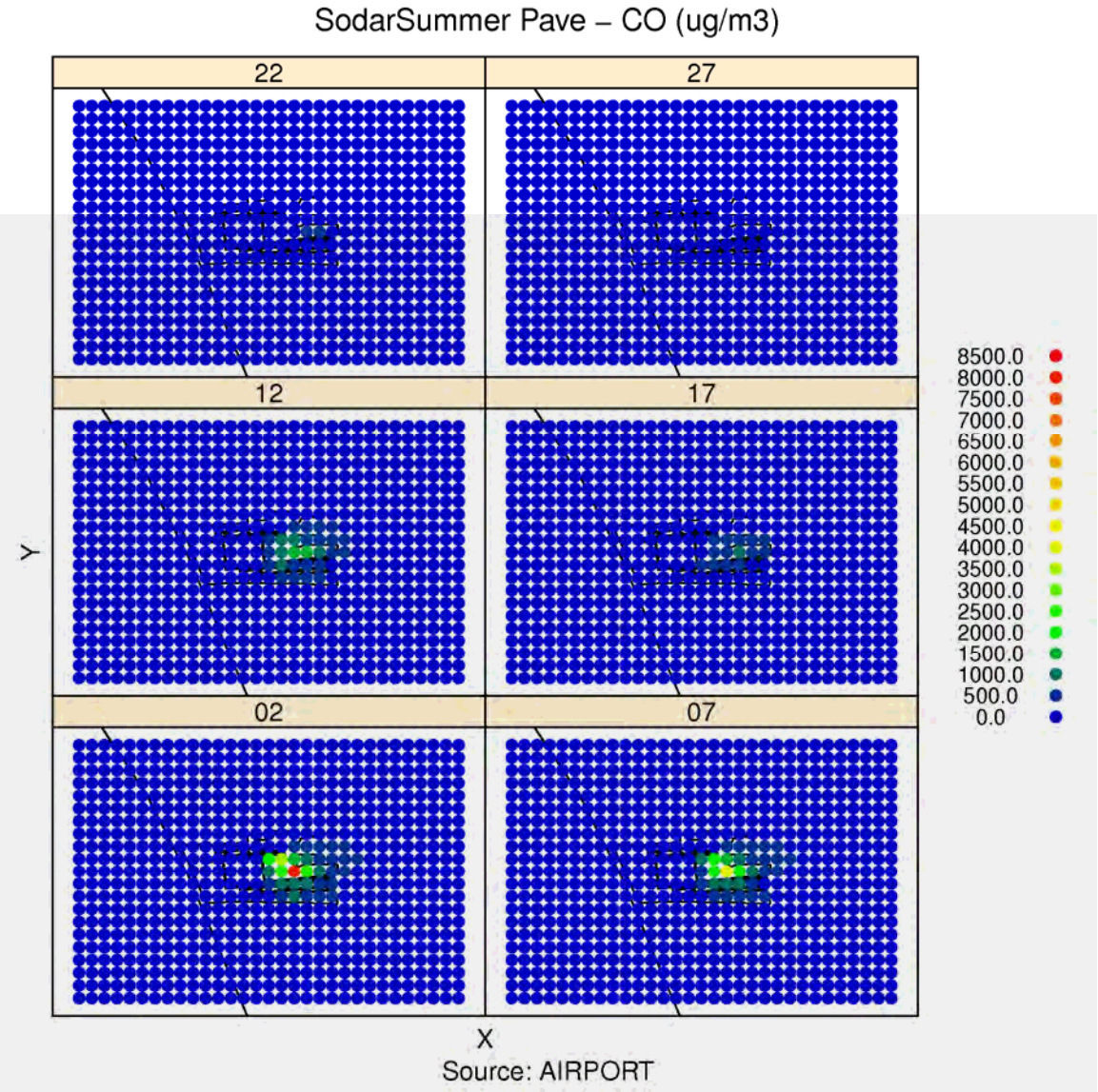

Figure 9A-108: Modeled period average CO concentrations from airport-related sources at flag-pole receptors at heights of 2m, 7m, 12m, 17m, 22m and 27m in Cartesian Grid of receptors during Summer Season.

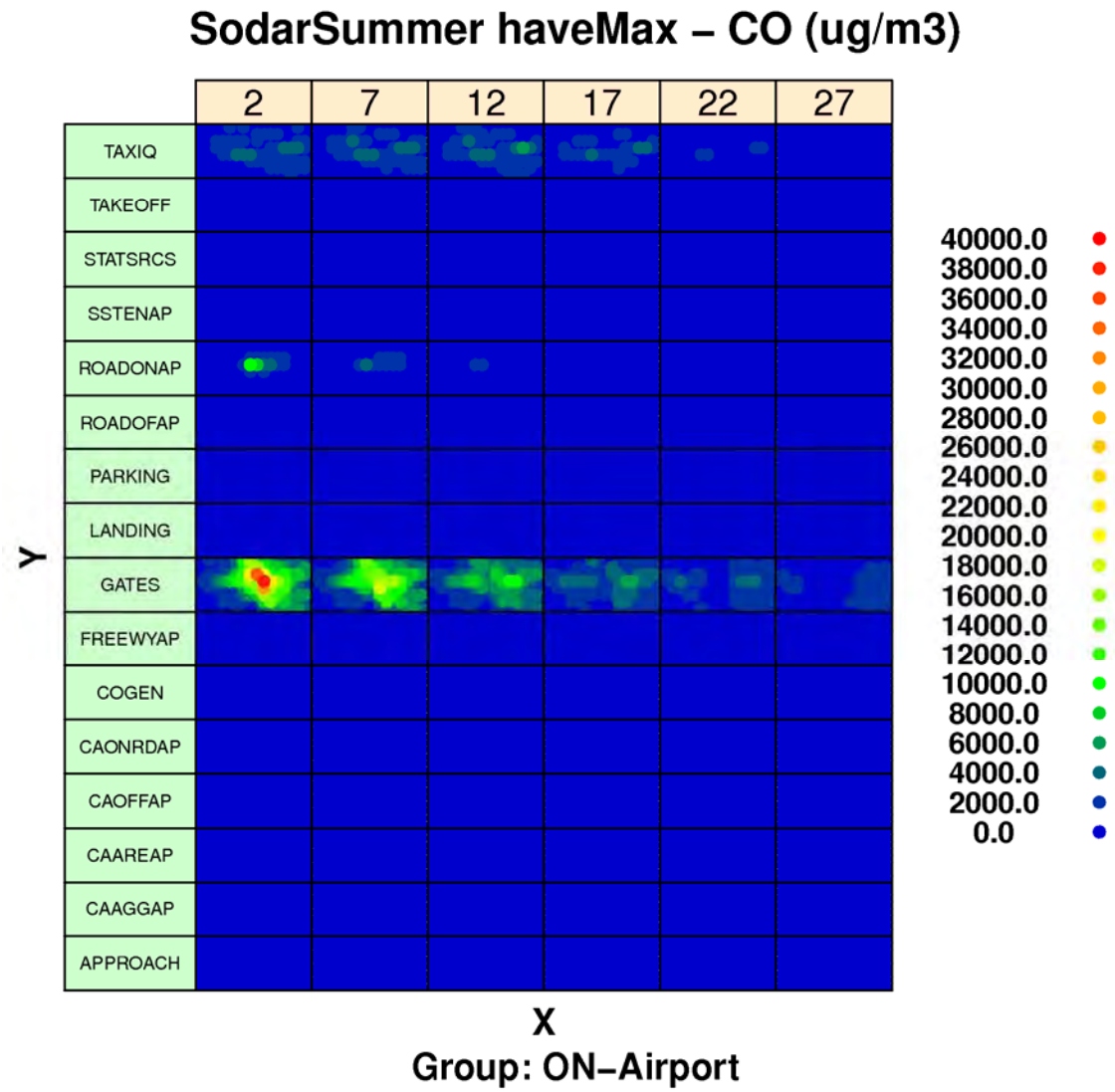

Figure 9A-109: Modeled hourly maximum CO concentrations from airport-related sources by source sector at flag-pole receptors at heights of 2m, 7m, 12m, 17m, 22m and 27m in Cartesian Grid of receptors during Summer Season.

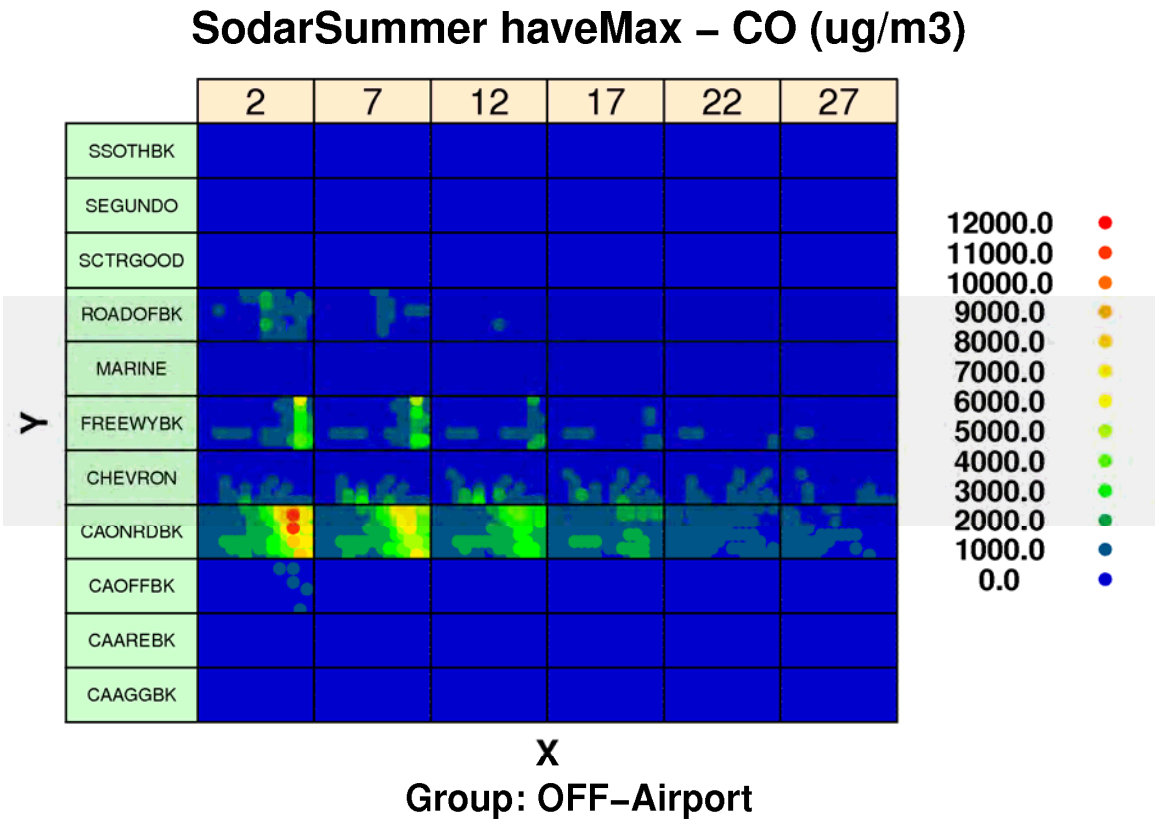

Figure 9A-110: Modeled hourly maximum CO concentrations from background sources by source sector at flag-pole receptors at heights of 2m, 7m, 12m, 17m, 22m and 27m in Cartesian Grid of receptors during Summer Season.

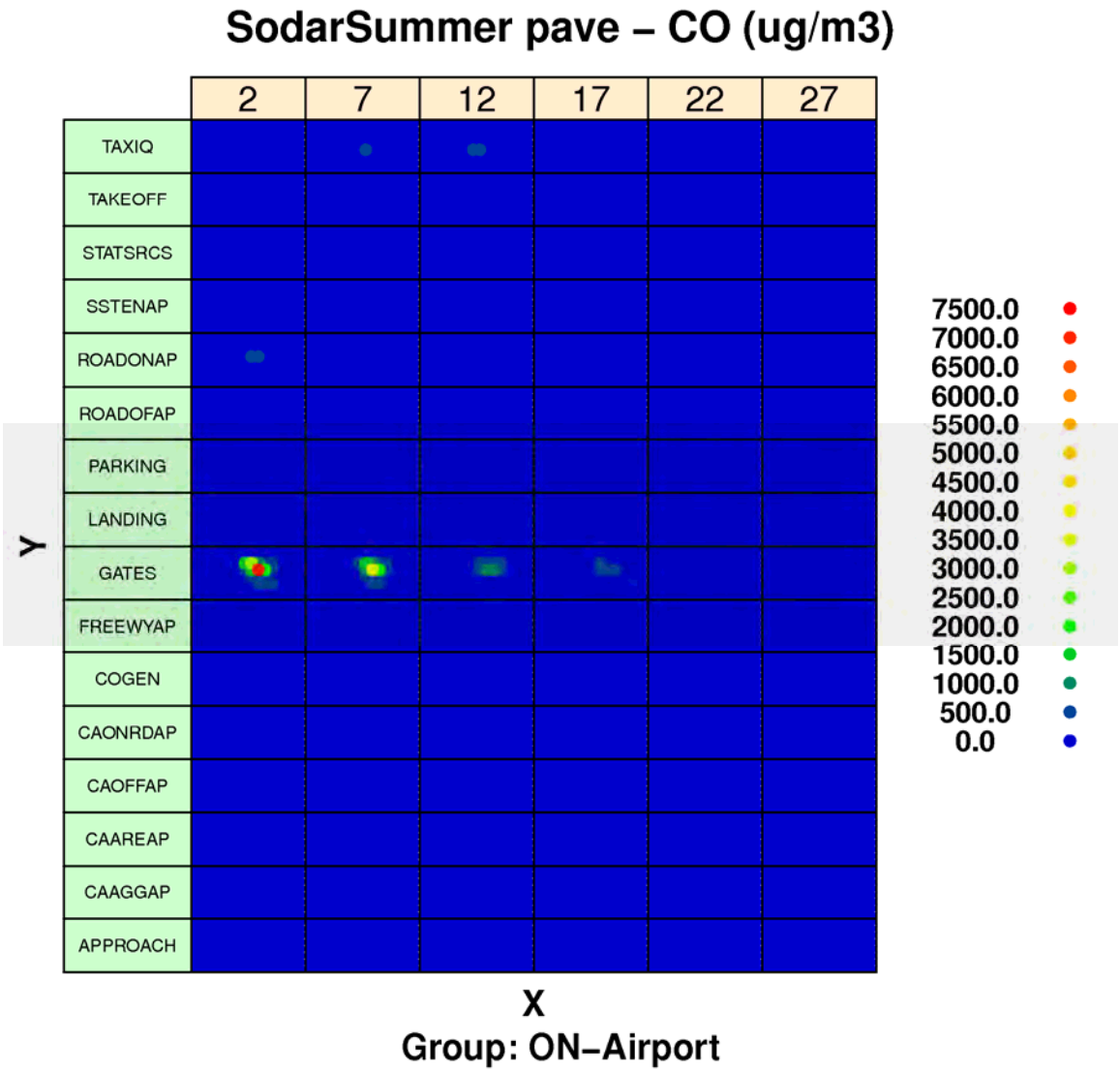

Figure 9A-111: Modeled period average CO concentrations from airport-related sources by source sector at flag-pole receptors at heights of 2m, 7m, 12m, 17m, 22m and 27m in Cartesian Grid of receptors during Summer Season.

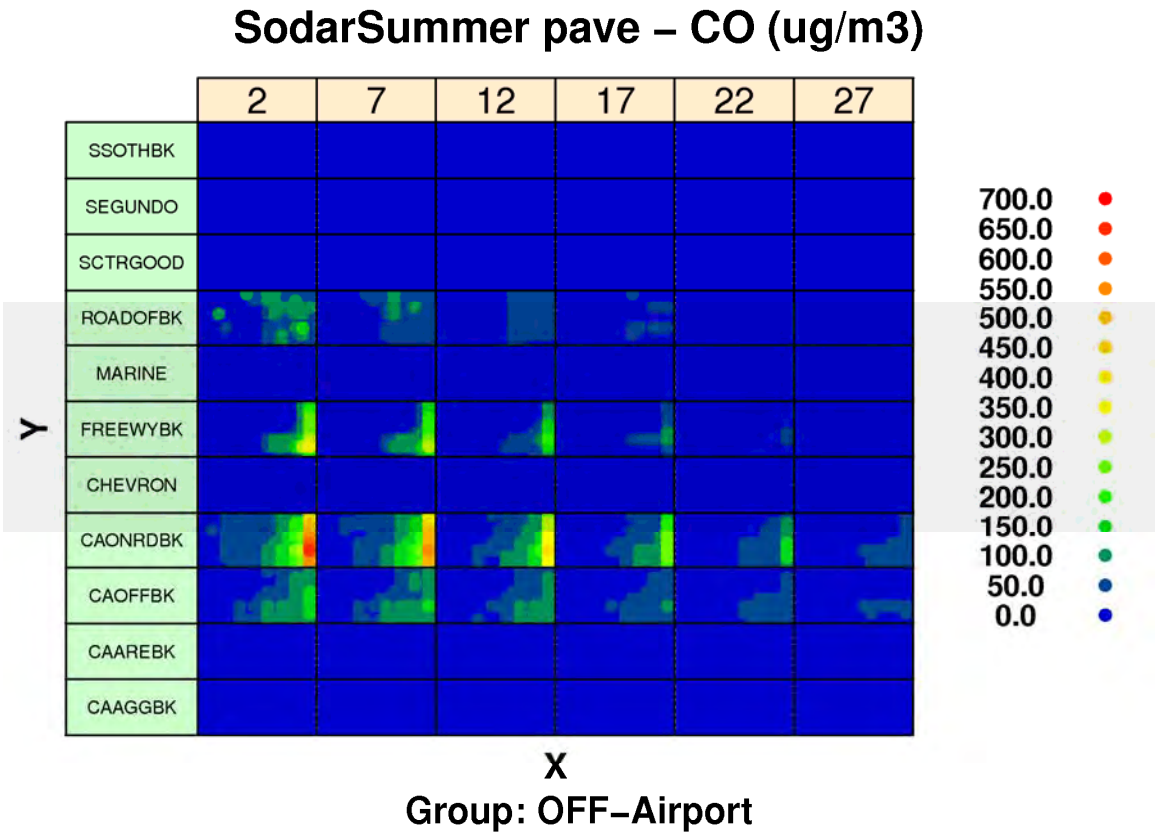

Figure 9A-112: Modeled period average CO concentrations from background sources by source sector at flag-pole receptors at heights of 2m, 7m, 12m, 17m, 22m and 27m in Cartesian Grid of receptors during Summer Season.

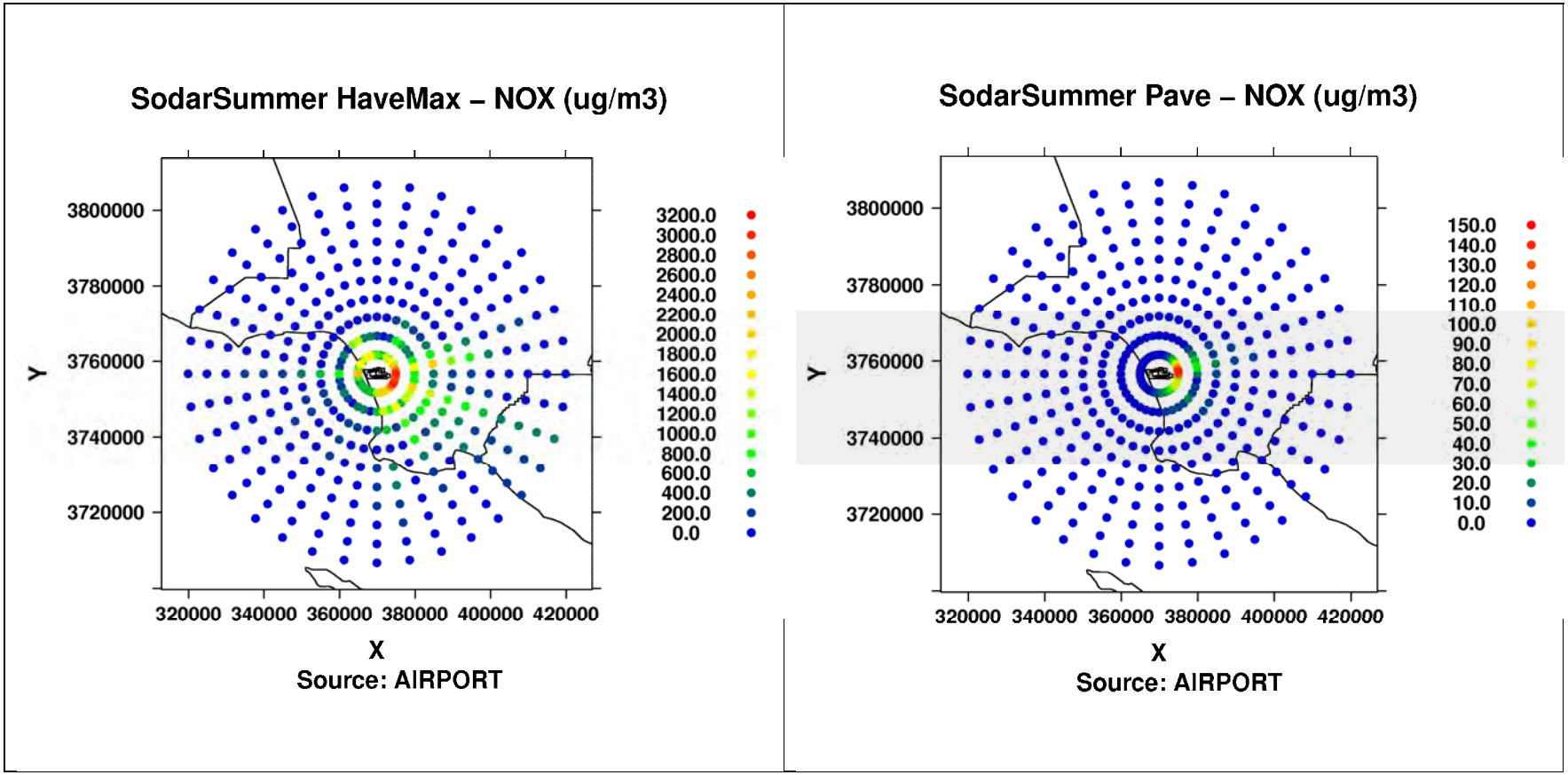

Figure 9A-113a: Modeled hourly max (left) and period average (right) NOx concentrations from airport-related in Polar Grid of receptors during Summer Season.

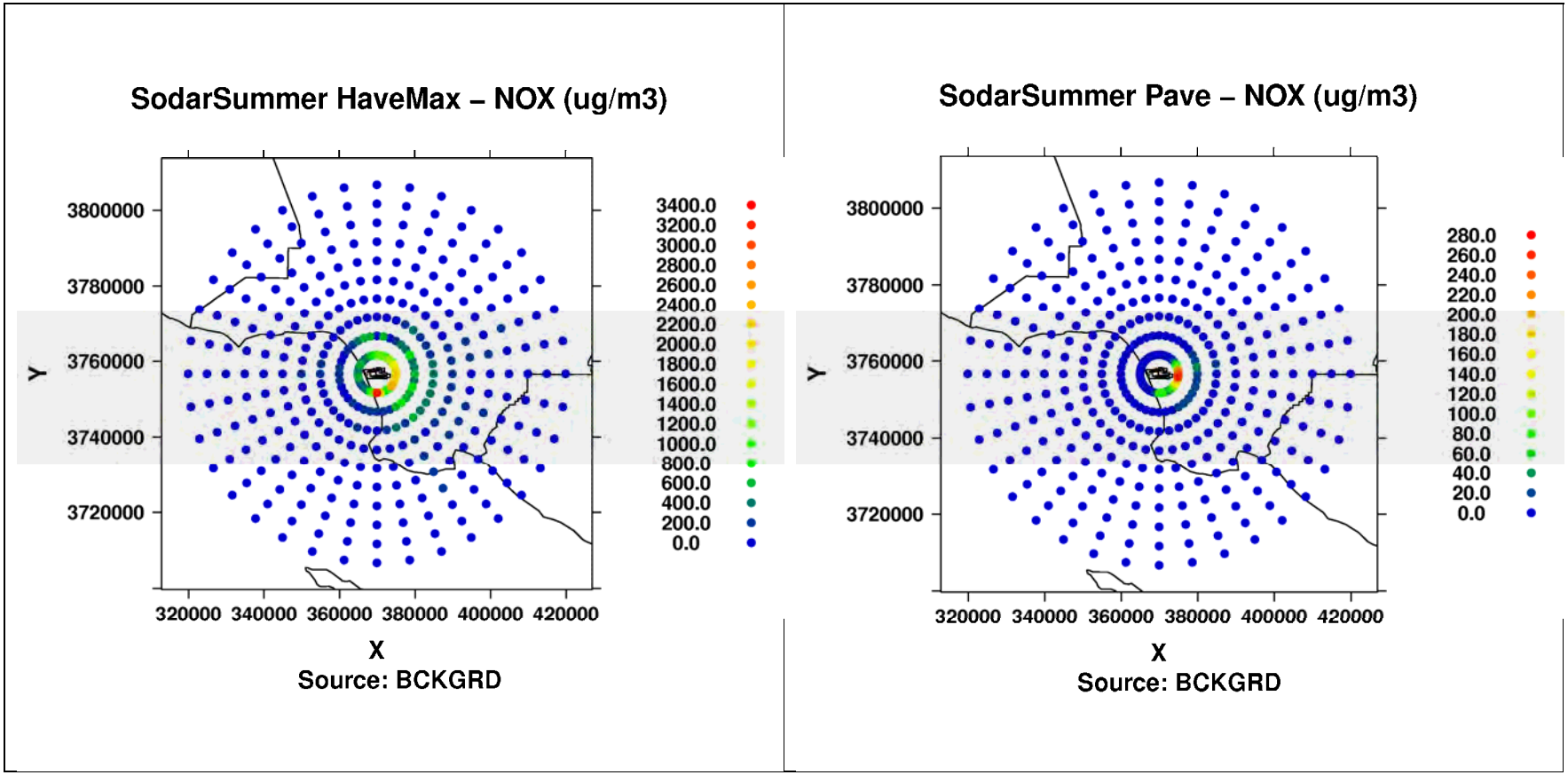

Figure 9A-113b: Modeled hourly max (left) and period average (right) NOx concentrations from background sources in Polar Grid of receptors during Summer Season.

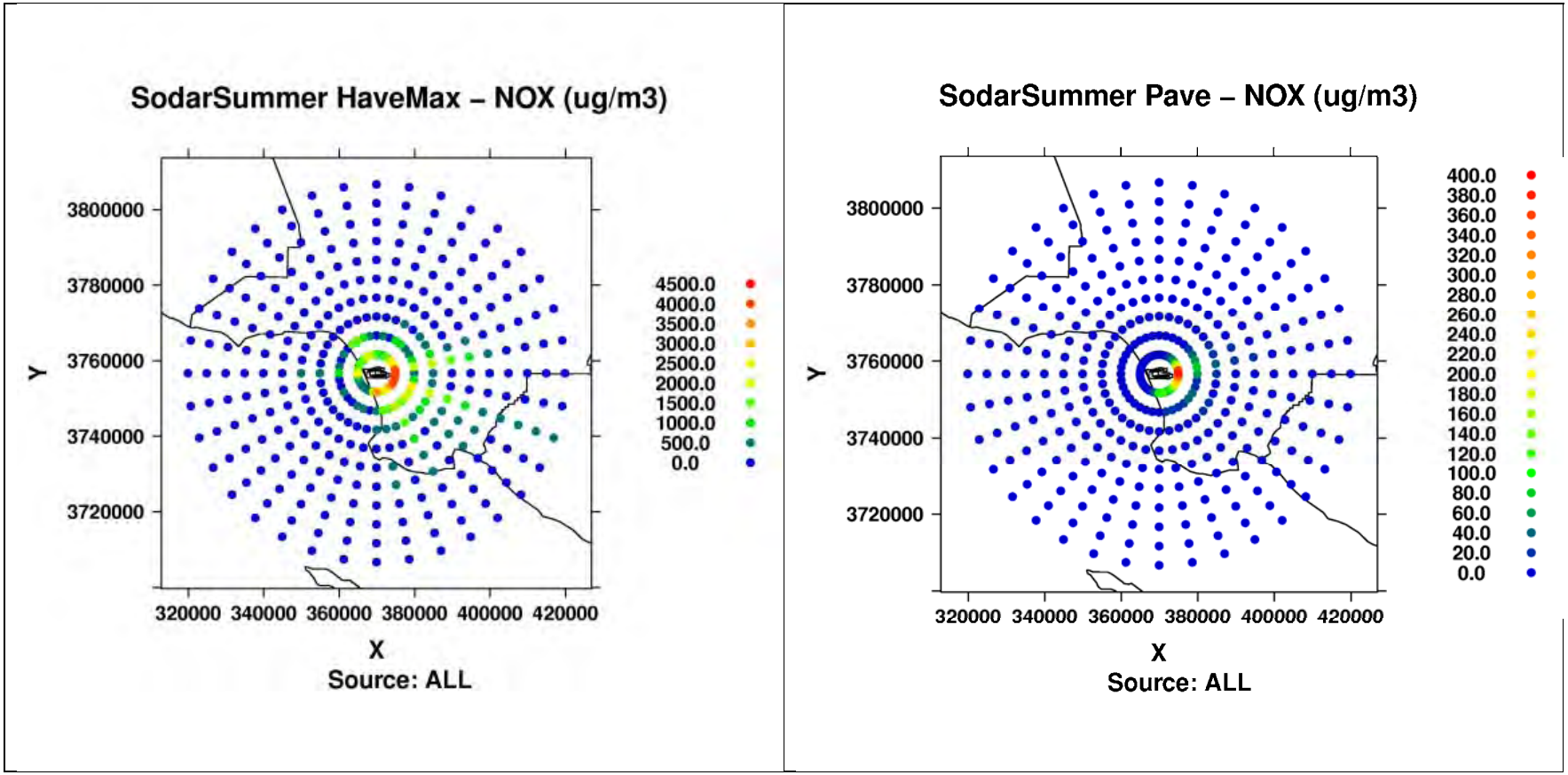

Figure 9A-113c: Modeled hourly max (left) and period average (right) NOx concentrations from ALL in Polar Grid of receptors during Summer Season.

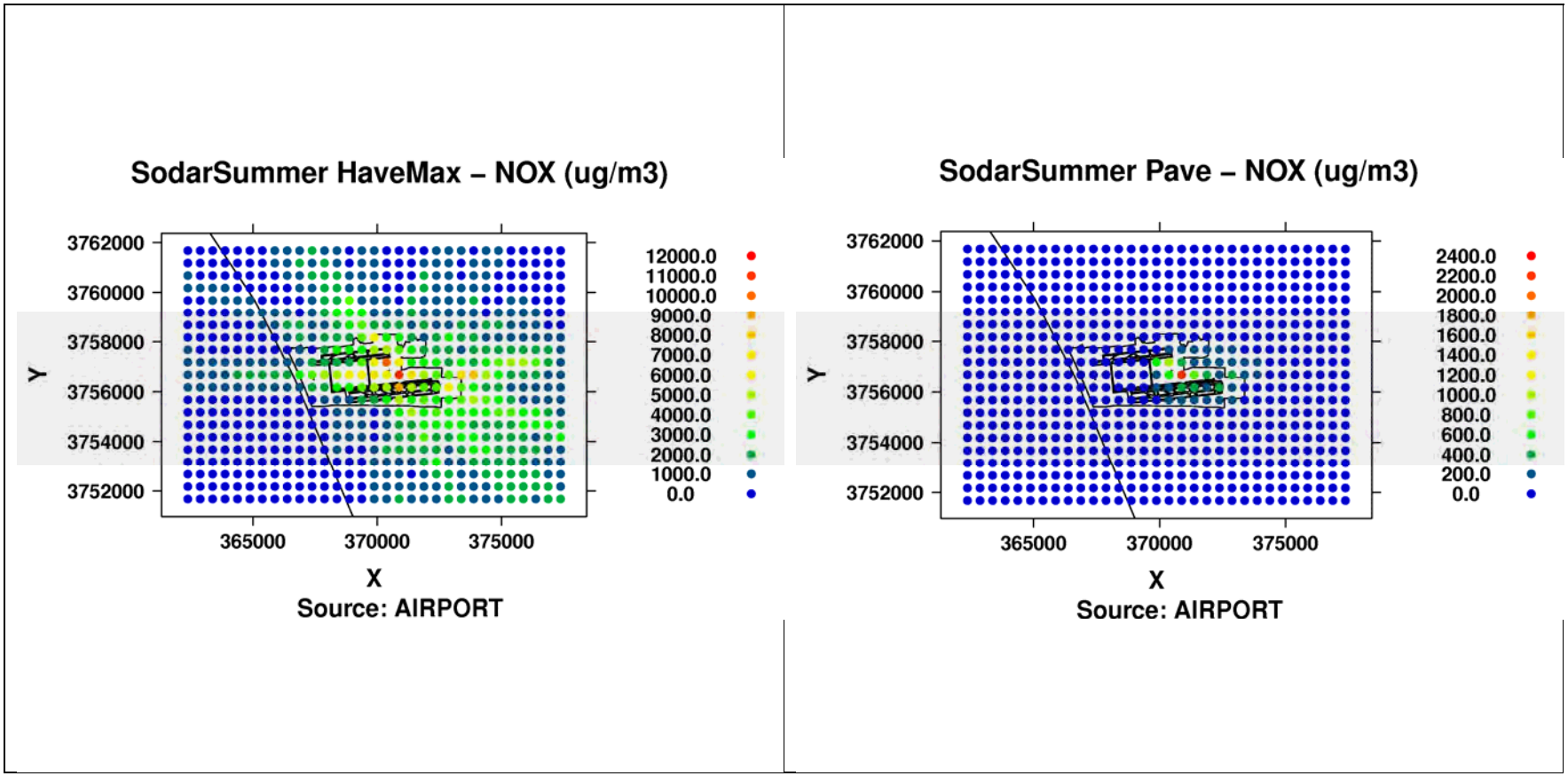

Figure 9A-114a: Modeled hourly max (left) and period average (right) NOx concentrations from airport-related in Cartesian Grid of receptors during Summer Season.

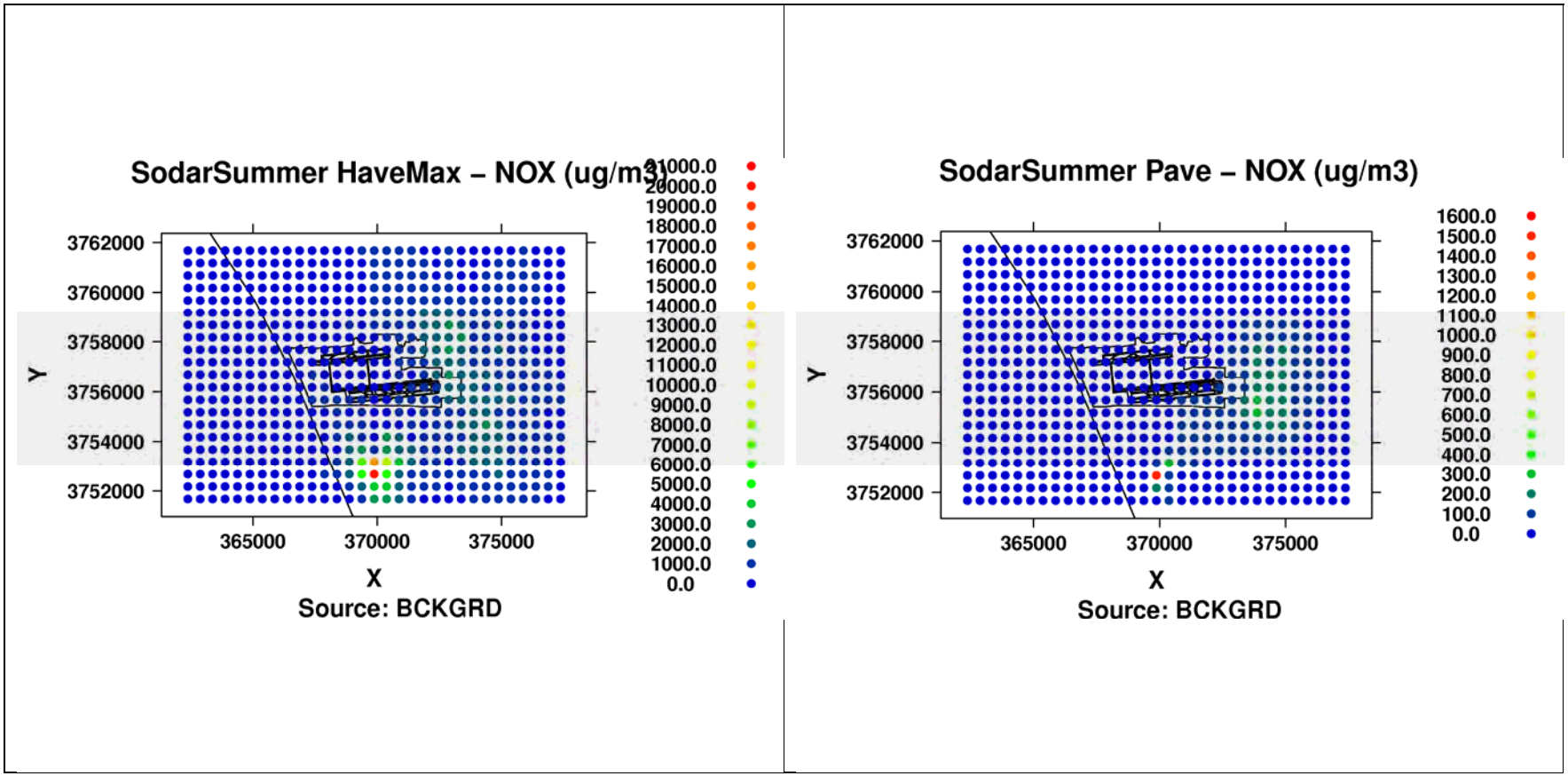

Figure 9A-114b: Modeled hourly max (left) and period average (right) NOx concentrations from background sources in Cartesian Grid of receptors during Summer Season.

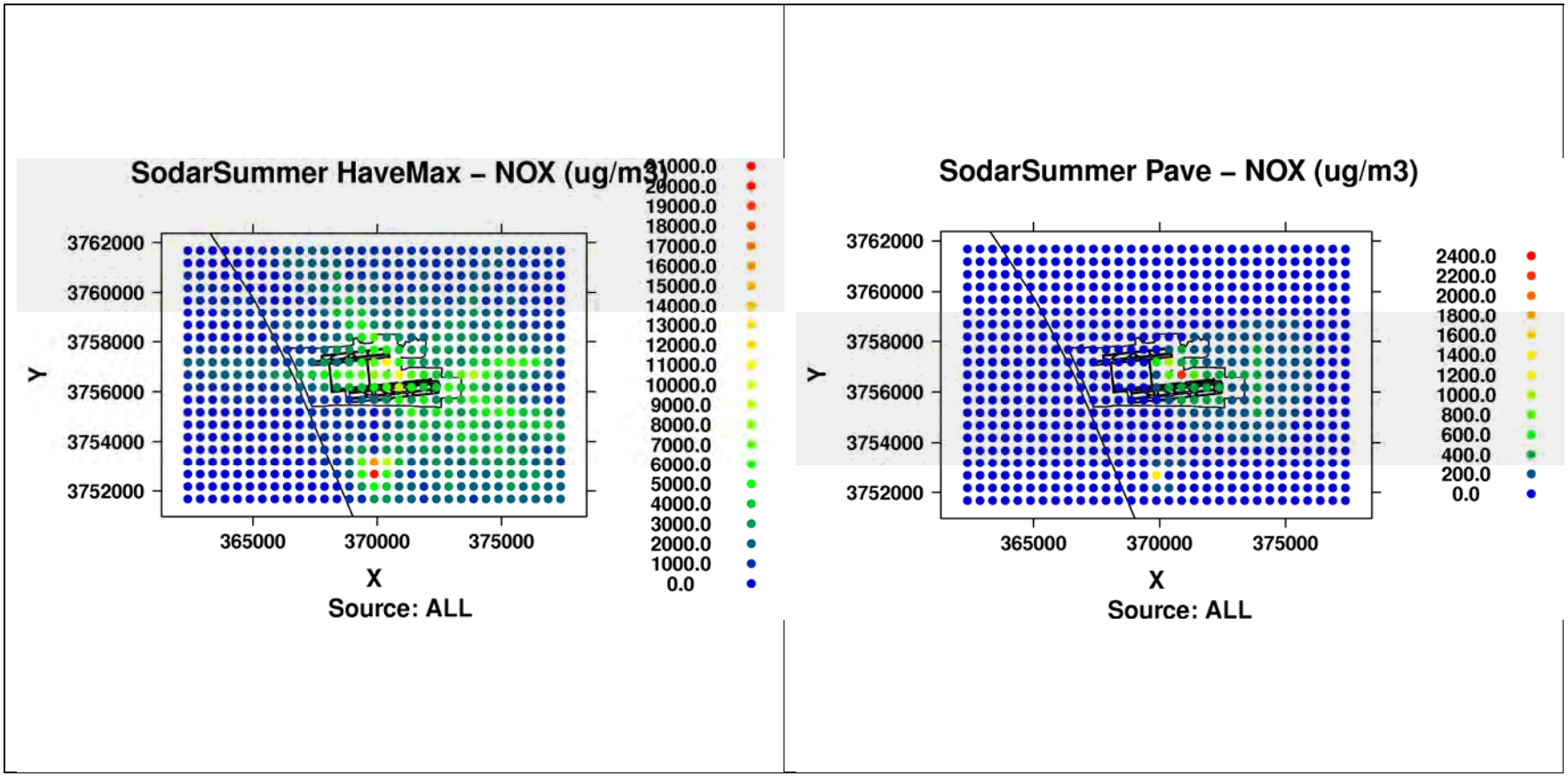

Figure 9A-114c: Modeled hourly max (left) and period average (right) NOx concentrations from ALL in Cartesian Grid of receptors during Summer Season.

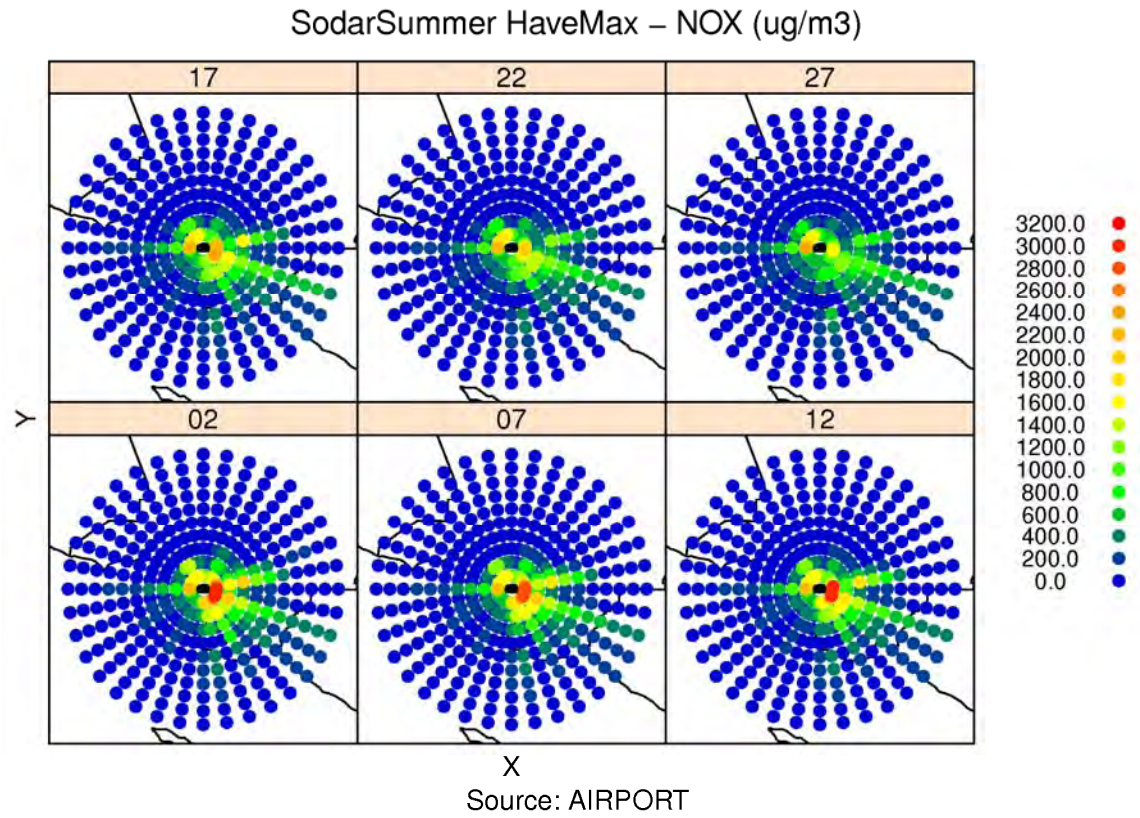

Figure 9A-115: Modeled hourly max NOx concentrations from airport-related sources at flag-pole receptors at heights of 2m, 7m, 12m, 17m, 22m and 27m in Polar Grid of receptors during Summer Season.

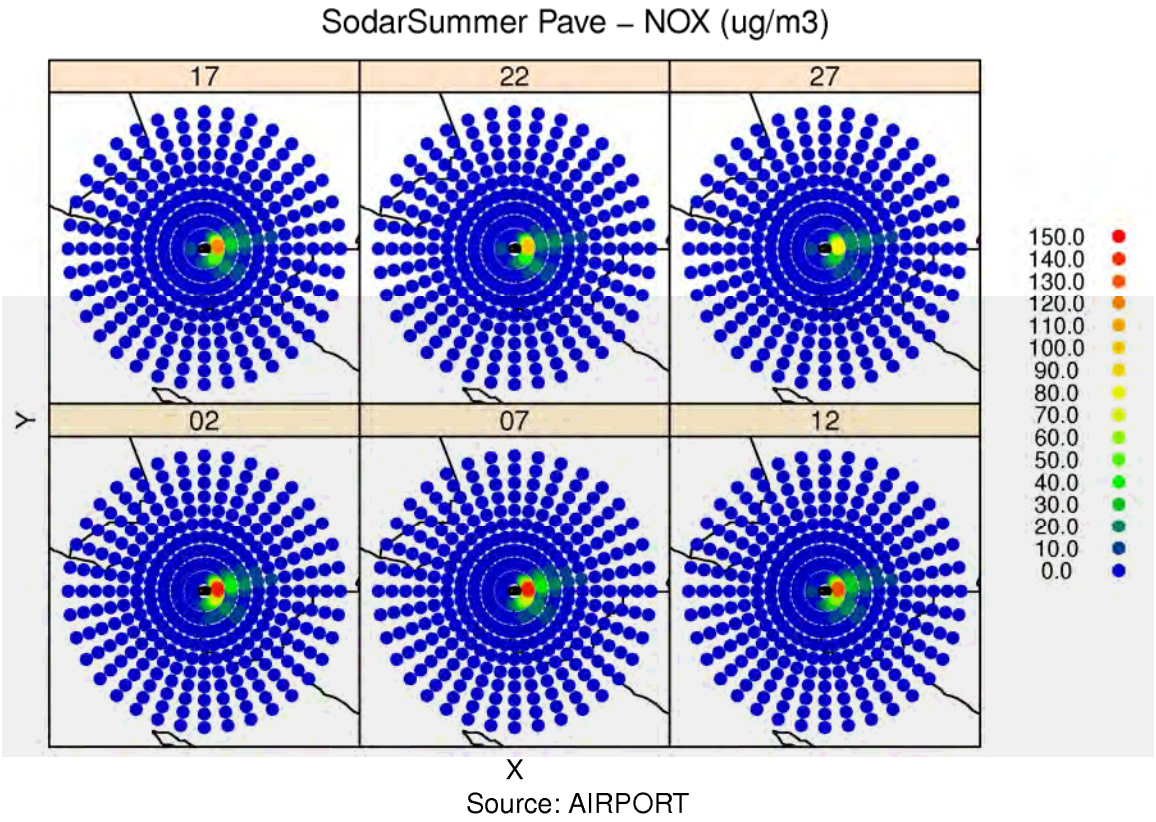

Figure 9A-116: Modeled period average NOx concentrations from airport-related sources at flag-pole receptors at heights of 2m, 7m, 12m, 17m, 22m and 27m in Polar Grid of receptors during Summer Season.

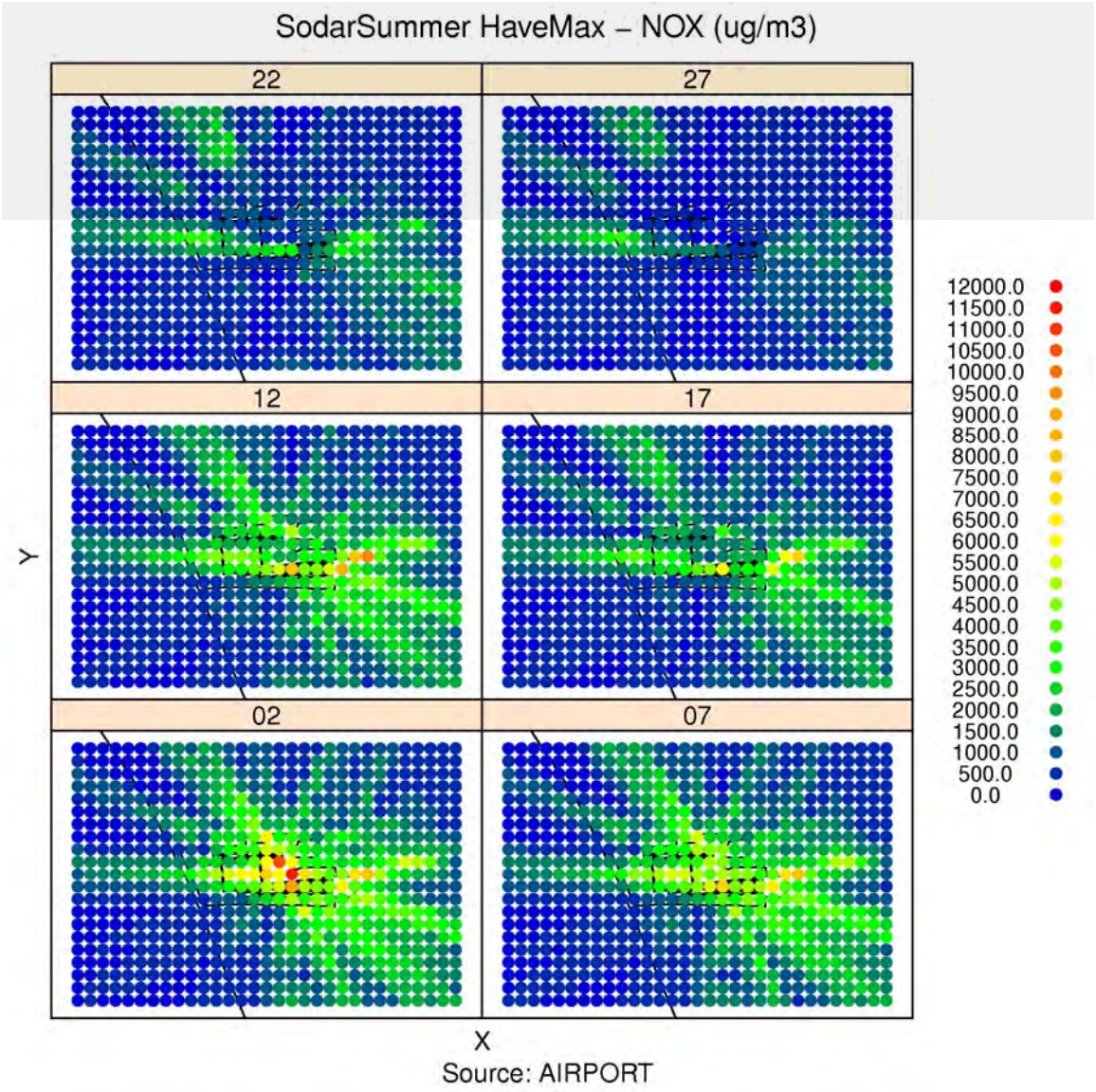

Figure 9A-117: Modeled hourly max NOx concentrations from airport-related sources at flag-pole receptors at heights of 2m, 7m, 12m, 17m, 22m and 27m in Cartesian Grid of receptors during Summer Season.

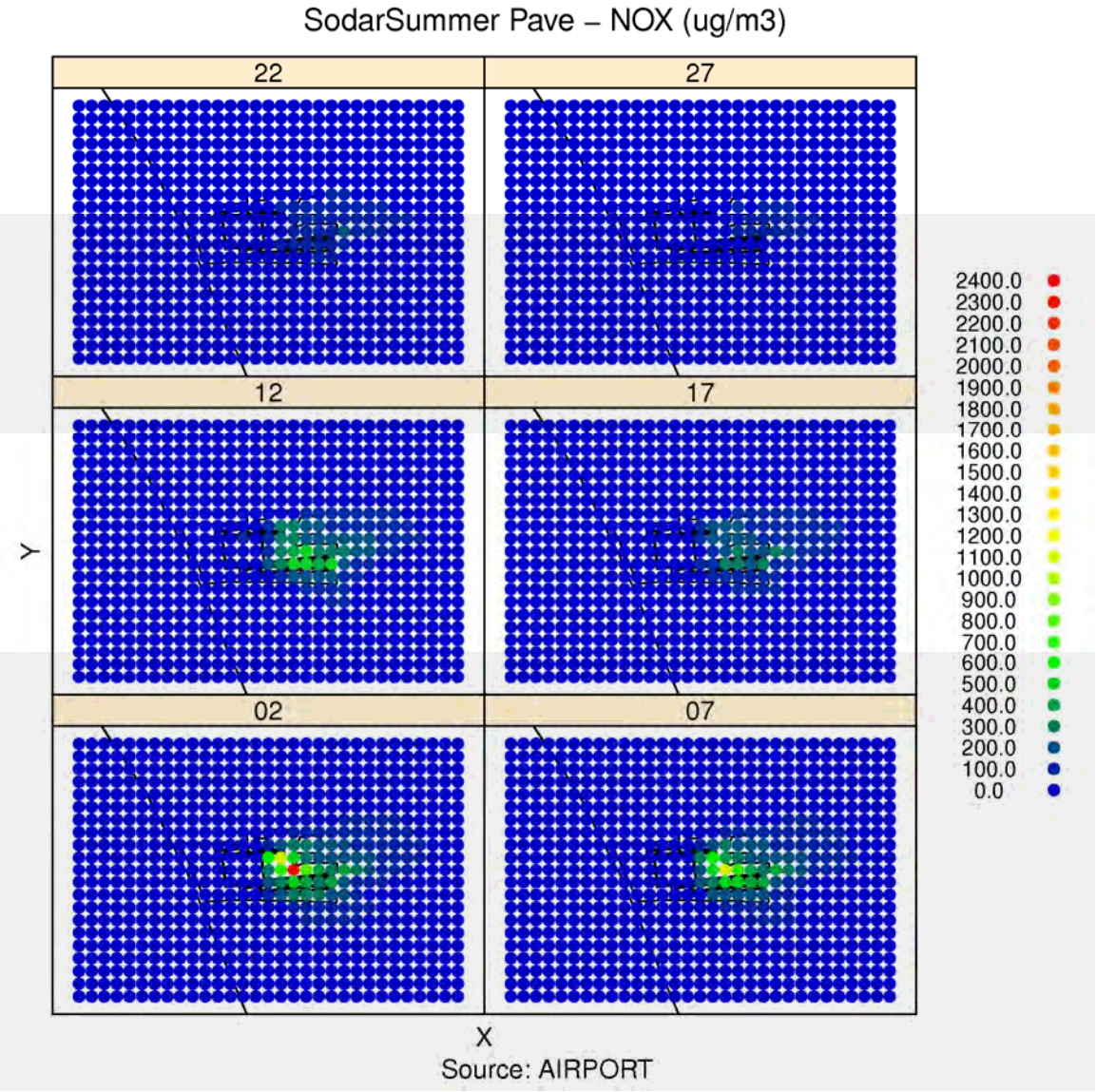

Figure 9A-118: Modeled period average NOx concentrations from airport-related sources at flag-pole receptors at heights of 2m, 7m, 12m, 17m, 22m and 27m in Cartesian Grid of receptors during Summer Season.

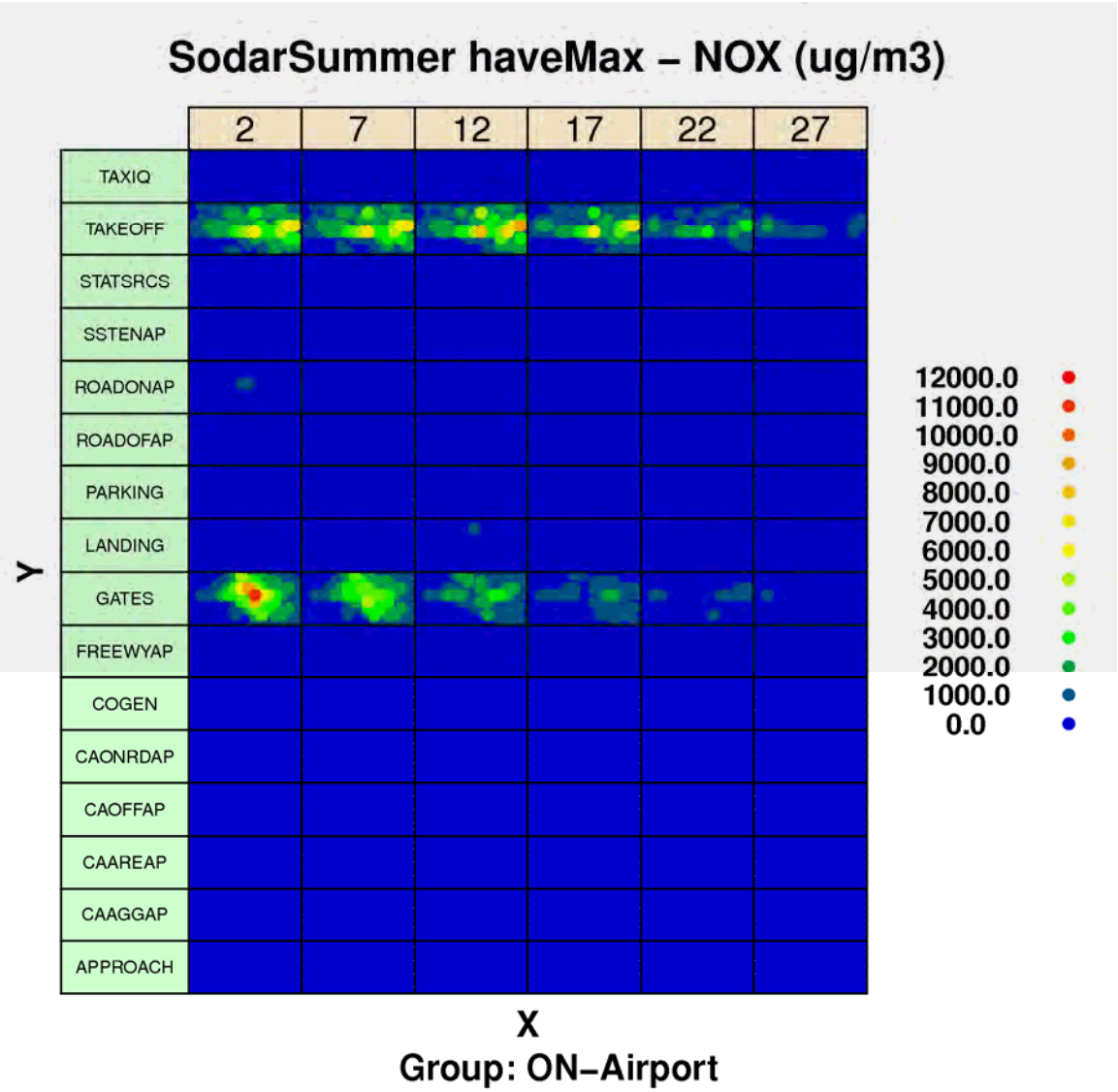

Figure 9A-119: Modeled hourly maximum NOx concentrations from airport-related sources by source sector at flag-pole receptors at heights of 2m, 7m, 12m, 17m, 22m and 27m in Cartesian Grid of receptors during Summer Season.

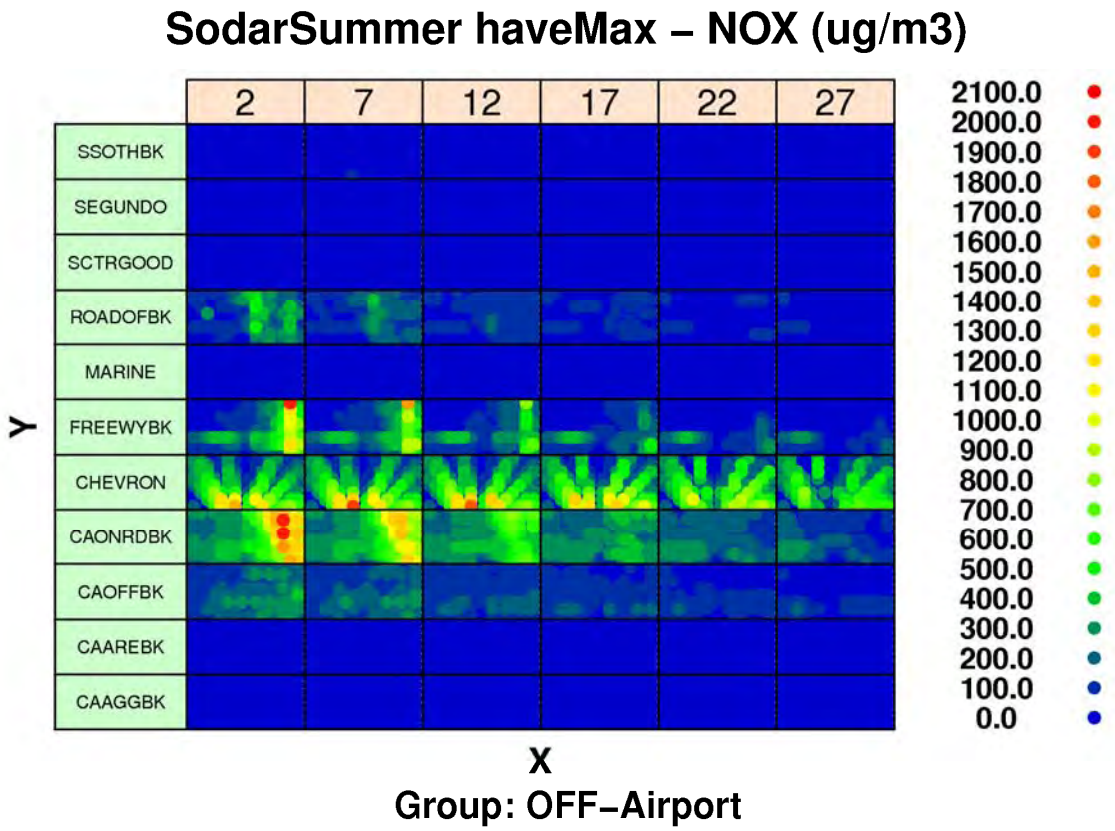

Figure 9A-120: Modeled hourly maximum NOx concentrations from background sources by source sector at flag-pole receptors at heights of 2m, 7m, 12m, 17m, 22m and 27m in Cartesian Grid of receptors during Summer Season.

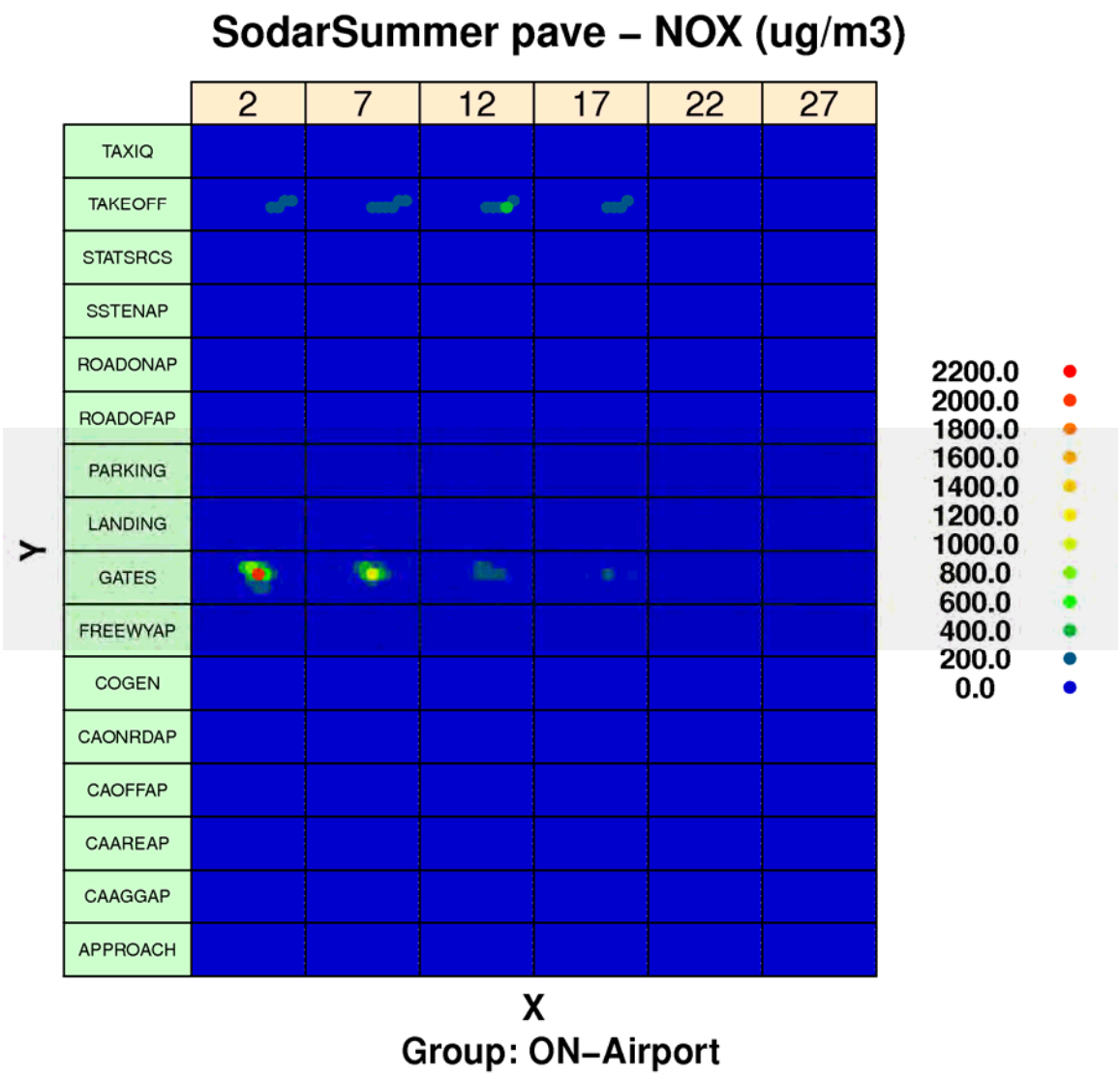

Figure 9A-121: Modeled period average NOx concentrations from airport-related sources by source sector at flag-pole receptors at heights of 2m, 7m, 12m, 17m, 22m and 27m in Cartesian Grid of receptors during Summer Season.

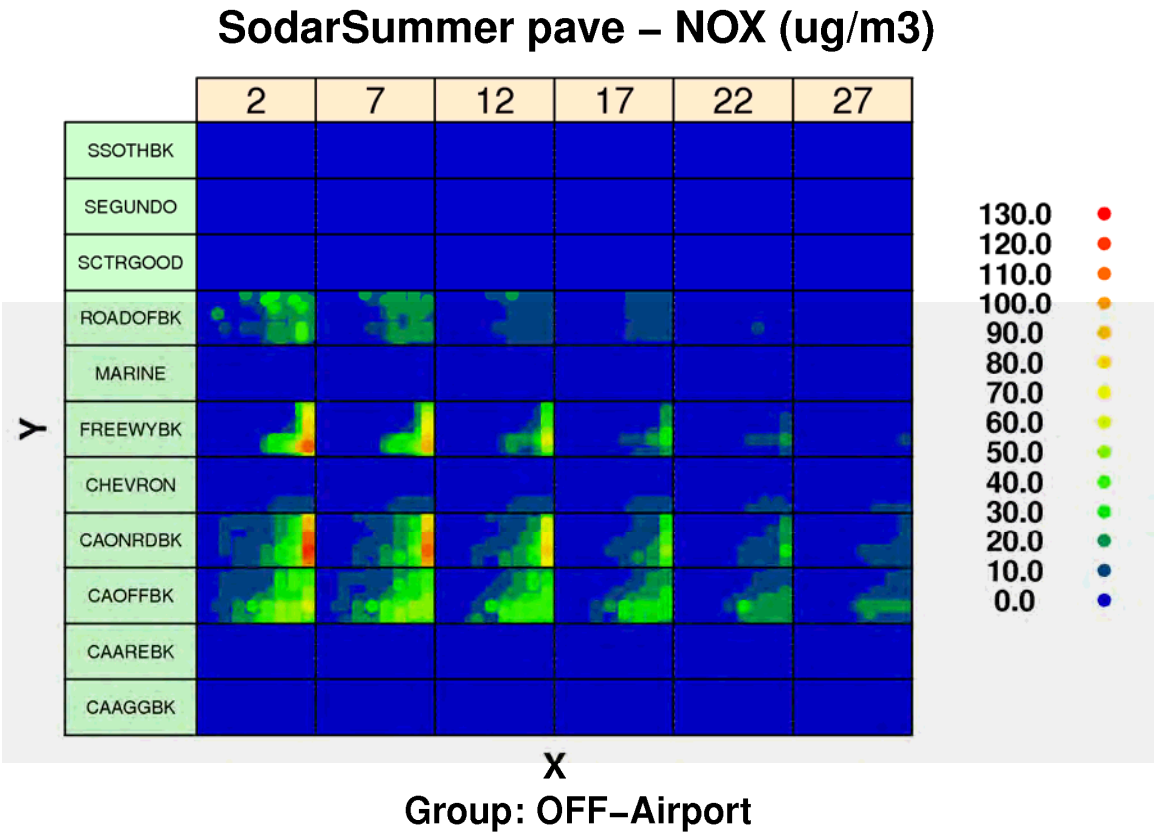

Figure 9A-122: Modeled period average NOx concentrations from background sources by source sector at flag-pole receptors at heights of 2m, 7m, 12m, 17m, 22m and 27m in Cartesian Grid of receptors during Summer Season.

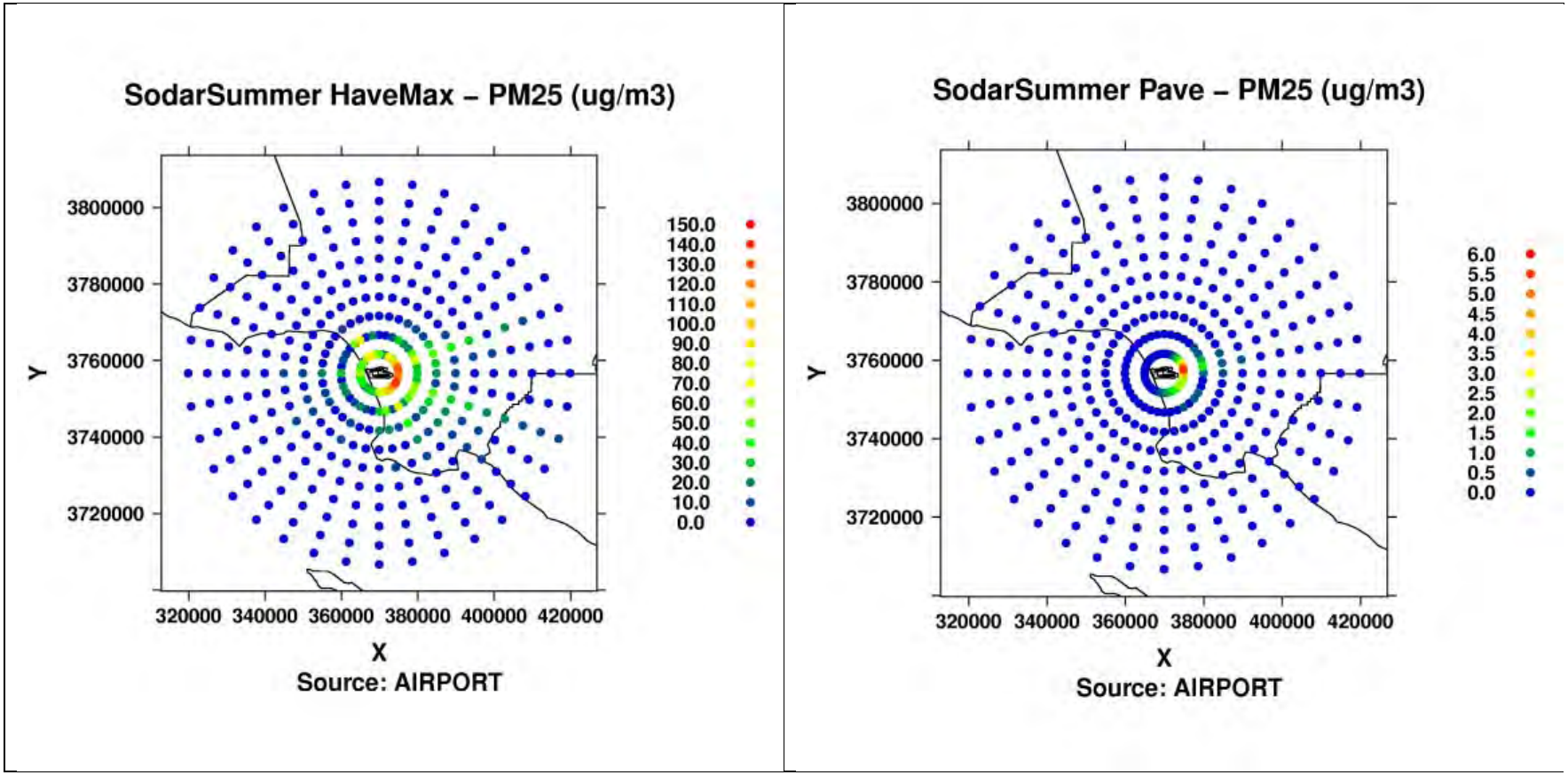

Figure 9A-123a: Modeled hourly max (left) and period average (right) $PM_{2.5}$ concentrations from airport-related in Polar Grid of receptors during Summer Season.

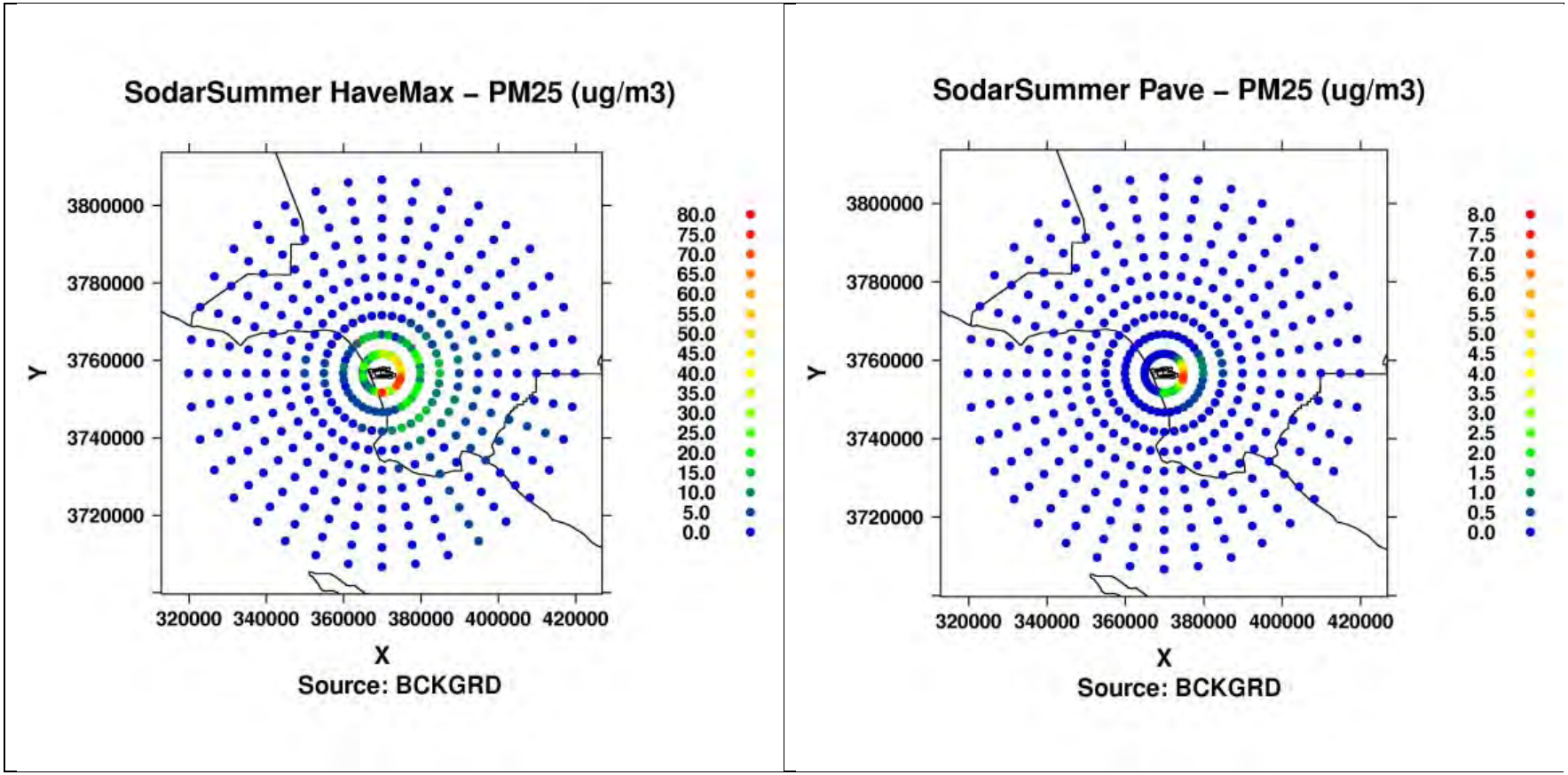

Figure 9A-123b: Modeled hourly max (left) and period average (right) $PM_{2.5}$ concentrations from background sources in Polar Grid of receptors during Summer Season.

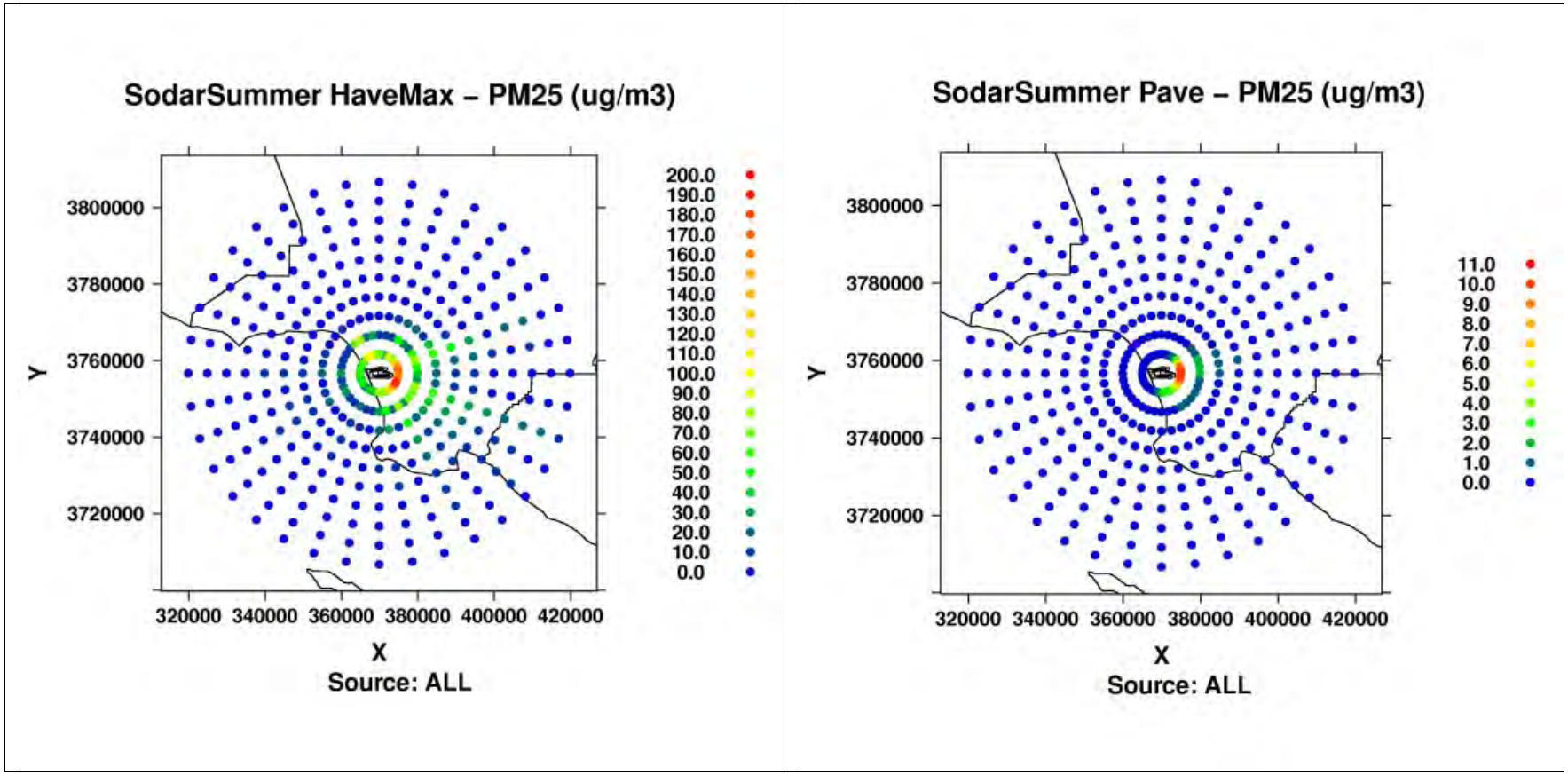

Figure 9A-123c: Modeled hourly max (left) and period average (right) $PM_{2.5}$ concentrations from ALL in Polar Grid of receptors during Summer Season.

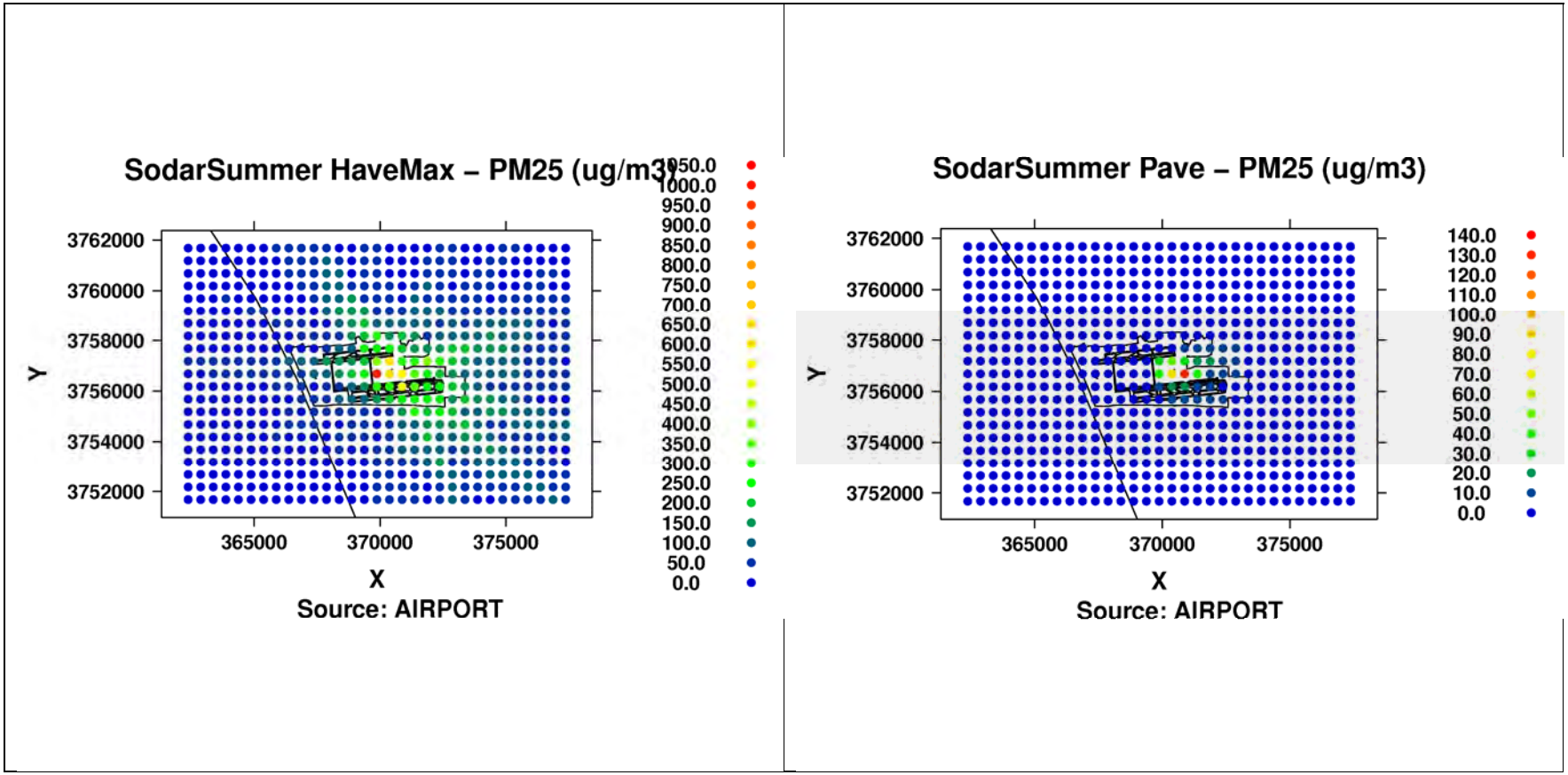

Figure 9A-124a: Modeled hourly max (left) and period average (right) $PM_{2.5}$ concentrations from airport-related in Cartesian Grid of receptors during Summer Season.

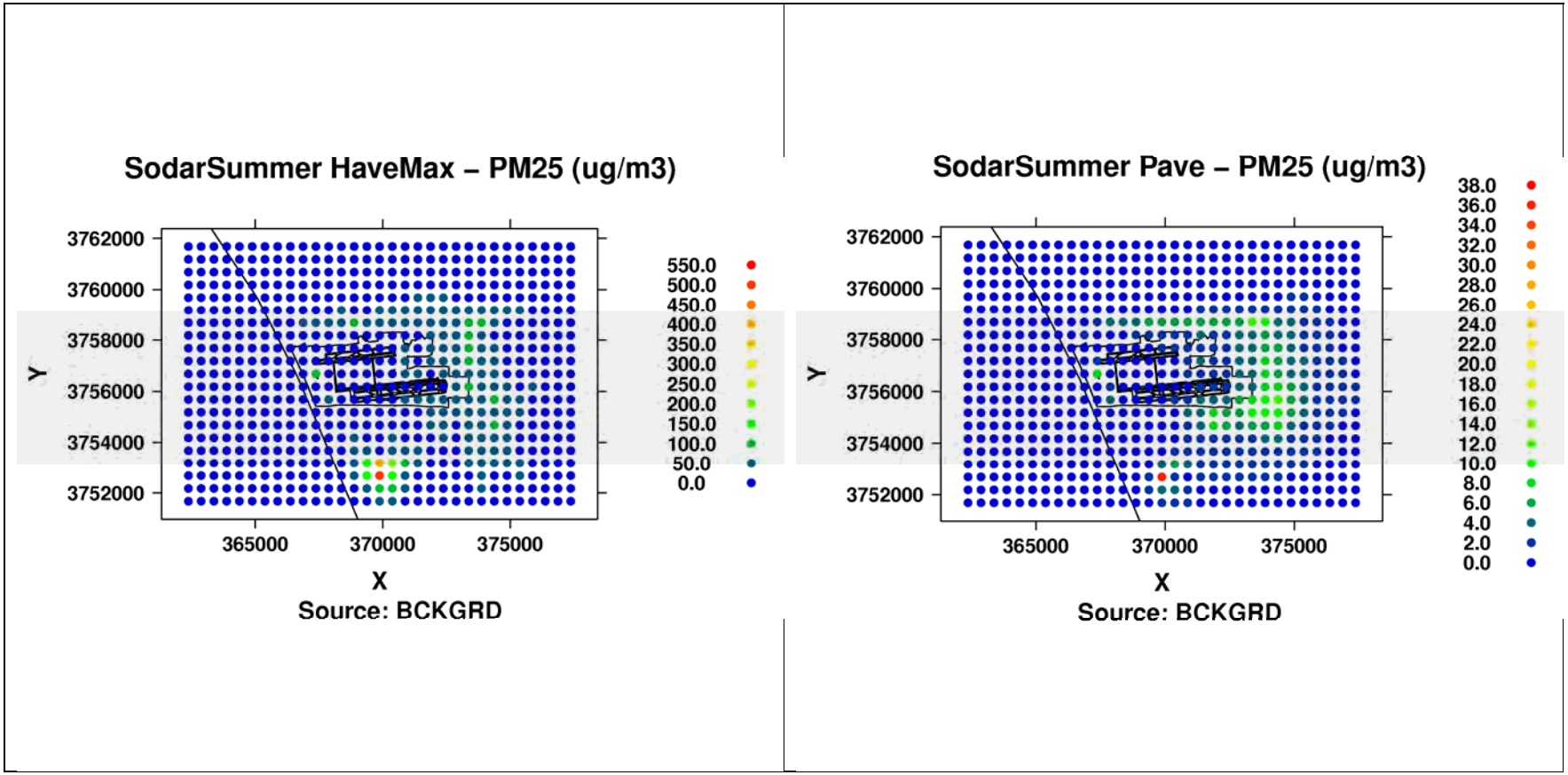

Figure 9A-124b: Modeled hourly max (left) and period average (right) $PM_{2.5}$ concentrations from background sources in Cartesian Grid of receptors during Summer Season.

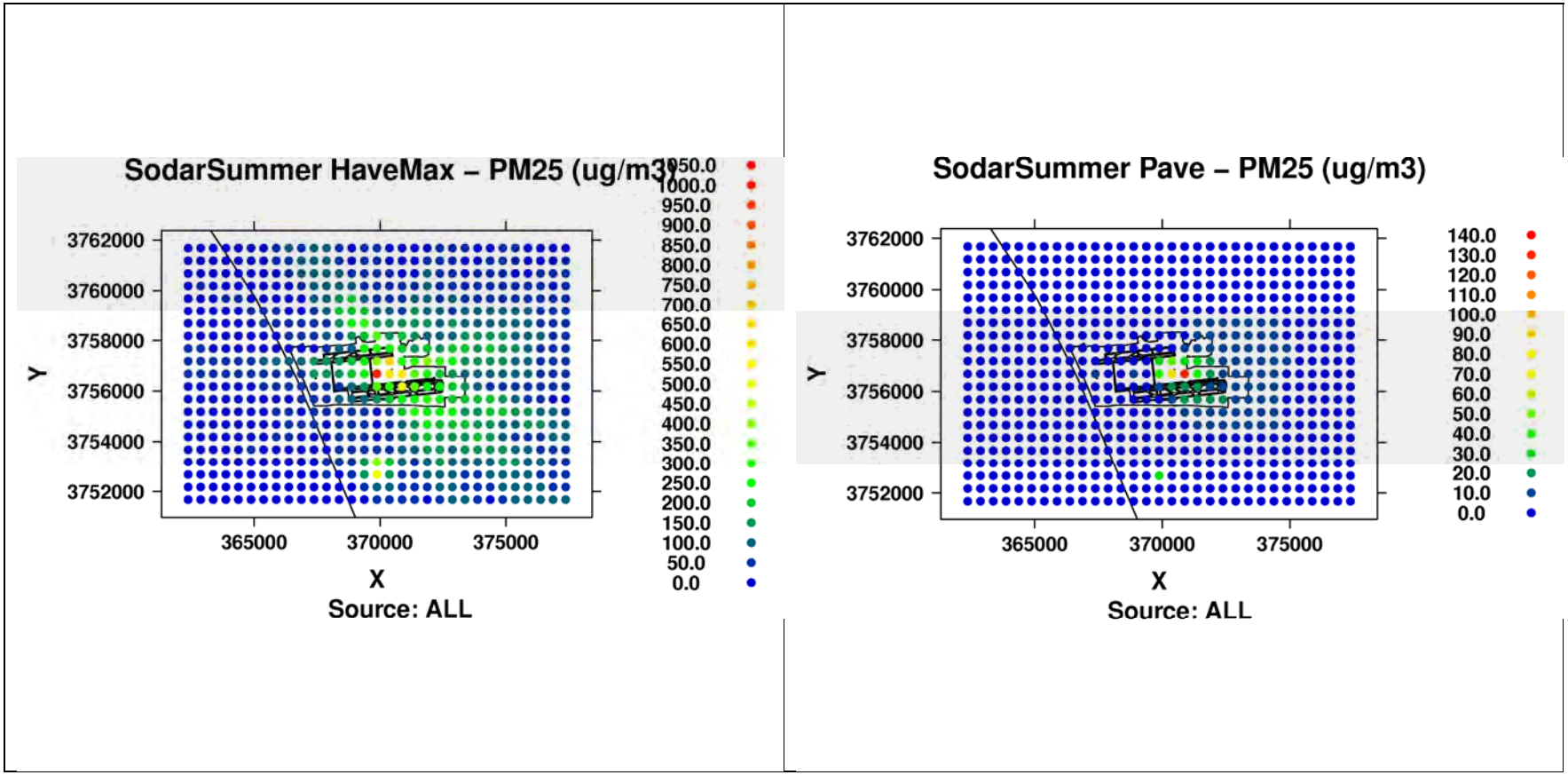

Figure 9A-124c: Modeled hourly max (left) and period average (right) $PM_{2.5}$ concentrations from ALL in Cartesian Grid of receptors during Summer Season.

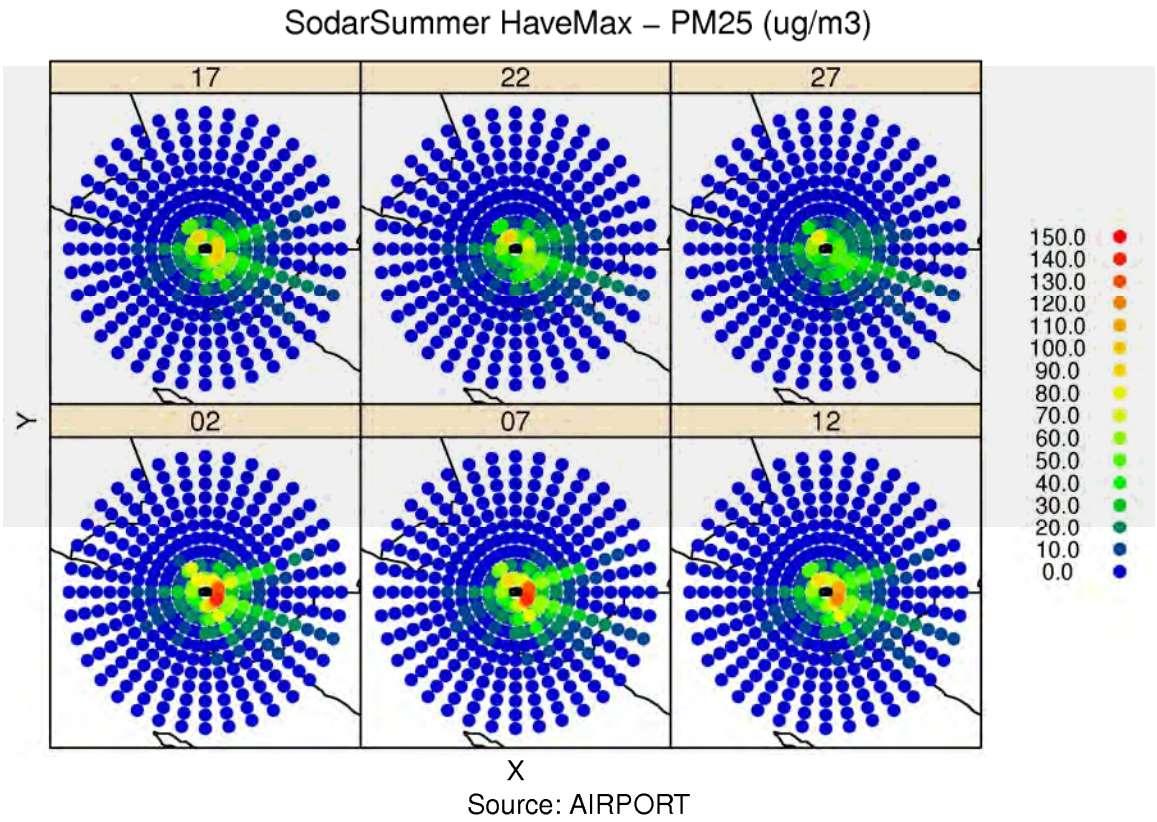

Figure 9A-125: Modeled hourly max $PM_{2.5}$ concentrations from airport-related sources at flag-pole receptors at heights of 2m, 7m, 12m, 17m, 22m and 27m in Polar Grid of receptors during Summer Season.

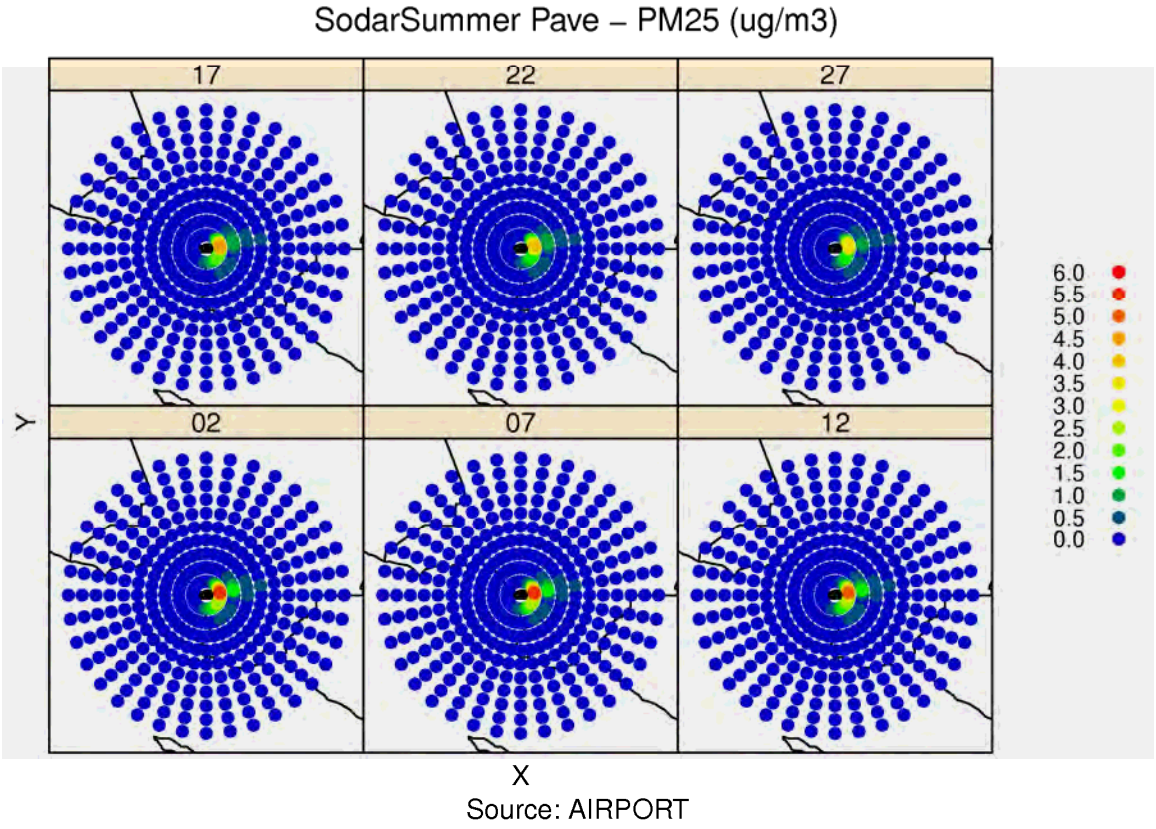

Figure 9A-126: Modeled period average $PM_{2.5}$ concentrations from airport-related sources at flag-pole receptors at heights of 2m, 7m, 12m, 17m, 22m and 27m in Polar Grid of receptors during Summer Season.

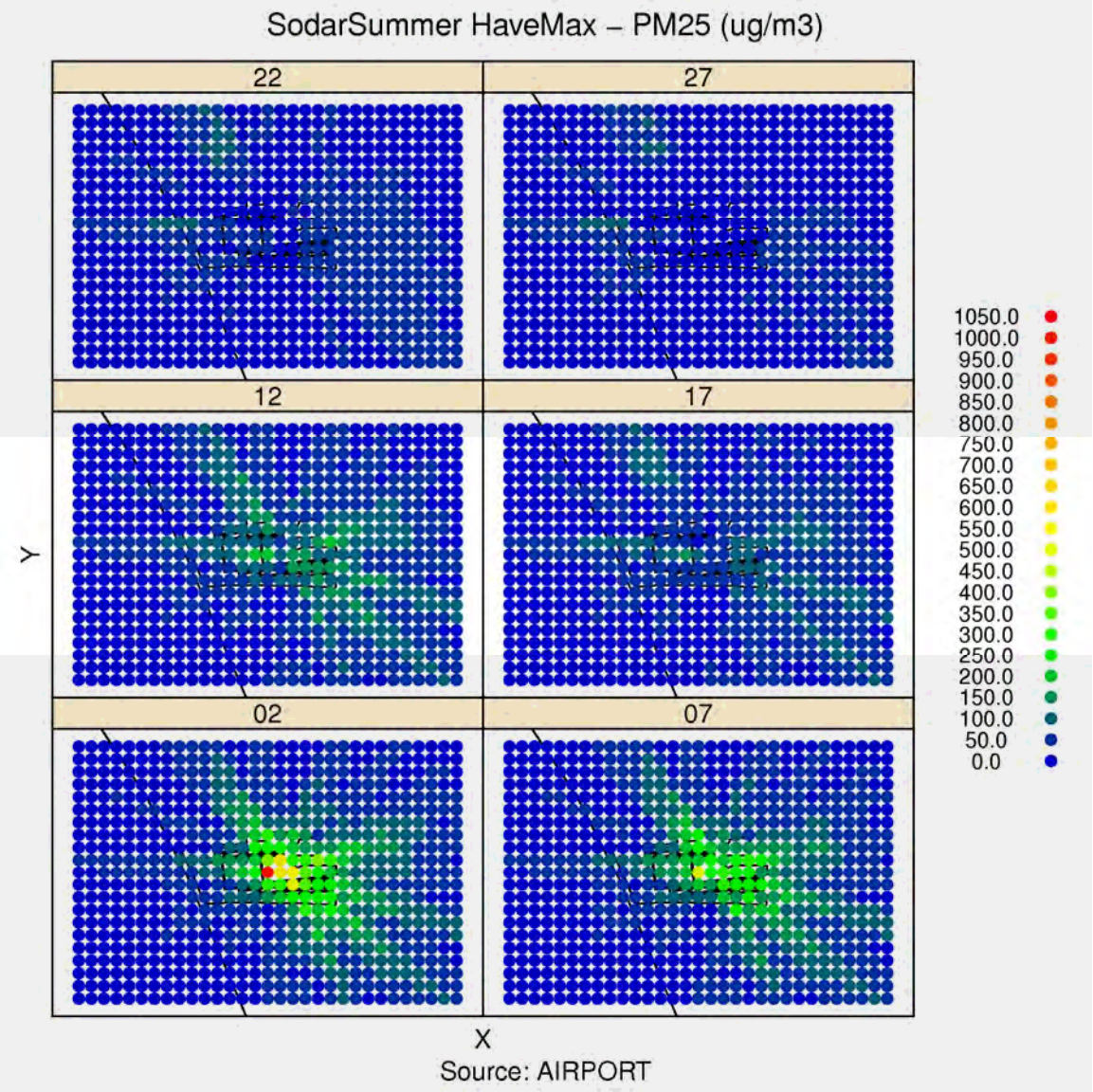

Figure 9A-127: Modeled hourly max $PM_{2.5}$ concentrations from airport-related sources at flag-pole receptors at heights of 2m, 7m, 12m, 17m, 22m and 27m in Cartesian Grid of receptors during Summer Season.

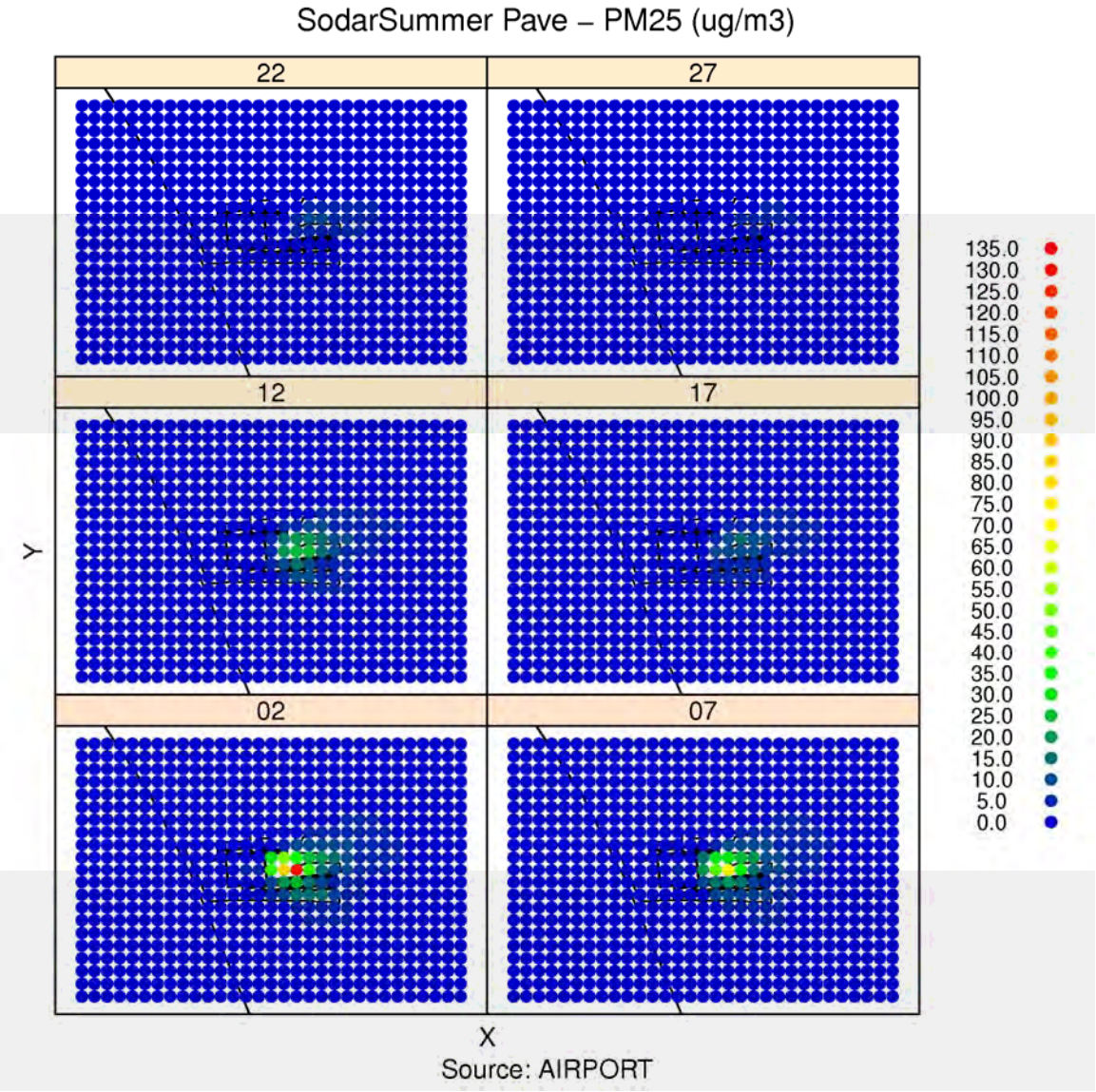

Figure 9A-128: Modeled period average $PM_{2.5}$ concentrations from airport-related sources at flag-pole receptors at heights of 2m, 7m, 12m, 17m, 22m and 27m in Cartesian Grid of receptors during Summer Season.

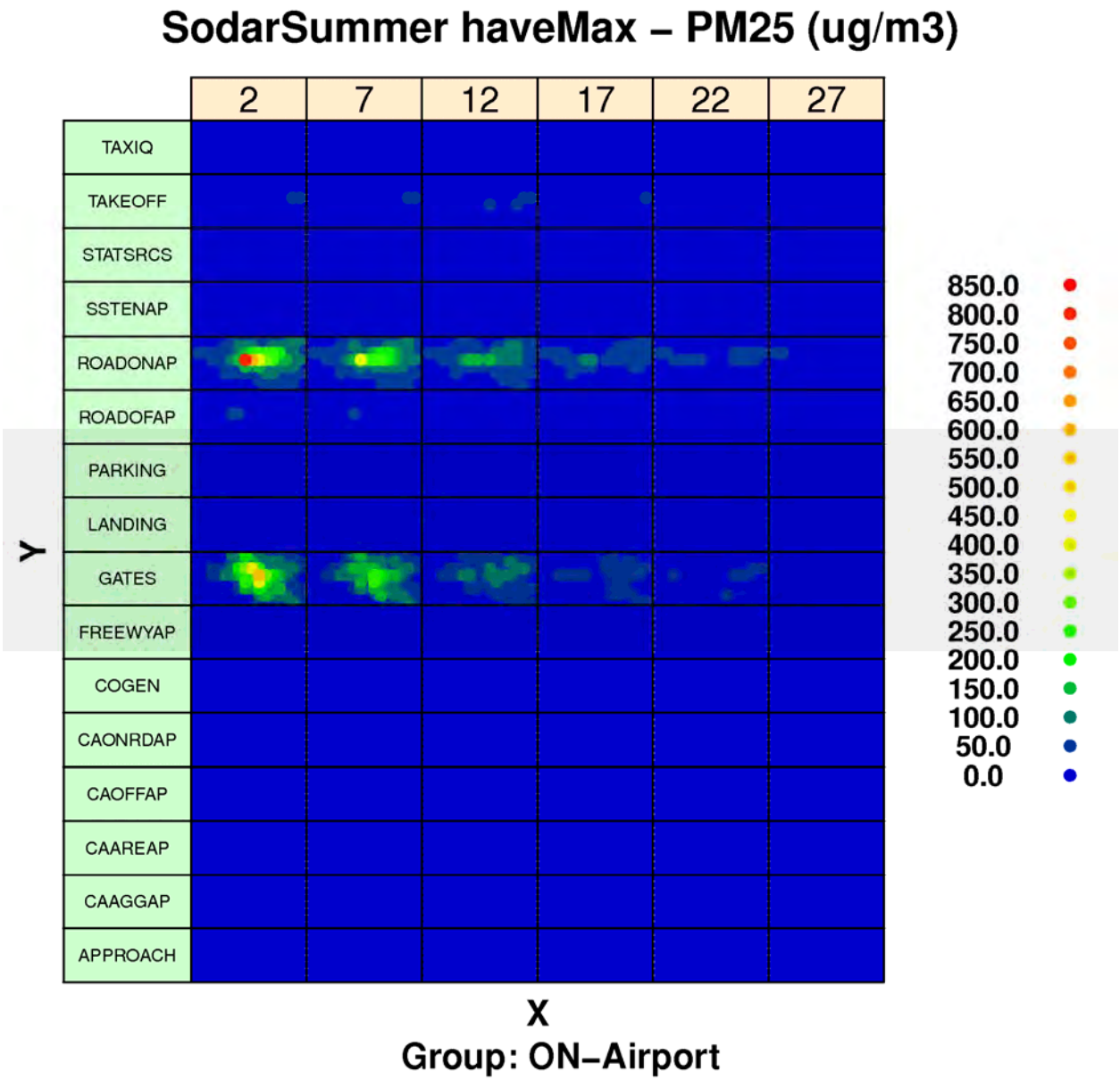

Figure 9A-129: Modeled hourly maximum $PM_{2.5}$ concentrations from airport-related sources by source sector at flag-pole receptors at heights of 2m, 7m, 12m, 17m, 22m and 27m in Cartesian Grid of receptors during Summer Season.

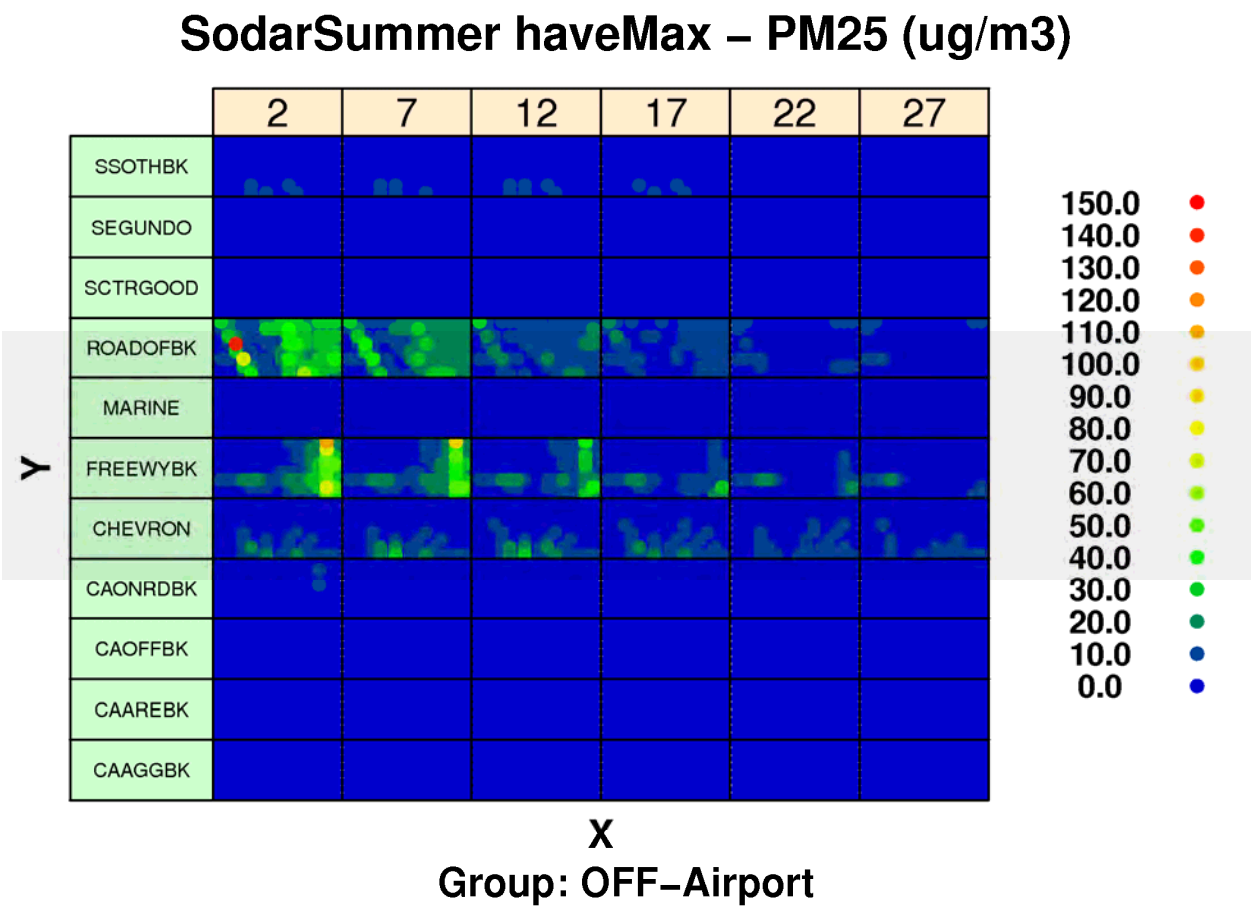

Figure 9A-130: Modeled hourly maximum $PM_{2.5}$ concentrations from background sources by source sector at flag-pole receptors at heights of 2m, 7m, 12m, 17m, 22m and 27m in Cartesian Grid of receptors during Summer Season.

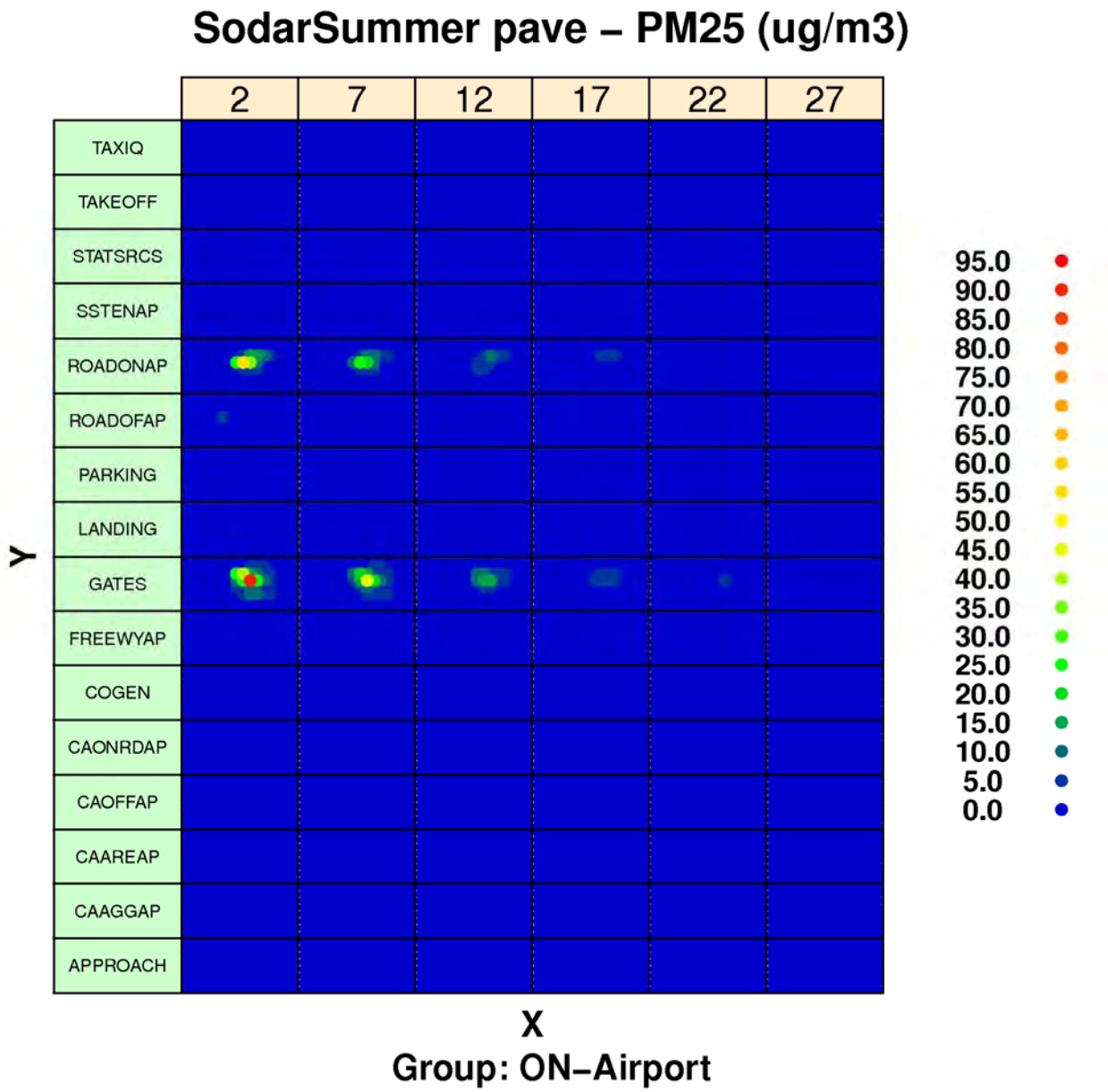

Figure 9A-131: Modeled period average $PM_{2.5}$ concentrations from airport-related sources by source sector at flag-pole receptors at heights of 2m, 7m, 12m, 17m, 22m and 27m in Cartesian Grid of receptors during Summer Season.

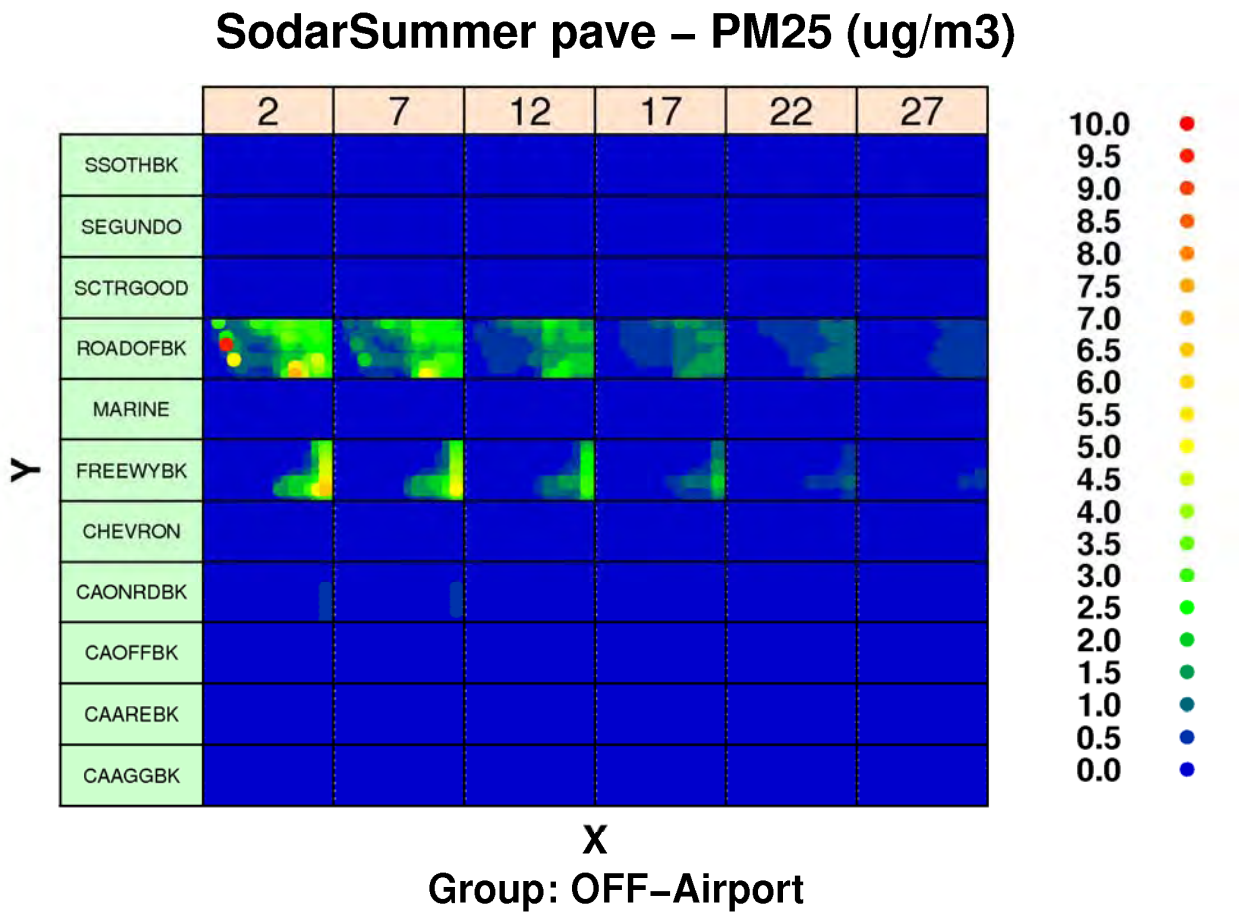

Figure 9A-132: Modeled period average $PM_{2.5}$ concentrations from background sources by source sector at flag-pole receptors at heights of 2m, 7m, 12m, 17m, 22m and 27m in Cartesian Grid of receptors during Summer Season.

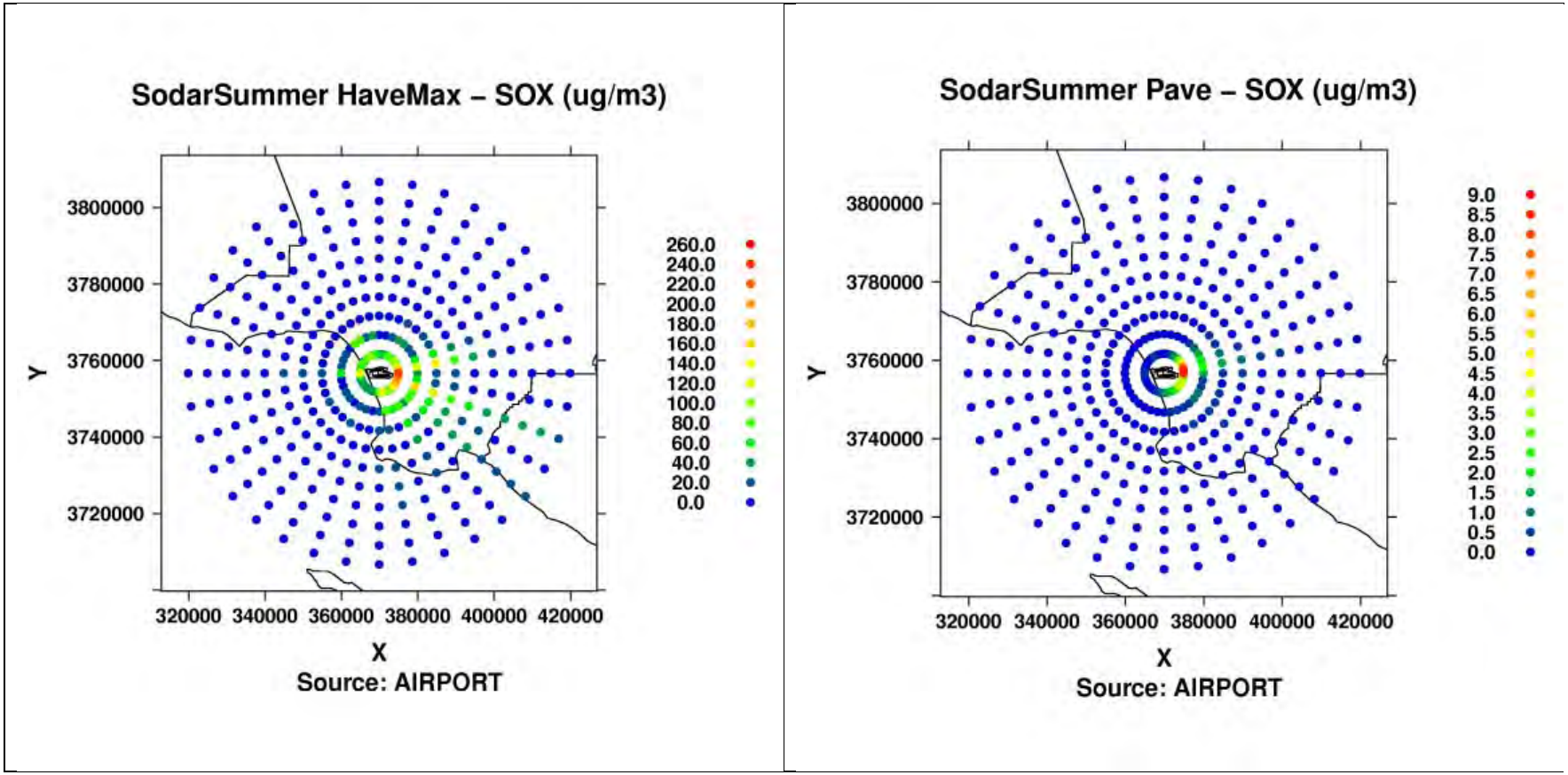

Figure 9A-133a: Modeled hourly max (left) and period average (right) SOx concentrations from airport-related in Polar Grid of receptors during Summer Season.

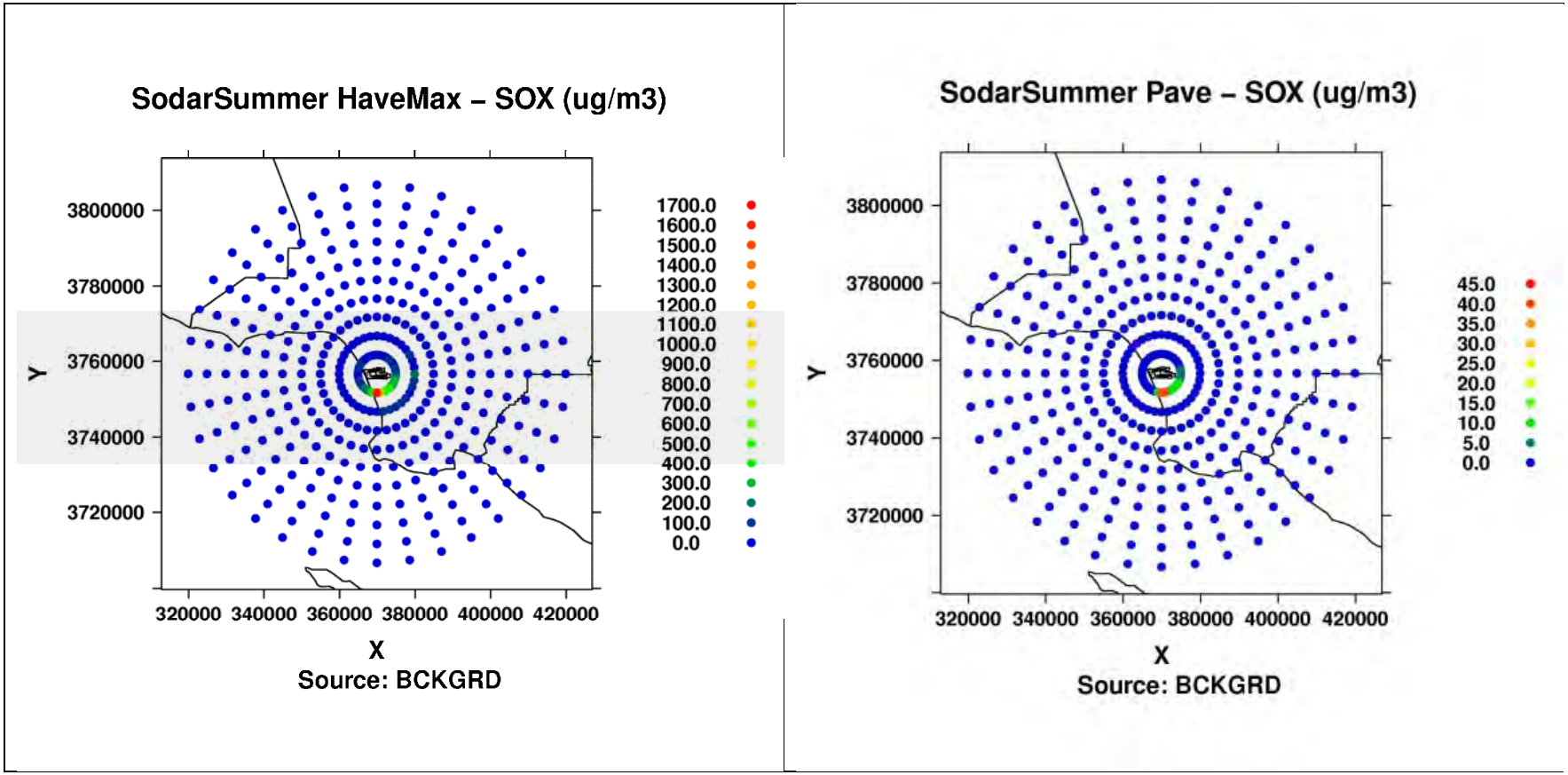

Figure 9A-133b: Modeled hourly max (left) and period average (right) SOx concentrations from background sources in Polar Grid of receptors during Summer Season.

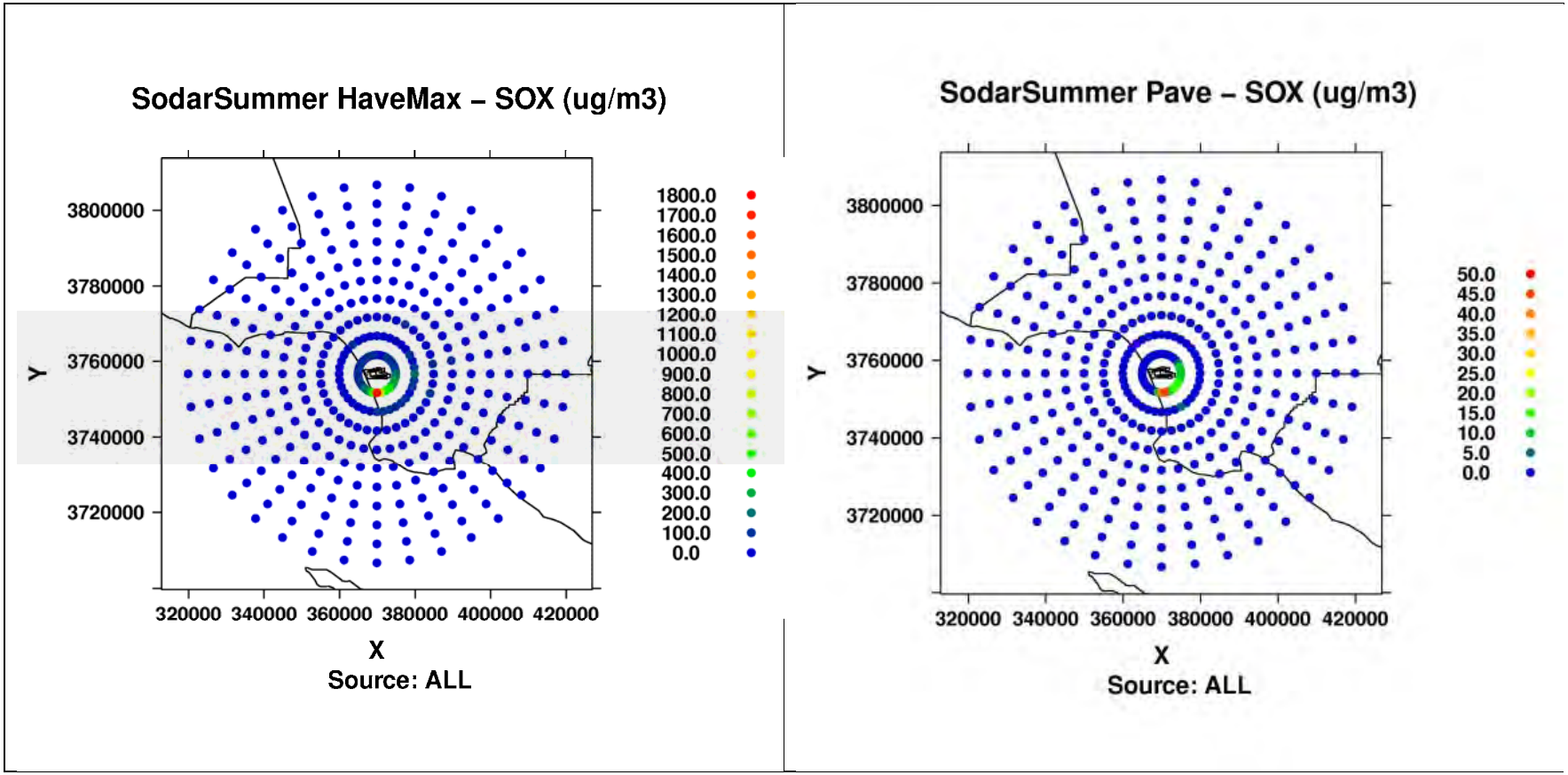

Figure 9A-133c: Modeled hourly max (left) and period average (right) SOx concentrations from ALL in Polar Grid of receptors during Summer Season.

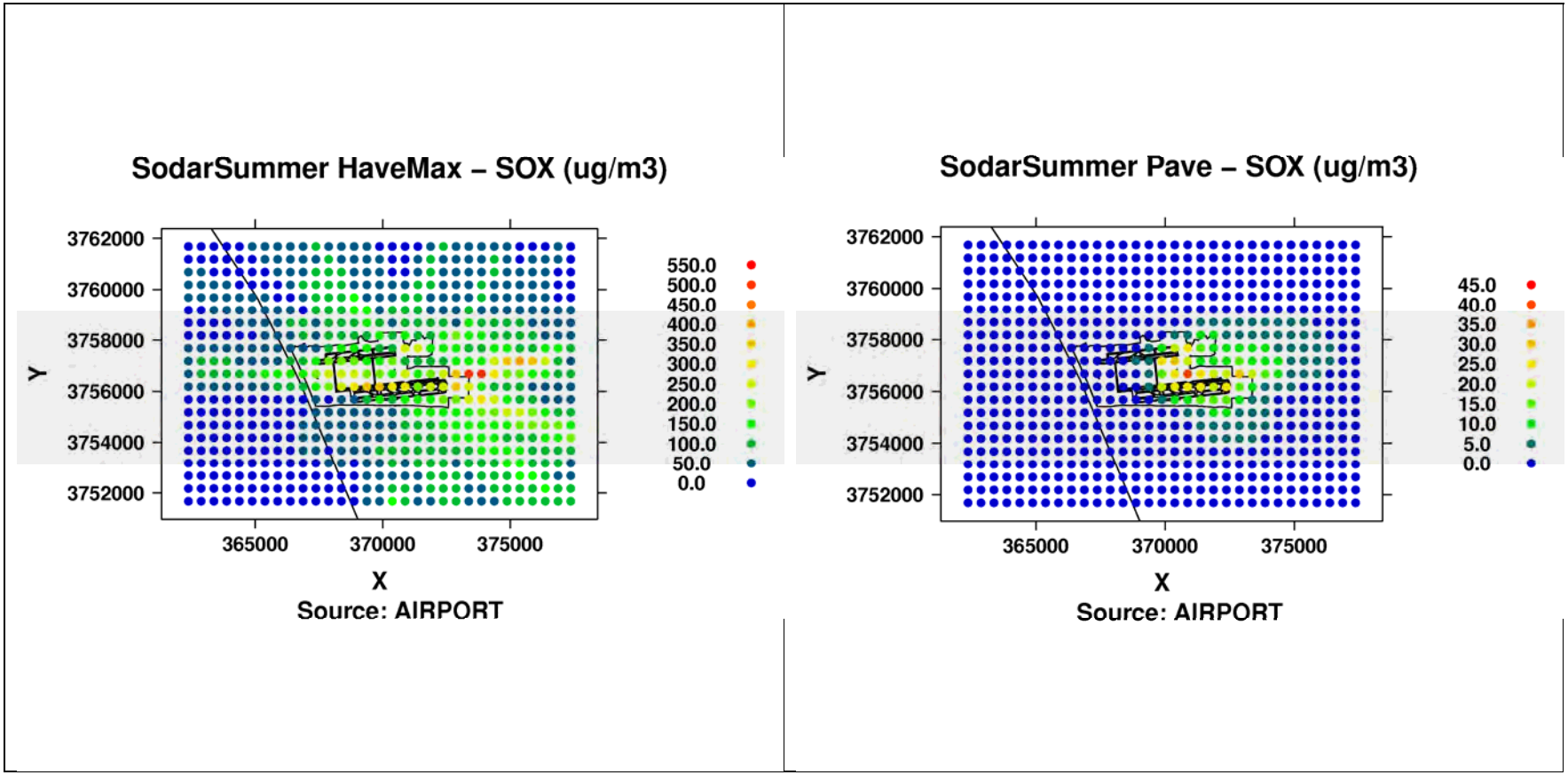

Figure 9A-134a: Modeled hourly max (left) and period average (right) SOx concentrations from airport-related in Cartesian Grid of receptors during Summer Season.

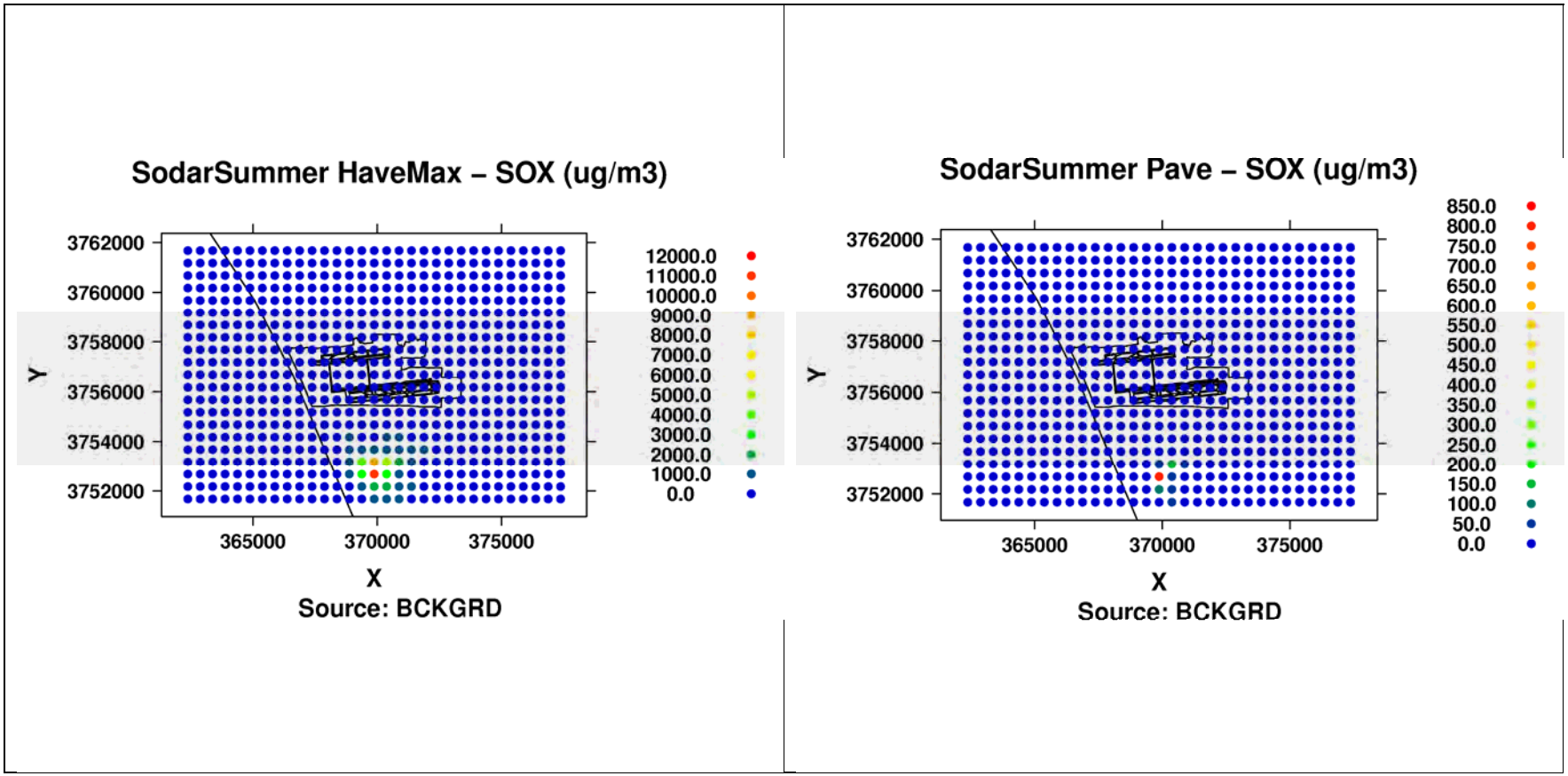

Figure 9A-134b: Modeled hourly max (left) and period average (right) SOx concentrations from background sources in Cartesian Grid of receptors during Summer Season.

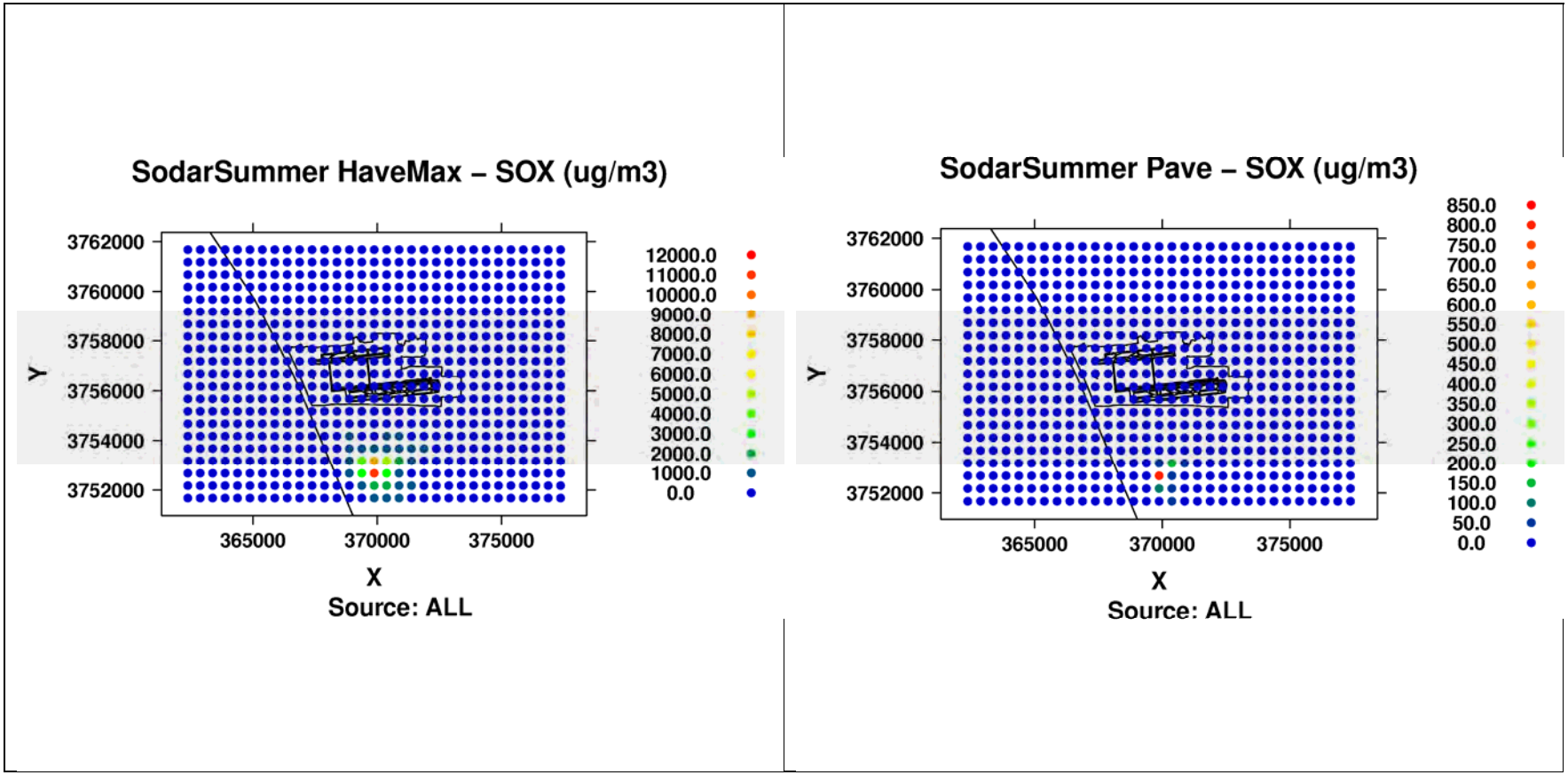

Figure 9A-134c: Modeled hourly max (left) and period average (right) SOx concentrations from ALL in Cartesian Grid of receptors during Summer Season.

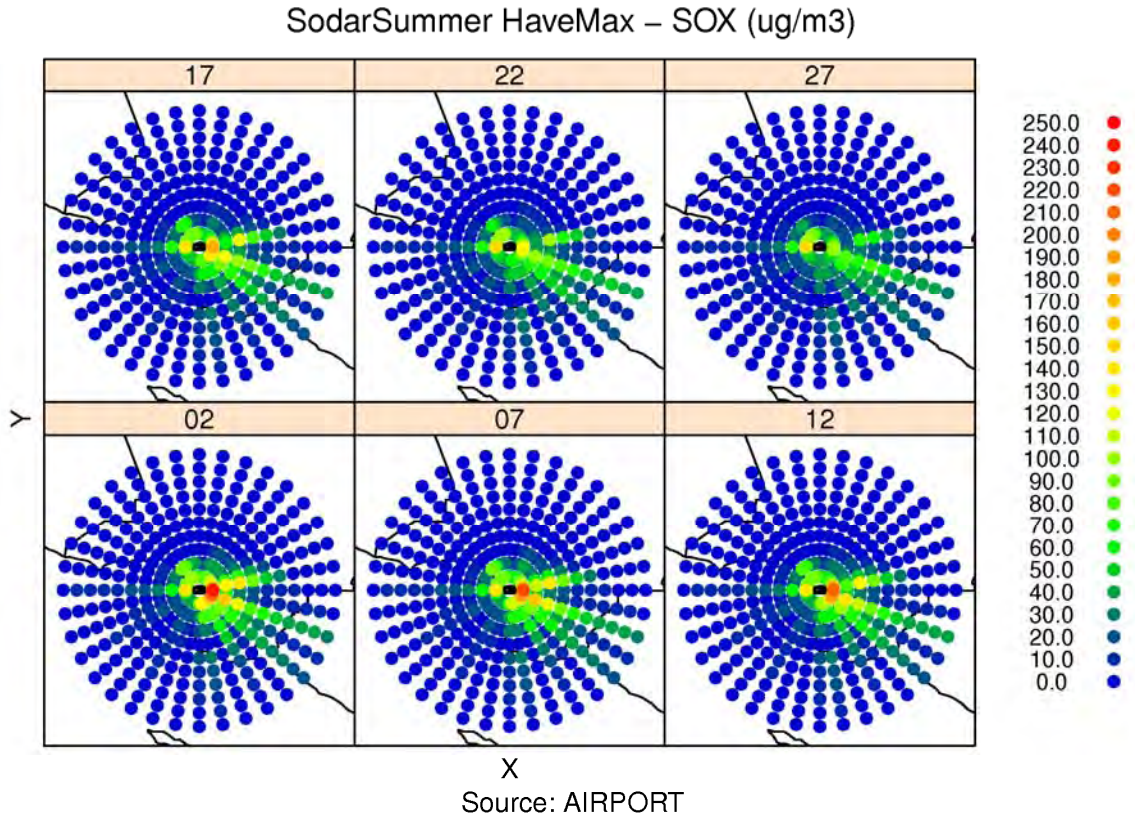

Figure 9A-135: Modeled hourly max SOx concentrations from airport-related sources at flag-pole receptors at heights of 2m, 7m, 12m, 17m, 22m and 27m in Polar Grid of receptors during Summer Season.

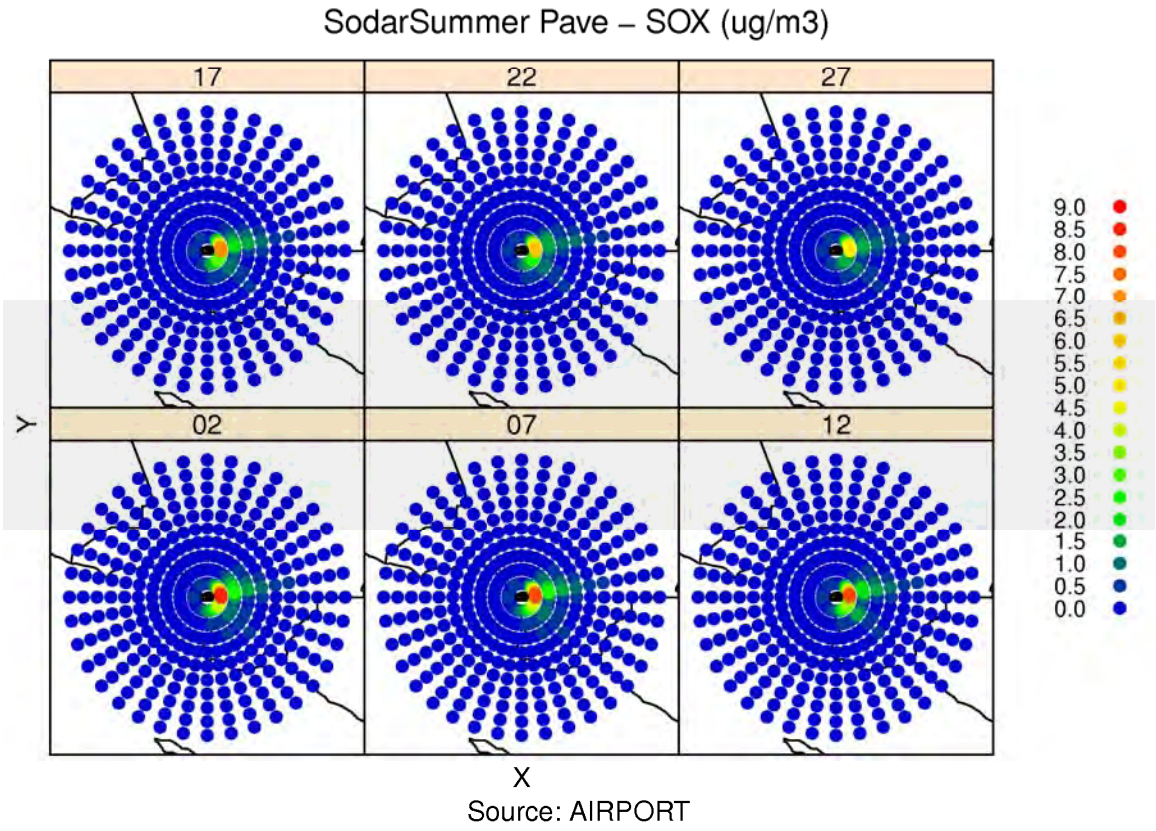

Figure 9A-136: Modeled period average SOx concentrations from airport-related sources at flag-pole receptors at heights of 2m, 7m, 12m, 17m, 22m and 27m in Polar Grid of receptors during Summer Season.

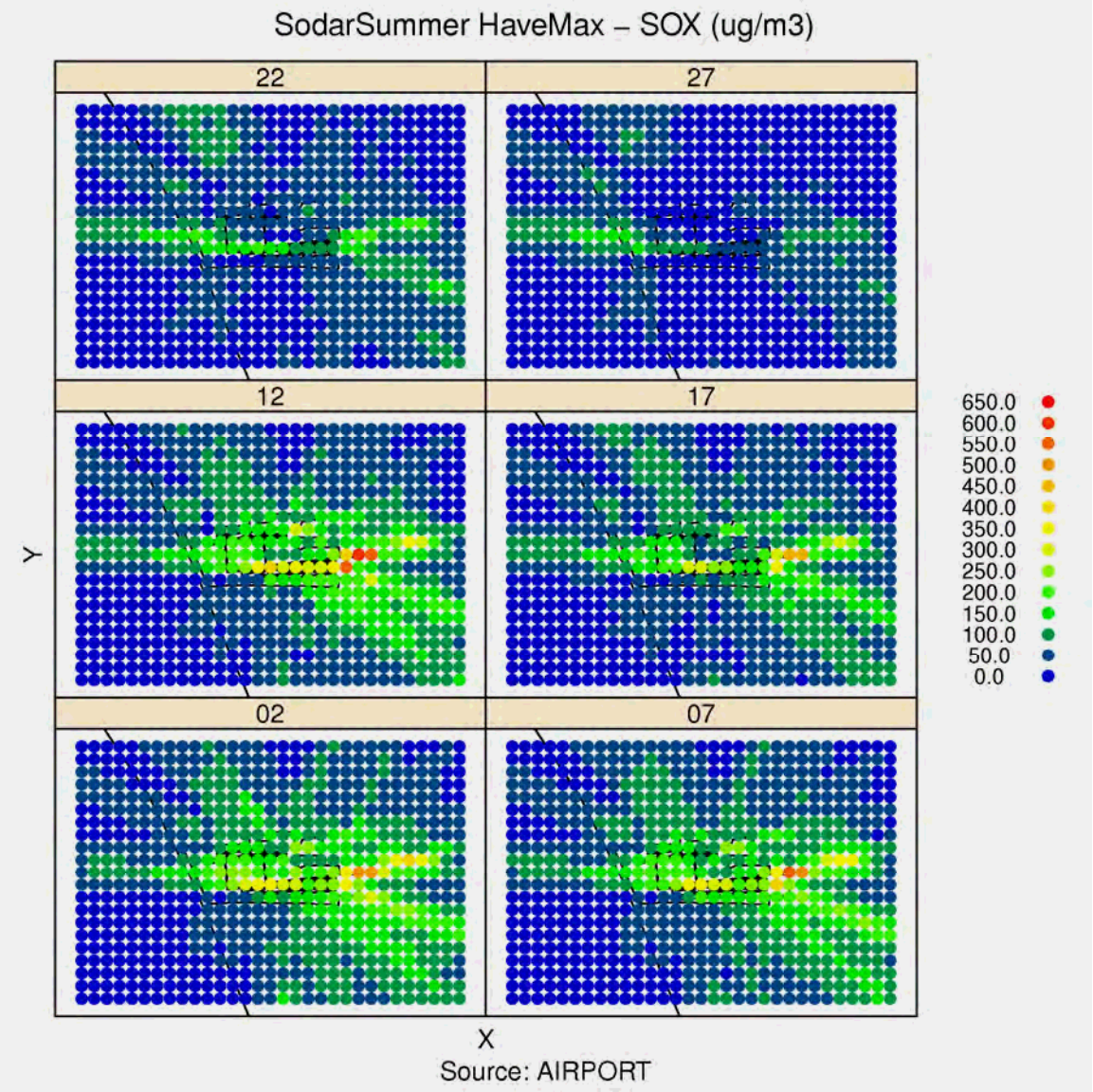

Figure 9A-137: Modeled hourly max SOx concentrations from airport-related sources at flag-pole receptors at heights of 2m, 7m, 12m, 17m, 22m and 27m in Cartesian Grid of receptors during Summer Season.

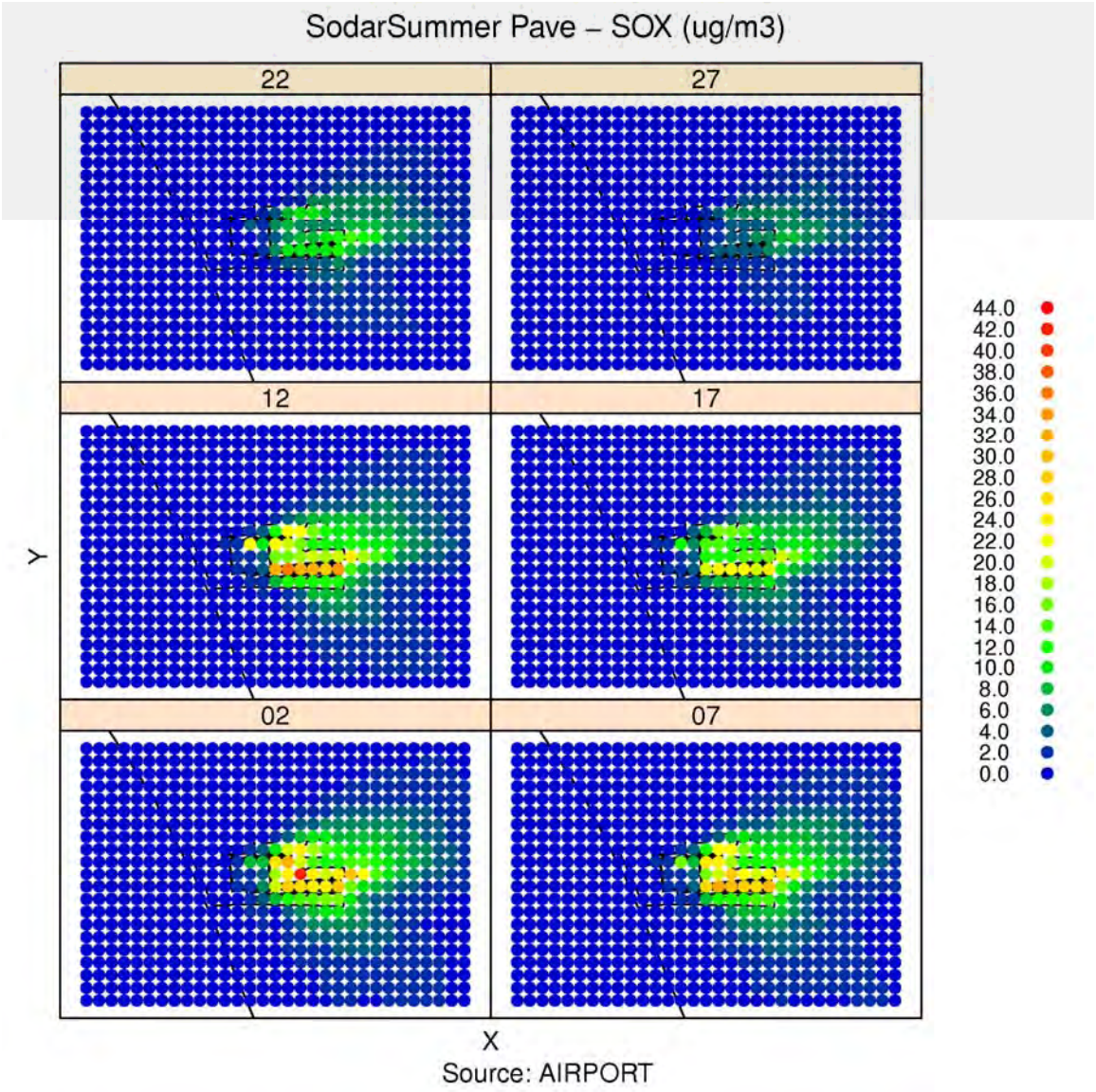

Figure 9A-138: Modeled period average SOx concentrations from airport-related sources at flag-pole receptors at heights of 2m, 7m, 12m, 17m, 22m and 27m in Cartesian Grid of receptors during Summer Season.

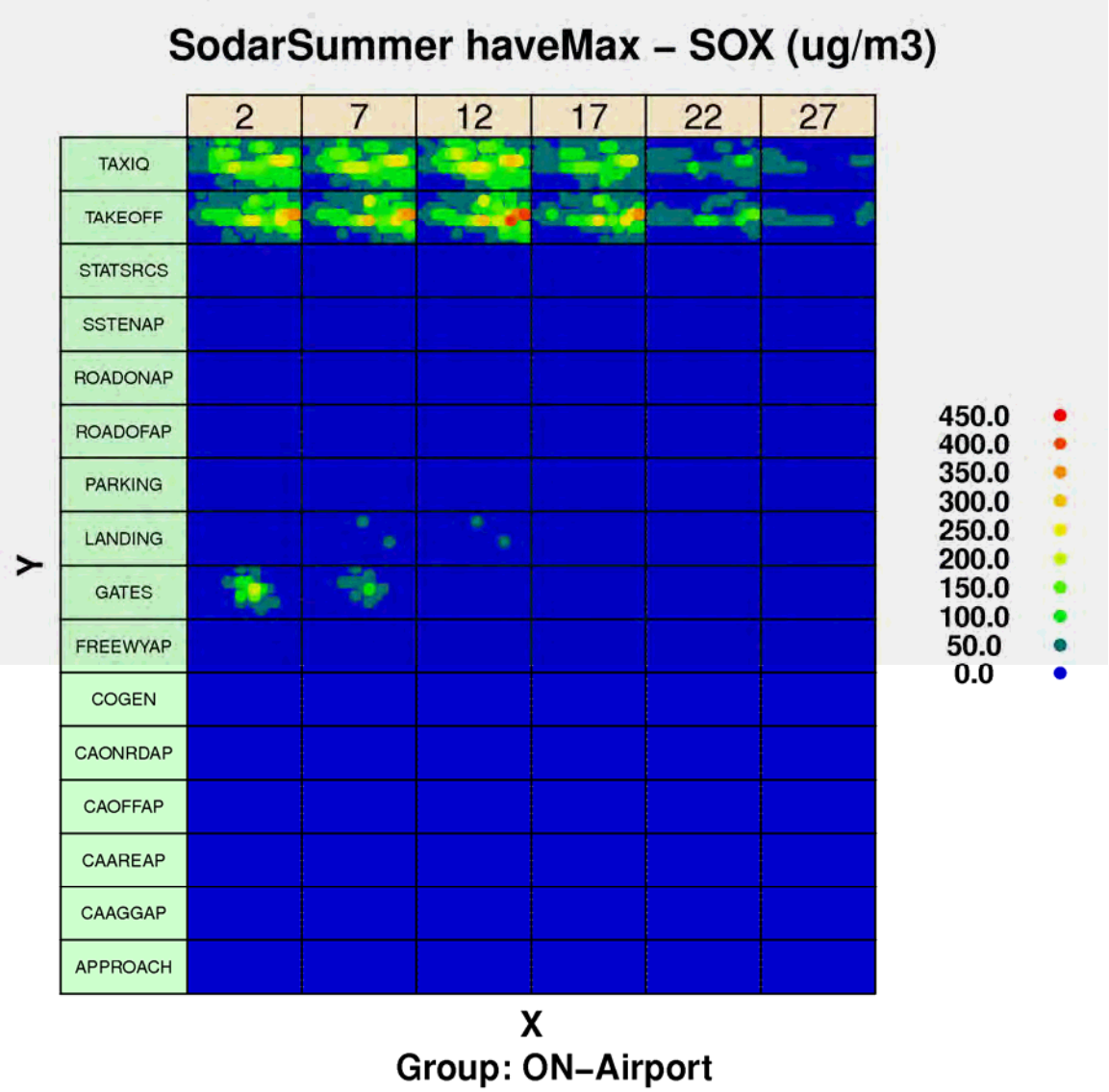

Figure 9A-139: Modeled hourly maximum SOx concentrations from airport-related sources by source sector at flag-pole receptors at heights of 2m, 7m, 12m, 17m, 22m and 27m in Cartesian Grid of receptors during Summer Season.

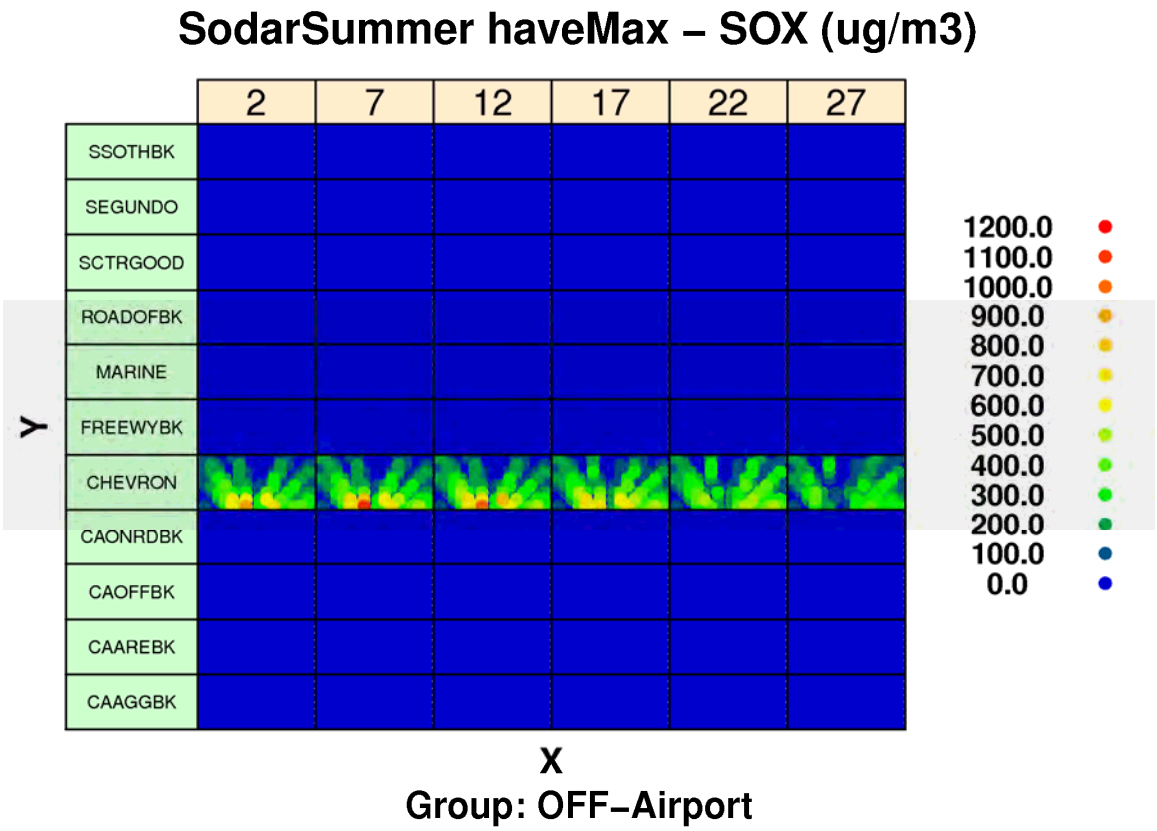

Figure 9A-140: Modeled hourly maximum SOx concentrations from background sources by source sector at flag-pole receptors at heights of 2m, 7m, 12m, 17m, 22m and 27m in Cartesian Grid of receptors during Summer Season.

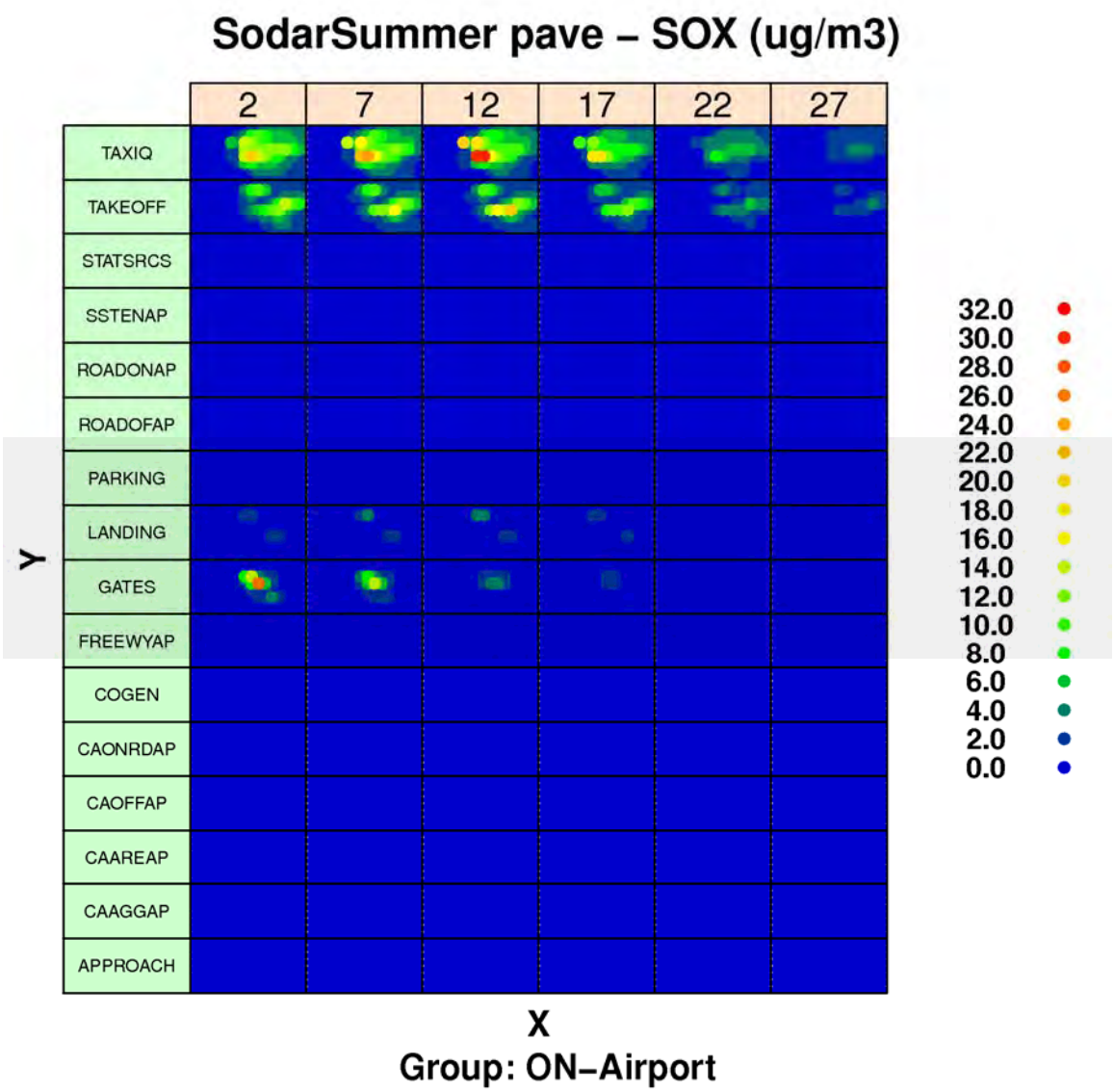

Figure 9A-141: Modeled period average SOx concentrations from airport-related sources by source sector at flag-pole receptors at heights of 2m, 7m, 12m, 17m, 22m and 27m in Cartesian Grid of receptors during Summer Season.

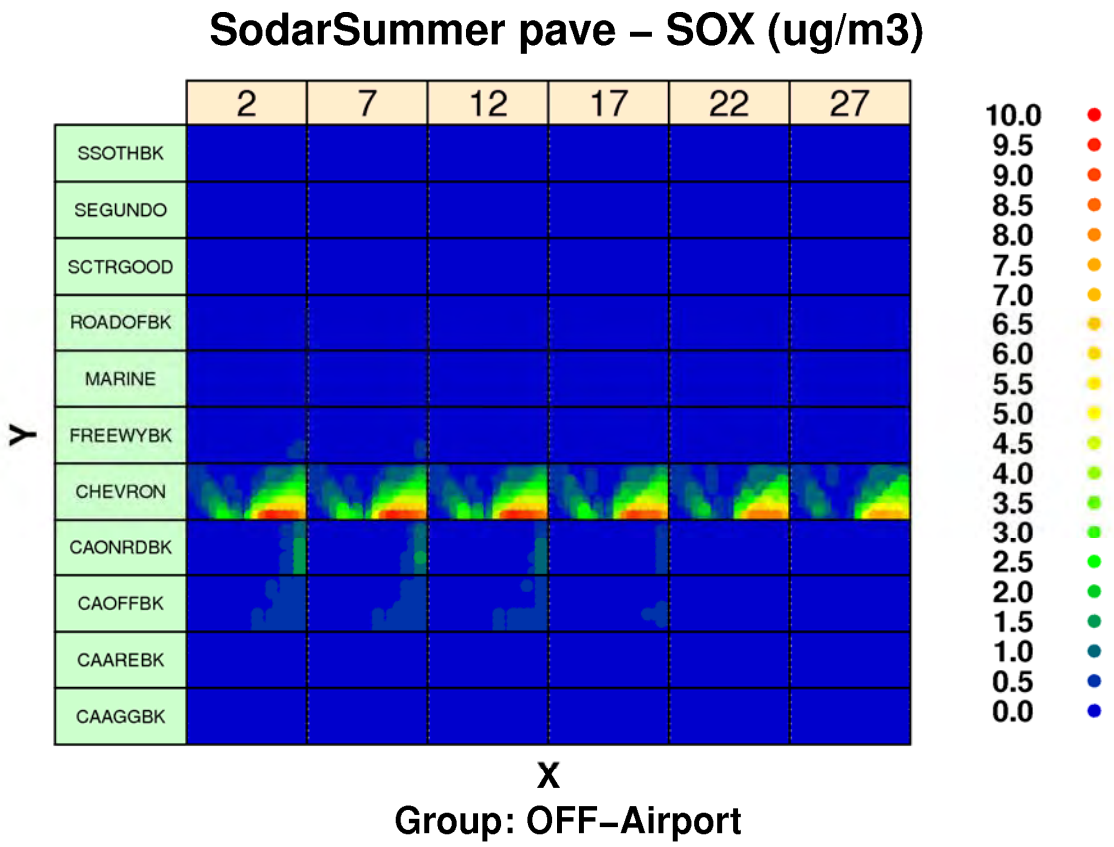

Figure 9A-142: Modeled period average SOx concentrations from background sources by source sector at flag-pole receptors at heights of 2m, 7m, 12m, 17m, 22m and 27m in Cartesian Grid of receptors during Summer Season.

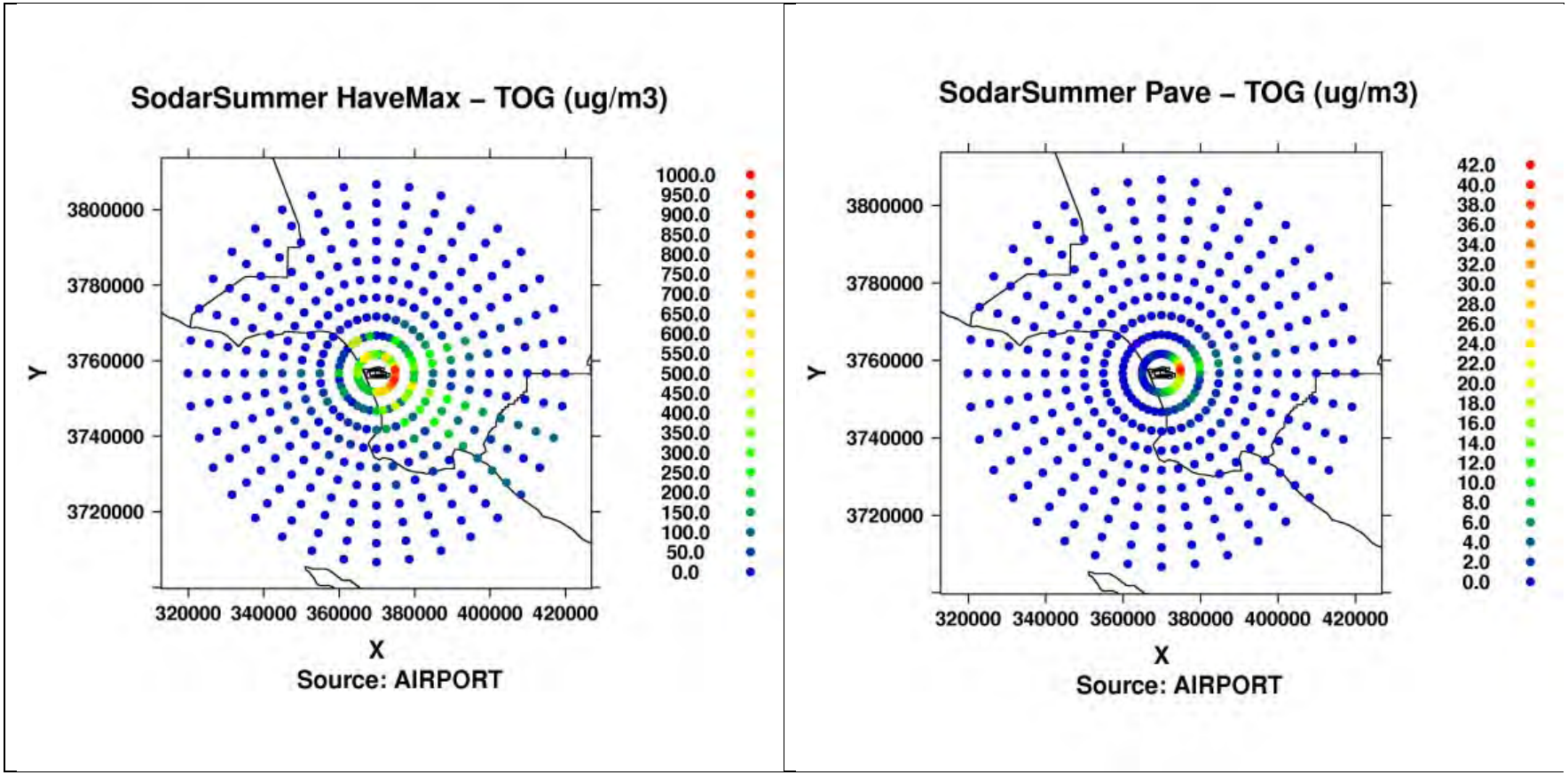

Figure 9A-143a: Modeled hourly max (left) and period average (right) TOG concentrations from airport-related in Polar Grid of receptors during Summer Season.

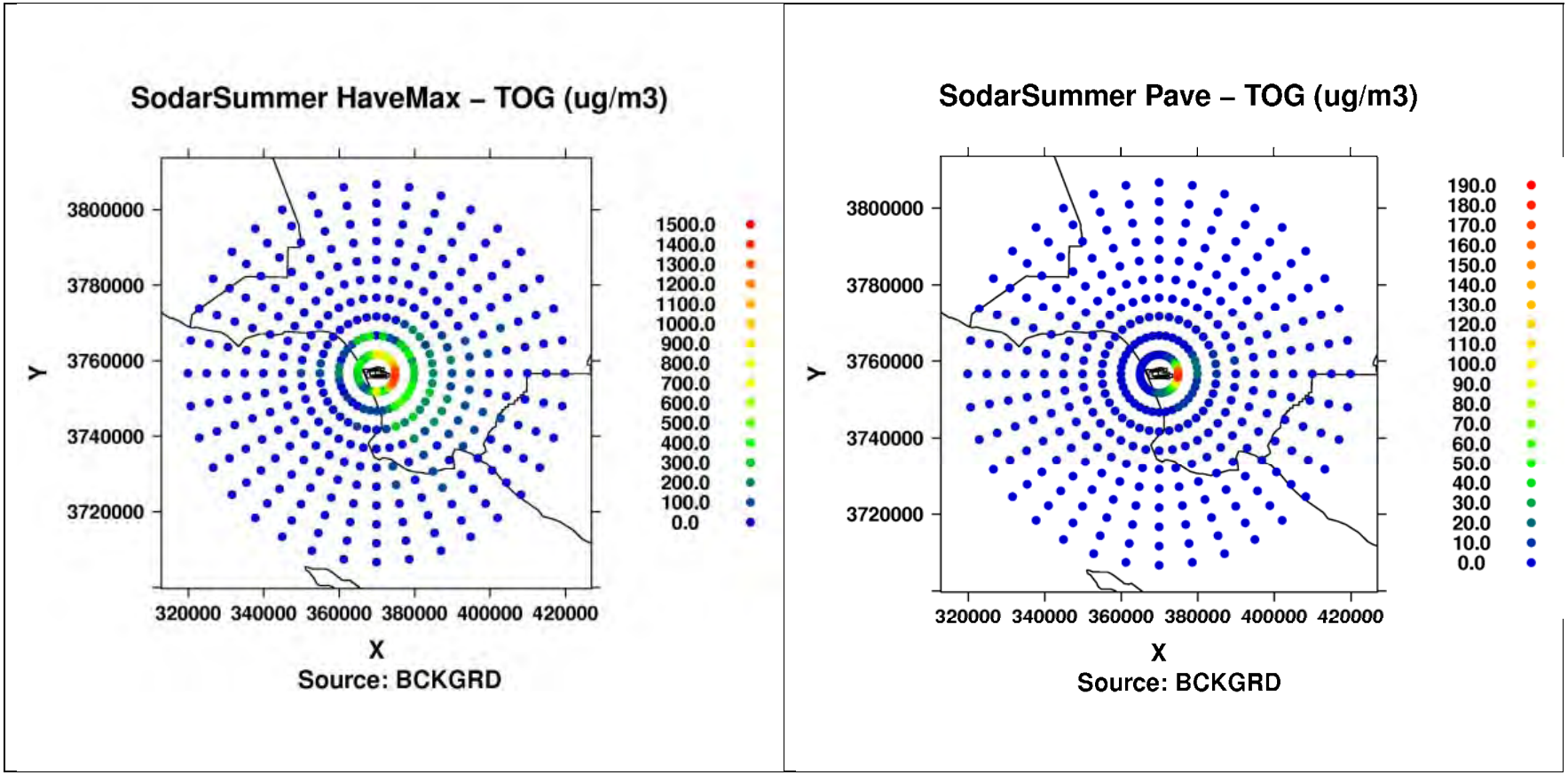

Figure 9A-143b: Modeled hourly max (left) and period average (right) TOG concentrations from background sources in Polar Grid of receptors during Summer Season.

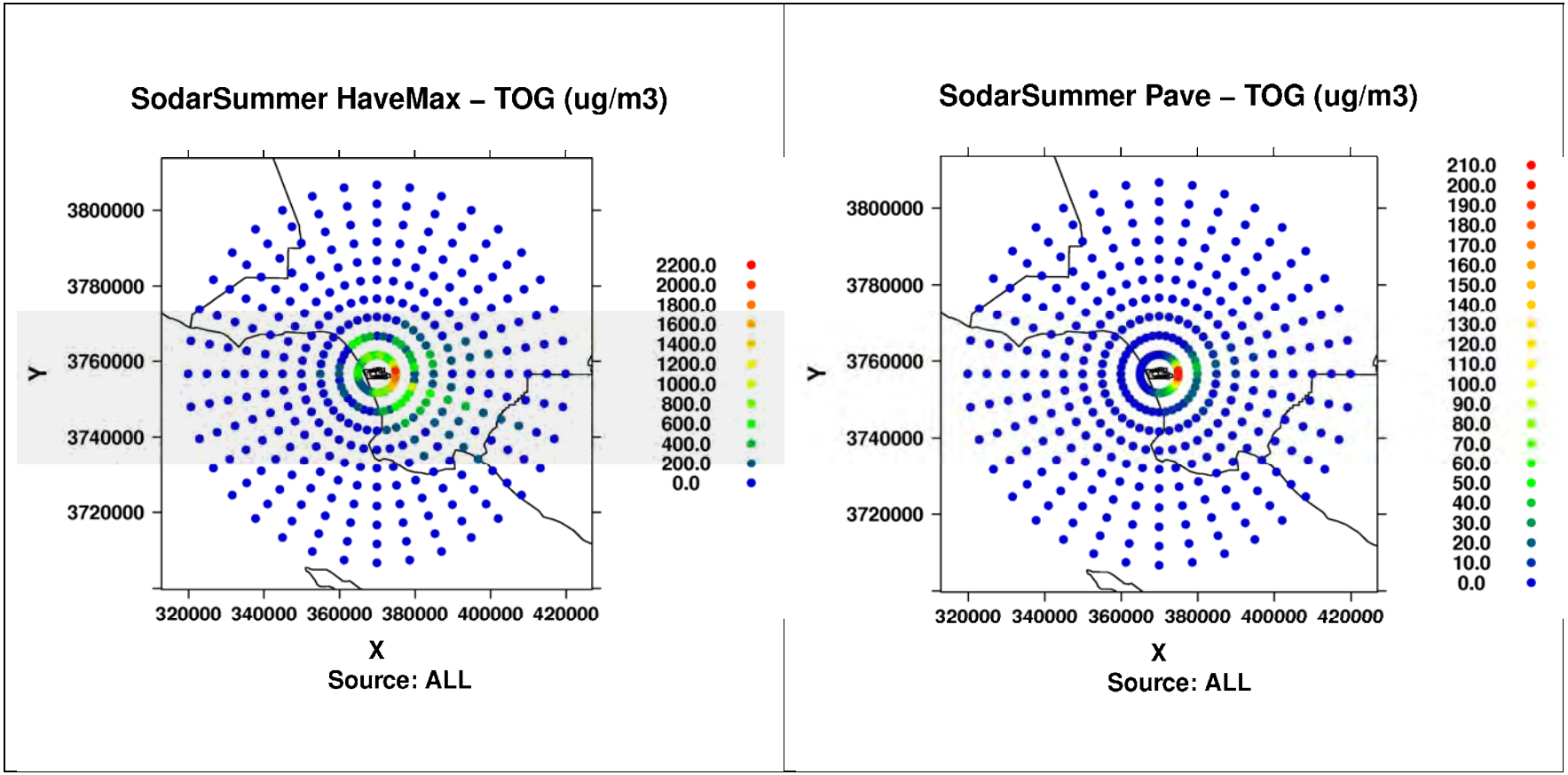

Figure 9A-143c: Modeled hourly max (left) and period average (right) TOG concentrations from ALL in Polar Grid of receptors during Summer Season.

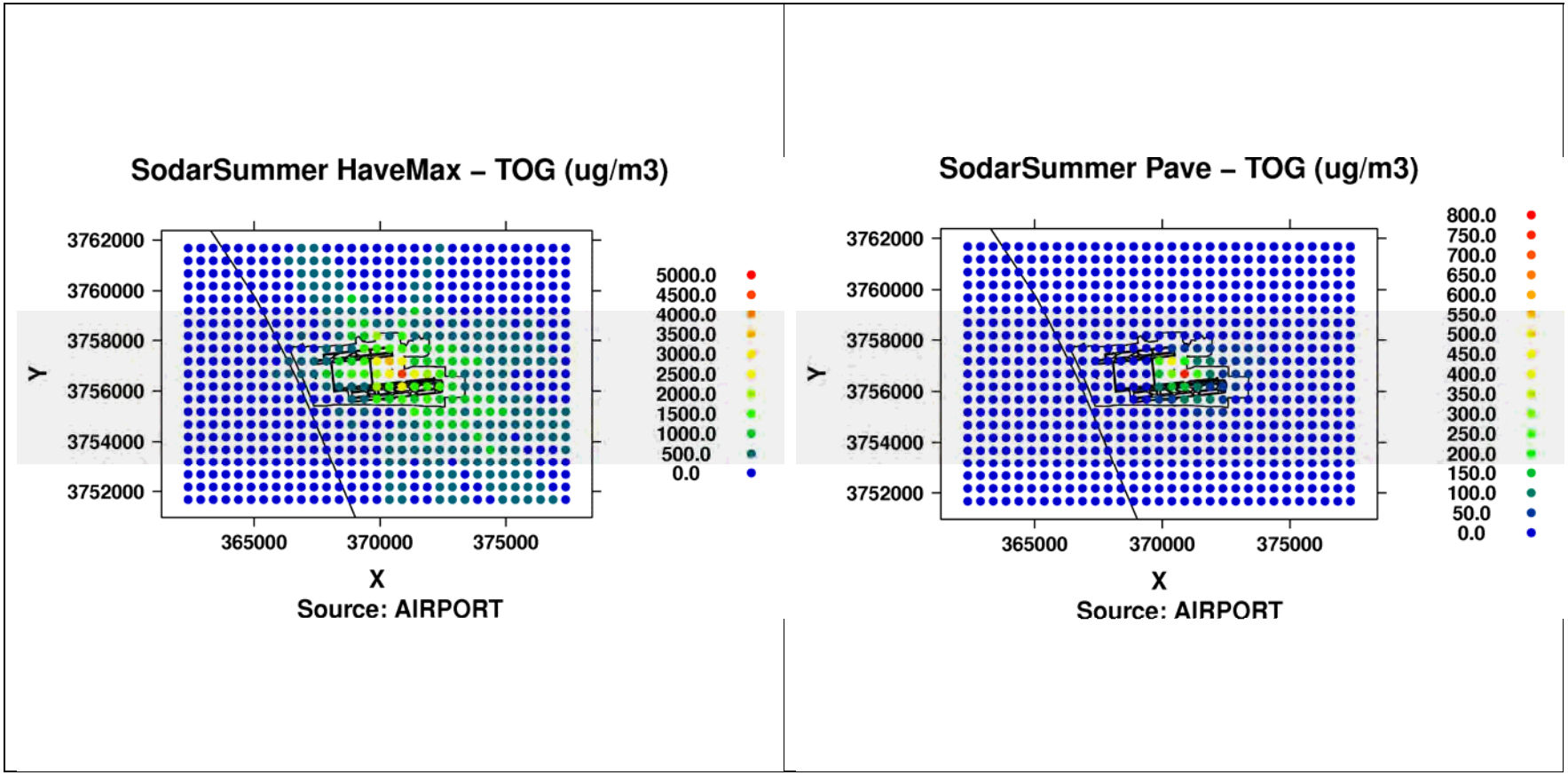

Figure 9A-144a: Modeled hourly max (left) and period average (right) TOG concentrations from airport-related in Cartesian Grid of receptors during Summer Season.

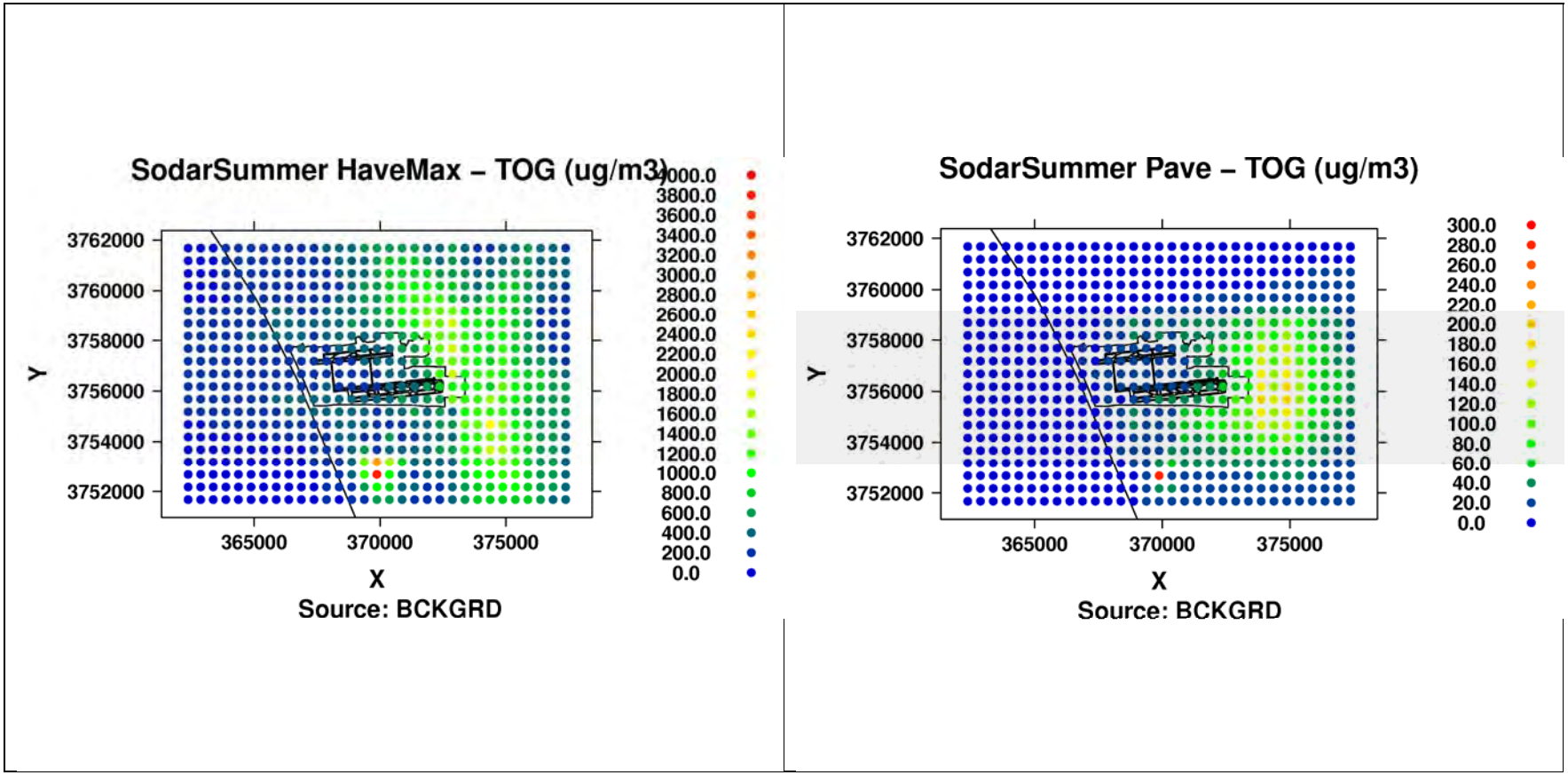

Figure 9A-144b: Modeled hourly max (left) and period average (right) TOG concentrations from background sources in Cartesian Grid of receptors during Summer Season.

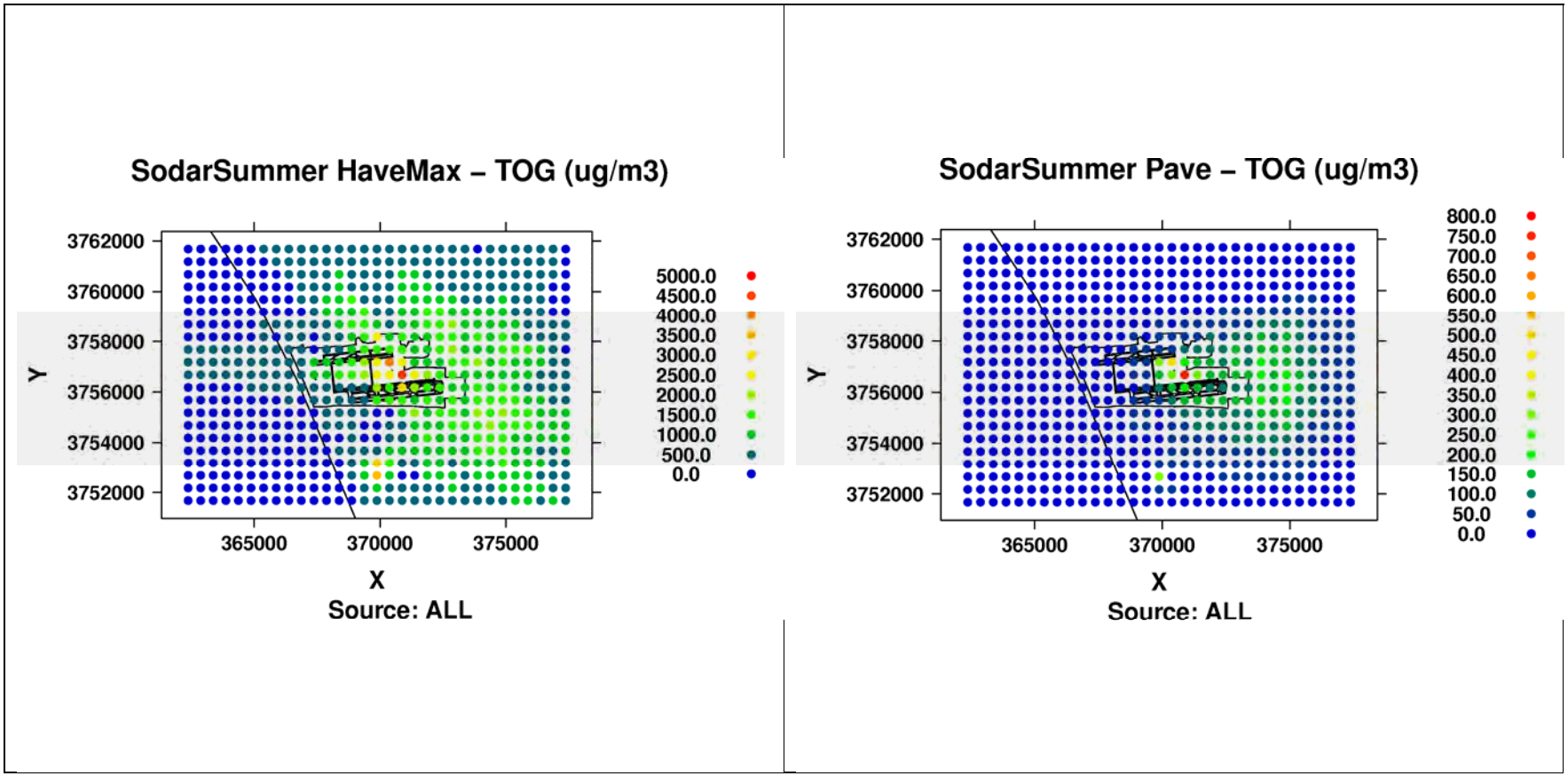

Figure 9A-144c: Modeled hourly max (left) and period average (right) TOG concentrations from ALL in Cartesian Grid of receptors during Summer Season.

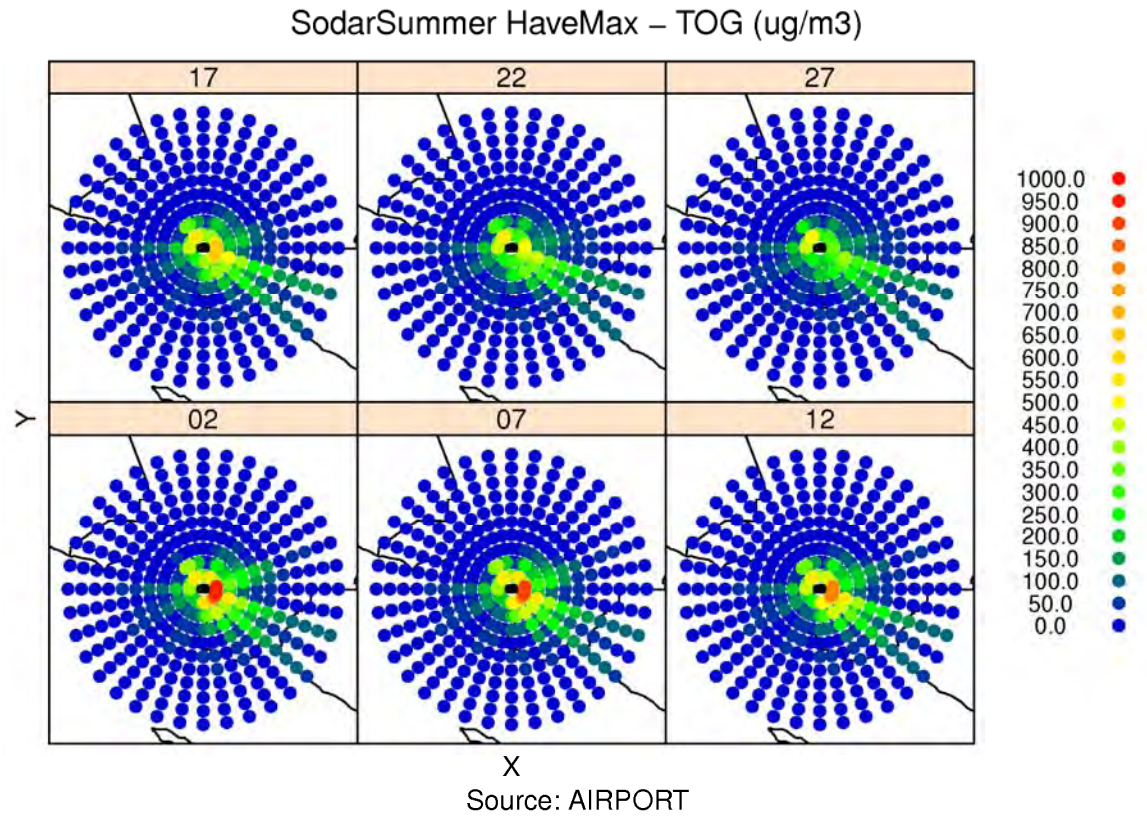

Figure 9A-145: Modeled hourly max TOG concentrations from airport-related sources at flag-pole receptors at heights of 2m, 7m, 12m, 17m, 22m and 27m in Polar Grid of receptors during Summer Season.

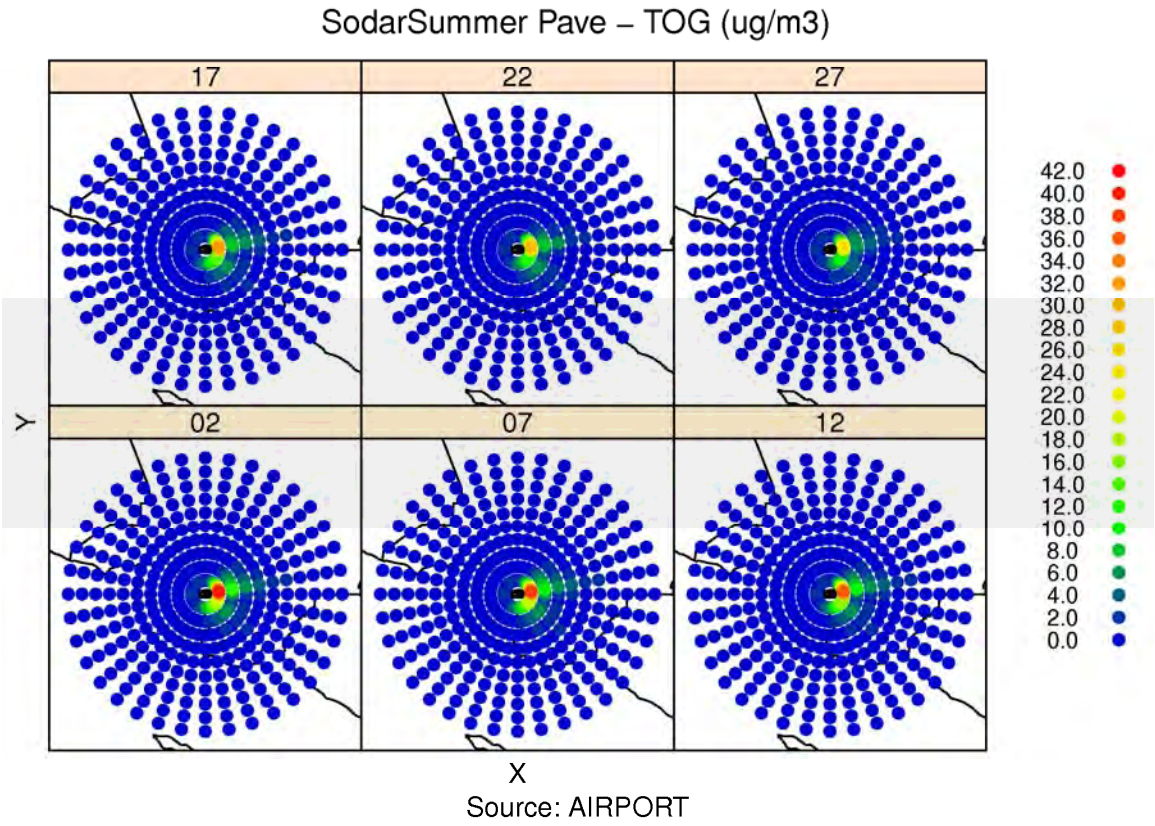

Figure 9A-146: Modeled period average TOG concentrations from airport-related sources at flag-pole receptors at heights of 2m, 7m, 12m, 17m, 22m and 27m in Polar Grid of receptors during Summer Season.

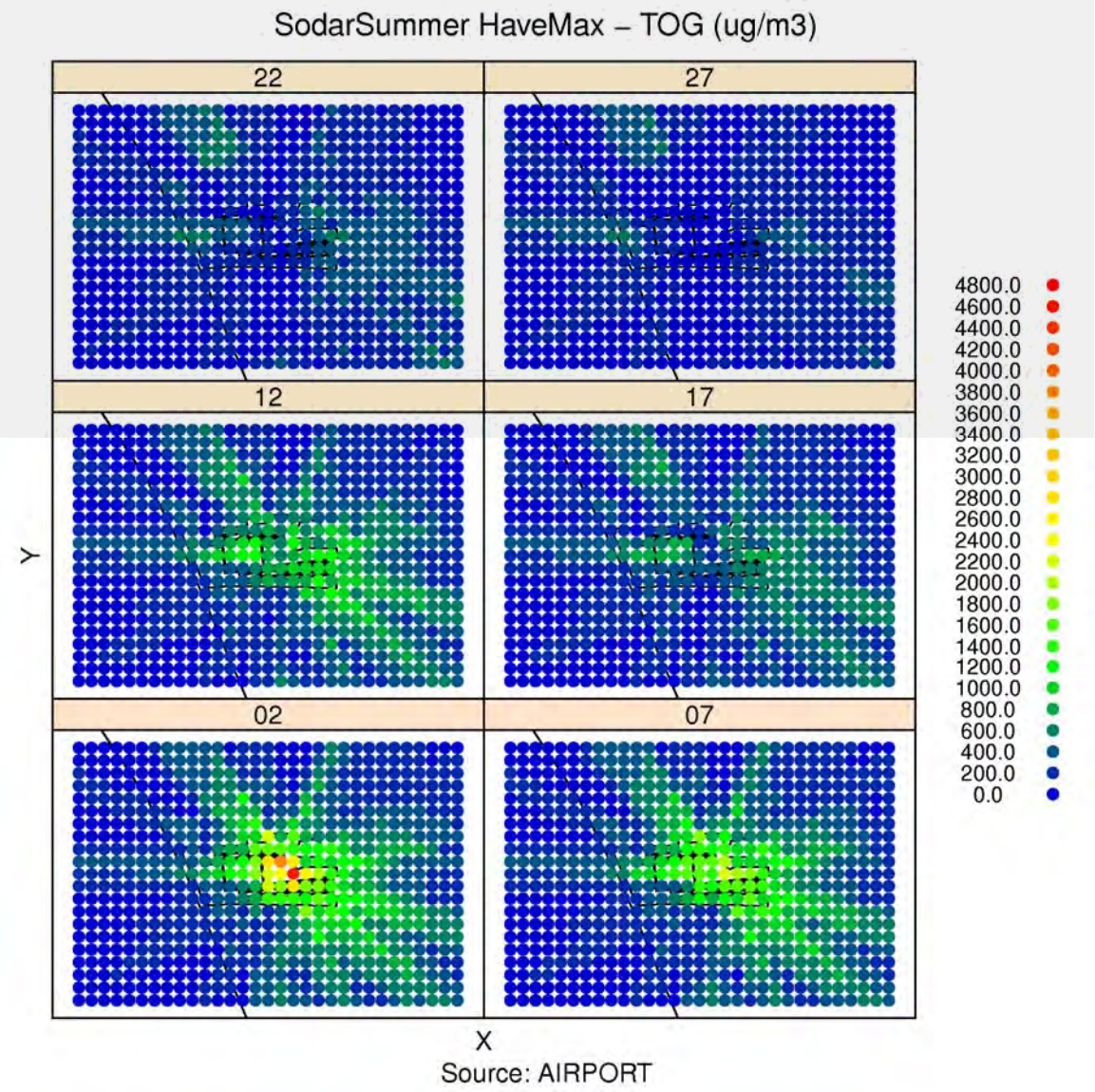

Figure 9A-147: Modeled hourly max TOG concentrations from airport-related sources at flag-pole receptors at heights of 2m, 7m, 12m, 17m, 22m and 27m in Cartesian Grid of receptors during Summer Season.

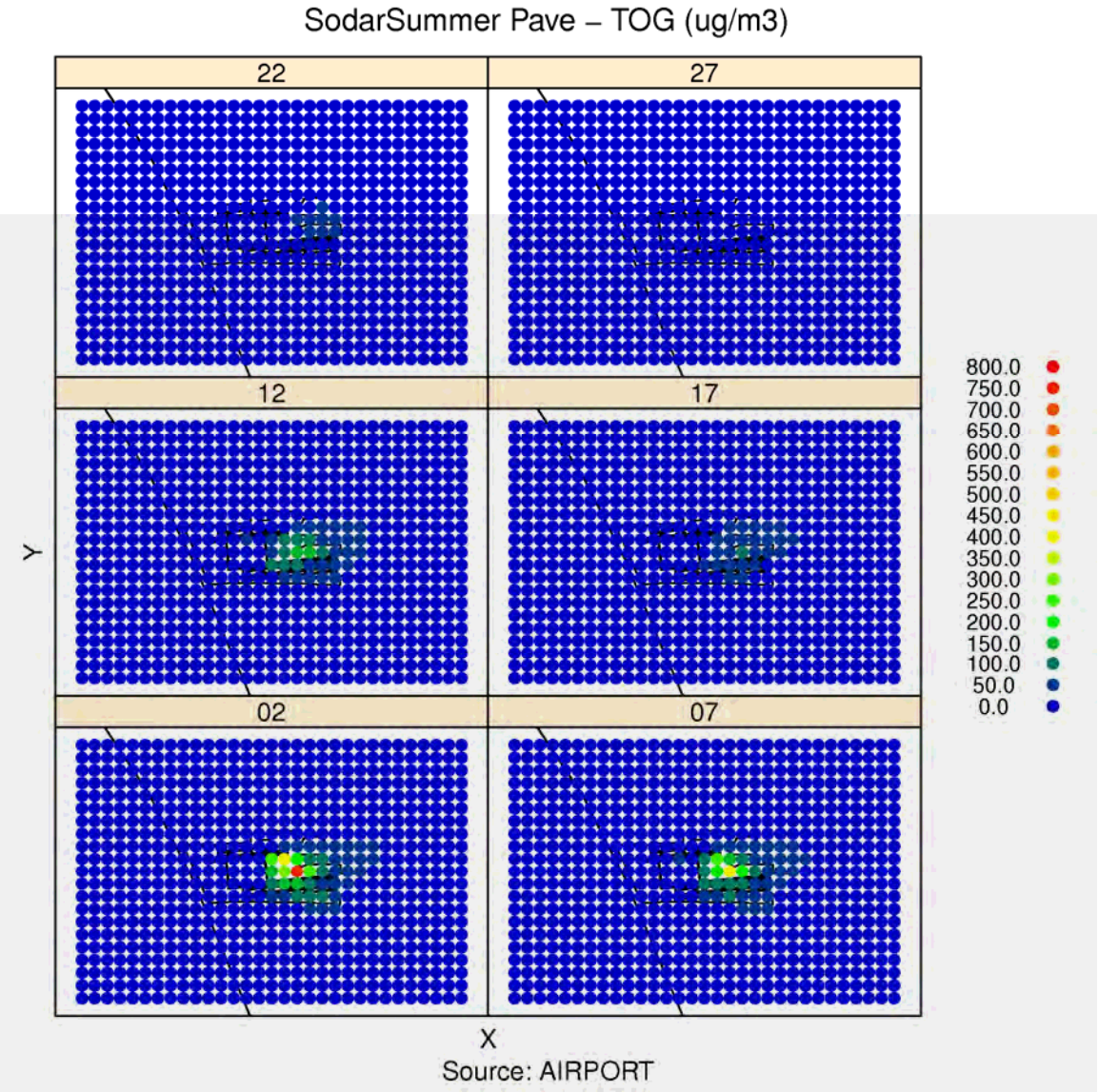

Figure 9A-148: Modeled period average TOG concentrations from airport-related sources at flag-pole receptors at heights of 2m, 7m, 12m, 17m, 22m and 27m in Cartesian Grid of receptors during Summer Season.

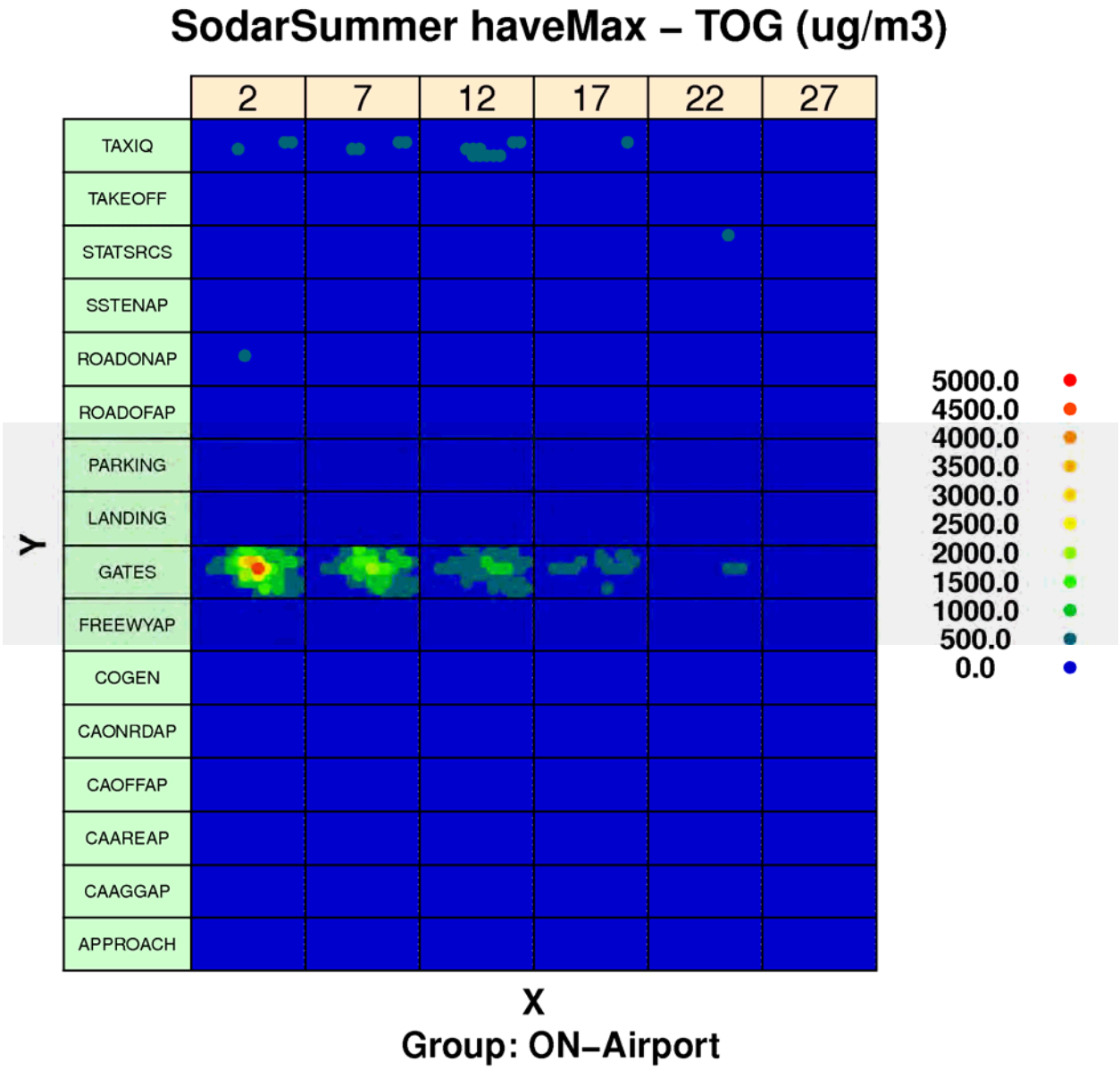

Figure 9A-149: Modeled hourly maximum TOG concentrations from airport-related sources by source sector at flag-pole receptors at heights of 2m, 7m, 12m, 17m, 22m and 27m in Cartesian Grid of receptors during Summer Season.

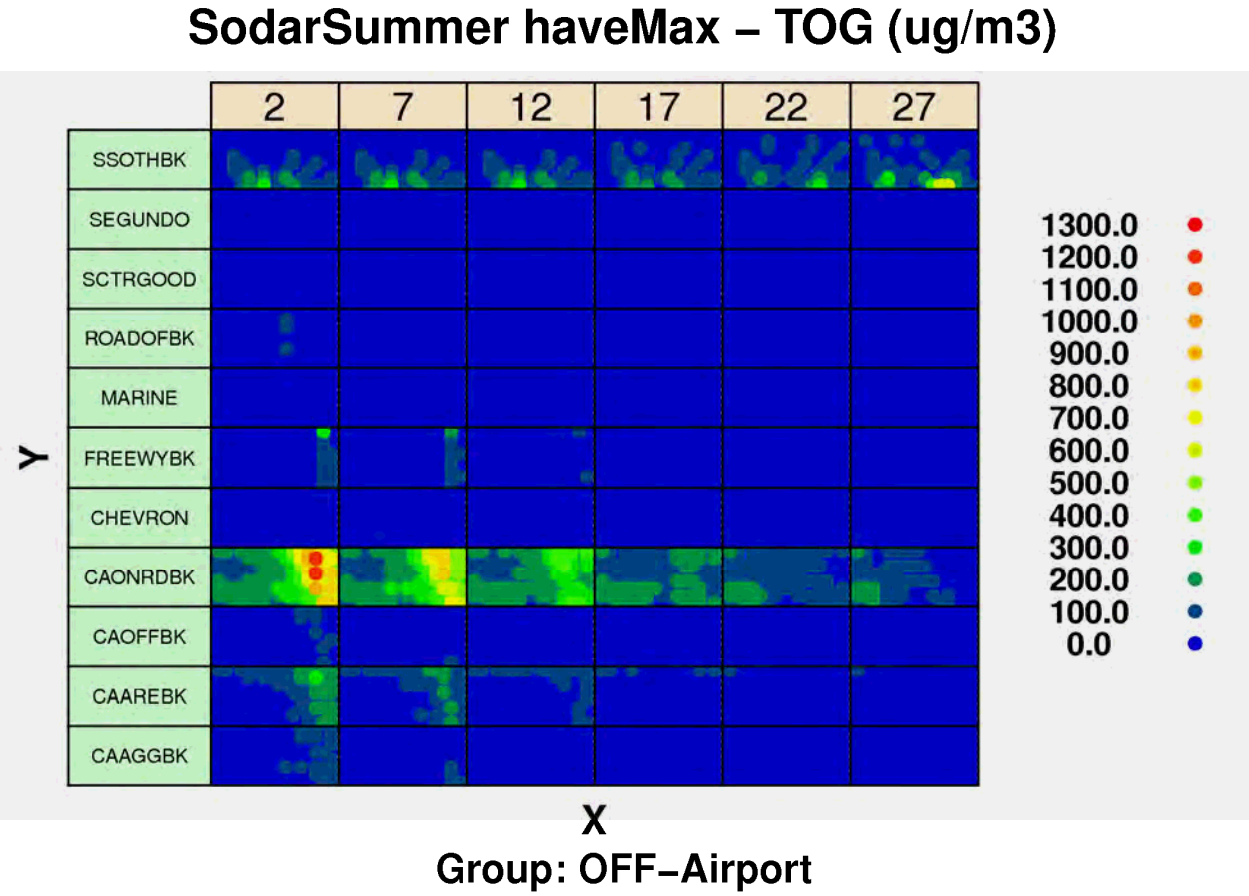

Figure 9A-150: Modeled hourly maximum TOG concentrations from background sources by source sector at flag-pole receptors at heights of 2m, 7m, 12m, 17m, 22m and 27m in Cartesian Grid of receptors during Summer Season.

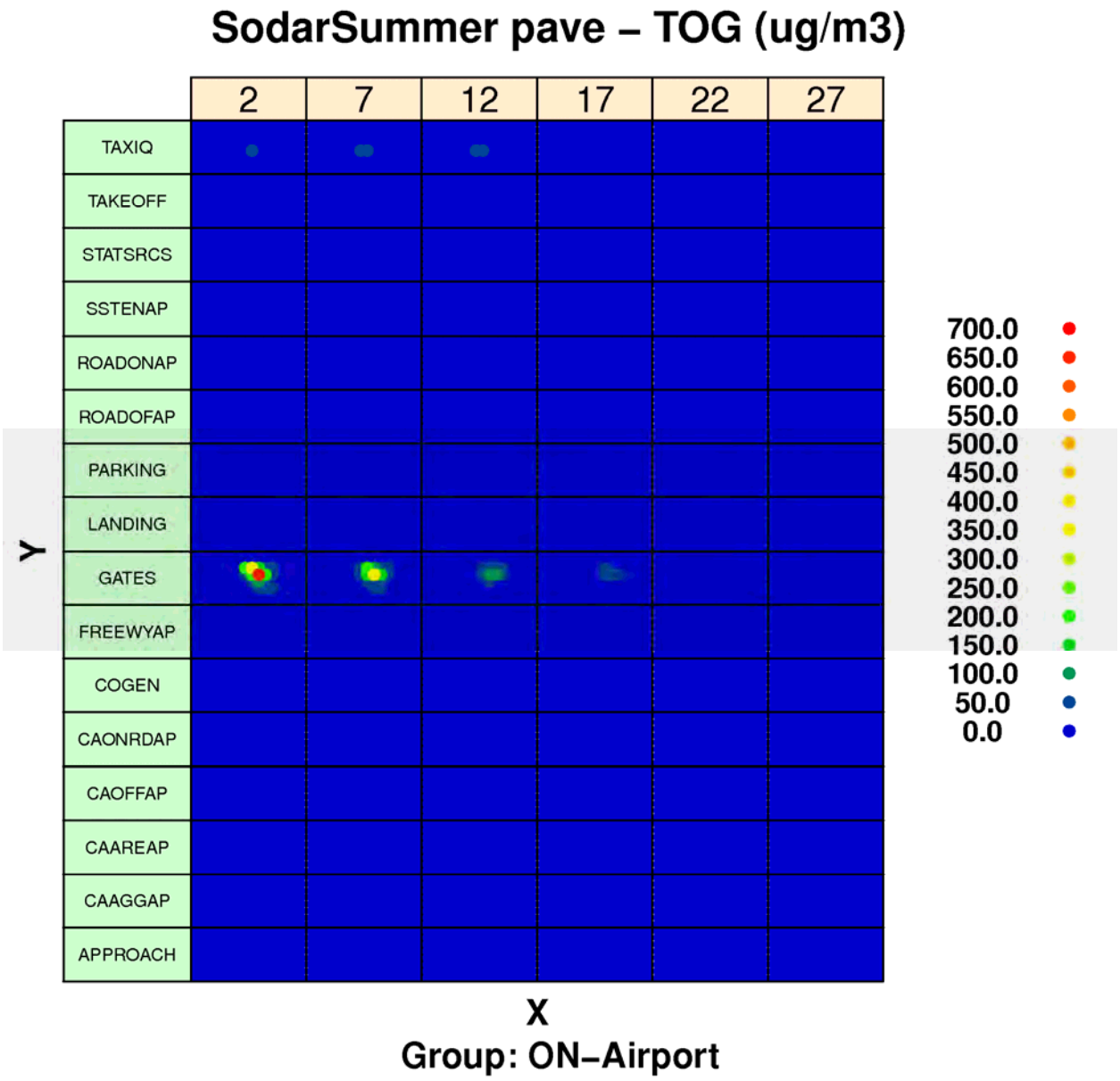

Figure 9A-151: Modeled period average TOG concentrations from airport-related sources by source sector at flag-pole receptors at heights of 2m, 7m, 12m, 17m, 22m and 27m in Cartesian Grid of receptors during Summer Season.

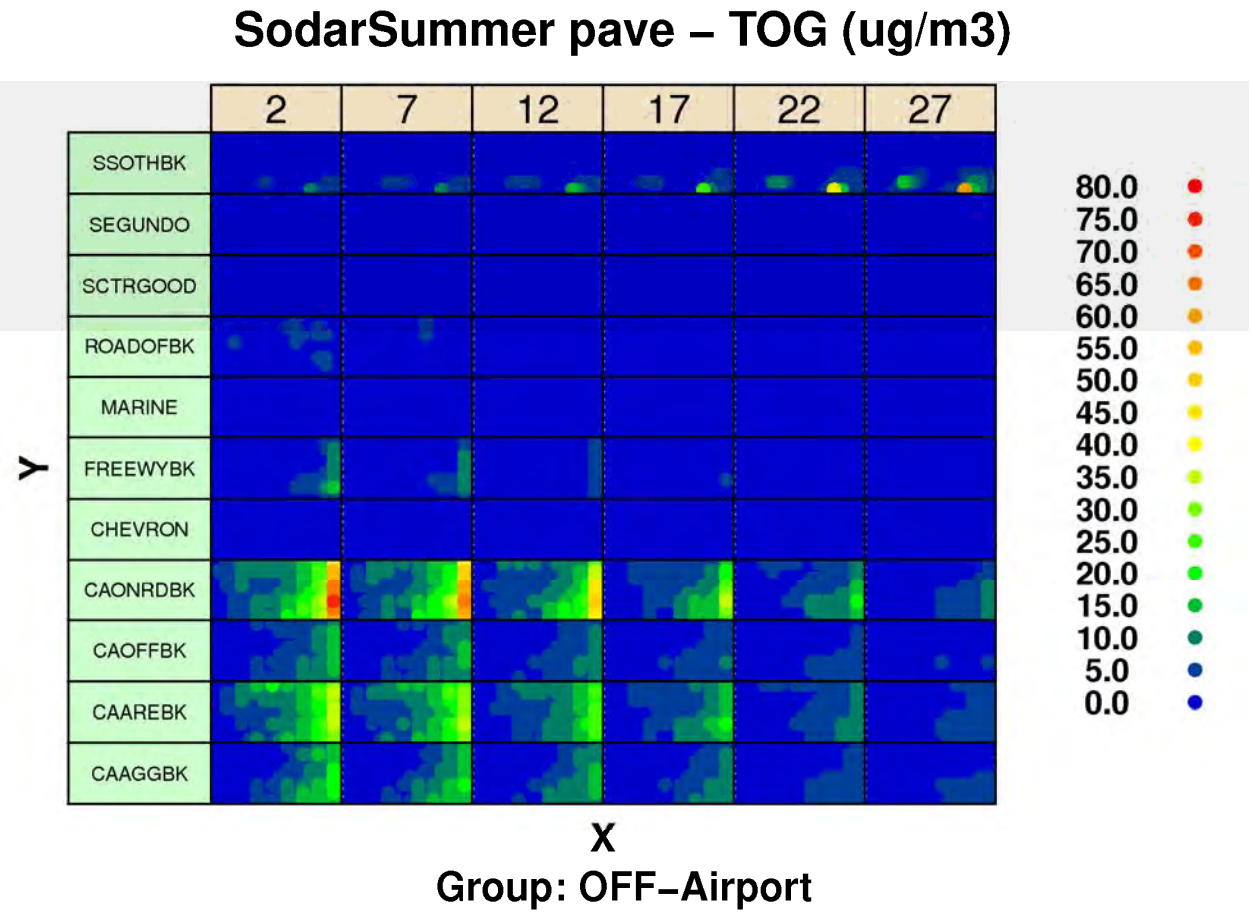

Figure 9A-152: Modeled period average TOG concentrations from background sources by source sector at flag-pole receptors at heights of 2m, 7m, 12m, 17m, 22m and 27m in Cartesian Grid of receptors during Summer Season.

II. Model Evaluation

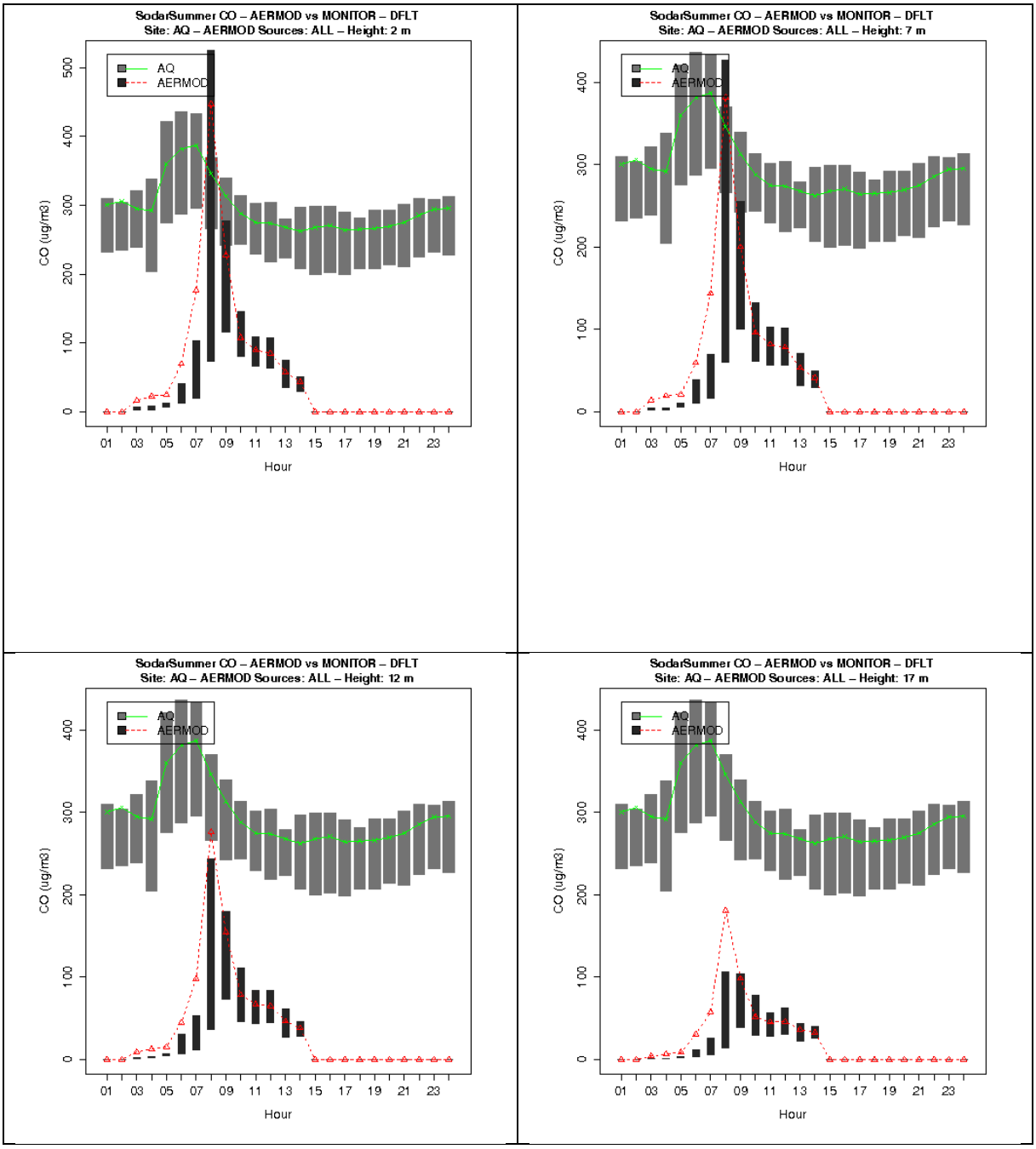

Figure 9A-153: Diurnal variability in observed and modeled CO concentrations at AQ Site from flagpole receptors at heights of 2m, 7m, 12m and 17m during Summer Season.

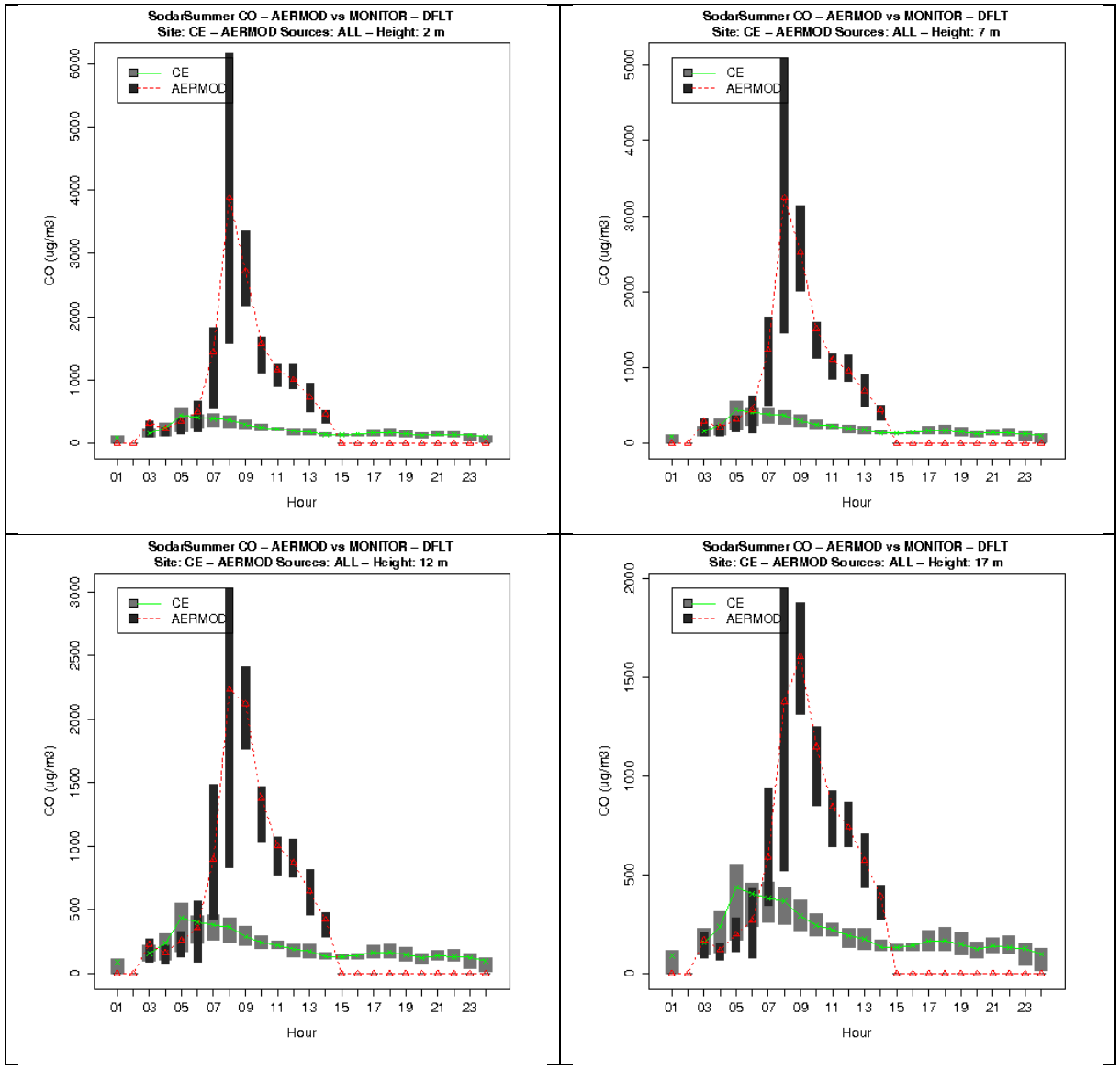

Figure 9A-154: Diurnal variability in observed and modeled CO concentrations at CE Site from flagpole receptors at heights of 2m, 7m, 12m and 17m during Summer Season.

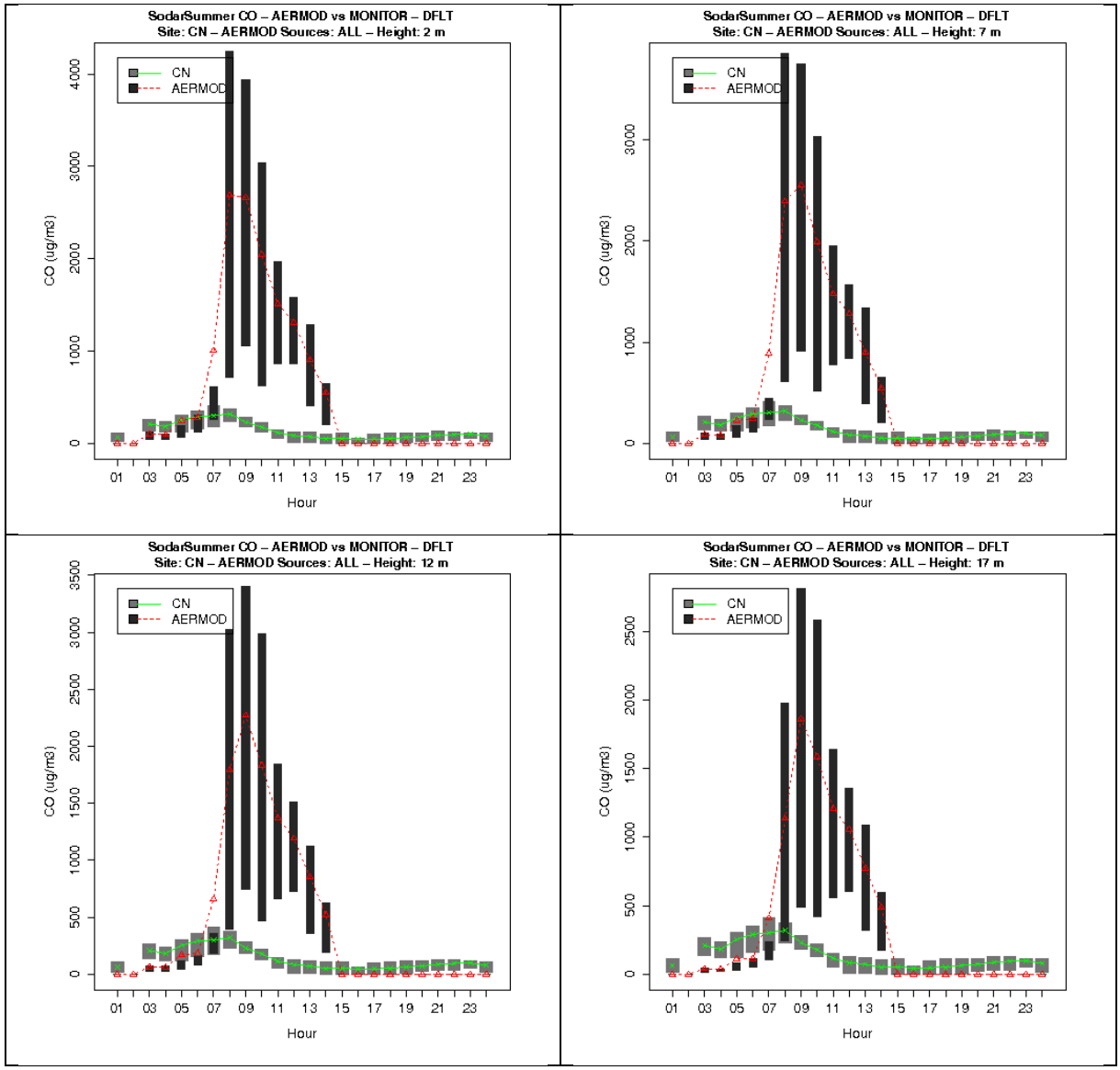

Figure 9A-155: Diurnal variability in observed and modeled CO concentrations at CN Site from flagpole receptors at heights of 2m, 7m, 12m and 17m during Summer Season.

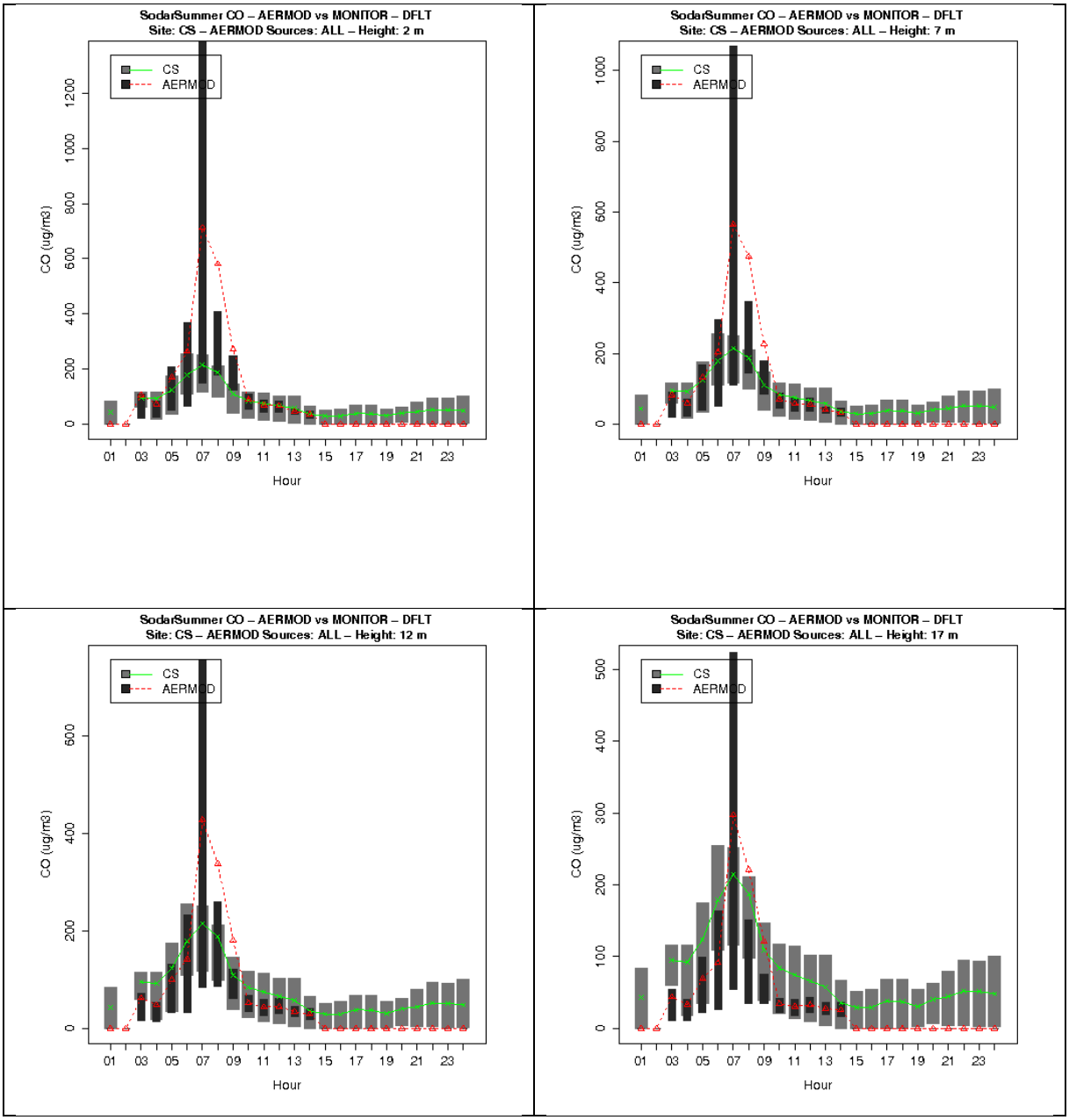

Figure 9A-156: Diurnal variability in observed and modeled CO concentrations at CS Site from flagpole receptors at heights of 2m, 7m, 12m and 17m during Summer Season.

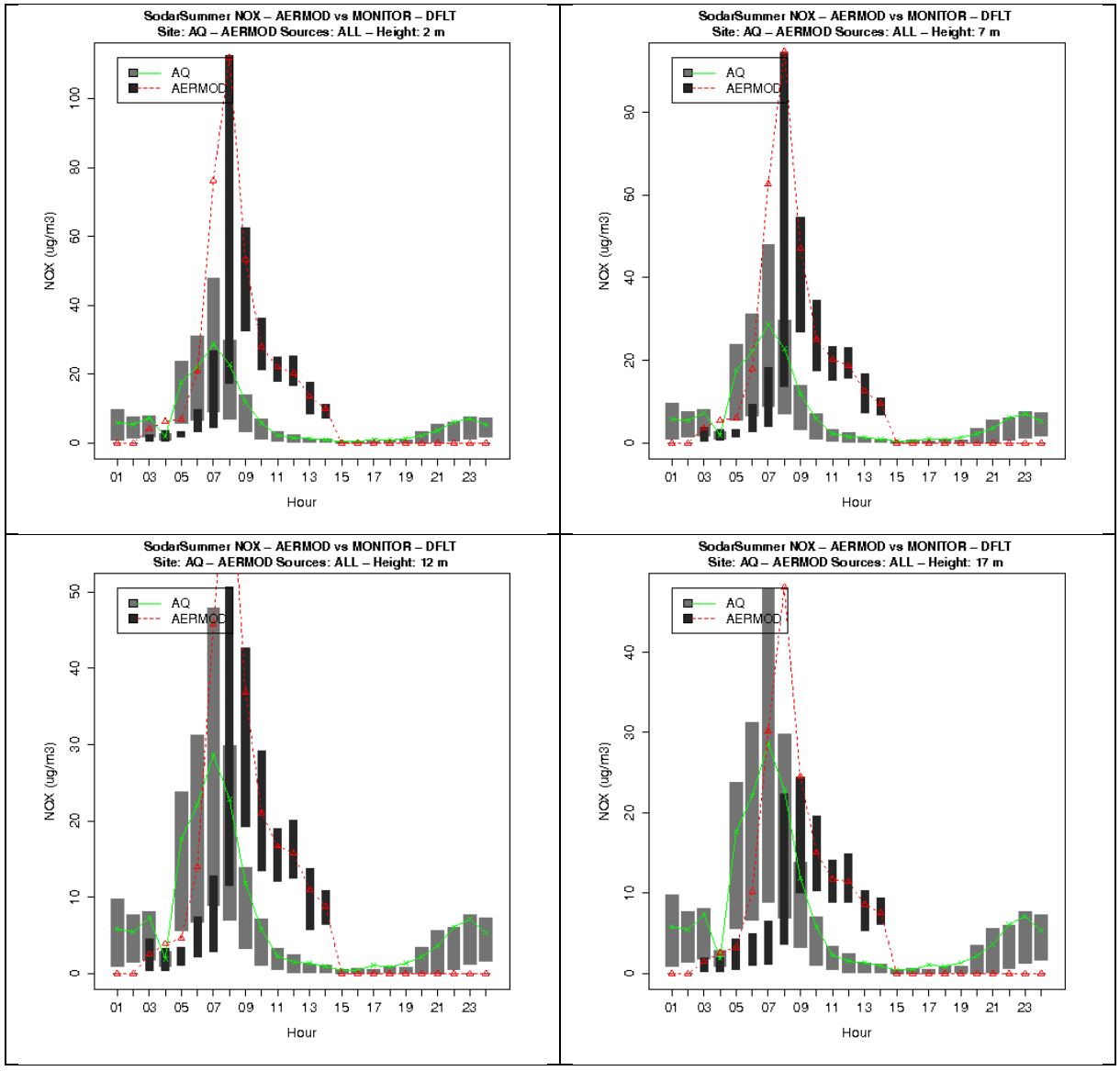

Figure 9A-157: Diurnal variability in observed and modeled NOx concentrations at AQ Site from flagpole receptors at heights of 2m, 7m, 12m and 17m during Summer Season.

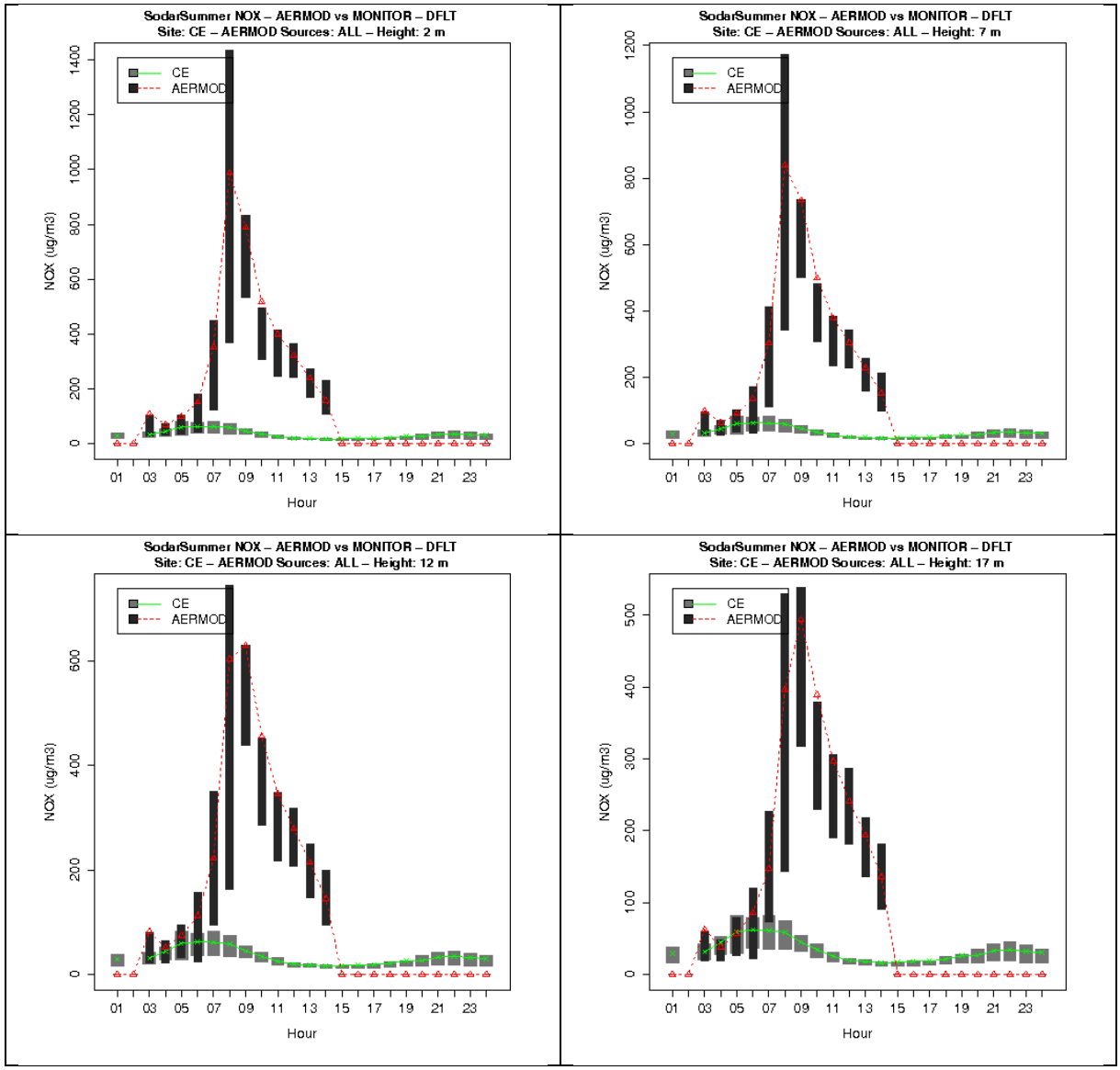

Figure 9A-158: Diurnal variability in observed and modeled NOx concentrations at CE Site from flagpole receptors at heights of 2m, 7m, 12m and 17m during Summer Season.

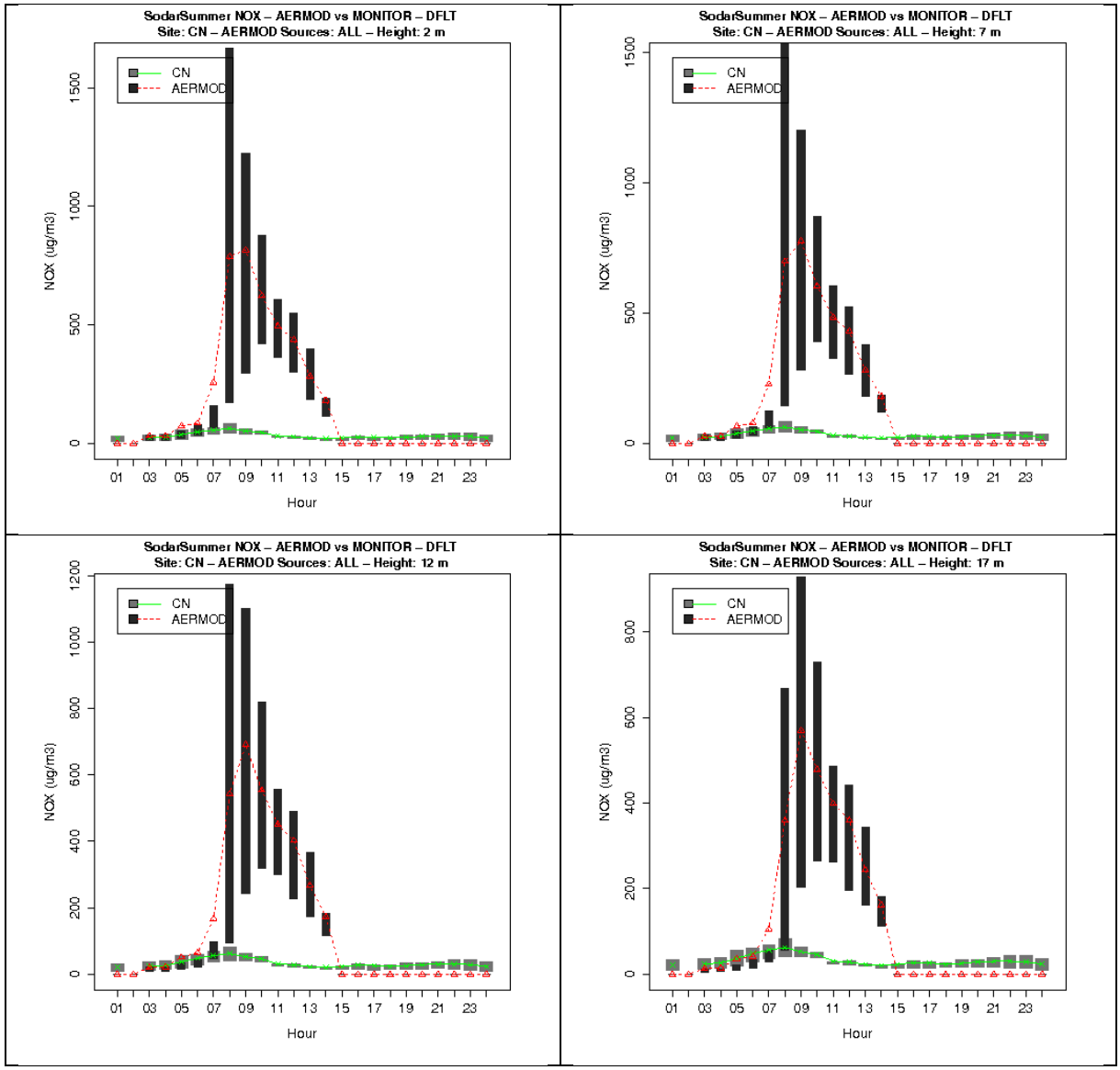

Figure 9A-159: Diurnal variability in observed and modeled NOx concentrations at CN Site from flagpole receptors at heights of 2m, 7m, 12m and 17m during Summer Season.

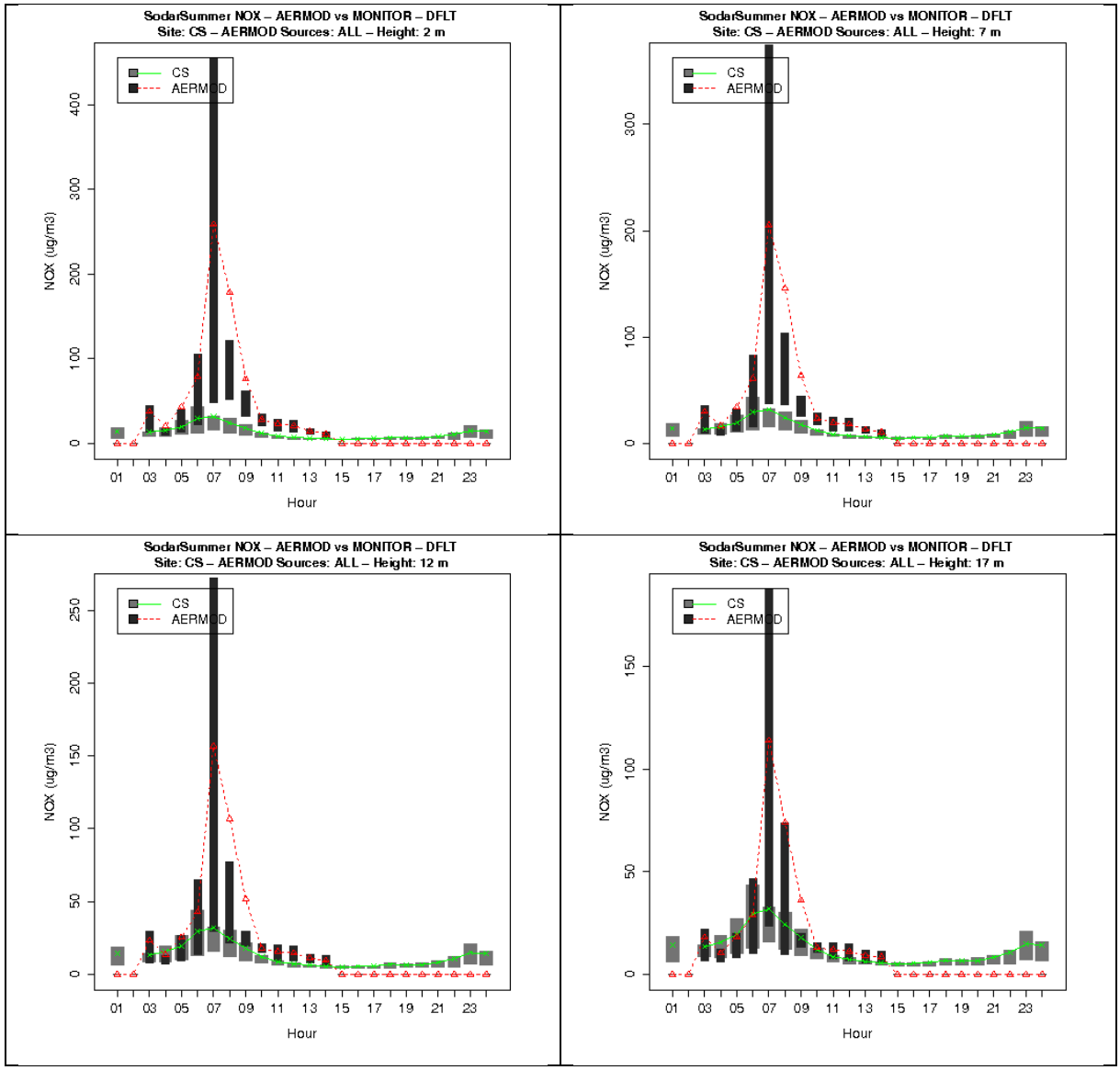

Figure 9A-160: Diurnal variability in observed and modeled NOx concentrations at CS Site from flagpole receptors at heights of 2m, 7m, 12m and 17m during Summer Season.

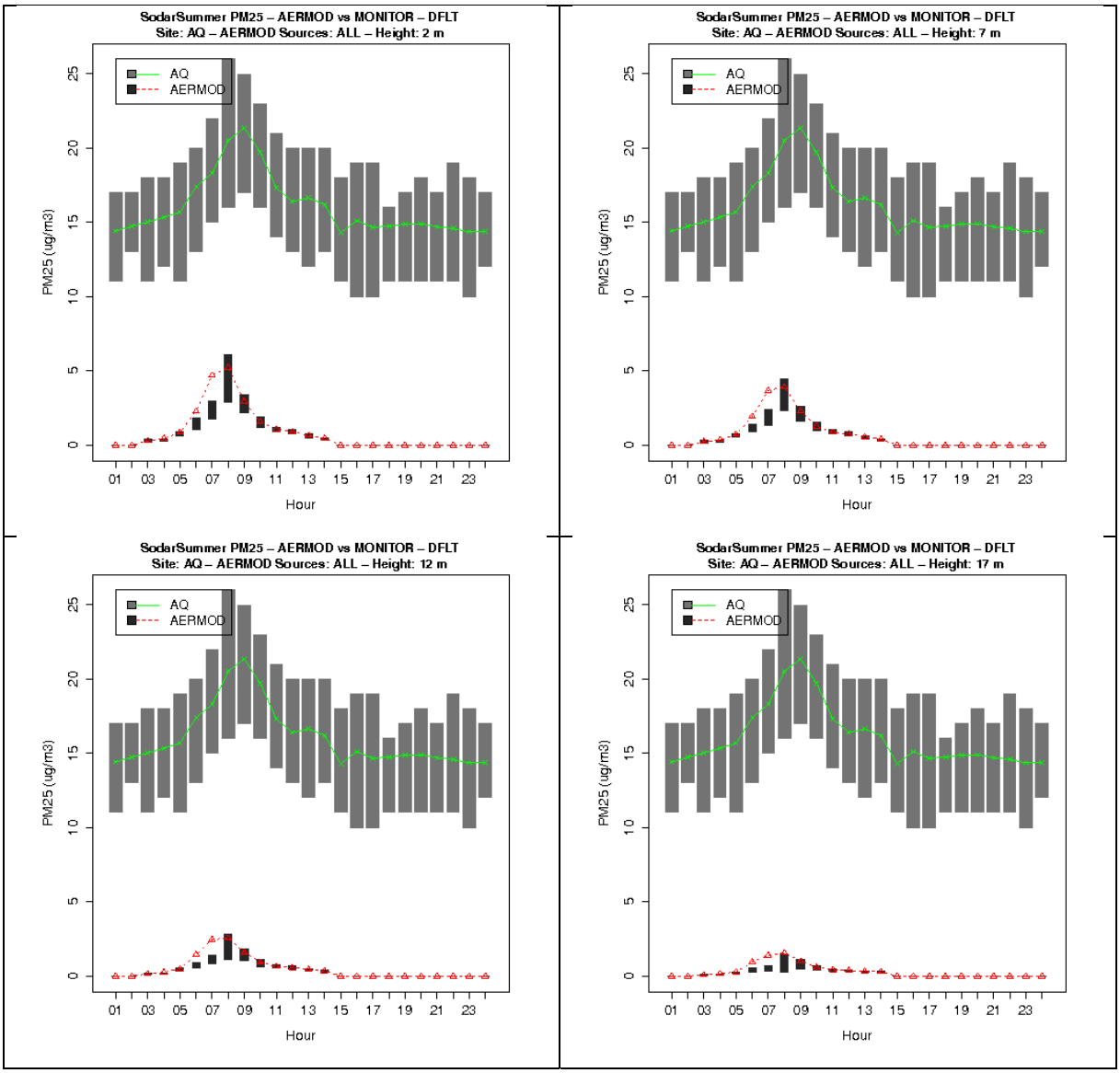

Figure 9A-161: Diurnal variability in observed and modeled $PM_{2.5}$ concentrations at AQ Site from flagpole receptors at heights of 2m, 7m, 12m and 17m during Summer Season.

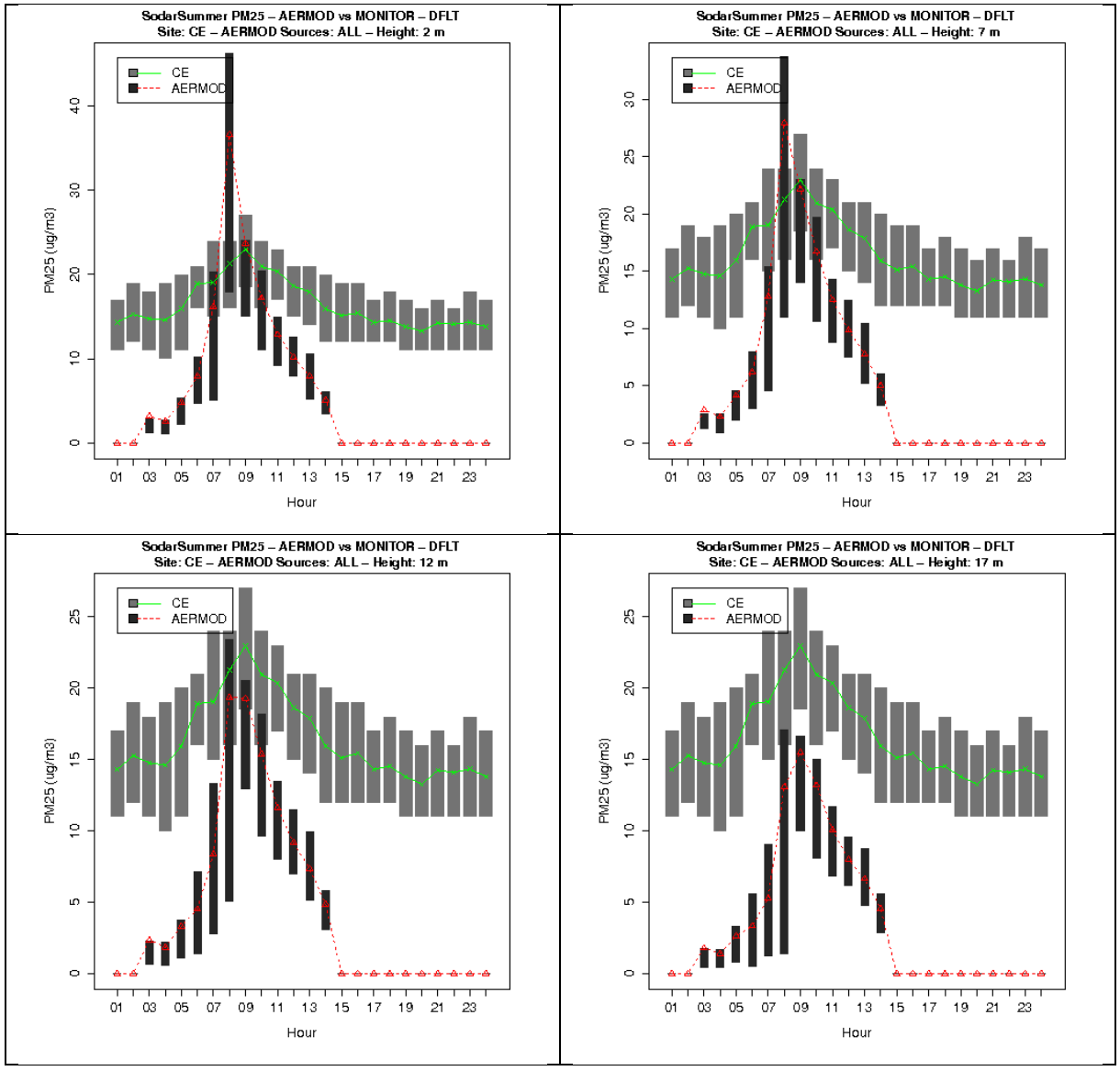

Figure 9A-162: Diurnal variability in observed and modeled $PM_{2.5}$ concentrations at CE Site from flagpole receptors at heights of 2m, 7m, 12m and 17m during Summer Season.

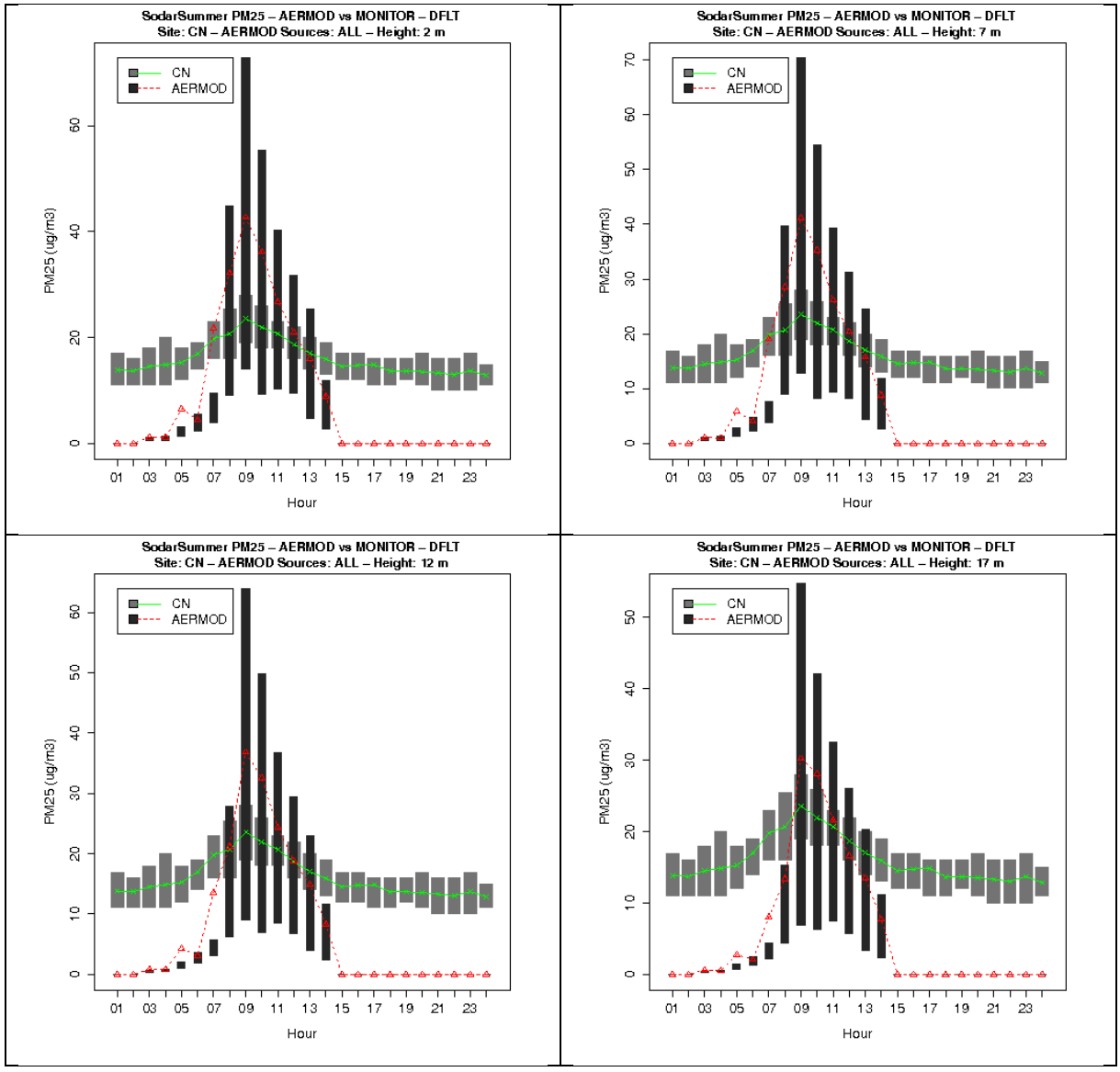

Figure 9A-163: Diurnal variability in observed and modeled $PM_{2.5}$ concentrations at CN Site from flagpole receptors at heights of 2m, 7m, 12m and 17m during Summer Season.

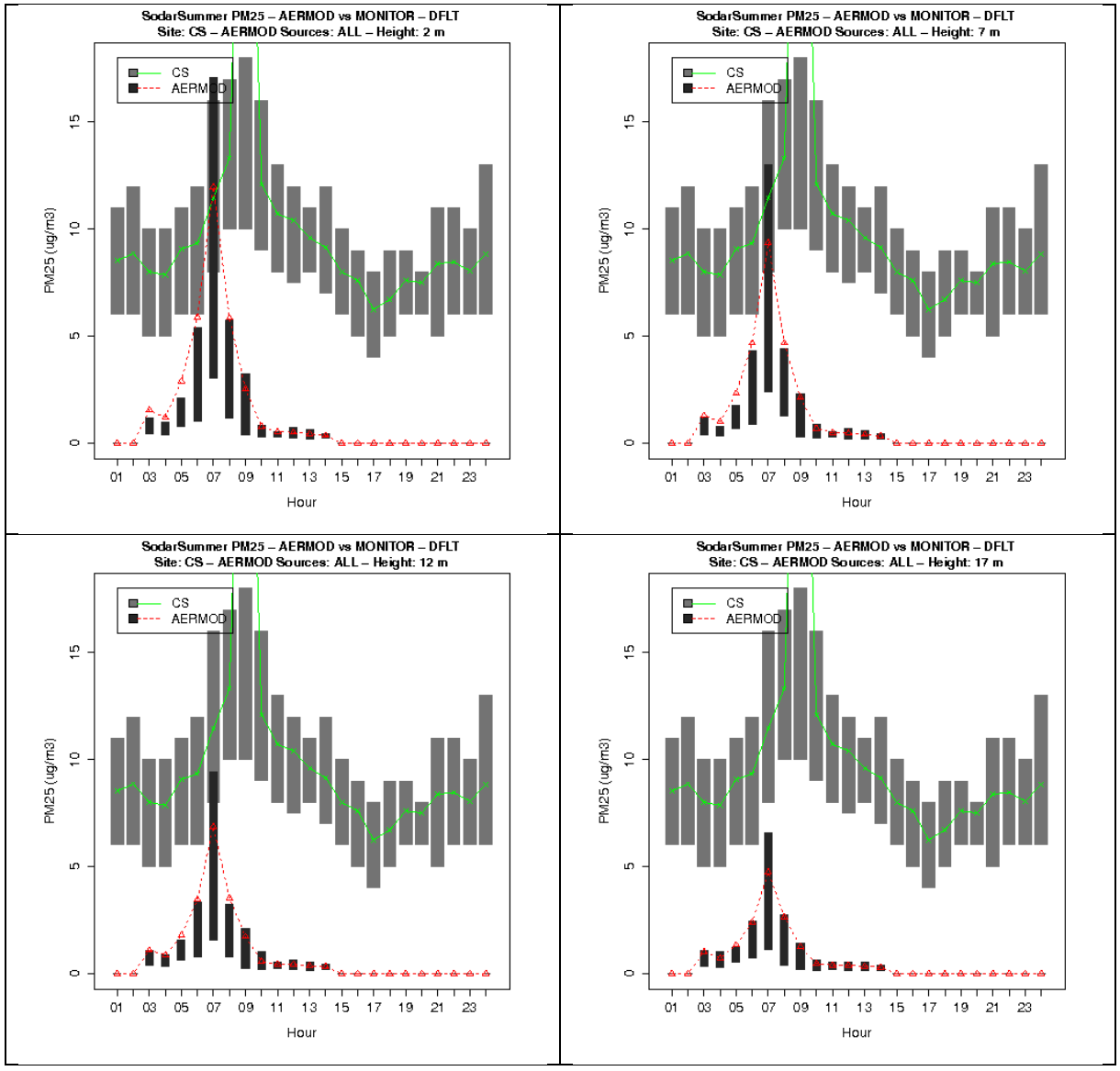

Figure 9A-164: Diurnal variability in observed and modeled $PM_{2.5}$ concentrations at CS Site from flagpole receptors at heights of 2m, 7m, 12m and 17m during Summer Season.

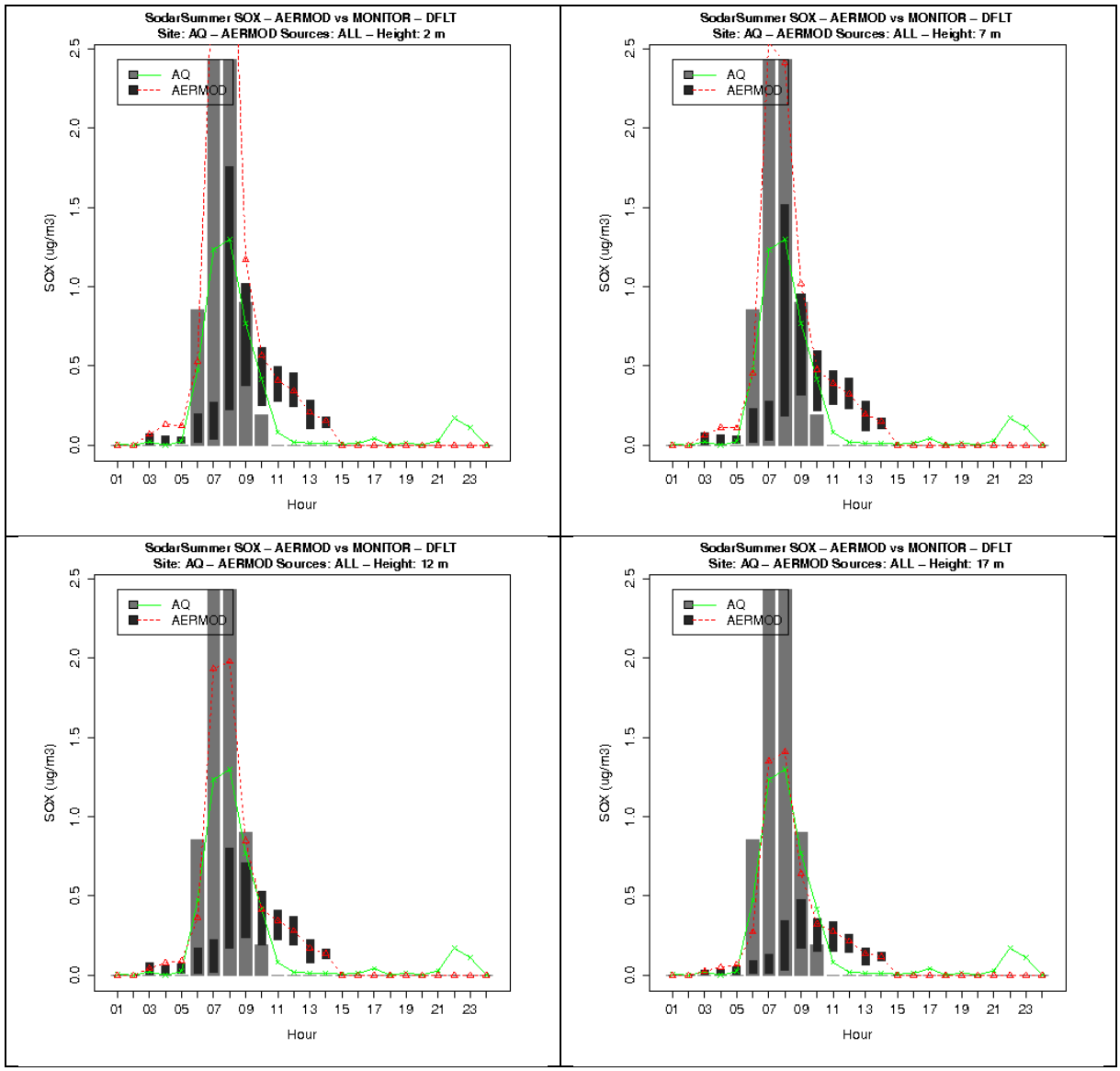

Figure 9A-165: Diurnal variability in observed and modeled SOx concentrations at AQ Site from flagpole receptors at heights of 2m, 7m, 12m and 17m during Summer Season.

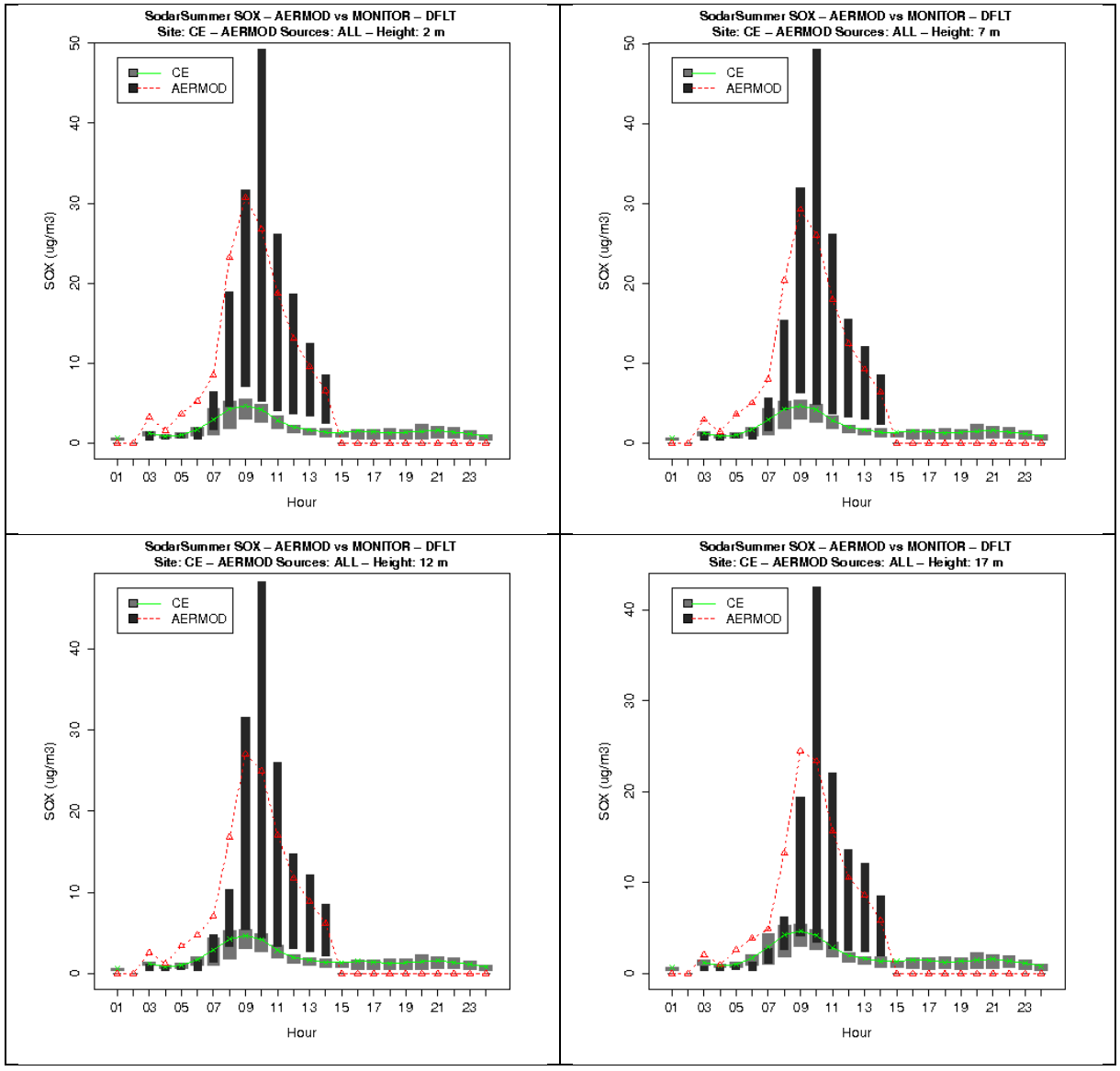

Figure 9A-166: Diurnal variability in observed and modeled SOx concentrations at CE Site from flagpole receptors at heights of 2m, 7m, 12m and 17m during Summer Season.

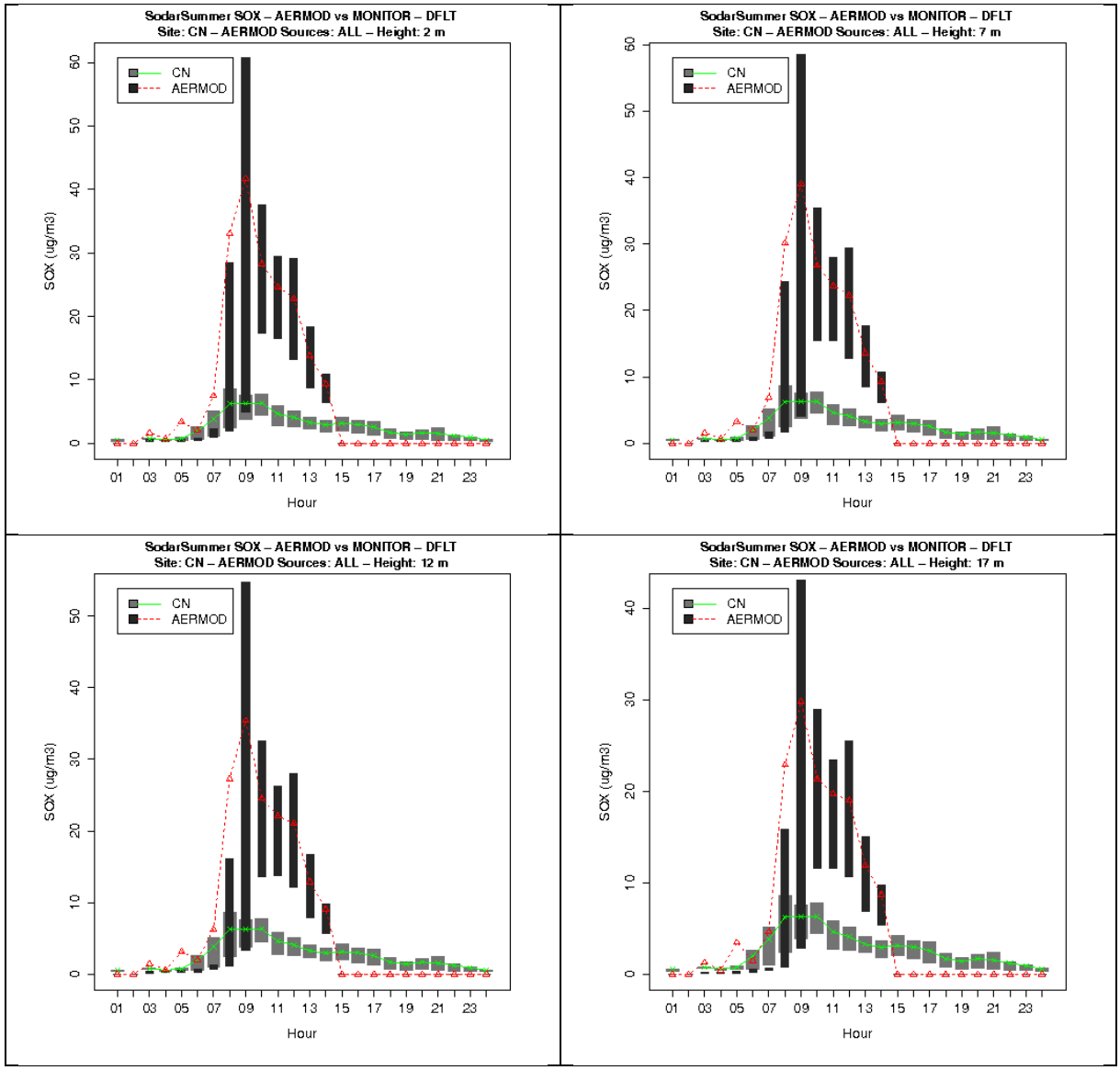

Figure 9A-167: Diurnal variability in observed and modeled SOx concentrations at CN Site from flagpole receptors at heights of 2m, 7m, 12m and 17m during Summer Season.

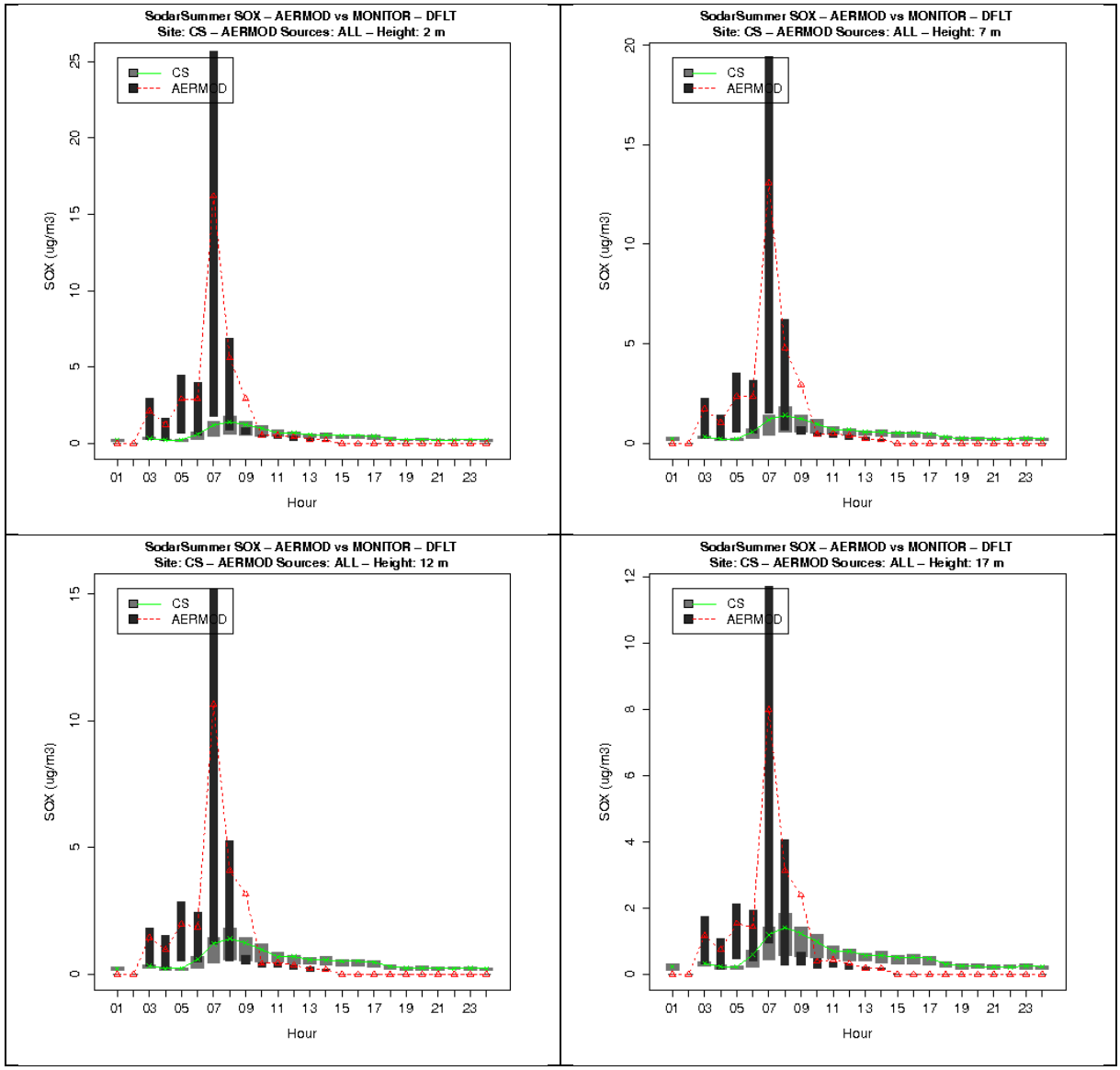

Figure 9A-168: Diurnal variability in observed and modeled SOx concentrations at CS Site from flagpole receptors at heights of 2m, 7m, 12m and 17m during Summer Season.

II. Source Attribution

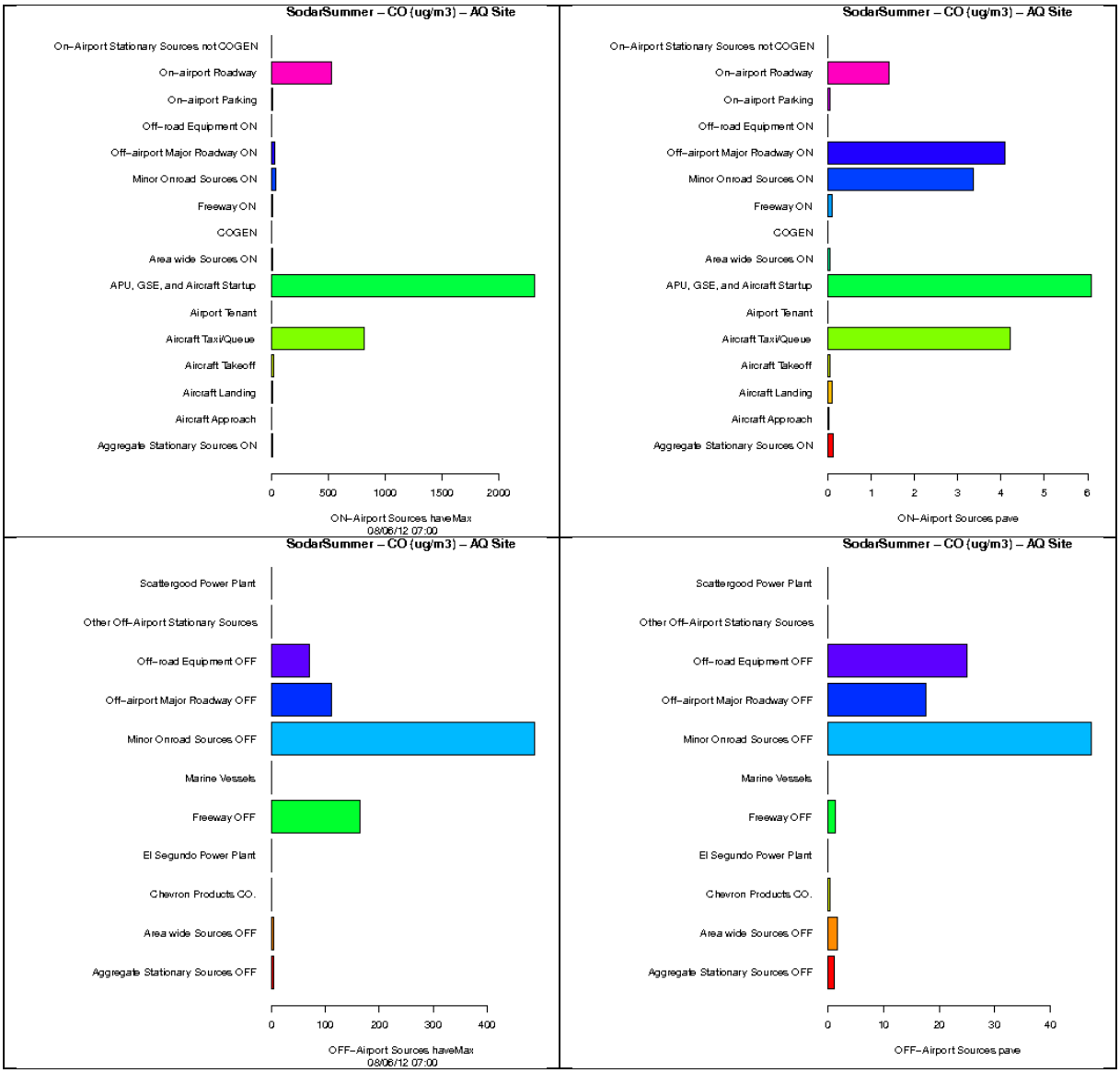

Figure 9A-169: Source-sector contributions to Hourly Maximum (left) and Period Average CO concentrations at AQ Site from airport-related sources (top) and background sources (bottom) during Summer Season. [The date and hour when the maximum 1-hour concentration was predicted is shown at the bottom of the figures on the left].

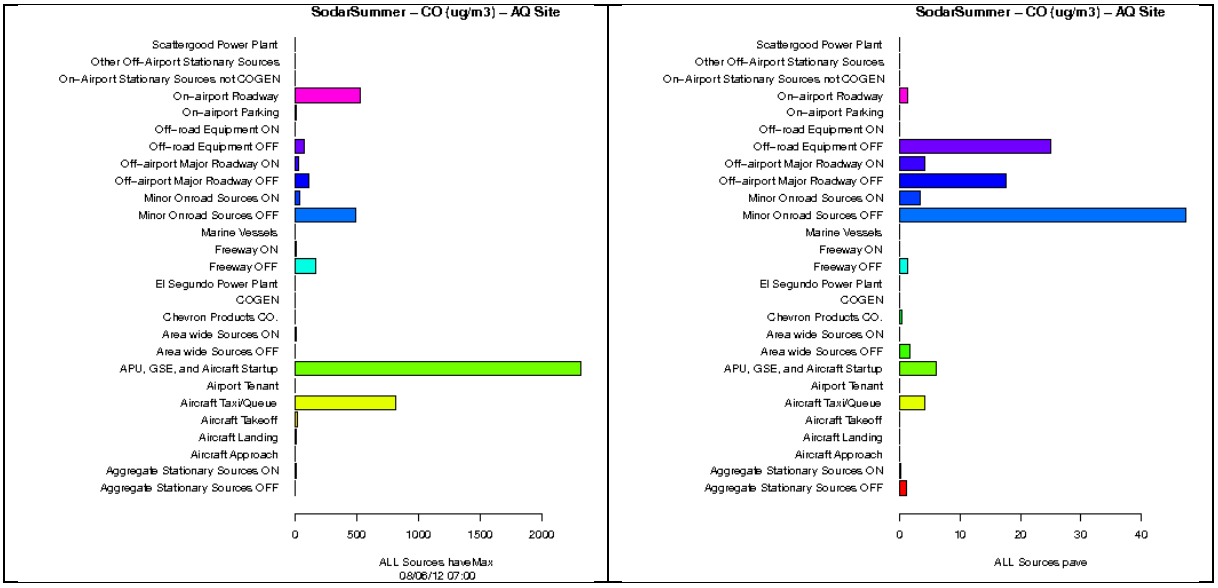

Figure 9A-170: Source-sector contributions to Hourly Maximum (left) and Period Average CO concentrations at AQ Site from ALL sources during Summer Season.

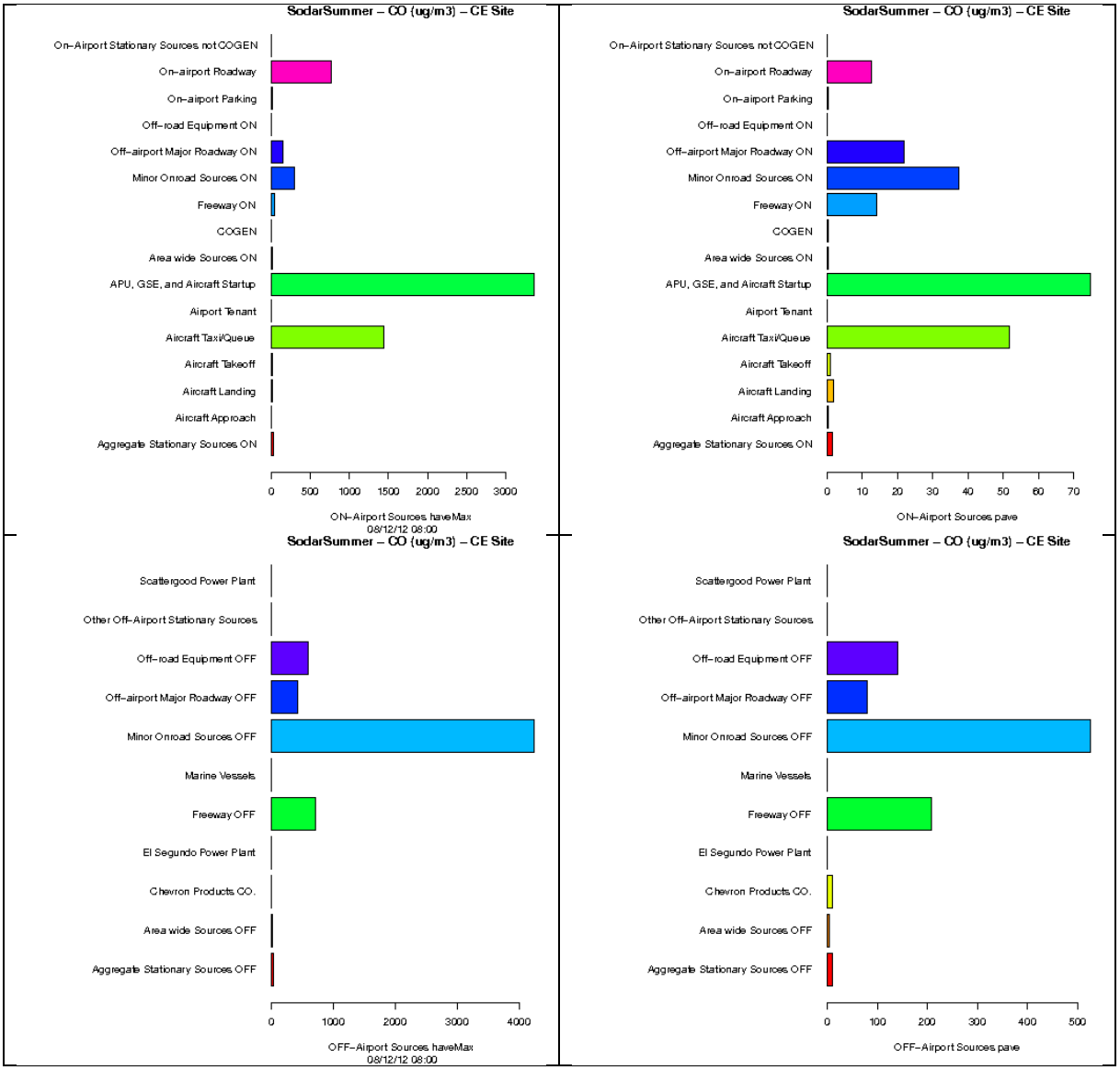

Figure 9A-171: Source-sector contributions to Hourly Maximum (left) and Period Average CO concentrations at CE Site from airport-related sources (top) and background sources (bottom) during Summer Season.

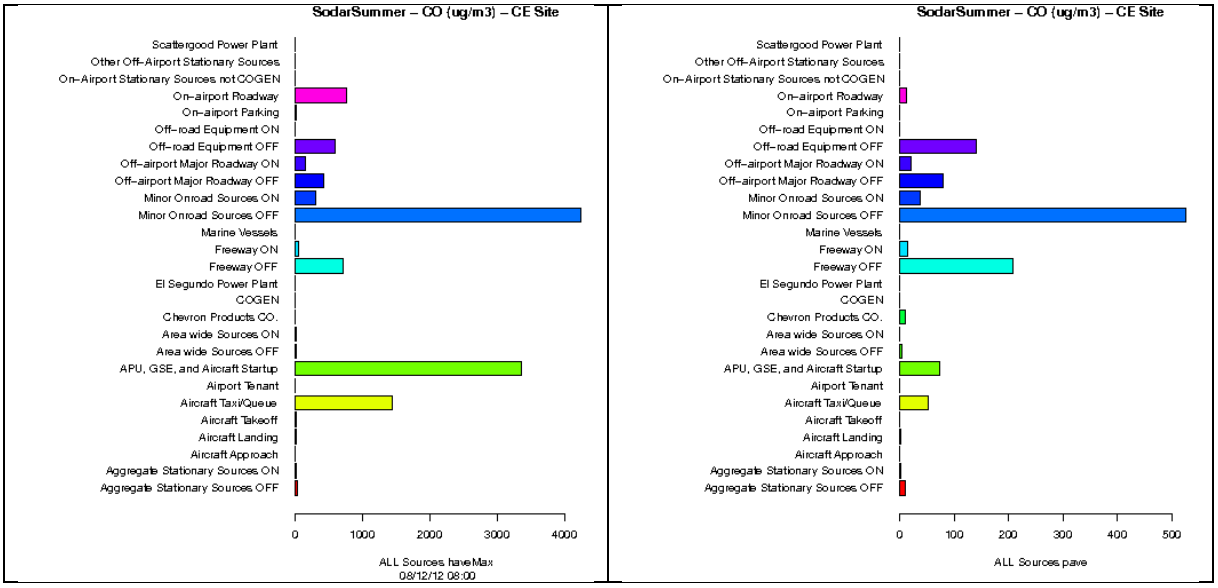

Figure 9A-172: Source-sector contributions to Hourly Maximum (left) and Period Average CO concentrations at CE Site from ALL sources during Summer Season.

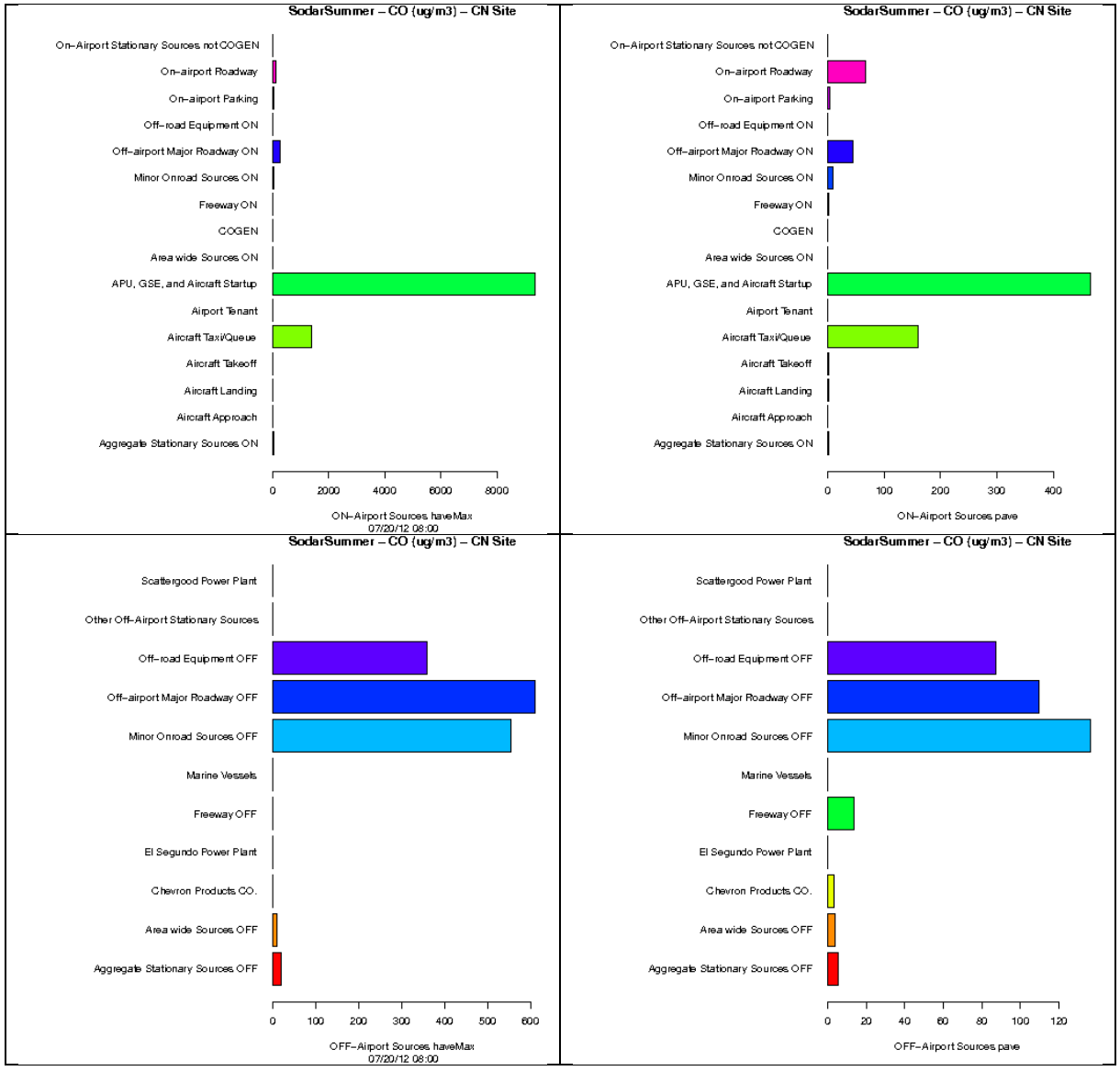

Figure 9A-173: Source-sector contributions to Hourly Maximum (left) and Period Average CO concentrations at CN Site from airport-related sources (top) and background sources (bottom) during Summer Season.

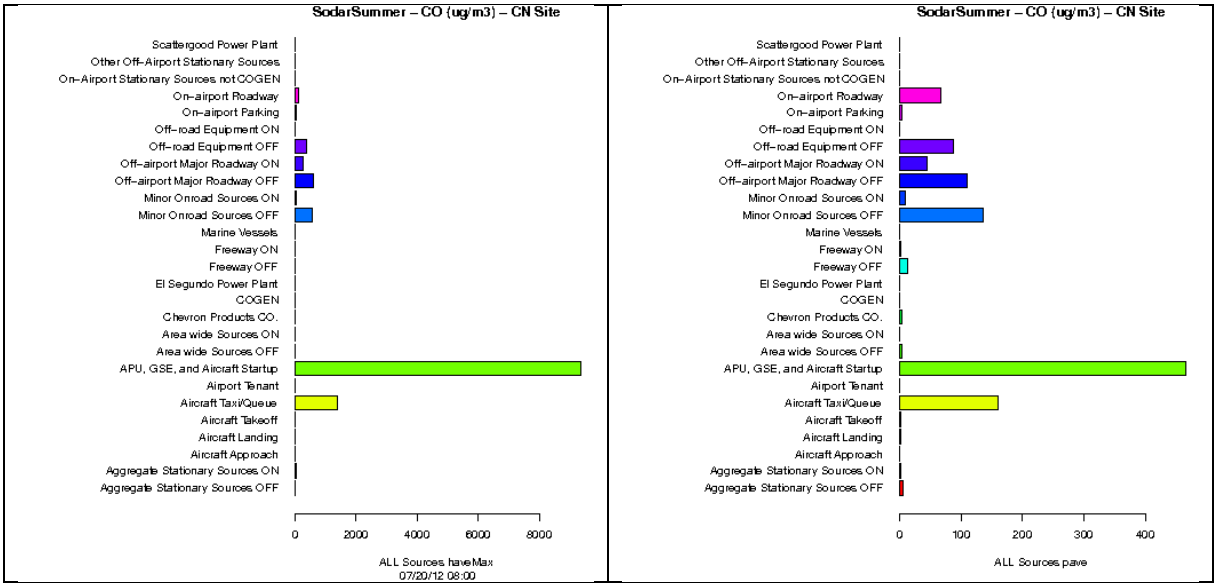

Figure 9A-174: Source-sector contributions to Hourly Maximum (left) and Period Average CO concentrations at CN Site from ALL sources during Summer Season.

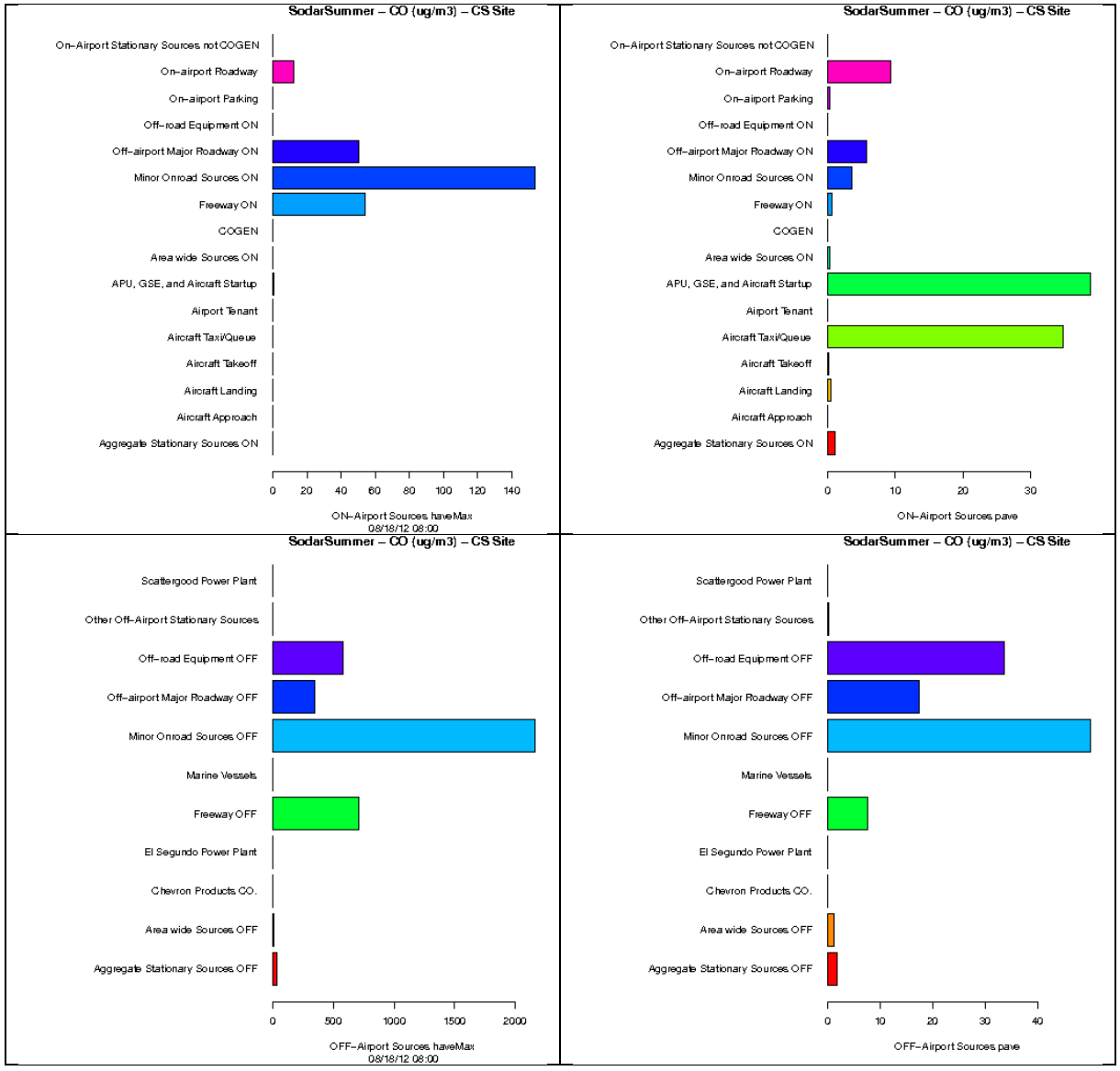

Figure 9A-175: Source-sector contributions to Hourly Maximum (left) and Period Average CO concentrations at CS Site from airport-related sources (top) and background sources (bottom) during Summer Season.

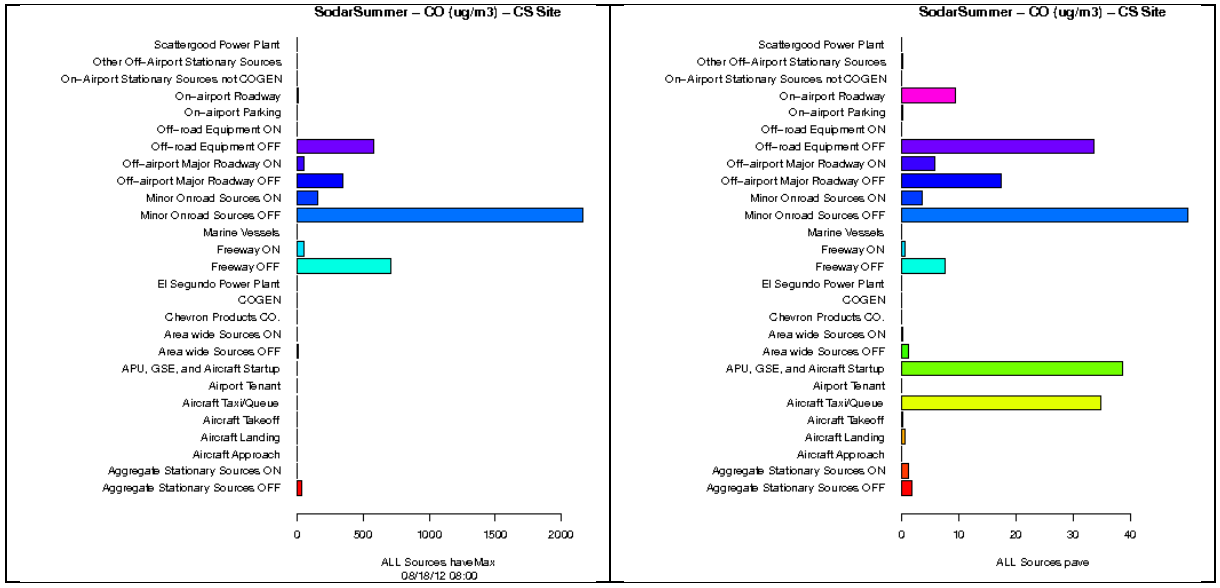

Figure 9A-176: Source-sector contributions to Hourly Maximum (left) and Period Average CO concentrations at CS Site from ALL sources during Summer Season.

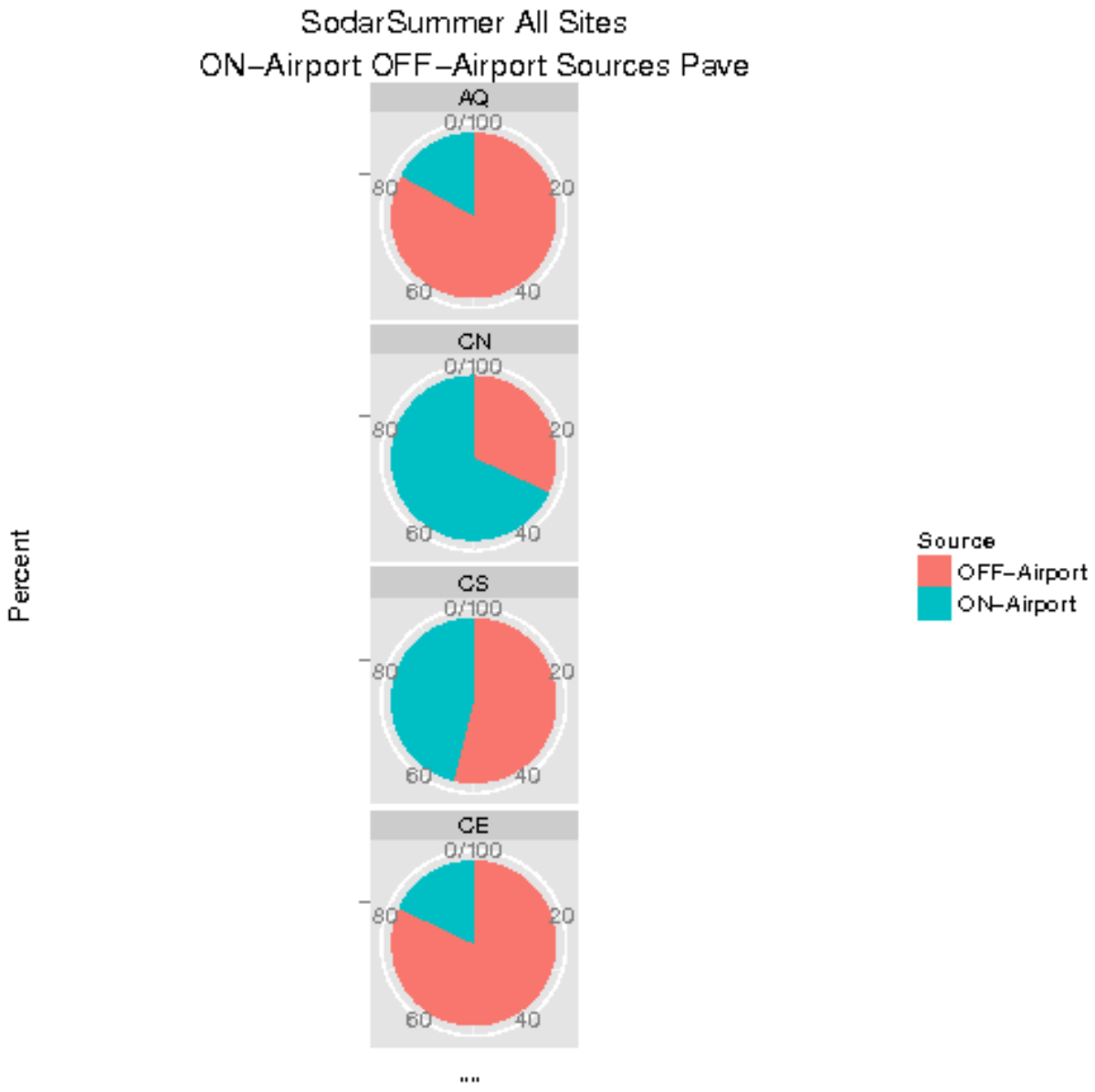

Figure 9A-177: Source-sector contributions to Period Average CO concentrations at each site from airport-related vs. background sources during Summer Season.

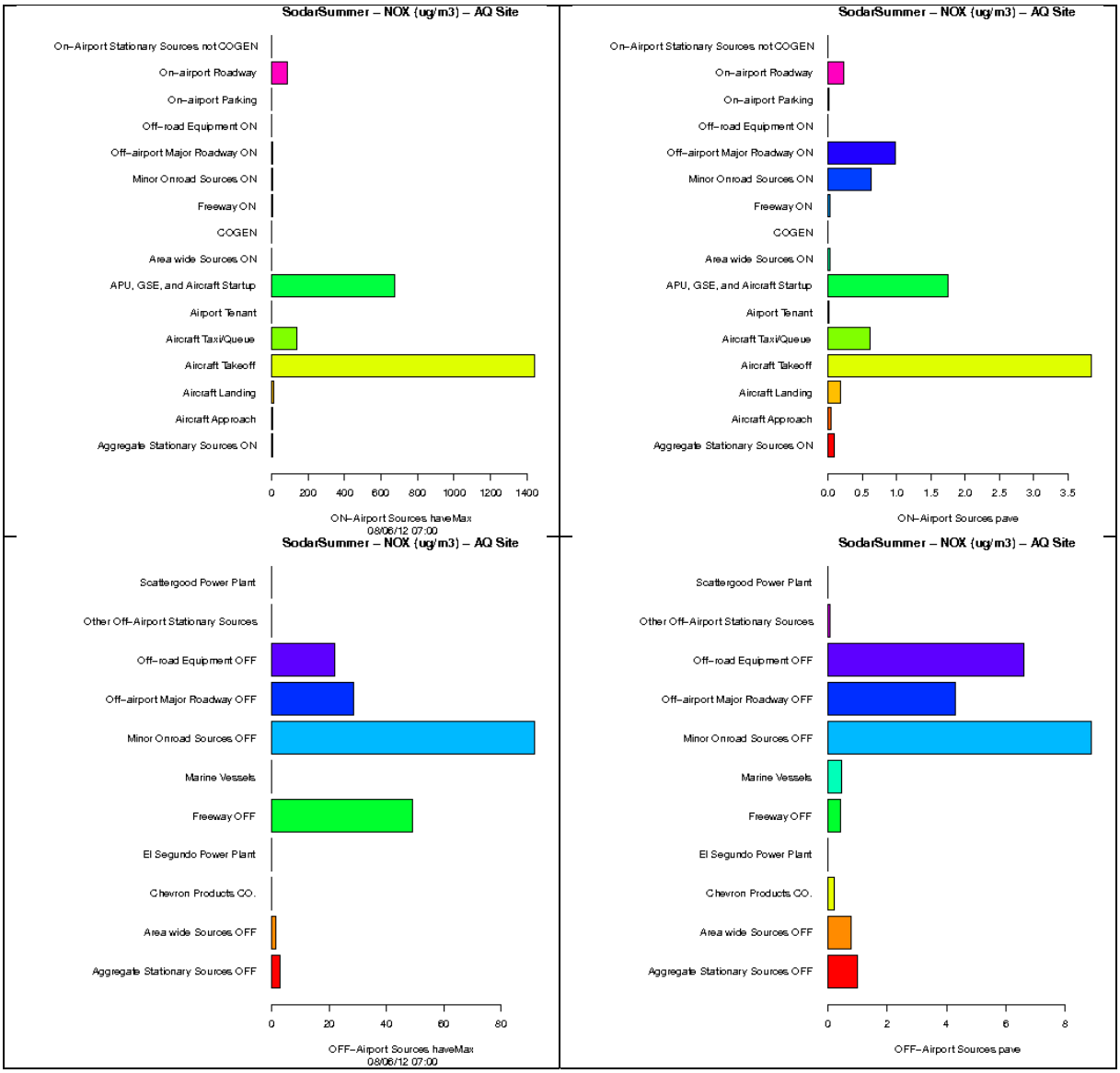

Figure 9A-178: Source-sector contributions to Hourly Maximum (left) and Period Average NOx concentrations at AQ Site from airport-related sources (top) and background sources (bottom) during Summer Season.

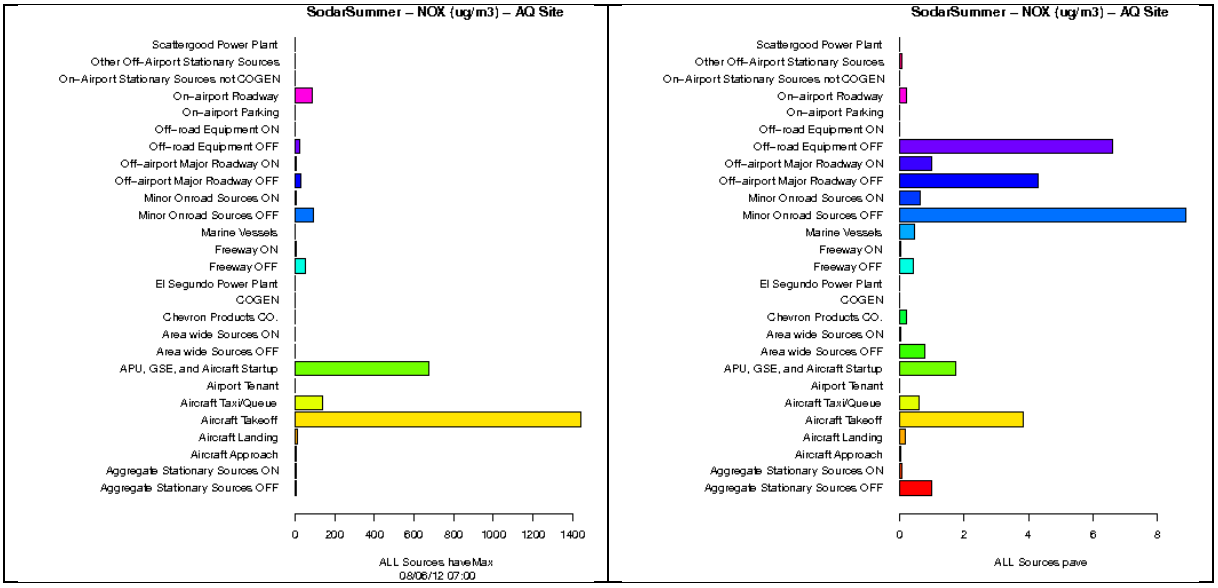

Figure 9A-179: Source-sector contributions to Hourly Maximum (left) and Period Average NOx concentrations at AQ Site from ALL sources during Summer Season.

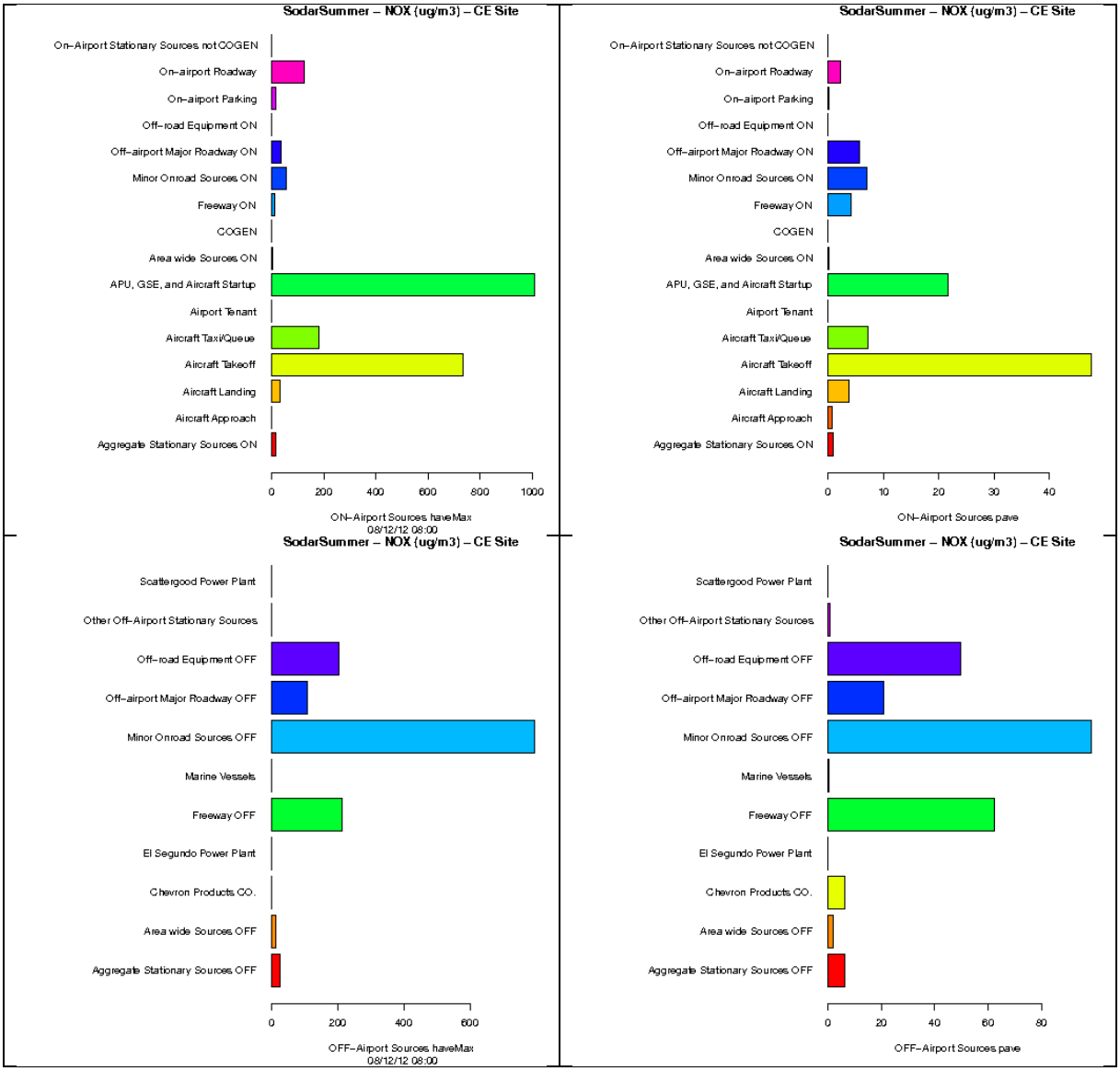

Figure 9A-180: Source-sector contributions to Hourly Maximum (left) and Period Average NOx concentrations at CE Site from airport-related sources (top) and background sources (bottom) during Summer Season.

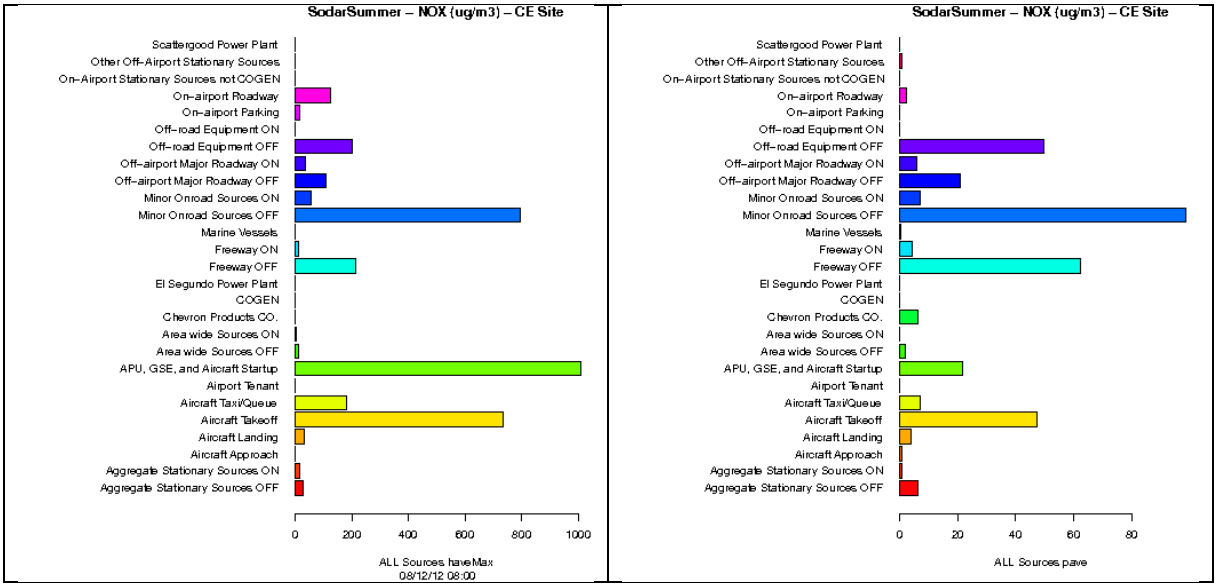

Figure 9A-181: Source-sector contributions to Hourly Maximum (left) and Period Average NOx concentrations at CE Site from ALL sources during Summer Season.

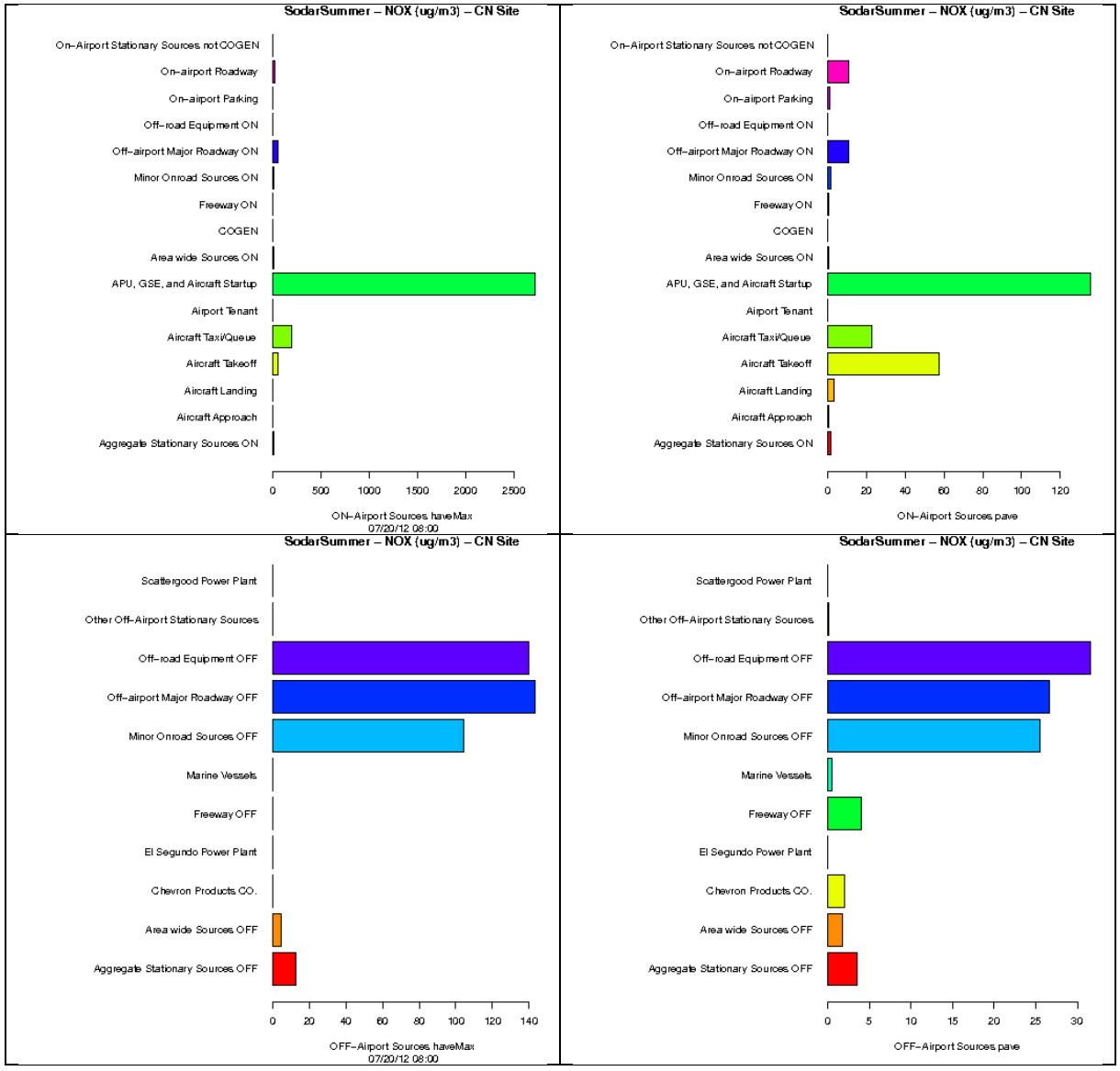

Figure 9A-182: Source-sector contributions to Hourly Maximum (left) and Period Average NOx concentrations at CN Site from airport-related sources (top) and background sources (bottom) during Summer Season.

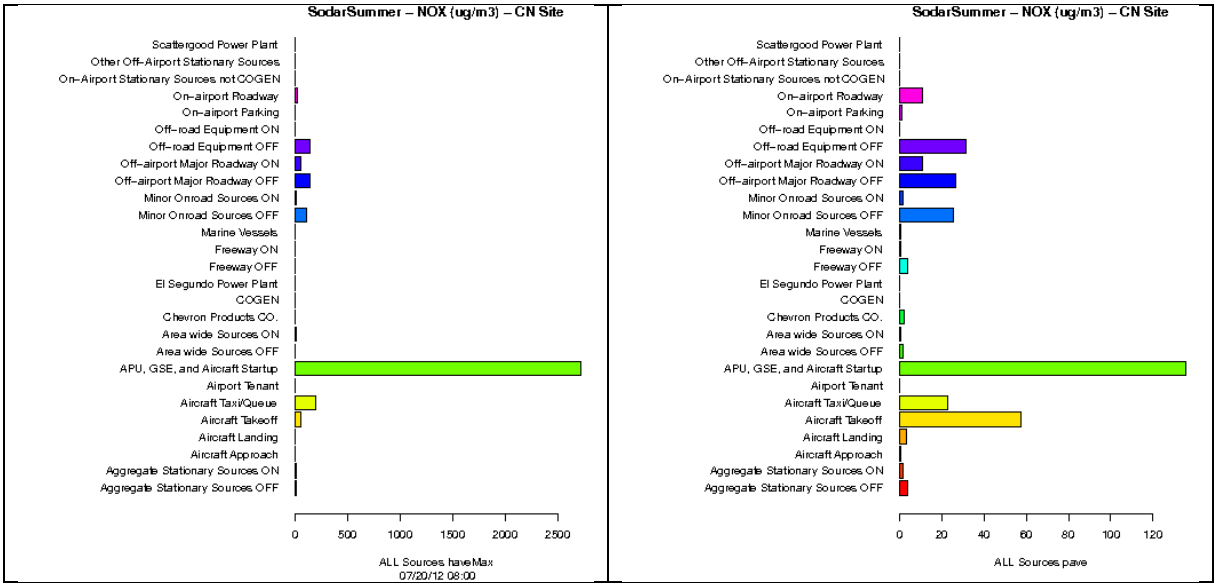

Figure 9A-183: Source-sector contributions to Hourly Maximum (left) and Period Average NOx concentrations at CN Site from ALL sources during Summer Season.

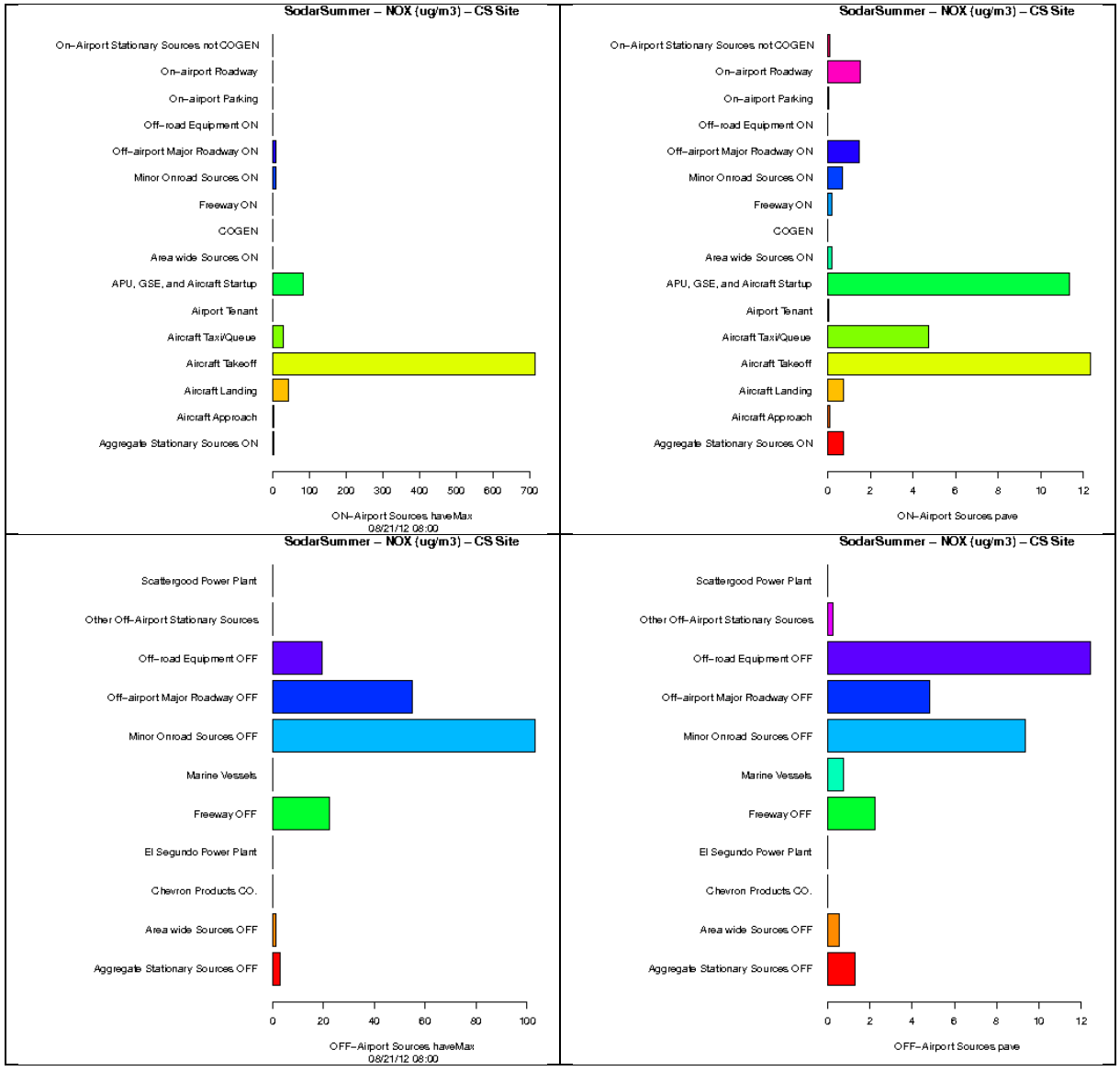

Figure 9A-184: Source-sector contributions to Hourly Maximum (left) and Period Average NOx concentrations at CS Site from airport-related sources (top) and background sources (bottom) during Summer Season.

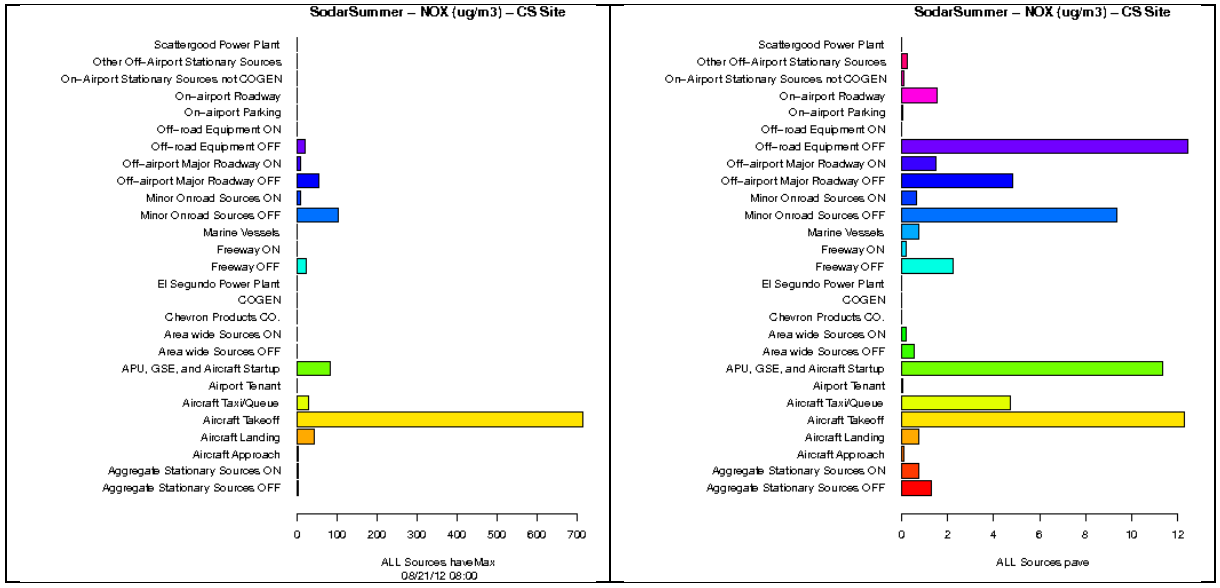

Figure 9A-185: Source-sector contributions to Hourly Maximum (left) and Period Average NOx concentrations at CS Site from ALL sources during Summer Season.

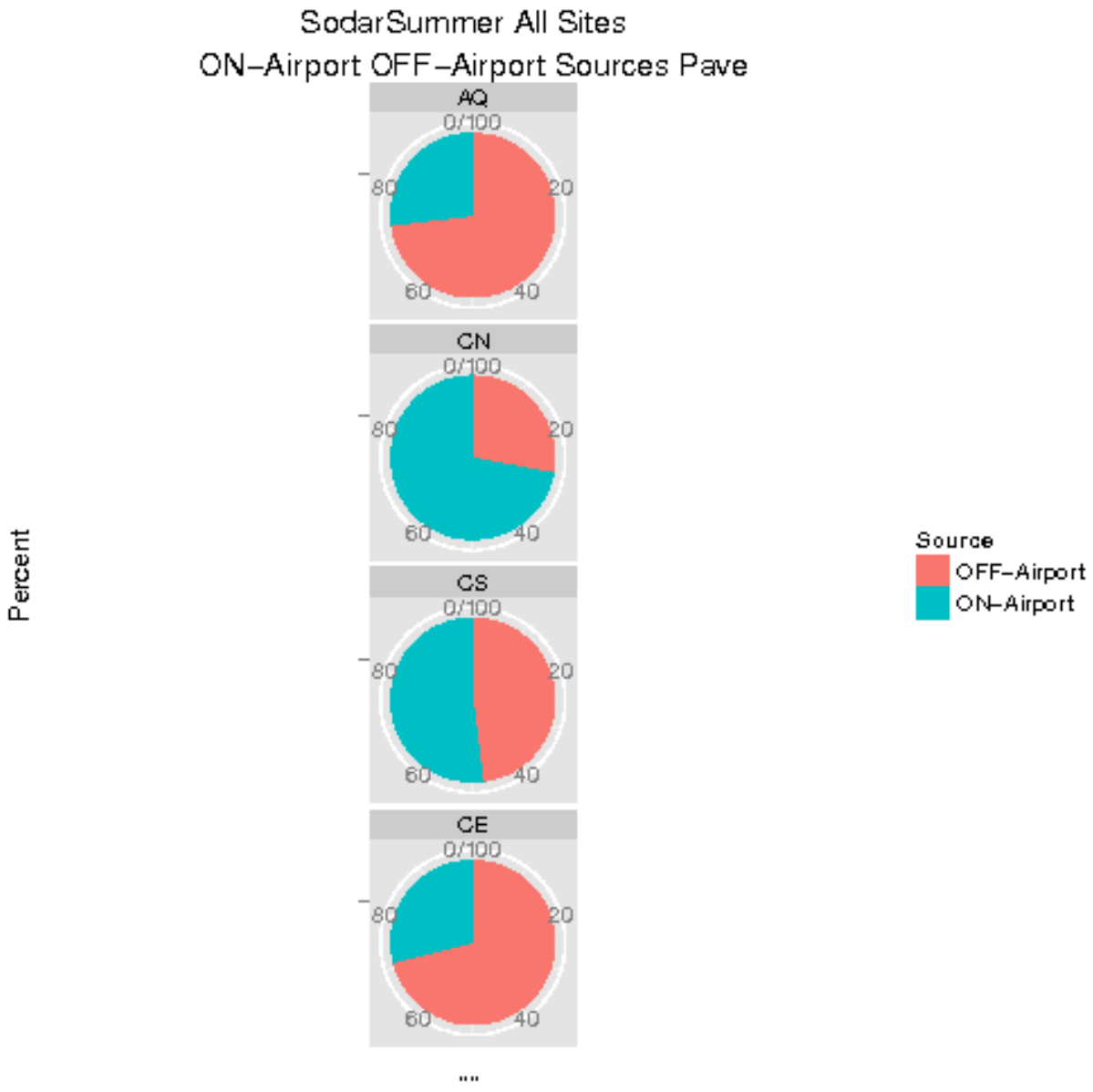

Figure 9A-186: Source-sector contributions to Period Average NOx concentrations at each site from airport-related vs. background sources during Summer Season.

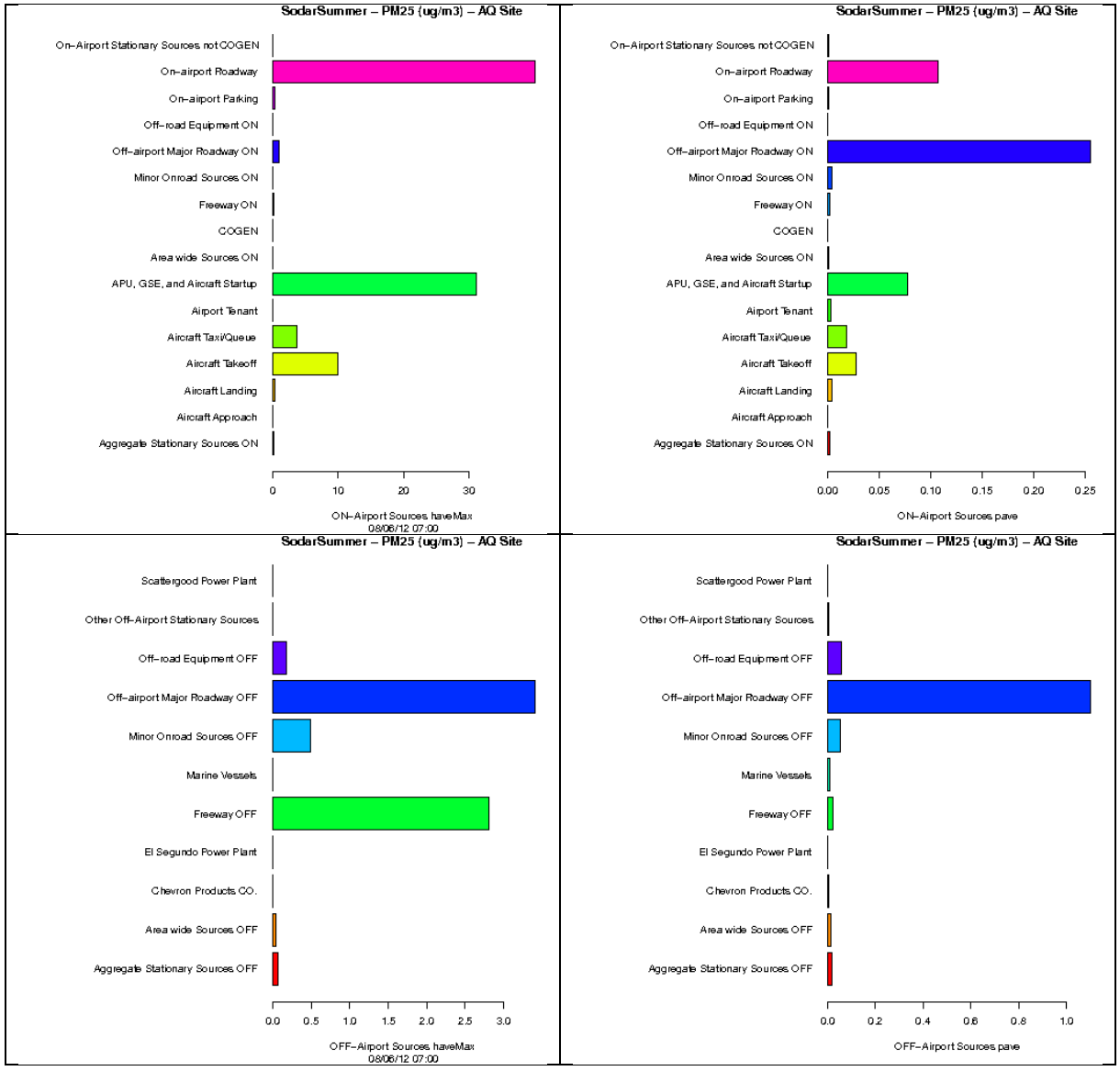

Figure 9A-187: Source-sector contributions to Hourly Maximum (left) and Period Average $PM_{2.5}$ concentrations at AQ Site from airport-related sources (top) and background sources (bottom) during Summer Season.

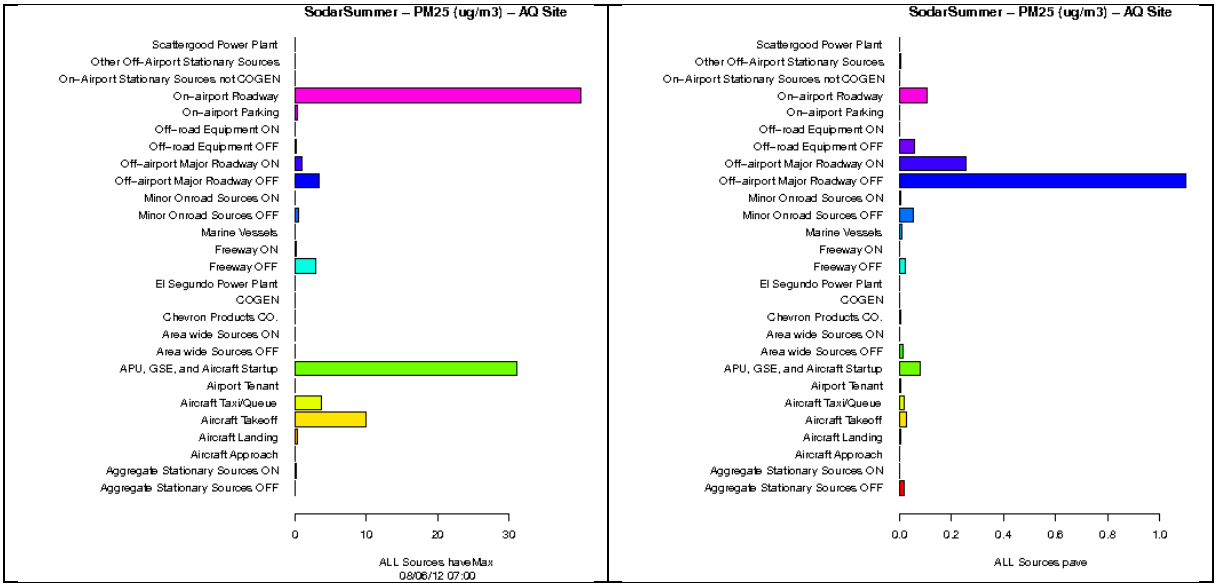

Figure 9A-188: Source-sector contributions to Hourly Maximum (left) and Period Average $PM_{2.5}$ concentrations at AQ Site from ALL sources during Summer Season.

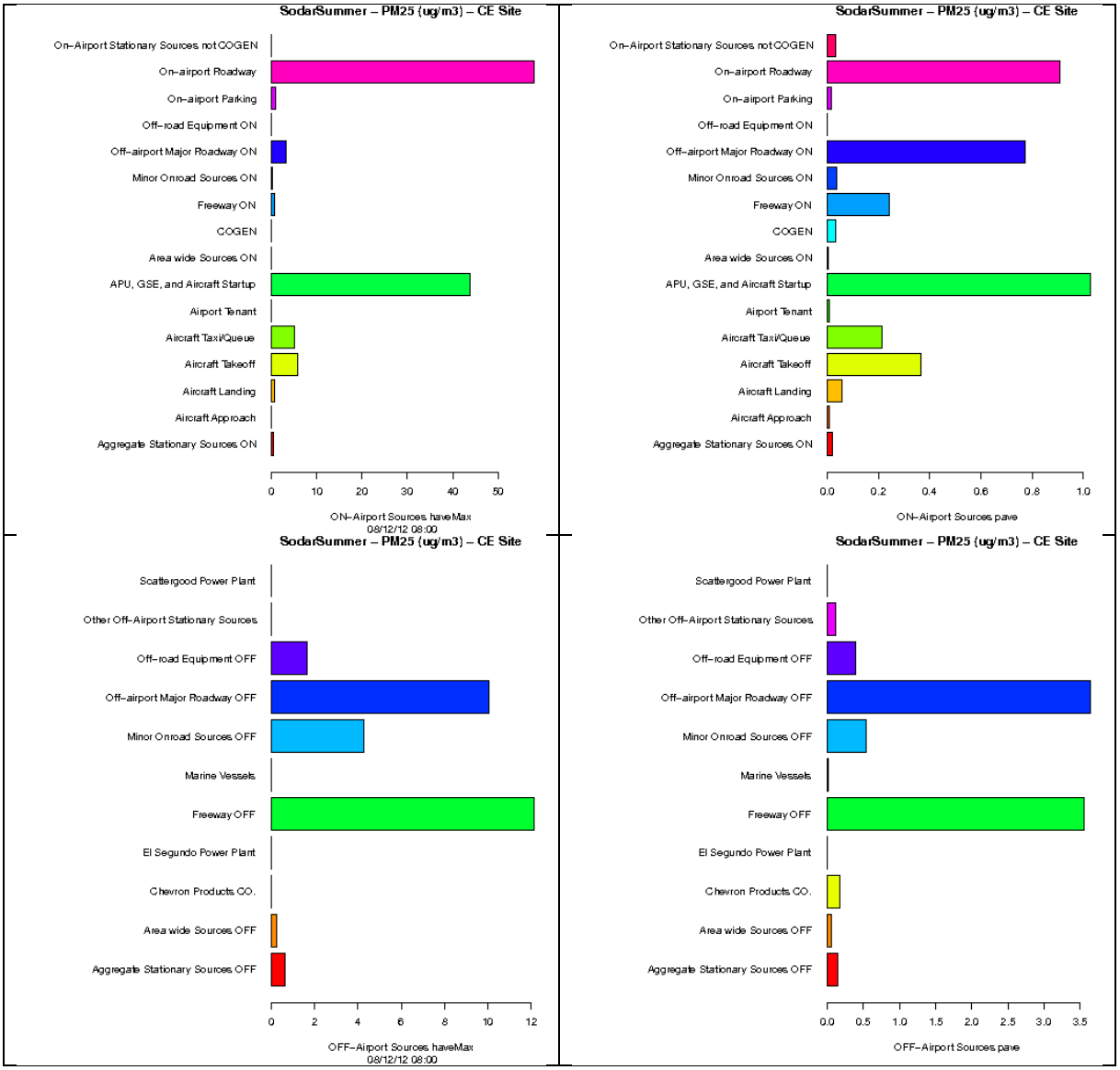

Figure 9A-189: Source-sector contributions to Hourly Maximum (left) and Period Average $PM_{2.5}$ concentrations at CE Site from airport-related sources (top) and background sources (bottom) during Summer Season.

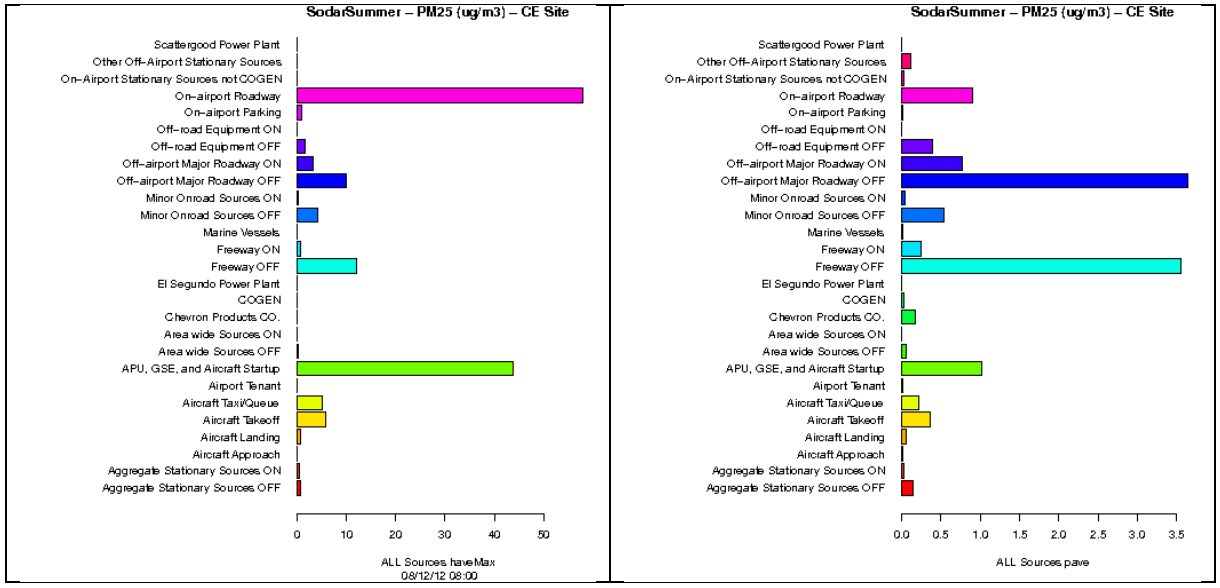

Figure 9A-190: Source-sector contributions to Hourly Maximum (left) and Period Average $PM_{2.5}$ concentrations at CE Site from ALL sources during Summer Season.

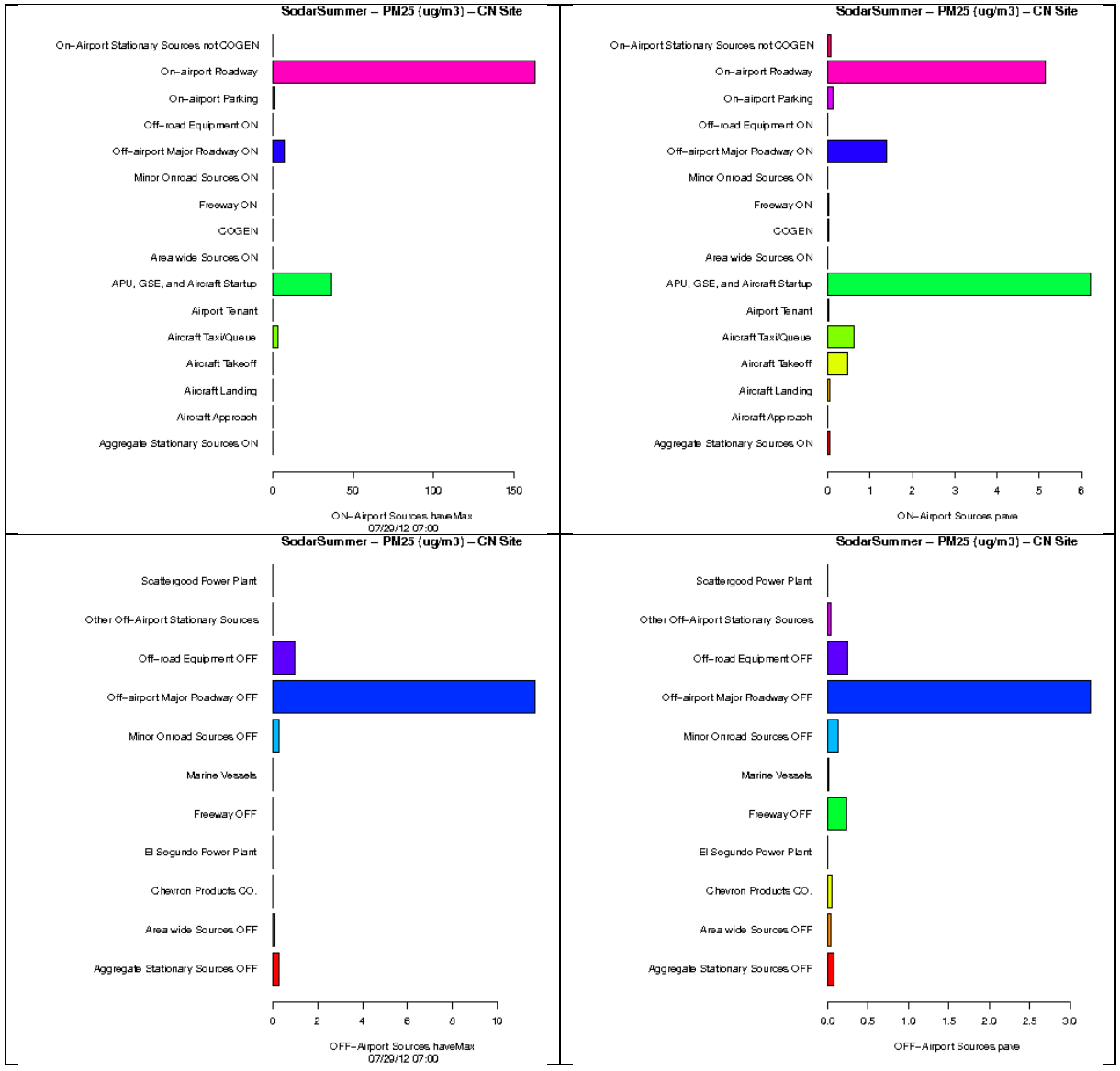

Figure 9A-191: Source-sector contributions to Hourly Maximum (left) and Period Average $PM_{2.5}$ concentrations at CN Site from airport-related sources (top) and background sources (bottom) during Summer Season.

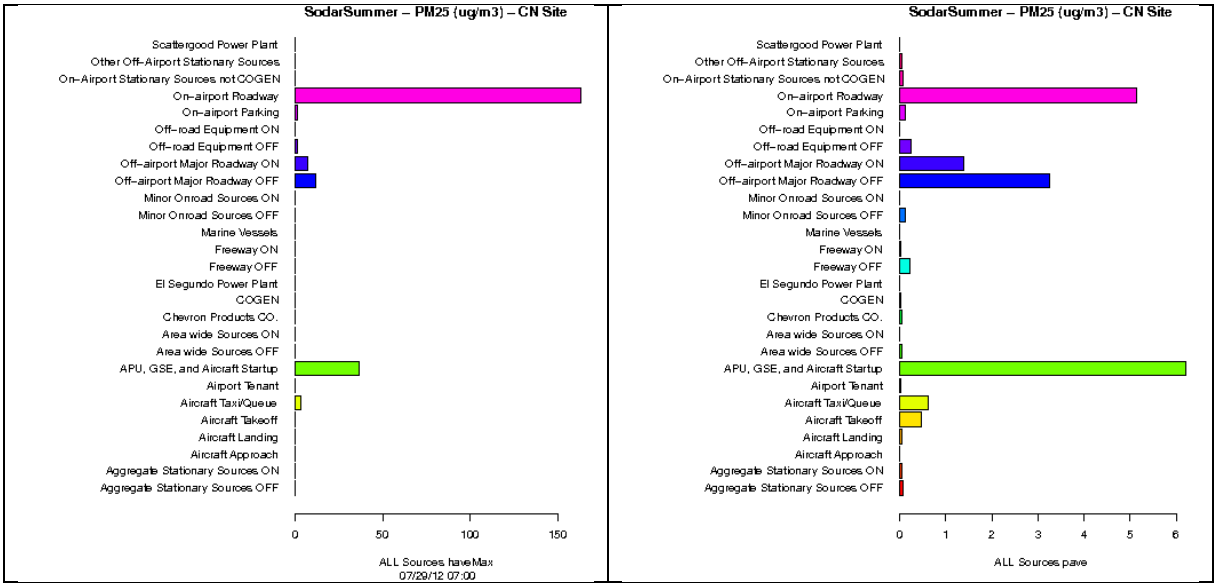

Figure 9A-192: Source-sector contributions to Hourly Maximum (left) and Period Average $PM_{2.5}$ concentrations at CN Site from ALL sources during Summer Season.

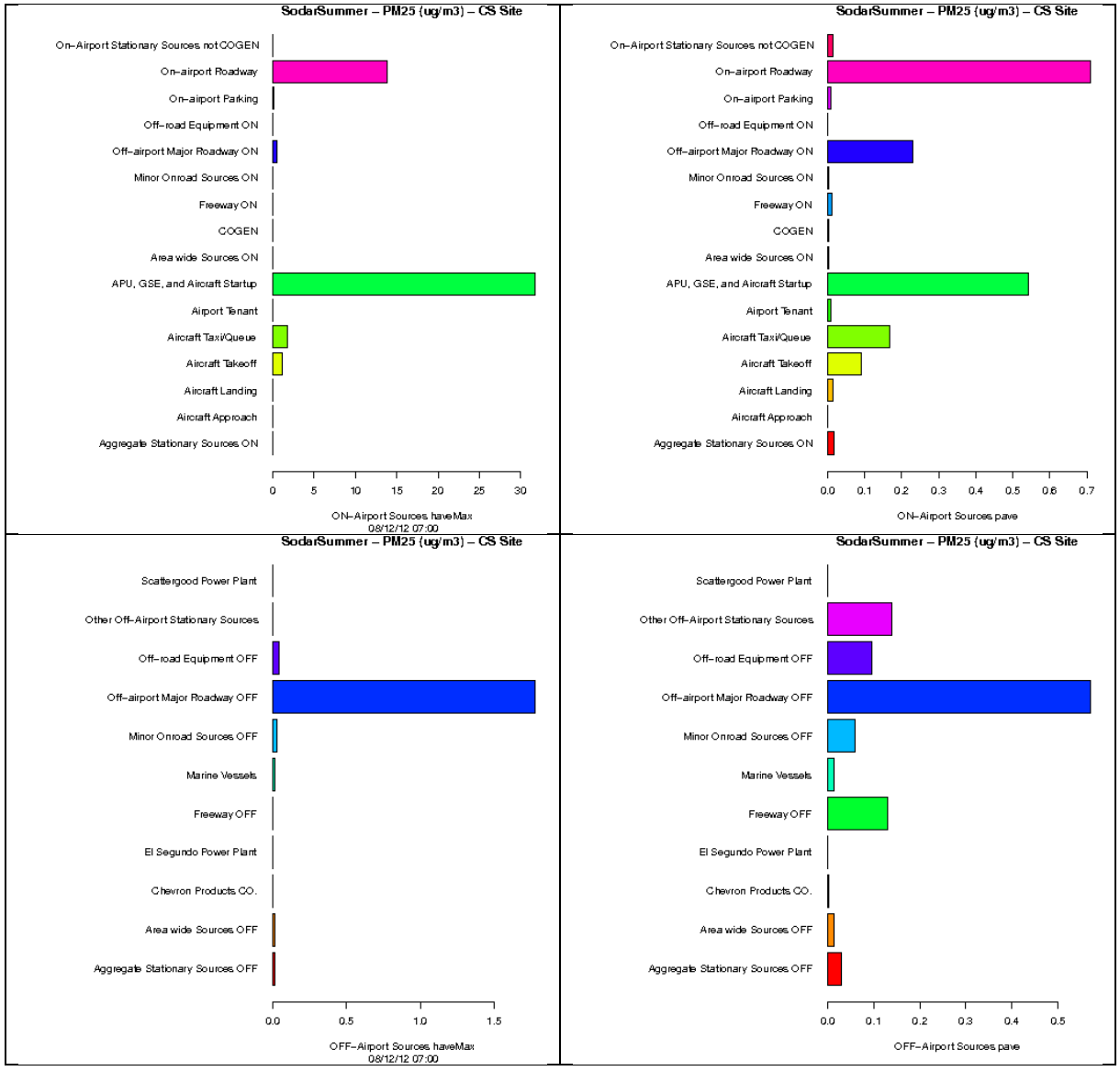

Figure 9A-193: Source-sector contributions to Hourly Maximum (left) and Period Average $PM_{2.5}$ concentrations at CS Site from airport-related sources (top) and background sources (bottom) during Summer Season.

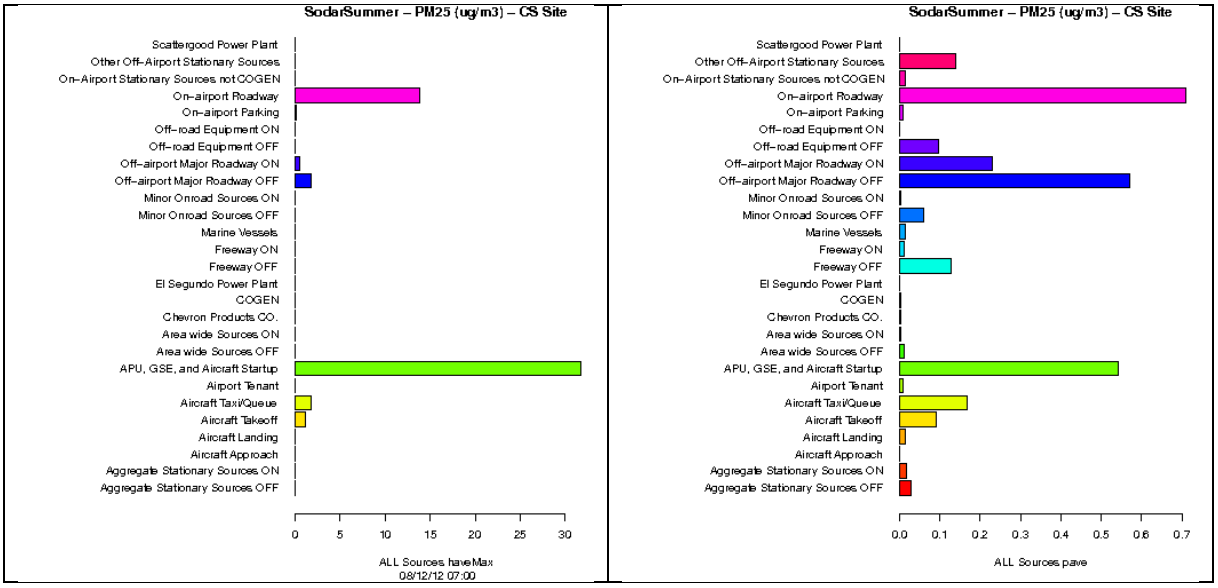

Figure 9A-194: Source-sector contributions to Hourly Maximum (left) and Period Average $PM_{2.5}$ concentrations at CS Site from ALL sources during Summer Season.

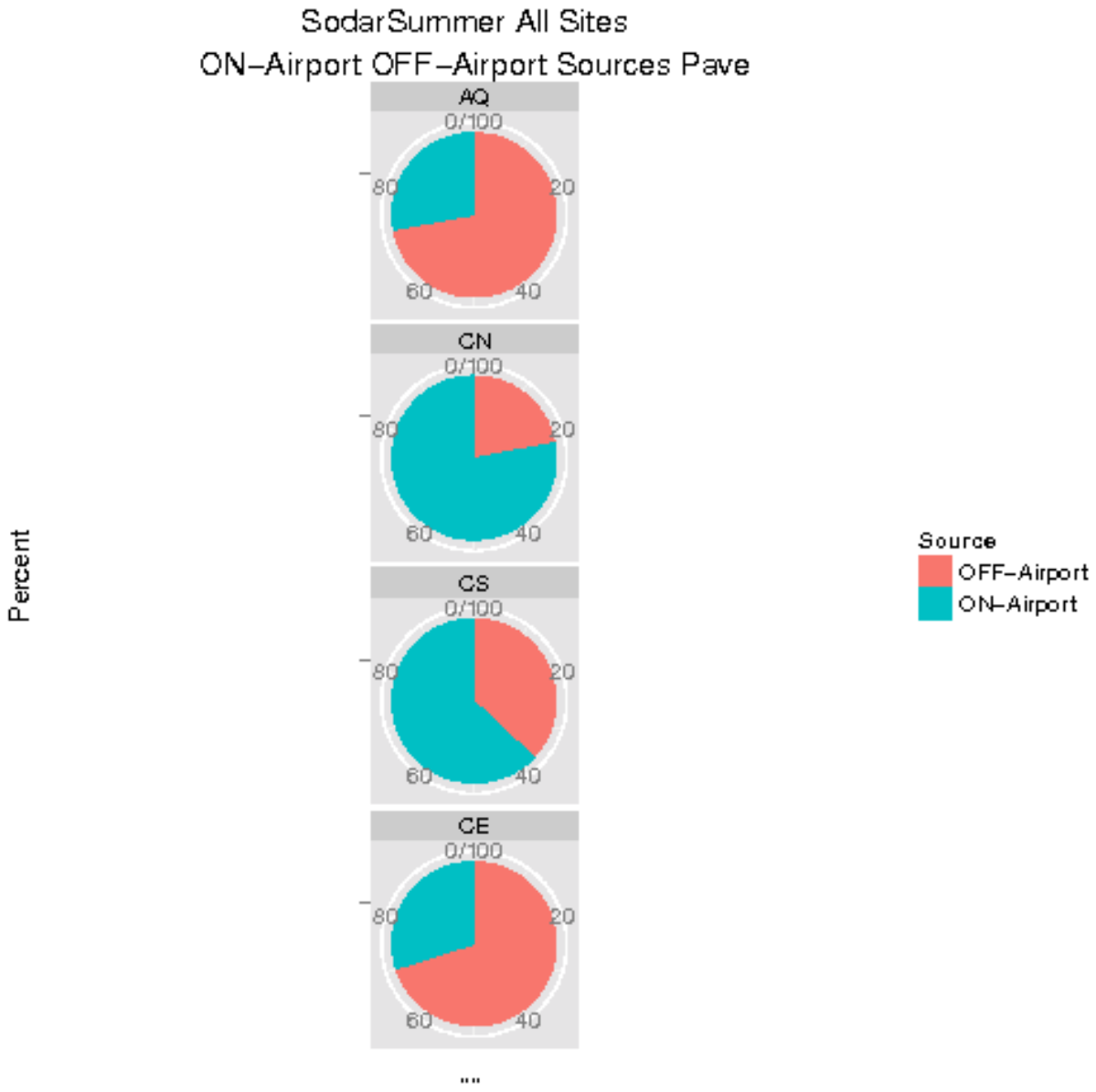

Figure 9A-195: Source-sector contributions to Period Average $PM_{2.5}$ concentrations at each site from airport-related vs. background sources during Summer Season.

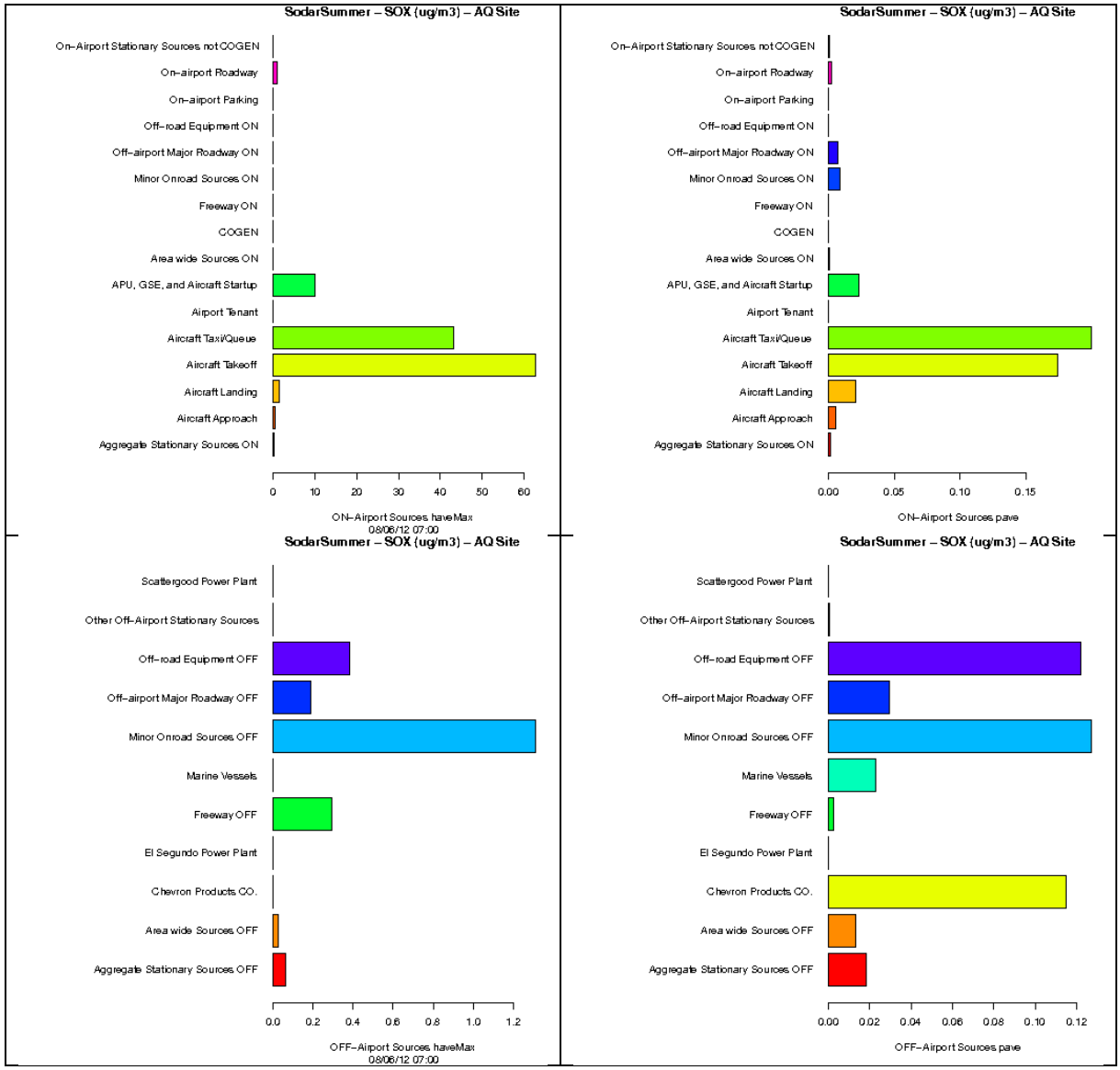

Figure 9A-196: Source-sector contributions to Hourly Maximum (left) and Period Average SOx concentrations at AQ Site from airport-related sources (top) and background sources (bottom) during Summer Season.

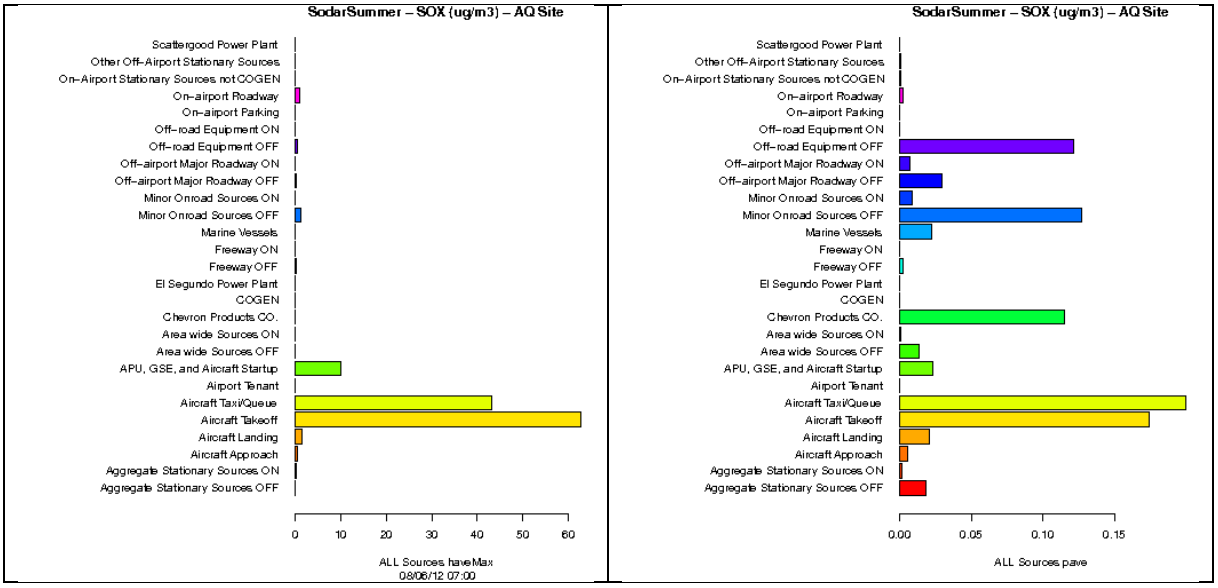

Figure 9A-197: Source-sector contributions to Hourly Maximum (left) and Period Average SOx concentrations at AQ Site from ALL sources during Summer Season.

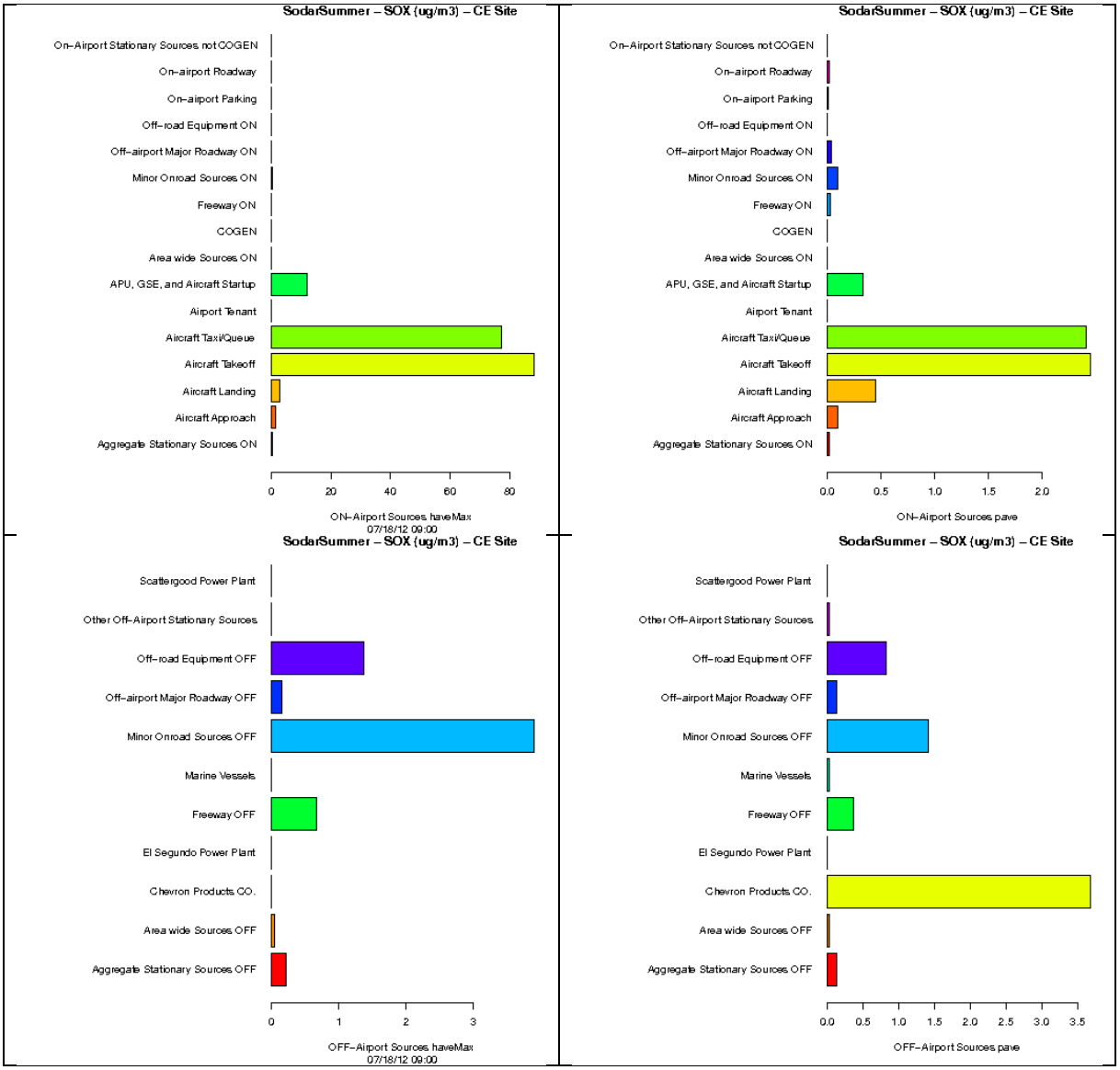

Figure 9A-198: Source-sector contributions to Hourly Maximum (left) and Period Average SOx concentrations at CE Site from airport-related sources (top) and background sources (bottom) during Summer Season.

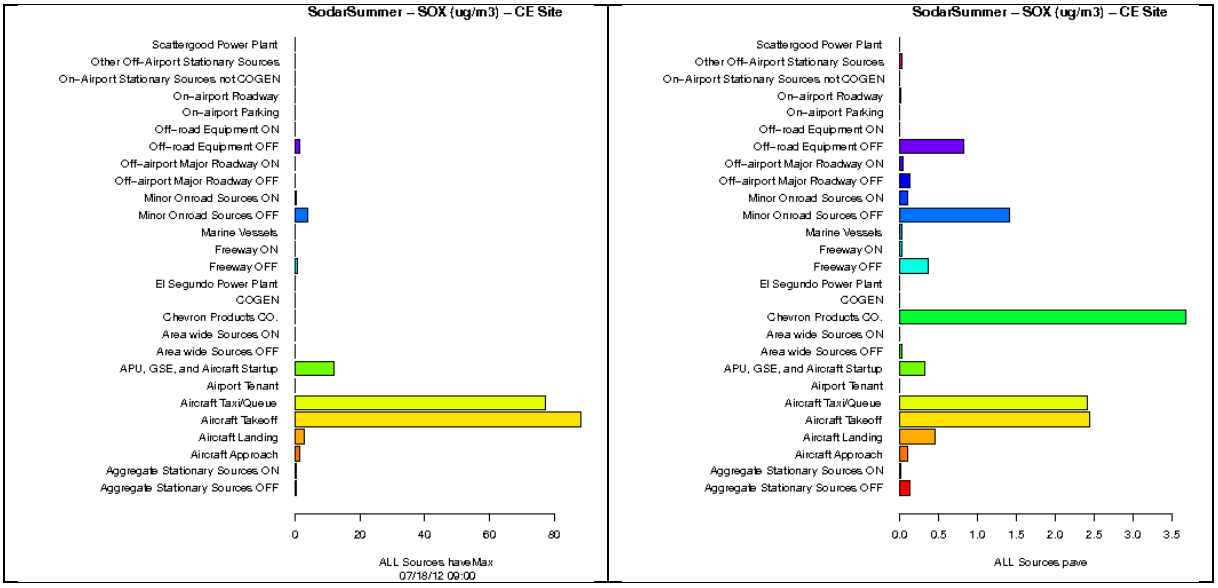

Figure 9A-199: Source-sector contributions to Hourly Maximum (left) and Period Average SOx concentrations at CE Site from ALL sources during Summer Season.

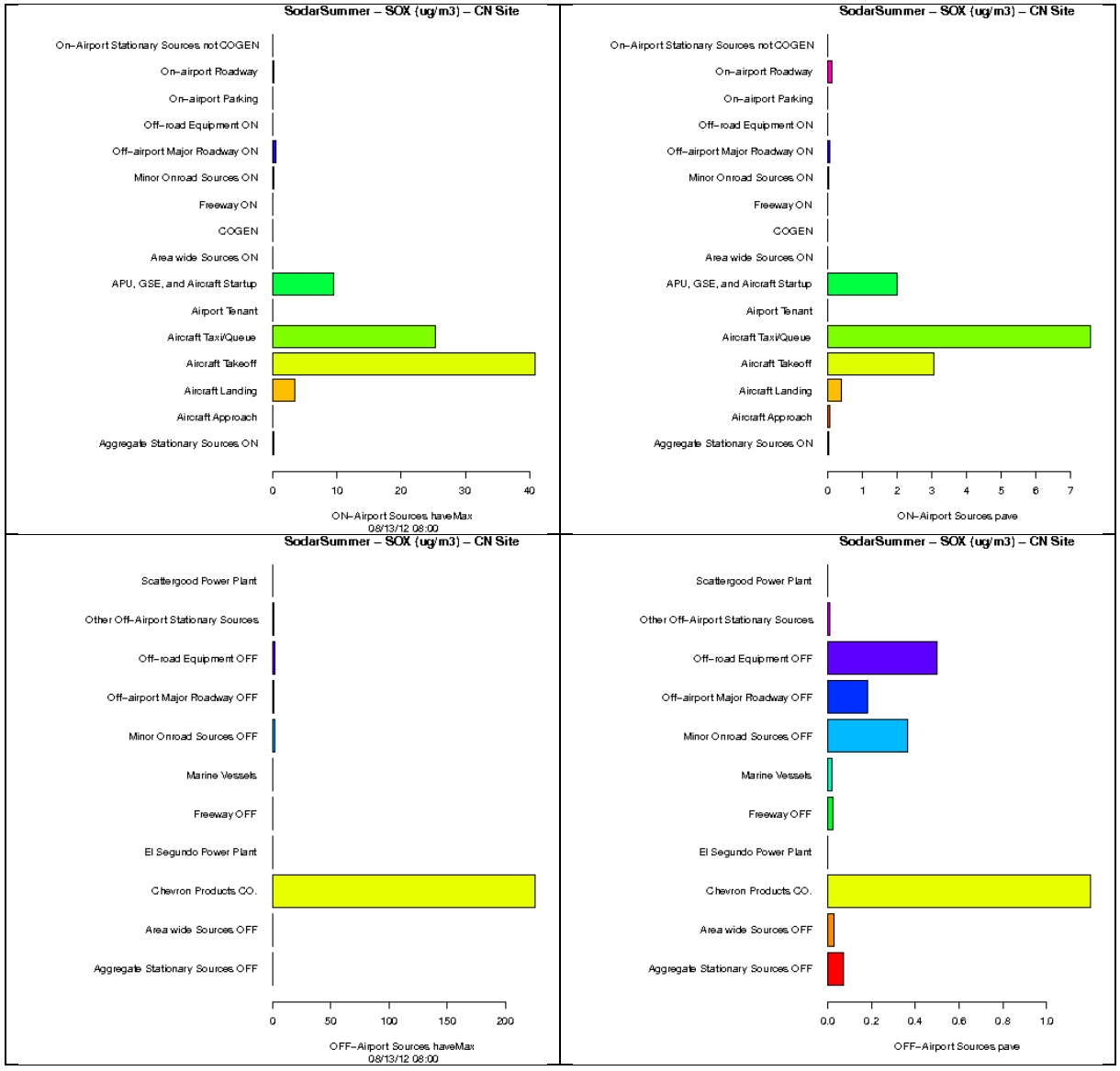

Figure 9A-200: Source-sector contributions to Hourly Maximum (left) and Period Average SOx concentrations at CN Site from airport-related sources (top) and background sources (bottom) during Summer Season.

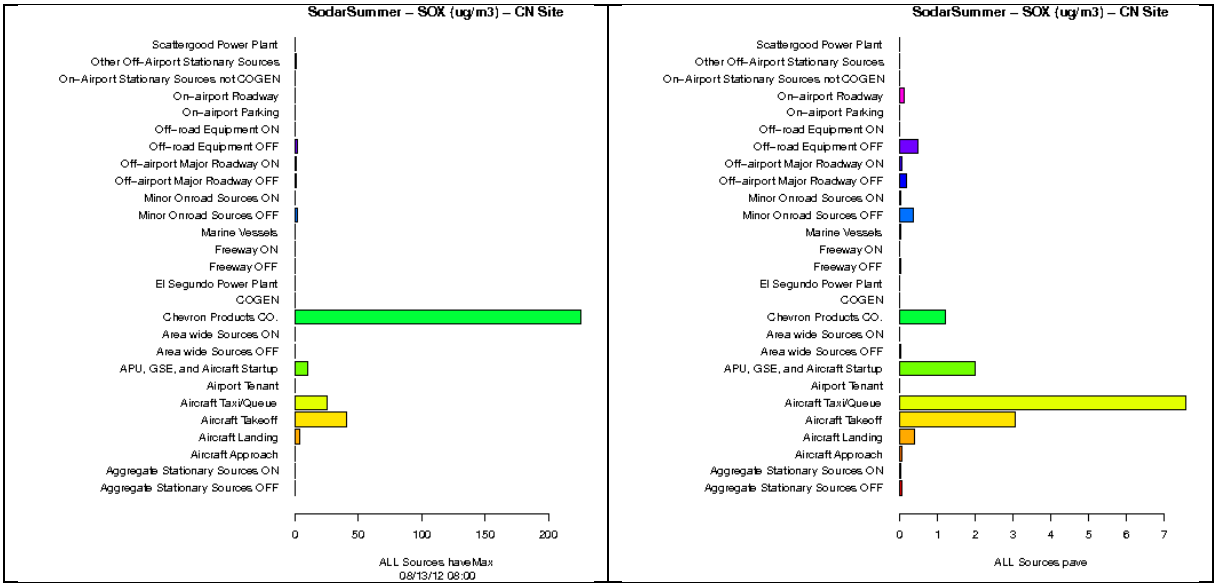

Figure 9A-201: Source-sector contributions to Hourly Maximum (left) and Period Average SOx concentrations at CN Site from ALL sources during Summer Season.

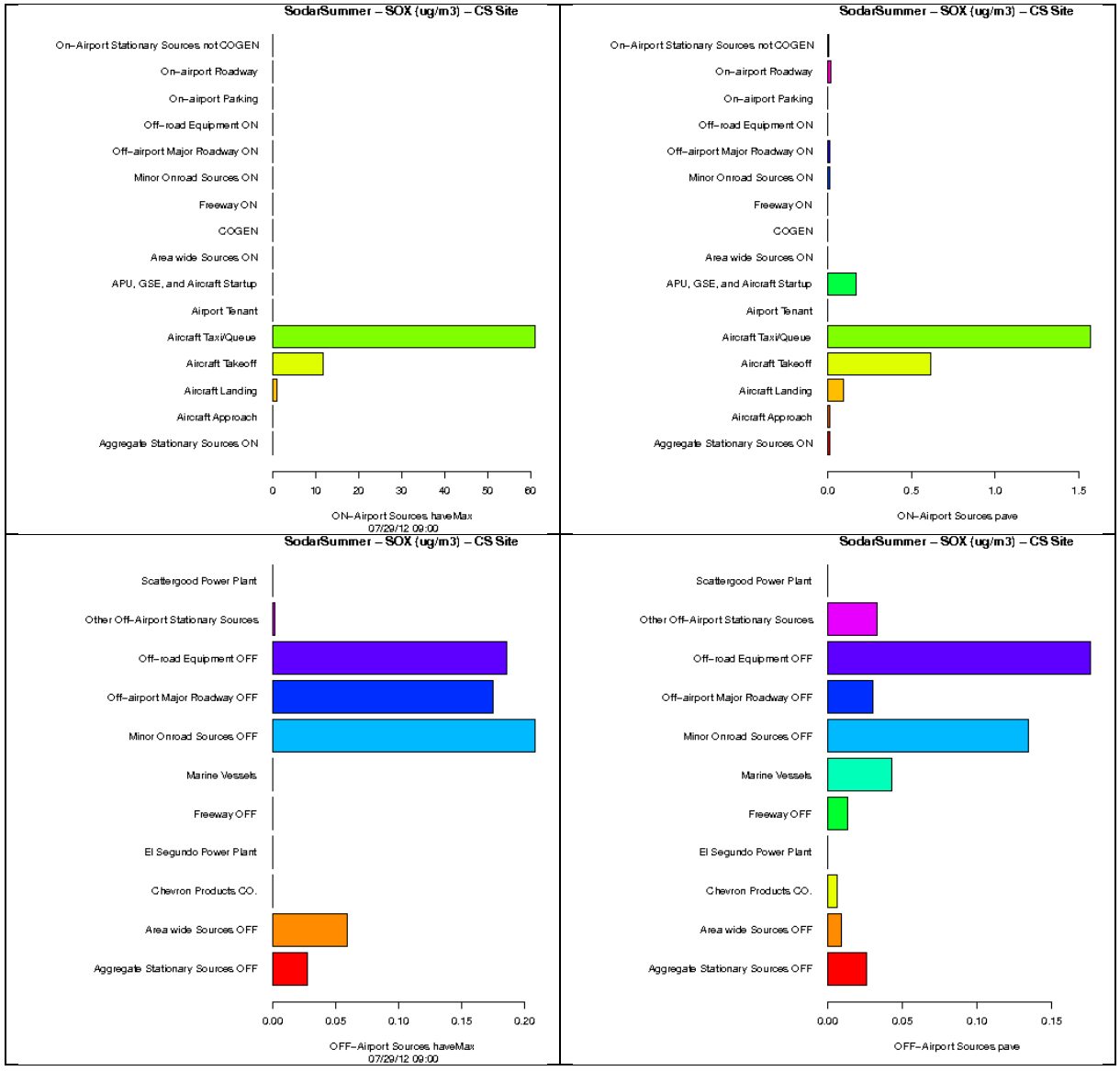

Figure 9A-202: Source-sector contributions to Hourly Maximum (left) and Period Average SOx concentrations at CS Site from airport-related sources (top) and background sources (bottom) during Summer Season.

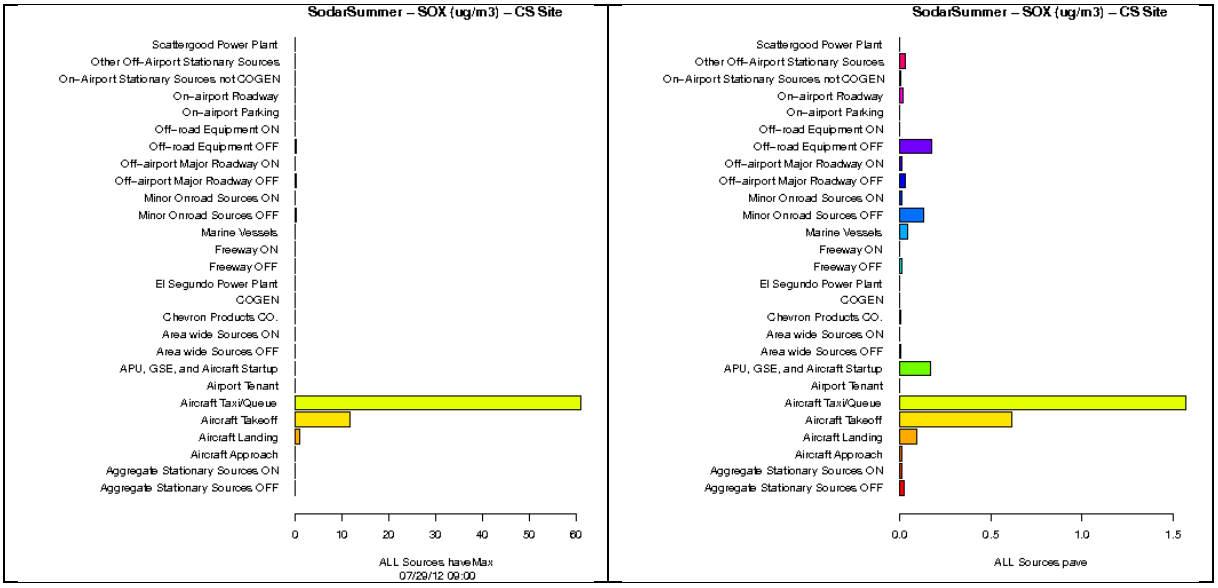

Figure 9A-203: Source-sector contributions to Hourly Maximum (left) and Period Average SOx concentrations at CS Site from ALL sources during Summer Season.

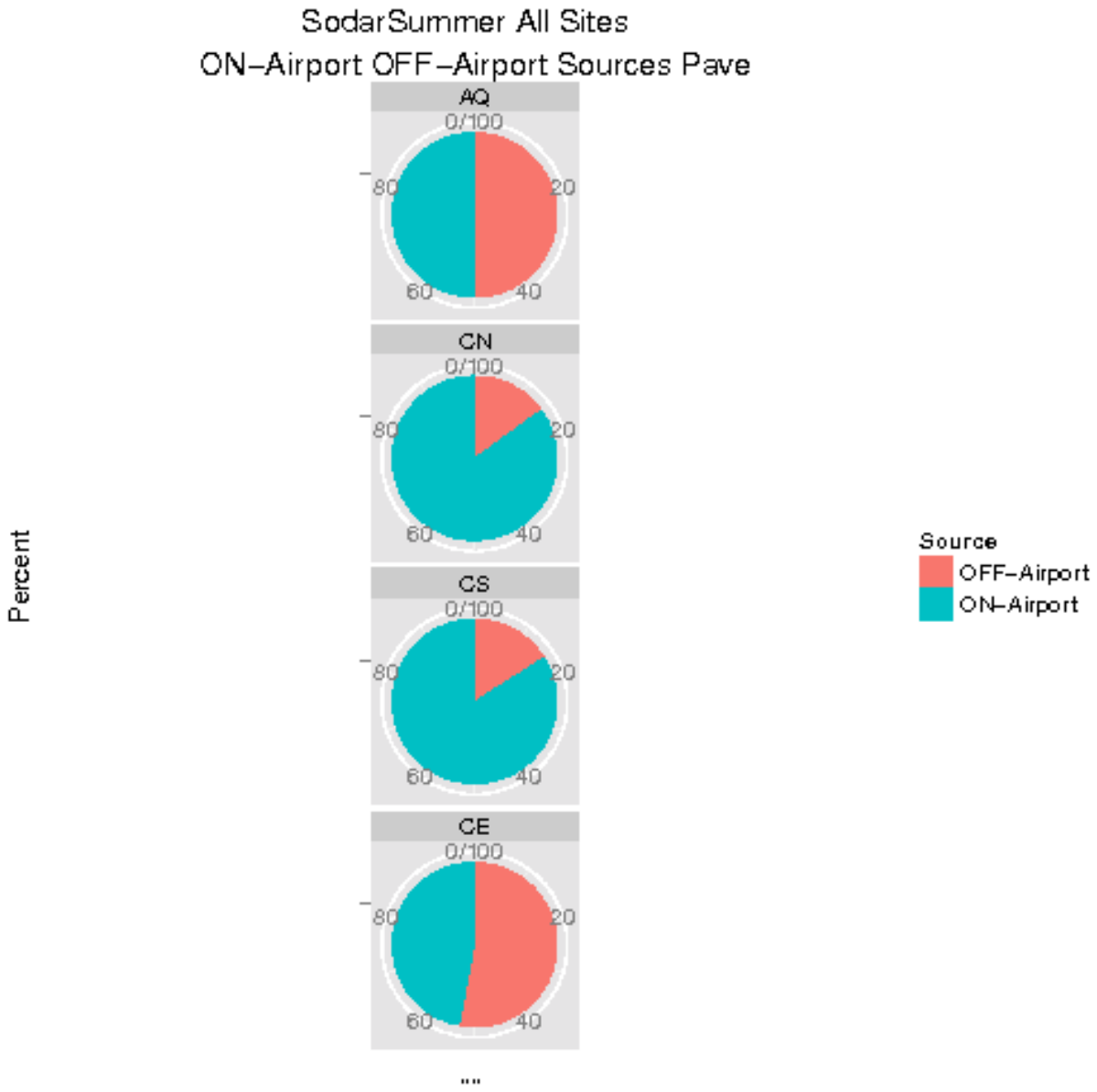

Figure 9A-204: Source-sector contributions to Period Average SOx concentrations at each site from airport-related vs. background sources during Summer Season.

IV. Sample AERMOD Input file

```
CO STARTING
CO TITLEONE  LAX Modeling Testcase
CO MODELOPT  CONC  FASTALL  ELEV
CO RUNORNOT  RUN
CO AVERTIME  1 24 MONTH PERIOD
CO POLLUTID  POLL
CO ERRORFIL ERRORS.OUT
CO FLAGPOLE
CO FINISHED

SO STARTING
SO ELEVUNIT  METERS
SO INCLUDED SO_SITE.DAT
SO INCLUDED EXTRAGROUPS.SO
SO FINISHED

RE STARTING
RE INCLUDED RECEPTORS.DAT
RE FINISHED

ME STARTING
ME SURFFILE  LAX_NKX_2012.SFC
ME PROFFILE  LAX_NKX_2012.PFL
ME SURFDATA  23174  2012
ME UAIRDATA  03190  2012
ME PROFBASE  38.40 METERS
ME STARTEND  2012  7  18  1  2012  8  28  24
ME FINISHED
OU STARTING
** AIRPORT Outputs
OU POSTFILE 1 AIRPORT PLOT 2012.POLL.AIRPORT.have.PLT
OU POSTFILE 24 AIRPORT PLOT 2012.POLL.AIRPORT.dave.PLT
OU POSTFILE MONTH AIRPORT PLOT 2012.POLL.AIRPORT.mave.PLT
OU POSTFILE PERIOD AIRPORT PLOT 2012.POLL.AIRPORT.pave.PLT
** ALL Outputs
OU POSTFILE 1 ALL PLOT 2012.POLL.ALL.have.PLT
OU POSTFILE 24 ALL PLOT 2012.POLL.ALL.dave.PLT
OU POSTFILE MONTH ALL PLOT 2012.POLL.ALL.mave.PLT
OU POSTFILE PERIOD ALL PLOT 2012.POLL.ALL.pave.PLT
** APPROACH Outputs
OU POSTFILE 1 APPROACH PLOT 2012.POLL.APPROACH.have.PLT
OU POSTFILE 24 APPROACH PLOT 2012.POLL.APPROACH.dave.PLT
OU POSTFILE MONTH APPROACH PLOT 2012.POLL.APPROACH.mave.PLT
OU POSTFILE PERIOD APPROACH PLOT 2012.POLL.APPROACH.pave.PLT
```

```
** BCKGRD Outputs
OU POSTFILE 1 BCKGRD PLOT 2012.POLL.BCKGRD.have.PLT
OU POSTFILE 24 BCKGRD PLOT 2012.POLL.BCKGRD.dave.PLT
OU POSTFILE MONTH BCKGRD PLOT 2012.POLL.BCKGRD.mave.PLT
OU POSTFILE PERIOD BCKGRD PLOT 2012.POLL.BCKGRD.pave.PLT
** CAAGGAP Outputs
OU POSTFILE 1 CAAGGAP PLOT 2012.POLL.CAAGGAP.have.PLT
OU POSTFILE 24 CAAGGAP PLOT 2012.POLL.CAAGGAP.dave.PLT
OU POSTFILE MONTH CAAGGAP PLOT 2012.POLL.CAAGGAP.mave.PLT
OU POSTFILE PERIOD CAAGGAP PLOT 2012.POLL.CAAGGAP.pave.PLT
** CAAGGBK Outputs
OU POSTFILE 1 CAAGGBK PLOT 2012.POLL.CAAGGBK.have.PLT
OU POSTFILE 24 CAAGGBK PLOT 2012.POLL.CAAGGBK.dave.PLT
OU POSTFILE MONTH CAAGGBK PLOT 2012.POLL.CAAGGBK.mave.PLT
OU POSTFILE PERIOD CAAGGBK PLOT 2012.POLL.CAAGGBK.pave.PLT
** CAAREAP Outputs
OU POSTFILE 1 CAAREAP PLOT 2012.POLL.CAAREAP.have.PLT
OU POSTFILE 24 CAAREAP PLOT 2012.POLL.CAAREAP.dave.PLT
OU POSTFILE MONTH CAAREAP PLOT 2012.POLL.CAAREAP.mave.PLT
OU POSTFILE PERIOD CAAREAP PLOT 2012.POLL.CAAREAP.pave.PLT
** CAAREBK Outputs
OU POSTFILE 1 CAAREBK PLOT 2012.POLL.CAAREBK.have.PLT
OU POSTFILE 24 CAAREBK PLOT 2012.POLL.CAAREBK.dave.PLT
OU POSTFILE MONTH CAAREBK PLOT 2012.POLL.CAAREBK.mave.PLT
OU POSTFILE PERIOD CAAREBK PLOT 2012.POLL.CAAREBK.pave.PLT
** CAOFFAP Outputs
OU POSTFILE 1 CAOFFAP PLOT 2012.POLL.CAOFFAP.have.PLT
OU POSTFILE 24 CAOFFAP PLOT 2012.POLL.CAOFFAP.dave.PLT
OU POSTFILE MONTH CAOFFAP PLOT 2012.POLL.CAOFFAP.mave.PLT
OU POSTFILE PERIOD CAOFFAP PLOT 2012.POLL.CAOFFAP.pave.PLT
** CAOFFBK Outputs
OU POSTFILE 1 CAOFFBK PLOT 2012.POLL.CAOFFBK.have.PLT
OU POSTFILE 24 CAOFFBK PLOT 2012.POLL.CAOFFBK.dave.PLT
OU POSTFILE MONTH CAOFFBK PLOT 2012.POLL.CAOFFBK.mave.PLT
OU POSTFILE PERIOD CAOFFBK PLOT 2012.POLL.CAOFFBK.pave.PLT
** CAONRDAP Outputs
OU POSTFILE 1 CAONRDAP PLOT 2012.POLL.CAONRDAP.have.PLT
OU POSTFILE 24 CAONRDAP PLOT 2012.POLL.CAONRDAP.dave.PLT
OU POSTFILE MONTH CAONRDAP PLOT 2012.POLL.CAONRDAP.mave.PLT
OU POSTFILE PERIOD CAONRDAP PLOT 2012.POLL.CAONRDAP.pave.PLT
** CAONRDBK Outputs
OU POSTFILE 1 CAONRDBK PLOT 2012.POLL.CAONRDBK.have.PLT
OU POSTFILE 24 CAONRDBK PLOT 2012.POLL.CAONRDBK.dave.PLT
OU POSTFILE MONTH CAONRDBK PLOT 2012.POLL.CAONRDBK.mave.PLT
OU POSTFILE PERIOD CAONRDBK PLOT 2012.POLL.CAONRDBK.pave.PLT
** CHEVRON Outputs
```

OU POSTFILE 1 CHEVRON PLOT 2012.POLL.CHEVRON.have.PLT
OU POSTFILE 24 CHEVRON PLOT 2012.POLL.CHEVRON.dave.PLT
OU POSTFILE MONTH CHEVRON PLOT 2012.POLL.CHEVRON.mave.PLT
OU POSTFILE PERIOD CHEVRON PLOT 2012.POLL.CHEVRON.pave.PLT
** COGEN Outputs
OU POSTFILE 1 COGEN PLOT 2012.POLL.COGEN.have.PLT
OU POSTFILE 24 COGEN PLOT 2012.POLL.COGEN.dave.PLT
OU POSTFILE MONTH COGEN PLOT 2012.POLL.COGEN.mave.PLT
OU POSTFILE PERIOD COGEN PLOT 2012.POLL.COGEN.pave.PLT
** FREEWYAP Outputs
OU POSTFILE 1 FREEWYAP PLOT 2012.POLL.FREEWYAP.have.PLT
OU POSTFILE 24 FREEWYAP PLOT 2012.POLL.FREEWYAP.dave.PLT
OU POSTFILE MONTH FREEWYAP PLOT 2012.POLL.FREEWYAP.mave.PLT
OU POSTFILE PERIOD FREEWYAP PLOT 2012.POLL.FREEWYAP.pave.PLT
** FREEWYBK Outputs
OU POSTFILE 1 FREEWYBK PLOT 2012.POLL.FREEWYBK.have.PLT
OU POSTFILE 24 FREEWYBK PLOT 2012.POLL.FREEWYBK.dave.PLT
OU POSTFILE MONTH FREEWYBK PLOT 2012.POLL.FREEWYBK.mave.PLT
OU POSTFILE PERIOD FREEWYBK PLOT 2012.POLL.FREEWYBK.pave.PLT
** GATES Outputs
OU POSTFILE 1 GATES PLOT 2012.POLL.GATES.have.PLT
OU POSTFILE 24 GATES PLOT 2012.POLL.GATES.dave.PLT
OU POSTFILE MONTH GATES PLOT 2012.POLL.GATES.mave.PLT
OU POSTFILE PERIOD GATES PLOT 2012.POLL.GATES.pave.PLT
** LANDING Outputs
OU POSTFILE 1 LANDING PLOT 2012.POLL.LANDING.have.PLT
OU POSTFILE 24 LANDING PLOT 2012.POLL.LANDING.dave.PLT
OU POSTFILE MONTH LANDING PLOT 2012.POLL.LANDING.mave.PLT
OU POSTFILE PERIOD LANDING PLOT 2012.POLL.LANDING.pave.PLT
** MARINE Outputs
OU POSTFILE 1 MARINE PLOT 2012.POLL.MARINE.have.PLT
OU POSTFILE 24 MARINE PLOT 2012.POLL.MARINE.dave.PLT
OU POSTFILE MONTH MARINE PLOT 2012.POLL.MARINE.mave.PLT
OU POSTFILE PERIOD MARINE PLOT 2012.POLL.MARINE.pave.PLT
** PARKING Outputs
OU POSTFILE 1 PARKING PLOT 2012.POLL.PARKING.have.PLT
OU POSTFILE 24 PARKING PLOT 2012.POLL.PARKING.dave.PLT
OU POSTFILE MONTH PARKING PLOT 2012.POLL.PARKING.mave.PLT
OU POSTFILE PERIOD PARKING PLOT 2012.POLL.PARKING.pave.PLT
** ROADOFAP Outputs
OU POSTFILE 1 ROADOFAP PLOT 2012.POLL.ROADOFAP.have.PLT
OU POSTFILE 24 ROADOFAP PLOT 2012.POLL.ROADOFAP.dave.PLT
OU POSTFILE MONTH ROADOFAP PLOT 2012.POLL.ROADOFAP.mave.PLT
OU POSTFILE PERIOD ROADOFAP PLOT 2012.POLL.ROADOFAP.pave.PLT
** ROADOFBK Outputs
OU POSTFILE 1 ROADOFBK PLOT 2012.POLL.ROADOFBK.have.PLT

```
OU POSTFILE 24 ROADOFBK PLOT 2012.POLL.ROADOFBK.dave.PLT
OU POSTFILE MONTH ROADOFBK PLOT 2012.POLL.ROADOFBK.mave.PLT
OU POSTFILE PERIOD ROADOFBK PLOT 2012.POLL.ROADOFBK.pave.PLT
** ROADONAP Outputs
OU POSTFILE 1 ROADONAP PLOT 2012.POLL.ROADONAP.have.PLT
OU POSTFILE 24 ROADONAP PLOT 2012.POLL.ROADONAP.dave.PLT
OU POSTFILE MONTH ROADONAP PLOT 2012.POLL.ROADONAP.mave.PLT
OU POSTFILE PERIOD ROADONAP PLOT 2012.POLL.ROADONAP.pave.PLT
** SCTRGOOD Outputs
OU POSTFILE 1 SCTRGOOD PLOT 2012.POLL.SCTRGOOD.have.PLT
OU POSTFILE 24 SCTRGOOD PLOT 2012.POLL.SCTRGOOD.dave.PLT
OU POSTFILE MONTH SCTRGOOD PLOT 2012.POLL.SCTRGOOD.mave.PLT
OU POSTFILE PERIOD SCTRGOOD PLOT 2012.POLL.SCTRGOOD.pave.PLT
** SEGUNDO Outputs
OU POSTFILE 1 SEGUNDO PLOT 2012.POLL.SEGUNDO.have.PLT
OU POSTFILE 24 SEGUNDO PLOT 2012.POLL.SEGUNDO.dave.PLT
OU POSTFILE MONTH SEGUNDO PLOT 2012.POLL.SEGUNDO.mave.PLT
OU POSTFILE PERIOD SEGUNDO PLOT 2012.POLL.SEGUNDO.pave.PLT
** SSOTHBK Outputs
OU POSTFILE 1 SSOTHBK PLOT 2012.POLL.SSOTHBK.have.PLT
OU POSTFILE 24 SSOTHBK PLOT 2012.POLL.SSOTHBK.dave.PLT
OU POSTFILE MONTH SSOTHBK PLOT 2012.POLL.SSOTHBK.mave.PLT
OU POSTFILE PERIOD SSOTHBK PLOT 2012.POLL.SSOTHBK.pave.PLT
** SSTENAP Outputs
OU POSTFILE 1 SSTENAP PLOT 2012.POLL.SSTENAP.have.PLT
OU POSTFILE 24 SSTENAP PLOT 2012.POLL.SSTENAP.dave.PLT
OU POSTFILE MONTH SSTENAP PLOT 2012.POLL.SSTENAP.mave.PLT
OU POSTFILE PERIOD SSTENAP PLOT 2012.POLL.SSTENAP.pave.PLT
** STATSRCS Outputs
OU POSTFILE 1 STATSRCS PLOT 2012.POLL.STATSRCS.have.PLT
OU POSTFILE 24 STATSRCS PLOT 2012.POLL.STATSRCS.dave.PLT
OU POSTFILE MONTH STATSRCS PLOT 2012.POLL.STATSRCS.mave.PLT
OU POSTFILE PERIOD STATSRCS PLOT 2012.POLL.STATSRCS.pave.PLT
** TAKEOFF Outputs
OU POSTFILE 1 TAKEOFF PLOT 2012.POLL.TAKEOFF.have.PLT
OU POSTFILE 24 TAKEOFF PLOT 2012.POLL.TAKEOFF.dave.PLT
OU POSTFILE MONTH TAKEOFF PLOT 2012.POLL.TAKEOFF.mave.PLT
OU POSTFILE PERIOD TAKEOFF PLOT 2012.POLL.TAKEOFF.pave.PLT
** TAXIQ Outputs
OU POSTFILE 1 TAXIQ PLOT 2012.POLL.TAXIQ.have.PLT
OU POSTFILE 24 TAXIQ PLOT 2012.POLL.TAXIQ.dave.PLT
OU POSTFILE MONTH TAXIQ PLOT 2012.POLL.TAXIQ.mave.PLT
OU POSTFILE PERIOD TAXIQ PLOT 2012.POLL.TAXIQ.pave.PLT
** EDMS Outputs
OU POSTFILE 1 EDMS PLOT 2012.POLL.EDMS.have.PLT
OU POSTFILE 24 EDMS PLOT 2012.POLL.EDMS.dave.PLT
```

OU POSTFILE MONTH EDMS PLOT 2012.POLL.EDMS.mave.PLT
OU POSTFILE PERIOD EDMS PLOT 2012.POLL.EDMS.pave.PLT
** ENGINES Outputs
OU POSTFILE 1 ENGINES PLOT 2012.POLL.ENGINES.have.PLT
OU POSTFILE 24 ENGINES PLOT 2012.POLL.ENGINES.dave.PLT
OU POSTFILE MONTH ENGINES PLOT 2012.POLL.ENGINES.mave.PLT
OU POSTFILE PERIOD ENGINES PLOT 2012.POLL.ENGINES.pave.PLT
** L06L Outputs
OU POSTFILE 1 L06L PLOT 2012.POLL.L06L.have.PLT
OU POSTFILE 24 L06L PLOT 2012.POLL.L06L.dave.PLT
OU POSTFILE MONTH L06L PLOT 2012.POLL.L06L.mave.PLT
OU POSTFILE PERIOD L06L PLOT 2012.POLL.L06L.pave.PLT
** L06L24R Outputs
OU POSTFILE 1 L06L24R PLOT 2012.POLL.L06L24R.have.PLT
OU POSTFILE 24 L06L24R PLOT 2012.POLL.L06L24R.dave.PLT
OU POSTFILE MONTH L06L24R PLOT 2012.POLL.L06L24R.mave.PLT
OU POSTFILE PERIOD L06L24R PLOT 2012.POLL.L06L24R.pave.PLT
** L06R Outputs
OU POSTFILE 1 L06R PLOT 2012.POLL.L06R.have.PLT
OU POSTFILE 24 L06R PLOT 2012.POLL.L06R.dave.PLT
OU POSTFILE MONTH L06R PLOT 2012.POLL.L06R.mave.PLT
OU POSTFILE PERIOD L06R PLOT 2012.POLL.L06R.pave.PLT
** L06R24L Outputs
OU POSTFILE 1 L06R24L PLOT 2012.POLL.L06R24L.have.PLT
OU POSTFILE 24 L06R24L PLOT 2012.POLL.L06R24L.dave.PLT
OU POSTFILE MONTH L06R24L PLOT 2012.POLL.L06R24L.mave.PLT
OU POSTFILE PERIOD L06R24L PLOT 2012.POLL.L06R24L.pave.PLT
** L07L Outputs
OU POSTFILE 1 L07L PLOT 2012.POLL.L07L.have.PLT
OU POSTFILE 24 L07L PLOT 2012.POLL.L07L.dave.PLT
OU POSTFILE MONTH L07L PLOT 2012.POLL.L07L.mave.PLT
OU POSTFILE PERIOD L07L PLOT 2012.POLL.L07L.pave.PLT
** L07L25R Outputs
OU POSTFILE 1 L07L25R PLOT 2012.POLL.L07L25R.have.PLT
OU POSTFILE 24 L07L25R PLOT 2012.POLL.L07L25R.dave.PLT
OU POSTFILE MONTH L07L25R PLOT 2012.POLL.L07L25R.mave.PLT
OU POSTFILE PERIOD L07L25R PLOT 2012.POLL.L07L25R.pave.PLT
** L07R Outputs
OU POSTFILE 1 L07R PLOT 2012.POLL.L07R.have.PLT
OU POSTFILE 24 L07R PLOT 2012.POLL.L07R.dave.PLT
OU POSTFILE MONTH L07R PLOT 2012.POLL.L07R.mave.PLT
OU POSTFILE PERIOD L07R PLOT 2012.POLL.L07R.pave.PLT
** L07R25L Outputs
OU POSTFILE 1 L07R25L PLOT 2012.POLL.L07R25L.have.PLT
OU POSTFILE 24 L07R25L PLOT 2012.POLL.L07R25L.dave.PLT
OU POSTFILE MONTH L07R25L PLOT 2012.POLL.L07R25L.mave.PLT

OU POSTFILE PERIOD L07R25L PLOT 2012.POLL.L07R25L.pave.PLT
** L24L Outputs
OU POSTFILE 1 L24L PLOT 2012.POLL.L24L.have.PLT
OU POSTFILE 24 L24L PLOT 2012.POLL.L24L.dave.PLT
OU POSTFILE MONTH L24L PLOT 2012.POLL.L24L.mave.PLT
OU POSTFILE PERIOD L24L PLOT 2012.POLL.L24L.pave.PLT
** L24R Outputs
OU POSTFILE 1 L24R PLOT 2012.POLL.L24R.have.PLT
OU POSTFILE 24 L24R PLOT 2012.POLL.L24R.dave.PLT
OU POSTFILE MONTH L24R PLOT 2012.POLL.L24R.mave.PLT
OU POSTFILE PERIOD L24R PLOT 2012.POLL.L24R.pave.PLT
** L25L Outputs
OU POSTFILE 1 L25L PLOT 2012.POLL.L25L.have.PLT
OU POSTFILE 24 L25L PLOT 2012.POLL.L25L.dave.PLT
OU POSTFILE MONTH L25L PLOT 2012.POLL.L25L.mave.PLT
OU POSTFILE PERIOD L25L PLOT 2012.POLL.L25L.pave.PLT
** L25R Outputs
OU POSTFILE 1 L25R PLOT 2012.POLL.L25R.have.PLT
OU POSTFILE 24 L25R PLOT 2012.POLL.L25R.dave.PLT
OU POSTFILE MONTH L25R PLOT 2012.POLL.L25R.mave.PLT
OU POSTFILE PERIOD L25R PLOT 2012.POLL.L25R.pave.PLT
** LD250240 Outputs
OU POSTFILE 1 LD250240 PLOT 2012.POLL.LD250240.have.PLT
OU POSTFILE 24 LD250240 PLOT 2012.POLL.LD250240.dave.PLT
OU POSTFILE MONTH LD250240 PLOT 2012.POLL.LD250240.mave.PLT
OU POSTFILE PERIOD LD250240 PLOT 2012.POLL.LD250240.pave.PLT
** LD6070 Outputs
OU POSTFILE 1 LD6070 PLOT 2012.POLL.LD6070.have.PLT
OU POSTFILE 24 LD6070 PLOT 2012.POLL.LD6070.dave.PLT
OU POSTFILE MONTH LD6070 PLOT 2012.POLL.LD6070.mave.PLT
OU POSTFILE PERIOD LD6070 PLOT 2012.POLL.LD6070.pave.PLT
** RL06L Outputs
OU POSTFILE 1 RL06L PLOT 2012.POLL.RL06L.have.PLT
OU POSTFILE 24 RL06L PLOT 2012.POLL.RL06L.dave.PLT
OU POSTFILE MONTH RL06L PLOT 2012.POLL.RL06L.mave.PLT
OU POSTFILE PERIOD RL06L PLOT 2012.POLL.RL06L.pave.PLT
** RL06R Outputs
OU POSTFILE 1 RL06R PLOT 2012.POLL.RL06R.have.PLT
OU POSTFILE 24 RL06R PLOT 2012.POLL.RL06R.dave.PLT
OU POSTFILE MONTH RL06R PLOT 2012.POLL.RL06R.mave.PLT
OU POSTFILE PERIOD RL06R PLOT 2012.POLL.RL06R.pave.PLT
** RL07L Outputs
OU POSTFILE 1 RL07L PLOT 2012.POLL.RL07L.have.PLT
OU POSTFILE 24 RL07L PLOT 2012.POLL.RL07L.dave.PLT
OU POSTFILE MONTH RL07L PLOT 2012.POLL.RL07L.mave.PLT
OU POSTFILE PERIOD RL07L PLOT 2012.POLL.RL07L.pave.PLT

```
** RL07R Outputs
OU POSTFILE 1 RL07R PLOT 2012.POLL.RL07R.have.PLT
OU POSTFILE 24 RL07R PLOT 2012.POLL.RL07R.dave.PLT
OU POSTFILE MONTH RL07R PLOT 2012.POLL.RL07R.mave.PLT
OU POSTFILE PERIOD RL07R PLOT 2012.POLL.RL07R.pave.PLT
** ROADS Outputs
OU POSTFILE 1 ROADS PLOT 2012.POLL.ROADS.have.PLT
OU POSTFILE 24 ROADS PLOT 2012.POLL.ROADS.dave.PLT
OU POSTFILE MONTH ROADS PLOT 2012.POLL.ROADS.mave.PLT
OU POSTFILE PERIOD ROADS PLOT 2012.POLL.ROADS.pave.PLT
** RT06L Outputs
OU POSTFILE 1 RT06L PLOT 2012.POLL.RT06L.have.PLT
OU POSTFILE 24 RT06L PLOT 2012.POLL.RT06L.dave.PLT
OU POSTFILE MONTH RT06L PLOT 2012.POLL.RT06L.mave.PLT
OU POSTFILE PERIOD RT06L PLOT 2012.POLL.RT06L.pave.PLT
** RT06R Outputs
OU POSTFILE 1 RT06R PLOT 2012.POLL.RT06R.have.PLT
OU POSTFILE 24 RT06R PLOT 2012.POLL.RT06R.dave.PLT
OU POSTFILE MONTH RT06R PLOT 2012.POLL.RT06R.mave.PLT
OU POSTFILE PERIOD RT06R PLOT 2012.POLL.RT06R.pave.PLT
** RT07L Outputs
OU POSTFILE 1 RT07L PLOT 2012.POLL.RT07L.have.PLT
OU POSTFILE 24 RT07L PLOT 2012.POLL.RT07L.dave.PLT
OU POSTFILE MONTH RT07L PLOT 2012.POLL.RT07L.mave.PLT
OU POSTFILE PERIOD RT07L PLOT 2012.POLL.RT07L.pave.PLT
** RT07R Outputs
OU POSTFILE 1 RT07R PLOT 2012.POLL.RT07R.have.PLT
OU POSTFILE 24 RT07R PLOT 2012.POLL.RT07R.dave.PLT
OU POSTFILE MONTH RT07R PLOT 2012.POLL.RT07R.mave.PLT
OU POSTFILE PERIOD RT07R PLOT 2012.POLL.RT07R.pave.PLT
** SHIPS Outputs
OU POSTFILE 1 SHIPS PLOT 2012.POLL.SHIPS.have.PLT
OU POSTFILE 24 SHIPS PLOT 2012.POLL.SHIPS.dave.PLT
OU POSTFILE MONTH SHIPS PLOT 2012.POLL.SHIPS.mave.PLT
OU POSTFILE PERIOD SHIPS PLOT 2012.POLL.SHIPS.pave.PLT
** T06L24R Outputs
OU POSTFILE 1 T06L24R PLOT 2012.POLL.T06L24R.have.PLT
OU POSTFILE 24 T06L24R PLOT 2012.POLL.T06L24R.dave.PLT
OU POSTFILE MONTH T06L24R PLOT 2012.POLL.T06L24R.mave.PLT
OU POSTFILE PERIOD T06L24R PLOT 2012.POLL.T06L24R.pave.PLT
** T06R Outputs
OU POSTFILE 1 T06R PLOT 2012.POLL.T06R.have.PLT
OU POSTFILE 24 T06R PLOT 2012.POLL.T06R.dave.PLT
OU POSTFILE MONTH T06R PLOT 2012.POLL.T06R.mave.PLT
OU POSTFILE PERIOD T06R PLOT 2012.POLL.T06R.pave.PLT
** T06R24L Outputs
```

```
OU POSTFILE 1 T06R24L PLOT 2012.POLL.T06R24L.have.PLT
OU POSTFILE 24 T06R24L PLOT 2012.POLL.T06R24L.dave.PLT
OU POSTFILE MONTH T06R24L PLOT 2012.POLL.T06R24L.mave.PLT
OU POSTFILE PERIOD T06R24L PLOT 2012.POLL.T06R24L.pave.PLT
** T07L Outputs
OU POSTFILE 1 T07L PLOT 2012.POLL.T07L.have.PLT
OU POSTFILE 24 T07L PLOT 2012.POLL.T07L.dave.PLT
OU POSTFILE MONTH T07L PLOT 2012.POLL.T07L.mave.PLT
OU POSTFILE PERIOD T07L PLOT 2012.POLL.T07L.pave.PLT
** T07L25R Outputs
OU POSTFILE 1 T07L25R PLOT 2012.POLL.T07L25R.have.PLT
OU POSTFILE 24 T07L25R PLOT 2012.POLL.T07L25R.dave.PLT
OU POSTFILE MONTH T07L25R PLOT 2012.POLL.T07L25R.mave.PLT
OU POSTFILE PERIOD T07L25R PLOT 2012.POLL.T07L25R.pave.PLT
** T07R Outputs
OU POSTFILE 1 T07R PLOT 2012.POLL.T07R.have.PLT
OU POSTFILE 24 T07R PLOT 2012.POLL.T07R.dave.PLT
OU POSTFILE MONTH T07R PLOT 2012.POLL.T07R.mave.PLT
OU POSTFILE PERIOD T07R PLOT 2012.POLL.T07R.pave.PLT
** T07R25L Outputs
OU POSTFILE 1 T07R25L PLOT 2012.POLL.T07R25L.have.PLT
OU POSTFILE 24 T07R25L PLOT 2012.POLL.T07R25L.dave.PLT
OU POSTFILE MONTH T07R25L PLOT 2012.POLL.T07R25L.mave.PLT
OU POSTFILE PERIOD T07R25L PLOT 2012.POLL.T07R25L.pave.PLT
** T24L Outputs
OU POSTFILE 1 T24L PLOT 2012.POLL.T24L.have.PLT
OU POSTFILE 24 T24L PLOT 2012.POLL.T24L.dave.PLT
OU POSTFILE MONTH T24L PLOT 2012.POLL.T24L.mave.PLT
OU POSTFILE PERIOD T24L PLOT 2012.POLL.T24L.pave.PLT
** T24R Outputs
OU POSTFILE 1 T24R PLOT 2012.POLL.T24R.have.PLT
OU POSTFILE 24 T24R PLOT 2012.POLL.T24R.dave.PLT
OU POSTFILE MONTH T24R PLOT 2012.POLL.T24R.mave.PLT
OU POSTFILE PERIOD T24R PLOT 2012.POLL.T24R.pave.PLT
** T25L Outputs
OU POSTFILE 1 T25L PLOT 2012.POLL.T25L.have.PLT
OU POSTFILE 24 T25L PLOT 2012.POLL.T25L.dave.PLT
OU POSTFILE MONTH T25L PLOT 2012.POLL.T25L.mave.PLT
OU POSTFILE PERIOD T25L PLOT 2012.POLL.T25L.pave.PLT
** T25R Outputs
OU POSTFILE 1 T25R PLOT 2012.POLL.T25R.have.PLT
OU POSTFILE 24 T25R PLOT 2012.POLL.T25R.dave.PLT
OU POSTFILE MONTH T25R PLOT 2012.POLL.T25R.mave.PLT
OU POSTFILE PERIOD T25R PLOT 2012.POLL.T25R.pave.PLT
** TAXI Outputs
OU POSTFILE 1 TAXI PLOT 2012.POLL.TAXI.have.PLT
```

```
OU POSTFILE 24 TAXI PLOT 2012.POLL.TAXI.dave.PLT
OU POSTFILE MONTH TAXI PLOT 2012.POLL.TAXI.mave.PLT
OU POSTFILE PERIOD TAXI PLOT 2012.POLL.TAXI.pave.PLT
** TF250240 Outputs
OU POSTFILE 1 TF250240 PLOT 2012.POLL.TF250240.have.PLT
OU POSTFILE 24 TF250240 PLOT 2012.POLL.TF250240.dave.PLT
OU POSTFILE MONTH TF250240 PLOT 2012.POLL.TF250240.mave.PLT
OU POSTFILE PERIOD TF250240 PLOT 2012.POLL.TF250240.pave.PLT
** TF6070 Outputs
OU POSTFILE 1 TF6070 PLOT 2012.POLL.TF6070.have.PLT
OU POSTFILE 24 TF6070 PLOT 2012.POLL.TF6070.dave.PLT
OU POSTFILE MONTH TF6070 PLOT 2012.POLL.TF6070.mave.PLT
OU POSTFILE PERIOD TF6070 PLOT 2012.POLL.TF6070.pave.PLT
OU FILEFORM EXP
OU FINISHED
```

(This page is intentionally blank)

APPENDIX 9-2: Figures for CMAQ Analyses

(This page is intentionally blank)

LIST OF FIGURES

Figure 9B-7. Modeled differences in seasonal mean speciated $PM_{2.5}$ between AQMD_AllAirp and AQMD_Zero scenarios during Winter Season.

Figure 9B-8. Modeled % differences in seasonal mean speciated $PM_{2.5}$ between AQMD_Jet and AQMD_Zero scenarios during Winter Season.

Figure 9B-9. Modeled % differences in seasonal mean speciated $PM_{2.5}$ between AQMD_HRE and AQMD_Zero scenarios during Winter Season.

Figure 9B-10. Modeled % differences in seasonal mean speciated $PM_{2.5}$ between AQMD_AllAirp and AQMD_Zero scenarios during Winter Season.

Figure 9B-11a. Modeled absolute (left) and % (right) differences in seasonal maximum daily average CO between AQMD_Jet and AQMD_Zero scenarios during Winter Season.

Figure 9B-11b. Modeled absolute (left) and % (right) differences in seasonal maximum daily average CO, NO_x and SO_2 between AQMD_Jet and AQMD_Zero scenarios during Winter Season.

Figure 9B-11c. Modeled absolute (left) and % (right) differences in seasonal maximum daily average SO_2 between AQMD_Jet and AQMD_Zero scenarios during Winter Season.

Figure 9B-12a. Modeled absolute (left) and % (right) differences in seasonal maximum daily average CO between AQMD_HRE and AQMD_Zero scenarios during Winter Season.

Figure 9B-12b. Modeled absolute (left) and % (right) differences in seasonal maximum daily average NO_x between AQMD_HRE and AQMD_Zero scenarios during Winter Season.

Figure 9B-12c. Modeled absolute (left) and % (right) differences in seasonal maximum daily average SO_2 between AQMD_HRE and AQMD_Zero scenarios during Winter Season.

Figure 9B-13a. Modeled absolute (left) and % (right) differences in seasonal maximum daily average CO between AQMD_AllAirp and AQMD_Zero scenarios during Winter Season.

Figure 9B-13b. Modeled absolute (left) and % (right) differences in seasonal maximum daily average NO_x between AQMD_AllAirp and AQMD_Zero scenarios during Winter Season.

Figure 9B-13c. Modeled absolute (left) and % (right) differences in seasonal maximum daily average SO_2 between AQMD_AllAirp and AQMD_Zero scenarios during Winter Season.

Figure 9B-14a. Modeled absolute (left) and % (right) differences in total $PM_{2.5}$ between AQMD_Jet and AQMD_Zero scenarios during Winter Season.

Figure 9B-14b. Modeled absolute (left) and % (right) differences in total $PM_{2.5}$ between AQMD_HRE and AQMD_Zero scenarios during Winter Season.

Figure 9B-14c. Modeled absolute (left) and % (right) differences in total $PM_{2.5}$ between AQMD_AllAirp and AQMD_Zero scenarios during Winter Season.

Figure 9B-15. Modeled differences in seasonal maximum daily average speciated $PM_{2.5}$ between AQMD_Jet and AQMD_Zero scenarios during Winter Season.

Figure 9B-16. Modeled differences in seasonal maximum daily average speciated $PM_{2.5}$ between AQMD_HRE and AQMD_Zero scenarios during Winter Season.

Figure 9B-17. Modeled differences in seasonal maximum daily average speciated $PM_{2.5}$ between AQMD_AllAirp and AQMD_Zero scenarios during Winter Season.

Figure 9B-18. Modeled % differences in seasonal maximum daily average speciated $PM_{2.5}$ between AQMD_Jet and AQMD_Zero scenarios during Winter Season.

Figure 9B-19. Modeled % differences in seasonal maximum daily average speciated $PM_{2.5}$ between AQMD_HRE and AQMD_Zero scenarios during Winter Season.

Figure 9B-20. Modeled % differences in seasonal maximum daily average speciated $PM_{2.5}$ between AQMD_AllAirp and AQMD_Zero scenarios during Winter Season.

Figure 9B-21a. Modeled absolute (left) and % (right) differences in seasonal mean CO between AQMD_Jet and AQMD_Zero scenarios during Summer Season.

Figure 9B-21b. Modeled absolute (left) and % (right) differences in seasonal mean NO_x between AQMD_Jet and AQMD_Zero scenarios during Summer Season.

Figure 9B-21c. Modeled absolute (left) and % (right) differences in seasonal mean SO_2 between AQMD_Jet and AQMD_Zero scenarios during Summer Season.

Figure 9B-22a. Modeled absolute (left) and % (right) differences in seasonal mean CO between AQMD_HRE and AQMD_Zero scenarios during Summer Season.

Figure 9B-22b. Modeled absolute (left) and % (right) differences in seasonal mean NO_x between AQMD_HRE and AQMD_Zero scenarios during Summer Season.

Figure 9B-22c. Modeled absolute (left) and % (right) differences in seasonal mean SO_2 between AQMD_HRE and AQMD_Zero scenarios during Summer Season.

Figure 9B-23a. Modeled absolute (left) and % (right) differences in seasonal mean CO between AQMD_AllAirp and AQMD_Zero scenarios during Summer Season.

Figure 9B-23b. Modeled absolute (left) and % (right) differences in seasonal mean NO_x between AQMD_AllAirp and AQMD_Zero scenarios during Summer Season.

Figure 9B-23c. Modeled absolute (left) and % (right) differences in seasonal mean SO_2 between AQMD_AllAirp and AQMD_Zero scenarios during Summer Season.

Figure 9B-24a. Modeled absolute (left) and % (right) differences in total $PM_{2.5}$ between AQMD_Jet and AQMD_Zero scenarios during Summer Season.

Figure 9B-24b. Modeled absolute (left) and % (right) differences in total $PM_{2.5}$ between AQMD_HRE and AQMD_Zero scenarios during Summer Season.

Figure 9B-24c. Modeled absolute (left) and % (right) differences in total $PM_{2.5}$ between AQMD_AllAirp and AQMD_Zero scenarios during Summer Season.

Figure 9B-25. Modeled differences in seasonal mean speciated $PM_{2.5}$ between AQMD_Jet and AQMD_Zero scenarios during Summer Season.

Figure 9B-26. Modeled differences in seasonal mean speciated $PM_{2.5}$ between AQMD_HRE and AQMD_Zero scenarios during Summer Season.

Figure 9B-27. Modeled differences in seasonal mean speciated $PM_{2.5}$ between AQMD_AllAirp and AQMD_Zero scenarios during Summer Season.

Figure 9B-28. Modeled % differences in seasonal mean speciated $PM_{2.5}$ between AQMD_Jet and AQMD_Zero scenarios during Summer Season.

Figure 9B-29. Modeled % differences in seasonal mean speciated $PM_{2.5}$ between AQMD_HRE and AQMD_Zero scenarios during Summer Season.

Figure 9B-30. Modeled % differences in seasonal mean speciated $PM_{2.5}$ between AQMD_AllAirp and AQMD_Zero scenarios during Summer Season.

Figure 9B-31a. Modeled absolute (left) and % (right) differences in seasonal maximum daily average CO between AQMD_Jet and AQMD_Zero scenarios during Summer Season.

Figure 9B-31b. Modeled absolute (left) and % (right) differences in seasonal maximum daily average NO_x between AQMD_Jet and AQMD_Zero scenarios during Summer Season.

Figure 9B-31c. Modeled absolute (left) and % (right) differences in seasonal maximum daily average SO_2 between AQMD_Jet and AQMD_Zero scenarios during Summer Season.
Figure 9B-32a. Modeled absolute (left) and % (right) differences in seasonal maximum daily average CO between AQMD_HRE and AQMD_Zero scenarios during Summer Season.

Figure 9B-32b. Modeled absolute (left) and % (right) differences in seasonal maximum daily average NO_x between AQMD_HRE and AQMD_Zero scenarios during Summer Season.

Figure 9B-32c. Modeled absolute (left) and % (right) differences in seasonal maximum daily average SO_2 between AQMD_HRE and AQMD_Zero scenarios during Summer Season.

Figure 9B-33a. Modeled absolute (left) and % (right) differences in seasonal maximum daily average CO between AQMD_AllAirp and AQMD_Zero scenarios during Summer Season.

Figure 9B-33b. Modeled absolute (left) and % (right) differences in seasonal maximum daily average NO_x between AQMD_AllAirp and AQMD_Zero scenarios during Summer Season.

Figure 9B-33c. Modeled absolute (left) and % (right) differences in seasonal maximum daily average SO_2 between AQMD_AllAirp and AQMD_Zero scenarios during Summer Season.

Figure 9B-34a. Modeled absolute (left) and % (right) differences in total $PM_{2.5}$ between AQMD_Jet and AQMD_Zero scenarios during Summer Season.

Figure 9B-34b. Modeled absolute (left) and % (right) differences in total $PM_{2.5}$ between AQMD_HRE and AQMD_Zero scenarios during Summer Season.

Figure 9B-34c. Modeled absolute (left) and % (right) differences in total $PM_{2.5}$ between AQMD_AllAirp and AQMD_Zero scenarios during Summer Season.

Figure 9B-35. Modeled differences in seasonal maximum daily average speciated $PM_{2.5}$ between AQMD_Jet and AQMD_Zero scenarios during Summer Season.

Figure 9B-36. Modeled differences in seasonal maximum daily average speciated $PM_{2.5}$ between AQMD_HRE and AQMD_Zero scenarios during Summer Season.

Figure 9B-37. Modeled differences in seasonal maximum daily average speciated $PM_{2.5}$ between AQMD_AllAirp and AQMD_Zero scenarios during Summer Season.

Figure 9B-38. Modeled % differences in seasonal maximum daily average speciated $PM_{2.5}$ between AQMD_Jet and AQMD_Zero scenarios during Summer Season.

Figure 9B-39. Modeled % differences in seasonal maximum daily average speciated $PM_{2.5}$ between AQMD_HRE and AQMD_Zero scenarios during Summer Season.

Figure 9B-40. Modeled % differences in seasonal maximum daily average speciated $PM_{2.5}$ between AQMD_AllAirp and AQMD_Zero scenarios during Summer Season.

Figure 9B-41. Modeled % differences in seasonal maximum daily average CO, NOx, $PM_{2.5}$ and SO_2 between AQMD_HRE and AQMD_Zero scenarios during Winter Season (entire domain shown).

Figure 9B-42. Modeled % differences in seasonal maximum daily average CO, NOx, $PM_{2.5}$ and SO_2 between AQMD_HRE and AQMD_Zero scenarios during Summer Season (entire domain shown).

Figure 9B-43. Modeled % differences in seasonal maximum daily average CO, NOx, $PM_{2.5}$ and SO_2 between AQMD_AllAirp and AQMD_Zero scenarios during Winter Season (entire domain shown).

Figure 9B-44. Modeled % differences in seasonal maximum daily average CO, NOx, $PM_{2.5}$ and SO_2 between AQMD_AllAirp and AQMD_Zero scenarios during Summer Season (entire domain shown).

Figure 9B-45. Incremental CO contributions modeled by CMAQ due to various emissions scenarios during Winter (left) and Summer (right).

Figure 9B-46. Incremental NO_x contributions modeled by CMAQ due to various emissions scenarios during Winter (left) and Summer (right).

Figure 9B-47. Incremental $PM_{2.5}$ contributions modeled by CMAQ due to various emissions scenarios during Winter (left) and Summer (right).

Figure 9B-48. Incremental SO_2 contributions modeled by CMAQ due to various emissions scenarios during Winter (left) and Summer (right).

I. Spatial Analyses

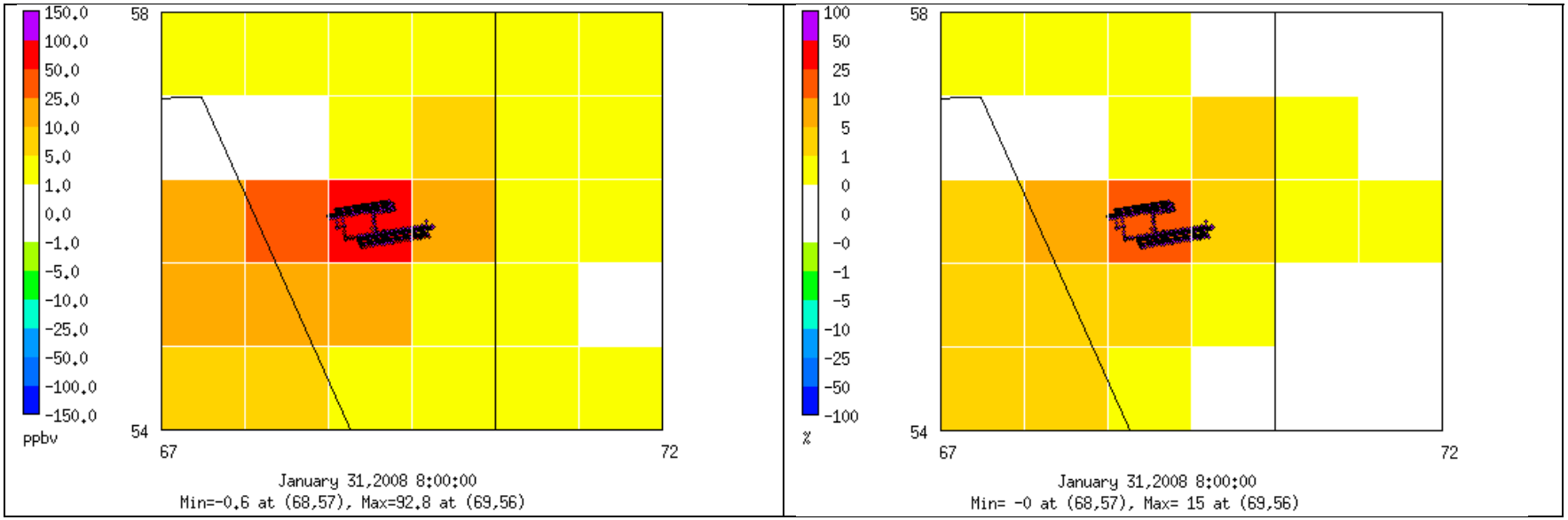

Figure 9B-1a. Modeled absolute (left) and % (right) differences in seasonal mean CO between AQMD_Jet and AQMD_Zero scenarios during Winter Season.

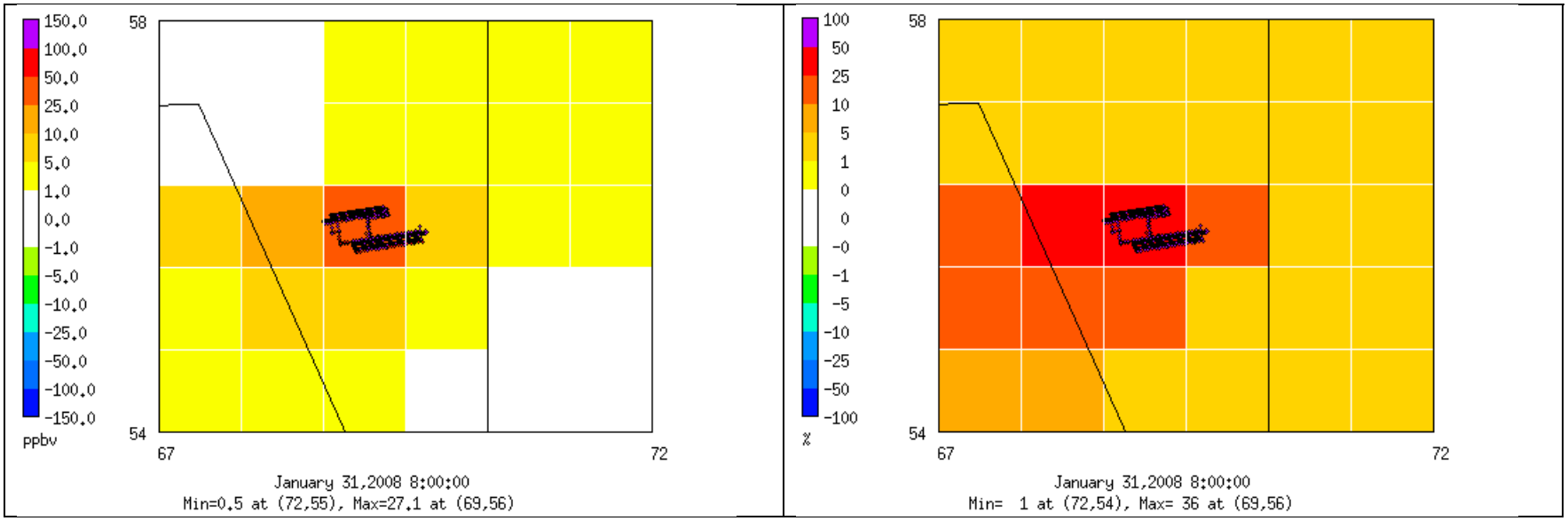

Figure 9B-1b. Modeled absolute (left) and % (right) differences in seasonal mean NO_x between AQMD_Jet and AQMD_Zero scenarios during Winter Season.

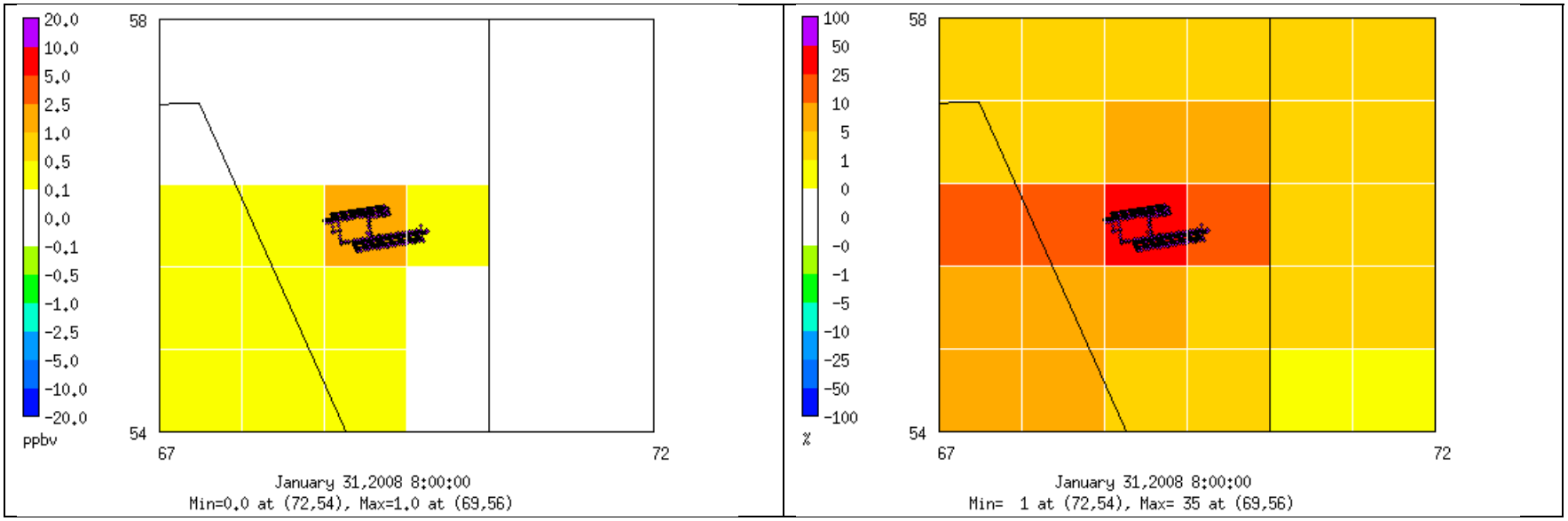

Figure 9B-1c. Modeled absolute (left) and % (right) differences in seasonal mean SO_2 between AQMD_Jet and AQMD_Zero scenarios during Winter Season.

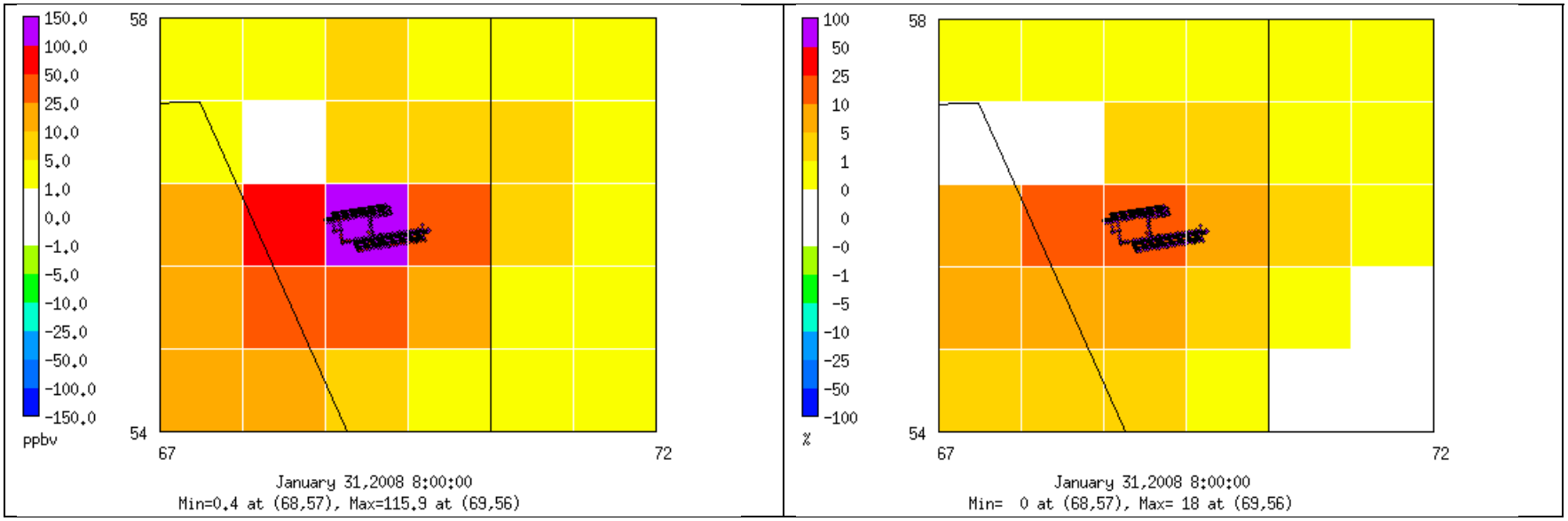

Figure 9B-2a. Modeled absolute (left) and % (right) differences in seasonal mean CO between AQMD_HRE and AQMD_Zero scenarios during Winter Season.

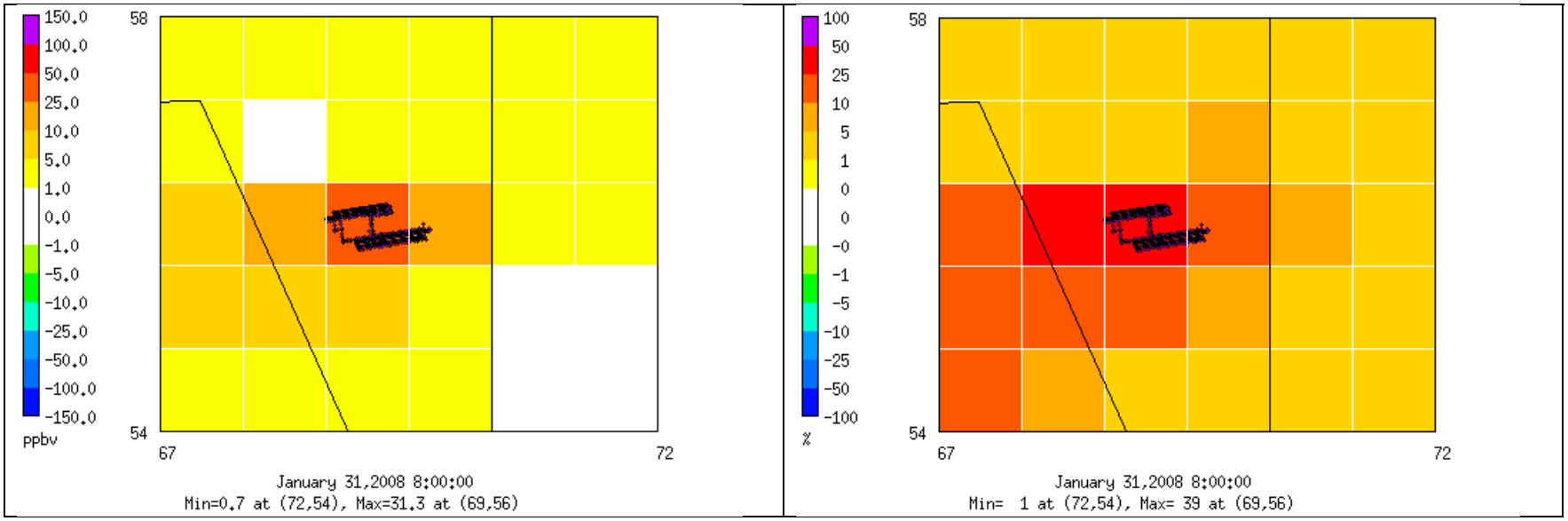

Figure 9B-2b. Modeled absolute (left) and % (right) differences in seasonal mean NO_x between AQMD_HRE and AQMD_Zero scenarios during Winter Season.

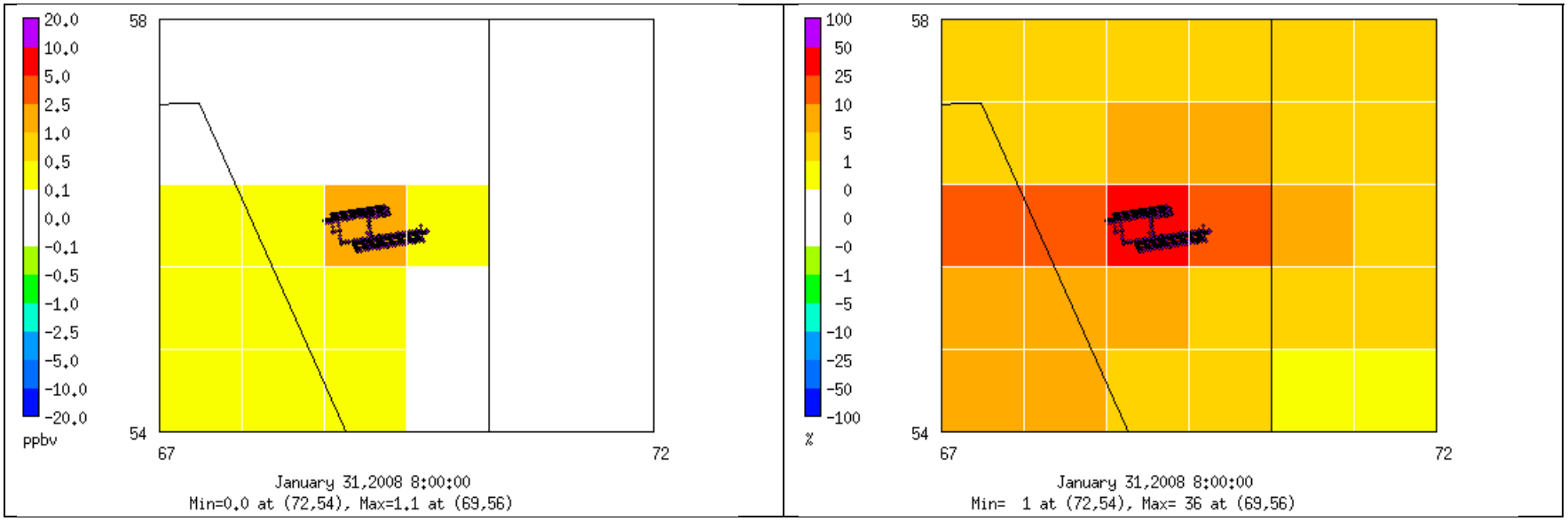

Figure 9B-2c. Modeled absolute (left) and % (right) differences in seasonal means SO_2 between AQMD_HRE and AQMD_Zero scenarios during Winter Season.

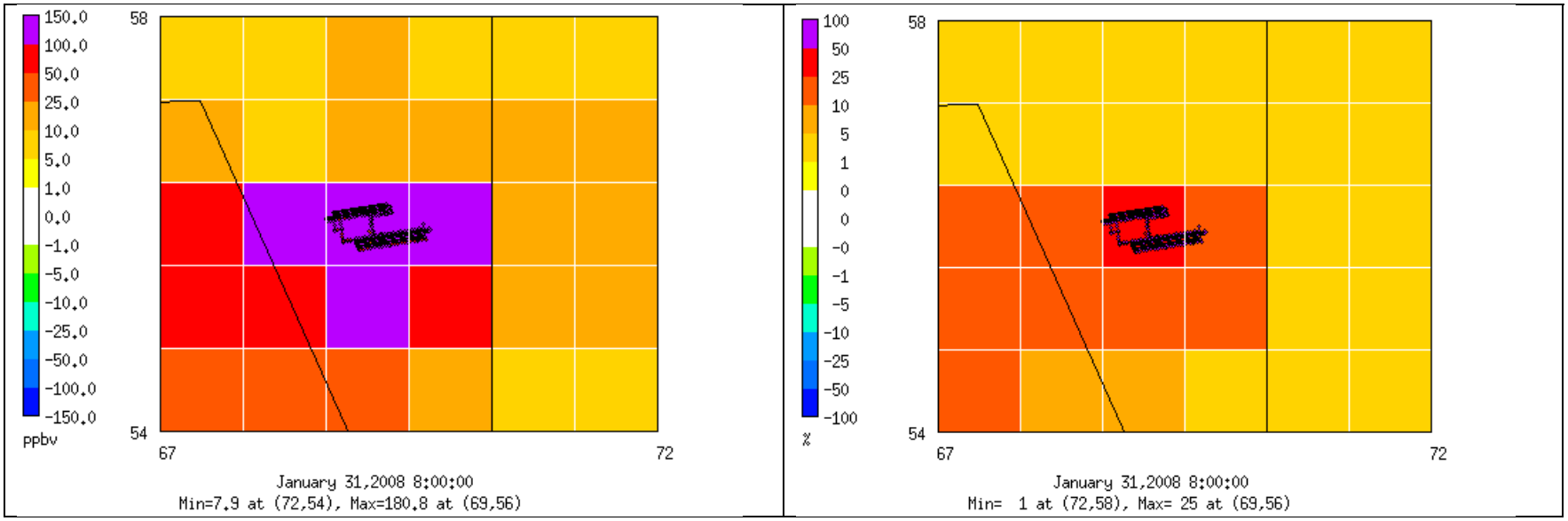

Figure 9B-3a. Modeled absolute (left) and % (right) differences in seasonal mean CO between AQMD_AllAirp and AQMD_Zero scenarios during Winter Season.

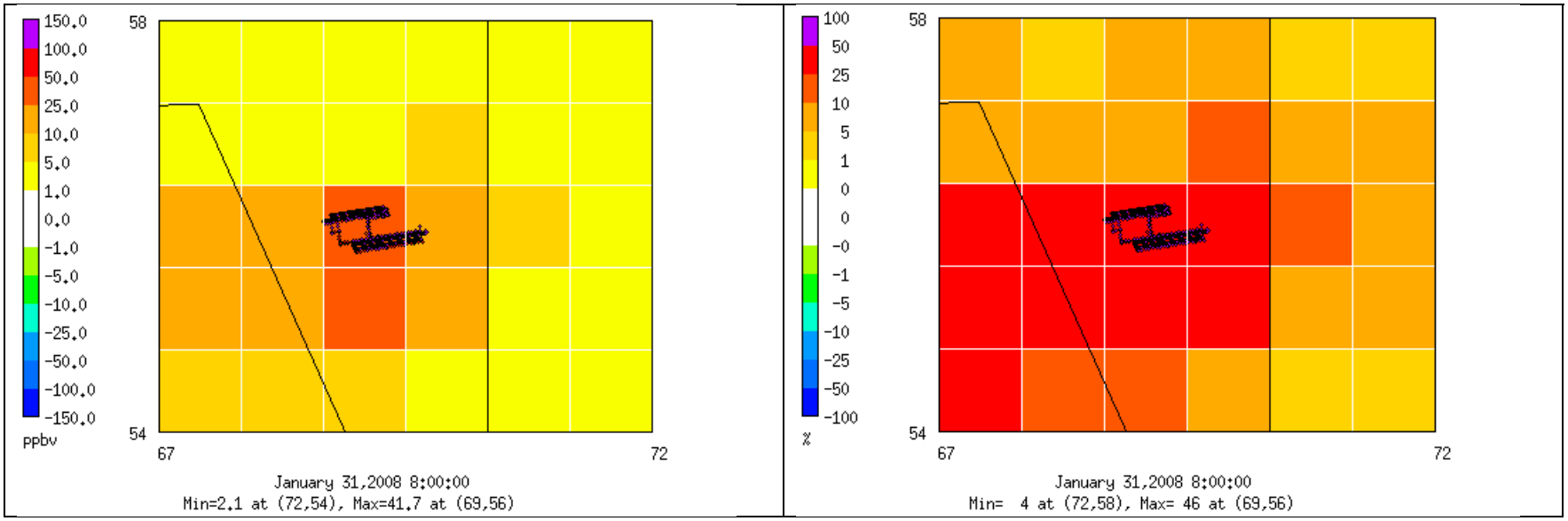

Figure 9B-3b. Modeled absolute (left) and % (right) differences in seasonal mean NO_x between AQMD_AllAirp and AQMD_Zero scenarios during Winter Season.

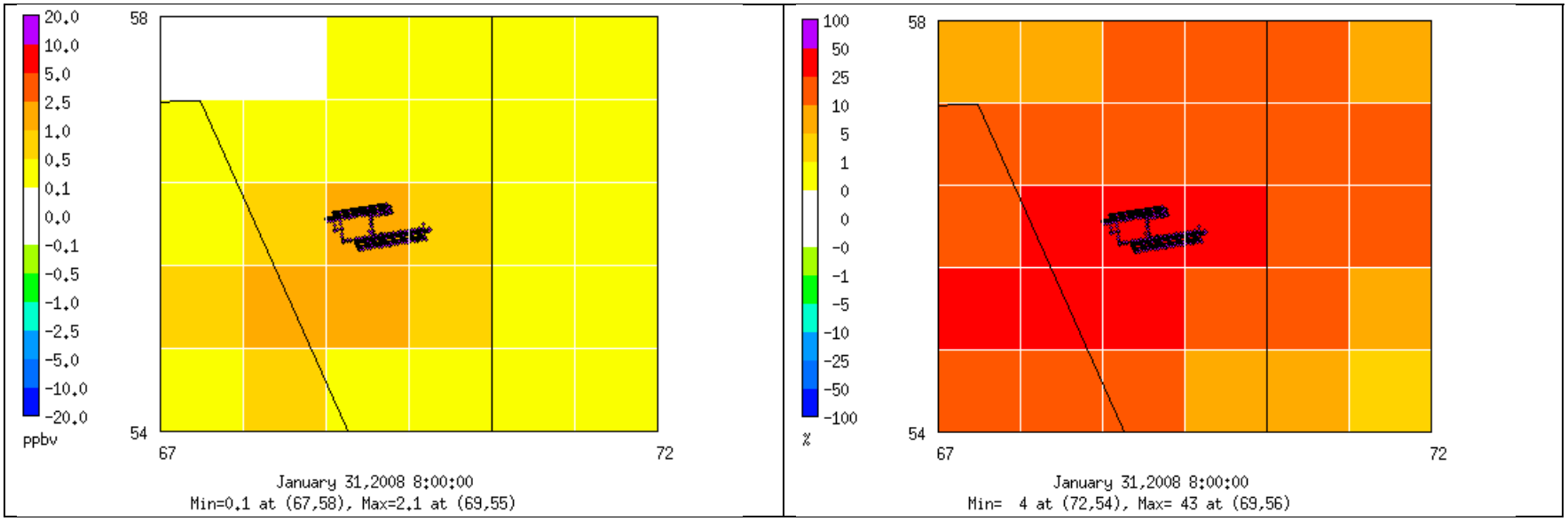

Figure 9B-3c. Modeled absolute (left) and % (right) differences in seasonal mean SO_2 between AQMD_AllAirp and AQMD_Zero scenarios during Winter Season.

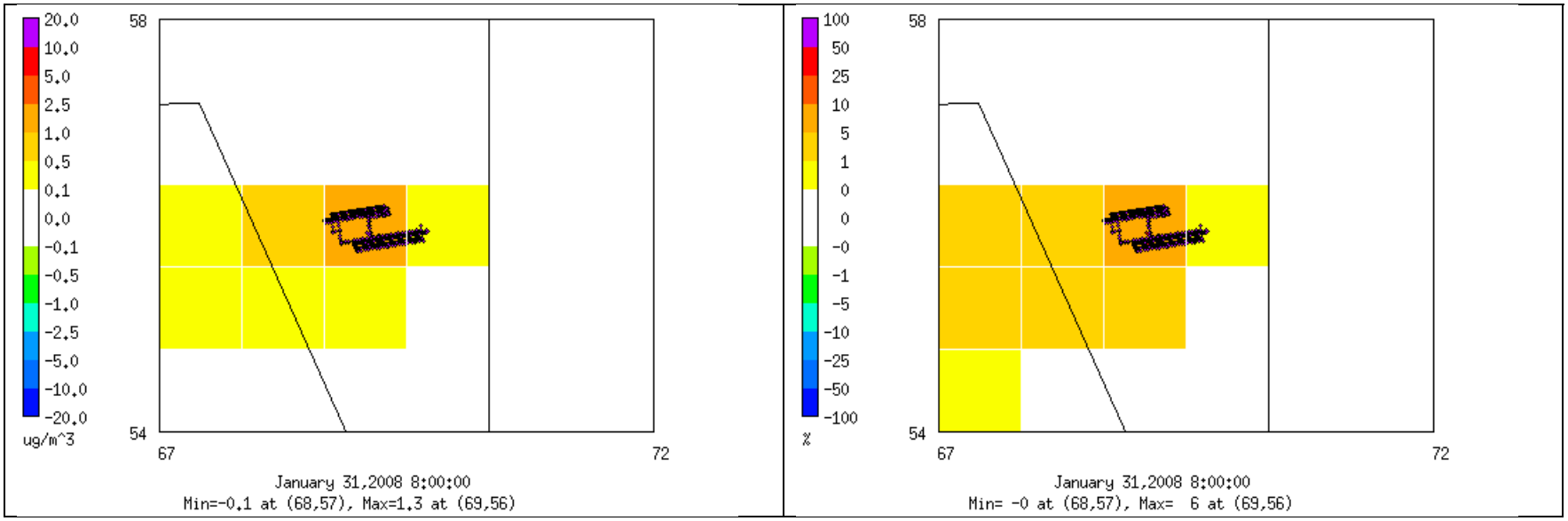

Figure 9B-4a. Modeled absolute (left) and % (right) differences in total $PM_{2.5}$ between AQMD_Jet and AQMD_Zero scenarios during Winter Season.

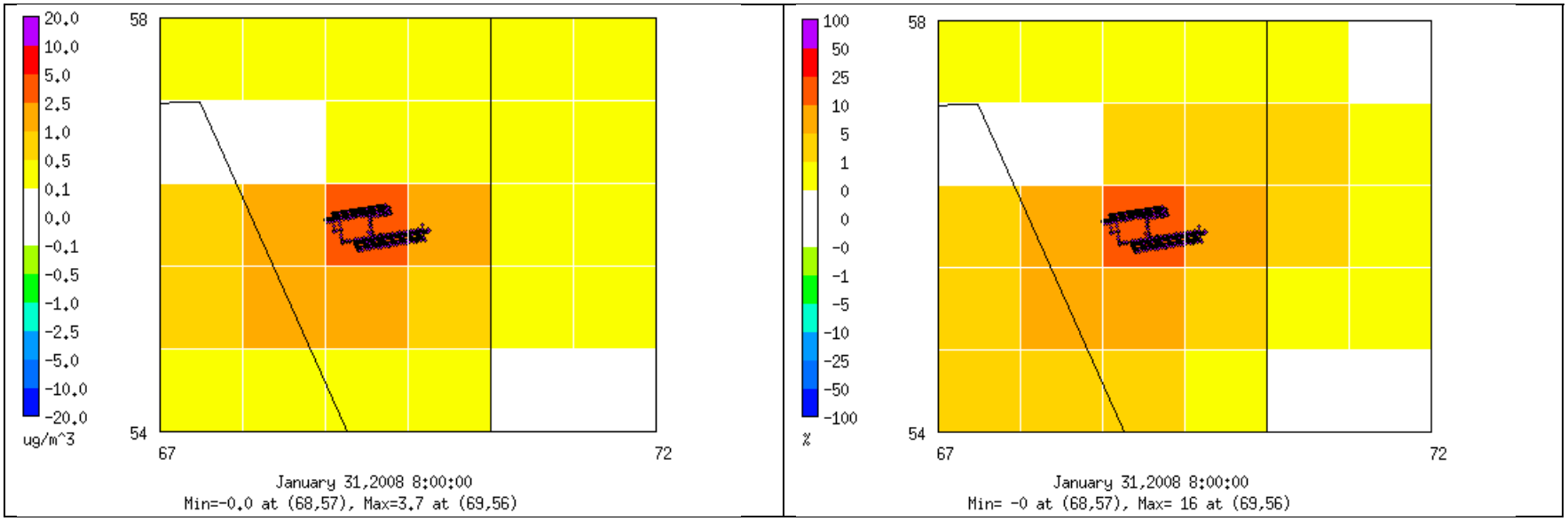

Figure 9B-4b. Modeled absolute (left) and % (right) differences in total $PM_{2.5}$ between AQMD_HRE and AQMD_Zero scenarios during Winter Season.

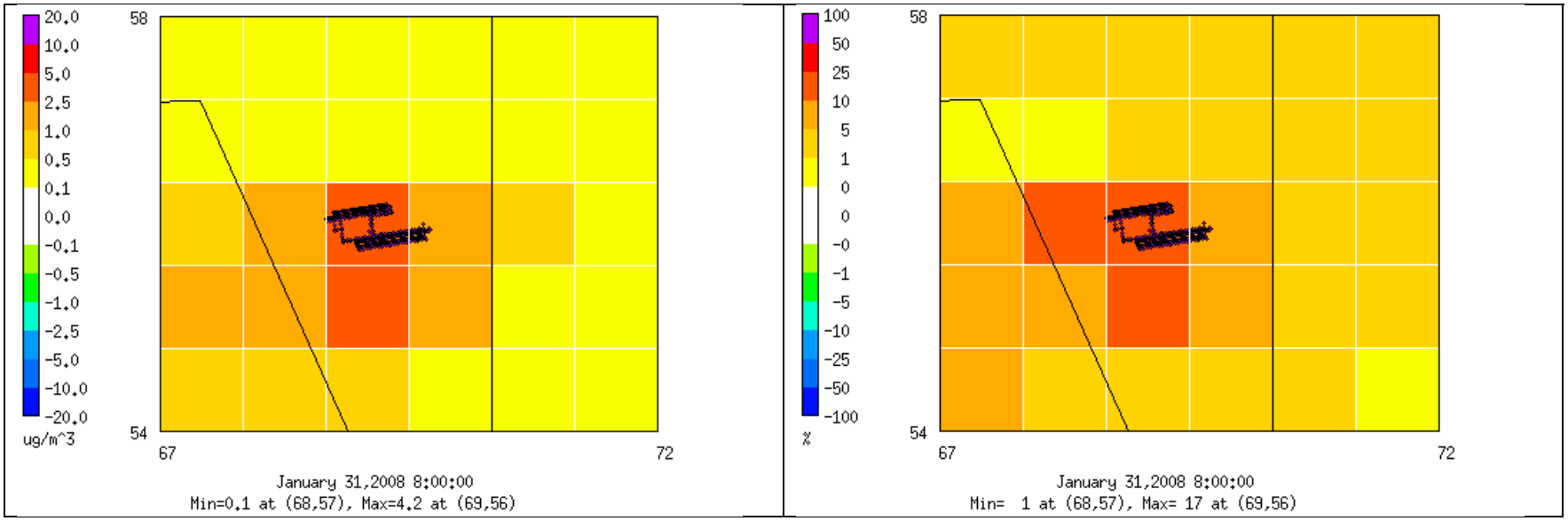

Figure 9B-4c. Modeled absolute (left) and % (right) differences in total $PM_{2.5}$ between AQMD_AllAirp and AQMD_Zero scenarios during Winter Season.

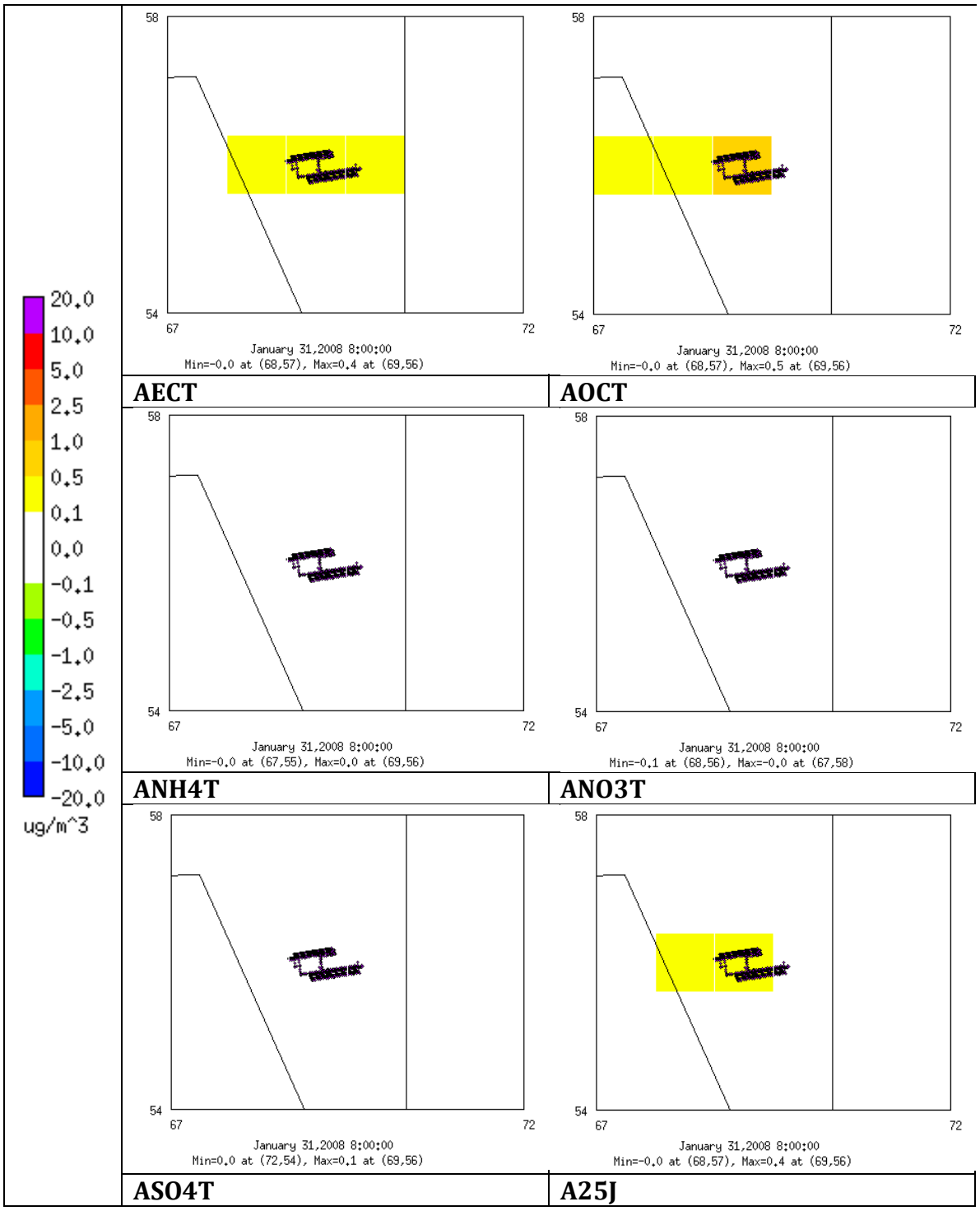

Figure 9B-5. Modeled differences in seasonal mean speciated $PM_{2.5}$ between AQMD_Jet and AQMD_Zero scenarios during Winter Season.

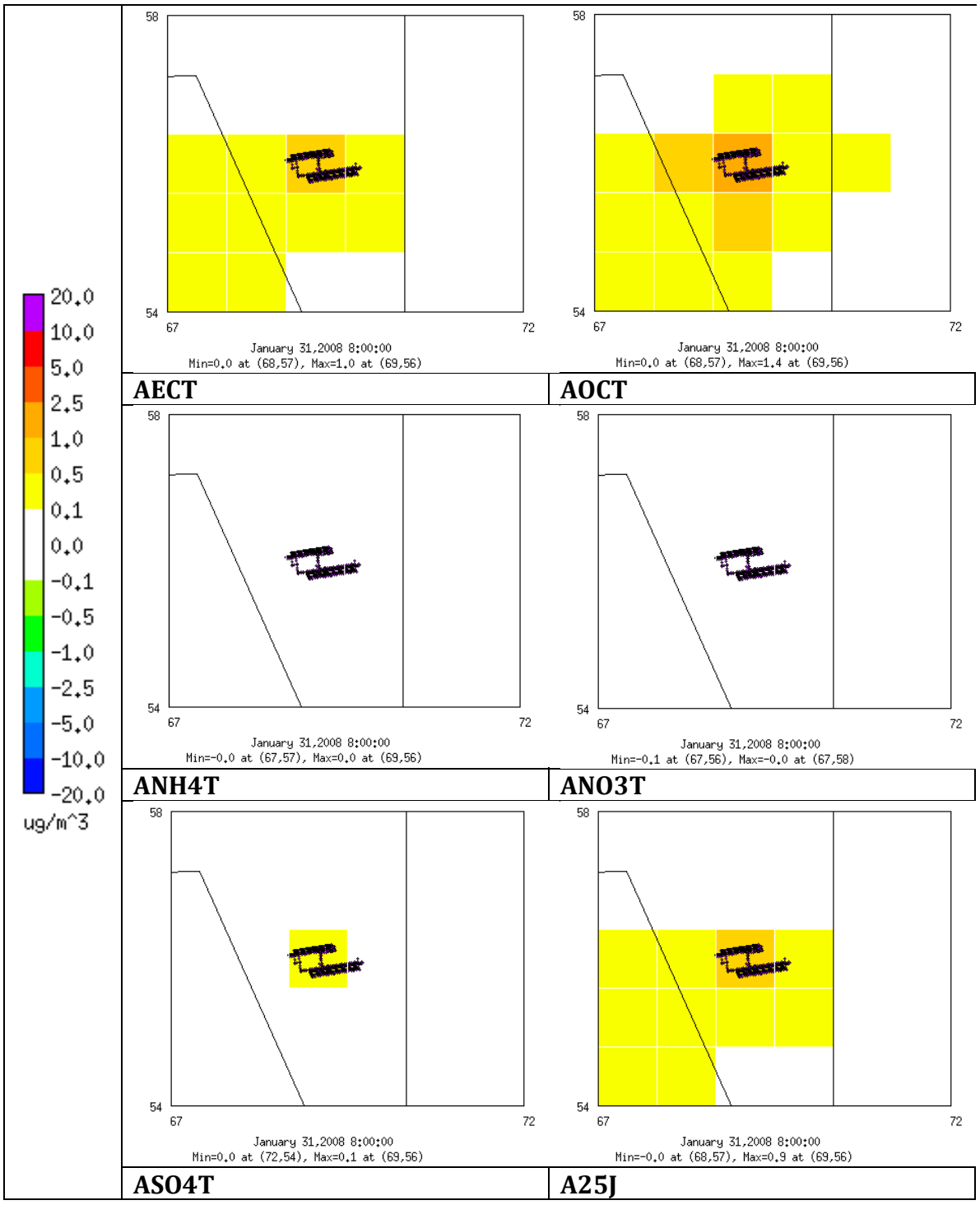

Figure 9B-6. Modeled differences in seasonal mean speciated $PM_{2.5}$ between AQMD_HRE and AQMD_Zero scenarios during Winter Season.

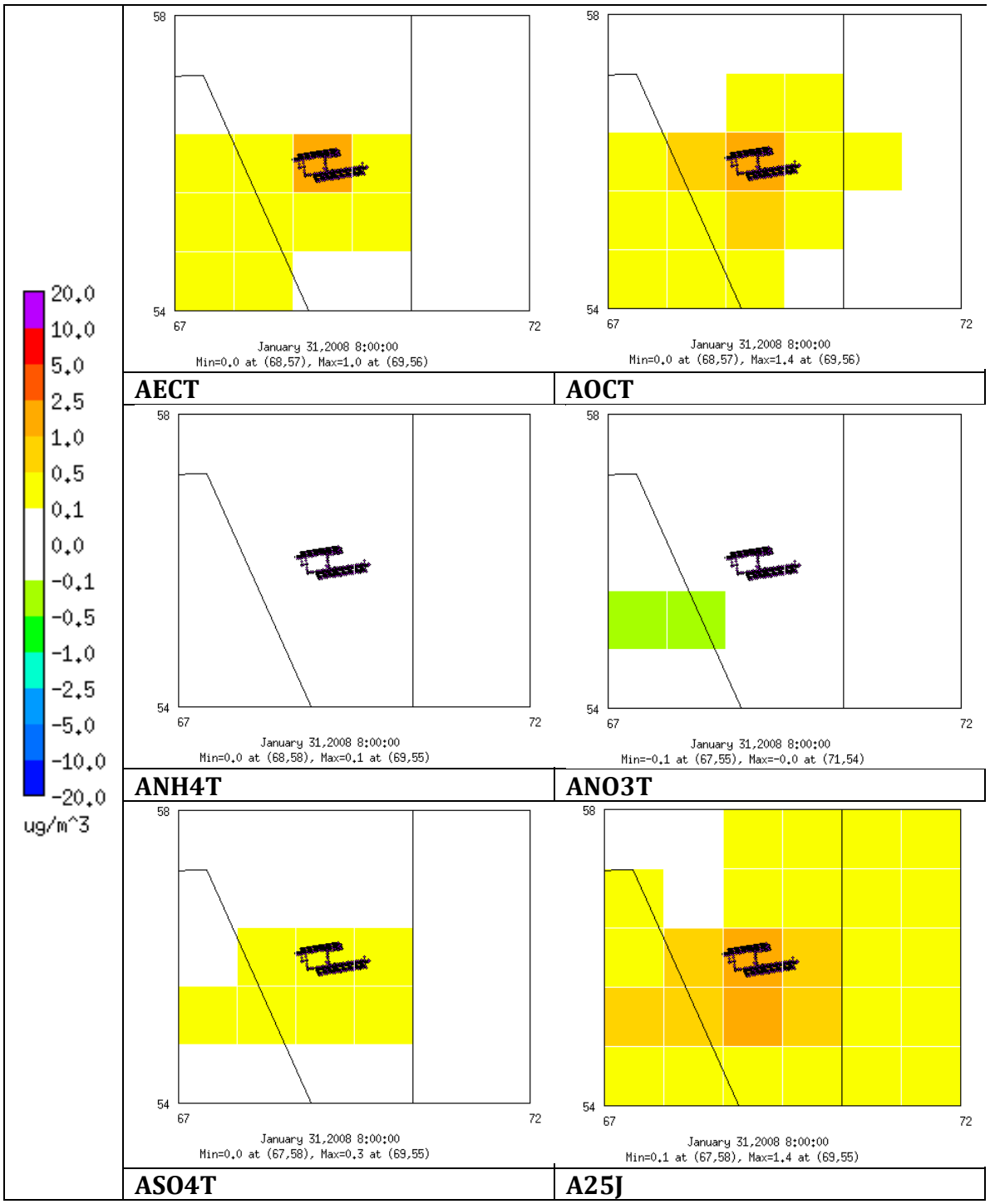

Figure 9B-7. Modeled differences in seasonal mean speciated $PM_{2.5}$ between AQMD_AllAirp and AQMD_Zero scenarios during Winter Season.

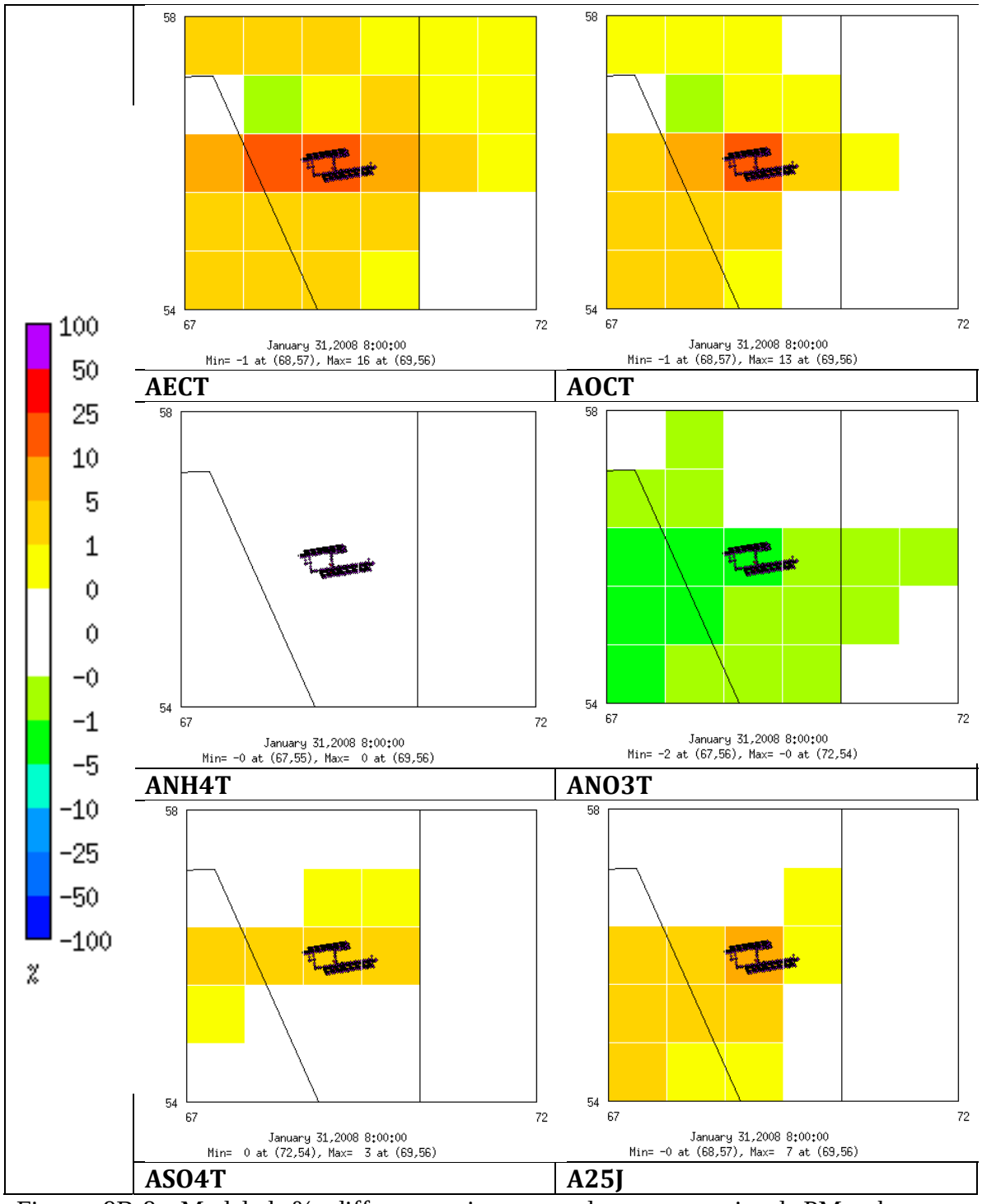

Figure 9B-8. Modeled % differences in seasonal mean speciated $PM_{2.5}$ between AQMD_Jet and AQMD_Zero scenarios during Winter Season.

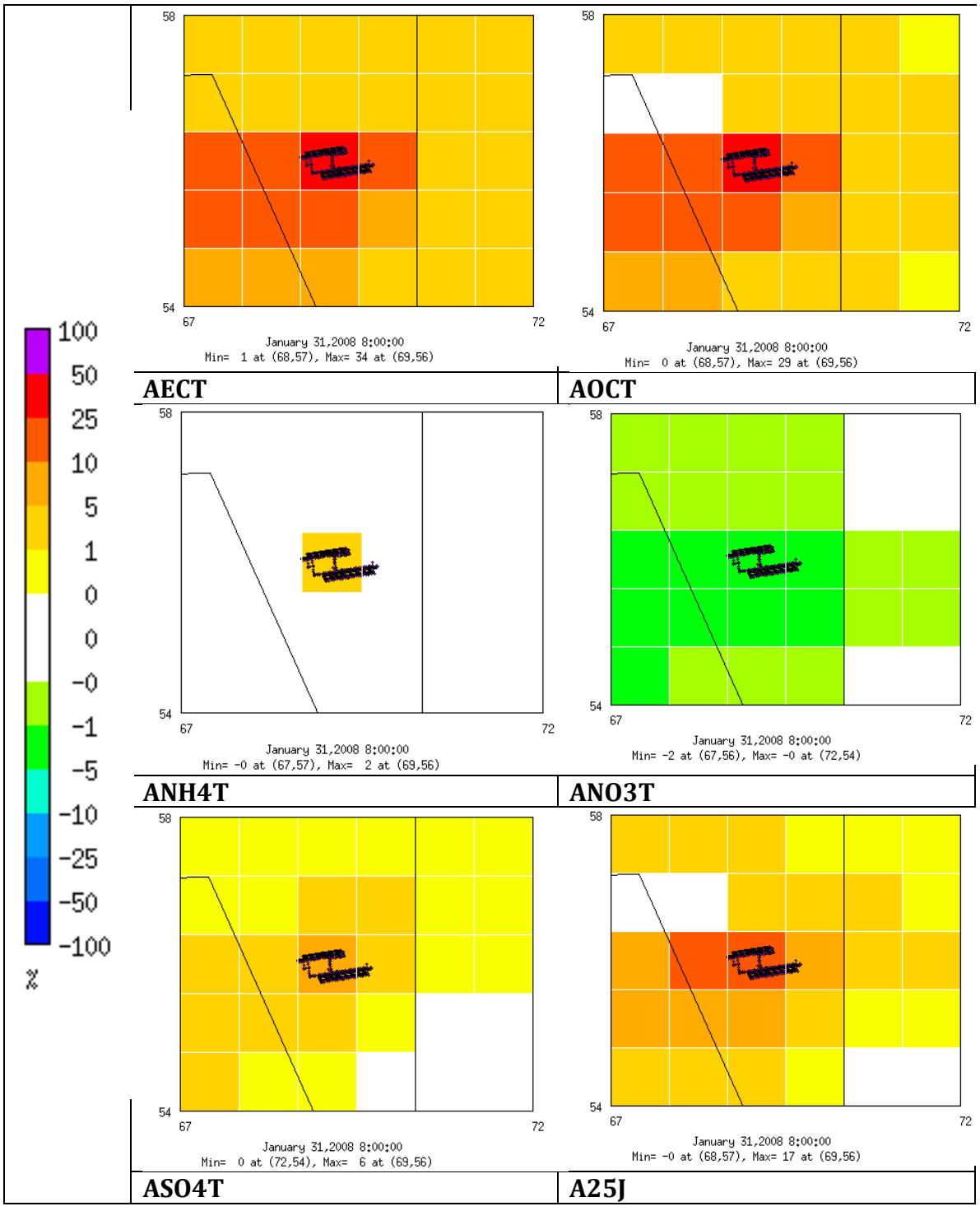

Figure 9B-9. Modeled % differences in seasonal mean speciated $PM_{2.5}$ between AQMD_HRE and AQMD_Zero scenarios during Winter Season.

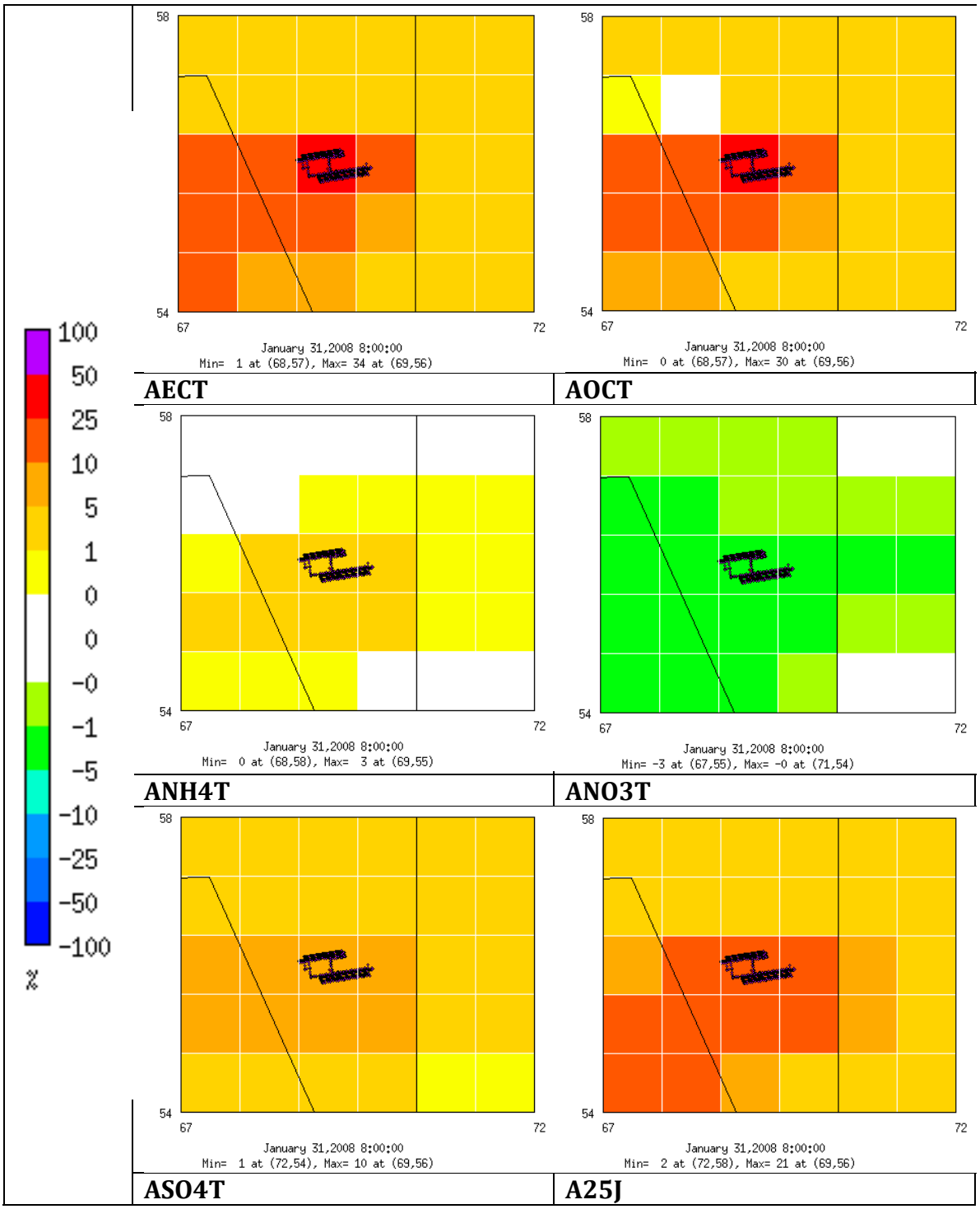

Figure 9B-10. Modeled % differences in seasonal mean speciated $PM_{2.5}$ between AQMD_AllAirp and AQMD_Zero scenarios during Winter Season.

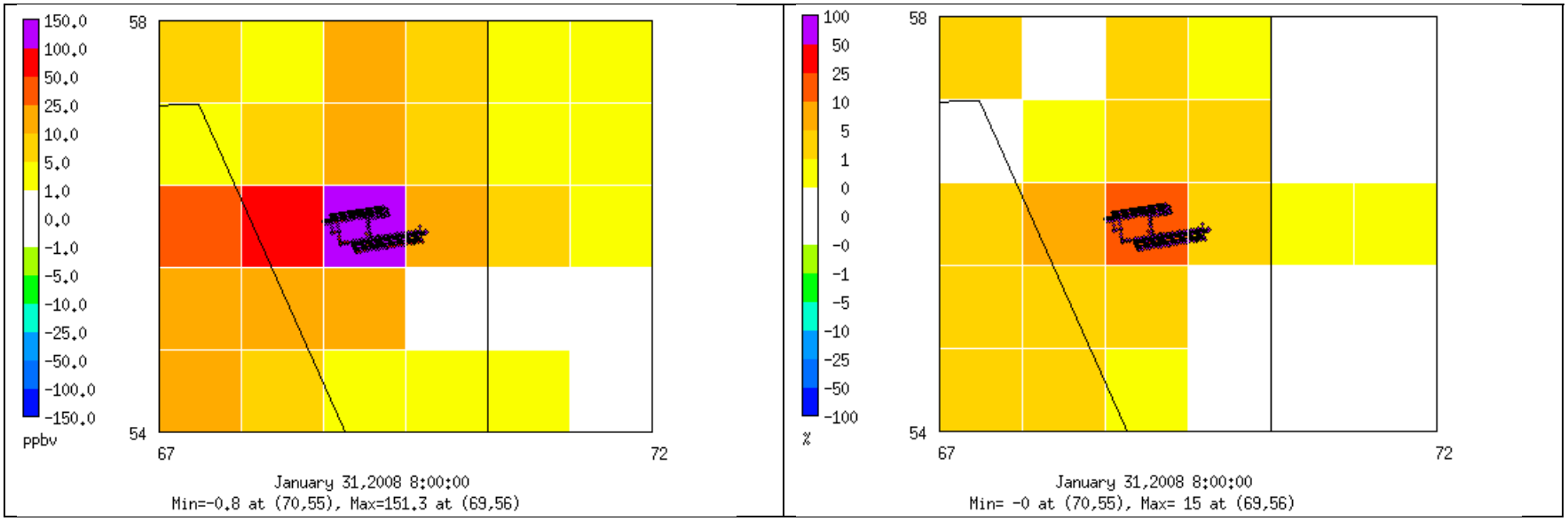

Figure 9B-11a. Modeled absolute (left) and % (right) differences in seasonal maximum daily average CO between AQMD_Jet and AQMD_Zero scenarios during Winter Season.

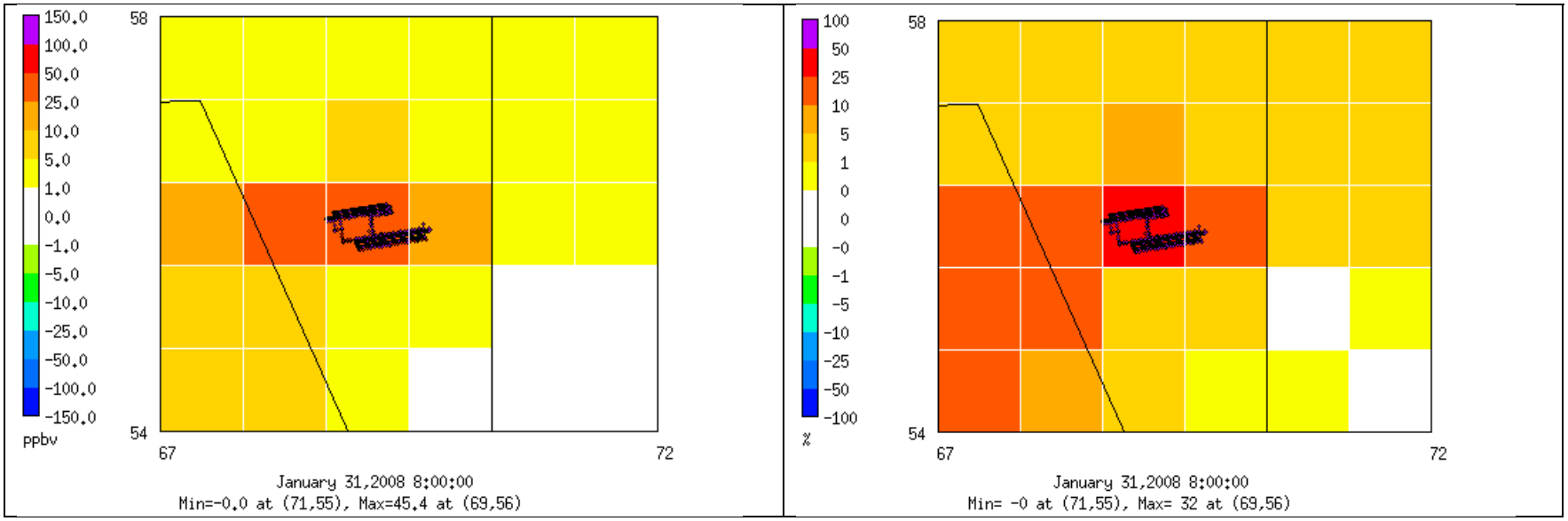

Figure 9B-11b. Modeled absolute (left) and % (right) differences in seasonal maximum daily average CO, NO_x and SO_2 between AQMD_Jet and AQMD_Zero scenarios during Winter Season.

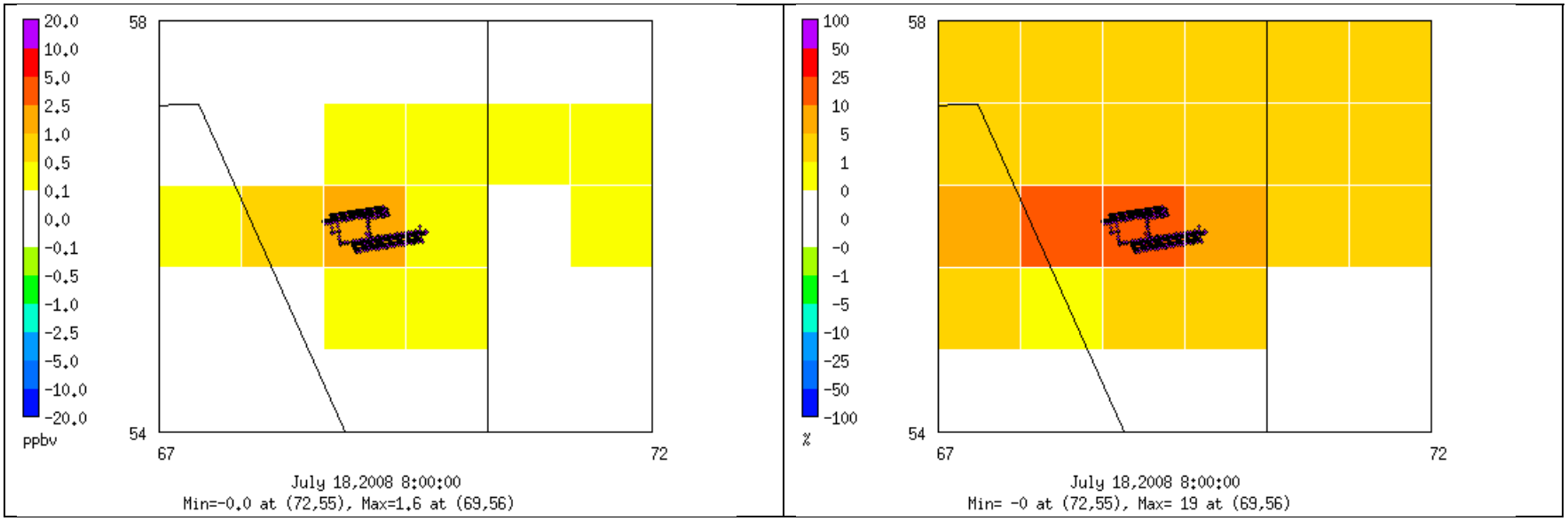

Figure 9B-11c. Modeled absolute (left) and % (right) differences in seasonal maximum daily average SO_2 between AQMD_Jet and AQMD_Zero scenarios during Winter Season.

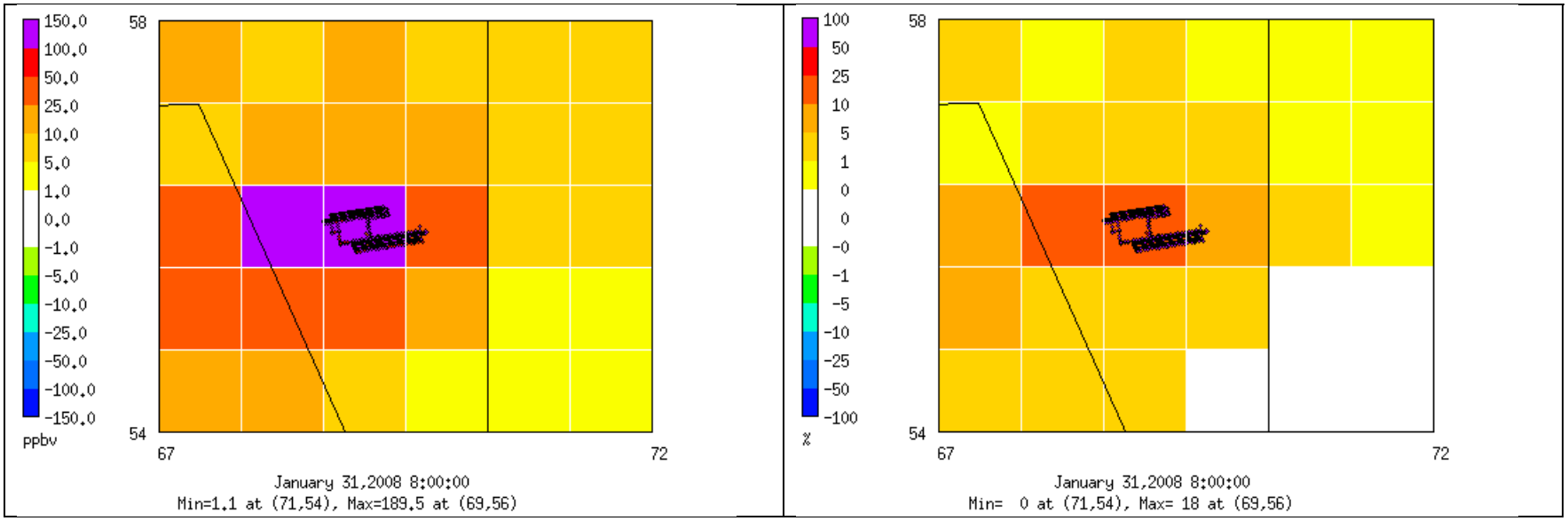

Figure 9B-12a. Modeled absolute (left) and % (right) differences in seasonal maximum daily average CO between AQMD_HRE and AQMD_Zero scenarios during Winter Season.

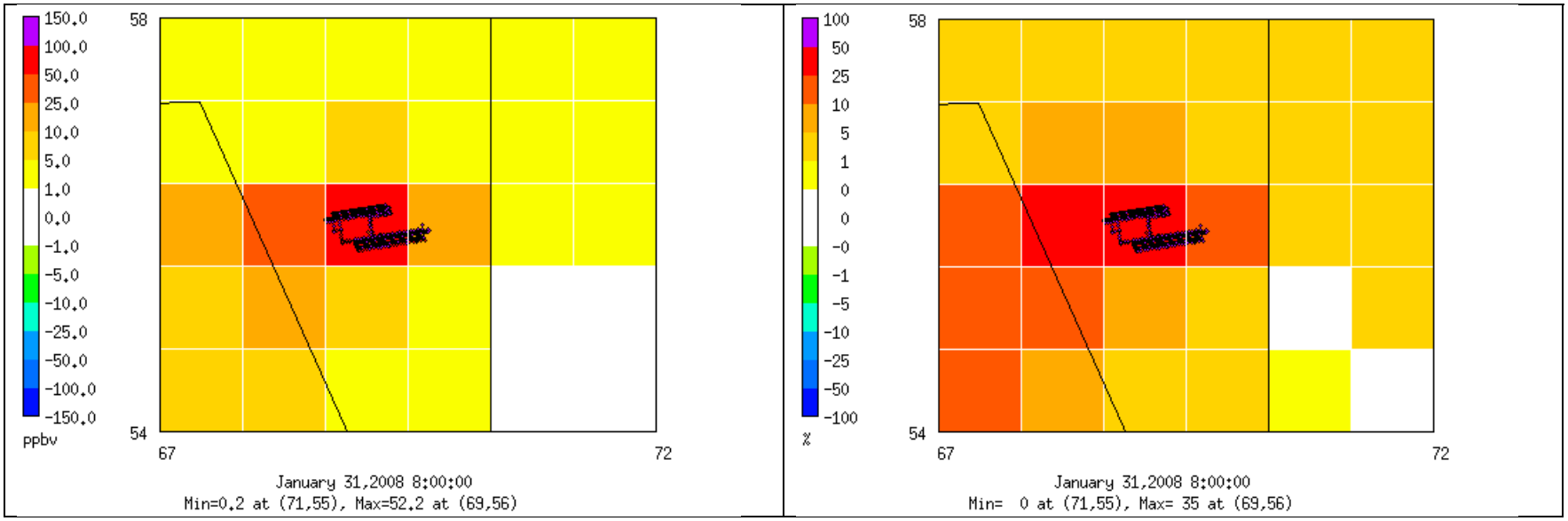

Figure 9B-12b. Modeled absolute (left) and % (right) differences in seasonal maximum daily average NO_x between AQMD_HRE and AQMD_Zero scenarios during Winter Season.

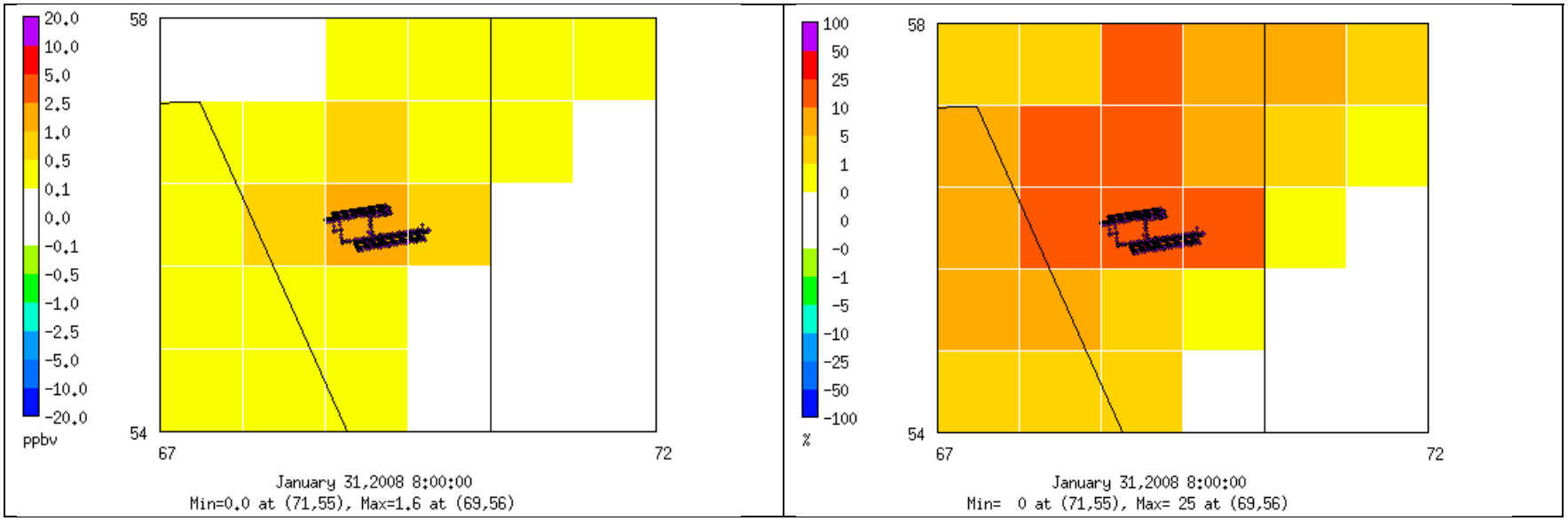

Figure 9B-12c. Modeled absolute (left) and % (right) differences in seasonal maximum daily average SO_2 between AQMD_HRE and AQMD_Zero scenarios during Winter Season.

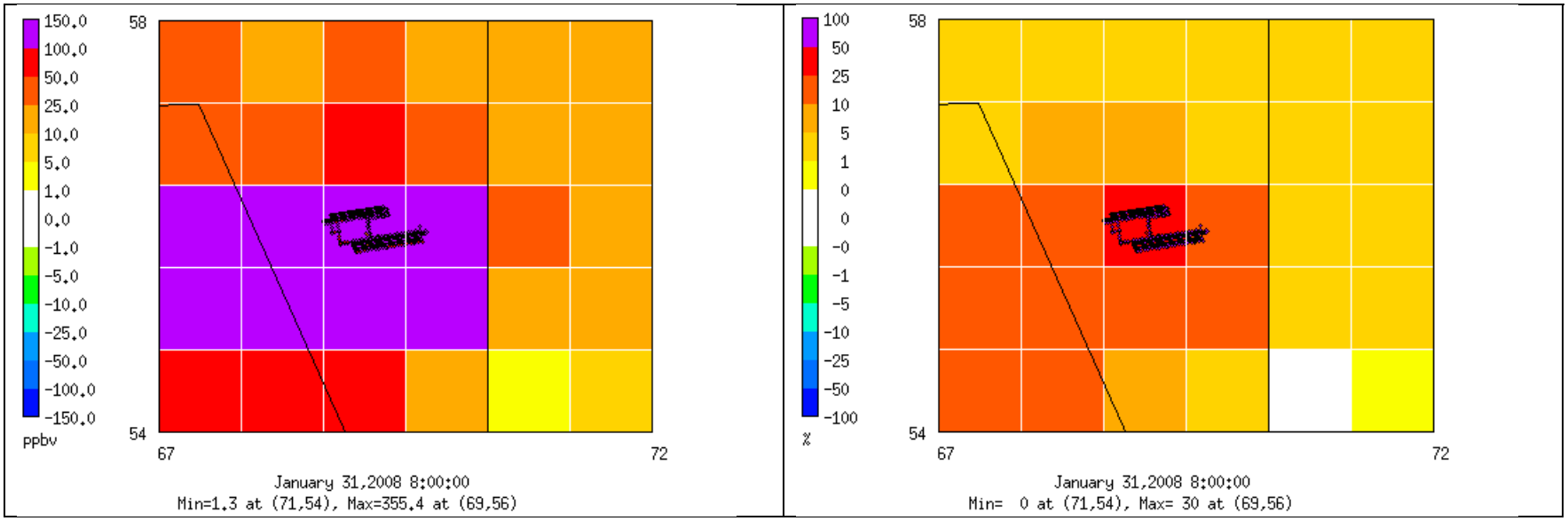

Figure 9B-13a. Modeled absolute (left) and % (right) differences in seasonal maximum daily average CO between AQMD_AllAirp and AQMD_Zero scenarios during Winter Season.

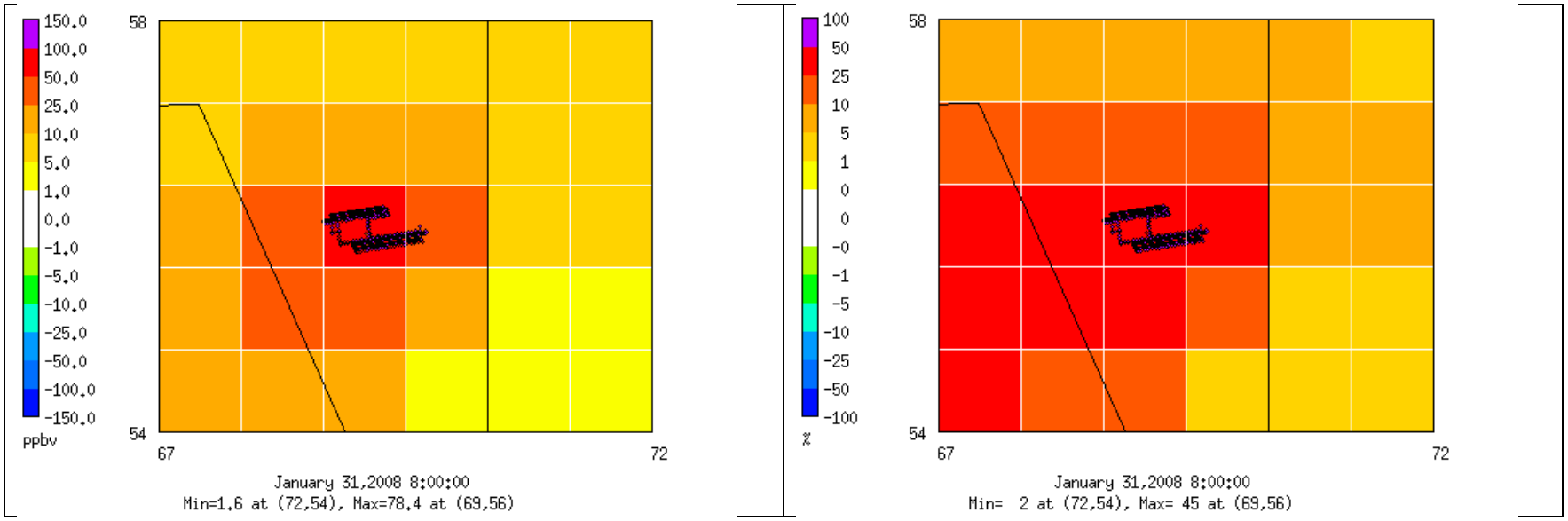

Figure 9B-13b. Modeled absolute (left) and % (right) differences in seasonal maximum daily average NO_x between AQMD_AllAirp and AQMD_Zero scenarios during Winter Season.

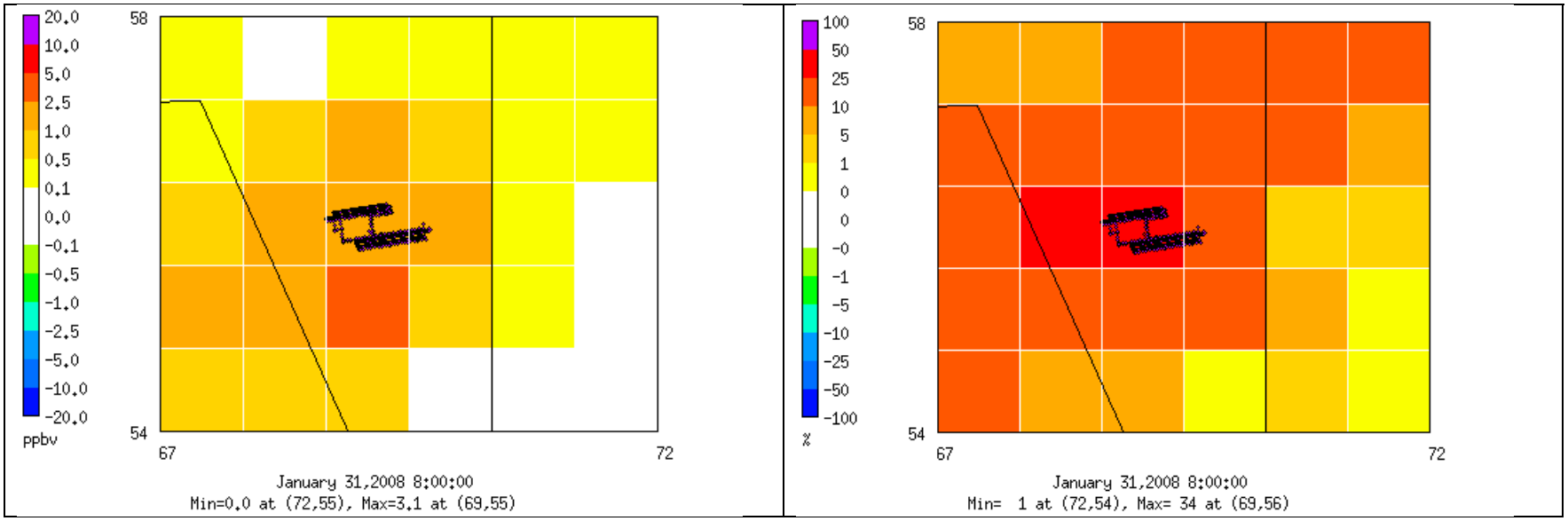

Figure 9B-13c. Modeled absolute (left) and % (right) differences in seasonal maximum daily average SO_2 between AQMD_AllAirp and AQMD_Zero scenarios during Winter Season.

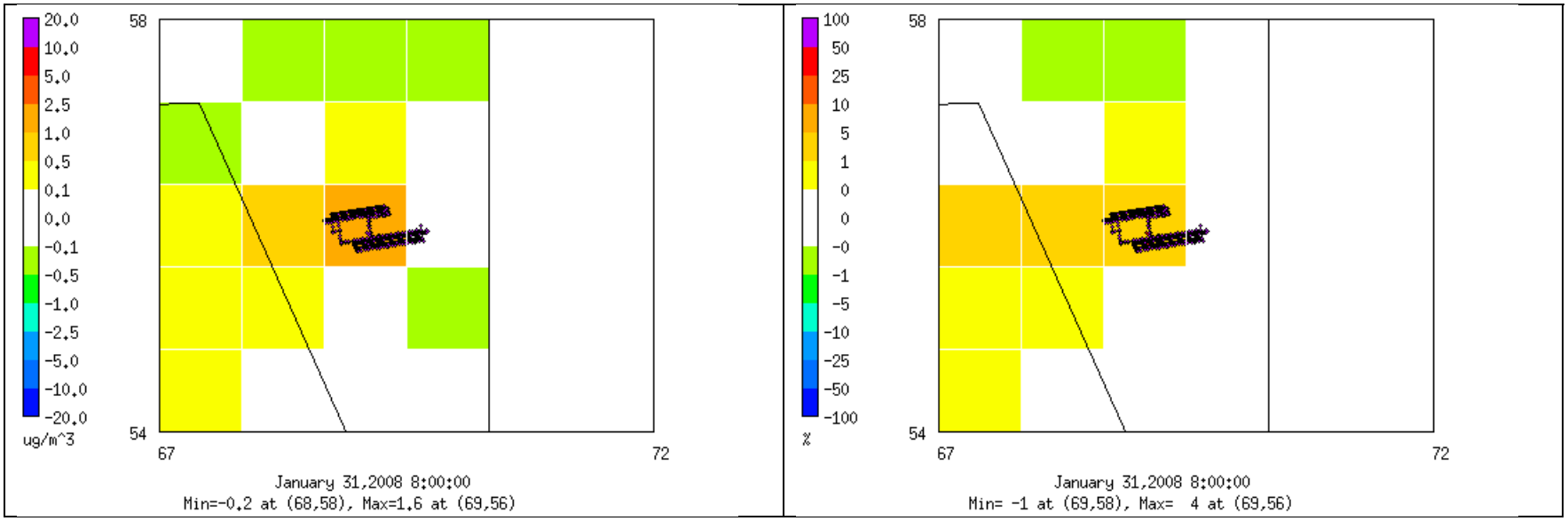

Figure 9B-14a. Modeled absolute (left) and % (right) differences in total $PM_{2.5}$ between AQMD_Jet and AQMD_Zero scenarios during Winter Season.

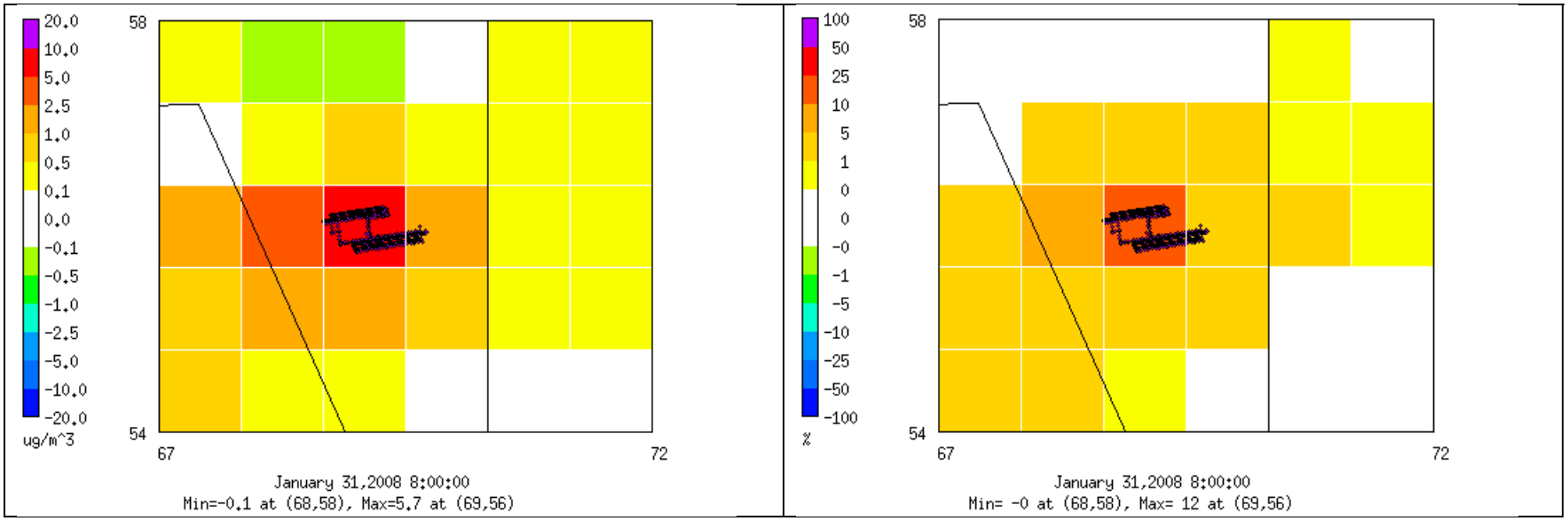

Figure 9B-14b. Modeled absolute (left) and % (right) differences in total $PM_{2.5}$ between AQMD_HRE and AQMD_Zero scenarios during Winter Season.

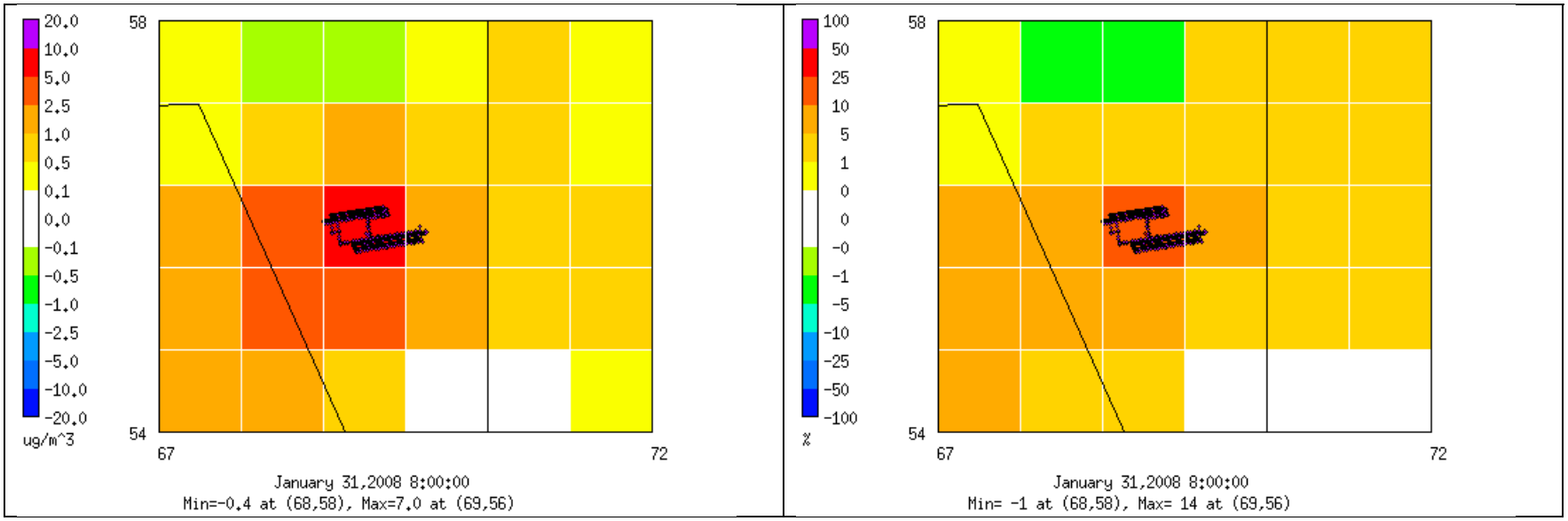

Figure 9B-14c. Modeled absolute (left) and % (right) differences in total $PM_{2.5}$ between AQMD_AllAirp and AQMD_Zero scenarios during Winter Season.

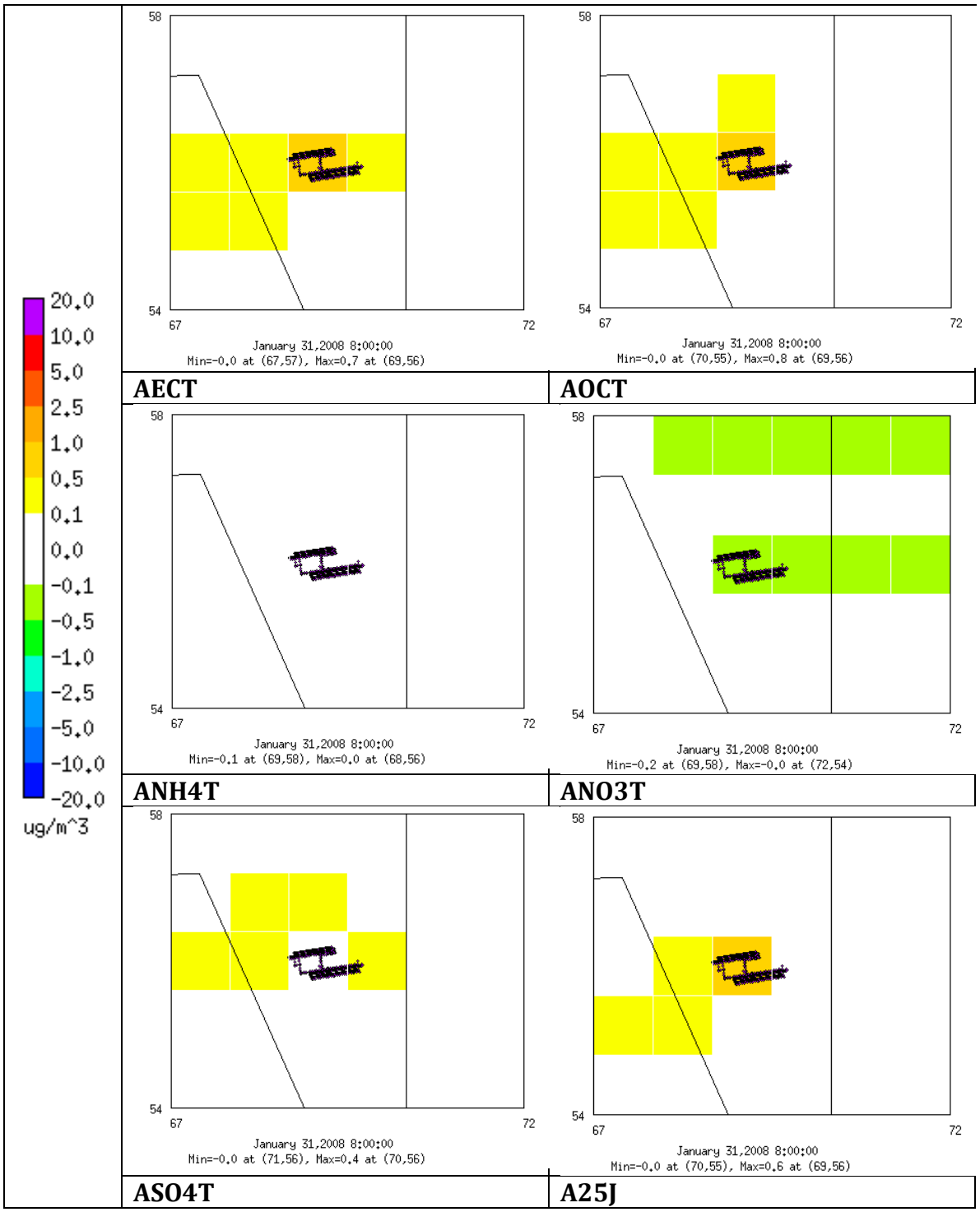

Figure 9B-15. Modeled differences in seasonal maximum daily average speciated $PM_{2.5}$ between AQMD_Jet and AQMD_Zero scenarios during Winter Season.

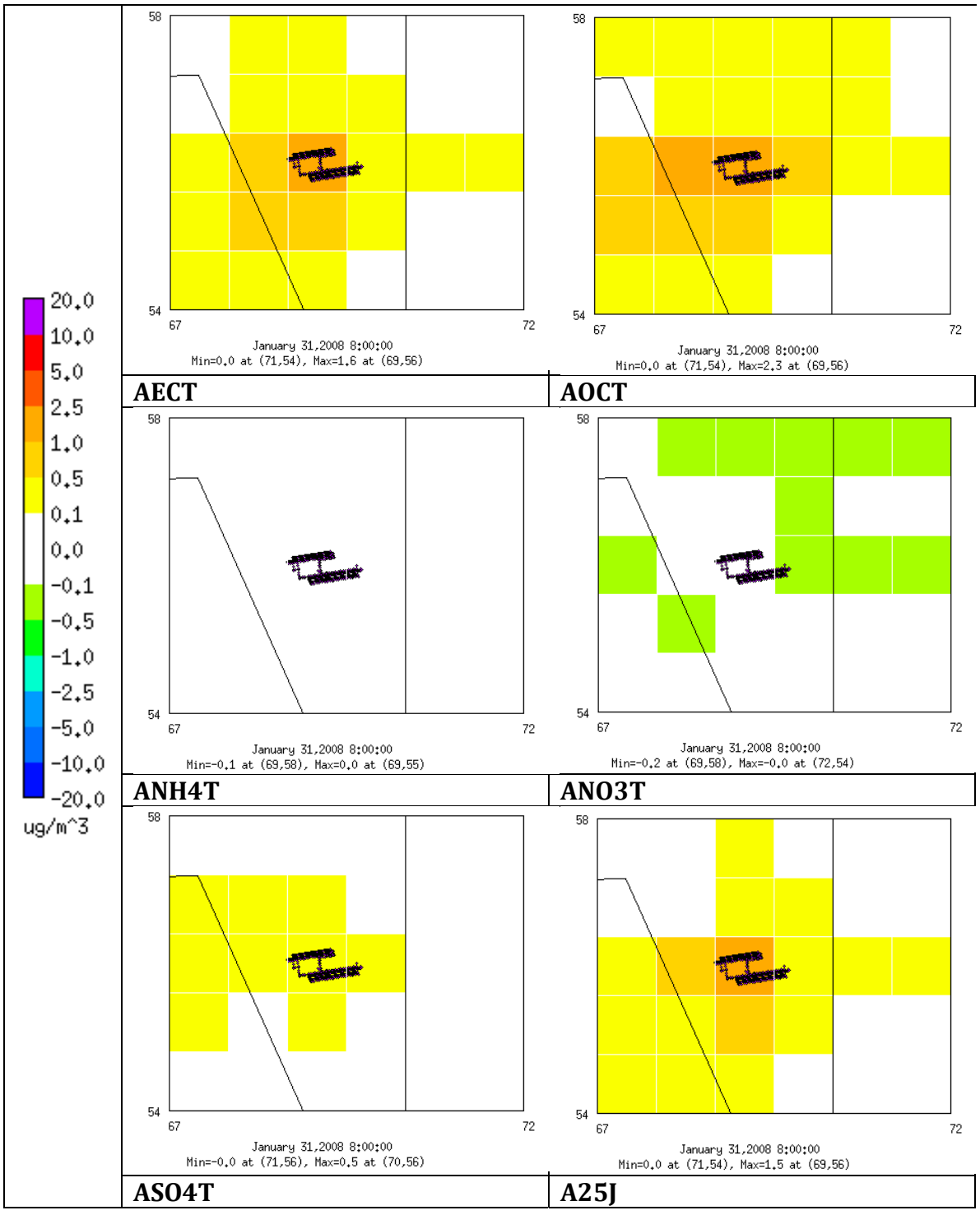

Figure 9B-16. Modeled differences in seasonal maximum daily average speciated $PM_{2.5}$ between AQMD_HRE and AQMD_Zero scenarios during Winter Season.

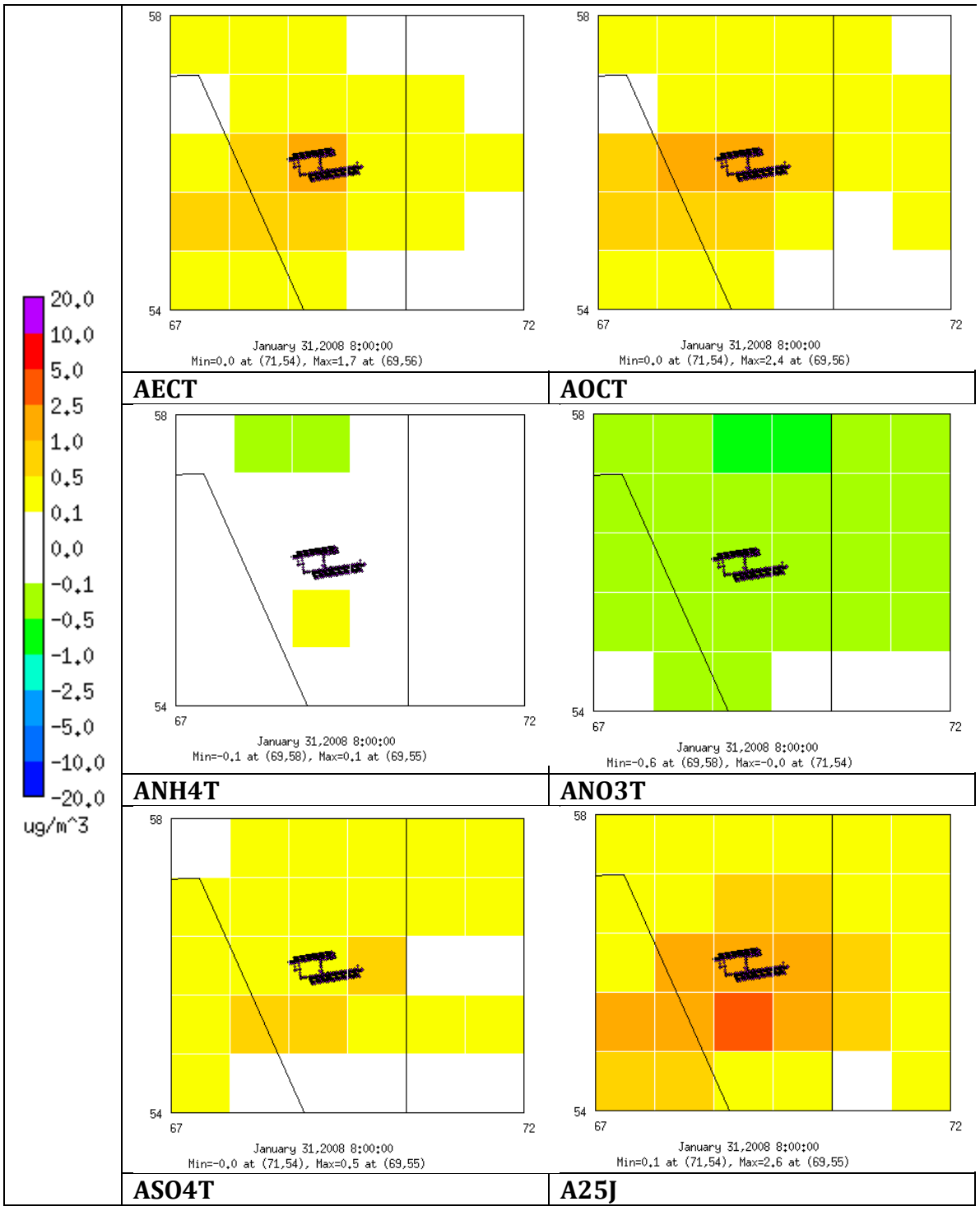

Figure 9B-17. Modeled differences in seasonal maximum daily average speciated $PM_{2.5}$ between AQMD_AllAirp and AQMD_Zero scenarios during Winter Season.

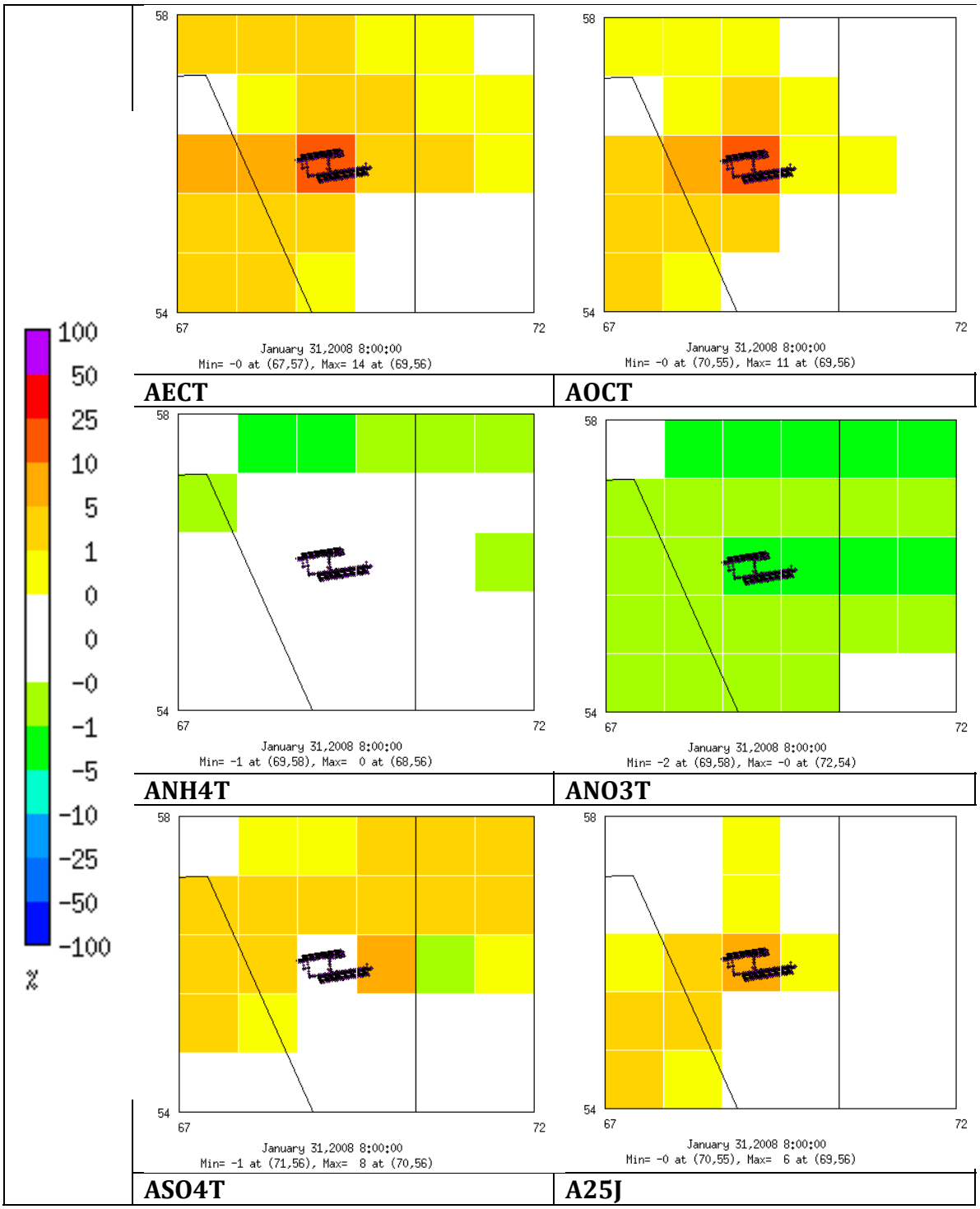

Figure 9B-18. Modeled % differences in seasonal maximum daily average speciated $PM_{2.5}$ between AQMD_Jet and AQMD_Zero scenarios during Winter Season.

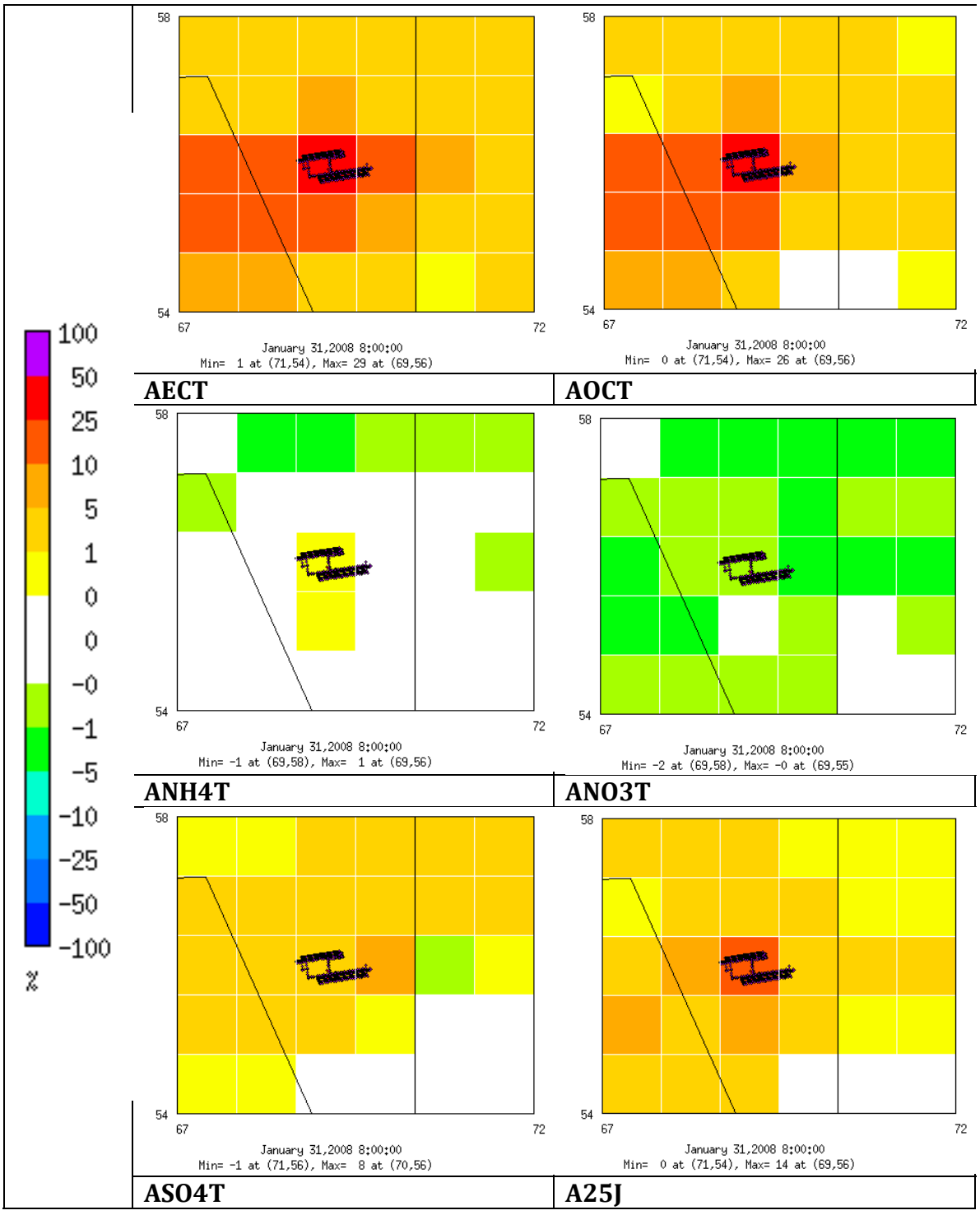

Figure 9B-19. Modeled % differences in seasonal maximum daily average speciated $PM_{2.5}$ between AQMD_HRE and AQMD_Zero scenarios during Winter Season.

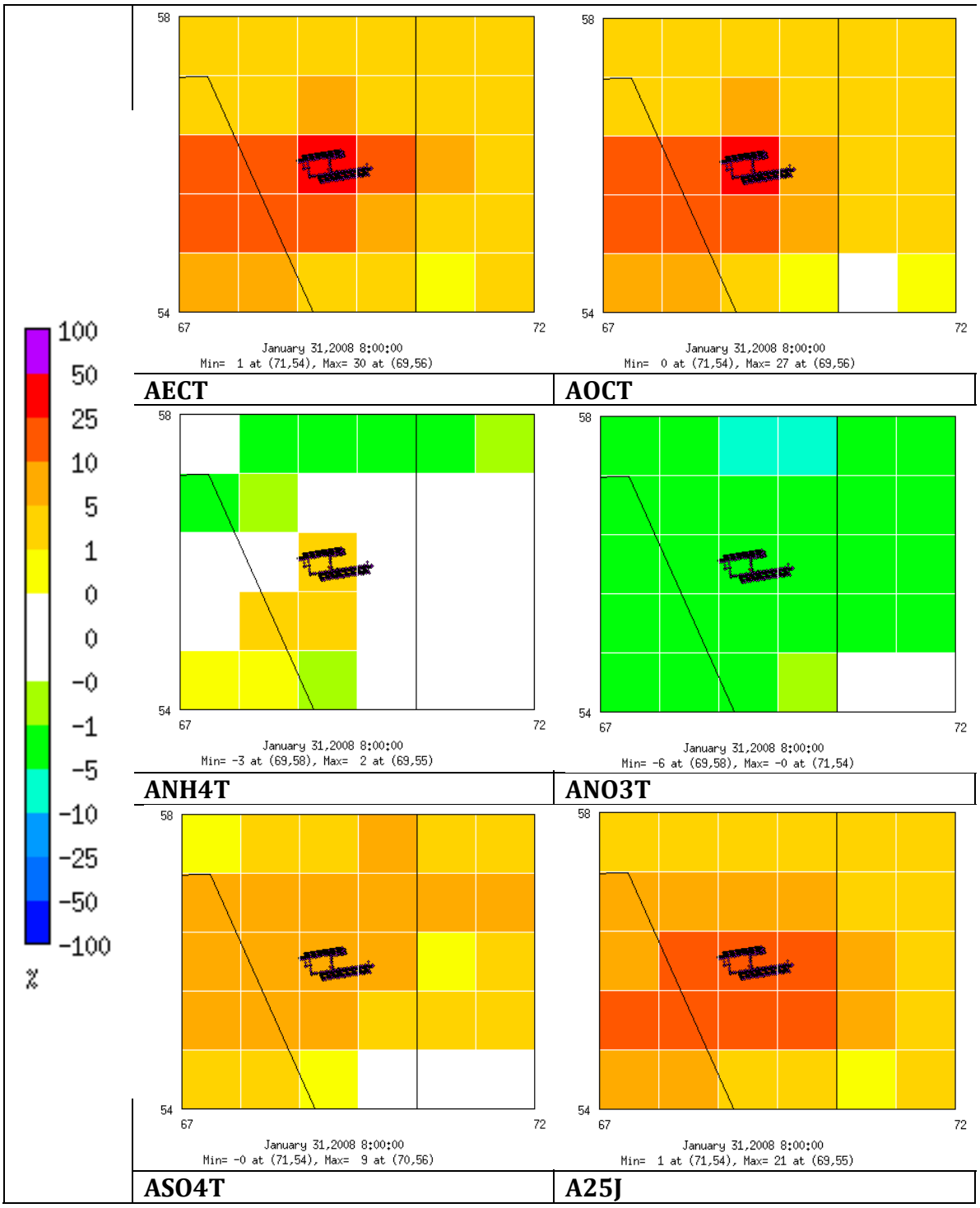

Figure 9B-20. Modeled % differences in seasonal maximum daily average speciated $PM_{2.5}$ between AQMD_AllAirp and AQMD_Zero scenarios during Winter Season.

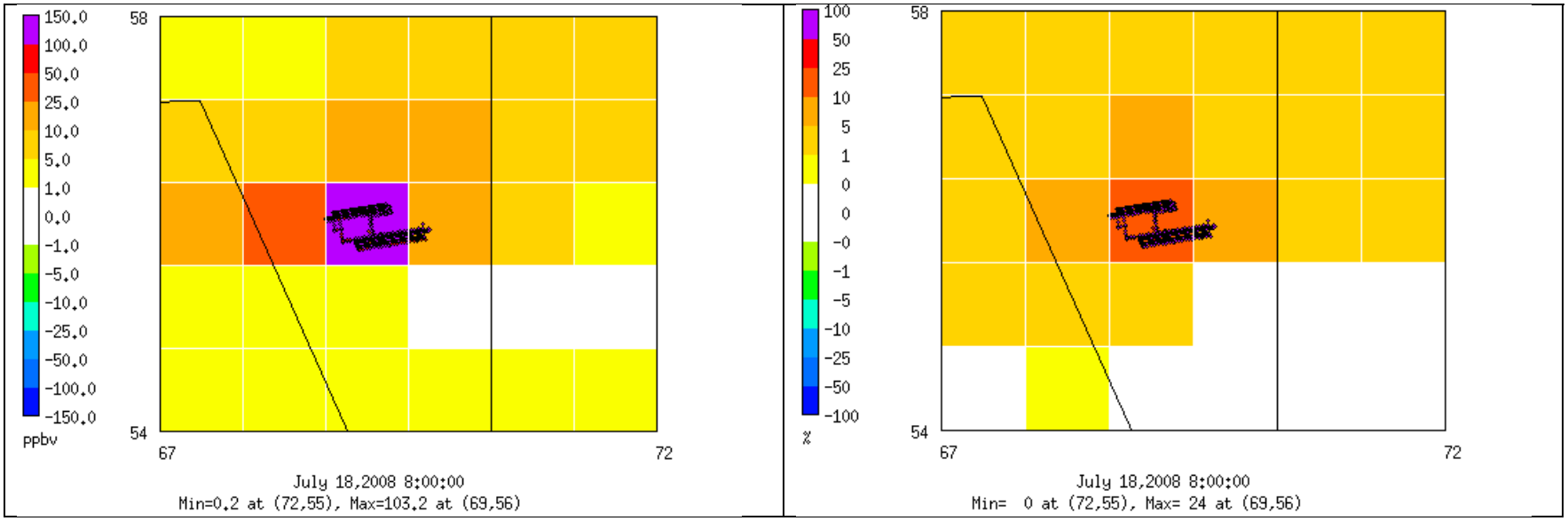

Figure 9B-21a. Modeled absolute (left) and % (right) differences in seasonal mean CO between AQMD_Jet and AQMD_Zero scenarios during Summer Season.

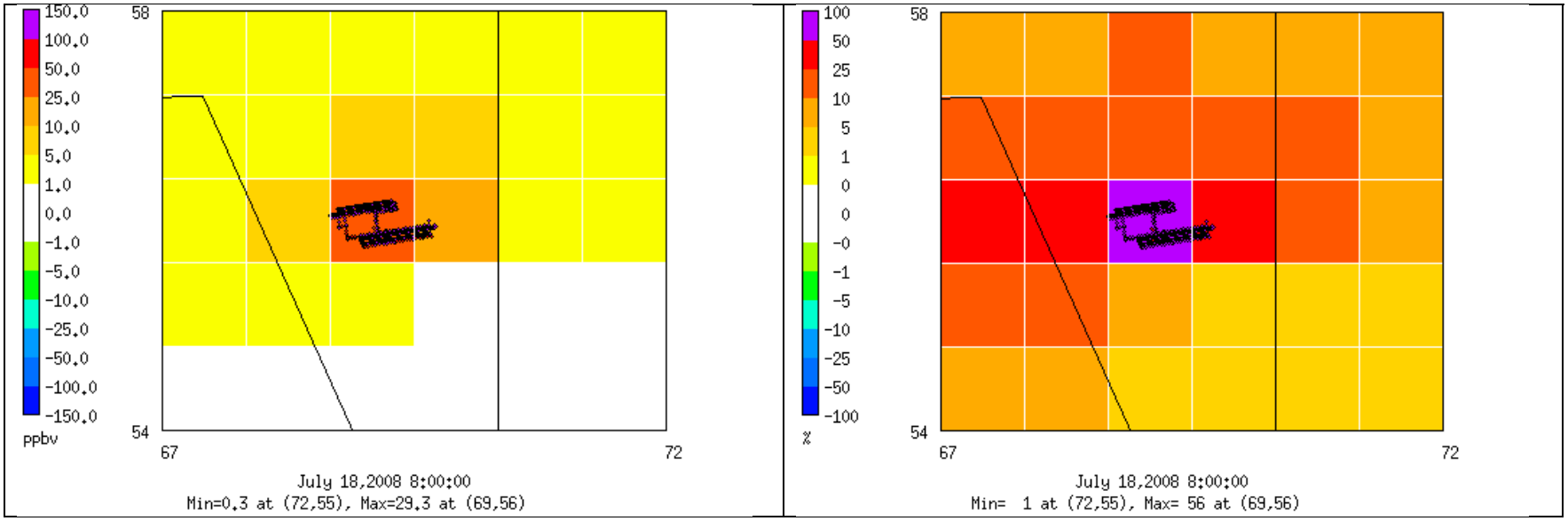

Figure 9B-21b. Modeled absolute (left) and % (right) differences in seasonal mean NO_x between AQMD_Jet and AQMD_Zero scenarios during Summer Season.

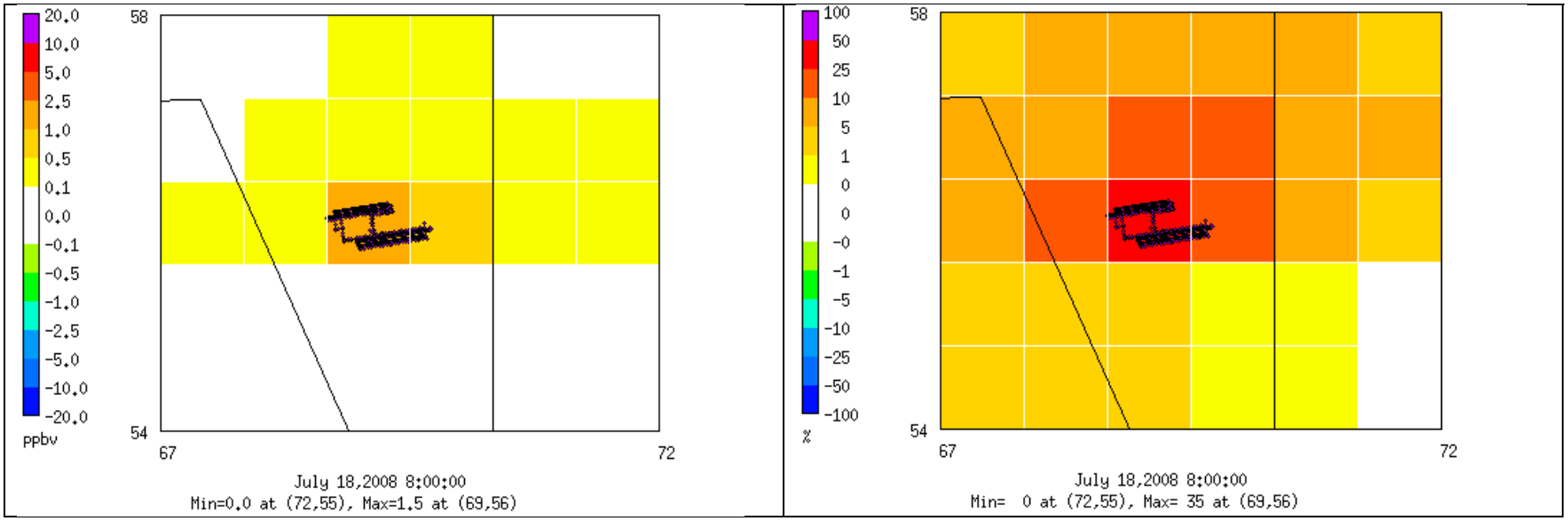

Figure 9B-21c. Modeled absolute (left) and % (right) differences in seasonal mean SO_2 between AQMD_Jet and AQMD_Zero scenarios during Summer Season.

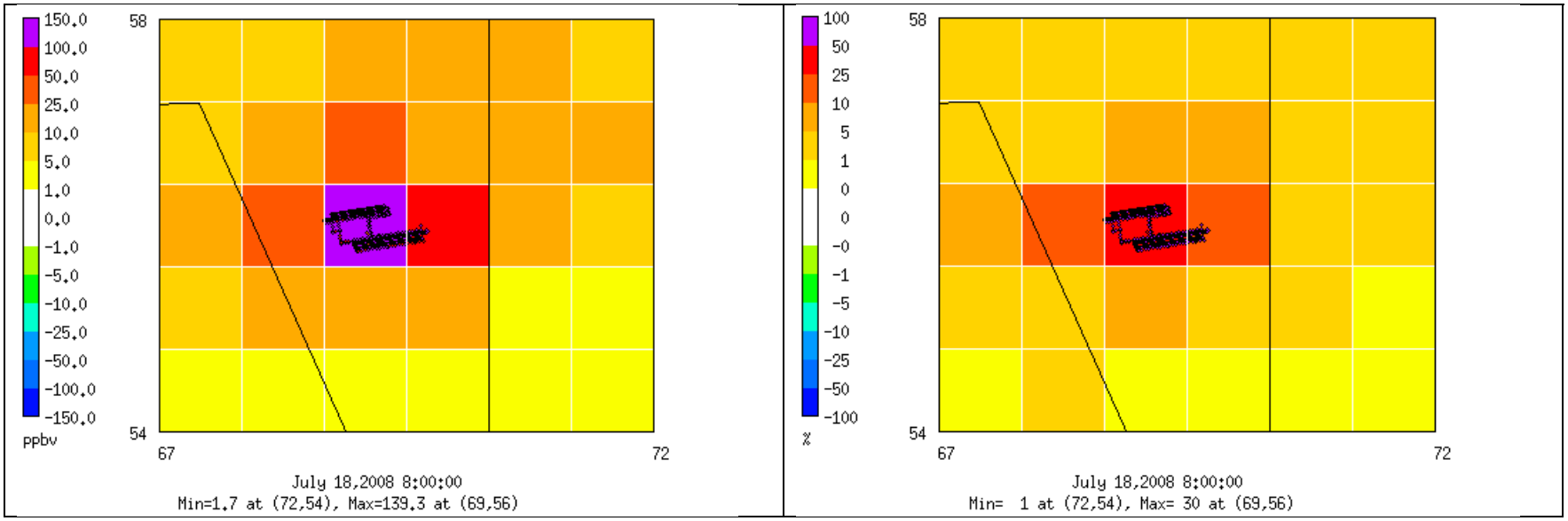

Figure 9B-22a. Modeled absolute (left) and % (right) differences in seasonal mean CO between AQMD_HRE and AQMD_Zero scenarios during Summer Season.

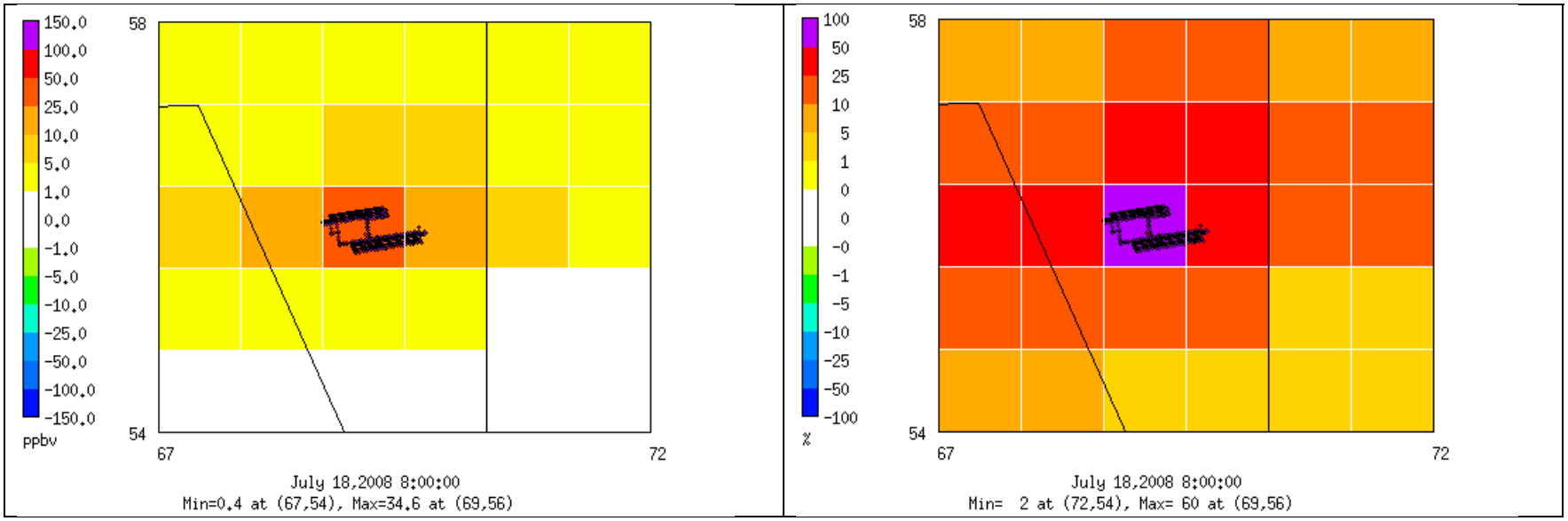

Figure 9B-22b. Modeled absolute (left) and % (right) differences in seasonal mean NO_x between AQMD_HRE and AQMD_Zero scenarios during Summer Season.

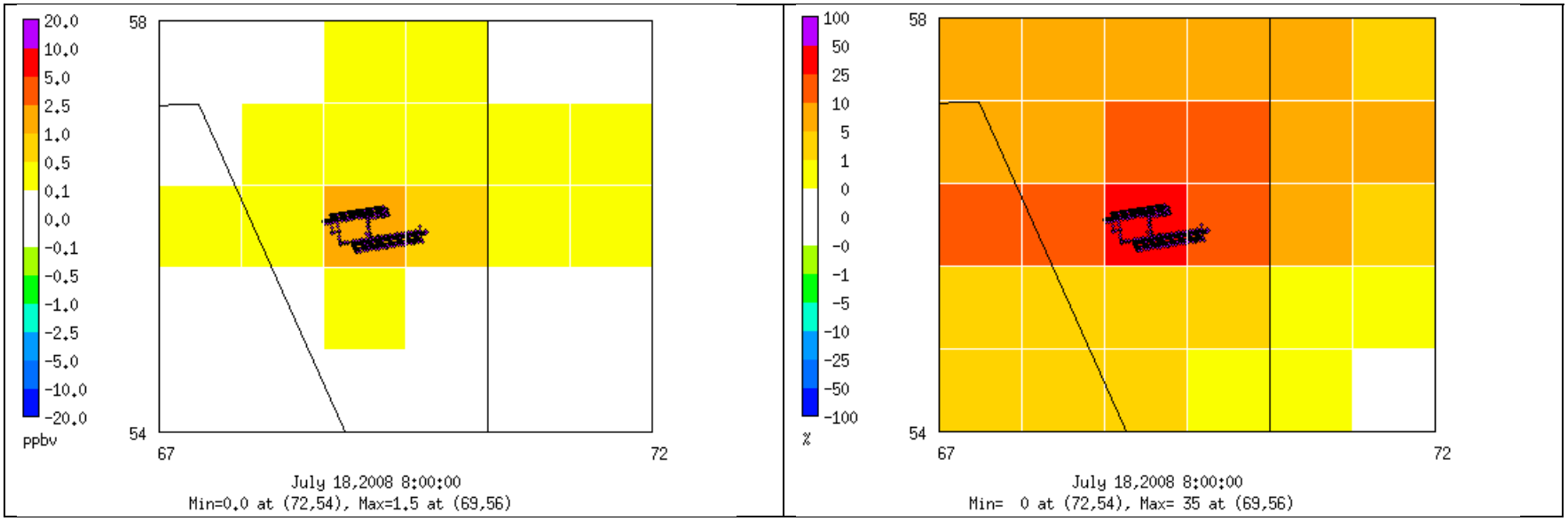

Figure 9B-22c. Modeled absolute (left) and % (right) differences in seasonal mean SO_2 between AQMD_HRE and AQMD_Zero scenarios during Summer Season.

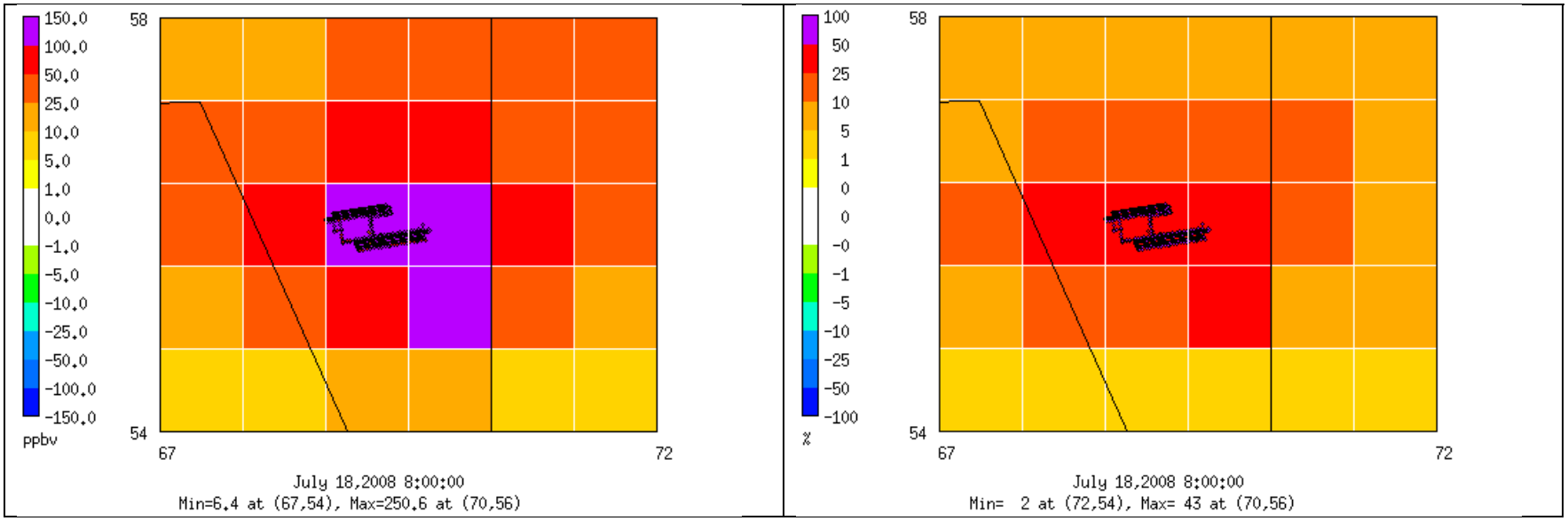

Figure 9B-23a. Modeled absolute (left) and % (right) differences in seasonal mean CO between AQMD_AllAirp and AQMD_Zero scenarios during Summer Season.

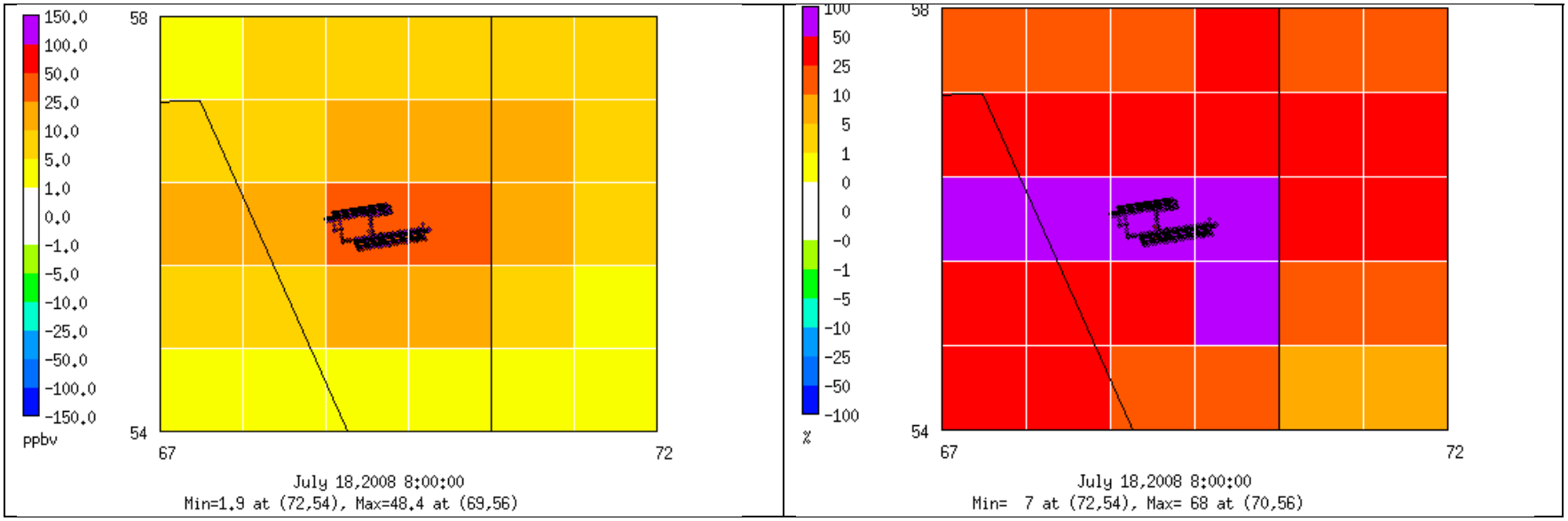

Figure 9B-23b. Modeled absolute (left) and % (right) differences in seasonal mean NO_x between AQMD_AllAirp and AQMD_Zero scenarios during Summer Season.

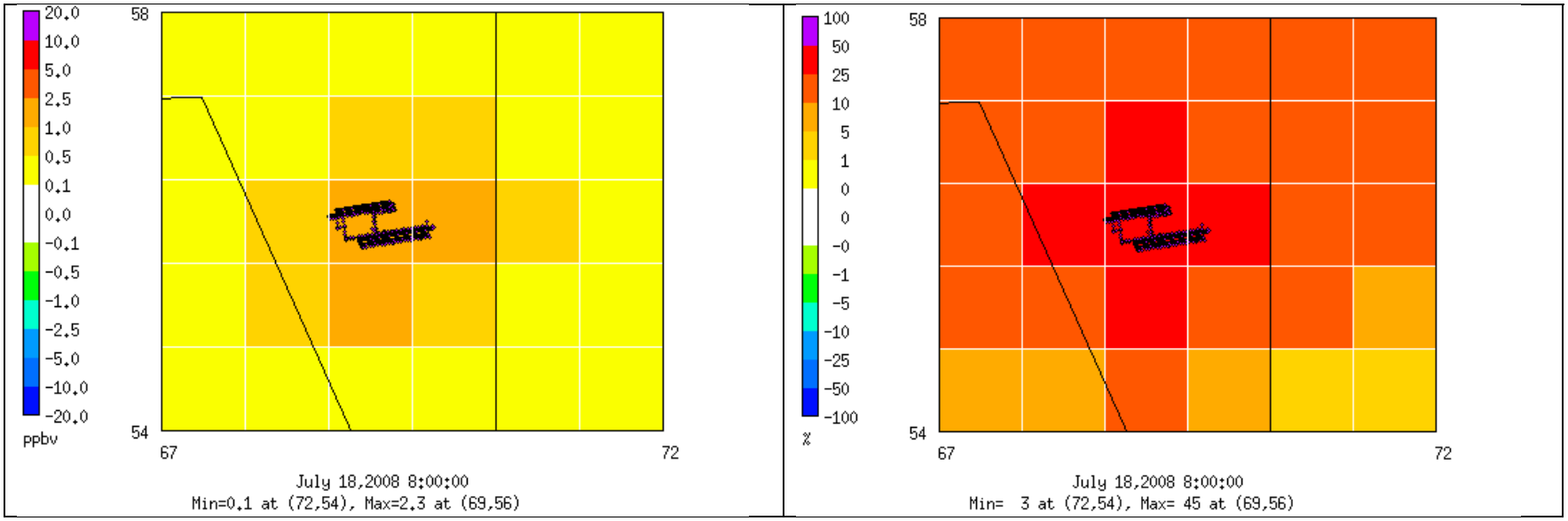

Figure 9B-23c. Modeled absolute (left) and % (right) differences in seasonal mean SO_2 between AQMD_AllAirp and AQMD_Zero scenarios during Summer Season.

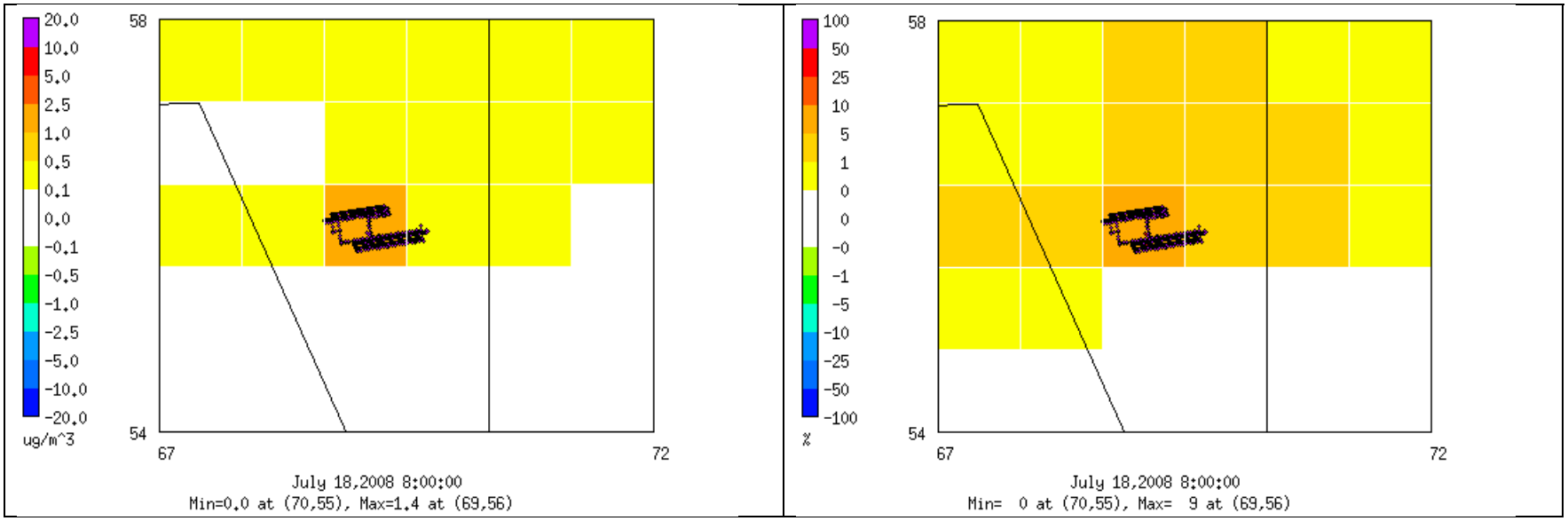

Figure 9B-24a. Modeled absolute (left) and % (right) differences in total $PM_{2.5}$ between AQMD_Jet and AQMD_Zero scenarios during Summer Season.

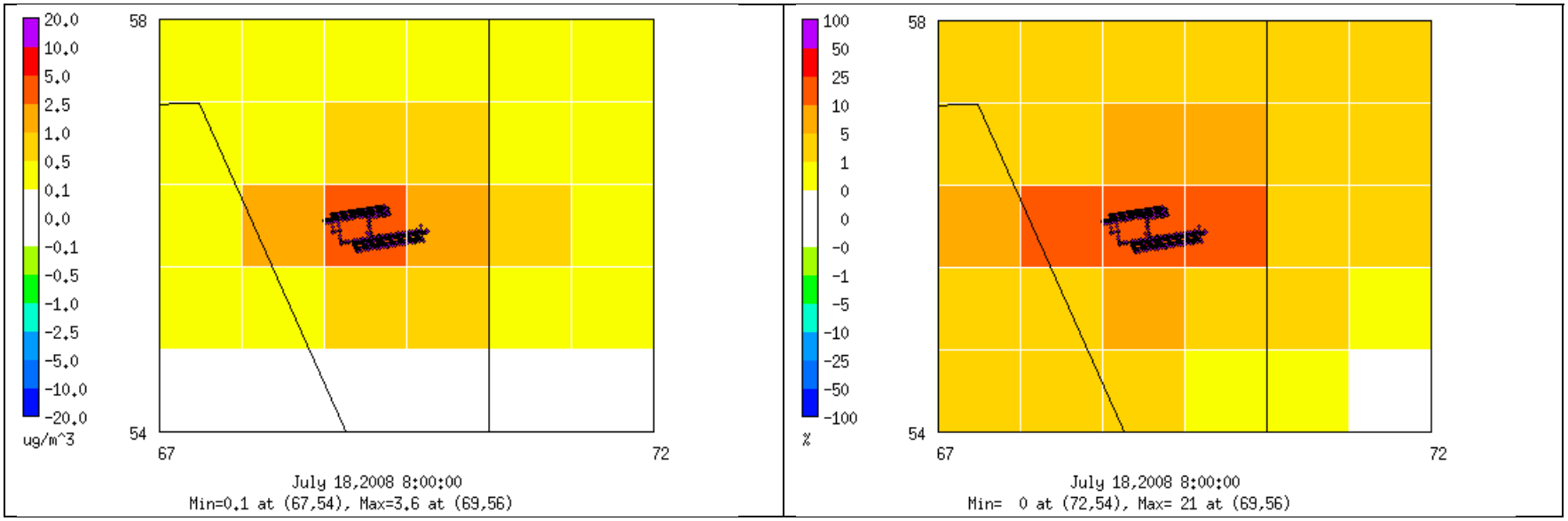

Figure 9B-24b. Modeled absolute (left) and % (right) differences in total $PM_{2.5}$ between AQMD_HRE and AQMD_Zero scenarios during Summer Season.

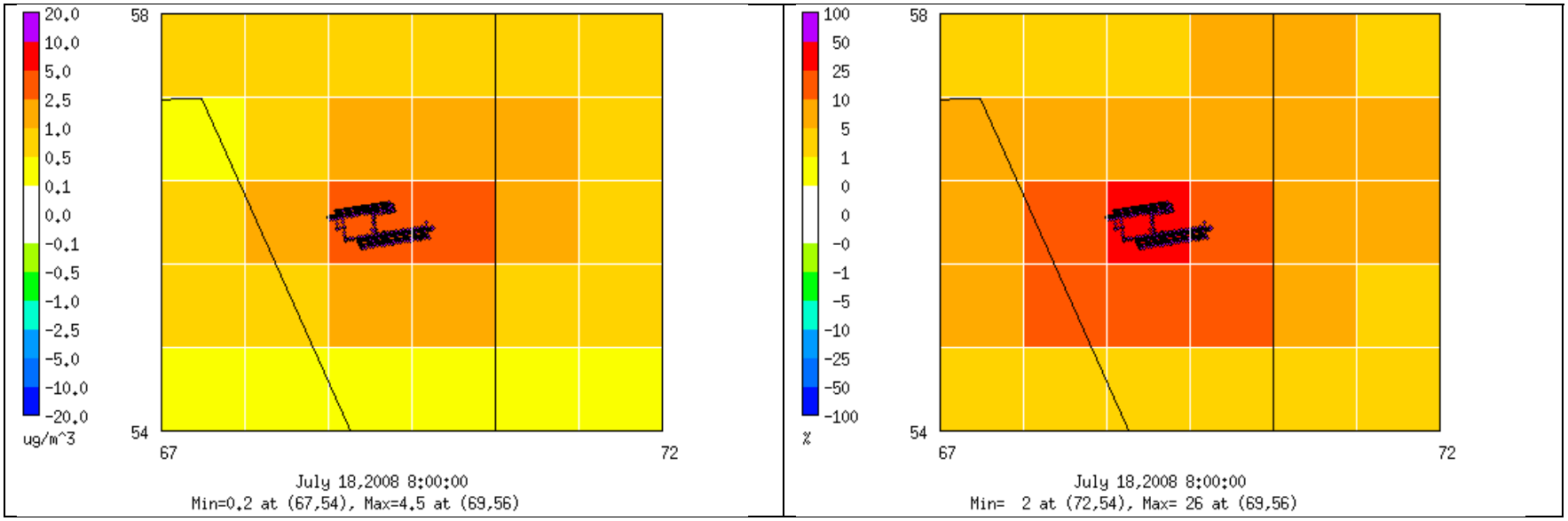

Figure 9B-24c. Modeled absolute (left) and % (right) differences in total $PM_{2.5}$ between AQMD_AllAirp and AQMD_Zero scenarios during Summer Season.

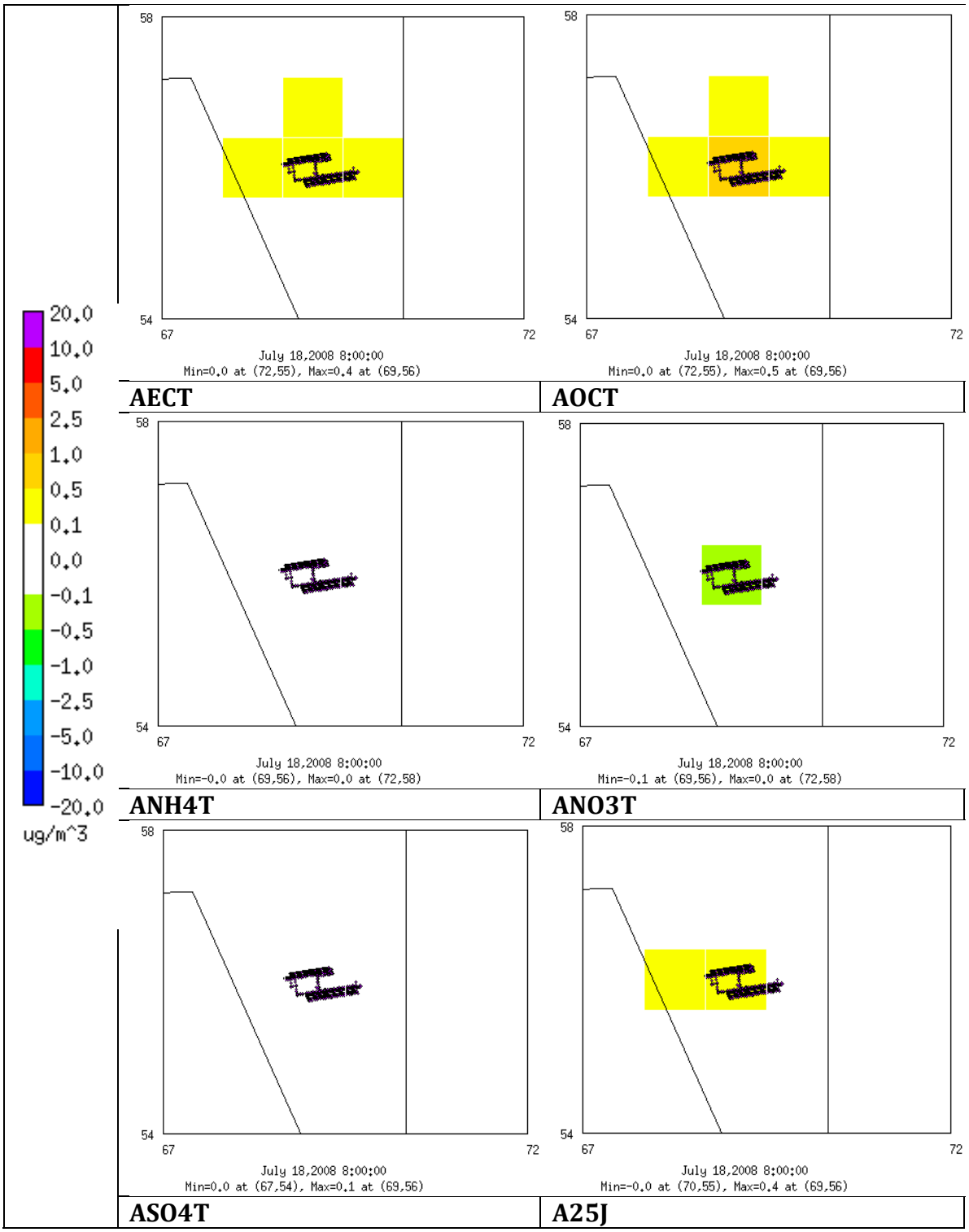

Figure 9B-25. Modeled differences in seasonal mean speciated $PM_{2.5}$ between AQMD_Jet and AQMD_Zero scenarios during Summer Season.

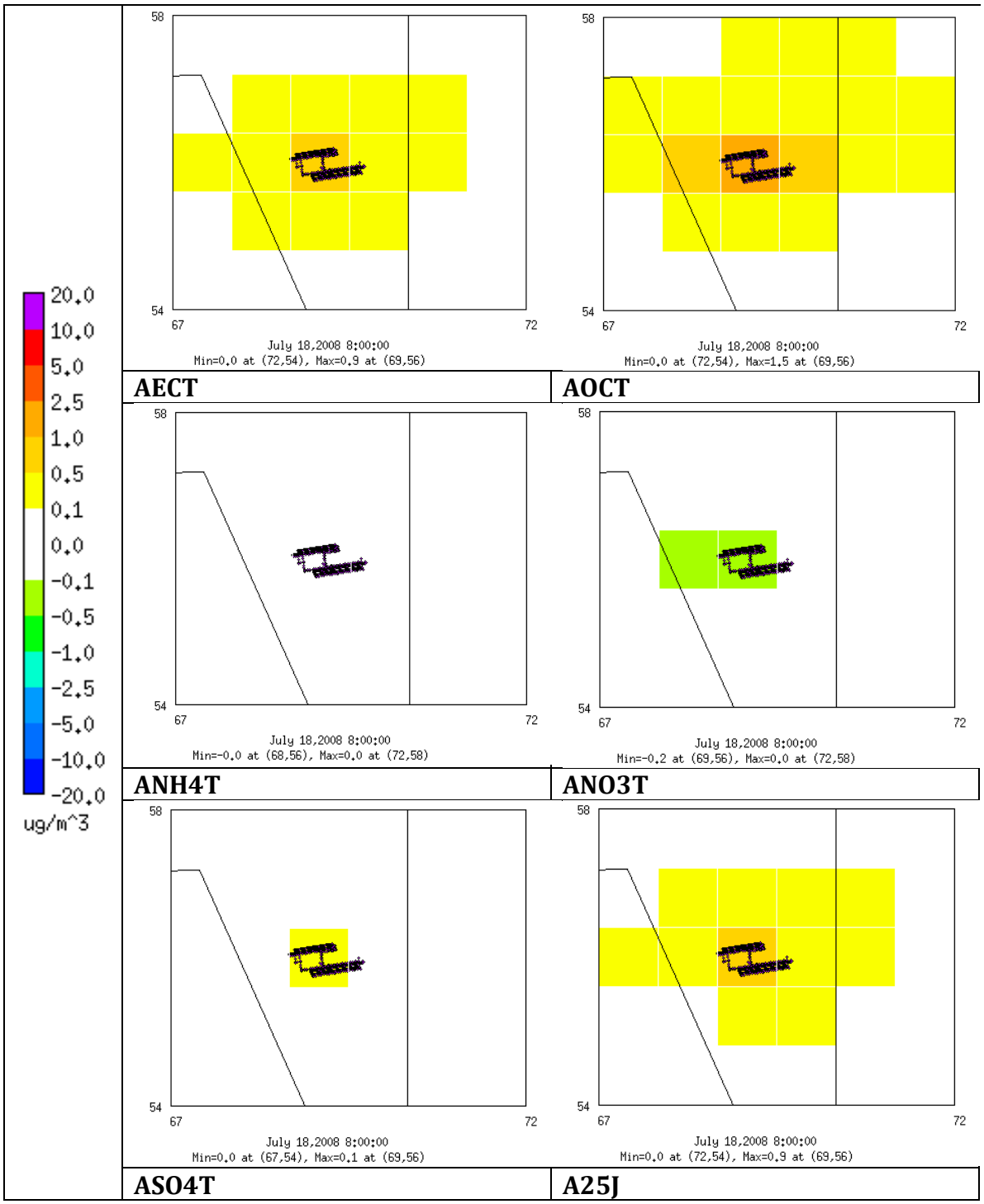

Figure 9B-26. Modeled differences in seasonal mean speciated $PM_{2.5}$ between AQMD_HRE and AQMD_Zero scenarios during Summer Season.

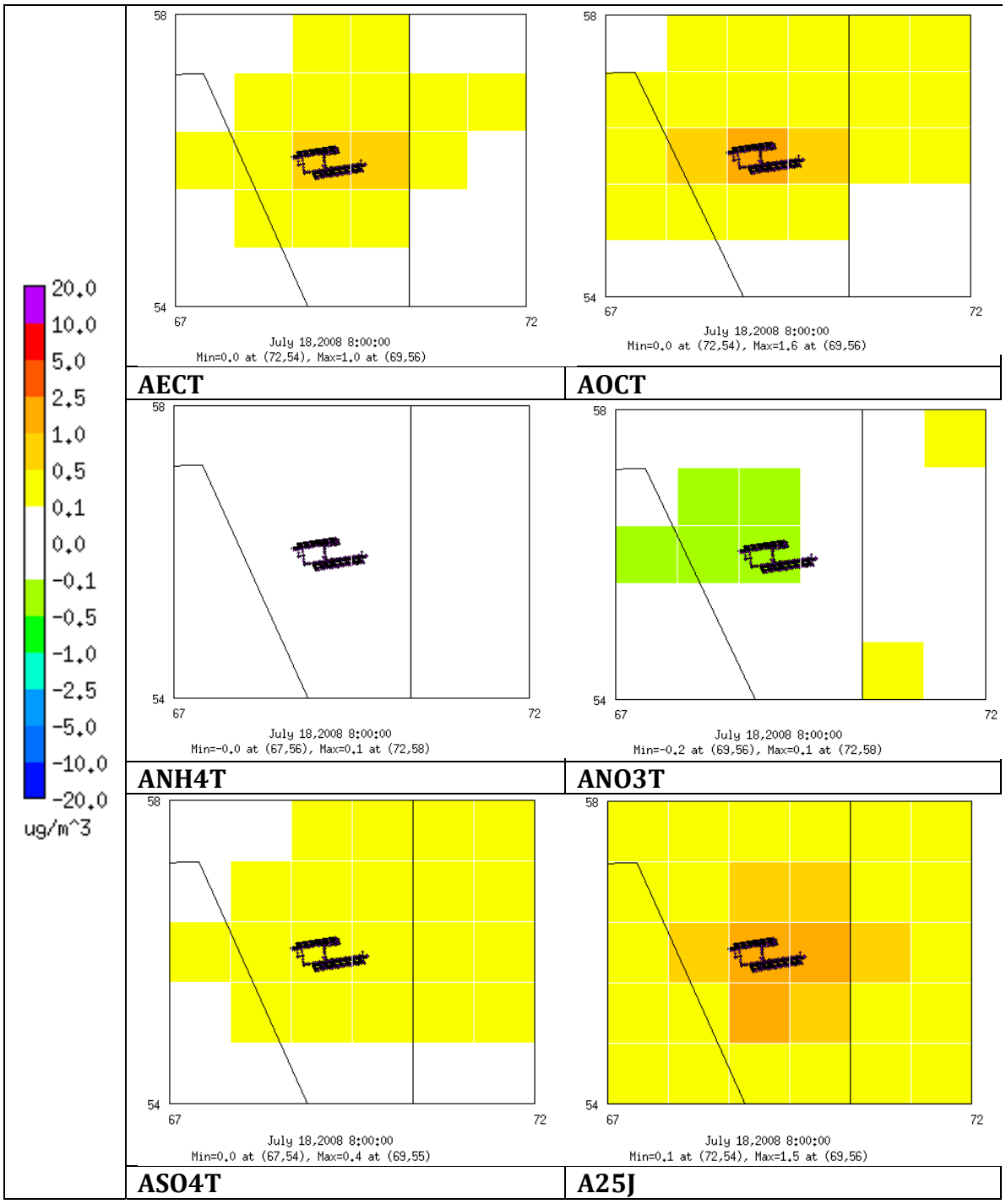

Figure 9B-27. Modeled differences in seasonal mean speciated $PM_{2.5}$ between AQMD_AllAirp and AQMD_Zero scenarios during Summer Season.

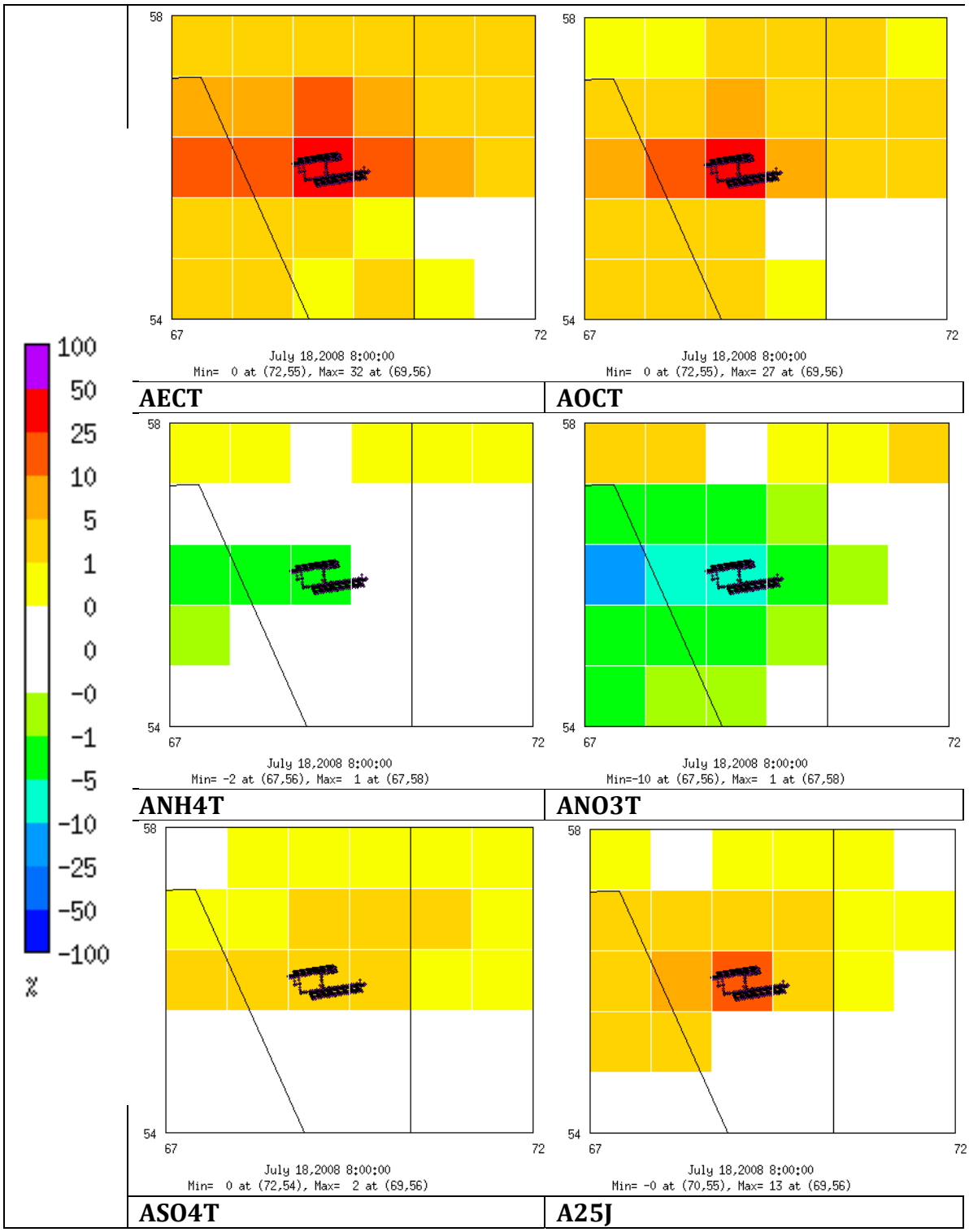

Figure 9B-28. Modeled % differences in seasonal mean speciated $PM_{2.5}$ between AQMD_Jet and AQMD_Zero scenarios during Summer Season.

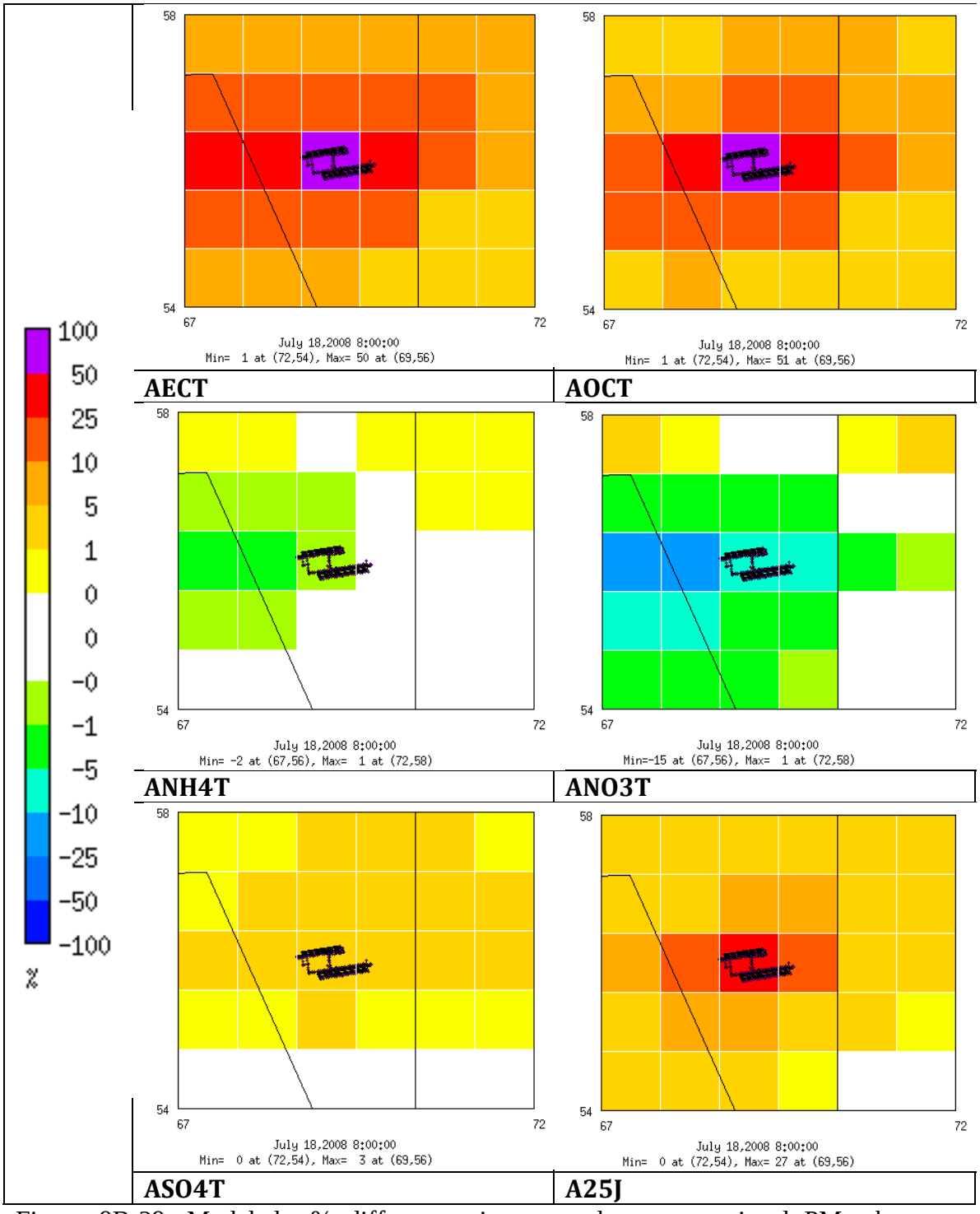

Figure 9B-29. Modeled % differences in seasonal mean speciated $PM_{2.5}$ between AQMD_HRE and AQMD_Zero scenarios during Summer Season.

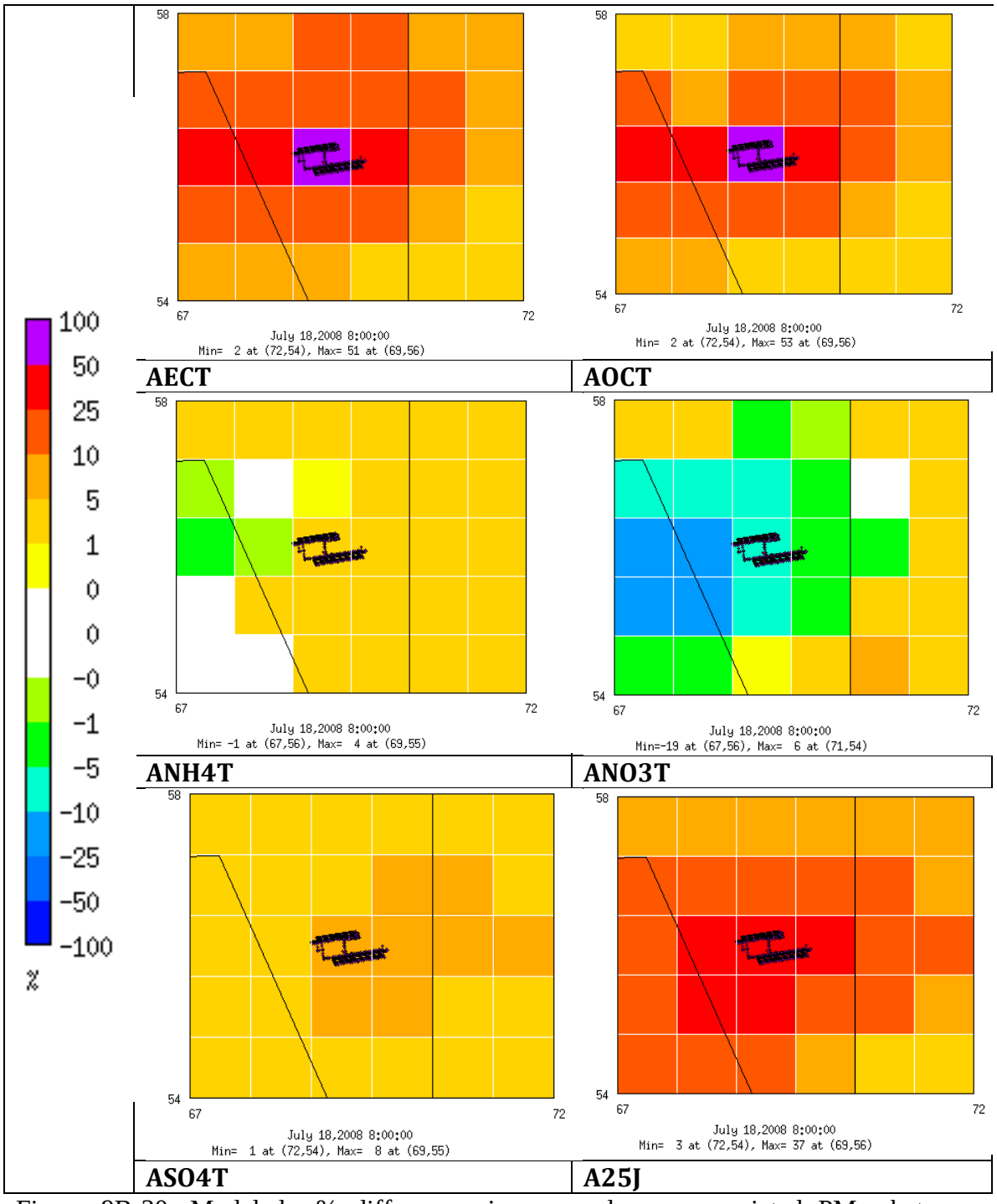

Figure 9B-30. Modeled % differences in seasonal mean speciated $PM_{2.5}$ between AQMD_AllAirp and AQMD_Zero scenarios during Summer Season.

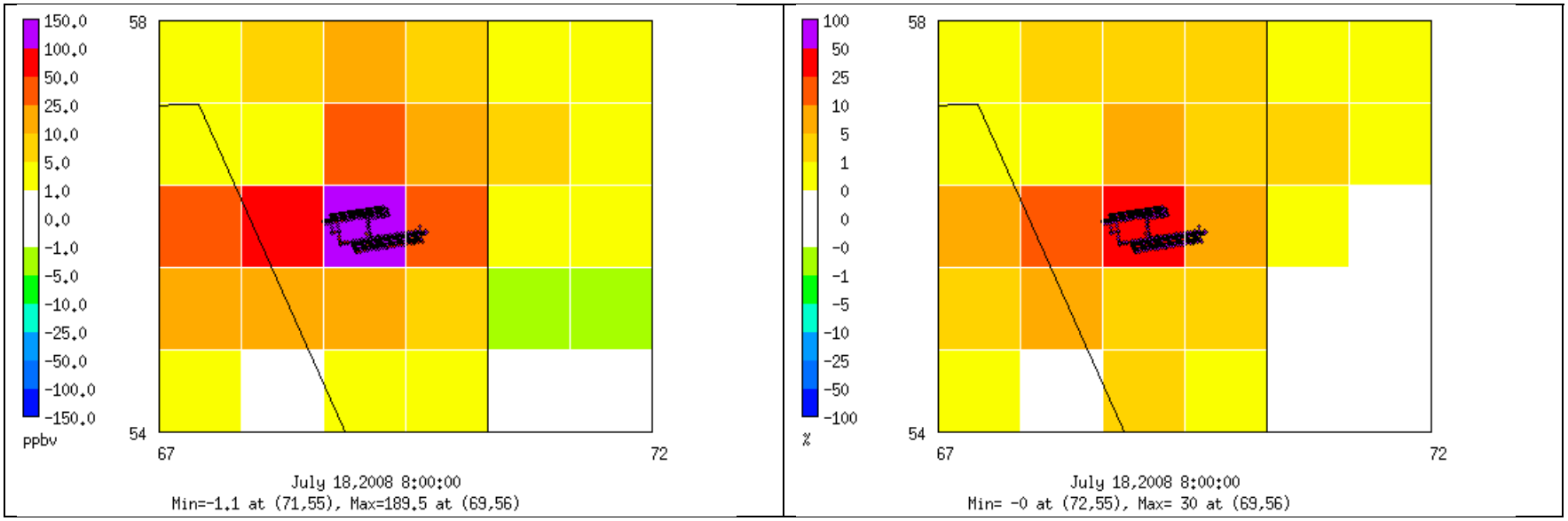

Figure 9B-31a. Modeled absolute (left) and % (right) differences in seasonal maximum daily average CO between AQMD_Jet and AQMD_Zero scenarios during Summer Season.

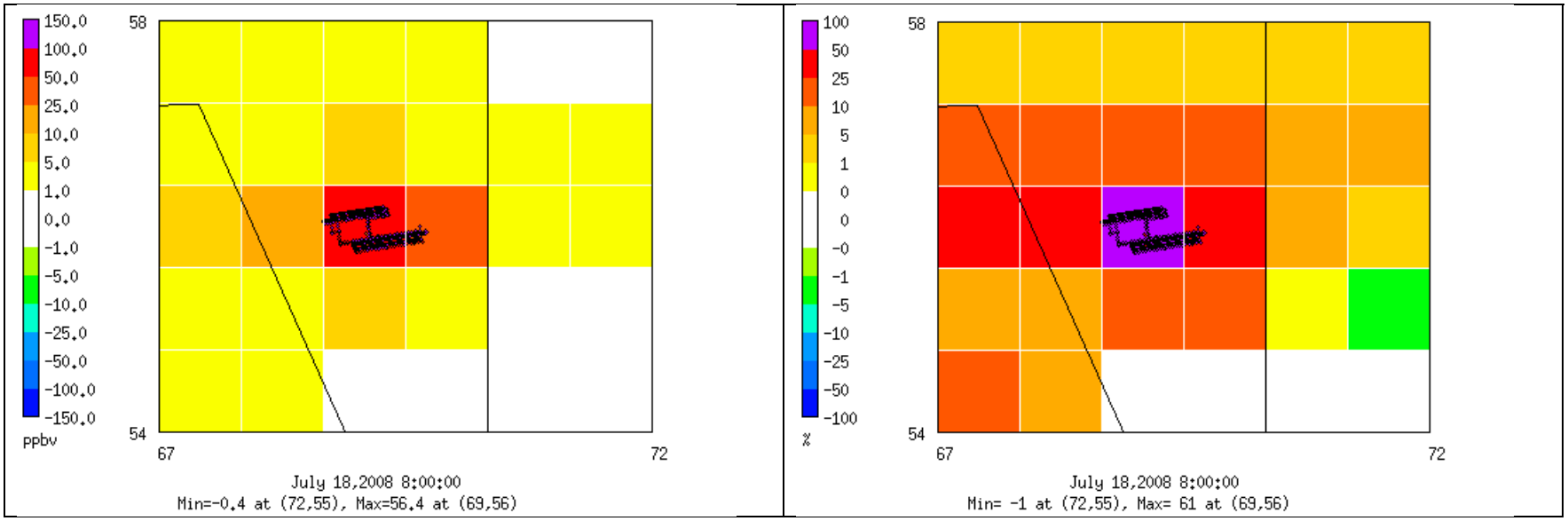

Figure 9B-31b. Modeled absolute (left) and % (right) differences in seasonal maximum daily average NO_x between AQMD_Jet and AQMD_Zero scenarios during Summer Season.

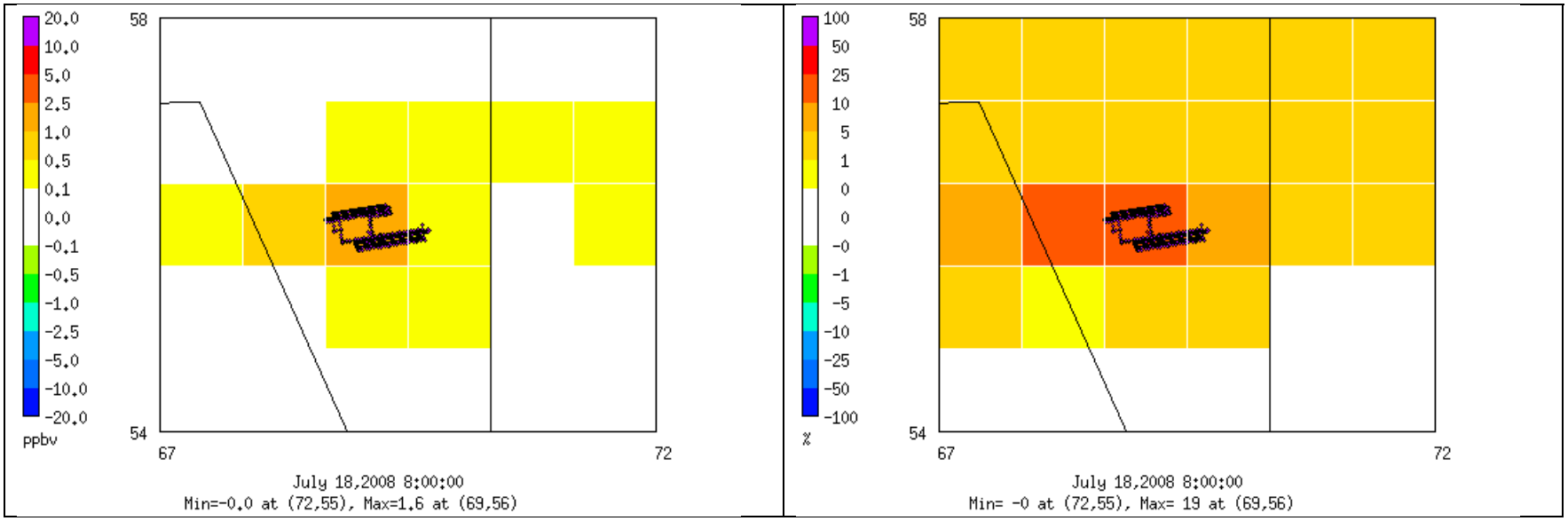

Figure 9B-31c. Modeled absolute (left) and % (right) differences in seasonal maximum daily average SO_2 between AQMD_Jet and AQMD_Zero scenarios during Summer Season.

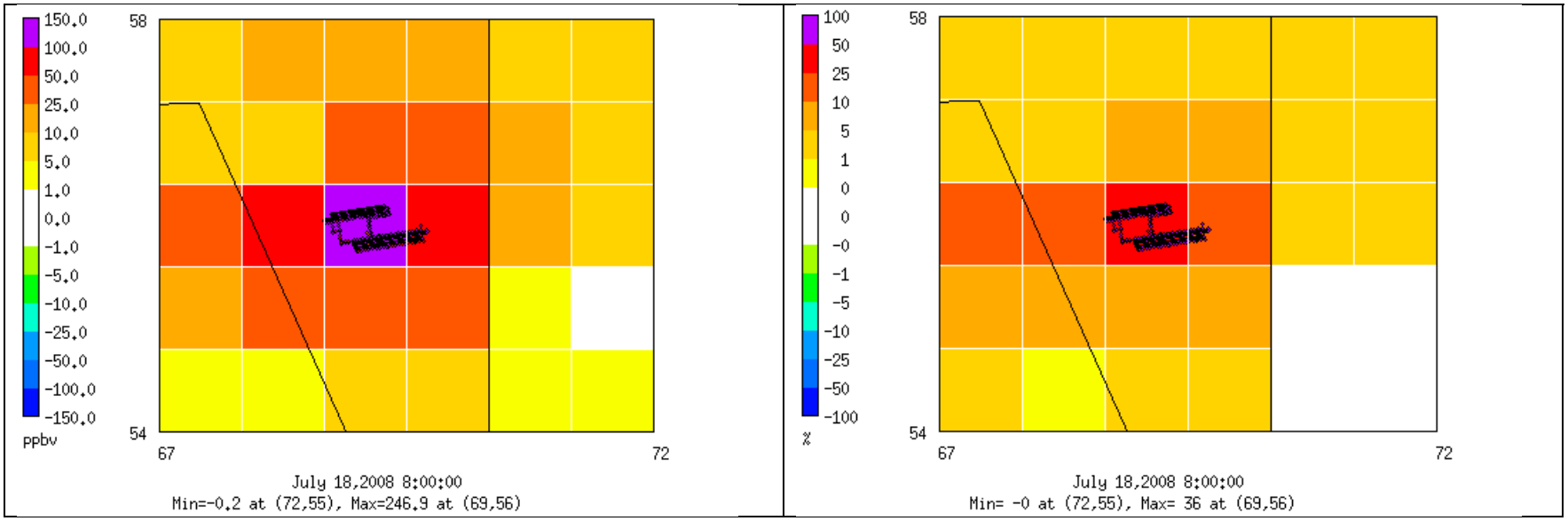

Figure 9B-32a. Modeled absolute (left) and % (right) differences in seasonal maximum daily average CO between AQMD_HRE and AQMD_Zero scenarios during Summer Season.

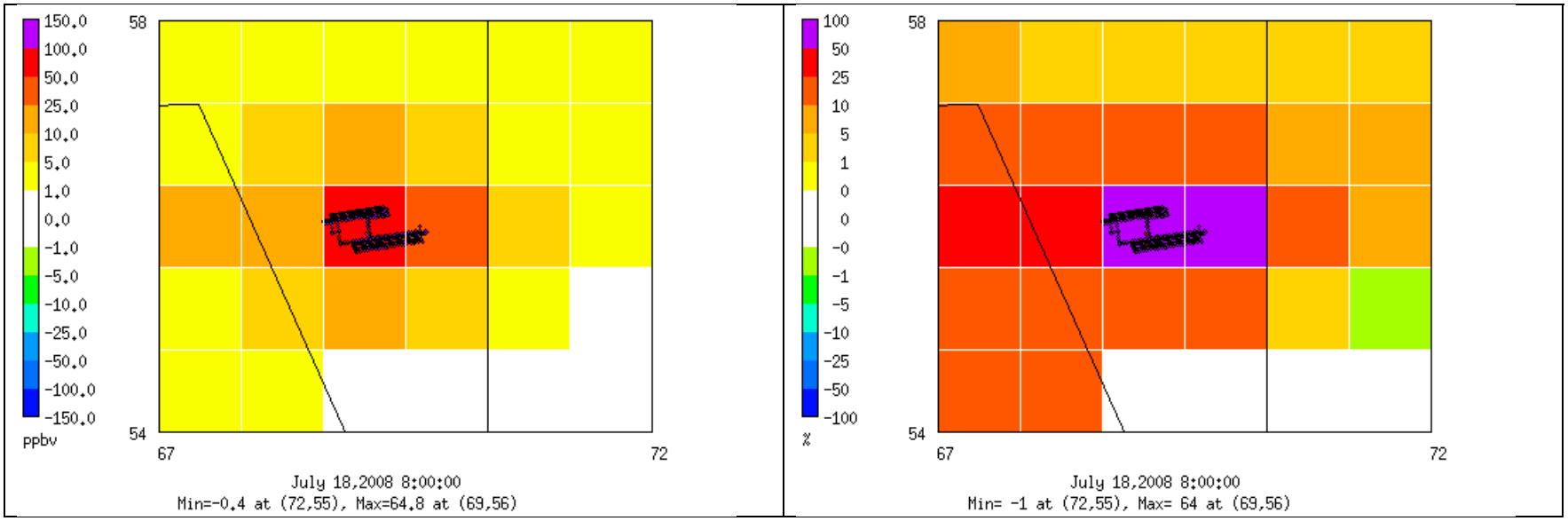

Figure 9B-32b. Modeled absolute (left) and % (right) differences in seasonal maximum daily average NO_x between AQMD_HRE and AQMD_Zero scenarios during Summer Season.

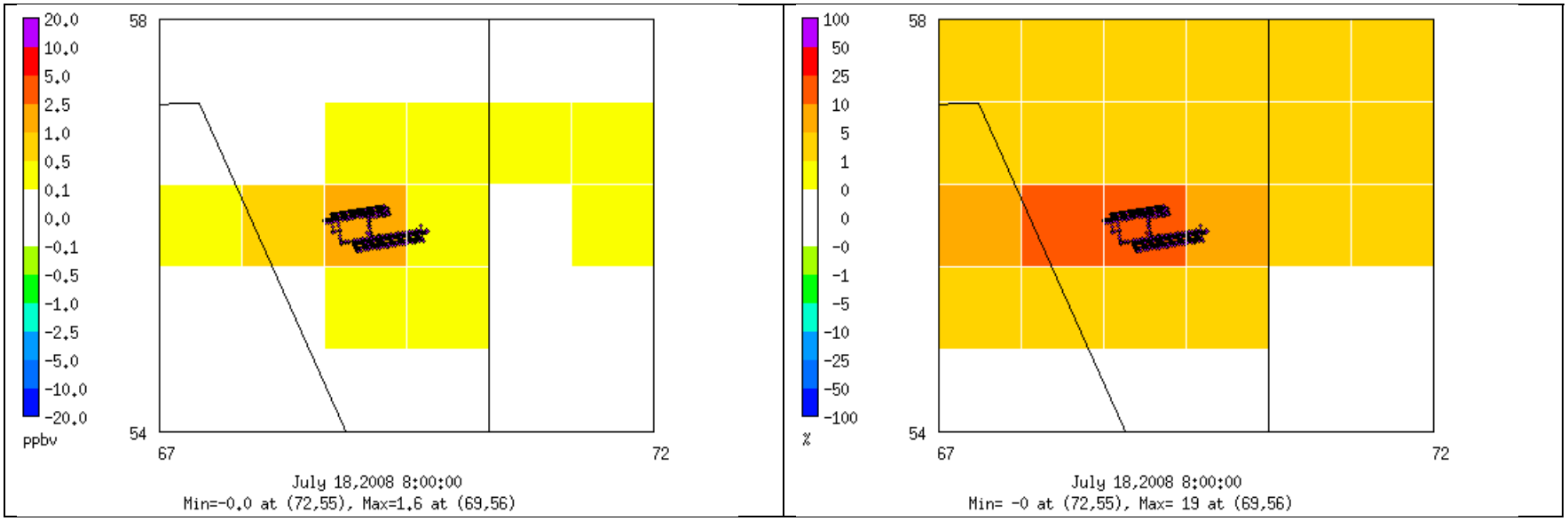

Figure 9B-32c. Modeled absolute (left) and % (right) differences in seasonal maximum daily average SO_2 between AQMD_HRE and AQMD_Zero scenarios during Summer Season.

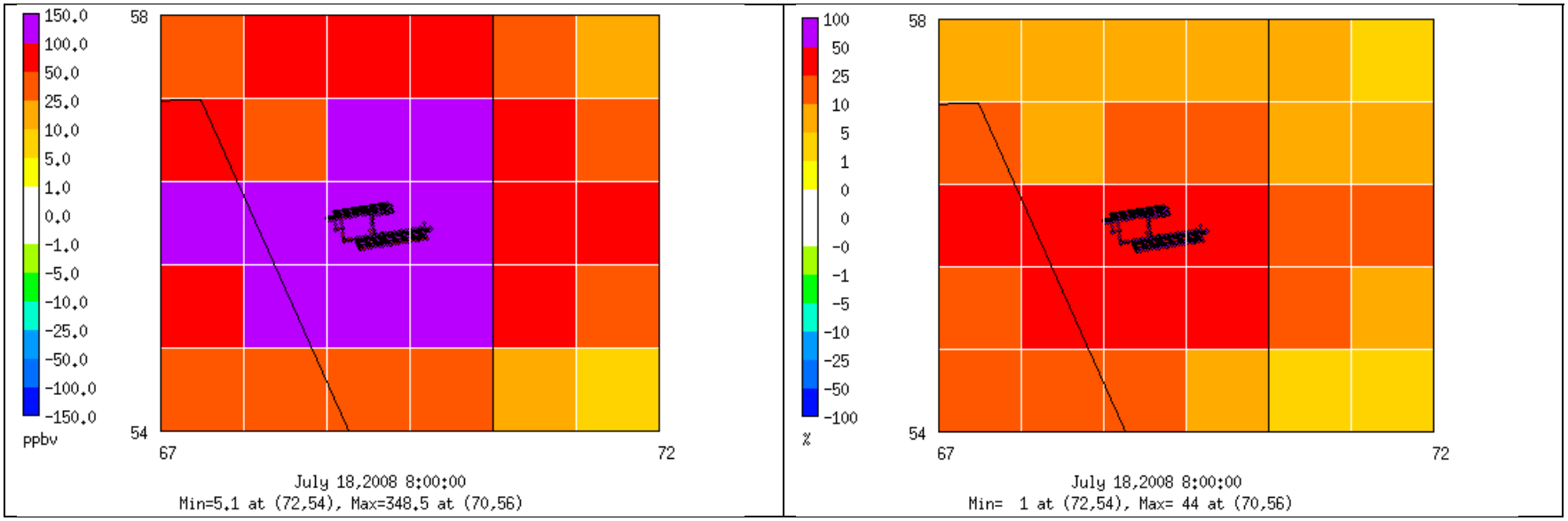

Figure 9B-33a. Modeled absolute (left) and % (right) differences in seasonal maximum daily average CO between AQMD_AllAirp and AQMD_Zero scenarios during Summer Season.

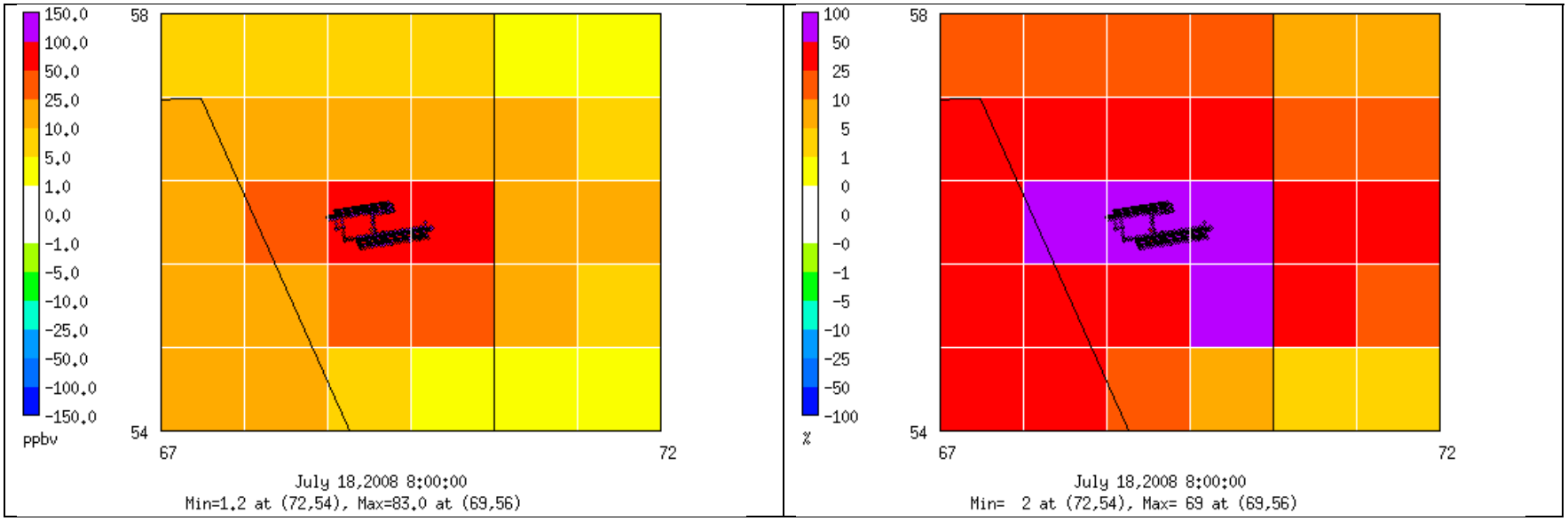

Figure 9B-33b. Modeled absolute (left) and % (right) differences in seasonal maximum daily average NO_x between AQMD_AllAirp and AQMD_Zero scenarios during Summer Season.

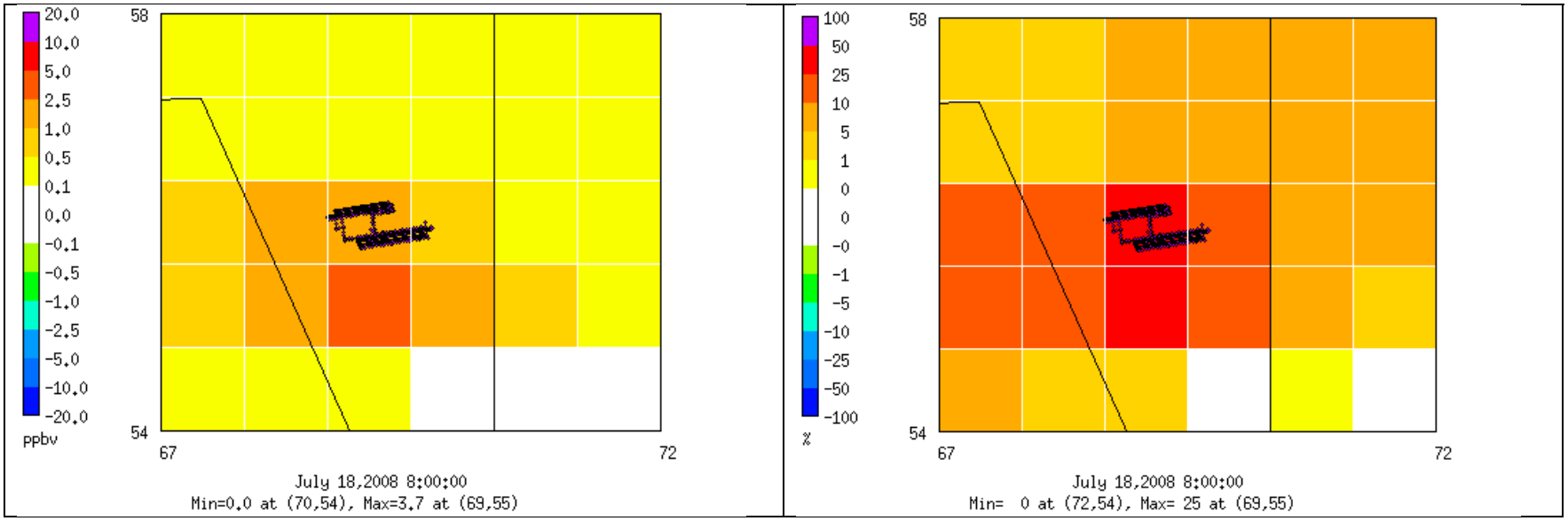

Figure 9B-33c. Modeled absolute (left) and % (right) differences in seasonal maximum daily average SO_2 between AQMD_AllAirp and AQMD_Zero scenarios during Summer Season.

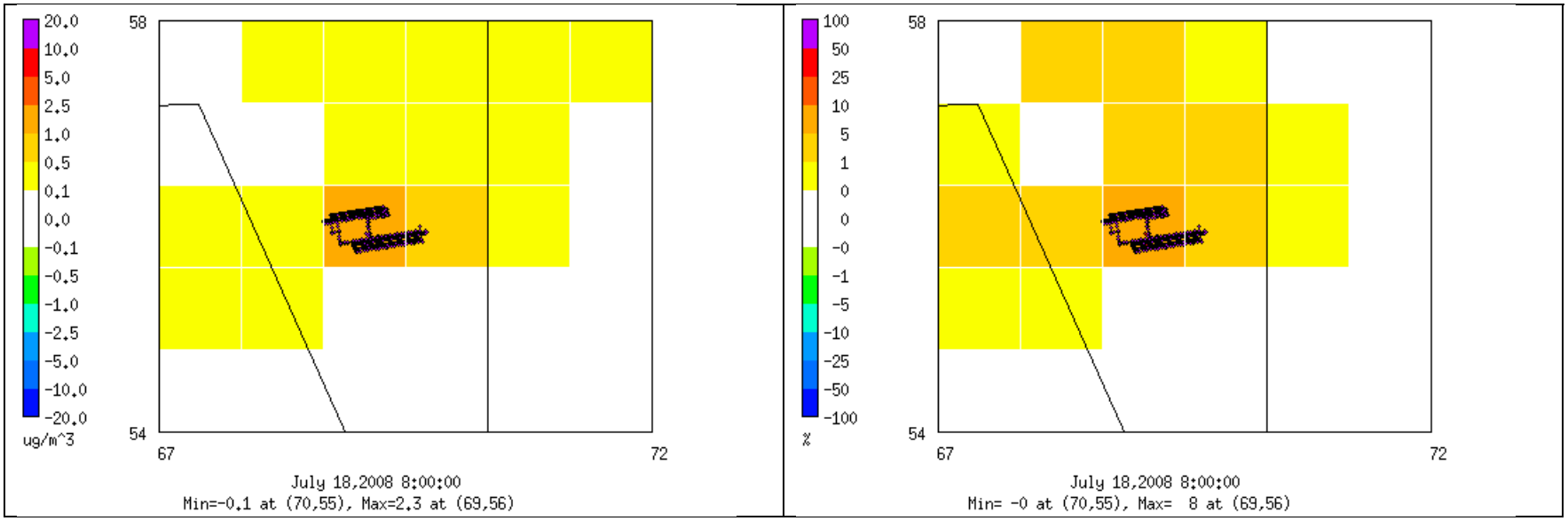

Figure 9B-34a. Modeled absolute (left) and % (right) differences in total $PM_{2.5}$ between AQMD_Jet and AQMD_Zero scenarios during Summer Season.

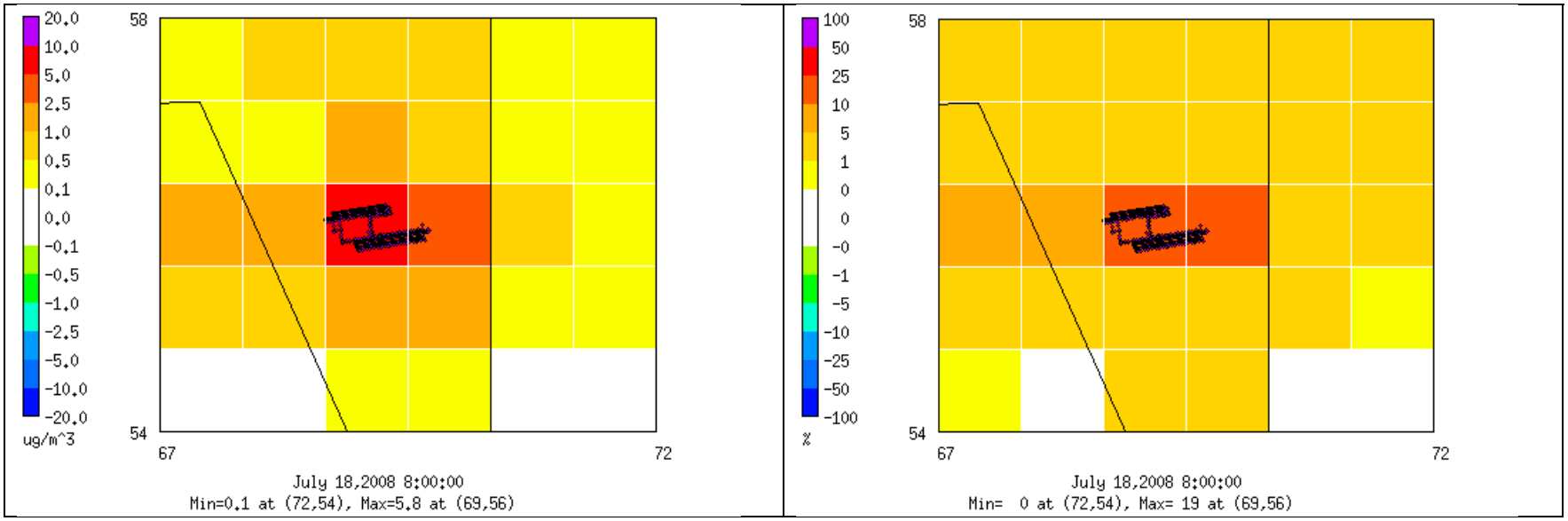

Figure 9B-34b. Modeled absolute (left) and % (right) differences in total $PM_{2.5}$ between AQMD_HRE and AQMD_Zero scenarios during Summer Season.

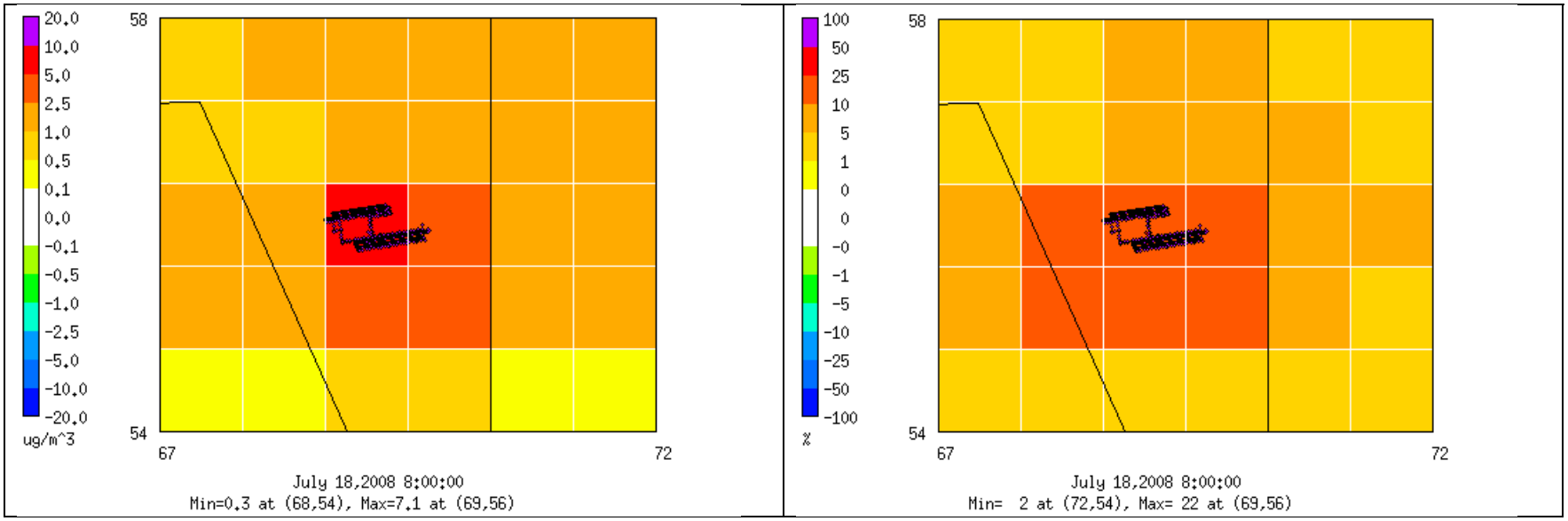

Figure 9B-34c. Modeled absolute (left) and % (right) differences in total $PM_{2.5}$ between AQMD_AllAirp and AQMD_Zero scenarios during Summer Season.

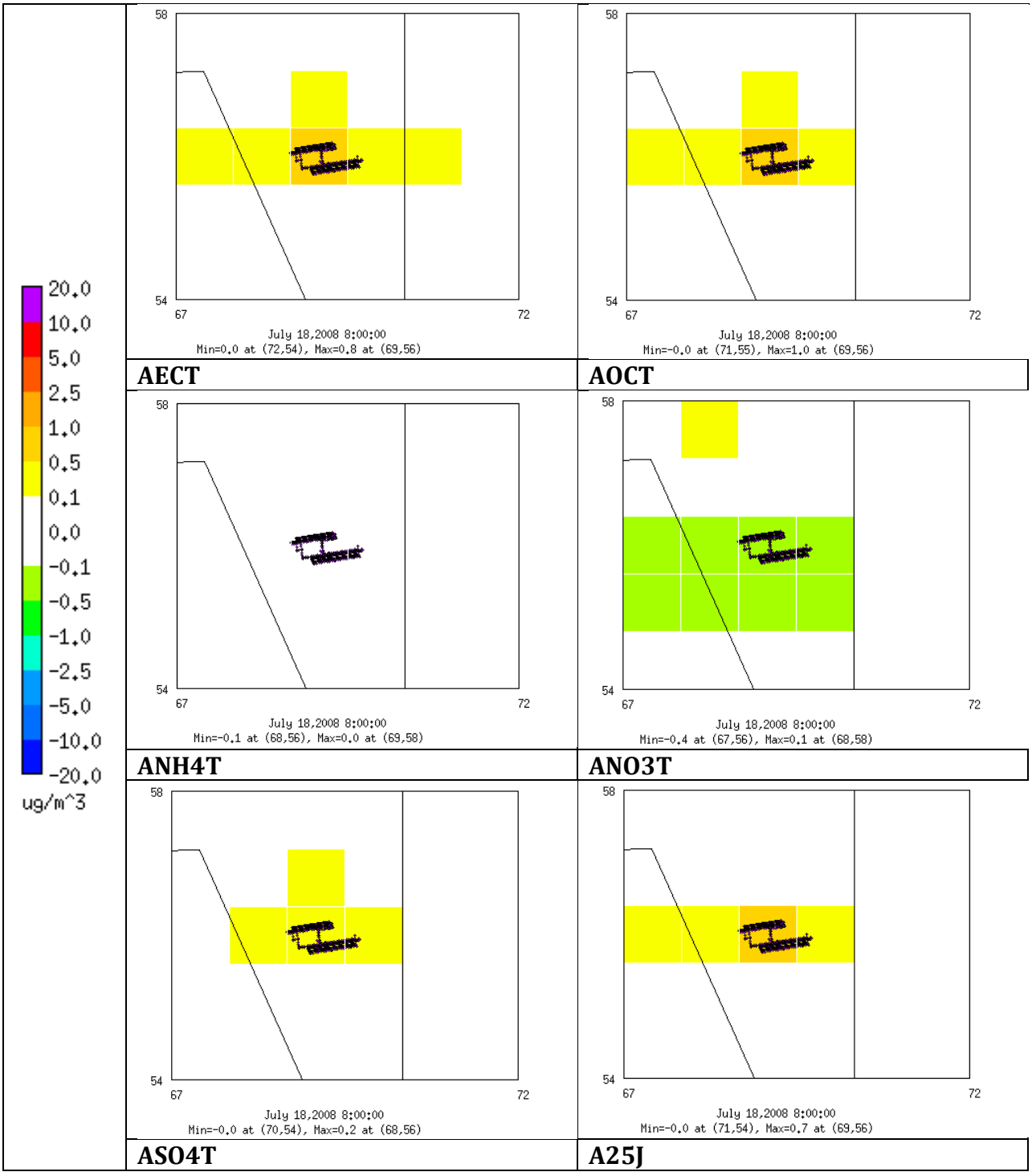

Figure 9B-35. Modeled differences in seasonal maximum daily average speciated $PM_{2.5}$ between AQMD_Jet and AQMD_Zero scenarios during Summer Season.

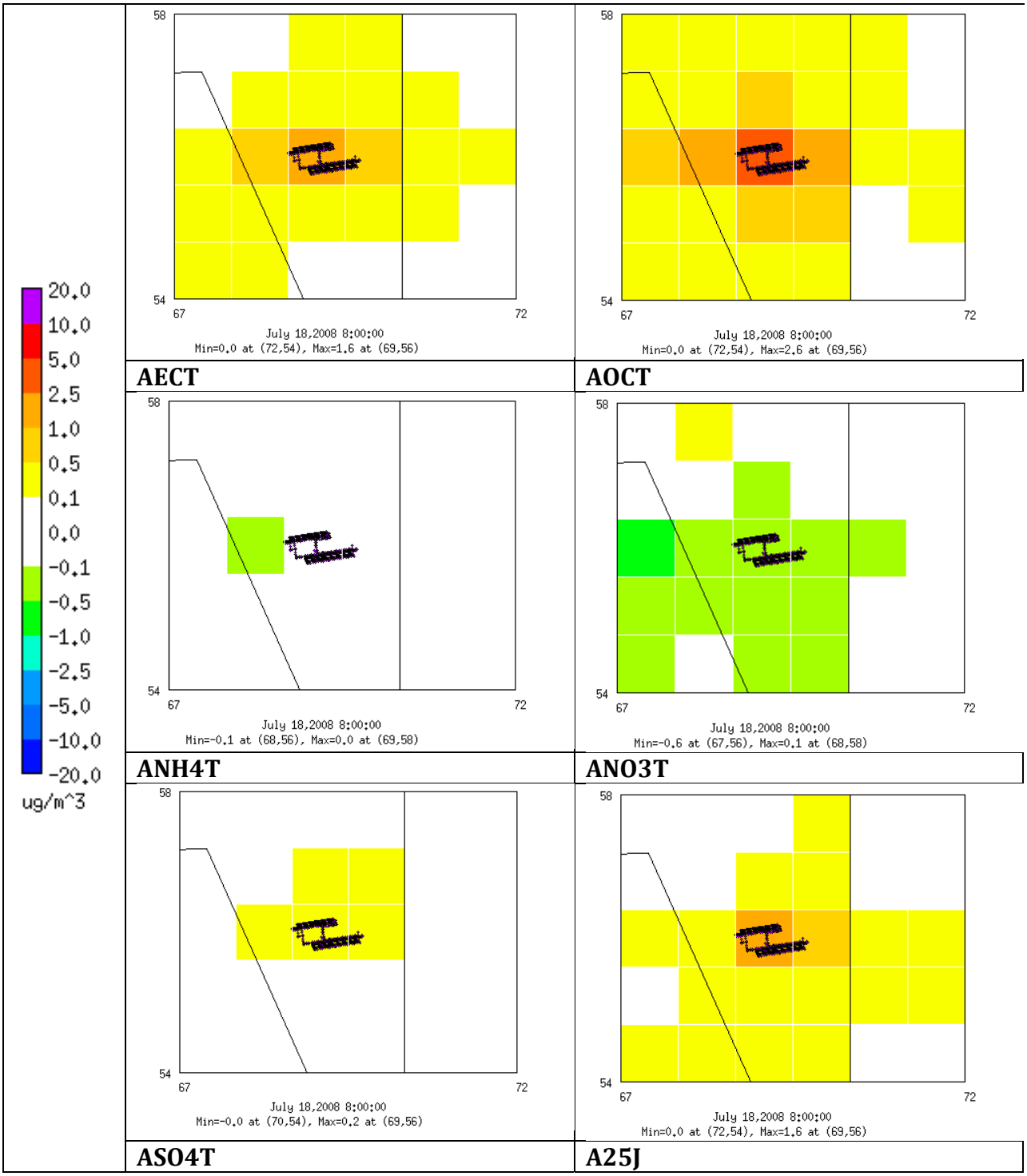

Figure 9B-36. Modeled differences in seasonal maximum daily average speciated $PM_{2.5}$ between AQMD_HRE and AQMD_Zero scenarios during Summer Season.

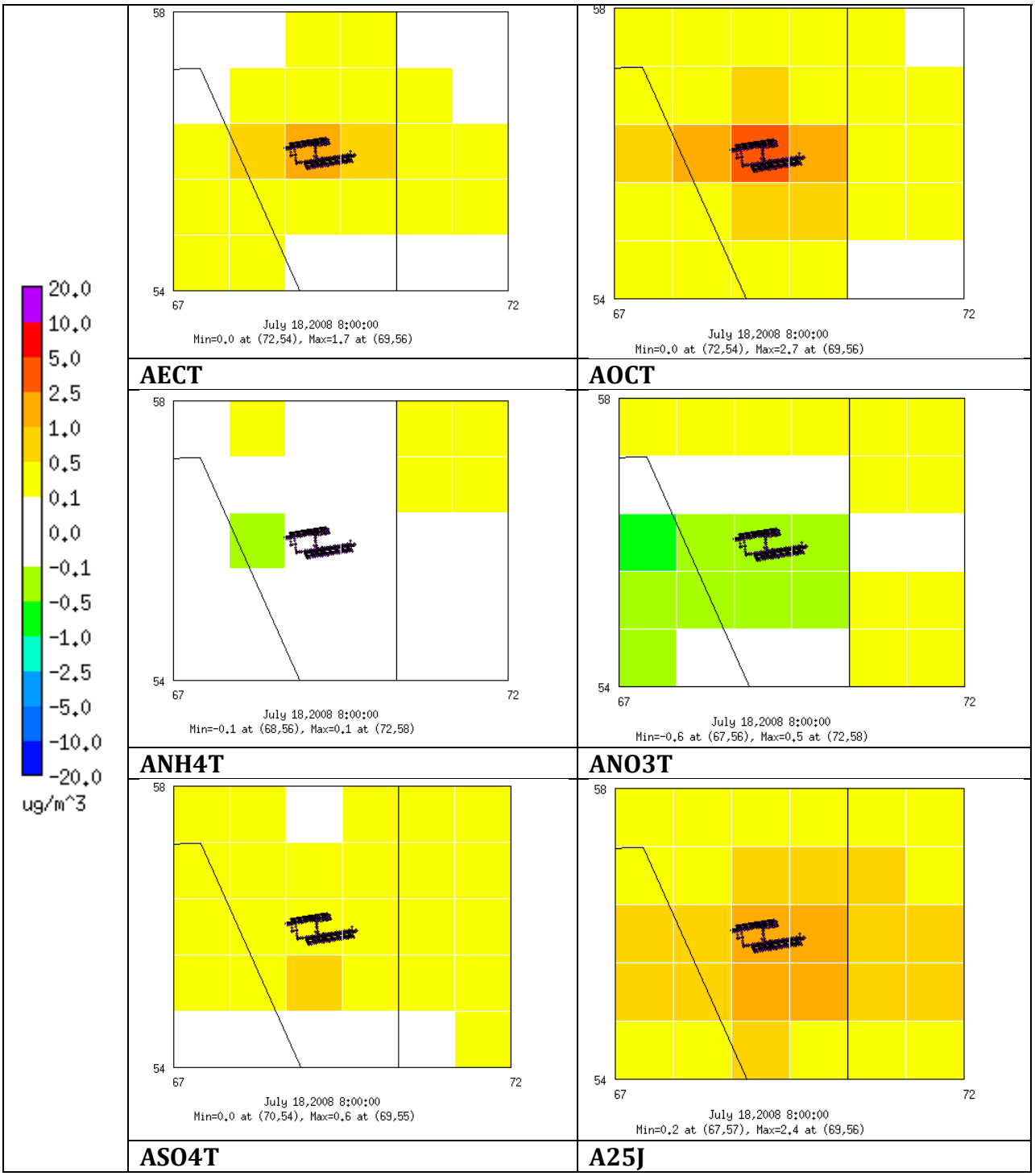

Figure 9B-37. Modeled differences in seasonal maximum daily average speciated $PM_{2.5}$ between AQMD_AllAirp and AQMD_Zero scenarios during Summer Season.

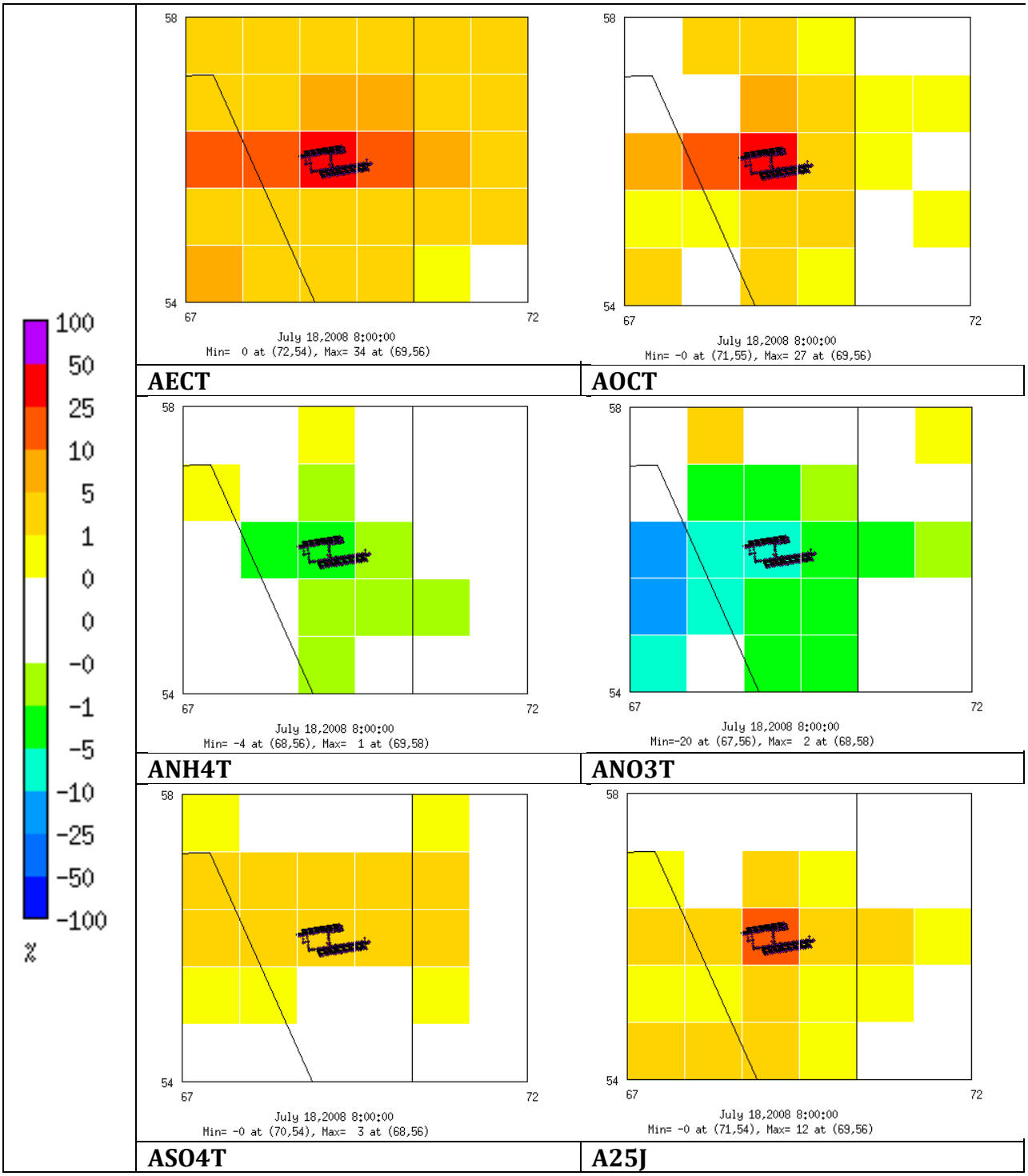

Figure 9B-38. Modeled % differences in seasonal maximum daily average speciated $PM_{2.5}$ between AQMD_Jet and AQMD_Zero scenarios during Summer Season.

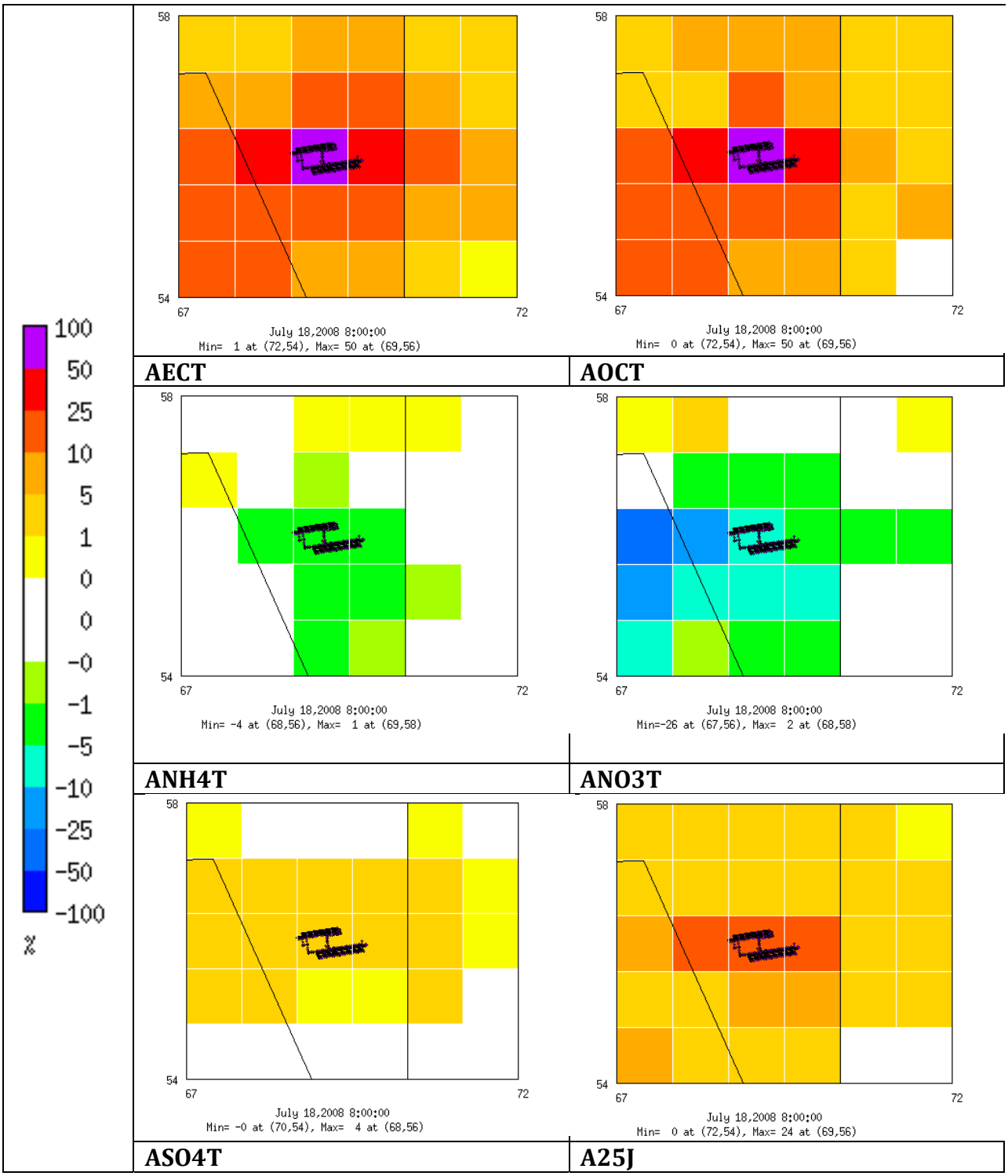

Figure 9B-39. Modeled % differences in seasonal maximum daily average speciated $PM_{2.5}$ between AQMD_HRE and AQMD_Zero scenarios during Summer Season.

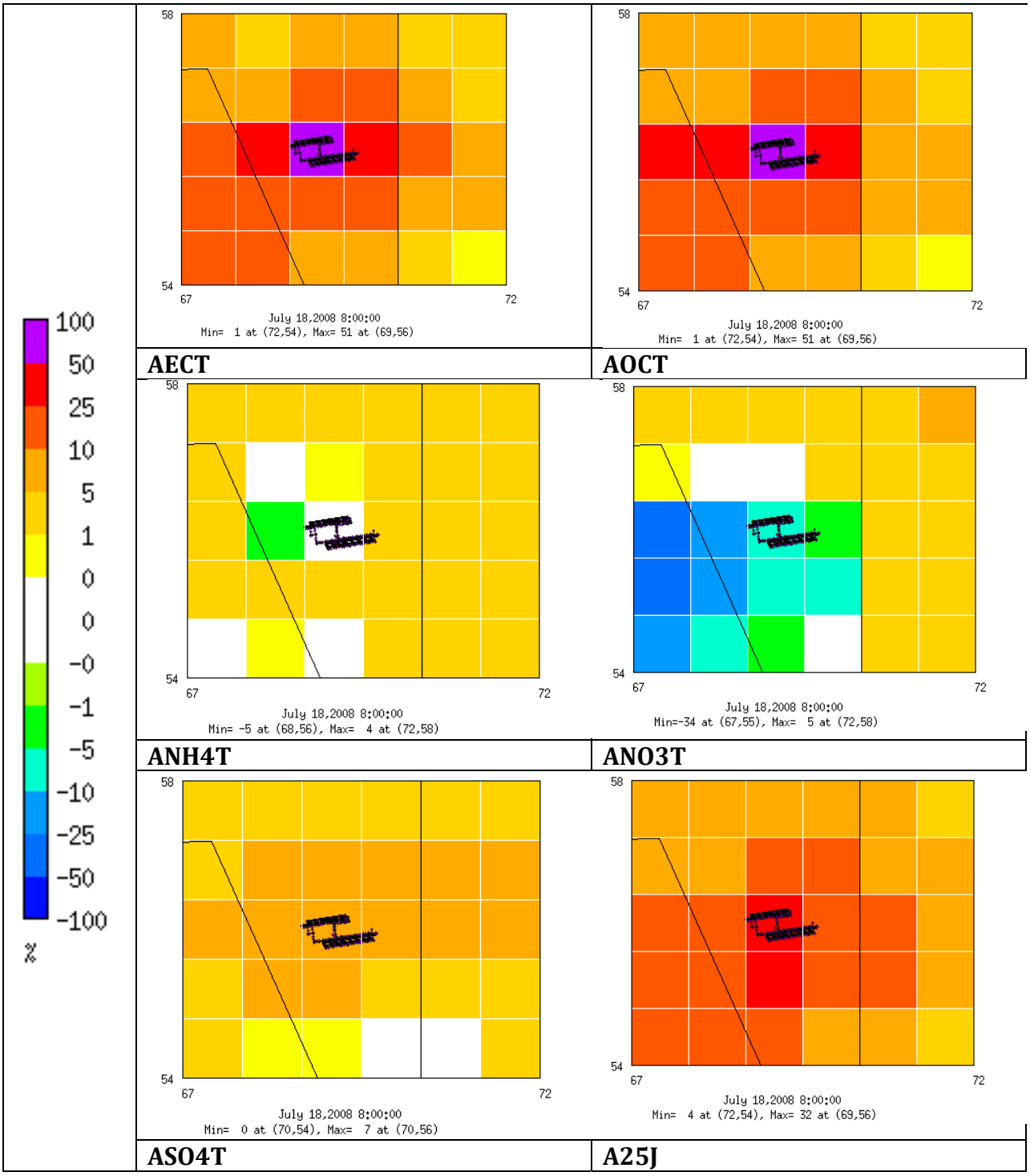

Figure 9B-40. Modeled % differences in seasonal maximum daily average speciated $PM_{2.5}$ between AQMD_AllAirp and AQMD_Zero scenarios during Summer Season.

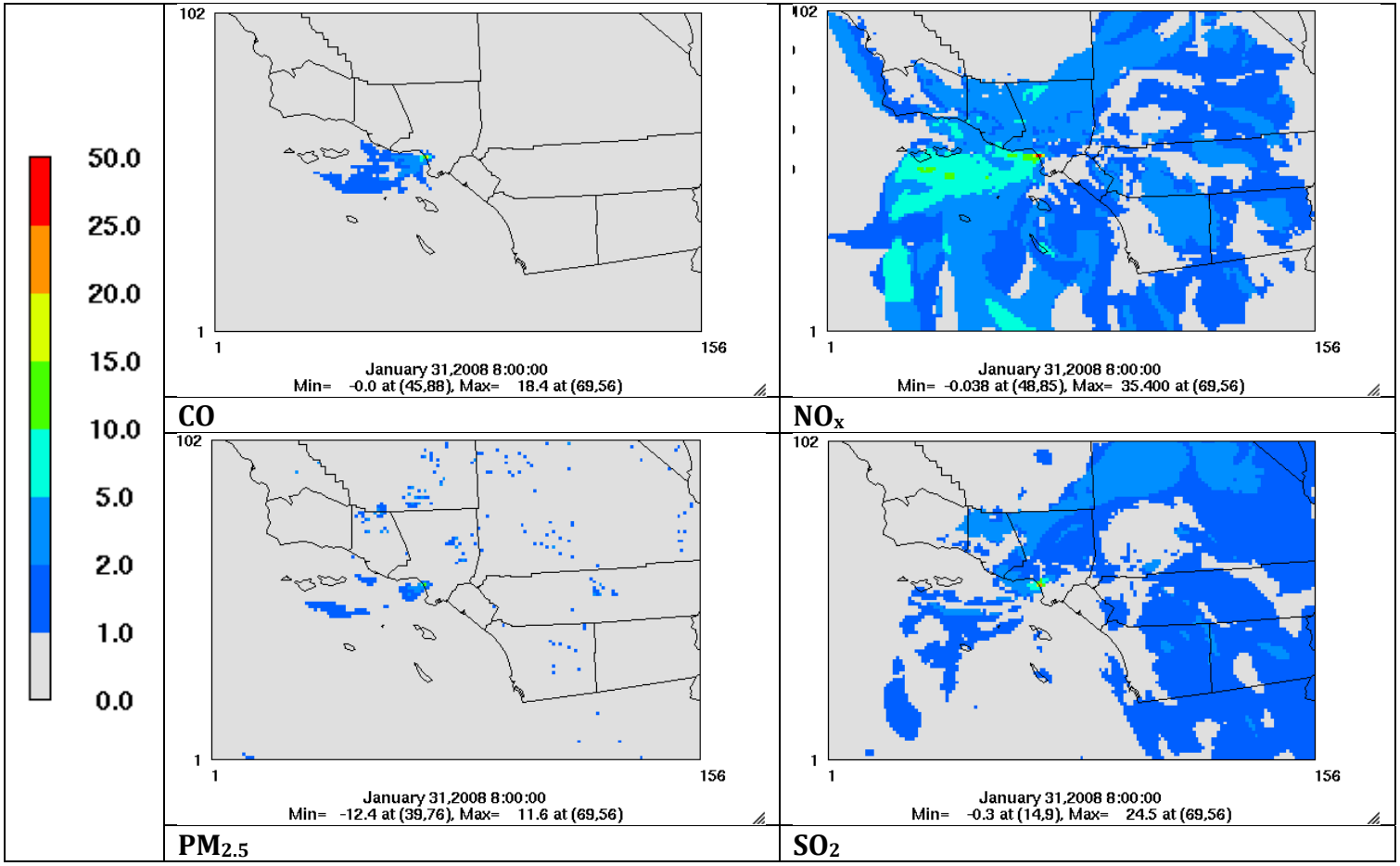

Figure 9B-41. Modeled % differences in seasonal maximum daily average CO, NOx, $PM_{2.5}$ and SO_2 between AQMD_HRE and AQMD_Zero scenarios during Winter Season (entire domain shown).

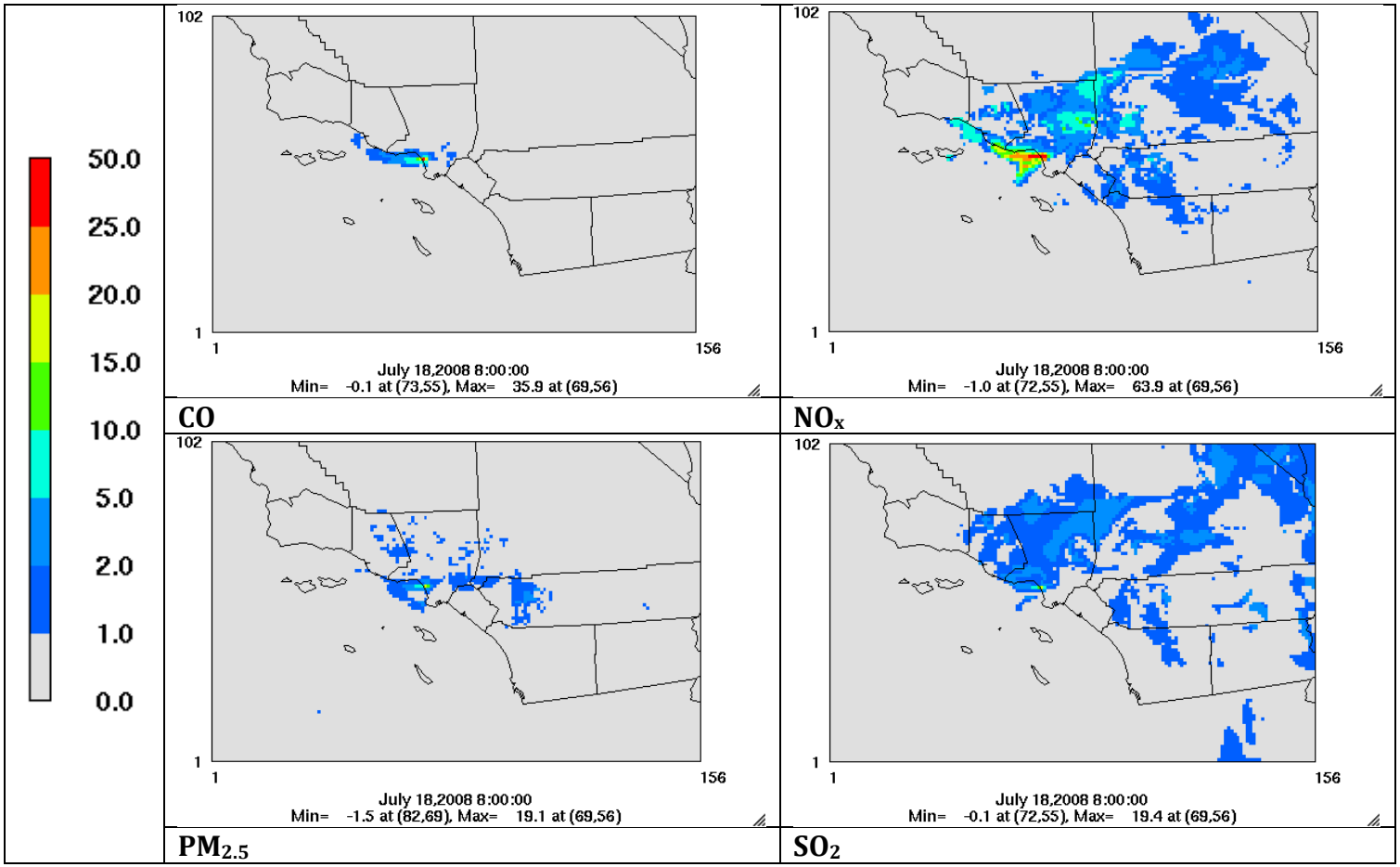

Figure 9B-42. Modeled % differences in seasonal maximum daily average CO, NOx, $PM_{2.5}$ and SO_2 between AQMD_HRE and AQMD_Zero scenarios during Summer Season (entire domain shown).

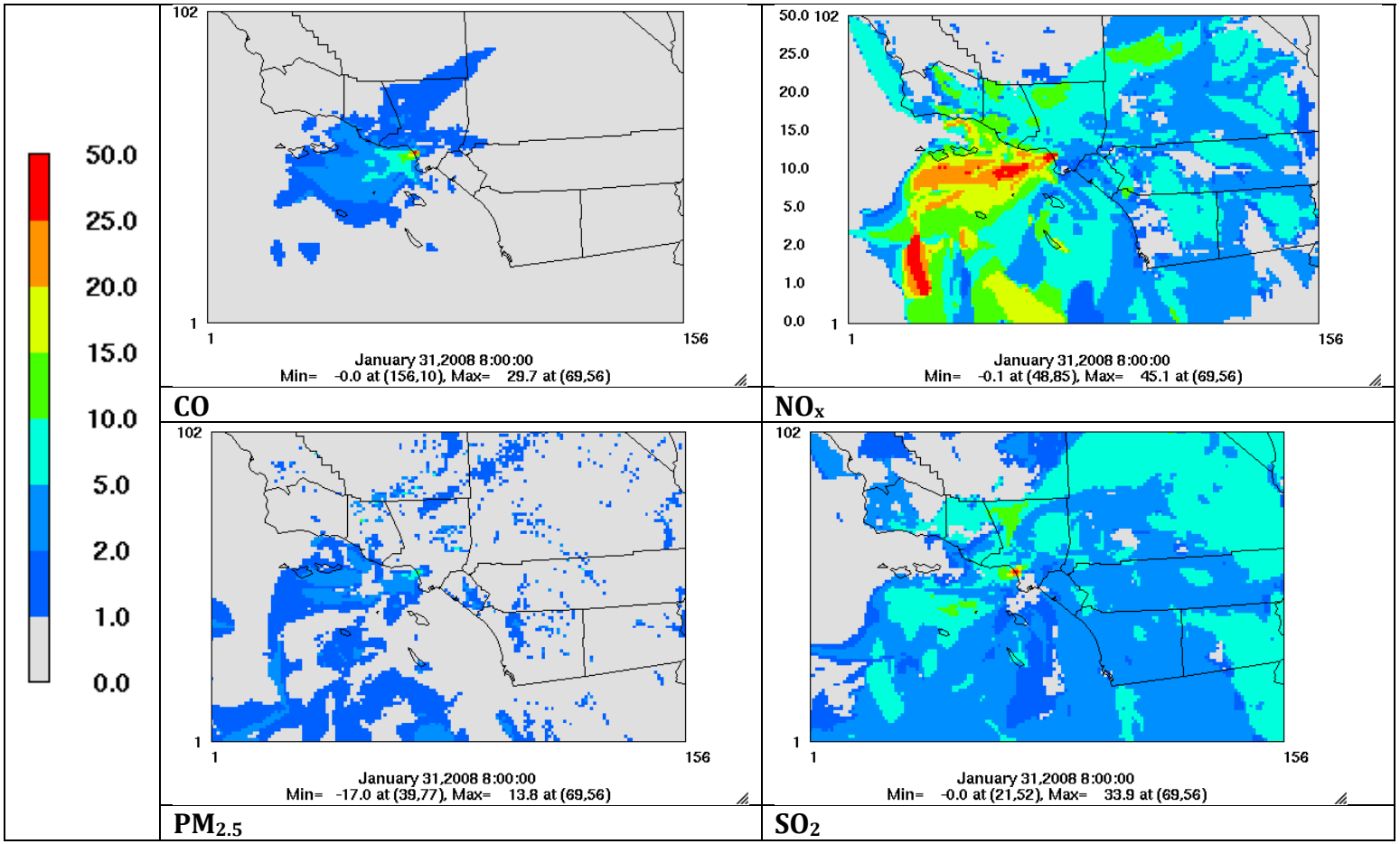

Figure 9B-43. Modeled % differences in seasonal maximum daily average CO, NOx, $PM_{2.5}$ and SO_2 between AQMD_AllAirp and AQMD_Zero scenarios during Winter Season (entire domain shown).

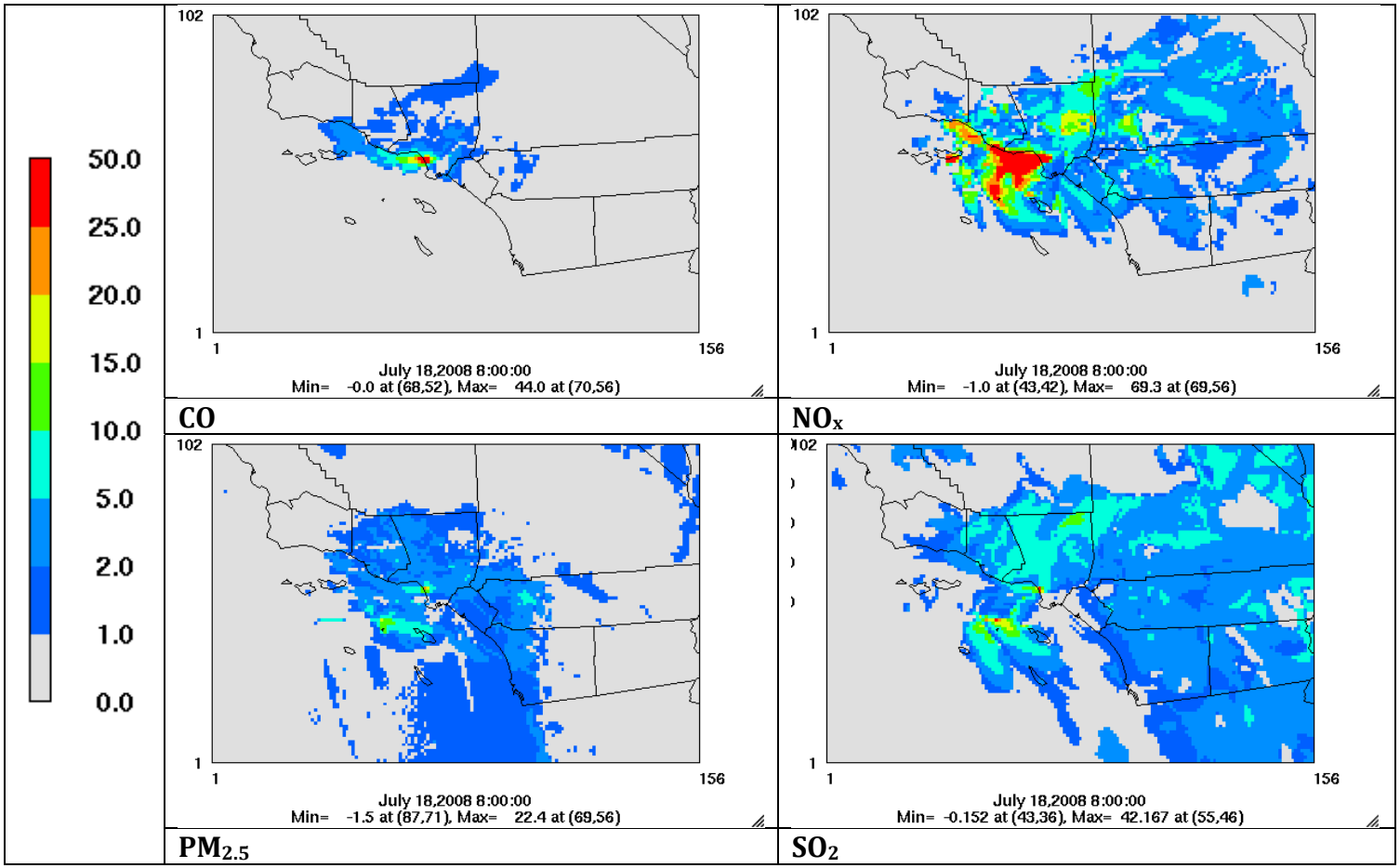

Figure 9B-44. Modeled % differences in seasonal maximum daily average CO, NOx, $PM_{2.5}$ and SO_2 between AQMD_AllAirp and AQMD_Zero scenarios during Summer Season (entire domain shown).

II. Source Apportionment

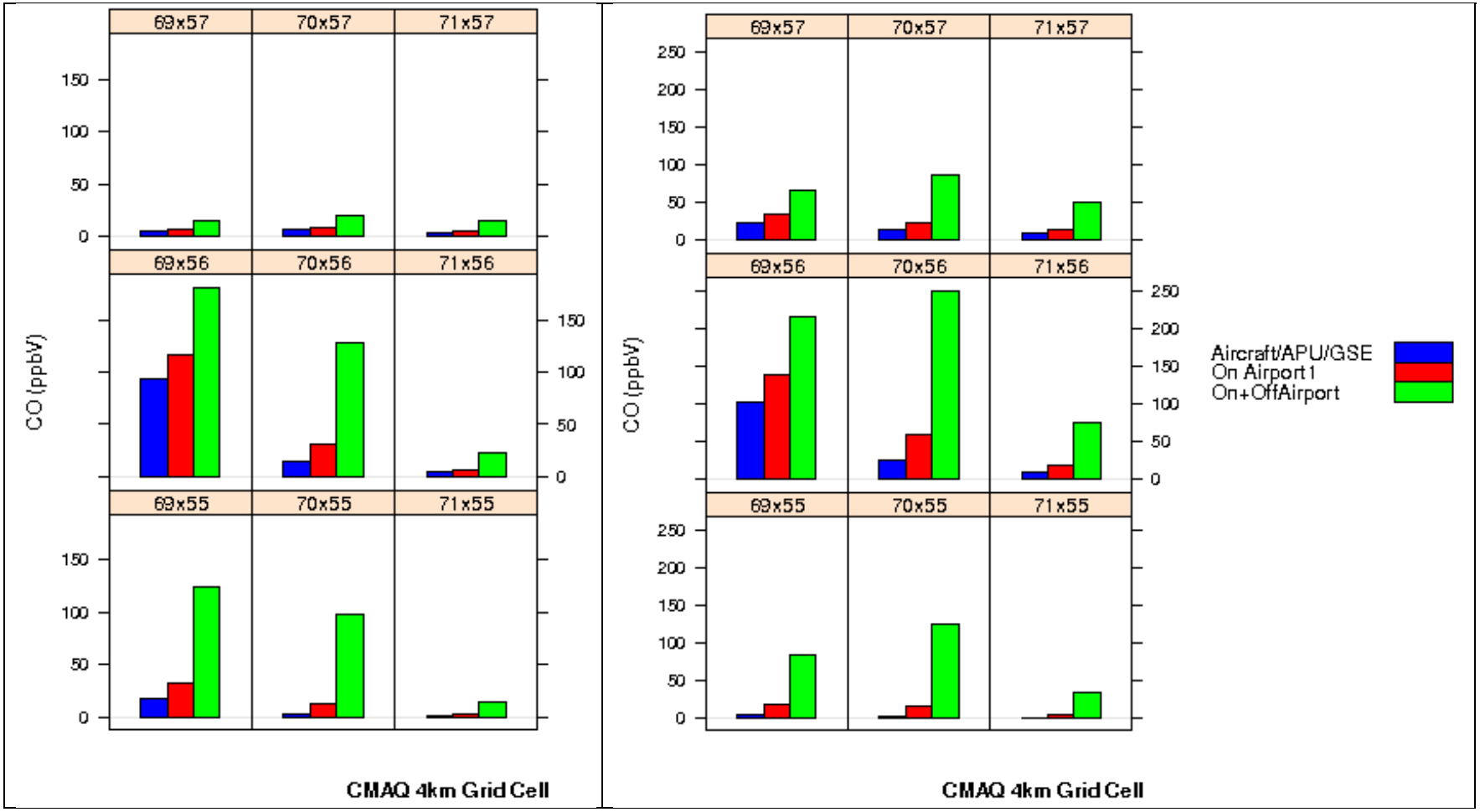

Figure 9B-45. Incremental CO contributions modeled by CMAQ due to various emissions scenarios during Winter (left) and Summer (right). [Numbers such as 69x57 indicate the Column, Row index of the CMAQ grid-cell]

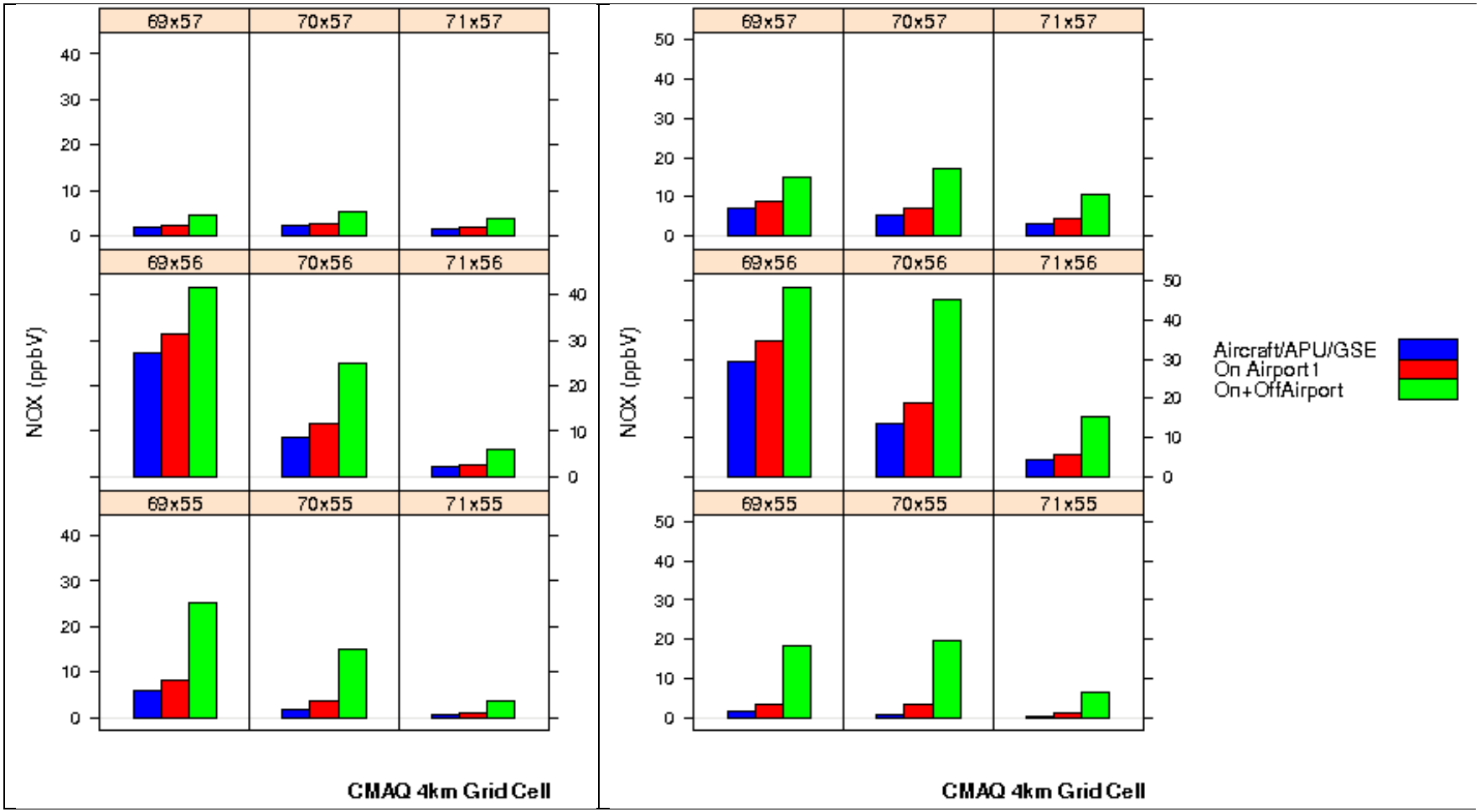

Figure 9B-46. Incremental NO_x contributions modeled by CMAQ due to various emissions scenarios during Winter (left) and Summer (right). [Numbers such as 69x57 indicate the Column, Row index of the CMAQ grid-cell]

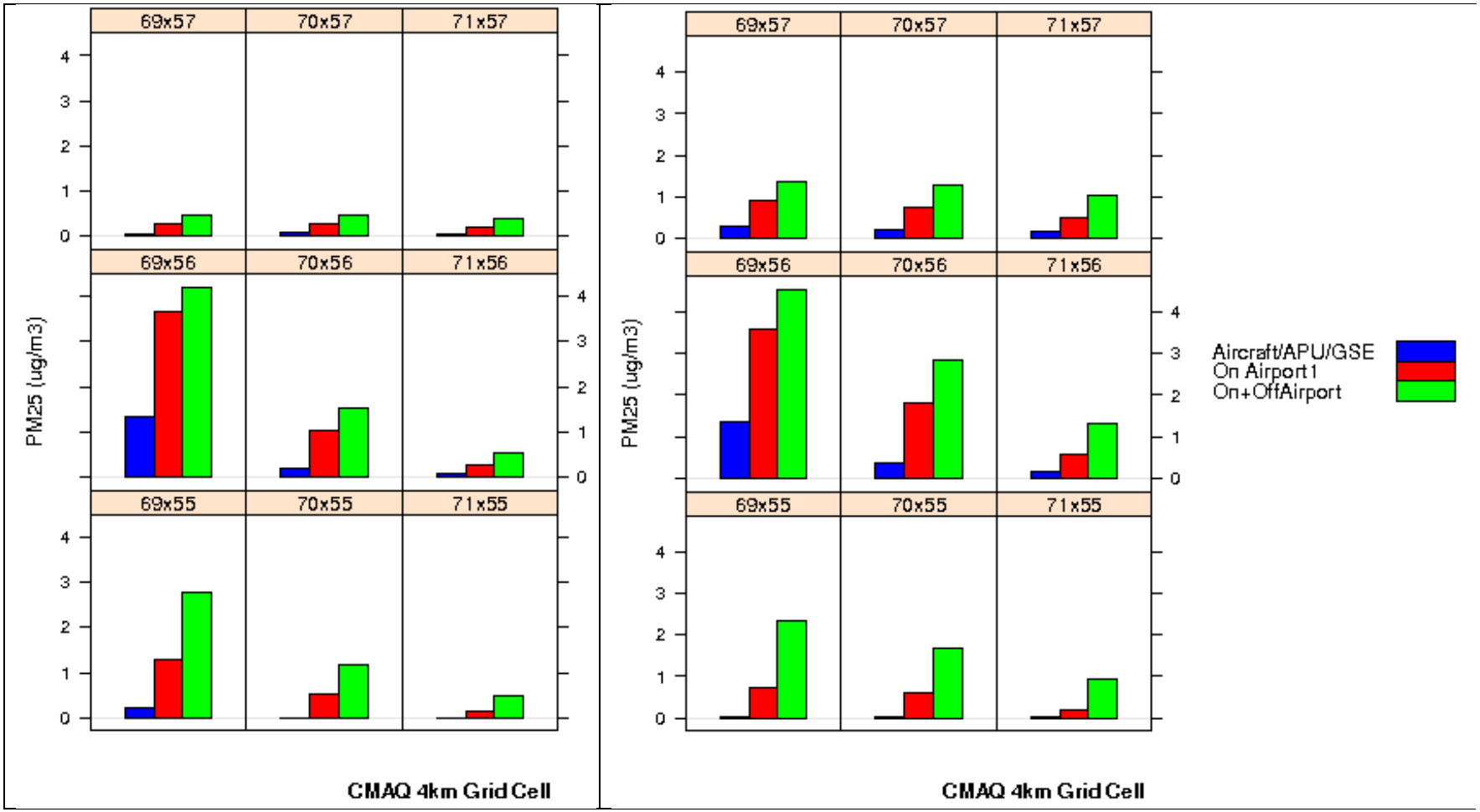

Figure 9B-47. Incremental $PM_{2.5}$ contributions modeled by CMAQ due to various emissions scenarios during Winter (left) and Summer (right). [Numbers such as 69x57 indicate the Column, Row index of the CMAQ grid-cell]

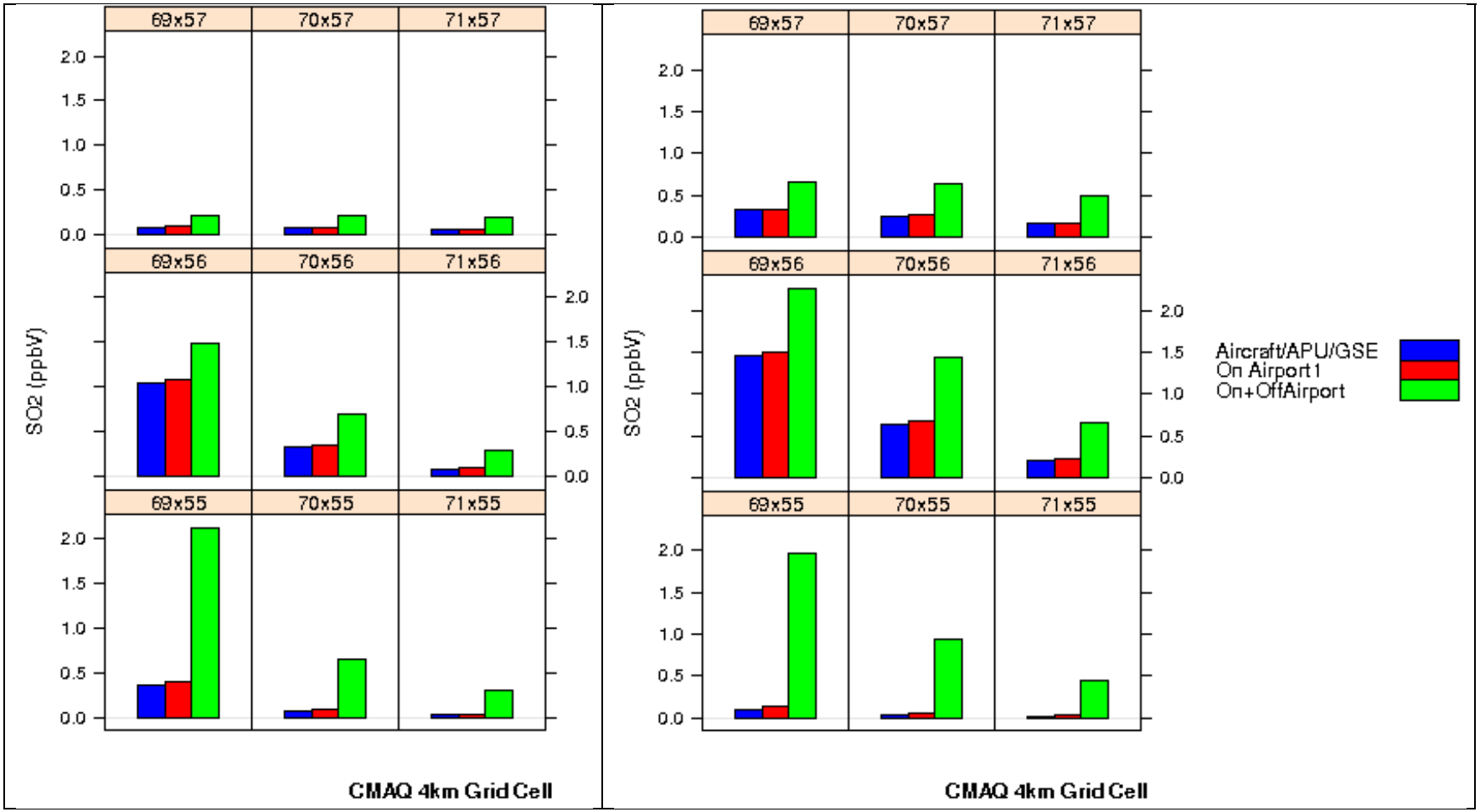

Figure 9B-48. Incremental SO_2 contributions modeled by CMAQ due to various emissions scenarios during Winter (left) and Summer (right). [Numbers such as 69x57 indicate the Column, Row index of the CMAQ grid-cell]

Section 10

KEY FINDINGS AND CONCLUSIONS OF THE LAX AQSAS

(This page is intentionally blank)

Table of Contents

List of Tables

List of Figures

(This page is intentionally blank)

10. KEY FINDINGS AND CONCLUSIONS OF THE LAX AQSAS

The Los Angeles International Airport (LAX) Air Quality and Source Apportionment Study (AQSAS) was conducted to determine the impact of airport operations on local air quality. This objective was achieved through field measurements taken during the Winter and Summer Seasons of the Study and the use of four modeling approaches, including two receptor-based models (Chemical Mass Balance [CMB] and Nonparametric Trajectory Analysis [NTA]), and two dispersion models (American Meteorological Society/U.S. EPA Regulatory Model [AERMOD] and the Community Multiscale Air Quality [CMAQ] model). The field measurements were used to determine the spatial and temporal variations in ambient air concentrations of gases and particulate matter (PM). Figure 10-1 shows the relationships between various components of the Study. Results and significant findings from the field measurements, emission inventory development, and modeling are presented in Sections 5 through 9. This section recaps and integrates the significant findings of the previous sections of the Study in Sections 10.2 through 10.4, and provides the summary of findings and conclusions of the Study in Sections 10.5 and 10.6.

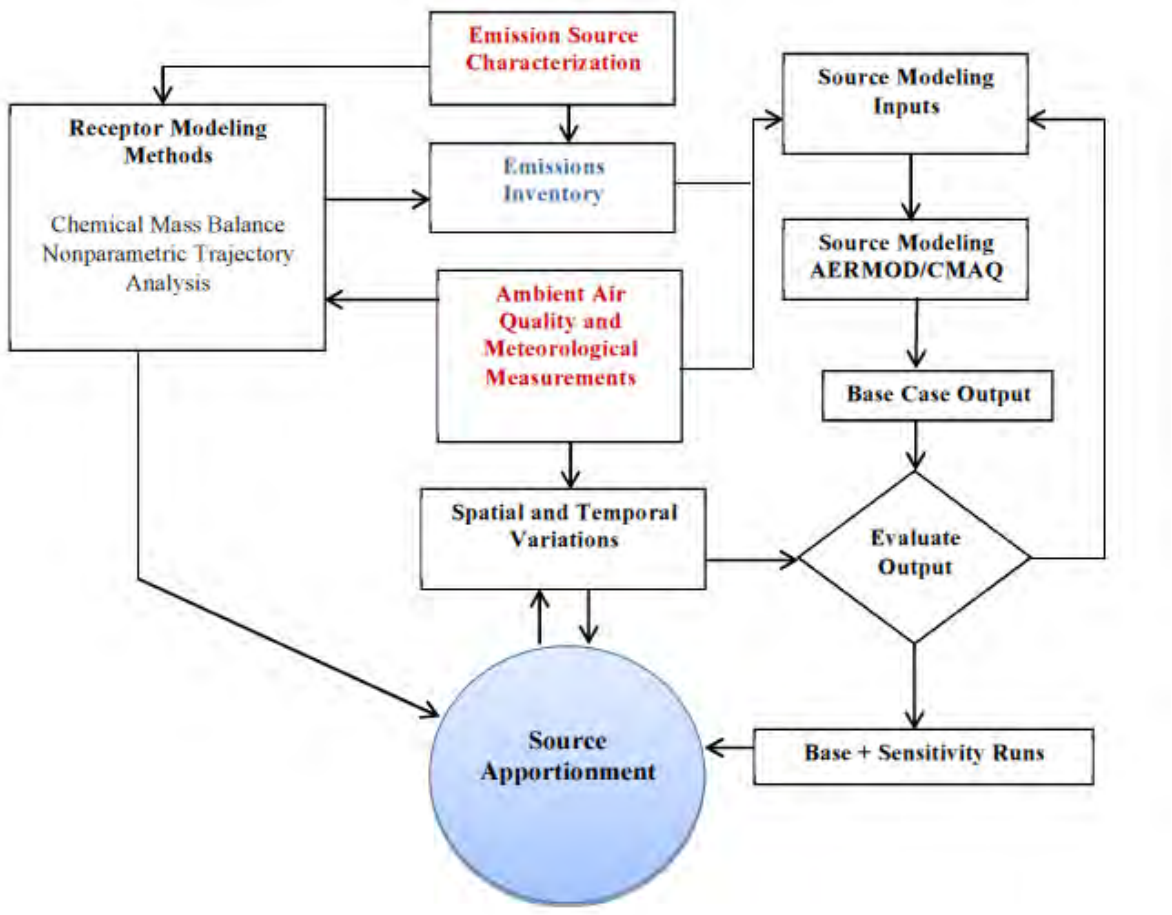

Figure 10-1. Links between field measurements (red), emission inventory development (blue), data analysis, and receptor and source modeling.

10.1 AIR QUALITY IN COMMUNITIES SURROUNDING LAX

Air quality monitoring for Phase III of the LAX AQSAS consisted of two six-week field measurement seasons: "Winter Monitoring Season" from January 31, 2012 to March 13, 2012 and "Summer Monitoring Season" from July 18, 2012 to August 28, 2012. A total of 17 sampling stations were deployed to provide data for spatial and temporal analyses as well as data for estimating the contributions of airport emissions to ambient pollutant concentration in adjacent communities. These stations included four community (or core) monitoring sites with continuous monitors, four satellite (i.e., supplemental community) monitoring sites equipped with passive and time-integrated samplers, and nine gradient (i.e., near-source) sites equipped with passive samplers. The four community (or core) sites were the Community East (CE) located in Lennox, Community South (CS) in El Segundo, Community North (CN) in Westchester, and South Coast Air Quality Management District (SCAQMD) Hastings site (AQ) in Playa Del Rey. Details of the measurement program are described in Section 3 and results presented in Section 5. The airport boundary, Study Area, and 17 monitoring sites, identified as core, gradient, or satellite sites, in the air monitoring network are shown in Figure 10-2.

The air pollutants studied in Phase III included both gases and fine particles. Fine particles ($PM_{2.5}$) were defined as those particles that are smaller than 2.5 micrometers (μm) in diameter and are capable of being inhaled into the lungs due to their size. Air quality standards have been established by the federal and state governments for some of the air pollutants included in the Study (see Table 10-1). No federal or state standards exist for the individual components of $PM_{2.5}$; however, they are regulated as a group based on total $PM_{2.5}$ mass. Ultrafine particles (UFP), which are particles smaller than 0.1 μm in diameter, are a subset of fine particles resulting from fuel combustion. While UFP can comprise a large portion of particle numbers, they normally contribute little to $PM_{2.5}$ mass due to their small size. Currently no air quality standard for UFP exists in the United States. Gaseous and particulate pollutants are either emitted directly from sources (primary pollutants, such as carbon monoxide [CO], sulfur dioxide [SO_2], nitrogen dioxide [NO_2], benzene, toluene, ethylbenzene, and xylenes [BTEX], 1,3-butadiene, black carbon [BC], elemental carbon [EC], polycyclic aromatic hydrocarbons [PAHs], UFP, and metals) or are formed in the atmosphere (secondary pollutants, such as NO_2, ammonium sulfate, ammonium nitrate, formaldehyde, and acetaldehyde).[1] Some pollutants are both primary and secondary pollutants. Examples include NO_2, formaldehyde, acetaldehyde, and sulfuric acid, which are the precursors to ammonium sulfate particles.

The CO, SO_2, and NO_2 levels measured in the communities surrounding the airport were lower than the levels of the National Ambient Air Quality Standards (NAAQS) during both monitoring seasons of the Study (see Table 10-2). The California Ambient Air Quality Standards (CAAQS) are more stringent than the national standards in some cases, and differ in the specific metric used to determine attainment. The CO, SO_2, and NO_2 levels were also lower than the CAAQS. Ambient levels of lead have been well below the air quality standards since it was phased out of gasoline. The maximum pollutant concentrations measured at the four core monitoring stations for Winter and Summer Seasons combined are shown in Figure 10-3.

[1] Although ozone is an important pollutant, it is formed over regions much larger than the Study Area for Phase III and was, therefore, not addressed in this Study.

Table 10-1. Air pollutants studied in Phase III.

Type of pollutant	Federal and State air quality standard exists	No air quality standard
Gases	CO (carbon monoxide) NO_2 (nitrogen dioxide) SO_2 (sulfur dioxide)	NO (nitric oxide) NO_x (oxides of nitrogen)[1] benzene, toluene, ethylbenzene, xylenes (BTEX) 1,3-butadiene formaldehyde, acetaldehyde, acrolein naphthalene and other volatile and semi-volatile polycyclic aromatic hydrocarbons (PAH)
Particles	$PM_{2.5}$ (fine particle mass) Lead	BC (black carbon), EC (elemental carbon)[2] OC (organic carbon) Soil (dust)[3] Ammonium Nitrate, Ammonium Sulfate UFP (ultrafine particles) Metals (e.g., Ni, V, Mn, Cr, Cd, As, Hg)

1. NO_x = NO + NO_2, NO and NO_2 convert chemically from one to the other in a matter of minutes, however NO_x concentrations can be considered to be conserved in this Study.
2. BC (from optical method) and EC (from thermal evolution method) are not identical, but for most purposes may be considered equivalent
3. Soil-derived elements, or dust, include aluminum, silicon, calcium, magnesium, iron, and potassium.

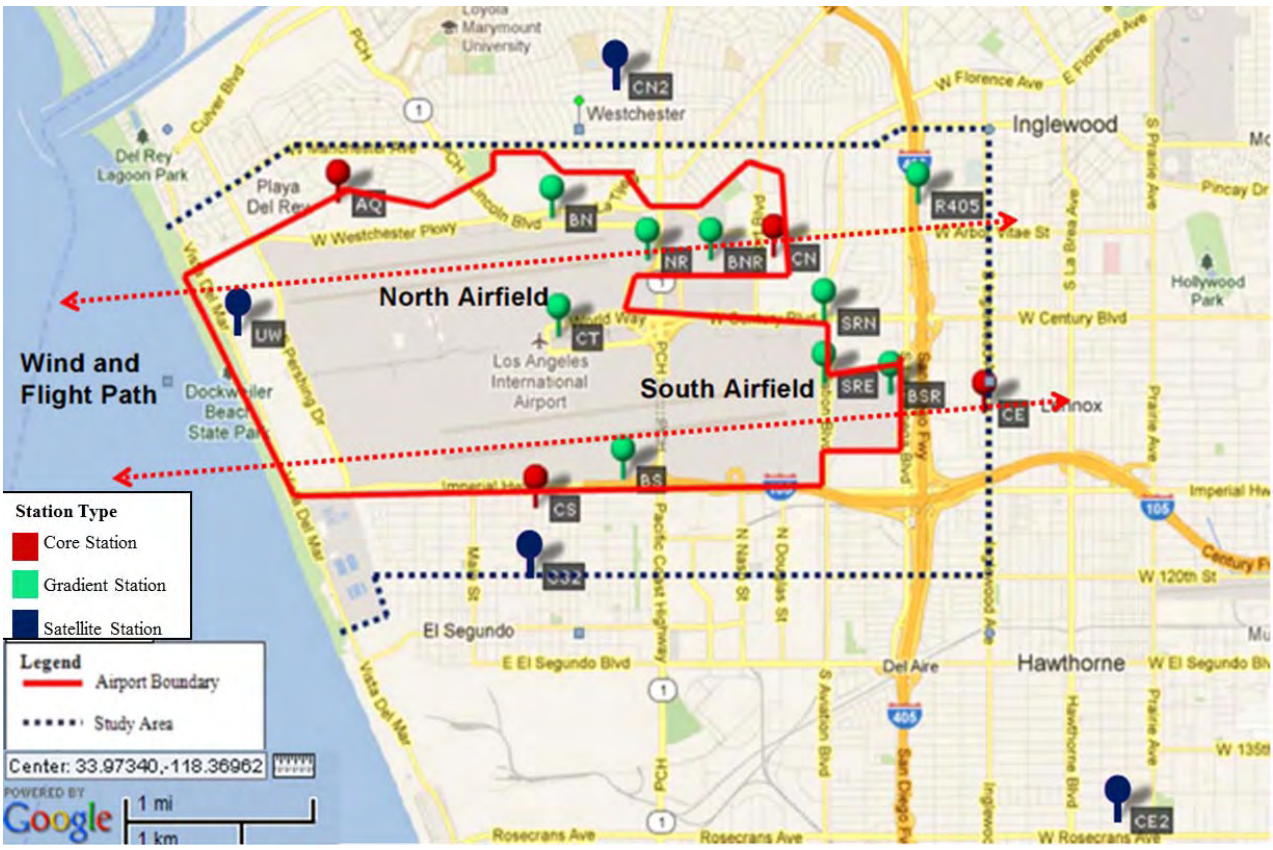

Figure 10-2. Locations of Phase III monitoring sites of the LAX AQSAS.

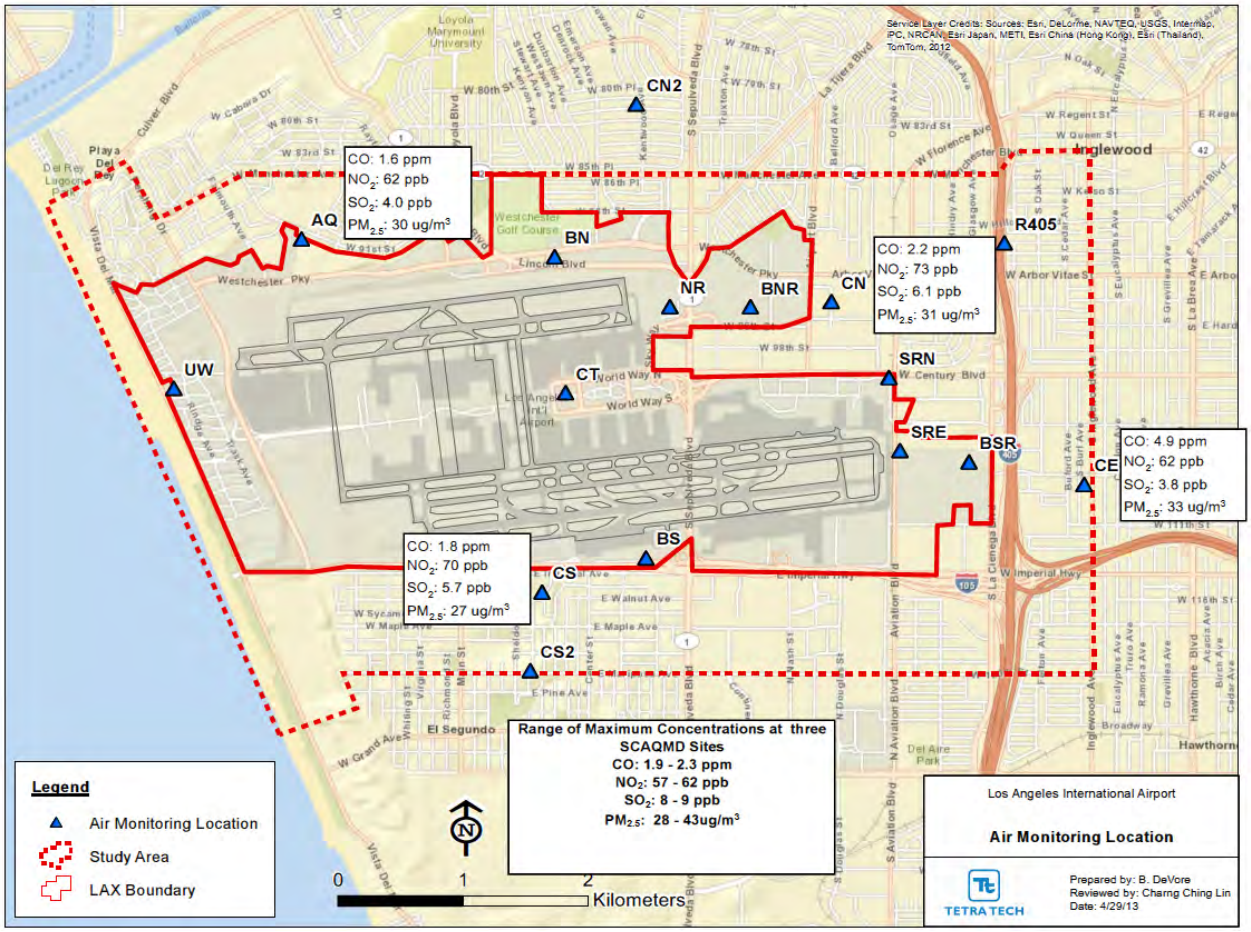

Figure 10-3. Maximum concentrations for CO, NO_2, SO_2, and $PM_{2.5}$ for Winter and Summer Seasons combined at the four core monitoring stations as compared to three SCAQMD sites.

$PM_{2.5}$ concentrations from the integrated filter-based samplers (e.g., seven-day Mini-Vol Portable Air Sampler, and 24-hour DRI Sequential Filter Sampler samples) were generally below the level of the annual NAAQS, while the Winter and Summer Season mean concentrations from the continuous Beta Attenuation Monitor[2] were at or higher than the level of the annual $PM_{2.5}$ standard. However, because the formation of secondary particles occurs over transport distances much greater than the Study Area, the large contributions (50 to 75 percent) of these secondary components of $PM_{2.5}$ indicate that the incremental contributions of airport-related emissions to ambient $PM_{2.5}$ concentrations at the community monitoring sites are likely small (see Table 6-17 in Section 6). For the four measured pollutants (CO, NO_x, SO_2, and $PM_{2.5}$) with air quality standards, the levels measured during the two seasons at the four core sites were comparable to those measured at the three nearest South Coast Air Quality Management District (SCAQMD) sites (i.e., Burbank, Los Angeles Main Street, and North Long Beach) within the South Coast Air Basin (SoCAB).

The concentrations of $PM_{2.5}$, EC, and metals are compared in Table 10-4 to data from SCAQMD Multiple Air Toxics Exposure Study III (MATES III) conducted from April 2004 to March 2006. Volatile organic air pollutants (i.e., BTEX, 1,3-butadiene, formaldehyde, and acetaldehyde) are

[2] Beta Attenuation Monitor provides measurements of ambient particle mass.

compared to MATES III data and the 2011 data from the California Air Resources Board (CARB) Air Toxics Monitoring Network in Table 10-5 which shows that concentrations measured during Phase III were comparable or lower than elsewhere in the SoCAB.

Table 10-2. Air pollutant concentrations for LAX AQSAS periods (Winter and Summer Seasons combined).[3]

	CO	**CO**	**NO_2**	**SO_2**	**$PM_{2.5}$**
	ppm	ppm	ppb	ppb	BAM $\mu g/m^3$
Hourly and Daily Federal and State Standards					
	1 hr max	8 hr max	1 hr max	1 hr max	24 hr max
NAAQS (Federal)	35	9	100	75	35
CAAQS (State)	20	9	180	250	*
Four Core Monitoring Stations					
CE (East)	4.9	< 4.9	62	3.8	33
CN (Northeast)	2.2	< 2.2	73	6.1	31
CS (South)	1.8	< 1.8	70	5.7	27
AQ (Northwest)	1.6	< 1.6	62	4.0	30
SCAQMD Monitoring Sites					
Burbank	2.3	< 2.3	57	8	34
Central LA	1.9	< 1.9	69	8	43
Long Beach	2.0	< 2.0	59	9	28

* There is no separate 24-hour $PM_{2.5}$ standard in California; however, the U.S. EPA promulgated a 24-hour $PM_{2.5}$ ambient air quality standard of 35 $\mu g/m^3$.

Notes: NAAQS levels are shown to provide context and are not directly comparable to the LAX AQSAS data statistics, which cover two measurement periods lasting 42 days each. The NAAQS are based on a full year of data and, in some cases, a running average of three years.

[3] Values in the table depict either the maximum value for Winter and Summer Season combined, or the mean value for Winter and Summer Seasons combined. This is indicated in the headings, such as 1-hr max, 8-hr max, etc., in the table.

Table 10-3. Seasonal mean NO_2, SO_2, $PM_{2.5}$ mass, EC and metal concentration data from 7-day passive and Mini-Vol aerosol sampling at the core and satellite community monitoring sites[1]

Site	units	CE	CE2	CN	CN2	CS	CS2	AQ	UW
Winter									
NO_2	ppb	25.56 ± 0.47	22.15 ± 0.41	27.28*	18.97 ± 0.35	21.09*	20.98 ± 0.40	19.12 ± 0.36	18.93 ± 0.35
SO_2	ppb	0.1± 0.39	0.07± 0.39	1.08*	0.16± 0.39	0.28*	0.13± 0.39	0.06± 0.39	0.06± 0.39
$PM_{2.5}$ mass	$\mu g/m^3$	11.97 ± 0.60	11.25 ± 0.56	10.11 ± 0.51	9.32± 0.47	9.74± 0.49	9.26± 0.46	9.3± 0.47	10.76 ± 0.54
EC	$\mu g/m^3$	1.13± 0.06	0.93± 0.05	1.13 ± 16.50	0.81± 0.04	1.01± 0.05	0.73± 0.05	0.76± 0.04	0.76± 0.04
Vanadium	ng/m^3	0.7± 0.2	0.9± 0.2	1.3± 1.1	0.8± 0.2	0.7± 0.2	0.8± 0.2	1.1± 0.2	0.8± 0.2
Chromium	ng/m^3	0.8± 0.3	0.6± 0.3	0.6± 1.5	0.5± 0.2	0.3± 0.3	0.4± 0.2	0.3± 0.2	0.5± 0.2
Manganese	ng/m^3	2.6± 0.2	3.5± 0.2	2.5± 1.1	2.1± 0.2	1.3± 0.2	1.9± 0.2	1.6± 0.2	2± 0.2
Nickel	ng/m^3	0.6± 0.2	0.8± 0.2	0.2± 1.1	0.5± 0.2	0.3± 0.2	0.5± 0.2	0.5± 0.2	0.3± 0.2
Lead	ng/m^3	0± 0.8	0.3± 0.8	0± 4.8	0.5± 0.8	0.1± 0.8	0.1± 0.8	0.7± 0.8	0.2± 0.8
Summer									
NO_2	ppb	15.62 ± 0.25	6.87± 0.12	13.50 ± 0.10	7.07± 0.11	5.82± 0.10	5.61± 0.10	4.54± 0.10	3.92± 0.10
SO_2	ppb	0.57± 0.39	0.27± 0.39	0.65± 0.10	0.41± 0.33	0.35± 0.10	0.29± 0.39	0.51± 0.39	0.41± 0.39
$PM_{2.5}$ mass	$\mu g/m^3$	9.8± 0.49	8.43± 0.42	5.91± 0.30	7.47± 0.37	7.04± 0.35	7.12± 0.36	7.06± 0.35	8± 0.40
EC	$\mu g/m^3$	0.58± 0.03	0.32± 0.02	0.53± 0.03	0.33± 0.02	0.28± 0.01	0.28± 0.01	0.23± 0.01	0.25± 0.01
Vanadium	ng/m^3	0.7± 0.1	0.8± 0.2	0.7± 0.1	0.7± 0.1	0.8± 0.1	0.8± 0.1	0.8± 0.1	1± 0.1
Chromium	ng/m^3	0.4± 0.1	0.2± 0.2	0± 0.1	0.1± 0.1	0.2± 0.1	0.1± 0.1	0.2± 0.1	0.2± 0.1
Manganese	ng/m^3	1± 0.1	0.8± 0.2	0.5± 0.1	0.6± 0.1	0.3± 0.1	0.6± 0.1	0.4± 0.1	0.5± 0.1
Nickel	ng/m^3	0.5± 0.1	0.3± 0.2	0.2± 0.1	0.3± 0.1	0.4± 0.1	0.4± 0.1	0.2± 0.1	0.4± 0.1
Lead	ng/m^3	0.1± 0.6	0.5± 0.8	0± 0.5	0.2± 0.5	0.4± 0.6	0.7± 0.6	0.5± 0.6	0.5± 0.5

1 Uncertainties for the LAX AQSAS data are uncertainties that are propagated through the sampling and analysis processes.

* No time-integrated samples were collected; therefore an average of continuous data was used. Only one valid Teflon sample was collected at the CN site during the Winter Monitoring Season due to equipment malfunction.

Table 10-4. Annual average $PM_{2.5}$ mass, EC, and metal concentration data from MATES III.[1]

MATES-III Apr 2005 - Mar 2006		MDL	Anaheim	Burbank	Los Angeles	Compton	N. Long Beach	W. Long Beach	Rubidoux
$PM_{2.5}$ mass	$\mu g/m^3$		17.7 ± 0.9	21.3 ± 1.2	19.4 ± 1.0	19.5 ± 1.0	18.5 ± 0.9	18.4 ± 0.9	23.4 ± 1.4
Elemental Carbon	$\mu g/m^3$		1.2 ± 0.1	1.8 ± 0.1	1.6 ± 0.1	1.6 ± 0.1	1.5 ± 0.1	2.0 ± 0.2	1.5 ± 0.1
Vanadium	ng/m^3	1.2	6.7 ± 0.4	4.1 ± 0.4	4.6 ± 0.4	7.5 ± 0.6	11.2 ± 0.8	19.2 ± 1.4	3.7 ± 0.3
Chromium	ng/m^3	2	2.0 ± 0.2	4.0 ± 0.3	4.0 ± 0.3	4.0 ± 0.4	4.0 ± 0.4	4.0 ± 0.5	5.0 ± 0.3
Manganese	ng/m^3	1	18.1 ± 1.3	22.7 ± 1.4	26.1 ± 1.2	25.0 ± 1.5	19.9 ± 1.2	29.9 ± 3.6	52.4 ± 2.3
Nickel	ng/m^3	1	4.0 ± 0.2	3.5 ± 0.2	5.4 ± 0.3	6.1 ± 0.3	6.9 ± 0.3	10.5 ± 0.6	3.9 ± 0.3
Lead	ng/m^3	5	6.2 ± 0.5	9.8 ± 0.5	14.6 ± 0.8	10.3 ± 0.7	8.4 ± 0.6	9.4 ± 0.7	11.4 ± 0.7
MATES-III Apr 2004 - Mar 2005									
$PM_{2.5}$ mass	$\mu g/m^3$		17.4 ± 0.9	20.6 ± 0.9	18.0 ± 0.9	18.2 ± 0.9	17.1 ± 0.9	18.3 ± 0.9	22.4 ± 1.3
Elemental Carbon	$\mu g/m^3$		1.5 ± 0.1	2.1 ± 0.1	2.0 ± 0.1	1.8 ± 0.1	1.5 ± 0.1	2.1 ± 0.2	1.8 ± 0.1
Vanadium	ng/m^3	1.2	6.9 ± 0.6	4.2 ± 0.4	4.8 ± 0.4	7.5 ± 0.5	11.7 ± 0.8	19.8 ± 1.4	4.0 ± 1.1
Chromium	ng/m^3	2	2.0 ± 0.2	4.0 ± 0.2	4.0 ± 0.3	4.0 ± 0.4	4.0 ± 0.5	5.0 ± 0.8	4.0 ± 0.3
Manganese	ng/m^3	1	19.0 ± 1.4	20.5 ± 0.9	25.2 ± 1.1	25.2 ± 1.4	19.4 ± 1.1	28.8 ± 1.9	47.7 ± 2.6
Nickel	ng/m^3	1	4.5 ± 0.3	4.4 ± 0.2	5.5 ± 0.6	6.4 ± 0.3	7.3 ± 0.4	12.1 ± 0.6	3.6 ± 0.2
Lead	ng/m^3	5	6.9 ± 0.5	10.7 ± 0.6	15.7 ± 0.8	13.0 ± 1.1	10.0 ± 0.7	12.0 ± 0.9	12.5 ± 1.1

[1] Uncertainties for MATES III data are standard errors of the means, where N is approximately 100 to 120 samples.

Table 10-5. Summary of volatile organic air contaminant concentration data from seven-day passive sampling at the Core and Satellite community monitoring sites[1] and annual average concentration from the CARB air toxics monitoring network for 2011 and MATES III.

Monitoring Program/Site	Benzene ppb	Toluene ppb	Xylenes ppb	Ethylbenzene ppb	1,3Butadiene ppb	Formaldehyde ppb	Acetaldehyde ppb
LAX AQSAS 2012							
Winter Season							
UW	0.29 ± 0.11	0.31 ± 0.15	0.15 ± 0.06	0.03 ± 0.02	0.000 ± 0.001	1.62 ± 0.03	0.74 ± 0.02
AQ	0.27 ± 0.11	0.23 ± 0.15	0.07 ± 0.06	0.01 ± 0.02	0.003 ± 0.001	1.52 ± 0.03	0.81 ± 0.02
CN2	0.71 ± 0.11	0.83 ± 0.15	0.45 ± 0.06	0.08 ± 0.02	0.005 ± 0.001	1.48 ± 0.03	0.84 ± 0.02
CN	0.82 ± 0.11	1.14 ± 0.15	0.57 ± 0.06	0.10 ± 0.02	0.004 ± 0.001	2.24 ± 0.05	1.14 ± 0.02
CS2	0.22 ± 0.11	0.27 ± 0.15	0.12 ± 0.06	0.02 ± 0.02	0.006 ± 0.001	1.77 ± 0.04	0.86 ± 0.02
CS	0.64 ± 0.11	0.73 ± 0.15	0.37 ± 0.06	0.06 ± 0.02	0.008 ± 0.001	1.72 ± 0.04	0.88 ± 0.02
CE	1.39 ± 0.11	1.64 ± 0.15	1.03 ± 0.06	0.17 ± 0.02	0.006 ± 0.001	2.14 ± 0.04	1.36 ± 0.03
CE2	1.37 ± 0.11	1.65 ± 0.15	0.78 ± 0.06	0.14 ± 0.02	0.006 ± 0.001	1.86 ± 0.04	1.20 ± 0.03
Summer Season							
UW	0.03 ± 0.11	0.01 ± 0.10	0.00 ± 0.02	0.00 ± 0.05	0.000 ± 0.008	0.92 ± 0.02	0.25 ± 0.01
AQ	0.05 ± 0.11	0.04 ± 0.10	0.00 ± 0.02	0.02 ± 0.05	0.000 ± 0.008	1.03 ± 0.02	0.29 ± 0.01
CN2	0.17 ± 0.11	0.18 ± 0.10	0.02 ± 0.02	0.12 ± 0.05	0.005 ± 0.008	1.08 ± 0.02	0.27 ± 0.01
CN	0.30 ± 0.11	0.25 ± 0.10	0.03 ± 0.02	0.22 ± 0.05	0.015 ± 0.008	1.53 ± 0.03	0.37 ± 0.01
CS2	0.17 ± 0.11	0.15 ± 0.10	0.02 ± 0.02	0.11 ± 0.05	0.000 ± 0.008	1.04 ± 0.02	0.31 ± 0.01
CS	0.11 ± 0.11	0.13 ± 0.10	0.01 ± 0.02	0.09 ± 0.05	0.003 ± 0.008	1.08 ± 0.02	0.32 ± 0.01
CE	0.25 ± 0.11	0.39 ± 0.10	0.04 ± 0.02	0.30 ± 0.05	0.016 ± 0.008	1.34 ± 0.03	0.44 ± 0.01
CE2	0.21 ± 0.11	0.24 ± 0.10	0.02 ± 0.02	0.09 ± 0.05	0.000 ± 0.008	1.08 ± 0.02	0.38 ± 0.01
ARB Air Toxic 2011							
Azusa	0.33 ± 0.03	0.98 ± 0.12	0.65 ± 0.04	0.30 ± 0.01	0.06 ± 0.01	3.01 ± 0.29	1.13 ± 0.14
Burbank	0.52 ± 0.06	1.43 ± 0.17	1.09 ± 0.07	0.20 ± 0.03	0.11 ± 0.02	3.52 ± 0.25	1.19 ± 0.15
Los Angeles N. Main	0.45 ± 0.05	1.08 ± 0.16	0.80 ± 0.07	0.16 ± 0.02	0.11 ± 0.01	3.01 ± 0.25	1.00 ± 0.13
N. Long Beach	0.44 ± 0.06	0.96 ± 0.15	0.63 ± 0.07	0.15 ± 0.02	0.10 ± 0.02	NA	NA
Rubidoux	0.28 ± 0.03	0.67 ± 0.09	0.50 ± 0.04	0.14 ± 0.01	0.05 ± 0.01	3.05 ± 0.34	1.10 ± 0.14
MATES-III Apr 2005 - Mar 2006							
Anaheim	0.42 ± 0.03	1.45 ± 0.12	0.86 ± 0.05	0.20 ± 0.02	0.04 ± 0.01	2.99 ± 0.12	1.31 ± 0.06
Burbank	0.69 ± 0.04	2.49 ± 0.15	1.56 ± 0.06	0.35 ± 0.02	0.12 ± 0.01	3.84 ± 0.15	1.95 ± 0.08
Los Angeles N. Main	0.57 ± 0.03	1.80 ± 0.10	1.13 ± 0.04	0.26 ± 0.01	0.09 ± 0.01	4.02 ± 0.17	1.69 ± 0.07
Compton	0.78 ± 0.06	2.72 ± 0.22	1.81 ± 0.09	0.41 ± 0.03	0.14 ± 0.02	2.94 ± 0.15	1.52 ± 0.09
San Bernardino	0.49 ± 0.02	1.69 ± 0.08	0.88 ± 0.03	0.22 ± 0.01	0.04 ± 0.00	3.81 ± 0.18	1.98 ± 0.09
North Long Beach	0.48 ± 0.03	1.40 ± 0.10	0.85 ± 0.04	0.20 ± 0.02	0.07 ± 0.01	3.56 ± 0.15	1.31 ± 0.06
Rubidoux	0.43 ± 0.02	1.49 ± 0.09	0.77 ± 0.03	0.19 ± 0.01	0.04 ± 0.01	3.53 ± 0.16	1.75 ± 0.08
West Long Beach	0.50 ± 0.03	1.56 ± 0.12	0.91 ± 0.04	0.22 ± 0.02	0.06 ± 0.01	3.36 ± 0.14	1.43 ± 0.08
MATES-III Apr 2004 - Mar 2005							
Anaheim	0.44 ± 0.03	1.55 ± 0.11	0.96 ± 0.04	0.20 ± 0.01	0.08 ± 0.01	2.91 ± 0.11	1.28 ± 0.06
Burbank	0.73 ± 0.04	2.68 ± 0.15	1.68 ± 0.06	0.34 ± 0.02	0.15 ± 0.01	3.73 ± 0.13	1.96 ± 0.08
Los Angeles N. Main	0.59 ± 0.03	1.84 ± 0.09	1.19 ± 0.04	0.25 ± 0.01	0.12 ± 0.01	4.47 ± 0.17	2.09 ± 0.10
Compton	0.82 ± 0.06	2.89 ± 0.24	1.97 ± 0.10	0.40 ± 0.03	0.20 ± 0.02	3.17 ± 0.12	1.56 ± 0.07
San Bernardino	0.49 ± 0.02	1.73 ± 0.10	0.97 ± 0.03	0.21 ± 0.01	0.08 ± 0.00	3.39 ± 0.18	1.79 ± 0.10
Huntington Park	0.76 ± 0.05	2.87 ± 0.18	1.79 ± 0.07	0.36 ± 0.03	0.17 ± 0.01	4.08 ± 0.14	1.33 ± 0.08
North Long Beach	0.56 ± 0.03	1.60 ± 0.10	1.04 ± 0.04	0.22 ± 0.02	0.12 ± 0.01	3.84 ± 0.14	1.30 ± 0.06
Pico Rivera	0.57 ± 0.03	1.97 ± 0.12	1.19 ± 0.04	0.26 ± 0.02	0.12 ± 0.01	3.49 ± 0.12	1.68 ± 0.07
Rubidoux	0.45 ± 0.02	1.53 ± 0.09	0.84 ± 0.03	0.18 ± 0.01	0.08 ± 0.01	3.47 ± 0.16	1.64 ± 0.08
West Long Beach	0.57 ± 0.04	1.98 ± 0.16	1.15 ± 0.06	0.27 ± 0.02	0.10 ± 0.01	3.19 ± 0.15	1.41 ± 0.07

1 Uncertainties for the LAX AQSAS data are propagated measurement uncertainties. Uncertainties for Air Toxics Network and MATES data are standard errors of the means (N is about 100 to 120).

10.2 SPATIAL AND TEMPORAL VARIATIONS IN POLLUTANT CONCENTRATIONS

The time-integrated saturation monitoring showed that the highest pollutant concentrations occurred near the North and South Airfield runways and roadways. The highest measured concentrations of NO and SO_2 occurred at the SRE monitoring site, which was a gradient site located 312 feet (95 meters) east of South Airfield Runway 25R, as shown in Figure 10-2. At locations 1,969 feet (600 meters) further east (BSR site), the measured concentrations were approximately ten percent of the values measured at the SRE site. Spatial variations in BTEX levels were more uniform, with higher levels near roadways. Average concentrations of benzene were 0.05 to 0.4 parts per billion (ppb) in the Summer Season and 0.3 to 1.5 ppb in the Winter Season at on-airport and off-airport monitoring sites. These values compare with upwind concentrations of 0.03 ppb in the Summer Season and 0.3 ppb in the Winter Season at Vista del Mar (UW). The average concentrations of volatile organic air contaminants increased from the UW site to east of the airport (CE site) with the highest average concentrations occurring adjacent to I-405 and east of I-405 (i.e., R405 site). Ambient concentrations of aldehydes were spatially uniform because the main sources were emissions from on-road vehicles and atmospheric formation from oxidation of precursor hydrocarbons (especially during the summer). Although there are no sources to the west, it has been shown that regional air pollution recirculates over the ocean with the off-shore evening winds and returns the next day when flow reverses. Therefore, the presence of fairly uniform aldehyde concentrations around the airport is consistent with the explanation that aldehydes are mostly due to a combination of vehicle exhaust and chemical transformation.

Comparisons of temporal (diurnal and day-of-week) variations in ambient pollutant concentrations (i.e., CO, NO_x, SO_2, $PM_{2.5}$, and BC) with corresponding temporal variations in vehicle traffic volumes and airport activity provided qualitative indications of the relative importance of airport-related emissions to the observed pollutant concentrations at the four core sites. During the Winter Season, morning winds were from the northeast, resulting in non-airport emissions having greatest impact at the CE and CN sites. Simultaneous peaks in CO, NO_x, and BC concentrations at these sites during the weekday morning commute period, and significantly lower concentrations during the same time period on Sundays, provide strong indication that the concentrations of these pollutants were mainly due to off-airport on-road mobile sources. In contrast, the SO_2 and UFP concentrations were low during the morning period at all sites except the CS site. SO_2 and UFP concentrations gradually increased throughout the day at both the CE and CN sites while near background concentrations levels were measured at both the CS and AQ sites. These results, coupled with the minimal weekday dependences for both SO_2 and UFP, indicate airport emissions were the main source of SO_2 and UFP at the CE and CN sites during the Winter Monitoring Season. The CS site was impacted during a relatively brief period, from about 06:00 to 10:00. Monitoring data from the AQ site showed little evidence of impact from airport emissions.

In contrast to the Winter Season, emissions from the airport were transported to the CN and CE sites during the daytime and nighttime of the Summer Season due to more persistent westerly winds. Consequently, SO_2 and UFP concentrations were higher earlier in the day during the Summer Season at both the CE and CN sites, while SO_2 and UFP concentrations at the CS site were much lower compared to the Winter Season. Pollutant concentrations were very low at

both the CS and AQ sites throughout the day and night. Diurnal patterns for NO_x, CO, and BC were similar during the Winter Season at the CE and CN sites, with concentrations observed to have morning peaks, very low midday levels and increasing during the evening starting around sunset. Daytime and early evening concentrations were lower for all pollutants at the CE and CN sites during the Summer Season due to greater vertical mixing and later development of the stable nocturnal inversion layer, which occurs in the summer after the evening commute. The substantially lower NO_x, CO, and BC levels at the CE and CN sites during the weekend mornings of both seasons are indications that off-airport on-road motor vehicles are likely the predominant source of these pollutants. Differences between the weekday and weekend were comparatively less for SO_2 and UFP number concentrations, and showed no day-of-week dependence, which suggest these pollutant concentrations are associated primarily with jet exhaust.

Diurnal variations in particle size distributions (PSD) provided useful insight regarding the relative importance of primary and secondary particles and their contributions to overall UFP number concentrations. UFP were separated into two size categories: freshly emitted or newly formed particles comprised the 7 to 30 nm range, while "aged" particles comprised the 30 to 160 nm size range. Furthermore, the day-of-week dependence of the diurnal variations of PSD and correlations of concentrations of particles in specific size ranges with concentration of other pollutants suggest the 7 to 30 nanometers (nm) and 30 to 160 nm particles may have different origins. Strong correlations of the 30 to 160 nm particles with CO, NO, and BC concentrations, and a strong weekday dependence of diurnal variations indicate an association of these particles with vehicle emissions. In contrast, the weaker correlation of the smaller 7 to 30 nm particles numbers with these mobile source pollutants (CO, NO, and BC) and stronger correlations with SO_2 and NO_2 concentrations suggest contributions of jet exhaust and, possibly, secondary particles.

A supplemental study was conducted at the end of the Summer Season to further investigate emission sources and the small particle size fraction of UFP. The volatility tandem differential mobility analyzer (VTDMA) measurements behind the blast fence at the end of the South Airfield Runway 25R, as described in Section 5.3.1, provided evidence of volatile sulfuric acid and ammonium sulfate in the smallest UFP size range. On average, about 30 to 50 percent of UFP were volatile. The concentrations of 14.5 nm particles measured at the CE site (about 1,600 m (or 1 mile) east of the South Airfield Runways) showed more spikes than corresponding measurements at the Trinity Lutheran Church Site (TLCS) site, which is located about 2,300 m (or 1.4 miles) south of the CE site, making it much less influenced by transport of pollutants from the airport during westerly winds. The average concentration of 14.5 nm particles at the CE site during the supplemental study period was approximately three times higher than particle concentrations at the TLCS site indicating frequent intermittent impact from jet engine exhaust.

10.3 IMPACT OF AIRPORT-RELATED EMISSIONS TO COMMUNITY AIR QUALITY

The airport contributions to ambient air quality were estimated by the Chemical Mass Balance (CMB) and Nonparametric Trajectory Analysis (NTA) receptor models, the American Meteorological Society/U.S. EPA Regulatory Model (AERMOD) Gaussian dispersion model, and the Community Multiscale Air Quality (CMAQ) grid-based air-quality simulation model. The receptor models use the measured pollutant concentrations to apportion the pollutants measured at a specific monitoring site to different source categories. The two source models use the emissions inventory estimates and the prevailing winds to estimate the downwind concentrations of the pollutants of interest. Analysis of the air quality data provided context and complemented the quantitative source apportionment results obtained by receptor and source modeling. Associations of spatial and time variations in pollutant concentrations with emission source activity and pollutant transport patterns were examined in this study as indications of the impacts of airport-related emission sources on local air quality. Special emphasis was given to the temporal variations in size distributions of UFP concentrations and correlations to other pollutants by time of day, day of week, varying meteorological conditions, and emission source activity.

Inventory of Airport and Non-Airport Related Emissions within the Study Area

The primary purpose of generating an emissions inventory was to quantify airport-related and non-airport related (or background) emissions. Airport-related emissions included: aircraft operations, auxiliary power units (APU)/ground support equipment (GSE), stationary sources, and motor vehicles (both on and off-airport). Non–airport related emissions included: off-airport motor vehicles, stationary sources (such as power plants, and Chevron El Segundo Refinery), marine vessels, aggregate stationary sources, and off-road equipment. The emissions inventories for the Winter and Summer Seasons for both airport and non-airport related sources are presented in Table 10-6. Generally, emission sources located outside the Study Area were not included in the emissions inventory, except for major emission sources located adjacent to the Study Area. Marine vessels in coastal waters to the west, the Scattergood Generating Station, the El Segundo Energy Center, and the Chevron El Segundo Refinery, are large emitters near enough to the Study Area to be included in the emissions inventory.

Table 10-7 shows the fraction of all emissions in the Study Area that are from airport sources, on average for both the Winter and Summer Seasons. All airport-related emission sources accounted for approximately 36 percent of CO, 25 percent of VOC, 36 percent of NO_x, 26 percent of SO_x, and 24 percent of $PM_{2.5}$ of all emissions, including emissions from marine vessels, refinery and power plants in the Study Area (average of both Winter and Summer Season). With the exclusion of emissions from marine vessels, refinery and power plants, the airport-related emission sources account for approximately 39 percent of CO, 34 percent of VOC, 64 percent of NO_x, 86 percent of SO_x, and 45 percent of $PM_{2.5}$ of the emissions in the Study Area. Table 10-7 shows that the marine vessels, power plants, and Chevron El Segundo Refinery, located outside the Study Area, are large contributors to emissions, especially NO_x and SO_x; although these sources may not be large contributors to ambient concentrations in the vicinity of the airport.

All motor vehicles (both airport and non-airport) within the Study Area accounted for 41 percent of CO, 20 percent of VOC, 13 percent of NO_x, 2 percent of SO_x and 14 percent of $PM_{2.5}$ of the total study area emissions. Ratios of the non-airport to airport-related traffic emissions are 2.3 for CO, 8.9 for VOC, 6.7 for NO_x, 7.7 for SO_x, and 2.3 for $PM_{2.5}$. As observed from the ratios, a majority of the motor vehicle emissions in the Study Area were not related to the airport. These results are based upon the data included in Section 8.

The emissions inventory for the LAX AQSAS was developed primarily as input for dispersion and air quality simulation modeling and cannot be used alone to infer source contributions at the monitoring stations. The ambient pollutant concentrations at community monitoring sites reflect the combined influences of local emissions and contributions of emissions from outside the Study Area, including the regional and urban background pollutant concentrations. Contributions of local emissions depend on proximity to the measurement sites and meteorological conditions that affect transport and dispersion of emissions.

Table 10-6. Emissions inventory of airport and non-airport related emissions for Phase III.

	Tons per Seasonal Period				
	CO	VOC	NO_x	SO_x	$PM_{2.5}$
Airport Related Emissions					
Winter Season					
Aircraft	225	41.5	362	29.7	3.3
APU/GSE	359	20.7	104	1.4	4.6
On-Airport Traffic	37.7	1.9	7.6	0.1	3.0
Off-Airport Traffic	74.0	5.7	17.3	0.2	1.4
Other	13.8	15.5	8.8	0.2	5.8
Total	709	85.3	499	31.6	18.0
Summer Season					
Aircraft	228	42.2	336	30	3.4
APU/GSE	329	19.0	95.8	1.4	4.4
On-Airport Traffic	48.0	2.2	8.3	0.1	3.5
Off-Airport Traffic	80.7	5.6	18.3	0.2	1.6
Other	12.6	14.5	7.2	0.1	5.3
Total	698	83.5	465	31.3	18.2
Non-Airport Related Emissions					
Winter Season					
Off-Airport Traffic	814	70.5	177	2.0	10.8
Chevron El Segundo Refinery	96.3	68.2	81.7	47.8	24.9
Marine	51.0	26.5	545	38.4	11.3
Other	308	101	107	3.1	11.9
Total	1,269	267	911	91.3	58.9
Summer Season					
Off-Airport Traffic	790	65.6	167	1.9	10.8
Chevron El Segundo Refinery	87.9	62.3	74.6	43.6	22.7
Marine	46.5	24.2	471	35.1	9.4
Other	285	93.2	98.3	2.9	11.3
Total	1,209	245	811	83.6	54.3
TOTAL					
Winter	1,978	352	1,410	123	77.0
Summer	1,907	329	1,276	115	72.4

Table 10-7. Fraction of Study Area emissions due to airport emissions sources, both with and without emissions from the Chevron refinery and marine vessels.

	% Airport Contribution to overall emission inventory within Study Area				
	CO	VOC	NO_x	SO_x	$PM_{2.5}$
Aircraft	12	12	26	25	5
APU/GSE	18	6	7	1	6
On/off-Airport Traffic	6	2	2	<1	6
Other Airport Sources	1	4	1	<1	7
Airport Contribution	36	25	36	26	24
Airport Contribution (without Chevron and marine vessels)	39	34	64	86	45

Chemical Mass Balance Receptor Modeling

The Chemical Mass Balance (CMB) model infers contributions from different source types. This is done by using multivariate measurements taken at receptor locations and the abundances of chemical components in source emissions. The model consists of a least-squares solution to a set of linear equations that expresses each receptor concentration of a chemical species as a linear sum of products of source profile species and source contributions. The source profile species and the receptor concentrations, each with uncertainty estimates, serve as input data to the CMB model. The CMB software applies the effective variance solution, which gives greater influence in the solution to chemical species that are measured more precisely in both source and receptor samples. The software also calculates uncertainties for source contributions from both the source and receptor uncertainties.

The CMB receptor model was used to estimate the source contributions to the ambient concentrations of $PM_{2.5}$, OC, EC, VOCs, and gaseous air toxics (e.g., BTEX) measured at three of the core community monitoring sites in Lennox (CE), Westchester (CN), and El Segundo (CS). CMB was not conducted for the AQ site because this site was not one of the three core sites with the chemical speciation data required for CMB analysis.[4] The ambient measurements used in the CMB receptor modeling (and also the NTA modeling described below) are representative of neighborhood scale in the range of 0.5 to 4 km (or 0.3 to 2.5 miles) and include both primary and secondary pollutants. CMB apportions source categories and cannot distinguish locations of emission sources that have the same chemical composition profile. For example, it is not possible for CMB to separately apportion airport- and non-airport-related vehicle emissions due to the similar vehicle emission profiles. The main CMB results are summarized below:

- Ammonium sulfate, ammonium nitrate, and unexplained organic matter, which were not apportioned by one of the source categories in the CMB calculation, comprised approximately half of the $PM_{2.5}$ mass at the CE and CN sites during the Summer Season and about two-thirds during the Winter Season. These three secondary components

[4] The AQ site was representative of a clean background with offshore airflow rather than airport or urban conditions. Samples collected at the AQ site were likely to have concentrations near or below CMB detection limits for many compounds of interest.

accounted for about a third of $PM_{2.5}$ at the CS site in the Winter Season and nearly all of the mass in the Summer Season.

- The sum of sea salt aerosol, soil derived fugitive dust and wood smoke account for an additional 20 to 30 percent of $PM_{2.5}$ mass.

- The contributions of jet exhaust to $PM_{2.5}$ mass were consistently small with Winter Season means ranging from 2 percent at the CE and CS sites to 2.5 percent at the CN site. Contributions during the Summer Season were below 1 percent at the CE and CS sites and slightly higher than 1 percent at the CN site.

- At the CE, CN, and CS sites, the average contributions to $PM_{2.5}$ mass of emissions from diesel vehicles accounted for 15 and 8 percent of the ambient $PM_{2.5}$ mass concentrations during the Winter and Summer Seasons, respectively. Emissions of gasoline vehicles accounted for 1.7 percent of the Winter Season and 0.3 percent of the Summer Season concentrations. While it is not possible for CMB to separately apportion airport- and non-airport-related vehicle emissions, the temporal and spatial analysis of ambient data suggests greater contributions from non-airport related traffic emissions. However, adjusting the total vehicle source contribution from the CMB results by 2.3 (which is the ratio of non-airport to airport-related vehicle emissions from the Study Area emissions inventory), the airport-related vehicle exhaust contributions to ambient $PM_{2.5}$ is estimated to be 4 to 9 percent.

- Table 10-8 is a summary of percent contribution of the sum of jet, diesel, and gasoline exhaust to the total observed ambient concentrations of $PM_{2.5}$, EC, and OC at the CE, CN, and CS sites.

Table 10-8. Summary of percent contribution of the sum of jet, diesel, and gasoline exhaust to the total observed ambient concentrations of $PM_{2.5}$, EC, and OC at the CE, CN, and CS sites.[5]

Site	$PM_{2.5}$		EC[6]		OC	
	Winter	Summer	Winter	Summer	Winter	Summer
CE	21.7±1.5	8.7±0.6	100	98	15.9±1.6	5.4±0.8
CN	20.8±1.2	9.7±0.6	100	100	15.9±1.4	7.4±0.8
CS	13.3±1.0	8.2±0.5	100	100	14.2±1.3	3.8±0.5

- Measurements of ambient lead and chromium concentrations were collected and the measured concentrations were in the range of 0.001 to 0.004 $\mu g/m^3$. These low levels have very high uncertainties; therefore, source contribution estimates for these compounds are highly uncertain. Note that the NAAQS for lead is a 3-month average of 0.15 $\mu g/m^3$, substantially higher than the measured lead values. Vanadium and PAH contributions were below detection.

[5] CMB was not conducted for the AQ site because this site was not one of the three core sites with the chemical speciation data required for CMB analysis.

[6] The airport does not comprise 100 percent of EC concentrations as these values are the sum of jet, diesel, and gasoline exhaust for sources that may not be related to the airport.

- The 55 Photochemical Assessment Monitoring Stations (PAMS) target hydrocarbons typically account for 70 to 80 percent of total nonmethane hydrocarbons in urban areas from all sources. The mean contributions of jet exhaust to the sum of these 55 target compounds ranged from a few percent to as much as 20 percent. The contributions of target hydrocarbons were greater during the Winter Season with a source contribution estimate (SCEs) of 12.3 $\mu g/m^3$ at the CE site; 12.7 $\mu g/m^3$ at the CS site; and 4.0 $\mu g/m^3$ at the CN site for jet exhaust. Benzene accounted for approximately 3 to 4 percent of the sum of PAMS species attributed to jet exhaust. Apportionment of toluene to jet exhaust was not significant. The apportionment results indicate that jet exhaust may contribute a significant fraction of the measured 1,3-butadiene in some cases, but with high uncertainty.

- On-road vehicles accounted for 25 to 40 percent of the sum of PAMS species and about 50 to 75 percent of the measured benzene. CMB cannot distinguish between airport and non-airport related vehicle emissions, so an unknown fraction of the on-road vehicle apportionment may be associated with airport ground support vehicles and vehicle traffic to and from the airport. However, vehicles in closer proximity to the monitoring sites can be expected to have greater influence on the measured VOC levels.

Nonparametric Trajectory Analysis

Nonparametric Trajectory Analysis (NTA) is a receptor model that can show the effects of nearby sources on the data and, at the same time, the sources of background pollutants can be located and quantified. This is completed by using one- to five-minute average pollutant concentrations and back-trajectories calculated using one- to five-minute average wind data. Averaging times on the order of minutes are required to be able to separate the effects of local sources. NTA estimates the conditional expected value of a pollutant at the receptor, given that the air has passed through a selected point prior to reaching the receptor.

NTA was applied to one-minute average air quality and meteorological data to determine the locations and contribution of nearby sources to air quality at the four core sites. In general, for this study, NTA has been projected to provide useful information for sources up to ten kilometers from a monitoring location. NTA relies on observations of airborne emittant concentrations as well as wind speed and direction values averaged over one to five minutes. It is important for the wind data to be representative of air movement in the local region at or near ground level. Table 10-9, Figure 10-4 and Figure 10-5, and the following discussion summarize the NTA estimates of the airport contributions to observed ambient concentrations of CO, NO_x, SO_2, BC, and UFP during the two study periods.

The source apportionment by NTA focused on criteria pollutants (CO, NO_x, and SO_2) and the non-criteria pollutant black carbon for two main reasons. First, the NTA method requires measurements with an averaging time of one to five minutes. CO, NO_x, SO_2, and black carbon were the only measurements taken during the Study with such short time averages. Other pollutants of concern, such as $PM_{2.5}$, benzene, and other organic gases, can only be measured with longer averaging times, making it impossible to apply NTA to determine the airport contributions to these pollutants. Second, over the last several years the U.S. EPA has been reviewing and, in some cases, dramatically tightening the National Ambient Air Quality Standards for criteria pollutants. Thus, the emphasis of the NTA source apportionment on criteria pollutants is prudent given this increased regulatory activity.

Table 10-9. Average percent of on-airport source contribution to the total observed ambient concentrations at four core stations as determined by NTA analysis of wind directions and measured concentrations.

Site	CO		NO_x		SO_2		BC		UFP	
	Winter	Summer	Winter	Summer	Winter	Summer	Winter	Summer	Winter	Summer
CE	14±9	40±10	17±9	51±5	43±10	64±10	28±6	52±5	<52	<80
CN	17±6	51±11	24±5	76±4	64±7	84±8	32±6	70±5	<69	<94
CS	17±10	11±3	22±12	18±7	36±7	9±4	34±8	19±3	n/a	<21
AQ	16±4	13±7	16±4	23±9	26±5	49±14	17±7	22±7	n/a	n/a

- Results from NTA analysis of the Winter Season show that the main sources of high concentrations of NO_x and CO are local traffic in the region north of the I-105 and east of the I-405 freeways. The highest concentrations of BC are associated with the same regions as CO and NO_x. The main source areas for SO_2 are the Central Terminal Area and North and South Airfields of the airport. The NTA results indicate only a possible minor offshore source of SO_2.

- Results from NTA analysis of the Summer Monitoring Season show that the main sources of high concentrations of CO, NO_x, BC, and SO_2 are located south of the I-105 freeway and east of the I-405 freeway. Since the region southeast of LAX is associated with high concentrations of all the species measured, and no obvious large sources are located within several kilometers of this region, the NTA results suggest a flow of the abovementioned pollutants into the Study Area from sources farther southeast of the airport. During the Summer Season, the wind direction was from the southeast about 10 percent of the time. Potential sources southeast of the Study Area include refineries and seaports. The possibility exists that some of the pollutants contained in the southeastern flow are re-circulated airport emissions from early morning winds from the north and northeast.

- The ranges in Table 10-9 are partly due to random variations in the data and partly due to assumptions in the calculations, known as bias.

- The contribution of on-airport and off-airport related sources was calculated for each minute that had concentration data at all core stations. The daily time variation of these source contributions showed that, except for SO_2 and UFP, the highest concentrations of pollutants occurred during times when the airport contribution was lowest.

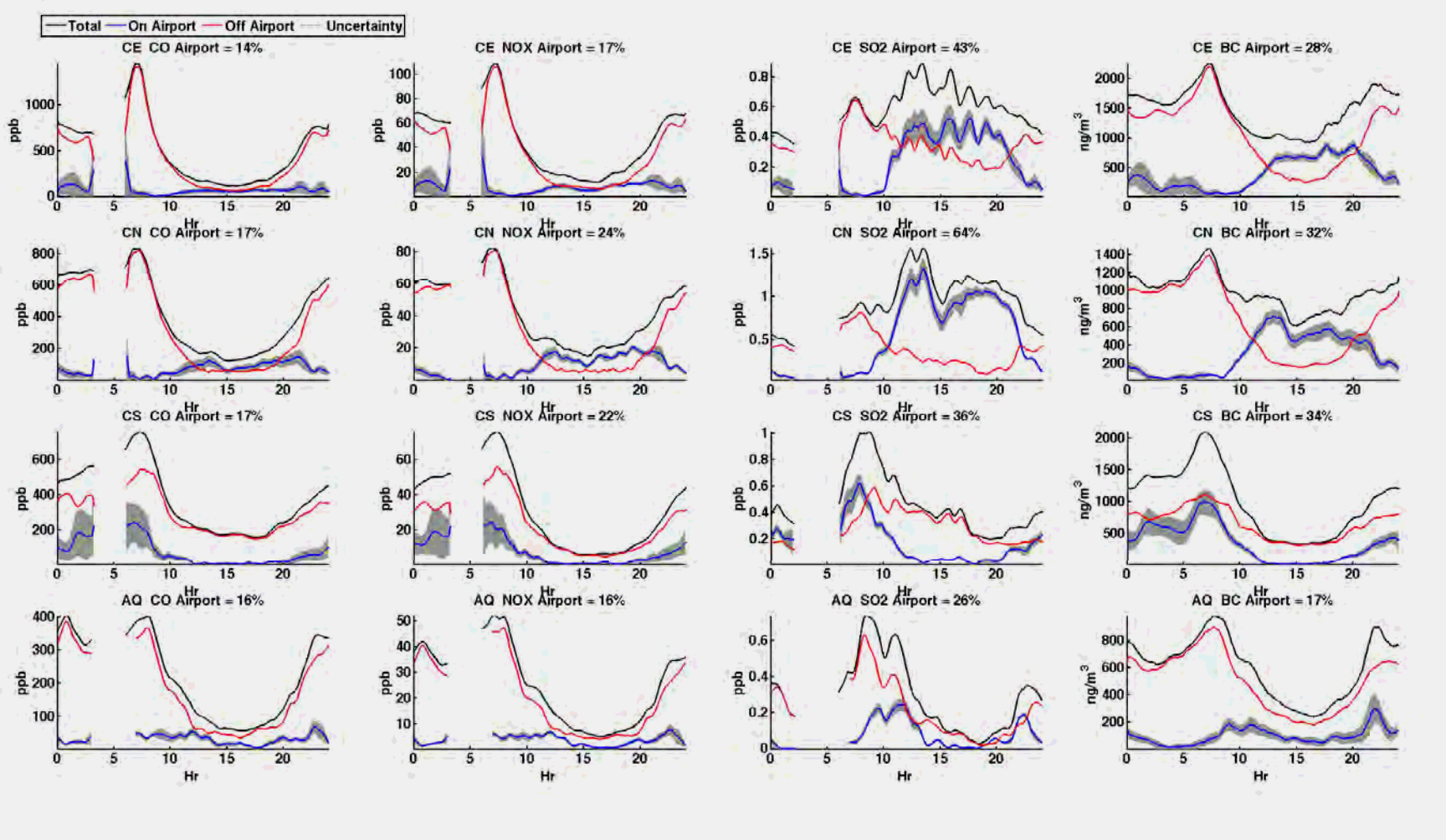

Figure 10-4. Hourly trajectory-based NTA source apportionment for the Winter Season. The black line is the total contribution, red is the off-airport contribution, and blue is the on-airport contribution. The on-airport contribution line contains the upper and lower limits (gray shaded), which include the estimated effects of random error and assumptions made in the computations. Breaks in the lines occur in the early morning hours when automatic calibration of the gas monitors occurs.

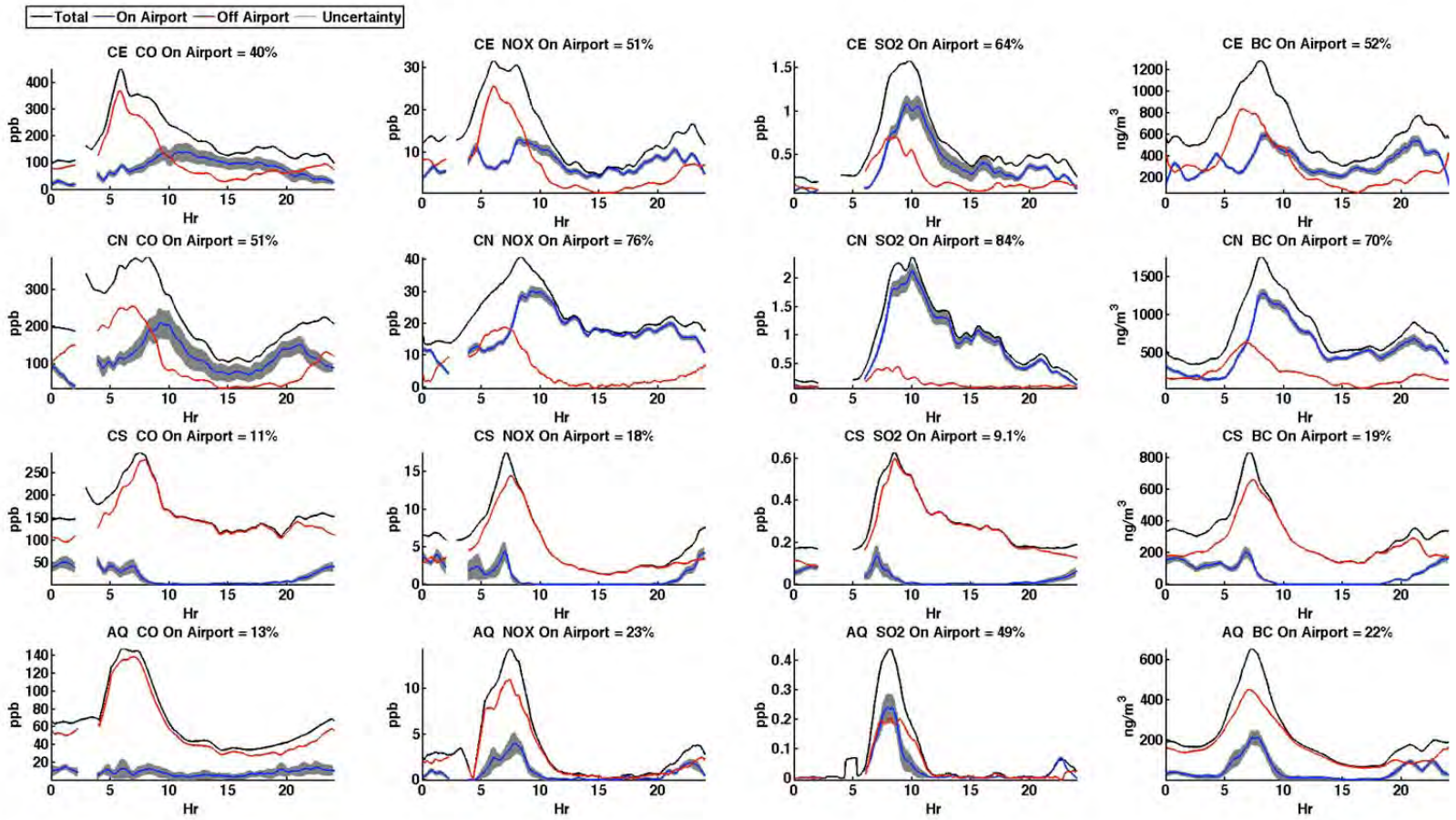

Figure 10-5. Hourly trajectory-based NTA source apportionment for the Summer Season. The black line is the total contribution, red is the off-airport contribution, and blue is the on-airport contribution. The on-airport contribution line contains the upper and lower limits (gray shaded), which include the estimated effects of random error and assumptions made in the computations. Breaks in the lines occur in the early morning hours when automatic calibration of the gas monitors occurs.

AERMOD Dispersion Modeling

The AERMOD dispersion model predicts the concentration impacts of different emission sources within the study domain[7] (i.e., the gridded area used for modeling by AERMOD) and permits comparison of the relative contributions from the modeled sources. It does not address chemical reactions that account for the formation of secondary pollutant along the transport trajectory, and also does not account for the regional or urban background contributions to the ambient pollutant concentrations at the receptor site. Thus, it can provide estimates of the airport contributions as a fraction of the total contributions from sources within the study domain, but not the fractions of the totals occurring downwind (since these totals also include contributions from sources outside the study domain).

The AERMOD model application for the Phase III Study uses a grid of ground receptors centered on the airport and spaced every 500 meters up to a distance of 5 kilometers. Flag-pole receptors at varying heights were used to allow for analysis of concentrations at the corresponding receptor grids and assigned heights (e.g., 2, 7, 12, 17, and 21 meters for Phase III). It is important to understand the concentrations in the elevated plume; however, that information was not used directly for source apportionment. Model outputs of maximum 1-hour and maximum season averages at the four core sites were used for estimating airport contributions to the local ambient air quality. The source apportionment results from the AERMOD dispersion modeling are summarized in Table 10-10.

Table 10-10. Average contributions from airport-related sources[8] for the Winter and Summer Season expressed as a percentage (%) of the total contributions from sources within the study domain.

Percent (%) airport-related contribution to total modeled impacts by AERMOD[9]								
Site	CO		NO_x		SO_2		$PM_{2.5}$	
	Winter	Summer	Winter	Summer	Winter	Summer	Winter	Summer
CE	21	18	32	29	42	48	30	31
CN	57	67	66	72	71	84	73	77
CS	28	45	34	52	21	84	44	63
AQ	48	17	57	27	53	49	59	28

- Pollutant concentrations predictions aloft were often higher than those at the 2-meter height. The highest concentrations for aircraft takeoff and landing, power plants, and marine sources were found aloft and not at the surface.

[7] Study domain is an array of gridded cells used in the grid model simulation, while Study Area (seen in Figure 10-2) is a physical geographic area.

[8] Airport-related sources for AERMOD consisted of those listed in the emission inventory. Extensive lists of the sources considered airport- and non-airport related may be found in Section 8, with summaries provided in Tables 8-34 through 8-37.

[9] AERMOD does not address chemical reactions that account for the formation of secondary pollutant along the transport trajectory, and also does not account for the regional or urban background contributions to the ambient pollutant concentrations at the receptor site; therefore, the estimated airport related contribution could be over-estimated.

- Results from AERMOD prediction for the Winter Season showed that more than 50 percent of total modeled impact from sources within the study domain on concentration of CO, NO_x, $PM_{2.5}$ and SO_2 at the CS and CE sites, were contributed by non-airport related sources located off-airport such as local stationary sources and off-airport roadway traffic not associated with the airport. For the AQ and CN sites, more than 50 percent of $PM_{2.5}$ and SO_2 from sources in the study domain were contributed by airport-related sources. The airport-related sources that were dominant at the AQ site included major roadway sources (e.g., airport-related traffic). The dominant contributions at the CN site were airport-related sources which included: APUs, GSE, and start-up emissions. Dominant non-airport related sources were off-road equipment at the AQ, CN, and CS sites and minor on-road sources at the CE site. These minor on-road sources were also observed at the AQ and CN sites.

- Results from AERMOD prediction for the Summer Season showed that more than 50 percent of the CO, NO_x, $PM_{2.5}$, and SO_x at the CE and AQ sites from study domain emission sources were contributed by non-airport related sources. Airport-related sources were the dominant contributors at the CS and CN sites, and comprised more than 75 percent for all pollutants from study domain sources impacting the CN site. Dominant airport-related sources were major roadway sources at the CS site and aircraft takeoff at the CE site.

CMAQ Modeling

The Community Multiscale Air Quality (CMAQ) model was used to estimate incremental concentrations contributed by airport-related sources to the total ambient concentrations. Unlike AERMOD, CMAQ also has the ability to estimate secondary aerosols that are formed inside as well as outside the Study Area, including sulfate, nitrate, and organic aerosols. Inputs to the CMAQ model were from the 2008 application files, such as emission rates, and meteorological files, provided by SCAQMD. The base case ($AQMD_{zero}$) was run with all on-airport emissions removed, which provided the background concentration.

Three additional emissions scenarios were modeled using CMAQ to estimate the incremental contributions of:

1) Jet exhaust, APU, and GSE,
2) All airport-related sources, and
3) All airport-related sources and non-airport related sources (i.e., local background sources) within the Study Area.[10]

CMAQ was run with a grid resolution of 4 kilometers by 4 kilometers (or 16 km^2), while the Study Area for Phase III is approximately 35 km^2 (8.5 km by 4.2 km). As a result, the entire Study Area lies mostly within two grid cells, with cell (69, 56) containing the AQ and CS sites and the adjacent cell (70, 56) to the east, containing the CN and CE sites. Furthermore, the coarse resolution of the grid cells used in CMAQ was unable to capture the spatial variability

[10] Please note that Sens3 may potentially double count the background sources since there was no way to separate those from the SCAQMD provided emissions inventories.

occurring on a finer scale that may be observed in and around the airport. Grid cells are named by (Column, Row) and are pre-determined in the CMAQ domain. The model predictions of the average air pollutant concentrations for only two grid cells do not capture the fine scale of spatial variability that may be observed in and around the airport. For example, ambient air quality measurements at the AQ site were generally low and near background levels, but the CMAQ-predicted concentrations at AQ site are the same as the center of the airport.

The CMAQ outputs were analyzed for an array of nine grid cells that included the two cells ([69, 56] and [70, 56]) centered on the airport. Airport contributions to ambient air quality based on CMAQ predictions were estimated using the adjacent cells as shown in Figure 10-6. This is a technique that is used often in CMAQ model evaluation, where an array of grid cells around a given monitoring location are reviewed to see if the model predicts reasonably well when a point measurement is compared with an array of grid cells. The estimated percent contributions to above-background modeled ambient concentrations in the two grid cells containing the airport and the four core sites are listed in Table 10-11 and are summarized below. As shown in Figure 10-7 and Figure 10-8, the CMAQ model predicts lower contributions in the other seven grid cells compared to grid cells (69,56) and (70,56) centered on the airport. The differences observed between the Winter and Summer Season for the average airport-related source apportionment as determined by CMAQ may be as a result of increased dispersion or the dominance of stronger onshore westerly winds during the Summer Season.

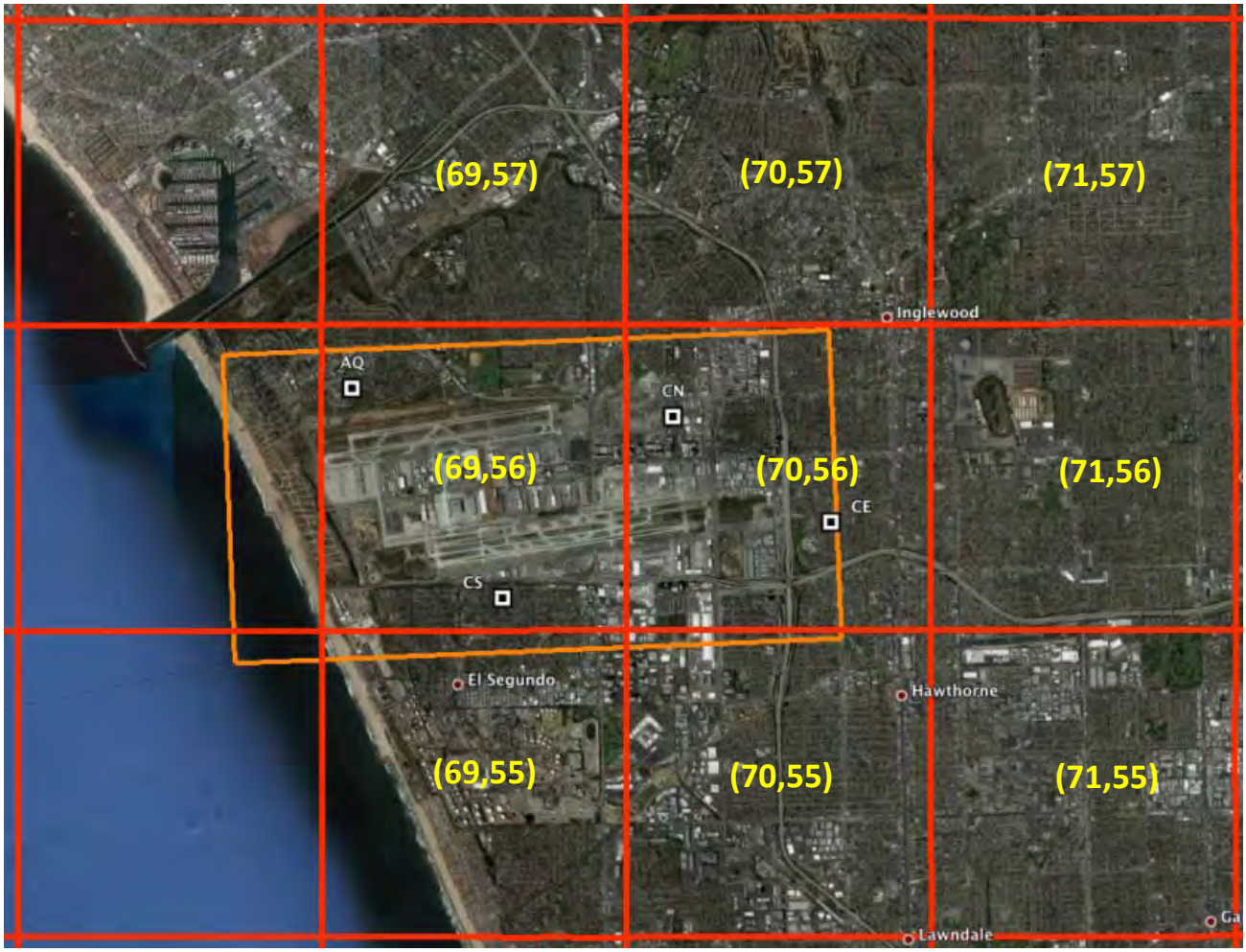

Figure 10-6. CMAQ modeling domain - nine grid cells and locations of the four core community monitoring sites.

Table 10-11. Average airport-related source apportionment for the Winter and Summer Season expressed as a percentage (%) above background concentrations by CMAQ modeling.

Percent (%)airport related contribution to CMAQ modeled ambient concentrations with background subtraction								
Grid Cell (Site)	CO		NO_x		SO_2		$PM_{2.5}$	
	Winter	Summer	Winter	Summer	Winter	Summer	Winter	Summer
70, 56 (CE and CN)	5	10	20	40	15	20	5	11
69, 56 (CS and AQ)	16	26	35	55	35	32	15	20

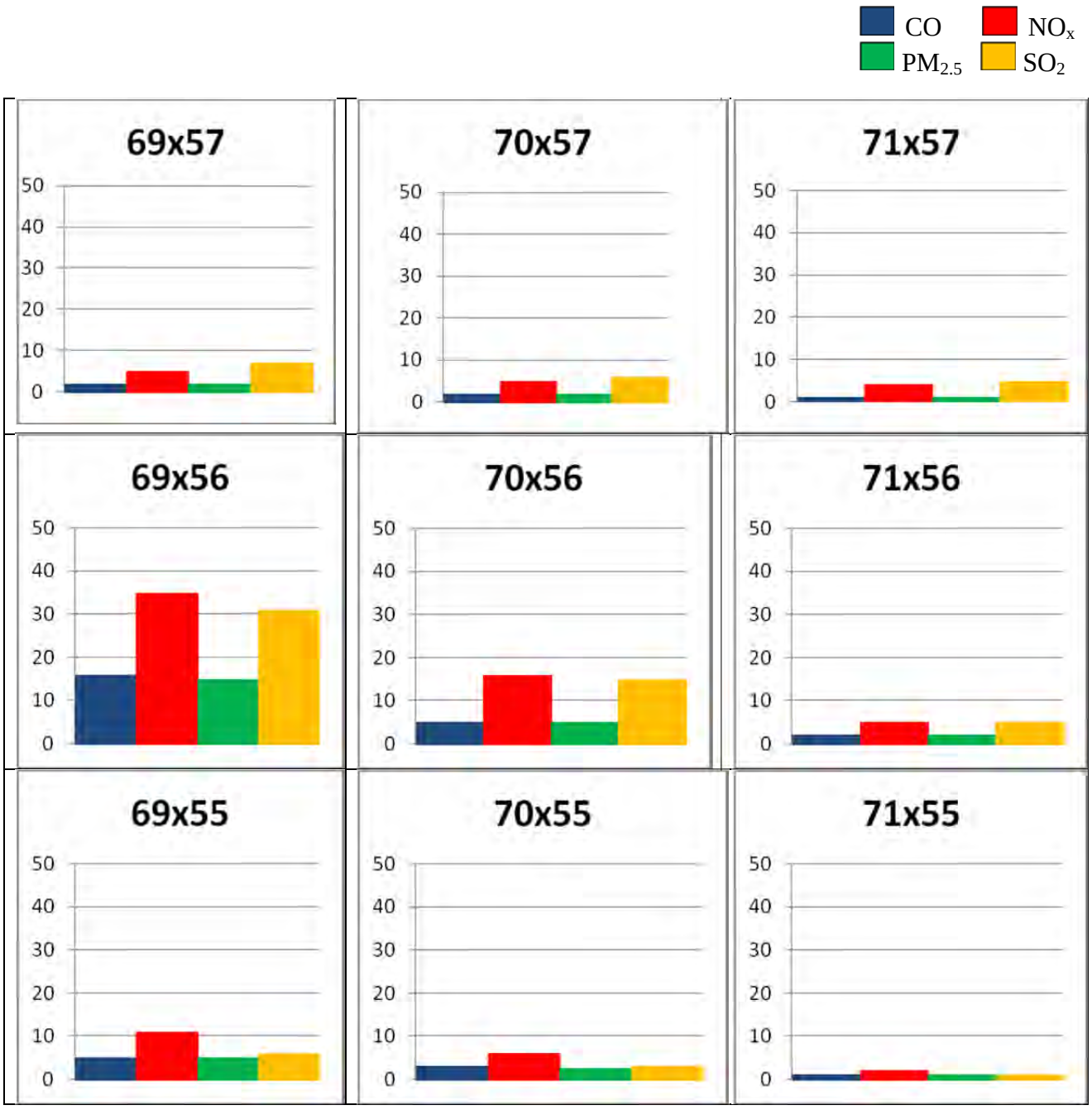

Figure 10-7. Incremental airport-related contribution above background modeled by CMAQ during the Winter Season (as percentage increase over background). The numbers at the top of each graph represent the corresponding grid cell as seen in Figure 10-6.

Figure 10-8. Incremental airport-related contribution above background modeled by CMAQ during the Summer Season (as percentage increase over background). The numbers at the top of each graph represent the corresponding grid cell as seen in Figure 10-6.

Summary of Source Contributions by Individual Air Pollutant

$PM_{2.5}$

From the emissions inventory analysis, all airport-related emission sources account for approximately 24 percent of the $PM_{2.5}$ of emissions from all sources in the Study Area. However, this estimate cannot be compared directly to source contribution estimates that are based upon ambient measurements since the later includes secondary components of $PM_{2.5}$. Secondary components accounted for 50 to 80 percent of $PM_{2.5}$ at the three core monitoring stations (CE, CN, and CS). Adjusting for secondary PM, the contribution of primary (directly emitted) airport-related emissions to ambient $PM_{2.5}$ concentrations is estimated to be 6 to 12 percent. The CMB analysis estimated that the contribution of jet exhaust to $PM_{2.5}$ mass was between 1 to 2 percent. Diesel exhaust contributed between 8 and 15 percent and gasoline vehicles contributed between 0.3 to 1.7 percent. CMB does not separately apportion airport- and non-airport-related vehicle emissions. The temporal and spatial analyses of ambient data suggest greater contributions from non-airport related traffic emissions. Adjusting the total vehicle source contribution from the CMB results by 2.3, the ratio of non-airport to airport-related vehicle emissions from the Study Area emissions inventory, the airport-related contribution to ambient $PM_{2.5}$ is estimated to be 4 to 9 percent. The CMAQ modeling assessment of the incremental contribution of airport-related emission sources to the background concentrations is approximately 5 to 20 percent for $PM_{2.5}$, depending on site location and season. Summaries for CMAQ cover all monitoring stations for both the Winter and Summer Seasons. For site specific summaries, please refer to Table 10-11.

CO, NO_x, and BC

Results from NTA analysis show that the main sources of high concentrations of NO_x, CO, and BC were local traffic in the region of the I-105 and I-405 freeways. The region southeast of LAX was associated with elevated concentrations of all the pollutants measured. Since no obvious large sources are located within the proximity of this region, the NTA results indicated a flow of the abovementioned pollutants into the Study Area from sources located southeast of the airport. Potential sources southeast of the Study Area include refineries and seaports. The possibility exists that some of the pollutants contained in the southeastern flow are re-circulated airport emissions from early morning winds from the north and northeast. Results from NTA analysis of wind directions and monitoring data indicate that, depending on location and the time of year, emissions from airport operations are responsible for 11 to 51 percent of the average measured CO concentrations, 16 to 76 percent of the average NO_x concentrations, and 17 to 70 percent of the average fine particle black carbon (soot) concentrations (note that these concentrations do not exceed either Federal or California Ambient Air Quality Standards). Please note that summaries for NTA cover all sites for both the Winter and Summer Seasons. For site specific summaries, please refer to Table 10-7. The CMAQ modeling assessment of the incremental contribution of airport-related emission sources to the background concentrations is about 2 to 25 percent for CO and about 2 to 50 percent for NO_x, depending on location and season.

SO_2

Results from NTA analysis showed that the main source areas for SO_2 are the Central Terminal Area, and the North and South Airfields of the airport (and at the freeways during the Summer Season). An analysis of wind direction and monitoring data indicates that, depending on location

and time of year, emissions from airport operations may contribute 9 to 84 percent of the average SO_2 concentrations (these concentrations did not exceed either Federal or California Ambient Air Quality Standards) during the two sampling seasons. It should be noted that this range is wide since the ambient concentrations of SO_2 are low; therefore, at times, the airport does contribute a large percentage to this low ambient concentration. The CMAQ modeling assessment of the incremental contribution of airport-related emission sources to the background concentrations is between 1 to 30 percent for SO_2, depending on location and season. Summaries for CMAQ cover all sites for both the Winter and Summer Seasons. For site specific summaries, please refer to refer to Table 10-11.

Ultrafine Particles (UFP)

Airport emission contributions to UFP, as determined by NTA, were between 52 and 94 percent depending on location and season. Sufficient UFP data were not collected at the AQ site and were only collected for one season at the CS site; therefore, they are not included in the aforementioned range. UFP number concentrations were approximately five times higher than typical urban levels at the CE site, which is located approximately one mile east of the South Airfield runways. Simultaneous measurements at a site approximately 1.4 miles south of the CE site (located at the Trinity Lutheran Church parking lot) showed that the UFP number concentrations were much lower, indicating that the frequent spikes and higher UFP number concentrations at the CE site are associated with jet exhaust from the South Airfield. UFP concentrations in the 7 to 30 nm range at the CE site were influenced more by airport activities than vehicle traffic, and were more associated with SO_2 concentrations. Supplemental Study measurements showed that 7-30 nm UFP likely consist of predominantly sulfuric acid aerosols, and contribute very little to $PM_{2.5}$ mass due to their small size. The larger UFP particles, 30 to 160 nm, comprised of "aged" particles, were correlated more strongly with pollutants that were more representative of vehicle traffic, including CO, NO_x, and BC.

PAMS Target Hydrocarbons

The mean contributions of jet exhaust to the sum the 55 Photochemical Assessment Monitoring Stations (PAMS) target hydrocarbons ranged from a few percent to as much as 20 percent, based on CMB results. Approximately 3 to 4 percent of the sum of the PAMS species attributed to jet exhaust was benzene. Apportionment of toluene to jet exhaust ranged from approximately 1 to 5 percent. The apportionment results indicate that jet exhaust may contribute a significant fraction of the measured 1,3-butadiene in some cases, but with high uncertainty. On-road vehicles accounted for 25 to 40 percent of the sum of the PAMS species and about 50 to 75 percent of the measured benzene. Knowing that CMB does not distinguish between airport and non-airport related vehicle emissions, an unknown fraction of the on-road vehicle apportionment is associated with airport ground support vehicles and vehicle traffic to and from the airport. From the emissions inventory analysis, all airport-related emission sources accounted for approximately 25 percent of volatile organic compounds (VOCs).

Reconciliation of Source Attribution Results

The estimation of the airport-related emissions contribution by the various receptor and/or source modeling techniques in this Study produced different results. Although the overall results from these different modeling approaches are generally similar in defining the impact of airport-related contribution, the range of values estimated by these different models for each pollutant is

wide. Therefore, no single value can be assigned to such contributions. It would be misleading to directly compare results from the various models. It should be noted that each model has its own limitations and unique features, such as modeling domain and required inputs. The following are examples of potential causes that contribute to differences in source contribution estimates observed by the various modeling approaches:

- Spatial scales. CMB and NTA use data collected at the core monitoring sites located in the communities that were representative of middle-scale (100 meters to 0.5 km) to neighborhood-scale (0.5 km to 4 km). AERMOD receptors had a resolution of 0.5 km, which is comparable to the middle to neighborhood scales used by CMB and NTA. However, CMAQ has a grid resolution of 4 km by 4 km (or 16 km^2). The Study Area for Phase III is approximately 35 km^2 (8.5 km by 4.2 km). The coarse resolution of the grid cells used in CMAQ was unable to capture the spatial variability occurring on a finer scale that may be observed in and around the airport. Nevertheless, the issue with CMAQ grid-resolution was addressed by expanding the analysis from two to nine grid cells centered on the airport to better capture the impacts of airport sources in the corresponding grid cells, as described above.

- Proximity of receptor sites to sources. Although aircraft emissions can be one of the largest emission sources at any airport, ambient concentrations observed at a specific receptor location tend to depend on distance from the sources. For example, the CN site is located directly downwind of the North Airfield runways for certain time periods and, therefore, is heavily influenced by airport operations during those periods. The CE site is located downwind of both the airport and the I-405 freeway and was influenced by airport operations, the freeway, and local traffic.

- Source category definitions. Different groupings of emission sources in the "on-airport" or "airport-related" and "off-airport" or "non-airport-related" categories used by various models may cause discrepancies in the modeling results. For example, airport-related source categories used in AERMOD and CMAQ included vehicle traffic emissions that occurred outside of the airport property but were related to airport operations. However, the NTA analysis used strictly an on-airport versus off-airport comparison. Therefore, it is important to keep this in mind when comparing various modeling results. The CMB model estimates the impacts of various emission source categories at specific receptor sites relative to the total air pollution concentrations occurring at those sites. This capability is due to the fact that CMB is tied directly to the ambient measurements made at the receptor sites and apportions those totals among each of the source types. However, CMB apportions source categories and cannot distinguish locations of the emission sources that have the same chemical composition profile. For example, CMB is unable to separately apportion on-airport and off-airport related vehicle emissions. The CMB analysis indicated that airport jet exhaust was responsible for 2 percent of the average fine particle mass concentrations and 3 to 8 percent of the average fine particle BC (soot) concentrations measured in surrounding communities. The sum of jet, diesel, and gasoline engine exhaust accounted for 8 to 22 percent of $PM_{2.5}$ mass, approximately all the fine particle BC concentrations, and 13 to 44 percent of the fine particle OC concentrations (the diesel and gasoline engine exhaust is emitted by local traffic, freeway traffic, and on-airport sources combined).

- Contribution of regional urban background. One of the important considerations when using dispersion modeling is to accurately estimate background concentrations when they are equal to or greater than the modeled concentrations. One of the main objectives of CMAQ is to provide regional background concentrations to allow for a proper estimate of incremental airport concentrations, which may not be accounted for in AERMOD, and to account for pollutants where secondary transformation is important. CMAQ provided assessments of the incremental contribution of airport-related emission sources to the background concentrations in 4 by 4 km grid cells surrounding the airport. These predictions for nine grid cells indicated incremental increases of about 2 to 25 percent for CO, about 1 to 30 percent for SO_2, about 2 to 50 percent for NO_x, and about 1 to 20 percent for $PM_{2.5}$, depending on location and season.

10.4 SUMMARY OF KEY FINDINGS

- The ambient concentrations of CO, NO_2, SO_2, and Pb within the communities adjacent to LAX were well below the threshold levels for exceedance of the national and state health-based ambient air quality standards during the study period. The highest pollutant concentrations were measured near emission sources (e.g., airport runways and major roadways). While high NO_x, SO_2, and black carbon (soot) levels were measured at the east end of the South Airfield, the concentrations dropped to approximately 10 percent of the peak values (i.e., near the surrounding urban background levels) within about 1,500 feet (500 meters) east of the runway.

- $PM_{2.5}$ levels were near the ambient air quality standard. Analysis of the chemical composition of the measured $PM_{2.5}$ concentrations show that about 50 to 75 percent of the ambient $PM_{2.5}$ mass was associated with ammonium nitrate, ammonium sulfate, and unapportioned organic matter (OM). The sum of sea salt aerosol, soil derived fugitive dust, and wood smoke account for an additional 20 to 30 percent of $PM_{2.5}$ mass. Consequently, the incremental airport contributions (jet exhaust and airport-related vehicle traffic) to $PM_{2.5}$ levels are relatively small. The CMB estimates of source contributions to ambient $PM_{2.5}$ mass were 1 to 2 percent for jet exhaust and 8 to 17 percent for the sum of diesel plus gasoline vehicle exhaust. It is not possible for CMB to separately apportion airport- and non-airport-related vehicle emissions because there is no difference in chemical signature between the two groups of vehicles. However, adjusting the total vehicle source contribution from the CMB results by 2.3 (which is the ratio of non-airport to airport-related vehicle emissions from the Study Area emissions inventory), the airport-related vehicle exhaust contributions to ambient $PM_{2.5}$ is estimated to be 4 to 9 percent.

- Results of the CMAQ air quality modeling indicated that the nitrate and sulfate and most of the residual OM are formed outside of the Study Area and associated with the regional urban background. The incremental airport contributions (jet exhaust and airport-related vehicle traffic) to $PM_{2.5}$ levels were estimated to be comparatively small (5 to 20 percent) in reasonable agreement with the adjusted CMB receptor modeling results.

- The contribution of airport-related emissions can vary by hour of the day, day of the week, and by season. Factors such as airport activity levels, wind direction, wind speed, ambient temperature, and other meteorological parameters, affect the contribution of airport-related emissions to local ambient air quality. Results from NTA analysis show that the main sources of high concentrations of NO_x, CO, and BC were local traffic in the region of I-105 and I-405 freeways. The NTA results show that the airport-related emissions contributions to the local ambient air quality were generally higher for a community station located directly east rather than north or south of the airport. During the winter, airport operations accounted for 15 to 22 percent for both CO and NO_x at all four core monitoring sites (CE, CN, CS, and AQ). While contributions were about the same during summer and winter at CS and AQ, the airport contributions at CE and CN were much higher during summer for CO (approximately 40 to 50 percent) and NO_x (approximately 50 to 75 percent). The airport contributions to black carbon show a similar seasonal pattern to CO and NO_x. Results from NTA analysis show that the main source area for SO_2 was the area encompassing the Central Terminal Area and the North and South Airfields of the airport (and the freeways during the Summer Season). Airport contributions to SO_2 were generally higher than for the other pollutants with less seasonal variation except at CS. The airport contributions to SO_2 during winter and summer were 40 to 80 percent at CE and CN, and 10 to 50 percent at CS and AQ. Airport contributions to UFP number concentrations, as determined by NTA, were between 52 and 94 percent at the CE and CN sites. The UFP number concentration is expected to decrease rapidly as a function of distance as shown in a recent gradient study conducted by SCAQMD at LAX.[11]

- The two-season average concentrations of key air toxics from the LAX AQSAS monitoring network are consistently lower than either the annual average concentrations for 2011 measured elsewhere in the basin or the average concentrations measured during the MATES-III study between 2004 and 2006.

- The ambient measurements showed that period average UFP number concentrations were about 3 to 5 times higher at the CE site than typical urban levels. Strong correlations of CO, NO, and BC with 30 to 160 nanometer (nm) UFP and distinct weekday versus weekend differences (i.e., lower on weekends compared to weekdays) in diurnal variations indicate these particles are most likely from vehicle exhaust-related emissions. In contrast, weak correlations of 7 to 30 nm UFP with CO, nitrogen oxide (NO), and BC, but strong correlation with SO_2 and NO_2, are indications of jet exhaust and potential secondary particles that are formed in atmosphere. Results of the Supplemental Study show that these particles are less than 30 nm in diameter and consist mostly of sulfuric acid aerosols. The spatial and temporal analyses as well as simultaneous sampling at the Trinity Lutheran Church School (TLCS) site, which was located 1.5 miles south of the CE site, indicated that the higher UFP number concentrations at the CE site were associated with jet exhaust from the South Airfield.

[11] Preliminary results from the SCAQMD Gradient Study conducted at LAX on September 11, 2012 show that UFP counts decreased approximately 70 percent at 300 meters and 80 percent at 460 meters from the source.

10.5 OVERALL CONCLUSIONS

In summary, the LAX AQSAS show that, with the exception of $PM_{2.5}$, the ambient concentrations of criteria pollutants within the communities adjacent to LAX were well below national and state health-based ambient air quality standards and ambient concentrations of air toxic contaminants were generally lower than measured elsewhere in the SoCAB. The generally lower pollutant concentrations in the LAX area can be attributed to its coastal location and the typical daytime sea breeze that helps to disperse local emissions. The concentrations of most measured pollutants were higher east of LAX compared to monitoring locations north or south of the airport.

Although $PM_{2.5}$ levels were near the standard, a substantial portion of the $PM_{2.5}$ mass is related to the regional urban background with airport-related emissions contributing a maximum of 5 to 20 percent. While UFP have negligible contributions to $PM_{2.5}$ mass, their number concentrations east of LAX were higher than typical levels in the SoCAB. Supplemental Study measurements at the CE site and behind the South Airfield blast fence indicate that the very small UFP, which have disproportionately higher contributions to particle number concentrations, are largely sulfuric acid aerosol from jet exhaust. The larger UFP, which have disproportionately higher contributions to mass concentrations, appear to be related to on-road vehicle exhaust from local traffic.

The health effects of UFP are largely unknown. A recent review of 300 studies of the health effects of ambient UFP funded by the Health Effects Institute (HEI Perspective 3, January 2013) concluded that experimental and epidemiologic studies provide suggestive, but no consistent evidence of adverse effects of short-term exposure to ambient UFP. [12] To date, the evidence linking UFP number concentrations with adverse health effects has not been sufficiently definitive to support a separate health-based ambient air quality standard for UFP. The expectation for the effects of UFP is based upon their potential to carry toxic material deep into the lungs. In contrast to UFP in vehicle emissions that may be composed of adsorbed organic compounds, UFP associated with jet exhaust are dominated by sulfuric acid aerosol that is rapidly neutralized to relatively benign ammonium sulfate and increases in size due to absorption of water vapor. [13] Future studies of the health impacts of airport emissions will need to consider these important chemical differences between UFP emissions from jet and vehicle exhaust.

[12] Health Effect Institute, January 2013. HEI Perspective 3 – Understanding the Health Effects of Ambient Ultrafine Particles. HEI Review Panel on Ultrafine Particles. Boston, MA

[13] Wyzga, R.E. 1995. Health Effects of Acid Aerosol. Water, Air and Soil Pollution, 85: 177-188

Appendix A

RESPONSES TO PUBLIC FEEDBACK

(This page is intentionally blank)

Prepared by:

CDM Smith
523 West Sixth Street, Suite 400
Los Angeles, CA 90014

Phase III of the LAX Air Quality and Source Apportionment Study

Appendix A
Responses to Public Feedback

Prepared for:

Los Angeles World Airports
Environmental Services Division

Project No. 99623

March 2014

Table of Contents

This page intentionally left bank.

Section 1
Background/History of Study

Feedback/Question:

1. What was the approximate cost of the Study?

Response:

The study cost was approximately $5 million for all three study phases.

Feedback/Question:

2. Please tell us if other air quality agencies contributed to study criteria and what criteria that is.

Response:

The government agencies involved with the study included the South Coast Air Quality Management District (AQMD), California Air Resources Board (CARB), U.S. Environmental Protection Agency (EPA), Federal Aviation Administration (FAA), and California Office of Environmental Health Hazard Assessment (OEHHA). These agencies participated as members of the Technical Working Group (TWG) providing input and guidance to the study design and implementation. LAWA and the TWG worked closely toward consensus-based decision-making and sought agreement among the respective participants on the scientific methods and processes used to conduct the study, including the general siting of monitoring stations, selection of pollutants to be measured, sample collection and analysis methods, modeling protocols, and interpretation of findings. The TWG members participated in over 20 meetings and conference calls beginning before the start of Phase I through completion of the Phase III Final Report. A summary of the Technical Working Group Composition can be found in the Final Report, Volume 3, Table 1-2 (page 1-9). The overall primary objective of the study was to assess potential air impacts frm the airport-related sources and operations on the local ambient air quality of the adjacent communities. The primary objectives of the study can be found in the Final Report, Volume 2, Section 1.1 (page 1-1).

Section 2
Overall Study Methodology/Approach

Feedback/Question:

3. Why aren't there any satellite stations on the East side of the airport?

Response:

There were a number of stations sited east of the airport. The locations of core, satellite and gradient sites are shown in the Final Report, Volume 2, Section 5, Figure 5-10 (page 5-22). Specifically, two of the core stations – Community East (CE) and Community North (CN); one satellite station – CE2; and five gradient stations – BNR, R405, SRN, SRE, and BSR, were located east of the airport.

Feedback/Question:

4. When conducting the air quality test, were the surrounding communities considered?

5. Since some of the runways operate over the school, why don't they have air quality sensors in schools to see how much the students get affected?

Response:

The communities surrounding the airport, including schools, were considered when sites were selected for this study. Several satellite and gradient sites were located on or near residences close to the airport. Several schools sites were considered, and one former school site was chosen (the Community South [CS] site). To obtain a conservative, meaning a high, estimate of the airport's contribution to air quality impacts, a number of sites around the airport were identified which were subjected to the study's site selection process. The monitoring network design, site selection, and objectives are discussed in the Final Report, Volume 2, Section 3.3 (beginning on page 3-4). The study was not a school air quality study or a health effects study; therefore, monitors were not placed in schools. However, the source apportionment results summarized in the Final Report, Volume 2, Section 10 represent conservative estimates of the airport's contribution to air quality impacts in the surrounding communities and nearby schools.

Feedback/Question:

6. Why wasn't the oil field included in the study ("Inglewood Deep" oil field just east of the 405)?

Response:

The Study Area is shown in the Final Report, Volume 1, Figure ES-1 (page ES-4), and was developed for purposes of conducting the airport source apportionment study. As noted in the Final Report, Volume 2, Section 1.2 (beginning on page 1-1), the Study Area for Phase III provided a focused area within which detailed air quality monitoring and modeling analyses could occur with particular attention given to the adjacent communities immediately to the north, east, and south of LAX. The Inglewood Oil Field is located outside of the Study Area.

Feedback/Question:

7. Why didn't your footprint include the cities of Hawthorne and Marina Del Rey or other areas such as Hollywood Park and LA County that are located near the airport?

8. Why does the Study Area only stop at Inglewood Avenue?

Response:

As noted in the Final Report, Volume 2, Section 1.2 (beginning on page 1-1), the Study Area for Phase III provided a focused area within which detailed air quality monitoring and modeling analyses could occur with particular attention given to the adjacent communities immediately to the north, east, and south of LAX. A number of sites around the airport were identified which were subjected to the study's site selection process. The monitoring network design, site selection, and objectives are discussed in the Final Report, Volume 2, Section 3.3 (beginning on page 3-4) and Appendix 3-1. Note that satellite monitoring station CE2 was located in Hawthorne (shown in Figure 5-19 of the Final Report, Volume 2, Section 5 (page 5-22).

Feedback/Question:

9. If the California Air Resources Board (CARB) will not set detailed values for engine pollution qualification tests, what component values have been assumed? Doesn't the test use only total particle darkening of paper target at a specific distance? (The question refers to measurement of particles from aircraft engines.)

Response:

The method for estimating particulate matter (PM) from aircraft engines includes PM_{10} and $PM_{2.5}$, based on the smoke number, which is determined from the particle coloring of a paper filter during an engine certification test. The FAA and the EPA conducted a number of studies to estimate the relative emissions of PM_{10} and $PM_{2.5}$ from those measurements and from analyzing actual engine emissions. From the measured engine smoke number and particulate matter emissions, these agencies have developed estimates of particulate matter emissions for most commercial aircraft engines. Those estimates are now included in the FAA's Emissions and Dispersion Modeling System (EDMS) model, which is the model used to calculate the emissions from the aircraft for this study. The aircraft engine emission inventories and methodology are discussed in the Final Report, Volume 2, Section 8.4 (beginning on page 8-9).

As part of the Chemical Mass Balance (CMB) analysis for this study, jet engine exhaust measurements were collected behind the Runway 25R blast fence. The chemical composition of $PM_{2.5}$ from these measurements was analyzed and included in the source profiles used in the CMB anlaysis. The CMB analysis is discussed in the Final Report, Volume 2, Section 6. The key source $PM_{2.5}$ profiles are listed in Table 6-7 (page 6-27), and distributions of $PM_{2.5}$ chemical marker compounds from these source types are summarized in Table 6-8 (page 6-28).

Feedback/Question:

10. What exactly are the off-airport area, industrial area and residential area?

Response:

The off-airport area is the area that is outside of the airport property line (fenceline), but still within the Study Area. Several larger sources that were actually outside the Study Area were included in the emission inventories. For instance, the power plants and the marine vessels were included because these sources were expected to have some contribution to the concentration within the Study Area.

Section 3
Air Quality Measurements

Feedback/Question:

11. The study should include information about particulates from automotive brakes and tires.

Response:

The emission inventories for roadways, freeways, and parking lots included estimates of tire wear and brake wear particulate matter emissions. The source profiles used in the CMB modeling included one created from analysis of surface dust collected adjacent to roadways in the area, which includes particles created by tire and brake wear. The study did not attempt to specifically identify those sources in the CMB analysis since they exist both on- and off-airport. The roadway emissions inventories are discussed in the Final Report, Volume 2, Sections 8.7, 8.8, 8.10, and 8.11 (beginning on page 8-28). The CMB analysis is discussed in the Final Report, Volume 2, Section 6. The key source $PM_{2.5}$ profiles are listed in Table 6-7 (page 6-27), and distributions of $PM_{2.5}$ chemical marker compounds from these source types are summarized in Table 6-8 (page 6-28).

Feedback/Question:

12. Because Community East measurements (of ultrafine particles) are greater than others, what conclusions were made related to other areas on airport, i.e., terminals, maintenance areas, etc.?

Response:

This study was developed to assess the potential contribution of airport activity to ambient pollutant concentrations, including ultrafine particle concentrations, at locations near the airport. The analyses in this study did not provide the data necessary to assess the contribution of pollutants from specific areas within the airport. For several pollutants, the source type (such as aircraft engines or automobile and truck engines) contribution could be estimated. However, this information still does not provide identification of the specific source areas within the airport.

For example, the measurements, modeling assessments and comparisons conducted for this study indicated that the smaller size category of ultrafine particles appears to be correlated with aircraft engine exhaust. However, the larger size category of ultrafine particles appears to be associated with on-road motor vehicle engines. Attempts were also made to get some information on the composition of ultrafines – via the supplemental study. However, the technology does not exist right now to do a detailed chemical analysis of the ultrafine particles in the manner that they were collected in this study.

Measurements of ultrafine particles are discussed in the Final Report, Volume 2, Section 5; with specific discussions of findings for ultrafine size distributions and correlations with other pollutants in Section 5.2.4 (beginning on page 5-72). The supplemental study conducted to provide information on possible sources of ultrafine particles is presented in the Final Report, Volume 2, Section 5.3 (beginning on page 5-99).

Feedback/Question:

13. Could you discuss microchip technology for measuring specific pollutants?

Response:

Microchip technology does exist and is advancing rapidly for making measurements of gaseous pollutants, like many of the criteria pollutants. There are hand held instruments or even items that can be clipped on to an iPhone that can make these measurements. At this time, those methods are not sufficiently accurate and precise to take the place of the kind of monitoring methods that were used in this study at the core sites. Desert Research Institute (DRI) has looked into this technology for doing the kind of saturation monitoring that was used in the study, however, it was not quite ready for full scale deployment when this study was started.

Feedback/Question:

14. UFP – Measurements from jet fuel variations due to changes in breeze: 1- no breeze, 2- breeze, 3 – change in flight patterns.

Response:

Potential correlations of ultrafine particles (UFP) with aircraft activity were assessed in the Final Report, Volume 2, Section 5.3 and Section 7.

Section 4
Air Quality Computer Modeling

Feedback/Question:

15. How is the study valid when it excluded the flight path over zip code 90045 which is essentially the airport area?

Response:

Airborne aircraft in the vertical were included in the Study. Emissions from each aircraft as it was approaching the airport (arrival mode), as well as departing from the airport (take-off and climb out modes) were included in the AERMOD and CMAQ modeling analyses. The study found that elevated concentrations were located aloft because aircraft operations above the ground were included. The emissions from aircraft operating at LAX are presented in the Final Report, Volume 2, Section 8.4, (beginning on page 8-9). The concentrations at various elevations above the ground are included in the Final Report, Volume 2, Section 9 – Appendix 9A (beginning on page 9A-1).

Feedback/Question:

16. Because there is no analysis for the general make-up of $PM_{2.5}$ particles that come from various sources, was there any effort to use $PM_{2.5}$ chemical make-up to estimate sources?

Response:

The CMB analysis that was presented in the Final Report was done using the chemical analysis of the $PM_{2.5}$ samples collected at the core sites and the community satellite sites. That data was used in the CMB process and in a more visual process of trying to connect the patterns of chemical species relative to activity patterns. The CMB analysis is discussed in the Final Report, Volume 2, Section 6. The key source $PM_{2.5}$ profiles are listed in Table 6-7 (page 6-27), and distributions of $PM_{2.5}$ chemical marker compounds from these source types are summarized in Table 6-8 (page 6-28).

Feedback/Question:

17. Were emission sources assumed or measured? If source values were used to work backwards, how were source values (magnitude and types of pollution) estimated without measurements of the source areas subsequently used to measure contributions?

Response:

The study used multiple methods to estimate airport-related contributions to ambient air quality near LAX. Several of these methods used measurements collected during the study near specific sources, while others relied on estimates of emissions based on measurements collected previously by other researchers or air agencies on other projects. So both measurements and estimates were used in developing airport contribution estimates.

In general, the "source-oriented" modeling methods (dispersion modeling with AMS/EPA Regulatory Model (AERMOD) or Community Multiscale Air Quality (CMAQ) rely on estimated emissions from each source type using emission factors developed from previous studies or measurements. For example, emissions from motor vehicles included in the inventories (Final Report, Volume 2, Section 8) were estimated using published emission factors, emission models and guidance developed by the California

Air Resources Board; and emissions from aircraft were estimated from emission indices published by the Federal Aviation Administration. However, continuous emissions monitoring data were available from a number of stationary sources within the Study Area; and the monitoring data was included in the emission inventories for those sources.

For one of the "receptor-oriented" models (CMB), measured concentrations from the core and satellite monitoring sites (the receptor sites) were used to estimate contributions from specific source types or categories (aircraft, motor vehicles, road dust, etc.). This model relies on a known distribution of specific chemicals and compounds in the source exhaust – this distribution is sometimes referred to as the source profile. Source profiles for many source types have been developed previously by air quality agencies and researchers – such as for gasoline or diesel motor vehicles. In addition, for this study the researchers collected data and developed several new profiles specific to LAX – aircraft engine exhaust and fugitive dust collected at the blast fence behind Runway 25R, gasoline and diesel liquid compounds, and gasoline vapor compositions collected from fuel suppliers around LAX.

The emissions inventories and methodologies for each source type are presented in the Final Report, Volume 2, Section 8 (beginning on page 8-1). The CMB analysis is discussed in the Final Report, Volume 2, Section 6. The key source $PM_{2.5}$ profiles are listed in Table 6-7 (page 6-27), and distributions of $PM_{2.5}$ chemical marker compounds from these source types are summarized in Table 6-8 (page 6-28). The key source VOC profiles are listed in Table 6-9 (page 6-34), and distributions of volatile organic compounds (VOC) marker compounds from these source types are summarized in Table 6-10 (page 3-35).

Feedback/Question:

18. How do you determine what is considered non-airport related sources and secondary aerosols when determining 90% of the ambient particulate matter is from non-airport sources?

Response:

Two of the source apportionment methods (CMB and CMAQ) were applied to obtain the airport and non-airport contributions to fine particulate matter ($PM_{2.5}$) which includes secondary aerosols. The CMB analysis included LAX-specific $PM_{2.5}$ and VOC profiles collected at the Runway 25R blast fence. From the CMB analysis, it was determined that approximately 1 to 2.5 percent of the $PM_{2.5}$ samples collected at the monitoring stations were attributable to aircraft engine exhaust (Final Report, Volume 2, Section 2, page 10-14, 2nd bullet point on the page). The estimated contribution of airport-related traffic to $PM_{2.5}$ concentrations ranged from 4 to 9 percent (Final Report, Volume 2, Section 10, page 10-14, 3rd bullet point on the page). Adding these ranges together to estimate the airport activity contributions to $PM_{2.5}$ concentrations indicates that approximately 5 to 11.5 percent is airport-related.

The CMAQ model has the capability of estimating secondary aerosol formation as well as estimating the dispersion of primary emissions from both airport and non-airport sources. The airport-related sources, besides aircraft, include the ground support equipment, several on-airport stationary sources, and traffic trips to and from the airport. From the CMAQ analysis, it was estimated that approximately 5 to 20 percent of the total $PM_{2.5}$ concentration was attributable to airport-related activities (Final Report, Volume 2, Section 10, Table 10-11, page 10-22). The CMAQ results provide a broader range of the potential airport contribution to $PM_{2.5}$, likely due to the inclusion of secondary aerosol formation associated with airport-related operations. In the symposium it was clarified that the range of airport related contributions to $PM_{2.5}$ concentrations at the core monitoring stations was 5 to 20 percent.

The CMB analysis is discussed in the Final Report, Volume 2, Section 6; the emissions inventories and methodologies are discussed in Section 8; and the CMAQ analysis is discussed in Section 9.2.

Feedback/Question:

19. Was there any construction activity at LAX considered during the studies?

Response:

The emissions inventories did account for construction, as well as landscaping equipment, trains, and other types of equipment that are considered off-road. The emission calculation methodology for these equipment types is discussed in the Final Report, Volume 2, Section 8.13 (beginning on page 8-61).

Feedback/Question:

20. If there is little correlation between fine particulates ($PM_{2.5}$) and ultrafine particulates, how were estimates made?

Response:

For this study, measurements were made of both ultrafine particles and of $PM_{2.5}$ concentrations, using different methods. In terms of any attempts to do source apportionment, the CMB analysis provided an estimate of aircraft contributions to $PM_{2.5}$; and the Nonparametric Trajectory Analysis (NTA) provided a rough estimate of UFP contributions from on-airport and off-airport locations. The CMB analysis is discussed in the Final Report, Volume 2, Section 6, and the NTA is discussed in Section 7.

Feedback/Question:

21. When estimating the percentage related to LAX, how were business activities that were related to LAX accounted for in the percentages, i.e., off-site cargo or car rental companies?

Response:

The emission inventory discussion in the Final Report, Volume 2, Section 8 provides a description of how the emission estimates were made. The study did not attempt to assign these source types to specific owners. The only differentiation regarding traffic was whether it was airport-related or non-airport traffic, and "airport-related" meant that the trip started or ended at the airport boundary. Airport-related vehicle emissions were identified in the emission inventory.

Feedback/Question:

22. Why is CMB fingerprinting not Source Orientated modeling?

Response:

The Source-oriented models start with emissions at the sources and then use the description of how the air is blowing and how the pollutants are dispersing (i.e., the meteorology) until the pollutants reach the receptor. The Source Oriented models attempt to predict concentrations at receptors based on actual or estimated emissions from the sources. The Chemical Mass Balance model and other receptor models, start with measurements at the receptor and then work backwards to try to determine the sources. Receptor-oriented models are forensic types of models – taking very detailed looks at the air pollutants measured at the receptors to piece together the most likely sources that contributed to those measurements based on known source profiles. Both approaches were used in this study.

Section 5
Overall Findings and Conclusions

Feedback/Question:

23. What is your data sharing policy?

Response:

The data is available on request to LAWA; it is at the Terabyte level and cannot be put on the website due to its size. Data requests may be submitted by email to airqualitystudy@lawa.org.

Feedback/Question:

24. Are there no regulatory standards for ultrafine particles (UFP)? But there are existing daily air quality standards. What are the sources of the daily air quality standards?

Response:

Ambient air quality standards have not been developed by either the U.S. EPA or the CARB for UFP. However, the U.S. EPA has developed a daily ambient air quality standard for fine particulate matter ($PM_{2.5}$). The measurements of $PM_{2.5}$ collected during the study were compared to this standard, as shown in the Final Report, Volume 1, Figure ES-4 (page ES-8).

Feedback/Question:

25. With regards to the conclusions, was there any correlation between measured values at ground level to that higher in the sky?

Response:

Measurements collected during this study were collected near ground level (typically within 2 to 4 meters of the surface). However, the air dispersion modeling analysis, using AERMOD, included receptor sites aloft. The modeled ground level concentrations provided an understanding of the pattern of surface concentrations around the airport. The modeled concentrations aloft were used to estimate whether concentrations were higher aloft or higher at the surface. The AERMOD results found that the estimated or predicted concentrations were higher aloft than at the surface, due to emissions from aircraft while above the ground. Results of pollutant modeling at various elevations above the ground are presented in the Final Report, Volume 2, Section 9 – Appendix 9A (beginning on page 9A-1).

Feedback/Question:

26. What assumptions were used to normalize requests and graph conclusions, 6(?) value time frames versus test readiness?

Response:

Although it is unclear as to what is meant by "normalize requests" and "6 value time frames versus test readiness", the following response describes how certain tabular data were presented as graphs and how various time-related pollutant measurements were normalized. Two types (formats) of information were included in the report: tables with actual numbers; and graphs for quick visual interpretation. It was anticipated other researchers would like to see the actual numbers, while other readers may prefer

more visual graphs and figures. The graph of maximum measured concentrations versus ambient air quality standards (Final Report, Volume 1, Figure ES-4 on page ES-8) was normalized to the most stringent standard for each pollutant and averaging period summarized on the graph. Specifically, the 1-hour CO results were normalized to the California Ambient Air Quality Standard (CAAQS) of 20 parts per million (ppm); the 1-hour NO_2 results were normalized to the National Ambient Air Qualty Standard (NAAQS) of 100 parts per billion (ppb), the 1-hour SO_2 results were normalized to the NAAQS of 75 ppb, and the 24-hour $PM_{2.5}$ results were normalized to the NAAQS of 35 micrograms per cubic meter ($\mu g/m^3$).

Feedback/Question:

27. Was there any Environmental Impact Report (EIR) done before building LAX and how in the EIR does this study results compare?

Response:

The process for preparing an EIR comes from the California Environmental Quality Act (CEQA), which was enacted in 1970; the construction of LAX predates CEQA. Therefore, no EIR was, or could have been, prepared for LAX before it was built, and it would not be possible to conduct the comparison referenced in the comment. Additionally, the AQSAS is a requirement of the LAX Master Plan Community Benefits Agreement and the LAX Master Plan Stipulated Settlement and is not tied to any specific LAX project.

Feedback/Question:

28. Where and when will this study be published? Will it be published "as is" or as a revised document that addresses all comments received during the comment period?

Response:

The study Final Report was published and posted to LAWA's website (http://www.lawa.org/AirQualityStudy/) on June 18, 2013, where it is currently available. Copies also were distributed to Councilmember Bill Rosendahl's District Office, located at 7166 W Manchester Avenue, Los Angeles, 90045 and at the following public libraries:

- Westchester-Loyola Village Branch Library, 7114 West Manchester Avenue, Los Angeles, CA 90045
- Inglewood Library, 101 West Manchester Boulevard, Inglewood, CA 90301
- El Segundo Library, 111 West Mariposa Avenue, El Segundo, CA 90245

LAWA initially accepted public feedback on the study until October 11, 2013, and LAWA subsequently extended the comment period to November 7, 2013. The questions raised at the public symposium, other public feedback received, and the associated responses were compiled into this appendix to the study. This appendix was posted to the website noted above in January 2014.

Feedback/Question:

29. What key findings will be shared or handed off to other government agencies, and when and to which government agencies or governing bodies?

Response:

The Final Report with all of the findings, including this appendix, are available to the public - including other public agencies - on the internet at: http://www.lawa.org/AirQualityStudy/. The monitoring data is available on request to LAWA; it is at the Terabyte level and cannot be put on the website due to its size. Data requests may be submitted by email to airqualitystudy@lawa.org.

Note that those agencies that were members of the Technical Working Group that oversaw this study were informed of the availability of the study report when it was completed.

Feedback/Question:

42. What does the study mean? As individual panel members, what are the conclusions that you draw from these results?

Response:

The Final Report with all of the findings, including this appendix, are available to the public - including other public agencies - on the internet at: http://www.lawa.org/AirQualityStudy/. The monitoring data is available on request to LAWA; it is at the Terabyte level and cannot be put on the website due to its size. Data requests may be submitted by email to airqualitystudy@lawa.org.

The key findings have been summarized in the Final Report, Volume 1 - Executive Summary. The general conclusions are noted below:

In summary, the LAX AQSAS shows that, with the exception of $PM_{2.5}$, the ambient concentrations of criteria pollutants within the communities adjacent to LAX were well below national and state health-based ambient air quality standards and ambient concentrations of air toxic contaminants were generally lower than measured elsewhere in the South Coast Air Basin (SoCAB). The generally lower pollutant concentrations in the LAX area can be attributed to its coastal location in the SoCAB and the typical daytime sea breeze that helps to disperse and transport local emissions inland toward the east. Consequently, the concentrations of most measured pollutants were higher east of LAX compared to monitoring locations north or south of the airport.

Although $PM_{2.5}$ levels were near the standard, a substantial portion of the $PM_{2.5}$ mass is related to the regional urban background with airport-related emissions contributing up to 5 to 20 percent. While UFP have negligible contributions to $PM_{2.5}$ mass, their number concentrations east of the LAX were higher than typical levels in the SoCAB. Supplemental Study measurements at the CE site and behind the South Airfield blast fence indicate that the very small UFP, which have disproportionately higher contributions to particle number concentrations, are largely sulfuric acid aerosol from jet exhaust. The larger UFP, which have disproportionately higher contributions to mass concentrations, appear to be related to on-road vehicle exhaust from local traffic.

The health effects of UFP are largely unknown. A recent review of 300 studies of the health effects of ambient UFP funded by the Health Effects Institute (HEI Perspective 3, January 2013) concluded that experimental and epidemiologic studies provide suggestive, but no consistent evidence of adverse effects of short-term exposure to ambient UFP. At present, a separate health based National Ambient Air Quality Standards (NAAQS) for UFP does not exist. The expectation for effects of UFP is based on their potential to carry toxic material deep into the lungs. In contrast to UFP in vehicle emissions that may be composed of adsorbed organic compounds, UFP associated with jet exhaust are dominated by sulfuric acid aerosol that is rapidly neutralized to relatively benign ammonium sulfate and increases in size due to absorption of water vapor. Future studies of the health impacts of airport emissions will need to consider these important chemical differences between UFP emissions from jet and vehicle exhaust.

Section 6
Other – Noise Pollution

Feedback/Question:

30. I would like to see noise pollution included in the study, without air there is no noise.

Response:

This study was developed solely as an air quality and source apportionment study. Noise was not part of the scope of this study.

Section 7
Other – Health Effects

Feedback/Question:

31. During the public symposium, mention was made to inconclusive results pertaining to UFPs. This question is in regards to not establishing regulatory standards at this point and you said a later study may be conducted. Which study are you referring to? Is it a Health Risk Study?

Response:

Conclusions about the significance of the ultrafine particle number concentrations that were measured cannot be made at this time relative to health or general air quality until more research is done to define what that relationship is. A recent review of the potential UFP health effects was published by the Health Effects Institute in January 2013. That study is available on the internet at: http://pubs.healtheffects.org/getfile.php?u=893. That study is titled "Understanding the Health Effects of Ambient Ultrafine Particles," (accessed on December 16, 2013).

Feedback/Question:

32. Has there been an Epidemiological Study to ascertain the health impacts?

33. What health studies will be or have been done?

34. Wouldn't it be prudent to consider the Precautionary Principal when considering the elevated ultrafine particle levels?

35. Do the chemicals that are higher near the airport affect the health of the people that live near the airport? Why or why not?

41. What are the projected health impacts to humans both on and off airport property? How do government agencies interact with each other on this issue?

Response:

This study was designed and developed to be an air quality source apportionment study; no health effects, impact analysis, or risk assessment was included. However, this study generated a lot of ambient air quality data that could be used by other researchers interested in air quality and health effects near the airport, meeting the secondary objective of the study noted in the Final Report, Volume 2, Section 3, Appendix 3-1 (i.e., the Final Scope of Work, Section 2.1.2, page 2-1).

Feedback/Question:

44. I felt that data was presented clearly as well the communities, but what about those with schools and children with [their] health and the account on the contamination occurring in their locations? I also found it helpful that we can ask questions and have them answered.

Response:

The communities surrounding the airport, including schools, were considered when sites were selected for this study. Several satellite and gradient sites were located on or near residences close to the

airport. Several schools sites were considered, and one former school site was chosen (the Community South [CS] site). As noted in the Final Report, Volume 2, Section 1.2 (beginning on page 1-1), the Study Area for Phase III provided a focused area within which detailed air quality monitoring and modeling analyses could occur with particular attention given to the adjacent communities immediately to the north, east, and south of LAX. A number of sites around the airport were identified which were subjected to the study's site selection process. The monitoring network design, site selection, and objectives are discussed in the Final Report, Volume 2, Section 3.3 (beginning on page 3-4).

The measurements collected also meets the secondary objective of the study noted in the Final Report, Volume 2, Section 3, Appendix 3-1 (i.e., the Final Scope of Work, Section 2.1.2, page 2-1), specifically to provide data for future studies, in terms of outdoor human exposures, meteorological effects on pollutant transport, dispersion and chemical transformation and development of a baseline for evaluating effectiveness of control strategies.

Section 8
Other – Additional Air Quality Studies

Feedback/Question:

36. Please project findings to 2030 when LAX is projected to have one million operations per year as opposed to current 600,000.

37. Based on the pollutant data that you have observed to date (e.g., SO_x), do you recommend a study which would examine possible role of bio-jet fuels made from municipal solid fuels?

38. Will any AQ studies be continued in the CE area? I ask because it had the highest $PM_{2.5}$ levels.

39. What opportunities or plans are there for continuing the LAWA air quality measurements post LAWA AQSAS and how are surrounding communities being informed?

Response:

The scope of this study included measuring the existing (current) ambient air quality around LAX and estimating the airport's contribution to those measurements. It was not part of this study's scope to estimate future impacts or to develop recommendations for future studies or continuous monitoring.

Section 9
Other - Mitigation

Feedback/Question:

40. So much pollution is generated when aircraft are in queue. Why isn't there a priority on fixing this?

43. How can the interpreted results and conclusions translate into policy modifications and other changes that will benefit those most affected by the air contaminants?

Response:

The scope of this study included measuring the existing (current) ambient air quality around LAX and estimating the airport's contribution to those measurements.